



John Campbell

# Complete Casting

## Handbook

Metal Casting Processes, Metallurgy, Techniques and Design



# Complete Casting Handbook

Metal Casting Processes,  
Metallurgy, Techniques  
and Design

*To Sheila once again. She really deserves it.*

# Complete Casting Handbook

Metal Casting Processes,  
Metallurgy, Techniques  
and Design

**John Campbell**

**OBE FREng DEng PhD MMet MA**

*Emeritus Professor of Casting Technology,  
University of Birmingham, UK*



ELSEVIER





Butterworth-Heinemann is an imprint of Elsevier  
The Boulevard, Langford Lane, Kidlington, Oxford OX5 1GB, UK  
225 Wyman Street, Waltham, MA 02451, USA

First edition 2011

Copyright © 2011 John Campbell. Published by Elsevier Ltd. All rights reserved.

The right of John Campbell to be identified as the author of this work has been asserted in accordance with the Copyright, Designs and Patents Act 1988

No part of this publication may be reproduced, stored in a retrieval system or transmitted in any form or by any means electronic, mechanical, photocopying, recording or otherwise without the prior written permission of the publisher

Permissions may be sought directly from Elsevier's Science & Technology Rights Department in Oxford, UK: phone (+44) (0) 1865 843830; fax (+44) (0) 1865 853333; email: [permissions@elsevier.com](mailto:permissions@elsevier.com). Alternatively you can submit your request online by visiting the Elsevier web site at <http://elsevier.com/locate/permissions>, and selecting *Obtaining permission to use Elsevier material*

#### Notice

No responsibility is assumed by the publisher for any injury and/or damage to persons or property as a matter of products liability, negligence or otherwise, or from any use or operation of any methods, products, instructions or ideas contained in the material herein. Because of rapid advances in the medical sciences, in particular, independent verification of diagnoses and drug dosages should be made

#### British Library Cataloguing in Publication Data

A catalogue record for this book is available from the British Library

#### Library of Congress Cataloging-in-Publication Data

A catalog record for this book is available from the Library of Congress

ISBN-13: 978-1-85617-809-9

For information on all Butterworth-Heinemann publications visit our web site at [books.elsevier.com](http://books.elsevier.com)

Printed and bound in the UK

11 12 13 14 15 10 9 8 7 6 5 4 3 2 1

Working together to grow  
libraries in developing countries

[www.elsevier.com](http://www.elsevier.com) | [www.bookaid.org](http://www.bookaid.org) | [www.sabre.org](http://www.sabre.org)

ELSEVIER

BOOK AID  
International

Sabre Foundation

# Contents

Preface .....	xix
Introduction from <i>Castings</i> 1st Edition 1991 .....	xxiii
Introduction to <i>Castings</i> 2nd Edition 2003.....	xxv
Introduction to <i> Casting Practice: The 10 Rules of Castings</i> 2004 .....	xxvii
Introduction to <i>Castings Handbook</i> 2011 .....	xxix
Acknowledgments.....	xxxii

## **VOLUME I CASTING METALLURGY**

---

<b>CHAPTER 1 The melt.....</b>	<b>3</b>
1.1 Reactions of the melt with its environment .....	5
1.2 Transport of gases in melts.....	9
1.3 Surface film formation.....	13
1.4 Vaporization .....	16
<b>CHAPTER 2 Entrainment .....</b>	<b>19</b>
2.1 Entrainment defects .....	24
2.1.1 Bifilms .....	24
2.1.2 Bubbles .....	28
2.1.3 Extrinsic inclusions .....	32
2.2 Entrainment processes .....	42
2.2.1 Surface turbulence.....	42
2.2.2 Oxide skins from melt charge materials.....	52
2.2.3 Pouring.....	54
2.2.4 The oxide lap defect I: Surface flooding .....	57
2.2.5 The oxide lap defect II: The confluence weld.....	60
2.2.6 The oxide flow tube.....	64
2.2.7 Microjetting .....	65
2.2.8 Bubble trails .....	67
2.3 Furling and unfurling.....	77
2.4 Deactivation of entrained films.....	88
2.5 Soluble, transient films .....	92
2.6 Detrainment.....	92
2.7 Evidence for bifilms.....	94
2.8 The importance of bifilms .....	100

<b>CHAPTER 3 Flow</b> .....	<b>105</b>
<b>3.1</b> Effect of surface films on filling.....	105
3.1.1 Effective surface tension.....	105
3.1.2 The rolling wave.....	106
3.1.3 The unzipping wave.....	108
<b>3.2</b> Maximum fluidity (the science of unrestricted flow).....	110
3.2.1 Mode of solidification.....	113
3.2.2 Effect of velocity.....	126
3.2.3 Effect of viscosity (including effect of entrained bifilms).....	128
3.2.4 Effect of solidification time $t_f$ .....	130
3.2.5 Effect of surface tension.....	140
3.2.6 Effect of an unstable substrate.....	143
3.2.7 Comparison of fluidity tests.....	144
<b>3.3</b> Extended fluidity.....	148
<b>3.4</b> Continuous fluidity.....	151
<b>CHAPTER 4 Molds and cores</b> .....	<b>155</b>
<b>4.1</b> Molds: Inert or reactive.....	155
<b>4.2</b> Transformation zones.....	156
<b>4.3</b> Evaporation and condensation zones.....	159
<b>4.4</b> Mold atmosphere.....	164
4.4.1 Composition.....	164
4.4.2 Mold gas explosions.....	166
<b>4.5</b> Mold surface reactions.....	168
4.5.1 Pyrolysis.....	168
4.5.2 Lustrous carbon film.....	170
4.5.3 Sand reactions.....	171
4.5.4 Mold contamination.....	171
4.5.5 Mold penetration.....	173
<b>4.6</b> Metal surface reactions.....	178
4.6.1 Oxidation.....	178
4.6.2 Carbon (pick-up and loss).....	179
4.6.3 Nitrogen.....	181
4.6.4 Sulfur.....	181
4.6.5 Phosphorus.....	181
4.6.6 Surface alloying.....	182
4.6.7 Grain refinement.....	182
4.6.8 Miscellaneous.....	183
<b>4.7</b> Mold coatings.....	183
4.7.1 Aggregate molds.....	183

4.7.2 Permanent molds and metal chills .....	185
4.7.3 Dry coatings .....	186
<b>CHAPTER 5 Solidification structure .....</b>	<b>187</b>
5.1 Heat transfer .....	187
5.1.1 Resistances to heat transfer .....	187
5.1.2 Increased heat transfer .....	202
5.1.3 Convection .....	219
5.1.4 Remelting .....	219
5.1.5 Flow channel structure .....	220
5.2 Development of matrix structure .....	224
5.2.1 General .....	224
5.2.2 Nucleation of the solid .....	225
5.2.3 Growth of the solid .....	228
5.2.4 Disintegration of the solid (grain multiplication) .....	236
5.3 Segregation .....	241
5.3.1 Planar front segregation .....	242
5.3.2 Microsegregation .....	245
5.3.3 Dendritic segregation .....	247
5.3.4 Gravity segregation .....	250
<b>CHAPTER 6 Casting alloys .....</b>	<b>255</b>
6.1 Zinc alloys .....	255
6.2 Magnesium .....	260
6.2.1 Films on liquid Mg alloys and protective atmospheres .....	261
6.2.2 Strengthening Mg alloys .....	266
6.2.3 Microstructure .....	268
6.3 Aluminum .....	269
6.3.1 Oxide films on Al alloys .....	271
6.3.2 Entrained inclusions .....	273
6.3.3 Grain refinement (nucleation and growth of the solid) .....	274
6.3.4 DAS and grain size .....	278
6.3.5 Modification of eutectic Si in Al–Si alloys .....	279
6.3.6 Iron-rich intermetallics .....	298
6.3.7 Other intermetallics .....	303
6.3.8 Thermal analysis of Al alloys .....	305
6.3.9 Hydrogen in Al alloys .....	306
6.4 Copper .....	309
6.4.1 Surface films .....	310
6.4.2 Gases in Cu-based alloys .....	310
6.4.3 Grain refinement .....	315

<b>6.5</b>	Cast iron .....	315
6.5.1	Reactions with gases .....	316
6.5.2	Surface films on liquid cast irons .....	318
6.5.3	Cast iron microstructures .....	332
6.5.4	Flake graphite iron (FGI) and inoculation .....	334
6.5.5	Nucleation and growth of the austenite matrix .....	343
6.5.6	Coupled eutectic growth of graphite and austenite .....	345
6.5.7	Spheroidal graphite iron (SGI) (ductile iron) .....	347
6.5.8	Compacted graphite iron (CGI) .....	355
6.5.9	Chunky graphite (CHG) .....	357
6.5.10	White iron (iron carbide) .....	359
6.5.11	General .....	360
6.5.12	Summary of structure hypothesis .....	360
<b>6.6</b>	Steels .....	362
6.6.1	Carbon steels .....	362
6.6.2	Stainless steels .....	363
6.6.3	Inclusions in carbon and low-alloy steels (general background) .....	365
6.6.4	Entrained inclusions .....	367
6.6.5	Primary inclusions .....	370
6.6.6	Secondary inclusions and second phases .....	374
6.6.7	Nucleation and growth of the solid .....	377
6.6.8	Structure development in the solid .....	380
<b>6.7</b>	Nickel-base alloys .....	382
6.7.1	Air melting and casting .....	383
6.7.2	Vacuum melting and casting .....	383
<b>6.8</b>	Titanium .....	386
6.8.1	Ti alloys .....	387
6.8.2	Melting and casting Ti alloys .....	387
6.8.3	Surface films on Ti alloys .....	389
<b>CHAPTER 7</b>	<b>Porosity .....</b>	<b>391</b>
<b>7.1</b>	Shrinkage porosity .....	391
7.1.1	General shrinkage behavior .....	391
7.1.2	Solidification shrinkage .....	392
7.1.3	Feeding criteria .....	399
7.1.4	Feeding: The five mechanisms .....	403
7.1.5	Initiation of shrinkage porosity .....	418
7.1.6	Growth of shrinkage pores .....	436
7.1.7	Shrinkage pore structure .....	436

7.2	Gas porosity .....	443
7.2.1	Entrained (external) pores .....	443
7.2.2	Blow holes .....	445
7.2.3	Gas porosity initiated in situ .....	445
7.3	Porosity diagnosis .....	461
<b>CHAPTER 8</b>	<b>Cracks and tears .....</b>	<b>465</b>
8.1	Hot tearing .....	465
8.1.1	General.....	465
8.1.2	Grain boundary wetting by the liquid.....	469
8.1.3	Pre-tear extension .....	470
8.1.4	Strain concentration.....	472
8.1.5	Stress concentration.....	473
8.1.6	Tear initiation .....	474
8.1.7	Tear growth.....	476
8.1.8	Prediction of hot tearing susceptibility .....	479
8.1.9	Methods of testing.....	483
8.1.10	Methods of control .....	489
8.1.11	Summary of the conditions for hot tearing and porosity .....	493
8.1.12	Hot tearing in stainless steels.....	494
8.1.13	Predictive techniques.....	495
8.2	Cold cracking.....	495
8.2.1	General.....	495
8.2.2	Crack initiation.....	496
8.2.3	Crack growth .....	497
<b>CHAPTER 9</b>	<b>Properties of castings.....</b>	<b>499</b>
9.1	Test bars .....	499
9.2	The statistics of failure .....	504
9.2.1	Background to the use of Weibull analysis .....	507
9.2.2	Two-parameter Weibull analysis.....	510
9.2.3	Three-parameter Weibull analysis.....	511
9.2.4	Bi-Weibull distributions .....	512
9.2.5	Limits of accuracy.....	514
9.2.6	Extreme value distributions.....	516
9.3	Effect of defects.....	516
9.3.1	Inclusion types and diagnosis .....	517
9.3.2	Gas porosity.....	520
9.3.3	Shrinkage porosity.....	525
9.3.4	Tears, cracks, and bifilms.....	526

<b>9.4</b>	Tensile properties .....	529
9.4.1	Microstructural failure.....	529
9.4.2	Ductility .....	533
9.4.3	Yield strength .....	539
9.4.4	Ultimate tensile strength .....	553
<b>9.5</b>	Fracture toughness .....	555
<b>9.6</b>	Fatigue.....	561
9.6.1	High cycle fatigue .....	561
9.6.2	Low cycle and thermal fatigue.....	571
<b>9.7</b>	Elastic (Young’s) modulus and damping capacity .....	573
<b>9.8</b>	Residual stress.....	574
<b>9.9</b>	High-temperature tensile properties .....	575
9.9.1	Creep.....	575
9.9.2	Superplastic forming .....	576
<b>9.10</b>	Oxidation and corrosion resistance .....	578
9.10.1	Internal oxidation .....	578
9.10.2	Corrosion .....	579
9.10.3	Pitting corrosion .....	582
9.10.4	Filiform corrosion .....	584
9.10.5	Intergranular corrosion.....	585
9.10.6	Stress corrosion cracking .....	586
<b>9.11</b>	Leak-tightness .....	587
<b>9.12</b>	Surface finish .....	591
9.12.1	Effect of surface tension .....	591
9.12.2	Effects of a solid surface film.....	593
<b>9.13</b>	Quality indices .....	594
References.....		RI-1

## VOLUME 2 CASTING MANUFACTURE

---

### Section 1

<b>CHAPTER 10</b>	<b>The 10 Rules for good castings.....</b>	<b>605</b>
<b>10.1</b>	Rule 1: ‘Use a good-quality melt’ .....	607
10.1.1	Background .....	607
<b>10.2</b>	Rule 2: ‘Avoid turbulent entrainment’ (the critical velocity requirement).....	614
10.2.1	Introduction .....	614
10.2.2	Maximum velocity requirement.....	615
10.2.3	The ‘no-fall’ requirement.....	619

<b>10.3</b>	Rule 3: ‘Avoid laminar entrainment of the surface film’ (the non-stopping, non-reversing condition).....	623
	10.3.1 Continuous expansion of the meniscus .....	623
	10.3.2 Arrest of forward motion of the meniscus .....	624
	10.3.3 Waterfall flow; the oxide flow tube .....	625
	10.3.4 Horizontal stream flow .....	627
	10.3.5 Hesitation and reversal.....	629
	10.3.6 Oxide lap defects.....	630
<b>10.4</b>	Rule 4: ‘Avoid bubble damage’ .....	631
	10.4.1 The bubble trail .....	631
	10.4.2 Bubble damage.....	632
	10.4.3 Bubble damage in gravity filling systems .....	633
	10.4.4 Bubble damage in counter-gravity systems.....	634
<b>10.5</b>	Rule 5: ‘Avoid core blows’ .....	635
	10.5.1 Background .....	635
	10.5.2 Outgassing pressure in cores.....	647
	10.5.3 Core blow model study .....	653
	10.5.4 Microblows.....	654
	10.5.5 Prevention of blows.....	655
	10.5.6 Summary of blow prevention.....	659
<b>10.6</b>	Rule 6: ‘Avoid shrinkage damage’ .....	659
	10.6.1 Definitions and background .....	659
	10.6.2 Feeding to avoid shrinkage problems.....	660
	10.6.3 The seven feeding rules .....	661
	10.6.4 The new feeding logic.....	688
	10.6.5 Freezing systems design (chills and fins).....	692
	10.6.6 Feeding – the five mechanisms.....	692
	10.6.7 Computer modeling of feeding .....	694
	10.6.8 Random perturbations to feeding.....	694
	10.6.9 The non-feeding roles of feeders .....	695
<b>10.7</b>	Rule 7: ‘Avoid convection damage’ .....	696
	10.7.1 The academic background .....	696
	10.7.2 The engineering imperatives.....	697
	10.7.3 Convection damage and casting section thickness.....	701
	10.7.4 Countering convection .....	704
<b>10.8</b>	Rule 8: ‘Reduce segregation damage’ .....	705
<b>10.9</b>	Rule 9: ‘Reduce residual stress’ .....	707
	10.9.1 Introduction .....	707
	10.9.2 Residual stress from casting .....	708
	10.9.3 Residual stress from quenching .....	712



10.9.4	Controlled quenching using polymer and other quenchant	716
10.9.5	Controlled quenching using air	719
10.9.6	Strength reduction by heat treatment	720
10.9.7	Distortion	722
10.9.8	Heat treatment developments	723
10.9.9	Beneficial residual stress	724
10.9.10	Stress relief	725
10.9.11	Epilogue	728
<b>10.10</b>	<b>Rule 10: ‘Provide location points’</b>	<b>728</b>
10.10.1	Datums	729
10.10.2	Location points	730
10.10.3	Location jigs	736
10.10.4	Clamping points	736
10.10.5	Potential for integrated manufacture	737

## Section 2 Filling system design

### CHAPTER 11 Filling system design fundamentals ..... 741

11.1	The maximum velocity requirement	741
11.2	Gravity pouring – The ‘no-fall’ conflict	741
11.3	Reduction or elimination of gravity problems	745
11.4	Surface-tension-controlled filling	751

### CHAPTER 12 Filling system components ..... 757

12.1	Pouring basin	757
12.1.1	The conical basin	757
12.1.2	Inert gas shroud	760
12.1.3	Contact pouring	761
12.1.4	The offset basin	762
12.1.5	The offset step (weir) basin	762
12.1.6	The sharp-cornered or undercut basin	769
12.1.7	Stopper	771
12.2	Sprue (down-runner)	772
12.2.1	Multiple sprues	778
12.2.2	Division of sprues	780
12.2.3	Sprue base	781
12.2.4	The well	782
12.2.5	The radial choke	785
12.2.6	The radius of the sprue/runner junction	785
12.3	Runner	787
12.3.1	The tapered runner	792

12.3.2	The expanding runner .....	793
<b>12.4</b>	<b>Gates .....</b>	<b>795</b>
12.4.1	Siting .....	795
12.4.2	Direct and indirect.....	795
12.4.3	Total area of gate(s) .....	796
12.4.4	Gating ratio.....	797
12.4.5	Multiple gates.....	798
12.4.6	Premature filling problem via early gates .....	798
12.4.7	Horizontal velocity in the mold.....	799
12.4.8	Junction effect .....	800
12.4.9	The touch gate.....	803
12.4.10	Knife gate .....	805
12.4.11	The pencil gate.....	806
12.4.12	The horn gate .....	806
12.4.13	Vertical gate.....	809
12.4.14	Direct gating into the mold cavity.....	809
12.4.15	Flow channel structure .....	810
12.4.16	Indirect gating (into an up-runner/riser) .....	811
12.4.17	Central versus external systems.....	814
12.4.18	Sequential gating.....	815
12.4.19	Priming techniques.....	817
<b>12.5</b>	<b>Surge control systems.....</b>	<b>819</b>
<b>12.6</b>	<b>Vortex systems .....</b>	<b>823</b>
12.6.1	Vortex sprue.....	823
12.6.2	Vortex well or gate.....	824
12.6.3	Vortex runner (the offset sprue).....	825
<b>12.7</b>	<b>Inclusion control: Filters and traps.....</b>	<b>826</b>
12.7.1	Dross trap (slag trap).....	827
12.7.2	Slag pockets .....	828
12.7.3	Swirl trap.....	829
<b>12.8</b>	<b>Filters .....</b>	<b>833</b>
12.8.1	Strainers.....	833
12.8.2	Woven cloth or mesh .....	834
12.8.3	Ceramic block filters.....	838
12.8.4	Leakage control.....	840
12.8.5	Filters in running systems .....	846
12.8.6	Tangential placement .....	848
12.8.7	Direct pour .....	850
12.8.8	Sundry aspects.....	851
12.8.9	Summary .....	852

<b>CHAPTER 13 Filling system design practice .....</b>	<b>853</b>
<b>13.1</b> Background to the methoding approach .....	854
<b>13.2</b> Selection of a layout.....	854
<b>13.3</b> Weight and volume estimate .....	854
<b>13.4</b> Pressurized versus unpressurized .....	857
<b>13.5</b> Selection of a pouring time .....	862
<b>13.6</b> Thin sections and slow filling .....	865
<b>13.7</b> Fill rate.....	866
<b>13.8</b> Pouring basin design.....	867
<b>13.9</b> Sprue (down-runner) design .....	867
<b>13.10</b> Runner design.....	871
<b>13.11</b> Gate design .....	873

### **Section 3 Processing (melting, molding, casting, solidifying)**

<b>CHAPTER 14 Melting .....</b>	<b>879</b>
<b>14.1</b> Batch melting.....	879
14.1.1 Liquid metal delivery.....	879
14.1.2 Reverberatory furnaces.....	880
14.1.3 Crucible melting (electric resistance or gas heated) .....	881
14.1.4 Induction melting .....	882
14.1.5 Automatic bottom pouring.....	882
<b>14.2</b> Continuous melting.....	883
14.2.1 Tower (shaft) furnaces.....	883
14.2.2 Dry hearth furnaces for non-ferrous metals .....	884
<b>14.3</b> Holding, transfer and distribution .....	885
14.3.1 Holder failure modes.....	887
14.3.2 Transfer and distribution systems .....	888
<b>14.4</b> Melt treatments .....	888
14.4.1 Degassing .....	888
14.4.2 Detrainment (cleaning) .....	896
14.4.3 Additions .....	901
14.4.4 Pouring .....	902
<b>14.5</b> Cast material .....	905
14.5.1 Liquid metal .....	905
14.5.2 Partially solid mixtures .....	905
<b>14.6</b> Remelting processes .....	909
14.6.1 Vacuum arc remelting (VAR) .....	909
14.6.2 Electro-slag remelting (ESR).....	910

<b>CHAPTER 15 Molding.....</b>	<b>911</b>
<b>15.1 Inert molds and cores .....</b>	<b>911</b>
15.1.1 Permanent metal molds (dies) .....	912
15.1.2 Salt cores .....	914
15.1.3 Ceramic molds and cores.....	915
15.1.4 Magnetic molding .....	917
<b>15.2 Aggregate molding materials .....</b>	<b>918</b>
15.2.1 Silica sand .....	919
15.2.2 Chromite sand .....	920
15.2.3 Olivine sand.....	920
15.2.4 Zircon sand.....	921
15.2.5 Other minerals.....	921
15.2.6 Carbon .....	922
<b>15.3 Binders .....</b>	<b>923</b>
15.3.1 Greensand.....	923
15.3.2 Dry sand .....	924
15.3.3 Chemical binders.....	924
15.3.4 Effset process (ice binder) .....	929
15.3.5 Loam.....	929
15.3.6 Cement.....	930
15.3.7 Fluid (castable) sand .....	930
<b>15.4 Other aggregate mold processes.....</b>	<b>931</b>
15.4.1 Precision core assembly .....	931
15.4.2 Machined-to-form .....	931
15.4.3 Unbonded aggregate molds.....	931
<b>15.5 Rubber molds.....</b>	<b>931</b>
<b>15.6 Reclamation and recycling of aggregates .....</b>	<b>932</b>
15.6.1 Aggregate reclamation in an Al foundry.....	932
15.6.2 Aggregate reclamation in a ductile iron foundry .....	935
15.6.3 Aggregate reclamation with soluble inorganic binders.....	936
15.6.4 Facing and backing sands .....	937
<b>CHAPTER 16 Casting.....</b>	<b>939</b>
<b>16.1 Gravity casting.....</b>	<b>939</b>
16.1.1 Gravity pouring of open molds.....	939
16.1.2 Gravity pouring of closed molds .....	940
16.1.3 Two-stage filling (priming techniques).....	944
16.1.4 Vertical stack molding .....	945
16.1.5 Horizontal stack molding (H process).....	945
16.1.6 Postscript to gravity filling.....	945

16.2	Horizontal transfer casting .....	946
16.2.1	Level pour (side pour).....	946
16.2.2	Controlled tilt casting.....	948
16.2.3	Roll-over as a casting process .....	955
16.2.4	Roll-over after casting (sometimes called inversion casting) .....	957
16.3	Counter-gravity .....	960
16.3.1	Low-pressure casting.....	963
16.3.2	Liquid metal pumps .....	968
16.3.3	Direct vertical injection .....	974
16.3.4	Programmable control.....	977
16.3.5	Feedback control .....	977
16.3.6	Failure modes of low-pressure casting .....	978
16.4	Centrifugal casting.....	979
16.5	Pressure-assisted casting.....	985
16.5.1	High-pressure die casting (HPDC) .....	986
16.5.2	Squeeze casting .....	991
16.6	Lost wax and other ceramic mold casting processes.....	997
16.7	Lost foam casting .....	1001
16.8	Vacuum molding (V process).....	1005
16.9	Vacuum-assisted casting .....	1008
16.10	Vacuum melting and casting .....	1009
<b>CHAPTER 17</b>	<b>Controlled solidification techniques .....</b>	<b>1013</b>
17.1	Conventional-shaped castings.....	1013
17.2	Directional solidification (DS) .....	1014
17.3	Single crystal solidification .....	1016
17.4	Rapid solidification casting .....	1018
<b>CHAPTER 18</b>	<b>Dimensional accuracy.....</b>	<b>1025</b>
18.1	The concept of net shape.....	1029
18.1.1	Effect of casting process .....	1030
18.1.2	Effect of expansion and contraction .....	1032
18.1.3	Effect of cast alloy .....	1032
18.2	Mold design .....	1033
18.2.1	General issues.....	1033
18.2.2	Assembly methods .....	1035
18.3	Mold accuracy .....	1038
18.3.1	Aggregate molds .....	1038
18.3.2	Ceramic molds .....	1041
18.3.3	Metal molds (dies) .....	1042
18.4	Tooling accuracy.....	1045

18.5	Casting accuracy.....	1046
18.5.1	Uniform contraction.....	1046
18.5.2	Non-uniform contraction (distortion).....	1053
18.5.3	Process comparison.....	1061
18.5.4	General summary.....	1063
18.6	Metrology.....	1063
<b>CHAPTER 19</b>	<b>Post-casting processing.....</b>	<b>1067</b>
19.1	Surface cleaning.....	1067
19.2	Heat treatment.....	1069
19.2.1	Homogenization and solution treatments.....	1070
19.2.2	Heat treatment reduction and/or elimination.....	1072
19.2.3	Blister formation.....	1073
19.2.4	Incipient melting.....	1074
19.2.5	Fluid beds.....	1075
19.3	Hot isostatic pressing.....	1077
19.4	Machining.....	1080
19.5	Painting.....	1083
19.6	Plastic working (forging, rolling, extrusion).....	1083
19.7	Impregnation.....	1085
19.8	Non-destructive testing.....	1086
19.8.1	X-ray radiography.....	1086
19.8.2	Dye-penetrant inspection (DPI).....	1087
19.8.3	Leak testing.....	1087
19.8.4	Resonant frequency testing.....	1088
	References.....	RII-1
	Appendix 1.....	1091
	Appendix 2.....	1095
	Appendix 3.....	1099
	Index.....	1103

This page intentionally left blank

# Preface

Metal castings are fundamental building blocks, the three-dimensional integral shapes indispensable to practically all other manufacturing industries.

Although the manufacturing path from the liquid to the finished shape is the most direct, this directness involves the greatest difficulty. This is because so much needs to be controlled simultaneously, including melting, alloying, molding, pouring, solidification, finishing, etc. Every one of these production steps has to be correct since failure of only one will probably cause the whole product to be unacceptable to the customer. In contrast, other processes such as forging or machining are merely single-step processes. It is clearly easier to control each separate process step in turn.

It is no wonder therefore that the manufacture of castings is one of the most challenging of technologies. It has defied proper understanding and control for an impressive five thousand years. However, there are signs that we might now be starting to make progress.

Naturally, this claim for the possible existence of progress appears to have been made by every writer of textbooks on castings for the last several hundred years. Doubtless, it will continue to be made in future generations. In a way, it is hoped that it will always be true. This is what makes casting so fascinating. The complexity of the subject invites a continuous stream of new ideas and new solutions.

The author trained as a physicist and physical metallurgist, and is aware of the admirable and powerful developments in science and technology that have facilitated the progress enjoyed by these branches of science. These successes have, quite naturally, persuaded the Higher Educational Institutes throughout the world to the adoption of *physical metallurgy* as the natural materials discipline required to be taught.

This work makes the case for *process metallurgy* as being a key discipline, inseparable from physical metallurgy. It can explain the properties of metals, in some respects outweighing the effects of alloying, working and heat treatment that are the established province of physical metallurgy. In particular, the study of casting technology is a topic of daunting complexity, far more encompassing than the separate studies, for instance, of fluid flow or solidification (as necessary, important and fascinating as such focused studies clearly are). It is hoped therefore that, in time, casting technology will be rightly recognized as a complex and vital engineering discipline, worthy of individual focus.

Prior to writing this book, the author has always admired those who have published only what was certain knowledge. However, as this work was well under way, it became clear to him that this was not achievable in this case. Knowledge is hard to achieve, and often illusive, fragmentary, and ultimately uncertain. This book is offered as an exercise in education, more to do with thinking and understanding than learning. It is an exercise in grappling with new concepts and making personal evaluations of their worth, their cogency, and their place amid the scattering of facts, some reliable, others less so. It is about research, and about the excitement of finding out for oneself.

Thus the opportunity has been taken in this new book to bring the work up to date, particularly in the new and exciting areas of surface turbulence, the recently discovered compaction and unfurling of folded film defects (the bifilms). Additional new concepts of alloy theory relating to the common alloy eutectics Al–Si and Fe–C will be outlined. These are particularly exciting. Perhaps these new paradigms can never be claimed to be ‘true’. They are offered as potentially valuable theories allowing us to codify and classify our knowledge until something better comes along. Newton’s theory of



gravitation was a welcome and extraordinarily valuable systematization of our knowledge for several hundred years until surpassed by Einstein's General Relativity.

Thus the author has allowed himself the luxury of hypothesis, that a skeptic might brand speculation. This book is a first attempt to codify and present what I like to call the 'New Metallurgy'. It cannot claim to be authoritative on all aspects at this time. It is an introduction to the new thinking of the metallurgy of cast alloys, and, by virtue of the survival of many of the casting defects during plastic working, wrought alloys too.

The intellectual problem that some have in accepting the existence of bifilms is curious. The problem of acceptance does not seem to exist in processes such as powder metallurgy, and the various spray-forming technologies, where everyone immediately realizes 'bifilms' exist if they give the matter a moment's thought. The difference between these particle technologies and castings is that the particulate routes have rather regular bifilm populations, leading to reproducible properties. Similar rather uniform but larger-scale bifilms can be seen in slowly collapsing metallic foams, in which it is extraordinary to watch the formation of bifilms in slow motion as one oxide film settles gently down on its neighbor (Mukherjee 2010). Castings in contrast can have coexisting populations of defects sometimes taking the form of fogs of fine particles, scatterings of confetti and postage stamps, and sometimes sheets of A4 and quarto paper sized defects.

The new concept of the bifilm involves a small collection of additional terms and definitions which are particularly helpful in designing filling and feeding systems for castings and understanding casting failure mechanisms. They include critical velocity, critical fall distance, entrainment, surface turbulence, the bubble trail, hydrostatic tensions in liquids, constrained flow, and the naturally pressurized filling system. They represent the software of the new technology, while its study is facilitated by the new hardware of X-ray video radiography and computer simulation. These are all powerful investigative tools that have made our recent studies so exciting and rewarding.

Despite all the evidence, at the time of writing there appear to be many in industry and research still denying the existence of bifilms. It brings to mind the situation in the early 1900s when, once again despite overwhelming evidence, many continued to deny the existence of atoms.

The practice of seeking corroboration of scientific concepts from industrial experience, used often in this book, is a departure that will be viewed with concern by those academics who are accustomed to the apparent rigor of laboratory experiments and who are not familiar with the current achievements of industry. However, for those who persevere and grow to understand this work it will become clear that laboratory experiments cannot at this time achieve the control over liquid metal quality that can now be routinely provided in many industrial operations. Thus the evidence from industry is vital at this time. Suitable confirmatory experiments in laboratories can catch up later.

The primary aim remains, to challenge the reader to think through the concepts that will lead to a better understanding of the casting process – the most complex of forming operations. It is hoped thereby to improve the professionalism and status of casting technology, and with it the castings themselves, so that both the industry and its customers will benefit.

As I mentioned in the preface to *CASTINGS 1991*, and bears repeat here, the rapidity of casting developments makes it a privilege to live in such exciting times. For this reason, however, it will not be possible to keep this work up to date. It is hoped that, as before, this new edition will serve its purpose

for a time; assisting foundry people to overcome their everyday problems and metallurgists to understand their alloys. Furthermore, I hope it will inspire students and casting engineers alike to continue to keep themselves updated. The regular reading of new developments in the casting journals, and attendance at technical meetings of local societies, will encourage the professionalism to achieve even higher standards of castings in the future.

**JC**  
**Ledbury, Herefordshire, England**  
23 November 2010

This page intentionally left blank

# Introduction from *Castings*

## 1st Edition 1991

Castings can be difficult to get right. Creating things never is easy. But sense the excitement of this new arrival:

The first moments of creation of the new casting are an explosion of interacting events; the release of quantities of thermal and chemical energy trigger a sequence of cataclysms.

The liquid metal attacks and is attacked by its environment, exchanging alloys, impurities, and gas. The surging and tumbling flow of the melt through the running system can introduce clouds of bubbles and Sargasso seas of oxide film. The mould shocks with the vicious blast of heat, buckling and distending, fizzing with the volcanic release of vapours that flood through the liquid metal by diffusion, or reach pressures to burst the liquid surface as bubbles.

During freezing, liquid surges through the dendrite forest to feed the volume contraction on solidification, washing off branches, cutting flow paths, and polluting regions with excess solute, forming segregates. In those regions cut off from the flow, continuing contraction causes the pressure in the residual liquid to fall, possibly becoming negative (as a tensile stress in the liquid) and sucking in the solid surface of the casting. This will continue until the casting is solid, or unless the increasing stress is suddenly dispelled by an explosive expansion of a gas or vapour cavity giving birth to a shrinkage cavity.

The surface sinks are halted, but the internal defects now start.

The subsequent cooling to room temperature is no less dramatic. The solidified casting strives to contract whilst being resisted by the mould. The mould suffers, and may crush and crack. The casting also suffers, being stretched as on a rack. Silent, creeping strain and stress change and distort the casting, and may intensify to the point of catastrophic failure, tearing it apart, or causing insidious thin cracks. Most treacherous of all, the strain may *not quite* crack the casting, leaving it apparently perfect, but loaded to the brink of failure by internal residual stress.

These events are rapidly changing dynamic interactions. It is this rapidity, this dynamism, that characterises the first seconds and minutes of the casting's life. An understanding of them is crucial to success.

This new work is an attempt to provide a framework of guidelines together with the background knowledge to ensure understanding; to avoid the all too frequent disasters; to cultivate the targeting of success; to encourage a professional approach to the design and manufacture of castings.

The reader who learns to guide the production methods through this minefield will find the rare reward of a truly creative profession. The student who has designed the casting method, and who is present when the mould is opened for the first time will experience the excitement and anxiety, and find himself asking the question asked by all foundry workers on such occasions: 'Is it all there?' The casting design rules in this text are intended to provide, so far as present knowledge will allow, enough predictive capability to know that the casting will be not only all there, but all right!

The clean lines of the finished engineering casting, sound, accurate, and strong, are a pleasure to behold. The knowledge that the casting contains neither defects nor residual stress is an additional powerful reassurance. It represents a miraculous transformation from the original two-dimensional form on paper or the screen to a three-dimensional shape, from a mobile liquid to a permanently shaped, strong solid. It is an achievement worthy of pride.

The reader will need some background knowledge. The book is intended for final year students in metallurgy or engineering, for those researching in castings, and for casting engineers and all associated with foundries that have to make a living creating castings.

Good luck!

# Introduction to *Castings* 2nd Edition 2003

I hope the reader will find inspiration from this work.

What is presented is a new approach to the metallurgy of castings. Not everything in the book can claim to be proven at this stage. The author has to admit that he felt compelled to indulge in what the hard line scientist would dismissively label 'reckless speculation'. Ultimately however, science works by proposing hypotheses, which, if they prove to be useful, can have long and respectable lives, irrespective whether they are 'true' or not. Newton's theory of gravitation was such a hypothesis. It was, and remains, respectable and useful, even though eventually proven inaccurate. The hypotheses relating to the metallurgy of cast metals, proposed in this work, are similarly tendered as being at least useful. Perhaps we may never be able to say for certain that they are really 'true', but in the meantime it is proposed as a piece of knowledge as reliable as can now be assembled (Ziman 2001). Moreover, it is believed that a coherent framework for an understanding of cast metals has been achieved for the first time.

The fundamental starting point is the bifilm, the folded-in surface film. It is often invisible, having escaped detection for millennia. Because the presence of bifilms has been unknown, the initiation events for our commonly seen defects such as porosity, cracks and tears have been consistently overlooked.

It is not to be expected that all readers will be comfortable with the familiar, cosy concepts of 'gas' porosity and 'shrinkage' porosity relegated to being mere consequences, simply macroscopic and observable outcomes, growth forms derived from the new bifilm defect, and at times relatively unimportant compared to the pre-existing bifilm itself. Many of us will have to re-learn our metallurgy of cast metals. Nevertheless, I hope that the reader will overcome any doubts and prejudice, and persevere bravely. The book was not written for the faint-hearted.

As a final blow (the reader needs resilience!), the book nowhere claims that good castings are easily achieved. As was already mentioned in the Preface, the casting process is among the most complex of all engineering production systems. We currently need all the possible assistance to our understanding to solve the problems to achieve adequate products. In particular, it follows that the section on casting manufacture is mandatory reading for metallurgists and academics alike.

For the future, we can be inspired to strive for, and perhaps one day achieve defect-free cast products. At that moment of history, when the bifilm is banished, we shall have automatically achieved that elusive goal, targeted by every foundry I know, '*highest quality together with minimum costs*'.

This page intentionally left blank

# Introduction to *Casting Practice:* *The 10 Rules of Castings* 2004

The second book is effectively my own checklist to ensure that no key aspect of the design of the manufacturing route for the casting is forgotten. The Ten Rules are first listed in summary form. They are then addressed in more detail in the following ten chapters with one chapter per Rule.

The Ten Rules listed here are proposed as necessary, but not, of course, sufficient, for the manufacture of reliable castings. It is proposed that they are used in addition to existing necessary technical specifications such as alloy type, strength, and traceability via international standard quality systems, and other well known and well understood foundry controls such as casting temperature etc.

Although not yet tested on all cast materials, there are fundamental reasons for believing that the Rules have general validity. They have been applied to many different alloy systems including aluminium, zinc, magnesium, cast irons, steels, air- and vacuum-cast nickel and cobalt, and even those based on the highly reactive metals titanium and zirconium. Nevertheless, of course, although all materials will probably benefit from the application of the Rules, some will benefit almost out of recognition, whereas others will be less affected.

The Rules originated when emerging from a foundry on a memorable sunny day together with indefatigable Boeing enthusiasts for castings, Fred Feiertag and Dale McLellan. The author was lamenting that the casting industry had specifications for alloys, casting properties, and casting quality checking systems, but what did not exist but was most needed was a *process specification*. Dale threw out a challenge: 'Write one' The Rules and this book are the outcome. It was not perhaps the outcome that either Dale or I originally imagined. A Process Specification has proved elusive, proving so difficult that I have concluded that it will need a more accomplished author.

The Rules as they stand therefore constitute a first draft of a Process Specification; more like a checklist of casting guidelines. A buyer of castings would demand that the list were fulfilled if he wished to be assured that he was buying the best possible casting quality. If he were to specify the adherence to these Rules by the casting producer, he would ensure that the quality and reliability of the castings was higher than could be achieved by any amount of expensive checking of the quality of the finished product.

Conversely, of course, the Rules are intended to assist the casting manufacturer. It will speed up the process of producing the casting right first time, and should contribute in a major way to the reduction of scrap when the casting goes into production. In this way the caster will be able to raise standards, without any significant increase in costs. Quality will be raised to the point at which casting a quality equal to that of forgings can be offered with confidence. Only in this way will castings be accepted by the engineering profession as reliable, engineered products, and assure the future prosperity of both the casting industry and its customers.

A further feature of the list of Rules that emerged as the book was being written was the dominance of the sections on the design of the filling systems of castings. It posed the obvious question 'why not devote the book completely to filling systems?' I decided against this option on the grounds that both caster and customer require products that are good in *every* respect. The failure of any one aspect may endanger the casting. Therefore, despite the enormous disparity in length, no Rule could be eliminated; they were all needed.

Finally, it is worth making some general points about the whole philosophy of making castings.



For a successful casting operation, one of the revered commercial goals is the attainment of product sales being at least equal to manufacturing costs. There are numerous other requirements for the successful business, like management, plant and equipment, maintenance, accounting, marketing, negotiating etc. All have to be adequate, otherwise the business can suffer, and even fail.

This text deals only with the technical issues of the quest for good castings. Without good castings it is not easy to see what future a casting operation can have. The production of good castings can be highly economical and rewarding. The production of bad castings is usually expensive and damaging.

The 'good casting' in this text is defined as one that meets or exceeds the customer's specification.

It is also worth noting at this early stage, that we hope that meeting the customer's specification will be equivalent to meeting or exceeding service requirements. However, occasionally it is necessary to live with the irony that the demands of the customer and the requirements for service are sometimes not in the harmony one would like to see. This is a challenge to the conscientious foundry engineer to persuade and educate the customer in an effort to reconcile the customer's aims with our duty of care towards casting users and society as a whole.

These problems illustrate that there are easier ways of earning a living than in the casting industry. But few are as exciting.

**JC**  
**West Malvern**  
03 September 2003

# Introduction to *Castings Handbook* 2011

Revised and expanded editions of *Castings* and *Castings Practice* were planned in a more logical format as *Casting Metallurgy* and *Casting Manufacture*. However, Elsevier suggested that the two might beneficially be combined as a single *Complete Castings Handbook*. I have warmed to this suggestion since encompassing both the science and the technological application will be helpful to students, academics, and producers. The origin of the division of the Handbook into volumes 1 and 2 therefore remains clear: Volume 1 is the metallurgy of castings, formally outlining for the first time my new proposals for an explanation of the metallurgy of Al–Si alloys, cast irons, and steels; Volume 2, manufacture, divides into the 10 Rules, manufacturing design, and finally the various processing steps.

As I have indicated previously, the numerous processing steps make casting a complex technology not to be underestimated. It is our task as founders to make sure the world, happily ignorant of this significant challenge, takes castings for granted, having never an occasion to question their complete reliability.

**JC**  
**Ledbury, Herefordshire, England**  
23 November 2010

This page intentionally left blank

# Acknowledgments

It is a pleasure to acknowledge the significant help and encouragement I have received from many good friends. John Grassi has been my close friend and associate in Alotech, the company promoting the new, exciting Ablation castings process. Ken Harris has been an inexhaustible source of knowledge on silicate binders, aggregates and recycling. His assistance is clear in Chapter 15. Clearly, the casting industry needs more chemists like him. Bob Puhakka has been the first regular user of my casting recommendations for the production of steel castings, which has provided me with inspirational confirmation of the soundness of the technology described in this book. Murat Tiryakioglu has been a loyal supporter and critic, and provided the elegantly written publications that have provided welcome scientific support. Naturally, many other acknowledgments are deserved among friends and students whose benefits have been a privilege to enjoy. I do not take these for granted. Even if not listed here they are not forgotten.

The American Foundry Society is thanked for the use of a number of illustrations from the Transactions.

This page intentionally left blank

# Casting metallurgy

# 1

1	The melt .....	3
2	Entrainment.....	19
3	Flow .....	105
4	Molds and cores.....	155
5	Solidification structure.....	187
6	Casting alloys.....	255
7	Porosity.....	391
8	Cracks and tears.....	465
9	Properties of castings.....	499

This page intentionally left blank

# The melt

Some liquid metals may be really pure liquid. Such metals may include pure liquid gold, possibly some carbon–manganese steels whilst in the melting furnace at a late stage of melting. These, however, are rare.

Many liquid metals are actually so full of sundry solid phases floating about, that they begin to more closely resemble slurries than liquids. This slurry-type nature can be seen quite often as some metals are poured, the melt overflows the lip of the melting furnace as though it were a cement mixture. In the absence of information to the contrary, this awful condition of a liquid metal should be assumed to apply. Thus many of our models of liquid metals that are formulated to explain the occurrence of defects neglect to address this fact. As techniques have improved over recent years there has been growing evidence for the real internal structure of liquid metals, revealing melts to be crammed with defects. Some of this evidence is described below. Much evidence applies to aluminum and its alloys where the greatest effort has been focused, but evidence for other metals and alloys is already impressive and is growing steadily.

It is sobering to realize that many of the strength-related properties of metals can only be explained by assuming that the original melt was full of defects. Classical physical metallurgy and solidification science that has considered metals as merely pure metals currently cannot explain aspects of the important properties of cast materials such as the effect of dendrite arm spacing; it cannot explain the existence of pores and their area density; it cannot explain the reason for the cracking of precipitates formed from the melt. These key aspects of cast metals will be seen to arise naturally from the assumption of a population of defects.

Any attempt to quantify the number and size distribution of these defects is a non-trivial task. McClain and co-workers (2001) and Godlewski and Zindel (2001) have drawn attention to the unreliability of results taken from polished sections of castings. A technique for liquid aluminum involves the collection of inclusions by forcing up to 2 kg of melt through a fine filter, as in the PODFA and PREFIL tests. The method overcomes some of the sampling problems by concentrating the inclusions by a factor of about 10 000 times (Enright and Hughes 1996, Simard et al. 2001). The layer of inclusions remaining on the filter can be studied on a polished section. The total quantity of inclusions is assessed as the area of the layer as seen under the microscope, divided by the quantity of melt that has passed through the filter. The unit is therefore the curious quantity  $\text{mm}^2 \text{kg}^{-1}$ . (It is to be hoped that at some future date this unhelpful unit will, by universal agreement, be converted into some more meaningful quantity such as volume of inclusions per volume of melt. In the meantime, the standard provision of the diameter of the filter in reported results would at least allow a reader the option to do this.)

To gain some idea of the huge range of possible inclusion contents, an impressively dirty melt might reach  $10 \text{ mm}^2 \text{kg}^{-1}$ , whereas an alloy destined for a commercial extrusion might be in the range 0.1 to 1, foil stock might reach 0.001, and computer discs  $0.0001 \text{ mm}^2 \text{kg}^{-1}$ . For a filter of 30-mm diameter these



figures approximately encompass the range of volume fraction  $10^{-3}$  (0.1%) down to  $10^{-7}$  (0.1 part per million by volume).

Other techniques for the monitoring of inclusions in Al alloy melts include LIMCA (Liquid Metal Cleanness Analyser) (Smith 1998), in which the melt is drawn through a narrow tube. The voltage drop applied along the length of the tube is measured. The entry of an inclusion of different electrical conductivity into the tube causes the voltage differential to rise by an amount that is assumed to be proportional to the size of the inclusion. The technique is generally thought to be limited to inclusions approximately in the range 10 to 100  $\mu\text{m}$  or so.

Although widely used for the casting of wrought alloys, the author regrets that the LIMCA technique has to be viewed with great reservation. Inclusions in light alloys are often oxide bifilms up to 10 mm diameter, as will become clear. Such inclusions do find their way into the LIMCA tube, where they tend to hang, caught up at the mouth of the tube, and rotate into spirals like a flag tied to the mast by only one corner. These are torn free from time to time and sediment in the bottom of the sampling crucible of the LIMCA probe, where they have the appearance of a heap of spiral Italian noodles (Asbjornson 2001). It is to be regretted that most workers using LIMCA have been unaware of these serious problems. Because of the air enfolded into the bifilm, the defects in the LIMCA probe have often been thought to be bubbles, which, probably, they sometimes partly are, and sometimes completely are. One can see the confusion.

Ultrasonic reflections have been used from time to time to investigate the quality of melt. The early work by Mountford and Calvert (1959) is noteworthy, and has been followed up by considerable development efforts in Al alloys (Mansfield 1984), Ni alloys and steels (Mountford et al. 1992). Ultrasound is efficiently reflected from oxide bifilms (almost certainly because the films are double, and the elastic wave cannot cross the intermediate layer of air, and thus is efficiently reflected). However, the reflections may not give an accurate idea of the size of the defects because of their irregular, crumpled form and their tumbling action in the melt. The tiny mirror-like facets of a large, scrambled defect reflect back to the source only when they happen to rotate to face the beam. The result is a general scintillation effect, apparently from many minute and separate particles. It is not easy to discern whether the images correspond to many small or a few large defects.

Neither LIMCA nor the various ultrasonic probes can distinguish any information on the types of inclusions that they detect. In contrast, the inclusions collected by pressurized (forced) filtration can be studied in some detail, although even here the areas of film defects are often difficult to discern. In addition to films, many different inclusions can be found as listed in Table 1.1.

Nearly all of these foreign materials will be deleterious to products intended for such products as foil or computer discs. However, for shaped castings, those inclusions such as carbides and borides may not be harmful at all. This is because having been precipitated from the melt, so they are usually therefore in excellent atomic contact with the matrix. These well-bonded non-metallic phases are thereby unable to act as initiators of other defects such as pores and cracks. Conversely, they may act as grain refiners. Furthermore, their continued good bonding with the solid matrix is expected to confer on them a minor or negligible influence on mechanical properties. (However, we should not forget that it is possible that they may have some influence on other physical or chemical properties such as machinability or corrosion.)

Generally, therefore, this book concentrates on those inclusions that have a major influence on mechanical properties, and that can be the initiators of other serious problems such as pores and cracks.

**Table 1.1** Types of inclusions in Al alloys

Inclusion type		Possible origin
Carbides	$\text{Al}_4\text{C}_3$	Pot cells from Al smelters
Boro-carbides	$\text{Al}_4\text{B}_4\text{C}$	Boron treatment
Titanium boride	$\text{TiB}_2$	Grain refinement
Graphite	C	Fluxing tubes, rotor wear, entrained film
Chlorides	NaCl, KCl, $\text{MgCl}_2$ , etc.	Chlorine or fluxing treatment
Alpha alumina	$\alpha\text{-Al}_2\text{O}_3$	Entrainment after high-temperature melting
Gamma alumina	$\gamma\text{-Al}_2\text{O}_3$	Entrainment during pouring
Magnesium oxide	MgO	Higher Mg containing alloys
Spinel	$\text{MgOAl}_2\text{O}_3$	Medium Mg containing alloys

Thus the attention will center on *entrained surface films*, which exhibit unbonded interfaces in the melt, and lead to a spectrum of problems. Usually, these inclusions will be oxides. However, carbon films are also common, and occasionally nitrides, sulfides and other compounds.

The pressurized filtration tests can find many of these entrained solids, and the analysis of the inclusions present on the filter can help to identify the source of many inclusions in a melting and casting operation. However, the only inclusions that remain undetectable but are enormously important are the newly entrained films that occur on a clean melt as a result of surface turbulence. These films are commonly entrained during the pouring of castings. They are typically only 20 nm thick, and so remain invisible under an optical microscope, especially if draped around a piece of refractory filter that when sectioned will appear many thousands of times thicker. The only detection technique for such inclusions is the lowly Reduced Pressure Test. This test opens the films (because they are always double, and contain air, as will be explained in detail in Chapter 3) so that they can be seen. Metallographic sections (or radiographs) of the cast test pieces clearly reveal the size, shape, and numbers of such important inclusions, as has been shown by Fox and Campbell (2000). The test will be discussed in detail later.

## 1.1 REACTIONS OF THE MELT WITH ITS ENVIRONMENT

A liquid metal is a highly reactive chemical. It will react both with the gases above it and if there is any kind of slag or flux floating on top of the melt, it will probably react with that too. Many melts also react with their containers such as crucibles and furnace linings.

The driving force for these processes is the striving of the melt to come into equilibrium with its surroundings. Its success in achieving equilibrium is, of course, limited by the rate at which reactions can happen, and by the length of time available.

Thus reactions in the crucible or furnace during the melting of the metal are clearly seen to be serious, since there is usually plenty of time for extensive changes. The pick-up of hydrogen from damp refractories is common. Similar troubles are often found with metals that are melted in furnaces heated by the burning of hydrocarbon fuels such as gas or oil.

We can denote the chemical composition of hydrocarbons as  $C_xH_y$  and thus represent the straight-chain compounds such as methane ( $CH_4$ ), ethane ( $C_2H_6$ ), and so on, or aromatic ring compounds such as benzene ( $C_6H_6$ ) etc. (Other more complicated molecules may contain other constituents such as oxygen, nitrogen, and sulfur, not counting impurities which may be present in fuel oils such as arsenic and vanadium.)

For our purposes we will write the burning of fuel taking methane as an example



Clearly the products of combustion of hydrocarbons contain water, so the hot waste gases from such furnaces are effectively wet.

Even electrically heated furnaces are not necessarily free from the problem of wet environment: an electric resistance furnace that has been allowed to stand cold over a weekend will have had the chance to absorb considerable quantities of moisture in its lining materials. Most furnace refractories are hygroscopic and will absorb water up to 5–10% of their weight. This water is released into the body of the furnace over the next few days of operation. It has to be assumed that the usual clay/graphite crucible materials commonly used for melting non-ferrous alloys are quite permeable to water vapor and/or hydrogen, since they are designed to be approximately 40% porous. Additionally, hydrogen permeates freely through most materials, including steel, at normal metallurgical operating temperatures of around 700°C and above.

This moisture from linings or atmosphere can react in turn with the metal M:



Thus a little metal is sacrificed to form its oxide, and the hydrogen is released to equilibrate itself between the gas and metal phases. Whether it will, on average, enter the metal or the gas above the metal will depend on the relative partial pressure of hydrogen already present in both of these phases. The molecular hydrogen has to split into atomic hydrogen (sometimes called ‘nascent’ hydrogen) before it can be taken into solution, as is described by the simple relation

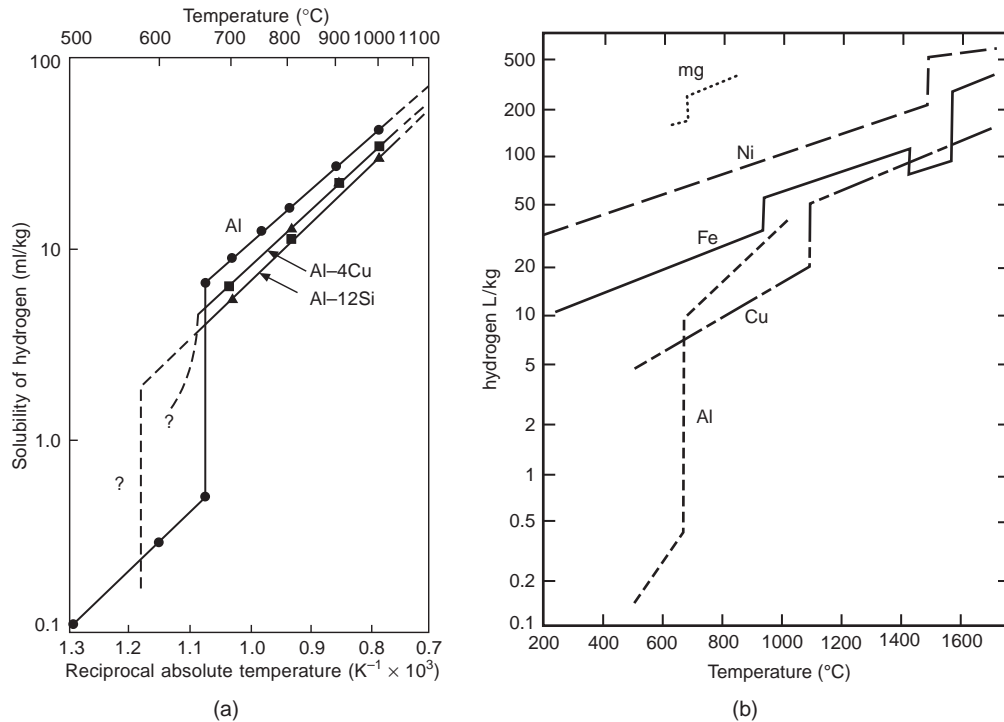


The equation predicting the partial pressure of hydrogen in equilibrium with a given concentration of hydrogen in solution in the melt is:

$$[H]^2 = kP_{H_2} \quad (1.4)$$

where the constant  $k$  has been the subject of many experimental determinations for a variety of gas-metal systems (Ransley and Neufeld 1948, Brandes 1983). It is found to be affected by alloy additions (Sigworth and Engh 1982) and temperature. The relation is a statement of the famous Sievert’s law, which describes the squared relation between a diatomic gas concentration and its pressure; for instance if the gas concentration in solution is doubled, its equilibrium pressure is increased by four times. A further point to note is that when the partial pressure of hydrogen  $P = 1$  atmosphere, it is immediately clear that  $k$  is numerically equal to the solubility of hydrogen in the metal at that temperature. Figure 1.1a shows how the solubility of hydrogen in aluminum increases with temperature.

Figure 1.1b shows that although many metals dissolve more hydrogen than aluminum, it is aluminum that suffers most from hydrogen porosity because of the huge difference in solubility

**FIGURE 1.1**

(a) Hydrogen solubility in aluminum and two of its alloys, showing the abrupt fall in solubility on solidification; (b) hydrogen solubility for a number of metals.

between the liquid and the solid. The solid can hold only about 1/20th of the gas in the liquid (corresponding to a partition coefficient of 0.05) so that there is a major driving force for the rejection of nearly all the hydrogen on solidification, creating significant porosity. This contrasts with magnesium and many other metals, where the partition coefficients are closer to 1.0, so that their higher hydrogen content is, in general, not such a problem to drive the nucleation of pores, even though it may contribute significantly to the growth of pores because of its high rate of diffusion, draining the hydrogen content from significantly greater volumes of the alloy. These factors are discussed at length in Section 7.2 relating to the growth of gas porosity.

Moving on to the concepts of equilibrium, it is vital to understand fully the concept of an equilibrium gas pressure associated with the gas in solution in a liquid. We shall digress to present a few examples to illustrate the concept.

Consider a liquid containing a certain amount of hydrogen atoms in solution. If we place this liquid in an evacuated enclosure then the liquid will find itself out of equilibrium with respect to the environment above the liquid. It is supersaturated with respect to its environment. It will then gradually lose its hydrogen atoms from solution, and these will combine on its surface to form hydrogen molecules, which will escape into the enclosure as hydrogen gas. The gas pressure in the enclosure will

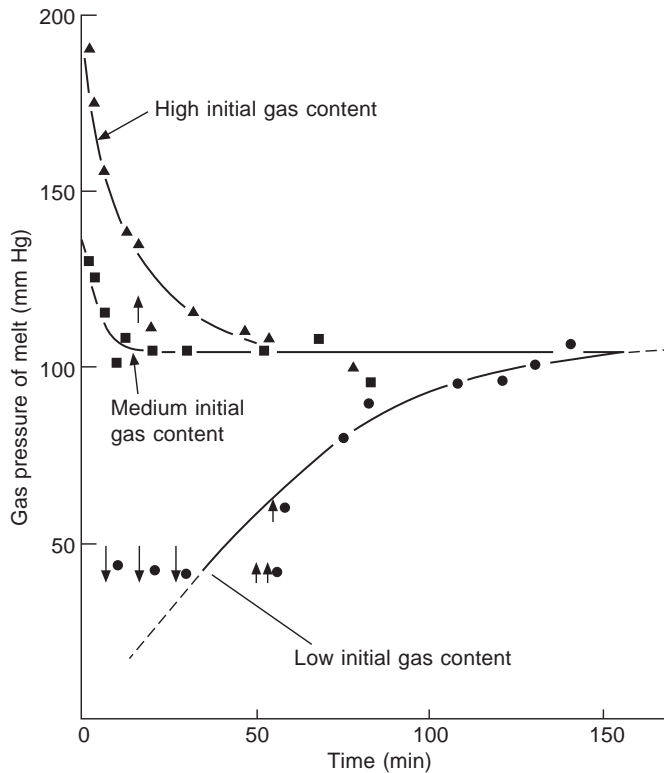


**FIGURE 1.2**

Hydrogen content of liquid aluminum bronze held in a gas-fired furnace, showing how the melt equilibrates with its surroundings. Data from Ostrom et al. (1975).

therefore gradually build up until the rate of loss of hydrogen from the surface becomes equal to the rate of gain of the liquid from hydrogen that returns, re-converting to individual atoms on the surface and re-entering solution in the liquid. The liquid can then be said to have come into equilibrium with its environment. The effective hydrogen pressure in the liquid has become equal to the hydrogen pressure in the region over the melt.

Similarly, if a liquid containing little or no gas (and therefore having a low equilibrium gas pressure) were placed in an environment of high gas pressure, then the net transfer would, of course, be from gas phase to liquid phase until the equilibrium partial pressures in both phases were equal. Figure 1.2 illustrates the case of three different initial concentrations of hydrogen in a copper alloy melt, showing how initially high concentrations fall, and initially low concentrations rise, all finally reaching the same concentration, which is in equilibrium with the environment.

This equilibration with the external surroundings is relatively straightforward to understand. What is perhaps less easy to appreciate is that the equilibrium gas pressure in the liquid is also effectively in operation *inside* the liquid.

This concept can be grasped by considering bubbles of gas which have been introduced into the liquid by stirring or turbulence, or which are adhering to fragments of surface films or other inclusions that are floating about. Atoms of gas in solution migrate across the free surface of the bubbles and into their interior to establish an equilibrium pressure inside.

On a microscopic scale, a similar behavior will be expected between the individual atoms of the liquid. As they jostle randomly with their thermal motion, small gaps open momentarily between the atoms. These embryonic bubbles will also therefore come into equilibrium with the surrounding liquid.

It is clear, therefore, that the equilibrium gas pressure of a melt applies both to the external and internal environments of the melt.

We have so far not touched on those processes that control the rate at which reactions can occur. The kinetics of the process can sometimes over-ride the thermodynamics and can exert control over the reaction.

Consider, for instance, the powerful reaction between the oxygen in dry air and liquid aluminum: no disastrous burning takes place; the reaction is held in check by the surface oxide film which forms, slowing the rate at which further oxidation can occur. This is a beneficial interaction with the environment. Other beneficial passivating (i.e. inhibiting) reactions are seen in the melting of magnesium under a dilute SF<sub>6</sub> (sulfur hexafluoride) gas, as described, for instance, by Fruehling and Hanawalt (1969).

A further example is the beneficial effect of water vapor in strengthening the oxide skin on the zinc alloy during hot-dip galvanizing so as to produce a smooth layer of solidified alloy free from 'spangle'. Without the water vapor, the usual protective atmosphere formed from a clean hydrogen–nitrogen mix provides an insufficient thickness of oxide, with the result that the growth of surface crystals disrupts the smoothness of the liquid zinc film to reveal the sharply delineated crystal patterns (Hart et al. 1984).

Water vapor is also known to stabilize the protective gamma alumina film on aluminum (Cochran et al. 1976, Impey et al. 1993), reducing the rate of oxidation in moist atmospheres. Theile saw this effect first in 1962. His results are replotted in Figure 1.3. Although his curve for oxidation in moist air is seen to be generally lower than the curves for air and oxygen (which are closely similar), the most important feature is the very low *initial* rate, the rate at very short times. Entrainment events usually create new surface that is folded in within milliseconds. Obtaining oxidation data for such short times is a problem.

The kinetics of surface reactions can also be strongly influenced on the atomic scale by surface-active solutes that segregate preferentially to the surface. Only a monolayer of atoms of sulfur will slow the rate of transfer of nitrogen across the surface of liquid iron. Interested readers are referred to the nicely executed work by Hua and Parlee (1982).

---

## 1.2 TRANSPORT OF GASES IN MELTS

Gases in solution in liquids travel most quickly when the liquid is moving, since, of course, they are simply carried by the liquid.

However, in many situations of interest the liquid is stationary, or nearly so. This is the case in the boundary layer at the surface of the liquid. The presence of a solid film on the surface will hold the surface stationary, and because of the effect of viscosity, this stationary zone will extend for some distance into the bulk liquid, although, of course, the thickness of the boundary layer will be

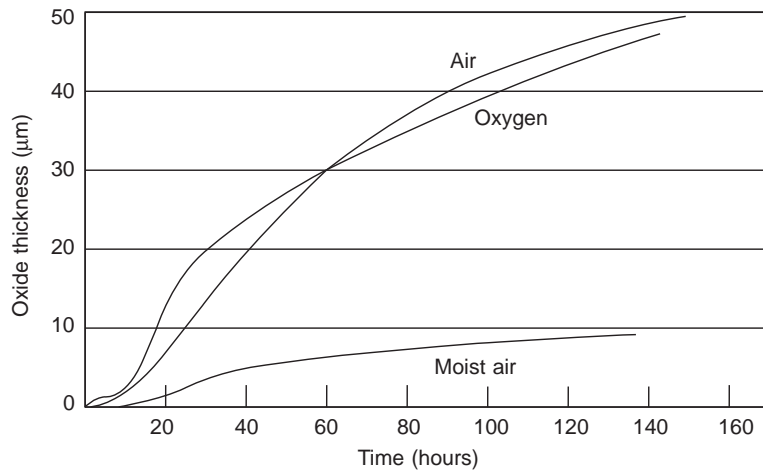


**FIGURE 1.3**

Growth of oxide on 99.9 Al at 800°C in a flow of oxygen, dry air, and moist air. Data from Theile (1962).

reduced if the bulk of the liquid is violently stirred. However, within the stagnant liquid of the boundary layer the movement of solutes can occur only by the slow process of diffusion, i.e. the migration of populations of atoms by the process of each atom carrying out one random atomic jump at a time.

Another region where diffusion is important is in the partially solidified zone of a solidifying casting, where the bulk flow of the liquid is normally a slow drift. In the solid state, of course, diffusion is the only mechanism by which solutes can spread.

The average distance  $d$  to which an element can diffuse (whether in a liquid, solid, or gas) in time  $t$  is given by the simple order of magnitude relation

$$d = (Dt)^{1/2} \quad (1.5)$$

where  $D$  is the coefficient of diffusion, measured in  $\text{m}^2/\text{s}$ . This simple formula, together with the values of  $D$  taken from Figure 1.4, is often extremely useful to estimate, if only relatively roughly, the distances involved in reactions. We shall return to the use of this equation many times throughout this book.

There are two broad classes of diffusion processes, each having quite a different value of  $D$ : one is *interstitial diffusion*, and the other is *substitutional diffusion*. *Interstitial diffusion* is the squeezing of small atoms through the *interstices* between the larger matrix atoms. This is a relatively easy process and thus interstitial diffusion is relatively rapid, characterized by a high value of  $D$ . *Substitutional diffusion* is the exchange, or *substitution*, of the solute atom for a similar-sized matrix atom. This process is more difficult (i.e. has a higher activation energy) because the solute atom has to wait for a gap of sufficient size to be created before it can jostle its way among the crowd of similar-sized individuals to reach the newly created space. Thus for substitutional diffusion  $D$  is relatively small.

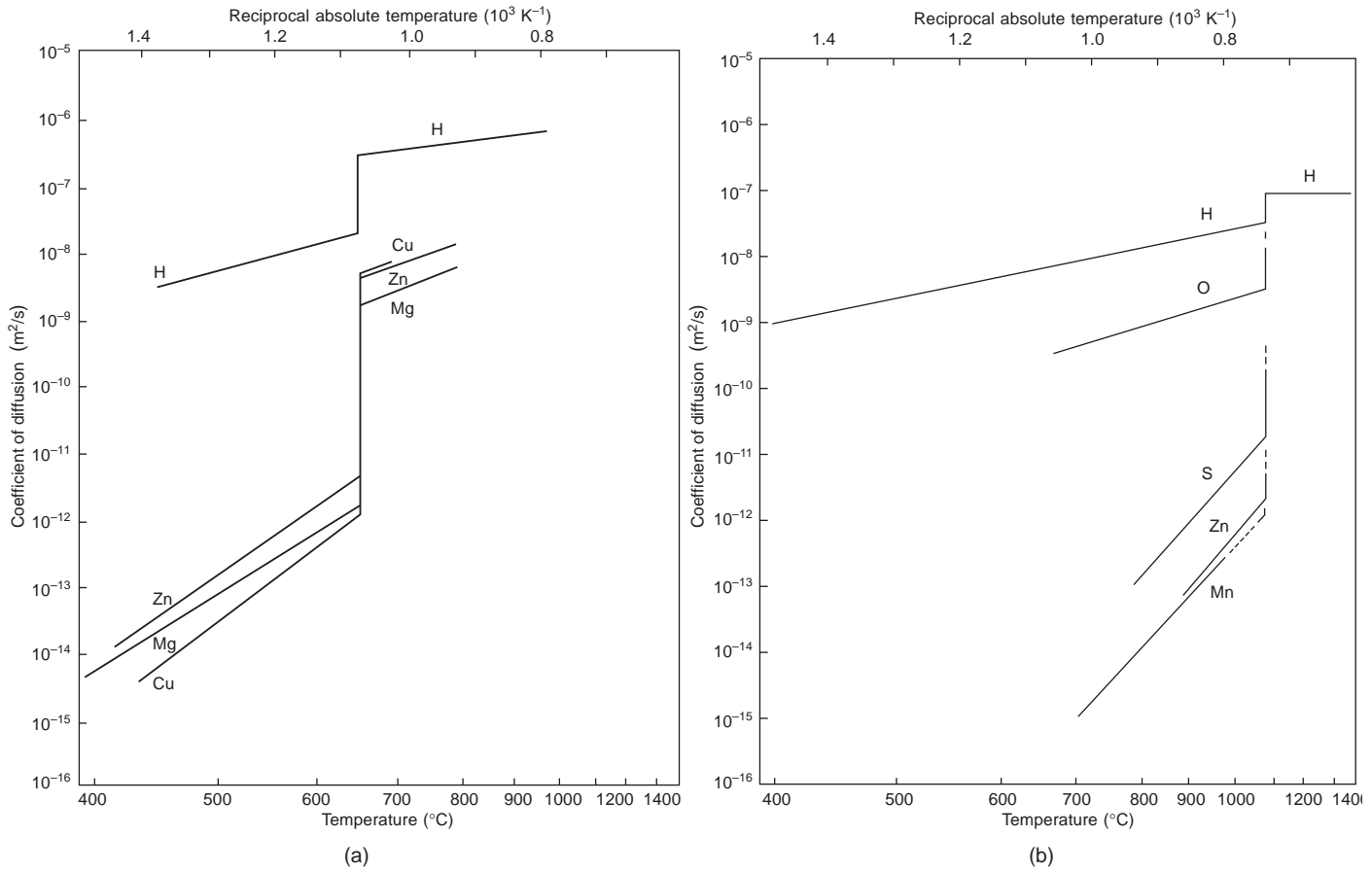


**FIGURE 1.4**

Diffusion coefficients for elements in solution in (a) Al, (b) Cu, and (c) Fe. (Data sources listed in *Castings*, 2nd Edition 2003.)



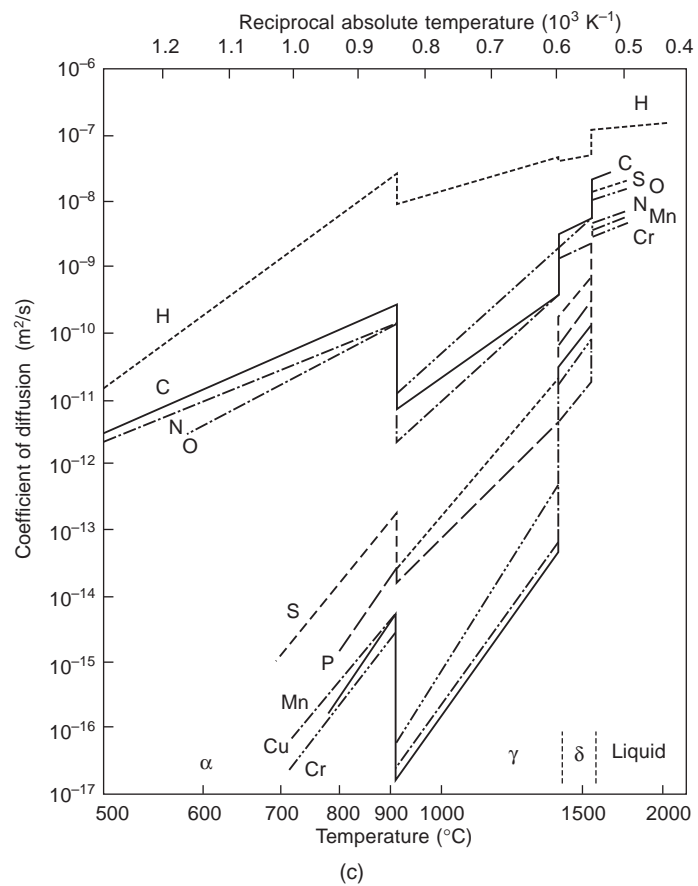


FIGURE 1.4 (continued).

Figure 1.4 shows the rates of diffusion of various alloying elements in the pure metals, aluminum, copper, and iron. Clearly, hydrogen is an element that can diffuse interstitially because of its small size. In iron, the elements C, N, and O all behave interstitially, although significantly more slowly than hydrogen.

The common alloying elements in aluminum, Mg, Zn, and Cu, clearly all behave as substitutional solutes. Other substitutional elements form well-defined groups in melts of copper and iron (Figures 1.4b and 1.4c).

However, there are a few elements that appear to act in an intermediate fashion. Oxygen in copper occupies an intermediate position. The elements sulfur and phosphorous in iron occupy an interesting intermediate position; a curious behavior that does not appear to have been widely noticed.

Figure 1.4c also illustrates the other important feature of diffusion in the various forms of iron: the rate of diffusion in the open body-centered cubic lattice (alpha and delta phases) is faster than in the more closely packed face-centered cubic (gamma phase) lattice. Furthermore, in the liquid phase diffusion is fastest of all, and differences between the rates of diffusion of elements that behave widely differently in the solid become less marked.

These relative rates of diffusion using Equation 1.5 and the data from Figure 1.4 will be referred to often in relation to many different phenomena throughout this book.

---

## 1.3 SURFACE FILM FORMATION

When the hot metal interacts with its environment many of the reactions result in products that dissolve rapidly in the metal, and diffuse away into its interior. Some of these processes have already been described. In this section we shall focus our attention on the products of reactions that remain on the surface. Such products are usually films.

Whether there is any tendency for a film to form or not depends on its stability, which can be quantified by its free energy of formation. A diagram for oxides showing this energy as a function of temperature was famously promoted by Ellingham and is shown in Figure 1.5. The extremely stable oxides are at the base, and those easily reduced back to their component metals are high on the graph. This concept of stability is based on an estimate of thermodynamic equilibrium.

In reality of course, the kinetics of the formation of oxides (and other compounds) depends on the rate at which components can arrive, and the rate at which they can be processed. The processing rate depends in turn on the structure of the crystal lattice as it develops.

Oxide films usually start as simple amorphous (i.e. non-crystalline) layers, such as  $\text{Al}_2\text{O}_3$  on Al, or MgO on Mg and Al-Mg alloys (Cochran et al. 1977). Their amorphous structure probably derives necessarily from the amorphous melt on which they nucleate and grow. However, they quickly convert to crystalline products as they thicken, and later often develop into a bewildering complexity of different phases and structures. Many examples can be seen in the studies reviewed by Drouzy and Mascre (1969) and in the various conferences devoted to oxidation (for instance Microscopy of Oxidation 1993). Some films remain thin, some grow thick. Some are strong, some are weak. Some grow slowly, others quickly. Some are heterogeneous and complex in the structure, being lumpy mixtures of different phases.

The nature of the film on a liquid metal in a continuing equilibrium relationship with its environment needs to be appreciated. In such a situation the melt will always be covered with the film. For

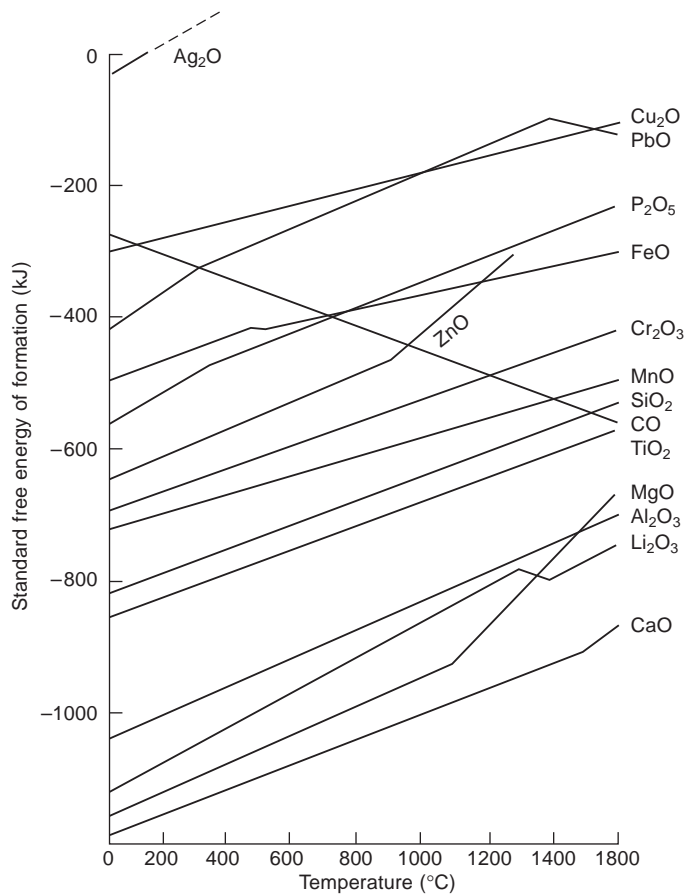


**FIGURE 1.5**

The Ellingham diagram, illustrating the free energy of formation of oxides as a function of temperature.

instance if the film is skimmed off it will immediately re-form. A standard foundry complaint about the surface film on certain casting alloys is that ‘You can’t get rid of it!’

Furthermore, it is worth bearing in mind that the two most common film-forming reactions, the formation of oxide films from the decomposition of moisture, and the formation of graphitic films from the decomposition of hydrocarbons, both result in the increase of hydrogen in the metal. The comparative rates of diffusion of hydrogen and other elements in solution in various metals are shown in Figure 1.4. These reactions will be dealt with in detail later.

The *noble metals such as gold, platinum, and iridium* are, for all practical purposes, totally film-free. These are, of course, all metals that are high on the Ellingham diagram, reflecting the relative instability of their oxides, and thus the ease with which they are reduced back to the metal.

*Iron* is an interesting case, occupying an intermediate position in the Ellingham diagram. Liquid irons and steels therefore have a complicated behavior, having a film which may be liquid or solid,

depending on the composition of the alloy and its temperature. Its behavior is considered in detail in Section 6.5 devoted to cast irons and steels.

*Liquid silver* is analogous to copper in that it dissolves oxygen. In terms of the Ellingham diagram (Figure 1.5) it is seen that its oxide,  $\text{Ag}_2\text{O}$ , is just stable at room temperature, causing silver to tarnish (together with some help from the presence of sulfur in the atmosphere to form sulfides), as every jeweler will know! However, the free energy of formation of the oxide is positive at higher temperatures, appearing therefore above zero on the figure. This means that the oxide is unstable at higher temperatures. It would therefore not be expected to exist at higher temperatures except in cases of transient non-equilibrium.

The *light alloys, aluminum, and magnesium* have casting alloys characterized by the stability of the products of their surface reactions. Although one reaction product is hydrogen, which diffuses away into the interior, the noticeable remaining reaction product is a surface oxide film. The oxides of the light alloys are so stable that once formed, in normal circumstances, they cannot be decomposed back to the metal and oxygen. The oxides become permanent features for good or ill, depending on where they come to final rest on or in the cast product. This is, of course, our central theme once again.

A wide range of other important alloys exist whose main constituents would not cause any problem in themselves, but which form troublesome films in practice because their composition includes just enough of the above highly reactive metals. These are discussed later in the metallurgical section, Chapter 6.

*Al-Mg alloy family*, where the magnesium level can be up to 10 weight per cent, are widely known as being especially difficult to cast. Along with aluminum bronze, those aluminum alloys containing 5–10% Mg share the dubious reputation of being the world's most uncastable casting alloys! This notoriety is, as we shall see, ill-deserved. If well cast, these alloys have enviable ductility and toughness, and take a bright anodized finish much favored by the food industry, and those markets in which decorative finish is all-important.

*Aluminum bronze* itself can contain up to 10% Al, and the casting temperature is of course much higher than that of aluminum alloys. The high aluminum level and high temperature combine to produce a thick and tenacious film of  $\text{Al}_2\text{O}_3$  that makes aluminum bronze one of the most difficult of all foundry alloys. Some other high-strength brasses and bronzes that contain aluminum are similarly difficult.

*Ductile irons* (otherwise known as spheroidal graphite or nodular irons) are markedly more difficult to cast free from oxides and other defects when compared to gray (otherwise known as flake graphite) cast iron. This is the result of the minute concentration of magnesium that is added to spheroidize the graphite, resulting in a solid magnesium silicate surface film that is easily entrained during pouring to create bifilms and dross.

In the course of this work we shall see how in a few cases the chemistry of the surface film can be altered to convert the film from a solid to a liquid, thus reducing the dangers that follow from an entrainment event. More usually, however, the film can neither be liquefied nor eliminated. It simply has to be lived with. A surface entrainment event therefore usually ensures the creation of a permanent defect.

Entrained films form the major defect in cast materials. Our ultimate objective to avoid films in cast products cannot be achieved by eliminating the formation of films. The only practical solution to the elimination of entrainment defects is the elimination of entrainment. The simple implementation of an improved filling system design can completely solve the problem. This apparently obvious solution is

so self-evident that it has succeeded to escape the attention of most of the casting community for the last several thousand years.

The techniques to avoid entrainment during the production of cast material represent an engineering challenge that occupies much of the second volume of this book.

## 1.4 VAPORIZATION

When melting and casting metals, temperatures are often sufficiently high that some alloy components will be evaporating all the time. The evaporation of elements from melts can be severe, and has consequences of which it is useful to be aware. Although examples will occur repeatedly throughout the book, a number of instances are gathered here to illustrate how common the effect is.

Figure 1.6 illustrates how volatile sodium is, so that additions to Al–Si alloys to modify the eutectic are only short-lived, because of the sodium evaporating from the melt within 15 or 20 minutes.

Zinc similarly evaporates from Cu–Zn alloys, and can oxidize, creating the familiar zinc flare. The wind of vapor blowing away from the melt seems responsible for the lack of gas porosity problems in the zinc-containing brasses, since gases such as hydrogen in the environment are continuously flushed away. This interesting and useful phenomenon is dealt with in more detail in Section 6.4.

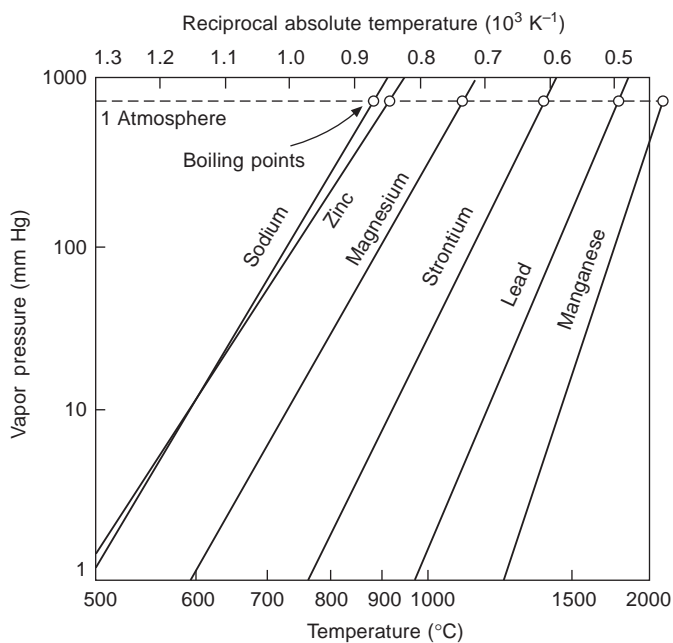


**FIGURE 1.6**

Increase in the pressure of vapor of some of the more volatile elements as temperature increases. Data from Brandes (1983).

When melting and holding magnesium alloys in a low-pressure casting machine, it is essential to suppress the evolution of vapor by the presence of some air, or other actively protective gas or flux above the melt. The experimental use of an inert gas, argon, above the melt to avoid oxidation led to the atmosphere becoming high in magnesium vapor, such that when the unfortunate operator opened the door to charge more ingots, admitting air, he was killed in the explosion. When vaporization is properly suppressed, the use of magnesium alloys in low-pressure casting machines is perfectly safe.

In the production of ductile iron, magnesium is actually above its boiling point when added to cast iron. The addition reaction is therefore so energetic that the boiling action requires special techniques, often involving special reactor vessels to prevent the melt erupting out of the container.

Alloys of copper and iron that contain lead are a particular problem because of the toxicity of lead. Thus leaded copper alloys and leaded free-cutting steel are now being phased out. The casting of these alloys into sand molds led to increasing amounts of lead that had condensed in the sand, causing the contamination of nearly everything in the foundry.

Manganese vapor from manganese steels similarly condenses in the molding sand, and is thought to be responsible for the enhanced wetting and penetration of molds by manganese steels.

Evaporation is a particular problem from alloys melted in vacuum. The charge make-up has to allow for the losses by evaporation. Furthermore, the condensation of the metal vapors on the cold walls of the vacuum chamber usually ignites when the chamber is opened to the air; the fine black metallic dust then burns, with a flame that licks its way around the chamber walls. If not burned on each occasion, the dust can accumulate to a thickness that might become dangerous. Even when the dust is oxidized, it is black, dirty, and can be a health hazard. Thus vacuum melting and casting requires special personal care. Melting and casting in an inert gas such as argon greatly reduces the rate of evaporation, and consequently reduces these problems.

This page intentionally left blank

# Entrainment

If perfectly clean water is poured, or is subject to a breaking wave, the newly created liquid surfaces fall back together again, and so impinge and mutually assimilate. The body of the liquid re-forms seamlessly. We do not normally even think to question such an apparently self-evident process.

However, the same is not true for many common liquids, the surface of which is not a liquid, but a solid, often invisible film of extreme thinness. Aqueous liquids often exhibit films of proteins or other large molecular compounds.

Liquid metals are a special case. The surface of most liquid metals comprises an oxide film. If the surface happens to fold, by the action of a breaking wave, or by droplets forming and falling back into the melt, the surface oxide becomes entrained in the bulk liquid (Figure 2.1).

The *entrainment process* can be a folding action as seen in Figure 2.1. Alternatively, also shown in the figure, parts of the flow can impinge, as droplets falling back into the liquid. In both cases the film necessarily comes together dry side to dry side. The submerged surface films are therefore *necessarily always double*.

Also, of course, because of the negligible bonding across the dry opposed interfaces, the defect now *necessarily resembles and acts as a crack*. Turbulent pouring of liquid metals can therefore quickly fill the liquid with cracks. The cracks have a relatively long life, and in many alloys can survive long enough to be frozen into the casting. We shall see how they have a key role in the

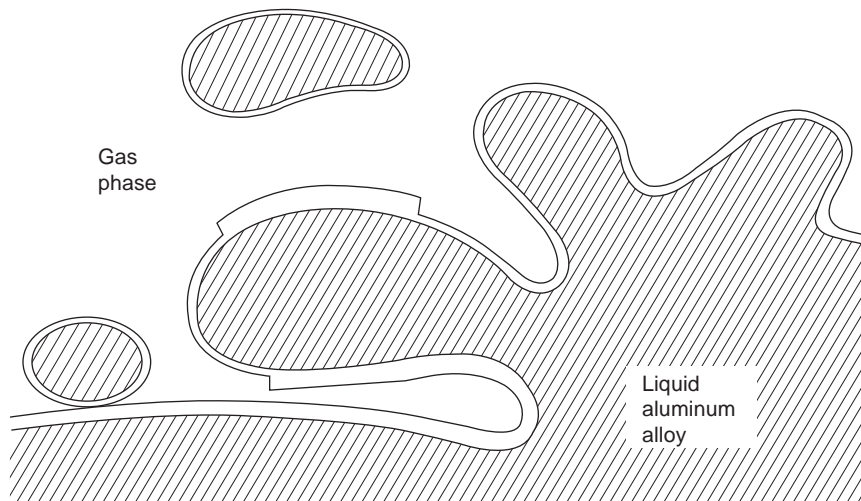


**FIGURE 2.1**

Sketch of a surface entrainment event.



creation of other defects during the process of freezing, and how they degrade the properties of the final casting.

Entrainment does not necessarily occur only by the dramatic action of a breaking wave as seen in Figure 2.1. It can occur simply by the contraction of a ‘free liquid’ surface. In the case of a liquid surface that contracts in area, its area of oxide, being a solid, is not able to contract. Thus the excess area is forced to fold in a concertina-like fashion. Considerations of buoyancy (in all but the most rigid and thick films) confirm that the fold will be inwards, and so entrained (Figure 2.2). Such loss of surface is common during rather gentle undulations of the surface, the slopping and surging that can occur during the filling of molds. Such gentle folding might be available to unfold again during

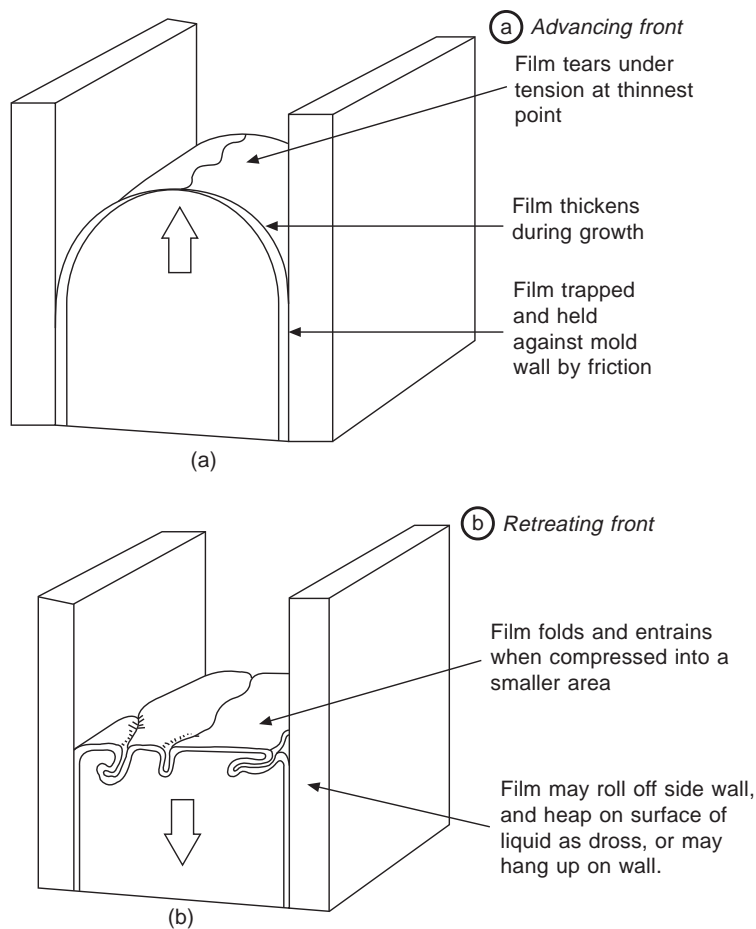


**FIGURE 2.2**

Modes of filling: (a) a liquid metal advancing by the splitting of its surface oxide (this may occur via a transverse unzipping wave); (b) the retreat of a surface illustrating the consequent entrainment of the surface oxide.

a subsequent expansion, so that the entrained surface might almost immediately detrain once again. This potential for reversible entrainment may not be important compared to the probability that much enfolded material will remain enfolded and entrained. Masses of entrained oxides will entangle and adhere to cores and molds, but more severe bulk turbulence may tear it away and transport it elsewhere.

With regard to all film-forming alloys, accidental entrainment of the surface during pouring is, unfortunately, only to be expected. This phenomenon of the degradation of liquid metals by pouring is perfectly natural and fundamental to the quality and reliability issues for cast metals. Because these defects are inherited by wrought metals nearly all of our engineering metals are degraded too. It is amazing that such a simple mechanism could have arrived at the twenty-first century having escaped notice of thousands of workers, researchers, and teachers.

Anyway, it is now clear that the entrained film has the potential to become one of the most severely damaging defects in cast products (and, as we shall see, in wrought products too). It is essential, therefore, to understand film formation and the way in which films can become incorporated into a casting so as to damage its properties. These are vitally important issues.

It is worth repeating that a surface film is not harmful while it continues to stay on the surface. In fact, in the case of the oxide on liquid aluminum in air, it is doing a valuable service in protecting the melt from catastrophic oxidation. This is clear when comparing with liquid magnesium in air. Since the magnesium oxide is not so protective the liquid magnesium can burn, generating its characteristic brilliant flame until the whole melt is converted to oxide. In the meantime so much heat is evolved that the liquid melts its way through the bottom of the crucible, through the base of the furnace, and will continue down through a concrete floor, taking oxygen from the concrete to sustain the oxidation process until all the metal is consumed. This is the incendiary bomb effect. Oxidation reactions can be impressively energetic!

A solid film grows from the surface of the liquid, atom by atom, as each metal atom combines with newly arriving atoms or molecules of the surrounding gas. Thus for an alumina film on the surface of liquid aluminum the underside of the film is in perfect atomic contact with the melt, and can be considered to be 'well wetted' by the liquid. (Care is needed with the concept of *wetting* as used in this instance. Here it refers merely to the perfection of the atomic contact, which is evidently automatic when the film is grown in this way. The concept contrasts with the use of the term *wetting* for the case where a sessile drop is placed on an alumina substrate. Perfect atomic contact is now unlikely to exist where the liquid covers the substrate, so that at its edges the liquid will form a large contact angle with the substrate, indicating, in effect, that it does not wish to be in contact with such a surface. Technically, the creation of the liquid–solid interface raises the total energy of the system. The *wetting* in this case is said to be poor.)

The problem with the surface film only occurs when it becomes *entrained* and thus submerged in the bulk liquid.

When considering submerged oxide films, it is important to emphasize that the side of the film which was originally in contact with the melt will continue to be well wetted, i.e. it will enjoy its perfect atomic contact with the liquid. As such it will adhere well, and be an unfavorable nucleation site for volume defects such as cracks, gas bubbles, or shrinkage cavities. When the metal solidifies the metal–oxide bond will be expected to continue to be strong, as in the perfect example of the oxide on the surface of all solid aluminum products, especially noticeable in the case of anodized aluminum.

The upper surface of the solid oxide as grown on the liquid is of course dry. On a microscale it is known to have some degree of roughness. In fact the upper surfaces of oxide films can be extremely

rough – some, like MgO, being microscopically akin to a concertina, others like a rucked carpet or plowed field, or others, like the spinel  $\text{Al}_2\text{MgO}_4$ , an irregular jumble of crystals.

The other key feature of surface films is the great speed at which they can grow. Thus in the fraction of a second (probably between 10 and 100 ms) that it takes to cause a splash or to enfold the surface, the expanding surface, newly creating additional area of liquid, will react with its environment to cover itself in new film. The reaction is so fast as to be effectively instantaneous for the formation of oxides.

Other types of surface films on liquid metals are of interest to casters. Liquid oxides such as silicates are sometimes beneficial because they can detrain by balling-up under the action of surface tension and then easily float out, leaving no harmful residue in the casting. Solid graphitic films seem to be common when liquid metals are cast in hydrocarbon-rich environments. In addition, there is some evidence that other films such as sulfides and oxychlorides are important in some conditions. Fredriksson (1996) describes TiN films on alloys of Fe containing Ti, Cr, and C when melted in a nitrogen atmosphere. Nitride films may be common in irons and steels.

In passing, in the usual case of an alloy with a solid oxide film, it is of interest to examine whether the presence of oxide in a melt necessarily implies that the oxide is double. For instance, why cannot a single piece of oxide be simply taken and immersed in a melt to give a single (i.e. non-double) interface with the melt? The reason is that as the piece of oxide is pushed through the surface of the liquid, the surface film on the liquid is automatically pulled down either side of the introduced oxide, coating both sides with a double film, as illustrated schematically in Figure 2.3a. Thus the entrainment mechanism necessarily results in a submerged film that is at least double. If the surface film is solid, it therefore always has the nature of a crack. Figures 2.3b and 2.3c illustrate the problem of introducing solid particles to a melt when attempting to manufacture a metal/matrix composite (MMC). Each particle, or cluster of particles only succeeds to penetrate the surface if it takes with it a ‘paper bag’ of surrounding oxide. The dry side of the oxide faces the introduced particle, enclosing a remnant of air. Thus the introduced particle is not actually in contact with the liquid, but remains effectively surrounded by a layer of air enclosed within an oxide envelope. Bonding between the particle and the melt is therefore difficult, or even impossible, greatly limiting the mechanical properties of such MMCs.

Finally, it is worth warning about widespread inaccurate and vague concepts that are heard from time to time, and where clear thinking would be a distinct advantage. Two of these are discussed below.

For instance one often hears about ‘the breaking of the surface tension’. What can this mean? Surface tension is a physical force in the surface of the liquid that arises as a result of the atoms of the liquid pulling their neighbors in all directions. Atoms deep in the liquid experience forces in all directions resulting, of course, in zero net force. However, for atoms at the surface, there are no neighbors above the surface, so that these atoms experience a net inward force from atoms below in the bulk. This net inward force is the force we know as surface tension. It is always present. It cannot make any sense to consider it being ‘broken’.

Another closely related misconception describes ‘the breaking of the surface oxide’, implying that this is some kind of problem. However, the surface oxide, if a solid film, is always being broken during normal filling. This must occur as the liquid surface expands to form waves and droplets. However, the film is being continuously reformed as fresh liquid surface is created. As the melt fills a mold, rising up between its walls, an observer looking down at the metal will see its surface oxide tear apart and slide sideways across the meniscus towards the walls of the casting, eventually becoming the skin of the casting (Figure 2.2a). However, of course, the surface oxide is immediately and continuously

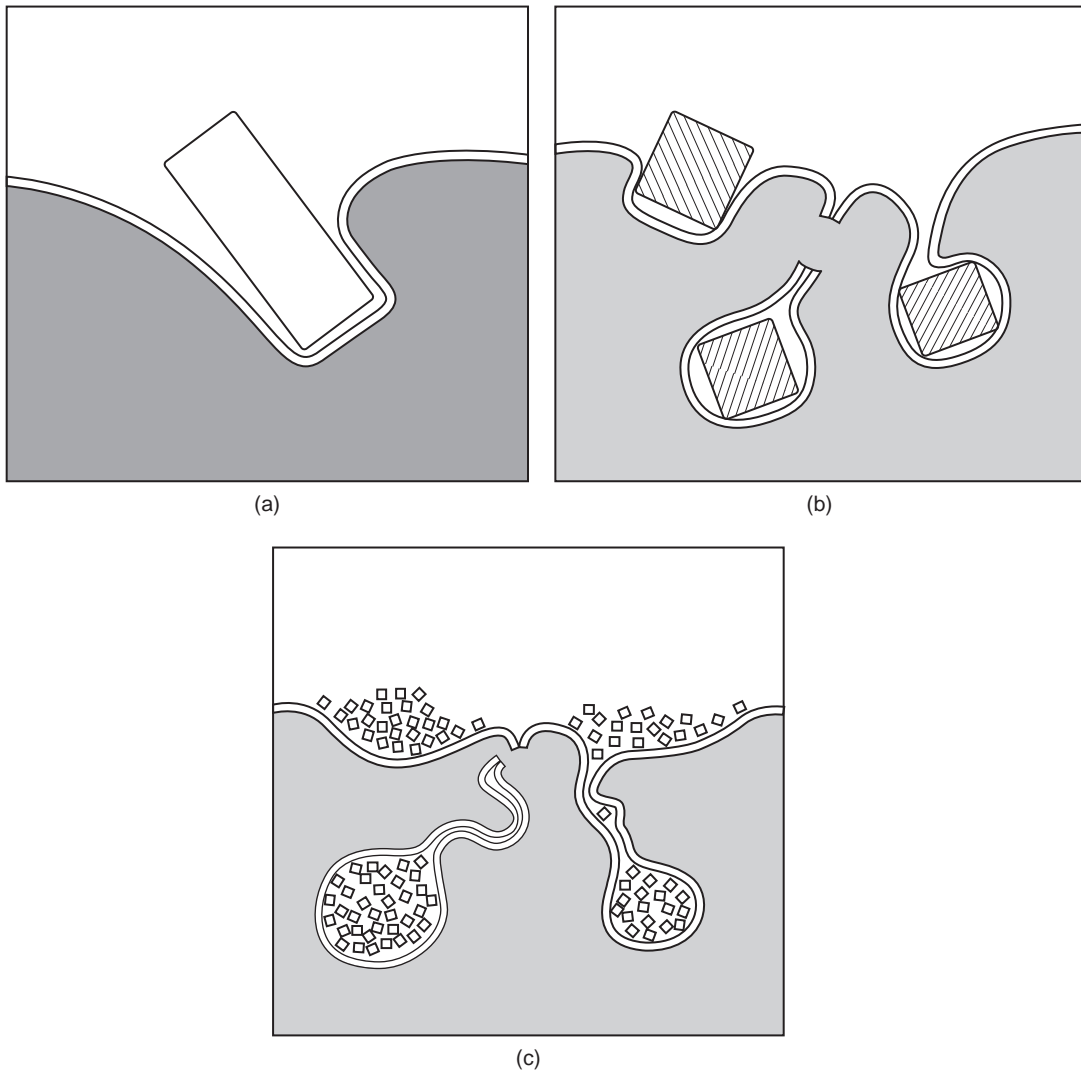


**FIGURE 2.3**

Entrainment of solids into liquid metals: (a) the introduction of melt charge materials; (b) optimum production of MMCs; (c) usual production of MMCs.

reforming, as though capable of infinite expansion. This is a natural and protective mode of advancement of the liquid metal front. It is to be encouraged by good design of filling systems.

As a fine point of logic, it is to be noted that the tearing and sliding across the open surface is driven by the friction of the casting skin, pressed by the liquid against the microscopically rough mold wall. Since this part of the film is trapped and cannot move, and since the melt is forced to rise, the film on

the top surface is forced to yield by tearing. This mode of advance is the secret of success of many beneficial products that enhance the surface finish of castings. For instance, coal dust replacements in molding sands encourage the graphitic film on the surface of liquid cast irons, and the graphitic film (not the relatively weak surface tension) mechanically bridges surface imperfections with a smooth solid film, improving surface finish, as will be detailed later.

As we have explained above, the mechanism of entrainment is the folding over of the surface to create a submerged, doubled-over oxide defect. This is the central problem. The folding action can be macroscopically dramatic, as in the pouring of liquid metals, or the overturning of a wave or the re-entering of a droplet. Alternately, it may be hardly noticeable, like the contraction of a gently undulating liquid surface.

The concept of the entrainment of the surface to form double films (bifilms) is so vital, and so central to the whole problem of the manufacture of castings, that it has been brought to the front of this publication. I found myself unable to write this text without introducing this issue first.

---

## 2.1 ENTRAINMENT DEFECTS

### 2.1.1 Bifilms

The entrainment mechanism is a folding-in of the surface or impingement action between two liquid surfaces. Figure 2.4 illustrates how entrainment can result in a variety of submerged defects. In the case of the folding-in of a solid film from the surface of the liquid the defect will be called a *bifilm*. This convenient short-hand denotes the *double* nature of the film defect, as in the word *bicycle*. The name is also reminiscent of the type of marine shellfish; the *bivalve*, whose two leaves of its shell are hinged, allowing it to open and close. (The pronunciation is suggested to be similar to bicycle and bivalve, so that ‘bifilm’ would be pronounced ‘*bifilm*’ as in ‘bye-film’ and not with a short ‘i’, that might suggest the word was ‘biff-ilm’.)

If the entrained surface is a solid film the resulting defect is a crack (Figure 2.4a) that may be only a few nanometers thick, and so be invisible to most inspection techniques. Figure 2.4a illustrates the important feature that entrained films usually constitute a main bifilm from which transverse bifilms emerge at intervals. This structure is a consequence of the two impinging surfaces being of different areas, the side having the larger area having to contract and thus forming the transverse folds. Naturally, the transverse bifilms are mainly on the one side, the side enclosed by the film of larger area. This expected natural behavior has interesting consequences for the structure of faults in some important second phases as we shall see.

Other consequences of the entrainment of the surface oxide film are seen in Figure 2.4 to be (b) the entrainment of bubbles as integral features of the bifilm being simply local regions where the two films have not come together because of the presence of entrapped gas; or (c) the entrainment of a surface liquid flux, or (d) solid debris, or (e) molding sand, or finally (f) an entrained old oxide, possibly from the surface of the ladle or furnace, in which sundry debris has accumulated by falling on to the surface from time to time and has been incorporated into the oxide structure.

It is as well to keep in mind that a wide spectrum of sizes and thicknesses of oxide film probably exist. With the benefit of hindsight provided by much intervening research, a speculative guess dating from the first edition of *Castings* (1991) is seen to be a reasonable description of the real situation (Table 2.1). The only modification to the general picture is the realization that the very new films can

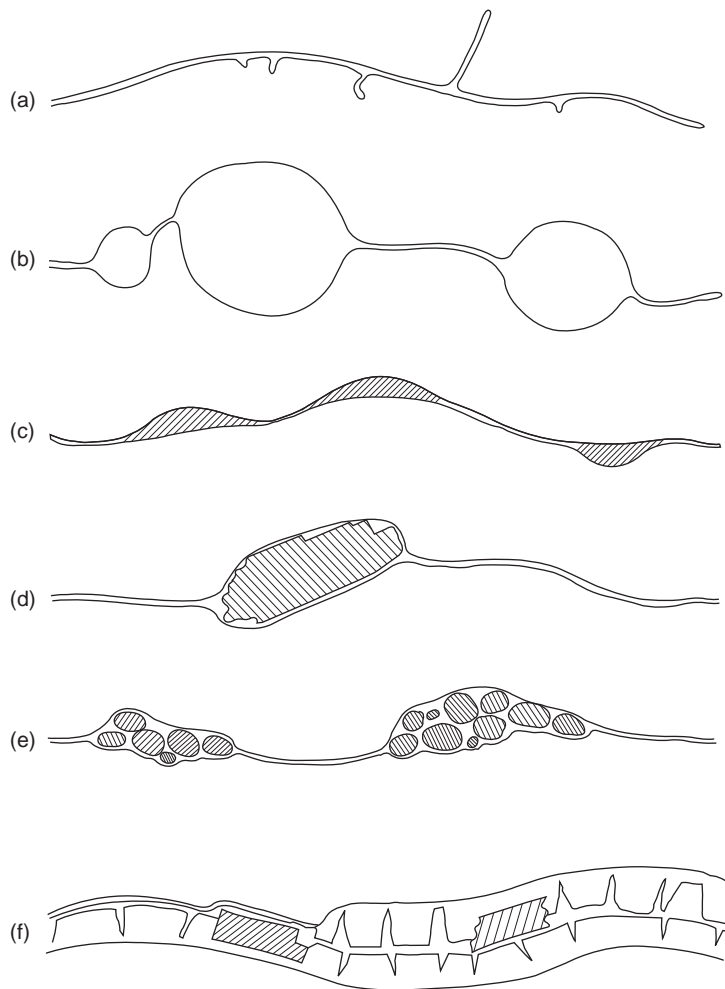


**FIGURE 2.4**

Entrainment defects: (a) a new bifilm; (b) bubbles entrained as an integral part of the bifilm; (c) liquid flux trapped in a bifilm; (d) surface debris entrained with the bifilm; (e) sand inclusions entrained in the bifilm; (f) an entrained surface film containing integral debris.

be even thinner than was first thought. Thicknesses of only 20 nm seem common for films in many aluminum alloys. The names ‘new’ and ‘old’ (probably better stated ‘young’ and ‘old’) are a rough-and-ready attempt to distinguish the types of film, and have proved to be a useful way to categorize the two main types of film.

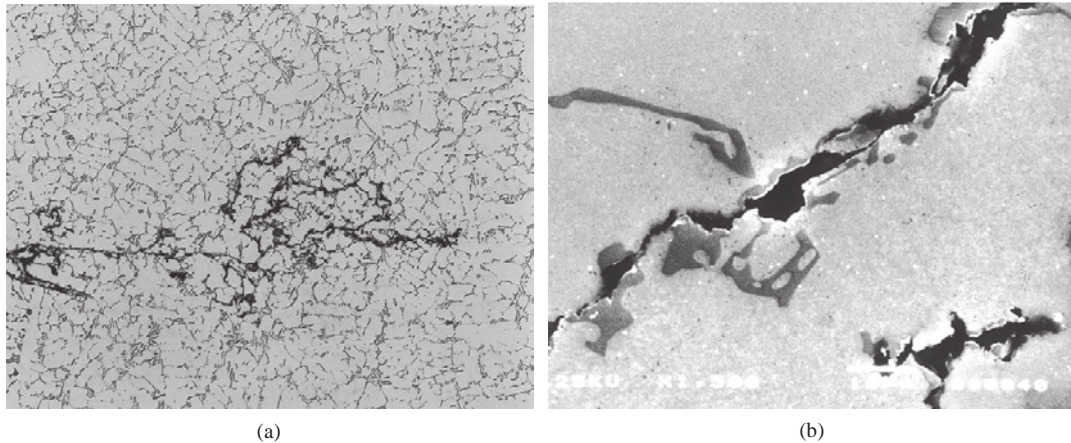
The limited thickness of a newly created surface film is a consequence of its rapid formation, the film having little time to grow and thicken. Research quoted by Birch (2000) on Zn–Al pressure die casting defects using a cavity fill time from 20–100 ms can be back-extrapolated to indicate that in the

Growth time	Thickness	Type	Description	Possible source
0.01–1 s	1 nm–1 $\mu\text{m}$	New	Confetti-like fragments	Pour and mold fill
10 s to 1 min	10 $\mu\text{m}$	Old 1	Flexible, extensive films	Transfer ladles
10 min to 1 hr	100 $\mu\text{m}$	Old 2	Thicker films, less flexible	Melting furnace
10 hr to 10 days	1000 $\mu\text{m}$	Old 3	Rigid lumps and plates	Holding furnace

case of this alloy the surface films formed in times of about 10 ms. Most recent work on entrained young oxides find a limiting thinness in the region of 20 nm. Thus these films are only about ten molecules thick.

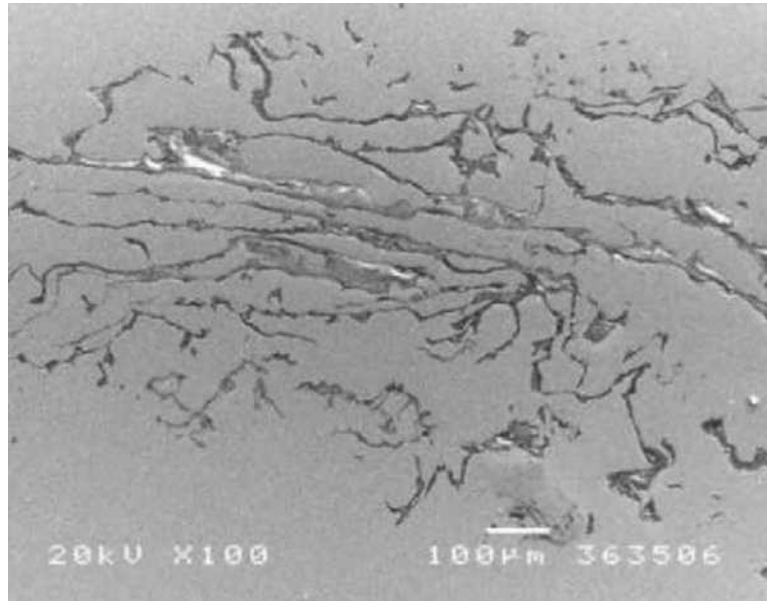
To emphasize the important characteristic crack-like feature of the folded-in defect, the reader will notice that it will be often referred to as a ‘bifilm crack’ or ‘oxide crack’. A typical entrained film is seen in Figure 2.5a, showing its convoluted nature. This irregular form, repeatedly folding back on itself, distinguishes it from a crack resulting from stress in a solid; its morphology distinguishes it as a defect that could only have formed in a turbulent liquid. At high magnification in the scanning electron microscope (Figure 2.5b) the gap between the double film looks like a bottomless canyon. This layer of air (or other mold gas) is nearly always present, trapped partly by the irregular folds and partly by the microscopic roughness of the film as it folds over.

Figure 2.6 is an unusual polished section photographed in an optical microscope in the author’s laboratory by Divandari (2000). It shows the double nature of the bifilm, since by chance the section happened to be at precisely the level to take away part of the top film, revealing underneath the smooth, glossy surface of a second, clearly unbonded film. Such confirmations of the double nature of the bifilm, and its unbonded central interface, are relatively common, but in the past have generally been overlooked.



**FIGURE 2.5**

(a) Convoluted bifilm in Al–7Si–0.4Mg alloy; (b) close-up reported by Green (Green and Campbell 1994) to appear ‘canyon-like’ in the SEM.



**FIGURE 2.6**

Polished surface of Al-7Si-0.4Mg alloy breaking into a bifilm, showing upper part of the soluble film removed, revealing the inside of the lower film (Divandari 2000).

As we have mentioned, the surface can be entrained simply by a contraction of the surface so as to create a problem of too much area of film for the area of surface available. However, if more severe disturbance of the surface is experienced, as typically occurs during the pouring of liquid metals, pockets of air can be accidentally trapped by chance creases and folds at random locations in the double film, since the surface turbulence event is usually chaotic (waves in a storm rarely resemble sine waves). The resultant scattering of porosity in castings seems nearly always to originate from these pockets of entrained air. This appears to be the most common source of porosity in castings (so-called 'shrinkage', and so-called 'gas' precipitating from solution are only additive effects that may or may not contribute additional growth). The creation of this source of porosity has now been regularly observed in the study of mold filling using X-ray radiography. It explains how this rather random distribution of porosity typical in many castings has confounded the efforts of computers programmed to simulate only solidification. Such porosity is commonly mis-identified as 'shrinkage porosity'. In reality it is nearly always tangled masses of oxide bifilms. For such defects, often observed on radiographs, we need to practice saying not 'it is shrinkage' but 'it *appears* to be shrinkage', preferably followed by the phrase 'but most likely *not* shrinkage'. Gradually, we shall appreciate that the porosity observed on radiographs is *rarely* shrinkage because in general foundry personnel know how to feed castings, so that in general, genuine shrinkage problems are not expected.

Once entrained, the film may sink or float depending on its relative density. For films on dense alloys such as copper-based and ferrous materials, the entrained bifilms float. In very light materials such as magnesium alloys and lithium alloys the films generally sink. For aluminum oxide in liquid



aluminum the situation is rather balanced, with the oxide being denser than the liquid, but its entrained air, entrapped between the two halves of the film, often brings its density close to neutral buoyancy. The behavior of oxides in aluminum is therefore more complicated and worth considering in detail.

Initially of course, enclosed air will aid buoyancy, assisting the films to float to the top surface of the melt. However, as will be discussed later, the enclosed air will be slowly consumed by the continuing slow oxidation (followed by the slow nitridation as discovered by Raiszadeh and Griffiths in 2008) of the surfaces of the central interfaces exposed to the entrapped air. Thus the air is gradually consumed and the buoyancy of the films will slowly be lost providing the hydrogen content of the melt is low. These authors found that when the hydrogen content of the melt was  $8 \text{ ml kg}^{-1}$  or more the diffusion of hydrogen into the bifilm more than compensated for the loss of air, so that the bifilm would expand. This complicated behavior of the bifilm explains a commonly experienced sampling problem, since the consequential distribution of defects in suspension at different depths in aluminum furnaces makes it problematic to obtain good-quality metal out of a furnace.

The reason is that after some time although most oxides sink to the bottom of the furnace, a significant density of defects collects just under the top surface. Naturally, this makes sampling of the better-quality material at intermediate depth rather difficult.

In fact, the center of the melt would be expected to have a transient population of oxides that, for a time, were just neutrally buoyant. Thus these films would leave their position at the top, would circulate for a time in the convection currents, taking up residence on the bottom as they finally lost their buoyancy. Furthermore, any disturbance of the top would be expected to augment the central population, producing a shower, perhaps a storm, of defects that had become too heavy, easily dislodged from the support of their neighbors, and which would then tumble down to the bottom of the melt. Thus in many furnaces, although the mid-depth of the melt would probably be the best material, it would not be expected to be completely free from defects.

### 2.1.2 Bubbles

*Small bubbles* of air entrapped between films (Figure 2.4b) are often the source of *microporosity* observed in castings. Round micropores would be expected to decorate a bifilm, the bifilm itself often being not visible on a polished microsection. Samuel (1993) reports reduced pressure test samples of aluminum alloy in which bubbles in the middle of the reduced pressure test casting are clearly seen to be prevented from floating up by the presence of oxide films.

*Large bubbles* are another matter, as illustrated in Figure 2.7. The entrainment of larger bubbles is envisaged as possible only if fairly severe surface turbulence occurs. The powerful buoyancy of those larger pockets of entrained air, generally above 5 mm diameter, will give them a life of their own. They may be sufficiently energetic to drive their way through the morass of other films as schematically shown in Figure 2.7. They may even be sufficiently buoyant to force a path through partially solidified regions of the casting, powering their way through the dendrite mesh, bending and breaking dendrites. Large bubbles have sufficient buoyancy to continuously break the oxide skin on their crowns, powering an ascent, overcoming the drag of the *bubble trail* in its wake. Bubble trails are an especially damaging consequence of the entrainment process, and are dealt with later. Large bubbles that are entrained during the pouring of the casting are rarely retained in the casting. This is because they arrive quickly at the top surface of the casting before any freezing has had time to occur. Because their buoyancy is sufficient to split the oxide at its crown, it is similarly sufficient to burst the oxide skin of

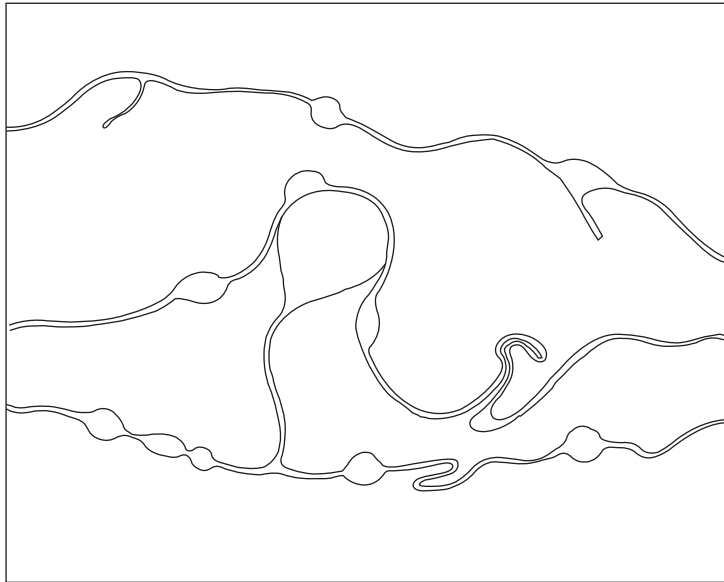


**FIGURE 2.7**

Schematic illustration of bifilms with their trapped microbubbles and active buoyant macrobubbles.

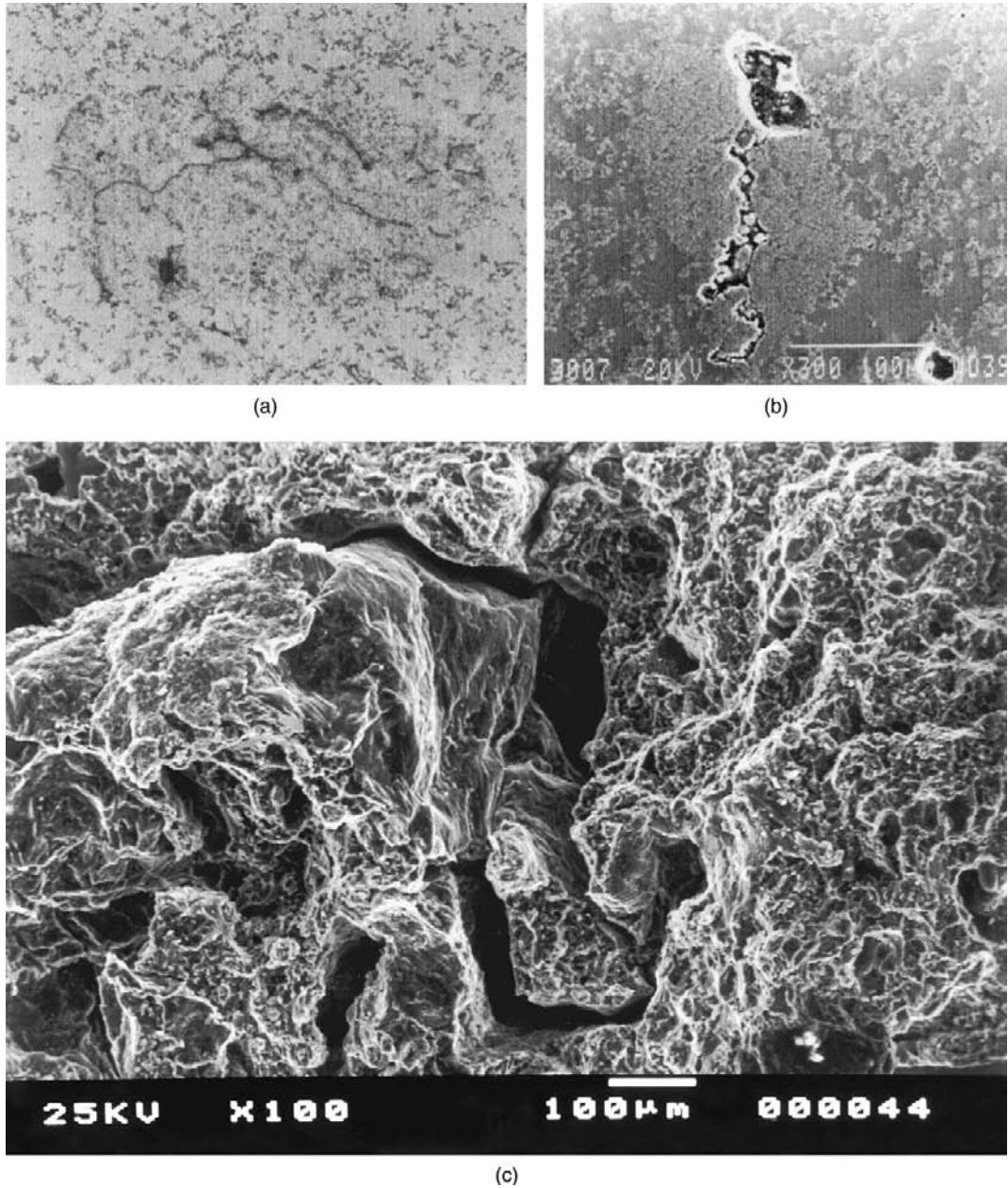
the casting that constitutes the last barrier between them and the atmosphere, and so escape. This detrainment of the bubble itself leaves the legacy of the bubble trail.

Bubble trails are a kind of elongated bifilm. However, when scrambled and raveled together they are practically indistinguishable from ordinary bifilms, as will be described later (see Figure 2.34).

Masses of bubbles can be introduced to the casting by a poor filling system design, so that bubbles arriving later are trapped in the tangled mesh of trails left by earlier bubbles. Thus a mess of oxide trails and bubbles is the result. I have called this mixture of bubbles and oxide bubble trails *bubble damage*. In the author's experience, bubble damage is the most common defect in castings, accounting for perhaps 80% of all casting defects. It is no wonder that the current computer simulations cannot predict the problems in many castings. (In fact, it seems that relatively few of our important defects are attributable to the commonly blamed 'gas' or 'shrinkage'.)

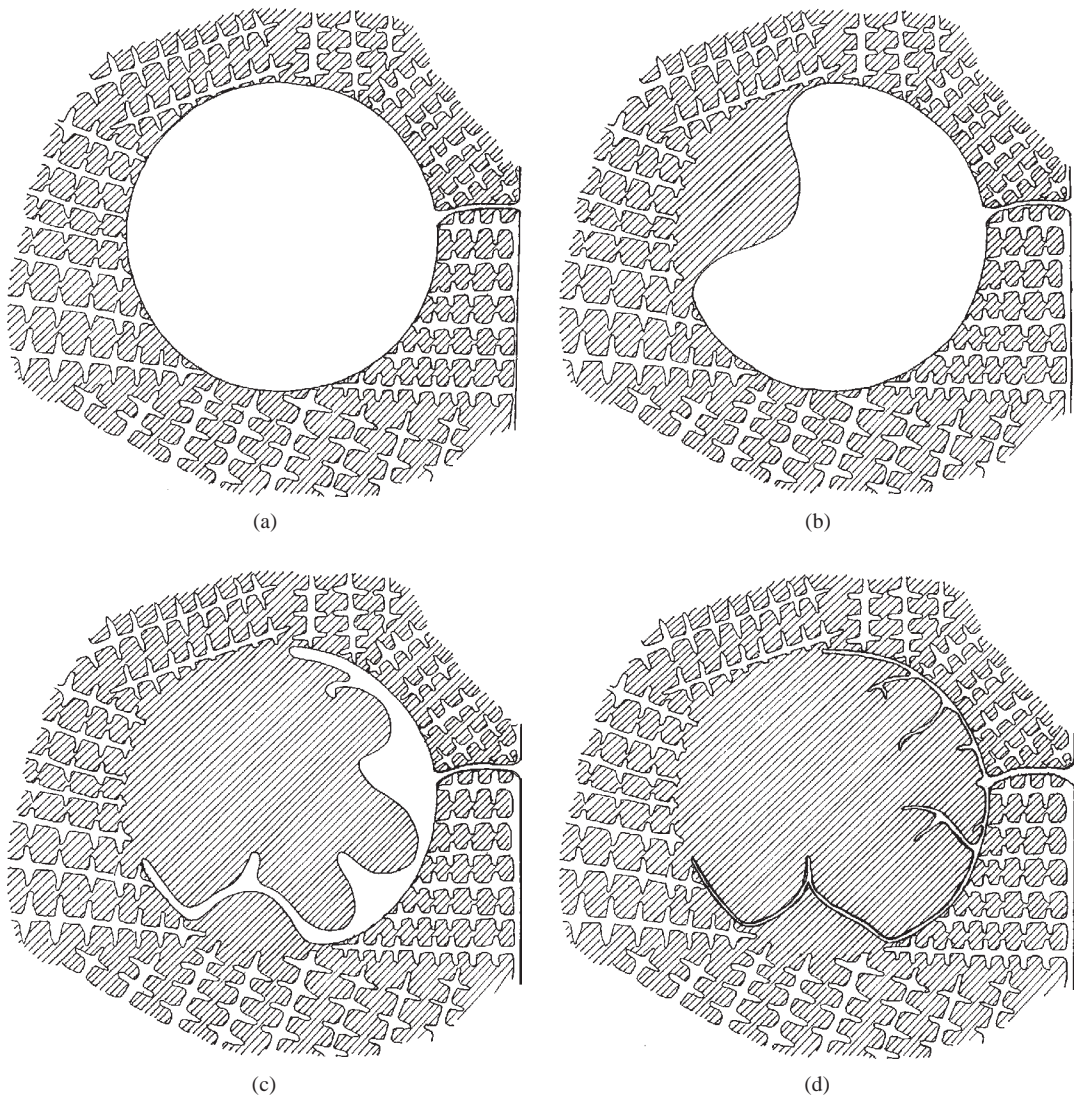
Pockets of air, as bubbles, are commonly an integral feature of the bifilm as we have seen. However, because the bifilm is itself an entrainment feature, there is a possibility that the bifilm or its bubble trail can form a leak path connecting to the outside world, allowing the bubble to deflate if the pressure in the surrounding melt rises. Such collapsed bubbles are particularly noticeable in some particulate metal matrix composites as shown in the work of Emamy and the author (1997), and illustrated in Figures 2.8 and 2.9. The collapsed bubble then becomes an integral part of the original bifilm, but is characterized by (i) a thicker oxide film because of its longer exposure to a plentiful supply of air, and (ii) a characteristically convoluted shape within the ghost outline of the original bubble.

Larger entrained bubbles are always somewhat crumpled, like a prune. The reason is almost certainly the result of the deformation of the bubble during the period of intense turbulence whilst the mold is filling. A spherical bubble would have a minimum surface area. However, when deformed its



**FIGURE 2.8**

Collapsed bubbles in Al-TiB<sub>2</sub> MMC (a) and (b) show ghost outlines of collapsed bubbles; (c) the resulting bifilm intersecting a fracture surface (Emamy and Campbell 1997).

**FIGURE 2.9**

Schematic illustration of stages of the collapse of a bubble, losing its entrained air via a leak path to the surface, showing the residual double film and the volume of dendrite-free interdendritic liquid.

area necessarily increases, increasing the area of oxide film on its surface. On attempting to regain its original spherical shape the additional area of film is now too large for the bubble, so that the skin becomes wrinkled. As the forces of turbulence hammer the bubble, each deformation of its shape would be expected to add additional area. (A further factor, perhaps less important, may be the reduction in volume of the bubble as the system cools, and as air is consumed by on-going oxidation

and nitridation. In this case the analogy with a large shiny round plum shrinking to become a smaller wrinkled prune, may be relatively accurate.)

The growth of the area of oxide as the surface deforms seems a general feature of entrainment. It is a one-way, irreversible process. Once formed, the area of the oxide cannot be reduced, so that as the liquid surface attempts to contract, for instance as the disturbance passes, the oxide has no choice but to wrinkle. The consequent crinkling and folding of the surface is a necessary characteristic of entrained films formed on a turbulent liquid surface, and is the common feature that assists to identify films on fracture surfaces. Figure 2.10a is a good example of a thin, probably young, film on an Al–7Si–0.4Mg alloy. Figure 2.10b is typical of the much thicker films on an Al–5Mg alloy, displaying the concertina-like corrugations of a film that has grown too large for the area available. A typical thick and granular older film on an Al–11Si alloy is seen in Figure 2.10c. The extreme thinness of some films can be seen on a fracture surface of an Al–7Si–0.4Mg alloy (Figure 2.11) that reveals a film folded multiple times but in its thinnest part measures just 20 nm thick.

The irregular shape of bubbles has led to them often being confused with shrinkage pores. Furthermore, perfectly round gas bubbles have been observed by video X-ray radiography of solidifying castings to form initiation sites for shrinkage porosity; bubbles appear to expand by a ‘furry’ growth of interdendritic porosity as residual liquid is drawn away from their surface in a poorly fed region of a casting. Such developments obscure the key role of the entrained bubble as the originating source of the problem.

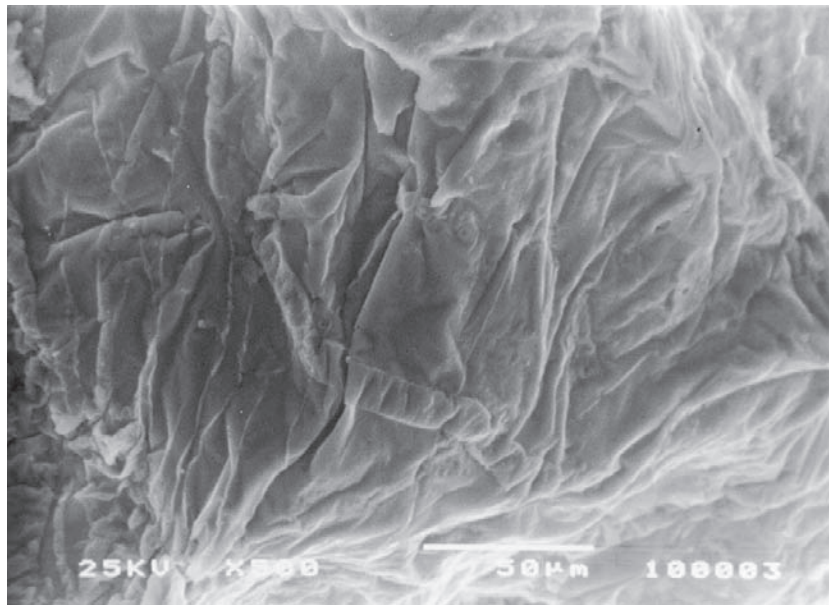
### 2.1.3 Extrinsic inclusions

In addition to bifilms (cracks) and bubbles (porosity), there are a number of other, related defects that can be similarly entrained (i.e. introduced into the matrix from the outside). These externally introduced features are variously but aptly called *entrained inclusions*, *extrinsic inclusions*, or *external inclusions* (they are also occasionally known by the equally accurate but awkward term *exogenous inclusions* which we shall avoid). Such features are, of course, completely different in character to second phases that precipitate from the melt as part of the cooling and solidification processes. The differences warrant careful examination, and are discussed below.

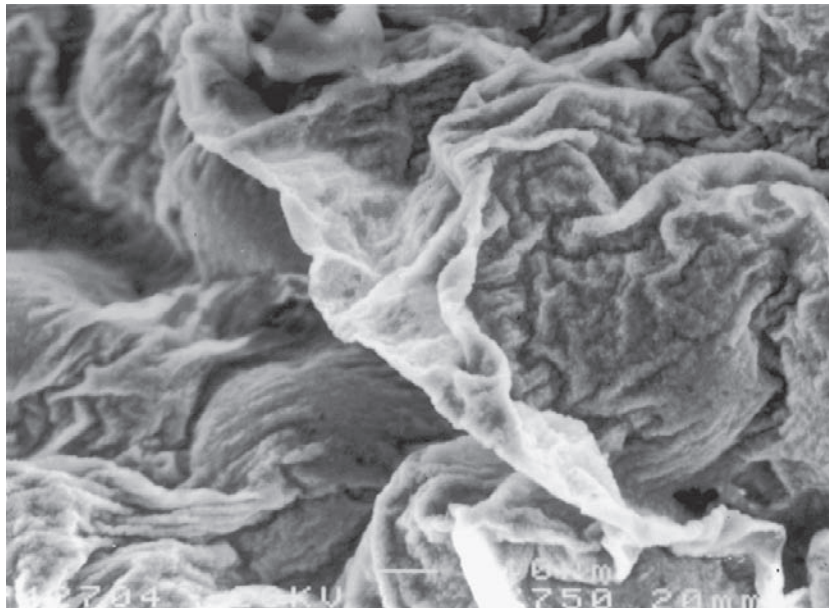
#### ***Flux and slag inclusions***

Fluxes containing chlorides or fluorides are relatively commonly found on machined surfaces of light alloy cast components. Such fluxes are deliquescent, so that when opened to the air in this way they absorb moisture, leading to localized pockets of corrosion and the unsightly exudation of corrosion products on machined surfaces. During routine examination of fracture surfaces, the elements chlorine and fluorine are quite often found as chlorides or fluorides on aluminum and magnesium alloys. The most common flux inclusions to be expected are NaCl and KCl.

However, chlorine and fluorine, and their common compounds, the chlorides and fluorides, are insoluble in aluminum, presenting the problem of how such elements came to be located in the matrix. This can probably only be explained by assuming that such materials were originally on the surface of the melt, but have been mechanically entrained, wrapped in the surface oxide film (Figure 2.4c). Thus flux inclusions on a fracture surface indicate the presence of a bifilm, probably of considerable area, although the presence of its single remaining half on one of the fracture surfaces will probably be not easily seen on the fracture.



(a)

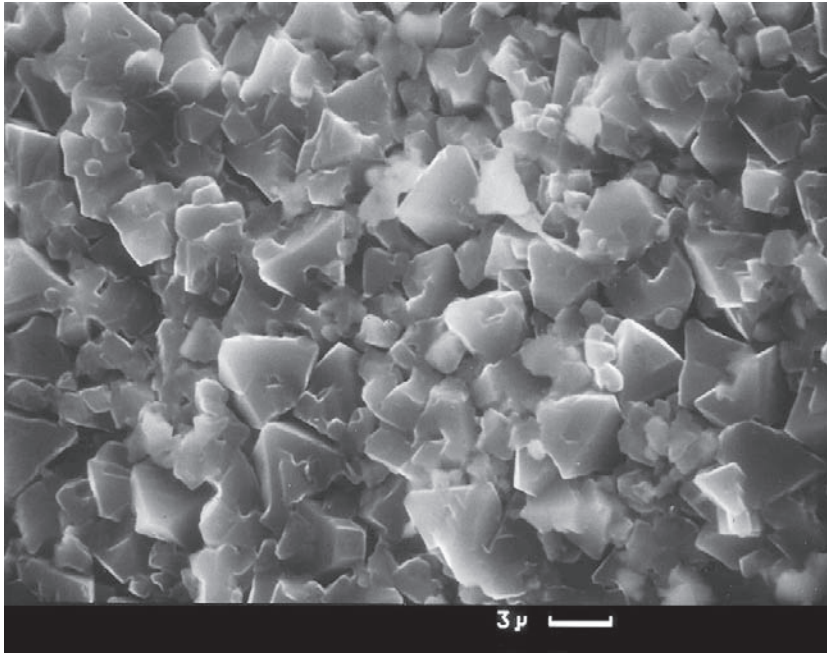


(b)

**FIGURE 2.10**

Fracture surfaces showing (a) a fairly thin film on an Al-7Si-0.4Mg alloy; (b) a thick but flexible film on Al-5Mg alloy (courtesy Divandari 2000); and (c) a thick granular spinel film on Al-7Si-0.6Mg alloy (courtesy Philip Bell 1981).





(c)

FIGURE 2.10 (continued).

Also, because flux inclusions are commonly liquid at the temperatures of liquid light alloys, and perfectly immiscible, why do they appear in the matrix and not spheroidize and rapidly float out, becoming lost from the surface of the melt? It seems that rapid detrainment does not occur. The explanation lies in the presence of the bifilm: the flux would originally have sat on the oxide surface of the melt. Surface turbulence folded in the surface, forming a flux sandwich in an entrained oxide bifilm. This package is slow to float or settle because of its extended area. The consequential long residence times allow transport of these contaminants over long distances in melt transfer and launder systems. Sokolowski and colleagues (2000) find that chloride flux inclusions travel distances of tens of meters in launders, whereas if they were simply spherical droplets they would be expected to completely separate from the melt within a meter or so of travel along a launder. They found that the electromagnetic pumps at the end of the launder system were eventually blocked by a mix of oxides and fluxes depositing in the working interiors of the pumps. It is likely that the inclusions are forced out of suspension by the combined centrifugal and electromagnetic body forces in the pump. It is hardly conceivable that fluxes themselves, as relatively low-viscosity liquids, could form a blockage. However, the accretion of a mixture of solid oxide films bonded with a sticky liquid flux would be expected to be highly effective in choking the system.

When bifilms are created by folding into the melt, the presence of a surface liquid flux would be expected to have a powerful effect by effectively causing the two halves of the film to adhere together by viscous adhesion. This may be one of the key mechanisms explaining why fluxes are so effective in

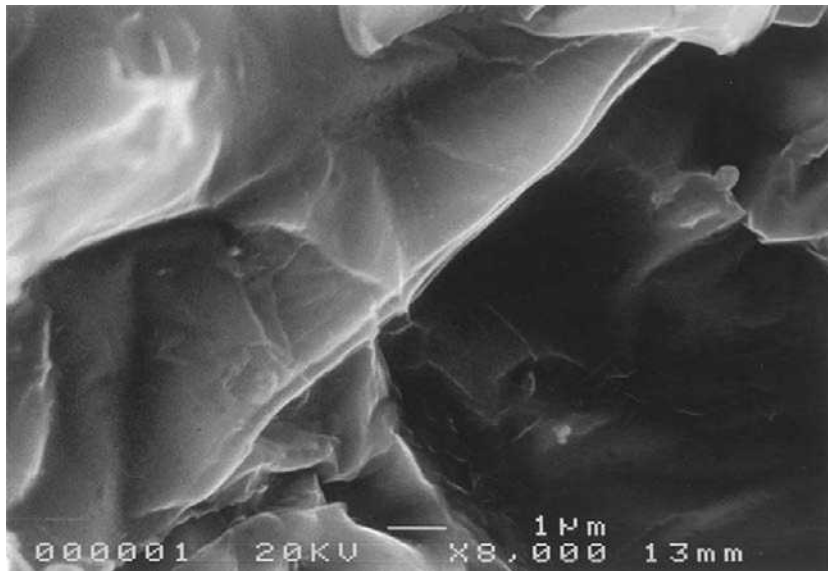


**FIGURE 2.11**

Multiply folded film on the fracture surface of an Al-7Si-0.4Mg alloy (courtesy of NR Green).

reducing the porosity in aluminum alloy castings. The bifilms may be glued shut. At room temperature the bonding by the solidified flux may aid strength and ductility to some extent. On the other hand, the observed benefits to strength and ductility in flux-treated alloys may be the result of the reduction in films by agglomeration (because of their sticky nature in the presence of a liquid flux) and flotation. These factors will require much research to disentangle.

Whether fluxes are completely successful to prevent oxidation of the surface of light alloys does not seem to be clear. It may be that a solid oxide film always underlies the simple chloride fluxes and possibly some of the fluoride fluxes. Even if an underlying oxide film were unstable, and gradually dissolving in the flux, the early entrainment of the melt surface prior to the complete solution of the oxide would explain the oxide presence despite any thermodynamic instability.

Even now, some foundries successfully melt light alloys without fluxes. Whether such practice is really more beneficial deserves to be thoroughly investigated. What is certain is that the environment would benefit from the reduced dumping of flux residues from so-called cleansing treatments.

There are circumstances when the flux inclusions may not be associated with a solid oxide film simply because the oxide is rapidly soluble in the flux. Such fluxes include cryolite  $\text{AlF}_3 \cdot 3\text{NaF}$  as used to dissolve alumina during the electrolytic production of aluminum, and the family of other fluorides  $\text{K}_2\text{TiF}_6$ ,  $\text{KBF}_4$ ,  $\text{K}_3\text{TaF}_7$ , and  $\text{K}_2\text{ZrF}_6$ . Thus the surface layer may be a uniform liquid phase in these special cases, provided the temperature is sufficiently high for the flux itself to be above its melting point.

For irons and steels when a liquid slag layer is present it is normally expected to be liquid throughout. Where a completely liquid slag surface is entrained Figure 2.12 shows the expected detrainment of the slag and the accidentally entrained gases and entrained liquid metal. Such



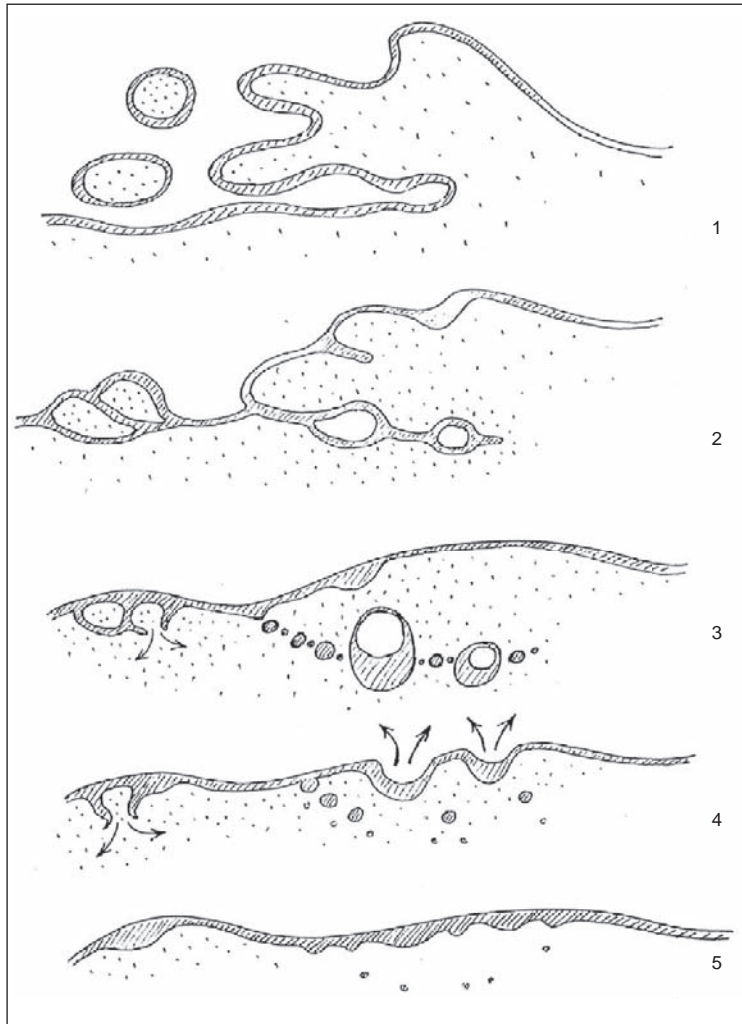


**FIGURE 2.12**

Entrainment of a liquid surface film, showing the subsequent detrainment of metal, gases, and most of the entrained droplets of liquid. No bifilm is formed. The cast metal remains essentially free from any serious permanent entrained damage.

spheroidization of fluid phases is expected to occur in seconds as a result of the high surface energy of liquid metals and their rather low viscosity.

A classical and spectacular break-up of a film of liquid is seen in the case of the granulation of liquid ferro-alloys (Figure 2.13). A ladle of alloy is poured onto a ceramic plate sited centrally above a bath of water. On impact with the plate the jet of metal spreads into a film that thins with distance from the center. The break-up of the metal film is seen to occur by the nucleation of holes in the film,

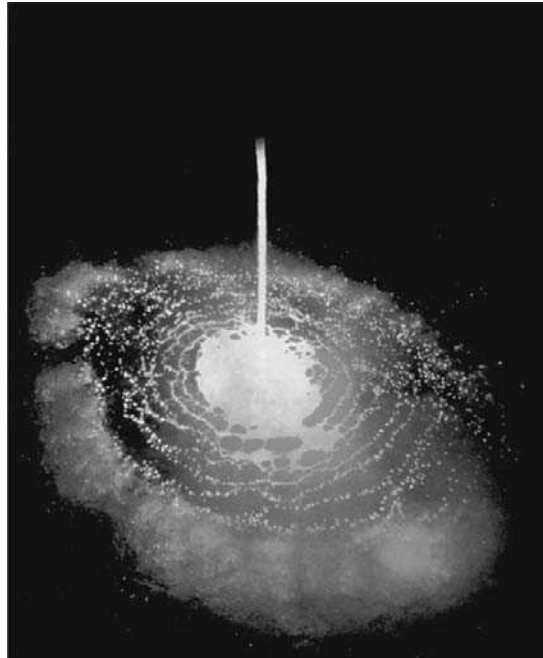


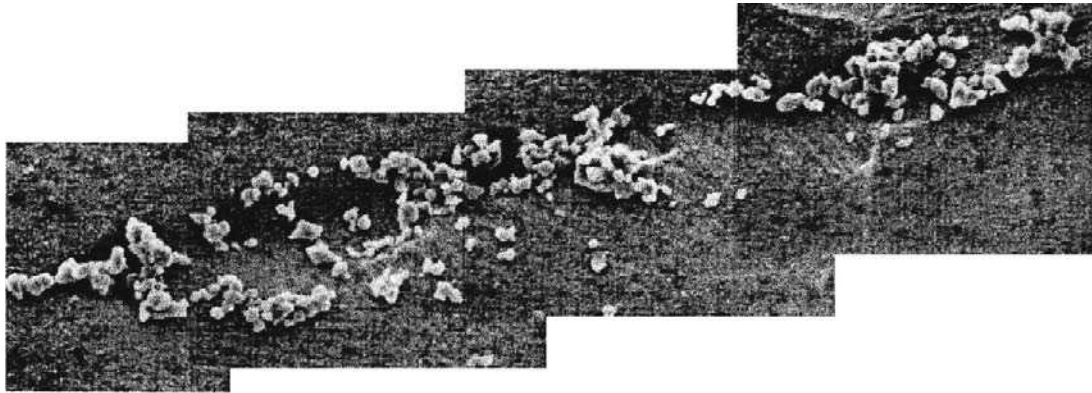
**FIGURE 2.13**

Granulation of liquid ferromanganese poured on to a flat ceramic target, showing the characteristic mode of fragmentation of a film into ligaments, then into droplets, and finally being cooled in a bath of water (courtesy of Uddeholm Technology, Sweden, 2001).

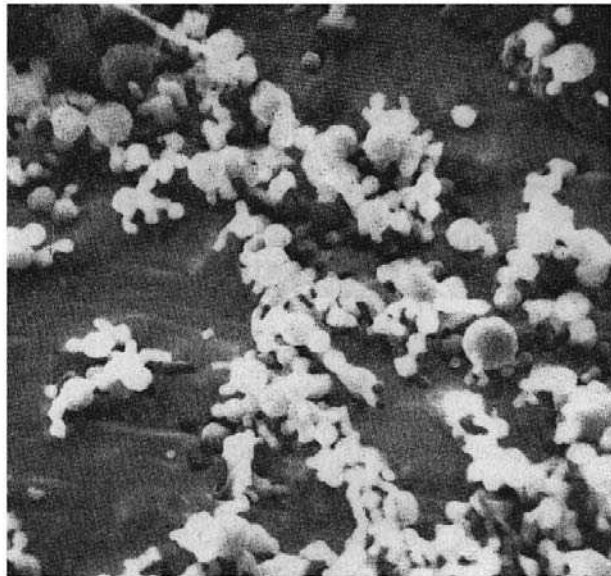
followed by the thinning of ligaments between holes, and finally by the break-up of the ligaments into droplets. This is the classical mode of break-up of a thinning liquid film.

A similar pattern of fragmentation of thin films may not only occur for liquid films. It seems possible that alumina is first entrained into liquid steel as solid films (the melting point of alumina being over 2000°C). However, once entrained, the films would be expected to spherodize. This is because the solid films are extremely thin, and the temperature will be sufficiently high to encourage rapid surface diffusion, leading to break-up of the films into roughly spherical particles. The spherodization will be driven by the high interfacial energy that is typical of high-temperature metallic systems. The clusters and stringers of isolated alumina inclusions in rolled steels might have formed by this process, the rolling action being merely to further separate and align them along the rolling direction (Figure 2.14a). This suggestion is supported by observations of Way (2001) that show the blockage of nozzles of steels in continuous casting plants to be the result of arrays of separate granular alumina inclusions (Figure 2.14b). It seems certain that such inclusions were originally alumina films (separate inclusions seem hardly conceivable) formed by the annular back-flow of oxidizing air inside the lower regions of the nozzle where the flow detaches from the nozzle wall. Properly tapered nozzles (instead of parallel bore nozzles) avoid this problem.

In contrast, a film of liquid flux on aluminum alloys is not, in general, expected to have this simple completely liquid structure. It seems certain that in most instances a solid alumina film will underlie



(a)



(b)

**FIGURE 2.14**

(a) Alumina stringers in deep-etched rolled steel; (b) alumina particles from a blocked tundish nozzle from a steel continuous casting plant (Way 2001).

the liquid flux. Thus this composite film will behave as a sticky solid layer, and will be capable of permanently entraining bubbles and liquid flux. Spheroidization of the liquid flux will be impossible.

### ***Old oxides***

Figures 2.3 and 2.4d represent one of many different kinds of extrinsic or external inclusion, such as a piece of refractory from the wall of a furnace or ladle or a piece of old surface oxide from the same

source. External inclusions can only be entrained together with a wrapping of young surface film. Attempts to introduce inoculants of various kinds into aluminum alloys have been made from time to time. All of these attempts are seen to be undermined by the problem of the surrounding young oxide with its associated layer of air, preventing the introduced particle from ever making contact with the melt as in Figure 2.3. This behavior necessarily occurs despite attempts by such authors as Mohanty and Gruzleski (1995) to add  $\text{TiB}_2$  particles to liquid aluminum beneath the surface of the melt. They found that such particles did not nucleate grains, but were pushed by dendrites to the grain boundaries. This is completely unexpected behavior for a  $\text{TiB}_2$  particle in good atomic contact with the melt. A particle of  $\text{TiB}_2$  in contact with the matrix is expected to be incorporated into the growing solid, and actually nucleate new solid grains. However, being pushed ahead of the solidification front is the behavior expected for any particle microscopically separated from its surrounding melt by a layer of air held in place by a film of oxide, and thus effectively completely non-wetted (i.e. not in contact with the melt, and so actually remaining 'dry').

Similarly, the vortex technique for the addition of particles to make a particulate metal matrix composite (MMC) is similarly troubled. It is to be expected that the method would drag the oxide film down into the vortex, together with the heaps of particles supported on the film, so that the clumping of particles, now nicely and collectively packaged, wrapped in film, is probably unavoidable. The 'clumping' of particles observed in such MMCs survives even long periods of vigorous stirring (Figure 2.3c). Such features are seen in the work by Nai and Gupta (2002) in which the central particles in clumps of stirred-in SiC particles are observed to have fallen out during the preparation of the polished sample, leaving small cave-like structures lined with SiC particles that are somehow still held in place. In addition, whether in clumps or not, during the preparation of the mixture the particles are almost certainly held in suspension by the network of bifilms that will have been introduced, in the same way that networks of films have been observed to hold gas bubbles in suspension (Samuel 1993). It seems also likely that the oxide network will reduce the fluidity of the material, and reduce the achievable mechanical properties, as discovered by Emamy and co-workers (2009).

In a further example, the manufacture of aluminum alloy MMCs based on aluminum alloy containing SiC particles introduced under high vacuum was investigated by Emamy and Campbell (1997). These authors found that under the hydrostatic tension produced by poor feeding conditions the SiC–matrix interface frequently decohered. This contrasted with the behavior of an Al– $\text{TiB}_2$  MMC in which the  $\text{TiB}_2$  particles were created by a flux reaction and added to the matrix alloy without ever having been in contact with the air. These particles exhibited much better adhesion at the particle–matrix interface when subjected to tension. Relatively few pores were initiated when subjected to the hydrostatic tensile stress generated by the poor feeding.

Figure 2.4d illustrates the entrainment of a piece of *old oxide*, probably from an earlier part of the melting or holding process. Such oxide, if very old, will have grown thick, and no longer justifies description as a film. It can be crusty or even plate-like. It is simply just another external inclusion. A typical example is seen in Figure 2.10c. If entrained during pouring, its passage through the liquid surface will ensure that it becomes wrapped in a new thin film, its entrained air film separating the old inclusion from contact with the melt. This wrapping will allow the matrix to 'decohere' easily from the inclusion, leading to the initiation of porosity or cracks. However, if the old oxide was entrained some time previously during the melting or holding process, its entrained wrapping will itself become old, having lost the majority of its air layer by continued reaction. In this case it will have become fairly 'inert' in the sense that it cannot easily initiate porosity; all its surfaces will have reacted with the melt

and thus have come into good atomic contact; its air layer will have become largely lost and welded closed.

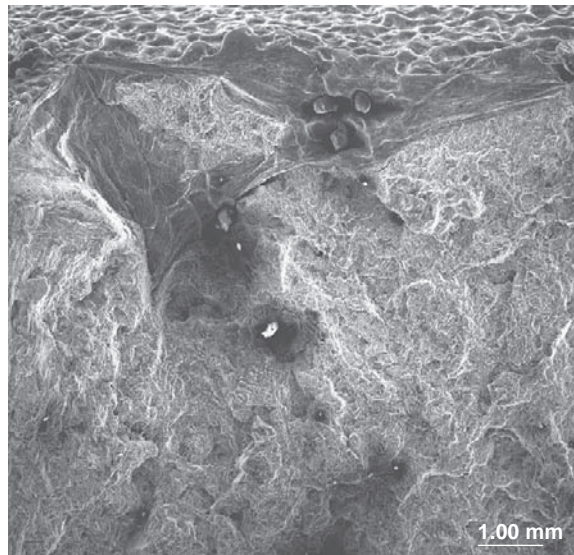
### ***Sand inclusions***

Molding sand inclusions are perhaps the most common extrinsic inclusion (Figures 2.3c and 2.4e), but whose mechanism of entrainment is probably rather complicated. It is not easy to envisage how minute sand grains could penetrate the surface of a liquid metal against the repulsive action of surface tension, and the presence of an oxide film acting as a mechanical barrier. The penetration of the liquid surface would require the grain to be fired at the surface at high velocity, like a bullet. However, of course, such a dramatic mechanism is unlikely to occur in reality. Although the following description appears complicated at first sight, a sand entrainment mechanism can occur easily, involving little energy, as described below.

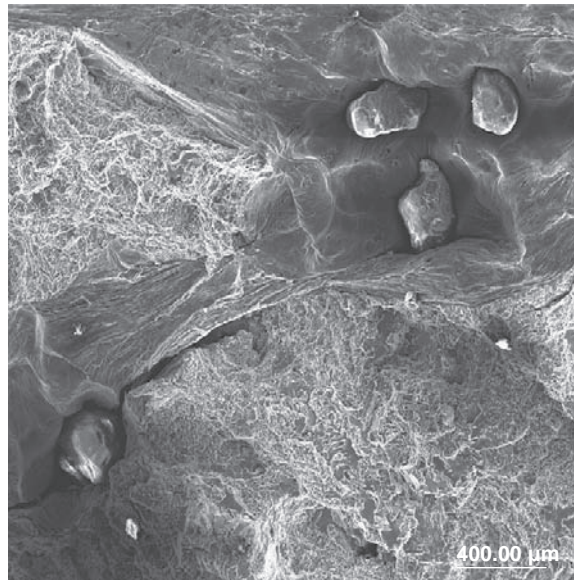
In a well-designed filling system for a sand casting, the liquid metal entirely fills the system, and its hydrostatic pressure acts against the walls of the system to gently support the mold, holding sand grains in place. Thus the mold surface will become hot. If bonded with a resin binder, the binder will often first soften, then harden and strengthen as volatiles are lost. The sand grains in contact with the metal will finally have their binder degraded (pyrolyzed) to the point at which only carbon remains, now hardened and rigid, like coke, forming strong mechanical links between the grains. The carbon layer remaining on the grains has a high refractoriness. It continues to protect the grains since it in turn is protected from oxidation because, at this late stage, most of the local oxygen has been consumed to form carbon monoxide. The carbon forms a non-wetted interface with the metal, thus enhancing protection from penetration and erosion.

The situation is different if the filling system has been poorly designed, allowing a mix of air to accompany the melt. This problem commonly accompanies the use of filling systems that have oversized cross-section areas, and thus remain unfilled with metal. In such systems the melt can ricochet backwards and forwards in the channel. The mechanical impact, akin to the cavitation effect on a ship's propeller, is a factor that assists erosion. However, other factors are also important. The contact of the melt with the wall of the mold heats the sand surface. As the melt bounces back from the wall, air is drawn through the mold surface, and on the return bounce, the air flow is reversed. In this way air is pumped backwards and forwards through the heated sand, and so burns away the binder. The burning action is intensified akin to the air pumped by bellows in the blacksmith's forge. When the carbon is finally burned off the surface of the grains, the sand is no longer bonded to its fellow grains in the mold. Furthermore, the oxide on the surface of the melt can now react with the freshly exposed silica surface of the grains, and thus adhere to them. If the melt now ricochets off the sand surface once again, the oxidized liquid surface peeling away from the mold is now covered with adhering grains of sand. As the surface folds over, the grains are thereby enfolded into an envelope of oxide film, as wrapped in a paper bag (Figure 2.15). Under the microscope, such oxide films can practically always be seen enfolding clusters of sand inclusions. Similarly, sand inclusions are often found on the inner surfaces of bubbles.

Sand inclusions are therefore a sure sign that the filling system design is poor, involving significant surface turbulence. Conversely, sand inclusions can nearly always be eliminated by attention to the filling system, not the strength or the variety of the sand binder. A rash of sand inclusions is a common ailment in foundries. The best solution lies neither with the sand plant operator nor the binder supplier, but in the hands of the designer of the filling system of the casting.



(a)



(b)

**FIGURE 2.15**

Fracture surface of Al-7Si-0.4Mg alloy showing (a) the sand-cast surface (top) with a surface-connected oxide film; (b) close-up showing the sand inclusions entrained in their 'paper bag' of oxide film (courtesy of S Fox 2002).

Finally, Figure 2.4f is intended to give a glimpse of the complexity that is likely to be present in many bifilms. Part of the film is new and thin, forming an asymmetrical thick/thin double film. (Reactions of the melt with the bifilm, as discussed at many points later in this work, often lead to asymmetrical precipitation of reactants if one side of the bifilm is more favorable than the other.) It would be expected that other parts of the defect would be fairly symmetrical thin double films. Elsewhere both halves may be old, thick and heavily cracked. In addition, the old film contains debris that has become incorporated, having fallen onto the surface of the melt at various times in its progress through the melting and distribution system.

Entrained material is probably always rather messy.

---

## 2.2 ENTRAINMENT PROCESSES

The entrainment of surface films, leading to the creation of a double film in the liquid, can occur in very different ways, and lead to quite different types of bifilm crack:

- (i) by surface turbulence, in which the bulk liquid and the liquid meniscus are in general traveling in at least approximately the same direction; the motion of the liquid front ensures that the breaking and re-forming of the surface film gives limited time for film growth, so these entrained films are thin, small, irregular and numerous, and occur widely during all types of pouring;
- (ii) by submergence of charge material used to make the melt; these films are often thick, with large area, especially if returns from a sand casting operation are employed; they are probably most easily removed by treatment with small bubbles as in rotary degassing;
- (iii) by laminar flow, in which the bulk liquid is in general flowing parallel to the meniscus, and the meniscus is stationary. The stationary meniscus then grows a thick surface film even though the melt may be traveling at high speed. The thick asymmetric films form large horizontal cracks or vertical tubes, and are therefore also common in top-gated castings;
- (iv) by the passage of bubbles or air or mold gases through the melt, creating the long bubble trail as a collapsed tube. Since most running systems entrain up to 50% air, there is no shortage of these damaging leak paths between ingates and the top of the casting.

### 2.2.1 Surface turbulence

As liquid metal rises up a vertical plate mold cavity, with the meniscus constrained between the two walls of the mold, an observer looking down from above (suitably equipped with protective shield of course!) will see that the liquid front advances upwards by splitting the surface film along its center. This occurs because the earlier area of the film is trapped between the wall of the mold and the liquid surface, effectively held in place by friction, and therefore cannot rise with the rising liquid. Thus film on the rising surface is torn apart, moving to each side, to become the skin of the casting, which is pinned in place against the mold walls (Figure 2.2a). As the surface tearing happens, of course, the surface film is continuously renewed so that the process is effectively continuous.

It seems that this vertical advance actually occurs by the action of one or more horizontal transverse traveling waves (I call them 'unzipping waves') that wander backwards and forwards along a meniscus rising between walls. This interesting phenomenon will be discussed in detail later.

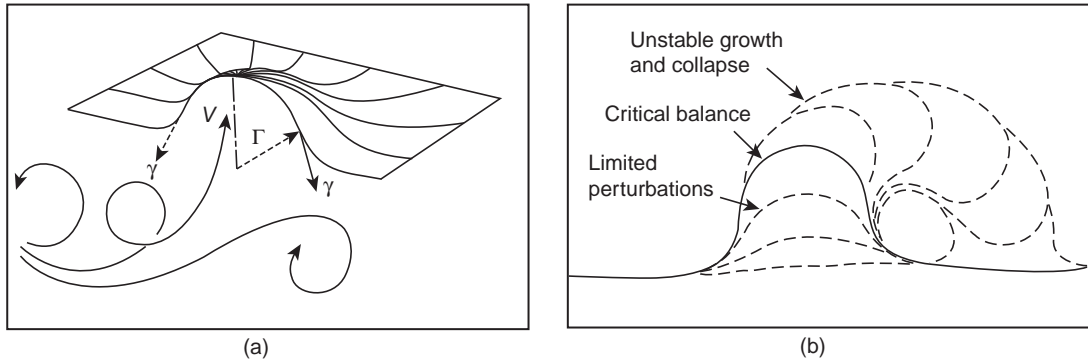


**FIGURE 2.16**

(a) The balance of forces in the liquid surface; (b) perturbations of the surface by inertial forces in the melt remain reversible up to the critical hemispherical limit, after which the surface becomes unstable and irreversibly deforms, introducing the danger of the entrainment of the surface.

The important feature of this form of advance of the liquid front is that the surface film never becomes entrained in the bulk of the liquid. Thus the casting remains potentially perfect. If this is not already perfectly understood at this point, all readers are encouraged to learn this fact by heart before proceeding to the remainder of the book.

A problem arises if the velocity of flow is sufficiently high at some locality for the melt to rise enough above the general level of the liquid surface so that it subsequently falls back under gravity, thus entrapping a portion of its own surface. This is the action of a breaking wave. It is represented in Figure 2.16. This process of entrainment of the liquid surface, and in particular its surface film, has been modeled by computer simulation by a number of workers. The various approaches have been reviewed by the author (Campbell 2006).

To gain some insight into the physics involved we can carry out the following analysis. The pressure tending to perturb the surface is the inertial pressure  $\rho V^2/2$  where  $\rho$  is the density of the melt, and  $V$  is the local flow velocity. The action of the surface tension  $\gamma$  tends to counter any perturbation by tensioning the surface, pulling the surface flat. The maximum pressure that surface tension can hold back is achieved when the surface is deformed into a hemisphere of radius  $r$ , giving a pressure  $2\gamma/r$  resisting the inertial pressure (Figure 2.16). Thus in the limit that the velocity is just sufficiently high to push the surface beyond the hemisphere, and so just exceeding the maximum restraint that the surface tension can provide, we have  $\rho V^2/2 = 2\gamma/r$ , so that the critical velocity  $V_{\text{crit}}$  at which the surface will become unstable, and start to suffer *surface turbulence* (my name for the phenomenon of breaking waves and entrainment of the surface into the bulk), is

$$V_{\text{crit}} = 2(\gamma/r\rho)^{1/2} \quad (2.1)$$

Subsequent experiments have shown that in spite of its rough derivation this is a surprisingly accurate result. However, the approach is unsatisfactory in the sense that the radius  $r$  has to be assumed, but there is little wrong with the physics, so the derivation is reproduced here because of its directness and simplicity.

Equation 2.1 is not an especially convenient equation since the critical radius of curvature  $r$  of the front at which instability occurs is not known independently. However, we can guess that it will not be



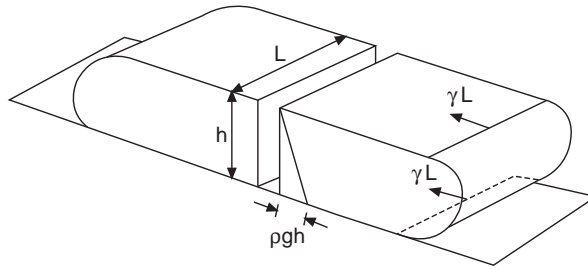


FIGURE 2.17

Balance of forces in a sessile drop sitting on a non-wetted substrate.

far from a natural radius of the front as defined, for instance, by a sessile drop. (The word ‘sessile’ means ‘sitting’, and is used in contrast to the ‘glissile’, or ‘gliding’ drop.) The sessile drop sitting on a non-wetted surface exhibits a specific height  $h$  defined by the balance between the forces of gravity, tending to flatten it, and surface tension, tending to pull the drop together to make it as spherical as possible. We can derive an approximate expression for  $h$  considering a drop on a non-wetted substrate as illustrated in Figure 2.17. The pressure to expand the drop is the average pressure  $\rho gh/2$  acting over the central area  $hL$ , giving the net force  $\rho gh^2L/2$ . For a drop sitting quietly, with its forces in equilibrium, this force is equal to the net force due to surface tension acting over the length  $L$  on the top and bottom surfaces of the drop,  $2\gamma L$ . Hence

$$\rho gh^2L/2 = 2\gamma L$$

giving

$$h = 2(\gamma/\rho g)^{1/2} \quad (2.2)$$

Assuming that  $h = 2r$  approximately, and eliminating  $r$  from Equation 2.1 we have

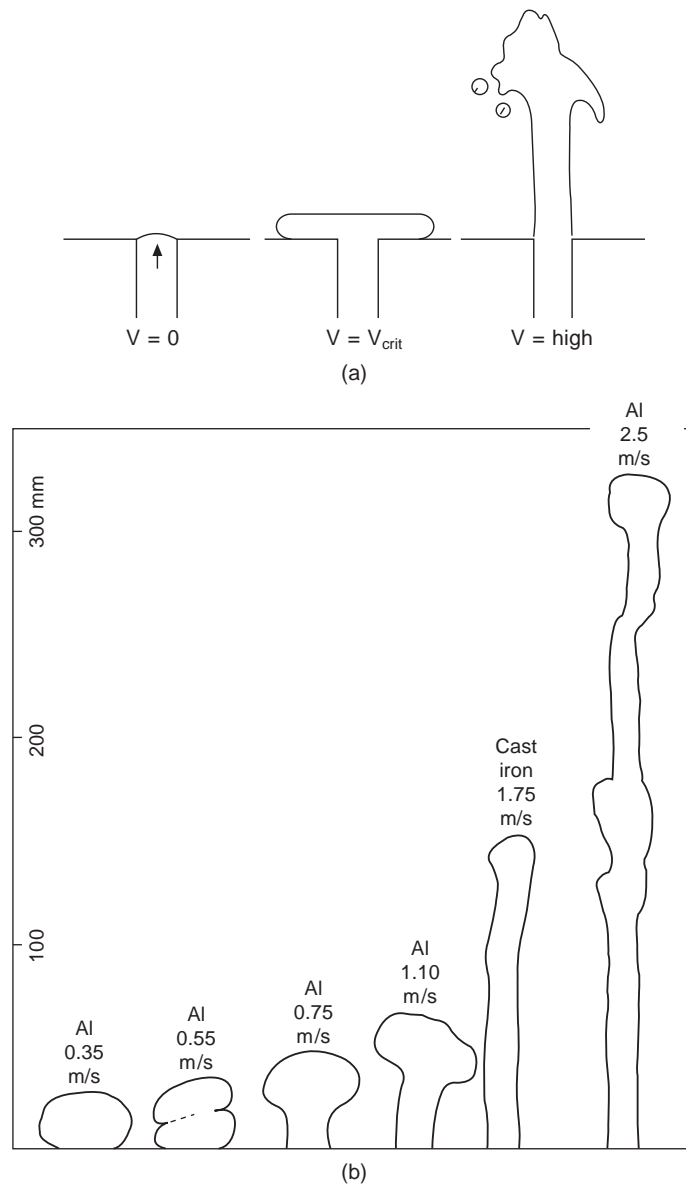
$$V_{\text{crit}} = 2(\gamma g/\rho)^{1/4} \quad (2.3)$$

This is the more elegant way to derive the critical velocity involving no assumptions and no adjustable parameters. It is analogous to the concept illustrated in Figure 2.18 in which liquid metal rises through a vertical ingate to enter a mold.

Clearly, for case (a) in Figure 2.18a, when the velocity at the entrance to the gate is zero the liquid is perfectly safe. There is no danger of enfolding the liquid surface. However, of course, the zero velocity filling condition is unfortunately not particularly useful for the manufacture of castings.

In contrast, case (c) can be envisaged in which the velocity is so high that the liquid behaves as a jet. The liquid is then in great danger of enfolding its surface during its subsequent fall. Regrettably, this condition is common in castings.

The interesting intermediate case (b) illustrates the situation where the melt travels at sufficient velocity to rise to a level that is just supported by its surface tension. This is the case of a sessile drop. Any higher, and the melt would subsequently have to fall back, and would be in danger of enfolding its surface. Thus the critical velocity required is that which is only just sufficient to project the liquid to the height  $h$  of the sessile drop. This height is simply that derived from conservation of energy,

**FIGURE 2.18**

(a) Concept of liquid emerging into a mold at zero, critical and high velocities; (b) experimentally observed profiles of liquid Al and cast iron emerging from an ingate at various speeds (Runyoro et al. 1992).

equating kinetic energy gain to potential energy loss,  $mV^2/2 = mgh$ , we obtain  $h = V^2/2g$ . Substituting this value in the value for the height of the sessile drop above (Equation 2.2) gives the same result for the critical velocity (Equation 2.3).

**Table 2.2 The critical heights and velocities of some liquids** (densities and surface tension adopted from Brandes and Brook 1992)

Liquid	Density $\text{kgm}^{-3}$	Surface tension $\text{Nm}^{-1}$	Critical height $h$ mm	Critical velocity $\text{ms}^{-1}$
Ti	4110	1.65	12.8	0.50
Al	2385	0.914	12.5	0.50
Mg	1590	0.559	16.0	0.42
Fe	7015	1.872	10.4	0.45
Ni	7905	1.778	9.6	0.43
Cu	8000	1.285	8.1	0.40
Zn	6575	0.782	7.0	0.37
Pt	19 000	1.8	6.2	0.35
Au	17 360	1.14	5.2	0.32
Pb	10 678	0.468	4.2	0.29
Hg	13 691	0.498	3.9	0.27
Water	1000	0.072	5.4	0.33

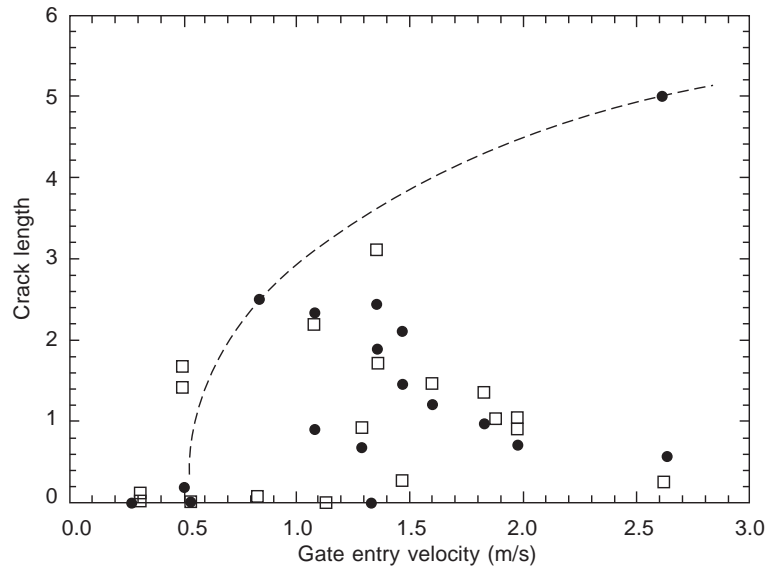
From Equation 2.2 we can find the height from which the metal can fall, accelerated by gravity, before it reaches the critical velocity given by Equation 2.3. When falling from greater heights, the surface of the liquid will be in danger of being entrained in the bulk liquid. The critical fall heights for entrainment of the surface are listed in Table 2.2. (Physical properties of the liquids have been taken at their melting points from Brandes and Brook (1992), since the values change negligibly with temperature. The values will be expected to be influenced somewhat by alloying of course.)

At first sight it seems surprising that nearly all liquids, including water, have a critical velocity in the region of  $0.3\text{--}0.5 \text{ms}^{-2}$ . This is a consequence of the fact that the velocity is a function of the *ratio* of surface tension and density, and, in general, both these physical constants change in the same direction from one liquid to another. Furthermore, the effect of the one-quarter power in Equation 2.3 further suppresses differences. Most of the important engineering metals have critical velocities close to  $0.5 \text{ms}^{-1}$  so that this value I now generally assume in the calculation of filling systems for castings of all metals and alloys.

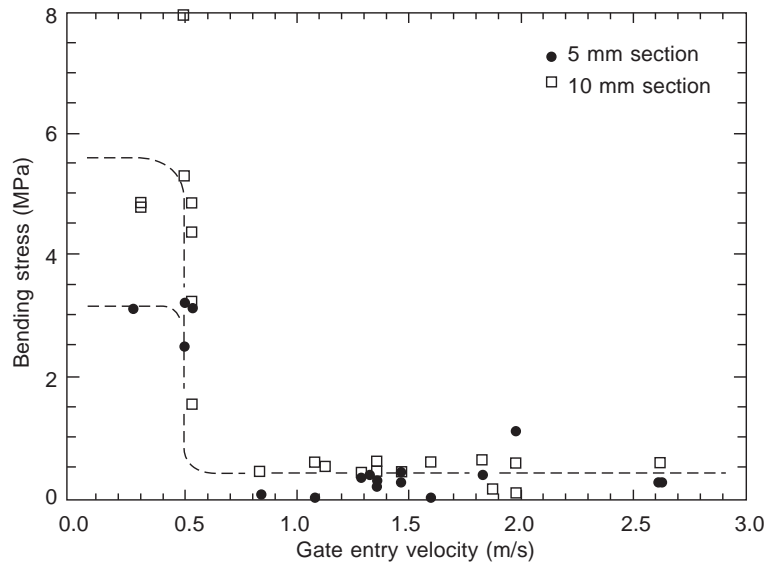
The value of  $0.5 \text{ms}^{-1}$  for liquid aluminum has been confirmed experimentally by Runyoro et al. (1992). They observed by video the emergence of liquid aluminum at increasing speeds from an ingate in a sand mold. An outline of some of the melt profiles is given in Figure 2.18b. At just over the critical velocity, at  $0.55 \text{ms}^{-1}$ , the metal falls back only slightly, forming its first fold, taking on the appearance of a traditional English bread called a cottage loaf. At progressively higher velocities the potential for damage during the subsequent fall of the jets is evident.

In further work shown in Figure 2.19, Runyoro (1992) observed a dramatic rise in surface cracks identified by dye penetrant testing, and the precipitous fall in bend strength of castings filled above  $0.5 \text{ms}^{-2}$ . I was so shaken by the alarming nature and clarity of this result that I completely changed the direction of research work at the University of Birmingham for the next decade, focusing on the role of surface turbulence generated by filling system design on the mechanical performance of castings.

For instance, the critical velocity for Cu–10Al alloy at  $0.4 \text{ms}^{-1}$  was subsequently confirmed by Helvae and Campbell (1996), and a similar value for ductile cast irons shown in Figure 2.20 was



(a)



(b)

**FIGURE 2.19**

(a) Crack lengths by dye penetrant testing in Al alloys cast at different ingate velocities; and (b) the bend strength of the same plate castings (Runyoro et al. 1992).

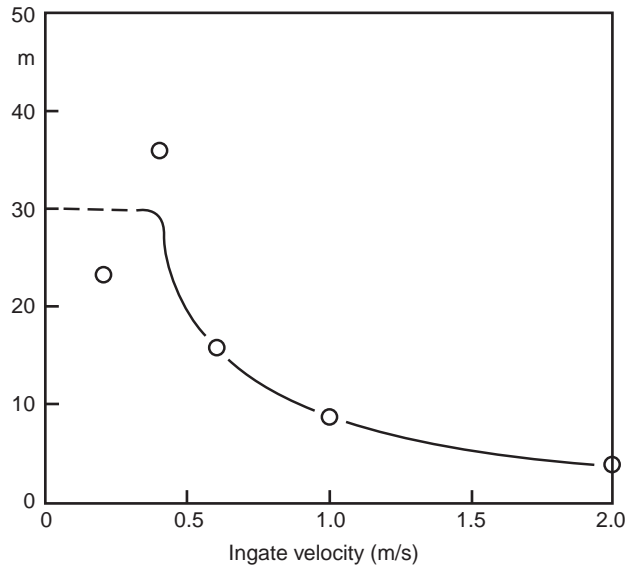


**FIGURE 2.20**

Reliability of ductile iron cast at different ingate velocities in terms of the two-parameter Weibull modulus  $m$  (Campbell 2000).

reported by the author (2000). The critical velocity for aluminum has been explored by computer simulation (Lai et al. 2002) in which area of the melt surface was computed as a function of increasing ingate velocity. Assuming the same values for physical constants as used here, a value of precisely  $0.5 \text{ ms}^{-1}$  was found (Figure 2.21), providing reassuring confirmation of the concept of critical velocity by a totally independent technique.

Since those early days further confirmations of the critical entry velocity into molds has been found for magnesium (Bahreinian 2005) to be in the range  $0.25\text{--}0.50 \text{ ms}^{-1}$ . Mirak and co-workers (2011) located a value for the Mg–9Al–1Zn alloy of  $0.30 \pm 0.05 \text{ ms}^{-1}$ . Furthermore, in much subsequent industrial work in foundries, in which filling systems have been redesigned to reduce ingate velocities to near  $0.5 \text{ ms}^{-1}$ , the improvements in quality of castings has been demonstrated in metals and alloys of all types, from light alloys to high-temperature alloys, steels, and titanium-based alloys.

### **Weber number**

The concept of the critical velocity for the entrainment of the surface by what the author has called *surface turbulence* is enshrined in the *Weber Number*,  $We$ . This elegant dimensionless quantity is defined as the ratio of the inertial pressure in the melt, assessed as  $\rho V^2/2$ , with the pressure due to surface tension  $\gamma(1/r_1 + 1/r_2)$  where  $r_1$  and  $r_2$  are the radii of curvature of the surface in two perpendicular directions. If only curved in one plane the pressure becomes  $\gamma/r$ , or for a hemisphere where the orthogonal radii are equal,  $2\gamma/r$ . Thus

$$We = \rho LV^2/\gamma \quad (2.4)$$

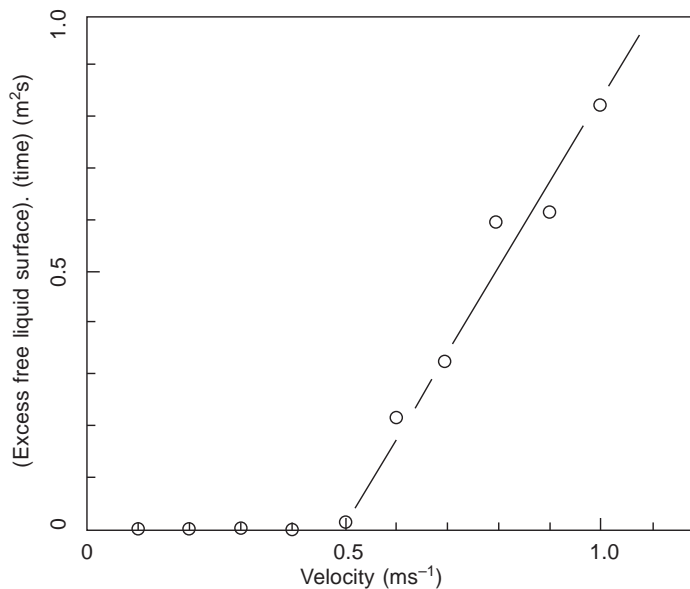


**FIGURE 2.21**

Computer simulation of the filling of a mold with Al, showing the excess free area of the melt as a function of ingate velocity (Lai et al. 2002).

Only the dimensioned quantities are included in the ratio, the scalar numbers (the factors of 2) are neglected, as is usual for a dimensionless number which is used over many orders of magnitude. The radius term becomes the so-called ‘characteristic length’ parameter,  $L$ . For flows in channels,  $L$  is typically chosen to be the hydraulic radius, defined as the ratio of the occupied area of the channel to its wetted perimeter. For a filled cylindrical channel this is half the radius of the channel (diameter/4). For a filled thin slot, it is approximately half of the slot width. As will be appreciated, the hydraulic radius is a concept closely allied to that of ‘geometrical modulus’ as commonly used by ourselves as casting engineers.

When  $We = 1$  the inertial and surface forces are roughly balanced. From the definition of  $We$  in Equation 2.4, and assuming for liquid aluminum a height of 12.5 mm for a sessile drop, giving a radius  $L = 12.5/2$  mm we find  $V = 0.25 \text{ ms}^{-1}$ , a value only a factor of 2 different from the critical velocity found earlier. When it is recalled that the real value of dimensionless numbers lies in their use to define numbers to the nearest order of magnitude (i.e. the nearest factor of ten), this is impressively in close agreement. The agreement is only to be expected, of course, since the condition that  $We < 1$  defines those conditions where the liquid surface is tranquil, and  $We > 1$  defines the conditions in which surface turbulence is expected.

The  $We$  number has been little used in casting research. This is a major omission on the part of researchers. It is instructive to look at the values that  $We$  can adopt in some casting processes.

Work on aluminum bronze casting has shown empirically that these alloys retain their quality when the metal enters the mold cavity through vertical gates at speeds of up to  $60 \text{ mm s}^{-1}$ . However, this extremely cautious velocity is almost certainly in error as a result of confusion introduced from other faulty parts of the filling system (notably problems with the pouring basin, and the well at the sprue/

runner junction). Helvae 1996 confirmed the theoretical predicted critical velocity for aluminum bronze of  $0.4 \text{ ms}^{-1}$ . However, if we accept the low-velocity  $0.060 \text{ ms}^{-1}$  into the mold cavity, we can assume that the radius of the free liquid surface is close to 5 mm (corresponding to half of the height of the sessile drop given in Table 2.2), the density approximately  $8000 \text{ kg m}^{-3}$ , and surface tension is approximately  $2.3 \text{ Nm}^{-1}$ , then  $We$  in this case is seen to be approximately 0.1, representing a condition dominated by surface tension, and thus ultra safe from any danger of surface turbulence.

In a mold of section thickness of 5 mm fitted with a glass window, Nieswaag observed that a rising front of liquid aluminum just starts to break-up into jets above a speed of approximately  $0.37 \text{ ms}^{-1}$ . This is reasonably close to our theoretical prediction of  $0.5 \text{ ms}^{-1}$  (Table 2.2). Assuming that the radius of the liquid front is 2.5 mm, and taking  $2400 \text{ kg m}^{-3}$  for the density of liquid aluminum, the corresponding critical value of  $We$  at which the break-up of the surface first occurs is therefore seen to be approximately 0.9. The users of vertically injected squeeze casting machines now commonly use  $0.4 \text{ ms}^{-1}$  as a safe filling speed (for instance Suzuki 1989), corresponding to  $We$  close to 2.0.

UK work in the 1950s (IBF Subcommittee 1960) showed that cast iron issues from a horn gate as a fountain when the sprue is only about 125 mm high and the gate about 12 mm in diameter (deduced from careful inspection of the photograph of the work). We can calculate, therefore, that  $We$  is approximately 80 for this well-advanced condition of surface turbulence.

Going on to consider the case of a pressure die casting of an aluminum alloy in a die of section thickness 5 mm and for which the velocity  $V$  might be  $40 \text{ ms}^{-1}$ ,  $We$  becomes approximately 100 000. It is known that the filling conditions in a pressure die casting are, in fact, characterized by extreme surface fragmentation, and possibly represent an upper limit which might be expected whilst making a casting. Owen (1966) noted from examination of the surfaces of zinc alloy pressure die castings that the metal advanced into the mold in a series of filaments or jets. These advanced splashes were subsequently overtaken by the bulk of the metal, although they were never fully assimilated. These observations are typical of much work carried out on the filling of the die during the injection of pressure die castings.

In summary, it seems that  $We$  numbers in the range 0–2.0 define the range of flow conditions that are free from surface turbulence. Although 1.0 is theoretically perfectly safe, it seems that a value nearer 2.0 appears to be transitional, indicating that a safe working critical velocity might be as high as  $1.0 \text{ ms}^{-1}$ . By the time the Weber number reaches 100, surface turbulence is certainly a problem, with jumping and splashing to a height of 100 mm or so. However, at values of 100 000 the concept of surface turbulence has probably given way to modes of flow characterized by jets and sprays, and eventually atomization.

### ***Froude number (Fr)***

The Froude number is another useful dimensionless quantity. It assesses the propensity of conditions in the liquid for making gravity waves. Thus it compares the inertial pressures  $\rho V^2/2$  that are perturbing the surface with the restraining action of gravity,  $\rho gh$ , where  $g$  is the acceleration due to gravity, and  $h$  is the height of the wave. Thus the Froude number is defined as

$$Fr = V^2/gh \quad (2.5)$$

It is important to emphasize the regimes of application of the  $We$  and  $Fr$  numbers. The Weber number deals with small-scale surface effects such as ripples, droplets, and jets. This is in contrast to the Froude number, which deals with larger-scale gravity waves, including such effects as slopping and surging in more open vessels, and in the ‘see-saw’ oscillations of flow observed in U-tube conditions of

some filling systems. We shall see later how  $Fr$  is useful to assess conditions for the formation of the hydraulic jump, a troublesome feature of the flow in large runners.

In the meantime, however, Froude number is useful to assess conditions where the undulation of the surface may cause its surface area to contract, forcing an entrainment condition. This concept has been so far overlooked as a major potential role in entrainment. The continued expansion of the advancing front is a necessary and sufficient condition for the avoidance of entrainment. Conversely, the contraction of the front in the sense of a loss of area of the 'free surface' of the liquid is a necessary and sufficient condition for the entrainment of bifilms.

Interestingly, the Weber number condition, indicating the onset of surface turbulence in the form of a potentially breaking wave, is a sufficient but not necessary condition for entrainment of bifilms. However, it is most probably a necessary condition for the entrainment of bubbles and perhaps some other surface materials. It is also likely that the surface turbulence condition aids the permanent entrainment of material entrained by surface contraction that might otherwise detrain. Thus the surface turbulence condition in the form of the critical velocity criterion remains a major influence on casting quality.

### **Reynolds number ( $Re$ )**

Many texts deal with turbulence, especially in running and gating systems, citing Reynold's number  $Re$ :

$$Re = \rho VL/\mu \quad (2.6)$$

where  $V$  is the velocity of the liquid,  $\rho$  is the density of the liquid,  $L$  is a characteristic linear dimension of the geometry of the flow path, and  $\mu$  is the viscosity. The definition of Reynolds number follows from a comparison of inertial pressures  $C_d\rho V^2/2$  (where  $C_d$  is the drag coefficient) and viscous pressures  $\mu V/L$ . The reader can confirm that the ratio of these two forces does give the dimensionless number  $Re$  (neglecting, of course, the presence of numerical factors  $2C_d$ ). The characteristic length  $L$  is, as before, usually defined as the hydraulic radius.

Clearly, the inertial forces are a measure of those effects that would cause the liquid to flow in directions dictated by its momentum. These effects are resisted by the effect of viscous drag from the walls of the channel containing the flow. At values of  $Re$  below about 2000, viscous forces prevail, causing the flow to be smooth and laminar, i.e. approximately parallel to the walls. At values of  $Re$  higher than this, flow tends to become turbulent; the walls are too far away to provide effective constraint, so that momentum overcomes viscous restraint, causing the flow to degenerate into a chaos of unpredictable swirling patterns.

It is vital to understand, however, that all of this flow behavior takes place in the bulk of the liquid, underneath the surface. During such turbulence in the bulk liquid, therefore, the surface of the melt may remain relatively tranquil. Turbulence as predicted and measured by  $Re$  is therefore strictly *bulk turbulence*. It does not apply to the problem of assessing whether the surface film will be incorporated into the melt. This can only be assessed by the concept of *surface turbulence* associated with  $We$  and  $Fr$ .

Flow in running systems is typically turbulent as defined by Reynolds number. Even for very narrow running systems designed to keep surface turbulence to a minimum, bulk turbulence would still be expected. In this case for a small aluminum alloy casting where  $V = 2 \text{ ms}^{-1}$ , in a runner only 4 mm high, hence  $L = 2 \text{ mm}$ ,  $Re$  is still close to 7000. For a fairly small steel casting weighing a few kg where the melt is flowing at  $2 \text{ ms}^{-1}$  in a runner 25 mm high, giving approximately  $L = 10 \text{ mm}$ , and assuming  $\mu = 5.5 \times 10^{-3} \text{ Nsm}^{-2}$  and  $\rho = 7000 \text{ kg m}^{-3}$ ,  $Re$  is approximately 20 000. For a large casting a meter



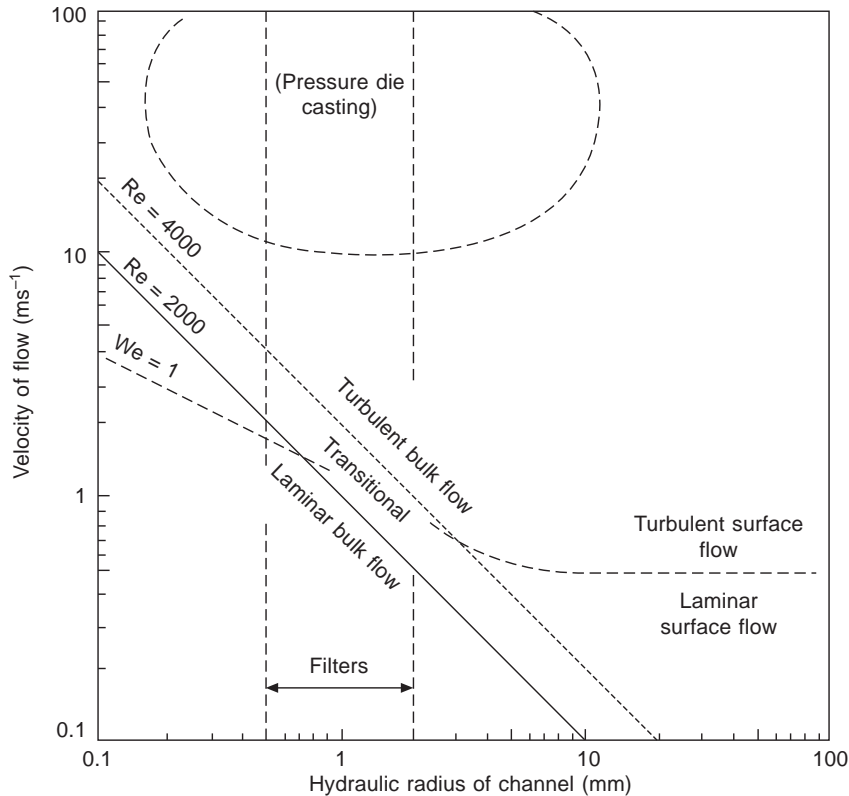


**FIGURE 2.22**

Map of flow regimes in castings.

or more high and weighing several tonnes it is quickly shown that  $Re$  is in the region of 2 000 000. Thus bulk turbulence exists in running systems of all types, and can be severe.

Only in the very narrow pores of ceramic foam filters is flow expected to be laminar as indicated in Figure 2.22. For velocities of  $2 \text{ ms}^{-1}$  for liquid aluminum in a filter of pore diameter 1 mm,  $Re = 2000$ . For liquid steel, which is somewhat more viscous,  $Re = 500$ . These values show that the flow is not far from an unstable turbulent condition even in the narrowest of channels found in most running systems. Only moderate increases in speed of flow would promote turbulence even in these very small channels.

The map of flow regimes presented in Figure 2.22 is a guide to our thinking and our research about the very different flow behavior that liquids can adopt when subjected to different conditions of speed and geometry.

### 2.2.2 Oxide skins from melt charge materials

Prior to melting, the charge materials need to be selected and weighed. The oxide originally on the charge material (we shall call such oxides 'skins') becomes necessarily submerged, to become part of

the melt when the underlying solid melts. For dense metals such as irons and steels the oxide skins submerged in this way often separate quickly to form a dross or slag that can be removed from the top of the melt.

For Al alloys for which the submerged oxide necessarily entrains with it a layer of air as a bifilm, the oxide skins are nearly neutrally buoyant so the melt clears only with great reluctance. Problems of the introduction of skins from the surfaces of charge materials are most commonly seen in the melting of aluminum and its alloys. Whether or not the skins on the charge materials find their way into the liquid metal depends on the type of furnace used for melting.

Furnaces in which the solid charge materials are added directly into a melting furnace or into a liquid pool produce a poor quality of melt. Problem melters include crucible furnaces among others. For such melting practice, all the oxide skins on the charge necessarily finish floating about in the melt.

In the case of charge materials such as ingots that have been chill cast into metal molds the surface oxide skin introduced in this way is relatively thin. However, charges that are made from sand castings that are to be recycled (usually called 'foundry returns') represent a worst case. The oxide skins on sand castings have grown thick during the extended cooling period of the casting in the aggressively moist and oxidizing environment of the sand mold. The author has seen complete skins of cylinder head castings dragged out of the liquid metal, complete with clearly recognizable combustion chambers and ports. The melt can become so bad as to resemble a slurry of old sacks. Unfortunately this is not unusual.

In a less severe case where normal melting was carried out repeatedly on 99.5% pure aluminum Panchanathan (1965) found that progressively poorer mechanical properties were obtained. By the time the melt had been recycled eight times, the high elongation of relatively pure Al had fallen from approximately 30% to 20%. This is easily understood if the oxide skin content of the metal is progressively increased by repeated casting.

Dry hearth furnaces can, in principle, give a significantly improved quality. Such units are often based on a tower or shaft design to provide a classical counter-flow heat exchange process; the charge is preheated during its course down the tower, while furnace waste gases flow upwards. The base of such a tower is usually a gentle slope of refractory on which the charge in the tower is supported. The slope is known as the dry hearth. Such a design of melting unit is not only thermally efficient, but has the advantage that the oxide skins on the surface of the metallic charge materials are mainly left in place on the dry hearth. The liquid metal flows, practically at its melting point, out of the skin of the melting materials, down the hearth, traveling through an extended oxide tube, and into the bulk of the melt. Here it needs to be brought up to a useful casting temperature. The oxide tube forms as the liquid flows, and finally collapses, more or less empty, when the flow is finished. The oxide content of melts from this variety of furnace is low. (The melting losses and gas content might be expected to be a little higher in this design of melter, but because of the protective nature of the oxide that forms in fuel waste gas atmosphere with high water content, the reaction between the melt and the waste gases is surprisingly low.)

The additional advantage of a dry hearth furnace for aluminum alloys is that foundry returns that contain iron or steel cast-in inserts (such as the iron liners of cylinder blocks or valve seats in cylinder heads) can be recycled. The insets remain on the hearth and can, from time to time, be raked clear, together with all the dross of oxide skins from the charge materials, via a side door into a skip. (A dross consists of oxides with entrapped liquid metal. Thus most dross contains between 50 and 80% metal, making the recovery of aluminum from dross economically valuable.)

The benefits of melting in a dry hearth furnace are, of course, eliminated at a stroke by the misguided enthusiasm of the operator, who, thinking he is keeping the furnace clean and tidy, and that the heap of remaining oxide debris sitting on the hearth will all make good castings, shoves the heap into the melt. Unfortunately, it is probably slightly less effort to push the dross downhill, rather than rake it out of the furnace through the dross door. The message is clear, but requires re-stating frequently. Good technology alone will not produce good castings. Good training and vigilant management remain essential.

### 2.2.3 Pouring

During the pouring of some alloys, the surface film on the liquid grows so quickly that it forms a tube around the falling stream. The author calls this an oxide flow tube.

A patent dating from 1928 by Beck describes how liquid magnesium can be transferred from a ladle into a mold by arranging for the pouring lip of the ladle to be as close as possible to the pouring cup of the mold, and to be in a relatively fixed position so that the semi-rigid oxide pipe which forms automatically around the jet is maintained unbroken, and thus protects the metal from contact with the air (Figure 2.23a).

A similar phenomenon is seen in the pouring of aluminum alloys and other metals such as aluminum bronze, ductile iron, and stainless steels.

However, if the length of the falling stream is increased, then the shear force of the falling liquid against the inner surface of the oxide tube increases. This drag may become so great that after a second or so the oxide tears, allowing the tube to detach from the lip of the ladle. The tube then accompanies the metal into the mold, only to be immediately replaced by a second tube, and so on. A typical 10-kg aluminum alloy casting poured in about 10 seconds can be observed to carry an area of between 0.1 and 2.0 m<sup>2</sup> of oxide into the melt in this way. This is an impressive area of oxide to be dispersed in a casting of average dimensions only 100 × 200 × 500 mm, especially when it is clear that this is only one source. The oxide in the original metal, together with the oxides entrained by the surface turbulence of the pour, will be expected to augment the total significantly.

#### ***The critical fall height***

The critical fall height is that height from which the melt falls to gain just sufficient energy to enfold its surface, creating an entrainment defect. This height happens to be identical to the height of the sessile drop of the melt.

Why is the critical fall height the same as the height of a sessile drop? The critical fall height can be seen to be a kind of re-statement of the critical velocity condition. It is because the critical velocity  $V$  is that required to propel the metal vertically upwards to the height at which it is still just supported by surface tension (Figure 2.18). This is the same velocity  $V$  that the melt would have acquired by falling from that height. (A freely traveling particle of melt starting from a vertical ingate would execute a parabola, with its upward starting and downward finishing velocities identical.)

When melts are transferred by pouring from heights less than the critical heights predicted in Table 2.2 (the heights of the sessile drop) there is no danger of the formation of entrainment defects. Surface tension is dominant in such circumstances, and can prevent the folding inwards of the surface, and thus prevent entrainment defects (Figure 2.23a). It is unfortunate that the critical fall height is such a minute distance. Most falls that an engineer might wish to design into a melt handling system, or

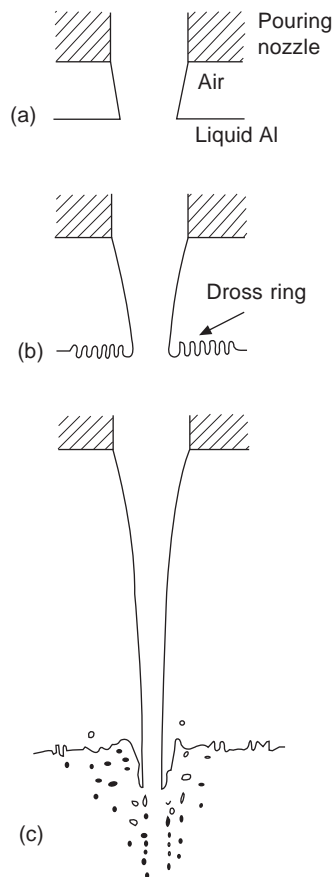


**FIGURE 2.23**

Effect of increasing height of a falling stream of liquid illustrating: (a) the oxide flow tube remaining intact; (b) the oxide flow tube successively detached and accumulating to form a dross ring; and (c) the oxide film and air being entrained in the bulk liquid.

running system, are nearly always greater, if not vastly greater. However, the critical fall height is one of those extremely inconvenient facts that we casting engineers have to learn to live with.

However, even above this theoretical height, in practice the melt may not be damaged by the pouring action. The mechanical support of the liquid by the surface film in the form of its surrounding oxide tube can still provide freedom from entrainment, although the extent of this additional beneficial regime is perhaps not great. For instance, if the surface tension is effectively increased by a factor of 2 or 3 by the presence of the film, the critical height may increase by a factor  $3^{1/4} = 1.3$ . Thus perhaps 30% or so may be achievable, taking the maximum fall from about 12 to 16 mm for aluminum. This seems negligible for most practical purposes.

At slightly higher speed of the falling stream, the tubes of oxide concertina together to form a dross ring (Figure 2.23b). Although this represents an important loss of metal on transferring liquid

aluminum and other cross-forming alloys, it is not clear whether defects are also dragged beneath the surface and thereby entrained.

At higher speeds still, the dross is definitely carried under the surface of the liquid, together with entrained air, as shown in Figure 2.23c. Turner (1965) has reported that, above a pouring height of 90 mm, air begins to be taken into an Al alloy melt with the stream, to reappear as bubbles on the surface. Experiments by Din and the author (2003) on Al-7Si-0.4Mg alloy have demonstrated that in practice the damage to the tensile properties of castings caused by falls up to 100 mm appears controlled and reproducible provided the melt has first gone through a ceramic foam filter. (However, above 200 mm, random damage was certain.)

These heights are well above the critical fall heights predicted above, and almost certainly are a consequence of the some stabilization of the surface of the falling jet by the presence of a film. The mechanical rigidity of the tubular film holds the jet in place, and effectively delays the onset of entrainment by the plunging action greatly in excess of the predicted 30%. It may be that the surface film stabilizes the surface, maintaining the smoothness of the jet, so avoiding entrainment of the surface oxide as it plunges into the melt as described below. Clearly, more work is required to clarify the allowable fall heights of different alloys.

In a study of water models, Goklu and Lange (1986) found that the quality of the pouring nozzle affects the surface smoothness of the plunging jet, which in turn influences the amount of air entrainment. They found that the disturbance to the surface of the falling jet is mainly controlled by the turbulence ahead of and inside the nozzle that forms the jet.

During the pouring of a casting from the lip of a ladle via an offset stepped basin kept properly full of metal, then the above benefit will apply: the oxide will probably not be entrained in the pouring basin if the pouring head is sufficiently low, as is achievable during lip pouring. However, in practice it seems that for fall distances of more than perhaps 50 or 100 mm freedom from damage cannot be relied upon. The pouring basin will always represent a threat to a filling system from this source.

Clearly, the benefits of defect-free pouring are easily lost if the pouring speed into the entry point of the filling system is too high. This is often observed when pouring castings from unnecessary height. A succession of increasingly bad pouring conditions can be listed as current examples: In aluminum foundries pouring is often by robot. In iron foundries it is commonly via automatic pouring systems from fixed launders sited over the line of molds. In steel foundries it is common to pour from bottom-poured ladles that contain over a meter depth of steel above the exit nozzle (the situation for steel from bottom-teemed ladles is further complicated by the depth of metal in the ladle decreasing progressively). In a practical instance of a jet plunging at  $10 \text{ ms}^{-1}$  into steel held in a 4-m diameter ladle, Guthrie (1989) found that the Weber number was  $2.7 \times 10^6$  whereas the Froude number was only 2.5. Thus despite very little slopping and surging, the surface forces were being overwhelmed by inertial forces by nearly two million times greater, causing the creation of a very dirty re-oxidized steel.

In all types of foundries the surface oxide is automatically entrained and carried into the casting if a simple conical pouring bush is used to funnel the liquid stream into the sprue. In this case, of course, practically all of the oxide formed on the stream will enter the casting. It has to be admitted that pouring basins of sophisticated design are not without their problems and their limitations, but the current widespread use of conical pouring basins undermines all other attempts to improve casting quality. Conical basins have to be eliminated if casting quality can have any chance to improve.

In summary, it is clear that the lower the pour heights the less damage is suffered by the melt. In addition, of course, less metal is oxidized, thus directly saving the costs of unnecessary melt losses.

Ultimately, however, it is, of course, best to avoid pouring altogether. In this way losses are reduced to a minimum and the melt is maintained free from damage.

The adoption of counter-gravity designs for foundries, in which metal is never poured at any point of the process, is no longer a pipe dream, but a practical and economical technique for casting production that is already in use in a number of foundries worldwide. It is an ultimate solution that cannot be recommended too strongly.

### 2.2.4 The oxide lap defect I: Surface flooding

The steady, progressive rise of the liquid metal in a mold may be interrupted for a number of reasons. There could be (i) an inadvertent break during pouring, or (ii) an overflow of the melt (called elsewhere in this work a ‘waterfall effect’) into a deep cavity at some other location in the mold, or (iii) the arrival of the front at a very much enlarged area, thus slowing the rate of rise nearly to a stop.

If the melt stops its advance the thickness of the oxide on the melt surface is no longer controlled by the constant splitting and re-growing action. It now simply thickens. If the delay to its advance is prolonged, the surface oxide may become a rigid crust.

When filling restarts (for instance when pouring resumes, or the overflow cavity is filled) the fresh melt may be unable to break through the thickened surface film. When it eventually builds up enough pressure to force its way through at a weak point, the new melt will flood over the old, thick film, sealing it in place. Because the newly arriving melt will roll over the surface, laying down its own new, thin film, a double film defect will be created, creating a bifilm. The bifilm will be highly asymmetrical, consisting of a lower thick film and an upper thin film.

Asymmetric films are interesting, in that precipitates sometimes prefer one film as a substrate for formation and growth, but not the other. Examples are briefly described later in the sections relating to confluence welds and oxide flow tubes. The asymmetric bifilm is a common defect in castings.

A key aspect of the stopping of the front is that the double film defect that is thereby created is a single, huge planar defect, extending completely through the product. Also, its orientation is perfectly horizontal. (Notice it is quite different from the creation of double film defects by surface turbulence. In this chaotic process the defects are random in shape, size, orientation, and location in the casting.) Flooding over the surface in this way is relatively common during the filling of castings, especially during the slow filling of alloys which form strong films.

From an exterior view of the casting, the newly arriving melt flooding over the thick stationary oxide will only have the pressure of its own sessile drop height as it attempts to run into the tapering gap left between the old meniscus and the mold wall. Thus this gap is imperfectly filled, leaving a horizontal lap defect clearly visible around the perimeter of the casting. This surface lap defect corresponding to the arrest of the progress of the melt is the only external sign of a major defect that extends probably completely through the casting.

Notice that in this way (assuming oxidizing conditions) we have created an *oxide lap*. If the arrest of the advance of the melt had been further delayed, or if the solidification of the melt had been accelerated (as near a metal chill, or in a metal mold) the meniscus could have lost so much heat that it had become partially or completely solid. In this case the lap would take on the form of a *cold lap* (the name ‘cold shut’ is recommended to be consigned to the scrap heap of unhelpfully descriptive jargon. I hate jargon.)

The distinction between oxide laps and cold laps is sometimes useful, since whereas both may be eliminated by avoiding any arrest of progress of the liquid front, only the cold lap may be cured by increasing the casting temperature, whereas the oxide lap may become worse.

For mold surfaces which are horizontal, the advance of the front takes an unstable dendritic form, with narrow streams, like dendrites, progressing freely ahead of the rest of the melt. This is because while the molten metal advances quickly in the mold the surface film is being repeatedly burst and moved aside. The faster the metal advances in one location, the thinner and weaker the film, so that the rate of advance of the front becomes less impeded. If another part of the front slows, then the film has additional time to strengthen, further retarding the local rate of advance. Thus in film-forming conditions fast-moving parts of the advancing front advance faster, and slow-moving parts advance slower, causing the advance of the liquid front to become unstable (Campbell 1988). This is a classic type of instability condition that gives rise to finger-like dendritic extensions on an advancing front.

Figure 2.24 shows the filling pattern of a thin-walled box casting such as an automotive sump or oil pan. The vertical walls fill nicely because of the organizing effect of gravity. However, problems arise on the horizontal top section. If the streams continue to flow, so as to fill eventually the whole of the horizontal section, the confluence welds (see Section 2.2.5) abutting the oxides on the sides of the streams will constitute cracks through the complete thickness of the casting. When highly strained, such castings are known to fail along the lines of the confluence welds outlining the paths of the original filling streams. In effect, each of the flowing streams generates a kind of oxide flow tube as is discussed in the next section.

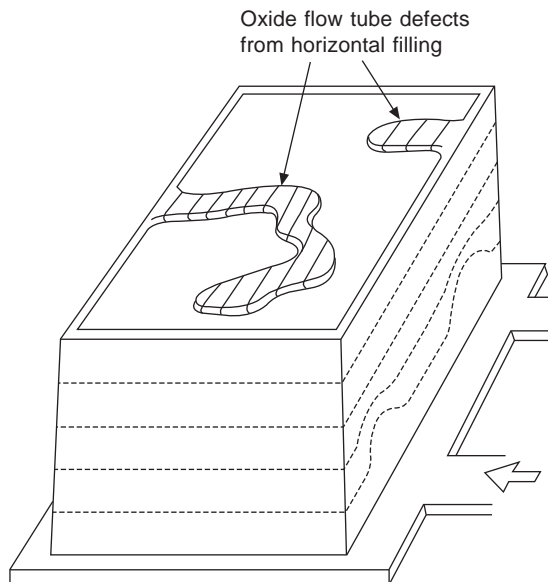


**FIGURE 2.24**

Filling of a thin-walled oil pan casting, showing the gravity-controlled rise in the walls, but the unstable meandering flow across horizontal areas leading to the danger of confluence weld type through-wall cracks.

For the case of vertical filling, when the advance of the front has slowed to near zero, or has actually momentarily stopped, then the strength of the film and its attachment to the mold will prevent further advance at that location. If the filling pressure continues to build up, the metal will burst through at a weak point, flooding over the stationary front. In a particular locality of the casting, therefore, the advance of the metal will be a succession of arrests and floods, each new flood burying a double oxide film (Figure 2.25).

This very deleterious mode of filling can be avoided by increasing the rate of filling of the mold.

The problem can, in some circumstances, also be tackled by reducing the film-forming conditions. This is perhaps not viable for the very stable oxides such as alumina and titania when casting in air. It is the reason for vacuum casting those alloys which are troubled by films; although the oxides cannot be prevented from forming by casting in vacuum, their rate of formation is reduced. The thin double film is expected, in principle, to constitute a crack as serious as that of thick double film (because the entrained layer of air is expected to have the same negligible strength). However, there are additional reasons why the thin film may be less damaging. A film that is mechanically less strong is more easily torn and more easily raveled into a more compact form. Internal turbulence in the melt will tend to

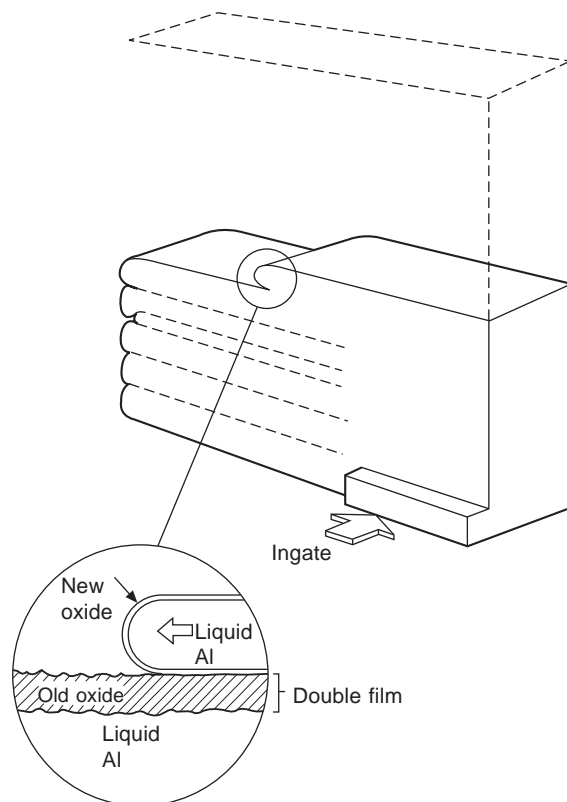


**FIGURE 2.25**

Unstable filling of a mold showing the formation of laps containing an asymmetric bifilm crack.



favor the settling of the defect into stagnant corners of the mold. Here it will be quickly frozen into the casting before it has chance to unfurl significantly.

Films on cast iron for instance are controllable to some extent by casting temperature and by additions to the sand binder to control the environment in the mold (Sections 4.5 and 6.5). Films on some steels are controllable by minor changes to the deoxidation practice (Section 6.6).

### 2.2.5 The oxide lap defect II: The confluence weld

Even in those castings where the metal is melted and handled perfectly, so that no surface film is created and submerged, the geometry of the casting may mean that the metal stream has to separate and subsequently join together again at some distant location. This separation and rejoining necessarily involves the collision of the films on the advancing fronts of both streams, with the consequent danger of the streams having difficulty in rejoining successfully. I called this junction a confluence weld (Campbell 1988). Most complex castings necessarily contain dozens of confluence welds, and it is important to recognize that the confluence weld does not necessarily, or even commonly, lead to any significant defect. However, occasionally it does lead to a severe defect. The conditions in which these issues arise are discussed below.

The author recalls that in the early days of the Cosworth Process, a small aluminum alloy pipe casting was made for very-high-pressure service conditions. At that time it was assumed that the mold should be filled as slowly as possible, gating the metal in at the bottom of the pipe, and arriving at the top of the pipe just as the melt was about to freeze to encourage directional feeding. When the pipe was finally cast it looked perfect. It passed radiographic and dye penetrant tests. However, it failed catastrophically under a simulated service test by splitting longitudinally, exactly along its top, where the metal streams were assumed to join. The problem defeated our team of casting experts, but was solved instantly by our foundry manager, George Wright, the company's very own dyed-in-the-wool traditional foundryman. He simply turned up the filling rate (neglecting the niceties of setting up favorable temperature gradients to assist feeding). The problem never occurred again. Readers will note a moral (or two) in this story.

Figure 2.26 shows various situations where confluence problems occur in castings. Such locations have been shown to be predictable in interesting detail by computer simulation (Barkhudarov and Hirt

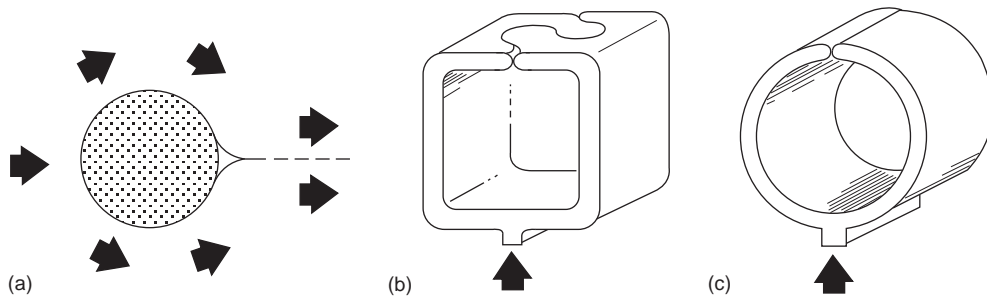
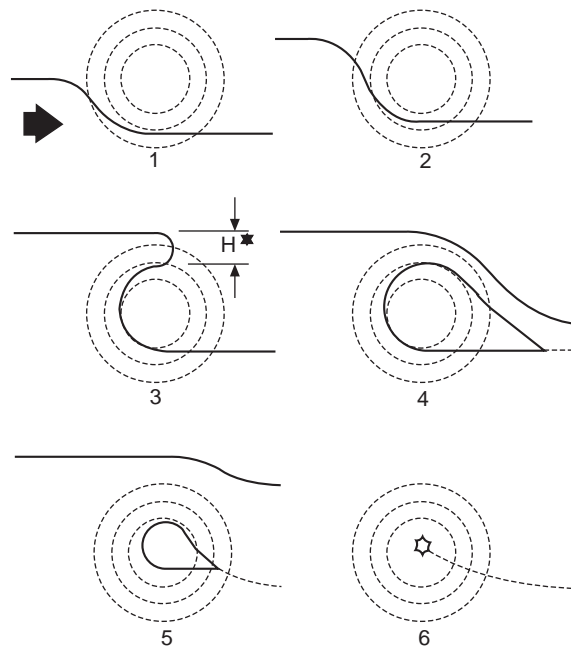


FIGURE 2.26

Confluence weld geometries: (a) at the side of a round core; (b) randomly irregular joins on the top of a bottom-gated box; (c) a straight join on the top of a bottom-gated round pipe (Campbell 1988).



**FIGURE 2.27**

Local thin area denoted by concentric contours in an already thin wall, leading to the creation of a filling instability, and a confluence weld ending in a point discontinuity (Campbell 1988).

1999). The weld ending in a point illustrated in Figure 2.27 is commonly seen in thin-walled aluminum alloy sand castings; the point often has the appearance of a dark, upstanding pip. The dark color is usually the result of the presence of sand grains, impregnated with metal. The metal penetration of the mold occurs at this point as a result of the conservation of momentum of the flow, concentrated and impacted at this point. (The effect is analogous to the implosion of bubbles on the propeller of a ship: the bubble collapses as a jet, concentrating the momentum of the in-falling liquid. The repeated impacts of the jet cause fatigue cracks to initiate in the metal surface, finally causing failure in the form of cavitation damage.) The problem has been called in US foundries ‘the black plague defect’, which seems somewhat over-melodramatic, but does emphasize the founder’s exasperation of having to deal with the unsightly marks by additional surface dressing.

Returning to the issue of the confluence weld, a complete spectrum of conditions can be envisaged:

1. The two streams do not meet at all.
2. The two streams touch, but the joint has no strength.
3. The joint has partial strength.
4. The joint has full strength because the streams have successfully fused, resulting in a joint that is indistinguishable from bulk material.

For conditions (1) and (2) the defects are either obvious, or are easily detected by dye penetrant or other non-destructive tests. If the problem is seen it is usually not difficult to cure as described below.

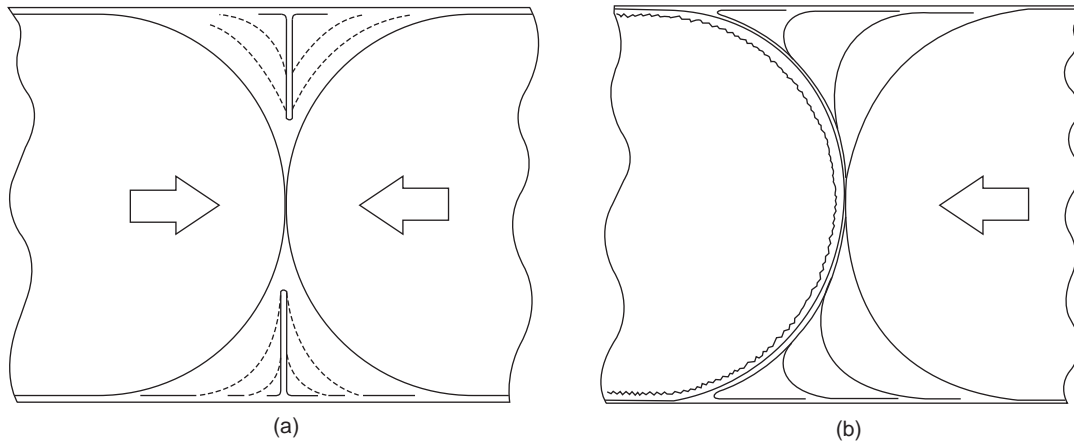


**FIGURE 2.28**

Mechanism of the confluence weld: (a) in the case of the meeting of two moving fronts which fuse to create a perfect weld (the residual entrained bifilms flatten against the walls of the casting); (b) a through-thickness crack because one front has stopped.

Condition (4) is clearly the target in all cases, but up till now it is not certain how often it has been achieved in practice. This can now also be clarified.

As with many phenomena relating to the mechanical effects of double oxide films, the understanding is rather straightforward. The concept is illustrated in Figure 2.28.

In the case of two liquid fronts that progress towards each other by the splitting and re-forming of their surface films, the situation just after the instant of contact is fascinating and key to the understanding of this problem. At this moment the splitting will occur at the point of contact because the film is necessarily thinnest at this point but no oxygen can access the microscopic area where the metal is in contact. As the streams continue to engage, the oxide on the surfaces of the two menisci continue to slide back from the point of contact, but because of the exclusion of oxygen from the contact region, no new film can form here. Remnants of the double film occupy a quarter to a third of the outer part of the casting section, existing as a possible crack extending inward from each surface. This is most unlikely to result in a defect because such films will be thin because of their short growth period. Having little rigidity, being more akin to tissue paper of gossamer lightness, it will be folded against the oxide skin of the casting by the random gusts and gales of internal turbulence. There it will attach, adhering as a result of little-understood atomic forces; probably van der Waal forces. Any such forces, if they exist, are likely to be only weak but the vanishingly thin and weak films will not need strong forces to ensure their permanent capture. Thus, finally, the weld is seen to be perfect. This situation is expected to be common in castings.

The case contrasts with the approach of two liquid fronts, in which one front comes to a stop, while the other continues to advance toward it. In this case the stationary front builds up the thickness of its oxide layer to become strong and rigid. When the 'live' front meets it, the thin film on the newly arriving front is now pinned against the rigid, thick film and is held in place by friction. Thus the continuously advancing stream expands around the rigidized meniscus, forcing its oxide film to split and expand, as the moving front wraps itself around the stationary front, causing a layer of thin new

film to be laid down on the old thick substrate. Clearly, a double film defect constituting a crack has been created completely across the wall of the casting. Again, the double film is asymmetrical.

Note once again that for the conditions in which one of the fronts is stationary, the final defect is a lap defect in which the crack is usually in a vertical plane (although, of course, other geometries can be envisaged). This contrasts with the surface flooding defect, lap defect type I, where the orientation of the crack is substantially horizontal.

The meandering cracks formed in the conditions of filling shown in Figure 2.24 are long confluence weld defects. Some other examples of different kinds of confluence welds are given below.

A location in an Al alloy casting where a confluence weld was known to occur was found to result in a crack. When observed under the scanning electron microscope the original thick oxide could be seen trapped against the tops of dendrites that had originally flattened themselves against the double film. The poor feeding in that locality had drained residual liquid away from the defect, sucking large areas of the film deeply into the dendrite mesh. One of the remaining islands of film pinned in its original place by the dendrites is shown in Figure 2.29. The draped appearance suggesting the dragging action of the surrounding film as it was pulled and torn away while the surrounding film disappeared into the depths.

Garcia and colleagues (2007) studied the problem of severe leakage defects in an Al alloy cylinder head casting, discovering the problem to be a confluence weld formed as a result of the back pressure of gas in the mold causing the advancing front to stop momentarily. They noted alpha-Fe intermetallics had nucleated on the stopped front, but the 'live' front was clear of precipitates. (Their successful identification

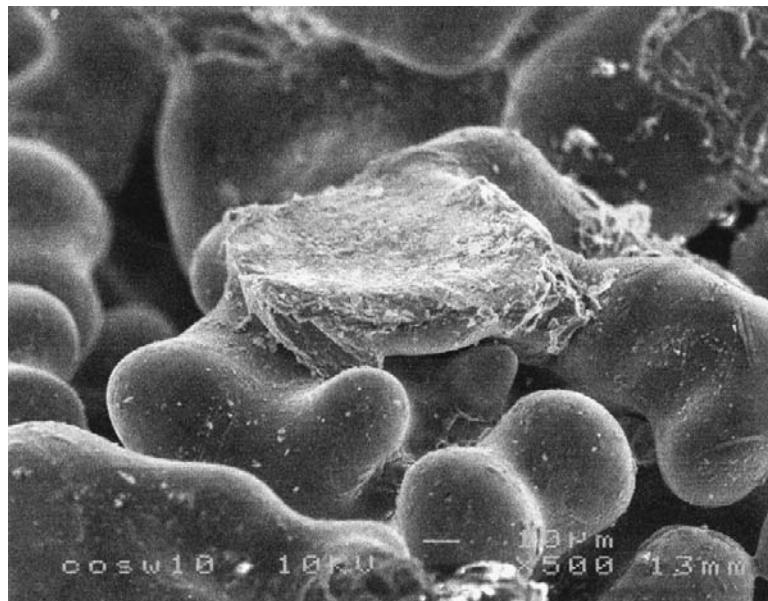


**FIGURE 2.29**

SEM fractograph of a confluence weld at a stopped front. An island of thick oxide remains, the rest having withdrawn into the depths of the dendrite mesh, retreating with residual liquid because of local feeding problems in the casting.

of a confluence weld defect contrasts with the study by Lett (2009) in which neither advancing liquid front was designed to stop. The result was no clear identification of the formation of confluence welds.)

Pellerier and Carpentier (1988) are among the few who have studied a confluence weld defect in a cast iron, almost certainly formed from a carbon film on the advancing meniscus (although it seems likely that the carbon film had itself formed on a precursor oxide film as illustrated in Figure 2.2c). Their thin-walled ductile iron casting was poured in a mold containing cores bonded with a urethane resin. They found a thin film (but did not appear to have noticed whether the film might have been double) of graphite and oxides through the casting at a point where two streams met. The bulk metal matrix structure was ferritic (indicating an initial low carbon content in solution) but close to the film was pearlitic, indicating that some carbon from the film was going into solution. The authors did not go on to explore conditions under which the defect could be avoided.

In summary, if the two fronts can be kept ‘alive’ the confluence is expected to be a perfect weld. If one front stops, the result is a crack. Thus the problem can be eliminated by keeping the liquid fronts moving. This is simply ensured by casting at a rate which is sufficiently high. Care is needed of course to avoid casting at too high a rate at which surface turbulence may become an issue. Providentially, there is usually a comfortably wide operational window in which the fill rate can meet the requirements to avoid all defects.

### 2.2.6 The oxide flow tube

The oxide tube around a flowing jet, if encapsulated in the casting, can form a cylindrical bifilm as the melt rises around it to entrain it. It becomes therefore a major geometrical crack. The cylindrical crack is an almost unbelievably unexpected form. Any metallurgical engineer familiar with normal fairly planar stress cracks would be hard pressed to believe it, and even more hard pressed to explain it.

The stream might be a falling jet, commonly generated in a waterfall condition in the mold, as in Figure 2.30. The stream does not need to fall vertically. Streams can be seen that have slid down gradients in such processes as tilt casting when carried out under poor control. Part of the associated flow tube is often visible along the surface of the casting.

Oxide flow tube defect from a fall

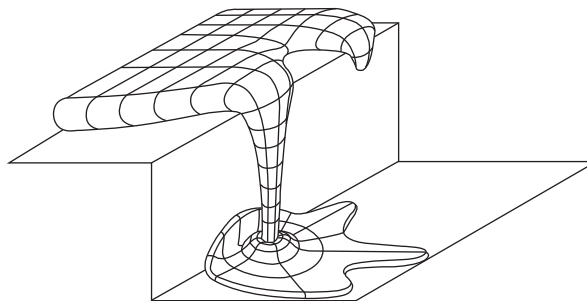


**FIGURE 2.30**

Waterfall effect in a casting causing: (i) a stationary top surface forming a horizontal lap and crack defect; (ii) a falling jet creating a cylindrical oxide flow tube leading to a cylindrical crack; and (iii) random surface turbulence damage in the lower levels of the casting.

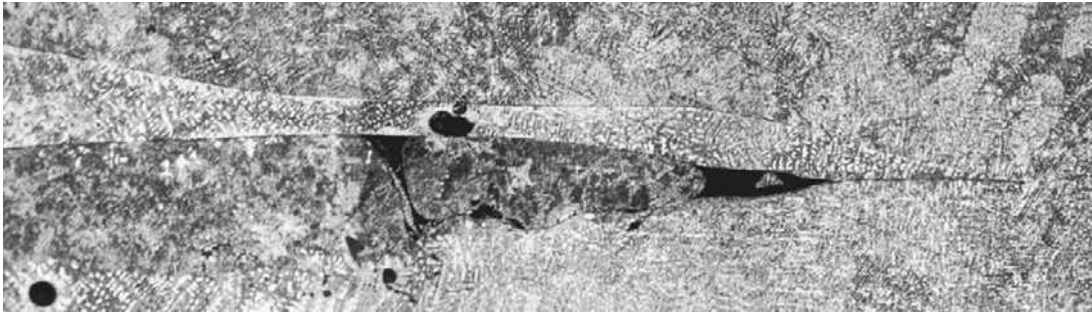


**FIGURE 2.31**

Oxide flow tubes separating regions of the solidifying structure of a high-pressure Al alloy die casting (courtesy of Ghomashchi and Chadwick 1986).

Alternatively, a wandering horizontal stream can define the flow tube, as is commonly seen in the spread of liquid across a horizontal surface. Figure 2.24 shows how, in a thin horizontal section, the banks of the flowing stream remain stationary whilst the melt continues to flow. When the flow finally fills the section, coming to rest against the now-rigid banks of the stream, the banks will constitute long meandering bifilms as cracks, following the original line of the flow.

The jets of flow in high-pressure die castings can be seen to leave permanent legacies as oxide tubes as seen in section in Figure 2.31. Many authors have noted such defects: Lavelle (1962) found such a density of oxide laps in a high-pressure die casting that the casting fractured with a fibrous appearance. More recently, Ahmed and Kato (2008) using a scanning acoustic microscope noted the damage to fatigue properties by ‘cold flakes’ that could detach to reveal a crack.

All these examples illustrate how unconstrained (i.e. free from contact with guiding walls) *gravity filling* or *horizontal filling* both risk the formation of serious defects. (The unconstrained filling of molds without risk can only be achieved by *counter-gravity* filling.)

Both falling and horizontal streams exhibit surfaces that are effectively stationary, and thus grow a thick oxide. When the rising melt finally entrains such features, the new thin oxide that arrives, rolling up against the old thick oxide, creates a characteristic asymmetrical double film. On such a double film in a vacuum cast Ni-based superalloy, the author has seen sulfide precipitates formed only on one side of the defect, indicating that only one side of the double film was favorable to nucleation and growth (microphotographs were not released for security reasons). Too little work was carried out to know whether the thick or thin side of the bifilm was the active substrate in this case.

In all cases it will be noticed that in such interruptions to flow, where, for any reason, the surface of the liquid locally stops its advance, a large, asymmetric double film defect is created. These defects are always large, and always have a recognizable, predictable geometrical form (i.e. they are cylinders, planes, meandering streams, etc.). They are quite different to the random size and shape of double films formed in the chaos of surface turbulence.

### 2.2.7 Microjetting

Where the advance of the liquid front occurs in very narrow sections, the smooth form of the meniscus can disappear, becoming chaotic on a microscale. Jets of liquid issue from the front, only to

be caught up within a fraction of a second by the general advance of the front, and so become incorporated back into the bulk liquid. The jets, of course, become oxidized, so that the advancing liquid will naturally be expected to become contaminated with a random assortment of tangled double films.

Such behavior was observed during the casting of Al-7Si-0.4Mg alloy in plaster molds (Evans and Campbell 1997). In this experiment the wall thickness of the castings was progressively reduced to increase the effect of surface tension to constrain the flow, reducing surface turbulence, and thus increasing reliability. As predicted, properties were clearly improved as the section was reduced from 6 to 3 mm. However, as the section was reduced further to increase the benefit, instead of the reliability increasing further as expected, it fell dramatically.

An explanation of this surprising behavior came from direct video observation of the meniscus of the casting as it traveled towards the camera in these smaller sections. The smooth profile of the meniscus was observed to be punctured by cracks, through which tiny jets of metal spurted ahead, only to be quickly engulfed by the following flow. The image could be likened to advancing spaghetti.

It seems likely that the effect is the result of the strength of the oxide film on the advancing front in thin section castings. In thin sections, the limited area of the front limits the number of defects present in the film. (The effect seems analogous to the behavior of metal whiskers, whose remarkable strength derives from the fact that they are too small to contain any significant defects.) Following this logic, a small area of film may contain no significant defect, and so may resist failure. Pressure therefore builds up behind the film, until finally it ruptures, the split releasing a jet of liquid. (To explain further, the effect is not observed in thick sections because the greater area of film assures the presence of plenty of defects, so the film splits easily under only gentle pressure so that the advance of the melt is therefore smooth.)

Similar microjets have been observed to occur during the filling of Al alloy castings via 2-mm-thick ingates. Single or multiple narrow jets, a millimeter or so in diameter, have been seen to shoot 100 mm or more across the mold cavity from the narrow slot ingates prior to the arrival of the main flow of metal (Cunliffe 1994).

Microjetting has also been observed in detail under the scanning electron microscope (Storaska and Howe 2004). When small droplets of Al-Si alloy have been melted in the electron beam the expansion of the liquid causes the oxide skin of the droplet to be subject to a massive stress in the region of 15 GPa. Some droplets are sufficiently small to have a good chance of not containing any defect in their skin, with the result that the skin slowly creeps to gradually reduce the internal pressure. Others, however, are seen to fracture suddenly, shooting out the compressed liquid as a jet.

The microjetting mechanism of advance of liquid metals in castings has so far only been observed in aluminum alloys, and the precise conditions for its occurrence are not yet known. It does not seem to occur in all narrow channels. The gaseous environment surrounding the flow may be critical to the behavior of the oxide film and its failure mechanism. Also, the effect may only be observed in conditions where not only the thickness but the width of the channel is also limited, thus discouraging the advance of the front by the steady motion of transverse waves (the unzipping mode of advance to be discussed later).

Where it does occur, however, the mechanical properties of the casting are seriously impaired. The reliability falls by up to a factor of 3 as casting sections reduce from 3 to 1 mm. Unless microjetting can be understood and controlled, the effect might impose an ultimate limit on the reliability of very thin

section castings. This would be a bitter disappointment, and hard to accept. To avoid the risk of this outcome more research is needed.

### 2.2.8 Bubble trails

Entrainment defects can be caused by the folding action of the (oxidized) liquid surface. Sometimes only oxides are entrained, as doubled-over film defects that we call bifilms. Sometimes the bifilms themselves contain small pockets of accidentally enfolded air, so that the bifilm is decorated by arrays of trapped bubbles. Much, if not all, of the microporosity observed in castings either is or has originated from a bifilm.

Sometimes, however, the folded-in packet of air is so large that its buoyancy confers on it a life of its own. This oxide-wrapped bubble is a massive entrainment defect that can become important enough to power its way through the liquid and sometimes through the dendrites. In this way it develops its own distinctive damage pattern in the casting. Most bad filling system designs are capable of generating such bubbles, and not just one; sometimes hundreds of large bubbles are generated. Unfortunately this is all too common in castings.

The passage of a single bubble through an oxidizable melt is likely to result in the creation of a bubble trail as a double oxide crack, a long bifilm, in the liquid. A bubble trail is the name I coined to describe the defect that was predicted to remain in a film-forming alloy after the passage of a bubble through the melt (Campbell 1991). Therefore, even though the bubble may be lost by bursting at the liquid surface, the trail remains as permanent damage in the casting.

The bubble trail occurs because the trail necessarily starts at the point where the bubble was first entrained in the liquid. The enclosing shroud of oxide film covering the crown of the bubble attempts to hinder its motion. This restraint is so large that bubbles of diameter less than about 5 mm are held back, unable to float freely to the surface. They remain tethered like balloons on a string. However, if the bubble is larger, its upward buoyancy force will split this restraining cover. Immediately, of course, the oxide re-forms on the crown, and splits and re-forms repeatedly. The expanding region of film on the crown effectively slides around the surface of the bubble, continuing to expand until the equator of the bubble is reached. At this point the area of the film is a maximum. Although the film was able to expand by splitting and re-forming, it is, of course, not able to contract its area since the film is a solid. Further progress of the bubble causes the film to continue sliding around the bubble, gathering together in a mass of longitudinal pleats under the bubble, to form a trail that leads back to the distant point at which the bubble was first entrained as a packet of gas. Any spiraling motion of the bubble will twist and additionally tighten the rope-like tether that continues to lengthen as the bubble rises.

The structure of the trail is a kind of collapsed tube. In section it is star-like but with a central portion that has resisted complete collapse because of the small residual rigidity of the oxide film (Figure 2.32). This is expected to form an excellent leak path if it joins opposing surfaces of the casting, or if cut into by machining. The leak path is non-trivial since it can stretch from the bottom to the top of the casting. In addition, of course, the coming together of the opposite skins of the bubble during the formation of the trail ensure that the films make contact dry side to dry side, and so constitute our familiar classical bifilm crack, but cutting through the casting as a sword through butter.

Since air, water vapor, and other core gases are normally all highly oxidizing to the liquid metal, a bubble of any of these gases will react aggressively, oxidizing the metal as it progresses, and leaving in its wake the collapsed tube of oxide like an old sack.



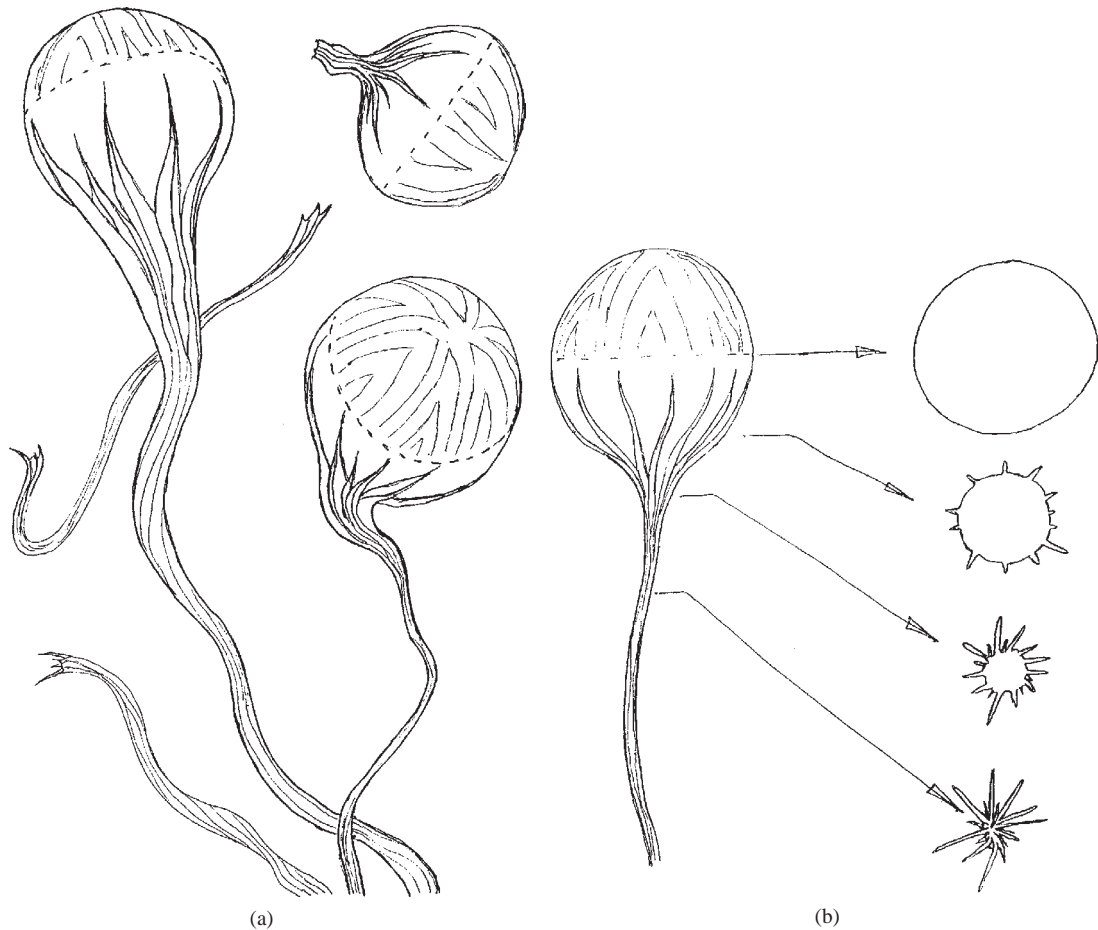


**FIGURE 2.32**

(a) Schematic illustration of rising bubbles and associated trails; (b) cross-sections illustrating the progressive collapse of the bubble trail.

Occasionally the bubble trail may break. At the top of Figure 2.32 is shown a bubble that has been torn free from its trail. Such bubbles, with the stump of their trail showing the bubble to be tumbling irregularly as it rises, have been directly observed by X-ray video.

In cast irons containing resin-bonded cores, core gases initially contain significant quantities of water vapor so that bubble trails originally form from oxides. These oxides are mainly silicates, and have rather low melting points, thus eventually succumbing, raveling, and compacting into formless heaps of slag in the tornado of escaping gases that blasts its way through the wall of the casting to form a permanent open link: a leakage defect. However, after the core has become sufficiently hot to drive off all its moisture, the supply of oxidizing gases is exhausted and the evolving gases become carbon-containing volatiles. At that stage of gas evolution, graphite bubble

trails start to form (Campbell 2008). Examples of such complicated bubble damage in cast irons are given in Section 10.4.

### ***Bubble damage***

Poor designs of filling systems can result in the entrainment of much air into the liquid stream during its travel through the filling basin, during its fall down the sprue, and during its journey along the runner. In this way dozens or even hundreds of bubbles can be introduced into the mold cavity.

When so many bubbles are involved the later bubbles have problems to rise through the maze of bubble trails that remain after the passage of the first bubbles. Thus the escape of late-arriving bubbles is hampered by the tangled accumulation of earlier trails. If the density of trails is sufficiently great, fragments of bubbles remain entrapped as permanent features of the casting. This messy mixture of bifilm trails and bubbles is collectively called 'bubble damage'. In the experience of the author, bubble damage is probably the most common defect in castings, but up to now has been almost universally unrecognized.

Bubble damage is nearly always mistaken for shrinkage porosity as a result of its irregular form, usually with characteristic cusp-like morphology. When seen on polished sections, the cusp forms that characterize bubble damage are often confused with cusps that are associated with the shapes of interdendritic shrinkage porosity. However, they can nearly always be distinguished with complete certainty by their difference in size. Careful inspection of the dendrite arm spacing will usually reveal the cusps that would have formed around dendrites as the residual interdendritic liquid is sucked into the dendrite mesh. The interdendritic cusps are usually up to ten times smaller than the cusps that are caused by the folds of oxide in bubble trails (Figure 2.33). Clearly, the two are totally unrelated and quite distinct.

Bubble damage is commonly observed just inside and above the first (or sometimes the last) ingate from the runner (Figure 2.33). The large bubbles have sufficient buoyancy to escape up the first ingate, but smaller bubbles can be carried the length of the runner, to appear through the farthest ingate. Alternatively, they can even be carried back once again to an earlier ingate if there is a back wave. This non-uniform distribution associated sometimes with first and sometimes with some other ingate position is a common feature of bubble damage. However, it does not always occur simply because of the presence of cores, and sometimes strong flows of metal inside the mold cavity, that can cause the bubble path to deviate a long way from a direct vertical path to the surface. Highly indirect paths are commonly observed in video radiography studies. Nevertheless, the common feature of bubble damage is its non-uniform distribution; it tends to be clustered along favored flow paths.

If the bubbles completely escape, the remaining trails can float around, finally settling sometimes at great distances from their source. Irregular masses of oxides in odd corners of castings have been positively identified as groups of tangled bubble trails (Figure 2.34). The work by Divandari (Figure 2.34) confirms that bubble trails, in filtered melts known to be free from oxide tangles, can detach and float freely, finally appearing at distant locations. The bubbles have moved on and escaped from the casting, but their trails have remained in suspension. They have broken free from their moorings (the point at which the bubble was first entrained) and have traveled, tumbling and raveling as they go, carried by the sweeping and circulating flow of the liquid during the filling process. Texan founders will recognize an analogy with tumbleweed.

Another common feature of bubble damage is the entrapment of small bubbles just under the cope skin of the casting (Figure 2.33). They are prevented from escaping only by the thickness of the oxide

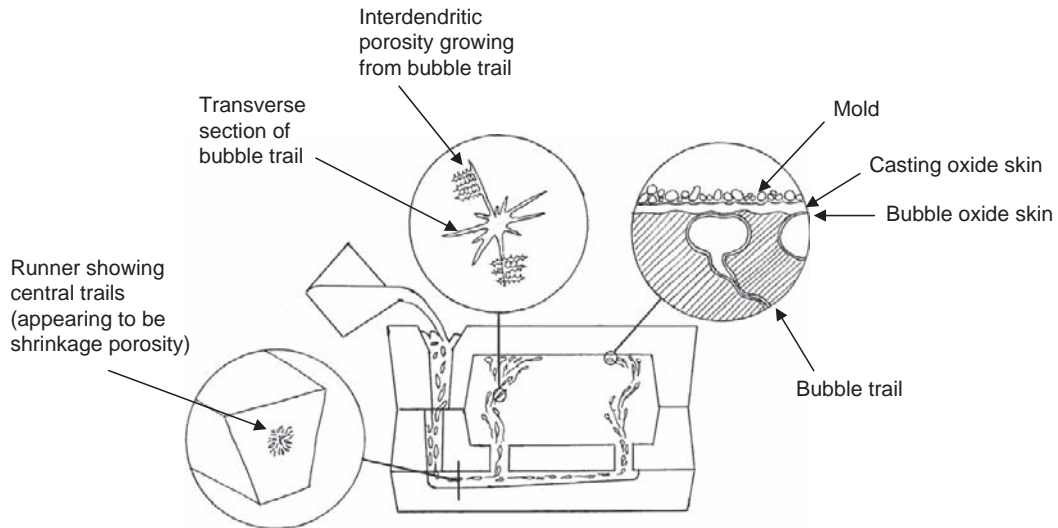


**FIGURE 2.33**

Pattern of bubble damage in a casting: (a) dendrites push trails into the centers of runners (misleadingly appearing as center-line shrinkage porosity); (b) trails invisible in radiography are usually visible on transverse sections; (c) entrained air bubbles smaller than about 5 mm diameter appear as immediately subsurface porosity, having insufficient buoyancy to break the double oxide barrier to escape to atmosphere.

skin on the casting and their own oxide skin (a double oxide film feature as usual!). Both these films must be broken before the bubble can escape to the outside world. (This is achieved by larger bubbles because of their greater buoyancy forces, but not by smaller bubbles. The dividing line between large and small bubbles seems to be in the region of 5 mm diameter for both light and dense alloys.) Such small bubbles are commonly observed in video radiographic studies to float up and sit under the top surface, resting only a double thickness of oxide depth under the skin of the casting. This sub-surface porosity is, of course, easily broken into when shot blasting, or when taking the first machining cut.

Close optical examination of the interiors of bubbles and bifilms in an aluminum alloy casting often reveals some shiny dendrite tips characteristic of shrinkage porosity. This adds to confusion of identification, because the action of a fall in pressure due to solidification shrinkage will often expand an existing bubble to give it a dendritic appearance. Alternatively, shrinkage may act to expand an existing bifilm, unfurling and opening it, and finally sucking its oxide films deep into the dendrite mesh. Whether the origin of the cavity was a bubble or a bifilm subsequent examination will usually reveal only fragments of the originating oxides among the dendrites.

This process has been observed in video radiographic studies of castings. An unfed casting has been seen to draw in air bubbles at a hot spot on its surface. The bubbles floated up in succession, initially bursting and disappearing at the top of the casting. However, later bubbles became trapped during their rise by dendrites growing in from the walls. As solidification progressed, shrinkage caused the originally spherical air bubbles to gradually convert to shrinkage cavities. The perfectly round and

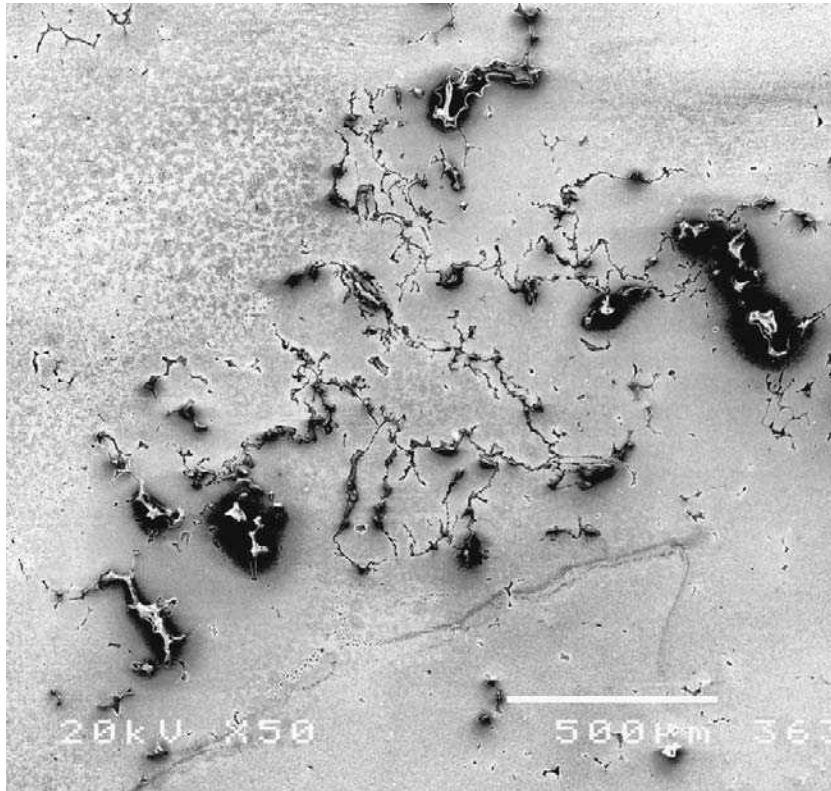


**FIGURE 2.34**

SEM metallographic section showing apparently normal entrained bifilms which are in fact a cluster of bubble trails (Divandari 2000).

sharp radiographic images were seen to become ‘furry’ and indistinct as the liquid meniscus was sucked into the surrounding mesh of dendrites. Finally, the defect resembled extensive shrinkage sponge; its origin as a gas bubble no longer discernible.

Other real-time radiography has shown bubbles entrained in the runner, and swept through the gate and into the casting. The upward progress of one bubble in the region of 5 mm diameter appeared to be arrested, the bubble circulating in the center of the casting, behaving like a balloon on a string. The string, of course, was the bubble trail acting as a tether. Other bubbles of various sizes up to about 5 mm diameter in the same casting were observed to float to the top of the casting, coming to rest under the oxide skin of the cope surface. These bubbles had clearly broken free from their tethers, probably as a result of the extreme turbulence during the early part of the filling process. The central bubble was marginally just too small to tear free from its trail. In addition, it may have lost some buoyancy as a result of loss of oxygen during its rise, or perhaps more likely, it ascended as far as it did because of assistance from the force of the flow of the melt. When the force of the flow abated higher in the mold cavity, its buoyancy alone was insufficient to split its crown of oxide skin, so that its upward progress was halted.

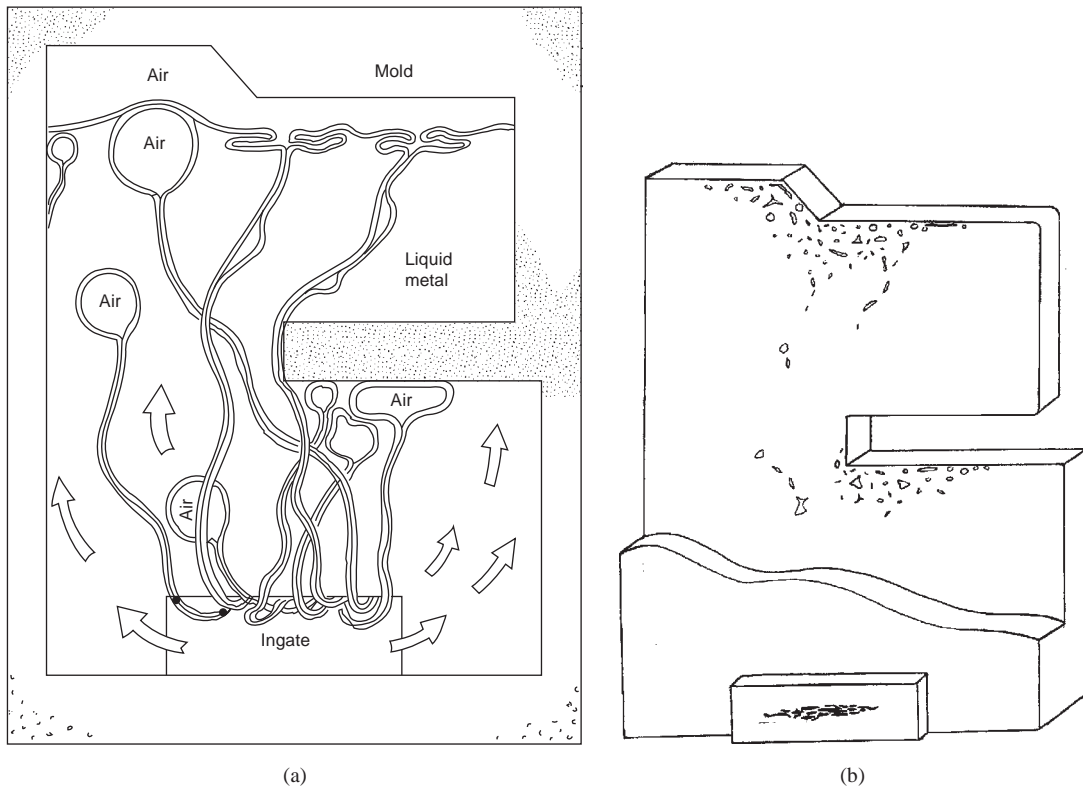


**FIGURE 2.35**

Schematic illustration of (a) bubbles entering a casting, and (b) the resulting permanent damage of residual bubbles and cracks. The residual bifilms remain invisible. The bubble trails in the runner are pushed and concentrated by the freezing front into the center of the section.

A scenario such as that shown in Figure 2.35 is common. The bubbles are entrained early in the filling system, arriving as a welter of defects, boiling up with the liquid as it fills the mold cavity. Many of the early bubbles will have sufficient buoyancy to escape. When the casting is finally solidified the appearance on a radiograph is expected to be something like that shown in Figure 2.35b. Porosity and cracks may be detected in regions above the ingate. The large number of remaining trails is likely to be invisible. The reader will recall, this mix of residual bubbles, oxides and cracks is usefully termed *bubble damage*.

Where many bubbles have passed through an ingate into the mold, a cross-section of the ingate will reveal some central porosity. Close examination will confirm that this porosity is not shrinkage porosity, but a mass of double oxide films, the bubble trails. The trails are pushed ahead of the dendrites growing out from the walls, and so concentrated in the center of the ingate section. In Al alloys they appear as a series of dark, non-reflective oxidized surfaces interleaved like the flaky, crumpled pages of an old newspaper, sepia-colored as a result of stains from mold gases.

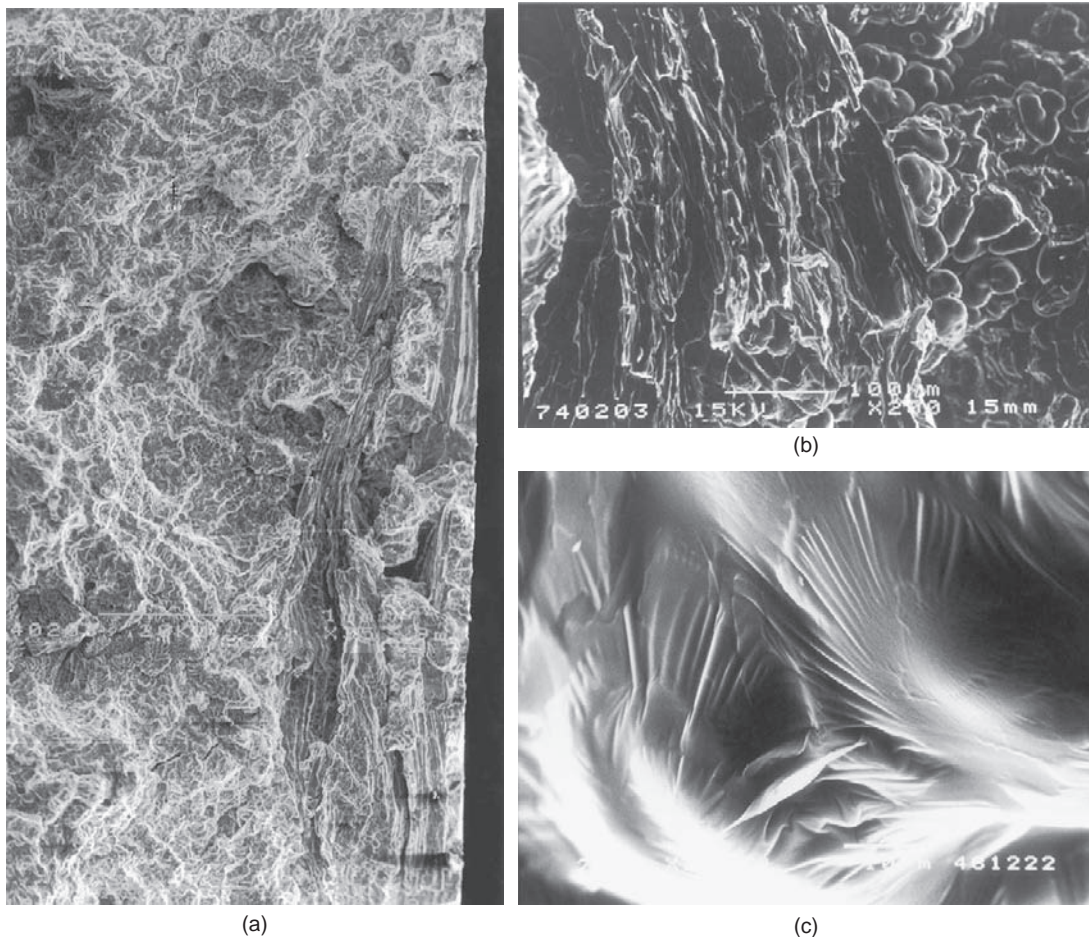


**FIGURE 2.36**

SEM fractographs of: (a) bubble trail in Al-7Si-0.4Mg alloy; (b) close-up showing area of shrinkage porosity grown from the trail; (c) the oxide film of the trail draped over dendrites, on the point of being sucked back into the dendrite mesh because of a slight shrinkage condition in the casting (Divandari 2000).

Divandari (1999) was the first to study systematically the formation of bubble trails in aluminum castings by X-ray video technique. He introduced air bubbles artificially into a casting, and was subsequently able to pinpoint the location of the trails and fracture the casting to reveal the defect. Figure 2.36a shows the inside of a trail in Al-7Si-0.4Mg alloy. The longitudinally folded film is clear, as is the presence of shrinkage cavities that have expanded away from the defect because the casting was not provided with a feeder. The small amount of shrinkage has sucked back the residual liquid among the dendrites seen in Figure 2.36b, and in places stretching the film over the dendrites as seen in Figure 2.36c. The thicker, older part of the film is seen pulled in tight creases, and where torn is seen to be replaced by newer, thinner film.



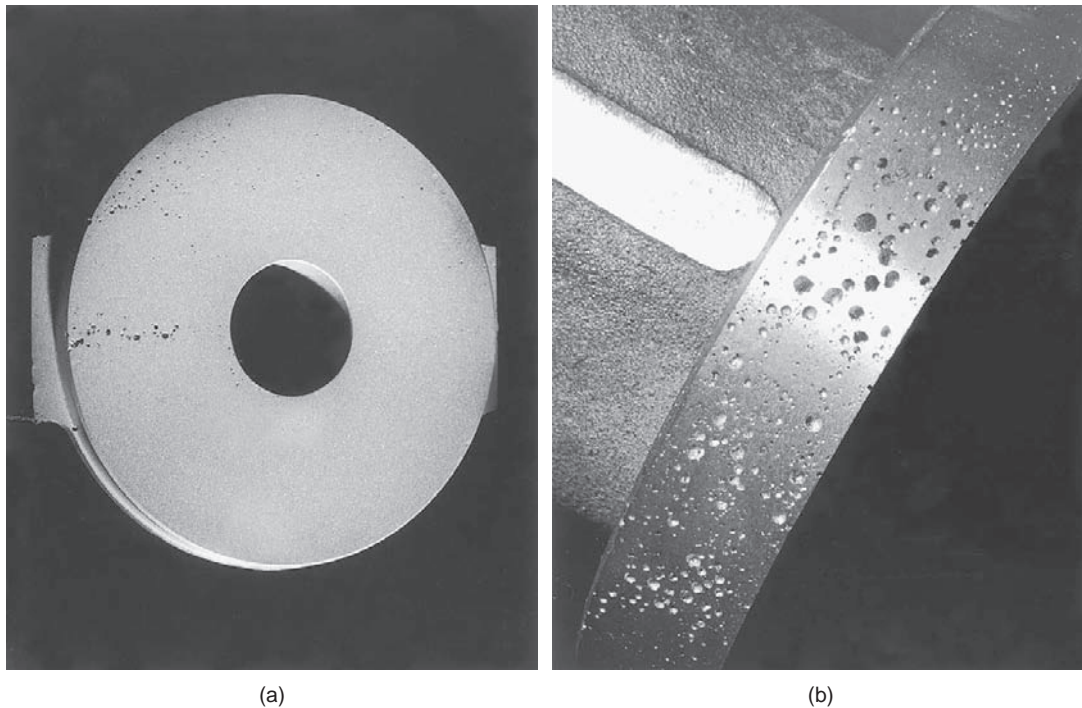


**FIGURE 2.37**

Bronze casting after machining revealing entrained air bubbles on (a) the front face and (b) the top edge of the flange.

Figure 2.37a shows a bronze casting that has suffered a highly turbulent filling process. The bubbles entrained by this turbulence can be seen to be grouped along a horizontal line (a site of a poor joint between cope and drag, allowing a cooling fin to create a line of dendrites inside the casting that had caught many of the bubbles) and towards the top of the casting in the ‘skeins of geese’ mode that characterizes these defects in bronzes. The skeins are probably the directionality to the visible defects provided by the arrays of invisible oxide bifilms, streaming like tattered banners in the wind, and funneling bubbles along their surfaces to create the ‘skeins’ on machined surfaces. Figure 2.37b is a close-up of the top of the same casting after defects have been revealed by machining.

A radiograph of a nearly pure copper casting that has also suffered bubble entrainment in its filling system is shown in Figure 2.38. This casting was thin-walled, and extensive, so that it continued to receive bubbles late into pouring, with the result that they have become trapped in the solidifying casting. The author has seen similar extensive arrays of bubbles in aluminum alloy oil pan castings.

During the radiography of some stainless steels I have witnessed an area initially identified as shrinkage porosity, but under the microscope was seen to be a mixture of bubbles and cracks. Such classic bubble damage is a remarkable combination that without the concept of the bubble trail would be extremely difficult to explain; tensile stress cannot have been present in the liquid phase because the bubbles would simply have expanded to relieve the stress, thus how can stress cracks have arisen? The



**FIGURE 2.38**

Radiograph of a thin-wall copper statue showing extensive bubble damage.

answer, of course, is that the cracks are not due to stress but are bifilms in the form of bubble trails, and have no problem to sit side-by-side with bubbles. In these strong steels the high cooling strain leads to high stresses that open up the bifilms to reveal their true nature as cracks.

In gray iron cylinder blocks the bubbles and their trails are sometimes formed from an oxide (a glassy silicate) and sometimes from a lustrous carbon film, depending on the composition of the gases in the bubble (Campbell 1970). The carbon film appears to be somewhat more rigid than most oxide films, and so resists to some extent the complete collapse of the trail, and retains a more open center. In effect, the bubbles punch holes through the cope surfaces of the casting, so that their trails form highly efficient leak paths. The subject of core blows in cast iron is dealt with in more detail under Rule 5 for good castings in Section 10.5.

Bubble trails are known in low-pressure casting if the riser tube is not pressure-tight, allowing bubbles of the pressurizing gas to leak through, rising up the riser tube and so directly entering the casting. The author has observed such a trail in a radiograph of an aluminum alloy casting. In the quiescent conditions after filling, the resulting trail was smooth and straight, rising through the complete height of the casting. When concentrating on the examination of the radiograph for



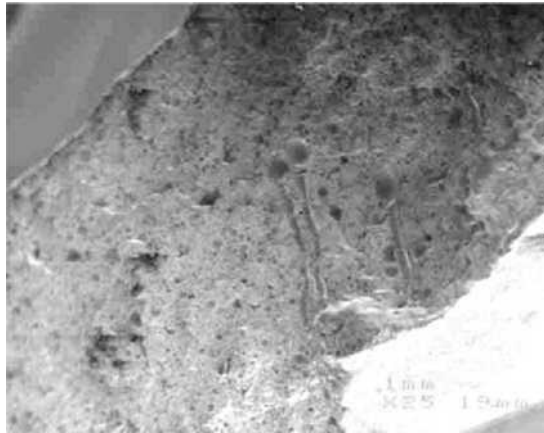


**FIGURE 2.39**

SEM fractograph of a zinc alloy pressure die casting revealing a bubble with an open trail (Divandari 2000).

minute traces of porosity or inclusions such extensive geometric features are easy to overlook, appearing to be the shadows of integral structural parts of the casting!

In general the bubble trail is a collapsed, or nearly closed, tube. However, completely open bubble trails have been observed by Divandari in pressure die castings (Figure 2.39). In this process the very high injection velocities, of the order of 10–100 times the critical velocity for entrainment, naturally entrain considerable quantities of air and mold gases. The very high pressure (up to 100 MPa, or 15 000 psi) applied during casting is mainly used to compress these unwanted gases to persuade them to take up the minimum volume in the casting. If, however, the die is opened before the casting is fully solidified, as is usual to maximize productivity, the entrained bubbles may experience a reduction in their surrounding mechanical support. The bubbles and their trails containing the highly pressurized gas can be suddenly released from their constraining pressure, and so expand, opening like powerful springs, whilst the casting is still in a plastic state. Such open bubble trails in pressure die cast components are expected to be serious sources of leakage, particularly when broken into by machining operations. In more extreme cases, it is common for a high-pressure die casting to explode if the die is opened too soon. These problems are of course greatly reduced (although perhaps never quite eliminated) by sacrificing some productivity, allowing the castings to solidify more completely before opening the die.

Finally, it is worth considering what length a bubble trail might reach. If we assume a bubble of 10 mm diameter rising through liquid aluminum, and if aluminum oxide grows to a thickness of 20 μm, it is not difficult to estimate that the 20% oxygen in the air is used up after creating a trail of about 0.5 m. This is quite sufficient to cause a major problem in most castings. However, this estimate is uncertain because Raiszadeh and Griffiths (2008) show that after the oxygen is consumed in a bubble, the nitrogen then starts to react to form aluminum nitride. Thus the maximum trail length might be nearer 2.5 m.

For castings poured in vacuum (actually corresponding only to dilute air of course!) vacuum bubbles are still to be expected to form, although the situation is a little more complicated. The entrained atmosphere in this case will be at a pressure somewhere between  $10^{-3}$  and  $10^{-6}$  atmospheres

(1 torr to  $10^{-3}$  torr). (The local vacuum inside the mold at the instant of pouring is likely to be much higher than the pressure indicated on the vacuum gauge of the furnace as a result of mold out-gassing.) Thus, considering the case of the vacuum casting of Ni-base superalloys, at a nominal depth of 100 mm in the liquid of density close to  $8000 \text{ kg m}^{-3}$ , a bubble of 20 mm diameter will collapse down to somewhere in the region of 5 mm to 0.5 mm diameter before its internal pressure rises to equal that of the surrounding melt. (We are neglecting the somewhat balancing effects of (i) a small reduction in size because of surface tension, and (ii) a small increase in size from the expansion of the mold gases, since molds for investment casting of Ni-based alloys are already at  $1000^\circ\text{C}$  or more.) The bubbles will be smaller at greater depths, and larger towards the top of the casting of course. Their considerably reduced concentration of oxygen will reduce the potential lengths of trails, or tend to generate more nitride-film-based trails. (It is known that Ni-based superalloys suffer from time to time from nitride problems.) It is not easy to predict what form a bubble trail may take in these circumstances, if the bubble is able to rise at all. There seems no shortage of research to do yet.

---

## 2.3 FURLING AND UNFURLING

Throughout its life, the bifilm undergoes a series of geometrical rearrangements. An understanding of these different forms is essential to the understanding of the properties of castings. The stages in the life cycle of the bifilm are

- (i) entrainment by surface turbulence;
- (ii) immediate furling by bulk turbulence; and
- (iii) slow unfurling in the stillness of the liquid after the filling of the casting is complete.

The verb ‘to furl’ is used in the same sense that a sailing boat will *furl* its sails, gathering them in; or it may *unfurl* them, letting them out to adopt their full area and fill with wind.

We shall show later that if the surface of the liquid suffers turbulence (i.e. the Weber number is significantly in excess of unity) the liquid is likely to enfold our familiar bifilm defects. Their size will probably depend on the strength (i.e. the tear resistance) of the film and the power of the turbulent flow. For some high-duty stainless steels the size might be 100 mm across. For Al–Si alloys containing low levels of Mg the bifilms seem to be more usually in the range 0.1–1 mm and occasionally up to 10 or 15 mm diameter.

Once submerged, the bifilms will be subjected to the conditions of bulk turbulence beneath the surface of the liquid. This is because Reynolds number,  $Re$ , is nearly always over the critical value of 2000 in liquid metal filling systems as is clear from Figure 2.22. (Exceptions may be counter-gravity and tilt pouring systems.) The launching of our delicate, gossamer-thin double film into a maelstrom of vortices in this heavy liquid will ensure that it is pummeled and raveled into a compact, convoluted form almost immediately. In this form it will be effectively reduced in shape and size from a planar crack of diameter perhaps 1–10 mm to a small ragged ball of perhaps a tenth of this size, i.e. a diameter in the range 0.1–1 mm. These are the sizes of small shadows of crumpled dross-like defects seen by Fox (2000) by radiography (Figure 2.40a) and commonly seen on polished metallographic sections of aluminum alloy castings (Figure 2.5a).

It is worth emphasizing that although the bifilm now has a highly contorted form; crumpled, convoluted, and raveled in an untidy random manner. Although it has not lost its crack-like character,

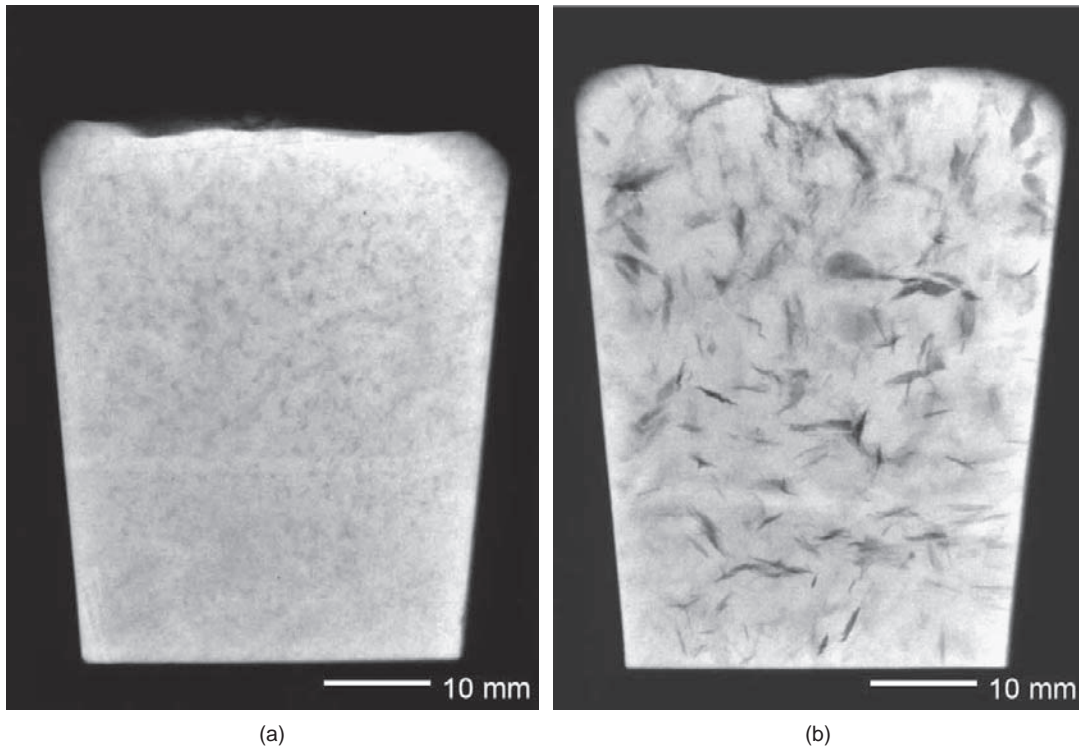


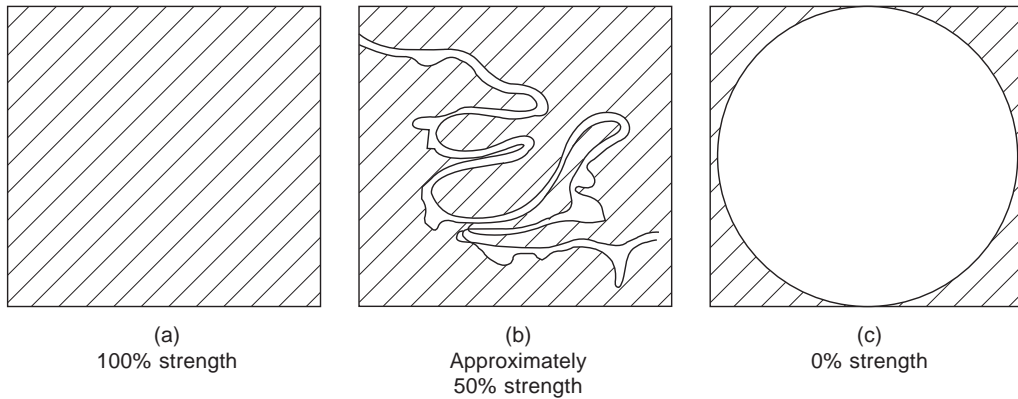
**FIGURE 2.40**

Radiographs of reduced pressure test samples of the same as-melted Al-7Si-0.4Mg alloy solidified under pressure of (a) 1 atmosphere and (b) 0.01 atmospheres (Fox and Campbell 2000).

its form contrasts sharply with the types of cracks familiar to the metallurgist. Clearly this bears no resemblance to a crack formed by the application of stress. It is a crack morphology unique to liquid metals and castings.

It seems also worth underlining the fact that the double film is unlikely to become separated once again into single films. This is because where the two halves are in contact, interfacial forces will be important, and inter-film friction will ensure that both films of the bifilm will move as one. In addition, the continued oxidation, thickening the films, will reduce the volume of air in the inter-film gap, reducing the pressure between the films. The exterior atmospheric and metallostatic pressures will thereby pressurize the two halves together, ensuring that the films continue their association as a pseudo-single entity, despite the absence, or near-absence, of bonding forces between the halves.

In this compact form, bifilms are able to pass through filters of normal pore size in the region of 1 mm diameter. Some will be arrested as a result of untidy trails of film that may become caught by the filter, since the compact forms will be winding and unwinding continuously in a random manner in the turbulent flow. Inside the filter the constraint of the narrow channels probably promotes laminar flow (Figure 2.22). It is possible that many compact bifilms will be unraveled and flattened against the internal surfaces of the filter if they become hooked up somewhere in a laminar flow stream. This

**FIGURE 2.41**

Relative strengths of (a) solid matrix; (b) convoluted bifilms; and (c) pores.

seems likely to be a potentially important filtration mechanism whereby compacted bifilms become caught at one point and straightened by the flowing stream.

At practically all other locations, during the whole of the voyage into the mold, the bulk turbulence will ensure that the bifilms are continuously tumbled, entering the mold in a relatively compact form.

Thus the casting initially finds itself with a distribution of compact, convoluted bifilms. Their tensile strength will, on average, be about half that of a pore of the same average diameter as the bifilm ball because of the effect of the mechanical interlinking of the crumpled crack as seen in Figure 2.41. If the convoluted crack is subject to a tensile stress it cannot come apart easily. There is much interlocking of sound metal, so that much plastic deformation and shearing will be involved in the failure.

Because of the combination of a certain amount of strength together with their compact size, the convoluted bifilms are rendered as harmless as possible at this stage. As a result the casting will enjoy maximum strength.

However, once the filling of the casting is complete, the bifilm now finds itself in a new, quiescent environment. If there is any movement of liquid because of solute or thermally driven convection, such movements are relatively gentle, occurring at low values of  $Re$ .

Conditions are now right for the bifilm to unfurl, opening, unfolding progressively, fold after fold, and effectively growing in size by about a factor of 10 on average, to its original size in the range of 1–10 mm or so. By this action the defect now re-establishes itself as a planar crack, and so can impair the strength and ductility of the metal to the maximum extent. This astonishing ability of the bifilm to open like a flower explains many of the problems of castings, as will become clear throughout this book.

What causes the bifilm to open again?

Interestingly, there are a number of potential driving forces. Although they will be considered in detail in later sections of the book, they are listed briefly here. The evidence mainly comes from recent studies of aluminum alloys where the effects have been most thoroughly studied to date. They include:

- (i) The precipitation of hydrogen in the gas film between the oxide interfaces, thus inflating the defect. The inflation is likely to take place in two main stages. The first we may call microinflation, with short lengths inflating individually. These short lengths are defined and

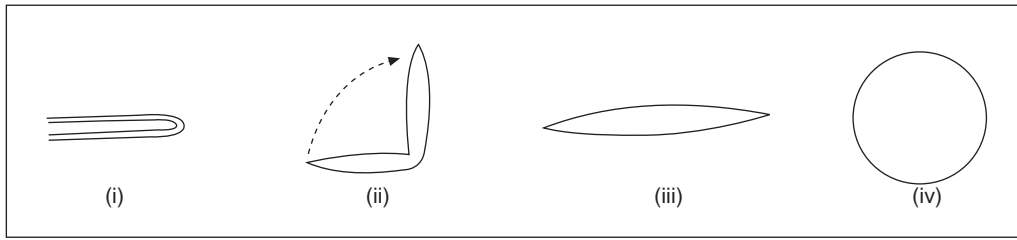
separated from adjacent lengths by the crease lines of adjacent folds. When sufficiently inflated, these short lengths will start to exert an unfolding pressure on adjacent lengths. As gas continues to inflate the bifilm, the bifilm will unfold progressively from one fold to the next fold, and so on. Thus the unfurling acting will probably be rather jerky and irregular, until the whole bifilm is unfolded. At this stage, of course, if enough hydrogen continues to precipitate, the planar bifilm crack will eventually inflate into a spherical pore. The stages of growth are illustrated in Figure 2.42a for a simply folded bifilm. Figure 2.42b illustrates the stages for a more convoluted bifilm.

If much gas precipitates, either because there is much gas in solution, or because there is plenty of time for diffusion, thereby aiding the collection of gas from a wide region, the gas pore may eventually outgrow its original bifilm to become a large spherical pore as shown in Figure 2.42c if growing freely in the liquid, or as in Figure 2.42d if growing later during freezing, appearing now as an interdendritic pore. Note that in this situation the two very different morphologies (c) and (d) are both hydrogen gas pores. On sectioning the pore it is probable that the originating fragment of bifilm will never be found.

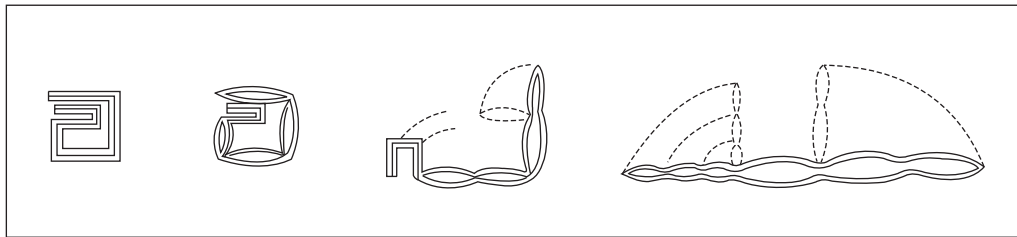
Interestingly, at the stage at which the pore starts to outgrow the boundaries of its originating bifilm, it will extend its own oxide film using its own residual oxygen gas (probably derived from the original bifilm). The new area of the defect will then consist of new, very thin film. It is possible to imagine that if all the oxygen were consumed in this way that eventually the pore would grow by consumption of the residual nitrogen in the air as discovered by Raiszadeh and Griffiths (2008). If this were also entirely consumed, growth might occur by adding clean, virgin metal surface. The many round pores in cast metals indicate that the linear dimensions of many bifilms are probably smaller than the diameters of such pores. It is a reminder of the wide spread of bifilm sizes to be expected.

- (ii) Shrinkage acts to unfurl bifilms because it can reduce the pressure in a local region of the casting. Thus in this region it may suck the two halves of the bifilm apart. If this happened at an early stage of freezing the defect would grow no differently to a hydrogen pore, the inflation process proceeding from one fold to the next. Exactly this effect is seen in Figure 2.40 in which small furled bifilms are seen to unfurl, becoming significant cracks up to 15 mm long. If the shrinkage effect was severe, the final stage of unfurling would be followed by the bifilm eventually growing to be more or less spherical, as seen in Figures 2.42a and 2.42c. If the opening took place at a late stage of freezing the defect would attempt to open when surrounded by dendrites as shown in Figure 2.42d. Both of these modes of opening could be driven by gas or shrinkage or both working in cooperation. Thus the rounded and interdendritic forms are not reliable indicators of the driving force for the growth of pores. In reality the round form is a reliable indicator that the pore grew prior to the arrival of dendrites, while the dendritic pore is a reliable indicator that this pore was a late arrival. No more can be concluded.

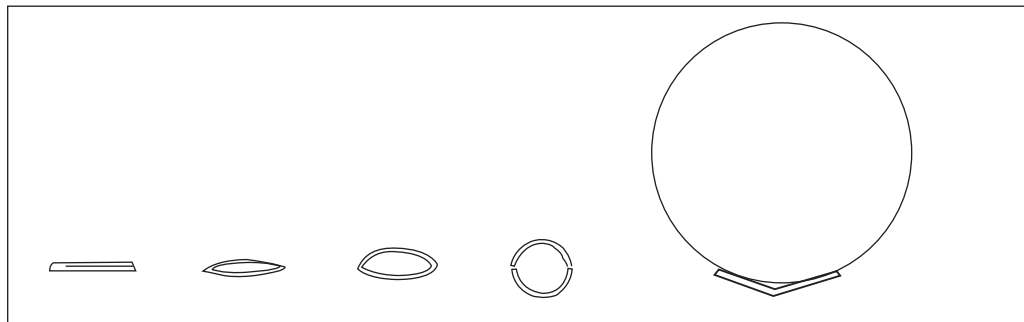
In the case of the dendritic morphology, withdrawal of the residual liquid (being either pushed by gas from inside the pore, or pulled by reduced pressure outside the pore) would stretch the film over surrounding dendrites (Figure 2.36c), and pull the bifilm halves into the interdendritic regions. The originating films might eventually be detected as fragments draped over some dendrites (Figure 2.29), or may be sucked completely out of sight deep into the dendrite mesh (Figure 2.42d).



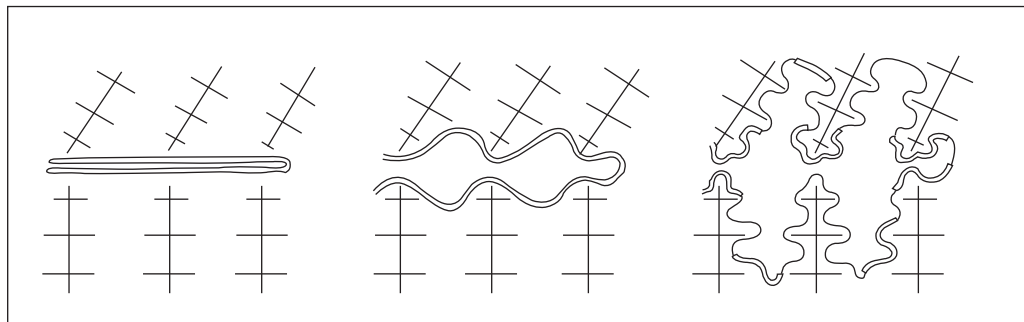
(a)



(b)



(c)



(d)

**FIGURE 2.42**

(a–d) Stages of unfurling and inflation of bifilms.

- (iii) Intermetallics in Al–Si alloys, such as Si and Fe-rich phases, nucleate and grow on the outer, wetted surfaces of the bifilm. The  $\beta$ Fe particles,  $\text{Al}_3\text{FeSi}$ , are particularly good examples. Initially, when the  $\beta$ Fe crystals are no more than a few nanometers thick, the crystals can follow the curvature and creases of the crumpled double film. However, as the crystals grow in thickness they quickly develop rigidity (because the rigidity of a beam in bending mode is proportional to its thickness to the third power). Thus as the precipitates thicken and rigidize, they *force* the straightening of the bifilm. The result is the familiar  $\beta$ Fe plate seen on polished sections, straight as a needle. (Occasional curved  $\beta$ Fe plates are probably the result of restraint at the two ends of the plate, so that the plate has been unable to straighten fully, remaining stressed like an archer's bow.) The  $\beta$ Fe plates sometimes exhibit a crack along their centerline (if  $\beta$ Fe has precipitated on both sides of the bifilm) or between the  $\beta$ Fe and the matrix, showing apparent decohesion from the matrix (if the  $\beta$ Fe has precipitated only on one side of the bifilm). It seems likely that all  $\beta$ Fe particles are cracked or decohered in this way because of the presence of the originating bifilm. The straightening of bifilms by intermetallics in Al alloys is dealt with in detail in Section 6.3.6.

The cracks may not always be seen on a polished section, especially if the casting is well fed. Keeping up the pressure on the bifilms during freezing will ensure that the two halves of the bifilm remain closely together and thus becoming an effectively invisible crack. Moderately poor feeding, or some hydrogen in solution, will part the films, allowing them to be seen on a polished metallurgical specimen. Research on this topic requires, paradoxically, to be carried out on poorly fed sample castings, in contrast to the foundry person who requires his castings to at least appear as sound as possible.

- (iv) Oxides are pushed ahead of growing dendrites essentially because they are unable to grow through the layer of air between the films. The result is the bifilms are automatically unraveled and flattened, effectively teased out and organized into planar areas among dendrite arrays. The teasing action is all the more effective because the bifilms are usually attached to the side walls of the casting, adjacent to the roots of the dendrites. Thus as the dendrites grow, pushing ahead the heap of films, those that are attached near their roots are stretched into flatness between the rows of dendrites (Figure 2.43). In addition, oxides are pushed into interdendritic and grain boundary regions. This is an important mechanism since it can occur in all cast alloys that have solid surface films. The pushing sideways or ahead results in large flat facets on fracture surfaces, or, occasionally, regularly undulating hilly regions of a fracture surface marking the tips of dendrites separated from the matrix by the heap of bifilm cracks (Figure 2.43b).

A room-temperature fracture surface is seen in Figure 2.44 for an Al–4.5Cu alloy (Mi 2000) in which the fracture surface is completely covered in thin alumina films, as ‘half’ of the original double film, or bifilm. The films have been pushed from ‘East’ and ‘West’ by the advance of dendrites. The heaps of excess film pushed ahead of the dendrites are clearly seen forming the central ‘North–South’ ridge. Images (a), (b), (c), and (d) of this figure show fracture surfaces of test bars taken from the same casting; test bar failing by fracture (a) was observed by video radiography to suffer a major turbulent breaking wave during mold filling, whereas (c) was observed to fill smoothly. The surface of (c) exhibited only rather small bifilms from the population that existed in original melt and which caused the scattered microporosity between regions of ductile dimple fracture surface. The ductile dimples indicated that there had been real metal-to-metal contact between the two halves of the fracture surface, in complete contrast to

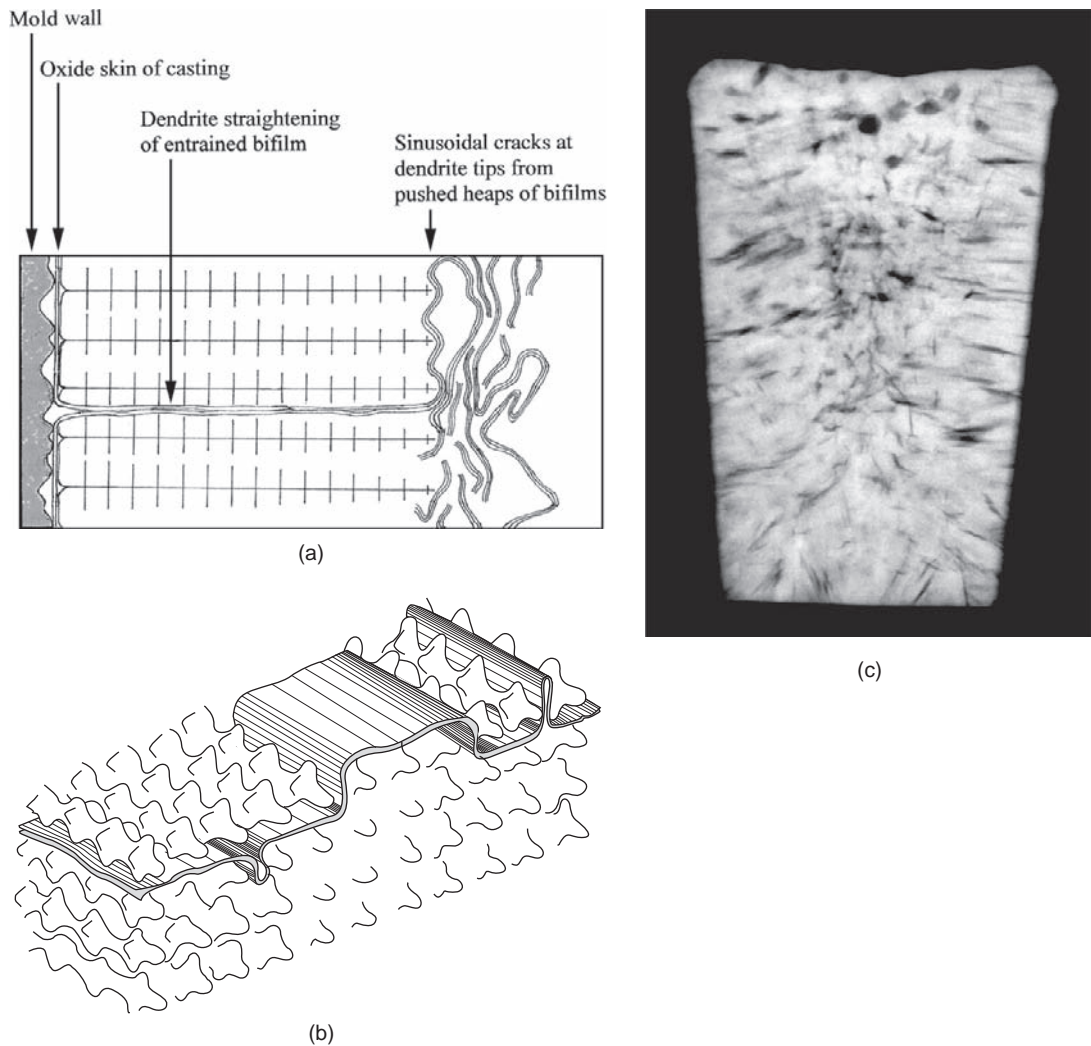


**FIGURE 2.43**

Dendrite flattening of bifilms: (a) the pushing action; (b) the flattened bifilm; (c) radiograph of RPT showing dendrite-flattened cracks grown inwards from the surface of the cast sample.

surface (a) where not a single ductile dimple could be found, indicating no metal-to-metal contact over its whole area. In fact its surface had been entirely covered with bifilms and was therefore effectively completely pre-cracked. This explained its elongation of only 0.3%, compared to the 3% of specimen (c).

Close examination of (a) was required to reveal tiny clues that the dendrite surface was actually covered with an oxide film derived from the turbulent liquid surface, and which had constituted half of the original bifilm; the arrow in Figure 2.44(b) indicates a small area where the film had been



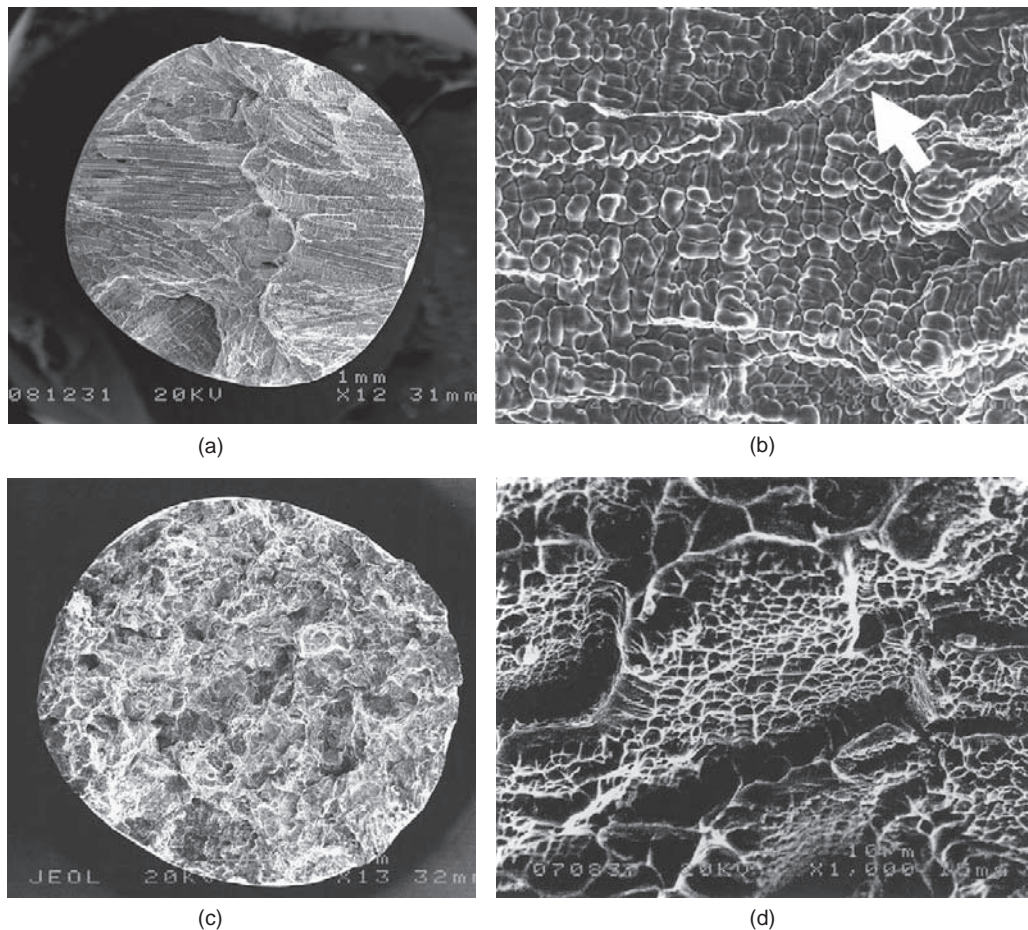


**FIGURE 2.44**

(a) Tensile fracture of Al-4.5Cu alloy that had suffered an entrainment effect observed by video X-ray radiography, showing large new bifilms straightened by large grains grown in from both sides, and heaps of spare film pushed into central areas. (b) The close-up shows a thin doubly folded area (arrowed). (c) Elsewhere in the same casting shows evidence of a population of small bifilm defects interspersed between ductile matrix, showing (d) ductile dimples on fracture (courtesy of Mi 2000).

folded over twice, confirming that the oxide film was not merely an oxide grown on the dendrites in the solid state (for instance, after fracture). Other samples from this research exhibited rather thicker oxide bifilms that were much easier to discern (Figure 2.45). In fact it seems in this image that a second oxide lies beneath the top fractured oxide, thus possibly originally constituting a *double bifilm* (i.e. originally four layers of oxide).

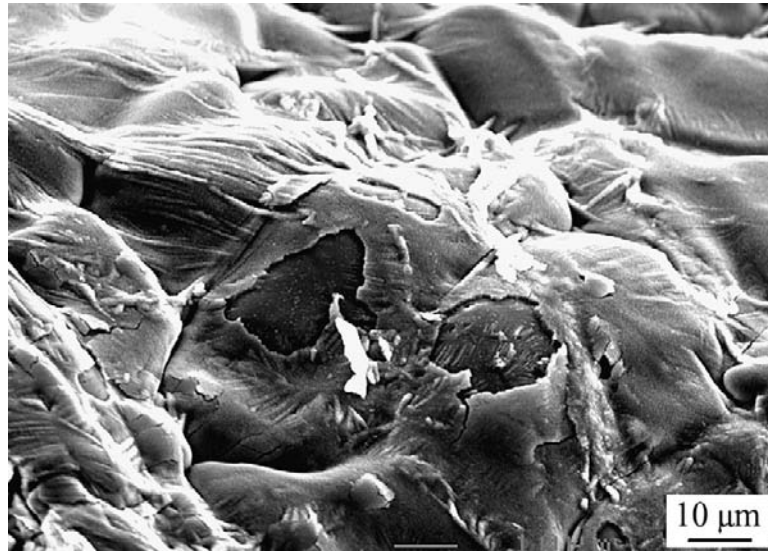


**FIGURE 2.45**

An area of the fracture seen in Figure 2.44a in which the film is thicker, revealing a second bifilm underneath. The parallel markings are deformation twins always seen in stretched alumina film (courtesy of Mi 2000).

In Figure 2.46 an AlN or Al<sub>2</sub>O<sub>3</sub> film is probably the cause of the planar boundaries seen in the fracture surface of a vacuum cast and HIPped Ni-base alloy IN939 (Cox 2000). In the case of the vacuum-cast alloy the castings had suffered surface turbulence during filling, but, significantly, the planar boundary features on the fracture surfaces were *not* observed in control castings made without turbulence. The planar features were also observed to be associated with poor tensile ductility. In Section 6.5 further planar defects created by dendrite straightening are discussed for cast irons, and in Section 6.6 probable examples in steels are proposed.

In all cases where large bifilms are found to have experienced dendrite straightening, the grain size always appears to be large. It seems reasonable to suppose that in a solidifying casting in which large bifilms are present, the natural action of convection would be prevented. Thus the normal eddies of high- and low-temperature metal destabilizing the growth of dendrites causing their arms to melt off and thus promoting grain multiplication, would be suppressed. The barriers to flow would be present across the complete casting section, in contrast to other regions of the casting which contained only confetti-like bifilms in suspension. These would convect freely, and thus naturally generate a refined grain size.

Clearly, the driving forces for the unfurling of bifilms are all those factors that are already known to the casting metallurgist as precisely those factors that impair ductility; including hydrogen in solution, shrinkage, iron contamination in Al alloys, and large grain size. Thus the only common factor implicated in the loss of ductility is the presence of bifilms.

However, in practice, we need to bear in mind that it will take time for the unfurling processes to occur. In a casting that is frozen quickly, the bifilms are frozen into the casting in their compact form,

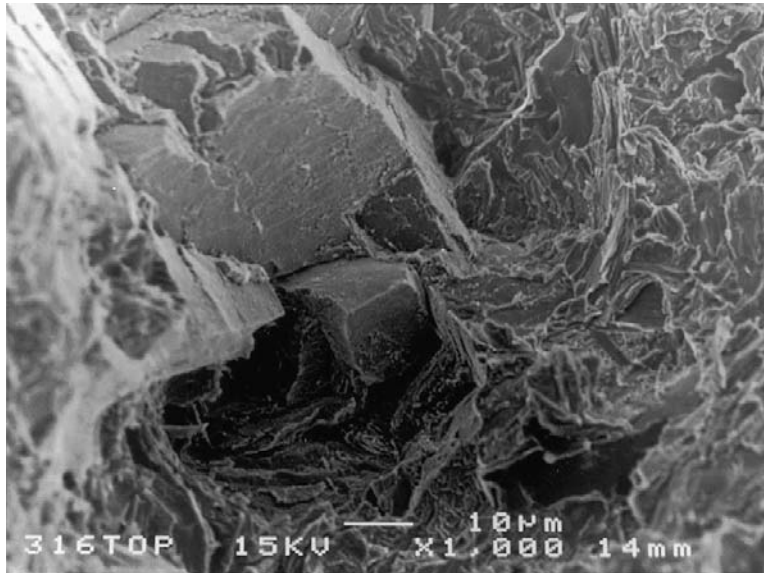


**FIGURE 2.46**

Tensile fracture surface of a turbulently cast, vacuum-melted and cast HIPped Ni-base alloy, showing apparently brittle grain boundaries. Such features were not observed in quiescently cast material.

with the result that most casting alloys that are chilled rapidly are strong and ductile, as all foundry engineers know.

Conversely, castings that have suffered lengthy solidification times exhibit shrinkage problems, higher levels of gas porosity, or large grain size. In addition, all exhibit reduced properties, particularly reduced ductility. The action of slow freezing impairing ductility is, once again, well known to the casting metallurgist.

In summary, it is clear that all the factors that refine DAS improve the mechanical properties of cast aluminum alloys (Figure 2.47). This is almost certainly not primarily the result of action of the DAS alone, as has been commonly supposed. The DAS is mainly a measure of the local freezing time, which is the time available for the inflation and unfurling of defects. If the growth of area of the defect was not bad enough, its inflation, causing its surfaces to separate, transforming it from a crack that can enjoy some tensile strength into a pore which has none, makes the defect even more damaging. Thus its strength falls further as is illustrated in Figure 2.41. It is both (i) the growth of area and (ii) the growth of volume of the defects that combine to inflict so much damage to the mechanical properties as solidification time increases. Increases in DAS are not the cause of the loss of ductility; the DAS is merely an indicator of the time involved. It is the built-in, independent clock.

Returning to the pivotal role of the entrainment defects, it seems clear from practical work in foundries that the highest velocities and maximum turbulence is in the sprue, runner, and gates, where Reynolds numbers of  $10^4$  to  $10^5$  are easily attained, indicating severe bulk turbulence. Bifilms entrained in these parts of the running system will therefore be highly compacted, and, at least initially, have less damaging consequences for mechanical properties.

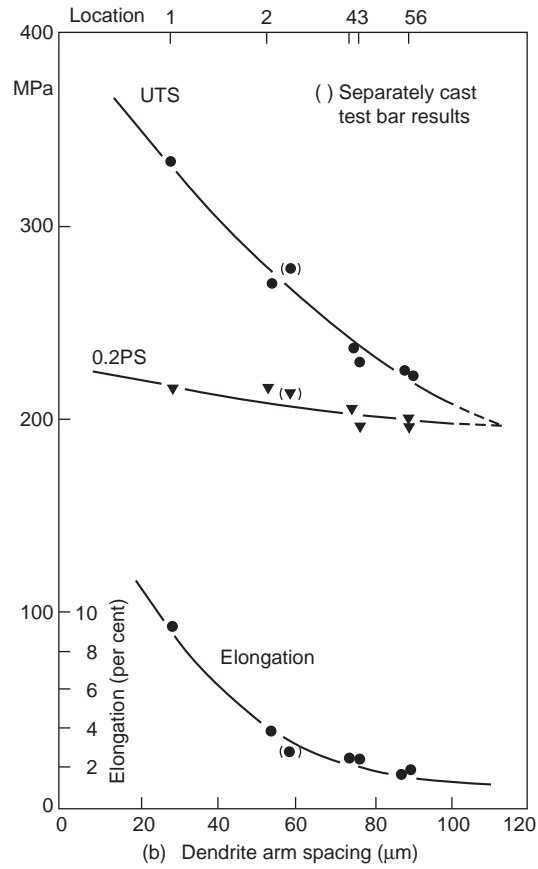
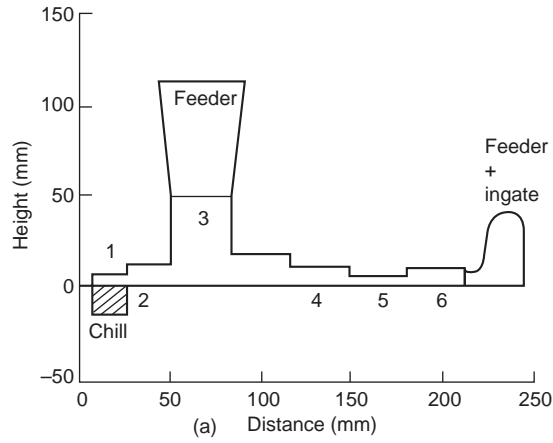


FIGURE 2.47

(a) Al-7Si-0.4Mg alloy casting and (b) its mechanical properties. (Data from Miguelucci 1985.)

The less severe surface turbulence and bulk turbulence in the mold cavity are, paradoxically, a concern. Reynolds numbers in a nicely filled mold cavity fall to values in the region of  $10^3$ , so that little energy is available to make the films more compact. Thus any bifilm entrained in the mold cavity itself will probably remain substantially open, maximizing its area. This in itself will cause maximum damaging effect, but will be additionally enhanced by the hydrogen diffusion to the enlarged area, inflating the defect, and so further reducing any limited load-carrying capacity it may once have enjoyed. It follows that the control of surface turbulence in the mold cavity itself is the most important factor to yield reliable properties.

It is almost certain that in some circumstances the bifilms will be unable to unfurl despite the action of some or all of the above driving forces. This is because they will sometimes be glued shut. Such glues will include liquid fluxes. If present on the surface of the melt, they will find themselves folded into the bifilm, and so form a sticky center to the sandwich, holding the bifilm closed, but the excess flux weeping or squeezed to its outer edges will aid the pinning of folds. The extreme thinness of bifilms will mean that even weak glues such as molten fluxes will be effective welds. Such action may explain part of the beneficial effect of fluxes. The melt may not be significantly cleaned by the flux, but its inclusions merely rendered less damaging by being unable to unfurl.

A similar action may explain the effect of low melting point additions such as bismuth to aluminum alloys. Although Papworth and Fox (1998) attribute the benefits of the Bi addition to the disruption of the integrity of alumina films, it seems more likely that a low melting point Bi-rich liquid will be inert towards the oxide, and that its action is passive, being merely an adhesive.

Whilst bifilms remain a feature of our processing techniques for aluminum alloys, fluxes, or low melting point metals might be a useful ploy, even if it is effectively ‘papering over the cracks’ of our current metallurgical inadequacies.

For the future, the very best cast material will be made free from bifilms in foundries specifically designed to deliver perfect-quality metal. Such concepts are already on the drawing board and may be realized soon. When this utopia is achieved we shall be able to make castings with any DAS, solidified fast or slow, all with perfect properties. There is already evidence that this prediction is accurate, as is explained in Section 9.4. Its routine achievement is a day to which we can look forward.

---

## 2.4 DEACTIVATION OF ENTRAINED FILMS

Once submerged, the inside of the bifilm will act as a thin reservoir of air. Air will exist in pockets, in bubbles trapped between the films, and in folds of the films, especially for films that have grown somewhat thicker, because their greater rigidity will bridge larger cavities among the folds. In addition, most oxides are microscopically rough, so that the opposed roughness of the surfaces themselves will constitute part of the reservoir, and assist to convey the gas to all parts of the inter-layer. A particularly rough oxide that takes a corrugated form is MgO as seen on Al-5Mg alloy (Figure 2.10b).

Nevertheless, of course, the bifilm is not likely to know that it is submerged. The oxides on its interior surfaces will therefore be expected to continue their growth regardless, under the impression that they are still in the fresh air. Thus, the layer of air in the bifilm will be gradually consumed as the oxygen is used up. As soon as all the oxygen has reacted, the nitrogen will then be converted to nitrides as demonstrated by Raiszadeh and Griffiths (2008).

In aluminum alloys, although the nitride of aluminum is not so stable as the oxide, and will therefore not form in competition with the oxide, it is nevertheless very stable. It is therefore likely to grow, if only slowly on Al alloys. In contrast, on molten ferrous alloys aluminum nitride forms rapidly at the much higher temperatures. Thus in a bifilm the layer of air is expected to disappear in time, but depending on the alloy and its impurities, at different rates. In steels this would be rapid, but in aluminum alloys it would be expected to be sluggish. In either case the 1% remnant of argon in the air would be likely to continue to remain as a gas because of its nearly perfect insolubility in molten metals (Boom 2000).

During the final stages of the disappearance of the gas layer the opposed oxides would be expected to grow together to some extent. Any resultant bonding may not be particularly strong, but may confer some improvement in strength compared to the layer of air. Additional limited strength would be expected from the mechanical interlocking of the opposed crystalline or otherwise rough surfaces.

If it is true that the gas layer will eventually be consumed, and if some diffusion bonding has occurred, then the most deleterious effects of the bifilm will have been removed. In effect, the potential of the defect for causing leaks, or nucleating bubbles, cavities, or cracks, will have been greatly reduced. This has been confirmed by Nyahumwa, Green and the author (1998 and 2000) who found that porosity in the fatigue fracture surfaces of Al-7Si-0.4Mg alloy appeared to be linked often with new oxides, but not old oxides. Raiszadeh and Griffiths (2007) observed bridging between the leaves of the bifilm after solution treatment.

Further evidence for the growing together of bifilms with time is provided by the work of Huang and co-workers (2000) who examined fragments of bifilms detached by ultrasonic vibration from polished metallographic sections. These revealed that the bifilms of alumina, in the process of transforming to spinel, appeared to be extensively fused together. Figure 2.48 is a re-interpretation of their observations. Their work is separately interesting since it indicates that bifilms of different numbers and sizes are associated with different alloys.

The automatic deactivation of bifilms with time may be relatively fast for new, thin films. This would explain the action of good running systems, where, after the fall of the liquid in the down-runner, the metal is allowed to reorganize for perhaps a second or so before entering the gates into the mold cavity. In general, such castings do appear to be good, although this speculation has not been followed by any formal study to explore whether the effect is real or not.

However, the deactivation of bifilms seems certain to be encouraged in cases where the metal is subjected to pressure, since mechanical properties of the resulting castings are so much improved, becoming significantly more uniform and repeatable, and pores and cracks of all types appear to be greatly reduced if not eliminated. Even if the air film in bifilms is not completely eliminated, it seems inevitable that the oxygen and nitrogen will react at a higher rate and so be more completely consumed, and any remaining gases be compressed. In addition, if the pressure is sufficient, liquid metal may be forced through the permeable oxide so as to fuse with, and thus weld to, metal exuding through faults in the far side of the film. The crack-like discontinuity would then have effectively been 'stitched' together, or possibly 'tack welded'. Pressurizing treatments that would promote such assisted deactivation include:

1. The solidification of the casting under an applied pressure. This is seen in the case of squeeze casting, where pressures of 50–150 MPa (500–1500 atmospheres) are used. However, significant benefits are still reported for sand and investment castings when solidified under pressures obtainable from a normal compressed-air supply of only 0.1–0.7 MPa (1–7 atmospheres). Berry

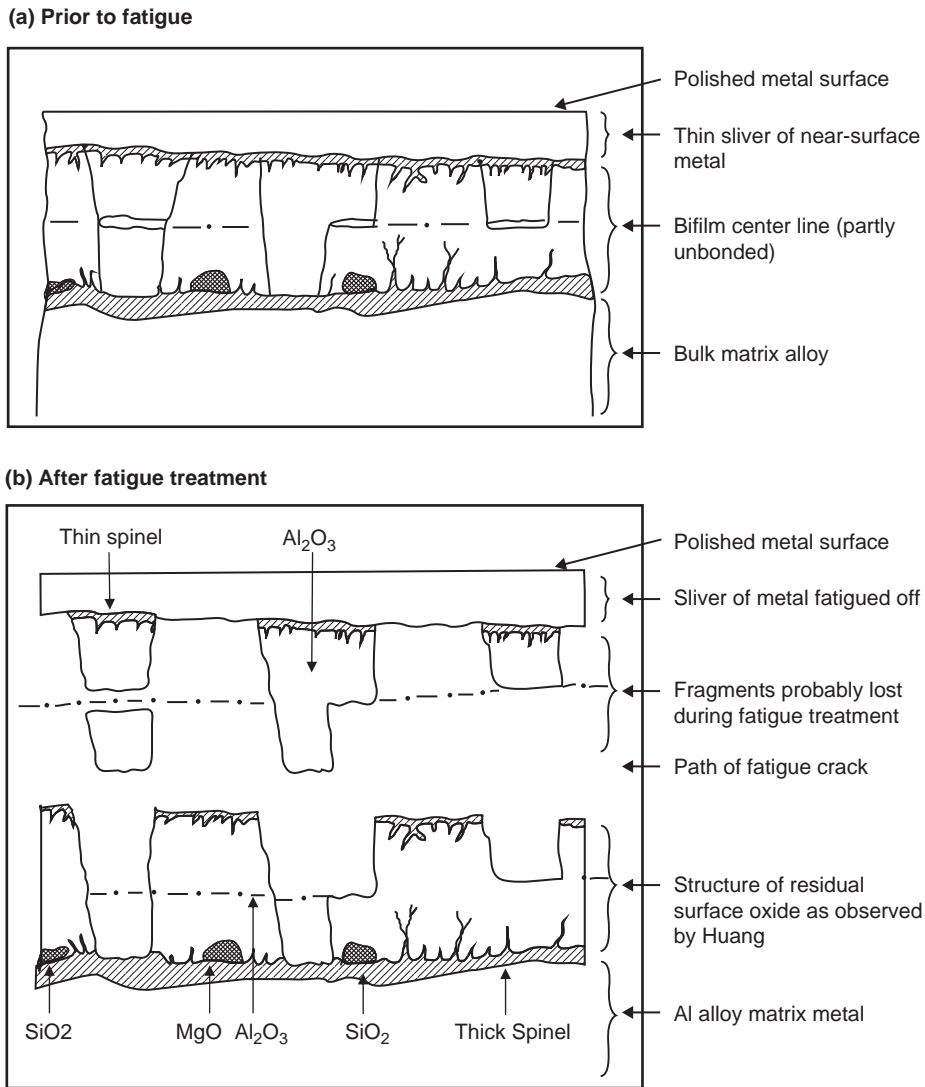


FIGURE 2.48

Interpretation of observations by Huang et al. (2000) showing (a) a section of double film near the surface of the cast Al-7Si-0.4Mg alloy with (b) fragments separated by fatigue when applying ultrasonics.

and Taylor (1999) review these attempts. It is interesting to reflect that the reduced pressure test, commonly used as a porosity test in aluminum alloy casting, further confirms the importance of this effect but uses exactly the same principle in the opposite direction: the pressure on the solidifying casting is lowered to maximize porosity so that it can be seen more easily (Dasgupta et al. 1998, Fox and Campbell 2000).

2. Hot isostatic pressing (hipping) is a solid state deactivation process, which, by analogy with the liquid state, appears to offer clues concerning the mechanism of deactivation processes in the liquid. The hipping of (solid) castings is carried out at temperatures close to their melting point to soften the solid as far as possible. Pressures of up to 200 MPa (2000 atmospheres) are applied in an attempt to compress flat all the internal volume defects and weld together the walls of the defects by diffusion bonding. It is clear that in the case of hipping aluminum alloys, the aluminum oxide that encases the gas film will not weld to itself, since the melting point of the oxide is over 2000°C and a temperature close to this will be required to cause any significant diffusion bonding.

The fact that hipping is successful at much lower temperatures, for instance approximately 530°C in the case of Al–7Si–0.4Mg alloy, indicates that some additional processes are at work. For instance, some diffusion bonding of oxides may occur in the presence of reactions in the oxide. In the case of Al alloys that have less than 0.10 wt%Mg, the oxide will be a variety of alumina, and so very stable and unlikely to bond. For higher Mg alloys, above about 1.0 wt% Mg (particularly the Al–5Mg and Al–10Mg alloys), the oxide involved in this case is MgO, and so, like alumina, is stable and unlikely to take part in any bonding action. For alloys with an intermediate Mg content in the range approximately 0.1–1.0 wt%Mg, after time at temperature, the initially formed alumina film absorbs Mg from the matrix, converting the oxide to a spinel structure. During the atomic rearrangements required for the reconstruction of this quite different lattice, some diffusion bonding will be favored.

In an elegant experiment, Aryafar, Raiszadeh and Shalbazadeh (2010) showed that no bonding across the Al<sub>2</sub>O<sub>3</sub> of bifilms occurred until all of the oxygen and nitrogen was consumed. After this, some weak patchy bonding resulted from the conversion of Al<sub>2</sub>O<sub>3</sub> to spinel, MgAl<sub>2</sub>O<sub>4</sub>, in a short time. After longer times stronger bonding resulted from the conversion of spinel to MgO. Bakhtiarani and Raiszadeh (2010) studied Al–4.5Mg melts, finding that after entrainment the bifilms continued to grow for several hours, the oxide spinel gradually converting to MgO. The atomic rearrangement resulted in some bonding across impinging regions of the bifilm, a process resembling the action of diffusion bonding, but occurring, of course, at temperatures hundreds of degrees lower than that at which true diffusion bonding of oxides could occur.

3. Finally, it should be noted that if the entrained solid film is partially liquid, some kind of bonding is likely to occur much more readily, as has been noted in Section 2.1. This may occur in light alloy systems where fluxes have been used in cleaning processes, or contamination may have occurred from traces of chloride or fluoride fluxes from the charge materials or from the crucible. Such fluxes will be expected to cause the surfaces of the oxide to adhere by the mechanism of viscous adhesion when liquid, and as a solid binder when cold. The beneficial action of fluxes in the treatment of liquid Al alloys may therefore be not the elimination of bifilms but their partial deactivation by assisting bonding. The fact that flux inclusions can appear commonly on machined surfaces of Al alloy castings is an indication that the rapid detrainment of fluxes by flotation as would be expected for a liquid inclusion has been inhibited by the flux being wrapped in a much larger bifilm.

Similarly, as we have noted previously, the observations by Papworth (1998) might indicate that Bi acts as a kind of solder in the bifilms of Al alloys. The metal exists as a liquid to 271°C, so that when subjected to the pressure of squeeze casting, it would be forced to percolate and in-fill bifilms. The



consequential resistance of bifilms to deformation and separation would be expected to be improved if only by their generally increased mechanical rigidity (i.e. not by any chemical bonding effect). If proven to be true, this effect could be useful.

In the case of higher-temperature liquid alloys, particularly steels, some oxides act similarly, forming low-melting-point eutectic mixtures. These valuable systems will be discussed in detail in Chapter 6.

---

## 2.5 SOLUBLE, TRANSIENT FILMS

Although many films such as alumina on aluminum are extremely stable, and completely insoluble in the liquid metal, there are some alloy/film combinations in which the film is soluble. This is of course especially true for the higher-melting-point metals where the higher temperatures and the reduced stability of the films encourage this behavior.

Transient films are to be expected in many cases in which the arrival of film-forming elements (such as oxygen or carbon) at the surface of the liquid exceeds the rate at which the elements can diffuse away into the bulk metal. If such a film is then entrained, the film may be folded in to create a crack, a hot tear, or initiate shrinkage porosity. However, after the initiation of this consequential 'secondary' defect, the originating bifilm then quietly goes into solution, never to be seen again.

It is to be expected that many oxide and nitride films might be soluble in some irons and steels.

Such behavior is commonly seen in gray cast irons. If a lustrous carbon film forms on the iron and is entrained in the melt, after some time it will dissolve. The rate of dissolution will be rather slow because the iron is already nearly saturated with carbon. The longer the time available the greater is the chance that the film will go into solution. Thus there are various conditions that can be envisaged:

- (i) In a thin section the lustrous carbon will be frozen in place, constituting a bifilm defect to reduce strength or create a leak path.
- (ii) In an intermediate section the entrained bifilm may last just long enough to initiate some other longer-lived and more serious defect, such as a hot tear or shrinkage porosity, prior to its disappearance.
- (iii) In heavy-section gray iron castings entrained lustrous carbon films are usually never seen, having plenty of time to go into solution.

Titanium alloys, including titanium aluminide alloys, have a high solubility for oxygen, so that oxide films, if they form, are almost certainly soluble. These issues are discussed in the section on Ti alloys (Section 6.8).

---

## 2.6 DETRAINMENT

In a liquid metal subjected to surface turbulence, many of the defects *entrained* by the folding and impingement actions can find themselves eliminated (*detrained*) from the melt at a later stage. These detrainment events take a variety of forms.

If the oxide surface film is particularly strong, it is possible that even if entrained by a folding action of the surface, the folded film may not be free to be carried off by the flow. It is likely to be attached to

part of the surface that remains firmly attached to some piece of hardware such as the sides of a launder, or the wall of a sprue. Thus the entrained film might be detrained, being pulled clear once again. This detrainment process is so fast that the film hardly has time to consider itself entrained.

Even if not completely detrained, a strong film, strongly attached to the wall of the mold may simply remain hanging in place, flapping in the flow in the melt delivery system, but fortunately never entering the casting, and so remaining harmless.

Beryllium added at levels of only 0.005% to reduce oxidation losses on Al–Mg alloys probably act in this way. On attempting to eliminate Be for environmental and health reasons, difficulties have been found in the successful production of wrought alloys by continuous (Direct Chill usually abbreviated to DC) casting. The beneficial action of Be that was originally unsuspected, but subsequently highlighted by this problem, is thought to be the result of the strengthening of the film by the low levels of Be, thus encouraging the hanging up of entrained films in the delivery system to the mold rather than their release into the flowing stream.

Large bubbles have sufficient buoyancy to break their own oxide film, and the casting surface oxide skin (once again, the two films constituting a double oxide barrier of course; the double film phenomenon appearing to be a fundamental and recurring film condition in casting technology) between them and the outside world at the top of the casting. They can thus detrain (Figure 2.33). If successful, this detrainment is not without trace, however, because of the presence of the bubble trail that remains to impair the casting.

Small bubbles of up to about 5 mm diameter have more difficulty to detrain. They are commonly trapped immediately under the top skin of the casting, having insufficient buoyancy to break through the double film barrier. Thus they are unable to allow their contents to escape to atmosphere. They are the bane of the life of the machinist, since they lodge just under the oxide skin at the top of a casting, and become visible only after the first machining cut. In iron and steel castings requiring heat treatment, this thin surface oxidizes away to reveal the sub-surface porosity. Similarly, shot blasting will also often reveal such defects as a result of their nearness to the outside surface.

The most complete and satisfactory detrainment is achieved if the liquid metal has a liquid oxide film. This is because, once entrained, the liquid oxide spherodizes to form droplets, and floats out with maximum speed (Figure 2.12). On arrival at the liquid oxide surface the liquid oxide droplets are simply re-assimilated in the surface liquid layer, and disappear. This is the mechanism by which steels finally deoxidized with Ca + Al achieve such high levels of cleanness in comparison with steels deoxidized with the usual Si, Mn, and Al. The oxides CaO and Al<sub>2</sub>O<sub>3</sub> form a low-melting-point eutectic which, when entrained, simply balls up and floats out. Those very small fragments of the entrained oxides that do not have sufficient Stokes velocity to reach the surface remain entrapped in the steel as minute, nicely spherical droplets. Steel metallurgists call this 'inclusion shape control', usually overlooking the main benefit of the detrainment of the larger inclusions.

Liquid fluxes in Al alloys may suffer a different fate. The liquid flux, if composed of a chloride mixture, does not dissolve the extremely stable aluminum oxide. Thus the liquid flux will remain on the surface of the melt, sitting on top of the solid oxide film. When entrained during stirring or pouring the solid film wraps up some of the flux, preventing it from spherodizing. In addition, the much larger area of the film greatly reducing its Stokes velocity. Thus alumina films containing a central flux layer can remain in suspension for long periods. This is known from the experience in the Nematik, Windsor foundry. Mold filling was automated by electro-magnetic pumps, sited at the ends of long launder systems that delivered liquid metal to the casting stations. The pumps would commonly sit in the melt

without problem for several months. However, when chlorine gas was introduced in the rotary degassing units the pumps blocked within 24 hours from a mixture of chloride flux and oxides. The chloride flux alone could never have made the long journey (several tens of meters) from the degassers since detrainment would have been expected for spherical droplets within seconds or minutes, clearing the melt within a meter or so of progress along the launder system. However, if entrained in an alumina film the flux could remain in suspension for hours. It would finally be detrained by the high body forces experienced by the liquid metal in the pump, and thus building up on the inner walls of the pump to block it with maximum efficiency.

Detrainment of bifilms in suspension in the melt can be encouraged by a number of means:

- (i) Filtration. The wide use of filters indicates there are benefits, even though the effectiveness of filters is extremely variable in different situations. The problems are discussed in more detail in Section 12.8.
- (ii) Rotary degassing treatment. As for filters, rotary degassing is a mixed blessing. Although a key benefit has been the stabilization of melt quality in foundries, its action probably far from being fully optimized at the time of writing (see Section 14.4).
- (iii) Sedimentation. The simple holding of melts and doing nothing but wait is an effective means to detrain many different kinds of melts in many different kinds of casting operation.

This important natural benefit is enjoyed by steel makers in the steel-making furnace, but who go to lengths to ruin their metal by pouring it through a fall of several meters into a ladle. Subsequently, thanks to the large density difference between the steel and its oxides, the quality is rescued by detrainment of many of the entrained inclusions by flotation. This detrainment can be so rapid that much entrained material has floated out to the surface of the ladle, adding to the surface slag, during the several minutes that are required for the ladle to be lifted out of the casting pit and transported to the casting station. This rapid detrainment cannot occur for Al-deoxidized steels, since the stable bifilms of alumina remain in suspension for much longer times, and create problems in the cast material.

In Al alloys the significant benefits of sedimentation are similarly not achieved because of the long periods of near-zero Stokes velocity of suspended alumina bifilms. However, if grain-refining additions are made, the relatively heavy TiB particles precipitate on the bifilms, dropping them out like stones. If the sediment of oxides and Ti-rich compounds is not disturbed at the bottom of the melt, the extremely clean metal above this can be decanted to create castings of high mechanical properties. Note that much if not nearly all of the improvement is due not to the grain refinement but to the absence of bifilms. This important effect is described in detail in Section 6.3.

---

## 2.7 EVIDENCE FOR BIFILMS

The evidence for bifilms actually constitutes the entire theme of this book. Nevertheless, it seems worthwhile to devote some time to highlight some of the more direct evidence.

It is important to bear in mind that the double oxide film defects are everywhere in metals. We are not describing occasional single 'dross' or 'slag' defects or other occasional accidental extrinsic types of inclusions. The bifilm defect occurs naturally, and in copious amounts, every time a metal is poured.

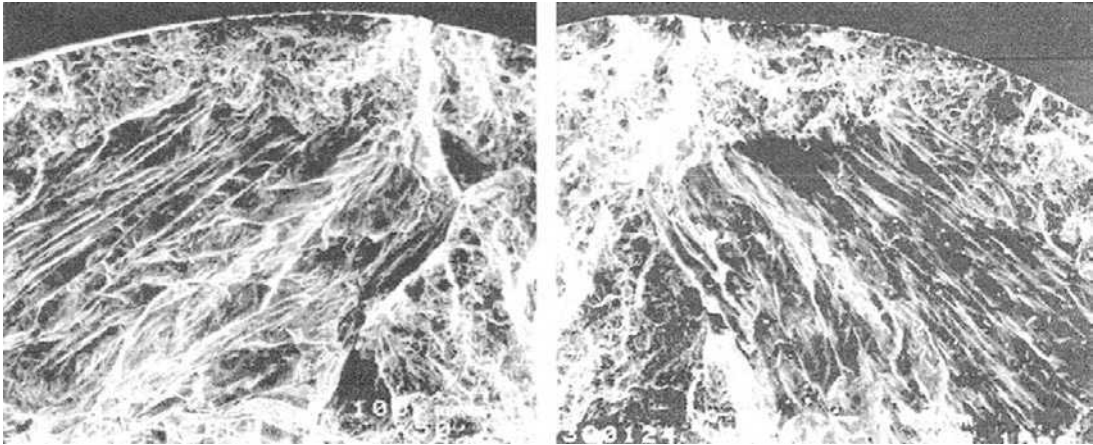


**FIGURE 2.49**

The secondary electron image of the near-mirror-images of the spinel bifilm halves on each half of the tensile failure surface of an Al-11.5Si alloy (courtesy of Cao 2010).

Many metals are crammed with bifilm defects. The fact that they are usually so thin has allowed them to evade detection for so long. Until recently, the ubiquitous presence of these very thin double films has not been widely accepted because until recently no single metal quality test has been able to resolve such thin but extensive defects.

Even so, over recent years there have been many significant confirmations.

The presence of bifilms is easily seen on fracture surfaces, particularly if a good scanning electron microscope (SEM) is available. If a bifilm is present, its component halves appear on each half of the fracture with nice butterfly wing symmetry (Figure 2.49). Griffiths and Lai (2007) show such symmetry on all of their fractured tensile bars of Mg alloy. Each oxide film is characterized by absence of metallic features, and appearance of folds and creases, even though the folds and creases may be so thin as to be difficult to see except under the best operating conditions of an SEM.

Another clear example of bifilms is seen in the use of the reduced pressure test (RPT) for aluminum alloys. The technique is also known, with slight variations in operating procedure, as the Straube Pfeiffer test (Germany), Foseco Porotec test (UK), and IDECO test (Germany). At low gas contents many operators have been puzzled by the appearance of hair-line cracks, often extending over the whole section of the RPT casting. They had problems to understand the cracks since the test is commonly only assumed to be an assessment of hydrogen porosity. An example of the cracks is seen in Figure 2.40. However, as gas content rises, the defects expand to become lens-shaped, and finally, if expansion continues, become completely spherical, fulfilling at last the expectation of their appearance as hydrogen pores. Such an effect of thin cracks transforming into spherical bubbles has been widely observed by many foundry people many times (e.g. Rooy 1992), and can only be explained reasonably by the presence of bifilms. Figure 2.50 illustrates examples of cracks and pores from different melts.

In a variant of the reduced pressure test to determine the quantity known as the density index, two small samples of a melt are solidified in thin-walled steel crucibles, one in air and one under a partial vacuum, respectively. A comparison of the densities of the two samples gives the so-called density

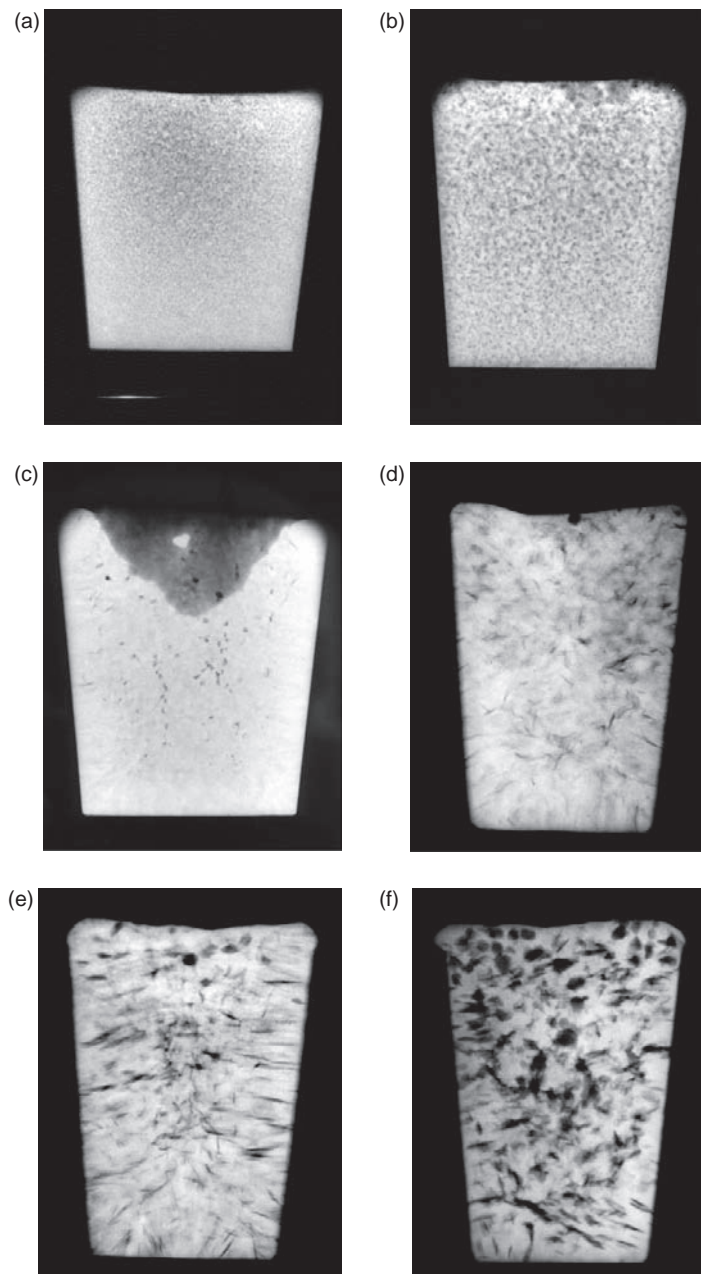


**FIGURE 2.50**

Radiographs of reduced pressure test samples of Al-7Si-0.4Mg alloy illustrating different bifilm populations (courtesy of S Fox).

index. However, in this simple form the density index is not particularly reproducible. The comparison is complicated as a result of the development of shrinkage porosity in the sample solidified in air. A better comparison is found by taking the lower half of the air-solidified sample and discarding the top half containing the shrinkage porosity. The fairly sound base is then compared to the sample frozen under vacuum. This gives a more accurate assessment of the porosity due to the combined effect of gas and bifilms. Without bifilms the hydrogen cannot precipitate, leading to a sound test casting, so that filtered metal always appears less 'gassy', giving the curious (and of course misleading) impression that the hydrogen can be 'filtered' out of liquid aluminum.

A recent novel development of the reduced pressure test has been made that allows direct observation of bifilms (Fox and Campbell 2000). The rationale behind the use of this test is as follows. The bifilms are normally difficult or impossible to see by X-ray radiography when solidified under one atmosphere pressure. If, however, the melt is subjected to a reduced pressure of only 0.1 atmosphere, the entrained layer of air should expand by ten times. Under 0.01 atmosphere the layer should expand one hundred times, etc. In this way it should be possible to see the entrained bifilms by radiography. A result is shown in Figure 2.40.

In this work a novel reduced pressure test machine was constructed so that tests could also be carried out using chemically bonded sand molds to make test castings as small slabs with overall dimensions approximately 50 mm high, 40 mm wide and 15 mm thick. The parallel faces of the slabs allowed X-ray examination without further preparation. The slower solidification provided by the sand mold was advantageous to allow a good unfurling response throughout the sample. (The placing of the usual thin steel cup on an insulating ceramic paper base acts almost as well.)

Figure 2.40 shows radiographs of plate castings from a series of tests that were carried out on metal from a large gas-fired melting furnace in a commercial foundry. Figure 2.40a shows a sample that was solidified in air indicating evidence of fine-scale low-density regions appearing as dark, faint compact images of the order of one millimeter in diameter. As the test pressures were lowered, the compact regions unfolded and grew into progressively longer and thicker streaks, finally reaching 10–15 mm in length at 0.01 atmosphere (Figure 2.40b).

The 'streak-like' appearance of the porosity is due to an edge-on view of an essentially planar defect (although residual creases of the original folds are still clear in some bifilm images). The fact that these defects are shown in such high contrast at the lowest test pressure suggests that they almost completely penetrate the full 15 mm thickness of the casting, and may only be limited in size by the 15 mm thickness of the test mold. The more extensive areas of lower-density porosity are a result of defects lying at different angles to the major plane of the casting.

At 0.01 atmosphere the thickness of bifilms as measured on the radiographs for those defects lying in the line of sight of the radiation was in the range 0.1–0.5 mm. This indicates that the original thickness of bifilms at one atmosphere was approximately 1–5  $\mu\text{m}$ .

These samples containing large bifilms are shown here for clarity. They contrast with more usual samples in which the bifilms appear to be often less than 1 mm in size, and when solidified at 1 atmosphere pressure are barely visible on radiographs. The work by Fox and the author (2000) on increasing the hydrogen content of such melts in the RPT at a constant reduced pressure typically reveals the inflation of clouds of bifilms, first becoming unfurled and slightly expanded by the internal pressure of hydrogen gas, and finally resulting in the complete inflation of the defects into expanded spheres at high hydrogen levels. Figure 2.50 shows a variety of RPT results for different melts, showing a range of different bifilm populations.

A much earlier but critical observation of the action of bifilms was so many years ahead of its time that it remained unappreciated until recently. In 1959 at Rolls-Royce, UK, Mountford and Calvert observed the echoes of ultrasonic waves that they directed into liquid aluminum alloys held in a crucible. What appeared to be an entrapped layer of air was observed as a mirror-like reflection of ultrasound from floating debris. (Reflections from other fully wetted solid phases would not have been so clear; only a discontinuity like a crack containing a layer of air which completely reflected the waves could have yielded such strong echoes.) Some larger particles could be seen to rotate, flashing reflections like a beacon when turning face on after each revolution. Immediately after stirring, the melts became opaque with a fog of particles. However, after a period of 10–20 minutes the melt was seen to clear, with the debris forming a deep layer at the base of the crucible. If the melt was stirred again the phenomenon could be repeated.

Stirred melts were found to give castings containing oxide debris together with associated porosity. It is clear that the macroscopic pores observed on their polished sections appear to have grown from traces of micropores observable along the length of the immersed films. Melts that were allowed to settle and then carefully decanted from their sediment gave castings clear of porosity.

Other interesting features that were observed included the precipitation of higher-melting-point heavy phases, such as those containing iron and titanium, onto the floating oxides as the temperature was lowered. This caused the oxides to drop rapidly to the bottom of the crucible. Such precipitates were not easy to get back into suspension again. However, they could be poured during the making of a casting if a determined effort was made to disturb the accumulated sludge from the bottom of the container. The resulting defects had a characteristic appearance of large, coarse crystals of the heavy intermetallic phases, together with entrained oxide films and associated porosity. These observations have been confirmed more recently by Cao and Campbell (2000) on other Al alloys.

Over subsequent years there has been significant development of the ultrasonic technique for the study of bifilms in Al alloys and steels (Mountford and Sommerville 1997 and 1993, respectively).

It is clear, therefore, from all that has been presented so far that a melt cannot be considered to be merely a liquid metal. In fact, the casting engineer must think of it as a slurry of various kinds of debris, mostly bifilms of various kinds, all containing entrained layers of air or other gases.

In a definitive piece of research into the fatigue of filtered and unfiltered Al–7Si–0.4Mg alloy by Nyahumwa, Green and Campbell (1998, 2000), test bars were cast by a bottom-filling technique and were sectioned and examined by optical metallography. The filtered bars were relatively sound. However, for unfiltered castings, extensively tangled networks of oxide films were observed to be randomly distributed in almost all polished sections. Figure 2.5 shows an example of such a network of oxide films in which micropores (assumed to be residual air from the chaotic entrainment process) were frequently observed to be present. In the oxide film networks, it was observed that oxide film defects constitute cracks showing no bond developed across the oxide–oxide interface. In the higher magnification view of Figure 2.5 the width between the two dry surfaces of folded oxide film is seen to vary between 1 and 10  $\mu\text{m}$ , in confirmation of the low-pressure test results described above. However, widths of cracks in places approached 1 mm where the bifilm had opened sufficiently to be considered as a pore.

A polished section of a cast aluminum alloy breaking into a tangled bifilm is presented in Figure 2.6. The top half of the bifilm happens to meet the polished surface, and has been polished away, revealing the inside surface of the underlying remaining half of the bifilm, demonstrating the oxide film to be a *double* film, with little or no bonding between the two films.

The detachment of the top halves of bifilms to reveal the underlying half is a technique used to find bifilms by Huang et al. (2000). They subjected polished surfaces of aluminum alloy castings to ultrasonic vibration in a water bath. Parts of bifilms that were attached only weakly were fatigued off, revealing strips or clouds of glinting marks and patches when the polished surface was observed by reflected light. They found that increasing the Si content of the alloys reduced the lengths of the strips and the size of the clouds, but increased the number of marks. The addition of 0.5 and 1.0 Mg reduced both the number and size of marks. Their fascinating polished sections of the portions of the bifilms that had detached revealed fragmentary remains of the double films of alumina apparently bonded together in extensive patches, appearing to be in the state of partially transforming to spinel (Figure 2.48).

The scanning electron microscope (SEM) has been a powerful tool that has revealed much detail of bifilms in recent years. One such example by Green (1995) is seen in Figure 2.11, revealing a film folded many times on the fracture surface of an Al-7Si-0.4Mg alloy casting. Its composition was confirmed by microanalysis to be alumina. The thickness of the thinnest part appeared to be close to 20 nm. It was so thin that despite its multiple folds the microstructure of the alloy remained clearly visible through the film.

There are varieties of bifilms in some castings that are clear for all to see. These occur in lost foam castings, and are appropriately known as fold defects. Some of these are clearly pushed by dendrites into interdendritic spaces of the as-cast structure (Tschapp et al. 2000). The advance of the liquid metal into the foam is usually sufficiently slow that the films grow thick and the defects huge, and are easily visible to the unaided eye. Other clear examples, but on a finer scale, are seen in high-pressure die castings. Ghomashchi (1995) has recorded that the solidified structure is quite different on either side of such features. For instance the jets of metal that have formed the casting are each surrounded by oxides (their 'oxide flow tubes' as discussed in Section 2.2.6) seen in Figure 2.31. Between the various flowing jets, each bounded by its film, the boundaries naturally and necessarily come together as double films, or bifilms. They form effective barriers between different regions of the casting, permitting different regions to solidify at different rates, each region therefore having its own appropriate dendrite arm spacing.

As an 'opposite' or 'inverted' defect to a flow tube is the bubble trail. It constitutes a long bifilm of rather special form. The passage of air bubbles through aluminum alloy melts has been observed by video radiography (Divandari 1998). The bubble trail caused by the flow path of the bubbles has been initially invisible on the video radiographic images. However, the prior solidification of the outer edges of the observed plate casting imposed a tensile stress on the interior of the plate that increased with time. After a few minutes the level of stress in the central region of the plate had risen sufficiently to open the bifilm; it flashed into view in a fraction of a second, expanding as a long crack, following the path taken by the bubbles, carving a path through what had appeared previously to be featureless solidifying metal.

Evidence for bifilms in zinc-based alloys, copper-based alloys, gray iron, ductile iron, steels, and high-temperature nickel-based alloys will be presented in later portions of the book.

Finally, it is salutary to consider the potential for metals if bifilms were not present. Gold is one such example. It can be beaten or pounded into foil (known as gold leaf) thinner than that of any other metal. This is because, since it is uniquely free of oxides, its malleability is not impaired. Thus thicknesses of 0.1  $\mu\text{m}$  are possible, which are so thin that it is possible to see through the metal, even though the golden luster of the metal is not lost. This contrasts with metals such as aluminum where



foils are generally in the range 200 to 4  $\mu\text{m}$ , but below about 25  $\mu\text{m}$  the foil starts to show pinholes as a result of the presence of inclusions, particularly oxide bifilms. In highly specialized applications in ribbon microphones, Al foil might be as thin as about 1  $\mu\text{m}$ , which is still ten times thicker than the thinnest gold. If other face centered cubic (fcc) metals (aluminum, silver, copper, etc.) could be made free from entrained oxides, foils of thickness similar to that of gold would, I assume, be easily produced.

The evidence for bifilms and the benefits of bifilm-free metals have been with us all for many years.

---

## 2.8 THE IMPORTANCE OF BIFILMS

Although the whole of this work is given over to the concept of bifilms, so that, naturally, much experimental evidence is presented as a matter of course, this short section lists the compelling logic of the concept and the inescapable and important consequences.

Since the folded oxides and other films constitute cracks in the liquid, and are known to be of all sizes and shapes, they can become by far the largest defects in the final casting. They can easily be envisaged as reaching from wall to wall of a casting, causing a leakage defect in a casting required to be leak-tight, or causing a major structural weakness in a casting requiring strength or fatigue resistance.

In addition to constituting defects in their own right, if they are given the right conditions during the cooling of the casting, the loosely encapsulated gas film can act as an excellent initiation site for the subsequent growth of gas bubbles, shrinkage cavities, hot tears, cold cracks, etc. The nucleation and growth of such consequential damage will be considered in later sections. The important message to take on board at this stage is that without the presence of bifilms, such defects would probably be impossible. Liquid metals free from bifilms could make castings free from defects. This is a message never to be forgotten.

Entrainment creates bifilms that may never come together properly and so constitute air bubbles immediately; alternatively, they may be opened (to become thin cracks, or opened so far as to become bubbles) by a number of mechanisms:

- (i) Precipitation of gas from solution creating gas porosity;
- (ii) Hydrostatic strain, creating shrinkage porosity;
- (iii) Uniaxial (tensile) strain, creating hot tears or cold cracks;
- (iv) In-service strain, causing failure by fracture in service.

Thus bifilms can be seen to simplify and rationalize the main features of the problems of castings. For those who wish to see the logic laid out formally this is done in Figure 2.51 for metals (i) without films, such as liquid gold, (ii) with films that are liquid, (iii) with films that are partially solid, and (iv) with films that are fully solid.

Note that the defects on the right of Figure 2.51 cannot, in general, be generated without starting from the bifilm defect on the left. The necessity for the bifilm initiator follows from the near impossibility of generating volume defects by other mechanisms in liquid metals, as will be discussed in later sections of this book. The classical approach using nucleation theory predicts that nucleation of any type (homogeneous or heterogeneous) is almost certainly impossible. Only surface-initiated defects (i.e. porosity or cracks growing into the casting from locations on the casting surface) appear to

Example Melt	Melt surface state during pour (Surface turbulence $We > 1$ ) (Bulk turbulence $Re > 2000$ )	Quiescence $We \ll 1$ $Re < 1000$	Casting Defect State
	Entrainment and furling	Flotation and unfurling	
Pure liquid gold, Pt, Ir, etc.	Film-free surface	Rapid flotation of bubbles	No defects
Al+Ca deoxidized carbon steel	Liquid surface film	Rapid flotation of liquid droplets	Few defects (only small spherical inclusions)
General carbon steels Al alloys + flux	Partially liquid film	Rapid flotation of large sticky bifilms, effectively welded permanently into compact form	Complex macroinclusions on cope surface
Al alloys Mg alloys Al bronzes Ductile irons Ni-based superalloys Stainless steels	Solid surface film	Rapid flotation of buoyant bubbles	Air bubbles ('gas') Bubble trails (potential leakage defects)
		Suspended furled bifilms with simultaneous unfurling + inflation driven by	General leakage defects.
		1. Gas precipitation	Gas microporosity
		2. Hydrostatic (3D) tensile strain	Shrinkage porosity (macro and micro)
		3. Uniaxial (1D) tensile strain	Hot tears and cold cracks
		4. Intermetallic crystal growth (unfurling only)	Centerline cracks in particles Matrix decohesion from particles
		5. Dendrite pushing (unfurling only)	Interdendritic failures Grain boundary failures

**FIGURE 2.51**

Overview of defect formation in alloys: Framework of logic linking surface conditions, flow and solidification conditions to the final form of the spectrum of entrainment defects.

be possible without the action of bifilms. In contrast to the difficulty of homogeneous or heterogeneous nucleation of defects, the initiation of defects by the simple mechanical action of the opening of bifilms requires nearly zero driving force; it is so easy that in all practical situations it is the only initiating mechanism to be expected.

We are therefore forced to the fascinating and enormously significant conclusion that in the absence of bifilms castings cannot generate defects that reduce strength or ductility. In other words, defects that lead to mechanical impairment are not produced by solidification, but only by casting. To restate once again for emphasis, in general, there is no such thing as a solidification defect. There are only casting defects.

As noted above, this hugely important fact has to be tempered only very slightly, since porosity, and possibly cracks, can also be generated easily by surface-initiation if a moderate pressurization of the interior of the casting is not provided by adequate feeders. However, of course, adequate feeding of the casting is widely understood and applied in foundries, and we can therefore assume its application here.

The wide application of good feeding, especially since the advent of good computer simulations, means that shrinkage porosity is *not* to be expected in castings. In fact nearly all porosity I see in castings or on radiographs is usually *never* shrinkage, despite its appearance. It is usually a mess of bifilms and their associated tangled layers of air resulting from a poor filling technique. It is extremely important therefore for the reader never to utter the phrase 'It is shrinkage'. The reader is urged to learn by heart and repeat often the phrase 'It *appears* to be shrinkage' but then add the rider 'but probably is not!'

The author has the pleasant memories of the early days (circa 1980) of the development of the Cosworth Process, when the melt in the holding furnace had the benefit of days to settle, becoming clear from bifilms, since production at that time did not occupy more than a few production shifts per week. The melt was therefore unusually free from bifilms, and the castings were found to be completely free from porosity. As the production rate increased during the early years the settling time was progressively reduced to only a few hours, causing a disappointing reappearance of microporosity, and a corresponding reduction of mechanical properties. This link between melt cleanness and freedom from porosity is well known. One of the first demonstrations of this fact was the simple and classic experiment by Brondyke and Hess (1964) that showed that filtered metal exhibited reduced porosity.

An important point to note is that a subsequently generated defect, which may be large in extent, may be simply initiated by and grow from a small bifilm. On the other hand, the bifilm itself may be large, so that any consequential defect such as a pore or a hot tear actually *is* the bifilm, but simply opened up. In the latter case no growth of area of the subsequent defect is involved, only separation of the two halves of the bifilm. Both situations seem possible in castings.

Standing back for a moment to view the larger scene of the commercial supply of castings, it is particularly sobering that there is a proliferation of standards and procedures throughout the world to control the observable defects such as gas porosity and shrinkage porosity in castings. Although once widely known as 'Quality Control' (QC) the practice is now more accurately named 'Quality Assurance' (QA). However, as we have seen, the observable porosity and shrinkage defects are often negligible compared to the likely presence of bifilms, which are difficult, if not impossible, to detect with any degree of reliability. They are likely to be more numerous, more extensive in size, and have more serious consequences.

The significance of bifilms is clear, and worth repeating. They are often not detectable by normal non-destructive testing (NDT) techniques, but can be more important than observable defects. They are often so numerous and/or so large that they can control the properties of castings, sometimes outweighing the effects of alloying and heat treatment.

The conclusion is inescapable: it is more important to specify and control the casting process to *avoid* the formation of bifilms than to employ apparently rigorous QA procedures, searching retrospectively (and possibly without success) for any defects they may or may not have caused.

Castings free from bifilms probably do not exist at this time. However, in principle, technologies exist that would enable the production of products with significantly reduced bifilm contents, possibly actually bifilm-free. Such products would be expected to be significantly stronger, totally reliable, and ultimately lower in cost than those made by our current production techniques. The first steps are being demonstrated for a number of alloy systems as I write.

Furthermore, there are good reasons for believing that Griffith's cracks, universally blamed for the start of failures of all our engineering metals, may cease to exist if bifilms can be eliminated, since it seems atomic-sized voids and cracks are not easily formed in metals because of the extremely high inter-atomic forces. There are good reasons for believing that every Griffith's crack originates from a bifilm, as I have argued in detail elsewhere (Campbell 2011). No other volume defect seems available or possible. This conclusion would revolutionize the science of metallurgy and the attainments of engineering. It is an awesome and fascinating thought, and even now possibly within the grasp of currently available technology. Our new generation of casting engineers will probably have the pleasure and satisfaction to achieve this long-sought goal.

This page intentionally left blank

# Flow

As the liquid metal flows into an empty mold cavity, its surface can exert considerable influence over the filling behavior.

As a pure metal surface (for instance if we were casting pure gold) the surface tension would be important when attempting to penetrate into small cavities or thin walls. This is the classical phenomenon of capillary repulsion (the opposite effect of capillary attraction that draws water up a glass tube; water wets glass, but molds are designed to be non-wetting by liquid metals).

If the metal reacts with its environment to create some kind of surface film, the action of the surface becomes even more dominant. Penetration of narrow sections and small holes is now even more problematic. Furthermore, the whole mode of advance of the liquid into the mold now has to change because of the mechanical strength of the surface film which is to some extent tending to hold back the advance.

The *unzipping wave* is the fascinating behavior of the *vertical* advance of a filmed liquid front only by *sideways* travel of *transverse waves*. Fortunately it appears this type of advance is usually harmless to the casting, even though each horizontal traverse of the wave leaves a horizontal witness on the surface of the casting. It seems likely that all vertical advance of film-forming liquids occurs by unzipping waves, although their action is not always obvious.

The elusive phenomenon of the *rolling wave* is examined and found only to occur when the underlying matrix gains strength by freezing. Fortunately, therefore is it not a common mode of advance of the liquid front. If rolling can be induced to occur, the entrainment of the oxide creates a serious bifilm, otherwise known as a lap defect, and possibly in this case, more specifically, a cold lap defect.

Finally, as sections become very thin, any advance of the front becomes increasingly difficult. The small area of the surface oxide ensures, statistically, that few defects are contained, so the surface oxide starts to develop the high strength of a defect-free material. When the pressure is sufficiently high to burst the film, the miniscule jet that issues through the fracture in the film can appear as a single thin, high-speed stream. Alternatively, successive fractures under pressure can accumulate to become a forest of jets, each separated from the others by its own cylindrical oxide film. This is the curious and little-researched phenomenon of *microjetting* described in Section 2.2.7.

---

## 3.1 EFFECT OF SURFACE FILMS ON FILLING

### 3.1.1 Effective surface tension

When the surface of the liquid is covered with a film, especially a strong solid film, what has happened to the concept of surface tension?

It is true that when the surface is at rest the whole surface is covered by the film, and any tension applied to the surface will be borne by the surface film (not the surface of the liquid; actually, there will be a small contribution towards the bearing of the tension in the surface by the effect of the interfacial tension between the liquid and the film, but this can probably be neglected for most practical purposes). This is a common situation for the melt when it is arrested by capillary repulsion at the entrance to a narrow section. Once stopped, the surface film will thicken, growing to be a mechanical barrier holding back the liquid.

The case of a stationary meniscus is commonly observed when multiple ingates are provided from a runner into a variety of sections, as in some designs of fluidity test. The melt fills the runner, and is arrested at the entrances to the narrower sections, the main liquid supply diverting to fill the thicker sections that do not present any significant capillary repulsion. During this period, the melt is held stationary at the entrances to the thinner sections initially by the repulsive effect of surface tension, but with increasing time the meniscus quickly develops a thick strong oxide layer that acts as a barrier to further progress. A short time later, when the heavier sections are finally filled, the melt in the runner pressurizes. By this time the thin sections require an additional tension in their surfaces to overcome the tensile strength of the thickened oxide film before the metal can burst through. For this reason fluidity tests with multiple sections from a single runner are always found to give an effective surface tension typical of a stationary surface, being two or three times greater than the surface tension of the liquid. Results of such tests are described in Section 3.2.4.

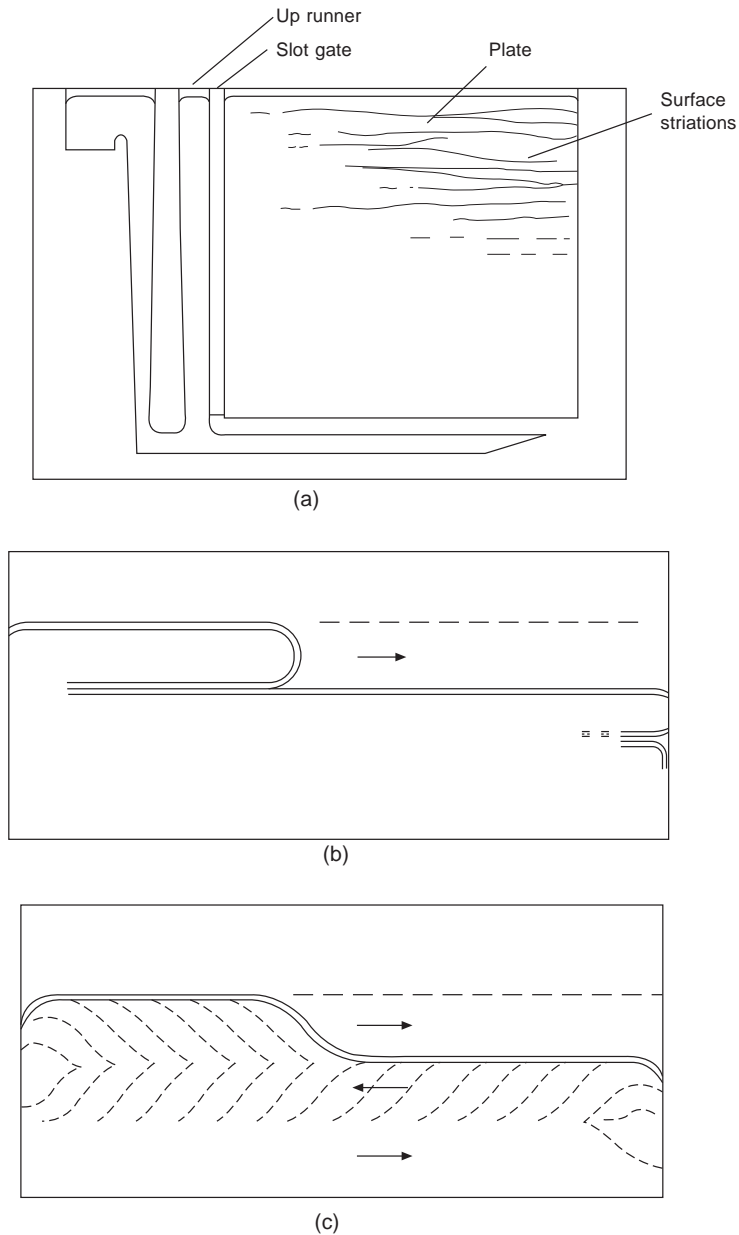
Turning now to the dynamic situation where the front of the melt is moving, new surface is continuously being created as the old surface is pinned against the mold wall by friction, becoming the outer skin of the casting (as in an unzipping type of propagation as described below). The film on the advancing surface continuously splits, and is continuously replaced. Thus any tension in the surface of the melt will now be supported by a strong chain (the surface film) but with weak links (the fresh liquid metal) in series. The maximum stress in the surface is therefore limited to the strength of the weak link, the surface tension of the liquid, in this instance. The strong solid film merely rides as pieces of loose floating debris on the surface, as rather flat icebergs on a polar sea. Thus normal surface tension would be expected to apply in the case of a dynamically expanding surface, as applies for instance to the front of an advancing liquid.

During the turbulent filling of a casting the dynamic surface tension is the one that is applicable, since new casting surface is being created with great rapidity. It is clear that the critical velocities for liquid metals calculated using the dynamic surface tension actually agree accurately with experimental determinations, lending confidence to the use of surface tension of the liquid for expanding liquid surfaces.

### 3.1.2 The rolling wave

Lap-type defects are rather commonly observed on castings that have been filled slowly (see Figure 2.25). It was expected therefore that a lap-type defect would be caused by the melt rolling over the horizontal, oxidized liquid surface, creating an extensive horizontal double-film defect (Figure 3.1b). Interestingly, an experiment set up to investigate the effect (Evans et al. 1997) proved the expectation wrong.

As a background to the thinking behind this search, notice the difference between the target of the work and various similar defects. The authors were not looking for (i) a cold lap (the old name 'cold

**FIGURE 3.1**

(a) Side-gated plate casting used to explore transverse wave effects (Evans et al. 1997); (b) rolling wave that may only occur on a partially frozen surface; and (c) an unzipping wave that may leave no internal defect, only a faint superficial witness on the casting surface.



shut' is an unhelpful piece of jargon, and is not recommended) since no freezing had necessarily occurred. They were not searching for (ii) a randomly incorporated film as generated by surface turbulence, or (iii) a rolling backwards wave seen in runners, where the tumbling of the melt over a fast under-jet causes much turbulent entrainment of air and oxides.

This was a careful study of several aluminum alloys, over a wide range of filling speeds. It seems conclusive that a rolling surface wave to cause an oxide lap does not exist in most situations of interest to the casting engineer. Although Loper and Newby (1994) do appear to claim that they observe a rolling wave in their experiments on steel the description of their work is not clear on this point. It does seem that they observed unzipping waves (see below). A repeat of this work would be useful.

The absence of the rolling wave at the melt surface of aluminum alloys is strong evidence that the kind of laps shown in Figure 2.25 and 3.1b must be cold laps. Rolling waves that form cold laps in aluminum alloy castings can probably only form when the metal surface has developed sufficient strength by solidification to support the weight of the wave. Whether this is a general rule for all cast metals is not yet clear. It does seem to be true for steels, and possibly aluminum alloys, continuously cast into direct chill molds as described in the following section.

### 3.1.3 The unzipping wave

Continuing our review of the experiment by Evans (1997) to investigate surface waves using the mold design shown in Figure 3.1a, as is normal, the mold initially filled rather quickly but became progressively slower as the meniscus approached the top of the mold. However, at a level part-way up the mold an unexpected discontinuous filling behavior was recorded. The front was observed to be generally horizontal and stationary, and its upward advance occurred not upward, but sideways. A transverse wave traveled swiftly along the length of the meniscus (Figure 3.1c), raising the level by the height of the wave, until reaching the most distant point. The speed of propagation of the wave was of the order of  $100 \text{ mm s}^{-1}$ . On arrival at the end of the plate, the wave was observed to be reflected back. Waves coming and going appeared to cross without difficulty, simply adding their height as they passed.

What was unexpected was the character of the waves. Instead of breaking through and rolling over the top of the surface, the wave broke through the oxide from underneath, and propagated by splitting the surface oxide as though opening a zip (Figure 3.1c). The splitting action occurred only locally at the point where the wave increased its height. Elsewhere, both ahead and behind the wave front, the melt surface was pinned in place by its oxide film, unable to advance vertically.

The propagation of these meniscus-unzipping waves was observed to be the origin of faint lines on the surface of the casting that indicated the level of the meniscus from time to time during the filling process. They probably occurred by the transverse wave causing the thickened oxide on the meniscus to be split, and subsequently displaced to lie flat against the surface of the casting. The overlapping and tangling of these striations appeared to be the result of the interference between waves and out-of-phase reflections of earlier waves.

The surface markings are, in general, quite clear to the unaided eye, but are too faint to be captured on a photograph. A general impression is given by the sketch in Figure 3.1. The first appearance of the striations seems to occur when the velocity of rise the advancing meniscus in liquid 99.8% purity Al falls to  $60 \pm 20 \text{ mm s}^{-1}$  or below. At that speed the advance of the liquid changes from being smooth and steady to the unstable discontinuous mode. Most of the surface of the melt is pinned in place by its

surface oxide, and its vertical progress occurs only by the passage of successive horizontal transverse waves. At the wave front the surface oxide on the meniscus is split, being opened out and laid against the surface of the casting, where it is faintly visible as a transverse striation.

Since this early work, the author has seen the unzipping wave traveling in a constant direction around the circumference of a cylindrical feeder, spiraling its way to the top. Even more recently, the surfaces of continuously cast cylindrical ingots of 300 mm diameter have been observed to be covered with spirals. Some of these are grouped, showing that there were several waves traveling helically around the circumference, leaving the trace of a 'multi-start thread'. Clearly, different alloys produced different numbers of waves, indicating a different strength of the oxide film. The cylindrical geometry represents an ideal way of studying the character of the wave in different alloys. Such work has yet to be carried out.

In the meantime, it is to be noted that there are a great many experimental and theoretical studies of the meniscus marks on steels. Particularly fascinating are the historical observations by Thornton (1956). He records the high luminosity surface oxide promoting a jerky motion to the meniscus, and the radiant heat of the melt causing the boiling of volatiles from the mold dressing, creating a wind that seemed to blow the oxide away from the mold interface. The oxide and the interfacial boiling are also noted by Loper and Newby (1994).

Much more work has been carried out recently on the surface ripples on continuously cast steels. Here the surface striations are not merely superficial. They often take the form of cracks, and have to be removed by scalping the ingot before any working operations can be carried out. It seems that in at least some cases, as a result of the presence of the direct chill mold, the meniscus freezes, promoting a rolling wave, and a rolled-in double oxide crack. Thus the defect is a special kind of cold lap.

An example is presented from some microalloyed steels that are continuously cast. Cracking during the straightening of the cast strand has been observed by Mintz and coworkers (1991). The straightening process occurs in the temperature range from 1000 down to 700°C, which coincides with a ductility minimum in laboratory hot tensile tests. The crack appears to initiate from the oscillation marks on the surface of the casting, and extends along the grain boundaries of the prior austenite to a distance of at least 5–8 mm beneath the surface. The entrainment event in this case is the rolling over of the (lightly oxidized) meniscus onto the heavily oxidized and probably partly solidified meniscus in contact with the mold. Evidence that entrainment occurs by a rolling wave is provided by the inclusion of traces of mold powder in the crack. The problem is most noticeable with microalloyed grades containing niobium. The fracture surfaces of laboratory samples of this material are found to be faceted by grain boundaries, and often contain mixtures of AlN, NbN, and sulfides.

Other typical early researches are those by Tomono (1983) and Saucedo (1983). The problems of the solidifying meniscus are considered by Takeuchi and Brimacombe (1984). Later work is typified by that of Thomas (1995) who has considered the complexities introduced by the addition of flux powder (which, when molten, acts as a lubricant) to the mold, and the effects of the thermal and mechanical distortion of the solidified shell.

All this makes for considerable complication. However, the role of the non-metallic surface film on the metal being entrained to form a crack seems in general to have been overlooked as a potential key defect-forming mechanism. In addition, the liquid steel melt in the mold cannot be seen under its cover of molten flux, so that any wave traveling around the inside of the mold, if present, is perfectly concealed. In addition, it must be remembered that continuously cast steels are usually actively withdrawn from the mold on a regular cycle, compared to continuously cast Al alloys which are

normally withdrawn from the mold smoothly and continuously. Thus the spiral traces of the traveling waves, so clearly seen on Al ingots, are not to be expected on steels, where the traveling waves, if present, will be forced to travel intermittently, along horizontal paths, leaving horizontal traces on the cast steel strand.

Finally, as a general feature of all vertical advance of melts in the apparent absence of any obvious unzipping phenomena, it is possible that all vertical advance of the meniscus may be the action of mini, ultra-short unzipping events, in which the oxide is split in some regions, while repairing in other, closely adjacent regions. Thus on a microscale the vertical advance may be ‘patchy’, or rather, may oscillate between closely adjacent regions. Such a concept avoids the obvious conceptual difficulties associated with the assumption that the mechanism involved in a rising meniscus is the simultaneous splitting and repairing of the surface film. Here is another question for which research would be illuminating.

---

## 3.2 MAXIMUM FLUIDITY (THE SCIENCE OF UNRESTRICTED FLOW)

Getting the liquid metal out of the crucible or melting furnace and into the mold is a critical step when making a casting: it is likely that most casting scrap arises during the few seconds of pouring of the casting.

The series of funnels, pipes, and channels to guide the metal from the ladle into the mold constitutes our liquid metal plumbing, and is known as the running system. Its design is crucial; so crucial, that this important topic requires treatment at length, describing the practical aspects of making castings. Thus Chapters 10–13 are required reading for all casting engineers. As a result of learning these chapters by heart, the reader will know how to introduce the melt into the running system, so that the running system is now nicely primed, having excluded all the air, allowing the melt to arrive at the gate, ready to enter the mold cavity at a safe speed. Up to this point everything has performed well.

The question now is, ‘Will the metal fill the mold?’

There is always the concern that the filling system might freeze prematurely, starving the casting of metal. Alternatively, the melt may not reach all parts of the mold before it loses its heat and stops.

For these reasons, as has been mentioned before, immediately after the pouring of a new casting, everyone assembles around the mold to see the mold opened for the first time. The casting engineer that designed the filling system, and the pourer, are both present, about to have their expertise subjected to the ultimate acid test, while colleagues, some sceptical, some hopeful, all look on. There is a question asked every time, reflecting the general hush of concern amid the foundry din, and asked for the benefit of defusing any high expectations and preparing for the worst: ‘Is it all there?’

This is the aspect of flow dealt with in this section. The ability of the metal to flow is influenced by many factors, including films, both those on the surface and those entrained, and by the rate of heat flow and the metallurgy of solidification. In different ways these factors all limit the distance to which the metal can progress without freezing. We shall examine them in turn.

The ability of the metal to run some distance to fill a mold is known as its *fluidity*. We shall see how pure metals and eutectics have high fluidity because of their smooth freezing fronts, allowing the melt to slip past with minimum hindrance, and so maximizing fluidity.

Conversely, long-freezing-range alloys have only a fraction, perhaps a half or a quarter of the fluidity of their pure metal components because of the friction to flow provided by the solidification front, now no longer smooth, but dendritic, and extending up to twice the distance into the flow.

Oxides in suspension in the melt can partially or completely block the entrance to thin sections, thus directly reducing flow in the thin section. However, in general, the role of oxides is more complicated. For instance in Al–Si alloys oxides will act as substrates for the growth of Si particles and beta-iron particles. These particles grow as rigid plate-like solids which, naturally, greatly interfere with the flow, reducing fluidity. When Sr (or Na) is added to inhibit precipitation of these pre-eutectic phases, the solidification now occurs at a lower temperature with a smooth eutectic front, greatly increasing fluidity. However, the oxide bifilms, now redundant as favored substrates, float aimlessly in the melt possibly raising the viscosity a little, but the effect is probably negligible because the bifilms are so flimsy and raveled by the turbulence of the flow, so posing little restriction to the liquid. However, at a later stage of freezing, the bifilms can now impair interdendritic flow by bridging between dendrite meshes to form impenetrable barriers (analogous to the blocking of flow into thin sections), while opening to initiate porosity. Thus interdendritic porosity becomes a danger. This complicated scenario is described in more detail in Section 6.3.5. It seems likely that the role of oxides has contributed (probably together with variations in test pieces, and the effect of poor filling system designs) to the wide scatter in experimental results that is evident historically.

The provision of unstable foundations for the growth of dendrites allows them to break off, and tumble along with the flow, thereby reducing the overall impediment to flow, as when acetylene smoke is applied to the mold (to be described later in Section 3.2.6) or possibly when vibration is applied to the mold.

Clearly, anything that impedes flow will reduce fluidity (it seems necessary to state the obvious from time to time). Thus one can see that the concept of *good fluidity* is seen to be simply the science of *unimpeded flow*. The more impediments we can remove, and the smoother the flow channel that can be provided, the greater the fluidity distance.

Ultimately therefore, careful application of casting science should allow us now to know that not only will the casting be all there, but it will be all right.

### **Fluidity definition**

The ability of the molten metal to continue to flow while it continues to lose temperature and even while it is starting to solidify is a valuable feature of the casting process. There has been much research into this property, with the result that a quantitative concept has evolved, which has been called ‘fluidity’. In terms of casting alloys, the fluidity is defined as the *maximum* distance to which the metal will flow in a standard mold. Thus fluidity is simply a length denoted here as  $L_f$ , measured, for instance, in millimeters. (The use of the foundry term *fluidity* should not be confused with its use in physics, where fluidity is defined as the reciprocal of viscosity.)

A second valuable quantitative concept that has often been overlooked was introduced by Feliu (1962). It is the parameter  $L_c$ , which Feliu called the critical length. Here, however, we shall use the name *continuous-fluidity length*, to emphasize its relation to  $L_f$ , to which we could similarly give the full descriptive name of *maximum-fluidity length* (although, in common with general usage, we shall keep the name ‘fluidity’ for short!). In this section we shall confine our attention to  $L_f$ , dealing with the equally important  $L_c$  in a following section.

Although fluidity (actually maximum fluidity, remember!) has therefore been measured as the (maximum) length to which the metal will flow in a long horizontal channel, this type of mold is inconveniently long for regular use in the foundry. If the channel is wound into a spiral, then the mold becomes compact and convenient, and less sensitive to leveling errors. Small pips on the pattern at regular spacings of approximately 50 mm along the centerline of the channel assist in the measurement of length. Figure 3.2 shows a typical fluidity spiral with a basin provided with a channel to a cup-shaped overflow basin to ensure a constant head height during the pouring process. Also shown is a horizontal channel that has been used for laboratory investigations into the fluidity of metals in narrow glass tubes. In this case the transparent mold allows the progress of the flow to be followed from start to finish.

There has been much work carried out over decades on the fluidity of a variety of casting alloys in various types of fluidity test molds, mostly of the spiral type. The wide variety of mold types and the sensitivity of fluidity to numerous variables have prevented fluidity from achieving the status of an internationally accepted material parameter. This is not too much of a disadvantage, since most fluidity work is at least internally consistent. Fundamental insights have been gained mainly from the great bulk of work carried out at MIT under the direction of Merton C Flemings. He has given useful reviews of his work several times, notably in 1964, 1974, and 1987.

The work of the many different experimenters in this field is difficult to review in any comprehensive way because almost each new worker has in turn introduced some new variant of the spiral test. A noteworthy effort to reduce problems so far as possible is seen in the test by Sabatino and others (2005). Other workers have gone further, introducing completely new tests usually with the emphasis on the casting of thin sections.

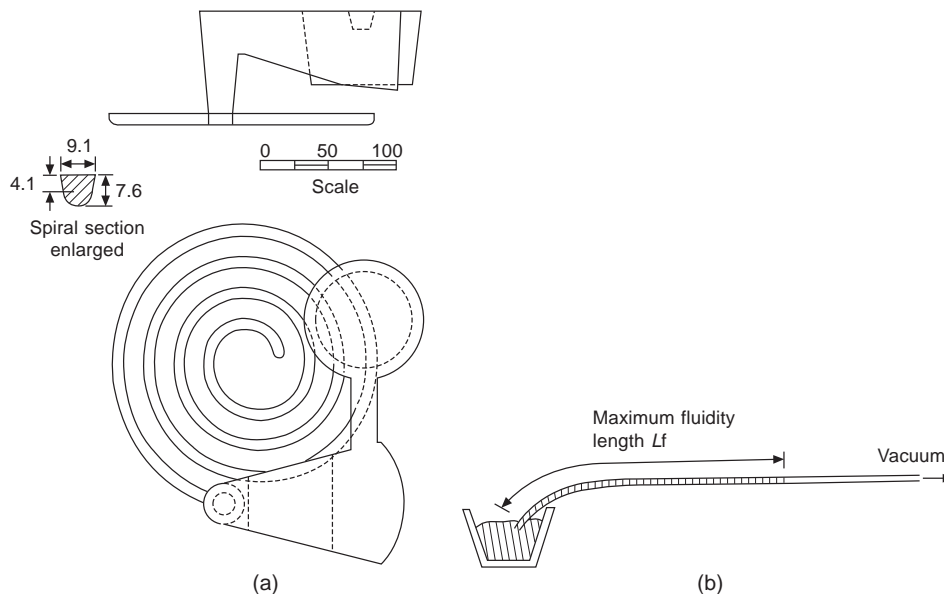


**FIGURE 3.2**

Typical fluidity tests for (a) foundry and (b) laboratory use.

Here we attempt to review the data once again, with the aim on this occasion of emphasizing the unity of the subject because of the basic, common underlying concepts. The various fluidity tests of the spiral, tube, or strip types are shown not to be in opposition. On the contrary, if proper allowance is made for the surface tension and modulus effects, these very different tests are shown to give exactly equivalent information.

It will become clear that the fluidity of metals is mainly controlled by the effects of fluid mechanics, solidification, and surface tension. This is a reassuring demonstration of good science.

### 3.2.1 Mode of solidification

Flemings (1974) demonstrated that the fluidity of pure metals and eutectics, which freeze at a single temperature, is different to that of alloys that freeze over a range of temperatures. These two different solidification types we shall call skin freezing and pasty freezing for short.

For a skin-freezing material the mode of solidification of the stream in a fluidity test appears to be, as one might expect, by planar front solidification from the walls of the mold towards the center (Figure 3.3a). The freezing occurs at some point along the length of the channel, after the metal has lost its initial superheat (the excess temperature above its melting point). The solidified region actually migrates downstream somewhat as the leading edge of the material is re-melted by the incoming hot metal, and re-freezing occurs further downstream. It is clear that the stream can continue to flow until the moment at which the freezing fronts meet, closing the flow channel. Note that this choking of flow happens far back from the flow front. In addition, solidification needs to be 100% complete at this location for flow to stop. Assuming the liquid has an approximately constant velocity  $V$ , then if its freezing time in that section is  $t_f$ , we have the flow distance

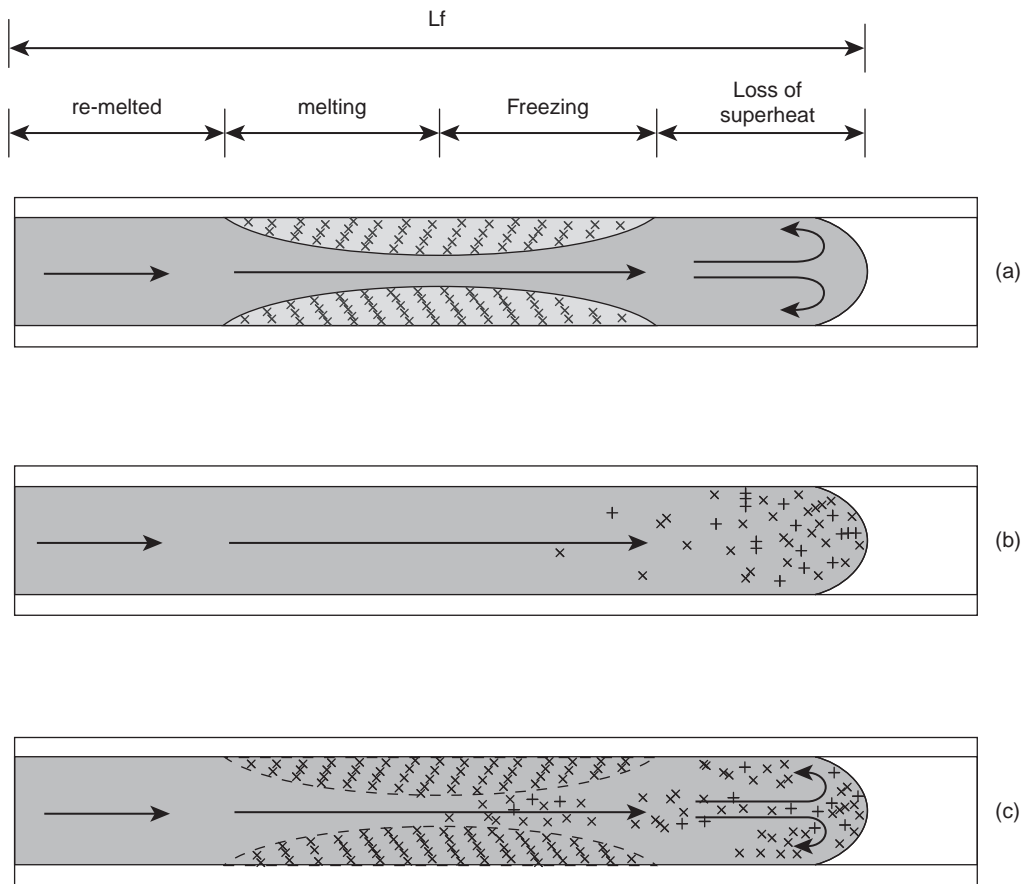
$$L_f = V \cdot t_f \quad (3.1)$$

This is an approximate equation first proposed by Flemings and co-workers (1963). It overestimates  $L_f$  because the velocity does reduce somewhat as the channel becomes constricted, giving a smaller measured fluidity. Nevertheless Equation 3.1 is surprisingly accurate, probably as a result of the acceleration of freezing as the channel closes, as described in Section 5.1 (see Figure 5.10). We shall assume the applicability of Equation 3.1 here.

The pattern of solidification of short-freezing-range material can be confirmed from the evidence of the microstructure of cross-sections of the castings. Columnar crystals are seen to grow from the sides of the mold, angled inwards against the flow, and meeting in the middle of the section. Confirmation of the presence of liquid cut-off by the meeting of the solidification fronts is clear from the shrinkage cavity at the tip of the casting; a pipe (or collapsed exterior) forms in the unpressurized region near the liquid tip. An internal pipe (or a general collapse of the casting) usually grows back nearly to the point at which the flow was blocked. Thus the mechanism of arrest of flow for skin-freezing materials is known with some certainty and in some detail.

The same situation does not apply to long-freezing-range alloys.

The pattern of solidification of longer-freezing-range materials is not so easily interpreted by metallography of the cast test piece. It turns out to be quite different to that of the skin-freezing material described above. Clearly, the dendrites growing from the mold wall at an early stage of freezing are somehow fragmented by the flow so that the stream develops as a slurry of tumbling dendritic fragments. These equiaxed dendrites are carried in the central flow to congregate at the liquid

**FIGURE 3.3**

Flow arrest in pure metals and coupled eutectics by complete solidification (after Matsuda and Ohmi 1981); (b) early model for long-freezing-range alloys; (c) new model proposed here.

front (Figure 3.3b). It has been assumed that when the amount of solid in suspension exceeds a critical percentage, the dendrites start to interlock, making the mixture unflowable (Flemings et al. 1961). This theory gives some cause for concern because the critical concentration to stop flow appears to depend on the applied head of metal and varies over the wide range of 20–50%. The arrest of flow occurs therefore when there is only approximately 20–50% solidification, thus reducing fluidity by this corresponding amount. Thus there is wide potential inaccuracy in the predictions that this theory is unable to explain. Furthermore, the concept of a clutter of equiaxed grains at the tip of the flow overlooks the fact that such grains usually originate from the fragmentation of dendrites (although it is just possible that the effect might occur if effective grain refinement were carried out). Since dendrites usually grow into the flow from the mold surface, the presence of stationary features in the flow would be expected to be much more of a hindrance to flow than grains freely tumbling along.

A possibly more accurate arrest mechanism is therefore proposed in Figure 3.3c. Here the freezing front proceeds to advance towards the center of flow, outlined by the dotted line. However, of course, the freezing region is now not solid, but is a permeable array of dendrites. This permeable array is a fixed hazard to traffic. If flow were steady, the dendrites would angle into the flow as they grew, as elegantly researched by Turchin (2007a), but would continue to grow stably and steadily. However, flow is rarely stable. Hot and cold vortices will swirl through the mesh, together perhaps with the devastating mechanical disruption caused by occasional bubbles (to be expected in most fluidity tests). The dendrite arms will therefore melt off during pulses of heat and shear forces, releasing fragments into the stream. (As an aside; the breakup of dendrites at only low velocities in the region of  $0.2 \text{ m s}^{-1}$  seen by Turchin (2007b) is clearly the result of the extreme turbulence developed by his displacement of the experimentally observed volume into a recess, instead of being aligned with the streamlines of the flow.)

In a more conventional fluidity test channel, the fragments would be carried forward by the flow as illustrated in Figure 3.3c, concentrating near the front of the stream where they are particularly visible. Their concentration in this region has been previously assumed to arrest flow. Much more probably the flow is slowed by the viscous drag in the fixed mesh of dendrites far back from the flow front, although the equiaxed grains accumulating near the flow front may make some contribution. Some discriminating research would clarify this, probably revealing that the answer is different for different alloys.

Conditions in the permeable dendrite mesh are likely to be complicated, if not chaotic. It is possible that the restraining mesh might partially collapse, consolidating the dendrites and impeding flow even further. Free-floating crystals might jam in the mesh. Oxide films would wrap around dendrites or might bridge and thereby block whole sections of the mesh, thus causing much more restriction than their volume fraction might suggest. Thus for pasty freezing systems, the prior turbulence in the filling system, creating areas of oxide bifilms that would help to block the mesh, would be expected to have a disproportionately high effect. Such complications might help to explain the significant differences between different fluidity research results. Overall, the development of the mesh and its disintegration into fragments may not be a particularly reproducible phenomenon.

Whatever the detailed mechanism for arresting flow, it follows that for long-freezing-range alloys flow stops when much less total solid has formed. Equation 3.1 therefore becomes

$$L_f = 0.2V.t_f \text{ to } 0.5V.t_f \quad (3.2)$$

Equation 3.2 reflects a feature that appears to be common to all alloy systems, and yet does not seem to have been widely recognized; long freezing range alloys have only one-fifth to one-half of the fluidity enjoyed by skin-freezing materials. These are big effects. The precise values should be predictable from the geometry of the dendrite mesh, but this also has yet to be researched. As an instance, Figure 3.4 illustrates the profound effect of a small amount of Sn on pure Al, causing the excellent fluidity of pure Al to fall by a factor between 3 and 4.

A similar effect is seen in Figure 3.5 illustrating the lead/tin system at  $50^\circ\text{C}$  above its liquidus. The fluidity of the intermediate alloys is dramatically different from the straight line interpolation of the fluidity of the two pure elements. The curve joining the lower data points is based on the fluidity of the long-freezing-range alloys being approximately one-fifth of the short-freezing-range alloys when lead-rich, from the available data points. There are no equivalent data points on the tin-rich side of the diagram, so here we have guessed that the longer-freezing-range alloys might have only approximately



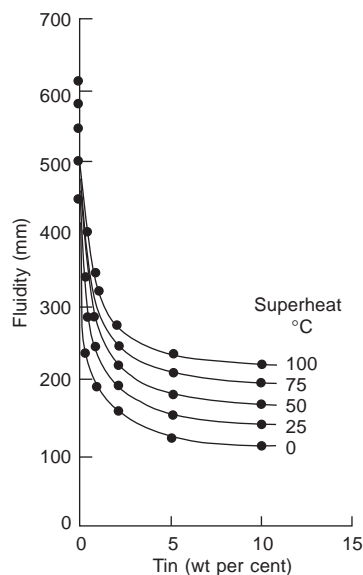


**FIGURE 3.4**

Variation of fluidity with composition of Al-Sn alloys (data from Feliu et al. 1960).

half fluidity, because the freezing range is narrower, and the one data point is consistent with this. More experimental points would have removed this uncertainty.

The fluidity of the eutectic in Figure 3.5 appears to be over 50% higher than the straightforward method of mixtures of its components (i.e. the straight line joining the fluidities of the two pure metals). This may be understandable if the pure metals may be exhibiting some dendritic growth, probably due to the presence of some impurity. This would suppress the fluidity of the pure constituents, but not necessarily the eutectic (especially if the main ‘impurities’ in each of the pure constituents consisted of the other ‘pure constituent’, i.e. if Pb were contaminated with Sn, and Sn were contaminated with Pb).

The Al-Zn system is more in line with expectations: the eutectic fluidity is very close to the straight line interpolation of the pure constituents (Figure 3.6), but the constant temperature result gives the interesting appearance of enhanced fluidity as predicted later in this section. Exasperatingly, the widely used commercial pressure die casting alloy Zn-4%Al alloy resides almost in the center of the fluidity minimum. What is worse, Friebe and Roe (1963) find that the fluidity falls further as a result of the level of 3%Cu in the alloy, normally present to add strength. It seems that the efforts of metallurgists to optimize alloys have paid minimal attention to the potentially huge benefits to castability from more fluid compositions, allowing thinner and lighter castings to be made, currently one of the biggest disadvantages currently faced by the zinc pressure die casting industry.

Impressively early work by Portevin and Bastien (1934) suggests the shape of precipitating solid crystals affects the flow of the remaining liquid; smooth crystals of solidifying intermetallic compounds creating less friction than dendritic crystals. Their famous result for the Sb-Cd system poured at

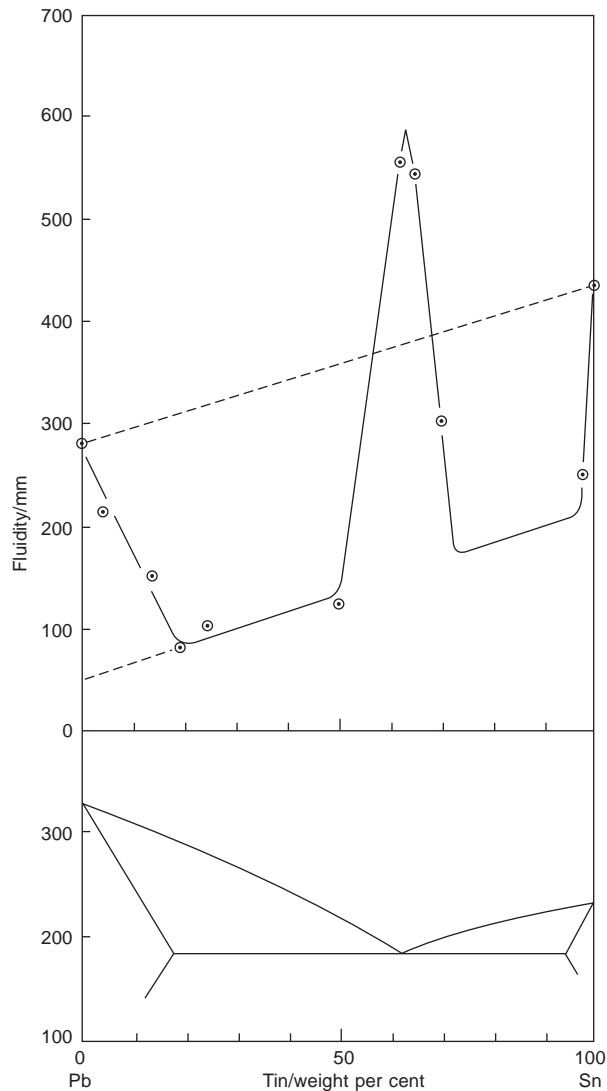


**FIGURE 3.5**

Fluidity of Pb-Sn alloys at 50°C superheat determined in the glass tube fluidity test. (Data from Ragone et al. 1956.)

a constant superheat of 100°C is shown in Figure 3.7 and appears to illustrate this convincingly. The greater fluidity of intermetallic compounds and eutectics with respect to their pure constituent elements seems to be true for this system in agreement with the Pb-Sn result but not with the Al-Zn fluidity. Perhaps more careful work with purer, bifilm-free constituents might help to resolve the question whether eutectics do have some special advantage over their constituent elements.

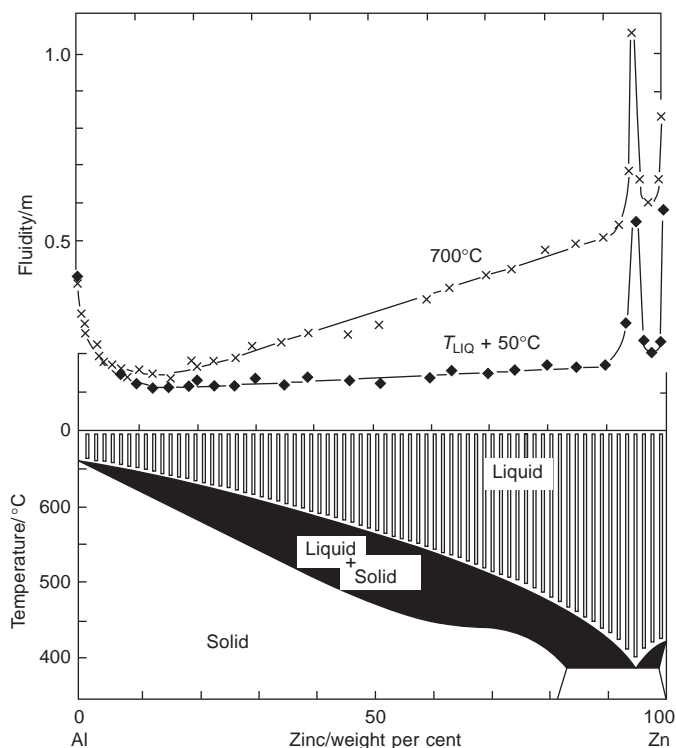


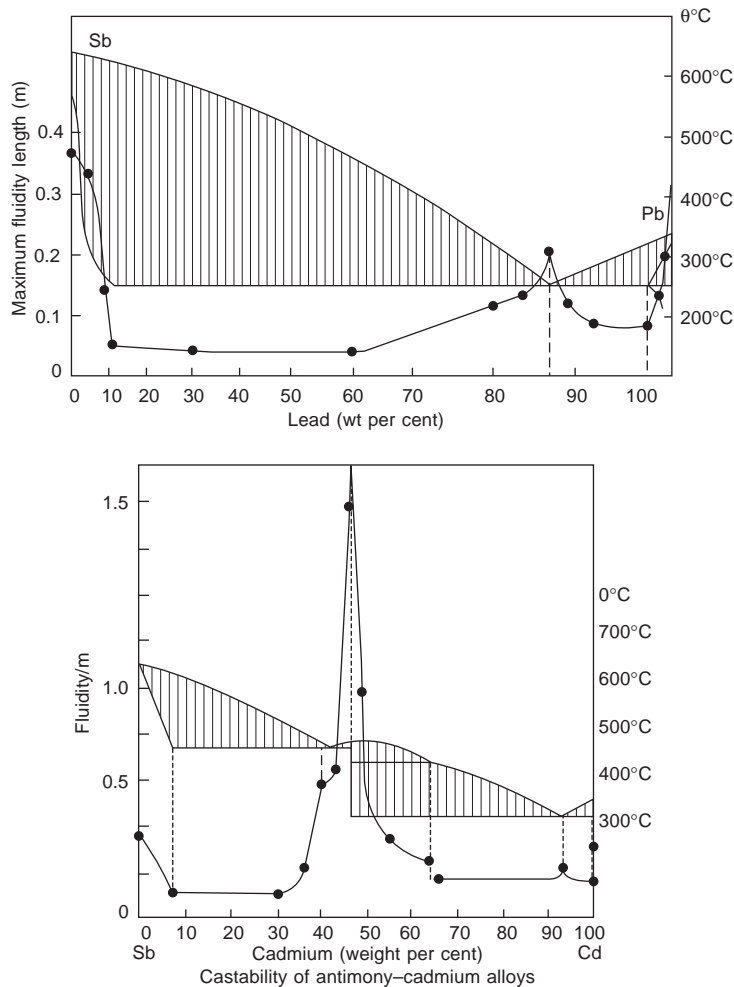
**FIGURE 3.6**

Al-Zn alloys poured into a straight cast iron channel showing fluidity at constant superheat, and the enhanced fluidity of the eutectic when cast at constant temperature (Lang 1972).

Incidentally, the details of this classic work are rarely questioned, but deserve close attention. For instance, the peritectic reaction shown in Figure 3.7 at approximately 63%Cd is found not to exist in later versions of this binary phase diagram (Brandes and Brook 1992). Thus the small step in fluidity, carefully depicted at this point, seems likely to be attributable to experimental error. Furthermore, at the Sb-rich end of the figure, the fall in fluidity will probably be steeper than that shown, so that the plateau minimum will be reached sooner than the limit of solid solution as assumed by the authors. This will be as a result of non-equilibrium freezing. More importantly, given the existence of some modest scatter in the results, it seems likely that the high-fluidity peak is actually not centered on the compound SbCd but is generated by the adjacent eutectic. However, these are minor quibbles of an otherwise monumental and enduring piece of work, years ahead of its time.

It needs to be emphasized that the fluidity of a complete alloy system at constant temperature will always be expected to favor the eutectic fluidity; their effectively higher superheat enhances the advantage to eutectics, although it reduces the advantage to intermetallic compounds. This effect is seen later in Figures 3.8 and 3.9.

We can usefully generalize these important effects of composition in the following way. Figure 3.8 shows a schematic illustration of a simple binary eutectic system. The fluidity at zero

**FIGURE 3.7**

Fluidity of Sb–Pb and Sb–Cd alloys showing the high fluidity of the eutectics determined by casting at a constant superheat into a cast iron fluidity spiral (Portevin and Castien 1934).

superheat is linear with composition for the skin-freezing metals and alloys (the pure metal A, the AB eutectic, and the pure metal B), whereas it is assumed to be about half of this for the long-freezing alloys. The resulting relationship of fluidity with composition is therefore seen to be the cusped line in Figure 3.8(i). This would be the expected form of the fluidity/composition relation for a constant superheat.

If, however, the alloys are cast at a constant temperature,  $T_c$ , there is an additional contribution to fluidity from the superheat that now varies with composition as indicated in Figure 3.8(ii). To find the total fluidity as a function of composition, curves (i) and (ii) are added (the addition in these simplified

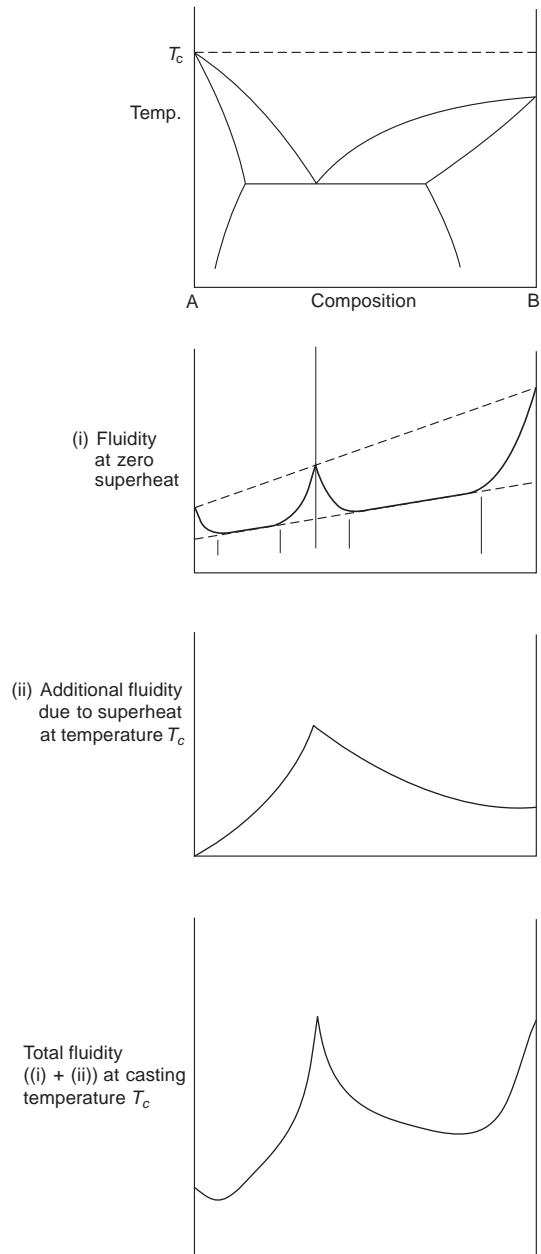


**FIGURE 3.8**

Schematic illustration of the different behaviors of eutectics when tested at constant superheat or constant temperature.

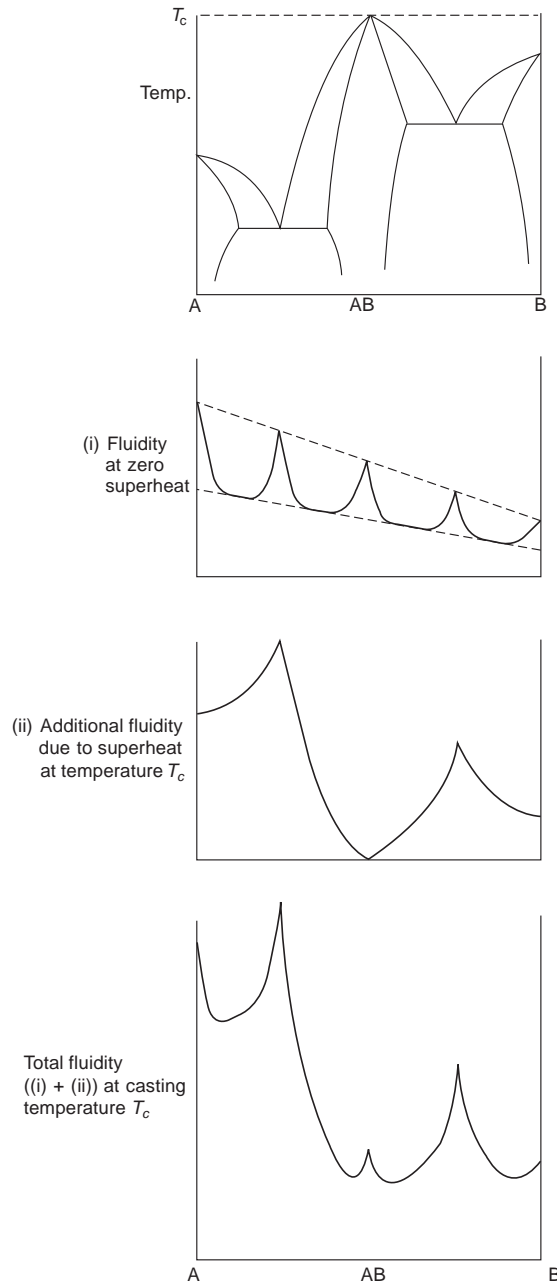


**FIGURE 3.9**

Schematic illustration of the different behaviors of high-melting-point intermetallics when tested at constant superheat or constant temperature.

illustrative examples neglects any differences of scale between the two contributions). The effect seen in (iii) is to greatly enhance the fluidity at the eutectic composition.

The same exercise has been carried out for a high-melting-point intermetallic compound, AB, in Figure 3.9. The disappointing total fluidity predicted for the intermetallic (summing (i) and (ii)) explains some of the problems that are found in practice with attempts to make shaped castings in such alloys. It explains why intermetallic compounds are rarely used as natural casting alloys, compared to eutectics and near-eutectics, which are common.

The expected poor fluidity of intermetallics underlines the suggestion by Portevin and Bastien that the high fluidity of intermetallics that they observe, although at constant superheat as seen in Figure 3.7, is nevertheless in fact strongly influenced by some other factor, such as the shape of the solidifying crystals. Alternatively, as suggested above, they have mistakenly attributed the high fluidity to the intermetallic, whereas perhaps it was really the result of the adjacent eutectic.

Another interesting and important lesson is to be gained from the predictions illustrated in Figures 3.8 and 3.9. The peaks in fluidity are impressively narrow. Thus for certain eutectic alloys the fluidity is awesomely sensitive to small changes to composition, particularly when it is realized that Figures 3.8 and 3.9 are simple relationships. Many alloy systems are far more complicated, crowding the cusps of fluidity closer and so making their slopes steeper. Dramatic changes of fluidity performance are to be expected therefore with only minute changes in composition. Perhaps this is the reason why fluidity research earns its reputation for being not reproducible. Perhaps it is also the reason why some castings can sometimes be filled, and at other times not; some batches of alloy cast well, but some nominally identical alloys cast poorly. Clearly, to maximize reproducibility we must improve the targeting of peak performance. The unattractive alternative is to forsake the peaks and devise more easily reproducible alloys in the troughs of mediocre fluidity. A good compromise, possible, would be to target the broader peaks, where the penalties of missing the peak are less severe.

The approach illustrated in Figures 3.8 and 3.9 can be used on more complex ternary alloy systems. In more complex multicomponent alloy systems the understanding that pure metals and eutectics exhibit a fluidity at least twice that of their long-freezing-range intermediate alloys is a key allowing even sparse and apparently scattered data on alloy systems to be rationalized. This was the background of Figure 3.10a, b and c that showed results for the Al–Cu–Si system that could not be drawn by its investigators, but was only unraveled in a subsequent independent effort (Campbell 1991). However, I learned only later, while my 1991 paper was in the process of publication, that Portevin and Bastien had already accomplished a similar evaluation of the Sn–Pb–Bi ternary system as early as 1934. In this prophetic work they had constructed a three-dimensional wax model of their fluidity response as a function of composition, showing ridges, peaks, and valleys.

In practice, it is important to realize that the improved fluidity of short- versus long-freezing-range materials forms the basis of much foundry technology.

The enormous use of cast iron compared to cast steel is in part a reflection of the fact that cast iron is a eutectic or near-eutectic alloy and so has excellent fluidity. Steel, in general, has a longer freezing range and relatively poor fluidity. Additionally, of course, the higher casting temperatures of steel greatly increase the practical problems of melting and casting, and cause the liquid metal to lose its heat at a faster rate than iron, further reducing its fluidity by lowering its effective fluid life,  $t_f$ . For instance, Figure 3.11a shows that a 1%C steel has zero fluidity at approximately 1450°C whereas a cast iron will run like water over a distance of 1.3 m at this temperature. Alternatively, the figure illustrates

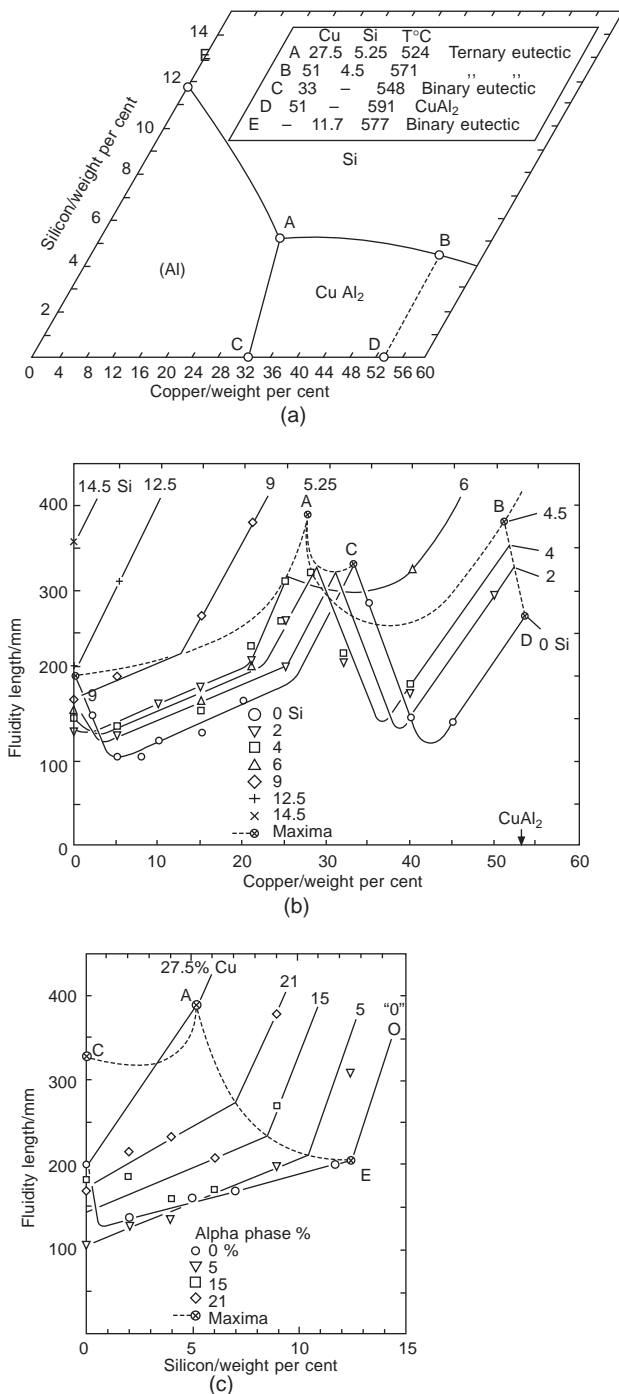
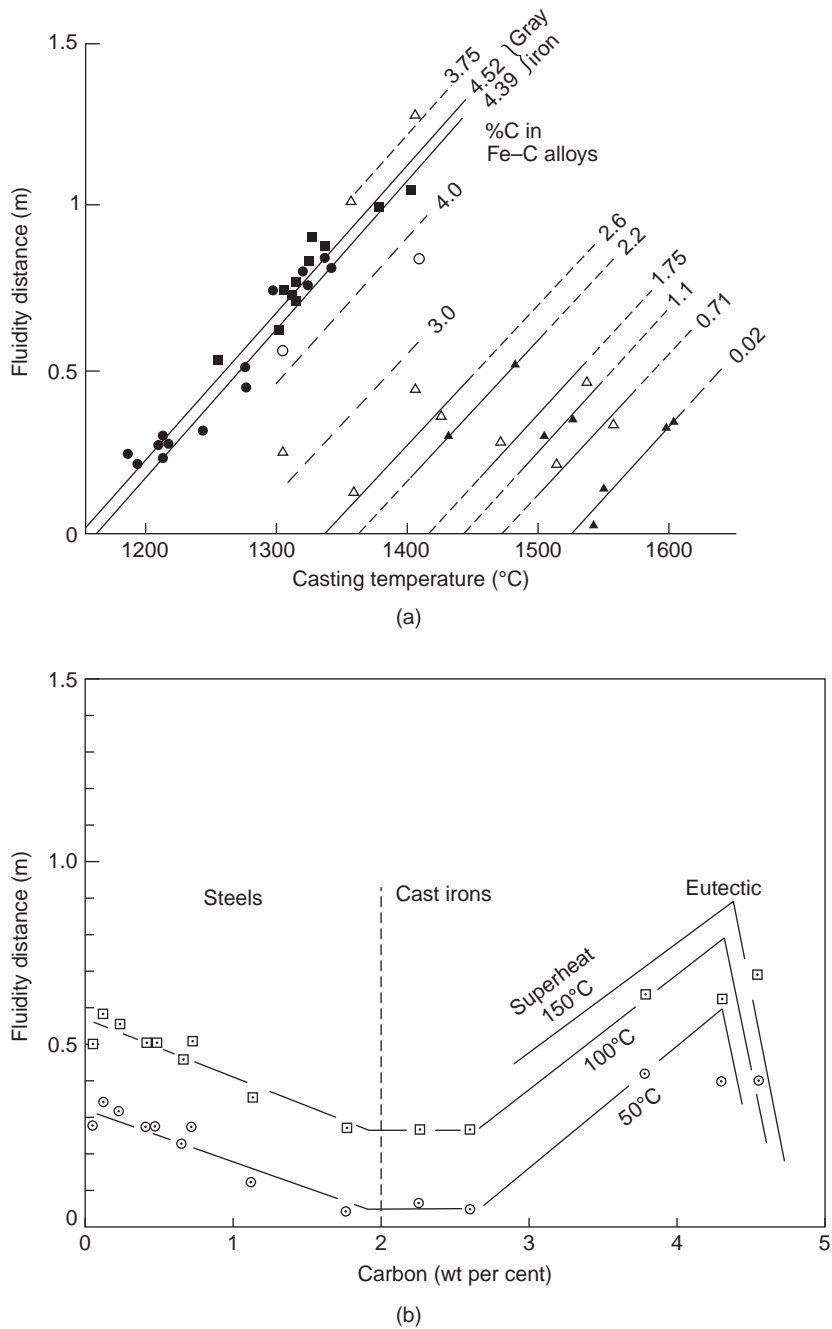


FIGURE 3.10

Phase diagram and fluidity of the Al-Si-Cu system. (Data from Garbellini et al. 1990; interpretation by Campbell 1991.)





**FIGURE 3.11**

(a) Effect of temperature and carbon content on the fluidity of Fe-C alloys; (b) the same data plotted as a function of composition. (Data from Berger 1932, Andrew et al. 1936, Evans 1951, Porter and Rosenthal 1952.)

that if a fluidity of 500 mm is required to fill a mold, a gray iron would achieve this at a temperature lower than 1300°C whereas a 0.5%C steel would require 1600°C.

The work by Porter and Rosenthal (1952) nicely illustrates the peak of fluidity at the eutectic composition, approximately 4.5 wt% carbon equivalent (Figure 3.12). As in many fluidity studies, this work is beautifully self-consistent, probably as a result of carefully carried out experiments with their own particular variety of fluidity test mold and their own particular set of compositions of their iron alloys. The results therefore do not fit particularly well with the earlier results presented in Figure 3.11, but this is probably as good agreement as one can expect. The essential features, including the high peak at the eutectic, are supported by all studies.

Fluidity can be affected by changes in composition of the alloy in other ways. For instance, the effect of phosphorus additions to gray iron are well known: the wonderful artistic castings, of statues, fountains, railings, and gates produced in the nineteenth and early twentieth century Europe were made in high-phosphorus iron because of its excellent fluidity. The effect is quantified in Figure 3.13a. The powerful effect of phosphorus on cast iron is solely the result of its action to reduce its freezing point. This is proven by Evans (1951), who found that when plotted as a function of superheat (the casting temperature minus the liquidus), the phosphorus addition hardly affects the fluidity (Figure 3.13b).

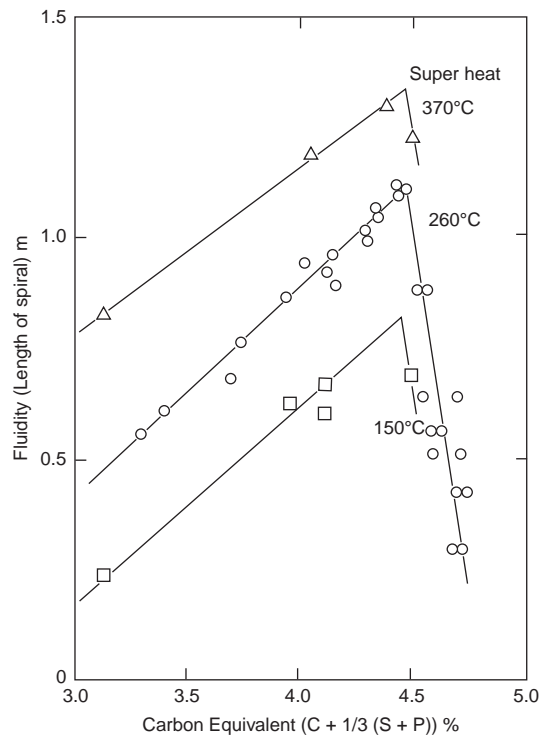


**FIGURE 3.12**

The excellent fluidity results for gray iron by Porter and Rosenthal (1952).

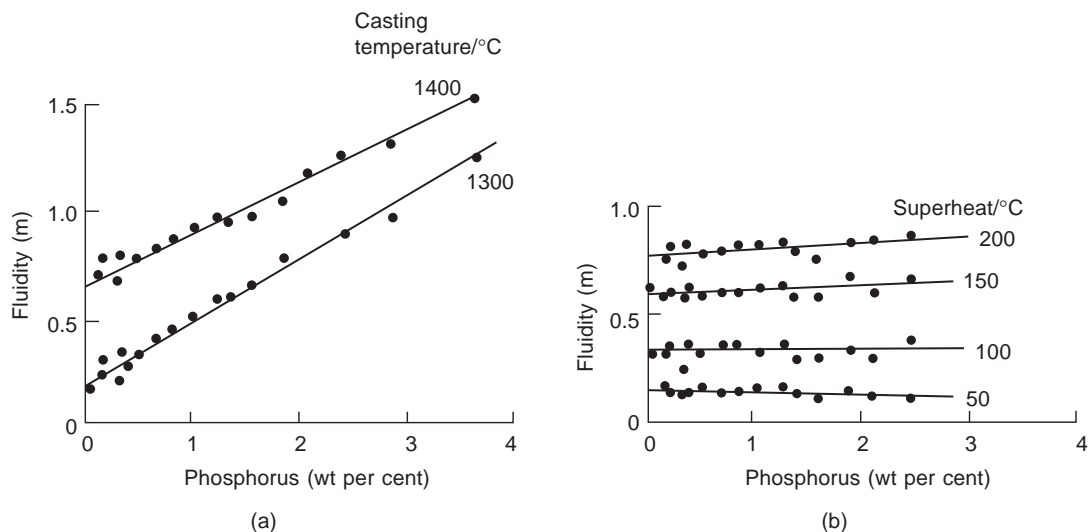


**FIGURE 3.13**

Effect of phosphorus on the fluidity of gray iron plotted as a function of (a) phosphorus addition and (b) superheat above the liquidus (Evans 1951).

Flemings has taken up this point, suggesting that the good fluidity of cast irons compared to steels is only a function of the higher superheat which can be used for cast iron. However, this is only part of the truth. Figure 3.11 shows data re-plotted from early work by Evans (1951) and Porter and Rosenthal (1952) on gray iron and Andrew (1936) on steels. The reasonably linear plots of fluidity against casting temperature (Figure 3.11a) are important and interesting in themselves. However, they can be redrawn as in Figure 3.11b. Here the horizontal flat portions of the curves show that the long-freezing-range alloys have constant fluidity at a given superheat, in agreement with Flemings and confirming the similar effect of phosphorus that we have already witnessed; any increase in fluidity is only the result of increases in superheat as the composition changes. However, as either the pure metal, Fe, or the eutectic at 4.3% carbon is approached there is clear evidence of enhanced flowability, showing that there is an additional effect at work here, almost certainly relating to the mode of solidification as we have discussed above. This effect was found as long ago as 1932 by Berger. Other binary alloy systems exhibit a similar special enhancement of fluidity at the eutectic as illustrated in Figures 3.5–3.7. The effect is also seen in a ternary system in Figure 3.10.

Interestingly, the effect of freezing range on fluidity is not confined to metals. Bastien et al. (1962) have shown that the effect is also clearly present in molten nitrate mixtures and in mixtures of organic compounds. It is to be expected that the effect will be significant in other solidifying systems, such as water-based solutions and molten ceramics, etc.

### 3.2.2 Effect of velocity

The velocity is explicit in Equations 3.1 and 3.2 for fluidity. It is all the more surprising therefore that it has not been the subject of greater attention. However, most workers in the field have used fluidity tests

with relatively small head heights, usually not exceeding 100 mm, so that velocities during test are usually fixed, and rather modest, under  $2 \text{ ms}^{-1}$ .

It might seem reasonable to expect that fluidity would increase linearly with increase in velocity, particularly in view of the forecasts of Equations 3.1 and 3.1. However, with regret, this appears to be a mistake. It is this erroneous belief that causes many casting engineers to assume that to fill thin-section casting the melt has to be thrown into the mold at maximum speed. These attempts to improve filling usually fail to produce good castings because of the complicating effects of bulk and surface turbulence.

For instance, as head height  $h$  of a casting is increased in a filling system free from friction effects, we might expect that because  $V = (2gh)^{1/2}$ , fluidity would increase proportionally to  $h^{0.5}$ . However, the resistance to flow from turbulence in the bulk of the liquid rise according to  $(1/2)\rho V^2$ . Thus losses rise rapidly with increased velocity  $V$ , causing it to be increasingly difficult to create high velocities, particularly in narrow channels. In fact Tiryakioglu and co-authors (1993) find experimentally that fluidity of 355 aluminum alloy rises at a much lower rate, which seems proportional to only  $h^{0.1}$ . This is almost certainly the result of the rapidly increasing drag effects on the motion of the liquid as velocity increases. Thus attempts to increase fluidity by increasing pressurization and/or velocity are subject to the law of rapidly diminishing returns.

Furthermore, at high speeds, it becomes increasingly difficult to keep surface turbulence under control. Thus the jetting and splashing of the flow entrains air, and creates oxide laps. The oxide laps occur because of the disintegration of the flow front. Splashes or surges of melt ahead of the general liquid front have to await the arrival of the main flow in order to be re-assimilated into the casting. During this time their surface oxidizes, so that re-assimilation is difficult, or impossible, resulting in an oxide lap. If the arrival of the main flow takes longer, the awaiting material might freeze. Thus the splash and its droplets might become a cold lap. On seeing these problems, the reaction of some casting engineers is to increase the filling speed, with predictably lamentable results.

In contrast, at more modest speeds, if the melt is introduced so that the liquid front remains smooth and intact, the air is not mixed in, but is pushed ahead, and the front has no isolated fragments. The very integrity of the front acts to keep itself warm. Both oxide laps and cold laps are avoided since the front probably advances by harmless unzipping perturbations. The casting is as sound as the filling system can make it.

In confirmation of these problems, Zadeh and the author (2001) have demonstrated how the fall of melts down sprues 500 mm high have resulted in good fluidity lengths, with apparently good castings judging by their external appearance. We thought we had success until we viewed the test pieces by X-ray radiography. To our dismay, the fluidity strip castings were found to be full of entrained bubbles and films. They would have been totally unsaleable as commercial products. It was necessary to introduce ceramic filters with an integral bubble trap to regain control over the integrity of the flow to give good-quality castings. Having done this, the fluidity distance was then no better than if the melt had been poured from 100 mm. I have never forgotten the lesson of this experience.

Thus, in general, up to small head heights of the order of 100 mm fluidity will be expected to rise linearly with increase in speed of flow. However, further increases in speed with current filling system designs appear to be counter-productive if castings relatively free from defects are required.

In summary of the effects of velocity therefore, it is essential to fill the mold without surface turbulence for the majority of alloy systems. The importance of this fact cannot be overstated. There is no substitute for a good filling system that will give a controlled advance of the liquid front.

Essentially, this means it is counter-productive to attempt to increase the velocity of filling for the production of sound castings.

### 3.2.3 Effect of viscosity (including effect of entrained bifilms)

Loper (1992) made the point that the variations of viscosity of liquid metals with temperature and with composition are relatively minor, and not capable of explaining the variations of fluidity seen across alloy systems. Furthermore, the viscosity of the melt does not even appear in the fundamental equations for fluidity (Equations 3.1 and 3.2). Thus the theoretical prediction is that fluidity should not depend on viscosity. This surprising prediction has been shown to be remarkably accurate.

It is instructive to compare the fluidity observed for semi-solid (strictly ‘partly solid’) and MMC cast materials. For concentrations  $\Phi$  of solids up to about 20% (0.2 fraction) the formula by Einstein dating from 1906 and in its modified form from 1911, for the viscosity  $\eta$  of a mixture of liquid plus solid, is sufficiently accurate for our purpose

$$\eta = (1 + 0.5\Phi)/(1 - \Phi)^2$$

A mix with 20% solid would be expected to have a viscosity about double that of the pure liquid. This is the concentration level of many MMCs. However, their fluidity as measured by the spiral or other fluidity test is hardly impaired. In fact, quite extensive and relatively thin-walled castings of most MMCs can be poured by gravity without too much difficulty. For instance, Kolsgaard and Brusethaug (1994) are among many who have found that the fluidity of well-made metal matrix composites (MMCs) of Al-7Si-0.3Mg alloy containing up to 20 volume per cent SiC particles remained unchanged. (‘Well made’ in this instance refers to the particulate component of the MMC being mixed into the liquid metal under extremely high vacuum, so as to reduce the entrainment of surface oxides.)

In contrast to the nearly zero effect of added particles or changes in alloy composition that might affect viscosity, there is a profound effect quickly generated by the presence of films in suspension in the liquid. This appears to be associated with the large effect on flow resulting from the large area of films, despite the negligible volume fraction of material that the films represent. Thus when melts become highly viscous, taking on the behavior and appearance of porridge (a Scottish dish of oats boiled in water and strongly flavored with salt) this cannot be the effect merely of the addition of solid particles since this can only explain a rise in viscosity by a factor of 2. If water is taken as unit viscosity, most metals are in the region of 2–5. All these are expected to flow like water.

When the melt becomes as viscous as a thick syrup, the viscosity is now in the region of 1000 to 10 000 times that of water. Many MMCs take on the appearance of such flow behavior. This viscous behavior cannot be explained merely by the presence of solid particles in suspension. Such high viscosities are only explicable if copious quantities of films are present in suspension in the liquid. With such extremely high viscosity, fluidity as measured by a spiral flow test is now impaired a little, but not as seriously as might be expected. Timelli and Bonollo (2007) studied pressure die casting alloys, confirming the high percentage of foundry returns in a charge did lower fluidity, and the effect was due to oxide films as identified by metallographic studies.

Fluidity to fill castings does start to be reduced because the entrained films can bridge dendrite meshes, and can bridge the entrance to narrow sections of castings, forming impenetrable barriers. Emamy (2009a,b) found that fluidity of his MMCs produced by vortex stirring was limited by oxides

introduced by the stirring process. The oxides, as bifilms of course, also reduced the mechanical properties of the cast mixtures.

It was found by Groteke (1985) that a filtered aluminum alloy was 20% more fluid than a 'dirty' melt. This finding was even more impressively confirmed by Adufeye (1997) who added a ceramic foam filter to the filling system of his fluidity mold. He expected to find a reduction in fluidity because of the added resistance of the filter. To his surprise, he observed on average approximately 100% increase of fluidity.

It seems, therefore, in line with common sense that the presence of films in the liquid causes filling problems for the casting. In particular, the entry of metal from thick sections into thin sections would be expected to require good-quality liquid metal, because of the possible accumulation and blocking action of the solids, particularly films, at the entry into the thin section. Thin sections attached to thick, and filled from the thick section, are in danger of breaking off rather easily as a result of layers of films across the junction. Metal flash on castings will often break off cleanly if there is a high concentration of bifilms in a melt. Flash adhering to a casting but which is resistant to be broken off because of its ductility might therefore be a useful quick test of the cleanness and resulting properties of the alloy. As an aside, an abrupt change of section, of the order of 10 mm down to 1 or 2 mm, is such an efficient film-concentrating location that it is a good way to locate and research the structure of films on fracture surfaces by simply breaking off the thin section. Bifilms are easily revealed and opened by this technique.

Dirty alloys suffer from a wide dispersion of sizes of inclusions. It is almost certainly the large films that are effective in bridging, and therefore blocking, the entrances to narrow sections. It is common to see that dirty melts produce castings free from flash, despite a relatively poor mold assembly resulting from ill-fitting cores. Conversely, the casting of clean metal produces a casting bristling with flash, and which bends rather than breaks. It is therefore a pain to get off. Good metal quality is going to require good tooling to obtain nicely fitting core assemblies.

After grain refinement additions to an aluminum melt the casting often exhibits significantly more flash. This is the result of the melt cleaning action. The heavy titanium-rich intermetallics precipitate on the oxide bifilms suspended in the melt and cause them to precipitate out, rapidly forming a layer of sludge on the bottom of the furnace or ladle. Thus the most important aspect of the grain refinement of Al alloys is the cleaning of the melt. This effect almost certainly exceeds the effect of grain refinement itself. There is no doubt, therefore, that the filling of extremely thin sections and fine detail is strongly dependent on the cleanness of the melt.

In support of this conclusion, it is known from experience, if not from controlled experiment, that melts of the common aluminum alloy Al-7Si-0.4Mg that have been subjected to treatments that are expected to increase the oxide content have suffered reduced fluidity as a result. The treatments include:

1. Repeated remelting of the same material;
2. High content of foundry returns (especially sand cast materials) in the charge;
3. The pouring of excess metal from casting ladles back into the bulk metal in the casting furnace, particularly if the fall height is allowed to be great;
4. Recycling in pumped systems where the returning melt has been allowed to fall back into the bulk melt (recirculating pumped systems that operate entirely submerged probably do not suffer to nearly the same extent, providing the air is not entrained from the surface);
5. Degassing with nitrogen from a submerged lance for an extended period of time (for instance a 1000-kg furnace subjected to degassing for several days).

These treatments, if carried out to excess, can cause the melt to become so full of dispersed films that the liquid assumes the consistency of a concrete slurry. As a consequence the fluidity is reduced. More serious still, the mechanical properties, particularly the ductility, of the resulting castings is nothing short of catastrophic.

Treatments of the melts to reduce their oxide content by flushing with argon, or treatments with powdered fluxes introduced in a carrier gas via an immersed lance, are reported to return the situation to normality. Much work is required to be carried out in this important area to achieve a proper understanding of these problems.

Finally, it seems likely that computer models, renowned for having to increase their viscosity values by a factor of up to 1000, achieve a more realistic flow simulation. This apparently shocking fudge seems likely to be the result of assuming a value for pure metals, but have to adjust the viscosity to that of a real metal, usually full of oxide bifilms. When we founders learn to cast purer melts the computer models will have to revert to the viscosity values for pure metals.

### 3.2.4 Effect of solidification time $t_f$

From Equation 3.1 it is clear that the greater the solidification time,  $t_f$ , the further the metal will run before freezing. This is a far more satisfactory way to improve the filling of castings than increasing the velocity, since control over surface turbulence is not necessarily lost.

For conditions in which the mold material controls the rate of heat loss from the casting, such as in sand casting, quoting Flemings (1963), the freezing time is approximately

$$t_f = \frac{\pi}{4K_m\rho_m C_m} \left\{ \frac{V}{A} \right\}^2 \left\{ \frac{\rho_s H}{(T_m - T_o)} \right\} \quad (3.3)$$

where symbols are defined in the appendix. Showman (2006) shows how small localized patches of lightweight aggregate of low heat diffusivity  $K_m\rho_m C_m$  in a sand mold can significantly extend fluidity, as expected from the above equation. These ‘patches’ are blown as cores, and incorporated into the mold by inserting them into the mold core boxes and blowing them integrally with the mold cores.

For conditions of freezing in chill molds where the interface resistance to heat flow is dominant, we may quote the alternative analytical equation for the freezing time due to Flemings

$$t_f = \rho_s H V / \{h(T_m - T_o)A\} \quad (3.4)$$

The main factors that increase  $t_f$  are clear in these equations. The factors are dealt with individually in the following subsections.

#### **Modulus**

Greaves in 1936 made the far-sighted suggestion that fluidity length was a function of modulus  $m$ .

The effect of the thickness, or shape of the channel, on the time of freezing of the metal in the channel, is nicely accounted for by Chvorinov’s rule (implicit in Equations 3.3 and 3.4). We can define the modulus  $m$  as the ratio ‘volume/cooling area’ of the casting, which is in turn of course equivalent to the ratio ‘area/cooling perimeter’ of the cross-section of a long channel. Remember that modulus has

dimensions of length, and is most conveniently quoted, therefore, in millimeters. Restating Equation 3.3 gives

$$t_f = k_m m^2 \quad (3.5)$$

The relation applies where the heat flow from the casting is regulated by the thermal conductivity of the mold (as is normal for a chunky casting in a reasonably insulating sand mold). The value of the constant  $k_m$  can be determined by experiment in some convenient units, such as  $\text{s mm}^{-3}$ . To gain some idea of the range of  $k_m$  in normal castings: for steel in green sand molds it is approximately 0.40; for Al-7Si alloys in dry sands it is 5.8; and for Al-3Cu-5Si it is  $11.0 \text{ s mm}^{-3}$ . It is worth noting that Equation 3.5 applies nicely to chunky castings in sand molds, and other reasonably insulating molds such as investment molds.

For the case where interfacial heat transfer dominates heat flow, as in chill molds, or thin-walled sand castings, Equation 3.4 becomes

$$k_f = k_i m / h \quad (3.6)$$

where  $k_i$  is a constant, and  $h$  is the rate of flow of heat across the air gap for a given temperature difference across the gap, and for a given area of interface. The parameter  $h$  is known as the heat-transfer coefficient. We shall see later how  $h$  starts to dominate in thin section castings, so that Equation 3.6 is often found to apply not only to chill castings but also to thin section sand castings.

In his experiments on sand molds, Feliu (1964) appeared to find a relation between fluidity and (modulus)<sup>3/2</sup> for thin section sand castings in the range 0.7–2 mm modulus (section thickness 1.4–4 mm). However, he did not allow for the effect of surface tension in reducing the effective head of metal. When this is allowed for, as will be illustrated in the exercise in the following section, it indicates that a linear relation between fluidity and section thickness as suggested by Equation 3.6 actually applies reasonably well. Barlow (1970) confirms that over a range of Pyrex tubes from 1–4 mm diameter the fluidity of both Al-10Si and Cu-10Al is closely linear with channel section.

Restating Equation 3.1 in terms of the relations 3.5 and 3.6, we have for sand molds

$$L_f / m = k V m \quad (3.7)$$

and for dies (and thin section sand molds)

$$L_f / m = k' V / h \quad (3.8)$$

We now have two simple but powerful formulae to assist in the prediction of whether a mold will fill. Interestingly, it seems that Equation 3.8 has rather general validity. Clearly, interfacially controlled heat flow is rather more common than is generally thought, especially in thin sections, where freezing times are short.

Applying Equation 3.8 to thin-walled sand castings shows that the ratio of fluidity to modulus,  $L_f / m$ , is a constant for a given mold material. For instance in Al alloys cast into thin-section sand molds, shop floor experience indicates the *fluidity to section thickness* ratio is around 100 (i.e. a section thickness of 4 mm should allow the metal to flow 400 mm prior to arrest by freezing). This is a really useful relation. For instance, if the ratio of thickness to distance to be run is only 50 the casting is no problem to make. When the ratio is 100 the casting is not to be underestimated; it is near the limits. When the ratio is 150 the casting cannot be made by flowing metal through the mold cavity from a single gate entry point; a completely different filling system is required. This is therefore a useful



guide as a quick check which can be made at the drawing stage as to whether a design of casting might be castable or not. We can restate the critical *fluidity to section thickness ratio* = 100 in terms of the more universal *fluidity to modulus ratio* = 200, allowing us to transfer this useful ratio to any shape of interest to a fair approximation.

The value of the concept of modulus,  $m$ , is that any shape of channel can be understood and compared with any other shape. For instance, straight tubes can be compared with trapezoidal spirals, or with thin flat strips. All that matters for the control of solidification time is the modulus (we are neglecting for the moment the refinements that allow for the slight inaccuracies of the simple modulus approach).

### **Heat transfer coefficient**

A reduction in the rate of heat transfer will benefit fluidity (as will become clearer when we look into the relation between the rate of heat transfer and the rate of solidification in Chapter 4). For this reason insulating ceramic coatings are applied to all gravity and low-pressure dies. The work of Rivas and Biloni (1980) illustrates the benefit to fluidity from the application of a white-oxide-based coating to a steel die. This is confirmed by Hiratsuka et al. (1994) from work in which metal is drawn into tubes of quartz, copper, and stainless steel.

For sand molds, acetylene black is applied from a sooty flame (Flemings et al. 1959) giving very substantial increases in fluidity, by a factor of 2 or 3. This dramatic improvement in fluidity is used in some precision sand foundries, allowing thin-walled castings to be filled that could not otherwise be cast. Similar results are reported for permanent mold foundries casting Al alloys and casting cast irons. Although attempts have been made to develop other fluidity-enhancing coatings, none has even approached a similar effectiveness. However, the unfortunate greasy black pollution caused by the soot in the foundry is unwelcome, causing the whole foundry environment to become blackened by soot. However, this severe disadvantage continues to be tolerated whilst alternatives are unavailable, since many castings cannot be filled without this practice.

The action of the carbon deposit was for many years thought to be an insulating effect; the carbon acting to reduce the heat transfer coefficient. This is now known not to be true as explained later.

### **Superheat**

Increases in casting temperature benefit fluidity in a direct way, as shown for example in Figures 3.14–3.17 and many other examples in this book. In fact, all investigations of fluidity have confirmed that the fluidity increases linearly with the superheat (defined here as the excess of casting temperature over liquidus temperature).

The effect of superheat is therefore valuable in itself. In addition, however, it can help us to understand the special fluid properties of eutectics, and the poor flow capabilities of most high-melting-point intermetallics as explained earlier in this section.

As a reminder, in Figure 3.6 obtained by Lang (1972) for the Al–Zn system, at constant superheat the fluidity of the eutectic is almost exactly that expected from the rule of mixtures, interpolating between the fluidities of the pure elements Al and Zn. (A rule of mixtures would have predicted the fluidity of the pure elements and the eutectic to lie on a straight line.) When determined at a constant temperature of 700°C, however, the eutectic now has the advantage of a large effective superheat, and the fluidity of the eutectic is correspondingly enhanced, becoming significantly higher than that of either Al or Zn as explained in the derivation of Figure 3.8.

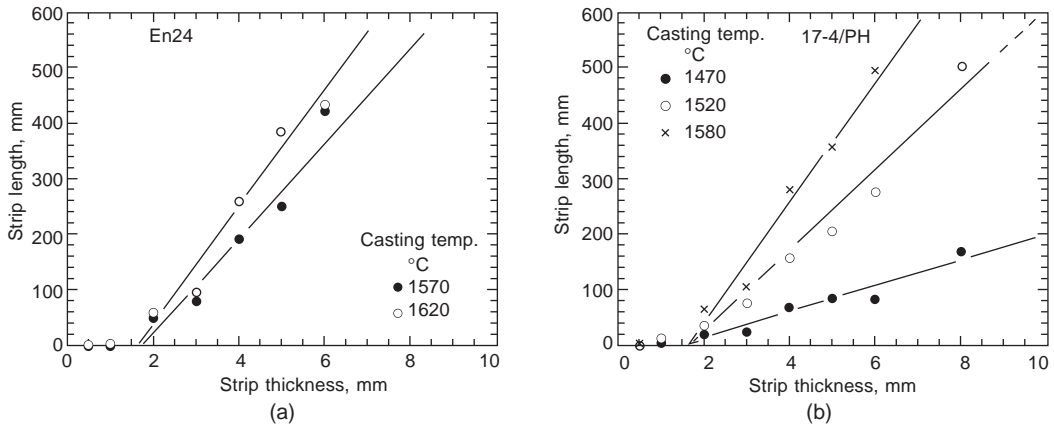


**FIGURE 3.14**

(a) Fluidity data for a low-alloy steel; and (b) a stainless steel poured in a straight-channel, furan-bonded sand mold (Boutorabi et al. 1990).

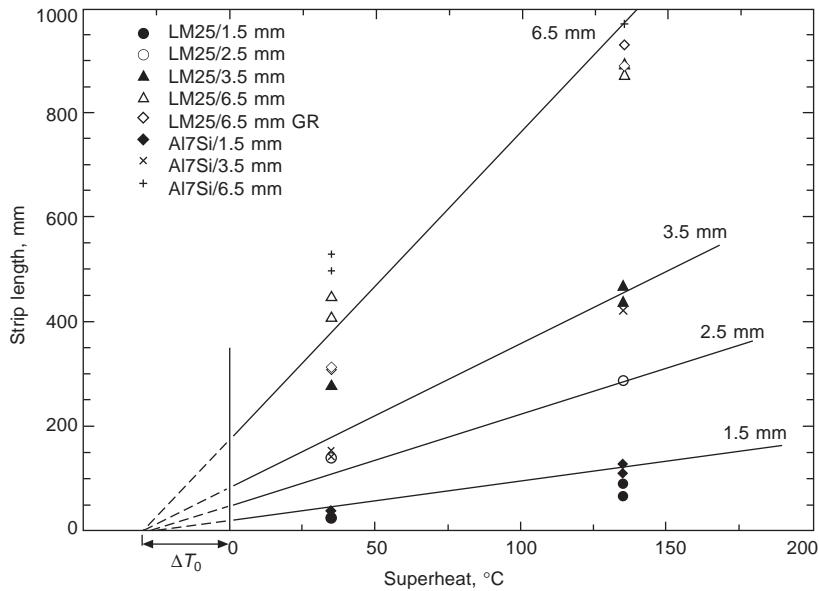


**FIGURE 3.15**

Fluidity of a variety of Al-7Si alloys, one grain refined (GR), showing linear increase with section thickness and casting temperature (Boutorabi et al. 1990).

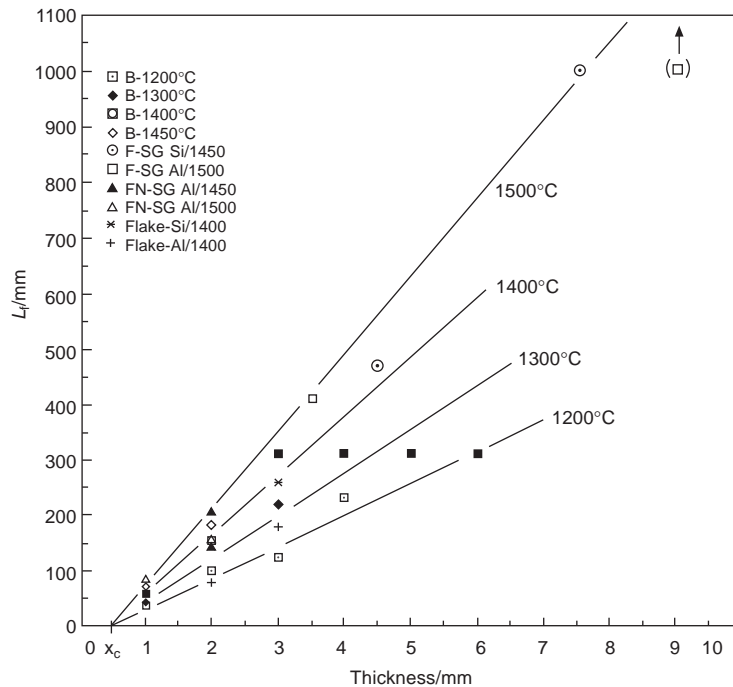


**FIGURE 3.16**

Fluidity of a variety of gray and ductile irons showing linear increase with section thickness and casting temperature (Boutorabi et al. 1990).

### Latent heat $H$

The latent heat given up on solidification will take time to diffuse, thereby delaying solidification, and extending fluidity. Much has been made of this point (see for instance Arnold et al. 1963) in explaining the claims for the good fluidity of the hypereutectic Al–Si alloys since pure silicon has a latent heat of solidification 4.65 times greater than that of aluminum (data from Brandes 1992).

Equation 3.3 is not likely to be particularly accurate. Nevertheless, when used in a comparative way, it is likely to give somewhat better results. Thus to find the improvement, for instance, in changing from pure Al to pure Si, we can see that the comparative freezing times are simply given by the ratio

$$\frac{t_{\text{Si}}}{t_{\text{Al}}} = \left\{ \frac{T_{\text{Al}} - T_0}{T_{\text{Si}} - T_0} \right\}^2 \left\{ \frac{\rho_{\text{Si}}}{\rho_{\text{Al}}} \right\}^2 \left\{ \frac{H_{\text{Si}}}{H_{\text{Al}}} \right\}^2 \quad (3.9a)$$

$$= \{0.460\}^2 \times \{0.867\}^2 \times \{4.65\}^2 \quad (3.9b)$$

$$= 3.4 \quad (3.9c)$$

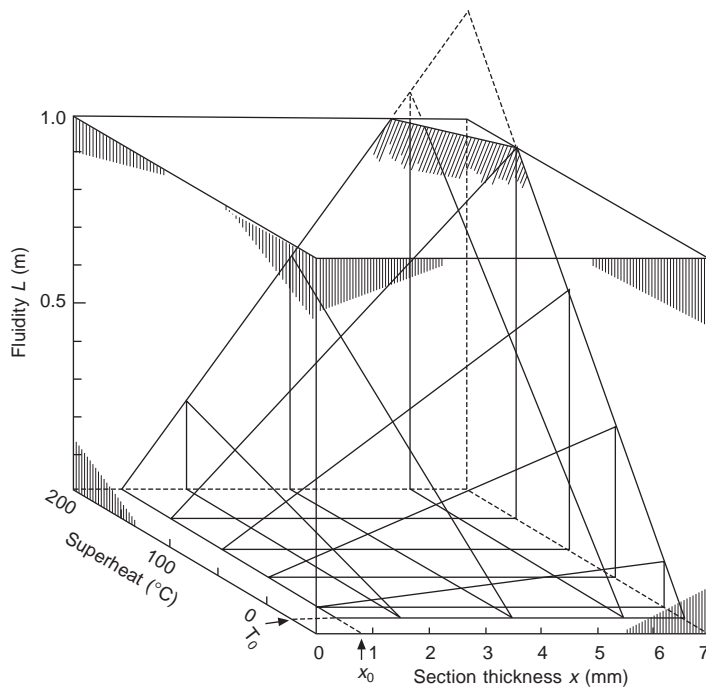


**FIGURE 3.17**

Fluidity results for Al–7Si alloys from Figure 3.1 re-presented in three-dimensional format.

Thus from Equation 3.9b, pure Si would have been expected to have 22 times the fluidity of pure aluminum as a result of its higher latent heat. However, silicon’s rate of heat loss, seen to be five times faster as a result of its higher freezing temperature, reduces this significantly. The low density of silicon also reduces the effect somewhat further. The final result, Equation 3.9c, is that pure silicon would be expected to deliver effectively 3.4 times the fluidity of pure aluminum. (Rather paradoxically, this conclusion will only be accurate at low concentrations of Si in Al because the other terms in Equation 3.3 then are not significantly changed, and thus properly cancel to give Equation 3.9 accurately.)

We can now construct a relation to examine the effect of the latent heat of Si on the fluidity of Al–Si alloys in sand molds as in Figure 3.18. It is clear that although the upward trend assignable to the latent heat effect is noticeable, the real contribution to the increased fluidity of the so-called hypereutectic alloys is mainly the result of the move of the equilibrium eutectic to higher Si content corresponding to a non-equilibrium eutectic. This conclusion appears to be supported by additional data by Lang (1972) in which he studies the effect of the addition of Na to the alloys. This stabilizes the eutectic, and creates clear peaks corresponding to an effective eutectic at approximately 14.5%Si, significantly higher than the expected equilibrium eutectic near 11.5%Si. The existence of a maximum in fluidity at about 14.5%Si has been confirmed by a number of researchers, for instance Pan and Hu (1996) and Adefuye (1997). In addition, the presence of a peak can be interpolated in the work of Parland (1987) who missed the peak, but whose data points on either side corroborate its existence.

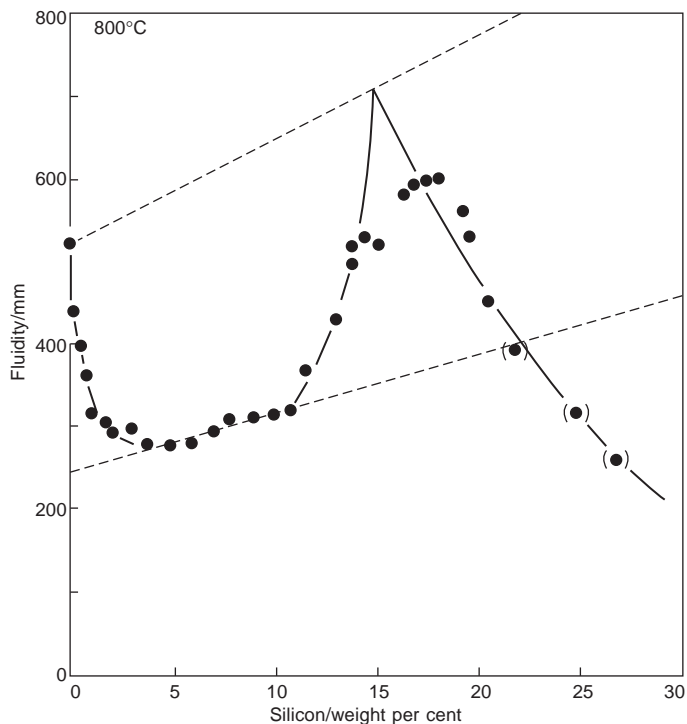


**FIGURE 3.18**

Fluidity of Al–Si alloys showing the theoretical increase in fluidity as Si is increased, as a result of the high latent heat of freezing of Si. Experimental data from Lang (1972). The fall at high Si is uncertain mainly as a result of working with Al alloys at unusually high temperatures.

The fall in fluidity at higher Si levels seems doubtful. Some authors find this (e.g. Pan and Hu) but others find the good fluidity to be maintained (e.g. Adefuye and the result on the Al–Cu–Si system in Figure 3.10 showing that the maximum is not a cuspid peak but merely a change of slope). Such discrepancies are probably to be expected when working at such high superheats in this difficult range of the Al–Si system. In particular, the rapid formation of oxides would be a troubling problem.

The undercooling behavior of this eutectic, encouraging the simultaneous precipitation of both aluminum dendrites and primary silicon, are probably additional complications. Further work is clearly required to clarify the behavior of this important eutectic system.

The use of the extraordinary Al–17Si alloy, developed around 1970 under the leadership of John Jorstad in the USA, with phosphorus additions to aid the nucleation of primary silicon particles, is well known for its use on automotive engine blocks, even though less use has been made of the alloy for blocks than it appears to deserve. It has, however, found many other uses for which it was never designed, and for which it is not perhaps really optimum, for instance for gearbox housings and other castings as a probable result of its availability (Jorstad 1996). The more rational use of this and other alloys would be welcome.

It is a further curious illogicality that most of the common Al–Si casting alloys are in the range of 4–10%Si, and are therefore concentrated in the region of mediocre fluidity properties between the high fluidity of pure Al and the high fluidity of the non-equilibrium eutectic (see below). Contrary to the claims of practically every writer on this subject, it is quite clear that the silicon *reduces* the fluidity at these intermediate compositions. (Almost certainly a confusion has arisen with the well-known, but less easily defined concept of *castability*. The improved castability of Al–Si alloys is probably a result of the benefits of their greater quantity of eutectic, and possibly a more benign oxide film, compared to many other Al alloy systems. Again, more research to clarify the contributions of these factors would be really helpful.)

The real benefit of silicon in relation to fluidity is only seen nearer to 14.5%Si, and possibly above, corresponding, probably, to the composition of the non-equilibrium eutectic. It is possible to modify these so-called hypereutectic alloys with sodium or strontium to stabilize the eutectic form of the silicon (avoiding the usual addition of phosphorus, and so avoiding the usual chunky primary silicon particles that give difficulties for machining). However, these compositions have not yet been promoted by suppliers nor have they been taken up by the users (Smith 1981).

In an interesting parallel with Zn-rich alloys from the Zn–Al–Cu system, as mentioned above, Friebel and Roe (1963) point out from their fluidity results that the commonly used pressure die casting alloys at 4%Al hardly benefit from the huge fluidity peak at 5%Al, whereas the famous ZA series alloys with 8, 12, and 27%Al all have completely missed all trace of benefit, and consequently have only mediocre flow properties. The ZA series have clearly sacrificed fluidity for strength, but the pressure die casting alloys have no such excuse; for their market, targeted at the manufacture of castings requiring intricate detail, they simply have a really disappointing non-optimum composition.

From time to time I cannot help reflecting on the irony that the great interest in fluidity exhibited by foundry people and researchers is curiously at odds with alloy users, who persist in ignoring the huge benefits in fluidity on offer at no cost, but perversely select and continue to use alloys exhibiting the most mediocre of flow properties.

Even in the twenty-first century, it seems that casting compositions with promise of good fluidity, mechanical properties, and machinability, remain to be properly developed. They promise exciting potential. The challenge will be to sell these substantial benefits to the conservative customer.

### ***Mold temperature***

For most casting processes mold temperature is fixed at or close to room temperature. For such processes, there is little or nothing that can be done to mold temperature to affect fluidity. Although many molds for irons and steels are surface dried prior to casting, the relatively small rise in temperature is unlikely to benefit fluidity (even though it is vital for reduction of volatile gases of course).

The intermediate temperatures of gravity and high-pressure dies, usually at around 300–400°C, do contribute modestly to the increase of fluidity in these casting processes. Die temperatures are sometimes raised a little to gain a little extra filling capability. However, the natural working temperature of a die is only changed by a significant, and therefore unpopular, technical effort.

However, for investment casting the ceramic shell allows a complete range of temperatures to be chosen without difficulty. From Equation 3.3 it is seen that the freezing time is proportional to the difference between the freezing point of the melt and the temperature of the mold. The few

tests of this prediction are reasonably well confirmed, for instance by Campbell and Olliff in 1971 (Figures 3.19–3.21).

One important prediction is that when the mold temperature is raised to the melting point of the alloy, the fluidity becomes infinite; i.e. the melt will run for ever! Actually of course, this self-evident conclusion needs to be tempered by the realization that the melt will run until stopped by some other force, such as gravity, surface tension, or the mold wall! All this corresponds to common sense. Even so, this elimination of fluidity limitations is an important feature widely used in the casting of thin-walled aluminum alloy investment castings, where it is easy to cast into molds held at temperatures in excess of the freezing point of the alloys at approximately 600°C. Single crystal turbine blades in nickel-based alloys are also cast into molds heated 1450°C or more, again well above the freezing point of the alloy.

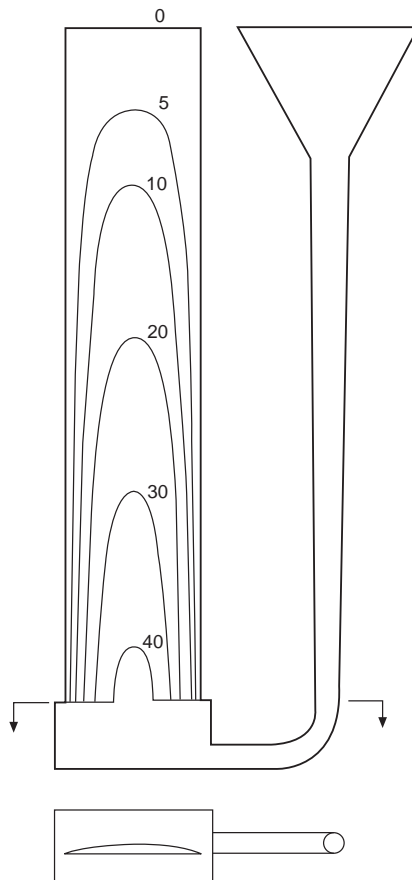


**FIGURE 3.19**

Aerofoil fluidity test for investment casting. The outlines of the cast shape are computed for increasing values of  $\gamma/\rho gh$ , units in millimeters (Campbell and Olliff 1971).

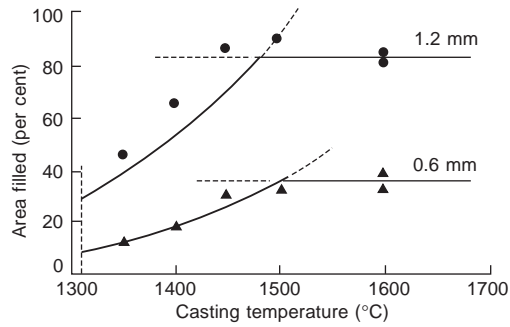


**FIGURE 3.20**

Results from the aerofoil test for an Ni-base superalloy. Lines denote theoretical predictions; points are experimental data.

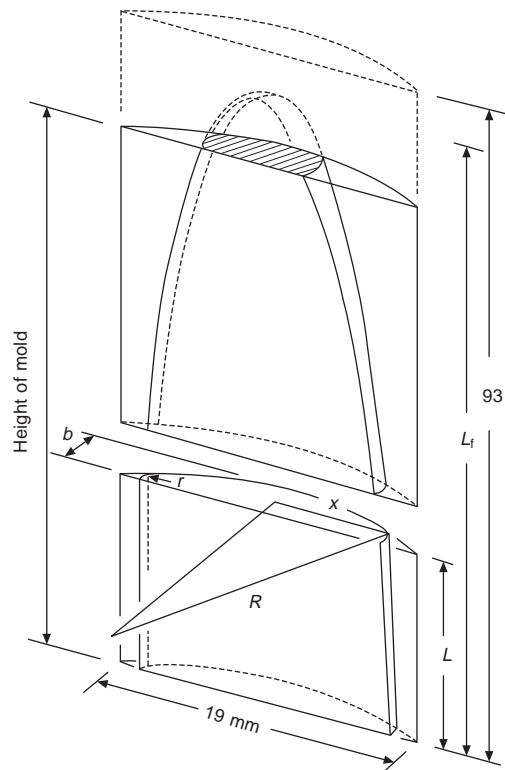


**FIGURE 3.21**

Geometry of a typical aerofoil cast test piece.



Any problems of fluidity are thereby avoided. Having this one concern removed, the founder is then left with only the dozens of additional important factors that require to be controlled for the success of the casting. Solving one problem completely is a valued step forward, but still leaves plenty of challenges for the casting engineer!

### 3.2.5 Effect of surface tension

If metals wetted the molds into which they were cast, then the metal would be drawn into the mold by the familiar action of capillary attraction, as water wets and thus climbs up a narrow-bore glass tube.

In general, however, metals do not wet molds. In fact mold coatings and release agents are designed to resist wetting by metals. Thus the curvature of the meniscus at the liquid metal front leads to capillary repulsion; the metal experiences a back pressure resisting entry into the mold. The back pressure due to surface tension,  $P_{ST}$ , can be quantified by the simple relation, where  $r$  and  $R$  are the two orthogonal radii which characterize the local shape of the surface, and  $\gamma$  is the surface tension

$$P_{ST} = 2\gamma\{(1/r) + (1/R)\} \quad (3.10)$$

When the two radii are equal,  $R = r$ , as when the metal is in a cylindrical tube, then the liquid meniscus takes on the shape of a sphere of radius  $r$ , and Equation 3.10 takes on the familiar form

$$P_{ST} = 2\gamma/r \quad (3.11)$$

Alternatively, if the melt is filling a thin, wide strip, so that  $R$  is large compared with  $r$ , then  $1/R$  becomes negligible and back pressure becomes dominated by only one radius of curvature,  $r$ , since the liquid meniscus now approximates the shape of a cylinder

$$P_{ST} = \gamma/r \quad (3.12)$$

At the point at which the back pressure due to capillary repulsion equals or exceeds the hydrostatic pressure,  $\rho gh$ , to fill the section, the liquid will not enter the section. This condition in the thin, wide strip is

$$\rho gh = \gamma/r \quad (3.13)$$

This simple pressure balance across a cylindrical meniscus is useful to correct the head height, to find the net available head pressure for filling a thin-walled casting. In the case of the filling of a circular section tube (with a spherical meniscus) do not forget the factor 2 for both the contributions to the total curvature as in Equation 3.11. In the case of an irregular section, an estimate may need to be made of both radii, as in Equation 3.10.

The effect of capillary repulsion, repelling metal from entering thin sections is clearly seen by the positive intercept in Figure 3.14 for a medium alloy steel and a stainless steel, in Figure 3.16 for cast iron, and in Figure 3.22 for a zinc alloy. Thus the effect appears to be quite general, as would be expected. The effective surface tension can be worked out in all these cases from an equation such as 3.13. In each case it is found to be around twice the value to be expected for the pure metal in a vacuum. Again, this high effective value is to be expected as explained in Section 3.1.1.

In larger round or square sections, where the radii  $R$  and  $r$  both become large, in the range of 10–20 mm, the effects of surface tension become sufficiently small to be neglected for most purposes. Large sections are therefore filled easily.

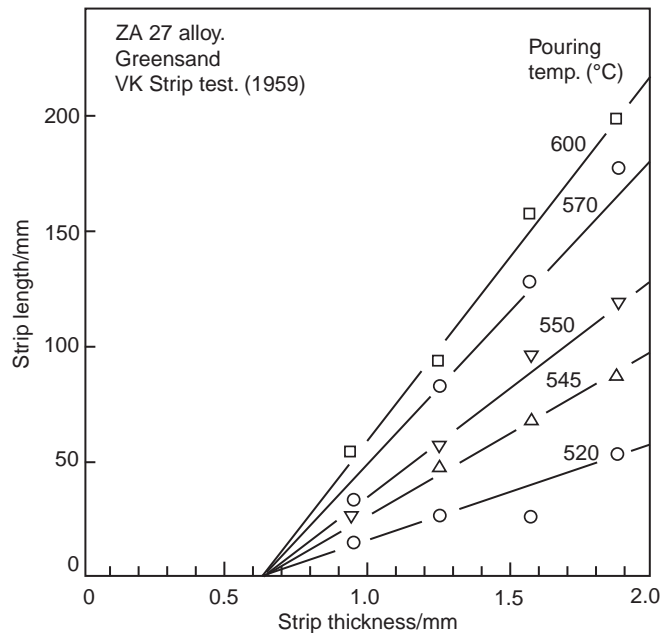


**FIGURE 3.22**

Fluidity of Zn–27Al alloy cast in greensand using the VK fluidity strip test (data from Sahoo and Whiting 1984).

### ***Flowability and fillability***

In the filling of many castings the sections to be filled are not uniform; the standard complaint in the foundry is ‘the sections are thick and thin’. This does sometimes give its problems. This is especially true where the sections become so thin in places that they become difficult to fill because of the resistance presented by surface tension. Aerofoils on propellers and turbine blades are typical examples.

To investigate the filling of aerofoil sections that are typical of many investment casting problem shapes, an aerofoil test mold was devised as shown in Figure 3.19. (This test mold also included some tensile test pieces whose combined volume interfered to some extent with the filling of the aerofoil itself; in later work the tensile test pieces were removed, giving considerably improved reproducibility of the fluidity test.)

Typical results for a vacuum-cast nickel-based superalloy are given in Figure 3.20 (Campbell and Olliff 1971). Clearly, the 1.2-mm section fills more fully than the 0.6-mm section. However, it is also clear that at low casting temperature the filling of both sections is limited by the ability of the metal to flow prior to freezing. At these low casting temperatures the fluidity improves as temperature increases, as expected.

However, above a metal casting temperature of approximately 1500°C further increases of temperature do not further improve the filling. As the metal attempts to enter the diminishing sections of the mold, the geometry of the liquid front is closely defined as a simple cylindrical surface. Thus it is not difficult to calculate the thickness of the mold at any point. Half of this thickness is taken as the radius of curvature of the liquid metal meniscus (Figure 3.21). It is possible to predict, therefore, that

the degree of filling is dictated by the local balance at every point around the perimeter of the meniscus between the filling pressure due to the metal head, and the effective back pressure due to the local curvature of the metal surface. In fact, if momentarily overfilled because of the momentum of the metal as it flowed into the mold, the repulsion effect of surface tension would cause the metal to ‘bounce back’, oscillating either side of its equilibrium filling position, finally settling at its balanced, equilibrium state of fullness.

The authors of this work emphasize the twin aspects of filling such thin sections; *flowability* limited by heat transfer, and *fillability* limited by surface tension.

At low mold and/or metal temperatures, the first type of filling, flowability, turns out to be simply classical fluidity as we have discussed above. Metallographic examination of the structures of aerofoils cast at lower temperatures shows columnar grains grown at an angle into the direction of flow, typical of solidification occurring whilst the metal was flowing. The flow length is controlled by solidification, and thus observed to be a function of superheat and other thermal factors, as we have seen.

The second type of filling, fillability, occurs at higher mold and/or metal temperatures where the heat content of the system is sufficiently high that solidification is delayed until after filling has come to a stop. Studies of the microstructure of the castings confirm that the grains are large and randomly oriented, as would be expected if the metal were stationary during freezing. Filling is then controlled by a mechanical balance of forces. The mode of solidification and further increases of temperature of the metal and the mold play no part in this phase of filling.

In a fluidity test of simpler geometry consisting of straight strips of various thickness, the linear plots of fluidity  $L_f$  versus thickness  $x$  and superheat  $\Delta T_s$  are illustrated in Figures 3.15 and 3.16 for Al-7Si alloy and cast iron in sand molds. It is easy to combine these plots giving the resultant three-dimensional pyramid plot, as is shown for the Al alloy data in Figure 3.17. In terms of the pressure head  $h$ , and the intercepts  $\Delta T_0$  and  $x_0$  defined on fluidity plots 3.15 and 3.16, the equation describing the slightly skewed surface of the pyramid is

$$L_f = C(\Delta T_s + \Delta T_0)(x - (2\gamma/\rho gh)) \quad (3.14)$$

where  $C$  is a constant with dimensions of reciprocal temperature. For the Al alloy,  $C$  is found from Figure 3.15 to have a value of about  $1.3 \pm 0.1 \text{ K}^{-1}$  and  $\Delta T_0 = 30 \pm 5 \text{ K}$ . The surface tension of pure liquid Al is close to  $1.0 \text{ Nm}^{-1}$  but is seen in this work to be effectively  $\gamma = 2 \text{ Nm}^{-1}$  because of the contribution of oxide film to the surface tension. Other values are  $\rho = 2500 \text{ kg m}^{-3}$ ,  $g = 10 \text{ ms}^{-2}$  and  $h = 0.10 \text{ m}$ . We can then write an explicit equation for fluidity (mm) in terms of superheat (degrees Celsius) and section thickness (mm)

$$L_f = 1.3(\Delta T_s + 30)(x - 1.6)$$

For a superheat  $\Delta T_s = 100^\circ\text{C}$  and section thickness  $x = 2 \text{ mm}$  we can achieve a flow distance  $L_f = 68 \text{ mm}$  for Al-7Si in a sand mold. If the head  $h$  were increased, fluidity would be higher, as indicated by Equation 3.14 (but noting the limitations discussed in Section 3.2.2).

As we have seen, in these thin-section molds both heat transfer and surface tension contribute to limit the filling of the mold, their relative effects differ in different circumstances. This action of both effects causes the tests to be complicated, but, as we have seen, not impossible to disentangle. Further practical examples of the simultaneous action of heat transfer and surface tension will be considered in Section 3.2.7.

### 3.2.6 Effect of an unstable substrate

In 1980 Southin and Romeyn investigated the amazing benefit to fluidity that followed from the blackening of molds by the soot of a lazy acetylene flame, and the similar benefit from painting the mold with a hexachlorethane-containing coating. They found a complicated behavior. For aluminum alloys up to 1%Cu the use of carbon black or hexachlorethane mold coatings *reduced* the fluidity because the planar (or cellular) growth front appeared to be stable, so that the strong, compact freezing front easily stopped the flow at an early stage as a result of an *enhanced* thermal transfer of the carbon coating. However, at higher copper contents the fluidity was increased because the dendritic front was fragmented by the flow, and the dendritic fragments were carried along in the flowing stream, giving a fine grain size and good fluidity.

The authors suggested that these results were only explained if (i) the rate of heat transfer was *increased*; and (ii) the coating mechanically destabilized the growing dendrites. This action was thought to occur by the unstable support of the growing dendrites, because of the mechanical collapse of the coating as the heavy melt ran over the fragile carbon deposit, probably aiding the oxidation of this fluffy deposit so as to further weaken support. The collapse of the substrate on which the dendrites were growing would destabilize, recrystallize, and release dendrites. The release mechanism is probably that proposed by Vogel, Doherty, and Cantor (1977) in which, after the plastic deformation at the dendrite root, recrystallization would occur, with the result that the newly formed high-angle grain boundary that formed across the root was favorably wetted and therefore penetrated by the melt, allowing the dendrite to detach. Thus instead of the dendrites growing into the stream to obstruct its flow, they were released to tumble along with the stream. The increased rate of heat loss, although usually reducing fluidity, was in this case more than countered by the effect of the undermining of the dendrite barrier.

Cupini and Prates (1977) similarly investigated the effect of hexachlorethane mold coatings. The release of chlorine from the breakdown of this chemical was found to refine the grain size of 99.44Al from the range of between 2 and 20 mm down to 0.2 mm. The effect seemed to be the result of the microscopic disturbance of the surface of the casting, where the dendritic grains were starting to grow, in general supporting the work by Southin and Romeyn, although they did not go on to study the fluidity of the alloy.

The work by Southin and Romeyn seems to me to be critical to the proper understanding of the fluidity of long-freezing-range alloys. In Section 3.2.1 the standard assumption was the long-freezing alloys arrest flow when the grains in the partly molten slurry start to impinge to form a solid network. We are now in a position to reassess this theory.

Southin and Romeyns' work shows that the real blockage to flow is not the cluster of equiaxed grains near the flow front (Figure 3.3b), but the forest of fixed dendrites (Figure 3.3c), probably growing roughly in the same geometrical envelope as the solidification front of the short freezing range alloys (Figure 3.3a).

It seems that the real scenario is that arms are melted off the dendrites and so tumble along with the stream, but while tumbling freely along do not constitute any serious threat to fluidity. Although such a slurry will have high effective viscosity, as we have seen, viscosity has very little effect on fluidity. These tumbling grains are swept more or less effortlessly along the central channel and conveyed to the front of the flow where they have been thought to block further flow when their density rose sufficiently high. Thus the equiaxed grains immediately behind the flow tip, studied by experimenters for

years on the assumption they constituted the blockage, appear to be largely irrelevant as obstacles to flow. I summarize what seems to be a more realistic model of flow blockage in Figure 3.3c.

The carbon blacking technique is widely used in precision sand foundries casting thin-walled parts in aluminum and magnesium alloys. However, the author has also seen its use for the casting of cast iron in gray cast iron molds, coated with a zircon wash, followed by a topping of carbon black from an acetylene flame. Incidentally, the technique of blacking molds and cores in this way requires good local extraction of smoke. Otherwise, after a year or so, the whole foundry simply goes a deeper shade of black.

Apparent evidence put forward from time to time that grain refinement increases fluidity (e.g. Alsem 1992) is not straightforwardly understood. This is because the addition of grain refiners might, if anything, increase the solids content of the flowing melt and so reduce fluidity. However, the cleaning effect of grain refinement, causing the Ti and B intermetallics to precipitate on bifilms in the furnace or ladle, causing the bifilms to drop out of suspension prior to casting is probably the overriding factor (Tiryakioglu and Campbell 2007). The clean melt, unhindered by its normal population of bifilms, can now flow more freely (mechanical properties of the casting are also increased, of course, but the grain-refining action would be expected to be only a small contributor to this improved performance).

### 3.2.7 Comparison of fluidity tests

Kondic (1959) proposed the various thin-section cast strip tests (called here the Voya Kondic (VK) Strip Test) as an alternative fluidity test because it seemed to him that the spiral test was subject to unacceptable scatter (Betts and Kondic 1961).

There has been some justification for these concerns, since the effect of pouring head, and sprue shape, among other parameters, were never well optimized. This situation continues to this day, although workers in Norway (Sabatino 2005, 2006) have made some progress to improve the specification of the test.

For a proper interpretation of all types of strip or spiral test results they need to be corrected for the back pressure due to surface tension at the liquid front. As we have seen, this effectively reduces the available head pressure applied from the height of the sprue. The resulting cast length will correspond to that flow distance controlled by heat transfer, appropriate to that effective head and that section thickness. These results are worked through as an example below.

Figure 3.22 shows the results by Sahoo and Whiting (1984) on a Zn–27Al alloy cast into strips, 17 mm wide, and of thickness 0.96, 1.27, 1.58, and 1.88 mm.

The results for the ZA27 alloy indicate the minimum strip thickness that can be entered by the liquid metal using the pressure head available in this test is  $0.64 \pm 0.04$  mm. Using Equation 3.13, assuming that the metal head is close to 0.1 m,  $R = 17/2$  mm and  $r = 0.64/2$  mm, and liquid density close to  $5720 \text{ kg m}^{-3}$ , we obtain the effective surface tension  $\gamma = 1.90 \text{ Nm}^{-1}$ . (If the  $R = 17/2$  curvature is neglected, the surface tension then works out to be  $1.98 \text{ Nm}^{-1}$  and therefore is negligibly different for our purpose.) This is an interesting value, over double that found for the surface tension of pure Zn or pure Al. It almost certainly reflects the presence of a strong oxide film.

It suggests that the liquid front was, briefly, held up by surface tension at the entry to the thin sections, so that an oxide film was grown that assisted to hold back the liquid even more. The delay is typical of castings where the melt is given a choice of routes, but all initially resisting entry, so that the

sprue and runner have to fill completely before pressure is raised sufficiently to break through the surface oxide. If the melt had arrived without any choice, and without any delay to pressurization, the melt would probably have entered with a resistance due only to surface tension. In such a condition,  $\gamma$  would be expected to have been close to  $1.0 \text{ Nm}^{-1}$ .

It suggests that, to be safe, values of at least double the surface tension be adopted when allowing for the possible loss of metal head in filling thin-section castings.

The ability to extrapolate back to a thickness that will not fill is a valuable feature of the VK Fluidity Strip Test. It allows the estimation of an effective surface tension. This cannot be derived from tests, such as the spiral test, that only uses one flow channel. The knowledge of the effective surface tension is essential to allow the comparison of the various fluidity tests that is suggested below.

The data from Figure 3.22 are cross-plotted in Figure 3.23a at notional strip thickness of 1.0, 1.5, and 3.0 mm. (These rounded values are chosen simply for convenience of reporting. The accurate values were employed for calculation purposes.) The individual lengths in each section have been plotted separately, not added together to give a total as originally suggested by Kondic. (Totalling the individual lengths seems to be a valid procedure, but does not seem to be helpful, and simply adds to the problem of disentangling the results.) Interestingly all the results extrapolate back to a common value for zero fluidity at the melting point for the alloy,  $490^\circ\text{C}$ . This is a surprising finding for this alloy. Most alloys extrapolate to a finite fluidity at zero superheat because the metal still takes time to give up its latent heat, allowing the metal time to flow. The apparent zero fluidity at the melting point in this alloy requires further investigation.

Also shown in Figure 3.23a are fluidity spiral results. An interesting point is that despite his earlier concerns, I am sure VK would have been reassured that the percentage scatter in the data was not significantly different to the percentage scatter in the strip test results.

The further obvious result from Figure 3.23a shows how the fluidity length measurements of the spiral are considerably higher than those of the strip tests. In a qualitative way this is only to be expected because of the great difference in the cross-sections of the fluidity channels. We can go further, though, and demonstrate the quantitative equivalence of these results.

In Figure 3.23b, the spiral and strip results are all reduced to the value that would have been obtained if the spiral and the strip tests all had sections of  $2 \text{ mm} \times 17 \text{ mm}$ .

This is achieved by reducing the spiral results by a factor 4.44 to allow for the effect of surface tension and modulus, making the results equivalent to those in the 2-mm-thick cast strip. The 2-mm section results remain unchanged of course. The 1.5 and 1.0 mm results are increased by factors of 1.75 and 4.12, respectively. These adjustment factors are derived below.

Taking Equation 3.1 (Equation 3.2 can be used in its place, since we are about to take ratios), together with Equations 3.6 and 3.7, and remembering that the velocity is given approximately by  $(2gH)^{1/2}$  then we have for sand molds

$$\begin{aligned} L_f &= km^n (2gH)^{1/2} \\ &= km^n (2g(H - (\gamma/r\rho g)))^{1/2} \end{aligned} \quad (3.15)$$

where  $n$  is 1 for interface controlled heat flow, such as in metal dies and thin sand molds, and  $n$  is 2 for mold control of heat flow, such as in thick sand molds.

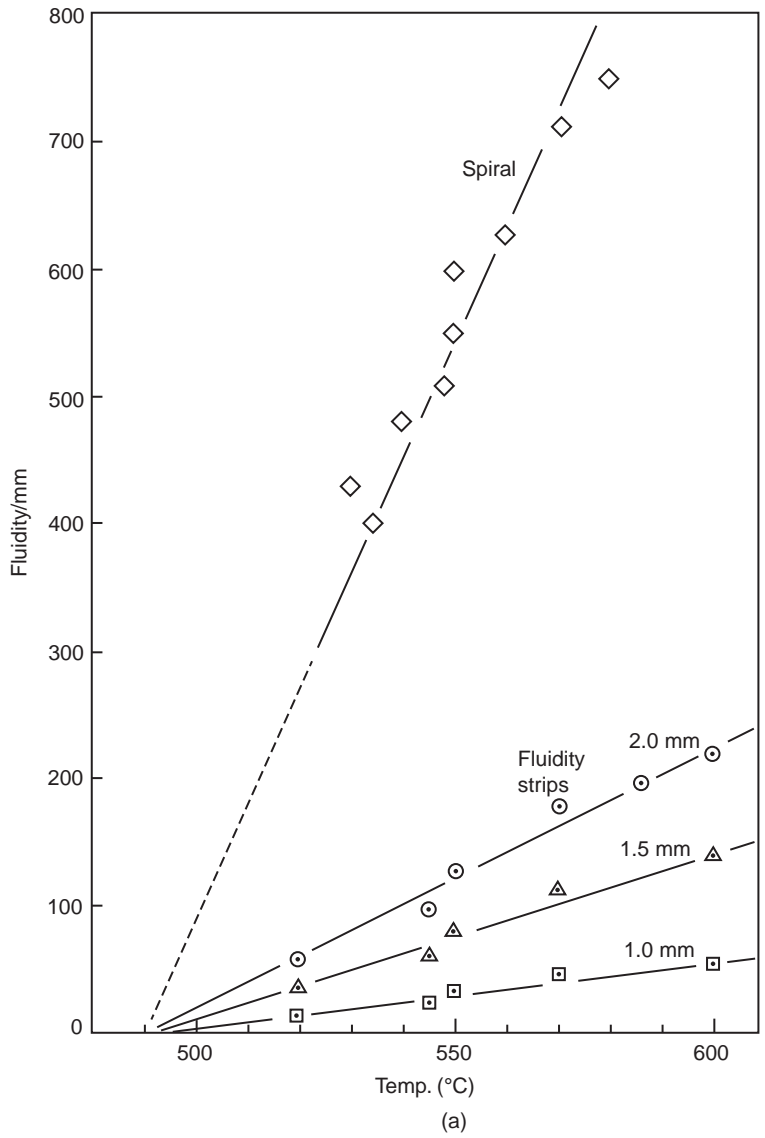


FIGURE 3.23

(a) Results from Figure 3.22 replotted to show the effect of superheat explicitly, as though from strips of thickness 1.0, 1.5, and 2.0 mm, together with results from the spiral test. (b) Data from the spiral and strip tests shown in (a) reduced by the factors shown in the figure to simulate results as though all the tests had been carried out in a similar size mold of section 2 mm × 17 mm. All the results are seen to agree, confirming the validity of the comparison.

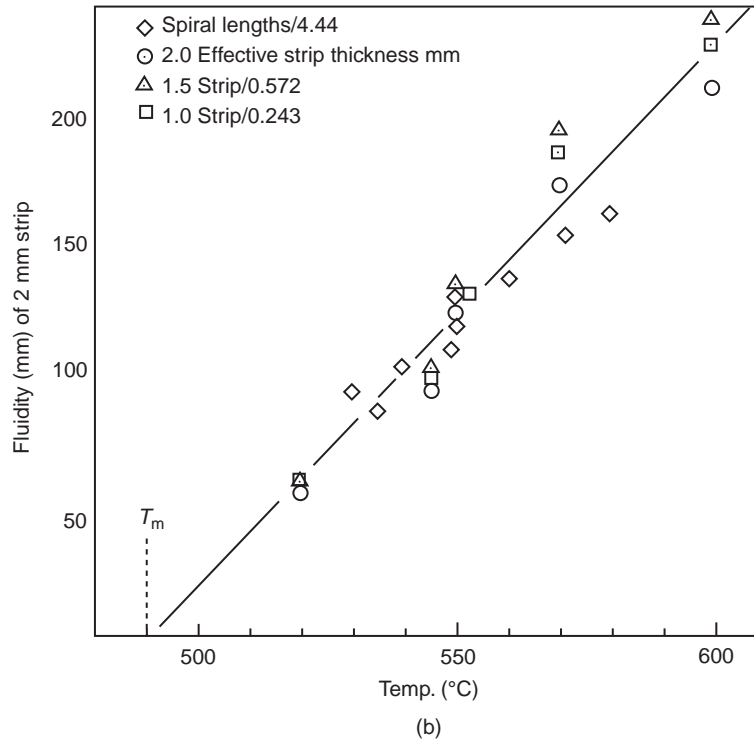


FIGURE 3.23 (continued).

Returning now the comparison of fluidity tests, then by taking a ratio of Equation 3.15 for two tests numbered 1 and 2, we obtain

$$\frac{L_1}{L_2} = \left(\frac{m_1}{m_2}\right)^n \left\{ \frac{H_1 - (\gamma/r_1\rho g)}{H_2 - (\gamma/r_2\rho g)} \right\}^{1/2} \quad (3.16)$$

For the work carried out by Sahoo and Whiting on both the spiral and strip tests, the ratio given in Equation 3.16 applies as accurately as possible, since the liquid metal and the molds were the same in each case. Assuming the moduli were 1.74 and 0.895 mm respectively, and the radii were 4 and 1 mm respectively,  $\gamma = 1.9 \text{ Nm}^{-1} = 5714 \text{ kg m}^{-3}$ , and the height of the sprue in each case approximately 0.1 m, it follows

$$\begin{aligned} \frac{L_{f1}}{L_{f2}} &= \left\{ \frac{1.74}{0.895} \right\}^2 \left\{ \frac{0.1 - 0.00847}{0.1 - 0.0339} \right\}^{1/2} \\ &= 3.77 \times 1.18 \\ &= 4.44 \end{aligned}$$

The calculation is interesting because it makes clear that the largest contribution towards increased fluidity in these thin-section castings derives from their modulus (i.e. their increased solidification



time). The effect of the surface tension is less important in the case of the comparison of the spiral with the 2-mm section. If the spiral of modulus 1.74 mm had been compared with a thin-section fluidity test piece of only 1 mm thick, then

$$L_{f1}/L_{f2} = 13.6 \times 1.68 = 9.25$$

Thus although the surface tension factor has risen in importance from 1.18 to 1.68, the effect of freezing time is still completely dominant, rising from 3.77 to 13.6.

The dominant effect of modulus over surface tension appears to be a general phenomenon in sand molds as a result of the (usually) small effect of surface tension compared to the head height.

The accuracy with which the spiral data are seen to fit the fluidity strip test results for the Zn-27Al alloy when all are adjusted to the common section thickness of 2 mm × 17 mm (Figure 3.23b) indicates that, despite the arguments that have raged over the years, both tests are in fact measuring the same physical phenomenon, that we happen to call fluidity, and both are in agreement.

---

### 3.3 EXTENDED FLUIDITY

We have examined metallurgical techniques in which fluidity can be extended, such as cleaning the melt from suspended oxides; reducing the rate of heat transfer by mold material or mold coat; and providing a coating to confer an unstable substrate for freezing. All these approaches involve flow of liquid in channels that are sufficiently narrow that the flow is constrained to be essentially unidirectional.

The casting technique for extending fluidity presented in this section involves multi-directional flow in which the cool metal at the flow tip is diverted away from the general direction of advance, allowing fresh, hot metal to take its place at the flow tip so that the total flow distance can be extended.

Such an effect is common in castings, and happens naturally if the flow channel is sufficiently wide so that the melt arriving at the front is diverted sideways to freeze, leaving a central flow channel open (see Figures 5.24 and 3.24a). This flow channel phenomenon is easily identified in the structure of the casting as a lengthy region of coarse grains, and sometimes some porosity, in contrast with the sides of the casting which are fine-grained and dense. Tol and co-workers (1997) notice this effect in their computational fluid dynamic (CFD) studies of flow in a narrow strip casting; as the number of cells across the thickness was increased the predicted fluidity distance increased because of the formation of a flow channel along the center of the strip (Figure 3.24a).

A less desirable multi-directional effect can occur in some fluidity test sections if they are sufficiently wide to allow an oxide flow tube to progress up one side of the fluidity channel, breaking through to the other side and flowing to back-fill (Figure 3.24b). This diverted flow takes away some of the cold metal from the tip, allowing the front to move ahead once again, but such extension to the fluidity cannot be recommended because a bifilm crack will extend through the cast section, separating these flow channels. In the absence of close walls to constrain the flow front in this fluidity channel, which at 40 mm is unusually wide, the bursting of the oxide on the front dictates a randomness that gravity is powerless to control in this horizontal channel. The result can at times become quite chaotic as seen in Figure 3.24c.

Hiratsuka and colleagues (1998) describe an artificial technique for extending fluidity, by providing overflows or 'flow-offs' at intervals along the length of a long casting. Their purpose was to extend the

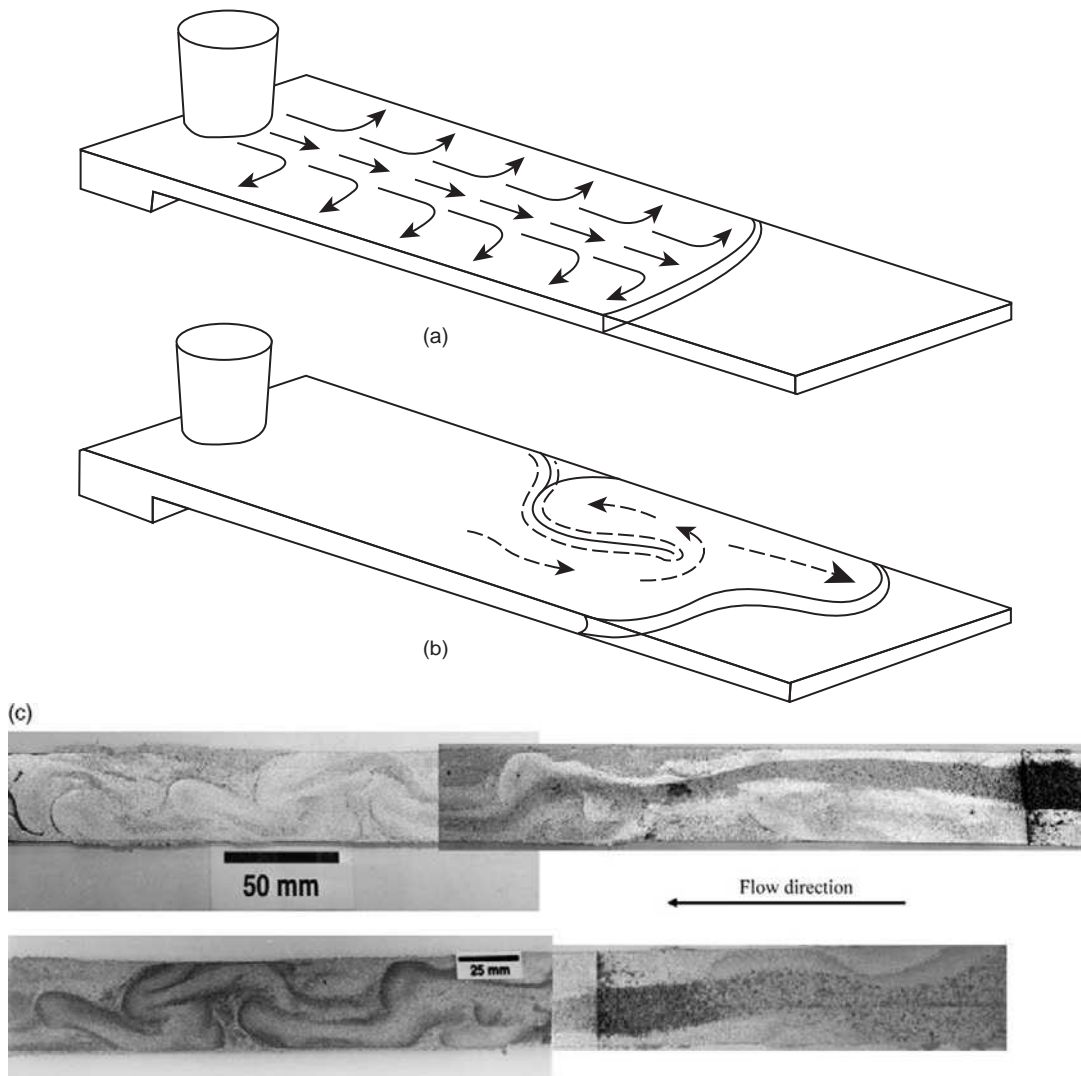


**FIGURE 3.24**

Flow patterns of Al-Si alloy on (a) a 4-mm-thick plate cast at 700°C; (b) a 3-mm-thick fluidity strip cast at 750°C; (c) photographs of the strip cast in (b) showing flow channel behavior and lap defects formed by the irregularities of the slowing flow. (Courtesy of A Habibollahzadeh 2004.)

gray zone in a long gray cast iron casting, 3 mm thick  $\times$  60 mm wide, pushing the white, chilled iron beyond the length required for good machinability. Figure 3.25 shows the way in which one overflow of 20 mm length increased the flow distance by 30 mm, showing a positive gain in efficiency of the addition. However, the three overflows totalling 60 mm of overflow increased the flow length of the casting by almost exactly 60 mm.

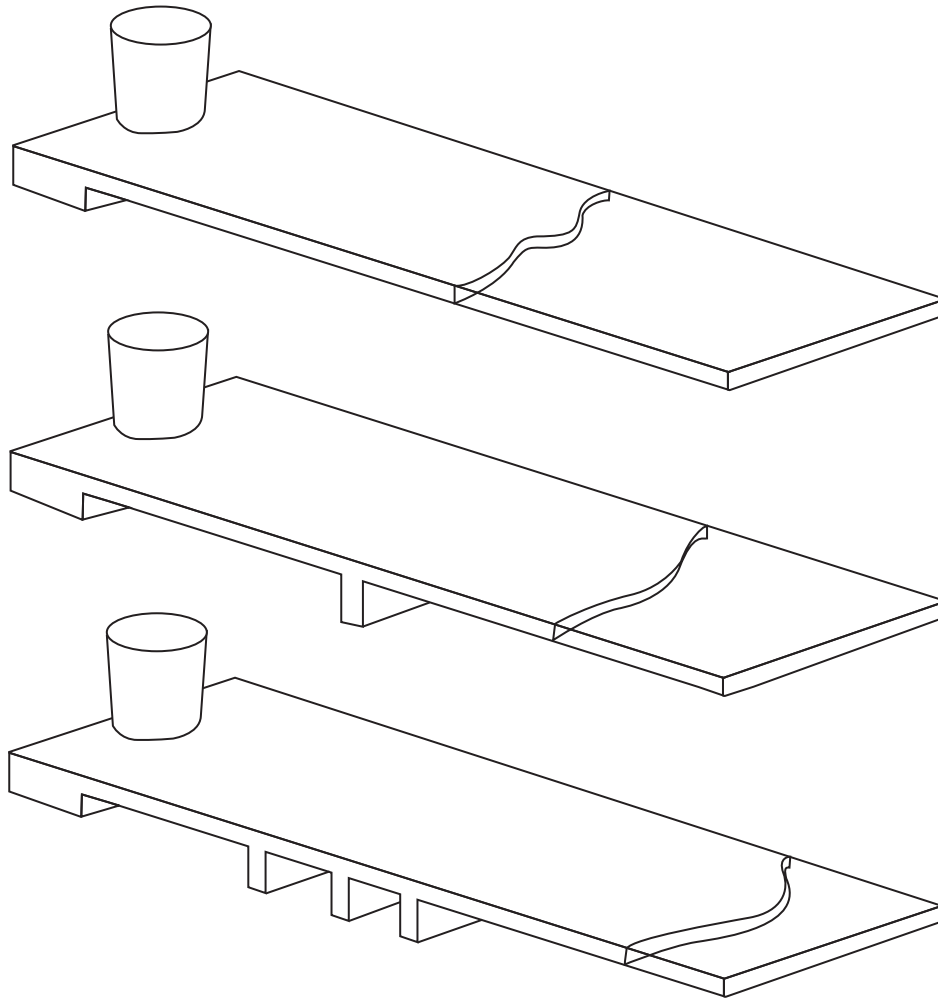


**FIGURE 3.25**

Flow distances of gray iron in a long plate enhanced by the provision of flow-offs to take away the cool front metal, allowing it to be replaced by hotter metal (Hiratsuka et al. 1998).

One of the reasons that Hiratsuka's extension technique was successful was the extreme narrowness of the sections, so that problems of circulating or reverse flow that might threaten to bring the cold liquid back into the casting were avoided.

The positioning of the overflows in Hiratsuka's work is curious, and would not be expected to result in an optimum effect. The authors give no reason for this. It seems there is plenty of scope for research to find rules for optimum positioning of overflows to obtain maximum benefit.

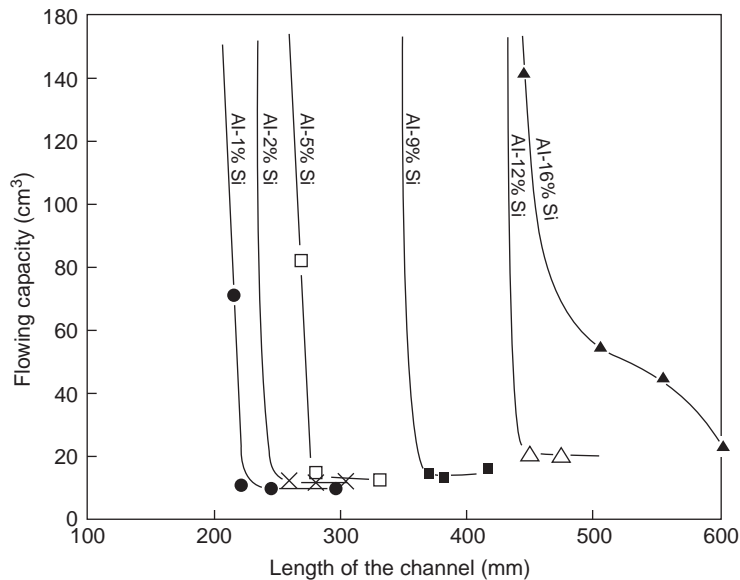


**FIGURE 3.26**

Flow capacity of the channel as a function of the length of the channel (Feliu 1962).

### 3.4 CONTINUOUS FLUIDITY

In a series of papers published in the early 1960s Feliu introduced a concept of the volume of flow through a section before flow was arrested. He carried out this investigation on, among other methods, a spiral test pattern, molded in green sand. He made a number of molds, cutting a hole through the drag by hand to shorten the spiral length. The metal that poured through the escape hole was collected in a crucible placed underneath, and weighed together with the length of the cast spiral. As the flow distance was progressively reduced by cutting progressively nearer to the start on a succession of molds, he discovered that at a critical flow distance the metal would continue flowing indefinitely (Figure 3.26). Clearly, any metal that had originally solidified in the flow channel was subsequently remelted by the continued passage of hot metal.

The conditions for remelting in the channel so as to allow continuous flow are illustrated in Figure 3.27. The concept is essential to the understanding of running systems, whose narrow sections would otherwise prematurely block with solidified metal. It is also clearly important in those cases where a casting is filled by running through a thin section into more distant heavy sections.

Because of its importance, I have coined the name 'Continuous Fluidity Length' for this measurement of a flow distance for which flow can continue to take place indefinitely. It contrasts with the normal fluidity concept, which to be strict should perhaps by more accurately named as 'Maximum Fluidity Length'.

The results by Feliu shown in Figure 3.28a seem typical. The *maximum* fluidity length has a finite value at zero superheat. This is because the liquid metal has latent heat, at least part of which has to

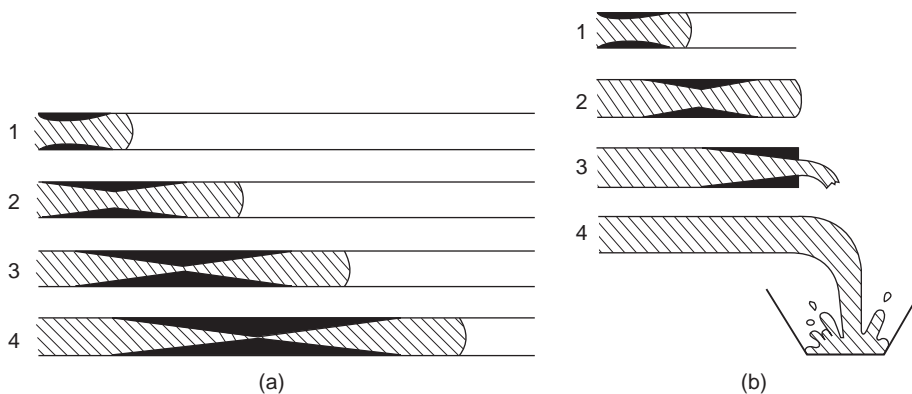


**FIGURE 3.27**

Concepts of (a) maximum fluidity length showing the stages of freezing leading to the arrest of the flow in a long mold; and (b) the continuous flow that can occur if the length of the mold does not exceed a critical length, defined as the continuous fluidity length.

be lost into the mold before the metal ceases to flow. *Continuous fluidity*, on the other hand, has zero value until the superheat rises to some critical level. (Note that in Figures 3.28a,b,c, the liquidus temperature  $T_m$  has been reduced from that of the pure metal by 5–10°C to allow for the presence of impurities.)

Figures 3.28a,b,c display three zones; (i) a zone in which the flow distance is sufficiently short, and/or the temperature sufficiently high, that flow continues indefinitely; (ii) a region between the maximum and the continuous fluidity thresholds where flow will not flow indefinitely, but will continue for increasingly long periods as distance decreases, or temperature rises; and (iii) a zone in which the flow distance cannot be achieved, bounded on its lower edge by the maximum fluidity threshold.

Examining the implications of these three zones in turn; Zone (i) is the regime in which most running systems operate; Zone (ii) is the regime in many castings, particularly if they have thin walls; Zone (iii) is the regime of bitter experience of costly redesigns, often after all the budget has been expended on the patternwork, and it is finally acknowledged that the casting cannot be made. Fluidity really can therefore be important to the casting designer and to the founder.

As a detail that may have some importance, whereas the curves derived by Feliu exhibit abrupt vertical turns when the continuous fluidity starts, this behavior is not shown for rather pure metals (and possibly eutectics) as seen in Feliu's original publication (1962) for both Al–Si and Al–Cu alloys. This is probably the result of the smoother growth front, consisting of planar or cellular growth being more resistant to remelting, whereas heat transfer to an array of dendrites is probably fast, promoting rapid remelting.

The author is aware of little other experimental work relating to continuous fluidity. An example worth quoting because of its rarity is that of Loper and LeMahieu on white irons in green sand dating from 1971. (Even so, the interested reader should take care to note that freezing time is not measured directly in this work.)

There is a nice computer simulation study carried out at Aachen University (Wu 1997, Sahn 1998) that confirms the principles outlined here. More work is required in this important but neglected field.

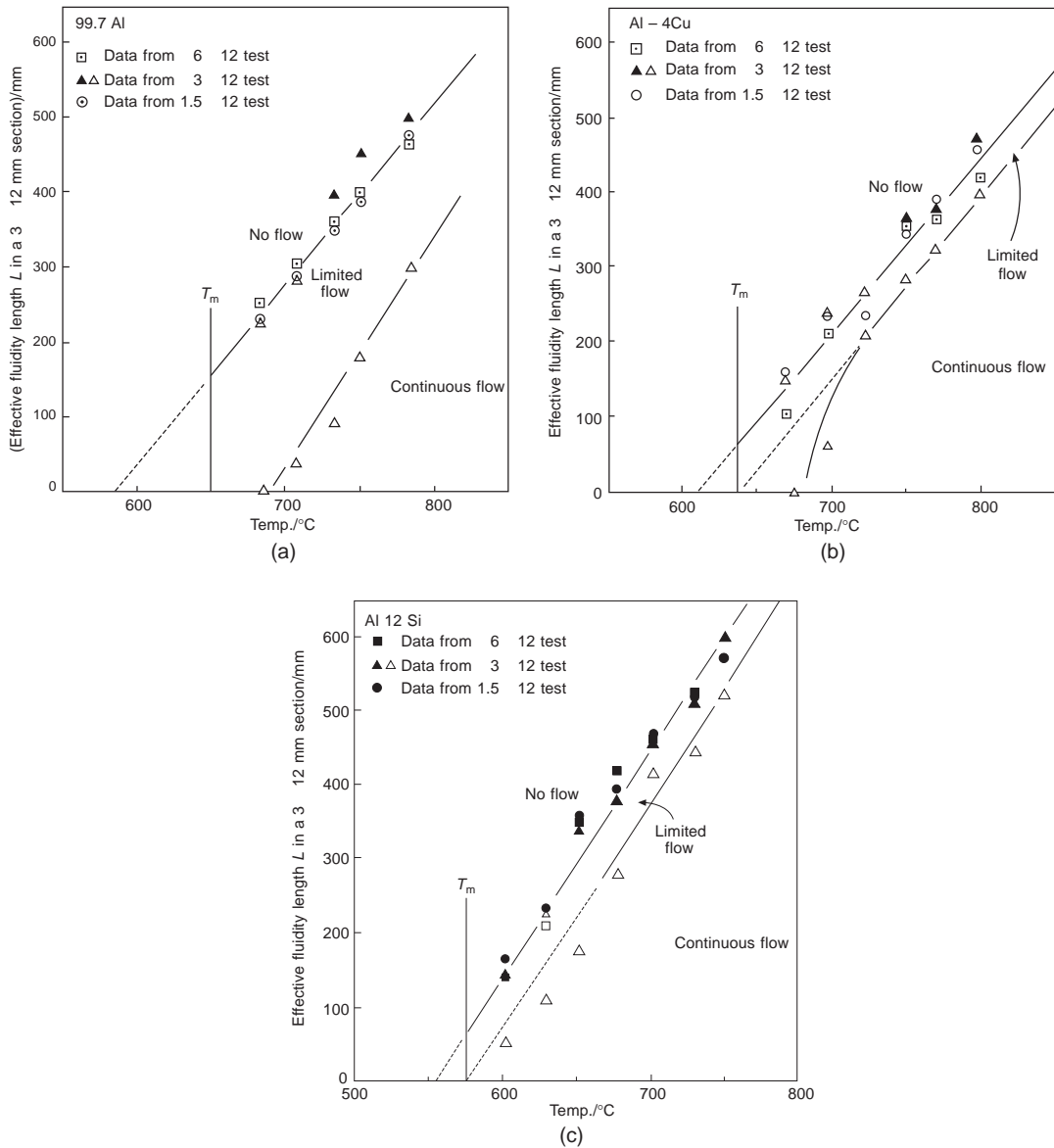


**FIGURE 3.28**

(a) Maximum and continuous fluidity data by Feliu for 99.7Al cast into greens and molds of section  $6 \times 12$ ,  $3 \times 12$  and  $1.5 \times 12$ , all reduced for presentation in this figure as though cast only in a section  $3 \times 12$  mm. (b) Data for Al-4Cu alloy by Feliu recalculated as though only from section  $3 \times 12$  mm. (c) Data for Al-12Si alloy by Feliu recalculated as though only from section  $3 \times 12$  mm.

This page intentionally left blank

# Molds and cores

As in so much technology, the production of molds and cores is a complex subject that we can only touch upon here. Although this text is about the metallurgy of the casting, the mold can be profoundly influential. The mold and the casting co-exist for sufficiently long, and at a sufficiently high temperature, that the two cannot fail to have an important mutual impact. Essentially, this section is about the *science* of mold and casting interactions.

In the later part of the book, 'Casting Manufacture' we concentrate on the *technology* of molds and castings, outlining the main benefits and problems of the various types of molds and cores to allow a user to make a more informed choice of manufacturing route.

## 4.1 MOLDS: INERT OR REACTIVE

Very few molds and cores are really inert towards the material being cast into them. However, some are very nearly so, especially at lower temperatures. This short section merely lists those types of molds and cores that in general do not react with their cast metals.

The usefulness of a relatively inert mold is emphasized by the work of Stolarczyk (1960), who suffered 4.5% porosity in gunmetal test bars cast in greensand molds compared to 0.5% porosity for identical castings into steel-lined molds. This simple experiment confirms one of the most important advantages of metal molds: they are impressively inert towards their liquid metal and cast product. Thus all of the gravity and low-pressure dies (permanent molds) are reassuringly inert.

Unfortunately the inertness of high-pressure die-casting dies, and some squeeze-casting dies, is compromised by die coolants and lubricants which definitely impair the casting to varying degrees.

Greensand molds that have been dried in an oven (i.e. dry sand molds) have been found to be largely inert, as shown by Locke and Ashbrook (1950).

This behavior contrasts with that of the original greensand in its various forms. The water and hydrocarbon contents of greensand mixes lead to masses of outgassing, and very rapid attack leading to oxidation or deposit of carbon on the liquid metal front, plus the generation of copious amounts of lower hydrocarbons (such as methane) and even more hydrogen. At first sight it is perhaps amazing that any useful casting could be produced by such a reactive system. However, greensand remains, justifiably, the most important volume producer of good castings worldwide. Its many benefits, particularly its unbeatable molding speed, are discussed in more detail in Chapter 15.

Whereas the various resin binders used for sand molds do not outgas as impressively as greensand, the quantities and nature of the various volatiles that are attempting to escape during the dramatic early seconds and minutes of attack by the melt are seen in Figures 4.1 and 4.2. Clearly, there is plenty of chemistry involved, and the high temperatures ensure that this is energetic.



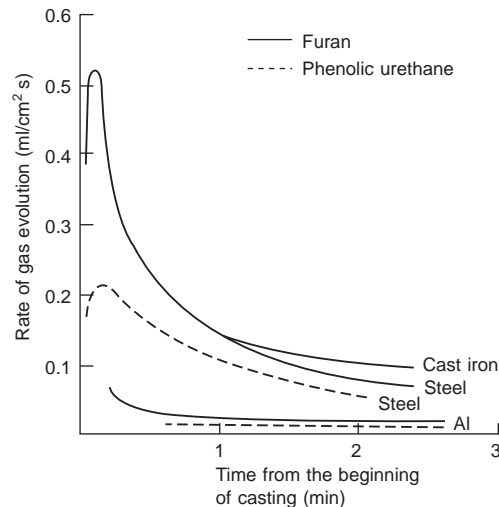


**FIGURE 4.1**

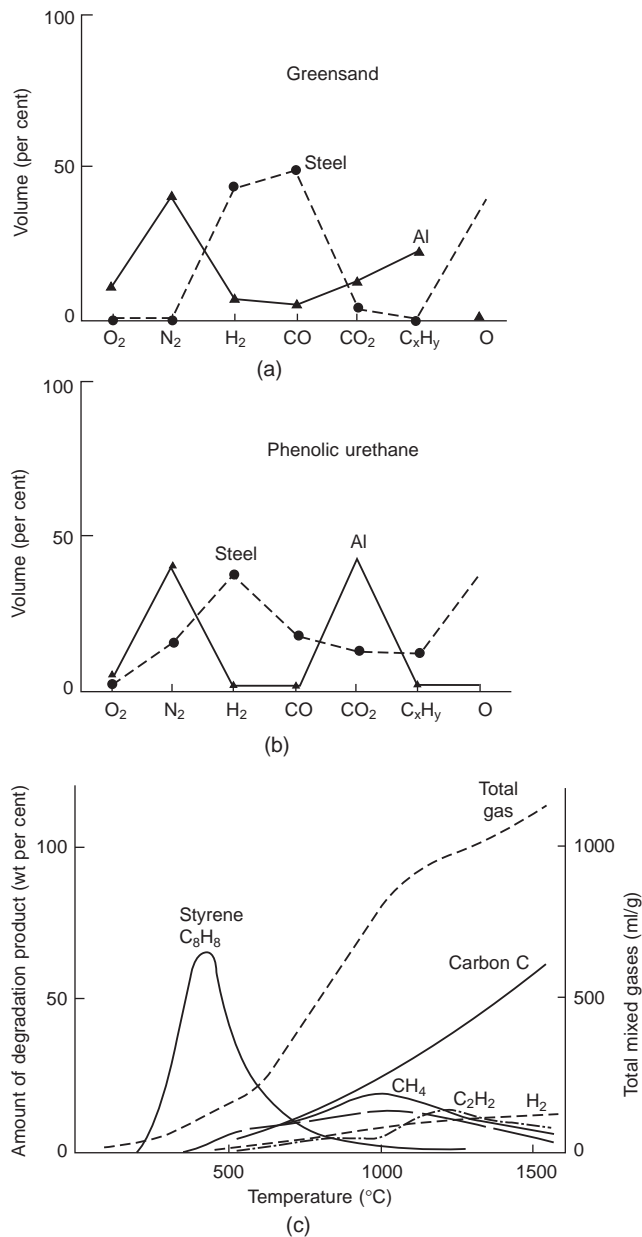
Measured gas evolution rates from castings of aluminum, iron, and steel, in chemically bonded sand molds (Bates and Monroe 1981).

## 4.2 TRANSFORMATION ZONES

Clearly, as the hot metal is poured into a greensand mold, the blast of heat from the melt at temperature greatly exceeding the boiling point of water very rapidly heats the surface of the mold, boiling off the water (and other volatiles). As the heat continues to advance into the mold the moisture continues to migrate, only to condense again in the deeper, cooler parts of the mold. As the heat continues to diffuse, the water evaporates again and migrates further. This is of course a continuous process. Dry and wet zones travel through the mold like weather systems in the atmosphere. The evaporation of water in greensand molds has been the subject of much research.

Looking at these in detail, four zones can be distinguished, as shown in Figure 4.3.

- (i) The dry zone is where the temperature is high and all moisture has been evaporated from the binder. It is noteworthy that this very-high-temperature region will continue to retain a relatively stagnant atmosphere composed of nearly 100% water vapor. However, of course, some of this superheated and very dry steam will be reacting at the casting surface to produce oxide and free hydrogen.
- (ii) The vapor transport zone, essentially at a uniform temperature of 100°C, and at a roughly constant content of water, in which steam is migrating from the casting.
- (iii) The condensation zone, where the steam recondenses. This zone was for many years the subject of some controversy as to whether it was a narrow zone or whether it was better defined as a front. The definitive theoretical model by Kubo and Pehlke (1986) has provided an answer where direct measurement has proved difficult; it is in fact a zone, confirming the early measurements by Berry, Kondic, and Martin (1959). This zone gets particularly wet. The raised water content

**FIGURE 4.2**

Composition of mold gases (a) from greensand (Chechulin 1965); (b) from phenolic urethane (Bates and Monroe 1981) and (c) from thermally decomposing expanded polystyrene (Goria et al. 1986).

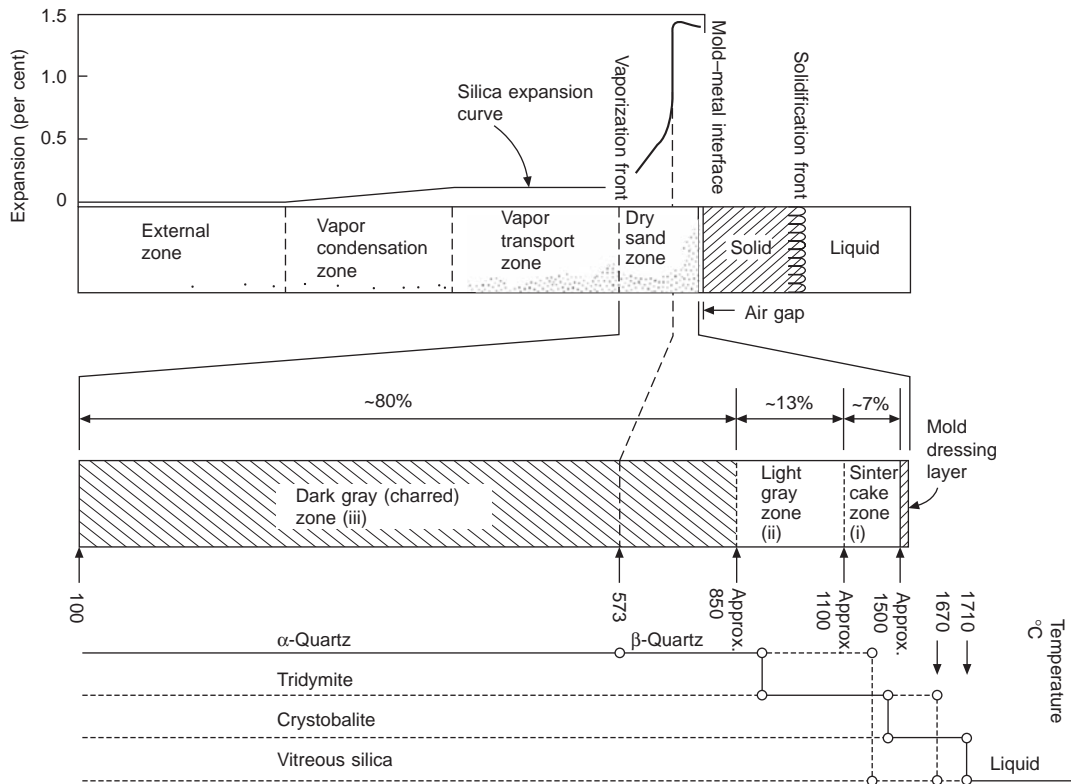


**FIGURE 4.3**

Structure of the heated surface of a greensand mold against a steel casting; and the forms of silica (after Sosman 1927) with solid lines denoting stable states, and broken lines denoting unstable states.

usually greatly reduces the strength of greensand molds, so that mechanical failure is most common in this zone.

(iv) The external zone where the temperature and water content of the mold remain as yet unchanged.

It is worth taking some space to describe the structure of the dry sand zone. When casting light alloys and other low-temperature materials, the dry sand layer has little discernible structure.

However, when casting steel it becomes differentiated into various layers that have been detailed from time to time (e.g. Polodurov 1965; Owusu and Draper 1978). These are, counting the mold coating as number zero:

1. Dressing layer of usually no more than 0.5 mm thickness, and having a dark metallic luster as a result of its high content of metal oxides.
2. Sinter cake zone, characterized by a dark brown or black color. It is mechanically strong, being bonded with up to 20% fayalite, the reaction product of iron oxide and silica sand. The remaining silica exists as shattered quartz grains partially transformed to tridymite and

crystalite, which is visible as glittering crystals (explaining the origin of the name cristobalite). This layer is largely absent when casting gray iron at ordinary casting temperatures.

3. Light-gray zone, with few cracked quartz grains and little cristobalite. What iron oxides are present are not alloyed with the silica grains. This zone is only weakly bonded, and disintegrates on touch.
4. Charred zone, of dark-gray color, of intermediate strength, containing unchanged quartz grains but significant levels of iron oxide. Polodurov speculates that this must have been blown into position by mold gases.

The pattern of these zones is further complicated by convection effects inside the mold or core for a relatively long period after casting, carrying carbonaceous vapors back into the heated zones, chemically ‘cracking’ the compounds to release hydrogen and depositing carbon. The inner layers therefore become black, with the sand grains seen under the microscope to be coated with a kind of fibrous, furry layer of graphite. Churches and Rundman (1995) studying a phenolic urethane mold found this reaction to occur between 15 minutes and 3 hours, and at temperatures down to about 540°C for their gray iron castings. Highly heated cores had lost up to 50% of their carbon after finally cooling to room temperature.

The changes in form of the silica sand during heating are complicated. An attempt to illustrate these relations graphically is included in Figure 4.3. This complexity, and particularly the expansion accompanying the phase change from alpha to beta quartz, has prompted a number of foundries to abandon silica sand in favor of more predictable molding aggregates. This advantageous move is expected to become more widespread in future.

---

### 4.3 EVAPORATION AND CONDENSATION ZONES

As the heat diffuses from the solidifying casting into the mold (Figure 4.4), the transformation zones migrate deeper into the mold. We can follow the progress of the advance of the zones by considering the distance  $d$  that a particular isotherm reaches as a function of time  $t$ . The solution to this simple one-dimensional heat-flow problem is  $d = (Dt)^{1/2}$  where  $D$  is the coefficient of diffusion. This solution is of course equivalent to the solute diffusion given earlier (Equation 1.5).

In the case of the evaporation front, the isotherm of interest is that at 100°C. We can see from Figures 4.4 and 4.5 that the value of  $D$  is close to  $1 \text{ mm}^2 \text{ s}^{-1}$ . This means that the evaporation front at 1 s has traveled 1 mm, at 100 s has traveled 10 mm, and requires 10 000 s (nearly 3 hours!) to travel 100 mm. It is clear that the same is true for aluminum, as well as steel. (This is because we are considering a phenomenon that relies only on the rate of heat flow in the mold – the metal and its temperature are not involved.)

For the condensation zone the corresponding value of  $D$  is approximately  $3 \text{ mm}^2 \text{ s}^{-1}$ , so that the position of the front at 1, 100, and 10 000 s is 1.7, 17, and 170 mm respectively.

These figures are substantiated to within 10 or 20% by the theoretical model by Tsai et al. (1988). This work adds interesting details such as that the rate of advance of the evaporation front depends on the amount of water present in the mold, higher water contents making slower progress. This is to be expected, since more heat will be required to move the front, and this extra heat will require extra time to arrive. The extra ability of the mold to absorb heat is also reflected in the faster cooling rates of castings made in molds with high water content. Measurements of the thermal conductivity of various molding sands by Yan et al. (1989) have confirmed that the

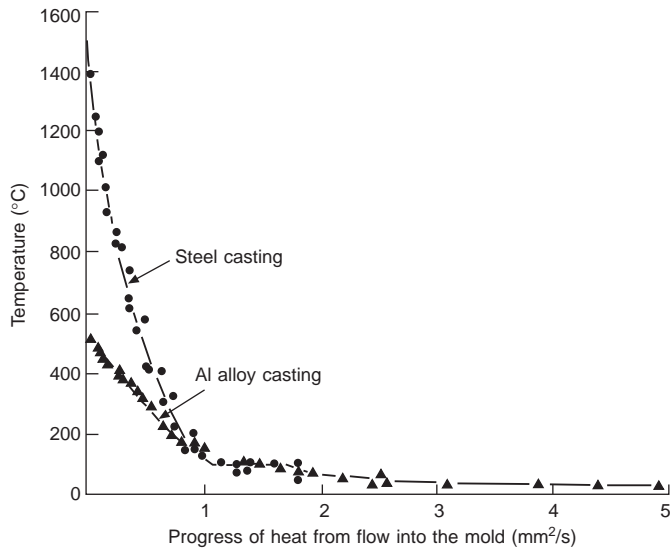


**FIGURE 4.4**

Temperature distribution in a greensand mold on casting an aluminum alloy (Ruddle and Mincher 1949–50) and a steel (Chvorinov 1940).

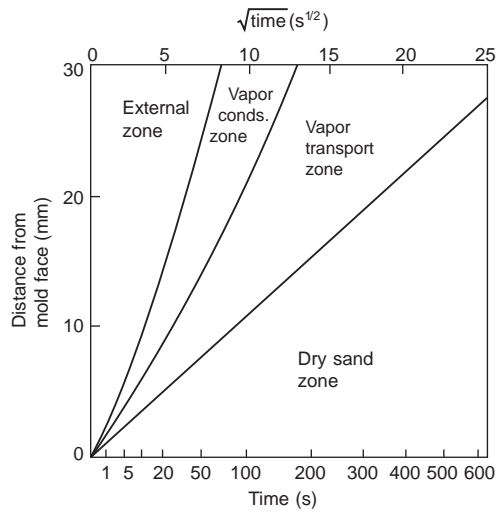


**FIGURE 4.5**

Position of the vapor zones after casting aluminum in a greensand mold (data from Kubo and Pehlke 1986).

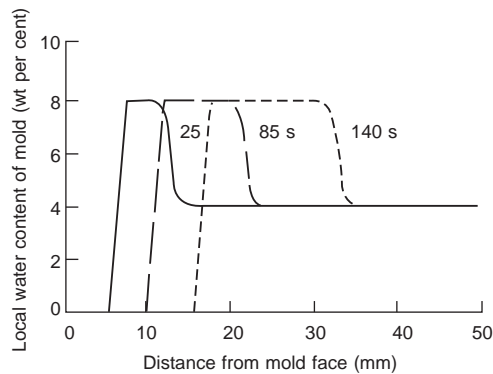


**FIGURE 4.6**

Water content of the vapor transport zone with time and position (smoothed computed results of Capp et al. 1974).

apparent thermal conductivity of the moisture-condensation zone is about three or four times as great as that of the dry sand zone.

An earlier computer model by Cappy et al. (1974) also indicates interesting data that would be difficult to measure experimentally. They found that the velocity of the vapor was in the range of  $10\text{--}100\text{ mm s}^{-1}$  over the conditions they investigated. Their result for the composition and movement of the zones is given in Figure 4.6. Kubo and Pehlke calculate flow rates of  $20\text{ mm s}^{-1}$ . These authors go on to show that moisture vaporizes not only at the evaporation front, but also in the transportation and condensation zones. Even in the condensation zone a proportion of the water vaporizes again at temperatures below  $100^\circ\text{C}$  (Figure 4.5).

The pressure of water vapor at the evaporation front will only be slightly above atmospheric pressure in a normal greensand mold. However, because the pressure must be the same everywhere in the region between the mold–metal interface and the evaporation front, it follows that the dry sand zone must contain practically 100% water vapor. This is at first sight surprising. However, a moment's reflection will show that there is no paradox here. The water vapor is very dry and hot, reaching close to the temperature of the mold–metal interface. At such high temperatures water vapor is highly oxidizing. There is no need to invoke theories of additional mechanisms to get oxygen to this point to oxidize the metal – there is already an abundance of highly oxidizing water vapor present (the breakdown of the water vapor also providing a high-hydrogen environment, of course, to enter the metal, and to increase the rate of heat transfer in the dry sand zone).

Kubo and Pehlke (1986) confirm that gas in the dry sand and transportation zones consists of nearly 100% water vapor. In the condensation zone the percentage of air increases, until it reaches nearly 100% air in the external zone (water vapor would be expected to be present at its equilibrium vapor pressure, 32 mmHg or 42 mb at  $30^\circ\text{C}$ ).

It is found that similar evaporation and condensation zones are present for other volatiles in the greensand mold mixture. Marek and Keskar (1968) have measured the movement of the vapor transport zone for benzene and xylene. The evaporation and condensation fronts of these more volatile materials travel somewhat faster than those of water. When such additional volatiles are present they

will, of course, contribute to the 1 atmosphere of gas pressure in the dry zone, helping to dilute the oxidizing effect of water vapor, and helping to explain part of the beneficial effect of such additives. In the following section we will see that many organics decompose at these high temperatures, providing a deposit of carbon, which further assists, in the case of such metals as cast iron, in preventing oxidation and providing a non-wetting metal surface of carbon which contains the liquid iron and helps to prevent its contact with the sand mold.

It is to be expected that vapor transport zones will also be present to various degrees in chemically bonded sands. The zones will be expected to have traces of water mixed with other volatiles such as organic solvents. Little work appears to have been carried out for such binder systems, so it is not easy to conclude how important the effects are, if any. In general, however, the volatiles in such dry sand systems usually total less than 10% of the total volatiles in greensand, so that the associated condensation zones will be expected to be less than one-tenth of those occurring in greensand. It may be, therefore, that they will be unimportant. However, at the time of writing we cannot be sure. It would be nice to know.

What is certain is that silicate binders appear to have a high chilling effect in ferrous castings because of their water content. The loss of the water will create evaporation and condensation zones that will carry heat away from the casting.

All of the above considerations on the rate of advance of the moisture assume no other flows of gases through the mold. This is probably fairly accurate in the case of the drag mold, where the flow of the liquid metal over the surface of the mold effectively seals the surface against any further ingress of gases. A certain amount of convection is expected in the mold, but this will probably not affect the conditions in the drag significantly.

In the vertical walls of the mold, however, convection may be significant. Close to the hot metal, hot gases are likely to diffuse upwards and out of the top of the mold, their place being taken by cold air being drawn in from the surroundings at the base of the mold, or the outer regions of the cope.

General conditions in the cope, however, are likely to be more complicated. It was Hofmann in 1962 that first emphasized the different conditions experienced during the heating up and outgassing of the cope. He pointed out that the radiated heat from the rising melt would cause the cope surface of the mold to start to dry out before the moment of contact with the melt. During this pre-contact period two different situations can arise:

1. If the mold is open, as the cope surface heats up the water vapor can easily escape through the mold cavity and out via the opening (Figure 4.7). The rush of water vapor through an open feeder can easily be demonstrated by holding a piece of cold metal above the opening. It quickly becomes covered with condensate. The water vapor starts its life at a temperature of only 100°C. It is therefore a relatively cool gas, and is thus most effective in cooling the surface of the mold as it travels out through the surface of the cope on its escape route.
2. If the mold is closed, the situation is quite different. The air being displaced and expanded by the melt will force its way through the mold, carrying away the vapor from the interface (Figure 4.7). The rate of flow of air is typically in the range  $10\text{--}100\text{ l s}^{-1}\text{ m}^{-2}$  (the reader is encouraged to confirm this for typical castings and casting rates). This is in the same range of flow rate as the transport of vapor given in computer models. Thus if the casting rate is relatively low, then the vapor transport zone is likely to be relatively unaffected, although perhaps a little accelerated in its progress. When the casting rate is relatively high, then the vapor transport zone will be effectively blown away, diluted with the gale of air so that no condensation can occur.

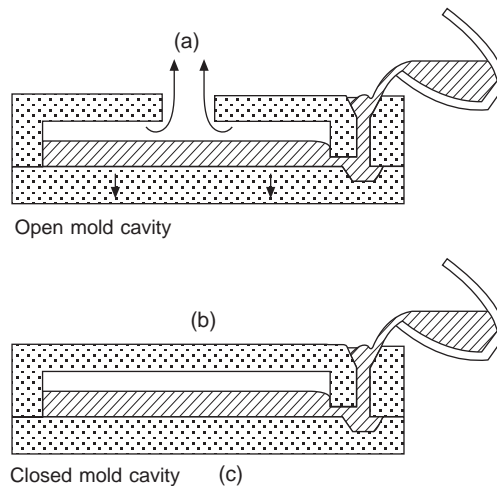


**FIGURE 4.7**

Three conditions of vapor transport in molds: (a) unrestricted free evaporation from the cope; (b) evaporation from the cope constrained to occur via the cope mold; (c) evaporation from the drag confined by the cover of metal, and possibly confined by the substrate on which the mold sits, and possibly at its sides by a molding box, leaving no option but for bubbling through the metal (partly from Hofman 1962).

Because the water vapor is driven away from the surface and into the interior of the mold, its beneficial cooling effect at the surface is not felt, with the result that the surface reaches much higher temperatures as a result of the direct radiation of heat from the melt, as is seen in Figure 4.8. The prospect of the failure of the cope surface by expansion and spalling of the sand is therefore much enhanced.

However, the rate of heating of the surface by radiation from the melt may be reduced by a white mold coat, such as a zircon- or alumina-based mold wash, now widely applied for large castings of iron and steel. Boenish (1967) confirmed that light-colored mold coats resist scabbing for up to 400% longer than the jet-black graphitic surfaces commonly used for cast iron.

One final aspect of vapor transport in the mold is worth a note. There has been much discussion over the years about the contribution of the thermal transpiration effect to the flow of gases in molds.

Although it appears to have been widely disputed, the effect is certainly real. It follows from the kinetic theory of gases, and essentially is the effect of heated gases diffusing away from the source of heat, allowing cooler gases to diffuse up the temperature gradient. In this way it has been argued that oxygen from the air can arrive continuously at the casting to oxidize the surface to a greater degree than would normally have been expected.

Williams (1970) described an experiment that demonstrated this effect. He took a sample of clay approximately 50 mm long in a standard 25-mm diameter sand sampling tube. When one end was heated to 1000°C and the other was at room temperature, he measured a pressure difference of 10 mmHg if one end was closed, or a flow rate of 20 ml per minute if both ends were open. If these results are typical of those that we might expect in a sand mold, then we can make a comparison as follows. The rate of thermal transpiration is easily shown to convert to  $0.53 \text{ l s}^{-1} \text{ m}^2$  for the conditions of temperature gradient and thickness of sample used in the experiment. From the model of Cappy



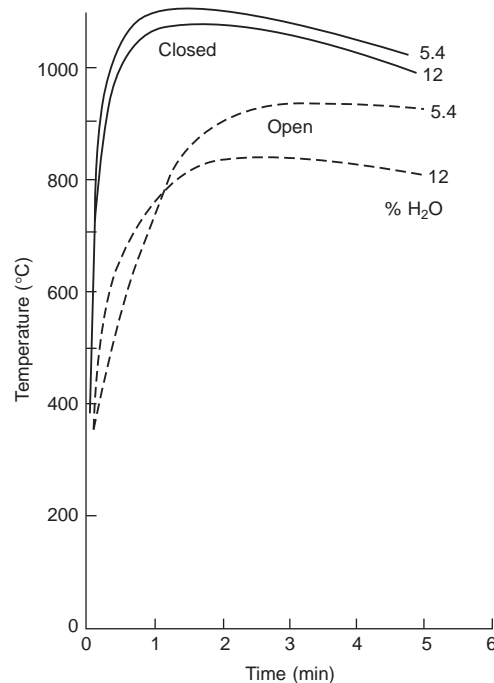


**FIGURE 4.8**

Temperature in the cope surface seen to be significantly lowered by open molds and high moisture levels (data from Hofman 1962).

et al. (1974), we obtain an estimate of the rate of transport of vapor of  $100 \text{ l s}^{-1} \text{ m}^2$  at approximately this same temperature gradient through a similar thickness of mold. Thus thermal transpiration is seen to be less than 1% of the rate of vapor transport. Additional flows like the rate of volume displacement during casting, and the rate of thermal convection in the mold, will further help to swamp thermal transpiration.

Thermal transpiration does seem to be a small contributor to gas flow in molds. It is possible that it may be more important in other circumstances. More work is required to reinstate it to its proper place, or lay it to rest as an interesting but unimportant detail.

## 4.4 MOLD ATMOSPHERE

### 4.4.1 Composition

On the arrival of the hot metal in the mold, a rich soup of gases boils from the surface of the mold and the cores. The air originally present in the cavity dilutes the first gases given off but this is quickly expelled through vents or feeders, or may diffuse out through the cope. Subsequently, the composition of the mold gas is relatively constant.

In the case of steel being cast into greensand molds, the mold gas mixture has been found to contain up to 50% hydrogen (Figure 4.2). The content of hydrogen depends almost exactly on the percentage of water in the sand binder, with dry sand molds having practically no hydrogen as found by Locke and Ashbrook (1950, 1972). Other changes brought about by increased moisture in the sand were a decrease in oxygen, an increase in the CO/CO<sub>2</sub> ratio, and the appearance of a few per cent of paraffins (it is not clear whether these originated from the use of lubricant sprayed on to the pattern). The presence of cereals in the binder was found to provide some oxygen, even though the concentration of oxygen in the atmosphere fell because of dilution with other gases (Locke and Ashbrook 1950). Chechulin (1965) describes the results for greensand when aluminum alloys, cast irons, and steels are cast into them. His results are given in Figure 4.2a. Irons and steels produce rather similar mold atmospheres, so only his results for steel are presented.

The high oxygen and nitrogen content of the atmosphere in the case of molds filled with aluminum simply reflects the high component of residual air (originally, of course, at approximately 20% oxygen and 80% nitrogen). The low temperature of the incoming metal is insufficient to generate enough gas and expand it to drive out the original atmosphere. This effective replacement of the atmosphere is only achieved in the case of iron and steel castings.

The atmosphere generated when ferrous alloys are cast into chemically bonded sand molds is, perhaps rather surprisingly, not so different from that generated in the case of greensand (Figure 4.2b). The mixture consists mainly of hydrogen and carbon monoxide.

The kinetics of gas evolution have been studied by a number of researchers. Jones and Grim (1959) found some clays evolved significant water at just over 100°C, particularly Western bentonite, although Southern bentonite results went wildly off scale. A second peak of evolution at around 550°C was relatively unimportant. Scott and Bates (1975) found that hydrogen evolution peaked within 4 to 5 minutes for most chemical binders. However, for the sodium silicate binder a rapid burst of hydrogen was observed, which peaked in less than 1 minute.

Scarber and co-workers (2006) measured 200 ml of gas from about 100 g (they do not give the exact weight of their samples) of a core bonded with some resin binders, which rose to over 500 ml if the core was coated with a water-based wash even though the core had been thoroughly dried. Even this paled into insignificance when compared to the outgassing of greensand which they found to be nearly ten times that from resin-bonded sands. In addition they found multiple peaks associated with solvent evaporation, and, probably, water evaporation. The process seemed to be complicated by the re-condensation of these volatiles in the cooler centers of cores, and their final re-evaporation (a re-enactment of the condensation and evaporation zones already discussed in Section 4.3). Yamamoto and colleagues (1980) described the variation in output they observed as: (i) Peak I attributed to the expansion of air plus the evaporation of free moisture and other volatiles in the core when the core was first covered with liquid metal; (ii) Peak II after about 30 seconds identified as the release of combined water (water of crystallization) in the binder and/or aggregate; and finally (iii) a broad smooth Peak III, constituting a nearly constant pressure output period for about 50–80 seconds, attributed to the general breakdown of the organics in the binder. They confirmed that Peak II was much higher for sodium silicate/CO<sub>2</sub> cores.

Lost-foam casting, where the mold cavity is filled with polystyrene foam (the ‘full mold’ process), is a special case. Here it is the foam that is the source of gases as it is vaporized by the molten metal. At aluminum casting temperatures the polymerized styrene merely breaks down into styrene, but little else happens, as is seen in Figure 4.2c. It seems that the liquid styrene soaks into the ceramic surface

coating on the foam, so that the coating will temporarily become completely impermeable. This unhelpful behavior probably accounts for many of the problems suffered by aluminum alloy castings made by the lost foam process.

At the casting temperatures appropriate for cast iron, more complete breakdown occurs, with the generation of hydrogen and considerable quantities of free carbon. Rao and Lee (1984) show how even methane is largely decomposed at these temperatures, forming less than 1% of a C-H<sub>2</sub>-O<sub>2</sub> mixture at 1 atmosphere. The carbon deposits on the advancing metal front as a pyrolytic form of carbon widely known as 'lustrous carbon'. Once formed, the layer is rather stable at iron-casting temperatures, and can therefore lead to serious defects if entrained in the metal. The problem has impeded the successful introduction of lost foam technology. For steel casting the temperature is sufficiently high to cause the carbon to be taken into solution. Steel castings of low or intermediate carbon content are therefore contaminated by pockets of high-carbon alloy. This problem has prevented lost-foam technology in the form of the full mold process being used for low- and medium-carbon steel castings.

Lost-foam iron castings are not the only type of ferrous castings to suffer from lustrous-carbon defects. The defect is also experienced in cast iron made in phenolic urethane-bonded molds, and at times can be a serious headache. The absence of carbon is therefore a regrettable omission from the work reported in Figure 4.2a. At the time Chechulin carried out this study, the problem would not have been known. Later, Gloria (1986) does report carbon as a product of decomposition of polystyrene foam.

It seems reasonable to expect that carbon may also be produced from the pyrolysis of other binder systems. More work is required to check this important point.

#### 4.4.2 Mold gas explosions

The various reactions of the molten metal with the volatile constituents of the mold, particularly the water in many molding materials, would lead to explosive reactions if it were not for the fact that the reactions are dampened by the presence of masses of sand in mold materials or cores. Thus although the reactions in the mold are fierce, and not to be underestimated, in general they are not of explosive violence because the 90% or more of the materials involved are inert (simply sand and nitrogen) and have considerable thermal inertia. Taleyarkhan (1998) draws attention to the important role of non-condensable gases (e.g. nitrogen) in the suppression of explosive reactions. Outgassing reactions are therefore rather steady and sustained.

When carrying out a series of experiments in about 1992 in which liquid aluminum was poured while the interior of a PU-bonded mold was recorded by video through a glass window, Helvae was surprised to note that in every case, on arrival of the metal in the mold, a flicker of flame licked across the mold cavity, sometimes more energetically than others. On no occasion was there an explosion. Much earlier, in 1948, Johnson and Baker recorded similar flashes of light when recording the filling of open greensand molds by molten steel at 1650°C. It seems such phenomena might be common, or even normal.

It is noteworthy that the gases from the outgassing of an aggregate mold may contain a number of potentially flammable or explosive gases. These include a number of vapors, for example hydrocarbons such as methane, other organics such as alcohols, and a number of reaction products such as hydrogen and carbon monoxide.

Because of the presence of these gases, explosions sometimes occur and sometimes not. The reasons have never been properly investigated. This is an unsatisfactory situation because the

explosion of a mold during casting can be an unpleasant event. The author has witnessed this a number of times in furan-bonded boxless molds when casting an aluminum alloy casting weighing over 50 kg: there was a muffled explosion, and large parts of the sand mold together with liquid metal flew apart in all directions. After several repeat performances the operators developed ways of pouring this component at the end of long-handled ladles, so as to keep as far away as possible, never knowing whether or not the mold would explode. The cause always remained a mystery. Everyone was relieved when the job came to an end.

Explosions in and around molds containing iron or steel castings are relatively common. One of the most common is from under the mold, between the mold and its base plate, after the casting has solidified, so that there is less danger either to personnel or casting. The sound of muffled explosions from the mix of CO and air under molds is common in many greensand foundries.

With subsequent experience, and in the absence of any other suggestions, the following is suggested as a possible cause of the problem in the case of the light alloy casting.

Explosions can, of course, only happen when the flammable components of the gas mix with an oxidizing component such as oxygen from the air. The mixing has to be efficient, which suggests that turbulence is important. Also, the mix often has to be within close compositional limits, otherwise either no reaction occurs, or only slow burning takes place. The limits for the carbon monoxide, oxygen, and inert (carbon dioxide and nitrogen) gas mixtures are shown in Figure 4.9.

In the author's experience, the mixing with air, which is essential for explosions, only occurs in molds in certain conditions. These are molds that are (i) open to air because of open feeder heads, or (ii) poured with oversize sprues that allow the ingress and entrainment of air, or (iii) the use of double pouring, using two sprues, where the start of pour is not easy to synchronize, with the result that air is taken down one sprue at the time that metal enters down the other, (iv) occasionally associated with Al-Si whose reactivity to convert moisture to hydrogen gas has been enhanced by addition of Sr as

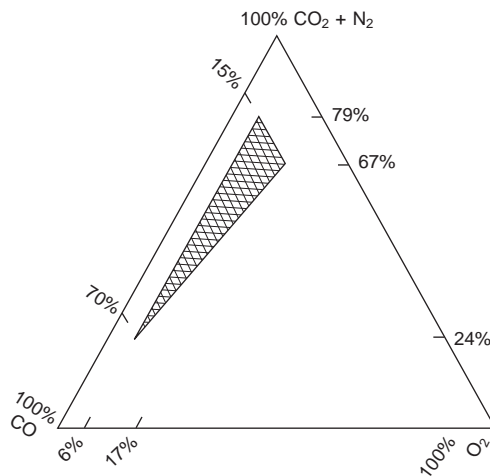


**FIGURE 4.9**

Shaded region defines the explosive regime for mixtures of CO, O<sub>2</sub>, and a mixture of CO<sub>2</sub> + N<sub>2</sub> (Ellison and Wechselblatt 1966).

a modifier. Thus eliminating open feeders by the use either of blind feeders or chills promises to be a useful step. The provision of a properly calculated single sprue should also help, as might the reduction or elimination of Sr addition.

‘What happens to the air already in the mold?’ is the next question. In a single-sprue system filling quiescently from the bottom upwards, the outgassing of the mold and cores will provide a spreading blanket of gas over the liquid. There will be almost no air in this cover, so that no burning or explosion can occur. The air will be displaced ahead, and will diffuse out of the upper parts of the mold. Where the flammable gas blanket meets the air it is expected to be cool, well away from the liquid metal. Thus any slight mixture that will occur at the interface between these layers of gases is not likely to ignite to cause an explosion.

In the case of the casting poured from two sprues, the second stream of metal might arrive to spark the spreading front of gases from the first stream. In the case of an open feeder, the cold draught of fresh air into the mold is likely to penetrate and mix with the flammable blanket, and be sufficiently close to the molten metal to be ignited. A poorly designed turbulent filling system will undo all the good described above. The splashing of hot droplets and jets of metal through the vapor blanket, mixing it with the air, will give ideal conditions to spark an explosion.

That the event occurs from time to time in a random manner is to be expected. It is partly as a result of the randomness introduced by the turbulent mixing, and partly the sensitivity of the composition of the mixture, since Figure 4.9 confirms that only a limited compositional range is explosive.

---

## 4.5 MOLD SURFACE REACTIONS

### 4.5.1 Pyrolysis

When the metal has filled the mold the mold becomes hot. A common misconception is to assume that the sand binder then burns. However, this is not true. It simply becomes hot. There is insufficient oxygen to allow any significant burning. What little oxygen is available is consumed in a minor, transient oxidation which quickly comes to a stop. What happens then to the binder is not burning, but pyrolysis.

Pyrolysis is the decomposition of compounds, usually organic compounds, simply by the action of heat. Oxygen is absent, so that no burning (i.e. high temperature oxidation) takes place. Pyrolysis of various kinds of organic binder components to produce carbon is one of the more important reactions that take place in the mold surface. Carbon is poorly wetted by many liquid metals, so the formation of carbon on the grains of sand, as a pyrolyzed residue of the sand binder, produces a non-wetted mold surface, which can lead to an improved surface finish to the casting (although, as will become clear, the effect of the surface film on the liquid metal is probably more important).

This non-wetting feature of residual carbon on sand grains is at first sight curious, since carbon is soluble in many metals, and so should react, and should therefore wet. Cast iron would be a prime candidate for this behavior. Why does this not happen?

In the case of ductile iron, sand cores do not need a core coat, since the solid magnesium-oxide-rich film (probably a magnesium silicate) on the surface is a mechanical barrier that prevents penetration of the metal into the sand.

In the case of gray cast iron in a greensand mold the atmosphere may be oxidizing, causing the melt surface to grow a film of liquid silicate. This is highly wetting to sand grains, so that the application of

a core coating such as a refractory wash may be necessary to prevent penetration of the metal into the core.

However, in the case of gray iron cast in a mold rich in hydrocarbons (i.e. greensand with sufficient additions of coal dust, or certain resin-bonded sands) metal penetration is prevented when the hydrocarbons in the atmosphere of the mold pyrolyze on the surface of the hot liquid metal to deposit a thin film of solid carbon on the liquid. Thus the reason for the robust non-wetting behavior is that a solid pyrolyzed carbon film on the liquid contacts a solid, pyrolyzed carbon layer on the sand grains of the mold surface. This carbon-against-carbon behavior explains the excellent surface finish that gray irons can achieve if bottom-gated and filled in a laminar fashion.

For the casting of iron, powdered coal additions or coal substitutes are usually added to greensands to improve surface finish in this way, providing a carbon layer to both the sand grains and the liquid surface. The reactions in the pyrolysis of coal were originally described by Kolorz and Lohborg (1963):

1. The volatiles are driven out of the coal to form a reducing atmosphere.
2. Gaseous hydrocarbons break down on the surface of the liquid metal. (Kolorz and Lohborg originally thought the hydrocarbons broke down on the sand grains to form a thin skin of graphite, but this is now known to be not true.)
3. The coal swells, and on account of its large expansion, is driven into the pores of the sand. This plastic phase of the coal addition appears to plasticize the binder temporarily and thereby eases the problems associated with the expansion of the silica, allowing its expansion to be accommodated without the fracture of the surface. As the temperature increases further and the final volatiles are lost, the mass becomes rigid, converting to a semi-coke. The liquid metal is prevented from contacting and penetrating the sand by this in-filling of carbon that acts as a non-wetted mechanical barrier.

Kolorz and Lohborg recommend synthetically formulated coal dusts with a high tendency to form anthracitic carbon, of good coking capacity and with good softening properties. They recommend that the volatile content be near 30%, and sulfur less than 0.8% if no sulfur contamination of the surface is allowable. If some slight sulfurization is permissible, then 1.0–1.2% sulfur could be allowed. Peterson and Blanke (1980) emphasize the bituminous nature and low ash content of desirable coals.

In the case of phenolic urethane and similar organic chemical binders based on resin systems, the thermal breakdown of the binder assists the formation of a good surface finish to cast irons and other metals largely in the manner described above. The binder usually goes through its plastic stage prior to rigidizing into a coke-like layer. The much smaller volume fraction of binder, however, does not provide for the swelling of the organic phase to seal the pores between grains. So, in principle, the sand remains somewhat vulnerable to penetration by the liquid metal. The second aspect of non-wettability is discussed below.

The founder should be aware of binder pyrolysis reactions that can have adverse effects on the surface quality of the casting. These are more likely to occur with binders that contain nitrogen (phenol urethanes and some furans), which can be converted to cyanide and amine gases. In the case of furans, problems may arise from the use of the sulfonic acid or phosphoric acid catalysts and will become cumulative, being least when new sand is used and progressively more concentrated as the content of conventionally reclaimed sand in the mix increases. Sulfonic acids react with iron and iron oxide residues in the sand, with feldspars, with limestone often present in poor-quality sand, and with certain

types of coatings, to form the corresponding sulfonates. These will in turn be reduced to sulfides during casting and these may then cause sulfide damage to cast parts.

Phosphoric acid damage is caused by a different mechanism, since phosphates are stable under casting conditions. It seems that the damage caused by phosphoric acid is primarily due to the reaction of its vapor with iron<sup>II</sup> oxide (or chromite) dust, leading to the formation of iron<sup>II</sup> phosphate which coats the sand grains. Both the phosphoric acid vapor and the iron<sup>II</sup> phosphate can interact with components in the (ferrous) metal being cast.

#### 4.5.2 Lustrous carbon film

The carbonaceous gases evolved from the binder complete their breakdown at the white hot surface of the advancing front of liquid metal, giving up carbon and hydrogen to the advancing liquid front. For steel, the carbon dissolves quickly and usually causes relatively little problem. For cast iron, the carbon dissolves hardly at all, because the temperature is lower, and the metal is already nearly saturated with carbon. Thus the carbon cannot dissolve away quickly into the liquid iron so that it accumulates on the surface as a film. The time for dissolution seems to be about the same as the time for mold filling and solidification. Thus the film has a life sufficiently long to affect the flow of the liquid.

As the liquid iron rolls out on the surface of the mold, it lays down its surface film as the liquid progresses. This laying down of the surface film can be likened to the laying down of the tracks of a track-laying vehicle. The film confers a non-wetting behavior on the liquid itself because the liquid is effectively sealed in a non-wetting skin. The skin forms a mechanical barrier between the liquid and the mold. The barrier is laid down as the liquid progresses because of friction between the liquid and the mold, the friction effectively stretching the film and tearing it at the meniscus where it immediately re-forms to continue the process (Figure 2.2). The strength and rigidity of the carbon film helps the liquid surface to bridge unsupported regions between sand grains or other imperfections in the mold surface. By this mechanism the surface of the casting is smoothed to a significantly finer finish than could be achieved by surface tension alone attempting to bridge between the sand grains.

It should be noted that the benefits of laying out a solid film as the liquid iron rolls out on the mold surface is only achieved if the liquid is encouraged to fill progressively, as a rolling action up against the mold surface. The casting surface can then take on an attractive, smooth, glossy shine. However, if the melt is top-poured, splashing and hammering the mold, no benefit is obtained; in fact the liquid penetration can be severe giving a casting surface so spiky, sharp and rough to take the skin off your hands. It makes sense to fill the casting nicely using a properly designed bottom-gated technique.

The mechanism for the improvement of surface finish can only operate effectively if the progress of the meniscus is steady and controlled, i.e. in the absence of surface turbulence.

In addition to surface finish problems, a further problem arises if surface turbulence causes the carbon film to become entrained in the liquid. The film will necessarily become entrained as a double film, a carbon bifilm (since single films cannot be entrained) constituting a serious crack-like defect. Fortunately in heavy section castings the entrained double film defect has time to dissolve, and never seems to be a problem. Light section castings should only be attempted using binder systems that produce little lustrous carbon since defects will not have time to dissolve and will therefore be effectively permanent. Alternatively, a preferable strategy would of course be the use of a running system that could guarantee the absence of surface turbulence.

It is worth mentioning that the lustrous carbon film, in contrast to all other surface films on other metals that I know, appears to detach easily from the iron during cooling. This curious behavior means that after breaking the casting out of the mold, the film is sometimes seen attached to the surface of the mold, covering the surface as a smooth, glossy sheet, leading many observers to the mistaken conclusion that the film had initially formed on the mold surface (Naro 2004). This is clearly not possible, of course, because pyrolysis reactions can only occur in high-temperature conditions, such as on the melt surface, in contrast to the sand grains which are relatively cold.

### 4.5.3 Sand reactions

Other reactions in the mold surface occur with the sand grains themselves. The most common of sand reactions is the reaction between silica ( $\text{SiO}_2$ ) and iron oxide (Wustite,  $\text{FeO}$ ) to produce various iron silicates, of which the most commonly quoted (but not necessarily the most common or the most important) is fayalite ( $\text{Fe}_2\text{SiO}_4$ ). This happens frequently at the high temperatures required for the casting of irons and steels. It causes the grains to fuse and collapse as they melt into each other, because the melting point of some of the silicates is below the casting temperature. (The much-quoted melting point of fayalite at only  $1205^\circ\text{C}$  may be an error, since fayalite may have a significantly higher melting temperature. A more likely candidate to melt is Grunerite,  $\text{FeSiO}_3$ .) The reacted grains adhere to the surface of the casting because of the presence of the low-melting-point liquid 'glue'. This is known as burn-on.

The common method of dealing with this problem is to prevent the iron oxidizing to form  $\text{FeO}$  in the first place. This is usually achieved by adding reducing agents to the mold material, such as powdered coal to greensand, or aluminum-powder additions to mold washes and the like. The problem is also reduced in other sands that contain less silica, such as chromite sand. However, the small amounts of silica which are present in chromite can still give trouble in steel castings, where the extreme temperature causes the residual silica to fuse with the clay. At these temperatures the chromite may break down, releasing  $\text{FeO}$  or even droplets of  $\text{Fe}$  on the surface of the chromite sand grains. Metal penetration usually follows as the grains melt into each other, and the mold surface generally collapses. The molten, fused mass is sometimes known as 'chromite glaze'. It is a kind of burn-on, and is difficult to remove from steel castings (Petro and Flinn 1978). Again, carbon compounds added to the molding material are useful in countering this problem (Dietert et al. 1970).

Peterson and Blanke (1980) draw attention to the potential role of hydrogen released during the pyrolysis of coal dust in greensand, proposing that hydrogen plays an important part in avoiding the formation of oxides and silicates, explaining its contribution to good surface finish and the avoidance of burn-on.

### 4.5.4 Mold contamination

There are a few metallic impurities that find their way into molding sands as a result of interaction between the cast metal and the mold. We are not thinking for the moment of the odd spanner or tonnes of iron filings from the steady wearing away of sand plant. (Such ferrous contamination is retrieved in most sand plants by the provision of a powerful magnet located at some convenient point in the recirculating sand system. The foundry maintenance crew always have interesting stories to tell of items found from time to time attached to the magnet.) Nor are we thinking of the pieces of tramp



metal such as flash and other foundry returns. Our concern is with the microscopic traces of metallic impurities that lead to a number of problems, particularly because of the need to protect the environment from contamination.

Foundries that cast brasses find that the grains of their molding sand become coated with a zinc-rich layer, with lead-rich nodules on the surface of the zinc (Mondloch et al. 1987). The metals are almost certainly lost from the casting by evaporation from the surface after casting. The vapor condenses among the cool sand grains in the mold as either particles of metallic alloy, or reacts with the clay present, particularly if this is bentonite, to produce Pb–Al silicates. If there is no clay present, as in chemical binder systems such as furan resins, then no reaction is observed so that metallic lead remains (Ostrom et al. 1982). Thus ways of reducing this problem are: (1) the complete move, where possible in simple castings, to metal molds; (2) the complete move, where possible, from lead-containing alloys; or (3) the use of chemical binders, together with the total recycling of sand in-house. This policy will contain the problem, but the sand will have a fair degree of toxicity. If the metallic lead can be separated from the sand in the sand-recycling plant the proceeds might provide a modest economic return, and the sand toxicity could be limited.

There has been a suggestion that iron can evaporate from the surface of a ferrous casting in the form of iron carbonyl  $\text{Fe}(\text{CO})_5$ . This suggestion appears to have been eliminated on thermodynamic grounds; Svoboda and Geiger (1969) show that the compound is not stable at normal pressures at the temperature of liquid iron. Similar arguments eliminated the carbonyls of nickel, chromium, and molybdenum. These authors carry out a useful survey of the existing knowledge of the vapor pressures of the metal hydroxides and various sub-oxides but find conclusions difficult because the data are sketchy and contradictory. Nevertheless they do produce evidence that indicates vapor transport of iron and manganese occurs by the formation of the sub-oxides  $(\text{FeO})_2$  and  $(\text{MnO})_2$ . The gradual transfer of the metal by a vapor phase, and its possible reduction back to the metal on arrival on the sand grains coated in carbon might explain some of the features of metal penetration of the mold, which is often observed to be delayed, and then occur suddenly. More work is required to test such a mechanism.

The evaporation of manganese from the surface of castings of manganese steel is an important factor in the production of these castings. The surface depletion of manganese seriously reduces the surface properties of the steel. In a study of this problem, Holtzer (1990) found that the surface concentration of manganese in the casting was depleted to an impressive non-trivial depth of 8 mm and the concentration of manganese silicates in the surface of the molding sand was increased.

The process of Mn evaporation can be observed to occur from a drop of liquid steel placed on a water-cooled copper substrate. A ‘halo’ is seen to develop around the drop indicating mainly Mn condensation, although Cr and Fe can also contribute (Nolli and Cramb 2008).

Figure 6.26 confirms that the vapor pressure of manganese is significant at the casting temperature of steel. However, the depth of the depleted surface layer is nearly an order of magnitude larger than can be explained by diffusion alone. It seems necessary to assume, therefore, that the transfer occurs mainly while the steel is liquid, and that some mixing of the steel is occurring in the vicinity of the cooling surface.

It is interesting that a layer of zircon wash on the surface of the mold reduces the manganese loss by about half. This seems likely to be the result of the thin zircon layer heating up rapidly, thereby reducing the condensation of the vapor. In addition, it will form a barrier to the progress of the manganese vapor, keeping the concentration of vapor near the equilibrium value close to the casting surface. Both mechanisms will help to reduce the rate of loss. If, however, the protective wash is

applied after the molding sand has already become significantly contaminated with Fe and Mn oxides in the recycling process, the underlying sand may partially melt and collapse (Kruse 2006). This instability of the underlying sand will cause mechanical penetration of the zircon wash, and extensive permeation of the metal into the underlying partially melted sand. The carry-over of such contamination should be eliminated by careful control of the recycling process or revised selection of molding aggregate (see Section 4.7.1).

Gravity die casters that use sand cores (semi-permanent molds) will be all too aware of the serious contamination of their molds from the condensation of volatiles from the breakdown of resins in the cores. The build-up of these products can be so severe as to cause the breakage of cores, and the blocking of vents. Both lead to the scrapping of castings. The blocking of vents by tar-like deposits in permanent molds is the factor that controls the length of a production run prior to the mold being taken out of service for cleaning. On carousels of dies in Al alloy cylinder head production, a die may need to be taken out of service every 10th or 15th casting. The absence of such problems in sand molds is a natural advantage of sand molding that is usually overlooked.

#### 4.5.5 Mold penetration

Svoboda (1994) reviews the wide field of mold penetration by melts, and concludes that (i) liquid state penetration occurs in 75% of cases, in which the effect is merely the mechanical balance between the driving pressure and capillary effects, (ii) in 20% of cases penetration is driven by chemical reactions, (iii) vapor-state reactions may control 5% of penetration problems. We shall examine his categories in detail below. In addition, the time dependence of penetration is an interesting behavior that requires explanation.

##### ***Liquid penetration: Effect of surface tension and pressure***

Any liquid will immediately start to impregnate a porous solid if the solid is wetted by the liquid. The effect is the result of capillary attraction. For this reason, molding materials are selected for their non-wetting behavior, so that penetration by liquid metals is resisted; the effect is known as capillary repulsion.

It was the French workers Portevin and Bastien (1936) that first proposed that capillary forces should be significant for the penetration of liquid metals into sand. However, this prediction was neglected until the arrival of Hoar and Atterton (1950) who first set out the basic physics, creating a quantitative model in which the surface tension  $\gamma$  of the melt would hold back the penetration of a liquid subjected to gradually increasing pressure against the surface of a porous, non-wetted aggregate. The liquid interface bridging the inter-particle spaces would gradually swell out, bulging to a steadily greater curvature until it became hemispherical (radius  $r$  in Figure 4.11). Up to this critical value the melt could be held back, but above this pressure, further advance of the meniscus would cause the radius of curvature to increase as indicated by the formula below, lowering the resistance. The balance condition at the critical pressure for penetration is that quoted in Equation 3.11,  $P = 2\gamma/r$ .

If we substitute  $\rho gH$  for pressure due to depth  $H$  in a metal of density  $\rho$  we have the critical depth of metal for penetration

$$H = 2\gamma/r\rho g \quad (4.1)$$

Thus, beyond this critical point, penetration would instantly occur as a run-away effect; Figure 4.10 shows the meniscus expanding rapidly away after the narrowest point between sand grains is passed. Penetration might subsequently only be stopped by the advancing front losing its heat and freezing. Such elementary physics is helpful to understand why finer grain size of the aggregate, or the provision of any extremely fine-grained surface coating, are both helpful to reduce penetration (increase  $H$ ) by this simple mechanical model.

The resistance of penetration until some critical pressure is achieved has been demonstrated many times. For instance, Draper and Gaindhar (1975) find a metal depth of approximately 300 mm is required for steel to penetrate consistently into greensand molds in their experiment. This critical depth

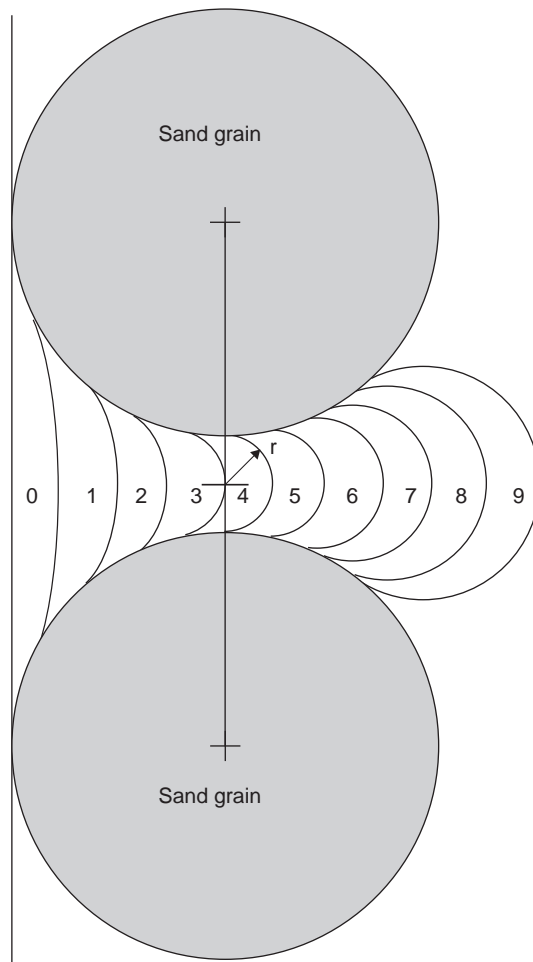


**FIGURE 4.10**

Metal penetration between two cylinders to simulate two sand grains. Surface tension resists the applied pressure up to the minimum radius  $r$ . Beyond this curvature penetration is a run-away instability.

was influenced to some degree by mold compaction, oxidizing conditions, and the temperature of mold hot-spots. If we assume a density of  $7000 \text{ kg m}^{-3}$ , surface tension approximately  $2 \text{ N m}^{-1}$  and acceleration due to gravity of about  $10 \text{ m s}^{-2}$ , we find the radius  $r$  is approximately  $0.02 \text{ mm}$ , indicating the inter-particle diameter to be roughly  $40 \text{ }\mu\text{m}$  in their molds, which seems a reasonable value.

All of the discussion so far has assumed perfect non-wetting between the metal and the mold (i.e. a contact angle of  $180^\circ$ ). Hayes and co-workers (1998) go to some lengths to emphasize the effect of conditions intermediate between wetting and non-wetting, taking account of the contact angle between the melt and its substrate. They find a good correlation between the contact angle and the penetration of liquid steel into silica sand molds. Petterson (1951) suggests that the penetration of steel into sand molds would be aided by a gradual fall in the contact angle as is commonly seen between liquids and substrates. There may be some truth in this in some situations, particularly for some alloys where vapor transport or chemical reactions are occurring. However, Hayes and colleagues measure the change in contact angle in their work and find the change insignificant. In their careful study the penetration appeared to be a simple mechanical process involving varying degrees of capillary repulsion.

Levelink and Berg have investigated and described conditions in which they suggested dynamic conditions were important (Figure 4.11). They claimed that iron castings in greensand molds were subject to a problem that they suggested was a water explosion. This led to a severe but highly localized form of mold penetration by the metal.

However, careful evaluation of their work indicates that it seems most likely that they were observing a simple conservation of momentum effect. As the liquid metal fills their conical mold it accelerates as the area of the cone decreases. As the melt nears the tip, it reaches its maximum velocity, slamming the melt into the ever-decreasing space. The result is the generation of a high shock pressure, forcing metal into the sand. The effect is similar to a cavitation damage event associated with the collapse of a bubble against a ship's propeller. Although they cite the presence of bubbles as evidence of some kind of explosion, the oxides and bubbles present in many of their tests seem to be the result of entrainment in their rather poor filling system, rather than associated with any kind of explosion.

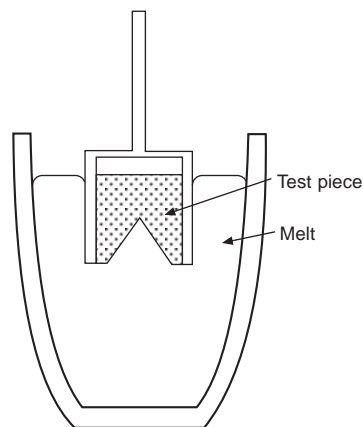


**FIGURE 4.11**

Water hammer (momentum effect) test piece (Levelink and Berg 1971).

The impregnation of the mold with metal in the last regions to fill is commonly observed in all metals in sand molds. A pressure pulse generated by the filling of a boss in the cope will often also cause some penetration in the opposite drag surface of a thin-wall casting. The point discontinuity shown in Figure 2.27 will be a likely site for metal penetration into the mold. If the casting is thin-walled, the penetration on the front face will also be mirrored on its back face. Such surface defects in thin-walled aluminum alloy castings in sand molds are highly unpopular, because the silvery surface of an aluminum alloy casting is spoiled by these dark spots of adhering black sand (sometimes called ‘the black plague’!) and thus will require the extra expense of being removed by hand, or blasting with shot or grit.

Levelink and Berg (1968) report that the problem is increased in greensand by the use of high-pressure molding. This may be the result of the general rigidity of the mold accentuating the concentration of momentum (weak molds will yield more generally, and thus dissipate the pressure over a wider area). They list a number of ways in which this problem can be reduced:

1. Reduce mold moisture.
2. Reduce coal and organics.
3. Improve permeability or local venting; gentle filling of mold to reduce final filling shock.
4. Retard moisture evaporation at critical locations by local surface drying or the application of local oil spraying.

The reduction in the mechanical forces involved by reduced pouring rates or by local venting are understandable as reducing the final impact forces. Similarly, the use of a local application of oil will reduce permeability, causing the air to be compressed, acting as a cushion to decelerate the flow more gradually.

The other techniques in their list seem less clear in their effects, and raise the concern that they may possibly be counter-productive! It seems there is plenty of scope for additional studies to clarify these problems.

Work over a number of years at the University of Alabama, Tuscaloosa (Stefanescu et al. 1996), has clarified many of the special issues relating to the penetration of sand molds by cast iron. Essentially, this work concludes that hot-spots in the casting, corresponding to regions of isolated residual liquid, are localized regions in which high pressures can be generated in the residual liquid inside the casting by the expansion of graphite, forcing the liquid out via microscopic patches of unfrozen surface, and causing local penetration of the mold. The pressure can be relieved by careful provision of ‘feed paths’ to allow the expanding liquid to be returned to the feeder. The so-called ‘feed paths’ are, of course, allowing residual liquid to escape, working in reverse of normal feeding.

Naturally, any excess pressure inside the casting will assist in the process of mold penetration. Thus large steel castings are especially susceptible to mold penetration because of the high metallostatic pressure. This factor is in addition to the other potential high-temperature reactions listed above. This is the reason for the widespread adoption in steel foundries of the complete coating of molds with a ceramic wash as an artificial barrier to penetration.

### ***Natural barriers to penetration***

We have seen above that in some conditions cast iron can develop a strong carbon film (the lustrous carbon film) on its advancing meniscus which is pulled down into the gap between the mold and the

metal. Here it effectively separates the liquid from the aggregate, providing a mechanical barrier to prevent penetration, and retain a smooth shiny surface on the casting. Also, as we shall see, oxidizing conditions can eliminate the carbon film replacing it with a liquid silicate. Penetration in oxidizing conditions can then be practically guaranteed.

In copper-based foundries, the alloy aluminum bronze is renowned for its ability to resist penetration of the mold. The reason is also certainly the mechanical barrier presented by the strong alumina film; the high content of Al, in the range 5–10%, and the high temperature combine to create one of the most tenacious films in the casting world. In contrast, those bronzes not protected by a strong film in the liquid state, tin-, lead-, and phosphor-bronze, all suffer penetration problems.

Similarly, Gonya and Ekey (1951) compared the behavior of the common copper–base alloy 85–5–5 and the Al–5Si alloy, investigating a number of molding variables. However, their most significant result related to pressure. They gradually increased pressure, finding penetration in the copper alloy at a critical pressure 17 kPa (2.5 psi) whereas the Al alloy continued to resist penetration up to the maximum they were able to provide in their experiment, about 30 kPa (4.5 psi). The presence of the alumina film is clearly a major benefit (if, of course, retained on the surface instead of being entrained in the melt!).

#### ***Temperature and time dependence of penetration***

Clearly, the metal cannot penetrate the mold if the metal has solidified. Taking this impressively undeniable basic logic to heart, Brookes et al. (2007) draw attention to the importance of the mold temperature. By both computer model and experiment they were able to demonstrate that as the mold surface increased on contact with the melt, and later decreased during cooling, penetration of liquid steel did not occur until the mold temperature exceeded a critical value. The penetration subsequently continued, causing the penetration effect to worsen while the temperature remained above the critical temperature. Penetration finally stopped when the temperature fell once again below the critical value. It is interesting that this relatively simple model appears to provide an explanation for the time dependence of penetration as has been known for many years (Jones 1948, Shirey and Williams 1968).

It should be noted, however, that the reduction of contact angle, i.e. progressively increasing effectiveness of wetting, also has been observed for many metal/mold combinations to be a function of time (for instance Wu et al. 1997, Shen et al. 2009). Also, of course, mold atmosphere greatly affects wetting ability, and this too is a function of time. Thus a reducing or neutral atmosphere is useful to reduce penetration in low-carbon steels in greensand molds, whereas an oxidizing atmosphere encouraged penetration as found by Draper and Gaindhar in 1975.

#### ***Chemical interactions***

There seems little doubt that the contact angle between the mold particles and the melt can change with both time and temperature. Hayes and colleagues (1998) noted a reduction of the contact angle of liquid steel on silica sand from 110 to 93° over a period of 30 minutes. However, this lengthy period and relatively small change are not likely to greatly affect most steel castings since the majority will have frozen in this time.

To effect a major change in behavior would require a major change in contact angle over a relatively short period such as a few minutes. The penetration of gray irons into silica sand molds in oxidizing condition is exactly such a candidate as has already been noted above.

***Effects of vapor transport***

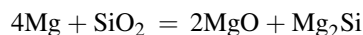
For a general overview of the knowledge of vapor transport the reader is referred to the excellent review by Svoboda and Geiger (1969). It is salutary to reflect that it seems relatively little additional knowledge on this important subject has been gained since this early date.

On a microscale, the effects of vapor transport are likely to be complicated. Ahn and Bergehan (1991) studied the infiltration of liquid Sn, Pb, and Cu inside metal capillaries using SEM. They found evidence of the deposition of metal vapors over a region up to 0.1 mm ahead of the advancing front. Clearly, the presence of this freshly deposited metal influenced the effect of the wetting of the liquid that followed closely behind.

Shen and colleagues (2009) drew similar conclusions from experiments with sessile drops in vacuum. They found that the contact angle of a zirconium/copper-based alloy on an alumina substrate fell from about 90 to 0° in about 10 minutes. They found Zr adsorption at the liquid/solid interface, followed by a Zr–Cu precursor film that accounted for the excellent wetting.

On a macroscale, vapor transport from metals into molds is a common feature in foundries, and will be referred to repeatedly elsewhere in this book. To give just two contrasting instances here:

- (a) Foundries casting magnesium into plaster molds filled with vacuum assistance (Sin et al. 2006) find that Mg diffuses into the plaster, reacting with the SiO<sub>2</sub>, taking the oxygen to form MgO, and reducing the Si to Mg<sub>2</sub>Si according to the reaction



- (b) Bronze foundries casting classical tin-bronzes and lead-bronzes find that both alloys suffer mold penetration. However, only lead has any significant vapor pressure at the casting temperature, its pressure being between 100 and 1000 times greater than tin (see Figure 6.26). We can conclude therefore that in this particular case, vapor pressure is seen to be of minor, if any, importance; a high vapor pressure does not necessarily lead to enhanced penetration. The expected absence of any significant mold reactions or any strong surface films leaves only the relatively weak action of surface tension to inhibit penetration. Thus mold penetration for these alloys seems possible only by mechanical means: the provision of a fine mold aggregate, or a ceramic surface coat.

---

## 4.6 METAL SURFACE REACTIONS

Easily the most important metal/mold reaction is the reaction of the metal with water vapor to produce a surface oxide and hydrogen, as discussed in Chapter 1.

However, the importance of the release of hydrogen and other gases at the surface of the metal, leading to the growth of porosity in the casting, is to be dealt with in Chapter 6. Here we shall devote ourselves to the many remaining reactions. Some are reviewed by Bates and Scott (1977). These and others are listed briefly below.

### 4.6.1 Oxidation

Oxidation of the casting skin is common for low-carbon-equivalent cast irons and for most low-carbon steels. It is likely that the majority of the oxidation is the result of reaction with water vapor from the

mold, and not from air, which is expelled at an early stage of mold filling as shown earlier. Carbon additions to the mold help to reduce the problem.

The catastrophic oxidation of magnesium during casting, leading to the casting (and mold) being consumed by fire, is prevented by the addition of so-called inhibitors to the mold. These include sulfur, boric acid, and other compounds such as ammonium borofluoride. More recently, much use has been made of the oxidation-inhibiting gas, sulfur hexafluoride ( $\text{SF}_6$ ), which is used diluted to about 1 or 2% in air or other gas such as  $\text{CO}_2$  to prevent the burning of magnesium during melting and casting. However, since its identification as a powerful ozone-depleting agent,  $\text{SF}_6$  is being discontinued for good environmental reasons. A return is being made to dilute mixtures of  $\text{SO}_2$  in  $\text{CO}_2$  and other more environmentally friendly atmospheres are now under development.

In any case, the burning of Mg alloys during pouring of the mold is almost certainly the result of surface turbulence. For instance, if liquid Mg can be introduced into a mold quiescently, so that it rises steadily with a substantially flat liquid surface in the mold, the huge heat of oxidation released on the surface is rapidly conveyed away into the bulk of the melt so that the surface temperature never rises to a dangerous level. Such a quiescent fill is therefore safe. Conversely, if the melt is jumping and splashing, the heat of oxidation will diffuse into the thin liquid splash from both sides of the splash surface, and quickly heats the small amount of metal in the splash. The ignition temperature of the melt is quickly exceeded, with disastrous results. There is a saying, which regrettably probably reflects some truth, that the few Mg foundries in existence nowadays is the result of most of them having burned down. True or not, the turbulent handling of Mg alloys is clearly dangerous but mostly avoidable.

Titanium and its alloys are also highly reactive. Despite being cast under vacuum into molds of highly stable ceramics such as zircon, alumina, or yttria, the metal reacts to reduce the oxides, contaminating the surface of the casting with oxygen, stabilizing the alpha phase of the alloy. The 'alpha case' usually has to be removed by chemical machining.

#### 4.6.2 Carbon (pick-up and loss)

Mention has already been made of the problem of casting titanium alloy castings in carbon-based molds. The carburization of the surface again results in the stabilization of the alpha phase, and requires to be subsequently removed.

The difficulty is found with stainless steel of carbon content less than 0.3% cast in Croning resin-bonded shell molds (McGrath 1973). The relatively high resin binder content of these molds, generally in the region of 2.5–3.0 wt%, causes steels to suffer a carburized layer between 1 and 2 mm deep. Tordoff (1996) also found significant carbon pick-up in stainless steels from phenolic urethane binders which rarely exceed 1.0–1.2 wt% BOS (based on sand). The carburization, of course, appears more severe the lower the carbon content of the steel. Naturally, the problem is worse on drag than on cope faces as a result of the casting sitting hard down on the drag face of the mold, and contracting away from the upper surfaces. Tordoff also found that iron oxide in the molding sand reduced the effect, whereas the use of a furan resin eliminated pick-up altogether. The author could not find a record of the effect of silicate-based binders, although their usually low content of organics would be expected to give minimal problems.

Carbon pick-up is the principal reason why low carbon steel castings are not produced by the lost-foam process. The atmosphere of styrene vapor, which is created in the mold as the polystyrene



decomposes, causes the steel to absorb carbon (and presumably hydrogen). The carbon-rich regions of the casting are easily seen on an etched cross-section as swathes of pearlite in an otherwise ferritic matrix.

In controlled tests of the rate of carburization of low-carbon steel in hydrocarbon/nitrogen mixtures at 925°C (Kaspersma 1982), methane was the slowest and acetylene the fastest of the carburizing agents tested, and hydrogen was found to enhance the rate, possibly by reducing adsorbed oxygen on the surface of the steel. At high ratios of  $H_2/CH_4$  at this temperature, hydrogen decarburizes steel by forming methane ( $CH_4$ ). This may be the important reaction in the casting of steel in greensand sand molds containing only low carbonaceous additions.

Surface decarburization of steels is often noted with acid-catalyzed furan resin binders (Naro and Wallace 1992).

In the investment casting of steel, the decarburization of the surface layer is particularly affected because atmospheric oxygen persists in the mold as a consequence of the inert character of the mold, and its permeability to the surrounding environment. Doremus and Loper (1970) have measured the thickness of the decarburized layer on a low-carbon steel investment casting and find that it increases mainly with mold temperature and casting modulus. The placing of the mold immediately after casting into a bin filled with charcoal helps to recarburize the surface. However, Doremus and Loper point out the evident danger that if the timing and extent of recarburization is not correct, the decarburized layer will still exist below a recarburized layer!

In iron castings the decarburization of the surface gives a layer free from graphite. This adversely affects machinability, giving pronounced tool wear, especially in large castings such as the bases of

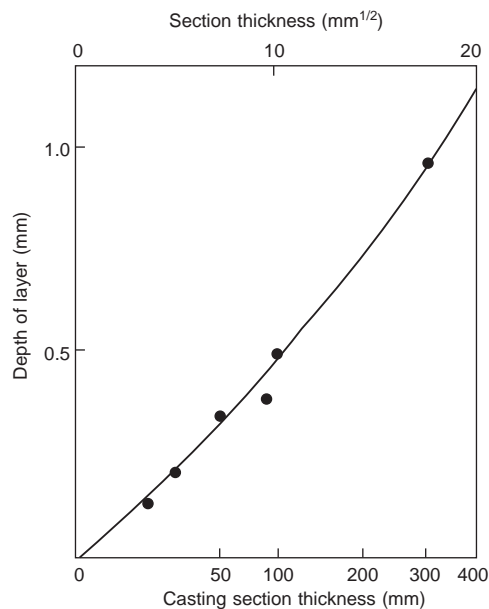


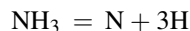
FIGURE 4.12

Depth of decarburization in gray iron plates cast in greensand (data from Rickards 1975).

machine tools. The decarburization seems to be mainly the result of oxidation of the carbon by water vapor since dry molds reduce the problem. An addition of 5 or 6% coal dust to the mold further reduces it. Rickards (1975) found that the reaction seems to start at about the freezing point of the eutectic, about 1150°C, and proceeds little further after the casting has cooled to 1050°C (Figure 4.12). Stefanescu and co-workers (2009) find that the depth of the casting skin in ductile iron is controlled by diffusion to only about 0.5 mm if the liquid in the casting is relatively quiescent, whereas the strong convection currents during solidification of larger castings causes mixing, increasing the skin depth to nearly 3 mm.

### 4.6.3 Nitrogen

Nitrogen pick-up in gray cast irons appears to be directly related to the nitrogen content of mold binders (Graham et al. 1987). Ammonia is released during the pyrolysis of urea and amines contained in hot box and Croning shell systems when they become recycled into a greensand system. Ammonia appears to be reversibly absorbed by the bentonite clays, and is released on heating. The pyrolysis of ammonia releases nascent nitrogen and nascent hydrogen by the simple decomposition



Graham and co-workers confirmed that subsurface porosity and fissures in irons do not correlate well with the total nitrogen content of the sand, but were closely related to the total ammonia content. Lee (1987) confirms the usefulness of an ammoniacal nitrogen test, which in his work pointed to wood flour as a major contributor of ammonia in his greensand system.

The link of ammonia and the so-called nitrogen fissures in iron castings suggests the formation of nitride bifilms which might be opened, becoming visible, opening by inflation with the copious amounts of hydrogen released by the decomposition of ammonia.

At the other end of the casting value system, vacuum-cast Ni-based superalloys suffer severely from nitrogen pick-up from the moment the door of the vacuum furnace is opened, allowing air to rush in and react while the casting is still hot. Casting returns in such foundries are known to contaminate the new melts, although the contamination would be expected not to be nitrogen in solution, but nitride bifilms in suspension. These conjectures require more research to clarify the situation.

### 4.6.4 Sulfur

The use of molds bonded with furane resin catalyzed with sulfuric and/or sulfonic acid causes problems for ferrous castings because of the pick-up of sulfur in the surface of the casting (Naro and Wallace 1992). This is especially serious for ductile iron castings, because the graphite reverts from spheroidal back to flake form in this high-sulfur region. This has a serious impact on the fatigue resistance of the casting.

### 4.6.5 Phosphorus

The use of molds bonded with furane resin catalyzed with phosphoric acid leads to the contamination of the surfaces of ferrous castings with phosphorus (Naro and Wallace 1992). In gray iron the presence

of the hard phosphide phase in the surface causes machining difficulties associated with rapid tool wear.

#### 4.6.6 Surface alloying

There has been some Russian work (Fomin 1965) and Japanese work (Uto 1967) on the alloying of the surface of steel castings by the provision of materials such as ferrochromium or ferromanganese in the facing of the mold. Because the alloyed layers that have been produced have been up to 3 or 4 mm deep, it is clear once again that not only is diffusion involved but also some additional transport of added elements must be taking place by mixing in the liquid state. Omel'chenko further describes a technique to use higher-melting-point alloying additions such as titanium, molybdenum, and tungsten, by the use of exothermic mixes. Predictably enough, however, there appear to be difficulties with the poor surface finish and the presence of slag inclusions. Until this difficult problem is solved, the technique does not have much chance of attracting any widespread interest.

#### 4.6.7 Grain refinement

The use of cobalt aluminate ( $\text{CoAl}_2\text{O}_4$ ) in the primary mold coat for the grain refinement of nickel and cobalt alloy investment castings is now widespread, as described in early reports by Rappoport (1964) and Watmough (1980). The mechanism of refinement is not yet understood. It seems unlikely that the aluminate as an oxide phase can wet and nucleate metallic grains. The fact that the surface finish of grain-refined castings is somewhat rougher than that of similar castings without the grain refiner indicates that some wetting action has occurred. This suggests that the particles of  $\text{CoAl}_2\text{O}_4$  decompose to some metallic form, possibly  $\text{CoAl}$ . This phase has a melting point of  $1628^\circ\text{C}$ . It would therefore retain its solid state at the casting temperatures of Ni-based alloys. In addition it has an identical face-centered-cubic-crystal structure to nickel. On being wetted by the liquid alloy it would constitute an excellent substrate for the initiation of grains.

Watmough also investigates a number of other additives to coatings for Ni-base high-temperature alloy castings including cobalt oxide,  $\text{CoO}$ . Since oxides are almost certainly not effective nuclei for solid formation, and since  $\text{CoO}$  is not especially stable (Llewelyn and Ball 1962), it is likely that the compound decomposes at casting temperature forming metallic cobalt, which would be expected to be an effective nucleus for the alloy. Although its melting point is not significantly higher than the alloy, the fact that the Co particles sit at the mold wall will ensure that they remain cool and therefore will resist melting, and continue to act as nucleating particles.

It is to be expected that there can be no refinement if all the  $\text{CoAl}$  particles are either melted or dissolved, or if the newly nucleated grains are themselves re-melted. Unfortunately, such remelting problems are common in investment castings as a result of (i) casting at too high a temperature; and (ii) convection problems that have so far been overlooked. It is regrettable that the beautifully fine grain structure produced by these techniques is often lost by subsequent convection in the casting, conveying so much heat from hotter regions that parts of the surface in the path of the flow re-melt, destroying the nuclei and the early grains, and replacing these with massive grains of uncontrolled size. In addition, the small depth of grain refinement (Watmough reports only 1.25 mm) is another probable consequence of uncontrolled convection. It is expected that control and suppression of convection in investment castings would greatly improve cast structures in polycrystalline high-temperature alloy

castings. These issues are dealt with later in 'Casting Manufacture' in Casting Rule 7 'Avoiding Convection'.

Cobalt addition to a mold coat is also reported to grain-refine malleable cast iron (Bryant 1971), presumably by a similar mechanism to that enjoyed by the vacuum-cast Ni-base alloys.

The use of zinc in a mold coat by Bryant and Moore to achieve a similar aim in iron castings must involve a quite different mechanism, because the temperature of liquid iron (1200–1450°C) greatly exceeds not only the melting point, but even the boiling point (907°C) of zinc! It may be that the action of the zinc boiling at the surface of the solidifying casting disrupts the formation of dendrites, detaching them from the surface so that they become freely floating nuclei within the melt. Thus the grain-refining mechanism in this case is grain multiplication rather than nucleation.

The zinc-containing coating and others listed below all appear to induce grain multiplication as a result of the rafts of dendrites attempting to grow on an unstable, moving and collapsing substrate. The effect seems analogous to that described in Section 3.2.6 for the enhancement of the fluidity of Al alloy castings by coatings of acetylene black or hexachlorethane on molds.

Nazar and co-workers (1979) report the use of hexachlorethane-containing coatings for the grain refinement of Al alloys.

#### 4.6.8 Miscellaneous

Boron has been picked up in the surfaces of stainless steel castings from furane-bonded molds that contain boric acid as an accelerator (McGrath, 1973).

Tellurium is sometimes deliberately added as a mold wash to selected areas of a gray iron casting. This element is a strong carbide former, and will locally convert the structure of the casting from gray to a fully carbidic white iron. Chen and co-workers (1989) describe how TeCo surface alloying is useful to produce wear-resistant castings.

In other work, the carbide-promoting action of Te is said to reduce local internal shrinkage problems, although its role in this respect seems difficult to understand. It has been suggested that a solid skin is formed rapidly, equivalent to a thermal chill (Vandenbos 1985). The effect needs to be used with caution: tellurium and its fumes are toxic, and the chilled region causes difficulties in those parts requiring to be machined.

The effect of tellurium converting gray to white irons is used to good purpose in the small cups used for the thermal analysis of cast irons. Tellurium is added as a wash on the inside of the cup. During the pouring of the iron it seems to be well distributed into the bulk of the sample, not just the surface, so that the whole test piece is converted from gray to white iron. This simplifies the interpretation of the cooling curve, allowing the composition of the iron to be deduced.

## 4.7 MOLD COATINGS

### 4.7.1 Aggregate molds

Although we have dealt at length with reactions that can occur between the metal and the mold, the purpose of a mold coating is to prevent such happenings by keeping the two apart. It has to be admitted that for many formulations, these attempts are of only limited success. Some useful reviews of coatings from which the author has drawn are given by Vingas (1986), Wile and colleagues (1988), and Beeley

(2001). Vingas in particular describes techniques for measuring the thickness of coatings in the liquid and solid states. All describe the various ways in which coatings can be applied by dipping, swabbing, brushing, and flow-over. These issues will not be dealt with here.

An important aspect to bear in mind, as with the provision of feeders, and the best action (if possible) is to avoid coatings. There are many reasons for avoiding coatings. Disadvantages include:

1. Cost of materials, especially those based on expensive minerals such as zircon.
2. Potential loss of accuracy because of difficulty of controlling coat thickness and coating penetration.
3. Possibility of cosmetic defects from runs and drops.
4. Floor space for coating station.
5. Energy cost to dry and possible capital cost and floor space for drying ovens and extraction ducting and fans.
6. Floor space to dry if dried naturally (this might exceed molding space since drying is slow).
7. Drying time can severely reduce productivity.
8. Cores appear to be never fully dried, despite all attempts, after the application of a coating, so that there is enhanced danger of blow defects if the core cannot be vented to the atmosphere.

At this time many coatings are still alcohol (ethanol) based, and so burned off rather than dried. This requires minimal floor space and energy, but does add to the loading of VOCs (volatile organic compounds) in the environment. This approach is likely to be banned under future legislation, forcing the use of water-based coatings. The water-based coatings pose a significantly increased drying problem. Puhakka (2009) describes the novel use of a remote infra-red camera to monitor the drying process, since while water is still evaporating the surface will remain cool. Only when fully dry will the surface temperature of the mold rise to room temperature.

The advantages of coatings include:

1. Reduction of cleaning costs because of improved surface finish (finer surface, reduced or eliminated veining, reduced penetration and/or burn-on and reduced reactions between metal and mold, for instance between (i) manganese steel and silica sand, and (ii) binder gases such as sulfur compounds from furan binders).
2. Improved shake-out because of improved sand peel.
3. Reduced machining time and tool wear.

Coating costs for the foundry are usually justified on (1) and (2) above and should be based on the dry refractory deposited. Naturally, costs are directly related to the surface area to volume ratio of the castings, and so will vary from foundry to foundry. Alternatively, surface area per ton of castings is a useful measure.

Coatings are not required in general for the lower-melting-point metals such as the zinc-based alloys and the light metals, Al- and Mg-based alloys but are widely used for cast iron, copper-based alloys and steels.

With regard to the definition of a coating, it is a creamy mixture made up from of a number of constituents:

1. *Refractory*, usually oxides of many kinds ground to a particle size of 50  $\mu\text{m}$  or less, but for cast irons carbonaceous material is common in the form of graphite or ground coke etc.

2. *Carrier* nowadays becoming more commonly water (alcohols and chlorinated hydrocarbons have environmental problems). This has to be removed after the coating has been applied, usually requiring the application of heat.
3. *Suspension agent* required to maintain a uniform dispersion of the refractory. Commonly used materials include sodium bentonite clay or cellulose compounds. Beeley (2001) describes a problem with the clay addition, as a result of the water soaking into the mold surface, but being hindered during the subsequent drying because of the presence of the impervious clay coat. The development of a coating without the clay addition doubled the rate of drying.
4. *Binder* which is often the same as that used for bonding molds. Thus organic resins, colloidal silica, and sodium-silicate-based binders are common. Interesting incompatibilities are sometimes experienced, such as the fact that magnesite coatings for steel castings may be difficult to use with sand bonded with furan resins because of its acid content, whereas they perform excellently when used in conjunction with silicate-bonded molds and cores.
5. *Sundry chemicals* including surfactants to improve wettability, antifoaming agents, and bactericides.

The use of coatings on cores to prevent core blows is usually a mistake. Although the coating does reduce the permeability of the surface, assisting to keep in the expanding gases, the additional volatiles from the coat, which appear to be never completely removed by drying, are usually present in excess to overwhelm the coating barrier.

Another interesting mistake is the use of coatings to prevent sand erosion. The presence of sand defects in a casting is never, in my experience, the fault of the sand. It immediately signals that the filling system is faulty. A turbulent filling system that entrains air will splatter and hammer against the sand surface, oxidizing away any binder, and so erode away cores and molds. Although, of course, a coating will reduce the problem, it is often less costly and more effective to upgrade the filling system to a naturally pressurized design. In this way the molds and cores are at all times gently pressurized by the melt, causing the sand grains of the mold to be held safely in place. An additional bonus is a better casting, enjoying more reliable properties and freedom from other defects such as porosity and cracks.

#### 4.7.2 Permanent molds and metal chills

Permanent molds or chills in gray iron or steel are practically inert, so any mold coat is not required to prevent chemical reactions between the two. A coat will help to:

1. protect the mold from thermal shock;
2. avoid the premature chilling of the metal that might result in cold lap defects;
3. confer some 'surface permeability' on the impermeable surface to allow the melt to flow better over the surface, and allowing the escape of any volatiles or condensates (particularly from the surface of chills).

It is often seen that two different mold coatings are used on a permanent mold. A thin smooth coating is applied to the mold cavity which forms the casting, whereas a thick, rough, insulating coating is applied to the running system in an effort to avoid temperature losses during mold filling. This is a mistake. The metal is in the running system for perhaps only 1 or 2 seconds (because its velocity is in the range of meters per second, and the distance involved is usually only a meter or less) that any loss of temperature is negligible. Furthermore, the roughness of this coat endangers the flow because of the

consequential turbulence. It is far better, much less trouble, less time-consuming, less costly, simply to coat the whole die with the same thin, smooth coat. The probability is that the castings will be improved.

### 4.7.3 Dry coatings

Dry coatings are of course an attractive concept because no drying is involved and there is no danger of introducing additional volatiles into molds or cores.

Greensand molds have benefited somewhat from the use of dusting powders of various kinds, and more recently by the electrostatic precipitation of dry zircon flour (precoated with an extremely thin layer of thermosetting resin, activated by the heat of the metal during casting). This development appears to have been resistant to extension to dry sand processes because of the generally poorer electrical conductivity of dry sand molds particularly when bonded with a phenol-urethane resin. It would be interesting to know whether more success might be expected from molds made with materials having higher electrical conductivity such as sand bonded with silicates or alkaline phenolics, or with chromite sand.

A successful technique for the application of dry coatings to dry sand molds has therefore proved elusive. Simply dusting on dry powder, or attempting to apply it in a fluidized bed, suffers from most of the powder being blown off as clouds of dust when the mold is cleaned by blowing out with compressed air prior to closure.

A Japanese patent (Kokai 1985) describes how fine refractory powder in a fluid bed is drawn into the surface pores of an aggregate mold or core by applying a vacuum via some far location of the mold or core. However, of course, despite probably being useful for simple geometries, this technique fails for complex shapes. Another Japanese patent describes how fine powder in a fluid bed is forced into the pores of a mold by a mechanical brushing action. A Canadian automotive foundry has developed a fluid bed containing a mixture of the fine coating powder together with relatively heavy zircon grains. The jostling of the zircon grains effectively hammers the powder into the mold pores.

These dry coating techniques deserve wider use. When correctly applied, the coating simply fills the interstices between the surface grains of the mold, not adding any thickness of deposit. Thus the technique has the advantage of preserving the accuracy of the mold, while improving surface finish with no drying time penalty.

# Solidification structure

In this chapter we consider how the metal changes state from the liquid to the solid. The importance of control over solidification is emphasized by Heusler and colleagues (2001) who point out in their work to improve the properties of an Al alloy cylinder block casting that strong local cooling has a strong positive effect on the mechanical properties that can be of a similar importance as the influence of the alloy.

The chapter outlines how the solid develops its structure. It is a widely accepted piece of dogma, often quoted, that the properties of the casting are controlled by its structure. This seems to me to be largely untrue for most non-ferrous alloys. For instance in meeting mechanical property specifications of an Al alloy casting its solidification structure, its grain size or dendrite arm spacing (DAS) bear only a superficial relation to the properties. The feature really in control is the bifilm population. The fact that the grain size and DAS appear to be important seems mainly in relation to the way in which they influence the bifilm unfurling and bifilm distribution. More of this later.

In a later chapter we consider the problems of the volume deficit on solidification, and the so-called shrinkage problems that lead to a set of void phenomena, sometimes appearing as porosity, even though, as we shall see, such problems are actually relatively rare in castings (mainly because foundry people understand how to avoid shrinkage porosity). Most of the problems attributed to shrinkage are either not shrinkage problems at all, or are only secondarily shrinkage problems. Most problems that *appear* to be ‘shrinkage’ are actually oxides, actually bifilms.

When we understand how shrinkage voids can form, we are then in a better position to understand the development of the pore structure due to the precipitation of gas. Both these sets of defects form generally from bifilms of course.

These issues highlight the problem faced by the author. The problem is how to organize the descriptions of the complex but inter-related phenomena that occur during the solidification of a casting. This book could be organized in many different ways. For instance, naturally, the gas and shrinkage contributions to the overall pore structure are complementary and additive, and both rely on the presence and character of the pre-existing population of bifilms.

The reader is requested to be vigilant to see this integration. I am conscious that whilst spelling out the detail in a didactic dissection of phenomena, emphasizing the separate physical mechanisms, the holistic vision for the reader is easily lost. Take care not to lose the overall coherence of our fascinating field.

---

## 5.1 HEAT TRANSFER

### 5.1.1 Resistances to heat transfer

The hot liquid metal takes time to lose its heat and solidify. The rate at which it can lose heat is controlled by a number of resistances described by Flemings (1974). We shall follow his clear treatment in this section.



The five main resistances to heat flow from the interior of the casting (starting at zero for convenience of numbering later) are:

0. The liquid.
1. The solidified metal.
2. The metal–mold interface.
3. The mold.
4. The surroundings of the mold.

All these resistances add, as though in series, as shown schematically in Figure 5.1.

As it happens, in nearly all cases of interest, resistance (0) is negligible, as a result of stirring by forced convection during filling and thermal convection during cooling. The turbulent flow and mixing quickly transport heat and so smooth out temperature gradients. This happens quickly since the viscosity of the melt is usually low, so that the flow of the liquid is fast, and the heat is transported out of the center of large ingots and castings in a time that is short compared to that required by the remaining resistances, whose rates are controlled by diffusion.

In many instances, resistance (4) is also negligible in practice. For instance, for normal sand molds the environment of the mold does not affect solidification, since the mold becomes hardly warm on its outer surface by the time the casting has solidified inside.

However, there are, of course, a number of exceptions to this general rule, all of which relate to various kinds of thin-walled molds, which, because of the thinness of the mold shell, are somewhat sensitive to their environment. Iron castings made in Croning shell molds (the Croning shell process is

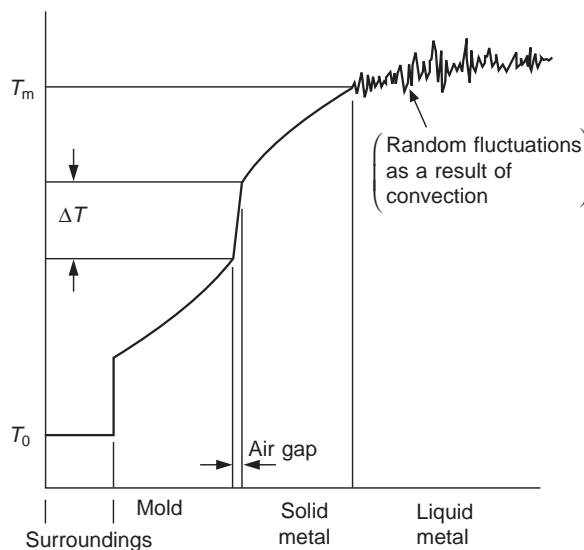


FIGURE 5.1

Temperature profile across a casting freezing in a mold, showing the effect of the addition of thermal resistances that control the rate of loss of heat.

one in which the sand grains are coated with a thermosetting resin, which is cured against a hot pattern to produce a thin, biscuit-like mold) solidify faster when the shell is thicker, or when the shell is thin but backed up by steel shot. Conversely, the freezing of steel castings in investment shell molds can be delayed by a thick backing of granular refractory material around the shell, all preheated to high temperature. Alternatively, without a backing, cooling is relatively fast, radiating heat away freely to cooler surroundings. Naturally, aluminum alloys in iron or steel dies can be cooled even faster when the back of the dies are cooled by water.

Nevertheless, despite such useful ploys for coaxing greater productivity, it remains essential to understand that in general the major fundamental resistances to heat flow from castings are items (1), (2), and (3). For convenience we shall call these resistances 1, 2, and 3.

The effects of all three simultaneously can nowadays be simulated with varying degrees of success by computer. However, the problem is both physically and mathematically complex, especially for castings of complex geometry.

There is therefore still much understanding and useful guidance to be obtained by a less ambitious approach, whereby we look at the effect of each resistance in isolation, considering only one dimension (i.e. unidirectional heat flow). In this way we can define some valuable analytical solutions that are surprisingly good approximations to casting problems. We shall continue to follow the approach by Flemings.

### ***Resistance 1: The casting***

The rate of heat flow through the casting, helping to control the freezing time of the casting, applies in the case of such examples as Pb–Sb alloy cast into steel dies for the production of battery grids and terminals; the casting of steel into metal molds; or the casting of hot wax into metal dies as in the injection of wax patterns for investment casting. It would be of wide application in the plastics industry.

However, it has to be admitted that this type of freezing regime does not apply for many metal castings of high thermal conductivity such as the light alloys or Cu-based alloys.

For the unidirectional flow of heat from a metal poured exactly at its melting point  $T_m$  against a mold wall initially at temperature  $T_0$ , the transient heat flow problem is described by the partial differential equation, where  $\alpha_s$  is the thermal diffusivity of the solid

$$\frac{\partial T}{\partial t} = \alpha_s \frac{\partial^2 T}{\partial x^2} \quad (5.1)$$

The boundary conditions are  $x = 0$ ,  $T = T_0$ ; at  $x = S$ ,  $T = T_m$ , and at the solidification front the rate of heat evolution must balance the rate of conduction down the temperature gradient, i.e.

$$H\rho_s \left( \frac{\partial S}{\partial t} \right) = K_s \left( \frac{\partial T}{\partial x} \right)_{x=S} \quad (5.2)$$

where  $K_s$  is the thermal conductivity of the solid,  $H$  is the latent heat of solidification, and for which the solution is:

$$S = 2\gamma\sqrt{\alpha_s t} \quad (5.3)$$

The reader is referred to Flemings for the rather cumbersome relation for  $\gamma$ . The important result to note is the parabolic time law for the thickening of the solidified shell. This agrees well with

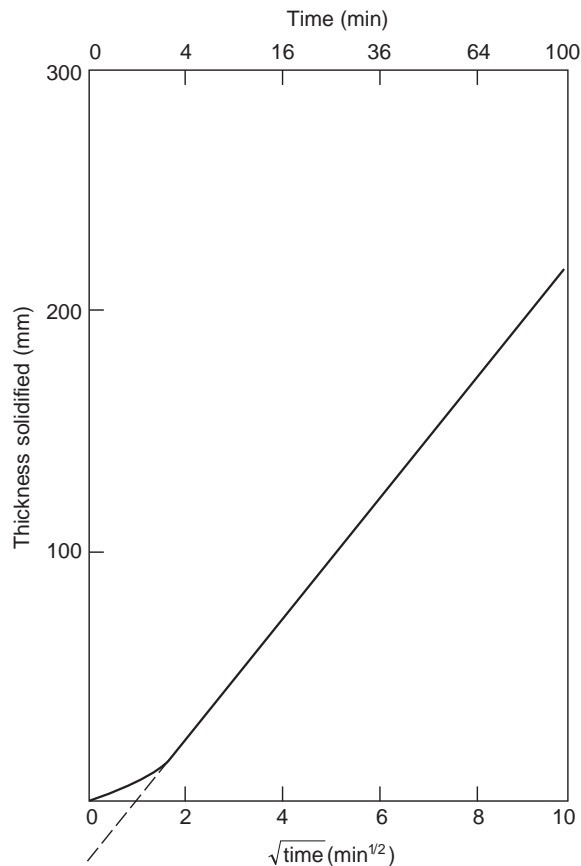


**FIGURE 5.2**

Unidirectional solidification of pure iron against a cast iron mold coated with a protective wash. (From Flemings 1974.)

experimental observations. For instance, the thickness  $S$  of steel solidifying against a cast iron ingot mold is found to be:

$$S = at^{1/2} - b \quad (5.4)$$

where the constants  $a$  and  $b$  are of the order of 3 and 25 respectively when the units are millimeters and seconds. The result is seen in Figure 5.2.

The apparent delay in the beginning of solidification shown by the appearance of the constant  $b$  is a consequence of the following: (i) The turbulence of the liquid during and after pouring, resulting in the loss of superheat from the melt, and so slowing the start of freezing. (ii) The finite interface resistance further slows the initial rate of heat loss. Initially the solidification rate will be linear, as described in the next section (and hence giving the initial curve in Figure 5.2 because of this plot using

the square root of time). Later, the resistance of the solidifying metal becomes dominant, giving the parabolic relation (shown, of course, as a straight line in Figure 5.2 because of the plot using the square root plot of time).

### **Resistance 2: The metal–mold interface**

In many important casting processes heat flow is controlled to a significant extent by the resistance at the metal–mold interface. This occurs when both the metal and the mold have reasonably good rates of heat conductance, leaving the boundary between the two the dominant resistance. The interface becomes overriding in this way when an insulating mold coat is applied, or when the casting cools and shrinks away from the mold (and the mold heats up, expanding away from the metal), leaving an air gap separating the two. These circumstances are common in the die casting of light alloys.

For unidirectional heat flow the rate of heat released during solidification of a solid of density  $\rho_s$  and latent heat of solidification  $H$  is simply:

$$q = -\rho_s H A \frac{\partial S}{\partial t} \quad (5.5)$$

This released heat has to be transferred to the mold. The heat transfer coefficient  $h$  across the metal–mold interface is simply defined as the rate of transfer of energy  $q$  (usually measured in watts) across unit area (usually a square meter) of the interface, per unit temperature difference across the interface. This definition can be written:

$$q = -hA(T_m - T_0) \quad (5.6)$$

assuming the mold is sufficiently large and conductive not to allow its temperature to increase significantly above  $T_0$ , effectively giving a constant temperature difference  $(T_m - T_0)$  across the interface. Hence equating 5.5 and 5.6 and integrating from  $S = 0$  at  $t = 0$  gives:

$$S = \frac{h(T_m - T_0)}{\rho_s H} \cdot t \quad (5.7)$$

It is immediately apparent that since shape is assumed not to alter the heat transfer across the interface, Equation 5.7 may be generalized for simple-shaped castings to calculate the solidification time  $t_f$  in terms of the volume  $V$  to cooling surface area  $A$  ratio (the geometrical modulus) of the casting:

$$t_f = \frac{\rho_s H}{h(T_m - T_0)} \cdot \frac{V}{A} \quad (5.8)$$

All of the above calculations assume that  $h$  is a constant. As we shall see later, this is perhaps a tolerable approximation in the case of gravity die (permanent mold) casting of aluminum alloys where an insulating die coat has been applied. In most other situations  $h$  is highly variable, and is particularly dependent on the geometry of the casting.

### The air gap

As the casting cools and the mold heats up, the two remain in good thermal contact while the casting is still liquid. When the casting starts to solidify, it rapidly gains strength, and can contract away from the mold. In turn, as the mold surface increases in temperature it will expand. Assuming for a moment that

this expansion is *homogeneous*, we can estimate the size of the gap  $d$  as a function of the diameter  $D$  of the casting:

$$d/D = \alpha_c \{T_f - T\} + \alpha_m \{T_{mi} - T_0\}$$

where  $\alpha$  is the coefficient of thermal expansion, and subscripts  $c$  and  $m$  refer to the casting and mold, respectively. The temperatures  $T$  are  $T_f$  the freezing point,  $T_{mi}$  the mold interface, and  $T_0$  the original mold temperature.

The benefit of the gap equation is that it shows how straightforward the process of gap formation is. It is simply a thermal contraction–expansion problem, directly related to interfacial temperature. It indicates that for a steel casting ( $\alpha_c = 14 \times 10^{-6} \text{ K}^{-1}$ ) of 1-meter diameter which is allowed to cool to room temperature the gap would be expected to be of the order of 10 mm at each of the opposite sides simply from the contraction of the steel, neglecting any expansion of the mold. This is a substantial gap by any standards!

Despite the usefulness of the elementary formula in giving some order-of-magnitude guidance on the dimensions of the gap, there are a number of interesting reasons why this simple approach requires further sophistication.

In a thin-walled aluminum alloy casting of section only 2 mm the room temperature gap would be only 10  $\mu\text{m}$ . This is only one-twentieth of the size of an average sand grain of 200  $\mu\text{m}$  diameter. Thus the imagination has some problem in visualizing such a small gap threading its way amid the jumble of boulders masquerading as sand grains. It really is not clear whether it makes sense to talk about a gap in this situation.

Woodbury and co-workers (2000) lend support to this view for thin wall castings. In horizontally sand cast aluminum alloy plates of 300 mm square and up to 25 mm thickness, they measured the rate of transfer of heat across the metal–mold interface. They confirmed that there appeared to be no evidence for an air gap. Our equation would have predicted a gap of 25  $\mu\text{m}$ . This small distance could easily be closed by the slight inflation of the casting because of two factors. (i) The internal metal–lostatic pressure provided by the filling system (no feeders were used). (ii) The precipitation of a small amount of gas; for instance it can be quickly shown that 1% porosity would increase the thickness of the plate by at least 70  $\mu\text{m}$ . Thus the plate would swell by creep with minimal difficulty under the combined internal pressure due to head height and the growth of gas pores. The 25  $\mu\text{m}$  movement from thermal contraction would be so comfortably overwhelmed that a gap would probably never have chance to form.

Our simple air gap formula assumes that the mold expands *homogeneously*. This may be a reasonable assumption for the surface of a greensand mold, which will expand into its surrounding cool bulk material with little resistance. A more rigid chemically bonded sand would be subject to rather more restraint, thus preventing the surface from expanding so freely. The surface of a metal die will, of course, be most constrained of all by the surrounding metal at lower temperature, but the higher conductivity of the mold will raise the temperature of the whole die more uniformly, giving a better approximation once again to homogeneous expansion.

Also, the sign of the mold movement for the second half of the equation is only positive if the mold wall is allowed to move outwards because of small mold restraint (i.e. a weak molding material) or because the interface is concave. A rigid mold and/or a convex interface will tend to cause inward expansion, reducing the gap, as shown in Figure 5.3. It might be expected that a flat interface will often be unstable, buckling either way. However, Ling, Mampaey, and co-workers (2000) found that both

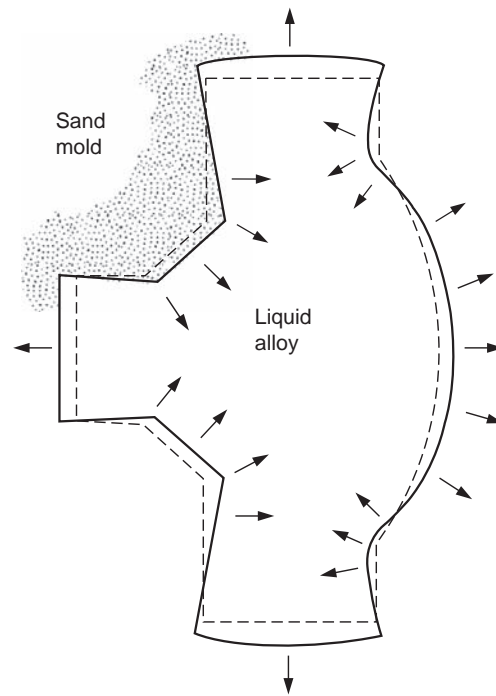


**FIGURE 5.3**

Movement of mold walls, illustrating the principle of inward expansion in convex regions and outward expansion in concave regions.

theory and experiment agreed that the walls of their cube-like mold poured with white cast iron distorted always outwards in the case of greensand molds, but always inwards in the case of the more rigid chemically bonded molds.

There are further powerful geometrical effects to upset our simple linear temperature relation. Figure 5.4 shows the effect of linear contraction during the cooling of a shaped casting. Clearly, anything in the way of the contraction of the straight lengths of the casting will cause the obstruction to be forced hard against the mold. This happens in the corners at the ends of the straight sections. Gaps cannot form here. Similarly, gaps will not occur around cores that are surrounded with metal, and onto which the metal contracts during cooling. Conversely, large gaps open up elsewhere. The situation in shaped castings is complicated and is only just being tackled with some degree of success by computer models. Even so, Kron (2004) is skeptical of the computer models to date. Few attempt to allow for the mechanical factors influencing the air gap. Even where such allowance is attempted, there is no agreement on a suitable constitutive equation for mechanical deformation of solids at temperatures near their melting points. The swelling of the casting in the mold due to the hydrostatic pressure in the liquid, and the friction of the rather soft casting against the mold are additional complicating factors.

Richmond and Tien (1971) and Tien and Richmond (1982) demonstrate via a theoretical model how the formation of the gap is influenced by the internal hydrostatic pressure in the casting, and by the

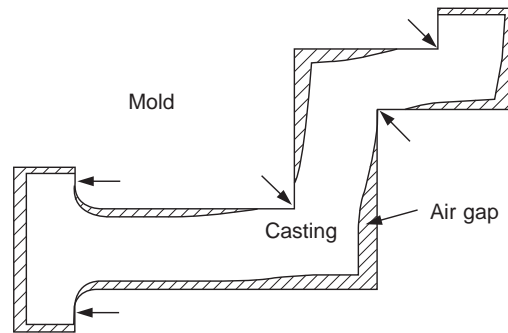


**FIGURE 5.4**

Variable air gap in a shaped casting: arrows denote the probable sites of zero gap.

internal stresses that occur within the solidifying solid shell. Richmond (1990) goes on to develop his model further, showing that the development of the air gap is not uniform, but is patchy. He found that air gaps were found to initiate adjacent to regions of the solidified shell that were thin, because, as a result of stresses within the solidifying shell, the casting–mold interface pressure first dropped to zero at these points. Conversely, the casting–mold interface pressure was found to be raised under thicker regions of the solid shell, thereby enhancing the initial non-uniformity in the thickness of the solidifying shell. Growth becomes unstable, automatically moving away from uniform thickening. This rather counter-intuitive result may help to explain the large growth perturbations that are seen from time to time in the growth fronts of solidifying metals. Richmond reviews a considerable amount of experimental evidence to support this model. All the experimental data seem to relate to solidification in metal molds. It is possible that the effect is less severe in sand molds.

Lukens et al. (1991) confirmed that increased feeder height increased the heat transfer at the base of the casting. Furthermore, for a horizontal cylinder 91 mm diameter in a chromite greensand mold, as the cylinder contracted away from the mold, gravity caused the cylinder to sit at the bottom of the mold, therefore contacting the mold purely along the line of contact along its base. Thus for this rather larger casting than the 25-mm-thick plate cast by Woodbury, it seems an air gap definitely occurs in a sand mold. This result confirms Lukens' earlier result (1990) in which most heat appears to be extracted through the drag, and increased head pressure enhances metal–mold contact.

Attempts to measure the gap formation directly (Isaac et al. 1985, Majumdar and Raychaudhuri 1981) are difficult to carry out accurately. Results averaged for aluminum cast into cast iron dies of various thickness reveal the early formation of the gap at the corners of the die where cooling is fastest, and the subsequent spread of the gap to the center of the die face. A surprising result is the reduction of the gap if thick mold coats are applied. (The results in Figure 5.5 are plotted as straight lines. The apparent kinks in the early opening of the gap reported by these authors may be artefacts of their experimental method.)

It is not be easy to see how the gap can be affected by the thickness of the coating. The effect may be the result of the creep of the solid shell under the internal hydrostatic pressure of the feeder. This is more likely to be favored by thicker mold coats as a result of the increased time available and the increased temperature of the solidified skin of the casting. If this is true then the effect is important

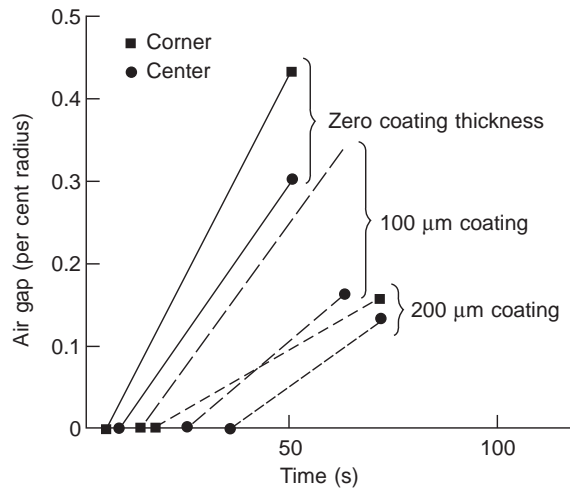


**FIGURE 5.5**

Results averaged from various dies (Isaac et al. 1985), illustrating the start of the air gap at the corners, and its spread to the center of the mold face. Increased thickness of mold coating is seen to delay solidification and to reduce the growth of the gap.

because the hydrostatic head in these experiments was modest, only about 200 mm. Thus for aluminum alloys that solidify with higher heads and times as long or longer than a minute or so, this mechanism for gap reduction will predominate. It seems possible, therefore, that in gravity die casting of aluminum the die coating will have the major influence on heat transfer, giving a large and stable resistance across the interface. The air gap will be a small and variable contributor. For computational purposes, therefore, it is attractive to consider the great simplification of neglecting the air gap in the special case of gravity die casting of aluminum.

It is probably helpful to draw attention to the fact that the name ‘air gap’ is perhaps a misnomer. The gap will contain almost everything except air. As we have seen previously, mold gases are often high in hydrogen, containing typically 50%. At room temperature the thermal conductivity of hydrogen is approximately 5.9 times higher than that of air, and at 500°C the ratio rises to 7.7. Thus, the conductivity of a gap at the casting–mold interface containing a 50:50 mixture of air and hydrogen at 500°C can be estimated to be approximately a factor of 4 higher than that of air. In the past, therefore, most investigators in this field have probably chosen the wrong value for the conductivity of the gap, and by a substantial margin!

This effect has been used by Doutré (1998) who injected helium gas, with a conductivity nearly identical to hydrogen (approximately 7 times the conductivity of air), into the air gap of a large Al alloy intake manifold cast in a permanent mold. The gas was introduced 30 s after pouring at a rate in the region of 10 ml s<sup>-1</sup>. In a full-scale works trial the production rate of the casting was increased by 25%. An even larger potential productivity increase, 45%, was found by Grandfield’s team (2007) when casting horizontal ingots in an open iron ingot mold. Gebelin and Griffiths (2007) found a reduced effect when attempting to cast resin-bonded sand molds in an evacuated chamber back-filled



with He. The explanation of the poor result in this latter case is almost certainly the result of the outgassing of sand molds under vacuum. This outward wind of volatiles would prevent the ingress of the He.

In passing, it seems worth commenting that He is expensive, and world supplies are limited. Naturally pure hydrogen introduced into the gap would perform similarly, but involve an unacceptable danger in the work place. Almost the same effect would be expected if steam, or better still, a water mist, were introduced into the air gap of a permanent mold. It would react with the metal to form hydrogen in situ, precisely where it is needed. Alternatively, many sand molds, such as greensand or sodium-silicate-bonded sands, have sufficient water that the hydrogen atmosphere is provided automatically, and free of charge.

### The heat-transfer coefficient

The authors Ho and Pehlke (1984) from the University of Michigan have reviewed and researched this area thoroughly. We shall rely mainly on their analytical approach for an understanding of the heat transfer problem.

When the metal first enters the mold the macroscopic contact is good because of the conformance of the molten metal to the detailed shape of the mold. Gaps exist on a microscale between high spots as shown in Figure 5.6. At the high spots themselves, the high initial heat flux causes nucleation of the solid metal by local severe undercooling (Prates and Biloni 1972). The nucleated solid then spreads to cover most of the surface of the casting because the thin layer of liquid adjacent to the cool mold surface will be expected to be undercooled. Conformance and overall contact between the surfaces is expected to remain good during all of this early period, even though the mold will now be starting to move rapidly because of distortion.

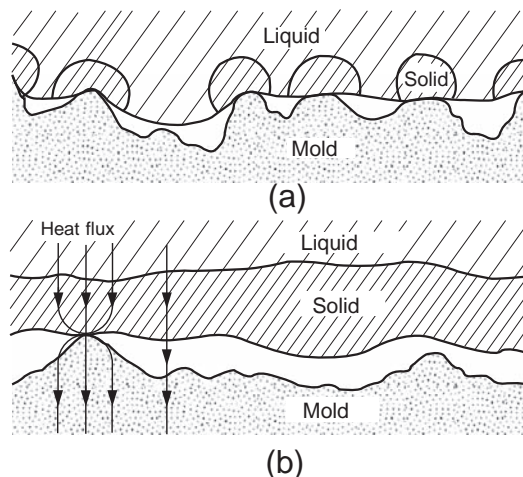


**FIGURE 5.6**

Metal–mold interface at an early stage when solid is nucleating at points of good thermal contact. Overall macroscopic contact is good at this stage (a). Later (b) the casting gains strength, and casting and mold both deform, reducing contact to isolated points at greater separations on non-conforming rigid surfaces.

After the creation of a solidified layer with sufficient strength, further movements of both the casting and the mold are likely to cause the good fit to be broken, so that contact is maintained across only a few widely spaced random high spots (Figure 5.6b). The total transfer of heat across the interface  $h_t$  may now be written as the sum of three components:

$$h_t = h_s + h_c + h_r$$

where  $h_s$  is the conduction through the *solid* contacts,  $h_c$  is the conduction through the *gas* phase, and  $h_r$  is that transferred by *radiation*. Ho and Pehlke produce analytical equations for each of these contributors to the total heat flux. We can summarize their findings as follows:

1. While the casting surface can conform, the contribution of solid–solid conduction is the most important. In fact, if the area of contact is enhanced by the application of pressure, then values of  $h_t$  up to  $60\,000\text{ Wm}^{-2}\text{ K}^{-1}$  are found for aluminum in squeeze casting. Such high values are quickly lost as the solid thickens and conformance is reduced, the values falling to more normal levels of  $100\text{--}1000\text{ Wm}^{-2}\text{ K}^{-1}$  (Figure 5.7).
2. When the interface gap starts to open, the conduction via any remaining solid contacts becomes negligible. The point at which this happens is clear in Figure 5.7b. (The actual surface temperature of the casting and the chill in this figure are reproduced from the results calculated by Ho and Pehlke.) The rapid fall of the casting surface temperature is suddenly halted, and reheating of the surface starts to occur. An interesting mirror image behavior can be noted in the surface temperature of the chill, which, now out of contact with the casting, starts to cool. The estimates of heat transfer are seen to simultaneously reduce from over 1000 to around  $100\text{ Wm}^{-2}\text{ K}^{-1}$  (Figure 5.7c).
3. After solid conduction diminishes, the important mechanism for heat transfer becomes the conduction of heat through the gas phase. This is calculated from:

$$h_c = k/d$$

where  $k$  is the thermal conductivity of the gas and  $d$  is the thickness of the gap. An additional correction is noted by Ho and Pehlke for the case where the gap is smaller than the mean free path of the gas molecules, which effectively reduces the conductivity. Thus heat transfer now becomes

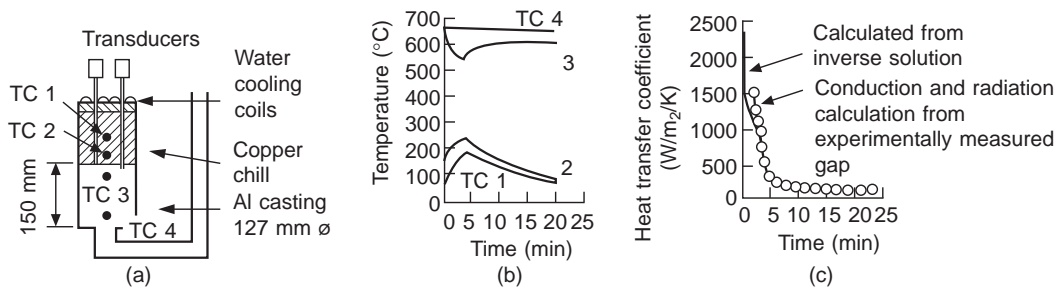


**FIGURE 5.7**

Results from Ho and Pehlke (1984) illustrating the temperature history across a casting–chill interface, and the inferred heat transfer coefficient.

a strong function of gap thickness. As we have noted above, it will also be a strong function of the composition of the gas. Even a small component of hydrogen will greatly increase the conductivity. Note also that it is assumed, almost certainly accurately, that the gas is stationary, providing heat flow by conduction only, not by convection.

For the case of light alloys, Ho and Pehlke find that the contribution to heat transfer from radiation is of the order of 1% of that due to conduction by gas. Thus radiation can be safely neglected at these temperatures.

For higher-temperature metals, results by Jacobi (1976) from experiments on the casting of steels in different gases and in vacuum indicate that radiation becomes important to heat transfer at these higher temperatures.

Turning now to experimental work on the effect of die coatings on permanent mold on heat transfer coefficients, a comprehensive review has been made by Nyamekye et al. (1994). Chiesa (1990) found that the conductance of a black coat was roughly twice that of a white coat of moderate thickness in the region of 120  $\mu\text{m}$ . Also, the insulating effect of a white coat increased only marginally with thickness. Their findings that coats with high surface roughness were more effective insulators have been confirmed by the calculations of Hallam and Griffiths (2000) for the case of Al alloy castings. They demonstrate excellent predictions based on the assumption that the resistance of the die coating is mainly due to the gas voids between the casting and the coating surface. Thus the character of the coating surface was a highly influential factor in determining the heat transfer across the casting–mold interface.

The effect of gravity on the contact between the casting and mold has already been discussed above. Woodbury (1998) finds that for a lightweight horizontal plate casting of only 6 mm thickness the heat transfer settles to a constant level of  $70 \text{ W m}^{-2} \text{ K}^{-1}$ . However, for a 25-mm-thick plate the heat transfer from the top is approximately unchanged at 70, but the value from the underside of this heavier plate is now approximately doubled at  $140 \text{ W m}^{-2} \text{ K}^{-1}$ .

For sand molds the use of pressure to enhance metal–mold contact is of course limited by penetration of the metal into the sand. The use of pressure has no such limitation in the case of metal molds. Tadayon (1992) reports the freezing time of a squeeze casting to be 84 s at zero applied pressure, but reducing to 56 s at 5 MPa. A further increase of pressure to 10 MPa reduced the time only minimally further to 54 s.

Finally, it seems necessary to draw attention to the comprehensive review by Woolley and Woodbury (2007). These authors critically assess the vast literature on the determination of heat transfer coefficients, concluding that they are skeptical of the accuracy of all of the published data, and cite a number of key reasons for unreliability. In a later paper (2009), for instance, these authors find that the use of thermocouples to measure heat flow in these experiments alone introduces an error of 65%. Clearly, we still have a long way to go to achieve reliable heat transfer coefficients.

### ***Resistance 3: The mold***

The rate of freezing of castings made in silica sand molds is generally controlled by the rate at which heat can be absorbed by the mold. In fact, compared to many other casting processes, the sand mold acts as an excellent insulator, keeping the casting warm. However, of course, ceramic investment and plaster molds are even more insulating, avoiding premature cooling of the metal, and aiding fluidity to give the excellent ability to fill thin sections for which these casting processes are renowned. It is a pity

that the extremely slow cooling generally contributes to rather poorer mechanical properties, but this is to some extent a self-inflicted problem. If the metal were free from bifilms it is predicted that mechanical properties would be not noticeably affected by slower rates of freezing (see Section 9.4).

Considering the simplest case of unidirectional conditions once again, and metal poured at its melting point  $T_m$  against an infinite mold originally at temperature  $T_0$ , but whose surface is suddenly heated to temperature  $T_m$  at  $t = 0$ , and that has thermal diffusivity  $\alpha_m$ , we now have:

$$\frac{\partial T}{\partial t} = \alpha_m \frac{\partial^2 T}{\partial x^2} \quad (5.9)$$

Following Flemings, the final solution is:

$$S = \frac{2}{\sqrt{\pi}} \left( \underbrace{\frac{T_m - T_0}{\rho_s H}}_{\text{metal}} \right) \underbrace{\sqrt{K_m \rho_m C_m}}_{\text{mould}} \sqrt{t} \quad (5.10)$$

This relation is most accurate for the highly conducting non-ferrous metals, aluminum, magnesium and copper. It is less good for iron and steel, particularly those ferrous alloys that solidify to the austenitic (face-centered cubic) structure that has especially poor conductivity. The relation quantifies a number of interesting outcomes as discussed below.

Note that at a high temperature heat is lost more quickly, so that a casting in steel should solidify faster than a similar casting in gray iron. This perhaps surprising conclusion is confirmed experimentally, as seen in Figure 5.8.

Low heat of fusion of the metal,  $H$ , similarly favors rapid freezing because less heat has to be removed. Therefore despite their similar freezing points, magnesium castings freeze faster than similar castings in aluminum.

The product  $K_m \rho_m C_m$  is a useful parameter to assess the rate at which various molding materials can absorb heat. The reader needs to be aware that some authorities have called this parameter the heat diffusivity, and this definition was followed in *Castings* (Campbell 1991). However, originally the definition of heat diffusivity  $b$  was  $(K_m \rho_m C_m)^{1/2}$  as described for instance by Ruddle (1950). In subsequent years the square root seems to have been overlooked in error. Ruddle's definition is therefore accepted and followed here. However, of course, both  $b$  and  $b^2$  are useful quantitative measures. What we call them is merely a matter of definition. (I am grateful to John Berry of Mississippi State University for pointing out this fact. As a further aside from Professor Berry, the units of  $b$  are even more curious than the units of toughness; see Table 5.2.)

For simple shapes, if we assume that we may replace  $S$  with  $V_s/A$  where  $V_s$  is the volume solidified at a time  $t$ , and  $A$  is the area of the metal–mold interface (i.e. the cooling area of the casting), then when  $t = t_f$  where  $t_f$  is the total freezing time of a casting of volume  $V$  we have:

$$\frac{V}{A} = \frac{2}{\sqrt{\pi}} \left( \frac{T_m - T_0}{\rho_s H} \right) \sqrt{K_m \rho_m C_m} \sqrt{t_f} \quad (5.11)$$

and so:

$$t_f = B(V/A)^2 \quad (5.12)$$

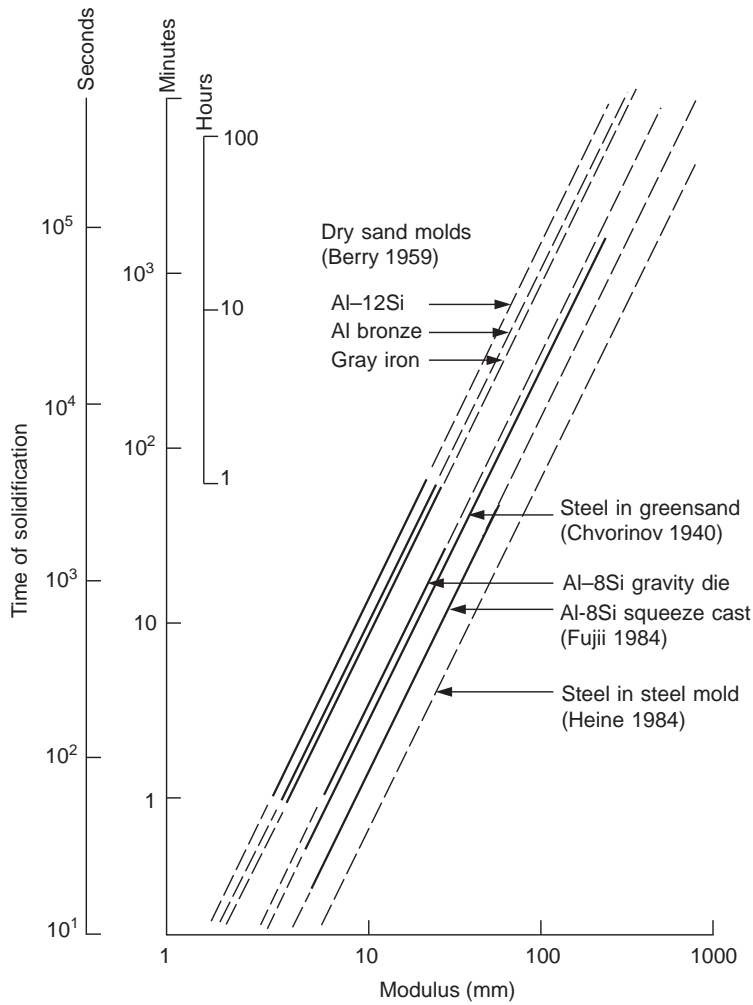


**FIGURE 5.8**

Freezing times of plate-shaped castings in different alloys and molds.

where  $B$  is a constant for given metal and mold conditions. The ratio  $(V/A)$  is the useful parameter generally known as the *modulus*  $m$ ; thus Equation 5.12 indicates that the parameter  $m^2$  is the important factor that controls the solidification time of the casting.

Equation 5.12 is the famous Chvorinov rule. Convincing demonstrations of its accuracy have been made many times. Chvorinov himself showed in his paper published in 1940 that it applied to steel castings from 12 to 65 000 kg weight made in greensand molds. This superb result is presented in Figure 5.9. Experimental results for other alloys are illustrated in Figure 5.8.

Chvorinov's rule is one of the most useful guides to the student. It provides a powerful general method of tackling the feeding of castings to ensure their soundness.

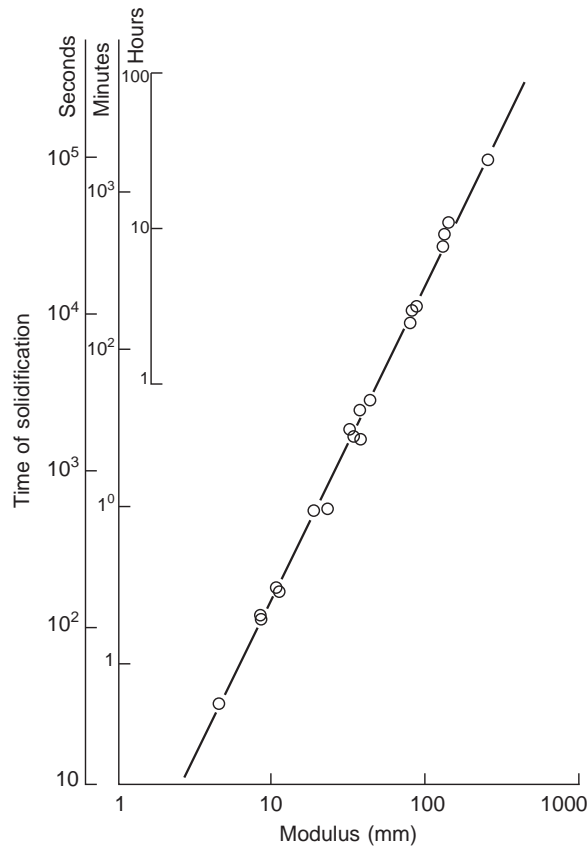


**FIGURE 5.9**

Freezing time of steel castings in greensand molds as a function of modulus (Chvorinov 1940).

However, the above derivation of Chvorinov's rule is open to criticism in that it uses one-dimensional theory but goes on to apply it to three-dimensional castings. In fact, it is quickly appreciated that the flow of heat into a concave mold wall will be divergent, and so will be capable of carrying away heat more rapidly than in a one-dimensional case. We can describe this exactly (without the assumption of one-dimensional heat flow), following Flemings once again:

$$\frac{\partial T}{\partial t} = \alpha_m \left( \frac{\partial^2 T}{\partial r^2} + \frac{n \partial T}{r \partial r} \right) \quad (5.13)$$

where  $n = 0$  for a plane, 1 for a cylinder, and 2 for a sphere. The casting radius is  $r$ . The solution to this equation is:

$$\frac{V}{A} = \left( \frac{T_m - T_0}{\rho_s H} \right) \left( \frac{2}{\sqrt{\pi}} \sqrt{K_m \rho_m C_m} \sqrt{t_f} + \frac{n K_m t_f}{2r} \right) \quad (5.14)$$

The effect of the divergency of heat flow predicts that for a given value of the ratio  $V/A$  (i.e. a given modulus  $m$ ) a sphere will freeze quickest, the cylinder next, and the plate last. Katerina Trbizan (2001) provides a useful study, confirming these relative freezing rates for these three shapes. For aluminum in sand molds, Equation 5.14 indicates these differences to be close to 20%. This is part of the reason for the safety factor 1.2 recommended when applying Chvorinov's feeding rule, since the feeding rules tacitly assume that all shapes with the same modulus freeze at the same time.

It should be noted that the simple Chvorinov link between modulus and freezing time is capable of great sophistication. One of the great exponents of this approach has been Wlodawer (1966), who produced a famous volume devoted to the study of the problem for steel castings. This has been a source book for the steel-castings industry ever since.

The subject has been advanced further by the work of Tiryakioglu in 1997 (interestingly using his deceased father's excellent PhD research at the University of Birmingham, UK, in 1964) that showed secondary, but important, effects of shape, volume, and superheat on the freezing time of the casting.

A final aspect relating to the divergence of heat flow is important. For a planar freezing front, the rate of increase of thickness of the solidified metal is parabolic, gradually slowing with thickness, as described by Equations such as 5.3 and 5.4 relating to one-dimensional heat flow. However, for more compact shapes such as cylinders, spheres, cubes, etc. the heat flow from the casting is three-dimensional. Thus initially for such shapes, when the solidified layer is relatively thin, the solid thickens parabolically. However, at a much later stage of freezing, when little liquid remains in the center of the casting, the extraction of heat in all three directions greatly accelerates the rate of freezing. Santos and Garcia (1998) show that the effect, accurately predicted theoretically by Adams in 1956, is general. Whereas in a slab casting the velocity of the front slows progressively with distance according to the well-known parabolic law, for cylinders and spheres the growth rate is similar until the front has progressed to about 40% of the radius. From then onwards the front accelerates rapidly (Figure 5.10).

This increase of the rate of freezing in the interior of many castings explains the otherwise baffling observation of 'inverse chill' as seen in cast irons. Normal intuition would lead the caster to expect fast cooling near the surface of the casting, and this is true to a modest degree in all castings. From this point onwards the front slows progressively in uniform plate-like sections. But in bars and cylinders, as the residual liquid shrinks in size towards the center of the casting, the front speeds up dramatically, causing gray iron to change to carbide white iron. The accelerated rate has been demonstrated experimentally by Santos and Garcia on a Zn-4Al alloy by measurement of the increasing fineness of dendrite arm spacing towards the center of a cylindrical casting.

It is interesting that the effect of accelerated freezing appears never to have been seen in Al alloys. This seems to be the result of the high thermal conductivity of these alloys, causing dendritic freezing over the whole cross-section of the casting, and thus smoothing and obscuring the acceleration of solidification towards the center of castings. However, a small pulse of heat at the end of freezing can be detected on a sensitive cooling curve.

### 5.1.2 Increased heat transfer

In practice, the casting engineer can manipulate the rate of heat extraction from a casting using a number of tricks. These include the placement of chill blocks in the mold, adjacent to the casting, or fins attached to the casting to increase the surface area through which heat can be dissipated. These techniques will be described below.

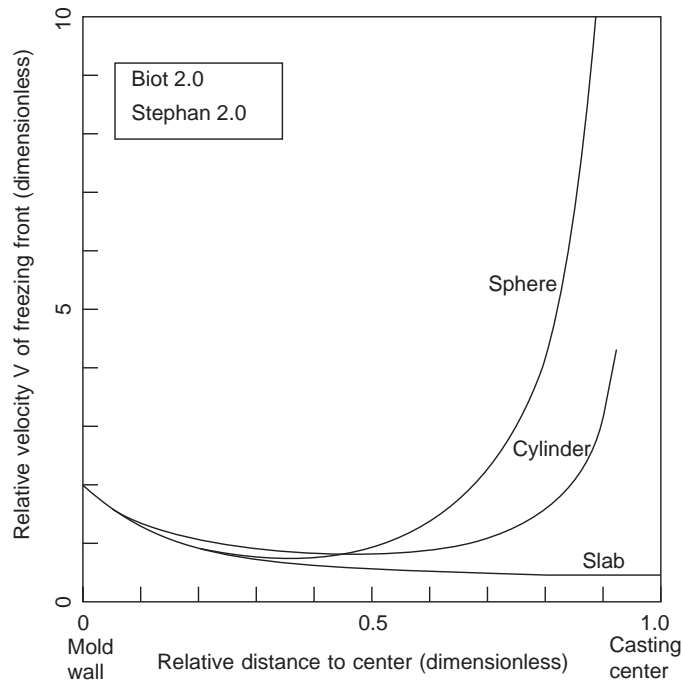


**FIGURE 5.10**

Acceleration of the freezing front in compact castings as a result of 3-D extraction of heat (sphere and cylinder curves calculated from Santos and Garcia 1998).

The action of chills and fins can provide localized cooling of the casting to assist directional solidification of the casting towards the feeder, thus assisting in the achievement of soundness. This is one of the important actions of these chilling devices. It is, however, not the only action, as discussed below.

Chills also act to increase the ductility and strength of that locality of the casting. It seems most probable that this occurs because the faster solidification freezes in the bifilms in their compact form before they have the chance to unfurl. (Recall that the bifilms are compacted by the extreme bulk turbulence during pouring and during their travel through the running system. However, they subsequently unravel if they have sufficient time or sufficient driving force, opening up in the mold cavity when conditions in the melt become quiet once again.) However, there is a small contribution towards strength and ductility from the refinement of structure. Al-Si alloys and Mg-based alloys particularly benefit. The remaining Al alloys and other fcc-structured metals such as Cu-based alloys and austenitic steels would not be expected to benefit usefully from finer grain or finer DAS.

The interesting corollary of this fact is that if chills are seen to increase ductility and strength of these alloys, it confirms that the cast material is defective, containing a high percentage of bifilms. Another interesting corollary is that if the alloy can be cast without bifilms, its properties will already be high, so that chilling should not increase its properties further. This rather surprising prediction is



fascinating, and, if true, indicates the huge potential for the increase of the properties of cast alloys. All castings without bifilms are therefore predicted to have extraordinary ductility and strength. It also explains our lamentable current condition in which most of us constantly struggle in our foundries to achieve minimum mechanical properties for castings even when the casting is plastered in chills. Some days we win, other days we continue to struggle. The message is clear, we need to focus on technologies for the production of castings with reduced bifilm content, preferably zero bifilm content. The rewards are huge.

Another action of chills is to straighten bifilms. This action occurs because the advancing dendrites cannot grow through the air layer between the double films, and so push the bifilms ahead. Those that are somehow attached to the wall will be partially pushed, straightened, and unraveled by the gentle advance of grains. This effect is reported in Section 2.3 on furling and unfurling of bifilms. Thus although a large percentage of bifilms will be pushed ahead of the chilled region, concentrating (and probably reducing the properties) in the region immediately ahead, some bifilms will remain aligned in the dendrite growth direction, and so be largely perpendicular to the mold wall. The mechanism is presented in Figure 2.43a and b, and an example is seen in the radiograph in Figure 2.43c.

The overall effects on mechanical properties of the pushing action are therefore not easily predicted. The reduction in density of defects close to the chill will raise properties, but the presence of occasional bifilms aligned at right angles to the surface of the casting would be expected to be severely detrimental. These complicated effects require to be researched. However, we can speculate that they seem likely to be the cause of troublesome edge cracking in the rolling of cast materials of many types, leading to the expense of machining off the surface of many alloys before rolling can be attempted. The superb formability of electroslag remelted compared to vacuum arc remelted alloys is almost certainly explained in this way. The ESR process produces an extremely clean material because oxide films are dissolved during remelting under the layer of liquid slag, and will not re-form in the solidifying ingot. In contrast, the relatively poor vacuum of the VAR process ensures that the lapping of the melt over the liquid meniscus at the mold wall will create excellent double oxide films. If considerable depths of the VAR ingot surface are not first removed (a process sometimes called 'peeling') oxide lap defects will open as surface cracks when subjected to forging or rolling.

Although, as outlined above, the chilling action of chills and fins is perhaps more complicated than we first thought, the chilling action itself on the rate of solidification is well documented and understood. It is this thermal aspect of their behavior that is the subject of the remainder of this section.

### ***External chills***

In a sand mold the placing of a block of metal on the pattern, and subsequently packing the sand around it to make the rest of the mold in the normal way, is a widely used method of applying localized cooling to that part of the casting. A similar procedure can be adopted in gravity and low-pressure die-casting by removing the die coat locally to enhance the local rate of cooling. In addition, in dies of all types, this effect can be enhanced by the insertion of metallic inserts into the die to provide local cooling, especially if the die insert is highly conductive (such as made from copper alloy) and/or artificially cooled, for instance by air, oil, or water.

Such chills placed as part of the mold, and that act against the outside surface of the casting, are strictly known as external chills, to distinguish them from internal chills that are cast in, and become integral with, the casting.

In general terms, the ability to chill is a combination of ability to absorb heat and to conduct it away. It is quantitatively assessed by

$$\text{heat diffusivity} = (K\rho C)^{1/2}$$

where  $K$  is the thermal conductivity,  $\rho$  the density, and  $C$  is the specific heat of the mold. It has complex units  $\text{Jm}^{-2} \text{K}^{-1} \text{s}^{1/2}$ . Take care not to confuse with

$$\text{thermal diffusivity} = K/\rho C$$

normally quoted in units of  $\text{m}^2 \text{s}^{-1}$ .

It is clear that the various refractory mold materials – sand, investment, and plaster – do not act effectively as chilling materials. The various chill materials are all in a league of their own, having chilling powers orders of magnitude higher than the refractory mold materials. They improve marginally, within a mere factor of 5, in the order steel, graphite, and copper.

The heat diffusivity value indicates the action of the material to absorb heat when it is infinitely thick, being unconstrained in the amount of heat it can conduct away and store in itself, i.e. as would be reasonably well approximated by constructing a thick-walled mold from such material.

This behavior contrasts with that of a relatively small lump of cast iron or graphite used as an external chill in a sand mold. A small chill does not develop its full potential for chilling as promised by the heat diffusivity because it has limited capacity for heat. Thus although the initial rate of freezing of a metal may be in the order given by the above list, for a chill of limited thickness its cooling effect quickly becomes limited because it becomes saturated with heat; after a time it can absorb no more. The amount of heat that it can absorb is defined as its heat capacity. We can formulate the useful concept of heat capacity per unit volume  $\rho C$  in terms of its density  $\rho$  and its specific heat  $C$ , so that the heat capacity of a chill of volume  $V$  is simply

$$\text{Volumetric heat capacity} = V\rho C$$

In the SI system its units are  $\text{JK}^{-1}$ . Figure 5.11 illustrates the fact that if chills are limited by their relatively low heat capacity, there is little difference between copper, graphite, and iron. However, for larger chills that are able to conduct heat away without saturating, copper is by far the best material. The next best, graphite, is only half as good, and iron is only a quarter as effective. For situations intermediate between small and large chills conditions part-way between the extremes can be read off the nomogram.

Aluminum chills are interesting, in that if rather small, they are relatively poor compared to steel, graphite, and copper, whereas larger blocks capable of carrying heat away without saturation are better than steel or graphite, but still only half as good as copper.

The results by Rao and Panchanathan (1973) on the casting of 50-mm-thick plates in Al–5Si–3Cu reveals that the casting is insensitive to whether it is cooled by copper, graphite, or steel chills, provided that the volumetric heat capacity of the chill is taken into account. We can conclude that their chills were rather limited in size, and so limited by their heat capacity.

These authors show that for a steel chill 25 mm thick its heat capacity is  $900 \text{ JK}^{-1}$ . A chill with identical capacity in copper they claimed to be 32 mm thick, and in graphite 36 mm. These values originally led the author to conclude that copper may therefore not always be the best chill material (*Castings* 1991). However, using somewhat more accurate data (Figure 5.11) copper is found, after all, to be the most effective whether limited by heat diffusivity or heat capacity.

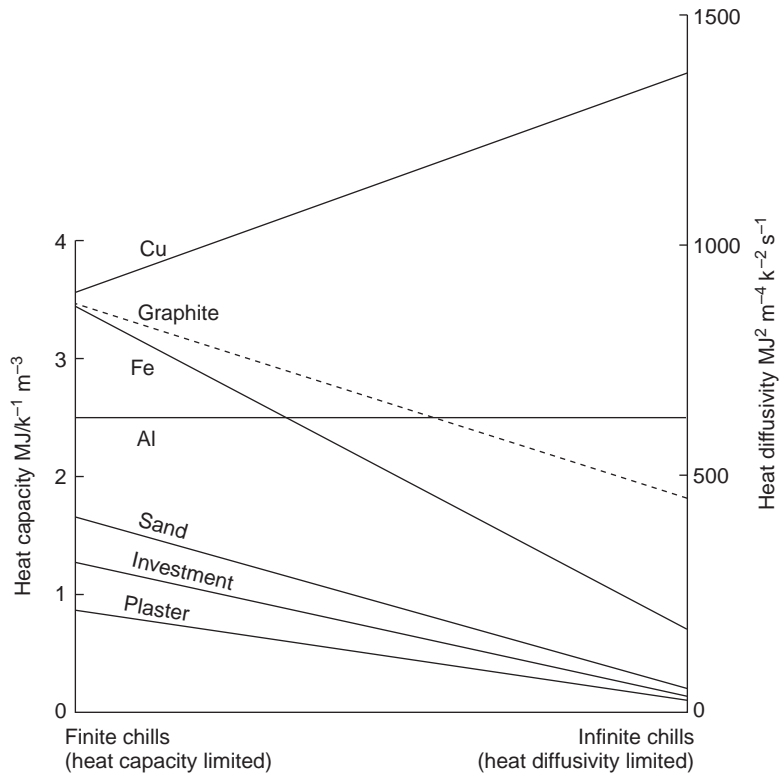


**FIGURE 5.11**

Relative diffivities (ability to diffuse heat away if a large chill) and heat capacities (ability to absorb heat if relatively small) of chill materials.

Lerner and Kouznetsov (2004) confirm for copper and iron chills on a 20-mm-thick Al alloy casting the rather surprising fact that the volume of external chills is far more important than their surface area of contact with the casting.

Figure 5.12 illustrates that the chills are effective over a considerable distance, the largest chills greatly influencing the solidification time of the casting even up to 200 mm (four times the section thickness of the casting) distant. This large distance is perhaps typical of such a thick-section casting in an alloy of high thermal conductivity, providing excellent heat transfer along the casting. A steel casting would respond less at this distance. This work by Rao and Panchanathan (1973) reveals the widespread sloppiness of much present practice on the chilling of castings. General experience of the chills generally used in foundrywork nowadays shows that chill size and weight are rarely specified, and that chills are in general too small to be fully effective in any particular job. It clearly matters what size of chill is added.

Computational studies by Lewis and colleagues (2002) have shown that the number, size, and location of chills can be optimized by computer. These studies are among the welcome first steps towards the intelligent use of computers in casting technology.

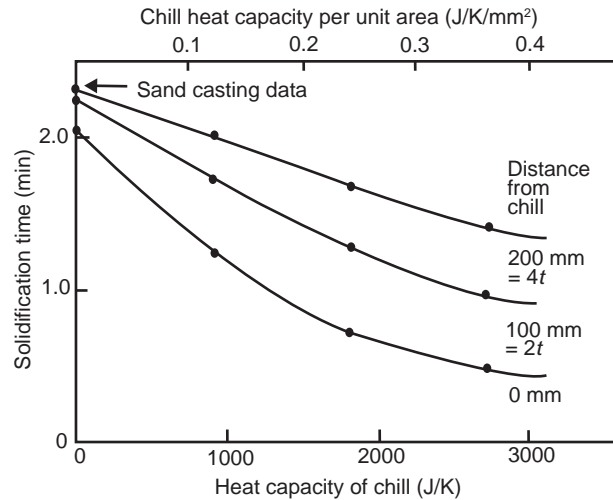


**FIGURE 5.12**

Freezing times of a plate  $225 \times 150 \times 50$  mm in Al-5Si-3Cu alloy at various distances from the chill is seen to shrink steadily as the chill is approached and as the chill size is increased (Rao and Panchanathan 1973).

Finally, in detail, the action of the chill is not easy to understand or to predict. The surface of the casting against the chill will often contract, distorting away and thus opening up an air gap. The chilled casting surface may then reheat to such an extent that the surface remelts. The exudation of eutectic is often seen between the casting and the chill (Figure 5.13). The new contact between the eutectic and chill probably then starts a new burst of heat transfer and thus a new rapid phase of solidification of the casting. Thus the history of cooling in the neighborhood of a chill may be a succession of stop/start, or slow/fast events.

### **Internal chills**

The placing of chills inside the mold cavity with the intention of casting them in place is an effective way of localized cooling. Such chills are usually carefully chosen to be of the same chemical composition as the melt so that they will be essentially invisible when finally frozen into the casting. The technique is an excellent solution to the challenge of making sound a heavy boss or thick section in the center of a complex casting that cannot be accessed by conventional feeding, especially if the center of the boss, together with the internal chill, is to be subsequently machined out.

Internal chills take a great variety of shapes as illustrated in Figure 5.14.

When estimating what size of chill might be required (i.e. its weight), the simple method of mixtures approach (Campbell and Caton 1977) indicates that to cool superheated pure liquid iron to its freezing point, and freezing a proportion of it, will require various levels of addition of cold, solid low-carbon steel depending on the extent that the addition itself actually melts. These estimations take no account of other heat losses from the casting. Thus for normal castings the predictions are likely to be incorrect by up to a factor of 2. This is broadly confirmed by Miles (1956), who top-poured steel into

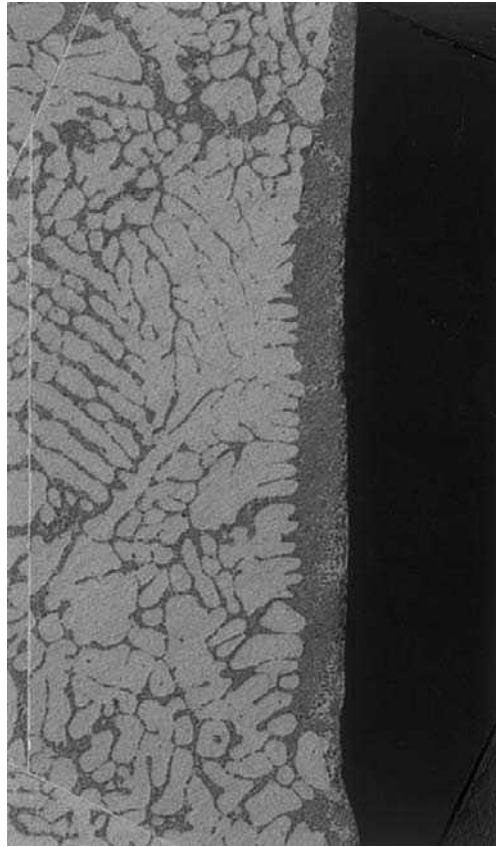


**FIGURE 5.13**

Al-Si eutectic liquid segregation by exudation at a chilled interface of an Al-7Si alloy.

dry sand molds 75 mm square and 300 mm tall. In the center of the molds were positioned a variety of steel bars ranging from 12.5 mm round to 25 mm square, covering a range of chilling from 2 to 11% solid addition. His findings reveal that the 2% solid addition nearly melted, compared to the predicted value for complete melting of 3.5% solid. The 11% solid addition caused extensive (possibly total) freezing of the casting judging by the appearance of the radial grain structure in his macrosections. He found 5% addition to be near optimum; it had a reasonable chilling effectiveness and caused relatively few defects.

These additions are plotted in graphical form in Figure 5.15. They illustrate that additions up to about 3.5% completely melt and disappear (although clearly cool the melt by this process). Further additions linearly increase the amount of liquid that is solidified, finally becoming completely frozen at about 10% addition.

In the case of additions above 10%, where the heat input is not sufficient to melt the chill, the fusing of the chill surface into the casting has to be the result of a kind of diffusion bonding process. This

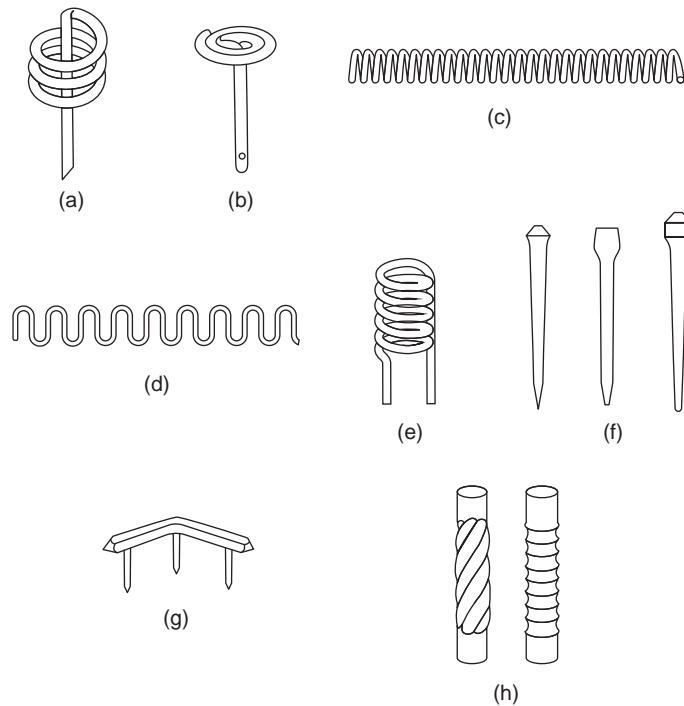


**FIGURE 5.14**

A variety of internal chills (from Heine and Rosenthal 1955).

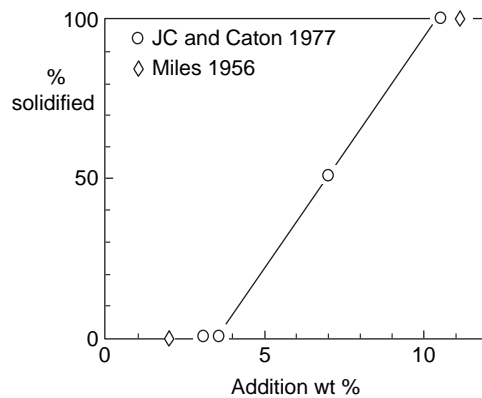


**FIGURE 5.15**

The addition of increasing percentage of cold mild steel particles to liquid mild steel cools the melt by melting of the additions up to about 4% addition, then starts to promote freezing, finally causing complete freezing of the melt at about 10% addition.

would emphasize the need for cleanness of the surface, requiring the minimum presence of oxide films or other debris against the chill during the filling of the mold. If Miles had used a better bottom-gated filling technique he may have reduced the observed filling defects further, and found that higher percentages were practical.

The work by Miles does illustrate the problems generally experienced with internal chills. If the chills remain for any length of time in the mold, particularly after it is closed, and more particularly if closed overnight, then condensation is likely to occur on the chill, and blow defects will be caused in the casting. Blows are also common from rust spots or other impurities on the chill, such as oil or grease. The matching of the chemical composition of the chill and the casting is also important; mild steel chills will, for instance, usually be unacceptable in an alloy steel casting.

Internal chills in aluminum alloy castings have not generally been used, almost certainly as a consequence of the difficulty introduced by the presence of the oxide film on the chill. This appears to be confirmed by the work of Biswas et al. (1985), who found that at 3.5% by volume of chill and at superheats of only 35°C the chill was only partially melted and retained part of its original shape. It seems that over this area it was poorly bonded. At superheats of above 75°C, or at only 1.5% by volume, the chill was more extensively melted, and was useful in reducing internal porosity and in raising mechanical properties. The lingering presence of the oxide film from the chill (now having floated off to lurk elsewhere in the casting) remains a concern, however.

The development of a good bond between the internal chill and the casting is a familiar problem with the use of chaplets – the metal devices used to support cores against sagging because of weight, or floating because of buoyancy. A one-page review of chaplets is given by Bex (1991). To facilitate the bond for a steel chaplet in an iron or steel casting the chaplet is often plated with tin. The tin serves to prevent the formation of rust, and its low melting point (232°C) and solubility in iron assists the bonding process.

There has been much work carried out on the casting of steel inserts into cast irons. Xu (2007) studied thin steel chill plates in a heavy gray iron block casting, measuring the diffusion of alloying elements between them. He notes that carbon content is smoothed across the interface, but the silicon concentration forms a sharp step at the interface. This is behavior to be expected in terms of the rates of diffusion given in Figure 1.4c.

Noguchi (1993) used a thermally sprayed Ni-based self-fluxing alloy on mild steel inserts in both flake and ductile iron. Although he reports that the bonding of inserts is sensitive to the volume ratio of the poured metal and insert (as we have seen in Figure 5.15) and the pouring temperature, the thermal spray greatly expands the regime of successful bonding. In later work, Noguchi (2005) cast steel sleeves and end rings into cast irons, avoiding the use of sprayed interlayers. In this work he raised the temperature of the insert higher than could be achieved by simple immersion. He arranged for an extended period of flow of hot metal around the insert, in some cases running the excess metal into flow-offs. He found that if he could raise the interface temperature to 1150°C, the melting point of the iron, he could achieve what appeared to be a perfect bond over large areas of the insert.

The bond between steel and titanium inserts in Al alloy castings has been investigated in Japan (Noguchi et al. 2001) who found only a 10- $\mu$ m silver coating was effective to achieve a good bond, although even this took up to 5 minutes to develop at the Al–Ag eutectic temperature 566°C. Attempts to achieve a bond with gold plating and Al–Si sprayed alloy were largely unsuccessful.

Biswas and co-workers (1994) have researched Al alloy chills in Al alloys as a function of relative volume and casting superheat. However, these authors overlook the problem of the oxide films, not

appreciating that it represents an ever-present danger. It will persist as a double film (having acquired its second layer during the immersion of the chill by the liquid) and so pose the risk of leakage or crack formation. Such risks are only acceptable for low-duty products.

Brown and Rastall (1986) take advantage of the oxide on the surface of heavy aluminum inserts in aluminum castings, using this to avoid any bonding between the casting and the insert. They use a cast aluminum alloy core inside an aluminum alloy casting to form re-entrant details that could not easily be provided in a pressure die cast product. Also, of course, because the freezing time is shortened, productivity is enhanced. The internal core is subsequently removed by disassembly or part machining, or by mechanical deformation of the core or casting.

### ***Fins***

If we add an appendage such as a fin to a casting, we inevitably form a T-junction between the two. Depending on the thickness of the appendage, the junction may be either a hot spot or a cold spot. Therefore, before we look specifically at fins on castings, it is worth spending some time to consider the concepts involved in junctions of all types.

Kotschi and Loper (1974) were among the first to evaluate junctions. Their results are summarized in Figures 5.16 and 5.17 and further interpreted in Figure 5.18 to show the complete range of junctions and their effect on the residual liquid in the main cast plate. Considering the range in Figure 5.18, starting at the thinnest appendage:

1. When the wall forming the upright of the T is thin, it acts as a cooling fin, chilling the junction and the adjacent wall (the top cross of the T) of the casting. We shall return to a more detailed consideration of fins shortly.
2. When the upright of the T-section has increased to a thickness of half the casting section thickness, then the junction is close to thermal balance, the cooling effect of the fin balancing the hot-spot effect of the concentration of metal in the junction.

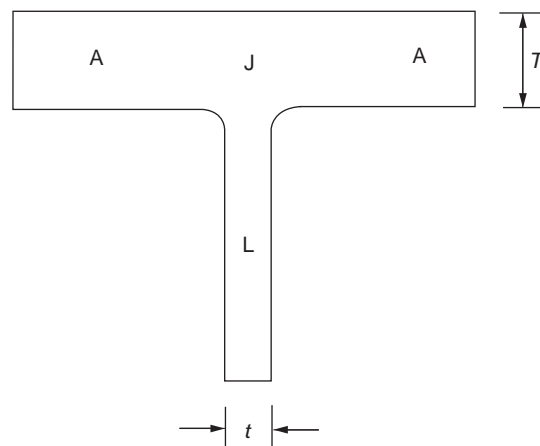


**FIGURE 5.16**

Geometry of a T-shaped junction.



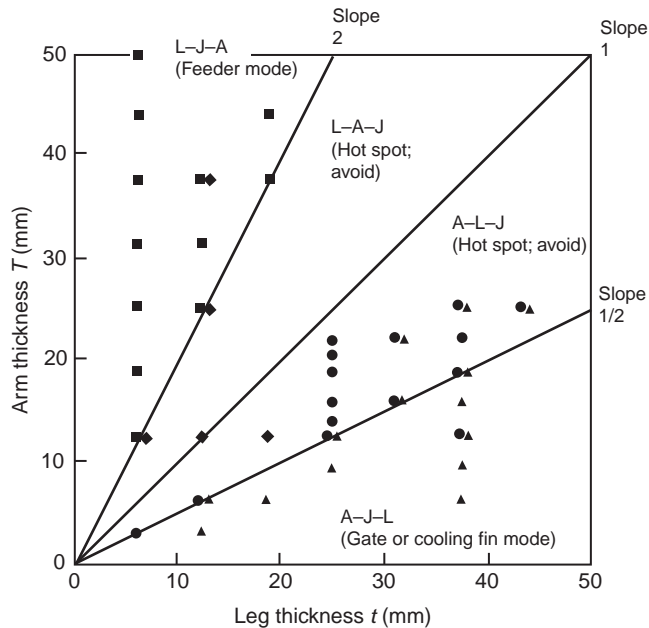


**FIGURE 5.17**

Solidification sequence for T-shaped castings (A = arm, J = junction, L = leg). Experimental data from Hodjat and Mobley (1984).

- By the time that the upright of the T has become equal to the casting section, the junction is a hot spot. This is common in castings. Foundry engineers are generally aware that the 1:1 T-junction is a problem. It is curious therefore that castings with uniform wall thickness are said to be preferred, and that designers are encouraged to design them. Such products necessarily contain 1:1 junctions that will be hot spots. (Techniques for dealing with these are dealt with later when considering the feeding of castings; see Chapter 6.)
- When finally the section thickness of the upright of the T is twice the casting section, then the junction is balanced once again, with the casting now acting as the mild chill to counter the effect of the hot spot at the junction. We have considered these junctions merely in the form of the intersections of plates. However, we can extend the concept to more general shapes, introducing the use of the geometric modulus  $m = (\text{volume})/(\text{cooling area})$ . It subsequently follows that an additional requirement when a feeder forms a T-junction on a casting is that the feeder must have a modulus two times the modulus of the casting. The hot spot is then moved out of the junction and into the feeder, with the result that the casting is sound. This is the basis behind Feeding Rule 4 discussed later.

Pellini (1953) was one of the first experimenters to show that the siting of a thin 'parasitic' plate on the end of a larger plate could improve the temperature gradient in the larger plate. However, the parasitic plate that he used was rather thick, and his experiments were carried out only on steel, whose conductivity is poor, reducing useful benefits.

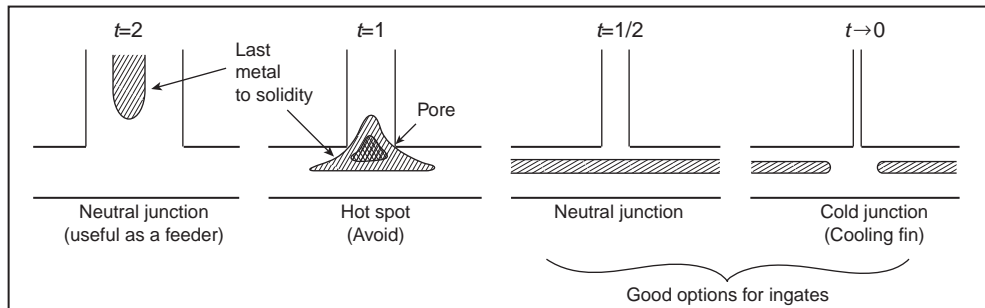


**FIGURE 5.18**

Array of T-junctions showing the thermal effects at the junction with different relative thickness of casting.

Figure 5.19 shows the results from Kim et al. (1985) of pour-out tests carried out on 99.9% pure aluminum cast into sand molds. The faster advance of the freezing front adjacent to the junction with the fin is clearly shown. (As an aside, this simple result is a good test of some computer simulation packages. The simulation of a brick-shaped casting with a cast-on fin should show the cooling effect by the fin. Some relatively poor computer algorithms do not take into account the conduction of heat in the casting, thus predicting, erroneously, the appearance of the junction as a hot spot, clearly revealed by the contours near the junction curving the wrong way.)

Creese and Sarfaraz (1987) demonstrate the use of a fin to chill a hot spot in pure Al castings that was difficult to access in other ways. They cast on fins to T- and L-junctions as shown in Figure 5.20. The reduction in porosity achieved by this technique is shown in Figure 5.21. For these casting sections of 50 mm there was no apparent difference between fins of 2.5 and 3.3 mm thickness so these results are treated together in this figure. These fins at 5 and 6% of the casting section happen to be close to optimum as is confirmed below. The reason that they conduct away perhaps less effectively than might be expected is because of their unfavorable location at  $45^\circ$  between two hot components of the junction.

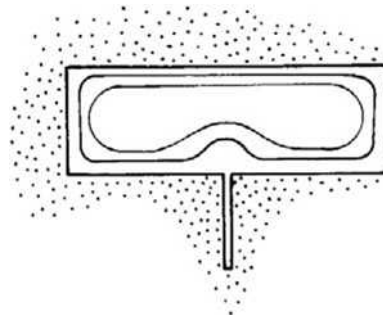


**FIGURE 5.19**

T-junction casting in 99.9Al by Kim et al. (1985) showing successive positions of the solidification front.

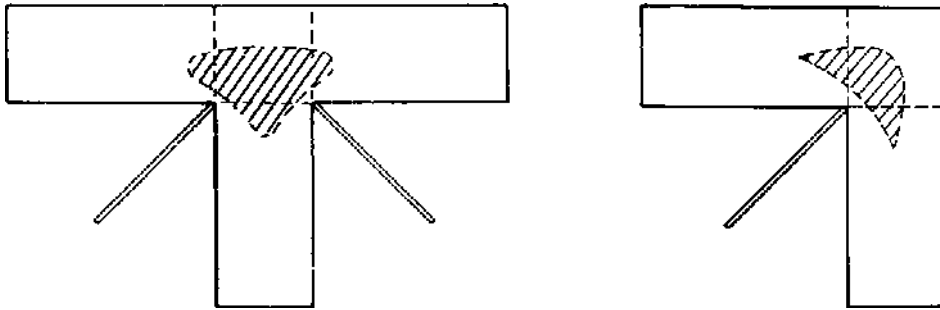


FIGURE 5.20

T- and L-junctions in pure aluminum cast in oil-bonded greensand. The shape of porosity in these junctions is shown, and the region of the junction used to calculate the percentage porosity is shown by the broken lines. The position of fins added to eliminate the porosity is shown. Results are presented in Figure 5.21.

Returning to the case where the upright of the T is sufficiently thin to act as a cooling fin, one further case that is not presented in Figure 5.18 is the case where the fin is so thin that it does not exist. This, you will say, is a trivial case. But think what it tells us. It proves that the fin can be too thin to be effective, since it will have insufficient area to carry away enough heat. Thus we arrive at the important conclusion that there is an optimum thickness of fin for a given casting section.

Similarly, an identical argument can be made about the fin length. A fin of zero length will have zero effect. As length increases, effectiveness will increase, but beyond a certain length, additional length will be of reducing value. Thus the length of fins will also have an optimum.

These questions have been addressed in a preliminary study by Wright and the author (1997) on a horizontal plate casting with a symmetrical fin (Figure 5.22). Symmetry was chosen so that thermocouple measurements could be taken along the center line (otherwise the precise thermal center was not known so that the true extension in freezing time may not have been measured accurately). In addition the horizontal orientation of the plate was selected to suppress any complicating effects of convection so far as possible. The thickness of the fin was  $tH$  and the length  $LH$  where  $t$  and  $L$  are the dimensionless numbers to quantify the fin in terms of  $H$ , the thickness of the plate. From this study it was discovered that there was an optimum thickness of a fin, and this was less than one tenth of  $H$ . Figure 5.22a interpolates an optimum in the region of 5% of the casting section thickness. The optimum length was  $2H$ , and longer lengths were not significantly more effective (Figure 5.22b). For the optimum conditions the freezing time of the casting was increased by approximately ten times. Thus the effect is useful. However, the effect is also rather localized, so that it needs to be used with caution. Eventually, non-symmetrical results for a chill on one side of the plate would be welcome.

Even so, the practical benefits to the use of a fin as opposed to a chill are interesting, and possibly even compelling. They are:

1. The fin is always provided on the casting, because it is an integral part of the tooling. Thus, unlike a chill, the placing of it cannot be forgotten.
2. It is always exactly in the correct place. It cannot be wrongly sited before the making of the mold. (The incorrect positioning of a chill is easily appreciated, because although the location of the chill

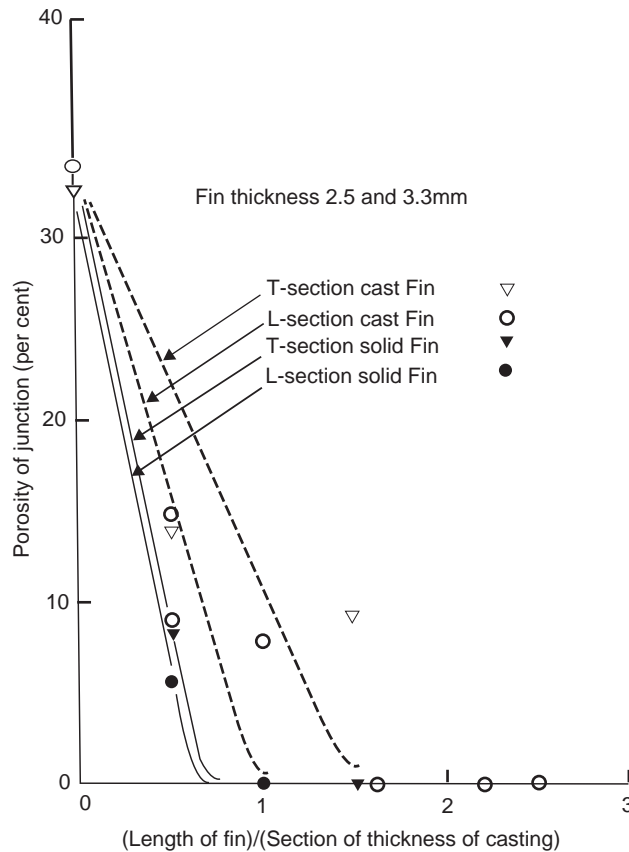


**FIGURE 5.21**

Results from Creese and Sarfaraz (1987, 1988) showing the reduction in porosity as a result of increasing length of fins applied as in Figure 5.21.

is normally carefully painted on the pattern, the application of the first coat of mold release agent usually does an effective job in eliminating all traces of this. Furthermore, of course, the chill can easily move during the filling of the molding box with sand.)

3. It cannot be displaced or lifted during the making of the mold. If a chill lifts slightly during the filling of the tooling with sand, the resulting sand penetration under the edges of the chill, and the casting of additional metal into the roughly shaped gap, makes an unsightly local mess of the casting surface. Displacement or complete falling out of the chill from the mold is a common danger, sometimes requiring studs to support the chill if awkwardly angled or on a vertical face. Displacement commonly results in sand inclusion defects around the chill or can add to defects elsewhere. All this is costly to dress off.
4. An increase in productivity has been reported as a result of not having to find, place and carefully tuck in a block chill into a sand mold (Dimmick 2001).

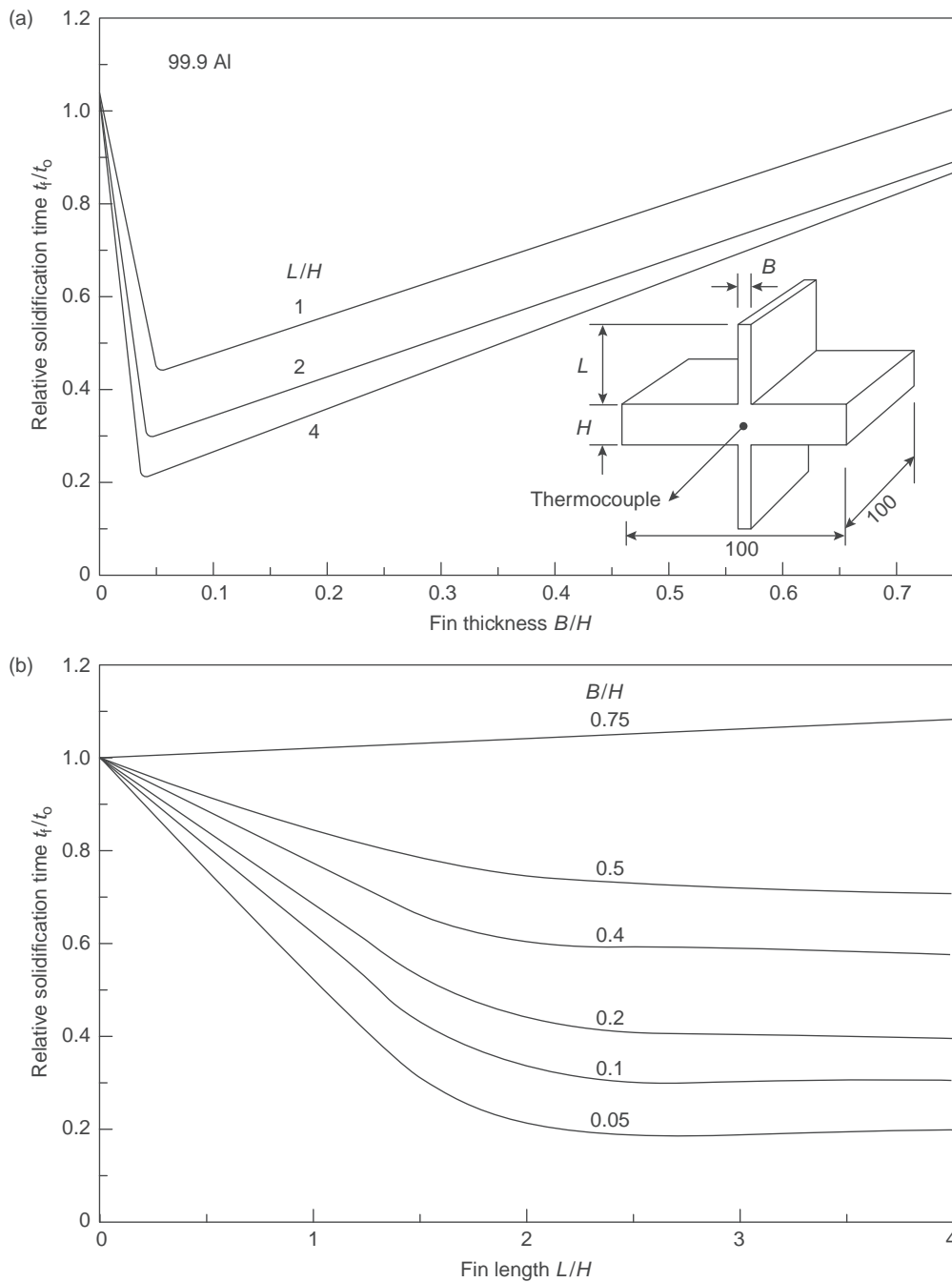


**FIGURE 5.22**

The effect of a symmetrical fin on the freezing time at the center of a cast plate of 99.9Al as a function of the length and thickness of the fin (averaged results of simulation and experiment from Wright and Campbell 1997).

5. The fin is easily cut off. In contrast, the witness from a chill also usually requires substantial dressing, especially if the chill was equipped with v-grooves, or if it became misplaced during molding, as mentioned above.
6. The fin does not cause scrap castings because of condensation of moisture and other volatiles, with consequential blow defects, as is a real danger from chills.
7. The fin does not require to be retrieved from the sand system, cleaned by shot blasting, stored in special bins, re-located, counted, losses made up by re-ordering new chills, casting new chills (particularly if the chill is shaped) and finally ensuring that the correct number in good condition, re-coated, and dried, is delivered to the molder on the required date.
8. The fin does not wear out. Old chills become rounded to the point that they are effectively worn out. In addition, in iron and steel foundries, gray iron chills are said to 'lose their nature' after some use. This seems to be the result of the oxidation of the graphite flakes in the iron, thus impairing the thermal conductivity of the chill. This is understandable in terms of Figure 5.11 since graphite has significantly better conductivity than pure iron or steel which would materially affect sufficiently large chills.
9. Sometimes it is possible to solve a localized feeding problem (the typical example is the isolated boss in the center of the plate) by chilling with a fin instead of providing a local supply of feed metal. In this case the fin is enormously cheaper than the feeder, and sometimes the feeder would be located where it cannot be subsequently removed, and its continued presence would be objectionable to the customer. The customer might accept a fin remaining in an obscure part of the casting, or the fin might be more easily removed.

This lengthy list represents considerable costs attached to the use of chills that are not easily accounted for, so that the real cost of chills is often underestimated.

Even so, the chill may be the correct choice for technical reasons. Fins perform poorly for metals of low thermal conductivity such as zinc, Al-bronze, iron, and steel. The computer simulation result in Figure 5.23 illustrates for the rather low thermal conductivity material, Al-bronze, that there are extensive conditions in which the chill is far more effective. Lerner and Kouznetsov (2004) compare the action of chills and fins, concluding that the two are sometimes interchangeable but the action of the fin is necessarily rather localized, whereas the chill gives a better distribution of cooling effect.

The kind of result shown in Figure 5.23 would be valuable if available for a variety of casting alloys varying from high to low thermal conductivity, so that an informed choice could be made whether a chill or fin were best in any particular case. Such data have yet to be worked out and published.

Fins are most easily provided on a joint line of the mold, or around core prints. Sometimes, however, there is no alternative but to mold them at right angles to the joint. From a practical point of view, these upstanding fins on patternwork are of course vulnerable to damage. Dimmick (2001) records that fins made from flexible and tough vinyl plastic solved the damage problem in their foundry. They would carry out an initial trial with fins glued onto the pattern. If successful, the fins would then be permanently inserted into the pattern. In addition, only a few standard fins were found to be satisfactory for a wide range of patterns; a fairly wide deviation from the optimum ratios did not seem to be a problem in practice.

Safaraz and Creese (1989) investigated an interesting variant of the cast-on fin. They applied loose metal fins to the pattern, and rammed them up in the sand as though applying a normal external chill, in the manner shown in Figure 5.20. The results of these 'solid' or 'cold' fins (so called to distinguish

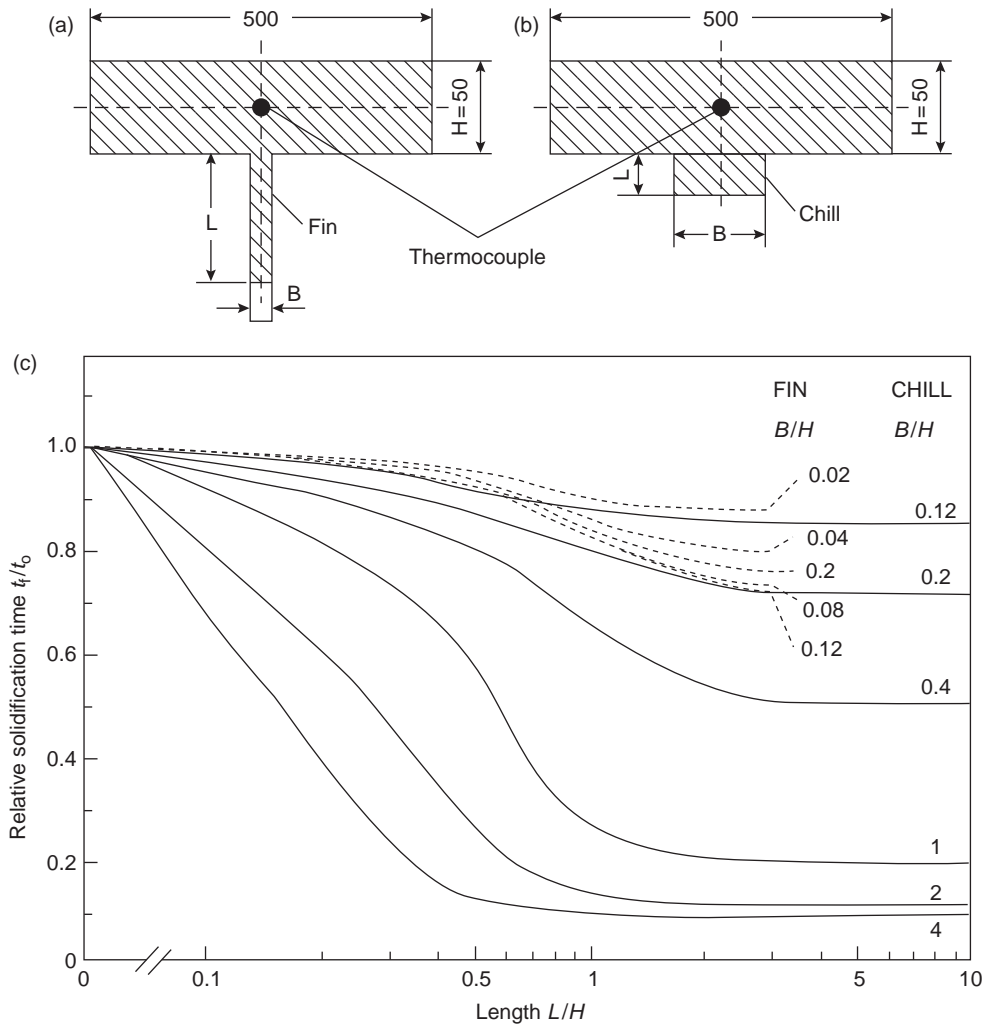


FIGURE 5.23

Comparison of the action of chills and cooling fins in Al bronze alloy AB1 (Wen, Jolly, and Campbell 1997).

them from the empty cavity that would, after filling with liquid metal, effectively constitute a ‘cast’ or ‘hot’ fin) are also presented in Figure 5.21. It is seen that the cold fins are more effective than the cast fins in reducing the porosity in the junction castings. This is the consequence of the heat capacity of the fin being used in addition to its conducting role. It is noteworthy that this effect clearly over-rides any disadvantage of heat transfer resistance across the casting/chill interface.

The cold fin is, of course, really a chill of rather slim shape. It raises the interesting question, that as the geometry of the fin and the chill is varied, which can be the most effective. This question has been tackled in the author’s laboratory (Wen et al. 1997) by computer simulation. The results are

summarized in Figure 5.23. Clearly, if the cast fin is sufficiently thin, it is more effective than a thin chill. However, for normal chills that occupy a large area of the casting (effectively approaching an 'infinite' chill as shown in the figure), as opposed to a slim contact line, the chill is massively more effective in speeding the freezing of the casting.

Other interesting lessons to be learned from Figure 5.23 are that a chill has to be at least equal to the section thickness of the casting to be really effective. A chill of thickness up to twice the casting section is progressively more valuable. However, beyond twice the thickness, increasingly thick chills show progressively reducing benefit.

It is to be expected that in alloys of higher thermal conductivity than aluminum bronze, a figure such as Figure 5.23 would show a greater regime of importance for fins compared to chills. The exploration of these effects for a variety of materials would be instructive and remains as a task for the future.

The business of getting the heat away from the casting as quickly as possible is taken to a logical extreme by Czech workers (Kunes et al. 1990) who show that a heat pipe can be extremely effective for a steel casting. Canadian workers (Zhang et al. 2003) explore the benefits of heat pipes for aluminum alloys. The conditions for successful application of the principle are not easy, however, so I find myself reluctant at this stage to recommend the heat pipe as a general purpose technique in competition to fins or chills. In special circumstances, however, it could be ideal.

### 5.1.3 Convection

Convection is the bulk movement of the liquid under the driving force of density differences in the liquid. In Section 5.3.4 we shall consider the problems raised by convection driven by solutes; heavy solutes cause the liquid to sink, and the lighter solutes cause flotation. In this section we shall confine our discussion simply to the effects of temperature: hot liquid will expand, becoming less dense, and will rise; cool liquid will contract, becoming denser, and so will sink.

The existence of convection has been cited as important because it affects the columnar to equiaxed transition (Smith et al. 1990). There may be some truth in this. However, in most castings, grain structure is of no importance. Hardly any customer specifies the grain structure of their castings, the only critical feature being soundness. Only in very few castings is grain size specified or is in any way noticeably significant in terms of affecting properties. Turbine blades are the exceptional example.

It is of course understood that soundness is of vital importance to nearly every casting, but it is not well known that in certain circumstances convection can give severe soundness problems. This is especially true in counter-gravity systems, and sometimes in investment castings. This important phenomenon is dealt with at length in Chapter 10, Rule 7 for the manufacture of good castings. It is recommended reading.

### 5.1.4 Remelting

When considering the solidification of castings it is easy to think simply of the freezing front as advancing. However, there are many times when the front goes into reverse! Melting is common during the filling and solidification of castings and needs to be considered at many stages.

On a microscale, melting is known to occur at different points on the dendrite arms. In a temperature gradient along the main growth direction of the dendrite the secondary arms can migrate down the temperature gradient by the remelting of the hot side of the arms and the freezing of the cold side.



Allen and Hunt (1979) show how the arms can move several arm spacings. Similar microscopic remelting occurs as the small arms shrink and the larger arms grow to reduce the overall energy of the system. This is the mechanism of dendrite arm coarsening, leading to the dendrite arm spacing (DAS) being a useful indicator of the solidification time of a casting.

Slightly more serious thermal perturbations can cause the secondary dendrite arms to become detached when their roots are remelted (Jackson et al. 1966). The separated secondaries are then free to float away into the melt to become nuclei for the growth of equiaxed grains. If, however, there is too much heat available, then the growth front stays in reverse, with the result that the nuclei vanish, having completely remelted!

On a larger scale in the casting, the remelting of large sections of the solidification front can occur. This can happen as heat flows are changed as a result of changes in heat transfer at the interface, as the casting flexes and moves in the mold, changing its contact points and pressures at different locations and at different times. It is likely that this can happen as parts of the mold, such as an undersized chill, become saturated with heat, while cooling continues elsewhere. Thus the early rapid solidification in that locality is temporarily reversed.

Local remelting of the solid is seen to occur as a result of the influx of fresh quantities of heat from forced convection during filling. The so-called ‘flow lines’ seen on the radiographs of magnesium alloy castings are clearly a result of the local washing away of the solidification front, as a curving river can erode its outer bank. These features appear quite distinct from other linear defects such as hot tears or cracks as a result of their smooth outlines and gradual shading of radiographic density (Skelly and Sunnucks 1954, Lagowski 1967). Interestingly, no damaging loss of properties has ever been reported from such linear features of castings.

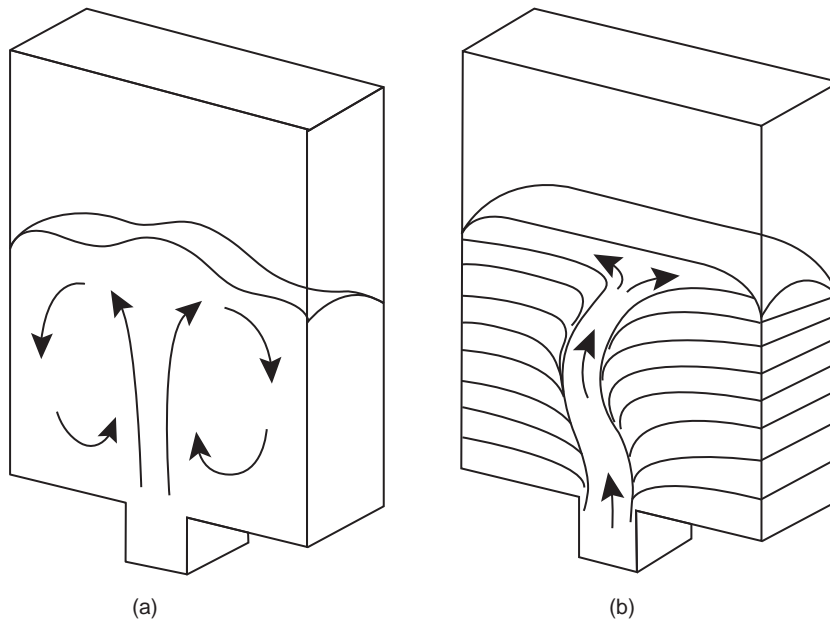
The existence of continuous fluidity is a widely seen effect resulting directly from the remelting of the solid material that has formed in the filling system, keeping the metal flowing despite an unfavorable modulus. Without the benefits of this phenomenon it would be difficult to make castings at all!

Other convective flows produced by solute density gradients in the freezing zone take time to get established. Thus channels are formed by the remelting action of low-melting-point liquid flowing at a late stage of the freezing process. The A and V segregated channels in steel ingots, and freckle defects in nickel- and cobalt-based alloys, are good examples of this kind of defect.

### 5.1.5 Flow channel structure

Consider the direct-gated vertical plate shown in Figure 5.24a. If this casting is filled quickly, the twin rotating vortices ensure that the plate fills with liquid at a uniform temperature. This may now be a problem to feed, and might exhibit the usual problems of distributed microporosity or surface sinks, etc.

This scenario contrasts with that of the slow filling of the casting, perhaps being filled slowly to reduce the potential for surface turbulence. In this case slow filling means *filling in a time commensurate with the solidification time of the section being filled*. If the filling rate were reduced to the point that the metal just reached the top of the mold by the time the metal had just cooled to its freezing point, then it might be expected that the top of the casting would be at its coldest, and freezing would then progress steadily down the plate, from the top to the gate. (At that time the gate would be assumed to be hot because of the preheating effect of the hot metal that would have passed through.) Nothing could be further from the truth.

**FIGURE 5.24**

(a) Fast filling showing mixing by vortices, giving a uniform temperature in the filled plate. (b) Slow filling, showing layered freezing during filling and the development of a central flow channel.

In reality, the slow filling of the plate causes metal to flow sideways from the gate into the sides of the plate (Figure 5.24b), cooling as it goes, and freezing near the walls. Thus while more distant parts of the casting are freezing, layers of fresh hot metal continue to arrive through the gate. The successive positions of the freezing front are shown in Figure 5.24b. The final effect is a flow path kept open by the hot metal through a casting that by now has mainly solidified. The well-fed panels either side of the flow channel are usually extremely sound and fine grained, and contrast with the flow channel. The final freezing of the flow channel is slow because of the preheated mold around the path, and so its structure is coarse and porous. The porosity will be encouraged by the enhanced gas precipitation under the conditions of slow cooling, and shrinkage may contribute if local feeding is poor because either the flow path is long or it happens to be distant from a source of feed metal. Rabinovich (1969) describes these patterns of flow in thin vertical plates, calling them *jet streams*. *Flow channel* is suggested as a good name, if somewhat less dramatic.

Figure 5.25 shows an extreme example. This figure is a radiograph of an Al-7Si-0.4Mg alloy plate cast in an acid catalyzed furan bonded silica sand mold. The flow channel is outlined by minute bubbles (most probably of hydrogen) that appear to have formed just under the surface of the casting as a result of reaction with the mold, but have floated upwards to rest against and decorate the upper surface of the channel. They have probably grown sufficiently large to become significantly buoyant because of the extra time and temperature for reaction in the flow channel region. Those parts of the casting that have solidified quickly do not show bubbles on the radiograph. The flow channel in this

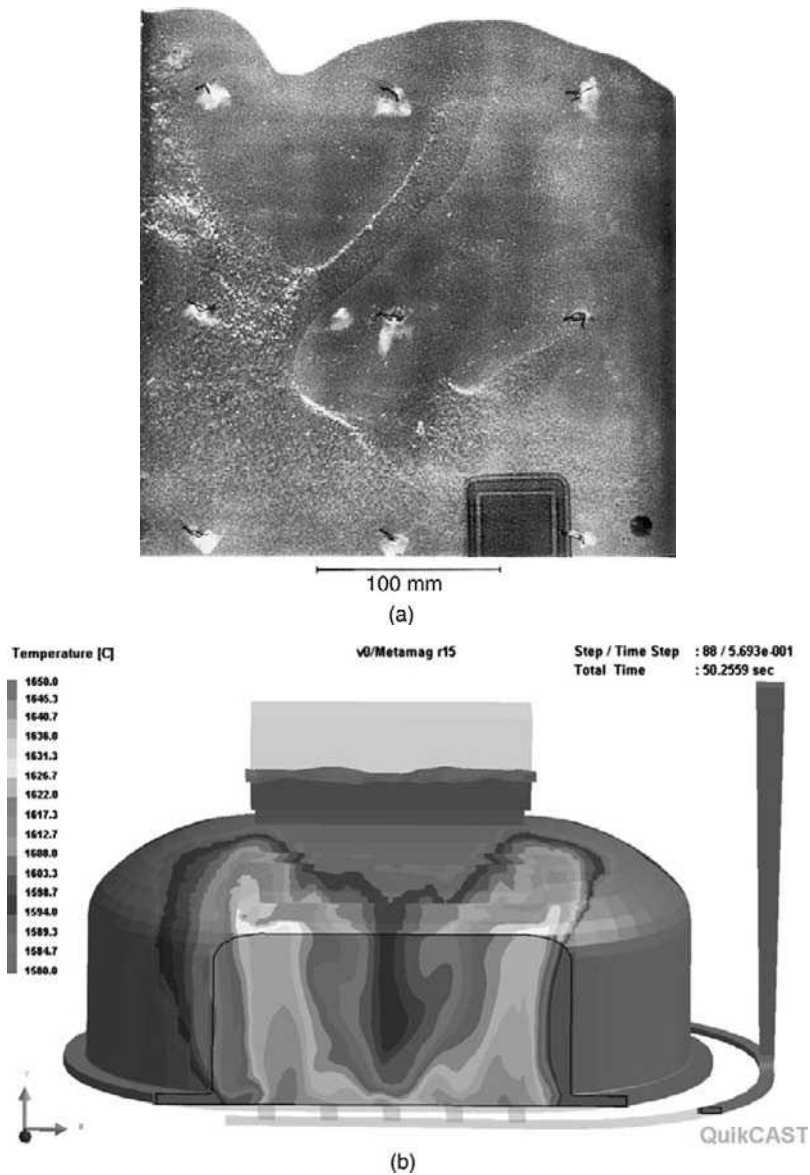


**FIGURE 5.25**

(a) Radiograph of an Al-7Si-0.4Mg alloy vertical plate filled via a side riser and slot gate shown in Figure 3.1a, showing unexpected flow channel filling behavior when cast particularly cool. Remains of thermocouples can be seen (Runyoro 1992). (b) Computer simulation of two flow channels developing in the walls of a gray iron casting despite the provision of five ingates in an effort to spread heat as evenly as possible (courtesy of R Puhakka 2009).

case arises because the casting was made at a particularly low pouring temperature, causing the channel to flow with a partly solidified slurry. It therefore adopted the form of a magma vent in the earth's crust, the pasty material resembling viscous lava, forming a volcano-like structure at the top surface.

Although Figure 5.25 illustrates a clear example because of the metal/mold reaction, in general the defect is not easily recognizable. It can occasionally be seen as a region of coarse grain and fine porosity in radiographs of large plate-like parts of castings. The structure contrasts with the extensive areas of clear, defect-free regions of the plate on either side. It is possible that many so-called shrinkage problems (for which more or less fruitless attempts are made to provide a solution by extra feeders or other means) are actually residual flow channels that might be cured by changing ingate position or size, or raising fill rate. No research appears to have been carried out to guide us out of this difficulty.

The flow channel structure is a standard feature of castings that are filled slowly from their base. This serious limitation to structure control seems to have been largely overlooked, and is one of the phenomena that limit the choice of a very long filling time.

Nevertheless, in general, the problem is reduced by filling faster, if that is possible without introducing other problems. More precisely, the velocity into the mold is initially controlled below approximately  $0.5 \text{ m s}^{-1}$  to avoid jetting through the ingate. After the base of the mold is covered to a sufficient depth the velocity can be ramped up. This is easily accomplished with a counter-gravity system, or even gravity system using a surge control design of filling system. A sufficiently high velocity will drive large circulating eddies (Figure 5.24) and finer-scale circulating eddies (bulk turbulence) beneath the relatively tranquil surface. In this way the temperature of a large area, if not the whole casting, will be relatively uniform, completely free of a flow channel.

However, even fast filling does not cure the other major problem of bottom-gating, which is the adverse temperature gradient, with the coldest metal being at the top and the hottest at the bottom of the casting, particularly concentrated in the ingate. Where feeders are placed at the top of the casting this thermal regime is clearly unfavorable for efficient feeding. However, of course, feeding can be made to be effective by oversized, if inefficient, feeders.

The problems of directly gating into the casting arise because the hot metal has to travel through the casting to reach all parts. One solution is *not* to gate into the casting but create a separate flow path called an *up-runner*, *outside* the casting. The melt is transferred by sideways flow off the up-runner via a slot gate into the mold cavity. The technique is described in Section 12.4.16. Another technique to counter adverse temperature gradient as a result of filling is the inversion of the casting after filling. This is an effective technique recommended for volume production.

It is well to remember that on occasions remelting to create flow channels can occur without the transfer of heat. The channels seen commonly in Ni-base superalloys, known as 'freckles' because of their appearance when etched revealing the random orientations of fragments of grains, and the 'A' and 'V' segregates in heavy steel castings and ingots, have been formed by residual liquid, strongly segregated in C, S, and P, that has a lower melting point than the matrix (Section 5.3.4). The matrix therefore melts when in contact with this liquid as a result of the diffusion of alloying elements into the matrix, lowering its melting point. Melting therefore occurs in this case by the transfer of solutes rather than the transfer of heat.

## 5.2 DEVELOPMENT OF MATRIX STRUCTURE

### 5.2.1 General

The liquid phase can be regarded as a randomly close-packed heap of atoms, in ceaseless random thermal motion, with atoms vibrating, shuffling, and jostling a meandering route, shoulder to shoulder, among and between their neighbors. The motion of individual atoms has been likened to the drunkard's walk.

In contrast, the solid phase is an orderly array, or lattice, of atoms arranged in more or less close-packed rows and layers called a lattice. Atoms arranged in lattices constitute the solid bodies we call crystals. Iron in its alpha phase takes on the body-centered-cubic (bcc) lattice known as ferrite (Figure 5.26a). This is a rather less close-packed lattice than the face-centered-cubic (fcc) lattice known as the gamma-phase, or as austenite. Figure 5.26b shows only a single 'unit cell' of the lattice. The concept of the lattice is that it repeats such *unit cells*, replicating the symmetry into space millions of times in all directions. Macroscopic lattices can sometimes be seen in castings as crystals having sizes from 1  $\mu\text{m}$  to 100 mm, representing arrays  $10^3$  to  $10^8$  atoms across.

The transition from liquid to solid, the process of solidification, is not always easy, however. For instance, in the case of glass, the liquid continues to cool, gradually losing the thermal motion of its atoms, to the point at which it becomes incapable of undergoing sufficient atomic rearrangements for it to convert to a lattice. It has therefore become a supercooled liquid, capable of remaining in this state for ever.

Metals, too, are sometimes seen to experience this reluctance to convert to a solid, despite on occasions being cooled hundreds of degrees Celsius below their equilibrium freezing temperature. This is easily demonstrated for clean metals in a clean container, for instance liquid iron in an alumina crucible.

If and when the conversion from liquid to solid occurs, it is by a process first of nucleation, and then of growth.

*Nucleation* is the process of the aggregation of clusters of atoms that represent the first appearance of the new solid phase. *Growth* is, self-evidently, getting bigger. However, this process is subject to factors that encourage or discourage it as we shall discuss.

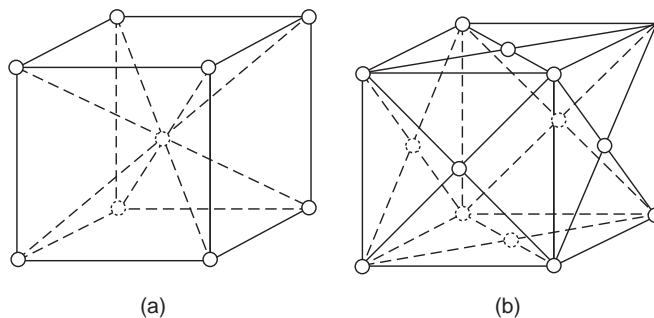


FIGURE 5.26

Body-centered cubic form of  $\alpha$ -iron (a) exists up to 910°C. Above this temperature, iron changes to (b) the face-centered-cubic form. At 1390°C the structure changes to  $\beta$ -iron, which is bcc once again (a).

In fact, the complexities of the real world dictate not only that the main solid phase appears during solidification, but also that alloys and impurities concentrate in ways to trigger the nucleation and growth of other phases. These include solid and liquid phases that we call second phases or inclusions, and gas or vapor phases which we call gas pores or shrinkage pores. It is convenient to treat the solid and liquid phases together as condensed (i.e. practically incompressible) matter that we shall consider in this chapter. The gas and vapor phases, constituting the non-condensed (and very compressible) matter such as gas and shrinkage porosity respectively, will be treated separately in Chapter 7.

For those readers who are enthusiastic about nucleation theory, there are many good formal accounts, some highly mathematical. A readable introduction relating to the solidification of metals is presented in Flemings (1974). We shall consider only a few basic aspects here; enough to enable us to understand how the structures of castings originate.

### 5.2.2 Nucleation of the solid

At first, as the temperature of a liquid is reduced below its freezing point, nothing happens. This is because in clean liquids the conversion to the solid phase involves a nucleation problem. We can gain an insight into the nature of the problem as follows.

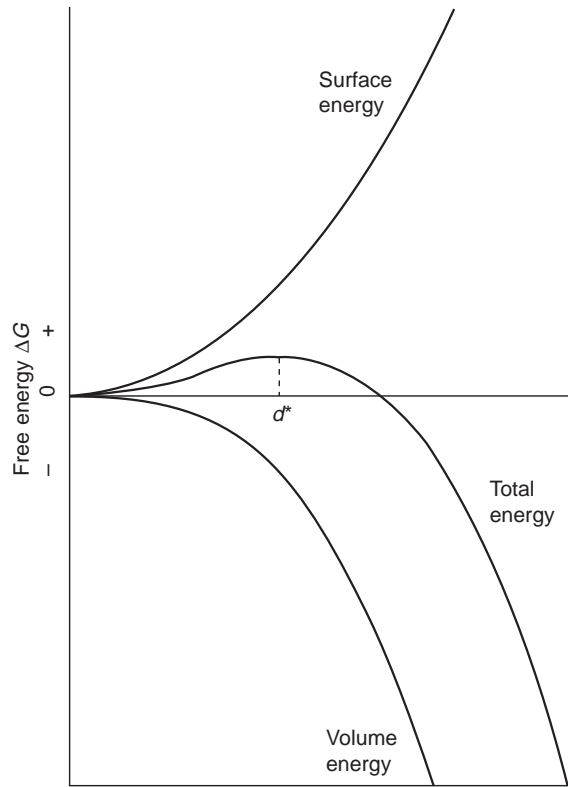
As the temperature continues to fall, the thermal agitation of the atoms of the liquid reduces, allowing small random aggregations of atoms into crystalline regions. For a small cubic cluster of size  $d$  the net energy to form this new phase is reduced in proportion to its volume  $d^3$  and the free energy per unit volume  $\Delta G_v$ . At the same time, however, the creation of new surface area  $6d^2$  involves extra energy because of the interfacial energy  $\gamma$  per unit area of surface. The net energy to form our little cube of solid is therefore:

$$\Delta G = 6d^2\gamma - d^3\Delta G_v \quad (5.15)$$

Figure 5.27 shows plots of the factors in this equation, showing that the net energy to grow the embryo increases at first, reaching a maximum. Embryos that do not reach the maximum require more energy to grow, so normally they will shrink and redissolve in the liquid.

Only when the temperature is sufficiently low to allow a chance chain of random additions to grow an embryo above the critical size will further growth be encouraged by a reduction in energy; thus growth will enter a 'runaway' condition. The temperature at which this event can occur is called the *homogeneous nucleation temperature*. For metals like iron and nickel it is hundreds of degrees Celsius below the equilibrium freezing point as has been demonstrated many years ago by Walker (1961) and by many more recent researchers such as Valdez and colleagues (2007).

Such low temperatures may in fact be attained when making castings, because the liquid metal sits inside its own surface oxide film, never making contact with its container. At microscopic points of contact of the filmed metal with the container, for molds with high conductivity, the cooling through the surface film may be so intense that homogeneous nucleation in the liquid may occur. Nucleation is not likely to be a heterogeneous event in this situation because the liquid contained in its oxide skin is not in actual atomic contact with the surface of the mold, and its oxide is not a favorable nucleating substrate. (We shall see later that although oxides, such as some crucible materials, are *not* good heterogeneous nuclei to initiate nucleation of the solid, they are *excellent* nuclei for many second phases, and are efficient, indirectly as bifilms, for the initiation of porosity and cracks. These two

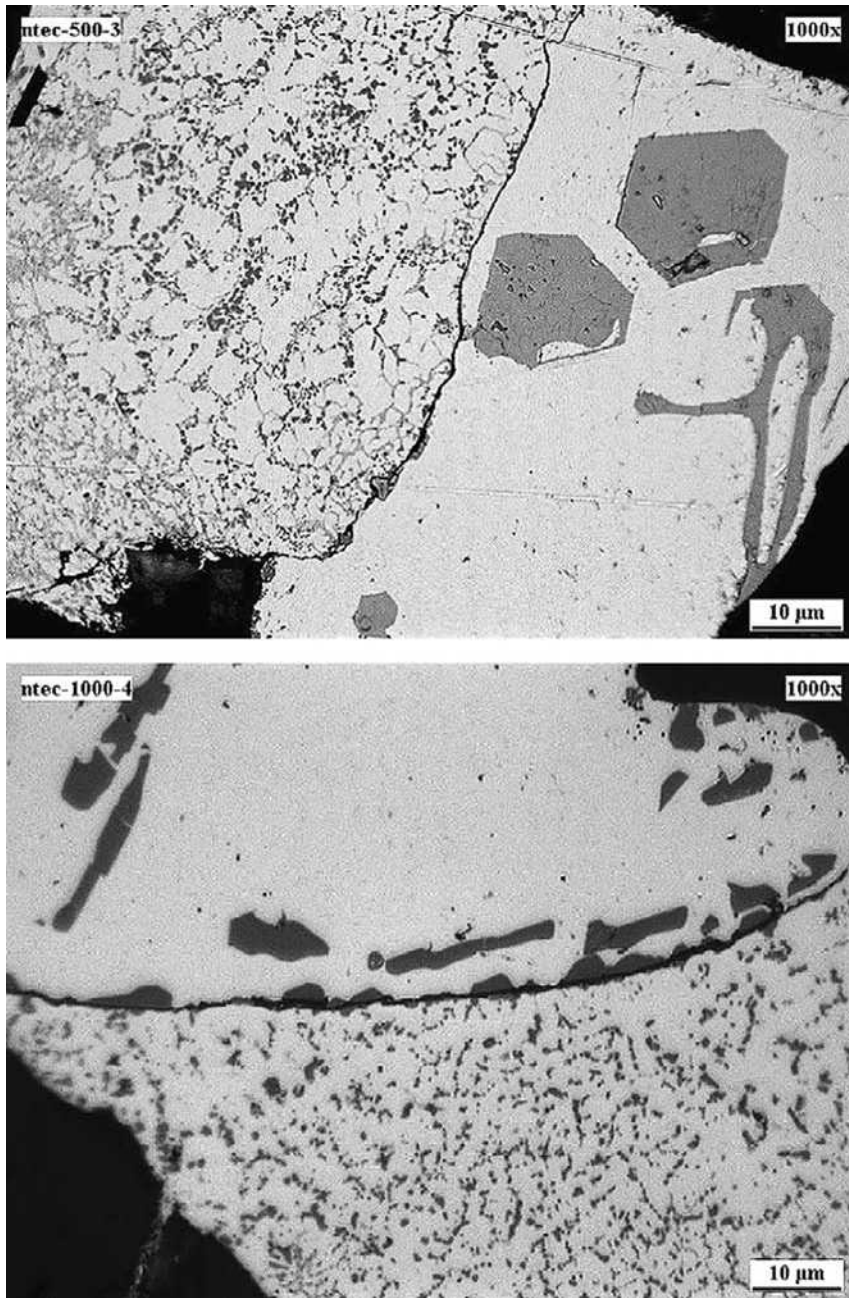


**FIGURE 5.27**

Surface and volume energies of an embryo of solid growing in a liquid give the total energy as shown. Below the critical size  $d^*$  any embryos will tend to shrink and disappear. Above  $d^*$  increasing size reduces the total energy, so growth will be increasingly favored, becoming a runaway process.

entirely different behaviors of oxides are a major factor in the development of cast structure which will be returned to repeatedly.)

Dispinar and Campbell (2007) have reported evidence of massive undercoolings in comparatively large aluminum alloy castings. The observations that drew our attention were studies of solidified filters from the filling systems of castings, in which adjacent regions of melt, separated by an apparent grain boundary, had vastly different DAS on either side of the boundary (Figure 5.28). This seemingly indicated the impossible situation of two different rates of freezing in adjacent regions of metal. The fine microstructure was finally interpreted as undercooled regions isolated from the bulk melt by oxide bifilms. Thus some of these separated regions had a high probability of containing no suitable inclusion on which to nucleate. The surrounding matrix, having solidified some time previously and so much cooler, acted as an efficient chill when freezing finally occurred. The enclosed droplet therefore exhibits its quenched-in, rapidly frozen, fine dendritic structure. This phenomenon, first seen in regions of melt trapped among oxide film inclusions, has now been identified in many castings poured

**FIGURE 5.28**

The separation and isolation of regions of Al-7Si alloy by oxide bifilms, resulting in (a) widely different solidification conditions, and (b) formation of Si particles on the bifilms (Dispinar 2007).



turbulently (including, for instance, in Ni-base superalloys cast in vacuum), where droplets from splashes cannot be re-assimilated by the melt because of their surface (double) oxide, and consequently have their own independent freezing behavior.

It is more common for the liquid to contain other solid particles in suspension on which new embryo crystal can form. In this case the interfacial energy component of Equation 5.15 can be reduced or even eliminated. Thus the presence of foreign nuclei in a melt can give a range of heterogeneous nucleation temperatures; the more effective nuclei requiring less undercooling. It is even conceivable that some solid might exist on an extremely favorable substrate at temperature above its freezing point. This seems to be the case, for instance, with silicon particles nucleating on AlP particles on oxide bifilms in Al–Si alloys. Graphite flakes appear to form similarly above the general Fe–graphite eutectic in cast irons. These examples will be discussed further in Chapter 6.

Nevertheless, it is important to keep in mind that not all foreign particles in liquids are favorable nuclei for the formation of the solid phase. In fact it is likely that the liquid is indifferent to the presence of much of this debris. Only rarely will particles be present that reduce the interfacial energy term in Equation 5.15. Thus, as far as most metals are concerned, oxides are not good nuclei. It is worth noting that it makes no difference whether the lattice structure and spacing of the oxide and metal are closely matched. The oxides are not wetted. This indicates that their electronic contribution to the interfacial energy with the metal is not favorable for nucleation. The covalently bonded oxides sit reluctantly against the metallic bonds of the metals.

### ***Grain refinement***

Materials with more metallic properties are good nuclei for the initiation of the solid phase. For the nucleation of steels, these include some borides, nitrides, and carbides. For Al alloys, an intermetallic compound,  $\text{TiAl}_3$ , is the key inoculant, together with  $\text{TiB}_2$ . These details are discussed in the section on casting alloys in Chapter 6.

It seems, however, that the action of an effective grain-refining addition to a melt is not only that of nucleating new grains. An important secondary role is that of inhibiting the rate of growth of grains, thereby allowing more grains the opportunity to nucleate.

Even so, as a cautionary note, the addition of  $\text{TiB}_2$  to Fe–3Si alloys (Campbell and Bannister 1975) exhibited a profound grain refinement action, almost certainly enhanced by the thick layer of borides that surrounded each grain. The mechanical properties were expected to be seriously impaired by this brittle grain boundary phase, illustrating the probability that not all grain refinement of cast alloys is beneficial.

For more complex systems, where many solutes are present, the rate of growth of grains was assumed by Greer and colleagues (2001) to be controlled by the rate at which solute can diffuse through the segregated region ahead to the advancing front. They carried out a detailed exercise for aluminum alloys, using a *growth restriction parameter*. This concept was refined by Australian workers (St John et al. 2007) as reported in Section 6.3.3.

### **5.2.3 Growth of the solid**

Once nucleated, the primary solid will spread relatively quickly through the undercooled liquid in contact with the face of the mold to form a solid skin that envelops the casting. The interesting question now is ‘How does it then continue its progress into the melt?’

Progress will only occur if heat is extracted through the solid, cooling the freezing front below the equilibrium freezing point. The actual amount of undercooling experienced at the freezing front is usually several degrees Celsius. If the rate of heat extraction is increased, the temperature of the solidification front will fall further, and the velocity of advance,  $V_s$ , of the solid will increase correspondingly.

For pure metals (assuming relative freedom from over-enthusiastic grain-refining additions), as the driving force for solidification increases, so the front is seen to go through a series of transitions. Initially it is planar; at higher rates of advance it develops deep intrusions, spaced rather regularly over the front. These are parts of the front that have been left far behind. At higher velocities still, this type of growth transforms into cigar-like projections called cells, which finally develop complex geometry involving side branches (Figure 5.29). These tree-like forms have given them the name dendrites (after the Greek word for tree, *Dendros*).

For the more important case of alloys, however, the three growth forms (planar, cellular, and dendritic) are similarly present (Figure 5.29). However, the driving force for instability is a kind of

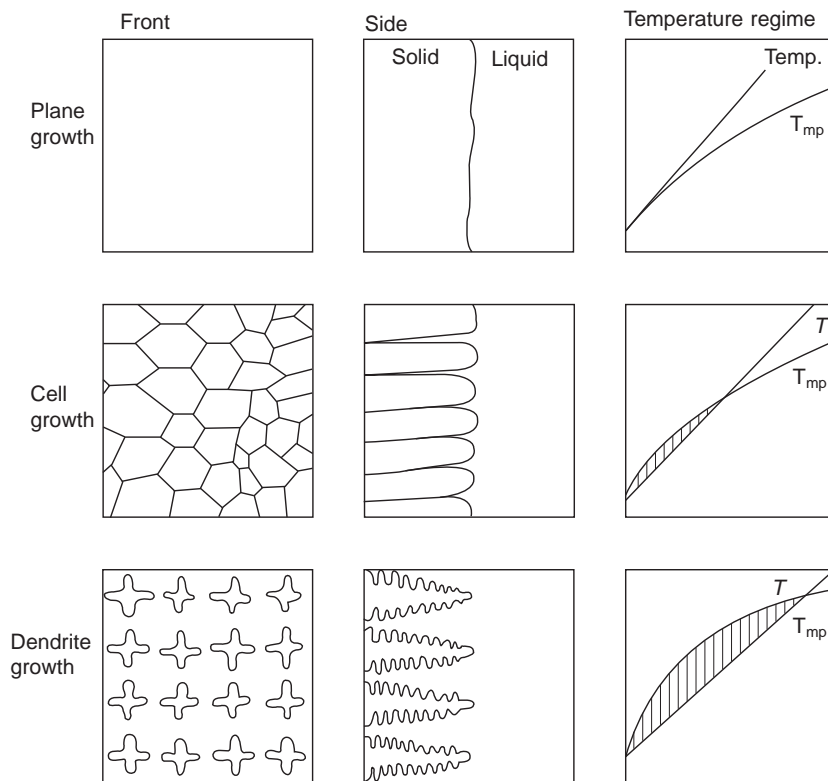


**FIGURE 5.29**

Transition of growth morphology from planar, to cellular, to dendritic, as compositionally induced undercooling increases (equivalent to  $G/V$  being reduced).

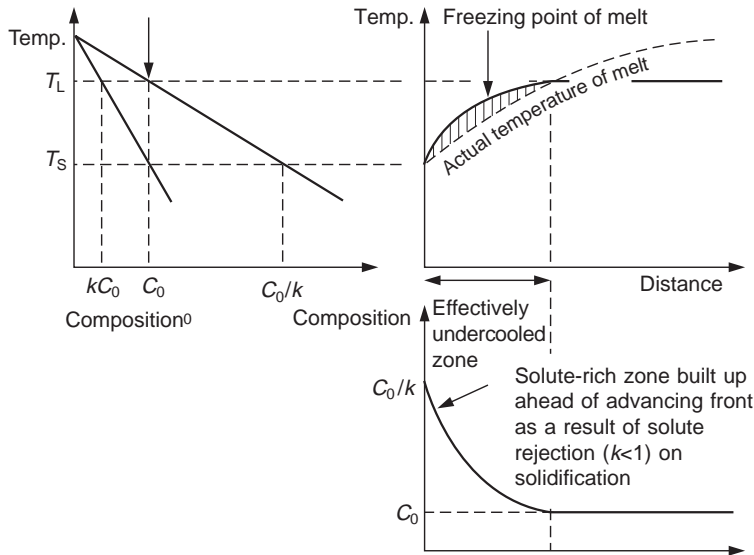


**FIGURE 5.30**

Link between the constitutional phase diagram for a binary alloy, and constitutional undercooling on freezing.

effective undercooling that arises because of the segregation of alloying elements ahead of the front. The presence of this extra concentration of alloying elements reduces the melting point of the liquid. If this reduction is sufficient to reduce the melting point to below the actual local temperature, then the liquid is said to be locally *constitutionally undercooled* (that is, effectively undercooled because of a change in the constitution of the liquid).

Figure 5.30 shows how detailed consideration of the phase diagram can explain the relatively complicated effects of segregation during freezing. It is worth examining the logic carefully.

The original melt of composition  $C_0$  starts to freeze at the liquidus temperature  $T_L$ . The first solid to appear has composition  $kC_0$  where  $k$  is known as the partition coefficient. This coefficient  $k$  usually has a value less than 1 (although the reader needs to be aware of the existence of the less common but important cases where  $k$  is greater than 1). For instance, for  $k = 0.1$  the first solid has only 10% of the concentration of alloy compared to the original melt; the first solid to appear is therefore usually rather pure.

In general,  $k$  defines how the solute alloy partitions between the solid and liquid phases. Thus:

$$k = C_S/C_L \quad (5.16)$$

For those equilibrium phase diagrams for which the solidus and liquidus lines are straight,  $k$  is accurately constant for all compositions. However, even where they are curved, the relative matching of the curvatures often means that  $k$  is still reasonably constant over wide ranges of composition. When  $k$  is close to 1, the close spacing of the liquidus and solidus lines indicates little tendency towards segregation. When  $k$  is small, then the wide horizontal separation of the liquidus and solidus lines warns of a strongly partitioning alloying element.

On forming the solid that contains only  $kC_0$  amount of alloy, the alloy remaining in the liquid has to be rejected ahead of the advancing front. Thus although the liquid was initially of uniform composition  $C_0$ , after an advance of about a millimeter or so the composition of the liquid ahead of the front builds up to a peak value of  $C_0/k$ . The build-up effect is like that of snow ahead of a snow plow. This is the steady-state condition shown in Figure 5.30.

In common with all other diffusion-controlled spreading problems, we can estimate the spread of the solute layer ahead of the front by the order-of-magnitude relation for the thickness  $d$  of the layer. If the front moves forward by  $d$  in time  $t$ , this is equivalent to a rate  $V_s$ . We then have:

$$d = (Dt)^{1/2} \text{ where } V_s = d/t$$

so:

$$d = D/V_s \quad (5.17)$$

where  $D$  is the coefficient of diffusion of the solute in the liquid. It follows that constitutional undercooling will occur when the temperature gradient,  $G$ , in the liquid at the front is:

$$G \leq -\frac{T_L - T_S}{D/V_s} \quad (5.18)$$

or

$$G/V_s \leq -(T_L - T_S)/D \quad (5.19)$$

from Figure 5.30, assuming linear gradients. Again, from elementary geometry which the reader can quickly confirm, assuming straight lines on the equilibrium diagram, we may eliminate  $T_L$  and  $T_S$  and substitute  $C_0$ ,  $k$  and  $m$ , where  $m$  is the slope of the liquidus line, to obtain the equivalent statement:

$$\frac{G}{V_s} = \frac{-mC_0(1-k)}{kD} \quad (5.20)$$

which is the classical solution derived from more rigorous diffusion theory by Chalmers in 1953, nicely summarized by Flemings (1974). This famous result marked the breakthrough in the history of the understanding of solidification by the application of physics. It marked the revolution from *qualitative description* to *quantitative prediction*. Computers have encouraged an acceleration of this new thinking.

Figure 5.29 illustrates how the progressive increase in constitutional undercooling causes progressive instability in the advancing front, so that the initial planar form changes first to form cells, and with further instability ahead of the front will be finally provoked to advance as dendrites.

Notice that the growth of dendrites is in response to an *instability condition* in the environment ahead of the growing solid, not the result of some influence of the underlying crystal lattice (although, of course, the crystal structure will subsequently influence the details of the shape of the dendrite). In the same way stalactites will grow as dendrites from the roof of a cave as a result of the destabilizing effect of gravity on the distribution of moisture on the roof. Icicles are a similar example; their forms being, of course, independent of the crystallographic structure of ice. Droplets running down window panes are a similar unstable-advance phenomenon that can owe nothing to crystallography. There are numerous other natural examples of dendritic advance of fronts that are not associated with any

long-range crystalline internal structure. It is interesting to look out for such examples. Remember also the converse situation that the planar growth condition also effectively suppresses any influence that the crystal lattice might have. It is clear therefore that the constitutional undercooling, assessed by the ratio  $G/R$ , is the factor that measures the degree of stability of the growth conditions, and so controls the type of growth front (*not*, primarily, the crystal structure).

Figure 5.31 shows a transition from planar, through cellular, to dendritic solidification in a low-alloy steel that had been directionally solidified in a vertical direction. The speeding up of the solidification front has caused increasing instability. Figures 5.32 and 5.33 show different types of dendritic growth. Both types are widely seen in metallic alloy systems. In fact, dendritic solidification is the usual form of solidification in castings.

A columnar dendrite nucleated on the mold wall of a casting will grow both forwards and sideways, its secondary arms generating more primaries, until an extensive 'raft' has formed (Figure 5.34). All these arms will be parallel, reflecting the internal alignment of their atomic planes. Thus on solidification the arms will 'knit' together with almost atomic perfection, forming a single-crystal lattice known as a grain. A grain may consist of thousands of dendrites in a raft. Alternatively a grain may consist merely of a single primary arm, or, in the extreme, merely an isolated secondary arm.

The boundaries formed between rafts of different orientation, originating from different nucleation events, are known as grain boundaries. Usually these are high-angle grain boundaries, so-called to distinguish them from the low-angle boundaries within grains that result from small imperfections in the way the separate arms of the raft may grow, or suffer slight mechanical damage, so that their lattices join slightly imperfectly, at small but finite angles.

Given a fairly pure melt, and extremely quiescent conditions, it is not difficult to grow an extensive dendrite raft sufficient to fill a mold having dimensions of 100 mm or so, producing a single crystal. Nordland (1967) describes an unusual and fascinating experiment in which he solidifies bismuth at high undercooling and high rates, but preserves the fragile dendrite in one piece. He achieves this by adding weights to the furnace that contained his sample of solidifying metal, and suspends the whole assembly in mid-air, using long lengths of polypropylene tubing from the walls and ceiling of the room. In this way he was able to absorb and dampen any outside vibrations.

In a review of the effects of vibration on solidifying metals, the author (1981) confirms that Nordland's results fall into a regime of frequency and amplitude where the vibrational energy is too low for damage to occur to the dendrites (Figure 5.35).

### ***Dendrite arm spacing (DAS)***

In the metallurgy of wrought materials, it is the *grain size* of the alloy that is usually the important structural feature. Most metallurgical textbooks therefore emphasize the importance of grain size.

In castings, however, grain size is sometimes important (as will be discussed later), but more often it is the *secondary dendrite arm spacing* (sometimes shortened merely to *dendrite arm spacing*, DAS) that appears to be the most important structural length parameter.

The mechanical properties of most cast alloys are usually seen to be strongly dependent on secondary arm spacing. As DAS increases, so ultimate strength, ductility, and elongation fall. Also, since homogenization heat treatments are dependent on the time required to diffuse a solute over a given average distance  $d$ , if the coefficient of diffusion in the solid is  $D$ , then from the order-of-magnitude

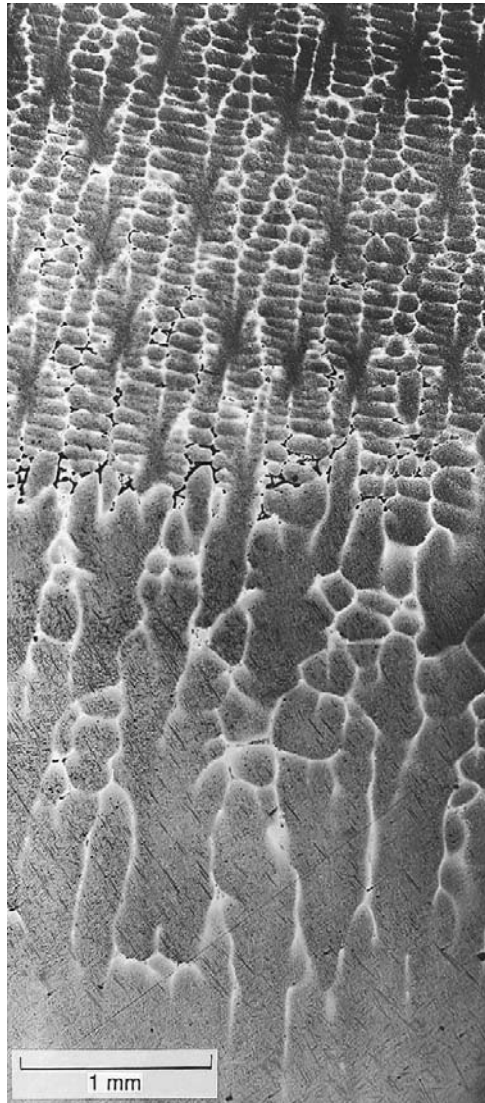


**FIGURE 5.31**

Structure of a low-alloy steel subjected to accelerating freezing from bottom to top, changing from planar, through cellular, to dendritic growth.

relation, Equation 1.5, we predict, quantitatively, the finer DAS to give us specifically shorter homogenization times, or better homogenization in similar times; the cast material is more responsive to heat treatment, giving better properties or faster treatments.

It is now known that the secondary DAS is controlled by a coarsening process, in which the dendrite arms first grow at very small spacing near the tip of the dendrite. As time goes on, the

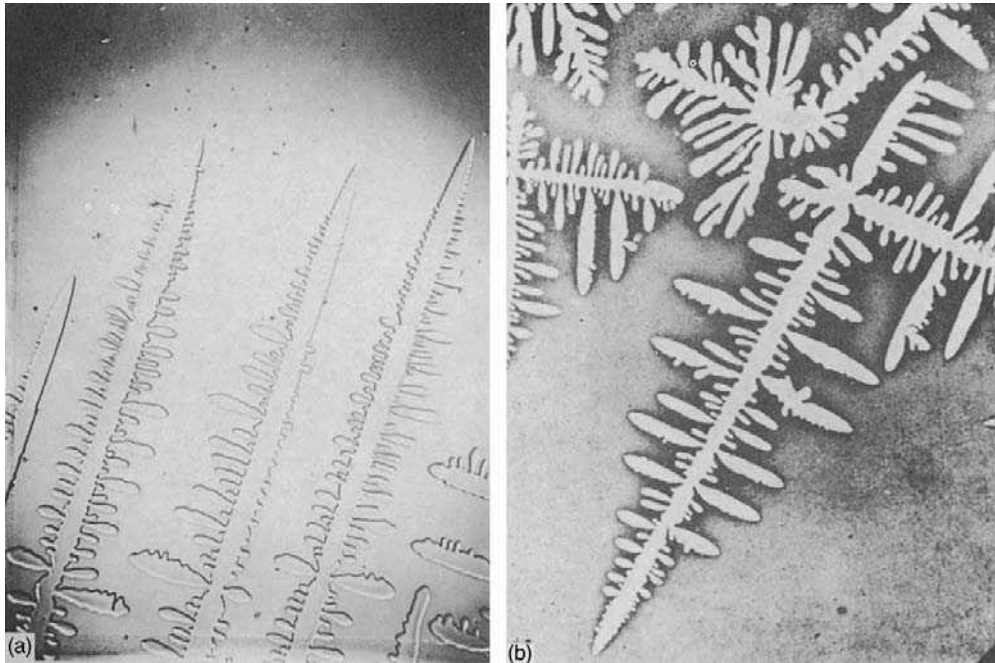


**FIGURE 5.32**

Transparent organic alloy showing dendritic solidification. Columnar growth (a) and equiaxed growth (b) with a modification to the alloy by the addition of a strongly partitioning solute, with  $k \ll 1$ , which can be seen to be segregated ahead of the growing front. Courtesy of JD Hunt; see Jackson et al. (1966).

dendrite attempts to reduce its surface energy by reducing its surface area. Thus small arms preferentially go into solution whilst larger arms grow at their expense, increasing the average spacing between arms. The rate of this process appears to be limited by the rate of diffusion of solute in the liquid as the solute transfers between dissolving and growing arms. From a relation such as Equation 1.5, and assuming the alloy solidifies in a time  $t_f$ , we would expect that DAS would be proportional to  $t_f^{1/2}$ , since  $t_f$  is the time available for coarsening. In practice it has been observed that DAS is actually proportional to  $t^n$  where  $n$  usually lies between 0.3 and 0.4 (Young and Kirkwood 1975). Figure 5.36 shows the magnificent research result, illustrating the relation between DAS and  $t_f$  continuing to hold for Al–4.5Cu alloy over eight orders of magnitude (Bower et al. 1966). Interestingly, however, a plot of grain size on the same figure shows that grain size is completely scattered above the DAS line. Clearly, grain size is completely independent of solidification time. In addition, of course, a grain cannot be smaller than a single dendrite arm, but can grow to unlimited size in some situations.

The primary DAS is of course significantly coarser than the secondary DAS, and appears controlled by rather different parameters. Young and Kirkwood (1975) proposed it is proportional to the parameter  $(GV)^{-1/2}$  where  $G$  is the temperature gradient and  $V$  is the rate of advance of the solidification front. A little later, Hunt and Thomas (1977) present more accurate analytical solutions as a function of

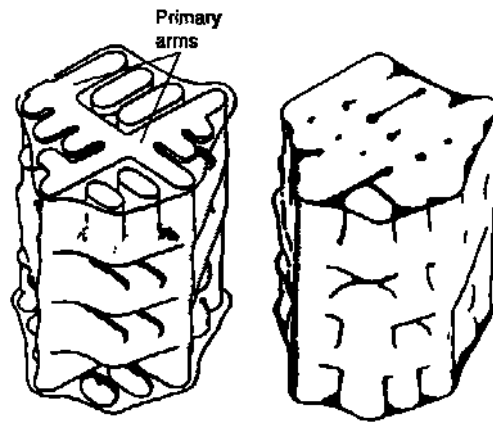


**FIGURE 5.33**

Rather irregular dendrites common in aluminum alloys at (a) 50 and (b) 90% solidified. The secondary arms spread laterally, joining to form continuous plates. After Singh et al. (1970).

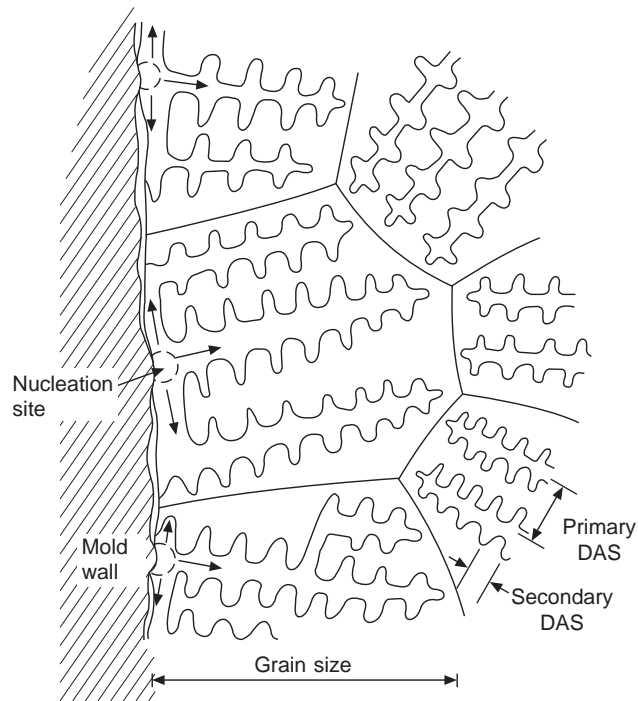


**FIGURE 5.34**

Schematic illustration of the formation of a raft of dendrites to make grains. The dendrite stems within any one raft or grain are all crystallographically related to a common nucleus.



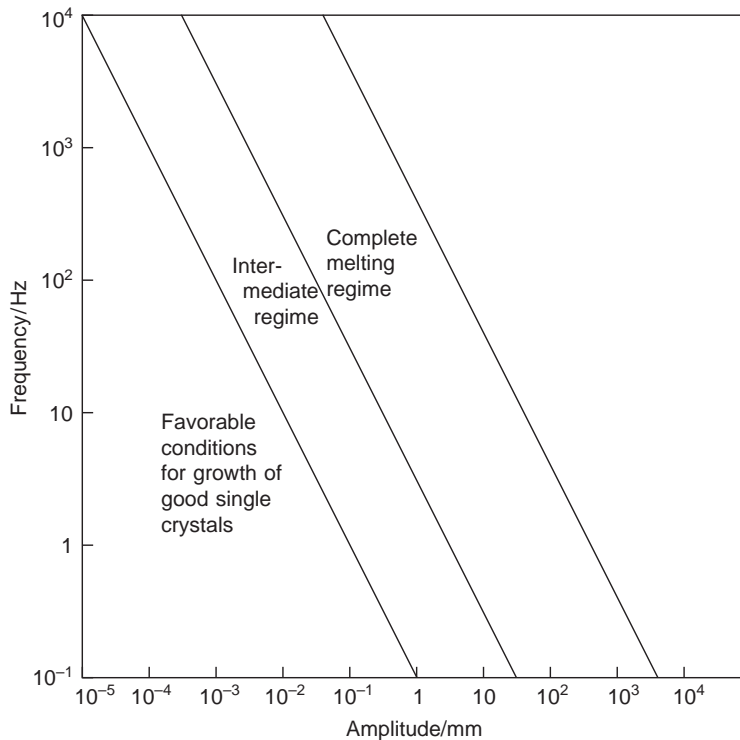


**FIGURE 5.35**

Grain refinement threshold as a function of amplitude and frequency of vibration (Campbell 1981).

$G$ ,  $V$ , and  $k$ , which were fitted to the results generated by a sophisticated computer program. Readers are recommended to the original papers for details of this piece of exemplary work.

In summary, primary DAS appears linked to solidification parameters and secondary DAS is controlled by solidification time. Grain size, on the other hand, is controlled by a number of quite separate processes, some of which are discussed further in the following section.

### 5.2.4 Disintegration of the solid (grain multiplication)

As the growers of single-crystal turbine blades know only too well, a single knock or other slight disturbance during freezing can damage the growing dendrite, breaking off secondary arms that then constitute nuclei for new separate grains. The growing crystal is especially vulnerable when strongly partitioning alloys are present that favor the growth of dendrites with secondary arms with weak roots. Thus some single crystals are fragile, and much more difficult to grow than others.

Figure 5.35 indicates that for any disturbance that can be characterized by a vibration of frequency  $f$  and/or amplitude  $a$ , a critical threshold exists at which the grains are fragmented. In a review of the mechanism of fragmentation by vibration (Campbell 1981) it was not clear whether the dendrite roots melted, or whether they were mechanically sheared, since these two processes could not be

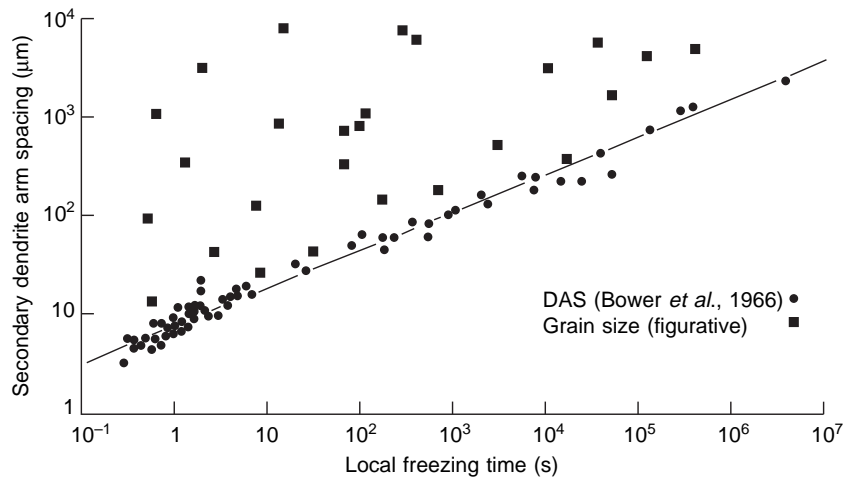


**FIGURE 5.36**

Relation between dendrite arm spacing (DAS), grain size, and local solidification time for Al-4.5Cu alloy.

distinguished by the experimental results. Whatever mechanism was operating, the experimental results on a wide variety of metals that solidify in a dendritic mode from Al alloys to steels could be summarized to a close approximation by

$$f.a. = 0.10 \text{ mm s}^{-1}$$

This relation describes the product of frequency (Hz) and amplitude (mm) that represents a critical velocity threshold for grain fragmentation. It seems to be valid over the complete range of experimental conditions ever tested, from subsonic to ultrasonic frequencies, and from amplitudes of micrometers to centimeters. Thus at ultrasonic frequency 25 kHz the amplitude for refinement is only 4 nm, whereas at the frequency of mains electricity 50 Hz the amplitude needs to be 2 mm.

In single-crystal growth it seems that the damage to a dendrite arm may not be confined to breaking off the arm. Simply bending an arm will cause that part of the crystal to be misaligned with respect to its neighbors. Its subsequent growth might be in a direction favorable for its continued growth, causing it to grow to the size of a significant defect. Vogel and colleagues (1977) propose that given a sufficiently large angle of bend, the plastically deformed material will recrystallize rapidly. The newly formed high-angle grain boundary, having a high energy, will be preferentially wetted by the melt, so that liquid will therefore propagate along the boundary and detach the arm. The arm now becomes a free-floating grain.

In the pouring of conventional castings, Ohno (1987) has drawn attention to the way in which the grains of some metals grow from the nucleation site on the mold wall. The grains grow from narrow stems that are vulnerable to plastic deformation and detachment. Thus as metal washes over the mold surface, thousands of crystals are swept into the melt. The nucleation sites with their remnant of dendrite root continue to be attached to the mold wall, quickly re-growing to seed strings of replacement crystals, one after another. There is an element of runaway catastrophe in this process; as one dendrite is felled, it will lean on its neighbors and encourage their fall.

The fragments of crystals that are detached in this way may dissolve once again as they are carried off into the interior of the melt if the casting temperature is too high. The interior of the casting may therefore become free of so-called equiaxed grains. If so, the structure of the casting will consist only of columnar grains that grow inwards from the mold wall.

However, if the casting temperature is not too high, then the detached crystals will survive, forming the seeds of grains that subsequently grow freely in the melt. The lack of directionality and the *equal* length of the *axes* of these crystals has given them the name 'equiaxed' grains. At very low casting temperatures, perhaps together with sufficient bulk turbulence, the whole of the casting may solidify with an equiaxed structure.

In mixed situations where modest quantities of equiaxed grains exist, they may be caught up as isolated grains in the growing forest of columnar dendrites. The directional heat flow that they will then experience will grow them unidirectionally, converting them to columnar grains. However, a sufficient deluge of equiaxed grains will swamp the progress of the columnar zone, converting the structure to equiaxed.

The *columnar-to-equiaxed transition* has been the subject of much solidification research. In summary it seems that the transition is controlled by the numbers of equiaxed grains that are available. The recent model by Bisuola and Martorano (2008) indicates that the advance of the columnar zone is blocked when only 20% of the liquid ahead has transformed to equiaxed grains. The modeling work by Spittle and Brown (1989) illuminates the concepts admirably (Figure 5.37).

In large steel ingots the columnar grains can reach lengths of 200 mm or more. These long cantilevered projections from the mold wall are under considerable stress as a result of their weight, and the additional weight of equiaxed grains, en route to the bottom of the ingot, that happen to settle, clustering on their tips. Under this weight, the grains will therefore bend by creep, possibly recrystallizing at the same time, allowing the grains that grow beyond a certain length to sag downwards at various angles. This mechanism seems consistent with the structure of the columnar zone in large castings, and explains the so-called *branched columnar zone*. The straight portions of the columnar crystals near the base have probably resisted bending by the support provided by secondary arms, linked to form transverse web-like walls, providing the excellent rigidity of a box-girder supporting structure.

The bending of dendrites under their own weight when growing horizontally is not confined to steel ingots. Newell and colleagues (2009) found that dendrites of Ni-base superalloys growing across the horizontal platforms of turbine blade single-crystal castings sagged under their own weight, but remaining straight as if creating a 'hinge' at their base, causing misalignments of up to 10°.

Growing dendrites can be damaged or fragmented in other ways to create the seeds of new grains.

Mold coatings that contain materials that release gas on solidification, and so disturb the growing crystals, are found to be effective grain refiners (Cupini et al. 1980). Although these authors do not find any apparent increase of gas take-up by the casting, it seems prudent to view the 10% increase in strength as hardly justifying such a risk until the use of volatile mold dressings is assessed more rigorously.

The application of vibration to solidifying alloys is also successful in refining grain size. The author admits that it was hard work reviewing the vast amount of work in this area (Campbell 1981). It seems that all kinds of vibration, whether subsonic, sonic, or ultrasonic, are effective in refining the grain size of most dendritically freezing materials providing the energy input is sufficient (Figure 5.35). The product of frequency and amplitude has to exceed  $0.01 \text{ mm s}^{-1}$  for 10% refinement,  $0.02 \text{ mm s}^{-1}$  for

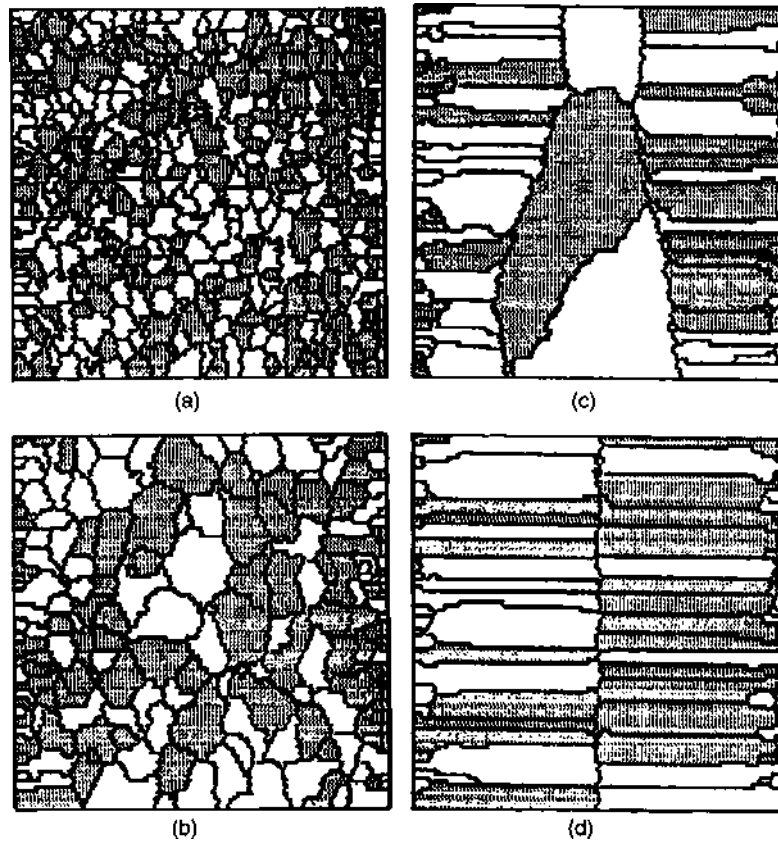


**FIGURE 5.37**

Computer-simulated macrostructure of growth inwards from the sides of an ingot for progressively increasing casting temperature (a) to (d). Reprinted with permission from J. Materials Science, Chapman & Hall, London.

50% refinement, and  $0.1 \text{ mm s}^{-1}$  for 90% refinement (Campbell 1980). It is possible that at the free liquid surface of the metal the energy required to fragment dendrites is much less than this, as Ohno (1987) points out. This is sometimes known as *shower nucleation*, as proposed by the Australian researcher Southin (1967), although it is almost certainly not a nucleation process at all. Most probably it is a dendrite fragmentation and multiplication process, resulting from the damage to dendrites growing across the cool surface liquid. These are possibly actually attached to the floating oxide film, or growing from the side walls, but are disturbed by the washing effect of the surface waves.

If we return to Figure 5.36 grain sizes are dotted randomly all over the upper half of the diagram, above the DAS size line. Occasionally some grains will be as small as one dendrite arm, and so will lie on the DAS line. No grain size can be lower than the line. This is because, if we could imagine a population of grains smaller than the DAS, and which would therefore find itself below the line, then in the time available for freezing, the population would have coarsened, reducing its surface energy to

grow its average grain size up to the predicted size corresponding to that available time. Thus although grains cannot be smaller than the dendrite arm size, the grain size is otherwise independent of solidification time. Clearly, totally independent factors control the grain size.

It is clear, then, that the size of grains in castings results not only from nucleation events, such as homogeneous events on the side walls, or from chance foreign nuclei, or intentionally added grain refiners. Grain nuclei are also subject to further chance events such as re-solution. Further complications, mostly in larger-grained materials, result from chance events of damage or fragmentation from a variety of causes.

A further effect should be mentioned. The grains formed during solidification may not continue to exist down to room temperature. Many steels, for instance, as discussed in Section 6.6, undergo phase changes during cooling. Even in those materials that are single phase from the freezing point down to room temperature can experience grain boundary migration, grain growth, or even wholesale recrystallization. Figure 5.38 shows an example of grain boundary migration in an aluminum alloy.



**FIGURE 5.38**

Micrograph of Al-0.2Cu alloy showing porosity and interdendritic segregation. Some grain boundary migration during cooling is clear. (Electropolished in perchloric and acetic acid solution and etched in ferric chloride. Dark areas are etch pitted.)

It bears emphasizing once again that dendrite arm spacing is controlled principally by freezing time, whereas grain size is influenced by many independent factors.

Before leaving the subject of the as-cast structure, it is worth giving warning of a few confusions concerning nomenclature in the technical literature.

Firstly, there is a widespread confusion between the concept of a grain and the concept of a dendrite. It is necessary to be on guard against this.

Secondly, the word 'cell' has a number of distinct technical meanings that need to be noted:

1. A cell can be a general growth form of the solidification front, as used in this book.
2. Cell is the term used to denote graphite 'rosettes' in gray cast irons. Strictly, these are graphite grains; crystals of graphite which have grown from a single nucleation event. They grow within, and appear crystallographically unrelated to, the austenite grains that form the large dendritic rafts of the gray iron structure.
3. The term 'cell count' or 'cell size' is sometimes used as a measure of the fineness of the microstructure, particularly in aluminum alloys. In Al alloys the distinction between primary arm, secondary arm, and grain is genuinely difficult to make in randomly oriented grains, where primary and secondary arms are not clearly differentiated (see Figure 5.33). To avoid the problem of having to make any distinction, a count is made of the number of rounded, bright features (that could be primary or secondary arms or grains) in a measured length. This is arbitrarily called 'the cell count', giving a measure of something called a 'cell size'. In these difficult circumstances it is perhaps the only practical quantity that can be measured, whatever it really is!

---

## 5.3 SEGREGATION

Segregation may be defined as any departure from uniform distribution of the chemical elements in the alloy. Because of the way in which the solutes in alloys partition between the solid and the liquid during freezing, it follows that all alloy castings are segregated to some extent.

Some variation in composition occurs on a microscopic scale between dendrite arms, known as microsegregation. It can usually be significantly reduced by a homogenizing heat treatment lasting only minutes or hours because the distance, usually in the range 10–100  $\mu\text{m}$ , over which diffusion has to take place to redistribute the alloying elements is sufficiently small. Equation 1.5 can assist to estimate times required for homogenization for different spacings.

Macrosegregation cannot be removed. It occurs over distances ranging from 1 cm to 1 m, and so cannot be removed by diffusion without geological time scales being available! In general, therefore, whatever macrosegregation occurs has to be lived with.

In this section we shall consider explicitly only the case for which the distribution coefficient  $k$  (the ratio of the solute content of the solid compared to the solute content of the liquid in equilibrium) is less than 1. This means that solute is rejected on solidification, and therefore builds up ahead of the advancing front. The analogy, used repeatedly before, is the build-up of snow ahead of the advancing snow plow. (It is worth keeping in mind that all the discussion can, in fact, apply in reverse, where  $k$  is greater than 1. In this case extra solute is taken into solution in the advancing front, and a depleted layer exists in the liquid ahead. The analogy now is that of a domestic vacuum cleaner advancing on a dusty floor, and sucking up dust that lies ahead.)

For a rigorous treatment of the theory of segregation the interested reader should consult the standard text by Flemings (1974), which summarizes the pioneering work in this field by the team of researchers at the Massachusetts Institute of Technology. We shall keep our treatment here to a minimum, just enough to gain some insight into the important effects in castings.

### 5.3.1 Planar front segregation

There are two main types of normal segregation that occur when the solid is freezing on a planar front; one that results from the freezing of quiescent liquid, and the other of stirred liquid. Both are important in solidification, and give rise to quite different patterns of segregation.

Figure 5.39 shows the way in which the solute builds up ahead of the front if the liquid is still (Quiescent liquid, Case 1). The initial build-up to the steady-state situation is called the initial transient. This is shown rather spread out for clarity. Flemings (1974) shows that for small  $k$  the initial transient length is approximately  $D/V_s k$  where  $D$  is the coefficient of diffusion of the solute in the liquid and  $V_s$  is the velocity of the solidification front. In most cases the transient length is only of the order of 0.1–1 mm.

After the initial build-up of solute ahead of the front, the subsequent freezing to solid of composition  $C_0$  takes place in a steady, continuous fashion until the final transient is reached, at which the liquid and solid phases both increase and segregate. The length of the final transient is even smaller than that of the initial transient since it results simply from the impingement of the solute boundary layer on the end wall of the container. Thus its length is of the same order as the thickness of the solute boundary layer  $D/R$ . For many solutes this is therefore between 5 and 50 times thinner than the initial transient.

For the case where the liquid is stirred, moving past the front at such a rate to sweep away any build-up of solute, Figure 5.39 (Stirred liquid Case 2) shows that the solid continues to freeze at its original low composition  $kC_0$ . The slow rise in concentration of solute in the solid is, of course, only the result of the bulk liquid becoming progressively more concentrated.

The important example of the effect of normal segregation, building up as an initial transient, is that of subsurface porosity in castings. The phenomenon of porosity being concentrated in a layer approximately 1 mm beneath the surface of the casting is a clear case of the build-up of solutes. The nucleation and growth of gas pores is discussed in Chapter 7.

Moving on now to consider an example of segregation where the liquid is rapidly stirred, the classic case was that of the rimming steel ingot seen in Figure 5.40. Although rimming steels are now a phenomenon of the past, their behavior is instructive. During the early stages of freezing, the high temperature gradient favored a planar front. The rejection of carbon and oxygen resulted in bubbles of carbon monoxide. These detached from the planar front and rose to the surface, driving a fast upward current of liquid, effectively scouring the interface clean of any solute that attempted to build up. Thus the solid continued to freeze with its original low impurity content, forming the pure iron ‘rim’, giving the steel its name. At lower levels in the ingot there was a lower density of bubbles to scour the front, so some bubbles succeeded in remaining attached, explaining the array of wormhole-like cavities in the lower part of the ingot. During this period the incandescent spray from the tops of the ingots as the bubbles emerged and burst at the surface was one of the great spectacles of the old steelworks, almost ranking in impressiveness with the blowing of the Bessemer converters. A good spray was said to indicate a good rimming action. I have fond memories of these times from my early days in the steel industry.

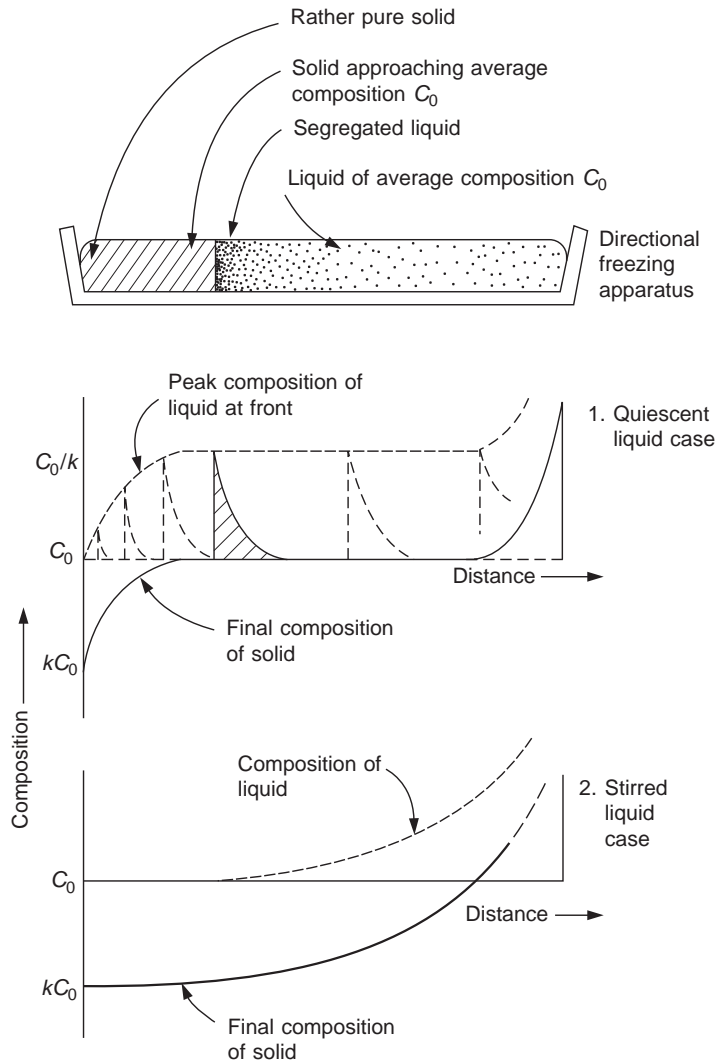


**FIGURE 5.39**

Directional solidification on a planar front giving rise to two different patterns of segregation depending on whether solute is allowed to build up at the advancing front or is swept away by stirring.

As the rim thickened, the temperature gradient fell so that the front started to become dendritic, retaining both bubbles and solute. Thus the composition then adjusted sharply to the average value characteristic of the remaining liquid, which was then concentrated in carbon, sulfur and phosphorus.

Rimming steel was widely used for rolling into strip, and for such purposes as deep drawing, where the softness and ductility of the rim assisted the production of products with high surface finish.



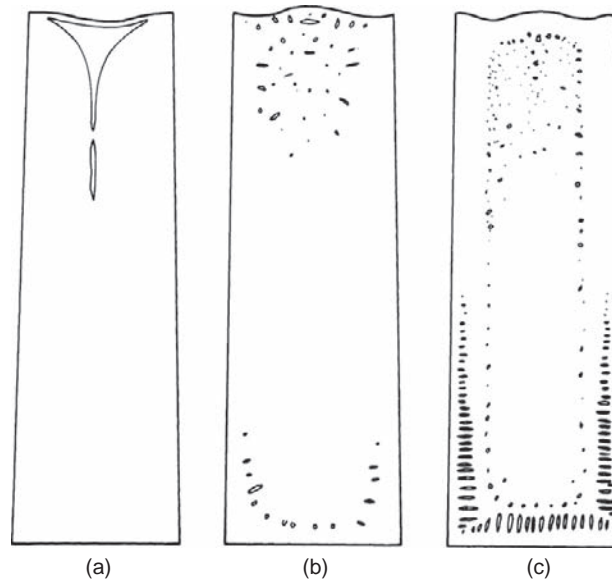


**FIGURE 5.40**

Ingot structures: (a) a killed steel; (b) a balanced steel; and (c) a rimming steel.

The oxygen levels in rimming steels were in excess of 0.02%, and were strongly dependent on the carbon and manganese contents. Typically these were 0.05–0.20 C and 0.1–0.6 Mn, giving a useful range of hardness, ductility, and strength.

With the development of continuously cast steel, the casting of steel into ingots has now become part of steelmaking history. The challenge to the deep-drawing qualities was to regain so far as possible the benefits of the rimmed steel from a continuous casting process, where the rimming action could no longer be used. This has been achieved by attention to the surface quality and inclusion content of the new steels.

As an interesting diversion it is worth including at this point the two other major classes of steel that were produced as ingots, since these still have lessons for us as producers of shaped castings. The two other types of ingots were produced as (a) killed steels and (b) balanced steels (Figure 5.40).

The balanced, or semi-killed steel, was one that, after partially deoxidizing, contained 0.01–0.02% oxygen. This was just enough to cause some evolution of carbon monoxide towards the end of freezing, to counter the effect of solidification shrinkage. The deep shrinkage pipe that would normally have been expected in the head of the ingot, requiring to be cropped off and remelted, was replaced with a substantially level top. The whole ingot could be utilized. The great advantage of this quality of steel was the high yield on rolling, because the dispersed cavities in the ingot tended to weld up. For this reason bulk constructional steel could be produced economically. However, it was a difficult balancing act to maintain such precise control of the chemistry of the metal. It was only because balanced steels were so economical that such feats were routinely attempted. Some steelmakers were declared foolhardy for attempting such tasks!

In contrast, killed steels were easy to manufacture. They included the high-carbon steels and most alloy steels. They contain low levels of free oxygen, normally less than 0.003% because of late additions of deoxidizers such as Si, Mn, and Al. The Al addition was often made together with other components such as Ca, and sometimes Ti, etc. Consequently there was no evolution of carbon monoxide on freezing, and a considerable shrinkage cavity was formed as seen in Figure 5.40. If allowed to form in this way, the cavity opened up on rolling as a fish-tail, and had to be cropped and discarded. Alternatively the top of the ingot was maintained hot during solidification by special hot-topping techniques. Either way, the shrinkage problem involved expense above that required for balanced or rimming steels. Fully killed steels were generally therefore reserved for higher-priced, low- and medium-alloy applications.

### 5.3.2 Microsegregation

As the dendrite grows into the melt, and as secondary arms spread from the main dendrite stem, the solute is rejected, effectively being pushed aside to concentrate in the tiny regions enclosed by the secondary dendrite arms. Since this region is smaller than the diffusion distance, we may consider it more or less uniform in composition. The situation, therefore, is closely modeled by Figure 5.39, case 2. Remember, the uniformity of the liquid phase in this case results from diffusion within its small size, rather than any bulk motion of the liquid.

The interior of the dendrite therefore has an initial composition close to  $kC_0$ , while, towards the end of freezing, the center of the residual interdendritic liquid has a composition corresponding to the peak of the final transient. This gradation of composition from the inside to the outside of the dendrite earned its common description as ‘coring’ because, on etching a polished section of such dendrites, the progressive change in composition is revealed, appearing as onion-like layers around a central core. The concentration of chromium and nickel in the interdendritic regions of the low-alloy steel shown in Figure 5.31 has caused these regions to be relatively ‘stainless’, resisting the etch treatment, and so causing them to be revealed in the micrograph.

Some diffusion of solute in the dendrite will tend to smooth the initial as-cast coring. This is often called back-diffusion. Additional smoothing of the original segregation can occur as a consequence of other processes such as the remelting of secondary arms as the spacing of the arms coarsens.

The partial homogenization resulting from back-diffusion and other factors means that, for rapidly diffusing elements such as carbon in steel, homogenization is rather effective. For plain carbon steels, therefore, the final composition in the dendrite and in the interdendritic liquid is not far from that predicted from the equilibrium phase diagram. The maximum freezing range from the phase diagram is clearly at about 2.0% carbon and would be expected to apply.

Even so, in steels where the carbon is in association with more slowly diffusing carbide-forming elements, the carbon is not free to homogenize: the resulting residual liquid concentrates in carbon to the point at which the eutectic is formed at carbon contents well below those expected from the phase diagram. In steels that contained between 1.3 and 2.0% manganese the author found that the eutectic phase first appeared between 0.8 and 1.3% carbon (Campbell 1969) as shown in Figure 5.41. Similarly, in 1.5Cr–1C steels Flemings et al. (1970) found that the eutectic phase first appeared at about 1.4% carbon (Figure 5.42). This point was also associated with a peak in the segregation ratio,  $S$ , the ratio of the maximum to the minimum composition; this is found between the interdendritic liquid and the

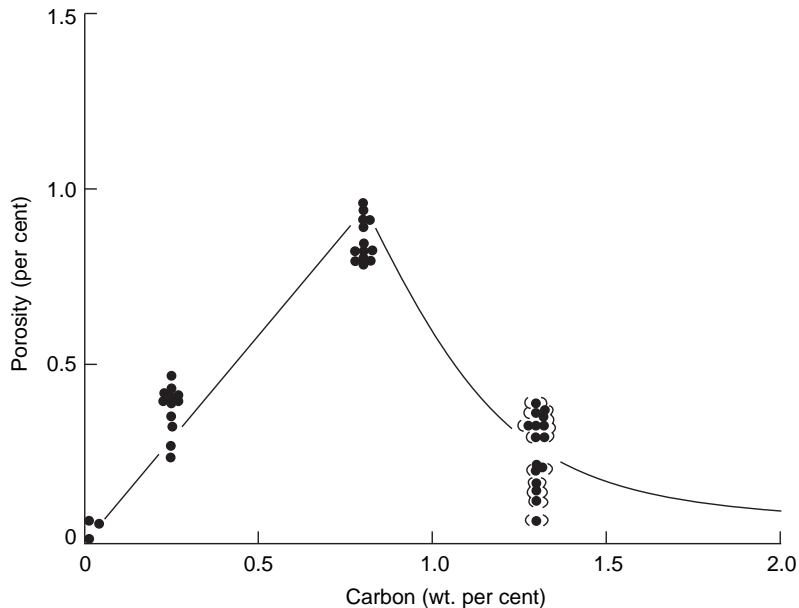


**FIGURE 5.41**

Porosity in Fe–C–Mn alloys, showing the reduction associated with the presence of non-equilibrium eutectic liquid (data points in brackets) (Campbell 1969).

center of the dendrite arm. (N.B. The interpretation of these diagrams as two separate curves intersecting in a cusp rather than a smoothly curved maximum is based on the fact that the two parts of the curve are expected to follow different laws. The first part represents the solidification of a solid solution; the second part represents the solidification of a solid solution plus some eutectic. As we have seen before, this is much more common in freezing problems than appears to have been generally recognized.)

The segregation ratio  $S$  is a useful parameter when assessing the effects of treatments to reduce microsegregation. Thus the progress of homogenizing heat treatments can be followed quantitatively.

It is important to realize that  $S$  is only marginally affected by changes to the rate of solidification in terms of the rates that can be applied in conventional castings. This is because although the dendrite arm spacing will be reduced at higher freezing rates, the rate of back diffusion is similarly reduced. Both are fundamentally controlled by diffusion, so that the effects largely cancel. (During any subsequent homogenizing heat treatment, however, the shorter diffusion distances of the material frozen at a rapid rate will be a useful benefit in reducing the time for treatment.)

Where microsegregation results in the appearance of a new liquid interdendritic phase, there are a number of consequences that may be important:

1. The appearance of a eutectic phase reduces the problem for fluid flow through the dendrite mesh. Shrinkage porosity is thereby reduced after the arrival of the eutectic, as seen in Figure 5.41. This important effect on porosity is discussed in greater detail in Chapter 7.

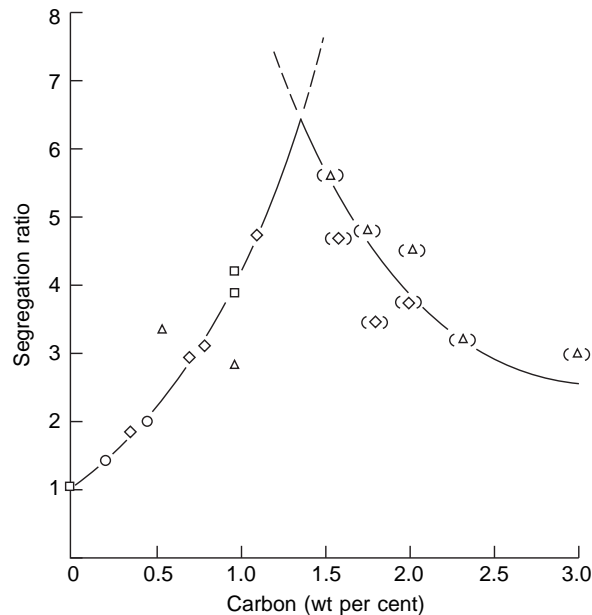


**FIGURE 5.42**

Severity of microsegregation in C–Cr-bearing steels, illustrating the separate regime for structures containing eutectic (points in brackets). Data from Flemings et al. (1970).

2. The alloy may now be susceptible to hot tearing, especially if there is only a very few percent of the liquid phase. This effect is discussed further in Chapter 8.
3. A low-melting-point phase may limit the temperature at which the material can be heat-treated.
4. A low-melting-point phase may limit the temperature at which an alloy can be worked, since it may be weakened, disintegrating during working because of the presence of liquid in its structure.

### 5.3.3 Dendritic segregation

Figure 5.43 shows how microsegregation, the sideways displacement of solute as the dendrite advances, can lead to a form of macrosegregation. As freezing occurs in the dendrites, the general flow of liquid that is necessary to feed solidification shrinkage in the depths of the pasty zone carries the progressively concentrating segregate towards the roots of the dendrites.

In the case of a freely floating dendrite in the center of the ingot that may eventually form an equiaxed grain, there will be some flow of concentrated liquid towards the center of the dendrite if in fact any solidification is occurring at all. This may be happening if the liquid is somewhat undercooled. However, the effect will be small, and will be separate for each equiaxed grain. Thus the build-up of long-range segregation in this situation will be negligible.

For the case of dendritic growth against the wall of the mold, however, the temperature gradient will ensure that all the flow is in the direction towards the wall, concentrating the segregation here. Thus the presence of a temperature gradient is necessary for a significant build-up of segregation.

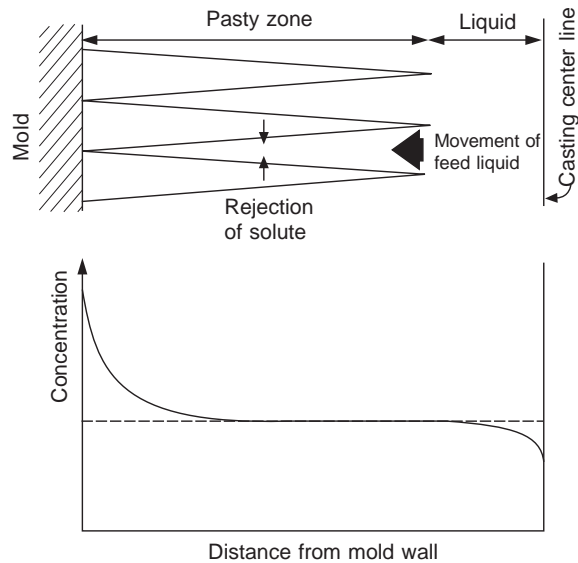


**FIGURE 5.43**

Normal dendritic segregation (usually misleadingly called inverse segregation) arising as a result of the combined actions of solute rejection and shrinkage during solidification in a temperature gradient.

It will by now be clear that this type of segregation is in fact the usual type of segregation to be expected in dendritic solidification. The phenomenon has in the past suffered the injustice of being misleadingly named 'inverse segregation' on account of it appearing anomalous in comparison to planar front segregation and the normal pattern of positive segregation seen in the centers of large ingots. In this book we shall refer to it simply as 'dendritic segregation'. It is perfectly normal and to be expected in the normal conditions of dendritic freezing.

Dendritic segregation is observable but is not normally severe in sand castings because the relatively low temperature gradients allow freezing to occur rather evenly over the cross-section of the casting; little directional freezing exists to concentrate segregates in the direction of heat flow.

In castings that have been made in metal molds, however, the effect is clear, and makes the chill casting of specimens for chemical analysis a seriously questionable procedure. Chemists should beware! The effect of positively segregating solutes such as carbon, sulfur, and phosphorus in steel is clearly seen in Figure 5.44 as the high concentration around the edges and the base of the ingot; all those surfaces in contact with the mold.

In some alloys with very long freezing ranges, such as tin bronze (liquidus temperature close to  $1000^{\circ}\text{C}$  and solidus close to  $800^{\circ}\text{C}$ ), the contraction of the casting in the solid state and/or the pressure in the liquid due to the metallostatic head, plus perhaps the evolution of dissolved gases in the interior of the casting causes almost neat eutectic liquid to be squeezed out on to the surface of the casting. This exudation is known as *tin sweat*. It was described by Biringuccio in the year 1540 as a feature of the manufacture of bronze cannon. Similar effects can be seen in many other materials; for instance when

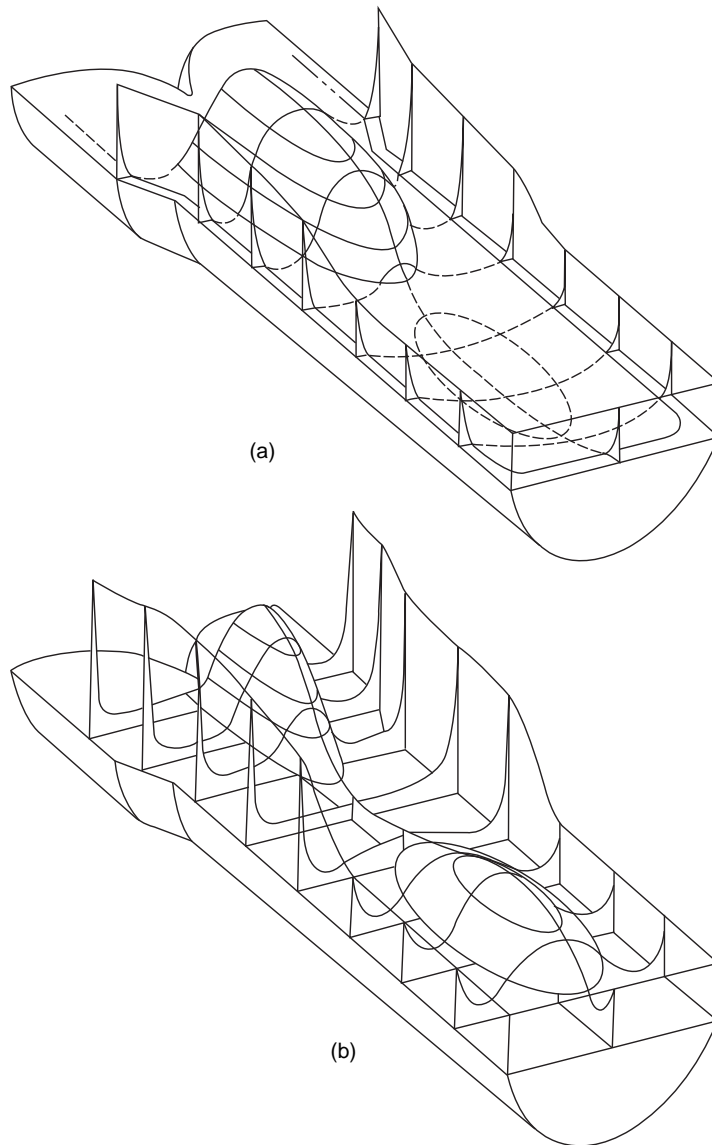


**FIGURE 5.44**

Segregation of (a) solutes and (b) inclusions in a 3000-kg sand cast ingot. Information mainly from Nakagawa and Momose (1967).

making sand castings in the commonly used Al–7Si–0.3Mg alloy, eutectic (Al–11Si) is often seen to exude against the surface of external chills (Figure 5.13). In a study by Thevik (1999) on direct chill (semi-continuous) casting of an Al–4.8Cu alloy the expected surface concentration in the matrix of the ingot was 5.0%Cu. However, as a result of surface exudation of this Cu-rich liquid the concentration just below the surface fell to only 4.5%Cu. This significant variation in Cu content was driven by only the rather modest pressure due to the 50 mm head of metal. The surface exudation of eutectic liquid gives problems during the manufacture of Ni-base superalloy single crystal turbine blades as is discussed in the section on Ni-based alloys.

### 5.3.4 Gravity segregation

In the early years of attempting to understand solidification, the presence of a large concentration of positive segregation in the head of a steel ingot was assumed to be merely the result of normal segregation. It was simply assumed to be the same mechanism as illustrated in Figure 5.39, case 1, where the solute is concentrated ahead of a planar front.

This assumption overlooked two key factors: (1) the amount of solute that can be segregated in this way is negligible compared to the huge quantities of segregate found in the head of a conventional steel ingot; and (2) this type of positive segregation applies only to planar front freezing. In fact, having now realized this, if we look at the segregation that should apply in the case of dendritic freezing then an opposite pattern (previously called inverse segregation) applies such as that shown in Figure 5.43! Clearly, there was a serious mismatch between theory and fact. The fact that this situation had been overlooked for so long illustrates how easy it is for us to be unaware of the most glaring anomalies. It is a lesson for us all in the benefits of humility!

This problem was brilliantly solved by McDonald and Hunt (1969). In work with a transparent model, they observed that the segregated liquid in the dendrite mesh moved under the influence of gravity. It had a density that was in general different from that of the bulk liquid. Thus the lighter liquid floated, and the heavier sank.

In the case of steel, they surmised that as the residual liquid travels towards the roots of the dendrites to feed the solidification contraction, the density will tend to rise as a result of falling temperature. Simultaneously, of course, its density will tend to decrease as a result of becoming concentrated in light elements such as carbon, sulfur, and phosphorus. The compositional effects outweigh the temperature effects in this case, so that the residual liquid will tend to rise. Because of its low melting point, the liquid will tend to dissolve dendrites in its path as solutes from the stream diffuse into and reduce the melting point of the dendrites. Thus as the stream progresses it reinforces its channel, as a flooding river carves obstructions from its path. This slicing action causes the side of the channel that contains the flow to be straighter, and its opposite side to be somewhat ragged. It was noted by Northcott (1941) when studying steel ingots that the edge nearest to the wall (i.e. the upper edge) was straighter. This confirms the upward flow of liquid in these segregates.

The ‘A’ segregates in a steel ingot are formed in this way (Figure 5.45). They constitute an array of channels at roughly mid-radius positions and are the rivers that empty segregated, low-density liquid into the sea of segregated liquid floating at the top of the ingot.

At the same time these channels are responsible for emptying the debris from partially melted dendrites into the bulk liquid in the center of the ingot. These fragments tumble along the channels, finally emerging in the sea of segregation in the head of the ingot, from where they subsequently fall

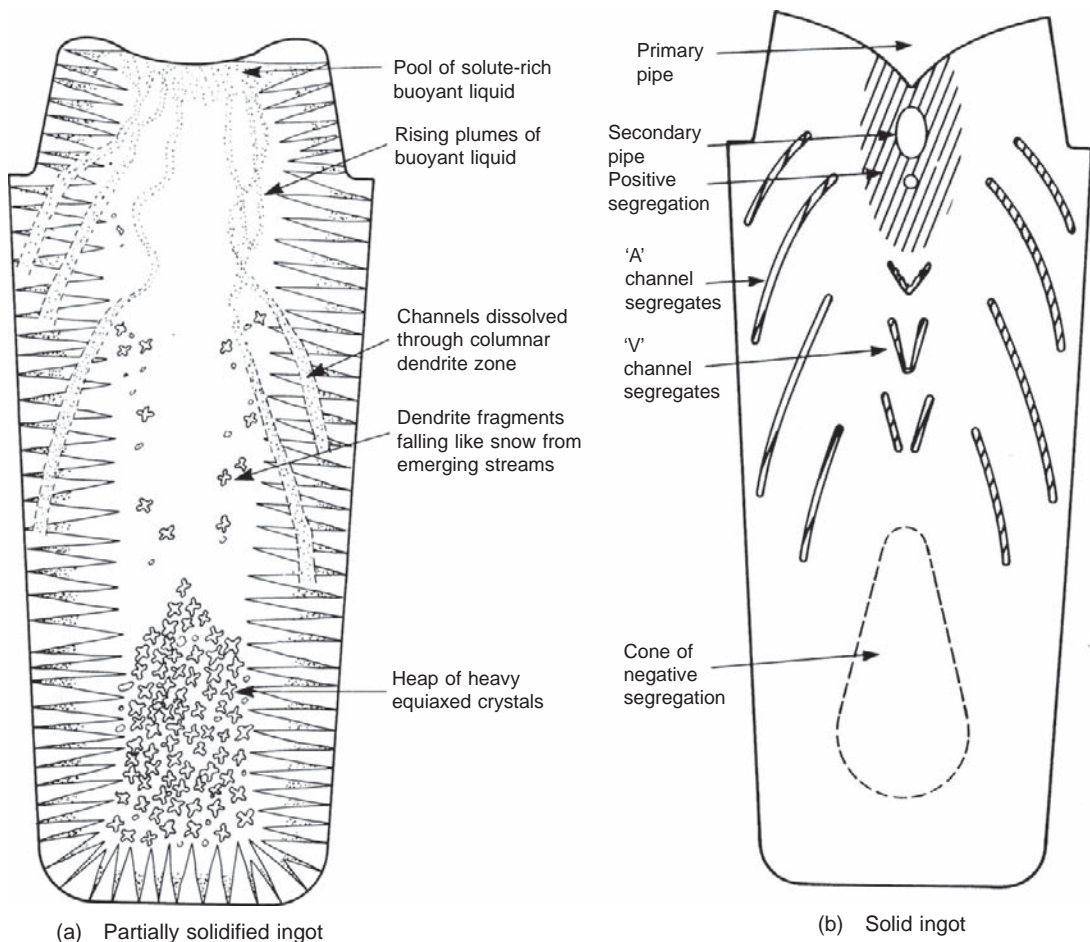


**FIGURE 5.45**

Development of segregation in a killed steel ingot (a) during solidification and (b) in the final ingot.

down the center of the ingot at a rate somewhere between that of a stone and a snowflake. They are likely to grow as they fall if they travel through the undercooled liquid just ahead of the growing columnar front, possibly by rolling or tumbling down this front. The heap of such fragments at the base of the ingot has a characteristic cone shape. In some ingots, as a result of their width, there are heaps on either side, forming a double cone. Because such cones are composed of dendritic fragments their average composition is that of rather pure iron, having less solute than the average for the ingot. The region is therefore said to exhibit *negative segregation*. It is clearly seen in Figure 5.44a. The equiaxed cone at the base of ingots is a variety of gravity segregation arising as a result of the sedimentation of the solid, in contrast with most other forms of gravity segregation that arise because of the gravitational response of the liquid.



A further contributing factor to the purity of the equiaxed cone region probably arises as a result of the divergence of the flow of residual liquid through this zone at a late stage in solidification, as suggested by Flemings (1974).

The 'V' segregates are found in the center of the ingot. They are characterized by a sharply delineated edge on the opposite side to that shown by the A segregates. This clue confirms the pioneering theoretical work by Flemings and coworkers that indicated that these channels were formed by liquid flowing downwards. It seems that they form at a late stage in the freezing of the ingot, much later than the formation of the 'A' segregates, when the segregated pool of liquid floating at the top of the ingot is drawn downwards to feed the solidification shrinkage in the center and lower parts of the ingot.

On sectioning the ingot transversely, and etching to reveal the pattern of segregation, the A and V segregates appear as a fairly even distribution of clearly defined spots, having a diameter in the range 2–10 mm. Probably depending on the size and shape of the ingot, they may be concentrated at mid-radial to central positions in zones, or evenly spread. The central region of positive segregation is seen as a diffuse area of several hundred millimeters in diameter. In both areas the density of inclusions is high. These channel segregates, seen as spots on the cross-section, survive extensive processing of the ingot, and may still be seen even after the ingot has been rolled and finally drawn down to wire!

It is interesting to note that in alloys such as tool steels that contain high percentages of tungsten and molybdenum, the segregated liquid is higher in density than the bulk liquid, and so sinks, creating channel segregates that flow in the opposite direction to those in conventional carbon steels. The heavy concentrated liquid then collects at the base of the ingot, giving a reversed pattern to that shown in Figure 5.44.

In nickel-based and high-alloy steel castings the presence of partially melted and collapsed crystals in the channels has the effect of a localized grain refinement, so that on etching longitudinal sections of the castings, the channels seem to sparkle with numerous grains at different angles. In this industry, channel segregates are therefore widely known as 'freckle defects'. The production rate of nickel-based ingots weighing many tonnes produced by secondary remelting processes, such as electroslag and vacuum arc processes, is limited by the unwanted appearance of freckles. It is their locally enhanced concentration of inclusions such as sulfides, oxides, and carbides, etc., that make freckles particularly undesirable. Valdes (2010) proposes a condition to predict freckle formation based on the following assumptions (i) the Rayleigh number; (ii) Darcy flow through the pasty zone; and (iii) the condition by Flemings and Nereo (1967) that the liquid flow from colder to hotter regions is faster than the rate of crystal growth. This comprehensive approach to this complex problem appears to yield impressive results.

Channel segregates are also observed in Al–Cu alloys. In fact workers at Sheffield University (Bridge et al. 1982) have carried out real-time radiography on solidifying Al–21Cu alloy. They were able to see that channels always started to form from defects in the columnar dendrite mesh. These defects were regions of liquid partially entrapped by either the sideways growth of a dendrite arm, or the agglomeration of equiaxed crystals at the tips of the columnar grains. Channels developed both downstream and upstream of these starting points.

The author has even observed channel defects on radiographs of castings in Al–7Si–0.3Mg alloy. Despite the small density differences in this system, the conditions for the formation of these defects seem to be met in sand castings of approximately 50-mm cross-section.

Although few ingots are cast in modern steelworks, large steel castings continue to be made in steel foundries. Such castings are characterized by the presence of channel segregates, in turn causing extensive and troublesome macrosegregation. Channel segregates can be controlled by:

1. Decreasing the time available for their formation by increasing the rate of solidification.
2. Adjusting the chemical composition of the alloy to give a solute-rich liquid that has a more nearly neutral buoyancy at the temperature within the freezing zone.

In practice, both these approaches have been used successfully.

For the sake of completeness, we should perhaps mention that the effective viscosity of the liquid metal can be artificially raised to such a degree that the weak forces of convection are suppressed, so that chemical segregation of the liquid can be eliminated. This can occur in an enhanced gravitational field such as during centrifuging, or in a strong magnetic field (Nikrityuk 2009). However, neither of these approaches is easy to envisage outside of the laboratory.

This page intentionally left blank

# Casting alloys

The metallurgy of the casting alloys is presented here for the first time as interpreted according to bifilm theory.

It has to be recognized that at the time of writing the bifilm interpretation is more speculative than I would wish. However, it is a theory that fits the facts with uncanny accuracy. It has to be kept in mind that theories are useful only if they can explain and if they can predict. As a well-known instance, the flat earth theory was useful, being accurate to predict both distances and directions while humans could only walk limited distances on the earth's surface. It is a theory that served mankind for thousands of years until the arrival of global travel. The bifilm approach is similarly presented as a useful theory until the time that it is proven inadequate. However, at this time, it seems more than adequate to provide many useful insights into the behavior of liquid metals and castings.

The reader is invited to form his or her own opinion as the metals are described in turn below. For traditional reviews of the metals listed in this section, but not including bifilm theory, nor the benefits of improved methoding techniques such as naturally pressurized filling systems, the reader is recommended the interesting and detailed accounts in the *ASM Handbook* 2008, Volume 15 'Casting'.

The very low melting point metals are not dealt with here. We shall concentrate on the structural engineering metals. Even so, in passing we should note that the casting of lead and its alloys for battery grids is currently a major application that should not be overlooked. The new area of lead-free solders is also of interest, noting that an Sn-based solder containing Ag and Cu exhibits planar voids at the base of ductile dimples on a fracture surface, suggestive that the bifilms in this alloy had been straightened by their formation on the planar intermetallic  $\text{Ag}_3\text{Sn}$  at the base of each dimple. It seems probable that for all metals, not only the high-melting-point engineering metals, the theory of the control of microstructure and properties of castings by bifilms remains applicable.

## 6.1 ZINC ALLOYS

For a general introduction to zinc casting alloys, particularly covering the practical details of routine melting and casting, the reader is strongly recommended to the readable account by Arthur C Street in his famous work *The Diecasting Book* (1986) since approximately 80% of zinc alloys are cast by high-pressure die casting (HPDC).

Relatively little is continuously cast, or gravity cast into permanent or sand molds. The alloy Kirksite is used for prototypes for cast tooling for sheet metal working and plastic injection molding. The higher-strength zinc–aluminum ('ZA') alloys are similarly sometimes used for low-volume products cast in permanent or sand molds. Graphite molds are sometimes machined from solid blocks for ease and relatively low cost for low-volume molds.

Zinc alloys were first cast by pressure die casting in about 1914. However, these early days were plagued by quality problems which undermined public confidence. The problems were eventually claimed to be brought under some kind of control from research carried out by Brauer and Peirce and published in 1923. As a result, modern zinc-based casting alloys are made from 99.99% pure Zn in an attempt to guard against the problems of contamination from the heavy elements including Pb, Bi, Tl, Cd, In, and Sn, which were found to migrate to grain boundaries, and seemed to be associated with the loss of mechanical properties, particularly under conditions of heat or moisture. We shall return to this issue below.

A feature of most Zn-based alloys is that practically all contain Al. The two major hot chamber casting alloys were developed in the 1920s as the ZAMAK 3 and ZAMAK 5 alloys (Z = zinc; A = aluminum; MA = Magnesium; K = Kopper being the German for copper). These are denoted alloys A and B respectively in UK specifications. They all contain 4%Al. Alloy A is most common, but alloy B contains a little Cu and is significantly harder. The nominal compositions of the casting alloys are given in Table 6.1. The US 'Alloy No.' system, Nos. 2, 3, 5, and 7, coincide approximately at Nos. 3 and 5 with the ZAMAK 3 and 5, and Alloys A and B.

The addition of Al to the hot chamber casting alloys appears to have originally been designed to reduce the attack of the mild steel crucible and swan neck components of the pressure die-casting machine because of the development of the thin, protective oxide formed by the Al. Also, the 4%Al addition produced an alloy close to the Zn/Al eutectic at 5%Al, and thus making a useful reduction in the melting temperature from 419°C to 382°C, and at the same time giving a valuable increase in strength.

The International Zinc Association have recently publicized a recent development in an effort to achieve even thinner-walled castings, to aid its competition with the light-pressure die-cast alloys based on Al and Mg. Whereas the traditional 4%Al alloys are claimed to be limited to 0.75-mm-thickness sections, the new composition claims 0.3 mm section thickness potential (Goodwin 2009). Clearly, some benefit will have arisen from the new composition at 4.5%Al being nearer to the eutectic at 5%Al as is clear from Figure 6.1. Furthermore, the limit imposed on the copper content at only 0.07% seems

**Table 6.1** Zn Casting Alloys

Alloy	Nominal Composition (wt %)	Comments
Alloy 2	4Al0.03Mg3Cu	'Kirksite' if gravity cast
Zamak 3 (Alloy A)	4Al0.03Mg	Common hot chamber alloy
Zamak 5 (Alloy B)	4Al0.05Mg1Cu	Common hot chamber alloy
Alloy 7	4Al0.01Mg0.01Ni	
Internat Zn Assoc	4.5Al0.01Mg0.07Cu	Eutectic fluid alloy
ZA8	8Al0.02Mg1Cu	Hot chamber, or gravity cast
ZA12	11Al0.02Mg1Cu	Cold chamber, or gravity in permanent mold or sand
ZA27	27Al0.015Mg2Cu	
AlCuZinc 5	4Al < 0.05Mg5Cu	General Motors creep-resistant alloys
AlCuZinc 10	4Al < 0.05Mg10Cu	
Superplastic zinc	22Al0.01Mg0.5Cu	(Wrought alloy)
ZM 11	22Al1.5Si0.5Cu0.3Mn	Mitsubishi, high-strength, high-damping, lightweight alloys
ZM 3	40Al3.0Si1.0Cu0.3Mn	
Super Cosmal	60Al6.0Si1.0Cu0.3Mn	

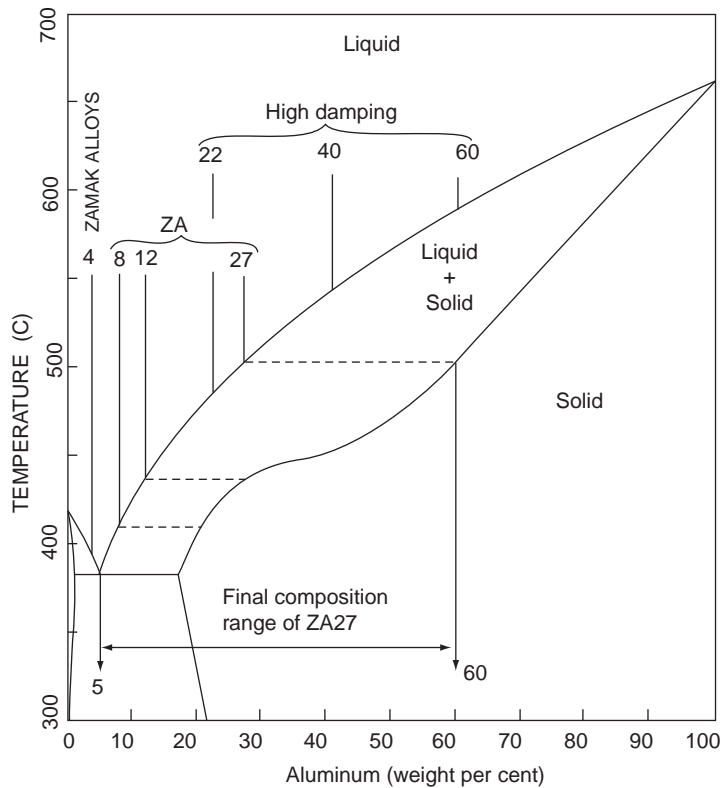


**FIGURE 6.1**

The Zn–Al phase diagram with some common zinc-based casting alloys.

also to be intended to limit the development of a freezing range which would have inhibited fluidity as explained in Chapter 3. This alloy has yet to prove itself commercially at this time, but it has a good chance, because the logic of its design seems sound.

The ZA hypereutectic series of alloys containing 8, 12, and 27%Al were a significant advance achieved by research carried out in the late 1960s. Their high strength, toughness and bearing properties increasing with increasing Al content make these alloys among the strongest and toughest of commonly available low-cost casting alloys. ZA27 can achieve 440 MPa in the as-cast condition, which is higher than practically all Al and Mg alloys even after expensive heat treatments.

The microsegregation and macrosegregation accompanying the solidification of the higher ZA alloys is impressive and can be troublesome. ZA27 starts as a homogeneous liquid of 27%Al, but the first metal to solidify contains 60%Al, whereas the final liquid to solidify contains 5%Al (Figure 6.1). These wide differences lead to a highly cored dendritic structure that a homogenizing heat treatment is sometimes used to encourage some limited redistribution of Al.

Although ZA8 can be cast by the hot chamber pressure die-casting process, the higher temperatures required for ZA12 and ZA27 would result in unacceptable rates of attack of the casting unit. The liquidus temperature for ZA27 is 500°C.

The superplastic zinc should not really be included in the casting alloys, since it needs plastic working and heat treatment to reduce its grain size before it can develop its full superplastic properties. It is included here simply to illustrate its interesting similarity with Zn casting alloys. The spectacular 1000% elongation that this alloy can develop is limited by microscopic cavitation, almost certainly the result of oxide bifilms entrained during melting and casting. Better melting and casting might deliver even better properties. Its composition is nevertheless close to other casting alloys, indicating that perhaps heat treatment might deliver some part of the superplastic properties, giving a huge benefit to toughness. This does not seem to be generally recognized.

One of the standard problems with Zn-based alloys is their poor creep resistance; the relaxation of steel bolts in holes threaded in Zn-based castings, especially at slightly raised temperatures in the region of 100–150°C, has been a central issue for automotive application in the engine compartment of vehicles. Research by General Motors (Rashid and Hanna 1989) has resulted in the two high-copper alloys in the table that exhibit improved creep performance.

A related problem is the continued aging of zinc alloys at room temperature over a period of weeks or months. This change of structure is accompanied by changes in properties, and by minute changes in the size of the casting. The size issues are discussed in Chapter 18.

In a separate quest, this time to optimize noise reduction in vehicles by improving the damping properties of zinc alloys, Mitsubishi has proposed three new alloys at very high levels of Al, 22, 40, and 60% (Mae and Sakonooka 1987). These are, of course, really Al-based alloys, their volume additions corresponding approximately to 40, 60, and 80% respectively, explaining their improved strength and increased lightness.

Unfortunately, however, from the point of view of the casting quality, the formation of the alumina film on the surface of the liquid alloys gives the standard problems, involving the entrainment of air bubbles and films during the extreme surface turbulence of filling. Although the melting and casting temperatures of zinc pressure die-casting alloys are low, therefore restricting the rate of thickening of films, making them even less visible than in Al alloys, this effectively merely sweeps the problem out of sight. The films have to be double, necessarily have an unbonded inner interface, and therefore still perform efficiently as cracks, even though less detectable than those in Al alloys.

The high level of Al in the three Mitsubishi alloys probably means the alloys contain high levels of aluminum oxide in the form of bifilms, so it may be the bifilms that are the reason for the high damping properties; during the shearing across the bifilm as the matrix is strained (see Chapter 9) the friction involved will dissipate energy in the form of heat. The elastic stiffness (Young's modulus) of the alloy is similarly significantly reduced by bifilms (as demonstrated by Hall and Shippen 1994 for a bronze alloy). It seems reasonable to conclude therefore that although the damping properties may be found to disappear if the alloys are cleaned from oxides, the alloys will benefit in other ways: their tensile and corrosion properties are likely to improve. They might then enjoy a wider commercial acceptance.

Bifilms seem almost certainly present in Figure 2.31, as witnessed by the sharp changes in microstructure across the boundaries formed by oxide flow tubes around the jets of metal that filled the die. In many situations the continued flow over previous jets that have solidified can remelt the solid, allowing it to lose its grip on its oxide tube, which is stripped away in the flow. The prior solidified jet then continues to remelt back somewhat, blurring the original sharp divisions between jets. The longitudinal layering of structures in HPDC products is common, being a characteristic feature of HPDC zinc alloys (Goodwin 2008).

Romankiewicz (1976) found that zinc alloys can contain up to 1 or 2% of oxides. These reduced mechanical properties. Furthermore, in damp conditions they became a source of selective corrosion. He offered no explanation for this behavior. Clearly, in terms of bifilms, the answer is that the films when entrained by turbulence are actually double and act as cracks, and will usually be pushed by dendrite growth into the interdendritic or intergranular regions. In damp conditions the corrosion can penetrate into the matrix along the unbonded interiors of the bifilms. The corrosion will be enhanced by the precipitation of other elements on the back of the films, explaining the effects of heavy elements such as Pb in promoting the often catastrophic degradation of properties over time. The degradation is often called intercrystalline or intergranular corrosion. It is easily demonstrated after only 10 days of testing in steam (Colwell 1973) or perhaps as long as a year in tropical locations.

The deterioration of properties with time, eventually causing the casting to fail, is an experience most of us have with such items as zip fasteners on travel goods, handles on briefcases, and window fasteners in the home. Thus although the research of Brauer and Pierce made huge improvements to Zn alloys, the problems are clearly not totally solved.

Other Canadian workers (Dionne et al. 1984) found that toughness of ZA27 was limited by brittle CuZn<sub>4</sub> following high-temperature homogenization treatment. This is typical behavior of a compound precipitating on bifilms (otherwise the failure by cracking is difficult to explain).

Blisters commonly form on the surface of pressure die cast alloys immediately after opening the die. Kaiser and Groenveld (1975) describe how when the die is opened the wall of the hot casting may be insufficiently strong to withstand the pressure of gases entrapped in the casting during die filling. Although the authors report that the defect can be controlled by reducing metal and die temperatures to increase the strength of the casting wall, they do not recommend this practice. Temperatures may rise in service to allow the alloy to creep, slowly forming a blister.

Blisters are known to form on Zn alloys at ambient temperature in the open air after a period varying from 1 to 6 months. The blisters almost certainly grow by the pressure of gases trapped in defects just under the surface of the casting. The defects are most likely bifilms and/or porosity (there really is practically no difference between the two!). The origin of the high pressure of gas inside the defect is less certain:

- (i) high pressures of air or other gases entrained during the turbulence of die filling;
- (ii) high levels of hydrogen from plating processes are common in many plated zinc castings;
- (iii) hydrogen generated from surface corrosion processes can diffuse into the metal. The presence of moisture creates a gently corroding environment, releasing hydrogen that will diffuse into the metal, precipitating in the centers of bifilms and/or bubbles.

The blister may grow by the gradual precipitation and increasing pressure in the defect, leading to the gradual creep of the alloy. A flow of hydrogen into the defect seems necessary, since after the initial expansion of the blister, the pressure will be expected to fall rapidly with increasing volume, bringing the rate of growth to a stop. In practice the blisters appear to continue to grow over a period of months or years.

The fact that Birch (2000) finds that the properties fall as dendrite arm spacing increases is further evidence that Zn die casting alloys, particularly Alloy 3, contain bifilms that have chance to straighten, reducing properties, as the time for solidification lengthens. This effect is discussed in more detail in Section 9.4.3.

A quite different problem arises in heavy section castings. As the Al content of the ZA series of alloys increases some casting problems emerge which are unique, and which is found in all these



alloys, but particularly ZA27. During solidification the Al-rich dendrites form first and float to the top of the casting. Thus the Zn-rich liquid, being much denser than the Al, is displaced to the bottom of the casting. Because of its much lower melting point, the Zn-rich liquid freezes much later, and therefore forms a shrinkage cavity on the base of the casting (completely opposite to a normal casting where the shrinkage would be concentrated in a top feeder). It is known as *underside shrinkage*. Naturally, this problem is more severe in heavier sections and where freezing times are long because of the use of a sand mold as opposed to a metal die.

Canadian workers have explored a variety of alloy additions that appear capable of eliminating underside shrinkage, of which the most practical and cost effective is Sr (Sahoo et al. 1984, 1985). This worked well provided an adequate feeder was sited on the top of the casting. These authors were not able to explain why Sr was effective, but surmised that a skin of metal formed on the base of the casting which was sufficiently strong to withstand collapse (even though an internal cavity was now likely to occur in place of the external sink). The pressurization of the casting interior by a generous feeder will assist to prevent collapse during the early stages of solidification. Furthermore, the pressurization of the casting skin against the drag surface of the mold will increase the rate of heat transfer, helping to thicken and strengthen the skin. The detailed action of Sr remains a mystery, even though it is tempting to draw an analogy with the modification of Al–Si alloys in which Sr acts to suppress nucleation of the solid ahead of the freezing front, thereby straightening the front, and so forming a stronger solidified skin.

The hot chamber pressure die cast Zn-based alloys yield relatively small components of high accuracy, good finish requiring no machining and thin walls. It also has unequaled productivity and fulfills the requirements of a wide market. Larger castings at somewhat slower rates are produced by the cold chamber pressure die technique. Both types of HPDC parts have practically unique features that make them popular with designers, such as integrally cast rivets or cast threads to facilitate joining, or integrally cast steel inserts to eliminate assembly.

However, even at this date it is clear that there remains great scope for the improvement of the properties and behavior of Zn alloys. In my opinion this centers on the problem to reduce oxide bifilms by improved melt handling and casting. Here once again there is plenty of work to do.

---

## 6.2 MAGNESIUM

Magnesium is the lightest structural metal with a density of only  $1738 \text{ kg m}^{-3}$  at room temperature. Its light weight drives exploration of the use of its alloys for automotive and aerospace in competition with aluminum-based alloys. The competition is finely balanced, with Mg having the highest specific stiffness, and relatively high specific strength, with good damping characteristics (i.e. quiet castings), but remains limited in some applications because its relatively low strength means that full advantage cannot usually be taken of its attractive low density. Numerous other factors weigh against Mg compared to Al.

Historically, the relative volatility of the cost of Mg has been a serious disadvantage in comparison with Al for volume applications. Even so, the aircraft industry in particular finds Mg alloys essential to its designs of numerous castings, and the electronics and communications industries (e.g. mobile telephones) opt for Mg for weight saving of chassis and frames.

Another major factor hampering the wider use of Mg at this time is the difficulty of recycling Mg alloys. Rapid oxidation and the numerous alloys all in relatively small quantity make recycling

problematic. This contrasts with Al alloys for which an efficient worldwide recycling industry is already in place, making a big contribution towards the reduction in costs of Al castings.

The relatively poor corrosion resistance of some Mg alloys means that expensive surface protection is required for some components. However, the more recent introduction of a purer variety of AZ91 alloy (Mg–9Al–1Zn) has made a major contribution towards the growth potential of a volume Mg market. It seems likely that if Mg could be cast without bifilm defects corrosion resistance would be enhanced further at practically zero cost. This prediction remains to be put into practice.

In the meantime, for readers who want a wealth of practical advice on the melting and casting of Mg alloys, two works stand out *Principles of Magnesium Technology* by Emley (1966) and *Product Design and Development for Magnesium Die Castings* by the Dow Chemical Company (1985). For a more detailed and more up-to-date account of the metallurgy of Mg alloys the excellent text by Polmear (2006) is recommended. Even so, it is necessary to bear in mind that these renowned texts include neither the concept of bifilms nor such concepts as naturally pressurized filling systems for castings. Thus the reader needs caution.

In fact, when starting to consider the metallurgy of the light casting alloys, Al- and Mg-based, the role of oxide films appears so fundamental that it seems sensible to make a start with first understanding the oxides to be expected on such melts.

### 6.2.1 Films on liquid Mg alloys and protective atmospheres

In their comprehensive review of the oxidation of liquid metals made in 1969, Drouzy and Mascre mention some of the benefits of oxidation, but caution ‘*oxidation is something of a hindrance in the handling of liquid metals, particularly in casting*’. This masterpiece of understatement ‘*something of a hindrance*’ seemed worth quoting. Such disarming and admirable restraint summarizes the awesome, towering importance of perhaps the central problem in metallurgy.

The oxidation of solid magnesium metal in air is not easily studied, because the metal often ignites even before it reaches its melting point. (This emphasizes that for foundries, the metal has to be handled at all times in an atmosphere and in a manner that helps to suppress ignition.)

The oxide, MgO, has a density greater than that of solid Mg, with the result that the prediction based on the Pilling-Bedworth ratio is less than 1, with the consequence that the oxide does not cover the metal from which it forms, and therefore does not protect it (the values in this table are only rather approximate, being based on densities at room temperature, but are probably sufficiently accurate for our purpose, since the *ratios* are not expected to differ significantly at melting temperatures). Clearly, these considerations only strictly apply to solid Mg and its alloys, but require to be kept in mind during the heating of the Mg charge in the furnace prior to melting.

Once molten, it has been traditional to protect the metal by fluxes based on chlorides and fluorides. However, this practice is less popular today as a result of the widespread problems of the entrainment of flux inclusions in the castings, and as a result of the contamination of the environment with spent fluxes.

There has therefore been a major move to so-called ‘dry melting’, using protection from gases, plus possibly a little sprinkled sulfur. One of the gases used to suppress the burning of Mg has been sulfur hexafluoride (SF<sub>6</sub>). At a dilution of only 0.1–1.0% in air or other gas such as CO<sub>2</sub>, the mixture was extremely effective. Xiong and Liu (2007) found that the film of MgO on the melt surface was supplemented by islands of MgF<sub>2</sub> under the oxide. The islands gradually spread to over about 50% of the

total area. Although SF<sub>6</sub> is now rightly outlawed because of its huge effect on the earth's ozone layer, other chlorine- and/or fluorine-containing gases are being actively evaluated that are less harmful to the environment, and their mode of action may be similar (International Magnesium Association 2006). Polmear (2006) describes the use of the refrigerant gas HFC 134a, one of the several forms of tetrafluoroethane. Another promising new protective atmosphere contains BF<sub>3</sub> (boron trifluoride); the toxicity problems of this gas are addressed by using the gas in extreme dilutions generated in line from a solid fluoroborate (Revankar 2000). Other developments are under way, and appear to be having some success to refine further the effectiveness of the traditional dilute SO<sub>2</sub> mixtures in CO<sub>2</sub>. Perhaps the old remedies will be proven best after all.

The action of CO<sub>2</sub> alone is perhaps more active than might be expected since it is reduced by Mg (to form MgO) in two stages: (i) CO<sub>2</sub> is reduced to CO; and (ii) CO is reduced to carbon (Wightman and Fray 1983). It is possible that the deposition of carbon may help to suppress the rate of oxidation although the formation of magnesium carbide would also be expected to complicate the situation further. Cochran and colleagues (1977) confirmed that CO<sub>2</sub> strongly inhibited the onset of breakaway oxidation although the mechanism appeared mysterious; they looked for but failed to find any carbon-containing phase in the surface of the metal after solidification. For low-Mg alloys, they found even a small amount of CO<sub>2</sub> was valuable to reduce oxidation, although the amount required was sensitive to the Mg content and the temperature of the melt.

An important detail is that magnesium alloys are known to give off magnesium vapor at normal casting temperatures, the oxide film growing by oxidation of the vapor, effectively growing 'from the top downwards'. This mechanism seems to apply not only for magnesium-based alloys (Sakamoto 1999) but also for Al alloys containing as little as 0.4 wt% Mg (Mizuno 1996).

The microscopic structure of MgO films on AZ91 alloy has been studied by Mirak and colleagues (2007) in the limited oxidation conditions offered by the interior of bubbles trapped in the melt. The films are thick and are characterized by much fine-scale wrinkling, clearly capable of entrapping much air. Their general appearance is indistinguishable from that shown for the Al-5Mg alloy in Figure 2.10b.

In some admirably comprehensive experiments to compare protective atmospheres for melting Mg alloys, Frueling and Hanawalt (1969) noted that a CO<sub>2</sub> atmosphere was better than N<sub>2</sub> or Ar in preventing the 'smoking' of Mg. The 'smoke' is almost certainly the condensation of Mg vapor to Mg metal and its oxidation to MgO (or possibly the direct oxidation of the vapor to oxide) in the atmosphere over the melt. In fact the attempted protection of molten Mg by Ar is potentially hazardous. I recall a tragic fatal accident in which an experimental low-pressure furnace containing Mg alloy was provided with an atmosphere of Ar. Unknown to anyone, including the operator, the furnace had filled with Ar vapor. On opening the door to top up the furnace with additional Mg alloy ingots, air entered and mixed with the vapor, triggering a massive explosion. Such accidents do not happen when the furnace atmosphere comprises some oxidizing fraction, such as air, CO<sub>2</sub>, SO<sub>2</sub>, and/or gases such as freon containing chlorine and/or fluorine. The clear lesson is (no apologies for spelling this out) the treatment of Mg requires knowledge, expertise, possibly and preferably humility, but certainly caution.

A rather different approach to the protection of Mg melts from oxygen in the air has been proposed by Rossmann (1982) which used Ar in a way that appears to be free from the dangers mentioned above. He pours liquid argon directly on to the surface of the melt contained in a crucible in the open air. One liter of liquid argon will generate 836 L of argon gas at 1 atmosphere and 15°C, so that very small volumes of liquid argon are required to entirely eliminate oxygen from the surface of the melt. The

heaviness of argon is a help to keep it on the surface of the melt, but may not be totally proof against air. At  $-233^{\circ}\text{C}$  the density of Ar gas is 1.66, at  $20^{\circ}\text{C}$  it is 1.28, and at  $700^{\circ}\text{C}$  it is  $1.12\text{ kg m}^{-3}$ . Thus it becomes a little less dense than air at  $20^{\circ}\text{C}$ , approximately  $1.20\text{ kg m}^{-3}$ . Even so, the laminar spreading of the liquid Ar over the melt, and its action as a wind to keep air away as it boils, may continue to be effective in keeping air away from the melt surface.

Other approaches to developing resistance to burning include the addition of Ca to the Mg alloy at levels in the region of 1% (Sakamoto 1996). The oxide film on the melt consisted of two layers; a mix of MgO and CaO on the lower layer, and a CaO-rich layer on the top. The development of the modified oxide increased the ignition temperature of the alloy by approximately 250 K. It seems curious that two metals that both fail the Pilling-Bedworth criterion when mixed appear to satisfy it nicely. It is not clear, and perhaps is not likely, that the benefits of such alloying additions can be extended to the more useful engineering alloys such as AZ91. Although such benefits might be welcome, there are, as we have seen, other approaches to the control of Mg ignition that are already available.

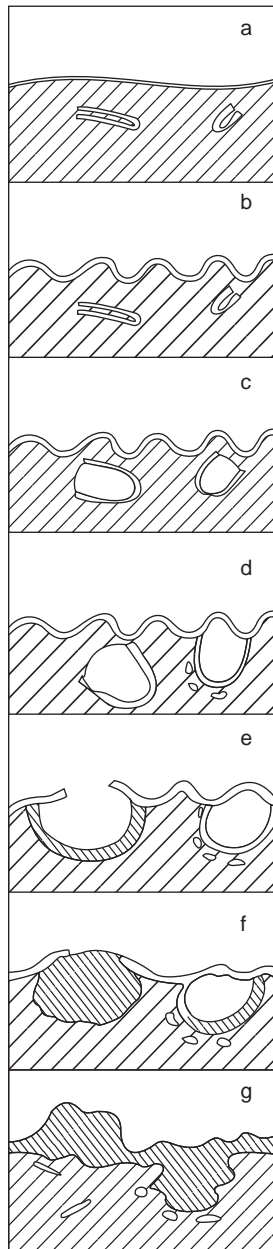
For sand molds, the addition of inhibitors is universal. In particular, for silica-based greensands containing perhaps 4% clay and 3 or 4% water, additions of 2% boric acid plus 2% sulfur are typical. For a self-setting resin-bonded silica sand the level of inhibition is similar. However, of course, heavier castings might require more, and lighter castings less (Mandal 2000). Furthermore, the skill of the designer of the filling system is also likely to influence the required amount of inhibition, as described below.

One final aspect of the ignition of Mg alloys is critically important. It is predictable that if a mold was filled with a liquid Mg alloy, but the filling was carried out without surface turbulence, so that the melt surface was at all times undisturbed, the alloy would probably not ignite. This proposal is based on the fact that the huge heat of formation of the oxide is easily conducted away into the bulk of the melt, limiting the rise of temperature of the metal surface to some trivial few degrees. However, if the melt surface is subjected to jumping and splashing, as occurs often when poured under gravity, each splash and droplet has a mass of only a few grams, and is only a few millimeters in thickness or diameter. Thus a sliver of liquid metal when traveling through the air would experience oxidation from both sides, the huge heat of oxidation now saturating the small mass and limited diffusion distance, with the result that the sliver, jet, or droplet now reaches a huge temperature, well above the ignition temperature. Thus surface turbulence initiates burning.

If the melt starts to burn, its reactivity will cause it to take oxygen from the silica sand of the mold, and thus will consume its way through the mold, possibly continuing through the concrete floor, taking oxygen from the concrete, until the Mg is entirely oxidized. Only then will the burning stop. The next clear lesson for the handling of Mg alloys is that it is absolutely necessary to ensure that burning of the metal does not start.

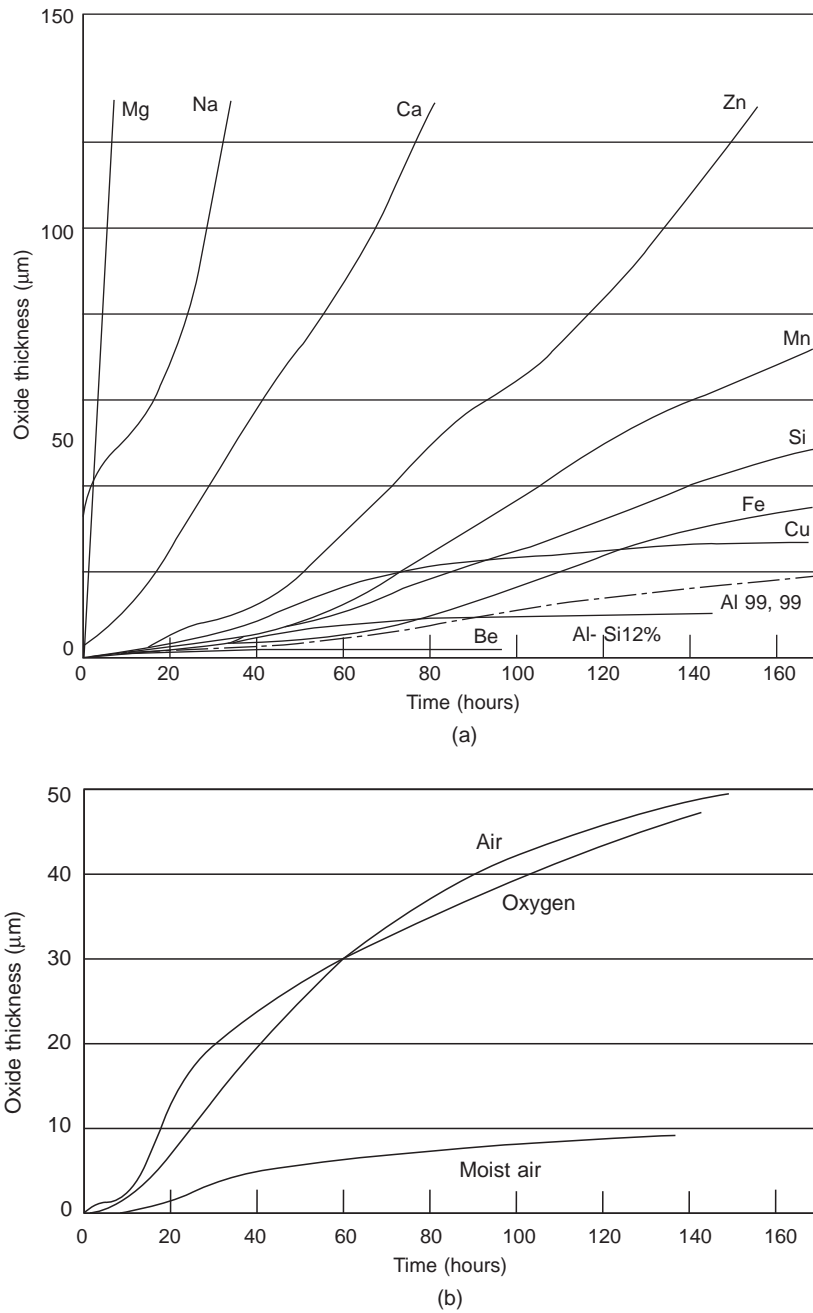
We shall turn now to the behavior of Al-Mg alloys in the range of approximately 2–20%Mg. These Al-Mg alloys are so dominated by the oxidation of Mg that they act practically as though they were pure Mg. We shall therefore include them in this section on Mg.

Provided burning can be successfully suppressed, as would be normal for the competent handling of Al-Mg alloys, the surface oxide initially develops as a thin layer of amorphous MgO (Figure 6.2a). After an incubation time that seems to depend on chance events to nucleate a change, the oxide crystallizes to MgO and some spinel, the name for the mixed MgO and  $\text{Al}_2\text{O}_3$  oxide, magnesium aluminate, which can be written  $\text{MgAl}_2\text{O}_4$  (Cochran 1977). This stage of oxidation is fast (Figure 6.3), particularly if the atmosphere is moist air, creating so much oxide that the film has to corrugate as in



**FIGURE 6.2**

The stages in oxidation of Al-5Mg alloy. (a) MgO film on surface and folded into the melt; (b) growth of surface film leads to corrugations; (c) in moist air  $\text{OH}^-$  ions diffuse through film, giving  $\text{H}^+$  ions in the melt, swelling bifilms with  $\text{H}_2$ ; (d) bubbles rise, disrupting surface film and starting break-away oxidation; (e) spinel  $\text{MgAl}_2\text{O}_4$  (dark shaded) forms; (f) and (g) complete conversion to thick, irregular spinel film (experimental data from Rault et al. 1996).

**FIGURE 6.3**

(a) Growth of oxide on Al and its alloys containing 1 at% alloying element at 800°C. (b) Growth of oxide on 99.9Al at 800°C in a flow of oxygen, and dry and moist air (data from Theile 1962).

a concertina (Figure 6.2b). The development of the oxidation process proposed in Figure 6.2 is based on an interpretation of the observations by Rault (1996) and Haginoya (1976). These authors find that the hydrogen released into the melt by the surface oxidation causes some of the subsurface bifilms to inflate and float, coming into contact with the underside of the surface film. Here they can break open the surface leading to irregular masses of spinel formation. However, Haginoya noticed that those films that were more deeply immersed in the liquid, and for some reason unable to float, perhaps being attached to a submerged surface of the casting, remained as films. This is perhaps to be expected, since they will probably require at least a part of the bifilm near to the surface to be successful to gain any hydrogen.

### 6.2.2 Strengthening Mg alloys

Magnesium metal, like most pure metals, is naturally rather weak, and requires strengthening for most engineering applications. The Mg-based alloys can be complicated (Unsworth 1988), and only a brief summary can be included here. In general, in common with the other family of low-melting-point alloys based on zinc, the magnesium-based alloys are not only mainly wanting in strength, but tend to creep rapidly as temperatures are raised.

Alloying with Al and Zn has produced a series of useful alloys, known as the AZ series including AZ31, AZ63, and AZ91. The latter alloy (its letters standing for 9wt% aluminum and 1 wt% zinc) is widely popular. Many of these alloys contain up to 0.4%Mn, as also is the case for the Al and Mn containing alloys AM50 (Mg–5Al–0.4Mn) and AM60 (Mg–6Al–0.4Mn). Other Al- and/or Zn-containing alloys include Mg–Al–Si, Mg–Al–Rare Earth, and Mg–Zn–Cu. The introduction of high-purity variants of these alloys, with lower levels of Fe, Cu, and Ni has significantly improved corrosion resistance. The common sand casting alloy AZ91C has now been largely replaced by AZ91E, its high-purity equivalent which has about 100 times better corrosion resistance. The alloy ZC63 (Mg–6Zn–3Cu–0.5Mn) was developed as an easy-to-process material for engine castings such as cylinder blocks and oil pans.

So far as possible, it is important to grain refine the structure of Mg alloy castings. A typical grain-refining action might reduce the grain size from 250  $\mu\text{m}$  down to 50  $\mu\text{m}$ . The reason for the importance of grain refinement is that the yield strength  $\sigma_y$  in Mg alloys is strongly related to the grain size by the Hall-Petch relationship

$$\sigma_y = \sigma_o + K_Y d^{-1/2} \quad (6.1)$$

The relationship is strong for Mg alloys because of their hexagonal close-packed (hcp) crystal structure. The only plane allowing relatively easy slip is the basal 0001 plane. All other directions in the crystal represent significant difficulty to initiate slip. Thus, because it will be unlikely for two adjacent grains to have their basal planes aligned, propagating slip from one grain to the next will normally be difficult. Thus the  $K_y$  factor in the Hall-Petch equation for Mg alloys is unusually large. (This contrasts with  $\alpha$ Al alloys, where the effect of grain size is relatively weak because  $K_y$  is small. This follows because propagating slip from one grain to another is easy in the aluminum face-centred cubic (fcc) lattice as a result of its high symmetry; an fcc crystal has many slip possibilities in all directions.)

Unfortunately, the grain refinement of Mg alloys is an unsatisfactory list of recipes of traditional practices, with no convincing science to provide explanations. For instance, the mysterious nature of

the grain refinement of Mg–Al alloys by superheating to around 850°C is widely practiced, but not understood. The role of carbon dissolved from the steel crucibles has been suspected. A rather wider range of alloys can be grain refined by carbon additions, most popularly by hexachlorethane plunged into the melt to effect some simultaneous degassing action. Other black art to grain refine these alloys is listed by Emley (1966). Zhang et al. (2010) describe a new grain-refining technique for AZ91 consisting of bubbling a mixture of Ar + CO<sub>2</sub> through a melt contained in a rotary degassing unit. The treatment takes 30 minutes, after which the grain size reduction seems better than competitive treatments. Although the authors suggest aluminum carbide, Al<sub>4</sub>C<sub>3</sub>, may be the effective nucleating agent, they neglect the fact that the melt is almost certainly full of oxide films. Despite this, they report increased tensile strengths increased by up to 20% and elongation by up to 100%.

### ***The Mg–Zr alloys***

A completely different class of Mg alloys was opened up by the discovery of the Mg–Zr alloys by Sauerwald in 1947. This has been an outstanding development for Mg, giving alloys with enhanced properties at both room and elevated temperatures. The alloys derive their properties from the remarkable grain-refining action of Zr.

Zirconium is only slightly soluble in Mg having a limit of only 0.60%Zr, and it is necessary to saturate the melt with Zr since only the Zr in solution at the time of casting is effective in refining the grain size. On solidification, undergoing a peritectic transformation close to 650°C (the available phase diagrams are not clear in this region), it appears that Zr-rich particles precipitate in the melt. The Zr-rich particles form an extremely effective nucleus for Mg as a result of their similar hexagonal lattice structure, and their nearly identical lattice spacings. The particles are often seen at the centers of Mg grains, confirming their role as nuclei for grain refinement. (The action of Zr is only useful in those alloys that do not contain Al because Al and Zr form a stable compound that effectively eliminates all free Zr from solution. Similar reactions occur with Mn, Si, Fe, Ni, Co, Sn, and Sb.)

The main effect of Zr on the strength of Mg alloys (in those alloys free from the above list of elements) is probably not the result of the usual mechanisms of precipitation hardening or solute hardening, etc., but its impressive action on the refinement of grains according to Equation 6.1. Grain size is typically reduced from 2 mm to 0.05 mm. This dramatic grain-refining action appears to be the result not only of the presence of effective nuclei, but of a significant contribution to the subsequent restriction of the growth of the grains by other solutes, as made clear by St John (2005).

Historically, the addition of Zr to an Mg melt has proved to be difficult because of the low solubility of Zr and its loss by reaction with air and reaction with Fe from the steel crucible, particularly as the temperature increases from 730 to 780°C (Cao et al. 2004). Traditionally one of the most successful techniques for the addition of Zr has been through the use of a master alloy containing Mg and 30%Zr, plus residual heavy flux, ‘weighted down’ often with a dense chloride such as BaCl<sub>2</sub>. The alloy and its content of entrained chlorides and fluorides has to be ‘puddled’ (i.e. mechanically pummelled or stirred) and then left to settle again. It sits in excess at the base of the crucible to act as a reservoir of Zr, maintaining saturation as nearly as possible, replacing that being continuously lost by oxidation and by reaction with the iron crucible. The melt is poured leaving 10 or 20% of the melt with its residual flux undisturbed at the bottom of the crucible. (This material can be recycled in other Mg–Zr alloys.)

During studies of the separation of flux from Mg alloys Reding (1968) confirmed that the flux settles to the bottom of the melt, but remains as separate droplets which refuse to coalesce into a single



drop. This seems consistent with the drop being entrained through the surface and thus being enclosed within a tenacious oxide skin. The SEM EDX studies revealing high Fe and Zr content at the drop-matrix interface corroborating the presence of an oxide skin on which Fe-rich and possibly Zr-rich intermetallics precipitate as on a favored substrate (see the analogous behavior in Al alloys, Section 6.3). The report by Reding makes sobering reading and is recommended to readers as a wake-up call in the problems of making Mg–Zr alloys. It is a concern in the Mg–Zn–Zr alloy that he studies that the flux droplets appear not to settle but remain dispersed uniformly through the melt. This suggests the presence of a network of large films, probably of MgO, that are resisting the settling of the flux. Whether this behavior is exclusive to this alloy seems unlikely, and may reflect poor handling or melting practice. We have much to learn about Mg alloys.

In view of these uncertainties it is perhaps surprising that the flux technique for the addition of Zr has been more or less successful for the production of Mg–Zr alloys for many years (Emley 1966). A more recent development by Qian (2003) showing Zr dissolution working well at only 730°C, stirring for only 2 minutes, and using melts protected from contamination from their iron crucibles by a simple wash of boron nitride (BN) promises future hope of a more controlled manufacture of these useful alloys.

### 6.2.3 Microstructure

The microstructural development of the very many Mg-based alloys is a complex and vast subject beyond our scope. However, some general points can be made about the simplest alloys, particularly the Mg–Al alloys.

The solid grains forming in a liquid Mg alloy melt have a flat (i.e. two-dimensional), hexagonal form, closely resembling the forms of snowflakes. These contrast with the dendritic forms of the cubic-structured metals, whose dendrites are three-dimensional stars, with three sets of axes at right angles, their positive and negative directions creating six primary arms.

Slow cooling of the Mg–Al alloys causes a coarse precipitate of  $Mg_{17}Al_{12}$  to precipitate at grain and dendrite boundaries (Figure 6.4). This curiously complex phase is commonly met in Mg alloys. At lower temperatures still, the particles become surrounded by a fine lamellar eutectoid precipitate of Mg and  $Mg_{17}Al_{12}$ .

Whereas with Al alloys that have enjoyed massive attention from researchers, so that the central role of oxide bifilms in the control of microstructure and properties has now been established beyond doubt, Mg alloys have hardly started on this path. Nevertheless, it is interesting to take an overview of an authoritative text like Emley's *Principles of Magnesium Technology* (1966) to see that most of the defects are films. At that time, of course, it was not known that all such films were in fact bifilms. It is tantalizing therefore to consider that Mg alloys might similarly be controlled by the presence of bifilms, since the bifilms are to be expected in Mg alloys. A few early hints that this may be so are listed below.

At this time there is little evidence that  $Mg_{17}Al_{12}$  nucleates on the outer surfaces of bifilms, even though closely analogous behavior in Al-based and other alloy systems would lead us to expect this. Also, the presence of central linear features, including voids, and the well-known brittleness of this compound are not easily explained in the absence of bifilms.

Srinivasan and colleagues (2006) investigated the structure and properties of AZ91 alloy to which had been added 0.5Si in an effort to improve high-temperature strength and creep resistance by the precipitation of  $Mg_2Si$  particles. They found that the  $Mg_2Si$  formed as coarse 'Chinese script' and

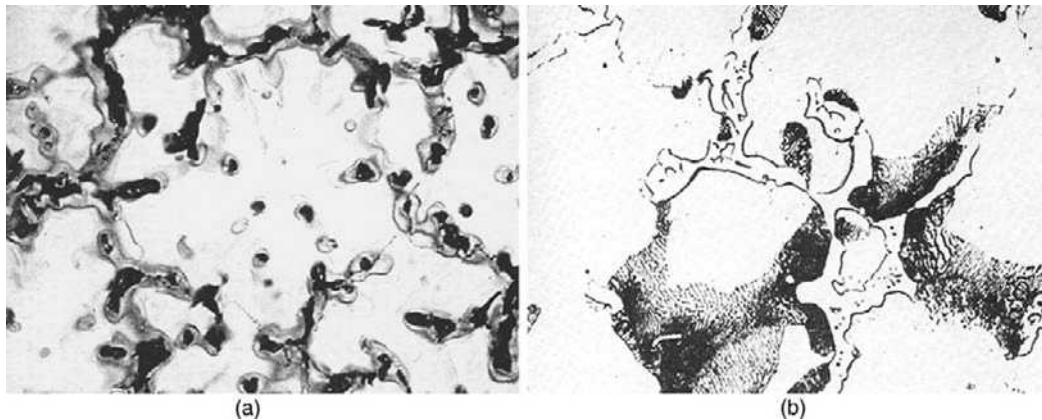


**FIGURE 6.4**

(a) Microstructure of chill cast Mg-8Al-0.5Zn-0.25Mn. The common intermetallic compound  $Mg_{17}Al_{12}$  (dark) and interdendritic coring (gray) is shown by the electrolytic polish. (b) Slowly cooled alloy showing eutectoid precipitate from decomposition of Al-rich solid solution (nital etch) (Emley 1966).

actually slightly reduced properties, but 0.1Sr addition made a radical change to the microstructure, changing the  $Mg_2Si$  from Chinese script to a refined form, evenly distributed along the grain boundaries.

It is tempting to draw a comparison with Al alloys, where it is fairly certain that Sr deactivates oxide bifilms, preventing the nucleation and growth of other phases on the bifilms, and thereby forcing the formation of these phases at lower temperatures in eutectic growth modes. In this case, it seems probable therefore that  $Mg_2Si$  is precipitating on bifilms, and taking a Chinese script form. After Sr addition,  $Mg_2Si$  no longer precipitates on bifilms and thus seeks the next most energetically favorable mode of precipitation, which appears to be a eutectic form associated with the grain boundaries. Other work on the addition of Sr at levels of only 0.01–0.02 wt% to AZ91 is reported by Aliravci (1992) reporting a number of changes such as finer grain size, reduced porosity, and improved mechanical properties. These issues are unexplained and clearly require a significant further research effort.

The next few years may reveal the true role of bifilms in Mg metallurgy. It is not yet clear whether bifilms are in control, although this is strongly suggested by the work of Griffiths and Lai (2007) who find large butterfly mirror images of bifilms on every tensile fracture surface and facets aligned by dendrites, suggesting bifilms cover practically the whole of their fracture surfaces. They also find the strength of top-filled compared to bottom-gated castings have a Weibull modulus reduced from 12 to 4.

It seems likely therefore that when founders start to cast Mg alloys without bifilms we should expect surprises.

## 6.3 ALUMINUM

The Al alloys have enjoyed a huge expansion over the past few decades as a result of their accessible casting temperatures and light weight. Although the alloys have been presumed easily processable,

probably as a result of their low melting temperature compared to cast iron, the industry has paid a high price for this presumption. Processing the alloys in the way that cast iron has been traditionally handled has resulted in major problems for Al castings and for the fledgling Al casting industry; the surface oxide has become entrained, leading to numerous and serious bifilm problems, and the hydrogen gas in solution in the liquid metal is partitioned uniquely strongly during solidification, inflating bifilms to become porosity. Thus there have been important and unsuspected problems with attempts to make castings in Al and its alloys. The metallurgical aspects of these issues will be dealt with in this section, and the practical engineering aspects of metal handling and casting later in Chapter 10 onwards.

Al metal, when pure, is surprisingly weak and soft. The strengthening of the metal has led to the development of three families of casting alloys.

- (i) The Al–Si alloys form the mainstream of the industrially important engineering cast alloys. Additions of Mg promote the precipitation of  $Mg_2Si$  in precipitation hardening heat treatments. One of the most widely used structural engineering alloys is Al–7Si–0.4Mg. Cu addition to Al–Si alloys similarly will precipitate and harden by the precipitation of  $CuAl_2$  although the Cu addition impairs the corrosion resistance of the alloy. The Al–Si alloys, with perhaps Mg and/or Cu additions, will feature significantly in this section. The presence of hard, metallic Si particles in the alloys gives the alloys the character of an in situ metal/matrix composite (MMC).

In contrast to the two-phase Al–Si alloys, two essentially single-phase solid solution alloys are also important, and have very different properties.

- (ii) The Al–Mg series, in which the Mg content may rise to around 10 wt% are reasonably strong ductile alloys with significant corrosion resistance, and capable of taking a bright white anodizing coat much loved by the food industry. The choice of Mg levels is typically 5 or 6 wt %. The strongest Al–10Mg alloy has been generally avoided over recent years, people fearing rumors of it becoming brittle with age, particularly in warm conditions such as in the tropics or in engine compartments of cars. This is a travesty of the facts, and it is a pity that this excellent alloy has suffered such unjust criticism; it is true that it loses a little of its huge ductility after some years, possibly as a result of the precipitation of  $Mg_5Al_8$  (or perhaps  $Mg_2Al_3$ ) in grain boundaries (probably on bifilms – suggesting a remedy by eliminating bifilms). Even so, its generous reserves of ductility ensure that it always remains ductile, in fact, usually more ductile than most of the Al–Si alloys even when at their best. Much of its ductility arises as a result of its uniform single-phase solid solution structure (contrasting sharply with the MMC structure of the Al–Si alloys). When liquid, the Al–Mg alloys react strongly with their environment, and usually require to have inhibitors in the mold to reduce metal/mold reactions if cast into sand.
- (iii) The second important series of single-phase solid solution alloys is that based on Al–Cu. Copper contents up to about 5.0 wt% are possible, with many alloys with a nominal composition around 4.5%. These alloys, when subjected to solution treatment and aging can achieve high strength and ductility. A famous alloy, A201, contains approximately 0.7%Ag, and is one of the strongest and toughest of all the cast Al alloys. Unfortunately, having silver lying about in the foundry introduces a security headache, adding to the founder's daily problems he could do without.

A special feature of the Al alloy market is that the metal is divided into primary and secondary markets, in which the primary alloys are those made from metal freshly won from the ore, whereas

secondary alloys are based on recycled material, thus economizing on the huge energy required to smelt Al from its ore, since melting it for the second time requires only about 5% of that energy. This economy is of course offset by the greater oxide and impurity contents, particularly iron. The Al alloy casting alloys for most applications are based on secondary metal. Only relatively few applications for aerospace and safety-critical items might specify primary alloys. Otherwise, most primary metal goes for wrought applications such as sheet and foil.

Finally, these issues should not take our focus away from the central problem with the casting of all Al alloys; during the turbulence of pouring, the incorporation of the surface oxide into the bulk of the alloy, where it constitutes a bifilm crack that impairs properties. Al alloys have therefore gained a reputation for unreliability. It is necessary to understand this problem to ensure that it is effectively avoided. This is the reason for starting the next section with the oxidation of the melt.

### 6.3.1 Oxide films on Al alloys

Considering first the reaction of liquid aluminum with oxygen, the equilibrium solubility of oxygen in aluminum is extremely small; less than one atom in about  $10^{35}$  or  $10^{40}$  atoms. This corresponds to less than one atom of oxygen in the whole world supply of the metal since Al was discovered and extraction began. Even allowing for the dynamic effects described in Chapter 1 in which the metal can have much higher levels of oxygen in solution, we can safely approximate its solubility to zero. Yet everyone knows that aluminum and its alloys are full of oxides. How is this possible? The oxides certainly cannot have been precipitated by reaction with oxygen in solution. Oxygen can only reach and react with the metal surface. Furthermore, the surface can only access the interior of the metal if it is entrained, or folded in. This is a mechanical, not a chemical, process. The presence of oxygen in aluminum thereby has to be understood not in terms of chemistry but in terms of mechanical entrainment.

It makes sense therefore to start with an understanding of the reactions at the surface of the metal. For the process and mechanisms of oxidation, the reader is referred to the few original sources concerned with the oxidation of liquid aluminum alloys (Theile 1962, Drouzy and Mascré 1969). This short review of the oxidation of Al-based alloys is based on these works.

For the case of pure liquid aluminum, the oxide film forms initially as an amorphous variety of alumina that quickly transforms into a crystalline variety, gamma-alumina. These thin films, probably only a few nanometers thick, their thickness consisting of only a few molecules, inhibit further oxidation. However, after an incubation period the gamma-alumina in turn transforms to alpha-alumina, which allows oxidation at a faster rate. Although many alloying elements in aluminum, including iron, copper, zinc, and manganese have little effect on the oxidation process (Wightman and Fray 1983), other alloys mentioned below exert important changes.

Figure 6.3 shows, approximately, the rate of thickening of films on aluminum and some of its alloys based on weight gain data by Theile (1962). The extremes are illustrated by the rate of thickening of Al-1.0 atomic %Mg at about  $5 \times 10^{-9} \text{ ms}^{-1}$  that is over a thousand times faster than the 1 atomic %Be alloy. Interestingly, Theile found that water vapor in an oxidizing environment inhibited the rate of oxidation of Al (Figure 1.3). This finding seems to be in accord with shop floor experience of operating furnaces in which the incoming Al alloy charge is preheated by the spent furnace gas (flue gas necessarily containing much water vapor). Although Al melts would be normally expected to increase their hydrogen content in proportion to the water vapor in the environment, over a certain

concentration of moisture the oxide film appears to become protective, inhibiting further uptake (but regrettably Cochran (1977) finds this benefit does not extend to high-Mg melts) so that high levels of hydrogen are not experienced in the melted metal from such furnaces.

The Al–Mg system is probably typical of many alloy systems that change their behavior as the percentage of alloying element increases. For instance, where the aluminum alloy contains less approximately 0.005 weight% magnesium the surface oxide is pure alumina. Above this limit the alumina can convert to spinel,  $\text{Al}_2\text{MgO}_4$ . It is important to note for later reference that the spinel crystal structure is quite different from any of the alumina crystal structures. Finally, when the alloy content is raised to above approximately 2%Mg, then the oxide film on Al converts to pure magnesia, MgO (Ransley and Neufeld 1948). These critical compositions change somewhat in the presence of other alloying elements.

In fact, the majority of aluminum alloys have some magnesium in the intermediate range so that although a pure alumina film forms almost immediately on a newly created surface, in time, it will usually be expected to convert to a spinel film.

The films have characteristic forms under the microscope. The newly formed alumina films are smooth and thin (Figure 2.10a). If they are distorted or stretched they show fine creases and folds that confirm the thickness of the film to be typically in the range 20–50 nm. The magnesia films are corrugated, as a concertina, and typically ten times thicker (Figure 2.10b). The spinel films are different again, resembling a jumble of crystals that look rather like coarse sandpaper (Figure 2.10c).

Rough measurements of the rate of thickening of the spinel film on holding furnaces show its growth to be impressively fast, approximately  $10^{-9}$  to  $10^{-10}$   $\text{kg m}^{-2} \text{s}^{-1}$ . Although these speeds appear to be small, they are orders of magnitude faster than the rates of growth of protective films on solid metals. Since the oxide itself is fairly impervious, its rate of growth expected to be controlled by the rate of diffusion of ions through the oxide lattice, how can further growth occur quickly after the first layer of molecules is laid down?

It seems that this happens because the film is permeated with liquid metal. Fresh supplies of metal arrive at the surface of the film not by diffusion, which is slow, but by flow of the liquid along capillary channels, which is, of course, far faster. The structure of the spinel film as a porous assembly of oxide crystals percolated through with liquid metal, as coffee percolates through ground beans, may be an essential concept for the understanding of its behavior.

We have already seen that progressive Mg additions to Al change the oxide from alumina, to spinel, and finally to magnesia. A cursory study of the periodic table to gain clues of similar behavior that might be expected from other additives quickly indicates a number of likely candidates. These include the other group IIA elements, the alkaline earth metals including beryllium, calcium, strontium, and barium. The Ellingham diagram (Figure 1.5) confirms that these elements have similarly stable oxides, so stable in fact that in sufficient concentration, alumina can be reduced back to aluminum and the new oxide takes its place on the surface of the aluminum alloy. The disruption or wholesale replacement of the protective alumina or spinel film can have important consequences for the melt.

In the case of additions of beryllium at levels of only 0.005%, the protective qualities of the film on Al–Mg alloy melts is improved, with the result that oxidation losses are reduced as Figure 6.3 indicates. Low-level additions of Be have been found to be important for the successful production of wrought alloys by continuous (direct chill) casting possibly because of a side effect of the strengthening of the film, causing it to ‘hang up’ on the mold or ladle, and so avoid entering the casting, as discussed earlier.

Attempts to measure the strength of films on Al alloys have been made from time to time (Kahl and Fromm 1984, 1984, Syvertsen 2006) but the measurements are not easy to make, and the results seem of uncertain value at this time.

Strontium is added to Al–Si alloys to refine the structure of the eutectic in an attempt to confer additional ductility to the alloy. However, strontium has a significant effect on the oxidation behavior of an Al–7Si–0.4Mg alloy as determined by Dennis et al. (2000). Strontium, like magnesium, seems also to form a spinel, its oxide combining with that of aluminum to form  $\text{Al}_2\text{O}_3\cdot\text{SrO}$  alternatively written  $\text{Al}_2\text{SrO}_4$ . In addition, the resistance to tearing of the film is probably also increased, affecting the entrainment process. Because of this additional powerful effect on the oxide film, the action of Sr as an addition to Al alloys is complicated. It is therefore dealt with separately in Section 6.3.5.

Sodium is also added to modify the microstructure of the eutectic silicon in Al–Si alloys. In this case the effect on the existing oxide film is not clear, and requires further research. Sodium will have much less of an effect in sensitizing the melt to the effect of moisture because it is less reactive than strontium. In addition, sodium is lost from the melt by evaporation because the melt temperatures used with aluminum alloys, typically in the range 650–750°C, approach its boiling point of 883°C. The wind of sodium vapor issuing from the surface of the melt will act to sweep moisture vapor and hydrogen away from its environment. Both the reduced reactivity and the vaporization would be expected to reduce any hydrogen problems associated with Na treatment compared to Sr treatment, corresponding to general foundry experience.

However, Wightman and Fray (1983) find that all alloys that vaporize disrupt the film and increase the rate of oxidation. The additions they tested included sodium, selenium, and (above 900°C) zinc. The disruption of the film acts in opposition to the benefit of the wind of vapor purging the environment in the vicinity of the melt. Thus the total effect of these opposing influences is not clear. It may be that at these low concentrations of solute any beneficial wind of vapor is too weak to be useful, allowing the disruption of the film to be the major effect. However, the overall rate is in any case likely to be dominated by the reduced reactivity of Na with moisture compared with Sr.

Experience of handling liquid aluminum alloys in industrial furnaces indicates that the character of the oxide film is visibly changed when sodium, strontium, or magnesium is added. For instance, as magnesium metal is added to an Al–Si alloy, the surface oxide on the melt is seen to take on a glowing red hue that spreads out from the point that the addition is made. This appears to be an effect of emissivity, not of temperature. Also, the oxide appears to become thicker and stronger. The beneficial effects found for the improved ductility of Al–Si alloys treated with sodium or strontium may be due not only therefore to the refined silicon particle size, as discussed in Section 6.3.5.

### 6.3.2 Entrained inclusions

When the surface of the melt becomes folded in, the doubled-over films take on a new life, setting out on their journey as bifilms. The scenario has been discussed in some detail in Chapter 2 in the description of liquid metal as a slurry of defects.

As an overview of these complicated effects, Figure 6.5 gives an example of the kinds of populations of defects that may be present. This figure is based on a few measurements by Simensen (1993) and on some shop floor experiences of the author. Thus it is not intended to be any kind of accurate record, it is merely one example. Some melts could be orders of magnitude better or worse than the figures shown here. However, what is overwhelmingly impressive, and clearly shown, are the

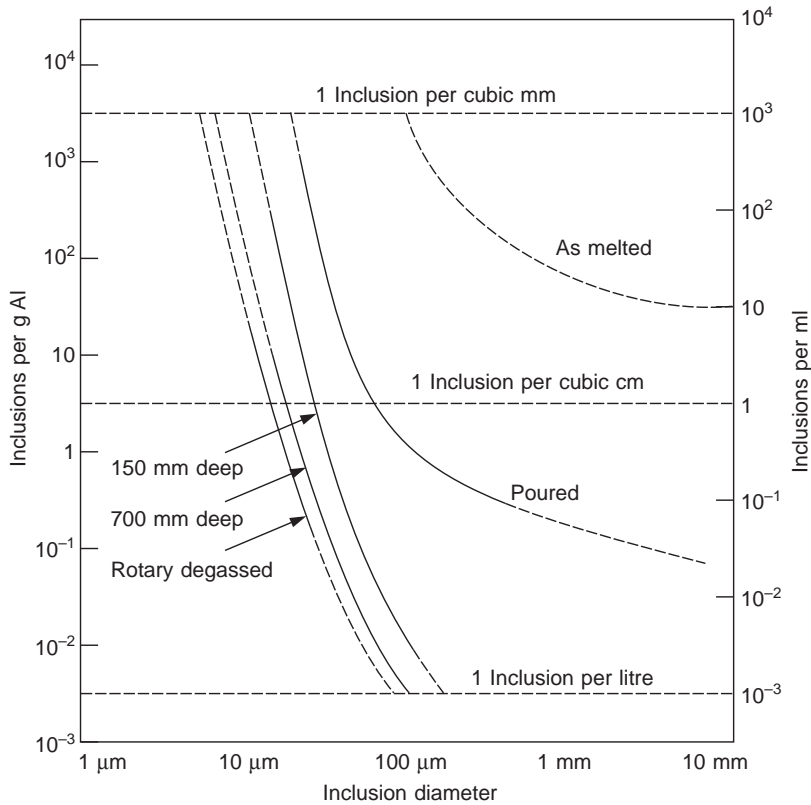


**FIGURE 6.5**

An example of inclusion content in an Al alloy.

vast differences that can be experienced. Melts can be very clean (1 inclusion per liter) or dirty (1000 inclusions per cubic millimeter). This difference is a factor of a thousand million. It is little wonder that the problem of securing clean melts has presented the industry with a practically insoluble problem for so many years. These problems are only now being resolved in some semi-continuous casting plants, and even in this case, many of these plants are not operating particularly well. It is hardly surprising therefore that most foundries for shaped castings have much to achieve. There is much to be gained in terms of increased casting performance and reliability. The mechanics of cleaning the melt, eliminating the oxides, and then ensuring that the oxides are not re-introduced prior to casting are dealt with in detail in Chapter 10 and the following chapters.

### 6.3.3 Grain refinement (nucleation and growth of the solid)

There are many reasons given for refining the grain size of castings. Yield strength and toughness are increased; microsegregated phases are more evenly distributed at grain boundaries; the susceptibility to hot tearing is reduced. The Al alloys are well behaved in this respect, so that the grain-refining action

is now thought to be relatively well understood and appears to be under good control. Even here, however, everything is not what it seems, since the immense importance of bifilms, strongly influencing these processes, has been mainly overlooked.

The addition of titanium in various forms into aluminum alloys has been found to have a strong effect in nucleating the primary aluminum phase. It is instructive to consider the way in which this happens.

Sigworth and Kuhn (2007) describe a well-accepted theory in which the addition of Ti to Al alloys raises the melting point by 5°C. At the same time the first phase to form is rich in Ti as a result of the relatively rare condition in which the partition coefficient is more than unity, causing solute to be preferentially absorbed by the growing solid rather than being segregated ahead. They point to elegant micrographic studies revealing Ti-rich dendritic shapes in the centers of refined grains as evidence of the correctness of the theory. All this experimental evidence is certainly in line with expectations from the phase diagram (Figure 6.6), but does not explain *refinement*.

The fundamental reason for the nucleation of grains appears to be the prior existence of TiAl<sub>3</sub> nuclei. There is no doubt that TiAl<sub>3</sub> is an active nucleus for aluminum because TiAl<sub>3</sub> is found at the centers of aluminum grains, and there is a well-established orientation relationship between the lattices of the two phases (Davies et al. 1970). These nuclei are stabilized by the huge undercooling of hundreds of degrees Celsius (Figure 6.6). At such high undercoolings the TiAl<sub>3</sub> phase might even form by homogeneous nucleation. It seems quite probable that this could happen in the melt during the Ti addition, when the local Ti concentrations around the dissolving Ti addition start as extremely high Ti levels, well into the TiAl<sub>3</sub> undercooled region of the phase diagram, prior to dispersing and falling to lower ineffective levels. Equally probably, the TiAl<sub>3</sub> particles are likely to be added ready-made in the grain-refining addition.

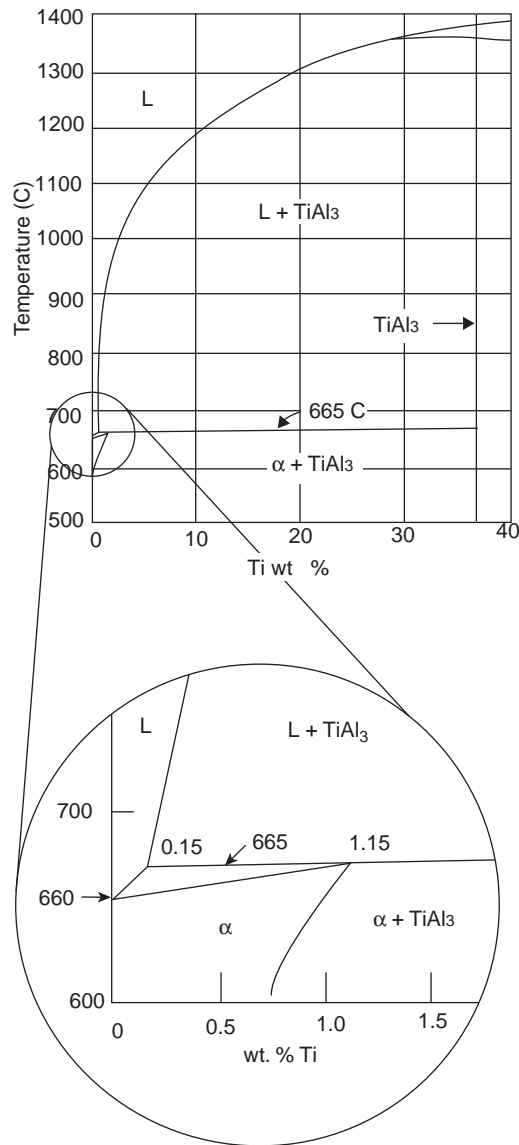
TiAl<sub>3</sub> in the liquid metal at a Ti concentration above about 0.15 wt% would be expected to be stable (Figure 6.6). However, many Al alloys contain Ti but at levels lower than this, so there is the danger that the TiAl<sub>3</sub> can disappear into solution in the melt. This is probably the mechanism for the ‘fade’ of the grain refinement effect with time.

Results of several researchers shown in Figure 6.7 illustrate that the effect of titanium in the grain refinement of aluminum starts at concentrations well below 0.10Ti. How titanium can be effective at concentrations anything lower than 0.15% has remained a mystery in Al–Ti liquid solutions until the epoch-making research by Schumacher and Greer (1993, 1994). These researchers carried out their studies on an amorphous aluminum alloy, as an analog of the liquid state. Nucleation is more easily observed since the kinetics of reaction are 10<sup>16</sup> times slower. Using TEM (transmission electron microscopy) they observed that TiAl<sub>3</sub> was present as adsorbed layers on titanium boride (perhaps more accurately, titanium diboride) (TiB<sub>2</sub>) crystals, and so its existence was stabilized at lower levels of Ti than would be expected from the phase diagram, and it was thereby effective in nucleating aluminum for far longer periods as a result of the near-insolubility of TiB<sub>2</sub>.

Effective grain refinement, however, seems to require more than simply the nucleation of new grains. A second important factor is the suppression of their growth. If growth is fast, grains can grow large before others have chance to nucleate. Conversely, if growth rates can be suppressed, greater opportunity exists for more grains to nucleate. For complex systems, where many solutes are present, the rate of growth of grains is assumed by Greer and colleagues (2001) to be controlled by the rate at which solute can diffuse through the segregated region ahead to the advancing front. They use a *growth restriction parameter Q* based on the concentration head of the front, defined as:

$$Q = m(k - 1)C_0 \quad (6.2)$$



**FIGURE 6.6**

Binary Al-Ti phase diagram.

Although they note that this relation should be modified by the rate of diffusion  $D$  of the solute, these factors are not well known for many solutes. They therefore assume that the rates of diffusion are fairly constant for all solutes of interest in aluminum (this is not far from the truth for the substitutional solutes shown in Figure 1.4a). Thus the potentially more accurate summation of the effects of different

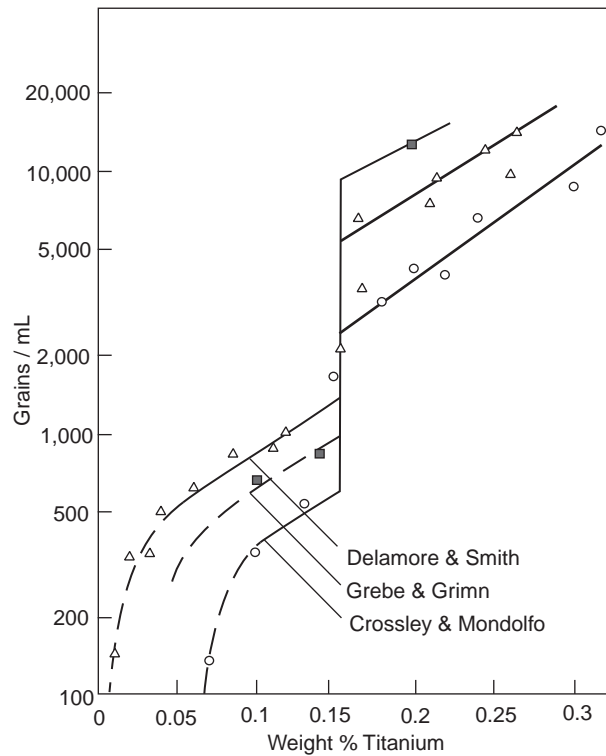


**FIGURE 6.7**

Increase in grain refinement with increasing titanium addition, especially at the peritectic 0.15Ti as found by several researchers.

solutes in solution, weighted inversely by their diffusivities as proposed by Hodaj and Durand (1997), is neglected in favor of a simple summation of  $Q$  values. The effect is shown in Figure 6.8. Initially, grain size clearly decreases with increasing total values of  $Q$ . With negligible values of growth restraint grains are seen to grow to nearly 1 mm diameter. As restraint is increased grain size reduces to nearly one-tenth of this, but can get no smaller. After this minimum, increasing  $Q$  now results in grain size returning to 1 mm.

The subsequent apparent growth of grains with increasing  $Q$  above about 20 is thought by Greer (2002) to be the result of the special effect of Si in ‘poisoning’ the grain refinement action of Ti at Si contents over 3%. The higher  $Q$  data are defined only by alloys with Si contents above 3%. For other solutes at high  $Q$ , particularly Cu, it is thought that the grain size remains small. Anyway, it seems that the attainment of fine grain size in Al–Si casting alloys has fundamental limitations, the attainable sizes being 5–10 times larger than those in some other casting alloys and in most wrought alloys.

Sigworth and Kuhn (2007) report practical tests in Al–Si, Al–Si–Cu, Al–Cu, Al–Mg, and Al–Zn–Mg alloys. They find a more confusing overall picture in which the grain-refining response is different for each alloy system. With today’s powerful Al–Ti–B refiners, they suggest there is no reason for large additions of soluble titanium in most alloys. In fact, they suggest it is more accurate to

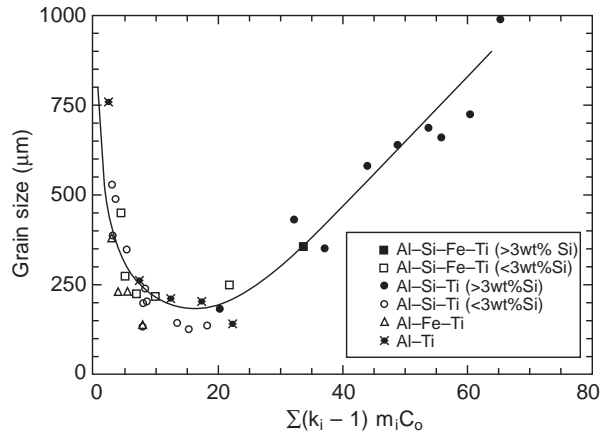


**FIGURE 6.8**

Effect of the growth restriction factor on the grain size of various Al alloys (Greer 2001)

consider that we grain refine with boron, not titanium. The recommended addition is 10–20 ppm of boron, preferably in the form of Al–5Ti–1B or Al–3Ti–1B rod. Lower dissolved titanium levels provide better grain refinement and an improved resistance to hot cracking in some alloys.

However, copper-containing Al–Si casting alloys are the exception in their work. In alloys such as 319 or 355, they find it is best to have a minimum of about 0.1%Ti, which is of course in line with our earlier discussion in this section, but Chen and Fortier (2010) recommend that Ti should be near but not exceed 0.10% for all Al–Si alloys (see also Section 5.2.2). Clearly, we still have much to learn about optimizing grain refinement.

### ***Melt cleaning by grain refinement***

We cannot leave the subject of grain refinement without adding a major caution to the reader. It is certain that the grain-refining additives act to precipitate and grow on oxide bifilms, which then become heavy and sediment to the bottom of the melt. The newly cleaned melt will then result in castings with improved properties. If the sediment is stirred in an (unfortunately misguided) effort to maximize the amount of grain refiner transferred to the casting then the bifilms with their precipitates of titanium-rich compounds will enter the casting, and properties are likely to be impaired. Thus it must be kept in mind that the major benefits of grain refinement are usually only marginally or even negligibly associated with the refining of grains, but everything to do with the cleaning of the melt from oxide bifilms. This important aspect is discussed more fully in Chapter 9 on properties.

Other nucleation and growth effects are happening during the solidification of many Al alloys as a result of the many solutes that are present, both intended and unintentional.

### **6.3.4 DAS and grain size**

In Figure 5.36 we can see the close link between freezing time and DAS, and in Figure 2.47 the close link between DAS and improved tensile properties. This is the reason, of course, for the strong motivation to chill castings to increase their strength and ductility.

In general, DAS is controlled by freezing rate alone (alloying has a minor effect that can be usually ignored). However, there is an interesting benefit to DAS from the action of grain refinement in removing bifilms from suspension. This occurs because the thermal conductivity of the melt increases when the bifilm barriers to heat flow are removed. Thus heat can be extracted more quickly from the casting, and DAS is consequently reduced.

In contrast, grain size is controlled mainly by the chemistry of grain-refining additions, plus any mechanical action that will fragment grains, leading to an effect sometimes called grain multiplication. The combined and contrasting effects of DAS and grain size on mechanical properties are dealt with in Chapter 9.

### 6.3.5 Modification of eutectic Si in Al–Si alloys

The *modification* of Al–Si alloys is the refinement of the Si eutectic phase by the addition of a small amount of a *modifier* such as Na or Sr. Figure 6.9 illustrates the dramatic change in structure which can be achieved.

When Al–Si alloys are solidified the eutectic silicon is seen on polished sections to consist of coarse, sharp-edged plates (Figure 6.9a). These have usually been thought to be detrimental to mechanical properties, being assumed to act as crack initiators. For this reason, for alloys containing above about 5–7%Si, the addition of sodium or strontium to the melt has been favored to refine the eutectic silicon phase, converting, as if by magic, the coarse Si flakes into an attractively fine eutectic (Figure 6.9b). Modification usually benefits the mechanical properties. However, life is rarely so simple. This straightforward scenario is beset with contradictions and complications. We shall try to unravel some of these problems here as a salutary and instructive exercise in the influence of bifilms on behavior of melts and cast products. The patience of the reader is requested while we plow through what appears to be an essentially simple mechanism, but clouded by a long history of misconceptions.

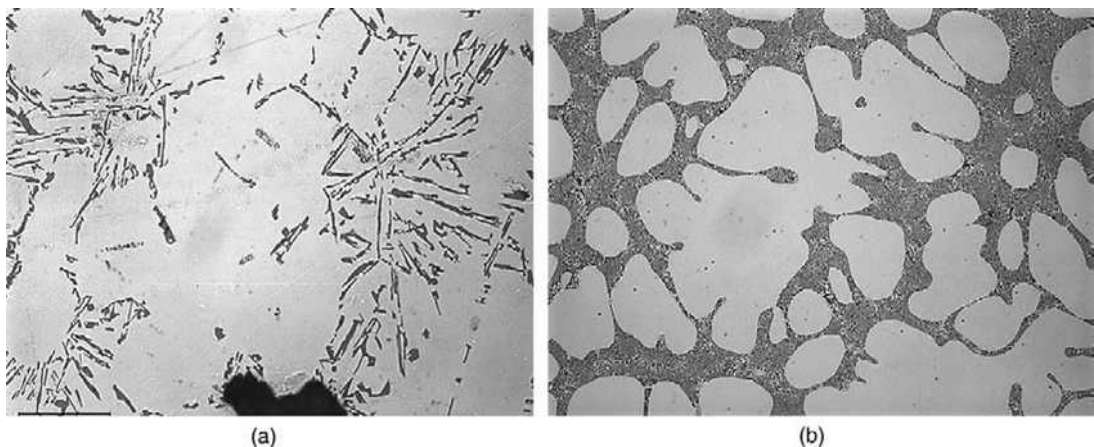


**FIGURE 6.9**

(a) An unmodified Al–Si eutectic in Al–7Si alloy; (b) the alloy modified by Sr addition.

### ***Hypereutectic Al–Si alloys***

In *hypereutectic* Al–Si alloys the primary silicon forms as compact polyhedral shapes. Here the nucleant is most definitely an aluminum phosphide, most probably AIP (although there is the possibility that the nucleus is actually  $\text{AlP}_3$  as suggested by Dahle and co-workers (2008)). The particle has an epitaxial relation with Si as is clear from the images recorded by Arnold and Presley in 1961 (Figure 6.10).

The study by Cho (2008) confirms that an aluminum phosphide (assumed here for simplicity to be AIP) is the preferred nucleant for Si, suggesting that when P is added to be present in sufficiently high concentration the AIP probably nucleates homogeneously in the melt. As small particles, the precipitating Si can wrap completely around them, therefore taking up a compact form.

However, of course, at the same time the presence of a copious quantity of oxide bifilms will ensure that plenty of AIP particles will also precipitate on these bifilm substrates. The Si that precipitates on the nuclei attached to the oxides will not be able to wrap around completely, since at least one side of the AIP will be firmly in contact with the oxide bifilm. Thus the Si will wrap around as far as it can, but subsequently proceed to grow out along the bifilm, straightening it somewhat during its progress, and thereby progressively reducing mechanical properties. It seems that the oxide bifilm is not a sufficiently good substrate to encourage nucleation of the Si phase (although it seems just possible that this may occur if P concentration is sufficiently low), but contact with the Si reduces the overall energy of the combination sufficiently to encourage growth. The final alloy microstructure is now mixed, with some Si forming as particles wrapped around free-swimming AIP particles but much Si continuing to grow as plates on the substantial population of bifilms. This is typical of a hypereutectic Al–Si structure. Figure 6.11c shows the compact primary Si particles with surrounding Si primary platelets.

Please take note of this new observation that appears to be an important universal principle for new phases that grow freely in the liquid: *the new phase takes on the morphology of its substrate*. This disarmingly simple principle helps to explain many features of cast microstructures. Thus primary Si can adopt two quite distinct forms:

- (i) a compact polyhedral particle when it grows on AIP particles, and
- (ii) a plate-like form when it grows on planar features such as bifilms.

(We shall see similar behavior in other intermetallics and in the Fe–C eutectics.)

### ***Hypoeutectic Al–Si alloys***

Part of the action of modification was first explained by Flood and Hunt in 1981. They interrupted the solidification of unmodified and Na-modified Al–Si eutectic alloy by quenching part-way through solidification to study the form of the growth front. Sections of their castings are seen in Figure 6.12. In the case of the unmodified alloy they found the growth front appeared ragged, with some nucleation of eutectic phase apparently ahead of the freezing front, but after the addition of sodium, a smooth planar growth of the eutectic front was found. The effective length of solidification front was now a factor of 17 times shorter than the irregular front. Thus for the same given quantity of heat extracted by the mold over a given area, Flood and Hunt suggested that the interface in the case of the planar front would advance 17 times faster, and therefore have a much finer structure than the unmodified alloy.

The smoothing action of Na on the eutectic front has been confirmed by Crossley and Mondolfo (1966). In their excellent thoughtful, classical paper they conclude that AIP as a nucleant is



**FIGURE 6.10**

(a) Primary Si particles nucleated on AlP showing the clear crystallographic relationship (Arnold and Presley 1961); (b) the aluminum phosphide particle nucleating on an oxide bifilm. The subsequent nucleation and growth of Si straightens the bifilm, effectively extending and flattening the crack, thus reducing properties in this unmodified condition.

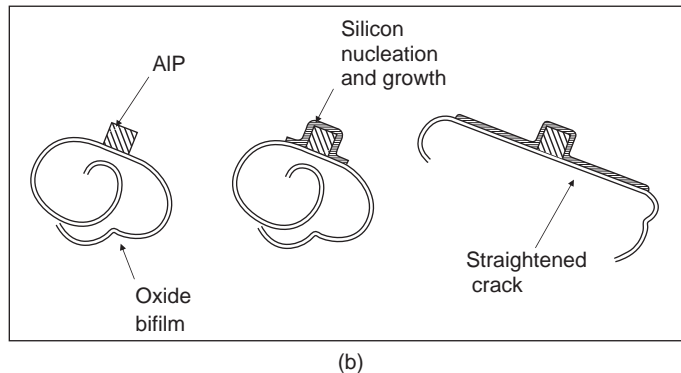


FIGURE 6.10 (continued).

neutralized, and observe that instead of Si crystals taking the lead in the freezing of the eutectic in unmodified alloys, after modification, Al dendrites take the lead. This clear thinking and accurate reporting was well ahead of its time.

Interestingly, in contrast with the *planar* front resulting from the Na addition, the form of the freezing front for the Sr-modified eutectic alloy is usually *cellular* in the freezing conditions commonly found in castings. This fairly smooth modified front has been studied by Anson et al. (2000). The intermediate (cellular) condition between extremely ragged (roughly dendritic) and perfectly smooth explains the intermediate performance of Sr. The cellular pattern is seen occasionally on the surface of Sr-modified castings that have suffered some degree of poor feeding, encouraging the loss of some residual liquid from around the cell, and so giving slight depressions on a cast surface that outline the cell boundaries (Figure 6.13).

This smoothing of the solidification front by Na to give a uniform and strong casting skin is used to good effect in most gravity die casting (permanent mold) shops. As the operator takes each casting from the die, he will check it for any sign of the drawing-in of the casting surface at a hot spot. This local collapse occurs because of the sucking-in of the surface that in places will have liquid near to the surface as a result of the ragged form of the freezing front, thinning and weakening the outer surface of the casting. On finding such a 'draw' or 'sink' the operator will add sodium to the melt. The local collapsing of the surface is instantly cured, only to return some time later, after the sodium has evaporated from the melt. However, the operator is watching for this event, and when he judges that a sink has become almost unacceptable, he adds sodium once again, straightening the freezing front and thus strengthening the solidifying wall of the casting, and the surface perfection is renewed.

The cellular structure of the front may lead to problems of feeding Sr-modified castings as suggested by McDonald and co-workers (2004). The cellular growth creating possible feeding problems is contrasted with the smooth front resulting from modification by Na. Surface-initiated porosity is favored by modification with Sr because of weak patches of the casting surface between the cells, whereas modification with Na creates a smooth, uniformly strong cast surface.

Flood and Hunt appreciated that the ragged interface in the unmodified condition could be explained by nucleation of silicon ahead of the general solidification front, but they admitted that the nature of the nucleus was at that time unknown.



(a)

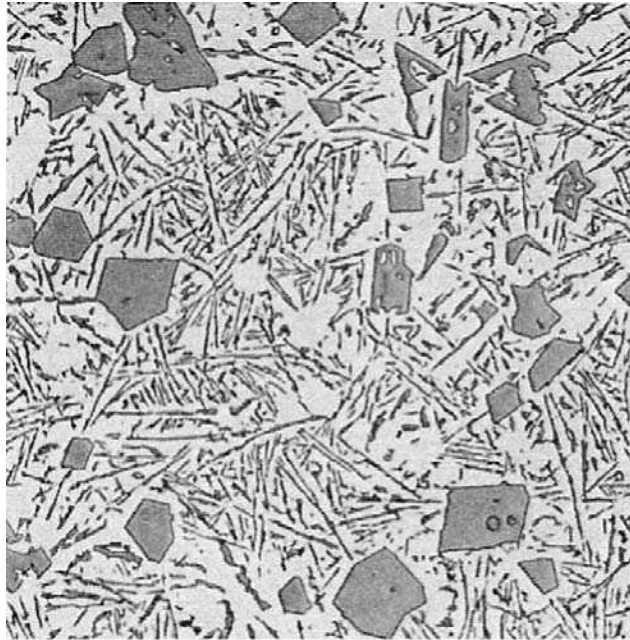


(b)

**FIGURE 6.11**

(a) The microstructure of a hypereutectic alloy, showing a mix of primary particles and unmodified eutectic silicon with relatively few AIP nuclei. (b) The cracks associated with growth on oxide bifilms can be clear, especially if solidification occurs unfed or with high hydrogen. (c) The hypereutectic alloy modified with additional phosphorus, as can be seen from the AIP nuclei in the centers of refined primary particles.





(c)

FIGURE 6.11 (continued).

### ***Nucleation of Si***

The paper by Cho and co-workers (2008) on the effect of Sr and P on Al–Si alloys presents excellent experimental data, confirming the nucleation of Si on AlP nuclei. However, the authors overlook the probability that the phosphides will themselves nucleate on oxide bifilms (in common with many other intermetallics that appear to favor precipitation on oxide bifilms). In this case, if Si particles now form on the phosphides as illustrated in Figures 6.10 and 6.11c, then the subsequent continued growth of the Si will naturally follow the oxide substrate on which the phosphide particle is sitting, illustrated schematically in Figure 6.10b.

Although at this time these authors dismiss the possibility of a double oxide substrate because no central crack can be discerned in the particles (as in Figure 6.11b by Ghosh and Mott (1964)), it has to be kept in mind that the central crack will only obligingly reveal itself if opened by shrinkage or gas. In a well-fed and well-degassed sample the crack will remain firmly closed, and essentially invisible, as in Figure 6.11a. It may appear mischievous to make an apparently perverse recommendation for the use of deliberately poorly fed castings for such research to make bifilms clearly identifiable, but it would help to clarify many issues. (The alternative use of higher gas levels to open and reveal bifilms will be less reliable because of the difficulty of control of hydrogen levels, and the rapidity of the changes of hydrogen content as a result of its rapid rate of diffusion either in or out of the sample. The use of shrinkage pressure to open bifilms is subject to fewer uncertainties.)

A potentially important observation can be discerned in Figure 6.14a in the paper by Cho and colleagues (2008). A transmission electron microscope (TEM) image of P-rich particles surrounded by

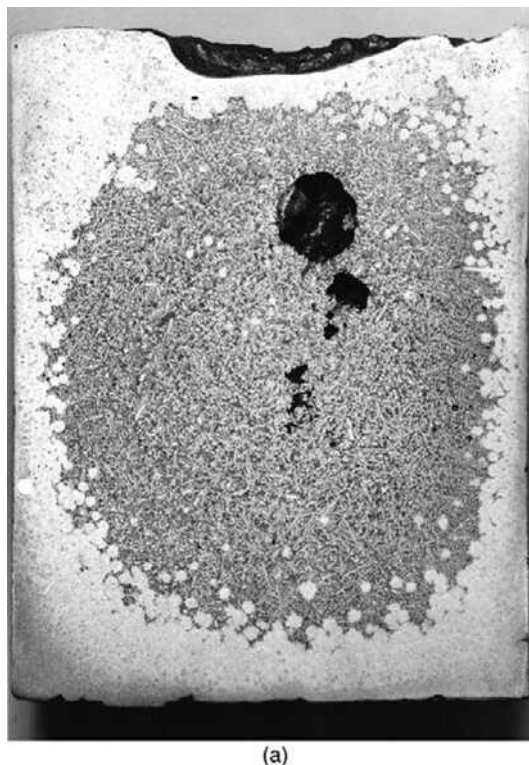


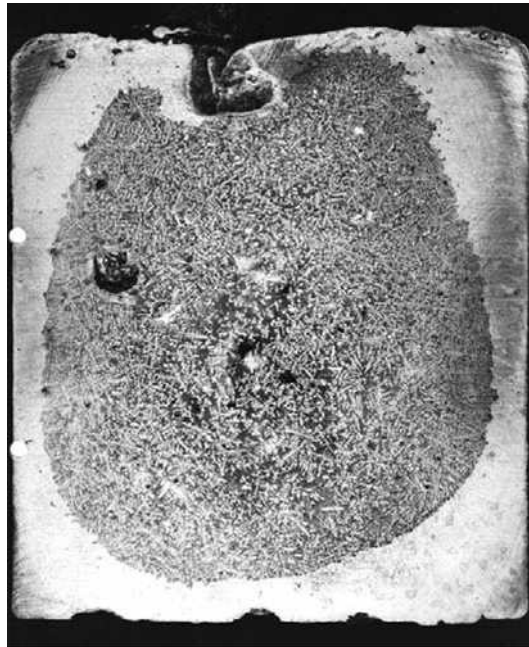
**FIGURE 6.12**

(a) A laboratory sample of unmodified Al-12Si alloy showing nucleation of eutectic ahead of the general solidification front; (b) the alloy modified with Na, showing suppression of nuclei in the melt, resulting in the advance of a planar solidification front (Flood and Hunt 1981).

$\text{Al}_2\text{Si}_2\text{Sr}$  are significantly, perhaps, arranged on an impressively straight line. This has all the hallmarks of being an oxide bifilm. This is an interesting possibility since bifilms are rarely imaged successfully in the TEM. The line is also characterized by fine pores (probably fragments of the interior unbonded interface of the bifilm) and by clear discontinuities in the strain bands, as would be expected across the plane of a crack. Since the original AIP precipitates occur prior to the general solidification of dendrites it is suggestive that the alignment is the result of the AIP particles having formed on the planar substrate of an oxide bifilm (corroborating the increasing evidence that nearly all intermetallics seem to favor formation on oxide bifilm substrates).

An optical image by Pennors (1998) from a quite different study shows a line-up of AIP particles on a bifilm, implied by Figure 6.14b. The presence of the beta-Fe particle implies the prior location of an oxide bifilm. One can infer that the beta-Fe particle occupies one side of the bifilm and the AIP particles occupy the other.

In many Al-Si alloys, P is already present in small concentrations. Because of the relatively low concentration of P, no free particles of AIP would be expected apart from those already precipitated on



(b)

FIGURE 6.12 (continued).

bifilms, favoring the subsequent growth of Si on bifilms, thus forming the typical plate-like primary Si particles that we know as the *unmodified* Al–Si structure (Figure 6.9a).

However, Cho (2008) finds that AIP can be deactivated (i.e. poisoned) by the addition of Sr to the melt; the mechanism of deactivation being the precipitation of  $\text{Al}_2\text{Si}_2\text{Sr}$  on its surface. Thus all the microscopic nuclei of AIP attached to bifilms would then be deactivated, preventing any formation of Si on bifilms.

(I had originally thought that the bifilms acted as nucleating substrates, and the addition of Sr or Na caused modification by deactivating the bifilms as nuclei. However, the finding by Cho that the precipitation of  $\text{Al}_2\text{Si}_2\text{Sr}$  on AIP causes the deactivation of the AIP nucleant now appears to me to be convincing. Thus the concept of a hierarchy of nucleating substrates, first AIP, then oxide bifilms, then some lower-temperature nucleus for the eutectic, now requires to be modified since bifilms appear to act only weakly or not at all. Nevertheless, of course, the bifilms remain as important growth substrates.)

When sufficient Sr has been added so there are no longer phosphide nuclei or oxide growth substrates that can operate to form Si particles or plates, a third process now comes into play. Si is forced to grow as a eutectic, probably nucleated on a boride such as CrB as suggested by Felberbaum and Dahle (2011), in the regions of significant undercoolings on or near the mold walls or near the melt surface. The Al–Si eutectic now grows as a coupled eutectic at an even greater undercooling (compared with phosphide or oxide-supported growth) as has often been observed (for instance Glenister and Elliott (1981)).

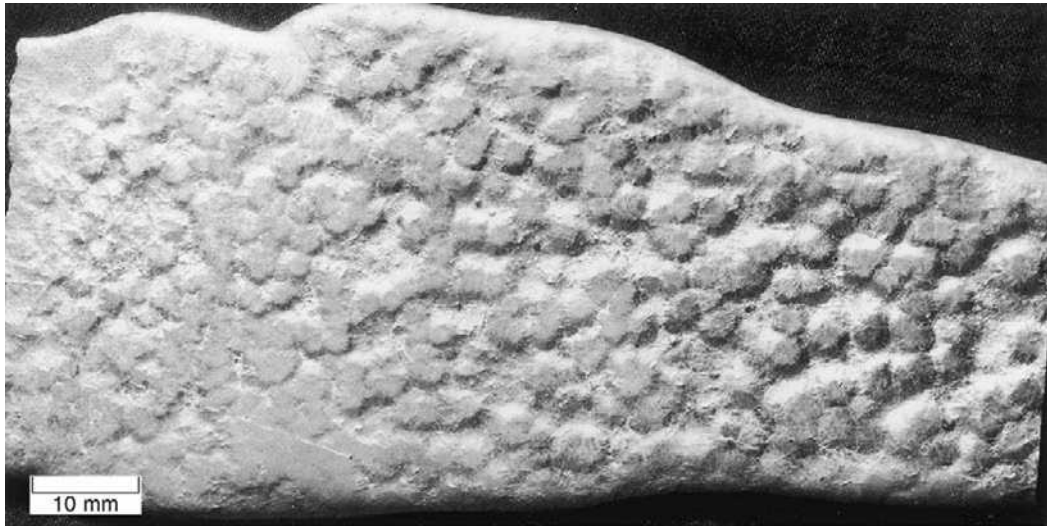


**FIGURE 6.13**

Thin casting of Al-7Si alloy modified with Sr, its unfed condition reveals its cellular growth form.

### ***Al-Si phase diagram***

The scenario can be described in terms of the Al-Si phase diagram in Figure 6.15. For normal melts of Al-Si alloys, which would all be expected to contain a generous population of bifilms, the eutectic freezing point would be  $577^{\circ}\text{C}$ , and the growth of the Si particles would follow the bifilms, forming large irregular plates. Interestingly, the eutectic composition appears to be not well defined, as might be expected with the melts freezing on rather variable, uncontrolled substrates. The diagram is based on the composition being 11.5%Si, although other works (Brandes and Brook 1992) suggest 12.6%Si. This unmodified eutectic is marked 'U' in the figure.

On addition of Sr, deactivating the AlP nuclei on the bifilms by coating them with  $\text{Al}_2\text{Si}_2\text{Sr}$  causes the melt to undercool to the point at which the modified eutectic forms at point M. This point is located at  $14.5 \pm 0.5\%$ Si, as identified from the maximum fluidity clearly recorded many studies of fluidity of modified Al-Si alloys (see Chapter 3), indicating an undercooling in the region of  $28^{\circ}\text{C}$ . This figure is subject to significant uncertainty because of the uncertainties in the compositions, and might therefore have a value somewhere between extremes of about  $12\text{--}33^{\circ}\text{C}$ . Whatever its exact value, it is a significant undercooling. In thermal analysis techniques, undercooling is used to monitor the effectiveness of a modifying addition.

As an aside, it is probable that non-modified Al-Si alloys would also record a maximum fluidity in the region of 14.5%Si because the bifilms will be compacted during this period of rapid flow, and will have little time to unfurl in the fairly rapid freezing associated with a fluidity test casting.

Although the reader with scientific interests will know that eutectic growth has been assumed to occur in a regime below the liquidus, or the extrapolation of the liquidus, at some point in a region skewed to the right under point U, in view of the new form of the phase diagram in which two eutectics are now clearly separated, it seems likely that eutectic growth actually takes place in the region MAB

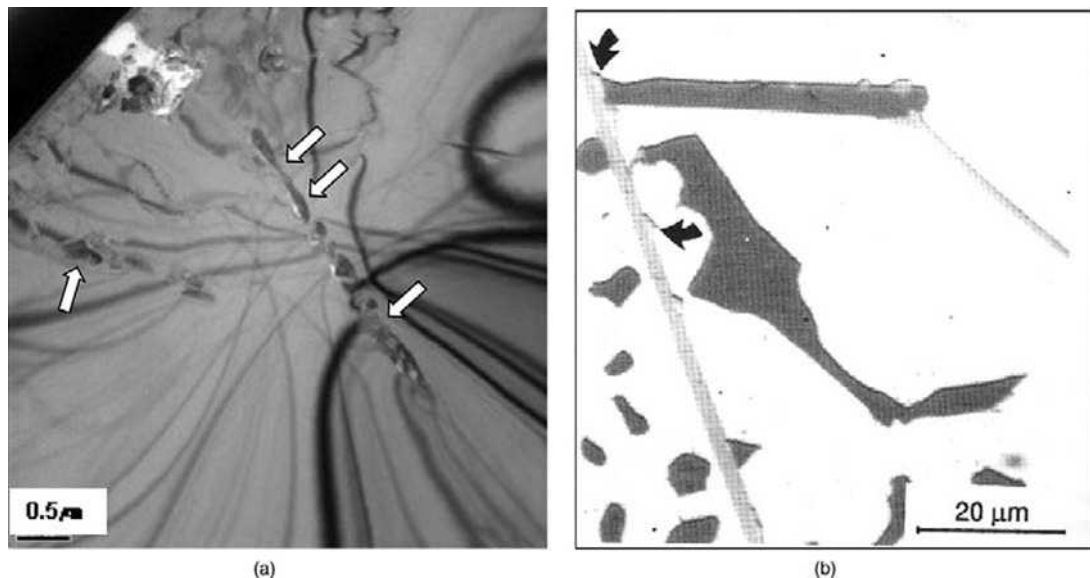


**FIGURE 6.14**

(a) TEM image by Cho (2008) of  $\text{Al}_2\text{Si}_2\text{Sr}$  phase containing P-rich particles (arrowed) and (b) SEM image by Pennors (1998) showing a row of AIP particles (arrowed) apparently on a  $\beta\text{-Fe}$  particle (courtesy of F H Samuel 2009).

which is simply under both liquidus lines. No complex argument to explain a skewed region may be necessary.

The consistent picture that emerges is of a succession of nucleation and growth processes operating at progressively lower temperatures. Summarizing:

- (i) With adequate P addition, AIP particles may form freely in the melt, and will nucleate Si particles (Figures 6.10 and 6.11c).
- (ii) At the same time (and at more normal lower P concentrations) AIP particles will nucleate on oxide bifilms if present in suspension in the melt. These will form a favored growth substrate for Si (Figures 6.10b, 6.11c), the growth starting at the AIP particle on the film; the eutectic freezing at U.
- (iii) The addition of Sr coats the AIP nucleus with  $\text{Al}_2\text{Si}_2\text{Sr}$  and deactivates its nucleating potential. Such a surface mechanism, concentrating the action of the modifier onto microscopic areas, would explain why only parts per million of Sr in solution can be effective.
- (iv) Thus neither AIP nor bifilms can operate to nucleate Si particles or grow Si plates. The melt will continue to cool without precipitation of Si until a new nucleus finally becomes effective to nucleate the eutectic phase at M. Felberbaum and Dahle (2011) find that borides such as CrB can nucleate the eutectic. The eutectic grows cooperatively with the Al phase on a substantially planar front (if modified with Na as in Figure 6.15b) or on a cellular front (if modified by Sr) (Figure 6.16). The Si now takes on the form of a fine, fibrous eutectic seen

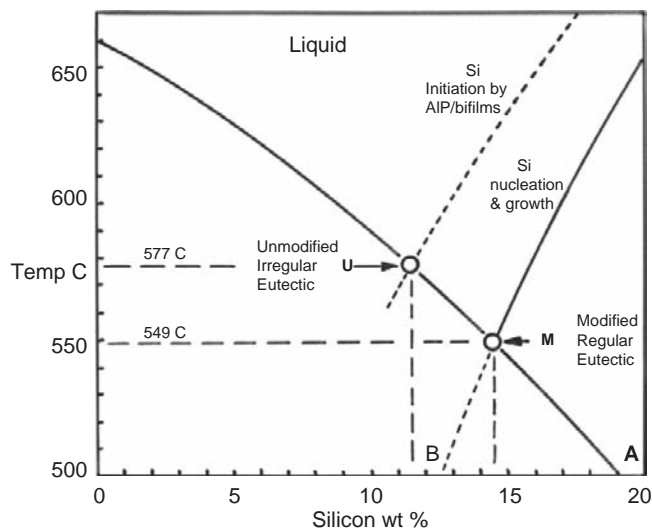


**FIGURE 6.15**

The Al-Si phase diagram showing the two eutectics, one at high temperature forming Si platelets on bifilms in suspension in the liquid; the other at low temperature as a classical coupled eutectic.

deep-etched in Figure 6.17 and in its more familiar optical micrographic structure as a fine, rod-like eutectic phase (Figure 6.9) that we know as a *modified* structure.

For (iv), after modification by the addition of Sr or Na, the Si can now no longer form at high temperature in the liquid and is now nucleated at a much lower temperature to grow as a fine, fibrous eutectic, the inter-phase distance being controlled by diffusion in the liquid, which we call a 'modified' structure. A feature of all such eutectics that contain a phase that grows in a crystalline, faceted fashion is that the phase wishes to grow in a single direction, but is forced to continuously modify its growth direction because of the close proximity of its neighbors. The result is a fibrous, 'coral' structure resulting from the necessity to continuously generate growth defects, usually twins (Figure 6.17). Thus such eutectic phases will naturally be expected to contain a high density of twin and other defects. This has been often reported, for instance as described by Steen and Hellawell (1975) and Song and Hellawell (1989), and in the absence of other explanations was once thought to explain the phenomenon of modification, even though no-one could quite understand why. Contrary to all previous authors, we can conclude that the high density of growth twinning is not a *cause* of the coral morphology but a natural *consequence*. The heavily twinned coral structure contrasts with the internal perfection of the primary crystals that grow freely, unrestricted in liquid ahead of the front.

This final change from (ii) formation as coarse plates on oxides freely suspended in the melt to (iv) growth in undercooled liquid (often from the highly cooled liquid against the walls of the mold) as a finely spaced eutectic appears to be the process we call 'modification'.

Note that the eutectic is a continuously growing phase, thus although its nucleation site is not currently known, its main distinguishing feature is its *continuous growth* leading to the development of



(a)

**FIGURE 6.16**

(a) Growth front of the high-temperature unmodified Al–Si eutectic showing Si growth as platelets in the liquid phase; (b) the relatively compact planar front of the modified alloy growing as a classical coupled eutectic (courtesy of Shu-Zu Lu and John Hunt 2010).

*continuous lengths* of branching coral of Si. It grows as a ‘classical’ eutectic. It contrasts with the discontinuous growth of irregularly sized platelets on uncontrolled bifilm substrates.

Formation mechanisms (i) to (ii) explain the plate-like morphology and comparative crystallographic perfection of plate-like Si, since at this stage of growth Si follows the extensive planar substrates which are sufficiently flexible to provide minimum mechanical constraint, so that the crystal grows essentially freely in the liquid. The mode of deposition of Si contrasts with those morphologies that emerge at higher temperatures such as plates, which are essentially separate particles. The growth of hypereutectic Si on AIP nuclei is another example of separated growth on particulate substrates. The eutectic morphologies that grew separated and necessarily not crystallographically related have been traditionally known as *irregular* or *anomalous* eutectics in contrast to *regular* or *normal* eutectics. The first has second-phase particles that are irregular, whereas the normal eutectic, being controlled by diffusion, is highly ordered and predictable.

### ***Practical application of Sr modification***

In practice, the choice between the use of sodium or strontium for modification depends on the circumstances. The sodium is usually lost fairly quickly from a melt as a result of evaporation



(b)

FIGURE 6.16 (continued).

because the sodium is close to its boiling point. For instance, for a 200-kg crucible furnace an Na addition is lost within a time of the order of 15–30 minutes. Strontium, on the other hand, is a normal, stable, alloy in liquid Al alloys. Although it is slowly lost by oxidation at the surface, and sometimes can soak away into refractory furnace linings until they saturate, the alloy will usually survive several remeltings.

The addition of strontium to the melt is an expensive option, but is taken in an effort to improve the ductility of the alloy. However, the results are not always straightforward to understand, and are accompanied by a number of problematical factors.

#### ***Effect of modification on mechanical properties***

The precipitation and growth of Si on the originally crumpled and compact bifilm will force the straightening of the bifilm because the Si, as a diamond cubic lattice, has a distinct favored growth morphology, taking on the form of a plate. This is the reason that unmodified alloys are generally associated with poor properties, because the Si has become attached to the bifilm, so that its planar growth necessarily straightens the bifilm, forcing them to unravel, unfolding them to become serious planar cracks that can lower properties. The Si particle has always been assumed to be brittle, but the observed cracking behavior is certainly associated with the presence of their internal bifilm cracks incorporated during their growth.



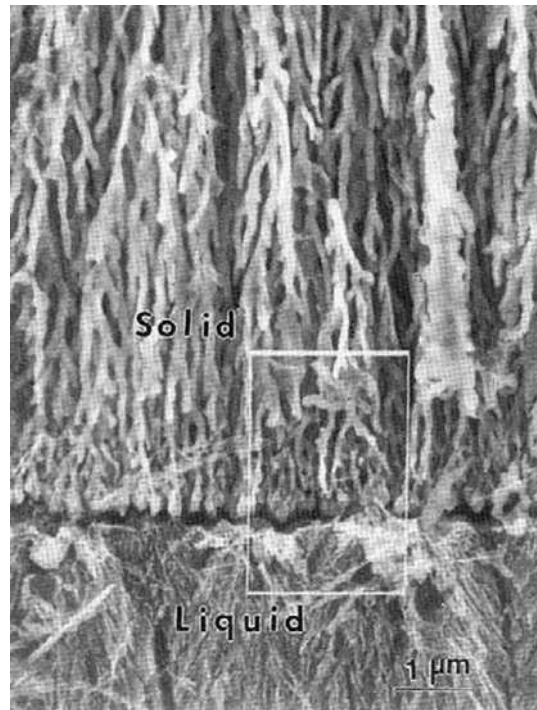


**FIGURE 6.17**

A magnified image of a quenched interface of the coupled eutectic (growing downwards in this image) illustrating the typical coral form of the silicon.

If the bifilms in the liquid no longer act as substrates, they are no longer straightened, and remain in their original, crumpled, compact state. Because the defects now remain compact, the mechanical properties remain reasonably high. This appears to be the mechanism whereby modification tends in most cases to improve mechanical properties. To re-state this conclusion in different words, modification appears only to raise the properties of those alloys whose properties are already low because of the presence of compact oxides, but are lowered further by the growth of unmodified Si. Modification is a technique for avoiding the worsening of poor properties. We shall discuss the considerable evidence for this later.

### ***Sr modification and porosity***

Much confusion has existed over whether strontium can be successfully added without the deleterious effect of hydrogen pick-up. Amid the confusion, the hydrogen already in solution in the strontium master alloy addition has often been blamed for this problem. However, we can, with some certainty, dismiss this minute source as negligible. What alternative possibilities remain?

Some have doubted that Sr leads to any increase in the gas content of Al–Si melts. However, there are good fundamental reasons why Sr would be expected to lead to an increase in hydrogen in the melt,

given the correct conditions of water vapor or other sources of hydrogen in the immediate environment. The enhanced reactivity of Sr will lead to enhanced reaction with environmental water vapor, leading to the oxidation of Sr and the release of hydrogen into the melt (Equation 1.2).

Even so, it is certainly the case that some foundries experience no problems because they happen to enjoy conditions for minimal uptake of hydrogen because of multiple factors:

- (i) low hydrogen content, usually associated with low humidity, of the local environment of the melt;
- (ii) protection of the melt from its environment (as for instance in an enclosed low-pressure casting unit);
- (iii) when undisturbed, the melt may continue to be protected from the environment by its oxide and create little additional surface oxide by reaction with water vapor or hydrocarbon gases with the associated release of hydrogen. Dennis and colleagues (2000) found that Al-7Si-0.4Mg alloy with 250 ppm Sr exhibited a short-term increase in the rate of oxidation, but over several hours exhibited a longer-term dramatic decrease in rate. Thus undisturbed melts will practically become inert, whereas melts subjected to disturbance of the surface will react rapidly. The stabilization of the oxide by moisture as seen in Figure 1.3 is a further factor to strengthen this behavior, although the continuous disturbance of the melt surface by continuous bubble degassing will undermine such benefits.

The elegant research led by Gruzleski (1986) and Dinayuga (1988) employed minimal disturbance of the surface of the melt, and so minimized pick-up of hydrogen, whereas Zhang et al. (2001) find a major uptake of hydrogen when regularly disturbing the surface by repeated sampling of their melt after Sr addition.

In an industrial furnace the stirring and ladling actions would be expected to fracture the protective oxide and so allow further reaction, encouraging the ingress of hydrogen in a furnace open to the atmosphere. In these conditions the addition of strontium will usually be accompanied by an increase in hydrogen content of the melt. The hydrogen naturally increases with increasing strontium content, temperature, time, and environmental water. This makes it practically impossible to add strontium without an increase in porosity in most foundry melting systems. In the experience of the author a single 0.05 wt% addition to a 1000-kg holding furnace caused the gas level to rise to such a high level that gas porosity caused the castings to swell, solidifying oversize because of their generous pick-up of gas, and had to be scrapped. It took three days of waiting for the melt to return to a castable quality. (The arrival of rotary degassing has, thankfully, eliminated such lengthy waits nowadays.) The absorption of hydrogen can, of course, be reduced by reducing the time available for absorption, for instance, by the casting of the whole melt immediately after the strontium treatment. Treating the strontium as a late addition in this way has been adopted successfully (Valtierra 2001).

Strontium is, however, generally used with success in low-pressure casting furnaces where the melt is transferred immediately after treatment into an enclosed furnace that excludes any environmental moisture. It may then be held indefinitely, provided that the pressurizing gas that is introduced into the furnace from time to time is dry or inert, and that the furnace lining is already saturated with strontium from previous additions.

So far we have examined the role of Sr in the increase in hydrogen content of the melt, leading to increased porosity. There appear to be additional factors at work.

A mechanism for the additional enhancement of porosity due to Sr has been put forward by Campbell and Tiriyakioglu (2009). Briefly, their argument is as follows: After an Sr addition, the bifilms are no longer favored substrates for the precipitation of Si. Thus the bifilms are no longer encapsulated inside the Si plates, but remain floating freely in suspension in the melt. These are now available for:

- (i) blocking interdendritic channels, reducing the permeability of the dendrite mesh practically to zero, as convincingly demonstrated by Fuoco and co-workers (1997, 1998) (Figure 6.18a). It is easily envisaged that piles of bifilms will be sucked into the dendrite mesh, where they will accumulate to block interdendritic channels. Furthermore, the bifilm at the base of the heap, experiencing the reduced pressure due to shrinkage, will open, effectively decohering from its other half because of its lack of bond, to create the start of a shrinkage pore (Figure 6.18b).

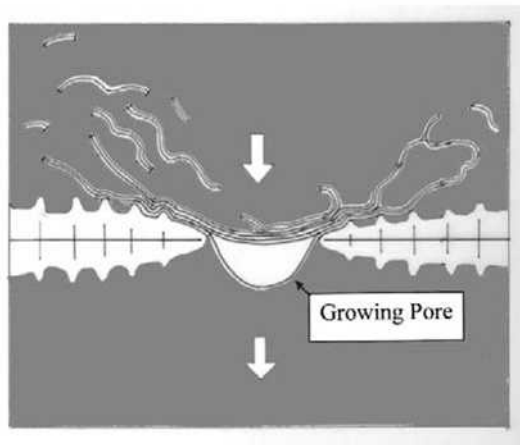
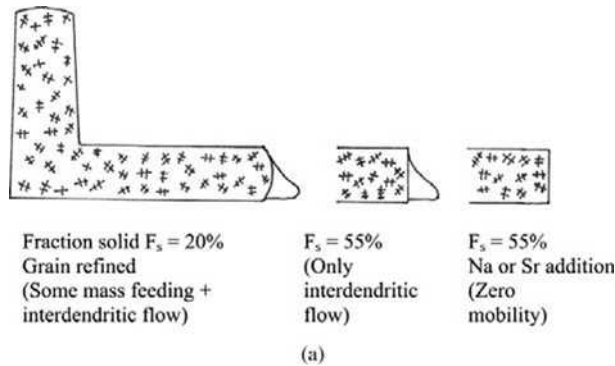


FIGURE 6.18

(a) Results by Fuoco (1997/8) revealing that the small amount of interdendritic flow at 55% fraction solid was completely stopped by eutectic modification; (b) the probable reason being the release of bifilms that would choke flow and have the potential to initiate porosity.

- (ii) The precipitation of hydrogen into the central crack, expanding the bifilm into a pore (recall that pores are volume defects and cannot therefore be initiated by solidification alone; they have to be initiated from an entrainment defect such as a bubble or bifilm). Thus the freely floating bifilms can initiate the creation of hydrogen pores. Although they do not confirm this precise mechanism, Lui et al. (2003) affirm that oxides are responsible for pore formation in Sr-modified alloys. Zhang (2001) describes how fissure-like pores gradually swell to become rounded after Sr addition, effectively describing the expansion of relatively large bifilms by the absorption of gas. Other authors only report the development of rounded pores immediately after the addition of Sr, indicating that their population of bifilms had a distribution of much smaller sizes, and thus less evidently initiating as cracks.

These bifilm actions leading to impairment of feeding, leading in turn to shrinkage problems, and their effectiveness as initiation sites for both shrinkage and gas pores, simply add to the already serious uptake of hydrogen possible under some conditions as we have seen. Thus the association of porosity with Sr modification has many aspects which have confused and resisted attempts at simplistic explanations for many years. The above discussion, like much of foundry science, is seen to be non-trivial, and may yet be far from complete. It is hardly piety, but simply an admission that at times it is necessary to respect the natural complexity of the world.

Outside of the Al–Si system, the mechanism whereby Sr deactivates bifilm substrates for Si appears to be a standard mechanism applicable in other alloy systems. The approach explains for instance how the refinement of the structure of the Al alloys containing  $Mg_2Si$  precipitates is modified by the addition of lithium metal (Hadian 2009).

### ***Mixed experience with Sr***

It is possible that modification, with its fine structure of the silicon phase in the Al–Si eutectic, may have better properties than the coarse unmodified structure. There are many results of published work that cite the benefits to strength and ductility following modification which have been thought to be the result of the finer Al–Si eutectic. However, despite eutectic refinement, some researchers have reported only mediocre improvements. Some have reported no benefit. A few have reported reductions in properties. This confusion of experience requires some examination.

Different foundries require massively different levels of addition to achieve a useful measure of modification. This variable performance between foundries can be understood in terms of the deactivation by Sr of AIP and possibly oxide bifilms as favored substrates for Si. Those with higher residual P contents, or possibly greater surface area of oxide per volume of melt, will require more Sr for deactivation.

Conventional foundries might typically require 300–500 ppm Sr to achieve modification. This is the situation in many small foundries and research laboratories where the processing of the melt in small batches makes melt quality practically impossible to control. Furthermore, probably all castings and test pieces will have been cast under gravity, mostly using relatively poor filling system designs, and thus their material will be expected to be impaired with new oxide films. For such poor melt quality the action of Sr in preventing the straightening of a large proportion of the oxide bifilms is a major advantage, and benefits are likely to be experienced.

On the other hand, a good casting operation may achieve relatively low levels of oxides and so require treatment with much lower levels of Sr, perhaps in the region of 50 ppm.

For a more ideal casting operation, taking for instance the counter-gravity filling of sand molds to cast engine blocks, such a system may have very few new films because of the relatively quiescent handling, and the possibility of gentle counter-gravity filling. Using such a process Hetke and Gundlach (1994) found their castings suffered a reduction in strength and ductility after Sr addition, and porosity was significantly increased. Similarly, Byczynski and Cusinato (2001) re-confirmed this finding in the Cosworth Process foundry operated by Ford/Nemak in Windsor, Ontario. Almost certainly these near-ideal operations do not need to discourage the straightening of bifilms because there are few bifilms to straighten. In fact these better foundries find that Sr impairs the mechanical properties of their castings, almost certainly because, with no favorable effects of Sr, only its unfavorable effects are now experienced. Any increase in the hydrogen content would cause the few bifilms to open by hydrogen precipitation, thus suffering an impairment mechanism due to inflation (instead of the other impairment mechanism of crystallographic straightening) and so increasing microporosity, and reducing properties.

The pickup of hydrogen is more serious in sand foundries, as described above, because there is a significant influx of hydrogen from the sand binder during mold filling, and the slower solidification gives greater time for the inflation of the bifilms by hydrogen diffusion. The hydrogen level will rise during the flow of melt into the mold because of the reaction with the organic sand binder, in the same way that hydrogen increases in greensand molds as observed by Chen (1994). In heavy sections, there will be several minutes for the hydrogen to diffuse into the casting sections. From Figure 1.4a the coefficient of diffusion of hydrogen is seen to be close to  $10^{-6} \text{ m}^2 \text{ s}^{-1}$ . From Equation 1.5, for a typical time around 100 s the average diffusion distance for hydrogen in aluminum is close to 10 mm. Thus the gas will easily penetrate the thickest sections of castings such as automotive cylinder blocks. The degradation of the sand binder will always raise the hydrogen level at the worst moment, as the melt enters the mold.

In permanent mold foundries, the hydrogen influx from the mold is reduced (although it remains from any cores of course) and the time for expansion of the bifilms is reduced. Thus the significant disadvantages of Sr are greatly reduced, allowing the beneficial aspects to dominate. Thus Sr may now show a net benefit, and will particularly show a benefit if the melt has a poor quality (i.e. has a high residual P and high density of oxide bifilms). In this case, the amount of the addition will have to be sufficiently high to treat the melt as we have noted above.

In summary, the most likely explanation of the action of Sr is that most operators using poorly designed gravity filling systems will benefit because the new bifilm defects introduced by pouring are prevented from forming plate-like silicon particles. Some will enjoy a useful net benefit if the increase in hydrogen can be controlled. In contrast, those operators using a process such as the Cosworth Process will have few new films, and so will automatically achieve a high level of mechanical properties despite the automatically higher hydrogen level and longer freezing time in the sand mold. This high level of properties cannot be raised much further because there are practically no defects to deactivate, and will only suffer negatively from the problem of extra porosity. The refinement of the eutectic, much sought-after by metallurgists and assumed to be the main mechanism of property enhancement, appears to have little effect either way.

It seems inescapable therefore that the really important quality requirement should perhaps be the absence of bifilms. This means really clean metal and excellent designs of melt handling. If such conditions were achieved expensive additions of Sr would achieve nothing, and could be abandoned.

### ***Summary of the modification mechanism***

We can summarize the evidence, laying out the steps of the logic for the central role played by oxide bifilms; this is a long and detailed list of explanations of the different facets of the modification phenomena.

1. Bifilms are to be expected in our Al alloys because of the way our metals are handled in our cast houses and foundries.
2. The bifilm has two important morphologies; (i) a compact original state in which the bifilm has been crumpled by internal turbulence in the liquid, becoming a fairly harmless defect; and (ii) a later condition in which it may become straightened to become a serious planar crack.
3. All intermetallics studied so far (including Si, alpha-Fe, beta-Fe, and Mg<sub>2</sub>Si, etc.) appear to precipitate and grow on bifilms. The cracked morphology of the intermetallic cannot be explained by solidification (which is incapable of creating such volume defects because of the effectively unbreakably powerful interatomic forces that hold the melt, the solid, and the interfaces in close atomic contact). The cracks can only originate by entrainment mechanisms (i.e. introduced externally from the liquid), explaining their necessary association with bifilms.
4. The known nucleation sites for Si are AIP particles. The AIP nuclei are most likely formed on oxide bifilms.
5. The Si particles are intermetallic with a diamond cubic crystal structure that forces its growth morphology to take up a plate-like form, attaching to the bifilm and therefore straightening the crumpled substrate into a flat planar bifilm. Thus the central bifilm crack now takes on the form of a large flat crack that has a serious effect on properties. The rather straight cracks sometimes observed in the centers of primary Si and beta-Fe particles are thereby explained, together with the *apparent* 'weakness and brittleness' of these strong particles (see also later in Figure 6.19).
6. The dilute addition of Sr (or Na) deactivates the AIP as a favorable nucleant for Si, and may consequently also deactivate oxide bifilms as favored substrates.
7. Early and easy nucleation of Si particles on bifilms can no longer occur. Thus the bifilms remain in suspension in the melt in their crumpled form (they are no longer straightened out by the plate-like growth of Si) so that properties are not degraded.
8. Having removed the oxide bifilms as nuclei, the next available opportunity for Si to form is as a eutectic at a significantly lower growth temperature, possibly nucleating on particles such as CrB. The eutectic spacing is now controlled by diffusion, and so is significantly finer and controlled by the rate of heat extraction. Its coral-type morphology is a consequence of dense twinning, forced by the continuous change of direction of the Si fibers as a result of the constraint of neighbors.
9. The non-straightening of the bifilms (the retention of the bifilms in their original fairly harmless compact form) by the addition of Sr is expected to be the major benefit to mechanical properties, particularly increased strength and ductility. (The finer spacing of the eutectic is expected to be a minor contribution to any increased strength, as illustrated by the experiments of Cho and Loper (2000) who demonstrate with Bi additions how properties are unaffected by the modification of the structure of an A356 alloy.)
10. The addition of Sr has the potential disadvantage of increasing porosity in the casting. This effect is the result of (i) the enhanced reactivity of the melt, resulting in the danger of increased hydrogen pick-up in some circumstances; and (ii) the bifilms, no longer encased in Si, remain free-floating in the melt, where they can block interdendritic feeding and initiate porosity, although it is predicted that faster freezing and lower gas-content molds can reduce these disadvantages.

### ***Non-chemical modification***

The bifilm hypothesis would predict that perfectly clean Al–Si melts would be automatically modified without any necessity for additions. This is an interesting and testable proposition that appears in fact to have good support. Jian and colleagues (2005) used ultrasonics to drive bifilms out of suspension, causing modification without the aid of any chemical additions. Similar observations at the University of Windsor have been noted using electromagnetic stirring to centrifuge Al–Si melts clear of bifilms, producing a beautifully modified eutectic (Sokolovski 2002). Wang et al. (2007), using what appears to be extremely clean Al–Si produced by direct electrolysis, find that a fully modified structure can be retained up to 16%Si. Above this level of Si these authors find that primary Si is formed, but this does not seem to be a fundamental limitation, but was probably the result of the introduction of oxides because the additional Si was added using a master alloy containing 50%Si, which would be certain to contain generous quantities of oxide.

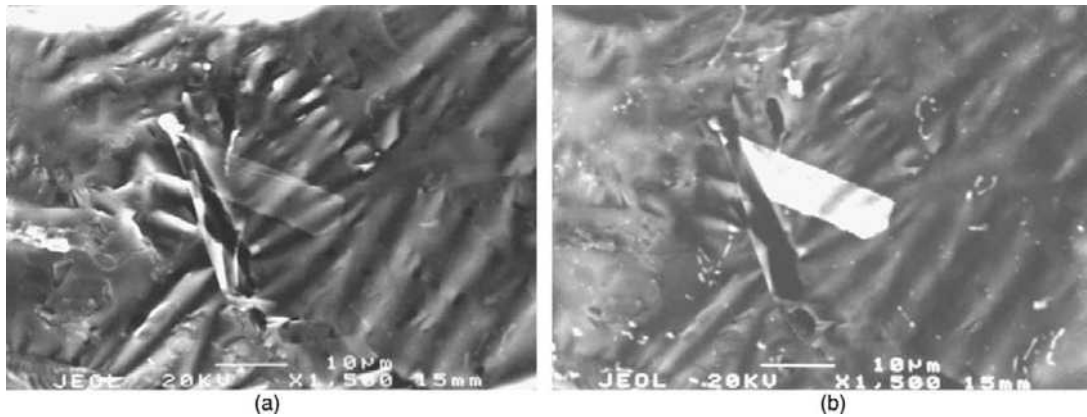
It seems true that for very clean Al–Si alloys primary Si will be unable to precipitate, and the structure will therefore be automatically modified without the intervention of Na or Sr.

### **6.3.6 Iron-rich intermetallics**

In addition to Si, it seems that most intermetallics also find oxides to be favored substrates for growth. The iron-rich intermetallics alpha-iron ( $\text{Al}_{15}\text{Fe}_3\text{Si}_2$ ) and beta-iron ( $\text{Al}_5\text{FeSi}$ ) are included in this list.

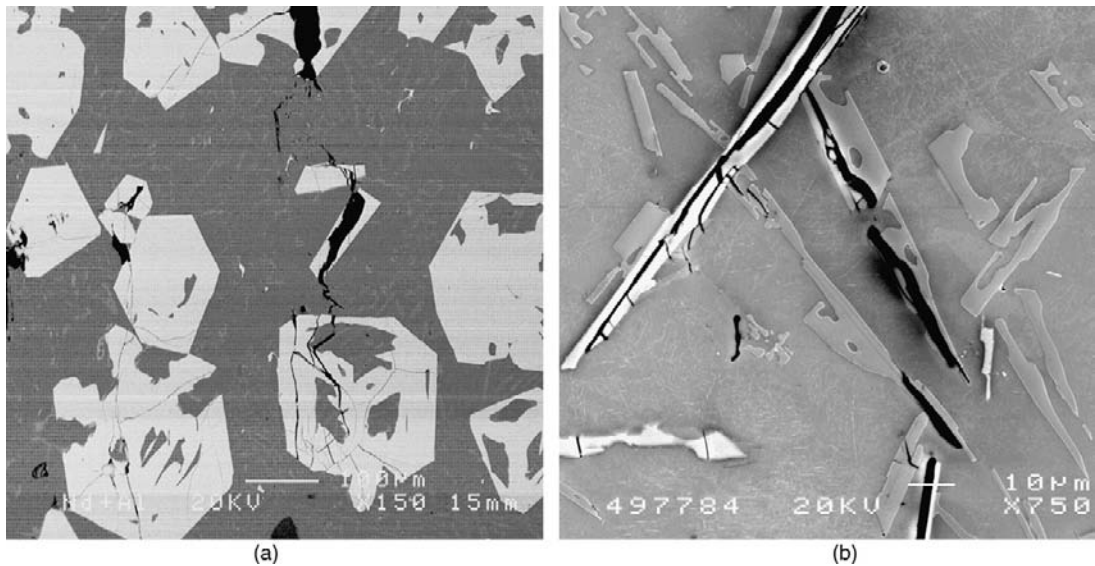
A number of authors have concluded that beta-iron first nucleates on AIP particles (Cho et al. 2008). If so, it would be expected, as in the case of Si nucleation, that the AIP particles would be already sited on oxide bifilms. Pennors and colleagues (1998) use elegant metallography to show AIP in a straight line, apparently attached to a beta-iron platelet (Figure 6.14b). Since the AIP appears to precipitate first, it seems reasonable to conclude that AIP must have aligned itself against a bifilm, since no other extensive planar solids are known to be present at that stage of solidification. The beta-iron will arrive later, sited on the other side of the bifilm, and so, perhaps, in no way connected to the AIP. It seems most probable therefore that both AIP and beta-iron form on bifilms, but these are independent and unrelated events. They only appear to be related when the AIP forms on one side of the bifilm and the beta-Fe forms on the opposing side; since the bifilm is usually not easily seen, it appears that the AIP particles are sitting on the beta-Fe.

Cao and Campbell (2000) discovered that  $\beta\text{Fe}$  plates in Al–Si alloys precipitated on the wetted outside surfaces of bifilms. Later work by these authors in 2003 indicated that a wide variety of oxide substrates might be effective, including  $\alpha\text{Al}_2\text{O}_3$ ,  $\gamma\text{Al}_2\text{O}_3$ ,  $\text{MgAl}_2\text{O}_4$ , and  $\text{MgO}$ . During the early stages of the growth of the precipitate, the  $\beta\text{Fe}$  particle is sufficiently thin that it can follow the folds of the bifilm. On a fracture surface the iron-rich phase can be clearly seen through the thin oxide film that represents one half of the bifilm (Figure 6.19). At this early stage it is faithfully following the undulations of the oxide film. However, as the  $\beta\text{Fe}$  particle thickens, the particle becomes increasingly rigid, taking on its preferred crystalline plate-like form, and so forcing the film to straighten. Finally, the bifilm is often seen as a crack aligned along the center of the  $\beta\text{Fe}$  particle (Figure 6.20b), or along the matrix–particle interface if the  $\beta\text{Fe}$  happened to nucleate only on one side of the bifilm (Figure 6.21). The cracks are not always seen because the individual halves of the bifilm are usually extremely thin, and are often tightly closed together. It usually requires some opening mechanism to come into play before the cracks are easily seen.



**FIGURE 6.19**

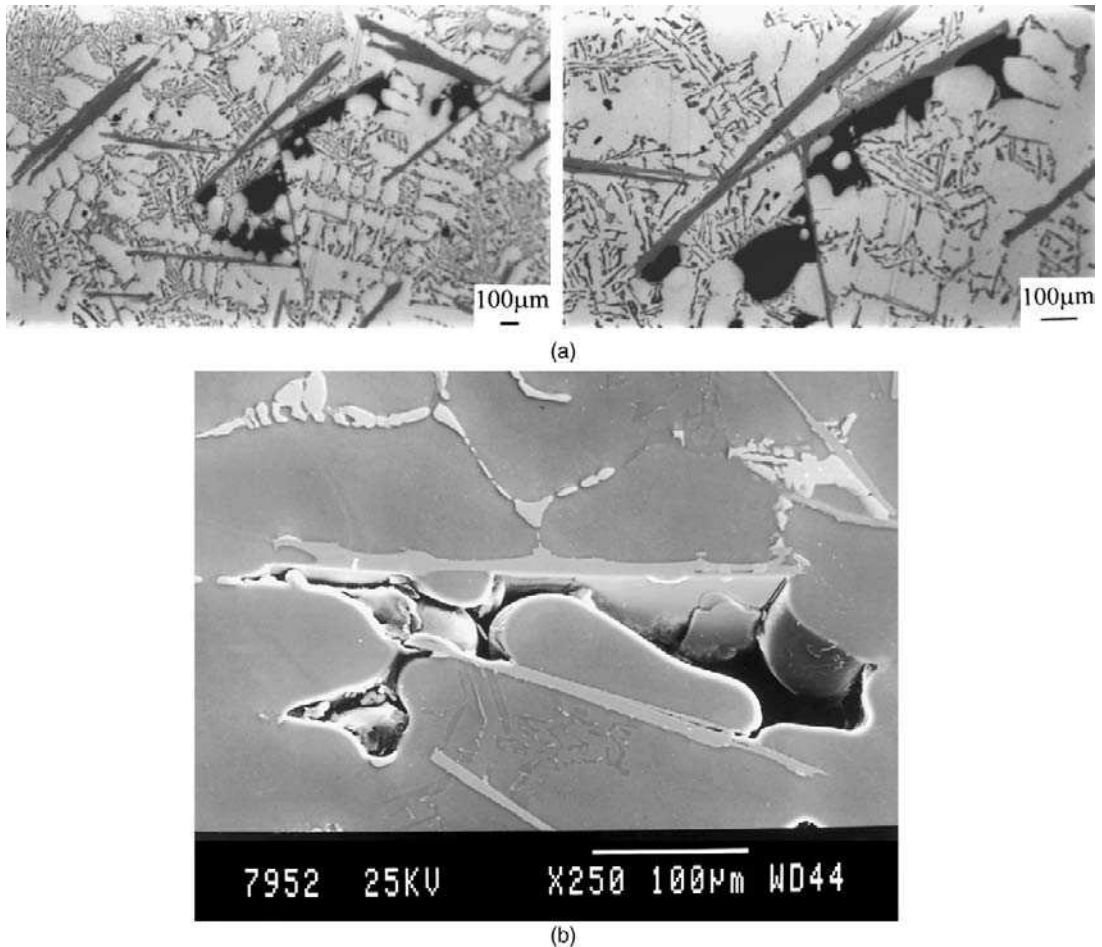
SEM image of an iron-rich particle nucleated on the underside of a thin alumina film imaged by (a) secondary electrons and (b) back-scattered electrons (Cao 2000).



**FIGURE 6.20**

Fe-rich particles in an Al-12Si alloy growing on oxide bifilms, showing (a) alpha-Fe with its cubic symmetry wrapping around and sealing in situ compact bifilms, thereby maintaining properties; and (b) beta-Fe with its monoclinic crystal structure, and silicon particles with their diamond cubic structure, growing as platelets, flattening bifilms, thereby straightening cracks and reducing properties (Cao 2000).



**FIGURE 6.21**

Platelets of  $\beta$ Fe showing pores opened by shrinkage or gas, initiated by the bifilm ((a) courtesy of Cao 2000; (b) courtesy of Samuel et al. 2001, Internat J Cast Metals Research).

Thus gas can inflate the bifilm, or shrinkage can pull it apart, as can stress applied during or after freezing.

The weakening effect of the straightened cracks seriously reduces the mechanical properties of the metal. This is the mechanism whereby iron is the most damaging impurity in Al alloys; it weakens the alloy as a result of its effectiveness in straightening oxide bifilms. It is important to remember that such inclusions as the  $\beta$ Fe particle are probably extremely strong and resistant to fracture, in common with many intermetallics. The observed cracks are not the result of intrinsic brittleness but the result of the presence of the oxide bifilm. The strong effect of Fe in reducing the properties of Al alloys is heightened because although the iron content is low, the size of both alpha- and beta-iron inclusions is

disproportionately large because its volume is increased five-fold by the content of aluminum, the formula having a five-to-one ratio in both  $\text{Al}_{15}\text{Fe}_3\text{Si}_2$  and  $\text{Al}_5\text{FeSi}$  respectively.

Wang and colleagues (2009) observe the formation of beta-Fe particles directly in a solidifying Al alloy using synchrotron radiation. They note that the beta-Fe nucleates at a temperature between 550 and 570°C. This is a surprisingly large range for a well-characterized crystal, and strongly suggests that the problem lies not with the crystal but with the variability of its messy and fragmented oxide substrates, each one of which will be different.

Figure 6.21 illustrates different views of the bifilm on one side of the particle has been inflated, growing away by gas precipitation or pulled away by shrinkage forces, opening a pore on one side of the  $\beta\text{Fe}$  plate. Because it has been common to observe an association between pores and  $\beta\text{Fe}$  particles, it has in the past been assumed that the  $\beta\text{Fe}$  particles blocked the movement of feed liquid along interdendritic channels, and so caused shrinkage porosity. However, in view of the three-dimensional access routes for feed liquid, and in view of the strong probability that pores probably cannot be formed without bifilms, restriction of feeding is almost certainly less important than the presence of bifilms. An observation by Miresmaeili (2006) in which platelets of  $\beta\text{Fe}$  were scattered and randomly oriented over a wide array of dendrites illustrated that the associated porosity at the sides of many of the plates were randomly oriented with respect to the dendrite direction and feeding direction. If the plates had been blocking the flow the pores should all have been sited 'downstream' of the plates. Their random siting indicated that the association was not the result of blockage of feed metal, but more likely the result of the decoherence of the bifilm from one side of the plate, growing into a pore.

Intermetallics with the closer-packed cubic symmetries (fcc, bcc) have such a high degree of symmetry that they often show little or no strong growth morphology. Any direction of growth is as favorable as any other. The alpha-Fe phase has a hexagonal lattice which is close to cubic, so it can grow in practically any direction. For this reason, the alpha-Fe phase is usually seen to grow in a meandering fashion, following around the irregular form of the bifilm in its original crumpled state. In this way the compact, convoluted form, with its associated central crack, is sealed in place, achieving a minimal impact on properties. This is why alpha-Fe as 'Chinese script' is generally encouraged by metallurgists. On polished microsections the convoluted forms of alpha-Fe are often seen to contain a skeleton of convoluted cracks – the trace of the originating crumpled bifilm sealed in situ (Figure 6.20a).

The conversion of the extended planar crack of the beta-Fe particles (Figure 6.20b) into convoluted compact cracks inside the Chinese script particles (Figure 6.20a) is one of the key techniques for reducing the deleterious impact of iron impurity in Al alloys. There have been a very large number of research programs to determine the best metallurgical solution to this problem. The common approach has been to use 0.5Mn addition for every 1.0Fe content (all in weight percent). Many other alloying solutions have been explored: Mahta and colleagues (2005) find the 1.0Fe level can be converted with 1.0Co or 0.33Cr. (Interestingly, this work indicates that primary Si in the form of compact nodules appears also to be stabilized by these additions, indicating that in addition to AIP there may be other effective nuclei for nodular Si based on transition metals.)

All of these alloying approaches to the control of beta-Fe come with the built-in disadvantage that the Mn addition increases the total volume of unwanted intermetallic phases as pointed out by Crepeau in his 1995 review. Other elements have been used as listed by Crepeau. These include Be, Mo, Ni, and S. This is a most suspect list, suggesting wildly different mechanisms. For instance Ni may act as an alloying element similarly to the other transition metals. Mo seems unlikely to fit into this category and

remains a mystery. Be will almost certainly not act in solution but as a significant strengthener of the oxide film on the melt, reducing entrainment of bifilms by a 'hanging-up' mode during pouring, so reducing the total oxide bifilm content in the melt. Sulfur seems likely to be analogous to phosphorus and may provide or modify a nucleating substrate. Clearly, much more work remains to clarify this messy subject.

An alternative approach based on a further finding by Mahta may be important. The occurrence of the beta-Fe phase appears to be particularly sensitive to the rate of solidification. Although more rapid freezing makes most features of the microstructure finer, there may be a reason for the beta-Fe to be particularly sensitive. This is because for the particle to grow, the bifilm has to be mechanically unfurled as an extendable substrate against the viscous drag of the liquid. This means that the beta-Fe can only form at relatively slow cooling rates. The alpha-Fe phase can also be suppressed by faster freezing as would be expected, but is less sensitive, requiring higher rates of freezing to reduce its formation.

Silicon crystals also nucleate and grow on oxide films as is seen in Figure 5.28, and reported by Jorstad (2008) in the discussion between him, Sigworth and myself on the subject of the modification of Si by Sr in Al-Si alloys. Figure 6.10b illustrates how Si appears to nucleate on AIP particles which themselves form on the alumina bifilms. The growth of the Si then cannot surround the nucleating particle, but seems happy to grow out along the bifilm, straightening the bifilm, and thus reducing the properties of the alloy. The cracks in Figure 6.11 arise in this way. After the addition of Sr which effectively deactivates the AIP nuclei and the bifilms, the Al-Si eutectic subsequently grows as a coupled eutectic, disregarding the presence of the bifilms, which thus remain compact, and properties are generally improved.

The conventional description of such intermetallics as brittle and weak needs to be examined critically. It should be common knowledge that intermetallics are generally strong; in fact micrometer-sized intermetallic particles will be expected to be extremely strong. Intermetallic alloy castings are currently being developed for turbine blade production and other ultra-high-performance uses. Furthermore intermetallics are even likely to be ductile. There is evidence for this in occasional observations of intermetallics that have been plastically deformed (for instance the  $Mg_2Si$  intermetallic particle observed by Hadian (2009), Figure 6.22).

In addition, ductile behavior in hard crystals is well known in physics; a crystal of common salt is usually brittle when crushed in air, but when deformed in water becomes strong and ductile as a result of the dissolving away of surface defects that can lead to failure (Mendelson 1962). All strong crystals deposited and grown in a solvent, and stressed while remaining in their solvent, are expected to be similarly strong and ductile. This is the case for all intermetallics grown in situ in metal matrices.

Incidentally, this is not the case of MMCs made by *mechanical mixing*; i.e. stirring-in intermetallic particles into a melt of the matrix. Such introduced particles naturally entrain the surface film on the melt during entry to the melt, as though stepping into a paper bag when entering. They are therefore effectively isolated from the matrix by the surrounding film and its associated layer of air. The entrained particle does not contact the melt (Figure 2.3). Such particles are thus always associated with, if not actually surrounded by, bifilm cracks. The attainment of ductility in such mechanically mixed MMCs is thereby always limited as seen in the work of Emamy et al. (2009).

### ***Si and Fe competition for sites***

Caceres (2004) made a series of alloys of increasing Si and Fe contents. He found that as Si was increased the beta-Fe particles were refined. Conversely, Liu (2003) noted that for some common

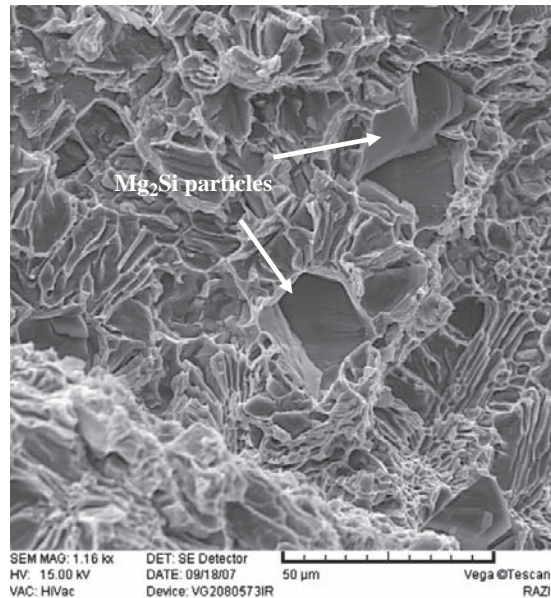


**FIGURE 6.22**

Fracture surface of an in situ Al–Mg<sub>2</sub>Si intermetallic MMC showing the ductile failure of the upper intermetallic particle (Hadian et al. 2009).

Al-based casting alloys higher Fe resulted in finer Si particles. This reciprocal relation between the formation of Si and beta-Fe particles reflects the fact that they are both competing for the same limited number of suitable substrates, as is clearly seen from their formation on bifilms in Figure 6.20b.

Shabestari and Gruzleski (1995) found that Sr suppressed the precipitation of Si (presumably on bifilms) but that beta-Fe particles still straightened and grew, but were slightly reduced in average length. This finding indicates that Sr is extremely effective in deactivating the precipitation of Si on the oxide substrate, possibly because of its action on the tiny AIP nuclei sitting on the oxide bifilms. The action of Sr is similar, but somewhat less effective for beta-Fe, possibly because the beta-Fe is nucleated directly on the oxide substrate, and this more extensive area may require deactivation by correspondingly more Sr. Mulazimoglu (1993) noted that Sr promotes the formation of more fragmented alpha-Fe particles in the form of a kind of Chinese script and coarsens the CuAl<sub>2</sub> phase in many copper-containing common Al alloys. His observations are again explained by the partial deactivation of the oxide substrates, resulting in fewer active substrates and consequently coarser precipitates.

Finally, it is significant that Caceres (2000) concludes that ductility of Al–Si alloys is controlled by the cracking of both Si and beta-Fe particles. Both phases nucleate and grow on the oxide bifilms in suspension in the alloy. Thus both naturally contain similar cracks.

### 6.3.7 Other intermetallics

Miresmaeili and co-workers (2005) studying Al–7Si–0.4Mg alloy with Sr additions found Al<sub>2</sub>Si<sub>2</sub>Sr precipitated on both  $\gamma$ Al<sub>2</sub>O<sub>3</sub> and MgO films. In addition, alignments of the precipitates indicated an

epitaxial relationship. The experimental technique was a model of simplicity. The melts were poured into a small steel cup the size of an eggcup. The outside surface of the casting was then studied by SEM. The intermetallics could easily be seen through the thickness of the oxide skin of the casting.

There is some evidence that  $\text{CuAl}_2$  intermetallic in Cu-containing Al alloys also forms on oxide bifilms (Campbell 2009). Thus the strong and tough Al–4.5Cu series of alloys, of which there are many, exhibit the  $\text{CuAl}_2$  phase along grain boundaries. On careful examination, although it seems clear that the Cu segregates to the interdendritic regions around every dendrite arm, the  $\text{CuAl}_2$  phase occurs only in some locations. It seems that the phase only precipitates when a bifilm is present, otherwise, the Cu merely remains in solution (Figure 6.23). (Although it is possible that the absence of the  $\text{CuAl}_2$  phase is the result of a locally lower Cu segregation, this seems unlikely because the interdendritic segregation appears to be especially uniform.) A further important observation is that, probably as a result of its cubic symmetry, the  $\text{CuAl}_2$  phase does not appear to have a strong straightening effect on the bifilm. Thus in contrast to Al–Si alloys in which the main alloying agent, Si, straightens the bifilms to reduce properties, this does not happen in Al–Cu alloys, explaining an important contribution to their excellent properties. (Another important contribution is its high Cu content creating the high precipitate density after heat treatment of course.)

Excess Ti in Al–Si alloys, often specified to be in the range 0.13–0.18%Ti, leads to the formation of  $\text{TiAl}_3$ -type intermetallics that form at temperatures well above the liquidus temperature of the alloy. These crystals can take up to 37%Si in solution, making a mixed intermetallic, usually written  $\text{Ti}(\text{AlSi})_3$ . They take either a blocky or a flake morphology (possibly as a result of the different sizes of bifilm on which they may nucleate). For optimum effect with modern grain refiners in most Al–Si alloys, including the popular Al–7Si types, Chen and Fortier (2010) recommend that 10–20 ppm B should be targeted, while the Ti level should be near, but not exceed, 0.10%. The reduction of Ti reduces the content of the Ti-rich intermetallics.

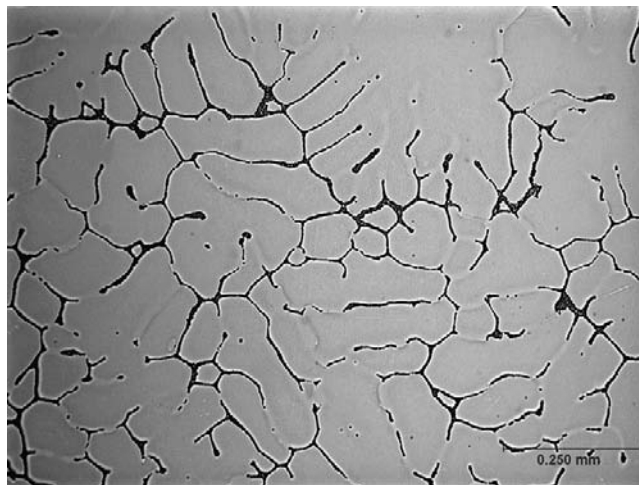


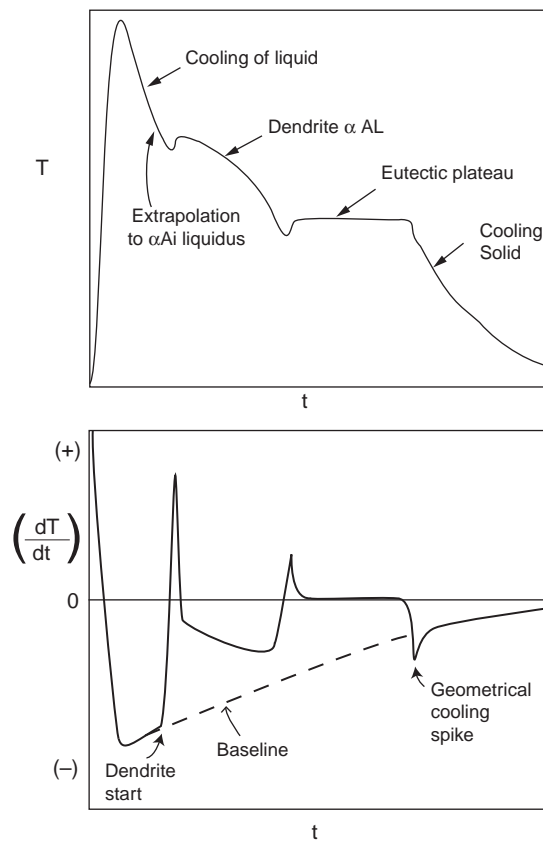
**FIGURE 6.23**

The as-cast Al–4.5Cu alloy showing  $\text{CuAl}_2$  phase at many but not all interdendritic boundaries even though Cu segregation can be visually discerned in all boundaries.

### 6.3.8 Thermal analysis of Al alloys

The cooling curve of a solidifying alloy can be informative, usually in several ways. This is a potentially large subject, and although useful for many alloys (particularly cast irons) we shall deal only with Al alloys as an example of features that can be observed. For a variety of cooling curves the reader is recommended the excellent book by Backerud, Chai, and Tamminen (1990) which gives clear curves for all the common Al casting alloys. In this short section we shall only consider an Al–7Si alloy as a particularly simple example. This is shown in Figure 6.24.

The cooling curve of temperature  $T$  versus time  $t$  shows the undercooling that is necessary to give the driving force to nucleate the alpha-Al dendrites. By the provision of grain refiners this undercooling can be reduced practically to zero, and so the under cooling can be used to assess the state of grain refinement of the melt prior to casting. Similarly the undercooling necessary to initiate the eutectic phase, and the steady-state growth temperature can be monitored to assess the state of modification of the eutectic. This



Thermal analysis for Al – 7 Si alloy

**FIGURE 6.24**

The thermal analysis of a simple Al–7Si alloy.

'plateau' is usually not so level in more complex alloys as a result of continued segregation during the course of the eutectic solidification, resulting in the 'plateau' taking on an increasing downward slope.

The differential curve  $dT/dt$  versus time  $t$  is similarly informative. Backerud shows how the area between the curve and the baseline can yield the heat evolved during the formation of that particular phase that is solidifying at the time. Thus if the heat of formation of the phases is known, the relative volumes of phases in the solidifying structure can be found.

The cooling curve and derivative can also be used to assess the quantity of Fe-rich phases in Al-Si alloys, since these evolve significant amounts of heat on solidification, significantly modifying the cooling curve.

An interesting feature often observed as a spike of cooling mysteriously diving down below the baseline, but which appears to be generally not understood, is the acceleration of freezing of the sample because of the geometrical effect as the residual melt dwindles to zero. In contrast with the rest of the thermal analysis, it has nothing to do with any metallurgical reaction. This effect is quantified in Section 5.1.2 and Figure 5.10.

### 6.3.9 Hydrogen in Al alloys

We turn now to the presence of hydrogen in aluminum. Hydrogen behaves quite differently to other solutes.

The aluminum-hydrogen system is a classic model of simplicity. The only gas that is soluble in aluminum in any significant amounts is hydrogen. (The magnesium-hydrogen system is similar, but rather less important in the sense that the hydrogen concentration increases only by a factor of about 1.4 on freezing, compared to a factor of about 20 for aluminum, so that dissolved gas in liquid magnesium is usually much less troublesome. Other systems are in general more complicated as we shall see later.)

Figure 6.25 is calculated from Equation 1.4 illustrating the case for hydrogen solubility in liquid aluminum. It demonstrates that on a normal day with 30% relative humidity, the melt at 750°C should approach about  $1 \text{ ml kg}^{-1}$  ( $0.1 \text{ ml } 100 \text{ g}^{-1}$ ) of dissolved hydrogen. This is respectably low for most commercial castings (although perhaps just uncomfortably high for aerospace standards). Even at 100% humidity the hydrogen level will continue to be tolerable for most applications. This is the rationale for degassing aluminum alloys by doing nothing other than waiting. If originally high in gas, the melt will equilibrate by losing gas to its environment (as is also illustrated by the copper-based alloy in Figure 1.2).

Further consideration of Figure 6.25 indicates that where the liquid aluminum is in contact with wet refractories or wet gases, the environment will effectively be close to one atmosphere pressure of water vapor, causing the concentration of gas in solution to rise to nearer  $10 \text{ ml kg}^{-1}$ . This spells disaster for most normal castings. Such metal has been preferred, however, for the production of many non-critical parts, where the precipitation of hydrogen as dispersed porosity can compensate to some extent for the shrinkage on freezing, and thus avoid the problem and expense of the addition of feeders to the casting. Traditional users of high levels of hydrogen in this way are the permanent mold casters of automobile inlet manifolds and rainwater goods such as pipes and gutters. Both cost and the practicalities of the great length to thickness ratio of these parts prevent any effective feeding.

Raising the temperature of the melt increases exponentially the solubility of hydrogen in liquid aluminum. At a temperature of 1000°C the solubility is over  $40 \text{ ml kg}^{-1}$ . However, of course, if there is

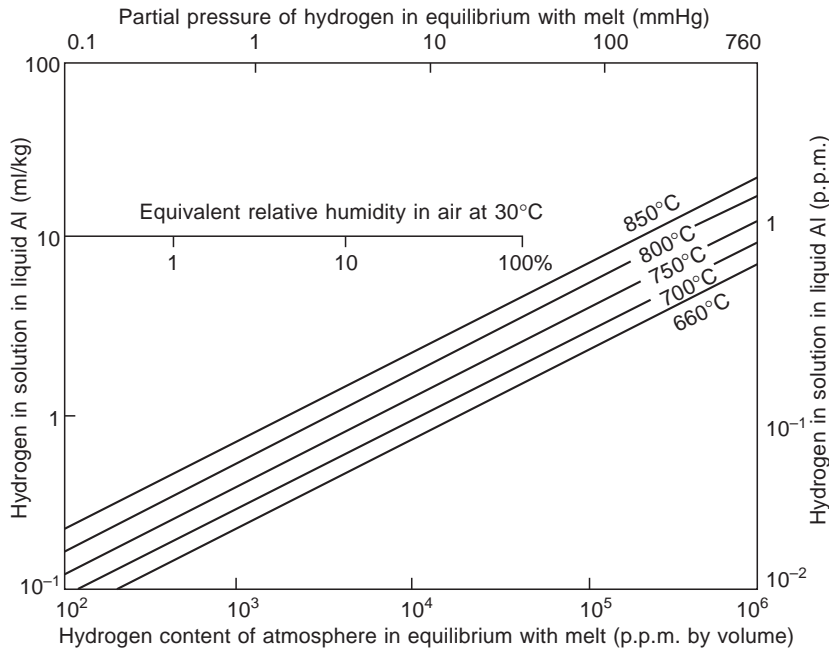


**FIGURE 6.25**

Hydrogen content of liquid Al shown as increasing with temperature and the hydrogen content of the environment as hydrogen gas or as water vapor.

no hydrogen available in its environment the melt will not be able to increase its gas content, no matter what its temperature is. This self-evident fact is easy to overlook in practice because there is nearly always some source of moisture or hydrogen, so that, usually, high temperatures are best avoided if gas levels are to be kept under good control. Most aluminum alloy castings can be made successfully at casting temperatures of 700–750°C. Rarely are temperatures in the range 750–850°C actually required, especially if the running system is good.

A low gas content is only attained under conditions of a low partial pressure of hydrogen. This is why some melting and holding furnaces introduce only dried air, or a dry gas such as bottled nitrogen, into the furnace as a protective blanket. Occasionally the ultimate solution of treating the melt in vacuum is employed (Venturelli 1981). This dramatically expensive solution does have the benefit that the other aspects of the environment of the melt, such as the refractories, are also properly dried. From Figure 6.25 it is clear that gas levels in the melt of less than  $0.1 \text{ ml kg}^{-1}$  are attainable. However, the rate of degassing is slow, requiring 30–60 minutes, since hydrogen can only escape from the surface of the melt, and takes time to stir by convection, and finally diffuse out. The time can be reduced to a few minutes if the melt is simultaneously flushed with an inert gas such as nitrogen.

For normal melting in air, the widespread practice of flushing the melt with an inert gas from the immersed end of a lance of internal diameter of 20 mm or more is only poorly effective. The useful flushing action of the inert gas can be negated at the free surface because the fresh surface of the liquid continuously turned over by the breaking bubbles represents ideal conditions for the melt to equilibrate



with the atmosphere above it. If the weather is humid the rate of re-gassing can exceed the rate of de-gassing.

Systems designed to provide numerous fine bubbles are far more effective. The free surface at the top of the melt is less disturbed by their arrival. Also, there is a greatly increased surface area, exposing the melt to a flushing gas of low partial pressure of hydrogen. Thus the hydrogen in solution in the melt equilibrates with the bubbles with maximum speed. The bubbles are carried to the surface and allowed to escape, taking the hydrogen with them. Such systems have the potential to degas at a rate that greatly exceeds the rate of uptake of hydrogen.

Rotary degassing systems can act in this way. However, their use demands some caution. On the first use after a weekend, the rotary head and its shaft will introduce considerable hydrogen from their absorbed moisture. Thus it is to be expected that the melt will get worse before it gets better. Thus degassing to a constant (short) time is a sure recipe for disaster when the refractories of the rotor are damp. In addition, there is the danger that if a vortex is formed at the surface of the melt, it may carry down air, thus degrading the melt by manufacturing oxides faster than they can be floated out. This is a common and disappointing mode of operation of a technique that has reasonable potential when used properly. The simple provision of a baffle board to prevent the rotation of the surface will suppress the vortex formation at reasonable rates of rotation. However, it is common to see such high rates that additional vortices are generated by the baffle board, making a bad situation worse.

High rates of loss of hydrogen during rotary degassing are entertaining because of the mass of flashes of blue flames of hydrogen burning as it is released from the melt surface.

Despite this, the major effect of rotary degassing may not be the degassing. The action of greatest importance is most probably the floating out of the major oxide films resulting from the skins of charge materials. These oxides are fractions of square meters in area. It is essential to eliminate them if castings of any integrity are to be achieved. It seems likely that these large area films will be eliminated within the first few minutes, but the danger that subsequently arises is the generation of millions of small oxide bifilms from the bursting of small degassing bubbles as they arrive at the surface of the melt. As they release their contents of inert gas plus any flushed-out hydrogen the waft of fresh air across the newly opened surface will oxidize the surface. Thus as the sides of the opened bubble collapse together, they will create a new oxide bifilm. Thus the original massive bifilms are replaced by millions of small bifilms. The compositions are likely to be different too; the old films will be mainly spinels but the new films will be relatively pure alumina. Only later will the alumina films convert to spinel if some Mg is available in the alloy. This behavior of rotary degassing is not fully researched and understood, so an optimum practical procedure is not easily recommended at this time.

One technique that has yielded good-quality metal is the use of rotary degassing together with the use of a flux. Once again, the action seems to be important for the wetting and elimination of oxides rather than any significant effect on hydrogen removal. Here too the recommended details are sketchy. The big Al producers of the world are known to have carried out their research, but keep the details a closely guarded secret.

### ***The rate of hydrogen pick-up***

When dealing with the rate of attainment of equilibrium in melting furnaces the times are typically 30–60 minutes. This slow rate is a consequence of the large volume to surface area ratio. We shall call this ratio the modulus. Notice that it has dimensions of length. For instance, a 10-tonne holding furnace would have a volume of approximately  $4 \text{ m}^3$ , and a surface area in contact with the atmosphere of

perhaps  $10 \text{ m}^2$ , giving a modulus of  $4/10 \text{ m} = 0.4 \text{ m} = 400 \text{ mm}$ . A crucible furnace of 200-kg capacity would have a modulus nearer 200 mm.

These values around 300 mm for large bodies of metal contrast with those for the pouring stream and the running system. If these streams are considered to be cylinders of liquid metal approximately 20 mm diameter, then their effective modulus is close to 5 mm. Thus their reaction time would be expected to be as much as  $300/5 = 60$  times faster, resulting in the approach towards equilibrium within times of the order of 1 minute. (This same reasoning explains the increase in rate of vacuum degassing by the action of bubbling nitrogen through the melt.) This is the order of time in which many castings are cast and solidified. We have to conclude, therefore, that reactions of the melt with its environment continue to be important at all stages of its progress from furnace to mold.

There is much evidence to demonstrate that the melt does interact rapidly with the chemical environment within the mold. There are methods available of protecting the liquid by an inert gas during melting and pouring which are claimed to reduce the inclusion and pore content of many alloys that have been tested, including aluminum alloys, and carbon and stainless steels (Anderson et al. 1989).

Ultimately, however, the gas in solution is normally not a problem to most alloys (steels might be an exception since the exact mechanism of hydrogen embrittlement is not yet understood) if it could be persuaded to remain in solution where it is normally perfectly harmless. This is largely achieved by such techniques as counter-gravity filling of molds; the reduction in entrained oxide bifilms by the elimination of pouring normally outweighs all other benefits.

---

## 6.4 COPPER

The ease of reducing copper from its ore has ensured copper and its alloys have enjoyed a long history, lasting thousands of years. Even so, copper and its alloys continue to be important at the present day for corrosion resistant cast products from domestic water fitting to high-strength marine applications in ships.

Pure copper castings are used for applications in which maximum thermal conductivity is required; a demanding application being blast furnace tuyeres. Similarly, pure copper is used in applications where maximum electrical conductivity is required such as heavy electrical switch gear and bus bars (although dilute additions of cadmium or chromium are often used to increase strength without reducing conductivity too much). 'Pure' copper and its dilute alloys have a reputation for being particularly difficult to cast, the castings often suffering hot tears and porosity. This is almost certainly the direct result of poor casting technique, leading to the entrainment of surface oxides, the products of impurities in the melt. The reader is recommended the sections of this work on casting manufacture for solutions to this common problem. The answer, as most often for castings, lies in the correct casting practice (for instance, not in the alloy composition or other metallurgical aspects).

The common brasses are red brass (70Cu30Zn) and yellow brass (60Cu40Zn), although many more complex and stronger brasses based on these alloys are also common.

Bronze alloys were traditionally solely alloys with tin (for instance bell metal is almost universally 77Cu23Sn), but nowadays aluminum bronze (5–10Al) and silicon bronze are important and widely used. Al bronze with additions of Fe, Ni, and Mn is used for ships' propellers.

Gunmetals are alloys in which Zn has been added to a tin bronze. For instance a 'Navy Gun Metal' was 88Cu8Sn4Zn. If lead is also added the alloy is known as 'leaded gunmetal'. One of the most

famous of these is *ounce metal*, so-called because it was made up of a pound of copper, an ounce of zinc, an ounce of tin and an ounce of lead, also known as 85–5–5–5 metal. The lead was useful because of its action to seal pores in these very long-freezing-range alloys. Leaded brasses and bronzes are used for plain bearings, the lead and tin-rich phases probably acting as high-pressure lubricants. However, lead has been phased out of domestic water fittings, and is being steadily eliminated from nearly all foundry alloys as a result of the toxicity of its fumes and contamination of sand molds during casting. Much exploratory work has been expended to investigate Si-containing alloys as a replacement in domestic water fittings (Fasoyinu 1998).

### 6.4.1 Surface films

Pure liquid copper in a moist, oxidizing environment, causes water molecules to break down on its surface, releasing hydrogen to diffuse away rapidly into its interior. This behavior is common to many liquid metals. The oxygen released in the same reaction (Equation 1.2), and copper oxide,  $\text{Cu}_2\text{O}$ , may be formed as a temporary intermediate product, but is also soluble, at least up to 0.14% oxygen. The oxygen diffuses and dissipates more slowly in the metal so no permanent film is created under oxidizing conditions unless the solubility limit is exceeded. If the solubility limit is exceeded at the melt surface, a surface film of  $\text{Cu}_2\text{O}$  will build up. However, this will dissolve away if the rate of input of oxygen falls below the rate of dissolution of the film. In reducing conditions no film of any kind is expected. Thus pure liquid copper is free from film problems in most circumstances. (Unfortunately this may not be true or in the presence of certain carbonaceous atmospheres that may create a carbonaceous film, as we shall see later. Carbon-based films on copper and its alloys do not appear to have been researched so far.)

Certain Cu alloys, particularly the various aluminum bronzes that contain typically 5–10 wt% Al are quite a different matter. The great reactivity of Al with oxygen in the atmosphere, and the high melting temperatures of these alloys, combine to create conditions for the growth of a thick, tough, and tenacious oxide that can give major problems if allowed to enter the casting.

### 6.4.2 Gases in Cu-based alloys

Copper-based alloys have a variety of dissolved gases and thus a variety of possible reactions. In addition to hydrogen, oxygen is also soluble. These elements in solution (denoted by square brackets below) can produce water vapor according to the reversible reaction



Thus water vapor in the environment of molten copper alloys will increase both hydrogen and oxygen contents of the melt. Conversely, on rejection of stoichiometric amounts of the two gases to form porosity, the principal content of the pores will not be hydrogen and oxygen but their reaction product, water vapor. An excess of hydrogen in solution will naturally result in an admixture of hydrogen in the gas in equilibrium with the melt. An excess of oxygen in solution will result in the precipitation of copper oxide.

Much importance is often given to the so-called *steam reaction*:



This is, of course, a nearly equivalent statement of Equation 6.3. The generation of steam by this reaction has been considered to be the most significant contribution to the generation of porosity in copper alloys that contain little or no deoxidizing elements. This seems a curious conclusion since the two atoms of hydrogen are seen to produce one molecule of water. If there had been no oxygen present the two hydrogen atoms would have produced one molecule of hydrogen, as indicated by Equation 1.3. Thus the same volume of gases is produced in either case. It is clear therefore that the real problem for the maximum potential of gas porosity in copper is simply hydrogen. Depending on how much oxygen is present in solution, dissolved hydrogen will produce either a molecule of water vapor or a molecule of hydrogen. The volumes of gas are the same in either case.

(However, as we shall see in later sections, the presence of oxygen will be important in the nucleation of pores in copper, but only if oxygen is present in solution in the liquid copper, not just present as oxide. The distribution of pores as subsurface porosity in many situations is probably good evidence that this is true. We shall return to consideration of this phenomenon later.)

Proceeding now to yet more possibilities in copper-based materials, if sulfur is present in solution then a further reaction is possible:



and for the copper–nickel alloys, such as the monel series of alloys, the presence of nickel introduces an important impurity, carbon, giving rise to an additional possibility:



Systematic work over the last decade at the University of Michigan (see, for instance, Ostrom et al. (1981)) on the composition of gases that are evolved from copper alloys on solidification confirms that pure copper with a trace of residual deoxidizer evolves mainly hydrogen. Brasses (Cu–Zn alloys) are similar, but because zinc is only a weak deoxidant the residual activity of oxygen in solution gives rise to some evolution of water vapor. Interestingly, the main constituent of evolved gas in brasses is zinc vapor, since these alloys have a melting point above the boiling point of zinc (Figure 1.6). Pure copper and the tin bronzes evolve mainly water vapor with some hydrogen. Copper–nickel monels with nickel above 1% have an increasing contribution from carbon monoxide as a result of the promotion of carbon solubility by nickel.

Thus when calculating the total gas pressure in equilibrium with melts of copper-based alloys, for instance inside an embryonic bubble, we need to add all the separate contributions from each of the contributing gases.

The brasses represent an interesting special case. The continuous vaporization of zinc from the free surface of a brass melt carries away other gases from the immediate vicinity of the surface. This continuous out-flowing wind of metal vapor creates a constantly renewed clean environment, sweeping away gases which diffuse out of the melt, carrying them from the alloy surface and preventing contamination of the local environment of the metal surface with furnace gases or other sources of pollution. For this reason cast brass is usually found to be remarkably free from gas porosity.

For alloys with more than 20%Zn, there is sufficient zinc vapor to burn in the air with a brilliant flame known as zinc flare. Flaring may be suppressed by a covering of flux. Similarly, aluminum is often added to brasses to reduce the loss of zinc, probably as a result of the formation of a dense alumina film. However, the beneficial degassing action is thereby suppressed, raising the danger of porosity, mainly from hydrogen.

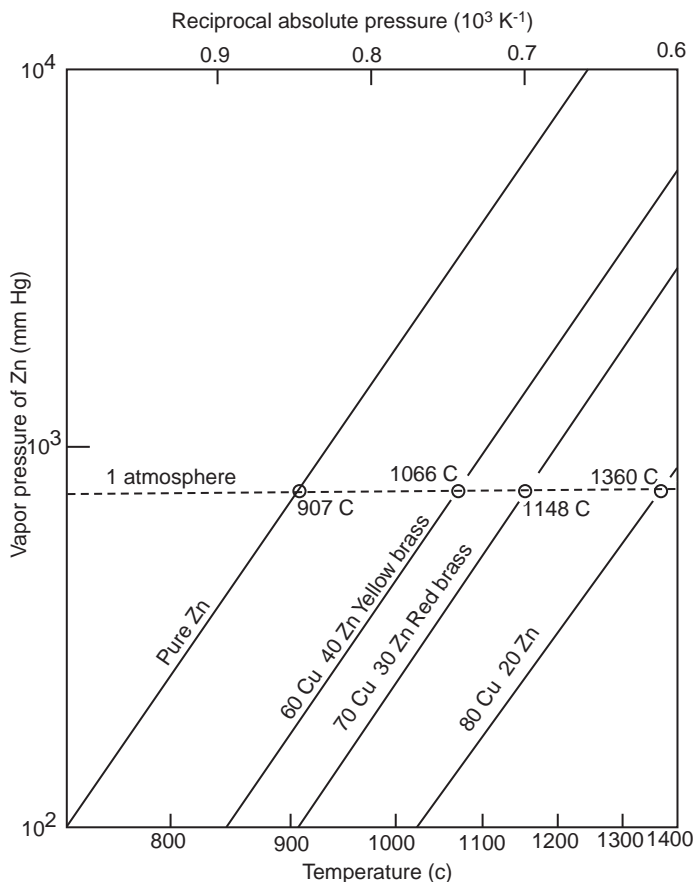


**FIGURE 6.26**

The vapor pressure of Zn and some brasses.

The boiling point of pure zinc is  $907^{\circ}\text{C}$ . But the presence of zinc in copper alloys does not cause boiling until higher temperatures because, of course, the zinc is diluted (strictly, its activity is reduced). Figure 6.26 shows the effects of increasing dilution on raising the temperature at which the vapor pressure reaches one atmosphere, and boiling occurs. The onset of vigorous flaring at that point is sufficiently marked that in the years prior to the wider use of thermocouples foundrymen used it as an indication of casting temperature. The accuracy of this piece of folklore can be appreciated from Figure 6.26 in which it is clear that the flaring temperatures increase in step with the increasing copper contents (i.e. at greater dilutions of zinc), and thus with the increasing casting temperatures of the alloys.

Around 1% of zinc is commonly lost by flaring and may need to be replaced to keep within the alloy composition specification. In addition, workers in brass foundries have to be monitored for the ingestion of zinc fumes.

Melting practice for the other copper alloys to keep their gas content under proper control is not straightforward. Below are some of the pitfalls.

One traditional method has been to melt under oxidizing conditions, thereby raising the oxygen in solution in the melt in an attempt to reduce gradually the hydrogen level. Prior to casting, the artificially raised oxygen in solution is removed by the addition of a deoxidizer such as phosphorous, lithium, or aluminum. The problem with this technique is that even under good conditions the rate of attainment of equilibrium is slow because of the limited surface areas across which the elements have to diffuse. Thus in fact little hydrogen may have been removed. Worse still, the original oxidation has often been carried out in the presence of furnace gases, so raising oxygen and (unwittingly) hydrogen levels simultaneously (Equation 1.2) high above the values to be expected if the two dissolved gases were in equilibrium. The addition of deoxidizer therefore may leave hydrogen at near saturation.

The further problem with this approach is that the deoxidizer precipitates out the oxygen as a suspension of solid oxide particles in the melt, or as surface oxide films. Either way, these by-products are likely to give problems later as non-metallic inclusions in the casting, and, worse still, as bifilm initiation sites to assist the precipitation of the remaining gases in solution, thus promoting the very porosity that the technique was intended to avoid. In conclusion, there is little to commend this approach.

An additional problem should be noted with respect to the relatively common practice of deoxidation with phosphorus. Gunmetals typically require only 0.01%P and Sn bronze typically 0.2%P (French 1957). If excess is used a liquid  $\text{Cu}_3\text{P}$  film forms on the top of the melt. If this is poured with the alloy it penetrates the mold leading to impaired surface finish and possibly entrained phosphide liquid.

A second reported method is melting under reducing conditions to decrease losses by oxidation. Hydrogen removal is then attempted just before casting by adding copper oxide or by blowing dry air through the melt. Normal deoxidation is then carried out. The problem with this technique is that the hydrogen-removal step requires time and requires the creation of free surfaces, such as bubbles, for the elimination of the reaction product, water vapor. Waiting for the products to emerge from the quiescent surface of a melt sitting in a crucible would probably take 30–60 minutes. Fumes from the fuel-fired furnace would be ever-present to help to reverse any useful degassing. Clearly therefore, this technique cannot be recommended either!

Marin and Utigard (2010) describe a variant of this technique in which they direct a flame of mixed  $\text{O}_2$  and  $\text{CH}_4$  (methane) on to the surface of the melt. Higher ratios of  $\text{CH}_4/\text{O}_2$  give higher reducing conditions that raise the rate of deoxidation of the copper. However, they note that hydrogen is simultaneously increased by this practice, eventually becoming so high that the melt ‘boils’ with the evolution of water vapor by reactions as in Equation 6.3. Boiling may now flush the melt to low levels of hydrogen, but the surface turbulence of the boil may now increase reaction with the air, increasing oxygen once again. All this resounds of lack of control.

A less dramatic and more straightforward technique involves a simple cover of granulated charcoal over the melt to provide the reducing conditions. This is a genuinely useful way of reducing the formation of drosses (dross is a mixture of oxide and metal, so intimately mixed that it is difficult to separate) as can be demonstrated from the Ellingham diagram (Figure 1.5), the traditional free energy/temperature graph. The oxides of the major alloying elements copper, zinc, and tin are all reduced back to their metals by carbon, which preferentially oxidizes to carbon monoxide (CO) at this high temperature. (The temperature at which the metal oxide is reduced, and carbon is oxidized to CO, is that at which the free energies for the formation of CO exceed that of the metal oxide, i.e. CO becomes more stable. This is where the lines cross on the Ellingham diagram.)

However, even here, it is as well to remember that charcoal contains more than just carbon. In fact, the major impurity is moisture, even in well-dried material that appears to be quite dry. An addition of charcoal to the charge at an early stage in melting is therefore relatively harmless because the release of moisture, and the contamination of the charge with hydrogen and oxygen, will have time to be reversed. In contrast, an addition of charcoal at a late stage of melting will flood the melt with fresh supplies of hydrogen and oxygen that will almost certainly not have time to evaporate out before casting. Any late additions of anything, even alloying additions, introduce the risk of unwanted gases.

Reliable routes for melting copper alloys with low gas content include:

1. Electric melting in furnaces that are never allowed to go cold.
2. Controlled use of flaring for zinc-containing alloys.
3. Controlled dry environment of the melt. Addition of charcoal is recommended if added at an early stage, preferably before melting. (Late additions of charcoal or other sources of moisture are to be avoided.)

In summary, the gases and vapors which can be present in the various copper-based alloys are:

Pure copper  $H_2$ ,  $H_2O$

Brasses, gunmetals  $H_2$ ,  $H_2O$ , Zn, Pb

Cupro-nickels  $H_2$ ,  $H_2O$ , CO, ( $N_2$ ?)

Various tests have been proposed from time to time for copper-based alloys. Dion (1979) recommends a test for oxygen by simply dipping a carbon rod into the melt. If the oxygen is high the rod 'sings' with the rapid evolution of microscopic bubbles of CO, producing a vibration that can be sensed by hand. This test can detect oxygen in solution down to a limit of about 0.01% at which the rod stops singing. The rod needs to be at the temperature of the melt since a cold graphite rod evolves gas. This raises the potential problem, of course, of the probability of moisture in the graphite, although it is possible that the test itself will assist to eliminate this providing the rod is reasonably dry. If the rod is dry it will also contribute to the flushing out of any hydrogen.

The total sum of gases has often been assumed to be testable using the Reduced Pressure Test (RPT) very similar to that used for Al alloys. Studies of the test are reported by numerous workers, including Matsubara (1972) and Ostrom (1974, 1976). The test is also described in the *ASM Handbook* (2008, vol 15). Analogously to the experience in Al alloys, the test has proved controversial and confusing for the same reason: the test is also highly sensitive to the presence of oxide bifilms. In reality, the test would be a better test of oxides than a test of gas, but with intelligent use, should give a useful indication of both.

Sub-surface pinholes in copper-base alloys have been widely researched. One of the more thorough reports is by Fischer (1988). The phenomenon appears to be exactly analogous to that observed in Al alloys. The pores arise as a result of a combination of factors, naturally leading to widespread confusion in the literature. The key factors include:

- (i) The gases in solution in the melt (of which, of course, there are several in copper alloys);
- (ii) The gases released by the mold binder material and which diffuse into the casting surface;
- (iii) The build up of gases ahead of the advancing freezing front, raising local concentration of the total gas content after a distance of 1 or 2 mm (i.e. just sub-surface);
- (iv) The presence of a population of oxide bifilms in suspension in the melt as a result of poor melting practice or poor casting practice. The bifilms act as initiation sites, and are themselves pushed

ahead of the front, so being in precisely the correct location for maximum effect of pore generation. The variation of difficulty of unfurling of the bifilms will give a spectrum of pore initiation times, giving a mix of round and dendritic pore morphologies corresponding to early and late arrivals respectively (see Figures 7.40 and 7.41).

### 6.4.3 Grain refinement

There has been much practical work carried out on the grain refinement of Cu-based alloys, but, it seems, little fundamental research so far.

It was Cibula in 1955 that used iron and cobalt borides, plus zirconium carbide and nitride, to grain-refine bronzes and gunmetals. As is usual with such work, hot tears were found to be reduced although porosity became more evenly dispersed or at times concentrated as layer porosity. Finer grains also appeared to be associated with reduced ductility and a lack of pressure tightness. These apparently perverse results are almost certainly the result of a high-oxide bifilm population in his cast material which is only to be expected from the awful casting techniques in general use at that time. Techniques such as those described later in this book should greatly assist to reduce these defect levels, and reverse such effects of loss of ductility and pressure tightness.

With similar poor casting methods, Couture and Edwards (1973) used Zr master alloys to successfully grain refine a variety of gun metals, finding improved strength and hot tear resistance, but confirmed Cibula's finding of a drastic reduction in elongation and pressure tightness.

Gould (1960) studied the grain refinement of pure copper, and found additions of Li and Bi to be effective, but many additions that were tried were of no use.

Clearly, copper alloys would benefit from additional work to understand the fundamentals of grain refinement. In addition, casting with improved filling system designs should help to remove the current confusion relating to loss of ductility and pressure tightness that has accompanied early work.

---

## 6.5 CAST IRON

Cast irons are nature's gift to foundrymen. They melt at accessible temperatures, requiring relatively low energy, they run like water, are strong enough for many engineering applications, and are relatively insensitive to poor casting techniques and so yield adequate castings despite sloppy and out-dated casting practices.

The commercial exploitation of simple gray irons was a major factor triggering the start of the Industrial Revolution, but the current spectrum of different cast irons is now dauntingly broad. It stretches from gray irons (so-called because of their fracture surface is colored gray from the graphite flakes that provide the fracture path) through compacted graphite irons, spheroidal graphite (known as ductile) irons, to white irons (the apparently brittle iron carbides providing a bright, white fracture surface) for wear resistance. Highly alloyed irons are commonly used for heat and oxidation resistance. Special heat treatments, particularly austempering, can provide high-performance irons with strengths approaching 1 GPa – the traditional reserve of high-strength steels.

For cast irons carbon is the key alloying element. In pure binary Fe–C alloys the minimum carbon content for a cast iron to distinguish it from a steel is close to 2%, but the liquidus temperature at this carbon content is high at 1290°C and the long freezing range of about 150°C and limited graphite



content would make feeding difficult. At a carbon content of approximately 4.3% the alloy is of eutectic composition, and the freezing temperature is comfortably low at 1150°C with negligible freezing range. This is also close to the composition at which the expansion due to graphite precipitation almost exactly counters the contraction due to austenite solidification, conferring on eutectic irons the enormous benefit of requiring little if any feeding. Beyond the eutectic composition the liquidus temperature rises once again and the precipitation of primary graphite prior to general solidification at the eutectic temperature means that graphite flotation in these hypereutectic irons can become a problem, limiting carbon contents usually to a maximum close to 4.5%.

With silicon as the next most common element in gray irons, equivalent structures can be achieved with reduced carbon, trading off C against increased Si. It is usual to quantify this relation by an *effective* carbon content, known as the *carbon equivalent* ( $C_E$ ) or sometimes the *carbon equivalent value* ( $CEV$ ). This is approximately

$$C_E = \%C + \%Si/3$$

A typical engineering quality of gray iron would consist of around 3.2C and 2.0Si, to give a  $C_E$  close to 3.9%C, just slightly hypoeutectic. In general, gray irons contrast with ductile irons which have a  $C_E$  commonly 4.2 to 4.4%.

In the days of making elaborate ornamental cast iron ware, or for certain wear-resistance applications, one or two percent of phosphorus was often added. This addition increased fluidity of the melt (Figure 3.13) and the hard phosphide phases added wear resistance to such applications as brakes. The %P acted similarly to the Si in its replacement of effective carbon, so that their combined effect gave approximately

$$C_E = \%C + [\%Si + \%P]/3$$

The reasonable cost, huge availability and attractive machinability of the graphitic irons, especially gray irons, guarantees the prosperous future of these alloys (despite all criticisms of its weight compared to Al alloy castings for instance).

Having said all this, it is true that cast irons have always been, and continue to be, the most used casting alloys, the most researched, but the least understood. This is why this section, perhaps unfortunately, is effectively pressurized into being the most speculative section in this book. For want of any other coherent explanation, I present my own approach to an understanding of the microstructures of irons in terms of the mechanisms of inoculation and nodularization. Until disproven, it is offered as no more than a potentially useful working hypothesis. In the meantime, we can look forward to the outcome of researches that might confirm the approach, or suggest an improved hypothesis.

### 6.5.1 Reactions with gases

Like copper-based alloys, the production of iron-based alloys is also complicated by the number of gases that can react with the melt, and that can cause porosity by subsequent evolution on solidification. Again, it must be remembered that all the gases present can add their separate contributions to the total pressure in equilibrium with the melt. We shall deal with the gases in turn.

Oxygen is soluble, and reacts with the high carbon content of cast irons. Carbon monoxide is the product, following Equation 6.5. Carbon dioxide is seen to be blamed by many experimenters who note bubbles in cast irons usually in association with oxide (usually silicate) slags. It has been assumed that the

high carbon content of the iron has reacted with the oxygen in the slag to create bubbles of CO. However, this is almost certainly an error. The slag is more usually the result not of carry-over from the ladle, but is created in situ in the mold by surface turbulence. The bubbles are much larger than could be generated by reaction, since the rate of reaction is limited by the rate of diffusion, which is necessarily rather slow, producing, as for the dispersed microporosity of Al alloys, bubbles of maximum diameter perhaps 0.5 mm. It would require the coalescence of 1000 of these bubbles to make the 5 mm diameter bubbles typical of those seen in irons. Thus it is certain that the bubbles are not the product of a diffusion-controlled reaction but are simply *air bubbles* introduced by the turbulence involved with the poor filling systems usually employed. Naturally, they will contain some traces of carbon monoxide. However, with a well-designed naturally pressurized filling system, both slag and so-called CO bubbles will disappear.

Carbon monoxide is still expected to be an important gas for the creation of porosity observed from time to time in cast irons, simply because of the high availability of both carbon and oxygen. However, it needs to be kept in mind that such bubbles will be expected to be fine, usually sub-millimeter in size, and evenly distributed.

CO can be encouraged to evolve from cast iron as a froth of bubbles, known as a carbon boil. Such an evolution of CO can be induced in molten cast iron, providing the silicon is low, simply by blowing air onto the surface of the melt (Heine 1951) thus reinforcing the fact, if not already obvious, that oxygen can be taken into solution in cast iron even though the iron already contains high levels of carbon. During subsequent solidification, in the region ahead of the solidification front, carbon and oxygen are concentrated still further. It is easy to envisage how, therefore, from relatively low initial contents of C and O, they can increase together so as to exceed a critical product  $[C].[O]$  to cause CO bubbles to form in the casting. The equilibrium equation, known as the solubility product, relating to Equation 6.5 is:

$$[C].[O] = kP_{CO} \quad (6.6)$$

We shall return to this important equation later. It is worth noting that the equation could be stated more accurately as the product of the activities of carbon and oxygen. However, for the moment we shall leave it as the product of concentrations, as being accurate enough to convey the concepts that we wish to discuss.

Hydrogen is soluble as in Equation 1.3, and exists in equilibrium with the melt as indicated in Equation 1.4. Although a vigorous carbon boil would reduce any hydrogen in solution to negligible levels by flushing it from the melt such techniques are not usual in iron melting. Thus any hydrogen will tend to remain in the melt. Even so, although some hydrogen might be present, it does not generally appear to lead to any significant problems in irons. This is probably the result of the hydrogen solubility being rather low, in contrast to steels, where higher melting temperatures lead to the possibility of high hydrogen levels in solution.

In addition, of course, the rate of diffusion of hydrogen is astonishingly high. Thus hydrogen might be quickly lost from a melt, probably only in a few minutes, if the melt has the benefit of a dry environment. Similarly, in the presence of moisture or hydrogen, the hydrogen content of a melt could rise quickly. It clearly pays to work with furnaces and their backup refractories that are always kept hot.

Nitrogen is also soluble in liquid iron. The reaction follows the normal law for a diatomic gas:

$$N_2 = 2[N] \quad (6.7)$$

and the corresponding equation to relate the concentration in the melt  $[N]$  with its equilibrium pressure  $P_{N_2}$  is simply:

$$[N]^2 = kP_{N_2} \quad (6.8)$$

As before, the equilibrium constant  $k$  is a function of temperature and composition. It is normally determined by careful experiment. As for hydrogen, in general it seems that nitrogen is probably not an important source of porosity in irons. Exceptional circumstances might include the reactions involving high-nitrogen binders since the decomposition of amines they contain appear to lead to such problems as nitrogen fissures (see the section ‘Nitride Films’ below). However, these seem to be as much surface nitride problems as nitrogen solution problems.

### 6.5.2 Surface films on liquid cast irons

When cast iron is held at a high temperature (e.g. 1500°C) in a furnace or ladle lined with a traditional refractory material such as ganister, a fascinating sight can be witnessed. The surface of the liquid iron is seen to be continuously punctuated by the silent and mysterious arrival of bright circular patches. These suddenly appear and spread from nothing to their full size of several centimeters within about a second. The patches drift around, coalesce with other patches, and finally attach themselves to the wall of the vessel where they cool and add to the solidified rim of slag. These patches are droplets of liquid refractory, melted from the walls and bottom of the vessel. As the vessel tips and empties, upstanding ‘stalactites’ on the base, and upward runs and drips on the walls, can usually be clearly seen, marking the sites where the drops detached.

In common with all the components of molten metal systems, the slag will be changing its composition rapidly as it interacts with the molten metal. At high temperature its contents of iron, manganese, and silicon will be reduced from their respective oxides and taken into solution in the liquid iron, whereas the remaining stable oxides, such as those of aluminum and calcium, will remain to accumulate as a dry slag, sometimes called a dross. These reactions will be explained further in the next section.

Such layers of slag on the surface of molten iron can be anything from 0.1 mm thickness upwards. (In the cupola, of course, the thickness is often around 100 mm or more.) It is not intended to consider such macroscopic surface-layer problems in this section. The following section considers only the microscopically thin surface film that, under certain conditions, will form automatically on the surface of the melt (no matter how good is the melting resistance of the lining material of the holding vessel).

#### ***Oxide films***

Work by Heine and Loper at the University of Wisconsin, dating from 1951, has done much to explain the complex formation of surface films on cast irons. A slightly later study by Merz and Marincek (1954) is also illuminating. Based on these studies we can explain the changes that occur as the temperature falls.

When the iron is at a high temperature, 1550°C, the Ellingham diagram indicates that CO is a more stable oxide than SiO<sub>2</sub>. Thus carbon oxidizes preferentially, and is therefore lost at a higher rate than silicon, as is seen in Figure 6.27. Here the blowing of air on to the surface of a small crucible of molten metal serves to accentuate the effect. Silicon is observed to fall only after all the carbon has been used up. At this high temperature no film is present on the melt – any silicon oxide, SiO<sub>2</sub>, would be immediately reduced to silicon metal, which would be dissolved in the melt, simultaneously forming CO, which would escape to atmosphere.

At around 1420°C the stability of the carbon and silicon oxides is reversed. The exact temperature of this inversion seems to be dependent on the composition of the iron as pointed out by Merz and

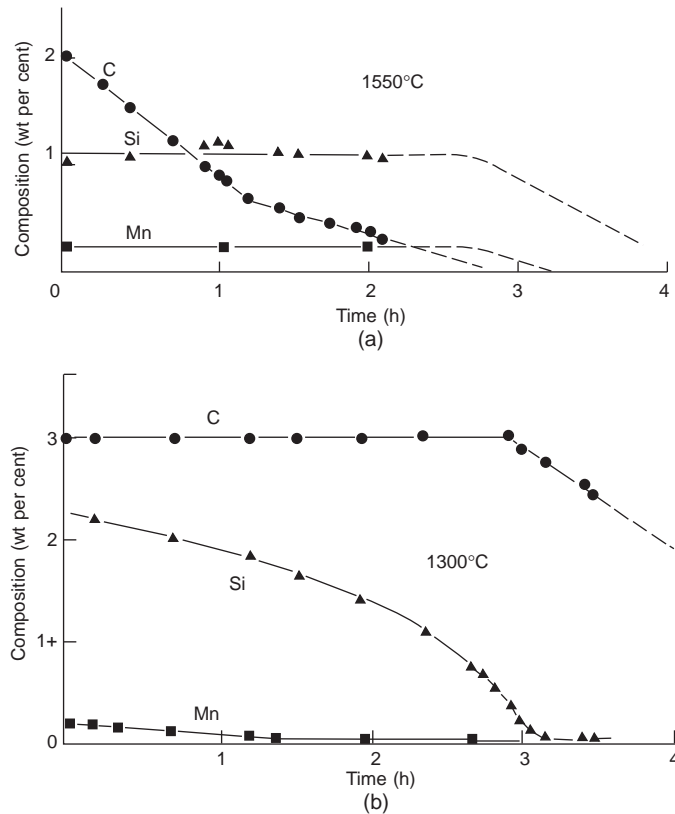


**FIGURE 6.27**

Change in composition of 3.6 kg of molten gray iron held in a silica crucible, whilst air was directed over its surface at the rate of  $22 \text{ ml s}^{-1}$  (a) melt at  $1550^\circ\text{C}$ ; and (b) melt at  $1300^\circ\text{C}$ . Data from Heine (1951).

Marincek; de Sy (1967) reports a range of  $1410\text{--}1450^\circ\text{C}$  for the irons that he investigated, whereas the Ellingham diagram (Figure 1.5) predicts an inversion temperature for pure Fe–C alloys of about  $1500^\circ\text{C}$ . The agreement is, perhaps, as good as can be expected because of compositional uncertainties. Below approximately  $1400^\circ\text{C}$ , therefore,  $\text{SiO}_2$  appears on the surface as a dry, solid film, rather gray in color. This film cannot be removed by wiping the surface, since it constantly reforms.

At a temperature of  $1300^\circ\text{C}$ , and in alloys that contain some manganese, it is clear from the Ellingham diagram that  $\text{MnO}$  is the least stable,  $\text{SiO}_2$  is intermediate, and  $\text{CO}$  the most stable. Thus manganese is oxidized away preferentially, followed by silicon, and finally by carbon. The contribution of  $\text{MnO}$  to the film at this stage may reduce the melting point of the film, causing it to become liquid.

At around  $1200^\circ\text{C}$ , iron oxide,  $\text{FeO}$ , contributes to the further lowering of the melting point at the ternary eutectic between  $\text{FeO}$ ,  $\text{MnO}$ , and  $\text{SiO}_2$ . If sulfur is also present in the iron then  $\text{MnS}$  will contribute to a complex eutectic of melting point  $1066^\circ\text{C}$  (Heine and Loper 1966).

The author finds that, in general terms, the above considerations nicely explain his observations in an iron foundry where he once worked. For a common grade of gray iron, the surface of the iron was

seen to be clear at 1420°C. As the temperature fell, patches of solid gray film were first observed at about 1390°C. These grew to cover the surface completely at 1350°C. The gray film remained in place until about 1280°C, at which temperature it started to break up by melting, finally becoming completely liquid at 1150°C.

When casting gray iron in an oxidizing environment, the falling temperature during the pour will ensure that the surface film will be liquid at the most critical late stage of the filling of the mold. If the film becomes entrained in the molten metal it will therefore quickly spheroidize into compact droplets. The droplets are of much lower density than the iron, and so will float out rapidly. On meeting the surface of the casting they will mutually assimilate, and be assimilated by, the existing liquid film, and so spread over the casting surface. The glassy sheen of some gray iron castings may be this solidified skin. The harmless dispersal of the oxide film in this way is the reason for the good-natured behavior of cast iron when cast into greensand molds; it is one of the very few metal–mold combinations that is capable of exhibiting tolerance towards surface turbulence. Even so, there appears to be some experience indicating the irons cast without turbulence exhibit improved properties. This confusing situation requires to be resolved by future research.

Only on one occasion has the accumulation of liquid oxide at a casting surface given the author some problems. This was in a gray iron casting where a small amount of surface turbulence was known to be present just inside the ingate, because it was not easy to lower the velocity below  $0.4 \text{ m s}^{-1}$  at this point, and was judged to be a negligible risk of any kind of internal defect. However, so much liquid surface was created at that location, and so many droplets of the entrained slag floated out at a point just downstream, that the layer of surface slag accumulated at the downstream location exceeded the machining allowance, scrapping the casting.

In *ductile irons* the entrainment of the surface is nearly always a serious matter. The small percentage of magnesium that is required to convert the iron from flake to the spheroidal graphite type dramatically alters the nature of the oxide film.

Above 1454°C Heine and Loper (1966) find that the surface of liquid ductile iron remains clear of any film. Below this temperature a film starts to form, increasing in thickness to 1350°C, at which point the surface exhibits solidified crusty particles. By the time the temperature has reached 1290°C the entire surface is covered with a dry dross. Magnesium vapor distils off through dross since the molten iron is above the boiling point of magnesium. Presumably the oxidation of the vapor to powdery MgO at the upper surface of the dross is a major contributor, causing the dross to grow quickly and copiously. The dross makes life difficult for the ductile iron foundryman, forming films, and agglomerating into dry, non-wetting heaps, that, if entrained, spoil otherwise excellent castings. Ductile iron is renowned for being difficult to cast cleanly, without unsightly dross defects. Surface films something like those on Al alloys are to be expected as in Figure 6.28.

### ***Oxide bifilms naturally in suspension in gray irons***

De Sy (1967) has shown that liquid cast iron generally contains significant quantities of oxygen in solution in excess of its solubility. He concluded, on the basis of careful and rigorous experiments, that the undissolved fraction of oxygen was present as SiO<sub>2</sub> particles. Interestingly, by heating to 1550°C he confirmed the expectation that the SiO<sub>2</sub> solids dissolved because they became less stable than CO, but reappeared on cooling once again. Hartman and Stets report for irons containing Mg not only the presence of SiO<sub>2</sub> in suspension, but also the more complex iron–magnesium–silicate, olivine, 2(Mg,Fe)O.SiO<sub>2</sub>. Hoffman and Wolf (2001) find a variety of oxides

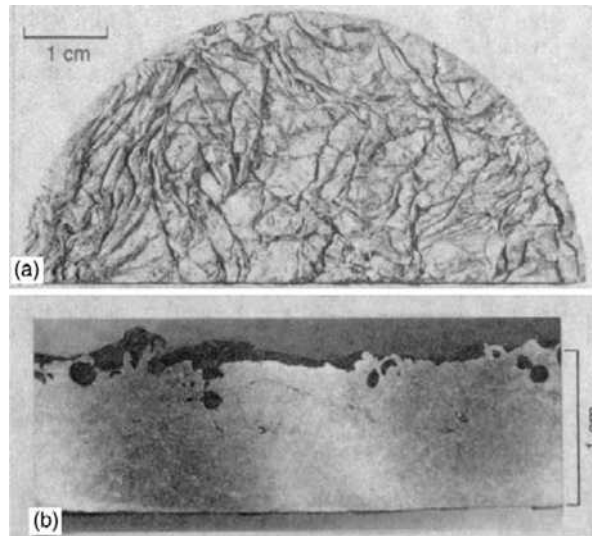


**FIGURE 6.28**

(a) Oxide skin on liquid Al-9Si-4Mg alloy wrinkled by repeated disturbance of the surface; and (b) a cross-section of the solidified metal. The appearance in both cases is extremely similar to graphite films on gray iron. (Courtesy of Agema and Fray 1990.)

including  $\text{SiO}_2$ ,  $\text{FeO}$ , and  $\text{MnO}$  among others, but superheating and holding at high temperature eliminated many of these. In their elegant study of the thermodynamics Mampaey and Beghyn (2006) show how mainly  $\text{SiO}_2$  together with some  $\text{FeO}$  forms in a typical melt when cooling from 1480 to 1350°C.

It seems reasonable to speculate that these oxides almost certainly would not be compact spheres, cubes, or rods, etc., but would most likely be in the form of *films*. Only films would have a sufficiently low Stokes velocity to remain in suspension for long periods of time associated with these experiments, and the long periods during which irons are held molten in holding furnaces.

In any case, of course, the *film* morphology is to be expected. During melting in the cupola as droplets of iron rain down, the natural folding-in of the surface film of  $\text{SiO}_2$  of each droplet would ensure a natural population of  $\text{SiO}_2$ -rich double films (bifilms). Additional treatments or handling such as pouring actions, stirring in induction furnaces, and the oxide introduced from the surface of the charge (whether steel, pig, or foundry returns) would increase this already large, natural population of oxide bifilms. Furthermore, it is well known that iron from electric furnaces is more liable to chill formation problems in thin sections than cupola iron, and this effect has been widely accepted as the loss of nuclei (in agreement with proposals made here), especially during extended time in holding furnaces or pouring systems.

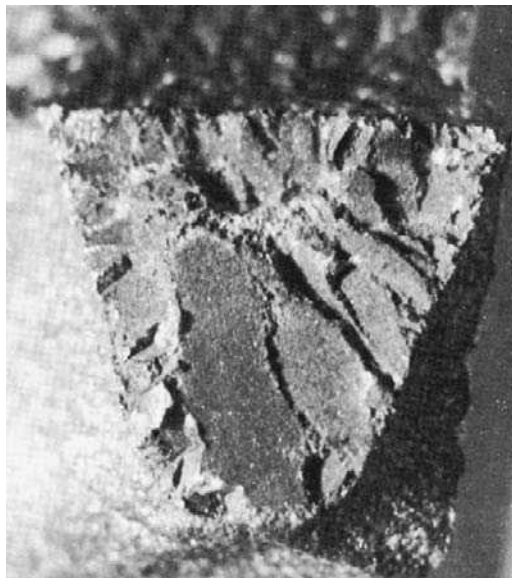
Thus there appear to be at least two quite different populations of oxide bifilms in suspension in liquid iron. (i) In gray irons the silica-rich bifilms are a natural population in equilibrium with the melt, the amount of silica-rich phase being predictable by thermodynamics. (ii) In ductile irons the magnesia-rich bifilms are the result of mechanical accidents involving the turbulent entrainment of the

surface film into the bulk liquid, resulting in non-reversible damage. We expand on this problem in ductile irons in this next section.

### ***Bifilms in ductile iron***

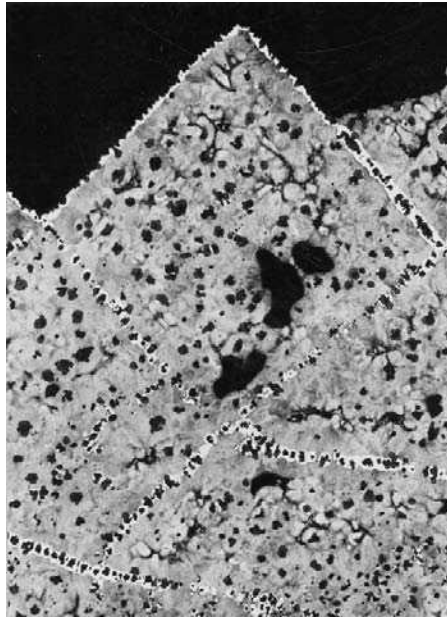
The population of oxide bifilms observed in ductile irons arise from the trauma of a turbulent filling system. In this case the presence of Mg stabilizes the magnesia, MgO, in the surface film, although Si might also contribute, thus forming a magnesium silicate,  $\text{MgO}\cdot\text{SiO}_2$  (also written as  $\text{MgSiO}_3$ ). Both magnesium oxide and magnesium silicate are extremely stable, and when entrained, represent permanent damage to the liquid metal and subsequently to the casting. Although the bifilms are known to have an initially compact morphology as a result of the turbulence during their formation, and so are relatively harmless as cracks, the subsequent straightening of these bifilms by various natural processes such as the growth of dendrites, creating extensive planar cracks, is common, resulting in the development of brittleness in the form of plate fracture (Figures 6.29 and 6.30) as discussed in more detail in the next section.

The ductile casting industry has referred to entrained surface films observed on polished microstructural samples as ‘dross stringers’ (Figure 6.31). This name, based on their one-dimensional appearance on a polished two-dimensional section, has led to a comforting self-deception, concealing their real nature as extensive planar defects in three-dimensional space in the form of films floating about in a sea of metal. The occasional appearance of clusters of graphite nodules that have floated up and been trapped under such ‘stringers’ corroborates their real nature as films; nodules would not be trapped under ‘strings’ but naturally collect under films. Also, as we are now aware, if the film is solid

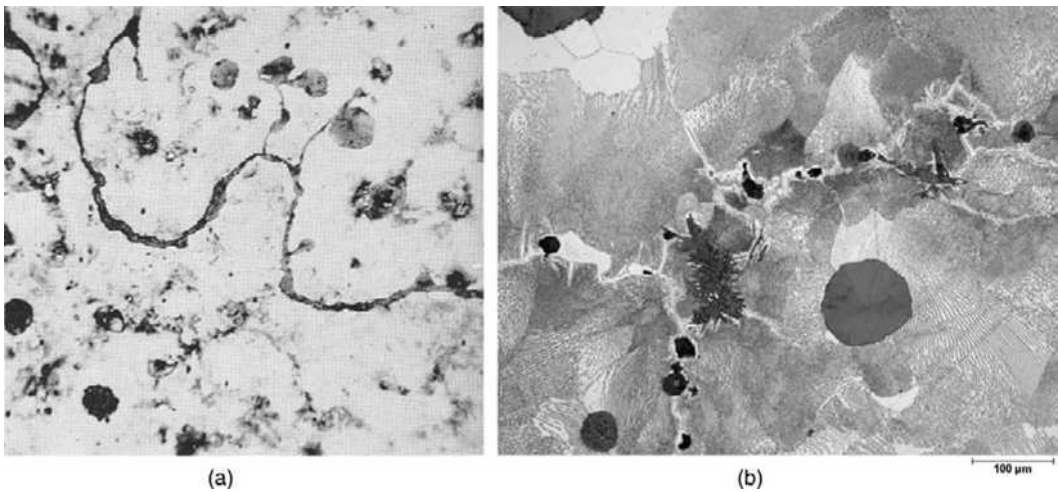


**FIGURE 6.29**

Plate fracture in the feeder neck of a ductile iron casting (Karsay 1980)

**FIGURE 6.30**

Polished microsection through the fracture (Barton 1985) (courtesy of Casting Technology International).

**FIGURE 6.31**

(a) So-called silicate 'stringer' in ductile iron (actually a visible silicate bifilm); (b) an alignment of mis-shaped nodules at a grain boundary in a pearlitic ductile iron, indicating the probable presence of an invisible bifilm.



(as it clearly is in this case), the entrainment process will fold them in dry side to dry side, thus forming a bifilm, a crack.

The films appear on the liquid metal only at low temperature as we have seen, and seem to be mainly magnesium silicate, probably with a thick upper layer of solid MgO. If the ductile iron is cast at a low temperature, and if the surface is entrained, the creation of seriously damaging bifilms is guaranteed. Naturally, as the hot liquid iron cools during its passage through the running system it is likely to cool to the temperature at which the solid film starts to form, so that defects will be expected in most filling systems in which surface turbulence is not controlled. Once entrained, the defects can, of course, lead to a variety of additional problems. One of these serious problems is discussed below.

The magnesium silicate dross 'stringers' (actually, we should immediately stop calling them 'stringers' and call them 'bifilms') are particularly thick bifilms, and very clear when seen on a polished microsection as seen in Figure 6.31a. Figure 6.31b probably also shows a bifilm in ductile iron, but the bifilm in this case is too thin to reveal its presence directly. We can be fairly sure a bifilm is present from the long line of particles of flaky graphite and mis-shapen spheroids, all typical of features that prefer to form on an oxide bifilm, and all apparently following a grain boundary, a common site for a bifilm. Elsewhere in this alloy, away from contact with the bifilm, the spheroids are beautifully formed.

### ***Plate fracture defect in ductile iron***

Like nitrogen fissures in gray irons, plate fracture in ductile irons has also never been satisfactorily explained. Ductile irons, should, of course, always exhibit a ductile mode of failure. Sometimes, however, a casting will exhibit poor strength and poor elongation to failure, with the fracture surface exhibiting large planar facets, the alloy appearing to consist of large embrittled grains. These unpredictable events give rise to serious concern that the material is not under the proper control that either the foundry or the customer would like to see. Everyone's faith is shaken. The question naturally arises, 'Is ductile iron a reliable engineering material?' This is the sort of question that should never arise, and that no-one wishes to hear.

Following the description given by Karsay (1980) and Gagne and Goller (1983), the features of the plate fracture are large, flat, apparently brittle fracture planes, in ductile irons that in normal circumstances would exhibit only ductile failure. The planar facets appear to grow mainly vertically at right angles to the bottom surface of the casting (Figure 6.29). When viewed closely in cross-section (Figure 6.30), the planes are seen to be studded with small, irregularly shaped graphite spheroids, arranged with an accuracy almost resembling a crystal lattice. When polished and etched the planes are characterized by a matrix that is somewhat lighter than the rest of the casting. Karsay suggests that the color difference may be the result of a higher Si content in this region, stabilizing the ferrite. Finally, in this region, there is a high incidence of small inclusions that appear to be mainly magnesium silicates.

All these features are consistent with the defect being an oxide bifilm, probably a magnesium silicate, explaining the high Si content, the high inclusion content, and possibly the malformed spheroids as a result of local loss of Mg. The planar form of the failure surface arises from the bifilm being pushed by the raft of austenite dendrites and organized into an interdendritic sheet, similar to that commonly seen in other alloy systems (Figures 2.43, 2.44a, 2.46). The vertical orientation is also understandable because of the greater rate of heat transfer from the base of the casting where gravity

retains the contact with the mold, so that grains growing vertically from the base grow fastest and furthest. In addition, the magnesium silicate bifilm will necessarily be trapped at the mold wall (otherwise dendritic straightening without some part of the film being anchored is not easily envisaged – only pushing bunches of film ahead will occur if the film is not anchored) and buoyancy will encourage its vertical orientation, and so assist the advancing dendrite to straighten the film. Spheroids in interdendritic regions would then be revealed at the regular spacing dictated by the dendrite arm size. During solidification and cooling at the high temperature the bifilm probably disintegrates to some extent because of its surface energy tending to spheroidize it. What remains are the changes in chemistry and numerous silicate fragments as inclusions plus remnants of the original central bifilm crack to encourage the direction of growth of the crack that finally causes failure.

Other features of plate fracture are its occurrence in slowly cooled regions, such as in a feeder neck. This may be the result of the lower rate of growth allowing the dendrites to straighten films more successfully (at high growth velocity, the drag resistance of films would resist dendrite growth, and resist film straightening).

Loper and Heine (1968) find that ‘spiking’ observed on fracture surfaces of both white and ductile irons is similar, and sometimes appears as oxidized facets. The occasional oxidation is easily understood if the bifilm connects to the surface and allows the ingress of air deep into the casting. Similar *internal oxidation* during heat treatment of irons is described in Section 9.10.

The less common appearance of plate fracture in irons of higher carbon equivalent and its reduction in resin-bonded sand molds reported by Barton (1985) is probably not so much the result of a more rigid mold as he suggests, but an indication that the entrainment of the oxide film is less damaging in this more carbonaceous environment.

Heine and Heine (1968) describe some fascinating observations and use telling language: ‘when iron is damaged by melting and pouring so that it solidifies “spikey” it will not permit feeding even though proper sized feeders are provided’. This description acknowledges the possibility of deterioration of the melt by improper melting and handling and the consequent faceted nature of the freezing pattern. Furthermore, the presence of extensive oxides, probably from wall to wall in the casting, and bridging the necks of feeders, act to prevent the flow of feed metal. I am always impressed by intuition of good foundrymen for understanding the underlying scientific mechanisms.

In passing, it is worth reminding ourselves of the possibility that other non-oxide bifilms are to be expected in cast irons.

### **Nitride bifilms**

Nitride bifilms probably form in cast irons giving rise to the ‘nitrogen fissure’ defects associated in the past with high-nitrogen binders. Nitrogen fissures in gray iron castings are large cracks, often measured in centimeters, which appear to have been associated with the use of sand binders that contain high levels of nitrogen. They are an enigma that has never been satisfactorily explained. The blame is normally given to high-nitrogen binders that contain amines, whose breakdown probably contributes both nitrogen and hydrogen to the liquid iron. However, although such binders are known to be associated with fissure defects, their use does not always result in fissures.

It seems most likely that entrained bifilms, perhaps consisting of nitride films, are also required, so that the filling system may also be highly influential. Any involvement of the filling system has not previously been suspected, but would explain the current confusion in the results of studies carried out so far. Once entrained, the combination of high hydrogen and nitrogen pressure in the iron might be

sufficient to inflate any nitride bifilms to some extent, opening the bifilms to revealing their presence as crack-like features.

### ***Carbon films (lustrous carbon)***

The liquid film present on cast iron at low temperature in an oxidizing environment has made iron easy to cast free from serious defects. This marvelous natural benefit of cast iron when cast into molds made from sand bonded with clay and water must have played an important part in the success of the Industrial Revolution. In general (although acknowledging a number of infamous and tragic exceptions) the bridges did not fall into the river, and the steam engines continued to power machinery. Later this benefit was to be extended to molds made using one of the first widely used chemical binders: sodium silicate. This environmentally friendly chemical is still widely used today as a low-cost sand binder for the production of strong molds (despite a number of significant disadvantages that some foundries have been prepared to live with, but which are now being successfully overcome).

However, it is one of those ironies of history that the arrival of modern chemical binders based on resins was to change all this.

Binders based on various kinds of resins, furan, phenolic, acrylic, polyurethane, etc., were heralded as the breakthrough of the twentieth century. Indeed, the new binders had many desirable properties, making accurate and stable molds, with excellent surface finish, good breakdown after casting, and at good rates of production from simple low-cost equipment.

However, when iron was poured into some of these early resin-bonded molds, especially those based on polyurethane, a new defect was discovered. It became known as lustrous carbon. Although it had been occasionally seen, especially if the volatile additions to greensand had been high, it was never so common nor so damaging. This shiny, black film resulted in casting skins wrinkled like elephant hide. Studies deduced from X-ray diffraction patterns (Draper 1976) concluded that it was pyrolytic carbon (a microcrystalline form) that was deposited from the gas phase on to hot surfaces in the temperature range of at least 650–1000°C. Being a form of pyrolytic carbon, similar to carbon black, it was unlike the nicely crystallographic regularity of graphite.

The hot surface was originally assumed to be the sand grains of the mold, and somehow the deposit was pushed ahead of the advancing liquid front, to become incorporated into the surface as folds (Naro and Tanaglio 1977). The explanation is clearly problematical on several fronts: in most instances the sand surface is rather cold, and thus incapable of chemically ‘cracking’ (i.e. breaking down) the polymeric gases to precipitate graphite. Also, it is difficult to imagine how a film deposited on the complex and rough sand grains could be detached from its grip on these three-dimensional shapes before the arrival of the liquid metal and so be pushed into rucks and folds. After the arrival of the metal the film would be assisted in keeping its place by being held against the surface of the sand grains by the pressure of the liquid. Clearly, this explanation cannot be correct.

The only explanation that fits all the facts is that the graphitic film forms on the surface of the molten metal itself. Photographs of lustrous-carbon defects, particularly those seen on the fracture surfaces of parts that have suffered brittle failure, beautifully reveal their origin as the surface film on the liquid metal (Bindernagel 1975, Naro and Tanaglio 1977). The caption to the photograph of the oxide skin on an aluminum alloy (Figure 6.28) could be changed to read that it was a carbonaceous skin on a gray iron; to the unaided eye the appearance of the two types of film is practically identical.

Part of the confusion that has surrounded the lustrous carbon film, and that has claimed that it deposited on sand grains dates from a misreading of the brilliant original work by Petrzela (1968). This

Czech foundry researcher devised a test in which he demonstrated that the vapors released from coal tar and other hydrocarbon additions to molding sands would decompose, depositing carbon as a shiny, silvery film on a metal strip, resistance heated to at least 1300°C. In his test, it happened that the sand was also heated to this temperature. Thus he observed carbon to be deposited directly onto the sand grains in addition to that deposited on the heated metal strip. The mistake of subsequent generations of researchers has been to assume that lustrous carbon always deposits onto sand grains, even though, at the instant that the metal is filling the mold, the sand is usually nowhere near the temperature at which a hydrocarbon vapor could be decomposed.

The reader is recommended to Petrzela's engaging chatty and candid account. He was clearly one of our great foundry characters. His writing contains other fascinating asides to some of his observations on the release of carbon from hydrocarbons. He describes a sooty deposit that had a fibrous, woolly appearance among sand grains that has been observed many times since, although not previously explained.

Other work has studied the generation of lustrous carbon in greensand molds. It is clear that the mold atmosphere can provide a hydrocarbon environment for the liquid metal if sufficiently high concentrations of hydrocarbons are added to the sand mixture. Such additives help the mold to resist wetting by the metal, and so improve surface finish, as appreciated in the original work of Petrzela (1968), and later by Bindernagel et al. (1975). Excess additions have sometimes been claimed to give lustrous carbon defects. One such defect is shown in Figure 6.32. However, it is certain that the defects form only if the surface turbulence can cause the film to be entrained. Otherwise, if the film is retained on the surface by careful uphill filling as in Figure 6.33, it is a valuable effect, significantly enhancing the surface finish of the casting. It is a pleasure to see iron castings that shine like new shoes.

The mechanism for the improvement of surface finish by the addition of hydrocarbons to the mold repays examination in some detail. The carbon film forms on the front of the advancing liquid. There is a suggestion by me (Campbell and Naro 2009) that the carbon deposits on a precursor oxide film (Figure 6.33), on the grounds that the surface graphite, Kish graphite, appears to do the same (as noted by Liu and Loper 1990) and flake graphite seems likely to form on oxides. Whether or not the film forms on a prior oxide film, it becomes trapped between the melt and the mold, and is held there by friction. Thus, as the meniscus advances, the film bridging the meniscus is forced to tear, splitting apart, but of course, immediately re-forming, as illustrated for the films on the advancing melts shown in Figures 2.2 and 6.33. The film is therefore continuously formed and laid down between the melt and the mold by the advancing metal, as though the advancing metal were rolling out its own track like a track-laying vehicle. The film forms a mechanical barrier between the metal and the mold. It is the mechanical rigidity of this barrier, helping to bridge the sand grains, that confers the improved smoothness to the cast surface. Thus, over the years, although there has been much talk about the action of surface tension bridging the gaps between sand grains (and this is clearly true to some extent) the main action in many alloys appears to be the result of the presence of the mechanically rigid surface film. The paper by Campbell and Naro (2009) beautifully illustrates the lustrous carbon film resembling a plate of steel, easily bridging sand grains and thus smoothing the surface of the casting (Figure 6.34a–d).

History now appears to have turned full circle because some resin binders for sands have recently been developed to yield iron castings with reduced incidence of lustrous carbon defects. At this stage it is not clear whether the surface finish of the castings has suffered as a result. If better filling systems using bottom-gating had been employed, the lustrous carbon would have been given its best chance to

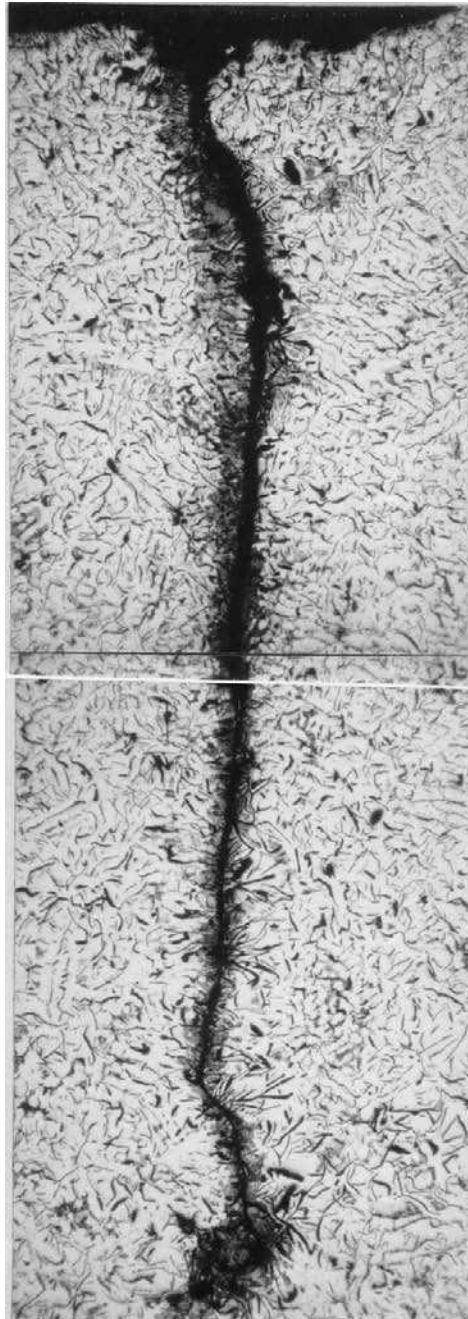


**FIGURE 6.32**

A folded-in lustrous carbon film, forming a carbon bifilm in gray iron.

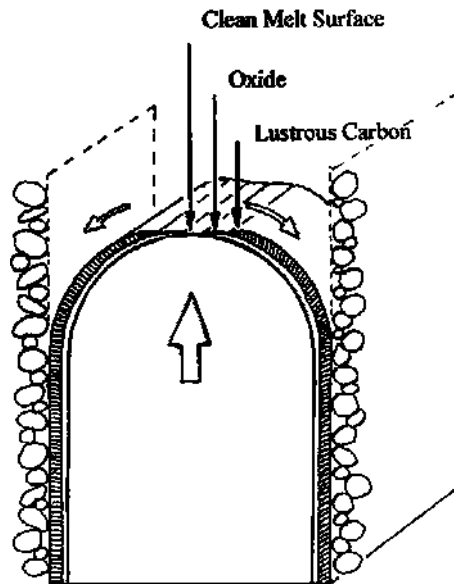


**FIGURE 6.33**

A schematic view of the advancing cast iron front causing the deposited films of oxide and carbon to be trapped between the mold and the metal, leading to the necessary splitting of the films at the advancing front.

enhance the surface finish of the casting with no danger of an entrainment defect. Thus the new reduced lustrous carbon binders need never have been developed.

In lost foam castings using polystyrene foam, lustrous-carbon films cause troublesome defects. In this situation the vaporization of the polystyrene to styrene, and the subsequent decomposition of the styrene to lower hydrocarbons and eventually to carbon, deposits thick carbonaceous films on the advancing surface of the iron (Figure 4.9 shows the decomposition products). Gallois et al. (1987) found the film to consist of three main layers: (1) an upper lustrous multilayered structure of amorphous carbon; (2) an intermediate layer of sooty fibers consisting of strings of crystallites; and (3) a layer adhering strongly to the surface of the iron consisting of polycrystalline graphite enriched in manganese, silicon, and sulfur. Clearly there has been some exchange of solutes from the iron into the film.

In sand castings the often-observed apparent decohesion of the carbon film from the metal surface and adhering to the surface of the mold (Figure 6.34) has previously led to much confused thinking, concluding that the lustrous carbon had formed on the mold. The decohesion of the carbon film from its original substrate had been difficult to explain because most if not all other films such as oxides strongly adhere to their originating matrix, as is demonstrated by anodized layers on Al alloys.

The presence of the woolly, fibrous carbon behind the film and among the sand grains in Figure 6.34a–d is illuminating and probably holds the explanation of this behavior. Clearly the fibrous carbon forms after the film is put in place against the mold wall. Thus it seems that the fibrous material forms at perhaps lower temperatures or at lower concentrations of hydrocarbons. The dense array of fibers, interconnected between the film and the grains, explains how the film, originally on the metal,

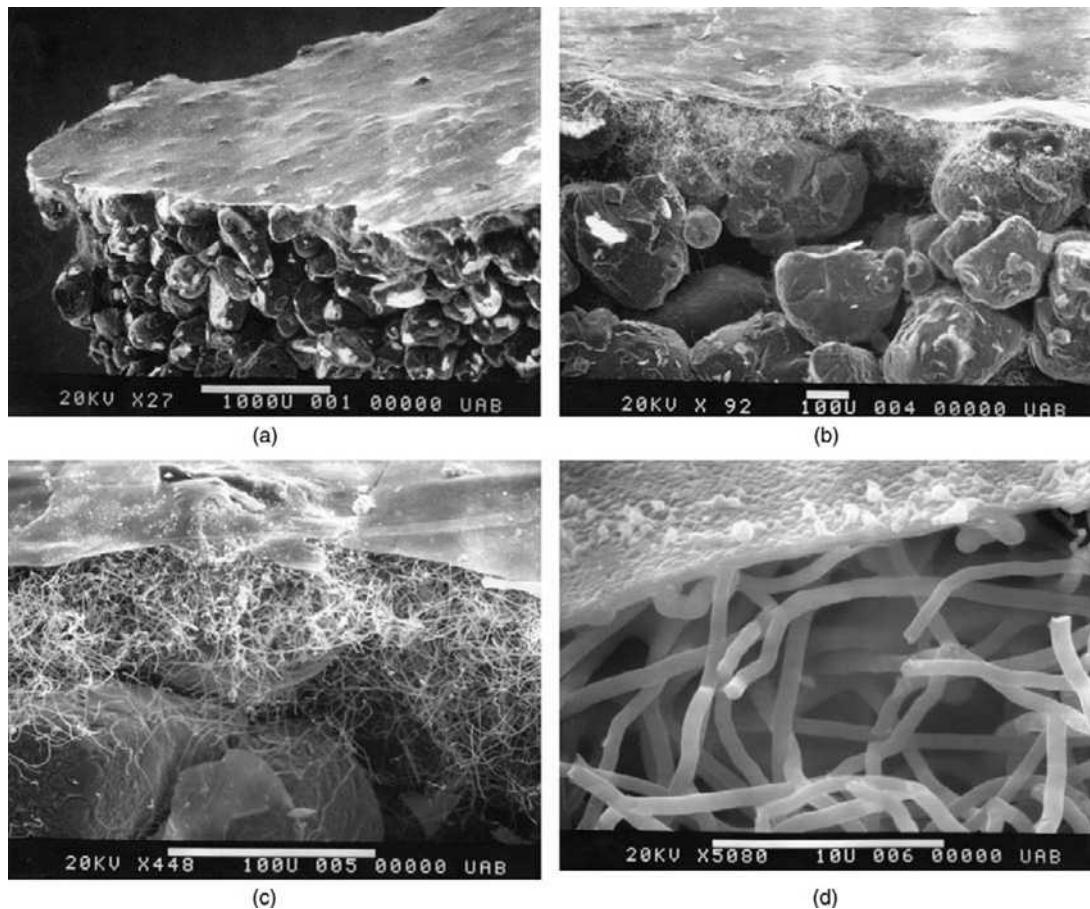


**FIGURE 6.34**

SEM images (a)–(d) illustrating the lustrous carbon film bridging sand grains.

can become rather firmly attached to the mold. Further encouragement for the film to detach from the casting will arise from the enormously different thermal contractions of the substrate casting and the carbon surface film.

Before moving on, it is probably worth reminding the reader that the visible evidence of the thermal decomposition of hydrocarbons  $C_xH_y$  on the surface of the melt is the surface film of remaining carbon. But there is also an invisible legacy: hydrogen will have dissolved in the liquid.

Graphite films that have grown on molten iron have been studied in the form of crystals formed on the surface of Fe–C alloys held in graphite crucibles, and so saturated with carbon before being allowed to cool (Sumiyoshi 1968). These shiny black sheets that float on the surface are analogous to the kish graphite that separates from hypereutectic cast irons during cooling, and are likely therefore to be growing on the underside of the surface oxide film. (For the scientifically minded, the graphite films in this research had interesting features. They were single crystals with numerous cracks along certain

crystal directions, and hexagonal growth steps on the underside that showed how the film grew by gradual deposition of carbon atoms, probably onto ledges from emergent screw dislocations.)

The growth of graphite on melts saturated with carbon, as above, is easy to understand; but how does graphite grow in the case of lustrous-carbon films where the composition of the iron is far from saturated? Such films should go into solution in the iron! Every student of metallurgy knows that at the eutectic temperature the carbon in solution in iron has to exceed 4.3 wt% before free (kish) graphite will precipitate. At higher temperatures the carbon concentration for saturation increases, following the liquidus line for the solidification of kish graphite in hypereutectic irons, as is clear from the Fe–C phase diagram. It seems unlikely that a graphite film can result from an equilibrium reaction. The explanation that follows is an example first mentioned in Section 2.5 relating to soluble films. It shows the effect relies on an interesting dynamic condition.

In an atmosphere containing hydrocarbons, if the rate of arrival of reactants at the free liquid surface is low, then both carbon and hydrogen can diffuse away from the surface into the bulk liquid. The free surface of the melt therefore remains clean.

However, in a highly concentrated environment of hydrocarbon gases the rate of arrival of reactants may exceed the rate of diffusion away into the bulk. Thus carbon will become concentrated on the surface (hydrogen less so, because its rate of diffusion is much higher) and may exceed saturation, allowing carbon to build up at the surface as a solid in equilibrium with the local high levels of carbon. Once formed, it would then take time to go into solution again, even if the conditions for growth and stability were removed. Thus it would appear to have a pseudostability, with a life just long enough so that in some conditions the film could be frozen into the casting if a chance event of surface turbulence were to enfold the surface into the melt.

The folding in of the graphitic film is known to result in the familiar lustrous carbon defect (Figure 6.32). This is, of course, simply a crack lined with the lustrous carbon films. In heavy sections such defects are not seen, probably because they will have time to go into solution before being frozen into the casting. In thinner sections of a ferritic matrix, or mixed ferrite/pearlite matrix, the films can be seen to be partly dissolved as indicated by the layers of the higher carbon content pearlite on either side of the defect.

More speculatively, many irons are poured so turbulently that it is to be expected that huge numbers of graphitic films will be entrained. This raises a distinct possibility that many of the graphite flakes seen on a polished section of gray iron will not be formed as a result of a metallurgical precipitation reaction, but may be the remnants of entrained graphitic bifilms. The occasional appearance on microsections of what seem to be isolated large flakes amid uniform smaller flakes is suggestive of the bi-modal distribution to be expected if such a mixed source of graphite were present.

Recent research has indicated that the conditions for the growth of the graphite film on liquid metals are similar to the conditions required for the growth of diamond films. Reviews by Bachmann and Messier (1984) and Yarborough and Messier (1990) list conditions for the growth of diamond as the breakdown of hydrocarbons and the presence of hydrogen. In the case of iron, the temperature is a little too high for diamond, and so would tend to stabilize the formation of graphite films. But for metals such as aluminum in a hydrocarbon environment, the conditions seem optimum for the creation of diamond on the metal surface. Prospectors and investors will be disappointed to note, however, that the rate of growth is slow, only one micrometer per hour. Thus in the time that most liquid metal fronts exist while pouring a casting, the diamond layers, if any, will be so thin as to be a disappointing investment.



### 6.5.3 Cast iron microstructures

The forms of graphite in cast irons have been the subject of intense interest and huge research efforts over many decades but a full understanding has been illusive. Readers are referred to the review by Loper (1999) for a wide-ranging synopsis covering many details not included in this study. Here, a rather different review is made of the literature, exploring the possibility of a unifying approach based on the hypothesis that oxide bifilms are present in liquid irons.

We have seen how a comprehensive understanding of the microstructure of Al–Si alloys has been proposed in terms of bifilms, explaining both the mechanism of modification and the structures of hypo- and hypereutectic alloys. Nakae and Shin (1999) among many others have drawn attention to the analogous features of Al–Si and Fe–C alloys. This section is an extension of the bifilm hypothesis, apparently valuable to an understanding of the Al–Si system, to a possible understanding of the various morphologies of carbon in the form of graphite and carbides in the Fe–C alloy system.

Adopting an analogous phase diagram to that shown in Figure 6.15 for Al–Si, the equivalent for the Fe–C system is shown in Figure 6.35a. The eutectic at 4.3%C and 1130°C seems fairly well established, although freezing point values up to 1150°C have also been commonly assumed. This seems to correspond to the formation of graphite as flakes on the silica bifilms (in detail, most probably nucleated not directly on the bifilms but on the nuclei already formed on the bifilms). If easy growth on silica is avoided by elimination of the silica, formation of graphite then occurs at some lower

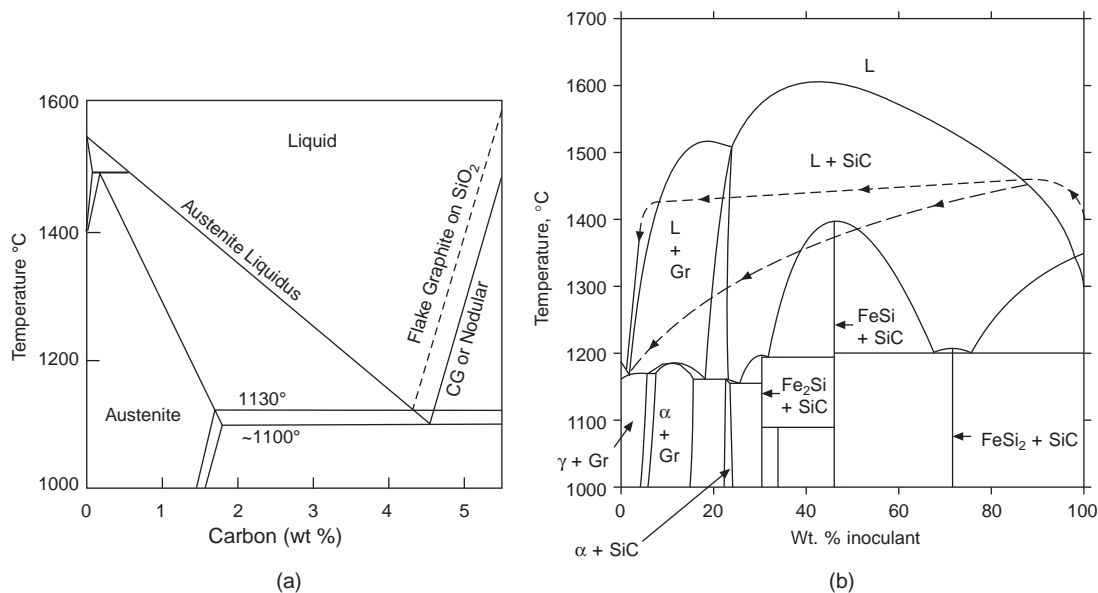


FIGURE 6.35

(a) Fe–C phase diagram showing (i) the high-temperature eutectic in which graphite forms on silica-rich bifilms in suspension in the melt, and (ii) the lower-temperature eutectic of Mg-treated iron in which the eutectic can take different forms in the partial or complete absence of bifilms. (b) The Fe–FeSi phase diagram showing possible melting and mixing routes for a dissolving FeSi inoculant particle (Harding et al. 1997).

temperature, growing as compacted or nodular forms as discussed below. The precise value of the lower temperature is not known at this time, but is probably in the region of 1100–1125°C, and will certainly be affected by the growth form as is clear from thermal analysis curves.

The eutectic composition is also moved to higher levels of carbon, so that the higher carbon levels typical of ductile irons may be at least partly the result of this effect, and not solely the result of the founder seeking greater graphite content to reduce feeding problems. Interestingly, the peak in fluidity, normally indicating the composition of a eutectic, are seen from the work by Porter and Rosenthal (1953) to be close to 4.5% C (Figure 3.11) even though this work was carried out with gray iron. This result indicates that rapidly flowing iron, which would contain turbulently raveling and retaining bifilms in their compact form, flows similarly to ductile iron which contains no bifilms, as might be expected.

### ***Graphite nuclei***

Mizoguchi and co-workers (1997) have demonstrated that austenite is ineffective in nucleating graphite. In fact they find that undercoolings below the liquidus of between 200 and 400°C are required to trigger nucleation by austenite. A more unfavorable nucleus than austenite would be difficult to imagine. The question therefore arises, ‘what does nucleate graphite?’ This question is all the more intriguing following the work by Mampaey and Xu (1997) in which they found that a single population of nuclei (whatever they might be) could explain both gray and ductile irons.

There is a growing consensus that both flake and spheroidal graphite nucleate on similar if not identical nuclei (for instance Warrick 1966) composed of particles of complex oxides and sulfides. This was the conclusion reached in the first study following the development in the UK of the microprobe analyzer (Jacobs 1974). Jacobs and colleagues were the first to carry out an elegant study suggesting that within graphite nodules there is a central seed of a mixed sulfide (they suggested Ca and Mg sulfide) surrounded by a mixed (Mg,Al,Si,Ti) oxide spinel. They found matching crystal planes between the central sulfide, the spinel shell, and the graphite nodule, indicating a succession of nucleating reactions. This exemplary work has been confirmed a number of times, most recently by Solberg and Onsoien (2001).

Many confirmations of this general conclusion have since been made (for instance Skaland 2001) suggesting that the oxy–sulfide mix of the various elements will have a spectrum of lattice spacings ensuring that at least part of the compound will match graphite, and therefore possibly constitute a favoured substrate. As an example of a recent study, while working on preconditioning treatments for gray irons (treatments involving small additions of elements such as Al prior to inoculation – possibly to enhance the population of naturally occurring nuclei in uninoculated irons), Riposan et al. (2008) define a three-stage model for the nucleation of graphite that differs in some details from that by Jacobs:

- (i) Small oxides (<2 μm) are formed in the melt (from preconditioner)
- (ii) Complex sulfides (<5 μm) nucleate on and wrap around the oxides (the presence of Mn and S is necessary; many authors have reported the beneficial effects of S, for instance Chisamera et al. (1996))
- (iii) Graphite nucleates on the sulfides (Ca, Sr, Ba in the sulfide assists nucleation), and, we shall suppose, will attempt to wrap itself around the sulfide particle.

Whether the details of the successive steps of nucleation follow exactly that described by Jacobs or by Riposan are not important for our understanding of the overall mechanism of inoculation. In the

following discussion the mechanisms proposed to explain the various morphologies of graphite are based on the possibility of:

- (i) *nucleation* on specific oxy-sulfide nucleating particles which are effective for all types of graphite,
- (ii) *growth* morphology of the graphite depends on the presence or absence of oxide bifilms of different types that can provide favorable growth substrates.

For a proper understanding of inoculation it will be essential for the reader to keep in mind the separate actions of nucleation and growth.

### 6.5.4 Flake graphite iron (FGI) and inoculation

The treatment of cast irons by the deliberate addition of material to aid the formation of graphite is generally called inoculation. Inoculation of cast irons is important to achieve a reproducible type and distribution of graphite, in order to give reproducible mechanical properties and machinability.

Uninoculated iron is characterized by poor control of the graphite flake morphology. Flakes occur, but are relatively few in number, and uncontrolled in size. The relatively few opportunities for the carbon to precipitate lead to relatively large regions of the iron elsewhere being supersaturated with carbon. Thus iron carbide ( $\text{Fe}_3\text{C}$ ) precipitation is likely in regions that are deficient in graphite nuclei. The mechanical properties of the iron are generally poor. In general, as will become clear during the progress of this account, it seems that some nuclei exist prior to inoculation, but their number and effectiveness cannot be relied on.

#### *The history of inoculation*

I am indebted to my friend Reginald Forrest for an account of the history of the inoculation process.

Ross and Meehan were co-owners of the Ross Meehan Foundry based in Chattanooga, Tennessee, USA (a city later to be immortalized by Glenn Miller with his swing band hit 'Chattanooga Choo Choo'). Gus Meehan was an inquisitive and observant foundryman. He was intrigued by the known benefits of 'treating' the melt with floor sweepings and put the treatment on a more controlled basis in his foundry. The practice became 'standard' in the Ross Meehan foundry and customers were happy. By chance an English foundryman working in Newcastle, UK, learned about this development and corresponded with Meehan to exchange experiences. This was Oliver Smalley, another observant, smart and practical foundryman. They experimented with various mixtures and materials and finally decided on calcium silicide as a major component of their mix, together with ferrosilicon fines and graphite. The mixtures were a closely guarded secret. All this time the consistency of the Ross Meehan cast iron castings was becoming widely known.

They decided to name their iron 'Meehanite' and later 'Meehanite Metal'. They patented their invention in 1922 and began a system of licensing foundries to produce iron castings from controlled (inoculated) liquid cast iron. This system, spearheaded by Smalley, who had the marketing flair, became progressively better controlled with measured response (wedge controls) and producing a spectrum of grades of gray iron known variously as Meehanite irons.

Smalley, the genius of marketing Meehanite, developed the concept of Meehanite as bridging the gap between steel and cast iron. Meehanite licensee foundries mushroomed in the USA and Europe; the issue of licenses being limited so far as possible to good, disciplined foundries who would follow the prescribed practices. Smalley realized that by reaching the end user (the engineers and designers)

and convincing them that Meehanite was a high-quality, consistent and reliable material and that castings produced by Meehanite-licensed foundries were to be trusted – he tapped into a rich vein. This was perhaps one of the first examples of technological foundry marketing.

Gus Meehan was the origin of the Meehanite name that became so famous in the cast iron industry – but Smalley was the real driving force in its commercial exploitation. The Americans and Smalley eventually went their separate ways, splitting the operation: Meehanite Metal Corporation controlled the American and Far East operations and International Meehanite Metal Company (IMMCO) based in the UK controlled European licensee operations. Materials & Methods Limited was the birth child of IMMCO and produced and marketed all of the inoculants and, later, nodularizers used by the licensed Meehanite foundries (and later sold openly to any foundry).

The gradual introduction of the inoculation process from 1922 onwards, and its continued development to the present day (for instance Skaland 2001 and Hartung et al. 2008), was found to greatly increase the number of nuclei available, giving a copious crop of graphite flakes of good uniformity of size, with a reduced tendency to carbide formation, and a consequent benefit to the mechanical properties and machinability of the iron. These benefits are now freely available to all cast iron foundries.

### ***The mechanism of inoculation***

Clearly, inoculation was some kind of process to provide the nucleation of graphite particles. However, the detailed mechanism remained unknown.

What was known was that successful inoculants include ferrosilicon (an alloy of Fe and Si, usually denoted as an inaccurate shorthand FeSi but usually containing approximately 75 wt% silicon), calcium silicide, and graphite. These were added to the melt as late additions, just prior to casting. Additions designed to work over a period of 15–20 minutes were used in a granular form, of size around 5 mm diameter, whereas very late additions (made to the pouring stream) were generally close to 1 mm. Late inoculation was favored because the inoculation effect gradually disappeared; a process known as ‘fade’.

Ferrosilicon is the normally preferred addition, and is known as a ‘clean’ inoculant. Calcium silicide is known to be a rather ‘dirty’ addition, almost certainly because the calcium will react with air to give solid CaO surface films (in contrast to FeSi that will cause liquid silicate films). The folding-in of CaO films during turbulent filling would create particularly drossy bifilm inclusions together with entrained air as porosity. The CaSi addition would probably have been much more acceptable with better-designed filling systems that reduce surface turbulence. (Ductile iron casters experience similar problems when using Mg as a nodulizer.)

It is immediately clear that the common inoculant FeSi does not perform any nucleating role itself. This is because liquid iron at its casting temperature (perhaps 1350–1400°C) is well above the melting point of the FeSi intermetallic compound (1210°C), so that the whole FeSi particle melts (Figure 6.35b).

The evidence now suggests that the molten inoculant continues to exist as a high Si region in the liquid iron. Although the Si-rich region is liquid, and the iron is liquid, and the two liquids are completely miscible, the two nevertheless take time to inter-diffuse. This time is probably the fade time. The Si-rich region slowly dissipates in the melt, eventually disappearing completely. However, during its short lifetime, it provides a local environment with a high effective carbon equivalent value (CEV). To get some idea of the scale and importance of this effect it is instructive (although admittedly

not really justified as we shall see) to calculate the carbon equivalent in one of these regions. For an iron of carbon content about 3%, assuming  $CEV = (\%C) + (\%Si/3)$  we have  $CEV = 3 + 75/3 = 28\%C$ . Extrapolating the carbon liquidus line on the equilibrium diagram to an iron alloy with the huge level of 28%C predicts a liquidus temperature in the region of several thousand degrees Celsius. (This is actually not surprising in view that graphite itself has an effective melting point of over 10 000°C.) Clearly therefore there seem to be good reasons for believing that the carbon in solution in the Si-rich regions is, in effect, enormously undercooled. It is a form of artificial constitutional undercooling (because the graphite is effectively undercooled as a result of a change in the constitution of the alloy).

Now, in reality, it is not appropriate to extrapolate the CEV beyond the eutectic value of 4.3%C. In fact, when this part of the equilibrium phase diagram is calculated, the liquidus surface is nothing like linear, as seen in Figure 6.35b (Harding, Campbell, and Saunders 1997). Even so, this figure shows the liquidus in the hypereutectic region to be very high, so that the essential concept is not far wrong. The path of the dissolving particle is marked on the figure, showing its gradual loss of silicon as the melted liquid region makes its way from right to left across the figure. Different paths can be envisaged for different rates of loss of temperature as are seen in the figure. This slowly disappearing liquid 'package' has to pass through regions where it will experience high undercooling, providing large driving forces for the precipitation of graphite.

The large undercooling, creating a substantial driving force in these liquid regions is almost certainly the reason why, over the years, so many different nuclei have been identified for the initiation of graphite. It seems that even nuclei that would hardly be expected to work at all are still coaxed into effectiveness by the extraordinary and powerful undercooling conditions that it experiences. Studies have shown that many particles that are found in the centers of graphite spherules, and thus appear to have acted as nuclei, whereas identical particles are also seen to be floating freely in the melt of the same casting, having nucleated nothing (Harding, Campbell, and Saunders 1997). This is understandable if the nuclei are not particularly effective. They will only be forced to act as nuclei if they happen to float through a region that is highly constitutionally undercooled.

Studies by quenching irons just after inoculation have revealed a complex series of shells around the dissolving FeSi particle. Hurum (1952, 1965) was the first to draw attention to this phenomenon but it has been studied by several others since (for instance, Fredriksson 1984). Although FeSi itself contains almost no carbon, the carbon in the cast iron diffuses into the liquid FeSi region quickly. Data from Figure 1.4c and Equation 1.5 indicate a time of 1 s for an average diffusion distance  $d = 0.1$  mm, but 100 s for  $d = 1$  mm. The flow resulting from the buoyancy of the high Si melt, and the internal flows of metal in the mold cavity, will smear the liquid Si-rich region into streamers, reducing the diffusion distance to give shorter estimated times for the homogenization of carbon. Thus the shell of SiC particles around a dissolving FeSi particle (Figure 6.36) appears logical as a result of the high undercooling in the part of the phase diagram where SiC should be stable (Figure 6.35b). It seems likely that the SiC nucleates homogeneously because of the high constitutional undercooling. In a shell further out from the center of the dissolving inoculant particle, graphite starts to form. It may be that graphite does not simply nucleate homogeneously as a result of the generous undercooling but can also form in this region by the decomposition of some of the SiC particles.

If all this were not already complicated enough, there is even more complexity. In addition to the dissolving FeSi particle providing (i) a local solute enrichment of Si there will also be (ii) a release of sundry complex inclusions including oxides and sulfides. Commercially available inoculants contain various impurities, and various deliberate additions that supplement the natural nucleating action in

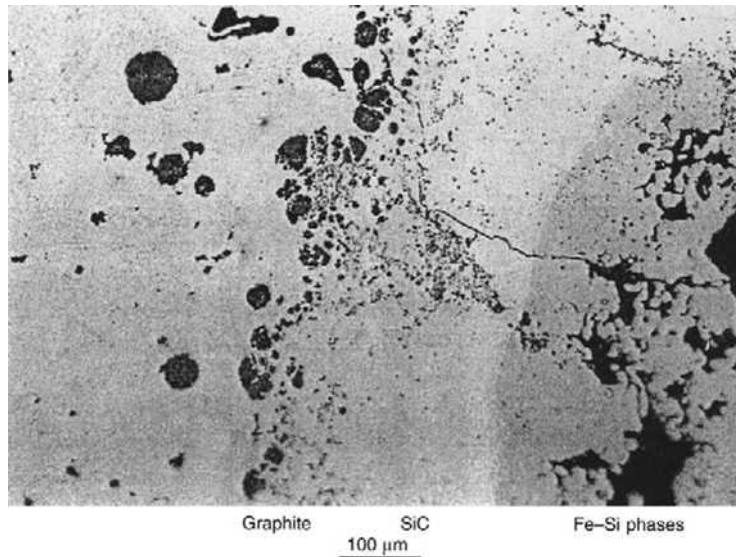


**FIGURE 6.36**

Microsection of a dissolving FeSi particle in a ductile iron, quenched from the liquid state (Bachelot 1997).

this way. These additions include Group 1A elements of the periodic table, Mg, Ca, Sr, and Ba, and often some rare earths such as La and Ce, that will react to create oxides and sulfides. At least some of these may be good heterogeneous nuclei for the formation of new graphite crystals (or perhaps new SiC crystals that may subsequently transform to graphite particles). Also, of course, these particles are provided exactly where they are needed, in the heart of the highly undercooled liquid region. These intentionally added particles will augment the naturally occurring population of nuclei already present in the melt. The overwhelming driving force explains the wide variation of successful nuclei, which, in other circumstances, would be expected to be of only mediocre, if any, effectiveness.

This action of the inoculating material in providing a combination of copious heterogeneous nuclei together with good growth conditions explains the action of graphitizers such as ferrosilicon, and the importance of the traces of impurities such as aluminum and rare earths that raise the efficiency of inoculation.

Ferrosilicon and calcium silicide are not, of course, the only materials that can act as inoculants. Silicon carbide (SiC) is also effective, as is graphite itself. Both of these materials can be seen to provide similar transient conditions consisting of pockets of liquid in suspension in the melt in which high constitutional undercooling promotes the nucleation of graphite in cast irons.

The chain of nucleating effects, oxides–sulfides–graphite, and only in the effectively supercooled regions, has the outcome that graphite particles exist in the melt at temperatures well above the eutectic. The prior existence of graphite particles in the liquid at high temperature, well above the temperature at which austenite starts to form is quite contrary to normal expectations based on the equilibrium phase diagram, but explains many features of cast iron solidification. The expansion of graphitic irons prior to freezing (the so-called ‘pre-shrinkage expansion’) has in the past always been

difficult to explain (Girshovich 1963). The existence of graphite spheroids growing freely in the melt above the eutectic temperature has been a similar problem, seemingly widely known, and seemingly widely ignored, but now provided with an explanation, even though it would be highly desirable to have some additional confirmation at some time in the future.

Harding and co-workers (1997) point out that once nucleated in the regions of high driving force for initiation, the graphite particles attached to their nuclei now will emerge into the general melt where they will become unstable and start to re-dissolve. Feest et al. (1980) find that although the Si-rich inoculant regions disperse relatively rapidly, the graphite formed rapidly in these regions is slow to re-dissolve.

While they were in the undercooled region, the graphite particles would have been expected to grow with extreme speed, thus adopting a thin and branching dendritic morphology. However, on leaving this rapid growth environment and entering a region where growth will suddenly be arrested, and resolution starts, the dramatic change will be expected to result not only in the arrest of growth but the coarsening of the graphite dendrite tips. This effect is seen in material quenched from this region (Figure 6.37) by Benaily (1998).

The observations by Loper and Heine (1961) confirm that graphite can form and survive in both hypo- and hypereutectic irons at 1400°C, well into the liquid range, high above the expected liquidus temperatures. Mampaey (1999) also confirms that graphite forms in the melt prior to the appearance of austenite. (These observations are quite contrary to expectations based on the equilibrium diagram. However, of course, the equilibrium diagram is based on the assumptions not only of (i) equilibrium behavior but also (ii) perfectly uniform composition, neither of which applies during the inoculation of cast irons.)

Thus nuclei will have initiated graphite nucleation in the *constitutionally undercooled* pockets of liquid, but will emerge and start to redissolve in the open melt. However, if they happen to pass through other undercooled regions the graphite will experience sudden bursts of growth, followed by slow dissolution in the bulk of the melt. Finally the graphite particle will approach the eutectic front, which

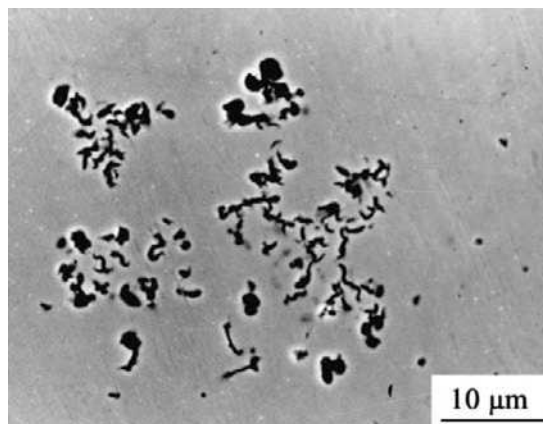


**FIGURE 6.37**

Coarsening of graphite particles on emerging from the undercooled FeSi region (Benaily 1998).

will be *thermally undercooled*, and so enjoy stability and a final spurt of growth before being frozen into the advancing eutectic.

Given sufficient time, all the inoculant particles will have melted and dispersed, leaving no pockets of undercooling floating about in the melt. This is almost certainly the phenomenon known to all foundry personnel as ‘fade’ of the inoculation effect, occurring within a time of approximately 5–20 minutes.

Assuming that the nucleated graphite particles survive, whether their subsequent growth occurs in the form of flakes or spheroids is a completely separate issue, unrelated to the nucleation/inoculation treatment. This is a growth problem. We shall deal with growth separately.

### **Growth of graphite**

Bearing in mind that many second phases and intermetallics precipitate on bifilms as preferred substrates, it seems reasonable to assume that these new graphite nuclei would also preferentially form on substrates provided by oxide bifilms. Having nucleated on the bifilm, the nucleus would in turn nucleate graphite. Figure 6.38 schematically shows a graphite nucleus formed on an oxide bifilm. As the bifilm by chance enters an undercooled region provided by a dissolving FeSi inoculant particle, the nucleus experiences a massive driving force as a result of hundreds of degrees of effective undercooling, forcing graphite to nucleate around the nucleus, and forcing rapid growth.

The newly forming graphite is not able to grow completely around the nucleating particle because the particle itself has grown on the planar bifilm substrate so that at least one of its faces is inaccessible (Figure 6.39). The silica-rich bifilm will form a ‘next best’ substrate for graphite, so although insufficiently favored to cause nucleation, it is sufficiently favored to support the further growth of the graphite. Thus in gray irons the graphite extends across the bifilm, leading to the fairly flat morphology

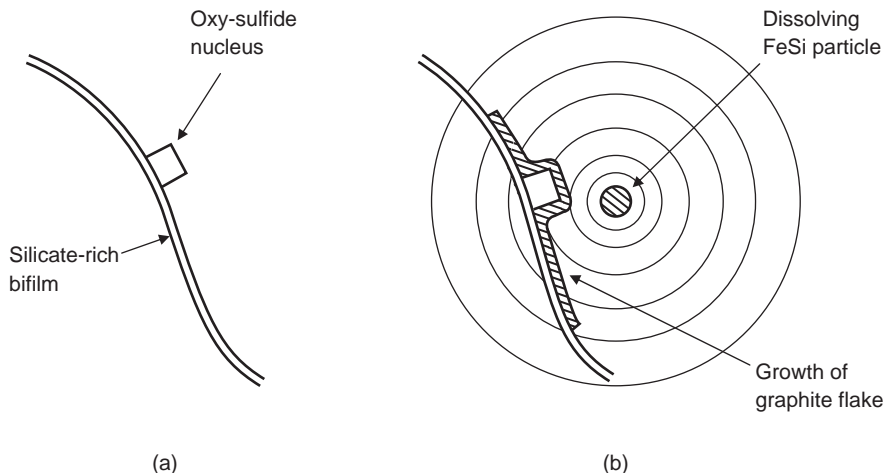


**FIGURE 6.38**

The mechanism of inoculation: (a) a bifilm in suspension in the melt, with oxy-sulfide nucleus (from trace impurities or preconditioners); and (b) the bifilm floating into a constitutionally supercooled region, causing graphite to nucleate and grow on the bifilm.



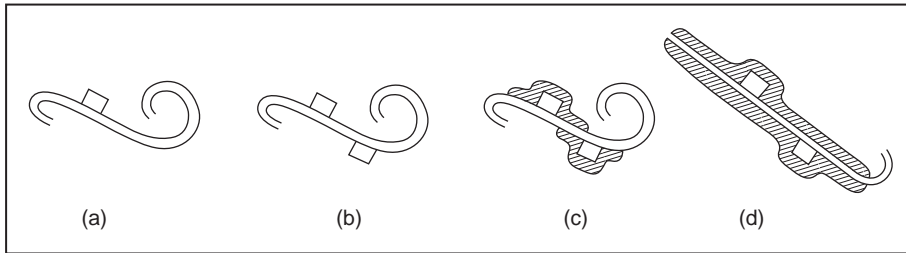


**FIGURE 6.39**

(a) A bifilm possibly supporting some initial nuclei; (b) additional nuclei provided by inoculant; (c) graphite forms on nuclei in supercooled regions; (d) graphite grows as fairly straight flake, straightening the bifilm to create a central crack.

of flakes in gray iron. The flakes grow in regions ahead of the solidification front (i.e. slightly above the general eutectic freezing temperatures) because of the energetically favored growth of graphite on the oxide substrates in suspension (Figure 6.40). The growth morphology of graphite, extending in the directions in its basal plane, would favor the straightening of the bifilm (Figure 6.39d). The bifilm would be expected to be extremely thin, possibly measure in nanometers, its minimal rigidity exerting negligible constraint of the advancing graphite crystal. The freedom from restraint would explain the development of relatively perfect crystals of graphite as observed growing in the liquid ahead of the coupled eutectic graphite (Figure 6.40).

The mechanism proposed above explains the growth of flake graphite from nucleating particles introduced by inoculation. Particles that appear to be nuclei for the initiation of flakes have often been observed, and seem likely to be a universal phenomenon in both flake and nodular irons (Rong and Xiang 1991).



**(10a) flake graphite;  $R = 1.2 \mu/s$**

**FIGURE 6.40**

A straight graphite flake formed on a bifilm freely floating in the melt is overtaken by the coupled growth of the eutectic, and incorporated into the solid (Li, Liu and Loper 1990).

Although a number of experimenters have concluded that graphite nucleates on silica (Tyberg and Graneholt 1970, Gadd and Bennett 1984, Nakae et al. 1991) this is probably an understandable error. In fact it is far more probable that they were observing *growth* of the graphite on silica. Nakea (1993) goes further, to identify the particular structural form of silica as cristobalite. It seems certain in fact that graphite nucleates on compact oxy-sulfide particles, but subsequently grows on silicon oxide bifilms, having the structure of cristobalite if Nakea is correct.

Eventually, the advancing solidification front will overtake those flakes growing on bifilms floating freely in suspension in the liquid. Thus eventually, these freely floating flakes will become incorporated into the solid as seen in the center of the solid in Figure 6.40 by Li, Liu and Loper (1990). Thus it would be expected to be common to see gray irons with two separate populations of flakes, (i) those formed as primary particles by free growth in the liquid, and (ii) those formed by coupled growth with austenite at lower temperatures. The coupled growth mode is discussed below. A bimodal distribution of graphite flakes is therefore to be expected in many microstructures. A bimodal distribution is suggested in Figure 6.40 but is more clearly seen in Figure 6.41. Less obvious but important bimodal distributions are probably common, as may be inferred from the work of Enright and colleagues (2000) using automated fractal analysis of microstructures.

### ***Practical experience with inoculation***

Goodrich (2008) attributes the *Type C* iron (ASTM A247), characterized by large, very straight flakes, with some branching, to the result of the growth of the flakes in the liquid, unencumbered by the presence of austenite. He calls these ‘pro-eutectic’ flakes. They originate in suspension in the melt and are therefore capable of flotation to the upper regions of a casting. The more common *Type A* graphite flakes are similar, displaying only minimal irregularity, suggesting a similar origin and behavior in the melt. Loper and Fang (2008) use deep etching to reveal what they call ‘pre-eutectic’ flakes with elegant hexagonal symmetry, and apparently largely free from defects. For many other irons, the presence of a dense mesh of austenite dendrites constrains the size and shapes of flakes and prevents any significant buoyancy problems (Loper 1999).



**FIGURE 6.41**

Two populations of flakes; one formed on bifilms and the other formed as a classical couple eutectic appearing as undercooled or coral form (Hillert and Rao 1967).

More usually in castings, the graphite flakes are seen to branch relatively frequently. In terms of the bifilm substrate this is straightforwardly understood from the irregular structure of the bifilms. During their entrainment from the liquid surface into the bulk melt they tend not to entrain as nicely parallel double films, but as randomly folded, messy structures. Thus folds leading to parts of the double film at irregular angles to the main bifilm fold are to be expected, and would account for the branching of growing flakes.

Experience of variable performance is also to be expected. For instance on the Monday morning, after the melt has been held for the weekend, operators commonly find the iron has poor graphite structure, despite attempts to provide nuclei by inoculation. We may speculate that this is the result of the gradual floating out of the bifilm substrates. Similarly, iron heated to high temperature suffers a similar degradation of graphite structure, almost certainly as a result of the dissolution of the bifilms because of the instability of  $\text{SiO}_2$  above about  $1450^\circ\text{C}$  in the presence of carbon. It would be interesting to know whether the melt, after losing its silica-rich bifilms at high temperature, would regain its good solidified structure when cooled once again, since although de Sy reports that the silica reappears in the melt on cooling, without some kind of surface turbulence the form of the silica may not be a bifilm, nor even a film, but may be a compact particle. As such, it is not likely to be a good substrate for the development of a good flake structure. Even so, the final pouring of the melt into the mold may provide sufficient turbulence to address this problem, making the problem essentially invisible to those attempting to study the effect.

In agreement with the prediction that graphite grows on oxide bifilms, the effect of oxygen addition to the melt during the pouring of iron into the mold is demonstrated by a number of authors. For instance Basdogan et al. (1980) and Chisamera et al. (1996) found oxygen to be highly effective in converting carbidic irons into beautifully 'inoculated' flake graphite irons. Liu and Loper (1990) found that oxygen was necessary to nucleate kish graphite on the surface of gray iron melts. Larger quantities of kish were formed at temperatures below  $1400^\circ\text{C}$ , below which  $\text{SiO}_2$  is stable, and kish was not observed in Si-free melts. Moreover, Johnson and Smart (1977) describe a critical experiment in which they use sophisticated Auger analysis to prove that two or three atomic layers of oxygen (and interestingly, sulfur) are present on fracture surfaces of the matrix adjacent to graphite flakes (fractured and observed in high vacuum) but the surfaces of the hollows left by spheroidal graphite nodules exhibited no oxygen. This is behavior consistent with a bifilm hypothesis, and with the assumption that the graphite itself may be strong, the presence of the bifilm gives it the appearance of weakness in tension. Briefly, if flake graphite formed on one side of an oxide bifilm the fracture surface would necessarily travel along the center of the oxide bifilm, revealing the oxide on both the graphite and the matrix, but oxides would be absent in the case of spheroidal graphite iron (as discussed below). Interestingly, if the graphite flake had nucleated on both sides of the oxide the fracture path would have passed through the flake, but would still have revealed the presence of oxygen, this time on both of the graphite faces. Johnson and Smart do not appear to have tested this condition.

Although all the above discussion relates to silica-based bifilms, there is evidence that alumina-based, or possibly Al-containing Si-based bifilms (for instance based on mullite or other stable aluminosilicate compound) exist. Carlberg and Fredriksson (1977) find that cast irons based on Fe-C-Si exhibit fine graphite structures, whereas those based mainly on Fe-C-Al display coarse graphite flakes. Chisamera (1996) confirms that conventional gray irons containing Al develop coarse graphite flakes.

The relatively poor mechanical properties of gray iron seems likely to be more to do with the presence of bifilm cracks down the centers of graphite flakes (or the sides of graphite flakes if graphite

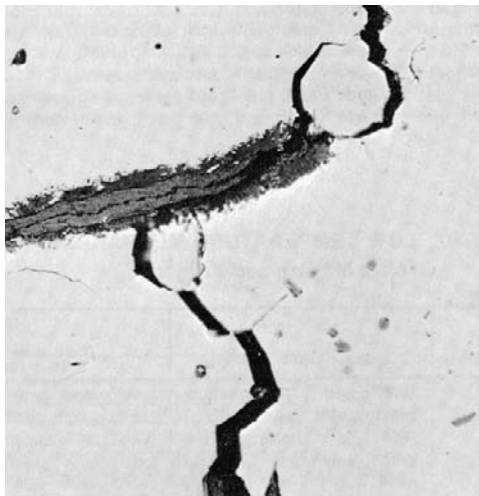
grows on only one side of the bifilm – the impression given that the flake has decohered from the matrix) rather than any intrinsic weakness of the graphite itself. (It seems possible that graphite is strong in tension perpendicular to its basal plane, while retaining its easy slip parallel to the basal plane.) A crack down the center of a flake is seen in Figure 6.42. In their studies of crack initiation and propagation in irons, Voigt and Holmgren (1990) report many centerline cracks in graphite flakes plus some decoherence from the matrix.

The above discussion relates to those graphite flakes growing freely in the melt giving rise to large, randomly oriented flakes which tend to float or settle irregularly, creating what has been called in the past an ‘anomalous’ or ‘irregular’ eutectic; i.e. a eutectic whose phases are not regularly sized and spaced, in contrast to a classical eutectic whose spacing is regularly ordered and controlled by diffusion.

### 6.5.5 Nucleation and growth of the austenite matrix

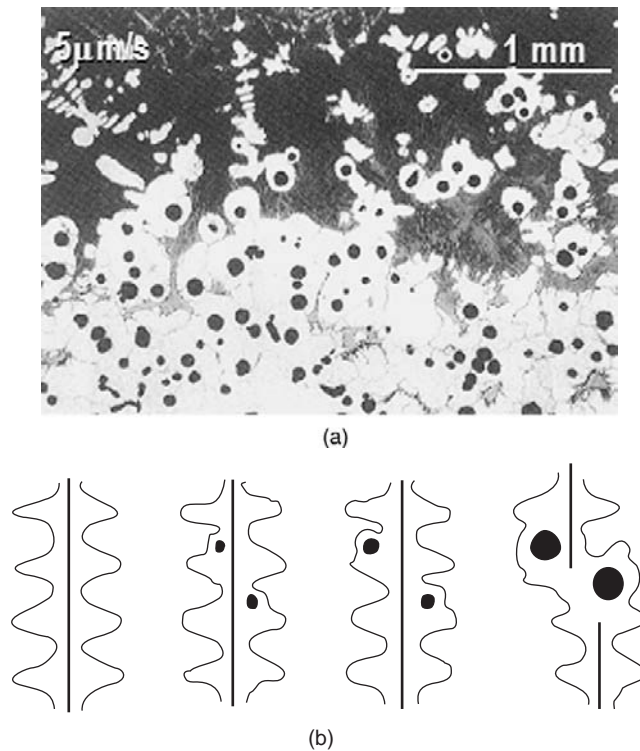
The nucleation of the austenitic matrix of cast irons has, to the author’s knowledge, never been researched. Furthermore, it is not especially clear that the problem is at all important. For instance, if a fine austenite grain size could be obtained, would it be beneficial? The answer to this question appears to be not known. Moreover, in the section on steels the grain refinement of austenite is seen to be unsolved. Thus in all this disappointing ignorance, we shall turn to other matters about which at least something is known.

Only recently, two different teams of researchers have revealed for the first time the growth morphology of the austenite matrix in which the graphite spherulites are embedded. Ruxanda et al. (2001) studied dendrites that they found in a shrinkage cavity, finding them to be irregular, each



**FIGURE 6.42**

Graphite flake exhibiting a central crack (the solid state precipitation of surrounding temper graphite is also fractured off) (Karsay 1971).

**FIGURE 6.43**

(a) The growth front of ductile iron (Li, Liu and Loper 1990); (b) the distortion of dendrites as a result of the internal expansion of nodules (after Hillert 1968).

dendrite being locally swollen and misshapen from many spherulites beneath their surfaces (Figure 6.43). Rivera et al. (2002) developed an austempering treatment directly from the as-cast state that revealed the austenite grains clearly. The grains were large, about 1 mm across, clearly composed of many irregular dendrites, several hundred eutectic cells, and tens of thousands of spherulites. The dendrites from both these studies have some resemblance to the aluminum dendrite shown in Figure 5.33.

It seems fairly certain, therefore, that the growth of the austenite dendrites occurs into the melt in which there exists a suspension of graphitic particles. The particles hover with what seems to be neutral buoyancy despite their very different density. This arises because their small size confers on them such a low Stokes velocity that they are carried about by the flow of the liquid: using Stokes relation it is quickly shown that a 1- $\mu\text{m}$ -diameter particle has a rate of flotation of only about  $1 \mu\text{m s}^{-1}$ , corresponding to a movement of the order of one dendrite arm spacing in a minute. Particles of 10  $\mu\text{m}$  diameter might have a more irregular form as in Figure 6.37. Thus despite their larger size, this would reduce their overall average density difference, and increase their viscous drag, so their flotation rate would hardly be higher. Thus many particles would have plenty of time to be incorporated into the dendrite structure.

Once trapped, the surrounding dendrite would be expanded and distorted by the continued growth of the graphite particle as in Figure 6.43, since, at these temperatures, the surrounding solid will be no barrier to the rapid diffusion of carbon to feed its growth. This micro-expansion of the dendrites translates of course to the macroscopic expansion of the whole casting, the expansion of the mold, and even the expansion of the surrounding steel molding box, if any. Sub-microscopic rearrangements of atoms can accumulate to become irresistible forces in the macroscopic world. This is *mold dilation* leading to an increased demand from feeders, or porosity in the casting.

### 6.5.6 Coupled eutectic growth of graphite and austenite

So far we have considered the separate nucleation and growth modes of graphite and austenite, as though these were unrelated. In fact the relation between the two is sometimes so poor as to make any eutectic relation hardly discernible. This rather loose relation between the two major phases has sometimes resulted in such eutectics being called ‘anomalous’ or ‘irregular’ as mentioned above. In this section we move the focus from ‘anomalous’ to the truly regular, ‘classical’ eutectic form, in which austenite and graphite grow in a closely cooperative mode, known as coupled growth.

In the absence of suitable nuclei that have formed on oxide substrates in suspension in the melt, the carbon in solution will be unable to precipitate. Thus the melt will continue to undercool until the undercooling finally becomes sufficient to provoke precipitation on some other (less favorable) substrate. Only relatively few such nuclei will operate, activating in those parts of the melt that are especially cool, such as those regions close to the mold walls. The subsequent evolution of heat will inhibit other nuclei from becoming active.

At modest undercoolings the coupled growth takes the form of rosettes, often called ‘cells’ (Figure 6.44). Thus it seems likely that a single initiation event on a nucleus, often sited on the mold

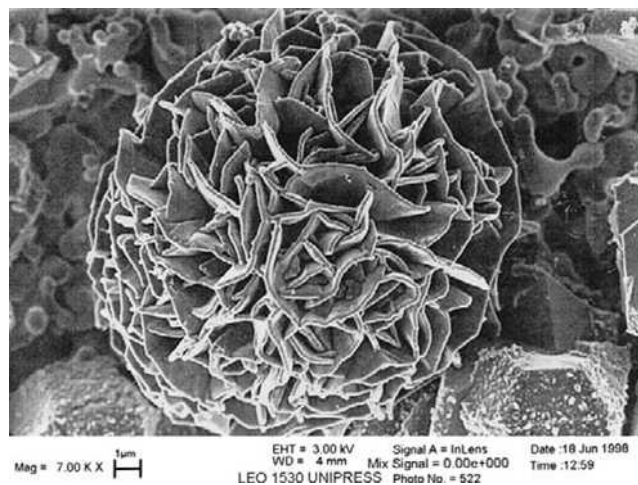


**FIGURE 6.44**

SEM image of deep - etched rosette of flake graphite, expanding to form a ‘cell’ or ‘eutectic grain’ (courtesy of Fraz, Gorney and Lopez 2007).

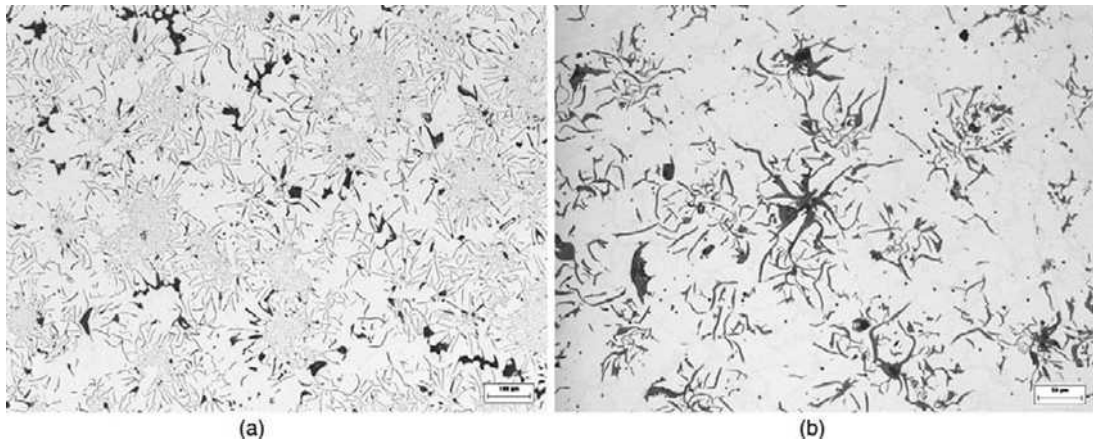


**FIGURE 6.45**

An array of cells (or eutectic grains) in a gray iron (optical micrographs courtesy of Serge Grenier QIT 2010).

wall, expands the coupled growth front as a hemisphere to form the rosettes or cells (Figures 6.44 and 6.45a). The cells are beautifully regular structures, with inter-flake distances now strictly controlled by diffusion in the boundary layer immediately ahead of the advancing front. The rosette form seems to be a strictly coupled growth, not requiring the presence of bifilms. It seems probable that it forms in the pockets of undercooled liquid that would impinge from time to time on an outside surface, thus the constitutional undercooling and the thermal undercooling near to the wall of the mold would be additive to promote nucleation on some marginally favorable particle. The strongly undercooled graphite at the centers of some rosettes seen in Figure 6.45a seems to confirm this suggestion for some conditions, but Figure 6.45b suggests conditions more gently undercooled on this occasion. The even spacing is easily understood if nucleation is prolific, because those nucleation events that occur too near to a neighbor will be less favored and may even remelt as its neighbors give off their heat of formation as they grow.

At still lower undercoolings, after initiation, the growth of the coupled eutectic is probably so fast that it will spread sideways to cover large undercooled regions at the mold wall. It will subsequently proceed on a substantially planar growth front, growing away from the wall. Thus only growth can now occur. It is the growth phenomenon that dominates the structure we call coral graphite (Figure 6.17). This fine, more highly undercooled eutectic, sometimes designated Type D or E according to ASTM specification A247, seems in general to have been avoided for general engineering castings. This is possibly because the inter-flake diffusion distance is now so small that only ferrite can be formed, limiting the strength of such irons.

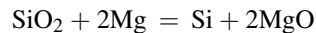
During coupled growth, flakes have to continually realign their growth direction because of the intrusion of their neighbors into their growth space. Since the growth direction of graphite is mainly parallel to the basal (0001) plane this means that the crystal has to develop faults to allow it to change direction. This explains the ‘coral’ type of graphite morphology, which is highly faulted (Zhu et al. 1985). We would expect therefore that types D and E graphite would be highly faulted, containing high defect densities, whereas rosette (or cell) graphite would represent an intermediate case as a result of

its larger spacing. Flake graphite, as mentioned above, would be expected to contain the least faults, growing without any significant restraint as an almost perfect crystal.

For interested readers, Nakae and Shin (1999) present beautiful micrographs to illustrate in detail the close similarity between the coral forms of Fe–C and Al–Si alloys (even though they fail to mention, and appear possibly not even to have noticed, the coral growth of Fe–C shown by their work).

### 6.5.7 Spheroidal graphite iron (SGI) (ductile iron)

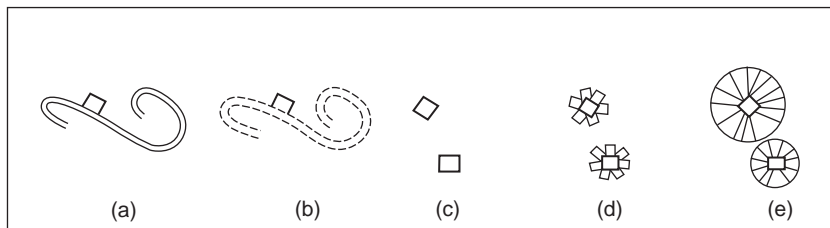
When excess magnesium is added to the melt, the oxide bifilms are completely eliminated. In the case of silica bifilms the silica will be reduced by magnesium to (i) silicon metal which will dissipate into solution in the matrix, and (ii) solid magnesium oxide that will precipitate probably on the pre-existing nuclei that originally sat on the films, possibly augmenting these original particles. The reaction is simply



The total loss of bifilms means that only solids remaining in suspension in the melt now are the original particulate nuclei, possibly augmented by additional MgO. If sulfur is also present in the melt, the MgO is likely to contain a component of MgS. These compact nuclei are now the only nucleation sites available for the precipitation of graphite. The precipitating graphite grows over the compact nucleus, wrapping completely around it so as to form a compact initiating morphology.

The disappearance of the bifilms and the initiation of spheroids are shown schematically in Figure 6.46. The ‘wrapping around’ process (Figure 6.46d) may consist of re-nucleation of many separate microscopic grains of graphite on favorable fragments of the oxy–sulfide surface. The growth mode is probably some kind of addition of carbon atoms to spiral growth steps generated by [0001] oriented screw dislocations (Figure 6.47). In this way the radial structure of graphite nodules develops from the graphite grains growing radially out from the compact nucleus to form the familiar approximately spherical nodule (Figure 6.48).

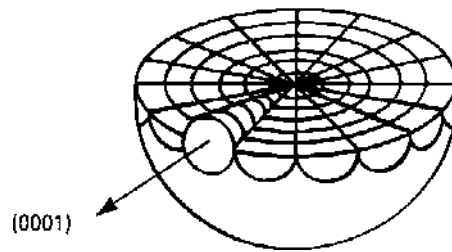
Johnson and Smart (1977) use the sophisticated and respected perturbation analysis by Mullins and Sekerka to suggest that interfacial energies are of importance in spheroidizing graphite nodules up to a diameter of perhaps 50 nm, after which the spherical form can no longer be stabilized. Thus much



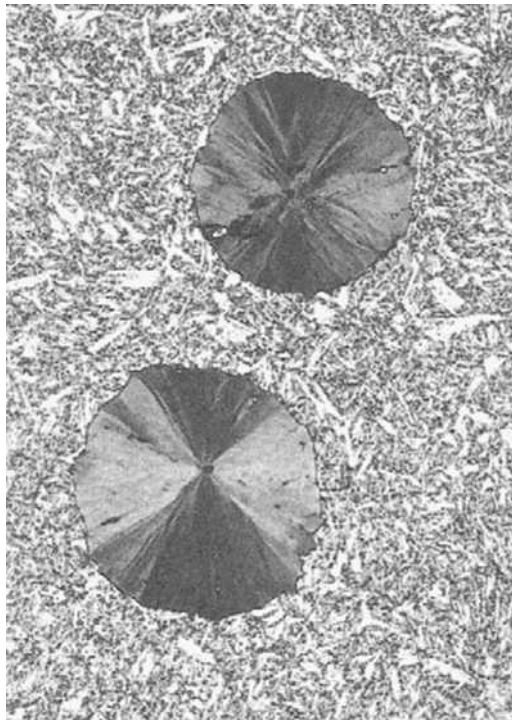
**FIGURE 6.46**

(a) The melt with a population of bifilms with sundry attached nuclei from impurities or preconditioning additions; (b) the elimination of the silica-rich bifilms by Mg; (c) the survival of the existing nuclei plus possible additional nuclei from inoculation; (d) the nucleation of graphite, wrapping completely around nuclei, particularly if they happen to pass through supercooled regions; (e) growth of spheroids.



**FIGURE 6.47**

The probable structure of a graphite nodule (Stefanescu 1988).

**FIGURE 6.48**

Graphite nodules in an austempered iron indicating nucleation on a small central inclusion followed by radial growth (Hughes 1988).

speculation by earlier authors that interfacial energies may be important in defining the shape of spheroidal graphite seems not relevant.

In his recent review, Stefanescu (2007) concludes that all the evidence points to nodules initially growing freely in the liquid, subsequently developing a shell of austenite, and finally contacting and

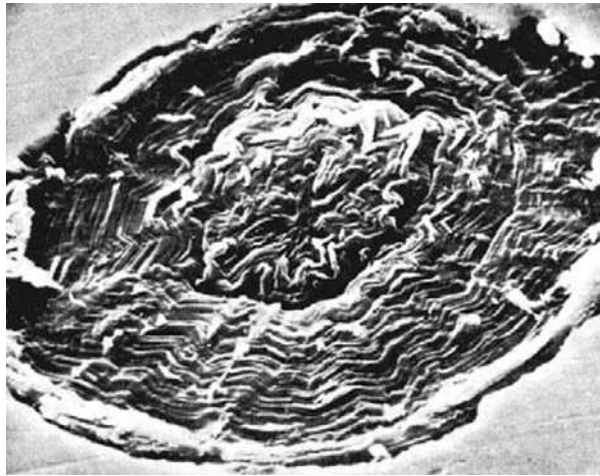


**FIGURE 6.49**

The chaotic growth structure of a graphite spherule, cathodically etched in vacuum, and viewed at a tilt of  $45^\circ$  in the SEM (Karsay 1985, 1992). Reprinted with permission of the American Foundry Society.

becoming incorporated into an austenite dendrite. A minor modification of this development may be envisaged, in which the graphite nodule does not grow a shell of austenite until it contacts an austenite dendrite. At that moment, a shell of austenite would be expected to wrap itself rapidly around the nodule. Painstaking metallography would be required to clarify this detail. Anyway, whatever the finer details of the encapsulation process, the shell of austenite seems a key feature associated with the growth of spheroids.

The separate nature of the growth problem can be appreciated from a close look at the graphite structure around some central nucleating particles. The structure in graphite spheroids close to the nucleating particle is sometimes seen to be highly irregular (Figure 6.49). The graphite form in this region appears chaotic, as perhaps might be expected if the effective undercooling leading to dramatically fast initial growth were to be in some kind of dendritic form (Figure 6.37). Clearly, after a very short growth distance, whatever original crystallographic orientation the graphite might have enjoyed with the oxy–sulfide nucleus is quickly lost in the rapid, chaotic growth. However, after a further small distance, the graphite organizes itself, and develops its nicely ordered radial grains typical of a good spheroid. Thus the organization of the growth takes time to develop, and is a macroscopic phenomenon. A strong analogy with the planar growth condition of a metal under conditions of low constitutional undercooling can be seen.

The spherical growth form almost certainly has at least some contribution from macroscopic influences. To influence the roundness of the growth form, a mechanism cannot be on an atomic scale, but must act on the scale of the spheroid itself. Such mechanisms might include (i) a low constitutional undercooling condition in the surrounding liquid when in the free-floating state, encouraging a smooth interface analogous to the planar growth of the metal at low driving force for growth, or (ii) a mechanical constraint imposed on the expanding sphere when surrounded by solid, but plastically deforming, austenite. It is just possible that (iii) some adsorption on the surfaces of the growing crystal,

limiting growth directions, may be important. There are no shortages of theories on this issue, and facts are hard to establish.

We shall attempt to evaluate here what seems to me to be perhaps the most likely mechanism: the mechanical constraint by the surrounding solid.

The spherical morphology of the graphite nodules may be encouraged by the mechanical constraint provided by the nodule having to force its growth against the resistance provided by its surrounding shell of austenite (Roviglione and Hermida 2004). A number of studies have clearly revealed the deformation of austenite dendrites by the growth of internal nodules (Figure 6.43). This lumpy morphology has been attributed to various mechanisms, all of which are likely to contribute to some degree:

- (i) Ruxanda and colleagues (2001) and Stefanescu (2008) assume the protrusions to be the natural growth shapes arising from cooperative growth of austenite and graphite by diffusion from the liquid.
- (ii) Buhrig-Polackzed and Santos (2008) indicate in a schematic illustration that the contact between nodules with their austenite shells and the austenite dendrites results in their mutual assimilation, to create a local bump on the dendrite. (Some subsequent surface smoothing driven by surface energy would be expected to occur rapidly.)
- (iii) Deformation of the dendrite by plastic flow, locally expanding the surrounding solid to accommodate the increasing volume occupied by the graphite has to be important. This effect appears to have been generally overlooked, but appears to be important and worthy of examination, as discussed below.

The pressure developed in a thick spherical shell (Figure 6.50) deforming plastically because of internal pressure is quantitatively expressed by (Chadwick 1963)

$$P = 2Y \ln b/a \quad (6.1)$$

where  $P$  is the internal pressure,  $Y$  is the yield stress, and  $b$  and  $a$  are the external and internal radii of the shell. The logic is as follows: if a perturbation to the spherical graphite shape were

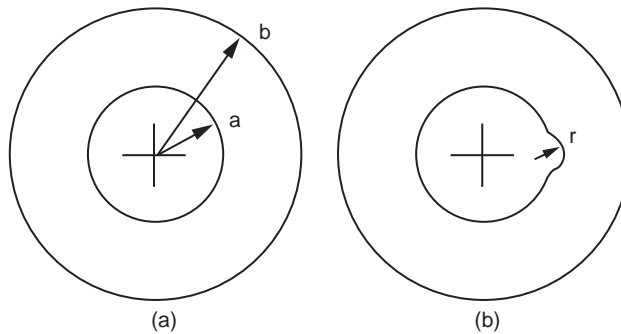


**FIGURE 6.50**

A thick shell expanding plastically because of internal pressure. A perturbation radius  $r$  is not favored because higher local pressure is required. Thus sphericity is encouraged.

to occur, having a necessarily smaller radius,  $r$ , the pressure to plastically extend the growth at this location would (according to equation 6.1) be increased (Figure 6.50b). Thus growth of the extension of smaller radius would be discouraged since additional pressure would be required to stabilize the perturbation. The easier spherical growth mode, simply expanding the uniform radius  $a$ , would therefore be encouraged. It seems therefore that there is some *qualitative* justification for believing that mechanical forces stabilize the spherical growth mode of the nodule.

However, it is useful to ascertain whether there is *quantitative* justification for this mechanism. If we take  $Y$  to be approximately 6 MPa (Campbell 1967) for austenite at the melting point of iron, and  $a = 2$  nm and  $b = 20$  nm, we find  $P = 30$  MPa approximately. Even at values of  $a = 20$   $\mu\text{m}$  and  $b = 200$   $\mu\text{m}$   $P$  is of course unchanged since the ratio  $a/b$  is the same, indicating that there is a substantial restraining pressure, approximately five times the yield stress, on the growth of the nodule during most of its life.

With regard to the possible asymmetric effect of a perturbation of radius  $r$ , taking  $r = a/2$  to  $a/10$  locally increases  $P$  to approximately between 35 and 60 Mpa, respectively. Thus a rounding effect due to mechanical smoothing of the forces to expand the austenite shell appears to be important. Although a creep model rather than the above plastic model might give a somewhat more accurate result, the above result can be relied upon to give us an order-of-magnitude estimate of the effect. I have found creep models and plastic flow models to give very similar answers provided the rates of deformation are similar (Campbell 1968a). Even so, clearly, more work is required to confirm this preliminary indication.

In general agreement with this conclusion, Jiyang et al. (1990) used color etching to reveal the austenite shells around graphite. They found that if the shell formed quickly and completely the nodule developed as a sphere, whereas slow-developing or non-enveloping shells led to mis-shapen nodules, in agreement with our estimates above.

As part of their work in the metals treatment industry, Lalich and Hitchings (1976) observed that some nuclei for nodules were far from round. They noted that the graphite originally wrapped completely around such curious shapes (in agreement with our assumptions in this book) but as growth of the nodule advanced, so the nodule quickly became progressively more round as would be expected from the effect of mechanical constraint encouraging smoothing described here.

In passing, it may be significant that on the addition of Mg causing dissolution of the silica-rich oxide bifilms, any residual gas trapped between the films is expected to be released. In this way it seems possible that clouds of fine bubbles, consisting mainly of argon, will be released into the melt. It seems likely that some Mg vapor will also diffuse into the bubbles. It is not easy to define the sizes of such bubbles with any accuracy. For instance a bifilm of 100  $\mu\text{m}$  square and average 1  $\mu\text{m}$  gas gap would yield a pore of approximately 20  $\mu\text{m}$  diameter. A similar bifilm of average 0.01  $\mu\text{m}$  gas gap would form a pore approximately 5  $\mu\text{m}$  diameter. A very small bifilm of 10  $\mu\text{m}$  square and 0.01  $\mu\text{m}$  average spacing would create a 1- $\mu\text{m}$ -diameter pore. Thus it seems that a fog of bubbles in the range of approximately 1 to 20  $\mu\text{m}$  is to be expected.

It is intriguing, but not perhaps relevant, that there is a theory proposing that nodules nucleate from Mg bubbles in suspension in the melt (Gorshov 1964, Itofugi 1996). However attractive this hypothesis might be to explain graphite coatings inside pores in solidified castings, as a result of the reduction in strain energy involved, any strain energy relief in the liquid state is zero, and the reduction of surface energy to encourage such precipitation in the liquid state seems negligible. Furthermore, the successful

incorporation of solid particulate oxide nuclei into the bubble depends critically on further reduction in interface energies. This is unlikely for particles of oxide formed by precipitation in situ in the liquid, which will be in atomic contact with the melt (i.e. will be well 'wetted', being a necessary condition for the particle to be a nucleating agent). Such particles will be energetically rejected by bubbles. Thus although a mechanism for the presence of extremely fine bubbles may be provided by the present analysis, it appears to be irrelevant to the formation of graphite nodules. It does not offer support to the gas bubble nucleation hypothesis.

A further interesting aside can be noted. The transformation of the planar cracks sandwiched inside the bifilms into clouds of fine bubbles that may float and escape from the alloy is the essence of the process by which apparently brittle gray iron becomes ductile. (Ductile iron only becomes embrittled once again, as noted below, if oxide bifilms are re-introduced by turbulence by handling of the melt or poor filling system design of the casting.)

Finally, curious observations such as that reported by Yamamoto and colleagues (1975) in which flake iron is converted into nodular iron by simply purging the melt with fine bubbles of nitrogen, argon, or carbon dioxide become explicable. From experience in the light metals industries, it is known that purging with gases can eliminate bifilms from melts. Thus spheroidization appears to be achievable via a purely mechanical route, replicating the condition achieved chemically by the addition of Mg. However, the observations by Aylen et al. (1965) in which the graphite structure of pig iron is refined by bubbling nitrogen through the melt is less easily explained. Perhaps nitride bifilms are active, or possibly sufficient oxygen contaminates the nitrogen to create thin silica films. Such observations are tantalizing, and will not be understood without incisive research.

### ***Mis-shapen spheroids***

The presence of ill-formed spheroids, particularly if present in large numbers, is widely known to be associated with the reduction in mechanical properties of nodular irons. Hughes (1988) describes how a good ductile iron can achieve at least 90% nodularity but less good irons can fall to as low as 50% or less and suffer reduced properties. The 50% or so component of flakes or other non-nodular shapes does not particularly affect properties such as proof strength but greatly reduces those properties related to failure, such as tensile strength and ductility. Hughes attributes this loss of fracture resistance to the sharp notches at the root of flakes. However, this widely held belief presupposes that the flakes act as cracks. This is probably only true if the flakes are formed on bifilms; the bifilm providing the crack. It is the presence of the crack that has to be viewed as the principal cause of failure.

In terms of the bifilm hypothesis, graphite would be expected to grow on oxide bifilms. Thus if Mg treatment were carried out to form spheroids, causing the oxygen content to fall to some residual level the silica-rich bifilm content of the melt would fall. Thus in a liquid now cleaned from transient silica-rich bifilms, spheroids would be created in suspension, floating upwards only very slowly as a result of their small size. However, many Mg addition techniques are extremely turbulent, so that large quantities of MgO and Mg silicates are expected to be created by the mechanical entrainment of the liquid surface. These new bifilms will be permanent defects formed from highly stable magnesia (MgO) or magnesium silicate (MgSiO<sub>3</sub>). Prior to pouring into the mold, some of these will fortunately float out in the ladle, adding to the Mg-rich slag. Thus, given a reasonable time for separation (an interesting and clearly important process variable that seems

not well researched) not all of these Mg-rich bifilms find their way into the castings to impair the structure and properties.

Unfortunately, on pouring into the mold, additional large quantities of Mg-rich oxide bifilms are likely to be re-introduced, particularly if the mold filling system is a rather poor design.

On contact with an oxide bifilm, a spheroid would tend to attach firmly to the film, thereby reducing the overall energy of the system. Further growth of the spheroid would then necessarily spread over the plane of the film. The symmetrical spherical constraint previously provided by the surrounding austenite is now also destroyed, aiding the non-spherical development. Thus the spheroid will grow to become significantly mis-shapen.

This effect can be seen in Figures 6.30 and 6.31b. In Figure 6.30 a number of oxide bifilms have been straightened by the growth of dendrites to lie along 100 planes. The nodules attached to the bifilms are clearly poorly shaped. Additional mis-shapen nodules are evident elsewhere in the structure which are expected to be lying on random areas of bifilm not straightened by dendrite growth. In Figure 6.31b it seems likely that the bifilm lies along the grain boundary, decorated with mis-shaped nodules, ferrite, and (probably) some scattering of porosity or cracks.

The phenomenon of mis-shapen nodules has up to now appeared a mystery. The effect is therefore predicted to be associated with either (i) insufficient dwell time for the damage introduced during Mg addition to float out, or (ii) poor casting practice, in which an otherwise nicely inoculated and spherodized melt is re-contaminated with bifilms.

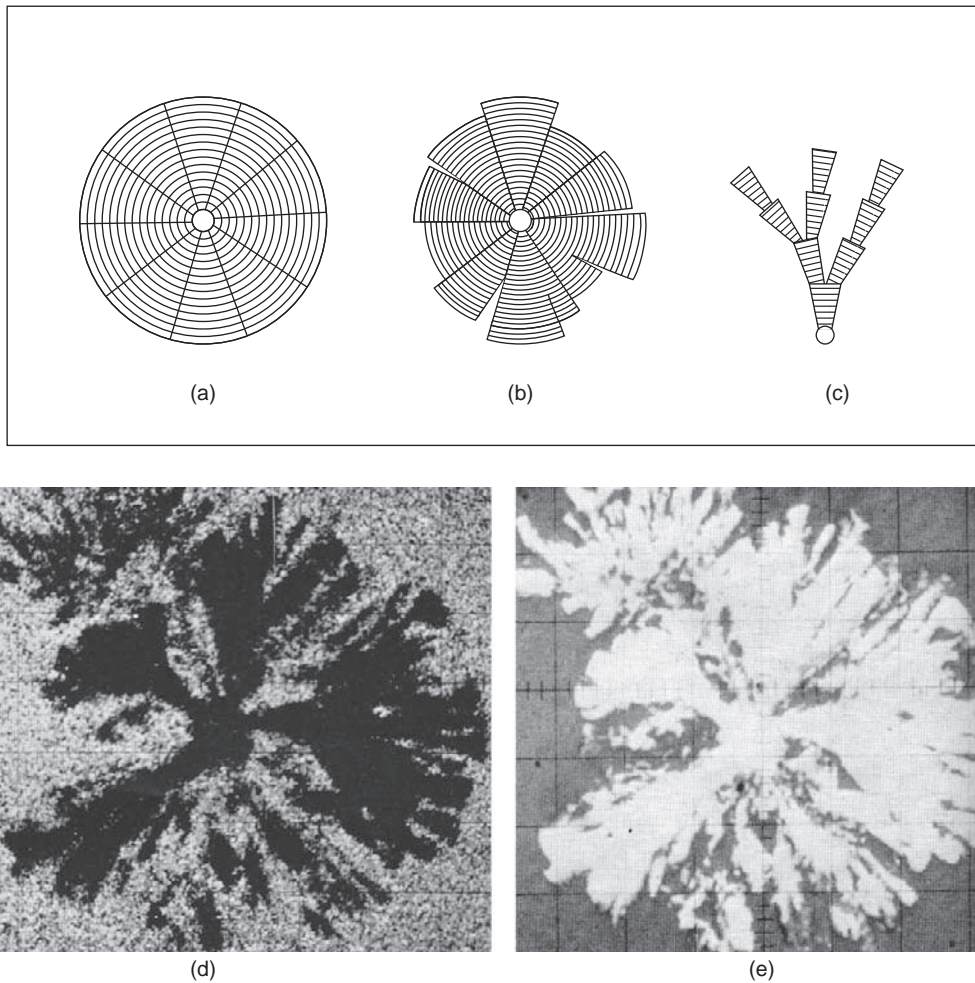
It is interesting to predict that more time after the spherodizing treatment to allow the melt to clear, together with a properly designed filling system, or counter-gravity filling system, should completely solve this problem. A step in the right direction is taken by Takita and colleagues (1999) who observe that nodules are converted from mis-shapes to spheroids by the use of a filter to take out the 'inclusions produced by inoculation'. This positive step contrasts with that taken by Liu and co-workers (1992) who, after the Mg addition, added 'post inoculants'. The post inoculants were highly successful to increase the nodule count, but led to a disastrous fall in nodularity. This was almost certainly a result of adding the inoculants through the melt surface. The inoculants would, of course, have their own oxide skins, which would have doubled up with the entrained surface oxide of the melt to create an asymmetrical bifilm with an alloy oxide on one side and a Mg-rich silicate on the other. On contact with growing graphite particles, this major source of fresh bifilm contamination would lead to the growth of non-spheroids.

Furthermore, of course, the significant reduction of properties associate with malformed spheroids cannot be the direct result of the shape of the spheroids, since they occupy such a small-volume fraction of the alloy. The loss of properties is predicted to be the result of the presence of the bifilms in the melt, occupying a vastly greater cross-sectional area than the spheroids. These extensive bifilms will act as cracks in the casting, significantly reducing properties.

### ***Exploded nodular graphite***

'Exploded' spheroids (Figure 6.51) are commonly seen in irons subject to graphite flotation, and especially if the composition of the iron is sufficiently hypereutectic (Sun and Loper 1983, Druschiz and Chaput 1993).

This undesirable morphology is not easily explained at this stage as a result of relatively little experimental work to clarify the problem. Cole (1972) suggested they had suffered remelting as a result of being carried by convection in and out of hot zones of the liquid. This seems most unlikely,

**FIGURE 6.51**

(a) Spheroid and (b) malformed spheroid; (c) chunky graphite (after Liu et al. 1983); (d) SEM iron image of an exploded spheroid; (e) electron image (Cole 1972).

however, since if the nodule had grown uniformly in a compact morphology the uniform graphite would be expected to have a substantially uniform rate of dissolution; solidification and re-melting would be expected to be reversible.

Since exploded nodules appear exclusively in the flotation region of hypereutectic irons two far more likely factors are:

- (i) Nodules growing in a sufficiently hypereutectic melt (Sun and Loper 1983) will experience an enhanced driving force for growth because of the carbon supersaturation that develops as the

melt cools. This will encourage growth instabilities leading to ‘dendritic’ rather than ‘planar’ growth, leading to exploded rather than smooth spheroid surfaces.

- (ii) The nodules may have nucleated early in the liquid phase and grown without the benefit of the mechanical constraint of the austenite. When not pressurized to remain spherical, the nodule will be free to grow more like a dendrite, developing instabilities that grow into projections to its growth front, finally developing the characteristic exploded forms. Evidence for mechanical restraint as a powerful effect is presented in the section on nodular graphite above.

### 6.5.8 Compacted graphite iron (CGI)

If the addition of magnesium is more carefully controlled to some level intermediate between spheroidal and flake iron, compacted (‘vermicular’ based on the Italian for ‘worm-like’) graphite is the result (Figure 6.52).

In our bifilm model it is clear that most of the oxide bifilms will be quickly dissolved by the addition of Mg. However, small patches may remain if the Mg addition is not too high; the tiny patches on which the original nuclei sat will be resistant to dissolution because they will be stabilized by their attachment to the nuclei. (Naturally, it will have been energetically favorable for the nuclei to attach to the bifilm, so that the combination of nucleus and film will enjoy a reduction in overall energy, stabilizing the combination.) Only half of the bifilm will be retained in this way, its distant ‘twin’ half not enjoying the protective influence of the nucleus will dissolve and disappear, since it is separated by an air gap. Only the small part of one half of the bifilm together with its unbonded interface, the remnants of the layer of air, will remain (Figure 6.53b).

The subsequent nucleation of graphite on the nucleus will result in rapid spreading of growth around the nucleus. On arrival at the non-wetted interface belonging to the residual patch of bifilm this spreading will be arrested (Figure 6.53c). The graphite has now grown to reach the residual layer of air on the remaining patch of half of the bifilm. The further growth of graphite is forced to occur not radially but in general unidirectionally away from the bifilm residue (Figure 6.53d). Clearly the growth cannot now be spherical, but its exact form is not possible to predict. Cole (1972) had observed a fine, unidirectional spiral structure similar to the worm-like growth mode clearly seen in Figure 6.52. Liu and colleagues (1980) find that the growth direction is along the C axis (0001 direction perpendicular to the basal planes) and appears to develop by a spiral dislocation mechanism as witnessed by the coarse and irregular spirals that they observe.

The great sensitivity of the compacted graphite morphology to magnesium concentration is corroborated by the proposed bifilm mechanism. If the Mg level is too low, residual bifilms will encourage flake graphite, whereas if the Mg level is too high, the limited stability enjoyed by the residual bifilm patches will be overcome, and the last remaining patches of bifilm will be dissolved, allowing the growth of totally spherical grains.

After nucleation of the compacted graphite form, a number of workers (for instance Su 1982, Mampaey 2000) find that the continued growth of the graphite appears to occur solely in the liquid. Because the graphite stays in contact with the liquid, it transfers its expansion directly to the liquid, reducing feeding requirements (Altstetter and Nowicki 1982). This welcome and valuable good behavior is in contrast to ductile iron in which the graphite transfers its expansion to its surrounding solidified shell, expanding the casting, and the mold, thereby increasing feeding requirements.



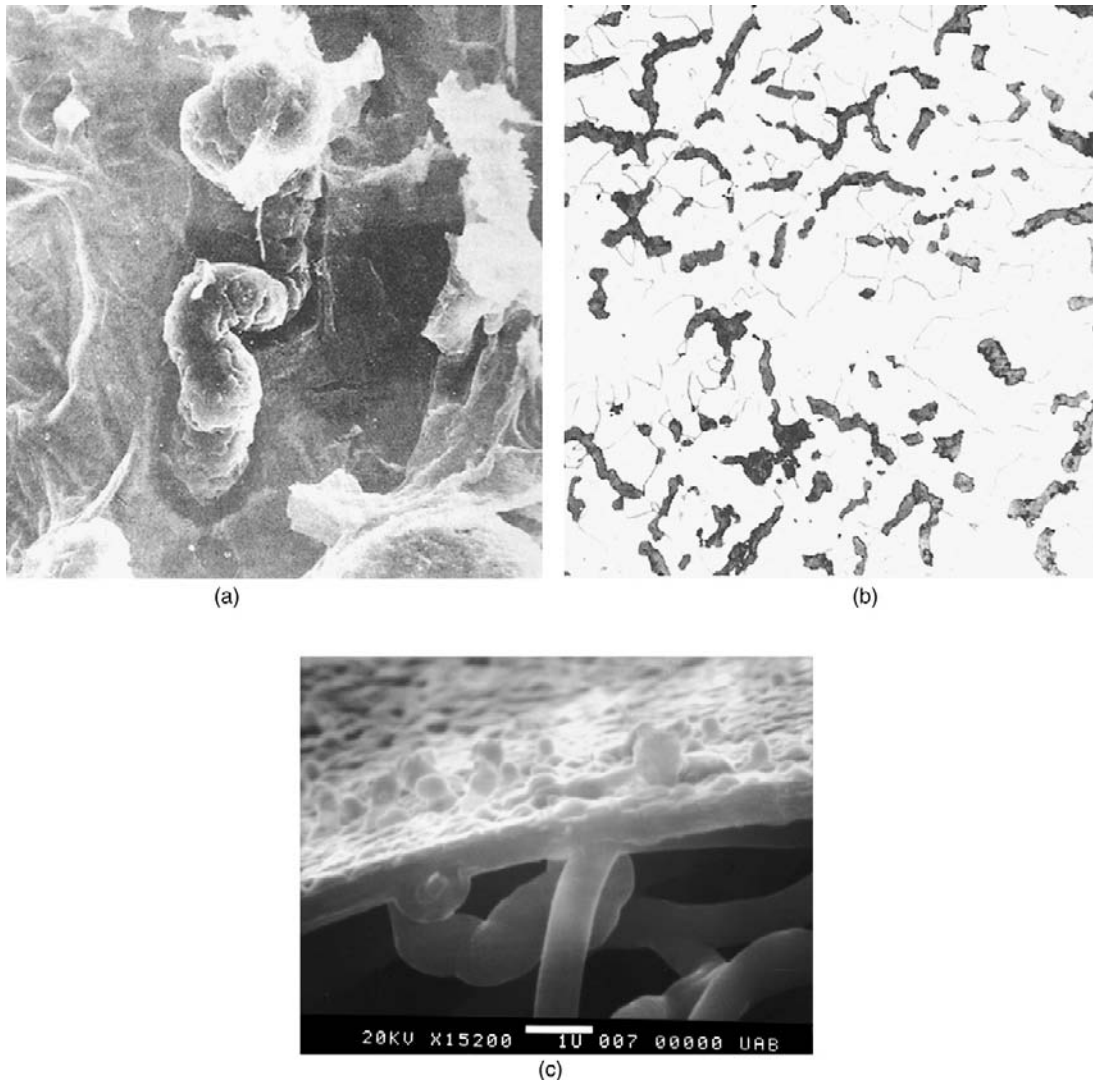


**FIGURE 6.52**

CGI viewed by (a) SEM deep etching and (b) optical metallography (Stefanescu et al. 1988) and (c) carbon wool fiber (growing off a lustrous carbon surface film on a gray iron) as a possible vapor phase equivalent of compacted graphite (Campbell and Naro 2010).

As a fascinating final thought concerning CGI, the fibrous graphite seen growing from the vapor phase in Figure 6.34, and shown in close-up in Figure 6.52b, appears to be identical in form to the graphite grown from the melt as CGI or ‘worm-like’ graphite, and might therefore be viewed as a three-dimensional model, giving an insight into the internal structure of CGI. These free-growing vapor growth phase and liquid growth phase forms of graphite appear to be identical. It is possible that

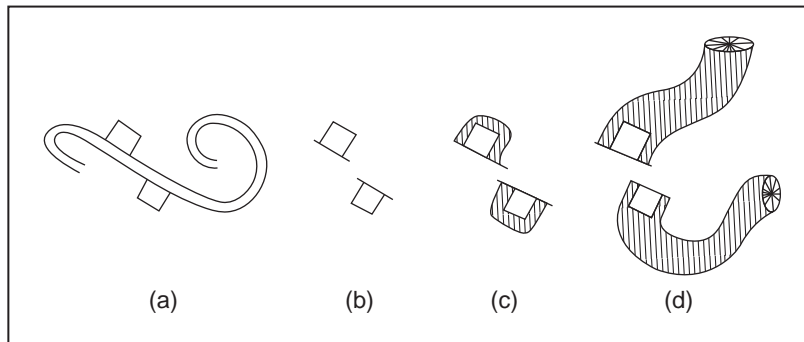


**FIGURE 6.53**

Formation of CGI by addition to (a) nuclei on bifilms of just sufficient Mg to (b) eliminate most of the silica-rich bifilms except for the remnant attached to the nuclei. (c) Inoculation promotes graphite initiation on the nuclei; (d) growth cannot occur by wrapping completely around the nucleus, so that initial growth cannot be spherically symmetrical, possibly favoring unidirectional growth.

the carbon concentration in each of these environments is similar, resulting in similar kinetics of deposition, and similar growth modes.

### 6.5.9 Chunky graphite (CHG)

Chunky graphite is often observed concentrated in the centers of heavy sections of nodular iron castings. ‘Chunky’ is not a particularly helpful descriptive adjective for this variety of graphite. Its ‘chunkiness’ is only apparent under the microscope at high magnification; otherwise it simply appears to be fine, irregular, branched and interconnected fragments (Figures 6.51c and 6.54). Once again, the properties of nodular iron are reduced. However, it seems the loss of properties may, once again, be at least partly associated with the short diffusion distances between branches of the graphite filaments, promoting the development of ferrite instead of the stronger pearlite eutectoid phase (Liu et al. 1983).

Liu and coworkers (1980, 1983) find evidence that chunky graphite grows along the C-axis direction, as does nodular graphite. Furthermore, they report observations on spheroids that exhibit gradual degeneration, gradually taking on the growth forms of chunky graphite. Thus they conclude that chunky graphite is a degenerate form of spheroidal graphite, and their work implies that chunky graphite grows out from spheroids. Itofugi and Uchikawa (1990) confirm the identical growth modes of spheroidal, compacted and chunky graphites as illustrated schematically in Figure 6.51.

All these workers observe the characteristic form of chunky graphite, as an apparently ‘stop/start’ growth in the C-direction consisting of nearly separate pyramidal ‘chunks’ linked by a narrow neck, like beads on a string (Figure 6.51c). The individual chunk sections are comprised of layers parallel to the basal plane, but only nanometers thick. This characteristically lumpy growth may be the result of a pulsating or irregular advance of the growth front, with the austenite advancing to nearly grow over the top of the graphite, forming the nearly pinched-off neck of the graphite, only to be overtaken again because the carbon in solution will now build up in the liquid ahead of the front,

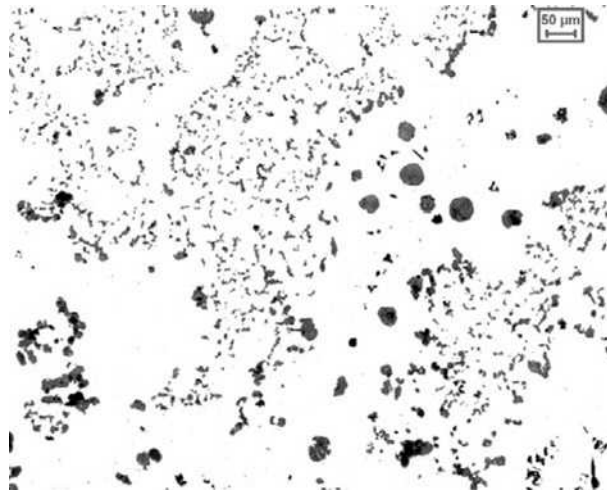


**FIGURE 6.54**

Graphite nodules and areas of fine, chunky graphite in the thermal center of a 200-mm cube casting (Kallbom et al. 2006).

accelerating the next phase of growth of the graphite until the local carbon concentration is depleted once again.

Observations by Kallbom and co-workers (2006) are consistent with an origin associated with bifilms. They observe the chunky graphite to be concentrated in the center of heavy sections, explained by the growth of the freezing front pushing bifilms ahead, and explaining their observations of ‘stringers’ of graphite nodules. These features are almost certainly sheets of oxides decorated with graphite nodules that have been nucleated on the oxide (analogously to those seen in Figure 6.31). The earlier paper by one of these authors (Kallbom 2005) describes how the outer several centimeters of the casting can be perfect, with good nodularity, good strength and ductility, but the structure can change abruptly, over a short distance equivalent to only a nodule diameter, to chunky graphite. Thus the central volume of the casting is weak and brittle. Because the problem is buried in the center of thick section castings it can be difficult to find by non-destructive methods.

All the above evidence that suggests chunky graphite requires the presence of bifilms combined with an absence of nuclei. It is possible to imagine a mechanism in which following a turbulent pour, many bifilms will be pushed ahead of the forest of growing dendrites, forming, at times, a distinct and abrupt separation of the outer dendritic region from the inner residual liquid. The presence of the concentration of bifilms in the center will suppress the normal pattern of free circulation that would ensure a good supply of nodules from the outer, cooler regions into the hot central region. Furthermore, because so much time is available, particles such as nuclei and nodules already in suspension in the center will have time to float out, or existing nodules to dissolve (since they will be unstable at these higher temperatures) depleting the centers of nuclei so that spheroids cannot form.

For those nuclei now floated out to the edge of this region of higher temperature and enhanced segregation, any nodules formed on the nuclei will not enjoy the benefit of a surrounding austenite shell, so that their growth mechanism will more nearly resemble that of an exploded spheroid. Since

these will be at the boundary of the central region, their growth is most likely to be an extension of the nodules along the C-axis (Liu et al. 1980) in the direction of the gradually advancing solidification front. In the absence of nuclei, the whole region would be expected to fill with this continuous growth form. The extended size of chunky graphite regions, much larger than cells of other types of graphite (Itofugi and Uchikawa 1990), corroborates the absence of nuclei in these regions.

The presence of bifilm cracks concentrated in the chunky graphite regions would explain the poor properties that are observed; it is difficult to see how otherwise a continuous graphite phase could reduce properties, particularly since in other irons (such as CGI) a continuous graphite phase is associated with excellent and reproducible tensile properties.

It is hoped that in the near future the explanation for the origin of chunky graphite might be clarified and confirmed by further careful experiments. The key word here is 'careful'. For instance the experiment by Asenjo and co-workers (2009) involving the placement of inoculants in different branches of a runner system to separate molds to compare the effects of mold inoculation in different heavy castings was a clever idea, but regrettably experimentally flawed. This was because, in common with most iron casting, the runners were not designed to be pressurized and fill on a single pass. Thus a reverse flow is likely to have contaminated the mold cavities, and all the cast material would have suffered from turbulence and air entrainment, therefore containing unknown quantities of oxide bifilms. Clearly, in the future, much greater sophistication of melting and casting will be required for experiments designed to clarify the solidification mechanisms for cast irons.

### 6.5.10 White iron (iron carbide)

Work by Rashid and Campbell (2004) has demonstrated the nucleation and growth of carbides on oxide bifilms in vacuum-cast Ni-base superalloys (seen later in Figures 6.62 and 6.63). It would be expected therefore that an analogous reaction would occur in Fe–C alloys, because the austenite forming during solidification also possesses a closely similar face-centered-cubic structure.

Carbides in irons appear to form preferentially at grain boundaries, and appear often to be associated both with residual graphite (sometimes as nodules, malformed nodules, or flakes aligned with the boundary) and pores all forming on the same boundaries (Figure 6.31b). This is a clue to the possible presence of an otherwise invisible bifilm.

Faubert et al. (1990) have studied carbides in heavy-section austenitic ductile iron (ADI). Towards the top of their castings they find degradation of properties more serious than they would have expected from the carbides themselves. They suspected that the real impairment was caused by the presence of films that had floated into this region. The 'films' would in fact have been 'bifilms'. Bifilms would segregate to grain boundaries, and possibly actually constitute the boundary. The presence of the bifilm is not only inferred from (i) the cracked carbides but also (ii) from the linear rows of nodules seen in micrographs from this work; (iii) from the pores as the residues of air bubbles trapped between the films; (iv) from the graphite flakes sitting in the boundary (called by the authors, unflatteringly, 'degenerate' graphite). Both graphite and carbides are expected to form on the wetted, outer surfaces of the bifilms. The presence of the central unbonded region (including the pores) between the films, constituting the crack through the interiors of the carbides, explains the *apparent* brittleness of the carbides. These intermetallic compounds would otherwise be expected to be strong, resistant to failure by cracking at the modest stresses that can be induced by solidification and cooling.

Stefanescu (1988) quotes the work of Hillert and Steinhauser (1960) in which the growth of iron carbide eutectic (ledeburite) occurs by the spreading of carbide (cementite) across a plane, followed by the development of a rod type of eutectic at right angles. It is tempting to consider that the original planar expansion would have been facilitated by growth across the surface of a bifilm. The bifilm would originally have been randomly crumpled, but would have been straightened by the progress of the carbide across its face, thus creating an essentially planar crack that would constitute a serious defect in the carbide. Associated branching cracks would have arisen from irregular folds in the bifilm.

Although carbides in gray irons are feared for their disastrous effect on machinability, they are of course desirable in those components required to withstand wear and abrasion. Furthermore, a complete white iron structure is required prior to subjecting the iron to malleablizing treatments. Although the role of malleable iron has been greatly eroded by the rise of ductile iron, for some products and some foundries the economics are not so different, so that at this time a respectable tonnage of malleable iron is still produced. It will be interesting to see the eventual outcome of this competition.

### 6.5.11 General

Several workers have noted that the initial stages of formation and growth of the graphite particles start with a spheroidal shape, regardless of whether these are destined to grow into spheroids or flakes, or any other type of graphite (for instance Jianzhong 1989, Itofugi et al. 1983). This observation is consistent with the scenarios portrayed in Figures 6.38, 6.39, and 6.46d. The spread of the graphite around the originating nucleus is always nearly spherical, or partly spherical. Even the partly spherical forms will appear spherical in some sections.

Overall, it seems clear that both nucleation and growth mechanisms influence graphite morphology, although these mechanisms dominate to different extents in different circumstances. For instance, nucleation dominates the formation of spheroids and deformed spheroids, whereas for flake graphite both nucleation and growth are influential. For compacted, undercooled coral and chunky graphites nucleation occurs once to initiate each cell, after which continuous growth dominates the development of the structure, leading to continuous branching morphologies. Indeed, the finer, fairly continuous forms, coral, chunky and compacted graphites, are so similar that they often seem to be confused in the casting literature (see Figure 6.55). They do seem similar in the sense that they all appear to be more-or-less coupled growth forms, advancing together with the austenite.

If, as proposed here, the various forms of graphite are significantly influenced by the presence or absence of bifilms, it would explain the historical resistance of the cast irons to explanation so far. This seems typical of bifilm phenomena.

Furthermore, it seems likely that the principal cause of reduced mechanical properties in all cases of non-spheroidal forms of cast irons is the presence of various kinds of oxide bifilms acting as cracks. Ductile iron owes its ductility to graphite that forms in the absence of oxide bifilms, but when oxide bifilms (mainly magnesia-rich) are entrained by poor casting technology, even ductile iron can be seriously reduced in ductility, possibly failing brittly by the 'plate fracture' mechanism as we have seen.

### 6.5.12 Summary of structure hypothesis

1. Cast iron melts normally contain oxide double films (mainly  $\text{SiO}_2$  bifilms) in suspension.
2. Inoculation produces oxy-sulfide particles which nucleate on silica-rich oxide bifilms.

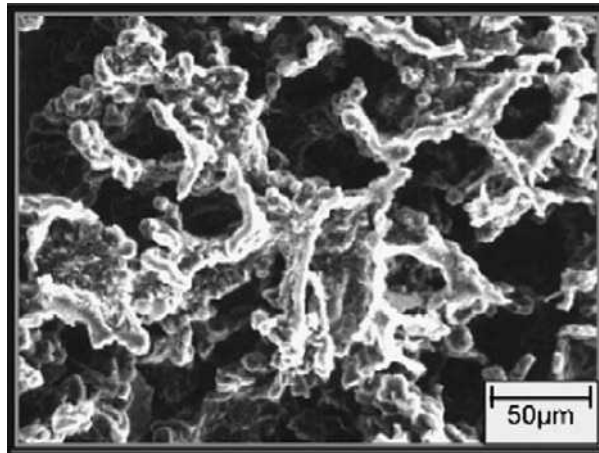


**FIGURE 6.55**

SEM image of deeply etched CGI closely resembling coupled eutectic coral structure, illustrating the overall similarity of these structures (courtesy of T Prucha, AFS 2009).

3. Graphite nucleates on the oxy–sulfide particles, and grows primary graphite, spreading over the bifilms, straightening the bifilms and forming flakes of crystallographically near-perfect graphite; the presence of the bifilms, as cracks, trapped inside or alongside graphite flakes accounts for the poor tensile properties of flake irons.
4. Compacted graphite nucleates on oxy–sulfide nuclei occupying bifilm residues. Growth occurs by fibrous filaments extending freely into the liquid.
5. Spheroidal graphite nucleates on oxy–sulfide nuclei free from bifilms. The spherical growth morphology is initiated by the freedom that the graphite has to wrap completely around the nucleus, but is later importantly encouraged by mechanical constraint of the austenite matrix; the absence of bifilms, eliminated by the Mg addition, explains the high mechanical properties.
6. Eutectic coral graphite nucleates on (currently unknown) nuclei at low temperatures, expanding to form cells of coupled growth with austenite, consisting of highly faulted continuous branching filaments of graphite in the austenite matrix; bifilms play no part in this growth mode.
7. Mis-shaped spheroids appear to be spheroids that have encountered an oxide (probably Mg-rich) bifilm, subsequently growing along the bifilm and losing sphericity. The presence of the bifilm destroys the symmetrical mechanical constraint of the austenite that favors sphericity.
8. Chunky graphite occurs in heavy-section ductile iron in regions. The central regions are isolated by, and probably full of, bifilms created by the poor casting technique. Thus convection and the redistribution of nuclei and nodules is suppressed, and existing nuclei can float out, so that the central region becomes devoid of nuclei. Graphite therefore develops akin to coral morphology. As such it may be a coupled eutectic form, and its ‘beads on a string’ morphology may result from an unstably advancing growth front.
9. Exploded spheroids may be the result of growth in the liquid, without the benefit of the mechanical constraint of an austenite shell. They are favored by (i) high CEV and (ii) the presence of oxide bifilm which interfere with the sphericity of growth.

10. Carbides form at very low temperatures on oxide bifilms. The presence of bifilms in the carbides explains the apparently brittle behavior of these strong intermetallics.

---

## 6.6 STEELS

There are such a wide variety of steels, of widely differing properties, that it is possible only to generalize with extreme caution. In general, we shall consider the simplest of steels; the carbon steels (often more accurately referred to as carbon/manganese steels, because Mn is such a common additional alloying element) and stainless steels. Stainless steels fall into main groups: ferritic, austenitic, and duplex (i.e. mixed ferrite and austenite).

Other steels are commonly known from their microstructures, including ferritic; austenitic; pearlitic; martensitic; and bainitic. Tool steels (another wide category) encompass forming and cutting tools often with high Mo or W additions to form hard carbides.

Although astonishing strengths available in the final worked and heat-treated products, sometimes approaching or even in the GPa range, from the point of view of the casting technologist, the key differences between the steels and the light alloys are:

- (i) the high melting and casting temperatures encouraging more severe and faster reaction with the environment and the possibility of acquiring a partly or completely melted surface oxide film;
- (ii) the higher strengths of the steels, so that higher internal stress can be sustained during freezing, leading more easily to the initiation of such defects as shrinkage porosity and hot tearing or cracking phenomena;
- (iii) the higher density of steels requiring stronger, often reinforced molds and cores to resist flotation, and heavy weights to prevent the lifting of copes.

### 6.6.1 Carbon steels

Steelmaking practice for the production of carbon steels traditionally starts from pig iron produced from the blast furnace. The high carbon in the iron, in the region of 3 or 4%, is the result of the liquid iron percolating down through the coke in the furnace stack. (A similar situation exists in the cupola furnace used in the melting of cast iron used by iron foundries.) Oxygen is added to oxidize the carbon down to levels more normally in the range of a few tenths of a percent. The bonus from the burning of the carbon is the huge and valuable increase of temperature that is needed to keep steels molten. Oxygen to initiate the CO reaction is added in various forms, traditionally as shovelfuls of granular FeO thrown onto the slag, but in modern steelmaking practice by spectacular jets of supersonic oxygen. The stage of the process in which the CO is evolved as millions of bubbles is so vigorous that it is aptly called a 'carbon boil'.

After the carbon is brought down into specification, the excess oxygen that remains in the steel is lowered by deoxidizing additions. Common deoxidizers have been manganese, silicon, and/or aluminum. In modern practice a more complex cocktail of deoxidizing elements is added as an alternative or in addition. These often contain small percentages of rare earths to control the shape of the non-metallic inclusions in the steel. It seems likely that this control of shape is the result of reducing the melting point of the inclusions so that they become at least partially liquid, adopting a more rounded form that is less damaging to the properties of the steel. Also, of course, such compact

spherical inclusions float out more rapidly than solid film-type deoxidation products, so that the steel is much cleaner, and properties are higher and more uniform as a result of the absence of bifilm-type cracks.

In most steel foundries, only *steel melting* is carried out from scrap steel (not made from pig iron, as in *steelmaking*). Because the carbon is therefore already low, there is often no requirement for a carbon boil.

The potentially significant problem that remains in the absence of a carbon boil is that hydrogen remains in the melt. In contrast to oxygen in the melt that can quickly be reduced by the use of a deoxidizer, there is no quick chemical fix for hydrogen. Hydrogen can only be encouraged to leave the metal by providing a dry and hydrogen-free environment. Hydrogen then will gradually evaporate off from the melt, tending to equilibrate with its surroundings. If a carbon boil can be induced, the loss of hydrogen will be rapid. However, if this cannot be induced, possibly in some artificial way, and if environmental control is insufficiently good, or is too slow, then the comparatively expensive last resort is vacuum degassing, although the use of argon–oxygen converters is now more common, which can efficiently flush hydrogen down to very low levels sometimes required for large castings whose dimensions (measured in large fractions of meters) exceed the distance that hydrogen can diffuse out during heat treatments.

### 6.6.2 Stainless steels

The percentage ferrite in cast stainless steels at room temperature depends mainly on the composition of the alloy. This is summarized in the Schoefer diagram presented in Figure 6.56. The equivalent Cr and Ni contributions are estimated from the weight percentage of alloying elements:

$$\text{Cr}_{\text{equiv}} = \% \text{Cr} + 1.5(\% \text{Si}) + 1.4(\% \text{Mo}) + \% \text{Nb} - 4.99$$

$$\text{Ni}_{\text{equiv}} = \% \text{Ni} + 30(\% \text{C}) + 0.5(\% \text{Mn}) + 26(\% \text{N} - 0.02) + 2.77$$

Fully austenitic and fully ferritic stainless steels suffer a number of cracking and intergranular corrosion problems that seem to me to be the result mainly of oxide bifilm problems, most probably as a result of dendrite straightening, leading to a population of cracks throughout the alloy.

However, most cast austenitic steels do not have the single-phase structure that their name implies; their structure is usually duplex. Ferrite in the range 5–25 volume percent is found to be valuable for (i) improved strength; (ii) improved weldability and castability (reducing cracking problems); and (iii) improved resistance to corrosion, stress corrosion cracking and intergranular corrosion attack in certain corrosive environments. It seems possible that the formation of the austenite during the growth of the primary ferrite dendrites might interrupt and hamper bifilm straightening in some way.

The advantages of the duplex structure are maximized at about 50/50 volume percent mixture (actually encompassing the small range of approximately 40–60 volume percent). It is *only* these steels that are known in the industry as ‘duplex stainless steels’.

An additional method of classifying stainless steels is according to their stainlessness, or ability to resist corrosion as quantified by their Pitting Resistance Equivalent (PRE). A commonly used equation for ranking stainless compositions is given by Davidson (1990):

$$\text{PRE} = \% \text{Cr} + 3.3(\% \text{Mo}) + 16(\% \text{N})$$



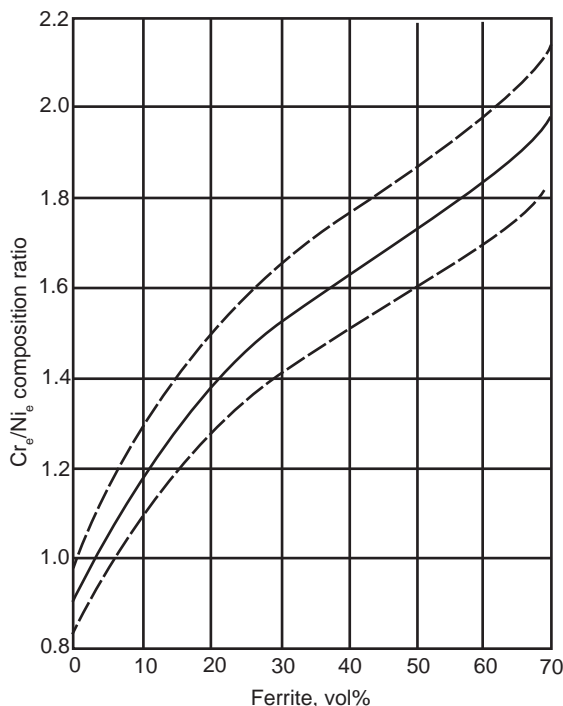


**FIGURE 6.56**

Schoefer diagram for estimating the ferrite content of steel castings in the composition range 16–26Cr, 6–14Ni, 0–4Mo, 0–2Mn, 0–2Si, 0–1Nb, 0–0.2C, 0–0.19N. Broken lines denote limits of uncertainty.

Four categories of improving levels of PRE can be listed (together with typical examples):

PRE	Example
1. 25 approx	(23Cr steels with zero Mo)
2. 30–36	(22Cr steels)
3. 32–40	(high-alloy 25Cr steels)
4. >40	(super duplex steels 25Cr–7Ni–4Mo)

One of the standard problems with many cast stainless steels is the formation of the infamous sigma phase ( $\sigma$ ) usually at grain boundaries. As with most intermetallics, the phase appears to be brittle, exhibiting cracks and leading to failure by cracking. Once again, this maligned intermetallic has all the familiar signs of having nucleated and grown on an oxide bifilm, thereby naturally exhibiting cracks in a material that would normally be expected to be strong and crack-free. Once again, the avoidance of this problem lies not necessarily in metallurgical control but in the use of appropriate casting technology. A naturally pressurized filling system is predicted to largely eliminate bifilms, removing these favored substrates, and thereby suppressing the formation of sigma phase. A large benefit to tensile

properties would result from the elimination of the bifilm cracks, and a perhaps smaller benefit from the presence of additional solutes in solution (since the sigma phase did not precipitate) that would enhance strength. The PRE might also improve, and possibly the resistance of some of the stainless steels to such other imponderables such as stress corrosion cracking.

### 6.6.3 Inclusions in carbon and low-alloy steels (general background)

Svoboda and colleagues (1987) report on a large program carried out in the USA in which over 500 macroinclusions were analyzed from 14 steel foundries. This valuable piece of work has given a definitive description of the types of inclusions to be found in cast steel, and the ways in which they can be identified. A summary of the findings is presented in Figure 6.57 and is discussed below.

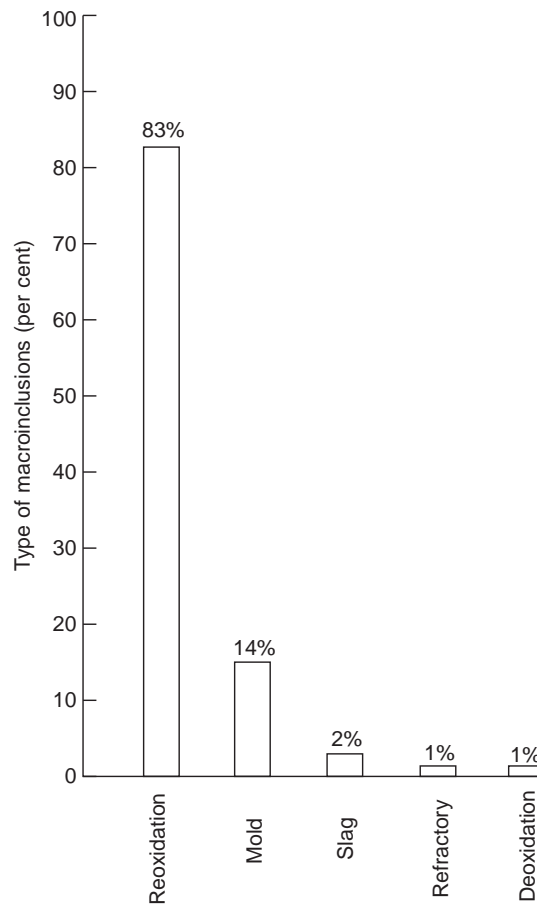


**FIGURE 6.57**

Distribution of types of macroinclusions in carbon and low-alloy steel castings, from a sample of 500 inclusions in castings from 14 foundries (Svoboda et al. 1987).

Each inclusion type can be identified by (1) its appearance under the microscope and (2) its composition.

1. Acid slags can be identified by their high FeO content (typically 10–25%), and glass-like microstructure.
2. Basic slags and furnace slags from high-alloy melts can be traced by the calcia (lime), alumina, and/or magnesia that they contain.
3. Refractories from furnace walls and/or ladles have characteristic layering, flow lines, and a pressed and sintered appearance including sintered microporosity. Their compositions are reminiscent of those of the refractories from which they originated (e.g. pure alumina, pure magnesia, phosphate-bonded aggregates, etc.).
4. Molding sand is identified from the shape of residual sand grains and from its composition high in silica.
5. Mold coat material is normally easily distinguished because of its composition (e.g. alumina or zircon).
6. Deoxidation products are always extremely small in size (typically less than 15  $\mu\text{m}$ ) and are composed of the strongest deoxidizers. These inclusions are likely to have formed at two distinct stages. (i) During the initial addition of strong deoxidizer to the liquid steel, when small inclusions will be nucleated in large numbers as a result of the high supersaturation of reactive elements in that locality of the melt. Any larger inclusions will have some opportunity to float out at this time. (ii) During solidification and cooling. These stages will be discussed further below.
7. Reoxidation products are large in size, usually 2–10 mm in diameter, and consist of a complex mixture of weak and strong deoxidizers. In carbon steels the mixture contains aluminum, manganese, and silicon oxides. In high-alloy steels the mixture often contains a dark silica-rich phase, and a lighter-colored Mn + Cr oxide-rich phase. Entrapped metal shot is found inside most of these inclusions. The shot is probably incorporated by turbulence (rather than by chemical reduction of the FeO by the strong deoxidizers). These larger inclusions have been previously known as ceroxide defects, as a result of their content of cerium and other powerful rare earth deoxidizers. The rare earth deoxidizers are used in an attempt to control the shape of sulfide inclusions.

Most research on the formation of inclusions in steels is directly, disappointingly, only at the diffusion reactions between the raw metallic deoxidizer, such as aluminum, and liquid steel. The inclusions generated in the supersaturation surrounding the deoxidants during its first seconds of melting and dispersing are interesting, including mixes of dendritic, star-like, and spherical forms (Tiekink 2010). Van Ende and co-workers (2010) do not comment on the presence of the crack that separates the liquid Al sitting upon their sample of liquid steel. This is clearly present in all their work. Even when bifilms are clear they are nearly always ignored. These interdiffusions between deoxidizers and liquid steel elucidate the processes occurring during deoxidation. The much more important processes involved in reoxidation, including entrainment during pouring, have mainly been overlooked so far.

It seems clear that the reoxidation products are bifilms of various sorts, somewhat scrambled, and often unable to reopen as a result of their formation from partially molten oxide mixtures. They confirm their identity by their droplets of metal and bubbles of residual air.

The reoxidation products are formed during the tapping of the furnace into the ladle. In general they will largely have floated out of the metal, forming the slag layer on the top of the melt in the ladle during the several minutes that it takes to lift the ladle out of the pit and travel to the casting station.

Only the pour into the mold is expected to create the reoxidation products that are observed. There is excellent evidence for this expectation; Melendez, Carlson, and Beckermann (2010) develop a computer model that predicts the locations of reoxidation inclusions in the mold. They achieve good descriptions of the awful mess castings become when, as they assume, the filling system design contains a conical funnel basin, uniform internal diameter refractory tubes for the sprue, runners, and ingates, and finally gates into parts of the casting that are not at the lowest points of the mold cavity.

These efforts to predict the distribution of reoxidation defects seem curiously misplaced when it is reasonably widely known (Kang 2005, Puhakka 2010) that if a properly designed filling system is applied to the casting the reoxidation inclusions disappear!

### 6.6.4 Entrained inclusions

Previously, most inclusions introduced from outside sources have been called exogenous inclusions, but this name, besides being ugly, is unhelpful because it is not descriptive. ‘Entrained’ indicates the mechanism of incorporation as an impact of opposed surfaces, as occurs in the incorporation of a droplet, or the folding-in of the surface. Also, the word ‘entrained’ draws attention to the fact that as a necessary consequence of their introduction to the melt, such inclusions have passed through its surface, and so will be wrapped in a film of its surface oxide. Depending on the dry or sticky qualities of the oxide, and the rate at which the wrapping may react with the particle, the entrained inclusion and its wrapping can act later as an initiation site for porosity or cracks. Metal, too, may become entrapped in the entraining action, and thus form the observed shot-like particles.

Svoboda has determined the distribution of types of macroinclusion in carbon and low-alloy cast steels from the survey (Figure 6.57). The results are surprising. He finds that reoxidation defects comprise nearly 83% of the total macroinclusions. These are our familiar bifilms created by the surface turbulence during the transfer of the melt from the furnace into the ladle, and from the ladle, through the filling system into the mold. In addition, he found nearly 14% of macroinclusions were found to be mold materials. Since we know that mold materials are also introduced to the melt as part of an entrainment process, it follows that approximately 96% of all inclusions in this exercise were entrainment defects resulting from damaging pouring actions.

Only approximately 4% of inclusions were due to truly extraneous sources; the carry-over of slag, refractory particles and deoxidation products.

This sobering result underlines the importance of the reaction of the metal with its environment after it leaves the furnace or ladle. The pouring, and the journey through the running system and into the mold, are opportunities for reaction of those elements that were added to reduce the original oxygen content of the steel in the furnace. The unreacted, residual deoxidizer remains to react with the air and mold gases. Such observations confirm the overwhelming influence of reactions during pouring or in the running system as a result of surface turbulence; these effects are capable of ruining the quality of the casting.

However, good running systems are not usually a problem for small steel castings. I used to think that large steel castings were a separate matter because of the high velocities that the melt necessarily suffers. This is partly a consequence of the use of bottom-pour ladles, and partly the result of the long fall of the melt down tall sprues. However, even these challenges are now known to be solvable.

The historical use of rather poor filling system designs has given steel the reputation for a high rate of attack on the mold refractories. Unfortunately, the solution has resulted in the use of pre-formed

refractory tubes for the running system. The joining of these standard pipe shapes means that nicely tapered sprues cannot easily be provided, with the result that much air goes through the running system with the metal. The chaos of surface turbulence in the runner, and the splashing, foaming, and bursting of bubbles rising through the metal in the mold cavity, will mean that reoxidation product problems are an automatic, unavoidable penalty.

It follows that a common feature of steel foundries is that the foundry often employs more welders in the 'upgrading' department than people in the foundry making castings. Common black jokes among steel foundry workers include 'More weld metal goes out of the foundry door than cast metal' and 'The drag is made in the foundry and the cope in the welding shop'. These regrettable jibes follow from the surface turbulence caused during pouring. The difficulties are addressed later in 'Casting Manufacture', in which better-molded systems are recommended, returning to sand molding for the front end of the filling system (a good pouring basin and tapered sprue combination is not usually harmed by the steel) whilst ceramic tubing might be acceptable and convenient for the remainder of the system if it can be properly accommodated. In the meantime, we shall examine the problems caused by the current poor filling systems.

### ***Solid oxide surface films***

Some liquid steels have strong, solid oxide films covering their surface. The high melting point of these oxides ensures that the surfaces of these liquid metals are covered with perfectly dry films. They occur on many stainless steels rich in chromium and molybdenum, especially the super duplex stainless steels. In castings above about 250 kg in weight the filling systems are sufficiently large to pass bifilms up to 100 mm across or more. Entrained air bubbles and surface turbulence in the mold cavity create even more films in situ in the forming casting. These are found to be arranged in clusters, often near the ingate, or just under the cope. They are identified on radiographs as resembling faint, dispersed microshrinkage porosity. When attempting to grind away such regions, hollowing out deep cavities in the casting in an effort to eliminate such apparently porous metal, it is common to check periodically with the red penetrant dye to ascertain whether the region is yet free from defects. The bifilms in these regions appear as an irregular red-colored spider's web. They are mainly at grain boundaries, of course, and are often somewhat opened up by cooling strains. When viewed under the optical microscope they have given rise to the description the 'loose grain effect' in some stainless steel foundries because the grains appear to be separated from each other by deep cracks at the grain boundaries, as though they might rattle if shaken. This is, of course, nearly true. The bifilms are segregated by the growing grains, being pushed ahead, and thus finally come to rest in the boundaries between grains. Thermal strains during cooling open the bifilms to give the crazed appearance of the microstructure. This maze of thin, deep cracks often has to be excavated completely through walls of 100 mm thickness and sometimes greater sections before these regions can be re-built by welding.

However, in small castings of these particular steels, there now seems to be evidence that the ingates can be sufficiently narrow (measured in millimeters) so that the strong, rigid plates of oxide cannot pass through (Cox et al. 1999). Thus, paradoxically, this notoriously difficult material can be used to make small castings that are relatively free from defects.

Low-carbon/manganese and low-alloy steels are typically deoxidized with Si, Mn, and Al in that order. They can suffer from a stable alumina film on the liquid if the final deoxidation with Al has been carried out too enthusiastically. This causes similar problems to those described above. In addition,

I have known ingots of high-alloy steels and Ni-base alloys to break up on the first stroke of a forging press after high levels of Al deoxidation have been used prior to casting. Those ingots that survived the forge usually cracked later during rolling or extrusion. When Al was reduced and Ca added (the effect of the Ca addition is explained below) the problem was solved for some alloys; the ingot forged and rolled like butter. For other alloys the solution has not worked. We need to do far more research into the achievement of liquid oxidation production on molten steels.

### ***Partly liquid surface oxide films***

When adding the usual level of final deoxidation with Al, approximately only 1 kg or less Al per 1000 kg steel, most low-carbon/manganese and low-alloy steels do not usually suffer severe internal defects. Because of the high melting temperatures of such steels, the surface oxides contain a mix of  $\text{SiO}_2$ ,  $\text{MnO}$ , and  $\text{Al}_2\text{O}_3$ , amongst other oxide components. The mix is usually partially molten. On being entrained during pouring the internal turbulence in the melt tumbles the films into sticky agglomerates. Because of the presence of the liquid phases that act as an adhesive, the bifilms cannot reopen, and grow by agglomeration. The matrix becomes therefore relatively free from defects in this way. Also, the oxide conglomerates are now rather compact. Their compactness and their low density causes them to float out rapidly, gluing themselves to the surface of the cope as a ‘ceroxide’ defect, so called because of the presence of cerium oxide as one of the more noticeable of the many phases in the inclusion. Cope defects are common *surface defects* in these steels. In castings weighing 10 000 kg or more the defects can sometimes grow to the size of a fist. They are, of course, labor-intensive to dig out and repair by welding. However, their compact form makes this job somewhat easier, and not quite in the league of the extensive webs of bifilms bridging the walls of super duplex stainless castings.

### ***Liquid surface oxide films***

Over recent years it has become popular to give a final deoxidation treatment with calcium in the form of calcium silicide (CaSi) or ferro-silicon-calcium because the steel has been found to be much cleaner. This is quickly understood from the following. Alumina and calcia both have melting points in excess of  $2000^\circ\text{C}$ . However, a roughly equal mixture of the oxides forms a low-melting-point eutectic. Thus the dry  $\text{Al}_2\text{O}_3$  surface oxide (if deoxidizing with only Al, plus possibly Si and Mn) is converted into a liquid oxide of approximate composition  $\text{Al}_2\text{O}_3\cdot\text{CaO}$  that has a melting point at or below  $1400^\circ\text{C}$ . Any folding-in of the liquid film that may now occur will quickly be followed by agglomeration of the bifilm into droplets. The compact form and low density of the droplets will ensure that they float out quickly and will be assimilated into the original liquid eutectic film at the surface, leaving the steel without defects. Any inclusions that remain will be small and spherical, and thus having a minimal impact on properties.

With a liquid surface film, entrainment of the surface no longer results in the creation of bifilms. Thus Lind and Holappa (2010) in their review of the effects of calcium additions to alumina in steels record the benefits to ductility and toughness of high-strength low-alloy (HSLA) steels and high-quality structural steels by Al + Ca deoxidation.

The reviewers go on to describe how MnS inclusions in flat-rolled plate and sheet grades of steels elongate to form stringers or platelets, lowering the through-thickness ductility and toughness. This behavior seems most likely to be the result of alumina bifilms forming elongated stringers or platelets, onto which manganese sulfide precipitates. The central alumina bifilms are too thin to see easily, but are the cracks that reduce the through-thickness properties.

### **Aluminum nitride**

In passing, it seems worth mentioning a class of defect that has been the subject of huge amounts of research, but which has never been satisfactorily explained. A tentative explanation is presented here. The phenomenon is the so-called ‘rock candy fracture’ appearance of some cast steel. This type of defect was seen when the ductility of the casting was especially low, despite the metal appearing to have precisely the correct chemistry and heat treatment. The fracture surface was characterized by intergranular facets that on examination in the scanning electron microscope were found to contain aluminum nitride. Naturally, the aluminum nitride was concluded to be brittle.

This defect seems most likely to be an entrained surface film. The film would probably originally consist of alumina, but would also contain some enfolded air. The nitrogen in the entrained air would be gradually consumed to form aluminum nitride as a facing to the crack. The defect would, of course, be pushed by the growing dendrites into the interdendritic spaces, particularly to grain boundaries. The central crack in the bifilm would give the appearance of the nitride being brittle. On examination, only the nitrogen is likely to be detected, constituting four-fifths of the air, and the oxygen being in any case not easily analyzed. The defect is analogous to the plate fracture defect in ductile irons, and the planar fracture seen in Al alloys and other alloy systems (Figures 2.44, 2.46, and 6.29).

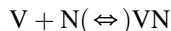
Thus in this case, despite the chemistry of the steel being maintained perfectly within specification, the defect would come and go depending on chance entrainment effects. Such chance effects could arise because of slight changes in the running system, or the state of fullness of the bottom-pour ladle, or the skill of the caster, etc. It is not surprising that the defect remained baffling to metallurgists and casters for so long.

### **6.6.5 Primary inclusions**

When the liquid alloy is cooling, new phases may appear in the liquid that precede the appearance of the bulk alloy. We shall deal with the formation of the primary metallic matrix phase in Section 6.6.7. Whether any newly forming dense phase gets called a phase or an inclusion largely depends on whether it is wanted or not: keen gardeners will appreciate the similar distinction between ‘plants’ and ‘weeds’!

New phases that precede the appearance of the bulk alloy are especially likely following the additions to the melt of such materials as deoxidizers or grain refiners, but may also occur because of the presence of other impurities or dilute alloying elements.

For instance, in the case of steel that has a sufficiently high content of vanadium and nitrogen, vanadium nitride, VN, may be precipitated according to the simple equation:



Whether the VN phase will be able to exist or not depends on whether the concentrations of V and N exceed the solubility product for the formation of VN. To a reasonable approximation the solubility product is defined as:

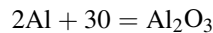
$$K = [\%V] \cdot [\%N]$$

where the concentrations of V and N are written as their weight percent. More accurately, a general relation is given by using, instead of weight percent, the activities  $a_V$  and  $a_N$ , in the form of a product of activities:

$$K' = a_V a_N$$

It is clear then that VN may be precipitated when V and N are present, where sometimes V is high and N low, and vice versa, providing that the product  $\%V \times \%N$  (or more accurately,  $a_V \times a_N$ ) exceeds the critical value  $K$  (or  $K'$ ). It is interesting to speculate that  $[N]$  may be high very close to the surface where the melt may be dissolving air. Thus the formation of a surface film of VN may be more likely. It is also necessary to bear in mind that even though all thermodynamic conditions for the formation of VN are met (in particular the solubility product is exceeded) the compound may still not form. This is because there is often a substantial nucleation problem that has to be overcome. This is achieved either by extremely high supersaturations of either V or N or both, or by the provision of a favorable nucleus. As we have seen repeatedly, oxide films are common substrates for the formation of many precipitating intermetallics. The film itself may not be the nucleant, but the nucleant will almost certainly have already nucleated on the film. Thus the film is the starting point for growth, starting at the site of a suitable incumbent nucleus, but spreading out over the film as its favored growth substrate.

In the case of deoxidation of steel with aluminum, the reaction is somewhat more complicated:

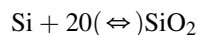


and the solubility product now takes the form:

$$K'' = [a_{Al}]^2 [a_O]^3$$

where the value of  $K''$  increases with temperature. Again, the surface conditions are likely to be different from those in the bulk, with the result that a surface film of AlN or  $Al_2O_3$  is to be expected, even if concentrations for precipitation in the bulk are not met.

Turpin and Elliot (1966) were among the first to study the problem of the nucleation of new dense phases from the melt. Using the approach of classical nucleation theory as illustrated in Equation 5.15, these authors used the standard free energy changes for the formation of oxides, which they took from the literature on thermodynamics, to find the energy for formation of a nucleus of the new material. We shall not follow their argument in detail, but merely quote their result in Figure 6.58 for the Fe–O–Si system. In this example two oxides are considered. The first is from the reaction:

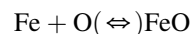


so that the equilibrium constant is now approximately:

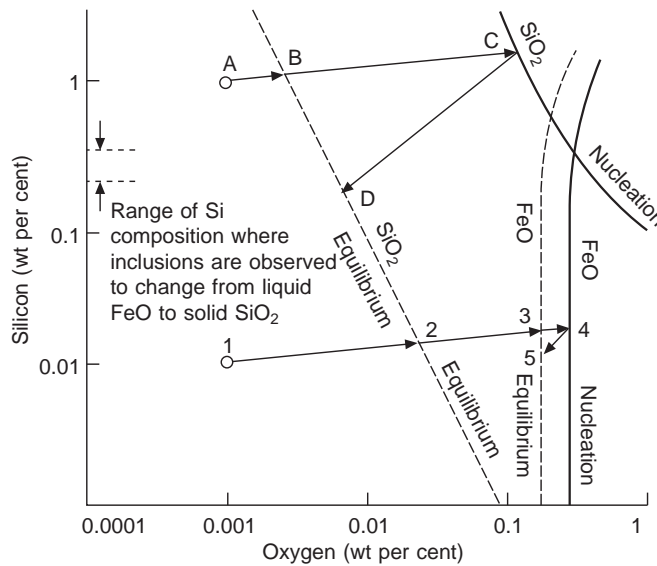
$$K''' = [\%Si][\%O]^2$$

Figure 6.58 shows this equilibrium threshold with its logarithmic slope of minus 2 (a negative slope of 2 means that an increase of a factor of 10 in oxygen concentration together with a decrease of a factor of 100 in silicon concentration will still result in the nucleation condition being satisfied). The higher threshold shown in Figure 6.58 corresponds to the concentrations required for nucleation, assuming a surface energy of the interface of  $1.3 \text{ N m}^{-1}$ . (We shall continue to use  $\text{N m}^{-1}$  in uniformity with the rest of this book. Otherwise, it would have been logical to quote surface energy in the identical units  $\text{J m}^{-2}$ .)

Turning now to the possibility of forming FeO in this system, the equation is:







**FIGURE 6.58**

Equilibrium and nucleation thresholds for silica and iron oxide inclusions in solidifying iron. Data on thresholds from Turpin and Elliot (1966).

This simple equation becomes even more simplified in its solubility product form,

$$K''' = [\%Fe] \cdot [\%O]$$

because the concentration of iron is very close to 100% (i.e. unity in the above equation). Thus the FeO can exist in equilibrium in an iron melt only if the oxygen concentration is high enough (since the iron concentration is already fixed at its maximum). Thus in Figure 6.58 the threshold for the formation of FeO is very nearly a vertical line. The parallel line denoting the threshold to overcome the resistance to the nucleation of FeO is quite close; this is because the surface energy of the interface is low, in the region of only  $0.25 \text{ N m}^{-1}$ .

Turpin and Elliott take their analysis further to show that a melt that has been allowed to come into equilibrium at a high temperature may reach a sufficient supersaturation to cause nucleation as the melt is cooled. They effectively work their analysis backwards, aiming for a nucleation at the freezing point of iron,  $1536^\circ\text{C}$ , and calculating what equilibrating temperature would have been required to achieve this. Their results are summarized in Figure 6.59.

These results demonstrate that it is possible, in principle, to predict the arrival and stability of particles in melts, as a function of temperature and composition. Turpin and Elliot were not able to confirm their theoretical predictions for this system because of experimental limitations. However, much work on the grain refinement of metals would surely benefit from a careful, formal approach of this kind.

We have considered examples of nucleation at various points in the book, especially in Section 5.2.2. At this stage we shall simply note that any primary inclusions form prior to the arrival of the

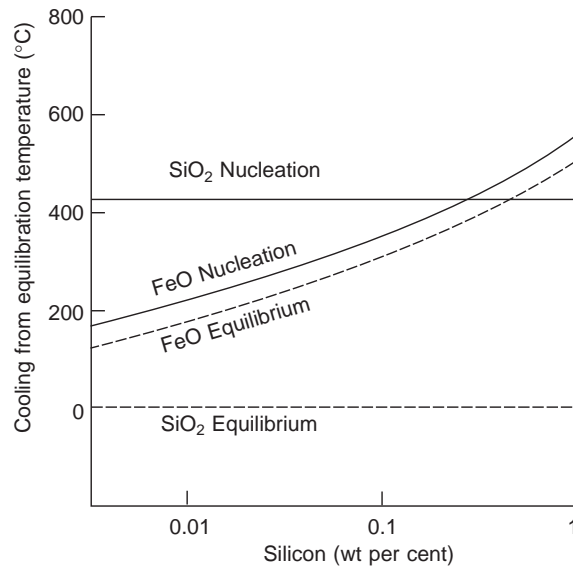


**FIGURE 6.59**

The cooling required, from a temperature where the system was allowed to come into equilibrium, down to the freezing point of iron (1536°C), to nucleate oxides in the Fe–O–Si system. From Turpin and Elliot (1966).

matrix primary phase. Thus they appear in a sea of liquid. During this ‘free-swimming’ phase, primary inclusions have been thought to grow by collision and agglomeration (Iyengar and Philbrook 1972). Whether this is true or not probably depends on the nature of the inclusions.

For instance it is not clear whether all liquid inclusions will coalesce even if they impinge. It seems probable that coalescence may be hindered by the presence of a surface film. However, if coalescence does occur, droplets would be expected to result in large spherical inclusions whose compact shape will enable them to float rapidly to the surface and become incorporated into a slag or dross layer which can be removed by mechanically raking off, or can be diverted from incorporation into the casting by the use of bottom-pouring ladles, or teapot spout ladles.

For solid inclusions, any agglomeration process that may occur might take the form of loosely adhering aggregates or clouds. However, agglomerations apply to particles. Entrained solid alumina films or other entrained solid films will not, in general, be particles but will be messy crumpled masses of double films that on a polished section might easily appear as a cloud of particles, particularly if parts of the alumina bifilm are so thin as to avoid detection, so that only thicker fragments are visible. Furthermore, at steel casting temperatures an extremely thin entrained and raveled alumina film may condense into arrays of compact particles, analogous to the way in which a sheet of liquid metal breaks up into droplets (a spectacular example is given in Figure 2.13), an effect driven by the reduction of surface energy. Subsequent working by rolling or extrusion will elongate films or arrays of separated particles thus explaining the observed alumina stringers often seen in wrought steels. The occasional cracks and pores associated with alumina inclusions will almost certainly be the residue of the central unbonded interface of the original alumina bifilm. (It will not be expected to be the result of so-called

brittleness of the alumina phase, nor its effect to initiate cracks in the matrix.) Work to clarify these possibilities would be welcome.

Hutchinson and Sutherland (1965) have studied the formation of open-structured solids. They find that flocs can form by the random addition of particles. If these particles are spherical and adhere precisely at the point at which they first happen to encounter the floc, then the floc builds up as a roughly spherical assembly, with maximum radius  $R$ , and about half the number of spheres within a region  $R/2$  from the centroid. The central core has an almost constant density of 64% by volume of spheres. Occasional added spheres will penetrate right into the heart of the floc. Graphite nodules in ductile iron appear to be a good example of this kind of flocculation; melts of hypereutectic ductile irons suffer a loss of graphite by the floating out of loose flocs of spherulites (Rauch et al. 1959).

We have only touched on examples of oxides and nitrides as inclusions in cast metals. Other inclusions are expected to follow similar rules and include borides, carbides, sulfides, and many complex mixtures of many of these materials. Carbo-nitrides are common, as are oxy-sulfides. In C-Mn steels the oxide inclusions are typically mixtures of  $MnO$ ,  $SiO_2$ , and  $Al_2O_3$  (Franklin et al. 1969) and in more complex steels deoxidized with ever more complex deoxidizers the inclusions similarly grow more complex (Kiessling 1978).

In his substantial review of inclusions in steels, Kiessling points out that steel that contains only as little as 1 ppm oxygen and sulfur will contain over 1000 inclusions  $g^{-1}$ . Thus it is necessary to keep in mind that steel is a composite product, and probably better named 'steel with inclusions'. Even so, steels are often much cleaner than light-alloy castings, that might contain 10 or 100 times more inclusions, partly helping to explain the relatively poor ductility and absence of a fatigue limit exhibited by Al-based casting alloys compared to steels.

Finally, of course, not all inclusions will be formed during the liquid phase. Many, if not most, will be formed later as the metal freezes. These are termed secondary inclusions, or second phases, and are dealt with in the following section.

### 6.6.6 Secondary inclusions and second phases

After the primary alloy phase has started to freeze, usually in the form of an array of dendrites, the remaining liquid trapped between the dendrite arms progressively concentrates in various solutes as these are rejected by the advancing solid. Because the concentration ahead of the front is increased by a factor  $1/k$ , where  $k$ , the partition coefficient, can often be a rather small number, greatly enhancing the segregation effect, the number of inclusions can be greatly increased compared to those that occurred in the free-floating stage in the liquid. However, the size population is usually different, being somewhat finer and more uniform as a result of the smoothing action of diffusion in the tiny volumes between the dendrites.

The secondary inclusions or second phases form at or close to the freezing front. One of the most common and important second phases is a eutectic. We have already seen how microsegregation can lead to the formation of eutectic at bulk compositions that are much below those expected from the equilibrium phase diagram.

For the remainder of this short section, we shall consider the arrival of other phases. Oxide inclusions in the Fe-O-Si system are taken as an example.

Take, for instance, a melt that contains 1% silicon and 0.001% oxygen, shown as point A on Figure 6.58. As freezing progresses and the concentration of the residual liquid region increases in both silicon and oxygen, the composition moves to B. This is the point at which silica is in stable

equilibrium with the melt. Thus silica could form if there were pre-existing silica or some other favorable nucleus present. However, in the effectively isolated pockets of liquid trapped between the dendrite arms the probability of a suitable substrate is low. Thus the liquid continues to supersaturate along the line BC. At C the concentration is sufficiently high to allow silica to nucleate without any assistance. It is said to nucleate homogeneously. Forward and Elliot (1967) calculated that the supersaturation required to nucleate silica occurs at about 98% solidification.

Once the new phase has been nucleated, the surrounding residual liquid will be quickly depleted of solutes. These will diffuse to the growing phase, causing the local concentrations to fall until they meet the equilibrium threshold at D. The concentration of those solutes will then remain stable in the local region, the inclusion only growing to take up any excess solute as it comes available because of rejection from the advancing dendrites.

If now we take a second example containing, for instance, only 0.01% silicon and 0.001% oxygen, we start at point 1 in Figure 6.58. At and beyond point 2, silica could form if there were any favorable nucleus or pre-existing silica. In the absence of this, on passing point 3, FeO could form if a favorable foreign substrate happened to be present. However, in the absence of pre-existing FeO or SiO<sub>2</sub> or any favorable nuclei for either of these phases, then point 4 will be reached. At this point FeO will nucleate spontaneously. Its subsequent growth will cause the supersaturation to fall until the local melt is once again in equilibrium with the new phase at point 5. (Because the path 4 to 5 on the composition map lies within the regime in which silica is stable, it is possible in principle that some silica may dissolve in the growing FeO particle, or might nucleate on it. However, in this particular case, nucleation of solid SiO<sub>2</sub> on liquid FeO seems highly unlikely.)

Turpin and Elliott go on to examine the Fe–O–Al system that contains, in addition to FeO and Al<sub>2</sub>O<sub>3</sub>, the mixed oxide hercynite FeO·Al<sub>2</sub>O<sub>3</sub>. Thus the succession of phases that can appear becomes more complicated. In real systems, of course, the situation is vastly more complex still, with very many alloying elements being concentrated in interdendritic regions, and all able to react with a number of fellow concentrates.

However, the nucleation of a first phase is likely to prevent the subsequent nucleation of any other phase that might also require one of the same elements for its composition. The availability of solute is clearly limited by a naturally occurring ‘first come first served’ principle.

In the subsequent observation of inclusions in cast steels, those that have formed in the melt prior to any solidification are, in general, rather larger than those formed on solidification within the dendrite mesh. The possible exceptions to this pattern are those inclusions that have formed in channel segregates, where their growth has been fed by the flow of solute-enriched liquid. Similarly, in the cone of negative segregation in the base of ingots the flow of liquid through the mesh of crystals would be expected to feed the growth of inclusions trapped in the mesh, like sponges growing on a coral reef feeding on material carried by in the current. In Figure 5.44 the peak in inclusions in the zone of negative segregation is composed of macro-inclusions that may have grown by such a mechanism. Elsewhere, particularly in the region of dendritic segregation around the edge of the ingot, there are only fine alumina inclusions.

### **Sulfides**

It would not be right to leave the subject of inclusions without mentioning the special importance of the role of sulfide inclusions in cast steel. The ductility of plain carbon steel castings is sensitive to the type of sulfide inclusions that form.

Type 1 sulfides have a globular form. They are produced by deoxidation with silicon.

Type 2 sulfides take the form of thin-grain boundary films that seriously embrittle the steel. They usually form when deoxidizing with aluminum, zirconium, or titanium.

Type 3 sulfides have a compact form, and do not seriously impair the properties of the steel. They form when an excess of aluminum or zirconium (but not apparently titanium!) is used for deoxidation.

Mohla and Beech (1968) investigated the relation between these sulfide types, and concluded that the change from type 1 to type 2 is brought about by a lowering of the oxygen content. Additionally, it seems that the new mixed sulfide/oxide phase has a low interfacial energy with the solid, allowing it to spread along the grain boundaries. Also, it might constitute a eutectic phase. Type 3 sulfides were thought by Mohla and Beech to be a primary phase. In common with all other investigators of sulfide embrittlement of steels, it is clear that these authors were less than happy with their tentative findings, since doubts and confusion still existed.

However, type 2 inclusions have all the hallmarks of an entrained film defect. It is significant that this type of inclusion forms only when the melt is deoxidized with Al or other powerful deoxidizers that are known to create solid films on the melt. The surface film might originally have been enriched with the other highly surface-active element, sulfur. The entrainment of an oxide film would in any case be expected to form a favorable substrate for the precipitation of sulfides. The film would naturally be pushed into the interdendritic regions by the growing dendrites, so that it would automatically sit at grain boundaries.

Even so, an explanation of type 3 sulfides remains elusive. These results illustrate the complexity of the form of inclusions, and the problems to understand their formation. Much additional research is required to elucidate the mechanism of formation of these defects.

A final question we should ask is 'How do inclusions in the liquid become incorporated into the freezing solid?'

It seems that for small inclusions, especially those that are in the relatively quiet region of the dendrite mesh, the particles are pushed ahead of the front, concentrating in interdendritic spaces.

For larger inclusions, generally above about 10  $\mu\text{m}$  diameter, trapping between dendrite arms is only likely if the inclusion is carried directly into the mesh by an inward-flowing current. This may be the mechanism by which large inclusions are originally trapped within the cone of negative segregation, where they subsequently grow to large size (Figures 5.44 and 5.45).

Where the front is relatively planar and strong currents stir the melt, the larger inclusions are not frozen into the advancing solid as a consequence of the velocity gradient at the front. Delamore (1971) found that those particles that do approach the interface cannot be totally contained within the boundary layer, and as a result spin or roll along it because of the torque produced by the velocity gradient. In this way the larger particles finally come to rest in the center of castings. Rimming steels benefited for the same reason from an absence of large inclusions in their pure rim.

Now for an absolutely final point about inclusions. Take care not to confuse those inclusions that arise from the melt or from freezing with those that occur as a result of later solid-state precipitation. Precipitation within the solid is usually on a scale at least a factor of 10 finer than anything that occurs when liquid phases are still present. This is the direct result of the considerably smaller rate of diffusion in the solid compared to the liquid.

For those readers who are interested in checking whether nitrides or other inclusions might occur in the solid, and particularly because of the problems of embrittlement when such precipitation occurs on grain boundaries, the logic of the approach is broadly the same as that presented above for the

nucleation in the liquid phase. In fact more accurate predictions are often possible because better data are usually available for reactions within solid metals.

### 6.6.7 Nucleation and growth of the solid

During the cooling of the liquid steel, a number of particles may pre-exist in suspension, or may precipitate as primary inclusions. The primary iron-rich dendrites will nucleate in turn on some of these particles. The work by Bramfitt (1970) illustrates how only specific inclusions act as nuclei for iron.

Bramfitt carried out a series of elegant experiments to investigate the effect of a variety of nitrides and carbides on the nucleation of solid pure iron from the liquid state. In this case, of course, the solid phase is delta-iron ( $\delta\text{Fe}$ ). In his work he found that his particular sample of iron froze at approximately  $39^\circ\text{C}$  undercooling (i.e.  $39^\circ\text{C}$  below the equilibrium freezing point). Of the 20 carbides and nitrides that were investigated, 14 had no effect, and the remaining six had varying degrees of success in reducing the undercooling required for nucleation.

The results are shown in Figure 6.60. They give clear evidence that the best nuclei are those with a lattice plane giving a good atomic match with a lattice plane in the nucleating solid. Extrapolating Bramfitt's theoretical curve to the value for the supercooling of his pure liquid iron indicates that any discrepancy between the lattices beyond approximately 23% means that the foreign material is of no help in nucleating solid iron from liquid iron.

Another interesting detail of Bramfitt's work was that a number of additions were ineffective because they either melted or dissolved in the liquid iron prior to it being cooled to promote freezing. This consequent lack of effectiveness was despite, in some cases, quite low values of discrepancy. This underlines the perhaps self-evident point (but often forgotten) that any addition has to be present in solid form for it to nucleate another solid. In addition, all of Bramfitt's work was concerned with the nucleation of  $\delta\text{Fe}$ , the body-centered-cubic form of iron.

The face-centered-cubic form of iron,  $\gamma\text{Fe}$ , or austenite, has been considerably more resistant to past attempts to nucleate it. It seems that no-one has yet succeeded to identify any prior-existing solid that may act as a nucleus for the  $\gamma\text{Fe}$  phase. The grain refinement of austenitic stainless steels remains a challenge to future metallurgists. It seems likely that only those cast austenitic stainless steels that solidify first to  $\delta\text{Fe}$ , prior to their subsequent transformation in the solid state to  $\gamma\text{Fe}$ , are able to benefit from grain refinement.

Suutala (1983) proposes a factor that allows the prediction of whether the steel will solidify to austenite or primary ferrite (delta iron); this is the ratio of the chromium equivalent to the nickel equivalent,  $\text{Cr}_{\text{eq}}/\text{Ni}_{\text{eq}}$ , where the chromium and nickel equivalents are calculated from (elements in weight percent):

$$\text{Cr}_{\text{eq}} = \% \text{Cr} + 1.5\text{Si} + 1.37\text{Mo} + 2\text{Nb} + 3\text{Ti}$$

$$\text{Ni}_{\text{eq}} = \% \text{Ni} + 22\text{C} + 0.31\text{Mn} + 14.2\text{N} + \text{Cu}$$

(Readers will note a close similarity with the definition of the Schoefer equations given earlier that define the structures of stainless steels at room temperatures.) Suutala proposes the ratio  $\text{Cr}_{\text{eq}}/\text{Ni}_{\text{eq}} = 1.55$  is the critical value; at values higher than this the solidification changes from primary austenite to ferrite. (This value applies for shaped castings and ingots. The equivalent value for welds because of their much faster rates of freezing is 1.43.) However, careful work by Ray and co-workers (1996)

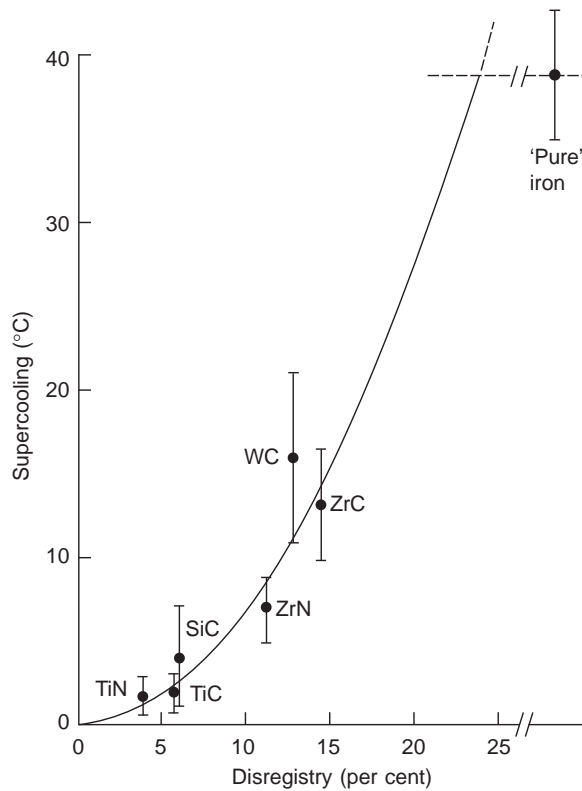


**FIGURE 6.60**

Supercooling of liquid iron in the presence of various nucleating agents. Data from Bramfitt (1970).

suggests that the division between austenite and ferrite is not sharp, but is better defined by a parameter the 'Ferrite Potential' (FP) that assesses the fraction of primary ferrite in austenitic stainless steels:

$$FP = 5.26(0.74 - Cr_{eq}/Ni_{eq})$$

Barbe and co-workers (2002) find that an FP value below 3.5 is useful for mainly ferritic steels, corresponding to a maximum  $Cr_{eq}/Ni_{eq} = 1.40$ . The retention of some austenite limits the grain growth of ferrite, and is suggested to reduce the susceptibility that ferritic steels have to 'clinking', i.e. cracking during continuous casting. When slabs are cooled to room temperature cracks are found on the slab edges. Sometimes the slabs crack into two. (This problem is reminiscent of problems in continuously cast direct chill (DC) aluminum alloys, particularly the strong 7000 series alloys. These appear to suffer from oxide bifilms entrained during the first few seconds of casting in which the metal falls and splashes turbulently during the early filling of the mold. The bifilm cracks created in this moment float randomly into higher regions of the ingot during the casting operation, causing it to crack catastrophically, sometimes weeks after being cast. It is dangerous to be near such an event. The high-Cr ferritic steels might be expected to behave analogously as a result of entrained Cr-rich films.)

Roberts et al. (1979) confirm that only ferritic material was refinable with titanium additions, and confirm that TiC and TiN have lattices that are good fits with ferrite, but poor fits with austenite. Baliktay and Nickel (1988) report that titanium additions can also refine the grain size of the widely used high-strength stainless steel 17-4-PH. However,  $Cr_{eq}/Ni_{eq} = 2$  approximately for this material, confirming that it solidifies to ferrite, in agreement with the finding by Roberts. More recent work (Wang et al. 2010) has demonstrated good refinement under laboratory conditions in a 12Cr steel ( $Cr_{eq}/Ni_{eq} = 25$ ) using an addition of Fe–Ti–N.

Japanese workers led by Mizumoto (2008) are perhaps the only people to claim to have successfully grain-refined an austenitic stainless steel (12Cr 18Ni with  $Cr_{eq}/Ni_{eq} = 0.83$ ). Even here the work was carried out only on a laboratory scale (melt weight 90 g) and had to be performed in seconds otherwise the niobium carbide (NbC) contained in their master alloy dissolved so quickly as to become ineffective. Again, no mechanical testing was carried out to ascertain whether there appeared to be any benefit to this procedure.

Let us stop this account of the grain refinement of cast steels, and stand back a little to take stock of the situation in which we find ourselves. Whereas it is common knowledge that the grain refinement of wrought steels is a valuable feature, the grain refinement of cast steels does not seem to be necessarily beneficial. Having recorded these struggles to achieve significant grain refinement in cast steels, the question arises, ‘Is it worth it?’ The answer is not clear as the following reports indicate.

Doubt is inferred from the work by Campbell and Bannister (1975) on the ferritic alloy Fe–3Si. They showed that the best refinement was obtained by the addition of TiB<sub>2</sub> to the melt. However, on metallographic examination the grain boundaries were found to be surrounded by a phase that appeared to be iron boride, which, like iron carbide, is brittle. The mechanical properties were not tested, but were likely to have been impaired. It would be valuable to explore further whether conditions could be found in which grain refinement would improve properties.

Encouragement that such useful results might be gained is given by Church et al. (1966), but even these results are not all good news. This work on a high-strength steel, 0.33C–0.7Mn–0.3Si–0.8Cr–1.8Ni–0.25Mo–0.040S–0.040P, revealed that although grain refinement was successfully accomplished with 0.60Ti, the benefit was negated by the presence of interdendritic films of titanium sulfide, causing severe embrittlement. However, toughness and ductility could be improved by smaller additions of titanium in the range 0.1–0.2%, which was still successful in achieving grain refinement. The doubt remains that much of this research was undermined by poor casting technique, introducing quantities of deleterious bifilm cracks, particularly at grain boundaries. Sulfur would be expected to precipitate preferentially on such substrates, giving the impression of brittle sulfide films at these locations.

Jackson (1972) lists a large number of additives that were unsuccessful in attempts to refine austenitic steels. His first success was the addition of FeCr powder together with floor sweepings! This impressively economic but hardly commendable formula caused him to persevere, searching for more scientifically chosen additions. He later found that calcium cyanamide (CaCN<sub>2</sub>) was quite useful, but required the nitrogen content in the alloy to be raised to 0.3% to be successful in 18:8 stainless steels. At this level of gas content severe nitrogen porosity is the unwelcome product. Jackson was able to define satisfactory conditions for 18/10/3Mo stainless steel, again providing that the nitrogen content was above 0.08 wt%. The modest improvement that he reports in mechanical properties he attributes not so much to the reduction in grain size as to the increase in the alloying effect of nitrogen! This work is further complicated by the expectation that the compound CaCN<sub>2</sub> will probably have decomposed at



steel casting temperatures. Thus a viable grain-refining agent for austenitic steel remains a challenge for future researchers.

In contrast to the limited success from attempts to nucleate grains, other approaches involving ‘seeding’, using granular metal additions of the same composition as the melt, have been repeatedly confirmed by different workers over the last half century as potentially successful (Jackson’s addition of FeCr powder is an instance, although the floor sweepings are probably not. Other genuine instances include Campbell and Caton (1977).)

Part of the reason for the overall disappointing progress on the grain refinement of cast steels, which might appear to be a potentially important metallurgical advance, lies in the special properties of steels. Firstly, many steels transform and recrystallize more than once to different crystal structures as they cool, thereby automatically providing a fine grain size at room temperature (even though, of course, the original segregated boundaries may still be in place). Secondly, unlike Al alloys with long-lived bifilm populations, they do not benefit from being ‘cleaned up’ by sedimentation of the bifilms by the grain-refining addition, since the high density of steels ensures they are already generally clean by flotation at the time of the grain-refining addition. No further cleaning is possible, thus the major advantage of grain refinement enjoyed by Al alloys is not necessary for steels.

### 6.6.8 Structure development in the solid

The grain structure of the steel that forms on solidification may turn out to be the same as that seen in the finished casting. However, this would be somewhat unusual. It happens only in those cases where the metal is a single phase from the freezing point down to room temperature. Examples include some austenitic stainless, and some ferritic stainless. However, even the ferritic stainless may undergo a transformation to martensite or bainite depending mainly on its carbon content. The transformer steel, Fe–3.25%Si, is a common steel that, on a polished and etched section, clearly displays at room temperature a structure that has changed little from that originating during solidification. For that reason it is a useful model alloy for research.

Even in these single-phase materials there is opportunity for grain boundary migration, possibly grain growth, and possibly recrystallization. Complete recrystallization would be expected in those parts of castings that had been subject to considerable plastic deformation during cooling. This would be expected, for instance, at junctions of flanges that restrain the contraction of the casting.

In materials that change phase during cooling to room temperature the situation can be very much more complicated. Low-carbon and low-alloy steels are a good example, illustrating the problems of understanding a structure that after freezing has undergone at least two further phase changes during cooling to room temperature. Figure 6.61 lists the changes.

- (a) The liquid solidifies to delta iron dendrites.
- (b) When solidification is complete, the principal grain boundaries (shown as full lines) have their positions delineated and to some extent fixed in position by segregates, particulate inclusions, and bifilms. The slight misalignments between parts of the dendrite raft result in a network of less important subgrain boundaries (shown as broken lines).
- (c) During cooling and differential contraction of the casting, the plastic strains will create dislocations that will migrate to form an additional network of new subgrain boundaries. These are, of course, all low-angle boundaries and may not be readily visible.

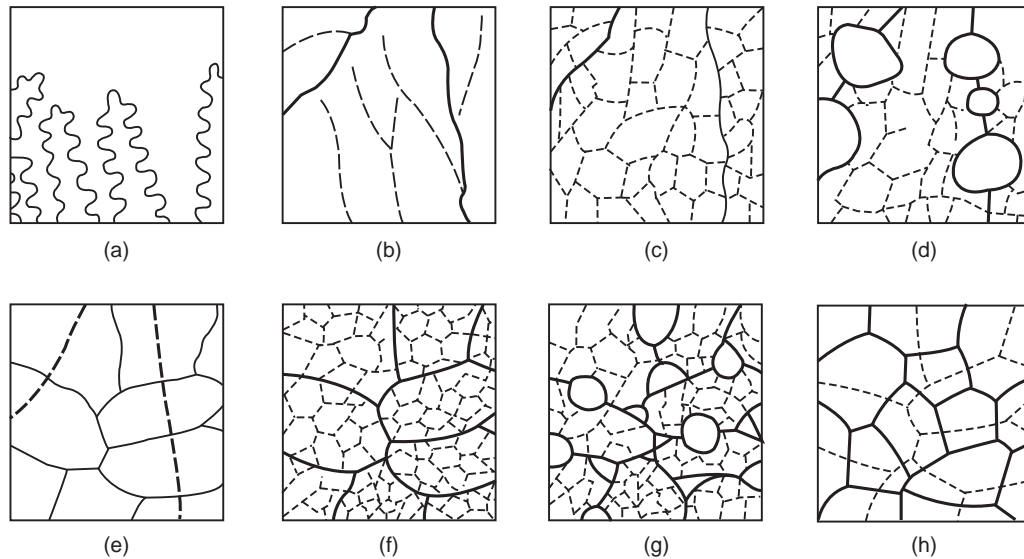


**FIGURE 6.61**

Successive stages of grain evolution in a low-carbon steel, from its freezing point to room temperature (see text for full explanation).

- (d) On reaching the temperature for the formation of the gamma-iron phase, austenite grains will nucleate on the original grain boundaries or other discontinuities. Their growth into the delta-grains will sweep away most traces of the subgrain network.
- (e) When the conversion to austenite is complete the original delta-grain boundaries (shown as broken lines) will still usually be discernible as ghost boundaries because of the fragmentary lines of segregates.
- (f) Further cooling strains will generate a new subgrain structure.
- (g) Austenite will start to convert to ferrite, usually nucleating at grain corners and boundaries, sweeping away the substructure once again.
- (h) The final ferrite grains will again show the ghost boundaries of the previous austenite grains because these will have experienced sufficient time at temperature to have gathered some segregates by diffusion to the boundary.
- (i) Subsequently, a further series of subgrains may be created, although by now the temperature is sufficiently low that any strains will generate fewer dislocations, and that such dislocations will not be sufficiently mobile at lower temperature to migrate into low-energy positions, forming low-angle boundaries. Thus the alloy will have become sufficiently strong to retain any further strain as elastic strain. The structure of the alloy will no longer be affected during further cooling, but elastic stresses will build up.

The final structure on a polished section will be a grain size that has been refined by two successive phase changes (but possibly coarsened a little by intervening grain growth) and may still retain ghost

boundaries of delta iron and austenite. The underlying structure of the original delta iron dendrites will probably still be present, as can be revealed by etching to highlight the differences in chemical composition.

This sequence of events neglects the other many phase changes that can occur in some steels. Thus transformation of austenite to pearlite is usual for carbon/manganese steels, or transformations to martensite or bainite is also possible at higher cooling rates.

For a formal review of the development of structure in castings, see Rappaz (1989). Further detailed work on cast structures has been carried out during extensive work on the structures of welds in steels. For a review of this work, see Sugden and Bhadeshia (1987). This work draws attention to the complicating effects of the formation of Widmanstätten and acicular ferritic structures, and the presence of martensite, bainite, pearlite, and retained austenite. The solidification morphology of the steel in this review of welding seems to be principally cellular, or possibly cellular/dendritic (i.e. dendrites without side branches). Also, of course, in successive weld deposits there are the additional effects of the subsequent heat treatment of the previous runs in the laying down of the subsequent deposits.

---

## 6.7 NICKEL-BASE ALLOYS

There are of course a wide range of Ni-base alloys, together with their cousins, the Co-base alloys. When alloyed with Cr, the alloys can achieve great resistance to heat and oxidation. For a special class of highly creep-resistant alloys, strong and oxidation-resistant at high temperature, the name 'high temperature alloy' or even 'superalloy' is often used. This class of alloy has, additionally, a few weight percent of Al as the major strengthening element (often together with some Ti), precipitating Ni<sub>3</sub>Al (the so-called gamma prime phase, written as the Greek letter  $\gamma$ ) as an extremely fine and stable second phase. Ti contributes together with Ti<sub>3</sub>Al. Many high-temperature alloys appear to contain most of the elements of the periodic table, making them probably more complex than any other metallic alloys.

Recent developments have seen the incorporation of many rare and expensive elements into high-temperature alloys. In particular, hafnium (Hf) has been used and noted for its action to reduce porosity. This somehow has been attributed to its lower coefficient of expansion (Chen and Knowles 2003) but seems much more likely to be the result of a stronger oxide on the surface of the liquid, thus holding up on the lip of the crucible or in the mouth of the mold, and so avoiding incorporation as bifilms into the casting.

The high quantity of highly oxidizable elements, Al, Cr, Ti, Hf, etc. in the high-temperature Ni-base alloys is the reason for the problems suffered by these alloys during casting. These elements all react rapidly with oxygen (and possibly with nitrogen) in the environment, creating solid films on the liquid surface. The entrainment of the solid surface film leads to bifilm creation, and hence pore and crack defects. As for steels, the conversion of the solid alumina-based surface film into a liquid surface film with the aid of Ca addition is a great help, avoiding bifilm formation, and thus raising properties, but does not seem to be effective for all alloys. For those alloys for which this phenomenon is effective the technique is important and is mentioned repeatedly below. Even here, it is possible that for some alloys where this would be helpful, Ca may be considered a harmful impurity for other reasons. This alloy system is complicated.

### 6.7.1 Air melting and casting

Many Ni-base alloys are melted and cast in air, both into ingots for subsequent working into plate, sheet, bar, tube and wire, etc. and into shaped castings. Such castings behave similarly to steels, so that deoxidizers such as Al require to be added to avoid a carbon boil reaction during freezing. Alternatively, Niu and colleagues (2003) describe how carbon is useful to deoxidize, eliminating more than 50% of the oxygen during the melting stage, even though Al is useful later to reduce the oxygen content further. Once again, as for steels, if Al would normally be used for deoxidation, a 50:50 mixture of Al and Ca is recommended to be used instead. For some Ni-base alloys this technique is valuable to avoid the embrittling effects of alumina bifilms, replacing these with liquid oxide eutectic that, even if entrained by poor casting technique, still has the chance to spheroidize and float out of the casting. At this time it is not clear which alloys respond successfully to this deoxidation technique. More research would be so welcome.

For a high-temperature alloy, its alloy content of Al means that no additional Al will be required for deoxidation since the alloy will naturally have a low oxygen content (although sometimes not so low as to prevent a carbon boil occurring during freezing). However, the alloy will definitely form a strong aluminum oxide bifilm on pouring; although there is only a few percentage of Al in the alloy, the high temperature encourages its extremely rapid growth. Thus a small addition of Ca immediately prior to pouring is valuable to liquefy the surface oxide, and thereby reduces cracking on solidification or during subsequent working.

### 6.7.2 Vacuum melting and casting

One of the principal castings made from Ni-base (and some Co-base) alloys is turbine blades mainly for aero engines, but also nowadays for power-generating turbines. As usual, these alloys contain aluminum and titanium as the principal hardening elements. Because such castings are produced by investment (lost wax) techniques, the running systems have been traditionally poor. It is usual for such castings to be top-poured, introducing severe surface turbulence, and creating high scrap levels. Even most bottom-gated filling systems, designed to fill the mold cavity in an uphill direction, are still poor; the defects introduced in the metal in the early part of such systems are simply carried over into the mold cavity to spoil the casting, or interfere with the progress of directional solidification or single crystal growth. When studying faults in single crystals, Carney and Beech (1997) find oxides at the root of most stray grains.

Turbine blades that have failed from major bifilm defects have caused planes to crash and have cost lives. Clearly, the problem is not trivial and the consequences are tragic. It is not satisfactory that we continue to live with gravity-poured blades fitted in aero engines. Such blades necessarily contain bifilm defects, many of which are not detectable by either X-ray radiography or by dye-penetrant inspection (DPI). In contrast, blades produced by counter-gravity filling could probably be guaranteed to be free from filling defects. Furthermore, perhaps we would have to check them neither by radiography nor by DPI. If we *have* to live with a defective production technique for parts for aircraft engines, more discriminating testing by multi-resonance techniques would ensure greater safety.

In an effort to reduce the scrap (i.e. castings that can be identified as defective), the alloys have been melted and cast in vacuum.

Melting in vacuum is useful to avoid loss of some critical elements by oxidation (although account has to be taken of losses by evaporation of such elements as Mn, Cr, and others). The melting crucible

therefore remains somewhat cleaner. Even so, a slag collar usually builds up from the accretion of oxides in suspension in the alloy. Some of these oxides are from the skins of the charge materials, but many are bifilms generated by the pouring of the alloy through drops of several meters, falling into long steel tubes when cast into rods by the alloy maker (again, of course, this occurs in vacuum, but the vacuum is not sufficiently good to prevent the creation of oxide bifilms).

Casting in vacuum is probably essential for such products as turbine blades. The wall thickness of these products is so small, becoming measured in micrometers at the trailing edges of blades, that any back-pressure of gas will inhibit filling.

It is quite clear, however, that casting in vacuum is not a complete solution. A good industrial vacuum is around  $10^{-4}$  torr (approximately  $10^{-2}$  Pa). This is not good enough to prevent the formation of bifilm defects (from entrainment of the surface oxide or nitride film) during pouring.

Considering oxides, equilibrium theory predicts that not even the vacuum of  $10^{-18}$  torr that exists in the space of near-earth orbit is good enough to prevent the formation of alumina (the most likely and most usual oxide) because  $10^{-40}$  torr is required to dissociate alumina. Recent research on pure liquid aluminum has revealed that this equilibrium prediction is hugely inaccurate as a result of the alumina dissociating to a sub-oxide  $\text{Al}_2\text{O}$ . This occurs at around  $10^{-6}$  torr, reducing to  $10^{-4}$  torr at approximately  $1000^\circ\text{C}$ , causing a 'wind' of  $\text{Al}_2\text{O}$  to flow away from any  $\text{Al}_2\text{O}_3$  on the surface of liquid Al, decomposing the  $\text{Al}_2\text{O}_3$  and conveying away its oxygen in the form of the suboxide. The wind of suboxide vapor prevents oxygen from arriving at the surface of the liquid metal (Giuranno 2006, Molina 2007). The aluminum surface can then slowly become perfectly clean, free from oxide.

Despite this beneficial evaporation of the aluminum oxide, it remains a fact that films are found entrained in vacuum cast alloys. Perhaps they are not oxides, but nitrides? This emphasizes, if emphasis is needed, that the real solution is not to attempt to prevent the formation of the surface film, but to avoid its entrainment. Thus top-pouring needs to be totally avoided. A well-designed bottom-gated filling system would be an improvement. However, the ultimate answer would be the complete avoidance of any type of pouring, using a counter-gravity system of filling. It would make beautiful castings that would probably not require expensive testing (the multi-resonance technique is fast and low cost). Furthermore, its easy automation would greatly lower costs and enhance quality further.

Considering further that the surface films on high-temperature Ni-based alloys might in some cases actually be AlN. The Ni-based superalloys are well known for their susceptibility to react with nitrogen from the air and so become permanently contaminated. It seems more likely that the contamination is actually a nitride film problem rather than a problem caused by nitrogen in solution. In any case, in air, the reaction to the nitride may be favored even if the rates of formation of the oxide and nitride are equal, simply because air is 80% nitrogen. Niu et al. (2002) report in many superalloys there are an order of magnitude more nitride than oxide inclusions. These authors report higher porosity and loss of rupture life with higher nitrogen, lending confirmation that the nitrogen is in the form of nitride bifilms.

Whatever the films are, oxides or nitrides, an example is seen in Figure 6.62 that happens in this case to be an oxide. Other examples of clear film-like defects in vacuum cast superalloys can be seen in the work of Ocampo (1999) and Malzer (2007). Ocampo describes a Co-base alloy with continuous grain boundary films decorated with porosity and carbides that are reluctant to dispersing even with treatment at  $1100^\circ\text{C}$ . Figure 6.63 also shows a bifilm crack surrounded by carbides. The study by

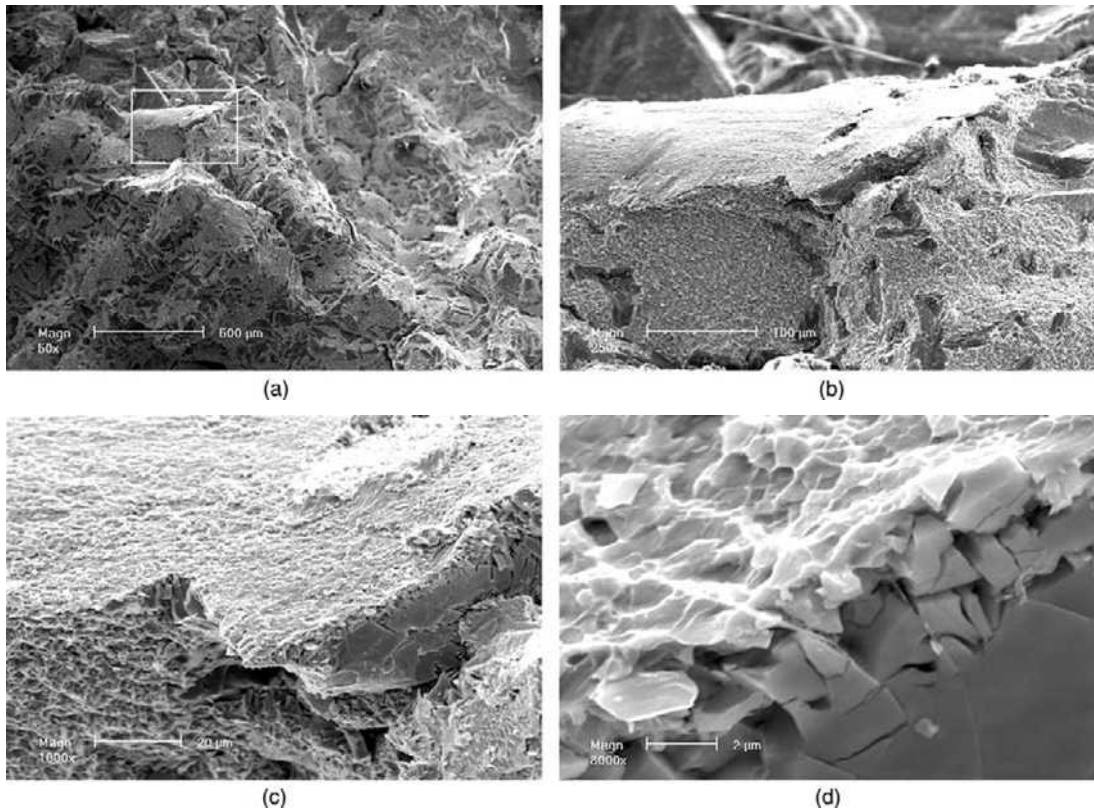


**FIGURE 6.62**

SEM image of a fracture surface of a Ni-based superalloy, melted and cast in vacuum. The light-gray oxide clearly occupies more than  $10 \text{ mm}^2$  of surface. The selected region, like a glacier, is only about  $1 \mu\text{m}$  thick, but has a  $20\text{-}\mu\text{m}$ -deep underlayer of carbides. At its high temperature of formation the oxide film has recrystallized (Rashid and Campbell 2004).

Malzer is interesting because the bifilms in his Ni-base superalloy are opened at regular intervals by the shrinkage conditions in the regular interdendritic spaces, creating lines of pores. The alignment of the bifilms and their pores in  $[001]$  directions reduces the creep life in the  $[110]$  directions at right angles.

These larger bifilm defects, clearly seen on fracture surfaces, may be less common than those that give rise to the ‘stars at night’ symptoms created by clouds of bifilm fragments that intersect the surface of vacuum investment superalloy castings (for instance reported by Wauby (1986)). However, it is difficult to be sure. The fluorescent dye can penetrate the folded bifilms, and so exude again during inspection with ultraviolet (UV) light. Some indications are large and bright, indicating large internal cavities. Others can appear on both the front and back of blades, possibly indicating that they penetrate the complete wall. A casting made with a good filling system (probably of lower cost than

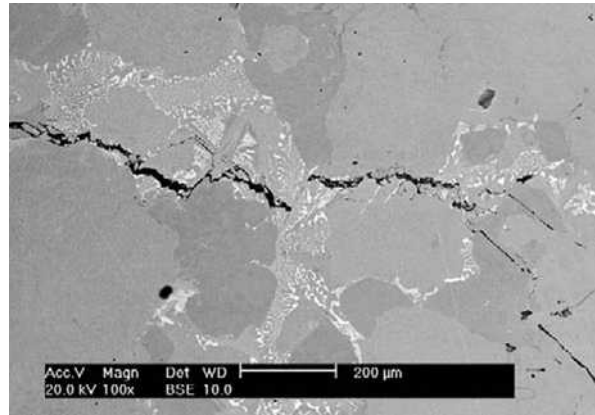


**FIGURE 6.63**

SEM image of an Ni-base alloy casting polished through a freckle containing segregated carbides precipitated on a bifilm crack (Rashid and Campbell 2004).

a conventional filling system, for those who assert that quality has to be paid for) can display zero indications. In the presence of a group of investment foundry personnel, I recall casting a blade that was put through the DPI process. It was then presented to an experienced inspector who, after a long and puzzled inspection, concluded it had not undergone immersion in the dye.

The grain refinement of the surface of Ni-base superalloys by a cobalt aluminate primary dip coat on the investment shell is dealt with in Chapter 10, Casting Rule 7. It is akin to a seeding process since it probably uses the intermetallic compound CoAl resulting from a thermal degradation of the aluminate. Rule 7 reminds us of the undermining action of convection in many investment molds that effectively redissolves our expensively manufactured refined grains and replaces them with huge, coarse grains.

Further important aspects of Ni-base alloys, particularly for turbine blades, are discussed in Chapter 17 ‘Controlled solidification techniques’.

## 6.8 TITANIUM

Titanium is a curious and special metal. In its liquid state it is practically impossible to handle without it reacting with everything. However, in its solid state it can be wonderfully resistant to oxidation and corrosion, whilst being impressively strong and having a density occupying an interesting ‘half-way house’, part-way between the Al alloys and the steels.

Its chemically inert behavior makes it favored for use for valves and fittings in the chemical industry, marine applications, and in prostheses for the human body, including replacement hip and knee joints. Its unique combination of lightness and strength make it ideal for aircraft, particularly undercarriage structures, and blades for some of the cooler parts of turbines.

Despite these glowing advantages, the whole technology of melting and casting of Ti and its alloys is, in my view, deeply disappointing as a result of poor melting and casting technology. Parallels with the casting of superalloy turbine blades are clear. For this reason I am risking unpopularity to state my

views, since I believe that the industry has the capability to develop what I believe to be the true, very much greater potential, of Ti and its alloys

### 6.8.1 Ti alloys

Naturally, the metallurgy of Ti alloys is an extensive subject that cannot be covered in any detail here. The reader is recommended to Polmear's book *Light Alloys 2006*. However, for a quick overview, the metallurgy of Ti is divided into the low-temperature  $\alpha$ -alloys generally stabilized by O, N, C, and slightly by Sn and Zr, and the higher temperature  $\beta$ -alloys, stabilized at room temperatures by Mo, V, Cr, Fe. Common  $\alpha$ -alloys include commercially pure Ti (actually a Ti-O alloy) and Ti-5Al-2.5Sn. Probably the most common of all Ti alloys is the mixed  $\alpha\beta$ -alloy Ti-6Al-4V (often known simply as 6-4 alloy).

Other important alloys include the titanium aluminides, TiAl and Ti<sub>3</sub>Al, both of which exist over a range of temperatures and are themselves significantly alloyed. They have excellent specific stiffness, oxidation resistance, and good creep resistance up to 700°C. Disadvantages include poor ductility. TiAl also suffers significant microsegregation as a result of the 'double cascade' effect of the two significant peritectic reactions that occur in series during its solidification. Despite these drawbacks, much development work is in progress with the aluminides because of their huge potential for weight reduction in gas turbines for aircraft.

### 6.8.2 Melting and casting Ti alloys

There is a fundamental challenge with the melting and casting of Ti and its alloys. Ti reacts with and dissolves practically everything, so there are few materials in which liquid Ti can be contained. In addition, the high melting temperature creates other technical problems, particularly rapid loss of temperature during casting.

Much Ti is therefore melted in a water-cooled copper crucible. Roberts (1996) describes the early history of the process in which melting was carried out in an inert atmosphere or vacuum by electric arc, electron beam, or by plasma in a hemispherical copper crucible. After the liquid metal had been poured out a hemispherical shell of frozen metal remained. When this was lifted out of the crucible its shape was remarked to be like a skull. Hence early workers referred to the process as 'melting in a skull' which was shortened to 'skull melting'.

One of the serious issues that arise as a result of melting in a cold crucible is that relatively little average superheat can be achieved in a melt. With modern induction heating typical average superheats in vacuum are around 15°C whereas an argon atmosphere seems to 'keep the melt warm' achieving around 35°C (Rishel 1999). These very limited values have promoted workers to adopt (erroneously in my view) techniques for extremely rapid filling of molds, such as centrifugal casting. The melt is poured down a central downsprue and radially out to the molds along spoke-like runners. Molds are arranged around the outside of a rotating platform, carefully balanced prior to spinning. All this happens in a large chamber providing an environment of vacuum or inert gas.

The disastrous turbulence generated by this approach ensures that castings are full of defects (Cotton 2006). Nevertheless, this problem seems to be accepted as normal in the Ti casting industry. Castings are repaired by grinding out defects and refilling by gas-tungsten-arc welding. Finally, all Ti alloy castings are subjected to hot isostatic pressing (hipping) as standard procedure. Hipping appears



to be especially effective for Ti alloys because pores are not only closed but also appear to be effectively welded, because any oxide or nitride film on the original pore is taken into solution. Thus the casting defects are mainly repaired by these additional (expensive) procedures.

Harding (2006) has demonstrated the casting of titanium aluminide (TiAl) by tilt pouring. Compared to centrifugal casting, this is a vast improvement in terms of reduced damage to the product. Even so, tilt is not an easy process at the low superheats available from a cold crucible. In addition, many castings have a geometry for which a tilt filling solution is impossible without a freefall at some point in the mold and consequent damage to the liquid.

My approach would be to use counter-gravity to fill the mold. This is a powerful filling technique that can apply to practically all geometries of castings. The melt is transferred vertically into the mold by dipping a riser tube into the center of the melt in the crucible, and applying a differential pressure. This is a simple technique. In addition, a gentle uphill fill would make good use of the limited superheat since most molds even up to a meter or so high could be filled within a very few seconds without exceeding 0.5 or perhaps  $1.0 \text{ m s}^{-1}$ . Such a technique would provide an essentially defect-free casting. Furthermore, of course, the castings would not require hiping, or, if hiping were insisted upon (as would be likely with many quality specifications apparently formulated without regard to logic) would not benefit further. Counter-gravity would ensure that the most frequent inclusions, solidified droplets of tungsten metal (W) from the splatter of weld electrodes in scrap and returned material, would remain sitting firmly on the bottom of the crucible, and thus not appear in the castings. The other major inclusion type, hard alpha particles, again mainly from foundry returns, are less easily dealt with, and largely invisible to X-rays. They can be detected by sophisticated ultrasound techniques.

It is doubtful if low melt temperature would be a problem when filling molds by counter-gravity. If temperature were a problem, I would opt to trial a CaO crucible (lime is one of the most-available and low-cost materials, in contrast with cerium oxide, which is a potentially highly suitable material, but rare and costly). This allows significantly greater temperatures to be reached in the melt. Perhaps more importantly, these temperatures are reached at lower power densities so the melt is subjected to much less turbulence (in a cold crucible the melt jumps about in the crucible, and may be a problem to prevent it jumping out of the crucible when using very high power in an effort to achieve a tolerable casting temperature). Thus much entrainment of the liquid surface will occur with all this violent activity of the surface. Although researchers are concerned for oxygen that will be picked up from the CaO by the melt, the real problem may be the pickup not of oxygen itself, but of oxide films. Thus the action of CaO to introduce oxygen into solution in the alloy may be harmless, or relatively harmless, whereas oxide films introduced by turbulent melting will act as cracks and will therefore seriously reduce properties, particularly ductility. As usual, there is no shortage of avenues to explore.

A further potential benefit of a ceramic crucible is that there is some chance of its accretion of sundry debris in suspension in the melt. Thus a melt would be expected to gradually become clean. This action occurs with practically all other ceramic and refractory containment of liquid metals; in fact the buildup of a collar of 'slag' is a common complaint with a melting process, but in reality is probably an unappreciated benefit. Such a scavenging action might be enhanced by the use of a very small amount of flux or slag. Such a liquid second phase afloat the main melt is a common technique to encourage suspended material to stick to, and be absorbed by, the second liquid.

Mold materials for Ti and its alloys are also problematic because of the high reactivity of Ti. Machined graphite molds were the first to be used for Ti in 1954 (Cotton 2006), soon to be followed by

rammed graphite (Antes 1958). More recently oxide-based materials that can be investment cast are becoming the norm. In all graphitic and oxide-based molds, reaction with the mold stabilizes the Ti alpha phase, thus converting the surface of the casting to this hard, brittle phase, known as the 'alpha skin'. The alpha skin has to be removed from the casting by machining or chemical dissolution. Unfortunately, this high-cost operation adds to the high cost of the alloy, the high cost of processing, and the high cost of hiping. The selection of Ti and its alloys for a casting requires a dedicated and determined buyer.

Permanent metal molds for simple shapes have the great advantage of avoiding the creation of an alpha skin, but such molds are often themselves expensive, consisting of alloys based on either Mo, W, or Nb (Choudry 1999).

### 6.8.3 Surface films on Ti alloys

Titanium alloys may not be troubled by a surface film at all. Certainly during the hot isostatic pressing (hipping) of these alloys any oxide seems to go into solution. Careful studies have indicated that a cut (and, at room temperature, presumably oxidized) surface of the intermetallic alloy, TiAl, can be diffusion bonded to full strength across the joint, and with no detectable discontinuity when observed by transmission electron microscopy (Hu and Loretto 2000). It seems likely, however, that the liquid alloy may exhibit a *transient film* in some conditions, like the oxide on copper and silver, and like the graphite film on cast iron. Transient films are to be expected where the film-forming element is arriving from the environment faster than it can diffuse away into the bulk. This is expected to be a relatively common phenomenon since the rates of arrival, rates of surface reaction, and rates of dissolution are not likely to be matched in most situations.

In conditions for the formation of a transient film, if the surface happens to be entrained by folding over, although the film is continuously dissolving, it may survive sufficiently long to create a legacy of permanent problems. These could include the initiation of porosity, tearing, or cracking, prior to its complete disappearance. In this case the culprit responsible for the problem would have vanished without trace.

Titanium alloys, including titanium aluminide alloys, have a high solubility for oxygen, so that oxide films, if they form, are almost certainly soluble. Mi (2002) has produced evidence that films do occur, and can occasionally be seen by careful examination under the scanning electron microscope in castings. However, previously Hu and Loretto (2000) had shown conclusively that even thick oxide films on TiAl alloys go into solution during hot isostatic pressing, leaving no metallographic trace. Thus in finished Ti alloy castings, all of which are usually hiped as part of the standard production process, entrained films are usually never seen. Only their consequentially created defects such as pores or cracks remain, and even these are likely to be closed by hiping (except of course for those pores or cracks connected to the surface).

Other consequences of the transient presence of bifilms in Ti alloys may be the morphology of the borides in some alloys of titanium aluminide. These are of extremely variable lengths in castings, short from some melts, but long from others, their lengths appearing to be bafflingly independent of casting parameters, and wildly out of the control of the metallurgist. This is typical of bifilm problems. In addition, on close examination the boride particles are often seen to be associated with crack-like porosity along their lengths, typical of that which would occur if a bifilm had started to separate a little during the growth of the boride over its surfaces (Figure 6.64). Cowen and Boehlert (2007) observe

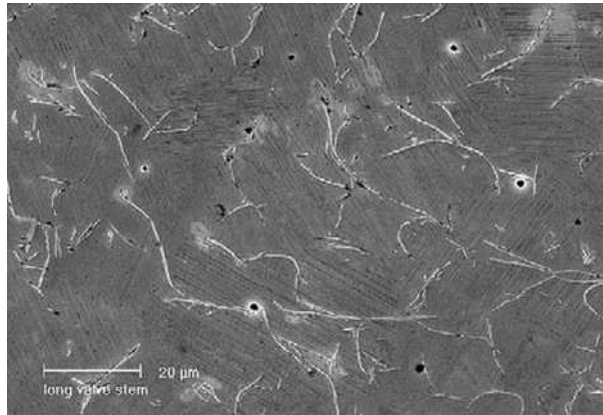


**FIGURE 6.64**

A titanium aluminide casting poured in argon atmosphere. Round pores may be argon bubbles, but all fine, crack-like pores are associated with platelet growth of borides (white linear features in image) and may indicate the bifilm substrates for the borides.

borides on the polished surfaces of specimens of Ti-22Al-26Nb alloy tested in creep. Immediately that the stress is applied they see the borides opening like cracks. As is often assumed for graphite, the borides may also be weak. Their strengths are not known, but may actually be high across transverse planes, in which case tensile failure would only be expected if the borides were formed on bifilms. Research is needed to clarify this.

# Porosity

## 7.1 SHRINKAGE POROSITY

There are so many ways to obtain porosity in a casting. Mainly, the porosity in castings seems to be entrained air bubbles, although sometimes it is a more uniform dispersion of bifilms partly or fully inflated with a gas from solution in the melt. At other times what appears to be shrinkage porosity is most often not shrinkage at all, but is a mass of oxides generated by the entrainment of the oxide surface in the turbulence of pouring. Finally some porosity is the result of mold or core blows, or even ‘microblows’ fired into the casting from microscopic pockets of volatile binder trapped in recesses in mold particles.

As should become clear, true shrinkage porosity is rather rare in castings as a result of founders knowing how to deal with this problem. Even so, we need to discuss it here to highlight some of the conceptual problems of shrinkage conditions, reduced or negative pressures that can initiate pores. These concepts are, frankly, complicated to explain. I shall do my best.

### 7.1.1 General shrinkage behavior

The molten metal in the furnace occupies considerably more volume than the solidified castings that are eventually produced, giving rise to a number of problems for the founder. The metal contracts at three quite different rates when cooling from the liquid state to room temperature, as Figure 7.1 illustrates.

- (i) As the temperature reduces, the first contraction to be experienced is that in the liquid state. This is the normal thermal contraction observed by everyone as a mercury thermometer cools; the volume of the liquid metal reduces almost exactly linearly with falling temperature. When making castings the shrinkage of the liquid metal is usually not troublesome; the extra liquid metal required to compensate for this small reduction in volume is provided without difficulty. It is usually not even noticed, being merely a slight extension to the pouring time if freezing is occurring while the mold is being filled. Alternatively, it is met by a slight fall in level in the feeder.
- (ii) The contraction on solidification is quite another matter, however. This contraction occurs at the freezing point, because (in general) of the greater density of the solid compared to that of the liquid. Contractions associated with freezing for a number of metals are given in Table 7.1. The contraction causes a number of problems. These include: (a) the requirement for ‘feeding’, which is defined here as any process that will allow for the compensation of solidification contraction by the movement of either liquid or solid; and (b) ‘shrinkage porosity’, which is the result of failure of feeding to operate effectively. These issues are dealt with at length in this chapter.

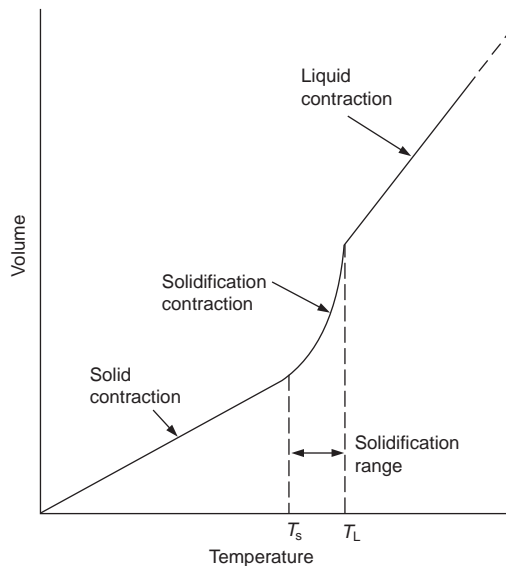


**FIGURE 7.1**

Schematic illustration of three shrinkage regimes: (i) in the liquid; (ii) during freezing; and (iii) in the solid.

- (iii) The final stages of shrinkage in the solid state can cause a separate series of problems. As cooling progresses, and the solidified casting attempts to reduce its size in consequence, it is rarely free to contract as it wishes. It usually finds itself constrained to some extent either by the mold, or often by other parts of the casting that have solidified and cooled already. These constraints always lead to the casting being somewhat larger than would be expected from free contraction alone. This is because of a certain amount of plastic stretching that the casting necessarily suffers. It leads to difficulties in predicting the size of the pattern since the degree to which the pattern is made oversize (the ‘contraction allowance’ or ‘patternmaker’s allowance’) is not easy to quantify. The mold constraint during the solid-state contraction can also lead to more localized problems such as hot tearing or cracking of the casting. The conditions for the generation of these defects are discussed in Chapter 8.

### 7.1.2 Solidification shrinkage

In general, liquids contract on freezing because of the rearrangement of atoms in the liquid structure changes from a rather open ‘random close-packed’ arrangement to a regular crystalline array of significantly denser packing in the solid.

The densest solids are those that have cubic close-packed (face-centered-cubic, fcc, and hexagonal close-packed, hcp) symmetry. Thus the greatest values for contraction on solidification are seen for these metals. Table 7.1 shows the contractions to be in the range 3.2–7.2%. The solidification shrinkage for the less closely packed body-centered-cubic (bcc) lattice is in the range 2–3.2%. Other materials that are less dense in the solid state contract by even smaller amounts on freezing.

**Table 7-1** Solidification shrinkage for some metals

Metal	Crystal structure	Melting point °C	Liquid density (kgm <sup>-3</sup> )	Solid density (kgm <sup>-3</sup> )	Volume change (%)	Ref.
Al	fcc	660	2368	2550	7.14	1
Au	fcc	1063	17 380	18 280	5.47	1
Co	fcc	1495	7750	8180	5.26	1
Cu	fcc	1083	7938	8382	5.30	1
Ni	fcc	1453	7790	8210	5.11	1
Pb	fcc	327	10 665	11 020	3.22	1
Fe	bcc	1536	7035	7265	3.16	1
Li	bce	181	528	-	2.74	4, 5
Na	bcc	97	927	-	2.6	4, 5
K	bcc	64	827	-	2.54	4, 5
Rb	bce	303	11 200	-	2.2	2
Cd	bep	321	7998	-	4.00	2
Mg	bep	651	1590	1655	4.10	3
Zn	sep	420	6577	-	4.08	2
Ce	bep	787	6668	6646	-0.33	1
In	tel	156	7017	-	1.98	2
Sn	tetrag	232	6986	7166	2.51	1
Bi	rbomb	271	10 034	9701	-3.32	1
Sb	rhomb	631	6493	6535	0.64	1
Si	diam	1410	2525	-	-2.9	2

The exceptions to this general pattern are those materials that expand on freezing. These include water, silicon, and bismuth (Table 7.1), and, of course, perhaps the most important alloy of all, cast iron.

Remember the ice cubes are always stuck fast, having expanded in the ice tray. Analogously, the success of ‘type metal’, a bismuth alloy used for casting type for printing, derives some of its ability to take up fine detail required for lettering because of its expansion on freezing. Graphitic cast irons with carbon equivalent above approximately 3.6 (Figure 7.2) similarly expand because of the precipitation of the low-density phase, graphite. The non-feeding requirements of gray irons are in sharp contrast to other cast irons that solidify ‘white’, i.e. containing the non-equilibrium carbide phase in place of graphite. In fact the white irons in general have solidification contractions similar to those of steels.

For the majority of materials that do contract on freezing it is important to have a clear idea of what happens in a poorly fed casting. As an ideal case of an unfed casting, it is instructive to consider the freezing of a sphere. We shall assume that the sphere has been fed via an ingate of negligibly small size up to the stage at which a solid shell has formed of thickness  $x$  (Figure 7.3). The source of supply of feed metal is then frozen off. Now as solidification continues with the freezing of the following onion layer of thickness  $dx$ , the reduced volume occupied by the layer  $dx$  compared to that of the original liquid means that either a pore has to form, or the liquid has to expand a little, and the surrounding solid correspondingly has to contract a little. If we assume for the moment that there is no favorable nucleus

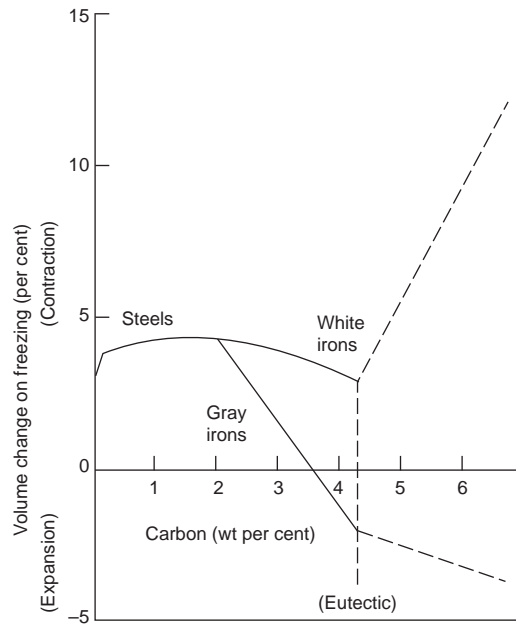


**FIGURE 7.2**

Volume change on freezing of Fe–C alloys. The relations up to 4.3% carbon are due to Wray (1976); higher carbon values are estimated by the author.

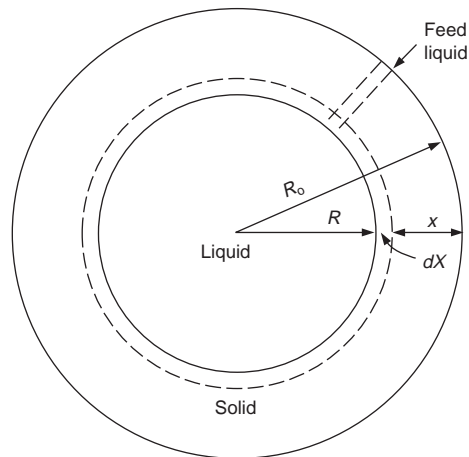


**FIGURE 7.3**

Solidification model for an unfed sphere.

available for the creation of a pore, then the liquid has to accommodate this by expanding, creating a state of tension, or negative pressure. At the same time, of course, the liquid is in mechanical equilibrium with the enclosing solid shell, effectively sucking it inwards. As more onion layers form, so the tension in the liquid increases, the liquid expands, and the solid shell is drawn inwards, initially suffering only elastic deformation, but as the stress rises, finally suffers plastic collapse.

The reader may find the solidifying sphere model easier to visualize by thinking of the exact converse situation of a material that expands on solidification: in this case the formation of solid squeezes the remaining liquid into a smaller volume. The compressed liquid therefore experiences a positive pressure. The internal positive pressure then clearly acts on the liquid to compress it. In turn, the liquid acts on the solid shell to expand it. It is an instructive exercise to go back and reverse this logic to ensure that the concept of negative pressure, or hydrostatic tension, in the liquid is fully understood before proceeding further with this chapter. However, if the reader finds this challenging, further examples to clarify the concept of negative pressures in liquids are presented in Section 7.1.2.1.

Calculations based on a solidifying sphere model were carried out by the author (Campbell 1967, 1968) that show the high tensile stresses in the residual liquid cause the solid to collapse plastically by a creep process. This inward movement of the solid greatly reduces the tension in the liquid. Even so it seems that negative pressures of  $-100$  to  $-1000$  atmospheres may be expected under ideal conditions. The liquid itself is easily able to withstand such stresses since the tensile strength of liquid metals is in the range of  $-10\,000$  to  $-100\,000$  atmospheres. Incidentally, the liquid–solid interface (whether planar or dendritic is immaterial) is also easily able to withstand the stress, because it is not a favorable site for failure by the nucleation of a cavity (see Section 7.1.5.3).

Even in situations that remain connected to feed metal, it can also be shown that the resistance to viscous flow of the residual liquid through a pasty zone can cause the pressure to fall, eventually becoming large enough for the casting to collapse by plastic or creep flow. This condition is described more fully later in the sections on interdendritic feeding and shrinkage porosity.

Thus, in many casting situations, the pressure in the solidifying metal can fall to low, zero or negative values. The negative values correspond to a hydrostatic stress that powers the formation of shrinkage porosity. However, at the same time, of course, the pressure gradient between the outside and inside of the casting is also the driving force for the various feeding mechanisms that help to reduce porosity.

Whether the driving force for pore formation wins over the driving force for feeding will depend on whether nuclei for pore formation exist. If not (i.e. if the metal is clean), then no pores will nucleate, and feeding is forced to continue until the casting is completely frozen and completely sound. If favorable nuclei are present, then pores will be created at an early stage before the development of any significant hydrostatic stress, with the result that little feeding will occur, and the casting will develop its full percentage of porosity as defined by the physics of the phase change (as given, for instance, in Table 7.1). In most cases the real situation is somewhere between these extremes, with castings displaying some evidence for partially successful liquid feeding in the form of feeder heads which have drawn down somewhat, and parts of the casting displaying evidence of some solid feeding (Figure 7.4) because of some surface sinks, but the interior exhibiting some porosity. Clearly in such cases feeding has continued under increasing pressure differentials, until the development of a critical internal stress at which some particular nuclei, or surface puncture, can be activated at one or more points in the casting. Feeding is then stopped at such a locality, and pore growth starts.

In those cases where a pore does form at an early stage of solidification, a freezing contraction of perhaps 3% does not at first sight appear to be of any great significance. However, the reader can easily



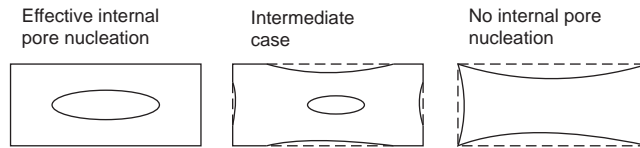


**FIGURE 7.4**

The three forms of shrinkage porosity: (a) internal; (b) mixed; and (c) external shrinkage porosity.

confirm that in a 100-mm-diameter sphere the corresponding cavity will be 31 mm in diameter. For an aluminum casting at 7% contraction, the cavity would be 41 mm in diameter. These considerable cavities require a dedicated effort to ensure that they do not appear in castings. This is especially difficult when it is realized that on occasions a substantial casting might be scrapped if it is found to contain a defect of only approximately 1 mm in size. (The scrapping of castings because of the imposition of unreasonably high inspection standards is a widespread injustice that would benefit from the injection of common sense.)

For the vast majority of cast materials, therefore, shrinkage porosity is one of the most important and common defects in castings. Paradoxically, this even includes gray cast irons because of the effect of mold dilation. This problem occurs if the mold is weak, allowing the benefits of the expansion of the graphite phase to be wasted on outwards expansion of the casting, rather than being used on inwards compression of cavities.

The serious consequences of the porosity occurring on the inside of the casting, where it causes a disproportionately large hole, contrasts with the occurrence of porosity on the outside of the casting. If our 100-mm-diameter sphere had a common solidification contraction in the region of 3%, and had no internal nuclei for the initiation of porosity, no pores would form here, and the solid would therefore be forced to collapse. The final casting would be slightly smaller by approximately 0.5 mm over its whole surface. This 1% reduction in diameter is sufficiently small to be not noticeable in most situations. If it were to be important for a casting requiring special accuracy, this small adjustment could be added to the patternmaker's shrinkage allowance. Thus the elimination of internal porosity and its displacement to the outside of the casting is a powerful technique that is strongly recommended.

Although shrinkage porosity can be reduced by improvements to the cleanness of the metal as mentioned above, this chapter deals later with the other major approach to this problem, the design and provision of good feeding, ensuring good conditions for easy accommodation of the volume change during freezing. The special case of provision of good liquid feeding, the usual way to deal with a feeding problem, is dealt with as a 'methoding' issue in Chapter 10 Rule 6 'Avoid shrinkage porosity.'

In the meantime, understanding negative pressure (hydrostatic tension) in castings is sufficiently critical to an appreciation of casting behavior that it will be valuable to divert to discuss examples before proceeding further.

### **7.1.2.1 Hydrostatic tensions in liquids**

In the original book *Castings* 1991 this section was to have been an appendix. However, it proved to be so interesting, and so central to the understanding of defect generation in castings, that the subject was included as part of the main text. The reader will understand why the subject is included here even though few of the examples described in this section are metal castings. Although most relate to water or other organic systems, the principles will be seen to apply perfectly to metals.

Liquids have been known to be able to withstand tension for many years. Mercury is an interesting case. In a clean glass barometer freshly filled with clean mercury, the liquid would adhere to the glass, 'hanging up', supporting the weight of the long length of the heavy liquid like a rope in tension. If the glass was tapped sharply, breaking the liquid away from the glass, the liquid would fall, opening up a vacuum above it. It would settle at the height at which it could be supported by the pressure of 1 atmosphere acting at its base. This height is approximately 760 mm; the barometric height. The so-called vacuum is of course not perfect. A tiny pressure due to the vapor pressure of mercury would operate, pushing the upper surface down about 1 micrometer at room temperature, which we shall ignore. Actually, if the glass and the metal had been really clean, in principle the mercury column could have hung from a height somewhere in the stratosphere, since the tensile strength of the liquid is extremely high.

The very high tensile strengths of liquid metals should not be a surprise. The interatomic distances in liquids, as random close-packed atomic structures, are only a few percent larger than the distances in solid metals, which have more regular close-packed structures. Thus the strengths would be expected to be similar, which is the case.

In 1850 Berthelot cooled various organic liquids in sealed glass tubes, watching until cavitation occurred as a shower of small bubbles. The number of bubbles was subsequently explained by Lewis (1961), who observed that the rupture was always associated with the sudden appearance and collapse of a single bubble, which was immediately followed by the formation of a large number of tiny bubbles along the length of the tube. The asymmetric collapse of the primary bubble would form an impacting jet and create a series of shock waves. These would be ideal conditions for the formation of additional bubbles. This simple experiment is of special interest, since it is analogous to the solidifying casting, with the internal solidifying liquid progressively occupying less volume, and with the surrounding solid gradually being pulled inwards, its elastic and plastic resistance to deformation steadily increasing, building up the tensile stress in the liquid, to the point at which the liquid fractures.

Berthelot's experiment has been repeated many times in different ways. For instance, Vincent and Simmons (1943) sealed their tube by freezing the liquid in the mouth of the capillary. They found that water would withstand  $-157$  atm and a mineral oil  $-119$  atm. This is a fascinating observation, since it indicates that the freezing interface will withstand high tensions; it is not necessarily a good nucleation site for pores, as has been indicated theoretically (Section 7.1.5). The facts reveal the error of those assumptions, widely presumed in the solidification literature, of ease of pore nucleation at the solidification front.

For a liquid sealed in a tube, Scott et al. (1948) calculated the build-up of tensile stress  $\Delta P$  as the liquid cools an amount  $\Delta T$ , using the coefficient of thermal expansion of the liquid  $\alpha$  and the glass  $\sigma$ , together with the modulus of rigidity  $G$  and the coefficient of compressibility  $\beta$  of the glass tube:

$$\Delta P = [(\alpha - \sigma)/(\beta - (1/G))]\Delta T$$

They also checked their results by measuring the length of the liquid columns after fracture. This work emphasizes the elastic strains built up in the liquid and the surrounding solid during the experiment.

Lewis (1961) found tensile strengths in water and carbon tetrachloride in excess of  $-60$  atm. Also, when water and carbon tetrachloride were introduced into the same tube the two liquids separated at a clear interface. Fracture was not observed to occur at the interface. The liquid-liquid interface seems as poor a nucleation site as the liquid-solid interface above. These observations confirm the expectations from classical nucleation theory as presented in Section 7.1.5.

Tyndall (1872) carried out experiments on the internal melting of ice by shining light through the ice. The light was absorbed by particles frozen inside. The heated particles then melted a small surrounding region of the shape of a snowflake (known nowadays as a Tyndall figure, or, occasionally, a negative crystal). However, because ice reduces in volume on melting, the liquid volume created in this way was under tension. As melting progressed, the tensile stress became so great that the liquid fractured with an audible click. The melted region was then observed to contain a small bubble. Kaiser (1966) demonstrated that the critical pressure for fracture was in excess of  $-150$  atm. Tyndall proved that the bubble was a vapor cavity containing practically no air by carefully melting the ice towards the figure, using warm water. As soon as a link was established with the bubble it collapsed and disappeared; no air bubble rose to the surface. The Tyndall figures are analogous to the isolated regions of metal castings, where vapor cavities are expected to be formed at critical stresses during solidification.

Briggs (1950) centrifuged water in a capillary tube, spinning it at increasing speed to stretch the water until it was observed to snap at a tensile stress of  $-280$  atm.

The early work on the determination of the tensile strengths of liquids held in various containers such as a Berthelot tube gave notoriously scattered results. This was probably to be expected from the different degrees of cleanness of the container, and any microscopic imperfections it may have had on its walls. Experiments to test the liquid away from the influence of walls have been carried out using ultrasonic waves focused in the center of a volume of liquid. The rarefaction (tensile) half of the vibration cycle can cause cavitation in the liquid. These experiments have been moderately successful in increasing the limits, but impurities in the liquid have tended to obscure results.

More recently, Carlson (1975) has reflected shock waves through a thin film of mercury and recorded strengths of up to  $-30\,000$  atm. This result is one of the first to give a strength value of the same order as that predicted by various theoretical approaches. Despite the dynamic nature of the test method, the result is not particularly sensitive to the length of the duration of the stress (varying only from  $-25\,000$  to  $-30\,000$  atm as the time decreased from  $1$  s to  $10^{-7}$  s). This again is to be expected, since nucleation is a process involving the rearrangement of atoms, where the atoms are vibrating about their mean positions at a rate of approximately  $10^{13}$  times per second.

An attempt to measure negative pressures in solidifying aluminum ingots directly was made by Ohsasa et al. (1988a, 1988b). They immersed a stainless steel disc into the top of a solidifying metal, so as to almost fill the top of the crucible in which the metal was held. When the solidification front reached the disc, a volume of liquid was effectively trapped underneath. As this volume solidified, the stress in the liquid was measured by a transducer connected to the disc. Stresses needed to cause pore formation were typically only about  $-0.1$  atm. However, occasionally stresses of up to  $-2.5$  atm were recorded. On these occasions the walls of the ingot were observed to suffer some inward collapse. Clearly, in this work the stresses were limited by the nucleation of cavities against the surface of the stainless steel disc. This would be poorly wetted as a result of the presence of the Cr-rich oxide on the steel. At the higher stresses that were measured, these were in turn limited by the inward plastic collapse of the solidified casting.

In general therefore, it seems that the various attempts to measure the strengths of mercury and the organic liquids have achieved results intermediate between the minimum predicted for a complex inclusion (potentially the weakest point in a liquid metal as explained in Section 7.1.5.3), and the maximum set for the prediction of homogeneous nucleation (Table 7.2). This is probably as good

**Table 7-2** Fracture pressures of liquids

Liquid	Surface tension (Nm <sup>-1</sup> )	Atomic diameter (nm)	$\Delta P^*$		
			From equation 6.1 (atm)	From fisher (atm)	Complex inclusion (atm)
Water	0.072	-	-	1320	16
Mercury	0.5	0.30	16 700	22 300	200
Aluminum	0.9	0.29	31 000	30 000	360
Copper	1.3	0.26	50 000	50 000	600
Iron	1.9	0.25	76 000	70 000	850

a result as can be expected. However, the one high result by Carlson is reassuring, suggesting that the physics seems basically correct, and really does apply to liquid metals.

### 7.1.3 Feeding criteria

Since the first half of this handbook is concerned with the metallurgy of cast metals, the practical aspects of feeding is taken up later, becoming an important feature from Chapter 10 onwards. However, it is desirable to indicate some central concepts, and some small amount of repetition will do no harm.

To allow for the fact that extra metal needs to be fed to the solidifying casting to compensate for the contraction on freezing, it is normal to provide a separate reservoir of metal. We shall call this reservoir a *feeder*, since its action is to *feed* the casting (i.e. to compensate for the solidification shrinkage). The American term *riser* is not recommended. It is not descriptive in a helpful way, and could lead to confusion with other features of the *rigging* such as vents, up which metal also rises. However, the American term *rigging* is helpful. It is a general word for the various appendages of runners, gates, and feeders, etc. No equivalent term exists in UK English.

The provision of a feeder can be complicated to get right. There are 7 Rules that the author has used to help in the systematic approach to a solution. Readers of the book *Castings* 1991 will note this is one more Rule than before. The additional Rule was cited in *Castings* but not elevated to the status of a Rule. The reader will appreciate that the new Rule 1 'Do not feed' has a valuable place in the new listing. Chapter 10, Section 6.4, explains that the Rule is not as perverse as it first seems.

More recently, Tiryakioglu (2001) has further simplified the 7 Rules as noted at the end of this section, but in more detail in Chapter 10, Section 6.5.

#### 7.1.3.1 The 7 feeding rules

**Rule 1.** The main question relating to the provision of a feeder on a casting is 'Should we have a feeder at all?' This is a question well worth asking, and constitutes Rule 1 'Do not feed (unless absolutely necessary)'.

The avoidance of feeding is to be greatly encouraged, in contrast to the teaching in most traditional foundry texts. There are several reasons to avoid the placing of feeders on castings. The obvious one is cost. Feeders cost money to put on, and money to take off. In addition, many castings are actually

impaired by the inappropriate placing of a feeder. This is especially true for thin-walled castings, where the filling of the feeder diverts metal from the filling of the casting, with the creation of a misrun casting. Probably half of the small and medium-sized castings made today do not need to be fed. Sometimes the casting suffers delayed cooling, impaired properties, and even segregation problems as a result of the presence of a feeder. Finally, it is easy to make an error in the estimation of the appropriate feeder size, with the result that the casting can be more defective than if no feeder were used at all.

However, there is one potential major problem if a feeder is not used, but where a feeding problem remains in the casting. The feeding problem will show itself as a region of reduced pressure in the casting at a late stage of freezing. The reduced pressure will act to open bifilms as in the Reduced Pressure Test (RPT) used for non-ferrous alloys. Thus in an aluminum alloy casting with medium-thickness sections, enhanced size and number of internal microshrinkage pores will be experienced if the sections are unfed. Whether this is important or not depends on the specification of microstructure and properties that the casting is required to meet. If the casting is required to have good elongation properties in a tensile test it is likely that feeding to maintain pressure during solidification (and thus keep the bifilms closed) will be needed to achieve this.

Just for the moment we shall assume that a feeder is required. The next question is ‘How large should it be?’

There is of course an optimum size. Figure 7.5 shows the results of Rao et al. (1975), who investigated an increasing feeder size on the feeding of a plate casting in Al–12Si alloy. Interestingly, when

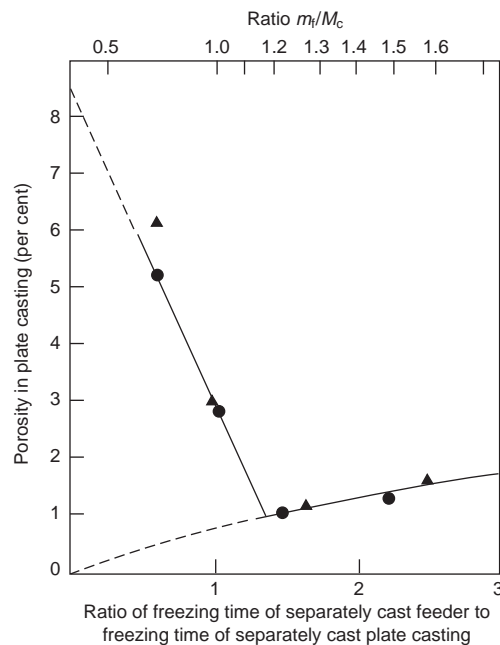


**FIGURE 7.5**

Effect of increasing feeder solidification time on the soundness of a plate casting in Al–12Si alloy. (Data from Rao et al. 1975.)

the data are extrapolated to zero feeder size the porosity is indicated to be approximately 8%, which is close to the theoretical 7.14% solidification shrinkage for pure aluminum (Table 7.1). At a feeder modulus of around 1.2 times the modulus of the casting, the casting is at its most sound. The residual 1% porosity is probably dispersed gas porosity. As the feeder size is increased further the solidification of the casting is now progressively delayed by the nearby mass of metal in the feeder. Thus while this excessive feeder is no disadvantage in itself, the delay to solidification of the whole casting increases the time available for further precipitation of hydrogen as gas porosity and the unfolding of bifilms. However, it is clear from this work that an undersized feeder will result in very serious porosity, whilst an oversized feeder causes less of a problem (although, of course, it does adversely influence the economics!).

The above work illustrates it is more important to deal with the shrinkage problems than with gas problems in castings. (This conclusion might raise the eyebrows of practiced foundry people. It needs to be kept in mind that most of what previously has been generally described as ‘gas’ in castings has actually been turbulently entrained *air bubbles* introduced by our poor filling systems. We shall deal with entrained air bubbles by the provision of non-entraining filling system designs.)

There is a vast literature on the subject of providing adequate-sized feeders for the feeding of castings. It is mainly concerned with two feeding rules. Numbering onwards from Rule 1 above, the conventional Rules are listed below.

**Rule 2.** The feeder must solidify at the same time as, or later than, the casting. This is the heat-transfer criterion, attributed to Chvorinov.

**Rule 3.** The feeder must contain sufficient liquid to meet the volume–contraction requirements of the casting. This is usually known as the volume criterion.

However, there are additional rules which are also often overlooked, but which define additional thermal, geometrical and pressure criteria that are absolutely necessary conditions for the casting to freeze soundly.

**Rule 4.** The junction between the casting and the feeder should not create a hot spot, i.e. have a freezing time greater than either the feeder or the casting. This is a problem that, if not avoided, leads to ‘under-feeder shrinkage porosity’. The junction problem is a widely overlooked requirement. The use of Chvorinov’s equation systematically gives the wrong answer for this reason, so the junction requirement is often found to override Chvorinov (Rule 1).

**Rule 5.** There must be a path to allow feed metal to reach those regions that require it. The reader can see why this criterion has been often overlooked as a separate Rule; the communication criterion appears self-evident! It is, nevertheless, often violated.

**Rule 6.** There must be sufficient pressure differential to cause the feed material to flow, and the flow needs to be in the correct direction, towards the region requiring the additional liquid (no apologies for blinding obviousness – it is surprising how often these rules are broken and the casting scrapped).

**Rule 7.** There must be sufficient pressure at all points in the casting to suppress the formation and growth of porosity. In Chapter 9 we shall see that the action of pressure also retains the good mechanical properties of the casting by suppressing the opening of bifilms. The bifilms effectively constitute a low background level of porosity (which may or may not be just visible) that is highly effective in reducing strength and ductility of castings.

It is essential to understand that all the Rules must be fulfilled if truly sound castings are to be produced. The reader must not underestimate the scale of this problem. The breaking of only one of the Rules may result in ineffective feeding, and a porous casting. The wide prevalence of porosity in castings is a sobering reminder that solutions are often not straightforward.

Because the calculation of the optimum feeder size is therefore so fraught with complications, is dangerous if calculated wrongly, and costs money and effort, the casting engineer is strongly recommended to consider whether a feeder is really necessary at all. This is Rule 1. You can see how valuable it is.

Of the remainder of castings that do suffer feeding demand, many could avoid the use of a feeder by the judicious application of chills and/or cooling fins.

This leaves only those castings that have heavy sections, isolated heavy bosses, or other features that *do* need to be fed with the correct size of feeder.

Finally, in a recent development of the concepts of feeding, it is worth drawing attention to the work of Tiryakioglu (2001). He has demonstrated that Rules 2, 3, and 4 can be gathered together under only one new criterion 'The thermal center of the total casting (i.e. the casting + feeder combination) should be in the feeder.' This deceptively straightforward statement has been shown to allow the calculation of optimum feeders with unprecedented accuracy. Discussion of this approach is detailed in Chapter 10 under Casting Rule 6.

### 7.1.3.2 Criteria functions

The development of computer software to predict the solidification of castings is not yet developed to predict the occurrence of porosity from first principles, i.e. calculating the pressure drop in the various parts of the casting, and thereby assessing the potential for nucleation and growth of cavities. This represents a Herculean task. As a useful short cut, therefore, many workers have searched for parameters that can be relatively easily calculated and enable an assessment of the potential for pore formation.

Niyama (1982) was perhaps the first to develop a useful criterion function. Dantzig and Rappaz (2009) give a rigorous and elegant account of his derivation. Based on a simple model assuming Darcy's law for the flow of residual liquid through the dendrite mesh he proposed the parameter  $G/R^{1/2}$  to assess the difficulty of providing feed liquid, where  $G$  is the temperature gradient at the solidus temperature and  $R$  the cooling rate. This is probably the most widely used criteria function. It has been found useful to predict the propensity for porosity in steels, often in the form assuming that porosity will occur when  $G/R^{1/2}$  falls below some critical value in the region of  $1 \text{ K}^{1/2} \text{ min}^{1/2} \text{ cm}^{-1}$ . The awful units of the critical Niyama criterion (quoted shamelessly by Dantzig and Rappaz) translate with sufficient accuracy into the respectable SI equivalent  $1 \text{ K}^{1/2} \text{ s}^{1/2} \text{ mm}^{-1}$  (for the purist  $1.00 \text{ K}^{1/2} \text{ s}^{1/2} \text{ mm}^{-1} = 1.29 \text{ K}^{1/2} \text{ min}^{1/2} \text{ cm}^{-1}$ ).

In their study of the formation of porosity in steel plates of thickness 5–50 mm, with and without end chills, Minakawa et al. (1985) confirmed that usefulness of the Niyama criterion in assessing the conditions for the onset of porosity in their castings. They also looked at  $G$  the temperature gradient along the centerline of the casting at the solidification front, and the fraction solid along the centerline. Neither of these alone was satisfactory.

In another theoretical study Hansen and Sahm (1988) support the usefulness of  $G/V_S^{1/2}$  for steel castings. However, in addition they go on to argue the case for the use of a more complex function  $G/V_S^{1/4} V_L^{1/2}$  where  $V_L$  is the velocity of flow of the residual liquid. They proposed this relation because they noticed that the velocity of flow in bars was five to ten times the velocity in plates of the same thickness, which, they suggest, contributes to the additional feeding difficulty of bars compared to plates. (A further contributor will be the comparatively high resistance to the plastic collapse of bars, compared to the efficiency of solid feeding in plates as will be discussed later.)

They found that  $G/V_S^{1/4} V_L^{1/2} <$  a critical value, which for steel plates and bars is approximately  $1 \text{ K s}^{3/4} \text{ mm}^{-7/4}$ . Their parameter is, of course, less easy to use than that due to Niyama, because it

needs flow velocities. The Niyama approach only requires data obtainable from temperature measurement in the casting.

Carlson and Beckermann (2010) proposed a dimensionless form of the Niyama criterion (especially useful in view of the difficult units  $K s^{3/4} mm^{-7/4}$ ) and find it to be useful for predicting shrinkage porosity in a steel, an Al alloy and an Mg alloy, demonstrating impressively wide applicability.

Unfortunately, however, there are many limitations of most of the other criteria functions that are widely overlooked. They include:

1. Strictly, they assess only the difficulty of interdendritic feeding.
2. They apply best to strong materials such as steels in cold molds. For steels in hot investment molds and for light alloys in cold molds where significant solid feeding can occur the criteria become inaccurate. Interdendritic feeding can become impossibly difficult, generating high internal tension in the casting, a condition that the computer would interpret as leading to porosity. However, the softer solid can yield plastically, collapsing slightly to give an internally sound casting.
3. Criteria functions cannot predict conditions for porosity arising as a result of the many other mechanisms for the production of porosity in castings. These include the major shrinkage pores as a result of the isolation of major liquid regions; the creation of surface-initiated porosity; and the mechanically entrained porosity originating from bubbles of air and mold gases introduced by poor filling systems. Experience shows that in general entrainment defects cause most of the porosity found in casting. Shrinkage porosity is actually quite rare because, in general, founders understand shrinkage and can avoid it. In fact this ability is continuously improving at this time because of the continuous development of prediction using computer models.
4. Sigworth et al. (1994) point out an obvious but often overlooked limitation of criteria functions that they cannot take account of the important effects of melt treatment, such as its oxide content in particular.

### 7.1.4 Feeding: The five mechanisms

During the solidification of a casting, the gradual spread and growth of the solid, often in the form of a tangled mass of dendrites, presents increasing difficulties for the passage of feeding liquid. In fact, as the freezing liquid contracts to form the solid, the pressure in the liquid falls, causing an increasing pressure difference between the inside and the outside of the casting. The internal pressure might actually fall far enough to become negative, as a hydrostatic tension.

The generation of such negative-pressure differentials, and even actual hydrostatic tension, is undesirable in castings. Such phenomena provide the driving force for the initiation and growth of volume defects such as porosity and surface sinks on castings, and the lowering of properties because of the unfurling and inflating of bifilms.

However, there appear to be at least five mechanisms by which hydrostatic tension can be reduced in a solidifying material, although, of course, not all five processes are likely to operate in any single case. Adequate feeding by one or more of these feeding processes will relieve the stress in the solidifying liquid and thus reduce the possibility of the formation of defects.

I first identified and described the five feeding mechanisms as set out in Figure 7.27 in 1969. Since then I see my drawing everywhere (I could draw better when I was younger). In the original publication, solid-state diffusion was added as a sixth effect that would cause pore shape to change



somewhat after solidification was complete. Shape changes in pores would occur because the forces of surface tension and mechanical stress are sufficient to cause material flow at temperatures near the melting point of the solid. Such changes to the pore shape and size are detectable under a microscope. However, these considerations are the reserve of the research scientist, and reflect the author's early interests, having been trained as a physicist. Nowadays, as a somewhat more practical foundryman trying to make good castings, the first five mechanisms are all that matter.

The mechanisms are dealt with in the order in which they might occur during freezing. The order coincides with a progressive but ill-defined transition from what might usefully be termed 'open' to 'closed' feeding systems.

#### 7.1.4.1 Liquid feeding

Liquid feeding is the most 'open' feeding mechanism and generally precedes other forms of feeding (Figure 7.6). It should be noted that in skin-freezing materials it is normally the only method of feeding. The liquid has low viscosity, and for most of the freezing process the feed path is wide, so that the pressure difference required to cause the process to operate is negligibly small. Results of a theoretical model of a cylindrical casting only 20 mm diameter (Figure 7.7) indicate that pressures of the order of only 1 Pa are generated in the early stages. By the time the 10 mm radius casting has a liquid core of radius 1 mm, corresponding to 99% solid, the pressure difference has increased only to 100 Pa which is approximately one-thousandth of an atmosphere and smaller than about one-tenth of the hydrostatic pressure due to depth. (It is worth emphasizing that the theoretical model represented in Figure 7.7 and elsewhere in this book represents a worst case. This is because the temperature gradient in the solidified shell has been neglected. The lower temperature of the outer layers of the shell will cause the shell to contract, compressing the internal layers of the casting, and thus reducing the internal hydrostatic tension. In some cases the effect is so large that the internal pressure can become positive, as shown in the excellent treatment by Forgac et al. (1979).)

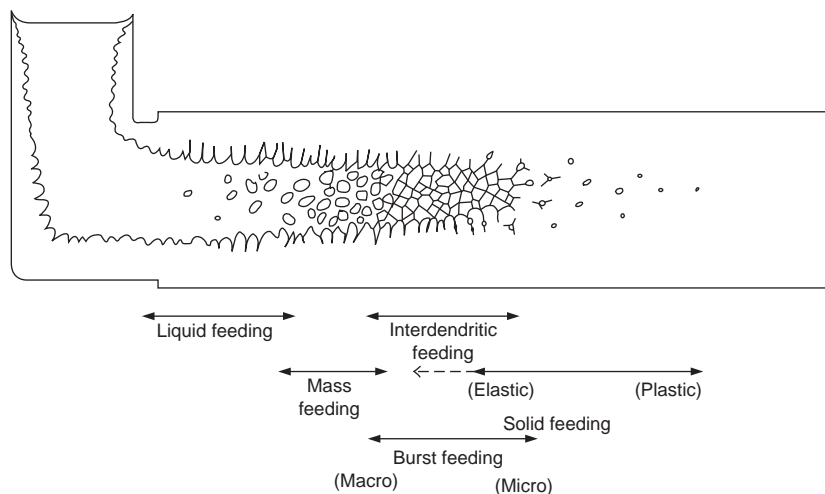
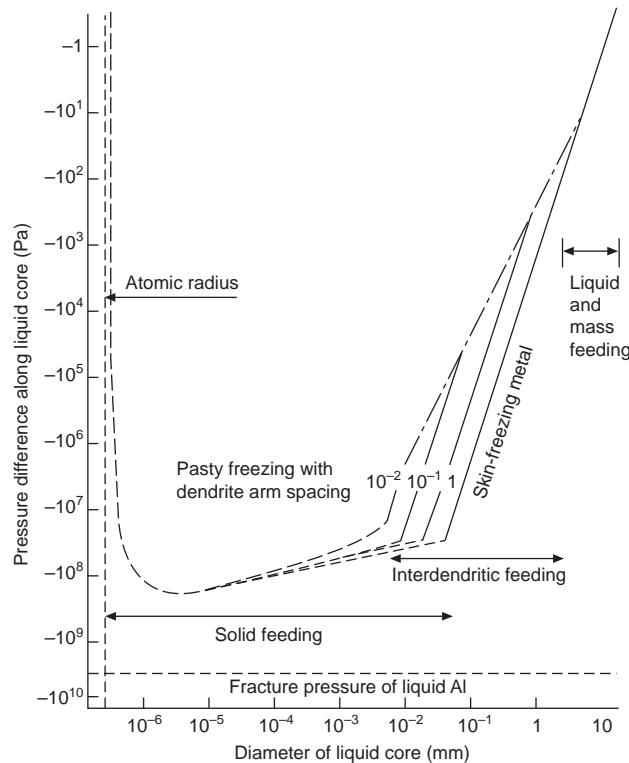


FIGURE 7.6

Schematic representation of the five feeding mechanisms in a solidifying casting (Campbell 1969).



**FIGURE 7.7**

Hydrostatic tensions in the residual liquid calculated for the various feeding regimes during the freezing of a 20-mm-diameter aluminum alloy cylinder (Campbell 1969).

For all practical purposes, therefore, liquid feeding occurs at pressure gradients that are so low that these gentle stresses will never lead to problems.

The rules for adequate liquid feeding are the seven feeding rules listed in Section 7.1.3.

Inadequate liquid feeding is often seen to occur when the feeder has inadequate volume. Thus liquid flow from the feeder terminates early, and subsequently only air is drawn into the casting. Depending on the mode of solidification of the casting, the resulting porosity can take two forms:

1. Skin-freezing alloys will have a smooth solidification front that will therefore result in a smooth shrinkage pipe extending from the feeder into the castings as a long funnel-shaped hole. In very short-freezing-range metals the surface of the pipe can be as smooth and silvery as a mirror.
2. Long-freezing-range alloys will be filled with a mesh of dendrites in a sea of residual liquid. In this case liquid feeding effectively becomes interdendritic feeding, of course. In the case of an inadequate supply of liquid in the feeder, the liquid level falls, draining out to feed more distant regions of the casting, and sucking in air to replace it. The progressively falling level of liquid will define the spread of the porosity, decreasing as it advances because of the decreasing volume fraction of residual liquid

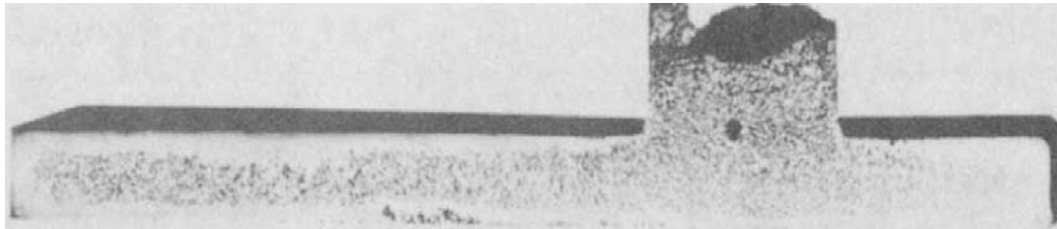


**FIGURE 7.8**

Porosity in the long-freezing-range alloy Cu–10Sn bronze, cast with an inadequate feeder, resulting in a spongy shrinkage pipe.

as freezing proceeds. The resulting effect is that of a partially drained sponge, as shown in the tin bronze casting in Figure 7.8. Sponge porosity is a good name for this defect.

When sectioned, the porosity resembles a mass of separate pores in regions separated by dendrites. It is therefore often mistaken for isolated interdendritic porosity. However, it is, of course, only another form of a primary shrinkage pipe, practically every part of which is connected to the atmosphere through the feeder. It is a particularly injurious form of porosity in castings that are required to be leak-tight, especially since it can be extensive throughout the casting, as Figure 7.8 illustrates. Furthermore this type of porosity is commonly found. It is an indictment of our feeding practice.

The author recalls an investigation into the nature of the porosity in the center of a balanced steel ingot. To ascertain whether the so-called secondary porosity was connected to the atmosphere via the shrinkage cavity in the top of the ingot, water was poured onto the top of the ingot. It created a never-forgotten drenching from the shower that issued from the so-called secondary pores. The lesson that the pores were perfectly well connected was not forgotten.

#### **7.1.4.2 Mass feeding**

Mass feeding is the term coined by Baker (1945) to denote the movement of a slurry of solidified metal and residual liquid. This movement is arrested when the volume fraction of solid reaches anywhere between 0 and 50%, depending on the pressure differential driving the flow, and depending on what percentage of dendrites are free from points of attachment to the wall of the casting. However, it seems that smaller amounts of movement can continue to occur up to about 68% solid, which is the level at which the dendrites start to become a coherent network, like a plastic three-dimensional space frame (Campbell 1969).

In thin sections, where there may be only two or three grains across the wall section, mass feeding will not be able to occur. The grains are pinned in place by their contacts with the wall. However, as the number of grains across the section increases to between five and ten the central grains are definitely free to move to some extent. In larger sections, or where grains have been refined, there may be 20–100 grains or more, so that the flow of the slurry can become an important mechanism to reduce pressure differential along the flow direction. Clearly, the important criterion to assess whether mass flow will occur is the ratio (casting section thickness)/(average grain diameter). This is probably one of the main reasons why grain refinement is useful in reducing porosity in castings (other important reasons being the greater dispersion of gases in solution, their reduced segregation, and the cleaning effect resulting from the sedimentation of bifilms).

At the point at which the grains finally impinge strongly and stop is the point at which feeding starts to become appreciably more difficult. This is the regime of the next feeding mechanism, interdendritic feeding.

In passing, we may note that in some instances mass feeding may cause difficulties. There is some evidence that the flow of the liquid/solid mass into the entrance of a narrow section can lead to the premature blocking of the entrance with the solid phase. Thus the feed path to more distant regions of the casting may become choked.

### 7.1.4.3 Interdendritic feeding

Allen (1932) was one of the first to use the term ‘interdendritic feeding’ to describe the flow of residual liquid through the pasty zone. He also made the first serious attempt to provide a quantitative theory. However, we can obtain an improved estimate of the pressure gradient involved simply by use of the famous equation by Poiseuille that describes the pressure gradient  $dP/dx$  required to cause a fluid to flow along a capillary:

$$\frac{dP}{dx} = \frac{8v\eta}{\pi R^4} \quad (7.1)$$

where  $v$  is the volume flowing per second,  $\eta$  is the viscosity, and  $R$  is the radius of the capillary. It is clear without going further that the resistance to flow is critically dependent on the size of the capillary. For a bunch of  $N$  capillaries, which we can take as a rough model of the pasty zone, the problem is reduced somewhat:

$$\frac{dP}{dx} = \frac{8v\eta}{\pi R^4 N} \quad (7.2)$$

For the sake of completeness it is worth developing this relation to evaluate a more realistic channel that includes the effect of simultaneous solidification so as to close it by slow degrees. The treatment is based on that by Piwonka and Flemings (1966) (Figure 7.9). Given that the average velocity  $V$  is  $v/\pi R^2$ , and, by conservation of volume, equating the volume flow through element  $dx$  with the volume deficit as a result of solidification on the surface of the tube beyond element  $dx$ , we have, all in unit time:

$$\pi R^2 V = 2\pi R(L-x) \left( \frac{\alpha}{1-\alpha} \right) \frac{dR}{dt} \quad (7.3)$$

By substituting and integrating, it follows directly that:

$$\Delta P = \frac{16\eta}{N} \left( \frac{\alpha}{1-\alpha} \right) \frac{dR}{dt} \cdot \frac{1}{R^3} \left( Lx - \frac{x^2}{2} \right) \quad (7.4)$$

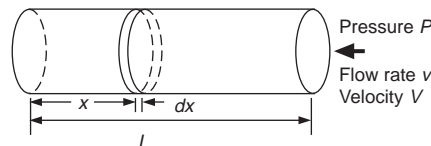


FIGURE 7.9

A tube of liquid, solidifying inwards, whilst being fed with extra liquid from the right.

We can find the maximum pressure drop  $\Delta P$  at the far end of the pasty zone by substituting  $x = 0$ . At the same time we can substitute the relation for freezing rate used by Pivonka and Flemings,  $dR/dt = -4\lambda^2/R$  approximately, where  $\lambda$  is their heat-flow constant. Also using the relation  $Nd^2 = D^2$  where  $d$  is the dendrite arm spacing and  $D^2$  is the area of the pasty zone of interest, we obtain at last:

$$\Delta P = 32\eta \left( \frac{\alpha}{1-\alpha} \right) \frac{\lambda^2 L^2 d^2}{R^4 D^2} \quad (7.5)$$

This final solution reveals that the pressure drop by viscous flow through the pasty zone is controlled by a number of important factors such as viscosity, solidification shrinkage, the rate of freezing, the dendrite arm spacing, and the length of the pasty zone. However, in confirmation of our original conclusion, the pressure drop is most sensitive to the size of the flow channels.

Additional refinements to this equation, such as the inclusion of a tortuosity factor to allow for the non-straightness of the flow, do not affect the result significantly. However, more recent improvements have resulted in an allowance for the different resistance to flow depending on whether the flow direction is aligned with or across the main dendrite stems (Poirier, 1987).

The overriding effect of the radius of the flow channel leads to  $\Delta P$  becoming extremely high as  $R$  diminishes. In fact, in the absence of nuclei that would allow pore formation to release the stress, the high hydrostatic stress near the end of freezing will be limited by the inward collapse of the solidified outer parts of the casting, as indicated in Figure 7.7. This plastic flow of the solid denotes the onset of 'solid feeding', the last of the feeding mechanisms. The natural progression of interdendritic feeding followed by solid feeding is confirmed by more recent models (Ohsasa et al. 1988a, 1988b).

### Effect of the presence of eutectic

The rapid increase of stress as  $R$  becomes very small explains the profound effect of a small percentage of eutectic in reducing the stress by orders of magnitude (Campbell 1969). This is because the eutectic freezes at a specific temperature, and progress of this specific isothermal plane through the mesh corresponds to a specific planar freezing front for the eutectic. The front occurs ahead of the roots of the dendrites, so that the interdendritic flow paths no longer continue to taper to zero, but finish, abruptly truncated as shown in Figure 7.10. Thus the part of the dendrite mesh most difficult to feed is eliminated.

Larger amounts of eutectic liquid in the alloy reduce  $\Delta P$  even further, because of the increased size of channel at the point of final solidification. As the percentage eutectic increases towards 100% the alloy feeds only by liquid feeding, of course, which makes such materials easy to feed to complete soundness.

Since most long-freezing-range alloys exhibit poor pressure tightness, the use of the extremely long-freezing-range alloy 85Cu–5Sn–5Zn–5Pb for valves and pipe fittings seems inexplicable. However, the 5% lead is practically insoluble in the remainder of the alloy, and thus freezes as practically pure lead at 326°C, considerably easing feeding by acting analogously to a eutectic, as discussed above.

The appearance of non-equilibrium eutectic in pure Fe–C alloys is predicted to be rather close to the equilibrium condition of 2%C (Clyne and Kurz 1981) because carbon is an interstitial atom in iron, and therefore diffuses rapidly, reducing the effect of segregation during freezing. However, in the presence of carbide-stabilizing alloys such as manganese, the segregation of carbon is enhanced to some extent, causing eutectic to appear not at the equilibrium 2%C but probably only somewhere near 1.0%C as seen in Figure 5.41. A similar result for 1%C1.5%Cr steels is shown in Figure 5.42.

In Al–Mg alloys, layer porosity is observed in increasing amounts as magnesium is increased, illustrating the growing problem of interdendritic feeding as the freezing range increases. However, at a critical composition close to 10.5%Mg the eutectic beta-phase is first seen in the microstructure and

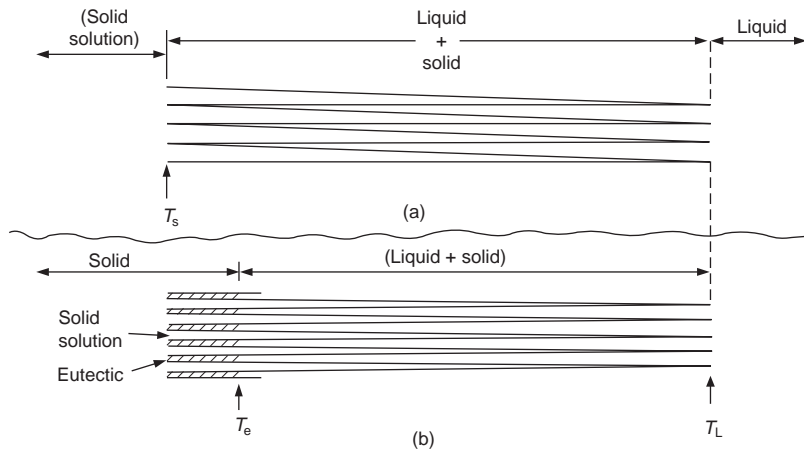


**FIGURE 7.10**

A diagrammatic illustration of (a) how the tapering interdendritic path increases the difficulty of the final stage of interdendritic feeding, and (b) how a small percentage of eutectic will eliminate this final and narrowest portion of the path, thereby greatly easing the last stages of feeding.

the porosity suddenly disappears (Jay and Cibula 1956). The arrival of eutectic at 10.5%Mg confirms the non-equilibrium conditions, and compares with the arrival composition 17.5%Mg predicted for equilibrium. Lagowski and Meier (1964) found a similar critical transition in Mg–Zn alloys as zinc is progressively increased. Their results are presented later in Figure 9.6.

However, one of the most spectacular displays of segregation of a solute element in a common alloy system is that of copper in aluminum. In the equilibrium condition, eutectic would not appear unless the copper content exceeded 5.7%. However, in experimental castings of increasing copper content, eutectic has been found to occur at concentrations as low as approximately 0.25%. This concentration corresponds to a peak in porosity, and the predicted peak in hydrostatic tension in the pasty zone (Figure 7.11).

Many property–composition curves are of the cuspid, sharp-peaked type (note that they are not merely a rounded, hump-like maximum). Examples are to be found throughout the foundry research literature (although the results are most often interpreted as mere humps!). For instance, in a series of bronzes of increasing tin contents Pell-Walpole (1946) was probably the first to conclude that the peak in porosity at 5%Sn, not 14% as expected from the equilibrium phase diagram, was the result of the maximum in the effective freezing range. Spittle and Cushway (1983) find a sharp maximum in the hot-tearing behavior of Al–Cu alloys at approximately 0.5–0.8%Cu (Figure 8.9). The analogous results by Warrington and McCartney (1989) can be extrapolated to show that their peak is nearer 0.5%Cu (Figure 8.6), close to the peak in porosity as described above.

#### 7.1.4.4 Burst feeding

Where hydrostatic tension is increasing in a poorly fed region of the casting, it seems reasonable to expect that any barrier might suddenly yield, like the bursting of a dam. Feed metal would then suddenly flood into the poorly fed region. This feed mechanism was proposed by the author simply as a logical possibility based on such straightforward reasoning (Campbell 1969). As solidification proceeds, both the stress and the strength of the barrier will be increasing together, but at different

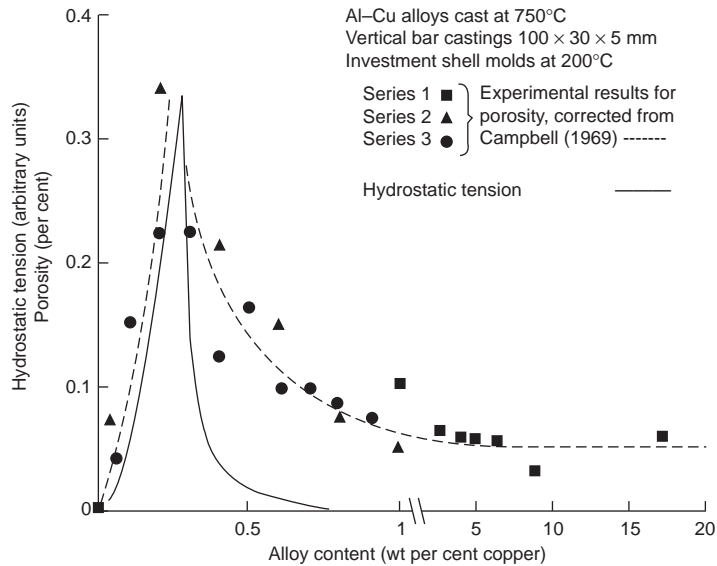


**FIGURE 7.11**

Predicted peak in hydrostatic tension in the pasty zone, and the measured porosity in test bars, as a function of composition in Al-Cu alloys (Campbell 1969).

rates. Failure will be expected if the stress grows to exceed the strength of the barrier. The barrier may be only a partial barrier, i.e. a restriction to flow, and failure may or may not be sudden.

In terms of Figure 7.12, the nucleation threshold diagram (explained later in Section 7.1.5.3; see Figure 7.21), the build-up of stress in the casting might be rapid, leading to the creation of a pore at P. However, if the casting is hotter, or is a weaker alloy, the development of stress will be somewhat slower, and might result in a burst of feed liquid by the collapse of a barrier to flow at point A. The internal stress will then be relieved, but after some additional build-up of gas in solution, the subsequent fall of pressure to B will result in a second burst event, once again relieving the internal stress, and returning the internal pressure to 1 atmosphere. The effect of these bursts is to prevent conditions reaching the nucleation threshold, so that porosity is avoided.

If the feeding barrier is substantial it may never burst, causing the resulting stress to increase and eventually exceed the nucleation threshold at P. This time the release of stress, returning the internal pressure to 1 atmosphere, corresponds to the creation and growth of a pore. There can be no further feeding of any kind in that region of the casting after a pore creation event; the driving force for feeding is suddenly eliminated.

Previously, the author has quoted the following observation as a possible instance of a kind of microscopic type of burst feeding. During observation of the late stages of solidification of the feeder heads of many aluminum alloy castings it is clearly seen that the level of the last portion of interdendritic liquid sinks into the dendrite mesh not smoothly, but in a series of abrupt, discontinuous jumps. It was thought that the jumps may be bursts of feeding into interdendritic regions. However, it now seems more likely that the jumps are the result of the repeated, sudden failure of the surface oxide film, caught and stretched between supporting dendrites at the surface. The liquid draining down into

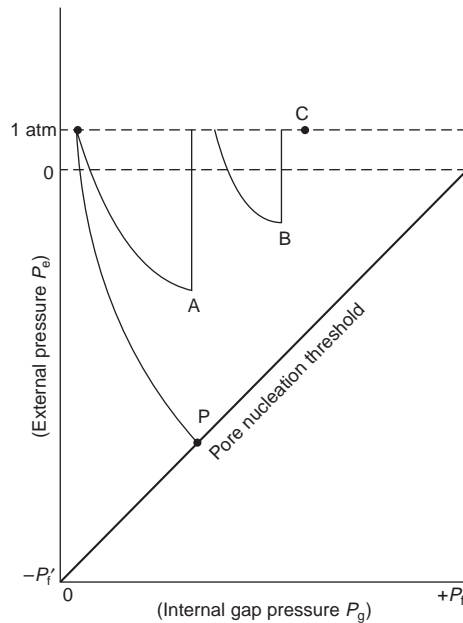


**FIGURE 7.12**

Gas-shrinkage map showing the path of development to early pore nucleation at P. In a contrasting case, slow mechanical collapse of the casting delays the build-up of internal tension, culminating in complete plastic collapse in the form of burst feeding processes at A and B. Such delay can be successful in avoiding pore nucleation, since conditions never reach the pore threshold if, for instance, freezing is complete at C.

the dendrite mesh will attempt to drag down its surface film, which will repeatedly burst and repair, resisting failure again for a time. The phenomenon is an illustration of the strength of the film, its capacity for stretching to some extent elastically, and the capacity of the solidified material at its freezing point to exhibit a certain amount of elastic recoil behavior.

A macroscopic type of barrier can be envisaged for those parts of castings where mass flow has occurred, causing equiaxed crystals to block the entrance to a section of casting.

Macroscopic blockages have been observed directly in waxes, where the flow of liquid wax along a glass tube was seen to be halted by the formation of a solidified plug, only to be restarted as the plug was burst. This behavior was repeated several times along the length of the channel (Scott and Smith 1985).

In iron castings such behavior was intentionally encouraged in the early twentieth century. Nearly all large castings were subjected to 'rodding' – one or two men would stand on the mold and ram an iron rod up and down through the feeder top. Extra feed metal might be called for and topped up from time to time. This procedure would last for many hours until the casting had solidified. Nowadays it is more common to provide a feeder of adequate size so that feeding occurs automatically without such strenuous human intervention!

On a microscale a type of burst feeding is the rupture of the casting skin, allowing an inrush of air or mold gases (Figure 7.19). However, this is, of course, a gaseous burst that corresponds to the growth of a cavity, not a feeding process. Pellini (1953) drew attention to this possibility in bronze castings. It is



expected that such surface-initiated porosity will be relatively common in castings of many long-freezing-range alloys.

In conclusion, it has to be admitted that whilst burst feeding might be an important feeding mechanism, it is not easy to quantify its effects by modeling. Despite some interest in using the concept of burst feeding as an explanation of some casting experiments, these uses remain speculative. The existence of burst feeding has never been unambiguously demonstrated. It therefore seems difficult to understand it and difficult to control it. At this stage we probably have to content ourselves with the conclusion that logic suggests that it does exist.

#### 7.1.4.5 Solid feeding

At a late stage in freezing it is possible that sections of the casting may become isolated from feed liquid by premature solidification of an intervening region.

In this condition the solidification of the isolated region will be accompanied by the development of high hydrostatic stress in the trapped liquid; sometimes high enough to cause the surrounding solidified shell to deform, sucking it inwards by plastic or creep flow. This inward flow of the solid relieves the internal tension, like any other feeding mechanism. In analogy with 'liquid feeding', the author called it 'solid feeding'. An equally good name would have been 'self feeding'.

When solid feeding starts to operate, the stress in the liquid becomes limited by the plastic yielding of the solid, and so is a function of the yield stress  $Y$  and the geometrical shape of the solid. (The yield stress  $Y$  is, of course, a function of the strain rate at these temperatures when assuming an elastic/plastic model. The procedure is practically equivalent to the assumption of a creep stress model, and results in similar order-of-magnitude predictions for stress (Campbell, 1968a, 1968b). For instance, for a sphere of radius  $R_0$ , with internal liquid radius  $R$  (Figure 7.3), the onset of complete plasticity is defined by:

$$P = 2Y \ln(R_0/R)$$

Mechanical engineers will recognize this relation as the classical formula for the failure of a thick-shell pressure vessel stressed by internal pressure to the point at which it is in a completely plastic state. This equation is expected to give maximum estimates of the hydrostatic tensions in castings because: (1) the shape is the most difficult to collapse inwardly; and (2) the equation neglects the opposing contribution of the thermal contraction of the solidified shell which will tend to reduce internal tension (Forgac et al. 1979). Nevertheless it is still interesting to set an upper bound to the hydrostatic tensions that might arise in castings.

This early model (Campbell 1967) used the concept that the liquid radius  $R$  had to be expanded to some intermediate radius  $R'$ , and the solid had to be shrunk inwards from its original internal radius  $R + dR$  to the new common radius  $R'$ . At this new radius the stress in the liquid equals the stress applied at the inner surface of the solid.

The working out of this simple model indicated that for a solidifying iron sphere of diameter 20 mm, the elastic limit at the inner surface of the shell was reached at an internal tensile stress of about 4 MPa (−40 atm); and by the time the residual volume of liquid was only 0.5 mm in diameter a plastic zone had spread out from the center to encompass the whole shell. At this point the internal pressure was in the range of approximately 20–40 Pa (−200 to −400 atm) and the casting was 99.998% solid. Solidification of the remaining drop of liquid increased the pressure in the liquid to approximately 100 MPa (−1000 atm). Later estimates using a creep model and cylindrical geometry confirmed similar figures for iron, nickel, copper, and aluminum (Campbell 1968a, 1968b).

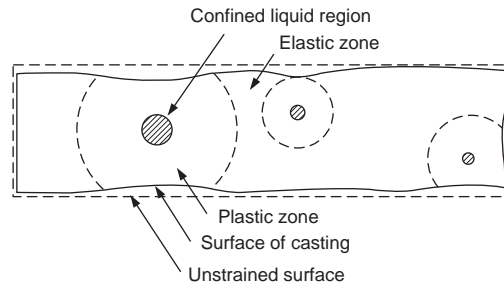


**FIGURE 7.13**

Plastic zones spreading from isolated volumes of residual liquid in a casting, showing localized solid feeding in action (Campbell 1969).

A minute theoretical point of interest to those of a scientific disposition is the effect of the solid–liquid interfacial tension. Although this is small, it starts to become important when the liquid region is only a few hundred atoms in diameter. The interfacial tension causes an inward pressure  $2\gamma_{LS}/R$  that starts to compress the residual liquid. This is the explanation for the theoretical curves to take an upward turn in Figure 7.7 as freezing nears completion, creating a limit to the maximum internal tension.

We have to bear in mind that these estimates of the internal tension are upper bounds, likely to be reduced by thermal contraction of the shell, and reduced by geometries that are easier to collapse, such as a cylinder or a plate. Also the predictions are in any case lower for smaller trapped volumes of liquid, as might occur, for instance, in interdendritic spaces. Figure 7.13 shows schematically the effect of plastic zones spreading from isolated unfed regions of the casting.

For an infinite, flat plate-shaped casting in a skin-freezing metal, the internal stress developed is zero, which is an obvious solution, since there can be no restraint to the inward movement of infinite flat plates separated by a solidifying liquid; the plates simply move closer together to follow the reduction in volume. For real plates, their surfaces are held apart to some extent by the rigidity of the edges of the casting, so the development of internal stress would be expected to be intermediate between the two extreme cases. The ease of collapse of the central regions of flat plates emphasizes the importance of geometry.

Figures 7.14 and 7.15 show results of some of my early experiments concerning porosity in small plates of an investment-cast nickel-based alloy. It happens to be an excellent example of solid feeding in action. At low mold temperatures the solid gains strength rapidly during freezing and therefore retains the rectangular outer shape of the casting, and the steep temperature gradient concentrates the porosity in the center of the casting. As mold temperature is increased, the falling yield stress of the solidified metal allows progressively more collapse of the center, solid feeding acting to reduce the total level of porosity. However, some residual porosity remains noticeable nearer the side walls, where geometrical constraint prevents full collapse. Note that these results were obtained in vacuum, with zero contribution from exterior positive atmospheric pressure. It follows, therefore, that all of the solid feeding in this case is the result of internal negative pressure. In fact, surface sinks are commonly seen in vacuum casting. Sinks are therefore not solely the consequence of the action of atmospheric pressure, as generally supposed.

Figure 7.16 shows solid-feeding behavior in spherical wax castings. The example is interesting because it is evident that sound castings can, in principle, be produced without any feeding in the

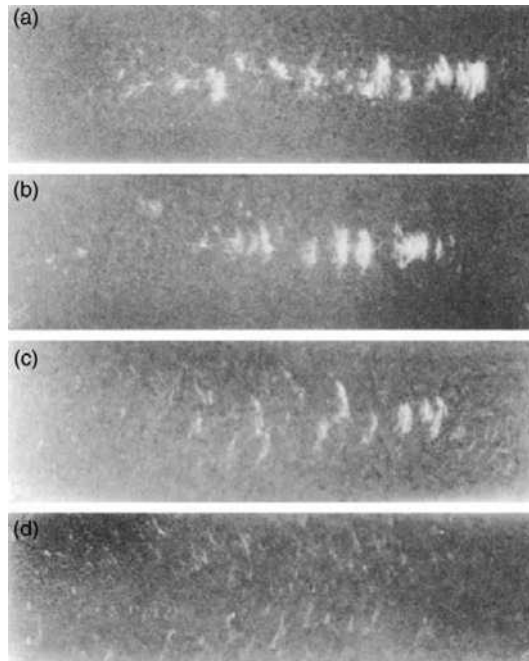


**FIGURE 7.14**

(a) Radiographs of bar castings  $100 \times 30 \times 5$  mm in nickel-based alloy cast at  $1620^\circ\text{C}$  in vacuum  $15 \mu\text{mHg}$  into molds at: (a)  $250^\circ\text{C}$ ; (b)  $500^\circ\text{C}$ ; (c)  $800^\circ\text{C}$ ; and (d)  $1000^\circ\text{C}$  (Campbell 1969). Centerline macroporosity is seen to blend into layer porosity, and finally into dispersed microporosity.

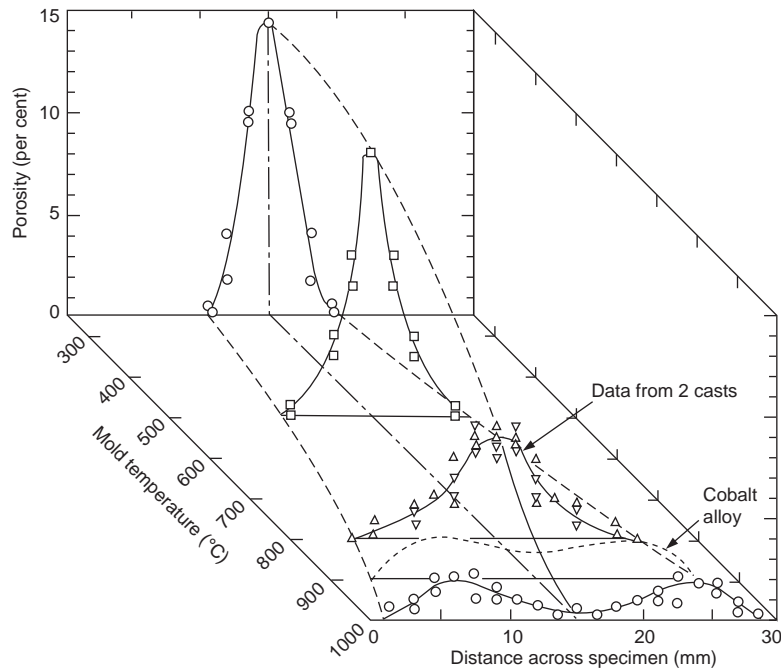
classical sense. In this case it is clear that feeding can be successfully accomplished by skillful choice of mold temperature to facilitate uniform solid feeding.

Figure 7.17 shows a similar effect in unfed Al–12Si alloy as a function of increasing casting temperature. The full 6 or 7% of internal shrinkage porosity at low casting temperature is gradually reduced by external collapse of the casting as casting temperature increases (Harinath et al. 1979).

If solid feeding is controlled so that it spreads itself uniformly in this way, then the accompanying movement of the outer surface of the casting becomes negligible for most purposes. For instance, the high-volume shrinkage of about 6% suffered by Al–Si alloys corresponds to a linear shrinkage of only 2% in each of the three perpendicular directions (i.e. 6% in 3-D corresponds to 2% in 1-D). For a datum in the center of the casting this means an inward wall movement of only 1% from each of the opposite surfaces. Thus a 25-mm-diameter boss would be 250 micrometers small on radius if it were entirely unfed by liquid.

In practice, of the 6% volume contraction in aluminum alloy castings, usually about 5% is relatively easily fed by liquid and interdendritic modes, leaving only about 1% as a feeding problem, and thus available to be provided by solid feeding. This corresponds to an inward movement of a surface of only 0.16%, which is only about 40 micrometers for our 25-mm-diameter casting. Thus dimensional errors resulting from solid feeding reduce to the point at which they become not measurable.

In contrast to the 0.25-mm worst-case reduction in radius for the 25-mm-diameter feature, if all the shrinkage were concentrated at the center of the casting, the internal pore would have a diameter of



**FIGURE 7.15**

Porosity across an average transverse section of vacuum-cast nickel-based alloy as a function of mold temperature, quantifying the effect shown in Figure 7.14. The effect of solid feeding by the plastic collapse of the section is clear from the shape of the porosity distribution at high mold temperatures.

10 mm. This point has been made before, but is worth repeating. The difference between the extreme seriousness of internal porosity, compared to its harmless dispersion over the exterior surfaces of the casting, is a key factor to encourage the development of casting processes that would automatically yield such benefits. The elimination of internal defects in the liquid that could nucleate a cavity is a major beneficial feature of a good casting process.

It is also worth emphasizing that solid feeding will occur at a late stage of freezing even if the liquid is not entirely isolated. The case has been discussed in the section on interdendritic feeding, and is part

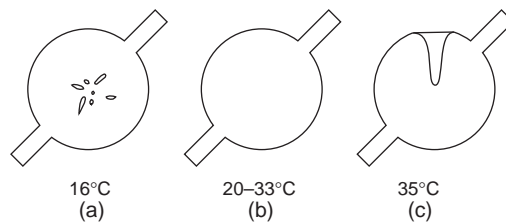


**FIGURE 7.16**

Cross-section of 25 mm diameter wax castings injected into an aluminum die at various temperatures.

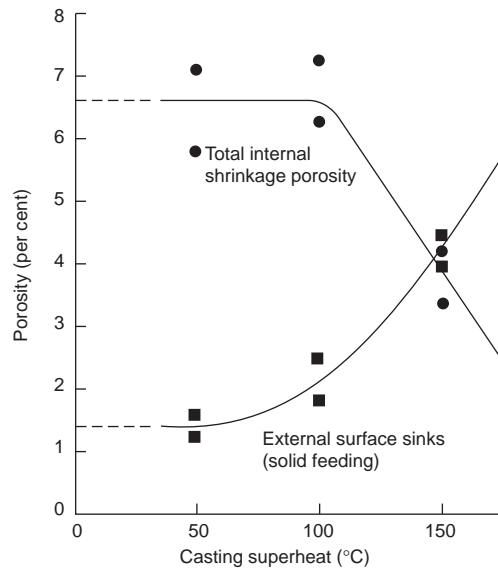


**FIGURE 7.17**

Al-12Si alloy cast into unfed shell molds showing the full 6.6% internal shrinkage porosity at low casting temperature, giving way to solid feeding at higher casting temperature. (Data from Harinath 1979.)

of the meaning of Figure 7.7. It is also clear in Figure 7.15. The effect is the result of the gradual build-up of tension along the length of the pasty zone because of viscous resistance to flow. At the point at which the tension reaches a level where it starts to cause the collapse of the casting the region is effectively isolated from the feeder. Although liquid channels still connect this region to the feeder they are by this time too small to be effective to feed.

An experimental result by Jackson (1956) illustrates an attempt to reduce solid feeding by increasing the internal pressure within the casting by raising the height of the feeder. Jackson was casting vertical cylinders 100 mm in diameter and 150 mm high in Cu 85-5-5-5 alloy in greensand. He employed a plaster-lined feeder of only 50 mm diameter (incidentally, failing Feeding Rules 2 and 3, which explains why he observed such high porosity in his castings). Nevertheless the beneficial effect of increasing the feeder height is clear in Figure 7.18. His data indicate that, despite the unfavorable geometry, if he had raised his feeder height to 250 mm, all exterior shrinkage would have been eliminated. The interior porosity would have fallen to about 2.0%, almost certainly being the residual effects from the combination of gas porosity, and the residual shrinkage from his poorly sized feeder.

In a study of two small shaped castings in three different Al-Si alloys, of short, medium, and long freezing ranges, Li, Jolly and Campbell (1998) measured the internal porosity of the castings by density, and the external porosity (the total surface sink effect) by measuring the volume of the casting in water. They found that the internal porosity in the castings in all three alloys was about the same at approximately 1 volume %. However, the external sinks grew from an average of 3.1 to 6.4-7.5 volume % for the short, medium, and long freezing range alloys. This significant increase in solid feeding for the long freezing range material probably reflects the easier collapsibility of the thinner solidified shell and its

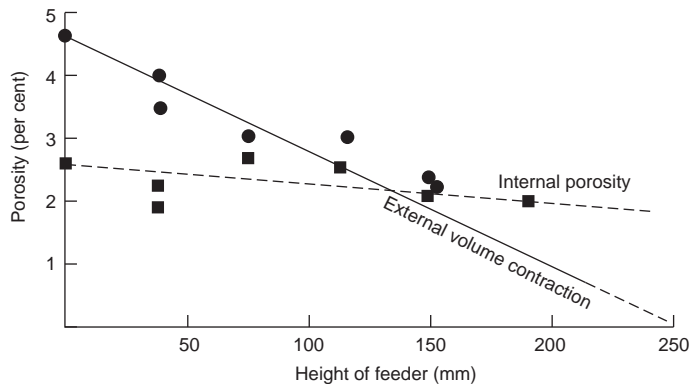


**FIGURE 7.18**

Gunmetal casting showing the reduction in solid feeding as liquid feeding is enhanced by extra height and volume of feed metal. (Data from Jackson 1956.)

internal mesh of dendrites. The more severe internal stress because of the greater difficulty in interdendritic feeding may also be a significant contributor. Conversely, of course, the absence of any corresponding increase in internal porosity confirms that feeding of the castings in the shorter-freezing-range alloys occurred by the simpler and easier more open liquid feeding mechanisms.

A reminder of the possible dangers accompanying solid feeding is probably worth summarizing. Clearly, if the liquid is free from bifilms, the casting will not contain internally initiated pores. However, it may generate:

- (i) Surface-initiated pores; or even
- (ii) Surface sinks.

In the presence of one or more easily opened bifilms, the situation changes significantly. The casting will now exhibit:

- (iii) A large interior shrinkage pore in the presence of a bifilm in the stressed region, if the hydrostatic stress becomes sufficiently high and if the stressed volume is large.
- (iv) A population of internal microscopic cracks. This is the subtle danger arising from the usual presence of a population of bifilms in the stressed liquid. In this situation the compact bifilms are subjected to a tensile stress in the liquid, providing a driving force to unfurl. The mechanical properties, especially the ductility and UTS, of the casting are thereby impaired in this region, even though there may be no visible indication if the bifilms are not opened sufficiently to reveal their presence. In a nearby region of the casting that had enjoyed better feeding, bifilms would have remained fairly furled, so the ductility and UTS would be expected to be better.

A final personal remark concerning solid feeding that is a source of mystery to the author, is the widespread inability of many to comprehend that it is a fact. This lack of comprehension is difficult to understand, in view of the obvious evidence for all to see as surface sinks (even in castings solidified in vacuum) and the fact that isolated bosses can be cast sound provided that the metal quality is good

(i.e. few nuclei to initiate internal pores). Foundries that convert poor filling systems to well-designed filling systems suddenly find that internal porosity and hot tears vanish, but the castings now require extra feeding to counter surface sinks (Tiryakioglu 2001). The increased solid feeding at higher mold temperatures is widely seen in investment castings. The easy collapse of flat plates, especially of alloys weak at their freezing points like Al alloys, explain their long and difficult-to-define feeding distances. The better-defined feeding distances of steels are the consequence of their better-defined resistance to collapse; their greater strength resisting solid feeding. Additionally, of course, hot isostatic pressing (hipping) is a good analogy of an enforced plastic collapse of the casting, as is also direct squeeze casting.

Who needs good imagination in the presence of all these facts?

### 7.1.5 Initiation of shrinkage porosity

In the absence of gas, and if feeding is adequate, then no porosity will be found in the casting.

Unfortunately, however, in the real world, many castings are sufficiently complex that one or more regions of the casting are not well fed, with the result that the internal hydrostatic tension will increase, reaching a level at which an internal pore may ‘pop’ into existence in a number of ways. Conversely, if the internal tension is kept sufficiently low by effective solid feeding, the mechanisms for internal pore formation are not triggered; the solidification shrinkage then appears on the outside of the casting. All this is discussed in more detail below.

#### 7.1.5.1 Internal porosity by surface initiation

If liquid from the feeder becomes cut off, the pressure inside the casting falls. Liquid that is still connected to the outside surface may then be drawn from the surface, causing the growth of porosity connected to the surface (Figure 7.13). The sucking of liquid from the surface in this way naturally draws in air, following interdendritic channels, spreading along these routes into the interior of the casting. The phenomenon is a kind of feeding by a fluid, where the fluid in this case is air. However, of course, this is hardly a feeding process but a pore growth process. This porosity in the interior of the casting is usually hard to distinguish from microporosity caused in other ways: on a polished section it appears to be a series of separate interdendritic pores, whereas in reality it is a single highly complex-shaped interconnected pore, linked to the surface. It is sometimes possible to identify its origins as surface-initiated porosity by its oxidized internal surface near to the surface of the casting. Deeper into the casting, away from the surface, the oxygen is totally consumed, so the surface film changes from an oxide to a nitride.

Figure 7.13 illustrates how the withdrawal of surface liquid is negligible in thin-section castings, explaining why thin sections require little feeding, or even no apparent feeding, but automatically exhibit good soundness. The effect is easily seen in gravity die castings because of their shiny surface when lifted directly from the die. In a section of intermediate thickness the experienced caster will often notice a local frosting of the surface. This dull patch is a warning that interdendritic liquid is being drained away from the surface indicating an internal feeding problem that requires attention (Figure 7.19).

Pericleous (1997) was the first to predict this form of porosity using a computer model of the freezing of a long-freezing-range alloy. His result is shown in Figure 7.20.

This pore-formation mechanism from the surface seems to be much more common than is generally recognized. It is especially likely to occur in long-freezing-range alloys at a late stage in

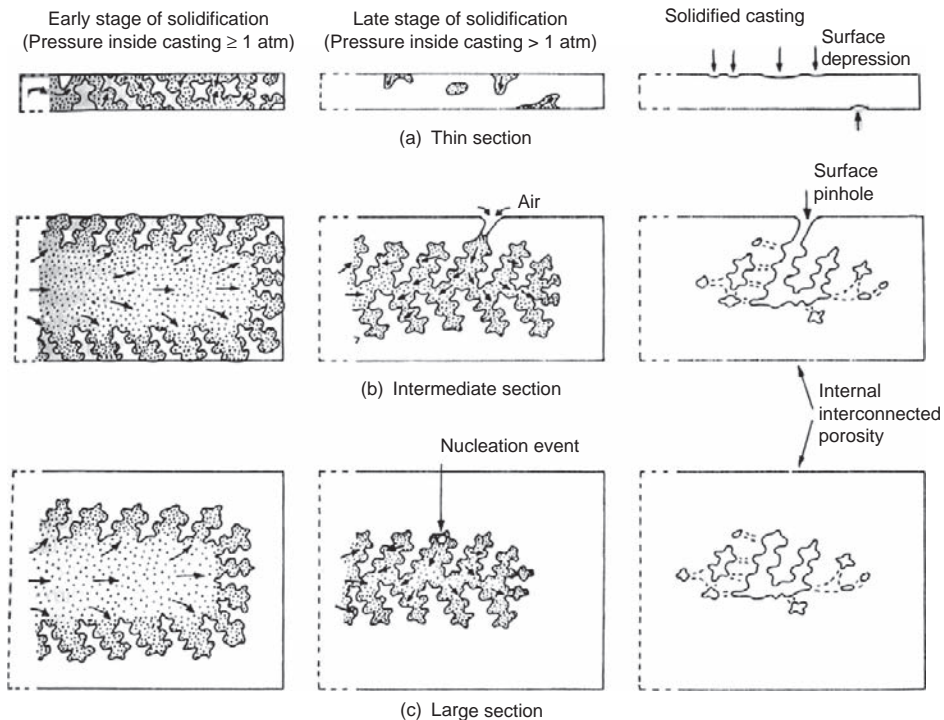


**FIGURE 7.19**

(a) Thin sections require little or no feeding since they can contain zero shrinkage porosity; (b) intermediate sections can develop surface connected porosity; (c) thick sections contain nucleated internal porosity (Campbell 1969).

freezing, when the development of the dendrite mesh means that drawing liquid from the nearby surface becomes easier than drawing liquid from the more distant feeder. The point at which liquid may be drawn from the surface may be anywhere (or practically everywhere) for an alloy of sufficiently wide freezing range.

However, in an alloy of intermediate freezing range, the initiation site is often a hot-spot such as an internal corner or re-entrant angle. As has been mentioned before, the gravity die caster pouring an Al-Si alloy looks for such defects on each casting as it is taken from the die. If such a 'draw' or cavity or frost-appearance is noticed in a re-entrant angle, he immediately doses the melt with sodium. The straightening of the solidification front (Figure 6.12b) strengthens the alloy at the corner so that it can better resist local collapse. The outcome is a pore hidden inside the casting if the melt quality is poor so that nucleation is easy. Alternatively, if the melt quality is good, no internal pore can easily form, so that the rise in internal tension will cause more general collapse of the casting. Solid feeding will have been encouraged.

The connection of two opposite surfaces of the casting by pores that are extensively connected internally is one of the major reasons why long-freezing-range alloys cannot easily be used for pressure-tight applications such as hydraulic valves or automobile cylinder heads. In such complex



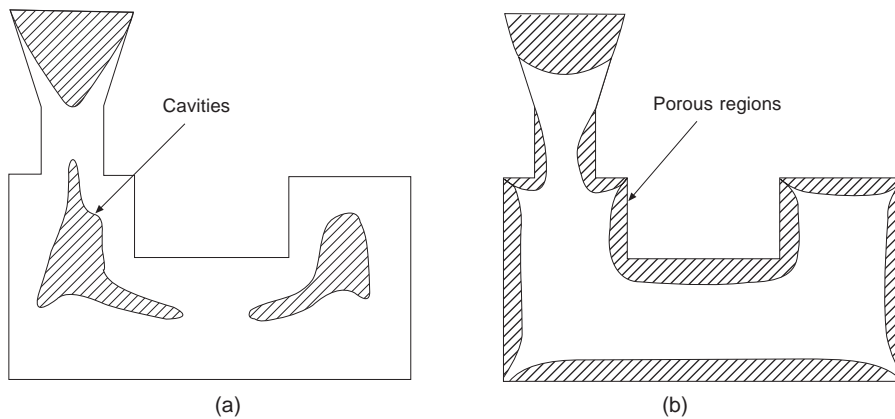


**FIGURE 7.20**

Regions of computer-simulated shrinkage porosity, (a) internally in a short-freezing-range alloy, and (b) externally (surface-initiated) in a long-freezing-range alloy. The latter was the first prediction of surface-initiated porosity by computer simulation (after Bounds et al. 1998).

castings it is often difficult to meet the essential requirement that the interior of the casting has a positive pressure at all locations so as to prevent surface-connected internal porosity.

#### **7.1.5.2 External porosity (surface sinks)**

If internal porosity is not formed (either by surface-linked initiation, or by nucleation events) then the lowering of the internal pressure will lead to an inward movement of the external surface of the casting. If the movement is severe and localized, then it constitutes a defect known as a 'sink' or a 'draw'. The feeding of the internal shrinkage by the inward flow of solid is, of course, 'solid feeding' or 'self feeding'.

Adequate internal pressure within the casting will reduce or eliminate solid feeding, so maintaining the shape of the casting and keeping it sound. In such favorable feeding conditions neither internal nor external porosity will occur.

If the remedy of the application of internal pressure is carried out too enthusiastically, the natural inward movement of solid feeding will be reversed, causing the casting to swell. Such growth is common in gray iron castings, and castings that have a high head of metal. Swelling of cast metal is also commonly seen in pressure die casting if the casting is removed from the die before it is fully solid. This is because the gas bubbles entrained by the extreme turbulence are under extremely high pressure. The technique is useful for identifying hot spots in the casting (i.e. regions last to freeze, and which therefore require additional local cooling in the die to raise productivity). Gas entrained in hot spots can cause the casting to locally explode when released early from the constraint of the die.

Returning to conventional gravity castings, in real situations it sometimes happens that a certain amount of external collapse of the casting will occur before the internal pressure falls to the level required to nucleate an internal pore. Once the pore is formed, the internal stress will be eliminated so that further solid feeding is arrested. The action of the remaining solidification shrinkage is simply to grow the pore. The final effect of solidification shrinkage on the casting is usually found to be partly

external and partly internal as illustrated in Figure 7.4. The balance between external and internal porosity can be widely seen in foundries. Examples are seen in Al–12Si (Figure 7.18) and in aluminum-based MMCs (Emamy and Campbell 1996).

### 7.1.5.3 Nucleation of internal porosity

Although the problem of the nucleation of cavities and bubbles is in principle similar to that of the nucleation of condensed phases such as the metal matrix and non-metallic inclusions, there are differences that make it worthwhile to look at non-condensed phases such as vacuums, vapors, and gases separately in some detail. In particular, we shall find that there are special difficulties with the nucleation of gas and void phases, forcing us to adopt new concepts. We shall deal first with shrinkage cavities, then gas pores, not forgetting that both can cooperate in both the formation and growth of such volume defects.

Short-freezing-range alloys, such as aluminum bronze and Al–Si eutectic, do not normally exhibit surface-connected porosity. They form a sound, solid skin at an early stage of freezing, and liquid feeding continues unhindered through widely open channels. Any final lowering of the internal pressure due to poor feeding towards the end of freezing may then create a pore by nucleation in the interior liquid. In this case there is clearly no connection to the outside surface of the casting, as illustrated in the larger section shown in Figure 7.13c. After nucleation, further solidification shrinkage will provide the driving force for growth of the pore, which, on sectioning or radiography, may be more or less indistinguishable from the surface-initiated type.

In alloys of short freezing range, therefore, porosity is probably normally nucleated, and is concentrated near the center of the casting, usually well clear of the casting surface. In castings of large length-to-thickness ratio this is widely referred to as centerline porosity. Thus unless subsequent machining operations cut into the porosity, castings in such alloys are normally leak-tight. (The leak paths commonly provided by folded oxide films or bubble trails generated during a turbulent fill are a separate problem requiring solution by other means such as improved filling, and/or the use of filters.)

Tiwari et al. (1985) have suggested a way of initiating internal porosity in specific regions of castings by the addition of nuclei in the form of fragments of refractory. These foreign particles contain much porosity, so that the growth of pores from such sites proceeds without difficulty. The result is a large internal pore, which, to some extent, can be sited in a chosen location in the casting. Additional feeders or chills are therefore not required, and internal porosity in an unwanted location is avoided. External porosity is also successfully avoided because internal pressure is prevented from falling to negative values. However, as inventive as this technique is, for the majority of castings that are required to be sound throughout, and are required to be free of pieces of refractory, it is, unfortunately, only of academic interest.

### Homogeneous nucleation

Following the beautifully elegant approach by Fisher (1948), we can quantify the conditions required for the formation of porosity in liquid metals. A quantity of work is associated with the reversible formation of a bubble in a liquid. If the local pressure in the liquid is  $P_e$ , we need to carry out an amount of work  $P_e V$  to push back the liquid far enough to create a bubble of volume  $V$ .

The formation and stretching out of the new liquid–gas interface of area  $A$  requires additional work  $\gamma A$ , where  $\gamma$  is the interfacial energy per unit area.

The work required to fill the bubble with vapor or gas at pressure  $P_i$  is negative and equal to  $-P_iV$ . (The negative sign arises because the pressure inside the bubble clearly helps the formation of the bubble, as opposed to the other work requirements, which tend to oppose bubble formation.) Thus the total work is:

$$\Delta G = \gamma A + P_e V - P_i V = 44\gamma\pi r^2 + (4/3)\pi r^3(P_e - P_i)$$

where clearly  $(P_e - P_i)$  is the pressure difference between the exterior and the interior of the bubble, which we may write as  $\Delta P$  for convenience. Similarly to dense-phase nucleation, a plot of  $\Delta G$  versus bubble radius  $r$  shows a maximum that constitutes an energy barrier to nucleation, as in Figure 5.27. The critical radius  $r^*$  in this case is:

$$r^* = 2\gamma/\Delta P^* \quad (7.6)$$

Since bubbles growing from the bulk liquid will grow an atom at a time as the result of statistical thermal fluctuations, it is evident that small bubbles with radii less than  $r^*$  will tend to disappear. Only exceptionally will a long chain of favorable energy fluctuations produce a bubble exceeding the critical radius  $r^*$ . When this rare event does happen, the embryonic bubble will then have the potential to grow to an observable size.

Fisher goes on to apply some delightfully elegant rate theory to derive values for the critical pressure difference  $\Delta P^*$  at which nucleation will occur. The reader is strongly recommended to consult Fisher's original paper. However, for our purposes we can obtain a sufficiently good estimate very easily and quickly using Equation 7.6. Using experimentally determined values of atomic sizes and surface energy  $\gamma$  for liquid metals. Assuming that the critical radius is perhaps in the region of an atomic diameter, we obtain Table 7.2.

The reasonable agreement between the calculated critical pressures is corroboration that the critical embryo is actually about two atoms across, and therefore occupies the volume of approximately eight atoms. However, whether or not these figures really are accurate is a detail that need not concern us here. The important message is that the pressures that are required for nucleation are *extremely* high, and reflect the real difficulty of homogeneous nucleation of pores in liquid metals. It is clear that the strengths of liquid metals are almost as high as those of solid metals (for liquid iron the fracture strength corresponds to nearly 8 GPa). This is hardly surprising since the atomic structure is similar, liquid metals being close-packed random structures, compared with solid metals being close-packed regular structures. In either case, the atoms are about the same distance apart, and it is similarly difficult to separate them; they are resistant to being forced apart to create a void.

It is certain that in practice the problem of nucleation is reduced by the presence of surface-active impurities in the melt. The non-metals oxygen, sulfur, and phosphorus are particularly active in iron melts: the presence of only 0.2 wt% of oxygen reduces the surface tension of liquid iron from 1.9 to approximately  $1.0 \text{ N m}^{-1}$ . This approximately halves the estimates of the pressure required for nucleation as shown by Equation 7.6. Similar reductions in surface tension (and therefore in fracture pressures) are to be found in liquid copper when contaminated with high levels of the non-metals, O, S, and P.

Such high concentrations of oxygen (and the other non-metals) are probably often found on solidification because of the concentration of solutes ahead of the freezing front. For the case of liquid iron once again, the partition coefficient for oxygen is approximately 0.05, giving a factor of 20 increase in concentration at the advancing front. Thus an average of only 0.01 wt% oxygen in the bulk melt can produce 0.2 wt% at the front.

If the levels of oxygen rise sufficiently to precipitate FeO as a liquid inclusion at the front, then the nucleation problem is reduced yet further because FeO has a surface tension of between 0.6 and 0.5 N m<sup>-1</sup>, depending on the oxygen content (Popel and Esin 1956). Thus a gas pore will preferentially nucleate in such a liquid inclusion, where the critical pressure is easily shown to be reduced to around 1.7 GPa. Effectively, this is still homogeneous nucleation in a pure liquid where in this case the pure liquid in the liquid Fe is in the form of regions, possibly minute droplets, of FeO.

Even this pressure is still so high as to be probably unattainable. What other possibilities are there?

It is possible that nucleation might occur on a solid impurity particle. A solid foreign substrate, if a poorly wetted surface, might make a location for nucleation. This is known as heterogeneous nucleation. If this poorly wetted solid surface happened to be inside the liquid FeO inclusion, we shall see how we can reduce the critical fracture pressure 1.7 GPa yet further in the following section.

### Heterogeneous nucleation

Fisher considers the case of the nucleation of a bubble against the surface of a solid substrate. The liquid is considered to make an angle  $\theta$  with the solid. This contact angle defines the extent of wetting;  $\theta = 0^\circ$  means complete wetting, whereas  $\theta = 180^\circ$  is complete non-wetting. The geometry is shown in Figure 7.21. Fisher shows that nucleation is easier by a factor:

$$P_{\text{het}}^*/P_{\text{hom}}^* = 1.12\{(2 - \cos\theta)(1 + \cos\theta)^2/4\}^{1/2} \quad (7.7)$$

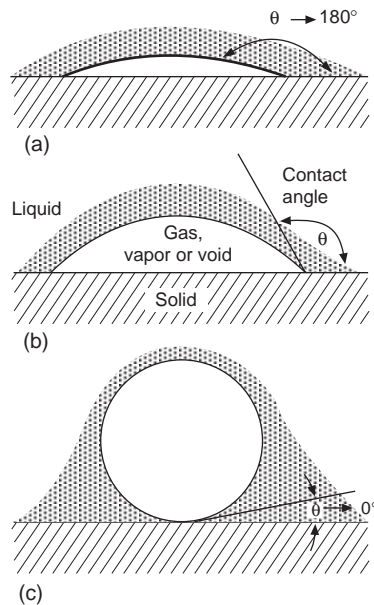


**FIGURE 7.21**

Geometry of a bubble in contact with a solid substrate showing (a) poor wetting and easy decohesion of liquid from the solid; (b) medium wetting; and (c) good wetting in which liquid cohesion to the solid is high, and the bubble is displaced out of contact with the solid.

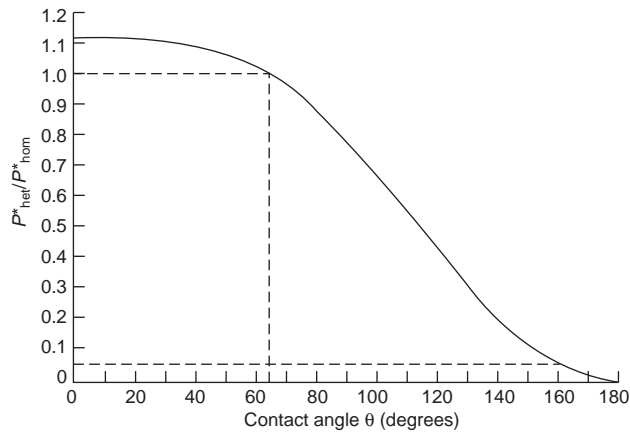


**FIGURE 7.22**

Relative difficulty of nucleating a pore as the contact angle with the solid changes from wetting to non-wetting. Only when the angle exceeds about  $65^\circ$  does heterogeneous nucleation on the solid become favorable.

The factor 1.12 arises because of the fewer sites for nucleation on a plane surface of atoms, compared to the greatly increased number of possibilities in the bulk liquid. This factor alone makes the nucleation of pores on wetted surfaces unfavorable. In fact, nucleation on solid surfaces does not become favorable until the contact angle exceeds  $60$  or  $70^\circ$ , as shown in Figure 7.22. For this reason the nucleation of pores against the growing solid such as a dendrite is *not* favored (since a melt wets the solid formed from itself).

This factor is contrary to those other factors that favor the nucleation of a pore close to a front. These favorable factors include the high gas contents and low surface tension usually present in the highly segregated liquid. Additionally there are likely to be inclusions present, pushed and concentrated by the advancing front into the residual liquid. Again, the inclusions that are pushed by the front are likely to be the non-wetted variety, and so will constitute good nuclei for pores. Contrary, therefore, to many published opinions elsewhere, the interface is theoretically *not* a favored site. Yet, paradoxically, pores will in practice nucleate there because of all the other favorable conditions that prevail adjacent to an advancing solidification interface. The received wisdom turns out to be correct for the wrong reasons!

It is also important to note that not all inclusions are good nucleation sites for porosity. Those that are well wetted will not be favored. These include the rather more metallic inclusions such as borides, carbides, and nitrides. (However, being well wetted, they are mostly good nuclei for the solid phase, and so can assist with grain refinement, as we have seen at several points in Chapter 5.)

The wetting requirements for the nucleation of pores are completely opposite: good nuclei must be not wetted. Such substrates include the non-metals such as oxides. However, the situation is especially bad for *entrained* oxides as will be described later in this chapter.

The reader should be aware that there is widespread misunderstanding of the important fact outlined above, that the nuclei required for the formation of a solid (i.e. for grain refinement) are quite different to the nuclei required for the formation of pores and voids.

A nice experiment was carried out by Gernez in 1867 in which he demonstrated that crystalline solids which had been grown in the liquid, and which had never been allowed to come into contact with

air, were incapable of inducing effervescence in a liquid supersaturated with gas. Otherwise identical solids that had surfaces which had been allowed to dry always caused effervescence.

Oelsen describes a related experiment that he carried out in 1936, in which he isolated a sample of liquid iron on all sides by a liquid slag. Since the iron contained 2% carbon and 0.035% oxygen it was supersaturated considerably in excess of equilibrium. In fact, Oelsen estimated that the internal pressure of carbon monoxide would be approximately 40 atm. When an iron rod was immersed in the melt to destroy the perfection of the containment, a violent eruption of gas immediately occurred, which ceased once again when the rod was withdrawn.

Figure 7.22 indicates that as the contact angle increases to  $180^\circ$  any difficulty of heterogeneous nucleation should fall to zero. In fact there are good reasons to believe that such perfect non-wetting is probably not possible, and that the maximum contact angle attainable in practice is perhaps close to  $160^\circ$ . Certainly no contact angle greater than this appears ever to have been observed (see, for instance, the work by Livingston and Swingley (1971)). Assuming this to be true, then from Figure 7.22 we see that heterogeneous nucleation on the most non-wetted solid known, having a contact angle of  $160^\circ$ , requires only about one-twentieth of the pressure required for nucleation in the bulk liquid.

Returning to our liquid FeO inclusion in solidifying iron; if a highly non-wetting inclusion were present inside the liquid FeO inclusion, then the lowest pressure for nucleation of a pore in this complex inclusion would be approximately  $1.7 \text{ GPa}/20 = 85 \text{ MPa}$ . Although this pressure is still high, it might now (just) be attainable in iron and steel castings. In Al and Mg alloys such a nucleation condition from an equivalent complex inclusion seems unlikely to be attained since these weaker materials would collapse plastically under the internal tension.

Similar reasoning can almost certainly be applied to other alloy systems: complex inclusions are likely to be present in all alloys. In fact it seems likely that most if not all inclusions are complex. The apparent simplicity of many inclusions may be an illusion; microscopic regions of impurities, perhaps only an atom or so thick, may be distributed in patches. It would be difficult to find such patches, and, conversely, difficult to prove that they did not exist.

Perhaps therefore these large fracture pressures predicted by the classical nucleation theory are to be expected to be always reduced by the presence of low surface energy liquid inclusions that in turn contain very poorly wetted solid particles. If this is the case, then assuming that all the values are reduced from their homogeneous nucleation values by the same total factor approximately 83 found for pure iron, the final column in Table 7.2 is estimated.

There is a natural concern that although these stresses are greatly reduced from those required for nucleation in the pure liquid, they are still probably too high to be attainable. Thus, in a nutshell, even fairly dirty liquid metals do not meet a reasonable criterion for fracture considering the classical nucleation theory.

Thus although the formation of pores by random, thermal atomic fluctuations within the liquid, and against plane solid surfaces, has been a problem in classical physics that has fascinated many scientists since the first attempt by Fisher in 1948, all of the solutions that have been found so far (see, for instance, the short review by Campbell (1968)) have shown that pores are difficult, and actually probably impossible, to nucleate, despite invoking the most active of heterogeneous substrates.

If liquid metals do not fracture, the internal initiation of porosity in castings is impossible. Nevertheless, the fact is that pores in castings are the norm rather than the exception. Clearly, there is a major mismatch between theory and fact. The failure of classical nucleation theory to account for

porosity is not widely appreciated. In this work, the fundamental inability of the classical theory has driven the search for other pore initiation processes as outlined below.

This conclusion is so important and so surprising that it is worth emphasizing by stating it another way. The student will usually have been persuaded that because classical homogeneous nucleation of pores in liquid metals is difficult, classical heterogeneous nucleation on a solid particle must therefore occur. The key conclusion from our above discussion is that this is almost certainly untrue. Classical nucleation of a cap-shaped bubble cannot occur even on the most non-wetted solid. This alarming fact forces a re-evaluation of initiation processes for porosity in castings.

Other potential processes are examined below in Section 7.1.5.4. However, it will become clear that the most likely candidate mechanism for pore initiation is entrainment defects, as will be described later in the Section 7.1.5.4.

### Nucleation conditions for shrinkage pores

The problem of the nucleation of shrinkage cavities has been widely overlooked. Somehow it has been assumed that they are fundamentally different to gas pores, and that they ‘just arrive’. After all, it is argued, they *must* occur in an unfed isolated volume of liquid, because the concept of shrinkage means that there is a volume deficit. It is assumed that this volume deficit *must* result in a cavity.

However, we shall go on to show in this section that there really is a difficulty in the initiation of a cavity in a liquid, as we have seen for various analogous systems described in Section 7.1.2.1 that demonstrate that the liquid can withstand hydrostatic tension, and may never fail. If we accept this, then it follows that the liquid is stretched elastically, and the surrounding solid drawn inwards, first elastically, then plastically, as the stress in the liquid increases (Campbell 1967). These predictions explain many common observations in the foundry, as will be referred to repeatedly in this work. Only when the stress in the liquid reaches the critical fracture pressure  $P_f$  will a pore appear, growing in milliseconds to a size which will dispel the stress. This is the instant at which the pore grows explosively, releasing the tension in the liquid.

Thus in case of any doubt, all the conclusions reached above for nucleation of pores in liquids, estimated by Fisher’s formula, apply to the nucleation of shrinkage cavities. Briefly these are summarized below.

Fracture strengths are, of course, reduced by the presence of weakly bonded surfaces in the liquid. Thus the above discussion on heterogeneous nucleation also applies. Shrinkage cavities are therefore expected to nucleate only on non-wetted interfaces.

Good nuclei for shrinkage cavities include oxides. Complex inclusions that consist of low-surface-tension liquid phases containing non-wetted solids might be especially efficient nuclei, as have also been discussed.

Unfavorable nuclei on which the initiation of a shrinkage cavity will *not* occur include wetted surfaces such as carbides, nitrides, and borides, and other metal surfaces such as the dendrites that constitute the solidification front. (Readers need to beware that many authors assume, incorrectly, that dendrites are good nuclei for pores although, perhaps somewhat perversely, pores often do nucleate at a dendritic front for other reasons as listed in earlier.) All these substrates are unfavorable for decohesion simply because the bonding between the atoms across the interface is so strong. This is reflected in the good wetting (i.e. small contact angle) of the liquid on these solids.

Interestingly, although oxides are included above as good potential nuclei for pores, this is only true of their non-wetted surfaces. Those surfaces that have grown off the melt, and are thereby in perfect

atomic contact with the melt, are not expected to be good nuclei. This illustrates the important distinction between wetting defined by contact angle, and wetting defined as being in perfect atomic contact with the liquid. Ultimately, it is the atom-to-atom contact, and the strong interatomic bonding, that is important.

### Nucleation conditions for combined gas and shrinkage pores

Following Fisher's analysis through once again, considering now that there is gas at pressure  $P_g$  on the inside of the pore effectively pushing, and a negative pressure  $P_s$  in the bulk liquid effectively pulling the embryonic pore into existence, the final result is:

$$P_f = P_g + P_s \quad (7.8)$$

This equation illustrates how gas and shrinkage cooperate to exceed the critical pressure for nucleation. The significance of this equation can perhaps be better appreciated by deriving an analogous relation as follows.

If we write the condition for simple mechanical equilibrium of a bubble of radius  $r$  in a liquid of surface tension  $\gamma$ , where the bubble has internal pressure  $P_i$  and external pressure in the liquid  $P_e$ , we have:

$$2\gamma/r = P_i - P_e \quad (7.9)$$

When the pore is of critical size, radius  $r^*$ , the internal pressure is the pressure of gas  $P_g$  in equilibrium with the liquid, and the external pressure  $P_e$  is the (negative) pressure due to shrinkage  $-P_s$ , then Equation 7.8 becomes the analog of Fisher's equation:

$$2\gamma/r^* = P_g + P_s \quad (7.10)$$

The fracture pressures of various liquid metals can then be estimated from this relation assuming that  $r$  is approximately one or two atomic diameters, giving the values presented in Table 7.2.

The cooperative action of gas and shrinkage quantified above in Equations 7.8 and 7.10 was predicted by Whittenberger and Rhines (1952). Their ground-breaking concept was enshrined by them in a nucleation diagram as shown in Figure 7.23. We shall devote some space here to a consideration of this insightful map and show how it can be developed to a fascinating degree of sophistication, greatly assisting the description of pore-forming conditions within a casting.

Turning now to a detailed consideration of Figure 7.23: for a well-fed casting,  $P_s = 0$ , and as freezing proceeds the gas is progressively concentrated in the residual liquid, raising the equilibrium gas pressure. Thus conditions in the casting progress along the line ADCE. At point E the conditions for heterogeneous nucleation of a gas pore on nucleus 1 are met, so that a gas pore will pop into existence at that instant. The initial rapid growth of the gas bubble will deplete its surroundings of excess gas in solution, so that conditions in the locality of the bubble will reverse off the nucleation threshold, back towards D. Thus a second pore will be unable to nucleate in the immediate neighborhood of the first pore. Other gas pores may nucleate elsewhere, beyond the diffusion catchment area of pore number 1.

Notice also that other heterogeneous nuclei are also present, floating about in the liquid (threshold 2 in Figure 7.23) but, being less favorable, are not activated.

We turn now to the quite different situation where the casting is free from gas, but is poorly fed. The internal pressure  $P_s$  in the casting falls because of the action of shrinkage, progressing along the line



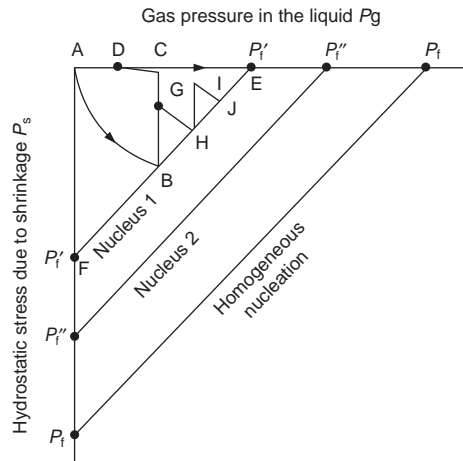


**FIGURE 7.23**

Gas-shrinkage map showing the path of conditions within the residual liquid in the casting in relation to the nucleation threshold for pore formation.

AF. At F the fracture pressure for nucleation on heterogeneous nucleus 1 is met, and a cavity forms. The hydrostatic tension is explosively released and conditions in the casting shoot back to point A.

In practice, both gas and shrinkage will be present to some degree in the average casting, and both will cooperate, causing the conditions to progress along a curve AB. In the absence of any foreign nuclei it is unlikely that the condition  $P_f$  would be met before the casting had solidified completely. This is because the homogeneous nucleation threshold is so far away. (Figure 7.23 is not to scale. If it had been, then the heterogeneous threshold would have been a minute triangle only a millimeter or two in size up at the top left hand corner of the page, making all the action undecipherable!) Thus the casting would have been sound if no favorable inclusions had been present. However, in the presence of nuclei 1 and 2, the combined gas and shrinkage pore will form at B on nucleus 1. Nucleus 2 will never be needed.

On the formation of a mixed pore at B, the pressure in the liquid immediately reverts to point C. Subsequent slower diffusion of gas into the pore will deplete the immediate surroundings of the pore, causing the local environment to progress to D. Outside this diffusion distance, conditions elsewhere in the casting continue to be free of stress, and may progress to point E at which many more gas pores may nucleate. These will add to the original mixed pore that will in the meantime have continued to grow under the combined action of shrinkage and gas.

The area of influence of the release of the hydrostatic tension due to shrinkage has been assumed in the above discussion to apply to the whole casting. In practice it is true that its influence is vastly greater than that of the depletion of gas. The distance over which shrinkage is depleted is probably a factor of 1000–10 000 times greater than that of gas. This is evident from the fact that diffusion distances of solutes in the liquid are usually measured in micrometers, whereas the distances between layers in typical layer porosity can be measured in millimeters or centimeters. As will be explained in Section 7.1.7.2, each layer in layer porosity represents a separate nucleation event, effectively isolated from its neighboring layer, because the threads of liquid that connect the two have become so fine as to be practically impassable because of viscous restraint.

Thus in terms of our nucleation diagram (Figure 7.23), the nucleation event at B may cause the reduction in tension in its own locality to drop to nearly zero at point C. However, at a distant location elsewhere, it may drop to only about a quarter of the original tension at G (as is explained in the case of the formation of layer porosity to be discussed in Section 7.1.7.2). A second nucleation event may then occur at H, leading via I to a third pore formation event at J, and so on.

The nucleation diagram is useful for visualizing the effect of such variables as casting under an applied pressure, so that the starting point A is raised, effectively making the nucleation threshold more distant. If it is sufficiently distant then there is a chance that it may not be reached before the casting has solidified.

The diagram also illustrates how it is of little benefit to the soundness of a casting to melt in vacuum and cast in vacuum (although it may be better for other reasons to cast in vacuum, to avoid any back pressure of gas that might resist the filling of very thin sections for instance. It may also be useful to avoid the entrainment of a protective gas such as argon, which cannot be subsequently diffused out, nor easily closed by hipping). This is because both the gas pressure and the pressure in the liquid are both shifted by one atmosphere, in the same direction, meaning that the pore nucleation threshold remains the same distance away, canceling any advantage. Conversely, melting under vacuum but solidifying under atmospheric pressure is seen to be a benefit, pushing the threshold away by 1 atmosphere pressure.

#### **7.1.5.4 Non-classical initiation of pores**

##### High-energy radiation

The radioactive decay of naturally occurring isotopes, and, unfortunately, contaminating artificial radioactive elements, occurs around us all at every point of our lives. Naturally occurring radioactive materials are relatively common in metals and alloys, and general radioactive contamination is presently increasing annually, arising from industrial and medical sources, and general fall-out since the first nuclear explosions in 1945. This is a sad outcome, but even if all future contamination of the environment were to be prevented, we will still have to come to terms with accepting the historical legacy of a radioactive environment as a fact of life.

Liquid metals are, in common with all other present-day materials, subjected to a constant barrage of high-energy particles from these internal radioactive decay processes. The passage of these high-energy particles through the liquid causes thermal or displacement spikes, the name given to regions of intense heating, or actual displacement of atoms, effectively raising the local temperature of the liquid to well above its boiling point. It is possible, therefore, that these transient heated regions might become vapor bubbles sufficiently large to satisfy Equation 7.1, and thus constituting effective nucleation sites for gas or shrinkage pores.

Johnson and Orlov in their review (1986) describe defect regions in solid metals of up to 100 atoms in diameter. Energy can be channeled away from such events along crystallographic directions in ordered solids, reducing the local damage. The lack of any long-range order in liquids means that no such safety valve is possible, so that energy deposition will be much more localized. It follows that the production of a bubble of 100 atoms diameter in liquid iron should be easy, giving an equivalent fracture pressure of approximately 1500 atm, much lower than that required for classical homogeneous nucleation. In liquid FeO the fracture pressure would be 400 atm. If the event occurred close to a non-wetted surface, then the fracture pressure would be only 20 atm. Such pressures would be much more easily met in castings.

Analogous events are actually observed directly in the bubble chamber, a device full of a transparent liquid that can be vaporized by a high-energy particle, and so define its path. It is sobering to note that a bubble chamber can only be constructed using steel made prior to 1945, in Europe commonly sourced from the German battleships on the seabed at Scapa Flow in the north of Scotland. Later steel introduces too much spurious background radiation.

Claxton (1967) has carried out a detailed study of the nucleation of vapor bubbles in liquid sodium subjected to a wide variety of different high-energy particles, including photons, electrons, protons, neutrons, alpha-particles, xenon, and strontium as fission fragments, and alpha-recoils. His preliminary analysis suggests that the only interactions capable of initiating nucleation of bubbles are 'knocked-on' atoms of the liquid produced by fast neutrons. Claxton (1969) suggests that for heavy recoils arising from alpha-particle decay the rate of energy transfer in liquid aluminum would be about three times higher than that in sodium, and in liquid iron should be about ten times, giving rise to the possibility of nucleation, depending on the isotope responsible.

Significantly, the micro-bubble spectrum in water is seen to be augmented when the water is irradiated with neutrons (Figure 7.24).

Additional factors that are likely to enhance any effects of the presence of radioactive isotopes in metals will be the concentration of such elements ahead of the freezing front. This is precisely where such events can be most effective. The region has high gas content, low surface tension, and high density of assorted solid debris, some of which may be effective nuclei.

Furthermore, if a particularly troublesome radio-active isotope happened to be present in the melt, as an alloy in solution, it would be fundamentally different in character from suspensions of bubbles or inclusions, in that it could not simply be eliminated by sedimentation or filtration. These uncertainties have never been investigated.

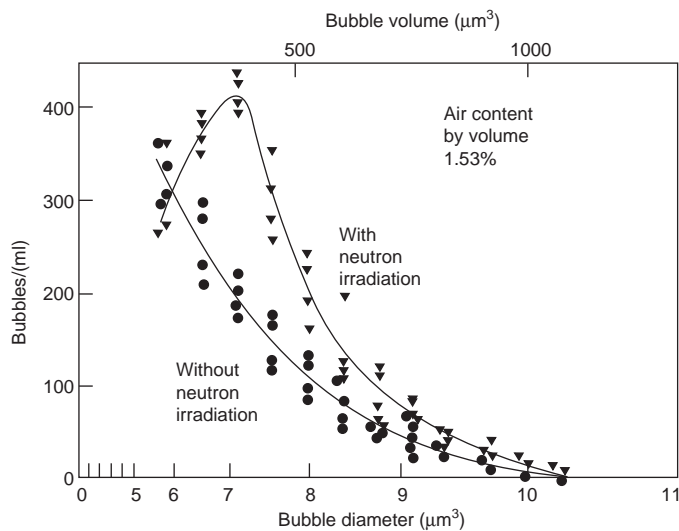


FIGURE 7.24

Microbubble spectrum in tap water with and without neutron irradiation (Hammit 1973).

Differences in the levels of contamination by trace isotopes may be just one of many possible reasons for the occasional different behavior from one batch of metal to the next that is often experienced in the foundry, and that often seems inexplicable. Kato (1999) is one of the first to record a check for the presence of alpha-emitters in his high-purity copper castings. It is a concern that one day such checks may have to become a routine.

### Pre-existing suspension of bubbles

A number of studies have indicated that there may be a microbubble spectrum in most liquids.

Studies on tap water have demonstrated that there seem to be approximately 300 bubbles of around 5  $\mu\text{m}$  diameter in each ml (Figure 7.24). Hammitt (1973) has carried out work that implies similar distributions of bubbles in liquid sodium circulating as coolant in atomic reactors. Even higher densities of bubbles have been measured by Outlaw et al. (1981) in vacuum-cast pure aluminum (Figure 7.25). Although, of course, we have to be careful not to assume that this pore distribution in the solid reflects that originally present in the liquid, the result does underline the fact that there are distributions of fine pores in circumstances where we may not have any reason to suspect their presence.

Chen and Engler (1994) examine the very old proposal that pores exist in irregular crevices of solid inclusions. They propose that for a conical cavity a gas pocket would have an indefinite existence (they neglect the complications of chemical reactions and dissolution that we shall consider below). In the case of old oxides, from the surfaces of melting or holding furnaces, that have been relatively recently entrained, this model is probably accurate. Even so, it seems likely that in most current situations, this source of inclusions will be of less importance than new films from more recent entrainment events. Bifilms are expected to exist in many liquid metals and alloys. They are not envisaged as a distribution

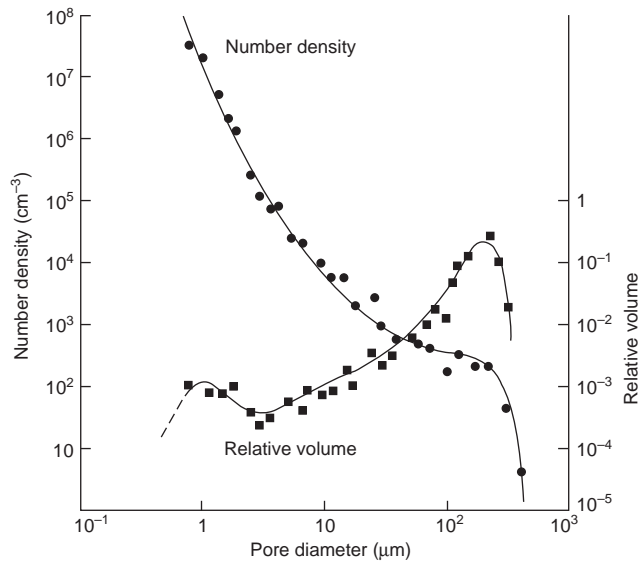


**FIGURE 7.25**

Hydrogen porosity in vacuum melted and cast 99.99Al. Total porosity is 0.71% (Outlaw 1981).

of spherical pores, but as a wide spectrum of sizes and shapes of films of air trapped between folded entrained surface films (the crack-like pores illustrated by Chen and Engler are good examples of bifilms in the early stages of opening). The films will usually be oxides, but may be a number of other non-metallic phases such as graphite or nitrides, etc. The bifilms are, of course, a kind of crevice, so that, to some extent, the theory elaborated by Chen and Engler remains appropriate. Even so, we shall see how the bifilm model as a somewhat flexible folded film, exhibiting some rigidity, and enclosing films and bubbles of entrained gas, in general, fits the facts more closely than that of a model of a solid particle with a gas-filled crevice.

For an entrained oxide film, the oxygen in the air entrapped in the folded film will be quickly consumed by reaction with the metal to form more oxide. The nitrogen may subsequently be consumed more slowly to form nitrides. Ultimately, however, there will be a tiny residue of only about 1% of the original volume of entrapped air, consisting mainly of argon. The inert gases are practically insoluble in liquid metals (Boom et al. 2000). Thus a spectrum of very fine volumes of inert gas, trapped within oxide fragments, will be expected to be rather stable over long periods of time.

Figure 7.26 shows the order of magnitude relation showing the size and number of bubbles equivalent to that volume percentage of porosity. For instance, 1% porosity can correspond to either a mere ten pores per ml when the pores are 1 mm diameter, or 10 million pores per ml when the pores are only 10  $\mu\text{m}$  diameter. (In Figure 7.26 the scale of gas content of the melt, assuming the melt to be aluminum, is of course only accurate at larger bubble sizes. It becomes increasingly inaccurate as sizes fall below 0.1 mm diameter because the internal gas becomes increasingly compressed by the action of surface tension.)

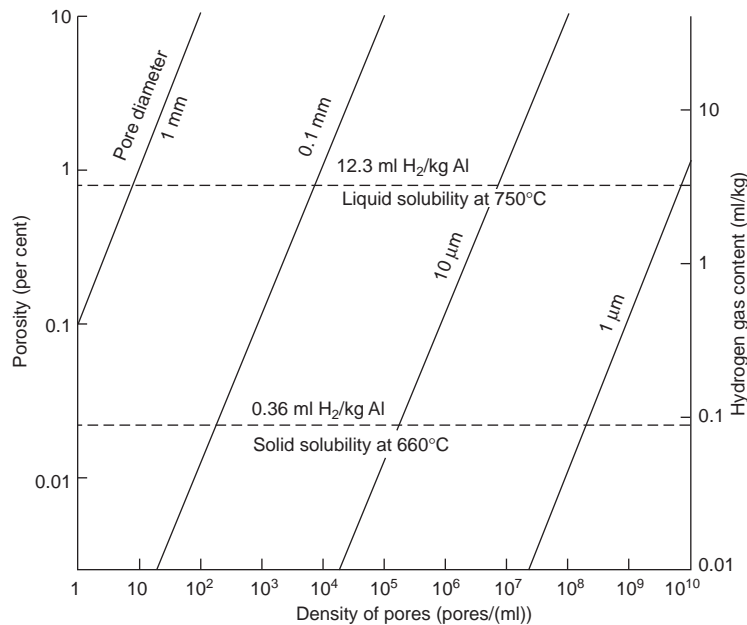


**FIGURE 7.26**

General relation between volume % porosity and number and size of pores. The solubility of hydrogen in aluminum is superimposed.

In other more reactive metals, such as liquid titanium, both oxygen and nitrogen have high solubility, leaving only the inert gases that may be insoluble. A micro-bubble distribution introduced on the surface oxide (if any) may be less stable in this material after the oxide has dissolved, since the bubbles would be more free to float out. Similarly, in other high-temperature liquids such as irons and steels the greater speed of reactions, the higher density of the melt and its higher surface tension will all tend to limit the lifetime and spread of sizes of any micro-bubble population introduced from this source. Nevertheless, enough of the population may still survive for long enough to cause problems in the short time needed to achieve solidification.

### Pore initiation on bifilms

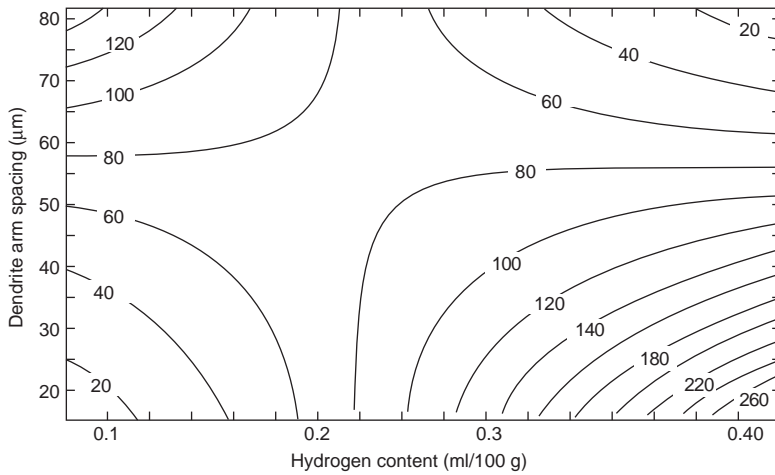
In contrast with all other pore initiation mechanisms, apart from the pre-existing population of pores with which this section has much in common, the bifilm is seen to possess the potential to initiate pores with negligible difficulty. It simply opens by the separation of its unbonded halves. Surface tension is not involved (as is usually assumed when nucleating a pore in a liquid). This is simply a mechanical action between parallel films of (effectively) vanishingly thin oxide separated by a vanishingly thin layer of gas. The acid test of any theory of pore initiation is its capability to explain the experimental data that have previously appeared to be inexplicable. Such data are described below.

The definitive research on the growth of porosity in aluminum alloy castings was that carried out at Alcan Kingston Laboratories by a team led by Fred Major (Tynelius 1993). In this exemplary work small tapered plates and end-chilled plates of Al-7Si-0.4Mg alloy were cast under varying conditions to separate the effects of gas content, alloy composition, freezing time, and solidus velocity on the growth of porosity in the castings. The reader is recommended to consult this impressively logical piece of work; the first of its kind, and not since repeated at the time of writing.

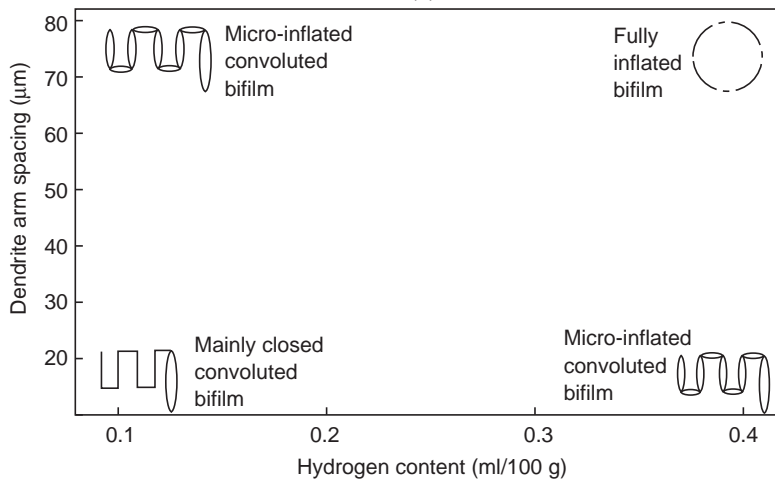
Normally, of course, the effects of solidification time, temperature gradient, and solidification rate are all so closely linked that they are effectively inseparable in most practical casting experiments. However, the experiment was cleverly designed so that the effect of casting geometry was separated out, revealing that the most appropriate thermal parameters to predict porosity were the solidification time and solidus velocity. These gave better results than any of the various temperature gradient terms. They also quantified the dominant effect of hydrogen, and the important contribution of strontium.

The outstanding mystery from this work was the parameter 'areal pore density' (i.e. the number of pores per unit area). The results are shown in Figure 7.27. It was found that at short solidification times the pore density *increased* with increasing hydrogen content. However, at long solidification times the pore density *decreased* as hydrogen content increased. The authors correctly surmised that this curious and baffling result must depend somehow on the nucleation processes at work. However, the finding has remained unexplained ever since. We shall see how the action of bifilms explains this enigma in a natural way.

We assume that conditions at the lower left corner of Figure 7.27 will be characterized by convoluted bifilms of which only the longest and most outside fold is inflated with sufficient gas to be seen as a pore on a polished section. With time (going vertically up the figure), or with additional concentration of gas (traveling along the bottom towards the right side of the figure) the bifilm will partly inflate additional sections, thus creating what would appear to be a cluster of small pores. Eventually, as the remaining sides of Figure 7.27a are traversed in progress towards the top right corner, the separate micro-inflated bifilm sections will become sufficiently inflated that the whole bifilm will unfurl, blowing up like a single spherical balloon.



(a)



(b)

**FIGURE 7.27**

(a) Experimental results by Tynelius et al. (1994) showing that pore density per cm<sup>2</sup> (the numbers in the figure) increases at fast freezing rates (small DAS) but decreases at slow freezing rates (large DAS); (b) interpretation by a bifilm model.

The interpretation of Figure 7.27a is outlined in Figure 7.27b. In the lower left-hand corner, gas content is so low, and time available so short, that any bifilms will be mostly still be closed, having been raveled up by the action of bulk turbulence. If anything, only the longest section of the bifilm at the outside of the compacted inclusion will be observable as a pore on a polished section because this part of the bifilm will open first, having the largest area to gain gas from solution, and being unshielded from the arrival of supplies of diffusing gas. (Internal folds within the convoluted film will be shielded from outside supply of gas until the defect unfolds.)

As we move from the lower left-hand corner up to the top left-hand corner, the increased solidification time will have allowed additional gas to diffuse to the bifilm, and will begin to open many of the folds. We can call this the micro-inflated stage. A polished section through the bifilm will give the appearance of about ten times the number of pores, in agreement with observations (Figure 7.27a). On the other hand, a move from the lower left corner directly to the lower right corner will similarly micro-inflate the bifilm. Although the time is still short, the amount of gas available is now sufficient to achieve this.

Finally, moving to the top right gives sufficient time and sufficient gas to power the complete inflation of the film. This is expected to occur by successive unfolding actions, as fold after fold opens out. Finally, the bifilm is fully inflated like a balloon. Thus on a polished section only one pore is seen. The main features of Figure 7.27a are thereby explained.

Keen readers can check the observed pore densities from the original publication, allowing a rough calculation of the number of bifilms in the original cast metal, and the size distribution of the final pores. A further check is the total fraction of porosity. Such checks confirm the consistency of the whole scenario.

The assumption that bifilms are present allows a description of porosity in terms of initiation and growth characterized by considerable sophistication and complexity; the important experimental work by Fred Major would probably otherwise remain unexplained and inexplicable.

As an additional related exercise we can gain some idea of the rate of unfurling of bifilms from a simple mechanical model as illustrated in Figure 7.28. We shall assume that the unfolding of the bifilm is resisted by a force  $F$  of the same type as that resisting the motion of a sphere in a viscous liquid (as in the derivation of Stokes' law). Thus the force would be  $3\pi\eta RV$  if it were evenly distributed over the square face of area  $R \times R$ . Since the velocity  $V$  is that at the tip of the bifilm, and the pivot of the bifilm is fixed, on average the resisting force is  $3\pi\eta RV/2$ . The opening force is that due to the pressure  $P$  in the gas phase of the bifilm, acting over the area  $hR$ . Equating moments we have

$$2PRh.(h/2) = 3\pi\eta RV.(R/2)$$

so that we can find the opening time  $t$  from the speed  $V$  and the distance traveled  $\pi R$ :

$$t = (3\pi^2/2)(\eta/P)(R/h)^2 = 15(\eta/P)(R/h)^2 \quad (7.11)$$

For viscosity  $\eta = 1.4 \times 10^{-3} \text{ N s m}^{-2}$ , and reasonable figures for  $P$  of about 0.2 atmosphere ( $0.2 \times 10^5 \text{ Pa}$ ) above ambient, and for  $R = 5 \text{ mm}$  and  $h = 5 \mu\text{m}$ ,  $t$  is only approximately 1 second. Whereas if  $R = 10 \text{ mm}$  and  $h = 1 \mu\text{m}$   $t$  is approximately 2 minutes. Thus the rate of opening is seen to be highly

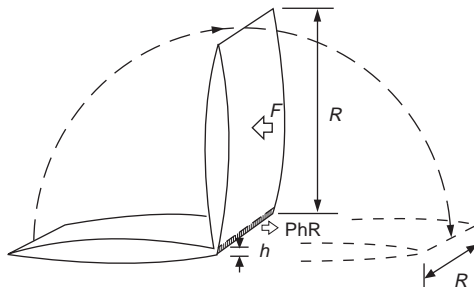


FIGURE 7.28

Model of the unfolding of a bifilm.



dependent on the geometry of the bifilm, as might be expected. Nevertheless, the rates are of the correct order of magnitude to explain the rate of loss of properties in most ordinary castings as the freezing time increases. This wide scatter in the performance of bifilms supports the interpretation of variable nucleation conditions surmised as a result of the sub-surface porosity described in Section 7.2.

### 7.1.6 Growth of shrinkage pores

For internal shrinkage pores that are nucleated within a stressed liquid, the initial growth is extremely fast; in fact it is explosive! The elastic stress in the liquid and the surrounding solid can be dissipated at the speed of sound. The tensile failure of a liquid is like the tensile failure of a strong solid; it goes with a bang.

On a more gentle scale, the audible clicks that are heard as pores nucleate within the melted Tyndall volumes in ice are an exact analogy, and a reminder of the smaller but not negligible tensile stress that is supported in the liquid water prior to a cavity being nucleated (see Section 7.2.2.1).

In the direct observation of the freezing of Pb–Sn alloys under a glass cover, Davies (1963) recorded the solidification of isolated regions of alloy on cine film at 16 frames per second. It was observed that as these regions shrank, a pore would suddenly appear in between frames. Thus the growth time for this initial growth phase had to be shorter than approximately 60 ms. Almost certainly it was very much faster than this. If in fact the rate of expansion is close to the speed of sound, close to  $6 \text{ km s}^{-1}$  in liquid aluminum, a pore 1 mm diameter will form a thousand times faster, in  $0.1 \mu\text{s}$ .

After this explosive growth phase the subsequent growth of the pore observed by Davies was more leisurely, occurring at a rate controlled by the rate of solidification. Thus this second phase of growth is controlled by the rate of heat extraction by the mold.

For pores that are surface-initiated, the initial stress is probably lower, and the puncture of the surface will occur relatively slowly as the surface collapses plastically into the forming hole. Thus the initial rapid growth phase will be less dramatic.

For shrinkage porosity that grows like a pipe from the free surface of the melt there is no initial fast growth phase at all. The cavity grows at all stages simply in response to the solidification shrinkage, the rate being dictated by the rate of extraction of heat from the casting.

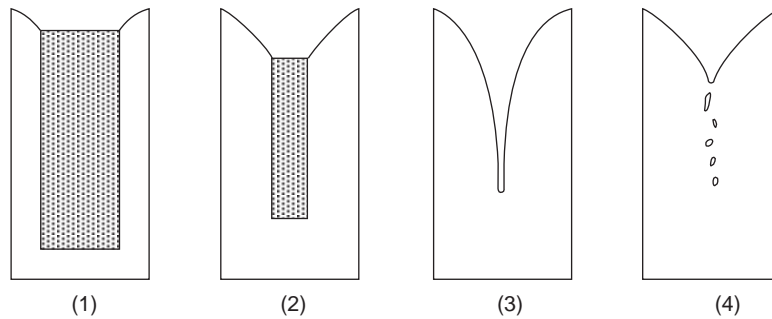
### 7.1.7 Shrinkage pore structure

#### 7.1.7.1 Shrinkage cavity or pipe

During liquid feeding, the gradual progress of the solidification front towards the center of the casting is accompanied by the steady fall in liquid level in the feeder. These linked advances by the solid and liquid fronts generate a smooth conical funnel as shown in Figure 7.29. This is a shrinkage pipe.

It is sometimes called a primary shrinkage pipe to distinguish it from so-called secondary shrinkage seen on sections cut through the casting. Secondary shrinkage appears to take the form of a scattering of disconnected pores below the primary pipe. Generally, however, it is easy to demonstrate that water, or a dye, poured in the top of the primary pipe will find its way into most, if not all, of the so-called secondary cavities. Thus in reality the secondary shrinkage cavities are an extension of the primary pipe. Thus the primary shrinkage cavity penetrates further into the casting than might be apparent at first sight, as Figure 7.29 makes clear.

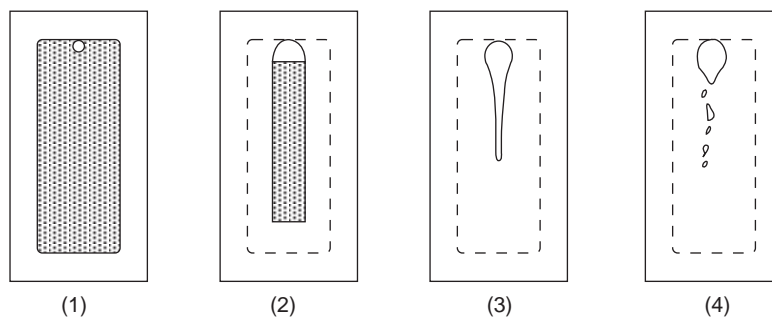
In the situation where the shrinkage problem is in an isolated central region of the casting, a narrow-freezing-range material will give a smooth single cavity. This is occasionally called a macropore to

**FIGURE 7.29**

Stages in the development of a primary shrinkage pipe. Stage (4) is the appearance of stage (3) on a planar cut section if the central pipe is not exactly straight (i.e. it is not a series of separate pores).

distinguish it from microporosity. There has been much written to emphasize the differences between these two forms of porosity. However, as will be clear from evidence presented in the next section, there seems to be no fundamental difference between them; one gradually changes into the other as conditions change from micro-volumes to macro-volumes of unfed regions, and from skin freezing to pasty freezing. Figure 7.8 illustrates a macropore in a bronze casting of very long freezing range, resulting in a single tapering cavity that has numerous branches, and appearing on a cut section to be thousands of separate cavities constituting a spongy structure.

In the case of the single isolated area of macroporosity, it is important to note that its final location will not be in the thermal center of the isolated region, as might at first be supposed. This is because the shrinkage pore could be nucleated anywhere within the volume of isolated, stressed liquid. However, immediately it is formed it will float to the top of the isolated liquid region. Conversely, of course, the situation can be viewed from the point of view of the liquid. This phase, being heavier, will sink, finding its own level in the bottom of the isolated region. The final position of the shrinkage cavity in this case will be as shown in Figure 7.30. Also, of course, the shape and the position of the porosity can

**FIGURE 7.30**

Stages in the development of an internal shrinkage cavity. Stage (4) is again the equivalent cut section to stage (3). Note that the porosity is not concentrated in the thermal center, but is off-set from the center of the trapped liquid region, by gravity.

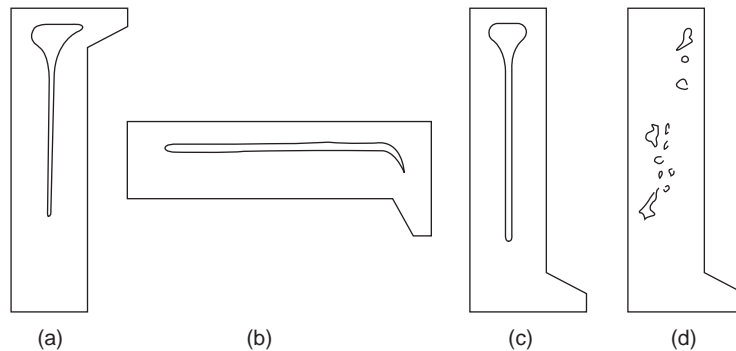


**FIGURE 7.31**

Shrinkage cavity in a short-freezing-range alloy as a function of orientation a, b, and c. Porosity shown in d illustrates some other source of porosity (it cannot be a shrinkage type because of its random form, not linked to the casting geometry).

be altered by changing the angle of the casting, since the pore floats (or the residual liquid finds its lowest level). An analogy is a stoppered bottle, partly filled with liquid, which is turned through different angles. The bottle corresponds to the outline of the isolated liquid volume in Figure 7.30.

Note once more that the long parallel walls of the casting give a corresponding long tapering extension of the shrinkage cavity. On a cut section, any slight out-of-straightness of this tubular cavity can once again be easily misinterpreted as dispersed porosity, so-called ‘secondary pipe’, as it weaves its way in and out of the plane of sectioning (Figure 7.30). In a casting of more complicated shape the shape of the shrinkage pore will take on a corresponding complexity.

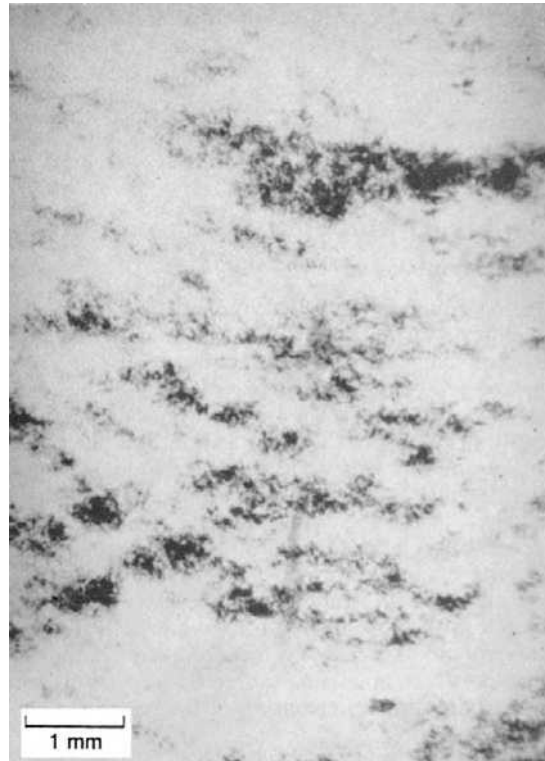
The effect of gravity on the final form and distribution of porosity is illustrated in Figure 7.31. Clearly, the porosity can be moved from one end of the casting to the other simply by making the casting in different orientations, a, b and c. (Figure 7.31d is simply slipped in to emphasize that porosity having no relation to the casting geometry cannot be shrinkage porosity.)

### 7.1.7.2 Layer porosity

Alloys of long freezing range are particularly susceptible to a type of porosity that is observed to form in layers parallel to the supposed positions of the isotherms in the solidifying casting. It is known as layer porosity.

Conditions favorable to the formation of layer porosity appear to be a wide pasty zone arising from long freezing range and/or poor temperature gradients. Poor gradients are typical of alloys of high thermal conductivity (such as the light alloys and copper-based alloys) and of molds having low rate of heat extraction either because of their high temperature (such as in investment casting) or low thermal conductivity (as in sand or plaster castings).

Given these favorable conditions for layer porosity, this variety of porosity has been observed in practically all types of casting alloys, including those based on magnesium (Lagowski and Meier 1964), aluminum (Pollard 1964), copper (Ruddle 1960), steels and high-temperature alloys based on nickel and cobalt (Campbell 1969). An example in steel is shown in Figure 7.32, and in a nickel-based vacuum cast alloy in Figure 7.15.

**FIGURE 7.32**

Radiograph of interdendritic porosity in a carbon steel (Campbell 1969).

It has been argued (Liddiard and Baker 1945, Cibula 1955) that layer porosity is the result of thermal contraction, in a manner analogous to hot tearing. Briefly, the theory goes that after the establishment of a coherent dendrite network by the impingement of the dendrite tips, subsequent cooling causes the structure to shrink, imposing tensile stresses on the network, causing the network to tear perpendicularly to the stress, i.e. parallel to the isotherms. If the tears are not filled by the inflow of residual liquid, then layers of porosity are frozen into the structure. Baker (1945) attempted to test whether the porosity was the result of thermal contraction on cooling by casting test pieces in a mold designed to accentuate hot tearing. However, no significant increase in layer porosity was found.

The negative result of Baker's critical experiment is substantiated by numerous observations, particularly the observations by Lagowski and Meier (1964) on Mg-Zn alloys covering the range of zinc contents up to 30% zinc. These clearly reveal that hot tearing peaks at 1%Zn, corresponding to the maximum of the thermal contraction, and well separated from layer porosity that peaks at 6%Zn (see Figures 8.8 and 9.6).

Finally, the thermal contraction model is seen in any case to be fundamentally flawed; it is not easy to envisage how such differential cooling could arise to pull apart the center, when the whole casting is solidifying in the absence of significant temperature differences. In any case, close inspection of the

pore structure reveals that it is not the dendrite mesh that is pulled apart; the mesh remains in place, and only the residual interdendritic liquid is missing.

I put forward a new explanation of layer porosity (Campbell 1968c). The new approach avoided the difficulties mentioned above because it was based not on thermal contraction in the solid as a driving force, but on the contraction of the liquid on solidification; the problem was interpreted as a feeding problem.

The sequence of events in the solidifying casting is shown in Figure 7.33. From Equation 7.5 it is clear that the hydrostatic tension increases parabolically with distance  $x$  through the pasty zone of length  $L$ , as shown in stage 1 (Figure 7.33). The stresses continue to increase with advancing solidification

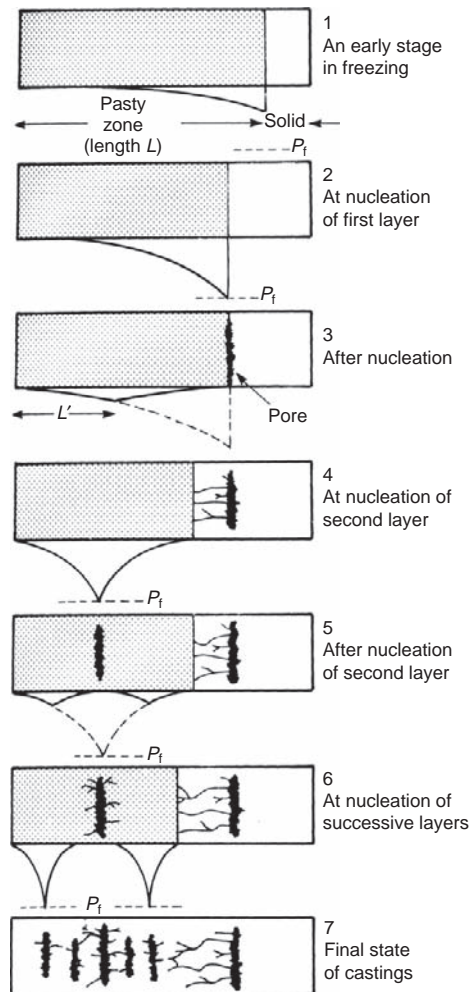


**FIGURE 7.33**

Schematic representation of the formation of layer porosity (Campbell 1968a, b).

(as  $R$  continues to decrease) until the local stress at some point along the parabola exceeds the threshold at which a pore will form (by either internal nucleation or surface puncture). This threshold is labeled the fracture pressure  $P_f$  in stage 2.

As soon as a pore is created by some mechanism, it will immediately spread along the isobaric surface (this surface of constant pressure also probably coincides with an isothermal surface, and an isosolid surface), forming a layer, and instantly dissipating the local hydrostatic tension. The elastic energy that is available for the initial explosive growth stage is proportional to the difference in areas under the pressure–distance curves before and after this growth. The energy is clearly proportional to the area  $L \times P_f$  under the curve. As we discussed in the previous section, this first stage of growth would last probably only microseconds, or at the most milliseconds.

As solidification proceeds further, the solidification contraction in the center of the remaining liquid region is now fed both from the feeder and by fluid (whether residual liquid, gas, or vapor) from the newly created pore. This is a slower growth phase for the new pore, extending via channels towards the region requiring feed metal. The new layer-shaped pore effectively provides a free liquid surface, adjacent to which no large stresses can occur in the liquid.

The maximum stress in the liquid has at this stage fallen by approximately a factor of 4, since the effective length  $L$  has now approximately halved. However, because of the progressive decrease in radius of the interdendritic channels,  $R$ , stress once again gradually increases with time until another pore formation event occurs as at stage 4.

Further nucleation and growth events produce successive layers until the whole casting is solidified. The final state consists of layers of porosity that have considerable interlinking.

Although these arguments have been presented for the case of porosity being formed only by the action of solidification shrinkage, the reader is reminded that the action of gas and shrinkage in combination also fits the facts well as discussed in Section 7.1.5.1 and illustrated in Figure 7.23.

It is important to observe that layer porosity is quite different to a hot tear. A hot tear is formed by the linear contraction of the casting pulling the grains and/or dendrites apart. When they are sufficiently separated there is insufficient residual liquid to fill the increasing volume, so that a true crack opens up. The crack, of course, supports no load, and represents a serious defect. In contrast, layer porosity is formed by the nucleation of a pore in the residual liquid. The liquid is in a state of hydrostatic tension, so that the pore spreads along the surface of maximum hydrostatic tension, through the liquid phase. The dendrites stay fixed in place. The final defect is a layer-like pore threaded through with dendrites. It is akin to a crack spot-welded at closely spaced spots, and so has considerable tensile strength. On a polished microsection therefore, a hot tear is clear, whereas porosity as part of a layer may or may not be easily identified. It only becomes really clear on a radiograph when the radiation is aligned with the plane of the layers.

Figure 7.15 shows layer porosity in an investment casting as a function of conditions that vary progressively from skin freezing to pasty freezing. It reveals that macroscopic centerline porosity, layer porosity, and microscopic dispersed porosity transform imperceptibly from one to the other as mold temperature alone is increased, effectively reducing the temperature gradient during solidification. It is clear, therefore, contrary to many widely held views, that there are no fundamental differences between the various types of macroporosity and microporosity. They are simply different growth forms of shrinkage porosity under different solidification conditions.

Similarly, Jay and Cibula (1956) carried out interesting work on Al–Mg alloys, in which they showed that as the gas content of the alloy was increased, the porosity changed gradually from layer

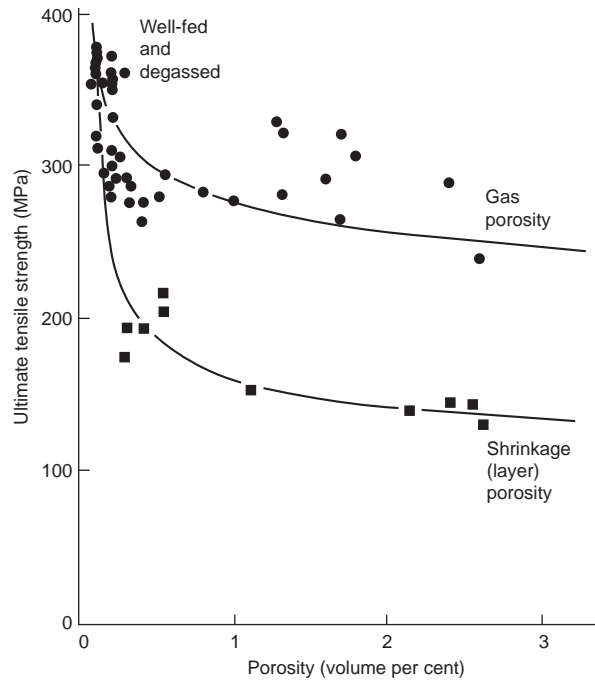


**FIGURE 7.34**

Reduction in UTS of an Al-11.5Mg alloy by dispersed porosity and by layer porosity (data from Jay and Cibula 1956).

porosity to dispersed pinhole porosity (Figure 7.34). Thus these two extreme categories of shrinkage and gas microporosity were demonstrated to be capable of being mixed, allowing a complete spectrum of possibilities from pure shrinkage layer type to pure dispersed gas type.

This merging and overlap of all the different types of porosity makes diagnosis of the cause of porosity sometimes difficult in any particular case. However, it is better to know of this difficulty, and thus be better able to guard against falling into the trap of being dogmatic. Section 7.3 gives some guidance on the diagnosis of the various types of porosity.

The above classical description of the formation of layer porosity was conceived prior to the discovery of bifilms. Thus the theory, based on the nucleation of pores by the accumulated build up tension because of the difficulty of interdendritic flow, and their subsequent growth along isobaric surfaces, seems to me probably still essentially correct. However, now that the presence of bifilms has been realized, it is necessary to take account of the effect they may have in such situations where interdendritic feeding is difficult. It seems likely that bifilms would interfere with the flow of residual liquid through the dendrite mesh. The close spacing of dendrites, providing support for the films, would ensure that they would be capable of resisting large pressure differences across their surface. Thus bifilms transverse to the flow would halt the upstream flow, but be sucked open by the downstream demand, creating a series of shrinkage cavities arranged generally transverse to the flow direction. Such a scenario is not greatly different from that of the classical theory presented above, and

might be difficult to separate experimentally, since the nucleation events in both explanations would be assumed to be bifilms. Ultimately, cleaning the melt will be a certain technique to eliminate layer porosity irrespective of its formation mechanism.

---

## 7.2 GAS POROSITY

### 7.2.1 Entrained (external) pores

Subsurface porosity in casting is a common fault. Sometimes, the subsurface pores are broken into by the loss of surface scale during heat treatment, as is common for steel castings, or are broken into during shot blasting to clean the castings. However, sometimes the problem is not seen until the first machining cut.

Subsurface pores can form as a result of the flotation of air bubbles that have been entrained during the pouring of a casting. If the bubbles are about 5 mm diameter or smaller they do not have sufficient buoyancy to break through the double oxide (their own oxide skin and the oxide skin on the surface of the casting) when they reach the surface of the casting. Thus they sit immediately under the surface of the casting, only two oxide thicknesses deep, and so extremely near to the surface, and extremely easily broken into. These bubbles are always clustered in specific sites, having floated into position, often above ingates, and have a spread of sizes, typically 1–5 mm in diameter.

This 5-mm limit on size is the result of a mechanical limitation and is a certain identification of these pores as being air bubbles entrained during the pouring of the casting. This size of bubble is too large to be generated by a diffusion reaction as described below, thus they are definitely not, for instance, hydrogen pores nucleated and grown in situ during the freezing of the casting.

There is a large research literature claiming that such bubbles in cast irons, associated with oxide slags, are the result of a reaction between the carbon in the iron and the oxygen in the slag, to create a CO bubble. This is clearly wrong for a variety of reasons:

- (i) The bubbles are nearly always too large to be produced by a diffusion reaction;
- (ii) The size range of bubbles corresponds to bubbles entrained by turbulent filling systems;
- (iii) The filling systems are always turbulent;
- (iv) The slag is nearly always generated in the filling system by the turbulent mixing of the melt and air, and so naturally occurs in association with the entrained air (although it is recognized that after swimming through the melt, the bubble will have acquired a contribution of CO, and probably H<sub>2</sub>).

It is important to recognize the subsurface bubbles generated by a turbulent filling system. They are quite different to those bubbles formed in situ during solidification, which are characterized by their uniform size (i.e. typically 0.5 mm diameter or smaller for castings up to a few hundred kg or so, hence normally smaller than one-tenth of the size of entrained air bubbles) and uniform distribution over much of the outer surface of the casting (in contrast with the clustering of entrained air bubbles). Sometimes in situ formed bubbles are uniformly distributed only on the upper parts of the casting because the pressure at greater depth suppresses the formation of bubbles.

A widely accepted theory of the origin of the in situ grown subsurface porosity has been summarized by Turkdogan (1986). He describes how subsurface porosity occurring in cast irons and steels poured into greensand molds is a consequence of metal–mold interaction. Gas bubbles form in



crevices of the mold in contact with the metal, and bubble into the metal, where they become trapped during the early stages of solidification. The action of alloying elements on the process is discussed in terms of their effect on the surface tension of the liquid metal; a lower surface tension allows bubbles to enter the metal more easily, thereby increasing the subsurface porosity.

The theory is similar to the micro-blow theory outlined in Chapter 10, Rule 5. However, micro-blows are probably effectively suppressed by the presence of a strong surface film, such as is normally found on many Al alloys, and irons and steels. Thus there are a number of difficulties with the theory as put forward by Turkdogan.

1. The metal does not in general enter the crevices of the mold. The high surface tension (plus the effect of a strong, fairly rigid surface film) causes the liquid to bridge between high spots, leaving the crevices empty. Mold washes that promote the wetting of the mold by the metal, such as those that are based on sodium silicate, actually reduce subsurface porosity.
2. The pressure required to force small bubbles (radius of 1 mm or less) into the liquid metal against the resistance of surface tension is high. Conversely, it is known that the pressures attainable at the surface of a mold, from which gas can easily migrate away through the mold to the atmosphere, are very low. Thus it seems unlikely that small bubbles could be forced into the metal in this way. (Large bubbles, with radius measured in centimeters, and therefore small pressure requirements, can be forced into the metal from outgassing cores; Chapter 10, Rule 5.)
3. Tellurium additions to cast iron reduce surface tension and should, according to the penetration theory, increase porosity. In fact tellurium additions are found to decrease porosity.
4. The theory is not capable of explaining the occurrence of subsurface porosity in inert molds such as investment molds, which are free from gas-forming materials such as moisture and hydrocarbons.

Features 1 and 2 may not always be relevant, because the micro-blow conditions may apply as described in Chapter 10, Rule 5. However, features 3 and 4 remain important damning evidence.

We shall therefore assume that in general the formation of subsurface porosity does not occur by mechanical penetration of the liquid surface by bubbles from the mold. We shall see how it is to be expected as the consequence of normal segregation ahead of the solidification front, and the normal processes of nucleation and growth of pores from gases in solution in the metal. A supply of gas diffusing from the mold into the casting surface will enhance the effect. Also, assuming the presence of bifilms completes a convincing model as we shall see.

We have seen in Section 5.3.1 how the early growth of the freezing front from the mold wall is planar because of the high temperature gradient. Thus the 'snow plow' build-up of solute occurs, starting from the original solute content  $C_0$ , and increasing over the first millimeter or so of travel of the front, until the solute reaches a level at which a pore may nucleate (Figure 5.39). Thus the gas content concentrated in this way is too low in the first millimeter or so to create significant porosity, whereas across all the central parts of the casting pores are possible. A typical form of this porosity is shown in Figure 7.35. It should perhaps be better named surface-layer-free porosity, since, if the gas content of the melt is sufficiently high, the porosity in such cases is rarely simply subsurface, but is distributed everywhere *except* in the surface layer as Figure 7.35 illustrates.

This microsegregation process is common in many alloy systems where the solute has a low partition coefficient  $k$ , resulting in a high concentration of solute ahead of the advancing front. (Recall from Section 5.3.1 that the maximum concentration of solute is  $C_0/k$ .) For these systems subsurface porosity is the standard form of gas porosity. It may or may not be the result of the release of gas from

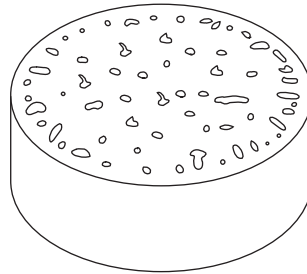


**FIGURE 7.35**

Subsurface porosity revealed on a cut section of a bar casting.

a metal–mold reaction that can subsequently diffuse into the casting. Such a source will certainly increase the gas available, and may in fact be the sole source of gas. However, it must not be forgotten that subsurface porosity is the normal appearance of gas porosity whether metal–mold reactions contribute or not.

For instance, Klemp (1989) describes subsurface porosity in a low-alloy steel cast into an investment mold. Such molds are fired at high temperature (commonly about 1000°C) and can be safely assumed to be dry and free from outgassing materials. In this case the subsurface porosity is definitely *not* the result of surface reaction; the gases were already in solution in the cast metal at the moment of pouring.

In contrast, but not in conflict, Turkdogan (1986) reports subsurface porosity in cast irons cast in greensand, but had no reports of any such defects in irons cast into iron molds. In this case the porosity in the greensand molds *is* the result of surface reaction; little gas was in solution in the cast metal.

It is not easy to make a clear separation in this account of the various gases, since all cooperate in some alloy systems, and many systems are analogous. However, a rough division will be attempted, the reader being requested to overlook the necessarily ragged edges between sections.

## 7.2.2 Blow holes

The avoidance of blow holes, bubbles blasted into castings from cores, and occasionally from molds, is dealt with at length in Chapter 10, Rule 5. However, this short note is simply included to ensure that we do not forget about ‘blows’ when we attempt to diagnose our porosity problems. An unvented core should always be viewed with suspicion.

## 7.2.3 Gas porosity initiated in situ

We have discussed the action of bifilms to initiate porosity in liquid metals in Sections 7.1.5.3 and 7.1.5.4. The interesting feature of the mechanical model for the opening of bifilms in relation to the growth of pores is illustrated in Equation 7.11. If the gas in solution in the liquid is assumed to be hydrogen, and assuming it to be approximately in equilibrium with the entrapped gas in the bifilm, the internal pressure will be proportional to  $[H]^2$  (other diatomic gases will act similarly of course, although their approach to equilibrium may be slower because of their slower rates of diffusion to the bifilm). The rate of unfurling is therefore especially sensitive to the amount of gas in solution in the alloy.

In the case of iron and steel where an important contributor to the internal pressure will be expected to be carbon monoxide, CO, the internal pressure will approach that dictated by the product of the activities of carbon and oxygen in the melt, approximately  $[C].[O]$ . In addition, of course, nitrogen and hydrogen will also contribute to the total pressure.

In one of the most exciting pieces of research ever published in this field, Tiberg (1960) describes the growth of carbon monoxide bubbles in liquid steel whilst actually observing the inside surface of the growing bubbles. He achieves this miracle by using high-speed cine film to record the nucleation and growth of bubbles on the inside wall of a fused silica tube that contained the steel. (One day, in the 1970s, I was introduced in passing to a pleasant young Scandinavian. His name turned out to be Tiberg. I enquired whether it was his work on observing bubble growth inside liquid steel, since this was the most exciting research I had ever read. He affirmed it was him, agreeing that it was the most exciting research he had ever carried out. We shook hands on such a warm and unexpected discovery of mutual interests. We had only time to bid each other farewell. We have never met since.)

The classical theories of pore growth assume that the geometry of the pore and its collection volume are spherical, and that growth is steady. This seems to be far from true in the experiment in which Tiberg tested these assumptions.

At high rates of growth he found that the speed of expansion of the bubble surface  $dr/dt$  was indeed constant from the time the bubble was first observed at a size of 30  $\mu\text{m}$ . However, after the addition of the deoxidizers, aluminum or silicon, the growth rate was slower and varied considerably from one bubble to another. In some bubbles growth suddenly halted and then continued at a slower rate. In fast-growing bubbles a small bright spot was observed.

The observation of the bright spot is interesting. It is most likely to have been an inclusion of alumina or silica (possibly actually in the form of a bifilm?), since this behavior was only observed after the addition of the corresponding deoxidizer. The transparency or translucency (or even its hollowness if in the form of a partially opened bifilm) of the inclusion would have allowed the interior of the inclusion to be visible, giving an observer a view into the interior of the melt. This would appear as a bright enclosure, the classical 'black body cavity' of the physicist, radiating a full spectrum corresponding to the temperature of the interior of the steel, and therefore appearing as a bright spot. (The remainder of the bubble surface radiating its heat away to the outside world via the transparent silica vessel, and partially reflecting the cooler outside environment from its surface, would therefore appear cooler.) We may speculate that the enhanced rate of transfer of gas into the bubble may have resulted from either (a) the short-circuiting of a surface layer that was hindering the transfer of gas into the bubble, or (b) the attached inclusion having a large surface area and a high rate of diffusion for gas. Its surface area would then act as a collecting zone, funneling the gas into the growing bubble through the small window of contact. A bifilm would have been expected to be especially effective in this way.

Tiberg's extraordinary observations link with work by the Japanese researcher Kita (1979), who studied the insides of pores in steels by SEM. He found that the inner surfaces of pores had curious markings, with radial 'petals', like flowers, suggestive that this may have been the site of gas leaking into the pores via some special route. The details of the markings were different for pores created by hydrogen, nitrogen, and carbon monoxide. In addition, some markings were clearly oxide inclusions.

It seems therefore that the growth of pores in steels, and perhaps in most liquid metals, is complicated, and far removed from the ideal spherical model assumed in all the theoretical approaches to the problem. This subject would greatly benefit from a more thorough study with modern equipment.

In the absence of more detailed information, we shall continue to assume that the growth of gas pores in liquid metals is controlled mainly by the rate of diffusion of gases through the liquid metal. There are many data in support of this, especially in simple systems such as the Al-H system. In general metal systems, however, the rate of growth is probably dominated by the rate of arrival of the fastest diffusing gas. From Figure 1.4c it is clear that in liquid iron, hydrogen has a diffusion coefficient approximately ten times higher than that of any other element in solution. Thus the average diffusion distance  $d$  is approximately  $(Dt)^{1/2}$  so that in comparison with other diffusing species, the radius over which hydrogen can diffuse into the bubble is  $(10/1)^{1/2} = 3$  times greater. Thus the spherical volume over which hydrogen can be collected by the bubble, in comparison with other diffusing species, is therefore  $3^3 = 30$  times greater. Thus it is clear that hydrogen has a dominant influence over the *growth* of the bubble.

It should be remembered that hydrogen makes a comparatively small contribution to the *nucleation* of the bubble, because it concentrates relatively little ahead of the advancing freezing front, in comparison with the combined effects of oxygen and carbon to form CO in liquid iron and steel. The situation is closely paralleled in liquid copper alloys, where oxygen controls the nucleation of pores because of the snow plow mechanism, whereas hydrogen contributes disproportionately to growth because of its greater rate of diffusion.

This clarification of the different roles of oxygen and hydrogen in copper and steel explains much early confusion in the literature concerning which of these two gases was responsible for subsurface pores. Zuihoff (1964, 1965) published the first evidence that confirmed the present hypothesis for steels. He succeeded in showing that aluminum deoxidation would control the appearance of pores. Clearly, if the oxygen was high, then pores could nucleate, but they would not necessarily grow unless sufficient hydrogen was present. Conversely, if hydrogen was high, pores might not form at all if no oxygen was present to facilitate nucleation. The hydrogen would therefore simply remain in solution in the casting. The same arguments apply, of course, to the roles of hydrogen and oxygen in copper-based alloys.

A useful simple test for steels which deserves wider use is proposed by Denisov (1965): a sample test piece was developed 110 mm high, and  $30 \times 15$  mm at the top, tapering down to  $25 \times 12$  mm at the base. A metal pattern of the sample quickly creates the shaped cavity in the sand, into which the metal is poured. Immediately after casting, the sample is knocked out and quenched in water. It is then broken into three pieces in a special tup. The entire process takes 1 to 2 minutes. It was found that the tapered test piece gave an accurate prediction of the risk of subsurface porosity; if such problems were seen in the sample they were seen in the castings and vice versa. The test therefore warned of danger, and avoiding action could be taken, such as the addition of extra deoxidizer to the ladle. This test for steel castings cast in greensand molds should be applicable to other alloy and sand systems prone to this problem. Although the simplicity and apparent usefulness of this test is commendable, perhaps the 'look and see' test by the author, described in Section 7.1.4 might be even simpler and quicker. Quick, reliable tests for use on the shop floor are very much needed. The reader is recommended to try these techniques.

In some alloy systems the rate of growth of pores is not expected to be simply dependent on the rate of diffusion in the matrix. The rate can also be limited by a surface film as discussed in Section 7.1.3.

Ultimately however, the maximum amount of gas porosity in a casting depends partly on simple mechanics, as illustrated by the well-known *general gas law*. The use of this law assumes that the gas

in the pore behaves as a perfect gas, which is an excellent approximation for our purposes. We shall also assume that all the gas precipitates (which is a less good approximation of course).

$$PV = nRT \quad (7.12)$$

where  $n$  is the amount of gas in gram moles<sup>-1</sup> (in much use of this equation,  $n$  is somewhat misleadingly assumed to be unity),  $R$  is the gas constant  $8.314 \text{ J K}^{-1} \text{ mol}^{-1}$ , and  $P$  is the applied pressure in  $\text{N/m}^2 = \text{Pa}$ .

The equation can be restated to give the volume  $V$  explicitly as:

$$V = nRT/P \quad (7.13)$$

It follows as a piece of rather obvious logic that the volume of the porosity is directly proportional to  $n$ , the amount of gas present in solution. This is graphically shown in Figure 7.36. The effect appears to have been well understood by Percy Riley, a well-known and irrepressible character in the early

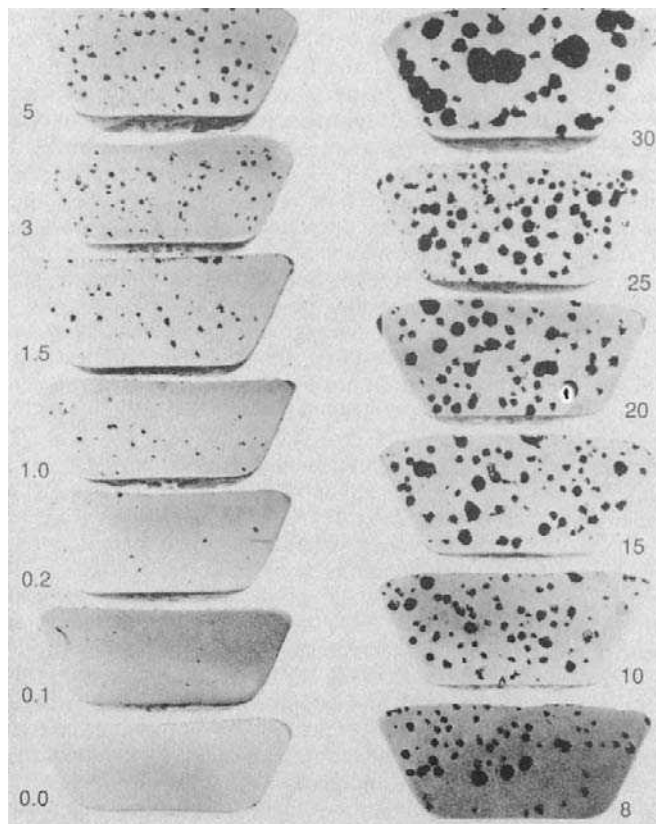


**FIGURE 7.36**

Gas porosity at various percentage levels in sectioned samples from the reduced pressure test. Courtesy of Stahl Speciality Co. (1990).

days of the development of the Al casting industry in the UK. He was an ex-Foseco employee working as a representative for Frankel Alloys Limited. He traveled around the country with a trunkload of potatoes in his car. All casting problems at that time were solved by adding potatoes to the melt. Clearly, the generous supply of hydrogen-expanded bifilms giving copious hydrogen porosity, but shrinkage problems were solved. Percy's approach is not necessarily recommended at this time.

The relation of hydrogen porosity to hydrogen content is revealed in Figure 7.36. This test shows cut sections of a small sample of melt cast into a metal cup about the size of an egg cup, and then solidified in vacuum. The test is sometimes known as the *Reduced Pressure Test (RPT)*, or the *Straube-Pfeiffer Test*. The solidification under reduced pressure expands the pores, making the test more sensitive and easier to use than the old foundry trick of pouring a small pancake of liquid onto a metal plate, and watching closely for the evolution of tiny bubbles (you need good eyes for this).

The general gas equation also shows that the volume of a gas is inversely proportional to the pressure applied to it. For instance, in the RPT, to determine the amount of hydrogen in a liquid aluminum alloy, the percentage porosity is commonly expanded by a factor of 10 by freezing at 0.1 atm (76 mmHg) residual pressure rather than at normal atmospheric pressure (760 mmHg).

This sensitivity to pressure needs to be kept in mind when using the test. For instance if the vacuum pump is overhauled and starts to apply not 76 mmHg but only 38 mmHg (0.05 atm) as a residual pressure, then the porosity in the test samples will be doubled, although, of course, the gas content of the liquid metal will be unchanged. Rooy and Fischer (1968) recommend that for the most sensitive tests the applied pressure should be reduced to 2–5 mmHg (approximately 0.003–0.006 atm). Clearly this will yield about a further ten-fold increase in porosity in the sample for any given gas content. However, care needs to be taken because these simple numerical factors are reduced by the additional loss of hydrogen from the surface of the test sample during the extra time taken to pump down to these especially low pressures, plus the losses of bubbles by bursting at the surface of the melt. In general, my experience is that a residual pressure of 76 mmHg (0.1 atm) is about right for all practical purposes, and most RPT kits operate at this value.

As has been mentioned before in the case of vacuum casting, the effect of pressure on pore growth is an excellent reason to melt and pour under vacuum, but to solidify under atmospheric pressure. It makes no sense to solidify under vacuum from the point of view of controlling porosity because pore expansion will act to negate the benefits of lower gas content (although solidification under vacuum may be important to prevent attack of the surface of the casting by nitrogen and oxygen if air is admitted to the vacuum chamber at an early stage). In terms of the general gas law, the pore volume  $V$  will be decreased by lower  $n$ , but increased correspondingly by low  $P$ . Whether the effects will exactly cancel will depend, among other things, on whether the melt has had time to equilibrate with the applied vacuum so as to reduce its gas content  $n$ . Taylor (1960) gives a further reason for not freezing under vacuum: For a nickel-based alloy containing 6% aluminum, the vapor pressure of aluminum at 1230°C is sufficient to form vapor bubbles at the working pressure of the vacuum chamber. He correctly concludes that the only remedy is to increase the pressure in the chamber immediately after casting. During the melting of TiAl intermetallic alloys at temperatures close to 1600°C, the evaporation of Al causes a loss of Al from the alloy, and a messy build-up of deposits in the vacuum chamber. Melting under an atmosphere of argon greatly reduces these problems. (However, pouring under argon cannot be recommended if the pouring is turbulent, because of the danger of the entrainment of argon bubbles; another reason for the adoption of counter-gravity filling of molds.)

If the rate of diffusion of the gas in the casting is slow, the volume of the final pore will be less than that indicated by the general gas law, and will be controlled by the time available for gas to diffuse into the pore. In Figure 7.5 the benefits of increasing feeder size seem to be enjoyed up to a critical size. After that any further increase in the feeder merely delays solidification of the casting so that gas porosity increases. The complete curve is therefore seen to be the sum of the effects of two separate curves. The first curve decreases linearly from about 7 to 0% porosity as shrinkage is countered by good feeding; and the second increasing parabolically from zero as more time is available for the diffusion of gas into pores as solidification time increases.

Although these general laws for the volume of a gas-filled cavity are well known and nicely applied in various models of pore growth (see for instance the elegant work by Kubo and Pehlke (1985), Poirier (1987) and Atwood and Lee (2000)) some researches have shown that the detailed mechanism of the growth of pores can be very different in some cases.

A direct observation of pore growth has been carried out for air bubbles in ice. At a growth rate of  $40 \mu\text{m s}^{-1}$ , Carte (1960) found that the concentration of gas built up to form a concentrated layer approximately 0.1 mm thick. He deduced this from observing the impingement of freezing fronts. When the bubbles nucleated in this layer, their subsequent rapid growth so much depleted the solution in the vicinity of the front that growth stopped and clear ice followed. The concentration of gas built up again and the pattern was repeated, forming alternate layers of opaque and clear ice.

On examination of the front under the microscope, Carte saw that the bubbles seemed to originate behind the front; the first 0.1 mm deep layer of solid appeared to be in constant activity; threads of air approximately  $10 \mu\text{m}$  in diameter spurted along what seemed to be water-filled channels, and were squeezed out of the ice. Sometimes bubbles arrived in quick succession, the first being pushed away and floating to the surface. Those bubbles that remained attached to the front would then expand, but finally be overtaken and frozen into the solid. It seems that pore growth might involve more turmoil than we first thought! Much of this activity arises, of course, from the expansion of the ice on freezing, and so forcing liquid back out of interdendritic channels. The opposite motion will occur in most metallic alloys as a result of the contraction on freezing. Also, it is to be expected that the movement in metals will be somewhat less frenetic. Nevertheless, no matter how the pore might grow in detail, we can reach some conclusions about the final limits to its growth.

Poirier (1987) uses the fact that the pore deep in a dendrite mesh will grow until it impinges on the surrounding dendrites. The radius of curvature of the pore is therefore defined by the remaining space between the dendrite arms. However, of course, although the smallest radius defining the internal pressure is now limited, the pore can continue to grow, forcing its way between the dendrite arms. Again, as has been mentioned before, an interdendritic morphology should not be taken as the definition of a shrinkage pore. Whether grown by gas or shrinkage, its morphology as spherical or interdendritic is merely an indication of the timing of its growth relative to the timing of the growth of the dendrites. Thus round pores have grown early. Interdendritic pores have grown late. Either can have been driven by gas or shrinkage, or both.

Fang and Granger (1989) found that hydrogen porosity in Al-7Si-0.3Mg alloy was reduced in size and volume percentage, and was more uniformly distributed, when the alloy was grain-refined. In this case the growth of bubbles will be limited by their impingement on grains. It may be that a certain amount of mass feeding may also occur, compressing the mass of grains and pores. In later work Poirier and co-workers (2001) confirm by a theoretical model that finer grains do reduce porosity to some degree.

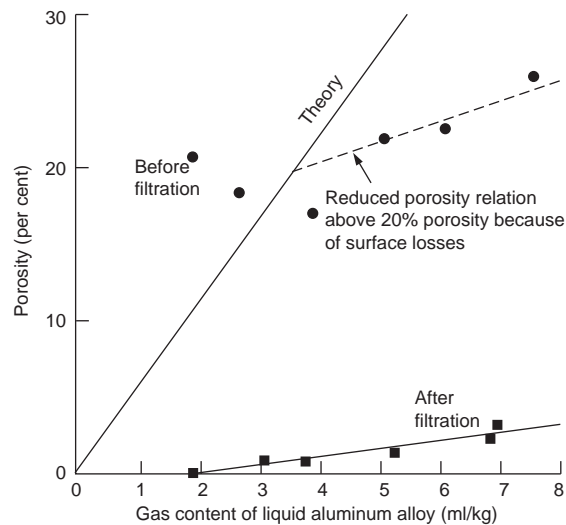


**FIGURE 7.37**

Porosity of Reduced Pressure Test samples frozen at 0.005 atm as a function of gas content. Data from Rooy and Fischer (1968).

Another limitation to growth occurs when the bubble can escape from the freezing front. This will normally happen when the front is relatively planar, and is typified by the example of the rimming steel ingot. In general, however, escape from a mesh of dendrites is likely to be rare.

A final limitation to growth is seen in those cases where the porosity reaches such levels that it cannot be contained by the casting. This occurs at around 20–30% porosity. During the freezing of the sample in the reduced pressure test, gas can be seen to escape by the bursting of bubbles at the surface of the sample. The effect is clearly seen in Figure 7.36. Also, Figure 7.37 shows that as gas is increased, measurements of porosity above 20% in such samples show a lower rate of increase of porosity than would be expected because of this loss from bubbles bursting at the surface, releasing their gas to the environment. (The theoretical curve in Figure 7.37 is based on 1% porosity in the solid being equal to 10 ml hydrogen in 1000 ml aluminum; this is equivalent to 10 ml hydrogen in 2.76 kg aluminum, or 0.362 ml hydrogen in 1 kg aluminum. Incidentally, Figure 7.37 also shows the enormous reduction in porosity as a result of increasing the difficulty of nucleation, because of the removal of nuclei by filtration. Clean metal makes better castings.)

It is worth drawing attention to the considerable volume of work over many years in which people have drilled into steel castings immersed in mercury or oil and have collected and analyzed the gases in pores. In almost every case the dominant gas was hydrogen. This led early workers to conclude that the bubbles were caused by hydrogen (see, for instance, the review of early work by Hultgren and Phragmen in 1939). This was despite calculations by Muller in 1879 that the CO pressure in pores in steel castings was up to 40 atmospheres, and the consequent correct deduction by Ledebur in 1882 that the hydrogen content of pores in steel castings at room temperature was the result of the continued accumulation of hydrogen after solidification was complete.



We can see that the high final hydrogen content of pores at room temperature is a natural consequence of the high rate of diffusion of hydrogen in both the liquid and solid states. Thus hydrogen is the dominant gas contributing to the growth of pores, and continuing to contribute additional gas during the cooling to room temperature.

Even after the casting reaches room temperature the growth of gas pores may still not be complete! Talbot and Granger (1962) showed that hydrogen in cast aluminum could continue to diffuse into pores in the solid state during a heat treatment at 550°C. Porosity was found to increase during this treatment, with pores becoming larger and fewer. With very long annealing in vacuum the hydrogen could be removed from the sample and the porosity could be observed to fall or even disappear.

Beech (1974) was perhaps the first to point out that the environment of a long bubble is not necessarily homogeneous. In other words, what may be happening at one end of the bubble may be quite different from what is happening at the other. This is almost certainly the case with the kind of subsurface porosity that continues to grow into an array of wormholes. The metal–mold reaction will continue to feed the base of the bubble, which of course remains within the diffusion distance of the surface. If the gas content of the melt is high the front of the bubble may also be gaining gas from the melt. However, if the melt has a low gas content, the front part of the bubble may lose gas. The bubble effectively acts as a diffusion short-circuit for the transfer of gas from the surface reaction to the center of the casting. The effect is shown in Figure 7.38.

Depending on the relative rates of gain and loss, the pore may grow, or even give off bubbles from the growing front. Alternatively it may stop growing and thus be overtaken by the dendrites and frozen into the thickening solid shell. The swellings and narrowings of these long bubbles probably reflect the variation in growth conditions, such as sudden variations in gap between the casting and the mold, or variations from time to time of convection currents within the casting.

The long CO bubbles in rimming steel ingots, cast into cast iron molds, were a clear case where the growing bubble was fed with gas from the growing front, and not from the mold surface.

Conversely, in aluminum bronze castings made in greensand molds Matsubara (1972) provides an elegant and clear demonstration of the feeding of the pore with gas from the mold, together with the combined effect of residual gas in the metal. Radiographs show wormhole porosity approximately 100 mm long. The amount of porosity was shown to increase as the gas content of the metal was increased, and as the water content of the molds was increased from zero to 8%. Halvae (1996)

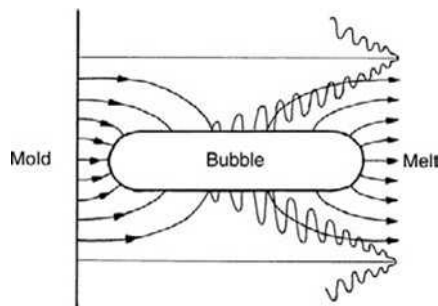


**FIGURE 7.38**

Subsurface pore growing in competition with dendrites, into a melt of low gas content. The pore gains gas by diffusion from the surface reaction, and loses it from its growing front (after Beech 1974).

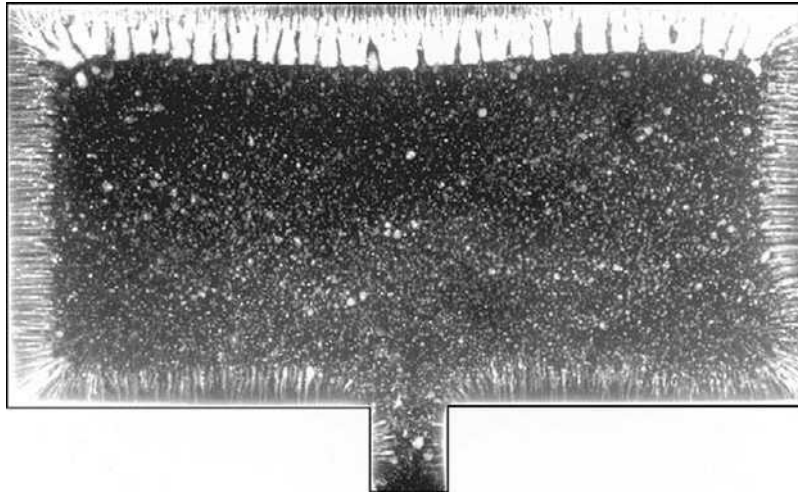


**FIGURE 7.39**

Radiograph of a Cu–10Al casting  $200 \times 100 \times 10$  mm with a high hydrogen content poured at  $1285^\circ\text{C}$  with gate velocity  $0.85 \text{ m s}^{-1}$  into a sand mold (Helvae 1997).

illustrates a similar structure for aluminum bronze cast into a sand mold bonded with a phenolic urethane resin (Figure 7.39). A proper melting procedure to give a low gas content in the melt prior to casting eliminated the porosity completely.

### Hydrogen porosity

It is important to remember that both water and hydrocarbons (which are available in abundance in most sand castings) can decompose at the metal surface, both releasing hydrogen. The surface of the melt and the casting will therefore have no shortage of hydrogen; in fact, from Section 4.4, it is seen that in general the mold atmosphere often contains up to 50% hydrogen, and may be practically 100% hydrogen in many cases.

What happens to this hydrogen?

Although much is clearly lost by convection to the general atmosphere in the mold, some will diffuse into the metal if not prevented by some kind of barrier (see later). If the hydrogen does manage to penetrate the surface of the casting, how far will it diffuse?

We can quickly estimate an average diffusion distance  $d$  from the useful approximate relation Equation 1.5,  $d = (Dt)^{1/2}$ . Some researchers increase the right-hand side of this relation by a factor of 2 in a token attempt to achieve a little more accuracy. We shall neglect such niceties, and treat this equation merely as an order of magnitude estimate. Taking the diffusion rate  $D$  of hydrogen as approximately  $10^{-7} \text{ m}^2 \text{ s}^{-1}$  for all three liquid metals, aluminum, copper, and iron (see Figures 1.4a–c), then for a time of 10 seconds  $d$  works out to be approximately 1 mm. For a time of 10 minutes  $d$  grows to approximately 10 mm.

Clearly, hydrogen from a surface reaction can diffuse sufficiently far in the time available during the solidification of an average casting to contribute to the formation and growth of subsurface porosity in most of our engineering metals.

The distance that the front has to travel before the solute peak reaches its maximum is actually identical to the figures we have just derived, as explained in Section 5.3.1. Thus conditions are exactly optimum for the creation of the maximum gas pressure in the melt at a point a millimeter or so under the surface of the casting. The high peak will favor conditions for the nucleation of pores whilst the closeness to the surface will favor the transport of additional gas, if present, from a surface reaction. Naturally, if there is enough gas already present in the melt, then contributions from any surface reaction will only add to the already existing porosity.

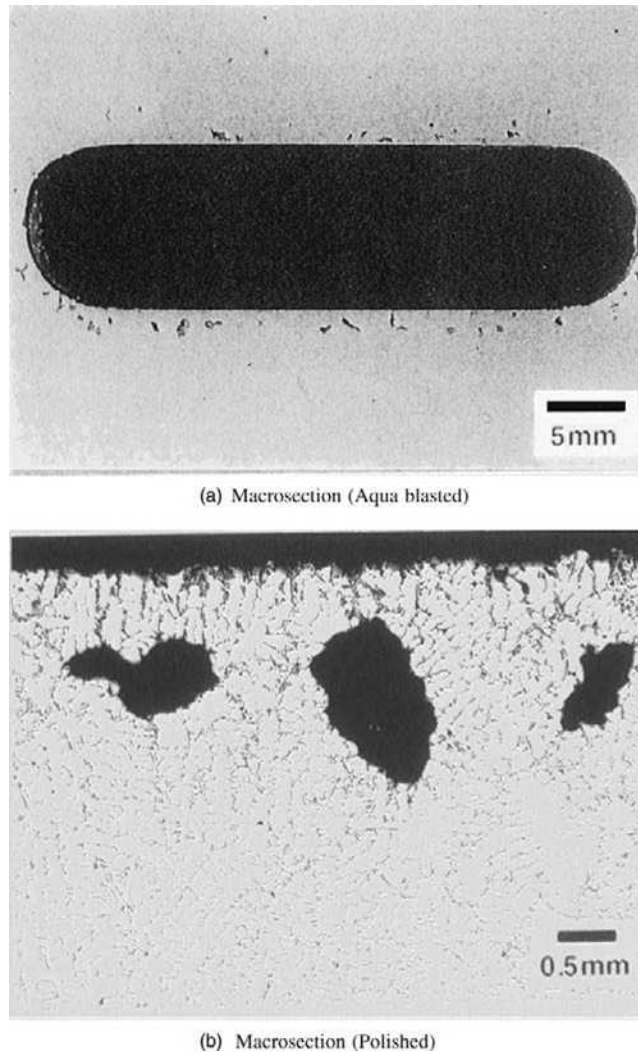
In an investigation of a wide variety of different binders for the molding sand, Fischer (1988) finds that subsurface porosity in copper-based castings is highly sensitive to the type of binder, although degassing and deoxidizing of the metal did help to reduce the problem. These observations are all in line with our expectations of contributing agencies.

In aluminum alloys where hydrogen gas in solution in the melt segregates strongly on freezing, the partition coefficient is approximately 0.05, corresponding to a concentrating effect of 20 times. Figure 7.40 shows subsurface porosity in an Al-7Si-0.4Mg alloy solidified against a sand core bonded with a phenolic urethane resin. The general gas content of the casting is low, so that pores are only seen close to the surface, within reach by diffusion of the hydrogen from the breakdown of the resin binder. Some of the pores in Figure 7.40a are clearly crack-like, and seem likely therefore to have formed on bifilms.

Close-up views of another casting showing subsurface porosity in the same alloy and same bonded sand (Figure 7.41a) confirms that the pores are of widely different form, some being perfectly round (Figure 7.41b), some dendritic (Figure 7.41c), and some of intermediate form (Figure 7.41d). It seems reasonable to assume that all the pores experienced the same environment, consisting of a uniform field of hydrogen diffusing into the melt from the degeneration of the core binder. Their growth conditions would therefore have been expected to be identical. Their very different forms cannot therefore be the result of growth effects (i.e. some are not shrinkage and others gas pores). The differences therefore must be a result of differences in ease of nucleation. The simple explanation is that the round pores nucleated early because of easy nucleation, and thus grew freely in the liquid. The dendrite-lined pores are assumed to have nucleated late, as a result of a greater difficulty to nucleate, so that they expanded when the matrix dendrites were already well advanced. The differences in ease of nucleation can be easily understood in terms of the randomly different conditions in which the nuclei, bifilms, are created. Some bifilms will come apart easily, whereas others will be raveled tightly, or may be partially bonded as a result of being older or being contaminated with traces of liquid salts from the surface of the melt.

The case of some subsurface pores initiating their growth very late, when freezing must have been 80% or more complete, raises an interesting extrapolation. If the bifilms had been even more difficult to open, or if not even present at all, then *no* pores would have nucleated. This situation may explain the well-known industrial experience, in which subsurface porosity comes and goes, is present one day, but not the next, and is more typical of some foundries than others. It is a metal quality problem.

Note that both round and dendritic pores can be both gas pores. They could also both be shrinkage pores, or both generated by combined gas + shrinkage contributions. Whether grown by gas or shrinkage, or both, the shape difference merely happens because of the timing of the pore growth in relation to the dendrite growth. Although it is common for gas pores to form early and so be rounded, and shrinkage pores to form late and so take on an interdendritic morphology, it is not necessary. It is very important not to fall into the standard trap of assuming that round pores result from gas and dendritic forms result from shrinkage.

**FIGURE 7.40**

(a) Polished section, lightly blasted with fine grit, showing subsurface porosity around a sand core in an Al-7Si-0.4Mg alloy casting of low overall gas content; and (b) an enlarged view of some pores on a polished section.

The work by Anson and Gruzleski (1999) describes particularly careful work in an attempt to distinguish between gas and shrinkage pores. Their study concentrated on the appearance and spacing of pores. They pointed out that on a polished section, groups of apparently separate, small interdendritic pores were almost certainly a single pore of irregular shape (Figure 7.42). Despite apparently clear differences in shape and spacing, it is finally evident in their case that all pores were gas pores,

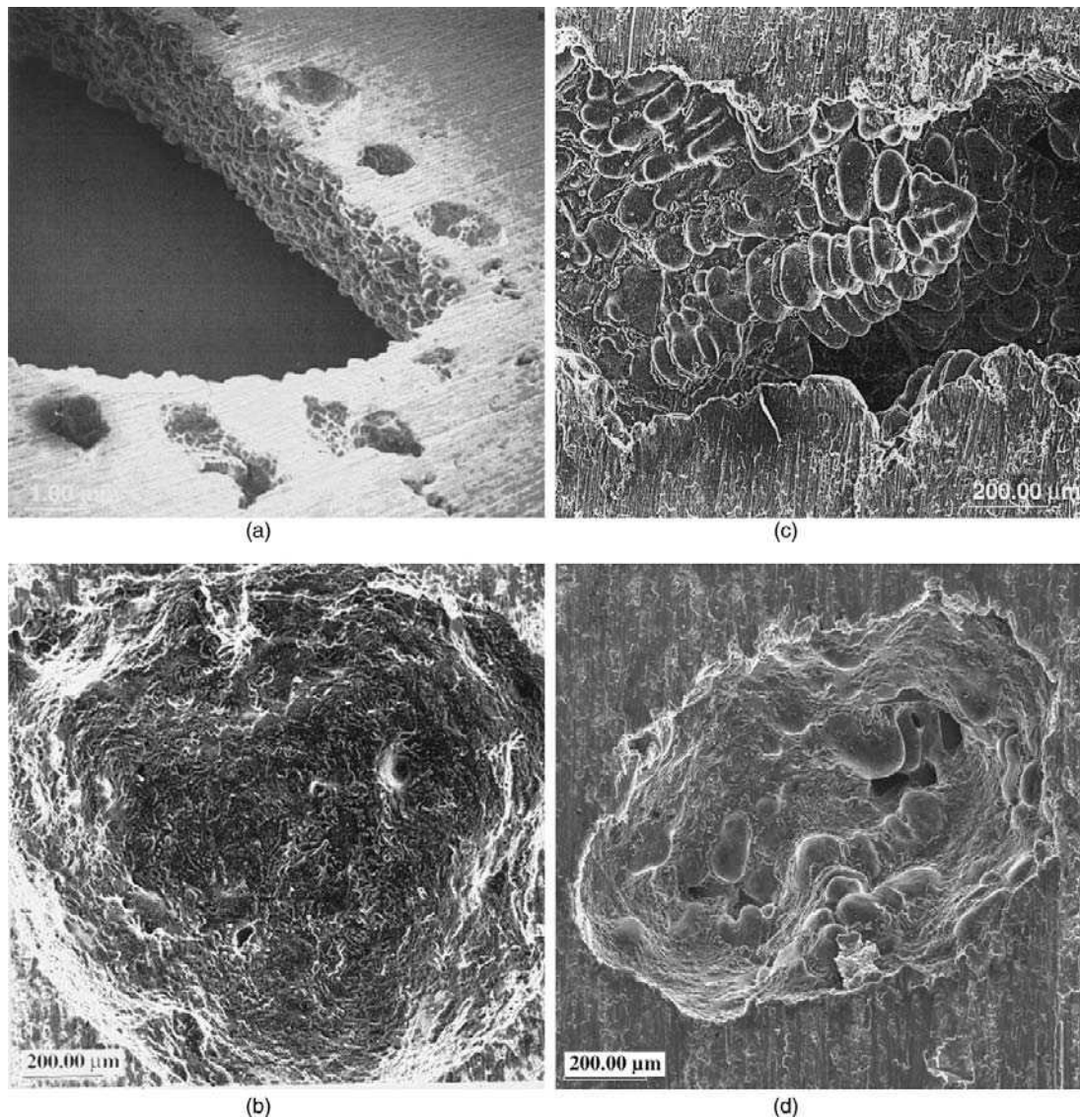


**FIGURE 7.41**

Thin slice of an Al-7Si-0.4Mg alloy casting taken from around a phenolic urethane bonded sand core.

(a) A general view, showing the sand-cast surface made by the core and several subsurface pores; and close-ups of (b) a spherical pore; (c) a dendritic pore; and (d) a mixed pore.

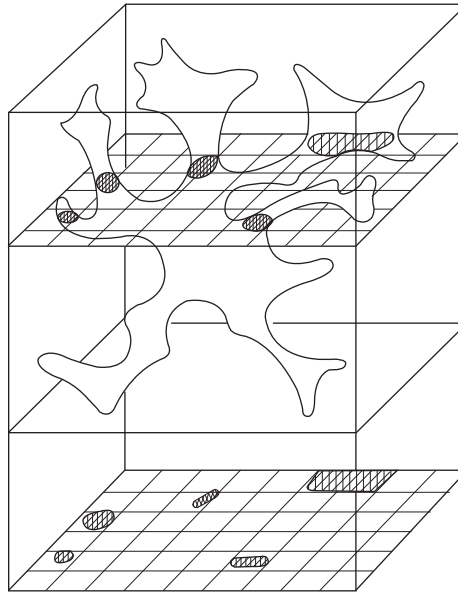


**FIGURE 7.42**

Complex interdendritic pore, appearing as a group of pores on a polished section (after Anson and Gruzleski 1999).

since they all grow at the same rate as hydrogen is increased. In this case the pores that were assumed to be shrinkage pores were almost certainly partially opened and/or late opened bifilms. Their irregular cuspid outlines probably derived partly from the irregular, crumpled form of the bifilms, together with their late opening in the interdendritic spaces. Such mis-identification of pore shapes is easily understood, and is common. We need to be on our guard against such mistakes.

### Carbon, oxygen, and nitrogen

For the case of the casting of aluminum alloys we have only to concern ourselves about hydrogen, the only known gas in solution.

For the case of copper-based alloys a number of additional gases complicates this simple picture. The rate of diffusion of oxygen in the liquid is not known, but is probably not less than  $10^{-8} \text{ m}^2 \text{ s}^{-1}$ . In the case of liquid iron-based alloys, oxygen and nitrogen diffuse at similar rates (Figure 1.4). Thus for all of these liquids the average diffusion distance  $d$  is 1–2.5 mm for the time span of 1–10 minutes. It seems therefore that all these gases can enter and travel sufficiently far into castings of all of these alloy systems to contribute to the formation of porosity.

In copper-based alloys the effect is widely seen and attributed to the so-called ‘steam reaction’ (Equation 6.3). It seems certain, however, that  $\text{SO}_2$  and  $\text{CO}$  will also contribute to the total pressure available for nucleation in copper alloys that contain the impurities sulfur and carbon. Carbon is an important impurity in Cu–Ni alloys such as the monels. Zinc vapor is also an important contributing gas in the many varieties of brasses and gunmetals.

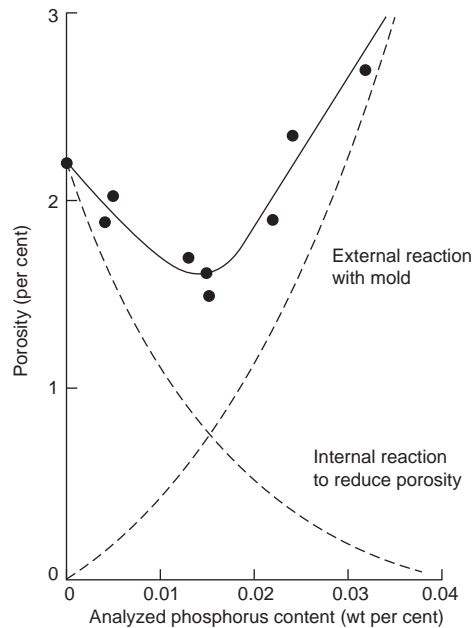


**FIGURE 7.43**

Effect of phosphorus on the porosity in 75-mm-thick plates of leaded gunmetal LG2 cast at 1100°C. Data from Townsend (1984).

From the point of view of nucleation the action of oxygen is likely to be central. This is because it is probably the most strongly segregating of all these solutes (with the possible exception of sulfur). Thus deoxidation practice for copper-based alloys is critical.

When gunmetal has been deoxidized with phosphorus, Townsend (1984) reports that an optimum rate of addition is required, as illustrated in Figure 7.43. Too little phosphorus allows too much oxygen to remain in solution in the melt, to be concentrated to a level at which precipitation of water vapor will occur as freezing progresses. Too much phosphorus will reduce the internal oxygen to negligible levels, suppressing this source of porosity. However, the melt will then have enhanced reactivity with its environment, the excess phosphorus picking up oxygen and hydrogen from a reaction at the metal surface with water vapor from the mold. The porosity in the cast metal is the result of the sum of these internal and external reactions, resulting in a minimum at approximately 0.015% phosphorus for the case of this particular sample of alloy.

A similar reaction occurs in gray iron in the presence of 0.005–0.02% aluminum or 0.04% titanium. The reaction is characterized by subsurface pores that have a shiny internal surface covered with a continuous graphite film. (The graphite film is present simply because the free surface provided by the pore allows the graphite to accommodate its volume expansion on precipitation most easily. Similarly, these pores are often seen to be filled with a frozen droplet of iron, again simply because the pore is an available volume into which liquid can be exuded during the period when the graphite expansion is occurring. Such droplets would be expected to be more common in casting

made in rigid molds, where the expansion could not be easily accommodated by the expansion of the mold.)

Carter (1979) describes the analogous problem caused by the presence of magnesium in *ductile iron*. Clearly, this double effect of the addition of a strong deoxidizer, resulting in an optimum concentration of the addition, is a general phenomenon.

In much of the work on *subsurface pores in irons and steels* the phenomenon is called *surface pinhole porosity*. This is almost certainly the result of the loss of the surface of the casting by a combination of oxidation and/or severe grit blasting, allowing the pores to be broken into, or simply uncovered. The *surface pinholes* almost certainly originated as *subsurface pinholes*.

In the case of low-carbon equivalent gray irons it is found that small surface pinholes occur that have an internal surface lined with iron oxide, and whose surrounding metal is decarburized, as witnessed by a reduction in the carbide content of the metal. Although Dawson (1965) and others make out a case for these defects to be the result of a reaction with slag, it seems more reasonable to suppose that once again the pores were originally subsurface, but the high oxygen content of the metal promoted early nucleation, with the result that the pores were extremely close to the surface of the casting. The thin skin of metal quickly oxidized, opening the pore to the air at an early stage, and allowing plenty of time for oxidation and decarburization whilst the casting was still at a high temperature. Tests to check whether the pores have been connected to the atmosphere do not appear to have ever been carried out.

Dawson reports that an addition of 0.02% aluminum usually eliminates the problem. This relatively high addition of aluminum is probably to be expected because the oxygen in solution in these low-carbon equivalent irons will be higher than that found in normal gray irons. However, if even higher levels of aluminum were added, the problem would be expected to return because of the increased rate of reaction with moisture in the mold, following the example in Figure 7.43.

Oxygen and carbon are important when CO is the major contributing gas, although, of course, in cast irons, where carbon is present in excess, the CO pressure is effectively controlled solely by the amount of oxygen present. This deduction is nicely confirmed for malleable cast irons by the Italian workers Molaroni and Pozzesi (1963), who found a strong correlation between their proposed 'oxidation index',  $I$ , defined as:

$$I = C + 4Mn + 1.5Si - 0.42FeO - 5.3$$

where the symbols for the elements carbon C, manganese Mn, etc., represent the weight percentage of the alloying elements in the iron. Compositions of irons that gave a positive index were largely free from pores, whereas those with an increasingly negative index were, on average, more highly porous.

In steels there are several gases that can be important in different circumstances. The most important are CO (Equation 6.5), N<sub>2</sub> (Equation 6.7), and H<sub>2</sub> (Equation 1.3). Since, at the melting point of iron, hydrogen has a solubility in the liquid of approximately 245 ml kg<sup>-1</sup> and in the solid of 69 ml kg<sup>-1</sup> (extrapolating slightly from Brandes (1983)), its partition coefficient is 69/245 = 0.28, with the result that it is concentrated ahead of the solidification front by a factor of 1.0/0.28 = 3.55. It therefore makes a modest contribution to the gas pressure for nucleation of pores in iron alloys.

Nitrogen seems to have a similar importance in nucleation. Its solubility at the melting point of iron is 0.0129 wt% in the solid and 0.044 wt% in the liquid (Brandes 1983), giving a partition coefficient 0.29, and a concentration effect for nitrogen ahead of the freezing front of approximately 3.4 times. Subsurface porosity is common when steels are cast into molds bonded with urea formaldehyde resin



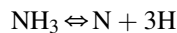
(Middleton 1970), or bonded with other amines that release ammonia,  $\text{NH}_3$ , on heating. These include hexamine in Croning shell molds (Middleton and Canwood 1967). The ammonia breaks down at casting temperatures to release both nitrogen and hydrogen. This situation has already been discussed in Sections 4.5 and 4.6 on metal–mold reactions.

Since  $k = 0.05$  for oxygen in iron, and  $k = 0.2$  for carbon in iron, the concentration factors are 20 and 5, respectively, so that when combined, the equilibrium CO pressure at the solidification front is  $20 \times 5 = 100$  times higher than in the bulk melt. (The distribution coefficients refer to bcc delta-iron; those for fcc gamma-iron would be nearer to unity, implying much less concentration ahead of the solidification front for solidification to austenite.) Because of the multiplying factor 100, oxygen in solution in the iron is the major contributing gas in the nucleation of CO gas pores during the solidification of many irons and steels.

### Nitrogen porosity

There has been a massive effort to understand the metal–mold reactions in which nitrogen is released. This gives problems in both iron and steel castings as subsurface pores. A review for steel castings is given by Middleton (1970).

The nitrogen problem in ferrous castings has resulted in the production of a whole new class of sand binders known as ‘low nitrogen’ binders. However, later work (Graham 1987) investigating the relation between total nitrogen content of the binder and the subsurface porosity and fissures in iron castings found no direct correlation. However, Graham did find a good correlation with the ammonia content of the binder. Ammonia is released during the pyrolysis of important components of many binders, such as urea, amines (including hexamine used in shell molds), and ammonium salts. The ammonia in turn will decompose at high temperature as follows:



thus nascent nitrogen and nascent hydrogen are released (the word *nascent* meaning *in the act of being born*, implying high reactivity of the atomic forms of these elements rather than their molecular forms). Both will contribute to the formation of pores in the metal. Both nitrogen and hydrogen will have a similar influence in the nucleation of a pore, concentrating strongly ahead of the freezing front. For the subsequent growth, however, hydrogen will be the major influence because of its much faster rate of diffusion. The fact that both gases are released simultaneously by ammonia explains the extreme effectiveness of ammonia in creating porosity. Nitrogen alone would not have been particularly effective. Even if it may have been successful in nucleating pores, without the additional help from hydrogen any subsequent growth would have been limited. The high rate of diffusion of hydrogen ensures that hydrogen dominates the growth of the pore. It is supplied by gas in solution in the liquid metal, and any fresh supply through the surface from a surface reaction.

It seems that ammonia can build up in greensand systems as the clays and carbons absorb the decomposition products of cores. Lee (1987) confirms that an ammoniacal nitrogen test on the molding sand was found to be a useful indicator of the pore-forming potential of the sand, even though the test was not a measure of total nitrogen.

The action of gases working in combination is illustrated by the work of Naro (1974) in his work on phenolic urethane–isocyanate binders. He showed that, from a range of irons, ductile iron (high carbon and low oxygen) was least susceptible and low-carbon equivalent irons (high oxygen) were most susceptible to porosity from the binder. Once again, it seems logical that the oxygen remaining in

solution in the iron plays a key role encouraging nucleation, nitrogen contributes modestly to both nucleation and growth, whereas hydrogen overwhelmingly dominates growth.

### Barriers to diffusion

In some unusual conditions, hydrogen appears to be prevented, or at least inhibited, from diffusing into some metals.

For magnesium alloys, potassium borofluoride ( $\text{KBF}_4$ ) has been known for many years to be an effective suppressant of metal–mold reactions for Mg alloys. In fact, if not added to the sand molds of some Mg castings both mold and casting will be consumed by fire – the ultimate metal–mold reaction! However, Al–5Mg and Al–10Mg casting alloys, and even Al–7Si–0.4Mg alloy, also benefit from  $\text{KBF}_4$  or  $\text{K}_2\text{TiF}_6$  additions to suppress reactions with the mold. We might speculate that liquid oxyfluorides, produced by the dissolution of the alumina film in the flux, assist to seal the surface of the liquid metal.

Naro (1974) confirms the widely reported fact that the addition of 0.25% iron oxide to phenolic urethane-isocyanate-bonded sands reduces subsurface pores in a wide range of cast irons. This is a curious fact, and difficult to explain at this time. One suggestion is that the oxide creates a surface flux, possibly an iron silicate. This glassy liquid phase is likely to reduce the rate at which gases can diffuse into the casting.

The rate of uptake of nitrogen in stainless steel is inhibited by the presence of silicon in the steel that, at certain oxidation potentials, forms  $\text{SiO}_2$  on the surface in preference to  $\text{Cr}_2\text{O}_3$  (Kirner 1988).

Even when the surface film consists only of a layer or so of adsorbed surface-active atoms, the presence of the layer reduces the rate at which gases can transfer across the surface. This happens, for instance, in the case of carbon steels: sulfur and other surface-active impurities hinder the rate at which nitrogen can be transferred. An excellent review of this phenomenon is given by Hua and Parlee (1982).

However, the precise mechanisms and effectiveness of many of these inhibition reactions are not clear at this time.

---

## 7.3 POROSITY DIAGNOSIS

### Gas porosity

To be able to take effective action to cure a porosity problem, the following table is designed to assist a diagnosis of the causes of porosity. The wide variety of gas porosity can usually be identified accurately with this guideline. Some care is needed where gas and shrinkage effects coincide, but these situations can also usually be identified with certainty (Table 7.3).

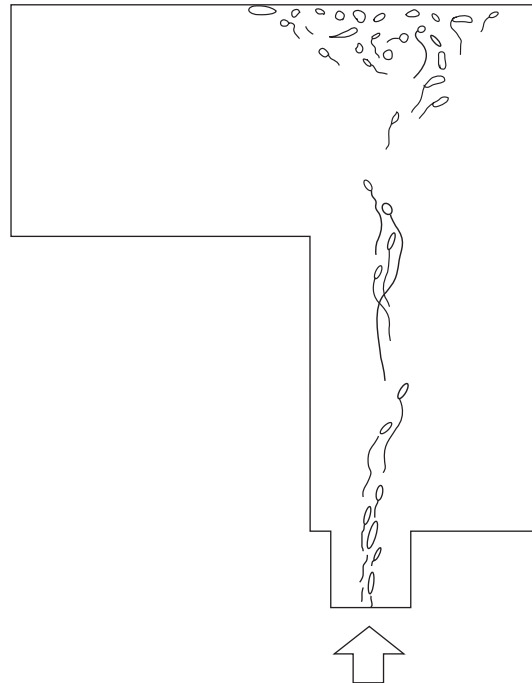
### Shrinkage porosity

The various forms of shrinkage cavity are summarized in Figure 7.46. Without exception, all the morphologies are dictated by (i) the *geometry* of the casting and (ii) *gravity*. These two key features allow shrinkage-dominated porosity to be clearly differentiated from other sources of porosity. The various forms that shrinkage porosity can take include:

1. Centerline porosity is formed in a skin-freezing alloy that has suffered an inadequate supply of liquid from the feeder. The geometry dictates that the pore is closely parallel to the thermal axis of the casting.

**Table 7.3** Porosity diagnosis summary

	Intrinsic (metallurgical defects)		Extrinsic (entrained casting defects)	
	Gas from solution in melt	Gas from mold reaction	Entrained air bubbles	Core blows
Spatial distribution	Uniform throughout casting	1–2 mm under surface	Clustered above ingates	Uniform depth under cope
Size (mm)	0.05–0.5	0.05–0.5	1–5	5–500
Features	Associated with bifilms in suspension in melt	Associated with bifilms in suspension in melt	Associated with oxides (solid oxides include bifilms + bubble trails) (liquid oxides include slags)	Connected by bubble trail to originating core
Examples		Figures 7.35, 7.45	Figure 7.44	

**FIGURE 7.44**

Good-quality melt, but turbulent filling creates air bubble pores and bubble trails concentrated above ingates.

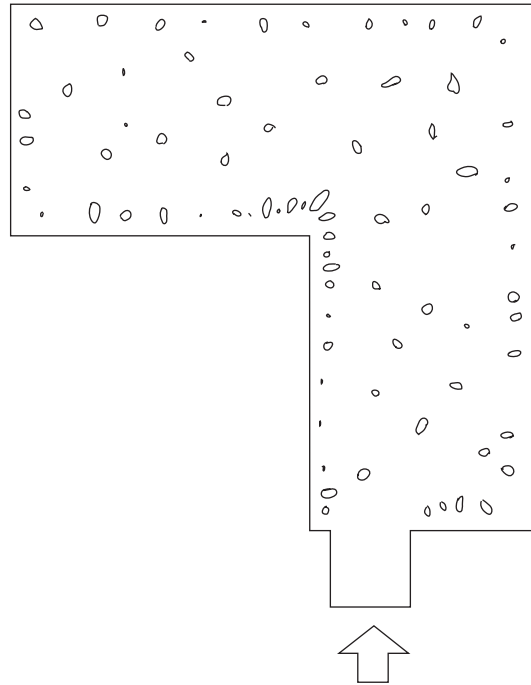


**FIGURE 7.45**

Good filling, but the bifilm population is inflated by higher hydrogen possibly originally in the melt, but supplemented by hydrogen from decomposition of the sand binder, leading to widespread porosity, with some concentration under the surface and especially near hot spots.

2. Sponge porosity. Formed in a long-freezing-range alloy, with adequate temperature gradient, but inadequate feed liquid from the feeder (e.g. Figure 7.8).
3. Layer porosity; the result of inadequate interdendritic feeding in a poor temperature gradient. The nucleation of internal porosity indicates a poor cleanness of the liquid metal. Geometry dictates that the pores are closely *at right angles* to the thermal axis of the casting.
4. Surface-initiated porosity generated in a long-freezing-range alloy in conditions of poor temperature gradient, but adequate cleanness of the melt.
5. Surface sink (external shrinkage porosity) formed in conditions of no liquid available from the feeder, but good cleanness of melt, in a relatively skin-freezing alloy, resulting in good solid feeding. Gravity dictates that the sink is usually sited on the cope surface of the casting.

Notice that the shrinkage pores are always influenced by the geometry of the casting, whether sometimes parallel to the axis of the casting as in centerline shrinkage, or (perhaps seemingly perversely) sometimes at right angles to the axis of the casting, as in layer porosity. Fortunately, the other major influence to the distribution of shrinkage porosity, gravity, is kinder to our intuition, acting only downwards.

If the porosity is clearly *not* strongly influenced by the shape of the casting and by gravity (for instance porosity in random locations, or well away from the thermal axis of the casting as in

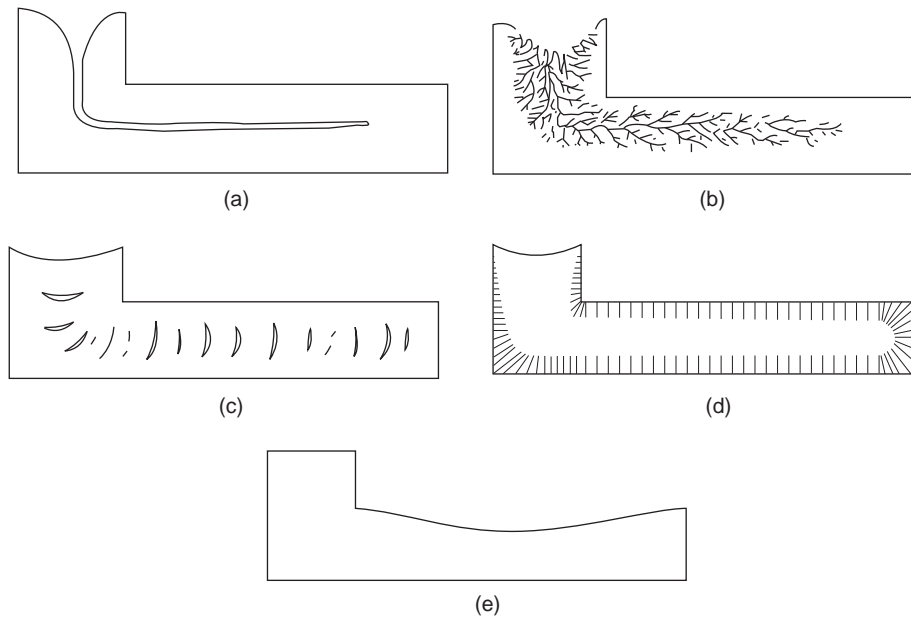


**FIGURE 7.46**

Summary of the various types of shrinkage porosity.

Figure 7.31d) we can conclude it is *not* shrinkage porosity. Very often, in fact most often, it will be porosity associated with masses of bifilms and bubble damage. This is a common variety of porosity that only ‘appears’ to be shrinkage porosity.

The casting engineer needs to keep at the forefront of the mind the fact that in *most* cases the pores are *not* shrinkage pores. Nearly all porosity I see identified on micrographs and labeled ‘shrinkage’ is actually oxides. The casting engineer needs to learn the phrase ‘It *appears* to be shrinkage’ and not ‘It is shrinkage’ bearing in mind that the pores are in nearly every case clusters of oxides together with entrained air, or bubble trails, introduced during the turbulence of the pour. These features disappear if the filling system design is good.

# Cracks and tears

# 8

## 8.1 HOT TEARING

### 8.1.1 General

A hot tear is one of the most serious defects that a casting can suffer. Although it has been widely researched, and is understood in a general way, it has remained a major problem in the foundries, particularly with certain alloys that are especially prone.

Over recent years the work by Rappaz (1999–2009) has provided illuminating details of the microscopic and mesoscopic behavior of metals leading to conditions in which hot tearing occurs. More will be said about this elegant work later in this chapter.

Even so, it has to be admitted that important insights into hot tearing behavior have emerged not only from scientific experiments in the laboratory, but from experience on the shop floor of foundries. However, these important shop floor findings have not been published in the scientific journals.

Briefly, for those that wish to read no further, the key result from the shop floor is that hot tearing can usually be eliminated in castings by simply improving the filling system. The improved systems are described in Chapter 10 onwards.

In the experience of the author, every hot tear, wherever it appears in a casting, can be eliminated by addressing the problems of the filling system. Once oxide bifilms are eliminated from the melt, the solidifying alloy cannot tear, reinforcing my conclusion that there is no such thing as a solidification defect; there are only casting defects. When subjected to a tensile strain by contraction of the casting, the material simply stretches, because metals are normally extremely soft and ductile at temperatures close to their melting points. It is essential to keep this basic piece of experience in mind while plowing through the details of this section. Thus while the traditional foundrymen cluster around the hot tear, discussing how the mold or core can be reduced in strength to reduce the stress on the contracting casting, my approach is to ignore the hot tear, simply taking it as the evid of a poor filling design. Thus the key action is to fix the filling design. The hot tear then disappears like magic. No action to reduce the strength of the mold or core is necessary.

This piece of practical experience appears to be disbelieved, or at least systematically overlooked, by every researcher in this field. This is a pity because there is much useful background that has been clarified by careful, systematic research over the years. This interesting background is reported here. It will become clear that it is consistent with the view that bifilms (as prior cracks suspended in the liquid) introduced by a poor running system are implicated as the fundamental cause, actually *becoming* the hot tear. Nevertheless, the patient reader will find it illuminating to review the experimental data, keeping in mind the fact that bifilms are the major underlying cause.

The reader should also note the large number of terms used for hot tearing, such as hot cracking, hot shortness, or hot brittleness. We shall use them interchangeably here.

### 8.1.1.1 Characteristics of a hot tear

The defect is easily recognized from one or more of a number of characteristics:

1. Its form is that of a ragged, branching crack, generally following intergranular paths. This is particularly clear on a polished section viewed under the microscope (Figure 8.1).
2. The failure surface reveals a dendritic morphology (Figure 8.1).
3. The failure surface is often heavily oxidized (prior, of course, to any subsequent heat treatment). This is more particularly true of higher temperature alloys such as steels.
4. Its location is often at a hot spot, and where contraction strain from adjoining extensive thinner sections may be concentrated.

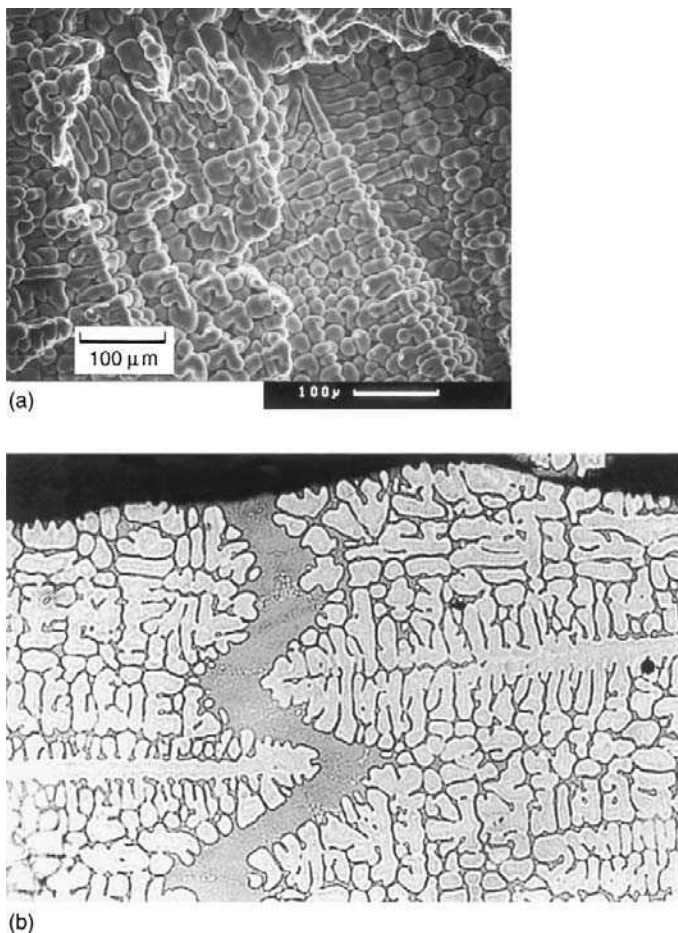


**FIGURE 8.1**

(a) SEM image of the surface of a hot tear in Al-7Si-0.4Mg alloy sand casting. (b) A filled hot tear in an Al-10Cu alloy (Spittle and Cushway 1983).

5. It does not always appear under apparently identical conditions; in fact it seems subject to a considerable degree of randomness in relation to its appearance or non-appearance, and to its extent.
6. The defect is highly specific to certain alloys. Other alloys are virtually free from this problem.

Before we go on to discuss the reasons for all this behavior, it is worth bearing in mind the most simple and basic observation:

*The defect has the characteristics of a tear.*

This disarmingly obvious characteristic immediately alerts us to a powerful clue about its nature and its origin. We can conclude that

*A hot tear is almost certainly a uniaxial tensile failure in a weak material.*

This may appear at first sight to be a trivial conclusion. However, it is fundamental. For instance, it allows us to make some important deductions immediately:

1. Those theories that assume hot tearing is the result of feeding difficulties can almost certainly be dismissed instantly. This is because feeding problems result in hydrostatic (i.e. a triaxial) stress in the residual liquid, causing pores or even layer porosity in the liquid phase. If the triaxial stress does increase to a level at which a defect nucleates, then the liquid separates and expands (triaxially) to create a pore among the dendrites. The dendrites themselves are not affected, and are not pulled apart. They continue to interlace and bridge the newly formed volume defect, as was discussed for layer porosity (Section 7.1.7.2).

This is in contrast to the hot tear, where it is clear from micrographs and X-ray radiographs (Figures 8.1b, 8.2) that the dendrites open up a pathway *first*. The opened gap drains free of liquid *later*.

The pulling apart of the dendrites, separating to form a eutectic-rich path through the structure (Figure 8.1b) probably brings with it no significant problems of loss of strength or other properties of the casting despite its alarming and unwelcome appearance on radiographs or cut sections. However, if the path had subsequently drained of eutectic liquid, a hot tear would have been formed, which would, of course, have seriously affected strength. This formation of an open tear might have been avoided if feed metal had been locally available to keep the interdendritic regions full of residual liquid.

A second confusion arises from the linking of hot tearing in general with the defect formed on the surface of the casting above a grossly underfed region. The collapse of the casting surface above this hot spot will deform the surface considerably, concentrating much strain in this local region. Thus a hot tear may form over this badly fed volume. The experimental arrangement described by Paray et al. (2000) is of this type. This special type of hot tear can also be solved by improving the local feeding.

2. If the defect is a tear then it has to be understood in terms of its initiation by exceeding a certain critical tensile stress, in common with all types of tensile failure. Rappaz and colleagues (1999) find a critical rate of tensile strain that will initiate a pore, finding that this gives a remarkably accurate estimate of the susceptibility to hot tearing. (The important work by Rappaz and his team will feature repeatedly in this review of the fundamentals of hot tearing.)



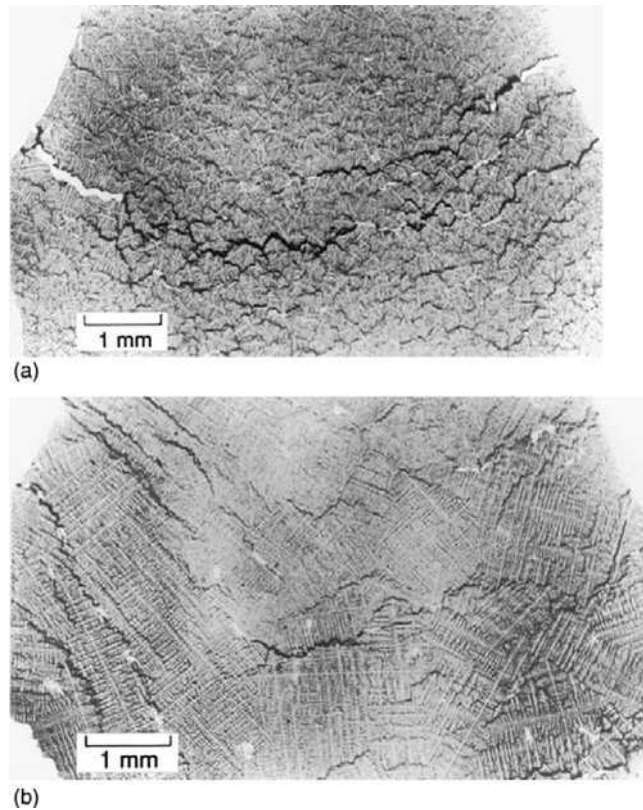


**FIGURE 8.2**

(a) Radiograph of a hot tear in an Al-6.6Cu grain-refined alloy. Dark regions are Cu-rich eutectic; white areas are open tears. (b) Radiograph of hot tears in Al-10Cu alloy not grain refined (Rosenberg et al. 1960. Courtesy of Merton C Flemings).

Keeping these general thoughts in mind will help us to keep the important features of the process in perspective, while we deal with a host of other aspects. It is not surprising that the research literature on this subject is confusing; the subject is genuinely complicated.

However, before proceeding with the details of the mechanisms associated with this defect, it is probably necessary to dismiss two other contenders for explanations of these hot failures. Dickhaus (1993) has proposed that the effect of surface tension, in the phenomenon of viscous adhesion, might explain hot strengths and the failure mechanisms of solidifying metals. However, simple order-of-magnitude estimates indicate that surface tension is perhaps capable of generating only one-hundredth, or even one-thousandth, of the stresses involved in hot tearing. In a quite different approach, Fredriksson (2005) has proposed that hot crack formation might occur because of the condensation of vacancies, expected to be present at concentrations of 0.01 to 0.1% in the metal lattice at these high temperatures. Vacancies are certainly present at maximum equilibrium concentrations at the melting point of metals, and certainly condense

during cooling. However, in practice, vacancies have never been observed to condense into volume defects such as cracks and pores. In every case examined, and in every metal studied so far, vacancy clusters collapse into either dislocation rings or stacking fault tetrahedra. These studies include direct observation in the electron microscope, and computer simulations of the behavior of large assemblies of atoms (known as molecular dynamics simulations). Basically, the forces between atoms are so great that pores or cracks cannot be opened up without the imposition of huge stresses in the GPa range. Solidifying metals are in general soft and ductile near their melting points, and so cannot generate and sustain such stresses (Campbell 2010).

This leaves us clear to study the more likely contenders for the generation of these defects.

### 8.1.2 Grain boundary wetting by the liquid

It was C S Smith who, over the years 1949 to 1952, first formulated the concept of the wettability of grain boundaries by the presence of a liquid phase in the boundary. Figure 8.3 summarizes his concept. The shape of the grain boundary particles is largely controlled by the relative surface energies of the grain-to-grain interface itself,  $\gamma_{gg}$ , and the grain-to-liquid interface,  $\gamma_{gL}$ . The balance of forces is:

$$\gamma_{gg} = \gamma_{gL} \cos \theta \quad (8.1)$$

It is clear that for most values of the equilibrium dihedral angle  $2\theta$  the grain boundary liquid assumes compact shapes. However, it will, of course, occupy a greater area of the boundary as its volume fraction increases. The relation between (1) the area of the boundary which is occupied by liquid, (2) the dihedral angle, and (3) the volume fraction of liquid present is a complicated geometrical calculation which the author was proud to identify and tackle (Campbell 1971), setting off the subsequent improved treatment by Tucker and Hochgraf (1973), and, finally, the comprehensive solution by Wray (1976). Hochgraf (1976) went on later to develop a fascinating study of the conditions for the spread of the liquid phase under non-equilibrium conditions, where the dihedral angle becomes effectively less than zero.

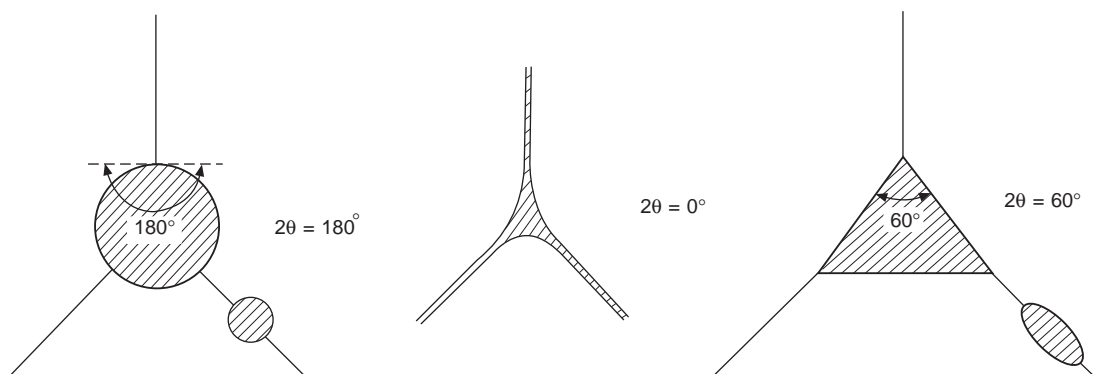


**FIGURE 8.3**

Shapes of the liquid phase at grain corners as a function of the dihedral angle (Smith 1948, 1952).

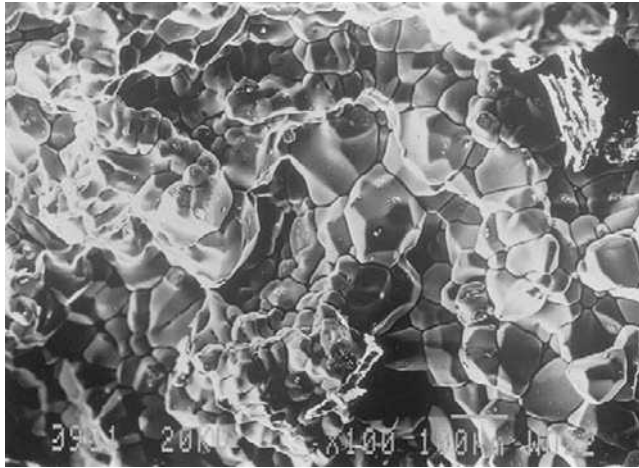


**FIGURE 8.4**

Hot tear surface of an Al-1%Sn alloy (courtesy of Chakrabarti 1999)

The importance of the dihedral angle being zero for complete wetting is illustrated in the work of Fredericksson and Lehtinen (1977). They observed the growth of hot tears in the scanning electron microscope. In Al-Sn alloys the liquid tin wetted the grain boundaries of the aluminum, leading to intergranular brittle failure when subjected to tension (Figure 8.4). In Al-Cd alloys, the liquid cadmium at the grain boundaries did not wet and therefore did not spread over the boundaries, but remained as compact pools, causing these alloys to fail by ductile fracture.

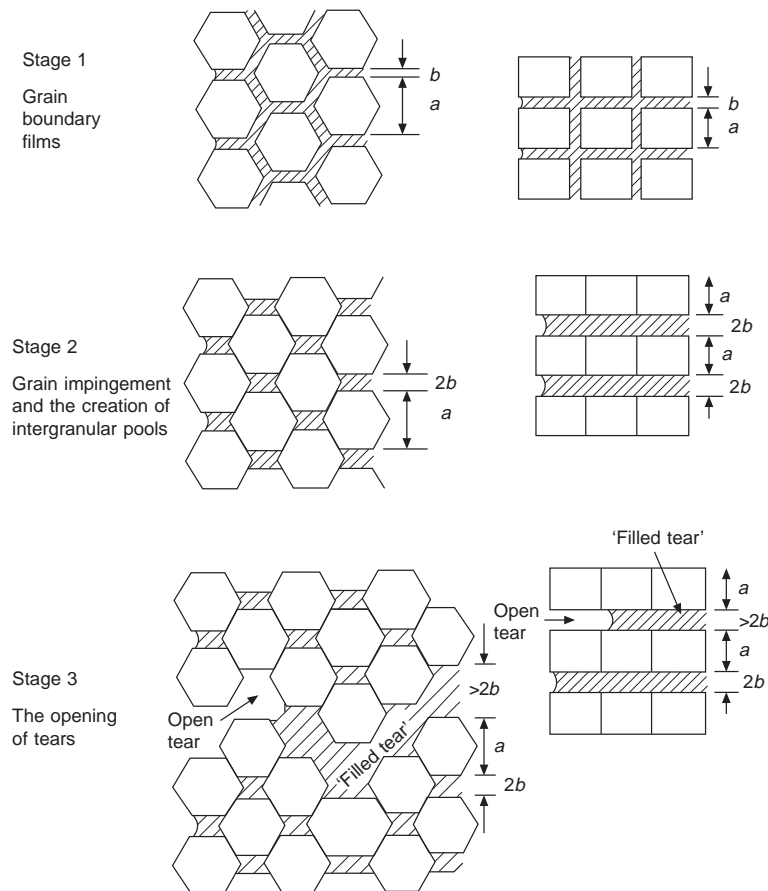
There have been a number of observations of failure by hot tearing where, on subsequent observation under the microscope, the fracture surface has been found to exhibit separate, nearly spherical droplets that appear to be non-wetting towards the fracture surface. This has been seen in systems as different as Al-Pb (Roth et al. 1980) and Fe-S (Brimacombe and Sorimachi 1977, Davies and Shin 1980). It seems certain that the liquid phase would wet a normal grain boundary. It is not clear therefore whether the observation is to be explained by the subsequent de-wetting of the liquid phase after the crack is exposed to the air, or because the boundary consists of a poorly wetted oxide bifilm.

### 8.1.3 Pre-tear extension

Whilst the casting is cooling under conditions in which liquid and mass feeding continue to operate, if the casting is contracting the solid grains swim about, maneuvering into new positions. In these conditions clearly no tearing can occur. The problem starts when grains grow to the point at which they finally collide firmly against each other, but are still largely surrounded by residual liquid.

Patterson and co-workers (1967) were among the first to consider a simple geometrical model of cubes. We shall develop this concept further as illustrated in Figure 8.5. It is clear that for grains of average diameter  $a$  separated at first by a liquid film of thickness  $b$ , the pre-tear extension  $\varepsilon$  is approximately:

$$\varepsilon = b/a \quad (8.2)$$

**FIGURE 8.5**

Stages of hot tearing using 2-D square and hexagonal grain models. Grains size ' $a$ ', are surrounded by a liquid film of thickness ' $b$ '. Stage 1: unstrained structure; stage 2 shows isolated regions of segregate; stage 3 shows open tears plus so-called 'filled' hot tears. Continued strain eventually will drain the liquid film completely, completing the tear.

For both the cube and the hexagon models in two dimensions the relation  $b/a = f_L/2$  can quickly be seen to be true, where  $f_L$  is the volume fraction of liquid. For a three-dimensional cube model the reader can easily confirm the further relation:

$$b/a = f_L/3 \quad (8.3)$$

Thus for between 3 and 6% residual liquid phase we have between 1 and 2% extension prior to the impingement of the grains. The pre-tear extension being proportional to the amount of liquid present is an observation confirmed many times by experiment. Furthermore, those alloys with large amounts of eutectic liquid during freezing, such as the Al-7Si and higher Si alloys, are usually free from hot tear

problems probably for this reason; there is plenty of extension that can be accommodated prior to any danger of the initiation of a tear.

Also, for a given amount of liquid present, the extension is inversely proportional to the grain size. Thus for finer grains, more strain can be accommodated by easy slip along the lubricated boundaries without the danger of cracking.

After the grains have impinged, a certain amount of grain boundary sliding may continue, as we shall discuss below, although this later phase may contribute only a very limited amount of further extension.

Even in the case of the solidification of pure metals, the grain boundaries are known to have a freezing point well below that of the bulk crystalline material (see, for example, Ho et al. (1985) and Stoltz et al. (1988)). The presence of liquid at the grain boundaries even in pure metals, but perhaps only a few atoms thick, may help to explain why some workers have found tearing behavior at temperatures apparently below the solidus temperature. However, many of the observations are also explainable simply by the presence of minute traces of impurities that have segregated to the grain boundaries. The two effects are clearly additive.

Because of the presence of the grain boundary film of liquid, bulk deformation of the solid will occur preferentially in the grain boundaries, so long as the strain is below a critical value (Burton and Greenwood 1970). This explains why the extension of the solid during fracture can be accounted for completely by the sum of the effects of (i) grain boundary sliding plus (ii) the extension due to the opening up of cracks (Williams and Singer 1968).

Later, during grain boundary sliding where the grains are now in contact over their complete surfaces, there has to be some deformation of the grains themselves. Novikov and Novik (1966) found by careful X-ray investigation that the deformation is confined to the surface of the sliding grains. In addition, at a temperature close to the melting point, recovery of the grains is so fast that they do not work harden. Because they remain in a relatively soft condition the general flow of the bulk material can continue relatively easily. Thus although the flow is now actually controlled by bulk deformation of the grains, the appearance under the microscope is simply that of the sliding of the grains along their boundaries.

It is necessary to keep in mind that the total extension due to the various kinds of grain boundary sliding (whether 'lubricated' or not) amount to only perhaps 1 or 2% strain. Further strain of at least this magnitude arises during the extension of the crack itself, as is discussed below.

### 8.1.4 Strain concentration

It was Pellini in 1952 who drew attention to the concentration of strain that could occur at a hot spot in a casting. It is instructive to quantify Pellini's theory by the following simple steps.

If the length of the casting is  $L$ , and if it has a coefficient of thermal expansion  $\alpha$ , during its cooling by  $\Delta T$  from the liquidus temperature it will contract by an amount  $\alpha\Delta TL$ . If all this contraction is concentrated in a hot spot of length  $l$ , then the strain in the hot spot is given by:

$$\varepsilon = \alpha\Delta TL/l \quad (8.4)$$

Clearly, in the hot spot the casting contraction strain is increased by the factor  $L/l$ .

For a casting 300 mm long and a hot spot of approximately 30 mm length at its end, the strain in the hot spot is concentrated ten times. This would be expected to be a fairly typical result – although it seems possible that strain concentrations of up to a hundred or more may sometimes occur.

It is interesting to note that the problem in the hot spot depends on the amount of strain concentrated in it, and this depends on the size of the adjacent casting and the temperature to which it has cooled while the hot spot remains hot and in a weak state.

We can clarify the size of the problem by evaluating an example of an aluminum casting. Assume that  $\alpha = 20 \times 10^{-6} \text{ C}^{-1}$  and that the casting has cooled  $100^\circ\text{C}$ . If its contraction is hindered, the strain that will result is, of course,  $20 \times 10^{-6} \times 100 = 0.002 = 0.2\%$ . This level of strain puts the material as a whole above the elastic limit even at room temperature. (In materials that do not show clear yield points, the yield stress is often approximated to the so-called proof stress, at which 0.1 or 0.2% permanent strain remains after unloading.) In the hot spot, therefore, if the strain concentration factor lies between 10 and 100, then the strain will be between 2 and 20%. These are strains giving an amount of permanent plastic extension that is relatively easily withstood by sound material. However, in material that is weakened by the presence of bifilms at the grain boundaries, and which can withstand typically only 1 or 2% of strain prior to failure, as we shall see below, it is no wonder that the casting fails.

In addition to the consideration of the amount of strain concentrated into the hot spot, it is also necessary to consider how many grain boundaries the hot spot will contain. If the grain size is coarse, the hot spot may contain only one boundary, with almost certain disastrous consequences, because all the strain will be concentrated in that one liquid film. If the hot spot contains fine grains, and thus many boundaries, then the strain per boundary is reduced. We may quantify this, since the number of grains in the length  $l$  of the hot spot is  $l/a$  for grains of diameter  $a$ . Hence if we divide the strain in the hot spot (Figure 8.4) by the number of boundaries in it, then we have the strain per boundary  $\varepsilon_b$

$$\varepsilon_b = \alpha \Delta T L a / l^2 \quad (8.5)$$

It is clear that to reduce the strain that is trying to open up the individual grain boundaries, the beneficial factors include (i) reduced temperature differences, (ii) smaller overall lengths between hot spots, and (iii) finer grain size. However, Equation 8.5 reveals for the first time that the most sensitive parameter is the length  $l$  of the hot spot; if this is halved, the grain boundary strain is increased four times.

### 8.1.5 Stress concentration

The problem of how sufficient stress arises during cooling to initiate and grow the hot tear may not be relevant. This is because the forces available during cooling are massive, greatly exceeding what is necessary to create a failure in the rather weak casting. Thus we may consider the forces available as being irresistible, forcing the casting to deform. Since this deformation will always occur, the question as to whether a hot tear will arise is clearly *not* controlled by stress, but must depend on other factors, as we shall discuss in this section.

Nevertheless, although overwhelmed, the forces of resistance offered by the casting are not quite negligible. Guven and Hunt (1988) have measured the stress in solidifying Al–Cu alloys. Although the stresses are small, they are real, and show a release of stress each time a crack forms. The loads at which failure occur are approximately 50 N in a section  $20 \text{ mm} \times 20 \text{ mm}$ . Thus the stresses are approximately 0.1 MPa (compared to a strength of over 100 MPa at room temperature). Also, as an interesting detail, a simultaneous change in the rate of heat transfer across the casting–mold interface was detected each time the force holding the casting against the mold was relaxed.

In rough agreement with Guven and Hunts' results, Forest and Berovici (1980) carried out careful tensile tests and found that an Al-4.2Cu alloy has a strength of over 200 MPa at 20°C, which falls to 12 MPa at 500°C, 2 MPa at the solidus temperature, and finally to zero at a liquid fraction of about 20%.

As we have mentioned before, the other stress that may be present could be a hydrostatic tensile stress in the liquid phase. Although this may contribute to the nucleation of a pore, which in turn might assist the nucleation of a tear, the presence of a *hydrostatic* stress is clearly not a necessary condition for the formation of a tear, as we have discussed earlier. We need a *uniaxial* tensile stress to create a tear.

One final point should be emphasized about stresses at these high temperatures. Because of the creep of the solid at high temperature, any stress will depend on the rate of strain. The faster the solid is strained, the higher will be the stress with which it resists the deformation.

Zhao and colleagues (2000) have determined the rheological behavior of Al-4.5Cu alloy, and thereby have determined the stress leading to the critical strain at which hot tearing will cause failure. This novel approach may require the densities of bifilms to be checked for similarity between their rheological sample and their hot tearing test piece, which is clearly poured rather badly. The elegant test piece devised by Rappaz and his team (Mathier 2009) has no defined filling technique, and one can only assume that the filling is poor, manufacturing entrainment defects that will confuse the results. It would be valuable to redefine this attractive-looking test to ensure that it could be filled without compromising the quality of the metal being tested.

### 8.1.6 Tear initiation

Probably the most important insight into the problem of tear initiation was provided by Hunt (1980) and Durrans (1981). Until this time the nucleation of a tear was not widely appreciated as a problem. The tear was assumed simply to form! The experiment by these authors is an education in profound insight provided by a simple technique.

These researchers constructed a transparent cell on a microscope slide that enabled them to study the solidification of a transparent analog of a metal. The cell was shaped to provide a sharp corner around which the solidifying material could be stretched by the turning of a screw. The idea was to watch the formation of the hot tear at the sharp corner.

The amazing outcome of this study was that no matter how much the solidifying material was stretched against the corner it was not possible to start a hot tear in clean material: the freezing mixture continued to stretch indefinitely, the dendrites continuing simply to move about and rearrange themselves.

However, on the rare occasion of the arrival of a small inclusion or bubble near the corner, then a tear opened up immediately, spreading between the dendrites and away from the corner. In their system, therefore, hot tearing was demonstrated to be a process dependent on nucleation. In the absence of a nucleus a hot tear did not occur no matter how much strain was applied. This fact immediately explains much of the scattered nature of the results of hot tearing work in castings: apparent identical conditions do not give identical tears, or at times even any tears at all.

It is necessary to remember that in the Hunt and Durrans' work the liquid would wet the mold, adhering to the sharp corner, and so would require a volume defect to be nucleated; the defect would not be created easily. In the case of a casting, however, a sharp re-entrant corner may have liquid

present at the casting surface, but the liquid will not be expected to wet the mold. In fact there is the complication that the liquid will be retained inside the surface oxide. The drawing of liquid away from this surface, analogous to the case of surface-initiated porosity, would represent the growth of the crack from the surface, and may involve a rather minimal nucleation difficulty. Thus in the case of cracks initiated at the surface, the Hunt and Durrans observation may not apply universally. However, the concept is still of value, as we shall discuss immediately below. In the case of internal hot tears their observation remains crucial. However, in the case of alloys that form strong oxide skins there may still be a difficulty in drawing inwards a rather rigid surface film, or of nucleating a tear on the underside of the surface oxide film; either way, surface initiation might be difficult in many casting alloys.

However, even at the surface of a casting in an alloy that does not form a surface film, the initiation of a tear may not be straightforward. It is likely that the tear will only be able to start at grain boundaries, not within grains. This is because the dendrites composing the grain itself will be interconnected, all having grown from a single nucleation site. Dendrites from neighboring grains will, however, have no such links, and in fact the growing together and touching of dendrite arms has not been observed in studies of the freezing of transparent models. The arms are seen to approach, but final contact seems to be prevented by the flow of residual liquid through the gap. Thus if a grain boundary is not sited conveniently at a hot spot, and where strain is concentrated, then a tear may be difficult to start. This will be more common in large-grained equiaxed castings, as suggested by Warrington and McCartney (1989).

If a grain boundary is favorably sited, it may open along its length. However, on meeting the next grain, which in general will have a different orientation, further progress may be arrested, at least temporarily. Thus a tear may be limited to the depth of a single grain. The effect can be visualized as the first stage of the spread of the tear in the hexagon grain model shown in Figure 8.5. Considerably more strain will be required to assist the tear to overcome the sticking point in its further advance beyond the first grain.

For the case of columnar grains, the boundaries at right angles to the tensile stress direction will provide conditions for easy initiation of a tear along such favorably oriented grain boundaries. The effect is analogous to the rectangular grain model in Figure 8.5.

For fine-grained equiaxed material where the grain diameter can be as small as 0.1–0.2 mm, the dispersion of the problem as a large number of fine tears, all one grain deep, is effectively to say that the problem has been solved. This is because the crack depth would then be only approximately 0.1 mm. This is commensurate with the scale of surface roughness, because average foundry sands also have a grain size in the range 0.1–0.2 mm. The fine-scale cracking would have effectively disappeared into the surface roughness of the casting.

Nevertheless it is fair to emphasize that the problem of the nucleation of tears has been very much overlooked in most previous studies. Nucleation difficulties would help to explain much of the apparent scatter in the experimental observations. A chance positioning of a suitable grain boundary containing, by chance, a suitable nucleus, such as a folded oxide film, would allow a tear to open easily. Its chance absence from the hot spot would allow the casting to freeze without defect; the hot spot would simply deform, elongating to accommodate the imposed strain.

In practice there is much evidence to support the assertion that most hot tears initiate from entrained bifilms. As has been mentioned above, the author has personally solved every hot tearing problem he has encountered in foundries by simply improving the design of the casting filling system. The proposal to use such an approach has generated almost universal disbelief and scorn. However, when implemented systematically in an aerospace foundry, all hot tearing problems in the difficult Al–4.5Cu–0.7Ag



(A201) alloy disappeared, to be replaced by surface sink problems. In comparison to the hot tears, the surface sinks were welcomed, and easily dealt with by improved feeding techniques (Tiryakioglu 2001).

The study by Chadwick and the author (1997) of A201 alloy poured by hand into a ring mold containing a central steel core showed that failure by hot tearing in such a constrained mold was almost guaranteed. Conversely, when the metal was passed through a filter, and caused to enter the mold uphill at a speed of less than  $0.5 \text{ m s}^{-1}$  to ensure the avoidance of defects, no rings exhibited hot tears. This was an amazing result, showing no failures in one of the world's most hot-tear-prone alloys, in a test designed to maximize hot tearing. (Memorably, when Chadwick arrived in my office to report the results of the hot tearing test, he declared the test a failure, saying 'What was the use of a hot tear test that did not hot tear?' I was speechless. A rare moment for me.)

A similar study was repeated for Al–1%Sn alloys by Chakrabarti (2000). Surfaces of hot torn alloys illustrate the brittle nature of the failure in this alloy (Figure 8.4). The alloy has such a large freezing range, close to  $430^\circ\text{C}$  (extending from close to pure Al at  $660^\circ\text{C}$  down to nearly pure Sn at  $232^\circ\text{C}$ ) that in the hot tear ring test the alloy appears even more susceptible to failure by hot tearing than A201 alloy. When subjected to the uphill filled version of the ring test most castings continued to fail. However, about 10% of the castings solidified without cracks. Once again, the existence of even one sound casting would be nothing short of amazing.

Further evidence can be cited from the work of Sadyappan et al. (2001) who demonstrated that their as-melted Al alloy gave many and large hot tears, whereas after cleaning the metal by degassing they observed only a few small tears. Dion et al. (1995) found that in their castings of yellow brass, the addition of aluminum to the alloy promoted hot tearing, as would be expected from the presence of the entrained alumina film resulting from their very turbulent filling system.

### 8.1.7 Tear growth

We have touched on the problem of tear growth in the previous section. However, it bears some repeating that (1) the birth of the hot tear and (2) its growth, sometimes to awesome maturity, are really separate phenomena.

The evidence is growing that tears are closely associated with bifilms. It remains to clarify the nature of the link. For instance (i) do tears initiate on bifilms and subsequently extend into the matrix alloy? or (ii) do bifilms constitute the tears, so that the growth of the tear is merely the opening of the bifilm, so that the defect is revealed, in fact becoming obvious? The evidence is accumulating that the important mechanism is (ii).

The easy growth in columnar grains where the direction of tensile stress is at right angles to the grain boundaries has been mentioned. Spittle and Cushway (1983) observed that the linear boundary formed between columnar crystals growing together from two different directions was an especially easy growth route for a spreading crack. This is confirmed by experience in the rolling industry, where the diagonal plane issuing from the corners of rectangular ingots, defining the joint plane of the two sets of columnar grains from the two adjacent sides, is a common failure plane during the early reduction passes. The problem is reduced by rounding the corners, or reducing the levels of critical impurities. In steel ingots the significant impurities are usually sulfur, and the so-called tramp elements such as lead and tin.

The explanation in terms of bifilms is that columnar grains push the bifilms into the intergranular spaces, so that failure along these surfaces is to be expected. The presence of an invisibly thin film

organized into position between dendrite arms explains the fracture surface seen in Figure 8.1a. The fracture follows the bifilm, the fracture surface exhibiting steps at integral numbers of dendrite arms, as explained in Figure 2.43. Naturally, the hot tear morphology is also seen in the room temperature fracture seen in Figures 2.44 and 6.30. Clearly, after being extended and flattened by the growth of dendrites, the bifilm is simply a hot tear waiting to be opened and so be revealed. If is not opened during solidification, then it can wait until opening later in a tensile test, or, more worryingly, opening to create a failure in service.

An X-ray radiograph of an Al alloy (Figure 2.43c) by Fox and Campbell (2000) in which the bifilms have been opened up by the action of reduced pressure show the bifilms near to the mold surface to be organized at right angles to the surface by the pushing action of the growing columnar grains.

In general, the bifilms and the consequential porosity are sited at grain boundaries. However, bifilms can traverse grains as illustrated in Figure 4.3. In all cases, however, the individual dendrites that constitute a grain never cross a bifilm. They cannot grow through air.

Warrington and McCartney (1989) confirm the findings of Spittle and Cushway (1983) when they find that fine equiaxed grains also promote easy growth conditions for a hot tear. This seems to be because the tear can propagate intergranularly along a path that, because of the fine grain size, can remain almost perpendicular to the applied stress on a macroscopic scale. In terms of bifilms, the result is simply the observation of the opening of that particular bifilm favorably oriented with respect to the stress direction, out of the many bifilms usually present between small grains.

Conversely, coarse equiaxed grains gave increased resistance to the spread of the crack. In this case the bifilms would be segregated to planes sometimes well away from the stress direction, causing greater plastic deformation in the attempted return of the crack to its average growth direction. In addition, of course, the distance traveled by the crack would be significantly increased.

The question of the amount of plastic work that is expended during the propagation of a tear is interesting. The work of deformation is easily shown to be of the order of at least  $10^4$  times greater than the work required to create the newly formed surfaces of the tear. Thus arguments based on the effect of the surface energy of the crack limiting its growth (as in the case of a classical Griffiths crack in a brittle solid such as glass) are clearly not relevant in the case of the failure of plastic solids such as metals at their melting points.

Novikov and Portnoi (1966) draw attention to the fact that, despite the rather brittle appearance of the fracture, the hot torn surfaces cannot usually be fitted back together again, confirming the expectation that considerable plastic deformation occurs during hot tearing. Furthermore, they found that the gap between the poorly fitting surfaces corresponded almost to the total elongation, indicating that the elongation was associated almost entirely with crack propagation in their work. The further implication was that (i) nucleation of the crack was easy, since high stresses would have given high elongations prior to cracking, and (ii) the pre-tear extension due mainly to grain boundary sliding was limited in their experiments. These observations are again consistent with propagation along a bifilm. The brittle, intergranular appearance of the fracture surface is typical of a crack that has followed the central fold of a double oxide film. The pre-existing film has been automatically pushed into grain boundaries during the growth of the grains.

Although high stresses cannot be envisaged at the stage of the nucleation of a crack (because crack nucleation will find easy start sites such as the opening up of bifilms), when the crack has started to grow the sharpness of its tip ensures that high stress is available locally at this point. For large-grained

material, therefore, the occasional absence of a favorably oriented grain boundary can be expected to result in further propagation by two means:

1. The continuation of the crack across the grain that attempts to block its path. Such occasional transgranular growth has been observed by Davies (1970) in models using low-melting-point Sn–Pb alloys. He saw that in such cases the crack followed the cell boundaries, which were clearly the next best route for the crack. Bifilms would be expected in both grain and cell interfaces, of course, and present a similarly cogent explanation.
2. The crack either renucleates a short distance ahead in a favorably oriented grain boundary or, more likely, travels around the grain by a path out of the plane of the section, appearing once again a little ahead. Fredriksson and Lehtinen (1977) have directly observed such behavior by pulling specimens of Al–Sn alloys in the scanning electron microscope. As the crack continues to open, the intervening region of obstructing grain is seen to deform plastically, as might a collapsing barrier. The stepwise propagation of the crack, linked by plastic barriers at the steps, explains the irregular, branching appearance that is a characteristic feature of hot tears. The failure of plastic bridges between randomly sited, disconnected bifilms explains the observations similarly.

Returning to our geometrical model, at the end of the pre-tear extension period the residual liquid is separated into pools between grains, as is seen in Stage 2 of Figure 8.5. The corresponding pools in the real casting are seen in Figure 8.2. These compact segregates must pose a problem for subsequent solution heat treatments, even though their existence does not seem to have been previously recognized. At this point further strain must cause some concentration of failure at a weak point in the structure of the solidifying casting. If a grain near the surface is separated from its neighbor by the presence of a bifilm, the growth of the crack can then occur with little further hindrance. The necessarily irregular nature of its progress mirrors that of the real crack; once again, compare Figures 8.2 and 8.5. Straighter portions of the crack resemble the cube model in Figure 8.5.

A potentially important feature of the hot tearing literature needs to be raised. From Figures 8.1, 8.2, and 8.5 it is quite clear that the portions of the cast structure in which the dendrites have separated but which still contain residual liquid have *always* contained residual liquid. This may seem self-evident. However, the casting literature is full of references to ‘healed’ hot tears, meaning tears containing residual liquid, but implying that the tears were once empty, and, fortuitously, were somehow subsequently filled by an inflow of liquid. Whether the term ‘healed hot tears’ is really intended to imply original emptiness and subsequent refilling is not clear but the term is misleading and would be better discontinued. The term ‘filled tear’ is more explicit. ‘Un-emptied’ tear would be even more accurate, but hardly an attractive name! The *filled tear* is simply the region between grains that have been separated by uniaxial strain, but which still remain full of intergranular liquid. If it solidifies while still full, as in Figure 8.1b, it will constitute a region of segregate, but will almost certainly still be as strong as the bulk of the casting, and so not constituting a defect that might impair its serviceability. It is *not* a hot tear, and has *never* been a hot tear.

Only if it becomes empty does it become a major defect meriting the name of hot tear. There are two quite separate mechanisms that could provide an empty tear.

1. The separation of the grains by continued strain to the point at which the residual liquid is no longer capable of keeping the tear filled. This is the mechanism displayed in our simple model

(Figure 8.5), and as seems to be shown in Figure 8.2a. The available liquid has been insufficient to keep the intergranular regions filled, and so has simply drained out of this region.

2. The above mechanism contrasts with the hot tear whose conditions for formation are identical (i.e. grains are separated by contraction strain) but the region between the grains now contains one or more bifilms that, on separation of the grains, also separates the halves of the bifilms. This creates a crack instantly and easily.

Both of these mechanisms seem possible. However, the first is expected to be more difficult to grow, the grains deforming plastically as the crack attempts to propagate from grain to grain. The presence of the bifilm in the second mechanism is expected to create a defect of a serious size with ease.

### 8.1.8 Prediction of hot tearing susceptibility

Over the years there have been many attempts to provide a useful working theory of hot tearing. Recently the attempts have narrowed to a few serious contenders. The exercise that has been found to be most useful to discriminate between them has been the attempt to predict susceptibility to hot tearing as a function of composition for binary alloys.

This is a useful test in alloy systems that display a eutectic. At zero-solute content the theory has to contend with a pure metal; at low-solute contents only solid solution dendrites are present; above a critical solute content eutectic liquid appears for the first time, steadily increasing to towards 100% as the solute content increases towards the eutectic composition. The ability to deal with all of these aspects across a single alloy system constitutes a searching test of any theory, and covers the majority of solidification conditions in real castings.

A typical experimental result is shown in Figure 8.6. It reveals a steeply peaked curve that Feurer (1976) has called a lambda curve, after the shape of the Greek capital letter  $\Lambda$ . The problem is to find a theoretical description that will allow the lambda curves to be simulated for different alloy systems.

It is salutary to note that for the Al–Cu alloy system any prediction based on the equilibrium diagram is completely wrong. Here the maximum freezing range would be predicted to be at 5.7Cu, which might lead the unwary to believe that the maximum problem in porosity and hot tearing should be at this copper content. From Figure 8.6 the problem in hot tearing is clearly centered on a rather dilute alloy of approximately only 0.5Cu. Any problems of hot shortness have almost disappeared on reaching 5.7Cu!

It is interesting to look at my early effort at prediction (Campbell 1969) that deals with the analogous problem of porosity in a spectrum of binary alloy compositions. Here the relative hydrostatic tension developed by the flow of feed metal through the dendrite mesh was calculated. The form of the relationship calculated for the Al–Cu system is shown in the figure. This particular result is based on the assumption that the residual liquid is 1% by volume. The peak is almost exactly in the correctly predicted location, confirming the fundamental importance of the arrival of eutectic liquid at that critical concentration of solute. The result closely agrees with the model by Rappaz (1999), as would be expected since both models are based on the development of hydrostatic tension at the root of the dendrites.

The remainder of the predictions based on hydrostatic tension follow this particular experimental data by Warrington and McCartney (1989) poorly, but follow the data by Spittle and Cushway (1983) rather more closely. This intermediate agreement reflects the general capability of the models to achieve fair agreement with experimental data that are in themselves of rather variable quality.

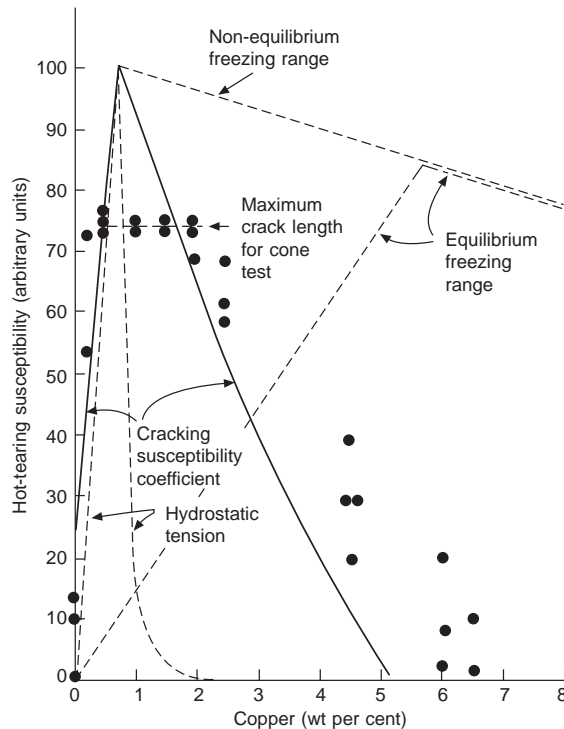


**FIGURE 8.6**

Hot tearing response of Al–Cu alloys showing a peak (necessarily extrapolated somewhat) at approximately 0.7Cu using the conical ring die test by Warrington and McCartney (1989), compared to various theoretical models. Freezing ranges and hydrostatic tension by Campbell (1989); CSC by Clyne and Davies (1977).

It is surprising that models based on hydrostatic tension agree as well as they do with hot tear initiation since they are not expected to be necessarily closely related, as we have mentioned above. The hydrostatic tension falls steeply with the arrival of eutectic liquid, dramatically reducing shrinkage porosity as seen in the original work, but not reducing hot tearing as found experimentally by Warrington and McCartney.

We also need to note that hot tearing is not well related to the non-equilibrium freezing range, as is also clear in Figure 8.6.

The theoretical approach by Feurer (1976) that appears to explain the form of the lambda curves can be similarly discounted because it is also based on the modeling of liquid flow and hence the development of hydrostatic stress, not uniaxial tension (Campbell and Clyne 1991).

An alternative theoretical approach to hot tearing was proposed by Clyne and Davies (1979). They implicitly assume that the failure is the result of uniaxial tension, but point out that strain applied during the stage of liquid and mass feeding is accommodated without problem by the casting. The problem of accommodating strain only occurs during the last stage of freezing, when the grains are no longer free to move easily. They define a cracking-susceptibility coefficient:

$$\text{CSC} = t_V/t_R \quad (8.6)$$

where  $t_R$  is the time available for stress–relaxation processes such as liquid and mass flow, and  $t_V$  is the vulnerable time period when cracks can propagate between grains. The concept is clear, but defining the limits of applicability of these various regimes for different alloy systems is not easy. However, as a first attempt the authors assume that the stress–relaxation period spans a fraction liquid  $f_L$  of approximately 0.6–0.1, and the vulnerable period spans  $f_V$  values 0.1–0.01. The predictions of the scheme for the Al–Cu system are shown in Figure 8.6 to fit the Warrington and McCarthy data better. For the Al–Si system they correctly predict a lambda curve with the correct form and peak at approximately 0.3Si, as found by their experiments. For the Al–Mg and Al–Zn systems they found the agreement less good. The agreement for Al–Mg was improved later by Katgerman (1982), who modified the CSC limits. For magnesium-based alloys Clyne and Davies (1981) use their model to predict a peak at 2.0Zn for the Mg–Zn system and 3.0Al for the Mg–Al system (Figure 8.7). The poorer tearing resistance of the zinc-containing alloy is the result of its considerably greater freezing range. However, from the ring test results shown in Figure 8.8 the peaks are actually observed to be at approximately 1.0Zn and 1.0Al. It is necessary to keep in mind that the experimental data will be significantly affected by the presence of bifilms, which will, in general, reduce the composition of the peak susceptibility, bringing agreement closer in line.

The approach therefore seems basically sound and useful, even though not always especially accurate in its predictions, as we have seen above. Thus, in common with most theories, it invites further development and refinement.

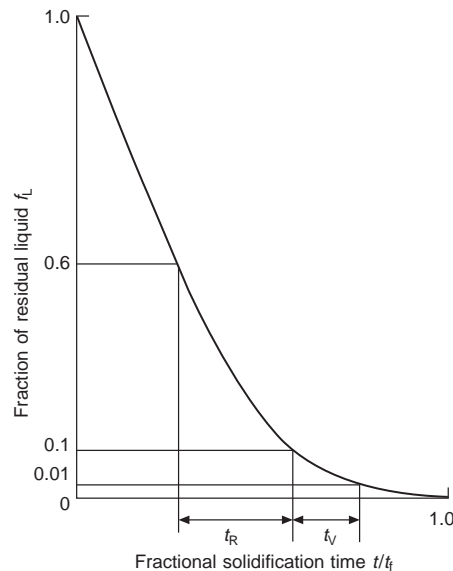


**FIGURE 8.7**

Model by Clyne and Davies (1977) for the regimes during which either stress relaxation or vulnerability to hot tearing occur.

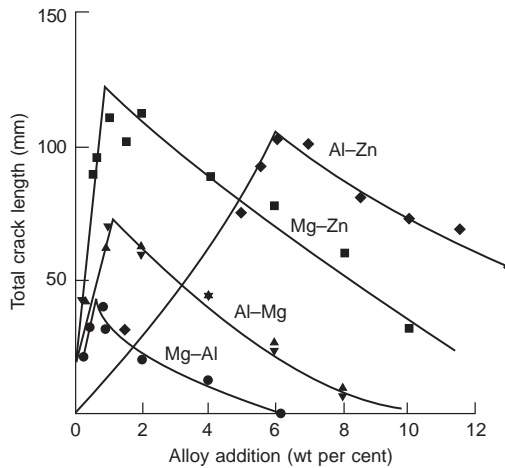


**FIGURE 8.8**

Hot tearing behavior of various alloys subjected to the ring die test. (Data from Dodd 1955, Dodd et al. 1955, Pumphrey and Lyons 1948, Pumphrey and Moore 1949.)

As a start it would seem useful to combine the cracking-susceptibility coefficient with Figure 8.5 derived above for the strain per boundary in the hot spot. This gives a modified CSC as:

$$CSC_b = \frac{\alpha \Delta T L a}{l^2} \bullet \frac{t_V}{t_R} \quad (8.7)$$

There is already considerable evidence to suggest that this more general equation is at least approximately accurate. Figure 8.9 shows how grain size is significant. Also, several researchers with different diameter ring tests confirm that the cracking susceptibility is proportional to the circumference of the ring (Isobe et al. 1978). This proportionality to length is implicit in the design of the various I-beam tests using graded lengths of beam (see below). Pekguleryuz (2010) compared a number of CSC parameters for Al–Si alloys and found Figure 8.7 to give the best correlation.

The CSC model has been extended to the cracking of steels (Clyne et al. 1982). In Fe–S alloys the prediction of a CSC peak at 0.1% S was observed to be accurately fulfilled in experiments by Davies and Shin (1980). Here, as a consequence of the complexity of iron-based alloys, the CSC model is extremely useful in providing a framework to understand the phenomena (Figure 8.10). For instance, Rogberg (1980) found that for stainless steels that solidified to delta-iron the alloys were insensitive to the impurities As, Bi, Pb, Sn, P, and Cu, whereas those that solidified to gamma iron suffered serious loss of hot ductility. Kujanpaa and Moisio (1980) confirmed that S and P embrittled gamma iron, but not delta-ferrite, but the best resistance to embrittlement was provided by a mixture of gamma- and delta-irons.

The most sophisticated development of attempts to predict the susceptibility to hot tearing has been the series of developments since 1999 by Rappaz and his colleagues. Initially their model assessed the linear contraction and volumetric shrinkage contributions to the hydrostatic tension, admitting that the model at that stage only predicted the formation of the initial pore, and did not extend to the

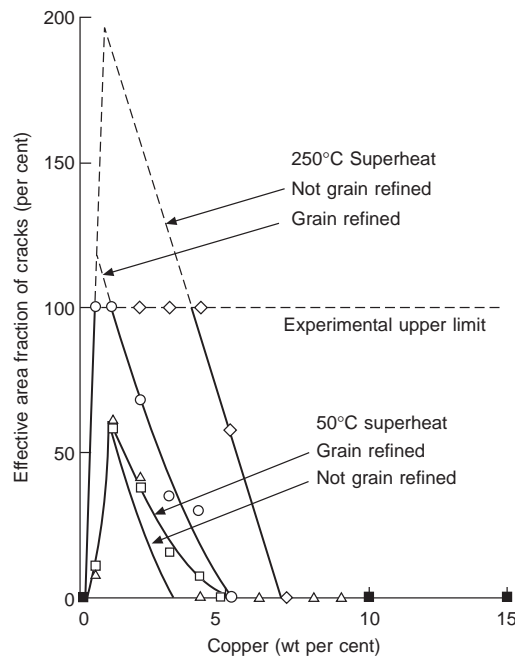


**FIGURE 8.9**

Hot tearing behavior of Al–Cu alloys using an I-beam-type test showing the benefits of low casting temperature and grain refinement (Spittle and Cushway 1983). Peaks are extrapolated to illustrate the close agreement with Figure 8.6.

development of a crack. A series of publications has followed since 2006 expanding the concept of a granular model, but one in which the grains were randomly distributed. This has been a great advance on the simplistic geometrical models discussed earlier, allowing the details of the nature of the pasty zone to be simulated during the progressive stages of freezing. The network of channels of residual liquid is seen in Figure 8.11. A result for an Al–1Cu alloy pasty zone is illustrated in Figure 8.12, and the highly non-uniform flow through the zone is shown in Figure 8.13. The authors summarize their work in the creation of morphological maps (Figure 8.14). Although at this stage these simulations are only 2-D, an extension to 3-D is claimed to be relatively easy. It will represent a major step forward in our understanding of the processes within the pasty zone. Even so, the presence of bifilms will complicate these already complex flow patterns still further. It is not surprising that the pasty zone sometimes will allow no flow whatever, as was demonstrated in Figure 6.17.

### 8.1.9 Methods of testing

A complete survey of the methods used to assess hot tearing is beyond the scope of this short book. The interested reader is recommended to various reviews, including historical accounts by Middleton (1953), Dodd (1955), and Hansen (1975), and more recently a number of briefer accounts by Guven and Hunt (1988) and Warrington and McCartney (1989).



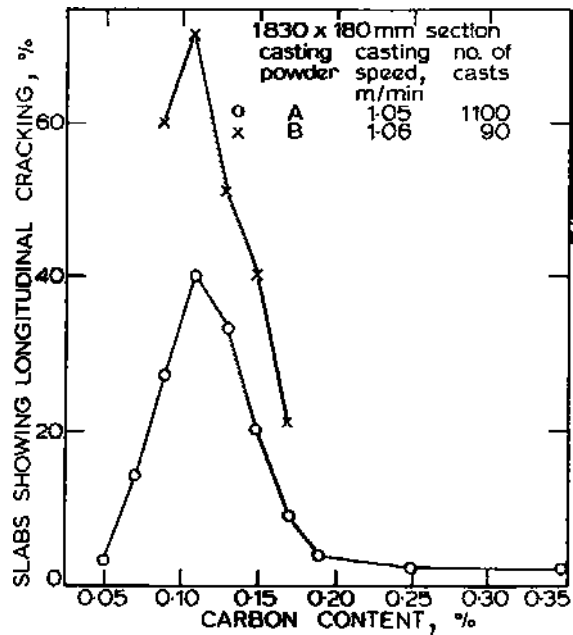


FIGURE 8.10

Effect of carbon content on the longitudinal cracking of continuously cast steels.

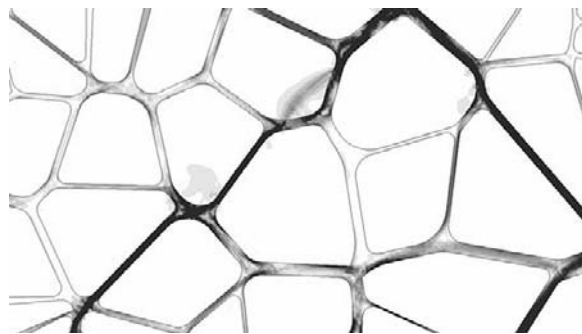
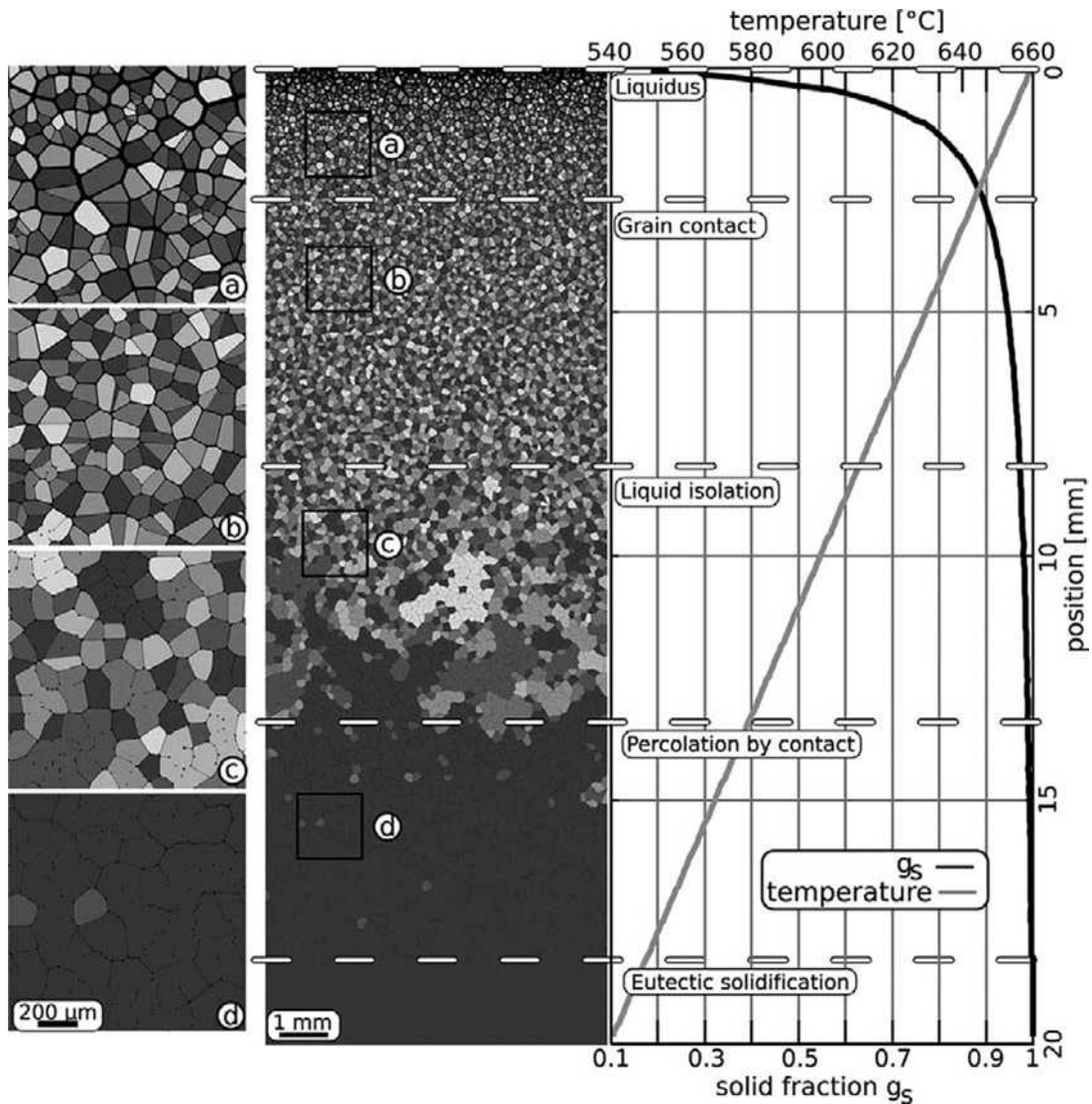


FIGURE 8.11

Preferred flow paths through a simulated intergranular mesh of equiaxed grains (Phillion et al. 2009).

The methods fall into two main groups; (i) the various tests of straight castings solidifying in molds in which the tensioned test piece is restrained at each end as an I-beam (sometimes known as 'dog bone') tests and (ii) the ring or conical mold tests. Both these types of tests use the occurrence of cracks as a measure of hot tearing propensity. Sundry other tests include the pulling of tensile test pieces



**FIGURE 8.12**

Calculated pasty zone of equiaxed grains for an Al-1%Cu alloy cooled at  $-1 \text{ K s}^{-1}$  in a gradient of  $6 \text{ K mm}^{-1}$ . Grains in mechanical contact are shaded the same gray level (Vernede et al. 2006).

during their solidification in a tensile testing machine as a direct measure of the resistance of the casting to failure.

The I-beam has many variants. One of the most common is the arrangement of various lengths of rod castings from a single runner. Each of the rods has a T-shaped end to provide a restriction to its

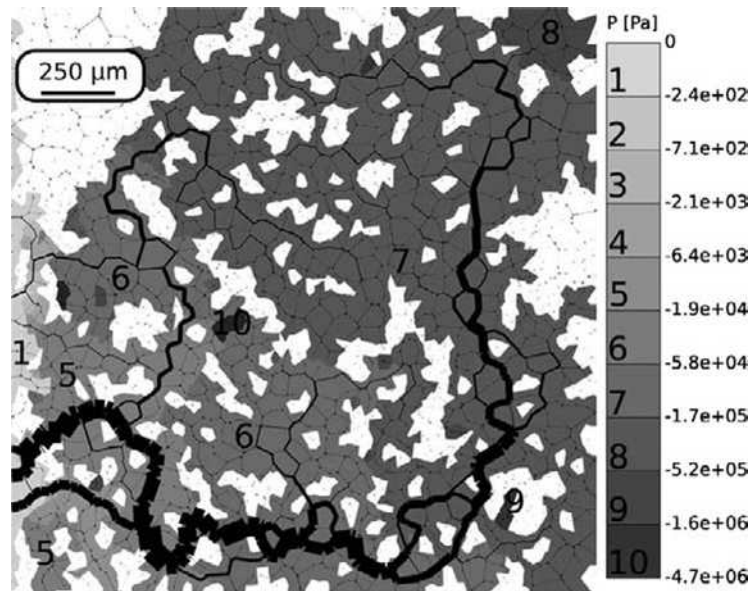


**FIGURE 8.13**

A model of the fluid flow and pressure distribution in an equiaxed pasty zone as a result of solidification shrinkage in Al-1%Cu alloy at 98.4% solid. The width of each channel is magnified in proportion to the local flow, and local pressure is indicated by the gray scale (Vernede et al. 2006).

contraction. When metal is poured, the contraction of the rods will take place with various degrees of constraint, those with rods greater than a critical length failing by tearing at the hot spot, which is the joint between the runner and the rod. From such a test, therefore, only one result is obtained, and its accuracy is limited by the increments by which the rods increase in length. The limited discrimination provided by the limited number of bars of different lengths in this test is further confounded by the fundamentally limited reproducibility of hot shortness tests.

Other sorts of I-beam test gain a potentially more discriminating result by measuring the lengths of cracks in the hot-spot region. However, even in this case the actual test volume of material is limited and the stress and strain distribution in the hot spot is far from uniform.

The ring test is a constrained geometry that could hardly be simpler. It is normally carried out in a steel die. Metal is poured into the open annulus between the inner and outer parts of the die. As it cools it contracts onto the inner steel core. The core also expands slightly as it heats up. The resulting constraint on the casting is severe, opening up transverse tears all around the ring in a susceptible alloy. In this respect the technique is useful in that it tests a large volume of material, subjecting it all to a uniform constraint condition. The method of assessment is by measuring the total length of cracks. This gives a reasonably large number that can be assessed accurately, making the test more discriminating. Thus despite the criticisms normally leveled at the ring test, it has many advantages, one of the most important of which is simplicity. In general the many different researches that have been carried out over the years by different workers using this approach are seen to agree tolerably

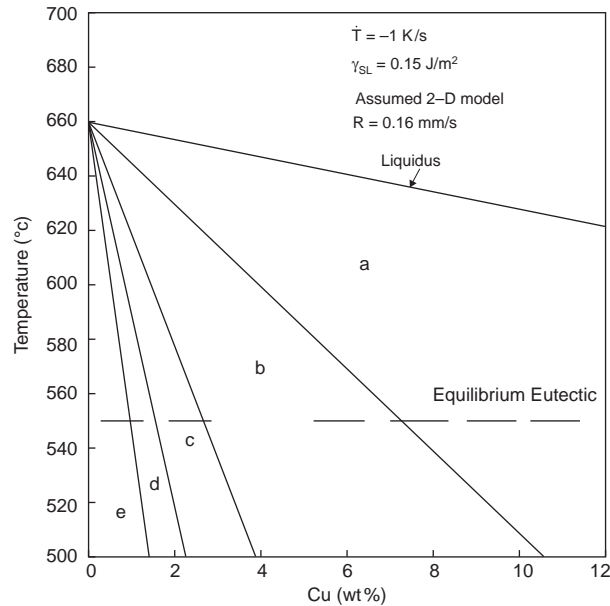


**FIGURE 8.14**

Map of the pasty zone based on the granular model by Vernede et al. (2006). Region (a) contains mostly isolated grains; (b) some grain contact leading to isolated clusters; (c) larger clusters containing some isolated liquid; (d) a continuous solid network but continuous films no longer exist; (e) solidification complete.

well. Pumphrey (1955) carried out a series of repeated checks with different workers over a period of months. These showed an impressive consistency. This is more than can be said for most other tests for hot tearing.

Another aspect of the ring test die is worth comment: the test is unusual in that its rigid restraint is sufficient to cause hot tearing in the absence of any real hot spot and in the absence of strain concentration.

Gruznykh and Nekhendzi (1961) and DiSylvestro and Faist (1977) describe similar ring tests for steels using sand molds.

The recent variant of the ring test by Warrington and McCartney (1989) provides a tapered center core that gives a constraint condition increasing linearly along the axis of the cone. This seems a useful test, but is clearly limited in very hot short materials to a maximum tear of the length of the side of the cone. This artificial cut-off is seen in Figure 8.6. More work would be helpful to confirm the limitations of reproducibility of the test. For instance, from Equation 8.7 it is to be expected that the width of the hot spot that the authors place along the cone by painting a strip of insulating wash down its length will be critical. It is not clear whether such a hot spot is necessary or even desirable in the test, but its presence is certain to have a major effect on results.

Trikha and Bates (1994) employ a nicely designed hot tearing test for steels that consist of opposed conical cores (Figure 8.15). The conical castings are gated at the horizontal joint defining a longitudinal

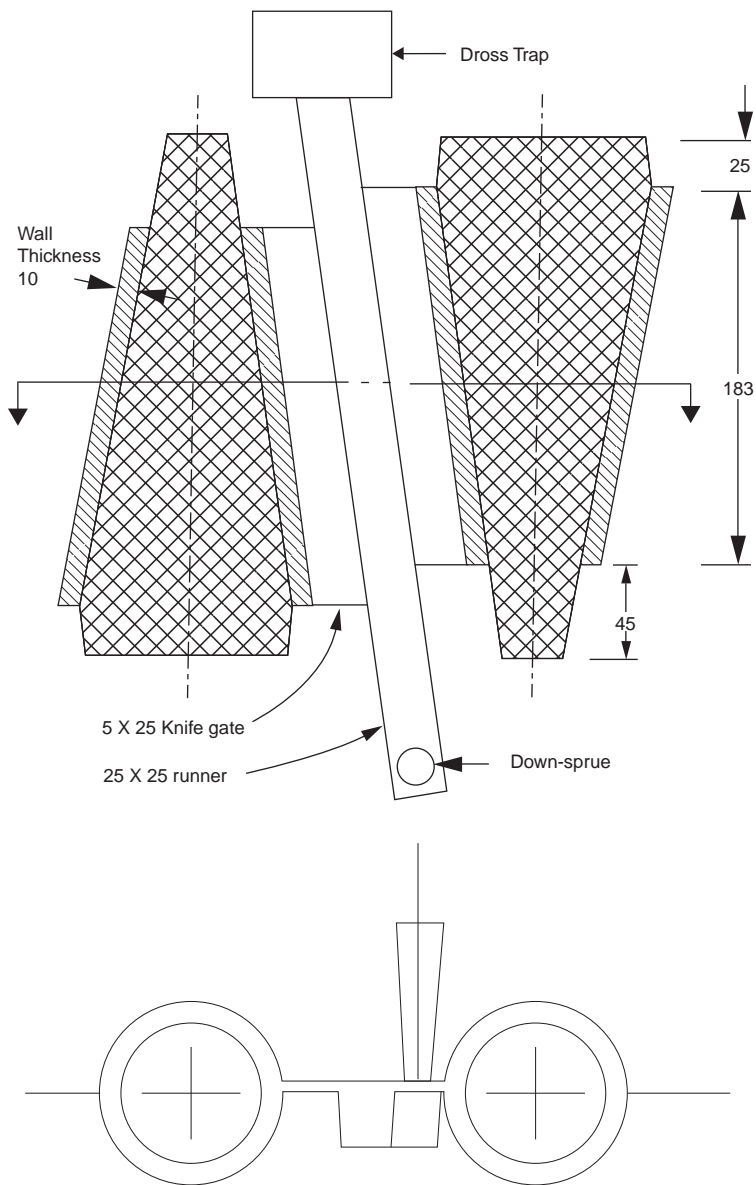


**FIGURE 8.15**

The hot tearing test of Trikha and Bates (1994) consisting of opposed cones, giving a pair of results that can be compared for reproducibility.

hot spot. Any cracks in the cores can be measured, giving a pair of values to assess the reproducibility of the results. The tearing can be assessed in terms of density of cores and binder materials.

A new approach to measure the strength of Al alloys in the mushy state (but, note, not necessarily a hot tearing test) is described by Mathier and co-workers (2008). A specially shaped tensile specimen is contained in a hot stainless steel mold and gradually cooled. The precise dimensions of the mold define a precisely shaped specimen, which in turn can be closely studied by carrying out, in parallel, a numerical simulation. In this way the information that can be generated by such a test is maximized. The only disappointment to the reporting of this interesting work is that the filling of the test mold is not specified, and has clearly been overlooked as being of critical importance to the integrity of the material under test.

### 8.1.10 Methods of control

The casting engineer can be reassured that there are a number of different approaches to tackling hot tearing problems in castings, or even, preferably, preventing such defects by appropriate precautions.

#### 8.1.10.1 Improved mold filling

In practice, as bears repeating any number of times, the author has never failed to deal with hot tearing by simply upgrading the filling system, ensuring that air is not entrained into the metal at any point. Whole foundries have been revolutionized in this way. Thus this is probably the single most important technique for dealing with hot tearing problems. It is the most convincing evidence that hot tears are strongly linked to the presence of bifilms. To the author's knowledge, sadly, this overwhelming evidence has not yet found its way into the scientific casting literature.

#### 8.1.10.2 Casting design

Much can be achieved at the design stage of the casting. A publication by Kearney and Raffin (1987) concerns itself almost exclusively with the prevention of hot tears by adjustments to the casting design. In general it can be summarized by saying:

- (i) Do not design sharp re-entrant corners;
- (ii) Do not provide a straight join between two potential hot spots; curve such members;
- (iii) Provide curves in gates so that deformation can be accommodated easily;
- (iv) Angle and off-set stiffeners and ribs to allow easier accommodation of strain;
- (v) For gravity die (permanent mold) casting the rapid removal of any internal steel core is recommended to reduce constraint.

The reader will appreciate the general philosophy, although this severe condensation hardly does justice to the original work of these authors.

It is also worth bearing in mind that flash on castings as the result of the poor fitting of molds and cores can be a major source of casting constraint. To identify the real sources of constraint it is necessary, therefore, to check the casting straight out of the mold (not after it has been nicely dressed to appear on the manager's table!).

All this list of dire warnings needs to be set into context. In the experience of the author the provision of sharp corners and other so-called geometrical dangers has never given a problem providing the liquid metal is of good quality, and provided the metal has not been impaired by a poor filling system design.

In any case, it is usual to find that the design is fixed, and any changes will involve significant negotiation with the customer and/or designer, and may eventually not be agreed. In such situations the casting engineer has to fall back on other options. These include the following.

### **8.1.10.3 Chilling**

The chilling of the hot spot is a useful technique. This reduces the temperature locally, thus strengthening the metal by taking it outside of its susceptible temperature range before any significant strain and stress is applied. By reducing the temperature locally nearer to that of the casting as a whole, the temperature differential that drives the process is reduced, and any strain concentration is redistributed over a larger region of the casting. Local chilling is therefore usually extremely effective.

In addition to this conventional explanation, recent research has revealed that the action of chills is more complex. Chills cause the solidification front to move away from the chill in a rapid, unidirectional movement. Bifilms, with their enclosed layer of air, are the ultimate barrier to dendrites since the solidification cannot progress through the air. The result is that the bifilms are pushed ahead of the front, and so pushed away from the vulnerable hot spot.

This is the reason that many entrainment defects, as opposed to genuine shrinkage problems, appear to be cured by the placing of a chill. The usual (and usually quite wrong) interpretation being that the chill has cured the 'shrinkage' porosity.

Some oxide bifilms appear, however, to be attached to the casting surface (possibly at the point at which they were originally folded-in) so that they are not completely free to be pushed ahead. Also, some are oriented so that some of the tips of the dendrites in the advancing dendrite raft pass either side of the bifilm, as seen in Figure 2.43. Either way, the bifilm is organized into a planar sheet, parallel to the dendrite growth direction, and then pinned in this position until solidified in place. Cracks at right angles to the chill surface can be seen in the radiograph shown in Figure 2.43. Such planes easily separate along the air layer as the result of a tensile strain. This may occur during freezing, in the form of a hot tear as shown in Figure 8.1. Alternatively, the planes and the characteristic steps can be seen in room-temperature tensile fracture surfaces as in Figures 2.44 and 2.46.

### **8.1.10.4 Reduced constraint**

A reduction in the stress on the contracting casting can be achieved by reducing the mold strength. As we have noted before, this is in principle relatively easily achieved. The options are: (1) reducing the level of binder in the sand core, although there is normally little scope for this, because those found not already operating at minimum strengths to reduce costs and ease shake-out are using strength as an insurance against core breakages and defects as a result of mishandling; and (b) weakening the core by using it in a less dense form (such as produced by blowing rather than by hand ramming), or modifying its design by making it hollow. Earlier shake-out from the mold, and more rapid decoring, may also be useful. However, Twitty (1960) found the opposite effect; his white iron castings suffered more hot tears when shaken out earlier as a result of the extra stresses put on the casting during the removal of the mold!

EI-Mahallawi and Beeley (1965) show how appropriate tests can be carried out on sands containing different binders. Their deformation/time test for sand under a gradient heating condition would be expected to provide a good assessment of the constraint imposed by different types of sand/binder systems. DiSylvestro and Faist (1977) use their sand-molded ring test to check the effect of different sand binders on the hot tearing in carbon steels. In later work on steel, SCRATA (1981) list the sand binders in increasing hot tearing tendency for casting sections of less than 30 mm. These are:

- Greensand (least hot tearing);
- Dry sand (clay bonded);
- Sodium silicate bonded (CO<sub>2</sub> and ester hardened types);
- Resin bonded shell sand;
- Alkyd resin/oil (perborate or isocyanate types);
- Oil sand;
- Phenol formaldehyde resin/isocyanate;
- Furan resin (worst tearing).

In the case of the worst sand binder, the furan resin, it is difficult to believe that the thermal and mechanical behavior of the binder is responsible for the increased incidence of hot tearing. It seems likely that the sulfur (or phosphorus) contained in the mixed binder will contaminate the surface of the steel casting, promoting grain boundary films of sulfides or phosphides, and thus rendering the metal more susceptible to tearing.

In thicker sections the greater amount of heat available causes more burning out of the binder, with better collapse of the sand mold. Organic binders benefit from this effect. Paradoxically the inorganic system based on sodium silicate in this list is also seen to benefit in a similar way. This is probably the result of the extra heat leading to greater general softening and/or melting of the binder at high temperature. As the binder cools, however, it is well known to become a fused, glassy mass, which can be difficult to remove from the finished casting. Even so, modern silicate binders contain breakdown agents that appear to have overcome this problem.

For ferrous castings the inclusion in the sand of material that will burn away rapidly, leaving spaces into which the sand can move, allows faster and greater accommodation of the movement of the casting. Common additions to greensand are wood flour, cellulose, and polystyrene granules. Slabs of polystyrene foam of 25–50 mm thickness have been inserted in the mold or core at approximately 6–12 mm away from the casting–mold interface, depending on the thickness of the casting. Conversely, reinforcing rods or bars in sand molds or cores greatly reduce the collapsibility of that part of the mold in which they are placed, and may cause local tearing.

In the case of gravity die casting, where the core may be made from cast iron or steel, it is common to construct the core so that it can be withdrawn or can be collapsed inwards as soon as possible after casting. Almost all aluminum alloy pistons are made in this way, with complex collapsible five-piece internal cores.

Ultimately, however, it has to be emphasized that removal of constraints after casting is not always a reliable technique. This is because the timing is difficult to control precisely; too early an action may result in a breakout of liquid metal, and too late will cause cracking. It is really better to rely on passive systems.

#### **8.1.10.5 Brackets**

The planting of brackets across a corner or hot spot can sometimes be useful. The brackets probably serve not only for strengthening but also as cooling fins. Perhaps predictably (because of the poorer conductivity of steel castings compared to those in aluminum, for instance), for steel castings they are generally less good at preventing tearing than are chills (SCRATA, 1981). Even so, some large steel castings are sometimes seen to be covered in ‘tear brackets’, the casting bristling like a porcupine. Such features confirm the existence of their poor filling system designs.



### **8.1.10.6 Grain refinement**

The grain refinement of the alloy is expected to be helpful in reducing crack initiation, as indicated by Equation 8.7. However, care is needed not to overlook the fact that if the conditions are spread between many boundaries, making initiation difficult, the subsequent growth of the crack may be easier, as discussed above. By similar reasoning, easy initiation on a favorably placed boundary between large grains will usually have problems to grow beyond the first grain.

Even so, in general, fine grains reduce the susceptibility to hot tears. Figure 8.9 shows the improved resistance to tearing by grain refinement of Al–Cu alloys. Davies (1970) finds a similar result for other Al alloys. Novikov and Grushko report the beneficial effects of refinement by Sc and Zr in Al–Cu–Li alloys. Twitty (1960) confirmed that his white cast iron alloyed with 30% chromium was severely hot short when not grain-refined, whereas 0.10–0.25Ti addition reduced the grain size and eliminated hot tearing.

However, in a really illuminating experiment to reduce hot cracking of a DC (Direct Chill ‘continuous’) Al alloy, Nadella and colleagues (2007) introduce grain refiner in the ladle prior to casting, successfully grain refining and eliminating cracking. However, when they added the same grain refiner into the metal stream during pouring into the mold, the casting was successfully grain-refined, but cracked. This is clearly an instance of the Ti-rich grain-refiner precipitating on bifilms in the ladle and sedimenting to the bottom of the ladle, so that the cast metal was clean. When the grain refiner was added to the launder bifilms were clearly unable to separate, and thus were carried over into the casting, creating excellent grain refinement, but also creating excellent conditions for cracking in the presence of cooling strains.

### **8.1.10.7 Reduced casting temperature**

Reduction of the casting temperature can sometimes help, as is seen clearly for Al–Cu alloys (Figure 8.9). This effect is likely to be the result of the achievement of a finer grain size. If, however, the effect also relies on the reorganization of bifilms, then the effect may be sensitive to geometry: some directions may become more prone to failure if bifilms are caused to lie across directions of tensile strain.

### **8.1.10.8 Alloying**

A variation of the alloy constituents, often within the limits of the chemical specification of the alloy, can sometimes help.

The addition of elements to increase the volume fraction of eutectic liquid can be seen to help by (i) increasing the pre-tear extension by lubricated grain boundary sliding, and (ii) decreasing the CSC. Couture and Edwards (1966) confirm that copper-based alloys benefit from increased amounts of liquid during the final stages of freezing.

Manganese in steels is well known for reacting with sulfur to form MnS, so that the formation of the deleterious FeS liquid at the grain boundaries is reduced.

For other more complicated alloy systems the answers are not so straightforward. For instance, in early work on the Al–Cu–Mg system by Pumphrey and Lyons (1948), the relation between hot tearing and composition is complex, as was confirmed by Novikov (1962) for various Al–Cu–X systems. Ramseyer et al. (1982) investigated the Al–Cu–Fe system and found that for certain ranges of composition increasing levels of iron were desirable to control tearing. This is a most surprising conclusion which most metallurgists would not have predicted; iron is usually an embrittling impurity in most high-strength aluminum alloys when assessed by room temperature tests of ductility. Later

work by Chadwick (1991) revealed that the effect of the iron is to provide a network of iron-rich crystals around the primary aluminum dendrites, as a scaffold framework that appears to support and reinforce the weaker dendrite array.

### 8.1.10.9 Reduced contracting length

Shortening the length over which the strain is accumulated is sometimes conveniently achieved by placing a feeder in the center of the length. Such a large concentration of heat in the center of the cooling section will allow the strain to be accommodated in the plastic region close to the feeder. Any opening up of intergranular pathways is likely to be easily fed from the nearby feeder. The careful siting of feeders in this way effectively splits up a casting into a series of short lengths. If each length is sufficiently short then strains that can cause a tear will be avoided. The siting of insulating coatings can also be used in the same way. In terms of Equation 8.5, the technique is equivalent to a method of reducing the strain concentration by multiplying the number of hot spots, and thus increasing the total length  $l$  of the hot spot whilst reducing the contracting length  $L$ .

### 8.1.11 Summary of the conditions for hot tearing and porosity

The findings of researches like those by Spittle and Cushway (1983) are summarized schematically in Figure 8.16a. The benefits of fine grain size are clear, but the benefits to be expected from clean metal are also emphasized as of overriding importance.

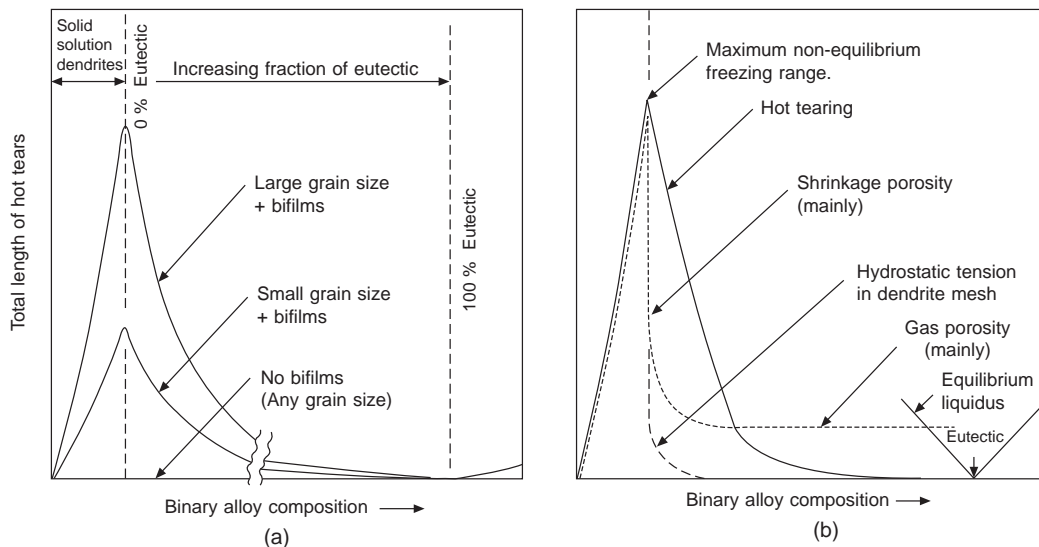


FIGURE 8.16

Summary of (a) the modest effects of grain size and the powerful effects of bifilms on hot tearing; and (b) the close and potentially confusing relation between the conditions for porosity (dependent on hydrostatic pressure) and hot tearing (mainly dependent on uniaxial strain).

The differences between the conditions for the occurrence of porosity and the occurrence of hot tearing has been mentioned a number of times. Figure 8.16b represents a summary of these conditions.

Clearly, porosity forms in the hydrostatic tension as a result of poor feeding, especially in the kind of conditions found in a pasty freezing alloy. The interdendritic feeding leads to a reduction in pressure described by the so-called Darcy relation, in which laminar flow through interdendritic channels suffers viscous drag, causing the pressure to fall. Thus these conditions exist in those alloys that solidify as a solid solution, and thus form dendrites whose interdendritic channels taper down to nothing, therefore maximizing viscous drag, and maximizing the potential for the creation of porosity.

Increasing the solute content of the alloy sufficiently to form some eutectic, particularly in non-equilibrium freezing conditions, the hydrostatic (triaxial) tension is immediately greatly reduced because the dendrite channels now no longer taper to a point, but are now truncated with a planar front of eutectic. The potential for porosity now falls precipitously as is clear in Figure 8.16b.

If any uniaxial tension exists, the potential for hot tearing at first increases similarly to the potential for pore formation, but the steep drop at the first appearance of the non-equilibrium eutectic liquid may or may not correspond to the hot tearing susceptibility depending on how this is measured experimentally.

The different regimes of triaxial and uniaxial tension correspond to the regimes for the incidence of porosity and hot tearing in alloy systems as illustrated in Figure 8.16. The continuing low level of porosity at higher solute contents approaching the eutectic is the result of a residual amount of gas porosity. This too, of course, usually only occurs because of the presence of a population of (usually) relatively small bifilms.

The maximum in the freezing range corresponds to the maximum potential for porosity and hot tearing (Campbell 1969, Rappaz 1999). Interestingly, this peak also corresponds closely to the compositions of many wrought alloys. This is because the wrought alloys have been optimized for maximum alloy content in solution, and avoiding the presence of hard eutectic phases which contribute little additional strength, and reduce other properties such as resistance to corrosion. Thus these alloys should suffer maximum hot tearing and cracking problems during casting. The only reason why such compositions are successful in practice is because of the great precautions taken by the wrought industry to cast metal as clean as possible, and under the highest temperature gradient possible provided by intense water cooling. Even so, the continuous casting industry is troubled by cracking of ingots, particularly of some of the stronger alloys, and particularly at the start of casting. This is because after all the cleaning of the melt, the cast is started by the melt being dropped several hundred millimeters into the mold where, of course, it re-creates huge bifilms. These cause the cracking of the cast material around the dovetail key at the top of the starter bar. Although, once the mold is filled, the remainder of the pour creates no further bifilms; the cracking troubles sometimes extend a long way up the length of the casting because of the mixing and progressive dilution of the original melt pool as the cast proceeds, spreading the original bifilms that are free to float far up the length of the product.

### 8.1.12 Hot tearing in stainless steels

The failure of stainless steel castings during solidification and cooling can be complicated by the phase changes that can occur during freezing. The critical parameter is the  $Cr_{eq}/Ni_{eq}$  ratio as discussed in some detail in Section 6.6. Nayal (1986) does not hesitate to make the useful, if obvious, point that it is the structure of the steel during freezing that is important, rather than the structure at room temperature. He categorizes the steels according to their structural reactions during freezing:

**A.**  $L \rightarrow L + \gamma \rightarrow \gamma$

$L \rightarrow L + \gamma \rightarrow L + \gamma + \delta \rightarrow \gamma + \delta$

**B.**  $L \rightarrow L + \delta \rightarrow L + \gamma + \delta \rightarrow \gamma + \delta$

**C.**  $L \rightarrow L + \delta \rightarrow \delta \rightarrow \gamma + \delta$

The range of solidification mode B occurs over values of  $Cr_{eq}/Ni_{eq}$  from 1.49 to 2.0. In later work together with Beech (1987) the researchers find in the case of freezing entirely in mode B no cracks were observed, whereas the presence of some component of A and C always led to some cracking.

The researchers Kujanpaa and Moisio (1980) find that P and S are particularly harmful in encouraging tearing in steels that solidify purely to austenite, but do not affect those that solidify with some delta ferrite. The division between the two steels is sharply defined at  $Cr_{eq}/Ni_{eq} = 1.5$ . Another Scandinavian worker, Rogberg (1980), confirms this general rule for the particular case of two steels pulled at high temperature in a tensile testing machine. The steel solidifying to austenite was sensitive to a wide range of impurities, but those containing ferrite seemed insensitive to these problems.

### 8.1.13 Predictive techniques

The ability to predict the occurrence of tearing in a casting would be valuable. This quest has driven a number of different approaches. One of the early attempts assuming the rheological behavior of solidifying alloys has been made by Qingchun et al. (1991) with some success. A not dissimilar viscoplastic model has benefited from the power of computers by Pokorny, Monroe, and Beckermann (2009) who have shown that the sites and severity of hot tears appear to be predictable in simulations of relatively complex light alloy castings. These forerunners of examples of early computing approaches are likely to become routine provisions of commercial computer simulations in due course. But for more scientific insights into the mechanisms of hot tearing the highly descriptive granular model under development by Rappaz and colleagues (1999–2009) is a likely contender as a future useful model to understand and predict tensile failure in the partly solidified state.

---

## 8.2 COLD CRACKING

### 8.2.1 General

Cold cracking is a general term used to emphasize the different nature of the failure from that of hot tearing. Whereas the word ‘hot’ in hot tearing implies a failure occurring at temperatures above the solidus, ‘cold’ simply means lower than the solidus temperature; in some cases, therefore, it can be rather warm! Solidus here means, of course, the real non-equilibrium solidus (not the value picked off an equilibrium phase diagram!).

The term ‘cracking’ is also to be contrasted with ‘tearing’. Whereas a tear is a ragged failure in a weak material, a crack is straighter and smoother, and occurs in strong materials. Because it represents the failure of a strong material, the stress required to nucleate and propagate the failure is correspondingly more significant (in hot tearing stress was less significant, whereas strain was important).

Occasionally a failure appears to fall somewhere between the tear and crack categories. Such borderline problems include the cracks that form in steels because of the presence of low-melting-point

residual elements, such as copper-rich phases, at the grain boundaries. The copper-bearing phase is liquid between 1000 and 1100°C, with its dihedral angle falling to zero in this temperature range, thus wetting the grains. Over this range of temperature, therefore, the steel is particularly susceptible to tensile failure (Wieser 1983). The temperature is well below the solidus (in terms of the Fe–C system), and cracking will not occur easily at higher temperatures because the liquid phase does not wet so well, and therefore does not cover such a large proportion of the grain boundary area.

Returning to the ‘cold’ crack, the driving force for the nucleation and spread of a cold crack is stress. The various ways in which stress can arise and be concentrated in castings have been dealt with previously and are not repeated here. However, one mechanism not pre-discussed is phase change in the solid state. In steels transforming from  $\delta$ - to  $\gamma$ -structure, the large volume reduction has been suggested as a potential source of stress because of the large strains involved (Gelperin 1946, Grill and Brimacombe 1973). In fact the volume change occurring during the collapse of the body-centered cubic ferrite phase to the close-packed austenite phase is close to 1.14%, corresponding to a linear contraction of 0.38% (being one-third of the volume contraction). This is a massive linear strain, well over the yield point (in the region of 0.05 to 0.1% strain), and so would be expected to open up any fragments of bifilms to form the nucleation sites of larger cracks that would propagate as the steel cooled, generating high stresses to propagate the cracks to observable size. This mechanism seems to be the cause of the widely experienced cracking of low-carbon and low-alloy steel continuously cast billets in the carbon range 0.10–0.15. Figure 8.10 is given as an example. The reduced cracking as carbon increases to 0.35 probably reflects the increasing proportion of the steel solidifying directly to austenite, avoiding the strains associated with the solid state transformation.

### 8.2.2 Crack initiation

Cracks start from stress raisers. A stress raiser can be an abrupt change of section in a casting. However, this problem is well known to designers, and in any case is not likely to cause increases of stress by much more than a factor of two.

More severe stresses are raised by sharper features such as folded oxide films (bifilms) that already constitute a kind of crack that has been cast into place at the time of the filling of the casting. These defects are all the more dangerous because they can occupy a large portion of the section of a casting, but at the same time are difficult to detect. Oxide bifilms are probably the most important initiators of cracks in light alloys. This is clear because from daily foundry experience, castings made with good running and gating systems are usually not sensitive to problems of cracking.

Turning now to the stresses involved during and after the solidification of a weld, these can be extremely high because of the constraint of the surrounding solid metal. This surrounding material is near to room temperature and thus very strong. In such a case Dixon (1987) has observed that cracks start from such innocuous sites as micropores. However, such small and relatively rounded defects are unlikely initiators despite the very high driving force. It is also most likely that the micropore is sited on a bifilm, and it is the bifilm that causes the initiation of the crack. Only very careful observation using the SEM would be capable of resolving such issues.

In the case of the strong 7000 series Al alloys Lalpoor and colleagues (2009) use finite element analysis to estimate the stresses in semi-continuously (DC) cast billets and slabs. Knowing the levels of stress, they estimate the critical defect sizes to initiate catastrophic failure. The diameters of such critical penny-shaped cracks need to be between 3 and 10 mm to initiate failure. Oxide bifilms are to be

expected easily exceeding this size as a result of the turbulent initial fill of the mold. In fact, bifilms up to 100 mm across would not be surprising. Thus sudden brittle failures are to be expected.

### 8.2.3 Crack growth

As the casting cools, stress–relaxation by creep becomes progressively slower, and eventually stops altogether. Thus from this stage onwards, further contraction only builds up elastic strain and consequent stress. The accumulating stress is available to grow the crack with great speed to large size. Lees (1946) reports the casting of a high-strength aluminum alloy into a sand mold designed to produce hot tearing by constraining the ends of the cast bars. If the restraint was not released before the castings cooled to 200°C then a loud crack was heard, corresponding to the complete fracture of the bar. Similar failures during the cooling of steel castings are also well known, as was, for instance, reported by Steiger as long ago as 1913.

After the strains of delta to austenite transformation above about 1440°C, during the further cooling of steel castings there is a succession of particularly vulnerable temperature ranges. The following list is not expected to be exhaustive.

1. Carbon steel castings will embrittle if they dwell for an excessive period between approximately 950 and 600°C (Harsem et al. 1968). Butakov et al. (1968) cite hydrogen, sulfur, and phosphorus as increasing embrittlement in the 900–650°C range, and the intergranular fracture surface as exhibiting various forms of sulfides, particularly MnS and FeS. Harsem (1968) adds carbides and AlN to this list. From our privileged gift of the wisdom of hindsight, it seems probable that many of these researches were influenced by the presence of bifilms. At least some of these problems are likely to be associated with the strains of the austenite to ferrite transition. New, clarifying researches are now needed.
2. Impure low-alloy steels suffer similarly in the range 550–350°C (Low 1969).
3. Low-carbon steels are susceptible to brittle failure if deformation occurs in the range 300–150°C, the so-called blue brittleness, or temper embrittlement range (Sherby 1962). In his review, Wieser (1983) lists the principal contributors to temper embrittlement as antimony, arsenic, tin, and phosphorus. These elements have been found to segregate to the prior austenite grain boundaries. Since these boundaries will in general coincide with the ferrite boundaries, then the crack will usually be intergranular once again. However, the effect of these and other elements in the various kinds of steels is complicated, not being the same in every case; for instance tin at concentrations up to 0.4% embrittles Ni–Cr–Mo–V steel but not 2.25Cr–1Mo steel. Copper, manganese, and silicon are also deleterious in some steels, whereas the effect of molybdenum is generally beneficial.
4. Most body-centered-cubic iron alloys become brittle at subzero temperatures, –150 to –250°C. This is often known as the cold brittleness range.

In steels, if the crack is open to the atmosphere, the color of its surface is a useful guide to when it formed: an uncolored metallic surface will indicate that the crack occurred at a temperature near to room temperature; the normal ‘temper colors’ (the light interference colors reflecting the thickness of the oxide) range from light straw, formed at somewhere near 300°C, through yellow, blue and finally to brown indicate greater exposure to time at temperature, with temperatures probably approaching 600 or 700°C for the darker colors.

This page intentionally left blank

# Properties of castings

# 9

Having made our casting, it may appear visually perfect, but the warm hopes encouraged by its comforting appearance can quickly be dashed when its properties are checked.

Very often the tensile properties reveal that the casting may be strong, passing the requirement for strength specified by the customer, but its ductility is below the specified requirement. This is common. Alternatively, everything appears to be fine, but the casting leaks. This is also common.

The customer can be impressively intransigent when it comes to demanding his specified properties. After all, when accepting the order from the customer, the foundry had agreed to provide the specified properties.

This section reviews some of the potential problems.

## 9.1 TEST BARS

Test bars are used to test the tensile properties of the cast metal. They are used in various ways:

- (i) To test a melt prior to or at the same time as the pouring of the casting (even though the test bar will probably require heat treatment, and so often be tested days after the pouring of the casting);
- (ii) To test the casting as a cast-on feature of the casting, accompanying the casting through heat treatment, and finally cut off and tested, sometimes in the presence of the customer's inspector;
- (iii) To test the casting as a specimen excised (i.e. cut out) from the casting as part of a destructive test of the casting.

The cast-on test bars and excised bars both will be tolerably representative of the material of the casting, and tend not to cause any serious problems of interpretation, even though exact simulation of conditions throughout the main body of casting are clearly not achieved and are probably not achievable. These bars are generally accepted as being sufficiently representative.

The main problems with test bars are with the separately cast bars. This section focuses on these.

Invariably, at the present day, type (i) test bars are poorly designed so that they give poor representations of the properties of the castings. To reduce their problems with obtaining reasonably representative bars, foundries will give the job of pouring to one particular person who is known to have a good pouring 'technique', and who can therefore achieve properties that are believed to be representative. Stories abound of those foundries that should pour test bars for each melt from day to day, but have poured a week's supply on Monday morning because they happened to know it was a good melt, and their expert pourer was available at the time. Such stories probably show my age; I have not heard of such practices in recent years.

The design of all current test bars pre-dates the concepts of surface turbulence, air entrainment and critical velocity, and pre-dates experimental verification of their filling action by such techniques as video X-ray radiography and computer simulation. Thus at the time of writing it is regrettable that all



our world standards of test bar designs are unsatisfactory. None can faithfully reproduce the actual quality of the melt; all impair the melt during the filling of the mold, explaining the scatter in properties that is usually observed. The scatter can be important, possibly causing a perfectly good batch of castings to be scrapped if properties appear (misleadingly) to be low.

Since all current national and international test bar molds known to the author appear to be designed to maximize defects, there seems to be no point in describing any of them. I am taking the initiative therefore to describe the features of one test bar mold below that has been properly developed and is known to give representative results.

### The 10 test bar mold

The concept is shown in Figure 9.1. The design has been proven by video X-ray radiography to be free from air entrapment

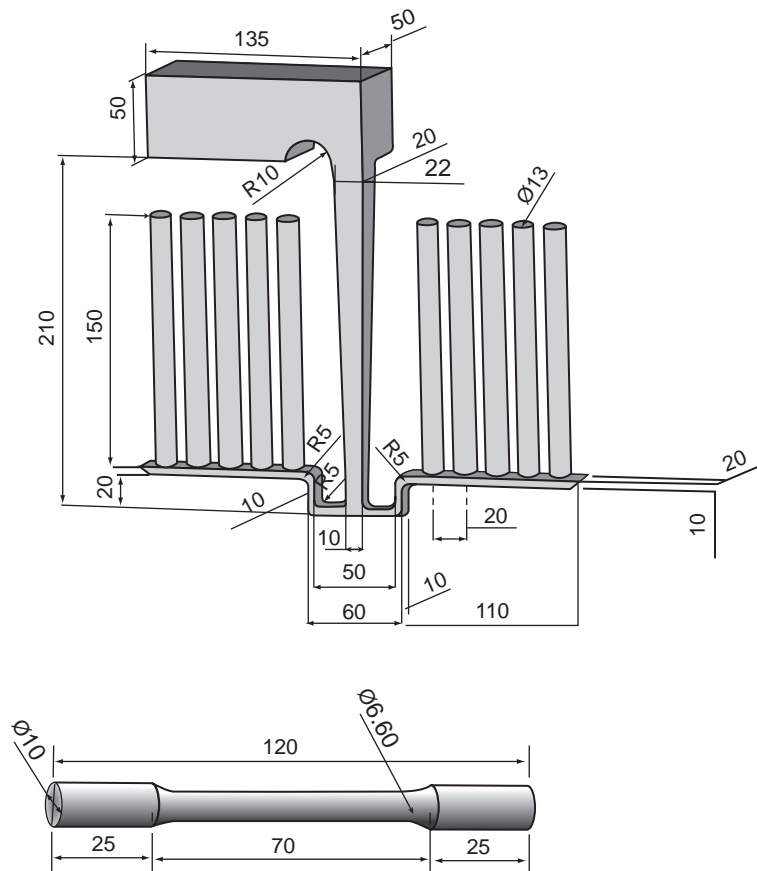


**FIGURE 9.1**

The Birmingham UK 10 test bar casting and test piece (Dispinar and Campbell 2005).

This mold casting ten bars at a time was specifically designed for research. The design was optimized by Dispinar and Campbell (2005) using Al–7Si–Mg alloy poured into resin-bonded sand molds viewed by X-ray radiographic video. All ten bars fill beautifully, so that their tensile properties have been found to be indistinguishable and to exhibit minimal scatter. This makes the mold ideal for carrying out studies on the optimization of heat treatment for instance, in which from only ten molds, 100 test bars are quickly produced, all with practically identical as-cast properties. Other studies requiring large numbers of bars for statistical purposes are also quickly generated from relatively few molds.

However, of course, even this design does not deliver a test bar free from damage. This is because the act of pouring metal into the pouring basin is somewhat damaging, and the initial stages of the priming of the down-sprue will be likely to be messy and additionally damaging. The damage in the down-sprue might be reduced by redesigning the assembly so that the bars were horizontal, thus much smaller fall heights would be suffered, giving much lower filling velocities and thus reduced damage to the metal. It would be useful to compare the results of vertical and horizontal molded systems. Ultimately, the pouring basin and the down-sprue damage could be totally eliminated if the mold were filled from a counter-gravity filling system. The adoption of counter-gravity filling systems is to be strongly encouraged. Only then would it be possible to achieve the filling of a test bar with metal that will be truly representative of the melt and the casting.

The mold works quite well for the Al–7Si–Mg alloys in a static pour mode (i.e. the mold is simply poured under gravity and left to cool). This design fulfills my Rule 1 for feeding – ‘Do not feed’. It seems to work adequately for most alloys, and especially light alloys in which solid feeding is relatively efficient, and where the alloys are of a reasonably good quality, i.e. a small population of small bifilms that are relatively resistant to opening under the reduction of pressure suffered without a feeder.

Early trials targeted at the production of a shaped test bar were abandoned because of the difficulty to ensure that the grip length furthest from the feeder was sound. The provision of a feeder to ensure soundness was probably possible, but was not straightforward without introducing other dangers of parallel filling systems and possible overspill between the different filling routes. The penalty that the bars all required to be machined was accepted.

The offset stepped basin and tapered sprue is designed to ensure that no air enters the mold (which appears to be the most serious criticism of current designs). The minimum depth in the basin used for the calculation of the filling system is 25 mm, thus the sprue is likely to start filling before the basin is filled to its minimum operational height unless a stopper is used in the sprue entrance. The stopper is only raised when the basin has been filled above the minimum level line. The basin is continued to be topped up after the removal of the stopper.

The mold works well as a sand mold. It would also be appropriate as a permanent metal mold, although the rather narrow channels would require to be increased in size to allow for the thickness of a mold coat.

Naturally, the design could be adapted for the casting of perhaps only two test bars at a time, making it more universally useful. Furthermore, the development at Birmingham showed, in line with expectations, that the design worked well for all types of metals from light alloys, via cast irons to steels.

However, for some alloys that are more difficult to feed, and probably as a prudent design where metal quality might be less than optimum, the bars would benefit from the enlargement of the horizontal runners from  $20 \times 10$  mm to  $20 \times 20$  mm, plus the provision of a feeder of at least  $20 \times 20$  mm

standing on each arm of the runner (a test bar on each side may need to be sacrificed to make room for the feeder). The feeder on each arm can then pressurize the runner and in turn maintain pressure in the 13-mm-diameter castings during freezing. An additional feature that is easily provided to aid feeding from an enhanced temperature gradient is the provision of a cooling fin at the top of each test bar. This is laid on the parting line, 2 mm thick with dimensions approximately  $20 \times 30$  mm and possibly open at the top of the mold to eliminate any back pressure (metal rarely fills all of the fin).

Alternatively, for alloys that are difficult to feed, a second variant of the 10 test bar mold is designed to be rolled over through  $180^\circ$  immediately after casting. In this case the runner bar is increased in section to  $25 \times 25$  mm to act as a feeder after the mold has been inverted. This is somewhat better for alloys which require much feeding, and, of course, reproduces more faithfully the conditions of those processes that use a roll-over mechanism such as the Cosworth operation. Most of the fatigue research from the Birmingham UK department has been performed with this casting technique.

The roll-over technique requires the use of a small pivoted cradle and hand crank (it is impressively primitive to look at!) for clamping the mold halves together and inverting the complete mold immediately after casting.

A practical inconvenience experienced with roll-over was the fact that the sprue emptied and poured over the floor. Originally we had suffered this, thinking that the ensuing mess was simply to be tolerated, and assuming that the casting would be unharmed because of the swan neck link to the runner/feeder bar, which would have prevented this vital feed metal from the runner bar being lost. However, this was not always true. The metal would sometimes siphon around the swan neck and empty from the runner/feeder which would then collapse inside its oxide skin like a punctured balloon.

Thus a refinement of technique which we found necessary to introduce was to take the sprue cut from the previous casting, and use this to plug and freeze the sprue of the current casting immediately prior to the roll-over. This was a slight inconvenience, but saved the mess on the floor, and retained the runner/feeder filled so that feeding could occur efficiently.

Once again, such practical inconveniences would be avoided by the adoption of a side-filled counter-gravity filling system with an integral roll-over facility. Counter-gravity is such a sensible, civilized and economic technology!

### K-mold test (evaluation of melt cleanness)

The K-mold test (Figure 9.3) is used not for the evaluation of mechanical properties but for the evaluation of the cleanness of molten aluminum. It was invented in Japan in 1973 by Kitaoka but not widely published until 2001. A description is given by Wannasin and colleagues (2007). The test is sensitive principally to large oxide bifilms. The test is valuable for assessing the quality of incoming metal to the foundry, and in optimizing melt treatments to raise melt quality.

The test is used in different ways by users. For instance one user defines a K-value (the number expressing the cleanness) in terms of the total number of oxide films observed on the fracture surfaces. Another user defines K as the number of fracture surfaces (made by breaking at the five V-grooves along the length of the bar) that contain oxides. If all five contain oxides then the rating is '5'. Most users, understandably, tend to ignore oxide defects smaller than some critical size, usually about 1 mm.

The fundamental feature of the K-bar test is that the fracture is forced to occur at the V-groove, thus the material is sampled at that point, whether there is a defect present or not. Thus the test checks

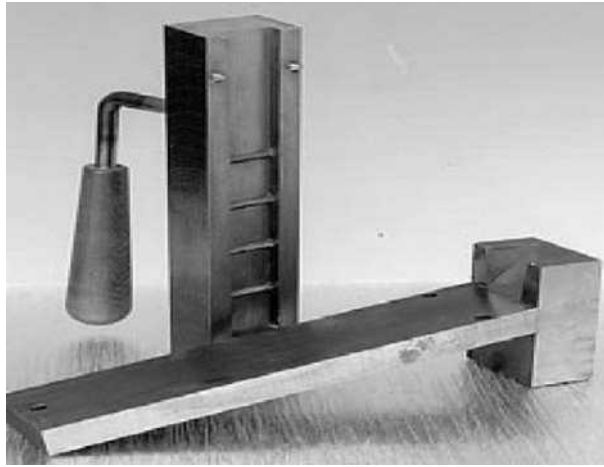


**FIGURE 9.2**

K-bar test mold (courtesy of N-Tec 2009).

random samples of the material. This differs from a test like the tensile test or a bend test in which failure occurs at the largest defect, giving a pessimistic indication of the general quality of the material.

It will be interesting in the future if material is made without a substantial population of bifilms. The familiar brittle fractures at the five V-notches should then become impossible. The material will simply bend, refusing to fracture.

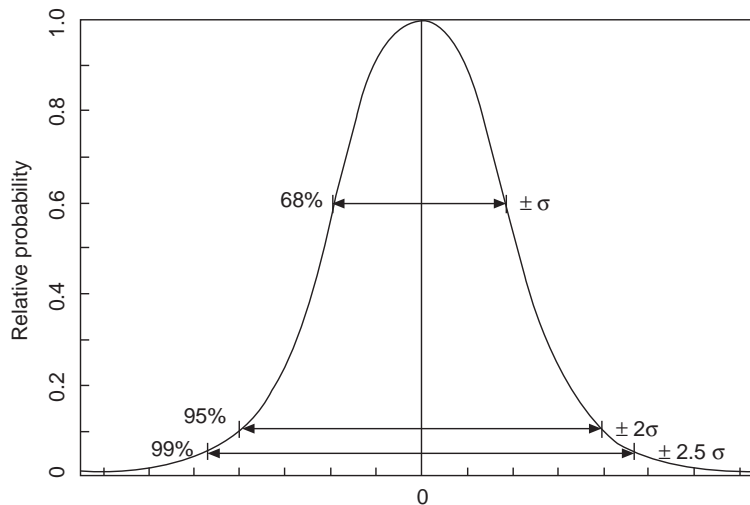


**FIGURE 9.3**

Gaussian distribution of strengths, showing assessment of scatter using different multiples of the standard mean deviation  $\sigma$ .

## 9.2 THE STATISTICS OF FAILURE

Unfortunately, the properties of materials are not accurately reproducible. Scatter of tensile and fatigue properties has been a particular problem with castings.

This is recognized by many of the world's standards for the testing of castings. If a tensile test bar falls below the strength value required by the specification, the specified procedure is to record the low properties with a record of any visible anomaly on the fracture surface and then break two additional test bars from the same production batch to show that the low property break was due to an inclusion or other anomaly and did not reflect the yield, elongation, and ultimate measurements of the metal.

Effectively, the failed result is discarded. The discarding of low values is a practice that has crept in to both foundries and laboratories. Somehow the low results are viewed as a mistake. We turn a blind eye to them. This approach is, of course, less than honest. Furthermore, it deprives us of valuable information on the real properties of the products we are making. It is a real result, illustrating how the properties reduce as a result of the presence of defects. Since all of the test bar results, 'good' or 'bad', are influenced by the population of defects, the 'outliers' are a good indication of the real spread of results.

When dealing with scattered property results, the common approach is simply to take an average. Occasionally, a standard deviation might also be calculated. The attempt to assess scatter by the use of a standard deviation, usually denoted sigma,  $\sigma$ , is of course much better than nothing, but does make the implicit assumption that the distribution of results is Gaussian, or Normal. The familiar bell-shaped distribution is shown in Figure 9.3. The value  $\pm\sigma$  encloses approximately 68% of the scattered results. The values  $\pm 2\sigma$  includes 95% and  $\pm 2.5\sigma$  includes 99%. Higher multiples of sigma, for instance  $3\sigma$  (99.73%) and  $4\sigma$  (99.994%), are less commonly used.

If instead we retain all results, good and bad, and plot them to reveal their distribution, we can obtain a histogram such as that in Figure 9.4a. The shape of the distribution curve is usually not the symmetrical Gaussian form but is skewed, as are many strength and fatigue life distributions. The skew form is to be expected, arising naturally because strength values cannot be higher than when the alloy is perfect. This defines a cut-off to strengths at an upper limit. However, depending on the size and location of defects, there is often no lower limit, so the low results exhibit a long 'tail'. A close approximation to the shape of the curve was derived theoretically by Weibull (1951). The curve (Figure 9.4a) can be plotted as the familiar cumulative distribution (Figure 9.4b) and by further mathematical manipulation the curved ends of this plot can be straightened in what is known as a Weibull plot (Figure 9.4c). In other words, a Weibull plot is simply another way of presenting a cumulative data distribution.

In general, the failure properties of metals are more accurately described by the Weibull distribution. There are good fundamental reasons for this. Although the original formulation by Weibull in 1951 was a purely mathematical description of scatter, it was Jayatilak and Trustrum in 1977 who explained that the formulation corresponded to the properties of a flaw size distribution of randomly inclined cracks. The strength distribution was accounted for by the probability of brittle fracture from the most severe defect, taking account of its size and orientation. It was a sophisticated development of the 'weakest link' concept.

In materials research, Weibull analysis was originally used almost exclusively for ceramics and glasses. The work by Green and Campbell (1993, 1994) illustrated the usefulness of this approach to castings.

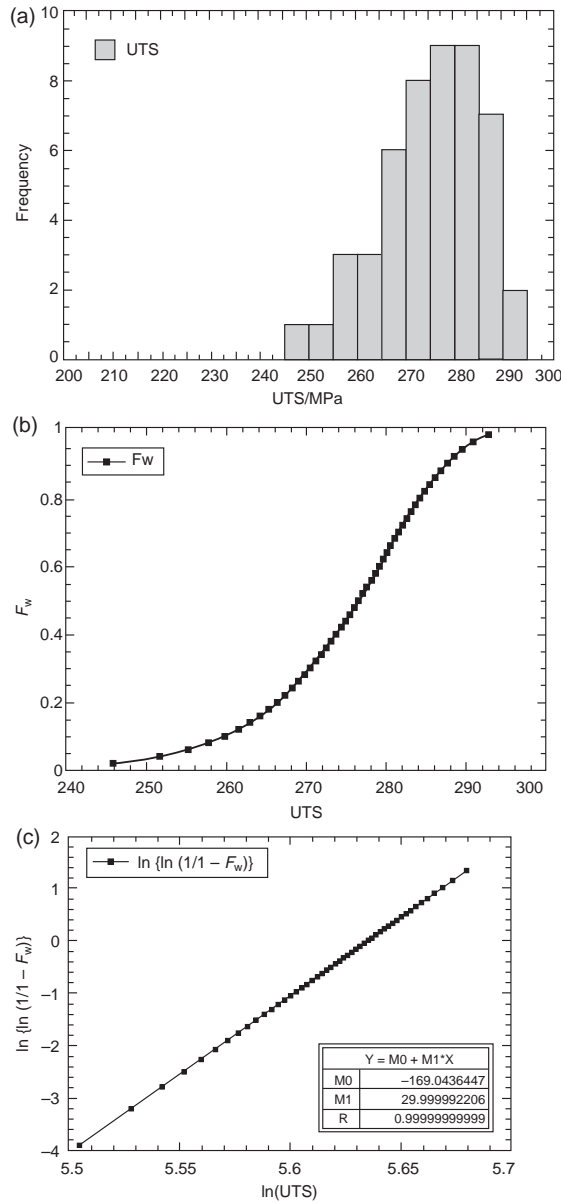


**FIGURE 9.4**

(a) Typical skewed distribution of tensile strengths as might be obtained from a cast Al–Si alloy (synthetic data by Green 1995). (b) Distribution identical to that in Figure 9.4a but replotted as a cumulative distribution (Green 1995). (c) Plot of the data in Figure 9.4b showing the simple straight line form of the two-parameter Weibull cumulative distribution (Weibull modulus  $m = 30$  and position parameter  $\sigma = 280$  MPa) (Green 1995).

The slope of the Weibull (pronounced ‘Vybl’ where ‘y’ is as in ‘why’) plot is a measure of the reproducibility of the data, and is known as the Weibull modulus,  $m$ . The other important parameters that are derived from a Weibull approach are the position parameter (a measure of the average strength) and the minimum threshold value. The threshold is that value below which no failures are expected; even though thousands of tensile tests might be performed, for a finite threshold no test would fail at a lower stress. The presence of a threshold is comforting. However, it can only be derived using the three-parameter Weibull analysis. If it is assumed that there is no threshold (i.e. it is assumed that strength can fall to zero on occasions) then the threshold can be neglected, allowing a simpler analysis using two-parameter Weibull. We shall present examples of these analyses later.

The Weibull analysis can, in principle, estimate the probable value of strength of the weakest casting in a sample of 100 typical castings, or perhaps the weakest 1 in 10 000. However, of course, when using extrapolations from limited data, the accuracy of the extrapolation needs to be carefully assessed. In addition, as with all extrapolations, uniformity of conditions when extending into the unknown is never certain so that extreme caution, if not outright skepticism, is required.

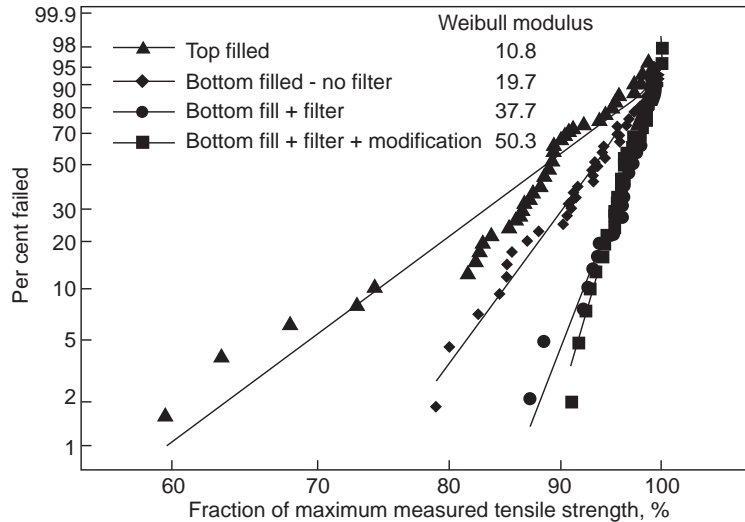
In much work using two-parameter Weibull, it has been found that for pressure die castings  $m$  is often between 1 and 10, whereas for many gravity-filled castings it is between 10 and 30. For good-quality aerospace castings a value between 50 and 100 is more usual. Values of 150–250 are probably somewhere near a maximum limit defined by the limits of accuracy of strength measurements (i.e. even if all strength results were perfectly identical, the expected modulus of infinity could not be demonstrated because the tensile testing machine would record slightly different strengths because of errors in the machine). It should be noted that all these Weibull parameters are based on the two-parameter interpretation of the Weibull analysis. The more accurate and complete three-parameter analysis is dealt with later in this chapter.

Figure 9.5 shows data for a single alloy cast in a variety of ways, showing the variation in reproducibility between different filling processes. The data are from sand castings poured variously ‘badly’ and ‘well’, giving a Weibull modulus varying between about 10 and 50. These kind of data are one of the simplest demonstrations of the importance of filling techniques on the reliability of cast products. It is also, of course, a clear demonstration of the action of entrainment defects.

Figure 9.6 shows the case of a bimodal distribution, i.e. two separate modes or distributions. Such multiple distributions are relatively common, and an indication of such an effect is to be seen in the poorest data shown in Figure 9.5. The various slopes are usually found to correspond to different distributions of defects. Several slopes can sometimes be distinguished, from the lowest to highest results, corresponding to pores, new bifilms, old bifilms, and sound material. The identification of the regimes of strength of each of these defect types can give a valuable insight into the causes of poor performance.

For instance, a bimodal distribution of strength results in many castings is to be expected. The melt will already contain a background population of bifilms, usually sub-millimeter size but in large number density, but if the melt enters the mold cavity turbulently the bifilms created at that late stage of filling are usually of large size, at least in the centimeter size range, giving quite different failure modes. A typical example is seen in Figure 2.44.

As a final caution, it is probably worth noting that all of the above analysis assumes reasonably brittle failure behavior. This seems to be a good assumption for most castings, where the failure of one part will lead to the failure of the whole component. This is not the case for ductile materials where crack blunting will occur. Ductile failure may be better described by a gamma distribution (Green



**FIGURE 9.5**

Two-parameter Weibull plot of strength results for Al-7Si-0.4Mg alloy cast in various ways (Green and Campbell 1994).

1994). The statistics of failure is an interesting and important area that holds many descriptions of distributions that would repay more widespread study.

### 9.2.1 Background to the use of Weibull analysis

The distribution of strengths of brittle materials was first formulated by Weibull (1951) who defined a probability of *survival*  $F_S$ . This section follows an approach described by Green (1993). The Weibull distribution is given by the expression

$$F_w = 1 - \exp\left\{-\left(\frac{x - \mu}{\sigma}\right)^m\right\} \quad (9.1)$$

where  $F_w$  is the cumulative fraction of *failures* up to a given value of  $x$ , say strength or fatigue cycles,  $\sigma$  is a position parameter where  $1 - 1/e$  of the samples survive ( $\sim 37\%$ ),  $\mu$  is a lower-strength boundary below which no specimen fails and  $m$  is a width parameter, referred to as the Weibull modulus. The greater the value of  $m$  the narrower is the range of strengths. This is the so-called three-parameter relation, in which the three parameters  $\sigma$ ,  $\mu$  and  $m$  are found by curve-fitting techniques.

The above expression is frequently used with the lower strength  $\mu$  set to zero, giving the so-called two-parameter Weibull approximation, so that

$$F_w = 1 - \exp\left\{-\left(\frac{x}{\sigma}\right)^m\right\} \quad (9.2)$$

In general the three-parameter relation should be used, or at least explored, prior to making the assumption that a lower threshold of values  $\mu$  does not exist. Forcing the Weibull fit to assume no



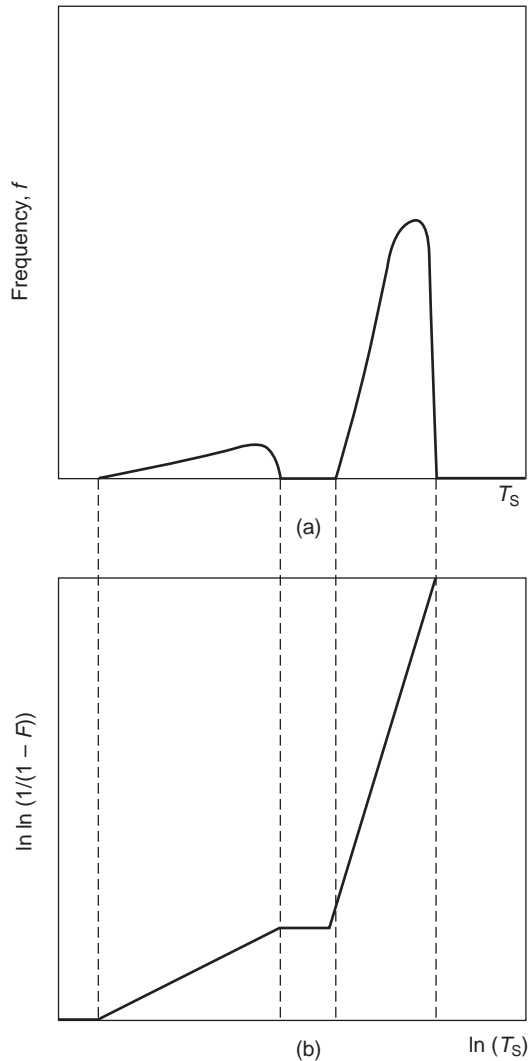


**FIGURE 9.6**

(a) Bimodal distribution and (b) its corresponding plot in terms of two separate two-parameter Weibull distributions.

threshold can give a misleading interpretation of the data. For instance Figure 9.7 showing top-poured material versus bottom-gated material shows the same data interpreted (a) as a two-parameter straight line plot or (b) a three-parameter curve. Clearly the three-parameter result is a more faithful representation of the data. Furthermore, the shape parameter ( $m$ ) and position parameter (scale parameter)  $\sigma$  are quite different, so that extreme caution needs to be exercised when attempting to compare the

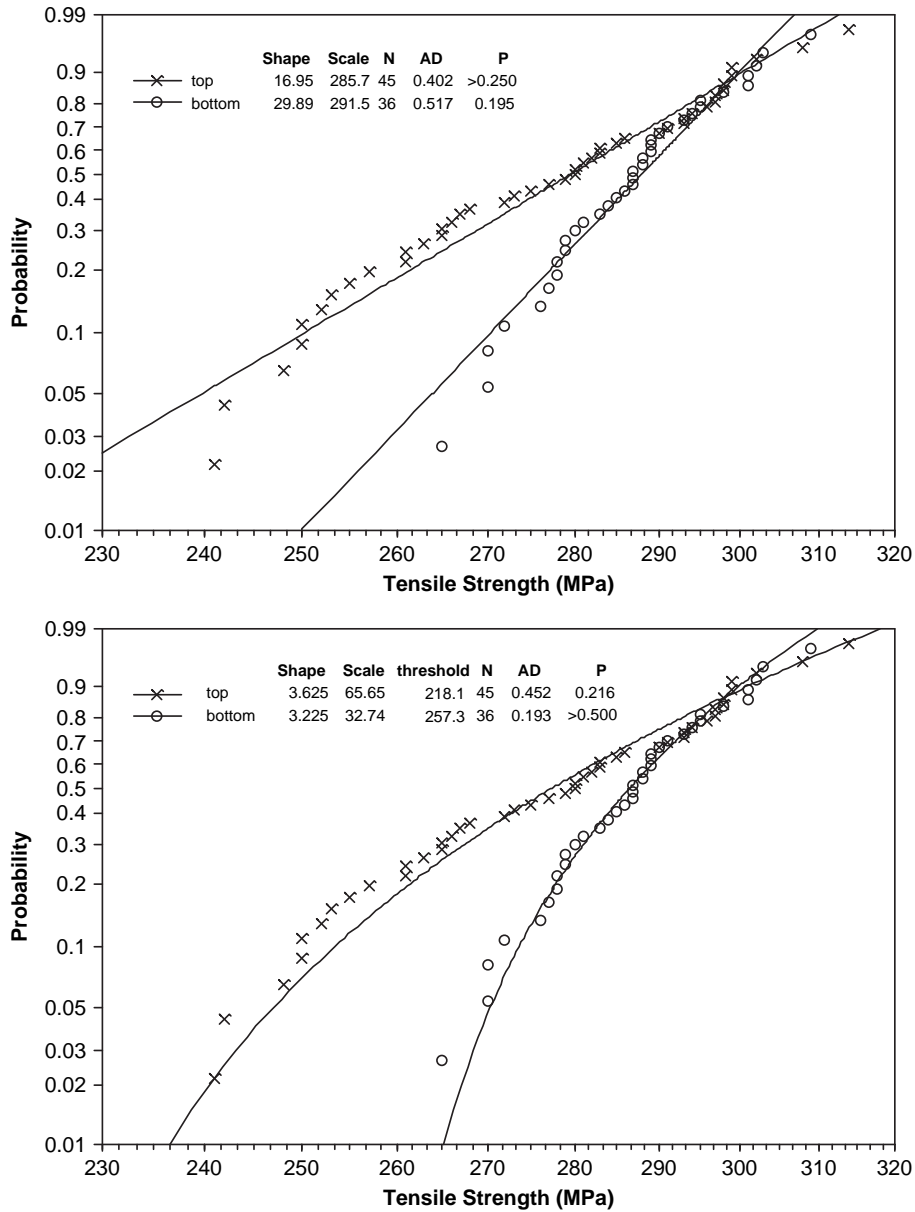


**FIGURE 9.7**

(a) A pair of strength distributions from top-poured versus bottom-gated castings, ill-fitted by a two-parameter Weibull analysis; (b) a three-parameter Weibull plot illustrating that both distributions have thresholds (lower limit values below which no results are expected) (courtesy of Tiryakioglu 2009).

parameters; it is essential to know whether the parameter refers to two- or three-parameter interpretations.

An example of a distribution of Weibullian failures described by Equation 9.2 is shown in Figure 9.4a. Unlike the normal distribution there is no reflective symmetry about the mean. To obtain the two-parameter Weibull modulus and position parameter from such a plot requires mathematical curve fitting. Alternatively, these can be found by reducing the cumulative distribution (Figure 9.4b) to a straight line plot (Figure 9.4c). To do this, we first eliminate the minus sign in the exponential term

$$\frac{1}{1 - F_w} = 1 - \exp\left\{\left(\frac{x}{\sigma}\right)^m\right\} \quad (9.3)$$

and taking natural logarithms twice gives

$$\ln\left\{\ln\left(\frac{1}{1 - F_w}\right)\right\} = m \ln(x) - m \ln(\sigma) \quad (9.4)$$

This can now be presented as a straight line by plotting  $\ln\left\{\ln\left(\frac{1}{1 - F_w}\right)\right\}$  as a function of  $\ln(x)$  giving the straight line with slope  $m$  and intercept  $-m \ln(\sigma)$ , the intercept giving the position parameter  $\sigma$ . The slope  $m$  and the position parameter  $\sigma$  are the two parameters to emerge from this approach, giving the name ‘two-parameter Weibull’ to this approach. The data of Figure 9.4b are replotted in Figure 9.4c with a straight line fitted to the data by simple regression analysis.

### 9.2.2 Two-parameter Weibull analysis

It is implicit in the Weibull distribution that the failure strength of a material is determined by the distribution of defects resulting from its manufacture. The Weibull distribution can be of great use because it is possible to extrapolate back to the very low probability of failure (high reliability) region, and to select a design stress to give a desired failure rate. The following procedure can be used when the volume effect is small.

1. Select an acceptable failure rate.
2. Rank the data in ascending order of strength (fatigue life, etc.) and assign corresponding ascending failure rank  $j$ .
3. Make the extrapolation from a sample of specimens to the population they are drawn from. This is required because the first specimens to fail in the sample tested has a probability of survival of 100% at a stress below its failure stress. However, there is a finite probability that if more specimens were tested one of them would fail at a lower stress. The most probable unbiased estimate of the probability of survival of the  $j$ th specimen in the ranked data is given by Tiryakioglu and Hudak (2008) as

$$F_j = \frac{j - a}{N + b}$$

where  $N$  is the total number of specimens tested and the parameters  $a$  and  $b$  are listed in Table 9.1.

4. Calculate  $\ln\left\{\ln\left(\frac{1}{F_s}\right)\right\}$  for each  $F_j$ .
5. Calculate  $\ln(x - \mu)$  for each  $(x - \mu)$ .

6. Plot  $\ln\left\{\ln\left(\frac{1}{F_s}\right)\right\}$  as a function of  $\ln(x - \mu)$  and regress through this a best-fit straight line. The Weibull modulus is the slope  $m$  of the line.
7. Calculate position parameter  $\sigma$  then back substitute into the Weibull equation (9.1 or 9.2) with  $F_s$ ,  $\sigma$  and  $m$  to calculate the design stress  $x$ .

### 9.2.3 Three-parameter Weibull analysis

Although the two-parameter Weibull approach has been widely used for the analysis of scatter in the mechanical test results of castings, there are plenty of instances where this approach is clearly not

**Table 9.1** Unbiased probability estimators (Tiryakioglu and Hudak 2008)

<b>N</b>	<b>a</b>	<b>b</b>
5	0.173	0.500
6	0.243	0.390
7	0.280	0.310
8	0.309	0.251
9	0.322	0.210
10	0.348	0.190
11	0.367	0.160
12	0.371	0.130
13	0.382	0.110
14	0.388	0.100
15	0.394	0.080
17	0.407	0.050
20	0.417	0.030
22	0.430	0.000
25	0.443	0.000
27	0.448	0.000
30	0.455	0.000
32	0.460	0.000
35	0.465	0.000
40	0.472	0.000
45	0.481	0.000
50	0.486	0.000
55	0.499	0.000
60	0.503	0.000
65	0.509	0.000
70	0.518	0.000
75	0.522	0.000
80	0.516	0.000
90	0.518	0.000
100	0.519	0.000

valid. If the two-parameter Weibull plot is not a straight line, the distribution is clearly not described by two-parameter Weibull assumptions. The real distribution might be one of several, but the most useful rapid check is to ascertain whether the original assumption making the minimum strength limit  $\mu$  equal to zero is correct. If in fact there is a minimum limit to strengths Equation 9.4 becomes:

$$\ln \left\{ \ln \left( \frac{1}{1 - F_w} \right) \right\} = m \ln(x - \mu) - m \ln \sigma \quad (9.5)$$

The Weibull plot then becomes a plot of the left-hand side of Equation 9.5 as the vertical axis, versus  $\ln(x - \mu)$  along the horizontal axis. The data then have to be fitted to give optimized values for the three parameters  $m$ ,  $\sigma$  and  $\mu$ , giving the appropriate appellation ‘three-parameter Weibull’ analysis.

Those casting processes and conditions that can deliver a distribution that is terminated by a minimum threshold are of enormous importance. It is not easy to predict at this early stage what feature of the casting process would lead to this key advantage. We may find the threshold is reproducible if the processing is carried out with attention to some key detail, such as, for instance, settling time prior to casting, or turbulence during the pour. A sharp cut-off to the distribution scatter may be an independent factor related to melt quality and turbulence, rather than some metallurgical factor such as cooling rate, chemistry, or heat treatment, etc.

Conversely, finding that the data indicate that  $\mu$  is actually zero, or even negative (i.e. the distribution of strengths or ductilities extrapolate to zero), is a salutary piece of information, which, if correct, warns of enormous danger for safety critical components, some of which will be expected to have zero strength or zero elongation.

Figure 9.8a shows strength distributions of two sets of castings. The castings with lower average strength follow a three-parameter Weibull distribution as confirmed by its  $p$  value being in excess of 0.05. Their threshold strength is 281 MPa. Thus although the average strength is low, possibly as a result of some inappropriate heat treatment, the castings exhibit a minimum strength below which no failures are expected.

### 9.2.4 Bi-Weibull distributions

An attempt has been made to fit the castings with higher average strength to a three-parameter Weibull plot without success, as indicated by the very low  $p$  value. The poor fit suggests a negative (i.e. zero in practical terms) threshold. However, the data strongly suggest that the data may follow a bi-Weibull distribution as indicated by the two separate regions of the curve. A bi-Weibull distribution is characterized by two different slopes for each part of the Weibull curve; this indicates the presence of two separate failure mechanisms, implying two different defect distributions.

Figure 9.8b shows the ductility results for the same two sets of castings. Both datasets follow three-parameter Weibull distribution as indicated by  $p$  values above 0.05. One set has a threshold value of 5.7% confirming that no castings from this population are expected to fail at an elongation below 5.7%. For the other castings, the threshold value is negative. Hence some castings from this source can be expected to fail without any elongation. Even here, although the  $p$  value indicates a reliable result, the appearance of the data in Figure 9.8b may indicate that a bi-Weibull distribution would be an even better description of the data. If so, even for these relatively poor data, a minimum threshold might be found to apply.

The bi-Weibull approach is too complex to present here. The interested reader is recommended to the guidelines set out by Tiryakioglu and Campbell (2010). However, the power and flexibility of this

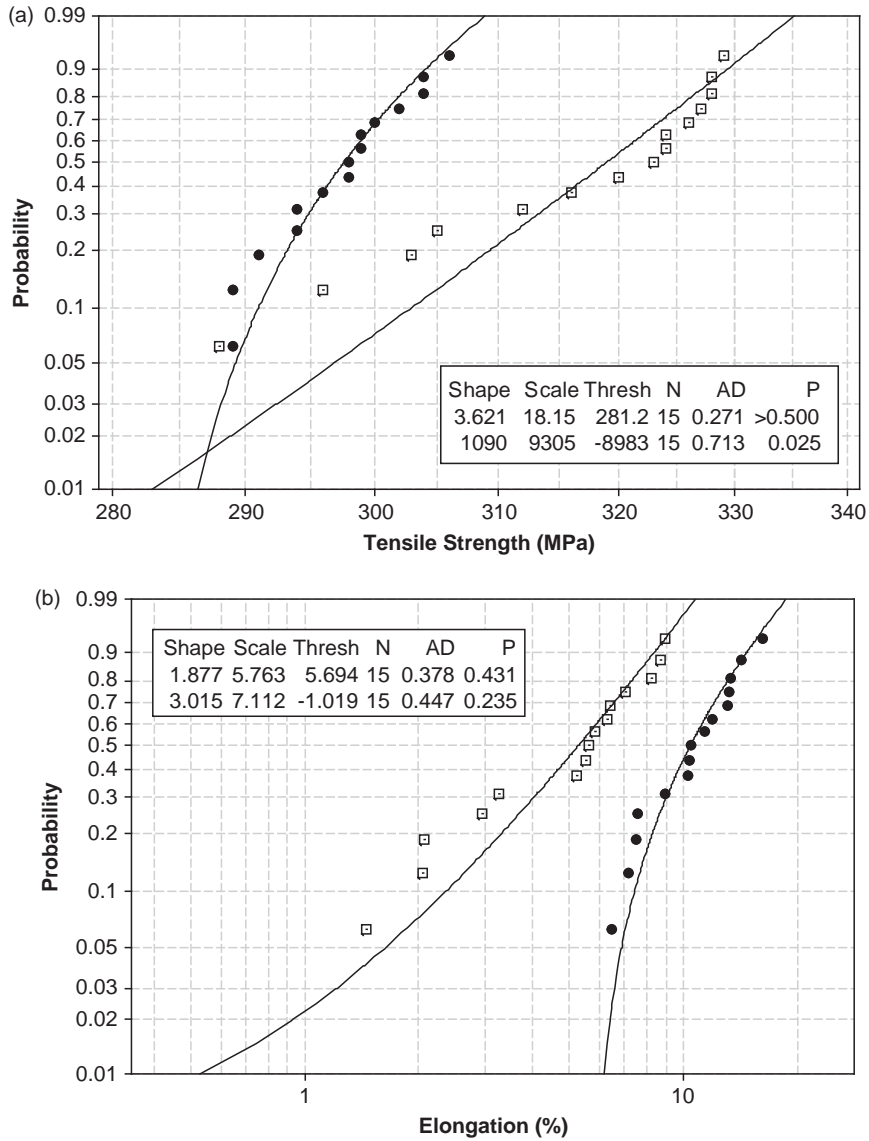


**FIGURE 9.8**

(a) A comparison of the strength distribution of two sets of castings by three-parameter Weibull. Those with the lower average strength had a minimum threshold of 281 MPa, whereas those with the higher average strength had a strength distribution that extrapolated to zero (actually indicating negative in the curve-fitted result). (b) Elongation results conveyed the message that one set of results, this time higher, were more reliable than those which extrapolated to zero. (Courtesy of Alotech Limited and M Tiryakioglu 2009.)

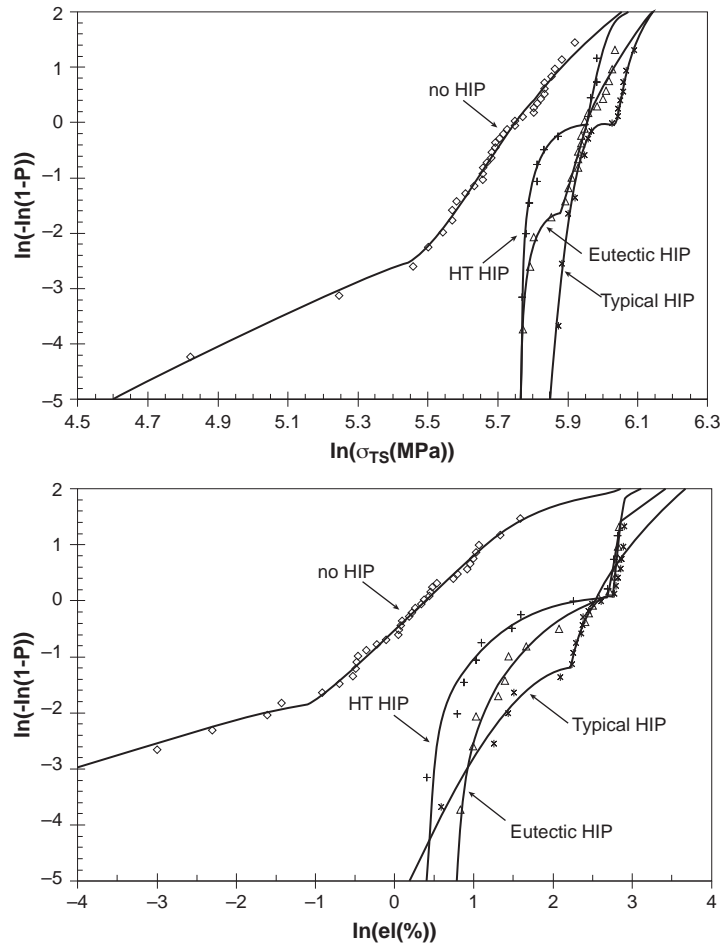


**FIGURE 9.9**

Three-parameter bi-Weibull plots of tensile strength and elongation for non-HIPped and castings with three different HIPping techniques showing at least two distributions of defects in each set (Staley et al. 2007).

technique to describe the complexity of property distributions in castings is illustrated by Figure 9.9. Sets of samples subjected to various hot isostatic pressing (HIP) routines were subjected to tensile tests. The distributions of the results illustrate that at least two defect populations appeared to be present in all the samples. In some results from this work there is even a suggestion that three populations were present, but more data would have been required to confirm this.

### 9.2.5 Limits of accuracy

Reliance on the precision of the Weibull moduli derived from a limited number of tests has to be viewed with some caution. For instance Tiryakioglu and Hudak (2008) have shown (Table 9.1) that for

a simulated result of 30 tensile tests that should have a true modulus  $m = 26.5$ , the actual experimental results to within 95% confidence limits (looking up  $\pm 0.025$  in Table 9.2 giving the fractional errors) will vary from 0.667 to 1.405 times the true result, equivalent to  $m = 17.7$  to 37.2. This is a soberingly wide spread, warning that the value of  $m$  is often less accurately estimated than we might like.

The use of about 30 samples has often been regarded as sufficient to obtain a valid Weibull plot. However, Tiryakioglu's cautionary analysis would indicate that an extrapolation of strength data to a failure rate of one in a hundred will give a corresponding expansion of the uncertainty in the extrapolated result. Despite these legitimate concerns the result does not further deteriorate too

**Table 9.2** Percentage points of the distribution of modulus  $m$  obtained by using the unbiased probability estimators in Table 9.1

<b>N</b>	<b>0.005</b>	<b>0.01</b>	<b>0.025</b>	<b>0.05</b>	<b>0.1</b>	<b>0.9</b>	<b>0.95</b>	<b>0.975</b>	<b>0.99</b>	<b>0.995</b>
5	0.292	0.325	0.381	0.434	0.504	1.630	2.014	2.458	3.169	3.653
6	0.320	0.358	0.418	0.475	0.549	1.555	1.852	2.189	2.694	3.052
7	0.356	0.391	0.445	0.501	0.579	1.502	1.747	2.031	2.462	2.753
8	0.374	0.409	0.470	0.530	0.602	1.480	1.705	1.950	2.293	2.579
9	0.392	0.427	0.488	0.545	0.618	1.444	1.650	1.836	2.126	2.371
10	0.404	0.447	0.504	0.563	0.638	1.419	1.605	1.791	2.051	2.298
11	0.429	0.465	0.529	0.582	0.652	1.399	1.574	1.746	2.003	2.194
12	0.436	0.484	0.539	0.593	0.662	1.380	1.543	1.690	1.892	2.042
13	0.450	0.488	0.550	0.610	0.677	1.362	1.510	1.644	1.837	1.982
14	0.459	0.503	0.560	0.618	0.687	1.350	1.493	1.631	1.792	1.930
15	0.462	0.503	0.568	0.625	0.695	1.334	1.465	1.603	1.769	1.900
17	0.491	0.528	0.594	0.643	0.708	1.324	1.449	1.574	1.735	1.859
20	0.523	0.557	0.611	0.664	0.728	1.299	1.412	1.514	1.644	1.760
22	0.536	0.575	0.635	0.683	0.746	1.282	1.384	1.480	1.610	1.714
25	0.565	0.597	0.648	0.697	0.754	1.266	1.363	1.447	1.568	1.643
27	0.559	0.601	0.652	0.702	0.762	1.254	1.341	1.430	1.538	1.613
30	0.576	0.611	0.667	0.716	0.773	1.241	1.328	1.405	1.493	1.565
32	0.592	0.633	0.684	0.729	0.781	1.234	1.311	1.384	1.480	1.537
35	0.612	0.645	0.690	0.738	0.790	1.226	1.300	1.369	1.453	1.523
40	0.632	0.662	0.708	0.749	0.798	1.207	1.276	1.342	1.424	1.486
45	0.633	0.670	0.723	0.764	0.813	1.196	1.260	1.320	1.388	1.440
50	0.654	0.684	0.734	0.773	0.820	1.190	1.250	1.303	1.374	1.420
55	0.670	0.700	0.748	0.785	0.830	1.183	1.239	1.291	1.355	1.406
60	0.676	0.709	0.749	0.790	0.833	1.174	1.229	1.277	1.332	1.380
65	0.691	0.720	0.762	0.798	0.841	1.168	1.218	1.266	1.321	1.361
70	0.703	0.731	0.769	0.804	0.845	1.159	1.210	1.259	1.312	1.348
75	0.704	0.735	0.776	0.810	0.850	1.158	1.207	1.252	1.304	1.347
80	0.713	0.740	0.780	0.817	0.855	1.150	1.197	1.238	1.289	1.327
90	0.723	0.755	0.790	0.824	0.862	1.141	1.184	1.222	1.273	1.304
100	0.742	0.769	0.805	0.834	0.870	1.132	1.173	1.211	1.250	1.287



drastically. For instance for our population of 30 tensile results with true  $m = 26.5$  the 0.01 and 0.99 columns of Table 9.1 give factors of 0.611 and 1.493, corresponding to a possible range of  $m = 16.2$  to 39.6.

However, further extrapolation to a rate of, for instance, one in a thousand seems likely to expand the uncertainty of the result to the point of it being worthless. To retrieve some precision many more tests, perhaps a hundred or more, will be needed depending on what accuracy is required.

### 9.2.6 Extreme value distributions

Previously, a measure of the uncertainty involved in such an extrapolation was sought by checking the standard deviation of the slope of the Weibull plot. This is clearly a respectable approach, but Tiryakioglu, Hudak, and Okten (2009) describe a more rigorous technique to be recommended when much is at stake.

There is often much interest in the extrapolation of results of a limited number of tests to assess the failure rate of a casting at a probability, for instance, of one in ten thousand or one in ten million. The design of safety-critical components on automobiles and aircraft falls into this category. Interestingly, there are techniques for dealing with such improbable extrapolations.

Beretta and Murakami (2001) developed a technique for the quantification of the probability of finding inclusion defects in very clean steels. This awesome task can be likened to the search for the occasional needle in the haystack, followed by the necessity of predicting precisely how many needles may be in other random haystacks. Their simple solution is the counting only of the maximum defects in any studied area of the sample, and analyzing these data with the largest-extreme-value distribution (also known as the Gumbel distribution after its inventor). They successfully use the technique for the study of pores and cracks.

Tiryakioglu (2008, 2009) has developed the science of extreme value distributions for application to the properties of castings. In particular, in an exercise (2008) to find the best description of the size of fatigue-initiating defects in cast Al alloys he assesses a wide variety of different distributions including Weibull, lognormal, Frechet, General Pareto, Gumbel, and General Extreme Value (GEV). He concludes that only Gumbel and GEV descriptions are accurate and appropriate. At this time these descriptions of distributions are hardly known in the casting community, but clearly deserve wider appreciation and use.

---

## 9.3 EFFECT OF DEFECTS

In general, any non-metallic discontinuity in the structure, whether a hard, soft, brittle, gas, or vapor phase, will probably impair the properties to some degree. Figure 9.10 is an excellent illustration.

However, of course, the more compact the defect the less damage will be suffered. At the point at which a defect is smaller than the microstructural features of the alloy (i.e. smaller than the DAS) it probably ceases to be important. It is important therefore to make a distinction between the less harmful defects considered in this section and the more extensive planar defects considered in the next section. (Very large planar defects can measure 10 to 10 000 times the linear dimensions of the DAS.)

However, the number of defects present in a given volume, i.e. the density of defects, is also important, and in some cases will override the effects of the compactness of the defect. We need to

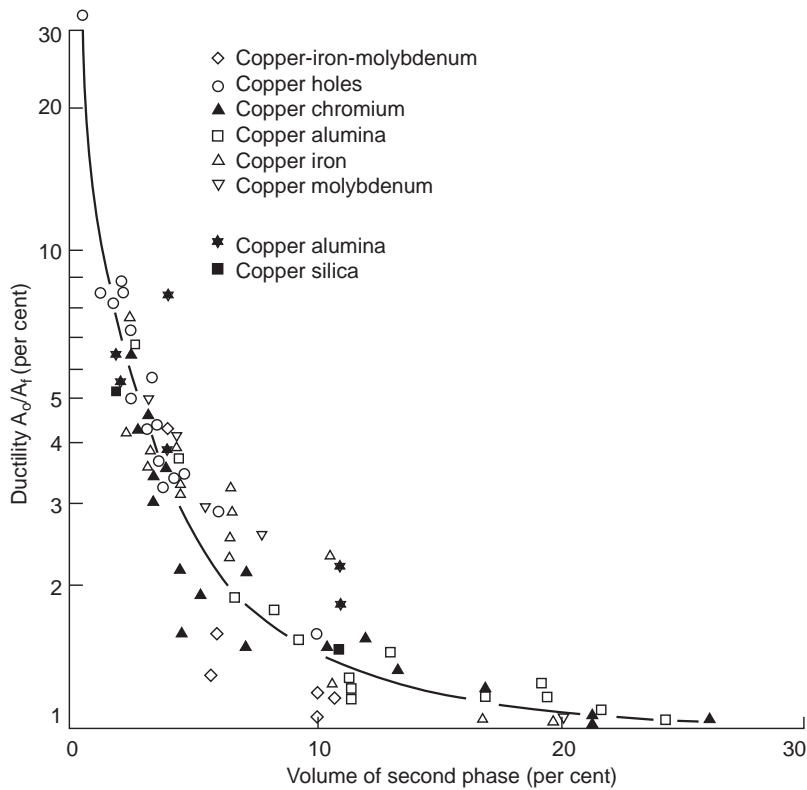


**FIGURE 9.10**

Ductility of copper containing a dispersion of second phases (data from Edelson and Baldwin 1962).

keep this in mind, since we shall look into the twin aspects of defect size and defect density in the section on properties.

It is noteworthy that defects considered here are not solidification defects. So far as shaped castings are concerned, there is no such feature as a *solidification defect*. Apart from such obvious features as shrinkage pipe or shrinkage porosity, which is comparatively rare, the only serious defects in castings are *casting defects*. These are all entrainment defects arising from surface turbulence prior to or during the filling of the mold.

### 9.3.1 Inclusion types and diagnosis

Inclusions vary widely in type both within an alloy type and between alloy bases from non-ferrous to ferrous. We shall quickly overview the compact inclusions in the various metal types; we shall consider film inclusions (possibly even more important than the compact inclusions) later.

In aluminum alloys the standard inclusions are isolated fragments of aluminum oxide. The fragments are too thick and chunky to be newly formed oxide, but are almost certainly particles carried

over from the melting furnace. To be included in the alloy they will have necessarily undergone an entrainment event, so that they will themselves be entrained in a new oxide envelope. If this entrainment was some minutes or hours prior to casting there is a good chance that the defect can be regarded as extensively if not completely 'old' oxide, with its new envelope more or less welded in place over much of its surface as a result of continuing oxidation by the entrained layer of air. Some sintering may also have occurred to supplement the welding process. Thus it will probably remain permanently compact, its welded patches inhibiting its relatively new envelope from re-opening in the mold cavity.

Such alumina inclusions are extremely hard. During machining they are often pulled out of the surface, forming long tears on the machined face. The ease of pulling out is almost certainly the direct result of the inclusion being unbonded to the matrix as a result of its surrounding envelope acquired during its entrainment into the liquid. These rock-like inclusions cause the machinist additional trouble by chipping the edge of the cutting tool. In magnesium alloys the oxide inclusions similarly have considerable nuisance value to the machinist.

Carbides, and sometimes borides, are also reported for some Al alloys, but these appear to have been little researched. It seems likely in any case that the precipitation of such phases may occur on oxide bifilms, so, in a way, it is perhaps more of a bifilm problem than a carbon contamination problem. Only further research will clarify this situation.

Flux inclusions are also troublesome in both Mg and Al alloys, reacting with moisture in the air and growing to create unsightly pustules of corrosion products on both the cast and machined surfaces. However, in addition, because of its high reactivity, magnesium has a mold-metal reaction product that is unique, and consists of reacted sand inclusions. Lagowski (1979) carried out a detailed study of these defects and their effects. It seems that the sand grains are detached from the mold wall and swept into the interior of the melt. The majority sink and sit on the drag surface of the casting. Here the 0.1–0.2-mm-diameter grains react with the magnesium, swelling, and dissolving, until finally only a nebulous halo of the order of 1 mm diameter remains. On a radiograph the residue can look like a snow storm. However, despite the alarming appearance, the mechanical properties appear to be hardly affected, provided the radiographic rating does not deteriorate beyond 4 on the ASTM radiographic standards. (The ASTM standard radiographs represent increasing severity of defects ranging from the least severe, rated 1, equivalent to a single inclusion of approximately 1 mm diameter in the representative 50 mm × 50 mm area, to the most severe, rated 8, depicting a blizzard.)

The rather limited types of inclusions in the light alloys contrast with the huge variety of inclusions found in the higher-melting-point materials. We shall take a brief look at carbon steels as representing an example of a material showing most of the inclusion types to be found in ferrous materials, despite the fact that compared to the light alloys they are usually impressively clean.

The sources of inclusions in steels are many and complicated. The liquid metal in the melting furnace is probably fairly clean at a late stage of melting because of the density difference between the non-metallic phases and the liquid steel, encouraging rapid flotation. However, prior to casting, the steel must be deoxidized by the addition of elements such as Si, Mn, and Al, etc. This reaction between the added elements and oxygen in solution in the melt creates a large population of fine inclusions in situ in the melt. A proportion of the inclusions generated from this action separate quickly by gravity. There has been much research on these in situ generated inclusions (see for instance Tiekink et al. (2010)).

Much less research has been carried out on the entrainment inclusions created during the two major pouring events. These are:

1. The transfer of the melt from the furnace into the transfer ladle will create a fresh, dense crop of inclusions, the air reacting with the exposed melt surface, oxidizing the deoxidizer additions that remain in solution in the steel. These surface inclusions, often in the form of a surface film, become entrained into the bulk melt by the action of the pour. They are known as re-oxidation inclusions. Fortunately, most of this contribution towards the loss of quality of the steel will float out in the time taken to lift the ladle out of the pit and transfer it to the casting station.
2. A second crop of re-oxidation inclusions is now entrained by the pouring action into the mold. Depending on the freezing time and geometry of the casting, this late crop of inclusions may have little or no time to float out.

Huge numbers of inclusions, generally known in the trade as re-oxidation products, result from these turbulent pouring processes, although, clearly, the second pour is far more damaging to the product than the first. The inclusions entrained in this way have been discussed in Section 6.6.

However, in addition to these sources, steels are also noted for the number of very fine additional inclusions that form later, during solidification. The remaining unreacted deoxidizing elements are concentrated in the interdendritic liquid, where more inclusions pop into being by a nucleation and growth process, as also described in Section 6.6. The interdendritic regions are small, limiting the size to which such inclusions can grow. Svoboda et al. (1987) observe that these inclusions are often also associated with small amounts of MnS. This is to be expected, since both manganese and sulfur will also be concentrated in the interdendritic spaces. It is possible that, because of their small size, some of the deoxidation products may be pushed ahead of the growing dendrites, and so become the nuclei for precipitates that arrive later.

As solidification proceeds, other inclusions may form by this concentration of segregated solutes in the interdendritic spaces. These may include nitrides such as TiN, carbides such as TiC, sulfides such as MnS, and oxy-sulfides, etc. The formation of these products is discussed in Section 6.6. In general they will be most concentrated and largest in size in the regions between grains, and in regions of the cast structure where segregation is highest, such as in channel segregates and the tops of feeders. They may also enjoy excursions into the casting as this remaining enriched metal from the feeder is sucked into the casting during the very last moments of feeding. The region under the feeder is known for its segregation problems resulting from the concentration of light elements, particularly carbon.

Later still, further precipitation of inclusions will occur in the solid state. In general, these are even finer. The driving force for their appearance is the decreasing solubility of the elements as temperature falls. Many hardening reactions are driven in this way, for instance the formation of aluminum and vanadium carbides and nitrides in steels and the precipitation of CuAl<sub>2</sub> phase in Al-4.5Cu alloy. The hardening is the consequence of the very fine size and spacing of the precipitate, making the inclusions effective as impediments to the movement of dislocations.

The precipitation of inclusions in the liquid and solid states creates populations of phases that are entirely different from entrained inclusions. Such intrinsically formed (in situ) inclusions grow atom by atom from the matrix and so are in perfect atomic contact with the matrix. They are probably therefore incapable of nucleating volume defects such as pores and cracks.

In contrast, the entrained inclusion is characterized by its unbonded wrapping of oxide, so it can easily nucleate pores and cracks from this lightly adherent coat; it easily peels away during subsequent

plastic working or creep. Alumina-rich inclusions in rolled steel are often seen to be associated with cavities. These are usually assumed to be the result of the brittle breakup of the inclusion during working, or the tearing away of the matrix from sharp corners acting as stress raisers. It seems likely to me that neither of these explanations is correct because alumina is strong, and volume defects are difficult to initiate in the solid state. The real explanation is most probably the fact that cracks and pores that are evident in such strings of inclusions are the fragments of the original alumina bifilm. This will never completely close despite much plastic working, partly as a result of the inert and stable nature of the ceramic phase, alumina, and partly as a result of the residual argon gas in the entrained layer of air. The residual argon is highly insoluble in metals.

### 9.3.2 Gas porosity

There are several different types of gas porosity, all of which are common in castings. They have to be diagnosed correctly, otherwise a wrong and consequently ineffectual treatment may be undertaken. The main categories are listed below.

#### 9.3.2.1 Gas precipitated from solution

I hesitate to call this ‘true gas porosity’, but that would convey the correct sense. It is porosity that arises as a result of gas, in solution in the liquid metal, which precipitates out during solidification. The subject is covered in detail in Section 7.2.

Also, it is necessary to re-emphasize the message given in Chapter 7, that the formation of pores is not necessarily easy. Pores cannot appear simply because the gas in solution has been rejected ahead of the advancing solidification front. If there were no nucleation sites present, the gas might exceed its solubility limit in the metal, but would still be unable to form a pore. The gas would simply remain in supersaturated solution. For aluminum alloys, the presence of supersaturated hydrogen in the solid does not appear to be harmful. For hydrogen in ferritic steels, however, the hydrogen may lead to the serious problem of hydrogen embrittlement. (Although even this does not seem to be certain. Even hydrogen embrittlement in steels may be a bifilm problem. If it is, this would explain why it has proven so difficult to understand over the many years that the phenomenon has been the subject of intensive research.)

In this section we shall assume that there are plenty of nuclei on which gases can precipitate during freezing. The only viable nuclei will normally be bifilms, since they offer such an easy precipitation site and minimal (if somewhat variable) resistance to unfurling.

In metals that solidify dendritically, the precipitated gas appears in the interdendritic spaces, and so is a well-dispersed, fine precipitate. This is its usual form. For castings of a few kg in weight the pores are usually in the range of 0.01–0.5 mm in diameter, and uniformly distributed throughout the whole casting. They can be up to a millimeter or so in diameter for larger castings. In general, however, these pores are so small that they are often invisible on a machined surface of an Al alloy because a cutting tool with a carbide tip will smear the metal over, concealing such microscopic defects. On the other hand, a diamond-tipped tool will cut cleanly, and thus render the defect visible, perhaps with the aid of a magnifying glass.

Al alloy automotive pistons in the UK used to be machined with carbide-tipped tools. On the introduction of polycrystalline diamond-tipped tools in the 1970s the piston foundries were brought to an alarming stop. They were unable to solve the sudden appearance of porosity in their castings (even

though, of course, the production process was unchanged). No customer was prepared to buy pistons that were clearly peppered with holes. The industry was forced to make a traumatic leap in the quality of its liquid metal, and lived to fight another day.

As a result of the requirement for the gas in solution to build up and concentrate before a precipitate can nucleate, there may be a sound skin over the outside of the casting. Thus the first pores appear usually 1 or 2 mm under the surface. This appearance of ‘subsurface porosity’ (Figure 7.35) is simply a variant to be expected when conditions are right for the freezing of a sound skin, as discussed in Section 7.2.3. It is a condition part-way between the completely uniform distribution of gas pores as discussed above, and the highly directional form that is to be discussed below.

In metals that solidify on a planar front the gas pores may grow, keeping pace with the growth of the front, causing long, tunnel-like defects that are sometimes called wormholes (Figure 7.38). They are often observed in ice cubes because tap water freezes on a fairly planar front. The pores may be up to 1 mm or so in diameter and of various lengths of up to 100 mm or more. An example of pores nearly 20 mm long is seen in Figure 7.39. This radiograph of an aluminum–bronze plate cast in a sand mold using non-degassed metal contrasts with a similar radiograph of a plate (not shown) cast from properly degassed melt, in which no defects at all could be seen.

All of these forms of gas porosity can be identified easily and with certainty.

It has to be kept in mind that the source of gas in solution can be that in the metal from the melting conditions. For a sand casting, additional gas in solution will have been acquired during its journey through the runner, and from continuing reaction with the mold during and after mold filling. All of these sources cooperate, and may raise the gas content of the metal over the threshold at which pores will initiate and grow.

### **9.3.2.2 Entrained air bubbles**

When the liquid metal tumbles into the mold in a ragged fashion, it necessarily entrains air or other mold gases. These will attempt to float out and separate from the metal if they have time, and if they are not hindered in some way. However, the oxide trails attached to the bubbles, and the oxide films that they encounter on their journey, or when they reach the surface of the casting, will all conspire to retain the bubbles in the casting. Such bubbles are common in film-forming systems, such as aluminum alloy castings, because the smaller bubbles do not have sufficient buoyancy to burst through (i) the oxide film at the surface of the casting, and (ii) its own oxide film (notice it is a double film every time that has to be ruptured) for the bubble to escape to atmosphere. The smaller bubbles therefore come to rest at a depth of only a double oxide skin thickness under the surface. Notice that this is another source of subsurface porosity, albeit usually localized rather than uniformly distributed over extensive areas of the surface as in the case of ‘real’ gas porosity as explained in the previous section. This subsurface location is so close to the surface that during shot blasting or heat treatment the thin surface is easily penetrated, giving the appearance of ‘surface porosity’.

The sizes of entrained bubbles range typically from 1 to 5 mm in diameter. Bubbles larger than 5 mm diameter have sufficient buoyancy to break through the double oxide barrier at the surface of the casting and so escape. Such defects are much less common in gray iron castings, where the surface film is often a liquid, and so allowing easier escape of buoyant defects.

Any prior solidification of the surface will further add to the difficulty of escape, but such extra hindrance is not common because the rate of rise of bubbles is fast, taking place usually before freezing. Exceptions are, of course, in thin-walled sections of castings that freeze during filling.

Pressure die castings are the extreme example that succeed to trap and retain the majority of the air in the die.

In gravity-filled castings, the bubbles will therefore be generally concentrated against the under-sides of cores, or in the highest parts of the casting, to which bubbles will rise after being introduced via the ingates. The distribution is far from uniform; their concentration over ingates is highly characteristic, and the remainder of the casting will often be perfectly free from defects (Figure 7.44). Sometimes the bubbles are concentrated over the first ingate on the runner, and sometimes over the last, depending on whether the runner is sufficiently deep to encourage a reverse flow to roll over the underlying incoming flow.

These concentrated accumulations of bubble defects are revealed after shot blasting, or, more inconveniently, after machining. They are typical consequences of a faulty running system.

Although often called ‘gas holes’, or ‘blow holes’, it is more helpful to call them ‘air bubbles’ to distinguish them from the finer and more well-distributed pores that precipitate from gas in solution in the liquid metal, and from true core ‘blow’ defects. Naturally, although the majority of gas in many of such defects will be air, there will be an increasing content of binder outgassing vapors as sand molds or cores heat up. Eventually, such bubbles may contain only mold vapors. Even so, the designation ‘air bubbles’ is sufficiently accurate for most purposes, and effectively describes their origin as entrainment defects.

Finally, of course, the bubble is not alone. It is accompanied by its bubble trail. This defect can extend from the bottom to the top of the casting. For a badly turbulent pour, there can be tangled masses of bubble trails, sometimes appearing on radiographs looking rather like regions of shrinkage porosity.

### **9.3.2.3 Core blows**

Blowhole defects have been dealt with in Section 7.2.2. A brief review plus some additional data are included in this section.

Blowhole defects are caused by the outgassing of a core, or occasionally of a mold. They are often characterized by huge size. The minimum diameter of bubble that can form on a core is perhaps 10–20 mm (Figure 10.12). However, if the core contains gas at sufficient pressure to overcome the hydrostatic pressure and cause a blow defect, then it will usually have enough volume to continue to blow for some time. In this way strings of bubbles from the core can accumulate to create a massive pore near the top of the casting. The diameter of this cavity can easily reach 100 mm. The author has seen the whole top half of a casting made hollow by this process. (It suggests an interesting manufacturing technique for hollow ware!)

Because the core will usually take time to absorb heat, and build up its pressure prior to blowing, the top of the casting may have had sufficient time to become partly frozen. Thus because of its late arrival, a core blow is often some distance beneath, with its upper surface parallel to, the surface of the casting. (Note that this behavior contrasts sharply with (i) ‘real’ gas porosity that starts only 1 or 2 mm subsurface, and contrasts with (ii) turbulence-entrained gases that arrive early, together with entry of the liquid metal into the mold, and which are prevented from escape only by the thickness of the surface oxide film.)

The site of a core blow is usually above the highest point of the core, especially if this is a sharply upward-pointed shape, like a steeple of a church. The bubbles will collect and detach preferentially upward from an upward-pointing shape. (It is the upside-down equivalent of the drop of water falling

preferentially from the tip of a downward-pointing stalactite.) Such shapes are therefore best avoided, or the mold assembly turned upside-down to avoid the problem. Core bubbles will, of course, detach from flat surfaces but with much greater difficulty. All cores benefit from being internally vented to reduce the build-up of pressure that might lead to blows, as is dealt with quantitatively in Section 10.5.

In film-forming alloys the passage of a bubble through the melt naturally creates a bubble trail. The passage of a large number of bubbles can therefore be highly damaging, leading to the development of a thickly oxidized trail that can form a highly efficient leakage path through the casting. Exfoliation-type defects can also be created where the bubbles break repeatedly the surface of the casting (Figure 10.13).

In sand molds it is common for blows to occur from chills or any other surfaces that are impermeable. For this reason the application of block chills to critical areas of mold sometimes gives disappointing results. The casting is often degraded by the boiling action of volatiles that have condensed on the chills.

Condensation on chills can occur prior to filling, especially if a sand mold is closed and stored overnight. The mold slowly cools during the night. The next morning the more rapid re-heating of the mold as the foundry environment warms up and drives moisture and other volatiles inwards, where the chill, still cold, surrounded by the insulating mold, now forms a convenient site for condensation.

Condensation on chills can also occur during filling. The progress of the hot metal through the mold produces clouds of volatiles that rush ahead, condensing on any cold surface.

The provision of surface vents on chills by (i) coating the chill with a permeable refractory and (ii) creating V-grooves in a hatched pattern are both useful measures to reduce the problem. The grooves also seem to enhance the chilling action, possibly by their additional area, but probably mainly by the enhanced contact during the contraction of the casting, which would normally have slid easily across the surface of the chill, but when grooved would drive the casting surface hard against the sides of the grooves. The effect may be aided by the expansion of the chill.

There is a further danger of blows off from some core repair pastes that are based on clays. The clays are composed of such fine particles that they are effectively completely impermeable. Although the repairs are dried, possibly by leaving in the air, or by gentle warming, the water of crystallization in the clay is not released until the clay reaches a temperature in the range 500–700°C. (The baking of the core at such high temperatures cannot, of course, usually be carried out because of the premature breakdown of the organic binder in the sand.) Thus the arrival of the melt causes this bonded moisture to boil out of the clay, and the released vapor, being unable to escape through the dried clay, is forced to escape through the melt. The creation of blow defects, and damage to mechanical properties and to leak tightness automatically results.

The repairing of cores with repair pastes based on clays seems in general therefore to be counter-productive.

#### **9.3.2.4 Layer porosity**

Layer porosity is that type of shrinkage porosity that forms in long-freezing-range alloys under conditions intermediate between those for concentrated macroporosity and dispersed microporosity. This important intermediate condition is clear from Figure 7.15. Whereas macroshrinkage in the form of a shrinkage pipe, or large central cavity, can be viewed as a compact defect, and dispersed micropores can be viewed as individual compact defects, the intermediate condition is more severe, in



the sense that a relatively small volume of porosity has formed itself into an extended defect by concentrating into a sheet or layer.

To form an opinion of the seriousness of this defect, it is helpful to recall the way in which layer porosity is formed. The pore spreads across a surface of constant tension that exists in the residual liquid in the dendrite mesh. This formation mechanism results in the unique structure of the defect. The layer is not exactly equivalent to a crack, since the dendrites are hardly disturbed during its growth; it is only the residual liquid that moves, opening up the planar defect. In fact the dendrites continue to bridge the pore as a dense array, effectively stitching the layer together with closely spaced threads. For this reason its effect on tensile properties seems to be intermediate between that of individual pores and a fully open hot tear or crack. This intermediate position is seen in its rather mild effects on mechanical properties illustrated in Figure 9.11.

The presence of layers is usually not easily discerned optically on a polished section because there are so many bridging dendrites that the overall pattern is almost hidden, causing the porosity to appear as normal dispersed microporosity. However, it is clearly revealed on radiographs if the view direction is oriented along the plane of the porosity.

A summary of gas pore diagnostic information is given in Table 7.3.

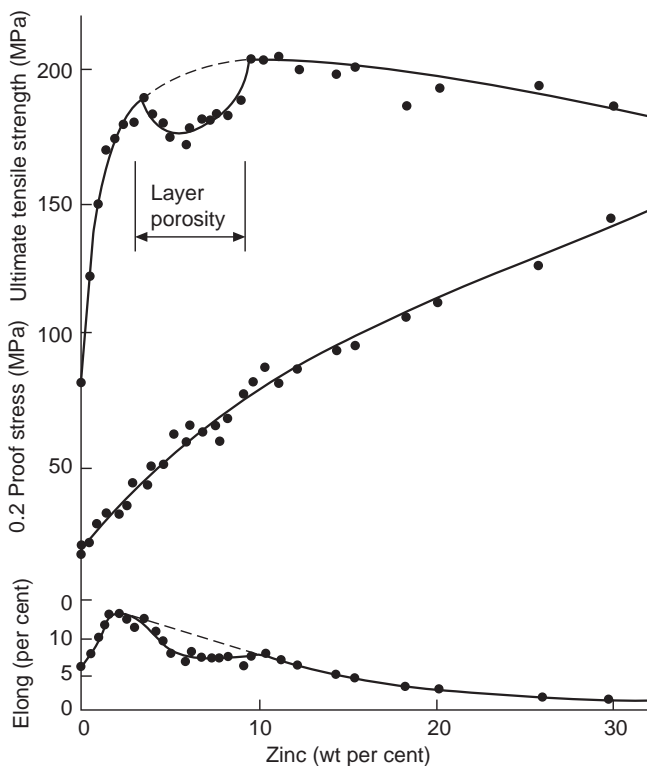


FIGURE 9.11

Effect of layer porosity on the mechanical properties of Mg-Zn alloys (data from Lagowski and Meier 1964).

### 9.3.3 Shrinkage porosity

#### Microshrinkage

The effect of shrinkage porosity on mechanical properties is probably practically identical to that of any other kind of porosity. On fracture surfaces, it is common to identify the pore as the origin of the failure. However, we have to keep in mind that a bifilm will almost certainly be associated with the pore, probably having initiated the formation of the pore, and will almost certainly be the starting point of the crack leading to failure. The relative likelihood of initiation by the pore or its associated bifilm is easily assessed by comparing the radius of curvature that each provides as a stress raiser. The radius of curvature of a shrinkage cavity will correspond to the curvature dictated by the curvature possible between dendrites, of the order of 10  $\mu\text{m}$  for a typical small casting. The curvature formed by the tip of a bifilm would be expected to be in the region between 10 and 1000 times smaller, thus being a significantly more threatening initiation site for a crack propagated by stress.

A further pitfall to bear in mind is that practically all shrinkage defects identified by radiography are actually not shrinkage defects but oxide film defects. A compact, convoluted bifilm, or tangled mass of many bifilms, containing some residual entrapped gas will appear identical to shrinkage porosity on a radiograph. Such attempted identifications should be labeled *not* 'shrinkage' but instead '*appears to be shrinkage*' (with the proviso 'but probably not' added for good measure). In my experience, most so-called 'shrinkage defects' turn out to be oxide defects introduced by poor filling systems.

True shrinkage defects are, in my opinion, rather rare. This is easily understood, because most foundry people understand shrinkage and the necessity for the provision of feeders. Thus most castings are reasonably well fed, and are unlikely to show shrinkage defects.

For those castings that do suffer some reduced internal pressure as a result of a poor feeding condition, if any part of the liquid is still in contact, or nearly in contact, with the outside skin of the casting, the skin might be sucked in, and a shrinkage pore grown by extension of this microscopic pipe drawn in from the outside surface. I have previously called this *externally initiated shrinkage porosity* (Figures 7.13 and 7.17). On a section cut through the casting it is indistinguishable from internally initiated porosity. However, of course, because it is externally linked, it constitutes a leak to the outside world. It would perform badly as a vacuum component, or would internally corrode, or harbor contamination in a food-processing or chemical plant. If machined into from the far side it would form a through-wall leak.

For other genuine shrinkage conditions in a long-freezing-range alloy, the microshrinkage pores can take the form of layer porosity (Figure 7.15) as has already been described in the previous section as also possibly formed by gas precipitation. As has been repeatedly mentioned throughout the book, both shrinkage and gas may have cooperated to form the porosity. It is probably not possible to detect the driving source of the porosity, both shrinkage and gas varieties, and the combined variety, would probably all appear identical if formed at the same stage of dendrite development in the casting.

#### Macroshrinkage (shrinkage pipe)

A macroshrinkage pipe, usually from a feeder head, can take the form of a smooth-walled cone for a eutectic alloy, or an extensive region of sponge porosity if a long-freezing-range alloy (Figure 7.8). The sponge appears to be separate interdendritic pores on a section, but the pouring of a colored liquid through the pores quickly illustrates how interconnected they are.

The various shapes of macro pores are very much influenced by gravity (effectively they float to the top of trapped liquid volumes – or perhaps we should say the residual liquid in the trapped liquid region naturally sits at the bottom of these volumes). Typical shapes are seen in Figures 7.30 and 7.31.

Such macro porosity is simply a sign of inadequate feeding. The rules for good liquid feeding are presented later in ‘Casting Manufacture’.

### 9.3.4 Tears, cracks, and bifilms

All planar defects such as cracks are capable of constituting extensive faults in the casting, and so are of great concern with regard to its strength. Not only do such features reduce the load-bearing area, but increase stress on the residual area even further because of the effect of stress intensification at the crack tip. The overall effect is significant, as is clear in Figure 9.12.

A fundamental, but not yet resolved issue needs to be raised at this point. It is possible that tears, cracks, and bifilms are all the same defect, all being simply bifilms. The difference is merely that tears

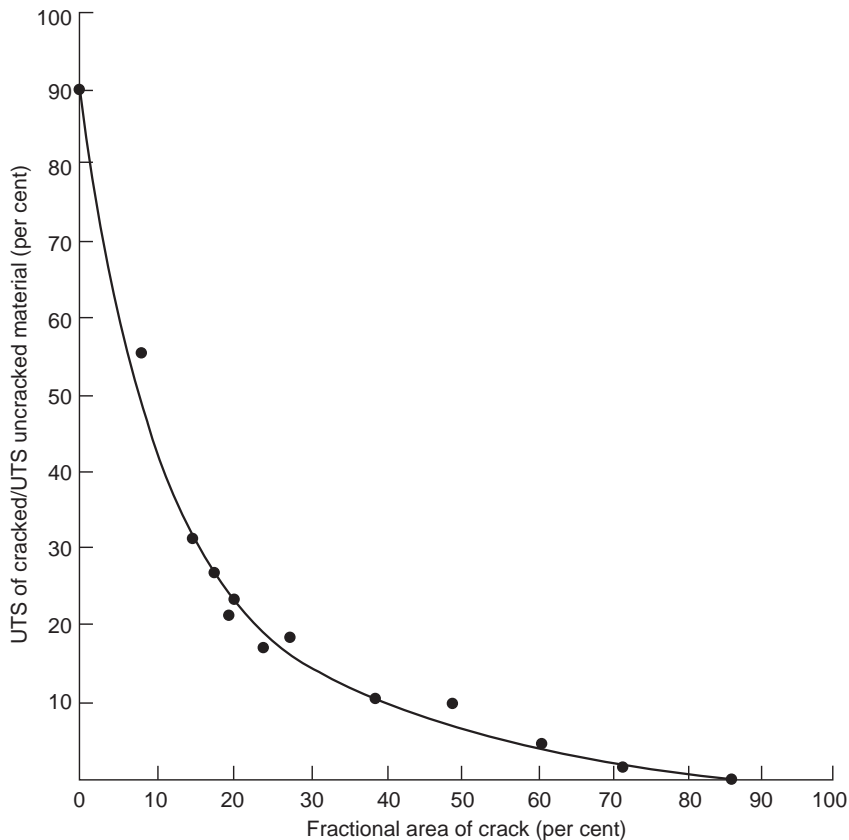


**FIGURE 9.12**

UTS of a casting as a function of the area of the crack (from Clyne and Davies 1975).

and cracks are bifilms that are open; tears have opened early, while the casting is still partly liquid, whereas cracks have opened late, after full solidification. Tears open with little or no stress, merely responding to strain, whereas cracks in the solid tend to only open after significant stress has accumulated, and possibly with an audible ‘crack’ as elastic energy is released. Bifilms are of course effectively cracks, but if they remain substantially closed they can remain undetected and unsuspected. It is frustrating that insufficient research has been carried out to ascertain whether the statement ‘All tears and cracks are originally bifilms’ is true. However, on balance, it seems to me to be likely to be true.

Hot tears and cold cracks open as a result of tensile strain and stress in the casting during cooling. They typically occur, therefore, across sections and in radii, where they will have an especially damaging effect on the serviceability of the casting. Their diagnostic features have already been discussed in Chapter 8. As open failures, they are naturally more serious defects than a closed bifilm. Although the bifilm can act as a crack, it may not have developed significant planar morphology by unfurling, and even if completely unfurled, and thus not capable of withstanding a tensile stress normal to itself, it will be able to withstand significant shear stress because of friction between the oxide halves, and because of jogs and creases that will provide mechanical obstruction to shear. Thus a closed crack, or closed bifilm, is a defect, but exhibits some strength. The open crack or opened bifilm is a serious weakening feature.

Such defects, especially if open, can extend to the whole casting cross-section, in which case, of course, the casting is already broken, and therefore fortunately identifiable as defective before being put into service!

However, a surface crack that may have formed and opened at high temperature may close again as the casting cools because of the normal development of compressive stress in the casting surface during the final stages of cooling, as discussed in Section 8.2. Such a crack, closed tightly under pressure, would be extremely difficult to detect by normal methods such as dye-penetrant testing and radiography. It is possible, therefore, that this is a common but rarely detected defect. It represents a serious concern in safety-critical components. Its detection might require pre-stressing to open the crack whilst being viewed by real-time radiography, or while being investigated by a penetrant dye. The writer is not aware that such testing techniques are ever used. However, for the most important of applications they would be well worth careful consideration.

It is worth restating that the extensive tear or crack-like defects are probably not so much initiated by bifilms, but actually *are* the bifilm. These entrainment defects can easily extend over the whole casting cross-section as we have seen. The visible presence of one of these defects will almost certainly warn of the presence of many more, less easily seen neighbors, and is the reason why it is sometimes futile to attempt to repair such defects by welding for instance.

The lesson remains clear. Intensive inspection and repair is no substitute for good metal, quiescently filled.

## Bifilms

The double film defect, the bifilm, is formed by the folding-in of a solid surface film during surface turbulence. Its composition is usually an oxide, nitride, or carbon. The bifilm defect can be small and negligible, or extensive, occupying the whole of a cross-section. Similarly its placing and orientation are random, so that either its chance placing, or its orientation, or its size, or all factors together, in a highly stressed region, may be damaging. It is the unpredictable nature of the double film defect that is such a concern.



**FIGURE 9.13**

Plates of 10-mm-thick cast in 99.5Al subjected to three-point bending (a) filled at an ingate speed greater than  $0.5 \text{ m s}^{-1}$ , and (b) less than  $0.5 \text{ m s}^{-1}$  (courtesy of Runyoro 1995).

I am often questioned why a sporadic defect such as a crack always appears at the same place in a particular casting. Clearly the pattern of stress concentration in the component is fixed. The random distribution of bifilms means that in the case of relatively few bifilms sometimes a bifilm will happen to be sited in the stressed region, and thus be opened by the strain. However, if there is a high concentration of bifilms, as often happens, there will then always be at least one in this region, with the result that all castings will exhibit a similar crack.

Figure 9.13 shows two simple plates 10 mm thick cast in 99.5%Al in the author's laboratory (Runyoro 1992). They were cast in a vertically parted mold via a bottom gate into the center of the long side at ingate speeds of above and below  $0.5 \text{ m s}^{-1}$  respectively and were afterwards subjected to a three-point bend test (later work progressed to use the much improved four-point bend test). The turbulently filled casting exhibited a number of cracks, none of which were along the line of the maximum stress. In fact the cracks were aligned in random orientations. The randomness is a strong clue to their origin as the products of surface turbulence; since turbulence means randomness, chaos, and essentially unpredictability. The material between the cracks is clearly highly ductile, as would be expected for rather pure cast aluminum. Also, interestingly, under the microscope the tips of the cracks are found to be blunt. They have been unable to propagate in the ductile aluminum, which constitutes a crack-blunting matrix. It follows that the cracks have not propagated but must have pre-existed as-cast, and have merely opened when subjected to bending. All these features are to be expected from entrained bifilms. The test plate (Figure 9.13b) cast at a speed at which entrainment is not possible is clearly free from bifilm defects.

If the bifilm is sufficiently large, and if it breaks the surface, then it *may* be detected by normal dye-penetrant methods. However, as a result of the bifilm being naturally tightly closed, or forced closed at the surface by surface compressive stress, the dye-penetrant approach is not reliable, indicating perhaps only a minute pinpoint contact. The 'stars at night' appearance of defects on vacuum-cast Ni-base alloys when the fluorescent penetrant dye is viewed under ultraviolet light are mostly defects

of this kind. This is easily demonstrated by putting on a well-designed filling system, after which the 'stars' all disappear! Bifilm defects are also difficult to detect by radiography unless the incidence of radiation happens to be in or near the plane of the defect, or unless the central region is sufficiently open to constitute an open crack, or the enclosing films sufficiently thick to appear as inclusions.

In contrast to the difficulty of observing bifilms non-destructively, they can sometimes be clearly seen on fracture surfaces. Very thin films require careful study of the fracture surface to reveal their minute characteristic signatures such as the tracery of fine folds. LaVelle (1962) studied the fracture surfaces of aluminum alloy pressure die castings and found layer upon layer of oxide films throughout the structure, giving the fracture a fibrous appearance. In some cases the surface contact of these extensive defects was minimal, indicating how unreliable their detection by a surface-penetrant dye technique could be.

Because film defects are potentially so damaging, and because they are practically impossible to detect by non-destructive methods with any certainty, the only suitable method to deal with this problem is not to attempt to inspect for them, but to set in place manufacturing techniques that guarantee their avoidance. At the present time no specification calls for specific manufacturing techniques that would eliminate film defects. This unsatisfactory situation has to change.

Only control of the quality of the melt and control of the filling of the casting will prevent film defects entering the mold. Once good-quality metal is in the mold, measures will be required to prevent the reintroduction of defects by such processes as the outgassing of cores, or other forms of surface turbulence after the filter (if any) in the runner. Only by carefully planned and monitored processing will bifilm creation be overcome with confidence.

Again, it bears plentiful repeats; the achievement of good castings lies not in inspection, but in process control.

---

## 9.4 TENSILE PROPERTIES

The fracture of metals is a complex subject that we can only touch on with respect to its castings aspects. Even so, the outline of knowledge presented here will be helpful to guide the casting engineer to achieve the best properties for his castings.

### 9.4.1 Microstructural failure

Three main varieties of microstructures and their mechanical behavior can be distinguished:

1. Where the matrix of the alloy is ductile, and the second phase, perhaps as hard particles, introduced by mixing (i.e. entrained), the added particles are not bonded to the matrix. When subjected to tensile strain the particles act like pores as seen in Figure 9.10. This is easily understood; the mix has isotropic properties, and the microscopic failure associated with each particle has no preferred directionality.
2. Where the second-phase particles have formed in situ in the alloy, if their formation was not associated with entrained particles, they would be perfectly bonded to the matrix. No fracture within the particles or decoherence at the interface could occur. This is perhaps more clearly seen in the precipitates formed in the solid, such as the GP zones in Al alloys, where debonding is inconceivable. Gall et al. (2000) use atomic simulations to estimate that the force to separate

Si from the Al matrix would probably exceed 30 GPa. This is 100 times a typical stress to cause tensile failure of an Al–Si alloy. Thus debonding (and we might also assume, cracking) will be impossible for Si particles.

3. For those second-phase particles that nucleate and grow on entrainment defects such as bifilms, the associated unbonded interface in the bifilm causes interesting specific failure modes. As always, Al–Si alloys are the most intensively studied system comprising an essentially non-metallic phase, silicon metal, in the soft metallic Al matrix. As such, the findings are instructive because it exhibits behavior typical of many in other such alloy systems, particularly the cast irons. We shall consider this system in detail.

When subjected to a tensile load, the silicon particles appear to either fracture or decohere from the matrix. In terms of bifilm theory, this behavior occurs if the silicon happens to have precipitated on both sides of the bifilm, with the crack in the center, or only on one side, with the crack between the particle and the matrix.

Some admirable evidence supporting this hypothesis comes from the work of Lopez and his team (Fras 2007) who painstakingly measured individual particles, noting their orientation to the tensile axis, and whether they fractured internally or decohered. Their fascinating results are presented in Figure 9.14.

Clearly at room temperature most particles fractured when the stress was at right angles to the plane of the particle. This is no surprise. However, it is interesting that no decohesion is reported for this orientation. In the case of the silicon particles, perhaps the tensile force operates on the extreme edges of the two particles to separate them successfully, whereas when operating on the edges of a vanishingly thin and weak half of the bifilm the strain might tweak the edges a little, but is not expected to pull the bifilm completely clear as in the case of the strong, rigid particle.

At 300°C the situation becomes more complex. The matrix now softens and can flow plastically under tensile load. Those particles aligned parallel to the stress direction and which have formed on only one side of a bifilm will now be subject to material shearing across and at 45° away from the particle, opening up the unbonded interface. When oriented at 45° to the stress the maximum resolved shear will be aligned parallel to the length of the particle, so that decohesion is no longer favored. Fracture of particles starts to occur at increasing angles of orientation, maximizing at 90° once again as would be expected.

As an interesting comparison, alpha-Fe particles were also checked for their sensitivity to orientation with respect to the tensile stress direction. As is clear from Figure 9.14d there is no favored direction. This is to be expected in view of their ability to wrap around convoluted bifilms, sealing in the convolutions, rather than straightening them as happens with Si particles and beta-Fe particles. The marked difference in behavior is clearly shown in Figure 6.19.

Turning now to a common feature of fracture surfaces, Figure 2.44d shows a typical so-called ductile fracture consisting of a dense array of ductile dimples. At the base of each dimple is a fractured Si particle. If the proposition is that Si particles are strong and resistant to fracture, then surely there must be a bifilm present in every ductile dimple? This reasoning indicates that huge, possibly unreasonably high, numbers of bifilms are present.

In practice, this appears to be only partly true. It seems there is a reasonable explanation of how such numerous fractures could occur from a much smaller population of bifilms as follows. Each bifilm will consist of one smooth side and one side with numerous transverse folds, constituting short

transverse cracks. An illustration is seen in Figure 6.19b showing a beta-Fe particle with one continuous length on one side of the main crack, and separate short lengths of crystal on the other side, separated by transverse cracks. This structure is to be expected in all bifilm formation since during the turbulence of folding in the surface, the impinging areas of surface are not likely to have the same area; the larger surface will be forced to adopt rucks, as transverse folds, while the opposite surface film will remain essentially unfolded.

During the solidification of the Al–Si coupled eutectic, the bifilms in suspension will tend to be dragged down into the hollows between the Al and Si phases. This will occur because the bifilms will be pushed ahead by the Al phase since the oxide is not preferentially ‘wetted’ by the alpha phase, but will preferentially attach to the Si phase, lowering the overall energy of the system. If it happens that the transverse cracks are on the side of the Al phase they will be pushed ahead, effectively flattened

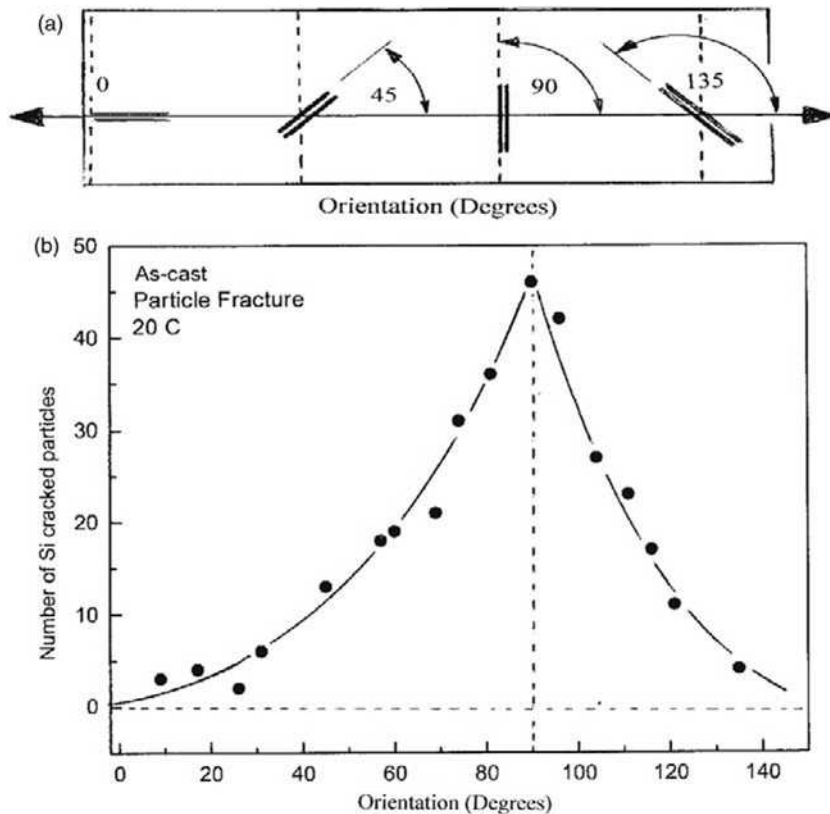


**FIGURE 9.14**

(a) Silicon particles in Al–Si alloy A319 subject to tensile stress. (b) At room temperature the particles mainly fracture when at 90° to the stress axis. (c) At 300°C ductile shear at 45° promotes decohesion, in addition to tensile failure continuing near 90°; (d) for alpha-Fe particles at room temperature their convoluted bifilms lead to fracture at random angles (Fras et al. 2007).



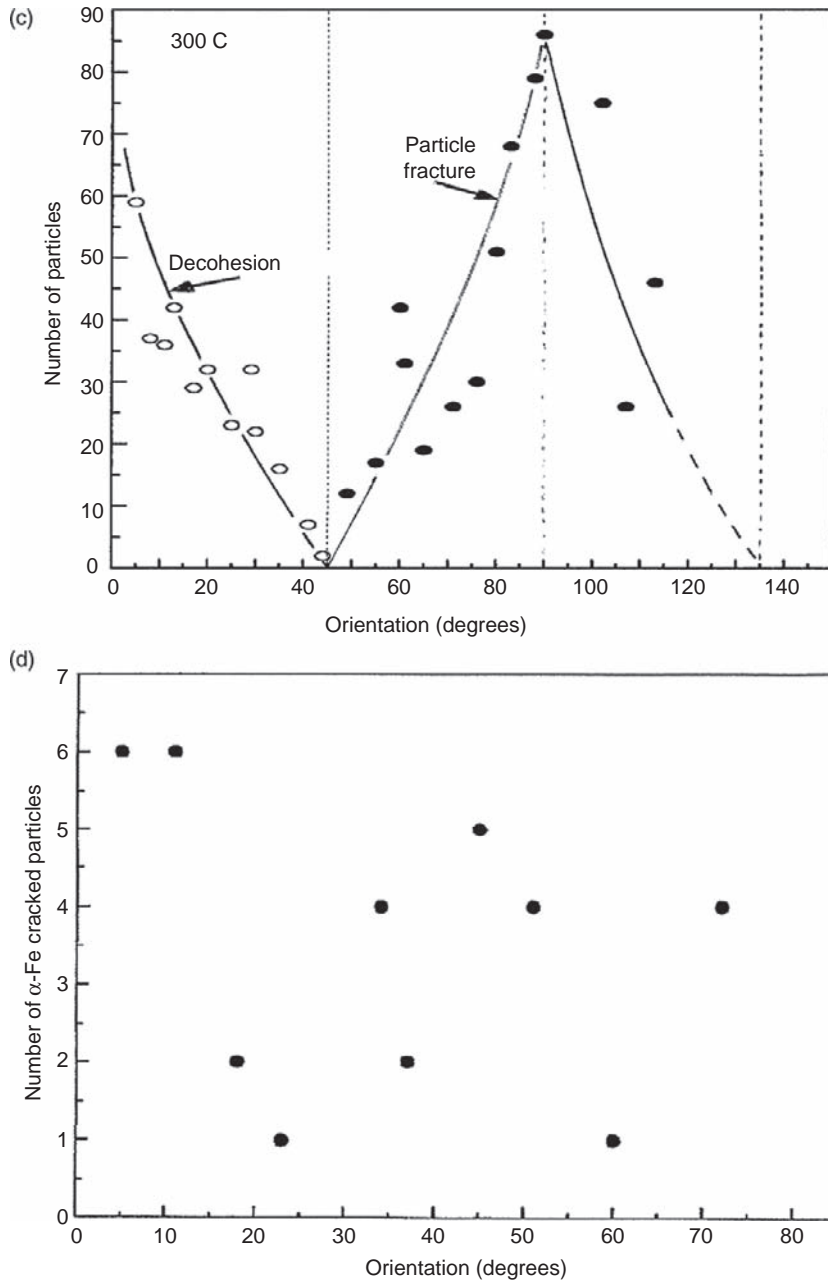


FIGURE 9.14 (continued).

against the advancing Si particles. Thus the Al phase will not be cracked, explaining the perfection of the plastic shear between Si particles, forming razor-sharp cusps of necked-down material. On the other hand, if the transverse cracks happen to be on the side of the Si particles, the Si will grow around these, incorporating them into the advancing Si crystal. Thus the advancing Si phase will be expected to be cracked repeatedly along its length. If Figure 6.19 is typical, we might expect to see transverse cracks every 10–20  $\mu\text{m}$ , which appears reasonably consistent with the observed fractures.

### 9.4.2 Ductility

Figure 9.10 is a famous result showing the ductility (in terms of reduction of area) of a basically highly ductile material, pure copper, being reduced by the addition of various kinds of second-phase particles, including pores. It is clear that the clean material has a ductility over 30%, but there is a large deleterious effect of the second phases, more or less irrespective of their nature. The lack of sensitivity to the nature of the particles or holes is almost certainly the result of the relatively easy decohesion of the particles from the matrix when deformation starts. Thus all particles act as holes.

This result is predictable if the particles are introduced into the melt by some kind of stirring-in process. As the particles penetrate the surface they necessarily take on the mantle of oxide that covers the liquid metal (Figure 2.3b). Thus all immersed particles will be expected to be coated with a layer of the surface oxide, with the dry side of the oxide adjacent to the particle. The absence of any bonding across this interface will ensure the easy decohesion that is observed. In practice, the submerged particles will often remain in clumps despite intense and prolonged stirring (Figure 2.3c). This seems to be most probably the consequence of the particles entering the liquid in groups, and being enclosed inside a packet of oxide. With time, the enclosing wrapping will gather strength as it thickens by additional oxidation, using up the enclosed air, and so gradually improve its resistance to being broken apart.

In castings the volume of pores rarely exceeds 1% (only occasionally are 2 or 3% found). For 1% porosity Figure 9.10 indicates that the ductility will have fallen from the theoretical maximum (which will be 100% reduction in area for a perfectly ductile material) to approximately 10%, an order-of-magnitude reduction! However, 10% elongation is fairly typical, if rather generous, for most light alloys, indicating the possibility of at least 1% by volume (or area) of defects normally present whether detected or not.

Why should an assembly of holes in the matrix affect the ductility so profoundly?

Figure 9.16 shows a simple model of ductile failure. For the sound material the extension to failure is of the order of the width  $l$  of the specimen, because of the deformation of the specimen along  $45^\circ$  planes of maximum shear stress. For the test piece with the single pore of size  $d$ , the elongation to failure is now approximately  $(l - d)/2$ . In the general case for a spacing  $s$  in an array of micropores we have

$$\begin{aligned} \text{Elongation} &= s - d \\ &= 1/n^{1/2} - (f/n)^{1/2} \\ &= (1 - f^{1/2})/n^{1/2} \end{aligned} \tag{9.7}$$

where  $n$  is the number of pores per unit area, equal to  $1/s^2$  and  $f$  is the area fraction of pores on the fracture surface, equal to  $nd^2$ .

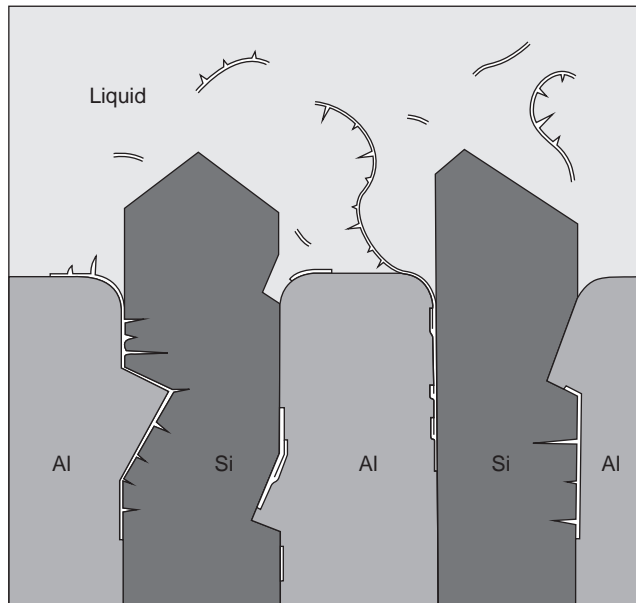


**FIGURE 9.15**

Bifilms with subsidiary transverse branches are entrained between the Al and Si phases during the growth of the Al-Si eutectic. Branches are pushed back and rejected by the Al phase, but are incorporated in the Si phase, leading to easy Si fracture and decoherence.

Equation 9.7 is necessarily very approximate because of the rough model on which it is based. (For a more rigorous treatment the reader is recommended to the pioneering work by Thomason (1968) and the more recent work by Huber (2005).) Nevertheless, our order-of-magnitude relation indicates the relative importance of the variables involved. It is useful, for instance, in interpreting the work of Hedjazi (1976), who measured the effect of different types of inclusions on the strength and ductility of a continuously cast and rolled Al-4.5Cu-1.5Mg alloy. From measurements of the areas of inclusions on the fracture surface, Hedjazi reached the surprising conclusion that the film defects were less important than an equal area fraction of small but numerous inclusions. His results are seen in Figure 9.17. One can see that for a given elongation, the microinclusions are about ten times more effective in lowering ductility. However, he reports that there were between 100 and 1000 times the number of microinclusions compared to film-type defects in a given area of fracture surface. From Equation 9.7, an increase in number of inclusions per unit area by a factor of 100 would reduce the elongation by a factor of 10, approximately in line with the observations.

The other observation to be made from Equation 9.7 is that ductility falls to zero when  $f = 1$ , for instance in the case of films which occupy the whole of the cross-section of the test piece. This self-evident result can easily happen for certain regions of castings where the turbulence during filling has been high and large films have been entrained. This is precisely the case for the example for the ductile alloy Al-4.5Cu that failed with 0.3% elongation, nearly zero ductility, seen in Figure 2.44a. This part of the casting was observed to suffer a large entrainment effect that had clearly created extensive

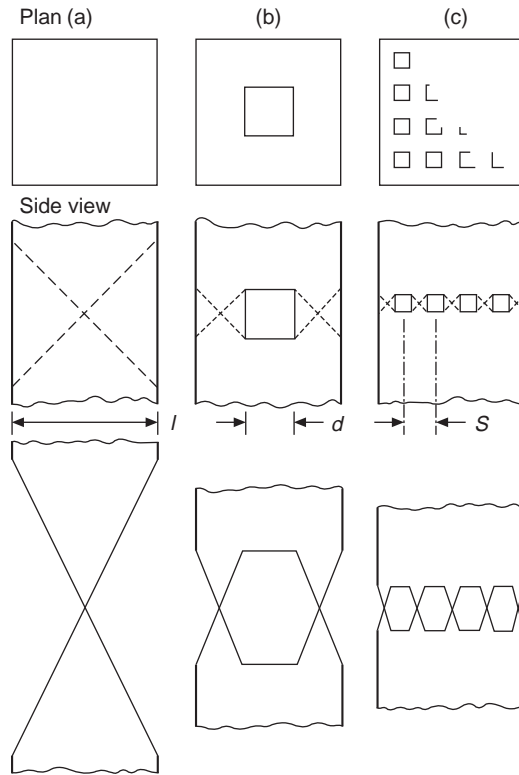


**FIGURE 9.16**

Simple ductile failure model, representing (a) sound specimen that necks down 100% reduction in area; (b) a single central pore reducing RA to about 50% with a single cup-and-cone fracture; and (c) multiple pores leading to poor elongation with ductile dimple fracture surface.

bifilms. Elsewhere, other parts of the same casting had filled quietly, and therefore contained no new bifilms, but only its background scatter of old bifilms inherited from the distribution already present in the melt. In this condition the ductility of the cast material rose to 3.5% (Figure 2.44b).

Pure aluminum is so soft and ductile that it is almost possible to tie a length of bar into a knot, and pull the knot tight. However, Figure 9.13 illustrates how the presence of bifilms has caused even this ductile material to crack when subjected to a three-point bend test. Notice the material close to the tips of the cracks is highly ductile, so the cracks could not have propagated as normal stress cracks, since the crack tips would have blunted (as confirmed under the microscope). Thus the only way for such cracks to appear in a ductile material like pure aluminum is for the cracks to have been introduced by a non-stress mechanism. The random accidents of the folding-in of the surface due to surface turbulence seems the only likely mechanism, corroborated by the random directions of the cracks, not necessarily aligned along the direction of maximum strain. The randomness of their direction and size is strong confirmation of their origin as the result of turbulence.

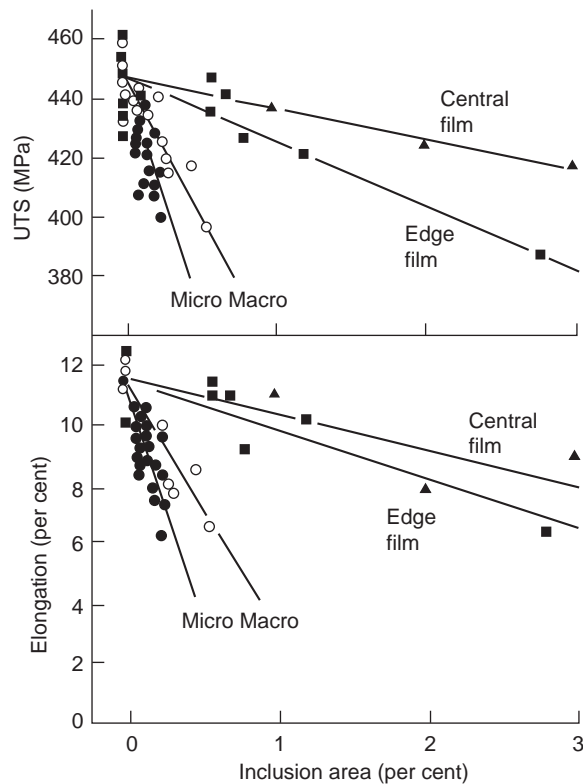


**FIGURE 9.17**

Strength and ductility of an Al-4.5Cu-1.5Mg alloy as a function of total area of different types of inclusions in the fracture surface. (Data from Hedhazi et al. 1976.)

Regardless of the inclusion content of a melt, one of the standard ways to increase the ductility of the casting is to freeze it rapidly. This is usually a powerful effect. Figure 2.47 illustrates an approximate ten-fold improvement as the dendrite arm spacing drops from 90 to 30  $\mu\text{m}$ . The effect follows directly from the freezing-in of bifilms in their compact form, reducing the time available for the operation of the various unfurling mechanisms. (There may also be some contribution from the dendrites pushing the bifilms away from surface regions, effectively sweeping the surface regions clear, and concentrating the bifilms in the center of the casting where they will be somewhat less damaging to properties as is clearly seen to happen in the channels, mainly the runner and gates, of filling systems of castings. This effect has not been investigated, but may be significantly affected if the bifilms are not quite cleared from the surface regions, but are organized into planar sheets by the columnar grains, as in Figure 2.43c, and whether therefore the benefits are now dependent on the direction of stress.)

The converse aspect of this benefit is that if the ductility of a casting from a particular melt quality is improved by chilling, this can be probably taken as proof that oxides are still present in the melt. (A simple quality control test can be envisaged based on this proposition.)

The great sensitivity of ductility to the presence of defects in the form of pores or cracks (or any other easily decohered interface such as those obligingly provided by bifilms) is the most powerful limitation to the attainment of good ductility. The awesome spread of ductilities of even aerospace castings is graphically illustrated in Figure 9.18a for Al-7Si-0.4Mg alloy by Tiryakioglu (2009a). As

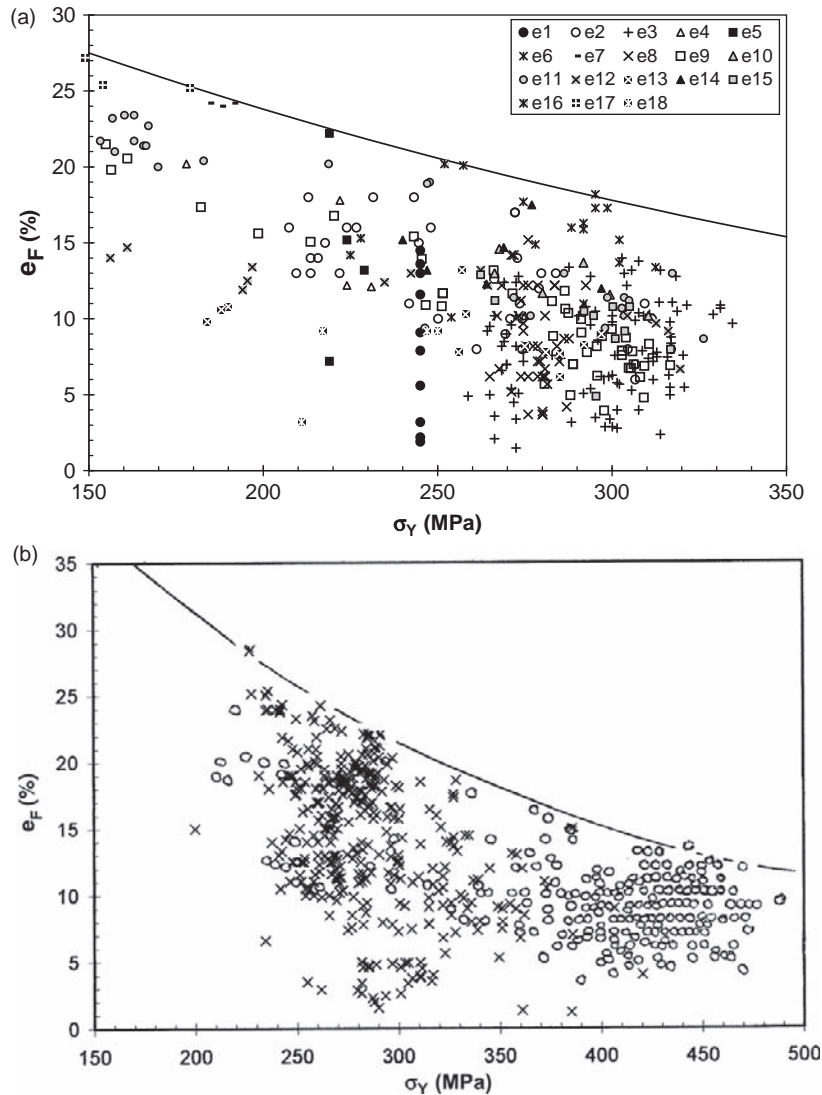


**FIGURE 9.18**

The scatter of uniform elongation to fracture results for (a) Al-7Si-Mg alloys (356 and 357 types) and (b) Al-4.5Cu alloys (201 and 206 types), reported mostly from aerospace foundries (Tiryakioglu et al. 2009). Clearly, the attainments of many fall far short of the potential available.

strength is increased by heat treatment, so the elongation of the alloy falls. However, the major effect can be seen to be not heat treatment, but some other arbitrary factor, causing many results to fall lamentably short of their potential. This scatter is attributed to the presence of bifilms. Tiryakioglu (2009b, 2009c) produces similar results for the higher-strength Al–4.5Cu-type casting alloys A206 and A201, the latter containing 0.7Ag (Figure 9.18b). It is clear that excellent properties could be achieved with simple, low-cost Al–Si alloys if they were sufficiently free from bifilms.

Furthermore, the limit shown in Figure 9.18 is only the limit of *uniform* elongation. After the initial extension of the test piece in a uniform manner, it then starts to *neck down*, beginning the *non-uniform* elongation regime. Alexopoulos and Tiryakioglu (2009) show that the total elongation is nearly doubled by the addition of the non-uniform elongation. The elongation associated with necking-down is expected to be an important feature of metals free from bifilms. When metals and alloys are produced free from bifilms they will be expected to achieve routinely 100% reduction in area (RA) as a demonstration of their perfection. The RA might become then a more common and discriminating measure of ductility.

Finally, there is the practical challenge of achieving the best ductility from a given batch of material. For instance the ductility falls with aging, but having reached a minimum at the peak hardening response, the ductility then rises once again. Thus occasionally over-aging is recommended equally with under-aging to achieve good ductility. Figure 9.19 illustrates that this is unfortunately not always true for the precipitation hardening of Al alloys. The under-aging treatment optimizes ductility for Al–Si–Mg alloys. However, the opposite appears to be true for an Al–Zn–Mg–Cu alloy (Figure 9.20).

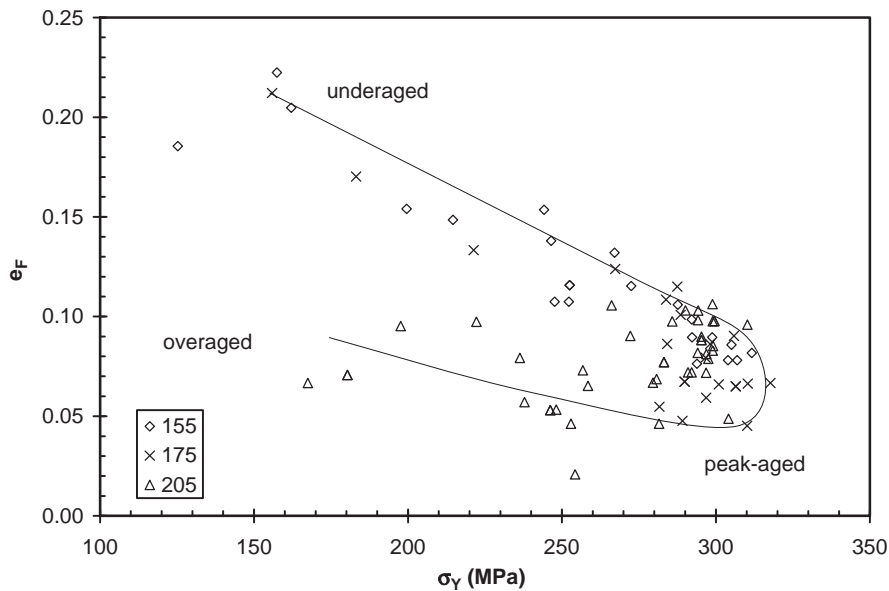
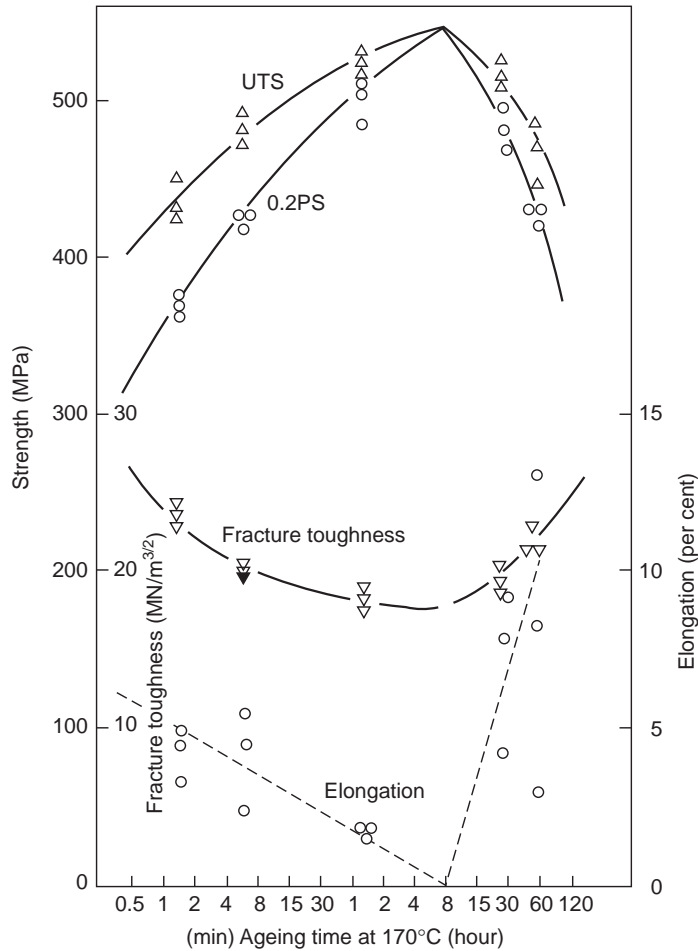


FIGURE 9.19

Elongation versus yield strength for Al–7Si–0.4Mg alloy showing under-aged strengths to be superior to those developed by over-aging (Alexopoulos and Tiryakioglu 2009).



**FIGURE 9.20**

Mechanical properties of a cast high-strength alloy Al-6Zn-2.7Mg-1.7Cu as a function of effective aging time at 170°C. (Data from Chen et al. 1984.)

### 9.4.3 Yield strength

Steels have a well-defined yield point separating elastic and plastic flow regions so the yield stress can be defined precisely. Al alloys show no such definitive behavior. The smooth and gradual transition between elastic and plastic behavior is so difficult to define that it forces us to define an effective yield stress in terms of a 'proof stress'. We shall assume that the 0.2% proof stress (0.2PS) is sufficiently equivalent for our purposes. (The 0.2PS is that stress at which reversible elastic deformation has just exceeded its limit, and a small amount, 0.2%, of permanent plastic deformation remains on unloading. Others define yield at 0.05PS and others at 0.1PS. All these definitions are closely similar to within a few MPa.)



Whereas both the ultimate strength and the ductility can be greatly damaged by defects, the yield strength is interestingly insensitive to their presence. This behavior is explained by the load-bearing area being reduced by the presence of the defect, thus increasing the stress in the matrix, and thereby causing work hardening due to local plastic flow. The increased strength of the matrix as a result of the work hardening to some extent counters the effect of the reduction in load-bearing area, keeping the yield point reasonably constant.

This insensitivity of yield to layer porosity is seen in Figure 9.11. The few percent or so loss of area due to the layer porosity, clearly reducing the UTS and elongation, cannot be detected in the scatter of the results for the 0.2PS. A similar result is seen in Figure 2.47.

In those cases where the yield stress *is* found to be significantly reduced, it is a warning that the material had lost a significant fraction of its load-bearing area. In the past it has not been easy to accept that the reduction of 0.2PS by 90% is the result of a crack occupying 90% of the area, especially when the fault is not easily seen, even on the fracture surface! (Figure 2.44a, which we have discussed several times before, is a clear example showing a fracture of a tensile specimen expected to show 10% elongation but in fact achieved close to zero elongation, corresponding to the nearly 100% loss of area provided by large bifilms.)

#### Microstructural size effects: The Hall-Petch relation

As the grain size  $d$  of a metal is reduced, its yield strength  $\sigma_y$  increases. The widely quoted formula to explain this result is that due to Hall and Petch (see, for instance, the derivation by Cottrell (1964)):

$$\sigma_y = a + bd^{-1/2} \quad (9.8)$$

where  $a$  and  $b$  are constants. The equation is based on the assumption that a slip plane can operate with low resistance across a grain, allowing one part of the grain to slide over the other, and so concentrating stress on the point where the slip plane impinges on the next grain. With the further spread of yielding temporarily blocked, the stress on the neighboring grain increases until it exceeds a critical value. Slip then starts in the next grain, and so on. The process is exactly analogous to the spreading of a crack, stepwise, halting at each grain boundary.

Although the Hall-Petch relation was originally conceived to explain the effect of grain size, its fundamental power is not limited to this particular mechanism for the hindering of slip planes. For instance, slip can be halted at strong precipitates that might reside in interdendritic regions or inside grains, as we shall see.

Gurland (1970) uses data from literature to show for a number of steels that their strength increases linearly with the inverse of the square root of the grain size for ferritic steels or the inter-particle spacing for pearlitic steels.

Similarly, for Al-Si alloys he shows the relationship between spacing and strength is the same for alloys containing 0% to 25%Si where the definition of spacing changes from (i) the grain size in pure aluminum, to (ii) the dendrite cell size in 1.6–2.5%Si alloys and (iii) the planar center-to-center nearest-neighbor distance between Si particles in 5.3–25%Si alloys.

The effects of metallurgical features such as grain size and dendrite arm spacing (DAS) on yield strength are such important metallurgical phenomena that, although they rely on the same basic mechanism as indicated above, they are given special, separate sections.

### 9.4.3.1 Grain size

#### General

The development of small grains during the solidification of the casting is generally an advantage. When the grain size is small, the area of grain boundary is large, leading to a lower concentration of impurities in the boundaries. The practical consequences that generally follow from a finer grain size are:

1. Improved resistance to hot tearing during solidification.
2. Improved resistance to cracking when welding or when removing feeders by flame cutting (for steel castings).
3. Reduced scattering of ultrasonic waves and X-rays, allowing better non-destructive inspection.
4. Improved resistance to grain boundary corrosion.
5. Higher yield strength (because of Hall-Petch relationship).
6. Higher ductility and toughness.
7. Improved fatigue resistance (including thermal fatigue resistance).
8. Reduced porosity and reduced size of pores. This effect has been shown by computer simulation by Conley et al. (1999). The effect is the consequence of the improved intergranular feeding and better distributed gas emerging from solution. Improved mass feeding will also help as described in Section 8.4.2.
9. Improved hot workability of material cast as ingots.

However, it would not be wise to assume that all these benefits are true for all alloy systems. Some types of alloys are especially resistant to attempts to reduce their grain size, whilst others show impaired properties after grain refinement. Furthermore, this impressive list is perhaps not so impressive when the effects are quantified to assess their real importance. These apparent inconsistencies will be explained as we go.

In addition, important exceptions include the desirability of large grains in castings that require creep resistance at high temperature. Applications include, in particular, ferritic stainless steel for furnace furniture, and high-temperature nickel-based alloy castings. Single-crystal turbine blades are, of course, an ultimate development of this concept. These applications, although important, are the exception, however. Because of the limitations of space, this section neglects those specialized applications that require large grains or single crystals, and is devoted to the more usual pursuit of fine grains.

Some of these benefits are explained satisfactorily by classical physical metallurgy. However, it is vital to take account of the presence of bifilms. These will be concentrated in the grain boundaries. The influence of bifilm defects is, on occasions, so important as to over-ride the conventional metallurgical considerations.

For instance, in the case of the propagation of ultrasonic waves through aluminum alloy castings, this was long thought to be impossible. Aluminum alloys were declared to be too difficult. They were thought to prevent ultrasonic inspection because of scatter of the waves from large as-cast grains; no back-wall echo could be seen amid the fog of scattered reflections. However, in the early days of the Cosworth Process, with long settling time of the liquid metal, and quiescent transfer into the mold, suddenly back-wall echoes could be seen without difficulty despite the absence of any grain-refining action. The clear conclusion is that the scatter was from the gas film between the oxide layers of the bifilms at the grain boundaries.

By extrapolation, it may be that the so-called 'diffraction mottle' that confuses the interpretation of X-ray radiographs, and usually attributed to the large grain size, is actually the result of the multitude of thin-section pores, or the glancing angle reflections from the air layer of bifilms at grain boundaries. It would be interesting to compare radiographs from material of similar grain size, but different content of bifilms to confirm this prediction.

The strong link between bifilms and microstructure, particularly grain size, is illustrated particularly well in Figure 2.44. The images (a) and (b) are the fracture surfaces of test bars taken from different parts of a single casting whose filling was observed by X-ray video radiography. The large grain size in the turbulently filled test bar (a) contrasts with the fine grain size in the quietly cast bar (b). The large grains are probably the result of reduced thermal convection in the casting because of the presence of the large obstructing bifilms, so that dendrites could grow without thermal and mechanical disturbance that is needed to melt off dendrite arms, and so lead to grain multiplication. In (b) the presence of numerous pockets of porosity suggests the presence of many smaller bifilms (that cannot be seen directly). These are older bifilms already present in the melt prior to pouring. The small bifilms will not be a hindrance to the flow of the melt, so that the small grain size is the result of grain multiplication because of convection during freezing.

Unfortunately, nearly all the experimental evidence that we shall cite regarding the structure and mechanical properties of castings is influenced by the necessary but unsuspected presence of bifilms. We shall do our best to sort out the effects so far as we can, although, clearly, it is not always possible. Only new, carefully controlled experiments will provide certain answers. At this time we shall be compelled to make our best guess.

### Grain refinement

The Hall-Petch equation has been impressively successful in explaining the increase of the strength of rolled steels with a reduction in grain size, and has been the driving force behind the development of high-strength constructional steels based on manufacturing processes, especially controlled rolling, to control the grain size. This is cheaper than increasing strength by alloying, and has the further benefit that the steels are also tougher – an advantage not usually gained by alloying.

The extension of these benefits to cast steels has been much less successful, as has been related in Section 6.6.

The development of higher-strength magnesium casting alloys with zirconium as the principal alloying element has also been driven by such thinking. The action of the zirconium is to refine the grain size, with a useful gain in strength and toughness. The sharp increase in yield strength as grain size is reduced is seen in Figure 9.21. The zirconium is almost insoluble in both liquid and solid magnesium, so that any benefit from other alloying mechanisms (for instance, solid solution strengthening) is negligible. The test to ensure that the zirconium has successfully entered the alloy is simply a check of the grain size. Yue and Chadwick (1991) used squeeze casting to demonstrate the impressive benefits of the grain refinement of magnesium castings. This is especially clear work that is not clouded by other effects such as the influence of porosity. It appears that magnesium benefits significantly from the effect of small grain size because factor  $b$  in the Hall-Petch equation is high. This is the consequence of the grain boundaries being particularly effective in preventing slip, because in hexagonal close-packed lattices there are few slip systems, and only on the basal plane, so that slip is not easily activated in a randomly oriented neighbor.

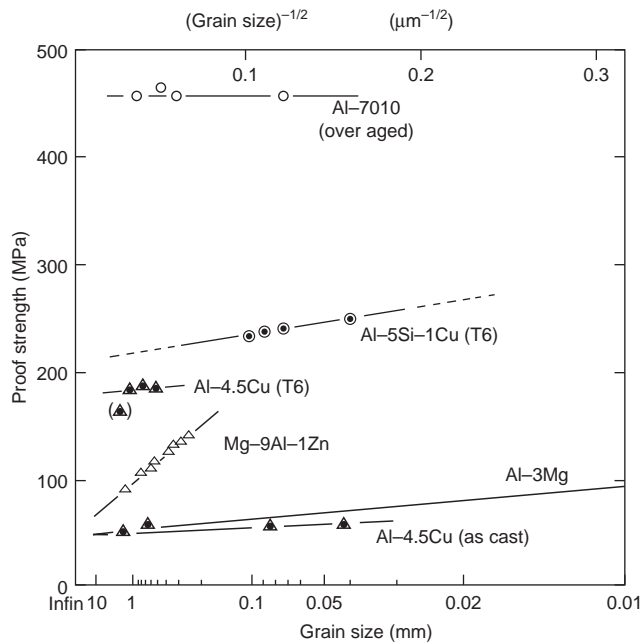


**FIGURE 9.21**

Hall-Petch plots of yield strength versus grain size<sup>-1/2</sup> illustrating (a) the relatively poor response of Al alloys contrasted with data for Mg alloys. (Data for 7070, Mg alloy, Al-4.5Cu from T M Yue and G A Chadwick 1991; Al-5Si-1Cu from Wierzbinska 2004; Al-3Mg from Lloyd and Court 2003.)

This behavior contrasts with that of face-centered-cubic materials such as aluminum, where the slip systems are numerous, so that there is always a slip system close to a favorable slip orientation in a neighboring grain. Thus although grain refinement of aluminum alloys is widely practiced, Flemings (1974) draws attention to the fact that its effects are generally over-rated. However, little useful work on the problem had been carried out at that time. Recent measurements by Hayes and co-workers (2000) reveal the quantitative benefits of fine grain size in an Al-3Mg. (Their work covers an impressive range of orders of magnitude of variation in grain size, so that its slight extrapolation into Figure 9.21 seems well justified.) They find huge increases in 0.2 Proof Stress of over 500 MPa when the grain size is only 0.2  $\mu\text{m}$ . However, of course, such fine grain sizes are not obtainable in normal-shaped castings. For normally attainable fine grain sizes in the range reducing from 1 mm down to 0.1 mm Figure 9.22 shows that the proof stress increases by approximately 10 MPa, indicating an extremely modest benefit.

The usual method of grain refinement of aluminum alloys is by the addition of titanium and/or boron. The effect has been discussed in Section 6.3.4. The practical difficulties of controlling the addition of grain-refining materials are discussed by Loper and Kotschi (1974), who were among the first to draw attention to the problem of fade of the grain-refinement effect. Sicha and Boehm (1948) investigated the effect of grain size on Al-4.5Cu alloy, and Pan et al. (1989) duplicated this for

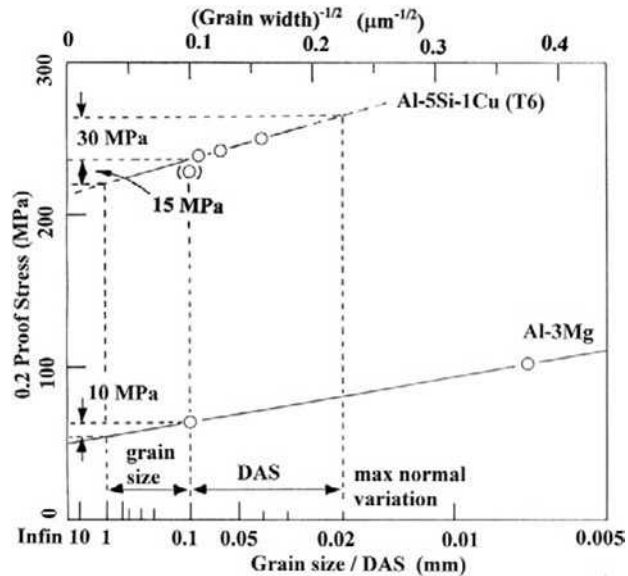


FIGURE 9.22

The poor strengthening effect of up to approximately 10 MPa for the best grain size reduction of Al-3Mg, with nothing for DAS refinement for this solid solution alloy; compared with 15 MPa for DAS plus 30 MPa for grain refinement of Al-Si alloys.

Al-7Si-0.4Mg alloy. However, both these pieces of work confirm the useful but relatively unspectacular benefits of refinement on strength. These authors suggest that the effects are complicated by the alloying effects of titanium, particularly the precipitation of large  $\text{TiAl}_3$  crystals at higher titanium levels since the expected linear increase in yield strength with  $(\text{grain diameter})^{-1/2}$  is not achieved. It seems likely, once again, that the presence of bifilms is complicating behavior. The large crystals of  $\text{TiAl}_3$  suggest precipitation on bifilms, and further suggest that the authors had stirred the melt in an effort to transfer as much Ti into the casting as possible. This counter-productive technique eliminates the benefits of the settling of bifilms by the weight of Ti-rich precipitates attached to them as discussed in Section 6.3.4.

It should not be assumed that the advantages, even if small, of fine grain size in wrought steels and cast light alloys automatically extend to other alloy systems. It is worth devoting some space to the difficulties and imponderables elsewhere.

For instance, steels that solidify to the body-centered-cubic (bcc) form of the iron lattice are successfully grain refined by a number of additives, particularly compounds of titanium and similar metals, as discussed in Section 6.6 (although not necessarily with benefits to the mechanical properties, as we shall see below). In contrast, steels that solidify to the face-centered-cubic (fcc) lattice do not appear to respond to attempts to grain refine with titanium, and are resistant to attempts to grain refine with most materials that have been tried to date.

The grain-refinement work carried out by Cibula (1955) on sand-cast bronzes and gunmetals showed that these alloys could be grain refined by the addition of 0.06% of zirconium. This was found

to reduce the tendency to open hot tears. However, this was the only benefit. The effect on strength was mixed, ductility was reduced, and although porosity was reduced in total, it was redistributed as layer porosity, leading to increased leakage in pressure-tightness tests. Although this was at the time viewed as a disappointing result, an examination of the tests that were employed makes the results less surprising. The test castings were grossly underfed, leading to greatly enhanced porosity. Had the castings been better poured and better fed, the result might have been greatly improved.

Remarkably similar results on a very different casting (but that also appears to have been underfed) were obtained by Couture and Edwards (1973). They found that various bronzes treated with 0.02Zr exhibited a nicely refined grain structure, and had improved density, hot tear resistance, yield, and ultimate strengths. However, ductility and pressure-tightness were drastically reduced. It is possible to conjecture that if the alloy had been better supplied with feed metal during solidification then pressure-tightness would not have been such a problem. The presence of copious supplies of bifilm defects are to be expected to complicate the results as a consequence of the poor casting technique.

The poor results by Cibula in 1955 have been repeatedly confirmed in Canadian research; Sahou and Worth (1990), Fasoyinu et al. (1998), Popescu et al. (1998) and Sadayappan et al. (1999) using, mainly, permanent mold test bars. These castings are not badly fed, so that the disappointing results by Cibula cannot be entirely ascribed to poor feeding. It seems likely that bifilms are at work once again.

There may be additional fundamental reasons why the copper-based alloys show poor ductility after grain refinement. Couture and Edwards noted that the lead- and tin-rich phases in coarse-grained alloys are distributed within the dendrites that constitute the grains. In grain-refined material the lead- and tin-rich phases occur exclusively in the grain boundaries. Thus it is to be expected that the grain boundaries are weak, reducing the strength of the alloy by: (1) offering little resistance to the spread of slip from grain to grain, and so effectively lowering the yield point; and (2) allowing deformation in their own right, as grain boundary shear, like freshly applied mortar between bricks. However, this seems unlikely to be the whole story since some of the poor results are found in copper-based alloys that contain no lead or tin. A further confusion probably exists because of the probability that the lead and tin phases may precipitate preferentially on bifilms, so that the observed grain boundary-weakening effect may not be directly the result of the metallic alloy additions.

Many of the above studies of copper-based alloys have used Zr for grain refinement. Thus it seems possible that they may have been seriously affected by the sporadic presence of zirconium oxide bifilms at the grain boundaries. Thus the loss of strength and ductility and the variability in the results would be expected as a result of the overriding damage caused by surface turbulence during the casting of the alloys.

As the reader will now appreciate, much of our research work on the strengths of cast alloys is, frankly, in a mess. Much of this work will require to be repeated with relatively bifilm-free material. We shall then benefit from understandable and reproducible data for the first time.

#### **9.4.3.2 Dendrite arm spacing**

Dendrite arm spacing (DAS) can refer to the spacing of the primary dendrite stems in those rather rare cases where no secondary arms exist. More usually, however, the DAS refers to the spacing between the secondary arms of dendrites. However, if tertiary arms are present at a smaller spacing, then it would refer to this.

If the DAS is reduced, then the mechanical properties of the cast alloy are usually improved. A typical result by Miguelucci (1985) is shown in Figure 2.47. Near the chill the strength of the alloy is

high, and the toughness is good. As the cooling rate decreases (and DAS grows), the ultimate strength falls somewhat. Although the decrease in itself would not perhaps be disastrous, the fall continues until it reaches the yield stress (taken as the proof stress in this case). Thus, on reaching the yield stress, failure is now sudden, without prior yield. This is disastrous. The alloy is now brittle, as is confirmed by elongation results close to zero.

Because of the effect of DAS, the effect of section size on mechanical properties is seen to be important even in alloys of aluminum that do not undergo any phase change during cooling. For ferrous materials, and especially cast irons, the effect of section size can be even more dramatic, because of the appearance of hard and possibly brittle non-equilibrium phases such as martensite and cementite in sections that cool quickly.

The improvement of strength and toughness by a reduction in DAS is such a similar response to that given by grain refinement that it is easy to see how these two separate processes have often been confused. However, the benefits of the refinement of grains and DAS cannot be the result of the same mechanisms. This is because when considering DAS no grain boundary exists between the arms of a single dendrite to stop the slide of a slip plane. A dislocation will be able to run more or less without hindrance across arm after arm, since all will be part of the same crystal lattice. Thus, in general, it seems that the Hall-Petch equation should not apply. Also, of course, Hall-Petch can only explain an increase in yield with an improved refinement, whereas refined DAS offers also offers an improved ductility.

Why then does a reduction in DAS increase both strength and toughness?

In the past, this question appears never to have been properly answered.

Classical physical metallurgy has been unable to explain the effect of DAS on mechanical properties. Curiously, this important failure of metallurgical science to explain an issue of central importance in the metallurgy of cast materials has been consistently and studiously overlooked for years.

In the first edition of *Castings* the author suggested that the answer seemed to be complicated, and to be the result of the sum of a number of separate effects, all of which seem to operate beneficially. These beneficial processes are listed and discussed below. However, after these effects have been reviewed and assessed, it will become clear that the major benefit from a refinement of DAS remains largely unexplained.

In this work, the action of bifilms will be presented as the dominant effect, capable of explaining for the first time the widely appreciated benefits of small DAS in castings, as we shall see.

### Residual Hall-Petch hardening

The near-perfection of the atomic lattice between adjacent dendrite arms would allow slip to progress from arm to arm without significant problem. This seems largely true for relatively pure Al and its solid solution alloys such as the low-magnesium Al-Mg alloys and many of the wrought alloys that are relatively low in solute. Thus there are fundamental reasons why the effect of Hall-Petch hardening should be negligible in these Al alloys, and in many other solid-solution, single-phase alloys (also including of course many stainless steels). The small or negligible benefit to the single-phase Al alloys is seen in Figure 9.21 for 7010, Al-4.5Cu and Al-3Mg alloys.

Slight faults during growth will cause the dendrite arms within a grain to become slightly misoriented. This will result in a low-angle grain boundary between the arms. The higher the degree of misorientation, the greater the resistance will be to the passage of a slip plane.

When studying the structure of a cast alloy under the microscope, most dendrite arms are seen to be, so far as one can tell by unaided observation, fairly true to their proper growth direction. Thus any boundary between the arms will have an almost vanishingly small misorientation, presenting a minimal impediment to slip across the boundary. However, it is also usually possible to see a proportion of arms at slight deviations of several degrees, perhaps as a result of mechanical damage. If mechanical disturbance during freezing is increased, for instance by stirring or vibration, then the number of misaligned arms, and their degree of misalignment, would be expected to increase.

Thus one might expect some small resistance to slip even from rather well-aligned dendrites because of the lack of perfection; the result of the existence of subgrains within the grains. Some contribution from Hall-Petch hardening might therefore be expected to be present at all times.

For those alloys that have interdendritic precipitates, however, there may be a positive action to arrest slip between dendrite arms. This is true in Al–Si alloys as is evident from the modest increase in strength noted in the impressive early work by Gurland (1970) and later by Wierzbinska and Sieniawski (2004) noted in Figures 9.22 and 9.23. Interestingly, for the Al–5Si–1Cu alloy there is a maximum potential benefit of about 15 MPa if very efficiently grain refined, plus a further maximum benefit from the refinement of DAS by chilling that might yield about 30 MPa. Thus by taking maximum advantage of refinement of grains and dendrites a total addition to strength could be 45 MPa. In practice, one would expect to achieve something rather less than this in most casting conditions, so that benefits to strength of Al–Si above 5 to 7%Si are not especially impressive, but worth having.

Comparing the benefits achievable in a single-phase solid-solution alloy such as Al–3Mg, Figure 9.22 illustrates that only about 10 MPa might be achieved by rapid solidification, but no benefit from grain refinement would be expected as a result of grain boundaries being easily traversed by slip planes in such materials. For most practical purposes this 10 MPa benefit is negligible.

We can conclude that in general, although the Hall-Petch mechanism is likely to be a contributor to increased strength, in most castings it will be negligibly small.

The final fact that eliminates the Hall-Petch effect as a major contributor to the DAS effect is the fundamental fact that Hall-Petch strengthening affects only the yield strength. Figure 2.47 and many similar results in the literature indicate that yield strength is hardly affected by DAS. The main effect of changes in DAS is seen in the ductility and ultimate strength values which Hall-Petch is not able to explain.

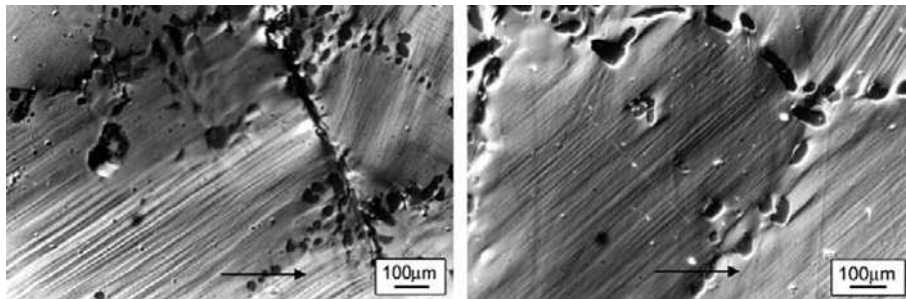


**FIGURE 9.23**

Change of slip band direction and intensity at interdendritic boundaries in Al–5Si–1Cu alloy (Wierzbinska and Sieniawski 2004).



### Restricted nucleation of interdendritic phases

As the DAS becomes smaller, the residual liquid is split up into progressively smaller regions. Although in fact these interdendritic spaces remain for the most part interconnected, the narrowness of the connecting channels does make them behave in many ways as though they were isolated.

Thus as solutes build up in these regions the presence of foreign nuclei to aid the appearance of a new phase becomes increasingly less probable as the number of regions is increased. As DAS decreases, the multiplication of sites exceeds the number of available nuclei, so that an increasing proportion of sites will not contain a second phase. Thus, unless the concentration of segregated solute reaches a value at which homogeneous nucleation can occur, the new phase will not appear.

Where the second phase is a gas pore, Poirier et al. (1987) have drawn attention to the fact that the pressure due to surface tension becomes increasingly high as the curvature of the bubble surface is caused to be squeezed into progressively smaller interdendritic spaces. The result is that it becomes impossible to nucleate a gas pore when the surface tension pressure exceeds the available gas pressure. Thus as DAS decreases there becomes a cut-off point at which gas pores cannot appear. Effectively, there is simply insufficient room for the bubble! The model by Poirier suggests that this is at least part of the reason for the extra soundness of chill castings compared to sand castings. Later work by Poirier (2001) and the theoretical model by Huang and Conley assuming no difficulty for the nucleation of pores confirms the improvement of soundness with increasing fineness of the structure.

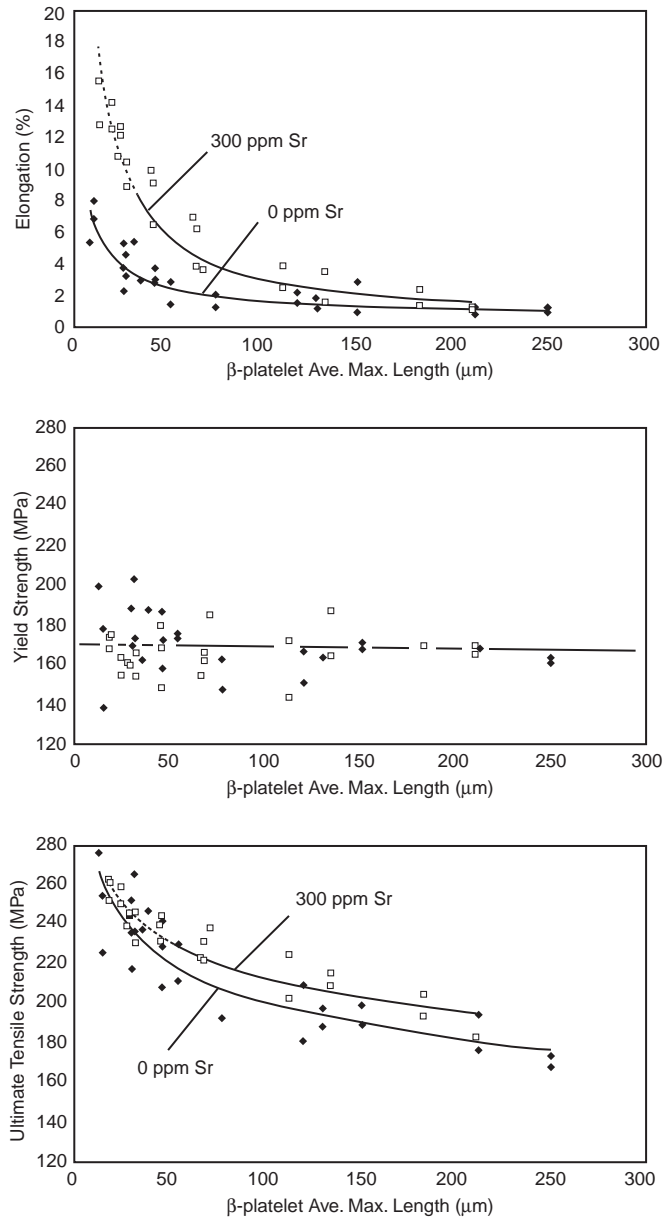
In summary, therefore, we can see that as DAS is reduced, the interdendritic structure becomes, on average, cleaner and sounder. These qualities may be significant contributors to improved properties.

### Restricted growth of interdendritic phases

Meyers (1986) found that for alloys of the Al–7Si system the strength and elongation were controlled by the average size of the silicon particles, although where the particles were uniformly rounded as in structures modified with sodium, the strength and elongation were controlled by the number of silicon particles per unit volume. These conclusions were verified by Saigal and Berry (1984), using a computer model. This important conclusion may have general validity for other systems containing hard, plate-like particles in a ductile matrix.

The highly deleterious effect of iron impurities in these alloys is attributed to the extensive plate-like morphology of the iron-rich phases. Vorren et al. (1984) have measured the length of the iron-rich plates as a function of DAS, and find, as might be expected, the two are closely related; as DAS reduces so the plates become smaller. From the work of Meyers, Saigal, and Berry we can therefore conclude that the strength and toughness should be correspondingly increased, as was in fact confirmed by Vorren. Ma and co-workers (2008) measure the lengths of the  $\beta$ -Fe particles in Al–7Si–0.4Mg alloy as a combined assessment of the increase of both Fe content and cooling time, plotting strength properties as a function of this length (Figure 9.24). They show how ductility is affected dramatically, tensile strength is somewhat reduced, but yield strength is hardly affected.

It seems likely that although there may be an element of cause and effect in the restriction of the growth of second phases by the dendrite arms, the major reason for the close relation between the size of secondary phases and DAS is that both are dependent on the same key factor, the time available for growth. Thus local solidification time controls the size of both dendrite arms and interdendritic phases.

**FIGURE 9.24**

(a) Properties of Al-7Si-0.4Mg alloy with 0 ppm and 300 ppm Sr as a function of average maximum length of  $\beta$ -Fe particles (Ma et al. 2008).

The reason underlying the importance of the large iron-rich plates in Al alloys is proposed in this work to be the result of the presence of oxide bifilms inside the plates, as has been stated in Section 6.3, and will be referred to below.

### Improved response to heat treatment

To summarize the effect of DAS on heat-treatment response: as DAS is reduced, so (i) the speed of homogenization is increased, allowing more complete homogenization, giving more solute in solution and so greater strength from the subsequent precipitation reaction. (ii) Speed of solution is also increased, allowing a greater proportion of the non-equilibrium second phase to be dissolved. The smaller numbers and sizes of remaining particles, if any, and the extra solute usefully in solution, will bring additional benefit to strength and toughness.

Even when the second-phase particles are equilibrium phases, the high-temperature homogenization and solution treatments have a beneficial effect even though the total volume of such phases is probably not altered. This is because the inclusions tend to spheroidize; their reduced aspect ratio, favoring improved toughness as discussed above. Any remaining pores will also tend to spheroidize, with similar benefit.

There is no doubt therefore that the improved response to heat treatment is a valuable benefit from refinement to DAS arising from the reduced presence of interdendritic phases (although, ironically, this effect is seen to reduce any Hall-Petch contribution) and possibly the additional solute now in solution. These real improvements to properties if heat treatment is carried out are a separate and additional factor to the important factor described below.

We need to keep in mind, however, that the improvements in properties as a result of refined DAS are enjoyed whether heat treatment is carried out or not. Thus there remains some other major factor at work, so far not considered. We consider this now.

### Effect of bifilms

The following examination of the effect of bifilms in the liquid alloy suggests that their effect on properties, as indicated by the DAS, is expected to be dominant.

Rather than consider that refined DAS improves properties, it is more accurate to start with the view that the properties of castings are good, but are degraded as DAS coarsens. This revised viewpoint is helpful as is explained below.

The importance of the presence of bifilms only becomes seriously damaging as solidification time is extended. This is due to the fact that the bifilms arrive in the casting in a compact form, tumbled into compactness by the bulk turbulence during the filling of the mold cavity. In this form their deleterious effects are minimized. They are small and rounded. Their effectiveness as defects grows as they slowly unfurl, gradually enlarging to take on the form of planar cracks up to approximately ten times larger diameter than the diameter of their original compact shape. As we have seen in Chapter 2, there are a number of driving forces for this straightening phenomenon. These include the precipitation of gas inside, or second phases (particularly iron-rich phases in Al alloys) outside, or the action of shrinkage to aid inflation, or the action of growing grains to push and thereby organize the films into interdendritic or intergranular planes.

The bifilms are seen therefore to evolve into serious defects, given time. Time is a crucial factor. Thus if there is little time, the defects will be frozen into the casting in a compact form of diameter in the range of 0.1–1 mm or less in smaller castings. However, given time, the bifilms will open to their

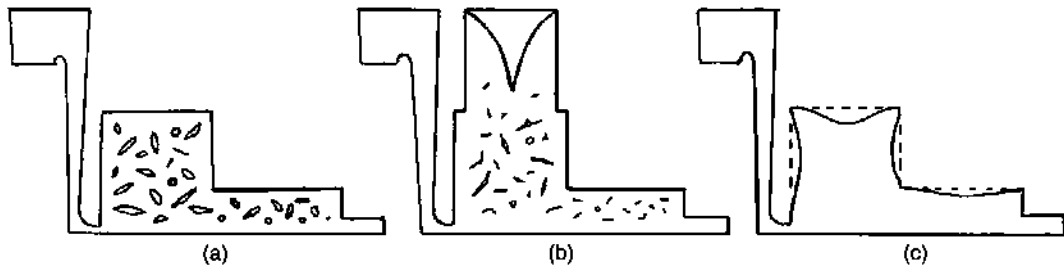


**FIGURE 9.25**

(a) Opened bifilms because of lack of feeding leading to poor ductility; (b) improved ductility from maintenance of pressure by a feeder; (c) excellent ductility irrespective of feeding or pressure in the absence of bifilms (however, possible external sinks in heavy sections as shown).

full size. This might be as large as 10–15 mm across in an Al alloy casting of 10–100 kg weight. In Al–bronze castings and some stainless steel castings weighing several tonnes bifilms in the size range of 50–100 mm are not uncommon. These constitute massive cracks that seriously degrade properties.

The fall of ductility with increasing DAS becomes clear therefore. It is not the DAS itself that is important. *The DAS is merely the indicator of the time available* for the opening of bifilms. The DAS is our independent clock. It is the opening of the bifilms into extensive planar cracks that is important in degrading properties.

The time required for the complete opening of bifilms depends, of course, on the rate at which they can open. This in turn depends on how raveled the bifilm is, and depends on the various driving forces available for opening. Thus the defects will open at variable rates depending somewhat on their geometry, but faster for higher concentration of gas in solution, poorer conditions for feeding, and, in aluminum alloys, higher iron contents.

A practical example is given in Figure 9.25. The sketch (a) shows the opening of bifilms in a poorly fed region whose solidification is delayed by its heavy section. In other regions of the casting the bifilms have no time to open, and are therefore frozen-in as compact and relatively harmless defects. The mechanical properties are good in the rapidly solidified regions, and poor in the slowly solidified and poorly fed regions. Sketch (b) illustrates the benefit of keeping some pressure on the solidifying liquid, in this case by the planting of a feeder onto the casting. The opening of the bifilms is thereby resisted to some extent, and improved properties are retained by the solidification under pressure, even though the pressure is quite modest. Sketch (c) illustrates the case where the metal is superbly clean. The properties are good everywhere regardless of cooling conditions and regardless of pressurization from a feeder. (The reader will notice some solid feeding, however, which would be avoided by the pressurization provided by a good-sized feeder.)

We can therefore make an interesting prediction for results such as those presented in Figure 2.47. The prediction is: if there were no bifilms in the liquid metal, the curves of UTS and Elongation to failure versus DAS would both be nearly horizontal lines. It is possible that a slight downward slope might be expected as a result of other factors, such as interdendritic regions becoming less clean, as discussed earlier. However, apart from such minor effects, properties would become essentially

*insensitive* to changes in DAS. In other words, in the absence of bifilms, properties would remain high regardless of how slowly or quickly the casting solidified.

Good evidence that this is true, that properties of clean metals are substantially independent of DAS, comes from widely different sources:

- (i) For steels, Polich and Flemings (1965) showed that low-alloy steels that had been subjected to directional solidification in an upward direction, encouraging the floating out and pushing ahead of bifilms, exhibited a constant elongation despite DAS increasing from 20 to 150  $\mu\text{m}$ . Conversely, equiaxed versions of the same steel, in which bifilms would not have separated, showed a fall in ductility as DAS increased (Figure 9.26).

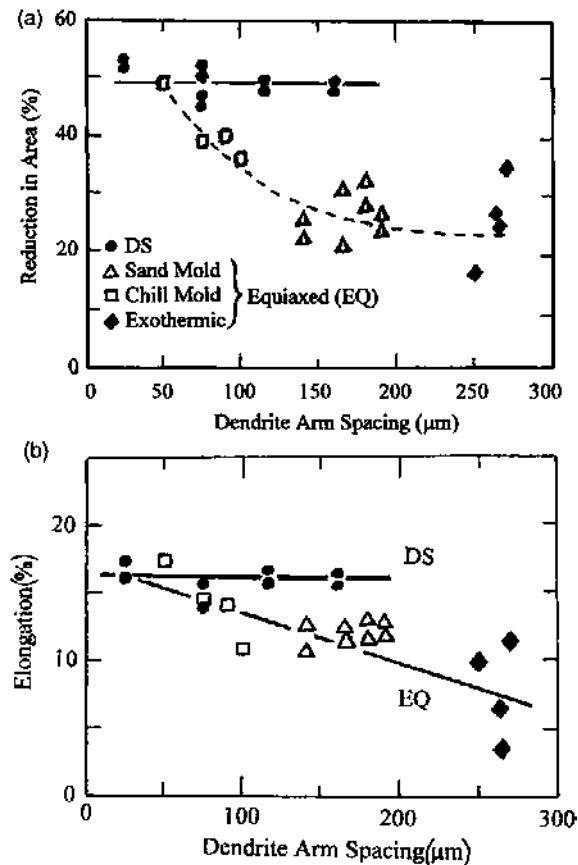


**FIGURE 9.26**

Vertically oriented directionally solidified (DS) low-alloy steel is expected to be relatively free from bifilms, and thus DAS has no influence on ductility; conventional equiaxed solidification traps bifilms, permitting DAS to control ductility measured as RA and Elongation by Polich and Flemings (1965).

- (ii) From early experience with the Cosworth Process, when Cosworth Engineering made its racing car engines from castings poured in conventional foundries, at least 50% of all the cylinder heads (four-valve-per-cylinder designs) failed by thermal fatigue between the exhaust valve seats. In 1980, when cylinder heads became available for the first time from the new process, characterized by quiescent transfer and counter-gravity filling, the failures fell immediately to zero. The DAS was hardly changed, and was in any case considerably larger than that available from permanent mold casting, for which resistance to thermal fatigue at that time was poor and variable. Thus DAS was not controlling in this case. It is difficult to avoid the conclusion that the action of bifilms was crucial in this experience.

The action of some casting customers specifying DAS to avoid thermal fatigue in critical locations like the exhaust valve bridge in cylinder heads is seen therefore to miss a valuable potential benefit. Certainly control of DAS will be important for casting systems that provide poor filling control and thus contain a high density of bifilms. However, in a process such as the Cosworth Process, specifically designed to provide good-quality metal, it is almost certainly an unnecessary complication and expense. In general, for casting processes as a whole, it would be more constructive to specify the reduction in bifilms by good processing techniques. This would achieve benefits throughout the whole casting, not merely in those designated regions where a limited DAS has been specified.

- (iii) The new ablation process completely separates any observable effect of DAS from properties. DAS can be huge if the application of the cooling water is delayed, allowing the dendrites to grow and coarsen. However, the properties can still remain high if the residual eutectic liquid is frozen quickly, thus retaining the bifilms small, the Fe-rich particles having no time to grow and straighten the bifilms and so reduce properties. Properties could remain adequate even when working with melts that were known to contain large populations of bifilms. Figure 9.27 is an example for an Al-7Si-0.4Mg-0.4Fe alloy showing the eutectic phase so fine as to be difficult to resolve, and Fe-rich platelets so small, approximately 1  $\mu\text{m}$  or less long, that they are difficult to find even at the highest optical magnifications.

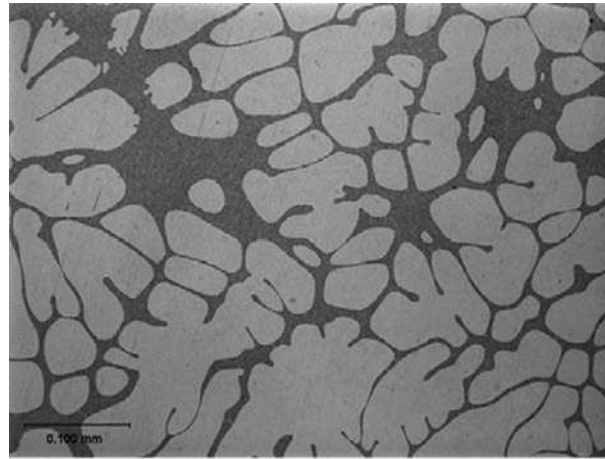
#### 9.4.4 Ultimate tensile strength

Ultimate tensile strength (TS) is a composite property composed of the total of (i) the yield stress plus (ii) additional strengthening from work hardening during the plastic yielding of the material prior to failure. These two components make its behavior more complicated to understand than the behavior of yield stress or ductility alone.

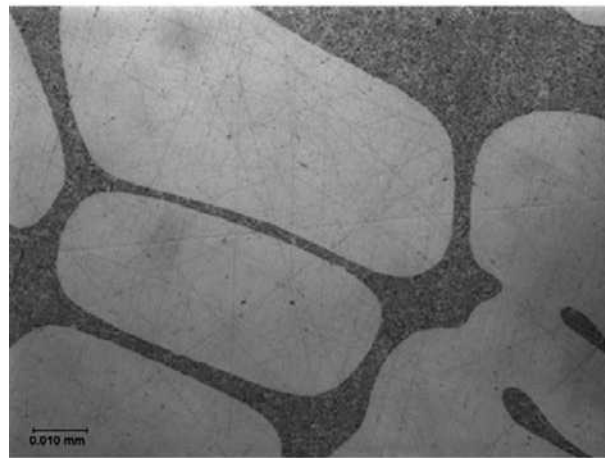
TS equals the yield, or proof, stress when (i) there is no ductility, as is seen in Figure 2.47 and Figure 9.20, and (ii) when the work hardening is zero. The zero work-hardening condition is less commonly met, but occurs often at high temperatures when the rate of recovery exceeds the rate of hardening.

The problem of determining the TS of a cast material is that the results are often scattered. The problems of dealing with this scatter are important, and are dealt with at length in Section 9.2. Section 9.2 is strongly recommended reading.

Generally, for a given alloy, proof strength is fixed. Thus as ductility is increased (by, for instance, the use of cleaner metal, or faster solidification) so TS will usually increase, because with the additional plastic extension, work hardening now has the chance to accumulate and so raise strength. The



(a)



(b)

**FIGURE 9.27**

Ablation cooled Al-7Si-0.4Mg-0.4Fe alloy showing Si particle size and spacing approximately  $1\ \mu\text{m}$ , and  $\beta$ -Fe particles too small to be easily found (courtesy of Alotech).

effect is again clear in Figure 2.47. For a cast aluminum alloy, Hedjazi et al. (1975) show that TS is increased by a reduction in defects, as shown in Figure 9.28. However, it seems probable that the response of the TS is mainly due to the increase in ductility, as is clear from the strong shift of the property region to the right rather than simply upwards.

The rather larger effect that layer porosity is expected to have on ductility will supplement the smaller effect due to loss of area on the overall response of TS. Figure 9.11 shows the reduction in TS and elongation in an Mg-Zn alloy system where the reduction in properties seems modest. In

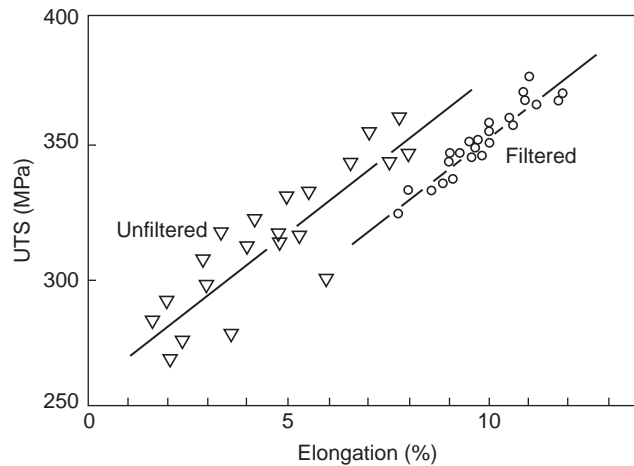


**FIGURE 9.28**

Mechanical properties of Al-4.5Cu-1.5Mg alloy in the unfiltered and filtered conditions, illustrating the strong response of ductility (data from Hedjazi et al. 1975).

Figure 7.34 the TS of an Al-11.5Mg alloy shows more serious reductions, especially when the porosity is in the form of layers perpendicular to the applied stress. Even so, the reductions are not as serious as would be expected if the layers had been cracks, a result emphasizing their nature as ‘stitched’, or ‘tack welded’ cracks, as discussed in Section 9.4.2.

When the layers are oriented parallel to the direction of the applied stress, then, as might be expected, Pollard (1965) has shown that layer porosity totaling even as high as 3% by volume has a practically undetectable effect on properties.

Finally it is clear that cracks or films occupying the majority of the cross-section of the casting will be highly injurious for TS as they are for ductility. The self-evident general understanding that the TS falls to zero as the crack occupies progressively more of the area under test is quantified by Clyne and Davies (1975) in Figure 9.12.

## 9.5 FRACTURE TOUGHNESS

Fracture toughness is a material property that is generally independent of the presence of gross defects (although it could be affected by a dense population of small defects, as will become clear). This is because it is assessed by the force required to extend a crack that has been artificially introduced in the material usually by extending a machined notch by fatigue. Thus fracture toughness measures the properties of the matrix at the point at which the notch is placed, i.e. it is a material property. It is not a property like tensile strength or ductility in which the crack finds its own start location, ensuring failure from the largest defect. When preparing the toughness assessment test piece the machining of a notch into the specimen at a pre-fixed location would be unlikely to encounter a major defect by chance.



Fracture toughness is the material property that allows the prediction of the shapes and sizes of defects that might lead to failure. It is a basic tenet of fracture mechanics that fracture may begin when the stress-intensity factor  $K$  exceeds a critical value, the fracture toughness  $K_{1C}$ . A detailed presentation of the concept of fracture toughness is beyond the scope of this book. The interested reader is recommended to an introductory text like that by Knott and Elliott (1979). Here we shall simply assume some basic equations and the experimental results.

Stress intensity  $K$  as well as fracture toughness has the dimensions of stress times the square root of length, and is most appropriately measured in units of  $\text{MN m}^{-3/2} = \text{MPa m}^{1/2}$ . (Care is needed with units of this property. Fracture toughness is sometimes measured less conveniently in  $\text{N mm}^{-3/2} = \text{MPa mm}^{1/2}$  that differ by a factor of  $(1000)^{1/2} = 31.6$ .) For a penny-shaped crack of diameter  $d$  in the interior of a large casting, the critical defect size at which failure will occur is approximately:

$$d = 2K_1C^2/\pi\sigma^2 \quad (9.9)$$

from which, for an aluminum alloy of fracture toughness  $32 \text{ MPa m}^{1/2}$  at its yield point of  $240 \text{ MPa}$ , the critical defect size  $d$  is  $11 \text{ mm}$ . For an edge crack, Equation 9.9 is modified by a factor of  $1.25$ , giving a corresponding critical defect size of  $9 \text{ mm}$ , indicating that edge cracks are somewhat more serious than center cracks, but in any event defects of about a centimeter across would be required, even at a stress at which the casting is on the point of plastic failure. These are comparatively large defects, which is reassuring in the sense that such large cracks may have a chance to be found by non-destructive tests prior to the casting going into service. However, they underline the conclusion that most current radiography standards which state ‘no linear defects’ of any size, or which reject aluminum alloy castings for flaws of only approximately  $1 \text{ mm}$  in size, may not be logical.

The important message to be learned from the concept of fracture toughness is that the maximum defect size that can be tolerated can be precisely calculated if the fracture toughness and the applied stress are both known.

Equation 9.9 can be used to indicate that at the limit, when the applied stress  $\sigma$  equals the yield stress  $\sigma_y$ , the greatest resistance to crack extension that can be offered by a material is controlled by the value of  $K_{1C}/\sigma_y$  (units most conveniently in  $\text{m}^{1/2}$ ). This parameter is a valuable measure of the defect tolerance of a material.

Figure 9.29 shows how the permissible defect size in ductile irons is large for low-strength irons, but diminishes with increasing strength because of the fall of fracture toughness. Thus for the stronger irons the permissible defect size is below  $1 \text{ mm}$ . This is particularly difficult to detect, and sets a limit to the stress at which a strong ductile iron casting may be used with confidence.

Steels can have high fracture toughness, with correspondingly good tolerance to large defects at low applied stress. However, because they are used in highly stressed applications, the permissible defect size is reduced, as Equation 9.12 indicates. Jackson and Wright (1977) discuss the serious problem of detecting flaws when the permissible size is small. At the time of writing most non-destructive testing methods have been found wanting in some respect. However, the technology of non-destructive techniques has improved significantly and is expected to continue to improve, allowing the detection of smaller defects with greater certainty, and so extending the range over which castings can be stressed whilst reducing the risk of failure. In this respect the most significant advance is probably the development of sophisticated resonance testing described in Chapter 19.

Nevertheless, Jackson and Wright’s conclusion is good advice: choose an alloy with a large critical flaw size, which can be detected, and measured accurately. Also, if the working load is fluctuating, it

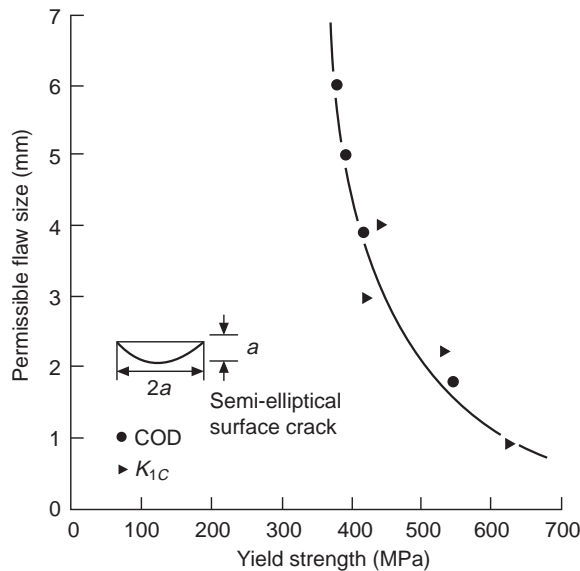


**FIGURE 9.29**

Permissible edge defect sizes in ductile irons of increasing strength. (Data from Seetharamu and Srinivasan 1985.)

will be necessary to calculate from crack propagation rate curves the time for a flaw to grow to the critical size. This can then be compared to the design life of the component.

To be safe, they recommend the following assumptions:

1. A string of cracks is equivalent to one long crack.
2. A group of flaws is one large flaw of size comparable with the envelope that circumscribes them.
3. Unless clearly seen to be otherwise, all flaws have a sharp aspect ratio.
4. All flaws reside on the surface.

A casting designed on this basis is likely to be somewhat over-designed, but perhaps not so much as if there had been no use of the principles of fracture mechanics.

There has been relatively little work carried out on the fracture toughness of cast Al alloys. Tiryakioglu and Hudak (2008) have therefore developed a relation between round notched tensile strength  $\sigma_{NT}$  and fracture toughness  $K_{1C}$ , both normalized by dividing by the yield stress  $\sigma_y$  as shown in Figure 9.30a for Al-7Si-0.6Mg alloy. The direct comparison between  $\sigma_{NT}$  and  $K_{1C}$  is given in Figure 9.30b showing limits of accuracy at 5% and 1% error to within 95% confidence. The best fit line is given by

$$K_{1C} = \beta \sigma_{NT} \quad (9.10)$$

where  $\beta = 6.33 \times 10^{-2} \text{ m}^{0.5}$  with  $R^2 = 0.72$  and standard mean deviation  $1.48 \text{ MPa}^2 \text{ m}$ . Round tensile test specimens with a circumferential sharp notch are easy and quick to produce, so the important parameter,  $K_{1C}$ , is suddenly made much more accessible.

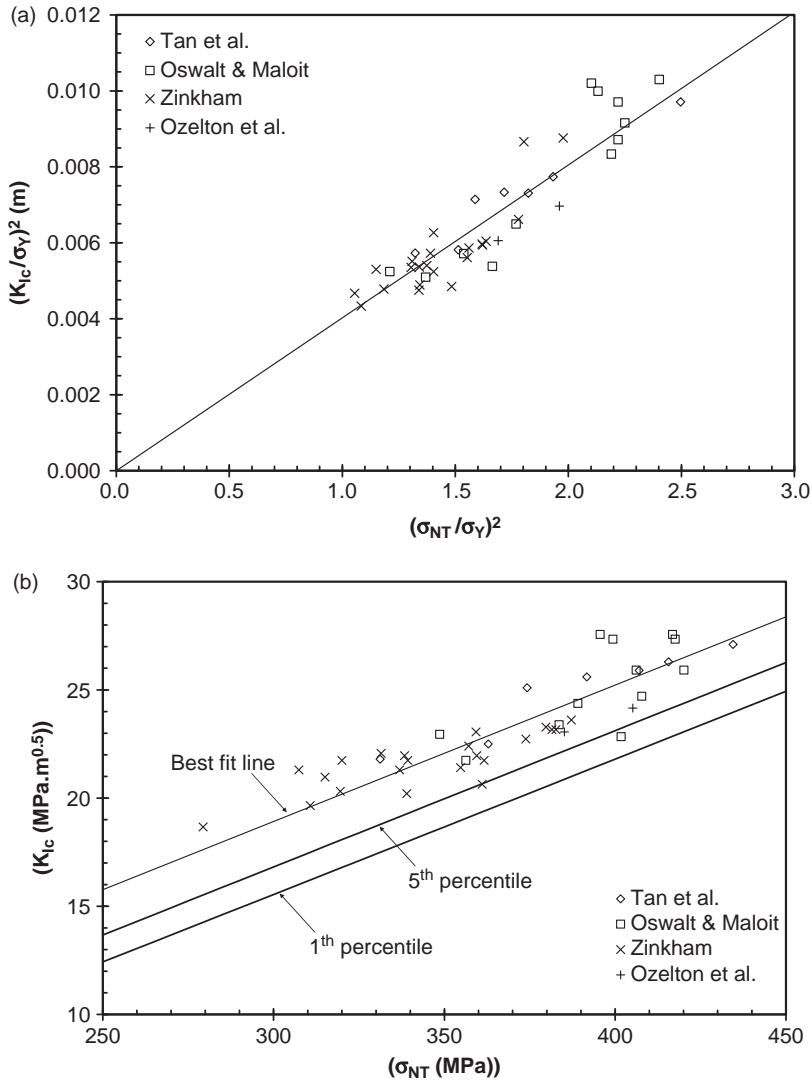


FIGURE 9.30

(a) Relation between  $(K_{1C}/\sigma_Y)^2$  and the square of notch tensile strength  $\sigma_{NT}$ /yield strength  $\sigma_Y$ . The best fit line goes through the origin, suggesting a convincing relationship. (b)  $K_{1C}$  values from is plotted versus notch-tensile strength (lower bounds at 95% and 99% confidence limits are also shown). (Tiryakioglu 2008.)

So far all the discussion has related to linear elastic fracture mechanics (LEFM), in which the fracture resistance of a material is defined in terms of the elastic stress field intensity near the tip of the crack. In fact, the fracture toughness parameter  $K_{1C}$  is valid only when the region of plastic yielding around the tip is small.

For lower-strength materials, plastic deformation at the tip of the crack becomes dominant, requiring the application of yielding fracture mechanics (YFM) and the concept of either (i) crack opening displacement (COD or  $\delta$ ), or (ii) the  $J$  integral, as a measure of toughness.

The critical COD is the actual distance by which the opposite faces of the crack separate before unstable fracture occurs. This critical opening is known as  $\delta_c$ . The critical flaw size is given by:

$$d_c = c(\delta_c/\varepsilon_y) \quad (9.11)$$

where  $c$  is a material constant and  $\varepsilon_y$  is the strain at yield. For materials that are on the borderline for treatment by LEFM or YFM, Jackson and Wright (1977) indicate that a unified test technique can be used to determine  $K_{1C}$  or  $\delta_c$  from a single test piece, and that the following useful relation may be employed:

$$\delta_c/e_y = (K_{1C}/\sigma_y)^2 \quad (9.12)$$

Hence the ratio  $\delta_c/e_y$  in YFM is comparable with  $(K_{1C}/\sigma_y)^2$  in LEFM, i.e. it is a measure of the defect tolerance of a material. It deserves to be much more widely used in the design and specification of castings.

The transition between  $K_{1C}$  and COD, when properly applied, is seen to give consistent predictions of the critical defect size. The results in Figure 9.29 for ductile irons show a region of smooth overlap between the two approaches.

Although the COD has a clear physical basis, in both its formulation and its application, there are empirical assumptions that are difficult to justify by the rigorous application of mechanics at this time. For this reason, more attention is being given to the use of the  $J$  integral in structural-integrity assessment, especially in the USA.  $J$  is a crack-tip driving force that, under certain conditions, can be applied to elastic–plastic situations to describe the onset of stable crack growth. For a given geometry of loading, size of test piece and size of defect,  $J$  is related directly to the area under the load–displacement curve obtained for the cracked body, where displacements are measured at the loading points.

A general overview of the fracture toughness and strength of cast alloys is given in Figure 9.31. This indicates the rather poor properties of flake irons, and the excellent properties of some steels, nickel alloys, and titanium alloys. Ductile irons occupy an interesting middle ground. In general it seems that most groups of alloys can exhibit either high strength and low toughness, or high toughness and low strength. The result is the hyperbolic shape of the curve as seen for ductile irons. As more results for other alloys are determined, Figure 9.31 will be expected to develop into a series of overlapping hyperbolic regimes containing the various alloy systems.

Figure 9.32 shows how the fracture toughness values can be translated into permissible flaw diameters, assuming a central penny-shaped crack, and a given level of applied tensile stress. Lalpoor and colleagues (2009) work out from computed stresses the sizes of critical flaws in a continuously cast high-strength Al alloy 7050, finding that the diameters of critical penny-shaped cracks are in the region of 20–50 mm. Since spontaneous failures of these products are relatively common (and expensive of course) it is clear that such large cracks do exist. It seems inescapable that these are bifilms introduced during the initial fall of the melt into the mold; the rest of the mold filling action is practically perfect and not capable of introducing such defects.

Figure 9.20 presents interesting results for the mechanical properties of a high-strength aluminum alloy that is not normally poured to make shaped castings. In this work it was cast and given a range of

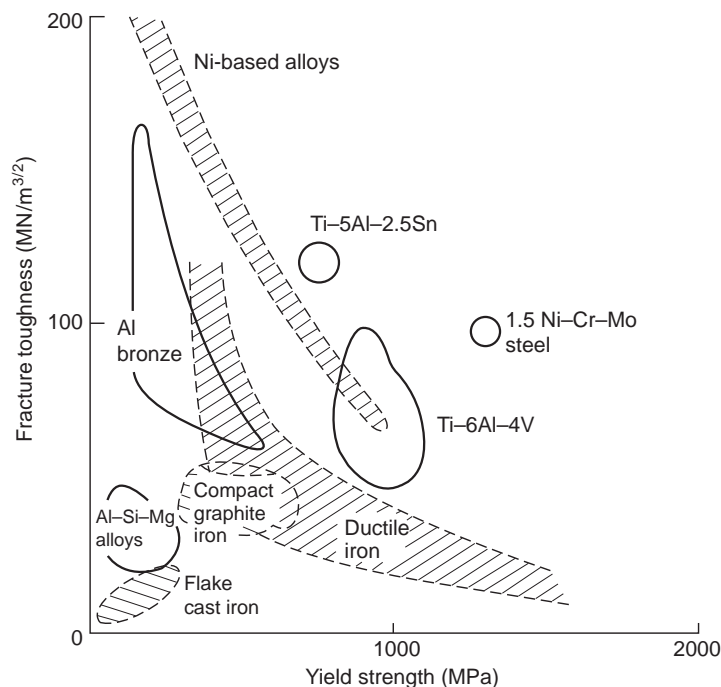


**FIGURE 9.31**

Map of fracture toughness versus yield strength for various cast alloys. (Data from Speidel 1982 and Jackson and Wright 1977.)

heat treatments covering the peak response condition. In the optimally hard state it had an elongation close to zero, and would not normally be used in this condition because a designer or user would be nervous about brittle failure. It is in the nature of brittle failure (i.e. failure without general plastic deformation) that there is no benefit from either (i) the redistribution of stress, or (ii) any prior warning of impending failure by the general plastic yielding of the casting. Nevertheless, the fracture toughness is clearly little influenced by aging, and retains a respectably high value regardless of the low ductility. This means that any crack or other defect will always have to exceed a certain critical size before failure occurs, even if such failure is eventually of a brittle character, and therefore probably catastrophic.

This general behavior is confirmed by Vorren and colleagues (1984) for the more common casting alloy Al-7Si-0.5Mg: although these researchers find the fracture toughness falls with increasing iron content in the alloy, the fall is significantly less than the fall in ductility, assessed by the reduction in area.

In those cases where general deformation of the casting cannot be tolerated, therefore, the use of fracture toughness is a more appropriate measure of the reliability of the casting than ductility. It seems that for many years we have been using the wrong parameter to assess the reliability of many of our castings.

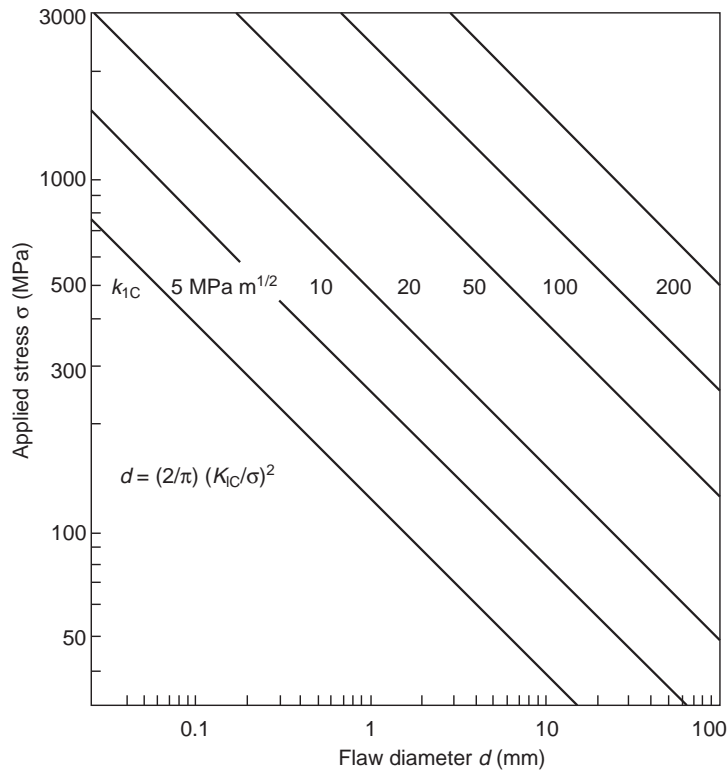


**FIGURE 9.32**

Relation between fracture toughness, applied stress and the critical defect size for failure in a material containing a central circular flaw.

## 9.6 FATIGUE

### 9.6.1 High cycle fatigue

A huge volume of work exists on the fatigue of castings. This lightweight and shallow condensation hardly scratches the surface therefore of a profound and increasingly mature discipline. We shall endeavor to mention some of the more important issues.

#### *Initiation*

A historically classical study of fatigue in a cast alloy Al-7Si-0.5Mg was carried out by Pitcher and Forsyth (1982). These workers were able to show that in general the fatigue performance of cast alloys was poor because the initiation of the fatigue crack during stage 1 of the fatigue process was short. This observation appears to have been confirmed for cast Al alloys many times, for instance recently by Wang, Apelian, and Lados (2001) who found no time was required for crack initiation, and that the fatigue life was the time merely for propagation of the crack. With the wisdom of hindsight, we can

conclude that this was almost certainly a consequence of the presence of bifilms. Thus the cast specimens were effectively pre-cracked. This conclusion is strongly indicated by the rather poor casting technique used for the preparation of test specimens, and additionally confirmed by the appearance of pores that appeared to be associated with films in some of their micrographs. Thus the size of initiating defects in their castings effectively eliminated stage 1.

However, Pitcher and Forsyth found that stage 2 of the growth of the crack, which is its stepwise propagation across the majority of the section, was remarkably slow compared to high-strength wrought alloys. The slow rate of crack propagation seemed to be the result of the irregular branching nature of the crack, which appeared to have to take a tortuous path through the as-cast structure. This contrasts with wrought alloys, where the uniformly even microstructure allows the crack to spread unchecked along a straight path. With the wisdom of hindsight we can speculate that the crack followed randomly oriented bifilms, as would have occurred if the sample shown in Figure 2.40b had been subjected to fatigue.

The results by Polich and Flemings (1965) on the solidification of steels is highly informative. They found that steels solidified unidirectionally, in which the growth direction was upwards, had properties significantly better than those solidified in a non-directional equiaxed mode. We can speculate that the equiaxed mode would have trapped bifilms between the growing grains, whereas the vertical solidification would have allowed bifilms to float clear, and even if encountered by the front, would have a chance to be pushed ahead and thus avoid incorporation in the solid. The absence of bifilms in the DS material is corroborated by the insensitivity of its ductility to wide changes in DAS (in contrast to equiaxed material) as seen in Figure 9.26. Furthermore, these authors found the properties of the DS material were also insensitive to the direction of grain growth, so that grain direction and grain boundary direction was, it seems, unimportant to the properties and the development of cracks. This important counter-intuitive finding further confirms that only the presence of bifilms at grain boundaries influences properties, and that otherwise, boundaries are practically as strong as the matrix so that cracks are hardly influenced by the presence of boundaries. (Despite widespread glib assertions of their weakness, grain boundaries are clearly strong, otherwise all our bridges would be in the rivers.)

One conclusion to be drawn from the work indicating that crack propagation is slow, but initiation takes no time, is that if initiation can be delayed, then fatigue lives of cast metals might be extended considerably, perhaps in excess of those of wrought alloys.

An indication of the general validity of this conclusion is confirmed by Pitcher and Forsyth. They shot-blasted their specimens to generate residual compressive stresses in the surface. This did help to slow initiation, and total fatigue lives were improved. For sand castings fatigue life was increased to that expected of chill cast material as shown in Figure 9.33. (It is a pity that the important high-stress/low-cycle part of the fatigue curve is often not investigated. It is interpolated here between the high-cycle results and the UTS values; i.e. the single cycle to failure result.) Chill-cast material is subject to a similar substantial improvement when shot blasted. For steel castings Naro and Wallace (1967) also found that shot peening considerably improved the fatigue resistance.

Although the improvement of fatigue resistance as a result of the compressive surface stresses introduced by shot peening is perhaps to be expected, the effect of grit blasting is less easy to predict, because the fine notch effect from the indentations of the grit particles would impair, whereas the induced compressive stresses would enhance fatigue life. From tests on aluminum alloys, Myllymaki (1987) finds that these opposing effects are in fact tolerably balanced, so that grit blasting has little net effect on fatigue behavior.

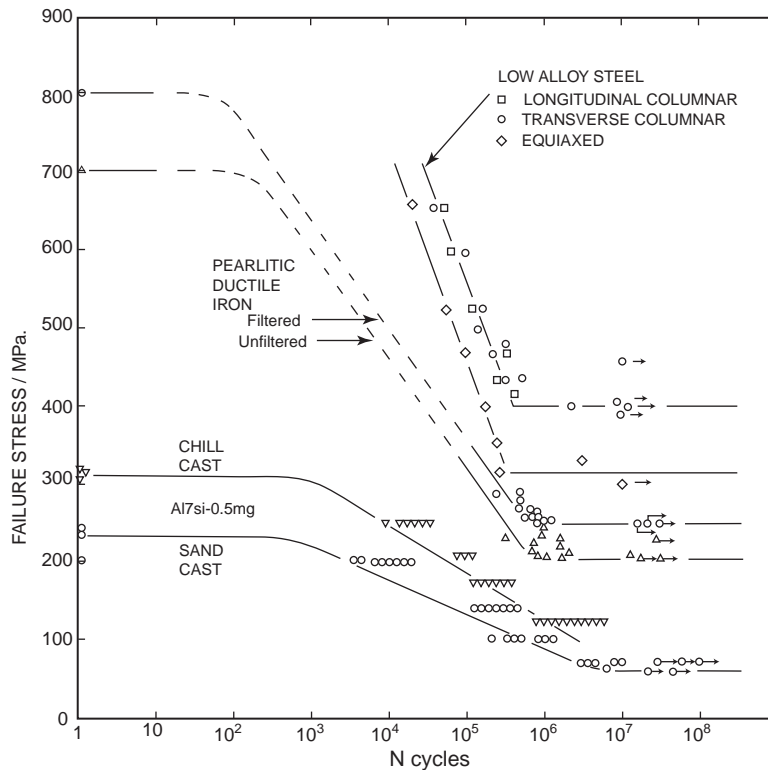


**FIGURE 9.33**

Fatigue data for an Al alloy (Pitcher and Forsyth 1982), a pearlitic ductile iron (Simmons and Trinkl 1987), and a low-alloy steel (Polich and Flemings 1965).

### ***Effect of defects***

Improvement is expected if cast defects are eliminated, so that the fatigue crack now needs to be initiated, thus introducing a lengthy stage 1. Figure 9.33 illustrates the case of a pearlitic ductile iron where consistently improved performance was obtained from the use of material with a reduced density of defects produced by filtering in the mold. The elimination of thermal fatigue cracking in the early Cosworth Process Al-7Si-0.4Mg alloy cylinder heads is another instance of the importance of the elimination of defects, so as to introduce a long stage 1 to the fatigue crack propagation.

This industrial experience has now been confirmed by a careful laboratory study by Nyahumwa, Green, and Campbell (1998, 2000) on Al-7Si-0.4Mg alloy castings. To vary the number density and size of oxide film defects in the castings, test bars were cast using bottom-gated filling systems with and without filtration. Test pieces were machined from the castings and were fatigue tested in pull-pull sinusoidal loading at maximum stresses of 150 MPa and 240 MPa under stress ratio  $R = +0.1$ .

The use of the pull-pull mode of testing (positive  $R$  ratio) is important for two reasons. (i) The fracture surface is undamaged (in contrast to the hammering that normal laboratory fatigue specimens



suffer) and so can be studied under the scanning electron microscope (SEM) in great detail. This is most important when searching for elusive features such as oxide films, and probably has been a significant factor explaining how such extensive defects have been overlooked until recently. (ii) In service conditions in many castings, the existence of residual tensile stress is a common feature because of inappropriate quenching practice after solution heat treatment. Some residual stress is to be expected even in carefully quenched castings. Thus fatigue failure is most likely to occur in regions already experiencing significant tensile loads. Thus pull–pull testing conditions will represent such regions more accurately. It follows that fatigue testing in laboratories using reversed loading (push–pull, with negative  $R$  ratios) should be reconsidered in favor of pull–pull.

Test bars of an Al–7Si–Mg alloy (2L99) were cast in chemically bonded silica sand molds. Two batches of test bars were cast using (i) a bottom-filling unfiltered system through which a liquid metal entered the ingate at a velocity greater than  $0.5 \text{ m s}^{-1}$ , and (ii) a bottom-filling filtered system through a ceramic foam filter with 20 pores per inch (corresponding to an average pore diameter of approximately 1 mm); in this system a liquid metal entered the ingate at a velocity less than  $0.5 \text{ m s}^{-1}$ . An SEM examination was carried out on the fracture surfaces of all the failed specimens to ascertain the crack initiator in every case. This was a huge exercise, probably never attempted previously.

Fatigue life data obtained from the filtered and unfiltered castings tested at 150 and 240 MPa are plotted in Figure 9.34. The probability of failure for each of the specimens in a sample was defined as the rank position divided by the sample size (i.e. the test results were ranked worst to best in ascending order; so, for instance, the 20th sample from the bottom in a total of 50 samples exhibited a 40% probability of failure).

Figure 9.35 shows the three main types of fracture surface observed: (a) oxide film defects which were categorized either as young, thin film or older, thicker film, based on the thickness of folds; (b) slip mechanisms indicated by a typical faceted transgranular appearance; and (c) fatigue striations, often called beach marks, denoting the step by step advance of the crack.

There was much to learn from this work. Figure 9.34 shows that for the unfiltered castings, most failures initiated from defects, sometimes pores, but usually oxides. The oxides were a mix of young and old. Only three specimens were fortunate to contain no defects. These exhibited ten times longer lives, and finally failed from cracks that had initiated by the action of slip bands that created interesting facets on the fracture surface. Thus these specimens had lives limited by the metallurgical properties of the alloy, although even in this case, an ‘ultimate’ attainment of life could not be assumed since it seems likely that entrainment defects had initiated the slip bands (Tiryakioglu, Nyahumwa, and Campbell 2011).

The filtered castings (bold symbols in Figure 9.34) were expected to be largely free from defects, but even these were discovered to have failed mainly as a result of defects, the defects consisting solely of old oxides that must have passed through the ceramic foam filter. There were no young oxides and no pores. A check of the equivalent initial flaw size (determined from the square root of the projected area of fatigue defect initiators) showed that 90% were in the range 0.1–1.0 mm, with a few as large as 1.6 mm. Thus most would have been able to pass through the filter without difficulty.

Again, those few samples of cast material free from oxides displayed an order of magnitude improved life, the best of which agreed closely with the best of the results from the unfiltered tests. This agreement confirms the relatively defect-free status of these few results.

The detrimental effect of mixed oxide films in the unfiltered castings is reflected by the lower fatigue performance compared to that of the filtered castings containing old oxide films. This indicates

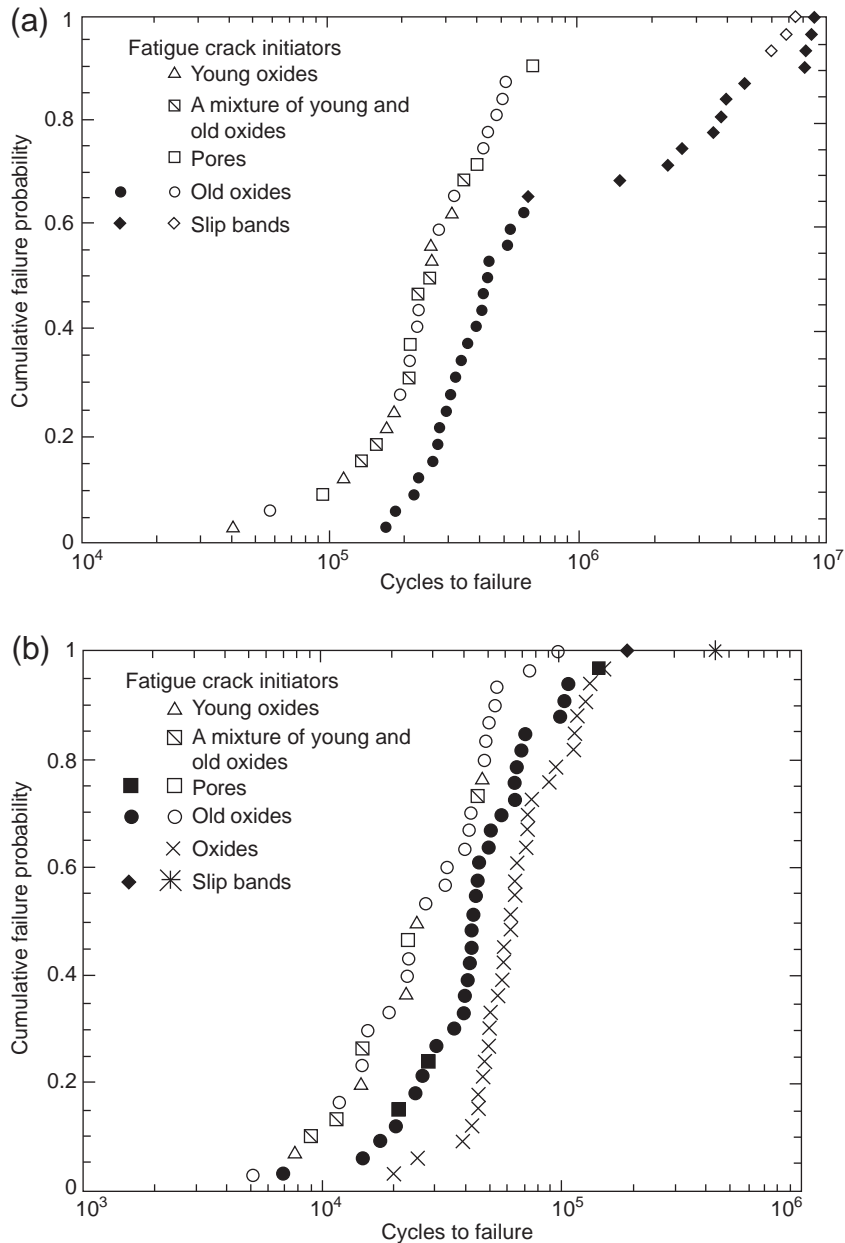
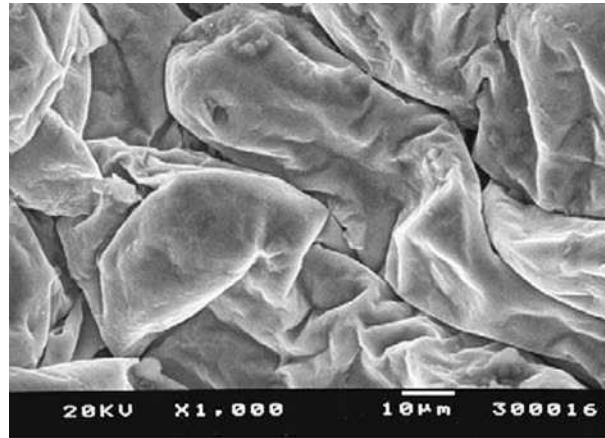
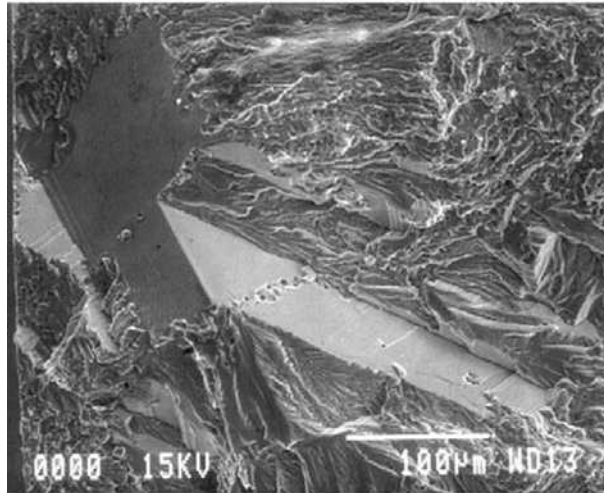


**FIGURE 9.34**

Fatigue life of unfiltered (open symbols), filtered (solid symbols) and unfiltered and HIPped (cross and star symbols) of Al-7Si-0.4Mg alloy castings tested in pull-pull at  $R = +0.1$  and (a) 150 MPa and (b) 240 MPa (Nyahumwa et al. 1998 and 2001).



(a)

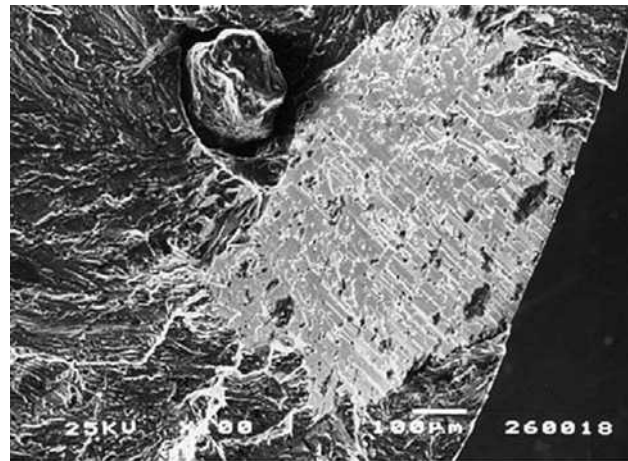


(b)

**FIGURE 9.35**

Fatigue fracture surfaces illustrating (a) oxide initiator; (b) slip plane generated facets; (c) bifilm facet with failure probably initiated from entrained sand particle; (d) close-up of sand particle showing it to be enveloped by an oxide film as a result of its entrainment; (e) mixed slip plane and bifilm facets; (f) 'beachmark' striations from the step-wise advance of the fatigue crack (Nyahumwa et al. 1998, 2001).

that the old oxide films, which were observed to act as fatigue crack initiators in the filtered castings, were less damaging than mixed oxide films. Clearly, we can conclude that the young films are more damaging, almost certainly as a result of their lack of bonding. This contrasts with the old oxide films that have benefited from a closing and partial re-bonding of the interface. This observation is consistent



(c)



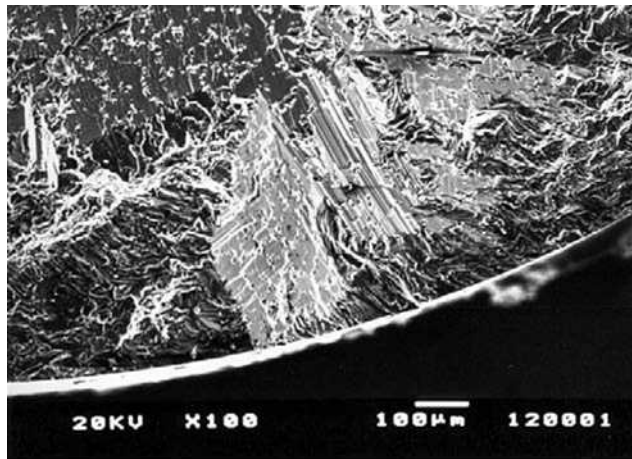
(d)

**FIGURE 9.35** (continued).

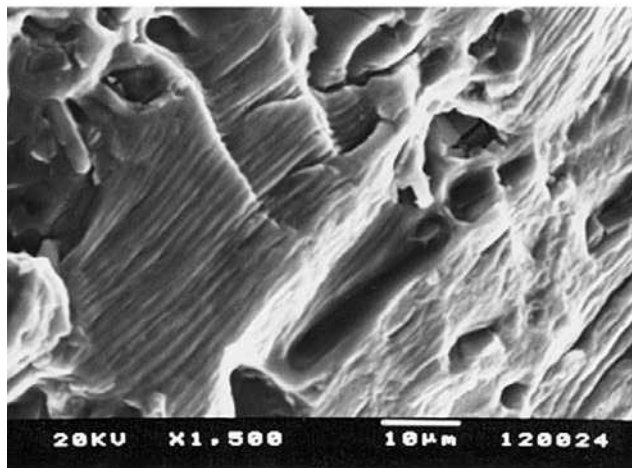
with the expectation that pores would be associated with new films, whose bifilm halves could separate to form pores, but not with old films, whose bifilm halves were (at least partly) welded closed.

These findings are confirmed in general by the results at the higher stress 240 MPa (Figure 9.34b). The fatigue failures of unfiltered castings are initiated from a mixture of pores, and old and new oxides; the 33 filtered castings initiated from 29 old oxides, three pores and one slip plane; and the 33 unfiltered and HIPped tests initiated from 32 old oxides and one slip plane. The various types of fracture surface are shown in Figure 9.35.

The presence of facets on the fracture surface is interesting. Whereas it has been usual to ascribe the formation of facets only to a slip plane mechanism, Tiryakioglu et al. (2011) have suggested that some



(e)



(f)

**FIGURE 9.35** (continued).

facets appear to have formed from straightened bifilms. There appear therefore to be two forms of facets which are quite distinct: (i) the slip plane generated facets have nearly flawless mirror-smooth planes with sharply defined edges and steps as seen in Figure 9.35d; (ii) the bifilm origin is less smooth, with no sharp steps or edges, but edges in places extending out from the facet to become contiguous with a crumpled oxide film, and its surface covered with small pores as would be expected to have been entrained together with the bifilm as is instanced in Figure 9.35e. Interestingly, both act as cracks, and both are of size dictated by the grain size of the casting, thus these authors found that their effect on fatigue life was effectively identical. Clearly, when these are observed the fatigue life is usually long, but does not represent an 'ultimate limit' as has previously been supposed.

Other workers (for instance Wang et al. 2001) using Al–7Si–0.4Mg alloy have in general confirmed that for a defect of a given area, pores are the most serious defects, followed by films of various types. This is to be understood in terms of the effect of bifilms that may be not only partly welded, but in any case always have some degree of geometrical interlocking as a result of their convoluted form as is clear from Figure 2.41.

However, the pre-eminence of pores in fatigue failure is not to be taken for granted. Nyahumwa found films to be most important in his work on this alloy. He had the advantage of having the latest techniques to search for and identify the full extent of films, whereas it is not known how thorough has been work elsewhere, and films are easy to overlook even with the best SEM equipment. In contrast, Byczynski (2002) working with the same techniques in the same laboratory as Nyahumwa found that pores were the most damaging defects in the more brittle A319 alloy used for automotive cylinder blocks. This difference may be explicable by the differences in ductility of the two alloys that were studied. Nyahumwa's alloy was ductile, and so required the stress concentration of bifilms acting as cracks. Byczynski's alloy was brittle, so that cracks could more easily occur from pores.

Thus we may tentatively summarize the hierarchy of defects that initiate fatigue in order of importance: these are pores and/or young bifilms, followed by old bifilms. It would be expected that in the absence of larger defects, progressively finer features of the microstructure would take their place in the hierarchy of initiators. However, it seems that such an attractively simple conceptual framework remains without strong evidence, even doubtful, at this time, as is described below.

The considerable work now available on Al alloys illustrates the present uncertainties. In Al alloys it has been thought that silicon particles may become active in the absence of other initiators. However, the action of bifilms is almost certainly involved in the occasional observations of the nucleation of cracks from these sources. For instance the observed decohesion of silicon particles from the matrix (Wang et al. 2001, part I) is difficult to accept unless a bifilm is present, as seems likely. The initiation of cracks from iron-rich phases occurs often if not exclusively from bifilms hidden in these intermetallics (Cao and Campbell 2002). The initiation of fatigue from eutectic areas, and reported many times (for instance Yamamoto and Kawagoishi 2000 and Wang et al. 2002, part II) is understandable if bifilms are pushed by growing dendrites into these regions. The fascinating fact that Yamamoto and Kawagoishi observe silicon particles sometimes initiating fatigue cracks and sometimes acting as barriers to crack propagation strongly suggests bifilms are present sometimes and not at other times, as would be expected. It is not easy to think of other explanations for this curious observation.

### ***Performance***

Figure 9.36 is intended to illustrate the panorama of performance that can be seen in castings. The poor results can sometimes be seen in pressure die castings, in which the density and size of defects can cause failure to occur on the first cycle. However, it is to be noted that the unpredictability of this process sometimes will yield excellent results if the defects are, by chance, or by manipulation, in an insensitive part of the casting, or where perhaps the bifilms are aligned parallel to the stress axis. The uncertainty of the effects of the certainly present bifilms in pressure die castings is the key reason why it is never easy to select such castings for safety-critical applications.

In terms of this panorama in Figure 9.36, the results of Nyahumwa are presented as 'fair' and 'good', respectively, showing a few tests that exhibit outstandingly good lives, reaching  $10^7$  cycles. Clearly, a series of ideal castings, free from defects, would display identical lives all at  $10^7$  cycles. The important lesson to draw from Figure 9.36 is that most engineering designs have to be based on the

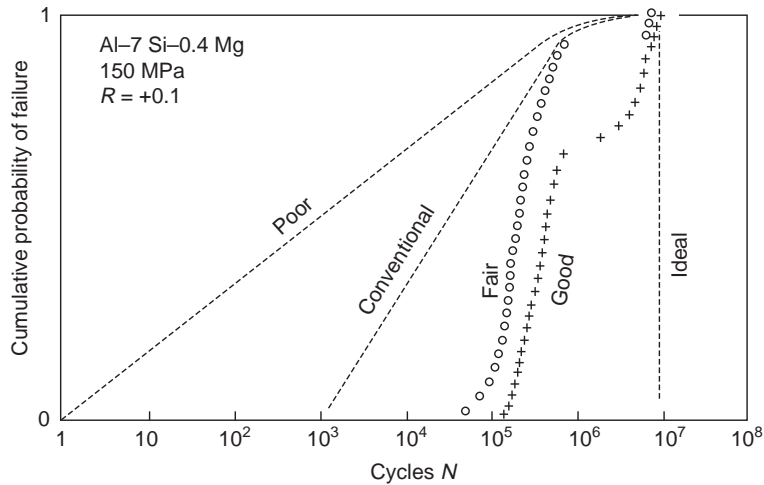


**FIGURE 9.36**

Schematic overview of the extreme range of fatigue performance found in structural Al alloy castings. There is recent evidence that the ‘ideal’ performance should be shifted substantially to the right (Tiryakioglu, Campbell, and Nyahumwa 2011).

minimum performance. It is clear therefore that even the castings designated ‘good’ in this figure have a potential to increase their lowest results by at least two orders of magnitude, i.e. 100 times. It means that for most of the aluminum alloy castings in use today we are probably using a maximum of only 1% of their potential fatigue life. To gain this hundred-fold leap in performance we do not need different or more costly alloys, we merely need to eliminate defects.

A curious phenomenon sometimes seen in fatigue failures is the development of a surface sink or hollow close to the initiation of the failure (Figure 9.37). This has been assumed by some authors to facilitate the initiation of fracture (see Jiang, Bowen, and Knott 1999). However, this is a natural phenomenon akin to ductile necking in the sound material between the defect and the surface of the sample, with the outcome that the surface plastically collapses inwards to meet the initiating crack or pore that is extending outwards. Similar hollows can be seen associated with many metallurgical failures. Whereas in this case the hollow is only 0.1 mm in size, macroscopic hollows measuring centimeters in diameter can be generated during tensile failure of tonnage-sized billets and extrusions.

As a closing update on the current understanding of the key aspects of fatigue, Tiryakioglu (2009) finds that the size distribution for fatigue-initiating defects in Al-7%Si-Mg alloys is described by an extreme value distribution known as the Gumbel distribution (and not Weibull or lognormal as has been commonly assumed). In addition the fatigue life model based on the Paris–Erdogan equation with no crack initiation stage provides respectable fits to the data he has been able to test so far. A new distribution function combining the size distribution of fatigue-initiating defects and fatigue life model provides fits to data that could not be rejected by goodness-of-fit tests, in contrast to two-parameter Weibull. Tiryakioglu has gone on to explain the use of Weibull and other distributions, providing helpful examples and illustrations of comparisons between different distribution models (Tiryakioglu 2010, 2011).

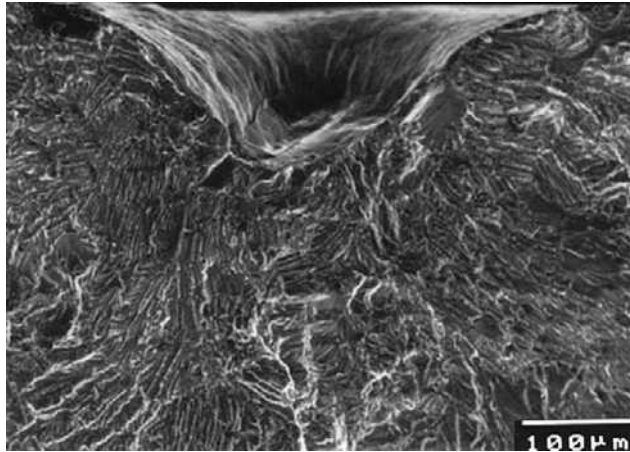


**FIGURE 9.37**

Surface collapse of a tensile or fatigue specimen causing a surface hollow as a plastic necking phenomenon adjacent to an internal crack. (The authors, Jiang, Bowen, and Knott, assumed that the collapse somehow initiated the failure.)

### 9.6.2 Low cycle and thermal fatigue

Thermal fatigue is a dramatically severe form of fatigue. Whereas normal *high cycle fatigue* occurs at *stresses* comfortably in the elastic range (i.e. usually well below the yield point) *thermal fatigue* is driven by thermal *strains* that force deformation well into the plastic flow regime. The maximum stresses, as a consequence, are therefore well above the yield point.

Thermal fatigue is common in castings in which part of the casting experiences a fluctuating high temperature whilst other parts of the casting remain a lower temperature. The phenomenon is seen in gray iron disc brakes, and aluminum alloy cylinder heads and pistons for internal combustion engines, particularly diesel engines and air-cooled internal combustion engines. It is also common in the casting industry with the crazing and sometimes catastrophic failure of high-pressure-die-casting dies made from steels, and gravity dies and ingot molds made from gray cast iron.

The valve bridge between the exhaust valves in a four-valve diesel engine is an excellent example of the problem, and has been examined in detail by Wu and Campbell (1998). In brief, the majority of the casting remains fairly cool, its temperature controlled by water cooling. However, the small section of casting that forms a bridge, separating the exhaust valves, can become extremely hot, reaching a temperature in excess of 300°C. The bridge therefore attempts to expand by  $\alpha\Delta T$  where  $\alpha$  is the coefficient of thermal expansion and  $\Delta T$  is the increase in temperature. For a value of  $\alpha$  about  $20 \times 10^{-6} \text{ K}^{-1}$  for an Al alloy we can predict an expansion of  $300 \times 20 \times 10^{-6} = 0.6\%$ . This is a large value when it is considered that the strain to cause yielding is only about 0.1%. Furthermore, since the casting as a whole is cool, strong, and rigid, the bridge region is prevented from expanding. It therefore suffers a plastic compression of about 0.6%. If it remains at this temperature for sufficient time (an hour or so) stress relief will occur, so that the stress will fall from above the yield point to somewhere near zero.



However, when the engine is switched off, the valve bridge cools to the temperature of the rest of the casting, and so now suffers the same problem in reverse, undergoing a tensile test, plastically extending by up to 0.6%.

The starting and stopping of the engine therefore causes the imposition of an extreme high strain and consequent stress on the exhaust valve bridge. For those materials, such as a poorly cast Al alloy, which has perhaps only 0.5% elongation to failure available, it is not surprising that failure can occur in the first cycle. What perhaps is more surprising is that any metallic materials survive this punishing treatment at all. It is clear that modern cylinder heads can undergo thousands of such cycles into the plastic range without failure.

The experience from the early days of setting up the Cosworth Process provided an illustration of the problem as described earlier. In brief, before the new process became available, the Cosworth cylinder heads intended for racing were cast conventionally, via running systems that were probably well designed by the standards of the day. However, approximately 50% of all the heads failed by thermal fatigue of the valve bridge when run on the test bed. These engines were, of course, highly stressed, and experienced few cycles before failure. From the day of the arrival of the castings made by the new counter-gravity process (otherwise substantially identical in every way) no cylinder head failed again. The presence of defects is seen therefore to be critical to performance, particularly when the metal is subjected to such extreme strains as are imposed by thermal fatigue conditions.

Thermal fatigue tests can be carried out in the laboratory on nicely machined test pieces resembling a tensile test piece. One of the interesting observations is that for some ductile Al alloys the repeated plastic cycling for those specimens that survive hundreds or thousands of cycles causes them to deform into shapeless masses. This gross deformation appears to be resisted more successfully for higher-strength alloys (Grundlach 1995). However, such tests require sophisticated and costly equipment which limits the number of investigations that can be carried out and the rate at which results can be achieved.

There are, however, other forms of test piece that are to be recommended for their extreme simplicity. Roehrig (1978) described three such tests, the simplest of which is shown in Figure 9.38. Such simple test pieces provide their own strain and stress development without the need for costly equipment. A typical testing scenario might be a stack of finned disc samples, bolted together through the central hole. The stack is immersed in a fluidized bed of alumina grit at near 1000°C for 5 seconds

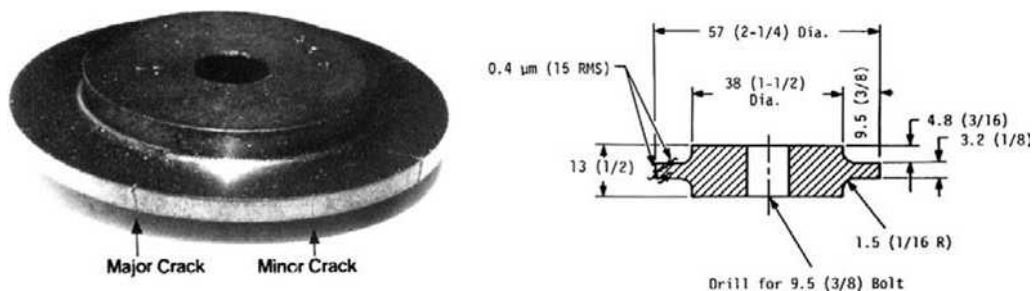


FIGURE 9.38

Simple and low-cost thermal fatigue specimen (Roehrig 1978).

followed by transferring into a second bed at near 100°C for 120 seconds. These conditions may be selected for the simulation of stresses in a particular design or new alloy intended for an automotive brake disc. Some samples and some alloys fail after only a few cycles, whereas others survive for 1000 cycles or more. Other tests described by Roehrig are designed to simulate conditions specifically in cylinder heads, and some raise the severity of the cooling by water quenching. Such tests are excellent to optimize the selection of alloy for a particular casting requiring a specific thermal cycle resistance.

---

## 9.7 ELASTIC (YOUNG'S) MODULUS AND DAMPING CAPACITY

In an engineering structure, the *elastic modulus* is the key parameter that determines the *rigidity* of the design. Thus steel with an elastic modulus of 210 GPa is very much preferred to the light alloys aluminum (70 GPa) and magnesium (45 GPa). However, of course, the specific modulus (the rigidity modulus divided by density) gives a somewhat more favorable comparison, since they are all closely similar at about 26 MPa m<sup>3</sup> kg<sup>-1</sup>.

Since the elastic properties of metals arise directly as a result of the interatomic forces between the atoms, there is little that can normally be done to increase this performance. Alloying, for instance, has practically no effect.

The one exception worth noting to this general rule is Al–Li, which creates such a large volume fraction of Al–Li intermetallics that the elastic modulus is raised by about 10%. At the same time the density is reduced by about 10%, resulting in an overall increase in specific elastic modulus of 20%. Even this triumph of metallurgical R&D is seen to be relatively modest when compared to the 200% increase provided by moving to the much cheaper alternative, steel.

It was all the greater surprise to the author, therefore, when he arranged for a computer simulation to be carried out on the largest bell in the UK. This was Great Paul, the 17 000 kg bell in St Paul's Cathedral, London. The investigators, Hall and Shippen (1994) found that agreement with the fundamental note and the harmonics could only be obtained by assuming that the elastic modulus was only 87 GPa, not 130 GPa expected for alloys of copper. This alarming 33% reduction was almost certainly the consequence of Great Paul being full of defects, mainly porosity and bifilms. This is true for most bells because, unfortunately, they are top poured via the crown of the bell. (The Liberty Bell in the USA is a famous example of a crack opened from the massive bifilm constituted by the oxide flow tube that can be seen to have formed around the sinuous flow of the falling metal stream, starting high on the shoulder of the bell, and continuing down the side to its lip.) At the time of writing, the one bell foundry in the world known to the author (Nauen, Tonsberg, Norway) that uses bottom-filling for its bells, placed mouth upwards, claims that it has never suffered a cracked bell, and its bells sound for twice as long as conventional bells. The longevity of the sound is understandable in view of the reduced quantity of bifilms to be expected, so reducing the loss of energy by internal friction between the rubbing surfaces of the bifilms as the bell vibrates.

It is clear therefore that many castings will suffer from a lower elastic modulus than expected because of their high content of bifilms. Furthermore, since elastic modulus is very rarely checked, this fact is not widely known. For the future, the full stiffness of the material will be gained only if the metal quality is good, and if the casting is poured with a minimum of surface turbulence.

The effect of a high density of bifilms in castings reducing the elastic modulus of the cast material is an interesting hypothesis that has a widely known and accepted metallurgical analogy that lends

convincing comparison. The example is that of flake cast irons compared to steels. The graphite flakes in cast irons act as cracks since they are unable to withstand significant tensile stress. The iron, behaving like a steel matrix laced with a multitude of cracks, finds its modulus reduced from 210 GPa to only 152 GPa, a reduction of 28%, a value comparable to the reduction expected for many defective cast materials. In addition, of course, flake graphite irons are renowned for their excellent damping capacity, its absorption of vibrations and deadening of noise making it an ideal choice for the beds of machine tools.

Sand cast plates of Mg alloy ZE41A-T5 showed variations in elastic modulus in the as-cast condition that could be plotted on a Weibull distribution, with measurements generally in the range 6% to 37% below the theoretical 44.7 GPa (Xinjin Cao 2009).

Further examples cannot be resisted.

Zildjian cymbals, much prized by percussionists and drummers, own much of their unique sound and mechanical resilience (lesser cymbals can turn inside out when struck) to the fact that their original cast preform is tested by striking to see if the material has a ring in its cast state. If it does not, it is remelted. Clearly, this example confirms our expectations that the effects of the presence of bifilm defects survive in some alloys even after the extensive working, applied in this case by forging and spinning into a thin disc.

The writer reveals his age when he admits to recalling the wheel tapper, moving along the side of the rail track, tapping the wheels of the train with his long handled hammer. He was checking that the 'ring' was correct. A cracked wheel would give a different note. Less romantically, but perhaps more reliably, the wheel tapper has now been superseded by the use of automated checking by ultrasonics while the wheels are rolled in a special checking station.

Ultimately therefore, although there are fundamental reasons why the elastic modulus of many castings and their alloys cannot be improved, the reader may be able to raise the elastic modulus of a badly poured casting by 20–30% with negligible cost, exceeding the achievements of the famous Al–Li alloy which cost a fortune to develop.

Elastic properties of castings can now be measured quickly and with great precision using such modern tools as vibration frequency spectrum analysis, as described in Section 19.8.

---

## 9.8 RESIDUAL STRESS

Unseen and often unsuspected, residual stress can be the most damaging defect of all. This is because the stress can be so large, outweighing all the benefits of heat treatment and expensive alloying, and outweighing even the effects of all other defects.

Residual stress is usually never specified to be low. This is a grave indictment of the quality of component specifications and of standards in general. It is also practically impossible to measure in a non-destructive way in the interior of a complicated casting. However, it can be controlled by correct processing – another vindication of prudent, intelligent manufacture compared to costly, difficult, and potentially unreliable inspection.

Also, of course, as will be noted in due course, in rare instances residual stress can be manipulated to advantage. However, in the general case it should be assumed for the sake of safety that somewhere in the finished part the retained stress will be in opposition to the strength of the casting. It can be viewed as subtracting from the casting's strength. Alternatively, it can be viewed as adding to the

applied stress. Either way the casting is subjected to a total stress near to its point of failure even when relatively trivial loads are applied. Unfortunately, a conservative assessment of residual stress would have to assume that it reached the yield stress.

The remedy is, of course, either (i) the avoidance of stress-raising treatments such as quenching castings into water following solution treatment (and so accepting the somewhat reduced strengths available from safer quenchants such as forced air) or (ii) the application of stress relief as already discussed (remembering, of course, that stress relief will effectively negate much or all of the strength gained from heat treatment). Either way, again, the use of the casting with lower internal stress and lower strength is vastly safer, more predictable and more reliable than a high-strength casting with high internal stress.

As an example of a part that suffered from internal stress, a compressor housing for a road-side compressor in Al-5Si-3Cu alloy (the UK specification LM4) was thought to require maximum strength and was therefore subjected to a full solution treatment, water quench and age (TF condition). Two housings exploded in service. Fortunately on these occasions, no one was near at the time so no one was hurt. The manufacturer was persuaded to carry out a heat treatment that would reduce the internal stress, but also, of course, reduce the strength. This was strenuously resisted, but finally very reluctantly agreed. However, on testing the parts to destruction, the implementation of a stress relief (TB7) treatment followed by air cooling gave a part with only half the strength but double the burst pressure. No failures have occurred since.

This sobering lesson is expanded as Rule 9 in the *10 Rules for Casting* dealt with in Chapter 10.

---

## 9.9 HIGH-TEMPERATURE TENSILE PROPERTIES

### 9.9.1 Creep

The gradual deformation of metals under load at high temperatures has been traditionally viewed as taking place in three stages:

1. Primary creep is the rapid early phase that gradually reduces in rate, eventually leading into stage two.
2. Secondary creep is the steady-state regime, in which creep rate is constant.
3. Tertiary creep is the final stage in which the rate of strain increases because of the growth of microscopic internal pores and tears that gradually link to cause the fracture of the whole component.

However, the reader should be aware that this traditional view is strongly criticized by Wilshire (see Wilshire and Scharning 2008, Williams et al. 2010) who proposes a revolutionary single mechanism and single equation to fit all parts of the extension versus time creep curve. Wilshire's argument is that primary creep is subject to a decreasing rate, whereas tertiary creep is subject to an accelerating rate, so that the so-called secondary creep is merely a region in which these two mechanisms overlap to give a minimum creep rate. Wilshire's approach allows an accurate interpolation and extrapolation from relatively few experimental data points for a number of quite different metals and alloys, suggesting it is a valuable new fundamental interpretation of creep behavior. We shall not delve deeper into the creep theory, but for our purposes, it is simply important to know that creep happens, and what we as founders might do to improve creep performance.

Components are said to have failed by creep if, during this slow deformation process, they exceed some critical size or shape. An example might be a turbine blade, whose length grows under the centrifugal stress so that it eventually scrapes the outer casing of the engine (although nowadays both blades and casings are designed to accept such problems). Alternatively, creep failure under tension might mean the fracture of the component at the end of tertiary creep.

Bifilms at grain boundaries are prime sites for the initiation of such catastrophic failures. Failure of the Ni-base alloy 718 described by Jo and colleagues (2001) appears to be precisely such a process initiated by oxide or nitride bifilms, judging from the micrographs published by these authors, although confirmatory evidence from the appearance and chemistry of the fracture surfaces was not carried out.

During the early development of the Pegasus engine for the Harrier Jump Jet 25 polycrystalline Ni-based alloy turbine blades that had previously been scrapped because of their content of porosity were subjected to hot isostatic pressing (hipping), and were fitted to a test engine alongside sound blades to evaluate whether hipping might be a satisfactory reclamation technique for blades that otherwise would be scrapped. The hipped blades failed within a few hours, damaging the engine and forcing a rapid shut down of the test. The failures had occurred by creep cavitation at the grain boundaries of recrystallized regions in the center of the castings. Almost certainly the original porosity would be caused by films rich in aluminum oxide entrained by the severe turbulence that is usual during the vacuum casting process. (The vacuum is known to contain plenty of residual air to ensure the growth of surface films.) The great stability of the films, formed at the high casting temperature, would ensure that they were resistant to any re-bonding action during hipping. The recrystallization would have happened because of the large plastic strains that were a necessary feature of the collapse of the porosity. The grains would grow, expanding until they reached local barriers such as bifilms. Thus the bifilms, effectively unbonded, and so acting as efficient cracks, were automatically located at the grain boundaries from where the failures were seen to occur.

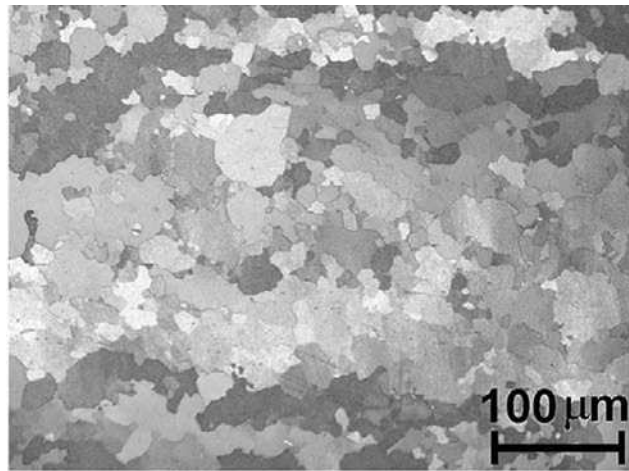
### 9.9.2 Superplastic forming

In a related phenomenon of the superplastic deformation, creep is deliberately induced at a high rate as a deformation process often involving 100% or more elongation. It is mainly useful for the shaping of sheet metals. The forming process is limited by the opening of microscopic voids, usually at grain boundaries, a process referred to in this field as 'cavitation'. A typical example in an Mg alloy is shown in Figure 9.39. The voids grow, causing the mechanical properties of the material to deteriorate, and progressively link, eventually causing complete failure.

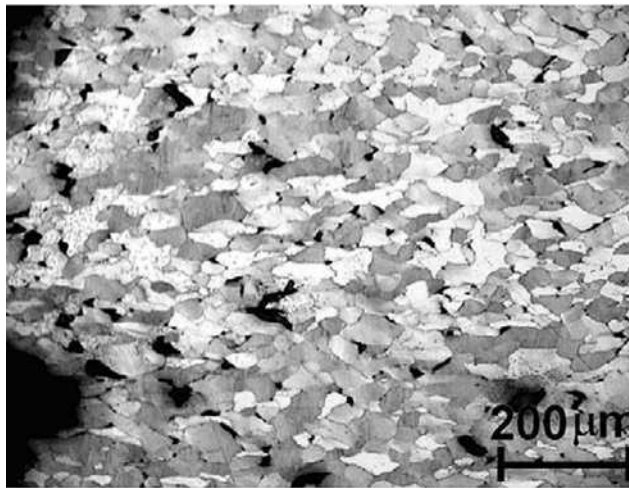
A number of Al alloys can be produced in a superplastic condition. Al–Zn alloys are common, although superplasticity has been developed in many Al alloys including Al–Li and Al–Mg varieties.

Chang (2009) describes how his Al–4.5Mg alloy cavitated at grain boundary precipitates of  $\text{Al}_6(\text{Mn,Fe})$  and Mg–Si particles, strongly suggesting these particles occupied sites on bifilms that happened to be in grain boundaries.

Even more direct evidence of a bifilm-controlled failure mechanism in this alloy is provided by the work of Kulas and co-researchers (2006). Their SEM observations confirmed that voids opened at grain boundary intermetallics during grain boundary sliding. The intermetallics seem to have formed on oxide bifilms, because close examination of the voids by these authors indicated the presence of 'filaments' aligned with the deformation direction, stretching across the voids. The filaments were not



(a)



(b)

**FIGURE 9.39**

Castings, solution treated, extruded 30:1 and finally subjected to tensile strain at  $10^{-3} \text{ s}^{-1}$  at  $200^\circ\text{C}$ . (a) Mg and (b) Mg–0.9Al alloy showing so-called cavitation; pore growth from the decoherence of grain boundaries (courtesy of Stanford et al. 2010).

analyzed (indeed, this would have been a problem because they were clearly extremely thin, perhaps only 100 nm or less) and did not receive further comment by the authors, but can hardly be anything other than alumina films; the remnants of the bifilms causing the failure.

Similar observations can be listed for steels. During creep at  $540^\circ\text{C}$  of a power plant steel (Perets 2004) containing 2.25Cr, 1Mo, 0.15C, carbides form on grain boundaries, where cracks and pores are

observed, together with decohesion of the matrix from the carbides. A 12Cr steel studied by Wu and Sandstrom (1995) showed cavity initiation so early in their creep tests that it seems likely the cavities were already present prior to testing. A super-austenitic stainless steel studied by Fonda (2007) using micro-tomography revealed that every sigma particle was associated with at least one void.

Intermetallic compounds are generally infamous for their brittle behavior, as reported by Yu and Sun for  $\text{Fe}_3\text{Al}$ . They produced this material by vacuum melting and vacuum pouring into a sand mold, but experienced the ingots cracking and sometimes falling into pieces during hot forging. They attributed this behavior to the large, coarse grains, but it seems certain to have been the result of alumina bifilms from the turbulence of the pour, since pour heights are high in typical vacuum furnaces. Figure 16.30 illustrates the problem. The large bifilms would suppress convection in the solidifying ingot and lead to the undisturbed growth of large grains, instead of the normal fine grains produced from grain multiplication in normal convection currents. Frommeyer (2002) reports superplastic behavior with elongations of 350% in  $\text{Fe}_3\text{Al}$  despite its grain size  $57\ \mu\text{m}$  (large for superplastic alloys), and even though more sensibly forming by extrusion and swaging, indicating there seems to be nothing fundamentally wrong with the formability of this intermetallic.

The implication of these creep and superplastic failures by the gradual accretion of grain boundary voids is that they would not occur if bifilms were not present. The failure mechanism would then probably be 100% ductile failure leading to 100% RA. If true, the prospects for improvement in these materials are awe inspiring.

---

## 9.10 OXIDATION AND CORROSION RESISTANCE

During the cooling of the casting in the mold, and to some extent after it has been extracted from the mold, and especially during high-temperature heat treatment, air can gain access to and can attack the interior of the casting via surface-connected bifilms. Similarly, if the casting experiences a corrosive environment, internal access of the corrodant can lead to a variety of problems. The role of the bifilm is central to the understanding of these important problems.

### 9.10.1 Internal oxidation

When a metal such as an aluminum alloy is heat treated, the external surface naturally develops a thick oxide skin. However, in addition, some researchers have noted the development of internal oxides.

How is this possible? Oxygen is insoluble in aluminum and its alloys, and so, in principle, is not able to penetrate the alloy.

Clearly, such internal oxidation can only occur if the oxidizing environment has access to the interior through some kind of hole. Surface-connected shrinkage porosity might create such a hole linked to extensive internal cavities. However, reasonably adequate pressurization of the metal in the casting by proper feeding will prevent the formation of surface-connected porosity. Much more probable is access via bifilms connected to the outside surface. In the case of machined castings, particularly test bars, the machined surface will certainly cut into many bifilms, opening up many points of access for penetration by gas or liquid and attack deep into the interior of the casting.

It is easy to understand therefore that when working with an Al–4Mg alloy subjected to a solution treatment at  $520^\circ\text{C}$  for several hours Samuel and co-workers (2002) expected to find the usual benefits

including not only the taking of solutes into solution, but fragmentation and spheroidizing of intermetallics, resulting in an improvement in mechanical properties. However, they reported the development of spinel (the  $\text{Al}_2\text{O}_3\cdot\text{MgO}$  mixed oxide) in the interior of the casting, and the reduction in tensile properties.

Fenn and Harding (2002) in the author's laboratory treated some as-cast ductile iron test bars at  $950^\circ\text{C}$  for 1 hour to eliminate carbides to allow them to be machined. The tensile properties turned out to be unexpectedly low, especially the ductility. Elongations in the region of 205 or more for this grade were to be expected, since ductile iron, as its name implies, is expected to be reliably ductile. It was a shock therefore to discover that elongations were highly scattered in the range of only 1–10%. Many specimens appeared to fail brittlely. SEM studies revealed thick uniform carpets of oxide on the fracture surfaces (Figure 9.40). These oxides clearly did not have the appearance of entrained films, and did not contain the content of Mg that would be expected if the oxides were bifilms entrained in the liquid metal during casting. It seems that the oxygen had penetrated the core of the bifilm, and added to the original magnesium silicate from which the original bifilm was constituted. The additional oxide appeared to be nearly pure iron oxide, as would be expected from a solid-state reaction. At the relatively low temperature of  $950^\circ\text{C}$  (low compared to the casting temperature of about  $1450^\circ\text{C}$ ) the magnesium in solution in the solid alloy would be fixed, being unable to diffuse to the surface of the bifilm to enhance the magnesium concentration in the oxide. A further confirmation of the solid-state thickening of these oxides is the fact that the graphite nodules appear through holes in the carpet. Clearly the iron oxide cannot thicken above the nodules, giving the curiously dimpled or quilted appearance of the surface of the oxide seen in Figure 9.40a. In Figure 9.40b the nodules themselves appear to be disintegrating as might be expected as their graphite oxidized away.

These internal oxidation problems are almost certainly common in cast alloys that have been subjected to heat treatment.

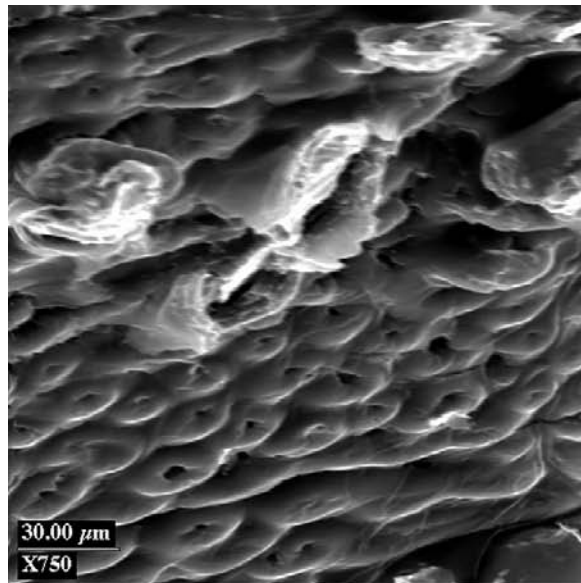
The same effect will occur, of course, automatically during the cooling of the casting in the mold. Additional oxidation of the originating bifilm will occur for surface-connected bifilms, thickening the film and possibly masking its original form. The original composition of the oxide may also be diluted and/or hidden by overgrowth of new oxide resulting from the solid-state reaction.

The solution to the avoidance of such internal oxidation is the avoidance of bifilms. Although this would be a complete solution, it may not be always practical. A next-best solution might be one of the many techniques to keep the bifilms closed, since, clearly, any action to open the bifilm, for instance by shrinkage, will enhance the access routes to the interior. It follows that a well-fed casting (i.e. pressurized by the atmosphere) or a casting artificially pressurized internally during solidification (as provided by some casting processes) will be less susceptible to the ingress of air during high-temperature treatment. It will therefore retain its mechanical properties relatively unchanged (whether originally good or bad of course).

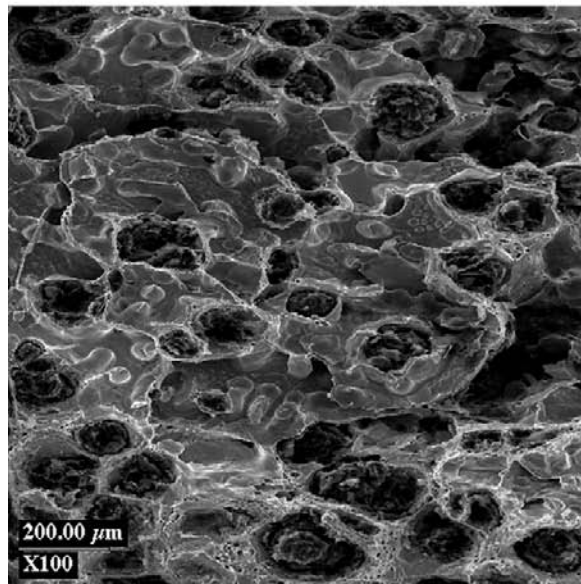
### 9.10.2 Corrosion

Corrosion of metals, particularly aluminum alloy castings and wrought products such as alloy plate and sheet, is a troublesome feature that has attracted much research in an effort to understand and control the phenomenon. Naturally, no comprehensive review of such a vast discipline can be undertaken here. The reader is referred to some recent reviews (Leth-Olsen and Nisancioglu 1998).





(a)



(b)

**FIGURE 9.40**

Fracture surface of a ductile iron damaged during annealing at 950°C for 1 hour by internal oxidation of a surface-connected bifilm, showing (a) the formation of a carpet of solid-state-grown oxide, and (b) oxidation of graphite nodules (Fenn and Harding 2002).

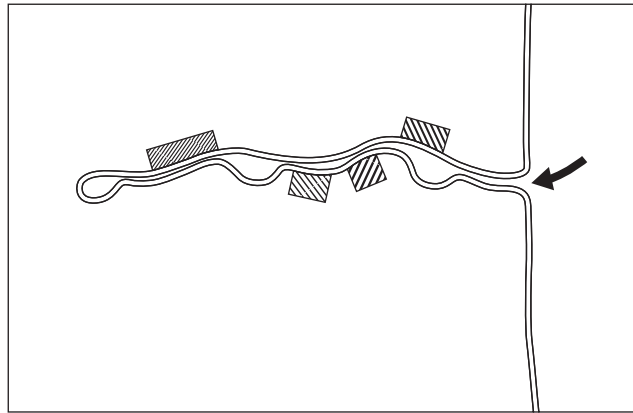


**FIGURE 9.41**

An image of a surface-connected bifilm, decorated with pockets of air and precipitated compounds of various kinds, is effectively open to the environment, and makes an effective and complex corrosion cell if any aqueous corrodant such as seawater or rainwater enters.

The purpose of this section is to present the evidence that a large number of possibly most corrosion problems, not only in shaped castings but also in wrought alloys, arise from casting defects.

All corrosion pits that the author has seen are the sites where bifilms happen to meet the surface. In the absence of bifilms it is proposed that there would probably be no corrosion of metals from surface pits. Corrosion might still be expected, but would probably be vastly reduced, having to occur uniformly over the whole surface of the metal. Alternatively, if localized sites were favored, localized corrosion might continue to occur on a reduced scale from other inclusions, grain boundaries, or from dislocations that intersect the surface.

Many of the current theories of the corrosion of metals have been principally concerned with environmental attack on an essentially continuous unbroken planar substrate, regarding the surface of the metal as a uniform reactive layer (Leth-Olsen and Nisancioglu 1998). The result has been that theories of filiform and intergranular corrosion of aluminum alloys are at a loss to explain many of the observed features of these phenomena, since these corrosion processes clearly do not exhibit uniformity of attack; the attack is extremely localized and specific in form.

The presence of bifilms generated in the pouring process has not, of course, been considered up to now as a factor contributing to the severity of corrosion. It will become clear in this section how bifilms help to explain many of the observed features of metallic corrosion. The link occurs since bifilms are, of course, often connected to the surface, allowing them to be detected by dye-penetrant techniques. Similarly, in a corrosive environment such bifilms will allow the local ingress of corrosive fluids between their unbonded inner surfaces (Figure 9.41). The presence of different varieties of second phases precipitated on the outer surfaces of bifilms will be expected to act as a further enhancement of the corrosion process by the creation of a corrosion couple, explaining the major differences observed, for instance, between Al alloys of different Fe, Mn, and Cu contents.

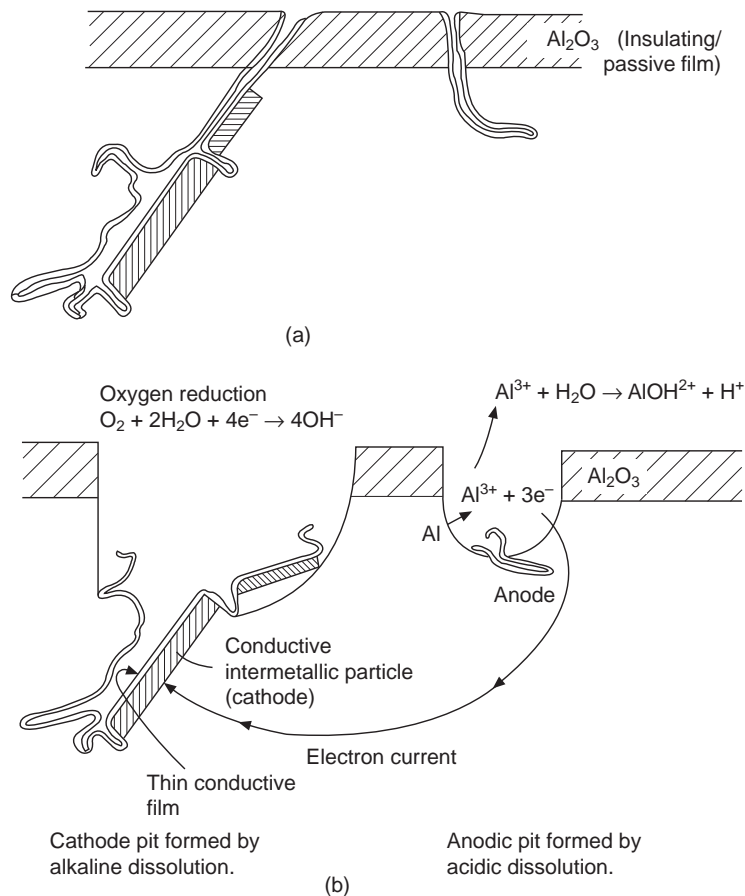


**FIGURE 9.42**

Mechanism of pitting corrosion (a) prior to and (b) during corrosion (adapted from Bailey and Davenport 2002).

The stages of corrosion, leading to some pits formed by cathodic action involving alkaline dissolution, and other pits formed by anodic action leading to acidic dissolution, are illustrated schematically in Figures 9.42a and b.

Direct and clear observations of oxide film tangles associated with corrosion sites have been made by Nordlien and Davenport (2000) and Afseth and co-workers (2000). Figures 9.43 and 9.44 are typical examples of seawater corrosion of a wrought Al alloy.

### 9.10.3 Pitting corrosion

Although there are many instances in which the corrosion of metals occurs uniformly across the whole surface, the special case of concentrated corrosion at highly localized sites, generating deep pits, is sometimes a serious concern. Most of the studies of pitting corrosion have been carried out on steels.

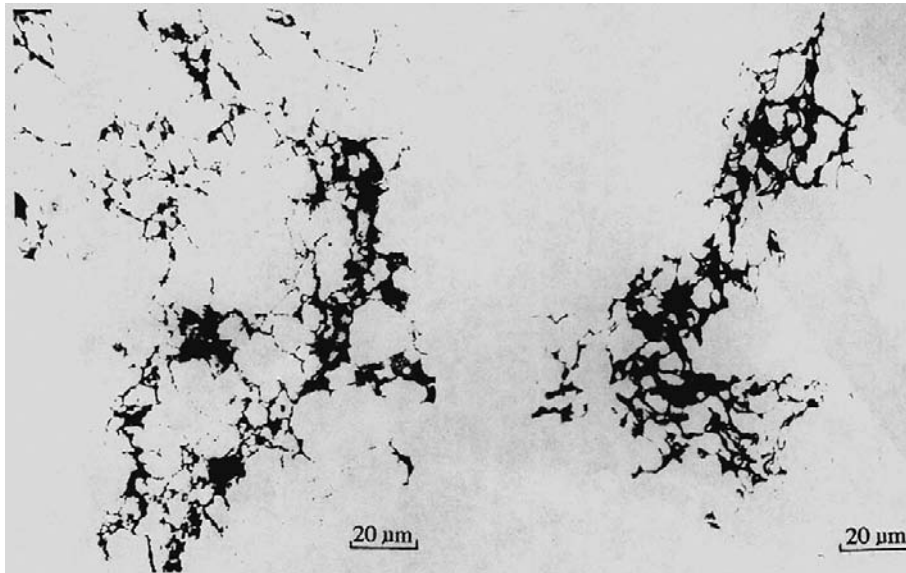


**FIGURE 9.43**

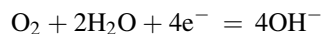
Two views of forged 7010-T736 alloy subjected to seawater corrosion (courtesy of P J E Forsyth 2000).

Because we cannot in this short work survey this vast subject, we shall take only Al and its alloys as an example, following the review by Szklarska-Smialowka (1999), and see how pitting corrosion relates to the cast structure.

The main message of this section is that, in general, the familiar corrosion pit is not, originally, the product of corrosion. It pre-exists, being the product of poor casting technology. This pre-existence appears to have been generally overlooked until now. Naturally, the corrosion process develops the pit, which is originally usually practically, if not actually, invisible, into a highly visible and deleterious feature.

The corrosion proceeds as illustrated in Figure 9.42 (Bailey and Davenport 2002). The intermetallic particle precipitated on the bifilm acts as a cathode, the electrical current passing through the electrolyte to anodic areas of the surface. It has been generally thought that the intermetallic particles provide the conductive path through the insulating alumina film. However, it is probable that the bifilm itself is sufficiently thin to be conductive, or will have been fractured during the cooling of the casting, so aiding this effect. The cathodic pit is the bifilm pit containing the intermetallic, whereas the anodic pits may be part of the same bifilm pits but distant from the intermetallic, or may be quite separate surface-intersecting bifilms that do not happen to contain intermetallics.

Oxygen is reduced at the cathode, demanding electrons, and so forming hydroxyl ions according to:



The alkaline conditions created by the hydroxyl ions assist to dissolve the material around the intermetallic, enlarging the pit. Conversely, at the anodic pit, conditions are acidic because of the generation of hydrogen ions as follows:

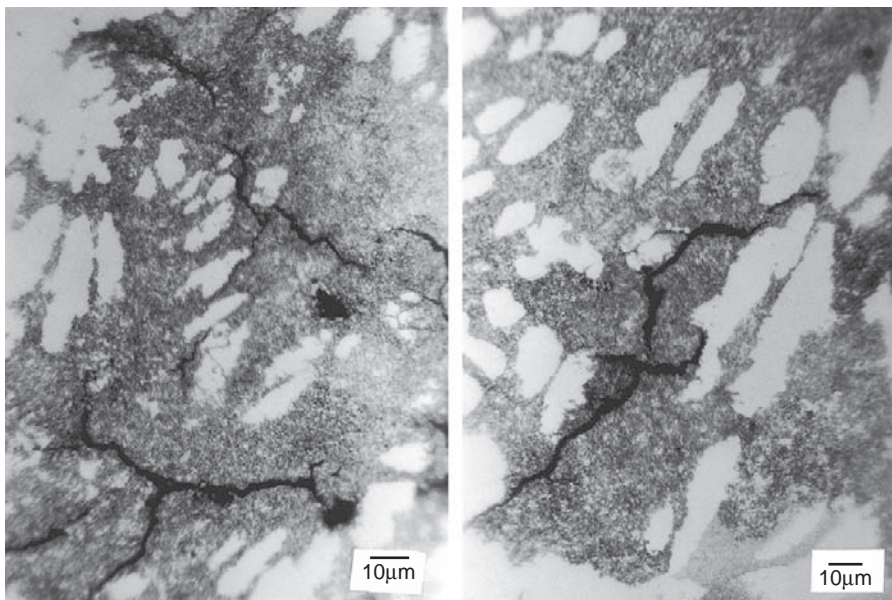
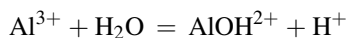
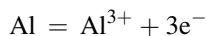


**FIGURE 9.44**

Typical polished and etched 7010 alloy in the solutionized condition subjected to seawater corrosion illustrating the interdendritic nature of the cracks (courtesy of P J E Forsyth 2000).



Thus this pit also enlarges as matrix material is dissolved. The electrical circuit is, of course, completed by electrons traveling through the aluminum matrix from the anode pit to the cathode pit.

The random nature of the creation of such defects, being linked to the action of surface turbulence at several stages of manufacture of the sheet, explains why the corrosion behavior is so variable, changing in severity from one supplier of metal to another, and from one production batch of alloy to the next. Also, of course, every pit will be different because of the random nature of the oxide tangles. The tangled geometry is indicated in Figures 9.43 and 9.44. This randomness has been a major problem to investigators.

The bifilms are expected to survive, and may even grow during plastic deformation, their residual entrained air continuing to oxidize any newly created elongation of the defect until supplies of air are exhausted. (Further extension of the defect may then weld.) Thus surface-linked cracks, possibly plated with intermetallics, will be characteristic not only of castings but also of wrought products.

#### 9.10.4 Filiform corrosion

In a standard corrosion scratch test, filiform corrosion takes the form of a high surface density of superficial corrosion paths, called filaments, which propagate extensively over the next few days from

a scribe mark on a test plate. The corrosion proceeds away from the scratch along filamentary lines aligned with the original rolling direction. They travel under any protective layer such as paint, occasionally tunneling beneath the metal surface, only to break out at the metal surface once again after a few millimeters or so. The lengthwise growth and subsequent sideways spreading of the filaments eventually causes any protective coating, such as a paint layer, to exfoliate. The length of filaments has been found to be generally in the range 1–10 mm. However, reviewers (Leth-Olsen and Nisancioglu 1998) confirm that quantification of the phenomenon suffers from significant scatter that has hampered these studies.

The concentration of corrosion at strictly localized sites (the filaments) is clear. However, it is important to observe that the great majority of the metal surface remains completely free from attack (despite the long and deep breach of the protective coating by the scratch). Also clear is the different behavior of different casting batches of nominally identical material, on different occasions giving filaments shallow or deep, or short (1 mm) or long (10 mm).

Growth of filaments stops when the length reaches some value between 1 and 10 mm. This has been suggested to be the result of chloride depletion in the head of the filament (Leth-Olsen and Nisancioglu 1998) but is clearly more likely to be that the bifilms that provide the easy path for corrosion are simply only that long, as is seen in direct observations of the melt (Section 3.5). In other words, the corrosion stops when it reaches the end of the bifilm.

In his review of the subject, Nordlien (1999) describes how the filaments of corrosion can grow at up to 5 mm per day. They occur on all families of aluminum alloys (1000, 2000, 3000, 5000, 6000, 7000, and 8000 series) and on all product forms (sheet, foil, extrusions).

Interestingly, a surface of rolled aluminum alloy sheet can be sensitized to the formation of filiform corrosion (in corrosion jargon it is 'activated') by annealing at 400°C. This effect can be understood as the growth of oxidation products on the internal surfaces of cracks, which will assist to open the cracks (see Section 9.10.1). The deactivation by etching probably corresponds to the preferential attack and removal of surface cracks and laminations. Reactivation by subsequent annealing seems likely to be the result of the opening of slightly deeper defects by oxidation. The removal of defects by etching removes only a few  $\mu\text{m}$  of depth of the surface. Considering the defects are commonly 1 mm to 10 mm in size, there will be no shortage of new defects to open on a subsequent reactivation cycle.

In severe cases of surface corrosion, the frequent observations of delamination (Leth-Olsen and Nisancioglu 1998) can be understood as the lifting of irregular fragments of bifilm that lie just under the metal surface. Other related observations of blistering (see Section 19.2) can also be understood as the inflation of just-subsurface bifilms by hydrogen evolved from the chemical reaction between the corrodant and the intermetallic compounds associated with the bifilm.

### 9.10.5 Intergranular corrosion

Intergranular corrosion in its various forms is also proposed to be associated in some cases with the newly identified bifilm defects, as a result of the natural siting of bifilms at grain boundaries in the cast structure.

Metcalfe (1945) records studies of the intercrystalline corrosion of the heads of rivets in an Al–Mg alloy from an aircraft that has been flown near marine environments. He concludes that the effect is one of stress corrosion cracking. Undoubtedly there would be residual stress that may have played a part in the failures that are described. More especially so since the cracks were observed to follow grain

boundaries sensitized by prolonged in-service aging, and the convoluted form of the crevices was due to the fact that the flattened grains themselves were distorted in this fashion by the complex flow pattern of the worked metal. Even so, a look at a section of one of the decapitated rivets in his work reveals a convoluted crack that can hardly have been propagated by stress. The stress would have been reduced to near zero after the spread of the first crack across the neck of the rivet. In fact, there is the trace of a crack which has repeatedly turned, spreading back and forth across the neck of the rivet at least five or six times. This type of crack is typical of a folded oxide defect. Its presence would ensure the stability of the convoluted form of the grain boundaries, which it would pin. Furthermore, in this vintage of alloy a high density of entrainment defects would be the norm. The defect has provided an easy path for the attack of corrodant.

Forsyth (1995, 1999) describes seawater corrosion leading to intergranular cracking in 7010 Al alloy. Corroded surfaces that have been polished back through the worst of the surface layer are presented in Figure 9.44. The intergranular and subgrainboundary cracks were, once again, typical of the localized tangled arrays of films that are normal in aluminum alloys produced via the melting and casting route. The cracks exhibit the typical irregular branching and changes of direction on a number of different size scales, often unrelated to the general size of the grain size of the matrix. Alloy material between such damaged regions was recorded to be completely free from attack. It is suggested that these observations are difficult to explain without the existence of random entrainment defects from the original casting.

When etching to reveal the dendrite structure, the cracks were seen (Forsyth 1999) to be confined to the interdendritic regions (Figure 9.44) as is expected from the dendrite pushing of oxide bifilms. The defects are therefore concentrated in the residual liquid in the interdendritic regions, and in grain boundaries.

Forsyth (1999) also investigated the corrosion of 7010 alloy in seawater as a result of machining or bruising of the surface. In the case of bruising, the deformation of the surface would be expected to open any entrained defects at or near the surface, creating highly localized and deeply penetrating intergranular pathways for attack.

Forsyth also draws attention to the especially damaging nature of the attack, in that despite rather little dissolution of material, complete blocks of material could be removed simply by the penetration of the attack along narrow planes in different directions. This observation corroborates his earlier report (Forsyth 1995) in which subsequent anodizing of the surface led to the incorporation of unanodized grains of metal in the corrosion debris remaining from such localized attack. The metal grains remained unanodized because they were found to be electrically isolated from their surroundings. This would not be surprising if double oxide films, separated by their inter-layer of air, surrounded the grains.

### 9.10.6 Stress corrosion cracking

Stress corrosion cracking (SCC) is a particularly serious form of failure. It seems to occur in conditions where both stress and corrosive environment combine. It is often unexpected, involving the corrosion of minute amounts of material, but producing extensive and sometimes disastrous cracks. There remains much research but few conclusive results. The problem remains a mystery.

Once again, the presence of bifilms might prove to be the unsuspected major influence in most of the research conducted so far. Two very different examples are presented below, one for an Mg alloy and the other for an austenitic stainless steel.

Winzer and Cross (2009) describe the stress corrosion cracking of Mg alloys containing  $\beta$  particles ( $\text{Mg}_{17}\text{Al}_{12}$ ). They describe how the consensus of opinion is growing that  $\beta$  particles are associated with the transgranular crack propagation, and suggest a number of mechanisms that might be involved without reaching any conclusions. However, the simplest explanation seems to be the association between  $\beta$  particles and bifilms. Bifilms will certainly be present, and  $\beta$  particles will be expected to form on them, and the bifilm crack will provide a route for the corrodants. It all seems so straightforward. However, it has yet to be proven.

Andresen and colleagues (2009) carried out work on an austenitic stainless steel intended for application as a core component in a nuclear light water reactor. The corrodant in this case was deaerated, demineralized water. Once again the authors admit to inconclusive results. However, the technique for the production of their samples, including vacuum induction melting and casting followed even more inappropriately by vacuum arc remelting (VAR) guarantees a generous population of oxide bifilm defects (as roundly criticized by me – Campbell (2010)). Several of the SEM images of the fracture surfaces showed clear examples of oxide films that had been formed on the melt. On occasions these filled the field of view of the image, and so could be deduced to be at least approximately 0.1–0.2 mm in size.

In conclusion, it seems there is considerable evidence that in the absence of bifilms, some types of corrosion and possibly stress corrosion cracking might be reduced or eliminated. The elimination of bifilms would revolutionize metals and improve the quality of our lives in many ways.

---

## 9.11 LEAK-TIGHTNESS

Leak-tightness has usually been dismissed as a property hardly worthy of consideration, being merely the result of ‘porosity’.

However, of all the list of properties specified that a casting must possess, such as strength, ductility, fatigue resistance, chemical conformity, etc., leak tightness is probably the most common and the most important. This might seem a trivial requirement to an expert trained in the metallurgy and mechanical strengths of materials. However, it is a critical requirement not to be underestimated.

A cylinder head for an internal combustion engine is one of the most demanding examples, requiring to be free from leaks across narrow walls separating pressurized water above its normal boiling point, very hot gas, hot oil at high pressure, and all kept separate from the outside environment. A failure at a single point is likely to spell failure for the whole engine. In this instance, as is common, leakage usually means ‘through leaks’, in which containment is lost because of a leak path completely through the containing wall.

However, leakage sometimes refers to surface pores that connect to an enclosed internal cavity inside a wall or boss. Such closed pores give problems in applications such as vacuum equipment, where outgassing from surfaces limits the attainment of a hard vacuum. Problems also arise in instances of castings used for the containment of liquids, where capillary action will assist the liquid to penetrate the pore. If the pore is deep or voluminous the penetrated liquid may be impossible to extract. This is a particular problem for the food-processing industry where bacterial contamination residing in surface-connected porosity is a concern. Similarly, in the decontamination of products used in the chemical, pharmaceutical, or nuclear industries, aggressive mechanical and chemical processes fail to achieve 100% decontamination almost certainly as a result of the surface contact with bifilms and



possibly with shrinkage cavities. Such industries require castings made from clean metal, transferred into molds with zero surface entraining conditions. Only then would performance be satisfactory.

It is true that leaks are sometimes the result of shrinkage porosity, especially if the alloy has a long freezing range, so that the porosity adopts a sponge or layer morphology. Clearly, any form of porous metal resulting from poorly fed shrinkage will produce a leak, especially after machining into such a region.

Leaks are seldom caused by gas porosity, i.e. bubbles of gas precipitated from solution in the liquid metal. The following logic provides an explanation.

Gurland (1966) studied the connections between random mixtures of conducting and non-conducting phases by measuring the electrical resistance of the mixture. He used silver particles in Bakelite, gradually adding more silver to the mix. He found the transition from insulating to conducting to be quite abrupt, in agreement with stochastic (i.e. random) models. The results are summarized as

% Ag	% Conducting
1	0
1.73	50
2.5	100

In the case of about 1–2% gas porosity in cast metals the metal must surely therefore be permeable to gas. Why is this untrue? It is untrue because the distribution of gas pores is not random as in Gurland's mixtures. Gas pores are distributed at specific distances, dictated by the diffusion distance for gas. In addition, the pores are kept apart by the presence of the dendrite arms. Thus leakage due to connections between gas pores cannot occur until there are impossibly high porosity contents in the region of 20–30% by volume (see Figure 7.16).

The only possible exception to this rule is the relatively rare occurrence of wormhole-type bubbles, formed by the simultaneous growth of gas bubbles and a planar solidification front. Such long tunnels through the cast structure naturally constitute highly effective leak paths (see Figures 7.38 and 7.39). Fortunately they are rare, and easily identified, so that corrective action can be taken.

In the author's experience, most leaks in light-alloy and aluminum bronze castings are the result of oxide inclusions. These fall into two main categories:

1. Some are the result of fragments of old, thick oxide films or plates which are introduced from the melting furnace or ladle, in suspension in the melt, and which become jammed, bridging between the walls of the mold as the metal rises. The leak path occurs because the old oxide itself suffered an entrainment event; as it passed through the surface it would take in with it some new surface oxide as a thin, non-wetting film covering. The leak path is the path between the rigid old oxide fragment and its new thin wrapping.
2. The majority of leaks are the consequence of new bifilms introduced into the metal by the turbulent filling of the mold. These tangled layers of poorly wetted surface films, folded over dry side to dry side, constitute major leak paths through the walls of castings. The leaks are mainly concentrated in regions of surface turbulence. Such regions are easily identified in Al alloys as areas of frosted or gray striations down the walls of top-gated gravity castings, outlining the path of the falling metal.

The remaining areas of walls, away from the spilling stream, are usually clear of any visible oxide striations, and are free from leaks. The reader should be able to confirm, and take pride in, the identification of de-gated top-poured aluminum alloy castings from a distance of at least 100 m! Unfortunately, this is not a difficult exercise, and plenty of opportunity exists to keep oneself in training in most light alloy foundries! It is to be hoped that this regrettable situation will improve.

An example of a sump (oil pan) casting, top poured into a gravity die (permanent mold), is shown in Figure 9.44. The leakage defects in this casting are concentrated in the areas that have suffered the direct fall of the melt. The surface oxide markings are seen on both the outside and inside surfaces of these parts of the casting walls (Figures 9.44a and b). Other distant areas where the melt has filled the mold in a substantially uphill mode are seen to be clear of oxide markings, and free from leaks. The precise points of leakage are found by the operator who inverts the casting, pressurizes it with air, and immerses it under water. He is guided by the stream of air bubbles emerging from leaks, and deals a rapid series of blows from a peening gun. This hammering action deforms the surface locally to close the leak. The peening marks are seen in closeup in Figure 9.44c.

The linkage between oxide films and leakage problems was noted by Burchell (1969), when he attempted to raise the hydrogen gas content of aluminum alloys by stirring with wood poles, dipped in water between use. The porosity of the castings increased as was intended to counter feeding problems, but so did the number of leaks. Burchell identified the presence of oxide films on the fracture surfaces of tensile test bars that were cast at the same time.

It is unfortunate therefore that the folded form of entrained surface films creates ideal opportunities for leak paths through the casting. This source of leakage is probably more common than leaks resulting from other kinds of porosity such as shrinkage porosity (although, of course, leaks from entrained films as a consequence of a poor filling system are usually mis-diagnosed as leaks from shrinkage because of poor feeding. This is a natural consequence of its appearance, because interdendritic porosity usually grows from the entrainment defect or actually *is* the entrainment defect.)

As an instance of the seriousness of leaks in castings that are required to be leak-tight, many foundries have been reluctant to cast aluminum manifolds and cylinder heads with sections less than 5 mm. This is because of the increased incidence of leaks that require the casting to be repaired or scrapped. The lack of pressure tightness relates directly to the presence of oxides whose size exceeds 5 mm (an interesting confirmation of the non-trivial size and widespread nature of these defects), and that can therefore bridge wall to wall across the mold cavity, connecting the surfaces by a leak path.

Leaks are often associated with bubble-damaged regions in castings. This is because all bubbles will have been originally connected to a surface as a necessary feature of their entrainment process. Some bubbles will have retained their bubble trail links to the outside world, whereas others will have broken away during the turmoil of filling. Bubble trails are particularly troublesome with respect to leak-tightness, since they necessarily start at one casting surface and connect to the surface above, and as part of their structure have a continuous pipe-like hollow center. The inflated bubble trails characteristic of high-pressure die castings (Figure 2.39) make excellent leak paths. A core blow also leaves a serious defect in the form of a collapsed bubble trail (Figure 2.32). Despite its collapsed form, the thickness and residual rigidity of its oxide will ensure that the trail does not completely close, so that a leak path is almost guaranteed.

In general, the identity of a leakage defect in a casting can be made with certainty by sawing the casting to within a short distance of the defect, and then breaking it open and studying the fracture

surface under the microscope. A new oxide film (probably from surface turbulence during pouring, or from a bubble trail) is easily identified from its folded and wrinkled appearance; an old oxide fragment (perhaps from the melting furnace or crucible) from its craggy form, like a piece of rock; and shrinkage porosity by its arrays of exposed dendrites. Fracture studies are a quick and valuable test and are recommended as one of the most powerful of diagnostic techniques. The reader is recommended to practice this often – despite its unpopularity with the production manager; the destruction of one casting will often save many.

### Leak detection

Turning now from the nature of leakage defects to methods of detection. Bubble testing has already been mentioned in which the inside of the casting is simply pressurized with air, the casting immersed in water, and any stream of bubbles observed. Even this time-honored and apparently simple technique is not to be underestimated, since providing effective and rapid sealing of all the openings from the cored internal cavity may not be easy in itself. It will almost certainly require careful planning to ensure that the correct amount of dressing has been carried out to eliminate troublesome flash and gating systems, etc., so that the sealing surfaces can be nicely accessed and sealed. Also, of course, the technique is slow, not quantifiable, and demands the constant attention of skilled personnel. After testing, the part often requires to be dried.

Hoffmann (2001) describes three basic methods of dry air leak testing suitable for production line applications: they measure (i) the rate of decay of gauge pressure, (ii) the rate of decay of differential pressure, and (iii) leakage rate directly in terms of mass flow. For highly specialized applications, helium mass spectrometry offers testing capability beyond the limits attainable by dry air methods.

- (i) The first technique, the rate of decay of gauge pressure, is the simplest and lowest cost, and is generally suitable where pressures do not exceed 2 bar and volumes do not exceed 100 ml.
- (ii) The differential pressure method pressurizes a non-leaking reference volume along with the test part. A transducer reads any difference in pressure that occurs over time. The differential technique reduces errors due to temperature changes, and is more accurate and faster than the direct pressure decay method. The technique is also well suited to applications specifying higher test pressures, exceeding 10 bar, and where relatively small cavities must be tested to a very low leak rate.
- (iii) The mass flow method pressurizes the test cavity, then allows any leakage to be compensated by actively flowing air into the cavity. The in-flowing air is measured directly by a mass flow meter in terms of volume per second. The method involves a single measurement, usually less than one second. (It avoids the taking of two measurements over a time interval – during which temperature may change for instance – that is required for the first two techniques, thus halving errors and increasing speed of response.) The method can tackle a wider range of volumes, and is accurate down to  $0.001 \text{ ml s}^{-1}$ .

For castings that are required to be leak tight to even greater standards, helium mass spectrometry can measure down to rates that are 10 000 times lower. This is principally because the helium atom is much smaller than molecules of nitrogen and oxygen, and so can penetrate much smaller pores.

Krypton gas has been used for the detection of very fine leaks, because of its content of 5% radioactive Krypton 85 (Glatz 1996). As before, the part to be tested is placed in an evacuated chamber to suck air out of the cavities. Krypton gas is then introduced to the chamber and allowed time to

penetrate the surface pores. The Krypton is then pumped out, ready for reuse, and air is admitted. The rate at which Kr is slowly released can be monitored to assess the volume of surface-connected internal pores. In addition, the spraying of the surface with a liquid emulsion of silver halide particles makes the surface sensitive to the low-energy beta particles given off by the radioactive decay of Kr85. After the emulsion is developed by conventional photographic techniques the part reveals the site and shapes of surface pores and cracks. The beta particles can penetrate approximately 1 mm of metal, revealing subsurface cracks (if connected to the surface elsewhere of course) and magnifying the width of pores and cracks that otherwise would be too small to see. The technique is more sensitive than dye-penetrant testing because the viscosity of gases is typically only 1/100 of that of liquids, making the test extremely searching.

Finally, it is worth emphasizing that a good melt quality combined with a good filling system will usually eliminate most of the leaks found in castings (providing core blows can be avoided by careful design or venting of cores). This conclusion is confirmed by foundries using intrinsically quiescent melt handling processes such as the Cosworth Process. These operations are so confident of the quality of their products that they do not even bother to test for leak tightness; none are ever found to leak.

---

## 9.12 SURFACE FINISH

There are two major aspects to the achievement of a good surface finish for castings; the first, applying to some metals, is surface tension of the liquid, and the second, important for many important alloys, the solid surface film on the liquid.

### 9.12.1 Effect of surface tension

It has been well understood for many years (Hoar 1953) that when in contact with many non-metals, liquid metals enjoy the benefit of capillary repulsion; the resistance felt by the metal when attempting to enter a small hole or channel.

(In passing we should note that if the liquid metal wetted the mold materials it would experience capillary attraction, effectively being sucked into the mold surface as water is sucked up a capillary tube. Mold materials are therefore selected, however, for their non-wettability. The founder goes to some lengths to avoid wetting conditions, which cause penetration of metal into the mold.)

Assuming therefore non-wetting conditions, when the pressure  $P$  in the liquid metal becomes sufficiently high, surface tension  $\gamma$  is no longer able to resist the penetration of the metal into the spaces between the sand grains of the mold. The size of the holes between the sand grains can be roughly estimated assuming that the radius of the inter-granular spaces  $r$  is only approximately 15.4% of the radius of the sand grains.

Following arguments already presented in the development of Equation 4.1, the resistance offered by surface tension is  $P = 2\gamma/r$ . If the pressure in the melt, density  $\rho$ , arises simply from its depth  $h$  then  $P = \rho gh$  where  $g$  is the acceleration due to gravity. From these equations the critical depth at which penetration first occurs can easily be estimated. For instance, for liquid steel where  $\gamma = 1.5 \text{ N m}$  and  $\rho = 7000 \text{ kg m}^3$ , a grain size of  $500 \mu\text{m}$  corresponding to a pore size of  $75 \mu\text{m}$  and radius  $37.5 \mu\text{m}$  indicates a critical depth at which penetration will occur as approximately 1.5 m. This static estimate

neglects the important dynamic problems created by a poor filling system in which the melt may violently impact the sand, and thus suffer additional transient penetration pressures.

The penetration of the mold in this way produces a 'furry' casting that may be quite unsaleable. The penetration may be only one grain deep, giving effectively an excessively rough surface. However, penetrations of 20–50 mm are not uncommon in large castings. In a classical series of experiments, Hoar and Atterton (1950–1956) demonstrate that once the critical pressure difference to force the metal into the sand is exceeded, then penetration occurs rapidly, within a second or so. Figure 4.10 illustrates that once the surface grains are penetrated, the penetration is a run-away effect. Ultimately, the depth of penetration is controlled by the freezing of the leading edge of the advancing metal when it reaches the freezing isotherm in the sand. Clearly, this distance is greater for larger castings. The mix of solid metal and sand is difficult to remove from such castings.

Attempts are made to resist such mold penetration by reducing the size of the pores by:

1. The use of finer sand for the mold or core. For cores this approach is limited by the requirement to maintain the permeability of the core material so that core gases can escape during casting. It is, however, widely used for vacuum (V) process molding, where the vacuum that is applied to maintain the rigidity of the mold assists in drawing the liquid metal into the pores between the sand grains. Thus, whereas normal sand castings have an average grain size in the range 250–500  $\mu\text{m}$ , sands for the V process are approximately 50–150  $\mu\text{m}$ . This can result in a dust nuisance when casting hotter metals such as iron, which is a pity since the vacuum molding process is otherwise good in its environmental benefits. Newer plants are improving their designs to tackle this problem. Croning shell process benefits surface finish by its fine grains, usually less than 200  $\mu\text{m}$ , but permeability is maintained in this case by the thinness of the shell mold, usually never more than 10 mm.
2. The application of a mold wash – a ceramic slurry applied as a paint to fill the spaces between the sand grains. The pores in the dried coating are one or two orders of magnitude smaller than the pores between the grains, thus, in line with Equation 2.2, enabling the mold surface to withstand 10–100 times greater pressures before metal penetration. Although the metal will often still succeed in penetrating the sand coating through cracks, the penetrated sand only adheres to the casting at the isolated points of failure of the coat, and so is relatively easy to remove. This action is generally used to counter metal penetration at the base of tall molds, which can sometimes be more than a meter high.

The application of a core wash is only marginally successful, however, in resisting metal penetration with the use of sand cores in low-pressure die casting. This seems to be the result of the rather poor pressure control on most low-pressure machines, and the additive effect of the momentum of the metal, giving a pressure peak at the instant when the liquid hits the top of the mold (see Section 3.1.2). Sand cores are only rarely used, therefore, in low-pressure die casting. For similar reasons, sand cores have proved impractical for high-pressure die casting. In this case other solutions such as water-soluble salt, glass, or ceramic cores have sometimes achieved success. In general, only withdrawable steel cores continue to be used successfully.

Filling pressures are high in pressure die casting. This is widely alleged to be for the purpose of increasing surface finish and definition, i.e. the ability of the metal to fill small radii so as to reproduce fine detail. Pressure die casting machines commonly operate at metal pressures of 1000 atm

(100 MPa). Equation 2.1 indicates that such pressures will force the liquid into radii of only 10 nm, approaching atomic dimensions! This is, of course, a vast overkill. The student should therefore be on his guard against such loose thinking. The high pressures are actually needed mainly to reduce the bubble defects produced by the turbulently entrained mold gases – the bubbles are simply squashed to acceptable dimensions. Consideration of Equation 2.1 reveals that a mere 10 atm (1 MPa) would reproduce a radius of about 1  $\mu\text{m}$ , which would be more than good enough for most purposes.

Filling pressures are enhanced for the genuine purpose of reproducing detail in the centrifugal casting of jewelry. A casting traveling at 10  $\text{m s}^{-1}$  on an arm of radius 1 m will experience an acceleration of 100  $\text{m s}^{-2}$ . This is close to 10  $g$ . In the absence of mold gases, and replacing the acceleration  $g$  due to gravity with the total acceleration  $(g + 10g) = 11g$  as the arm goes from the vertically up through the vertically down part of its stroke, Equation 2.3 predicts that an improvement in the fineness of detail by a factor of 11 should be achievable. These predictions are likely to be all the more accurate for jewelry alloys based on noble metals such as gold and platinum since they will not be troubled by surface oxides.

In engineering uses of centrifugal casting much higher accelerations are normally used, typically 50–100  $g$ . The high pressures in the liquid are, however, not normally needed for filling, since the molds are usually of simple shapes. The technique is valuable for totally unrelated reasons: (1) for pipes and cylinders and the like, because the centrifugal action avoids the requirement for a central cylindrical core to make a hollow shape; and (2) for enhancing the pressure in the casting during freezing to reduce porosity, and (3) centrifuging the oxides and similar less dense inclusions into the center of the bore, where, if necessary, they can be machined off. In this case, however, it has to be pointed out that the production of shaped castings by this route involves pouring the liquid metal down a central down-runner, and accelerating it out along radial runners, to arrive in the mold at such a high speed that considerable damage is done to both mold and metal. The high centrifugal pressures are then needed to help repair this damage constituted by entrained porosity and inclusions in the casting. Shaped castings would probably be cheaper and better if not centrifuged at all, but simply produced with a properly designed gravity-running system.

### 9.12.2 Effects of a solid surface film

The above considerations of the control of surface finish by surface tension do not apply to many metals and alloys that have strong, solid surface films. In this case there is no liquid on the surface of the melt, so penetrating the mold becomes difficult. Instead, the solid film has some rigidity, thus bridging the gaps between grains of aggregate, thereby creating a smooth surface. This effect is especially encouraged if the melt is caused to fill the mold in a counter-gravity mode, the metal rising upwards, rolling out its solid skin like a track-laying vehicle against the mold surface (Figure 2.2). The smoothness of the casting surface that is created reflects the smoothness of the surface of the original liquid meniscus at the time the original surface film formed.

Aluminum alloys enjoy this benefit because of its strong alumina film. These include aluminum bronzes (Cu–10Al, etc.) since the higher temperatures of these alloys give an even thicker and stronger oxide skin.

An Alcoa patent by DeYoung and Dunlay in 2002 describes how the addition of strontium (Sr) to aluminum alloys strengthens the surface oxide and consequently improves the surface of direct chill (DC) ingots.

Similarly, in 1989 Sare found that when melting the surface of cast irons by gas tungsten arc welding, gray iron produced a rough surface but ductile iron was smooth as a result of its small content of Mg that promoted a strong MgO surface film.

These chemical techniques for thickening and strengthening the oxide film on the liquid can be supplemented by giving the film more time to grow, as is easily achieved by proper bottom-gating of the mold cavity and ensuring that the melt rises lamina-ly, the film growing on the surface meniscus, but diverting sideways to become the skin of the casting (Figures 2.2 and 6.33). The thicker, more rigid skin is then able to bridge the sand grains or other surface imperfections of the mold, giving an enhanced surface finish. It seems possible that the quality of surface finish may be a function of the rate of rise of the liquid in the mold, since this would be expected to be directly related to the thickness and rigidity of the surface film.

Perhaps the most impressive demonstration of the benefits of a strong skin is shown by cast iron in molds that contain volatile carbonaceous additions such as coal dust. The hydrocarbons chemically decompose ('crack') on the surface of the rising hot metal, releasing hydrogen which escapes somewhere (it would be interesting to know where it goes; whether into the metal or the mold atmosphere) but certainly depositing carbon on the surface of the liquid in the form of a strong film. This is known as lustrous carbon (see Section 6.5.2 and Figure 2.2c). Iron castings that are nicely bottom-gated can emerge from the mold with a black, glossy surface almost like a mirror. Such a good finish is the sign of a good filling system.

It is clear with steel castings (Puhakka 2011) that those poured with poor filling systems display a poor finish with generous amounts of so-called 'burn-on'. The poor finish almost certainly arises from the impacting of the mold surface with high momentum, with little or no time for the development of a useful protective film barrier, thus leading to a dynamic penetration.

The poor surface contrasts with the surface of bottom-gated castings that have the benefit of a naturally pressurized filling system design. These castings exhibit an excellently smooth and glossy finish with zero burn-on. The bottom-gated, smoothly filled mold rolls out its surface oxide like a carpet against the mold wall, the pressure against the mold only increasing gently so as to allow the oxide good time to strengthen, and form an effective barrier against penetration. In this mode of filling the melt and mold never come into contact. Puhakka has demonstrated that even steel castings can achieve a surface finish that is so smooth to the touch as to be almost strokable.

---

## 9.13 QUALITY INDICES

The confusion of the interplay of properties between yield strength, tensile strength, and elongation, the strengths going up as the elongation reduces with different heat treatments and other factors, is solved by the brilliant concept of a Quality Index. This is a single figure indicating the quality of the cast material. However, so far, quality indices appear to be exclusively used in the Al alloy casting industry, and in particular for the widely used Al-7Si-Mg alloys.

The concept was invented by French researchers (Drouzy, Jacob, and Richard 1980) in the following form

$$Q_{DJR} = \sigma_{UTS} + 150 \log E$$

where the ultimate strength  $\sigma_{UTS}$  was in units of MPa and elongation  $E$  was in units of percent (%). The formulation as a single parameter is undoubtedly useful, and has become popular in the industry. Those castings achieving an index above 500 MPa were regarded as outstanding, but it is probably only a matter of time before techniques improve to yield even higher values.

Even though the single-parameter quality index concept has been recognized as excellent, the Drouzy formulation for a single parameter as a measure of quality has been criticized by a number of subsequent researchers. In particular the use of UTS and Elongation has elements of double counting, and was not based on the really essential engineering design parameter, yield strength  $\sigma_Y$  (or near equivalent such as 0.2% proof stress). Finally, the incorporation of the log term was inconvenient and in fact hardly necessary. The author's laboratory (Din, Rashid, and Campbell 1996) came up with the simpler:

$$Q_{DRC} = \sigma_Y + kE$$

where  $k$  is a constant determined from experiment to be 50 for both 356 and 357 alloys (respectively the low and high Mg versions of the Al-7Si alloys).

Both of these quality measures were based on empirical approaches which had no fundamental significance. In practice, a reader may wonder why there is even a specification on elongation because parts are designed to handle stresses well below the yield strength.

The answer on a legalistic level is put forward by the automotive companies who wish their components to bend rather than fracture in a crash, so that the component cannot be cited as a potential cause of the crash.

On a more general engineering level, it is clearly more desirable for a component to fail by plastic deformation than fracture because plastic deformation absorbs more energy. This statement points to the assessment of energy (or toughness as described by the energy under the true stress-strain curve) as a measure of quality. However, we all know that almost all part failures happen by fatigue fracture, although both fracture toughness and fatigue life are both strongly affected by defects. Therefore quality indices can give a measure of the severity of defects and would be expected therefore to be useful in giving an indication of fatigue life.

Tiryakioglu (2009) initially suggested a more rational assessment based on the energy to fracture. This could be closely approximated to the average  $(\sigma_{UTS} + \sigma_Y)$  multiplied by  $E$  (giving the area under the stress-strain curve). Since  $\sigma_Y$  is relatively fixed, and  $\sigma_{UTS}$  is a function of  $\sigma_Y$  and  $E$ , it follows that  $E$  is a dominant factor in this proposed assessment of quality. Finally therefore if  $E$  is measured at a known value of  $\sigma_Y$ ,  $E$  alone can give an excellent measure of the quality of the material.

Tiryakioglu and colleagues (2009) proposed from fundamental grounds that there should be an upper bound to the uniform elongation to fracture of Al alloys, since necking prior to fracture was generally never observed. Their theoretical predictions were revealed to be closely modeled by experimental data; the upper bound to elongation was revealed by plotting all the available data, mainly from aerospace alloy foundries. The result for the 356 and 357 alloys are shown in Figure 9.45a and the results for the Al-4.5Cu alloys A206 and A201 in Figure 9.45b. A measure of quality can now be defined immediately as

$$Q_T = E_{\text{measured}}/E_{\text{potential}}\%$$

The quality index now becomes the percentage of the maximum elongation attainable at that level of yield strength (for instance as resulting from a particular heat treatment). This formulation of the



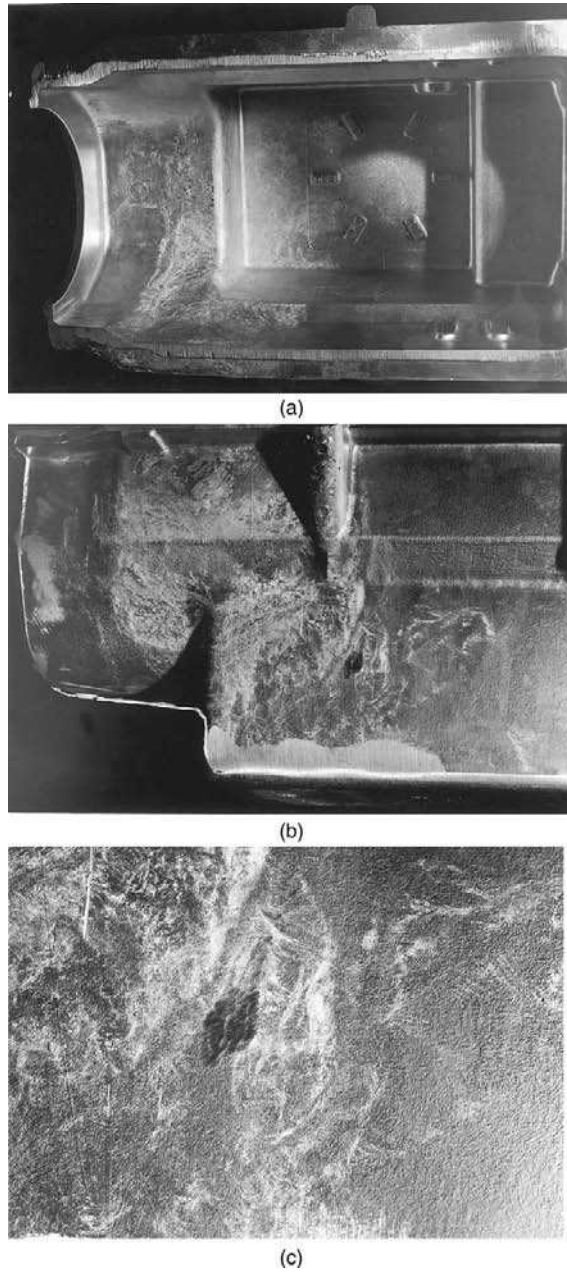


**FIGURE 9.45**

Views of (a) the inside and (b) the outside of a top-poured oil pan (sump) casting showing the light traces of entrained oxides and the corresponding lead defects repaired by peening, seen in close-up at (c).

quality concept using  $Q_T$  is strongly recommended as giving a direct measure of the level of attainment of potential quality. The new index is applicable to all Al-alloys and should be applicable to all cast alloys.

In fact, it is sobering to see the masses of mediocre or actually bad results compared with the maximum elongation that is possible in the alloy at each particular yield strength. Clearly, a few results are close to 100%, but many achieve only 50% or even only 5% of the potential value. There is plenty of scope for improvement in the industry.

This page intentionally left blank

# References – Volume I

- Abbas, M., Ray, N. K., Deb, P., & Mallick, J. P. (1993). *Indian Foundry Journal*, 39(9), 12–16.
- Adams, A. (2001). *Modern Castings*, 91(3), 34–36.
- Adams, C. M. (1958). ‘Thermal considerations in freezing.’ Chapter in ‘*Liquid Metals and Solidification*.’ ASM Cleveland Ohio, 187–217.
- Afseth, A., Nordlien, J. H., Scamans, G. M., & Nisancioglu, K. (2000). In *ASST 2000 (2nd International symposium Al surface science technology) UMIST* (pp. 53–58). Manchester UK: Alcan + Dera.
- Agema, K. S., & Fray, D. J. (1988). Agema PhD thesis, Department of Materials, Cambridge, UK.
- Adefuye, S. (1997). PhD thesis, University of Birmingham UK, ‘The fluidity of Al-Si alloys.’ Supervisor N. R. Green.
- Ahn, J.-H., & Berghezan (1991). *Materials Science and Technology*, 7(7), 643–648.
- Ahamed, A. K. M. A., & Kato, H. (2008). *International Journal of Cast Metals Research*, 21(1–4), 162–167.
- Alexopoulos, N. D., & Tiryakioglu, M. (2009). *Materials Science & Engineering A*. doi:10.1016/j.msea.2008.12.026.
- Ali, S., Mutharasan, R., & Apelian, D. (1985). *Metallurgical Transactions*, 16B, 725–742.
- Aliravci, C. A., Gruzleski, J. E., & Dimayuga, F. C. (1992). *TAFS*, 100, 353–362.
- Allen, D. I., & Hunt, J. D. (1979). Solidification and Casting of Metals. Sheffield Conference, 1977. Metals Society, 39–43.
- Allen, N. P. (1932). *Journal of the Institute of Metals*, 49, 317–346.
- Allen, N. P. (1933). *Journal of the Institute of Metals*, 51, 233–308.
- Allen, N. P. (1934). *Journal of the Institute of Metals*, 52, 192–220.
- Alsem, W. H. M., Wiggen, P. C. van, & Vader, M. (1992). Light Metals. In E. R. Cutshall (Ed.) (pp. 821–829). The Minerals, Metals and Materials Society USA.
- Altstetter, J. D., & Nowicki, R. M. (1982). *TAFS*, 90, 959–970.
- American Foundrymen’s Society. (1987). *Green Sand Additives*. Detroit, USA: AFS.
- Anderson G. R. (1985). In *Patt-Tech 85 Conference*, Oxford, UK.
- Anderson, G. R. (1987). *TAFS*, 95, 203–210.
- Anderson, J. V., & Karsay, S. I. (1985). *British Foundryman*, 492–498.
- Anderson, S. H., Foss, J. W., Nagan, R. M., & Jhala, B. S. (1989). *TAFS*, 97, 709–722.
- Andresen, P. L., Chou, P. H., Morra, M. M., Nelson, J. L., & Rebak, R. B. (2009). *Metallurgical & Materials Transactions A*, 40A(12), 2824–2836.
- Andrew, J. H., Percival, R. T., & Bottomley, G. T. C. (1936). *Iron and Steel Special Report*, 15, 43–64.
- Angus, H. T. (1976). *Cast Iron*. London: Butterworths.
- Anson, J. P., & Gruzleski, J. E. (1999). *Transactions of American Foundry Society*, 107, 135–142.
- Anson, J. P., Stucky, M., & Gruzleski, J. E. (2000). *Transactions of American Foundry Society*, 108, 419–426.
- Antes, H. W., Norton, J. T., & Edelman, R. E. (1958). *TAFS*, 66, 135–142.
- Appa Rao, G., Srinivas, M., & Sarma, D. S. (2004). *Materials Science & Technology*, 20, 1161–1170.
- Archibald, J. J., & Smith, R. L. (1988). In Volume 15 ‘Casting’ from *Metals Handbook*, ASM, pp. 214–221.
- Armbruster, D. R., & Dodd, S. F. (1993). *TAFS*, 101, 853–856.
- Arnold, F. L., Jorstad, J. L., & Stein, G. E. (1963). *Current Engineering Practice*, 6, 10–15.
- Arnold, F. L., & Prestley, J. S. (1961). *Transactions of American Foundry Society*, 69, 129–136.
- Aryafar, M., Raiszadeh, R., & Shalbazadeh, A. *Journal of Materials Science* published online 19 Feb 2010, DOI 10.1007/s10853-010-4308-8.
- Asbjornson (2001). PhD thesis, Department of Materials, University of Nottingham.
- Ashton M. C. (1990). In *SCRATA 34th Conference. Sutton Coldfield, paper 2*, Steel Castings Research and Trade Association, Sheffield, UK.

## RI-2 References

- Ashton, M. C., & Buhr, R. C. (1974). *Phys. Met. Div. internal Report PM-1-74-22*. Canada Dept Energy Mines and Resources.
- Askeland, D., & Holt, M. L. (1975). *TAFS*, 83, 99–106.
- Atwood, R. C., & Lee, P. D. (2000). *Modeling of Casting Welding and Advanced Solidification Processing Conference, Aachen*. In P. Sahm, & P. Hansen, (Eds.).
- Avey, M. A., Jensen, K. H., & Weiss, D. J. (1989). *TAFS*, 97, 207–212.
- Aylen, P., Foulard, J., & Galey, J. (1965). *TAFS*, 73, 311–316.
- Bachelot, F. (1997). MPhil thesis, University of Birmingham, UK.
- Backerud, L., Chai, G., & Tamminen, J. (1990). ‘Solidification characteristics of aluminum alloys’, vol. 2 *Foundry Alloys*, AFS/Skanaluminium, printed in USA.
- Bachmann, P. K., & Messier, R. (1984). *Chemical and Engineering News*, 67(20), 24–39.
- Bailey, A., & Davenport, A. J. (April 2002). *Final Year Project*. UK: University of Birmingham, Department of Metallurgy.
- Bak, C., Degois, M., & Schissler, J. M. (1980). *TAFS*, 88, 301–312.
- Baker, W. A. (1945). *Journal of the Institute of Metals*, 71, 165–204.
- Baker, W. F. (1986). *TAFS*, 94, 215–218.
- Bakhtiarani, F. N., & Raiszadeh, R. (2010). *Journal of Materials Science*. In press.
- Bahreini, F., Boutorabi, S. M. A., & Campbell, J. (2005). Shape Casting: The John Campbell Symposium. In M. Tiryakioglu, & P. N. Crepeau (Eds.), *TMS* (pp. 463–472).
- Baliktay, S., & Nickel, E. G. (1988). *Seventh World Conference Investment Casting. Munich*, paper 10.
- Barbe, L., Bultink, I., Duprez, L., & Cooman, B. C. De (2002). *Materials Science & Technology*, 18, 664–672.
- Barkhudarov, M. R., & Hirt, C. W. (1999). *Die Casting Engineer* (Jan-Feb), pp. 44–47.
- Barlow, G. (1970). PhD thesis, University of Leeds.
- Barrett, L. G. (1967). *TAFS*, 75, 326–329.
- Barton, R. (February 28 1985). *Foundry Trade Journal*, 117–126.
- Basdogan, M. F., Bennett, G. H. J., & Kondic, V. (1983). ‘Solidification Technology in the Foundry and Cast House’ *Warwick University Conference 1980*. Metals Soc. Publication. 240–247.
- Bastien, P., Armbruster, J. C., & Azou, P. (1962). In *29 International foundry congress* Detroit, pp. 400–409.
- Bates, C. E., & Monroe, R. W. (1981). *TAFS*, 89, 671–686.
- Bates, C. E., & Scott, W. D. (1977). *TAFS*, 85, 209–226.
- Bates, C., & Wallace, J. F. (1966). *TAFS*, 74, 174–185.
- Batty, O. (1935). *TAFS*, 43, 75–106.
- Bean, X., & Marsh, L. E. (1969). *Metal Progress*, 95, 131–134.
- Beck, A., Schmidt, W., & Schreiber, O. (1928). U.S. Patent 1,788,185.
- Beech, J. (April 1974). *The Metallurgist and Materials Technologist*, 129–232.
- Beeley, P. R. (2001). *Foundry Technology* (2nd ed.). London: Butterworth-Heinemann.
- Benaily, N. (1998). ‘Inoculation of flake graphite iron’ MPhil thesis, UK: University of Birmingham.
- Benson, L. E. (June 1938). *Foundry Trade Journal*, 527–528.
- Benson, L. E. (June 1938). *Foundry Trade Journal*, 543–544.
- Benson, L. E. (1946). *Journal of the Institute of Metals*, 72, 501–510.
- Beretta, S., & Murakami, Y. (2001). *Metallurgical & Materials Transactions B*, 32B, 517–523.
- Berger, R. (1932). *Fonderie Belge*, 17.
- Berry, J. T., Kondic, V., & Martin, G. (1959). *TAFS*, 67, 449–476.
- Berry, J. T., & Taylor, R. P. (1999). *TAFS*, 107, 203–206.
- Berry, J. T., & Watmough, T. (1961). *TAFS*, 69, 11–22.
- Berthelot, M. (1850). *Annali Di Chimica*, 30, 232.
- Bertolino, M. F., & Wallace, J. F. (1968). *TAFS*, 76, 589–628.

- Betts, B. P., & Kondic, V. (1961). *British Foundryman*, 54, 1–4.
- Bex, T. (1991). *Modern Casting*, November, p. 56.
- Biel, J., Smalinskas, K., Petro, A., & Flinn, R. A. (1980). *TAFS*, 88, 683–694.
- Bindernagel, I., Kolorz, A., & Orths, K. (1975). *TAFS*, 83, 557–560.
- Bindernagel, I., Kolorz, A., & Orths, K. (1976). *AFS International Journal of Cast Metals*, 1(4), 42–45.
- Birch, J. (March 2000). *Diecasting World*, 18–19.
- Birch, J. (September 2000). *Diecasting World*, 174(3570), 28.
- Bird, P. G. (1989). In *Foseco technical service report MMP1.89* 'Examination of the factors controlling the flow rate of aluminium through DYPUR units.' 1 March 1989.
- Bishop, H. F., Ackerlind, C. G., & Pellini, W. S. (1952). *TAFS*, 60, 818–833.
- Bishop, H. F., Myskowski, E. T., & Pellini, W. S. (1955). *TAFS*, 63, 271–281.
- Bisuola, V. B., & Martorano, M. A. (2008). *Metallurgical & Materials Transactions A*, 39A(12), 2885–2895.
- Biswas, P. K., Rohatgi, P. K., & Dwarakadasa, E. S. (1985). *British Foundryman*, 78, 511–516.
- Biswas, P. K., Pillai, R. M., Rohatgi, P. K., & Dwarakadasa, E. S. (1994). *Cast Metals*, 7(2), 65–83.
- Boenisch, D. (1967). *TAFS*, 75, 33–37.
- Boenisch, D. (1988). In *Conference 'Ensuring Quality Castings' BCIRA*, University of Warwick, 29–31 March 1988, paper 18.
- Boenisch, D., & Patterson, W. (1966). *TAFS*, 74, 470–484.
- Bonsak, W. (1962). *TAFS*, 70, 374–382.
- Boom, R., Dankert, O., Veen van, A., & Kamperman, A. A. (2000). *Metallurgical and Materials Transaction B*, 31B(5), 913–919.
- Bossing, E. (1982). *TAFS*, 90, 33–38.
- Bounds, S. M., Moran, G. J., Pericleous, K. A., & Cross, M. (1998). Modelling of Casting, Welding and Solidification Processing Conference VIII San Diego. In B. G. Thomas, & C. Beckerman (Eds.), *TMS* (pp. 857–864).
- Boutorabi, S. M. A., Din, T., & Campbell, J. (1990). University of Birmingham unpublished work.
- Bower, T. F., Brody, H. D., & Flemings, M. C. (1966). *AIME Transactions*, 236, 624.
- Bramfitt, B. L. (1970). *Metallurgical and Materials Transactions*, 1, 1987–1995.
- Brandes, E. A., & Brook, G. B. (Eds.). (1992). *Smithells Metals Reference Book* (7th ed.). Butterworths.
- Brauer, H. E., & Pierce, W. M. (1923). *Transactions of the American Institute of Mining and Metallurgy*, 68, 796–832.
- Bridge, M. R., Stephenson, M. P., & Beech, J. (1982). *Metals Technology*, 9, 429–433.
- Bridges, D. (1999). Wheels and axles. In *I. Mech. E. Seminar*, London.
- Briggs, L. J. (1950). *Journal of Applied Physics*, 21, 721–722.
- Briggs, C. W., & Gezelius, R. A. (1934). *TAFS*, 42, 449–476.
- Brimacombe, J. K., & Sorimachi, K. (1977). *Metallurgical and Materials Transactions*, 8B, 489–505.
- Bromfield, G. (July 1991). *The Foundryman*, 261–265.
- Brondyke, K. J., & Hess, P. D. (1964). *Transactions of the Metallurgical Society of AIME*, 230(7), 1542–1546.
- Brookes, B. E., Berckermann, C., & Richards, V. L. (2007). *International Journal of Cast Metals Research*, 20(4), 177–190.
- Brown, J. R. (1970). *British Foundryman*, 63, 273–279.
- Brown, N., & Rastall, D. (1986). *European Patent Application No 87111549.9 filed 10.08.87*. p. 9.
- Bryant, M. D., & Moore, A. (1971). *British Foundryman*, 64, 215–229, 306–307.
- Buhrig-Polackzek, A., & Santos de, A. (2008). *Metals Handbook Volume 15 Casting*. Ohio, USA: ASM. 317–329.
- Burchell, V. H. (1969). *British Foundryman*, 62, 138–146.
- Burton, B., & Greenwood, G. W. (1970). *Met. Sci. J.*, 4, 215–218.
- Butakov, D. K., Mel'nikov, L. M., Rudakov, I. P., & Maslova Yu, N. (1968). *Lit. Proizv*, 4, 33–35.

## RI-4 References

- Butler, C. J. (1980). U.K. *Patent GB 2020714*.
- Butler, T., & Lund, J. N. (February 2003). *Modern Castings*, 40–42.
- Byczynski, G. E., & Cusinato, D. A. (2001). *First international conference filling and feeding of castings 4-5 April University of Birmingham, UK, and International Journal Cast Metals Research* 2002 14(5), pp. 315–324.
- Caceres, C. H. (2000). *TAFS*, 108, 709–712.
- Caceres, C. H. (2004). Proc 9th Internat Conf Al Alloys. In J. F. Nie, et al. (Eds.), *Institute of Materials Engineering Australia Ltd* (pp. 1216–1221).
- Caine, J. B., & Toepke, R. E. (1966). *TAFS*, 74, 19–22.
- Caine, J. B., & Toepke, R. F. (1967). *TAFS*, 75, 10–16.
- Campbell, J. (1967). *Transactions of the Metallurgical Society of AIME*, 239, 138–142.
- Campbell, J. (1968). *The Solidification of Metals*. ISI Publication, 110, 19–26.
- Campbell, J. (1968a). *Transactions of the Metallurgical Society of AIME*, 242, 264–268.
- Campbell, J. (1968b). *Transactions of the Metallurgical Society of AIME*, 242, 268–271.
- Campbell, J. (1968c). *Transactions of the Metallurgical Society of AIME*, 242, 1464–1465.
- Campbell, J. (1969). *Journal of Cast Metals Research*, 5(1), 1–8.
- Campbell, J. (1969). *Trans AIME*, 245, 2325–2334.
- Campbell, J. (1971). *Metallography*, 4, 269–278.
- Campbell, J. (1980). ‘Solidification Technology in the Foundry and Casthouse’ *Warwick Conference*. Metals Soc Publication 1981, 273, 61–64.
- Campbell, J. (1981). *International Metals Reviews*, 26(2), 71–108.
- Campbell, J. (1988). *Materials Science and Technology*, 4, 194–204.
- Campbell, J. (1991). *Cast Metals*, 4(2), 101–102.
- Campbell, J. (1991). *Castings*. Butterworth-Heinemann.
- Campbell, J. (1994). *Cast Metals*, 7(4), 227–237.
- Campbell, J. (2000). *Ingenia*, 1(4), 35–39.
- Campbell, J. (2003). *Castings*. UK: Elsevier, Oxford. pp. (a) 178–181; (b) 161–162; (c) 158–160.
- Campbell, J. (2006). *Materials Science & Technology*, vol. 22(2), 127–145, and (8) 999–1008.
- Campbell, J. (2006). ‘Modeling of entrainment defects during casting’. In *TMS Annual Congress*, San Antonio, USA.
- Campbell, J. (2007). *AFS International Journal of Metalcasting*, 1(1), 7–20.
- Campbell, J. (2009). *Materials Science & Technology*, 25, 125–126.
- Campbell, J. (2009). *Metallurgical & Materials Transactions B*, 40B(6), 786–801, ‘A hypothesis for Graphite Formation in Cast Irons’.
- Campbell, J. (2009). *Metallurgical & Materials Transactions A*, 40A(7), 1510–1511, ‘Stress corrosion cracking of Mg alloys’.
- Campbell, J. (2010). *Metallurgical and Materials Transactions A*, 41A(5), 1101, only. ‘Stress corrosion cracking of stainless steels’.
- Campbell, J. (2011). In M. Tiryakioglu, P. Crepeau, & J. Campbell, (Eds.). ‘The Origin of Griffiths Cracks’ *Shape Casting Symposium TMS Annual Congress*, San Diego, CA.
- Campbell, J., & Bannister, J. W. (1975). *Metals Technology*, 2(9), 409–415.
- Campbell, J., & Caton, P. D. (1977). In *Institute of metals conference on solidification*, Sheffield UK (pp. 208–217).
- Campbell, J., & Clyne, T. W. (1991). *Cast Metals*, 3(4), 224–226.
- Campbell, J., & Isawa, T. (1994). U.K. *Patent GB 2,284,168 B (Filed 04-02-1994)*.
- Campbell, J., & Naro, R. L. (2010). Lustrous carbon in grey iron. *TAFS*, 114, 6, paper 10-36.
- Campbell, J., & Olliff, I. D. (1971). *AES Cast Metals Research Journal*, 55–61, June.
- Campbell, J., & Tiryakioglu, M. (2008). *Effect of Sr on porosity*. Submitted to *Metallurgical & Materials Transactions*.
- Campbell, H. L. (1950). *Foundry*, 78, 86, 87, 210, 212, 213.

- Cao, P., Qian, M., StJohn, D. H., & Frost, T. M. (2004). *Materials Science & Technology*, 20(5), 585–592.
- Cao, X. (2001). PhD thesis, Department of Metallurgy, University of Birmingham, UK.
- Cao, X. (2009). Personal communication.
- Cao, X., & Campbell, J. (2000). *American Foundry Society Transactions*, 108, 391–400.
- Cao, X., & Campbell, J. (2003). *Metallurgical & Materials Transactions A*, 34A(July), 1409–1420.
- Capello, G. P., & Carosso, M. (1989). In *AGARD report, May, No. 762*.
- Cappy, M., Draper, A., & Scholl, G. W. (1974). *TAFS*, 82, 355–360.
- Carlberg, T., & Fredriksson, H. (1979). *Solidification and Casting of Metals Conf, Univ Sheffield UK 1977*. pp. 115–124. The Metals Society.
- Carlson, G. A. (1975). *Journal of Applied Physics*, 46(9), 4069–4070.
- Carlson, K. D., & Beckermann, C. 'Shrinkage porosity prediction using a dimensionless Niyama criterion.' To be published 2010.
- Carne, C. A., & Beech, J. (1997). Solidification Processing. In J. Beech, & H. Jones (Eds.) (pp. 33–36). UK: Sheffield University.
- Carte, A. E. (1960). *Proc. Phys. Soc.*, 77, 757–769.
- Carter, S. F., Evans, W. J., Harkness, L. C., & Wallace, J. F. (1979). *TAFS*, 87, 245–268.
- Celik, M. C., & Bennett, G. H. J. (April 1979). *Metals Technology*, 138–144.
- Chadwick, G. A., & Yue, T. M. (1991). Southampton: Hi-Tech Metals R&D Ltd. Personal communication. (See Yue, T. M.)
- Chadwick, H. (1991). *Cast Metals*, 4(1), 43–49.
- Chadwick, P. (1963). *International Journal of Mechanical Sciences*, vol. 5, 165–182.
- Chalmers (1953). Quoted by Flemings, M. C. 1974.
- Chamberlain, B., & Zabek, V. J. (1973). *TAFS*, 81, 322–327.
- Chandley, G. D. (1983). *TAFS*, 91, 199–204.
- Chandley, G. D. (1989). *Cast Metals*, 2(1), 2–10.
- Chang, J.-K. B., Taleff, E. M., & Krajewski, P. E. (2009). *Metallurgical & Materials Transactions A*, 40A(13), 3128–3137.
- Charles, J. A., & Uchiyama, I. (1969). *Journal of the Iron and Steel Institute*, 207(July), 979–983.
- Chechulin, V. A. (1965). In B. B. Gulyaev (Ed.), *Gases in Cast Metals* (pp. 214–218). Consultants Bureau Translation.
- Chen, C. O., Ramberg, F., & Evensen, J. D. (1984). *Metal Science*, 18, 1–5.
- Chen, G. J., Liu, S. H., & Ren, B. L. T. (1989). *TAFS*, 97, 335–338.
- Chen, Q. Z., & Knowles, D. M. (2003). *Materials Science & Technology*, 19(4), 447–455.
- Chen, X. G., & Engler, S. (1994). *TAFS*, 102, 673–682.
- Chen, X.-G., & Fortier, M. (2010). *Journal of Materials Processing Technology*, 210, 1780–1786.
- Chiesa, F. (1990). *TAFS*, 98, 193–200.
- Chisamera, M., Riposan, I., & Barstow, M. (1996). *TAFS*, vol. 104, 581–588.
- Cho, J.-I., & Loper, C. R. (2000). *Transactions American Foundry Society*, 108, 359–367.
- Cho, Y. H., Lee, H.-C., Oh, K. H., & Dahle, A. K. (2008). *Metallurgical and Materials Transactions*, 39A(10), 2435–2448.
- Chung, Y., & Cramb, A. W. (2000). *Metallurgical and Materials Transactions B*, 31B, 957–971.
- Church, N., Wieser, P., & Wallace, J. F. (1966). *TAFS*, 74, 113–128, Also in *Br Found* 1966, 59, 349–363.
- Chvorinov, N. (1940). *Giesserei*, 10, 177–186, 201, 222 and 27 (May 31) 201–208.
- Cibula, A. Proceedings IBF 1955 45 A73-A90. Also in *Foundry Trade Journal*, 1955, 98, pp. 713–726.
- Clausen, C. (1992). *Modern Casting* (August). 39–39.
- Claxton, K. T. (1967). The Influence of Radiation on the Inception of Boiling in Liquid Sodium. In *UK Atomic Energy Authority Research Group Report AERE-R5308*. Also in *Proc. International Conference on the Safety of Fast Reactors (CAE)* (pp. II-B-;8–1). Aix-en-Provence, September 1967.



## RI-6 References

- Claxton, K. T. (1969). UKAEA, Harwell, UK. Private communication.
- Clegg, A. L., & Das, A. A. (1987). *British Foundryman*, 80, 137–144.
- Choudhury, A., Blum, M., Scholz, H., Jarczyk, G., & Busse, P. (February 1999). In *Proc 1999 International Symposium Liquid Metal Processing and Casting* (pp. 244–255). (Santa Fe, NM.)
- Churches, D. M., & Rundman, K. B. (1995). *TAFS*, 103, 587–594.
- Clyne, T. W. (1977). PhD thesis, University of Cambridge.
- Clyne, T. W., & Davies, G. J. (1975). *British Foundryman*, 68, 238–244.
- Clyne, I. W., & Davies, G. J. (1979). In *Solidification and Casting of Metals* (pp. 275–278). Sheffield: Metals Society Conference, 1977.
- Clyne, T. W., & Davies, G. J. (1981). *British Foundryman*, 74, 65–73.
- Clyne, T. W., & Kurz, W. (1981). *Metallurgical Transactions*, 12A, 965–971.
- Clyne, T. W., Wolf, M., & Kurz, W. (1982). *Metallurgical Transactions*, 13B, 259–266.
- Coble, R. L., & Flemings, M. C. (1971). *Metallurgical Transactions*, 2(Feb), 409–415.
- Cochran, C. N., Belitskus, D. L., & Kinosz, D. L. (1977). *Metallurgical Transactions*, 8B, 323–332.
- Cole, G. S. (1972). *TAFS*, 80, 335–348.
- Cole, G. S., Cisse, J., Kerr, H. W., & Bolling, G. F. (1972). *TAFS*, 80, 211–218.
- Colwell, D. L. (1963). *TAFS*, 71, 172–176.
- Cotton, J. D., Clark, L. P., & Phelps, H. R. (June 2006). *Journal of Metals*, 13–16.
- Cottrell, A. H. (1964). *The Mechanical Properties of Matter*. Wiley. p. 82.
- Couture, A., & Edwards, J. O. (1966). *TAFS*, 74, 709–721, 792–793.
- Couture, A., & Edwards, J. O. (1967). *AFS Cast Metals Research Journal*, 3(2), 57–69.
- Couture, A., & Edwards, J. O. (1973). *TAFS*, 81, 453–461.
- Cowen, C. J., & Boehlert, C. J. (2007). *Metallurgical & Materials Transactions A*, 38A, 26–34.
- Cox, M., Harding, R. A., Green, N. R., & Scholl, G. W. (2007). *Materials Science and Technology*, 23(9), 1075–1084.
- Cox, M., Wickins, M., Kuang, J. P., Harding, R. A., & Campbell, J. (2000). *Materials Science and Technology*, 16, 1445–1452.
- Creese, R. C., & Sarfaraz, A. (1987). *TAFS*, 95, 689–692.
- Creese, R. C., & Sarfaraz, A. (1988). *TAFS*, 96, 705–714.
- Creese, R. C., & Xia, Y. (1991). *TAFS*, 99, 717–727.
- Crossley, F. A., & Mondolfo, L. F. (1951). *Journal of Metals*, 3, 1143–1154.
- Cunliffe, E. L. (1996). 'The minimal gating of aluminium alloy castings.' PhD thesis, Metals and Materials Department, University of Birmingham, UK.
- Cunningham, M. (1988). *Stahl Speciality Co.* Kingsville, MO, USA: Private communication.
- Cupini, N. L., Galiza, J. A. de, Robert M. H., & Pontes, P. S. (1980). In *Solidification technology in the foundry and cast house. Metals society conference* (pp. 65–69).
- Cupini, N. L., & Prates de Campos Filho, M. (1977). *Sheffield conference 'solidification and casting of metals' Metals Soc 1979* (pp. 193–197).
- Dai, X., Yang, X., Campbell, J., & Wood, J. (2003). *Materials Science and Engineering*, A354(1–2), 315–325.
- Dantzig, J. A., & Rappaz, M. (2009). *Solidification*. Lausanne, Switzerland: EPFL Press. pp. 486–490.
- Dasgupta, S., Parmenter, L., & Apelian, D. (1998). In *AFS 5th International conference molten aluminum processing* (pp. 285–300).
- Datta, N., & Sandford, P. (1995). In *3rd AFS international permanent mold casting of aluminum conference, paper 3* (p. 19).
- Davidson, R. M. R. (1990). *Materials Performance*, 29(1), 57–62.
- Davies, G. J., & Shin, Y. K. (1980). In *Solidification technology in the foundry and casthouse. Metals Soc. conference, Warwick, paper 78*, pp. 517–523 (Published Metals Soc. 1983).

- Davies, I. G., Dennis, J. M., & Hellowell, A. (1970). *Metallurgical Transactions*, 1, 275–280.
- Davis, K. G. (1977 March). *AFS Internat. Cast Metals J*, 23–27.
- Davis, K. G., & Magny, J.-G. (1977). *TAFS*, 85, 227–236.
- Davies, V., & de, L. (1963). *Journal of the Institute of Metals*, 92, 127.
- Davies, V., & de, L. (1964-65). *Journal of the Institute of Metals*, 93, 10.
- Davies, V., & de, L. (1970). *British Foundryman*, 63, 93–101.
- Dawson, J. V., & Bcira, J. (1962). *IO* (4), pp. 433–437.
- Dawson, J. V., Kilshaw, J. A., & Morgan, A. D. (1965). *TAFS*, 73, 224–240.
- Daybell, E. (1953). *Proceedings of the Institute of British Foundryman*, 46, B46–B54.
- Delamore, G. W., & Smith, R. W. (1971). *Metallurgical Transactions*, 2, 1733–1743.
- Delamore, G. W., Smith, R. W., & Mackay, W. B. F. (1971). *TAFS*, 79, 560–564.
- Denisov, V. A., & Manakin, A. M. (1965). *Russian Castings Production*, 217–219.
- Dennis, K., Drew, R. A. L., & Gruzleski, J. E. (2000). *Aluminum Trans*, 3(1), 31–39.
- Devaux, H. (1987). Measurement and Control in Liquid Metals Processing. In R. J. Moreau (Ed.) (pp. 107–115). The Netherlands: Nijhoff.
- De Sy, A. (1967). *TAFS*, 75, 161–172.
- DeYoung, D. H., & Dunlay, M. J. (2002). U.S. Patent 6,334,978.
- Dickhaus, C. H., Ohm, L., & Engler, S. (1993). *TAFS*, 101, 677–684.
- Dietert, H. W., Doelman, R. L., & Bennett, R. W. (1970). *TAFS*, 78, 145–156.
- Dietert, H. W., Fairfield, H. H., & Brewster, F. S. (1948). *TAFS*, 56, 528–535.
- Dimayuga, F. C., Handiak, N., & Gruzleski, I. E. (1988). *TAFS*, 96, 83–88.
- Dimmick, T. (2001). *Modern Castings*, 91(3), 31–33.
- Din, T., & Campbell, J. (1994). University of Birmingham UK, unpublished work.
- Din, T., Kendrick, R., & Campbell, J. (2003). Paper 03-017. *TAFS*, 111.
- Din, T., Rashid, A. K. M. B., & Campbell, J. (1996). *Materials Science & Technology*, 12(3), 269–273.
- Dinayuga, F. C., Handiak, N., & Gruzleski, J. E. (1988). *TAFS*, 96, 83–99.
- Dion, J.-L., Couture, A., & Edwards, J. O. (1978). *TAFS*, 86, 309–314, and *AFS Internat Cast Metals J*, 4(2) 1979, 7–13.
- Dion, J.-L., Fasoyinu, F. A., Cousineau, D., Bibby, C., & Sahoo, M. (1995). *TAFS*, 103, 367–377.
- Dionne, P., Dickson, J. I., & Bailon, J. P. (1984). *TAFS*, 92, 693–701.
- Dispinar, D., & Campbell, J. (2004). *International Journal of Cast Metals Research*, 17(5), 280–286, and 278–294.
- Dispinar, D., & Campbell, J. (April 2005). University of Birmingham UK, unpublished work.
- Dispinar, D., & Campbell, J. (2006). *International Journal of Cast Metals Research*, 19(1), 5–17.
- Dispinar, D., & Campbell, J. (2007). *Journal of Materials Science*, 42, 10296–10298.
- DiSylvestro, G., & Faist, C. A. (1977). *TAFS*, 85, 627–642.
- Divandari, M. (1998). University of Birmingham UK, unpublished work.
- Divandari, M., & Campbell, J. (1999). In *AFS 1st international conference on gating filling and feeding of aluminum castings 11–13 Oct 1999* (pp. 49–63).
- Divandari, M., & Campbell, J. (2000). *Aluminum Trans*, 2(2), 233–238.
- Dixon, B. (1988). Solidification Processing Conference 1987. *Inst. Metals*, 381–383.
- Dodd R. A. (1950). PhD thesis, Department of Industrial Metallurgy, University of Birmingham, UK.
- Dodd, R. A. (1955). *Hot tearing of casting: a review of the literature. Department mines Ontario Canada, Research report PM184*. Also in *Foundry Trade Journal* (1956), 101, pp. 321–331.
- Dodd, R. A. (1955). *Hot Tearing of Binary Mg-Al and Mg-Zn Alloys*. Dept Mines Ontario Canada, Research Report PM191.
- Dodd, R. A., Pollard, W. A., & Meier, J. W. (1957). *TAFS*, 65, 100–117.

## RI-8 References

- Dong, S., Niyama, E., & Anzai, K. (1995). *ISIJ International*, 35, 730–736.
- Doremus, G. B., & Loper, C. R. (1970). *TAFS*, 78, 338–342.
- Doutre, D. (1998). Advances in Industrial Materials. In D. S. Wilkinson, W. J. Poole, & A. Alpes (Eds.), *The Metallurgical Soc of CIM*.
- Double, D. D., & Hellawell, A. (1974). *Acta Metallurgica*, 22, 481–487.
- Draper, A. B. (1976). *TAFS*, 84, 749–764.
- Draper, A. L., & Gaindhar, J. L. (1975). *TAFS*, 83, 593–616.
- Drezet, J. M., Commet, B., Fjaer, H. G., & Magnin, B. (2000). In P. R. Sahm, P. N. Hansen & J. G. Conley (Eds.), *Modeling of Casting, Welding and Advanced Solidification Processes IX*. (pp. 33–40).
- Drouzy, M., Jacob, S., & Richard, M. (1980). *Internat Cast Metals Journal*, 5(2), 43–45.
- Drouzy, M., & Mascré, C. (1969). *Metall Reviews*, 14, 25–46.
- Druschitz, A. P., & Chaput, W. W. (1993). *TAFS*, 101, 447–458.
- Durrans, I. (1981). Thesis, University of Oxford.
- Durville, P. H. G. (1913). *Brit Patent*, 23, 719.
- Eastwood, L. W. (1951). *AFS symposium on principles of gating* (pp. 25–30).
- Edelman, R. E., & Saia, A. (1968). *TAFS*, 76, 222–224.
- Edelson, B. J., & Baldwin, W. M. (1962). *Transactions of the ASM*, 55, 230.
- Einstein, A. (1906). *Ann Physik*, 19, 289 and 1911, 34, 591.
- El-Mahallawi, S., & Beeley, P. R. (1965). *British Foundryman*, 58, 241–248.
- Ellison, W., & Wechselblatt, P. M. (1966). *TAFS*, 74, 350–356.
- Emamy, G. M., Abbasi, R., Kaboli, S., & Campbell, J. (2009). ‘The fluidity of Al-based MMCs containing Al<sub>2</sub>O<sub>3</sub> and SiC particles’. *International Journal of Cast Metals Research*.
- Emamy, G. M., & Campbell, J. (1995). *International Journal of Cast Metals Research*, 8, 13–20.
- Emamy, G. M., & Campbell, J. (1995). *International Journal of Cast Metals Research*, 8, 115–122.
- Emamy, G. M., & Campbell, J. (1997). *Transactions of AFS*, 105, 655–663.
- Emamy, G. M., Kaboli, S., Razaghian, A., & Campbell, J. (2009). ‘The statistical analysis of tensile properties of A357/Al<sub>2</sub>O<sub>3</sub> MMCs’. *Materials Science & Technology*.
- Emamy, G. M., Taghiabadim, R., Mahmudi, M., & Campbell, J. (2002). *Statistical study of tensile properties of A356 aluminum alloy, using a new casting design. ASM 2nd Internat Al Casting Technology Symposium, 7–10 October 2002 Columbus Ohio*.
- Enright, N., Lu, S. Z., Hellawell, A., & Pilling, J. (2000). *TAFS*, 108, 157–162.
- Enright, P. (2001). Private communication.
- Enright, P., & Hughes, I. R. (November 1996). *The Foundryman*, 390–395.
- Evans, E. P. (1951). *BCIRA Journal*, 4,(319), 86–139.
- Evans, J., Runyoro, J., & Campbell, J. (1997). Solidification processing. In J. Beech, & H. Jones (Eds.) (pp. 74–78).  
Published by Dept. Engineering Materials, University of Sheffield.
- Fang, O. T., & Granger, D. A. (1989). *TAFS*, 97, 989–1000.
- Fasoyinu, F. A., Sadayappan, M., Cousineau, D., & Sahoo, M. (1998). *TAFS*, 106, 721–734.
- Fasoyinu, F. A., Sadayappan, M., Cousineau, D., Zavadil, R., & Sahoo, M. (1998). *TAFS*, 106, 327–337.
- Faubert, G. P., Moore, D. J., & Rundman, K. B. (1990). *TAFS*, 98, 831–845.
- Feest, E. A., McHugh, G., Morton, D. O., Welch, L. S., & Cook, I. A. (1983). ‘Solidification Technology in the Foundry and Cast House’, *Warwick University Conference 1980*. Metals Society Publication. pp. 232–239.
- Felberbaum, M., & Dahle, A. (2011). *Cast House Symposium*. San Diego, CA: TMS Annual Congress.
- Feliu, S. (1962). *TAFS*, 70, 838–844.
- Feliu, S. (1964). *TAFS*, 72, 129–137.
- Feliu, S., Flemings, M. C., & Taylor, H. F. (1960). *British Foundryman*, 53, 413–425.
- Feliu, S., Luis, L., Signin, D., & Alvarez, J. (1962). *TAFS*, 70, 838–844; (1964) 71, 145–157; (1964) 72, 129–137.

- Fenn, D., & Harding, R. A. (2002). University of Birmingham, UK, unpublished work.
- Fernandez, E., Musalem, P., Fava, J., & Flinn, R. A. (1970). *TAFS*, 78, 308–312.
- Feurer, U. (1976). *Giesserei*, 28, 75–80 (English translation by Alusuisse).
- Fischer, R. B. (1988). *TAFS*, 96, 925–944.
- Fisher, J. C. (1948). *Journal of Applied Physics*, 19, 1062–1067.
- Flemings, M. C. (1974). *Solidification Processing*. USA: McGraw-Hill.
- Flemings, M. C. (1963). In *30th International found congress Prague* (pp. 61–81) and *British Foundryman* (1964) 57, 312–325.
- Flemings, M. C., Conrad, H. F., & Taylor, H. F. (1959). *TAFS*, 67, 496–507.
- Flemings, M. C., & Nereo, G. E. (1967). *TMS-AIME*, 239, 1449–1461.
- Flemings, M. C., Kattamis, T. Z., & Bardes, B. P. (1991). *TAFS*, 99, 501–506.
- Flemings, M. C., Mollard, F. R., & Niyama, E. F. (1987). *TAFS*, 95, 647–652.
- Flemings, M. C., Niiyama, E., & Taylor, H. F. (1961). *TAFS*, 69, 625–635.
- Flemings, M. C., Poirier, D. R., Barone, R. V., & Brody, H. D. (April 1970). *Journal of the Iron and Steel Institute*, 371–381.
- Fletcher, A. J. (1989). *Thermal Stress and Strain Generation in Heat Treatment*. Elsevier.
- Flinn, R. A., Van Vlack, L. H., & Colligan, G. A. (1986). *TAFS*, 94, 29–46.
- Flood, S. C., & Hunt, J. D. (1981). *Metal Science*, 15, 287–294.
- Fomin, V. V., Stekol'nikov, G. A., & Omel'chenko, V. S. (1965). *Russian Castings Production*, 229–231.
- Fonda, R. W., Lauridsen, E. M., Ludwig, W., Tafforeau, P., & Spanos, G. (2007). *Metallurgical and Materials Transactions A*, 38A(11), 2721–2726.
- Forest, B., & Berovici, S., (1980). In *Solidification technology in the foundry and casthouse. Metals Society Conference Warwick, paper 93*, pp. 1–12.
- Forgac, J. M., Schur, T. P., & Angus, J. C. (1979). *Journal of Applied Mechanics*, 46, 83–89.
- Forslund, S. H. C. (1954). *21st International Foundry Congress*, Florence, paper 15.
- Forsyth, P. J. E. (1995). *Materials Science and Technology*, 11(3), 1025–1033.
- Forsyth, P. J. E. (1999). *Materials Science and Technology*, 15(3), 301–308.
- Forward, G., & Elliott, J. F. (1967). *Journal of Metals*, 19, 54–59.
- Fox, S., & Campbell, J. (2002). *International Journal of Cast Metals Research*, 14, 6.
- Franklin, A. G., Rule, G., & Widdowson, R. (September 1969). 1. *Iron Steel Institute*, 1208–1218.
- Fras, E., Gorny, M., & Lopez, H. F. (2007). *TAFS*, 115, 1–17.
- Fras, E., Wienczek, K., Gorny, M., & Lopez, H. F. (2007). *Metallurgical and Materials Transactions A*, 38A(2), 385–395.
- Frawley, I. J., Moore, W. F., & Kiesler, A. L. (1974). *TAFS*, 82, 561–570.
- French, A. R. (1957). *Institute of Metals Monograph & Report*, 22, 60–84.
- Freti, S., Bornand, J. D., & Buxmann, K. (June 1982). *Light Metal Age*, 12–16.
- Friebel, V. R., & Roe, W. P. (1963). *TAFS*, 71, 388–393.
- Fruehling, J. W., & Hanawalt, J. D. (1969). *TAFS*, 77, 159–590.
- Fredriksson, H. (1984). *Materials Science Engineering*, 65, 137–144.
- Fredriksson, H. (1996). 'Solidification Science and Processing'. In I. Ohnaka, & D. M. Stefanescu (Eds.). *The Minerals, Metals and Materials Society*.
- Fredriksson, H., Haddad-Sabzevar, M., Hansson, K., & Kron, J. (2005). *Materials Science & Technology*, 21(5), 521–529.
- Fredriksson, H., & Lehtinen, B. (1979). In *Solidification and Casting of Metals. Metals Society Conference* (pp. 260–267). Sheffield. Metals Soc.
- Frommeyer, G., Derder, C., & Jimenez, J. A. (2002). *Materials Science & Technology*, 18(9), 981–986.
- Fruehling, J. W., & Hanawalt, J. D. (1969). *TAFS*, 77, 159–164.

## RI-10 References

- Fuji, N., Fuji, M., Morimoto, S., & Okada, S. (1984). *Journal of Japan Institute of Light Metals*, 34(8), 446–453 (Met. Abstr. 51-1657).
- Fuji, M., Fuji, N., Morimoto, S., & Okada, S. (1986). *Journal of Japan Institute of Light Metals*, 36(6), 353–360 (Transl. NF 197).
- Fuoco, R., Correa, E. R., & Andrade Bastos, de, M. (1998). *TAFS*, 106, 401–409.
- Fuoco, R., Correa, E. R., & Correa, A. V. O. (1995). *TAFS*, 103, 379–387.
- Gadd, M. A., & Bennett, G. J. (1984). In H. Fredriksson, & M. Hillert, (Eds.). *The Physical Metallurgy of Cast Iron* North-Holland (p. 99).
- Gagne, M., & Goller, R. (1983). *TAFS*, 91, 37–46.
- Gagne, M., Paquin, M.-P., & Cabanne, P.-M. (2008). In *World Foundry Congress 68th* (pp. 101–106).
- Gall, K., Horstemeyer, M. F., van Schilfgaarde, M., & Baskes, M. I. (2000). *Journal of the Mechanics and Physics of Solids*, 48, 2183–2218.
- Gallois, B., Behi, M., & Panchal, J. M. (1987). *TAFS*, 95, 579–590.
- Gammelsaeter, R., Beck, K., & Johansen (1997). *Light Metals*, 1007–1011.
- Garbellini, O., Palacio, H., & Biloni, H. (1990). *Cast Metals*, 3(2), 82–90.
- Garcia-Garcia, O., Sanches-Araiza, M., Castro-Roman, M., & Escobedo, B. J. C. (2007). *Shape Casting: 2nd International Symposium*. In P. N. Crepeau, M. Tiryakioglu, & J. Campbell (Eds.), *TMS 2007* (pp. 109–116).
- Garnar, T. E. (1997). *TAFS*, 85, 399–416.
- Gebelin, J.-C., & Griffiths, W. D. (2007). *Proc 5th Decennial Internat Conference on Solidification Processing*. In H. Jones (Ed.) (pp. 512–516). UK: (SP07) Sheffield.
- Gebelin, J.-C., & Jolly, M. R. (2003). *Modeling of Casting, Welding and Solidification Processing Conference X*, Destin USA.
- Gebelin, J.-C., Jolly, M. R., & Jones, S. *INCAST* 13(11), (Dec) 22–27.
- Geffroy, P.-M., Lakehal, M., Goni, J., Beaugnon, E., Heintz, J.-M., & Silvain, J.-F. (2006). *Metallurgical and Materials Transactions A*, 37A, 441–447.
- Gelperin, N. B. (1946). *TAFS*, 54, 724–726.
- Genders, R., & Bailey, G. L. (1934). *The Casting of Brass Ingots*. The British Non-Ferrous Metals Research Association.
- Gentry, E. G. (1966). *TAFS*, 74, 142–129.
- Gernez, M. (1867). *Phil. Mag*, 33(4), 479.
- Geskin, F. S., Ling, E., & Weinstein, M. I. (1986). *TAFS*, 94, 155–158.
- Ghomashchi, M. R. (1995). *Journal of Materials Processing Technology*, 52, 193–206.
- Ghomashchi, M. R., & Chadwick, G. A. (1986). *Metals and Materials*, 477–482.
- Ghosh, S., & Mott, W. J. (1964). *Transactions of American Foundry Society*, 72, 721–732.
- Giese, S. R., Stefanescu, D. M., Barlow, J., & Pivonka, T. S. (1996). Part II. *TAFS*, 104, 1249–1257.
- Girshovich, N. G., Lebedev, K. P., & Nakhendzi Yu, A. (April 1963). *Russ. Castings Prodn*, 174–178.
- Giuranno, D., Ricci, E., Arato, E., & Costa, P. (2006). *Acta Materialia*, 54, 2625–2630.
- Glatz, J. (December 1996). *Materials Evaluation*, 1352–1362, *INCAST*, June 1997 1–7.
- Glenister, S. M. D., & Elliott, R. (1981). *Metal Science*, 15(4), 181–184.
- Godding, R. G. (1962). *BCIRA Journal*, 10(3), 292–297.
- Godlewski, L. A., & Zindel, J. W. (2001). *TAFS*, 109, 315–325.
- Goklu, S. M., & Lange, K. W. In *Proceedings conference process technology vol. 6 Washington USA April 1986* (pp. 1135-1146). Iron and Steel Society.
- Gonya, H. J., & Ekey, D. C. (1951). *TAFS*, 59, 253–260.
- Goodwin, F. E. (2008). *ASM Handbook*, pp. 1095–1099. Vol. 15 ‘Casting’.
- Goodwin, F. E. (2009). *Cast Metal & Diecasting Times*, 11(4), 14.

- Goria, C. A., Serramoglia, G., Caironi, G., & Tosi, G. (1986). *TAFS*, 94, 589–600 (these authors quote Kobzar A I, Ivanyuk E G; *Russian Castings Production* 1975, 7, 302–330).
- Gorshov, A. A. (1964). *Russian Castings Production*, 338–340.
- Gould, G. C., Form, G. W., & Wallace, J. F. (1960). *TAFS*, 68, 258–267.
- Gouwens, P. R. (1967). *TAFS*, 75, 401–407.
- Graham, A. L., Mizzi, B. A., & Pedicini, L. J. (1987). *TAFS*, 95, 343–350.
- Grandfield, J. F., Nguyen T. T., Rohan, P., & Nguyen, V. (2007). In Jones, H. (Ed.), *Proceedings 5th Decennial international conference on solidification processing (SP07) Sheffield, UK* (pp. 507–511).
- Gray, R. J., Perkins, A., & Walker, B. (1977). *Sheffield Conference 'Solidification & Casting of Metals'* (pp. 300–305) (published by Metals Soc 1979 Book 192).
- Grebe, W., & Grimm, G. P. (1967). *Aluminium*, 43, 673–683.
- Green, N. R. (1994). University of Birmingham UK, personal communication.
- Green, N. R. (1995). University of Birmingham UK, unpublished work.
- Green, N. R., & Campbell, J. (1993). *Materials Science and Engineering*, A173, 261–266.
- Green, N. R., & Campbell, J. (1994). *Transactions of AFS*, 102, 341–347.
- Green, R. A. (1990). *TAFS*, 98, 947–952.
- Green, R. A., & Heine (1990). *TAFS*, 98, 495–503.
- Greer, A. L., Bunn, A. M., Tronche, A., Evans, P. V., & Bristow, D. J. (2000). *Acta Materialia*.
- Greaves, R. H. (1936). In *ISI special report*, 15, 26–42.
- Grefhorst, C., & Crepaz, R. (2005). *Casting Plant and Technology International*, 1, 28–35.
- Griffiths, W. D., Cox, M., & Campbell, J. (2007). *Scholl G Materials Science and Technology*, 23(2), 137–144.
- Griffiths, W. D., & Lai, N. W. (2007). *Metallurgical and Materials Transactions A*, 38A, 190–196.
- Grill, A., & Brimacombe, J. K. (1976). *Ironmaking Steelmaking*, 3(2), 76.
- Grote, R. E. (1982). *TAFS*, 90, 93–102.
- Groteke, D. E. (1985). *TAFS*, 93, 953–960.
- Groteke, D. E. (2008). Personal communication to J.C.
- Grupke, C. C., Hunter, L. J., Leonard, C., Nath, R. H., & Weaver, G. J. (2011). *TAFS*, paper 11–036.
- Gruzleski, J., Handiak, N., Campbell, H., & Closset, B. (1986). *TAFS*, 94, 147–154.
- Gruznykh, I. V., & Nekhendzi Yu, A. (1961). *Russ. Castings Prodn*, 6, 243–245.
- Gurland, J. (1966). *AIME Transactions*, 236, 642–646.
- Gurland, J. (1979). *Application of the Hall-Petch Relation to particle Strengthening in Spherodized Steels and Aluminum-Silicon Alloys*. Proceedings of the 2nd Conf. on Strength of Metals and Alloys. pp. 621–625.
- Guthrie, R. I. L. (1989). *Engineering in Process Metallurgy*. Oxford UK: Clarendon Press.
- Guyen, Y. F., & Hunt, J. D. (1988). *Cast Metals*, 1(2), 104–111.
- Ha, M., Kim, W.-S., Moon, H.-K., Lee, B.-J., & Lee, S. (2008). *Metallurgical and Materials Transactions A*, 39(5), 1087–1098.
- Hadian, R., Emamy, M., & Campbell, J. (2009). The modification of cast Al-Mg<sub>2</sub>Si metal matrix composite by Li. *Metallurgical and Materials Transactions B*, 40(6), 822–832.
- Haginoya, I. (1976). *Journal of Japan Institute of Light Metals*, 26(3), 131–138, and *ibid.* 1981, 31, 769–774.
- Hall, F. R., & Shippen, J. (1994). *Engineering Failure Analysis*, 1(3), 215–229.
- Hallam, C. P., Griffiths, W. D., & Butler, N. D. (2000). In P. R. Sahm, P. N. Hansen, & J. G. Conley (Eds.), *Modeling of Casting, Welding and Advanced Solidification Processes IX*.
- Halvae, A., & Campbell, J. (1997). *TAFS*, 105, 35–46.
- Hammiti, F. G. (1974). In L. Bjorno (Ed.), *Finite-Amplitude Wave Effects in Liquids* (pp. 258–262). Proceedings 1973 Symposium Copenhagen: IPC Science and Technology Press, paper 3.10.
- Hansen, P. N. (1975). PhD thesis Part 2, Technical University of Denmark, Copenhagen 1975. (Lists 283 publications on hot tearing.)

## RI-12 References

- Hansen, P. N., & Rasmussen, N. W. (1994). In *BCIRA international conference*, UK: University of Warwick.
- Hansen, P. N., & Sahn, P. R. (1988). In A. F. Giamei, & G. J. Abbaschian (Eds.), *Modelling of Casting and Welding Processes IV*. The Mineral, Metals and Materials Society.
- Harding, R. A. (June 2006). *67th World foundry congress*, Paper 17. Harrogate, UK.
- Harding, R. A., Campbell, J., & Saunders, N. J. (1997). Inoculation of ductile iron. In J. Beech & H. Jones (Eds.), *Solidification processing 97 Sheffield conference 7–10 July 1997*.
- Harinath, U., Narayana, K. L., & Roshan, H. M. (1979). *TAFS*, 87, 231–236.
- Harper, S. (1966). *Journal Institute Metals*, 94, 70–72.
- Harris, K. P. (2004). *Foundry Practice (Foseco)*, 242(September), 01–07.
- Harris, K. P. (2005). Shape Casting: The JC Symposium. In M. Tiryakioglu & P. N. Creapeau (Eds.), *TMS annual congress, 2005*, pp. 433–442.
- Harris, K. P. (July 2005). *Modern Castings*, 36–38.
- Harsem, O., Hartvig, T., & Wintermark, H. (1968). *35th International foundry congress*. Kyoto, paper 15.
- Hart, R. G., Berke, N. S., & Townsend, H. E. (1984). *Metallurgical Transactions*, 15B, 393–395.
- Hartmann, D., & Stets, W. (2006). *TAFS*, 114, 1055–1058.
- Hartung, C., Ecob, C., & Wilkinson, D. (2008). *Casting Plant & Technology*, 2, 18–21.
- Hassell, H. J. (1980). *British Foundryman*, 73(4), 95.
- Hayes, J. S., Keyte, R., & Prangnell, P. B. (2000). *Materials Science & Technology*, 16, 1259–1263.
- Hayes, K. D., Barlow, J. O., Stefanescu, D. M., & Piwonka, T. S. (1998). *TAFS*, 106, 769–776.
- Hebel, T. E. (1989). *Heat Treating*. USA: Fairchild Business Publication.
- Hedjazi, D., Bennett, G. H. J., & Kondic, V. (1975). *British Foundryman*, 68, 305–309.
- Hedjazi, D. J., Bennett, G. H. J., & Kondic, V. (December 1976). *Metals Technology*, 537–541.
- Heine, H. J., & Heine, R. W. (1968). *TAFS*, 76, 470–484.
- Heine, R. W. (1951). *TAFS*, 59, 121–138.
- Heine, R. W. (1968). *TAFS*, 76, 463–469.
- Heine, R. W. (1982). *TAFS*, 90, 147–158.
- Heine, R. W., & Green, R. A. (1989). *TAFS*, 97, 157–164.
- Heine, R. W., & Green, R. A. (1992). *TAFS*, 100, 499–508.
- Heine, R. W., Green, R. A., & Shih, T. S. (1990). *TAFS*, 98, 245–252.
- Heine, R. W., & Loper, C. R. (1966a). *TAFS*, 74, 274–280.
- Heine, R. W., & Loper, C. R. (1966b). *TAFS*, 74, 421–428, and *British Foundryman* (1967), 60, 347–353.
- Heine, R. W., & Rosenthal, P. C. (1955). *Principles of Metal Casting*. NY, USA: McGraw-Hill Book Co Inc + AFS.
- Heine, R. W., & Uicker, J. J. (1983). *TAFS*, 91, 127–136.
- Heine, R. W., Uicker, J. J., & Gantenbein, D. (1984). *TAFS*, 92, 135–150.
- Henschel, C., Heine, R. W., & Schumacher, J. S. (1966). *TAFS*, 74, 357–364.
- Hernandes-Reyes, B. (1989). *TAFS*, 97, 529–538.
- Herrera, A., & Kondic, V. (1979). In *Solidification and Casting of Metals. Conference* (pp. 460–465). Sheffield, 1977: Metals Society London.
- Hess, K. (1974 March). *AFS Cast Metals Research Journal*, 6–14.
- Hetke, A., & Gundlach, R. B. (1994). *TAFS*, 102, 367–380.
- Heusler, L., Feikus, F. J., & Otte, M. O. (2001). *TAFS*, 109, 215–223.
- Heyn, E. (1914). *Journal of Institute Metals*, 12, 3.
- Hill, H. N., Barker, R. S., & Willey, L. A. (1960). *Transactions of American Society Metals*, 52, 657–671.
- Hillert, M. (1968). Recent Research on Cast Iron. In H. D. Merchant (Ed.) (pp. 101–127). Gordon and Breach NY.
- Hillert, M., & Steinhauser, H. (1960). *Jernkontorets Ann*, 144, 520–522.

- Hiratsuka, S., Niyama, E., Funakubo, T., & Anzai, K. (1994). *Transactions of Japan Foundryman's Society*, 13(11), 18–24.
- Hiratsuka, S., Niyama, E., Anzai, K., Hori, H., & Kowata, T. (1966). *4th Asian foundry congress* (pp. 525–531).
- Hiratsuka, S., Niyama, E., Horie, H., Kowata, T., Anzai, K., & Nakamura, M. (1998). *International Journal of Cast Metals Research*, 10(4), 201–205.
- Hirt, C. W. (2003). www.flow3d.com
- Ho, K., & Pehlke, R. D. (1984). *TAFS*, 92, 587–598.
- Ho, P. S., Kwok, T., Nguyen, T., Nitta, C., & Yip, S. (1985). *Scripta Metal*, 19(8), 993–998.
- Hoar, T. P., & Atterton, D. V. (1950). *Journal of Iron & Steel Institute*, 166, 1–7.
- Hoar, T. P., Atterton, D. V., & Houseman, D. H. (1953). *Journal of Iron & Steel Institute*, 175, 19–29.
- Hoar, T. P., Atterton, D. V., & Houseman, D. H. (1956). *Metallurgia*, 53, 21–25.
- Hochgraf, F. G. (1976). *Metallography*, 9, 167–176.
- Hodaj, F., & Durand, F. (1997). *Acta Materialia*, 45, 2121.
- Hodjat, Y., & Mobley, C. E. (1984). *TAFS*, 92, 319–321.
- Hoff, O., & Andersen, P. (1968). In *35th International foundry congress*, Kyoto, paper 8.
- Hoffman, E., & Wolf, G. (2001). *Giessereiforschung*, 53(4), 131–151.
- Hofmann, F. (1962). *TAFS*, 70, 1–12.
- Hofmann, F. (1966). *AFS Cast Metals Research Journal*, 2(4), 153–165.
- Hofmann, J. (2001). *Foundry Trade Journal*, 175(3578), 32–34.
- Hofmann, R., & Wittmoser, A. (1971). U.S. Patents 3619866 and 3620286 (16 Nov 1971).
- Holt, G. S., Mitchell, C. J., & Simmons, R. E. (July 1989). *BCIRA Report 1779; and BCIRA Journal*, 291–296.
- Holtzer, M. (March 1990). *The Foundryman*, 135–144.
- Hoult, F. H. (1979). *Transactions of AFS* 87, 237–240 and 241–244.
- Howe Sound Co – Superalloy Group USA 1965 British Patent 1,125,124.
- Hu, D., & Loretto, M. H. (2000). University of Birmingham, UK, personal communication.
- Hsu, W., Jolly, M. R., & Campbell, J. (2003).
- Hua, C. H., & Parlee, N. A. D. (1982). *Metallurgical Transactions*, 13B, 357–367.
- Huang, J., & Conley, J. G. (1998). *TAFS*, 106, 265–270.
- Huang, H., Lodhia, A. V., & Berry, J. T. (1990). *TAFS*, 98, 547–552.
- Huang, L. W., Shu, W. J., & Shih, T. S. (2000). *TAFS*, 108, 547–560.
- Huber, G., Brechet, Y., & Pardoën, T. (2005). *Acta Materialia*, 53, 2739–2749.
- Hughes, I. C. H. (1988). *Metals Handbook Vol. 15 Casting*. Ohio, USA: ASM, 647–666.
- Hultgren, A., & Phragmen, G. (1939). *Transactions of AIME*, 135, 133–244.
- Hull, D. R. (1950). *Castings of Brass and Bronze*. ASM.
- Hummer, R. (1988). *Cast Metals*, 1(2), 62–68.
- Hunsicker, H. Y. (1980). *Metallurgical Transactions*, 11A, 759–773.
- Hunt, J. D. (1980). University of Oxford, personal communication.
- Hunt, J. D., & Thomas, R. W. (1997). Proceedings 4th Decennial International Conference on Solidification Processing (SP97). In J. Beech, & H. Jones (Eds.) (pp. 350–353). UK: University of Sheffield.
- Hurum, F. (1952). *TAFS*, 60, 834–848.
- Hurum, F. (1965). *TAFS*, 73, 53–64.
- Hutchinson, H. P. (1965). Sutherland D. S. *Nature*, 206, 1036–1037.
- IBF Technical Subcommittee TS 17. (1948). *Symposium Internal Stresses in Metals and Alloys, London 1947*. Institute of Metals, pp. 179–188.
- IBF Technical Subcommittee TS 18. (1949). *Proceedings IBF*, 42, A61–A77.



## RI-14 References

- IBF Technical Subcommittee TS 32. (1952). *British Foundryman*, 45, A48–A56. *Foundry Trade Journal*, 93, 471–477.
- IBF Technical Subcommittee TS 32. (1956). *Foundry Trade Journal*, 101, 19–27.
- IBF Technical Subcommittee TS 32. (1960). *British Foundryman*, 53, 10–13 (but original work reported in *British Foundryman* 1952, 45, A48–A56).
- IBF Technical Subcommittee TS 35. (1960). *British Foundryman*, 53, 15–20.
- IBF Technical Subcommittee TS 61. (1964). *British Foundryman*, 57, 75–89, 504–508.
- IBF Technical Subcommittee TS 71. (1969). *British Foundryman*, 62, 179–196.
- IBF Technical Subcommittee TS 71. (1971). *British Foundryman*, 64, 364–379.
- IBF Technical Subcommittee TS 71. (1976). *British Foundryman*, 69, 53–60.
- IBF Technical Subcommittee TS 71. (1979). *British Foundryman*, 72, 46–52.
- Iida, T., & Guthrie, R. I. L. (1988). *The Physical Properties of Liquid Metals*. Oxford: Clarendon Press, p. 14.
- Impey, S., Stephenson, D. J., & Nicholls, J. R. (1993). *Microscopy of Oxidation 2. Cambridge conference*, pp. 323–337.
- International Magnesium Association (2006). 'Alternatives to SF<sub>6</sub> for magnesium melt protection.' EPA-430-R-06-007.
- Ionescu, V. (2002). *Modern Castings*, 92(5), 21–23.
- Isaac, J., Reddy, G. P., & Sharman, G. K. (1985). *TAFS*, 93, 29–34.
- Isawa, T. (1993). 'The control of the initial fall of liquid metal in gravity filled casting systems.' PhD thesis, University of Birmingham, Department of Metallurgy and Materials Science.
- Isawa, T., & Campbell, J. (1994). *Transactions of Japan Foundrymen's Society*, 13(Nov), 38–49.
- ISO Standard 8062. (1984). Castings – System of Dimensional Tolerances.
- Isobe, T., Kubota, M., & Kitaoka, S. (1978). *Journal of Japan Foundry Society*, 50(11), 671–676.
- Itamura, M., Murakami, K., Harada, T., Tanaka, M., & Yamamoto, N. (2002). *International Journal of Cast Metals Research*, 15, 167–172.
- Itamura, M., Yamamoto, N., Niyama, E., & Anzai, K. (1995). In Z. H. Lee, C. P. Hong, & M. H. Kim (Eds.). *Proceedings 3rd Asian foundry congress* (pp. 371–378).
- Itofugi, H. (1996). *TAFS*, 104, 79–87.
- Itofugi, H., & Uchikawa, H. (1990). *TAFS*, 98, 429–448.
- Iyengar, R. K., & Philbrook, W. O. (1972). *Metallurgical Transactions*, 3, 1823–1830.
- Jackson, K. A., Hunt, J. D., Uhlmann, D. R., & Seward, T. P. (1966). *AIME Transactions*, 236, 149–158.
- Jackson, R. S. (1956). *Foundry Trade Journal*, 100, 487–493.
- Jackson, W. J. (April 1972). *Iron and Steel*, 163–172.
- Jackson, W. J., & Wright, J. C. (September 1977). *Metals Technology*, 425–433.
- Jacob, S., & Drouzy, M. (1974). *International Foundry Congress 41 Liege, Belgium*. Paper 6.
- Jacobi, H. (1976). *Arch. Eisenhüttenwesen*, 47, 441–446.
- Jacobs, M. H., Law, T. J., Melford, D. A., & Stowell, M. J. (1974). *Metals Technology*, 1(11), 490–500.
- Jaquet, J. C. (1988). In *8th Colloque Europeen de la Fonderie des Metaux Non Ferreux du CAEF*.
- Jay, R., & Cibula, A. (1956). *Proc. Inst. Br. Found.*, 49, A126–A140.
- Jayatilaka, A., de, S., & Trustrum, K. (1977). *Journal of Material Science*, 12, 1426.
- Jeancolas, M., & Devaux, H. (1969). *Fonderie*, 285, 487–499.
- Jeancolas, M., Devaux, H., & Graham, G. (1971). *British Foundryman*, 64, 141–154.
- Jelm, C. R., & Herres, S. A. (1946). *Transactions of American Foundrymen's Association*, 54, 241–251.
- Jian, X., Xu, C., Meek, T., & Han, Q. (2005). *TAFS*, 113, 131–138.
- Jiang, H., Bowen, P., & Kntt, J. F. (1999). *Journal of Materials Science*, 34, 719–725.
- Jianzhong, L. (1989). *TAFS*, 97, 31–34.
- Jirsa, J. (1982). *Foundry Trade Journal* (Oct 7), 520–527.

- Jiyang, Z., Schmidt, W., & Engler, S. (1990). *TAFS*, 98, 783–786.
- Jo, C.-Y., Joo, D.-W., & Kim, I.-B. (2001). *Materials Science and Technology*, 17, 1191–1196.
- Johnson, A. S., & Nohr, C. (1970). *TAFS*, 78, 194–207.
- Johnson, R. A., & Orlov, A. N. (1986). *Physics of Radiation Effects in Crystals*. Elsevier North Holland.
- Johnson, S. B., & Loper, C. R. (1969). *TAFS*, 77, 360–367.
- Johnson, T. V., Kind, H. C., Wallace, J. F., Nieh, C. V., & Kim, H. J. (1989). *TAFS*, 97, 879–886.
- Johnson, W. C., & Smart, H. B. (1977). 'Solidification and Casting of Metals' *Sheffield Conf.*, pp. 125–130. Metals Soc Publication, 192, 1979.
- Johnson, W. H., & Baker, W. O. (1948). *TAFS*, 56, 389–397.
- Jolly, M. J., Lo, H. S. H., Turan, M., Campbell, J., & Yang, X. (2000). In P. R. Sahm, P. N. Hansen, & J. G. Conley (Eds.), *Modeling of Casting, Welding and Advanced Solidification Processing IX Aachen*.
- Jones, D. R., & Grim, R. E. (1959). *TAFS*, 67, 397–400.
- Jones, S. G. (April 1948). *American Foundryman*, 139.
- Jorstad, J. L. (1971). *TAFS*, 79, 85–90.
- Jorstad, J. L. (1996). *TAFS*, 104, 669–671.
- Kahl, W., & Fromm, E. (1984). *Aluminium*, 60(9), E581–E586.
- Kahl, W., & Fromm, E. (1985). *Metallurgical Transactions B*, 16B(3), 47–51.
- Kahn, P. R., Su, W. M., Kim, H. S., Kang, J. W., & Wallace, J. F. (1987). *TAFS*, 95, 105–116.
- Kaiser, G. (1966). *Berichte der Bunsengesellschaft für Physikalische Chemie*, 70(6), 635–639.
- Kaiser, W. D., & Groenveld, T. P. (1975). *8th Internat die casting congress, Detroit, Michigan, USA* (pp. 1–9), paper number G-T75-084.
- Kallbom, R., Hamberg, K., Wessen, M., & Bjorkegren, L. E. (2005). *Materials Science Engineering A*, A413–A414, 346–351.
- Kallbom, R., Hamberg, K., & Bjorkegren, L.-E. (2006). *World foundry congress, Harrogate, UK*, paper 184/1–10.
- Karsay, S. I. (1971). *Ductile Iron II; Engineering Design Properties Applications*. Canada: Quebec Iron & Titanium (QIT) Corporation.
- Karsay, S. I. (1980). *Ductile Iron: the state of the art 1980*. Canada: QIT-Fer et Titane Inc.
- Karsay, S. I. (1985). *Ductile Iron Production Practices*. Published by AFS.
- Karsay, S. I. (1992). *Ductile Iron Production Practices; the state of the art 1992 QIT Fer et Titane Inc. Canada; and 'Ductile Iron; the essentials of gating and risering system design' revised 2000*. Published by Rio Tinto Iron & Titanium Inc.
- Kaspersma, J. H., & Shay, R. H. (1982). *Metallurgical Transactions*, 13B, 267–273.
- Katgerman, L. (1982). *Journal of Metals*, 34(2), 46–49.
- Kasch, F. E., & Mikeloms, P. L. (1969). *TAFS*, 77, 77–89.
- Kato, E. *Metallurgical and Materials Transactions A*, 30A (September) 2449–2453.
- Kay, J. M., & Nedderman, R. M. (1974). *An Introduction to Fluid Mechanics and Heat Transfer* (3rd ed.). CUP. pp. 115–119.
- Kearney, A. L., & Raffin, J. (1987). *Hot Tear Control Handbook for Aluminium Foundrymen and Casting Designers*. USA: American Foundrymen's Soc., Des Plaines Illinois.
- Khalili, A., & Kromp (1991). *Journal of Material Science*, 26, 6741–6752.
- Khan, P. R., Su, W. M., Kim, H. S., Kang, J. W., & Wallace, J. F. (1987). *TAFS*, 95, 105–116.
- Kiessling, R. (1987). *Non-metallic inclusions in steel*. The Metals Society.
- Kihlstedt, D. (1988). *ASM Metals Handbook, Vol. 15, 273–274, Casting*.
- Kilshaw, J. A. (1963). *BCIRA Journal*, 11, 767.
- Kilshaw, J. A. (1964). *BCIRA Journal*, 12, 14.
- Kim, M. H., Loper, C. R., & Kang, C. S. (1985). *TAFS*, 93, 463–474.
- Kim, M. H., Moon, J. T., Kang, C. S., & Loper, C. R. (1993). *TAFS*, 101, 991–998.

## RI-16 References

- Kim, S. B., & Hong, C. P. (1995). *Modeling of casting, welding and advanced solidification processes VII* (pp. 155–162). TMS.
- Kirner, J. F., Anewalt, M. R., Karwacki, E. J., & Cabrera, A. L. (1988). *Metallurgical Transactions*, 19A, 3045–3055.
- Kita, K. (1979). *AFS Internat Cast Metals Journal*, 4(4), 35–40.
- Kitaoka, S. (2001). *Conference: Light Metals (Metaux Legers): International Symposium on Light Metals as held at the 40th Annual Conference of Metallurgists of CIM (COM 2001), Toronto, Ontario, Canada, 26–29 August 2001*. Canada: Published by Canadian Institute of Mining, Metallurgy and Petroleum, Xerox Tower Suite 1210 3400 de Maisonneuve Blvd. W, Montreal, PQ, Quebec H3Z 3B8, pp. 13–24.
- Klemp, T. (1989). *TAFS*, 97, 1009–1024.
- Knott, J. F., & Elliott, D. (1979). *Worked Examples in Fracture Mechanics. Inst. Metals Monograph 4*. London: Inst. Metals.
- Kokai, K. (1985). Japan patent application by Toyota 60 54244, 28 March 1985.
- Kolorz, A., & Lohborg, K. (1963). In *30th International foundry congress* (pp. 225–246.)
- Kolsgaard, A., & Brusethaug, S. (1994). *Materials Science & Technology*, 10(6), 545–551.
- Kondic, V. (1959). *Foundry*, 87, 79–83.
- Kono, R., & Miura, T. (1975). *British Foundryman*, 69, 70–78.
- Koster, W., & Goebing, K. (1941). *Giesserei*, 28(26), 521.
- Kotschi, T. P., & Kleist, O. F. (1979). *AFS International Cast Metals Journal*, 4(3), 29–38.
- Kotschi, R. M., & Loper, C. R. (1974). *TAFS*, 82, 535–542.
- Kotschi, R. M., & Loper, C. R. (1975). *TAFS*, 83, 173–184.
- Kotsyubinskii, O., & Yu. (1961–62). *Russian Castings Production*, 269–272.
- Kotsyubinskii, O., & Yu. (1963). In *30th International Foundry Congress*. (pp. 475–487).
- Kotsyubinskii, O., Yu, Gerchikov, A. M., Uteshev, R. A., & Novikov, M. I. (1961). *Russian Castings Production*, 8, 365–368.
- Kotsyubinskii, O., Yu, Oberman Ya, I., & Gerchikov A. M. (1962). *Russian Castings Production*, 4, 190–191.
- Kotsyuhinskii, O., Yu, Oberman Ya, I., & Gini, E. Gh. (1968). *Russian Castings Production*, 4, 171–172.
- Kotzin, E. L. (1981). *Metalcasting and Molding Processes*. Des Plaines, Illinois, USA: American Foundrymen's Soc.
- Krinitzky, A. I. (1953). *TAFS*, 61, 399–410.
- Kron, J., Bellet, M., Ludwig, A., Pustal, B., Wendt, J., & Fredriksson, H. (2004). *International Journal of Cast Metals Research*, 17(5), 295–310.
- Kruse, B. L., Richards, V. L., & Jackson, P. D. (2006). *TAFS*, 114, 783–795.
- Kubo, K., & Pehlke, R. D. (1985). *Metallurgical Transactions*, 16B, 359–366.
- Kubo, K., & Pehlke, R. D. (1986). *Metallurgical Transactions*, 17B, 903–911.
- Kujanpaa, V. P., & Moisio, T. J. I. (1980). *Solidification technology in the foundry and cast house, Warwick Conference* (pp. 372–375) (Metals Soc 1983).
- Kulas, M.-A., Green, W. P., Taleff, E. M., Krajewski, P. E., & McNelly, T. R. (2006). *Metallurgical & Materials Transactions A*, 37A, 645–655.
- Kunes, J., Chaloupka, L., Trkovsky, V., Schneller, J., & Zuzanak, A. (1990). *TAFS*, 98, 559–563.
- Kuyucak, S. (2002). *TAFS*, 110.
- Kuyucak, S. (February 2008). *68th World foundry congress*, pp. 483–487.
- Lagowski, B. (1967). *TAFS*, 75, 229–256.
- Lagowski, B. (1979). *TAFS*, 87, 387–390.
- Lagowski, B., & Meier, J. W. (1964). *TAFS*, 72, 561–574.

- Lai, N.-W., Griffiths, W. D., & Campbell, J. (2003). In D. M. Stefanescu, J. A. Warren, M. R. Jolly, & M. J. M. Krane (Eds.), *Modeling of casting, welding and solidification processes-X* (pp. 415–422).
- Laid, E. (1978). U.S. Patent application 16 Feb 1978 Number 878,309.
- Lalpoor, M., Eskin, D. G., & Katgerman, L. (2009). *Metallurgical & Materials Transactions A*, 40A(13), 3304–3313.
- Lalpoor, M., Eskin, D. G., & Katgerman, L. (2010). *Metallurgical & Materials Transactions A*, 41A(9), 2425–2434.
- Lane, A. M., Stefanescu, D. M., Piwonka, T. S., & Pattabhi, R. (1969). *Modern Castings* (October), 54–55.
- Lang, G. (1972). *Aluminium*, 48(10), 664–672.
- Larranaga, P., Asenjo, I., Sertucha, J., Suarez, R., Ferrer, I., & Lacaze, J. (2009). *Metallurgical & Materials Transactions A*, 40A, 654–661.
- Latimer, K. G., & Read, P. J. (1976). *British Foundryman*, 69, 44–52.
- LaVelle, D. L. (1962). *TAFS*, 70, 641–647.
- Lawrence, M. (February 1990). *Modern Castings*, 51–53.
- Ledebur, A. (1882). *Stahl und Eisen*, 2, 591.
- Leduc, L., Nadarajah, T., & Sellars, C. M. (July 1980). *Metals Technology*, 269–273.
- Lee, R. S. (1987). *TAFS*, 95, 875–882.
- Lees, D. C. G. (1946). *Journal of the Institute of Metals*, 72, 343–364.
- Lerner, Y., & Aubrey, L. S. (2000). *TAFS*, 108, 219–226.
- Lerner, S. Y., & Kouznetsov, V. E. (2004). *Modern Castings* (May), 37–41.
- Leth-Olsen, H., & Nisancioglu, K. (1998). *Corrosion Science*, 40, 1179–1194, and 1194–1214.
- Lett, R. L., Felicelli, S. D., Berry, J. T., Cuesta, R., & Losua, D. (2009). *TAFS*, 8, paper 09-043.
- Levelink, H. O. (1972). *TAFS*, 80, 359–368.
- Levelink, H. G., & van den Berg, H. (1962). *TAFS*, 70, 152–163.
- Levelink, H. G., & van den Berg, H. (1968). *TAFS*, 76, 241–251.
- Levelink, H. O., & van den Berg, H. (1971). *TAFS*, 79, 421–432.
- Levelink, H. O., & Julien, F. P. M. A. (June 1973). *AFS Cast Metals Research Journal*, pp. 56–63.
- Lewis, G. M. (1961). *Proceedings of the Physical Society (London)*, 71, 133.
- Li, Y., Jolly, M. R., & Campbell, J. (1998). Modeling of Casting, Welding and Advanced Solidification Processes VIII. In B. G. Thomas, & C. Beckermann (Eds.), *The Minerals, Metals and Materials Society* (pp. 1241–1253).
- Li, Y. X., Liu, B. C., & Loper, C. R. (1990). *TAFS*, 98, 483–488.
- Liass, A. M. (1968). *Foundry Trade Journal*, 124, 3–10.
- Liass, A. M., Borsuk. (18 Dec 1962) French Patent 1342529.
- Liddiard, E. A. G., & Baker, W. A. (1945). *TAFS*, 53, 54–65.
- Lin, H. J., & Hwang, W.-S. (1988). *TAFS*, 96, 447–458.
- Lin, J., Sharif, M. A. R., & Hill, J. L. (1999). *Aluminum Transactions*, 1(1), 72–78.
- Lind, M., & Holappa, L. (2010). *Metallurgical & Materials Transactions B*, 41B, 359–366.
- Ling, Y., Mampaey, F., Degrieck, J., & Wettinck, E. (2000). In P. R. Sahm, P. N. Hansen & J. G. Conley (Eds.), *Modeling of casting, welding and advanced solidification processes IX* (pp. 357–364).
- Liu, F., Zhao, D. W., & Yang, G. C. (2001). *Metallurgical & Materials Transactions B*, 32B, 449–460.
- Liu, L., Samuel, A. M., Samuel, F. H., Dowty, H. W., & Valtierra, S. (2002). The role of Sr oxide on porosity. *Transactions of AFS*, 110, 449–462.
- Liu, L., Samuel, A. M., Samuel, F. H., Doty, H. W., & Valtierra, S. (2003). The role of Fe in Sr-modified 319 and 356. *Journal of Materials Science*, 38, 1255–1267.
- Liu, L., Samuel, A. M., Samuel, F. H., Doty, H. W., & Valtierra, S. (2003). *International Journal of Cast Metals Research*, 16(4), 397–408.
- Liu, P. C., Li, C. L., Wu, D. H., & Loper, C. R. (1983). *TAFS*, 91, 119–126.

## RI-18 References

- Liu, P. C., Loper, C. R., Kimura, T., & Park, H. K. (1980). *TAFS*, 88, 97–118.
- Liu, S., & Loper, C. R. (1990). *TAFS*, 98, 385–394.
- Liu, S. L., Loper, C. R., & Witter, T. H. (1992). *TAFS*, 100, 899–906.
- Livingston, H. K., & Swingley, C. S. (1971). *Surface Science*, 24, 625–634.
- Llewellyn, G., & Ball, J. I. (1962). GB Patent application, Complete published 1965, 987,060.
- Lo, H., & Campbell, J. (2000). In P. R. Sahm, P. N. Hansen, & J. G. Conley (Eds.), *Modeling of Casting, Welding and Advanced Solidification Processes IX* (pp. 373–380).
- Locke, C., & Ashbrook, R. L. (1950). *TAFS*, 58, 584–594.
- Locke, C., & Ashbrook, R. L. (1972). *TAFS*, 80, 91–104.
- Locke, C., & Berger, M. J. (1951). The flow of steel in sand molds Part II. In *America research report, Steel Founders Society* 25.
- Longden, E. (1931–32). *Proceedings of IBF*, 25, 95–145.
- Longden, E. (1939–40). *Proceedings of IBF*, 33, 77–107.
- Longden, E. (1947–48). *Proceedings of IBF*, 41, A152–A165.
- Longden, E. (1948). *TAFS*, 56, 36–56.
- Loper, C. R. (1981). *TAFS*, 89, 405–408.
- Loper, C. R. (1992). *TAFS*, 100, 533–538.
- Loper, C. R. (1999). *TAFS*, 107, 523–528.
- Loper, C. R., & Fang, K. (2008). *TAFS*, paper 08-065 (05) pp. 8.
- Loper, C. R., & Heine, R. W. (1961). *TAFS*, 69, 583–600.
- Loper, C. R., & Heine, R. W. (1968). *TAFS*, 76, 574–554.
- Loper, C. R., Javaid, A., & Hitchings, J. R. (1996). *TAFS*, 104, 57–65.
- Loper, C. R., & Kotschi, R. M. (1974). *TAFS*, 82, 279–284.
- Loper, C. R., & LeMahieu, D. L. (1971). *TAFS*, 79, 483–492.
- Loper, C. R., & Miskinis. (1985). *TAFS*, 93, 545–560.
- Loper, C. R., & Newby, M. R. (1994). *TAFS*, 102, 897–901.
- Loper, C. R., & Saig, A. G. (1976). *TAFS*, 84, 765–768.
- Low, J. R. (1969). *Transactions of AIME*, 245, 2481–2494.
- Lubulin, I., & Christensen, R. J. (1960). *TAFS*, 68, 539–550.
- Lukens, M. C., Hou, T. X., & Pehlke, R. D. (1990). *TAFS*, 98, 63–70.
- Lukens, M. C., Hou, T. X., Purvis, A. L., & Pehlke, R. D. (1991). *TAFS*, 99, 445–449.
- Lumley, R. N., Sercombe, T. B., & Schaffer, G. B. (1999). *Metallurgical & Materials Transactions*, 30A, 457–468.
- Ma, Z., Samuel, A. M., Samuel, F. H., Doty, H. W., & Valtierra, S. (2008). *Materials Science and Engineering, A* 490, 36–51.
- Mae, Y., & Sakonooka, A. (1985). *Metallurgical Society of AIME*. TMS Paper 0197, pp. 7. (U.S. Patent 4808243 1987).
- Maeda, Y., Nomura, H., Otsuka, Y., Tomishige, H., & Mori, Y. (2002). *Internat Journal Cast Metals Research*, 15, 441–444.
- Maidment, L. J., Walter, S., & Raul, G. (1984). Detroit: 8th Heat Treating Conf.
- Malzer, G., Hayes, R. W., Mack, T., & Egglar, G. (2007). *Metallurgical & Materials Transactions A*, 38A(2), 314–327.
- Mampaey, F. (1999). *TAFS*, 107, 425–432.
- Mampaey, F. (2000). *TAFS*, 108, 11–17.
- Mampaey, F., & Beghyn, K. (2006). *TAFS*, 114, 637–656.
- Mampaey, F., Habets, D., Plessers, J., & Seutens, F. (2008). *International Foundry Research/Geissereiforschung*, 60(1), 2–19.

- Mampaey, F., & Xu, Z. A. (1997). *TAFS*, 105, 95–103.
- Mampaey, F., & Xu, Z. A. (1999). *TAFS*, 107, 529–536.
- Mandal, B. P. (2000). *Indian Foundry Journal*, 46(4), 25–28.
- Mansfield, T. L. (1984). Proc Conf ‘Light Metals’. *Metallurgical Society of AIME*, 1305–1327.
- Manzari, M. T., Lewis, R. W., & Gethin, D. T. (2000). ‘Optimum design of chills in sand casting process’. *Proceedings of IMECE 2000 International mechanical engineering congress Florida, USA DETC98/DAC-1234 ASME* (p. 8).
- Marck, C. T., & Keskar, A. R. (1968). *TAFS*, 76, 29–43.
- Marin, T., & Utigard, T. (2010). *Metallurgical & Materials Transactions B*, 41B(3), 535–542.
- Mariotto, C. L. (1994). *TAFS*, 102, 567–573.
- Martin, L. C. B., Keller, C. T., & Shivkumar, S. (1992). *3rd Internat Conf on Molten Aluminum Processing*. Orlando, FL: AFS, 79–91.
- Mathier, V., Grasso, P.-D., & Rappaz, M. (2008). *Metallurgical & Materials Transactions*, 39A, 1399–1409.
- Mathier, V., Vernede, S., Jarry, P., & Rappaz, M. (2009). *Metallurgical & Materials Transactions A*, 40A(4), 943–957.
- Matsubara, Y., Suga, S., Trojan, P. F., & Flinn, R. A. (1972). *TAFS*, 80, 37–44.
- Matsuda, M., & Ohmi, M. (1981). *AFS International Journal of Cast Metals*, 6(4), 18–27.
- Majumdar, I., & Raychaudhuri, B. C. (1981). *International Journal of Heat and Mass Transfer*, 24(7), 1089–1095.
- Maske, F., & Piwowarsky, E. (1929). *Foundry Trade Journal*, (March 28), 233–243.
- Mazed, S., & Campbell, J. (1992). Univ Birmingham, UK; unpublished work.
- McCartney, D. G. (1989). *International Materials Reviews*, 34(5), 247–260.
- McClain, S. T., McClain, A. S., & Berry, J. T. (2001). *TAFS*, 109, 75–86.
- McDavid, R. M., & Dantzig, J. (1998). *Metallurgical & Materials Transactions*, 29B, 679–690.
- McDonald, R. J., & Hunt, J. D. (1969). *AIME Transactions*, 245, 1993–1997.
- McDonald, R. I., & Hunt, J. D. (1970). *AIME Transactions*, 1, 1787–1788.
- McGrath, C., & Fischer, R. B. (1973). *TAFS*, 81, 603–620.
- McKim, P. E., & Livingstone, K. E. (1977). *TAFS*, 85, 491–498.
- McParland, A. J. (1987). ‘Solidification processing’ Institute of Metals, London 1988. In *Sheffield conference* (pp. 323–326).
- Medvedev Ya, I., & Kuzukov, V. K. (1966). *Russian Castings Production*, 263–266.
- Melendez, A. J., Carlson, K. D., & Beckermann, C. (2010). *International Journal of Cast Metals Research*, 23(5), 278–288.
- Mendelson, S. J. (1962). *Applied Physics*, 33(7), 2182–2186.
- Metcalf, G. J. (1945). *Journal Institute of Metals* (1029), 487–500.
- Mertz, J. M., & Heine, R. W. (1973). *TAFS*, 81, 493–495.
- Merz, R., & Marincek, B. (1954). *21st International foundry congress*. Paper 44, pp. 1–7.
- Meyers, C. W. (1986). *TAFS*, 94, 511–518.
- Mi, J., Harding, R. A., & Campbell, J. (2002). *International Journal of Cast Metals Research*, 14(6), 325–334.
- Micks, F. W., & Zabek, V. J. (1973). *TAFS*, 81, 38–42.
- Middleton, J. M. (1953). *TAFS*, 61, 167–183.
- Middleton, J. M. (1964). *British Foundryman*, 57, 1–19.
- Middleton, J. M. (1965). *British Foundryman*, 58, 13–24.
- Middleton, J. M. (1970). *British Foundryman*, 64, 207–223.
- Middleton I., M., & Canwood, B. (1967). *British Foundryman*, 60, 494–503.
- Midea, A. C. (2001). *TAFS*, 109, 41–50; and *Foundryman* (March 2003) 60–63.

- Miguelucci, E. W. (1985). *TAFS*, 93, 913–916.
- Mihaichuk, W. (February 1986). *Modern Castings*, pp. 36–38 and (March) pp. 33–35.
- Mikkola, P. H., & Heine, R. W. (1970). *TAFS*, 78, 265–268.
- Miles, G. W. (1956). *Proceedings of the Institute of British Foundrymen*, 49, A201–A210.
- Miller, G. F. (1967). *Foundry*, 95, 104–107.
- Minakawa, S., Samarasekera, I. V., & Weinberg, F. (1985). *Metallurgical Transactions*, 16B, 823–829.
- Mintz, B., Yue, S., & Jonas, J. J. (1991). *International Materials Reviews*, 36(5), 187–217.
- Mirak, A. R., Divandari, M., & Boutorabi, S. M. A. (August 2010). *Materials Science and Technology*.
- Mirak, A. R., Divandari, M., Boutorabi, S. M. A., & Campbell, J. (2007). *International Journal of Cast Metals Research*, 20(4), 215–220.
- Miresmaeili, S. M. (2006). University of Birmingham, UK; unpublished work.
- Miresmaeili, S. M., Campbell, J., Shabestari, S. G., & Boutorabi, S. M. A. (2005). *Metallurgical & Materials Transactions A*, 36A, 2341–2349.
- Miyagi, Y., Hino, M., & Tsuda, O. (1985). In 'R&D' Kobe steel engineering reports 1983 33 July (3) also published in Kobelco Technical Bulletin 1076 (1985).
- Mizoguchi, T., Perepezko, J. H., & Loper, C. R. (1997). *TAFS*, 105, 89–94, and *Materials Science & Engineering A* 1997, vol. A226–228, pp. 813–817.
- Mizumoto, M., Sasaki, S., Ohgai, T., & Kagawa, A. (2008). *International Journal of Cast Metals Research*, 21(1–4), 49–55.
- Mizuno, K., Nylund, A., & Olefjord, I. (1996). *Materials Science and Technology*, 12, 306–314.
- Mohanty, P. S., & Gruzleski, J. E. (1995). *Acta Metallurgica et Materialia*, 43, 2001–2012.
- Mohla, P. P., & Beech, J. (1968). *British Foundryman*, 61, 453–460.
- Molaroni, A., & Pozzesi, V. (1963). In *30th International foundry congress*, pp. 145–161.
- Molina, J. M., Voytovych, R., Louis, E., & Eustathopoulos, N. (2007). *International Journal of Adhesion & Adhesives*, 27, 394–401.
- Mollard, F. R., & Davidson, N. (1978). *TAFS*, 78, 479–486.
- Momchilov, E. (1993). *Journal of Materials Science and Technology, Institute for Metal Science, Bulgarian Academy of Sciences, Sofia*, 1(1), 5–12.
- Mondloch, P. A., Baker, D. W., & Euvrard, L. (1987). *TAFS*, 95, 385–392.
- Morgan, A. D. (1966). *British Foundryman*, 59, 186–204.
- Morgan, P. C. (1989). *Metals and Materials*, 5(9), 518–520.
- Morthland, T. E., Byrne, P. E., Tortorelli, D. A., & Dantzig, J. A. (1995). *Metallurgical and Materials Transaction B*, 26B, 871–885.
- Mountford, N. D. G., & Calvert, R. (1959–60). *Journal of Institute Metals*, 88, 121–127.
- Mountford, N. D. G., Sommerville, I. D., From, L. E., Lee, S., & Sun, C. (1992/93). *A measuring device for quality control in liquid metals*. Lulea, Sweden: Scaninject Conf.
- Mountford, N. D. G., & Sommerville, I. D. (1993). *Steel technology international* (pp. 155–169). London, UK.
- Mountford, N. D. G., Sommerville, I. D., Simionescu, A., & Bai, C. (1997). *TAFS*, 105, 939–946.
- Mukherjee, M., Garcia-Moreno, F., & Banhart, J. (2010). *Metallurgical & Materials Transactions B*, 41B(3), 500–504.
- Mulazimoglu, M. H., Handiak, N., & Gruzleski, J. E. (1989). *TAFS*, 97, 225–232.
- Mulazimoglu, M. H., Tenekedjiev, N., Closset, B. M., & Gruzleski, J. E. (1993).  *Casting Metals*, 6(1), 16–28.
- Muller, F. C. G. (1887). *Zeit. ver dent. Ingenieure*, 23, 493.
- Mutharasan, R., Apelian, D., & Romanowski, C. (1981). *Journal of Metals*, 83(12), 12–18.
- Mutharasan, R., Apelian, D., & Ali, S. (1985). *Metallurgical Transactions*, 16B, 725–742.
- Muthukumarasamy, S., & Seshan, S. (1992). *TAFS*, 100, 873–879.

- Myllymaki, R. (1987). In W. B. Young (Ed.), *Residual stress in design, process and materials selection* (pp. 137–141). ASM Conference USA.
- Nadella, R., Eskin, D., & Katgerman, L. (2007). *Materials Science & Technology*, 23(11), 1327–1335.
- Nai, S. M. L., & Gupta, M. (2002). *Materials Science & Technology*, 18, 633–641.
- Nakae, H., Koizumi, H., Takai, K., & Okauchi, K. (1992). *IMONO Either*, 64, 34–39.
- Nakae, H., & Shin, H. (1999). *International Journal of Cast Metals Research*, 11(5), 345–349.
- Nakae, H., Takai, K., Okauchi, K., & Koizumi, H. (1991). *IMONO*, 63, 692–703.
- Nakagawa, Y., & Momose, A. (1967). *Tetsu-to-Hagane*, 53, 1477–1508.
- Naro, R. L. <http://www.asi-alloys.com/DocsPDF/Naro.pdf> the first 2 paragraphs of p. 6.
- Naro, R. L. (1974). *TAFS*, 82, 257–266.
- Naro, R. L. (2004). *TAFS*, 112, 527–545.
- Naro, R. L., & Pelfrey, R. L. (1983). *TAFS*, 91, 365–376.
- Naro, R. L., & Tanaglio, R. O. (1977). *TAFS*, 85, 65–74.
- Naro, R. L., & Wallace, J. F. (1967). *TAFS*, 75, 741–758.
- Naro, R. L., & Wallace, J. F. (1992). *100*, 797–820.
- Nayal, G. El. (1986). *Materials Science & Technology*, 2, 803.
- Nayal, G. El., & Beech, J. (1987). *3rd International Conference Solidification Processing*. Sheffield: Inst Metals Publication 421, pp. 384–387.
- Nazar, A. M. M., Cupini, N. L., Prates, M., & Daview, G. J. (1979). *Metallurgical and Materials Transactions B*, 10B, 203–210.
- Neiswaag, H., & Deen, H. J. J. (1990). In *57 World foundry congress*, Osaka, Japan.
- Newell, M., D'Souza, N., & Green, N. R. (2009). *International Journal of Cast Metals Research*, 22(1–4), 66–69.
- Nguyen, T., & Carrig, J. F. (1986). *TAFS*, 94, 519–528.
- Nicholas, K. E. L. (1972). *British Foundryman*, 65, 441–451.
- Nicholas, K. E. L., & Roberts, R. W. (1961). *BCIRA Journal*, 9(4), 519.
- Nikolai, M. F. (1996). *TAFS*, 104, 1017–1029.
- Nikrityuk, P. A., Eckert, K., & Grandmann, R. (June 2009). *Metallurgical & Materials Transactions B*, 40B(3), 317–327.
- Nishida, Y., Droste, W., & Engler, S. (1986). *Metallurgical Transactions*, 17B, 833–844.
- Niu, J. P., Sun, X. F., Jin, T., Yang, K. N., Guan, H. R., & Hu, Z. Q. (2003). *Materials Science & Technology*, 19(4), pp. 435–349.
- Niu, J. P., Yang, K. N., Sun, X. F., Jin, T., Guan, H. R., & Hu, Z. Q. (2002). *Materials Science & Technology*, 18(9), 1041–1044.
- Niyama, E., & Ishikawa, M. (1966). In *4th Asian foundry congress*, pp. 513–523.
- Niyama, E., Uchida, T., Morikawa, M., & Saito, S. (1982). In *International foundry congress 49*, Chicago, paper 10.
- Noesen, S. J., & Williams H. A. (1966). In *4th national die casting congress*, Cleveland, Ohio, paper number 801.
- Noguchi, T., Horikawa, N., Nagate, H., Nakamura, T., & Sato, K. (2005). *International Journal of Cast Metals Research*, 18(4), 214–220.
- Noguchi, T., Kamota, S., Sato, T., & Sakai, M. (1993). *TAFS*, 101, 231–239.
- Noguchi, T., Kano, J., Noguchi, K., Horikawa, N., & Nakamura, T. (2001). *International Journal of Cast Metals Research*, 13, 363–371.
- Nolli, P., & Cramb, A. W. (2008). *Metallurgical & Materials Transactions*, 39B, 56–65.
- Noreo, G. E., Polich, R. F., & Flemings, M. C. (1965). *TAFS*, 73, 1–13, and 28–33.
- Nordland, W. A. (1967). *AIME Transactions*, 239, 2002–2004.
- Nordlien, J. H. (1999). *Aluminium Extrusion*, 4(4), 39–41.



- Nordlien, J. H., Davenport, A. J., & Scamans, G. M. (2000). In *ASST 2000 (2nd International symposium Al Surface Science Technology) UMIST Manchester UK* (pp. 107–112). Alcan + Dera.
- Northcott, L. (1941). *Journal of the Iron and Steel Institute*, 143, 49–91.
- Novikov, I. I. (April 1962). *Russian Castings Production*, 167–172.
- Novikov, I. I., & Grushko, O. E. (1995). *Materials Science & Technology*, 11, 926–932.
- Novikov, I. I., Novik, F. S., & Indenbaum, G. V. (1966). *Izv. Akad. Nauk. Metal*, 5, 107–110 (English translation in Russ. Metall. Mining, 1966, 5, 55–59).
- Novikov, I. I., Portnoi, V. K., & Russ (1996). *Castings Production*, 4, 163–166.
- Nyahumwa, C., Green, N. R., & Campbell, J. (1998). *TAFS*, 106, 215–223.
- Nyahumwa, C., Green, N. R., & Campbell, J. (2000). *Metallurgical & Materials Transactions A*, 31A, 1–10.
- Nyamekye, K., An, Y.-K., Bain, R., Cunningham, M., Askeland, D., & Ramsay, C. (1994). *TAFS*, 102, 127–131.
- Nyamekye, K., Wei, S., Askeland, D., Voigt, R. C., Pischel, R. P., Rasmussen, W., & Ramsay, C. (1994). *TAFS*, 102, 869–876.
- Ocampo, C. M., Talavera, M., & Lopez, H. (1999). *Metallurgical & Materials Transactions A*, 30A, 611–620.
- Oelsen, W. (1936). *Stahl u Eisen*, 56, 182.
- O'Hara, P. (February 1990). *Engineering*, pp. 41–42.
- Ohnaka. (2003). (Mould coat doubles the back-pressure in molds).
- Ohno, A. (1987). *Solidification: The Separation Theory and its Practical Applications*. Springer-Verlag.
- Ohsasa, K.-I., Takahashi, T., & Kobori, K. J. (1988a). *Japan Institute of Metals*, 52(10), 1006–1011 (Materials Abstr. 51-0785).
- Ohsasa, K.-I., Ohmi, T., & Takahashi, T. (1988b). *Bull. Fac. Eng. Hokkaido Univ*, 143 (in Japanese).
- Osborn, D. A. (1979). *British Foundryman*, 72, 157–161.
- Ostrom, T. R., Biel, J., Wager, W., Flinn, R. A., & Trojan, P. K. (1982). *TAFS*, 90, 701–709.
- Ostrom, T. R., Frasier, D. J., Trojan, P. K., & Flinn, R. A. (1976). *TAFS*, 84, 665–674.
- Ostrom, T. R., Trojan, P. K., & Flinn, R. A. (1974). *TAFS*, 82, 519–524.
- Ostrom, T. R., Trojan, P. K., & Flinn, R. A. (1975). *TAFS*, 83, 485–492.
- Ostrom, T. R., Trojan, P. K., & Flinn, R. A. (1981). *TAFS*, 89, 731–736.
- Outlaw, R. A., Peterson, D. T., & Schmidt, F. A. (1981). *Metallurgical Transactions*, 12A, 1809–1816.
- Owen, M. (1966). *British Foundryman*, 59, 415–421.
- Owusu, Y. A., & Draper, A. B. (1978). *TAFS*, 86, 589–598.
- Pakes, M., & Wall, A. (1982). Zinc Development Association UK.
- Pan, E. N., Hsieh, M. W., Jang, S. S., & Loper, C. R. (1989). *TAFS*, 97, 379–414.
- Pan, E. N., & Hu, J. F. (1996). In *4th Asian Foundry Congress*, pp. 396–405.
- Pan, E. N., & Hu, J. F. (1997). *TAFS*, 105, 413–418.
- Panchanathan, V., Seshadri, M. R., & Ramachandran, A. (1965). *British Foundryman*, 58, 380–384.
- Papworth, A., & Fox, P. (1998). *Materials Letters*, 35, 202–206.
- Patterson, W., Engler, S., & Kupfer, R. (1967). *Giesserei-Forschung*, 19(3), 151–160.
- Patterson, W., & Koppe, W. (1962). *Giesserei*, 4, 225–249.
- Parkes, T. W., & Loper, C. R. (1969). *TAFS*, 77, 90–96.
- Parkes, W. B. (1952). *TAFS*, 60, 23–37.
- Paray, F., Kulunk, B., & Gruzleski, J. E. (2000). *International Journal of Cast Metals Research*, 13, 147–159.
- Pattabhi, R., Lane, A. M., & Piwonka, T. S. (1996). Part III. *TAFS*, 104, 1259–1264.
- Patterson, W., Engler, S., & Kupfer, R. (1967). *Giesserei-Forschung*, 19(3), 151–160.
- Pekguleryuz, M. O., Lin, S., Ozbakir, E., Temur, D., & Aliravci, C. (2010). *International Journal of Cast Metals Research*, 23(5), 310–320.
- Pelleg, J., & Heine, R. W. (1966). *TAFS*, 74, 541–544.
- Pellerier, M., & Carpentier, M. (1988). *Hommes et Fonderie*, 184, 7–14.

- Pellini, W. S. (1952). *Foundry*, 80, 124–133, 194, 196, 199.
- Pellini, W. S. (1953). *TAFS*, 61, 61–80, and 302–308.
- Pell-Walpole, W. T. (1946). *Journal of the Institute of Metals*, 72, 19–30.
- Pennors, A., Samuel, A. M., Samuel, F. H., & Doty, H. W. (1998). *TAFS*, 106, 251–264.
- Perbet, D. (1988). *Hommes et Fonderie* (Mars) p. 15. French plus English Translation.
- Perets, S., Arbel, A., Ariely, Venkert, A., & Schneck, R. Z. (2004). *Materials Science & Technology*, 20(12), 1519–1524.
- Peterson, W. M., & Blanke, J. E. (1980). *TAFS*, 88, 503–506.
- Petro, A., & Flinn, R. A. (1978). *TAFS*, 86, 357–364.
- Petrzela, L. (1968). *Foundry Trade Journal* (Oct 31), 693–696.
- Pettersson, H. (1951). *TAFS*, 59, 35–55.
- Phillion, A. B., Vernede, S., Rappaz, M., Cockcroft, S. L., & Lee, P. D. (2009). *International Journal of Cast Metals Research*, 22(1–4), 1–5.
- Pillai, R. M., Mallya, V. D., & Panchanathan, V. (1976). *TAFS*, 84, 615–620.
- Pitcher, P. D., & Forsyth, P. J. E. The influence of microstructure on the fatigue properties of an Al casting alloy. In *Royal Aircraft Establishment Technical Report 82107* Nov. 1982.
- Piwonka, T. S., & Flemings, M. C. (1966). *Transactions of the Metallurgical Society of AIME*, 236, 1157–1165.
- Poirier, D. R. (1987). *Metallurgical Transactions*, 18B, 245–255.
- Poirier, D. R., Sung, P. K., & Felicelli, S. D. (2001). *TAFS*, 105, 139–155.
- Poirier, D. R., & Yeum, K. (1987). *Solidification Processing Conference Sheffield*. London: Institute of Metals.
- Poirier, D. R., & Yeum, K. (1988). In *Light Metals Conf USA* (pp. 469–476).
- Poirier, D. R., Yeum, K., & Maples, A. L. (1987). *Metallurgical Transactions*, 18, 1979–1987.
- Pokorny, M. G., Monroe, C. A., & Beckermann, C. (2009). In J. Campbell, P. N. Crepeau, & M. Tiryakioglu (Eds.), *Shape Casting: The 3rd International Symposium TMS*.
- Polich, R. F., & Flemings, M. C. (1965). *TAFS*, 73, 28–33.
- Pollard, W. A. (1964). *TAFS*, 72, 587–599.
- Pollard, W. A. (1965). *TAFS*, 73, 371–379.
- Polmear, I. J. (2006). *Light Alloys* (4th ed.). Butterworth Heinemann.
- Polodurov, N. N. (1965). *Russian Castings Production*, 5, 209–210.
- Pope, J. A. (1965). *British Foundryman*, 58, 207–224.
- Popel, G. I., & Esin, O. A. (1956). *Zh. Fiz. Khim*, 30, p. 1193.
- Portevin, A., & Bastien, P. (1934). *Journal of Institute Metals*, 54, 45–58.
- Portevin, A., & Bastien, P. (1936). *Institute of British Foundrymen*. 33rd Annual Conf Glasgow, pp. 88–116.
- Prates, M., & Biloni, H. (1972). *Metallurgical Transactions*, 3A, 1501–1510.
- Prible, J., & Havlicek, F. (1963) In *30th International foundry congress*, pp. 394–410.
- Prodhom, A., Carpenter, M., & Campbell, J. (1999). CIATF technical forum.
- Puhakka, R. (2009). *Modern Castings* (June), pp. 27–29.
- Puhakka, R. (November 2010). *Foundry Trade Journal*, 184(3679), 277–279.
- Pulkonik, K. J., Lee, W. E., & Rosenberg, R. A. (1967). *TAFS*, 75, 38–41.
- Pumphrey, W. I. (1955). *Researches into the Welding of Aluminium and its Alloys*. Research Report 27, Aluminium Development Association UK.
- Pumphrey, W. I., & Lyons, J. V. (1948). *Journal of the Institute of Metals*, 74, 439–455.
- Pumphrey, W. I., & Moore, D. C. (1949). *Journal of the Institute of Metals*, 75, 727–736.
- Qian, M., Graham, D., Zheng, L., StJohn, D. H., & Frost, M. T. (2003). *Materials Science & Technology*, 19(2), 156–162.
- Qingchung, L., Kuiying, C., Chi, L., & Songyan, Z. (1991). *TAFS*, 99, 245–253.
- Rabinovich, A. (March 1969). *AFS Cast Metals Research Journal*, 19–24.

- Ragone, D. V., Adams, C., & Taylor, H. (1956). *TAFS*, 64, 653–657.
- Raiszadeh, R., & Griffiths, W. D. (2008). *Metallurgical & Materials Transactions*, 39B, 298–303.
- Ramrattan, S. N., Guichelaar, P. J., Palukunnu, A., & Tieder, R. (1996). *TAFS*, 104, 877–886.
- Ramseyer, J. C., Gabathuler, J. P., & Feurer, U. (1982). *Aluminium*, 58(10), E192–E194 and 581–585.
- Ransley, C. E., & Neufeld, H. (1948). *Journal of the Institute of Metals*, 74, 599–620.
- Rao, G. V. K., & Panchanathan, V. (1973). *Cast Metals Research Journal*, 19(3), 135–138.
- Rao, G. V. K., Srinivasan, M. N., & Seshadri, M. R. (1975). *TAFS*, 83, 525–530.
- Rao, T. S. V., & Roshan, H. Md. (1988). *TAFS*, 96, 37–46.
- Rao, Y. K., & Lee, H. G. (1984). *Metallurgical Transactions*, 15B, 396–400.
- Rapoport, D. B. (1964). *Foundry Trade Journal*, 116, 169.
- Rappaz, M. (1989). *International Material Reviews*, 34(3), 93–123.
- Rappaz, M. Hot tearing developments.
- Rappaz, M., Drezet, J.-M., & Gremaud, M. (1999). *Metallurgical & Materials Transactions A*, 30A(2), 449–455.
- Vernede, S., Jarry, P., & Rappaz, M. (2006). *Acta Materialia*, 54, 4023–4034.
- Mathier, V., Grasso, P.-D., & Rappaz, M. (2008). *Metallurgical & Materials Transactions A*, 39A, 1399–1409.
- Mathier, V., Vernede, S., Jarry, P., & Rappaz, M. (2009). *Metallurgical & Materials Transactions A*, 40A(4), 943–957.
- Phillion, A. B., Vernede, S., Rappaz, M., Cockcroft, S. L., & Lee, P. D. (2009). *International Journal of Cast Metals Research*, 22(1–4), 1–5.
- Vernede, S., Dantzig, J. A., & Rappaz, M. (2009). *Acta Materialia*, 57, 1554–1569.
- Rashid, A. K. M. B., & Campbell, J. (2004). *Metallurgical & Materials Transactions*, 35A(7), 2063–2071.
- Rashid, M. S., & Hanna, M. D. In *North American Die Casting Association (NADCA) Conf Cleveland 1993 Paper T93-041* pp. 105–111 (U.S. Patent 4990310 1989).
- Rassenfoss, J. A. (1977). *TAFS*, 85, 583–596.
- Rauch, A. H., Peck, J. P., & Thomas, G. F. (1959). *TAFS*, 67, 263–266.
- Rault, L., Allibert, M., Prin, M., & Dubus, A. (1996). *Light Metals*, 345–355.
- Reddy, D. C., Murty, S. S. N., & Chakravorty, P. N. (1988). *TAFS*, 96, 839–844.
- Reding, J. N. (1968). *TAFS*, 76, 92–98.
- Rege, R. A., Szekeres, E. S., & Foreng, W. D. (1970). *Metallurgical Transactions*, 1, 2652–2653.
- Ren, X. C., Zhou, Q. J., Shan, G. B., Chu, W. Y., Li, J. X., Su, Y. J., & Qiao, L. J. (2008). *Metallurgical & Materials Transactions*, 39A, 87–97.
- Revankar, V., Baker, P., Schultz, A. H., & Brandt, H. (2000). *Light Metals*, 51–55.
- Rezvani, M., Yang, X., & Campbell, J. (1999). *TAFS*, 107, 181–188.
- Richins, D. S., & Wetmore, W. O. (1951). In *AFS Symposium on Principles of Gating* (pp. 1–24).
- Richmond, O., & Tien, R. H. (1971). *Journal of the Mechanics and Physics of Solids*, 19, 273–284.
- Richmond, O., Hector, L. G., & Fridy, J. M. (1990). *Journal of Applied Mechanics-Transactions of the ASME*, 57, 529–536.
- Rickards, P. J. (1975). *British Foundryman*, 68, 53–60.
- Rickards, P. J. (1982). *British Foundryman*, 75, 213–223.
- Riposan, I., Chisamera, M., Stan, S., Toboc, P., Ecob, E., & White, D. (2008). *Materials Science and Technology*, 24(5), 579–584.
- Rishel, L. L., Pollock, T. M., & Cramb, A. W. In *Proceedings 1999 International symposium liquid metal processing and casting; Santa Fe, NM February 1999* (pp. 287–299).
- Rivas, R. A. A., & Biloni, H. (1980). *Zeit. Metallk*, 71(4), 264–268.
- Rivera, G., Boeri, R., & Sikora, J. (2002). *Materials Science and Technology*, 18, 691–697.
- Roberts, R. J. (1996). *TAFS*, 104, 523–526.
- Roberts, T. E., Kovarik, D. P., & Maier, R. D. (1979). *TAFS*, 87, 279–298.

- Roedter, H. (1986). *Foundry Trade Journal International*, September 1986, p. 6
- Roehrig, K. (1978). *TAFS*, 86, 75–92.
- Rogberg, B. (1980). In *Solidification technology in the foundry and cast house, Warwick Conference*. pp. 365–371 (Metals Society 198).
- Rogers, K. P., & Heathcock, C. J. (1990). U.S. Patent 5,316,070, 31 May 1994.
- Romankiewicz, F. (1976). *AFS International Cast Metals Journal*, 1(4), 13–17.
- Romero, J. M., Smith, R. W., & Sahoo, M. (1991). *TAFS*, 99, 465–468.
- Rong De, L., & Xiang, Y. J. (1991). *TAFS*, 90, 707–712.
- Rosenberg, R. A., Flemings, M. C., & Taylor, H. F. (1960). *TAFS*, 68, 518–528.
- Rossmann, M., *Giesserei* (February 1982). 69(4), 102–103.
- Roth, M. C., Weatherly, G. C., & Miller, W. A. (1980). *Acta Materialia*, 28, 841–853.
- Rouse, J. (1987). In *54th International foundry congress, New Dehli. Paper 30*, p. 16.
- Roviglione, A. N., & Hermida, J. D. (2004). *Metallurgical & Materials Transactions B*, 35B, 313–330.
- Ruddle, R. W. (1956). *'The Running and Gating of Sand Castings' Monograph & Report Series No 19*. London: Institute of Metals.
- Ruddle, R. W. (1960). *TAFS*, 68, 685–690.
- Ruddle, R. W., & Cibula, A. (1957). *Institute of Metals Monograph*, Report 22 5–32.
- Ruddle, R. W., & Mincher, A. L. (1949–50). *Journal of the Institute of Metals*, 76, 43–90.
- Runyoro, J. (1992). PhD thesis, University of Birmingham, UK.
- Runyoro, J., Boutorabi, S. M. A., & Campbell, J. (1992). *TAFS*, 100, 225–234.
- Ruxanda, R., Sanchez, L. B., Massone, J., & Stefanescu, D. M. (2001). *Transactions of American Foundry Society*, 109, 37–48 (Cast Iron Division).
- Sabatino Di, M., Arnberg, L., Brusethaug, S., & Apelian, D. (2006). *International Journal of Cast Metals Research*, 19(2), 94–97.
- Sabatino Di, M., Syvertsen, F., Arnberg, L., & Nordmark, A. (2005). *International Journal of Cast Metals Research*, 18(1), 59–62.
- Sadayappan, M., Fasoyinu, F. A., Thomson, J., & Sahoo, M. (1999). *TAFS*, 107, 337–342.
- Sadayappan, M., Sahoo, M., Liao, G., Yang, B. J., Li, D., & Smith, R. W. (2001). *TAFS*, 109, 341–352.
- Saeger, C. M., & Ash, E. J. (1930). *TAFS*, 38, 107–145.
- Safaraz, A. R., & Creese, R. C. (1989). *TAFS*, 97, 863–870.
- Sahoo, M., & Whiting, L. V. (1984). *TAFS*, 92, 861–870.
- Sahoo, M., Whiting, L. V., & White, D. W. G. (1985). *TAFS*, 93, 475–480.
- Sahoo, M., & Worth, M. (1990). *TAFS*, 98, 25–33.
- Saia, A., & Edelman, R. E. (1968). *TAFS*, 76, 189–195.
- Saigal, A., & Berry, J. T. (1984). *TAFS*, 92, 703–708.
- Sakakibara, Y., Suzuki, T., Hayashi, H., et al. (1988). Japan Patent 17578/88, Europe patent EP0306841 A2.
- Sakamoto, M., Akiyama, S., & Ogi, K. (1996). *4th Asian foundry congress proceedings, Australia*, pp. 467–476.
- Samarasekera, I. V., Anderson, D. L., & Brimacombe, J. K. (1982). *Metallurgical Transactions*, 13B, 91–104.
- Sambasivan, S. V., & Roshan, H. Md. (1977). *TAFS*, 85, 265–270.
- Samuel, A. M., & Samuel, F. H. (1993). *Metallurgical Transactions A*, 24A, 1857–1868.
- Samuel, F. H., Samuel, A. M., Doty, H. W., & Valtierra, S. (2002). Submitted to Metal and Materials Transactions A, 15 November 2001, paper 01-616-A.
- Sandford, P. (March 1988). *The Foundryman*, 110–118.
- Sandford, P. (1993). *TAFS*, 101, 817–824.
- Santos, R. G., & Garcia, A. (1998). *International Journal of Cast Metals Research*, 11, 187–195.
- Sare, I. R. (1989). *Cast Metals*, 1(4), 182–190.

- Saucedo, I. G., Beech, J., & Davies, G. J. (1980). *Conference 'Solidification technology in foundry and cast house'* Warwick Univ. Metals Society Publication 1983, pp. 461–468.
- Scarber, P., & Bates, C. E. (2006). *TAFS*, 114, 37–44.
- Scarber, P., Bates, C. E., & Griffin. (2006). *TAFS*, 114, 435–445.
- Scheffer, K. D. (1975). *TAFS*, 83, 585–592.
- Schumacher, P., & Greer, A. L. (1993). *Key Engineering Materials*, 81–83, 631.
- Schumacher, P., & Greer, A. L. (1994). *Materials Science and Engineering*, A181/A182, 1335–1339.
- Schurmann, E. (1965). *Arch. Eisenh.*, 36, 619–631 (BISI Translation 4579).
- Sciama, G. (1974). *TAFS*, 82, 39–44.
- Sciama, G. (1975). *TAFS*, 83, 127–140.
- Sciama, G. (1993). *TAFS*, 101, 643–651.
- Schmidt, D. G., & Jacobson, A. E. (1970). *TAFS*, 78, 332–337.
- Scott, A. F., et al. (1948). *Journal of Chemistry Physics*, 16, 495–502.
- Scott, D., & Smith, T. J. (1985). Personal communication.
- Scott, W. D., & Bates, C. E. (1975). *TAFS*, 83, 519–524.
- Scott, W. D., Goodman, P. A., & Monroe, R. W. (1978). *TAFS*, 86, 599–610.
- Schrey, A. (2007). *Foundry Practice (Foseco)* 246 (June), pp. 01–07.
- SCRATA. (1981). *Hot tearing – Causes and Cures*, *Tech. Bull. No. 1*. Sheffield, UK: Steel Castings Research and Trade Association.
- Seetharamu, S., & Srinivasan, M. W. (1985). *TAFS*, 93, 347–350.
- Sexton, A. H., & Primrose, J. S. G. (1911). *The Principles of Ironfounding*. London: The Technical Publishing Co.
- Shabestari, S. G., & Gruzleski, J. E. (1995). *TAFS*, 103, 285–293.
- Shen, P., Zhen, X.-H., Lin, Q.-L., Zhang, D., & Jiang, Q.-P. (2009). *Metallurgical & Materials Transactions*, 40A(2), 444–449.
- Sherby, O. D. (1962). *Metals Engineering Quarterly* (ASM), May, 3–13.
- Ship Department Publication 18. (1975). *Design & Manufacture of Nickel-Aluminium-Bronze Sand Castings*. Bath, UK: Ministry of Defence (Procurement Executive) Foxhill.
- Shirey, D. R., & Williams, D. C. (1968). *TAFS*, 76, 661–674.
- Showman, R. E., & Aufderheide, R. C. (2003). 111, paper 145, p. 12.
- Showman, R. E., Aufderheide, R. C., & Yeomans, N. P. (August 2007). *Foundry Trade Journal*, 224–227.
- Sicha, W. E., & Boehm, R. C. (1948). *TAFS*, 56, 398–409.
- Sigworth, G. (1984). *Metallurgical Transactions*, 15A, 227–282.
- Sigworth, G. K., & Engh, T. A. (1982). *Metallurgical Transactions*, 13B, 447–460.
- Sigworth, G., Jorstad, J., & Campbell, J. (2009). *AFS International Journal of Metalcasting Correspondence*, 3(1), 65–77.
- Sigworth, G. K., & Kuhn, T. A. (2007). *International Journal of Metalcastings*, 1(1), 31–40.
- Sigworth, G. K., Wang, C., Huang, H., & Berry, J. T. (1994). *TAFS*, 102, 245–261.
- Simard, A., Proulx, J., Paquin, D., Samuel, F. H., & Habibi, N. (2001). American Found. In *Soc Molten Al processing conference, Orlando, Florida, November*.
- Simensen, C. J. (1993). *Zeit Metallkunde*, 84(10), 730–733.
- Simmons, W., & Trinkl, G. (1987). *BCIRA Conf*. UK: British Cast Iron Research Assoc.
- Sin, S. L., Dube, D., & Tremblay, R. (2006). *Materials Science & Technology*, 22(12), 1456–1463.
- Singh, S. N., Bardes, B. P., & Flemings, M. C. (1970). *Metallurgical Transactions*, 1, 1383.
- Sinha, N. P., & Kondic, V. (1974). *British Foundryman*, 67, 155–165.
- Sinha, N. P. (1973). PhD thesis. University of Birmingham, UK.
- Sirrell, B., & Campbell, J. (1997). *TAFS*, 105, 645–654.

- Skarbinski, M. (1971). *British Foundryman*, 44, 126–140.
- Skaland, T. (2001). *TAFS*, 105, 77–88.
- Skelly, H. M., & Sunnucks, D. C. (1954). *TAFS*, 62, 481–491.
- Smith, C. S. (1948). *Transactions AIME*, 175, 15–51.
- Smith, C. S. (1949). *Transactions AIME*, 185, 762–768.
- Smith, C. S. (1952). *Metal Interfaces*. Cleveland, Ohio: ASM. 65–113.
- Smith, D. D., Aubrey, L. S., & Miller, W. C. (1988). In B. Welch (Ed.), *'Light Metals' Conf* (pp. 893–915). The Minerals, Metals and Materials Soc.
- Smith, D. M. (1981). U.K. *Patent application GB 2,085,920,A*.
- Smith, R. A. (1986). U.K. *Patent GB 2,187,984,A*; priority date 21 February 1986.
- Smith, T. J., Lewis, R. W., & Scott, D. M. (1990). *The Foundryman*, 83, 499–507.
- Sokolowski, J. H. (2006). University of Windsor, Canada. Unpublished work.
- Sokolowski, J. H., Kierkus, C. A., Brosnan, B., & Evans, W. J. (2000). *TAFS*, 108, 497–503.
- Solberg, J. K., & Onsoien, M. I. (2001). *Materials Science and Technology*, 17, 1238–1242.
- Song, H., & Hellawell, A. (1989). *Light Metals*, 819–823.
- Sontz, A. (1972). *TAFS*, 80, 1–12.
- Sosman, R. B. (1927). The properties of silica. In *The Chemical Catalogue Co. USA, Am. Chem. Soc. Monograph Series*, pp. iv–45.
- Southam, D. L. (1987). *Foundry Management and Technology*, 7, 34–38.
- Southin, R. T. (1967). The solidification of metals. *Brighton Conference UK*, 305–308, ISI Publication 110.
- Southin, R. T., & Romeyn, A. (1980). *Warwick Conf 'Solidification Technology in the Foundry and Cast House'*. Metals Soc 1983, 355–358.
- Speidel, M. O. (1982). In *Sixth European Non-Ferrous Metals Industry Colloquium CAEF*, pp. 65–78.
- Spitaler, P. (1957). *Giesserei*, 44, 757–766.
- Spittle, J. A., & Brown, S. G. R. (1989). *Journal of Material Science*, 23, 1777–1781.
- Spittle, J. A., & Brown, S. G. R. (1989). *Journal of Material Science*, 5, 362–368.
- Spittle, J. A., & Cushway, A. A. (1983). *Metals Technology*, 10, 6–13.
- Spraragen, W., & Claussen, G. E. (1937). *Journal of American Welding Society (Supplement: Welding Research Committee)*, 16(11), 2–62.
- Srinagesh, K. (1979). *AFS International Cast Metals Journal*, 4(1), 50–63.
- Srinivasan, A., Pillai, U. T. S., & Pai, B. C. (2006). *TAFS*, 114, 737–746.
- Stahl, G. W. (1961). *TAFS*, 69, 476–478.
- Stahl, G. W. (1963). *TAFS*, 71, 216–220.
- Stahl, G. W. (1986). *TAFS*, 94, 793–796.
- Stahl, G. W. (1989). 'The gravity tilt pour process'. In *Processing AFS Internat Conference: Permanent Mold Castings, Miami*. Paper 2.
- Staley, J. T. (1981). *Metals Handbook*, pp. 675–718 (9th ed.), Vol. 4, Heat Treating. American Society for Metals, USA.
- Staley, J. T. (1986). *Aluminium Technology 86, Institute Metals UK Conference*, pp. 396–407.
- Stanford, N., Sabirov, I., Sha, G., La Fontaine, A., Ringer, S. P., & Barnett, M. R. (2010). *Metallurgical & Materials Transactions A*, 41A(3), 734–743.
- Steel Founders' Society of America (Anon) (1970). *Steel Castings Handbook* (4th edn.).
- Steel Founders' Society of America (Anon) (2000). *Foundry Trade Journal*, May, pp. 40–41.
- Steen, H. A. H., & Hellawell, A. (1975). *Acta Materialia*, 23, 529–535.
- Stefanescu, D. M. (1988). *Metals Handbook* (9th ed.), Volume 15, Casting. Ohio, USA: ASM, 168–181.
- Stefanescu, D. M. (2007). *Metallurgical & Materials Transactions A*, 38A(7), 1433–1447.
- Stefanescu, D. M., Giese, S. R., Piwonka, T. S., Lane, A. M., Barlow, J., & Pattabhi, R. (1996). *TAFS*, 104, 1233–1264.

- Stefanescu, D. M., Hummer, R., & Nechtelberger, E. (1988). *Metals Handbook* (9th ed.). Volume 15 Casting. Ohio, USA: ASM. pp. 667–677.
- Stefanescu, D. M., Wills, S., & Massone, J. (2009). *TAFS*, 20, paper 09-120.
- Stein, H., Iske, F., & Karcher, D. (1958). *Giesserei-Technisch-Wissenschaftliche Beihefte*, 21, 115–1124.
- Steiger, R., von. (1913). *Stahl und Eisen*, 33, 1442.
- StJohn, D. H., Easton, M. A., Cao, P., & Qian, M. (2007). *International Journal of Cast Metals Research*, 20(3), 131–135, and SP07 Proc 5th Decennial Internat Conf Solidification Processing. In H. Jones. (Ed.), Sheffield UK, July 2007, pp. 99–103.
- StJohn, D. H., Qian, M., Easton, M. A., Cao, P., & Hildebrand, Z. (2005). *Metallurgical & Materials Transactions A*, 36A, 1669–1679.
- Stolarczyk, J. E. (1960). *British Foundryman*, 53, 531–548.
- Stoltze, P., Norskov, I. K., & Landman, U. (1988). *Physical Review Letters*, 61(4), 440–443.
- Storaska, G. A., & Howe, J. M. (2004). *Materials Science and Engineering A*, 368, 183–190.
- Street, A. C. (1986). *The Diecasting Book* (2nd ed.). Redhill, UK: Portcullis Press. Chapter 8 on zinc alloys, pp. 170–194.
- Su, J. Y., Chow, C. T., & Wallace, J. F. (1982). *TAFS*, 90, 565–574.
- Sugden, A. A. B., & Bhadeshia, H. K. D. H. (1987). University of Cambridge, UK.
- Sullivan, E. J., Adams, C. M., & Taylor, H. F. (1957). *TAFS*, 65, 394–401.
- Sumiyoshi, Y., Ito, N., & Noda, T. (1968). *Journal of Crystal Growth* (3 and 4), 327–339.
- Sun, G. X., & Loper, C. R. (1983). *TAFS*, 91, 841–854.
- Sun, L., & Campbell, J. (2003). *TAFS*, paper 03–018. In press.
- Surappa, M. K., Blank, E., & Jaquet, J. C. (1986a). Conference Aluminium Technology. In T. Sheppard (Ed.), *Institute Metals* (pp. 498–504).
- Surappa, M. K., Blank, E., & Jaquet, J. C. (1986b). *Scripta Materialia*, 20, 1281–1286.
- Sutton, T. (June 2002). *The Foundryman*, 95(6), 223–231.
- Suutala, N. (1983). *Metallurgical Transactions*, 14A, 191–197.
- Suzuki, S. (1989). *Modern Castings*, 38–40, October.
- Svensson, I. L., & Dioszegi, A. (2000). In P. Sahm, P. Hansen & Conley (Eds.), *Modelling of casting, welding and advanced solidification processes IX*, pp. 102–109.
- Svensson, I., & Villner, L. (1974). *British Foundryman*, 67, 277–287.
- Svoboda, J. M. (1994). *TAFS*, 102, 461–471.
- Svoboda, J. M., & Geiger, G. H. (1969). *TAFS*, 77, 281–288.
- Svoboda, J. M., Monroe, R. W., Bates, C. E., & Griffin, J. (1987). *TAFS*, 95, 187–202.
- Swift, R. E., Jackson, J. H., & Eastwood, L. W. (1949). *TAFS*, 57, 76–88.
- Swing, E. (1962). *TAFS*, 70, 364–373.
- Sy, A. de (1967). *TAFS*, 75, 161–172.
- Syvertsen, M. (2006). *Metallurgical & Materials Transactions B*, 37B(6), 495–504.
- Szklarska-Smialowska, Z. (1999). *Corrosion Science*, 41, 1743–1767.
- Tadayon, M. R. (28th September 1982). ‘Finite element modelling of heat transfer and solidification in the squeeze forming process.’ PhD thesis, University College, UK: Swansea.
- Tadayon, M. R., & Lewis, R. W. (1988). *Cast Metals*, 1, 24–28.
- Tafazzoli-Yadzi, M., & Kondic, V. (1977). *AFS Internat. Cast Metals Journal*, 2(4), 41–47.
- Taft, D. J. (1968). *British Foundryman*, 61, 69–75.
- Talbot, D. E. G., & Granger, D. A. J. (1962). *Institute of Metals*, 91, 319–320.
- Taleyarkhan, R. P., Kim, S. H., & Gulec, K. (1998). *TAFS*, 106, 619–624.
- Taylor, C. M. Jr., & Taylor, H. F. (1953). Fundamentals of Riser Behavior. *AFS Transactions*, 686–693.
- Taylor, K. C., & Baier, A. (2003). *Casting Plant + Technology International*, 123(2), 36–46.

- Taylor, L. S. (1960). *Foundry Trade Journal*, 109(2287), 419–427.
- Thevik, H. J., Asbjorn, Mo, & Rusten, T. (1999). *Metallurgical & Materials Transactions B*, 30B(1), 135–142.
- Thiele von, W. (1962). *Aluminium (Germany)*, 38, 707–715, 780–786 (English translation by H Nercessian 29 April 1963, 5229, Alcan Banbury UK and Electricity Council Research Centre UK).
- Thomas, B. G., & Parkman, J. T. (1998). *1997 Conference 'Solidification'*. Indianapolis Indiana: The Minerals, Metals and Materials Society, pp. 509–520.
- Thornton, D. R. (1956). *Journal of Iron and Steel Institute*, 183(3), 300–315.
- Tiberg, L. (1960). *Jerkont. Ann*, 144(10), 771–793.
- Tiekink, W., Boom, R., Overbosch, A., Kooter, R., & Sridar, S. (2010). *Ironmaking and Steelmaking*, 37(7), 488–495.
- Tien, R. H., & Richmond, O. (1982). *Journal of Applied Mechanics-Transactions of the ASME*, 49, 481–486.
- Timelli, G., & Bonollo, F. (2007). *International Journal of Cast Metals Research*, 20(6), 304–311.
- Timmons, W. W., Spiegelberg, W. D., & Wallace, J. F. (1969). *TAFS*, 77, 57–61.
- Tiryakioğlu, E. (1964). 'A Study of the Dimensioning of Feeders for Sand Castings', Ph.D. thesis, University of Birmingham, UK.
- Tiryakioğlu, M. (2001). Personal communication.
- Tiryakioğlu, M. (2008). Statistical distributions for the size of fatigue-initiating defects. A comparative study. *Materials Science Engineering A*, 497, 119–125.
- Tiryakioğlu, M. (2009). The size of fatigue-initiating defects. *Material Science & Engineering*, 520, 114–120.
- Tiryakioğlu, M. (2011). In *Shape Casting: 'John Berry Honorary Symposium' IV San Diego, Ca, USA*. TMS Annual Congress.
- Tiryakioğlu, M., Askeland, D. R., & Ramsay, C. W. (1993). *TAFS*, 101, 685–691.
- Tiryakioğlu, M., & Campbell, J. (2007). *International Journal of Cast Metals Research*, 20(1), 25–29.
- Tiryakioğlu, M., Campbell, J., & Alexopoulos, N. D. (2009a). *Metallurgical & Materials Transactions A*, 40A, 1000–1007.
- Tiryakioğlu, M., Campbell, J., & Alexopoulos, N. D. (2009b). *Materials Science & Engineering A*, 506, 23–26.
- Tiryakioğlu, M., Campbell, J., & Nyahumwa, C. (2011). In Crepeau, P. et al. (Ed.), 'Fracture Surface Facets and Fatigue Life Potential of Castings'; *Shape Casting: The John Berry Honorary Symposium; TMS San Diego CA*.
- Tiryakioğlu, M., & Campbell, J. (2009c). *Materials Science & Technology*, 25(6), 784–789.
- Tiryakioğlu, M., & Hudak, D. (2008a). *Mater. Sci. & Engng A*, 498, 501–503.
- Tiryakioğlu, M., & Hudak, D. (2008). *Journal of Materials Science*, 43, 1914–1919.
- Tiryakioğlu, M., Hudak, D., & Okten, G. (2009). *Materials Science & Engineering A*, 527, 397–399.
- Tiryakioğlu, M., Tiryakioğlu, E., & Askeland, D. A. (1997a). *International Journal Cast Metals Research*, 9, 259–267.
- Tiryakioğlu, M., Tiryakioğlu, E., & Askeland, D. A. (1997b). *TAFS*, 105, 907–915.
- Tiwara, S. N., Gupta, A. K., & Maihotra, S. L. (1985). *British Foundryman*, 78(1), 24–27.
- Tokarev, A. I. (1966). *Iz.v VUZ Chern. Met*, 3, 193–200, BCIRA Translation T1190, January 1966.
- Tol, R., van, Katerman, L., & Akker, H. E. A., van der. (1997). *Solidification Processing (SP97)*, pp. 79–82. In J. Beech & H. Jones (Eds.), Conference, Sheffield UK.
- Thomason, P. F. (1968). *Journal of the Institute of Metals*, 96, 360–365.
- Tomono, H., Ackermann, P., Kurz, W., & Heinemann, W. (1980). *Solidification Technology in foundry and cast house*. Warwick Univ. Conf. Metals Society Publication 1983, pp. 524–531.
- Tordoff, E. G., Wolfram, T., Talwar, V., & Hysell, M. (1996). *TAFS*, 104, 461–466.
- Townsend, D. W. (1984). *Foundry Trade Journal*, 24, 409–414, May.
- Trbizan Katerina. (2001). *Casting simulation*. World Foundry Organisation (paper 4) 83–97.
- Travena, D. H. (1987). *Cavitation and Tension in Liquids*. Bristol: Adam Huger, Inst. Phys.



- Trikha, S. K., & Bates, C. E. (1994). *TAFS*, 102, 173–180.
- Trojan, P. K., Guichelaar, P. J., & Flinn, R. A. (1966). *TAFS*, 74, 462–469.
- Tsai, H. L., Chiang, K. C., & Chen, T. S. (1989). In A. F. Giamei, & O. J. Abbaschian (Eds.), *Modeling of Casting and Welding Processes IV* (pp. 1988). USA: The Minerals, Metals and Materials Society.
- Tschapp, M. A., Ramsay, C. W., & Askeland, D. R. (2000). *TAFS*, 108, 609.
- Tsuruya, S., Ishikawa, Y., & Sono, K. (1974). *Transactions of AFS*, 82, 27–34.
- Tucker, S. P., & Hochgraph, F. G. (1973). *Metallography*, 6, 457–464.
- Turchin, A. N., Eskin, D. G., & Katgerman, L. (2007). (a) *International Journal of Cast Metals Research*, 20(6), 312–318.
- Turchin, A. N., Eskin, D. G., & Katgerman, L. (2007). (b) *Metallurgical & Materials Transactions A*, 38A(6), 1317–1329.
- Turkdogan, E. T. (1988). Foundry Processes, Their Chemistry and Physics (International Symposium (1986)). In S. Katz, & C. F. Landefeld (Eds.) (pp. 53–100). Warren, Mich. USA: Plenum Press.
- Turner, A., & Owen, F. (1964). *British Foundryman*, 57, 55–61, 355–356.
- Turner, G. L. (1965). *British Foundryman*, 58, 504–505.
- Turpin, M. L., & Elliott, I. F. (1966). *Journal of Iron and Steel Institute*, 204, 217–225.
- Twitty, M. D. (1960). In BCIRA I., Report 575 (pp. 844–856). In C. F. Walton (Ed.) (1971). *Gray and Ductile Iron Casting Handbook*. Cleveland, Ohio: Gray and Ductile Iron Founders' Soc. Inc.
- Tyberg, B., & Graneholt, O. (1970). *37th International foundry congress 4*.
- Tyndall, J. (1872). *The Forms of Water*. New York: D. Appleton and Co.
- Unsworth, W. (1988 February). *Metals and Materials*, 83–86.
- Uto, Y., & Yamasaki D. (1967). U.K. *Patent Specification 1,198,700*.
- Valdes, J., King, P., & Liu, X. (2010). *Metallurgical & Materials Transactions A*, 41A(9), 2408–2416.
- Valdez, M. E., Uranga, P., & Cramb, A. W. (2007). *Metallurgical & Materials Transactions B*, 38B, 257–266.
- Vandenbos, S. A. (1985). *TAFS*, 93, 871–878.
- Van Ende, M. A., Guo, M., Proost, J., Blanpain, B., & Wollants, P. (2010). *Ironmaking and Steelmaking*, 37(7), 496–501.
- Venturelli, G., & Sant'Unione, G. (February 1981). *Alluminio* 100–106.
- Vernede, S., Dantzig, J. A., & Rappaz, M. (2009). *Acta Materialia*, 57, 1554–1569.
- Vernede, S., Jarry, P., & Rappaz, M. (2006). *Acta Materialia*, 54, 4023–4034.
- Vigh, L., & Bennett, G. H. J. (1989). *Cast Metals*, 2(3), 144–150.
- Villner, L. (1969). *British Foundryman*, 62, 458–468. Also published in *Giesserei* 1970 57(27), 837–844 and *Cast Metals Research Journal*, 1970, 6(3), 137–142.
- Vincent, R. S., & Simmons, G. H. (1943). *Proceedings Physical Society (London)*, 376–382.
- Vogel, A., Doherty, R. D., & Cantor, B. (1977). *Univ Sheffield Conference 'The solidification and casting of metals'*. Published Metals Soc 1979, pp 518–525.
- Voigt, R. C., & Holmgren, S. D. (1990). *TAFS*, 98, 213–225.
- Vorren, O., Evensen, J. E., & Pedersen, T. B. (1984). *TAFS*, 92, 459–466.
- Wakefield, G. R., & Sharp, R. M. (1992). *Journal of Materials Science and Technology*, 8, 1125–1129.
- Wakefield, G. R., & Sharp, R. M. (1996). *Journal of Materials Science and Technology*, 12, 518–522.
- Walker, J. L. (1961). *Physical Chemistry of Process Metallurgy II*. NY: Interscience, p. 845.
- Wall, A. J., & Cocks, D. L. (1980). *British Foundryman*, 73, 292–300.
- Wallace, J. F. (1988). *TAFS*, 96, 261–270.
- Wallace, J. F., & Hrusovsky, J. P. (1979), 87, 269–278.
- Wallace, J. F., & Kissling, R. J. (December 1962). *Foundry* 36–39, 1963 Jan 64–68.
- Wang, C., Gao, H., Dai, Y., Ruan, X., Wang, J., & Sun, B. (2010). *Metallurgical & Materials Transactions A*, 41A(7), 1616–1620.

- Wang, J., Lee, P. D., Hamilton, R. W., Li, M., & Allison, J. (2009). *Scripta Materialia*, 60(7), 516–519.
- Wang, Q. G., Apelian, D., & Lados, D. A. (2001 part I). *Journal of Light Metals*, 1(1), 73–84.
- Wang, Q. G., Apelian, D., & Lados, D. A. (2001 part II). *Journal of Light Metals*, 1(1), 85–97.
- Wang, R.-Y., Lu, W.-H., & Ma, Z.-Y. (2007). *TAFS*, 111, 8, paper 124.
- Wannasin, J., Schwam, D., & Wallace, J. F. (2007). *Journal of Materials Processing Technology*, 191(1–3), 242–246.
- Ward, C. W., & Jacobs, I. C. (1962). *TAFS*, 70, 332–337.
- Wardle, G., & Billington, J. C. (1983). *Metals Technology*, 10, 393–400 (October).
- Warrick, R. J. (1966). *TAFS*, 74, 722–733.
- Warrington, D., & McCartney, D. G. (1989). *Cast Metals*, 2(3), 134–143.
- Watmough, T. (1980). *TAFS*, 88, 481–488.
- Waudby, P. E., & George, G. H. *Twentieth EICF conference on investment casting brussels June 1986*, paper 12, pp. 19
- Way, L. D. (2001). *Materials Science and Technology*, 17(10), 1175–1190.
- Webster, P. D. (1964). *British Foundryman*, 57, 520–523.
- Webster, P. D. (1967). *British Foundryman*, 60, 314–319.
- Webster, P. D. (1966). *British Foundryman*, 59, 387–393.
- Webster, P. D. (1980). In *Fundamentals of Foundry Technology*. Portcullis Press.
- Wells, M. B., & Oleksa, J. T. (1988). *TAFS*, 96, 913–918.
- Wen, S. W., Jolly, M. R., & Campbell, J. (1997). *Solidification Processing conference SP97 Sheffield. 7–10 July 1997. Paper on 'Promotion of directional solidification...'*.
- Weibull, W. (1951). *Journal of Applied Mechanics*, 18, 293–297.
- Weiner, J. H., & Boley, B. A. (1963). *Journal of Mechanics Physics & Solids*, 11, 145–154.
- Weins, M. J., Bottom, J. L. S., & de, Flinn, R. A. (1964). *TAFS*, 72, 832–839.
- Wen, S. W., Jolly, M. R., Campbell, J. (1997). In J. Beech & H. Jones (Eds.), *Proceedings 4th Decennial international conference on solidification processing, Sheffield*, pp. 66–69.
- Whittenberger, E. J., & Rhines, F. N. (1952). *Journal of Metals*, 4(4), 409–420, and *Trans AIME*, 194, 409–420.
- Wieser, P. F. (1983). *TAFS*, 91, 647–656.
- Wieser, P. F., & Dutta, I. (1986). *TAFS*, 94, 85–92.
- Wieser, P. F., & Wallace, J. F. (1969). *TAFS*, 77, 22–26.
- Wightman, G., & Fray, D. J. (1983). *Metallurgical Transactions*, 14B, 625–631.
- Wildermuth, J. W., Lutz, R. H., & Loper, C. R. (1968). *TAFS*, 76, 258–263.
- Wile, L. E., Strausbaugh, K., Archibald, J. J., Smith, R. L., & Piwonka, T. S. (1988). *Metals Handbook* (9th ed.). Volume 15 Casting. ASM International. 240–241.
- Williams, D. C. (1970). *TAFS*, 78, 374–381, 466–467.
- Williams, J. A., & Singer, A. R. E. (1968). *Journal of the Institute of Metals*, 96, 5–12.
- Williams, S. J., Bache, M. R., & Wilshire, B. (2010). *Materials Science & Technology*, 26(11), 1332–1337.
- Wilshire, B., & Scharning, P. J. (2008). *Materials Science & Technology*, 24, 1–9.
- Winardi, L., Littleton, H. E., & Bates, C. E. (2007). *TAFS* paper 062 (04), pp. 10.
- Winter, B. P., Ostrom, T. R., Sleder, T. A., Trojan, P. K., & Pehlke, R. D. (1987). *TAFS*, 95, 259–266.
- Winzer, N., & Cross, C. E. (2009). *Metallurgical & Materials Transactions A*, 40A(2), 273–274.
- Wittmoser, A. (1975). *Transactions of AFS*, 83, 63–72.
- Wittmoser, A., Steinack, K., & Hofmann, R. (1972). *British Foundryman*, 65(February), 73–84.
- Wlodawer, R. (1966). *Directional Solidification of Steel Castings*. English translation by Hewitt L. D, Riley R. V. Pergamon Press.
- Wojcik, W. M., Raybeck, R. M., & Paliwoda, E. J. (1967). *Journal Metals*, 19(Dec), 36–41.
- Wolf, A., & Steinhauser, T. (2004). *Casting Plant & Technology Internat*, (3), 6–11.

- Woodbury, K. A., Chen, Y., Parker, J. K., & Piwonka, T. S. (1998). *TAFS*, 106, 705–711.
- Woodbury, K. A., Ke, Q., & Piwonka, T. S. (2000). *TAFS*, 108, 259–265.
- Woodbury, K. A., Piwonka, T. S., & Ke, Q. (2000). *Modeling of Casting, Welding and advanced solidification processes IX*. pp. 270–277, In P. R. Sahm, P. N. Hansen & J. G. Conley (Eds.).
- Woolley, J. W., & Woodbury, K. A. (2007). *TAFS*, 115, 18 (Paper 075(01)).
- Woolley, J. W., & Woodbury, K. A. (2009). *TAFS*, 117, 31–40.
- Worman, R. A., & Nieman, J. R. (1973). *TAFS*, 81, 170–179.
- Wray, P. J. (1976). *Acta Materialia*, 76, 125–135.
- Wray, P. J. (1976). *Metallurgical Transactions*, 7B, 639–646.
- Wright, T. C., & Campbell, J. (1997). *TAFS*, 105, 639–644, and *Modern Castings*, June 1997 (see also T Dimmick 2001, *Modern Castings*, 91(3), 31–33).
- Wu, C., Sahajwalla, & Pehlke, R. D. (1997). *TAFS*, 105, 739–744.
- Wu, M. (1997). *TAFS*, 105, 693–702.
- Wu, R., & Sandstrom, R. (1995). *Materials Science & Technology*, 11(6), 579–588.
- Xiong, S.-M., & Liu, X.-L. (2007). *Metallurgical & Materials Transactions A*, 38A, 248–434.
- Xu, Z. A. TMS, U.S.A. August, 2007.
- Xu, Z. A., & Mampaey, F. (1997). *TAFS*, 105, 853–860.
- Yamaguchi, K., & Healy, G. (1974). *Metallurgical Transactions*, 5, 2591–2596.
- Yamamoto, N., & Kawagoishi, N. (2000). *Trans AFS*, 108, 113–118.
- Yamamoto, S., Kawano, Y., Murakami, Y., Chang, B., & Ozaki, R. (1975). *TAFS*, 83, 217–226.
- Yamamoto, Y., Iwahori, H., Yonekura, K., & Nakamura, M. (1980). *AFS International Cast Metals Journal*, 5(2), 60–65.
- Yan, Y., Yang, G., & Mao, Z. (1989). *Journal of Aeronautical Material (China)*, 9(3), 29–36.
- Yang, X., & Campbell, J. (1998). Pouring basin. *International Journal of Cast Metals Research*, 10, 239–253.
- Yang, X., Din, T., & Campbell, J. (1998). Offset sprue. *International Journal of Cast Metals Research*, 11, 1–12.
- Yang, X., Jolly, M. R., & Campbell, J. (2000). Vortex flow runner. *Aluminum Trans*, 2(1), 67–80. In P. Sahm P. Hansen & Conley. (Eds.) (2000). *Modelling of casting, welding and advanced solidification processing IX*, pp. 420–427.
- Yaokawa, J., Miura, D., Anzai, K., Yamada, Y., & Yoshi, H. (2007). *Japan Foundry Engineering Society Materials Transaction*, 48(5), 1034–1041.
- Yarborough, W. A., & Messier, R. (1990). *Science*, 247, 688–696.
- Yazzie, K. E., Williams, J. J., Kingsbury, D., Peralta, P., Jiang, H., & Chawla, N. (2010). *Journal of Metals*, 62(7), 16–21.
- Yonekura, K., et al. (1986). *TAFS*, 94, 277–284.
- Youdelis, W. V., & Yang, C. S. (1982). *Metal Science*, 16, 275–281.
- Young, K. P., & Kirkwood, D. H. (1975). *Metallurgical Transactions*, 6A, 197–205.
- Young, P., & quoted Anon. (2002). *Foundry Trade Journal* (April), 27–28.
- Yu, X. Q., & Sun, Y. S. (2004). *Materials Science & Technology*, 20(3), 339–342.
- Yue, T. M., & Chadwick, G. A. Personal communication 1991 relating to the effect of grain size on the 0.2PS of 7010 Al alloy, AZ91 Mg alloy and Al-4.5Cu alloy.
- Zadeh, A. H., & Campbell, J. (2002). *TAFS* paper 02–020.
- Zang, Z., Bian, X., & Liu, X. (2001). *International Journal of Cast Metals Research*, 14(1), 31–35.
- Zeitler, H., & Scharfenberger, W. (1984). *Aluminium (Germany)*, 60(12), E803–E808.
- Zhang, C., Mucciardi, F., Gruzleski, J., Burke, P., & Hart, M. (2003). *AFS Trans*, paper 010–03.
- Zhang, E., Wnag, G. J., Xu, J. W., & Hu, Z. C. (2010). *Material Science Technology*, 26(8), 956–961.
- Zhao, L., Baoyin, Wang, N., Sahajwalla, V., & Pehlke, R. D. (2000). *International Journal of Cast Metals Research*, 13, 167–174.

- Zhu, P., Sha, R., & Li, Y. Effect of twin/tilt on the growth of graphite. In H. Fredriksson & M. Hillert. (Eds.), The physical metallurgy of cast iron, *Proc Materials Research Soc*, 34, p. 3.
- Zildjian Avedis Company cited in *Modern Castings* 2002 (May) page 68.
- Ziman, J. (2001). Physics department, University of Bristol. 'Non-instrumental roles of science'.
- Zuithoff, A. L. (1964). *31st International foundry congress Amsterdam 1964*, paper 29; and in *Geisserei* (1965) 52(9), 820–827.
- Zurecki, Z., & Best, R. C. *TAFS*, 104, 859–864.

This page intentionally left blank



John Campbell

# Complete Casting

## Handbook

Metal Casting Processes, Metallurgy, Techniques and Design



# Complete Casting Handbook

Metal Casting Processes,  
Metallurgy, Techniques  
and Design

*To Sheila once again. She really deserves it.*



# Complete Casting Handbook

Metal Casting Processes,  
Metallurgy, Techniques  
and Design

**John Campbell**

**OBE FREng DEng PhD MMet MA**

*Emeritus Professor of Casting Technology,  
University of Birmingham, UK*



ELSEVIER



Butterworth-Heinemann is an imprint of Elsevier  
The Boulevard, Langford Lane, Kidlington, Oxford OX5 1GB, UK  
225 Wyman Street, Waltham, MA 02451, USA

First edition 2011

Copyright © 2011 John Campbell. Published by Elsevier Ltd. All rights reserved.

The right of John Campbell to be identified as the author of this work has been asserted in accordance with the Copyright, Designs and Patents Act 1988

No part of this publication may be reproduced, stored in a retrieval system or transmitted in any form or by any means electronic, mechanical, photocopying, recording or otherwise without the prior written permission of the publisher

Permissions may be sought directly from Elsevier's Science & Technology Rights Department in Oxford, UK: phone (+44) (0) 1865 843830; fax (+44) (0) 1865 853333; email: [permissions@elsevier.com](mailto:permissions@elsevier.com). Alternatively you can submit your request online by visiting the Elsevier web site at <http://elsevier.com/locate/permissions>, and selecting *Obtaining permission to use Elsevier material*

#### **Notice**

No responsibility is assumed by the publisher for any injury and/or damage to persons or property as a matter of products liability, negligence or otherwise, or from any use or operation of any methods, products, instructions or ideas contained in the material herein. Because of rapid advances in the medical sciences, in particular, independent verification of diagnoses and drug dosages should be made

#### **British Library Cataloguing in Publication Data**

A catalogue record for this book is available from the British Library

#### **Library of Congress Cataloging-in-Publication Data**

A catalog record for this book is available from the Library of Congress

ISBN-13: 978-1-85617-809-9

For information on all Butterworth-Heinemann publications visit our web site at [books.elsevier.com](http://books.elsevier.com)

Printed and bound in the UK

11 12 13 14 15 10 9 8 7 6 5 4 3 2 1

Working together to grow  
libraries in developing countries

[www.elsevier.com](http://www.elsevier.com) | [www.bookaid.org](http://www.bookaid.org) | [www.sabre.org](http://www.sabre.org)

ELSEVIER

BOOK AID  
International

Sabre Foundation

# Contents

Preface .....	xix
Introduction from <i>Castings</i> 1st Edition 1991 .....	xxiii
Introduction to <i>Castings</i> 2nd Edition 2003.....	xxv
Introduction to <i> Casting Practice: The 10 Rules of Castings</i> 2004 .....	xxvii
Introduction to <i>Castings Handbook</i> 2011 .....	xxix
Acknowledgments.....	xxxi

## **VOLUME I CASTING METALLURGY**

---

<b>CHAPTER 1 The melt.....</b>	<b>3</b>
1.1 Reactions of the melt with its environment .....	5
1.2 Transport of gases in melts.....	9
1.3 Surface film formation.....	13
1.4 Vaporization .....	16
<b>CHAPTER 2 Entrainment .....</b>	<b>19</b>
2.1 Entrainment defects .....	24
2.1.1 Bifilms .....	24
2.1.2 Bubbles .....	28
2.1.3 Extrinsic inclusions .....	32
2.2 Entrainment processes .....	42
2.2.1 Surface turbulence.....	42
2.2.2 Oxide skins from melt charge materials.....	52
2.2.3 Pouring.....	54
2.2.4 The oxide lap defect I: Surface flooding .....	57
2.2.5 The oxide lap defect II: The confluence weld.....	60
2.2.6 The oxide flow tube.....	64
2.2.7 Microjetting .....	65
2.2.8 Bubble trails .....	67
2.3 Furling and unfurling.....	77
2.4 Deactivation of entrained films.....	88
2.5 Soluble, transient films .....	92
2.6 Detrainment.....	92
2.7 Evidence for bifilms.....	94
2.8 The importance of bifilms .....	100

<b>CHAPTER 3 Flow</b> .....	<b>105</b>
<b>3.1</b> Effect of surface films on filling.....	105
3.1.1 Effective surface tension.....	105
3.1.2 The rolling wave.....	106
3.1.3 The unzipping wave.....	108
<b>3.2</b> Maximum fluidity (the science of unrestricted flow).....	110
3.2.1 Mode of solidification.....	113
3.2.2 Effect of velocity.....	126
3.2.3 Effect of viscosity (including effect of entrained bifilms).....	128
3.2.4 Effect of solidification time $t_f$ .....	130
3.2.5 Effect of surface tension.....	140
3.2.6 Effect of an unstable substrate.....	143
3.2.7 Comparison of fluidity tests.....	144
<b>3.3</b> Extended fluidity.....	148
<b>3.4</b> Continuous fluidity.....	151
<b>CHAPTER 4 Molds and cores</b> .....	<b>155</b>
<b>4.1</b> Molds: Inert or reactive.....	155
<b>4.2</b> Transformation zones.....	156
<b>4.3</b> Evaporation and condensation zones.....	159
<b>4.4</b> Mold atmosphere.....	164
4.4.1 Composition.....	164
4.4.2 Mold gas explosions.....	166
<b>4.5</b> Mold surface reactions.....	168
4.5.1 Pyrolysis.....	168
4.5.2 Lustrous carbon film.....	170
4.5.3 Sand reactions.....	171
4.5.4 Mold contamination.....	171
4.5.5 Mold penetration.....	173
<b>4.6</b> Metal surface reactions.....	178
4.6.1 Oxidation.....	178
4.6.2 Carbon (pick-up and loss).....	179
4.6.3 Nitrogen.....	181
4.6.4 Sulfur.....	181
4.6.5 Phosphorus.....	181
4.6.6 Surface alloying.....	182
4.6.7 Grain refinement.....	182
4.6.8 Miscellaneous.....	183
<b>4.7</b> Mold coatings.....	183
4.7.1 Aggregate molds.....	183

4.7.2 Permanent molds and metal chills .....	185
4.7.3 Dry coatings .....	186
<b>CHAPTER 5 Solidification structure .....</b>	<b>187</b>
5.1 Heat transfer .....	187
5.1.1 Resistances to heat transfer .....	187
5.1.2 Increased heat transfer .....	202
5.1.3 Convection .....	219
5.1.4 Remelting .....	219
5.1.5 Flow channel structure .....	220
5.2 Development of matrix structure .....	224
5.2.1 General .....	224
5.2.2 Nucleation of the solid .....	225
5.2.3 Growth of the solid .....	228
5.2.4 Disintegration of the solid (grain multiplication) .....	236
5.3 Segregation .....	241
5.3.1 Planar front segregation .....	242
5.3.2 Microsegregation .....	245
5.3.3 Dendritic segregation .....	247
5.3.4 Gravity segregation .....	250
<b>CHAPTER 6 Casting alloys .....</b>	<b>255</b>
6.1 Zinc alloys .....	255
6.2 Magnesium .....	260
6.2.1 Films on liquid Mg alloys and protective atmospheres .....	261
6.2.2 Strengthening Mg alloys .....	266
6.2.3 Microstructure .....	268
6.3 Aluminum .....	269
6.3.1 Oxide films on Al alloys .....	271
6.3.2 Entrained inclusions .....	273
6.3.3 Grain refinement (nucleation and growth of the solid) .....	274
6.3.4 DAS and grain size .....	278
6.3.5 Modification of eutectic Si in Al–Si alloys .....	279
6.3.6 Iron-rich intermetallics .....	298
6.3.7 Other intermetallics .....	303
6.3.8 Thermal analysis of Al alloys .....	305
6.3.9 Hydrogen in Al alloys .....	306
6.4 Copper .....	309
6.4.1 Surface films .....	310
6.4.2 Gases in Cu-based alloys .....	310
6.4.3 Grain refinement .....	315

<b>6.5</b>	Cast iron .....	315
6.5.1	Reactions with gases .....	316
6.5.2	Surface films on liquid cast irons .....	318
6.5.3	Cast iron microstructures .....	332
6.5.4	Flake graphite iron (FGI) and inoculation .....	334
6.5.5	Nucleation and growth of the austenite matrix .....	343
6.5.6	Coupled eutectic growth of graphite and austenite .....	345
6.5.7	Spheroidal graphite iron (SGI) (ductile iron) .....	347
6.5.8	Compacted graphite iron (CGI) .....	355
6.5.9	Chunky graphite (CHG) .....	357
6.5.10	White iron (iron carbide) .....	359
6.5.11	General .....	360
6.5.12	Summary of structure hypothesis .....	360
<b>6.6</b>	Steels .....	362
6.6.1	Carbon steels .....	362
6.6.2	Stainless steels .....	363
6.6.3	Inclusions in carbon and low-alloy steels (general background) .....	365
6.6.4	Entrained inclusions .....	367
6.6.5	Primary inclusions .....	370
6.6.6	Secondary inclusions and second phases .....	374
6.6.7	Nucleation and growth of the solid .....	377
6.6.8	Structure development in the solid .....	380
<b>6.7</b>	Nickel-base alloys .....	382
6.7.1	Air melting and casting .....	383
6.7.2	Vacuum melting and casting .....	383
<b>6.8</b>	Titanium .....	386
6.8.1	Ti alloys .....	387
6.8.2	Melting and casting Ti alloys .....	387
6.8.3	Surface films on Ti alloys .....	389
<b>CHAPTER 7</b>	<b>Porosity .....</b>	<b>391</b>
<b>7.1</b>	Shrinkage porosity .....	391
7.1.1	General shrinkage behavior .....	391
7.1.2	Solidification shrinkage .....	392
7.1.3	Feeding criteria .....	399
7.1.4	Feeding: The five mechanisms .....	403
7.1.5	Initiation of shrinkage porosity .....	418
7.1.6	Growth of shrinkage pores .....	436
7.1.7	Shrinkage pore structure .....	436

7.2	Gas porosity .....	443
7.2.1	Entrained (external) pores .....	443
7.2.2	Blow holes .....	445
7.2.3	Gas porosity initiated in situ .....	445
7.3	Porosity diagnosis .....	461
<b>CHAPTER 8</b>	<b>Cracks and tears .....</b>	<b>465</b>
8.1	Hot tearing .....	465
8.1.1	General.....	465
8.1.2	Grain boundary wetting by the liquid.....	469
8.1.3	Pre-tear extension .....	470
8.1.4	Strain concentration.....	472
8.1.5	Stress concentration.....	473
8.1.6	Tear initiation .....	474
8.1.7	Tear growth.....	476
8.1.8	Prediction of hot tearing susceptibility .....	479
8.1.9	Methods of testing.....	483
8.1.10	Methods of control .....	489
8.1.11	Summary of the conditions for hot tearing and porosity .....	493
8.1.12	Hot tearing in stainless steels.....	494
8.1.13	Predictive techniques.....	495
8.2	Cold cracking.....	495
8.2.1	General.....	495
8.2.2	Crack initiation.....	496
8.2.3	Crack growth .....	497
<b>CHAPTER 9</b>	<b>Properties of castings.....</b>	<b>499</b>
9.1	Test bars .....	499
9.2	The statistics of failure .....	504
9.2.1	Background to the use of Weibull analysis .....	507
9.2.2	Two-parameter Weibull analysis.....	510
9.2.3	Three-parameter Weibull analysis.....	511
9.2.4	Bi-Weibull distributions .....	512
9.2.5	Limits of accuracy.....	514
9.2.6	Extreme value distributions.....	516
9.3	Effect of defects.....	516
9.3.1	Inclusion types and diagnosis .....	517
9.3.2	Gas porosity.....	520
9.3.3	Shrinkage porosity.....	525
9.3.4	Tears, cracks, and bifilms.....	526

<b>9.4</b>	Tensile properties .....	529
9.4.1	Microstructural failure.....	529
9.4.2	Ductility .....	533
9.4.3	Yield strength .....	539
9.4.4	Ultimate tensile strength .....	553
<b>9.5</b>	Fracture toughness .....	555
<b>9.6</b>	Fatigue.....	561
9.6.1	High cycle fatigue .....	561
9.6.2	Low cycle and thermal fatigue.....	571
<b>9.7</b>	Elastic (Young’s) modulus and damping capacity .....	573
<b>9.8</b>	Residual stress.....	574
<b>9.9</b>	High-temperature tensile properties .....	575
9.9.1	Creep.....	575
9.9.2	Superplastic forming .....	576
<b>9.10</b>	Oxidation and corrosion resistance .....	578
9.10.1	Internal oxidation .....	578
9.10.2	Corrosion .....	579
9.10.3	Pitting corrosion .....	582
9.10.4	Filiform corrosion .....	584
9.10.5	Intergranular corrosion.....	585
9.10.6	Stress corrosion cracking .....	586
<b>9.11</b>	Leak-tightness .....	587
<b>9.12</b>	Surface finish .....	591
9.12.1	Effect of surface tension .....	591
9.12.2	Effects of a solid surface film.....	593
<b>9.13</b>	Quality indices .....	594
References.....		RI-1

## VOLUME 2 CASTING MANUFACTURE

---

### Section 1

<b>CHAPTER 10</b>	<b>The 10 Rules for good castings.....</b>	<b>605</b>
<b>10.1</b>	Rule 1: ‘Use a good-quality melt’ .....	607
10.1.1	Background .....	607
<b>10.2</b>	Rule 2: ‘Avoid turbulent entrainment’ (the critical velocity requirement).....	614
10.2.1	Introduction .....	614
10.2.2	Maximum velocity requirement.....	615
10.2.3	The ‘no-fall’ requirement.....	619



<b>10.3</b>	Rule 3: ‘Avoid laminar entrainment of the surface film’ (the non-stopping, non-reversing condition).....	623
	10.3.1 Continuous expansion of the meniscus .....	623
	10.3.2 Arrest of forward motion of the meniscus .....	624
	10.3.3 Waterfall flow; the oxide flow tube .....	625
	10.3.4 Horizontal stream flow .....	627
	10.3.5 Hesitation and reversal.....	629
	10.3.6 Oxide lap defects.....	630
<b>10.4</b>	Rule 4: ‘Avoid bubble damage’ .....	631
	10.4.1 The bubble trail .....	631
	10.4.2 Bubble damage.....	632
	10.4.3 Bubble damage in gravity filling systems .....	633
	10.4.4 Bubble damage in counter-gravity systems.....	634
<b>10.5</b>	Rule 5: ‘Avoid core blows’ .....	635
	10.5.1 Background .....	635
	10.5.2 Outgassing pressure in cores.....	647
	10.5.3 Core blow model study .....	653
	10.5.4 Microblows.....	654
	10.5.5 Prevention of blows.....	655
	10.5.6 Summary of blow prevention.....	659
<b>10.6</b>	Rule 6: ‘Avoid shrinkage damage’ .....	659
	10.6.1 Definitions and background .....	659
	10.6.2 Feeding to avoid shrinkage problems.....	660
	10.6.3 The seven feeding rules .....	661
	10.6.4 The new feeding logic.....	688
	10.6.5 Freezing systems design (chills and fins).....	692
	10.6.6 Feeding – the five mechanisms.....	692
	10.6.7 Computer modeling of feeding .....	694
	10.6.8 Random perturbations to feeding.....	694
	10.6.9 The non-feeding roles of feeders .....	695
<b>10.7</b>	Rule 7: ‘Avoid convection damage’ .....	696
	10.7.1 The academic background .....	696
	10.7.2 The engineering imperatives.....	697
	10.7.3 Convection damage and casting section thickness.....	701
	10.7.4 Countering convection .....	704
<b>10.8</b>	Rule 8: ‘Reduce segregation damage’ .....	705
<b>10.9</b>	Rule 9: ‘Reduce residual stress’ .....	707
	10.9.1 Introduction .....	707
	10.9.2 Residual stress from casting .....	708
	10.9.3 Residual stress from quenching .....	712

10.9.4	Controlled quenching using polymer and other quenchant	716
10.9.5	Controlled quenching using air	719
10.9.6	Strength reduction by heat treatment	720
10.9.7	Distortion	722
10.9.8	Heat treatment developments	723
10.9.9	Beneficial residual stress	724
10.9.10	Stress relief	725
10.9.11	Epilogue	728
<b>10.10</b>	<b>Rule 10: ‘Provide location points’</b>	<b>728</b>
10.10.1	Datums	729
10.10.2	Location points	730
10.10.3	Location jigs	736
10.10.4	Clamping points	736
10.10.5	Potential for integrated manufacture	737

## Section 2 Filling system design

### CHAPTER 11 Filling system design fundamentals ..... 741

11.1	The maximum velocity requirement	741
11.2	Gravity pouring – The ‘no-fall’ conflict	741
11.3	Reduction or elimination of gravity problems	745
11.4	Surface-tension-controlled filling	751

### CHAPTER 12 Filling system components ..... 757

12.1	Pouring basin	757
12.1.1	The conical basin	757
12.1.2	Inert gas shroud	760
12.1.3	Contact pouring	761
12.1.4	The offset basin	762
12.1.5	The offset step (weir) basin	762
12.1.6	The sharp-cornered or undercut basin	769
12.1.7	Stopper	771
12.2	Sprue (down-runner)	772
12.2.1	Multiple sprues	778
12.2.2	Division of sprues	780
12.2.3	Sprue base	781
12.2.4	The well	782
12.2.5	The radial choke	785
12.2.6	The radius of the sprue/runner junction	785
12.3	Runner	787
12.3.1	The tapered runner	792

12.3.2	The expanding runner .....	793
<b>12.4</b>	<b>Gates .....</b>	<b>795</b>
12.4.1	Siting .....	795
12.4.2	Direct and indirect.....	795
12.4.3	Total area of gate(s) .....	796
12.4.4	Gating ratio.....	797
12.4.5	Multiple gates.....	798
12.4.6	Premature filling problem via early gates .....	798
12.4.7	Horizontal velocity in the mold.....	799
12.4.8	Junction effect .....	800
12.4.9	The touch gate.....	803
12.4.10	Knife gate .....	805
12.4.11	The pencil gate.....	806
12.4.12	The horn gate .....	806
12.4.13	Vertical gate.....	809
12.4.14	Direct gating into the mold cavity.....	809
12.4.15	Flow channel structure .....	810
12.4.16	Indirect gating (into an up-runner/riser) .....	811
12.4.17	Central versus external systems.....	814
12.4.18	Sequential gating.....	815
12.4.19	Priming techniques.....	817
<b>12.5</b>	<b>Surge control systems.....</b>	<b>819</b>
<b>12.6</b>	<b>Vortex systems .....</b>	<b>823</b>
12.6.1	Vortex sprue.....	823
12.6.2	Vortex well or gate.....	824
12.6.3	Vortex runner (the offset sprue).....	825
<b>12.7</b>	<b>Inclusion control: Filters and traps.....</b>	<b>826</b>
12.7.1	Dross trap (slag trap).....	827
12.7.2	Slag pockets .....	828
12.7.3	Swirl trap.....	829
<b>12.8</b>	<b>Filters .....</b>	<b>833</b>
12.8.1	Strainers.....	833
12.8.2	Woven cloth or mesh .....	834
12.8.3	Ceramic block filters.....	838
12.8.4	Leakage control.....	840
12.8.5	Filters in running systems .....	846
12.8.6	Tangential placement .....	848
12.8.7	Direct pour .....	850
12.8.8	Sundry aspects.....	851
12.8.9	Summary .....	852

**CHAPTER 13 Filling system design practice ..... 853**

- 13.1 Background to the methoding approach ..... 854
- 13.2 Selection of a layout..... 854
- 13.3 Weight and volume estimate ..... 854
- 13.4 Pressurized versus unpressurized ..... 857
- 13.5 Selection of a pouring time ..... 862
- 13.6 Thin sections and slow filling ..... 865
- 13.7 Fill rate..... 866
- 13.8 Pouring basin design..... 867
- 13.9 Sprue (down-runner) design ..... 867
- 13.10 Runner design..... 871
- 13.11 Gate design ..... 873

**Section 3 Processing (melting, molding, casting, solidifying)**

**CHAPTER 14 Melting ..... 879**

- 14.1 Batch melting..... 879
  - 14.1.1 Liquid metal delivery..... 879
  - 14.1.2 Reverberatory furnaces..... 880
  - 14.1.3 Crucible melting (electric resistance or gas heated) ..... 881
  - 14.1.4 Induction melting ..... 882
  - 14.1.5 Automatic bottom pouring..... 882
- 14.2 Continuous melting..... 883
  - 14.2.1 Tower (shaft) furnaces..... 883
  - 14.2.2 Dry hearth furnaces for non-ferrous metals ..... 884
- 14.3 Holding, transfer and distribution ..... 885
  - 14.3.1 Holder failure modes..... 887
  - 14.3.2 Transfer and distribution systems ..... 888
- 14.4 Melt treatments ..... 888
  - 14.4.1 Degassing ..... 888
  - 14.4.2 Detrainment (cleaning) ..... 896
  - 14.4.3 Additions ..... 901
  - 14.4.4 Pouring ..... 902
- 14.5 Cast material ..... 905
  - 14.5.1 Liquid metal ..... 905
  - 14.5.2 Partially solid mixtures ..... 905
- 14.6 Remelting processes ..... 909
  - 14.6.1 Vacuum arc remelting (VAR) ..... 909
  - 14.6.2 Electro-slag remelting (ESR)..... 910

<b>CHAPTER 15 Molding.....</b>	<b>911</b>
<b>15.1</b> Inert molds and cores .....	911
15.1.1 Permanent metal molds (dies) .....	912
15.1.2 Salt cores .....	914
15.1.3 Ceramic molds and cores.....	915
15.1.4 Magnetic molding .....	917
<b>15.2</b> Aggregate molding materials .....	918
15.2.1 Silica sand .....	919
15.2.2 Chromite sand .....	920
15.2.3 Olivine sand.....	920
15.2.4 Zircon sand.....	921
15.2.5 Other minerals.....	921
15.2.6 Carbon .....	922
<b>15.3</b> Binders .....	923
15.3.1 Greensand.....	923
15.3.2 Dry sand .....	924
15.3.3 Chemical binders.....	924
15.3.4 Effset process (ice binder) .....	929
15.3.5 Loam.....	929
15.3.6 Cement.....	930
15.3.7 Fluid (castable) sand .....	930
<b>15.4</b> Other aggregate mold processes.....	931
15.4.1 Precision core assembly .....	931
15.4.2 Machined-to-form .....	931
15.4.3 Unbonded aggregate molds.....	931
<b>15.5</b> Rubber molds.....	931
<b>15.6</b> Reclamation and recycling of aggregates .....	932
15.6.1 Aggregate reclamation in an Al foundry.....	932
15.6.2 Aggregate reclamation in a ductile iron foundry .....	935
15.6.3 Aggregate reclamation with soluble inorganic binders.....	936
15.6.4 Facing and backing sands .....	937
<b>CHAPTER 16 Casting.....</b>	<b>939</b>
<b>16.1</b> Gravity casting.....	939
16.1.1 Gravity pouring of open molds.....	939
16.1.2 Gravity pouring of closed molds .....	940
16.1.3 Two-stage filling (priming techniques).....	944
16.1.4 Vertical stack molding .....	945
16.1.5 Horizontal stack molding (H process).....	945
16.1.6 Postscript to gravity filling.....	945

16.2	Horizontal transfer casting .....	946
16.2.1	Level pour (side pour).....	946
16.2.2	Controlled tilt casting.....	948
16.2.3	Roll-over as a casting process .....	955
16.2.4	Roll-over after casting (sometimes called inversion casting) .....	957
16.3	Counter-gravity .....	960
16.3.1	Low-pressure casting.....	963
16.3.2	Liquid metal pumps .....	968
16.3.3	Direct vertical injection .....	974
16.3.4	Programmable control.....	977
16.3.5	Feedback control .....	977
16.3.6	Failure modes of low-pressure casting .....	978
16.4	Centrifugal casting.....	979
16.5	Pressure-assisted casting.....	985
16.5.1	High-pressure die casting (HPDC) .....	986
16.5.2	Squeeze casting .....	991
16.6	Lost wax and other ceramic mold casting processes.....	997
16.7	Lost foam casting .....	1001
16.8	Vacuum molding (V process).....	1005
16.9	Vacuum-assisted casting .....	1008
16.10	Vacuum melting and casting .....	1009
<b>CHAPTER 17</b>	<b>Controlled solidification techniques .....</b>	<b>1013</b>
17.1	Conventional-shaped castings.....	1013
17.2	Directional solidification (DS) .....	1014
17.3	Single crystal solidification .....	1016
17.4	Rapid solidification casting .....	1018
<b>CHAPTER 18</b>	<b>Dimensional accuracy.....</b>	<b>1025</b>
18.1	The concept of net shape.....	1029
18.1.1	Effect of casting process .....	1030
18.1.2	Effect of expansion and contraction .....	1032
18.1.3	Effect of cast alloy .....	1032
18.2	Mold design .....	1033
18.2.1	General issues.....	1033
18.2.2	Assembly methods .....	1035
18.3	Mold accuracy .....	1038
18.3.1	Aggregate molds .....	1038
18.3.2	Ceramic molds .....	1041
18.3.3	Metal molds (dies) .....	1042
18.4	Tooling accuracy.....	1045

18.5	Casting accuracy.....	1046
18.5.1	Uniform contraction.....	1046
18.5.2	Non-uniform contraction (distortion).....	1053
18.5.3	Process comparison.....	1061
18.5.4	General summary.....	1063
18.6	Metrology.....	1063
<b>CHAPTER 19</b>	<b>Post-casting processing.....</b>	<b>1067</b>
19.1	Surface cleaning.....	1067
19.2	Heat treatment.....	1069
19.2.1	Homogenization and solution treatments.....	1070
19.2.2	Heat treatment reduction and/or elimination.....	1072
19.2.3	Blister formation.....	1073
19.2.4	Incipient melting.....	1074
19.2.5	Fluid beds.....	1075
19.3	Hot isostatic pressing.....	1077
19.4	Machining.....	1080
19.5	Painting.....	1083
19.6	Plastic working (forging, rolling, extrusion).....	1083
19.7	Impregnation.....	1085
19.8	Non-destructive testing.....	1086
19.8.1	X-ray radiography.....	1086
19.8.2	Dye-penetrant inspection (DPI).....	1087
19.8.3	Leak testing.....	1087
19.8.4	Resonant frequency testing.....	1088
	References.....	R11-1
	Appendix 1.....	1091
	Appendix 2.....	1095
	Appendix 3.....	1099
	Index.....	1103

This page intentionally left blank



# Preface

Metal castings are fundamental building blocks, the three-dimensional integral shapes indispensable to practically all other manufacturing industries.

Although the manufacturing path from the liquid to the finished shape is the most direct, this directness involves the greatest difficulty. This is because so much needs to be controlled simultaneously, including melting, alloying, molding, pouring, solidification, finishing, etc. Every one of these production steps has to be correct since failure of only one will probably cause the whole product to be unacceptable to the customer. In contrast, other processes such as forging or machining are merely single-step processes. It is clearly easier to control each separate process step in turn.

It is no wonder therefore that the manufacture of castings is one of the most challenging of technologies. It has defied proper understanding and control for an impressive five thousand years. However, there are signs that we might now be starting to make progress.

Naturally, this claim for the possible existence of progress appears to have been made by every writer of textbooks on castings for the last several hundred years. Doubtless, it will continue to be made in future generations. In a way, it is hoped that it will always be true. This is what makes casting so fascinating. The complexity of the subject invites a continuous stream of new ideas and new solutions.

The author trained as a physicist and physical metallurgist, and is aware of the admirable and powerful developments in science and technology that have facilitated the progress enjoyed by these branches of science. These successes have, quite naturally, persuaded the Higher Educational Institutes throughout the world to the adoption of *physical metallurgy* as the natural materials discipline required to be taught.

This work makes the case for *process metallurgy* as being a key discipline, inseparable from physical metallurgy. It can explain the properties of metals, in some respects outweighing the effects of alloying, working and heat treatment that are the established province of physical metallurgy. In particular, the study of casting technology is a topic of daunting complexity, far more encompassing than the separate studies, for instance, of fluid flow or solidification (as necessary, important and fascinating as such focused studies clearly are). It is hoped therefore that, in time, casting technology will be rightly recognized as a complex and vital engineering discipline, worthy of individual focus.

Prior to writing this book, the author has always admired those who have published only what was certain knowledge. However, as this work was well under way, it became clear to him that this was not achievable in this case. Knowledge is hard to achieve, and often illusive, fragmentary, and ultimately uncertain. This book is offered as an exercise in education, more to do with thinking and understanding than learning. It is an exercise in grappling with new concepts and making personal evaluations of their worth, their cogency, and their place amid the scattering of facts, some reliable, others less so. It is about research, and about the excitement of finding out for oneself.

Thus the opportunity has been taken in this new book to bring the work up to date, particularly in the new and exciting areas of surface turbulence, the recently discovered compaction and unfurling of folded film defects (the bifilms). Additional new concepts of alloy theory relating to the common alloy eutectics Al–Si and Fe–C will be outlined. These are particularly exciting. Perhaps these new paradigms can never be claimed to be ‘true’. They are offered as potentially valuable theories allowing us to codify and classify our knowledge until something better comes along. Newton’s theory of

gravitation was a welcome and extraordinarily valuable systematization of our knowledge for several hundred years until surpassed by Einstein's General Relativity.

Thus the author has allowed himself the luxury of hypothesis, that a skeptic might brand speculation. This book is a first attempt to codify and present what I like to call the 'New Metallurgy'. It cannot claim to be authoritative on all aspects at this time. It is an introduction to the new thinking of the metallurgy of cast alloys, and, by virtue of the survival of many of the casting defects during plastic working, wrought alloys too.

The intellectual problem that some have in accepting the existence of bifilms is curious. The problem of acceptance does not seem to exist in processes such as powder metallurgy, and the various spray-forming technologies, where everyone immediately realizes 'bifilms' exist if they give the matter a moment's thought. The difference between these particle technologies and castings is that the particulate routes have rather regular bifilm populations, leading to reproducible properties. Similar rather uniform but larger-scale bifilms can be seen in slowly collapsing metallic foams, in which it is extraordinary to watch the formation of bifilms in slow motion as one oxide film settles gently down on its neighbor (Mukherjee 2010). Castings in contrast can have coexisting populations of defects sometimes taking the form of fogs of fine particles, scatterings of confetti and postage stamps, and sometimes sheets of A4 and quarto paper sized defects.

The new concept of the bifilm involves a small collection of additional terms and definitions which are particularly helpful in designing filling and feeding systems for castings and understanding casting failure mechanisms. They include critical velocity, critical fall distance, entrainment, surface turbulence, the bubble trail, hydrostatic tensions in liquids, constrained flow, and the naturally pressurized filling system. They represent the software of the new technology, while its study is facilitated by the new hardware of X-ray video radiography and computer simulation. These are all powerful investigative tools that have made our recent studies so exciting and rewarding.

Despite all the evidence, at the time of writing there appear to be many in industry and research still denying the existence of bifilms. It brings to mind the situation in the early 1900s when, once again despite overwhelming evidence, many continued to deny the existence of atoms.

The practice of seeking corroboration of scientific concepts from industrial experience, used often in this book, is a departure that will be viewed with concern by those academics who are accustomed to the apparent rigor of laboratory experiments and who are not familiar with the current achievements of industry. However, for those who persevere and grow to understand this work it will become clear that laboratory experiments cannot at this time achieve the control over liquid metal quality that can now be routinely provided in many industrial operations. Thus the evidence from industry is vital at this time. Suitable confirmatory experiments in laboratories can catch up later.

The primary aim remains, to challenge the reader to think through the concepts that will lead to a better understanding of the casting process – the most complex of forming operations. It is hoped thereby to improve the professionalism and status of casting technology, and with it the castings themselves, so that both the industry and its customers will benefit.

As I mentioned in the preface to *CASTINGS 1991*, and bears repeat here, the rapidity of casting developments makes it a privilege to live in such exciting times. For this reason, however, it will not be possible to keep this work up to date. It is hoped that, as before, this new edition will serve its purpose

for a time; assisting foundry people to overcome their everyday problems and metallurgists to understand their alloys. Furthermore, I hope it will inspire students and casting engineers alike to continue to keep themselves updated. The regular reading of new developments in the casting journals, and attendance at technical meetings of local societies, will encourage the professionalism to achieve even higher standards of castings in the future.

**JC**  
**Ledbury, Herefordshire, England**  
23 November 2010

This page intentionally left blank

# Introduction from *Castings*

## 1st Edition 1991

Castings can be difficult to get right. Creating things never is easy. But sense the excitement of this new arrival:

The first moments of creation of the new casting are an explosion of interacting events; the release of quantities of thermal and chemical energy trigger a sequence of cataclysms.

The liquid metal attacks and is attacked by its environment, exchanging alloys, impurities, and gas. The surging and tumbling flow of the melt through the running system can introduce clouds of bubbles and Sargasso seas of oxide film. The mould shocks with the vicious blast of heat, buckling and distending, fizzing with the volcanic release of vapours that flood through the liquid metal by diffusion, or reach pressures to burst the liquid surface as bubbles.

During freezing, liquid surges through the dendrite forest to feed the volume contraction on solidification, washing off branches, cutting flow paths, and polluting regions with excess solute, forming segregates. In those regions cut off from the flow, continuing contraction causes the pressure in the residual liquid to fall, possibly becoming negative (as a tensile stress in the liquid) and sucking in the solid surface of the casting. This will continue until the casting is solid, or unless the increasing stress is suddenly dispelled by an explosive expansion of a gas or vapour cavity giving birth to a shrinkage cavity.

The surface sinks are halted, but the internal defects now start.

The subsequent cooling to room temperature is no less dramatic. The solidified casting strives to contract whilst being resisted by the mould. The mould suffers, and may crush and crack. The casting also suffers, being stretched as on a rack. Silent, creeping strain and stress change and distort the casting, and may intensify to the point of catastrophic failure, tearing it apart, or causing insidious thin cracks. Most treacherous of all, the strain may *not quite* crack the casting, leaving it apparently perfect, but loaded to the brink of failure by internal residual stress.

These events are rapidly changing dynamic interactions. It is this rapidity, this dynamism, that characterises the first seconds and minutes of the casting's life. An understanding of them is crucial to success.

This new work is an attempt to provide a framework of guidelines together with the background knowledge to ensure understanding; to avoid the all too frequent disasters; to cultivate the targeting of success; to encourage a professional approach to the design and manufacture of castings.

The reader who learns to guide the production methods through this minefield will find the rare reward of a truly creative profession. The student who has designed the casting method, and who is present when the mould is opened for the first time will experience the excitement and anxiety, and find himself asking the question asked by all foundry workers on such occasions: 'Is it all there?' The casting design rules in this text are intended to provide, so far as present knowledge will allow, enough predictive capability to know that the casting will be not only all there, but all right!

The clean lines of the finished engineering casting, sound, accurate, and strong, are a pleasure to behold. The knowledge that the casting contains neither defects nor residual stress is an additional powerful reassurance. It represents a miraculous transformation from the original two-dimensional form on paper or the screen to a three-dimensional shape, from a mobile liquid to a permanently shaped, strong solid. It is an achievement worthy of pride.

The reader will need some background knowledge. The book is intended for final year students in metallurgy or engineering, for those researching in castings, and for casting engineers and all associated with foundries that have to make a living creating castings.

Good luck!

# Introduction to *Castings* 2nd Edition 2003

I hope the reader will find inspiration from this work.

What is presented is a new approach to the metallurgy of castings. Not everything in the book can claim to be proven at this stage. The author has to admit that he felt compelled to indulge in what the hard line scientist would dismissively label 'reckless speculation'. Ultimately however, science works by proposing hypotheses, which, if they prove to be useful, can have long and respectable lives, irrespective whether they are 'true' or not. Newton's theory of gravitation was such a hypothesis. It was, and remains, respectable and useful, even though eventually proven inaccurate. The hypotheses relating to the metallurgy of cast metals, proposed in this work, are similarly tendered as being at least useful. Perhaps we may never be able to say for certain that they are really 'true', but in the meantime it is proposed as a piece of knowledge as reliable as can now be assembled (Ziman 2001). Moreover, it is believed that a coherent framework for an understanding of cast metals has been achieved for the first time.

The fundamental starting point is the bifilm, the folded-in surface film. It is often invisible, having escaped detection for millennia. Because the presence of bifilms has been unknown, the initiation events for our commonly seen defects such as porosity, cracks and tears have been consistently overlooked.

It is not to be expected that all readers will be comfortable with the familiar, cosy concepts of 'gas' porosity and 'shrinkage' porosity relegated to being mere consequences, simply macroscopic and observable outcomes, growth forms derived from the new bifilm defect, and at times relatively unimportant compared to the pre-existing bifilm itself. Many of us will have to re-learn our metallurgy of cast metals. Nevertheless, I hope that the reader will overcome any doubts and prejudice, and persevere bravely. The book was not written for the faint-hearted.

As a final blow (the reader needs resilience!), the book nowhere claims that good castings are easily achieved. As was already mentioned in the Preface, the casting process is among the most complex of all engineering production systems. We currently need all the possible assistance to our understanding to solve the problems to achieve adequate products. In particular, it follows that the section on casting manufacture is mandatory reading for metallurgists and academics alike.

For the future, we can be inspired to strive for, and perhaps one day achieve defect-free cast products. At that moment of history, when the bifilm is banished, we shall have automatically achieved that elusive goal, targeted by every foundry I know, '*highest quality together with minimum costs*'.

This page intentionally left blank



# Introduction to *Casting Practice:* *The 10 Rules of Castings* 2004

The second book is effectively my own checklist to ensure that no key aspect of the design of the manufacturing route for the casting is forgotten. The Ten Rules are first listed in summary form. They are then addressed in more detail in the following ten chapters with one chapter per Rule.

The Ten Rules listed here are proposed as necessary, but not, of course, sufficient, for the manufacture of reliable castings. It is proposed that they are used in addition to existing necessary technical specifications such as alloy type, strength, and traceability via international standard quality systems, and other well known and well understood foundry controls such as casting temperature etc.

Although not yet tested on all cast materials, there are fundamental reasons for believing that the Rules have general validity. They have been applied to many different alloy systems including aluminium, zinc, magnesium, cast irons, steels, air- and vacuum-cast nickel and cobalt, and even those based on the highly reactive metals titanium and zirconium. Nevertheless, of course, although all materials will probably benefit from the application of the Rules, some will benefit almost out of recognition, whereas others will be less affected.

The Rules originated when emerging from a foundry on a memorable sunny day together with indefatigable Boeing enthusiasts for castings, Fred Feiertag and Dale McLellan. The author was lamenting that the casting industry had specifications for alloys, casting properties, and casting quality checking systems, but what did not exist but was most needed was a *process specification*. Dale threw out a challenge: 'Write one' The Rules and this book are the outcome. It was not perhaps the outcome that either Dale or I originally imagined. A Process Specification has proved elusive, proving so difficult that I have concluded that it will need a more accomplished author.

The Rules as they stand therefore constitute a first draft of a Process Specification; more like a checklist of casting guidelines. A buyer of castings would demand that the list were fulfilled if he wished to be assured that he was buying the best possible casting quality. If he were to specify the adherence to these Rules by the casting producer, he would ensure that the quality and reliability of the castings was higher than could be achieved by any amount of expensive checking of the quality of the finished product.

Conversely, of course, the Rules are intended to assist the casting manufacturer. It will speed up the process of producing the casting right first time, and should contribute in a major way to the reduction of scrap when the casting goes into production. In this way the caster will be able to raise standards, without any significant increase in costs. Quality will be raised to the point at which casting a quality equal to that of forgings can be offered with confidence. Only in this way will castings be accepted by the engineering profession as reliable, engineered products, and assure the future prosperity of both the casting industry and its customers.

A further feature of the list of Rules that emerged as the book was being written was the dominance of the sections on the design of the filling systems of castings. It posed the obvious question 'why not devote the book completely to filling systems?' I decided against this option on the grounds that both caster and customer require products that are good in *every* respect. The failure of any one aspect may endanger the casting. Therefore, despite the enormous disparity in length, no Rule could be eliminated; they were all needed.

Finally, it is worth making some general points about the whole philosophy of making castings.

For a successful casting operation, one of the revered commercial goals is the attainment of product sales being at least equal to manufacturing costs. There are numerous other requirements for the successful business, like management, plant and equipment, maintenance, accounting, marketing, negotiating etc. All have to be adequate, otherwise the business can suffer, and even fail.

This text deals only with the technical issues of the quest for good castings. Without good castings it is not easy to see what future a casting operation can have. The production of good castings can be highly economical and rewarding. The production of bad castings is usually expensive and damaging.

The 'good casting' in this text is defined as one that meets or exceeds the customer's specification.

It is also worth noting at this early stage, that we hope that meeting the customer's specification will be equivalent to meeting or exceeding service requirements. However, occasionally it is necessary to live with the irony that the demands of the customer and the requirements for service are sometimes not in the harmony one would like to see. This is a challenge to the conscientious foundry engineer to persuade and educate the customer in an effort to reconcile the customer's aims with our duty of care towards casting users and society as a whole.

These problems illustrate that there are easier ways of earning a living than in the casting industry. But few are as exciting.

**JC**  
**West Malvern**  
03 September 2003

# Introduction to *Castings Handbook* 2011

Revised and expanded editions of *Castings* and *Castings Practice* were planned in a more logical format as *Casting Metallurgy* and *Casting Manufacture*. However, Elsevier suggested that the two might beneficially be combined as a single *Complete Castings Handbook*. I have warmed to this suggestion since encompassing both the science and the technological application will be helpful to students, academics, and producers. The origin of the division of the Handbook into volumes 1 and 2 therefore remains clear: Volume 1 is the metallurgy of castings, formally outlining for the first time my new proposals for an explanation of the metallurgy of Al–Si alloys, cast irons, and steels; Volume 2, manufacture, divides into the 10 Rules, manufacturing design, and finally the various processing steps.

As I have indicated previously, the numerous processing steps make casting a complex technology not to be underestimated. It is our task as founders to make sure the world, happily ignorant of this significant challenge, takes castings for granted, having never an occasion to question their complete reliability.

**JC**  
**Ledbury, Herefordshire, England**  
23 November 2010

This page intentionally left blank

# Acknowledgments

It is a pleasure to acknowledge the significant help and encouragement I have received from many good friends. John Grassi has been my close friend and associate in Alotech, the company promoting the new, exciting Ablation castings process. Ken Harris has been an inexhaustible source of knowledge on silicate binders, aggregates and recycling. His assistance is clear in Chapter 15. Clearly, the casting industry needs more chemists like him. Bob Puhakka has been the first regular user of my casting recommendations for the production of steel castings, which has provided me with inspirational confirmation of the soundness of the technology described in this book. Murat Tiryakioglu has been a loyal supporter and critic, and provided the elegantly written publications that have provided welcome scientific support. Naturally, many other acknowledgments are deserved among friends and students whose benefits have been a privilege to enjoy. I do not take these for granted. Even if not listed here they are not forgotten.

The American Foundry Society is thanked for the use of a number of illustrations from the Transactions.

This page intentionally left blank

# Casting manufacture

# 2

## Section 1

10	The 10 Rules for good castings .....	605
----	--------------------------------------	-----

## Section 2: Filling System Design

11	Filling system design fundamentals .....	741
12	Filling system components .....	757
13	Filling system design practice .....	853

## Section 3: Processing (Melting, Molding, Casting, Solidifying)

14	Melting .....	879
15	Molding .....	911
16	Casting .....	939
17	Controlled solidification techniques .....	1013
18	Dimensional accuracy .....	1025
19	Post-casting processing .....	1067

## **INTRODUCTION TO THE CASTING MANUFACTURING INDUSTRY**

---

*The foundry world never ceases to amaze me with its kaleidoscopic mix of metals and processes. It has to be one of the most, if not the most, complex industries. Its complexity makes it a challenge to describe, but all the more interesting.*

*The main metal divisions are, perhaps naturally, ferrous and non-ferrous. This split is presented in some detail in the accompanying Figure 10.01. It is somewhat artificial in the sense that Ni and Co base alloys share much similar technology, and grade smoothly into the various varieties of stainless steels. Even so, tradition has it that Ni and Co are not ferrous, and it has to be admitted that as face-centered-cubic metals, they share many properties in common with Cu and Al.*

*The alternative common approach to categorizing the casting industry is in terms of its mold making, with greensand easily holding its magnificent first place in terms of productivity, but a wide variety of alternative molding processes each designed for its own niche, and the niches sometimes of huge size, such as pressure die casting, and the manufacture of Al alloy wheels by low-pressure permanent mold (Figure 10.02).*

*The main process divisions for manufacturing castings include molding and casting. It is an interesting exercise to set up a matrix with a vertical list of molding options, and a horizontal list of casting options. Correlating these can be seen to fill nearly every box of the matrix, although there are interesting gaps that the reader can quickly discover.*

*However, the description of casting manufacture is not that simple, because in addition to the main processing steps of molding and casting, there are very many other process steps including melting and solidification which add complexity, so that the two-dimensional matrix quickly multiplies into a multi-dimensional array. Thus it has not been possible in this account to tackle a description of the industry as a matrix. The processes are, so far as possible, discussed as separate features.*

*The processes include: (i) melting; (ii) molding; (iii) casting; (iv) solidification control (sometimes); and (v) many post-casting processing operations. Each processing step has yet more options, making the attempt to summarize the industry even more problematic. Many of these processing steps have generally been selected for such laudable features as their rate of production, acceptable efficiency or low cost.*

*However, with regret, the above choices of (i) melting and (iii) casting processes have usually been selected badly; these are the weakest links in the production sequence. In fact, it has to be admitted that most of our melting operations and most casting operations in the casting industry are awful. Few are selected for the quality of the product even though all will admit that a system that consistently produces nearly zero or actually zero scrap would constitute a major advantage. This major feature has been consistently overlooked. We shall go out of our way not to overlook it here.*

*Finally, before even the processing is considered, the casting technique has to be designed correctly. This is a non-trivial task. Thus the next three chapters are devoted to getting this right. The new Rules listed in Chapter 10, and the procedures for the design of the filling systems for the castings, are, with regret, often in conflict with much traditional practice simply because the result of new technology available for the research of these processes has revealed many of the*



The structure of the casting industry (1) by metal

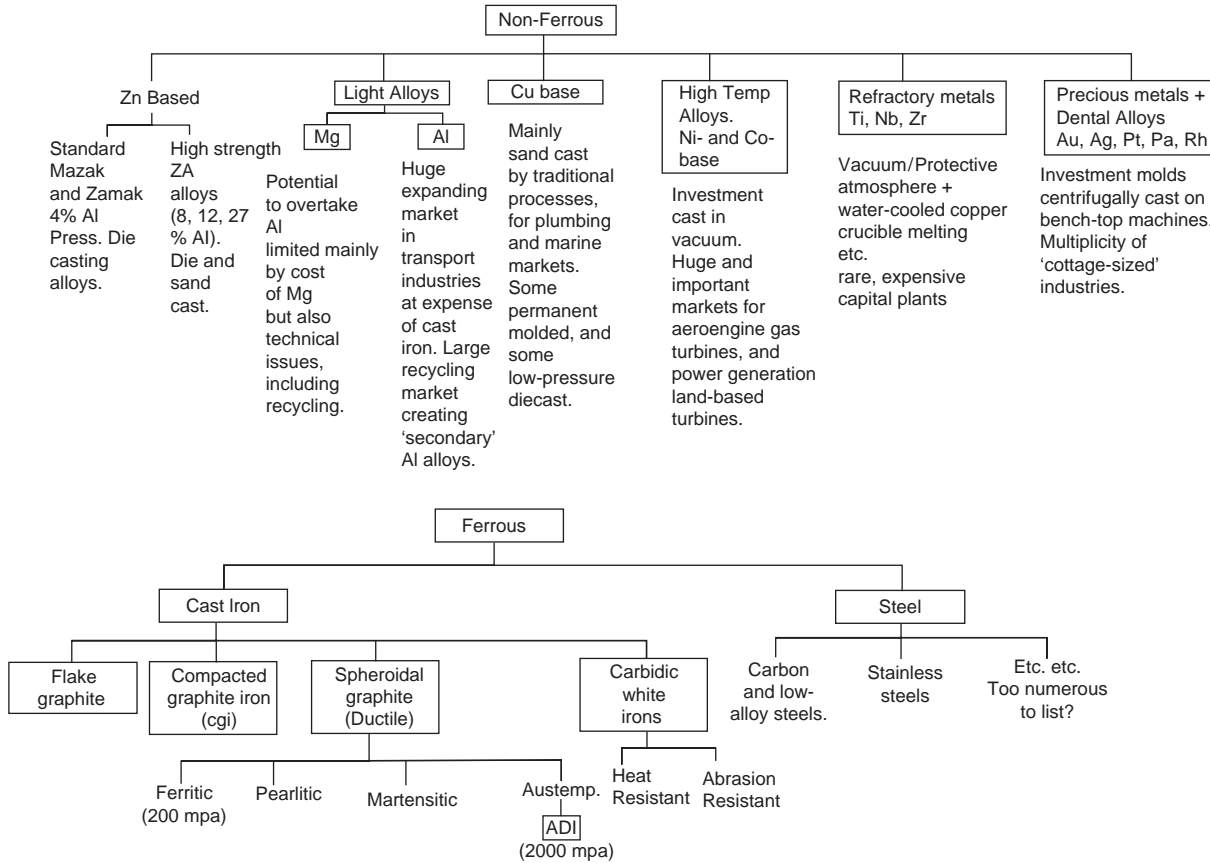


FIGURE 10.01

The structure of the casting industry (1) by metal.

The structure of the casting industry (2) by molding technology

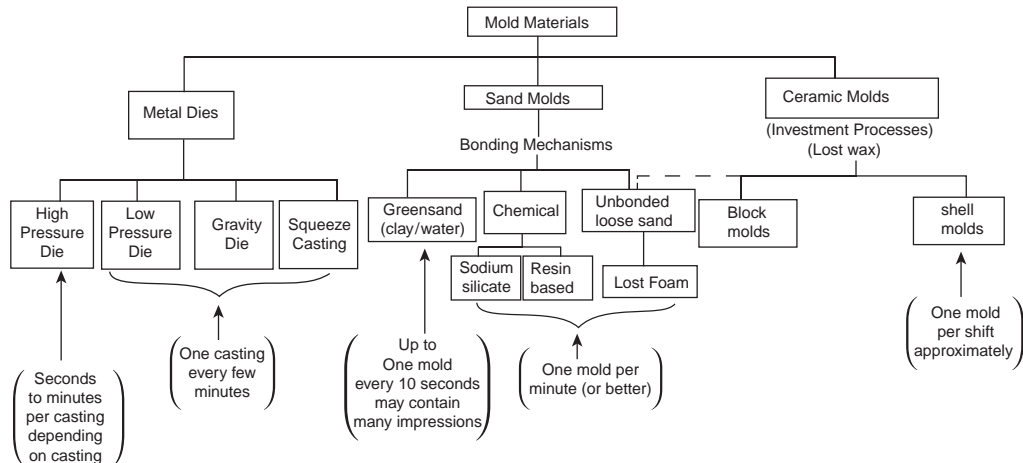


FIGURE 10.02

The structure of the casting industry (2) by molding technology.

reasons for the poor performance of tradition systems, and has pointed the way to substantial potential improvements.

The central problem within the metal casting industry is pouring. It happens at multiple stages of our production processes. We have been lulled into complacency from the innocent images in our minds of pouring a glass of water or a cup of tea, but have failed to appreciate that liquid metals are greatly damaged by such actions. The use of pouring under gravity as an aid to making castings is a two-edged sword: gravity pouring is easy, but gravity accelerates our metals to unwanted and damaging speeds. Ultimately, we have to re-think our processing to eliminate pouring at every stage. This may sound alarming, but in fact is not such a daunting engineering challenge. An increasing number of foundries are now successful in eliminating their reliance on pouring.

In the meantime there are some strategies for reducing the damage inflicted by pouring that will be helpful while more revolutionary systems can be put in place. The improved systems are repaying careful application in a number of foundries. I am glad to report that the new systems recommended in this book come with warm recommendations from their users, and even their accountants.

JC  
Ledbury  
25 November 2010

---

**SECTION**

**1**

**10** The 10 Rules for good castings .....605

This page intentionally left blank

# The 10 Rules for good castings

# 10

The 10 Rules are my personal checklist (Campbell 2004), ensuring that I have not forgotten any essential aspect of casting manufacture. It cannot be emphasized too strongly that the failure of only one of the Rules can result in total failure of the casting. This is not meant to be alarmist, but simply practical. No-one has ever promised that making castings would be easy. However, following the rules is a great help.

We start off with a quick summary, followed by a detailed assessment of each rule in turn in the remainder of this section.

## Rule 1. Start with a good-quality melt

Immediately prior to casting, the melt shall be prepared, checked, and treated, if necessary, to bring it into conformance with an acceptable minimum standard. Prepare and use so far as possible only near-defect-free melt.

## Rule 2. Avoid turbulent entrainment of the surface film on the liquid

This is the requirement that the liquid metal front (the meniscus) should not go too fast. Maximum meniscus velocity is approximately  $0.5 \text{ m s}^{-1}$  for most liquid metals. This requirement also implies that the liquid metal must not be allowed to fall more than the critical height corresponding to the height of a sessile drop of the liquid metal. The maximum velocity may be raised to  $1.0 \text{ m s}^{-1}$  or even higher, and the critical fall height might be correspondingly raised to approximately 50 mm, in sufficiently constrained running systems or thin section castings.

## Rule 3. Avoid laminar entrainment of the surface film on the liquid

This is the requirement that no part of the liquid metal front should come to a stop prior to the complete filling of the mold cavity. The advancing liquid metal meniscus must be kept 'alive' (i.e. moving) and therefore free from thickened surface film that may be incorporated into the casting. This is achieved by the liquid front being designed to expand continuously. In practice this means progress only *uphill* in a continuous *uninterrupted* upward advance; i.e. in the case of gravity poured casting processes, from the base of the sprue onwards. This implies:

- Only bottom gating is permissible.
- No falling or sliding downhill of liquid metal is allowed.
- No horizontal flow of significant extent.
- No stopping of the advance of the front due to arrest of pouring or waterfall effects, etc.

#### Rule 4. Avoid bubble entrainment

No bubbles of air entrained by the filling system should pass through the liquid metal in the mold cavity. This may be achieved by:

- Properly designed off-set step pouring basin; fast back-fill of properly designed sprue; preferred use of stopper; avoidance of the use of wells and all other volume-increasing features of filling systems (such as expanding channels sometimes known as ‘diffusers’); small volume runner and/or use of ceramic filter close to sprue/runner junction; possible use of bubble traps. A naturally pressurized filling system fulfills most of these criteria.
- No interruptions to pouring.

#### Rule 5. Avoid core blows

- No bubbles from the outgassing of cores or molds should pass through the liquid metal in the mold cavity. Cores to be demonstrated to be of sufficiently low gas content and/or adequately vented to prevent bubbles from core blows.
- No use of impermeable clay-based core or mold repair paste.

#### Rule 6. Avoid shrinkage

- No feeding uphill in larger section thickness castings. Feeding against gravity is unreliable because of (i) adverse pressure gradient and (ii) complications introduced by convection.
- Demonstrate good feeding design by following all seven Feeding Rules, by an approved computer solidification model, and by test castings.
- Once good feeding is attained, fix the temperature regime by controlling (i) the level of flash at mold and core joints; (ii) mold coat thickness (if any), and (iii) temperatures of metal and mold.

#### Rule 7. Avoid convection

Assess the freezing time in relation to the time for convection to cause damage. Thin and thick section castings automatically avoid convection problems. For intermediate sections either (i) reduce the problem by avoiding convective loops in the geometry of the casting and rigging, (ii) avoid feeding uphill, or (iii) eliminate convection by roll-over after filling.

#### Rule 8. Reduce segregation

Predict segregation to be within limits of the specification, or agree out-of-specification compositional regions with customer. Avoid channel segregation formation if possible.

#### Rule 9. Reduce residual stress

No quenching into water (cold or hot) following solution treatment of light alloys. (Polymer quenchant or forced air quench may be acceptable if casting stress can be shown to be acceptable.)

#### Rule 10. Provide location points

All castings to be provided with location points for pick-up for dimensional checking and machining. Proposals to be agreed with quality auditor, machinist, etc.

## 10.1 RULE 1: 'USE A GOOD-QUALITY MELT'

### 10.1.1 Background

The melt needs to be demonstrated to be of good quality. A good-quality liquid metal is one that is defined as:

- (i) Substantially free from suspensions of non-metallic inclusions in general, and bifilms in particular.
- (ii) Relative freedom from bifilm-straightening and bifilm-opening agents. These include certain alloy impurities in solution such as hydrogen or other gases, and Fe in Al alloys.

It should be noted that the good quality of the melt should not be taken for granted, and, without proper treatment, is almost certain to be not attained.

There are a few exceptions in which good quality might be assumed. Such metals may include pure liquid gold, iridium, platinum, perhaps mercury, and possibly some liquid steels whilst in the melting furnace at a late stage of melting. These instances are, however, either rare, or tantalizingly inaccessible such as the steel in the melting furnace; in the process of getting it out of the furnace much damage is done to the liquid by the pouring that is currently an integral feature of our conventional steel foundries.

An important distinction is useful to identify two major oxide inclusion types:

- (i) The oxide skins from the charge materials. I sometimes call these 'primary oxides'. These are usually massive oxide bifilms, having the dimensions of the originating pieces of charge, and will therefore be measured in fractions of meters; and
- (ii) The population of much smaller oxides from the matrix of the charge materials. These would be expected to be confetti-size fragments over a wide size range of at least micrometers to centimeters.

Clearly, the major task is to eliminate the macroscopic films. However, for reliable properties, it is also essential to eliminate the majority of the larger fraction of mesoscopic and microscopic films.

Regrettably, many liquid metals are actually so full of sundry solid phases floating about, that they begin to more closely resemble slurries than liquids. In the absence of information to the contrary, this condition of a liquid metal should be assumed to apply. The evidence for the real internal structure of liquid metals being crammed with defects has been growing over recent years as investigation techniques have improved. Some of this evidence is described below. Much of the evidence applies to aluminum and its alloys where the greatest research effort has been. Evidence for other materials is presented elsewhere in this book.

It is sobering to realize that many of the strength-related properties of metals can only be explained by assuming that the initial melt is full of defects. Many of our theoretical models of liquid metals and solidification that are formulated to explain the occurrence of defects neglect to address this critical fact. Classical physical metallurgy and solidification science has been unable to explain the important properties of cast materials such as the effect of dendrite arm spacing and the ease of formation of pores and cracks. The problem of the anomalously rapid growth of short cracks despite the low stress intensity during the early stage of fatigue is easily explained if the cracks pre-exist. We shall see that in general the behavior of cast metals arises naturally from the population of defects.

However, it has to be admitted that is often not easy to confirm the presence of non-metallic inclusions in liquid metals, and even more difficult to quantify their number and average size or spread of sizes. McClain and co-workers (2001) and Godlewski and Zindel (2001) have drawn attention to the unreliability of the standard approach studying polished sections of castings. A technique for liquid aluminum involves the collection of inclusions by pressurizing up to 2 kg of melt, forcing it through a fine filter, as in the PODFA and PREFIL tests. Pressure is required because the filter is so fine. The method overcomes the sampling problem by concentrating the inclusions by a factor of about 10 000 times (Enright and Hughes 1996, Simard et al. 2001). The layer of inclusions remaining on the filter can be studied on a polished section. (The total quantity of inclusions is assessed as the area of the layer as seen in section under the microscope, divided by the quantity of melt that has passed through the filter. The unit is therefore the curious quantity  $\text{mm}^2 \text{kg}^{-1}$ . We can hope that at some future date this unhelpful unit will, by universal agreement, be converted into some more meaningful quantity such as volume of inclusions per volume of melt. In the meantime, the standard provision of the diameter of the filter in reported results would at least allow readers the option to do this for themselves.)

To gain some idea of the range of inclusion contents an impressively dirty melt might reach  $10 \text{ mm}^2 \text{kg}^{-1}$ , an alloy destined for a commercial extrusion might be in the range 0.1 to 1, foil stock might reach 0.001, and computer discs  $0.0001 \text{ mm}^2 \text{kg}^{-1}$ . For a filter of 30 mm diameter these figures approximately encompass the range  $10^{-3}$  (0.1%) down to  $10^{-7}$  (0.1 part per million) volume fraction.

Other techniques for the monitoring of inclusions in Al alloy melts in the past included LiMCA (Smith 1998), in which the melt is drawn through a narrow tube. The voltage drop applied along the length of the tube is measured. The entry of an inclusion of different electrical conductivity (usually non-conducting) into the tube causes the voltage differential to rise by an amount that is assumed to be proportional to the size of the inclusion. The technique is generally thought to be limited to inclusions approximately in the range 10 to 100  $\mu\text{m}$ , and generally presuming that the inclusions are particles. Although once widely used for the casting of wrought alloys, the author regrets that technique has to be viewed with great reservation. As we have mentioned, the key inclusions in light alloys are not particles but (double) films, and although often extremely thin, can be up to 10 mm (1 cm) in diameter. Such inclusions sometimes succeed to find their way into the LiMCA tube, where they tend to hang in the metal stream, caught up at the mouth of the tube, and rotate into spirals like a flag tied to the mast by only one corner. Asbjornson (2001) has reported piles of helical oxides in the bottom of the LiMCA crucible. It is to be regretted that most workers using LIMCA have been unaware of these serious problems. However, the general disquiet about the appropriateness of this technique has finally caused the LiMCA device to be dropped by the manufacturer. It seems unlikely to be used significantly in the future.

Ultrasonic reflections have been used from time to time to investigate the quality of melts. The early work by Mountford and Calvert (1959) is noteworthy, and has been followed up by considerable development efforts in Al alloys (Mansfield 1984), Ni alloys and steels (Mountford et al. 1992). Ultrasound is efficiently reflected from oxide films (almost certainly because the films are double, and the elastic wave cannot cross the intermediate layer of air, and thus is reflected with mirror-like efficiency). However, the reflections may not give an accurate idea of the size of the defects because the irregular, crumpled form of such defects, and their tumbling action in the melt. The tiny mirror-like facets of large defects reflect back to the source only when the facets happen to rotate to face the beam. The result is a general scintillation effect, apparently from many minute and separate particles. It is not easy to discern whether the images correspond to many small or a few large bifilms.



Neither LiMCA nor the various ultrasonic probes can distinguish any information on the types of inclusions that they detect. In contrast, the inclusions collected by pressurized filtration can be studied in some detail. In aluminum alloys many different inclusions can be found. Table 1.1 lists some of the principal types.

Nearly all of these foreign materials will be deleterious to products intended for such products as thin foil or computer discs. However, for engineering castings, those inclusions such as carbides and borides are probably not harmful at all (although they would be unpopular with machinists). This is because, having been precipitated from elements in solution in the melt, they would be expected to be in excellent atomic contact with the matrix alloy. These non-metallic phases enjoy well-bonded interfaces and are thereby unable to act as initiators of void-type or volume defects such as pores and cracks. On the contrary, they may act as grain refiners. Furthermore, their continued good bonding with the solid matrix is expected to confer on them a minor or negligible deleterious influence on mechanical properties. They may strengthen the matrix to some degree.

Generally, therefore, this book concentrates on those inclusions that have a major detrimental influence on mechanical properties, because of their action to initiate other serious problems such as pores, cracks and localized corrosion. Thus the attention will center on *entrained surface films, known as bifilms*. Usually, these inclusions will be oxides. However, carbon films are also common, and occasionally nitrides, sulfides and other substances. These entrained films exhibit a unique structure, with outer faces that are in atomic contact with the melt, but have an inner interface that is unbonded, and thus lead to the spectrum of problems all too familiar to foundry people.

The pressurized filtration tests can find some of these entrained solids, and the analysis of the inclusions present on the filter can help to identify the source of many inclusions in a melting and casting operation. However, films that are newly entrained into the melt as a result of surface turbulence remain undetectable but can be enormously important. These films are commonly entrained during the pouring of castings, and so, perhaps, are not normally subjected to detection or assessment in a melting and distribution operation at this late stage. They are typically only 20 nm thick, and so remain invisible under an optical microscope, especially in a ceramic filter, since they will be difficult to discern when draped around a piece of the filter that when sectioned appears many thousands of times thicker.

The only fairly reliable detection technique for such inclusions is the lowly Reduced Pressure Test (RPT). This test opens the films (because they are always double, and contain residual entrapped air) so that they can be seen by eye on a polished section or on a radiograph. The radiography of the cast test pieces reveals the size, shape and numbers of such important inclusions, as has been shown in studies by Fox and Campbell (2000) and Dispinar and Campbell (2006). A central slice of the small cylindrical RPT casting to yield a parallel section gives an improved radiographic result (Figure 10.1). Viewing this work in retrospect the approach using X-rays now appears somewhat over the top, and probably unnecessary. Simply viewing a polished section by unaided eye has subsequently proved almost equally effective, and vastly cheaper and quicker.

Figure 10.2 shows how a quality map can be constructed to show the total length and total number of bifilms on a polished RPT section. The large central square might form a suitable quality window for an operation making 'space filling' components for which filling and feeding are not critical as a result of relatively low requirements from the casting. The '50 × 50' regime might be a minimum requirement for parts requiring some strength and toughness. The Cosworth foundry used a window '3 × 3' during my time, and quite often achieved '0 × 0', giving castings of exceptional soundness and high properties.

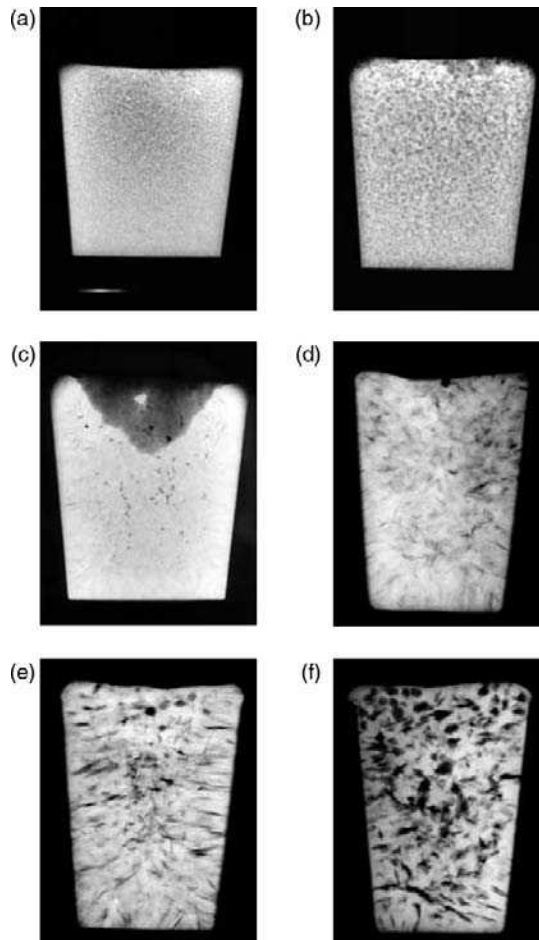


**FIGURE 10.1**

Radiographs of RPT samples of Al-7Si-0.4Mg alloy illustrating different bifilm populations (courtesy of S Fox).

However, even the RPT technique probably only reveals the more extensive bifilms, between perhaps 0.1 and 10 mm diameter. This is because the effective tensile opening stress can only be a maximum of one atmosphere (0.1 MPa). In a tensile test of a solidified metal the stress can easily reach a thousand times greater than this and so is capable of opening much smaller bifilms. For instance, in some Al-Si alloys cracked Si particles at the base of many ductile dimples indicate the failure of the particle by cracking. If we assume this failure can only occur because of the presence of a bifilm then a true density of defects might approach  $10^{15} \text{ m}^{-3}$  (corresponding to  $10^6 \text{ mm}^{-3}$ ) at a diameter of between 1 and  $10 \mu\text{m}$ . This is a huge density of defects, but is consistent with the direct ultrasonic observation of a melt by Mountford and Calvert (1959) in which they describe a dirty melt appearing as a fog. After the inclusions were allowed to settle (aided by precipitating heavy

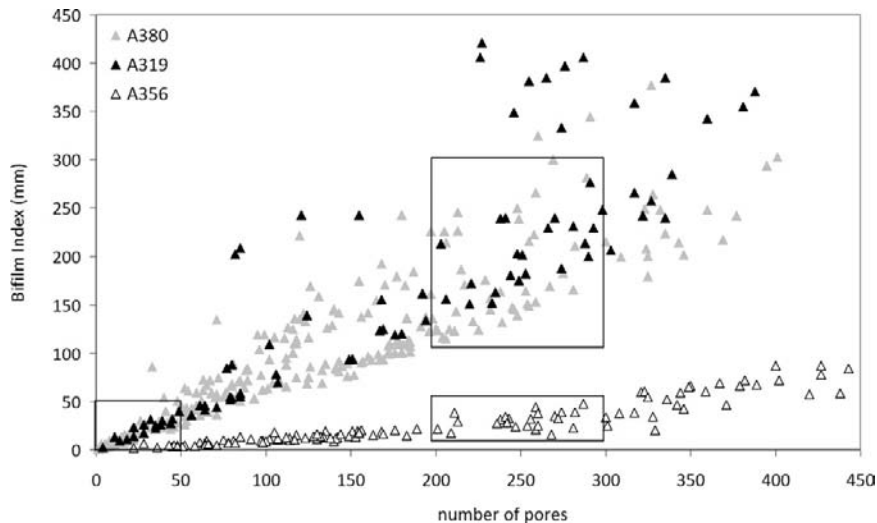


**FIGURE 10.2**

RPT results for three casting alloys, showing number and total length of bifilms on the polished section (Dispinar and Campbell 2011).

grain-refining titanium-rich compounds on them) the melt cleared completely so that a clear back-wall echo could be seen. They were able to repeat this phenomenon simply by stirring up the melt to recreate the fog, and watch the weighed-down oxides clearing once again.

It is unfortunate that many melts start life with poor, sometimes grossly poor, quality in terms of their content of suspended bifilms. The 'fog' persists in most alloys because the bifilms are usually neutrally buoyant. Figure 10.1 gives several examples of different poor qualities of liquid aluminum alloy. The figures show results from RPT samples observed (somewhat unnecessarily as has already been noted!) by X-ray radiography. Since the samples are solidified under only one tenth of an atmosphere (76 mm residual pressure compared to the 760 mm of full atmospheric pressure) any gas-containing defects, such as bubbles, or bifilms with air occluded in the centers of their sandwich structures, will be expanded by ten times. Thus rather small defects can become visible for the first time.

We shall assume that pores are always initiated by bifilms, giving initially crack-like or irregular pores. The formation of rounded pores simply occurs as a result of the bifilm being opened beyond this initial condition by excess precipitation of gas, finally achieving a pore diameter greater than the original length of the bifilm. Thus the RPT is an admirably simple device for assessing (i) the number of bifilms; (ii) their average size (even though this might be somewhat of an overestimate if much hydrogen is present); and (iii) gas content is assessed by the degree of opening of the bifilms from thin crack-like forms to fairly spherical pores, at the same time lowering the average density of the cast sample.

If the melt contained no gas-containing defects the cut and polished section (or in this case the radiographs) of the RPT would be clear.

However, as we can see immediately, and without any benefit of complex or expensive equipment, the melts recorded in Figure 10.1 are far from this desirable condition. Figure (a) shows a melt with

small rounded pores that indicates that the bifilms that initiated these defects were particularly small, of the order of 0.1 mm or less. The density of these defects, however, was high, between 10 and 100 defects per cubic cm. Sample (b) has a similar defect distribution, but with slightly higher hydrogen content. Sample (c) illustrates a melt that displayed a deep shrinkage pipe, normally interpreted to mean good quality, but showing that it contained a scattering of larger pores, probably as a result of fewer bifilms, so that the available gas was concentrated on the fewer available sites. Melt (d) has considerably larger bifilms, of size in the region of 5 mm in length, and in a concentration of approximately 1 per cm<sup>3</sup>. Samples (e) and (f) show similar samples but with increasing gas contents that have inflated these larger bifilms to reasonably equiaxed pores.

Naturally, it would be of little use for the casting engineer to go to great lengths to adopt the best designs of filling and feeding systems if the original melt was so poor that a good casting could not be made from it.

Thus this section deals with some of the aspects of obtaining a good-quality melt.

In some circumstances it may not be necessary to reduce both bifilms and bifilm-opening agents. An interesting possibility for future specifications for aluminum alloy castings (where residual gas in supersaturated solution does not appear to be harmful) is that a double requirement may be made consisting of (i) the content of dissolved gas in the melt to be high, but (ii) the percentage of gas porosity to be low. The meeting of this interesting double requirement will ensure to the customer that bifilms are not present. Thus these damaging but undetectable defects will, if present, be effectively labeled and made visible on X-ray radiographs and polished sections by the precipitation of dissolved gas. It is appreciated that such a stringent specification might be viewed with dismay by present suppliers. However, at the present time we have mainly only rather poor technology, making such quality levels out of reach. We shall not necessarily suffer such backward processing for ever.

The possible future production of Al alloys for aerospace, with high hydrogen content but low porosity, is a fascinating challenge. As our technology improves such castings may be found not only to be manufacturable, but offer a guaranteed reliability of fatigue life, and therefore command a premium price.

The prospect of producing ultra-clean Al alloys that can be demonstrated in this way to be actually extremely clean raises the issue of contamination of the liquid alloy from the normal metallurgical additions such as the various master alloys, and grain refiners, modifiers, etc. It may be that for super-clean material, normal metallurgical additions to achieve refinement of various kinds will be found unnecessary, and possibly even counter-productive because of the unavoidable addition of oxide films at least from the outer surfaces of the master alloy additions.

The improvement of Al alloys by melting with dry hearth furnaces to eliminate the primary oxide skins of the charge, simply by scraping these off the hearth through a side door, is to be strongly recommended. The subsequent treatment of the melt with Ti-rich grain refiners is recommended, not necessarily to grain refine, but to precipitate heavy Ti-rich inclusions on oxide bifilms to sediment these from the melt. It seems likely that extremely clean Al might be obtained in this way. These and other sedimentation techniques are discussed in more detail under the section on melting.

For steels, the content of hydrogen may be a more serious matter, especially if the section thickness of the casting is large. In some steel castings of section thickness above about 100 mm up to 1000 mm or more, the hydrogen cannot escape by diffusion during the time available for cooling or during the time of any subsequent heat treatments. Thus the high hydrogen content retained in these heavy

sections can lead to hydrogen embrittlement, and the catastrophic failure of the section by cracking. When making very large steel castings, such as back-up rolls for rolling mills, it is common practice to induce a carbon boil to reduce the hydrogen content. Having done this, it is necessary to work quickly to cast the metal since the hydrogen content tends to rise rapidly once again, re-establishing its equilibrium with its environment such as damp atmospheres and/or damp refractories in ladles etc. Although Ren and colleagues (2008) claim that hydrogen might nucleate voids with the aid of vacancies, it is difficult to avoid what appears to be the more probable speculation that the hydrogen cracking might initiate by hydrogen precipitating into, and forcing open, bifilms.

For ductile iron production the massive amounts of turbulence that accompanies the addition of magnesium in some form, such as magnesium ferro-silicon, are almost certainly highly damaging to the liquid metal. It is expected that immediately after such nodularization treatment the melt will be massively dirty. It will be useful therefore to ensure that the melt can dwell for sufficient time for the entrained magnesium-oxide-rich films to float out. The situation is analogous to the treatment of cast iron with CaSi to effect inoculation (i.e. to achieve a uniform distribution of graphite of desirable form). In this case the volumes of calcium-oxide-rich films are well known, so that the CaSi treatment is known as a 'dirty' treatment compared to FeSi inoculation. The author is unsure about in-mold treatments with such oxidizable elements as Ca and Mg. Do they give results as good as external treatments? If so, how is this possible? Some work to clarify this situation would be valuable.

For nickel-based superalloys melted and cast in vacuum, it is with regret that the material is, despite its apparently clean melting environment, found to be sometimes as crammed with oxides (and/or nitrides) as an aluminum alloy (Rashid and Campbell 2003). This is because the main alloying element in such alloys is aluminum, and the high temperature favors rapid formation and thickening of the surface film on the liquid even in vacuum, because the vacuum is only, of course, dilute air. If the film becomes entrained, the liquid and any subsequent casting is damaged. The process for the production of these alloys designed for remelting to make castings in foundries involves, unfortunately, melting and pouring processes that leave much to be desired.

The melting and alloying process in the manufacture of Ni-based alloys starts in an induction crucible furnace, and is poured under gravity via a series of sloping launders, falling several times, and finally falling one or two meters or more into steel tubes that act as molds. This awfully turbulent primary production process for the alloy impairs all the downstream cast products. More recent moves to increase productivity using larger diameter tubes to make larger diameter alloy billets have only made the bad situation worse. An alternative recent move towards the production of Ni-base alloy bar by horizontal continuous casting is to be welcomed as the first step towards a more appropriate production technique for these key ingredients of our modern aircraft turbines. Production of improved material is currently limited, but should be the subject of demand from customers.

Even so, the subsequent melting and gravity casting operations in the investment casting foundries to produce Ni- and Co-base turbine blade castings are also currently extremely disappointing, so that good quality starting material would at this time probably be a waste. The aircraft industry has been trapped within its rigid procedures designed to ensure safety, but which have inhibited the rational engineering development of improved casting techniques that could deliver far safer castings.

Melting systems and melt treatments designed to provide improved melt quality are dealt with in more detail in Volume 3 'Melting'.

---

## 10.2 RULE 2: 'AVOID TURBULENT ENTRAINMENT' (THE CRITICAL VELOCITY REQUIREMENT)

### 10.2.1 Introduction

The avoidance of surface turbulence is probably the most complex and difficult Rule to fulfill when dealing with gravity pouring systems.

The requirement is all the more difficult to appreciate by many in the industry, since everyone working in this field has always emphasized the importance of working with 'turbulence-free' filling systems for castings. Unfortunately, despite all the worthy intentions, all the textbooks, all the systems, and all the talk, so far as the author can discover, it seems that no-one appears to have achieved this target so far. In fact, in traveling around the casting industry, it is quite clear that the majority (at least 80%) of all defects are directly caused by turbulence. Thus the problem is massive; far more serious than suspected by most of us in the industry.

In fact, Johnson and Baker concluded from their experiments in 1948 that 'gating systems did not function as commonly supposed', and 'no gating system prevented turbulence'. It seems we have all been warned for a long time.

To understand the fundamental root of the problem, it will become clear in Section 2.1 that any fall greater than the height of the sessile drop (of the order of 10 mm) causes the metal to exceed its critical velocity, and so introduces the danger of defects in the casting. Since most falls are in fact at least 10 or 100 times greater than this, and since the damage is likely to be proportional to the energy involved (i.e. proportional to the square of the velocity) the damage so created will usually be expected to be in the range 100 to 10 000 times greater. Thus in the great majority of castings that are poured simply under the influence of gravity, there is a major problem to ensure its integrity. In fact, the situation is so bad that the best outcome of many of the filling system design solutions proposed in this book are merely damage limitation exercises. Effectively, it has to be admitted that at this time it seems impossible to guarantee the avoidance of some damage when pouring liquid metals.

This somewhat depressing conclusion needs to be tempered by a number of factors.

First, the world has come to accept castings as they are. Thus any improvement will be welcome. This book describes techniques that will create very encouraging improvements.

Second, this book is merely a summary of what has been discovered so far in the development of filling system design. Better designs are to be expected now that the design parameters and filling system concepts (such as critical velocity, critical fall height, entrainment, bifilms, etc.) are defined and understood.

Third, there *are* filling systems that can yield, in principle, perfect results.

Of necessity, such perfection is achieved by fulfilling Rule 2 by avoiding the transfer of the melt by pouring. Thus considering the three directions of filling a mold:

- (i) Downhill pouring under gravity;
- (ii) Horizontal transfer into the mold (achieved by tilt casting in which the tilt conditions are accurately controlled), or by the 'level pour' or 'level transfer' techniques);
- (iii) Uphill (counter-gravity) casting in which the melt is caused to fill the mold in only an uphill mode.

Only the last two processes have the potential to deliver castings of near perfect quality. In my experience, I have found that in practice it is often difficult to make a good casting by gravity, whereas

by a good counter-gravity process (i.e. a process observing all the 10 Rules) it has been difficult to make a bad casting. The jury is still out on horizontal transfer by tilting. This approach has great potential, but requires a dedicated effort to achieve the correct conditions. Horizontal transfer has great potential but unfortunately has fallen into disuse.

Thus in summary, filling of molds can be carried out down, along, or up. Only the 'along' and 'up' modes totally fulfill the non-surface turbulence condition.

However, despite all its problems, it seems more than likely that the *downward* mode, *gravity casting*, will continue to be with us for the foreseeable future. Thus in this book we shall devote some considerable length to the damage limitation exercises that can offer considerably improved products, even if, unfortunately, those products cannot be ultimately claimed as perfect.

Most will shed no tears over this conclusion. Although potential perfection in the *along* and *up* modes is attractive, the casting business is all about making adequate products; products that meet a specification and at a price a buyer can afford.

The question of cost is interesting; perhaps the most interesting. Of course the costs have to be right, and often gravity casting is acceptable and sufficiently economical. However, more often than might be expected, high quality and low cost can go together. An improved gravity system, and certainly one of the better counter-gravity systems, can be surprisingly economical and productive. Such opportunities are often overlooked. It is useful to watch out for such benefits.

### 10.2.2 Maximum velocity requirement

One day, I was seated in the X-ray radiograph viewing room using an illuminated viewing screen to study a series of radiographic films of cylinder head castings made by our counter-gravity casting system at Cosworth, at that time only recently developed. Each radiograph in turn was beautiful, having a clear, 'wine glass' perfection that every founder dreams of. I was at peace with the world. However, suddenly, a radiograph appeared on the screen that was a total disaster. It had gas bubbles, shrinkage porosity, hot tears, cracks and sand inclusions. I was shocked, but sensed immediately what had happened. I shot out of the viewing room into the foundry to query Trevor, our man on the casting station. 'What happened to this casting?' He admitted instantly 'Sorry, governor, I put the metal in too fast.'

This was a lesson that remained with me for years. This chance experiment by counter-gravity, using an electromagnetic pump allowing independent control of the ingate velocity, had kept all the other casting variables constant (including temperature, metal quality, alloy content, mold geometry, mold aggregate type, binder type, etc.), showing them to be of negligible importance. Clearly, the ingate velocity was dominant. By only changing the speed of entry of metal we could move from total success to total failure. This was a fundamental lesson. Clearly, it applies to all casting processes.

Thinking further about this lesson, common sense tells us all that there is an optimum velocity at which a liquid metal should enter a mold. The concept is outlined in Figure 2.18. At a velocity of zero the melt is particularly safe (Figure 2.18a), being free from any danger of damage. Regrettably, this stationary condition for the melt is not helpful for the filling of molds. In contrast, at extremely high velocities the melt will enter the mold like a jet of water from a fire-fighter's hosepipe (Figure 2.18c), and is clearly damaging to both metal and mold. At a certain intermediate velocity the melt rises to just that height that can be supported by surface tension around the periphery of the spreading drop (Figure 2.18b). The theoretical background to these concepts is dealt with at length in Chapter 2. For nearly all liquid metals this critical velocity is close to  $0.5 \text{ m s}^{-1}$ . This value is of central importance in

the casting of liquid metals, and will be referred to repeatedly in this section and when designing filling systems for castings.

Japanese workers optimizing the filling of their design of vertical stroke pressure die casting machine using both experiment and computer simulation (Itamura 1995) confirm the critical velocity of  $0.5 \text{ m s}^{-1}$  for their Al alloy, finding at velocities above this value that air bubbles have a chance to become entrained. (These workers go further to define the amount of liquid that needs to be in the mold cavity to suppress entrainment at higher ingate velocities.)

Looking a little more closely at the detail of critical velocities for different liquids, it is close to  $0.4 \text{ m s}^{-1}$  for dense alloys such as irons, steels and bronzes and about  $0.5 \text{ m s}^{-1}$  for liquid aluminum alloys. The value is  $0.45\text{--}0.60 \text{ m s}^{-1}$  for Mg and its alloys. Taking an average of about  $0.5 \text{ m s}^{-1}$  for all liquid metals is usually good enough for most purposes related to the design of filling systems for castings, and will be generally used throughout this book.

Returning to Figure 2.18b showing the liquid metal emerging close to its critical velocity, and spreading slowly from the ingate. The shape of the drop is closely in equilibrium, its surface tension holding its compact shape, and just balancing the head of pressure due to its density that would, if acting alone, spread the drop out infinitely thin. As the ingate steadily supplies metal at close to  $0.5 \text{ m s}^{-1}$  the steadily growing drop closely resembles the shape of a *sessile drop* (from the Latin word for ‘sitting’. The word contrasts with *glissile drop*, meaning a gliding or sliding drop.) A sessile drop of Al sitting on a non-wetted substrate is always approximately 12.5 mm high. Corresponding values for other liquids are Fe 10 mm, Cu 8 mm, Zn 7 mm, Pb 4 mm, water 5 mm.

Recent research has demonstrated that if the liquid velocity exceeds the critical velocity there is a danger that melt will overshoot the height supportable by surface tension, so that on falling back again the surface of the liquid metal may be folded over. This *entrainment* of the liquid surface I have called *surface turbulence*. At risk of overly repeating this important phenomenon, this entrainment of the surface can occur if there is sufficient energy in the form of velocity in the bulk liquid to perturb the surface against the smoothing action of surface tension. In addition, notice that damage is not *necessarily* created by the falling back of the metal. The falling is likely to be chaotic, so that any folding action may or may not occur. The significance of the critical velocity is clear therefore: below the critical velocity the melt is safe from entrainment problems; above the critical velocity there is the danger, but not the necessity, of surface entrainment leading to defect creation.

To be more precise about the entrainment action, actually any disturbance of the surface of the liquid that extends its surface is irreversible without some entrainment occurring. This is because the surface oxide film forms almost instantly, but once formed cannot be reduced once again in area without crumpling in some way, leading to the folding in of some of the surface oxide (see for instance Figure 2.2b). Thus even below the critical velocity some entrainment may be occurring, but, clearly, above the critical velocity the rate of entrainment suddenly increases.

Thus we see there is a chance that if the speed of the liquid exceeds about  $0.5 \text{ m s}^{-1}$  its surface film may be folded into the bulk of the liquid. This folding action is an *entrainment* event. It leads to a variety of problems in the liquid that we can collectively call *entrainment defects*. The major entrainment defects are:

- (i) Bubbles as, of course, air bubbles (but widely misinterpreted as reaction products of solidification such as hydrogen porosity, or reaction products between oxide slag and graphite in cast iron to create CO bubbles).



- (ii) Bifilms, as doubled-over oxide films. The author has named these folded-in films 'bifilms' to emphasise their double, folded-over nature. Because the films are necessarily folded dry side to dry side, there is little or no bonding between these dry interfaces, so that the double films act as cracks. The cracks (alias bifilms) become frozen into the casting, lowering the strength and fatigue resistance of the metal. Bifilms may also create leak paths, causing leakage failures.

The folding-in of the oxide is a random process, leading to scatter and unreliability in the properties on a casting to casting, day to day, and month to month basis during a production run.

The different qualities of metals arriving in the foundry will also be expected to contain populations of bifilms that will differ in type and quantity from batch to batch. Thus the performance of the foundry will suffer additional variation. The foundry needs to have procedures in place to smooth variations of its incoming raw material so far as possible so as to fulfill Rule 1.

The maximum velocity condition effectively forbids top gating of castings (i.e. the planting of a gate in the top of the mold cavity, causing the metal to fall freely inside the mold cavity). This is because liquid aluminum reaches its critical velocity of about  $0.5 \text{ m s}^{-1}$  after falling only 12.5 mm under gravity. The critical velocity of liquid iron or steel is exceeded after a fall of only about 10 mm. (These are, of course, the heights of the sessile drops.) Naturally, such short fall distances are always exceeded in practice in top gated castings, leading to the danger of the incorporation of the surface films, and consequent porosity, leakage and crack defects.

Castings that are made in which velocities everywhere in the mold never exceed the critical velocity are consistently strong, with high fatigue resistance, and are leak-tight (we shall assume they are properly fed, of course, so as to be free from shrinkage porosity).

Experiments on the casting of aluminum have demonstrated that the strength of castings may be reduced by as much as 90% or more if the critical velocity is exceeded. The corresponding defects in the castings are not always detected by conventional non-destructive testing such as X-ray radiography or dye penetrant, since, despite their large area, the folded oxide films are sometimes extremely thin, and do not necessarily give rise to any significant surface or X-ray indications.

The speed requirement automatically excludes conventional pressure die castings as having significant potential for unreliability, since the filling speeds are usually 10–100 times greater than the critical velocity. Even so, over recent years there have been welcome moves, introducing some special developments of high-pressure technology that are capable of meeting this requirement. These include the vertical injection squeeze casting machine, and the Shot Control techniques. Such techniques can, in principle, be operated to fill the cavity through large gates at low speeds, and without the ingress of air into the liquid metal. Such castings require to be sawn, rather than broken, from their filling systems of course. Unfortunately, the castings remain somewhat impaired by the action of pouring into the shot sleeve. Even here, these problems are now being addressed by some manufacturers, with consequent benefits to the integrity of the castings, but involving technical, maintenance and cost challenges that are not easily overcome.

Other uphill filling techniques such as *low-pressure* filling systems are capable of meeting Rule 2. Even so, it is regrettable that the critical velocity is practically always exceeded during the filling of the low-pressure furnace itself because of the severe fall of the metal as it is transferred into the pressure vessel, damaging the melt prior to casting. In addition, many low-pressure die casting machines are in fact so poorly controlled on flow rate that the speed of entry into the die can greatly exceed the critical velocity, thus negating one of the most important potential benefits of the low-pressure system.

Processes such as the Cosworth Process avoid these problems by never allowing the melt to fall at any stage of processing, and control its upward speed into the mold by electromagnetic pump. These processes are to be discussed in greater detail in the Processing Section 16 'Casting'.

Metals that can also suffer from entrained surface films include the ZA (zinc–aluminum) alloys and ductile irons. For a few materials, particularly alloys based on the Cu–10Al types (aluminum- and manganese-bronzes) the critical velocities were originally thought to be much lower, in the region of only  $0.075 \text{ m s}^{-1}$ . However, from recent work at Birmingham (Halvae and Campbell 1997) this low velocity seems to have been a mistake probably resulting from the confusion caused by bubbles entrained in the early part of the filling system. With well-designed filling systems, the aluminum bronzes accurately fulfill the theoretically predicted  $0.4 \text{ m s}^{-1}$  value for a critical ingate velocity.

Some ferrous alloys have similarly dry oxide films that give classical, unbonded bifilm defects, although in certain irons and steels the entrained bifilms agglomerate as a result of being partially molten and therefore somewhat sticky. These sticky masses of oxide therefore remain more compact, and float out more easily to form surface imperfections in the form of slag macroinclusions on the surface. The subject of entrainment is described more extensively in the metallurgy of cast steels (Section 6.6).

Because of the central importance of the concept of critical velocity, the reader will forgive a re-statement of some aspects in this summary.

- (i) Even if the melt does jump higher than the height of a sessile drop, when it falls back into the surface there is no certainty that it will enfold its surface film. These tumbling motions in the liquid can be chaotic, random events. Sometimes the surface will fold badly, and sometimes not at all. This is the character of surface turbulence; it is not predictable in detail. The key aspect of the critical velocity is that at velocities less than the critical velocity the surface is always safe. Above the critical velocity there is always the *danger* of entrainment damage. The critical velocity criterion is therefore seen to be a necessary but not sufficient condition for entrainment damage.
- (ii) If the whole, extensive surface of a liquid were moving upwards at a uniform speed, but exceeding the critical velocity, clearly no entrainment would occur. Thus the surface disturbance that can lead to entrainment should more accurately be described not merely as a velocity but in reality a velocity difference. It might therefore be defined more accurately as a critical velocity gradient measured across the liquid surface. For those of a theoretical bent, the critical gradient might be defined as the velocity difference achieving the critical velocity along a distance in the surface of the order of the sessile drop radius (approximately half its height) in the liquid surface. To achieve reasonable accuracy, this approach allows for the reduction in drop height with velocity. Hirt (2003) solves this problem with a delightful and novel approach, modeling the surface disturbances as arrays of turbulent eddies, and achieves convincing solutions for the simulation of entrainment at hydraulic jumps and plunging jets. Such niceties are neglected here. The problem does not arise when considering the velocity of the melt when emerging from a vertical ingate into a mold cavity. In that situation, the ingate velocity and its relation to the critical velocity is clear.
- (iii) If the melt is traveling at a high speed, but is constrained between narrowly enclosing walls, it does not have the room to fold over its advancing meniscus. Thus no damage is suffered by the liquid despite its high speed, and despite the high risk involved. This is one of the basic

reasons underlying the design of extremely narrow channels for filling systems that are proposed in this book. Very narrow filling channels have the great advantage of filling the running system in *one pass*, the melt filling the channel with its meniscus operating as a piston to push the air ahead. In this way, despite its high speed it retains its quality. (This contrasts with oversize channels in which there is sufficient room for the melt to jet and splash, rebounding and churning to flow counter to the incoming melt, mixing with the air to degrade the melt prior to entering the mold cavity.)

### 10.2.3 The 'no-fall' requirement

It is quickly shown that if liquid aluminum is allowed to fall more than 12.5 mm then it exceeds the critical  $0.5 \text{ m s}^{-1}$ . The critical fall height can be seen to be a kind of re-statement of the critical velocity condition. Similar critical velocities and critical fall heights can be defined for other liquid metals. The critical fall heights for all liquid metals are in the range 3–15 mm.

It follows immediately that practically all pouring of metals is bad. Figure 10.3 shows an all too common and lamentably efficient destruction of the melt quality. Clearly, neither the employee, manager, nor designer of the plant knew they were engaged in such destruction of quality.

It also follows similarly that *top gating* of molds, almost without exception, will lead to a violation of the critical velocity requirement. In addition, for many forms of gating that enter the mold cavity at the mold joint, if any significant part of the cavity is below the joint, these will also violate this requirement.

In fact, for conventional sand and gravity die casting, it has to be accepted that some fall of the metal is necessary. Thus it has been accepted that the best option is for a single fall, concentrating the total fall of the liquid at the very beginning of the filling system, and causing the fall to be surrounded by a close-fitting, tapered conduit known as a *sprue*, or *down-runner*. This conduit brings the melt to the lowest point of the mold. The damage potential of the fall is limited if the sprue is as narrow as possible, so as to constrain the melt, giving it little chance to damage itself by folding in its oxide surface. Thus the sprue is designed to have a cross-section only just large enough to take the required flow rate to fill the casting in the target fill time. The distribution system from the point that the melt hits the base of the sprue, consisting of runners and gates, should progress only *horizontally* or preferably *uphill*. The metal should never suffer a further drop.

Considering the mold cavity itself, the no-fall requirement effectively rules that all gates into the mold cavity enter at the bottom level, known as *bottom gating*. The siting of gates into the mold cavity at the top (*top gating*) or at the joint (*gating at the joint line*) are not options if safety from surface turbulence is required.

Also excluded are any filling methods that cause waterfall effects in the mold cavity (Figure 2.30). This requirement dictates the siting of a separate ingate at every isolated low point on the casting.

Even so, the concept of the critical fall distance does require some qualification. If the critical limit is exceeded it does not mean that defects will necessarily occur. It simply means that there is a risk that they may occur. This is because for falls greater than the critical fall distance the energy of the liquid is sufficiently high that the melt is potentially able to enfold in its own surface. Whether a defect occurs or not is now a matter of chance. (This contrasts, of course, with falls of less than the critical height. In this case there is no chance that any serious defect can occur, the regime being comparatively safe.)

**FIGURE 10.3**

A typical melt transfer, seriously degrading the melt.

There is, however, further qualification that needs to be applied to the critical fall distance. This is because the critical value quoted above has been worked out for a liquid, neglecting the presence of any oxide film. In practice, it seems that for some liquid alloys, the surface oxide has a certain amount of strength and rigidity, so that the falling stream is contained in its oxide tube and so is enabled to better resist the conditions that might enfold its surface. This behavior has been investigated for aluminum alloys (Din, Kendrick, and Campbell 2003). It seems that although the original fall distance limit of 12.5 mm continues to be the safest option, fall heights of up to about 100 mm might be allowable in some instances. In the unusual circumstances of a ceramic foam filter being inserted into the flow, the fall distance downstream of the filter might be increased to approximately 200 mm without undue damage to the melt as explained in Section 11.2. However, falls greater than 200 mm definitely entrain defects; the velocity of the melt in this case is over  $2 \text{ m s}^{-1}$  so that entrainment seems unavoidable. Also, of course, other alloys may not enjoy the benefits of the support of a tube of oxide

around the falling jet. This benefit requires to be investigated in other alloy systems to test what values beyond the theoretical limits may be used in practice.

The initial fall down the sprue in gravity filled systems does necessarily introduce some oxide damage into the metal. The damage is concentrated during the first few seconds during which the sprue is priming. This period of fall of the metal can be very messy. The period can be shortened by the use of a stopper to ensure the pouring basin is filled prior to the sprue being allowed to fill. Even so, it seems reasonable to conclude that gravity poured castings will never attain the degree of reliability that can be provided by counter-gravity and other systems that can totally avoid surface turbulence.

Of necessity, therefore, it has to be accepted that the no-fall requirement applies to the design of the filling system downstream of the base of the sprue. The damage encountered in the fall down the sprue has to be accepted; although with a good sprue, good pouring basin and stopper this initial fall damage can be reduced to a minimum.

It is a matter of good luck that it seems that for some alloys much of the oxide introduced by the initial turbulence in the filling system does not appear to find its way through and into the mold cavity. It seems that much of it remains attached to the walls of the running system. This fortunate effect is clearly seen in many top gated castings, where most of the oxide damage (and particularly any random leakage problem) is confined to the area of the casting under the point of pouring, where the metal is falling, as is seen in Figure 9.44. Severe damage does not seem to extend into those regions of the casting where the speed of the metal front decreases, and where the front travels uphill, but there does appear to be some carry-over of defects. Thus the provision of a filter immediately after the completion of the fall is valuable. It is to be noted, however, that the filter will not take out all of the damage.

The requirement that the filling system should cause the melt to progress only uphill after the base of the sprue forces the decision that the runner must be in the drag and the gates must be in the cope for a horizontal single jointed mold (if the runner is in the cope, then the gates fill prematurely, before the runner itself is filled, thus air bubbles are likely to enter the gates. However, it has to be admitted that this preferred arrangement is not always possible.) The 'no-fall' requirement may also exclude some of those filling methods in which the metal slides down a face inside the mold cavity, such as some tilt casting type operations. This undesirable effect is discussed in more detail in the section devoted to tilt casting. As we shall see, sliding downhill is not a necessary filling mode for tilt casting; if feasible, horizontal transfer of the melt is strongly recommended for the tilt casting process.

It is noteworthy that these precautions to avoid the entrainment of oxide films also apply to casting in inert gas or even in vacuum. This is because the oxides of Al and Mg (as in Al alloys, ductile irons, or high temperature Ni-base alloys for instance) form so readily that they effectively 'getter' the residual oxygen in any conventional industrial vacuum, and form strong oxide films on the surface of the liquid.

Rule 2 in its 'no fall' embodiment applies to 'normal' castings with walls of thickness over 3 or 4 mm. For channels that are sufficiently narrow, having dimensions of only a few millimeters, the curvature of the meniscus at the liquid front can keep the liquid front from disintegration. As the section thickness of the casting decreases the effect of surface tension becomes ever more powerful. Thus the action of surface tension in narrow filling system geometries is valuable to conserve the liquid as a coherent mass, and so acting to push the air out of the system ahead of the liquid. The filling systems therefore fill in one pass.

A good filling action, pushing the air ahead of the liquid front as a piston in a cylinder, is a critically valuable action. Such systems deserve a special name such as perhaps 'One pass filling (OPF) designs'.

Although I do not usually care for such jargon, the special name emphasizes the special action. It contrasts with the turbulent and scattered filling often observed in systems that are over-generously designed, in which the melt can be traveling in two directions at once along a single channel; a fast jet travels under the return wave that rolls over its top, rolling in air and oxides at the boundary between the opposing streams.

For a wide, shallow, horizontal channel, any effect of surface tension is clearly limited to channels that have dimensions smaller than the sessile drop height for that alloy. Thus for Al alloys the maximum channel height would be 12.5 mm, although even this height would exert little influence on the melt, since the roof would just touch the liquid, exerting no pressure on it. Similarly, taking account that the effect of surface tension is doubled if the curvature of the liquid front is doubled by a second component of the curvature at right angles, a channel of square section could be 25 mm<sup>2</sup>, and be just contained by surface tension. In practice, however, for any useful restraint from the walls of channels, these dimensions require to be at least halved, effectively compressing the meniscus, as a mechanical spring, into the tight confines of the channel.

For very thin walled castings, of section thickness less than 2 mm, the effect of surface tension in controlling filling becomes predominant. The walls are so much closer than the natural curvature of a sessile drop that the meniscus is tightly compressed, and requires the application of pressure to force it into such narrow gaps. The liquid surface is now so constrained that it is not easy to break the surface; i.e. once again there is no longer room for splashing or droplet formation. Thus the critical velocity is higher, and metal speeds can be raised by approximately a factor of 2 without danger.

In very thin-walled castings, with walls less than 2 mm thickness, the tight curvature of the meniscus becomes so important that filling can sometimes be without regard to gravity (i.e. can be uphill or downhill) since the effect of gravity is swamped by the effect of surface tension. This makes even the uphill filling of such thin sections problematical, because the effective surface tension exceeds the effect of gravity. Instabilities therefore occur, whereby the moving parts of the meniscus continue to move ahead in spite of gravity because of the reduced thickness of the oxide skin at that point. Conversely, other parts of the meniscus that drag back are further suppressed in their advance by the thickening oxide, so that a run-away instability condition occurs. This dendritic advance of the liquid front is no longer controlled by gravity in very thin castings, making the filling of extensive sections, whether horizontal or vertical, a major filling problem.

The problem of the filling of thin walls occurs because the flow happens, by chance, to avoid filling some areas because of random meandering. Such chance avoidance, if prolonged, leads to the development of strong oxide films, or even freezing of the liquid front. Thus the final advance of the liquid to fill such regions is hindered or prevented altogether.

The dangers of a random filling pattern problem are relieved by the presence of regularly spaced *ribs* or other geometrical features that assist to organize the distribution of liquid. Random meandering is thereby discouraged and replaced by regular and frequent penetration of the area, so that the liquid front has a better chance to remain 'live', i.e. it keeps moving so that a thick restraining oxide is given less chance to form.

The further complicating effect of the microscopic break-up of the front known as micro-jetting observed in casting sections of 2 mm and less in sand and plaster molds is not yet understood. The effect has not yet been investigated, and may not occur at all in the dry mold conditions such as are found in gravity die casting. What little is known about this mysterious phenomenon is discussed briefly in Chapter 2.

---

## 10.3 RULE 3: 'AVOID LAMINAR ENTRAINMENT OF THE SURFACE FILM' (THE NON-STOPPING, NON-REVERSING CONDITION)

### 10.3.1 Continuous expansion of the meniscus

If the liquid metal front continues to *advance* at all points on its surface, effectively continuing to *expand* at all points on its surface, like a progressively inflating balloon, then all will be well. This is the ideal mode of advance of the liquid front. In general, this is the mode of advance of a counter-gravity filling system, which is why counter-gravity filling of castings is such a powerful technique for the production of good castings.

In fact, we can go further with this interesting concept of the requirement for continuous surface expansion. There is a sense in that if surface is lost (i.e. if any part of the surface experiences contraction) then, because the surface oxide cannot contract, some entrainment of the surface necessarily occurs. Thus this can be seen to be an all-embracing and powerful definition of the condition for entrainment of defects, simply that surface must not be lost. Clearly, surface is effectively lost by being *enfolded* (in the sense that the fold now disappears inside the liquid, as has been the central issue described under Rule 2), or by simply *shrinking*, i.e. *being lost* (necessarily leading to folding) as described below. Thus in a way this condition, 'Avoid loss of surface', can be seen to supersede the conditions of critical velocity or Weber number. It promises to be a useful condition that could be recognized in numerical simulation, and thus be useful for computer prediction of entrainment.

In practice, however, an uphill advance of the liquid front, if it can be arranged in a mold cavity, is usually a great help to keep the liquid front as 'alive' as possible, i.e. keeping the meniscus moving, and so expanding and continuously creating new oxide.

It seems possible that the condition for exceeding the critical velocity may lead to more severe entrainment than simple surface contractions, and that surface contractions might lead to entrained film that remains closely attached to the oxide on the surface, instead of becoming displaced into the deep interior of the casting as happens with surface turbulence. These distinctions remain to be clarified by research.

While the surface is being continuously expanded when filling the mold uphill, the casting has the benefit that the older, thicker oxide is continuously being displaced to the walls of the mold where it becomes the skin of the casting. Thus very old and very thick oxide does not normally have chance to form and become entrained. In fact, one of the great benefits of a good filling system is to ensure that the older oxides on the surface of the ladle or pouring basin etc. do not enter the mold cavity. For instance, in the tilt pouring of aluminum alloy castings, the filling of a new casting can be checked by dropping a fragment of paper on the metal surface as the tilt commences. This marker should stay in place, indicating that the old skin on the metal was being retained by the runner, so that only clean metal underneath could flow into the mold cavity. If the paper disappears into the runner, the runner is not doing its job. In a way, the use of the tea-pot pouring ladle and bottom-pour ladles common in the steel casting industry are in response to the acute form of these same problems, in which the high rates of reaction with the environment at such high temperatures encourages the surface oxide to grow from microscopic to macroscopic thickness, to constitute the familiar slag layer.

### 10.3.2 Arrest of forward motion of the meniscus

Problems arise if the front becomes pinned by the rate of advance of the metal front being too slow, or if it stops or reverses.

If the liquid front stops, a thick surface film has chance to form. Figure 10.4a shows a common way in which this can happen; by the abrupt enlargement of area at some stage during the filling of the mold. The stationary surface film may become so thick and strong that if pressure increases later to encourage flow to re-start, the front finds itself pinned in place, no longer able to move. As the advance re-starts elsewhere in the mold the melt may overflow and submerge the thick stationary film, forming an entrainment defect (Figure 2.25). As the new metal rolls over the old film a new fresh oxide is laid down over the old thick oxide, forming our familiar double film, with dry side facing dry side so that the double layer forms an unbonded interface, as a crack. On this occasion the bifilm is a thick/thin asymmetric variety. This mode of creation of a bifilm can constitute a large geometrical defect, sometimes in the form of a horizontal crack extending across the whole casting, or as a horizontal lap around its complete perimeter.

A good name for this defect is an *oxide lap*. (It is to be distinguished from the solidification defect that often has a superficially similar appearance, called here a *cold lap*, caused not necessarily by the strength of the oxide film but by the freezing in place of the liquid front. The method of treating these

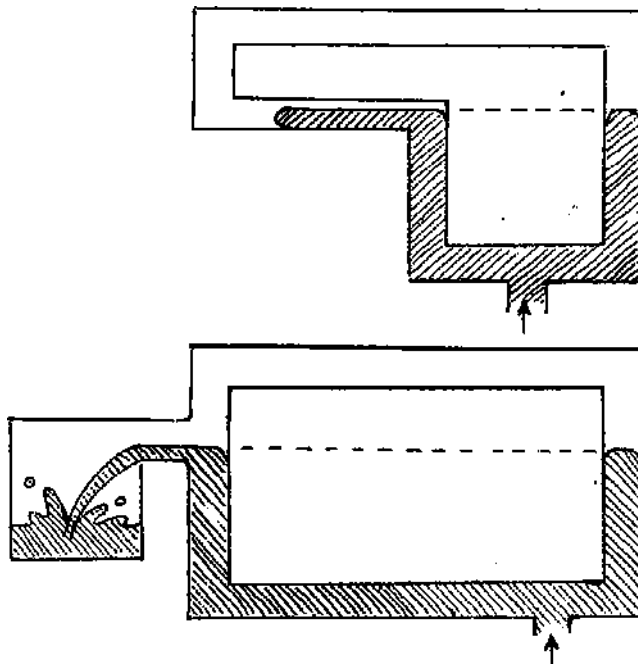


FIGURE 10.4

Two common filling situations in which the general advance of the melt is stopped, introducing the danger of a lap defect.



defects is quite different. A cold lap can be cured by increasing the casting temperature, whereas increasing the temperature of an oxide lap is likely to make it worse.)

### 10.3.3 Waterfall flow; the oxide flow tube

Instead of a large horizontal defect, a curious but major geometrical defect in the form of a cylindrical tube that I call an *oxide flow tube* can form in several ways.

If the liquid falls vertically, as a plunging jet, the falling stream is surrounded by a tube of oxide (Figure 10.4b). Despite the high velocity of the falling metal inside, the oxide tube remains stationary, thickening with time, until finally surrounded by the rising level of the metal in the mold cavity. This rising metal rolls up against the oxide tube, forming a double oxide crack (once again of a highly asymmetrical thick/thin form). Notice the curious cylindrical form of this crack and its largely vertical orientation. The arrest of the advance of the front in this case occurred by the curious phenomenon that although the metal was traveling at a high speed parallel to the jet, its transverse velocity, i.e. its velocity at right angles to its surface, was zero. It is the zero velocity component of a front that allows the opportunity for a thick oxide skin to develop.

These oxide flow tubes are often seen around the falling streams of many liquid metals and alloys as they are poured. The defects are also commonly seen in castings. Although occasionally located deep inside the casting where they are not easily found, they are often clearly visible if formed against the casting surface.

A patent dating from 1928 (Beck) describes how liquid magnesium can be transferred from a ladle into a mold by arranging for the pouring lip of the ladle to be as close as possible to the pouring cup of the mold, and to be in a relatively fixed position so that the semi-rigid oxide flow tube which forms automatically around the jet is maintained unbroken, and thus protects the metal from contact with the air (Figure 2.23a). A similar phenomenon is seen in the pouring of aluminum alloys and other metals such as aluminum bronze.

In a large Ni-base superalloy turbine blade, cast in vacuum, and destined for a land-based turbine, the top pouring of this blade via the root had almost certainly created a cluster of vertically oriented oxide flow tubes as the melt poured in a series of separate streams through the root, to start its long fall towards the blade tip. When the transverse grooves of the fir-tree root were machined by grinding, vertical cracks were observed which were argued to be grinding cracks from over-enthusiastic grinding. However, their origin as oxide flow tubes was corroborated by the observation under the microscope of a series of sulfide precipitates with an alignment that was characteristic of occupying one side of a vertical oxide film. Micrographs could not be released for security reasons, so a sketch to illustrate the effect is seen in Figure 10.5a. The interpretation of the micrograph is shown in Figure 10.5b. The presence of the bifilm in the form of an oxide flow tube explains both the vertical cracking during grinding, and the vertical alignment of the sulfides which have clearly grown only on one side of an interface. Precipitates have been reported to form on only one side of an asymmetric bifilm, as seen in a confluence weld (Garcia 2007). (The air gap between the two oxide films shown in Figure 10.5b is exaggerated for clarity. Clearly in practice the two films will be in contact, and the air gap will be comprised only of the air trapped in the microscopic roughness of the two contacting surfaces.)

The stream does not need to fall vertically. Streams can be seen that have slid down gradients in such processes as tilt casting when carried out under poor control. Part of the associated flow tube is

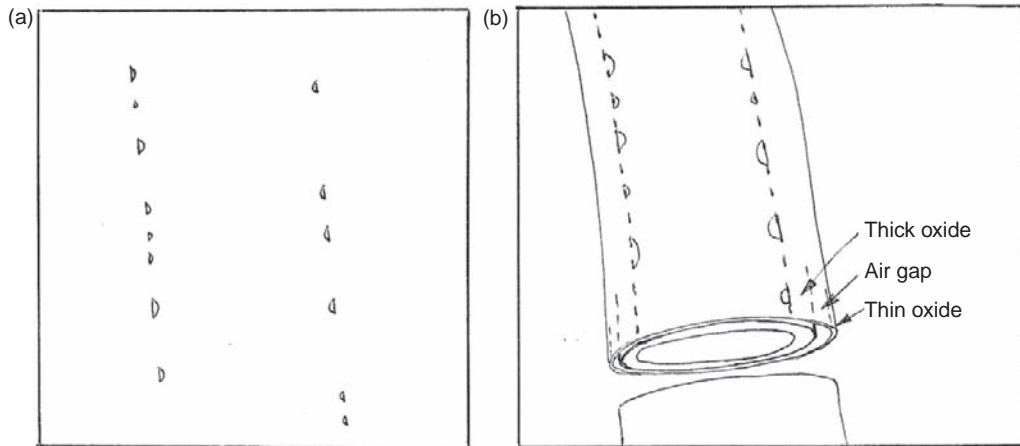


**FIGURE 10.5**

(a) Vertical lines of sulfide inclusions seen on a polished section of a vacuum top-poured Ni-base superalloy.  
 (b) Interpretation in terms of precipitation on an oxide flow tube (oxide thicknesses and air gap are greatly exaggerated for clarity, whereas in reality they are so thin as to be invisible).

often visible on the surface of the casting, as a witness to the original presence of the metal stream. Alternatively, a wandering horizontal stream can define the flow tube, as is commonly seen in the spread of liquid across a horizontal surface. Figure 2.24 shows how, in a thin horizontal section, the banks of the flowing stream remain stationary whilst the melt continues to flow. When the flow finally fills the section, coming to rest against the now-rigid banks of the stream, the banks will constitute long meandering asymmetrical bifilms as cracks, following the original line of the flow.

The jets of flow in pressure die castings can sometimes be seen to leave permanent legacies as oxide tubes as seen in section in Figure 2.31.

Even with the best design of gravity-poured system, the rate of fill of the mold may be far from optimum at certain stages during the fill. For instance, Figure 10.4 shows two common geometrical features in castings that cause the advance of the liquid metal to come to a stop. The heavy section filled downhill will cause the metal front to stop, possibly causing a lap-type defect at points on the casting well away from the real cause of the problem. Until the recess is filled by the pouring metal, the remainder of the liquid front cannot advance. There are several reasons for avoiding any 'waterfall' action of the metal during the filling of the mold.

- (i) A cylindrical oxide flow tube forms around the falling stream. If the fall is from a reasonable height, the tube is shed from time to time, and plunges into the melt where it will certainly contribute to severe random defects. The periodic shedding of oxide flow tubes into the melt is a common sight during the pouring of castings. Several square meters of oxide area can be clearly seen to be introduced in this way during the filling of the mold.
- (ii) The plunging jet is likely to exceed the critical velocity. Thus the metal that has suffered the fall is likely to be impaired by the addition of randomly entrained bifilms generated near the point of impact.

- (iii) As the melt rises around the tube, supporting it to some degree and reducing the height of the fall, the flow tube remains in place and simply thickens. As the general level of the melt rises around the tube, the new oxide rolls up against the surface of the cylinder, forming the curious cylindrical bifilm that acts as a major cylindrical crack around a substantially vertical axis.
- (iv) During the period of the waterfall action, the general rise of the metal in the rest of the mold will be interrupted, causing an oxide to form across the whole of the stationary level surface. If this has time to thicken significantly, it may be too strong to move when the levels equalize. Thus rising melt will overflow the film, as the flooding over an ice sheet, rolling a second thin film into place on top of the thick stationary layer. Thus a major horizontal lap defect may be created as a horizontal bifilm. The bifilm will be highly asymmetrical, with one thick and one thin film facing each other as described earlier.

Defects (i) and (ii) above are the usual fragmented and chaotic type of bifilm. Defects from (iii) and (iv) are the major geometrical bifilms.

Waterfall problems are usually easily avoided by the provision of a gate into the mold cavity at every low point in the cavity. Occasionally, deep recesses can be linked by channels through the mold or core assembly; the links being removed during the subsequent dressing of the casting.

#### 10.3.4 Horizontal stream flow

If the melt is allowed to spread without constraint across a horizontal thin-walled surface, gravity can play no part in persuading the flow to propagate on a broad stable front, as would happen naturally in a vertical or sloping plate (Figure 2.24). The front propagates unstably in the form of a river bounded by river banks composed of thickening oxide.

A fascinating example of a flow tube can be quoted from observations of flow up a sloping open channel driven by a traveling magnetic field from a linear motor sited under the channel. When used to drive liquid aluminum alloy uphill, out of a furnace and into a higher-level receiver, the traveling melt is seen to flow inside its oxide tube. When the magnetic field is switched off, the melt drains out of the oxide tube and back into the furnace, the tube collapsing flat on the bottom of the channel. However, when the field is switched on again, the same oxide tube magically refills and continues to pass metal as before. Clearly the tube has considerable strength and resilience. It is sobering to think that such features can be built into our castings, but remain unsuspected and almost certainly undetectable. Clearly, the casting methods engineer requires vigilance to ensure that such defects cannot be formed.

The vertical oxide flow tube is probably more common than any of us suspect. The example given below is simply one of many that could be described.

Figure 10.6 illustrates the bronze bell, sometimes known as the 'Freedom Bell' as a larger-sized replica of the Liberty Bell, hung outside the railway station in Washington DC. Horizontal weld repairs, etched for enhanced clarity by rain water, record for all time the fatal hesitations in the pouring process that led to the horizontal oxide bifilms that would have appeared as horizontal laps. Perhaps these were the points at which the pouring ladles were changed. The vertical weld repairs record the passage of the falling stream that created the vertical flow tube that led to cracks through the thickness of the casting. These vertical cracks were opened by the hoop stress created by the casting contracting onto its core. This is a common source of failure for bells, nearly all of which are top-poured through the crown. The renowned Liberty Bell (the only survivor of three attempts, all of which cracked)



**FIGURE 10.6**

Inspection of the Freedom Bell outside the railway station in Washington DC, unfortunately spoiled by welds from an attempt to repair cracks caused by vertical oxide flow tubes from top pouring and horizontal oxide bifilms from filling hesitations (photograph by Sheila).

reveals a magnificent example of a flow tube defect that starts at the crown, curves sinuously around and over the shoulder, and finally falls vertically down the skirt to the mouth of the bell. Although there are many examples of bells that exhibit these long cracks, it is perhaps all the more surprising that any bells survive the top pouring process. It seems likely that in the majority of cases of bells of thicker section the oxide flow tube is not trapped between the walls of the mold to create a through-thickness pair of parallel cracks. In such thicker sections the tube is more likely to be detached and carried away, crumpling into a somewhat smaller defect that can be accommodated elsewhere. It is to be hoped that the new resting place of the defect will not pose any serious future threat to the product. Clearly, the top pouring of castings is a risky manufacturing technique.

Oxide flow tubes are common defects seen in a wide variety of castings that have been filled across horizontal sections or down sloping downhill sections. The deleterious oxide flow tube structures described above that form when filling *downwards* or *horizontally* cannot form when filling *vertically upwards*, i.e. in a *counter-gravity* mode. The requirement that the meniscus only travels uphill is sacred.

Although molds can be filled substantially without risk only by *counter-gravity filling*, even in this case vigilance is still required to avoid other filling defects. Even in this favorable mode of filling, a related *oxide lap* defect, or even a *cold lap* defect, can still occur if the advance of the meniscus is stopped at any time as we have seen. Such defects constitute the well-known *confluence weld* defect.

In all cases it will be noticed that such interruptions to flow, where, for any reason, the surface of the liquid locally stops its advance, a large, asymmetric double film defect is created. These defects are always large, and always have a recognizable, predictable geometrical form (i.e. they are cylinders, planes, meandering streams, etc.). They are quite different to the double films formed by surface turbulence, which are random in size and shape, often extremely thin or of variable thickness, but essentially completely unpredictable as a result of their chaotic origin.

### 10.3.5 Hesitation and reversal

If the meniscus stops at any time, it is common for it to undergo a slight reversal. Minor reversals to the front occur for a variety of reasons:

- A reversal will practically always occur when a waterfall is initiated. This occurs because at the point of overflow, the liquid will be at a level slightly above the overflow, dictated by the curvature of its meniscus, i.e. for a liquid Al alloy it will be about 12.5 mm above the height of the overflow since this is the height of the sessile drop. However, immediately after the overflow starts, the general liquid level drops, no longer supported by the surface tension of the meniscus. In the case of liquid aluminum alloy this fall in general level of the liquid will be perhaps about 6 mm, just enough to flatten the more distant parts of the meniscus against the rest of the mold walls.
- Hesitations to an advancing flow will often be accompanied by slight reversals because of inertial effects of the flow. Momentum perturbations during filling will cause slight gravity waves, the surface therefore experiencing minor slopping and surging motion, oscillating gently up and down.

These minute reversals of flow flatten the oxidized surface of the meniscus. When advancing, the meniscus adopts a rounded form, but when flattened, the oxidized surface now occupies less area. A fold necessarily develops, wrinkling the surface, endangering the melt with the possibility that the entrainment of this excess oxide is permanent; the entrainment folding action is not reversed once the melt is able to continue its advance. The folding in of a small crack attached to the surface of the casting is illustrated in Figure 10.7. Such shallow surface cracks occurring as a result of hesitation

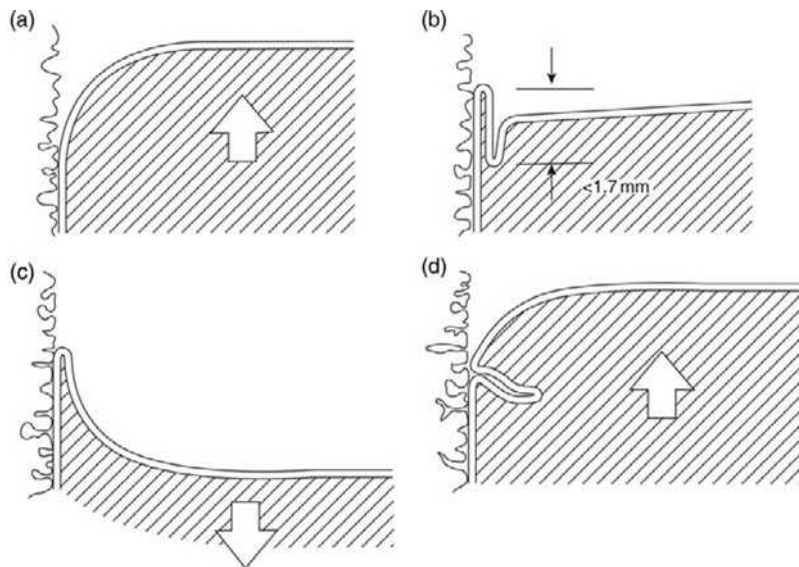


**FIGURE 10.7**

The creation of bifilm cracks of the order of mm deep by the reversal of the front, causing the meniscus to flatten and enfold the excess surface area of film.

and/or reversal of the front are common in aluminum alloys, and are revealed by dye penetrant testing.

It is instructive to estimate the maximum depth that such oxide folds might have. Following Figure 10.7, if the front of the liquid in Figure 10.7a is a cylinder of radius  $r$ , the perimeter of the quarter of a cylinder is  $\pi r/2$ , so that the maximum length of excess surface if the melt level now drops a distance  $r$  to become horizontal is  $\pi r/2 - r = r((\pi/2) - 1) = r/2$  approximately. The radius of the meniscus  $r$  is approximately 6 mm for liquid aluminum (as a result of the total height of a sessile drop being approximately 12 mm), giving the excess length 3 mm. If this is folded just once to create a bifilm, its potential depth is therefore found to be approximately 1.5 mm. This may not seem a lot, but an appearance of such a crack during the NDT examination of a casting by dye penetrant will almost certainly fail any safety critical casting. Clearly, the depth of the crack cannot easily be known during the DPI inspection, and in any case might genuinely be serious for a highly stressed part experiencing fatigue.

If the melt continues its downward oscillation the defect can be straightened out as shown in Figure 10.7c. Alternatively, if the bifilm created in this way holds itself closed, possibly because of viscous adhesion (i.e. the trapped liquid metal takes time to escape from between the films) or possibly as the result of other forces such as Van der Waals forces, then there is the danger that the fold is not reversible, and additional folds may be created on each oscillation cycle.

In fact, many of these defects are not as deep as the maximum estimate of 1.5 mm for several reasons. (i) The melt surface may not drop the full distance  $r$ ; (ii) the film may be folded more than once, creating a greater number of shallower folds; and (iii) the fold-like crack may hinge to lie flat against the surface of the casting. The action of internal forces as a result of flow of the liquid, surging through the mold sections, may be helpful in this respect. For these reasons such defects are usually only a fraction of a millimeter deep, so that they can often be removed by grit blasting. Only relatively rarely do they reach the maximum possible depth approaching 1.5 mm. Even so, for castings requiring total integrity, requiring resistance to high stress or fatigue, these minor oscillations of the front are very real threats that are best avoided.

The ultimate solution, as we have emphasized here, is that the melt should be designed to be kept on the move, advancing steadily forwards at all times. All we foundry people should be deeply grateful for the simplicity of this solution.

### 10.3.6 Oxide lap defects

The flooding of the melt over a large oxide film that has grown as a result of a hesitation in the vertical rise of the liquid, and the problem of joining of flows if one has stopped, are essentially equivalent. The first is usually a horizontal double film, where the second is usually vertical. Both are highly asymmetrical, consisting of a thick film (grown on the stationary interface) and a thin film (grown on the moving front).

These very deleterious defects, as major cracks, can be avoided by increasing the rate of filling of the mold. Care is needed of course to avoid casting at too high a rate at which surface turbulence may become an issue. However, providentially, there is usually a comfortably wide operational window in which the fill rate can meet all the requirements to avoid defects. This is another simple solution for which we are all grateful.

---

## 10.4 RULE 4: 'AVOID BUBBLE DAMAGE'

Entrainment defects are caused by the folding action of the (oxidized) liquid surface. Sometimes only oxides are entrained, as doubled-over film defects, called bifilms. Sometimes the bifilms themselves contain small pockets of accidentally enfolded air, so that the bifilm is decorated by arrays of trapped bubbles. Much, if not all, of the microporosity observed in castings either is, or has originated from, a bifilm.

Sometimes, however, the folded-in packet of air is so large that the buoyancy of the newly created bubble confers on it a life of its own. This oxide-wrapped piece of air that we call a bubble is a massive entrainment defect. It can be sufficiently buoyant to power its way through the liquid and sometimes through the dendrites. In this way it develops its own distinctive damage pattern in the casting.

### 10.4.1 The bubble trail

The passage of a single bubble through an oxidizable melt is likely to result in the creation of a bubble trail as a double oxide crack, a long bifilm, in the liquid. A bubble trail is the name coined (Campbell 1991) to describe the defect that was predicted to remain in a film-forming alloy after the passage of a bubble through the melt. Thus even though the bubble may be lost by bursting at the liquid surface, the trail remains as permanent damage in the casting.

The bubble trail occurs because the trail is nearly always attached to the point where the bubble was first entrained in the liquid. The enclosing shroud of oxide film covering the crown of the bubble attempts to hinder its motion. This restraint is so large that bubbles having relatively little buoyancy, of diameter less than about 5 mm, are held back, unable to rise. However, if the bubble is larger, its upward buoyancy force will split this restraining cover. Immediately, of course, the oxide re-forms on the crown, and splits and re-forms repeatedly. The expanding region of film on the crown effectively slides around the surface of the bubble, continuing to expand until the equator of the bubble is reached. At this point the area of the film is a maximum. Figure 10.8 shows residual fragments on such a bubble in a Ti alloy (also shown in this figure is some shrinkage porosity that has grown from the underside of the bubble presumably because the casting had been poorly fed. The bubble trail is just visible below this region.) Although the film was able to expand by splitting and re-growing, it is not able to contract since it is a solid. Further progress of the bubble causes the film to continue sliding around the bubble, gathering together in a mass of longitudinal pleats under the bubble, forming a trail that leads back to the point at which the bubble was first entrained as a packet of gas. Any spiraling motion of the bubble will twist and additionally tighten the rope-like tether that continues to lengthen as the bubble rises.

The structure of the trail is a kind of collapsed tube. In section it is star-like but with a central portion that has resisted complete collapse because of the small residual rigidity of the oxide film (Figure 2.32). This is expected to form an excellent leak path if it joins opposing surfaces of the casting, or if cut into by machining. In addition, of course, the coming together of the opposite skins of the bubble during the formation of the trail ensure that the films make contact dry side to dry side, and so constitute our familiar classical bifilm crack.

Poor designs of filling systems can result in the entrainment of much air into the liquid stream during its travel through the filling basin, during its fall down the sprue, and during its journey along the runner. In this way dozens or even hundreds of bubbles can be introduced into the mold cavity.

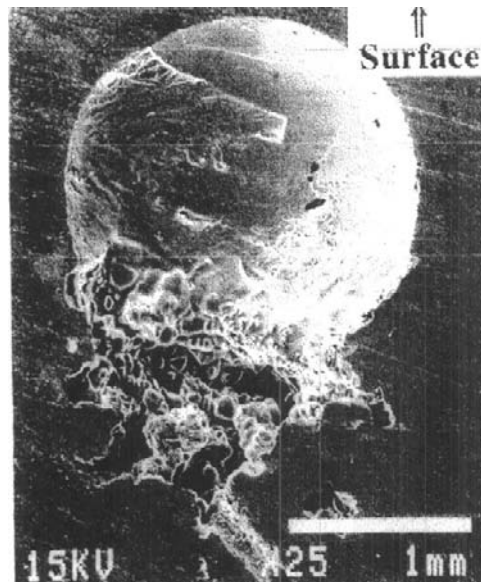


**FIGURE 10.8**

A bubble in a centrifugally cast Ti-6Al-4V alloy by Susuki et al. (1996), showing oxide slipping around its surface, and some shrinkage porosity clustered around the start of its bubble trail in the bottom of the image.

### 10.4.2 Bubble damage

Bubble damage is usually a mixture; the residue of bubbles and bubble trails. It is a typical entrainment mess.

When many bubbles are involved the later bubbles have problems rising through the morass of bubble trails that remain after the passage of the first bubbles. Figure 10.9 shows counts of the number of bubbles per cubic centimeter arising in a small experimental casting as a result of the provision of a 'well' at the base of the sprue. Clearly, hundreds of bubbles are generated, and only die away after several seconds. Larger castings would be expected to generate many times this number, and have their production persist for proportionately longer. Furthermore, if this were not bad enough, even more bubbles are created in the pouring basin (requiring the offset step basin to keep many of these out of the filling system) and many more are generated at the base of the sprue and in the running system unless these are designed to be naturally pressurized.

It is easy to understand that the free flotation and escape of late-arriving bubbles is hampered by the accumulation of the tangle of residual bifilms. If the density of films is sufficiently great, fragments of bubbles remain entrapped as permanent features of the casting. This mass of fragments of bifilm trails and bubbles is collectively called 'bubble damage'. In the experience of the author, bubble damage is probably the most common defect in castings, but up to now has been almost universally unrecognized.

Bubble damage in the form of masses of trails is nearly always mistaken for shrinkage porosity as a result of the irregular form of the air porosity that it encloses, usually with characteristic cusp-like morphology. Another common feature of bubble damage is its non-uniform distribution. Unlike



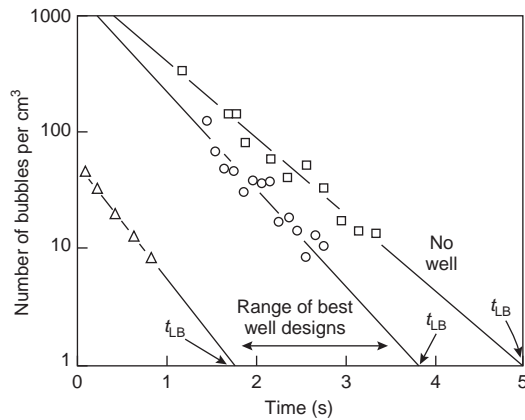


**FIGURE 10.9**

Water model of bubbles entrained by surface turbulence in a well (Isawa and Campbell 1994) for runners twice the area of the sprue, showing their decrease with time for different well designs, extrapolated to the time for the last bubble  $t_{LB}$ .

shrinkage porosity, it is often not in areas where shrinkage porosity might be expected. For instance shrinkage porosity would be expected in hot spots, but oxide damage resembling shrinkage porosity can be found almost anywhere in the casting.

In some stainless steels the phenomenon is seen under the microscope as a mixture of bubbles and cracks. (A remarkable combination! Without the concept of the bifilm such a combination would be extremely difficult to explain; with bubbles that would naturally expand to relieve and eliminate stresses, and cracks that therefore could not form because their formation would need stresses.) In these strong materials the high cooling strain leads to high stresses that open up the double oxide bubble trails.

### 10.4.3 Bubble damage in gravity filling systems

In gravity filled running systems the requirement to reduce bubbles in the liquid stream during the filling of the casting calls for offset stepped basins, or other non-entraining filling system such as contact pouring for instance. (The conventional conical or funnel-shaped pouring basin is the worst possible filling device for concentrating 50% or more of air in the metal.)

The sprue is required to be tapered, the taper calculated to match, or very slightly compress, the natural form of the falling stream; the stream naturally narrows during its fall because of its acceleration under the action of gravity. By tailoring the shape of the sprue to the natural shape of the stream the melt has the best chance to avoid the entrainment of air.

Parallel or reversed taper sprues are not recommended. Elliott and Mezoff (1948) show that their parallel slot sprues entrain air bubbles, finding that at low casting temperatures their Mg alloy castings exhibit bubbles, whereas at high casting temperatures the castings exhibit mainly oxide films. Although the authors conclude that the air is consumed by the Mg alloy, which will certainly be partly if not wholly true, it seems also likely that many larger bubbles would have time to escape at high

temperatures prior to the formation of a solidified skin. The authors are clearly not aware of the seriousness of these residual oxides.

Special precautions are needed to reduce the damage introduced if a parallel or reverse tapered sprue design has to be used. Such features include the radial choke or a filter at the entrance to the sprue.

At one time it was mandatory that each sprue had a sprue well at its base. The designs of filling systems recommended in this book explicitly avoid wells. This departure from tradition is possible only because the new filling systems are characterized by runners of approximately the same area as that of the sprue exit. It is to be noted that the traditional choice of sprue exit/runner/gate ratios of 1:2:2 and 1:2:4, etc. are automatically bad. The runner is too large to fill completely, regrettably entraining air and so ensuring bubble damage problems.

A beneficial consequence of the avoidance of a well is the addition of friction to the liquid provided by the additional solid surface of the mold at the point impacted by the metal as it turns the corner, so slowing the velocity of the melt to the greatest extent. If the sprue/runner junction is nicely formed, bubbles are formed for precisely zero seconds. This awkward way of making a simple statement that no bubbles are formed is deliberate. It emphasizes the contrast with filling systems that have been accepted as conventional up to now. Nowadays it is not necessary to accept a design that introduces any bubbles at all.

It is mandatory that no interruption to the pour occurs that leads to the lowering of the melt in the pouring basin below the minimum design level. If the sprue entrance is unpressurized in this way air will enter the running system. In the worst instance of this kind, if the basin level drops to the point that the sprue entrance becomes uncovered this has to be viewed as a disaster. A provision must be made for the foundry to reject automatically any castings that have suffered an interrupted pour, or slow pour that has allowed the basin to empty to a level below the designed minimum level.

To be safe, it is worth ensuring that basins are provided that are up to twice the required minimum depth to keep the sprue filled, and ensuring that the pourer keeps the basin topped up as highly as possible, well above the minimum level. In this way the casting may run a little faster, but air will be excluded and bubble damage avoided.

#### 10.4.4 Bubble damage in counter-gravity systems

Pumped systems such as the Cosworth Process, or low-pressure castings systems into sand molds or dies, are highly favored as having the potential to avoid the entrainment of bubbles if, and only if, the processes are carried out under proper control. The reader needs to be aware that good control of a *potentially* good process should not be assumed; it requires to be demonstrated.

Although low pressure filling systems can in principle satisfy the requirement for the complete avoidance of bubbles in the metal, a leaking riser tube in a low-pressure casting machine can lead to a serious violation (Figure 10.10a). The stream of bubbles from a leak in a defective riser tube will float directly up the tube and enter the casting. Unfortunately, this problem is not rare. Thus regular checks for such leakage, and the rejection of castings subjected to such consequent bubble damage, will be required. If the melt in the pressurized vessel becomes too low a huge amount of gas can erupt up the riser tube (Figure 10.10b).

For pumped systems, bubbles can be released erratically from the interior wall of a sloping tube launder system, especially if it is not cleaned with regular maintenance. Bubbles can become trapped and

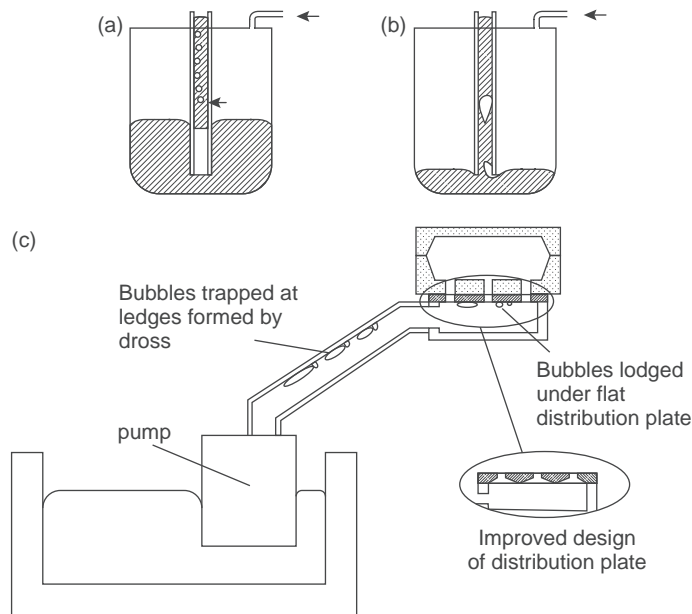


**FIGURE 10.10**

Bubbles introduced by defective counter-gravity systems. (a) Leak in a riser tube of a low-pressure casting unit; (b) the dangerous ingestion of massive bubbles if the melt level is too low; (c) bubbles entrapped by dross and poor design features of some pumped systems, creating bubbles that are released erratically.

escape from time to time from the underside of a badly designed distribution plate used in some counter-gravity systems such as the early variants of the low-pressure sand (LPS) system (Figure 10.10c).

All counter-gravity filling systems need to be designed to avoid the ingress of air or the trapping of air bubbles that might be randomly released.

## 10.5 RULE 5: 'AVOID CORE BLOWS'

### 10.5.1 Background

When sand cores are surrounded by liquid metal, the heating of the sand and its binder causes gas to be generated in the core. Normally, the core will be designed so that the gas can escape through the core prints and so be dissipated in the mold so that high gas pressure inside the core can be avoided.

In some circumstances, however, the pressure of gas in the cores may rise to a level higher than that in the liquid, with the result that a bubble may be forced out into the melt. This forcing of gas into the liquid can be nearly explosive. The gas bubble is *blown* into existence. *Blow defect* is therefore a good name for this type of gas pore.

The reader needs to be aware that the name 'blow-hole' is, unfortunately, widely misused to describe almost any kind of hole in a casting. In this work the name 'blow-hole, blowhole', or simply

'blow', is strictly reserved solely for those defects which are forced, (actually 'blown') into the liquid metal via the mechanical penetration of the liquid surface. The term is therefore quite specific and accurately descriptive. (The term excludes pores nucleated internally by the precipitation of gas dissolved in the liquid, or diffusing in from the surface, and also excludes bubbles entrained by surface turbulence.) The reader is encouraged to use the name 'blowhole' with accuracy.

The contribution of surface tension to increasing the pressure required is practically negligible in the case of *core blows* because of the large size of the bubbles that are formed in this process. Core blow bubbles are large, lazy, wobbling bubbles, containing gas at low pressure. They are quite unlike microblows, if these exist, to be discussed later, which are envisaged as small, hard spheres having a likeness to mini ball bearings.

Core blow bubbles create trails as they rise through a melt. The trails are, of course, a similar form of bubble damage to that of turbulence-entrained bubbles discussed under Rule 4. However, they are sufficiently distinct that they benefit from separate consideration.

For instance bubble damage arising from surface turbulence in the filling system takes quite a different form. The bubbles are generated by the high velocities in the front end of the system (in the basin, sprue or runner). The high shear stresses in the melt ensure that the bubbles are chopped mainly into small sizes, in the range 1–10 mm diameter. Some of the smaller bubbles have been observed in video radiographic studies to coalesce in the gate. These coalesced bubbles float quickly, before any significant solidification has taken place, and so burst at the liquid surface and escape. A bubble smaller than about 5 mm diameter has only a tenth of the buoyancy of a 10-mm bubble, and cannot force the splitting of the oxide films that bars its escape. Bubble 'A' in Figure 10.11a illustrates such a case. If such a bubble succeeds to reach the top of the casting it therefore remains trapped at a distance only a double oxide skin depth beneath the surface of the casting.

The bubble given off by the outgassing of a core is quite different. These bubbles are large. In irons and steels the single core blow bubble is about 13 mm diameter. In light alloys the effective bubble diameter is approximately 20 mm (Figure 10.12). Although these large bubbles have high buoyancy, they are not produced immediately. The timing of their eruption into the melt determines the kind of defect that is formed in the casting.

If, in relatively thick sections, the bubble detaches prior to any freezing, the repeated arrival of bubbles at the surface of the casting can result in repeated build-up of bubble skins, forming multiple leaves of oxide, well named as an *exfoliation defect* (Figure 10.13a). Exfoliated structures are those that have been expanded and delaminated, like puff pastry, or like the conversion of slate rock into vermiculite, or like leaves from a book.

Exfoliated dross defects are recorded for steels containing 0.13C, 1Cr, 0.5Mo, and 0.4Al (Frawley et al. 1974), and for ductile iron (Loper and Saig 1976). The content of film-forming elements in these alloys is of central significance. For ductile iron (containing magnesium) the defect is described as a wrinkled or pastry-like area, and when chipped out appears to be a mass of tangled flakes resembling mica that can be easily peeled away. Polished microsections of the defect confirmed its structure as composed of tangled films, and contrasted with the structure of the rest of the casting, which was reported as excellent.

More usually, the core takes time to warm up, and takes further time to build up its internal pressure. This significant delay in the creation of a bubble allows time for some freezing of the casting to occur. Thus by the time the bubble is finally forced into existence, it rises to find itself trapped under the frozen layer of solid (Figure 10.13b).

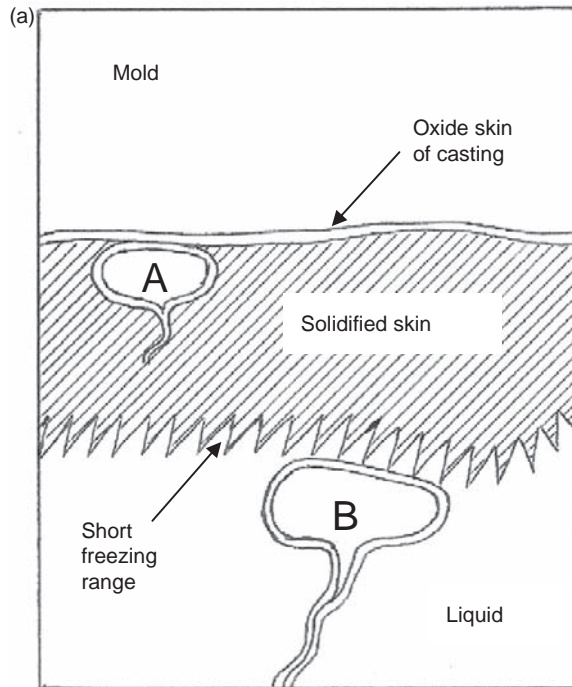


**FIGURE 10.11**

Bubbles arriving at the cope in (a) a skin-freezing alloy, and (b) a long-freezing-range alloy. Bubbles 'A' arrive early, probably originating from entrainment during pouring. Bubbles 'B' arrive late; in the dendritically freezing alloy the bubble now grows interdendritically, but can, of course, be grown either by additional gas or by shrinkage.

Once a core has blown its first bubble, additional bubbles are easily formed, since the bubble trail seems usually to remain intact, and keeps re-inflating to pass an additional bubble along its length. The bubbles contain a variety of gases, including water vapor, that are aggressively oxidizing to metals such as aluminum and higher melting point metals. Bubble trails from core blows are usually particularly noteworthy for their characteristically thick and leathery double oxide skin, built up from the passage of many bubbles. This thick skin is part of the reason why core blows result in such efficient leak defects through the upper sections of castings. Bubble trails from core blows are particularly damaging because they are, of course, automatically connected from a cored volume of the casting, and often penetrate to the adjacent core (since little solidification will usually have occurred between cores to stop it). Alternatively, in thicker sections, they travel from the core to the very top of the casting.

After the emergence of the first blow into the melt, the passage of additional bubbles contributes to the huge growth of some blow defects. Often the whole of the top of a casting can be hollow. The size

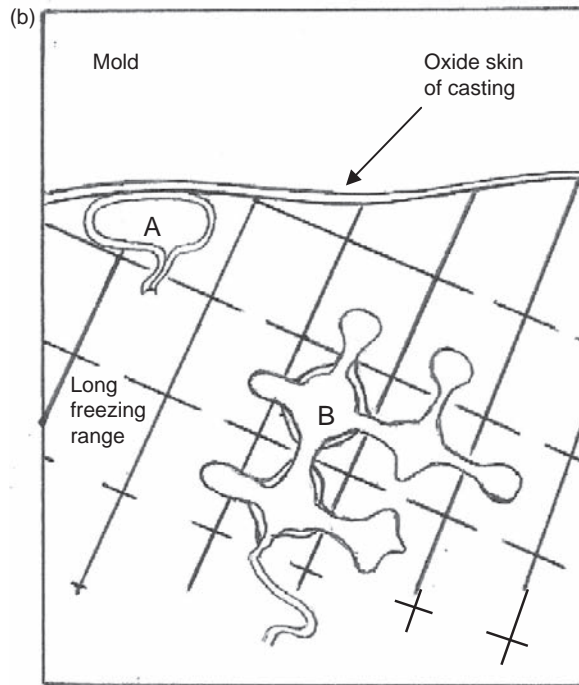
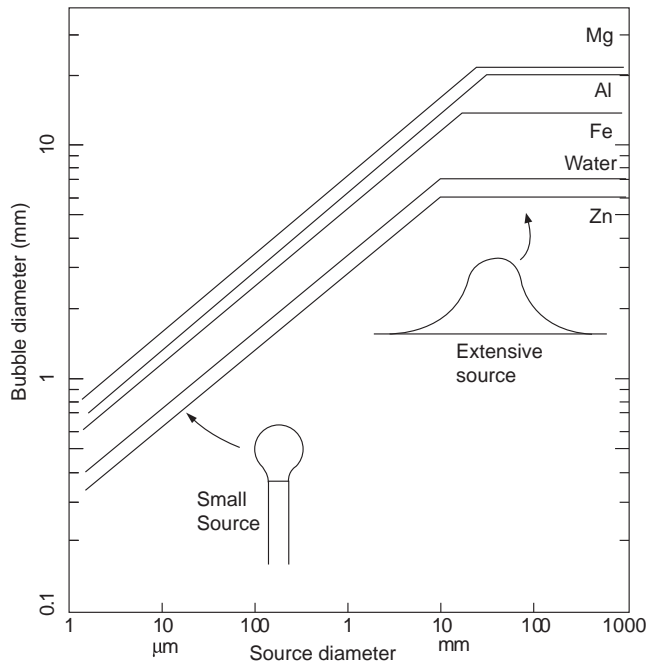


FIGURE 10.11 (continued).

of the defect can sometimes be measured in fractions of meters. An accumulating bubble will spread under the dendrites, as, inversely, a large limp balloon would float down to sag on the tips of conifer trees.

These trapped bubbles are recognizable in castings by their size (often measured in centimeters or even decimeters!), their characteristic flattened shape, and their position several millimeters under the uppermost surfaces of local regions of the casting (Figure 10.13b). In addition, of course, they will faithfully follow the contours of the upper surface of the casting. Like the bubble trail mentioned earlier, the core blow defect is sometimes so impressively extensive as to be difficult to perceive on a radiograph.

As an example, the author remembers making a delightful compact aluminum alloy cylinder block for a small pump engine. At first sight the first casting appeared excellent, and unusually light. It seemed that the designer had done a good job. A close study of the radiograph revealed it to be clear of any defects. However, on standing back to take a more general view it was noticed that a curious line effect, as though from a wall thickness, could not be found on the designer's drawing. It took some time to realize the casting was completely hollow; the smooth and extensive form of the core blow faithfully followed the contours of the casting. The prolific outgassing of the water jacket core around the bores of the block was found to be the source. The water jacket core was stood upright on its core prints (the only vents) that located in the drag. The problem arose because of the very slow filling



**FIGURE 10.12**

Size of bubbles detaching from a range of sizes of source in a variety of liquids.

velocity that had been chosen. Vapors were driven ahead of the slowly rising metal, concentrating in the tip of the water jacket core (unfortunately unvented at its top). Thus by the time the melt arrived at the top, it was unable to cover the core because of the rate of gas evolution. One unhelpful suggestion was that the technique seemed an excellent method for making ultra-lightweight hollow castings. The problem was solved by simply increasing the fill rate, covering the core by the melt before outgassing started. Core gasses were then effectively sealed into the core, and were vented in the normal way via the prints at the base of the core.

A lesson is clearly drawn from this experience, that it is far better if possible to vent cores from their top. A somewhat slow filling rate is then not such a danger.

In the case of core blows completely through thin walls, the bubble has no chance to grow to a large size before it has penetrated the wall. Thus the 'bubble trail' becomes merely a hole in the wall of a thin wall casting. Figure 10.14a shows a fracture surface made through a core blow defect in a gray iron casting that provided a leak path through the wall thickness (the left- and right-hand edges of the wall can be seen in the figure). The other images in this figure illustrate progressively closer views of this defect, revealing its astonishing detailed structure. The bubble trails are formed from an oxide in the form of a glassy iron silicate. Figure 10.14c shows the unusual form of these trails, since they appear to reveal clusters of paths made by individual bubbles. Cast iron appears unique in that its bubble trails appear to detach from the matrix. (Similar behavior has been noted for the lustrous carbon film that forms on the liquid iron meniscus, but becomes trapped against the mold during mold filling, and

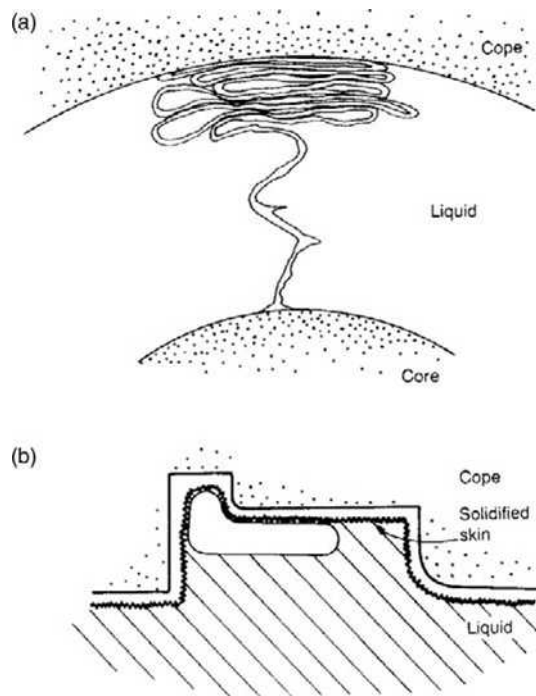


**FIGURE 10.13**

(a) An exfoliated dross defect produced by copious gas from a core blow prior to any solidification; (b) trapped gas from a core blow evolved some time after solidification.

finally detaches from the casting and adheres to the mold surface after the casting is shaken out – see Section 6.5.)

At other times the bubble trails are formed from a lustrous carbon film (Figure 10.15). The carbon film appears to be somewhat more rigid than most oxide films, as suggested by its characteristic smooth surface shown in Figure 10.15b, c, resisting the complete collapse of the trail, and retaining a more open center. In effect, the bubbles punch holes through the cope surfaces of the casting, so that their more open trails, as irregular tubes, form highly efficient leak paths.

The core blow seen in Figure 10.15a has caused a severe leak through the wall of an iron casting. The detail is revealing: the region A is a carbon-based bubble trail; C is a portion of matrix iron, whereas B is an irregular mass of iron silicates that was probably the original series of bubble trails when the emerging gases from the core blow were mainly expanding air and water vapor, both highly oxidizing, and thus creating glassy silicate trails at that early stage. While the water vapor is evaporating from the core, the temperature of the core is held down at close to 100°C. When the core is finally dry, its temperature now increases sufficiently to drive off carbonaceous volatiles. These would now react on contact with the matrix to create carbonaceous bubble trails. However, in the meantime, the original glassy silicates would partially melt and be churned by the continuing and possibly accelerating maelstrom of gases into irregular masses of



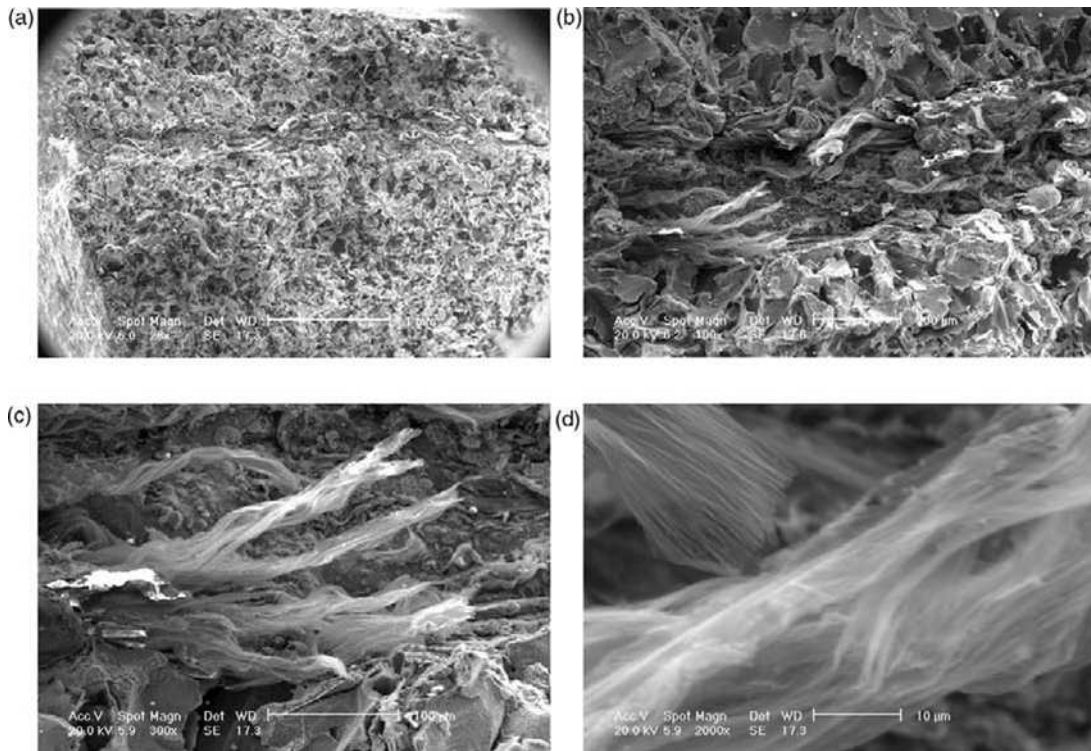


**FIGURE 10.14**

A leakage defect from a core blow through a 4-mm wall in gray iron. (a) Secondary electron image of a fracture through the defect, showing the leakage channel only about 300  $\mu\text{m}$  diameter; (b) an irregular group of glassy silicate bubble trails near the center of the leak path; (c) closer view of the twisted form of some silicate trails; (d) close-up of translucent glassy fluted trails (foreground trail is necessarily out of focus).

slag (the iron silicates). The finding of slag in castings, especially in bubble trails, is usually the result of the local generation of slag by local oxidation of the melt; in my experience, especially when using a good offset step basin, the appearance of slag is rarely the result of the ingress of slag from the poured metal; it is the result of in situ creation of oxides by entrained air or core gases.

Blows can sometimes form from molds. Whereas founders are familiar with the problem of blows from cores, blows from molds are rarely considered. In fact this is a relatively common problem (even though this section remains entitled 'Core Blows' as a result of common usage). The huge volumes of gas that are generated inside the mold have to be considered. They need room to expand and escape. Any visitor to an iron or steel foundry will be impressed with the jets of burning gases issuing from the joints of molding boxes. Effectively the gases and volatiles will be fighting to get out. It is prudent therefore to provide them with escape routes, since the alternative escape route via the liquid metal in the mold cavity can spell disaster for the casting.

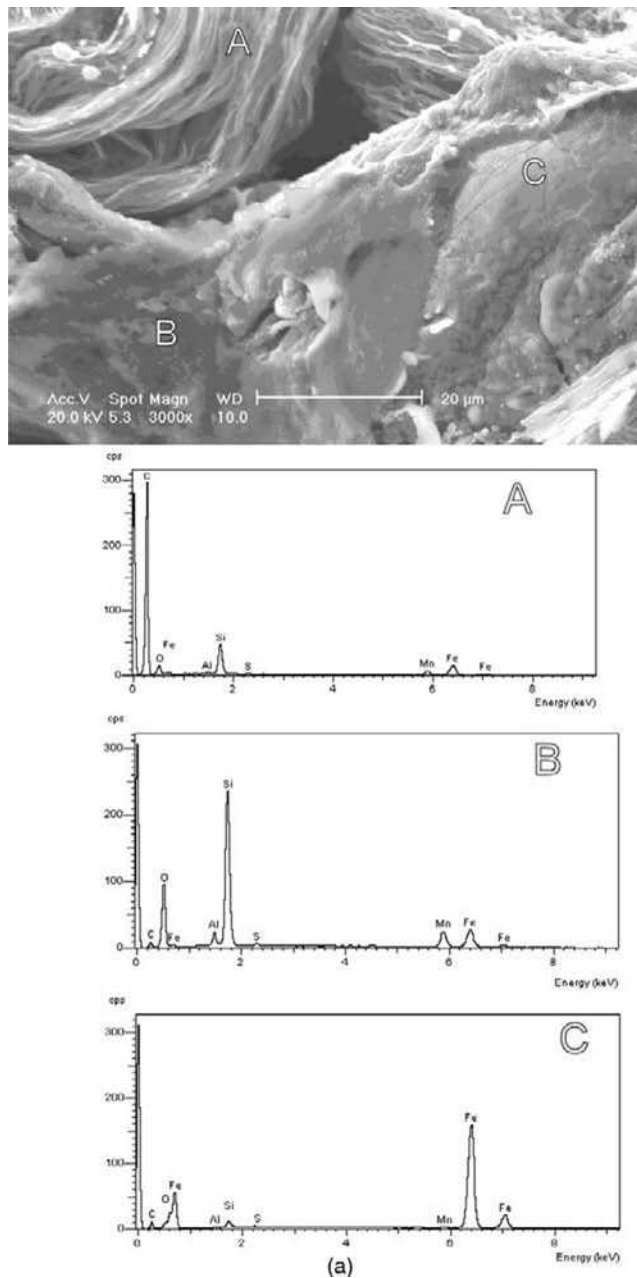
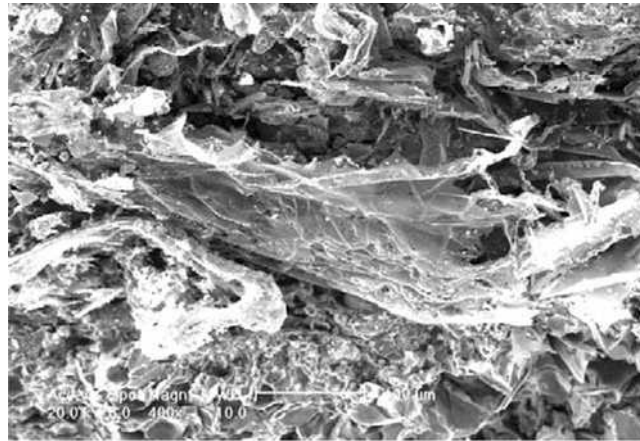
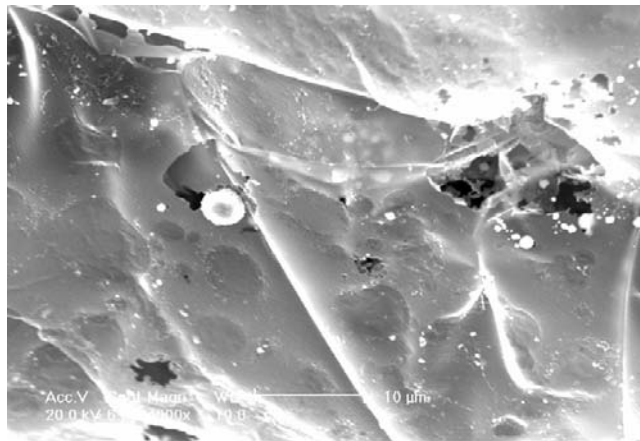


**FIGURE 10.15**

Bubble trail that had caused a leak, probably formed later by core blow in gray iron. (a) General view inside trail showing 'A' carbon films, 'B' oxides (silicates) and 'C' marix alloy; (b) other areas of carbon film; (c) close-up of plate-like carbon film.



(b)



(c)

Mold blows form most easily from upward pointing features (Figure 10.16). The effect is the upside-down equivalent of the droplet of water detaching from the tip of a stalactite. Thus the removal of upwardly pointing features, or the inverting of the whole casting, is often a useful tactic. A mold blow forms most easily if the mold is enclosed, generating high mold pressures, as shown in Figure 10.17. In this figure the bubbles are shown meandering up through the casting, lodging under a core, and finally accumulating under the solidified skin forming the cope of the casting.

However, on occasions, blows can even form from large flat regions of molds. The build-up of pressure in the drag has been observed by the author to lead to severe blow defects in meter-square flat plates of a bronze alloy, particularly towards the far end of the plate where the condensation of volatiles driven ahead of the melt adds to the amount already available from the sand binder (Figure 10.18). The provision of woven nylon vent tubes through the drag was quite inadequate; the enormous quantities of

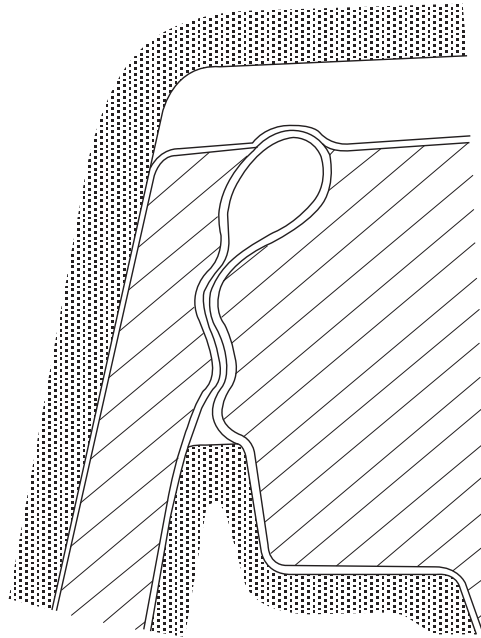


**FIGURE 10.16**

Detachment of a bubble from the top of a core, bequeathing a bubble trail as a permanent legacy of its journey. This bubble, unusually, may be early enough to escape at the free surface of the rising metal.

gas simply overwhelmed this painstaking but useless provision. The drag needed to vent from the whole of its lower surface area by standing the mold clear of the ground, or standing it on a deeply ridged base plate.

Theory indicates (Campbell 1970) that the size of a detaching bubble is linked to the size of the source. The results of calculated bubble diameters are shown in Figure 10.12, and reveal that even though a bubble might detach from a horizontal surface, and so be of maximum size, its size is limited to 10–15 mm or so, depending on the liquid. However, final sizes of core blow defects vary in size typically from 10–100 mm in diameter, showing that they are usually the accumulation of many bubbles, or possibly even the result of a constant stream of gas funneled along a single bubble trail, arriving and coalescing under the solidifying skins of castings.

Blows are evolved from sources other than the cores and mold.

Blows from the explosive volatilization of core adhesives is well known.

Less well known is the fact that considerable volumes of water vapor are given off from clay-based core repair and mold repair pastes. This is because the clay contains water of crystallization, so that even after thoroughly drying the core repair at 100 or 200°C, the water bound in the structure of the clay remains unchanged, only being released at a high temperature, in the region of perhaps 600°C. Thus the water is released only when the clay contacts the liquid metal. This is particularly unfortunate, because the clay is composed of such fine particles that it is substantially impermeable, preventing the escape of the water into the core or mold, so that the water is forced to boil off through the

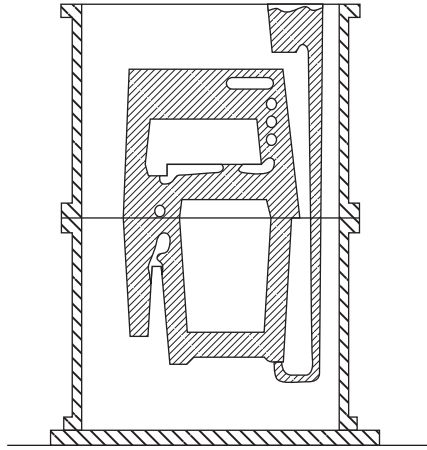


**FIGURE 10.17**

Casting in a close-fitting steel mold box on an unvented flat steel plate, showing blows from an upwardly oriented feature on the lower part of the mold.

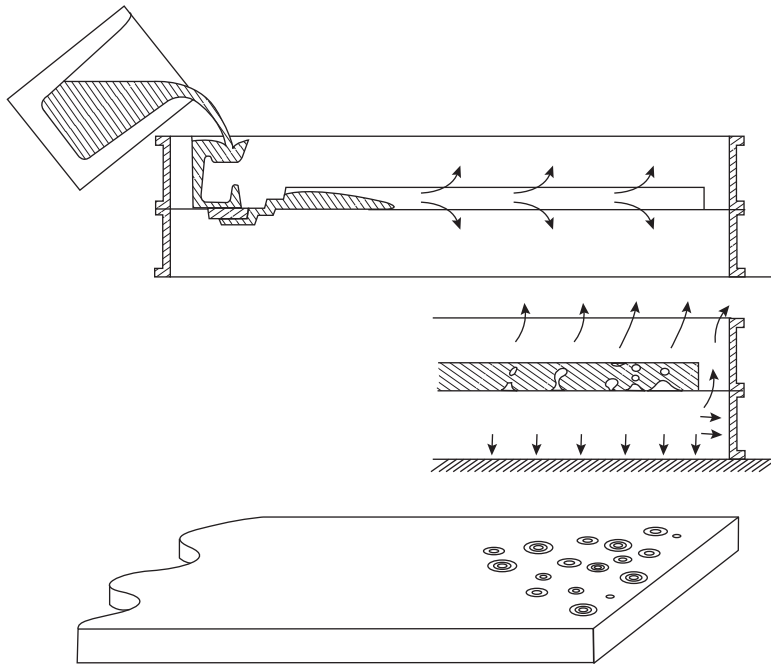


**FIGURE 10.18**

A large flat plate casting with an enclosed drag. Volatiles are driven ahead and condense in the cooler distant mold, exacerbating defects at the far end.

metal. Repair of cores with clay-based pastes therefore generally leads automatically to blow defects. The wide use of core repair pastes illustrates that this danger is little known. The use of such materials is to be avoided unless followed by baking at a temperature that can be demonstrated to avoid the generation of blows in the melt.

The generation of blows off metal chills is the result of an almost identical process. When a block metal chill is placed in a bonded aggregate mold, the pouring of the metal causes a rapid outgassing of the volatiles in the aggregate/binder mixture. The volatiles, particularly water vapor, are driven ahead of the spreading liquid metal, and condense on any cold surface, such as a metal chill. When the liquid metal finally arrives and overruns the chill the condensates boil off. Since the chill is impermeable, the vapor is forced to bubble through the melt.

The prevention of blows from condensation on chills is widely known and generally well applied. The chill should normally be coated with a ceramic wash or spray that is afterwards thoroughly dried to give an inert, permeable and non-wetted surface layer. If this coat has residual surface roughness so much the better. The effective permeability of the surface can be further enhanced by providing deep V-grooves in a criss-cross pattern. The grooves are bridged to some degree by the action of the surface tension of the melt, so that the bottoms of the grooves act as surface vents, tunneling the expanding vapors to freedom ahead of the advancing melt. Additionally, the V-grooves are thought to enhance the effectiveness of the chilling action by increasing the contact between the casting and the chill, particularly during the cooling and contraction of the surface of the casting, forcing the grooved cast surface sideways against the walls of the grooves on the chill.

To demonstrate that a chill, a core, or assembly of cores, does not produce blows may require a procedure such as the removal of all or part of the cope or overlying cores, and taking a video recording of the filling of the mold. If there are any such problems, the eruption of core gases will be clearly observable, and will be seen to result in a boiling action, creating a froth of surface dross that would of course normally be entrapped inside the upper walls of the casting. A series of video recordings might be found to be necessary, showing the steady development of solutions to a core-blowing problem, and recording how individual remedies resulted in progressive elimination of the problem. The video recording requires to be retained by the foundry for inspection by the customer for the life of the component. Any change to the filling rate of the casting, or core design, or the core repair procedure, should necessitate a repeat of this exercise.

For castings with a vertical joint where a cope cannot be conveniently lifted clear to provide such a view, a special sand mold may be required to carry out the demonstration that the core assembly does not cause blows from the cores at any point. This will have to be constructed as part of the tooling to commission the casting, and justified as an investment in quality assurance.

It should be noted that the danger of forming blows (bubbles in the melt) only arises if the liquid metal is subjected to the pressure in the mold (or core) and the pressurized gas has no option but to escape via the melt.

For instance, the general build-up of pressure in the mold cavity during filling is not usually a problem from the point of view of creating bubbles in the melt. In fact, for a fast-filling mold, the build-up of back-pressure inside the mold cavity can be useful in slowing the final stages of filling, reducing the mold penetration that can occur because of the impact at the final instant of filling. Naturally, the converse is true for some difficult-to-fill castings, where mold back-pressure can be sufficient to prevent the complete filling of molds. The escape of gases entrapped in the mold cavity is made more difficult by the application of mold coats, so that pressures can easily be doubled (Ohnaka

2003). Thus the internal pressure in the mold cavity may affect the filling of the mold positively or negatively, but will never usually lead to the creation of bubbles.

The build-up of pressure within the body of the mold can lead to problems. It can be severe in molds that are enclosed in steel boxes, and which are sat on a steel plate or on a concrete floor. The gases are relatively free to escape from the cope, but gases attempting to escape from the drag are sealed in by the overlying liquid in the mold cavity (Figures 10.17 and 10.18). The problem is enhanced if the casting is a tight fit in the molding box, as is usually the case of course since the casting engineer is always trying to get as much value as possible out of each box. In fact the build up of pressure inside sand molds crammed into tight-fitting steel boxes has, in the author's experience, contributed to a number of spectacularly defective castings, and in one instance to a casting that persistently refused to fill its mold because the back-pressure of gases rose so high.

Fortunately mold back-pressure is easily dealt with by the provision of one or more whistlers. These are narrow, pencil-shaped vents connecting the mold cavity to the outside world via the cope.

Finally, it is worth commenting on the curiously misguided but common provision of whistler vents through the top of the mold in an effort to eliminate 'gas' porosity in the casting. When the founder sees a core blow he will often apply a mold vent. Clearly, this action is of no use. A moment's reflection reveals the self-evident fact that the pores (i.e. the entrained air bubbles) are already in the metal, and the metal itself would have to rise up the vent to eliminate the porosity from the casting. The error in thinking arises because of the confusion between gas entrapped in the mold cavity and gas entrained in the melt. When these are separated into their logically separate categories, confusion disappears, and the correct remedy can be identified.

### 10.5.2 Outgassing pressure in cores

The sudden heat from the liquid metal causes the volatile materials in the mold to evaporate fiercely. In greensand molds and many other binder systems the main component of this volatilization is water. Even in so-called dry-binder systems there is usually enough water to constitute a major contribution to the total volume of liberated gas. On contact with the hot metal, much of the water is decomposed to surface oxide films and to hydrogen. The high hydrogen contents of analyzed mold gases are clearly seen in the measurements of Scott and Bates (1975).

In the case of the mold, the generation of copious volumes of gas is usually not a problem. The gas has plenty of opportunity to diffuse away through the bulk of the mold. The pressure build-up in a greensand cavity during mold filling is normally only of the order of 100 mm water gauge (0.01 atm) according to measurements by Locke and Ashbrook (1972). This corresponds to merely 10 mm or so head pressure of liquid iron or steel. However, even this rather modest pressure might have been overestimated because their experimental arrangement corresponded to a closely fitting steel molding box, and escape for mold gases only via the cope. Even so, in greensand systems where the percentage of fines and clay and other constituents is high, the permeability of the mold falls to levels at which the ability of the mold volatiles to escape becomes a source of concern. The venting of the cope by needling with wires of about 3 mm diameter is a time-honored method of re-introducing useful levels of permeability.

Chemically bonded molds are usually of no concern from the point of view of generating a back-pressure during the filling of the mold. This is because the sand is usually bought in as ready washed, cleaned and graded into closely similar sizes (a 'three pan sand'). In addition, usually only a one or two volume percent of binder is used, leaving an open, highly permeable bonded mold. A single

measurement by the author using a water manometer showed a pressure rise during the filling of a cylinder head mold of less than 1 mm water gauge. Even this completely negligible rise seemed to decay to nothing within a second or less.

In the case of cores, however, once the core is covered by liquid metal, the escape of the core gases is limited to the area of the core prints, if the metal is not to be damaged by the passage of bubbles through it. Furthermore, the rate of heating of the core is often greater than that of the mold because it is usually surrounded on nearly all sides by hot metal, and the volume of the core is, of course, much less. All these factors contribute to the internal pressure within the core rising rapidly to high values.

Many authors have attempted to provide solutions to the pressure generated within cores. However, there has until recently been no agreed method for monitoring the rate or quantity of evolved gases that corresponds with any accuracy to the conditions of casting. A result of one method by Naro and Pelfrey (1983) is shown in Figure 10.19. (This method is an improvement on earlier methods in which the water and other volatiles would condense in the pipework of the measuring apparatus, reducing the apparent volume of gases, and thereby invalidating the experimental results.) The really important quantity given

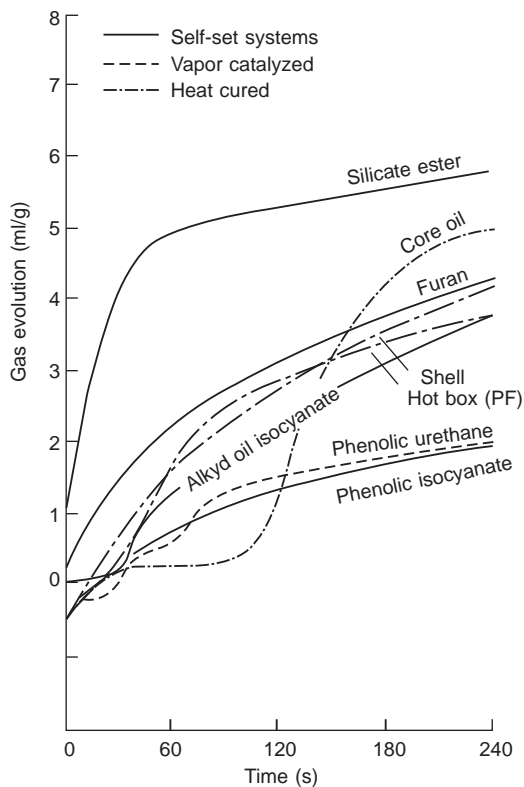


**FIGURE 10.19**

Gas evolution from various binder systems using an improved test procedure that includes the contribution from water and other volatiles (Naro and Pelfrey 1983).



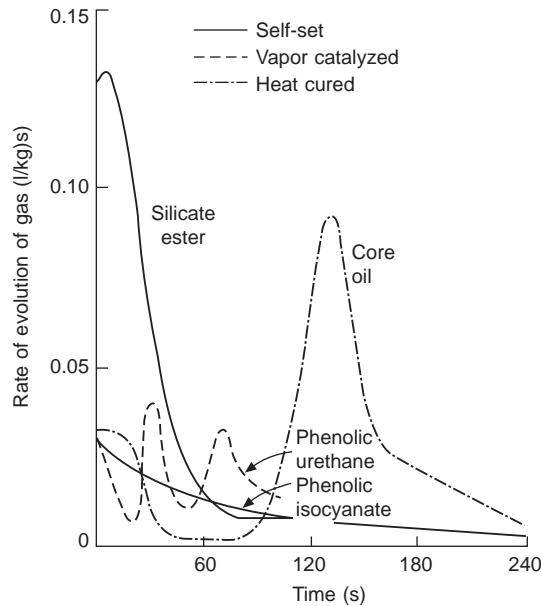


**FIGURE 10.20**

Rates of gas evolution from various sand binders based on the slopes of the curves shown in Figure 10.19.

by these curves is the *rate* of evolution of gas. The rates, of course, are equal to the slope of the curves in Figure 10.19, and are presented in Figure 10.20. Only a few results are presented for clarity.

It is sufficient to note that the rates of outgassing are very different for different chemical binder systems. The initial high rate for the silicate is the result of its water content evolved at relatively low temperature during the early stages of the heating of the core. Other organic binders evolve their carbonaceous gases at a variety of temperatures, and apart from core oil, generally show much gentler rates that are more easily vented.

Anyway, taking these recent estimates of  $Q$ , the rate of volume of gas generated from a given weight of core in  $\text{m L g}^{-1} \text{s}^{-1}$  (or preferably the identical-sized value in the equivalent unit  $\text{L kg}^{-1} \text{s}^{-1}$ ) as being of tolerable relevance to the real situation in castings, we can construct a core outgassing model. We shall roughly follow the method originally pioneered by Worman and Nieman (1973).

We first need to define the concept of permeability. This is a measure of the ease with which a fluid (the core gas in our case) can flow through a porous material (the core in our case). Permeability  $P_e$  is defined as the rate of gas flow  $Q$  (as a volume per unit time) through a permeable material of area  $A$  and length  $L$  and driven by a pressure difference  $\Delta P$ :

$$P_e = QL/A\Delta P$$

The SI units of  $P_e$  are quickly seen to be:

$$\begin{aligned} [P_e \text{ units}] &= [\text{liter s}^{-1}] [\text{m}]/[\text{m}^2] [\text{Pa}] \\ &= \text{L s}^{-1} \text{m}^{-1} \text{Pa}^{-1} \end{aligned}$$

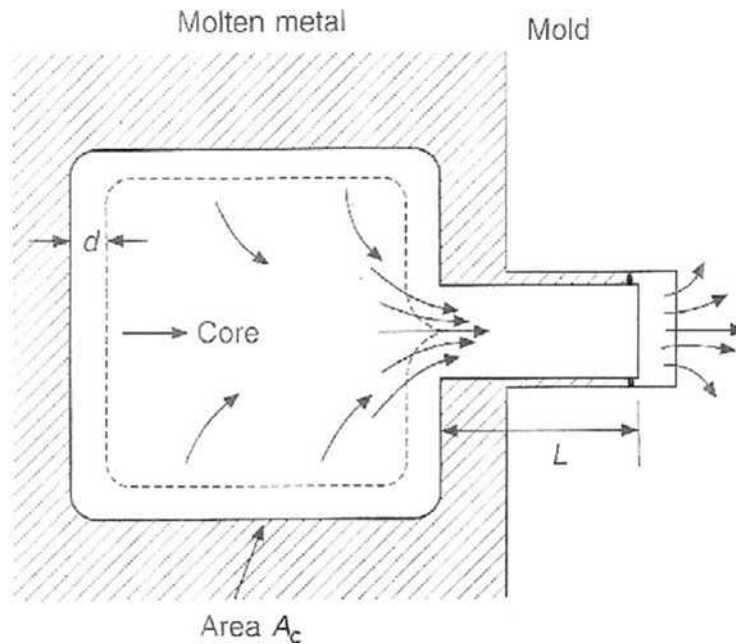


**FIGURE 10.21**

Core model, showing heated layer thickness  $d$  outgassing via its print. In this particular case, metal flash along the sides of the print force gas to exit only from the end area  $A$ .

Consider now our simple model of a core shown in Figure 10.21. The measured volume of gas evolved per second from a kilogram of core material is  $Q$ . If we allow for the fact that this will have been measured at temperature  $T_1$ , usually above  $100^\circ\text{C}$  ( $373\text{K}$ ) to avoid condensation of moisture, and the temperature in the core at the point of generation is  $T_2$ , then the volume of gas produced in the core is actually  $QT_2/T_1$  where  $T$  is measured in degrees K. For the casting of light alloys the temperature ratio  $T_2/T_1$  (in K remember) is about 3, whereas for steels it is nearly 6.

If we multiply this by the weight of sand heated by the liquid metal, then we obtain the total volume of gas evolved per second from the core. Thus if the heated layer is depth  $d$ , the core area  $A_c$  and density  $\rho$ , then the volume of gas evolved per second is  $QdA_c\rho T_2/T_1$ . If the core is surrounded by hot metal, this volume of gas has to diffuse to the print and force its way through the length  $L$  of the print of area  $A_p$ . We shall assume that the pressure drop experienced by the gas in diffusing through the bulk of the core is negligible in comparison with the difficulty of diffusing through the print (this is of course not always accurate depending on the shape of the core). Considering then the permeability definition for only the pressure drop along the print, we obtain the pressure in the core (above the ambient pressure at the outside tip of the print):

$$P = QdA_c\rho.LT_2/A_pT_1P_e$$

This simple model emphasizes the direct role of permeability  $P_e$  and of  $Q$ , the rate of gas evolution on the generation of pressure in the core. It is to be noted that the high casting temperature for steels is seen to result in values for  $P$  approximately twice that for aluminum alloys. Thus cores in steel castings will be twice as likely to create blows than cores in aluminum alloy castings. For this reason, an enclosed core that would give no problems in an aluminum alloy casting may cause blows when the same pattern is used to make an equivalent bronze or iron casting.

Our model also highlights the various geometrical factors of importance. In particular, the area ratio of the core and the print,  $A_c/A_p$ , is a powerful multiplier effect, and might multiply the pressure by anything between 10 and 100 times for different core shapes. Also emphasized is the length  $L$  of the core print. If the print is a poor fit then  $L$  may be unnecessarily lengthened by the flashing of the metal into the print so as to enclose the flow path in an even longer tunnel. If the liquid metal completely surrounds the end of the print too, then, of course, all venting of gases is prevented. Gases are then forced to escape through the molten metal, with consequential bubble damage to the casting.

The provision of a vent such as a drilled hole along the length of the print will effectively reduce  $L$  to zero; the model predicts that the internal pressure in the core will then be eliminated (the only remaining pressure will, of course, be the much smaller pressure to overcome the resistance to flow through the core itself). The value of vents in reducing blowing from cores has been emphasized by many workers. Caine and Toepke (1966), in particular, estimate that a vent will reduce the pressure inside a core by a large factor, perhaps 5 or 10. This is an important effect, far outweighing all other methods of reducing outgassing pressure in cores.

Vents can be molded into the core, formed from waxed string. The core is heated to melt out the wax, and the string can then be withdrawn prior to casting. This traditional practice was often questioned as possibly being counterproductive, because of the extra volatiles from the wax that, on melting, soaks into the core. Such fears are seen to be happily unfounded. The technique is completely satisfactory because the presence of the vent completely overrides the effect of the extra volatile content of the core.

A final prediction from the model is the effect of temperature. In theory a lowering of the casting temperature will lower the internal core pressure. However, this is quickly seen to be a negligible effect within the normal practical limits of casting temperatures. For instance, a large change of 100 K in the casting temperature of an aluminum alloy will change the pressure by a factor of approximately 100/900. This is only 11%. For irons and steels the effect is smaller still. It and can therefore be abandoned as a useful control measure.

We shall now move on to some further general points.

Cores are almost never made from greensand because the volatile content (particularly water, of course) is too high and the permeability (because of its 5 or 10% clay and other fines) is too low. In addition, the cores would be weak, and unable to support themselves on small prints; they would simply sag. If greensand is used at all then it is usually dried in an oven, producing 'dry sand' cores (their name should perhaps use the past tense, and so be more accurately 'dried sand' cores). These are relatively free of volatiles, and are mechanically strong. But because they retain the poor permeability of the original greensand they therefore usually require good venting. This is usually time-consuming and labor-intensive.

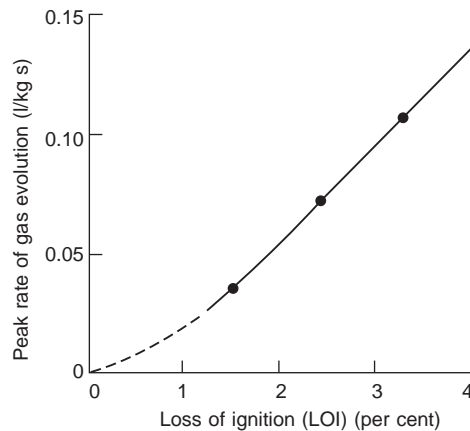
Sand cores are therefore not nowadays made from dried sand, but generally chemically bonded from clean, washed and dried silica sand that is closely graded in size to maintain as high a level of

permeability as is possible. The limit to the size of sand grains and the permeability is set by the requirements of the casting to avoid (i) penetration by the metal, and (ii) the production of internal surfaces of the casting that are unacceptably rough.

These cores are bonded with a chemical binder that is cured by heat or chemical reaction to produce a rigid, easily handled shape. The numerous different systems in use all have different responses to the heat of the casting process, and produce gases of different kinds, in different amounts, at different times, and at different rates as illustrated in Figures 10.19 and 10.20. These results are not to be taken as absolute in any sense. The manufacturers' products are changing all the time for a variety of reasons: health and safety; economics; commercial; changes in world markets and supplies of raw materials, etc. Thus binder formulations change and new systems are being developed all the time. At present the phenolic urethane systems are among the lowest overall producers of volatiles, which explains their current wide use for intricate cores, for instance in the case of water jackets for automobile cylinder heads and blocks.

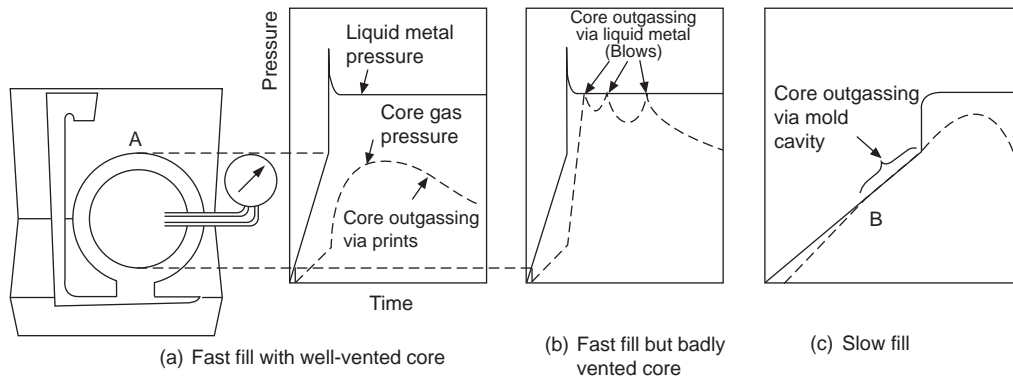
Part of the reason for the historical success enjoyed by the phenolic urethane binders is their high strength, which means that the addition levels needed to achieve an easily handled core are low. This is one of the important factors in explaining their position near the bottom of Figure 10.19; the volume of gas evolved is, of course, proportional to the amount of binder present. This self-evident fact is clearly substantiated in the work of Scott et al. (1978), shown in Figure 10.22. (If allowance is made for the fact that these workers used a core sample size of 150 ml, corresponding to a weight of approximately 225 g, then the rate of evolution measurements converted to  $1 \text{ kg}^{-1} \text{ s}^{-1}$  agree closely with those presented in Figure 10.20. This is despite the significant differences in the techniques. The data in Figure 10.20 may therefore be of more universal application than is apparent at first sight.)

Renewed interest these days is being taken in inorganic binders based on salts. Preferably the salts should contain no water, particularly water bound up in the crystalline structure that could be evolved at the high temperature required for casting. It will repay us all to monitor these developments closely.



**FIGURE 10.22**

Increase in the peak rate of outgassing as loss on ignition (LOI) increases. Data recalculated from Scott et al. (1978).

**FIGURE 10.23**

Effect of fill rate on core outgassing (adapted from Campbell 1950).

### 10.5.3 Core blow model study

Campbell (1950) (not the author) devised a useful test that assessed the pressure in cores compared to the pressure in the liquid metal. A modified version of his test is shown in Figure 10.23 and the following is a modification and further development of his explanation.

If the mold is filled quickly then the hydrostatic pressure due to depth in the liquid metal is built up more rapidly than the pressure of gas in the core. This dominance of metallostatic pressure can persist throughout filling and solidification. The higher metal pressure effectively suppresses any bubbling of gas through the core at point A as illustrated in Figure 10.23a. Bubbles will form at A only if the core pressure reaches the metal pressure because either the venting of the core is poor (Figure 10.23b) or the core is covered too slowly (Figure 10.23c).

If the mold is filled slowly, the gas pressure in the core exceeds the metal pressure at B and remains higher during most of the filling of the mold. Gas escapes through the top of the core during the late stages of the filling, so that, although the metal pressure in Figure 10.23c finally exceeds the gas pressure in this case, it is doubtful whether the gas will stop flowing. This is because, in practice, when the liquid metal reaches the top of the casting at A it is prevented from closing and joining together by the constant evolution of gas. The migration of volatiles ahead of the slowly rising metal front also concentrates the gas source near A, and the creation of a well-established, well-oxidized bubble trail will further hinder the welding and closing together of the meniscus at this point. Gas issuing from the top of a submerged core can be seen to cause the melt to tremble and flutter against the surface of the core, the melt attempting to close together to stop the flow, but repeatedly failing in this attempt as drossy surface films thicken.

Figure 10.23b illustrates the case in which the pressure in the core rises only just above the metal pressure, with the result that a limited number of bubbles escape. If the casting has started to solidify, then although the bubble may be forced into the melt, it is unlikely to be able to escape from the upper surface of the casting.

### 10.5.4 Microblows

It is conceivable that small pockets of volatiles on the surface of molds might cause a small localized explosive release of vapor that would cause gas to be forced through the (oxidized) liquid surface of the casting to form an internal bubble. Poorly mixed sand containing pockets of pure resin binder might perform this. Alternatively, sand particles with small cavities filled with a volatile binder material might act as cannons to blast pockets of vapor into the metal. Figure 10.12 indicates that for the blowing of bubbles of less than 1 mm diameter in some common liquid metals the source of the high-pressure gas needs to be only a few micrometers diameter. The pressures inside such minute bubbles is easily shown to be high, of the order of 1 MPa (10 atm).

Evidence for microblows comes from the strip casting of steel between twin rolls (Ha et al. 2008). ‘Dent’ defects are observed that are 0.3–1.5 mm in diameter and up to 0.5 mm deep. Sometimes taking the form of a simple depression, but sometimes a characteristic form of a blow defect, connected to the surface with a narrow neck linked to an internally spherical shape. These miniature gas pockets were found to be the result of the roughness of the roll surface, so that gases entrapped in microscopic depressions in the roll surface expanded on arrival of the melt, causing a gas bubble to be driven into the liquid.

For sand castings there is no direct evidence for this mechanical mechanism of subsurface pore formation. The mechanism for the creation of subsurface porosity remains obscure. It awaits creative and discriminating experiments to separate the problem from classical processes such as diffusion, in which the gases travel from the mold, across the mold/metal interface into the casting as separate atoms, albeit in swarms, the interface being mechanically undisturbed by this inward flow of elements. Such diffusive transfer is assumed in most of the remainder of this work. However, the reader should be aware of the possibility of mechanical transfer of gases, possibly as eruptive events, disrupting the casting interface as minute explosions.

An observation of a surface interaction that is worth reporting, but whose cause is not yet known, is described below. It may therefore have been allocated to the wrong section of the book. It is hoped that future research will provide an answer.

In the study of interactions between chemically-bonded sand molds and liquid metals, a novel and simple test was devised in the author’s laboratory (Mazed 1992). It was prosaically named the ‘wait and see’ test. It consisted simply of a flat horizontal surface of a bonded aggregate onto which a small quantity of metal was poured to give a puddle of 50–100 mm diameter. The investigator then waited to see what happened. If anything was going to happen it was not necessary to wait long.

When Al–7Si alloy was poured on to the flat surface of either a phenolic-urethane (PF) or furane/sulfonic acid (FS) bonded silica sand the liquid alloy maintained its mirror smooth upper surface. The same was true when Al–7Si–0.4Mg alloy was poured on PF-bonded sand. When the puddles of liquid metal had finally solidified they had retained their top mirror-like surfaces and after sectioning were found to be sound.

However, when the Al–7Si–0.4Mg alloy was poured on the FS-bonded sand the effect was startlingly different. After several seconds a few bubbles not exceeding 1 mm diameter were observed to arrive at the surface, underneath the surface oxide film, raising up minute bumps on the mirror surface. After a few more seconds the number increased, finally becoming a storm of arriving and bursting bubbles, destroying the mirror. The final sessile drop was found to be quite porous throughout its

depth, corroborating the expectation that the bubbles had entered the drop at its base because of a reaction with the sand binder.

The fact that this reaction was only observed with certain binders and with certain alloys originally suggested to the author a chemical mechanism. At the time of the work this was thought unlikely because the diffusive transfer of gas into the melt would result in gas in solution. Having an equilibrium pressure of only about 1 atmosphere (since the pressure at the mold surface was originally thought to be limited to this level) it would have been difficult to nucleate small bubbles. However, it has been more recently realized that the presence of bifilms in the alloy practically eliminates the nucleation problem, and so might make the process feasible. This will be especially true since some melts will, partly by accident and partly as a result of alloy susceptibility, have different quantities and different qualities of bifilms. The 0.4Mg-containing alloy would have been expected to contain a different concentration and a different type of bifilm.

Even so, a mechanical process cannot be ruled out at this stage. For instance the presence of Mg in the Al-7Si alloy may cause MgO formation at the metal/mold interface leading to a convoluted and microscopically fractured surface oxide film that may be more easily penetrated by high-pressure gas. High local pressures might arise particularly if the FS binder was not as well mixed as the PF binder, leaving minute pockets of pure binder in the sand mixture of the plate core. Thus the quality of mixing may be important.

Clearly, there is no shortage of important factors to be researched. Probably it will always be so. In the meantime, the best we can do is be aware of the possible effects and possible dangers, and have patience to live with uncertainty until the truth is finally uncovered.

### 10.5.5 Prevention of blows

By far the best solution to the evolution of gases from cores is the use of a sand binder for the core that has little or no evolution of gas as the core becomes hot. This would represent a perfect solution. The best hopes here are the inorganic binders that contain no water of crystallization. However, the few binders that have so far been developed to meet this criterion are usually not satisfactory in other ways. At the time of writing the perfect core binder has yet to be developed!

In the meantime, one of the best actions to avoid blows from cores (or more occasionally from molds) is to increase the permeability of the core by the use of a coarser aggregate and/or by the use of venting.

Since the core print is usually the area where all the escaping gas has to concentrate, a simple hole through the length of the print makes a huge impact on the problem, as has been shown previously by the author (*Castings* 2003). For some aluminum alloy castings this can be a complete solution. However, of course, if the vent hole can be continued to the center of the core this is even better. The further provision of easy escape for gases through the mold and out to the atmosphere is necessary for copper-based and iron and steel castings where the outgassing problem becomes severe because of the higher temperatures. In iron and steel foundries many readers will have seen the vigorous jets of burning carbon monoxide issuing from vents in molds for many minutes after pouring. Figure 10.24 illustrates a succession of improved venting techniques.

For low-volume production involving the making of cores by hand, a vent can be provided along a curved path through a core by laying a waxed rope inside whilst it is being made. The core is subsequently heated to melt the wax so that the rope can be pulled out. The concerns that the wax itself,

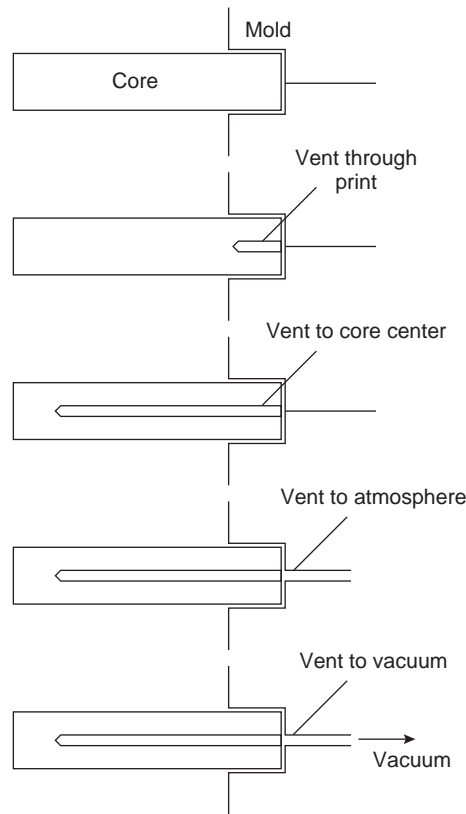


**FIGURE 10.24**

Venting of a core, illustrating progressively more effective techniques.

now percolated into the core, would add to the volatiles and so counter any benefit is, thankfully, unfounded. The provision of the vent is an overwhelming benefit.

For more delicate low-volume work, the author has witnessed long curved cores for aerospace castings being drilled by hand, using a drill bit fashioned from a length of piano wire held in a three-jaw rotary chuck driven by a small motor. The tip of the high-carbon-steel wire is hammered flat, and ground to a sharp point shaped like an arrow head. The core is drilled by hand in a series of straight lengths, the piano wire drill buzzing quickly through the core. Each hole is targeted to intersect the previous hole, the straight holes emerging on the bends, where the openings are subsequently plugged by a minute wipe of refractory cement (Figure 10.25). The complete vent is checked to ensure that it is continuous, and free from leaks, by blowing smoke into one of the vent openings, and watching for the smoke to emerge freely at the far opening. Only when the smoke emerges freely at the far end, and from no other location, is the core accepted for use. It is then stored in readiness for mold assembly.

Occasionally, instead of an opening to the atmosphere, it is necessary to link the outside opening to a vacuum line. This is relatively common practice in gravity die (permanent mold) casting, increasing the efficiency of the extraction of gases from a resin-bonded sand core. However, the evolution of



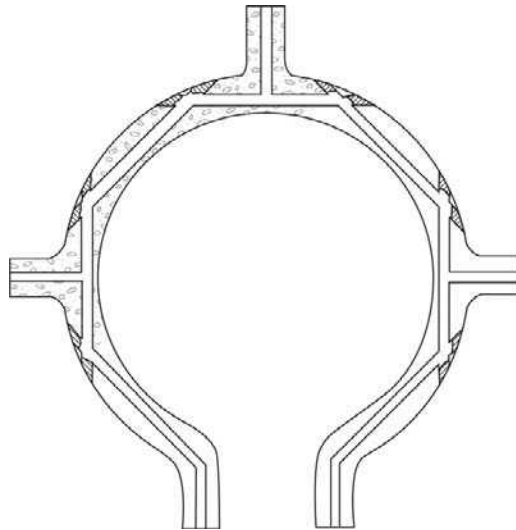


**FIGURE 10.25**

Drilled and plugged holes to vent a narrow ring-shaped core.

volatiles from the binder creates problems by condensing as sticky resins and tars in the vacuum line, so that, for long production runs, regular attention is required to avoid blockage, often dictating the timing of the withdrawal of the tooling for maintenance.

The reader is advised to exercise caution with regard to the application of a vacuum line to aid venting. The author once tried this on an extensive thin-section core with a single small area print around which was poured liquid stainless steel at 1600°C. The resulting rapid build-up of pressure was so dramatic that it blew off the vacuum connection with a bang! However, the discerning reader will notice the extreme circumstances described here, and rightly conclude that in this case the author was testing the patience of Providence.

The application of vacuum connections to core prints is widely practiced in the gravity die casting of Al alloy automotive cylinder heads. The water jacket core is particularly difficult to vent without such extreme measures. However, because of the wide use of resin-based binders for this core, the vacuum line quickly becomes blocked by condensing resins and tars. Thus after perhaps only a dozen castings the die may have to be withdrawn from service to clean out the vacuum lines.

If there is an option, it is far better to arrange that the core vents through prints that are directed vertically upwards (Figure 10.26). This is because as the melt rises in the mold, the volatiles migrate through the core ahead of the metal, concentrating in the last part of the core. If the core is vented at its base this is a potential disaster. The volatiles are too far from the print, and will continue to be pushed ahead, finally being pushed into the form of an eruption of bubbles from the top of the core. This problem can be reduced by covering the core with liquid metal as quickly as possible. Venting from the base is then given its best chance.

Even so, a print allowing outgassing from the top of the core is ideal. If a vent cannot be provided up the center of the top print, a top print is still valuable, even though it may contain no central vent,

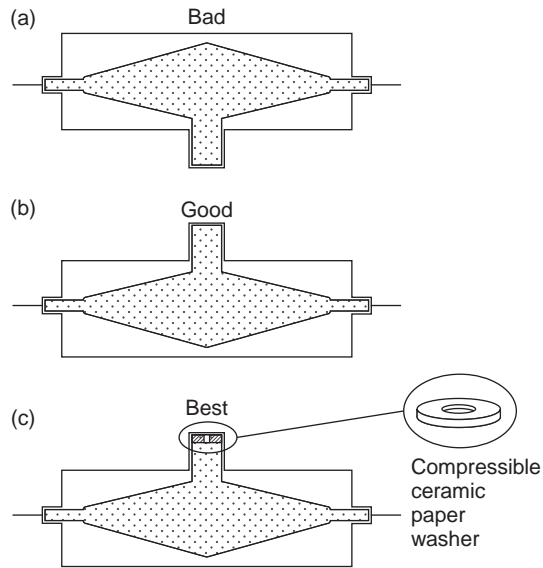


**FIGURE 10.26**

Vertical upwards venting, preferably with a soft print, is ideal. However, the addition of a central hole through the core print, or even down into the center of the core, would be better.

because the volatiles will travel up the core surface. This can be seen on core prints that emerge from the tops of aluminum alloy castings. The melt is seen to flutter, trembling against the side of the core print as gas rushes up in the form of minute, high frequency waves, causing ripples to radiate out across the surface of the melt.

The provision of soft ceramic paper gaskets, preferably with a central hole, shaped like a washer, placed on the end of core prints is an excellent provision for the escape of gases. This simple remedy prevents the melt from flashing over the end of the print to block the vent (Figure 10.26). The compressible washer allows for the sealing of the core print against ingress by liquid metal, but allows closure of the mold without danger of the crushing of the core.

Finally, if the core can be covered quickly with liquid metal, and the pressure in the metal quickly raised to be at all times greater than the internal pressure generated inside the core, then bubble formation will be suppressed. Thus simply filling the mold faster is often a quick and complete solution. The provision of an additional top feeder to increase hydrostatic pressure needs care, since if the feeder has large volume the delay in the rise of pressure to fill it may be counter-productive. If feeding of the casting is not really required, the sprue and pouring basin can provide the early pressurization that is needed, it would be better to leave well alone and not be tempted to provide a top feeder.

Eventually, it is hoped, we can look forward to the day when computer simulation will provide an accurate description of each core and mold, allowing in detail for the effect of outgassing of cores of intricate geometries and the complicating effect of rate of filling. A welcome start has been made by Maeda (2002) who demonstrate a computer simulation of the flow of gas through an aggregate core,

and Starobin (2010) who investigate water jacket cores for cylinder blocks. Perhaps we can now look forward to such studies becoming a commonplace feature of the design of a new casting.

### 10.5.6 Summary of blow prevention

The various actions that can be taken to eliminate blow holes are:

1. Use a core binder that has minimal outgassing (i.e. minimize the binder so far as possible) or delayed outgassing (change to a late outgassing material).
2. Improve the permeability of the core aggregate.
3. Provide vents, particularly through the print.
4. If possible, vent the core from its top-most point.
5. Apply a vacuum to the core prints.
6. Redesign the core (or invert the casting) to avoid upward-pointing features.
7. Fill quickly to cover the core with liquid metal as soon as possible, before its internal pressure rises high enough to force a bubble into the melt.
8. Use a high hydrostatic head of liquid metal to suppress the evolution of gas from the surface of the core.
9. Raise the casting temperature. This is a last resort. The technique is quite commonly applied. It has the effect of giving more time for the core to outgas through the liquid metal before a solidified shell can form, so that bubbles will not be trapped by the growth of the solid skin of the casting. The approach can only be recommended with some reluctance, perhaps justifiable in an emergency, or perhaps only for gray iron cast with dry sand cores. In most situations the passage of the bubbles through the melt will, even if the bubbles escape, result in damage to the casting in the form of the creation of bubble trails, leading possibly to both leakage and dross defects.

---

## 10.6 RULE 6: 'AVOID SHRINKAGE DAMAGE'

### 10.6.1 Definitions and background

Before getting launched into this section, we need to define some terms.

There is widespread confusion in parts of the casting industry, particularly in investment casting, between the concepts of *filling* and *feeding* of castings. It is essential to separate these two concepts.

- *Filling* is self-evidently the short period during the pour, and refers to the filling of the filling channels themselves (sometimes called the *priming* of the running system) and the filling of the mold cavity. This may only last seconds or minutes.
- *Feeding* is the long, slow process that is required during the contraction of the liquid that takes place on freezing. This process takes minutes or hours depending on the size of the casting. It is made necessary as a result of the solid occupying less volume than the liquid, so the difference has to be provided from somewhere. This contraction on solidification is a necessary consequence of the liquid being a structure resembling a random close-packed array of atoms, compared to the solid, which has the denser regular close packing in a structure known as a crystal lattice.

Chapter 7 is required reading. It reminds the reader that three separate stages of contraction accompany the cooling of a liquid metal down to room temperature, but the linear contraction of the liquid and of the solid are of little consequence for feeding; we shall concentrate here on the solidification contraction. This contraction gives a volume deficit that can result in problems for the casting.

The volume contraction during freezing can be fed by a number of mechanisms, but mainly by liquid feeding from a feeder. If for some reason liquid metal to feed the contraction cannot easily be supplied, the contraction starts to act on the surrounding solid, drawing it in by plastic deformation (solid feeding) and at the same time stretching the liquid metal. This elastic expansion of the liquid is naturally accompanied by the development of a hydrostatic tension, a negative pressure, which can provide the driving force for the nucleation and growth of porosity. These concepts of negative pressure are not easily understood. The reader is strongly recommended to visit Chapter 7 where this phenomenon is described in detail.

### 10.6.2 Feeding to avoid shrinkage problems

To allow ourselves the luxury of some repeated emphasis and further definitions: To provide for the fact that extra metal needs to be fed to the solidifying casting to compensate for the contraction on freezing, it is normal to provide a separate reservoir of metal. We shall call this reservoir a *feeder*, because its action is to *feed* the casting, i.e. to compensate for the solidification shrinkage (obvious really!).

In much casting literature the reservoir is known, non-obviously, as a *riser*; and worse still, may be confused with other channels that communicate with the top of the mold, such as vents, or whistlers, since metal *rises* up these openings too. The author reserves the name *riser* for (i) the special kind of feeder that is connected to the side of the casting via a slot gate, and in which metal rises up at the same time as it rises in the mold cavity; and (ii) the ‘surge riser’ designed to avoid the surge of first metal into the ingate.

If a feeder is *not* placed on a casting (necessarily a rather chunky casting that definitely requires feed metal) then we can expect a significant shrinkage problem. Figure 10.27 illustrates for an Al casting the absence of a feeder would result in a pore volume of up to 7%. That is a big porosity problem. However, as the feeder size increases in proportion to the casting, the resulting porosity reduces, eventually reaching a minimum at a feeder to casting modulus ratio of about 1.25. The porosity in the casting at this minimum depends on the gas content; at zero gas the casting will be sound. At higher gas levels the porosity rises, but it is clear that gas porosity does not raise the total porosity level so significantly as an undersized feeder. Although there is much discussion concerning the dangers of overfeeding of castings, the figure illustrates that an oversize feeder is far less damaging than an undersized feeder.

It is most important to be clear that the filling system (sometimes called the running system) is not normally required to provide any significant feeding. The filling system and the feeding system have two quite distinct roles: one fills the casting so its role is completed quickly, and the other feeds the shrinkage during solidification, whose role is more time consuming requiring the casting to freeze. (On occasions it is possible and valuable to carry out some feeding via the filling system, but this is somewhat unusual and requires special precautions. We shall deal with this later.)

Where computer modeling is not carried out, the following of the *seven feeding rules* by the author is strongly recommended. Even when computer simulation is available, the seven rules will be found to

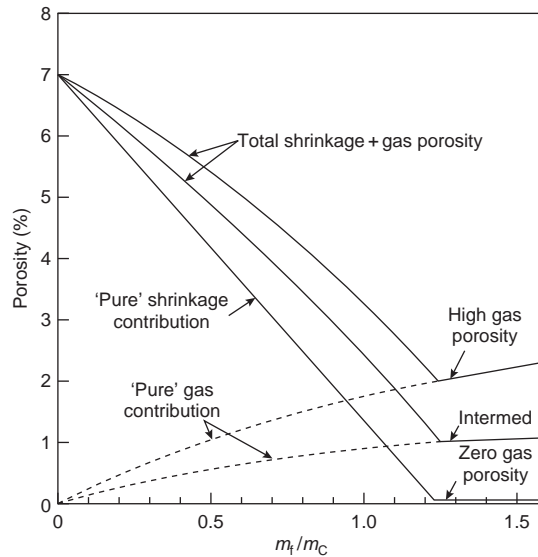


**FIGURE 10.27**

Generalized relation between gas and shrinkage as feeder size is increased in terms of the modulus ratio, based on particular results by Rao et al. (1975) shown in Figure 7.5.

be good guidelines. For the computer itself, the following of Tiryakioglu's reduced rules constitutes the most powerful logic and is recommended, although the same rules also constitute a useful check for those who determine feeder sizes by pen and paper.

In addition to observing all the requirements of the Rules for feeding, the use of all *five mechanisms* for feeding (as opposed to only liquid feeding) should also be used to advantage. These, once again, are described at length in Chapter 7. They will be found to be especially useful when attempting to achieve soundness in an isolated boss or heavy section where the provision of feed metal by conventional techniques may be impossible. However, a reminder of the attendant dangers of the use of solid feeding is presented later.

### 10.6.3 The seven feeding rules

The *Feeding Rules* have already been outlined in Volume 1 but are presented here in greater detail.

It is essential to understand that all of the Rules must be fulfilled if castings are to be produced that require soundness, accuracy and high mechanical properties. The reader must not underestimate the scale of this problem. The breaking of only one Rule may result in ineffective feeding, and a defective casting. The wide prevalence of porosity in castings is a sobering reminder that solutions are often not straightforward. Because the calculation of the optimum feeder size is therefore so fraught with complications, is dangerous if calculated wrongly, the casting engineer is strongly recommended to consider whether a feeder is really necessary at all. (For instance many modest feeding problems are easily dealt with by the provision of a chill or cooling fin rather than a feeder. Many thin walled

castings do not even require this, since thin sections in general act good naturedly as though self feeding.)

### **10.6.3.1 Feeding Rule 1: 'Do not feed' (unless necessary)**

This first and most important question relating to the provision of a feeder on a casting is 'Should we have a feeder at all?' It is a question well worth asking.

For instance, most castings I see being produced in foundries are covered in feeders when it is evident there is no real shrinkage problem. The so-called 'shrinkage' being actually a mass of bifilms and bubbles because of a poor filling system.

Another practice which deserves a separate Feeding Rule of its own is the topping up of feeders with hot metal after the mold has been filled. This is a seriously damaging practice; the minimal aid to feeding temperature gradient by this addition of hot metal is vastly countered by the serious damage done to the casting by the surface oxide on the feeder being dragged down by the falling metal. This entrained oxide is carried down through the feeder and enters the casting, producing serious defects that *appear* to be shrinkage just below the feeder. Thus if a feeder is to be provided to a casting, we should adopt the additional feeding rule 'Never top up feeders.'

The avoidance of feeding is to be greatly encouraged, in contrast to the teaching in most traditional foundry texts. There are several reasons to avoid the placing of feeders on castings. The obvious one is cost. They cost money to put on, and money to take off. In addition, many castings are actually impaired by the inappropriate placing of a feeder. This is especially true for thin-walled castings, where the filling of the feeder diverts metal from the filling of the casting, with the creation of a misrun casting.

Probably half of the small and medium-sized castings made today do not need to be fed. This is especially true as modern castings are being designed with progressively thinner walls. In fact, as we have already mentioned, the siting of heavy feeders on the top of thin-walled castings is positively unhelpful for the filling of the casting, since the slow filling of the feeder delays the filling of the thin sections at the top of the casting, with consequent misruns. Sometimes the casting suffers delayed cooling, impaired properties, and even segregation problems as a result of the presence of a feeder. Finally, it is easy to make an error in the estimation of the appropriate feeder size, with the result that the casting can be more defective than if no feeder were used at all.

As a general rule, therefore, it is best to avoid the placing of feeders on thin-walled castings. The low feed requirement of thin walls can be partly understood by assuming that of the total of 7% solidification shrinkage in an aluminum casting, 6% is easily provided along the relatively open pathway through the growing dendrites. Only about the last 1% of the volume deficit is difficult to provide. Thus if this final percentage of contraction on freezing has to be provided by solid feeding, moving the walls of the casting inwards, this becomes, at worst, 0.5% per face, which on a 4 mm thick wall is only 20  $\mu\text{m}$ . This small movement is effectively not measurable since it is less than the surface roughness. If this deficit does appear as internal porosity then it is in any case rather limited, and normally of little consequence in commercial castings. (It may require some attention in castings for safety-critical and aerospace applications.)

The other feature of thin-walled castings is that considerable solidification will often take place during pouring. Thus the casting is effectively being fed via the filling system. The extent to which this occurs will, of course, vary considerably with section thickness and pouring rate. If the section thickness (or rather modulus; see below) of the filling system is similar to that of the casting, then

feeding via the filling system might be a valuable simplification and cost saving. This important and welcome benefit to cost reduction is strongly recommended.

Because the calculation of the optimum feeder size is so fraught with complications, is dangerous if calculated wrongly, and costs money and effort, the casting engineer is strongly recommended to consider whether a feeder is really necessary at all. Rule 1 is probably the most valuable rule.

Of the remainder of castings that do suffer some feeding demand, many could avoid the use of a feeder by the judicious application of chills or cooling fins. The general faster freezing of the casting might then allow the provision of sufficient residual feeding via the filling system as indicated above. Minor revisions, opening up restrictions to the feed path along the length of the filling system, may provide valuable (and effectively 'free') feeding from the pouring basin.

However, this still leaves a reasonable number of castings that have heavy sections, isolated heavy bosses, or other features which cannot easily be chilled and thus *do* need to be fed with the correct size of feeder. The remainder of the Rules are devoted to getting these castings right.

### 10.6.3.2 Feeding Rule 2: The heat-transfer requirement

Chvorinov's heat transfer requirement for successful feeding can be stated as follows: *The feeder must solidify at the same time as, or later than, the casting.*

Nowadays this problem can be solved by computer simulation of solidification of the casting. Nevertheless it is useful for the reader to have a good understanding of the physics of feeding, so that computer predictions can be checked. We need to keep in mind that the computer simulation may not be especially accurate since much of the basic input data are sometimes not well known or wrongly inputted. Also, of course, computer time could be usefully avoided in sufficiently simple cases. In this chapter we shall concentrate on approaches which do not require a computer.

The freezing time of any solidifying body is approximately controlled by its ratio (volume)/(cooling surface area) known as its modulus,  $m$ . Thus the problem of ensuring that the feeder has a longer solidification time than that of the casting is simply to ensure that the feeder modulus  $m_f$  is larger than the casting modulus  $m_c$ . To allow a factor of safety, particularly in view of the potential for errors of nearly 20% when converting from modulus to freezing time, it is normal to increase the freezing time of the feeder by 20%, i.e. by a factor of 1.2. Thus the heat-transfer condition becomes simply:

$$m_f > 1.2 m_c \quad (10.1)$$

It is important to notice that the modulus has dimensions of length. Using SI units it is appropriate to use millimeters. (Take care to note that in French literature the normal units are centimeters, and in the USA at the present time, to the despair of all those promoters of the welcome logic of SI units (the *Système International*), a confusing mixture of millimeters, centimeters, inches and feet. It is essential therefore to quote the length units in which you are working.)

Figure 10.27 confirms the optimum feeder modulus of factor approximately 1.2 times the casting modulus. The danger of insufficient feeding is clear, whereas overfeeding is clearly preferable. The contribution of gas porosity to the total unsoundness of the casting is also seen superimposed on the feeding response.

The modulus of a feeder can be artificially increased by the use of an insulating or exothermic sleeve. It can be further increased by an insulating or exothermic powder applied to its open top surface after casting. Recent developments in such exothermic additions have attempted to ensure that after the exothermic reaction is over, the spent exothermic material continues in place as a reasonable thermal

insulator. These products are constantly being further developed, so the manufacturer's catalog should be consulted when working out minimum feeder sizes when using such aids. However, as a guide as to what can be achieved at the present time, a cylindrical feeder in an insulating material is only  $0.63D$  in diameter compared with the diameter  $D$  in sand. This particular insulated feeder therefore has only 40% of the volume of the sand feeder. Useful savings can therefore be made, but have, of course, to be weighed against the cost of the insulating sleeve and the organizational effort to purchase, store, and schedule it, etc. However, a further benefit that is easily overlooked from the use of a more compact feeder is the faster pressurization of thin sections that may aid filling, and so reduce losses due to occasional incomplete filling of mold cavities, and the faster pressurization of cores to reduce the chance of blows.

When working out the modulus of the casting it is necessary to consider which parts are in good thermal communication. These regions should then be treated as a whole, characterized by a single modulus value. Parts of the casting that are not in good thermal communication can be treated as separate castings.

For instance, castings of high thermal conductivity such as those of aluminum- and copper-based alloys can nearly always be treated as a whole, since when extensive thin sections cool attached thicker sections and bosses, the thin sections act as cooling fins for the thicker sections. Conversely, of course, the thick sections help to maintain the temperature of thinner sections. The effect of thin sections acting as cooling fins extends for up to approximately ten times the thickness of the thin section.

However, for castings of low thermal conductivity materials such as steel and nickel-based alloys (and surprisingly the copper-based Al-bronze), practically every part of the casting can be treated as separate from every other. Thus a complex product can be dealt with as an assembly of primitive shapes: plates, cubes, cylinders, etc. (making allowance, of course, for their common mating faces, which do not count as cooling area in the modulus estimate).

Table 1.1 lists some common primitive shapes. Familiarization with these will greatly assist the estimation of appropriate feeder modulus requirements.

### 10.6.3.3 Feeder Rule 3: Mass transfer (volume) requirement

The second, widely understood and well-used Rule, usually known as the volume criterion, is as follows: *The feeder must contain sufficient liquid to meet the volume-contraction requirements of the casting.*

At first sight it may seem surprising that when the heat transfer requirement above is satisfied then the volume requirement is not automatically satisfied also. However, this is definitely not the case. Although we may have provided a feeder of such a size that it would theoretically contain liquid until after the casting is solid, in fact it may still be too small to deliver the volume of feed liquid that the casting demands. Thus it will be prematurely sucked dry, and the resulting shrinkage cavity will extend into the casting.

Different metals and alloys need significantly different amounts of feed metal. Figure 10.28a illustrates a section of a feeder on a plate casting in which the required shrinkage volume is just nicely concentrated in the feeder. This is the success we all hope for. However, success is not always easily achieved, and Figure 10.28b, c and d show the complication posed by the different shrinkage behavior of different alloys. The pure Al and the Al-12Si alloy are both short freezing range, and contrast with the Al-5Mg alloy which is a long freezing range material.



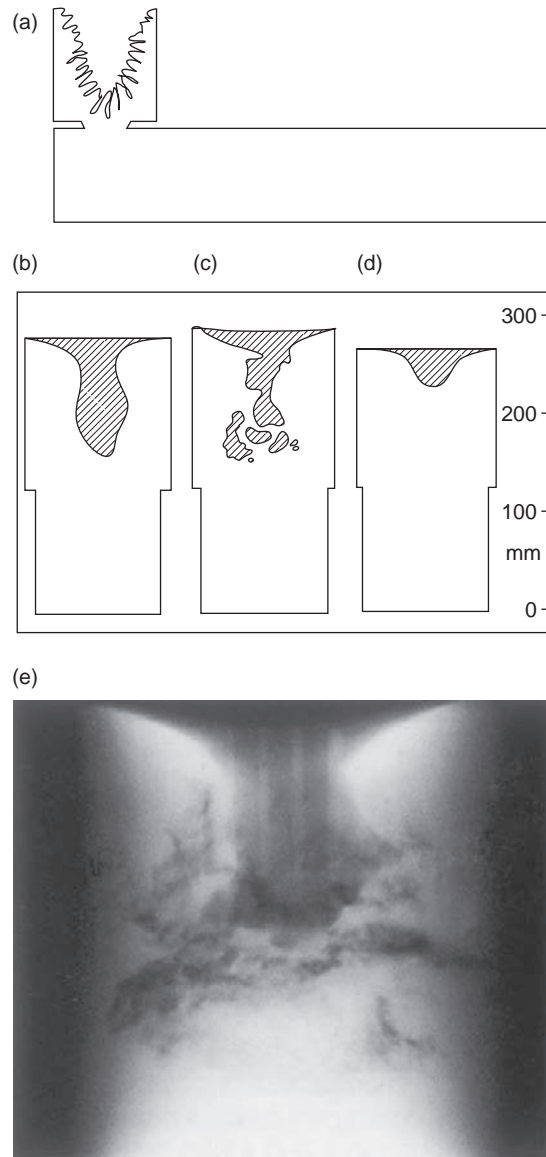


**FIGURE 10.28**

Cross-section of (a) simple plate casting, nicely fed, with all its shrinkage porosity concentrated in the feeder; (b) 99.5Al; (c) Al-12Si; (d) Al-5Mg; radiograph of Al-12Si alloy feeder (courtesy of Foseco 1988).

Some additional points of complexity in the operation of feeders in real life need to be emphasized.

- (i) The Mg containing alloy in Figure 10.28d will almost certainly contain some fine, scattered microporosity that will have acted to reduce the apparent shrinkage cavity. Thus in practice the demand from the feeder will vary with the gas content of the metal.
- (ii) The complicated form of the pipe in Al–12Si alloy (Figure 10.28c and e) almost certainly reflects the presence of large oxide films that were introduced by the pouring of the castings. These large planar defects fragment both the heat flow and the mass flow in the feeder, and the short freezing range and surface tension conspire to round off the cavities in the separated volumes of liquid isolated by the planes of oxide. In addition, the oxide, together with the solidifying crust on the top surface of the feeder also has some strength and rigidity, again complicating the collapse of the feeder top, and influencing the shape of the shrinkage pipe as it, and its associated oxide skin, gradually expands downwards. These effects are additional reasons for the 20% safety factor often used for the calculation of feeder sizes. Feeders often do not have the simple carrot-shaped shrinkage pipe predicted by the computer. The radiograph of the feeder in Figure 10.28e is an excellent example of the action of large bifilms fracturing and diverting the melt draining from a feeder.

Figure 10.28 illustrates that normal feeders are relatively inefficient in the amount of feed metal that they are able to provide. This is because they are themselves freezing at the same time as the casting, depleting the liquid reserves of the reservoir. Effectively, the feeder has to feed both itself and the casting. We can allow for this in the following way. If we denote the efficiency  $e$  of the feeder as the ratio (volume of available feed metal)/(volume of feeder,  $V_f$ ), then the volume of feed metal is, of course,  $eV_f$ . Since the liquid contracts by an amount  $\alpha$  during freezing, then the feed demand from both the feeder and casting together is  $\alpha(V_f + V_c)$ , and hence:

$$eV_f = \alpha(V_f + V_c) \quad (10.2)$$

or:

$$V_f = (e - \alpha)V_c \quad (10.3)$$

For aluminum where  $\alpha = 7\%$  approximately (see Table 7.2 for values of  $\alpha$  for other metals), and for a normal cylindrical feeder of  $H = 1.5D$  where  $e = 14\%$ , we find:

$$V_f = V_c \quad (10.4)$$

i.e. there is as much metal in the feeder as in the casting! This is partly why the yield (measured as the weight of metal going into a foundry divided by the weight of good castings delivered) in many aluminum foundries is rarely above 50%. Metal in the running system and scrap allowance will reduce the overall yield of good castings even further so that overall yields are often closer to 45%. (In comparison, the economic benefits of higher-yield casting processes such as counter-gravity casting, in which metallic yields of 80–90% are common, appear compellingly attractive, especially for high-volume foundries.)

For steels the value of  $\alpha$  lies between 3 and 4%, depending on whether solidification is to the body-centered-cubic or face-centered-cubic structures. For pure Fe–C steels the fcc structure applies above 0.1% carbon where the melt solidifies to austenite. For  $\alpha = 4$  and  $e = 14\%$ , Equation 10.3 gives:

$$V_f = 0.40V_c$$

and for steel that freezes to the bcc structure (delta ferrite) with  $\alpha = 3$ , and using a feeder of 14% efficiency we have:

$$V_f = 0.27V_c$$

Thus, compared to Al alloys, the smaller solidification shrinkage of ferrous metals reduces the volume requirement of the feeder considerably. For graphitic cast irons the value reduces even further of course, becoming approximately zero in the region of 3.6–4.0% carbon equivalent. Curiously, a feeder may still be required because of the difference in *timing* between feed demand and graphite expansion, as will be described later.

The interesting reverse tapered feeder (Figure 10.29c) has been promoted for many years (Heine 1982, Creese and Xia 1991) and is currently widely used for ductile iron castings. Even so, the reader needs to be aware that in the opinion of the author, Figure 10.29 may not be as accurate we would like. At this time, the extent of the uncertainties is not known following the recent work of Sun and Campell (2003). This investigation of the effect of positive and negative tapers on the efficiencies of feeders, found that the reverse tapered feeder (Figure 10.29c) appeared to be less efficient than parallel sided cylindrical feeders, or even feeders with a slight positive taper. These doubts are an unwelcome sign of the extent of our ignorance of the best feeder designs at this time.

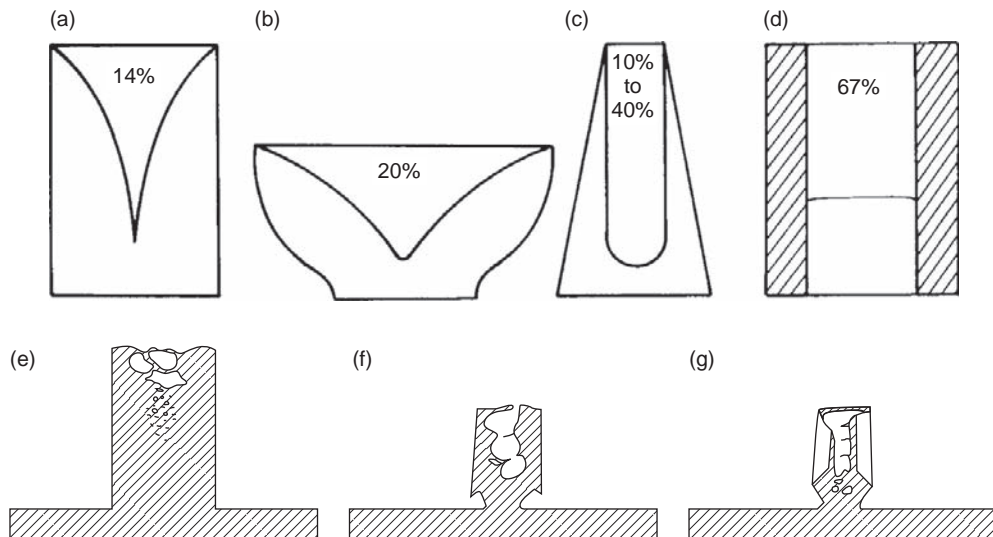


**FIGURE 10.29**

Metal utilization of feeders of various forms molded in sand. The (a) cylindrical and (b) hemispherical heads have been treated with normal feeding compounds; (c) efficiency of reverse tapered feeders depends on detailed geometry (Heine 1982, 1983); (d) exothermic sleeve (Beeley 1972); metal utilization for ductile iron plates with (e) cylindrical sand feeder; (f) insulating feeder; and (g) cruciform exothermic feeder (after Foseco 1988).

Whether the size of the feeder is dictated by the thermal or volume requirement is related to the geometry of the casting. Figure 10.30 shows a theoretical example, calculated neglecting non-cooling interfaces for simplicity. Curve A is the minimum feeder volume needed to satisfy the thermal condition  $m_f = 1.2m_c$ ; and curve B is the minimum feeder volume needed to satisfy the feed demand criterion based on 4% volume shrinkage and 14% metal utilization from the feeder. Figure 10.30 reveals that chunky steel plates up to an aspect ratio of about 6 or 7 length to thickness are properly fed by a feeder dictated by freezing time requirements. However, thin section steel plates above this critical ratio always freeze first, and so require a feeder size dictated by volume requirements.

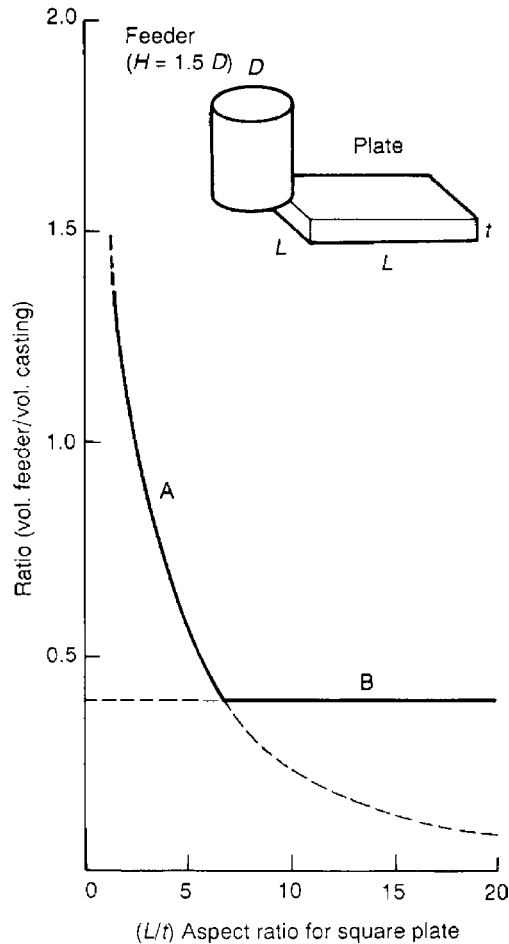


**FIGURE 10.30**

Feeder volume based on a feeder mold in sand, and calculated neglecting non-cooling interfaces for simplicity. Curve A is the minimum feeder volume to satisfy  $m_f = 1.2m_c$  and curve B is the minimum volume to satisfy the feed demand of 4% volume shrinkage and 14% utilization of the feeder.

In fact the shape of the shrinkage pipe in the feeder is likely to be different for each of these conditions. For instance, the feeder efficiencies shown in Figure 10.29 are appropriate for the feeding of chunky castings because the continuing demand of feed metal from the casting until the feeder itself is almost solid naturally creates a long, tapering shrinkage pipe, resembling a carrot.

In the case of the more rapid solidification of thin castings, the relatively large diameter feeder needed to provide the volume requirement will give a shallowly dished shape in the top of the feeder, since the feed metal is provided early, before the feeder itself has solidified to any great extent. The efficiency of utilization of the feeder will therefore be expected to be significantly higher, as confirmed by Figure 10.30.

Research is needed to clarify this point. In the meantime, the casting engineer needs to treat the present data with caution, and conclusions from Figures 10.29 and 10.30, for instance, have to be viewed as illustrative of general principles rather than numerically accurate. Clearly, it is desirable to achieve smaller, more cost-effective feeders. The change of feeder efficiency depending on whether freezing or volume requirements are operating requires more work to clarify this uncertainty. In the meantime, this problem illustrates the power of a good computer simulation to avoid the necessity for simplifying assumptions.

A further use of feeders where the casting engineer requires care is the use of a blind feeder sited low down on the casting. The problems are compounded if such a low-sited blind feeder is used together with an open feeder placed higher. It must be remembered that during the early stages of freezing the top feeder is supplying metal to the blind feeder as well as the casting. The blind feeder has to be treated as though it is an integral part of the casting. The size of the top feeder needs to be enlarged accordingly.

The blind feeder only starts to operate independently when the feed path from the top feeder freezes off. This point occurs when the solidification front has progressed a distance  $d/2$ , where  $d$  is the thickness of the thickest casting section between the top and the blind feeders. Thus the volume of the blind feeder is now reduced by the  $d/2$  thickness layer of solid that has already frozen around its inner walls.

If this caution were not already enough, a further pitfall is that the thickness of solid shell inside the blind feeder may now exceed the length of the atmospheric vent core, creeping over its end and sealing it from the atmosphere. The blind feeder is therefore prevented from breathing, and is unable to provide any feed metal. In fact it now works in reverse, to suck metal out of the casting.

There are therefore subtleties in the operation of blind feeders that make success illusive. It is easy to make a mistake in their application, and the correct operation of the atmospheric vent is not always guaranteed, so it is difficult to recommend their use on smaller castings. For larger castings, where the size of the blind feeder is large, the collapse of the top of the feeder is more predictable, so that the action of the blind feeder becomes more reliable.

Whereas the size of feeders for alloys such as those based on alloys that shrink in a conventional fashion on freezing are straightforward to understand and work with, graphitic cast irons are considerably more complicated in their behavior. They are therefore more complicated to feed, and the estimate of feeder sizes subject to more uncertainty.

The amount of graphite that is precipitated depends strongly on factors that are not easy to control, particularly the efficiency of inoculation. In addition, the expansion of the graphite can lead to an expansion of the casting if the mold and its container are not rigid. Since a mold and a molding box can never be perfectly rigid, this leads to a larger volume casting that requires more metal to feed it, with

the danger that the feeder is now insufficient to provide this additional volume. Shrinkage porosity as a result of mold dilation is a common feature of iron castings.

One of the ways to reduce (but, of course, never to eliminate) this problem is to use very dense, rigid mold in rigid, well-engineered boxes. Furthermore, the expansion of the graphite can be accommodated without swelling the casting by allowing the excess melt to exude out of the casting and back into the feeder. The provision of a small feeder is therefore essential to the production of many geometries of small iron castings. This small feeder provides essential feed metal during the time that normal shrinkage occurs, but also acts as an overflow during graphite expansion. It follows therefore that subsequent examination of the feeder indicates, mysteriously, that no net volume of liquid has flowed out from the feeder.

Ductile cast irons commonly use a reverse-tapered feeder such as that shown in Figure 10.29c. If the feeder remained full for too long, its top would freeze over, isolating it from the atmosphere, and so preventing the delivery of any liquid. It is logical therefore to encourage the feeder to start feeding almost immediately, concentrating the action of shrinkage throughout the casting all on the small area at the top of the feeder. In this way the level of liquid in the top of the feeder falls quickly, becoming surrounded by hot metal, so very soon there is no danger of it freezing over. For this to happen it is essential that no feeding continues to be provided via the running system. This would keep the feeder full for too long. Thus it is necessary to design the ingate to freeze quickly. The feeder then works well.

This feeding technique, although at this time used exclusively in the ductile iron industry so far as the author is aware, would be expected to be applicable to a wide variety of metals and alloys.

#### **10.6.3.4 Feeding Rule 4: The junction requirement**

The junction problem is a pitfall awaiting the unwary. It occurs because the simple act of placing a feeder on a casting creates a junction. As we shall see in Section 12.4.8, a junction with an inappropriate geometry will lead to a hot spot. The hot spot may cause a shrinkage cavity that extends into the casting.

We shall see later (in the section on filling system design, dealing with the design of ingates) that it is easy to create a junction, planting either a feeder or a gate on to a casting, only to find that it has created a hot spot, and so leads to a localized feeding problem at the junction. After the feeder or gate is cut off a shrinkage cavity is found extending into the casting. This occurs when the ratio of modulus of the addition (the feeder or gate) to the modulus of the casting is close to 1:1.

The simplest example illustrating the problem clearly is that of the feeding of a cube. The cube casting has the reputation of being notoriously difficult to feed. This is because the casting technologist, carefully following Rule 2, calculates a feeder of 1.0 or perhaps 1.2 times the modulus of the cube. If the cube has side length  $D$ , then the feeder of 1:1 height to diameter ratio works out to have a diameter of  $1.2D$ . Thus the cube appears to require a feeder of rather similar volume sitting on top. However, the cube and its feeder are now a single compact shape that solidifies as a whole, with its thermal center in the centre of the new total cast shape, i.e. approximately in the centre of the junction. The combination therefore develops a shrinkage cavity at the junction, the hot spot between the casting and feeder. When the casting is cut off from the feeder, the porosity that is found is generally called ‘under-feeder shrinkage porosity’. This rather pompous pseudo-technical jargon clouds the clear conclusion that *the feeder is too small*.

The junction rules, developed later in the section on design of ingates, indicate that to avoid creating a hot spot we need to ensure that the feeder actually has twice the modulus of the casting. Thus the cube should have had a feeder of side length  $2D$ . The shrinkage cavity would then have been concentrated only in the feeder.

The junction problem is a widely overlooked requirement. The use of Chvorinov's equation systematically gives the wrong answer for this reason, so the junction requirement is often found to override Chvorinov. This is an important result that has caused much trouble for methoding engineers over the years and requires us all to update our thinking.

However, in some cases the junction problem can be avoided. The simplest solution is not to place the feeder directly on the casting so as to create a junction. It happens that this rule is not easily applied to a cube because there is no alternative site for it.

However, in the case of a plate casting, there are options. The feeder should not be placed directly on the plate, but should be placed on an extension of the plate.

The general rules to solve the junction problem are therefore as follows:

- (i) Appendages such as feeders and ingates should not be planted on the casting so as to create a T (or an L-) junction (although the L-junction is rather less detrimental than the T-junction). They are best added as extensions to a section, as an elongation to a wall or plate, effectively moving the junction off the casting.
- (ii) If there is no alternative to the placing of the feeder directly on the casting, then to avoid the hot spot in the middle of the junction, the additional requirement that the feeder must meet is, if a T-junction,

$$m_f > 2m_c \quad (10.5)$$

or if an L-junction

$$m_f > 1.33m_c \quad (10.6)$$

The value of the constants is taken from Sciana (1974).

Note that no safety factor of 1.2 has been applied to these feeder sizes. This is because the shrinkage cavity does not occur exactly at the geometric center of the freezing volume trapped at the thermal center; the cavity 'floats' to the top, and the feed liquid finds its level at the base of the isolated region. Thus the final shrinkage cavity is naturally displaced above the junction interface, giving a natural 'built-in' safety factor.

Note that we have assumed that the feeder is above the casting, so as to feed downwards under gravity. This is the recommended safe way to use feeders. If the feeder (or large gate) were placed *below* the casting, gravity would now act in reverse, so that any shrinkage cavity caused by the junction would float into the casting (in other words, the residual liquid metal in the casting drains into the feeder). This action illustrates one of the dangers of attempting to feed uphill.

Although it is not a good idea to make the feeder any larger than is really required, if it is only marginally adequate, the root tip of porosity seen in Figures 10.28 and 10.29 may on occasions just enter the casting, and may therefore be unacceptable. This necessitates the application of a safety factor, giving a feeder of larger size on average, but still just acceptable even when all the variables are loaded against it. It is common to use the safety factor 1.2 for the estimation of its modulus.

### 10.6.3.5 Feeding Rule 5: Feed path requirement (the communication requirement)

There must be a path to allow feed metal to reach those regions that require it. It is clearly no use having feed metal available at one point on the casting, unable to reach a more distant point where it is needed. Clearly there has to be a way through. The reader can see why this criterion has been often overlooked as a separate Rule; the communication criterion appears self-evident! Nevertheless it does have a number of geometrical implications which are not so self-evident, and which will be discussed.

In a valuable insight, Heine (1968) has drawn attention to the fact that the highest-modulus regions in a casting are either potential regions for shrinkage porosity if left unfed, or may be feeding paths if connected to feed metal. He recommends the identification of feed paths that will transport feed metal through castings of complex geometry, such as the hot spots at the T-junctions between plates

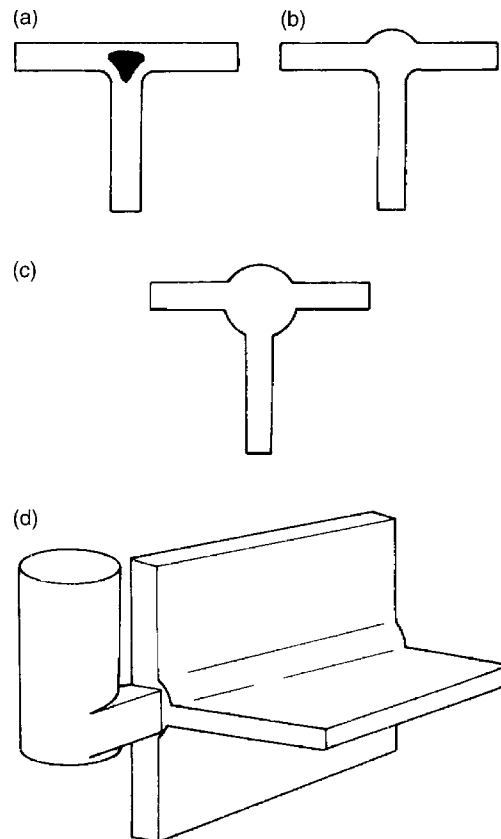


**FIGURE 10.31**

(a) T-junction with normal concave fillet radius; (b) a marginal improvement to the feed path along the junction; (c) convex fillets plus pad that doubles feeding distance along the junction; and (d) practical utilization of a T-junction as a feed path (Mertz and Heine 1973).



(Figure 10.31). (He also draws attention to the fact that certain locations are never feed paths. These include corners or edges of plates, or the ends of bars and cylinders.)

The various ways to help to ensure that feed paths remain open are considered in this section.

#### Directional solidification towards the feeder

If the feeder can be placed on the thickest section of the casting, with progressively thinner sections extending away, then the condition of progressive solidification towards the feeder can usually be achieved.

A classical method of checking this due to Heuvers can be used in which circles are inscribed inside the casting sections. If the diameters of the circles increase progressively towards the feeder then the condition is met (Figure 10.32). Lewis and Ransing (1998) draw attention to the fact that Heuvers' technique is only two-dimensional, and that the condition would be more accurately represented in three dimensions by a progressive change in the radius of a sphere, effectively equivalent to the progressive increase in casting modulus towards the feeder. The fundamental reason for tapering the casting in this way is to achieve taper in the liquid flow path (Sullivan et al. 1957). For convenience we shall call this the modulus gradient technique.

Failure to provide sufficient modulus gradient towards the feeder can be countered in various ways by (i) re-siting the feeder, (ii) providing additional feeder(s), or (iii) modifying the modulus of the casting. Ransing describes a further option, (iv) in which he proposes a change in heat transfer coefficient. The latter technique is a valuable insight because it is easily and economically computed by a geometrical technique, and so contrasts with the considerable computing reserves and effort required by finite element and finite difference methods. If  $R$  is the radius of the inscribed sphere, the local solidification time  $t$  is proportional to  $R^2/h$  where  $h$  is the heat transfer coefficient at the metal–mold interface. Thus at locations 1 and 2 we have  $h_2 = h_1(R_1/R_2)^2$ . This relation allows an estimate of

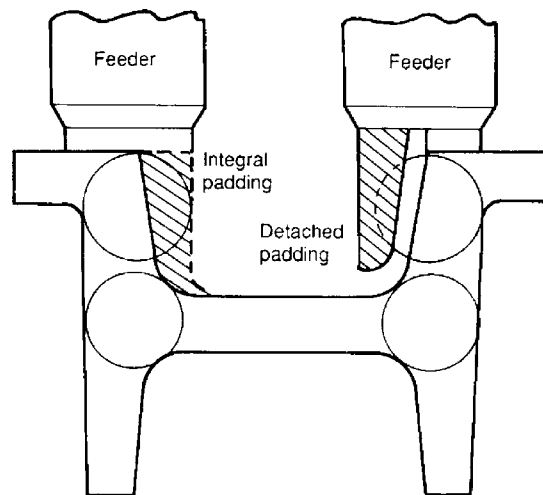


**FIGURE 10.32**

Use of Heuvers circles to determine the amount of attached padding (Beeley 1972) and the use of detached (or indirect) padding described by Daybell (1953).

the change of  $h$  that is required to ensure that the freezing time increases steadily towards the feeder. Ransing uses a change of 10% increase of solidification time for each different geometrical section of the casting (i.e. for feeding via a thin section to a thick distant section he increases the freezing time of the thin section over that of the thick by 10%). The technique can be usefully employed in reverse, in the sense that known values of  $h$  produced by a chill can quickly be checked for their effectiveness in dealing with an isolated heavy section. In every case the target is to eliminate the local hot spot, and ensure a continuous feed path back to the feeder. This simple technique has elegance, economy and power and is strongly recommended.

The casting modulus can be modified by providing either a chill or cooling fin to speed solidification locally, or by providing extra metal to thicken the section and delay solidification locally. The provision of extra metal on the casting is known as padding. The addition of padding is most usefully carried out with the customer's consent, so that it can be left in position as a permanent feature of the casting design. If consent cannot be obtained then the caster has to accept the cost penalty of dressing off the padding as an additional operation after casting.

Occasionally this problem can be avoided by the provision of detached, or indirect, padding as shown in Figure 10.32. Daybell (1953) was probably the first to describe the use of this technique. The author has found it useful in the placement of feeders close to thin adjacent sections of casting, with a view to feeding through the thin section into a remote thicker section.

The principle of progressive increase of modulus towards the feeder, although generally accurate and useful, is occasionally seen to be not quite true. Depending on the conditions, this failure of the principle can be either a problem or a benefit, as shown below. (Even so, the Ransing technique described above is unusual since it successfully takes this problem into account.)

In a re-entrant section of a casting the confluence of heat flow into the mold can cause a hot spot, leading to delayed solidification at this point, and the danger of local shrinkage porosity in an alloy that shrinks during freezing, such as an Al alloy. Alternatively, in an alloy that expands such as a high carbon-equivalent cast iron, the exudation of residual liquid into the mold as a result of the high internal pressure created during the precipitation of graphite can cause penetration of the aggregate mold material, with unwelcome so-called *burned-on* sand in a particularly inaccessible region. Such a hot spot can occur despite an apparent unbroken increase in modulus through that region towards the feeder. This is because the simple estimation of modulus takes no account of the geometry of heat flow away from cooling surfaces; all surfaces are assumed to be equally effective in cooling the casting. Such a hot spot requires the normal attention such as extra local cooling by chill or fin, or additional feed via extra padding or feeders.

The failure of the modulus gradient technique can be used to advantage in the case of feeder necks to reduce the subsequent cut-off problem. Feeders are commonly joined to the main casting via a feeder neck, with the modulus of the neck commonly controlled to be intermediate between that of the casting and the feeder; the moduli of casting, neck and feeder are in the ratio 1.0:1.1:1.2 (Beeley 1972). However the neck can be reduced considerably below this apparently logical lower limit, because of the hot spot effect, and because of the conduction of heat from the neighboring casting and feeder that helps to keep the neck molten for a longer period than its modulus alone would suggest. This point is well illustrated by Sciamia (1975), and his results are summarized in Figure 10.33. The results clearly demonstrate that for steel, feeder necks can be reduced to half of the diameter  $D$  of the feeder, providing that they are not longer than  $0.1D$ . The higher thermal conductivity copper- and aluminum-based materials can have necks almost twice as long without problems.

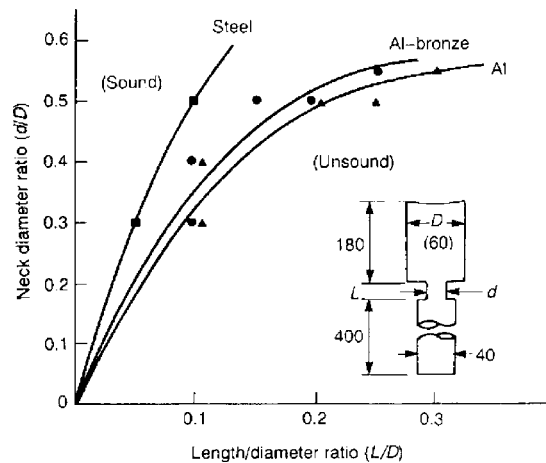


**FIGURE 10.33**

Effect of a constricted feeder neck on soundness of steel, aluminum bronze, and 99.5Al castings. The experimental points by Sciama (1975) denote marginal conditions.

By extrapolation of these results towards smaller neck sizes, it seems that a feeder neck in steel can be only  $0.25D$  in diameter, providing it is no more than approximately  $0.03D$  in length. Similarly, for copper and aluminum alloys the  $0.25D$  diameter neck can be up to  $0.06D$  long. These results explain the action of the Washburn core, or breaker core, which is a wafer-thin core with a narrow central hole, and which is placed at the base of a feeder, allowing it to be removed after casting by simply breaking it off. In separate work the dimensions of typical Washburn cores is recommended to be a thickness of  $0.1D$  and a central hole diameter of  $0.4D$  (work by Wlodawer summarized by Beeley 1972). The hole size and thickness appear to be very conservative in relation to Sciama's work. However, Sciama may predict optimistic results because he uses a feeder of nearly 1.5 times the modulus of casting, which would tend to keep the junction rather hotter than a feeder with a modulus of only 1.2 times that of the casting (it would be valuable to repeat this work using a more economical feeder). Also, of course, conservatism may be justified where feeding conditions are less than optimum for other reasons in the real foundry environment.

The aspect of conservatism because of the real foundry environment is an interesting issue. For instance, the feeder neck could, in the extreme theoretical case, be of zero diameter when the thickness of the feeder neck core was zero. The *reductio ad absurdum* argument illustrates that an extreme is not worth targeting, especially when sundry debris in suspension, such as rather rigid bifilms, could close off a narrow aperture.

In fact, this danger appears to be very real for metals that commonly suffer a high population of bifilms, such as the light alloys. During the rapid filling of the mold the bifilms swarm into the feeder, propelled by the momentum of the flow. However, during feeding, the gradual settling of bifilms inside the feeder will pile up the bifilms over the exit, especially if this is narrow, and may prevent feeding by the simple mechanical action of the lowest bifilm opening, its lower half expanding away into the casting as the metal is sucked down, whereas the pile-up of bifilms above the feeder exist may be

sufficiently rigid to support the weight of metal in the feeder, thus preventing feeding. The eventual outcome is the mysterious case of the full feeder with a large shrinkage cavity immediately underneath. The pompous ‘under-riser shrinkage porosity’ jargon now no longer means the feeder was too small, but the melt was too dirty to allow feeding.

### Minimum temperature gradient requirement

Experiments on cast steels have found that when the temperature gradient at the solidus (i.e. the temperature gradient at which the final residual liquid freezes) falls to below approximately  $0.1\text{--}1\text{ K mm}^{-1}$  then porosity is observed even in well-degassed material. Although there is much scatter in other experimental determinations, it seems in general that the corresponding gradients for copper alloys are around  $1\text{ K mm}^{-1}$  and those for aluminum alloys are around  $2\text{ K mm}^{-1}$  (Pillai et al. 1976). It seems therefore that the temperature gradient defines a critical threshold of a non-feeding condition. As the flow channel nears its furthest extent, and becomes vanishingly narrow, it will become subject to small random fluctuations in temperature along its length. This kind of temperature ‘noise’ will occur as a result of small variations in casting thickness, or of density of the mold, thickness of mold coating, blockage or diversion of heat flow direction by random entrained films etc. Thus the channel will not reduce steadily to infinite thinness, but will terminate when its diameter becomes close to the size of the random perturbations.

There has been some discussion about the absolute value of the critical gradient for feeding on the grounds that the degree of degassing, or the standard of soundness, to which the casting was judged will affect the result. These are certainly very real problems, and do help to explain some of the wide scatter in the results.

Hansen and Sahm (1988) draw attention to a more fundamental objection to the use of temperature gradients as a parameter that might correlate with feeding problems. They indicate that the critical gradient required to avoid shrinkage porosity in a steel bar is five to ten times higher than that required for a plate, and point to other work in which the critical gradient in a cylindrical steel casting is a function of its diameter. Thus the concept of a single gradient which applies in all conditions seems too simplistic. It seems the rate of flow of the residual feeding liquid is also important.

### Feeding distance

It is easy to appreciate that in normal conditions it is to be expected that there will be a limit to how far feed liquid can be provided along a flow path. Up to this distance from the feeder the casting will be sound. Beyond this distance the casting will be expected to exhibit porosity.

This arises because along the length of a flow channel, the pressure will fall progressively because of the viscous resistance to flow (Section 7). When the pressure falls to a critical level, which might actually be negative (simply becoming a tensile stress in the liquid) then porosity may form. Such porosity may occur from an internal initiation event (such as the opening of a bifilm), or from the drawing inwards of feed metal from the surface of the casting, since this may now represent a shorter and easier flow path than supply from the more distant feeder.

There has been much experimental effort to determine feeding distances. The early work by Pellini and his co-workers (summarized by Beeley (1972)) at the US Naval Materials Laboratory is a classic investigation that has influenced the thinking on the concept of feeding distance ever since. They discovered that the feeding distance  $L_d$  of plates of carbon steels cast into greensand molds depended on the section thickness  $T$  of the casting: castings could be made sound for a distance from the feeder

edge of  $4.5T$ . Of this total distance,  $2.5T$  resulted from the chilling effect of the casting edge; the remaining  $2.0T$  was made sound by the feeder. The addition of a chill was found to increase the feeding distance by a fixed 50 mm (Figure 10.34). They found that increasing the feeder size above the optimum required to obtain this feeding distance had no beneficial effects in promoting soundness. The feeding distance rule for their findings is simply:

$$L_d = 4.5T \quad (10.7)$$

Pellini and colleagues went on to speculate that it should be possible to ensure the soundness of a large plate casting by taking care that every point on the casting is within a distance of  $2.5T$  from an edge, or  $2.0T$  from a feeder.

Note that all the semi-empirical computer programs written since have used this and the associated family of rules as illustrated in Figure 10.34 to define the spacing of feeders and chills on castings. However, the original data relate only to steel in greensand molds, and only to rather heavy sections ranging from 50–200 mm. Johnson and Loper (1969) have extended the range of the experiments down to section a thickness of 12.5 mm and have re-analyzed all the data. They found that for plates the data, all in units of millimeters, appeared to be more accurately described by the equation:

$$L_d = 72m^{1/2} - 140 \quad (10.8)$$

and for bars:

$$L_d = 80m^{1/2} - 84 \quad (10.9)$$

where  $m$  is the modulus of the cast section in millimeters. The revised equations by Johnson and Loper have usually been overlooked in much subsequent work. What is also overlooked is that all the relations apply to cast mild steels in greensand molds, not necessarily to any other casting alloys in any other kinds of mold.

In their nice theoretical model, Kubo and Pehlke (1985) find support for Pellini's feeding distance rules for steel castings, but it is a concern that no equivalent rule emerged for Al–4.5Cu alloy that they also investigated.

In fact, colleagues of Flinn (1964) found that whereas the short-freezing-range alloys manganese bronze, aluminum bronze, and 70/30 cupro-nickel all had feeding distances that increased with section thickness, the long-freezing-range alloy tin bronze appeared to react in the opposite sense, giving a reduced feeding distance as section thickness increased. (The nominal composition of this classical long-freezing-range material is 85Cu, 5Sn, 5Zn, 5Pb. It was known among traditional foundrymen as 'ounce metal' since to make this alloy they needed to take one pound of copper to which one ounce of tin, one ounce of zinc, and one ounce of lead was added. This gives, allowing for small losses on addition, the ratios 85:5:5:5.)

Kuyucak (2002) reviews the relations for estimating feeding distance in steel castings, and finds considerable variation in their predictions. This makes sobering reading.

Jacob and Drouzy (1974) found long feeding distances, greater than  $15T$ , for the relatively long-freezing-range aluminum alloys Al–4Cu and Al–75i–0.5Mg, providing the feeder is correctly sized.

All this confusion regarding feeding distances remains a source of concern. We can surmise that the opposite behavior of short- and long-freezing-range materials might be understood in terms of the ratio *pasty zone/casting section*. For short-freezing-range alloys this ratio is less than 1, so the solidified skin

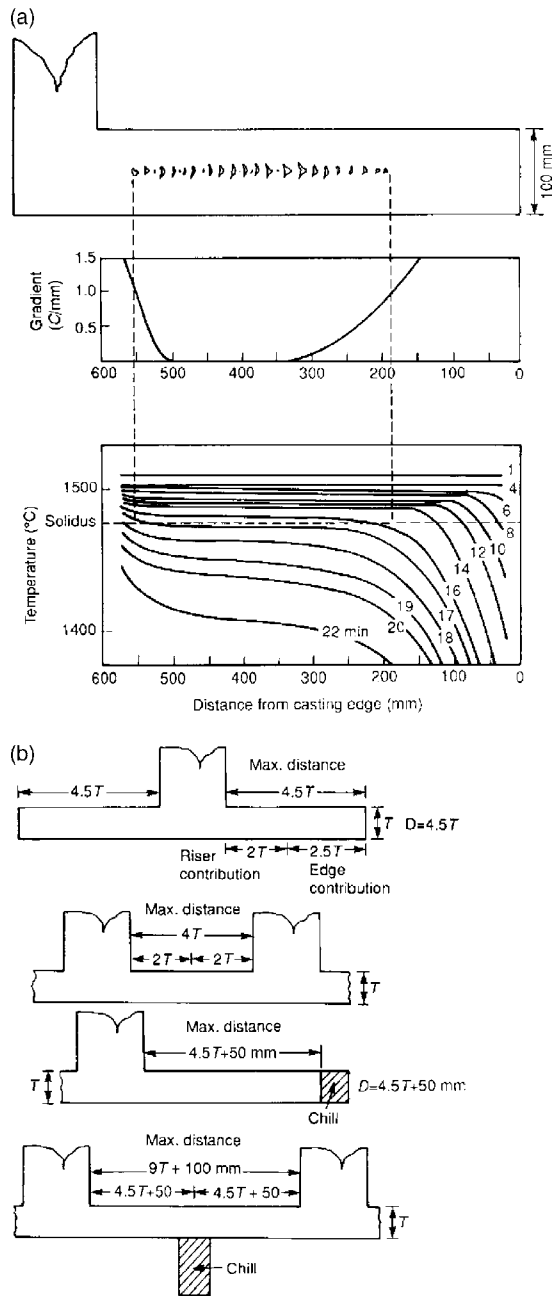


FIGURE 10.34

The famous results by Pellini (1953) for (a) the temperature distribution in a solidifying steel bar; and (b) the feeding distances for steel plates cast in greensand.

of the alloy is complete, dictating feeding from the feeder, and thus normal feeding distance concepts apply.

For the case of long-freezing-range materials where the pasty zone/casting section ratio is greater than 1, and in fact might be 10 or more, the outer solid portions of the casting are far from solid for much of the period of solidification. The connections of liquid through to the outer surface will allow flow of liquid from the surface to feed solidification shrinkage if flow from the more distant feeder becomes more difficult. In addition, the higher temperature and lower strength of the liquid/solid mass will allow general collapse of the walls of the casting inwards, making an important contribution to the feeding of the inner regions of the casting by the 'solid feeding' mechanism. It is for this reason that the higher conductivity and lower strength alloys of Al and Cu can be characterized by practically infinite feeding distances, particularly if the alloys are relatively free from bifilms. For clean metal, internal porosity simply does not nucleate, no matter how distant the casting happens to be from the feeder; the outer walls of the casting simply move inwards very slightly.

Thus although the general concept of feeding distance is probably substantially correct, at least for short-freezing-range alloys, and particularly for stronger materials such as steels, it should be used, if at all, with great caution for non-ferrous metals until it is better understood and quantified. In summary it is worth noting the following:

- The data on feeding distances have been derived from extensive work on carbon steels cast in greensand molds. Relatively little work has been carried out on other metals in other molds.
- The definition of feeding distance is sensitive to the level of porosity that can be detected and/or tolerated.
- It is curious that the feeding distance is defined from the edge of a feeder (not its centerline).
- The quality of the cast metal in terms of its gas and oxide content would be expected to be crucial. For instance, good quality metal achieved by the use of filters and good degassing and casting technique (i.e. having the benefit of a low bifilm content) would be expected to yield massive improvements in feeding distance. This has been demonstrated by Romero et al. (1991) for Al-bronze. Berry and Taylor (1999) report a related effect, whilst reviewing the benefit to the feeding distance of pressurizing the feeder. This work is straight forwardly understood in terms of the pressure on the liquid acting to suppress the opening of bifilms.

A final note of caution relates to the situation where the concept of feeding distance applies to an alloy, but has been exceeded. When this happens it is reported that the sound length is considerably less than it would have been if the feeding distance criterion had just been satisfied. If true, this behavior may result from the spread of porosity, once initiated, into adjacent regions. The lengths of sound casting in Figure 10.34a are considerably shorter than the maximum lengths given by Equations 10.7–10.9, possibly because the feeding distance predicted by these equations has been exceeded and the porosity has spread. Mikkola and Heine (1970) confirm this unwelcome effect in white iron castings.

### Criteria functions

For a discussion of the use of criteria functions to assess the difficulty to feed, and the propensity of the metal to develop porosity, please refer to the earlier Section 7.1.3.2.

### 10.6.3.6 Feeding Rule 6: Pressure gradient requirement

Although all of the previous feeding rules may be met, including the provision of feed liquid and a suitable flow path, if the pressure gradient needed to cause the liquid to flow along the path is not available, feed liquid will *not* flow to where it is needed. Internal porosity may therefore occur.

One of the most usual causes of failure to feed is not taking advantage of gravity. As opposed to *filling uphill* (which is of course quite correct) *feeding* should only be carried out *downhill* (using the assistance of gravity).

Attempts to feed uphill, although possible in principle, can be unreliable in practice, and may lead to randomly occurring defects that have all the appearance of shrinkage porosity. In castings of modest size feeding uphill appears to be successful as will be discussed later as the technique 'Active Feeding'. In many castings, particularly larger castings, problems occur when attempting to feed uphill because of the difficulties caused by various effects: (i) adverse pressure gradient as discussed below; (ii) danger of upward floating of gas or air bubbles into the casting; and (iii) adverse density gradient leading to convection as dealt with in Rule 7 of the 10 Rules.

A positive pressure gradient from the outside to the inside of the casting will help to ensure that the feed material (either solid or liquid) travels along the flow path into those parts of the casting experiencing a shrinkage condition. The various feeding mechanisms are seen to be driven by the positive pressure such as atmospheric pressure and/or the pressure due to the hydrostatic head of metal in the feeder. The other contributor to the pressure gradient, the driving force for flow, is the reduced or even negative pressure generated within poorly fed regions of some castings. All of these driving forces happen to be additive; the flow of feed metal is caused by being pushed from the outside and by being pulled from the inside.

Figure 10.35 illustrates the feeding problems in a complicated casting. The casting divides effectively into two parts either side of the broken line. The left-hand side has been designed to be fed by an open feeder F1 and a blind feeder F2. The right-hand side was intended to be fed by blind feeder F3.

Feeder F1 successfully feeds the heavy section S1. This feeder is seen to be comparatively large. This is because it is required to provide feed metal to the whole casting during the early stages of freezing, while the connecting sections remain open. At this early stage of interconnection of the whole casting, the top feeder is also feeding both blind feeders.

Feeder F2 feeds S5 because it is provided with an atmospheric vent, allowing the liquid to be pressurized by the atmosphere as in the coffee cup experiment illustrated in Figure 10.35, so forcing the metal through into the casting. (The reader is encouraged to try the coffee cup experiment.)

The identical heavy sections S3 and S4 show the unreliability of attempting to feed uphill. In S4 a chance initiation of a pore has created a free liquid surface, and the internal gas pressure within the casting happens to be close to 1 atmosphere. Thus the liquid level in S4 falls, finding its level equal to that in the feeder F2. The surface-initiated pore in S2 has grown from the hot spot that has weakened and broken through the corner of the casting. The pore has grown, equalizing its level exactly with that in the feeder F2, since both surfaces are subject to the same atmospheric pressure. In Section S3, by good fortune, no pore initiation site is present, so no pore has occurred, with the result that atmospheric pressure via F2 (and unfortunately also via the puncture by the atmosphere at the hot spot in the re-entrant section S2) will feed solidification shrinkage here, causing the section to be perfectly sound.



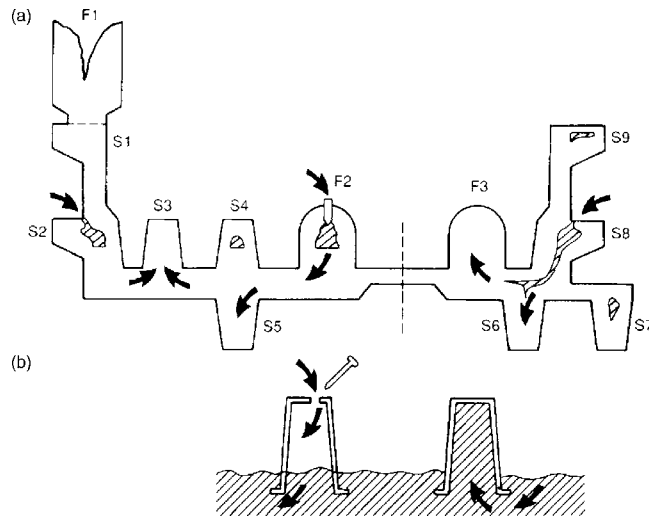


**FIGURE 10.35**

Castings with blind feeders; F2 is correctly vented but has mixed results on section S3 and S4. Feeder F3 is vented and therefore does not feed. The unfavorable pressure gradient draws liquid from a fortuitous skin puncture in section S8. See text for further explanation. (b) The plastic coffee cup analog; the air is held in the upturned cup and cannot be released until air is admitted via a puncture. The liquid it is holding is then immediately released.

Turning now to the right-hand part of the casting, although feeder F3 is of adequate size to feed the heavy sections S6, S7, and S8, unfortunately its atmospheric vent has been forgotten. This is a serious mistake. The plastic coffee cup experiment shows that such an inverted air-tight container cannot deliver its liquid contents. The pressure gradient is now reversed, causing the flow to be in the wrong direction, from the casting to the feeder! The detailed reasoning for this is as follows. The pressure in the casting and feeder continues to fall as freezing occurs until a pore initiates, either under the hydrostatic tension, or because of a build-up of gas in solution, or because of the inward rupture of the surface at a weak point such as the re-entrant angle in section S8. The pressure in section S8 is now raised to atmospheric pressure whilst the pressure in the feeder is still low, or even negative. Thus feed liquid is now forced to flow from the casting into the feeder as freezing progresses. A massive pore then develops because feeder F3 has a large feed requirement, and drains section S8 and the surrounding casting. The defect size is worse than that which would have occurred if no feeder had been used at all!

Section S6 remains reasonably sound because it has the advantage of natural drainage of residual liquid into it. Effectively it has been fed from the heavy section S8. The pressure gradient due to the combined actions of gravity, shrinkage and the atmosphere from S8 to S6 is positive. The only reason why S6 may display any residual porosity may be that S8 is a rather inadequate feeder in terms of either its thermal requirement or its volume, or because the feed path may be interrupted at a late stage.

Section S7 cannot be fed because there is no continuous feed path to it. S9 is similarly disadvantaged. This has been an oversight in the design of the feeding of this casting. In a sand casting it is

likely that S7 and S9 will therefore suffer porosity. This will be almost certainly true for a steel casting, but less certain if the casting is a medium-freezing-range aluminum alloy. The reason becomes clear when we consider an investment casting, where, if a high mold temperature is chosen, and if the metal is clean, will allow solid feeding to operate, allowing the sections the opportunity to collapse plastically, and so become internally sound, provided that no pore-initiation event interrupts this action. Solid feeding is often seen in aluminum alloy sand castings, but more rarely in steel sand castings because of the greater rigidity of the solidified steel, which successfully resists plastic collapse in cold molds.

The exercise with the plastic coffee cup shows that the water will hold up indefinitely in the upturned cup until released by the pin causing a hole. The cup will then deliver its contents immediately (but not before!). Blind feeders are therefore often unreliable in practice because the atmospheric vent may not open reliably. Such feeders then act to suck feed metal from the casting, making any porosity worse.

If a blind feeder is provided with an effective atmospheric vent, then the available atmospheric pressure may help it to feed uphill. The atmosphere is capable of holding up several meters of head of metal. For liquid mercury the height is approximately 760 mm, being the height of the old-fashioned atmospheric barometer of course. Equivalent heights for other liquid metals are easily estimated allowing for the density difference. Thus for liquid aluminum of specific gravity 2.4 compared to liquid mercury of 13.9, the atmosphere will hold up about  $(13.9/2.4) \times 0.76 = 4$  meters of liquid aluminum or  $(13.9/7.0) \times 0.76 = 1.5$  m liquid iron.

Summarizing the maximum heights supportable by one atmosphere for various pure liquids near their melting points:

Mercury	0.760 m (the barometric height 760 mm = 1 atmosphere)
Steel	1.48 m
Zinc	1.58 m
Aluminum	4.36 m
Magnesium	6.54 m
Water	10.40 m

Whilst no pore exists, the tensile strength of the liquid will in fact allow the metal, in principle, to feed to heights of kilometers, since in the absence of defects the liquid can withstand tensile stresses of thousands of atmospheres. The liquid can, in principle, hang up in a tube, its great weight stretching its length somewhat. However, the random initiation of a single minute pore will instantly cause the liquid to 'fracture', causing the liquid in the tube to fall, finally stabilising at the level at which atmospheric pressure can support the liquid. Thus any height above that supportable by one atmosphere is clearly at high risk.

Moreover, there is even worse risk. If when attempting to feed against gravity there is a leak path to atmosphere, allowing atmospheric pressure to be applied in the liquid metal inside the solidifying casting, the melt will then fall further, the action of gravity tending to equalize levels in the mold and feeder. Thus, if the feeder is sited below the casting, the casting will completely empty of residual liquid. Regrettably, this is an efficient way to cast feeders of excellent soundness, but seriously porous castings.

Clearly, the initiation of a leak path to atmosphere (via a double oxide film, or via a liquid region in contact with the surface at a hot spot) is rather easy in many castings, making the whole principle of

uphill feeding so risky that it should not be attempted in circumstances where porosity cannot be tolerated. It is a pity that the comforting theories of pushing liquid uphill by atmospheric pressure or even hanging it from vast heights using the huge tensile strength of the liquid cannot be relied upon in practice.

For all practical purposes, the only really reliable way to feed is *downhill*, using gravity.

Thus feeding uphill is not altogether reliable, and cannot be recommended as a general technique. To restate the reasons briefly, this is because any initiation of a shrinkage or gas pore, or any inward rupture of the casting surface, will release the internal stress of the casting, removing the pressure difference between the casting and feeder. With the pressures in casting and feeder equalized, the metal level in the casting will fall, and that in the feeder will rise so as to equalize the levels if possible. The result is a porous casting. Blind feeders that are placed low on the casting can be unreliable in practice for this reason.

This loss of pressure difference cannot occur if the feeder is placed above the general level of the casting so that feeding always takes place with the assistance of gravity. Feeder F2 in Figure 10.35 would have successfully fed sections S2 and S4 either if it was taller or if it had been placed at a higher location, for instance on the top of S4.

It is clear that F3 may not have fed section S8 if the corner puncture occurred, even if it had been provided with an effective vent, because the pressure gradient for flow would have been removed. A provision of an effective vent, and the re-siting of the base of the feeder F3 to the side of S8, would have maintained the soundness of both S6 and S8 and would have prevented the surface puncture at S8. S7 and S9 would still have required separate treatment.

The conclusion to these considerations is: *place feeders high to feed downhill*. This is a general principle of great importance. It is of similar weight to the general principle discussed previously, *place ingates low to fill uphill*. These are fundamental concepts in the production of good castings.

### 10.6.3.7 Feeding Rule 7: Pressure requirement

The final rule for effective feeding is a necessary requirement like all the others. Sufficient pressure in the residual liquid within the casting is required to suppress both the initiation and the growth of cavities both internally and externally.

This is a *hydrostatic* requirement relating to the suppression of porosity, and contrasts with the previous pressure gradient requirement that relates to the *hydrodynamic* requirements for flow (especially flow in the *correct* direction!).

A fall in internal pressure may cause a variety of problems:

- Liquid may be sucked from the surface. This is particularly likely in long-freezing-range alloys, or from re-entrant angles in shorter-freezing-range alloys, resulting in internal porosity initiated from, and connected to, the outside.
- The internal pressure may fall just sufficiently to unfurl, but not fully open the population of bifilms. The population of bifilms will therefore remain effectively invisible. The result will be an apparently sound casting but, inexplicably, the mechanical properties will be poor, particularly the elongation and fatigue performance. (It is possible that some so-called 'diffraction mottle' may be noted on X-ray radiographs as a result of the newly appearing population of slightly opened cracks.)

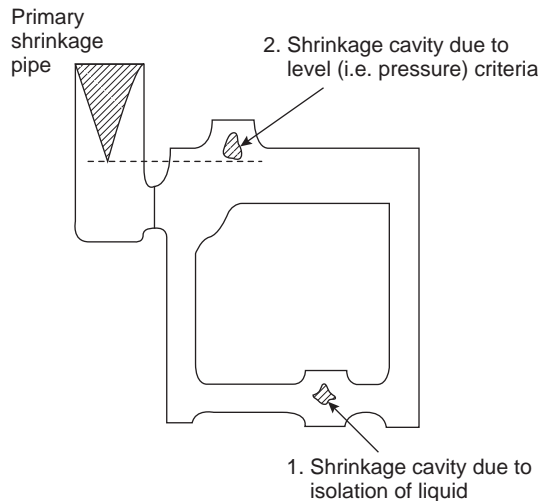


**FIGURE 10.36**

Pressure loss situations in castings leading to the possibility of shrinkage porosity.

- The internal pressure may fall sufficiently to open bifilms, so that a distribution of fine and dispersed microporosity will appear. The mechanical properties will be even lower. (For the technically fastidious, the mechanical opening of bifilms is driven not so much by pressure reduction, a *stress* phenomenon, but by the progression of shrinkage, a *strain* phenomenon experienced by the liquid.)
- The internal shrinkage may cause macro-shrinkage porosity to occur, especially if there are large bifilms present as a result of poor filling of the casting. Properties may now be in disaster mode and/or large holes may appear in the casting. Figure 10.36 illustrates pressure loss situations in castings that can result in shrinkage porosity. Figure 10.37 illustrates the common observation in Al alloy castings in which a glass cloth is placed under the feeder to assist the break-off of the feeder after solidification. Bafflingly, it sometimes appears that the cloth prevents the feeder from supplying liquid, so that a large cavity appears under the feeder. The truth is that double oxide films plaster themselves against the underside of the cloth as the feeder fills, keeping the bifilms in the casting, and ensuring that the feeder contains clean metal. The half of the bifilm against the cloth tends to weld to the cloth, possibly by a chemical fusing action, or possibly by mechanical wrapping around the fibers of the cloth. Whatever the mechanism, the action is to hold back the liquid above, whilst the lower half of the (unbonded) double film is easily pulled away by the contracting liquid, opening the void that was originally the microscopically thin interface of air inside the bifilm. Once again, bifilms are seen to interfere with the action of a feeder, and create the curious phenomenon of shrinkage porosity immediately under a feeder which remains completely full of (clean) metal.
- If there is insufficient opportunity to open internal defects, the external surface of the casting may sink to accommodate the internal shrinkage. (The occurrence of *surface sinks* is occasionally referred to elsewhere in the literature as ‘cavitation’; a misuse of language to be deplored. Cavitation properly refers to the creation and collapse of minute bubbles, and the consequent erosion of solid surfaces such as those of ships’ propellers.)

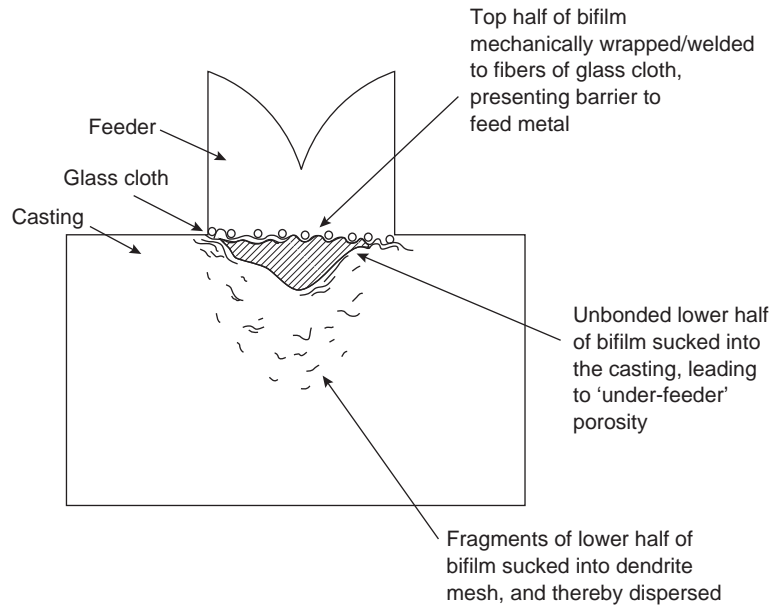


**FIGURE 10.37**

Apparent blocking of feed metal by a glass cloth strainer in an Al alloy casting because of bifilms collected on the underside of the cloth.

Often, of course, the distribution of defects observed in practice is a mixture of the above list. The internal pressure needs to be maintained sufficiently high to avoid all of these defects.

Finally, however, it is worth pointing out that over-zealous application of pressure to reduce the above problems can result in a new crop of different problems.

For instance, in the case of long-freezing-range materials cast in a sand mold, a high internal pressure, applied for instance to the feeder, will force liquid out of the surface-linked capillaries, making a casting having a 'furry' appearance. Overpressures are not easy to control in low-pressure sand casting processes, and are the reason why these processes often struggle to meet surface-finish requirements. Work at the University of Alabama (Stefanescu et al. 1996) on cast iron castings has shown that the generation of excess internal pressure by graphite precipitation can lead to exudation of the residual liquid via hot spots at the surface of the casting, leading to penetration of the sand mold. Later work on steels has shown analogous effects (Hayes et al. 1998).

In short-freezing-range materials the inward flow of solid can be reversed with sufficient internal pressure. Too great a pressure will expand the casting, blowing it up like a balloon, producing unsightly swells on flat surfaces (Figures 10.37 and 10.38).

### Feeding of cast iron castings by control of pressure

The successful feeding of cast irons is perhaps the most complex and challenging feeding task compared to all other casting alloys as a result of the curious and complicating effect of the expansion of graphite during freezing. The effects are most dramatically seen for ductile irons.

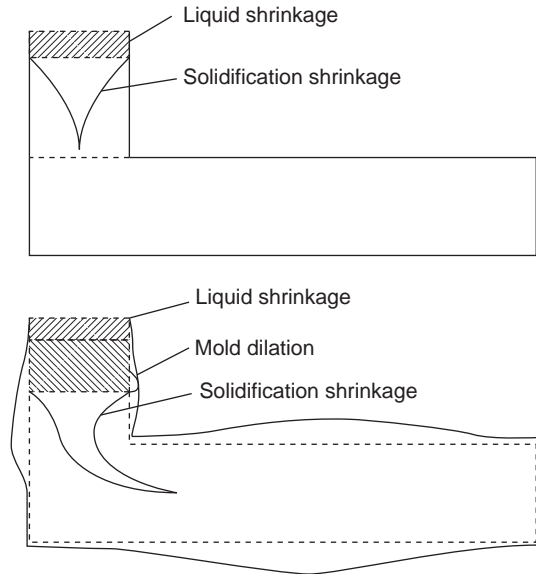


**FIGURE 10.38**

Comparison between the external size and internal shrinkage porosity in a casting as a result of (a) moderate pressure in the liquid, and adequately rigid mold; and (b) too much pressure and/or a weak mold.

The great prophet of the scientific feeding of ductile irons was Stephen Karsay. In a succession of engaging and chattily written books he outlined the principles that applied to this difficult metal (see for instance Karsay 1992, 2000). He drew attention to the problem of the swelling of the casting in a weak mold as shown in Figure 10.38, in which the valuable expansion of the graphite was lost by enlarging the casting, causing the feeder to be inadequate to fill the increased volume. He promoted the approach of making the mold more rigid, and so better withstanding stress, and at the same time reducing the internal pressure by providing feeders that acted as pressure relief valves. The feeder, after some initial provision of feed metal during the solidification of austenite, would reverse its action, back-filling with residual liquid during the expansion of the solidification of the eutectic graphite, relieving the pressure thus preventing mold dilation. The final state was that *both* the casting and feeder were substantially sound. (Occasionally, one hears stories that such sound feeders have been declared to be evidently useless, having apparently provided no feed metal. However, their removal would immediately cause all subsequent castings to become porous!)

The reproducibility of the achievement of soundness in ductile iron castings is, of course, highly sensitive to the efficiency of the inoculation treatment, because the degree of expansion of graphite is directly affected. This is notoriously difficult to keep under good control, and makes for one of the greatest challenges to the iron founder.

Roedter (1986) introduced a refinement of Karsay's pressure relief technique in which the pressure relief was limited in extent. Some relief was allowed, but total relief was prevented by the premature freezing of the feeder neck. In this way the casting was slightly pressurized, elastically deforming the

very hard sand mold, and the surrounding steel molding box (if any). The elastic deformation of the mold and its box would store the strain energy. The subsequent relaxation of this deformation would continue to apply pressure to the solidifying casting during the remainder of solidification. Thus soundness of the casting could be achieved, but without the danger of unacceptable swells on extensive flat surfaces. Even so, the use of strain energy is clearly seen to be vulnerable, because it can reverse only a very small amount of deformation as is explained below.

For somewhat heavier ductile iron castings, however, it has now become common practice to cast completely without feeders. This has been achieved by the use of rigid molds, now more routinely available from modern greensand molding units. Naturally, the swelling of the casting still occurs, since, ultimately, solids are incompressible. However, as before, the expansion is restrained to the minimum by the elastic yielding of the mold and its container, and distributed more uniformly. Thus the whole casting is a few percent larger. If the total net expansion was 3 volume %, this corresponds to 1 linear % along the three orthogonal axes, so that from a central datum, each point on the surface of the casting would be approximately 0.5% oversize. This uniform and very reproducible degree of oversize is usually negligible. However, of course, it can be compensated, if necessary, by making the pattern 0.5% undersize.

The use of the elastic strains to re-apply pressure is strictly limited because such strains are usually limited to only 0.1 linear % or so. Thus only a total of perhaps 0.3 volume % can be compensated by this means. This is, as we have seen above, only a fraction of the total volume change that is usual in a graphitic iron, and which permanently affects the size and dimensions of the casting. The judgment of feeder neck sizes to take advantage of such small margins is not easy.

With the steady accumulation of experience in a well-controlled casting facility, the casting engineer can often achieve such an accuracy of feeding that even such a modest gain is considered a valuable asset. Even so, the reader will appreciate that the feeding of graphitic irons is still not as exact a science and still not as clearly understood as we all might wish.

### Active feeding

Most feeding systems on castings are passive. They work by themselves without outside intervention. (Even those counter-gravity systems to which pressure is applied to enhance feeding are not considered to be 'active' in the sense discussed below.)

There has recently been introduced a novel system of feeding in which a side feeder is pressurized from an outside source of pressure and is thus encouraged to feed uphill (Figure 10.39). This approach to feeding was developed for use with automatic molding where molds could not be inverted through 180° after pouring. The concept appears to have proved useful within the context of fast, automatic greensand molding for aluminum alloy castings in a vertically parted mold, where the application of the pressurizing tubes can be automated, and where the casting sizes and weights are limited. Current problems with repeatability may be the teething problems of the new technique that remain to be completely solved by additional effort.

The counter-gravity filling of such molds has been a considerable advance in terms of attaining a high quality of metal in the mold cavity. It has also been useful because the space taken by the down sprue is now released as additional molding area.

The provision of small, compact feeders has been a similar benefit, saving mold space, although this is countered to some extent by the need for a direct line of access for the pressurizing tube to the top of the feeder. Greensand molds have been shown to develop useful temperature gradients in

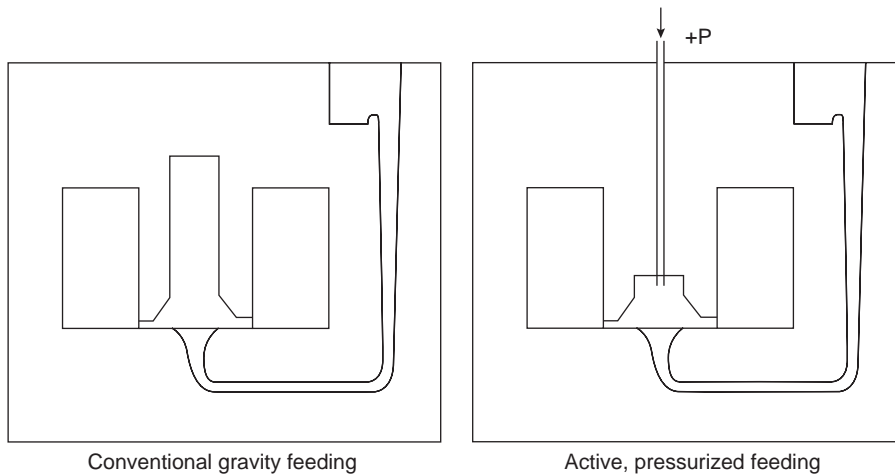


**FIGURE 10.39**

Active feeding in a vertically parted automatic greensand molding machine.

thin-walled aluminum alloy castings (Rasmussen et al. 1995). This natural gradient, the consequence of a good bottom-gating technique, is exploited by the bottom feeder.

It seems that the danger of convection reversing these advantages is small if the castings are of limited wall thickness and weight, which is the case for most casting produced on vertically-parted automatic molding machines. At the time of writing, the limits are not yet known. Clearly, at some point of increasing wall thickness and casting weight an extended solidification time will encourage the development of convection, and feeding uphill in such circumstances will become problematic, if not actually impossible.

Thus although active feeding has been investigated by computer simulation and shown to have attractive advantages, its application to sections of 15 mm thickness in Al alloys (Hansen 1994) seems likely to be close to, if not actually over, a limit at which convection will start to undo the benefits.

#### 10.6.4 The new feeding logic

Much of the formal calculation of feeders has been of poor accuracy because of a number of simplifying assumptions that have been widely used. Tiryakioğlu has pioneered a new way of analyzing the physics of feeding, having, in addition, the good fortune to have as a critical test the exemplary experimental data on optimum feeder sizes determined by his late father, Ergin Tiryakioğlu, many years earlier (1964). This was carried out at the University of Birmingham, UK, where Ergin and I shared an office for a time while we were both researching for our PhDs. The reader is recommended to the original papers by Murat Tiryakioğlu (1997–2002) for a complete description of his admirable logic. We shall summarize his approach only briefly here, following closely his excellent description (Tiryakioğlu et al. 2002).

As we have seen in Rules 2 to 4, an efficient feeder should (i) remain molten until the portion of the casting being fed has solidified (i.e. the solidification time of the feeder has to be equal to, or exceed, that of the casting), (ii) contain sufficient volume of molten metal to meet the feeding demand of that



same portion of the casting, (iii) not create a hot spot at the junction between feeder and casting. An optimum feeder is then defined as the one with the smallest volume, for its particular shape, to meet these criteria. A feeder that is less compact or that has less volume than the optimum feeder will result in an unsound casting.

The standard approaches to solve these problems have usually been based on the famous rule by Chvorinov (1940) for the solidification time of a casting is:

$$t = B(V/A)^n \quad (10.10)$$

where  $B$  is the mold constant,  $V$  is the casting volume,  $A$  is the surface area through which heat is lost, and  $n$  is a constant (2 in Chvorinov's work for simple shaped castings in silica sand molds). The  $V/A$  ratio is known as the modulus  $m$ , and has been used as the basis for a number of approaches to determining the size of feeders for the production of sound castings, as described in Feeding Rule 2.

Despite its wide acceptance, Chvorinov's Rule has limitations because of the underlying assumptions used in deriving the equation. As a result of these limitations, the exponent,  $n$ , fluctuates between 1 and 2, depending on the shape and size of the casting, and the mold and pouring conditions. One of the reasons for this anomaly is that Chvorinov's Rule originally did not take the shape of the casting into consideration. A new geometry-based model (Tiryakioğlu et al. 1997) proved that the modulus includes the effect of both casting shape and size. These two independent factors were separated from each other by the use of a shape factor  $k$  where

$$t = B' k^{1.31} V^{0.67} \quad (10.11)$$

and  $B'$  is the mold constant. The shape factor,  $k$ , is the ratio (the surface area of a sphere of same volume as the casting)/(the surface area of the casting). In Equation 10.11,  $V$  assesses the amount of heat that needs to be dissipated for complete solidification, and  $k$  assesses the relative ability of the casting shape to dissipate the heat under the given mold conditions:

$$k = A_s/A = 4.837V^{2/3}/A \quad (10.12)$$

where  $A_s$  is the surface area of the sphere.

Adams and Taylor (1953) were the first to consider *mass transfer* from feeder to casting. They realized that during solidification, a mass of  $\alpha V_c$  needs to be transferred from the feeder to the casting ( $\alpha$  is fraction shrinkage of the metal). However, as Tiryakioğlu (2002) explains, their development of the concept unfortunately introduced errors so that the final solution was not accurate.

Moreover, the lack of knowledge about the effect of *heat transfer* between a feeder and a casting has led the researchers to the mindset of considering the feeder and casting separately. In other words, almost all feeder models have been based on calculation of solidification times for the feeder and casting independently, and then assuming that the same solidification characteristics will be followed when they are combined. However, it should be remembered that the feeder is also a portion of the mold cavity and the solidifying metal does not know (or care) which portion is the casting and which is the feeder.

The objective of the foundry engineer when designing a feeding system is to have the thermal center of the total casting (the feeder-casting combination) in the feeder. In fact, all three requirements for an efficient feeder listed (i) to (iii) above can be summarized as a single requirement: *the thermal center of the feeder-casting combination will be in the feeder*. This new approach, which treats the casting-feeder combination as a single, total casting constitutes the foundation of Tiryakioğlu's new approach to characterize heat and mass transfer between feeder and casting.

The new approach

Let us consider a plate casting that is fed effectively by a feeder. Knowing that the solidification contraction of the casting is  $\alpha V_c$ , this volume is transferred from the feeder to the casting, resulting in the final volume of the feeder being  $(V_f - \alpha V_c)$ . Solidification contraction of the feeder is ignored since it does not change the heat content of the feeder. If the feeder has been designed according to the rules for efficient feeding, the last part to solidify in this combination is the feeder. In other words, the thermal center of the casting-feeder combination (the total casting) is in the feeder. Therefore the solidification time of the total casting is exactly the same as the feeder, and both have the same thermal center.

This is not true for the casting, however. The thermal center of the casting is also in the feeder, but its solidification time may or may not be equal to that of the total casting. Hence

$$k_t^{1.31} V_t^{0.67} = k_f^{1.31} (V_f - \alpha V_c)^{0.67} \quad (10.13)$$

where subscript  $t$  refers to the total casting. So far we have ignored the heat transfer between the casting and the feeder. Using optimum feeder data obtained by systematic changes in feeder size for an Al–12wt%Si alloy (Tiryakioğlu 1964) the solidification times of casting and feeder are compared in Figure 10.40a and total casting and feeder in Figure 10.40b. Figure 10.40a shows the  $(t_c - t_f)$  relationship when mass transfer is taken into account and heat transfer is ignored. It should be kept in mind that the scatter in Figure 10.40a is not due to experimental error since all values were calculated. Figure 10.40b shows the relationship between the solidification times of feeder and total casting (feeder + casting combination). Although the agreement in Figure 10.40b is encouraging, at low values the error is up to 30%. However, solidification time should be identical for the feeder and the total casting. The error is due to the neglect of the heat exchange between feeder and casting. Mass is transferred from the feeder to the casting throughout the solidification process. Solidification takes place over a temperature range, so that subtracting  $\alpha V_c$  from  $V_f$  adjusts for mass exchange completely, but for heat exchange this treatment assumes isothermal conditions, and therefore is not sufficient. Hence the feeder solidification time needs to be adjusted for the heat exchange with the casting. We can treat this heat exchange as if it were superheat extracted from/given to the feeder. For the superheat model, we will use the model by E. Tiryakioğlu (1964) for its simplicity and its independence from actual pouring temperature. Equation 10.13 can now be rewritten as:

$$k_t^{1.31} V_t^{0.67} = k_f^{1.31} (V_f - \alpha V_c)^{0.67} e^{\xi \Delta T_f} \quad (10.14)$$

where  $\xi$  is a constant dependent on the alloy ( $0.0028^\circ\text{C}^{-1}$  for Al–Si eutectic alloy (Tiryakioğlu 1964) and  $0.0033^\circ\text{C}^{-1}$  for Al–7%Si (Tiryakioğlu et al. 1997b)),  $\Delta T_f$  is the temperature change (rise or fall) in feeder because of the heat exchange, and can be easily calculated using Equation 10.14. The sum of change in heat content of the feeder and casting is zero (heat lost by one is gained by the other). Therefore

$$C (V_f - \alpha V_c) \Delta T_f + C (V_f + \alpha V_c) \Delta T_c = 0 \quad (10.15)$$

where  $C$  is the specific heat of the metal. Hence

$$\Delta T_c = (V_f - \alpha V_c) \Delta T_f / (V_f + \alpha V_c) \quad (10.16)$$

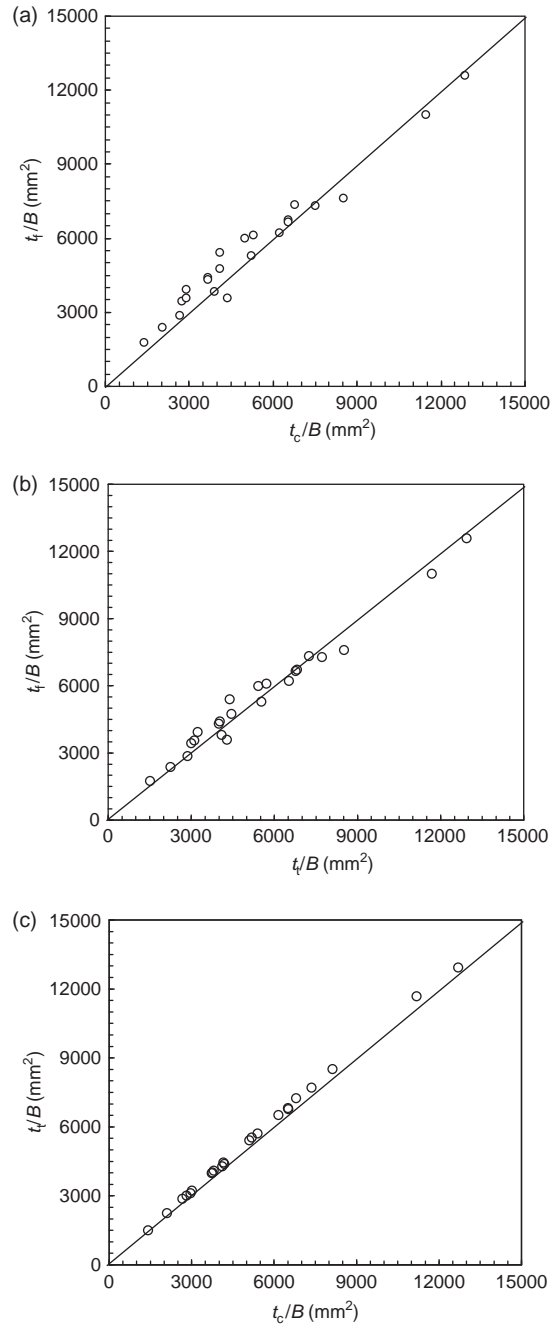


**FIGURE 10.40**

Comparison of calculated solidification times of (a) casting and feeder; (b) total casting and feeder; (c) total casting (or feeder) versus casting after adjustment to account for heat transfer between feeder and casting (Tiryakioglu et al. 2002).

The total solidification time of the casting can now be written as

$$t_c = k_c^{1.31} (V_f + \alpha V_c)^{0.67} e^{\xi \Delta T_c} \quad (10.17)$$

The solidification times of feeder and casting can now be compared. This comparison is presented in Figure 10.40c, which shows a practically perfect fit and a relationship that can be expressed as:

$$t_t = t_f = \alpha t_c \quad (10.18)$$

The data for Al–Si alloy shown in Figure 10.40c give  $\alpha = 1.046$ .

In a separate exercise, using the data for steel by Bishop and co-workers (1955) assuming  $\xi$  of  $0.0036^\circ\text{C}^{-1}$  for steel (Tiryakioğlu 1964), a similar excellent relationship is obtained where  $\alpha$  is found to be 1.005 (Tiryakioğlu 2002). Thus the solidification time of optimum-sized feeders in the feeder–casting combination was found to be only a few percent longer than that of castings both for Al–Si alloy and steel castings.

We can conclude that for an accurate description of the action of a feeder, both mass and heat transfer from feeder to casting during solidification have to be taken into account simultaneously. Previous feeder models that account for mass transfer assume that the transfer takes place isothermally and at the pouring temperature. This previous assumption overestimates the additional heat brought into the casting from the feeder. The new model incorporates the effect of superheat and is based on the equality of solidification times of feeder and total casting.

The requirements for efficient feeders – (i) solidification time; (ii) feed metal availability; and (iii) prevention of hot spot at the junction – can be combined into a single requirement when the casting–feeder combination is treated as a single, total casting. The three criteria reduce to the simple requirement: ‘The thermal center of the total casting should be in the feeder.’

The disarming simplicity of this conclusion conceals its powerful logic. It represents the ideal criterion for judging the success of a computer model of a casting and feeder combination.

### 10.6.5 Freezing systems design (chills and fins)

In this section on feeding, we are of course mainly concerned with the action of chills and fins to provide localized cooling of the casting. This is my first choice to avoid the planting of a feeder on a hot spot. I always try to avoid feeding.

Chills (or fins) can assist directional solidification of the casting towards the feeder, thus assisting in the achievement of soundness. Details of this thermal action are presented in Section 5.1.2 on Increased Heat Transfer.

Chills (or fins) also act to increase the ductility and strength of that locality of the casting. For some alloys this benefit to mechanical properties results from the well-known Hall-Petch effect associated with shortening slip distances, and the difficulty of re-initiating slip in the adjacent grain. However, it is more likely that most alloys will benefit most from the freezing of bifilms in their compact state. This justification of this conclusion is outlined in Section 9.4 on the mechanical properties of castings.

### 10.6.6 Feeding – the five mechanisms

The five feeding mechanisms – liquid, mass, interdendritic, burst and solid feeding – are different ways in which cast material can flow to feed the solidification contraction. The mechanisms are dealt with in

detail in Chapter 7. In general it is fair to state that only liquid, interdendritic and solid are important for our purposes of making sound castings. However, when relying on solid feeding for soundness there are precautions that it is wise to observe.

### Dangers of solid feeding

The great benefit of solid feeding is that a casting can be made sound, even though it demands feed metal but cannot be fed by liquid from a conventional feeder. In favorable conditions, the casting can collapse plastically; the shrinkage volume is merely transferred from the inside to the outside of the casting. Here, if the volume is distributed reasonably evenly over a large area of the casting, the shrinkage will cause only a negligible and probably undetectable reduction in the size or shape of the casting.

This feeding benefit is commonly gained in light alloy castings, which are relatively weak at their freezing points, and so collapse rather easily; no large internal tensile stresses are generated so that pores are not necessarily created internally. Similarly, the easy collapse of weak solid is found in many ferrous and higher temperature alloys in investment casting, where the high mold temperature retains the plasticity of the solidified skin of the casting.

There are, however, dangers in relying on solid feeding for the soundness of a casting, as are illustrated in Figure 9.25c.

1. If the outside shrinkage is not distributed so favorably, but remains concentrated in a local region, a surface sink is the result. This may, of course, result in a portion of the casting being out of tolerance, possibly no longer cleaning up on machining, so that the casting is scrapped.
2. When operating without feeders, a second possibility is the formation of shrinkage pores, grown from initiation sites (almost certainly bifilms), so that solid feeding immediately fails. It seems that such events tend to be triggered by rather large bifilms such as arise from random variations in pouring techniques. The achievement of soundness using solid feeding then becomes a hit-and-miss affair.
3. A further possibility is that much smaller bifilms will be common, but not easily perceived. If the melt has a distribution of small, possibly microscopic, bifilms, these will be unfurled to some extent by the reduced pressure in the unfed region thus being converted from crumpled compact features of negligible size to flat thin extensive cracks. Thus although the casting may continue to appear perfectly sound in the unfed region, and solid feeding declared to be a complete success, the mechanical properties of this part of the casting will be reduced. In particular, although the yield strength of the region will be hardly affected, that part of the casting will exhibit reduced strength, ductility and fatigue resistance.
4. If the localized shrinkage problems are even more severe, the distribution of small bifilms will develop further. After unfurling to become flat cracks, additional reduction of pressure in the liquid will open them further to become visible microporosity. The pores may even grow to such a size that they become visible on radiographs. This situation is common in steel castings where the high strength of the solidified skin creates large internal stresses, providing irresistible forces to open bifilms and thus bring solid feeding to a halt.

In contrast to these dangers, the action of a feeder to pressurize the melt and so help to resist the unfurling and even the inflating of bifilms is seen to be some kind of benefit. The bifilms, although still present, remain out of sight. Using a domestic analogy from home decoration, there is a very real sense in which adding feeders to castings is almost literally 'papering over the cracks'.

However, this rather severe censure is not completely valid, in the sense that closed bifilms in a casting do exhibit some strength because they can withstand shear stress (although, of course, not tensile stress at right angles to the bifilm). The pressure provided by the (liquid) feeder has a valuable role in keeping the bifilms closed.

### 10.6.7 Computer modeling of feeding

Good computer models have demonstrated their usefulness in being able to predict shrinkage porosity with accuracy, and have therefore brought about a revolution within the industry. A simulation using a reliable modeling software package should now be specified as a prior requirement to be carried out before work is started on making the tooling for a new casting. This minor delay has considerable benefits in shortening the overall development time of a new casting, and greatly increases the chance of being 'right first time'.

However, the limitations of some computer simulations require to be recognized. For instance these include:

- (i) no allowance for the effect of thermal conduction in the cast metal (rare nowadays);
- (ii) no allowance for the important effects due to convection in the liquid (common);
- (iii) neglect of, or only crude allowance for, the effect of the heating of the mold by the flow of metal during filling (now commonly addressed);
- (iv) no capability of any design input. Thus gating and feeding designs will be required as inputs (just beginning to be addressed at this time).

For the future, it is to be expected that software packages will evolve to provide intelligent solutions to all these requirements. Examples of a good start in this direction are shown by Dantzig and co-workers (Morthland 1995, McDavid 1998). In the meantime, it remains necessary to use computer models with some discretion. For instance in the work by the Morthland team they warn that the results are specific to the feeding criterion used. If a more stringent temperature gradient criterion were used (for instance  $2 \text{ K cm}^{-1}$  instead of  $1 \text{ K cm}^{-1}$ ) the feeder would have been larger.

The above approaches to the optimization of the feeding requirements of castings have involved the use of numerical techniques such as finite element and finite difference methods. Ransing et al. (2003) propose a geometrical method based on an elegant extension of the Heuvers circle technique. This technique was described above in the section describing the feed path requirements for feeding.

### 10.6.8 Random perturbations to feeding

It is helpful if the computer simulation indicates that the casting solution is as robust as possible. This is because on the foundry floor, a number of practical issues conspire to change the casting conditions, and thus threaten the quality of the casting.

In aluminum castings, flash of approximately 1 mm thickness and only 10 mm wide has been demonstrated to have a powerful effect on the cooling of local thin sections up to 10 mm thick, speeding up local solidification rates by up to ten times. The effect is so much reduced in ferrous castings because of their much lower thermal conductivity that any effect of cooling by fins is practically negligible.

Thus for high conductivity alloys flash has to be controlled, or used deliberately, since, in moderately thick sections, it has the potential to cut off feeding to more distant sections. The erratic appearance of flash in a production run may therefore introduce uncertainty in the reproducibility of feeding, and the consequent variability of the soundness of the casting. Flash on very thick sections is usually less serious because convection in the liquid in thick sections conveys the local cooled metal away, effectively spreading the cooling effect over other parts of the casting, giving an averaging effect over large areas of the casting. In general, however, it is desirable that these uncertainties are reduced by good control over mold and core dimensions.

The other known major variable affecting casting soundness in sand and investment castings is the ability of the mold to resist deformation. This effect is well established in the case of cast irons, where high mold hardness is a condition for soundness. However, there is evidence that such a problem exists in castings of copper-based alloys and steels. A standard system such as statistical process control (SPC), or other technique, should be seen to be in place to monitor and facilitate control of such changes. Permanent molds such as metal or graphite dies are relatively free from such problems. Similarly many other aggregate molding materials are available that possess much lower thermal expansion rates, and so produce castings of greater accuracy and reproducibility. Many of these are little, if any, more expensive than silica sand. A move away from silica sand is already under way in the industry, and is strongly recommended.

The solidification pattern of castings produced from permanent molds such as gravity dies and low pressure dies may be considerably affected by the thickness and type of the die coat which is applied. A system to monitor and control such thickness on an SPC system should be seen to be in place.

For some permanent molds, pressure die casting and some types of squeeze casting the feeding pattern is particularly sensitive to mold cooling. After the development and acceptance of the casting, any further changes to cooling channels in the die, or to the cooling spray during die opening, will have to be checked to ensure that corresponding deleterious changes have not been imposed on the casting. The quality of the water used for cooling also requires to be seen to be under good control if deposits inside the system are not to be allowed to build up and so cause changes in the effectiveness of the cooling system with time.

### 10.6.9 The non-feeding roles of feeders

Feeders are sometimes important in other ways than merely providing a reservoir to feed the solidification shrinkage during freezing.

We have already touched on the effect that feeders can have on the metallurgical quality of cast metal by assisting to restrain the unfurling and opening of bifilms by maintaining a pressure on the melt. This action of the feeder to pressurize the casting therefore helps to maintain mechanical properties, particularly ductility and fatigue strength.

A further key role of many feeders, however, is merely as a flow-off or kind of dump. Many filling system designs are so poor that the first metal entering the mold arrives in a highly damaged condition. The presence of a generous feeder allows some of this metal to be floated out of the casting. This role is expected to be hindered, however, in highly cored castings where the bifilms will tend to attach to cores in their journey through the mold.

In general, experience with the elimination of feeders from Al alloy castings has resulted in the casting 'tearing itself apart'. This is a clear sign of the poor quality of metal probably resulting mainly

from the action of the poor running system. The inference is that the casting is full of serious bifilm cracks. These remain closed, and so invisible, whilst the feeder acts to pressurize the metal. If the pressurization from the feeder is removed the bifilms will be allowed to open, becoming visible as cracks. This phenomenon has been seen repeatedly in X-ray video radiography of freezing castings. It is observed that good filling systems do not lead to the casting tearing itself apart, even though the absence of a feeder has created severe shrinkage conditions. In this situation the casting shrinks a little more (under the action of solid feeding) to accommodate the volume difference.

The action of the feeder to pressurize the melt during solidification is useful in further ways. Both summarizing and thinking further we have:

- (i) As we have seen, pressurization raises mechanical properties, particularly ductility.
- (ii) Pressurization together with some feeding helps to maintain the dimensions of the casting. Although the changes in dimensions by solid feeding are usually small, and can often be neglected, on occasions the changes may be outside the dimensional tolerance. A feeder to ensure the provision of liquid metal under some modest pressure is then required.
- (iii) Pressurization can delay or completely prevent blow defects from cores.

In summary, providing the filling system design is good so as to avoid creating large bifilms, and provided the solidification rate is sufficiently fast to retain the inherited population of bifilms compact, castings that do not require feeders for feeding should not be provided with feeders.

## 10.7 RULE 7: 'AVOID CONVECTION DAMAGE'

### 10.7.1 The academic background

Convection is the flow phenomenon that arises as a result of density differences in a fluid.

In a solidifying casting the density differences in the residual liquid can be the result of differences in solute content as a consequence of segregation. This is a significant driving force for the development of channel defects known as the 'A' and 'V' segregates in steel ingots and as freckle trails in nickel- and cobalt-base investment castings. The name 'freckles' comes from the appearance of the etched components that shows channels containing randomly oriented grains that have been partly remelted in the convecting flow and detached from their original dendrites. Although, for many reasons, channel defects are unwelcome, they are usually not life threatening to the product. These defects are discussed earlier in Section 5.3.4 and are not discussed further here.

Convection can also arise as a result of density differences that result from temperature differences in the melt. There have been numerous theoretical studies of the solidification of low-melting-point materials in simple cubical molds, of which one side is cooled and the other not. The resulting gentle drift of liquid around the cavity, down the cool face and up the non-cooled face, changes the form of the solidifying front. A schematic example is shown in Figure 10.41. These are interesting exercises, but give relatively little assistance to the understanding of the problems of convective flow in engineering systems.

The results due to Mampaey and Xu (1999) who studied the natural convection in an upright cylinder of solidifying cast iron showed that the thermal center of the liquid mass was shifted upwards, and graphite nodules in spheroidal graphite irons were transported by the flow. Such studies reflect the gentle action of convection in small, simple-shaped, closed systems; the kind of action one would



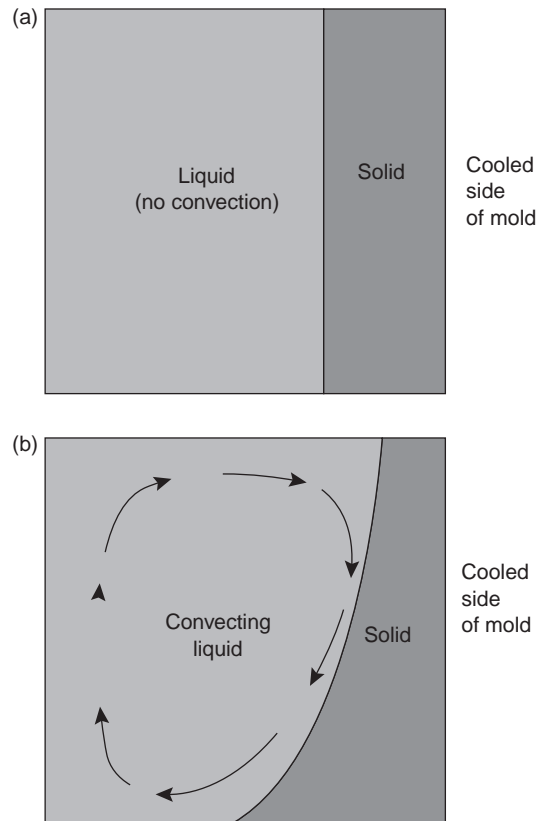


**FIGURE 10.41**

Solidification in a 2-D box of which only the right-hand side is cooled: (a) planar front growth in the case of no convection; (b) the distortion caused by convective flow.

expect to see in a cooling cup of tea. These facts have lulled us into a state of false security, assuming convection to be essentially harmless and irrelevant. We need to think again.

### 10.7.2 The engineering imperatives

Convection was practically unknown as an important factor in shaped castings until the early 1980s. Even now, it is not widely known or understood. However, it can be life and death to a casting, and has been the death of a number of attempts to develop counter-gravity casting systems around the world. Most workers in this endeavor still do not know why they failed. The Cosworth Casting Process nearly foundered on this problem in its early days, only solving the problem by its famous (infamous?) roll-over system.

Thus convection is not merely a text-book curiosity. The casting engineer requires to come to terms with convection as a matter of urgency. The problem can be of awesome importance, and can lead to major difficulties, if not impossibilities, to achieve a sound and saleable casting.

Convection enhances the difficulty of uphill feeding in medium section castings, making them extremely resistant to solution. In fact increasing the amount of (uphill) feeding by increasing the diameter of the feeder neck, for instance, makes the feeding problem worse by increasing the opportunity for convection. Many of the current problems of low-pressure casting systems derive from this source.

In contrast, having feeders at the top of the casting, and feeding downwards under gravity is completely stable and predictable, and gives reliable results.

The instability of convective problems when filling and feeding uphill is worth emphasizing. Because the heavy, cool liquid overlays the hotter less dense liquid, the situation is metastable. If the stratified layers of liquid are not disturbed there is a chance that the heavy liquid will remain wobbling around on the top, and may solidify in place without incident. However, a small disturbance may upset the delicate balancing act. Once started, the cold melt will slip sideways, plunging downwards to the bottom, and the hot liquid surge upwards, so that a convective circulation will quickly establish. In practice therefore, a number of castings may be made successfully if the metastable equilibrium is not disturbed, but, inexplicably, the next may exhibit massive remelted and unfed regions.

Triggers to initiate the unstable flow could arise from many different kinds of uncontrolled events. A significant trigger could be an event such as the rising of a bubble from a core blow, as a result of an occasionally ill-fitting of a core print, leading to the chance sealing of the core vent by liquid metal.

Momchilov (1993) gives one of the very few accounts of the exasperating randomness of convection problems. He found that with the use of two riser tubes from a furnace containing liquid metal into one die cavity, successive castings could be observed to have completely different internal temperature histories. The first casting might be fine. However, the subsequent casting would suffer a die temperature inexplicably overheating by 120°C and the temperature in the furnace simultaneously dropping by 65°C. These are powerful and important exchanges of heat between the die and the crucible below. These changes caused the second casting to be partially remelted.

The use of twin riser tubes by Momchilov raises an important feature of convection. Convective flows require to be continuous, as in a circulation. Thus in the case of two riser tubes into one die cavity, the conditions for a circular flow, up one tube and down the other, are ideal. It is likely that Momchilov would have solved his problem, or at least greatly reduced it, simply by blocking off one of the tubes.

The elimination of ingates in this way to solve convection problems in counter-gravity *fed* castings should be considered as a standard *first* step. This was found to be a useful measure in the early days of the Cosworth Process when it operated merely as a static low-pressure casting process. (The later development of the roll-over concept represented a welcome total solution.)

The only other description of the problems of convection ever discovered by the author comes from a patent by Rogers and Heathcock (1990). They fall foul of convection during the attempt to make an aluminum alloy cylinder block casting in a counter-gravity filled permanent mold. They found that as the mold heated up the problem became worse, and the rate of flow of the convection currents increased. The microstructure of the casting was unacceptable in the area affected by convection. They dealt with the problem by providing strong cooling just above the ingates. This solution clearly threatened the provision of feed metal whilst the casting was solidifying, and so was a risky strategy. There is no record that the patent was ever implemented in production. Perhaps convection secured another victim.

Castings that employ a third mold part to site the running system under the casting are at risk of convective effects causing the melt to circulate up some ingates and down others via the casting above and the runner underneath. This is especially dangerous if the runner is a heavy section. Pressurizing the runner with an adequate feeder is a way of maintaining the net upward movement of metal required for the feeding of the casting, thus reducing the deleterious effects of the convection to merely that of delaying freezing. In this case the worst that happens is the development of a locally coarser structure.

Investment casting often provides numerous convective loops in wax assemblies, as a result of attaching the wax patterns at more than one point to increase the strength of the complete wax assembly. A typical wax assembly for the casting of polycrystalline Ni-base turbine blades is illustrated in Figure 10.42a. The central upright is surrounded by six blades (only two are shown in the section), so that in addition to its heavy section designed to act as a feeder, it is kept even hotter by the presence of the surrounding blade castings that prevents loss of heat by radiation. Conversely, of course, the blades cool quickly because they can radiate heat freely to the cool surroundings. A convective loop is therefore set up, with hot metal rising up the central feeder, and falling through

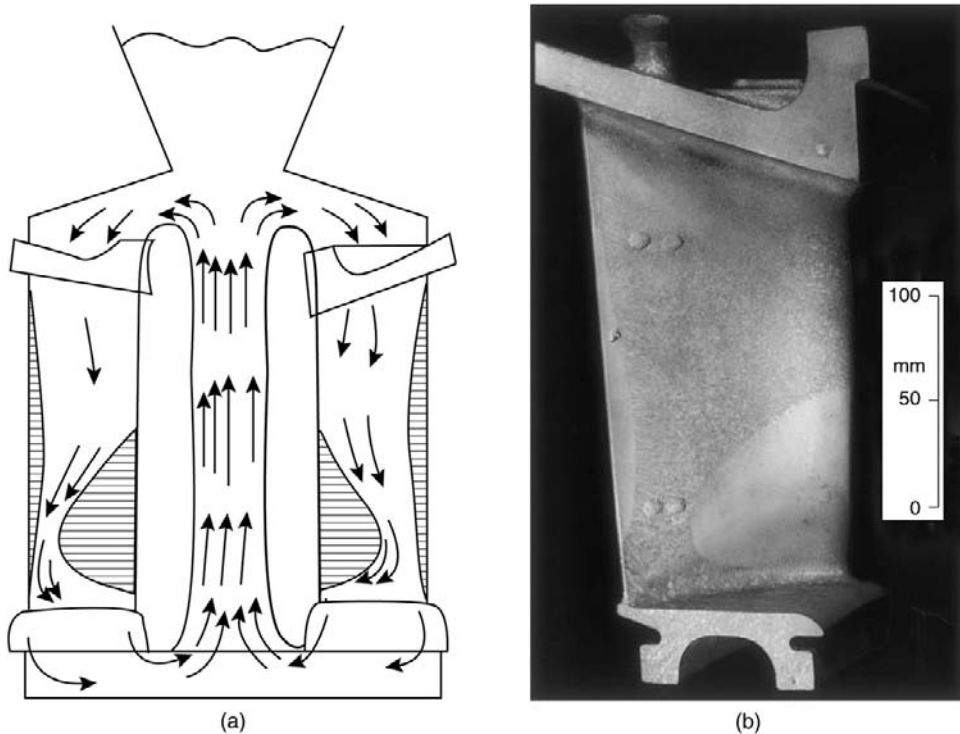


**FIGURE 10.42**

(a) Lost wax assembly of six Ni-base turbine blades around a central feeder, showing the expected convective loops; (b) an etched blade showing the remelting of the fine surface grains created by the cobalt-aluminate nucleant in the mold surface, and the subsequent growth of coarse grains that define the patches where the flow paths impinged on the casting surface.

the cooling castings. The final grain structure seen on the etched component reveals the path of the flow (Figure 10.42b). The casting is designed to have fine surface grains nucleated by the cobalt-aluminate addition to the primary coat of the mold. However, because hot metal enters the mold cavity from the top, sweeping down through the casting after the chill grains are formed, the original chill grains are remelted in those patches where the flow brushes against the walls. The flow becomes a concentrated channel as it exits the base of the blade. The very narrow section of the trailing edge of the casting is not penetrated, and so escapes remelting, as does the large region in the bottom right that the flow has missed.

Very large blades for the massive land-based turbines for power generation are sometimes cast horizontally. In this case each end of the casting is subject to convective problems as is seen in Figure 10.43.

The cutting of convective links in wax assemblies is recommended, and cries out for wide attention in most current investment casting operations. The strengthening of wax assemblies by wax links inadvertently provides convective links and should be avoided. Ceramic rods can provide strengthening, or, if wax connections are used, they should be plugged with a ceramic disc to avoid metal flow. These simple modifications to the wax assembly will completely change the mode of solidification of the castings, allowing for the first time an accurate understanding of filling and feeding effects.

Other problems in sand castings are illustrated in Figure 10.44. Gravity die (permanent mold) castings are less prone to these problems because of their more rapid rate of heat extraction by the metal mold. For castings in metal molds the sections have to be considerably larger before convection starts to be a threat. Figure 10.45 shows the convection effects from side or bottom feeding, compared to the relative stability of top feeding.

It is evident that many computer predictions of heat flow and the feeding of castings will be quite inadequate to deal with convection problems, since it is usual to consider the loss of heat from castings

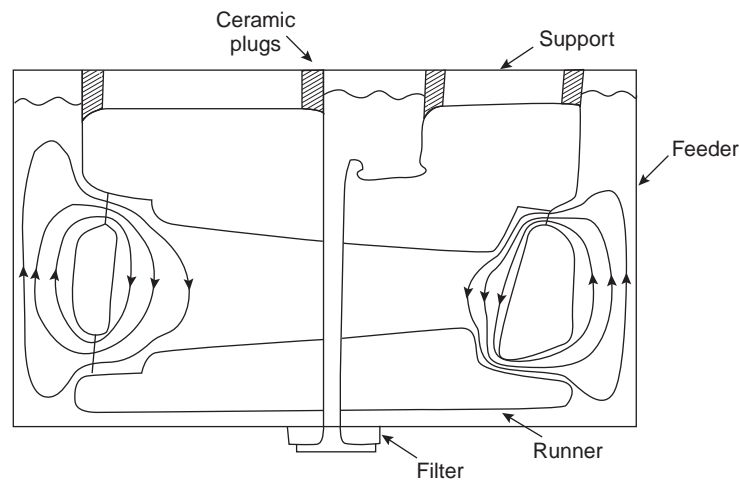


**FIGURE 10.43**

Horizontal orientation of a large investment-cast turbine blade, illustrating convective loops in the root and shroud. The flows convey heat from the cylindrical feeders, remelting regions of the casting.

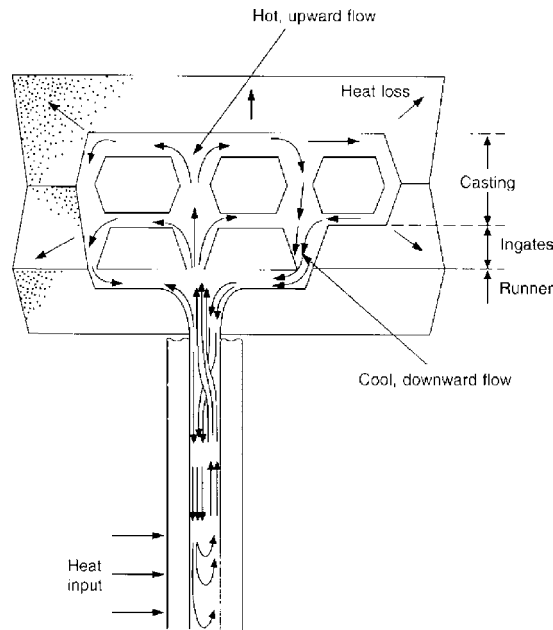


**FIGURE 10.44**

Convection-driven flow within a solidifying low-pressure sand casting.

simply by conduction. Clearly, thicker sections in a loop will cool more quickly than the computer would predict, since convection allows them to export their heat. Conversely, of course, thin sections in the same loop will suffer the arrival of additional heat that will greatly delay their solidification. In fact, if the hot section has an independent source of heating, such as the electrical heating provided in many counter-gravity systems, the sections in the loop can circulate for ever. The computer would have particular difficulty with this.

Even so, the greater speed and sophistication of computing will eventually provide the predictions containing the contribution of convection that are so badly needed. It is hoped that future writers and founders will not need to lament our poor abilities in this area.

### 10.7.3 Convection damage and casting section thickness

If the solidification time of the casting is similar to the time taken for convection to become established, extensive remelting can be caused by convective flows. Serious damage to the micro- and macro-structure of the casting can then occur. The time for convection to start appears to be in the region of 1 or 2 minutes. In 3 or more minutes convection can become well established, causing extensive remelting and a major redistribution of heat in castings.

Castings that freeze in a time either shorter than 1 minute, or longer than perhaps 10 minutes, are expected to be largely free from convection problems as indicated below.

Thin section castings are largely free from convection difficulties. They can therefore be fed uphill simply because the thin section gives (i) the viscous restraint of its nearby walls makes any convective

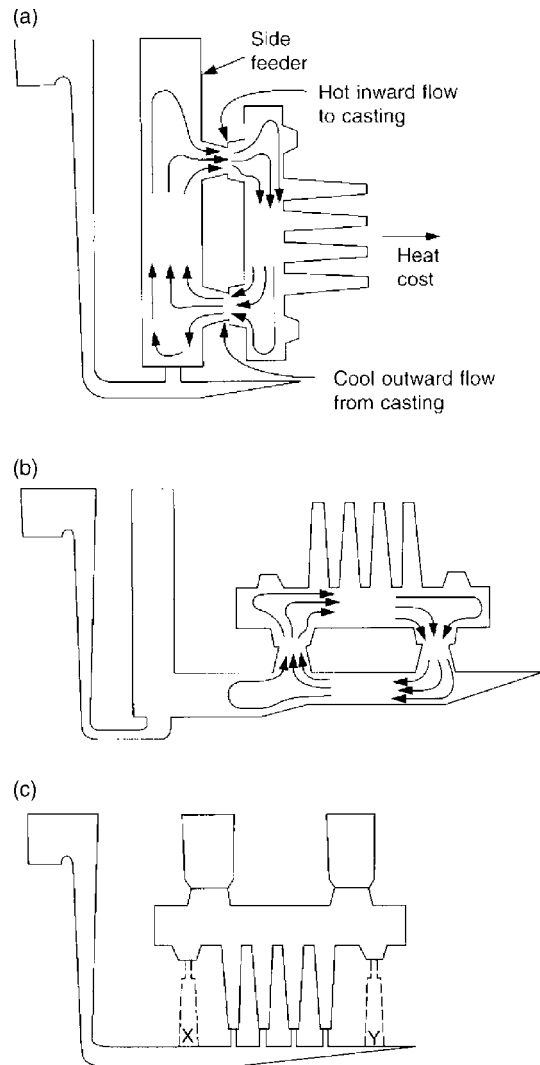


**FIGURE 10.45**

Encouragement of thermal convection by (a) side feeding; (b) bottom feeding; (c) its near elimination by top feeding.

tendency more difficult, and (ii) more rapid freezing allows convection less time to develop and wreak damage in the casting. Thus instability is (i) suppressed and (ii) given insufficient time, respectively, so that satisfactory castings can be made.

Conversely, thick section castings taking perhaps 10 minutes to 10 hours to freeze are also relatively free from convection problems, because the long time available before freezing allows the metal

plenty of time to convect, re-organizing itself so that the hot metal floats gently into the feeders at the top of the casting, and the cold metal slips to the bottom. All this activity occurs and is complete before any significant amount of solidification has occurred. Thus the system reaches a stable condition before damage can be caused. Once again, castings are predictable.

In what can only be described as a perverse act of fate, convection does its worst in the most common sizes of castings, the problem emerging in a serious way in the wide range of intermediate section castings. These include the important structural castings such as automotive cylinder heads, cylinder blocks and wheels, and the larger investment cast turbine blades in nickel-based alloys amongst many others. Convection can explain many of the current problems with difficult and apparently intractable feeding problems with such common products. The convective flow takes about one or two minutes to gather pace and organize itself into rapidly flowing plumes. This is occurring at the same time as the casting is attempting to solidify. The flows cut channels through the newly solidified material, remelting volumes of the casting.

The channels will contain a coarse microstructure because of their greatly delayed solidification, and in addition may contain shrinkage porosity if unconnected to feed metal. This situation is likely if the feeders solidify before the channels as undoubtedly happens on occasions, because the channels derive their energy for flow from some other heat source, such as a very heavy section low down on the casting, or the ingate attached to the riser tube of a counter-gravity system for instance.

For conventional gravity castings that require a lot of feed metal, such as cylinder heads and blocks, and which are bottom gated, but top fed, this will dictate large top feeders, because of their inefficiency as a result of being furthest from the ingates, and so containing cold metal. This is in contrast to the ingate sections at the base of the casting that will be nicely preheated. The unfavorable temperature regime is of course unstable because of the inverted density gradient in the liquid, and thus leads to convective flow, and consequent poor predictability of the final temperature distribution and effectiveness of feeding. It is the standard legacy of bottom filling: the favorable filling conditions leading to the worst feeding conditions. Life was never easy for the casting engineer.

The upwardly convecting liquid within the flow channels usually has a freezing time close to that of the pre-heated section beneath, which is providing the heat to drive the flow. In the case of many low-pressure systems, the metal supply system is artificially heated, leading to a constant heat input, so that the convecting streams rising out of these regions never solidify. This is what happened to the Cosworth system in the early days of its development. When the mold and casting (which should by now have been fully solidified) was hoisted from the casting unit liquid poured from the base of the mold, emerging from such remelted channels to the amazement of onlookers who had assumed that after the appropriate length of time for solidification, no liquid could possibly still be present, and present in such quantity.

When removing a convecting casting from a counter-gravity filling system in this way, the draining of liquid from the interdendritic regions leaves regions in the casting that appear convincingly like shrinkage defects, and are usually confused as such.

The convection of hot metal up and the simultaneous movement of cold metal down the riser tube of a low-pressure casting unit delays the freezing of the casting in the mold above, and can lead to a significant reduction in productivity. A thermocouple in the riser tube reveals the chaotically varying temperature of the swirling eddies of hot and cold pockets of liquid.

The author is aware of a casting being made on a low-pressure machine whose freezing time kept increasing as the melt was subjected to increasingly thorough rotary degassing treatment. It

seems that each rotary degassing treatment reduced the amount of bifilms in suspension. As the effective viscosity of the melt was progressively reduced in this way the convection increased, extending the time taken for the casting to solidify. Thus clean metal is free to convect, whereas melt with an internal semi-rigid lattice of bifilms will be more resistant to flow. It is perhaps superfluous to add that reliance on the inhibition of convection by filling the liquid with oxides to increase viscosity cannot be recommended.

#### 10.7.4 Countering convection

Solutions to the problems of convection are summarized as follows.

##### Roll-over

The inversion of the mold after casting effectively converts the preheated bottom ingate filling system into a top feeding system, thus gaining a really efficient feeding system.

Furthermore, of course, the massive technical benefit of the inversion of the system to take the hot metal to the top, and the cold at the bottom, confers stability on the thermal regime. Convection is eliminated. For the first time, castings can be made reliably without shrinkage porosity.

Batty (1935) was well ahead of this time, using the roll-over technique for steel castings. He showed by careful measurement of the temperature gradient the reasons for his success to convert 'troublesome' steel castings to 'reliable' steel castings.

The massive productivity and economic benefit of this technique when applied to Al aggregate molded castings follows because the mold now contains its liquid metal all below the entry point, allowing the mold to be removed from the casting station without waiting for the casting to freeze (which is of course the standard productivity delay suffered by most counter-gravity casting processes). In this way cycle times can be reduced from about 5 minutes to below 1 minute. This is a powerful and reliable system used by such operations as the Cosworth Process which achieved the casting of a mold containing two cylinder blocks every 45 seconds. We can hope that techniques involving roll-over *immediately after* casting will become the norm for most medium-sized castings in the future.

##### Tilt casting

Those tilt casting processes in which the roll-over is used *during* casting actually to effect the filling process can also satisfy the top feeding requirement.

However, in practice care is needed because many geometries are accompanied by waterfall effects, if only by the action of the sliding of the metal in the form of a stable, narrow stream down the sloping side of the mold. Thus meniscus control is, unfortunately, often poor. Where the control of the meniscus can be improved to eliminate entrainment problems, tilt casting techniques are valuable. Ultimately, if the tilt is controlled to perfection, a kind of horizontal transfer of the melt can be achieved. This system does not seem difficult or costly to attain, and is to be recommended strongly.

##### Cut convective loops

Explore the elimination of ingates on counter-gravity feeding of castings. The widespread use of convective loops in investment castings wax assemblies should be reduced by the wider use of ceramic supports and stops.



## 10.8 RULE 8: 'REDUCE SEGREGATION DAMAGE'

Section 5.3 describes the many mechanisms whereby concentration of solutes can be enhanced or depleted in some regions of the casting during the short time of solidification.

Microsegregation between dendrite arms is, as we have seen, a necessary consequence of normal freezing of an alloy, but the fine scale of the effect allows a significant amount of redistribution during subsequent homogenizing and solutionizing heat treatments.

The various forms of macrosegregation, on the other hand, are irreversible and have to be lived with. They can sometimes be sufficiently serious to threaten the serviceability of the casting, and in any case will threaten to scrap the casting if the composition is found to be outside the specification limits in places, whether or not this is important for the function of the casting. (At this time the founder has to live with the injustice of castings rejected for illogical or unreasonable objections, even though destructive testing to simulate service conditions would in principle provide evidence of the complete harmlessness of most deviations from overtight specifications.)

One of the most common of macrosegregation problems is that arising from dendritic freezing, in which the positively partitioning solute is concentrated against a cooling surface. In sand castings the effect is rarely a problem because of the relatively small temperature gradients, but can be serious in metal molds and when using metallic chills. Thus the use of chills requires caution in those alloys prone to segregation. In addition, the use of a fin or a pin can simulate the action of a chill so as to give a local segregation effect.

For Al alloys segregation is not usually a problem, especially in alloys such as those based on the Al-Si-Mg system. However, for those Al alloys that contain Cu, particularly if the Cu content is in the region of 4.5 to 5.5%Cu, the variations in Cu content throughout a casting can be serious.

Figure 10.46a gives an instance. Dendritic segregation will lead to a concentration of Cu at a chill face, but an opposite pattern adjacent to the feeder. Both regions can easily be well outside specification. A reduced section thickness can act as a cooling fin, and so simulate the action of a chill, causing a peak in Cu segregation adjacent to the fin as shown in Figure 10.46b. However, just inside the fin, the conditions are those of a thin section casting joined on to a heavy section, thus delaying freezing, so that the opposite pattern of segregation is to be expected. This steep change in composition

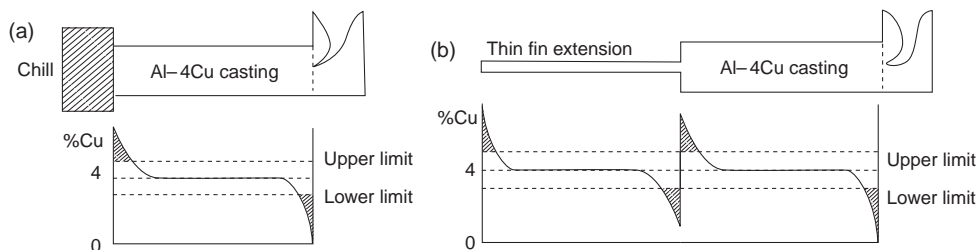


**FIGURE 10.46**

(a) Dendritic segregation pattern, concentrating solute against a chilled face; (b) analogous pattern produced by a reduction in section thickness acting as a cooling fin.

will, of course, result in a correspondingly large variation in mechanical properties, particularly after heat treatment. It is a concern that these large changes in strength, possibly from brittle to ductile behavior, are concentrated at the change in section at which externally applied stress will also be concentrated. These effects do not appear to have been investigated so far, but clearly should be explored. Design rules for avoiding or reducing these problems would be welcome.

The other macrosegregation effect that is troublesome in slowly cooled castings is the channel defect. This arises from the effect of gravity on the solute in the dendrite mesh, causing liquid high in solute to migrate, organizing its flow into channels that remelt a pathway through the mesh. The effect has been countered in some alloy developments by the design of more neutral buoyancy into the segregated melt. However, this luxury is not normally open to the majority of castings that have to conform to a chemical specification, even though the specification is often rather arbitrary and rarely of any consequence for the satisfactory operation of the product in service.

Channel segregates appear also to concentrate bifilms, as evidenced by the numbers of cracks that can occur in these lengthy pencil-like channels. The bifilms will be pushed into these regions. Later, when most of the casting is solid, the highly segregated liquid in the channel will remain liquid as a result of its low melting point. The local high gas content in solution, and the local reduction in pressure due to the problems of feeding down such long channels, partly blocked by tumbling melted-off grains (the 'freckles' when viewed by sectioning and etching) will combine to unfurl and expand the bifilms, creating planar cracks across the width of the channel. The cracks are, of course, much more serious than the segregates themselves.

The vigorous operation of channel segregates in heavy steel castings funnels low density solutes, mainly high in carbon, into the feeder head of the casting. Unfortunately this segregated liquid accumulating in the feeder is not harmlessly put away, but awaits its turn to degrade the casting at a later stage, when the feeder comes into operation to feed the solidification shrinkage in the body of the casting. At this stage the high carbon liquid is drawn down into the casting, giving a carbon-rich region immediately below the feeder (Figure 10.47). The effect is countered to some degree by the diameter of the feeder. Clearly, in the extreme, a feeder of the same diameter of the casting would cause minimal segregation. However, this is clearly not a particularly useful solution but may indicate that a modest increase in feeder diameter might be helpful, and a narrow orifice breaker core may do more harm than good. Faster freezing of the casting would help most. The founder needs to be aware of this solute pattern, and may ultimately have to target the fine balance between too little carbon in the steel and too much beneath the feeder. Our computer programs are not capable of simulating these effects at this time. Once again, the foundry engineer would greatly benefit from some quantitative guidance from a program of carefully conducted research.

The under-feeder segregation is compared and contrasted with the opposite thermal condition: an under-fin condition giving some more complexity overall, but similar results, if on a smaller scale, in the casting (Figure 10.47b). Naturally, and under-chill condition is similar. The fin and pin actions are not likely to be noticeable in steel castings as a result of the poor thermal conductivity, but the situation is likely to be non-trivial in Al, Mg and many Cu alloys.

A final observation on segregation is important. All segregations take time to build up. Thus reducing the time available by almost any method is a valuable and powerful general strategy to reduce macrosegregation. The provision of additional chills arranged to reduce the temperature gradients that would have been set up by a single chill, especially using internal chills if possible, is strongly recommended. If the customer would agree, a move to a less segregating alloy would also be an effective strategy.

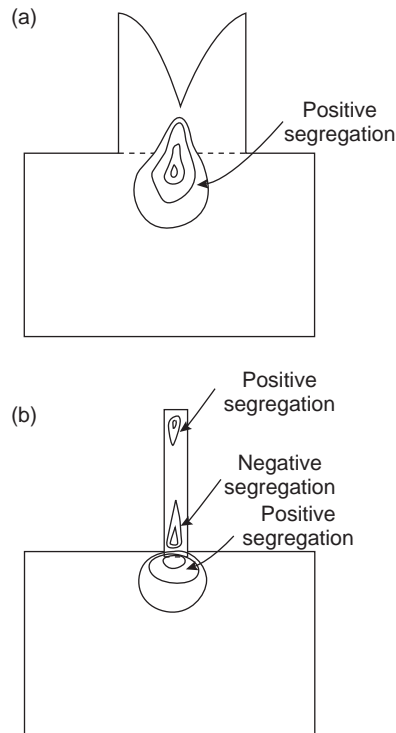


**FIGURE 10.47**

(a) Positive segregation under a feeder; (b) positive segregation under a cooling fin, but negative closely adjacent inside the fin. These extremes of concentration of solute are both close to a vulnerable change in section, where stress may be concentrated.

## 10.9 RULE 9: 'REDUCE RESIDUAL STRESS'

### 10.9.1 Introduction

Unfortunately, it seems that in general the engineering community have not been made aware of the potentially awesome importance of residual stress in the manufacturing of engineering components. All manufactured components contain internal stress, often high. The problem is that this very real danger is invisible.

Most foundries and machining operations have stories about the casting that flew into pieces with a bang when being machined, or even when simply standing on the floor! Benson (1946) describes one such event. The author and several colleagues narrowly missed the shrapnel from an aluminum alloy compressor housing that exploded in their midst while being cut on a band saw.

It is easy to disregard such stories. However, they should be viewed as warnings. They warn that, in certain conditions, castings can have such high stresses locked inside that they are dangerous and unfit for service. In fact they can act like small bombs. We are unaware that the casting may be on the brink of catastrophic failure because, of course, the problem is invisible; the casting looks perfect.

There are those metallurgists within the industry, some eminent, and whose opinions on other matters I respect, that have taken issue with me. They have argued that the presence of residual stresses, particularly those from quenching, are actually irrelevant since the whole component is in balance with its own stresses. The question of overall balance is certainly true. However, this argument overlooks the fact that the *distribution* of stress is usually far from uniform, and parts of the component may be near to their failure stress even prior to the application of any service stress. Usually, as we shall see, the major tensile stress is in the center, and it is this part of the component that fails first under tensile load.

Admittedly, not all components are necessarily endangered by internal stress. Indeed, in some cases the stress can be beneficial (some examples are given below). However, in general, the risk exists that the stress may not be beneficial. The residual stress may add to the service stress and so promote premature failure at only low service stress, to the bewilderment of the designer who imagines the material of his component to be uniform and who has completely overlooked the possibility that the part contains invisible threats from stresses. Because of the complexity of some castings, and the complexity of the state of stress, it is usually not easy to estimate the magnitude of either the internal residual stress or its precise action. Often, however, it is at least equal to or exceeds the yield stress. Thus it is not trivial. In fact at this level it will dominate all other designed loads. If the casting is in a fatigue condition, it will certainly lead to early failure. It is ignored at our peril.

This section takes a look at the wide spectrum of stresses in castings, and attempts to clarify those that are important and which should be controlled, in contrast to those that can be safely neglected.

### 10.9.2 Residual stress from casting

There have been a number of test pieces that have been used over the years to help assess the parameters affecting the residual stress in castings. Most of these are based on the form of the three-bar frame casting shown in Figure 10.48.

In practice the stress remaining in the casting is usually assessed by scribing two lines on the central bar and accurately measuring their spacing. The bar, of length  $L$ , is then cut between the lines, and, usually, the cut ends spring apart as the cut is completed. The distance between the lines is then measured again and the difference  $\Delta L$  is found. The strain  $\epsilon$  is therefore  $\Delta L/L$  and the stress  $\sigma$  is simply found, assuming the elastic (Young's) modulus  $E$ , by the definition:

$$E = \sigma/\epsilon \quad (10.18)$$

Such studies have revealed that the residual stress in castings is a function of the cooling rate in the mold, as shown for aluminum alloy castings from the effect of water content of the mold in Figure 10.49. Dodd (1950) cleverly illustrated that this effect is not the result of the change of mold strength by preparing greensand molds with various water contents, then drying each carefully so that they all had the same water content. This gave a series of molds with greatly differing strengths. When these were cast and tested there was found to be no difference in the residual stress in the castings. This result was further confirmed by testing castings made in molds rammed to various levels of hardness. Again, no significant difference in residual stress was found.

Dodd (1950) also checked the effect of casting temperature, and noted a small increase in residual stress as casting temperature was increased.

As with cases of the constraint of the casting by the mold, removing the casting from the mold at an early stage would be expected to be normally beneficial in reducing residual stress. Figure 10.50 shows

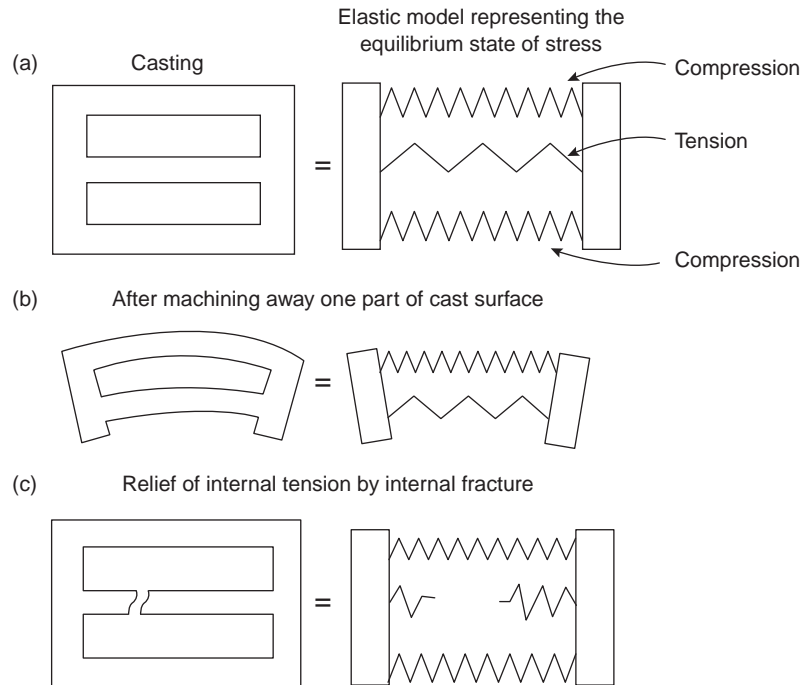


**FIGURE 10.48**

Heyn's (1914) model of the balance of internal stresses after rapid cooling: (a) quenched casting showing high internal tensile stress and relatively low external compressive stress; (b) the distortion of the casting after one side is machined away; and (c) the common condition of internal tensile failure.

the result for iron and a high-strength aluminum alloy. The higher residual stress for cast iron reflects its greater rigidity and strength. The effects of percentage water in the sand binder, and of stripping time and casting temperature, have been confirmed in other work on high strength aluminum alloys and gray iron using a rather different three-bar frame (IBF Technical Subcommittee 1949, 1952). It is noteworthy that all these direct measurements show casting stresses to be modest; only approximately 10% of the yield strength.

All these observations appear to be explainable assuming that the main cause of the development of residual stress is the interaction of different members of the casting cooling at different rates. Beeley (1972) presents a neat solution to the problem.

The strain  $\Delta L/L$  due to differential contraction is determined by the temperature difference  $\Delta T$  and the coefficient of thermal expansion of the alloy  $\alpha$ . Thus we have the strain

$$\varepsilon = \Delta L/L = \alpha \Delta T \quad (10.19)$$

and so from Equation 10.18 the stress is

$$\sigma = \alpha E \Delta T \quad (10.20)$$

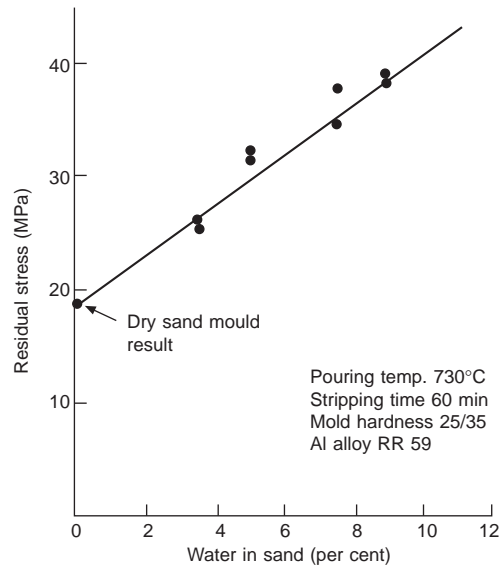


**FIGURE 10.49**

Internal stress in the center member of a three-bar frame as a function of water content of the greensand mold (Dodd 1950).

The stress therefore depends on the temperature difference between members. It is also worth noting that the stress is independent of casting length  $L$ .

A rather different result illustrating the influence of the geometry of the three-bar frame casting was found by Steiger (1913). He measured the increase of stress in the center bar of gray iron castings after increasing the rigidity of the end cross members. He found that a center bar of more than twice the diameter of the outer bars would suffer a residual stress of over 200 MPa, sufficient to fracture the bar during cooling. Working Equation 10.20 backwards, it is quickly shown that the temperature difference was only about 100°C to produce this failure stress. Clearly, such temperature differences will be common in castings, and often exceeded. Thus high stresses may be expected for some castings. Even so, this conclusion was reached from very early work (1913), and should really be confirmed with modern techniques and equipment before we place too much faith in this result.

In ferrous castings that experience a gamma to alpha (austenite to ferrite) phase change during cooling, any stresses that are built up prior to this event are probably reduced, their memory diluted by the plastic flow that the transformation causes. It seems probable therefore that the temperature differences and cooling rates applying below the gamma-alpha-transformation temperature that are the most important for the final remaining levels of stress in these steels.

This fact prompts Kotsyubinskii (1961) to recommend that heavy sections of ferrous castings be cooled by forced air or chills to equalize their cooling rates with those of the thinner sections, up to the point at which the pearlite reaction occurs. Below this temperature, little can be done to avoid the build-up of stress. This is because the metal is largely elastic, and plastic relaxation, occurring only slowly by creep, becomes progressively less effective; thus cooling should at that stage be slow and even, so as to take advantage of as much natural stress relief as possible.

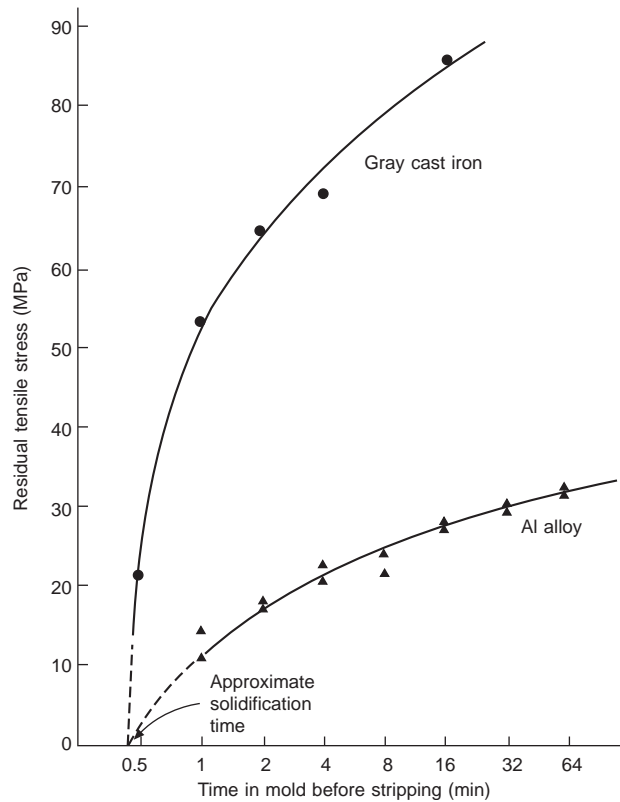


**FIGURE 10.50**

Residual stress in Al alloy and gray iron castings as a function of stripping time. Data from Dodd (1950) and IBF Technical Committee (1949).

In an aggregate mold, castings are cooled relatively slowly, so that the final internal stress in the product will normally be relatively low, and can often be neglected (although the possible exception warned by Steiger above is noted). It is true that the dimensions of the casting will often be changed by stress during cooling, but on shaking out from the mold the final, residual, stress will not normally be high. In addition, the distortions that have arisen during cooling in the mold are usually extremely reproducible. This is a consequence of the reproducible conditions of production, in which the mold is the same temperature each time, and the metal is the same temperature each time, so that the final shape is closely similar each time. This reproducibility is probably greater than for any other casting process.

This repeatable regime is not quite so well enjoyed by the various kinds of die casting, particularly gravity die (permanent mold) casting, as a result of many factors, but in particular the variability of mold size and shape as a result of variation of mold temperature. The somewhat faster cooling, particularly because of the earlier extraction of the casting from the mold, is an additional factor that does not favor low final stress.

In general, internal stress remaining from the casting process is rarely high enough to be troublesome but we cannot always be complacent about this. The ability to predict stresses using computer simulation will be invaluable to maintain a cautious watch for such dangers.

Ultimately, however, particularly for aluminum alloys, the stresses from casting are usually eliminated by any subsequent high temperature solution heat treatment which acts as an excellent stress-relieving treatment.

In confirmation, Benson (1938) made the important commonsense generalization that it is the last thermal treatment, and the rate of cooling from this final treatment, that is important so far as residual stresses are concerned. Thus the last treatment might simply be casting, or annealing, or quenching from a solution treatment. Having considered casting, we shall now turn our attention to subsequent treatments.

### 10.9.3 Residual stress from quenching

If, when quenching castings from a high temperature heat treatment, the time for cooling the outer sections of castings is shorter than the time required for heat to diffuse out from interior sections, the outer parts of the casting therefore cool to form a rigid frame that can contract to squash the hot, weak, plastic central features to shorter lengths. Later, the inner sections, now somewhat smaller in length, will cool, gathering strength and contracting further, but this late contraction will suffer the restraint of the outside sections that have by now become cold and rigid. Thus the interior sections, now also strong and rigid, go into tension, forcing in turn the outer parts into compression. Thus the major problems of internal tensile stress and distortion of the casting are usually created at this time.

Furthermore, the stresses are not significantly reduced by a subsequent aging treatment. The temperatures and times for aging treatments are too low to lead to stress relief.

It is unfortunate that many heat treatments require a quenching stage, intended to cool the casting sufficiently quickly to freeze solutes into a solid solution, thereby preventing them from precipitating too early, and thus still being available for controlled precipitation during the aging treatment. If the quench is slow some solute may be lost by precipitation from solution, thus making it unavailable for subsequent hardening reactions, so that the final strength of the casting is reduced. This reasoning has driven metallurgists to seek quenching rates as fast as possible.

The problem has been that all such research by metallurgists to optimize heat treatments has been carried out on test bars of a few millimeters in diameter that represent no problem to cool quickly. The outside and inside of the bars are in excellent thermal communication, and the high thermal conductivity of most metals ensures that the cooling throughout the section is essentially uniform. Thus the world's standards on heat treatment often dictate water quenching to obtain the highest material properties.

Quite clearly, the problem of larger components, or certain components of special geometrical complexity in which uniform cooling is an impossibility, has been overlooked. This is a most serious oversight. The performance of the whole component may therefore be undermined by the application of these techniques that have been optimized by research on small test bars, and which therefore are inappropriate, if not actually dangerous, for many large and complex components.

This is such a common problem that when a troubled casting user telephones me to say words to the effect 'My aluminum alloy casting has broken. What is wrong with it?' my standard, and rather tired, reply now is 'Do not bring the casting to me. I will tell you *now* over the telephone why it has failed.



It has failed because it has been poured badly and therefore contains bifilms that reduce its strength. However, in addition, you have carried out a solution heat treatment accompanied by a water quench.' The caller is usually stunned, incredulous that I know that water has quenched his casting, and asks how I know. My experience is this: in all my life investigating the causes of failure of perhaps hundreds of Al alloy castings, only one failed because of serious embrittlement caused as a result of the alloy being outside chemical specification. All the rest failed for only two reasons; (i) weakening by bifilms, together with (ii) massive internal stresses that have loaded the already weakened casting close to its failure stress even before any service stress was applied.

I have to record, with some sadness, that all the standard metallurgical investigations into casting failures that I see appear completely irrelevant; they include such costly and time-consuming activities as the determination of the chemical specification, the metallurgical structure, the mechanical properties such as hardness and other standard metallurgical tests. It underlines the importance of understanding the new metallurgy of cast metals in which the residual stresses and bifilms together play the dominating roles in the performance of engineering components, particularly cast engineering components. It is necessary to sympathize with the metallurgist attempting to carry out the traditional failure investigation, since both these dominating macroscopic defects are hard to detect: the stress is perfectly invisible, and the bifilms are mostly invisible.

Equation 10.20 explains why not all shapes and sizes of castings necessarily suffer a problem. Compact or small castings, and those for which the quenchant can easily reach all parts, are often not seriously affected, because  $\Delta T$  is necessarily small. It is essential to remember this: not all castings are seriously affected by quench stresses.

However, for those castings that are affected by uneven temperatures during cooling, it is salutary to estimate the actual magnitude of the strain  $\epsilon$ . For aluminum the coefficient of expansion  $\alpha$  is about  $20 \times 10^{-6} \text{ K}^{-1}$  and the temperature fall during a quench is approximately 500 K. The strain works out to be therefore approximately as  $20 \times 10^{-6} \times 500 = 10^{-2} = 1\%$ . For steels  $\alpha$  is approximately  $14 \times 10^{-6}$ , and the temperature change for quench from many heat treatments is in the region of 900 K, again giving a strain close to 1%. Since the yield (or proof) strain is only approximately 0.1%, these imposed quench strains are about *ten times* the yield strain. These dramatic strains can therefore be seen to take the component well into the plastic deformation range.

For steels with elongations to failure of perhaps 30–50%, the imposition of 1% strain is usually not a serious threat to the serviceability of the casting, even though the corresponding stress is very high. However, for many Al alloys, with only 1 or 2% elongation to failure, the imposition of 1% strain can be highly threatening. The comforting thought for the future is that as elongations for Al alloys approach those of steels because of the steady improvement of cleanness, the danger of residual stress in such castings will decrease.

In the meantime, casting geometries that are particularly susceptible include large, thick section castings, where the heat of the interior takes time to reach the outside of the casting, giving high  $\Delta T$ . Ingots or other block-type products can be seriously stressed for this reason. DC ingots (Direct Chill continuously cast) of aluminum alloys are severely cooled by water, but are often over 300 mm diameter. Whilst sitting on the shop floor waiting further processing the strong 7000 series alloy ingots have sometimes been known to explode like bombs. (As an aside, the length of time taken before the ingot decides to fail is curious and interesting. It seems likely that the failure under the high internal stresses is initiated from one of the large bifilms that is expected to be entrained during the turbulent start of casting. The gradual precipitation of hydrogen into the bifilm will gradually increase the

pressure in the bifilm crack, encouraging it to extend as a stress crack. The hydrogen may be already in solution in the metal, or may be gradually accrued by reaction with water vapor in the atmosphere during storage, especially if part of an extensive bifilm is near to the ingot surface where it can receive hydrogen by diffusion from the outside surface, but is therefore able to distribute the pressurized gas over the whole area of the bifilm to create significant stress at the sharp edges of the defect. Other penetrating contaminants may include air to cause additional internal oxidation, or fluxes, or traces of chlorine gas, or sulfides from greases, to act as surface active additions to reduce the surface energy of the metal and so further encourage crack growth. Research to clarify these possibilities would be valuable.)

Other varieties of castings that are susceptible to damaging levels of residual stress include those that are hollow, with limited access for the quenchant into the interior parts of the casting, and which also have interior geometrical features such as dividing walls and strengthening ribs (Figure 10.51). This latter series of geometrical requirements might seem to be an unlikely combination of features that would eliminate most castings. Perhaps surprisingly therefore, the list of castings that fulfill these requirements is rather long, and includes such excellent examples as automotive cylinder heads and blocks, and housings for components such as compressors and pumps. When immersed in the water quench, the water attempts to penetrate the entrances into the hollow interior of the casting. However, because the casting is originally above 500° C, any water that succeeds in entering will convert almost instantaneously to steam, blowing out any additional water that is attempting to enter. The result is that the outside of the casting in contact with the quenchant cools rapidly, whereas the interior can cool only at the rate that thermal conduction will conduct the heat along the tortuous path via interior walls of the casting to the outer surfaces.

The rate of conduction of heat from the interior to the exterior of the casting can be estimated from the order of magnitude relation

$$x = (Dt)^{1/2} \quad 10.21$$

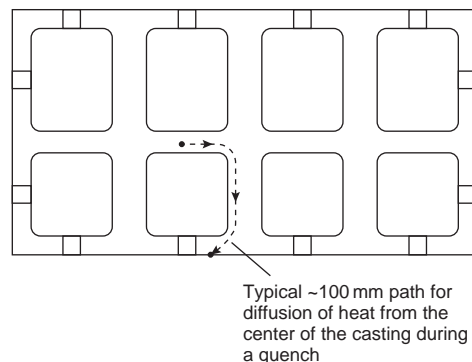


**FIGURE 10.51**

Schematic representation of a hollow casting with internal walls and small ports to the outside world, such as an automotive cylinder head, illustrating the long diffusion path for heat from its center during a quench, leading to internal residual tension.

where  $x$  is the average diffusion distance,  $D$  is the thermal diffusivity of the alloy, and  $t$  is the time taken. The thermal diffusivity is defined as

$$D = K/\rho C \quad 10.22$$

where  $K$  is the thermal conductivity, about  $200 \text{ W m}^{-1} \text{ K}^{-1}$  for aluminum, the density  $\rho$  is about  $2700 \text{ kg m}^{-3}$  and the specific heat  $C$  is approximately  $1000 \text{ J kg}^{-1} \text{ K}^{-1}$ . These values yield a value for the thermal diffusivity  $D$  close to  $10^{-4} \text{ m}^2 \text{ s}^{-1}$ . (The corresponding value for steel is approximately  $10^{-5} \text{ m}^2 \text{ s}^{-1}$ .) Equation 10.21 is used to generate Figure 10.52 in which the distance for diffusion of heat out of a product indicates the approximate boundaries of safe regimes constituting conditions in which sufficient time is available for the diffusion of heat from the interior during the quench. The time of cooling in different quenchants is provided by results such as those shown in Figure 10.53. These results were obtained by siting a thermocouple in the center of a 10-mm wall of an Al-7Si-0.4Mg alloy casting. Comparative results would be valuable for ferrous materials.

For Al alloys the temperature range of approximately  $500^\circ\text{C}$  down to  $250^\circ\text{C}$  appears to be the critically important range during cooling, since any beneficial effects of solute retention occur in this range and little can be affected at temperatures below  $250^\circ\text{C}$ .

For a solid aluminum bar of 20 mm diameter (approximately equivalent to a solid plate of 10 mm thickness) Figure 10.53 indicates that quenching in water will reduce the temperature in its center from  $500$  to  $250^\circ\text{C}$  in about 5 seconds. Substituting 5 s in Equation 10.21 shows that on average heat will have traveled 20 mm in this time. The 20-mm bar or 10-mm plate will both therefore enjoy a reasonably uniform temperature so that minimal stress will be generated.

As stated above, this situation is common in such castings as automotive cylinder heads, whose links between the internal sections and the outside world are via small holes in the outer walls and tortuous routes around the water jackets. The total distance that heat now has to diffuse is of the order of 100 mm. The walls of the casting are 10 mm or less, so that the cooling of the exterior of the casting will again occur in a time of the order of 5 seconds. However, Figure 10.53 indicates that approximately 100 seconds is required for the heat to diffuse the 100 mm distance from the inside to the

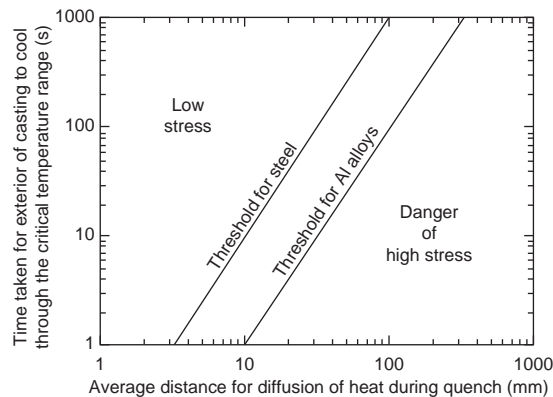


**FIGURE 10.52**

Regime for low stress in terms of quench rate and distance for heat flow.

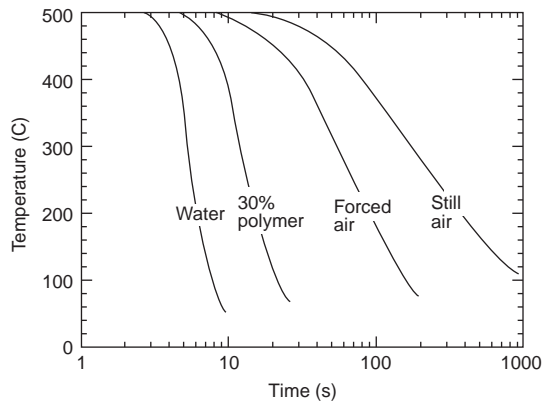


**FIGURE 10.53**

Quench rates in a 10-mm-thick Al plate casting in a variety of quench media.

outside. This long delay in the cooling and contraction of the interior of the casting will be expected to result in a high internal tensile stress.

#### 10.9.4 Controlled quenching using polymer and other quenchants

Figure 10.53 shows that there are other intermediate quenching rate options available. The use of water, whilst being cheap and environmentally pleasant, causes problems for the quenching of most alloys, whether light alloys or ferrous. The rapidity of the quench is not suitable for larger parts, especially hollow parts with internal structures, as we have seen above. In addition to this problem, water gives an uneven and non-reproducible quench because of its boiling action. When the parts are immersed in the water they are at a temperature hundreds of degrees above the boiling point. Thus the water in contact with the hot surface boils, coating it with a layer of vapor that conducts heat poorly, temporarily insulating that area whilst surrounding areas that may happen to remain in contact with the water continue to cool rapidly via a nucleate boiling regime (Figure 10.54; this figure is the result of an investigation by Xiao et al. (2010) with a window-frame-shaped casting of 122 mm<sup>2</sup> with sections of 10–25 mm). The pattern of contact varies rapidly and irregularly as the vapor film forms and collapses in the turbulent water. Agitation of the water is often used to even the cooling effect as far as possible. However, Figure 10.54 shows that agitation has an effect only on the vapor blanket stage but is not a major effect, and has no effect at all on the nucleate boiling stage when heat transfer occurs at maximum rate.

Thus the resulting stress pattern in the casting is complex and different from casting to casting. This is expected to be especially true when the castings are stacked closely in a heat treatment basket, since those in the center of the basket will experience quite different cooling conditions to those on the outside.

To overcome the blanketing action of the vapor, liquids with higher boiling point such as oils have been used. However, the flammability hazard and the smoke and fumes have caused such quenchants to become increasingly unacceptable. Cleaning of the casting after the quench is also an environmental problem. Water-based solutions of polymers have therefore become widely used. They are safer and

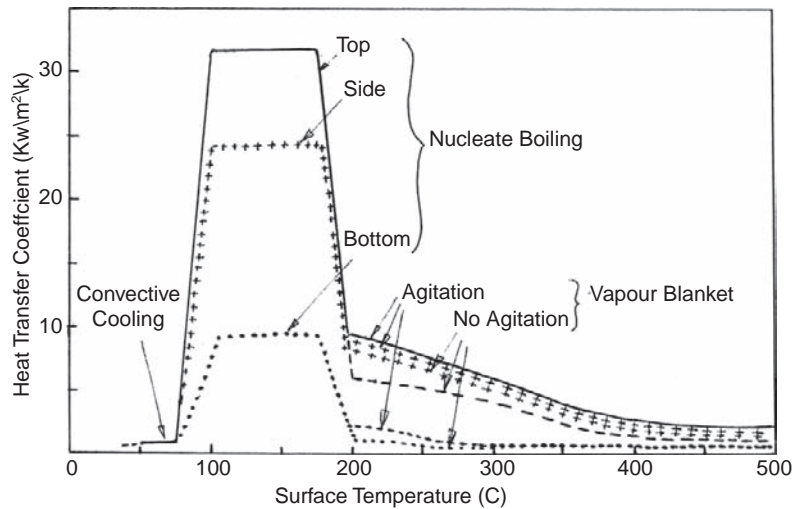


**FIGURE 10.54**

Heat transfer coefficient (HTC) measured for a small frame casting quenched into water at 50°C. HTC is a strong function of temperature and orientation, but is relatively little influenced by agitation except at high temperature (smoothed data from Xiao et al. 2010).

somewhat less unpleasant in use. Fletcher (1989) reviews their action in detail. We shall simply consider a few general points.

Some polymers are used in solution in water and appear to act simply by the large molecular weight and length of their molecules increasing the viscosity and the boiling point of the water. Such viscous liquids are resistant to boiling and so provide a more even quench, with the quenchant remaining in better contact with the surface of the casting.

Sodium polyacrylate solution in water produces cooling rates similar to those of oils. However, its action is quite different. It seems to stabilize the vapor blanket stage by enclosing the casting in a gel-like casing (Fletcher and Griffiths 1995).

Other polymers have a so-called reverse temperature coefficient of solubility. This lengthy technical description means that the polymer becomes less soluble as the temperature of the solution is raised. Many, but by no means all, of the polymers are based on glycol. One widely used polymer is polyalkylene glycol. This material becomes insoluble in water above about 70°C. The commercial mixtures are usually sold already diluted with water because the product in its pure form would be intractably sticky, like rather solid grease, and would therefore present practical difficulties on getting it into solution. It is usually available containing other chemicals such as antifoaming agents, corrosion inhibitors, and possibly anti-bacteriological components.

Such polymers have an active role during the quench. When the quenchant contacts the hot casting, the pure polymer becomes insoluble. It separates from the solution, and precipitates both on the surface of the casting and in the hot surrounding liquid as clouds of immiscible droplets. The sticky, viscous layer on the casting, and the surrounding viscous mixture, inhibit boiling and aid the uniform cooling condition that is required. When the casting has cooled to below 70°C, the polymer becomes

soluble once again in the bulk liquid, and can be taken back into solution. Re-resolution is unfortunately rather slow, but the agitation of the quench tank with, for instance, bubbles of air rising from a submerged manifold to scrub the sticky residue off the castings, reduces the time required.

Polymer quenchants have been highly successful in reducing stresses in those castings that are required to be quenched as part of their heat treatment. The properties developed by the heat treatment are also found to be, in general, more reproducible. Capello and Carosso (1989) has shown that the elongation to failure of sand-cast Al-75I-0.5Si alloy, using 2.5 times the standard deviation to include 99% of expected results, exhibits greater reliability as shown in Table 10.1. Thus the average properties that are achieved may be somewhat less than those that would have been achieved by a cold water quench, but the products have the following advantages:

1. The minimum values of the random distribution of strength values are raised.
2. With castings nearly free from stress the user has the confidence of knowing that all of the strength is available, and that an unknown level of internal stress is not detracting from the strength indicated (misleadingly) by a test bar.
3. The castings will have significantly reduced distortion.

These authors carried out quenching tests on an aluminum plate  $150 \times 100 \times 1.5$  mm, and found that, taking the distortion in cold water as 100%, a quench with water temperature raised to 80°C reduced the distortion only marginally to 86% of its previous value. Quenching in a mixture of 20% glycol in water gave a distortion of only 3.5%.

**Table 10.1** Elongation to failure results from different quenching media

	Elongation (%)	
	Minimum	Mean $\pm 2.5\sigma$
Hot-water quench (70°C)	2.01	4.73 $\pm$ 2.72
Cold-water quench	4.80	6.47 $\pm$ 1.67
Water-glycol quench	4.85	5.81 $\pm$ 0.96

For many castings, therefore, the use of a boiling water quench seems to be of limited help in reducing the stresses introduced by water quenching as discussed above. Thus although the rate of quench may be reduced by the use of hot or boiling water the results are not always reliable. This is almost certainly the consequence of the variability of the vapor blanket that forms around the hot casting. The blanket forms and disappears irregularly, depending on many factors including the precise geometry of the part, its inclination during the quench, and the proximity of other hot castings, etc. In addition, from a practical point of view, a hot water quench is costly to install, run and maintain.

For steels, other quenching routes to achieve a low stress casting have been developed involving the use of an intermediate quench into a molten salt at some intermediate temperature of approximately 300°C for approximately 20 s prior to the final quench into water (Maidment et al. 1984). Despite the advantages claimed by the authors, the expense and complexity of this double quench are likely to keep the technique reserved for aerospace components, if anything.

However, it is with regret to conclude that the polymer quench is not currently a long-term practical solution for production for an automotive product. The polymer solution has to be cleaned out of

internal cavities where it could lodge, otherwise it would become concentrated and carbonized during the subsequent aging treatment, creating copious fumes that pour from the aging furnace and spread throughout the foundry. In addition, any residual core sand in such locations would be effectively bonded into place by this concentrated polymer binder, and would be practically impossible to dislodge. Perversely, such bonded-in sand is likely to cause damage later in the life of the engine when it finally decides to free itself and starts to clog oil passages and destroy bearings. Finally, the use of polymer in the foundry environment is notoriously messy; splashes from the quench or from the rinse tank cause the surrounding equipment to become black and sticky, and footwear tends to stick to the floor.

In contrast to its problems with automotive castings, polymer is excellent for aerospace castings where the extra trouble to clean each casting individually does not outweigh the benefit of superb heat treatment response and reduced internal stress.

There seems little information on another quenchant that holds significant promise: a water/carbon dioxide solution. The mixture is of course highly environmentally friendly. Different concentrations of CO<sub>2</sub> provide different degrees of control over the rate and uniformity of the quench. It seems likely that at least some of the action of the solution is to break up the vapor blanket, thus making the quench more uniform. The gas supply companies have been investigating such CO<sub>2</sub> quenchants, combining them with inert nanoparticles such as alumina to form liquid muds. These are claimed to give sufficiently slow quenches to avoid the well-known problems of the quench-cracking of highly alloyed steels (Stratton 2010). More information on this interesting and attractive technique would be welcome.

### 10.9.5 Controlled quenching using air

The author recalls with pain memories of quenching complex cylinder heads into water, requiring the consequential banana-shaped products to be straightened with a huge 50 000-kg press specially bought in to rectify the damage. The castings subjected to straightening were those that appeared to have survived failure from cracking in the quench itself (although internal cracks inside the water jackets were often difficult to detect, being usually only found on subsequent return of service failures). In addition, it was found, the castings failed by fatigue in service after only short lives. (These were highly stressed racing cylinder heads so that the disappointment of failure was to some extent compensated by the rare, if not unique, benefit of rapid feedback of service life data.)

It was this experience that drove the author to the air quenching of cylinder head castings. When the cylinder head casting, considered above, was subjected to quenching in a blast of air, Figure 10.53 indicates that cooling was now a leisurely 100 seconds or so. Thus sufficient time was available for the internal sections to lose their heat to the outside so that the casting maintained a reasonably uniform temperature during the quench. The generation of high internal stress and resulting distortion was avoided.

Air quenching proved to be a complete solution for automotive castings. It was clean, quick, environmentally friendly, low cost and quickly and easily implemented in a series production environment. The castings retained their accuracy, and quench failures and fatigue failures disappeared. We were able to restore productivity and profitability (and sell the 50 000-kg straightening press to get our money back).

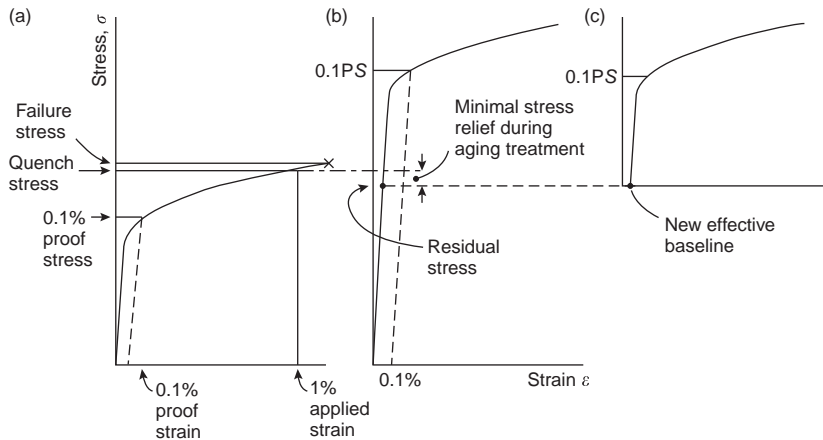


**FIGURE 10.55**

Evolution of the stress/strain properties of a precipitation-hardened Al alloy as heat treatment progresses: (a) after quench; (b) after aging to double the yield strength; (c) the final effective stress/strain relation after allowing for the presence of residual stress. Although clearly the alloy is stronger, the overall strength of the casting has been reduced.

### 10.9.6 Strength reduction by heat treatment

Figure 10.55 illustrates how the overall effective strength of a casting can be reduced by a heat treatment designed to strengthen the alloy.

Figure 10.55(a) shows the stress/strain curve for the alloy, and the imposition of 1% tensile strain on the inner parts of the casting as a result of a water quench. This quench strain results in a quench stress close to the failure stress of the material. If no aging treatment is carried out this stress is locked into the component for the rest of its life. Naturally, it has little residual strength left, and is likely to fail on the first application of a stress in service.

However, after an aging treatment designed to double the yield strength of the alloy, the situation is shown in Figure 10.55(b). Assuming the benefit of a small amount of stress relief (the amount indicated in the figure may be rather generous), the residual quench stress is only slightly lower; substantially unchanged. If additional service stress in tension is applied to the central parts of the casting, the residual tensile stress in these parts is effectively a starting point for the additional loading. Thus, effectively, the new stress/strain curve for the component is shown in Figure 10.55(c). It is clear that the new overall stress/strain capability of the casting has been reduced compared to the original unheat-treated material; thus, tragically, as a result of our lengthy, complex and expensive heat treatment the component is effectively weaker.

In summary, for certain sensitive castings such as automotive cylinder heads, the residual stress in aluminum alloy castings quenched into water in this way are well above the yield point of the alloy. Even after the strengthening during the aging treatment, the stress remains at between 30 and 70% of the yield stress, with a useful working approximation being 50%. Thus the useful strength of the alloy is reduced from its unstressed state of 100%, down to around 50%. This massive loss of effective



strength makes it inevitable that residual tensile stresses are a significant cause of casting failure in service, particularly fatigue failure, since the residual stress is always generously above the fatigue limit of the alloy.

Turning now to steels; in contrast to the behavior of Al alloys, the thermal diffusivity  $D$  is approximately ten times lower, of the order of only  $10^{-5} \text{ m}^2 \text{ s}^{-1}$ . The reader can quickly show that the corresponding distances to which heat can flow are 7 mm in 5 seconds but only 30 mm in 100 seconds. For a given rate of quench therefore, steels will suffer a higher residual stress (Figure 10.52). Nevertheless, they are much more able to withstand such disadvantages, having not only higher strength, but more particularly higher elongation to failure. Thus although the final internal stress is high, the steel product is nowhere near the failure condition experienced by the aluminum alloy casting. The aluminum alloy casting also experiences about 1% imposed elongation but has only a few percent, perhaps on occasions even less than 1% elongation prior to failure. Thus it can fail actually in the quench, or early in service. In contrast, the steel casting has ten or 20 times greater elongation (as a result primarily of its reduced bifilm content). Thus although the 1% or so of imposed quench strain resulting from unequal cooling may result in 1% or so of distortion of the steel casting, its condition is far from any dangerous condition that might result in complete failure, since enormously greater strain has to be imposed to reach a failure condition (Figure 10.56).

The above statements are so important they are worth repeating in different words for additional clarity. The rapid quenching of steels for metallurgical purposes (such as the stabilization of austenite for Hadfield Manganese steel) is not usually a problem. The reason is that most steels are particularly clean, because of the rapidity with which entrainment defects are deactivated and/or detrained after pouring. The result is that steels typically have an elongation to failure of 40 or 50%. In contrast, most

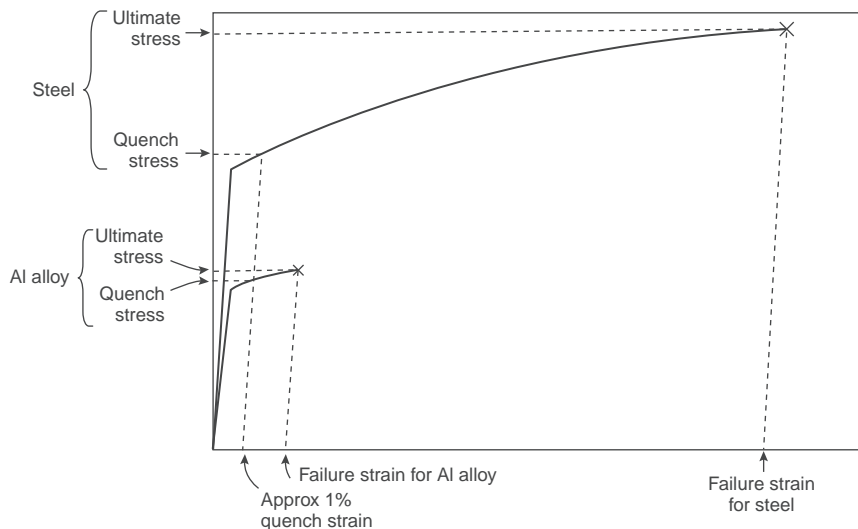


**FIGURE 10.56**

Comparison of the stress/strain relations for an Al alloy and a steel, illustrating the relatively dangerous condition of the Al alloy after a quench.

Al alloys (and probably most Mg alloys) do not enjoy this benefit; suffering from a high density of neutrally buoyant bifilms they typically achieve less than a tenth of this ductility. Thus the application of 1% strain takes the aluminum alloy close to, or even sometimes in excess of, its failure strain. For steels, even though the 1 % strain applied by the quench will take the part into the plastic region, causing huge stresses, the steel remains safe; its greater freedom from bifilms permits it to endure enormously greater extension before it will fail (Figure 10.56).

For the future, the production of Al alloys with low bifilm concentration promises to offer ductilities in the range of that of steels. Already, good foundries know that high strengths together with elongations of 10–20% are achievable, if good care is taken.

Slower quenching techniques are safer, although, of course, the strength attained by the heat treatment is somewhat reduced. Even so, the reduced mechanical strength when using slower and more controlled quenches such as a polymer or a forced air quench is more than compensated by the benefit of increased reliability from putting unstressed (or, more accurately, low-stressed) castings into service. Thus the casting designer and/or customer needs to accept somewhat reduced mechanical strength and hardness requirements in order to gain a superior performance from the product. The reductions of strength and hardness are expected to be in the range 5–10%, but the improvement in casting performance can be expected to be approximately 100% or more (as a result of avoiding the loss of the order of 50%). These are huge benefits to be gained at no extra cost.

The proper development of quenching techniques to give maximum properties with minimum residual stress is a technique known as quench factor analysis. It is also much used to optimize the corrosion behavior of aluminum alloys. The method is based on the integration of the effects of precipitation of solute during the time of the quench. In this way any loss of properties caused by slow quenching or stepped quenching can be predicted accurately. The interested reader is recommended to the nice introduction by Staley (1981), and his later more advanced treatment (Staley 1986).

### 10.9.7 Distortion

Residual stresses in castings are not only serious for parts that require to withstand stress in service. They are also of considerable inconvenience for parts that are required to retain a high degree of dimensional stability. This problem was understood many years ago, being first described as early as 1914 in a model capable of quantitative development by Heyn. His model was the three-bar casting shown in Figure 10.48. The internal stresses were represented by two outer springs in compression, each carrying half of the total load of internal compressive stress, and an inner spring in tension carrying all of the internal tensile stress. If one of the surfaces of the casting was machined away, one of the external stresses would be eliminated. It is predictable therefore that the casting would deform to give a concave curvature on the machined side as illustrated in the figure.

The distortion of castings both before and after machining is a common fault, and typical of castings that have suffered a water quench. Once again, it is a problem so frequently encountered that I have, I regret, wearied of answering the telephone to these enquires too. After all, it is difficult to understand how a casting could avoid distortion if parts of it are stressed up to or above its yield point.

For light alloy castings in particular, a more gentle quench, avoiding water (either hot or cold), and choosing polymer or air will usually solve the problem instantly. As mentioned briefly above, polymer

performs well for aerospace castings but is expensive and messy, whereas air is recommended as being clean, economical and practical for high volume automotive work. Otherwise, stress relieving of castings by heat treatment prior to machining is strongly recommended. In all cases, of course, some fraction of the *apparent* strength of the product has to be sacrificed.

### 10.9.8 Heat treatment developments

Although not strictly relevant to the question of reducing residual stresses, it is worth emphasizing the newer developments in heat treatments that give approximately 90% or more of total attainable strength, but with much reduced stress and greatly reduced cost. The reduced cost is always an attention-grabbing topic, and materially helps the introduction of technology that can deliver an improved product.

Figure 10.57 illustrates the progression of recent developments in heat treatment of Al alloys where the problem of stress is central.

The traditional full heat treatment of a precipitation-hardened alloy, which constitutes the bulk of cast structural components at this time, consists of a solution treatment, water quench and age as illustrated in Figure 10.57(a). The treatment results in excellent apparent strength for the material, but

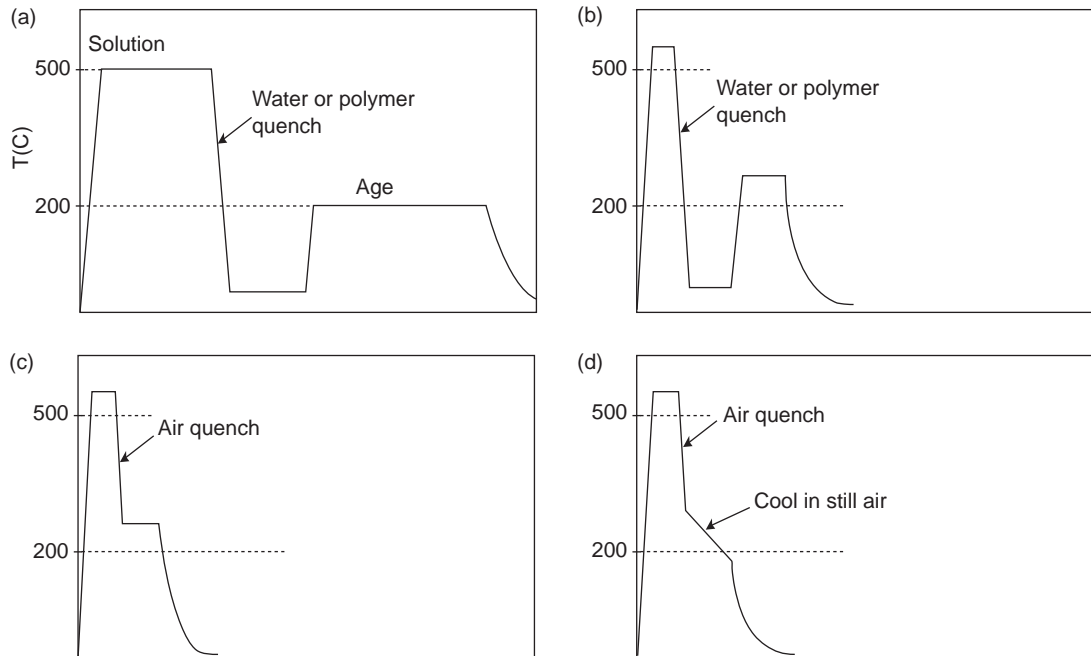


**FIGURE 10.57**

A progression of developments for the precipitation heat treatment of Al alloys. (a) Traditional full T6 heat treatment giving excellent properties but taking 12–24 hours; (b) shortened treatment giving nearly equivalent results; (c) use of air quench to reduce time, energy and residual stress; (d) a possible ultimate short and simple cycle, aging during the high temperature cool in still air.

is energy intensive in view of the long total times, and the water quench may be severely deleterious (depending on the geometry of the casting) as we have seen.

Figure 15.57(b) shows how the traditional treatment can be reduced significantly in modern furnaces that enjoy accurate control over temperature, thereby reducing the risk of overheating of the charge because of random thermal excursions. An increase in temperature by  $10^{\circ}\text{C}$  will allow, to a close approximation, an increase in the rate of treatment by a factor of 2. Thus times at temperature can be halved. These benefits are cumulative, such that a rise of  $20^{\circ}\text{C}$  will allow a reduction in time by a factor of  $2 \times 2 = 4$ , or a rise of  $30^{\circ}\text{C}$  a reduction in time of a factor  $2 \times 2 \times 2 = 8$  although, of course, there are clearly limits to how far this simple relation can be pushed. Even so, it seems to hold within acceptable accuracy over many decades of temperature change. The reader will appreciate that the tiny additional energy required by the higher temperature is of course completely offset by the huge savings in overall time at temperature.

Both (a) and (b) require separate furnaces for solution and aging treatments (if long delays waiting for the solution furnace to cool to the aging temperature are to be avoided). Thus floor space requirement is high. Floor space requirement is increased further by the quench station, and, if a polymer quench is used, by a rinsing tank station.

If an air quench is used to gain the benefits of reduced residual stress, the additional benefits to the overall cycle time are seen in Figure 15.57(c); the quench can now be interrupted and the product transferred to the aging furnace already at the correct temperature for aging, saving time and reheat energy. Additional benefits include the fact that the air quench is environmentally friendly; the castings are not stained by the often less-than-clean water; the conveyor is straightforward to build and maintain; there is no mechanism required for lowering into water that normally results in complex and rusting plant. As we have repeatedly emphasized, the products from this type of furnace have somewhat lower apparent strengths and hardness, but greatly improved performance in service.

Figure 15.57(d) shows an ultimate system that might be acceptable for some products. The aging treatment is simply carried out by interrupting the air quench slightly above the normal aging temperature, and allowing the part to cool in air (prior to final rapid cooling by fans if necessary). This represents a kind of natural aging process in which no aging furnace is required. Strengths will suffer somewhat, but the lower costs and simplicity of the process may be attractive, making the process suitable for some applications.

### 10.9.9 Beneficial residual stress

Not all residual stress need be bad.

Bean and Marsh (1969) describe a rare example, in which the stress remaining after quenching was used to enhance the service capability of a component. They were developing the air intake casing for the front of a turbojet engine. The casting has the general form of a wheel, with a center hub, spokes, and an outer shroud. In service the spokes reached  $150^{\circ}\text{C}$  and the shroud cooled to  $-40^{\circ}\text{C}$ . The expansion of the spokes and contraction of the shroud gave problems in service. With additional high loads from accelerations up to  $7g$  and other forces, some casings were deformed out of round, and some even cracked. In order to counter this problem the casting was produced with tensile stress in the spokes, and compressive loading in the shroud. This was achieved by wrapping the spokes in glass fiber insulation, whilst allowing the shroud to cool quickly at the full quenching rate, but the spokes to

cool and contract later. By this means approximately 40 MPa tensile stress was introduced into the spokes. This was tested by cutting a spoke on each fifteenth casting, and measuring the gap opening of approximately 2 mm.

Another method of equalizing quenching rates in castings is by the clamping of shielding plates around thinner sections to effectively increase their section. The method is described by Avey et al. (1989) for a large circular clutch housing in a high-strength aluminum alloy. The technique improved the fatigue life of the part by over 400%.

It may be significant that both of these descriptions of the positive use of residual stress relate to rather simple rotationally symmetric castings.

### 10.9.10 Stress relief

For traditional gray iron foundries of the last century, the original method of providing some stress relief in iron castings was simply to leave the castings in the foundry yard. Here, the long passage of time, of weeks or months, and the changeable weather, including rain, snow, frost and sun, would gradually do its work. It was well known that the natural aging outdoors was more rapid and complete than aging done indoors, presumably because of the more rapid and larger temperature changes.

Nowadays the more usual method of reducing internal stress is both faster and more reliable (although somewhat more energy intensive!). The casting is reheated to a temperature at which sufficient plastic flow can occur by creep to reduce the strain, and hence reduce the stress. This is designed to take place within a reasonable time, of the order of an hour or so. As pointed out earlier, it is then most important that stress is not reintroduced by cooling too quickly from the stress-relieving treatment.

An apparently perverse and quite exasperating feature of internal tensile stress in castings is that the casting will often crack while it is being reheated as part of the stress-relieving process to avoid the danger of cracks! This happens if the reheating furnace is already at a high temperature when the castings are loaded. The reason for this is that if the casting already has a high internal tensile stress, on placing the casting in a hot reheating furnace the outside will then be heated first and expand, before the center becomes warm. Thus the center, already suffering a high stress, will be placed under additional tensile load, the total being sometimes sufficient to exceed the tensile strength.

The problem is avoided by reheating sufficiently slowly that the temperature in the center is able to keep pace (within tolerable limits) with that at the outside. Consideration of the thermal diffusivity using Equation 10.21 will give some guidance of the times required.

Figure 10.58 shows the temperatures required for stress relief of various alloys. (Strictly, the figure shows results for 3 h, but the results are fairly insensitive to time, a factor of 2 reduction in time corresponding to an increase in temperature of 10°C, hardly moving the curves on the scale used in the figure.) It indicates that nearly 100% of the stress can be eliminated by an hour at the temperatures shown in Table 10.1.

Bhaumik (2010) describes experiments to prove an elegant and simple technique to determine the times and temperatures needed to achieve specific degrees of stress reduction. The technique is known as a stress relaxation test. A tensile test bar of the material is mounted in a tensile testing machine, and the test bar is enclosed by a heater. The test bar is loaded to near its yield stress while the heater is

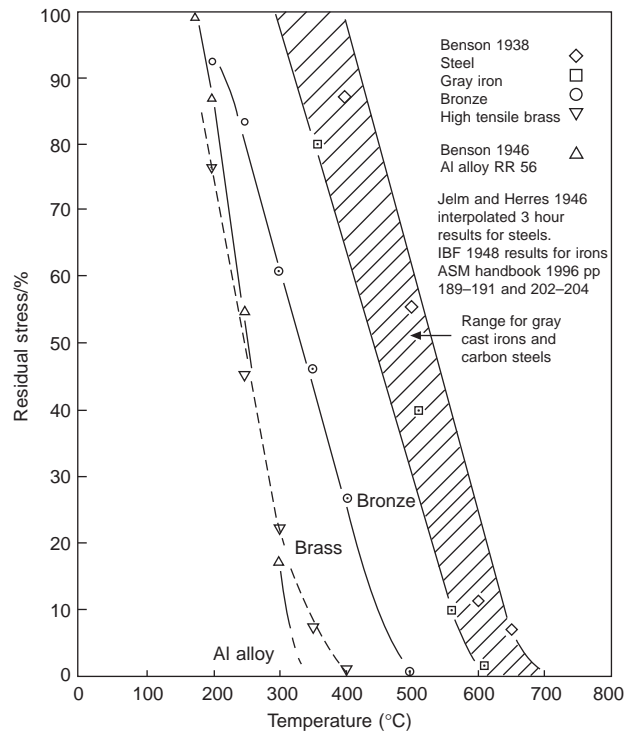


**FIGURE 10.58**

Stress relief of a selection of alloys treated for 3 hours at temperature. Data from Benson (1938), Jelm and Herres (1946) and Institute of British Foundrymen (1948).

raised to the test temperature. The tensile test machine will then automatically record the fall in stress with time. At low temperatures the times to achieve a 90 % drop in stress might take hours or days, whereas at high temperatures this degree of stress relief might take only minutes. This simple, accurate, quantitative test is strongly recommended.

There are numerous examples of the use of such heat treatments to effect a valuable degree of stress relief. One example is the work by Pope (1965) on cast iron diesel cylinder heads that were found to crack between the exhaust valve seats in service, despite a stress-relief treatment for 2 hours at 580°C. A modification of the treatment to 4 hours at 600°C cured the problem. From Figure 10.58 and Table 10.2 we can see that even 2 hours at 600°C would probably have been sufficient.

The work by Kotsyubinskii et al. (1968) highlights the fact that during the thermal stress relief the casting will distort. They carried out measurements on box-section castings in gray iron, intended as the beds of large machine tools, for which stress-relieving treatment is carried out after some machining of the top and base of the box section. He suggests that the degree of movement of the castings is approximately assessed by the factor  $(w_1 - w_2)/w_c$  where  $w_1$  and  $w_2$  are the weights of metal machined from the top and base of the casting respectively, and  $w_c$  is the weight of the machined casting. This interesting observation has, to the author's knowledge, never been confirmed.

**Table 10.2** Approximate stress-relieving temperatures

Alloy	Stress-relief temperature (°C)
Al-2.2Cu-1Ni-1Mg-1Fe-1Si-0.1Ti	300
Brass Cu-35Zn-1.5Fe-3.7Mn	400
Bronze Cu-10Sn-2Zn	500
Gray iron 3.4C-2Si-0.38Mn-0.1S-0.64P	600
Steel (C-Mn types)	700

Moving on now from heat treatment, there are other methods of stress relief that are sometimes useful. In simple castings and welds it is sometimes possible to effect relief by mechanical overstrain as described in the excellent review by Spraragen and Claussen (1937).

Kotsyubinskii (1962) describes a further related method for gray iron in which the castings are subjected to rapid heating and cooling between 300°C and room temperature at least three times. The differential rates of heating within the thick and thin sections produce the overstrain required for stress relief by plastic flow.

More drastic heating rates are required to effect stress relief by differential heating in aluminum alloys because of the thermal smoothing provided by the high thermal conductivity. Hill et al. (1960) describe an 'up-quenching' technique in which the casting is taken from cryogenic temperatures, having been cooled in liquid nitrogen, and is reheated in jets of steam. This thermo-mechanical treatment introduces a pattern of stresses into the casting that are opposite to those introduced by normal quenching. One of the benefits of this method is that it is all carried out at temperatures below normal aging temperatures, so that the effects of the final heat treatment and the resulting mechanical properties are not affected. One of the possible disadvantages that the authors do not mention is the enhanced tensile stress in the center of the casting during the early stages of the up-quench. Some castings would not be expected to survive this dangerous moment.

A variant of these approaches is stress relief by vibration. This is probably effective in some shapes, but it is difficult to see how the technique can apply to all parts of all shapes. This is particularly true if the component is treated at a resonant frequency. In this condition some parts of the casting will be at nodes (will not move) and some parts at antinodes (will vibrate with maximum amplitude). Thus the distribution of energy in the casting will be expected to be highly heterogeneous. Some investigators have reported the danger of fatigue cracks if vibrational stresses over the fatigue limit are employed (Kotsyubinskii 1961). The technique may require some skill in its application, since null results are easily achieved (IBF Technical Subcommittee 1960).

There may be greater certainty of a valid result with sub-resonant treatment. This technique emerged later as a possible method of stress relief (Hebel 1989). In this technique the casting is vibrated not on the peak of the frequency-amplitude curve, but low on the flank of the curve. At this off-peak condition the casting is said to absorb energy more efficiently. Furthermore, it is claimed that the progress towards complete stress relief can be monitored by the gradual change in the resonant frequency of the casting. When the resonant frequency ceases to change, the casting is said to be fully stress relieved. If this technique could be verified, then it would deserve to be widely used.

### 10.9.11 Epilogue

Although the *strength of the material* will therefore be lowered by a slower quench, the *strength of the component* (i.e. the failure resistance of the complete casting acting as a load-bearing part) in service will be increased.

If water quench is avoided with a view to avoiding the dangers of internal residual stress, it is common for the customer to complain about the 5% or so loss of apparent properties. In answer to such understandable questions, an appropriate reply to focus attention on the real issue might be ‘Mr. Customer, with respect, do you wish to lose 5% or 50% of your properties?’

In the experience of the author, a number of examples of castings that have been slowly quenched, losing 5 or 10% of their strength, are demonstrated to double their performance in service. This was the case for a road-side compressor casting subjected to a full T6 heat treatment. The compressor housing exploded in service, fortunately not resulting in any injury to passers-by. After the second explosion the manufacturer requested help. I recommended a stress relief treatment. This was declared to be impossible because it was claimed the compressor housing needed maximum strength. Despite the reservations of the manufacturer, stress-relieved castings (that had only half the strength of the fully heat treated product) were tested to destruction in comparison with fully heat treated castings. The stress-relieved products proved twice as resistant to failure under pressure compared to the fully heat treated parts with the metallurgically ‘strong’ alloy.

Finally therefore, it remains deeply regrettable, actually a scandal, that many national standards for heat treatment continue to specify water quenching without any warning of the dangers for certain geometries of casting. This disgraceful situation requires to be remedied. In the meantime the author deeply regrets to have to recommend that such national standards be set aside. It is easy for the casting supplier to take refuge in the fact that our international and national standards on heat treatment often demand quenching into water, and thereby avoid the issue that such a production practice is risky for many components, and in any case provides the user with a casting of inferior performance. However, the ethics of the situation are clear. We are not doing our duty as responsible engineers and as members of society if we continue to ignore these crucial questions. We threaten the performance of the whole component merely to fulfill a piece of metallurgical dogma that from the first has been woefully misguided.

The fact is that our inappropriate heat treatments have been costly to carry out, and have resulted in costly failures. It has to be admitted that this has been nothing short of a catastrophe for the engineering world for the past half century, and particularly for the reputation of light alloy castings, not to mention the misfortune of users. As a result of the unsuspected presence of bifilms they have suffered poor reliability so far, but as a result of the unsuspected presence of residual stress this has been made considerably worse by an unthinking quest for material strength that has on occasions reduced component performance.

---

## 10.10 RULE 10: ‘PROVIDE LOCATION POINTS’

This Rule, ‘Provide location points’, is added simply because the foundry can accomplish all the other nine Rules successfully, and so produce beautiful castings, only to have them scrapped by the machinist. This can create real-life drama if the castings have been promised in a just-in-time delivery system. This Rule is added to help to avoid such misfortunes, and allow all parties to sleep more soundly in their beds.



Before describing location points, their logical precursors are datum planes. We need to decide on our datums first (for language purists the plural of datum is data, but this would introduce unwelcome confusion with the conventional meaning of the word, thus we all need to grit our teeth with the inelegant plural 'datums').

### 10.10.1 Datums

A datum is simply a plane defining the zero from which all dimensions are measured.

For a casting design it is normal to choose three datum planes at right angles to each other. In this way all dimensions in all three orthogonal directions can be uniquely defined without ambiguity.

In practice, it is not uncommon to find a casting design devoid of any datum, there being simply a sprinkling of dimensions over the drawing, none of the dimensions being necessarily related to each other. On other designs the dimensions relate with great rigor to each other and to all machined features such as drilled holes etc., but not to the casting. In yet other instances that the author has suffered, datums on one face have not been related to datums on other views of the same casting. Thus the raft of features on one face of the casting shifts and rotates independently of the raft of features on the opposite face.

Figure 10.59(a) shows a sump (oil pan) for a diesel engine designed for gravity die casting in an aluminum alloy. The variations in die temperature and ejection time result in variability of the length of the casting that are well known with this process, and not easily controlled. The figure shows how the dimensioning of this part has made the part nearly unmanufacturable by this method. Three fundamental criticisms can be made:

- (i) The datum is at one end of the product. If the datum had been defined somewhere near the center of the part, then the variability produced by the length changes of the casting would have been approximately halved.
- (ii) There is only one feature on the component whose location is critical; this is the dipstick boss. If the boss is slightly misplaced then it fouls other components on and around the engine. It will be noticed that the dipstick boss is at the far end of the casting from the datum. Thus variability in length of the casting will ensure that a large proportion of castings will be deemed to have a misplaced boss. If the datum had been located at the other end of the casting, near to the boss, the problem would have been reduced to negligible proportions. If the datum had been chosen as the boss itself, the problem would have disappeared altogether, as in Figure 10.59(b).
- (iii) The datum is not defined with respect to the casting. It is centered on a row of machined holes, which clearly do not exist at the time the casting is first made and when it is first required to be checked and before any machining of the casting has taken place. Depending on whether the machinist decides to fix the holes in the center of the flange, or relate them by measurement to the more distant dipstick boss, or to the center of the casting averaged from its two ends, or any number of alternative strategies, the drilled holes could be almost anywhere, including partly off the flange or even completely off the flange!

Figure 10.59(b) shows how these difficulties are easily resolved. The datum is located against the side of the dipstick boss, and hence is fixed in its relation to the casting and goes some way to halving errors in the two directions from this plane. It also means that the dipstick boss itself is now impossible to

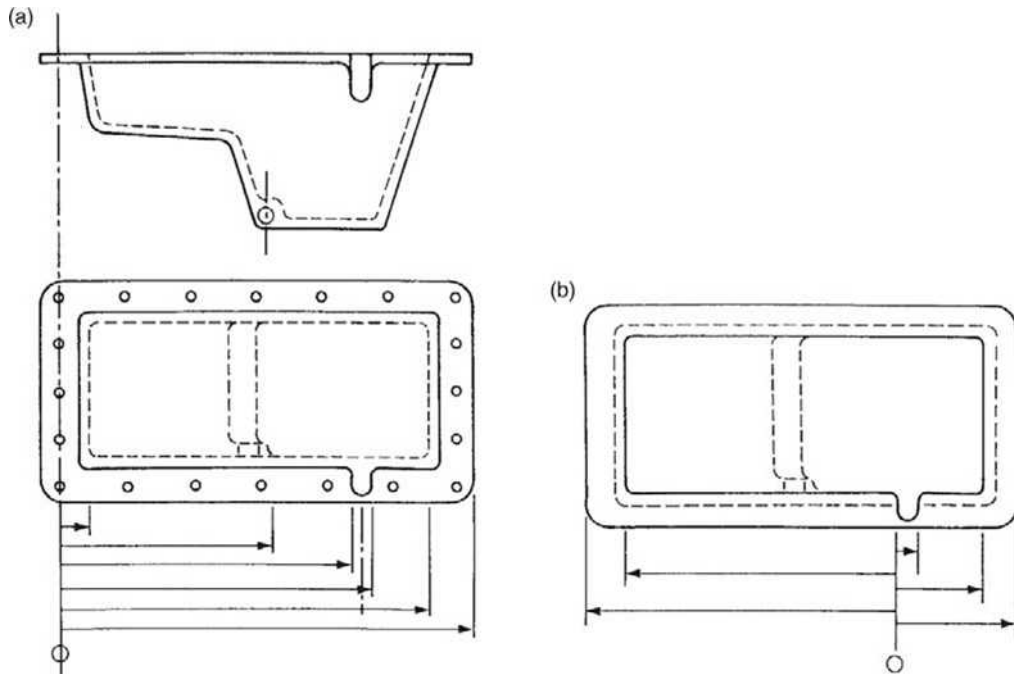


**FIGURE 10.59**

(a) A badly dimensioned sump casting, resulting in a casting manufactured only with difficulty and high scrap losses. (b) A change of datum to the most critical feature of the casting results in easy and efficient manufacture.

misplace, no matter how the casting size varies; all the other dimensions are allowed to float somewhat because movement of other points on the casting is not a problem in service. This part can then be produced easily and efficiently, without trauma to either producer or customer!

In summary, the rules for the use of datums (partly from Swing (1962)) are:

1. Choose three orthogonal datum planes.
2. Ensure the planes are parallel to the axes of motion of the machine tools that will be used to machine the part (otherwise unnecessary computation and opportunity for error are introduced).
3. Fix the planes on real casting features, such as the edges of a boss, or the face of a wall (i.e. not on a centerline or other abstract constructional feature). Choose casting features that are:
  - (a) critical in terms of their location, and
  - (b) as near the center of the part as possible.

### 10.10.2 Location points

Location points are those tiny patches on the casting that are used to locate the casting precisely and unambiguously in three dimensions. They are required by all parties involved in the manufacture of the product including:

- (i) the toolmaker, since he can construct the tooling with reference to them;

- (ii) the founder, to check the core and mold assembly if necessary and the casting once it has been made; and
- (iii) the machinist, who uses them to locate the casting prior to the first machining operations.

These features therefore integrate the manufacture of the product, ensuring its smooth transmission as it progresses from toolmaker to founder to machinist.

Whereas the casting datums are invisible planes that define the concept of a zero in the dimensional space in and around a casting, the tooling points are real bits of the casting. The datums are the software, whereas the tooling points are the hardware, of the dimensioning system.

It is useful, although not essential, for the datums to be defined coincident with the tooling points.

The location points are required to be *actual cast-on features* of the casting. This point cannot be over-emphasized. It is not helpful, for instance, to define a location feature as a centerline of a bore. This invisible feature only exists in space (perhaps we should say 'free air'). Virtual features such as centerlines have to be found by locating several (at least three) points on the internal as-cast solid surface of the bore, and its center thereby calculated. Clearly, these 'virtual' or 'free-air' so-called location points necessarily rely on their definition from other nearby as-cast surfaces. These ambiguities are avoided by the direct choice of as-cast location features.

The location features need to be cast nicely, without obscuring flash, or burned-on sand, and definitely should not be attacked by enthusiastic finishers wielding an abrasive wheel.

It is essential that the location points are *not* machined. If they are machined, the circumstance poses the infinitely circular question 'What prior datums were used to locate and position the casting accurately to ensure that the machining of the machining locations (from which the casting would be picked up for machining) were correctly machined?' Unfortunately, such indefensible nonsense has its committed devotees.

Location points are known by several different names, such as machining locations (which is a rather limiting name) or pick-up points. On drawings, TP for Tooling Point is used as the common abbreviation for the drawing symbol. Although in practice I tend to use all the names interchangeably it is proposed that 'Location Points' describes their function most accurately and will be used here.

Before the day of the introduction of location points in the Cosworth engine-building operation, I was accustomed to a complex cylinder head casting taking a skilled man at least 2 hours to measure to assess how to pick up the casting for machining. The casting was repeatedly re-checked, re-orienting it slightly with shims to test whether wall thicknesses were adequate, and whether all the surfaces required to be machined would in fact clean up on machining. After the 2 hours, it was common to witness our most expensive casting dumped on the scrap heap; no orientation could be found to ensure that it was dimensionally satisfactory and could be completely cleaned up on machining. All this changed on the day when the new foundry came on stream. A formal system of six location points to define the position of the casting was introduced. After this date, no casting was subjected to dimensional checking. All castings were received from the foundry and on entering the machine shop, and were immediately thrown on to a machine tool, pushed up against their location points, clamped, and machined. No tedious measurement time was subsequently lost, and no casting was ever again scrapped for machining pick-up problems.

It is essential that every casting has defined locations that will be agreed with the machinist and all other parties who require to pick up the casting accurately.

For instance, it is common for an accurate casting to be picked up by the machinist using what appear to be useful features, but which may be formed by a difficult-to-place core, or a part of the casting that requires some dressing by hand. Thus although the whole casting has excellent accuracy, this particular local feature is somewhat variable in location. The result is a casting that is picked up inaccurately, and does not therefore clean up on machining. As a result it is, perhaps rather unjustly, declared to be dimensionally inaccurate.

The author suffered precisely this fate after the production of a complex pump body casting for an aerospace application that achieved excellent accuracy in all respects, except for a small region of the body that was the site where three cores met. The small amount of flash at this junction required dressing with a hand grinder, and so, naturally, was locally ground to a flat, but at various slightly different depths beneath the curved surface of the pump body. This hand-ground location was the very site that that machinist chose to locate the casting. The result was disaster. Furthermore, it was not easily solved because of the loss of face to the machinist who then claimed that the location options suggested by the foundry were inconveniently awkward. The fault was not his of course. The fundamental error lay in not obtaining agreement between all parties before the part was made. If the location point used by the machinist really was the only sensible option for him, the casting engineer and toolmaker needed to ensure that the design of the core package would allow this.

Ultimately, this Rule is designed to ensure that all castings are picked up accurately and conveniently if possible, so that unnecessary scrap is avoided.

Different arrangements of location points are required for different geometries of casting. Some of the most important systems are listed below.

### Rectilinear systems

Six points are required to define the position of a component with orthogonal datum planes that is designed for essentially rectilinear machining, as for an automotive cylinder head or block. (Any fewer points than six are insufficient to define the position of the casting, and any more than six will ensure that one or more points are potentially in conflict.)

On questioning a student on how to use a six-point system to locate a brick-shaped casting, the reply was ‘Oh easy! Use four points around the outside faces and one top and one bottom.’ This shows how easy it is to get such concepts wildly wrong!

In fact, the six points are used in a 3, 2, 1 arrangement as shown in Figure 10.60. The system works as follows: three points define plane A, two define the orthogonal plane B, and one defines the remaining mutually orthogonal plane C. The casting is then picked up on a jig or machine tool that locates against these six points. Example (a) shows the basic use of the system: points 1, 2, and 3 locate plane A; points 4 and 5 define plane B; and point 6 defines plane C. Planes A, B, and C may be the datum planes. Alternatively, it is often just as convenient for them to be parallel to the datum planes, but at accurately specified distances away.

Clearly, to maximize accuracy, points 1, 2 and 3 need to define a widely based triangle, and points 4 and 5 similarly need to be as widely spaced as possible. A close grouping of the locations will result in poor reproducibility of the pick-up of the casting; tiny errors in the position or surface roughness of the tooling points will be magnified if they are not widely spaced.

Example (b) shows an improved arrangement whereby the use of a tooling lug on the longitudinal centerline of the casting allows the dimensions along the length of the casting to be halved. The largest dimension of the casting is usually subject to the largest variability, so halving its effect is a useful action.

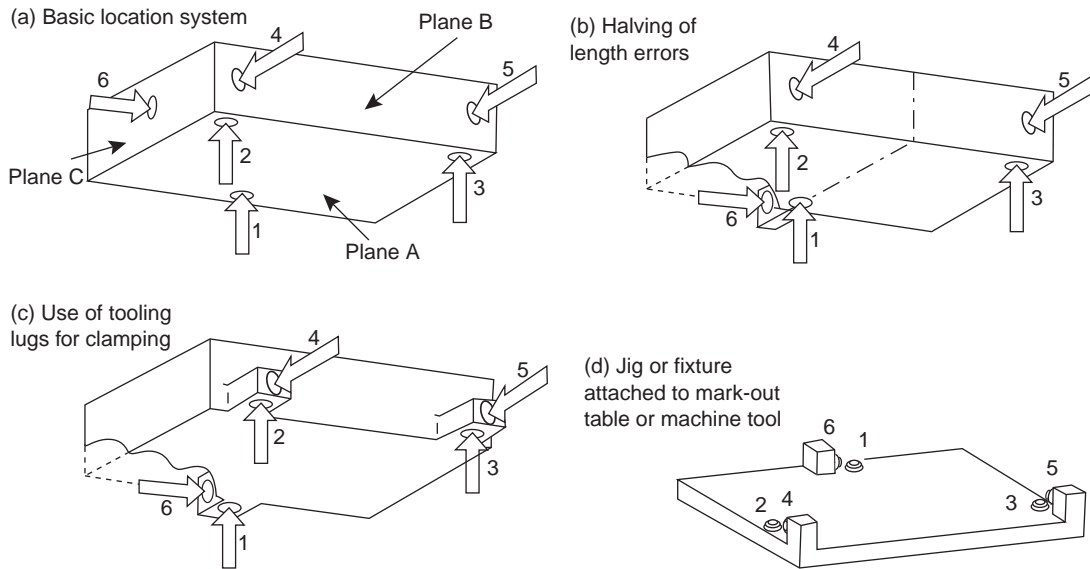


**FIGURE 10.60**

(a) The six-point location system; (b) halving of length errors; (c) use of lugs to combine tool location with clamping points; (d) a jig to cradle the casting during dimensional checking or machining (clamps are omitted for clarity).

Example (c) is a further development of this idea, creating lugs that serve the additional useful purpose of allowing the part to be clamped immediately over the points of support, and off the faces that require to be machined. In practice the lugs may be existing features of the casting, or they may be additions for the purpose of allowing the casting to be picked up for inspection or machining.

The final development, example (d), shows the use of lugs arranged on all the centerlines of the casting so as to halve the errors in all directions. Note that the casting is now inverted for pick-up if the tooling points are to be placed exactly on the horizontal centerline of the casting.

For maximum internal consistency between the tooling points, all points should be arranged to be in one half of the mold, usually the fixed or lower half, although sometimes all in the cope. The separation of points between mold halves, or having some defined from the mold and some from cores, will compromise accuracy. However, it is sometimes convenient and correct to have all tooling points in one internal core, or even one half of an internal core (defined from one half of the core box) if the machining of the part requires to be defined in terms of its internal features.

It is noteworthy that this introduces a small error of principle. The faces of tooling points 1, 2, and 3 are formed in the drag, whereas 4, 5, and 6 are formed in the cope. This is a small error in this case, because the cope/drag joint is among the most reliable of all the mold joints, introducing only a small error in the definition of the location of plane A. Although it is a good rule to place all six points in one piece of mold, often in the drag, so that they all relate to each other accurately, because of the small potential for cope/drag error, an exception may be allowable in this case.

Alternatively, a preferable solution would be to pick up from the underside of lugs 1, 2, and 3, and accept that the casting is now being defined from a plane which is off the casting centerline by the thickness of the lugs. This is a negligible problem, and retains the significantly greater accuracy of pick-up which will result from having all six points in one mold half.

In general it is useful if the tooling locations on the casting can remain in position for the life of the part. It is reassuring to have the tooling points always in place, if only to resolve disputes between the foundry and machine shop concerning failure of the part to clean up on machining. It is therefore good practice to try to avoid placing them where they will be eventually machined off. Using existing casting features wherever possible avoids the cost of additional lugs, and avoids the cost of subsequent removal if necessary.

The definition of the six-point locations, preferably on the drawing (nowadays the computer model), prior to the manufacture of the casting, is the only method of guaranteeing the manufacturability of the part.

### Cylindrical systems

Most cylindrical parts do not fall nicely into the classical six-point location systems as described above for rectilinear components. The errors of eccentricity and diameter both contribute to a rather poor location of the center using this approach. The unsuitability of the orthogonal pick-up system is analyzed nicely by Swing (1962).

In fact, the obvious way to pick up a cylinder is in a three-jaw chuck. The self-centering action of the chuck gives a useful averaging effect on any out-of-roundness and surface roughness, and is of course insensitive to any error of diameter.

In classical terms, the three-jaw chuck is equivalent to a two-point pick-up, since it defines an axis. We therefore need four more points to define the location of the part absolutely. Three points longitudinally abutting the jaws will define the plane at right angles to the center axis, and one final point will provide a 'clock' location. Figure 10.61 shows the general scheme.

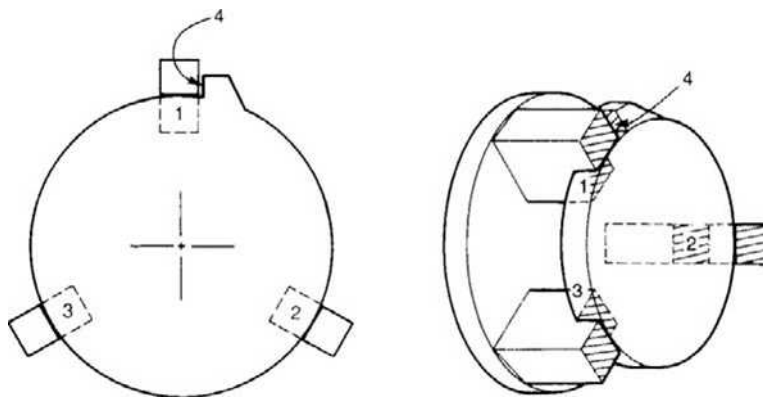


**FIGURE 10.61**

Use of a three-jaw self-centering chuck for casting location and clamping (note that location 4 is occasionally required as a 'clock' location).

Another location method that is occasionally useful is the use of a V block. This is a way of ensuring that a cylindrical part, or the round edge of a boss, is picked up centrally, averaging errors in the size and, to some extent, the shape of the part. The method has the disadvantage that errors in diameter of the part will cause the whole part to be shifted either nearer to or away from the block, depending on whether the diameter is smaller or larger. (The reader can quickly confirm these shifts in position with rough sketches.)

A widely used but poor location technique is the use of conical plugs to find the center of a cored hole. Even if the hole is formed by the mold, and so relatively accurately located, any imperfection in its internal surface is difficult to dress out, and will therefore result in mis-location. If a separate core forms the hole then the core-positioning error will add to the overall inaccuracy of location. Location from holes is not recommended.

It is far better to use external features such as the sides of bosses or walls, as previously discussed. These can be more easily cast and maintained clean.

### Triangular systems

For some suitable parts of triangular form, such as a steering gear housing, a useful and fundamentally accurate system is the cone, groove and plane method (Figure 10.62).

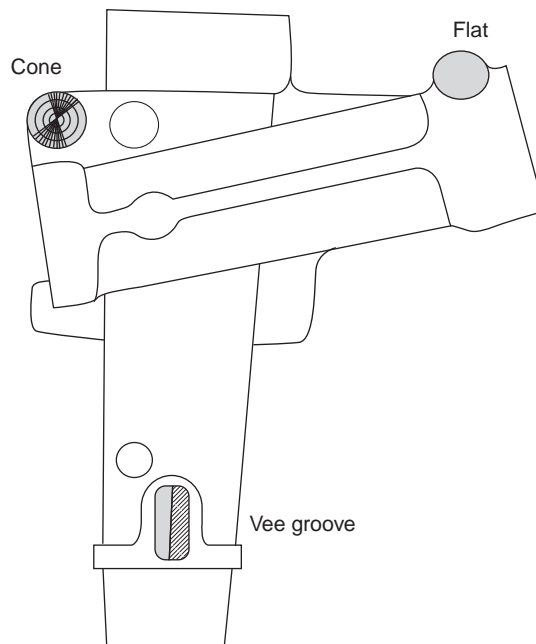


**FIGURE 10.62**

Plan view of a steering housing for an automobile, showing a flat, a groove, and a cone location system.

### Thin-walled boxes

For prismatic shapes, comprising hollow, box-like parts such as sumps (oil pans), the pick-up may be made by averaging locations defined on opposite internal or external walls. This is a more lengthy and expensive system of location often tackled by a sensitive probe on the machine tool, which then calculates the averaged datum planes of the component, and orients the cutter paths accordingly. This technique is especially useful where an average location is definitely desirable, as a result of the casting suffering different degrees of distortion of its relatively thin walls.

The industry and its customers very much need purchasing and manufacturing policies based on positive attitudes such as teamwork and cooperation, together with the adoption of integrated and fundamentally correct systems.

### 10.10.3 Location jigs

Figure 10.60(d) illustrates a basic jig that is designed to accept a casting with a six-point location system. The jig is simply a steel plate with a series of small pegs and blocks. It contrasts with many casting jigs, which are a nightmare of constructional and operational complexity.

Our simple jig is also simple to operate. When placing the casting on the jig, the casting can be slid about on locations 1, 2, and 3 to define plane A, then pushed up against locators 4 and 5 to define plane B, and finally slid along locators 4 and 5 until locator 6 is contacted. The casting is then fixed uniquely in space in relation to the steel jig plate. It can then be clamped, and the casting measured or machined. The six locations can, of course, be set up and fixed directly onto, effectively integrated into the machine tool that will carry out the first machining operation.

After the first machining operations it is normal to remove the casting from the as-cast locations and proceed with subsequent machining using the freshly machined surfaces as the new location surfaces. McKim and Livingstone (1977) go on to define the use of functional datums which may become useful at this stage. They are machined surfaces that normally relate to features locating the part in its intended final application.

Other jigs can easily be envisaged for cylindrical and other shaped parts.

### 10.10.4 Clamping points

During machining the forces on the casting can be high, requiring large clamping loads to reduce the risk of movement of the casting. Clamping points require to be planned and designed into the casting at the same time as the location points. This is because the application of high clamping loads to the casting involves the risk of the distortion of the casting, and of spring-back after the release of the clamps at the end of machining. Surfaces machined flat are apt to become curved after unclamping because of this effect.

The great benefit of using tooling lugs as shown in Figure 10.60(c) can therefore be appreciated. The location point and the clamping point are exactly opposed on either side of the lug. In this way the clamping loads can be high, without introducing the risk of the overall distortion of the casting.

Further essential details of the design of the clamping action include the requirement for the action to move the part on to, and hold it against, the location point.

For softer alloys that are easily indented, the clamp face needs to be 5–10 mm in diameter, similar to the working area of the tooling point. Even so, a high clamping load will typically produce an



indentation of 0.5 mm in a soft Al alloy, decreasing to 0.2 mm in an Al alloy hardened by heat treatment, and correspondingly less still in irons and steels.

### 10.10.5 Potential for integrated manufacture

As we have already emphasized, the tooling points should be defined on the drawing of the part (i.e. more usually on the computer model), and should be agreed by (i) the manufacturer of the tooling, (ii) the caster, and (iii) the machinist. It is essential that all parties work from *only* these points when checking dimensions and when picking the part up for machining.

The method allows an integrated approach right from the start of the creation of the tooling, because the pattern or tool maker can use the tooling points as the critical features of the tooling in relation to which all measurements will be defined. The foundry engineer can check his core and mold assembly, and will know how to pick up the casting to check dimensions after the production of the first sample castings. The machinist will use the same points to pick up the casting for machining. They all work from the same reference points. It is a common language and understanding between design, manufacture, and inspection of products. Disputes about dimensions then rarely occur, or if they do occur, are easily settled. Casting scrap apparently due to dimensioning faults, or faulty pick-up for machining, usually disappears.

This integrated manufacturing approach is relatively easily managed within a single integrated manufacturing operation. However, where the pattern shop, foundry and machinist are all separate businesses, all appointed separately by the customer, then integration can be difficult to achieve. It is sad to see a well-designed six-point pick-up system ignored because of apparent cussedness by one member of the production chain.

This page intentionally left blank

---

# Filling system design

# 2

11	Filling system design fundamentals.....	741
12	Filling system components .....	757
13	Filling system design practice.....	853

This page intentionally left blank

# Filling system design fundamentals

Getting the liquid metal out of the crucible or melting furnace and into the mold is a critical step when making a casting: it is likely that most casting scrap arises during this few seconds of pouring of the casting.

Recent work observing the liquid metal by video X-ray radiography as it travels through the filling system confirms that most of the damage is done to castings by poor filling system design. It is also worth reflecting on the fact that every gram of metal in the casting has, of necessity, traveled through the filling system. Leaving the design of the filling system to chance, or even to the patternmaker (with all due respect to all our invaluable and highly skilled patternmakers), is a risk not to be recommended.

It is fair to say that the avoidance of surface turbulence is probably the most complex and difficult requirement to fulfill when dealing with gravity pouring systems.

---

## 11.1 THE MAXIMUM VELOCITY REQUIREMENT

Casting Rule 2 described in some detail how a melt is safe from entrainment problems if its velocity is below the critical velocity, approximately  $0.5 \text{ m s}^{-1}$ . The danger of entrainment increases as its velocity increases to about  $1.2 \text{ m s}^{-1}$  after which entrainment damage is probably unavoidable. Acknowledging these limits, I find myself always targeting ingate speeds between  $0.5$  and  $1.0 \text{ m s}^{-1}$ . The situation is described further in the following section.

---

## 11.2 GRAVITY POURING – THE ‘NO-FALL’ CONFLICT

Although we have a Rule forbidding the fall of the metal, gravity pouring involves pouring, which necessarily means the metal falls. The obviousness of this pedantic statement emphasizes the fundamental problem faced when pouring castings under gravity. The whole design problem for filling systems revolves around the solution to this conflict.

When melts are transferred by pouring from heights less than the critical heights predicted in Table 2.2 (the heights of the sessile drop) there is no danger of the formation of entrainment defects. Surface tension is dominant in such circumstances, and can prevent the inward folding of the surface, and thus prevent the creation of entrainment defects. Critical velocities and critical fall heights can be defined for all liquid metals. The critical fall heights for all liquid metals are in the range 3–15 mm.

It is just possible to meet this stringent requirement for open top molds in the absence of a filling system (Figure 11.1) because the pouring ladle can be lowered to within a few millimeters of the bottom of the mold. This is probably why the world’s first metal engineering structure, the Iron Bridge

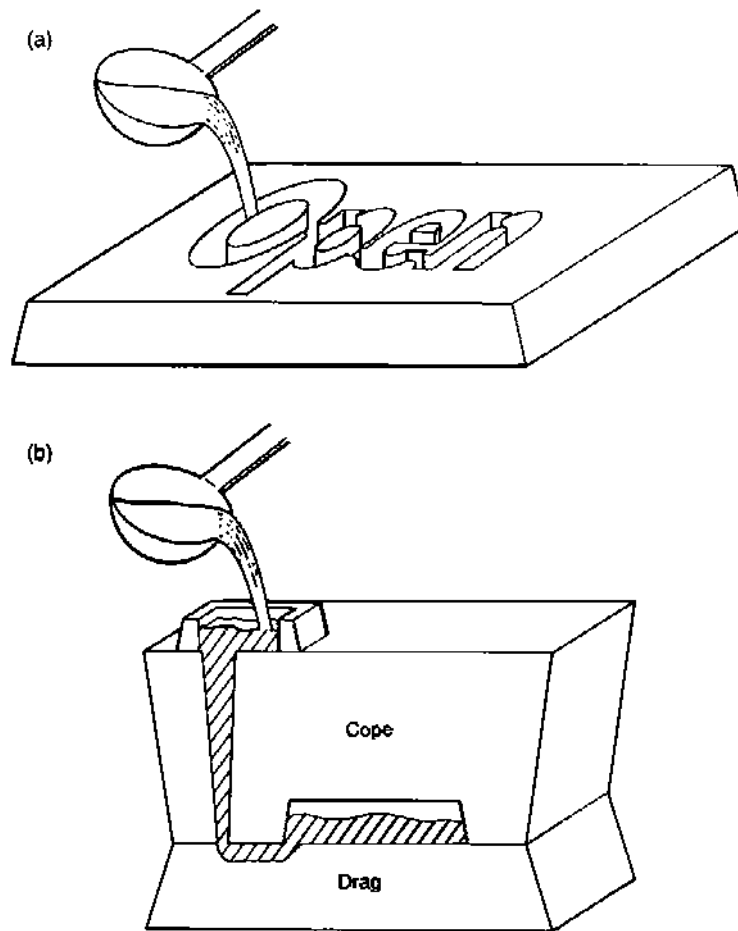


**FIGURE 11.1**

(a) An open and (b) a closed mold partially sectioned.

in the UK, with impressive 23-m-long spans, was so successful. In contrast, most molds nowadays are closed, and therefore require specially designed filling channels to lead the metal into the mold cavity.

It is unfortunate for foundry engineers that the critical fall height is such a minute distance. Most falls that an engineer might wish to design into a melt handling system, or running system, are nearly always greater, if not vastly greater. The small value of the critical fall height is one of those extremely inconvenient distances that we casting engineers have to learn to live with.

It follows immediately that *top gating* of a casting (Figure 11.2) almost without exception will lead to a violation of the critical velocity requirement. Many forms of gating that enter the mold cavity at the mold joint, if any significant part of the cavity is below the joint, will also violate this requirement.

Also excluded are any filling methods that cause waterfall effects in the mold cavity. This requirement dictates the siting of a separate ingate at every isolated low point on the casting.

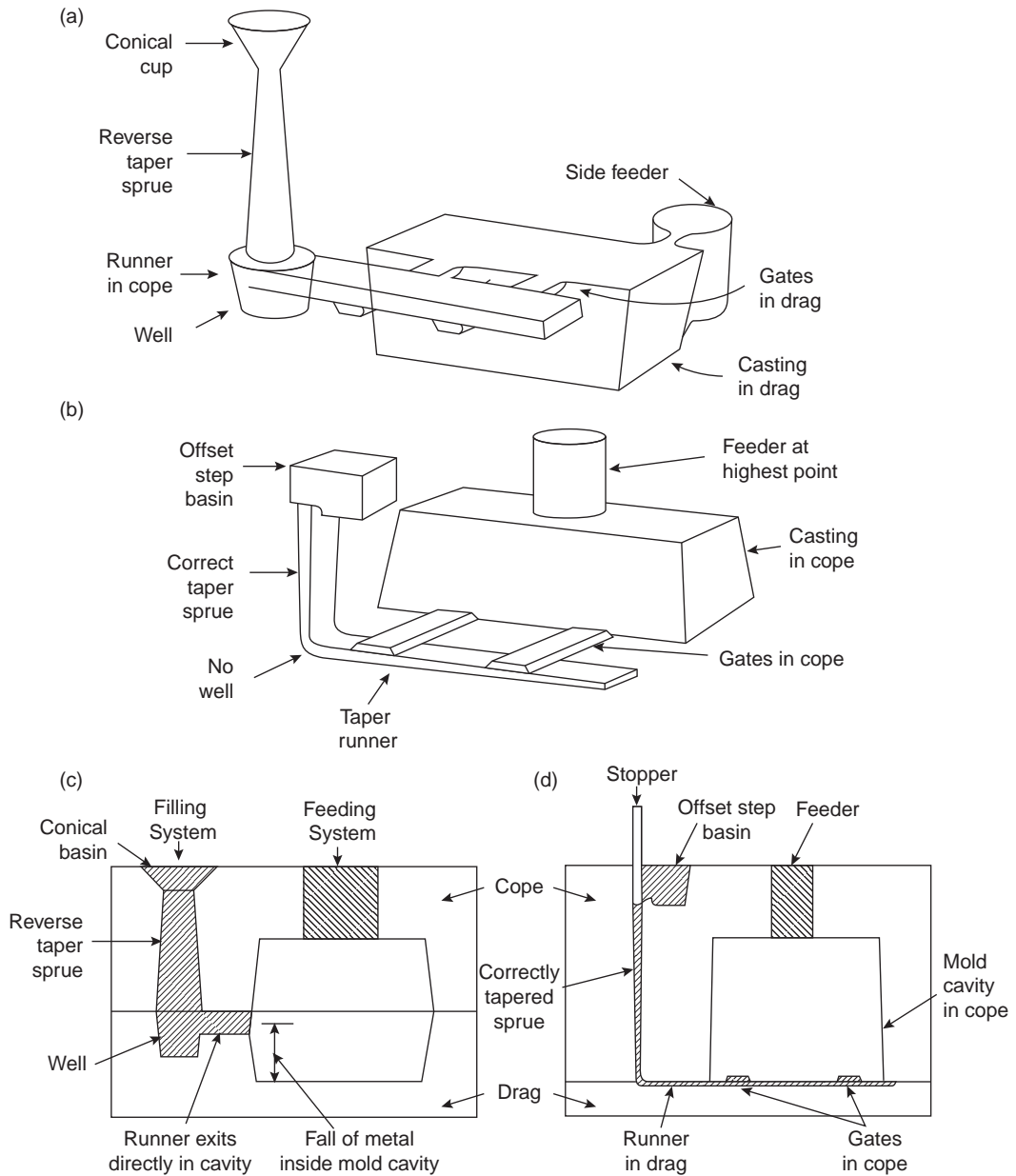


**FIGURE 11.2**

(a) Poor top-gated and side-fed running system, compared with (b) a more satisfactory bottom-gated and top-fed system; (c) poor system gated at joint and (d) recommended economical and effective system.

If the melt does fall as a stream into the surface of the liquid, and depending on the alloy and the flexibility of its oxide film, the tube of oxide that forms around it may form a cylindrical crack if it remains in place, or if it detaches may concertina together to form a dross ring (Figure 2.23b). Although this represents an important loss of metal on transferring liquid aluminum and other dross-forming alloys, it is not clear whether defects are also dragged beneath the surface and thereby entrained.

At higher speeds still, the dross is definitely carried under the surface of the liquid, together with entrained air, as shown in Figure 2.23c. Turner (1965) has reported that, above a pouring height of 90 mm, air begins to be taken into the melt with the stream, to reappear as bubbles on the surface.

Falls in excess of the critical heights have been investigated for aluminum alloys (Din, Kendrick, and Campbell 2003). The author's own tendency is often to allow himself up to  $1.0 \text{ m s}^{-1}$  gate velocity, but never beyond  $1.2 \text{ m s}^{-1}$  which appears to be the velocity at which problems first occur, corresponding to a 70-mm fall. Falls of 100 mm, corresponding to a falling velocity of  $1.4 \text{ m s}^{-1}$  appear always to entrain serious defects unless the melt is smoothed (the flow is 'laminized') by the use of a ceramic foam filter. In the case of a flow smoothed by a filter even a fall of even 200 mm ( $2 \text{ m s}^{-1}$ ) appears to be tolerable as clearly shown later in Section 12.8 on filtration. This is in general agreement with the water model results of Goklu and Lange (1986) who found that the internal turbulence within a plunging jet influenced its surface smoothness, which in turn influenced the amount of air entrainment. Practical maximum pour heights require to be investigated for other alloy systems to test what values beyond the theoretical limits may be used in practice.

Clearly, the benefits of defect-free pouring are easily lost if the pouring speed into the entry point of the filling system into the mold is too high. This is often observed when filling the pouring basins of castings from an unnecessary height. In aluminum foundries this is usually by robot. In iron foundries it is commonly via automatic pouring systems from fixed launders sited over the line of molds. In steel foundries it is common to pour from bottom-poured ladles that contain over a meter depth of steel above the exit nozzle (the pouring conditions for steel from bottom-teemed ladles are further complicated by the depth of metal in the ladle decreasing progressively from pour to pour). These three systems are all at risk of entraining defects in the pouring basin. However, the effect becomes sharply greater as we progress from filling the pouring basin by:

- (i) lip pouring to
- (ii) robot pouring to
- (iii) automatic pouring from overhead launders to
- (iv) bottom-poured ladles.

In fact the situation is so bad for bottom-poured ladles, or bottom teeming as it is sometimes known, that it seems to me that a pouring basin concept will never work satisfactorily for this mode of filling. Entrainment will be occurring at a rate faster than detrainment from the basin can occur. This is a serious situation that is not widely appreciated causing widespread problems in steel foundries. We shall deal with this problem later, and note that one of the few solutions to this serious issue is the elimination of the pouring basin and the implementation of contact pouring.

When the melt finally enters the down-sprue, the initial fall down the sprue in gravity-filled systems is nearly always a ragged and messy affair, necessarily introducing oxide damage into the metal. Some of this raggedness is reduced by the use of a stopper to pre-fill the pouring basin. However, it seems reasonable to conclude that gravity-poured castings will never attain the degree of reliability that can be provided by counter-gravity and other systems that can avoid surface turbulence. Of necessity,



therefore, it has to be accepted that the no-fall requirement applies to the design of the filling system downstream of the base of the sprue. The damage encountered in the fall down the sprue has to be accepted; although with a good sprue and pouring basin design this initial fall damage can be reduced to a minimum as we shall see.

---

## 11.3 REDUCTION OR ELIMINATION OF GRAVITY PROBLEMS

Over the years a number of valuable techniques have been developed to overcome the problems that gravity pouring involves. These will be dealt with as technological issues later in the Processing Section under 'Casting'. Essentially, they can be summarized as:

- (i) Accepting as inevitable the unwanted acceleration due to gravity, and thus designing filling systems to cope with the necessarily high velocities but, despite the great danger to the melt, attempting to reduce the opportunities for damage by entrainment. This is achieved mainly by constraining the melt in narrow channels, too slim to allow the melt to fold over on itself and thus enclose its own surface. This is the basis behind the 'naturally pressurized' filling system design described at length in this book.
- (ii) Using essentially horizontal transfer of various types, including so-called 'level pour' techniques, or a special approach to tilt casting controlled in such a way to encourage only horizontal transfer while the mold rotates.
- (iii) True counter-gravity filling, in which the melt is transferred only uphill against gravity, using either pressurization from below by gas pressure or pump system, or vacuum from above.
- (iv) Filling molds with such narrow walls and sections that the melt is constrained by surface tension which now controls the filling instead of gravity. This phenomenon is discussed later below.

At the time of writing most castings are made by pouring the liquid metal into the opening of the running system, as in (i) above, using the action of gravity to effect the filling action of the mold. This is a simple and quick way to make a casting. Thus *gravity sand casting* and *gravity die casting* (*permanent mold casting* in the USA) are important casting processes at the present time. Gravity castings have, however, gained a poor reputation for reliability and quality, simply because their running systems have in general been badly designed. Surface turbulence has led to porosity and cracks, and unreliability in leak-tightness and mechanical properties.

Nevertheless, as emphasized in this book, there are rules for the design of gravity-running systems that, although admittedly far from perfect, are much better than nothing. Such rules were originally empirical, based sometimes on water modeling work and some confirmatory tests on real castings. We are now a little better informed by access to real-time video radiography of molds during filling, and sophisticated computer simulation, so that liquid aluminum or liquid steel can be observed or at least simulated as it tumbles through the mold. Despite this, many uncertainties still remain. The rules for the design of filling systems are still not the mature science for which we all might wish. Even so, some rules are now evident, and their intelligent use allows castings of the highest quality to be made. They are therefore described at length (but not, we hope, ad nauseam) and constitute essential reading!

It is hoped to answer the questions 'Why is the running system so complicated?' and 'Why are there so many different features?' It is a salutary fact that the apparent complexity has led to much confused thinking.

An invaluable clarifying rule that I recommend to all those struggling with the understanding of running and gating systems is ‘If in doubt, visualize water.’ Most of us have clear perceptions about the mobility and general flow behavior of water in the gentle pouring of a cup of tea, the splat as it is spilled on the floor, the flow of a river over a weir, or the spray from a high-pressure hose pipe. A general feeling for this behavior can sometimes allow us to cut through the mystique, and sometimes even through the calculations! In addition, the application of this simple criterion can often result in the instant dismissal of many existing filling systems intended for the production of a reliable quality of casting as being clearly quite useless!

There are, of course, numerous ways to get the metal into the mold, but some are disastrously bad, some tolerable, some good. To appreciate the good we shall have to devote some space to the bad. If this reads like a sermon, then so be it. *The Good Running System* is a *Good Cause* that deserves the passionate concern of the casting engineer. Too many castings with hastily rigged running systems have appeared to be satisfactory in limited prototype trials, but have proved to have disastrous levels of scrap when put into production. This is normally the result of surface turbulence during filling that produces non-reproducible castings, some apparently good, some definitely bad. This result confirms the nature of turbulence. Turbulence implies chaos; and chaos implies unpredictability. When using a running system that generates surface turbulence a typical scrap rate for a commercial vehicle casting might be 15%, whereas with a turbine blade subjected to much more stringent inspection rejections can easily reach 75%.

In general, however, experience shows that foundries that use exclusively turbulent filling methods, such as most investment foundries, experience on average about 20–25% scrap, of which 5–10% is the total of miscellaneous minor processing problems such as broken molds, castings damaged during cut-off, etc. The remaining 15–20% is composed of random inclusions including mold fragments, random porosity, and misruns – the standard legacy of turbulent running systems: the inclusions are created by the battering of the mold and the folding of the liquid surface, as are the random pockets of porosity; and the misruns by the unpredictable ebb and flow in different parts of the casting during filling. In sand casting foundries, most of the so-called mold problems leading to sand inclusion are actually the result of the poor filling system designs. With good filling systems sand problems such as mold erosion and sand inclusions disappear.

In a foundry making a variety of castings, the 15% running system scrap is made up of difficult castings which might run at 85–95% scrap (almost never 100%!) and easy castings which run at 5% scrap (almost never zero!). The non-repeatable results continuously raise the characteristic false hope that the problems are solved, only to have the hopes dashed again by the next few castings. The variability is baffling, because the foundry engineer will often go to extreme lengths to ensure that all the variables believed to be under control are held constant.

Only a carefully worked out running system will give filling that is characterized by low surface turbulence, and which is therefore reproducible every time.

Interestingly, this can mean 100% scrap. However, this is not such a bad result in practice because the defect will be reproducibly repeated in every casting. It is therefore easy to identify and correct, and when corrected, stays corrected. After the first trials, the good running system should yield reliable, repeatable castings, and be characterized by a scrap rate close to zero.

A good running system, perhaps something like that shown in Figure 11.2b, will also be tolerant of wide variations in foundry practice, in contrast with the normal experience accompanying turbulent filling, in which pouring conditions are critical. Many foundries will have the experience that certain castings can only be poured successfully by certain operators.

In contrast, the good running system will ensure that filling of the casting will now be under the control of the running system, not the pourer, and casting temperature will no longer be dictated by the avoidance of misruns, but might be set independently to control, for instance, grain size without the addition of grain refiners. It is clear, therefore, that a good running system is a good ally in the creation of economical products of high quality.

The elements of a good system are:

1. Economy of size. A lightweight system will increase yield (the ratio of finished casting weight to total cast weight), allowing the foundry to make more castings from the existing melt supply. It may also help to get more castings into a given mold box. This has a big effect on productivity and economy. Also, critically, a slim system works better than an oversized system, delivering better castings.
2. The filling of the mold at the required speed. In the method proposed in this book, the whole running system is designed so that the velocity of the metal in the gates is below the critical value. This value varies negligibly from one alloy to another, being generally close to  $0.5 \text{ m s}^{-1}$ . There is now much experimental and theoretical data to support this value (Boutorabi 1991). Data on the density of castings produced by gating uphill have shown that air entrapment can occur above approximately  $0.5 \text{ m s}^{-1}$  (Suzuki 1989). In computer simulations of flow, Lin and Hwang (1988) show that when liquid aluminum enters the mold horizontally at  $1.1 \text{ m s}^{-1}$  it hits the far wall with such force that the reflected wave breaks, causing surface turbulence. These figures confirm the safety of  $0.5 \text{ m s}^{-1}$ , and the danger of exceeding  $1 \text{ m s}^{-1}$ . Even so, I often allow myself to work at velocities up to  $1 \text{ m s}^{-1}$  since the  $0.5 \text{ m s}^{-1}$  is often difficult to meet, and the  $1 \text{ m s}^{-1}$  is usually just sufficiently slow to avoid any serious problems.
3. The delivery of only liquid metal into the mold cavity, i.e. not other phases such as slag, oxide, and sand. However, in most cases the overwhelmingly important and unwelcome phase is air (probably contaminated with other mold gases of course). The design of filling systems to achieve the exclusion of air is a major preoccupation in this book. The main weapon here is pressurization of the metal in the filling system. The naturally pressurized filling system proposed in this work automatically fulfills this essential requirement.
4. The elimination of surface turbulence, preferably at an early stage in the runner system, but certainly by the time that the metal arrives in the mold cavity. The problem here is that by the time the metal has fallen the length of the sprue to reach the lowest level of the casting, its velocity is well above the critical velocity for surface turbulence. Despite this danger, the running system should, so far as possible, prevent the resulting fragmentation of the stream. Any fragmentation will result in permanent damage to the casting in most alloys. However, if fragmentation occurs, the best that can now happen is that it should be followed by an action to gather the stream together again. In this way the melt enters the mold as a coherent, compact spreading front, preferably at a velocity sufficiently low that the danger of any further break-up of the front is eliminated.
5. Ease of removal. Preferably the system should break off. As a next best option, it should be removable with a single stroke of a clipping press, or a straight cut on a saw. Curved cuts take more time and are more difficult to dress to finished size by grinding or finishing. Internal or shielded gates may need to be machined off, in which case the expense of setting up the casting for machining might be avoidable by carrying out this task later, during the general machining of the casting.

(Note that in general practice it is usually best to assume that there is no requirement for the filling system to act as a feeder, i.e. to compensate for the contraction on solidification. We should ensure that the feeding function if necessary at all, is carried out by a separate feeder placed elsewhere, preferably high up, on the casting (Figure 11.2b). Occasionally it is possible to use a running system that can also provide some feeding. This especially favorable option should be exploited whenever possible. It is worth noting that in investment casting the almost universal confusion between filling and feeding systems is deeply regrettable. In this book the two functions are treated totally separately.)

Because the above list of criteria has been so difficult to meet in practice, there has been a move away from gravity casting as a result of what have been believed to be insoluble barriers to the attainment of high quality and reliability.

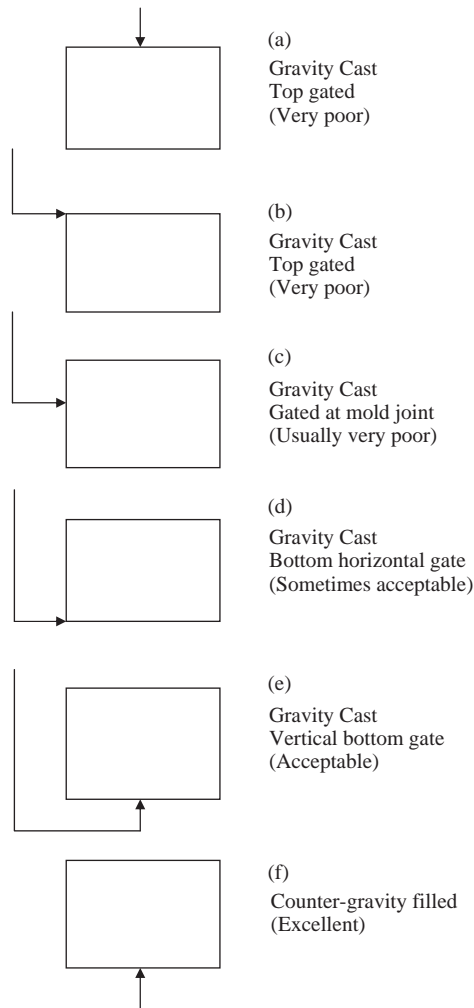
Uphill filling, against gravity, known as *counter-gravity casting*, has provided a solution for the elimination of surface turbulence. (Counter-gravity should not be confused with a variety of gravity pouring known as *bottom gating* as in Figures 11.2 and 11.3.) This development has therefore provided the impetus for the growth of low-pressure die casting, low-pressure sand casting, and various forms of counter-gravity filling of investment castings. A form of high-pressure die-casting has also been developed to take advantage of the quality benefits associated with counter-gravity filling followed by high-pressure consolidation. These different techniques of getting the metal into the mold will all be discussed later.

Although counter-gravity filling fulfills all the above requirements, our task when faced with gravity pouring is to optimize filling conditions so far as possible to meet this difficult set of criteria.

Requirement 3 above for good gating is important: only liquid metal should enter the casting. Thus all bubbles entrained by the surface turbulence characterizing the early part of the running system should have been eliminated by this stage. If the running system is poor, and bubbles are still present, their rise and bursting at the liquid surface in the mold violates Casting Rules 2 and 4. These violations result in a number of problems, including bubble trails, splash defects, and the retention of the scattering of smaller bubbles that remain trapped under the oxide skin of the rising metal. These cause concentrations of medium-sized pores (0.5–5 mm diameter) at specific locations in the casting, usually at upper surfaces of the casting above some of the ingates.

The other point in Requirement 3, that dross or slag does not enter the mold cavity, is interesting. In the production of iron castings it is normal for the runner to be placed in the cope and the gates in the drag, as is illustrated in Figure 11.2a. The thinking behind this design of system is that slag will float to the top of the runner, and thus will not enter the gates. Such thinking is at fault because it is clear that at least some of the first metal to enter the runner will fall down the first gate that it meets, taking with it not only the first slag but also air. This premature delivery of metal into the mold before the runner is full is clearly unsatisfactory. The metal has had insufficient time to settle down, to organize itself free from dross, oxide, and bubbles. The fact that such systems are widely used, and are found in practice to reduce bubble defects in the casting actually reveals how poor the front end of the running system is. Clearly, bubbles are being generated throughout the pour, so the off-take of gates at the base of the runner is valuable in this case.

A more satisfactory system is illustrated in Figure 11.2b. Here the runner is in the drag and the gates in the cope. In this system the runner has to fill first before the gates are reached. Thus the metal has a short but valuable time to rid itself of bubbles and dross, most of which can be trapped against the upper surface of the runner. Only a limited amount of slag or dross will be unfortunately placed to enter

**FIGURE 11.3**

Various direct gating systems applied to a box-shaped casting. (Note that all of the gravity systems shown here are poor: the sprue base connects directly with the ingate into the casting. All gravity systems need mechanisms (not shown for clarity) to reduce the velocity of the melt.)

the gate. Provided the velocity of the metal in the gate is not too high, even this slag still has a good chance of being held against the ceiling of the runner or gate, and thus not entering the casting. Figure 11.2c illustrates an optimum system designed to resist the entrainment of air at all stages of the system.

Statement 4 above is deceptively simple. However, the requirement of no surface turbulence is so important, and so central to the quest for good castings, that we have to consider it at length.

Texts elsewhere often refer to turbulence-free filling as laminar filling. The implication here is that turbulence as defined by Reynold's number is involved, and that the desirable criterion is that of laminar flow of the bulk. However, it is not bulk turbulence that is relevant since turbulent flow in the bulk liquid can still be accompanied by the desirable smooth flow of the surface. Our attention requires to be concentrated on the behavior of the liquid surface. Thus provided we ensure that by 'laminar fill' we mean 'surface laminar fill', then we shall have our concepts correct, and our thinking accurate.

Requirement 4 above is clearly violated by splashing during filling. It can be seen immediately that top gating will probably therefore always introduce some defects (the exception is very thin wall castings where surface tension takes over control of surface turbulence). Figure 11.3 illustrates the spectrum of gating options from very poor to excellent. The systems can be judged in the degree to which the metal is allowed to suffer a free fall into the mold cavity. Bottom-gated systems are always required if surface turbulence is to be eliminated. Counter-gravity is, of course, even more powerful than any bottom-gated gravity system because the velocity of the metal can be controlled at all times to be below critical.

However, although bottom gating is necessary, it is not a sufficient criterion. It is easy to design a bad bottom-gating system! In fact, it is possible to state the case more forcefully: a bad bottom-gated system is usually worse than most top-gated systems.

For instance, it is common to see bottom-gated systems proudly displayed with the base of the runner turned so that metal directly enters the mold (Figures 11.3d and 11.4). Such systems are compact, and appear economical until the percentage scrap figures are inspected. The sequence of events is clear if we consider the fall of the first liquid down the length of the sprue. The high velocity of the metal on its impact at its base is not contained. The resulting splash may be likened to an explosion of a high-velocity jet fired like a projectile directly into the mold. The bulk of the metal follows in an untidy fashion, as jet fragments mixed with air and mold gases. The jet ricochets from the far wall, causing more surface turbulence as the rebounding wave washes back, breaking and rolling over to entrain yet more surface oxide and more gas. The elimination of the entrained bubbles by bursting as they rise to the surface of the melt causes additional droplets to be created by splashing.

It is important, therefore, to design the down-sprue with care so that it will fill quickly, excluding air as quickly as possible, and to design the runner and gate to constrain the metal, avoiding any provision of room for splashing (Figure 11.5a). Further improvements might be allowable as in Figures 11.5b and 11.5c in which the fall heights down the sprue are progressively reduced, reducing velocities in the mold, by simply re-orienting the casting. This is a valuable technique.

The base of the sprue should be the lowest point in the whole system: having reached here, all subsequent flow of the liquid should be uphill, displacing the air ahead in a controlled and progressive advance. So far as possible, the liquid should be slowed as it goes, experiencing as much opportunity as possible to become quiescent before entering the mold. It should finally enter the mold at a velocity between  $0.5$  and  $1.0 \text{ m s}^{-1}$ . In this way a good and reproducible casting is favored.

It is important to note that these precautions to avoid the entrainment of oxide films also apply to casting in inert gas or even in vacuum. This is because the oxides of Al and Mg (as in Al alloys, ductile irons, or high-temperature Ni-base alloys for instance) form so readily that they effectively 'getter' the residual oxygen in any conventional industrial vacuum, and form strong films on the surface of the liquid.

The reader might notice that there is no emphasis in this book regarding the huge amount of research that has been carried out on the filling systems of castings, treating the flow of the metal as an

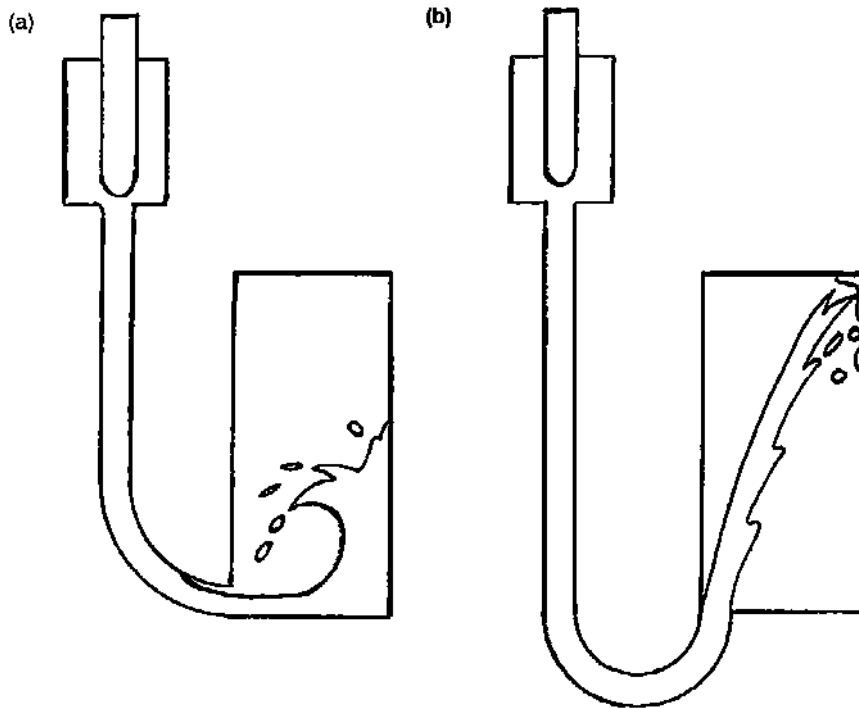


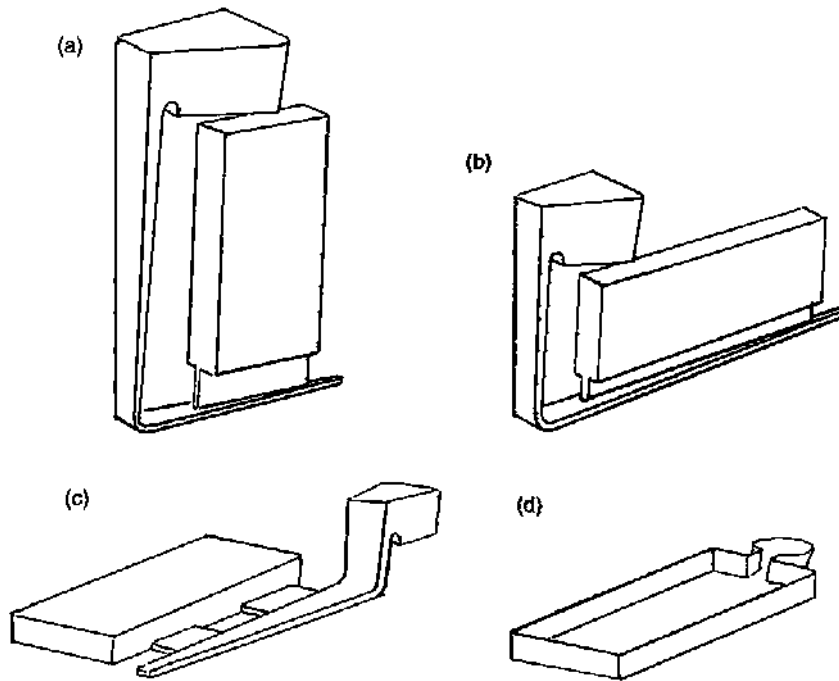
**FIGURE 11.4**

Two bottom-gated systems that behave poorly because of direct entry of metal into the mold cavity at an uncontrolled velocity (after Grube and Kura 1955).

exercise in hydraulics. Using this scientific method the friction factors and loss coefficients at bends and orifices etc. can be summed to find overall rates of flow (for instance see Bradley et al. 1992). In general, only perfectly filled channels are considered. This approach is neglected here only because the major problem for the filling systems of castings is flow in (at least initially) unfilled channels and unfilled molds, where surface turbulence can wreak damage. Even with a well-designed filling system the problem to obtain a good casting may be controlled by the priming of the system, in which the 100% of air has to be supplanted by, it is hoped, 100% of metal, without in the meantime harming the quality of the liquid metal. Thus the technology for casting is essentially different, and, it seems, significantly more difficult to solve. That is what this book is about.

## 11.4 SURFACE-TENSION-CONTROLLED FILLING

Casting Rule 2, the avoidance of pouring and therefore exceeding the critical velocity, applies to 'normal' castings with walls of thickness of 3 or 4 mm or more. It is important to consider the different circumstances for extremely thin-walled products.

**FIGURE 11.5**

Improved bottom-gated system; (a)–(c) progressively improved filling systems by height reductions down to (d) zero height by tilt casting.

For channels that are sufficiently narrow, having dimensions of only a few millimeters, the curvature of the meniscus at the liquid front can help to preserve the liquid front from disintegration. Thus narrow filling system geometries are valuable in their action to conserve the liquid as a coherent mass, and so acting to push the air out of the system ahead of the liquid. The filling systems therefore fill in one pass. Such a filling action, pushing the air ahead of the liquid front as a piston in a cylinder, is a ‘one pass filling (OPF) design’.

In some thin-walled castings the liquid may not be able to enter the mold at all. This is to be expected if the pressure is too low to force melt into the narrow section. It is an effect due to surface tension  $\gamma$ . If the liquid surface is forced to take up a sharp curvature to enter a non-wetted mold then it will be subject to a repulsive force that will resist the entry of the metal. Even if the metal manages to enter, it will still be subject to the continuing resistance of surface tension, which will tend to reverse the flow of metal, causing it to empty out of the mold if there is any reduction in the filling pressure. These are important effects in narrow-section molds (i.e. thin-section castings) and have to be taken into account.

We may usefully quantify our formulation of this problem with the well-known equation (stated in Chapter 3 as Equation 3.10 but restated here using different symbols)



$$P_i - P_e = \gamma(1/r_1 + 1/r_2) \quad (11.1)$$

where  $P_i$  is the pressure inside the metal, and  $P_e$  the external pressure (i.e. referring to the local environment in the mold). The two radii  $r_1$  and  $r_2$  define the curvature of the meniscus in two planes at right angles. The equation applies to the condition when the pressure difference across the interface is exactly in balance with the effective pressure due to surface tension. To describe the situation for a circular-section tube of radius  $r$  (where both radii are now identical), the relation becomes:

$$P_i - P_e = 2\gamma/r \quad (11.2)$$

For the case of filling a narrow plate of thickness  $2r$ , one radius is, of course,  $r$ , but the radius at right angles becomes infinite, so the reciprocal of the infinite radius equates to zero (i.e. if there is no curvature there is no pressure difference). The relation then reduces to the effect of only the one component of the curvature,  $r$ :

$$P_i - P_e = \gamma/r \quad (11.3)$$

We have so far assumed that the liquid metal does not wet the mold, leading to the effect of *capillary repulsion*. If the mold is wetted then the curvature term  $\gamma/r$  becomes negative, so allowing surface tension to assist the metal to enter the mold. This is, of course, the familiar phenomenon of *capillary attraction*. The pores in blotting paper attract the ink into them; the capillary channels in the wick of a candle suck up the molten wax; and the water is drawn up the walls of a glass capillary. In general, however, the casting technologist attempts to avoid the wetting of the mold by the liquid metal. Despite all efforts to prevent it, wetting sometimes occurs, leading to the penetration of the melt into sand cores and molds.

Continuing now in our assumption that the metal–mold combination is non-wetting, we shall estimate what head of metal will be necessary to force it into a mold to make a wall section of thickness  $2r$  for a gravity casting made under normal atmospheric pressure. If the head of liquid is  $h$ , the hydrostatic pressure at this depth is  $\rho gh$ , where  $\rho$  is the density of the liquid, and  $g$  the acceleration due to gravity. The total pressure inside the metal is therefore the sum of the head pressure and the atmospheric pressure,  $P_a$ . The external pressure is simply the pressure in the mold due to the atmosphere  $P_a$  plus the pressure contributed by mold gases  $P_m$ . The equation now is:

$$(P_a + \rho gh) - (P_a + P_m) > \gamma/r \quad (11.4)$$

giving immediately (reflecting the fact that atmospheric pressure acts uniformly everywhere, so effectively canceling)

$$\rho gh - P_m > \gamma/r \quad (11.5)$$

The back-pressure due to outgassing in the mold lowers the effective head driving the filling of the mold. It is good practice, therefore, to vent narrow sections, reducing this resistance to practically zero if possible.

It is also clear from the above result that, provided the mold is permeable and/or well vented, atmospheric pressure plays no part in helping or resisting the filling of thin sections in air, since it acts equally on both sides of the liquid front, canceling any effect. Interestingly, the same equation and reasoning applies to casting in vacuum, which, of course, can be regarded as casting under a reduced atmospheric pressure. Clearly, a *vacuum casting* is therefore not helpful in overcoming the resistance to filling provided by surface tension (although, to be fair, it may help by reducing  $P_m$  by outgassing the

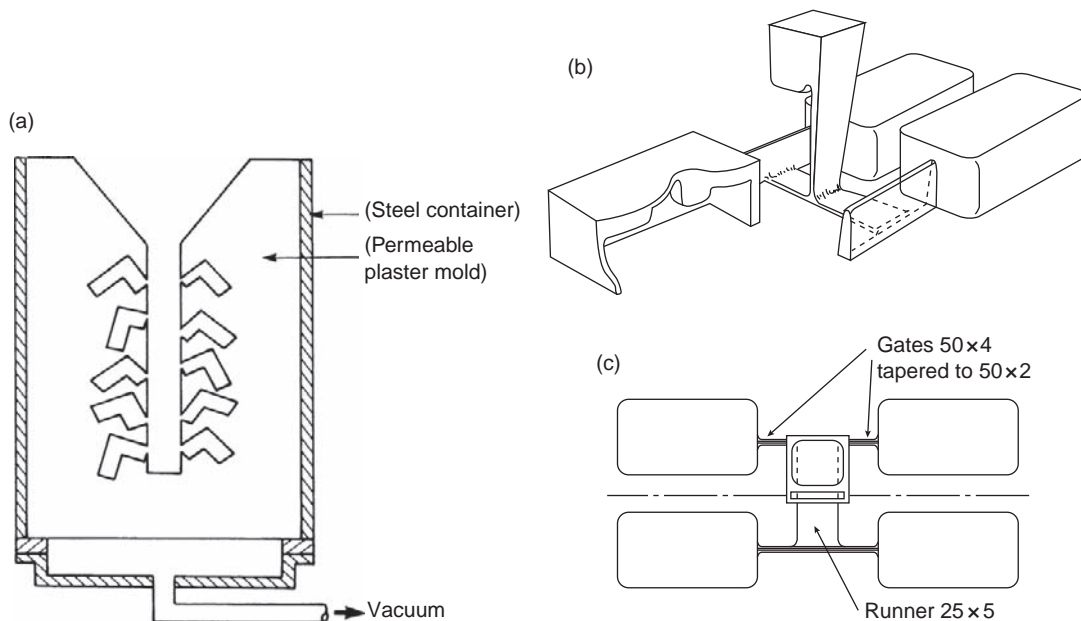


**FIGURE 11.6**

(a) A plaster mold encased in a steel box using vacuum-assisted filling through the base of the mold. No formal running system is required for such small thin-walled castings; (b) a perspective and plan view of a sand mold to make four cover castings, using narrow slot-filling system to maximize benefits from surface tension and wall friction.

mold to some extent prior to casting, and it will help where the permeability of the mold is low, where residual gases may be compressed ahead of the advancing stream. Vacuum casting may also help to fill the mold by reducing – but not eliminating – the effect of the surface film of oxide or nitride.)

The case of *vacuum-assisted filling* (not vacuum casting) is quite different, since the vacuum is not now applied to both the front and back of the liquid meniscus, thus canceling any benefit as above, but applied only to the advancing front as illustrated in Figure 11.6a. This application of a reduced pressure to one side of the meniscus creates a differential pressure that drives the flow. The differential pressure acts by atmospheric pressure continuing to apply to the liquid metal via the running system, but the atmospheric pressure in the mold is reduced by applying a (partial) vacuum in the mold cavity. This is achieved by drawing the air out either through the permeable mold, or through fine channels cut through to the section required to be filled (as is commonly applied to the trailing edge of an aerofoil blade section). In this way  $P_m$  is guaranteed to be zero or negligible, and  $P_a$  remains a powerful pressure to assist in the overcoming of surface tension as the equation indicates:

$$P_a + \rho gh > \gamma/r \quad (11.6)$$

It is useful to evaluate the terms of this equation to gain a feel for the size of the effects involved. Taking, roughly,  $g$  as  $10 \text{ m s}^{-2}$ , and the liquid aluminum density  $\rho$  as  $2500 \text{ kg m}^{-3}$  and  $\gamma$  as  $1.0 \text{ N m}^{-1}$

(for steels and high-temperature alloys the corresponding values are approximately  $7000 \text{ kg m}^{-3}$  and  $2.0 \text{ N m}^{-1}$ ), the resistance term  $\gamma/r$  works out to be 2 kPa for a 1-mm section (0.5-mm radius) and 10 kPa for a 0.1-mm radius trailing edge on a turbine blade.

For a head of metal  $h$  100 mm the head pressure  $\rho gh$  is 2.5 kPa, showing that the 1-mm section might just fill. However, the 0.1-mm trailing edge has no chance; the head pressure being insufficient to overcome the repulsion of surface tension. However, if vacuum assistance were applied (N.B. not vacuum casting, remember) then the additional 100 kPa of atmospheric pressure normally ensures filling. In practice it should be noted that the full value of atmospheric pressure is not easily obtained in vacuum-assisted casting; in most cases a value nearer half an atmosphere is more usual. Even so, the effect is still important: one atmosphere pressure corresponds to 4 m head of liquid aluminum, and approximately 1.5 m head of denser metals such as irons, steels, and high-temperature alloys. In modest-sized castings of overall heights around 100 mm or so, these valuable pressures to assist filling are not easily obtainable by other means. The pressure delivered by a feeder placed on top of the casting may only apply the additional head corresponding to its height of perhaps 0.1–0.4 m; only one-tenth of the pressures that can be applied by the atmosphere.

For those castings that have sections of only 1 or 2 mm or less, the surface tension wields a strong control over the tight radius of the front. Filling is only possible by the operation of additional pressure, such as that provided by the jeweler's centrifuge, or the application of vacuum assistance. Filling can occur upwards or downwards without problems, being always under the control of the surface tension, which is effectively so strong in such thin sections that it keeps the surface intact. Surface turbulence is thereby suppressed. The liquid has insufficient room to break up into drops, or to jet or splash. The integrity of the front is under the control of surface tension at all times. This special feature of the filling of very thin-walled castings means that they do not require formal running systems. In fact, such thin-walled plaster investment castings are made successfully by simply attaching wax patterns in any orientation directly to a sprue (Figure 11.6a). The metal flows similarly either with gravity or counter to gravity, and no 'runner' or 'gate' is necessary.

To gain an idea of the head of metal required to force the liquid metal into small sections, from Equation 2.6 we have:

$$\begin{aligned}\rho gh &= \gamma/r \\ h &= \gamma/r\rho g\end{aligned}\tag{11.7}$$

Using the values for aluminum and steel given above, we can now quickly show that to penetrate a 1-mm section we require heads of at least 80 and 60 mm, respectively, for these two liquids.

If the section is halved, the required head for penetration is, of course, doubled. Similarly, if the mold shape is not a flat section that imposes only one curvature on the meniscus, but is a circular hole of diameter 1 mm, the surface then has an additional curvature at right angles to the first curvature. Equation 11.2 shows the head is doubled again.

In general, because of the difficulty to predict the shape of the liquid surface in complex and delicate castings, the author has found that a safety factor of 2 is not excessive when calculating the head height required to fill thin sections. This safety factor is quickly used up when allowances for errors in the wall thickness and the likely presence of surface films are taken into account.

In Figure 11.6a the castings have a wall thickness of only 0.4 mm and because the sprue is only about 100 mm high, providing too little head pressure, the castings will not normally fill. This is the

reason for connecting the base of the mold on to a vacuum manifold that can deliver perhaps 0.5 bar reduction in pressure through the permeable mold. The 0.5 atmosphere suction is equivalent to nearly 2 m head of liquid Al alloy that encourages the castings to fill practically instantaneously.

The resistance to flow provided by surface tension can be put to good effect in the use of slot-shaped filling systems. In this case the slots are required to be a maximum thickness of only 1 or 2 (perhaps 3 at the most) mm thickness for engineering castings. (Although, clearly, jewelry and other widget-type products might require even thinner filling systems.) Figure 11.6b shows a good example of such a system. A similar filling system for a test casting designed by the author, but using a conical basin (not part of the author's original design!), was found to perform tolerably well, filling without the creation of significant defects (Groteke 2002). It is quite evident, however, when filling is complete such narrow filling channels offer no possibility of significant feeding. This is an important issue that should not be forgotten. In fact, in these trials, this casting never received the proper attention to feeding, and as a consequence suffered surface sinks and internal microporosity (the liquid alloy was clearly full of bifilms that were subsequently opened by the action of solidification shrinkage).

Finally, however, in some circumstances there may be fundamental limitations to the integrity of the liquid front in very thin sections.

- (i) There is a little-researched effect that the author has termed microjetting (*Castings* 2003). This phenomenon has been observed during the filling of liquid Al–7Si–0.4Mg alloy into plaster molds of sections between 1 and 3 mm thickness (Evans et al. 1997). It seems that the oxide on such small liquid areas temporarily restrains the flow, but repeatedly splits open, allowing jets of liquid to be propelled ahead of the front. The result resembles advancing spaghetti. The mechanical properties are impaired by the oxide films around the jets that become entrained in the maelstrom of progress of the front. Whether this unwelcome effect is common in thin-walled castings is unknown, and the conditions for its formation and control are also unknown. It is a concern that this turbulent advance in very thin sections will undermine the benefits we have discussed above. The reality is not known. Very thin-walled castings remain to be researched.
- (ii) In pressure die castings a high velocity  $v$  of the metal through the gate is necessary to fill the mold before too much heat is lost to the die. Speeds of between 25 and 50 m s<sup>-1</sup> are common, greatly exceeding the critical velocity of approximately 0.5 m s<sup>-1</sup> that represents the watershed between surface tension control and inertial control of the liquid surface. The result is that entrainment of the surface necessarily occurs on a large scale. The character of the flow is now dictated by inertial pressure, proportional to  $v^2$ , vastly exceeding the restraining influences of gravity or surface tension. This behavior is the underlying reason for the use of  $PQ^2$  diagrams as an attempt to understand the filling of pressure die castings. In this approach a diagram is constructed with a vertical axis denoting pressure  $P$ , and the horizontal axis denoting the flow rate  $Q$ . The parabolic curves are linearized by squaring the scale of the  $Q$  values on the horizontal axis. The approach is described in detail in much of the pressure die casting literature (see for instance Wall and Cocks 1980). In practice, it is not certain how valuable this technique is, now that computer simulation is beginning to be accepted as an accurate tool for the understanding of the process.

## 12.1 POURING BASIN

### 12.1.1 The conical basin

The in-line conical basin (Figure 11.2a), used almost everywhere in the casting industry, appears to be about as bad as could be envisaged. It is not recommended. It is probably responsible for the production of more casting scrap than any other single feature.

The problems with the use of the conical basin arise as a result of a number of factors:

1. The metal enters at an unknown velocity, and so making the estimation of the design of the remainder of the running system problematical.
2. The metal enters with a high, unchecked velocity. Since the main problem with running systems is to reduce the velocity, this adds to the difficulty of reducing surface turbulence.
3. Any contaminants such as dross or slag that enter with the melt are necessarily taken directly down the sprue.
4. The device works as an air pump, concentrating air into the flow (the action is analogous to other funnel-shaped pumps in which a fast stream of fluid directed down the center of the funnel is designed to entrain a second surrounding fluid. Good examples are steam ejectors and the vacuum suction device that can be driven from a compressed air supply.) The mix of air and metal in terms of volume is often about 50/50, corresponding to the widely quoted finding of 0.5 discharge coefficient. Because air is the single most important contaminant in running systems, this is the most severe disadvantage, yet, regrettably, is not widely appreciated to be a problem.

An example that the author has witnessed many times can be quoted. Bottom teemed steel ingots produced by the conventional arrangement that consisted of pouring the steel into a central conical cup, affixed to the top of a spider distribution system of ceramic tubes connected to the center of the base of a group of four or six surrounding ingot molds (Figure 12.1). Because the top of the ingot mold remained open during filling, the upwelling cascade of air bubbles in the center of the rising metal was clear for all to see. This boiling action of emerging air almost certainly undermines the quality of most present-day ingot casting (it is fortunate that most steel is now continuously cast, thereby avoiding this problem).

The small volume of the basin makes it difficult for the pourer to keep full (its *response time* is too short, as explained later), so that air is automatically entrained as the basin becomes partially empty from time to time during pouring. The pourer can be completely unaware of this, since, although it seems to the pourer that the sprue entrance remains covered, the aspiration of air usually takes place under the surface at the basin/sprue junction.

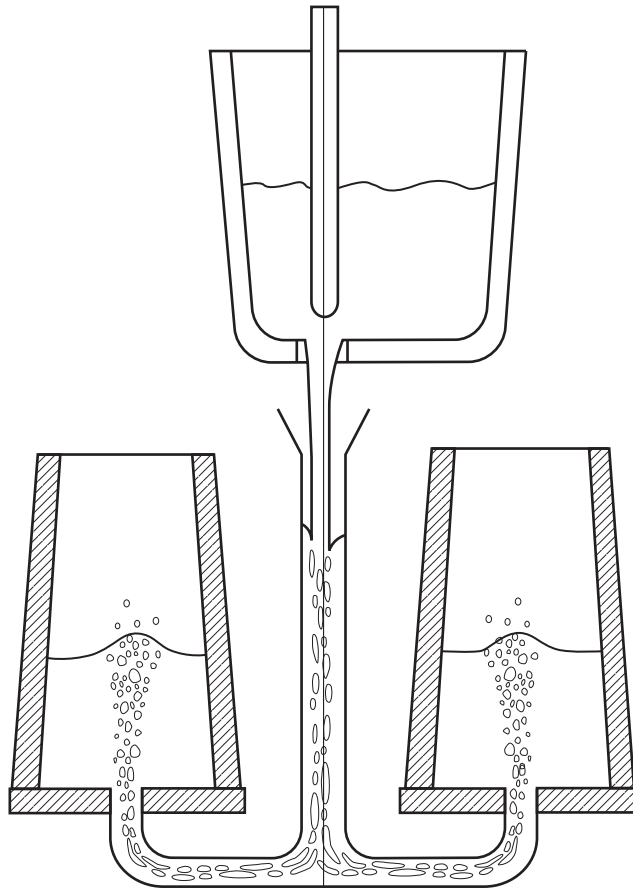


**FIGURE 12.1**

A common system for the casting of ingots, illustrating the entrainment problems created by a conical intake to the filling system.

1. The mold cavity fills differently depending on precisely where in the basin the pourer directs the pouring stream, whether at the far side of the cone, the center, or the near side. Computer simulations of these three filling modes clearly show that three castings are produced with quite different defect patterns. Thus the castings are intrinsically not reproducible.
2. This type of basin is most susceptible to the formation of a vortex, because any slight off-axis direction will tend to start a rotation of the pool. There has been much written about the dire dangers of a vortex, and some basins are provided with a flat side to discourage its formation. In fact, however, this so-called disadvantage would only have substance if the vortex continued down the length of the sprue, along the runner and into the mold cavity. This is unlikely. Usually, a vortex will 'bottom out', giving an air-free flow into the remaining runner system as

will be discussed later. This imagined problem is almost certainly the least of the difficulties introduced by the conical basin. In any case, the use of the offset step basin recommended below avoids any trace of vortex action.

All the above disadvantages are present if the conical basin is well made, fits the sprue entrance accurately, and is accurately placed, as shown in Figure 12.2a. This is the best situation, which is already unacceptably bad.

However, the already long list of damning faults is made even worse for a variety of reasons. A basin that is too large for the sprue entrance (Figure 12.2b) jets metal horizontally off the exposed ledge formed by the top of the mold, creating much turbulence and preventing the filling of the sprue. The problem is unseen by the caster, who, because he is keeping the basin full, imagines he is doing a good job. The cup shape of basin (Figure 12.2c) is bad for the same reason. The basin that is too small (Figure 12.2d) has painful memories for the writer: a casting with an otherwise excellent running system was repeatedly wrecked by such a simple oversight! Again, the caster thought he was doing a good job. However, the aspirated air caused a staggering amount of bubble damage in an aluminum sump casting; it was possible to push a finger through the papery wall into the bubble damaged areas.

The expansion of the sprue entrance to act as a basin (Figure 12.2e) may hold the record for air entrainment (however the author has no plans to expend effort investigating this black claim). Worse still, the top of this awful device is usually not sufficiently wide that the pourer can fill it because it is too small to hit with the stream of metal without the danger of much metal splashed all over the top of the mold and surrounding personnel. Thus this combined 'basin/sprue' necessarily runs partly empty for most of the time. Furthermore, the velocity of the melt is increased as the jet is compressed into the narrow exit from the sprue (this important point is discussed in detail later). The elongated tapered basin system has been misguidedly chosen for its ease of molding. There could hardly be a worse way to introduce metal to the mold.

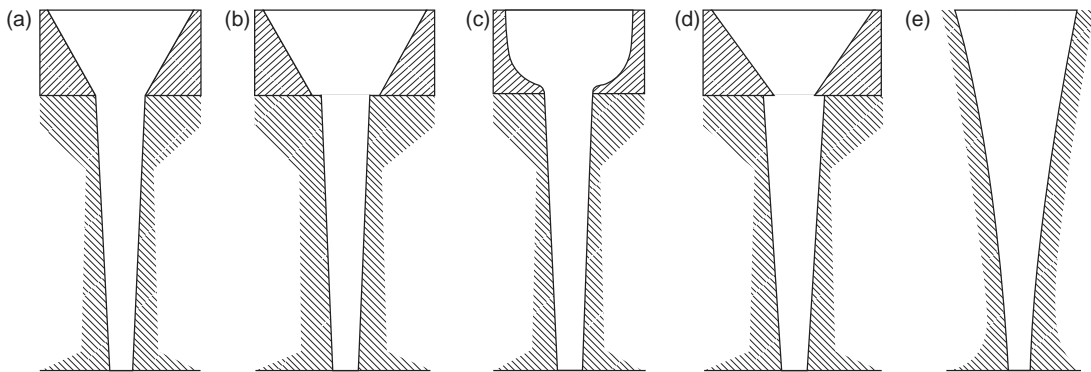


**FIGURE 12.2**

A rogues gallery of non-recommended scrap-generating conical basin and sprue combinations, showing (a) perhaps least damaging; (b) basin too large creating a ledge; (c) cup form creating a right angle edge; (d) basin too small creating an undercut; (e) enlarged sprue to act as a combined basin and sprue, greatly accelerating the flow.

For very small castings weighing only a few grams and where the sprue is only a few millimeters diameter, there is a strong element of control of the filling of the sprue by surface tension. For such small castings the conical pouring cup probably works tolerably well. It is simple and economical, and probably fills well enough. This is as much good as can be said about the conical basin. Probably even this is praising too highly.

Where the conical cup is filled with a hand ladle held just above the cone, the fall distance of about 50 mm above the entrance to the sprue results in a speed of entry into the sprue of approximately  $1 \text{ m s}^{-1}$ . At such speeds the basin is probably least harmful. On the other hand, where the conical cup is used to funnel metal into the running system when poured directly from a furnace, or from many automatic pouring systems, the distance of fall is usually much greater, often 200–500 mm. In such situations the rate of entry of the metal into the system is between 2 and 4 meters per second. From the bottom-poured ladles in steel foundries the metal head is usually over 1 m giving an entry velocity of  $5 \text{ m s}^{-1}$ . This situation highlights one of the drawbacks of the conical pouring basin; it contains no mechanism to control the speed of entry of liquid.

The pouring cup needs to be kept full of metal during the whole duration of the pour. If it is allowed to empty at any stage then air and dross will enter the system. Many castings have been spoiled by a slow pour, where the pouring is carried out too slowly, allowing the stream to dribble down the sprue, or simply poured down the center without touching the sides of the sprue, and without filling the basin at all (which is the trouble with the expanded sprue type, Figure 12.2e). Alternatively, harm can be done by inattention, so that the pour is interrupted, allowing the bush to empty and air to enter the down-sprue before pouring is restarted. Because of the small volume of the basin, it is not easily kept full so that these dangers are a constant threat to the quality of the casting.

Unfortunately, even keeping the pouring cup full during the pour is no guarantee of good castings if the cup exit and the sprue entrance are not well matched, as we have seen above. This is the most important reason for molding the cup and the filling system integral with the mold if possible.

The operator also has the task to aim the pour with great precision, since it is known that hitting the far side of the cone will give a different filling condition, and a different quality of casting, from a pour whose stream hits the near side of the cone, or falls directly down the axis of the sprue. Variations between these targets during the course of a pour will deliver a variety of different defects in successive castings, giving the foundry the familiar problem of generating scrap castings from time to time even though ‘nothing has been changed’.

Finally, even if the pour is carried out as well as possible, any witness of the filling of a conical basin will need no convincing that the high velocity of filling, aimed straight into the top of the sprue, will cause oxides and air to be carried directly into the running system, and so into the casting. For castings where quality is at a premium, or where castings are simply required to be adequate but repeatable, the conical basin can never be recommended.

### 12.1.2 Inert gas shroud

A shroud is the cloth draped as a traditional covering over a coffin. In the foundry the word is used to describe the draping of an inert gas, often contained within a metal enclosure, to shield and thereby protect the metal stream from oxidation by air.

It is commonly used during the pouring of steel castings, and is described in more detail in Section 14.4. Although undeniably useful to some extent, I have to admit to viewing the use of a shroud as



a vulnerable and incomplete solution for the exclusion of air. Thus I have preferred to put in place systems that offer more robust solutions to the avoidance of ingestion of gases into the filling system. These various systems are described below.

### 12.1.3 Contact pouring

The attempt to exclude air during the pouring of castings is carried to its ultimate logical solution in the concept of contact pouring. In this system the metal delivery system and the mold are brought into contact so that air is effectively sealed out. Reports of the use of contact pouring date back to 1962 (Jeancolas et al. 1962, Bracale 1962).

The direct contact system is of course necessary, and taken for granted in the case of counter-gravity systems, in which the mold is placed directly over a source of metal. The metal is then displaced upwards by pump or differential pressure.

Contact pouring is practiced in the Al casting industry by the use of bottom-pour ladles (Figure 12.3). These are generally rather small ladles containing 10 or 20 kg of metal. Their great advantage is that a robot can dip them vertically into the metal in a furnace, with the stopper open so that the ladle fills from underneath the metal surface. The stopper can be closed and the ladle lifted out and transferred to the mold. It is then set in place aligning with the sprue and the stopper raised to fill the mold. The ladle can be used to retain metal in the ladle as a heel, which can remain in the ladle between casts. Alternatively, if the speed of emptying is sufficient, the surface oxide skin in the ladle

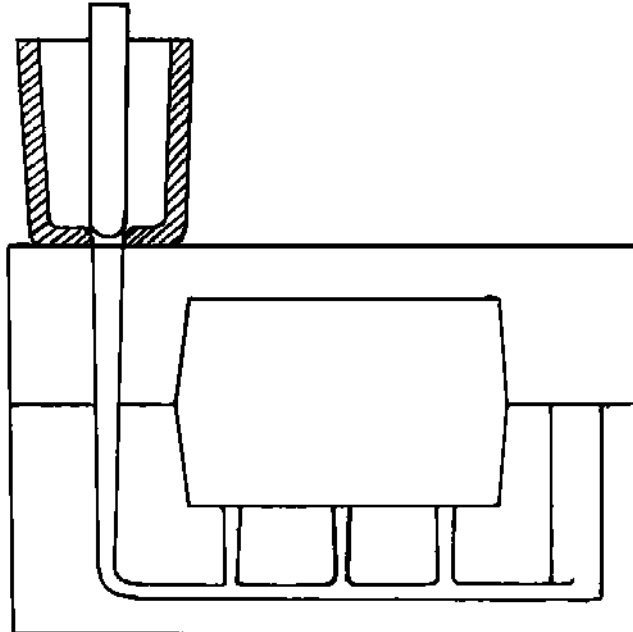


**FIGURE 12.3**

Contact pour, avoiding basin problems.

can be drawn out with the melt, so that the ladle remains clean, requiring no attention or cleaning between pours (the discarded oxide is the last to exit the ladle, and so sits harmlessly at the top of the sprue). Contact pour using a bottom-stoppered ladle handled by a robot deserves wider use, and would be far preferable to the current widespread use of dipping duck-type ladles and the messy filling and emptying operations they perform.

A high-volume operation (VAW, now Hydro Aluminium Limited, Dilligem, Germany) casting aluminum alloy transports the mold up to the underside of a launder, in the base of which is a nozzle closed by a stopper. When the mold is presented to and pressurized against the nozzle the stopper is opened. After the mold is filled the stopper is closed and the mold can be removed. This system works reliably and well.

The author has used contact pouring to make a 50 000 kg 4%Cr steel casting using the stopper in the base of the 50 000 kg bottom-poured ladle to deliver directly into the mouth of a sprue to make a highly successful back-up roll casting (Kang 2001).

Contact pouring has been used on automatic molding lines at hundreds of molds per hour for the pouring of cast iron (Disa 2002). The iron is poured into an intermediate pouring box fitted with a nozzle and stopper in its base. The box is planted on the mold and the stopper is raised to fill the mold. The system offers the lowest possible head pressure to enhance surface finish, and reduce speeds in the mold. When filling is complete the stopper is lowered and the box is lifted clear. The small amount of metal that drains is collected in a small indentation in the mold surface, generally shrinking back into the sprue as the metal solidifies. The top of the molds remain clean, instead of swimming with pools of metal, making a contribution to overall yield. The box is then refilled to its original level. The absence of a pouring basin in the mold further increases yield. Why anyone should want to use any other kind of gravity filling system is a mystery to me.

#### 12.1.4 The offset basin

Another design of *basin* (sometimes called a *bush*), which has been recommended from time to time, is the offset basin (Figure 12.4a).

The floor of this basin is usually arranged to be horizontal (but sometimes sloping). The intention is that the falling stream is brought to rest prior to entering the sprue. This, unfortunately, is not true. The vertical component of flow is of course zero, but the horizontal component is practically unchecked. This sideways jet across the entrance to the sprue prevents approximately half of the sprue from filling properly, so that air is entrained once again. The horizontal component of velocity continues beneath the surface of the liquid throughout the pour, even though the basin may be filled.

There has been research using this type of basin over the years, in which the discharge coefficients from sprues have been measured and found to be in the region of 50% or less. These low figures confirm that the sprue is only 50% or less filled, so that the major fluid being discharged is air. The quality of any castings produced from such devices must have been lamentable.

This type of basin is definitely not recommended.

#### 12.1.5 The offset step (weir) basin

The provision of a vertical step, or weir, in the basin (Figure 12.4b, c) brings the horizontal jet across the top of the sprue to a stop. It is an essential feature of a well-designed basin.

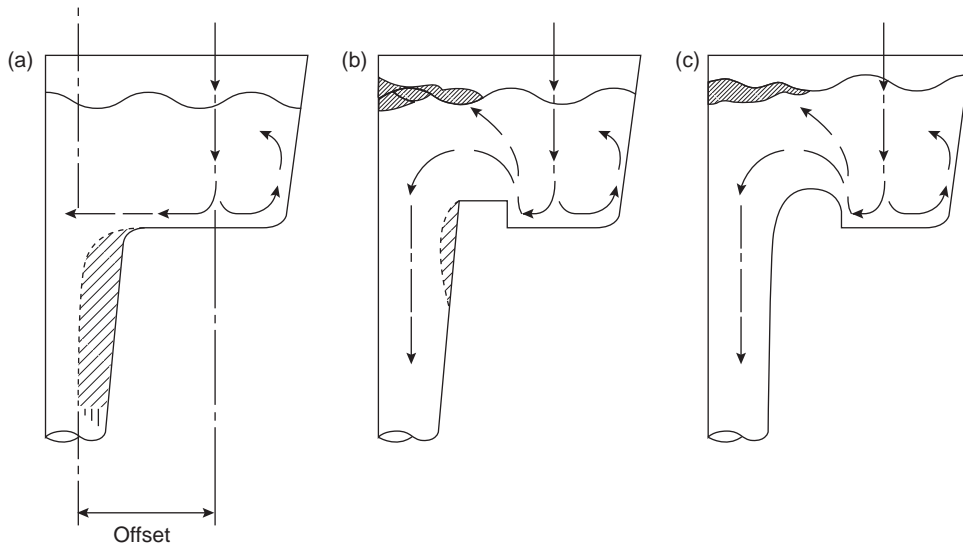


**FIGURE 12.4**

Offset pouring basins (a) without step (definitely not recommended); (b) sharp step (not recommended); (c) radiused step (recommended).

Interestingly, this basin has a long history. West describes the first use of a basin conforming almost exactly to the offset step concept even though the step is not quite as sharp as one would like. This was in 1882. Since then, the principle has become progressively lost. Sexton and Primrose described a closely similar design (but without a well-formed step) in their textbook on ironfounding published in 1911. If this basin is really valuable (as is recommended here) the reader will be curious why it has been known for so long, but has been extremely unpopular in foundries, whose experience of it has been discouraging. There are several reasons for this bad experience. Sometimes the basin has been made incorrectly, neglecting the important design features listed below. However, more serious than this, it has been common practice to place this excellent design of basin on a filling system that completely undoes all the benefits provided by the basin. Thus the benefits of the basin are never realized, and the basin is unjustly blamed.

Despite the revered age of this basin design, the precise function and importance of each feature of the design had not been investigated until recent computer studies by Yang and Campbell (1998). These studies make it clear that:

- (i) The *offset* blind end of the basin is important to bring the vertical downward velocity to a stop. The *offset* also avoids the direct *inline* type of basin, such as the conical basin, where the incoming liquid goes straight down the sprue, its velocity unchecked, and taking with it unwanted components such as air, dross and slag.

In older designs of this device the blind end of the basin was often molded as a hemispherical cup. This was not helpful, since metal could easily be returned, ejected upwards and out of the basin by the sloping sides. The spraying of melt all around the foundry is bad for yield and so

unpopular with the foundry accountant, but is also not recommended for operators. The flat floor and near-vertical sides of the basin were therefore significant advantages. In fact the use of sharp corners to the offset side of the basin is positively helpful to avoid metal being ejected by the basin.

- (ii) The *step (or weir)* is essential to eliminate the fast horizontal component of flow over the top of the sprue which would prevent it from filling fully. Basins without this feature commonly only about half fill the sprue, giving an effective so-called discharge coefficient of therefore only approximately 0.5 (how could it be higher if the sprue is only half full?). The provision of the step yields a further bonus since it reverses the downward velocity to make an upward curving flow in the basin, giving some opportunity for lighter phases such as slag and bubbles to separate out to the top surface of the melt in the basin prior to entering the sprue. Floating debris that has detrained in this way is shown schematically in Figure 12.4b, c. Early basin designs were less than ideal because the step was not vertical (Swift 1949) so that its effect was compromised. The step needs a vertical height at least equal to the height of the stream at that point to ensure that it brings the horizontal component of flow to a complete stop. Commonly, this height will be at least a few millimeters for a small casting, and might be 10–20 mm for a casting weighing several tonnes.
- (iii) Finally, the provision of a generous *radius* over the top of the step (Figure 12.4c), smoothing the entrance into the sprue, further aids the smooth, laminar flow of metal. Swift and co-workers (1949) illustrated this effect clearly in their water models of various basins. The effect is also confirmed by the computer study by Yang and Campbell (1998).

The action of the step in preventing the entrainment of bubbles into the sprue and encouraging detrainment is seen clearly in the water model by Kuyukak (2008). This model shows the great benefit of the step in detraining hundreds of buoyant bubbles. It needs to be kept in mind, of course, that non-buoyant or slowly buoyant defects such as oxide bifilms will not be detrained, but will be carried over into the casting. Thus a good fraction of the damage caused by the turbulence of filling the pouring basin will degrade the casting; it is sobering to conclude that the damage suffered by gravity pouring starts even before any metal enters the sprue. (This situation contrasts with that of the contact pour ladle, which can fill and discharge beautifully from its bottom nozzle with practically zero entrainment of air bubbles or bifilms.)

There are plenty of opportunities for getting important details of this basin design incorrect, so that it functions poorly. Figure 12.5 shows some of these. Figure 12.5a is a common fault in which an extended flat between the step and the sprue allows the melt to regain some of its horizontal component of velocity, and thus overshoots the sprue entrance and causing air entrainment. The use of basins from a store, and simply dropped onto all types of molds leads often to Figure 12.5b in which there is a mismatch, leading to serious air entrainment. Figure 12.5c shows a less serious but unnecessary shape fault that will cause some entrainment. The practice of placing a boom or dam across the top of the basin in Figure 12.5d to hold back floating debris is almost certainly counter-productive. It is seen to interfere with the natural circulation in the basin that would automatically favor the separation of buoyant phases. A dam is not recommended. The use of a completely open base Figure 12.5e is not a perfect solution, but may be acceptable since the velocities at the sprue entrance are not high if the basin is not too deep. The optimum design is seen in Figure 12.5f together with the bringing forward of the back wall to be flush with the sprue entrance, constraining the flow of the melt to enter the sprue exactly parallel to its axis.

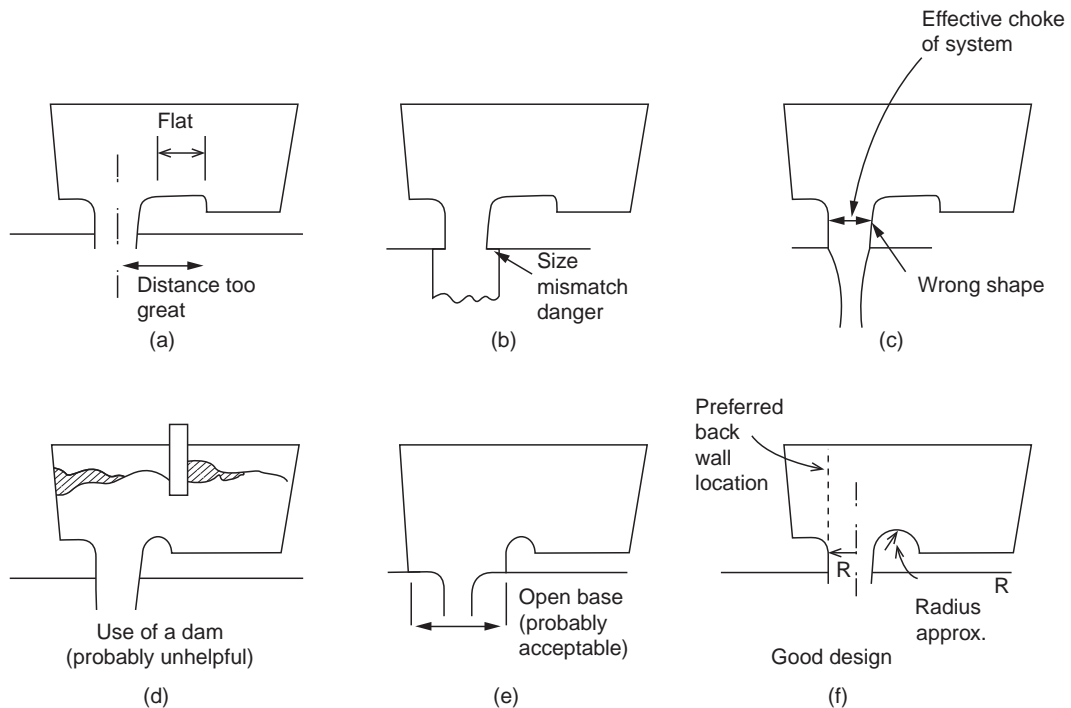


**FIGURE 12.5**

Offset basins (a) offset too large; (b) mismatch causing an undercut; (c) incorrect matching of tapers; (d) a dam prevents beneficial upward flow to encourage detrainment of bubbles and slag; (e) open base is acceptable if sprue entrance is radiused; (f) correctly designed basin, with further benefit if basin walls more closely wrapped around sprue entrance.

In practice, compared to the conical type, the offset step design of basin is so easy to keep full it becomes immediately popular with both caster and quality technologist alike. And, naturally, when teamed up with a well-designed filling system, the basin can demonstrate its full potential for quality improvement of the casting, even though it may not be holding back non-buoyant (i.e. bifilm) defects. The feature that makes the carry-over of bifilms acceptable is that they arrive in the mold cavity in a compact, convoluted form, and are therefore a minimal threat to properties, providing they are retained compact by either rapid freezing and/or good pressurization from a feeder.

An understandable criticism of offset basins is that they are so voluminous that they reduce yield and are therefore costly. The usual design is shown in Figure 12.6a. Clearly the yield criticism can be completely met by ensuring that the basin drains as completely as possible by arranging it to be sufficiently higher than the casting. However, of those cases where the basin has to be placed lower and will not drain, the problem is to some extent addressed by the design variants shown in Figure 12.6b, c. In addition to saving money, these basins work even better because they constrain the melt more effectively; they encourage the funneling of the melt into the sprue with excellent laminar directional

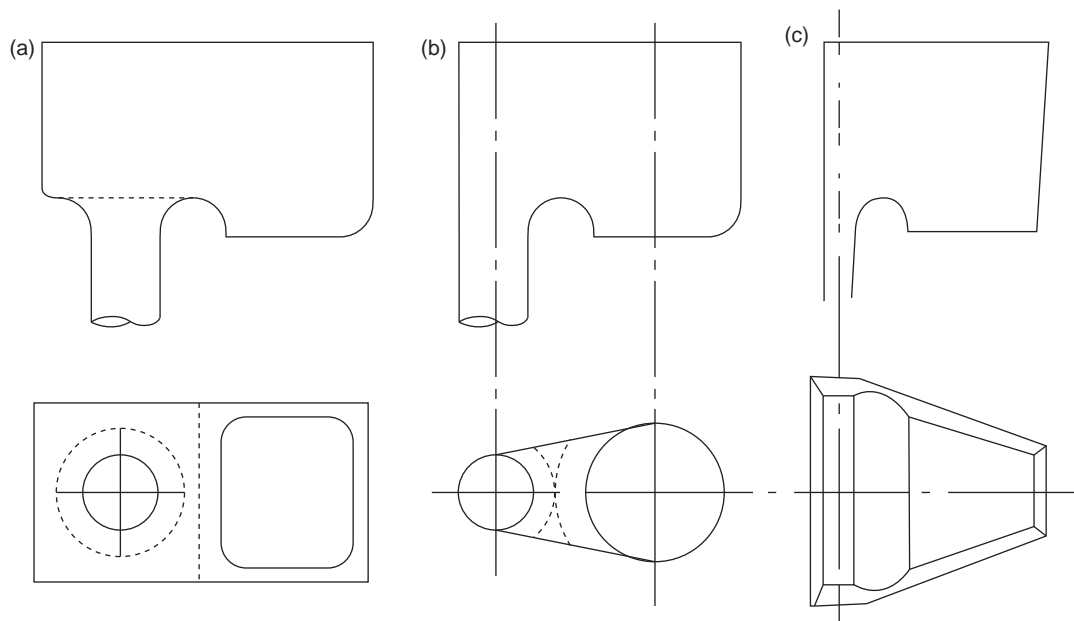


**FIGURE 12.6**

Side and plan views of offset basins (a) conventional rectangular; (b) slimmed shape to streamline flow and improve metal yield; (c) 'reverse delta' for high aspect ratio rectangular sprues (recommended by Puhakka 2010).

guidance. Even so, there is a limit to which these designs should be pushed in terms of reduced volume since the dwell time in the basin is useful for detrainment of defects.

These offset step basins can be made as separate cores, stored, and planted on molds, matching up with the sprue entrance when required. However, because they will be required for many different castings, and so will need to mate up with different sprue entrance diameters, there is a concern about any mismatch of the basin exit and the sprue entrance. However, the problem is much less acute than mismatch of conical basins, because the speed of the falling stream at this point is considerably lower, in fact only at about its critical velocity. In these circumstances surface tension is able to bridge modest outstanding ledges without significant entrainment of the liquid surface. An overhanging ledge is probably more serious and to be avoided. Thus a selection of stored basins with excess exit diameter is to be preferred. In fact it may be preferable to arrange the bush to have its base completely removed on the sprue side (Figure 12.5e). The bush will then fit practically any mold. Provided the entrance to the sprue on the top surface of the cope is nicely radiused, the metal will probably be adequately funneled into the sprue.

Ultimately, however, the author prefers to mold the basin integral with the sprue, and so avoiding the link-up and alignment problems. This is easily achieved with a vertical mold joint, but is less easy, but still possible, with a horizontally jointed mold.

The basin is easier to use, and in general works sufficiently effectively, if its *response time* is approximately 1 second. To the author's knowledge there is no definition of response time. I therefore

adopt a convenient measure as the time for the basin to empty completely if the pourer stops pouring. In practice, of course, the pourer does not usually stop pouring, so that the actual rate of change of level of the basin is usually at least double the response time as defined above. Such times are relatively leisurely, allowing the pourer to maintain a consistent level of melt in the basin. Different pourers or pouring systems may require times shorter or faster than this.

The volume of the basin  $V_b$  ( $\text{m}^3$ ) to give a response time  $t_r$  (in seconds) at a pouring rate  $Q$  ( $\text{m}^3$  per second) is given simply by

$$V_b = Q/t_r$$

Clearly, when  $t_r = 1$  second,  $V_b = Q$  numerically when using the recommended SI units. This is the volume of a '1-second basin'. Occasionally, if the quality of the casting demands it, I use a larger '2-second basin'.

Overall, the use of a basin is not altogether satisfactory from the point of view of the metal quality that is delivered into the casting, and is technically complicated, requiring such extras as pouring control using laser triangulation (Secom 2003). Contact pouring is far preferable.

#### Use of offset stepped basin with a bottom-pour ladle

Ladles equipped with a nozzle in the base are common for the production of large steel castings. Pouring from the base is sometimes known as 'teeming'. The benefits are generally described to be:

- (i) for large castings the tipping of a ladle to effect a lip pour becomes impractical, so that the bottom-teemed ladle is the only practical option;
- (ii) the accuracy of the placing and the vertical direction of the pour are valuable;
- (iii) the metal is delivered from beneath the surface of the melt, so avoiding the transfer of slag.

Even so it is widely known in the trade that steel foundries using bottom-pour ladles suffer dirtier castings than those steel foundries that use lip-pour ladles. This follows as a natural consequence of the great difference in pouring speeds into the conical basin, with the consequent great difference in the rate of entrainment of air by the intake cone acting as an air pump.

Although it might appear that the use of bottom-pour ladles with an offset stepped basin at the entry to the mold has the potential to avoid this central problem, the offset step basin has a problem to cope with the huge entrance velocity. Even more seriously, even if the offset step basin were used optimally, it is likely that steel casting free from oxides would still be unachievable. This serious condition arises because the high speeds of entry from the ladle into the basin entrain so much air and oxide that these defects cannot be detrained in the time available prior to entering the sprue. This is a massive disadvantage suffered by steel casters.

Kuyucak (2008) describes a water model illustrating the use of a nozzle extension applied to the nozzle exit on the ladle. The extension is introduced deep into the basin so as to remain submerged during the pour. This virtually eliminates all entrainment. It seems likely that a good seal would be required between the nozzle and the extension tube, otherwise air could be drawn into the stream at this point as experienced on occasions by the long silica tube extension used by Harrison Castings.

A problem with the use of the nozzle extension is the initial splash when the nozzle is first opened, causing metal to jet vertically out of the basin and fountain liberally around. Kuyucak illustrates how this can be reasonably controlled by sinking the tube exit into the 'well' sunk into the base of the basin. Interestingly, he does not use an undercut form around the base of the basin walls. His water model

indicates some residual entrainment action of any concave feature, whereas a convex surface, as an upturned cup, placed directly under the falling stream appeared to be helpful to control this initial transient.

For a successful use of the nozzle extension concept, it is necessary to examine how the offset step basin can be optimally filled. This in itself is not straightforward.

The common problem when using an offset stepped basin is that although a pourer using a lip-pour ladle can continue to adjust the rate of pour to maintain the level of liquid at the required height in the basin, this is easier said than done if the melt is being supplied from a bottom-pour ladle whose rate of delivery often cannot be controlled, the stopper may be either open or closed. Any attempt to adjust the rate of delivery results in sprays of steel in all directions.

In addition to this problem, as the bottom-teemed ladle gradually empties, it reduces its rate of delivery. In the case of pouring a single casting from a ladle, it is fortunate that the filling system for the casting actually requires a falling rate of delivery as the net head (the level in the basin minus the level of metal in the mold) of metal driving the flow around the filling system gradually falls to zero. Even so, it is clear that the two rates are independently changing, and may be poorly matched at times. The match of speeds might be so bad that the basin runs empty, but even if this disaster is avoided, well before this condition occurs, filling conditions can be expected to be bad. At a filling level beneath the designed fill level in the basin the top of the liquid will appear to be covering the entrance to the sprue, but underneath, the sprue will not be completely filled, and so will be aspirating air. It is essential therefore to ensure, somehow, that the level in the basin remains at least up to its designed level. At this time the problem of satisfactorily matching speeds can only be solved in detail by computer. Most software designed to simulate the filling of castings should be able to tackle this problem. However, it is perhaps more easily solved by simply having a basin with greatly increased depth, for instance perhaps up to four times the design depth. The ladle nozzle size is then chosen to deliver at a higher rate, causing the basin to overflow its design level, and so effectively running the casting at an increased speed. This increased speed is far preferable to the danger of under-filling of the basin with the consequential ingestion of air into the melt.

In general therefore, a greatly increased depth to the basin is very much to be recommended. The problem of overflowing and increased speed of running may not be as serious as it might first appear. The reason is quickly appreciated. If the height of metal in the pouring basin rises to a level twice the design depth, the rate of delivery from the ladle would be 40% higher (a factor of  $2^{1/2} = 1.414$ ). A basin four times the minimum height will accommodate delivery from the ladle at up to twice as fast as the running system was designed for. The increase in pressure that this provides will drive the filling system to meet the higher rate. (Notice that the narrow sprue exit is not acting as a so-called choke, illustrating how wrong this concept is.) Thus the system is, within limits, automatically self-compensating if the basin has been provided with sufficient freeboard. It is important therefore to make sure that offset stepped basins in collaboration with a bottom poured ladle do have sufficient additional height.

The preferred option to overflow the basin in terms of height is valuable in the other common experience of using a large bottom-pour ladle to fill a succession of castings. Let us take as an example a 20 000 kg ladle that is required to pour nine castings each of 2000 kg. (The final 2000 kg in the ladle will probably be discarded because it will pour too slowly, contain too much slag and be too low in temperature; there are sometimes real problems to pour successive castings from one ladle.) The first castings will be poured extremely rapidly because the head of metal in the ladle will be high. However,



the most serious problem is that the final castings in the sequence will be poured slowly, perhaps too slowly.

The important precaution therefore is to ensure that the minimum height in the pouring basin is still met so the final casting is still poured sufficiently quickly. This is a key requirement, and will ensure that the final casting is good. Thus all of the filling design should be based on the filling conditions for the last casting. Clearly, all the preceding castings will all be over-pressurized by increased heights of metal in their pouring basins, and so will fill correspondingly faster, with correspondingly higher velocities entering the mold. This should be checked to ensure that the velocities are not so very high as to cause unacceptable damage. Usually, this approach can be made to work out well.

In some cases the first castings may have their pouring basins filled high, but the metal has not yet arrived in the feeders to give a signal to the operator to stop pouring. In this case the only option seems to be to monitor the progress of the pour by some other factor, such as precise timing, or better still a direct read-out load cell on the overhead hoist carrying the ladle.

The matching of the speed of delivery from the ladle with the speed of flow out of the pouring basin is greatly assisted if the rate of delivery from the ladle is known. This is a complex problem dependent on the height of metal in the ladle, its diameter, and the diameter of the nozzle. The interaction of all these factors can be assessed using the nomogram provided in the Appendix. However, much of the problem of matching the rates out of the ladle and the rate out of the pouring basin is eliminated by eliminating the pouring basin; contact pouring has significant advantages.

### 12.1.6 The sharp-cornered or undercut basin

In addition to the matching of the rate of flow between the ladle and the casting, there are additional problems with the application of offset weir basins for use with bottom-poured ladles.

As we have discussed above, the velocity of the melt exiting the base of the bottom-poured ladle when the stopper is first opened is awesomely high. This is because the melt at the base of a full ladle is highly pressurized. Effectively it has fallen from the upper surface of the melt in the ladle; often as much as a meter or more. Thus the exit speed is often in the region of  $5 \text{ m s}^{-1}$ . This is so high that if this powerful jet is directed into the blind end of a step basin, the liquid metal flashes outwards over the base, hits the radii in the corners of the vertical sides, where it is turned upwards to spray all over the foundry (Figure 2.12a). Such spectacular pyrotechnic displays are not recommended; little metal enters the mold.

The small radii around the four sides of the off-axis well of the basin are extremely effective in redirecting the flow upwards and out of the basin. One solution to this problem is therefore simply the removal of the radii. The provision of sharp corners to all four sides reduces the splashing tendency to a minimum (the top of the weir step leading over to the sprue entrance should still be nicely radiused of course).

The sharp-cornered basin is a useful design. However, an ultimate solution to the splashing problem is provided by a simple re-entrant undercut at the base of the basin (Figure 12.7b). (I recall demonstrating such a basin in a steel foundry whilst foundry personnel hid behind pillars and doors. On the opening of the ladle stopper the stream gushed into the basin, but not a drop emerged. The pouring process was quiet; its intense energy tamed for the first time. The foundry personnel emerged from their hiding places to gaze in wonder.)

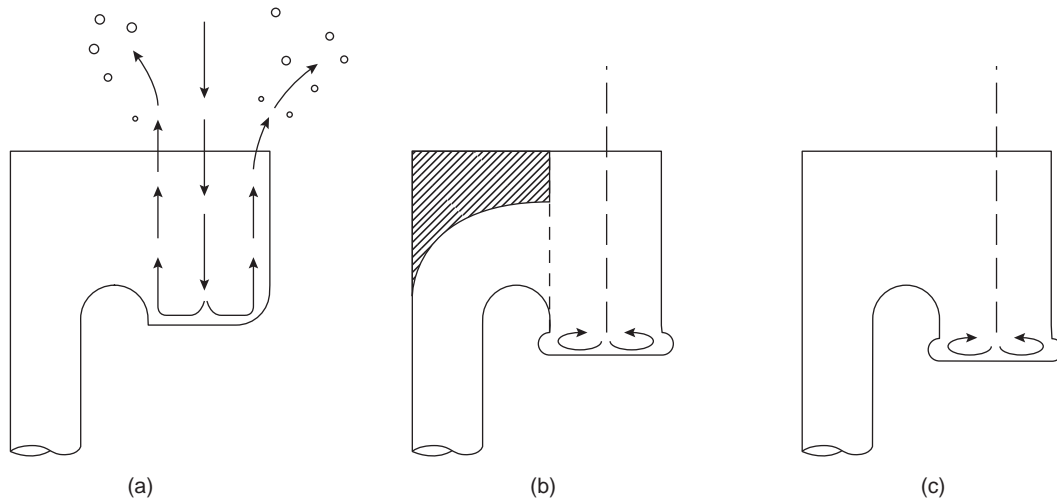


**FIGURE 12.7**

Offset basins for high velocity input. (a) No undercut empties spectacularly upwards (not recommended). (b) and (c) The provision of an undercut gives a basin that resists splashing. The shaded area can be molded in a vertical jointed mold to further improve flow and metal yield, and prevents any risk of pouring directly down the sprue. However, its use may be questionable since it leaves little room for detrainment action of buoyant phases.

The undercut is, of course, a problem for many greensand molding operations making horizontally parted molds. This is why the sharp-edged basin is so useful. Even so, where extreme incoming velocities are involved, an undercut edge to all four sides of the filling well of the basin may be the only solution.

The undercut may be difficult to mold, but it can be machined. The upgrading of a sprue cutter on a high-production greensand line to 3-D machining unit equipped with a ball-ended high-speed cutter would make short work of the basin, complete with its undercut and sprue entrance, and providing all this within the molding cycle time. Such a unit would be an expensive sprue cutter, but would be a good investment.

The undercut is not a problem for vertically jointed molds. Its use on machines such as Disamatics is popular and welcomed by the foundry operators. Its quiet filling is easily controlled, and there is complete absence of splashed metal (splashed metal is commonly seen as pools, sometimes nearly lakes, swimming around on the tops of molds). The reduction of pouring overspill is a significant contribution to the raising of metal yield in the foundry.

The precise depth of the undercut is important. It requires to be twice as deep as the incoming stream to allow for the depth of the reverse flow. If the depth is less than this the reversal cannot occur efficiently. If the depth is much greater the undercut will not fill and is likely to entrain air. Its depth can be estimated as follows.

Assuming the metal maintains its speed approximately after impacting on the floor of the basin, if the infalling jet of metal has diameter  $d$ , its area  $\pi d^2/4$  must equal the area of the stream after it has expanded and flattened to thickness  $t$  on reaching the perimeter of the basin. If the floor diameter is  $D$

the area of the perimeter flow at thickness  $t$  is  $\pi Dt$ . Equating these areas, assuming they correspond to approximately equal flow rates, we have  $\pi d^2/2 = \pi Dt$ . The thickness of the undercut  $2t$  is therefore simply  $d^2/D$ . This does require an estimate of the diameter of the metal stream exiting the ladle.

A note of caution surrounds the use of the undercut. More research is needed to ensure that the quality of the melt is not degraded by entrainment, since the design is based on the re-entrainment of the high-speed flow. However, entrainment below the surface seems likely to be an improvement on the massive entrainment suffered by a conical basin. It would be useful to see this expectation verified by careful practical measurements.

The molding of the sprue cover (the shaded region in Figure 12.7b) ensures that metal is never poured in error directly down the sprue, and saves a little metal. However, it is almost certainly counter-productive since the buoyant phases (slags and bubbles) now have practically no opportunity to detrain. Overall, therefore, it is not recommended. The additional metal cast in Figure 12.7c will be worth the small additional cost, and the larger area of the basin at the pouring end (seen in Figure 12.6b) will encourage the pourer to target the pour correctly.

If, having fulfilled all the above concerns, the offset stepped basin is successfully maintained full, the head of metal provided by the height of the down-runner will be steady, and the rate of flow will be controlled by the sprue. The filling rate will be no longer at the mercy of the human operator on that day. The running system will have the best chance to work in accord with the casting engineer's calculations.

### 12.1.7 Stopper

As a further sophistication of the use of the offset step basin, some foundries place a small sand core in the entrance to the sprue. The core floats only after the bush is full, and therefore ensures that only clean metal is allowed to enter the sprue. Alternatively, a wire attached to the core or a long stopper rod lifted by hand accomplishes the same task. For a large casting the raising of the stopper will require a more ruggedly engineered solution, involving the benefit of the action of a long lever to add to the mechanical advantage and keep the operator well away from sparks and splashes. However it is achieved, the delayed opening of the down-sprue is valuable in many foundry situations.

The early work on the development of filling systems at Birmingham concentrated on the use of the offset step basin. A stopper was not used because it was considered to be too much trouble. However, after about the first 12 months, as a gesture to scientific diligence, it was felt that the action of a stopper should be checked, if only once, by observing the filling of a sprue using the video X-ray radiographic unit, comparing filling conditions with and without a stopper. A stopper was placed in the sprue entrance, sealing the sprue. The metal was poured into the basin. When the basin was filled to the correct level the stopper was raised. The pouring action to keep the basin full was then continued until the mold was filled. The results were unequivocal. The use of a stopper improved the filling of the sprue to a degree that was amazing. It was with some resignation that the author affirmed this result. For every casting after that day, a stopper was always used.

Latimer (1976) demonstrated that the use of a stopper reduced the fill time by 60%. This is further proof that the system runs fuller (and indicates indirectly that without the stopper the system must be entraining more than 50% air).

There seems little doubt therefore that, despite the inconvenience, when the best-quality castings are required, a stopper is advisable. Thus the author always insists on its use for aerospace products.

In addition, the use of stoppers is particularly useful for very large castings where different levels of the filling system are activated by the progressive opening of stoppers as the melt level rises in the mold, so bringing into action new sources of metal to raise the filling speed.

---

## 12.2 SPRUE (DOWN-RUNNER)

The sprue has the difficult job of getting the melt down to the lowest level of the mold whilst introducing a minimum of defects despite the high velocity of the stream.

The fundamental problem with the design of sprues is that the length of fall down the sprue greatly exceeds the critical fall height. The height at which the critical velocity is reached corresponds to the height of the sessile drop for that liquid metal. Thus for aluminum this is about 13 mm, whereas for iron and steel it is only about 8 mm. Since sprues are typically 100–1000 mm long, the critical velocity is greatly exceeded. How then is it possible to prevent damage to the liquid? This question is not easily answered and illustrates the central problem to the design of filling systems that work using gravity. (Conversely, of course, counter-gravity systems can solve the problem at a stroke, which is their massive technical advantage.)

For the sprue at least, the problem is soluble. The secret of designing a good sprue is to make it as narrow as possible, so that the metal has minimal opportunity to break up and entrain its surface during the fall. The concept on protecting the liquid from damage is either (i) to prevent it from going over its critical velocity or, (ii) if the critical velocity has to be exceeded, to protect it by *constraining* its flow in channels as narrow as possible so that it is not able to jump and splash.

Theoretically a design of the sprue can be seen to be achieved by tailoring a funnel in the mold of exactly the right size to fit snugly around a freely falling stream of metal, carrying just the right quantity of metal per second (Figure 12.8). We call the funnel the down-runner, or sprue for short. Many old founders call it the spue, or spew (which, incidentally, does not appear to be a joke).

Most sprues are oversized. This is bad for metallic yield, and thus bad for economy. However, it is much worse for the metal quality, which is damaged in two important ways:

- (i) The sprue takes more time to fill. Air is therefore taken down with the metal, causing severe surface turbulence in the sprue because of the high velocity of the fall. This, of course, leads to a build-up of oxide in the sprue itself, and much consequential damage downstream in the running system and the casting from entrained oxide and air. The amount of damage to the metal caused by a poor basin and sprue can be quickly appreciated from the common observation of the blockage of filters. Even with good-quality liquid metal, a poor basin and sprue will create so much oxide that a filter is quickly overloaded and blocked. Such poor front ends to filling systems are so common that filter manufacturers give standard recommendations of how much metal a filter can be expected to take before becoming choked. However, in contrast to what the manufacturers say, with a good basin and sprue (and providing, of course, the quality of the melt is not too bad) a filter seems capable of passing any amount of liquid metal without problem.
- (ii) The free fall of the melt in an oversized sprue, together with air to oxidize away the binder in the sand, is a potent combined assault that is highly successful in destroying molds. The hot liquid ricochets and sloshes about, its high speed and agitation punishing the mold surface with a hammering and scouring action. At the same time the pockets of air in the rebounds of the

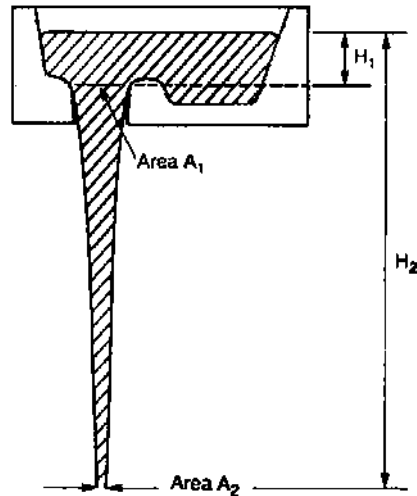


**FIGURE 12.8**

The geometry of the stream falling freely from a basin.

flow will displace air backwards and forwards through the sand like blasts from a blacksmith's bellows, causing the organic matter in the binder to glow, and, literally, to disappear in a puff of smoke! When the binder is burned away, reclaiming the sand back to clean, unbonded grains, the result is, of course, severe sand erosion. Figure 12.9 shows a typical result for an aluminum alloy casting in a resin-bonded sand mold. An oversize sprue is a liability.

Conversely, if the sprue is correctly sized the metal fills quickly, excluding air before any substantial oxidation of the binder has a chance to occur. The small amount of oxygen in the surface region of the mold is used up quickly by the burning of a small percentage of binder, but further oxidation has to

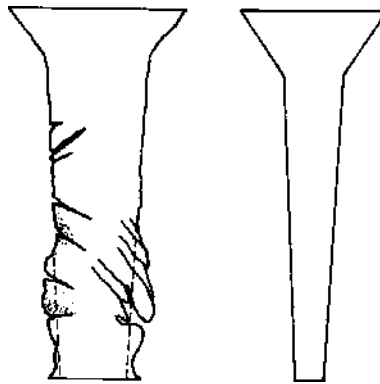


**FIGURE 12.9**

An oversize sprue that has suffered severe erosion damage because of air entrainment during the pour. A correctly sized sprue is usually well formed.

proceed at the rate at which new supplies of air can arrive by diffusion or convection through the body of the mold. This is, of course, slow, and is therefore not important for those parts of the mold such as the sprue, which are required to survive for only the relatively short duration of the pour. Furthermore, since the liquid metal now fills the volume of the sprue, the oxide film forming the metal–mold interface is stationary, protecting the mold material in contact with the sprue, and transmitting the gentle pressure of the steady head of metal to keep the mold surface intact. The result is a perfectly cast sprue (Figure 12.9), free from sand erosion and oxide laps. A correct-sized sprue for an aluminum alloy casting will shine like a new pin. (But beware, an undersized sprue will too!) Figure 12.2 illustrates some examples of good and bad systems. A test of a good filling system design in any metal is how well the running system has cast. It should be perfectly formed.

How then is it possible to be sure that the sprue is exactly the right size? The practical method of calculating the dimensions of the sprue is explained in Chapter 13. Basically, the sprue is designed to mimic the taper that the falling stream adopts naturally as a result of its acceleration due to gravity (Figure 12.10). The shape is complex, its area as a function of height is given by an equation for a hyperbola (interestingly, not a parabola as widely stated). Because most sprues have been traditionally formed by a straight taper, the curved sides of the stream cause the metal to become detached

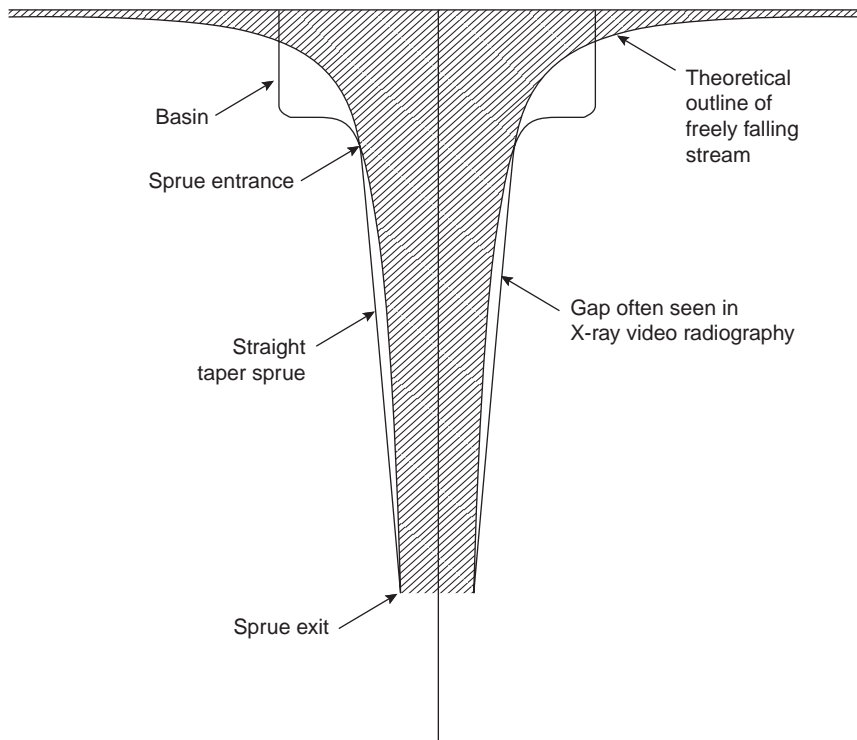


**FIGURE 12.10**

Theoretical hyperbola shape of the falling stream, illustrating the complicating effects of the basin and sprue entrance.

from the walls at about half-way down as shown in this figure. For modest-sized castings this (together with other errors, mainly due to the geometry and friction of the flow in the basin) is simply corrected by making the sprue entrance about 20% larger in area (corresponding of course to about a 10% increase in diameter). Thus straight-tapered sprues, especially if the entrance area is enlarged by 20%, appear to work reasonably satisfactorily.

For very tall castings the straight-tapered approximation to the sprue shape is definitely not satisfactory. In this case it is necessary to calculate the true diameter of the sprue at close intervals along its length. The correct form of the falling stream can then be followed with sufficient accuracy, keeping the stream in contact with the mold during the whole course of its fall, and air entrainment during the fall can be avoided.

Using this detailed approach the author has successfully used sand sprues for very large castings. An interesting example is a 50 000 kg steel casting 7 m high. The sprue was assembled from a stack of tubular sand cores, accurately located by an annular stepped joint. (Only one core box was required, but the central hole required a pile of separately turned loose pieces.) The conventional use of ceramic tubes for the building of filling systems for steel castings was thereby avoided, with advantage to the quality of the casting. As an interesting aside, the appearance of this sprue after being broken from the mold was at first sight disappointing. It seemed that considerable sand erosion had occurred, causing the sprue to increase in diameter by over 10 mm (about 10%). On closer examination, however, it became clear that no erosion had occurred, but the chromite sand had softened and been compressed, losing its air spaces between the grains to become a solid mass. It had partially softened probably as a result of the use of a silicate binder system; the silicate had reacted with the chromite to form a lower melting point phase. Since such a growth in diameter would necessarily have occurred by a kind of creep process, in which pressure, temperature, and time would be involved, it follows that much of this expansion would have happened after the casting had filled, since pressure was then highest, the sand fully up to temperature, and more time would be available because the time for the solidification of the sprue would be as much as ten times longer than the pouring time. Thus during the pour the sand-molded sprue would almost certainly have retained a satisfactory shape, as corroborated by the predicted fill time being fulfilled, and the cleanness of the metal rising in the mold cavity was clearly seen to be excellent.

Sand-molded filling systems for steel castings are, of course, prone to erosion if the system design is bad, and particularly if, as is usual, the system is oversized. In this case, however, the sand-molded hyperbolic sprue worked considerably better than the conventional refractory tube system. However, there would be no doubt that the refractory tubes would be excellent if they could be specifically designed and produced for the sprues for each individual steel casting. Naturally, at the present time this is not easily arranged. Even so, it may be found to be an economic option in view of the expensive sands and mold coatings required if sand is used alone. In addition, the refractory tubes are extremely easy and quick to incorporate into a sand mold, often avoiding the significant cost of creating a new joint line by adding a new mold part.

An interesting option might be the creation of sand cores to replace the refractory hollowware. Thus the foundry would be free to construct its own hollowware to fit each casting, using one core box with a variety of turned, central loose pieces to form the tapered internal form.

The cross-section of the sprue can be round or rectangular. Some authorities have strongly recommended square in the interests of reducing the tendency of the metal to rotate, forming a vortex, and so aspirating air. This probably *was* important in castings using conical pouring basins because any

out-of-line pouring would induce the rotation of the melt in the pouring cup. However, the author has never seen any vortex formation with an offset step basin. The problem seems not to exist with good basin design.

In addition, of course, the vortex appears to be unjustifiably maligned. The central cone of air will only act to introduce air to the casting if the central core extends into the mold cavity. This is unlikely, and in its use with the vortex sprue and other benign uses of vortices, the design is specifically arranged to suppress the possibility of air entering the casting. The vortex can be a powerful friend, as we shall see.

To summarize: for ease and safety of design at this time, the sprue should be a single, smooth, nearly vertical, tapering channel, containing no connections or interruptions of any kind. The rate of filling of the mold cavity should be under the absolute control of its cross-section area. If, therefore, the casting is found in practice to be filling a little too fast or too slow, then the rate can be modified without difficulty by slight adjustment of the size of the sprue.

Significantly, it is not simply the sprue exit that requires modification in this case. If correctly designed, the whole length of the sprue acts to control the rate of flow. This is what is meant by a naturally pressurized system. We can get the design absolutely correct for the sprue along its complete length. Although methoding engineers have been carrying out such calculations correctly for many years, somehow only the sprue exit has been considered to act as the choke. We need to take careful note of this widespread error, and perhaps take time to re-think our filling system concepts. The whole length of a filling system (sprue, runner, and gates) should be slightly pressurized, and so be making its contribution to the overall choking of the flow. The choke is localized in no particular place. We are now dealing with a *distributed* choke effect.

Turning now to a common problem with many automatic molding units for the manufacture of horizontally parted molds, we have already lamented that these units do not provide for a properly molded basin. (Despite such a basin being possible to be machined as mentioned above, cutting by machining is usually never actioned.)

Worse still, it is regrettable that a reverse-taper sprue is usually the only practical option. The sprue pattern needs to be permanently fixed to the pattern plate, and therefore has to be moldable (i.e. the mold has to be able to be withdrawn off the sprue when stripping the mold off the pattern) as seen in Figure 11.2b.

Although there is a strong case for believing that all our high-production molding lines are especially designed to make only defective castings, for the dedicated engineer, even when pitted against such odds, all is not yet lost. The strategies to reduce the problems that are suffered are detailed below.

The sprue entrance should be maintained at its correct calculated size, and the taper (now the wrong sign, remember) down the length of the sprue should be kept to a minimum. (A polished stainless steel sprue pattern can often work perfectly well with zero taper providing the stripping action is accurately square.) The sprue exit is now very much oversized of course, so that much turbulence is to be expected at the base of the sprue.

Even though all precautions are taken in this way to reduce the surface turbulence to a minimum, the consequential damage to the melt by a reverse or zero tapered sprue is preferably reduced further by the provision of:

- (i) A filter as soon as possible after the base of the sprue. The friction provided by the filter acts to hold back the flow, and thus assists the poorly shaped sprue to back-fill as completely and as quickly as possible, and so reduce the total damage. The filter will also act to filter out some



of the damage, although it has to be realized that this filtering action is not particularly efficient. The use of filters is dealt with in detail in Section 12.7.

- (ii) A radial choke. This is a clever ‘quick fix’ suggested by Groteke (2005) described in Section 12.2.5.

We need to dwell a little longer on the importance of the use of the correct taper, so far as possible, for sprues.

The effect of too little or even negative taper has been seen above to be detrimental to casting quality. Surely, one might expect that the opposite condition of too much taper would not be a problem, since it seems reasonable to assume that the velocity of the metal depends only on the distance of fall. However, this is not true. The head of metal in the pouring basin provides the driving force experienced by the melt entering the sprue. If the sprue taper matches the natural taper of the falling stream the only acceleration experienced by the melt is the acceleration due to gravity. If, however, the taper of the sprue is greater than this, the melt is correspondingly speeded up as the sprue constricts its area. This extra speed is unwelcome, since the task of the filling system designer is to reduce the speed. The effect of varying taper has been studied by video X-ray techniques. In experiments in which the sprue exit area was maintained constant, a doubling of the sprue entrance area was seen to nearly double the exit speed, with the generation of additional turbulence in the runner. Three times greater entrance area led to such increased velocities in the runner that severe bubble entrainment was created (Sirrell and Campbell 1994). This is one of the reasons why the elongated basin/sprue (Figure 12.2e) is so bad.

This effect is illustrated in Figure 12.11. For the negatively tapered sprue (a) and zero taper (b) the velocity at the sprue exit is merely that due to the fall of metal. The rate of arrival is of course

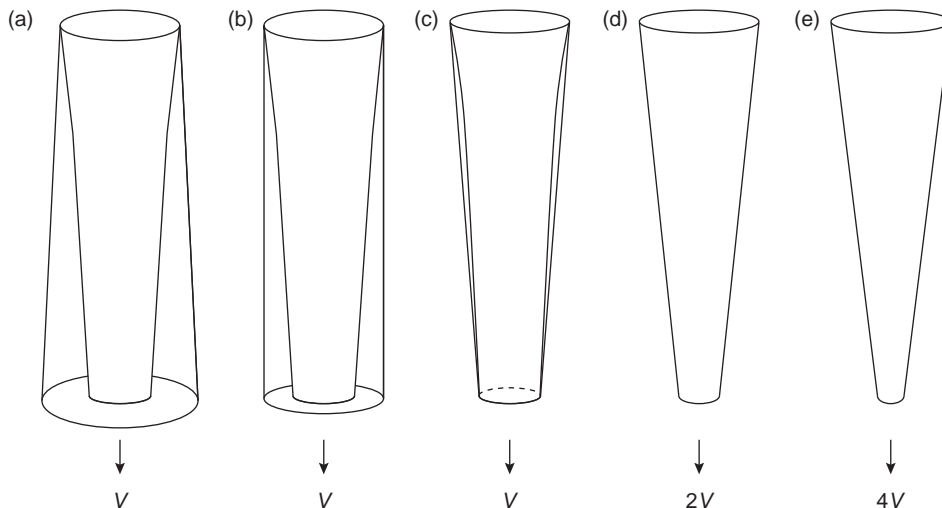


**FIGURE 12.11**

A variety of straight tapered sprues. Too little or too much taper is bad. Only the center form that matches the falling stream is recommended. Even this could be improved by either (i) 20% additional entrance area, or (ii) better still, shaped to the special hyperbolic curve to follow the shape of the stream.

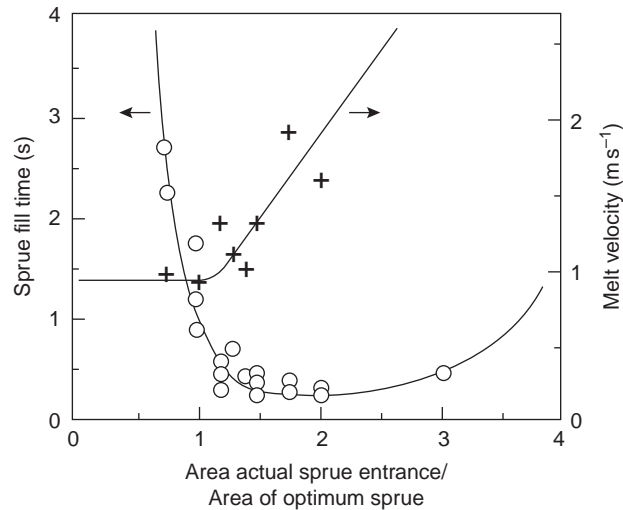


**FIGURE 12.12**

Experimental data from video radiographic observations of sprue filling time and velocity of discharge. A taper of 20% greater than the optimum taper (corresponding to 1.2 on the horizontal axis) is shown to be close to an optimum choice (Sirrell 1995).

controlled by the area of the sprue top, and the falling metal does not touch the walls of the sprue. For the correctly sized sprue (c) the velocity and rate of delivery are substantially unchanged, although it will be noticed that the whole of the length of the sprue is now contacting and controlling the stream, to the benefit of the melt quality. Those sprues with too much taper (d) and (e) continue to deliver metal at nearly the same rate (in  $\text{kg s}^{-1}$  for instance), but at much higher speed (in  $\text{m s}^{-1}$  for instance) in proportion to the reduction in area of the exit. Far from acting as an effective restraint, the narrow sprue exit merely increases problems.

These effects were studied using real-time X-ray radiography (Sirrell et al. 1995) to optimize the taper, measuring the time for the sprue to back-fill, and the speed of the exiting melt (Figure 12.12). This work confirmed that the long-used 20% increase of the area of the sprue entrance was a valuable correction. The consequential 20% increase in velocity into the runner was an acceptable penalty to ensure that the sprue primed faster and more completely, despite its straight-wall approximate shape.

Thus to summarize the effect of sprue taper; the taper has to be correct (within the 20% outlined above). Too little or too much taper both lead to damage of the melt.

### 12.2.1 Multiple sprues

In magnesium alloy casting the widespread use of a parallel pair of rectangular slots to act as the sprue seems to be due to the desire for the reduction in vortex formation (especially, as we have noted, if poor designs of pouring basin are employed). Swift et al. (1949) have used three parallel slots in their studies of the gating of aluminum alloys. However, the really useful benefit of a slot shape is probably associated with the reduction in stream velocity by the effect of friction on the increased surface area.

The slots can be tapered to tailor their shape to that of the falling stream. Such sprues would probably benefit the wider casting industry. A study to confirm the extent of this expected benefit would be valuable.

A really important benefit from the use of a slot sprue appears to have been widely overlooked. This is the accuracy with which it can be attached to a slot runner to give an excellent filling pattern. This benefit is described in detail in the section below concerning the design problems of the sprue/runner junction. It seems that we should perhaps be making much more regular use of slot sprues.

When pouring a large casting whose volume is greater than can be provided from the ladle, it is common to use more than one ladle. The sequential pouring of one ladle after the other into a single basin has to be carried out smoothly because any loss of metal level to below the design minimum level is almost certain to create defects in the casting. Simultaneous pouring is often carried out. Occasionally this can be accomplished with a single sprue, but using an enlarged pouring basin, often with a double end, either side of the sprue, allowing the ladles access from either side (Figure 12.13b).

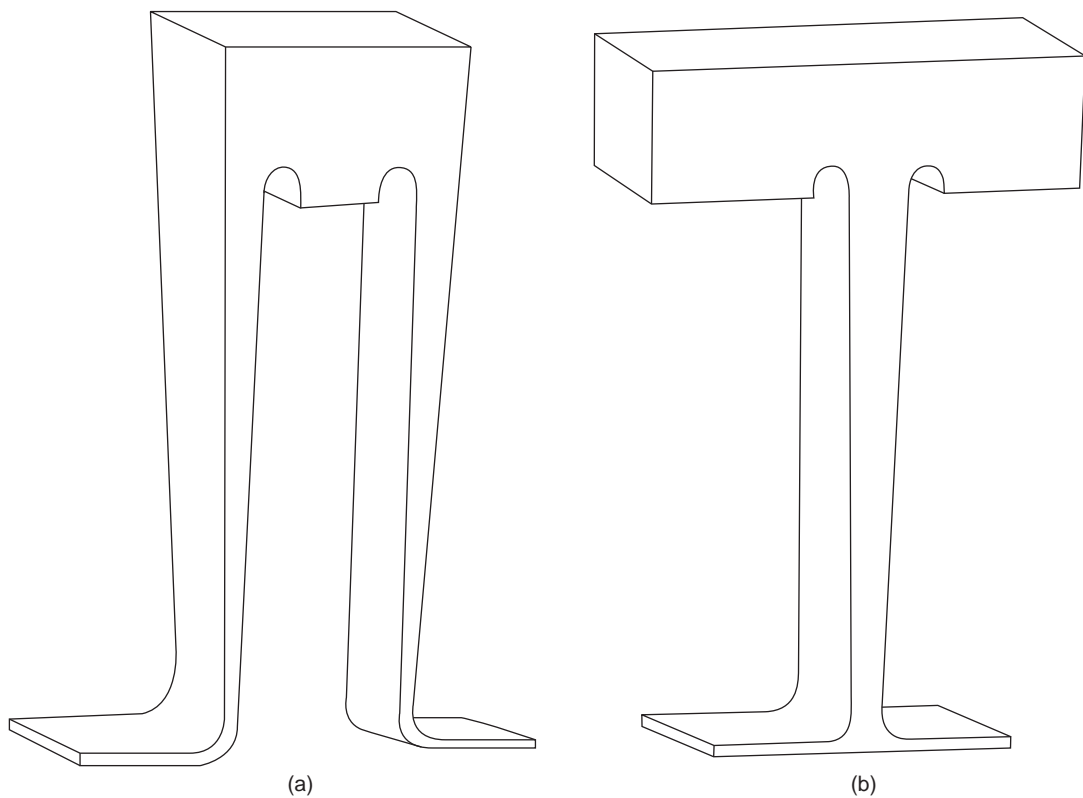


**FIGURE 12.13**

The filling of a runner splitting into two directions by (a) two sprues; or (b) a single sprue with a double ended basin to allow two pourers either together or pouring in series without a break.

Single pouring can still be conveniently used with a double sprue (Figure 12.13a). Often, however, two or more sprues are used, sited at opposite ends of the mold, so as to give plenty of accessibility for ladles and cranes, and reduce the travel distance for the melt in the filling system. When using more than one sprue the correspondingly smaller area of each channel is an advantage because they fill more easily and quickly, excluding their air more rapidly. Multiple sprues for larger castings are to be recommended and should be considered more often.

For very large castings, an interesting technique can be adopted. Several sprues can connect to runners that are arranged around the mold cavity at different heights. For instance in the pour of a 3-m-high iron casting weighing 37 000 kg described by Bromfield (1991), four sprues were arranged to exit from two pouring basins. The sprues were initially closed with graphite stoppers. The trough was first filled. The stoppers to the lowest-level runner were then opened. The progress of the filling was signaled by the making of an electrical contact at a critical height of metal in the mold. In other instances witnessed by the author, the progress of filling could be observed by looking down risers or sighting holes placed on the runners. When the next level of runner was reached, announced by the bright glow of metal at the base of the sighting hole, the next level of sprues was brought into action to deliver the metal to this level of runner. In the case of the casting that was witnessed, three levels of runners were provisioned by six sprues. The technique had the great advantage that the rate of pouring did not start too fast, and then slowly decrease to zero during the course of the very long duration of the pour. The rate could be maintained at a more consistent level by the action of bringing in additional sprues as required. In addition, the temperature of the advancing front of the melt could also be maintained by the fresh supplies of hot metal arriving at the different levels, thus reducing the need for excessive casting temperatures to avoid misruns. Again, the significant advantages of multiple sprues are clear.

## 12.2.2 Division of sprues

The attempt to provide gating or feeding off various parts of the sprue at various heights is almost always a mistake, and is to be avoided. Examples of poor junctions affecting the sprue are shown in Figure 12.14. Overflow from such channels can introduce metal into parts of the mold prematurely, where it can fall, splashing and damaging the casting and mold before the general arrival of the melt via the intended bottom gate. Small puddles and droplets often solidify and oxidize, and thus create lap-type defects in the casting since they cannot easily be remelted and assimilated. Even if the channels are carefully angled backwards to avoid premature filling, they then act to aspirate air into the metal stream. Thus divided sprues usually act either to let metal out or to let air in.

However, of course, sprues can be divided if this is carried out with extreme care. The extreme care is needed because of the extreme velocity in the sprue. Any slight error can create disproportionate amounts of entrainment damage. Division of sprues into separate sources of metal is required in vertically parted molds, especially those requiring to fill all cavities at the same time, so as to reduce the total filling time of the mold to a minimum figure corresponding to the filling time of a single cavity.

Figure 12.15a shows a technique for dividing up the flow of a sprue so that equal quantities reach all the branches. The figure shows a sprue design for six cavities. The area at  $A_0$  carries the total flow of course and is notionally divided into six equal areas. The areas  $A_1$ ,  $A_2$  and  $A_3$  are calculated assuming the free fall of the melt, taking off the appropriate fractions of the area of the flow at each level.

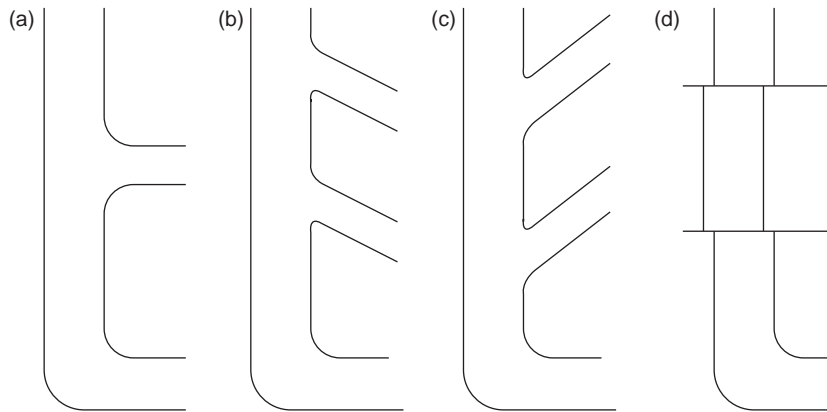


**FIGURE 12.14**

A variety of sprue/runner junctions. None are recommended. They all work badly, either entraining air or allowing metal to escape prematurely at a low and damaging rate, forming dribbles and drops.

The question nearly always arises, what about the sharp corners that are revealed after the taking off of each of the runners at the various levels. These seem to survive well, because the whole sprue volume fills quickly, after which all portions of the sprue wall are pressurized and therefore protected by the melt. Any attempt to round the corners to protect (beyond the millimeter or so radius to permit molding and stripping) is counter-productive, because such a region cannot be properly filled and pressurized, with the result that the mold is destroyed at this location, and sand inclusions will appear in the casting.

If only one division is required, for instance for four cavities, the sprue can be conveniently divided across the mold joint (Figure 12.15b). This technique works well, once again despite the sharp edges of sand which appear so vulnerable.

### 12.2.3 Sprue base

The point at which the falling liquid emerges from the exit of the sprue and executes a right-angle turn along the runner requires special attention. The design of this part of the liquid metal plumbing system has received much attention by researchers over the years, but with mixed results that the reader should note with caution.

Figure 12.16a illustrates a common round sprue to flat runner junction. This well-known and apparently innocuous system gives unbelievably bad results as shown in the simulations of Gebelin and colleagues (2005, 2006) and confirmed by video radiographic studies of the filling of castings. The ricochet behavior of the melt as it zigzags along the runner ensures that the runner never properly fills and the melt is subject to severe oxidation. Despite much research, there seems no way to optimize this particular type of junction. Clearly, it needs to be avoided.

The simple geometries shown in Figure 12.16b, c do not require a computer simulation to convince a reader that they have the potential to deliver metal essentially without turbulence. These simple designs are recommended.

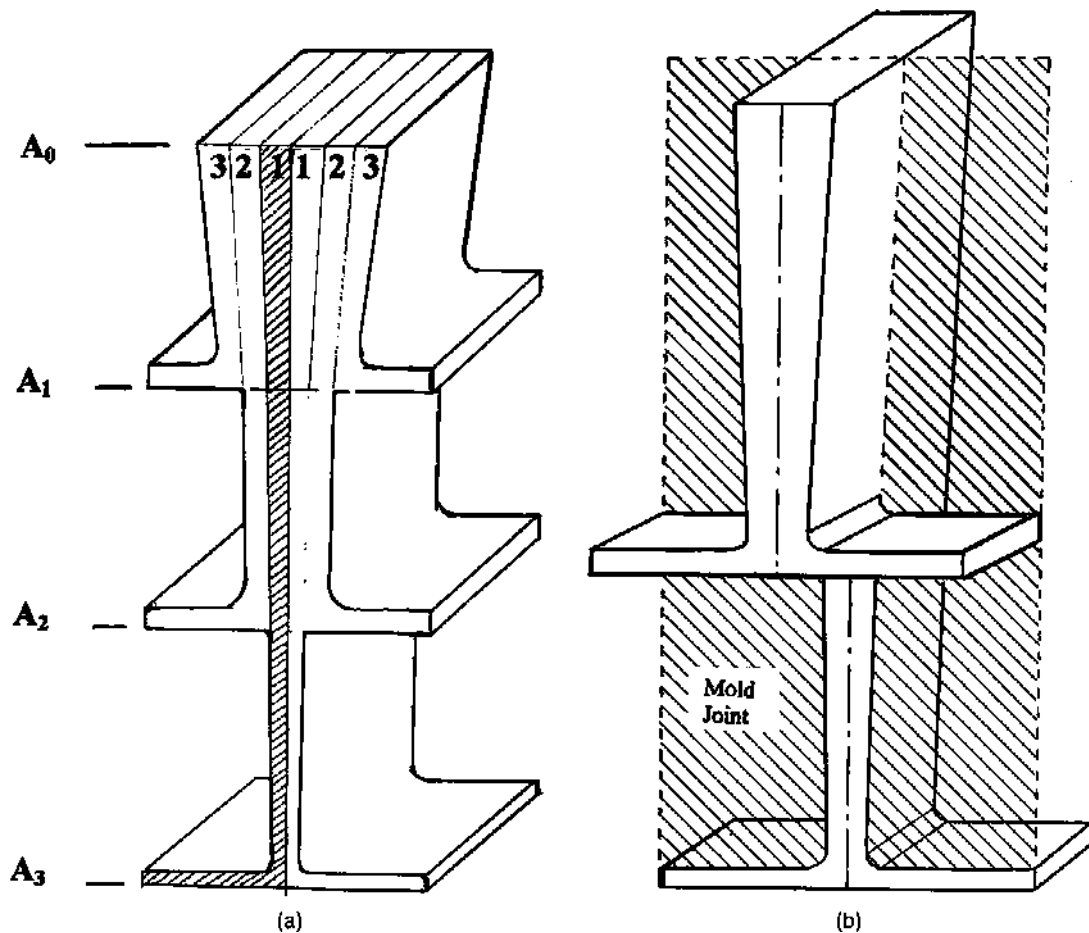
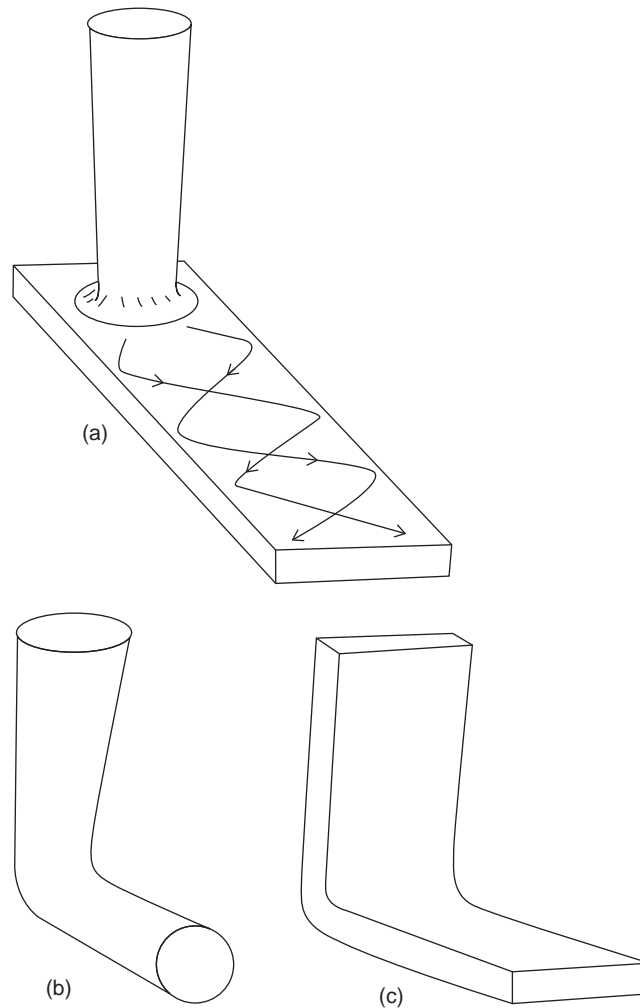


FIGURE 12.15

(a) A technique for splitting flow off from a sprue to fill multiple cavities in a vertically split mold at the same time. (The sharply molded corners survive well in the absence of entrained air.) (b) A single sprue split to fill cavities at the same time can be conveniently made across the mold joint.

### 12.2.4 The well

One of the widely used designs for a sprue base is a *well*. This is shown in Figure 12.17a. Its general size and shape have been researched in an effort to provide optimum efficiency in the reduction of air entrainment in the runner. The final optimization from early researches was a well of double the diameter of the sprue exit and double the depth of the runner. This optimization was confirmed in an elegant study by Isawa (1994) who found that the elimination of the hundreds and thousands of bubbles that were generated initially reduced exponentially with time. The exponential relationship gave a problem to define a finite time for the elimination of bubbles because the data could not be extrapolated to zero bubbles; clearly the extrapolation predicted an infinite time! He therefore cleverly



**FIGURE 12.16**

(a) There is no solution to the problem of joining a round sprue to a rectangular runner; the flow ricochets from wall to wall, never properly filling the runner. Simple sprue/runner junctions at (b) and (c) can work perfectly.

extrapolated back to the time required to arrive at the last bubble, and used ‘the time to the last bubble’ to compare different well designs.

However, it should be noticed that both this and all the research into wells had been carried out on water models, and all had used runners of large cross-section that were not easy to fill. The result was a well design that, at best, cleared the liquid of bubbles after about 2 seconds.

For small castings that fill in only a few seconds we have to conclude that such well designs are counter-productive. In these cases it is clear that much of the filling time will be taken up conveying

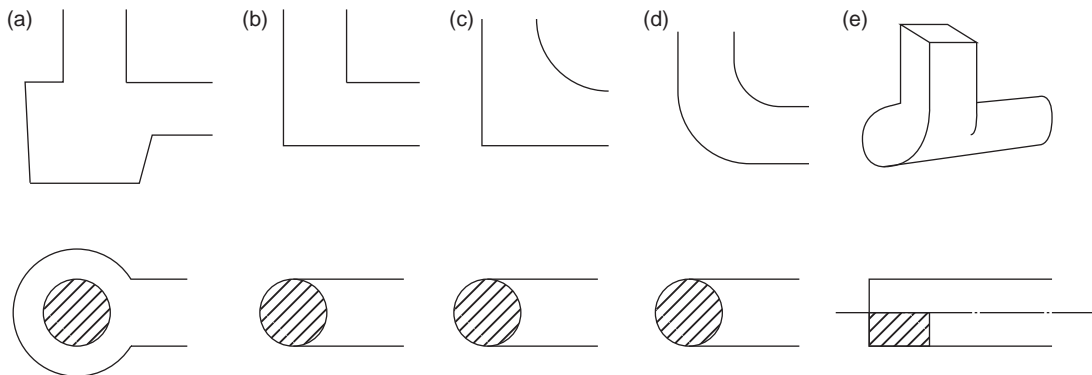


**FIGURE 12.17**

A variety of sprue/runner junctions in side and plan views from poorest (a) to best (d). The offset junction at (e) forms a vortex flow along the cylindrical runner. Early results suggest it performs well, but more research is probably needed (Section 12.6.3).

highly damaged metal into the mold cavity. Thus the comforting and widely held image of the well as being a ‘cushion’ to soften the fall of the melt is seen to be an illusion. In reality, the well was an opportunity for the melt to churn, entraining quantities of oxide and bubble defects.

Clearly, an abrupt right angle (Figure 12.17b) was not a satisfactory solution since it could be certain that plenty of bubbles would be entrained from the downstream portion of the vena contracta (Figure 12.18). This region of flow, at the trailing extremity of the air and vapor pocket, is particularly unstable and sheds bubbles into the flowing stream.

Systematic X-ray radiographic studies started in 1992 have been revealing. They have shown that in a sufficiently narrow filling channel with a good radius at the sprue/runner junction, the high surface tension of the liquid metal assists to retain the integrity of a compact liquid front, constraining the melt. These investigative studies on dramatically narrow channels in real molds with real metals quickly confirmed that the sprue/runner junction was best designed as a simple turn (Figure 12.17c, d), provided that the channels were of minimum area.

The minimum area condition is important. For instance if the inside radius seen in Figure 12.17c is approximately the same as the thickness of the sprue exit, the junction has a modest volume that is somewhere close to optimum. If the inside radius becomes much greater than twice this value the additional volume starts to introduce entrainment behavior. Furthermore, the liquid in the corner of the junction revolves like a ball bearing, reducing the friction experienced by the melt undertaking the turn. Thus the velocity of the melt out of the junction is closely equal to the entering velocity; very little energy is lost.

From this point of view the junction (Figure 12.17d) is a great improvement because the redundant volume in the sharp angle of the bend is eliminated, reducing entrainment problems. In addition, the outside wall of the bend, being stationary and microscopically rather rough, introduces friction into the turn, so that the exiting melt is somewhat reduced in speed. Reductions of 20% or so in velocity have been recorded. Any such speed reductions, even though small, are welcome. Thus it is useful, if possible, to also radius the outside of the bend to maintain a parallel channel.



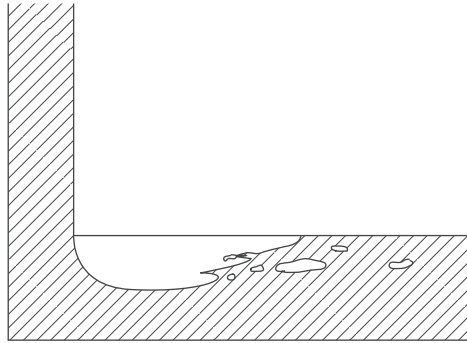


**FIGURE 12.18**

The vena contract problem at a right angle with inadequate radius. The downstream part of this decohered region of flow is unstable, shedding bubbles into the flow.

In summary, despite what was recommended by the author in *Castings* 1991, more recent research confirms that wells are no longer recommended. The simple turn, maintaining a uniform cross-section area as closely as possible, seems best.

### 12.2.5 The radial choke

This is a clever ‘quick fix’ for the evils of a reverse tapered sprue (especially one fitted with a well as in Figure 12.19a) suggested by Groteke (see Sikovski and Groteke 2005) in which a small cylinder can be planted on the drag pattern at the base of the sprue. It forms a narrow annulus through which the melt is constrained to flow in a radial direction (Figure 12.19b). No other changes to the pattern are usually made. The corrective action to the sprue, in getting it to fill in about half the time, is immediate and valuable. (As an interesting aside, the provision of a reduced volume at the base of the sprue as seen in Figure 12.19b is diametrically opposed to the concept of providing an enlarged volume in the form of a well. One works, the other is a disaster.)

Computer simulations of the detailed filling of the radial choke show it to be somewhat messy in practice, indicating that improvements to the concept can surely be made and would be desirable. An optimization study would be welcome. Even so, even in its current relatively undeveloped form, it is quick and easy to fit, and acts as an immediate and significant improvement over the unaided reverse tapered sprue. It can help a lot until an overall better system can be put in place.

### 12.2.6 The radius of the sprue/runner junction

It has been shown that for small castings, generally up to a few kg in weight, the melt can be turned through the right angle at the base of the sprue simply by putting a right-angle bend into the channel. However, if no radius is provided, the melt cannot follow the bend, so that a vena contracta is created (Figure 12.18). The trailing edge of this cavitated region is unstable, so that its fluttering and flapping action sheds bubbles into the stream.

The vena contracta is a widely observed phenomenon in flowing liquids. It occurs wherever a rapid flow is caused to turn through any sharp change of direction. An important example has already been

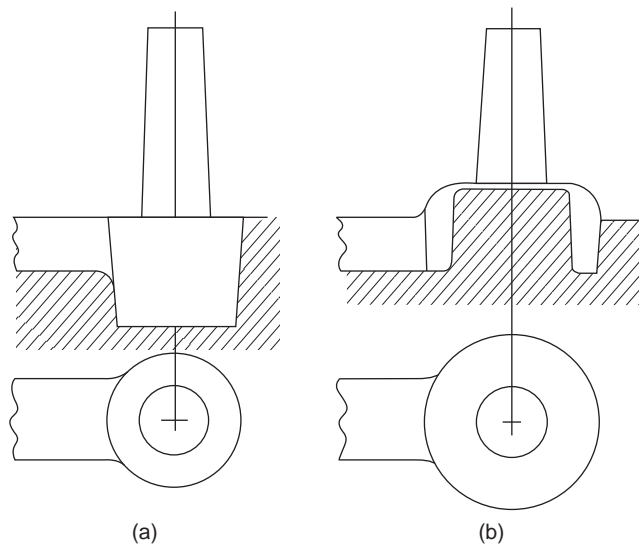


**FIGURE 12.19**

(a) Traditional well, nearly as deleterious as a conical basin; (b) radial choke, a substantial benefit compared to a 'well' but may benefit further from additional optimization.

met in the offset pouring basin if no step is provided (Figure 12.4a). This creates a vena contracta that showers bubbles down the sprue. However, the base of the sprue is probably an even more important example since the speeds are much higher here. The loss of contact of the stream from the top of the runner immediately after the turn has been shown to be the source of much air in the metal. Experiments with water have modeled the low-pressure effect here, demonstrating the sucking of copious volumes of air into the liquid as streams and clouds of bubbles (Webster 1967). This is expected to be particularly severe for sand molds, where the permeability will allow a good supply of air to the region of reduced pressure.

In fact, when pouring castings late at night, when the foundry is quiet, the sucking of air into the liquid metal can be clearly heard, a haunting sound in the darkness like bath water down the plug-hole! Such castings always reveal oxides, sand inclusions, and porosity above the gates, which are the tell-tale signs of air bubbles aspirated into the running system.

In contrast, provided that the internal corner of the bend is given a sufficiently large radius, the melt will turn the corner without cavitation or turbulence (Figure 12.17c). In fact, the action of the advancing metal is like a piston in a cylinder: the air is simply pushed ahead of the advancing front, never becoming mixed. To be effective, the internal radius of the bend needs to be at least equal to the diameter of the sprue exit, and possibly twice this amount, but probably not more. Too large a radius introduces too much redundant volume into the filling channel, allowing the development of surface turbulence and entrainment of air and oxides. The precise radius might benefit from further research. The action of the internal radius is significantly improved if the outside of the bend is also provided with a radius to maintain the parallel form of the channel (Figure 12.17d).

For larger castings where surface tension becomes progressively less important, the channels are filled only by the available volume of flow. Initially, during the first critical period as the filling system is priming, there is considerable danger of significant damage to the metal.

To limit such damage it is helpful to take all steps to prime the front end of the filling system quickly. This is assisted by the use of a stopper in the pouring basin. However, in *Castings* 1991 the author has considered the use of various kinds of chokes at the entrance to the runner as a possible solution to these problems. Again, recent research has not upheld these recommendations. It seems that any such constriction merely results in the jetting of the flow into the more distant expanded part of the runner.

This finding emphasizes the value of the concept of the *naturally pressurized* system. It is clearly of no use to expand the running system to fulfill some arbitrary formula of ratios, in the hope that the additional area will persuade the flow velocity to reduce. The flow tends to maintain its speed and direction (steadfastly ignoring any enlargement of area we may provide in the hope that the melt might fill this additional area and slow down).

The use of a *vortex sprue*, or even simply a *vortex base* or *vortex runner* (Figure 12.17e) in conjunction with a conventional sprue represent exciting and potentially important new developments in running system design. These concepts are described more fully in Section 12.6.

---

## 12.3 RUNNER

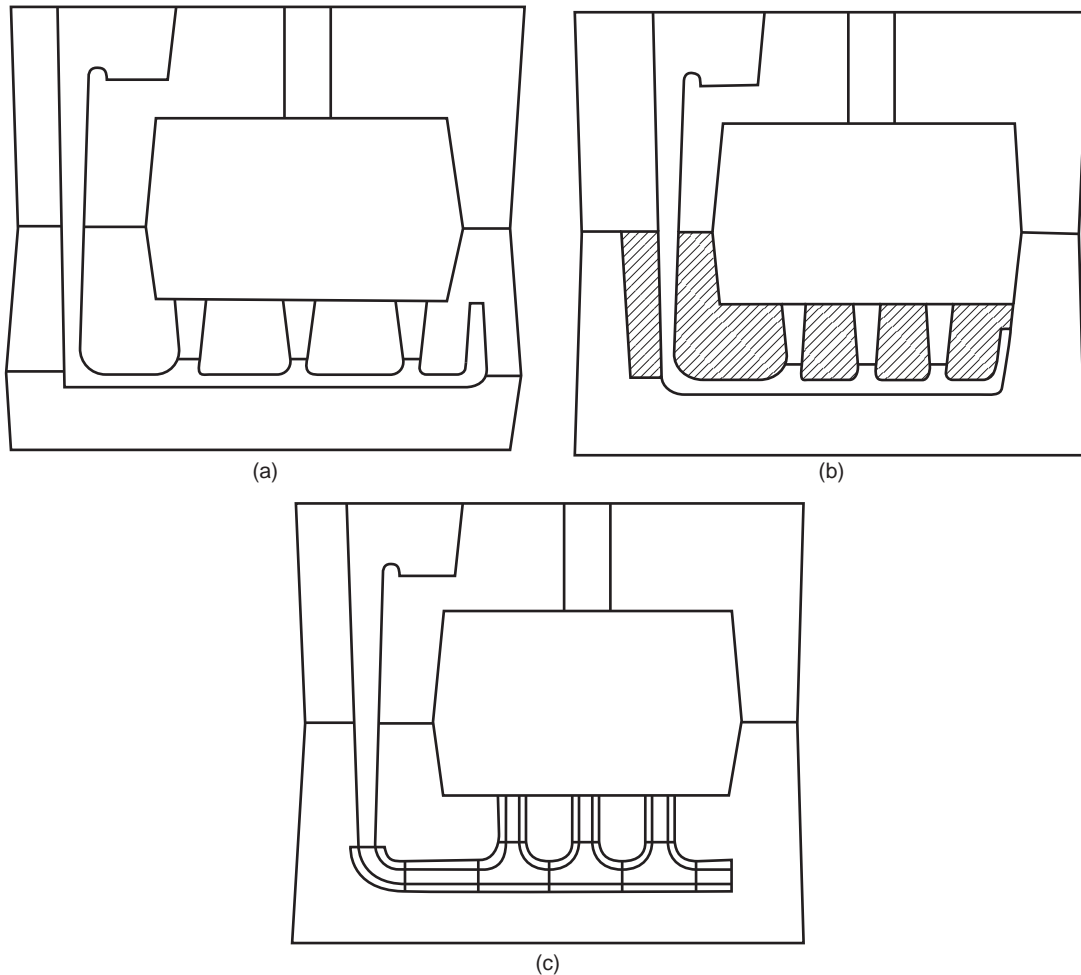
The runner is that part of the filling system that acts to distribute the melt horizontally either around or under the mold, reaching distant parts of the mold cavity quickly to reduce heat loss problems.

The runner is usually necessarily horizontal because it simply follows the normal mold joint in conventional horizontally parted molds. In other types of molds, particularly vertically jointed molds, or investment molds where there is little geometrical constraint, the runner would often benefit from being inclined uphill.

It is especially useful if the runner can be arranged under the casting, so that the runner is connected to the mold cavity by vertical gates. All the lowest parts of the mold cavity can then be reached easily this way. The technique is normally achieved only in a three-part mold in which the joint between the cope and the drag contains the mold cavity, and the joint between the lower mold parts (the base and the drag) contains the running channels (Figure 12.20a). The three-part mold is often a costly option. Sometimes the three-level requirement can be achieved by use of a large core (Figure 12.20b), or the distribution system can be assembled from refractory or sand core sections, and built into the mold as the molding box is filled with sand (Figure 12.20c). These options are often worth considering, and might prove an economic investment.

More usually, however, a two-part mold requires both casting and running system to be molded in the same joint between cope and drag. To avoid any falls in the filling system the runner has to be molded in the drag, and the casting and its gates in the cope (Figure 12.21).

The usual practice, especially in iron and steel foundries, of molding the casting in the drag (Figure 11.2a) is understandable from the point of view of minimizing the danger of run-outs. A leak at the joint or a burst mold is a possible danger and a definite economic loss. This was an important consideration for hand-molded greensand, where the molds were rather weak (and was of course the reason for the use of the steel molding box or flask). However, the placing of the mold cavity below the

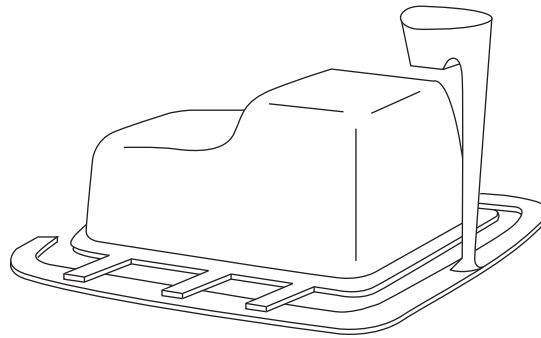


**FIGURE 12.20**

Bottom-gated systems achieved by (a) a three-part mold with accurately molded running system; (b) making use of a core; and (c) a two-part mold with preformed refractory channel sections molded into drag.

runner causes an uncontrolled fall into the mold cavity, creating the risk of imperfect castings. It is no longer such a danger for the dense, strong greensand molds produced from modern automatic molding machines, or for the extremely rigid molds created in chemically bonded sands. For products whose reliability needs to be guaranteed, the arrangement of the runner at the lowest level of the mold cavity, causing the metal to spread through the running system and the mold cavity only in an uphill direction is a challenge that needs to be met (Figure 12.21). Techniques to achieve this include the clever use of a core (Figure 12.20b) or for some hollow castings the use of central gating (Figures 12.22b and 12.23).

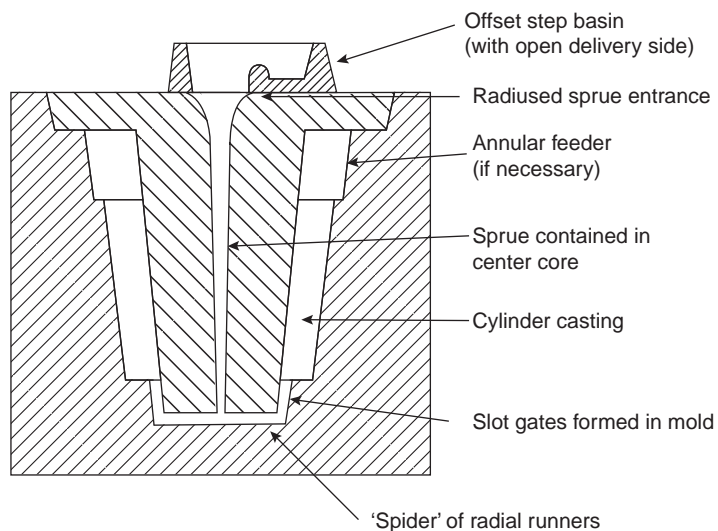
Webster (1964) carried out some early exploratory experiments to determine optimum runner sizes. We can summarize his results in terms of the comparative areas of the runner/sprue exit. He has found

**FIGURE 12.21**

An external running system arranged around an automotive sump (oil pan).

that a runner that has only the same area as the sprue exit (ratio 1) will have a metal velocity that is high. A ratio of 2 he claims is close to optimum since the runner fills rapidly and excludes air bubbles reasonably efficiently. A ratio of 3 starts to be difficult to fill; and a ratio of 4 is usually simply wasteful for most castings. Webster's work was a prophesy, foretelling the dangers of large runners that foundries have, despite all this good advice, continued to use.

For the best results, however, recent careful studies have made clear that even the expansion of the area of flow by a factor of 2 is not achieved without a serious amount of surface turbulence. This is now known from video X-ray radiographic studies, and from detailed examination of the scatter of mechanical properties of castings using a highly sensitive and quantifying technique, Weibull analysis.

**FIGURE 12.22**

Cross-section of an internal running system for the casting of a cylinder.

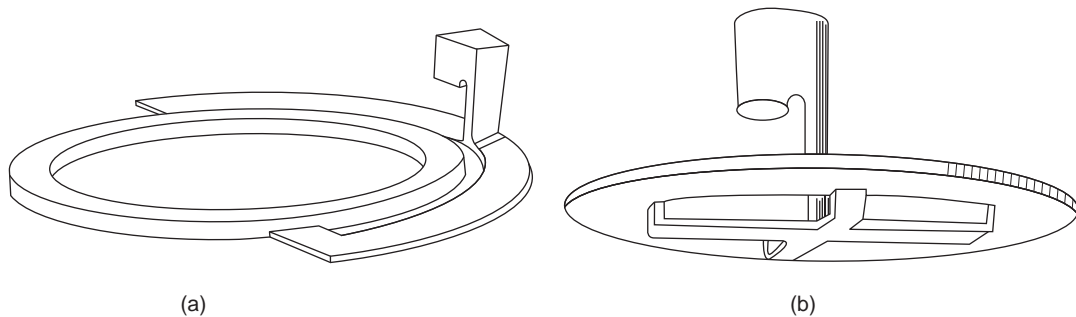


**FIGURE 12.23**

Ring casting produced using (a) an external and (b) an internal filling system.

The best that can easily be achieved without damage is merely the reduction of about 20% in velocity by the friction of the sprue/runner bend, necessitating a 20% increase in area of the runner as has been discussed above. Any greater expansion of the runner will cause the runner to be incompletely filled, and so permit conditions for damage.

Greater speed reductions, and thus greater opportunities for expansion of the runner, occur if the number of right-angle bends is increased, since the factor of 0.8 reduction in speed is cumulative from one bend to the next. After three such bends the speed is reduced by half ( $0.8 \times 0.8 \times 0.8 = 0.5$ ). Right-angle bends were anathema in filling system designs when large cross-sections were the norm. However, with very narrow systems, there is less room for surface turbulence. Even so, great care has to be taken. For instance video X-ray studies have confirmed that the bends operate best if their internal and external radii provide a parallel channel. The lack of an external radius can cause a reflected wave in larger channels.

One of the most effective devices to reduce the speed of flow in the runner is the use of a filter. The close spacing of the walls of its capillaries ensures a high degree of viscous drag. Flow rate can often be reduced by a factor of 4 or 5. This is a really valuable feature, and actually explains nearly all of the beneficial action of the filter (i.e. when using reasonable-quality metal in a well-designed filling system the filter does very little filtering; its really important action in improving the quality of castings is its reduction of velocity). The use of filters is considered later (Section 12.8).

There has over the years been a considerable interest in the concept of the separation of second phases in the runner. Jeancolas et al. (1969) carried out experiments on ferrous metals to show that at Reynolds numbers below the range 7000–12 000, suspended particles of alumina could be deposited in the runner but at values in excess of 15 000, they could not precipitate. Although these findings underline the importance of working with the minimum flow velocities wherever possible, it is quickly shown that for a steel casting of height 1 m, giving a velocity of flow of  $4.5 \text{ m s}^{-1}$ , for  $\eta = 5.5 \times 10^3 \text{ N s m}^{-2}$ , and for a runner of  $80 \text{ mm}^2$ ,  $Re$  is over 100 000. Thus it seems that conditions for the deposition of solid materials such as sand and refractory particles in runners will not be met. In general, therefore, it seems misguided to attempt to design filling systems that might be thought to encourage flotation of inclusions.

Even so, a worker in a foundry casting iron may protest that slag accumulates on the tops of runners, where it is much to be preferred than in the casting. He will point out that separation in this

case happens because of (i) the great difference in density between the slag and the metal; (ii) because of the large size of the slag droplets; and (iii) because of his large section runner that promotes slower flow. Although there may be a modicum of truth in all of this, it is certain that in most cases most of the slag does not arrive with the metal, since this is often via bottom-poured launder, but is generated in situ in the running system, mainly because the filling system channels are too large.

At this point, the reader might, among the confusing detail, be starting to appreciate the basic scenario and some of the major targets of the filling design:

- (i) The metal arrives in some chaos at the bottom of the sprue.
- (ii) After this initial trauma, it may be gathered together once again by the integrating action of a feature such as a filter or radial choke to provide some delay and back-pressure.
- (iii) It rises steadily against gravity, filling section after section of the running system.
- (iv) Finally it arrives in the mold in fair condition, not having suffered too much damage, and at a speed below the critical velocity.

It should be noted that such a logical system and its consequential orderly fill is not to be taken for granted. For instance, it is usually a problem if the runner is molded in the cope. This is mainly because the gates, which are in either the drag or the cope, will inevitably start to fill and allow metal into the mold cavity before the runner is full, as is clear from Figure 11.2a. The traditional running of cast iron in this way fails to achieve its potential in its intended separation of metal and slag. This is because the first metal and its load of slag (mainly generated in the sprue and early part of the runner) enters the gates immediately, prior to the filling of the runner, and thus prior to the chance that the slag can be trapped against the upper surface of the runner. In short, the runner in the cope results in the violation of the fundamental ‘no fall’ criterion. The runner in the cope is not recommended for any type of casting – not even gray iron! Despite all, the reader needs to be aware that regardless of all these good reasons and good intentions, it is sometimes highly inconvenient or sometimes impossible to site the runner in the drag.

The complexity of behavior of some filling system designs is illustrated by a runner in a gravity die, positioned in the cope, which acted to reduce the bubble damage in the casting (Figure 12.24). This result, apparently in complete contradiction to all the behavior warned above, arose because of the exceptionally tall aspect ratio of the runner, which was shaped like a vertical slot. This shape retained

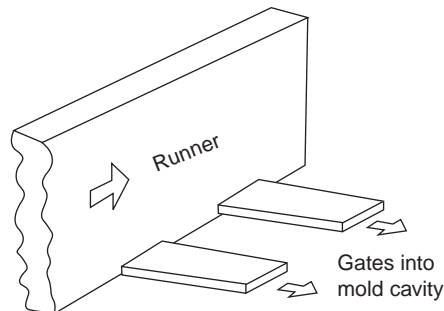


**FIGURE 12.24**

Tall slot runner with bottom gates.

bubbles high above the exits to the gates molded below. In fact it seems that the reduction in bubbles into the casting by placing the gates low in this way only really resulted because of the extremely poor front end of the filling system. The filling system was a bubble-manufacturing design, so that almost any remedy had a chance to produce a better result. However, there is a real benefit to be noted (running systems are perversely complicated) because the gates would prime slowly as a head of metal in the runner was built up, thus avoiding any early jetting through into the mold cavity. This is a benefit not to be underestimated, and highlights the problem of generalizing for complex geometries of castings and their filling systems that can sometimes contain not just liquid metal but emulsions of slag and/or air.

In gravity die castings the placing of the runner in the cope, and taking off gates on the die joint (Figure 11.2a), is especially bad. This is because the impermeable nature of the die prevents the escape of air and mold gases from the top of the runner. Thus the runner never properly fills. The entrapped gas floating on the surface of the metal will occasionally dislodge, as waves race backwards and forwards along the runner, and as the gases heat up and expand. Large bubbles will therefore continue to migrate through the gates from time to time throughout the pour. Some bubbles might dislodge from the runner and into the casting even later, not only causing bubble trails and splash problems, but also the advancing solidification front may trap whole bubbles.

This scenario is tempered if a die joint is provided along the top of the runner to allow the escape of air. Alternatively, a sand core sited above the runner can help to allow bubbles to diffuse away.

### 12.3.1 The tapered runner

It is salutary to consider the case where the runner has two or more gates, and where the stepping or tapering of the runner has been unfortunately overlooked. The situation is shown for three gates in Figure 12.25a. Clearly, the momentum of the flowing liquid causes the furthest gate, number 3, to be favored. The rapid flow past the opening of gate 1 will create a reduced-pressure region in the adjacent

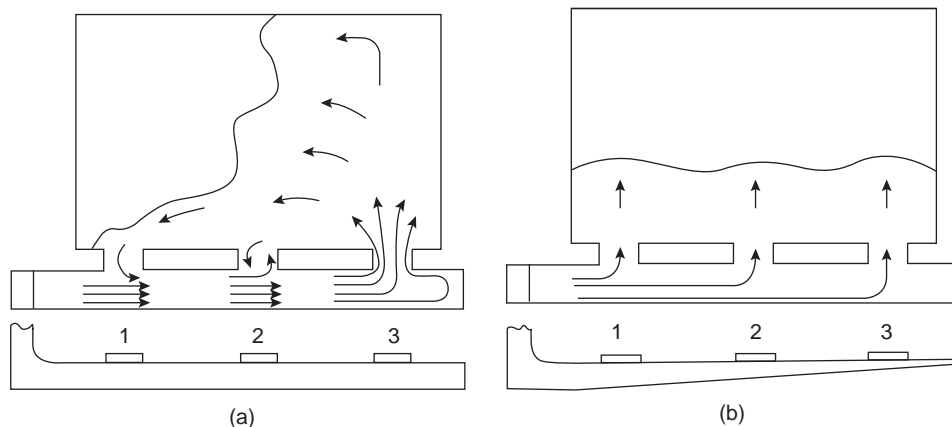


FIGURE 12.25

(a) An unbalanced delivery of melt into the mold as a result of an incorrect runner design; (b) a tolerably balanced system.



gate at this point, drawing liquid out of the casting! The flow may be either in or out of gate 2, but at such a reduced amount as to probably be negligible. In the case of a non-tapered runner it would have been best to have only gate 3.

Where more than one gate is attached to the runner, the runner needs to be reduced in cross-section as each gate is passed, as illustrated in Figure 12.25b.

In the past such reductions have usually been carried out as a series of steps, producing the well-known stepped runner designs. For three ingates the runner would be reduced in section area by a step of one-third the height of the runner as each gate was passed. However, real-time X-ray studies have noted that during the priming of such systems, the high velocity of the stream causes the flow to be deflected, leaping into the air when impacting the step, and ricocheting off the roof of the runner. Needless to say, the resulting flow is highly aerated, and does not achieve its intended even distribution. It has been found that simply reducing the cross-section of the runner gradually, usually linearly, giving a smooth, straight taper geometry does a reasonable job of distributing the flow evenly (Figure 12.25b).

Kotschi and Kleist (1979) allow a reduction in the runner area of just 10% more than the area of the gate to give a slight pressurization bias to help to balance the filling of the gates. However, they used a highly turbulent non-pressurized system that will not have encouraged results of general applicability. In contrast, computer simulation of the narrow runners recommended in this work has shown that the last gate suffers some starvation as a result of the accumulation of friction along the length of the runner. Thus for slim systems the final gates require some additional area, not less. Thus instead of tapering the runner to zero thickness, which is an overcorrection favoring most of the filling via gate 1, some compromise, such as tapering to 50% of the thickness, will usually be found to give a more even favoring of gates (Figure 12.25b). The taper can, of course, be provided horizontally or vertically (an important freedom of choice often forgotten).

Finally, at all times avoid tapering the runner to zero. The thinning section adds no advantage but to provide points on which people keep stabbing themselves in the foundry. It aids safety in the workplace to stop the taper at about five millimeters section thickness. Tapering to 50% of thickness usually gives a more satisfactory distribution.

### 12.3.2 The expanding runner

In an effort to slow the metal in its early progress in the runner, a number of methods of expanding the area of the runner have been tried. Such expanding sections of runners have often been graced by the name of 'diffuser'. It has to be admitted that none of these designs is successful. However, it is worth describing these attempts for our education.

The simple expansion of the runner at an arbitrary location along the runner is of no use at all (Figure 12.26a). The melt progresses without noticing the expansion, progressing as a central jet, and finally hitting the far end of the runner and creating backwaves, which in their reverse flow entrain bubbles and oxides where the flows shear side by side. Even expanding the runner directly from the near side of the sprue (shown as having a square section for clarity) is not helpful (Figure 12.26b). However, expanding the runner from the far side of the sprue (Figure 12.26c) does seem to work considerably better. But even here the front tends to progress in two main streams on either side of the central axis of the runner, leaving the center empty, or relatively empty, forming a low-pressure region some distance down-stream in the runner, similar to the pattern seen previously for a round sprue on

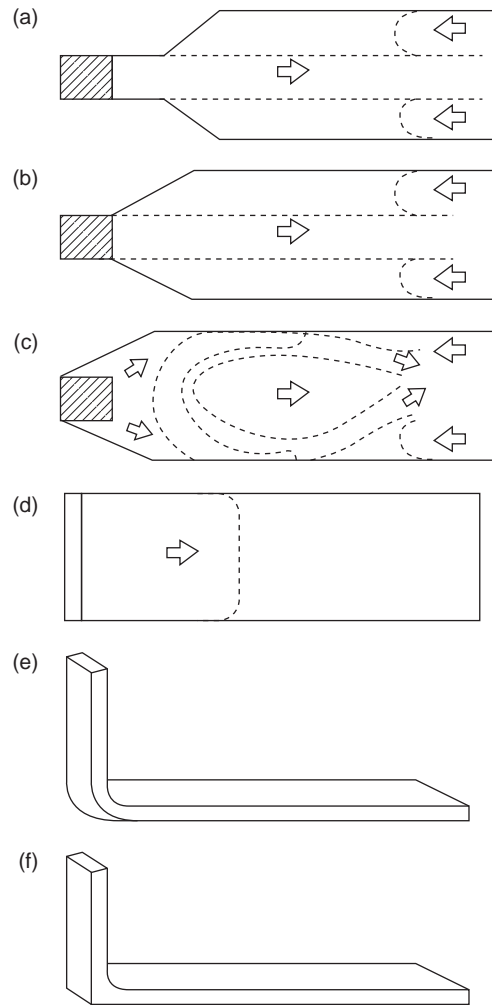


**FIGURE 12.26**

Plan views of a square section sprue connected to a shallow rectangular runner showing attempts to expand the runner (a and b) that fail completely. Attempt (c) is better, but flow that ricochets off the walls generates a central starved, low-pressure region; (d) a slot sprue and slot runner produce a uniform flow distribution in the runner shown in (e) (recommended) and (f) (usually acceptable).

a rectangular runner (Figure 12.16). This development of this double jet flow seems to be the result of the attempted radial expansion of the flow as it impacts on the runner, but finds itself constrained by and reflected from the walls of the runner. This situation for high-temperature liquids such as irons and steels leads to the downward collapse of the center of the runner in sand molds, since this becomes heated by radiation, and so expands (especially if mold consists of silica sand and its temperature is raised above its alpha/beta transition), but is unsupported by the pressure of metal. The closing down of

the runner in this way can be avoided by a central molded support, effectively separating the runner into two separate, parallel runners. In practice I have found that a slot runner about 100 mm wide for irons and steels is close to the maximum that can resist collapse in such a zigzag flow. It may be that large dimensions would be safe if the flow were parallel (Figure 12.26d, e, f).

The use of slot sprues linked to slot runners promises to be a complete solution to the problem of the sprue/runner junction problem and deserves wider exploitation. The use of such a geometry might permit the more uniform action of friction to assist a modest expansion of the runner to achieve a correspondingly modest speed reduction. This has yet to be tested.

What is certain is that most normal efforts to expand the runner to reduce speed not only fail, but as a result of the melt becoming depressurized and entraining gas the failure is a disaster for the casting quality. Much more research is needed to test what can be achieved. Successful and reliable speed reduction by expanding runners may prove impossible. To be safe in the meantime, and perhaps for ever, diffusers should probably be laid to rest.

---

## 12.4 GATES

The gates, or ‘ingates’, are those last feature of the filling system that introduce the metal into the mold cavity. They can have a profound effect on the melt flow into the cavity, for good or evil. Every part of the filling system has its own special purpose, and is critical to success. Every part has to be correct, including the gates.

### 12.4.1 Siting

When setting out the requirements for the site of a good gate, it is usual to start with the questions ‘Where can we get it on?’ and ‘Where can we get it off?’ Other practical considerations include ‘Gate on a straight side if possible’ and ‘Locate at the shortest flow distance to the key parts of the casting’.

This is a good start, but, of course, just the start. There are many other aspects to the design of a good gate.

### 12.4.2 Direct and indirect

In general, it is important that the liquid metal flows through the gates at a speed lower than the critical velocity so as to enter the mold cavity smoothly. If the rate of entry is too high, causing the metal to fountain or splash inside the mold cavity, then the battle for quality is probably lost. Turbulence inside the mold cavity is the most serious turbulence of all. Turbulence occurring early in the running system may or may not produce defects that find their way into the casting because many bifilms remain attached to the walls of the runners and many bubbles escape. However, any creation of defects in the mold cavity ensures unavoidable damage to the casting.

One important rule therefore follows very simply: Do not place the gate at the base of the down-runner so that the high velocity of the falling stream is redirected straight into the mold, as shown in Figure 11.4. In effect, this *direct* gating is *too direct*. An improved, somewhat *indirect* system is shown in Figure 11.2b illustrating the provision of a separate runner and gate, and thus incorporating a number of right-angle changes of direction of the stream before it enters the mold. These provisions

are all used to good effect in reorganizing the metal from a chaotic mix of liquid and gases into a coherent moving mass of liquid. Thus although we may not be reducing the entrainment of bifilms, we may at least be preventing bubble damage in the mold cavity.

As we have mentioned above, all of the oxides created in the early turbulence of the priming of the running system do not necessarily find their way into the mold cavity. Many appear to 'hang up' in the running system itself. This seems especially true when the oxide is strong as is known to be the case for Al alloys containing Be. In this case the film attached to the wall of the running system resists being torn away, so that such castings enjoy greater freedom from filling defects. The wisdom of lengthening the running system, increasing friction, especially by the use of right-angle bends, adds back-pressure for improved back-filling and reduces velocity. It also provides more surface to contain and hold the oxides generated during priming.

### 12.4.3 Total area of gate(s)

A second important rule concerns the sizing of the gates. They should be provided with sufficient area to reduce the velocity of the melt into the range  $0.5\text{--}1.0\text{ m s}^{-1}$ . The concept is illustrated in Figure 2.18. In the author's experience, velocities above  $1.2\text{ m s}^{-1}$  for Al alloys always seem to give problems. Velocities of  $2\text{ m s}^{-1}$  in film-forming alloys, unless onto a core as explained below, would be expected to have consequences sufficiently serious that they could not be overlooked. With even higher velocities the problems simply increase.

Occasionally, there is a problem to obtain a sufficient size of gate to reduce the melt speed to safe levels before it enters the mold cavity. In such cases it is valuable if the gate opens at right angles onto a thin (thickness a few millimeters) wall. This is because the melt is now forced to spread sideways from the gate, and suffers no splashing problems because the local section thickness of the casting is too small. As it spreads away from the gate it increases the area of the advancing front, thereby reducing its velocity. Thus by the time the melt arrives in a thicker section of the casting it is likely to be moving at a speed below critical. Effectively, the technique uses a thin wall section of the casting as an extension of the filling system.

This is a good reason for gating direct onto a core, but, once again, is contrary to conventional wisdom. In the past, gating onto a core was definitely bad. This was because of the amount of air entrained in the flow. The air assisted to hammer and oxidize the surface of the core and thus led to sand erosion and the local destruction of the core. With a good design of filling system, however, in which air is largely excluded, the action of the hot metal is safe. Little or no damage is done to the core despite the high velocity of the stream, because the melt merely heats the core whilst exerting a steady pressure that holds the core material in place. Thus, with a good filling system design, gating directly onto a core is recommended.

Returning to the usual gating problem whereby the gate opens into a large section casting, if the area of the gate is too small then the metal will be accelerated through, jetting into the cavity as though from a hosepipe. Figure 2.18 shows the effect. In many castings the jet speed can be so high that the metal bounces around the mold cavity, scouring roof and walls of the cavity. Historically, many castings have been gated in this way, including most steels and gray cast iron castings. The approach has enjoyed mediocre success whilst greensand molding has been employed, but it seems certain that better castings and lower scrap rates would have been achieved with less turbulent filling. In the case of cores and molds made with resin binders that cause graphitic films on the liquid iron, the pressurized

delivery system is usually unacceptable. The same conclusion is true for ductile irons in all types of molds.

We may define some useful quick rules for determining the total gate area that is needed. For an Al alloy cast at  $1 \text{ kg s}^{-1}$  assuming a density of approximately  $2500 \text{ kg m}^{-3}$  and assuming that we wish the metal to enter the gate at its critical speed of approximately  $0.5 \text{ m s}^{-1}$  it means we need approximately  $1000 \text{ mm}^2$  of gate area. The elegant way to describe this interesting ingate parameter is in the form of the units of area per mass per second; thus for instance ' $1000 \text{ mm}^2 \text{ kg}^{-1} \text{ s}$ '.

Clearly we may pro-rata this figure in different ways. If we wished to fill the casting in half the time, but at the same low ingate velocity, we would require  $2000 \text{ mm}^2$  and so on. It can also be seen that the area is quickly adjusted if it is decided that the metal can be allowed to enter at twice the speed, thus the  $1 \text{ kg s}^{-1}$  would require only  $500 \text{ mm}^2$ , or if directly onto a core in a thin section casting, perhaps twice the rate once again, giving only  $250 \text{ mm}^2$ .

Allowing for the fact that denser alloys such as irons, steels, and copper-based alloys have a density approximately three times that of aluminum, but the critical velocity is slightly smaller at  $0.4 \text{ m s}^{-1}$ , the ingate parameter becomes, with sufficient precision,  $500 \text{ mm}^2 \text{ kg}^{-1} \text{ s}$ .

The values of approximately  $1000 \text{ mm}^2 \text{ kg}^{-1} \text{ s}$  for light alloys and  $500 \text{ mm}^2 \text{ kg}^{-1} \text{ s}$  for dense alloys are useful parameters to commit to memory.

#### 12.4.4 Gating ratio

In its progress through the running system the metal is at its highest velocity as it exits the sprue. If possible, we aim to reduce this in the runner, and further reduce as it is caused to expand once again into the gates. The aim is to reduce the velocity to below the entrainment threshold (the  $0.4$  or  $0.5 \text{ m s}^{-1}$  if possible, but up to  $1.0 \text{ m s}^{-1}$  if necessary) at the point of entry into the mold cavity.

It is worth spending some time below describing the traditional ratio method of defining running systems which is widely used. It is to be noted that it is not recommended!

It has been common to describe running systems in terms of ratios based on the area of the exit of the sprue. For instance, a widely used area ratio of the sprue/runner/gates has been 1:2:4. Note that in this abbreviated notation the ratios given for both the runner and the gates refer back to the sprue, so that for a sprue exit of 'A', the runner area is 2A and the total area of the gates is 4A. It is clear that such ratios cannot always be appropriate, and that the real parameter that requires control is the velocity of metal entering the mold. Thus on occasions this will result in ratios of 1:1:10 and other unexpected values. The design of running systems based on ratios is therefore a mistake.

Having said this, I do allow myself to use the ratio of the area of sprue exit to the (total) area of the gates. Thus if the sprue is  $200 \text{ mm}$  tall (measured of course from the top of the metal level in the pouring basin) the velocity at its base will be close to  $2 \text{ m s}^{-1}$ . Thus a gate of 4 times this area will be required to get to below  $0.5 \text{ m s}^{-1}$ . (Note therefore that the old 1:2:4 and 1:4:4 ratios can be seen therefore to be applicable only up to  $200 \text{ mm}$  sprue height. Beyond this sprue height the ratios are insufficient to reduce the speed below  $0.5 \text{ m s}^{-1}$ . The reader should also notice the damaging increase in area of the runner which is implied in these figures.)

I am often asked what about the problem that occurs when the mold cross-sectional area reduces abruptly at some higher level in the mold cavity. The rate of rise of the metal will also therefore be increased suddenly, perhaps becoming temporarily too fast, causing jetting or fountaining as the flow squeezes through the constriction. Fortunately, and perhaps surprisingly, this is extremely rare in

casting geometries. In 40 years dealing with thousands of castings I have difficulty recalling whether this has ever happened. The narrowest area is usually the gate, so the casting engineer can devote attention to ensuring that the critical velocity is not exceeded at this critical location, not forgetting the danger just inside the mold because of the velocity of the sideways spreading flow (see below). If the velocities through the gate and across the floor of the mold cavity are satisfactory it usually follows that the velocity will be satisfactory at all other levels in the casting.

Even in a rare situation where a narrowing of the mold is severe, it would still be surprising if the critical velocity were exceeded, because the velocity of filling is at its highest at the ingate, and usually decreases as the metal level rises, finally becoming zero when the net head is zero, as the metal reaches the top of the mold.

Once again, of course, counter-gravity filling wins outright. In principle, and usually with sufficient accuracy in practice, the velocities can be controlled at every level of filling.

### 12.4.5 Multiple gates

As will become clear, there are a number of reasons why more than one gate may be desirable. This might be to (i) distribute heat more evenly in the mold, (ii) reduce horizontal velocities in the mold, (iii) reduce contact hot spots, (iv) reduce distortion of the casting, (v) provide liquid at all the lowest points in the mold cavity to avoid waterfall effects, (vi) provide greater gate area for heavier parts of the casting, and (vii) ease cut-off. These factors will be discussed.

### 12.4.6 Premature filling problem via early gates

Sutton (2002) applied Bernoulli's theorem to draw attention to the possibility that a melt traveling along a horizontal runner will partly enter vertical gates placed along the length of the runner, despite the fact that the runner may not yet have completely filled and pressurized (Figure 12.27). This arises as a result of the pressure gradient along the flow, and is proportional to the velocity of flow. In real casting conditions, the melt may rise sufficiently high in such gates that cavities attached to the gates might be partially filled with a slow dribble of upwelling metal prior to the filling of the runner, and therefore prior to the main flow up the vertical gates. These upward dribbles of metal in the cavity are poorly assimilated by the arrival of the main metal supply, and so usually constitute a lap defect resembling a mis-run or part-filled casting.

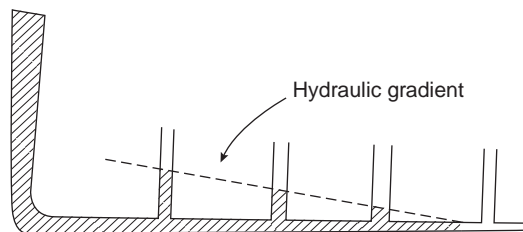


FIGURE 12.27

The partial filling of vertical ingates along the length of a runner as a result of the pressure gradient formed naturally by friction losses.

This same effect would be expected to be even more noticeable in horizontal gates molded in the cope, sited above a runner molded in the drag (Figure 11.2b). The head pressure required to simply cross the parting line and start an unwanted early filling of part of the mold cavity would be relatively small, and easily exceeded.

### 12.4.7 Horizontal velocity in the mold

When calculating the entry velocity of the metal through the gates, it is easy to overlook what happens to the melt once it starts to spread sideways into the mold cavity. The horizontal sideways velocity away from the gate can sometimes be high. In many castings where the ingate enters a vertical wall the transverse spreading speed inside the mold is higher than the speed through the gate, and causes a damaging splash as the liquid hits the far walls (Figure 12.28). We can make an estimate of this lateral velocity  $V_L$  in the following way.

The lateral travel of the melt will normally be at about the height  $h$  of a sessile drop. We shall assume the section thickness  $t$ , for a symmetrical ingate, area  $A_i$ . The melt enters the ingate at the velocity  $V_i$ , and spreads in both directions away from the gate. Equating the volume flow rates through the gate and along the base of the casting gives

$$V_i \cdot A_i = 2V_L \cdot h \cdot t$$

If we limit the gate velocity and the transverse velocity to the same critical velocity  $V_C$  (for instance  $0.5 \text{ m s}^{-1}$ ) and adopt a gate thickness  $t$  the same as that of the casting wall, the relation simplifies to the fairly self-evident geometrical relation in terms of the length of the ingate  $L_i$

$$L_i = 2h$$

The message from this simple formula is that if the length of the gate exceeds twice the height of the sessile drop, even if the gate velocity is below the critical velocity, the transverse velocity may still be too high, and surface turbulence will result from the impact of the transverse flow on the end walls of the mold cavity.

To be sure of meeting this condition, therefore, for aluminum alloys where  $h = 13 \text{ mm}$ , gates must always be less than 26 mm wide (remembering that this applies only to gates that have the same

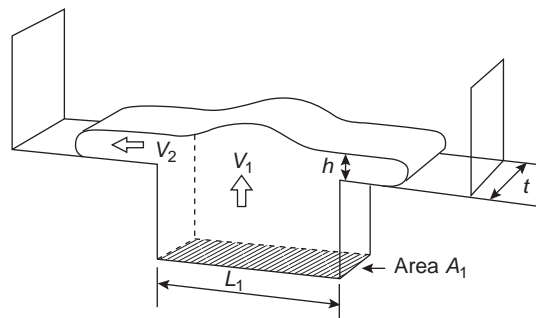


**FIGURE 12.28**

Sideways flow inside mold cavity.

thickness as the wall of the casting). For irons and steels gates should not exceed 16 mm wide. If we allow ourselves  $1 \text{ m s}^{-1}$  for both ingate and transverse flow inside the mold cavity the above figures remain unchanged.

Clearly, it is a concern that, in practice, gate lengths are often longer than these limits and may be causing unsuspected problems inside the mold cavity.

Since we often require areas considerably greater than can be provided by such short gates, it follows that multiple gates are required to achieve the total ingate area to bring the transverse velocity below critical. Two equally spaced gates of half the length will halve the problem, and so on. In this way the individual gate lengths can be reduced, reducing the problem correspondingly. Our relation becomes simply for  $N$  ingates of total ingate length  $L_i$

$$L_i/N = 2h$$

Or directly giving the number of ingates  $N$  that will be required to limit velocities to  $0.5 \text{ m s}^{-1}$

$$N = L_i/2h \quad (12.1)$$

These considerations based on velocity through the gate or in the casting take no account of other factors that may be important in some circumstances. For instance the number of ingates might require to be increased for a variety of reasons as listed at the beginning of this multiple gate section.

### 12.4.8 Junction effect

When the gates are planted on the casting they create a junction. This self-evident statement requires explanation.

Some geometries of junction create the danger of a hot spot. The result is that a shrinkage defect forms in the pocket of liquid that remains trapped here at a late stage of freezing. Thus when the gate is cut off a shrinkage cavity is revealed in the casting. This defect is widely seen in foundries. In fact, it is almost certainly the reason why most traditional molders cut such narrow gates, causing the metal to jet into the mold cavity with consequent poor results to casting quality.

The magnitude of the problem depends strongly on what kind of junction is created. Figure 12.29 shows the different kinds of junctions. An in-line junction (Figure 12.29c) is hardly more than an extension of the wall of the casting. Very little thermal problem is to be expected here. The T-junction (Figure 12.29a) is the most serious problem. It is discussed below. The L-junction (Figure 12.29b) is an intermediate case and is not further discussed. Readers can make their own allowances assuming conditions intermediate between the zero (in-line junction) and T-junction cases.

To help understand the hot-spot risk associated with the formation of a T junction it is instructive to recall the freezing patterns of T-sections. In the 1970s Kotschi and Loper carried out some admirable theoretical studies of T-junctions (Figure 5.16) using only simple calculations based on modulus. These studies pointed the way for experimental work by Hodjat and Mobley in 1984 that broadly confirmed the predictions. The data are interpreted in Figure 5.17 simply as a set of straight lines of slopes 2, 1, and 1/2. (A careful study of the scatter in the data shows that the predictions are not infallibly correct in the transitional areas, so that some caution is required.)

Figure 5.18 presents a simplified summary of these findings. It is clear that a gate (the upright leg of the T) of 1:1 geometry, i.e. a section equal to the casting section (the horizontal arm of the T), has a hot spot in the junction, and so is undesirable. In fact, Figure 5.18 makes it clear that any medium-sized



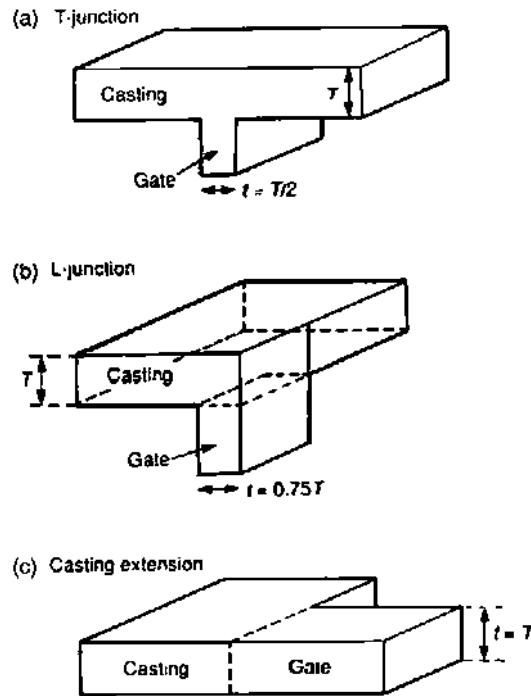


**FIGURE 12.29**

Maximum allowable gate thickness to avoid a hot spot at the junction with the casting.

gate less than twice as thick, or more than half as thick, will give a troublesome hot spot. It is only when the gate is reduced to half or less of the casting thickness that the hot-spot problem is eliminated. (Other lessons can be learned from the T-junction results: (1) an appendage of less than one-half of the section thickness will act as a cooling fin, locally enhancing the rate of cooling in the manner of a metal chill in a sand mold; and (2) an appendage of section double that of the casting will freeze later without a hot-spot problem. This is the requirement for a feeder when planted on a plate-like casting, as was discussed in Chapter 7 and in Rule 6 of the 10 Rules in Chapter 10.)

In the case of gates forming T-junctions with the casting (Figure 5.18), the requirement to make the gate only half of the casting thickness ensures that under most circumstances no localized shrinkage defect will occur, and almost no feeding of the casting will take place through the gate.

Slot gates much less than half the section of the casting act as cooling fins. This effect can be put to good use in setting up a favorable temperature gradient in the casting, encouraging solidification from a bottom gate towards a top feeder. Such cooling fin gates have been used to good effect in the production of aluminum and copper-based alloys because of their high thermal conductivity (Wen et al. 1997). (The effect is much less useful in irons and steels, to the point at which any benefit is practically unnoticed.) Also, the common doubt that the cooling effect would be countered by the preheating because of the flow of metal into the casting is easily demonstrated to be, in most cases, a negligible problem. The preheating only occurs for the relatively short filling time compared to the

time of freezing of the casting, and the thin gate itself has little thermal capacity. Thus following the completion of its role as a gate it quickly cools and converts to acting as a cooling fin.

Where a gate cannot conveniently be made to act as a cooling fin, the author has planted a cooling fin on the sides of the gate. (This is simple if the slot gate is on a joint line.) By this means the gate is strongly cooled, and in turn cools the local part of the casting.

The current junction rules have been stated only in terms of thickness of section. For gates and casting sections of more complex geometry it is more convenient to extend the rules, replacing section thickness by equivalent modulus. The more general rule that is inferred is 'the gate modulus should be half or less than the local casting modulus'.

It is worth drawing attention to the fact that not all gates form T-junctions with the casting. For instance, those that are effectively merely extensions of a casting wall may clearly be continued on at the full wall thickness without any hot-spot effect (Figure 12.29c).

Gates which form an L-junction with the wall of the casting are an intermediate case (Sciama 1974), where a gate thickness of 0.75 times the thickness of the wall is the maximum allowable before a hot spot is created at the junction (Figure 12.29b).

It is possible that these simple rules may be modified to some degree if much metal flows through the gate, locally preheating this region. In the absence of quantitative guidelines on this point it is wise to provide a number of gates, well distributed over the casting to reduce such local overheating of the mold. The Cosworth system devised by the author for the ingating of cylinder heads used ten ingates, one for every bolt boss. It contrasted with the two or three gates that had been used previously, and at least partly accounts for the immediate success of the gating design (although it did not help cut-off costs, of course!).

If the casting contains heavy sections that will require feeding then this feed metal will have to be provided from elsewhere. It is necessary to emphasize the separate roles of (i) the filling system and (ii) the feeding system. The two have quite different functions. In the author's experience attempts to feed the casting through the gate are to be welcomed if really possible; however, there are in practice many reasons why the two systems often work better when completely separate. They can then be separately optimized for their individual roles.

It is necessary to make mention of some approaches to gating that attempt to evaluate the action of running systems with gates that operate only partly filled (Davis 1977). The reader will confirm that such logic only applies if the gates empty downhill into the mold, like water spilling over a weir. This is a violation of one of our most important filling rules. Thus approaches designed for partially filled gates are not relevant to the technique recommended in this book. The placing of gates at the lowest point of the casting, and the runner below that, ensures that the runner fills completely, then the gates completely, and only then can the casting start to fill. The complete prior filling of the running system is a valuable aim to achieve; it avoids the carrying through of pockets of air as waves slop about in partially filled systems. Complete filling eliminates waves.

As in most foundrywork, curious prejudices creep into even the most logical approaches. In their otherwise praiseworthy attempt to formalize gating theory, Kotschi and Kleist (1979) omit to limit the thickness of their gates to reduce the junction hot spot, but curiously equalize the areas of the gates so as to equalize the flow into the casting. In practice, making the gates the same is rarely desirable because most castings are not uniform. For instance, a double flow rate might be required into part of the casting that is locally twice as heavy.

The design of gates may be summarized in these concluding paragraphs.

The requirement for gates to be limited to a maximum thickness naturally dictates that the gates may have to become elongated into a slot-type shape if the gate area is also required to be large. Limitations to the length of the slots to limit the lateral velocities in the mold may be required, dictating more than one gate. The limitation of lateral velocities in addition to ingate velocities is a vital feature.

The slot form of the gates is sometimes exasperating when designing the gating system because it frequently happens that there is not sufficient length of casting for the required length of slot! In such situations the casting engineer has to settle for the best compromise possible. In practice, the author has found that if the gate area is within a factor of 2 of the area required to give  $0.5 \text{ m s}^{-1}$ , then an aluminum alloy casting is usually satisfactory. Any further deviation than this would be cause for concern. Gray irons and carbon steels are somewhat more tolerant of higher ingate velocities.

As a final part of this section on gating, it is worth examining some traditional gating designs.

### 12.4.9 The touch gate

The touch gate, or kiss gate, is shown in Figure 12.30a. As its name suggests, it only just makes contact between the source of metal and the mold cavity. In fact there is no gate as such at all. The casting is simply placed so as to overlap the runner. The overlap is typically 0.8 mm for brass and bronze castings (Schmidt and Jacobson 1970, Ward and Jacobs 1962) although up to 1.2 mm is used. Over 2.5 mm overlap causes the castings to be difficult to break off, negating the most important advantage. The elimination of a gate in the case described by the authors was claimed to allow between 20 and 50% more castings in a mold. Furthermore, the castings are simply broken off the runner, speeding production and avoiding cut-off costs and metal losses from sawing. The broken edge is so small that for most purposes dressing by grinding is not necessary; if anything, only shot blasting is required.

A further benefit of the touch gate is that a certain amount of feeding can be carried out through the gate. This happens because (1) the gate is preheated by the flow of metal through it, and (2) the gate is so close to the runner and casting that it effectively has no separate existence of its own; its modulus is not that of a tiny slot, but some average between that of the runner and that of the local part of the casting to which it connects. Investigations of touch gate geometry have overlooked this point, with confusing results. More work is needed to assess how much feeding can actually be carried out. The result is likely to be highly sensitive to alloy type so that any study would benefit from the inclusion of short- and long-freezing-range alloys, and high- and low-conductivity metals.

Ward and Jacobs report a reduced incidence of misrun castings when using touch gating. This observation is almost certainly the result of the beneficial effect of surface tension control in preventing the penetration of the gates before the runner is fully filled and at least partly pressurized. Only when the critical pressure to force the metal surface into a single curvature of 0.4 mm is reached (in the case of the 0.8 mm overlap) will the metal enter the mold cavity. This pressure corresponds to a head of 30–40 mm for copper-based alloys.

The use of such narrow slots for gates might give a user some concern about the melt jetting through such a narrow constriction. In practice surface tension probably acts to avoid this, since the meniscus has to be compressed to a radius of only 400 micrometers when passing through a 0.8 mm overlap. Immediately after the narrowest point is passed, the surface tension acts to spring the meniscus back to a larger radius, closer to its sessile drop radius in the region of 5 mm or more. Thus the speed of advance of the front immediately reduces. The velocity is only high in

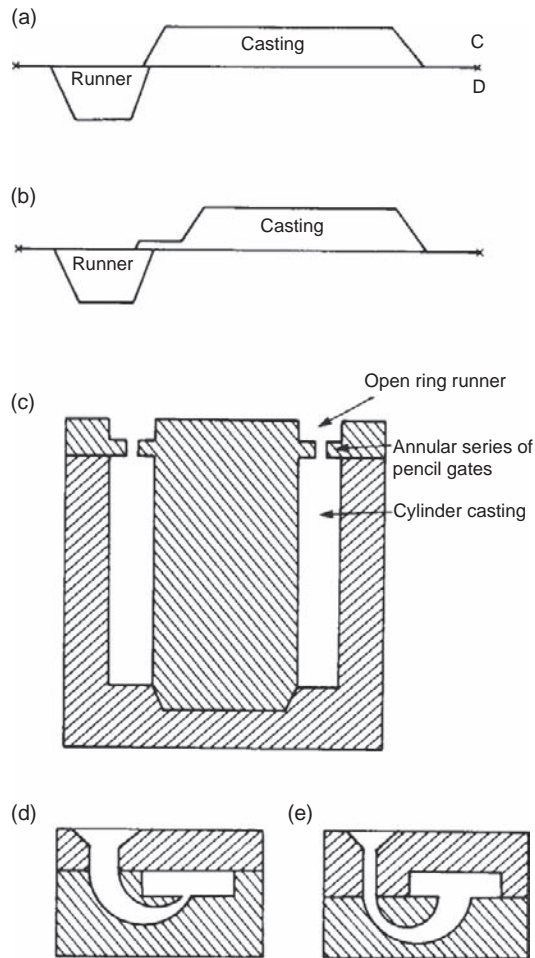


**FIGURE 12.30**

(a) Touch gate, (b) knife gate, (c) pencil gate, (d) normal and (e) reversed horn gates.

the very center of the gap, but becomes gentle once again after passing this point. Thus the mold fills relatively quiescently.

The only concern about jetting relates to the little-known phenomenon of ‘microjetting’. It is possible that for certain strongly oxidizing alloys such a mode of advance might occur in the narrow overlap, the microjets causing oxidation damage in the cavity prior to the arrival of the main body of liquid. This effect could easily be tested for each alloy with a partly open cavity. Any microjetting would be quickly seen.

Finally, with such a thin gate, variations of only 0.1 mm in thickness have been found to change performance drastically. With the runner in one half of the mold and the casting in the other, this is

clearly seen to be a problem from small variations in mismatch between the mold halves. This problem is solved below.

### 12.4.10 Knife gate

The above capillary repulsion problem arising as a result of the variable thickness of the touch gate can be countered in practice by providing a small gate attached to the casting, i.e. in the same mold half as the casting cavity (Figure 12.31b), so that the gate geometry is fixed regardless of mismatch. This is sometimes called a *knife gate*.

Although it is perhaps self-evident, touch and knife gates are not viable as knock-off gates on the modern designs of accurate, thin-walled, aluminum alloy castings. This is simply because the gate has a thickness similar to the casting, so that on trying to break it off, the casting itself bends! The breaking off technique only works for strong, chunky castings, or for relatively brittle alloys.

The system was said to be unsuitable for aluminum bronze and manganese bronze, both of which are strong film-forming alloys (Schmidt and Jacobson 1970), although this discouraging conclusion was probably the result of the runner being usually molded in the cope and the castings in the drag and a consequence of their poor filling system, generating quantities of oxide films that would threaten to choke gates. The unfortunate fall into the mold cavity would further damage quality, as was confirmed by Ward and Jacobs (1962). They found that uphill filling of the mold was essential to providing a casting quality that would produce a perfect cosmetic polish.

The system has been studied for a number of aluminum alloys (Askeland and Holt 1975), although the poor gating and downhill filling used in this work appears to have clouded the results. Even so, the study implies that a better quality of filling system with runner in the drag and casting impressions in the cope could be important and rewarding.

The fundamental fear that the liquid may jet through the narrow gate may be unfounded as has been discussed above. It is worthwhile to dwell a little more on this issue. As mentioned earlier, there may actually be no jetting problem at all as a result of the high surface tension of liquid metals. Whereas water might be expected to jet through such a narrow constriction, liquid aluminum is effectively compressed when forced into any section less than its natural sessile drop height of 12.5 mm. The action of a melt progressing through a thin gate, equipped with an even thinner section formed by a sharp notch was observed for aluminum alloys in the author's laboratory by Cunliffe (1994). The gate was 4 mm thick and the thickness under the various notches was only 1–2 mm. The progress of the melt along the section was observed via a glass window from above. The metal was seen to approach, cross the notch constriction, and continue on its way without hindrance, as though the notch constriction did not exist! This can only be explained if the melt immediately re-expands to fill the channel after passing the notch. It seems the liquid meniscus, acting like a compressed, doubled-over leaf spring, immediately expands back to fill the channel when the point of highest compression is passed.

If the surface turbulence through touch and knife gates is tolerable, or minimal, as expected, they deserve to be much more widely used. It would be so welcome to be able to end the drudgery of sawing castings off running systems, together with the noise and the waste. With good-quality metal provided by a good front end to the filling system, and uphill filling of the mold cavity after the gate, it seems likely that this device could work well. It would probably not require much work to establish a proper design code for such a practice.

### 12.4.11 The pencil gate

Many large rolls for a variety of industries are made from gray cast iron poured in greensand molds. They often contain a massive proportion of gray iron chills around the roll barrel to develop the white iron wear surface of the roll. It is less common nowadays to cast rolls in *loam molds* produced by strickling. (*Loam* is a sand mixture containing high percentages of clay and water, like a mud, which allow it to be formed by *sleeking* into place. It needs to be thoroughly dried prior to casting.) Steel rolls are similarly cast.

Where the roll is solid, it is often bottom-gated tangentially into its base. Where the roll or cylinder is hollow, it may be centrifugally cast, or it may be produced by a special kind of top-gating technique using pencil gates.

Figure 12.31c represents a cross-section through a mold for a roll casting. Such a casting might weigh over 60 000 kg, and have dimensions up to 5 m diameter by 5 m face length, with a wall thickness 80 mm (Turner and Owen 1964). It is cast by pouring into an open circular runner, and the metal is metered into the mold by a series of pencil gates. The metal falls freely through the complete height of the mold cavity, gradually building up the casting. The metal–mold combination of gray iron in greensand is reasonably tolerant of surface turbulence. In addition, the heavy-section thickness gives a solidification time in excess of 30 minutes, allowing a useful time for the floating out and separation of much of the oxide entrained by splashing. The splashing is limited by the slimness of the falling streams from the narrow pencil gates.

The solidification geometry is akin to continuous casting. The slow, controlled build-up of the casting ensures that the temperature gradient is high, and thus favoring good feeding. The feeder head on top of the casting is therefore only minimal, since much of the casting will have solidified by the time the feeder is filled. This beneficial temperature gradient is encouraged by the use of pencil gates: the narrow falling streams have limited energy and so do not disturb the pool of liquid to any great depth (a single massive stream would be a disaster for this reason).

Top gating in this fashion using pencil gates is expected to be useful only for the particular conditions of: (i) gray iron; (ii) heavy sections; and (iii) greensand or inert molds. It is not expected to be appropriate for any metal–mold combinations in which the metal is sensitive to the entrainment of oxide films, especially in thin sections where entrained material has limited opportunity to escape.

Even so, this top pouring, although occurring in the most favorable way possible as discussed above, still results in occasional surface defect in products that are required to be nearly defect-free. The use of bottom gating via an excellent filling system, entering the mold at a tangent to centrifuge defects away from the outer surface of the roll would be expected to yield a superior product. No matter what the casting method, there is no substitute for a good filling system.

### 12.4.12 The horn gate

The horn gate is a device used by a traditional greensand molder to make a quick and easy connection from the sprue into the base of the mold cavity without the need to make and fit a core or provide an additional joint line (Figure 12.31d). The horn pattern could be withdrawn by carefully easing it out of the mold, following its curved shape.

Although the ingenuity of the device can be admired, in practice it cannot be recommended. It breaks one of our fundamental rules for filling system design by allowing the metal to fall downhill. In addition, there are other problems.

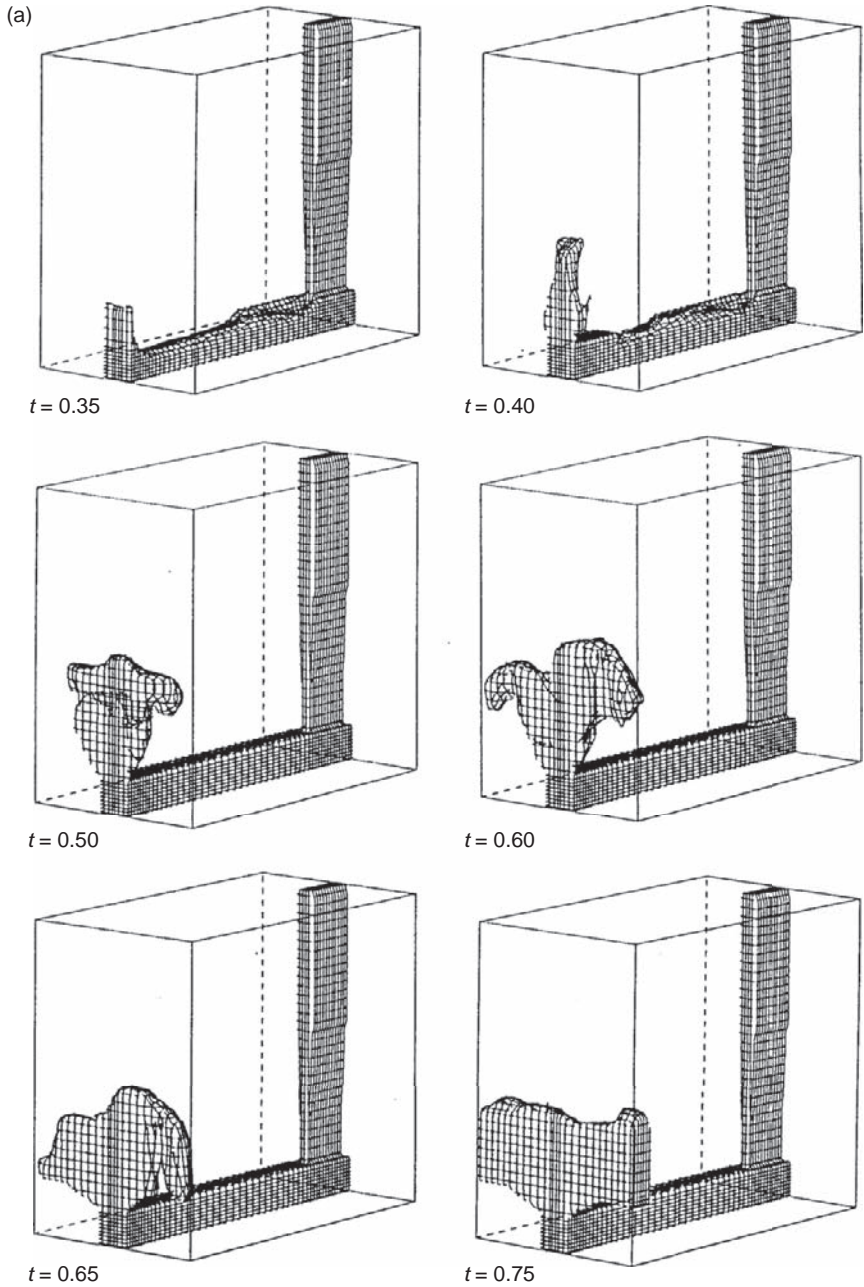


**FIGURE 12.31**  
A vertical fan gate at the end of a runner showing the difference in flow as a result of a (a) top connection, and (b) bottom connection to the runner.

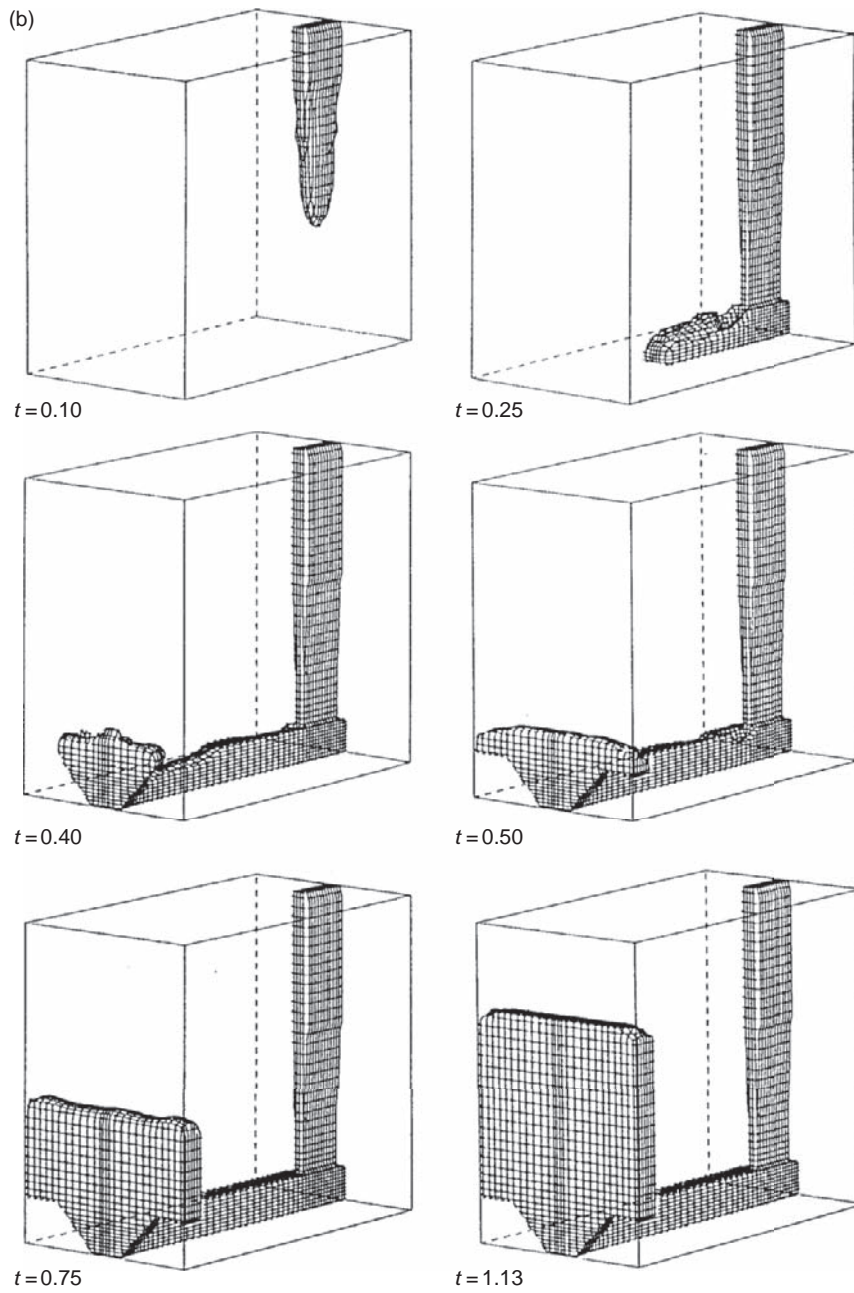


FIGURE 12.31 (continued).



When used with its narrow end at the mold cavity it causes jetting of the metal into the mold. This effect has been photographed using an open-top mold, revealing liquid iron emerging from the exit of the gate, and executing a graceful arc through the air, before splashing into a messy, turbulent pool at the far side of the cavity (Subcommittee T535 1960).

It has occasionally been used in reverse in an attempt to reduce this problem (Figure 12.31e). However, the irregular filling of the first half of the gate by the metal running downhill in an uncontrolled fashion and slopping about in the valley of the gate is similarly unsatisfactory. Furthermore, the large end junction with the casting now poses the additional problem of a large hot spot that requires to be fed to avoid shrinkage porosity.

The horn gate might be tolerable for a rough gray iron casting in greensand. Otherwise it is definitely to be avoided.

### 12.4.13 Vertical gate

Sometimes it is convenient to place a vertical gate at the end of a runner. Whereas the slowing of the flow by expanding the channel was largely unsuccessful for the horizontal runner, an upward-oriented expanding fan-shaped gate can be extremely beneficial because of the aid of gravity. As always, the application is not completely straightforward.

Figure 12.34a shows that if the fan gate is sited directly on top of a rectangular runner, the flow is constrained by the vertical sides of the runner, so that the liquid jets vertically, falling back to fill the fan gate from above.

Figure 12.34b shows that if the expansion of the fan is started from the bottom of the runner, the flow expands nicely, filling the expanding volume and so reducing in speed before it enters the mold cavity. This result is valuable because it is one of the very few successful ways in which the speed of the metal entering the mold cavity can be reduced.

The work in the author's laboratory (Rezvani et al. 1999) illustrates that this form of gate produces castings of excellent reliability. Compared to conventional slot gates, the Weibull modulus of tensile test bars filled with the nicely diverging fan gate was raised nearly four times, indicating the production of castings of four times greater reliability.

Itamura (2002) and co-workers have shown by computer simulation that the limiting  $0.5 \text{ m s}^{-1}$  velocity is safe for simple vertical gates, but can be raised to  $1.0 \text{ m s}^{-1}$  if the gate is expanded as a fan. However, expansion does not continue to work at velocities of  $2 \text{ m s}^{-1}$  where the flow becomes a fountain. Similar results have been confirmed in the author's laboratory by Lai and Griffiths (2003) who used computer simulation to study the expansion of the vertical gate by the provision of a generous radius at the junction with the casting. All these desirable features involve additional cutting off and dressing costs of course.

### 12.4.14 Direct gating into the mold cavity

If the casting engineer has successfully designed the running system to provide bottom gating with minimal surface turbulence, then the casting will fill smoothly without the formation of film defects. However, the battle for a quality casting may not yet be won. Other defects can lie in wait for the unwary!

For the majority of castings the gate connects directly into the mold cavity. I call this simply 'direct gating'. In most cases it is allowable, or tolerable, but it sometimes causes other problems because of the effect it has on the solidification pattern of the casting.

### 12.4.15 Flow channel structure

If the filling is slow, the melt may carve its own path through the solidifying casting, conveying hot metal up the flow channel, and allowing it to reach the advancing liquid front. The channel and the portion of the mold in contact with it become particularly hot, therefore taking significantly longer to cool. Thus within an otherwise excellent casting with fine microstructure and low porosity, the channel region is coarse grained and with noticeable porosity (Figure 5.25b). This structure may cause a casting made to a strict quality specification to be scrapped. It is possible that many so-called shrinkage problems (for which more or less fruitless attempts are made to provide a solution by extra feeders or other means) are actually residual flow channels that might be cured by changing ingate position or size, or raising fill rate. No research appears to have been carried out to guide us out of this difficulty.

The flow channel structure is a standard feature of castings that are filled slowly through a gate planted directly in their base but, amazingly, this serious limitation to structure control seems to have been widely overlooked. It is seen in a computer prediction of a thin-wall steel casting in Figure 12.32, and seen through a glass window for cast iron by Xu and Mampaey (1994). Elliott and Mezoff (1947) report the phenomenon in Mg alloys castings. This widespread effect is discussed in more detail in Section 5.1.5.

If the flow channel is particularly well developed it will almost certainly remain as an elongated hot spot in the thin wall, and so will require to be fed. This will probably mean the provision of a tall feeder sat on the runner bar, and the increase of the areas of the runner and gate to ensure that the feeder has a feed path to deliver feed metal to the base of the flow channel after much of the remainder of the casting has frozen. Such feeding uphill is not recommended since it is not always reliable, but in the case of a well-developed flow channel it is the only chance to recover some solidarity of the casting.

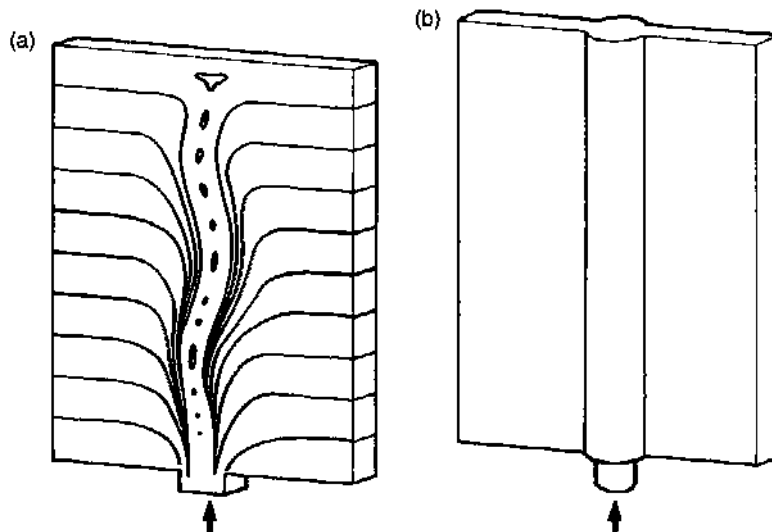


FIGURE 12.32

(a) Direct bottom-gated vertical plate, and (b) the use of a boss to assist feeding after casting is filled.

Nevertheless, in general, the problem is reduced by filling faster (if that is possible without introducing other problems). However, even fast filling does not cure the other major problem of bottom gating, which is the adverse temperature gradient, with the coldest metal being at the top and the hottest at the bottom of the casting. Where feeders are placed at the top of the casting this thermal regime is clearly unfavorable for effective feeding. If bottom gating into the mold cavity is used the unfavorable feeding regime simply has to be accepted, using enlarged, relatively inefficient feeders.

#### 12.4.16 Indirect gating (into an up-runner/riser)

There is an interesting gating system that solves the major features of the bottom gating and flow channel problem. The problem arises because the hot metal that is required to fill the casting is gated directly into the casting and has to travel through the casting to reach all parts.

The solution is *not* to gate into the casting: a main flow path is created *outside* the casting. It is called a *riser* or *up-runner*. Metal is therefore diverted initially away from the casting, through the riser, only entering subsequently by displacement sideways from the riser as fresh supplies of hot metal arrive. The fresh supplies flood up into the top of the riser, ensuring that the riser remains hot, and that the hottest metal is delivered to the top of the mold cavity. The system is illustrated in Figure 12.33. The system has the special property that the riser and slot gate combination acts not only to fill but also to feed. (The reader will notice that the use of the term ‘riser’ in this book is limited to this special form of feeder which also acts as an ‘up-runner’, in which the metal rises up the height of the casting. It is common in the USA to refer to conventional feeders placed on the tops of castings as risers. However, this terminology is avoided here; such reservoirs of metal are called feeders, not risers, following the simple logic of using a name that describes their action perfectly, and does not get confused with other bits of plumbing such as whistlers, up which metal also rises!)

The upper parts of the casting in Figure 12.33 will probably also require some feeding. This is easily achieved by planting a feeder on the top of the riser, as a kind of riser extension. This retains all the benefits of the system, since its metal is hot, and hotter metal below in the riser will convect into the feeder.

The disadvantages of the riser and slot gate system are as follows:

1. The considerable cut-off and finishing problem, since the gate often has to be sited on an exterior surface of the casting, and so requires much subsequent dressing to achieve an acceptable cosmetic finish.
2. There appears to be no method of predicting the width and thickness of the gate at the present time. Further research is required here. In the normal gate where it is required to freeze before the casting section to avoid the hot-spot problem in the junction, the thickness of the gate is held to half of the casting thickness or less. However, in this case the gate is really equivalent to a feeder neck, through which feed metal is required to flow until the casting has solidified. Whereas a thickness of double the casting thickness would then be predicted to avoid the junction hot spot under conditions of uniform starting temperature, the preheating effect of the gate due to the flow of metal through it might mean that a gate as narrow as half of the casting section may be good enough to continue feeding effectively. There are, unfortunately, no confirmatory data on this at the present time.

It is important to caution against the use of a gate which is too narrow for a completely different reason; if filling is reasonably fast then the resistance to flow provided by a narrow slot gate will cause the riser

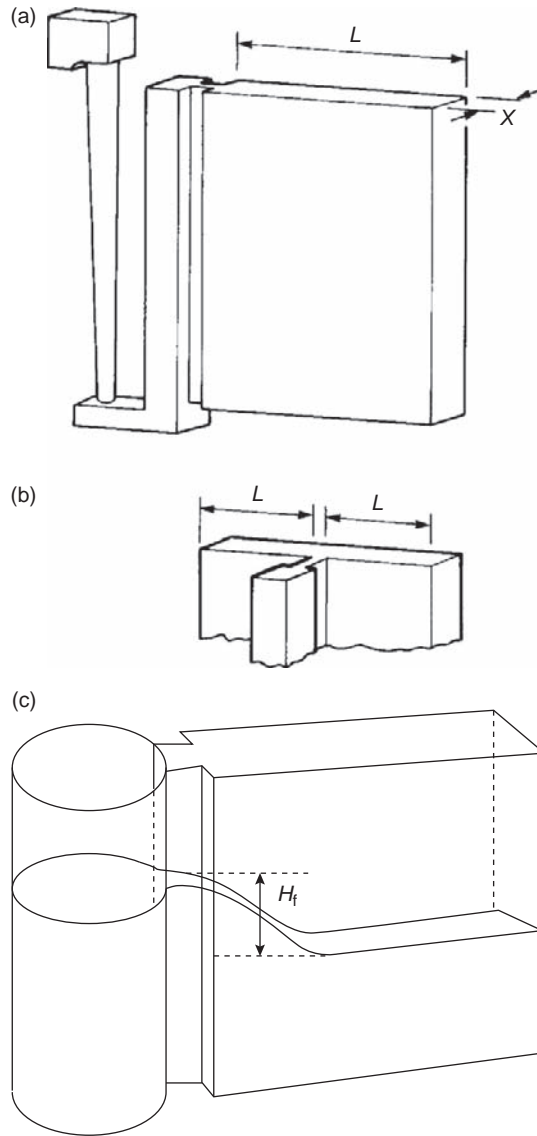


**FIGURE 12.33**

Riser and slot gate to both gate and feed a vertical plate from (a) its side, or (b) its center. (c) The danger of causing a drop  $H_f$  too severe if the slot gate is too narrow.

to fill up to a high level before much metal has had a chance to fill the mold cavity. The dynamics of filling and surface tension, compounded by the presence of a strong oxide film, will together conspire to retain the liquid in the riser for as long as possible. The metal will therefore spill through the slot into the casting from an elevated level (the height of fall  $H_f$  shown in Figure 12.33c). Again, our No-Fall Rule is broken. It is desirable, therefore, to fill slowly, and/or to have a gate sufficiently wide to present minimal resistance to metal flow. In this way the system can work properly, with the liquid metal in the riser and casting rising substantially together. Metal will then enter the mold gently.

It is also important for the gate not to be thinner than the casting when the casting wall thickness reduces to approximately 4 mm. A gate 2 mm thick would hold back the metal because of the effect of surface tension and the surface film allowing the metal head to build up in the riser. When the metal eventually breaks through, the liquid will emerge as a jet, and fall and splash into the mold cavity. For casting sections of 4 mm or less the gate should probably be at least as thick as the wall.

In general, it seems reasonable to assume that conditions should be arranged so that the fall distance  $h$  in Figure 12.33c should be less than the height of the sessile drop. The fall will then be relatively harmless.

For thinner-section castings (for instance, less than 2 mm thickness) made under normal filling pressure, the feeding of thin-section castings can probably be neglected (as will be discussed in Section 12.6). Thus any hot-spot problems can also be disregarded, with the result that the ingate can be equal to the casting thickness. Surface tension controls the entry through the gate and the further progress of the metal through the mold cavity, reducing the problems of surface turbulence. Fill speed can therefore be increased.

A further important point of detail in Figure 12.33 should be noted. The runner turns upward on entry to the riser, directing the flow upwards. A *substantial* upward step is required (the step shown in the figure is probably not sufficient) to ensure this upward direction to the flow. If the provision of this step is neglected causing the base of the runner to be level with the gate and the base of the casting, metal rushes along the runner and travels unchecked directly into the mold cavity as in Figure 11.4a. A flow path would then be set up so that the riser would receive no metal directly, only indirectly after it had circulated through the casting. The base of the casting would receive all the heated metal, and the riser would be cold. Such a flow regime clearly negates the reason for the provision of the system! Many such systems have failed through omitting this vital detail.

What rates are necessary to make the system work best? Again we find ourselves without firm data to give any guide. We can obtain some indication from the following considerations.

The first liquid metal to flow through the slot gate and along the base of the cavity travels as a stream. Being the first metal traveling over the cold surface of the mold, it is most at risk from freezing prematurely. Subsequent flow occurs over the top of this hot layer of metal, and therefore does not lose so much heat from its under surface. Thus if we can ensure that conditions are right for the first metal to flow successfully, then all subsequent flow should be safe from early freezing. In the limiting condition where the tip of the first stream just solidifies on reaching the end of the plate, it will clearly have established the best possible temperature gradient for subsequent feeding by directional solidification back towards the riser. Subsequent layers overlying this initial metal will, of course, have slightly less beneficial temperature gradients, since they will have cooled less during their journey. Nevertheless, this will be the best that we can do with a simple filling method; further improvements will have to await the application of programmed filling by pumped systems.

Focusing our attention, therefore, on the first metal into the mold, it is clear that the problem is simply a fluidity phenomenon. We shall assume that the height of the stream corresponds to the height  $h$  of the meniscus which can be supported by surface tension. If the distance to be run from the gate is  $L$ , and the solidification time of the metal is  $t_f$  in that section thickness  $x$ , then in the limiting condition where the metal just freezes at the limit of flow (thus generating the maximum temperature gradient for subsequent feeding):

$$t_f = L/V \quad (12.2)$$

where  $V$  is the velocity of flow ( $\text{m s}^{-1}$ ) of the metal stream. The corresponding rate of flow  $Q$  ( $\text{kg s}^{-1}$ ) for metal of density  $\rho$  ( $\text{kg m}^{-3}$ ) is easily shown to be:

$$\begin{aligned} Q &= Vhx\rho \\ &= Lhx\rho/t_f \end{aligned} \quad (12.3)$$

At constant filling rate the time  $t$  to fill a casting of height  $H$  is given by:

$$t = t_f(H/h) \quad (12.4)$$

Considering now the first length of melt to travel along the base of the mold, a 10-mm-thick bar in Al-7Si alloy would be expected to freeze completely in about 40 seconds giving a flow life for the solidifying alloy of perhaps 20 seconds. The meniscus height  $h$  is approximately 12.5 mm, and so for a casting  $H = 100$  mm high, 8 times the meniscus height, the pouring time would be  $8 \times 20 = 160$  seconds, or nearly 3 minutes. This is a surprisingly long time, and almost certain to be over-estimated, since the horizontal flows imagined for this exercise would probably result in some visible, but perhaps not especially important, horizontal laps.

Anyway, the conclusion is not likely to be particularly accurate, but does emphasize the important point that relatively thin cast sections do not necessarily require fast filling rates to avoid premature solidification. What is important is the steady, continuous advance of the meniscus.

Naturally, however, it is important not to press this conclusion too far, and the above first-order approximation to the fill time probably represents a time that might be achievable in ideal circumstances: in fact, if the rate of filling is too slow, then the rate of advance of the liquid front will become unstable for other reasons:

1. Surface film problems may cause instability in the flow of some materials in the form of unzipping waves, as is explained in Section 3.1. Film-free systems will not suffer this problem, and vacuum casting may also assist.
2. Another instability that has been little researched is the flow of the metal in a pasty mode (Figure 5.25a) shows the curious behavior in which flow channels take a line of least resistance through the casting, abandoning the riser.

### 12.4.17 Central versus external systems

Most castings have to be run via an external running system as shown in Figures 12.21 and 12.23a. While this is satisfactory for the requirements of the running system, it is costly from the point of view of the space it occupies in the mold. This is especially noticeable in chemically bonded molds, whose

relatively high cost is, of course, directly related to their volume, and whose volume can be modified relatively easily since the molds are not usually contained in molding boxes, i.e. they are boxless. Naturally, in this situation it would be far more desirable if the running system could somehow be incorporated inside the casting, so as to use no more sand than necessary.

This ideal might be achieved in some castings by the use of direct gating in conjunction with a filter as discussed later (Section 12.8.7).

For castings that have an open base, however, such as open frames, cylinders, or rings, an excellent compact and effective solution is possible. It is illustrated for the case of cylinder and ring castings in Figures 12.22 and 12.23. The runners radiate outwards from the sprue exit, and connect with vertical slot gates arranged as arcs around the base of the casting. Ruddle and Cibula (1957) describe a similar arrangement, but omit to show how it can be molded (with all due respect to our elder statesmen of the foundry world, their suggested arrangement looks unmoldable!), and omit the upward gates. The vertical gates are an important feature for success, introducing useful friction into the system, and making for easy cut-off.

The vertical gates have a further important function: they allow some flexibility so that the contraction of the radial spider runners do not pull the sides of the casting inwards as they cool. For this reason the vertical gates need to be as long as possible to reduce distortion to a minimum.

Feeders can be sited on the top of the cylinder if required. Alternatively, if the casting is to be rolled through 180° after pouring, the feeding of the casting can take the form of a ring feeder at the base (later to become the top, of course). This is especially valuable since it eliminates any distortion from the inwards pull of the radial runners.

Experience with internal running has found it to be an effective and economical way to produce hollow shapes. It is also effective for the production of other common shapes such as gearboxes and clutch covers, where the sprue can be arranged to pass down through a rather small opening in one half of the casting and then be distributed via a spider of runners and gates on the open side. Care is needed, however, because these long radial runners contract significantly, and may create distortion of the casting.

A final caution should be noted: it has been observed that aluminum alloy castings of 300 mm or more internal diameter containing a central sprue exhibit a patternmaker's contraction considerably less than that which would have been expected for an external system. This seems almost certainly to be the result of the expansion of the internal core as a result of the extra heating from the internal running system. For a silica sand core this expansion can be between 1 and 1.5%, effectively negating the patternmaker's shrinkage allowance, which is normally between 1 and 1.3%. The use of a non-silica aggregate for the core eliminates this concern.

### 12.4.18 Sequential gating

When there are multiple impressions on a horizontal pattern plate, it is usually unwise to attempt to fill all the cavities at the same time. (This is contrary to the situation with a vertically parted mold, in which many filling systems specifically target the filling of all the cavities at once to reduce pouring time.)

The reasoning in the case of the horizontal mold is simple. The individual cavities are filling at a comparatively slow rate, and not necessarily in a smooth and progressive way. In fact, despite an otherwise good running system design, it is likely that filling will be severely irregular, with slopping and surging, because of the lack of constraint on the liquid, and because of the additional tendency for

the flow to be unstable at low flow rates in film-forming alloys. The result will be the non-filling of a number of the impressions and doubtful quality of the others.

Loper (1981) has provided a solution to this problem for multiple impressions on one plate as shown in Figure 12.34a. He uses runner dams to retard the metal, allowing it time to build up a head of metal sufficient to fill the first set of impressions before overcoming the dam and proceeding to the next set of impressions, and so on.

The system has only been reported to have been used for gray iron castings in greensand molds. It may give less satisfactory results for other metal–mold systems that are more susceptible to surface turbulence. However, the design of the overflow (the runner down the far side of each dam) could be designed as a miniature tapered down-runner to control the fall, and so reduce surface turbulence as far as possible. Probably, this has yet to be tested.

Another sequential-filling technique, ‘horizontal’ stack molding, has also only so far been used with cast iron. This was invented in the 1970s by one of our great foundry characters from the UK, Fred Hoult, after his retirement at the age of 60. It is known in his honor as the ‘H Process’. Figure 12.34b

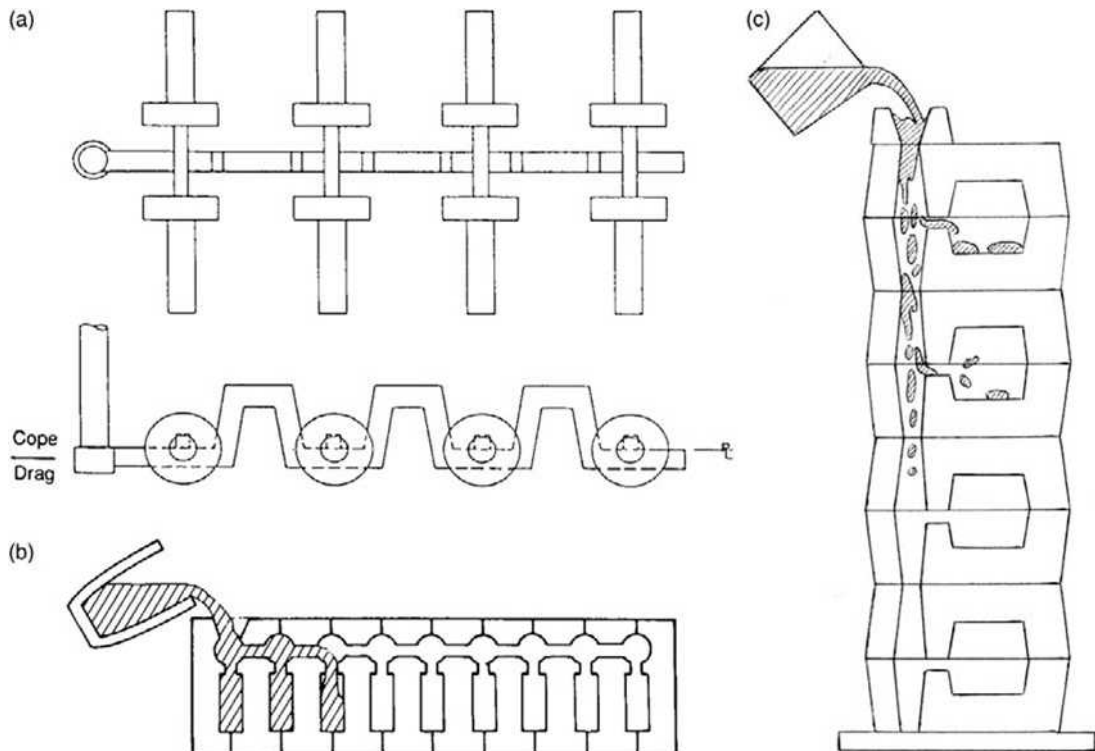


**FIGURE 12.34**

(a) Sequential filling for a number of impressions on a pattern plate (after Loper 1981), and (b) sequential filling for horizontal stack molded castings (H Process). (c) Vertical stack molding which has little to recommend it if good castings are required.



outlines his method. The progress of the metal across the top of those castings already filled keeps the feeders hot, and thus efficient. The length of the stack seems unlimited because the cold metal is repeatedly being taken from the front of the stream and diverted into castings. (The reader will note an interesting analogy with the up-runner and slot gate principle; one is horizontal and the other vertical, but both are designed to divert their metal into the mold progressively. The same effect is also used in the promotion of fluidity as described by Hiratsuka (1966).) Stacks of 20 or more molds can easily be poured at one time. Pouring is continued until all the metal is used up, only the last casting being scrapped because of the incomplete pour, and the remaining unfilled molds are usable as the first molds in the next stack to be assembled.

The size of castings produced by the H Process is limited to parts weighing from a few grams to a few kilograms. Larger parts become unsuitable partly because of handling problems, since the molds are usually stacked vertically during assembly, then clamped with long threaded steel rods, and finally lowered to the floor to make a horizontal line. Larger parts are also unsuitable because of the fundamental limitation imposed by the increase of defects as a necessary consequence of the increased distance of fall of the liquid metal inside the mold, and possibly greater opportunity to splash in thicker sections.

The benefits of the horizontal stacking of molds can be contrasted with the traditional stack molding technique, in which the stack is vertical (Figure 12.34c). This is a way of casting many identical molds at the same time. However, it is an awful technique, designed to make poor-quality castings. The sprue tapers cannot be organized into a single tapering channel, so the fall of the melt is extremely turbulent. Uncontrollable entrainment defects are therefore to be expected. The technique is not recommended.

### 12.4.19 Priming techniques

There have been a number of attempts over the years to introduce a two-stage filling process. The first stage consists of filling the sprue, after which a second stage of filling is started in which the runner and gates, etc. are allowed to fill.

The stopping of the filling process after the filling of the sprue brings the melt in the sprue to a stop, ensuring the exclusion of air. After a delay of a few seconds, the melt is then allowed to start flowing once again. This second phase of filling has the full head  $H$  of metal in the sprue and pouring basin to drive it, but the column has to start to move from zero velocity. It reaches its 'equilibrium' velocity  $(2gH)^{1/2}$  only after a period of acceleration. Thus the early phase of filling of the runner and gates starts from a zero rate, and has a gradually increasing velocity. The action is similar to our 'surge control' techniques described earlier.

The benefits of the exclusion of air from the sprue, and the reduced velocity during the early part of stage 2, are benefits that have been recorded experimentally for semi-solid (actually partly solid) alloys and for different types of metal matrix composite (MMC). These materials are otherwise extremely difficult to cast without defects, almost certainly because their entrainment defects cannot float out but are trapped in suspension because of the high viscosity of the mixture. Weiss and Rose (1993) and Cox et al. (1994) developed a system in which the advance of the Al alloy MMC was arrested at the base of the sprue by a layer of ceramic paper supported on a ceramic foam filter (Figure 12.35a). When the sprue was filled the paper was lifted from one corner by a rod, allowing the melt to flow through the filter and into the running system. These authors call their system 'interrupted pouring'. However, the

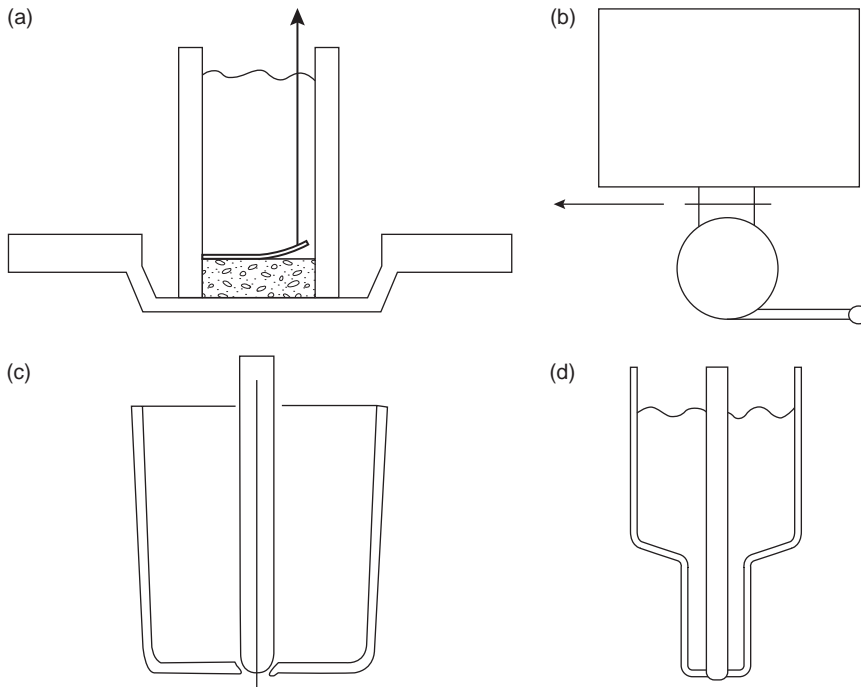


**FIGURE 12.35**

Two-stage filling techniques: (a) ceramic paper seal on top of ceramic foam filter, lifted by wire; (b) steel slide gate at entrance to runner; (c) stopper in the base of a ladle; (d) extended snorkel and stopper.

name ‘two-stage pour’ is recommended as being more positive, and less likely to be interpreted as a faulty pour as a result of an accident.

The two-stage pour was convincingly demonstrated as beneficial by Taghiabadi and colleagues (2003) for both partly solid and conventional aluminum casting alloys. These authors used Weibull statistics to confirm the reality of the benefits. They used a steel sheet to form a barrier, as a slide valve, in the runner. After the filling of the sprue the sheet was withdrawn, allowing the mold to fill.

Wildermuth (1968) used a sheet metal slide gate coated with fireclay to close the ingate to his sand molds (Figure 12.35b). This was successful to make significantly cleaner castings with fewer cope defects in both ductile iron and steel plate castings.

A second completely different embodiment of the two-stage filling concept is the *snorkel ladle*, sometimes known as the *eye-dropper ladle*. It is illustrated in Figure 12.35c. The device is used mainly in the aluminum casting industry, but would with benefit extend to other casting industries. Instead of transferring metal from a furnace via a ladle or spoon of some kind, and pouring into a pouring basin connected to a sprue, the snorkel dips vertically into the melt, and can be filled uphill through its base nozzle simply by dipping sufficiently deeply. The stopper is then lowered to close the nozzle and the ladle is lifted clear from the melt. It is then transferred to the mold where it can deliver its contents into a conventional basin and sprue system, or, in the mode recommended here, lowered down through

the mold to reach and engage with the runner. Only then is its stopper raised and the melt delivered to the start of the running system with minimal surface turbulence. It is a variety of the contact pour technique in which the contact is made not at the top of the sprue but at its base. Effectively the nozzle extension on the ladle is the sprue. In this way the damaging fall of the melt down the sprue is completely avoided. The approach is capable of producing excellent products.

Two-stage filling in its various forms seems to offer real promise for many castings.

---

## 12.5 SURGE CONTROL SYSTEMS

The flowing of metal past the gates and into some kind of dump has been widely used to eliminate the first cold metal, diverting it away, together with any initial contamination by sand or oxide. However, it is not the purpose of this section to discuss dross and slag traps, but explore techniques for avoiding the violent surge of melt into the mold if the sprue, runner, and gate link directly into the casting.

Usually, the first metal through the gate is a transient jet, the metal spurting through when the runner is suddenly filled. This is not a problem for castings of small height where the jet effect can be negligible, but becomes increasingly severe for those with a high head height. For a tall casting the velocity at the end of the runner is high so the momentum of the melt, shocked to an instant stop, causes the metal to explode through the far gate, and enter the cavity like a javelin. This damaging initial transient can occur despite the correct tapering of the runner, since the taper is designed to distribute the flow evenly into the mold only after the achievement of steady state conditions.

If the metal were simply to bypass the ingate and continued to travel along the runner, the natural build-up of back-pressure by friction along the length of the flow would slightly pressurize gates, and cause them to fill a little. The effect is seen in Figure 12.27. If this back-pressure could be increased in some way this gentle filling might be controlled to advantage.

The design of a *flow-off* device, diverting the initial flow away from the casting, is capable of some sophistication, and promises to be a key ingredient, particularly for large, expensive one-off castings. It is a valuable technique for the reduction of the shock of the sudden filling of the runner and the impact of metal through the gates. This section introduces the concept of surge control systems.

A gate that channels the initial metal into a dump *below* the level of the runner is probably the least valuable form of this technique (Figure 12.36a). The downward-facing gate will continue to fill without generating significant back-pressure, the metal merely falling into the trap, until the instant the trap is completely filled. At that instant, the shock of filling is then likely to create, albeit at a short time later, the spurting action into the mold that it was designed to avoid. However, by this time the gates and perhaps even the mold are likely to contain some liquid, so there is a chance that any deleterious jetting action will to some extent be suppressed. This flow-off dump has the benefit of working as a classical dross trap, of course.

A taper prior to the trap can be useful to prevent the back-wave reversing debris out of the trap, since there is only room for the inflow of metal (Figure 12.36c).

An improved form of the device is easily envisaged. A gate into a dump molded *above* from the runner has a more positive action (Figure 12.36d). It provides a gradual reduction in flow rate along the runner because it generates a gradually increasing back-pressure as it fills, building up its head height. When placed at the end of the runner, the gate acts to reduce temporarily the speed into the (real) gates by providing additional gate area, and is valuable to reduce the unwanted final filling shock by some

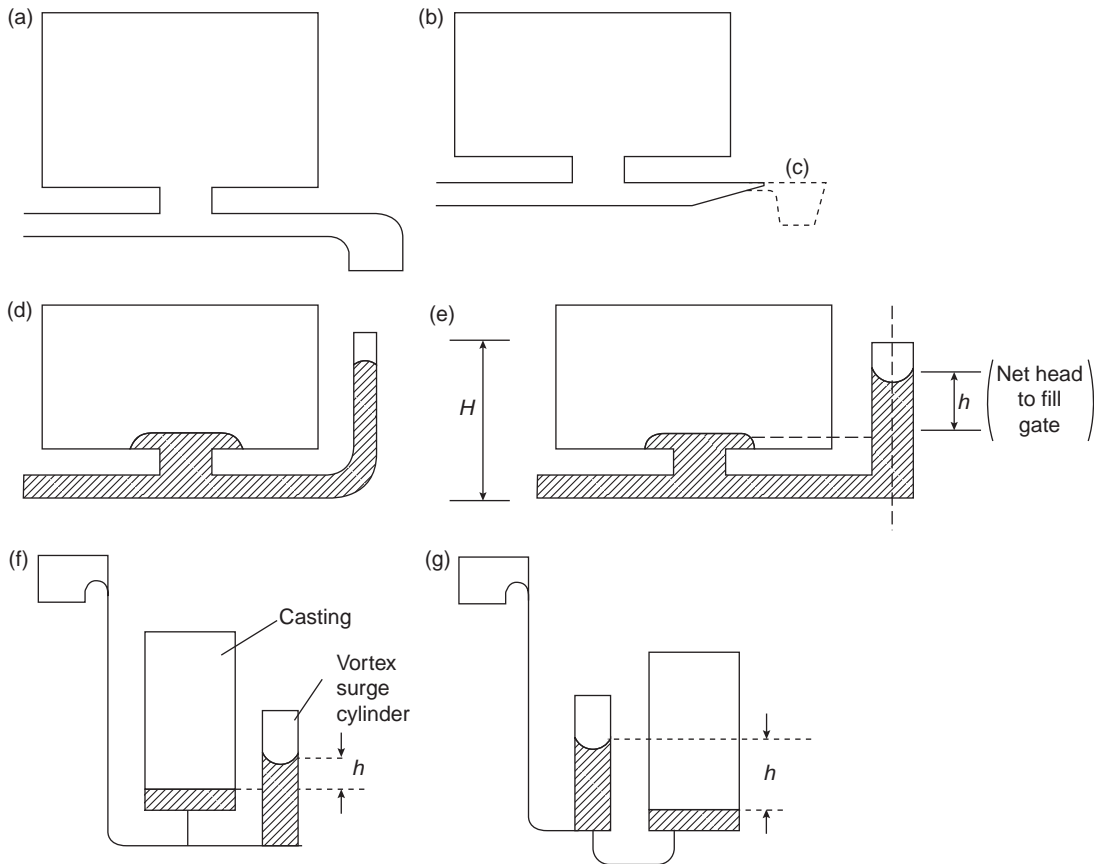


**FIGURE 12.36**

Bypass designs: (a) cross trap type not especially recommended; (b) without cross trap; (c) with non-return trap; (d) vertical runner extension for gravity deceleration (but care required to include damping of 'U-tube' oscillations); (e) and (f) surge control systems using a terminal vortex surge riser; (g) surge control system with in-line vortex and axial (central) outlet.

contribution to reducing speed. However, the narrow section seen in this image will fill so quickly that the desired gradual build-up of flow through the gate will be minimal. A further danger from something that resembles a simple runner extension is that such a device acts as a 'U' tube, so that the melt overshoots to a high level in the tube, falls back too far, rebounds to a high level, etc., oscillating wildly up and down. It is of no use to provide a steady back-pressure.

Additional volume of the dump is an advantage to delay the build-up of pressure to fill the gate. The economically minded casting engineer might find that some castings could be made as 'free riders' in the mold at the end of such gates. The quality may not be high, especially because of the impregnation of the aggregate mold by the momentum of the metal. Even so, the part may be good enough for some purposes, and may help to boost earnings per mold.

A more sophisticated design incorporates all the desirable features of a fully developed surge control system. It consists of extending the runner into the base of an upright circular cylinder, which the runner enters tangentially (Figure 12.36e, f). The height and diameter of the cylinder are calculated to raise the back-pressure into the gates at a steady rate (avoiding the application of the full head from the filling system) for a sufficient time to ensure that the gates and the lower part of the casting are filled to a depth  $d$  sufficient to suppress a damaging jump (Figure 12.37a). When the cylinder (a kind of vortex dump) is completely filled only then does the full pressure of the sprue come into operation to accelerate the filling of the mold cavity. The final filling of the dump may still occur with a ‘bang’ – the water hammer effect – announced by the shock wave of the impact as it flashes back along the runner at the speed of sound. However, this final filling shock will be considerably reduced from that produced by the metal impacting the end of a simple closed runner.

In practice the levels in the riser and casting would be expected to rise together, the level in the riser leading that in the casting by the height difference  $h$ , which might be only a little more than 50 mm to overcome the friction through the gate and give the driving force for the rate of rise in the mold of  $1 \text{ m s}^{-1}$ .

Although the surge technique actually controls the speed of metal through the ingate, it is not called a speed control since its role is over soon after the start of the pour. The name ‘surge control’ emphasizes its temporary nature.

An even more sophisticated variant that can be suggested is the incorporation of the surge control dump in line with the flow from the sprue (Figure 12.36g). The design of the dump as a vortex as before brings additional advantages: on arrival at the base of the sprue and turning into the runner at high speed, the speed is valuable to create a centrifugal action. This action is strongly organizing to the melt, retaining the integrity of the front rather than the chaotic splashing that would have occurred in an impact into a rectangular space for instance. The rotary action also assists to centrifuge the entrained air, slag (and possibly some oxides) into the center where they have opportunity to float if the cylinder is given sufficient height. The good-quality melt is taken off from the center of the base. The small fall down the exit of the surge cylinder is not especially harmful in this case because the rotational action assists the flow to progress with maximum friction down the walls of the exit channel. The system acts to take the first blast of high-velocity metal, gradually increasing the height in the surge cylinder. In this way a gradually increased head of metal is applied to the gates. Furthermore, of course, the metal reaching the gates should be free of air and other low-density contaminants.

Options for rotary surge risers are seen in Figure 12.37. Type (a) is a secondary surge design, so called because the surge riser comes second in line after the gate into the casting. Types (b) and (c) are primary surge systems, in which the exiting runner can emerge in either the cope or the drag as is convenient for the casting.

These surge control concepts promise to revolutionize the production of large steel castings, for which other good filling solutions are, in general, either not easy or not practical. The bypass and surge control devices represent valuable additions to the techniques of controlling not only the initial surge through the gates, but if their action is extended, as seems possible, they can make a valuable contribution to slowing velocities during the vulnerable early phase of filling.

The action of a bypass to double as a classical dross trap is described further in Section 12.7.

Finally, although the surge control concept can be valuable, it is probably an expensive option in terms of metal usage compared to the control of velocity using filters. However, the variety using no filter is almost certainly safer than the use of filters if the quality of the melt is in question. A blocked

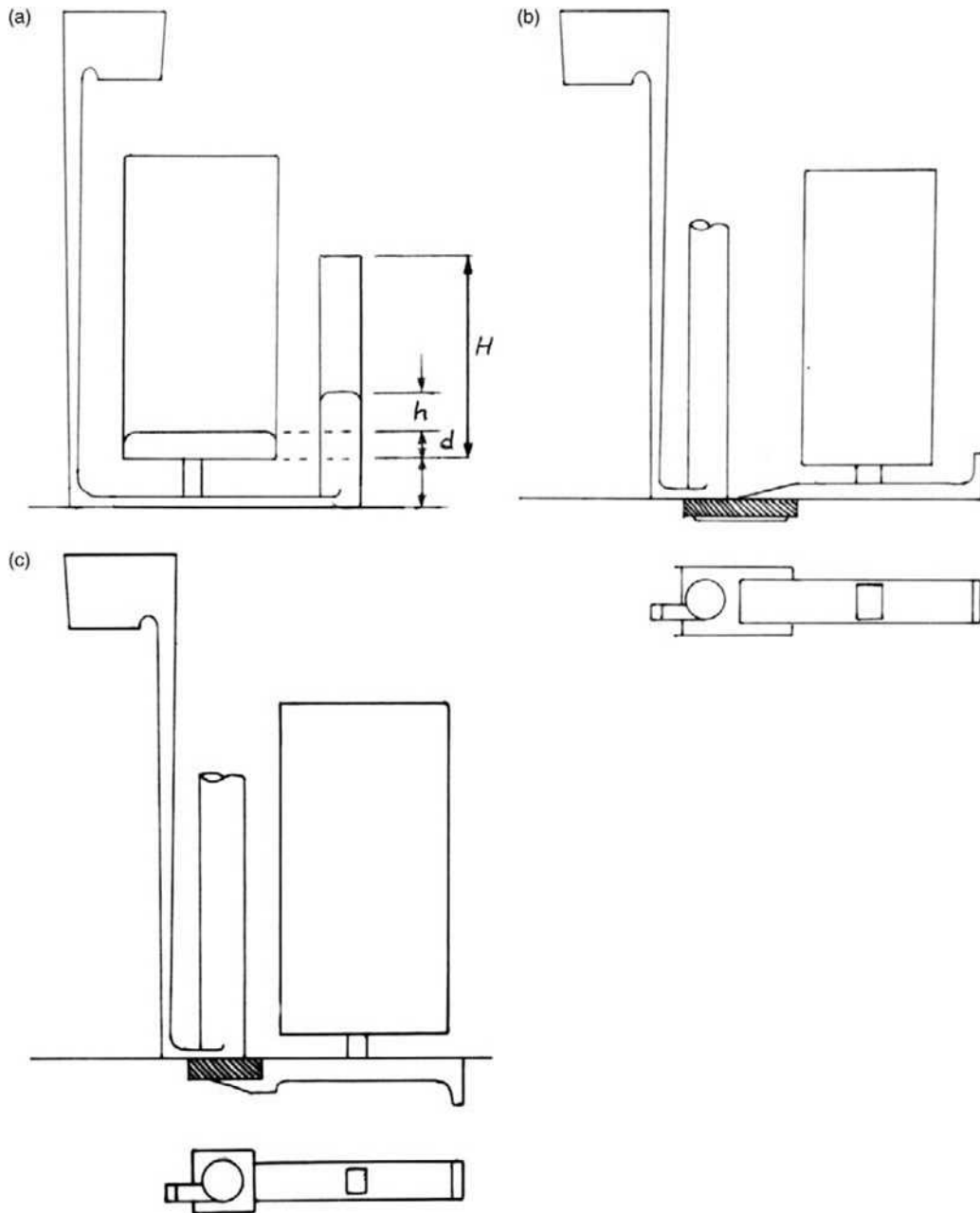


**FIGURE 12.37**

Surge control systems: (a) simplest system in which surge rise is placed 'second'; (b) primary position for surge rise, with runner in cope; (c) primary surge riser but runner in drag.

filter means a scrapped casting, whereas the secondary surge control will work despite any poor quality of the melt.

---

## 12.6 VORTEX SYSTEMS

The vortex has usually been regarded in foundries as a flow feature to be avoided at all costs. If the vortex truly swallowed air, and the air found its way into the casting, the vortex would certainly have to be avoided. However, in general, this seems to be not true.

The great value of the vortex is that it is a powerful organizer of the flow. Designers of water intakes for hydroelectric power stations are well aware of this benefit. Instead of the water being allowed to tumble haphazardly down the water intake from the reservoir, it is caused to spiral down the walls. At the base of the intake duct the loss of rotational energy allows the duct to back-fill to some extent. The central core of air terminates at the level surface of a comparatively tranquil pool, only gently circulating, near the base of the duct. Clearly, the spiraling central core of air terminates at the surface of the pool; it does not extend indefinitely through the system.

Several proposals to harness the benefits of vortices to running systems have originated in recent years from Birmingham, following the lead by Isawa (1994). They are potentially exciting departures from conventional approaches. Only initial results can be presented here. The systems merit much further investigation.

### 12.6.1 Vortex sprue

The benefits of the vortex for the action of a sprue were first explored by Campbell and Isawa (1994) as illustrated in Figure 12.38. An aluminum alloy was poured off-axis, being diverted tangentially into a circular pouring basin. The melt spun around the outside of the basin, gradually filling up and so progressing towards the central sprue entrance. As it progressed inwards, gradually reducing its radius, its rotation speeded up, conserving its angular momentum like the spinning ice skater who closes in outstretched arms. Finally, the melt reached the lip of the sprue, where, at maximum spinning speed, it started its downward fall.

The rationale behind this thinking is that the initial fall during the filling of the sprue is controlled by the friction of a spiral descent down the wall of the sprue. Once the sprue starts to fill, the core of the vortex terminates near the base of the sprue; it does not in fact funnel air into the mold cavity. The hydrostatic pressure generated by this system, driving the flow into the runner and gates, arises only from the small depth of liquid at the base of the vortex, so that the net pressure head  $h$  driving the filling of the mold is small. Because the level of the pool at the base of the vortex and the level of metal in the mold cavity both rise together, the net head to drive the filling of the mold remains remarkably constant during the entire mold-filling process. Thus the filling of the mold is necessarily gentle at all times.

Despite some early success with this system, it seems that the technique is probably not suitable for sprues of height greater than perhaps 200 or 300 mm, because the benefits of the spiral flow are lost progressively with increasing fall distance. More research may be needed to confirm the benefits and limitations of this design. For instance, the early work has been conducted on parallel cylindrical sprues, since the taper has been thought to be not necessary as a result of the melt adopting its own

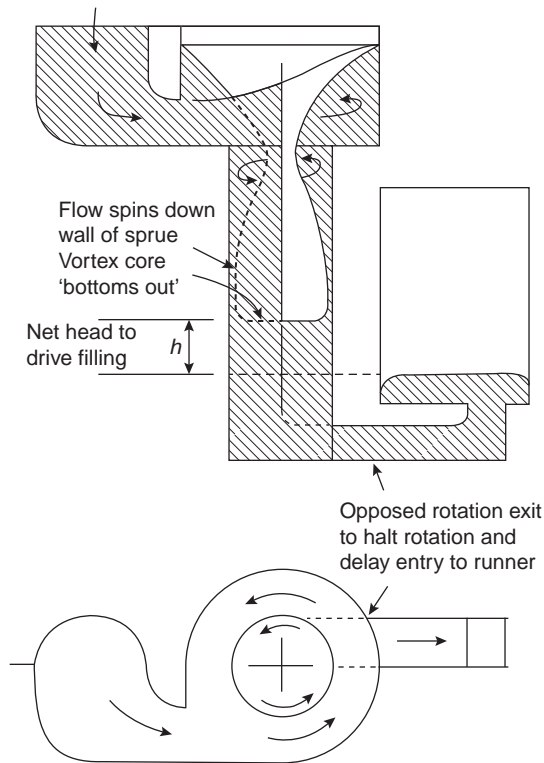


**FIGURE 12.38**

Vortex sprue (after Isawa and Campbell 1994).

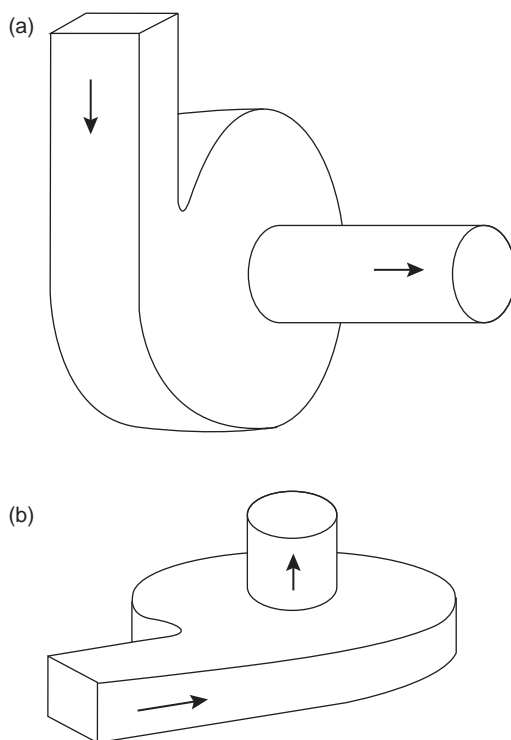
'taper' as it accelerates down the walls, becoming a thinner stream as it progresses. However, a taper may in any case be useful to favor the speeding up of the rate of spin, and so assisting to maintain the spin despite losses from friction against the walls. Also, of course, the provision of a taper will assist the sprue to fill faster and increase yield. Much work remains to be done to define an optimum system.

### 12.6.2 Vortex well or gate

The provision of a cylindrical channel at the base of the sprue, entered tangentially by the melt, is a novel idea with considerable potential (Hsu et al. 2003). It gives a technique for dealing with the central issue of the high liquid velocity at the base of the sprue, and the problem of turning the right-angle corner and successfully filling the runner. What is even better, it promises to solve all of these problems without significant surface turbulence.

A concept for a vortex well is seen in Figure 12.39a. The vertical orientation is often convenient because the central outlet from the vortex can form the entrance to the runner, allowing the connection to many gates. Alternatively, the horizontal orientation (Figure 12.39b) may be useful for delivery from a fast-delivering runner into a single vertical gate.



**FIGURE 12.39**

(a) Vortex well (with horizontal axis) and (b) vortex gate (with vertical axis).

Notice that the device works exactly opposite to the supposed action of a spinner designed to centrifuge buoyant inclusions from a melt. In the vortex well the outlet to the rest of the filling system is the outlet that would normally be used to concentrate inclusions. Thus the device certainly does not operate to reduce the inclusion content. However, it should be highly effective in reducing the generation of inclusions by surface turbulence at the sprue base of poorly designed systems.

Once again, these are early days for this invention. Early trials on a steel casting of about 4 m height have suggested that the vortex is extremely effective in absorbing the energy of the flow. In this respect its action resembles that of a ceramic foam filter. To enable the device to be used in routine casting production the energy-absorbing behavior would require to be quantified. There is no shortage of future tasks.

### 12.6.3 Vortex runner (the offset sprue)

The simple provision of an *offset sprue* causes the runner to fill tangentially, the melt spinning at high speed (Figures 12.17e and 12.40). The technique is especially suited to a vertically parted mold, where a rectangular cross-section sprue, molded on only one side of the parting line, opens into a cylindrical runner molded on the joint. The consequential highly organized filling of the runner is a definite

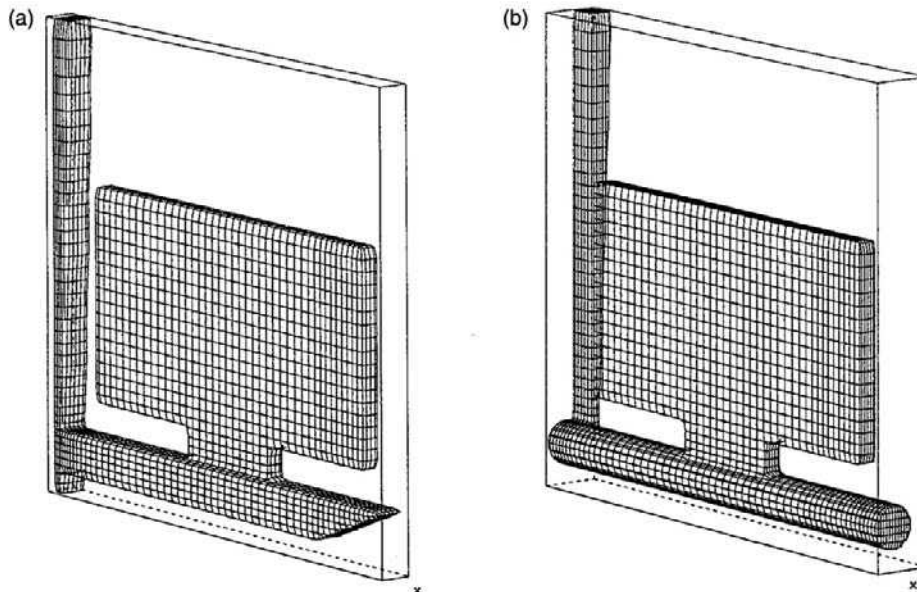


**FIGURE 12.40**

(a) A conventional runner, and (b) a vortex runner, useful on a vertically parted mold (courtesy of X Yang and Flow 3-D).

improvement over many poor runner designs, as has been demonstrated by the Weibull statistics of strengths of castings produced by conventional in-line and off-set (vortex) runners (Yang et al. 1998, 2000, 2003). The technique produces convincingly more reliable castings than conventional in-line sprues and runner systems.

Mbuya (2006) shows from mechanical test results analyzed by the Weibull technique that although the action of the vortex runner without a filter is better than the rectangular runner without a filter, it is less good than a rectangular runner with a filter. Such comparative studies would be helpful to decide whether other solutions such as the slot sprue/slot runner, or the vortex well, etc., might perform better. However, the vortex runner has the great benefit of simplicity (it is completely molded, requiring no delay to the molding cycle by the fitting of a filter) and low cost. It promises to be valuable for vertically parted molds; it deals effectively with the problem of high velocities of flow in such molds because of the great fall heights often encountered.

## 12.7 INCLUSION CONTROL: FILTERS AND TRAPS

The term ‘inclusion’ is a short-hand term generally used for ‘non-metallic inclusion’. However, it is to be noted that such defects as tungsten droplets from a poor welding technique can appear in some recycled metals, especially Ti alloys; these, of course, constitute ‘metallic inclusions’. Furthermore,

one of the most common defects in many castings is the bubble, entrained during pouring. This constitutes an 'air inclusion' or 'gas inclusion'.

The fact that bubbles are trapped in the casting from the filling stage is remarkable in itself. Why did the bubble not simply rise to the surface, burst and disappear? This is a simple but important question. In most cases the bubble will not have been retained by the growth of solid, because solid will, in general, not have time to form. The answer in practically all cases is that oxide films will also be present. In fact the bubbles themselves are simply sections of the oxide films that have been entrained by the folding of the surface, but not folded perfectly face to face. The bubbles decorate the irregularly folded double films, as inflated islands trapped in the folds. Thus many bubbles, entangled in a jumble of bifilms, never succeed to reach the surface to escape. Even those that are sufficiently buoyant to power their way through the tangle may still not burst at the surface because it is likely to accumulate layers of oxide that bar its final escape.

This close association of bubbles and films (since they are both formed by the same turbulent entrainment process; they are both *entrainment defects*) is called by me *bubble damage*. We need to keep in mind that the bubble is the visible part of the total defect. The surrounding region of bifilms to which it is connected act as cracks, and can be much more extensive and often invisible. However, the presence of such films is the reason that cracks will often appear to start from porosity, despite the porosity having a nicely rounded shape that would not in itself appear to be a significant stress raiser.

Whereas inclusions are generally assumed to be particles having a compact shape, it is essential to keep in mind that the most damaging inclusions are the films (actually always double, unbonded films, remember, so that they act as cracks), and are common in many of our common casting alloys. Curiously, the majority of workers in this field have largely overlooked this simple fact. It is clear that techniques to remove particles will often not be effective for films, and vice versa. The various methods to clean metals prior to casting have been reviewed in Section 12.1 as a fulfilment of Rule 1. The various methods to clean metals traveling through the filling systems of castings will be reviewed here.

### 12.7.1 Dross trap (slag trap)

The dross trap is used in light-alloy and copper-based alloy casting. In ferrous castings it is called a slag trap. For our purposes we shall consider the devices as being one and the same.

Traditionally, it has made good sense to include a dross trap in the running system. In principle, a trap sited at the end of the runner should take the first metal through the runner and keep it away from the gates. This first metal is both cold, having given up much of its heat to the running system en route, and will have suffered damage by oxide or other films during those first moments before the sprue is properly filled.

In the past, designs have been along the lines of Figure 12.36a. This type of trap was sized with a view to accommodating the total volume of metal through the system until the down-runner and horizontal runner were substantially filled. This was a praiseworthy aim. In practice, however, it was a regular joke among foundrymen that the best-quality metal was concentrated in the dross trap and all the dross was in the casting! What had happened to lend more than an element of truth to this regrettable piece of folk-law?

It seems that this rather chunky form of trap sets up a circulating eddy during filling. Dross arriving in the trap is therefore efficiently floated out again, only to be swept back along the runner on the back-wave, and finally through the gates and into the casting a few moments later! Ashton and Buhr (1974)

have carried out work to show that runner extensions act poorly as traps for dirt. They observed that when the first metal reached the end of the runner extension it rose, and created a reflected wave which then traveled back along the top surface of the metal, carrying the slag or dirt back towards the ingates. Such observations have been repeated on iron and steel casting by Davies and Magny (1977) and on many different alloys in the author's laboratory using real-time radiography of molds during casting. The effect has been confirmed in computer simulations. It seems, therefore, to be real and universal in castings of all types. We have to conclude that this design of dross trap cannot be recommended!

Figure 12.36b shows a simple wedge trap. It was thought that metal flowing into the narrowing section was trapped, with no rebound wave from the end wall, and no circulating eddy can form. However, video radiographic studies have shown that such traps can reflect a backward wave if the runner is sufficiently deep. Also, of course, the volume of melt that they can retain is very limited.

A useful design of dross trap appears to be a volume at the end of the runner that is provided with a narrow entrance (the extension shown in broken outline in Figure 12.36b) to suppress any outflow. It is a kind of wedge trap fitted with a more capacious end. In the case of persistent dross and slag problems, the trap can be extended, running around corners and into spare nooks and crannies of the mold. If the entrance section is substantially less than the height of a sessile drop, it will be filled by the entering liquid, but would be too narrow to allow a reflected wave to exit. It should therefore retain whatever material enters. In addition, depending on the narrowness of the tapered wedge entrance, to some extent the device should be capable of filling and pressurizing the runner in a progressive manner akin to the action of a gate. This is a useful technique to reduce the initial transient momentum problems that cause gates to fill too quickly during the first few seconds. This potentially useful benefit has yet to be researched more thoroughly so as to provide useful guidelines for mold design.

The device can be envisaged to be useful in combination with other forms of bypass designs such as that shown in Figure 2.37(e).

### 12.7.2 Slag pockets

For iron and steel castings the term 'slag pocket' is widely used for a raised portion of the runner that is intended to collect slag. The large size of slag particles and their large density difference with the melt encourages such separation. However, such techniques are not the panacea that the casting engineer might wish for.

For instance the use of traps of wedge-shaped design (Figure 12.41a) is expected to be almost completely ineffective because the circulation pattern of flow would take out any material that happened to enter. On the other hand, a rectangular cavity has a secondary flow into which buoyant material can transfer if it has sufficient time, and so remain trapped in the upper circulating eddy. This consideration again emphasizes the need for relatively slow flow for its effectiveness. Also, of course, none of these traps can become effective until the runner and the trap become filled with metal. Thus many filling systems will have passed much if not all such unwanted material before the separation mechanisms have chance to come into operation. A further consideration that causes the author to hesitate to recommend such traps is that they locally remove the constraint on the flow of the metal, allowing surface turbulence. At this time it is not clear whether traps cause more problems than they solve.

Davis and Magny (1977) observed the filling of iron and steel castings by video radiography. They confirmed that most slag retention devices either do not work at all, or work with only partial

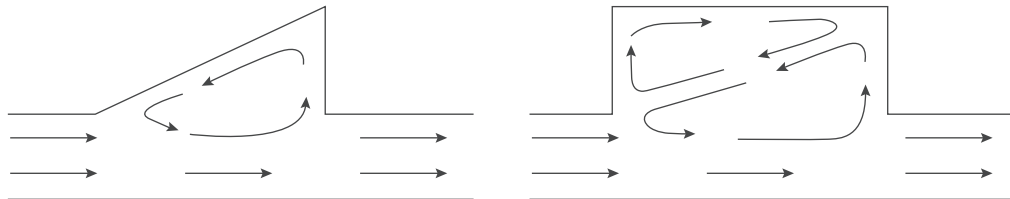


**FIGURE 12.41**

Various designs of slag pockets: (a) relatively ineffective self-emptying wedge; (b) rectangular trap stores buoyant phases in upper circulating flow. However, neither can be recommended since constraint over the flow is lost at these locations, and surface turbulence encouraged.

effectiveness. These authors made castings with different amounts of slag, and tested the ability of slag pockets sited above runners to retain the slag. They found that rectangular pockets were tolerably effective only if the velocity of flow through the runner was below  $0.4 \text{ m s}^{-1}$  (interesting that this is precisely the critical speed at which surface turbulence will occur, and so cause surface phases to be turbulently stirred back into the bulk liquid). For a casting only 100 mm high the metal is already traveling four times too fast. For such reasons the experience with slag pockets has been mainly disappointing.

In defense of the historical use of such traps it must be borne in mind that they were traditionally used with pressurized filling systems, often heavily choked at the gate, so that the runner was encouraged to fill as quickly as possible, making the trap effective at an early stage of filling. Also, if the choking action were sufficiently severe the speed of flow in the runner may have been sufficiently slow to ensure slag entrapment. However, this text does not recommend pressurized filling systems mainly because of the problems that follow from the necessarily high ingate velocities.

Perhaps, therefore, the slag trap has come to the end of its useful life.

### 12.7.3 Swirl trap

The centripetal trap is an accurate name for this device, but rather a mouthful. It is also known as a whirl gate, or swirl gate, which is shorter, but inaccurate since the device is not really a gate at all. Choosing to combine the best of both names, we can call it a swirl trap. This is conveniently short, and accurately indicates its main purpose for trapping rubbish.

The idea behind the device is the use of the difference in density between the melt and the various unwanted materials which it may carry, either floating on its surface or in suspension in its interior. The spinning of the liquid creates a centrifugal action, throwing the heavy melt towards the outside where it escapes through the exit, to continue its journey into the casting. Conversely, the lighter materials are thrown towards the center, where they coagulate and float. The centripetal acceleration  $a_c$  is given by:

$$a_c = V^2/r \quad (12.5)$$

where  $V$  is the local velocity of the melt, and  $r$  is the radius at that point. For a swirl trap of 50 m radius and sprue heights of 0.1 m and 1 m, corresponding to velocities of  $1.5$  and  $4.5 \text{ m s}^{-1}$  respectively, we find that accelerations of  $40$  and  $400 \text{ m s}^{-2}$  respectively are experienced by the melt. Given that the gravitational acceleration  $g$  is  $9.81 \text{ m s}^{-2}$ , which we shall approximate to  $10 \text{ m s}^{-2}$ , these values illustrate

that the separating forces within a swirl trap can be between 4 and 40 times that due to gravity. These are, of course, the so-called 'g' forces experienced in centrifuges.

So much for the theory. What about the reality?

Foundrymen have used swirl traps extensively. This popularity is not easy to understand because, unfortunately, it cannot be the result of their effectiveness. In fact the traps have worked so badly that Ruddle (1956) has recommended they should be abandoned on the grounds that their poor performance does not justify the additional complexity. One has to conclude that their extraordinarily wide use is a reflection of the fascination we all have with whirlpools, and an unshakeable belief, despite all evidence to the contrary, that the device should work.

Regrettably, the swirl trap is expected to be completely useless for film-forming alloys where inclusions in the form of films will be too sluggish to separate. Since some of the worst inclusions are films, the swirl trap is usually worse than useless, creating more films than it can remove. Worse still, in the case of alloys of aluminum and magnesium, their oxides are denser than the metal, and so will be centrifuged outwards, into the casting! Swirl traps are therefore of no use at all for light alloys (however, notice that the vortex sprue base, although not specifically designed to control inclusions, might have some residual useful effect for light alloys since the outlet is central). Finally, swirl traps seem to be difficult to design to ensure effective action. In the experience of the author, most do much more harm than good.

The inevitable conclusion is that swirl traps should be avoided.

The remainder of this section on swirl traps is for those who refuse to give up, or refuse to believe. It also serves as a mini-illustration of the real complexity of apparently simple foundry solutions. Such illustrations serve to keep us humble.

It is worthwhile to examine why the traditional swirl trap performs so disappointingly. On examination of the literature, the textbooks, and designs in actual use in foundries, three main faults stand out immediately:

1. The inlet and exit ducts from the swirl traps are almost always opposed, as shown in Figure 12.42a. The rotation of the metal as a result of the tangential entry has, of course, to be brought to a stop and reversed in direction to make its exit from the trap. The disorganized flow never develops its intended rotation and cannot help to separate inclusions with any effectiveness. Where the inlet and exit ducts are arranged in the correct tangential sense (Figure 12.42b) then Trojan et al. (1966) have found that efficiency is improved in their model results using wood chips in water. Even so, efficiencies in trapping the chips varied between the wide limits of 50 and 100%.
2. The inlet is nearly always arranged to be higher than the exit. This elementary fault gives two problems. First, any floating slag or dross on the first metal to arrive is immediately carried out of the trap before the trap is properly filled (Figure 12.42c). Second, as was realized many years previously (Johnson and Baker 1948), the premature escape of metal hampers the setting up of a properly developed spinning action. Thus the trap is slow to develop its effect, perhaps never achieving its full speed in the short time available during the pour. This unsatisfactory situation is also seen in the work of Jirsa (1982), who describes a swirl trap for steel casting made from preformed refractory sections. In this design the exit was again lower than the entrance, and filling of the trap was encouraged merely by making the exit smaller than the entrance. Much metal and slag almost certainly escaped before the trap could be filled and become fully operational. Since 90% efficiency was claimed for this design it seems probable that all of the

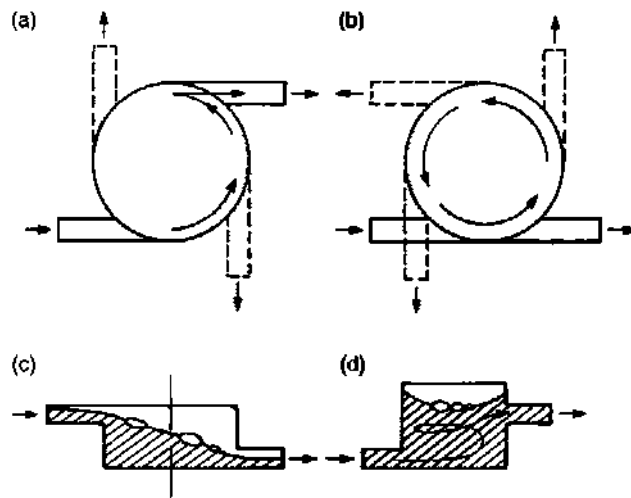


**FIGURE 12.42**

Swirl traps showing (a) incorrect opposed inlet and exit ducts; (b) correct tangential arrangements; (c) incorrect low exit; (d) correct high exit. Once again, I feel reluctant to recommend even a good design. They are all better avoided.

remaining 10% which evaded the trap did so before the trap was filled (in other words, the trap was working at zero efficiency during this early stage). Jeancolas et al. (1971) report an 80% efficiency for their downhill swirl trap for bronze and steel casting, but admit that the trap does not work at all when only partly full.

3. In many designs of swirl trap there is insufficient attention paid to providing accommodation for the trapped material. For instance, where the swirl trap has a closed top the separated material will collect against the center of the ceiling of the trap. However, work with transparent models illustrates clearly how perturbations to the flow cause the inclusions, especially if small, to ebb and flow out of these areas back into the main flow into the casting (Jeancolas 1971, Trojan 1966). Also, of course, traps of such limited volume are in danger of becoming completely overwhelmed, becoming so full of slag or dross that the trap effectively overflows its collection of rubbish into the casting.

Where the trap has an open top the parabolic form of the liquid surface assists the concentration of the floating material in the central 'well' as shown in Figure 12.42d. The extra height for the separated materials to rise into is useful to keep the unwanted material well away from the exit, despite variations from time to time in flow rate. Some workers have opened out the top of the trap, extending it to the top of the cope, level with the pouring bush. This certainly provides ample opportunity for slag to float well clear, with no danger of the trap becoming overloaded with slag. However, the author does not recommend an open system of this kind, because of the instability which open-channel systems sometimes exhibit, causing surging and slopping between the various components comprising the 'U'-tube effect between the sprue, swirl trap and mold cavity.

It is clear that the optimum design for the swirl trap must include the following features:

- (i) the entrance at the base of the trap,
- (ii) the exit to be sited at a substantially higher level,
- (iii) both entrance and exit to have similar tangential direction, and
- (iv) an adequate height above the central axis to provide for the accumulation of separated debris.

In most situations the only difference in height that can be conveniently provided in the mold will mean that the inlet will be molded in the drag, and the exit in the cope. This is the most marginal difference in level and will be expected to be completely inadequate. At the high speeds at which the metal will enter the trap the metal will surge over this small ledge with ease, taking inclusions directly into the casting, particularly if the inlet and outlet are in line as shown for one of the options in Figure 12.42b. This simplest form of cope/drag parting line swirl trap cannot be expected to work.

The trap may be expected to work somewhat more effectively as the angle of the outlet progresses from 90 to 180°. (The 270° option would be more effective still, except that some reflection will show it to be unmoldable on this single joint line; the exit will overlay the entrance ports! Clearly, for the 270° option to be possible, the entrance and exits have to be molded at different levels, necessitating a second joint line provided by a core or additional mold part.)

When using preformed refractory sections, or preformed baked sand cores, as is common for larger steel castings, the exit can with advantage be placed considerably higher than the entrance (Figure 12.42d).

These simple rules are designed to assist the trap to spin the metal up to full speed before the exit is reached, and before any floating or emulsified less-dense material has had a chance to escape.

For the separation of particulate slag inclusions from some irons and steels, *Castings* 1991 showed that a trap 100 mm diameter in the running system of molds 0.1 to 1 m high would be expected to eliminate inclusions of 0.2 to 0.1 mm, respectively. The conclusion was that, when correctly designed, the swirl trap could be a useful device to divert unwanted buoyant particles away from ferrous castings.

We have to remember, however, that it is not expected to work for film-type inclusions. Compared to particles, films would be expected to take between 10 and 100 times longer to separate under an equivalent field force. Thus most of the important inclusions in a large number of casting alloys will not be effectively trapped. Thus the alloys that most need the technique are least helped.

This damning conclusion applies to other field forces such as electromagnetic techniques that have recently been claimed to remove inclusions from melts. It is true that forces can be applied to non-conducting particles suspended in the liquid. However, whereas compact particles move relatively quickly, and can be separated in the short time available while the melt travels through the field, films experience the same force, but move too slowly because of their high drag, and so are not removed.

In summary, we can conclude that apart from certain designs of bypass trap, other varieties of traps are not recommended. In general they almost certainly create more inclusions than they remove. Even the bypass variety of trap is probably of little use with a nicely designed, naturally pressurized filling system. Thus, finally, we reach the conclusion that few traps work, and none are needed. This is another traditional foundry issue that should be laid to rest.



## 12.8 FILTERS

Filters take many forms: as simple strainers, woven glass or ceramic cloths, and ceramic blocks of various types. Naturally, their effectiveness varies from application to application, as is discussed here.

### 12.8.1 Strainers

A sand or ceramic core may be molded to provide a coarse array of holes, of a size and distribution resembling a domestic colander. A typical strainer core might be a cylinder 30–50 mm diameter, 10–20 mm long, containing ten or more holes, of diameter approximately 3–5 mm (Figure 12.43a). These devices are mainly used to prevent slag entering iron castings. The domestic colander used in the kitchen is usually used to strain aggregates such as peas. These represent solid spherical particles of the order of 5 mm diameter. Thus, when applied to most metal castings, the rather open design of strainers means that they can hardly be expected to perform any significant role as filters.

In fact, Webster (1966) has concluded that the strainer works by reducing the rate of flow of metal, assisting the upstream parts of the filling system to prime, and thereby allowing the slag to float. Slag can be given time to separate, and can be held against the top surface of the runner, or in special reservoirs placed above the strainers to collect the retained slag. Webster goes on to conclude that if the strainer only acts to reduce the rate of flow, then this can be carried out more simply and cheaply by the proper design of the running system.

This may not be the whole story. The strainer may be additionally useful to laminize the flow (i.e. cause the flow to become more streamlined).

However, whatever benefits the strainer may have, its action to create jets downstream of the strainer is definitely not helpful. The placing of a strainer in a geometry that will quickly fill the region at the back of the strainer would be a great advantage. Geometries to suppress jetting at the back of

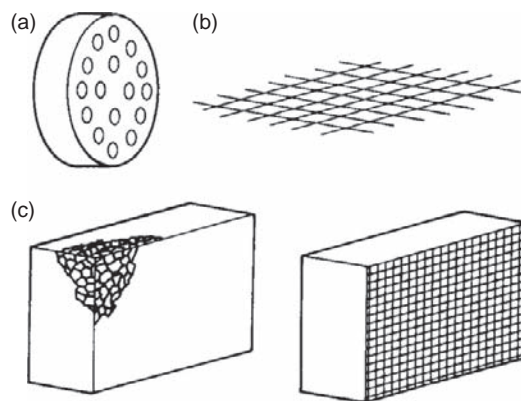


**FIGURE 12.43**

Various filters showing (a) a strainer core (hardly a filter at all); (b) woven cloth or mesh, forming a two-dimensional filter; (c) ceramic foam and extruded or pressed blocks, constituting three-dimensional filters.

filters appears to be a key aspect of the siting of an effective filter. This concept is discussed later. The extruded or pressed ceramic filters with their arrays of parallel pores are, of course, equivalent to strainers with a finer pore size.

Over the years there has been much work carried out to quantify the benefits of the use of filters. Nearly all of these have shown measurable, and sometimes important, gains in freedom from defects and improvements in mechanical properties. These studies are too numerous to list here, but include metals of all types, including Al alloys, irons, and steels. The relatively few negative results can be traced to the use of unfavorable siting or geometry of the filter print. For positive and reliable results, these aspects of the use of filters cannot be overlooked. Special attention is devoted to them in what follows.

### 12.8.2 Woven cloth or mesh

For light alloys, steel wire mesh or glass cloth is used to prevent the oxides from entering the casting. Cloth filter material has the great advantage of low cost. It can be bought in rolls up to 1 m wide and 100 m long, and is easily cut to size.

The surprising effectiveness of these rather open meshes is the result of the most important inclusions being in the form of films, which appear to be intercepted by and wrapped around the strands of the mesh. Openings in the mesh or weave are typically 1–2 mm which gives good results. Many investigators have remarked on the curious fact that the cloth appears to be effective in filtering out inclusions down to a tenth of this size range. This mystery is immediately explained by the realization that the filtered objects are films not particles. Significantly, the fact that such pore sizes are so effective is an independent confirmation of the large size of the majority of films that cause problems in castings, particularly in light alloys.

The use of steel wire mesh is also useful to retain films. It has the great advantage over cloth because of its rigidity. A steel mesh can be placed in a running system with the full confidence that it will not deform and allow the melt to bypass the filter. The steel does not have time to go into solution during the filling of aluminum alloy castings, so that the material of the casting is in no danger of contamination. However, of course, the steel presents a problem of iron contamination during the recycling of the running system. Even the glass cloth can sometimes cause problems during the break-up of the mold, when fragments of glass fiber can be freed to find their way into the atmosphere of the foundry, and cause breathing problems for operators. Both materials therefore need care in use.

Some glass cloth filters are partially rigidized with a ceramic binder, and some by impregnation with phenolic resin. (The outgassing of the resin can cause the evolution of large, centimeter-sized bubbles when contacted by the liquid metal. Provided the bubbles do not find their way into the casting the overall effect of the filters is definitely beneficial in aluminum alloys.) Both types soften at high temperature, permitting the cloth to stretch and deform.

A woven cloth based on a high-silica fiber has been developed to avoid softening at high temperatures, and might therefore be very suitable for use with light alloys. In fact at the present time its high-temperature performance usually confines its use to copper-based alloys and cast irons. There are few data to report on the use of this material. However, it is expected that its use will be similar to that of the other meshes, so that the principles discussed here should still apply.

Despite the attraction of low cost, it has to be admitted that, in general, the glass cloth filters are not easy to use successfully.

For instance, as the cloth softens and stretches there is a strong possibility that the cloth will allow the metal to bypass the filter. It is essential to take this problem into account when deciding on the printing of the filter. Clearly, it is best if it can be firmly trapped on all of its edges. If it can be held on only three of its four edges the vulnerability of the unsupported edge needs careful consideration. For instance, even though a cross-joint filter may be properly held on the edges that are available, the filter is sometimes defeated by the leading edge of the cloth bending out of straight, bowing like a sail, and thus allowing the liquid to jet past. All the filters shown in Figure 12.44 are at risk from this problem. It may be better to abandon cloth filtration if there is any danger of the melt jetting around a collapsing or ballooning filter.

When sited at the point where the flow crosses a joint as in Figure 12.44a, b, a greensand mold will probably hold the cloth successfully, the sand impressing itself into the weave, provided sufficient area of the cloth is trapped in the mold joint. In the case of a hard sand mold or metal die, the cloth requires a shallow print which must be deep enough to allow it room if the mold joint is not to be held apart. Also, of course, the print must not be too deep, otherwise the cloth will not be held tight, and may be pulled out of position by the force of the liquid metal. Some slight crushing of a hard sand mold is desirable to hold the cloth as firmly as possible.

A rigidized cloth filter can be inserted across the flow by simply fitting it into the pattern in a pre-molded slot across the runner and so molding it integral with the mold (Figure 12.44c). However, this is only successful for relatively small castings. Where the runner area becomes large and the time and temperature becomes too high, the filter softens and bows in the force of the flow. Even if it is not entirely pulled out of position it may be deformed to sag like a fence in a gale, so that metal is able to flow over the top. This is the reason for the design shown in Figure 12.44e. The edge of the filter crosses the joint line, either to sit in a recess accurately provided on the other half of the mold, or if the upstand is limited to a millimeter or so, to be simply crushed against the other mold half. (The creation of some loose grains of sand is of little consequence in the running system, as has been shown by Davies and Magny (1977); loose material in the runner is never picked up by the metal and carried into the mold. The author can confirm this observation as particularly true for systems that are not too turbulent. The laminizing action of the filter itself is probably additionally helpful.)

If the filter is introduced at an earlier stage of manufacture during the production of a sand mold, it can be placed in position in a slot cut in the runner pattern. When the sand is introduced the filter is automatically bonded into the mold (Figure 12.44d). Again, an upstand above the level of the joint may be useful. In any case, when using filters across runners, it also helps to arrange for the selvage (the reinforced edge of the material) of the cloth to be uppermost to give the unsupported edge most strength; the ragged cut edge has little strength, letting the cloth bend easily, and allowing some, or perhaps all, of the flow to avoid the filter. All the cloth filters used as shown in Figure 12.44 are defeatable, since they are held only on three sides. The fourth side is the point of weakness. Failure of the filter by the liquid overshooting this unsupported edge can result in the creation of more oxide dross than the filter was intended to prevent! Increasing the trapped area of filter in the mold joint can significantly reduce these risks.

Geometries that combine bubble traps (or slag or any other low-density phase) are shown in Figure 12.45 for in-line arrangements, and for those common occasions when the runner is required to be divided to go in opposite directions. With shallow runners of depth of a few millimeters there is little practical difference in whether the metal goes up or down through the filter. Thus several permutations of these geometries can be envisaged. Much depends on the links to the gates, and how the gates are to

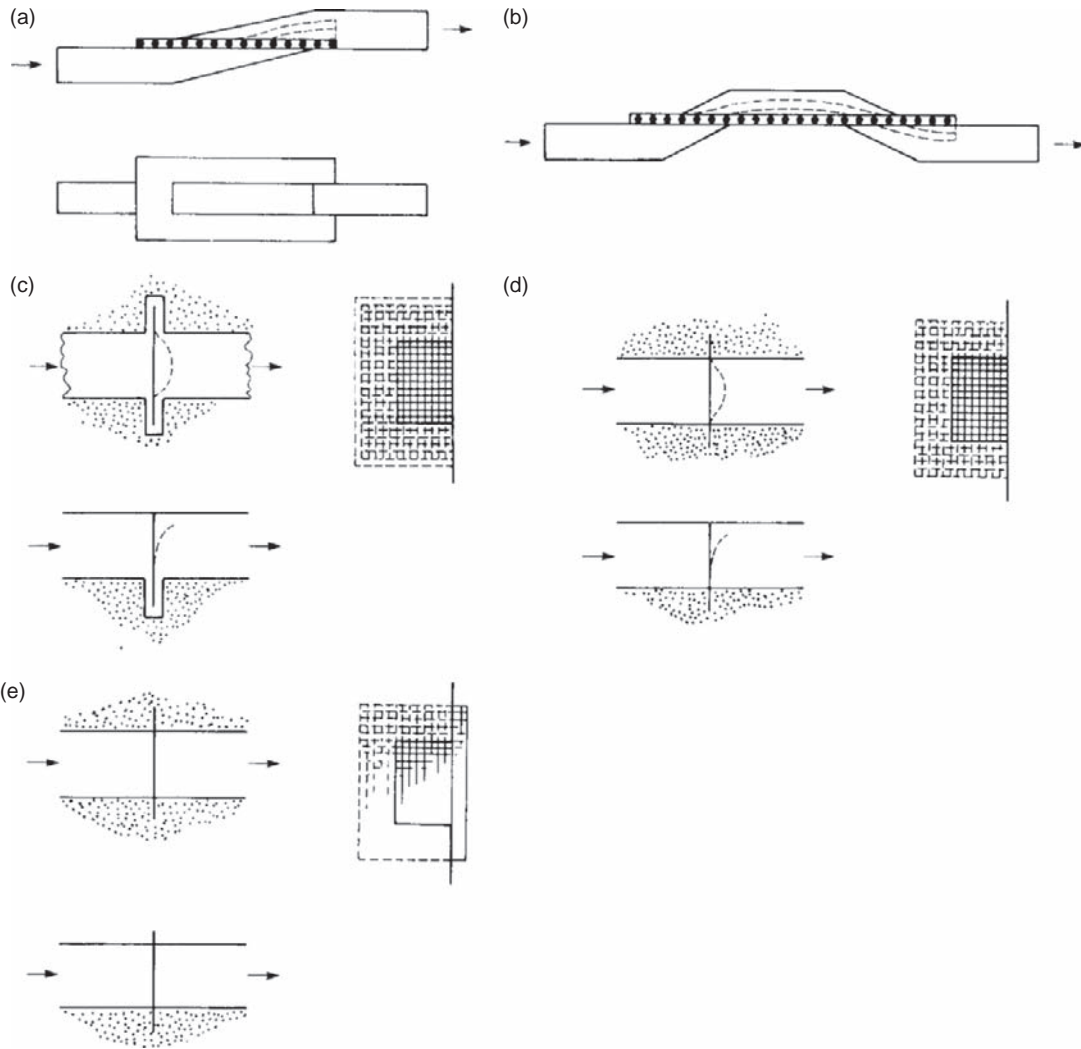


**FIGURE 12.44**

Siting of cloth filters (a) in the mold joint; (b) in a double crossing of the joint; (c) in a slot molded across the runner; (d) in a slot cut in the runner pattern; (e) with an additional upstand across the joint plane to assist sealing.

be placed on the casting. In general, however, I usually aim to have the runner exit from the filter below the joint.

Cloth filters are entirely satisfactory where they can be held around all four sides. This is the case at the point where gates are taken vertically upwards from the top of the runner. This is a relatively unusual situation, where, instead of a two-partted mold, a third mold part forms a base to the mold and

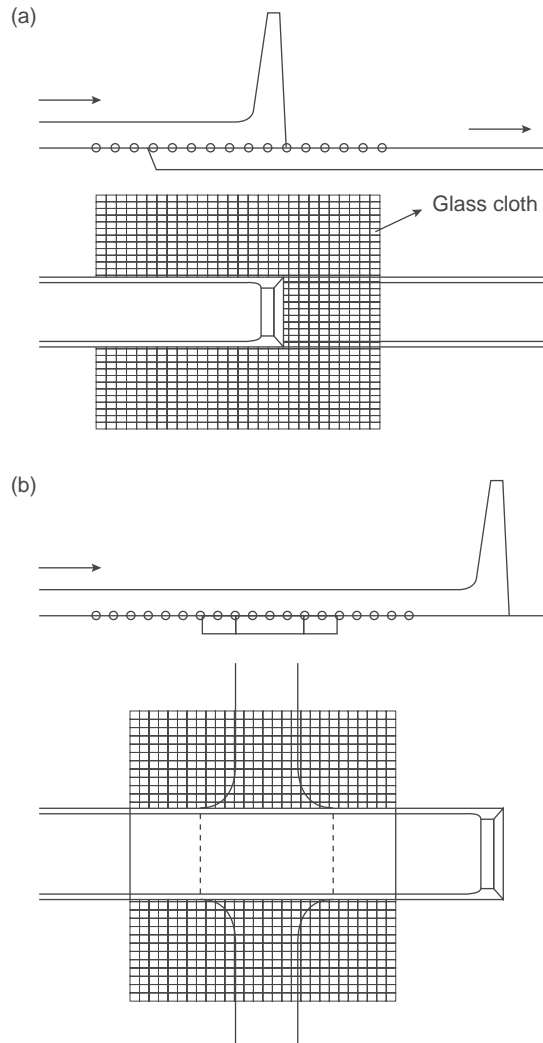


**FIGURE 12.45**

Uses of glass cloth filtration with a bubble trap (a) for an in-line runner; (b) for transverse runners.

allows the runner system to be located under the casting. Alternatively, a special core can be used to create an extra joint beneath the general level of the casting.

Another technique for holding the filter on all sides is the use of a 'window frame' of strong paper or cardboard that is bonded or stapled to the cloth. The frame is quickly dropped into its slot print in the mold, and gives a low-cost rigid surround that survives sufficiently long to be effective. The outgassing of the paper may not be a problem, since the gases have a chance to escape via the mold. Even so, it would be reassuring to see published an independent X-ray video investigation to check this.

### 12.8.3 Ceramic block filters

Ceramic block filters of various types introduced in about 1980 have become popular, and have demonstrated impressive effectiveness in many applications in running systems.

Unfortunately, much that has been written about the mechanisms by which they clean up the cast material appears to be irrelevant. This is because most speculation about the filtration mechanisms has considered only particulate inclusions. As has become quite clear over recent years, the most important and widespread inclusions are actually films. Thus the filtration mechanism at work is clearly quite different, and, in fact, easily understood.

In aluminum alloys the action of a ceramic foam filter to stop films has, in general, not been recognized. This is probably because the films are so thin; a new film may be only 20 nm thick, making the doubled-over entrained bifilm still only about 40 nm. Thus the oxide bifilm, a thin ceramic, of thickness measured in nanometers wrapped around another piece of ceramic measured in micrometers (i.e. a thousand times thicker) cannot easily be detected under the microscope. This partly explains the curious experience of finding that a filter has cleaned up a casting, but on sectioning the filter to examine it under the microscope, not a single inclusion can be found.

The contributing effect, of course, is that the filter acts to improve the filling behavior of the casting, so reducing the number of inclusions that are created in the mold during the filling process. This behavior was confirmed by Din et al. (2003) who found only about 10% of the action of the filter was the result of filtration, but 90% was the result of improved flow.

A further widespread foundry experience is worth a comment. On occasions the quantity of inclusions has been so great that the filter has become blocked and the mold has not filled completely. Such experiences have caused some users to avoid the use of filters. However, in the experience of the author, such unfortunate events have resulted from the use of poor front ends of filling systems (poor basin and sprue designs) that create huge quantities of oxide films in the pouring process. The filter has therefore been overloaded, leading either to its apparently impressive performance, or its failure by blockage. The general advice given to users by filter manufacturers that filters will only pass limited quantities of metal is seen to be influenced by similar experience. The author has not found any limit to the volume of metal that can be put through a filter, provided the metal is sufficiently clean and the front end of the filling system is designed to perform well.

Thus the secret of producing good castings using a filter is to team a good front end of the filling system together with the filter. (If the remainder of the filling system design is good, this will, of course, help additionally.) Little oxide is then entrained, so that the filter appears to do little filtration. However, it is then fully enabled to serve a valuable role as a flow rate control device. The beneficial action of the filter in this case is probably the result of several factors:

1. The reduction in velocity of the flow (provided an appropriately sized cross-section area channel is provided downstream of course). This is probably the single most important action of the filter. However, there are other important actions listed below.
2. Reduces the time for the back-filling of the sprue, thereby reducing entrainment defects from this source.
3. Smooths fluctuations in flow.
4. Laminizes flow, and thus aids fluidity a little.

5. The freezing of part of the melt inside the filter by the chilling action of the filter was predicted for Al alloys in ceramic foam filters by computer simulation and found by experiment by Gebelin and Jolly in 2002 and 2003. This phenomenon may be an advantage, because it may act to restrict flow, and so reduce delivery from the filter in its early moments. The metal eventually re-melts as more hot metal continues to pass through the filter, allowing the flow to speed up to its full rate later during filling. (Interestingly, this advantage did not apply to pre-heated ceramic molds where the pre-heat was sufficient to prevent any freezing in the filter.) This temporary freezing behavior requires to be properly researched.

There are different types of ceramic block filter.

1. Foam filters made by impregnation of open-cell plastic foams with a ceramic slurry, squeezing out the excess slurry, and firing to burn out the plastic and develop strength in the ceramic. The foam structure consists of a skeleton of ceramic filaments and struts defining a network of interconnecting passageways.
2. Extruded forms that have long, straight, parallel holes. They are sometimes referred to as cellular filters.
3. Pressed forms, again with long, straight but slightly tapered holes. The filters are made individually from a blank of moldable clay by a simple pressing operation in a two-part steel die. As die-formed products they are the most accurately reproducible sizes of all the block filter types.
4. Sintered forms, sometimes known as bonded filters, in which crushed and graded ceramic particles are mixed with a ceramic binder and fired.

In all types the average pore size can be controlled in the range 2 to 0.5 mm approximately, although the sintered variety can achieve at least 2 to 0.05 mm. Insufficient research (other than that funded by the filter manufacturers!) has been carried out so far to be sure whether there are any significant differences in the performance between them.

An early result of Khan et al. (1987) found that the fatigue strength of ductile iron was improved by extruded cellular filters, but that the foam filters were unpredictable, with results varying from the best to the worst. Their mode of use of the filters was less than optimum, being blasted by metal in the entrance to the runner, and with no back protection for the melt. (We shall deal with these aspects below.) The result underlines the probable unrealized potential of both types, and reminds us that both would almost certainly benefit from the use of recent developments. In general, we have to conclude that the published comparisons made so far are, unfortunately, often not reliable.

For aluminum alloys the results are less controversial, because the filters are highly effective in removing films which have, of course, a powerful effect on mechanical properties. Mollard and Davidson (1978) are typical in their findings that the strength of Al-7Si-Mg alloy is improved by 50%, and elongation to failure is doubled. This kind of result is now common experience in the industry.

For some irons and steels, where a high proportion of the inclusions will be liquid, most filter materials are expected to be wetted by the inclusion so that collection efficiency will be high for those inclusions. Ali et al. (1985) found that for alumina inclusions in steel traversing an alumina filter, once an inclusion made contact with the filter it became an integral part of the filter. It effectively sintered into place; this action probably reflects the fact that neither the filter nor the inclusions were entirely

solid at the temperature of operation because of the presence of impurities; they behaved as though they were 'sticky'. This behavior is likely to characterize many types of inclusion at the temperature of liquid steel.

In contrast with this, Wieser and Dutta (1986) find that whereas alumina inclusions in steel are retained by an alumina filter, even up to the point at which it will clog, deoxidation of steel with Mn and Si produces silica-containing products that are not retained by an extruded zirconia spinel filter. These authors also tested various locations of the filter, discovering that placing it in the pouring basin was of no use, because it was attacked by the slag and dissolved!

Block filters are more expensive than cloth filters. However, they are easier to use and more reliable. They retain sufficient rigidity to minimize any danger of distortion that might result in the bypassing of the filter. It is, however, important to secure a supply of filters that are manufactured within a close size tolerance, so that they will fit immediately into a print in the sand mold or into a location in a die, with minimal danger of leakage around the sides of the filter. Although all filter types have improved in dimensional control over recent years, the foam filter seems most difficult to control, the extruded is intermediate, whereas the pressed filter exhibits good accuracy and reproducibility as a result of it being made in a steel die; residual variation seems to be a result of less good control of shrinkage on firing.

The combination of a bubble trap together with a filter is often useful. If a filter is placed alone in a runner it will usually hold back the first bubbles that arrive. These will coalesce, and, if sufficient bubbles are in the flow, the front of the filter becomes nearly covered with a massive bubble. At that point the bubble is subjected to such a high pressure that it is forced through the filter and rattles up through the casting, creating damage. This is the reason for the placing of a bubble trap above the inlet side of a filter, so that bubbles can float clear of the face of the filter. In the bubble trap they are seen in X-ray video studies of Al alloys to shrink and disappear into the sand mold. Examples are shown in Figures 12.45, 12.46, and 12.48.

#### 12.8.4 Leakage control

It is essential to control the leakage past the filter. The danger of a leak is not so much the bypass of unfiltered metal but the fact that it is likely to jet through any narrow gap, causing turbulence downstream of the filter.

For instance Figure 12.46e shows a filter placement that at first sight appears simple and elegant. Unfortunately, it is a disaster. It crosses the mold joint, with the result that it has to be placed in the drag, sitting proud of the drag surface. The cope then has to be lowered so that the closing over the filter is carried out blind. It is not known whether the filter and/or mold is crushed, or whether the filter is a loose fit, encouraging jetting of metal around the top of its print. The danger of attempting to site a filter across the mold joint is avoided in all other filter illustrations shown here. Only Figure 12.46b shows a filter that slightly protrudes above the joint. This is designed to create a gentle crush against the cope, ensuring a seal. Any loose sand generated by such crushing techniques has never, to the author's knowledge, posed any threat of sand inclusions in the casting (sand inclusions are never picked up from a runner as observed by Davis and Magny in 1977, but are generated by poor filling systems in which extreme turbulence is accompanied by copious entrainment of air. Sand inclusions are always cured by eliminating the turbulence and air entrainment in the filling system.)



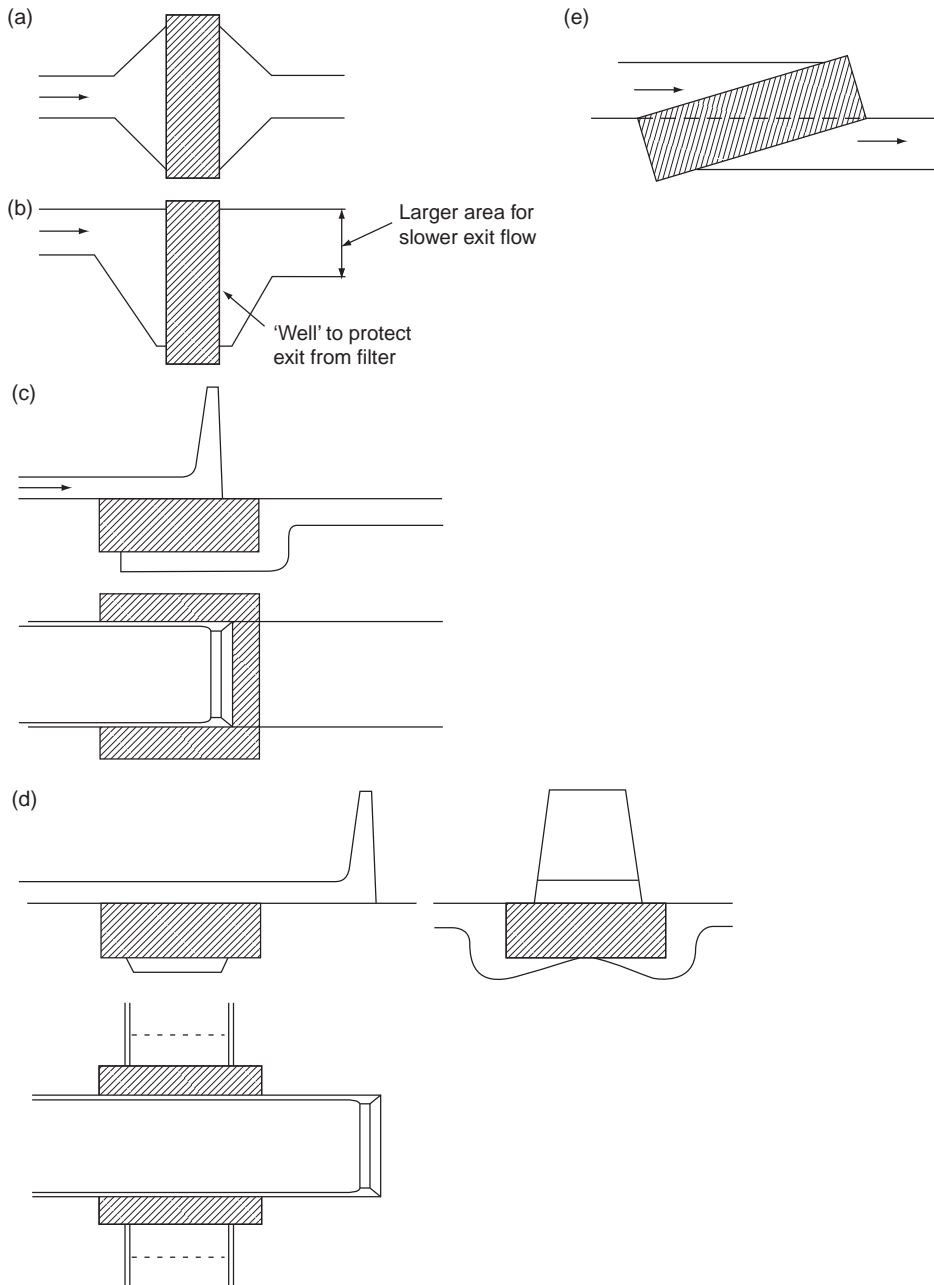


**FIGURE 12.46**

Ceramic foam filter printing (a) conventional; (b) improved early back protection of filter by melt; (c) tangential in-line filtration in runner; (d) three views of tangential transverse runners with reduced fall and well volume; (e) possible siting of filter across join (not recommended).

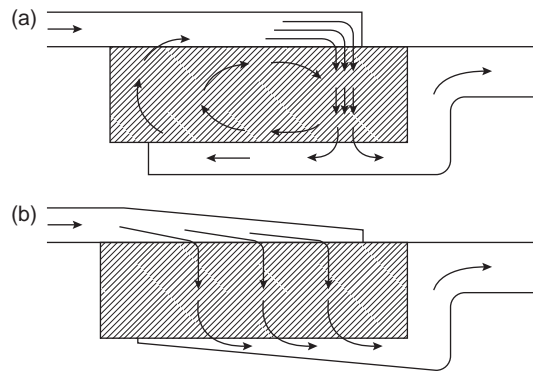
All filter techniques described in this book use filters that sit fully in the drag, so that they can be seen to fit well, giving some assurance that they will work as intended, or can be seen to fit badly, and corrective action taken in good time.

There are various techniques to reduce a leak bypassing a filter.

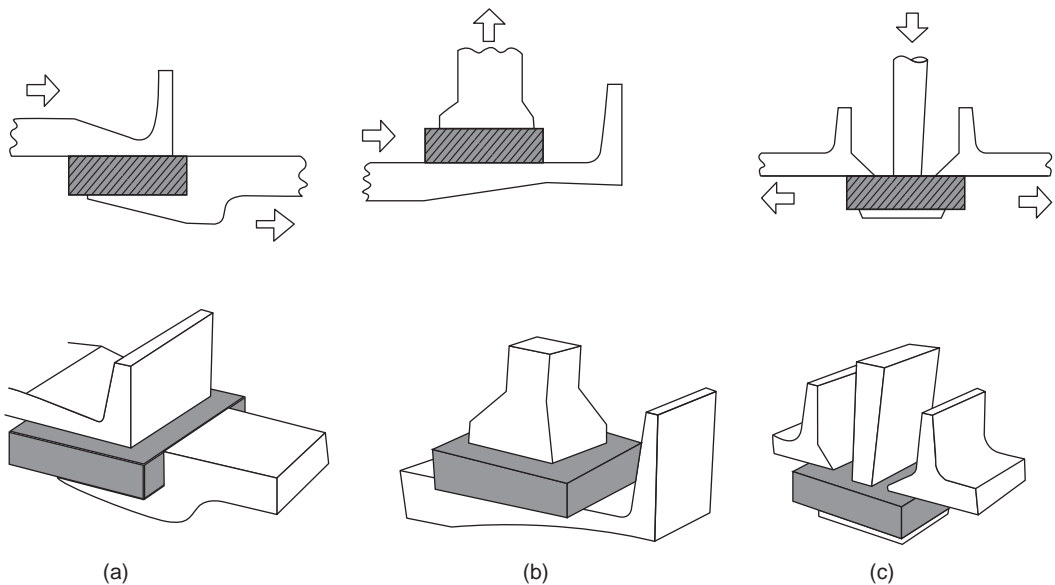
1. A seating of a compressible gasket of ceramic paper. This approach is useful when introducing filters into metal dies, where the filter is held by the closing of the two halves of the die. The variations in size of the filters, and the variability of the size and fit of the die parts with time and temperature, which would otherwise cause occasional cracking or crushing of the rather brittle filter, are accommodated safely by the gasket.
2. Molding the filter directly into an aggregate (sand) mold. This is achieved simply by placing the filter on the pattern, and filling the mold box or core box with aggregate in the normal way. The filter is then perfectly held. In greensand systems or chemically bonded sands the mold material seems not to penetrate a ceramic foam filter more than the first pore depth. This is a smaller loss than would be suffered when using a normal geometrical print. However, the technique often requires other measures such as the molding of the filter into a separate core, or the provision of a loose piece in the pattern to form the channel on the underside of the filter.
3. Use a filter printing geometry that is insensitive to leakage. Figures 12.48b and c are good examples where a leak past the filter is likely to be harmless. Any side leakage over the top of the filter from the sprue exit will be negligible because of the momentum of the flow, carrying most of the flow directly downwards through the filter. Contrast the situation with Figure 12.46a where an ill-fitting filter can easily allow a jet to force its way over the top of the filter. Figures 12.49 and 12.50 also illustrate good examples of robust filter geometries.

There are other aspects of the siting of filters in running systems that are worth underlining.

1. Siting a filter so that some metal can flow over or adjacent to the filter for a second or two (into a slag trap for instance) prior to priming the filter is suggested to have the additional benefit that the preheat of the filter and the metal reduces the priming problem associated with the chilling of the metal by the filter (Wieser and Dutta 1986). An example is seen in Figure 12.46d. The chilling effect of the filter can be important for some thin wall castings of large area.
2. The area of the filter needs to be adequate. There is much evidence to support the fact that the larger the area (thereby giving a lower velocity of flow through the filter) the better the effectiveness of the filter. For instance, if the filter area is too small in relation to the velocity of flow then the filter will be unable to retain foreign matter: the force of the flow will strip away retained films like sheets from the washing line in a hurricane; particles and droplets will follow a similar fate.
3. Many filter placements do not distribute the flow evenly over the whole of the filter surface. Thus a concentrated jet is unhelpful, being equivalent to reducing the active area of the filter. The tangential placement of a filter can also be poor in this respect, since the flow naturally concentrates through the farthest portion of the filter and might even circulate backwards through the filter (Figure 12.47a). This inefficient flow regime is countered by tapering the tangential entrance and exit flow channels as illustrated in Figure 12.47b thereby directing the flow more uniformly through the filter. The provision of a bubble trap reduces the effectiveness of the taper, but the presence of the trap is probably worth this sacrifice. (If the trap is not provided, bubbles

**FIGURE 12.47**

(a) Concentration and reverse flow in a foam filter; (b) tapered inlet and exit ducting to spread flow.

**FIGURE 12.48**

Filters with bubble traps: (a) in-line; (b) horizontal runner with filter beneath vertical gate; (c) recommended system for filter location at base of sprue. Several runners can be taken off in different directions.

arriving from entrainment in the basin or sprue gather on the top surface of the filter. When they have accumulated to occupy almost the whole of the area of the filter the single large bubble is then forced through the filter, and travels on to create severe problems in the mold cavity. The trap is expected to be similarly useful for the diversion of slag from the filter face during the pouring of irons and steels.)

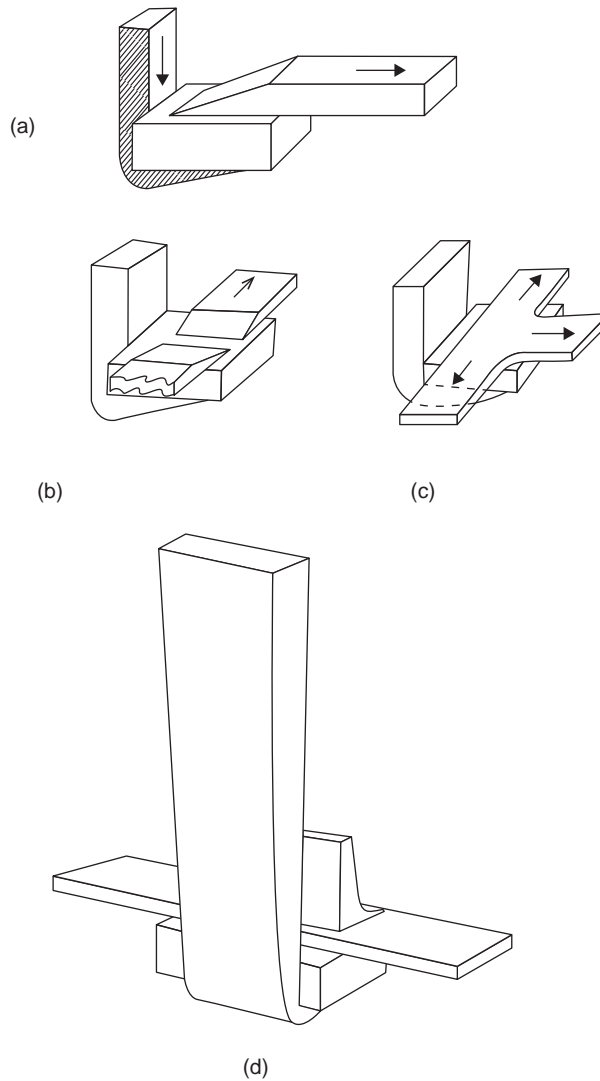


**FIGURE 12.49**

A possible connection of a sprue to a filter sited in the drag, with a, b and c showing 1, 2, and 3 runners taken off in the cope; (d) shows the use of a bubble trap.

Mutharasan et al. (1981) find that the efficiency of removal of  $\text{TiB}_2$  inclusions from liquid aluminum increased as the velocity through the filter fell from about  $10 \text{ mm s}^{-1}$  to  $1 \text{ mm s}^{-1}$ . Later, the same authors found identical behavior for the removal of up to 99% of alumina inclusions from liquid steel (Mutharasan et al. 1985). However, it is to be noted that these are extremely low velocities, lower than would be found in most casting systems. In the work by Wieser and Dutta (1986) on the filtration of

alumina from liquid steel, somewhat higher velocities, in the range  $30\text{--}120\text{ mm s}^{-1}$ , are implied despite the use of filter areas up to ten times the runner area in an attempt to obtain sufficient slowing of the rate of flow. Even these flow velocities will not match most running systems. These facts underline the poverty of the data that currently exist in the understanding of the action of filters.

Wieser and Dutta go on to make the interesting point that working on the basis of providing a filter of sufficient size to deal with the initial high velocity in a bottom-gated casting, the subsequent fall in velocity as the casting fills and the effective head is reduced implies that the filter is oversized during the rest of the pour. However, this effect may be useful in countering the gradual blockage of the filter in steel containing a moderate amount of inclusions.

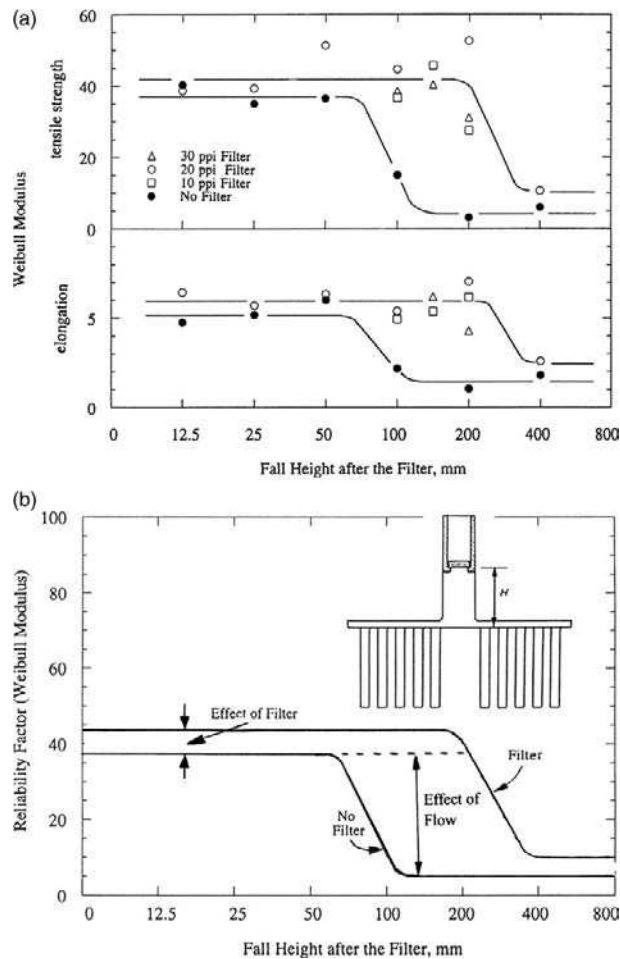


**FIGURE 12.50**

Direct pour filtration showing (a) the reduced reliability as the fall increases with and without a filter in place; (b) the interpretation of 'a'; (c) the reduced reliability as diameter of test bars is increased.

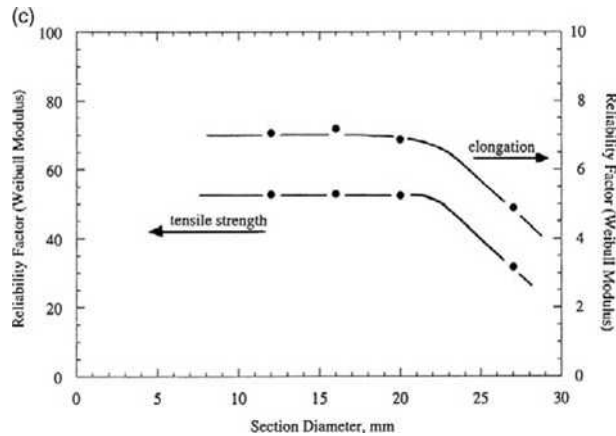


FIGURE 12.50 (continued).

### 12.8.5 Filters in running systems

Although we have seen above that filtration efficiency appears to be strongly dependent on inclusion and filter types, Ali (1985) confirms a strong effect of velocity, finding only at very low velocities (measured in  $\text{mm s}^{-1}$ ) was a high level (96%) of filtration achieved in steel melts. The casters of wrought Al alloys are aware of the necessity for the low velocities through filters, which is why their packed bed filters are so large, being nearly a cubic meter in volume. This snail pace flow rate to achieve good filtration performance by filters emphasizes the fact that filters in running systems generally cannot possibly filter significantly because speeds are far too high. The research by Din and Campbell (2003) clearly showed that only about 10% of the clean-up of a casting was the result of filtration by the filter, whereas 90% of the cleanliness benefit was the result of improved flow of the melt, avoiding the subsequent entrainment of oxide bifilms (see Figure 12.50 and Section 12.8.7).

This result further emphasizes another major concern for the use of filters. If the melt is allowed to jet from the back of a filter, the downstream quality of the melt can be ruined. Loper and colleagues (1996) were among the first to draw attention to this problem. They described the need for what they called a 'hydraulic lock', a region behind the filter that flooded quickly to suppress jetting through the air. We need to return to this critical aspect of the use of filters in running systems.

For relatively small castings, and where the cost of the filter is a major issue, the best location when using a single filter is near the entrance to the runner, immediately following the sprue. The resistance to penetration of the pores of the filter by the action of surface tension is an additional benefit, delaying the priming of the filter until the sprue has at least partially filled. The frictional resistance to flow through the filter once it is operational provides a further contribution to the reduction in speed of the flow. This frictional resistance has been measured by Devaux (1987). He finds the head loss to be large for filters of area only one or two times the area of the runner. He concludes that whereas a filter area of twice the runner area is the minimum size that is acceptable for a thick-section casting, the filter area has to be increased to four times the runner area for thin-section castings. The pressure drop through filters is a key parameter that is not known with the accuracy that would be useful. Midea (2001) has

attempted to quantify this resistance to flow but used only low-flow velocities useful for only small castings. A slight improvement is made by Lo and Campbell (2000) who study flow up to  $2.5 \text{ m s}^{-1}$ . Even so, at this time the author regrets that it remains unclear how these measurements can be used in a design of a running system. A clear worked example would be useful for us all.

The filter positioned at the entrance to the runner also serves to arrest the initial splash of the first metal to arrive at the base of the sprue. At the beginning of the runner the filter is ideally positioned to take out the films created before and during the pour.

For larger castings, particularly tonnage steel castings, the provision of several filters is useful; one filter per ingate. In this way the ingate velocity and quality can be optimized. Also, with dense melts, there is much less danger of the priming filling of one filter before the others are primed, with the result that the melt preferentially fills the casting via the first filter, travels through the mold cavity, and pours down the ingates to fill the remaining unprimed filters from the wrong side. There is increased danger of this occurring with the use of multiple filters in light alloys, because a higher head, perhaps over 100 mm in some cases, will be needed to prime the filter but the ingate height above the filter may be less than this, allowing the cavity to fill before pressure can be raised sufficiently high for the remaining filters to prime. The head to prime steel filters will only be about half of this value, reducing this danger.

The clean liquid can be maintained relatively free from further contamination so long as no surface turbulence occurs from this point onwards. This condition can be fulfilled if:

1. The melt proceeds at a sufficiently low velocity and/or is sufficiently constrained by geometry to prevent entrainment. This particularly includes the important provision to eliminate jetting from the rear face of the filter. This *essential* condition must be observed by only using those arrangements that ensure the melt covers and submerges the exit face of the filter as quickly as possible.
2. Every part of the subsequent journey for the liquid is either horizontal or uphill. The corollary of this condition is that the base of the sprue and the filter should always be at the lowest point of the running system and the casting. This excellent general rule is a key requirement.
3. A low velocity will be achieved if the cross-sectional area of the runner downstream of the filter is increased in proportion to the reduction in speed provided by the filter. Since the siting of a ceramic foam filter in a channel of a running system will reduce the flow rate as a result of the two factors:
  - (i) A reduction of the total cross-sectional area for flow by perhaps approximately 15% (since the porosity of the filter is roughly 85%).
  - (ii) Frictional loss. This is currently unknown, but might be at least a further 15%.

Thus the volume flow rate  $Q$  may be reduced by a total of approximately 30%. This may be revealed by an extension of the fill time by 30%. (Sufficient work has not been carried out on systems with and without filters to know whether this is accurate or not.)

In isolated observations of the velocity of flow through filters in generally non-pressurized flow conditions, the velocity appears to be reduced by approximately a factor of 5. If  $Q$  is reduced by a factor of 1.3 it follows that after the filter the area of the flow channel might be expanded by a factor of  $5/1.3 = 3.85$ .

If the filter had been placed in a filling system calculated to be naturally pressurized, it follows that the area downstream of the filter should remain (just) naturally pressurized after this expansion of 3.85.

(Clearly a factor of 4 expansion is slightly too much, and some pressurization might be lost. Although, fortunately, the danger downstream is much reduced as a result of the much reduced velocities, it seems prudent to recommend factors of expansion less than 4, even though a factor of 4 may be just workable in many situations.)

Although these areas are, I believe, essentially correct (although clearly some refinement of their accuracy might be needed if some good research on this subject were to be carried out) there are new dangers downstream. These include:

- (i) The melt may not initially fill the enlarged channel, but simply run along the bottom of the newly expanded runner, only reaching the correct velocity when the whole channel is finally filled;
- (ii) The upper parts of the filter may jet metal, thus oxidizing and contaminating the downstream melt, as a result of the channel being unfilled to the top, exposing the top of the filter for an extended time.

The above description applies to the siting of a filter in the main runner, usually immediately after the sprue/runner junction.

If now we turn to the quite different situation in which filters are placed in each ingate, the situation seems quite different.

For instance, the behavior of the filter in terms of the back-pressure it will generate is clearly a function of velocity  $V$ , and I suspect this function will in fact be  $V^2$ . Thus there is considerable change to the filling system as a whole with the filter immediately following the sprue where the velocity is high.

In contrast, in the ingates when using a naturally pressurized design, the velocities are significantly lower, so that back-pressure is greatly reduced. In any case the gate area into the filter has already been correctly sized, so no expansion on the output side is required. The use of filters in gates is best employed in vertical gates, since these ensure that the filter primes fully and is protected by liquid on its exit face.

Like so much of gating design, these important details of the correct use of filters would greatly benefit from some systematic work evaluating the effects on fill times, sprue heights, velocities, flow rates, filter placement in runners or gates etc. Preferably this would be carried out by computer simulation backed up by spot checks with real castings, and possibly even further backed up by more spot checks with video X-ray radiography or even water model systems.

### 12.8.6 Tangential placement

Filters have been seen to be open to criticism because of their action in splitting up the flow, thereby, it was thought, probably introducing additional oxide into the melt.

There is some truth in this concern. A preliminary exploration of this problem was carried out by the author (Din and Campbell 1994). Liquid Al alloy was recorded on optical video flowing through a ceramic foam filter in an open runner. The filter did appear to split the flow into separate jets; a tube of oxide forming around each jet. However, close observation indicated that the jets recombined about 10 mm downstream from the filter, so that air was excluded from the stream from that point onwards. The oxide tubes around the jets appeared to wave about in the eddies of the flow, remaining attached to the filter, like weed attached to a grill across a flowing stream. The study was repeated and the observations confirmed by X-ray video radiography. The work was carried out at modest flow velocities in the region of  $0.5\text{--}2.0\text{ m s}^{-1}$ . It is not certain, however, whether the oxides would continue



to remain attached if speeds were much higher, or if the flow were to suffer major disruption from, for instance, the passage of bubbles through the filter.

What is certain is the damage that is done to the stream after the filter if the melt issuing from the filter is allowed to jet into the air. Loper and co-workers (1996) call this period during which this occurs *the spraying time*. This is so serious a problem that it is considered in some detail below. Loper describes the limited volume at the back of the filter as a *hydraulic lock*, the word *lock* appearing to be used in a similar sense to a lock on an inland waterway. In England the length of water impounded between two locks is called a 'pound'. Alternatively an *air lock*, or a *vacuum lock*, is the impounded region of fluid (air or vacuum) between two gates or valves. Anyway, his meaning is clear. I discuss this problem in terms of the requirement to 'protect' the back of the filter with melt.

Unfortunately, most filters are placed transverse to the flow, simply straight across a runner and in locations where the pressure of the liquid is high (i.e. at the base of the sprue or entrance into the runner). In these circumstances, the melt shoots through a straight-through-hole type filter almost as though the filter was not present, indicating that such filters are not particularly effective when used in this way. When a foam filter suffers a similar direct impingement, penetration occurs by the melt seeking out the easiest flow paths through the various sizes of interconnected channels, and therefore emerges from the back of the filter at various random points. Jets of liquid project from these exit points, and can be seen in video radiography. The jets impinge on the floor of the runner, and on the shallow melt pool as it gradually builds up, causing severe local surface turbulence and so creating dross. If the runner behind the filter is long or has a large volume, the jetting or spraying behavior can continue until the runner is full, creating large volumes of seriously damaged metal.

Conversely, if the volume of the filter exit can be kept small and filled rapidly, the volume of damaged melt that can be formed is now reduced correspondingly. Although this factor has been little researched, it is certain to be important in the design of a good placement for the filter.

Figure 12.46a shows a common but poor filter print design that would lead to extensive downstream damage – an extended spraying time in Loper's words. An improved geometry that assists the back of the filter to be covered with melt quickly is shown in Figure 12.46b. Figure 12.46c is improved still further by placing the block filter tangentially to the direction of flow. The tangential mode has the advantage of the limitation of the exit volume under the filter, providing a geometrical form resembling a sump, or lowest point, so that the exit volume fills quickly. In this way the opportunity for the melt to jet freely into air is greatly reduced so that the remainder of the flow is protected. A further advantage of this geometry is the ability to site a bubble trap over filter (Figure 12.46c) providing a method whereby the flow of metal and the flow of air bubbles can be divided into separate streams. The air bubbles in the trap are found to diffuse away gradually into sand molds. For permanent molds, the traps may need to be larger.

The volume adjacent to the filter exit is seen to be well controlled in the case of Figures 12.48a and b, but Figure 12.49a could be a concern, because the single runner from the filter has to have sufficient area to retain the advantage of the flow reduction from the filter, and thus is rather thick. It may therefore not fill well, but may support spraying from the filter during most of the time to fill the complete length of the runner. Variant (b) is better with the 2-way runner being only half the height. (c) is probably excellent, with its 3-way runner, each one third height, so that the region above the filter would be expected to fill completely in a dynamic situation, with the melt proceeding along the runners, filling the whole cross-section of each of the runners.

An additional benefit is that the straight-through-hole extruded or pressed filters seem to be effective when used tangentially in this way. A study of the effectiveness of tangential placement in the author's laboratory (Prodham et al. 1999) has shown that a straight-through-pore filter could achieve comparable reliability of mechanical properties as could be achieved by a relatively well-placed ceramic foam filter (Sirrell and Campbell 1997).

Adams (2001) draws attention to the importance of the flow directed downwards through the filter. In this way buoyant debris such as dross or slag can float clear. In contrast, with upward flow through the filter the buoyant debris collects on the intake face of the filter and progressively blocks the filter.

The tapering of both the tangential approach and the off-take from the filters further reduces the volume of melt, and distributes the flow through the filter more evenly, using the total volume of the filter to best advantage. A variety of filter placements, illustrating many of these key advantages, are illustrated in Figures 12.48 and 12.50.

### 12.8.7 Direct pour

Sandford (1988) showed that a variety of top pouring could be used in which a ceramic foam filter was used in conjunction with a ceramic fiber sleeve. The sleeve/filter combination was designed to be sited directly on the top of a mold to act as a pouring basin, eliminating any need for a conventional filling system. In addition, after filling, the system continued to work as a feeder. This simple and attractive system has much appeal.

Although at first sight the technique seems to violate the condition for protection of the melt against jetting from the underside of the filter, jetting does not seem to be a problem in this case. Jetting is avoided almost certainly because the head pressure experienced by the filter is so low, and contrasts with the usual situation where the filter experiences the full blast of flow emerging from the base of the sprue.

Sandford's work illustrated that without the filter in place, direct pour of an aluminum alloy resulted in severe entrainment of oxides in the surface of a cast plate. The oxides were eliminated if a filter was interposed, and the fall after the filter was less than 50 mm. Even after a fall of 75 mm after the filter relatively few oxides were entrained in the surface of the casting. The technique was further investigated in some detail (Din et al. 2003) with fascinating results illustrated in Figure 12.50. It seems that under conditions used by the authors in which the melt emerging from the filter fell into a runner bar and series of test bars, some surface turbulence was suffered, and was assessed by measuring the scatter of tensile test results. The effect of the filter acting purely to filter the melt was seen to be present, but slight. The castings were found to be repeatable (although not necessarily free from defects) for fall distances after the filter of up to about 100 mm in agreement with Sandford. Above a fall of 200 mm reproducibility was lost (Figure 12.50a, b, c).

This interesting result explains the mix of success and failure experienced with the direct pour system. For modest fall heights of 100 mm or so, the filter acts to smooth the perturbations to flow, and so confers reproducibility on the casting. However, this may mean 100% good or 100% bad. The difference was seen by video radiography to be merely the chance flow of the metal, and the consequential chance location of defects.

The conclusion to this work was a surprise. It seems that direct pour should not necessarily be expected to work first time. If the technique were found to make a good casting it should be used,

since the likelihood would be that all castings would then be good. However, if the first casting was bad, then all should be expected to be bad. The site of the filter and sleeve should then simply be changed to some other location to seek a different pattern of filling. This could mean a site only a few millimeters or centimeters away from the original site. The procedure could be repeated until a site was found that yielded a good casting. The likelihood is that all castings would subsequently be good.

However, the technique will clearly not be applicable to all casting types. For instance, it is difficult to see how the approach could reliably produce extensive relatively thin-walled products in film-forming alloys where surface tension is not quite in control of the spread of metal in the cavity. For such products the advance of the liquid front is required to be steady, reproducible and controlled. Bottom gating in such a case is the obvious solution. Also, the technique works less well in thicker section castings where the melt is less constrained after its fall from the underside of the filter. Figure 12.50c illustrates the fall in reliability of products as the diameter of the test bars increases from 12 mm to above 20 mm. The larger sections would have offered reduced constraint to the falling metal, so suffering entrainment damage, and more scattered properties.

Even though the use and development of the direct pour technique will have to proceed with care, it is already achieving an important place in casting production. A successful application to a permanent molded cylinder head casting is described by Datta and Sandford (1995). Success here appears to be the result of the limited, and therefore relatively safe, fall distance.

A recent development of the direct pour technique is described by Lerner and Aubrey (2000). For the direct pouring of ductile iron they use a filter that is a loose fit in the ceramic sleeve. It is held in place by the force of impingement of the melt. When pouring is complete the filter then floats to the top of the sleeve and can be lifted off and discarded, avoiding contamination of recycled metal.

### 12.8.8 Sundry aspects

1. The dangers of using ceramic block filters in the direct impingement mode is illustrated by the work of Taylor and Baier (2003). They found that a ceramic foam filter placed transversely in the down-sprue worked better at the top of the sprue rather than at its base. This conclusion appears to be the result of the melt impact velocity on the filter causing jetting out of the back of the filter. Thus the high placement was favored for the reasons outlined in the section above on the direct pour technique. This result is unfortunate, because if the filter exit volume had been limited to a few ml (a depth beneath the filter limited to 2 or 3 mm) the lower siting of the filter would probably have performed best.
2. It is essential for the filter to avoid the contamination of the melt or the melting equipment. Thus for many years there appeared to be a problem with Al-Si alloys that appeared to suffer from Ca contamination from an early formulation of the filter ceramic. If this problem actually existed, it has in any case now been resolved by modification of the chemistry of the filter material. In addition, modern filters for Al alloys are now designed to float, so that they can be skimmed from the top of the melting furnace when the running systems are recycled. This avoids the costly cutting out and separation of spent filters from recycled rigging to avoid them collecting in a mass the bottom of the melting furnace.

Interestingly, the steel gauzes used for Al alloys do not contaminate the alloy entering the casting. This is almost certainly the result of the alloy wrapping a protective alumina film over the wires of the mesh as the meniscus passes through. However, the steel will dissolve later if recycled via a melting furnace of course.

The recent introduction of carbon-based filters for steel does add a little carbon to the steel, but this seems negligible for most grades. Experience suggests that even ultra-low carbon steels appear to avoid contamination from this source.

Xu and Mampaey (1997) report the additional benefit of a ceramic foam filter in an impressive 12-fold increase in the fluidity of gray iron poured at about 1400°C in sand molds. They attribute this unlooked-for bonus to the effect of the filter in (i) laminizing the flow and so reducing the apparent viscosity due to turbulence, and (ii) reducing the content of inclusions. One would imagine that films would be particularly important.

### 12.8.9 Summary

So far as can be judged at this time, among the many requirements to achieve a clean casting, the key practical recommendations for the casting engineer can be summarized as:

1. Do not allow slag and dross to enter the filling system. This task is solved by eliminating the conical pouring basin and substituting an offset step basin. Even better results would be expected from the various contact pouring options.
2. Use a good early part of the filling system (well-designed basin and sprue) to avoid the creation of additional slag or dross that may block the filter.
3. Integrate the filter with a buoyant trap. The bubble trap described earlier should also work as a slag trap. The presence of the filter significantly aids the separation of a buoyant and a heavy phase. Where particularly dirty metals are in use, the trap will, of course, require the provision of sufficient volume and height on its upstream side to accommodate retained material, allowing slag and dross to float clear, and leaving the filter area to continue working unhindered. The volume requirement does, however, require to be balanced by the shape of the trap, which needs a narrow aspect ratio; if it had a large open volume the turbulence of the melt thrashing around in this open space could generate sufficient oxide to block the filter. At all times the melt requires to be constrained (i.e. subject to a gentle pressurization).
4. Avoid the danger of the bypassing of the filter by poor printing. Mold-in the filter if possible.
5. Provide protection of the melt at the exit side of the filter, by rapid fill of this volume with liquid metal. A useful geometry to achieve this is the tangential placement of the filter, followed by a shallow well that can be filled quickly. For filters that fill uphill, the effective volume above should be as small as possible, so that an exit to a runner of thickness less than the sessile drop height is required, otherwise the whole runner may fill with jetted and damaged metal.

## Filling system design practice

## 13

In view of all the information on filling system components, and all the Casting Rules listed in earlier sections of the book, this section attempts to gather these together, to see how we might achieve a complete, practical solution to the design of a filling system. The ability to design a quantitative solution, yielding precise dimensions of the filling channels at all points, is a key responsibility, perhaps *the* key responsibility, of the casting engineer.

When I am asked ‘What is the most important feature of the filling system design?’ the reply is ‘Everything’. As has been stated before, all gravity filling systems run with such high velocities that they are hypersensitive to any small error of mismatch, sizing, or geometry. A small, innocent-looking expansion or ledge leads to a stream of entrainment defects. Every part of the system needs to be correct.

Naturally, computers are beginning to have some capability of optimizing the design of filling systems (McDavid and Dantzig 1989, Jolly et al. 2000). However, at this time it is clear that most computer simulations of filling have to employ the liquid viscosity as an adjustable parameter, commonly using values for the metal viscosity that are many times the viscosity of the pure metal. The reason for this is almost certainly the presence of a dense suspension of bifilms which are probably the only features that can have any significant effect on the viscosity of melts. This adjustment of the viscosity is unsatisfactory in the sense that melts are starting to be prepared with very different bifilm contents, so that filling simulations by computer can be unexpectedly found to be unsatisfactory if the appropriate viscosity for the melt condition is not known.

The other significant limitation of computer simulations is that thermal and solute-driven convection is highly computationally intensive, and is therefore generally neglected. Furthermore, of course, the damage that is introduced by oxides, which in some cases appear to be capable of completely blocking the operation of feeders, is far from being simulated, and may ultimately be practically impossible. The list of potentially important factors required for such a model is daunting. These will include the rate of strengthening of the oxide, and its fracture and tearing resistance, each of which is likely to be sensitive to alloy content, impurities, environment, and age of the oxide, etc. We are never likely to gather all the data that are needed, and never likely to have computers sufficiently powerful to take them all into account.

Anyway, until the time that the computer is tolerably proficient, it will be necessary for the casting engineer to undertake the duty of designing filling systems for castings. The complication of the procedure is not to be underestimated (if it were easy the procedure would have been developed years ago). Many factors need to be taken into account. This short outline cannot cover all eventualities, but will present a systematic approach that will be generally applicable.

---

### 13.1 BACKGROUND TO THE METHODING APPROACH

If a computer package is available to simulate the solidification of the casting, it is best to carry this out first. Most software packages are sufficiently accurate when confined to the simulation of solidification (it is the filling simulation and other sophisticated simulations such as that of stress, strain, and distortion that are more difficult, and the results often less accurate). A solidification simulation with the addition of no filling or feeding system will illustrate whether there are special problems with the casting. Figure 13.1 illustrates the formal logic of this approach. It lays out a powerful methodology that is strongly recommended.

If in fact there are no special problems it is good news. Otherwise, if problems do appear for a long-running part, and if they can be eliminated by discussion with the designer of the component at this initial stage, this is usually the most valuable strategy. Such actions often include the shift of a parting line, or the coring-out of a heavy section or boss. The purpose of a modest one-time design change is to avoid, so far as possible, the ongoing expense for the life of the product of special actions such as the provision of chills or feeders, or an extra core, etc.

If, despite these efforts, a problem remains, the various options including additional chills, feeders or cores will require detailed study to limit, so far as possible, the cost penalties. The following section provides the background for the next steps of the procedure.

---

### 13.2 SELECTION OF A LAYOUT

First, it will be necessary to decide which way up the part is to be cast (this may be changed later in the light of many considerations, including problems of core assembly, desirable filling patterns, subsequent handling, and de-gating issues, etc.). If a two-part mold is to be used, the form of the casting should preferably be mainly in the cope, allowing gating at the lowest parts of the casting. This may prove so difficult that a third box part may be selected through which the running system could be sited under the casting. If some solution to the challenge of lowest point gating cannot easily be found, the risk of filling the casting at some slightly higher point may need to be assessed. Some filling damage might have to be accepted for some castings. Even so, it is unwelcome to have to make such decisions because the extent of any such damage is difficult to predict.

A heavy section of the casting needs special attention. This may most easily be achieved by orienting this part of the casting at the top and planting a feeder here. Alternatively, other considerations may dictate that the casting cannot be oriented this way, so arrangements may have to be made to provide chills and/or fins to this section if it has to be located in the drag.

When a general scheme is decided, including the approximate siting of gates and runners, the provision of feeders, if any, and the location of the sprue, a start can be made on the quantification of the system.

---

### 13.3 WEIGHT AND VOLUME ESTIMATE

The weight of the casting will be known, or can be estimated. This is added to an estimate of the weight of the rigging (the filling and feeding system) to give an estimate of the total poured weight. Dividing this by the density of the liquid metal will give the total poured volume.

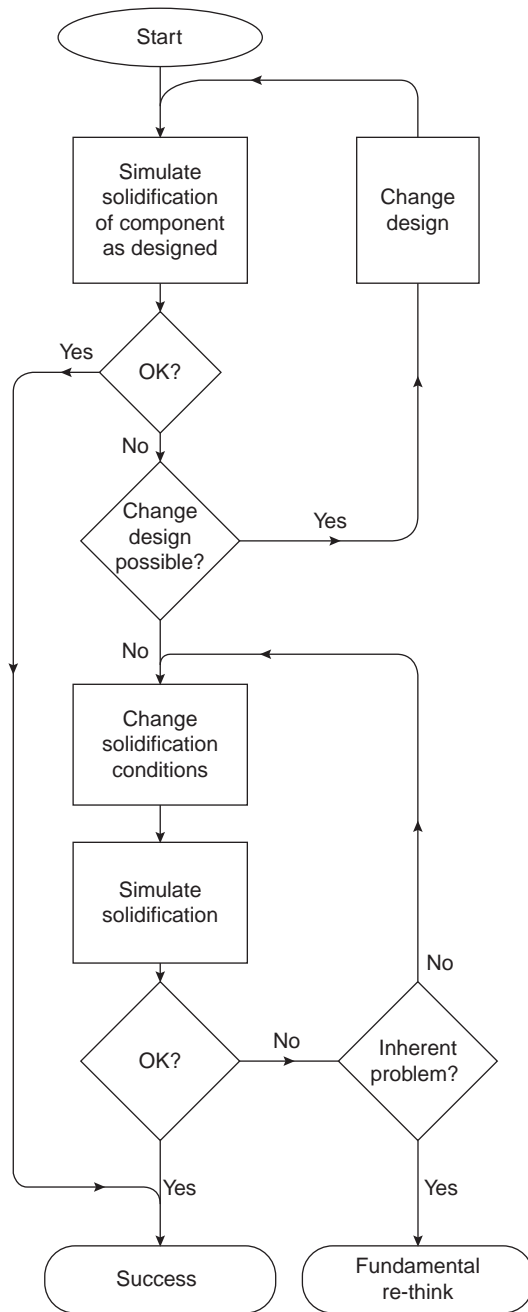


**FIGURE 13.1**

Methoding procedure for computer simulation.

Unfortunately, of course, the weight of the rigging is clearly not accurately known at this early stage because it has not yet been designed. However, an approximate estimate is nearly always good enough. Although a revised value can always be used in a subsequent iteration of the rigging design calculations to obtain an accurate value for the weight of the rigging, after some experience an additional iteration will be found to be hardly ever necessary. The outcome of an iteration when the correct total weight is known is usually a change of only a millimeter or two in many dimensions of the system and can often be neglected.

Another question that constantly arises is ‘Should the weight of metal in the pouring basin be included in the total poured weight?’ The answer depends on the precise pouring technique.

1. A common approach is to time the pour from the start of pouring from the ladle. In this way the melt is poured into the empty basin, gradually raising the level until the basin is sufficiently full. The stopper is raised to start the pour down the sprue, but pouring continues to maintain the basin continuously topped up until the moment that the mold is full. The average fill rate is simply the total weight poured divided by the total time.
2. Conversely, after the basin has been filled, the pour may be timed from the raising of the stopper. In some practices, there may be a delay to allow the basin to settle prior to the opening of the sprue. If the filling system has to avoid the draining of the basin (i.e. the level of metal in the basin is approximately equal to the maximum height of the casting + feeders) the weight of metal in the basin is no longer relevant to the calculation of the dimensions of the rest of the filling system. The average fill rate appropriate to the calculation of the filling system is the weight of metal poured (minus the weight in the basin) divided by the time for the filling of the mold (neglecting the time to fill the basin).
3. If the metal in the basin is held back by a stopper, giving it time to settle, and if the casting is formed by eventually draining the melt from the basin, then the filling time is clearly that time from raising of the stopper to the draining empty of the basin. The weight of metal in the basin requires to be included in the total weight poured. (This description neglects the usual desirability to keep a little metal above the sprue entrance if some residual head height is required.)
4. An alternative filling system practice is to arrange for the basin to hold the complete charge (plus a small margin as explained below) for the running system and casting. After the basin is filled, a short delay of a few seconds is beneficial to allow as much detrainment of bubbles and oxides as possible. The stopper is then raised and the complete contents of the basin disappear into the entrance to the down-sprue. The time to empty the basin is the pour time. In this case the average fill rate for the casting is the total weight of the casting plus rigging (minus any residual metal in the basin) divided by the fill time. A caution with this approach is to ensure that a sufficient head of metal remains in the basin at the end of filling to pressurize and fill out the upper parts of the mold cavity.

Those techniques including the draining of the pouring basin introduce an error in the design assumptions since the filling system is generally designed assuming a constant head pressure in the basin. Thus the draining of the basin will deliver a falling pressure at the end of the filling period. This is not usually serious since the filling system is not likely to depressurize sufficiently to introduce defects at this late stage, and the overall filling time is extended by only a second or so.

The draining does become a problem if the casting requires a relatively high fill rate during the last moments of the fill, or if it has narrow sections offering capillary repulsion to resist filling in top



parts of the casting. These features would be good reasons to maintain a full basin and accept the loss of metal yield.

---

## 13.4 PRESSURIZED VERSUS UNPRESSURIZED

It was the famous researchers from the US Navy Research Laboratory, Johnson, Bishop, and Pellini, who, in 1954, defined and classified filling systems as either pressurized or non-pressurized. This was a useful distinction.

In his book *Castings* 1991 the author recommended the achievement of velocity reduction by the progressive enlargement of the area of the flow channels at each stage, with the aim of progressively reducing the rate of flow. This is known as an *unpressurized* running system. The aim was to ensure that the gate was of a sufficient area to make a final reduction to the speed of the melt, so that it entered the mold at a speed no greater than its critical velocity. More recent research, however, with the benefit of video X-ray radiography and computer simulation has demonstrated that the enlargement of the system by, for instance, a factor of two to halve the velocity as the flow emerges from the exit of the sprue and enters the runner usually fails to have any effect on the velocity, so that the runner is only half filled with this fast jet of metal. Worse still, the jet hits the far end of the runner, bouncing back to create a wave that rolls over the incoming fast jet; at the junction between these opposite streams bubbles and oxides are efficiently entrained. Thus the unpressurized systems unfortunately behave poorly, degrading the metal, because much of the system runs only partly full. The other standard criticism (but incidentally of much less importance) was that unpressurized systems are heavy, thus reducing metallic yield, and thus costly.

In fact, video radiography reveals that at the abrupt increase in cross-section at the base of the sprue on the entry to the runner, the entrainment of air occurs with dramatic effectiveness. This is because the melt jets along the base of the runner (not filling the additional area provided) and hits the end of the runner. The return flow creates an especially damaging situation: the rolling back wave which is formed (Figure 13.2b) can be long-lived, developing into a stable flow structure that resembles a *hydraulic jump*. The bubbles travel along the interface between the two opposing streams (probably because of the presence of two non-wetting oxide films separating the two flowing streams) and progress to the ingate, usually collecting in a low-pressure zone on one side of the ingate, before proceeding to swim up through the metal in the mold cavity (Figure 13.2e). Naturally, these bubbles and oxides bequeath serious permanent damage to the casting (Figure 13.2f).

The cast iron foundryman had some justification therefore to champion his own favorite *pressurized* systems. For the benefit of the reader, the so-called *pressurized running system* is one in which the metal flow is *choked* (i.e. *limited by constriction*) at the gate; i.e. its rate of flow into the mold is to some extent controlled by the area of the gate, the last point in the running system (Figure 13.2a). This causes the running system to back-fill from this point, and become pressurized with liquid, forcing the system to fill and exclude air. Thus the system entrains fewer bubbles and oxides. However, it also forces the metal into the mold as a jet. Clearly this system violates one of our principal rules, since the metal is now entering the mold above its critical speed. The resulting splashing and other forms of surface turbulence inside the mold introduce their own spectrum of problems, different from those of the unpressurized system, but usually harming both the quality of the mold and the casting.

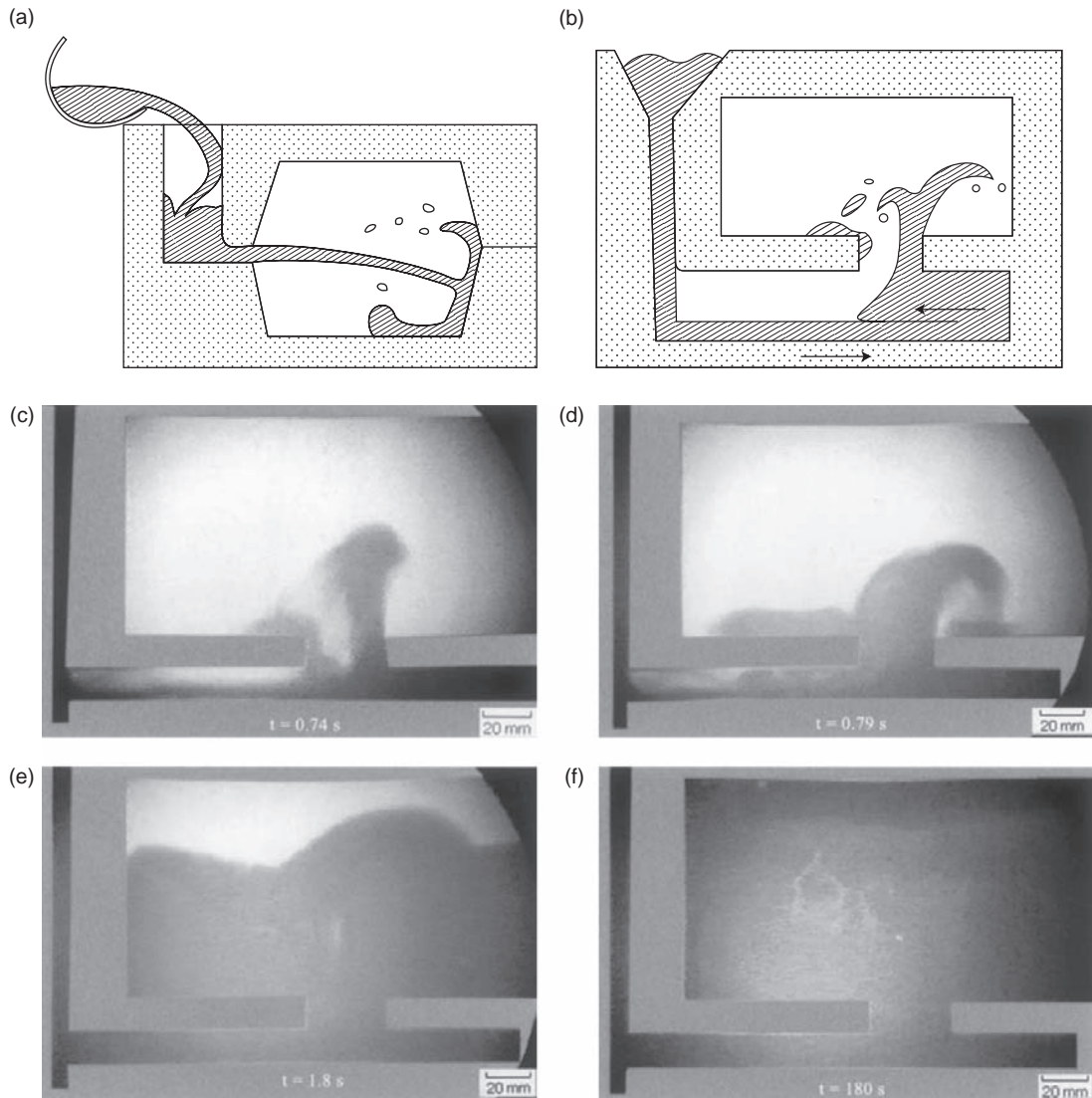


**FIGURE 13.2**

Mode of filling of (a) a pressurized system, showing the jet into the mold cavity; (b) an unpressurized system, showing the fast underjet, and the rolling back wave in the oversized runner; (c, d, e) X-ray video frames of an Al alloy filling a mold 100 mm high, 200 mm wide  $\times$  20 mm thick illustrating the unpressurized system; (f) the final casting showing subsurface bubbles and internal cracks.

Thus neither the unpressurized nor the pressurized traditional systems are seen to work satisfactorily. This is a regrettable appraisal of present casting technology.

Because for many years the pressurized systems were mainly used for cast iron, there were special reasons why the systems appeared to be adequate:

1. In the days of pouring gray iron into greensand molds the problems of surface turbulence were minimized by the tolerance of the metal–mold system. The oxidizing environment in the greensand mold produced the liquid silicate film on the surface of the liquid iron. Thus when this was turbulently entrained it did not lead to a permanent defect (*Castings* 2003). In fact, many good castings were produced by tipping the metal into the top of the mold, using no running system at all! Nowadays, with the use of certain core binders and mold additives that cause solid graphitic surface films on the metal, and consequently reduce its tolerance to surface turbulence, the pressurized systems are producing defects where once they were working satisfactorily. This problem has become more acute as it has become increasingly common for irons to have alloy additions such as magnesium (to make ductile iron) and chromium (for many alloyed irons) which lead to strong oxide films on the liquid surface, leading to serious defects if entrained.
2. Over recent years the standards required of castings has risen to an extent that the traditional foundryman is shocked and dazed. Whereas the pressurized system was at one time satisfactory, it now needs to be reviewed. The achievement of quality is now being seen to be not by inspection, but by process control. Turbulence during filling introduces a factor that will never be predictable or controllable. This ultimately will be seen as unacceptable. Reproducibility of the casting process will be guaranteed only by systems that fill the mold cavity with laminar surface flow. At one time this was achievable only with counter-gravity filling systems. Nowadays, as we shall see, we can achieve some success with gravity systems, provided they are designed correctly.

The conclusion given by the author in *Castings* 1991 was ‘*Unpressurized* systems are recommended therefore *Pressurized* are not.’ This bold statement now requires revision in the light of our recent research since we now find that neither system is really satisfactory.

In summary, the unpressurized system had the praiseworthy aim to reduce the gate velocity to below the critical velocity. Unfortunately, such systems usually ran only part-full, causing damage to the castings because of entrained air bubbles and oxides. The pressurized system probably benefited greatly from its ability to fill quickly and to run full, greatly reducing the damage from bubbles. However, the high velocity of the melt as it jetted into the mold created its own contribution to havoc. Further complications for both systems were the unsatisfactory pouring basin and sprue designs which simply added to the existing fundamental problems.

### The choke

Turning now to another hallowed precept of running system design that requires to be laid to rest. This was the concept of the *choke*. The choke was a local constriction designed to limit flow. In the non-pressurized system the choke was generally at the base of the sprue, whereas the pressurized system was choked at the ingates into the mold. Unfortunately, a choke is an undesirable feature. Flow rates are usually already too high in most filling systems at the base of the sprue. Providing a constriction speeds up the flow even more, causing it to emerge as a jet that does not expand to fill the downstream channel and so entrains air once again, with much consequential damage.

All the early unpressurized and pressurized systems were devised before the benefits of computer simulation and video X-ray radiography. They also pre-dated the development of the concepts of surface turbulence, critical velocity, critical fall height, and bifilms. It is not surprising therefore that all these traditional approaches to the design of filling systems gave less than satisfactory results.

In the history of the development of filling systems most of the early research was carried out in an effort to understand flow, but was of limited value because the emphasis was on steady state flow through fully filled pipework, following the principles of hydraulics. This does, of course, sometimes occur late during the filling process. However, the real problems of filling are associated with the *priming* of the filling system, i.e. its behavior before the filling system is filled. Thus these early studies give us relatively little useful background on which to base effective designs for real castings.

A completely new approach is described in this book that attempts to address these issues. We shall abandon the concept of a localized choke. The whole of the length of the filling system should experience its walls in permanent contact and gently pressurized by the liquid metal. Thus, effectively, the whole length of the running system should be designed to act like a choke; a kind of *continuous choke* principle. A useful name is 'naturally pressurized' system, because the new design concept is based on designing the flow channels in the mold so as to follow the *natural form* that the flowing metal wishes to take, and at the same time develop a *natural back-pressure* throughout the system as a result of the effect of frictional drag.

### Gating ratios

It is necessary to divert for a second short section to examine a second red herring, the filling system as defined by its traditional gating ratios. When considering the relative areas of the key parts of the filling system, the sprue exit area is conventionally taken as 1, the runner cross-section and the gate cross-section areas are listed as comparisons. Thus 1:2:4 is a typical series indicating that the runner has twice the area of the sprue exit, and the gate has four times the sprue exit area. Another common gating ratio was 1:2:2. These ratios are frankly unhelpful, and should be discarded.

Other series of ratios that might have some helpful aspects are discussed below. However, I never find myself defining the filling system using ratios; the ratios are a natural outcome of the filling system design. They are an outcome, not an input.

If we imagine that after the metal emerges from the sprue and takes its right angle bend into the runner, the stream would be expected to lose some energy so that its velocity would fall by some amount, say 20% (this amount is not claimed to be accurate, but is taken here for clarity of illustration). This would allow us to expand the channel by this amount. We shall assume that the runner can remain parallel, retaining its area of 1.2 along its complete length (although in reality the gradual accumulation of the effect of friction along its length might add a further reduction in speed, say 10%, allowing in principle the area of the runner to be increased to 1.3 times the area of the sprue exit. However, for simplicity at this stage we shall neglect this effect.) After turning through a further right-angle bend into the gate this turn might contribute a further velocity fall of 20%, giving a series of permissible area ratios of 1:1.2:1.4, although it will be noticed that the ingate velocity has only fallen by approximately 40% from that at the sprue exit.

If the assumed 20% expansion of area after each bend is not entirely allowed (for instance if only 10% expansion were provided after each bend) the stream will experience a gentle pressurization. If zero expansion of the runner was made after each bend the melt would experience an even greater pressurization. This pressurization is in fact only a fairly modest pressure against the walls of the

running system, but will be valuable to counter any effect of bubble formation and will act to support the walls of the running system against collapse (a special problem in large running systems for large castings). Thus to be more sure of maintaining the system completely full, and slightly pressurized, a ratio of 1:1.1:1.2 or perhaps even better 1:1:1 might be used.

From the ratios it is clear that the naturally pressurized system is part-way between the pressurized and unpressurized systems. The value of ensuring that the whole of the filling system is at least gently pressurized was first appreciated by Jeancolas and his colleagues in 1962, but seems to have been neglected until now. This prophetic insight is a feature that should be part of all computer simulations of filling systems. If any part of the surface area of the filling system reveals an absence of pressure, the system requires revision to address this. A refinement would be to illustrate the pressurization of the surface of the filling system, using contours of pressure. Any regions sufficiently low to present a risk of depressurization in practice could indicate the need for action to address this. A robustly pressurized system is the target.

In the interests of maximizing pressurization to avoid air entrainment, I nearly always select the runner area equal to the sprue exit. This avoids any choice of losses at this junction, which are in any case not precisely 20% and are probably not accurately known for the various different sprue/runner junctions that are used.

Moving on now to considerations of the area of the ingate, Table 13.1 indicates the ratios I normally use for a naturally pressurized system 1:1: $n$  where the value ' $n$ ' can take almost any value (although normally between approximately 4 and 10) if care is taken to distribute the melt over the whole area of the gate. This is not always straightforward, but we shall devote space to a full consideration of the decision-making required for  $n$ .

However, at this point in our progress of examining the evolution of our running system design the reader may already have noticed a major problem. The naturally pressurized system has no built-in mechanism for any significant reduction in velocity of the stream. Thus the high velocity at the base of the sprue is maintained (with only minor potential reduction due to frictional drag) into the mold. Thus the benefits of complete priming of the filling system to exclude air may be lost once again on entering the mold cavity.

This fundamental problem alerts us to the fact that the naturally pressurized approach requires completely separate mechanisms to reduce the velocity of the melt through the ingates. The options include:

- (i) the use of filters;
- (ii) the provision of specially designed runner extension systems such as flow-offs;

**Table 13.1** Examples of area ratios (sprue exit area:runner area:gate area)

	Examples of area ratios
Pressurized	1:0.8:0.6 1:1:0.8
Unpressurized	1:2:4 1:4:4
Naturally pressurized	1:1: $n$
Naturally pressurized with foam filter in gate	1:1:4
With speed reduction or by-pass designs	1:1:10

- (iii) a surge control system;
- (iv) the use of a vertical fan gate at the end of the runner.

Additional mechanisms might be possible in the future, when properly researched, such as:

- (v) the use of vortices to absorb energy whilst avoiding significant surface turbulence.

We shall consider all these options in detail in due course, but the reader needs to be aware that, unfortunately, at this time the use of naturally pressurized systems is in its infancy. In particular, the rules for such designs are not yet known for some features such as joining of round or square section sprues to rectangular runners. The rules for the incorporation of filters may even yet not be fully understood, and vortex systems in particular are definitely not yet understood, even though they appear to have much promise.

This creates a familiar problem for the foundry person: in the real world, the casting engineer has to take decisions on how to make things, whether or not the information is available at the time to help make the best choice. Thus insofar as the rules are presently understood for the majority of castings, they are set out below, for good or for bad. I hope they assist the caster to achieve a good result. One day I hope we in the industry will all have the better answers that we need.

In the meantime, computers are starting to be successful to simulate the flow of metal in filling systems. At the present time such simulations are highly computationally intensive, and therefore slow and/or not particularly accurate. It is necessary to be aware that some simulation packages are still highly inaccurate. However, time will improve the situation, to the great benefit of casting quality.

---

## 13.5 SELECTION OF A POURING TIME

A common concern is how can production rates be maintained high if metal velocities in the filling system need to be kept below the critical  $0.5 \text{ m s}^{-1}$ ? Fortunately, this is not usually a problem because the time to fill a casting is dependent on the rate of mold filling measured as a volume per second, and can be fixed at a high level. At the same time the velocity through the ingate can be independently lowered simply by increasing the area of the gate (simple in principle, but sometimes harder in practice!). These considerations will become clearer as we proceed.

When faced with a new design of casting, the first question asked by the casting engineer is ‘How fast should it be filled?’ The selection of a pouring time is one of the most interesting moments in the design of a filling system for a new casting.

Sometimes there is no choice. On a fast molding line making 360 molds per hour there are only 10 seconds for each complete cycle, of which perhaps only 5 seconds may be the available time for pouring. (Although it is worth keeping in mind that even here, as a last resort, the pour time might be doubled if two pouring facilities were to be installed.)

When there *is* a choice the pour time can often be changed between surprisingly large limits. Many castings are filled very much faster than necessary, and there are benefits to a reduction in this speed. One factor limiting the slowest speed is the rate of rise of the metal in some sections.

The surface of an Al casting becomes marked with striations due to the passage of transverse unzipping waves at a vertical rise velocity below  $60 \text{ mm s}^{-1}$  (Evans et al. 1997). Although they can leave their witness on the surface of the oxidized surface of the casting they are usually harmless to its internal structure. Even so, they may be unsightly on a cosmetically important casting, but if the alloy

has an extra strong surface oxide, or is partially freezing because of a cool pour, the waves may lead to such severe surface horizontal laps that the casting becomes beyond repair. Types of geometries where this problem is most often seen are illustrated in Figure 13.3. A hollow cylinder cast on its side is a common casualty (Figure 13.3a) because of the sudden increase in area to be filled, reducing the rate of rise as the metal reaches the top of the core. The problem is also found on the upper surfaces of tilt castings if the rate of tilt is too slow and if, at larger angles, the area of the metal surface increases to further reduce the rate of rise as is seen in Figure 13.3b.

Considerations that control the choice of rate of metal rise in steel castings indicate that these factors have yet to be properly researched (Forslund 1954, Hess 1974). In practice, a common rate of rise in a steel foundry making castings several meters tall and weighing several tonnes is  $20 \text{ mm s}^{-1}$ . A further limit to the fill time of a steel casting is the possible collapse of the cope when subjected to radiant heat of the rising metal for too long. This problem is reduced by generous venting of the top of the mold via a top feeder as explained for Figure 4.7, and is further reduced by the practice of providing

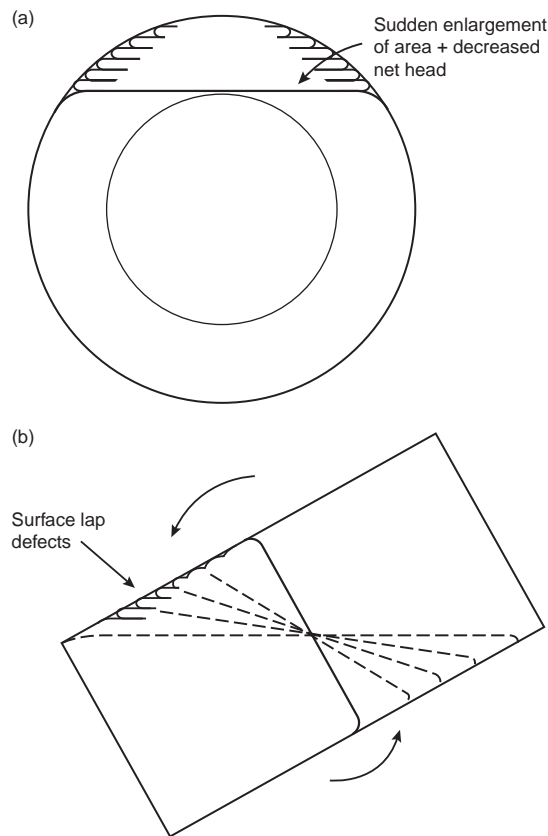


**FIGURE 13.3**

Common lap problems at reduced rates of rise, as a result of increased area of liquid surface in the mold (a) in a horizontal pipe or cylinder; (b) on the cope surface of a tilt casting.

a white mold coat based on a material such as alumina or zircon, thus absorbing much less of the incident radiation.

Alternatively another constraint on a choice of pour time is the consideration that it may be necessary to fill the mold before freezing starts in its thinnest section (or, more usefully, its smallest modulus). Thus an idea of the time available can be gained from Figure 13.4. (Readers are recommended to generate such diagrams for themselves for special casting conditions, using embedded thermocouples to determine the freezing times versus modulus relations, e.g. for cast iron in silicate-bonded sand molds, or aluminum-based alloys in investment molds at 600°C, etc.)

Having made our choice of an approximate minimum fill time for the casting, it is instructive to consider whether this time could be doubled, or even doubled again. It is surprising how often this is a possibility. Whereas the experienced foundryman will hesitate to extend the pouring time of

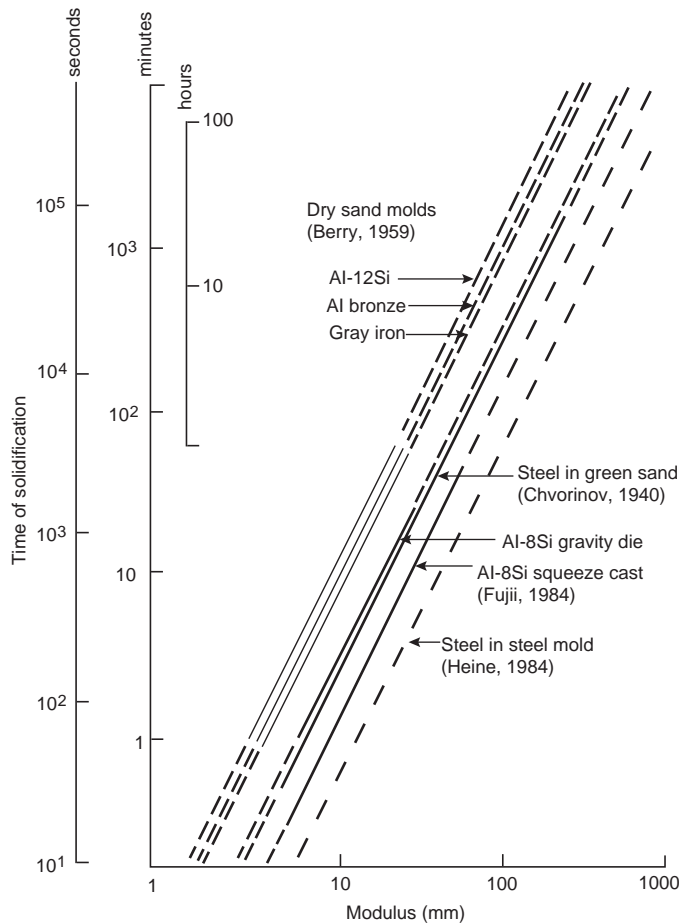


FIGURE 13.4

Freezing times for plates in different alloys and molds.



a familiar casting, his experience will be based usually on a poor filling system. Such systems generate problems such as slopping and surging, and splashes ahead of the main body of melt. This generation of lap-type defects will give the appearance of having been filled too slowly; the erroneous diagnosis leading to an erroneous corrective action that will make the problem worse.

In general, if there is a wide choice of time, for instance somewhere between 5 and 25 seconds, it is strongly recommended to opt for the maximum time, giving the minimum fill rate. This is because, compared to the faster fill rate, the selection of the slower rate reduces the cross-section area of all parts of the filling system, in this case by a factor of 5. This is economically valuable, giving a great boost to yield. The filling channels shrink from appearing 'chunky' to appearing like needles (with the confident but erroneous predictions by all experienced onlookers that such systems will never fill). In addition, there is the benefit that the slimmer filling system actually works better, improving the quality of the casting by giving less room for the metal to jump and splash. Random scrap from pouring defects is thereby reduced. These are important benefits.

On the arrival of a completely new design of casting, the choice of the time to fill the mold can sometimes be impressively arbitrary, with perhaps no-one in the foundry having any clear idea on the time to use. Nevertheless, a value that seems reasonable can be tried, and can always be modified, preferably extended, on a subsequent trial. Such modifications usually only require the filling system to be modified by a few millimeters.

An interesting benefit of lengthy filling times is the surface finish of the casting. The oxide on the surface of the melt has time to thicken, so that, if correctly bottom gated, as it slides around the rising meniscus to become the skin of the casting the liquid metal is mechanically protected from penetrating the mold. Also, of course, the metal pressure due to depth is also correspondingly reduced, further reducing penetration. The result is a beautiful shiny casting.

Another important fact to remember is that provided the pouring basin is kept filled to at least its designed level, the filling time is not allowed to vary by chance as in a hand-cut running system, and is not under the control of the pourer, but remains accurately under the control of the casting engineer.

---

## 13.6 THIN SECTIONS AND SLOW FILLING

It is perfectly normal to assume that thin sections will require to be filled as quickly as possible. However, we need to question this piece of conventional thinking.

It is certainly true that thin sections have to be filled prior to freezing if freezing would prevent the section filling. This much is obvious. However, the rest of the thinking is rather less obvious, but important for success. The factors that make slower filling usually more successful require to be properly understood.

1. If filling is extremely fast it is likely to be extremely turbulent. Entry through the gate at speeds much above the critical velocity of  $0.5 \text{ m s}^{-1}$  will probably result in such surface turbulence that jetting and splashing occur. Droplets of melt that jump far above the rising metal and attach to the walls of the mold will oxidize and may freeze. Thus when the bulk of the melt finally arrives the drops cannot be properly assimilated, forming an oxide lap or even a cold lap. An array of such lap features will lead the founder to think that the melt has been poured too cold, or too slowly, and may increase the temperature (unfortunately increasing the rate of oxidation)

or increase the filling speed (unfortunately enhancing the turbulence). Either action will, of course, make the problem worse.

- When filling at a speed at which the meniscus of the melt keeps itself together, the fact that the melt travels together means that it 'keeps itself warm'. This cosy thought is not the whole story, however. The mechanism of slow filling of extensive thin sections ensures that the hot metal travels through the casting in a fairly straight line directly to the front, spreading laterally on arrival behind the advancing meniscus (Figure 12.35). This effect is extremely powerful in achieving the filling of thin sections. The effect has, perhaps, a minor downside, in that the flow of hot metal through the section to reach the front continues to maintain an open *flow channel*. This channel then freezes late, and may lead to a coarser grain than is desirable (although such factors should not lead to any significant deterioration of properties providing the melt is clean). It may also lead to problems to obtain full soundness in this section, but once again cleanness is a big help to keeping these problems at bay.

---

## 13.7 FILL RATE

Having selected a fill time, the *average fill rate* is, of course, simply the total poured weight divided by the total time, expressed in a convenient unit such as  $\text{kg s}^{-1}$ . This requires to be converted to the average volume fill rate by dividing by the density of the liquid metal, giving a value in such units as  $\text{m}^3 \text{s}^{-1}$ .

Even this value cannot be used directly. This is because the filling system has to be sized to take the significantly higher rate of flow at the beginning of the pour. The *average fill rate* is, of course, less than the *initial fill rate* because the high initial rate is not maintained. The metal slows as the mold fills, the fill rate finally falling to zero if the metal level in the mold finally reaches the same level as that in the pouring basin. To make allowance for this effect, it is convenient to assume that the *initial fill rate* is a factor of approximately 1.5 times higher than the *average fill rate*. This factor is actually precisely correct if the casting is a uniform plate with its top level with the pouring basin, as shown in Appendix 1. However, in general, the factor is reasonably accurate for most castings, being not particularly sensitive to geometry, as can be demonstrated by such exercises as checking the fill times of extreme examples such as a cone filled via its base compared to inverting it and filling via its tip.

A further factor needs to be taken into account; it is found by experience for many castings that the frictional drag reduces flow rates in filling systems by approximately 30%, so that filling systems should be speeded up by the factor 1.3 to compensate. Combining the geometrical factor 1.5 with the friction factor 1.3

$$1.5 \times 1.3 = 2.0$$

Thus a *design fill rate* is almost exactly twice the *average fill rate*. When we allow for density, we obtain the *design volume flow rate*,  $Q$ , preferably in units  $\text{m}^3 \text{s}^{-1}$ . This is the value to be used for defining the size of all of the remaining features of the filling system that we require to calculate.

Incidentally, for a given volume flow rate, the mold will fill in the same time whether aluminum or iron is poured (Galileo would have known this). Thus the system described below applies to all metals and alloys, perhaps to the surprise of many of us who have unwittingly accepted the dogma that each metal and alloy requires its own special system.

Later, when the first mold is poured, the filling should be timed with a stopwatch as a check of the running system design. The actual time should be within 10% of the predicted time. In fact the agreement is often closer than this (Kotschi and Kleist 1979), to the amazement of doubters of casting science!

After the first casting is produced, it may be clear that it needs a casting rate either slower (allowing some solidification during pouring) or faster (to avoid cold lap-type defects). These modifications to the rate can be easily and quickly carried out by minor adjustment (usually only millimeters of changes to dimensions are usually required) to the size of the filling channels. Again, it is useful to emphasize, provided the pouring basin is kept correctly filled, which frankly is easy, such changes remain under the control of the casting technologist (not the pourer).

---

## 13.8 POURING BASIN DESIGN

If the basin is designed with a response time of 1 second, it means that if pouring stops the basin will empty in 1 second, we have the volume per second emptying from the basin of  $Q$ , so that this equals the working volume of the basin filled to its minimum depth. For convenience, if the basin is a cube of side  $A$ , its volume is  $A^3$ . Thus in one second  $Q = A^3$  or

$$A = Q^{1/3} \quad (13.1)$$

Naturally, a '2-second basin' is clearly double this volume. Having quickly found the overall dimensions, it is often convenient to adjust the shape by, for instance, halving the width and doubling the length. This gives the 'block' of liquid that the basin contains. It is important to remember now to double the height of the basin to give plenty of 'freeboard', so that the pourer can easily maintain the basin overfull, but never drop into the danger zone below the minimum height of liquid at which the filling system would become depressurized and thus be in danger of entrainment issues.

If a stopper is used and the basin is filled with the complete charge to fill the casting, the basin step becomes redundant since there is minimal transverse flow during the draining of the melt into the sprue. For this reason the step can be eliminated with the benefit that the basin, with the help of a sloping floor, can completely drain empty. Care is needed for such a technique to ensure that there remains sufficient head pressure to fill the outlying regions near the top of the casting. The condition for draining the basin but not losing head height by the melt dropping down the sprue has knife-edge criticality. For this reason a pyramid-shaped base to the basin allows nearly complete draining without significant loss of head condition to be less sensitively achieved.

Finally, the reader should not forget that all these concerns about basin design are eliminated at a stroke if the basin is eliminated. The basin should perhaps be considered an unnecessary evil. Contact pouring is a highly desirable system, not only eliminating the basin, but also eliminating the entrainment damage that inevitably occurs during the filling of the basin.

---

## 13.9 SPRUE (DOWN-RUNNER) DESIGN

Now that an initial rate of pouring has been chosen, how can we achieve it accurately, limiting the rate of delivery of metal to precisely this chosen value? Theoretically it can be achieved by tailoring

a funnel in the mold of exactly the right size to fit around a freely falling stream of metal, carrying just the right quantity (Figures 12.8 and 12.10). We call this our down-runner, or sprue.

The theoretical dimensions of the sprue can therefore be calculated as follows. If a stream of liquid is allowed to fall freely from a starting velocity of zero, then after falling a height  $h$  it will have reached velocity  $v$ . (The height  $h$  always refers to the height from the melt surface in the pouring basin. This zero datum is one of the great benefits of the offset basin compared to the conical basin, since the starting velocities can never be known with any accuracy when working with a conical basin.) Thus for a mass  $m$  falling with acceleration  $g$ , equating its loss of potential energy  $mgh$  with its gain in kinetic energy  $mv^2/2$ , we have

$$v = (2gh)^{1/2} \quad (13.2)$$

To obtain the sprue sizes it is necessary to realize that the low-velocity  $v_1$  at the top of the sprue must be associated with a large cross-sectional area  $A_1$ . At the base of the sprue the higher metal speed  $v_2$  is associated with a smaller area  $A_2$ . If the falling stream is continuous it is clear that conservation of matter dictates that:

$$Q = v_1A_1 = v_2A_2 = v_3A_3 \text{ etc.} \quad (13.3)$$

where subscript 3 can refer to any downstream location for the local values of the area of the stream and its velocity (for instance the area and velocity at the gates). Since the velocities are now known from the height that the melt has fallen (neglecting any losses due to friction at this stage), and  $Q$  has been decided, each of the areas of the filling system can now be calculated.

In nearly all previous treatises on running systems the important dimension of the sprue for controlling the precise rate of flow has been assumed to be the area of the exit. This part of the system has been assumed to act as 'the choke', regulating the rate of flow of metal throughout the whole running system. It is essential to revise this thinking. If the sprue is correctly designed to just touch the surface of the falling liquid at all points, the *whole sprue* is controlling (not just its exit). There is nothing special about the narrowest part at the sprue exit. We shall continue this concept so far as we can throughout the rest of the filling system, along the runner and through the gates; every section is providing some control. If we achieve the target of fitting the dimensions of the flow channels in the mold just to fit the natural shape of the flowing stream, it follows that no one part is exerting control. The whole system is all just as large as it needs to be; the channels of the filling system just touch the flowing stream at all points.

Even so, after such features as bends and filters and other complications, the energy losses are not known precisely. Thus there is a sense in which the sprue (not just its exit, remember) is doing a good job of controlling, but beyond this point the precision of control may be lost to some extent after those features that introduce imponderables to the flow. (In the fullness of time we hope to understand the features better. Even now, computers are starting to make useful inroads to this problem area.)

Thus, as long as the caster pours as fast as possible, attempting to fill the pouring basin as quickly as possible, and keeping the basin full during the whole of the pour, then he or she will have no influence on the rate of filling inside the mold; the sprue (the whole sprue, remember) will control the rate at which metal fills the mold.

For most accurate results it is best to calculate the sprue dimensions using the formulae given above, and using the alloy density to obtain the initial volume flow rate  $Q$ .

However, for many practical purposes we can take a short cut. It is possible to construct a useful nomogram for Al (Figure 13.5) assuming a liquid density of  $2500 \text{ kg m}^{-3}$  and for the dense alloys based on Fe and Cu assuming a liquid density around  $7500 \text{ kg m}^{-3}$  (these figures are not especially accurate, but allow for a simple nomogram without the introduction of unacceptable errors). Thus areas of sprues at the top and bottom can be read off, and the sprue shape formed simply by joining these areas by a straight taper. Preferably, it is simple to read off areas of the sprue at other intermediate levels to provide a more accurately defined sprue having a curved taper. Recall that the heights are measured in every case from the level of metal in the pouring basin, regarding this as the zero datum.

The nomogram is easy to use. For instance if we wish to pour an aluminum alloy casting at an average rate of  $1.0 \text{ kg s}^{-1}$ , corresponding, of course, to a design rate of  $2.0 \text{ kg s}^{-1}$ , Figure 13.5 is used as follows. The  $2.0 \text{ kg s}^{-1}$  rate with a depth in the basin (the top level down to the level of the sprue entrance) of

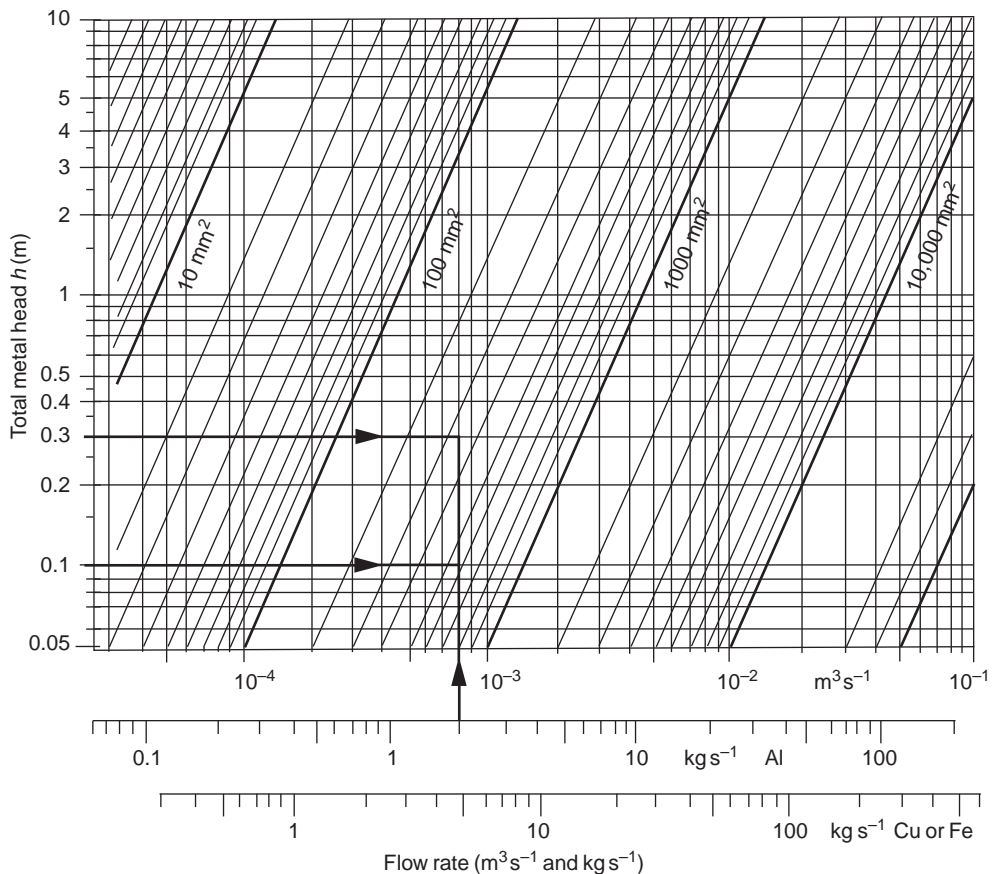


**FIGURE 13.5**

Nomogram giving approximate sprue areas ( $\text{mm}^2$ ) for light and dense metals as a function of flow rate and head height.

100 mm, and a sprue length of 200 mm (total head height from the top level of the melt in the basin = 300 mm), then its entrance and exit areas can be read from the figure as approximately 580 mm<sup>2</sup> and 330 mm<sup>2</sup> respectively. Remember that if the sprue shape is approximated to a straight taper, Section 12.2 advises to increase the area of the entrance by approximately 20% to compensate for errors, making the final straight taper sprue top close to 670 mm<sup>2</sup>. However, a better approach is to form a nicely shaped hyperbolically tapered sprue, which is easily defined from the nomogram, and is naturally accurate, avoiding any need for compensation for errors; it is not necessary to add the 20% to the sprue entrance area.

As a check on the nomogram read-outs for our aluminum alloy casting, we can now calculate the dimensions numerically using the equations given above. At 1.0 kg s<sup>-1</sup> average fill rate, corresponding to a design rate 2.0 kg s<sup>-1</sup>, assuming a liquid density of 2500 kg m<sup>-3</sup>, we obtain an initial volume flow rate  $Q = 2.0/2500 = 0.8 \times 10^{-3} \text{ m}^3 \text{ s}^{-1}$ . We can calculate that the falls of 100 mm and 300 mm are seen to cause the melt to accelerate to a velocity of 1.41 and 2.45 m s<sup>-1</sup>, giving areas of 566 and 327 mm<sup>2</sup> respectively. These values are in reasonable agreement with those taken directly from the nomogram.

The cross-section of the filling system can, of course, be round or square, or even some other shape, provided the area is correct (we are neglecting the small corrections required as a result of increased drag as sections deviate further from a circle). However, in view of making the best junction to the runner, a slot sprue and slot runner are strongly recommended for most purposes since they can be linked together in a way to preserve the streamlined flow. (Multiple sprues might be useful to connect to a number of runners. Several such sprues would be expected to work better than one large sprue as a result of improved constraint of the metal during its fall as discussed in Section 12.2.)

If we were to choose a slot shape for the sprue, convenient sizes might be in the region of 10 × 60 mm<sup>2</sup> entrance and 6.5 × 50 mm<sup>2</sup> exit. (If two sprues were used as shown in Figure 12.13a these areas would, of course, be halved.)

### Basin + sprue worked example

For a steel casting poured at an average rate 30 kg s<sup>-1</sup> and intended to be poured in 10 seconds:

$$\text{Average pour rate} = 3 \text{ kg s}^{-1}$$

$$\text{Design pour rate} = 6 \text{ kg s}^{-1}$$

$$\begin{aligned} \text{Volume flow rate } Q &= (6/7) \times 10^{-3} \text{ m}^3 \text{ s}^{-1} \text{ (density of liquid } 7 \times 10^3 \text{ kg m}^{-3}\text{)} \\ &= 0.86 \times 10^{-3} \text{ m}^3 \text{ s}^{-1} \end{aligned}$$

Assuming a basin with a minimum working depth  $h_1$  selected arbitrarily as 50 mm (but not forgetting that it would be safe to make this basin 100 mm deep, and aim to always fill above the 50 mm minimum):

$$\begin{aligned} \text{At sprue entrance velocity } V_1 &= (2gh_1)^{1/2} \\ &= (2 \times 9.81 \times 0.050)^{1/2} \\ &= (2 \times 10 \times 0.050)^{1/2} \text{ approximately (good enough to within 1\%)} \\ &= 1.0 \text{ m s}^{-1} \text{ (compared to the accurate result of } 0.99 \text{ m s}^{-1}\text{)} \end{aligned}$$

Since by definition we have  $Q = V \times A$

Where  $V$  is the velocity and  $A$  the area of the liquid stream, so that

$$\begin{aligned}\text{Sprue entrance area } A_1 &= Q/V_1 \\ &= 0.86 \times 10^{-3} / 1.0 \text{ m}^2 \\ &= 860 \text{ mm}^2 \\ &= 29 \text{ mm}^2 \text{ square or } 33 \text{ mm}^2 \text{ diameter}\end{aligned}$$

At sprue exit, if height of sprue is 200 mm, plus minimum height in basin 50 mm, total fall is 250 mm minimum.

$$\begin{aligned}\text{Velocity } V_2 &= (2 \times 10 \times 0.250)^{1/2} \\ &= 2.24 \text{ m s}^{-1}\end{aligned}$$

$$\begin{aligned}\text{Sprue exit area } A_2 &= Q/V_2 = 0.86 \times 10^{-3} / 2.24 \text{ m}^2 \\ &= 0.384 \times 10^{-3} \text{ m}^2 \\ &= 384 \text{ mm}^2 \\ &= 20 \text{ mm}^2 \text{ square or } 22 \text{ mm}^2 \text{ diameter}\end{aligned}$$

Instead of either a square or round sprue, it will be easier to make a good connection with the runner using a rectangular sprue. Taking therefore the entrance area as  $860 \text{ mm}^2$  we could use  $86 \times 10 \text{ mm}$ , but this is probably inconveniently wide. Hence we finally chose  $15 \times 60 \text{ mm}$  approximately (rounding up slightly) as an entrance. The exit area  $384 \text{ mm}^2$ , rounded up slightly to  $400 \text{ mm}^2$ , could then conveniently become  $10 \times 40$  approximately, giving a useful taper that will allow the sprue pattern to be molded easily, with a good draw angle on both faces of the rectangle.

If the decision were to go with the hyperbolic tapered sprue form, one of the few disadvantages is the reduction in draw angle as the sprue nears its base. For a tall sprue the bottom sections become nearly parallel, making withdrawal from a mold a challenge (but a worthwhile challenge of course!).

---

## 13.10 RUNNER DESIGN

Taking a simple turn from the sprue exit into the runner, we retain the same area  $400 \text{ mm}^2$  around the curve. The runner entrance will therefore have dimensions  $40 \text{ mm}$  wide by  $10 \text{ mm}$  deep. The inside radius of this turn should be at least approximately 1 or 2 times the thickness of the channel, thus we shall choose  $10 \text{ mm}$ , or if there is room on the pattern plate,  $20 \text{ mm}$ . Preferably the outside radius of the bend should be formed to give a parallel curve. If the outside curve cannot be molded and has to be left as a right angle, then the inside curve radius would be better reduced back to  $10 \text{ mm}$  to avoid the otherwise large volume that would be created in the right angle corner. Any unnecessary volume in the flow channels presents the risk of air bubble entrainment. The channels require to be as small as possible, while still delivering the required flow. Their small area will constrain the flow, preferably giving it no chance to fold over on itself, or jump or splash. It should fill the channel immediately, progressing as a piston to push the air ahead.

The melt will be traveling close to  $2.24 \text{ m s}^{-1}$ . The problem remains, 'How do we get the speed down from this value to at least  $1.0$  or preferably even  $0.5 \text{ m s}^{-1}$  at the gate *without* causing damage to

the flow en route?' This is *the* central problem for the design of a good filling system. This central problem seems in the past either to have been overlooked, or to have solutions proposed that do not work. At this point we need to appreciate the possible solutions with some care.

We only have a limited number of strategies for speed reduction. At this stage of the development of the technology the options appear to include:

- (i) Filtration.
- (ii) A number of right-angle bends in succession (Jolly et al. 2000). This reduces speed but is in great danger of introducing turbulent entrainment of air and oxides.
- (iii) A by-pass runner design acting in a surge control mode, calculated to introduce the melt through the gate at the correct initial rate for a sufficient time to cover the gate with a depth of metal. (The rate through the gate increases later of course when the surge container is full, but any jump or splash is now inhibited by the depth of metal in the mold above the gate.)
- (iv) The neglect of the problem of speed reduction in the runner, and simply tapering the runner to balance flow through a number of gates, making the total area of gates sufficient to correspond to, say,  $1 \text{ m s}^{-1}$ .

Considering our first option: if the filter reduces the flow rate by a factor of 5 then in principle the runner exit from the filter could be increased in area by a factor of five. We shall choose a value of 3 to give a good margin of safety, helping to ensure that if the filter is placed near the runner entrance, the downstream part of the runner is properly filled and slightly pressurized. Its area would then be  $3 \times 400 = 1200 \text{ mm}^2$ . The dimensions of the slot runner after the filter might then be  $12 \times 100 \text{ mm}$ . This is an unsatisfactory size of runner. The large width would be in danger of collapse because of mold expansion for a high melting point material such as an iron or steel cast in a silica sand mold (although the runner would be expected to survive for an Al alloy). In addition, the depth at 12 mm is too deep because the height of the progressing liquid, now moving at a modest speed under  $1.0 \text{ m s}^{-1}$ , will be only about 8 mm. Thus the runner will not initially fill the section, thus air cannot be pushed ahead in a kind of piston-like progression of the metal in the runner. This unsatisfactory size of runner forces us to abandon this approach.

It would perhaps be more convenient if the runner were divided into two runners of  $10 \times 60 \text{ mm}$ , or better still, three runners of dimensions  $8 \times 50 \text{ mm}$ . More runners would help to constrain the melt even more, helping to avoid air and oxide entrainment by encouraging the once-through filling mode (i.e. no room for the damaging action of reflected back-waves). Much depends on the layout of the mold and the filling system. Two runners might be more conveniently filled from two separate sprues, possibly exiting from the opposite ends of a suitably modified single basin, complete with a central pouring well and vertical steps either side as illustrated in Figure 12.13.

An alternative arrangement can be envisaged. Instead of placing the filter close to the runner entrance, the runner is continued at its  $10 \times 40 \text{ mm}$  size, and vertical gates rise from the runner, each containing a filter. The total area beyond the filters is required to be at least  $1200 \text{ mm}^2$  to ensure the melt enters the mold cavity without jetting. Care needs to be taken with this solution to ensure that the large gate areas do not create hot spots at the junction with the casting. The gates may therefore require to be slimmed down to narrow slots having half the thickness of the local thickness of the casting. The runner may require to be tapered depending on the particular geometry.

The second option, using a succession of right-angle bends, is only recommended if a good computer simulation package for flow in narrow filling systems is available to test the integrity of the



flow (most simulation packages do not predict flows accurately; most cannot cope with thin sections; and most cannot cope with surface tension). If a proven software package to simulate flow is available, a reasonable solution can be found largely by trial and error along the lines of the development described by Jolly et al. (2000). This approach is not described further here.

The third option can be a good solution. Figure 12.40 illustrates the layout. The gradual filling of the surge riser will cause the metal in the gate to experience a gradually higher filling pressure. At the point at which the surge riser is filled, the pressure comes on to the gate from the full height of the metal in the pouring basin. At this instant the casting should be filled to some depth at least 20 or 30 mm above the gate, so that any jetting into the mold when the full filling rate comes into effect will be to some extent suppressed. (The precise depth to suppress completely the formation of bifilms remains to be researched.)

As mentioned earlier, it is sensible to arrange the overflow, or surge riser, to be a cylinder and connected tangentially to the runner. In this way, by avoiding unnecessary turbulence and filling more progressively, the build-up of back-pressure to fill the gates is smoothed, and, not unimportantly, a better quality of metal is preserved in the cast surge riser for future recycling within the foundry.

The careful sizing of surge risers to suppress the early jetting of melt through the gates is strongly recommended. To the author's knowledge, the technique has been relatively little used so far. More experience with the technique will almost certainly lead to greater sophistication in its use. Unfortunately, it is complicated to calculate the dimensions of the components of this system. I recommend therefore that the dimensions for the system are first guessed on the basis of experience, and then tested by computer simulation. One or two iterations will normally result in a closely optimum solution.

Our fourth option, to accept the high speed in the runner, and simply work out the areas of gates needed to transfer melt into the mold at around  $1.0 \text{ m s}^{-1}$ , actually works satisfactorily well in a number of cases. These circumstances include:

1. Where the ingates are taken vertically off the runner into the casting the benefit of gravity to assist the gates to fill is useful, although the gates need to be reasonably long to gain the full benefit of this effect. I try always to make vertical gates at least 50 mm tall, but prefer 100 mm if I can get it.
2. Those instances where it is known the ingate velocity is not under good control, and still dangerously high, but the geometry inside the mold cavity does not allow significant turbulence. Thus if we can gate straight on to a core that defines a narrow wall section, the metal can spread under control of the narrow section, being too constrained to be able to jump or splash. The spreading front increases its area and consequently slows as it fills the narrow wall. This works well.

---

## 13.11 GATE DESIGN

In general, it is essential that the liquid metal flows through the gates at a speed lower than the critical velocity so as to enter the mold cavity smoothly. If the rate of entry is too high, causing the metal to fountain or splash in the mold cavity, the battle for quality has probably been lost.

The gate should enter at the very base of the casting, if possible at right angles onto a thin section, as has been described earlier. Gating horizontally directly across a flat floor of a casting is to be avoided if possible – a thin jet of metal skating across a flat surface is a recipe for mold expansion defects of

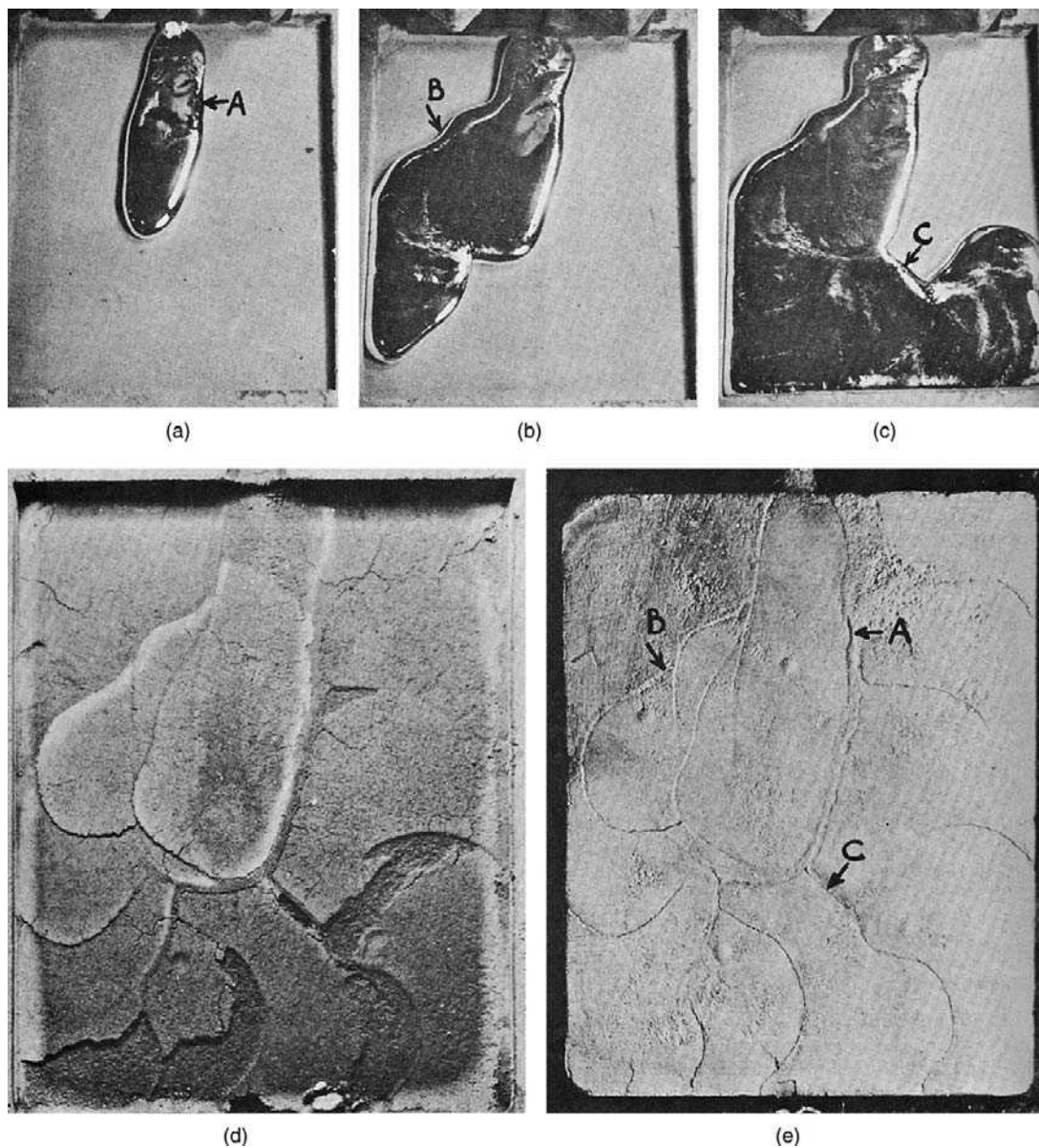


**FIGURE 13.6**

Relation between metal flow pattern over a horizontal surface and the development of rattails: (a, b, c) flow of metal; (d) the final mold surface; (e) the casting surface (image reversed to aid comparison) (Goad 1959).

various sorts that will spoil the surface of the casting as illustrated in Figure 13.6. The casting will also be at risk from the formation of an oxide flow tube that may constitute a serious internal discontinuity in the casting. A further risk is the filling of features on the far side of the casting from the gate; this metal is relatively cold and is vulnerable to the formation of cold laps. If possible, it is usually far better to ingate vertically into one edge of the casting, the melt emerging via slots in the floor of the casting. Such ingating causes the metal to swell slowly from the gate, roll nicely over the floor and up the walls of the casting, while keeping the advancing front warm by flow channel behavior, avoiding cold lap issues.

For our example casting, the velocity at the base of the sprue is  $2.45 \text{ m s}^{-1}$ . Thus to achieve  $0.5 \text{ m s}^{-1}$  through the gate(s), and if no friendly core is conveniently sited onto which to gate directly, we shall require an expansion of the area compared to that of the base of the sprue by a factor  $A_2/A_3 = 5$  approximately. In terms of the gating ratio much loved by the traditionalists among us, we are using 1:1:5 for this casting. The use of this size of gate assumes that we are gaining no advantage from a by-pass runner and surge rise design. If a good by-pass design could be devised an acceptable ratio might then become 1:1:1, effectively easing subsequent cut-off, and reducing any possible problems of hot spots or convection at this location.

Sometimes the by-pass cannot be provided. Even if available, it may be useful to use both the by-pass and the enlarged gate until such a time that our understanding of filling systems makes it clear that such belt-and-braces solutions are not required.

It is common for gates to be taken at right angles off a runner. Nafisi (2010) shows how the melt turns this right angle with difficulty, creating a vena contra and a vortex stirring pattern of flow in the gate. With gates at right angles to the runner it is necessary to reduce this problem by providing a generous radius to the inside of the bend. For the future, more sinuous designs of runner/gate connections will become the norm, like branches of a tree, or perhaps more appropriately, branches of a river. Such solutions have to be developed in terms of useful designs that the foundry person can implement easily and quickly. With the NC machining of tooling such options are looking attractive.

Where the gates form a T-junction with the casting, the maximum modulus of the gates should be half of that of the casting (if, as will be normal, no feeding is planned to be carried out via the gates). Thus, in general, the thickness of the gates needs to be less than half the thickness of the wall. This forces the shape of the gates to be usually of slot form. If made especially thin when casting alloys of good thermal conductivity, such as Al and Mg alloys, and some Cu alloys, the gate can sometimes be usefully employed to act as a cooling fin soon after the filling of the casting.

The other major consideration that must not be overlooked is the problem of the transverse, or lateral, velocity of the melt in the mold cavity as it spreads away from the ingate. This can easily exceed the critical velocity despite the velocity in the gate itself being correctly controlled. In this case a single gate may have to be divided to give multiple gates as described in Section 12.4.7.

The area of the gate required to reduce the gate velocity to below the critical velocity, and the limitations of its thickness, sometimes dictates a length of slot significantly longer than the casting. In this situation there is little choice but to revise the design of the filling system, selecting a correspondingly longer fill time so that the gate can be shortened to fit the length available. Alternatively, a by-pass runner design may be the solution. If a solution cannot be found, the conclusion has to be accepted that the casting as designed cannot be made so as to enjoy reliable properties and performance. A serious discussion with the designer will probably be required.

This page intentionally left blank

## SECTION

# Processing (melting, molding, casting, solidifying)

# 3

14	Melting .....	879
15	Molding.....	911
16	Casting.....	939
17	Controlled solidification techniques .....	1013
18	Dimensional accuracy.....	1025
19	Post-casting processing .....	1067

This page intentionally left blank

# Melting

# 14

The economics of melting is a key factor in foundry costing. For instance, if aluminum could be melted at 100% efficiency (i.e. no heat losses) to a temperature of 720°C, the energy required would be 320 kWh ton<sup>-1</sup>. For steel to 1600°C the requirement is nearly identical at 330 kWh t<sup>-1</sup>. Naturally, real furnaces tend to fall a long way from this ideal, so that although some achieve in the region of 650 kWh t<sup>-1</sup>, others are nearer double this. Furthermore, holding furnaces are essentially 100% *inefficient*, although for production and quality reasons their use may be valuable. In this account we shall not dwell much on the energy requirements and the economics, for it is the subject of many studies and publications.

In contrast, it is rare for the quality of melts to be considered. The quality can be significantly affected by the melting, holding and transfer techniques, and, of course, directly affects the quality and economics of production. This is the special subject of this section.

Steel foundries have a wide choice of melting furnaces. Nowadays only induction and arc type furnaces are generally employed in foundries. The older reverberatory roof designs such as the open hearth furnace are not generally used. Whatever the variety of furnace, from the point of view of quality of the liquid metal they produce, all varieties are probably capable of delivering a high-quality product. The special reason for this is the large density difference between liquid steel and its oxides in suspension, causing the oxides to float out relatively quickly.

It is regrettable that the oxides are usually efficiently re-introduced during the emptying of the furnace into the ladle, in which the melt performs a simulation of the Niagara Falls. The saving feature of this trauma is that much, but probably not all, of the damage detrains within minutes, floating to the surface to join the slag layer prior to the melt being cast.

The situation is quite different for aluminum alloys in which the oxides (and possibly nitrides) are similar in density to the melt, and so are resistant to separation by flotation or sedimentation. Thus aluminum and its alloys present special difficulties if a relatively clean melt is desired. We shall give some space below to an examination of this problem.

The lightweight magnesium alloys represent the opposite extreme, in which the oxide is significantly denser than the melt, and so sinks rapidly. The problem in this case is to avoid disturbing this sediment if a good melt quality is required.

---

## 14.1 BATCH MELTING

### 14.1.1 Liquid metal delivery

The delivery of liquid metal by tanker, often traveling many miles by road or rail from the smelter, is an obvious choice because it saves cost to the smelting company of having to solidify it into ingots, and saves the cost to the foundry of melting the material once again in-house. The logic seems inescapable.

For deliveries of liquid iron there may not be a problem. The author is aware of only one such example of iron in the UK that traveled about 30 km by railway.

For aluminum alloys, however, liquid delivery is much more common. Even so, the author remains concerned that the cost savings may be more apparent than real. It is worth discussing the issues below.

For those foundries that produce one-off castings, or small batches, especially if the castings are in the tonnage size range, the arrival of a large quantity of metal at one time would be ideal. However, these are the very organizations that prefer to organize their own supplies of melt, keeping timing and quality issues under their own control. Also, of course, from a melt supplier's point of view, a smelter needs a regular, predictable delivery schedule, not huge quantities at long and irregular intervals.

In high-volume operations the author favors melt systems in which the melt level never changes outside closely controlled limits. The abrupt arrival therefore of a huge mass of metal into the system is problematic. If uncontrolled it would cause large changes in metal level. Control measures involve costs in the form of large receiving furnaces that either tilt or are equipped with pumps or automatic ladling systems.

Typically, the melt is transferred from the tanker, empties down a chute, and cascades into a large holding furnace. The furnace is a large capital item, and its life not made easy by the washing of melt up and down its walls. Also, although melt losses from such units are not generally made known, one would expect a loss by the conversion of several percent of the melt to dross during this transfer. Up to half of the melting energy saving therefore disappears immediately in loss of metal. The depreciation, running and maintenance costs of the receiving furnace are a further loss.

For Al alloys, the loss that gives me most cause for concern, hidden and unsuspected, derives from the damage caused to the liquid metal by this traumatic transfer operation. The melt will be loaded with bifilms to the extent that it will be difficult to clean the melt sufficiently to make adequate castings. Downstream processes such as rotary degassing and sink-and-float holding furnaces can probably only eliminate a percentage of inclusions. If, for instance, the processing is successful to remove 90% of solids, the remaining 10% may still be sufficient to degrade the castings to the point of unacceptability in terms of its ductility.

Thus in summary, I find the supply of bulk liquid metals unattractive economically and technically.

### 14.1.2 Reverberatory furnaces

Melting in a shallow pool can most conveniently be carried out by heating from above. The use of flames to achieve this is not helpful if the flame is directed to impinge directly on the metal. In this way the melt is oxidized locally, and one would expect its hydrogen content to be increased. In addition, the transfer of heat in this way is not particularly efficient. Because the flame, directed across the melt tends to rise off the melt, it tends to heat the roof rather than the charge. This effect can be enhanced by ensuring that the flame is luminous (sometimes by adding carbonaceous additives to the fuel). In this way the roof becomes incandescent.

This is how the furnace got its name: heat from a luminous flame radiated to the refractory roof of a furnace is reverberated (i.e. reflected or re-radiated) to the melt below. The Siemens' open hearth furnace was an early example that made most of the high-quality steel in the world for many years. Later types of furnace using electrical heating elements in the roof have taken up the name of electrical reverberatory furnaces ('electric reverbs' for short!). Such furnaces for Al holding can typically transfer up to  $120 \text{ kW m}^{-2}$  to the melt.



The radiant roof principle has been useful for furnaces in which turbulence is at a minimum, since the melt is heated from the top, leaving the bottom significantly cooler, causing a stratified temperature gradient that promotes stable conditions, reducing convected stirring to a minimum.

Such stratified stability can be counter-productive on occasions. The author has vivid memories of working a 1000-kg resistance-heated radiant roof furnace containing nominally Al-7Si-0.4Mg alloy. An Al-10Mg ingot was slipped into the bath on a Friday evening to raise the Mg level from its low value of 0.3%Mg, where it had slowly fallen over the past week, back to 0.4%Mg. At the start of the next shift on Monday morning the Mg content of the furnace was checked. Everyone was aghast to discover that it had not changed, but if anything had fallen further. While we stood around baffled, a bright team member suggested that the ingot might have melted but its liquid metal might still be lying at the bottom of the furnace (its low temperature more than countering the fact that at 10%Mg the liquid might have been expected to float). This was found to be true. On stirring for a few minutes with a coated iron bar the whole melt rose to its expected 0.4%Mg content.

For Al alloy holding furnaces the stratification is eliminated by many users by a number of strategies; an immersed diffuser giving a train of bubbles will cause a local upwelling of the melt, and thus a gradual turnover. Other furnaces use more aggressive systems such as centrifugal or electromagnetic pumps particularly if melting is required to occur in the furnace; melting in holding furnaces is otherwise extremely slow because of the low thermal conductivity of liquid Al compared to solid Al. The author admits to all these uses being counter-productive to one of the main features of the Al alloy holding furnace; its utility in achieving some quiescence to allow the sink and float of inclusions, mainly bifilms of course, so as to achieve a good-quality melt.

The rotary furnace ensures no such stratification of the charge. These are occasionally seen in aluminum foundries. In addition to ensuring the homogeneity of the melt the design is thermally efficient because the heated roof is circulated under the melt where it can heat the charge most efficiently by direct contact. Such units can be useful for secondary smelters who wish to melt dross to recover the entrained aluminum alloy. The addition of a chloride flux based usually on common salt, sodium chloride, plus sometimes potassium chloride, significantly assists this process. For foundry use for Al alloys, however, the rotary furnace cannot be recommended because of the damaging amount of surface turbulence that it causes. The unit produces only rather poor-quality metal.

### 14.1.3 Crucible melting (electric resistance or gas heated)

In common with all bath and crucible-type melting processes, crucible melting necessarily includes everything that is 'thrown into the pot'. This self-evident fact is often overlooked, but in fact conceals the important feature of this melting technique; the surface oxide on the charge materials necessarily forms part of the melt. These primary oxide skins can represent a large content of thick oxides in suspension in the liquid metal. This is a good reason for not choosing a crucible furnace for metal supply in an aluminum foundry.

Panchanathan et al. (1965) found that when melting was carried out repeatedly on 99.5%Al progressively poorer mechanical properties were obtained. By the time the melt had been recycled eight times, the elongation values had fallen from approximately 30 to 20%. This is easily understood if the oxide content of the metal is progressively increased by repeated melting of castings.

The remelting of aluminum alloy sand castings probably represents one of the worst cases, since the oxide skin on a sand casting is particularly thick, having cooled from high temperature in the

aggressively moist oxidizing environment of the sand mold. When the skin is submerged in the melt it can float about, substantially complete. One day, when remelting scrapped cylinder heads by adding them to one end of a combined melting and holding furnace, the author has seen the skin of a complete cylinder head fished out from the opposite end of the furnace, complete with all details such as combustion chambers and ports. (Someone joked that we should fill it with liquid metal and re-sell it.) It is easy to understand how the condition of some melts can be so bad as to resemble a slurry of old sacks. Unfortunately this is not unusual.

The remelting of aluminum alloy gravity die (permanent molded) castings have an oxide skin that is much thinner, as a result of the relatively inert environment provided by the metal mold, and seem to give fewer problems. Whether this is a real or imagined advantage in view of the damage that can be caused by any entrained oxide skin, irrespective of its thickness, is not clear at this time.

A further problem with crucible melting is that the debris in suspension usually continues to circulate for long periods because the heating of the crucible is via its walls, creating an upward convective flow adjacent to the walls and down in the center of the melt. Although the rate of circulation is relatively gentle, the velocities will almost certainly exceed the Stokes settling velocity of the oxides. Thus oxides have little chance to separate by buoyancy, i.e. will be unable to sink or float.

A further aspect of crucible melting that has been little researched, and remains only a suspicion at this time, is the inexorable rise of iron contamination of Al alloys. Although iron tools are often blamed, many furnace operators take care to protect the implements from dissolution by a refractory wash coat. The suspicion is that at least some of the iron contamination arises from the reduction of iron impurities in the protective glazes or walls of some crucibles.

#### 14.1.4 Induction melting

Induction melting is another variety of crucible melting which suffers from the problem of all the surface oxide skins on the charge being included in the melt.

Although crucibles heated via their walls promote stirring of the melt, the induction furnace provides at least ten times the velocity of stirring. Thus the original surface oxides incorporated into the melt are efficiently maintained in suspension; the strong stirring component ensures that none separate by buoyancy. Furthermore, there remains the suspicion that the stirring action may be sufficiently vigorous to shred oxides, or even manufacture new surface oxide and entrain it in some way.

The particularly violent stirring in induction furnaces of high power to weight ratio (over approximately  $10 \text{ kW kg}^{-1}$ ) is seen in crucibles in which the melt is partially levitated by the inductive forces. This action almost certainly introduces oxide by the continuous fluctuations in the area of the surface as the melt shudders and wobbles like an unsupported jelly. These conditions typify melting in water-cooled copper crucibles known as the skull-melting process, so-called from the original hemispherical crucibles against which a shell of solid was solidified during the melting process. On lifting this from the crucible after pouring, the residue resembled a skull cap. Thus skull melting would be expected to introduce masses of oxides (although this fact has never been proven).

#### 14.1.5 Automatic bottom pouring

Automatic bottom pouring is a technique used in the investment casting industry for the vacuum melting and casting of lost-wax molds. It is a surprisingly simple process invented by Alec Allen in the

UK in 1966. A hole in the base of a refractory melting crucible was covered by a cylindrical slug of metallic charge (often steels or Ni-base alloys) that was a close fit in the crucible. The slug was melted rapidly by induction. The rapidity of the melting meant that a low-cost disposable sand crucible was normally adequate. The last part of the charge to melt was the portion over the hole. When this melted the liquid metal poured through into the mold below. A variant of the process used a small coin-sized disc that fitted into a recess above the hole. The temperature of the pour could be controlled by selection of the thickness of the disc.

However, of course, a significant issue is the procurement of a pre-alloyed charge of exactly the size to fit the crucible and exactly the weight required by the casting. Moreover, of course, the Achilles' heel of this approach is simply the pour. Practically all processes that pour metal create defects. Regrettably, casting technology needs to get away from pouring.

The push-up base crucible process is a similarly rapid 'just-in-time' melt production and casting technique that uses pre-prepared 'logs' for melting, but achieves the avoidance of pouring by a commendably elegant technique. It is described with the counter-gravity casting processes in Section 16.3.

## 14.2 CONTINUOUS MELTING

### 14.2.1 Tower (shaft) furnaces

The tower or shaft furnace is one of the most efficient melting units, since it is a true counter-current heat exchanger. Cold charge enters at the top of the tower and slowly descends, while spent gases from the melting zone pass up the tower, preheating the charge prior to its arrival in the melting zone, and cooling the gases before they emerge from the top of the shaft.

The cupola; a shaft furnace for iron

Iron foundries have had the benefit of such a furnace for many years in the form of the cupola. Because the melted iron passes over a deep bed of incandescent coke, it can be heated to a high temperature if necessary. The skilled furnace manager can manipulate and hold the metal temperature and composition with impressive precision.

Only recently has the coke-fired cupola started to give way to induction melting, mainly not because of inefficiency, but because of the twin problems of obtaining good-quality coke, and controlling the effluent into the environment from the top of the stack.

Some moves have been made towards the gas-fired cupola. Here the melting stack is supported not by coke, but by a bed of refractory spheres. Unfortunately, the spheres are eroded quickly by attempts to produce metal at a high temperature, greatly increasing costs. Thus the gas-fired cupola has much in common with dry hearth furnaces, in which liquid metal is produced at temperatures only just above the melting point of the metal or alloy. The gas-fired cupola is therefore said to be a good melter, but poor superheater of metal. A duplexing operation is an efficient solution in which an induction-heated holding furnace raises the temperature of the cupola iron to that required for casting.

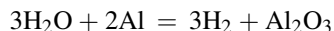
The sink and float issues that are so important in the melting of aluminum alloys hardly apply in the case of the melting of irons and steels. This is simply because of the great density difference that the heavy metals enjoy with respect to entrained defects. Detrainment of harmful entrained bifilms in these metals is fast not only because of the larger density difference, but also because of the much higher

temperatures, causing the entrained surface films to be molten or at least partially molten. Thus the entrainment defects are compact and resistant to any unfurling action, being either spherical liquid drops or compact sticky masses that can float out quickly despite strong convective stirring. Those microscopic silica-based bifilms that are predicted to be present in liquid iron seem, fortunately, to remain in suspension for much longer periods, although the Monday morning melt quality from an induction furnace usually requires some attention.

### 14.2.2 Dry hearth furnaces for non-ferrous metals

For aluminum alloys the vertical shaft furnace has become popular in recent years for good reason. The base of the tower is usually a gentle slope of refractory on which the charge in the tower is supported. In addition to its melting efficiency because of the excellent use of the heat available from the combustion gases, the unit can provide unusually clean metal. This is because the outer oxide skins on the charge do not enter the melt, but are left in place on the dry hearth; the pieces of charge collapse like punctured balloons as the melt escapes as a little stream via a hole in the skin, and flows as a cool liquid, practically at its melting point, out of the skin of the melting materials, down the hearth, traveling through an extended oxide tube, and into the bulk of the melt. After its arrival in a holding volume, where some homogenization of the melt can take place, it is also brought up to a useful casting temperature. The outer oxide skins pile up on the dry hearth and are raked off from time to time via a side door.

The concern that this type of furnace might result in a high hydrogen content in the melt from the volume of preheating 'wet' combustion gases seems unfounded. It is true that as the moisture content of the environment of an Al alloy melt increases, the hydrogen level of the melt increases because of the well-known reaction:



Thus one would expect from the thermodynamics that higher moisture would necessarily lead to higher hydrogen levels in the melt. However, above a certain limiting concentration of moisture, the character of the oxide on the solid metal in the charge changes, becoming more resistant to further oxidation and the consequent absorption of hydrogen. Thus, somewhat counter-intuitively, the very high moisture content of the spent gases acts to resist the rapid take-up of hydrogen by favorably affecting the kinetics, despite the unfavorable thermodynamics.

A variant of this type of melting furnace is the use of a reverberatory type of dry hearth unit in which the heat of the melting gases is recovered by the use of recuperative burners (i.e. burners that recoup, or recover, the heat). Such combustion units operate in pairs, with one burner firing at a time, the hot spent gases being used to preheat the recuperator system for the second burner. When the incoming gases for the first burner have cooled its recuperator sufficiently, the heating switches to the second burner and so on. The useful feature of this design is that similar melting efficiencies to the tower design can be achieved, but roof height requirements are greatly reduced, and the loading of the furnace can be achieved at floor level by fork lift truck.

The consequence of these benefits is that the author views the dry hearth tower and dry hearth recuperative melters as the best options for the melting of Al alloys.

These benefits have extended to the melting of copper in an Asarco-type furnace. Again, the design is a simple tower, gas heated at its base, and equipped with a dry hearth.

The remaining key feature of all the dry hearth melters is that they necessarily produce liquid metal at only just above its melting point. This may be an advantage or disadvantage depending on circumstances. Because of the very low temperature of the liquid metal, the melt has a relatively low gas content. For many casting systems, therefore, a second furnace or combined second chamber will be required to raise the temperature of the liquid up to a convenient casting temperature.

A second feature of the dry hearth is that the system can provide liquid metal 'on tap', i.e. as a just-in-time delivery system. Thus a large inventory of liquid metal is not required in the melt supply. It can be switched on or off, or simply increased or decreased in rate simply by turning up or down the burners at the base of the stack.

Some caution is required when using the furnace in this mode for those aluminum alloys containing high levels of copper. In this case there is a danger related to such changes in rate; the chemical analysis of the delivered metal changes somewhat. This follows because on slowing down the rate of delivery the eutectic continues to melt and flow for longer, causing the melt to become enriched in solute. Conversely, on speeding up the delivery rate the first metal to melt is now depleted in eutectic, and so is lower in solute.

For this reason the furnaces are better used continuously, with only gradual changes in rate so far as possible if high-Cu alloys are being used, or are necessarily connected to a holding furnace in which the melt can be homogenized as described below. Also, naturally, the furnace is designed to work at greatest efficiency when working near its maximum rate. Thus slow or zero rate melting will be costly if carried out to excess.

The additional advantage of a dry hearth furnace for aluminum alloys is that foundry returns that contain iron or steel cast-in inserts (such as the iron liners of cylinder blocks or valve seats in cylinder heads) can be recycled. The inserts remain on the hearth and can, from time to time, be raked clear, together with all the dross of oxide skins from the charge materials. (A dross consists of oxides with entrapped liquid metal. Thus most dross contains between 50 and 80% metal, making the recovery of aluminum from dross economically valuable.)

The benefits of melting in a dry hearth furnace are, of course, eliminated at a stroke by the misguided enthusiasm of the operator, who, thinking he is keeping the furnace clean and tidy, and thinking that the heap of remaining oxide debris sitting on the hearth will all make good castings, shoves the heap down the slope and into the melt. Unfortunately, it is probably slightly less effort to push the dross downhill, rather than rake it out of the furnace through the side door. The message is clear, but we require to remind ourselves frequently: Good technology alone will not produce good castings. Good training and vigilant management remain essential. My old foundry manager used to warn me 'You need at least six pairs of eyes to run a foundry.'

---

## 14.3 HOLDING, TRANSFER AND DISTRIBUTION

The function of a holder is generally well known. It is a reservoir intended to smooth rate changes between melt production and consumption, and allows the smoothing or adjustment of both composition and temperature. However, holding furnaces can have a significant effect on melt quality since they allow time for detrainment of defects by sedimentation or flotation.

However, the effectiveness of the holder in achieving these goals depends strongly on the method of heating, and the operating practice.

For Al alloys, a reverberatory (i.e. roof reflecting) furnace is always recommended. Here the heat transfer from electrical elements or from a fuel flame is obtained by heating the roof, which then radiates its heat down to the melt surface. The formation of dross is minimized by the uniform distribution of heat over the whole surface of the melt. (This action contrasts with the practice of directing a flame directly onto the surface of the melt. The higher local concentration of heat is suspected to lead to a higher rate of hydrogen pick-up. In addition, the higher temperature and the constant mechanical agitation of the surface will increase dross formation.)

However, heating from above causes a stratification of the metal in the bath. The stratification ensures that any added metal does not mix, but simply finds its own level according to its density, and then travels in a straight line to the exit point, by-passing all the other metal layers above and below, which remain stagnant in the furnace. Its composition is marginally smoothed by a small amount of turbulent mixing, and a minor contribution from diffusive interchange with layers above and below. However, clearly, the smoothing action is not achieved with the effectiveness that might be expected since most metal in the furnace remains unaware that any other metal has passed through the system.

This problem is not expected to arise with a more recent design of holder that uses immersion heaters. The immersed, close-ended tubes consist of a ceramic such as SiC that exhibits good thermal conductivity and good resistance to attack by liquid aluminum. The tubes can be heated internally by gas or by electrical elements. In this way heat is provided directly and at considerable depth in the melt, with the result that the melt against the walls of the heater tube generate a convective upwards flow that drives a circulation in the whole bath.

Other techniques to circulate the melt are common, by, for instance, the passage of bubbles of inert gas from a diffuser, or by the action of a rotary degasser. Other relatively common techniques include the use of an immersed electromagnetic pump, or electromagnetic pump sited on the outer wall of the furnace, but inducing a motion in the melt through the wall.

Holders for cast irons are generally heated by gas or induction or both. If induction is used the melt will certainly be well mixed.

For those holders that are stirred by some means any changes of temperature or chemistry are, of course, smoothed with maximum effectiveness. However, in the case of the production of Al alloy melts, such stirring action acts in opposition to one of the most valuable functions of the holding furnace, that of allowing inclusions to sink or float.

For Al alloys the principal and most damaging inclusion is the bifilm. Since this has close to neutral buoyancy, its settling velocity is often much less than a velocity that can be imposed by stirring. Thus if the melt is stirred the defect can remain in circulation, never settling. In the view of the author, the effects of small changes to the composition of the melt and its gas content are generally insignificant compared with the effect of the presence of bifilms. Thus our thinking regarding operation of a holding furnace is required to be re-thought. On balance, I am of the opinion that a holder should be left to itself, because most melt treatments are probably counter-productive. An Al alloy melt benefits from quiet neglect.

The Cosworth Process was perhaps the first to acknowledge that for liquid aluminum alloys the oxide inclusions in a holding furnace could be encouraged to separate simply by a sink and float principle; the metal for casting being taken by a pump from a point at about midway depth where the best-quality metal was to be expected. Degassing by argon bubbling was almost certainly counter-productive to melt quality by creating a circulation that retained bifilms in suspension.

The holding of melts in a closed pressurizable vessel for the low-pressure die casting of aluminum, or dosing the liquid metal, is usually impaired by the initial turbulent pour of the melt to fill the furnace. The total pour height is often of the order of a meter or more. Not only are new oxides folded into the melt in this pouring action, but those oxides that have settled to the floor of the furnace since the last filling operation are stirred into the melt once again.

A design by the author, patented by the company Alotech, illustrates that simple equipment such as a holding furnace for liquid aluminum is capable of considerable sophistication, leading to the production of greatly improved processing and products (Grassi and Campbell 2008). It avoids convection and the disadvantages of stratification by making the bath shallow. Degassing occurs passively by the diffusion of hydrogen out of the shallow layer of metal into a counter-current flow of nitrogen, thus avoiding any disturbance of the melt (such as would occur with rotary degassing for instance). The sedimentation of bifilms is encouraged to the maximum extent by the elimination of stirring. It takes the concept of melt cleaning and degassing to an ultimate level that might represent a limit to what can be achieved. In addition, the technique is simple, low capital cost, low running cost, has no moving parts and is operator-free. At this time the technique is being applied only to aluminum alloys.

The other feature of this technique for obtaining ultraclean and degassed metal is the transfer of the metal into the mold without the re-introduction of defects, necessitating a connection to a casting station by pipework with no moving parts, and casting by counter-gravity or another variety of non-turbulent transfer into molds.

### 14.3.1 Holder failure modes

Cracks in the refractory lining of the furnace, filled with liquid metal, give a high conductivity path for leakage of heat from the furnace, with the result that if the leak reaches the outer steel shell, that portion of the shell becomes extremely hot, and may be dangerous to touch. If the heat input to the furnace is limited, such leaks sometimes give problems to maintain temperature in the furnace. For this reason, furnaces with unheated extensions to form a pump well, or dipping area, are especially troublesome. I personally no longer favor holder designs of furnaces with unheated extensions because, on the development of a leak, they sometimes become so cool that despite maximum heat input to the main body of the furnace, threatening the refractories and the life of the furnace, casting still remains impossible. There is then no option but to shut down, drain the furnace and repair the lining. This usually takes a week or more.

A new lining dries quickly if numerous holes are provided all over and under the furnace body shell. Steam and sometimes water escapes from the holes to aid the drying process, which can otherwise take weeks, with metal remaining uncastable because of high hydrogen content. All holding furnaces should be specified with a mass of drying holes all over the steel shell, otherwise they are rarely provided by the furnace manufacturer.

It is best never to shut down a furnace. If a furnace is shut down, cooling and shrinking of the lining causes it to pull away from the crushable back-up insulation and create a gap between the hot face and back-up insulation. The loss of mechanical support endangers the lining. Most of the lining shrinkage is caused by the contraction of the aluminum in cracks of the lining. Aluminum alloys have a linear contraction of about 1.3% from the melting temperature down to room temperature. For this reason it is best to keep holding furnaces close to their operating temperature throughout their life. Over

shut-down periods the temperature might be reduced a little. It is safest to cool the furnace only to just below the solidus temperature so that no run-out disasters can occur while the furnace is unattended. The refractories therefore remain dry and ready for a quick start to production after the shut-down period.

### 14.3.2 Transfer and distribution systems

The tilting of large furnaces and the pouring of melts into ladles to be transported by overhead crane or forklift truck are damaging to the metal and dangerous to personnel. The melt losses on each pour are probably of the order of 1% each time, representing a significant hidden loss. If furnaces can remain static, and if melts can be piped around the foundry without moving parts, without damage to the melt, and never seen by operators, this is an ideal. This ideal standard is often not attained for a variety of reasons.

Siphons are widely used in Al reduction plants to transfer the newly won metal out of the reduction cells for further processing. Siphons have occasionally been used in foundries. However, although these devices might appear attractive at first sight, their design is generally poor, involving the displacement of the melt to a significant height by vacuum, only to allow it to cascade down a uniform tube into the awaiting vessel (Pechiney 1977). Thus the existing designs degrade the melt significantly.

For low-melting-point metals, such as lead and zinc, it is possible to arrange distribution conveniently and successfully via heated pipes. The concept of metal on tap at various points around the foundry has also been applied to a more limited degree for liquid magnesium alloys.

For liquid aluminum alloys, the distribution by pipe is less easily achieved, but can be arranged via a horizontal U-shaped channel generally known as a launder. These long horizontal channels resemble Roman aqueducts, and can be many tens of meters in length, and generally heated by an electrical resistance element in the roof lids.

Good insulation and tight-fitting lids ensure that the power consumption is only a kW or so per meter. In addition, the melt is protected from the atmosphere to some degree, reducing oxidation. The launder can connect melting and holding furnaces and all the casting stations without the need for human interference. Thus at the point of delivery of the melt the gentle flow will have had chance to detrain bifilms, and so is expected to be in excellent condition and at the correct temperature.

Naturally, a launder system is only of use in foundries casting one or perhaps two alloys. Also, any risk of loss of power requires an emergency generator. However, where appropriate, a launder distribution has many advantages (Sieurin 1974, 1975). In practice, it is a pity that the benefits of this excellent distribution system are often lost at the point of delivery by a waterfall into a mold, or by a turbulence-inducing dipping bucket system. It is not necessary to organize the foundry so badly.

---

## 14.4 MELT TREATMENTS

### 14.4.1 Degassing

Gases dissolved in melts are disadvantageous because they precipitate in bifilms and cause them to unfurl. Having unfurled and at that stage starting to behave as a slightly open crack, the precipitation of yet more gas might further inflate the bifilm to create porosity. Each of these stages is accompanied by the progressive reduction in the mechanical properties of the cast product.



The degassing treatments for steels include deoxidation by various chemical additives such as Si, Mn, and Al and possibly the use of a carbon boil to reduce hydrogen; the CO bubbles flushing the hydrogen from the melt. Alternatively the use of reduced pressure and the bubbling of inert gas through the melt in an argon/oxygen degassing (AOD) vessel is relatively widely used in steel foundries. These treatments are outlined in Section 6.6.

Degassing treatments for the various copper alloys are dealt with in Section 6.4.

The remainder of this section concentrates mainly on the various treatments for the Al- and Mg-based light alloys. For these metals there is no way to degass by chemical reaction. The only options are various physical techniques.

### Passive degassing

Degassing passively is degassing by doing nothing. One just waits. This is a technique that is generally surprisingly successful. It is based on the fact that even if the atmosphere is practically saturated with water vapor, the hydrogen content of the melt in equilibrium with the atmosphere is not especially high and remains suitable for most products.

It does require that the melt is not surrounded by a blanket of wet refractories in, for instance, a crucible furnace that has been allowed to sit unused for a day or more. Since refractories can absorb up to 10 wt% water the use of a furnace started up from cold is a serious risk. The outgassing of the refractories will provide a 100% water vapor atmosphere to surround the crucible, and will almost certainly permeate the crucible to attack the melt. Keeping furnaces hot to avoid moisture pick-up is to be recommended.

Even an induction furnace can continue to give a 100% water vapor environment to a melt for days or possibly weeks after the installation of a new lining. This is because the water is driven through the refractories, and condenses on the water-cooled induction coils. It can remain here for a long time, constituting a reservoir to maintain the 100% water vapor atmosphere that will permeate the refractories of the furnace.

The reader should note that these sources of water vapor in the body of the furnace counter those degassing processes that attempt to remove gases by protecting the melt surface or by bubbling through the bulk, as is discussed below. Whether these surface or bulk degassing processes will be effective will depend on whether they exceed the rate of regassing via the surfaces in contact with the refractories that contain the 100% water vapor. Even if the degassing process is reasonably successful, as soon as degassing is stopped, regassing will continue unabated, raising the gas levels yet again (Chen et al. 1994).

Clearly, there is no substitute for a dry furnace. Perhaps induction furnace suppliers could think about heating their induction coils until water is eliminated. It would be a great help to founders.

### Liquid argon shield

The dripping or pouring of a small stream of liquid argon onto the surface of a melt has been carried out for relatively small melts, particularly in investment foundries, for many years (Anderson et al. 1989). The liquefied gas is of course much lighter and perfectly immiscible with the liquid metal, but is heavier than air, and thus spreads over the surface of the melt. It boils off steadily, expanding by 600 times in its volume, thus carrying away volatile emissions from the environment of the surface. The technique has been applied with apparent success to melts of steels, Ni-base and Al-base alloys (Figure 14.1).

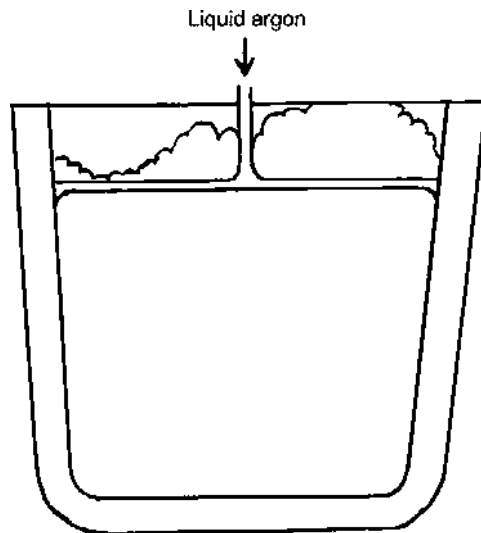


**FIGURE 14.1**

Protection of the surface of the melt by the addition of liquid argon.

Although the liquefied gas is at cryogenic temperatures, its effect on the cooling of the melt is negligible because of its low thermal capacity, and the relatively poor rate of heat exchange from the melt. The liquefied gas gains heat only by direct contact with the melt; the radiant heat passing through the transparent liquid ineffectively.

The method is not recommended for induction melting involving vigorous stirring in view of the danger of entrapping the liquefied gas under the melt to cause ejection or explosion of the melt. There is also claimed to be an occasional problem with the condensation of moisture from the atmosphere contaminating the addition (Zurecki and Best 1996).

### Gaseous argon shield

It is often found to be counter-productive to inject an inert gas onto the surface of a melt in the hope that this might somehow protect the melt and thus reduce its gas content. Usually the gas content increases. The reason for this is that the injected gas entrains with it at least an equal volume of air, which is now driven across the melt surface, equilibrating with the melt. Thus the indiscriminate addition of inert gas introduces the environmental gas, usually air, undermining any benefit.

Zurecki and Best (1996) describe the blanketing of ferrous and non-ferrous melts with gaseous argon. Significantly, the argon is injected tangentially against the melt surface, and is circulated and contained within a lightweight refractory cone (Figure 14.2). The injection of the gas parallel to the inner walls of the cone avoids the entrainment of air, and the swirling technique organizes the gas so that the rate of gas usage is highly efficient. The heated and expanded gas finally escapes from the top of the cone. The authors describe how the technique improves metal yield and the recovery of alloy additions. It also reduces slag build-up and crucible maintenance.

These techniques for degassing from the open surface of the melt rely, of course, on convection within the bulk to circulate the melt to within a diffusion distance of the surface.

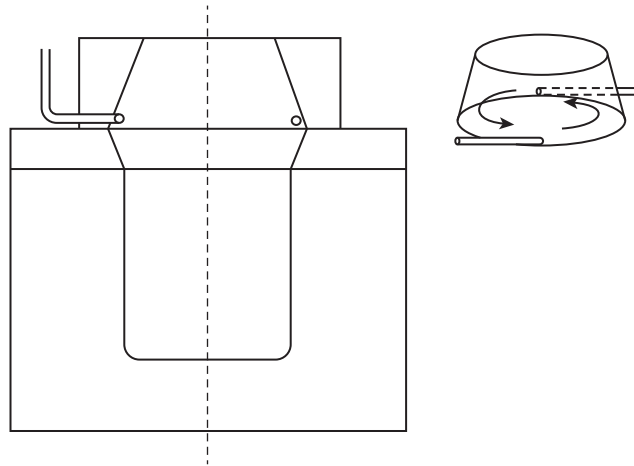


**FIGURE 14.2**

Protection of the surface of the melt by delivery of argon gas via a swirling action.

### Bulk degassing by bubbles

Traditionally the steel industry has used the naturally occurring bubble technique of a ‘carbon boil’, in which the creation and floating out of carbon monoxide bubbles from the melt carries away unwanted gases such as hydrogen (passively by simple flushing action) and oxygen (actively by chemical reaction with carbon). The nitrogen in the melt may go up or down depending on its starting value and the nitrogen content of the environment above the melt, since it will tend to equilibrate with the environment.

Hydrogen is a big issue for steel foundries making very large castings such as back-up rolls for rolling mills. These castings are too large, having diffusion distances too great for hydrogen, which could therefore not diffuse out and escape during subsequent heat treatments. The castings were therefore in danger of suffering failure by hydrogen cracking. To reduce the hydrogen level prior to casting, a typical practice would be to take a sample at melt-out to check the hydrogen content. If this was above 4 ppm, then a 0.4% carbon boil had to be induced, before taking off the oxidizing slag and recarburizing under a reducing slag. This had to be carried out as quickly as possible as the hydrogen would start to climb, threatening to return the analysis to its starting value while the furnace lining continued to deteriorate. The furnace hands would explain that these problems always seemed to occur on a Friday when everybody wanted an early finish.

The more recent oxygen steelmaking processes in which oxygen is injected into the melt certainly reduce hydrogen and nitrogen, but, of course, raise the oxygen in the melt. The oxygen requires to be subsequently reduced either chemically by reaction with C or other deoxidizers such as Si, Mn, or Al, etc., or use even more modern techniques such as AOD (argon-oxygen-decarburization) in special vessels. We shall not dwell further on these sophistications, since these specialized techniques, claimed to be well understood and well developed for steel, are almost unused elsewhere in the casting industry. Even so, there is some recent evidence that the simple use of non-entraining filling system designs for castings might eliminate the need for these complex and expensive treatments (Puhakka 2011). If proven to be true this would be a revolutionary step forward for steel casters.

By comparison, the approaches to the degassing of aluminum alloys, containing only hydrogen, has for many years been primitive. Only recently have more effective techniques been introduced, and even these involve some uncertainty and appear to introduce some counter-productive effects.

For instance until approximately 1980, aluminum was commonly degassed using immersed tablets of hexachlorethane ( $C_2Cl_6$ ) which thermally degrade in the melt to release large bubbles of chlorine and carbon (the latter as smoke). Alternatively, a primitive tube lance was used to introduce a gas such as nitrogen or argon. Again large bubbles of the gas were formed. These techniques involving the generation of large bubbles were so inefficient that little dissolved gas could be removed, but the creation of large areas of fresh melt to the atmosphere each time a bubble burst at the surface of the melt provided an excellent opportunity for the melt to equilibrate with the environment. Thus on a dry day the degassing effect might be acceptable. On a damp day, or when the flue gases from the gas-fired furnace were suffering poor extraction, the melt could gain hydrogen faster than it could lose it. This poor rate of degassing, combined with the high rate of re-gassing from interaction with the environment, led to variable and unsatisfactory results. Further complication arose from the significant entrainment of new oxides and chlorides from the melt surface, as a result of the major disturbance from the bursting of large bubbles of escaping gas. The creation of oxides was probably enhanced if the tablets were slightly damp. Overall, it is likely that most melts were significantly damaged by the use of hexachlorethane tablets. This primitive technique cannot be recommended.

The introduction of inert gas into a melt using a lance has mixed results. The technique is inefficient because of the large bubble size, giving a relatively small total area for the exchange of gases. In addition, the bursting of large bubbles at the melt surface creates opportunity for enhanced equilibration with the environment, plus the creation of fresh oxide bifilms as the bubble opens to the atmosphere.

The situation is greatly improved by the provision of a porous refractory diffuser on the end of the lance, or the setting of a porous brick diffuser in the base of the furnace or ladle. The much finer bubbles are significantly more effective in eliminating gas because of their significantly larger total surface area, and the smaller distance between bubbles reduces the diffusion distance for hydrogen to escape.

Even so, a considerable part of the benefit of degassing is not merely the degassing action. The action of the bubbles to eliminate oxide bifilms has in general been overlooked. It is assumed that the millions of tiny bubbles attach to oxides in the melt and float them to the top, where they can be skimmed off. Thus the melt is cleared, at least partially, of oxide bifilms. This will almost certainly result in a greater benefit to the castings than the mere reduction of gas content.

The size of bubbles in relation to the efficiency of removal of films is probably critical. For instance, large bubbles will displace large volumes of melt during their rise to the surface, their laminar streamlines displacing bifilms sideways, so that the bifilm and bubble never make contact (Figure 14.3). Haugland and Engh (1977) use a water model to observe particles sliding around a bubble surface in the boundary layer of the bubble, but still avoiding contact.

On the other hand, small bubbles will displace relatively little liquid, and so be able to impact on relatively large bifilms in their path. Thus large bifilms will be contacted, collecting smaller bubbles beneath them, and will be buoyed up to the surface. In this way the large oxide skins from the charge materials, measuring fractions of a meter across, are easily and quickly floated out. This is a major benefit that castings did not enjoy until the arrival of effective bubble techniques.

It follows that the smallest oxide that can be removed by a bubble is approximately the same size as the bubble, thus there is definitely an advantage to move to smaller bubbles to scavenge the melt clean

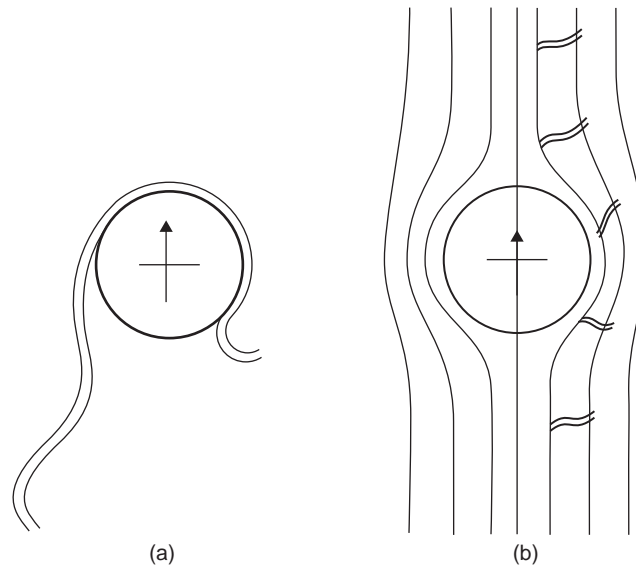


**FIGURE 14.3**

For given size of bubble (a) larger-sized bifilms are easily floated out, whereas (b) small bifilms follow the streamlines of the rising bubble, and so do not contact the bubble.

down to smaller oxide sizes. Since the smallest bubbles in melts are usually measured in millimeters as seen from Figure 10.12, it follows that oxides smaller than this will be expected to be unaffected by this flotation process.

The reader will by now appreciate that although these techniques are universally known as ‘degassing techniques’, since their use results in reduced porosity in the casting, a powerful but largely unappreciated benefit is the removal of significant quantities of oxide bifilms. This benefit was explicitly appreciated by the researchers Lasz and Laty as long ago as 1991. Curiously, however, this important fact remains stubbornly and consistently overlooked, to the great detriment of explanations of how bubble ‘degassing’ works to improve the soundness of castings.

### Rotary degassing of Al alloys

Rotary degassing appeared to come to the rescue of the Al casting industry. The use of a rapidly rotating rotor to chop jets of inert gas into fine bubbles that rose as clouds through the melt raised the rate of degassing in comparison with the normal rates of re-gassing. Thus effective degassing could be reliably achieved in times that were acceptable in a production environment.

The use of an ‘inert’ gas is a convenient untruth. Even sources of high-purity inert gas contain sufficient oxygen as an impurity to create an oxide film on the inside of the surface of the bubbles. Thus millions of very thin bifilms must be created during the degassing process. For a new rotor, or after a weekend, the rotor and its shaft will have absorbed considerable quantities of water vapor (most refractories can commonly absorb water up to 10% of their weight). Furthermore, the gas lines are usually not clean, or contain long rubber or plastic tubing. These materials absorb and therefore leak

large quantities of volatiles into the degassing line. Thus by the time the gas arrives in the melt it is usually not particularly inert. Also, of course, the bursting of bubbles at the surface of the melt is certain to introduce some oxides, and possibly nitrides. At this time no-one knows whether the inclusions created as by-products of degassing are negligible or whether they seriously reduce properties. What is known is that despite expected counter-productive effects such as the generation of millions of smaller oxides, aluminum alloys are usually improved by rotary degassing. Whether the counter-productive effects can be reduced to secure further improvements is not clear.

Rotary degassing was introduced as an attempt to reduce bubble size and therefore improve degassing effectiveness. This seems to have been achieved, but is but one benefit to be set against a number of disadvantages and uncertainties. Despite a great number of researches into rotary degassing many imponderables remain, especially concerning the oxide population of the melt, which most researchers overlook in their preoccupation with the gas content.

For instance, it seems that prior to degassing the melt contains mainly spinel bifilms, large but few in number, suggestive that these represent the oxide skins from the charge. After rotary degassing the melt contains masses of fine, pure alumina bifilms (Enright 1998). The masses of fine alumina bifilms created during the degassing process seem likely to be the reason why inclusion monitoring techniques such as pressurized filtration are overwhelmed and incapable of giving sensible answers for some minutes after treatment.

The alumina bifilms may have been created on the inner surfaces of bubbles from the oxygen and moisture impurities in the (so-called) inert gas (for instance, among other prolific sources, there will be much contamination from the inner channels of the rotary degasser). Alternatively, the pure alumina might originate from the waft of fresh air that will enter the bubble as it bursts at the melt surface. These questions remain unanswered at this time.

Also unanswered is the question of possible re-entrainment of oxides after having been carried to the surface. It is easy to imagine that large oxide skins will retain sufficient trapped bubbles to remain buoyant, allowing them to join the layer of dross as relatively permanent contributors, and thus be scraped off. However, it seems also possible to envisage that small oxides buoyed up by a bubble might easily re-entrain once their bubble buoyancy aid has burst.

Pouly and Wuilloud (1997) draw attention to the fact that some rotor designs work counter-productively, increasing the number and volume of inclusions as measured by PoDFA technique. Dispinar (2010) carried out some excellent experiments in which the number and size of oxide bifilms was counted in addition to measurements of the hydrogen content of an Al alloy. He first upgassed a melt by adding water vapor to the degasser while monitoring hydrogen and oxides. Both increased. He then degassed with pure inert gas, finding the hydrogen decreased, but the oxide content continued to increase. He attributed this result to the vortex formed around the central shaft of the degasser which was probably entraining air into the melt. However, further work might reveal that such behavior may be usual whether a vortex is formed or not. Water models of rotary degassers clearly show that even the baffle board introduced to arrest the rotation of the melt to avoid vortex formation can cause severe air entrainment in its own wake; it appears to be capable of creating more problems than it solves.

Pouly and Wuilloud also report that the use of chlorine (nowadays avoided for environmental reasons) was not always helpful. Martin and colleagues (1992) find that if nitrogen alone is used AlN is formed creating a 'wet' dross (i.e. a dross high in liquid aluminum alloy). It seems likely that the AlN is in the form of aluminum nitride bifilms, otherwise the retention of entrapped metal is not easily explained.

Other chemical interactions are noted by Khorasani (1995) who found 10% of the Sr in solution in the melt was lost within 3 minutes, indicating the huge rate of reaction either with the nitrogen used for degassing, or with oxygen from contamination of the gas or from bursting of bubbles at the surface.

There is no doubt that the addition of fluxes, mainly chlorides and fluorides, together with the bubble action greatly assists to clean the melt. This may be the result of the wetting of oxides, causing them to adhere and be assimilated by the liquid flux at the melt surface reducing re-entrainment. The result of this research, carried out by the world's large aluminum suppliers, is viewed to be too valuable to be allowed to be published for the benefit of society. This antisocial behavior is practiced even though it is well known that technical leads in industry can be held without patent protection for only a few years, after which competitive advantage is lost because all competitors have become aware of the technology.

After treatment, after the rotor has been raised out of the melt and the surface skimmed, a test of the efficiency of the cleaning action is simply to look at the surface of the melt. If the cleaning action is not complete, during the next few minutes small particles will be seen to arrive at the surface, under the surface oxide film, which is seen to pop upwards, announcing each new arrival. The 'degassing' treatment can be repeated until no further arrival of debris can be seen. The melt surface then retains its pristine mirror smoothness. The melt can then be pronounced as clean as the treatment can achieve. This probably means the elimination, or near elimination, of the primary spinel skins, but its replacement by millions of fine alumina bifilms.

The fact that pressure die castings benefit from reduced leakage problems if the melt has been treated by rotary degassing (Hairy 2003) is clear evidence for the action of rotary degassing to remove large oxides, probably primary skins from charge materials. (Leakage defects can have little to do with degassing, since hydrogen bubbles cannot be envisaged to affect leakage problems, whereas large oxide bifilms are excellent providers of leak paths.)

An experience by the author illustrates some of the misconceptions surrounding the dual role of hydrogen and oxide bifilms in aluminum melts. An operator used his rotary degasser for 5 minutes to degass 200 kg of Al alloy. The melt was tested with a reduced pressure test (RPT; see below) sample that was found to contain no bubbles. The melt was therefore deemed to be degassed. The melt was transferred in its ladle via fork lift truck to a low-pressure die casting furnace, into which it was poured. The melt in the low-pressure furnace was then tested again by RPT, and the sample found to contain many bubbles. The operator was baffled. He could not understand how so much gas could have re-entered the melt in only the few minutes required for the transfer.

The truth is more complicated, and unfortunately more uncertain. It may have been that the melt was insufficiently degassed with only 5 minutes of treatment. In fact with a damp rotor the gas level is likely to rise initially (getting worse before it gets better!). The RPT showed no bubbles *not* because the hydrogen was low, but because the short treatment had clearly been sufficiently successful to remove a large proportion of the bifilms that were the nuclei for the bubbles. This metal, still retaining a high level of hydrogen, was then poured from a considerable height, re-introducing copious quantities of oxide bifilms that act as excellent nuclei, so that the RPT could now reveal the high hydrogen content.

A second scenario is a possibility. If the melt was sampled for the RPT test immediately after the rotary degassing action the hydrogen may not have been reduced significantly, as in the above explanation. In addition, the remaining bifilms would at that early stage still have been uniformly

dispersed throughout the melt. Thus, in addition to the hydrogen content, the bifilm content may also have remained high. Thus a single sample from near the surface would have shown the presence of few, if any, bifilms, and thus few, if any, pore indications on the RPT sample. During transfer to the furnace the melt would have some time for the bifilm population to separate out, some sinking, some floating. Thus a second RPT a few minutes later would have shown a massive content of bifilms that had segregated close to the top surface. These would have been transferred to the furnace, adding to those created during the pour and those stirred up once again from the bottom of the furnace. After a delay of a few more minutes, a further RPT test taken from the top of the melt would sample the newly enhanced bifilm population that had segregated to the surface of the melt, creating numerous pore indications on the sample, and giving the impression of a higher gas content to anyone who was unaware of the possible changes in bifilm population.

Hu and co-workers (2008) are among the few to study the rotary degassing of Mg alloy, deriving a model for the rate of degassing as a function of parameters such as the rate of rotation of the rotor, etc. They point out that although Mg has a high solubility for hydrogen, the small difference in solubility in the solid (its partition coefficient 0.41 contrasts with that for Al, 0.05) causes it to be widely reported that there is little gas problem with Mg. They do report a problem in Mg alloys for the attainment of good ductility, although, as usual, these authors overlook the important distinction whether this is as a result of hydrogen gas or oxides.

I have to confess to feel diffident about this section concerning rotary degassing. The technique is widely used in the Al casting industry, and about which so much has been written, but so little is known. I personally am reluctant to use rotary degassing while its action is so obscure, and an optimum procedure for reduction of gas and oxides does not yet appear to have been defined. After so many years of research and development this situation is a disappointment. I look forward to it being remedied soon.

### Vacuum degassing

Treatments to reduce the gas content of melts include vacuum degassing. Such a technique has only been widely adopted by the primary steel and Ni-base alloy industry. If a melt were simply to be placed under vacuum the rate of degassing would be low because the dissolved gas would have to diffuse to the free surface to escape. The slow convection of the melt will gradually bring most of the volume near to the top surface, given time. The process is greatly speeded by the more powerful stirring action of induction melting. Additionally, the introduction of the flushing action from millions of small bubbles of inert gas via a porous plug stirs the melt rapidly to bring bulk liquid up to the surface, and the bubbles create additional degassing surface. The process is then accomplished rapidly.

The steel casting industry has in general dropped vacuum degassing and has taken up the more flexible AOD process mentioned above, and in more detail in Section 6.6.

### 14.4.2 Detrainment (cleaning)

#### Natural flotation and sedimentation

The very light metal, magnesium, is lighter than its oxide, MgO. Thus the oxide readily sinks, so that clean magnesium alloys are relatively easily achieved within a few minutes, provided stirring of sediments can be avoided.



The dense metal based on zinc, copper, and iron all have oxides that are lighter and therefore float to the surface of the melt. The higher melting point irons and steels achieve this especially effectively since their oxides are sometime liquid, and so float out as especially compact spherical droplets, or partially liquid, so that compact bifilms resemble sticky balls that cannot unfurl, thus remaining compact and achieving high flotation velocities, clearing the melt rapidly after a pouring or stirring action.

Thus steel melts in the furnace are probably of good quality, but are disastrously damaged during the pour into the ladle. The melt then recovers to some extent during the transfer of the ladle to the casting station, and during the usual subsequent wait to allow its temperature to fall to the casting temperature. Unfortunately, defects are again re-introduced during the final casting operation. Although many continuous casting operations do take precautions to avoid a final re-contamination with oxides, it seems probable that in practice even more care is really required. Clearly, we achieve cleaner steels than we deserve from our primitive bucket technology. For the future, really excellent steels should be attainable, cultivating the good natural behavior of this useful engineering material.

In the meantime, only the aluminum alloys remain reluctant to clean their melts by flotation or sedimentation. Although the oxide is slightly denser than the liquid, its structure as a bifilm containing some entrained air causes the oxides to be often of nearly neutral buoyancy. Thus Al alloys are renowned for retaining their population of oxide bifilms for hours or days. The retention is enhanced because of natural convection that characterizes all furnace designs, and can sometimes be further enhanced by such treatments as bubble degassing which cause effective stirring and over-turning of the whole melt.

Only the Alotech holding furnace for Al alloys is designed to eliminate convection (by a design protected by patent pending at the time of writing), and thus provide conditions for the natural and passive sedimentation of oxides. With the use of a counter-current of dry gas it also ensures the passive degassing of the melt. The use of passive systems for melt quality enhancement has been so far overlooked, but has to be one of the most attractive ways forward (Grassi and Campbell 2011).

#### Aided flotation

Flotation is a process widely used in the mineral-processing industry to float out specific components of a mixture. Such a process clearly operates during bubble degassing of metal, although the researches so far have concentrated on the removal of gas rather than the floating out of oxides. Other important features that have been neglected in all this work include the rate of re-gassing from the environment or from a damp rotor.

As has been described above, it is known that during the course of degassing of an Al melt with nitrogen the first oxides that are removed from the melt are mainly spinels, probably the oxide skins originating on the charge materials. After some minutes, the spinels are replaced by millions of fine, pure alumina films. Thus the bifilm population is completely changed by rotary degassing.

In terms of the general quality of the castings, mechanical properties would be improved because the old thick oxides would constitute massive defects. Their replacement by the smaller alumina bifilms, despite their enormously greater numbers, would be expected to unfurl less easily, and confer better properties because of the smaller maximum defect size. Nevertheless, it need hardly be emphasized that the properties are likely to be even better without this huge population of small cracks.

#### Aided sedimentation

The sedimentation of oxide bifilms in light alloy melts by the formation of heavy precipitates on them is the only example known to the author of the cleaning of melts by aided sedimentation. This

phenomenon is so important that we shall dwell on it at length, while noting that other examples may remain to be discovered in other alloy systems.

The sedimentation of oxides (actually bifilms of course) in an Al alloy by the formation of titanium-rich precipitates on them, causing them to drop like stones to the bottom of the melt, was observed by Mountford and Calvert in 1959. They looked into the melt by means of ultrasonic reflections, noting that on cooling the melt to cause Ti compounds to supersaturate and precipitate from solution, the liquid miraculously cleared of a fog of suspended particles, transferring to the bottom of the melt to form a layer of sediment, rich in oxides and Ti compounds. When the sediment was disturbed prior to pouring, polished sections of the castings exhibited tangles of oxides containing large Ti intermetallics and associated porosity.

While studying the 'fade' of grain refiners Schaffer and colleagues (2004) observe the strange settling behavior of grain-refining particles in Al alloys, surprisingly completing in only a few minutes, but offer no explanation. Chu (2002) finds the  $TiB_2$  particles are associated with spinel oxides and Srimanosaowapak and O'Reilly (2005) confirm that  $TiAl_3$  particles assist to sediment oxides during grain refinement. This effect has been used for many years (Cook 1997) to sediment impurities from electrical conductivity (EC) grade aluminum; Cook uses 3:1 TiB additions (instead of the more usual 5:1 TiB ratio) which precipitates as a boride-rich sludge, leaving the metal with high electrical conductivity. Vanadium borides were rather less effective than titanium borides, giving settling times of 5 or 6 hours. These long times may have been the result of rather more vigorous convection stirring in their experiment. Wuilloud (1994) describes how Alusuisse have cleaned melts in only 50 minutes by the addition of grain refiner. Without grain refiner, 80% of the 'impurities' still remained in suspension after this time.

Interestingly Wuilloud reports that the addition of the grain refiner to the launder to the DC casters resulted in a reduction in quality of the cast metal. Nadel and co-workers (2007) appear unaware of the Alusuisse technique, assuming that grain refinement would reduce the cracking observed in DC ingots. They found, in agreement with Wuilloud, that grain refinement in the furnace did grain refine the ingot, and did eliminate cracking. However, grain refinement in the rapidly moving stream of metal in the launder, transferring the melt to the DC caster, did, once again, grain refine, but the ingot was cracked. Clearly, when adding to the launder, the bifilms had no time to settle. Thus the elimination of cracking was the result of elimination of bifilms rather than the result of the finer grain size (Campbell 2008).

Following treatment by rotary degassing, Schaffer and Dahle (2009) find the loss of grain refinement was due to the sedimentation of  $TiB_2$  particles, presumably on oxides. This contrasts with the findings of Khorasani (1995) who found evidence of flotation of  $TiB_2$  in the dross layer. This somewhat messy situation might be explained by the sedimentation of large  $TiB_2$  precipitates on smaller oxides, but flotation of smaller  $TiB_2$  particles on larger oxides. Alternatively, the situation may be more complicated by some precipitation on spinels and some on the pure alumina particles.

Only a limited amount of work appears to have been carried out on Mg alloys to study the cleaning action of aided sedimentation. As long ago as 1969 Fruehling and Hanawalt studied the fracture surfaces of 12-mm diameter test bars, in a demonstration that a protective atmosphere could be at least as effective as a flux in achieving a clean melt. They showed that oxide skins would separate from Mg alloys, achieving metals with completely clean fractures, in only a matter of minutes. Simensen (1981) aided gravity by centrifuging both Al and Mg alloy melts, precipitating out  $TiB_2$  and  $VB_2$  in Al alloys and  $Al_4C_3$ ,  $Al_3Zr$ , and  $(Fe,Mn)_3Si$  in Mg alloys. Exceptions were low-density agglomerates of oxides

and chlorides which segregated to the rotation axis. The technique, although scientifically interesting, can hardly be judged a useful foundry tool.

### Filtration

Filtration is perhaps the most obvious way to remove suspended solids from liquid metals. However, it is not without its problems, as we shall see.

The action of a filter in the supply of liquid metal in the launder of a melt distribution system in a foundry or cast house (i.e. a foundry for continuous casting of long products) is rather different from its action in the running system of a shaped casting.

The filters used in the running systems of castings act for only the few seconds or minutes that the casting is being poured. The velocities through them are high, usually several meters per second, compared to the more usual  $0.1 \text{ m s}^{-1}$  rates in cast house launders. The filtration effect in running systems is further not helped by the concentration of flow through an area often a factor of up to 100 smaller than that used in launder systems. The total volume per second per unit area rates at which casting filters are used are therefore higher by a factor of at least 1000 times. It is hardly surprising therefore that any filtration action in the filling systems of castings is therefore practically zero. However, the effect on the flow is profound. The use of filters in running systems is dealt with in detail later in the book. We concentrate in this section on filters in launder systems, which, in this case, do appear to achieve some filtration.

The treatment of tonnage quantities of metal by filtration has been developed only for the aluminum casting industry. The central problem for most workers in this field is to understand how the filters work, since the filters commonly have pores sizes of around 1 mm, whereas, puzzlingly, they seem to be effective to remove a high percentage of inclusions of only 0.1 mm diameter. Most researchers expand at length, listing the mechanisms that might be successful to explain the trapping of such small solid particles. Unfortunately, these conjectures are probably not helpful, since without exception all the conjectures to the present day relate to the effect that filters may have on arresting *particles*. These conjectures are not repeated here. We have no interest in stopping particles. For engineering castings, particles generally have little or no influence on properties.

The fact is that the important solids being filtered in aluminum alloys are not particles resembling small solid spheres, as has generally been assumed. The important inclusions are *films* (actually always *double films* that we have called *bifilms*). Once this is appreciated the filtration mechanism becomes much easier to understand. The films are often of size 1–10 mm, and so are, in principle, easily trapped by pores of 1 mm diameter. Such bifilms are not easily seen in their entirety in an optical microscope, the visible fragments that happen to intersect the polished surface appearing to be much smaller, explaining why filters *appear* to arrest particles smaller than their pore diameters.

We need to take care. This explanation, whilst probably having some truth, may oversimplify the real situation. In Section 2.3, the life of the bifilm was described as starting as the folding in of a planar crack-like defect as a result of surface turbulence. However, internal turbulence wrapped the defect into a compact form, reducing its size by a factor of 10 or so. In this form it could pass through a filter; finally opening once again in the casting as the liquid metal finally comes to rest, and bifilm-opening (i.e. unfurling) processes start to come into action.

In more detail now, the trapping of compact forms of bifilms is explained by their irregular and changing form. During the compacted stage of their life, they will be constantly in a state of flux, raveling and unraveling as they travel along in the severely turbulent flow in the channels of the

running system. Two-dimensional images of such defects seen on polished sections always show loose trailing fragments. Thus in their progress through the filter, one such end could become attached, possibly wrapping over a web or wall of filter material. The rest of the defect would then roll out, unraveling in the flow, and be flattened against the internal surfaces of the filter, where it would remain fixed in the tranquil boundary layer. The thin oxide ceramic film would be essentially invisible against the coarse thickness of the body of the ceramic filter, explaining why polished sections of many filters appear free from inclusions after they appear to have completed a useful job of cleaning up a casting. The other reason why the filter often looks free from inclusions is that the major task of the filter is not filtration but the slowing of the velocity of flow, reducing the damage that the melt can do to itself from entering the mold cavity at too high a speed, so creating damaging oxide bifilms in the casting.

### Packed beds

In practice, in DC (direct chill) continuous casting plants, filters have been used for many years, sited in the launder system between the melting furnaces and casting units. Commonly, the filtration system is a large and expensive installation that may approach a cubic meter in volume. The filter system typically comprises at least one crucible furnace that is in two parts. One half is filled with refractory material such as alumina balls or tabular alumina. The flow of the melt down one half of the crucible, through a connecting port, and up through the deep packed bed of refractory particles. Such systems have been shown to be effective in greatly reducing the inclusion count (the number of inclusions per unit area). However, it is known that the accidental disturbance of such filter beds releases large quantities of inclusions into the melt stream. This has also been reported when enthusiastic operators see the rising upstream level of the melt indicating the filter is becoming blocked. They consequently stir the bed with iron rods to ease the flow of metal. It is not easy to imagine actions that could be more counter-productive.

Some work has been carried out on filtering liquid aluminum through packed beds of tabular or ball alumina (Mutharasan et al. 1981) and through bauxite, alumino-silicates, magnesia, chrome-magnesite, limestone, silicon carbide, carbon, and steel wool (Hedjazi et al. 1975). This latter piece of work demonstrated that all of the materials were effective in reducing macro-inclusions. This is perhaps to be expected as a simple sieve effect. However, only the alumino-silicates were really effective in removing any micro-inclusions and films, whereas the carbon and chrome-magnesite removed only a small percentage of films and appeared to actually increase the number of micro-inclusions. The authors suggest that the wettability of the inclusions and the filter material is essential for effective filtration.

An interesting application of a chemically active packed bed is that by Geskin et al. (1986), in which liquid copper is passed through charcoal to provide oxygen-free copper castings. It is certain, however, that the charcoal will have been difficult to dry thoroughly, so that the final casting may be somewhat high in hydrogen. Because of the low-oxide bifilm content, and possibly the low oxygen content in solution, it is likely that hydrogen pores will not be nucleated (Section 6.4). The hydrogen is expected therefore to stay in solution and remain harmless.

### Alternative varieties of filters

Other large and expensive filtration systems include the use of a pack of porous tubes, sealed in a large heated box, through which the aluminum is forced. The pores in this case are between 0.25 and 0.05 mm, with the result that the filter takes a high head of metal to prime it. However, the technique is not subject to failure because of disturbance, and guarantees a high quality of liquid metal.

Other smaller and somewhat cheaper systems that have been used include a box housing a large area (usually at least  $300 \times 300$  mm) ceramic foam filter sited permanently below the surface of the melt. The velocities through the filter are usually low, encouraged by the large area of the filter. The filter is only brought out into the air to be changed when the metal level either side of the filter box shows a large difference, indicating that the filter is becoming blocked.

The efficiency of many filtration devices can be understood when it is assumed that the important filtration action is the removal of films (not particles). Thus glass cloth is widely used to good effect in many different forms in the Al casting industry. A woven silica fiber cloth is similarly effective for cast iron.

### Practical aspects

It is typical of most filtration systems that the high quality of metal that they produce (often at considerable expense) is destroyed by thoughtless handling of the melt downstream of the filter.

Even the filter itself can give difficulties in this way. Many have wondered whether the filter itself causes oxides because the flow necessarily emerges in a divided state, and therefore must create double films in the many confluence events. Video observations by the author on a stream of aluminum alloy emerging from a ceramic foam filter with a pore diameter close to 1 mm have helped to clarify the situation. It seems true that the flow emerges divided as separate jets for even modest velocities around  $500 \text{ mm s}^{-1}$ . However, within a few mm (apparently depending on the flow rate of the metal) the separate jets merge. Thus the oxide tubes formed around the jets appear to be up to 10 m long but they remained attached to the filter. The oxide tubes did not extend further because, of course, after the streams merged oxygen was necessarily excluded. The forest of tubes was seen to wave about in the flow like underwater grass. It is possible that more rapid flows might cause the grass to detach as a result of its greater length and the higher speed of the metal. This seems possible in running systems of tall castings where the velocities can be extremely high. Further work will be necessary to clarify this.

In the meantime, the problem is avoidable by ensuring that the exit face of the filter quickly becomes covered, effectively protected by melt quickly after the filter becomes primed. This is an important aspect of the designing of effective filters into the running systems of shaped castings, as is discussed in Section 12.8.

### 14.4.3 Additions

Additions to melts are made for a variety of reasons. These can include additives for chemical degassing (as the addition of Al to steel to fix oxygen and nitrogen) or grain refinement (as in the addition of titanium and/or boron or carbon to Al alloys). Sometimes it seems certain that the poor quality of such materials (perhaps melted poorly and cast turbulently, and so containing a high level of oxides) can contaminate the melt directly.

Indirectly, however, the person in charge of making the addition will normally be under instructions to stir the melt to ensure the dissolution of the addition and its distribution throughout the melt. Such stirring actions can disturb the sediment at the bottoms of melts, efficiently re-introducing and re-distributing those inclusions that had spent much time in settling out. The author has vivid memories of wrecking the quality of early Cosworth melts in this way: the addition of grain refiners gave wonderfully grain-refined castings, and should have improved feeding, and therefore the soundness of

the castings. In fact, all the castings were scrapped because of a rash of severe microporosity, initiated on the stirred-up oxides that constituted the sediment in the holding furnace.

Additions of Sr to aluminum melts have often been accused of also adding hydrogen because of the porosity that has often been noted to follow such additions. Here again, it is unreasonable to suppose that sufficient hydrogen could be introduced by such a small addition. Section 6.3.5 describes how the action of Sr is particularly complicated. However, all the detailed mechanisms described there for enhanced porosity will be certainly made worse by stirred sediment.

#### 14.4.4 Pouring

Most foundries handle their metal from one location in the foundry to another by ladle. The metal is, of course, transferred into the ladle by pouring, and out of the ladle by pouring, into a further ladle or into the mold by pouring. At every pouring operation, it is likely that large areas of oxide film will be entrained in the melt. Furthermore, because pour heights are usually not controlled, the amount of oxide introduced in this way will vary from one occasion to the next (Prakash et al. 2009).

Not all pouring necessarily results in damage to melts. It is known that pours from heights less than the height of the sessile drop cannot entrain the surface oxide. However, such heights are very low, being 16 mm for Mg, 13 mm for Al, and only 8 mm for dense metals such as copper-base, and iron and steel alloys.

However, this theoretical limit, whilst absolutely safe, may be exceeded for some metals with minimum risk. As long ago as 1928 Beck described how liquid magnesium could be transferred from a ladle into a mold by arranging the pouring lip of the ladle to be as close as possible to the pouring cup of the mold, and be relatively fixed in position. In this way the semi-rigid oxide tube that formed automatically around the stream of pouring metal remained unbroken, and so protected the falling stream.

Early observations by Turner (1965) noted that air was taken into the melt, reappearing as bubbles on the surface when the pouring height exceeded about 90 mm. This was closely confirmed by Din, Kendrick and the author (2003) on Al-7Si-0.4Mg alloy, demonstrating that in practice the damage caused by falls up to 100 mm appears controlled and reproducible, although this good behavior was probably only achieved provided the melt had first gone through a ceramic foam filter. Above 200 mm, Din and colleagues found that random damage was certain whether a filter had been in place or not. At these high energies of the plunging jet bubbles are entrained, with the consequence that bubble trails add to the total damage in terms of area of bifilms. In summary, it seems that fall heights of perhaps 10–20 mm are completely safe, whereas up to 100 mm may be successful but are a risk, but somewhere in the region of 100–200 mm severe harm can be expected.

In steel foundries using bottom-pour ladles, the velocities of the pour are always in excess of  $4 \text{ m s}^{-1}$ , introducing the danger of massive air entrainment and oxide generation. This is the major challenge facing steel casters, and currently causes extensive damage to the casting, requiring costly upgrading procedures.

For this reason the inert gas shroud has been adopted in some steel foundries where it takes the form of a protective shield, rather like a collar, around the metal stream issuing from a bottom-poured ladle. It encloses an inert gas environment, usually argon (Figure 14.4). With its use Wells and Oleksa (1988) report a two-thirds reduction in oxides in steel castings, and reduced cleaning of the ladle

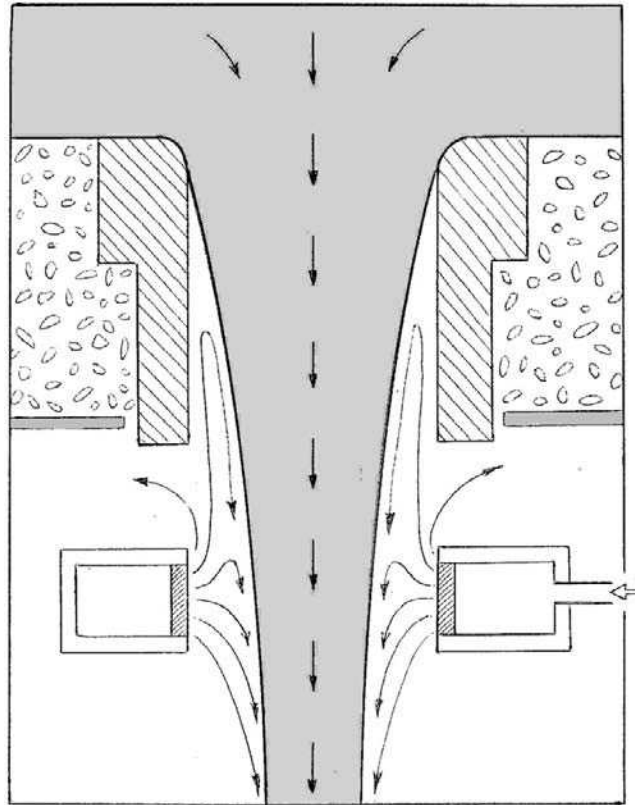


**FIGURE 14.4**

The use of a protective gas shroud (usually argon) around the metal stream from a bottom pour ladle, illustrating the entrainment of protective gas into the annular gap between the stream and a parallel bore nozzle, thus reducing oxidation in the nozzle.

nozzle. The Steel Foundry Society of America (SFSA 2000) reports further developments in which macroinclusions were reduced by 90% by use of a shroud.

In this figure the drawing of gas into the annular gap between the nozzle and the melt explains many of the problems of the blockage by oxide of those nozzles with an internally straight bore. The air in the annular gap is rapidly drawn down by contact with the falling jet. Consequently, air is drawn up to replace it. This extremely rapid circulation of air in this confined region explains the build-up of oxides and the blockage of the nozzle. The tapered nozzle avoids this problem by ensuring contact with the melt as it accelerates down the nozzle. Effectively, the tapered nozzle is a short sprue, and benefits from some pressurization of the melt against its walls to keep any gap closed, and keep air out.

It is difficult to believe that a user would think that the short distance between the ladle and the conical basin was influential in any substantial reduction of the oxidation of the melt. Usually, the time involved in this short journey will be probably only a few hundred milliseconds. It is not easy therefore

to escape the conclusion that users were in fact tacitly acknowledging the air pump action of the conical basin. The shroud therefore encourages argon to be sucked into the cone instead of air, assuming that the rate of delivery of argon is sufficient (since venturi pumps usually transfer roughly equal volumes of pumping fluid and entrained fluid).

The beneficial action of an argon shroud is that the reactive gas is simply replaced by an inactive gas. Thus although volumes of bubbles will continue to be entrained with the flow, they at least do not react to produce oxides or nitrides.

In fact, of course, the shroud will never be completely protective for various reasons: the gas itself will be contaminated with oxygen, water vapor and other gases and volatiles in the plumbing system that delivers the gas. More important still, the seal of the shroud around the stream cannot be made proof against leakage of air; and finally the outgassing from the mold, especially in the case of an aggregate (sand) mold, will normally totally overwhelm any attempt to provide a protective environment. Monroe and Blair (1995) draw attention to the mechanical sealing problems.

Even so, when used appropriately, the shroud is useful. It greatly reduces re-oxidation problems of steels during casting as demonstrated by research carried out by SFSA. The result emphasizes the damage done by the emulsion of steel and air bubbles that characterizes the average poorly designed casting system.

The shroud has been taken to an extreme form as a silica tube, over a meter long, mounted directly to the underside of a bottom-pour ladle (Harrison Steel, USA, 1999). The tube acts as a re-usable sprue, and is inserted through the cope and lowered carefully through the mold, so that its exit reaches the lowest point of the filling system. The stopper is then opened. If the seal between the ladle and tube is good, the filling rate of the mold is high. If leakage of air occurs at the seal the rate of mold filling is significantly reduced, implying the strong pumping action of the falling stream to create a vacuum in the upper part of the tube, drawing in air if it can, and thus diluting the falling stream with air. Several castings in succession can be poured from one tube. However, after the tube cools the silica cracks into fragments, and requires to be replaced. Although this solution to the protection of the metal stream from oxidation is to be admired for its ingenuity, it does appear to the author to be awkward in use. In addition, the leakage problem is always an attendant danger.

Moving on to the pouring issues in most foundries, it seems that the lower the pour heights the less damage is suffered by the melt. In addition, of course, because less metal is oxidized melt losses are directly reduced. Sometimes big savings can be achieved in the foundry by simply reducing pour heights. Ultimately, however, it is, of course, best to avoid pouring altogether. In this way losses are reduced to a minimum and the melt is maintained free from damage.

Until recent years, such concepts have been regarded as pipe dreams. However, the development of the Cosworth Process has demonstrated that it is possible for aluminum alloy castings to be made without the melt suffering any pouring action at any point of the process. Once melted, the liquid metal travels along horizontal heated channels, retaining its constant level through the holding furnace, and finally to the pump, where it is pressurized to fill the mold in a counter-gravity mode. Such technology might also be applied to magnesium alloys.

The potential for extension of this technology to other alloy base systems such as copper-based or ferrous alloys is less clear. This is because many of these other alloy systems either do not suffer the same problems from bifilms, or do not have the production requirements of some of the high-volume aluminum foundries. Thus, in normal circumstances, many irons and steels are relatively free from



bifilms because of the large density difference between the inclusions and the parent melt, encouraging rapid flotation. Alternatively, many copper-based and steel foundries are more like jobbing shops, where the volume requirement may make the justification of a counter-gravity system more difficult. The technical challenges are also non-trivial; high-technology pumps, if they were available, would have problems to survive the oxidation and thermal shock problems of a stop-go production requirement, although a low-pressure system delivering melt directly from the melting furnace into the base of molds seems a relatively straightforward and attractive option.

As a well-known instance, the counter-gravity Griffin Process has been impressively successful for the volume production of steel wheels for rail rolling stock. The process produces wheels that require no machining (apart from the center hub). The outer cast rim runs directly on the steel rail. The products out-perform forged steel wheels in terms of reliability in service, earning the process 80% of the freight rail wheel market in the USA. What a demonstration of the soundness of the counter-gravity concept, contrasting dramatically with steel castings produced world-wide by gravity pouring, in which defects and expensive upgrading of the casting are the norm.

---

## 14.5 CAST MATERIAL

### 14.5.1 Liquid metal

It has become fashionable to criticize the traditional approaches to the production of castings by the filling of a mold with liquid metal. The liquid casting approach probably deserves such criticism, earned by its abject failure on occasions to deliver castings of respectable quality. This has been a regrettable and lengthy 'dark ages' from which it is hoped the industry is gradually emerging. It will be long and hard for the casting community to reverse its unflattering image. A new professionalism will only be recognized by results in the form of on-time deliveries of good castings.

In the meantime, it is understandable that the casting of liquid metal has been thought to be fundamentally problematic (in contrast to the central message of this book). Thus huge expenditure and effort has been carried out on the casting of various partially solid alloys and liquid/solid mixtures (misleadingly named semi-solid mixtures since they are usually not 50% solid mixes), for which there are undoubted benefits.

Even so, the author remains convinced that despite all the well-known difficulties with the casting of liquid metals, the difficulties are worth living with, and ultimately the benefits to properties hard to beat. For this reason this book remains strongly committed to the production of castings by the casting of liquid metal, convinced that such a production route will provide the major benefits to the majority of customers for the foreseeable future.

This is not to deny the special features and advantages enjoyed by some non-liquid or, perhaps we should say, partially solid routes to casting manufacture.

### 14.5.2 Partially solid mixtures

Partially solid mixtures have been widely known as 'semi-solid' mixtures. I have to say I avoid such inaccurate names. Imprecision in our words can become wooliness in our thinking. I agree the accurate name does not alliterate to help it off the lazy tongue, but it is correct, and in my view therefore worth the effort.

The advantages of casting partially solid mixtures are well known, and include their use in high-pressure die casting (HPDC), in which the slurry seems more resistant to disintegration, and thus avoids the worst excesses of entrainment usually suffered by the HPDC technique when applied to liquid metals. Furthermore, because a significant fraction of the heat content has been removed from the mixture prior to casting, the metal dies run cooler, suffering reduced crazing due to thermal shock, and so lasting longer. Freezing is also faster, thus increasing productivity. Although reduced shrinkage porosity is also cited as an advantage because, once again, a significant fraction of the cast material has already solidified, this is almost certainly more apparent than real; the so-called shrinkage porosity in pressure die castings was mainly misdiagnosed entrainment problems including air and oxides. However, of course, there has to be some small component of reduced shrinkage problems, but in such thin-section castings this would be expected to be practically negligible. Anyway, the undoubted overall improved soundness confers improved and more reliable mechanical properties, and improved leak tightness.

The disadvantages of the processing of partially solid mixtures relates to the increased cost of processing of the mixtures, and for some approaches, the increased control necessary to form a correct mix (other approaches have automatic, intrinsic, built-in control, such as the approach by Rheometal (Granath 2008), using not temperature control but a method of mixtures based on enthalpy equilibration, melting a known amount of solid in a known amount of liquid. The oxide skin from the melted solid addition appears not to have raised any problems so far as is known to date, but probably requires further investigation.)

During the mixing processes in which the dendrites are grown and fragmented, some but not all of the processes tend to introduce air and oxides into the mixture. The result is, of course, a mix that now contains a dispersion of oxide bifilm that will limit the properties achievable from the final casting. The beneficial aspect of the defect dispersion is that it is probably rather uniform in its extent and the size of the individual defects. Thus the properties may not be optimum, but the product will probably be uniformly reliable.

### Rheocasting

Rheocasting is one such option, in which a partially solid alloy but flowable alloy is produced by careful cooling of the liquid alloy into the liquid + solid range while mechanically stirring to ensure that dendrites are broken up, forming compact, near-spherical forms. Such an approach was discovered by Spenser, Mehrabian, and Flemings at MIT in 1972. The process continues to find its niche in the industrial and commercial world in the second millennium.

### Thixocasting

Thixocasting was a variant of the Rheocasting approach in which the partially solid mixture was precast in the form of semi-continuously cast 'logs'. The logs required to be sawn to the correct length, reheated to the casting temperature, and finally cast. This approach has always suffered from the cost of the separate melting and Rheocasting process steps. Furthermore, the foundry returns (runners, feeders, and scrap castings) present a problem for recycling. The just-in-time processes for the production of partially solid mixes avoid both of these issues.

### Just-in-time slurry production

New concepts require agonisingly long development periods before they become accepted by users. Companies such as Alcan Canada (Doutre 2000, Lashkari 2007), Ube Japan (Lee and Kim 2007),

Idra Italy (Yurco 2003) and Rheometal, Sweden (Granath 2008), among others (Midson 2008), have continued to develop novel just-in-time slurry production techniques to counter one of the challenges of the process, the production of controlled qualities of slurry at commercially attractive production rates, and commercially attractive costs.

#### Strain-induced melt activation (SIMA)

SIMA produces a thixotropic condition by first deforming the solid alloy followed by a heat treatment into the mushy zone. The approach avoids melting and the entrainment of air and oxides suffered by competitive techniques for slurry production. Chen et al. (2010) describe its use for magnesium alloy AZ91, using equal channel angular pressing (ECAP) to produce a high but uniform strained condition, and thereby achieve impressive results. Even so, it seems likely its potential for commercial exploitation will be limited by its challenging economics, in common with other semi-solid routes.

#### Mg alloy slurry production from granules

The work by Fan (2007), Zerwinski (2008), and others has demonstrated the feasibility of producing Rheocastings in Mg alloys by the processing of alloy granules through a twin screw injection molding machine as part of a pressure die casting process. The processing of Mg granules via a route more normally associated with the processing of plastics is possible partly because of their low strength and hardness, and partly because Mg reacts with the steel screws to only a limited extent, compared, for instance, to Al alloys which dissolve iron readily. Once again, the uniform dispersion and shredding of the oxide skins from the original granules is seen to deliver a product that has uniformly reliable, if not optimum, properties. In fact the precipitation of the so-called  $\beta$ -Mg<sub>17</sub>Al<sub>12</sub> phase at grain boundaries in thixotropic Mg alloys containing over 7%Al has been cited (D'Errico 2008) as limiting ductility. It seems almost certain that this phase is precipitating on bifilms generated by the mixing process, and pushed ahead of the growing grains, so effectively pre-cracking the grain boundaries.

#### Metal/matrix composites (MMCs)

Solid/liquid mixtures can be made by the addition of particles of solid into the melt. The exploration of such mixtures was pioneered by Pradeep Rohatgi, who over the years since his time in 1965 in the International Nickel Company Laboratories, New York, has explored mixtures of practically everything with everything (see his Rohatgi Symposium reported by Gupta (2006)). Most matrices studied so far are those of Al alloys, but other work includes Zn, Mg and, later, superalloys (Rohatgi 1990). The particle additions include graphite, SiC, Al<sub>2</sub>O<sub>3</sub>, and low-cost additives such as fly ash, a waste product from power plants. Thousands of tonnes of such MMCs are now processed for use in the transport industries.

The process most used to make mixtures is the so-called vortex method in which the solid additions are fed into a central vortex made in a rapidly stirred liquid metal. Some work has also been carried out using particles in suspension in a carrier gas, introduced under the melt surface from a lance.

All processes that introduce particles from the outside into the interior of the melt suffer the problem of having to penetrate the oxide skin on the melt. This means that particles usually enter the matrix as clumps, each clump being enclosed by a wrapping of the oxide film necessarily entrained from the surface (Figure 2.3). The problem with such clumps is that the reservoir of air they contain continues to thicken and strengthen their surrounding oxide envelope. The vigorous stirring required to break these large agglomerates down into smaller agglomerates automatically introduces yet more

oxides into the melt via the central vortex. Tian and colleagues (1999) study clusters of alumina particles in liquid Al, finding clusters from one particle of 10  $\mu\text{m}$  diameter to clusters of particles 100  $\mu\text{m}$  diameter. In each case the clusters are enclosed by amorphous alumina films.

The MMC studies by Emany and co-workers (2009) also illustrate particle clusters inside oxide 'paper bags'. There is evidence from this work that the loss of fluidity with higher additions of particles is not primarily the result of the higher percentage of particles but the result of increased oxide bifilm content from the vortex stirring process. The huge increase in bifilm population in such vortex-produced MMCs is also seen to degrade ductility, even though, paradoxically, there may be some slight increase in strength.

Badia (1971) explores the production of MMCs in Al and Zn matrices by additions of a variety of solids including SiC,  $\text{Al}_2\text{O}_3$ ,  $\text{SiO}_2$ , and graphite. He found that coating of the particles with Ni was essential to achieve some kind of wetting so that the additions would remain in suspension, otherwise the additions appeared to surface once again, rejected from the melt as a dry powder. The action of the Ni is not completely clear, and may depend not only on its metallic nature but also on its powerful exothermic reaction with Al to form nickel aluminides. Any benefit to the MMC of the introduction of a lightweight phase is lost, however, because the 5  $\mu\text{m}$  Ni coat on particles 5  $\mu\text{m}$  diameter corresponds to an addition containing well over 50% Ni. Badia used the vortex addition technique and subsurface injection from a lance, but preferred the vortex approach because continued stirring with the rotor could maintain the addition in suspension.

Practically all of the above studies have focussed on the use of particle additions to a melt. Occasional exploratory studies have included a variety of fibers (Rohatgi 1990) and SiC whiskers (Das 1981) for which surprising gains in strength have been recorded for levels of only 0.5 volume % addition.

In contrast to these laboratory studies, in which the introduction of particles was attempted with relatively inefficient protective atmospheres, Alcan instigated a major production initiative in which they produced an Al alloy – SiC MMC in tonnage quantities in a high vacuum environment (Hammond 1989) – although at the time the production conditions were a commercial secret. The uniform dispersion of the particulate phase in Duralcan, as it came to be known, indicated its relative freedom from oxide films, although work by Emany and the author (1995) did reveal some residual bonding problems, even though these were much less than those commonly seen elsewhere. Later work (Hoover 1991) confirmed the excellent specific stiffness, good tensile properties including fatigue, and good retention of properties at elevated temperature.

### In situ MMCs

The formation of MMCs by the precipitation of the strong, hard particles in situ in the matrix by a metallurgical reaction during solidification is an attractive technique. In this case the strengthening particles suffer no poor cohesion with the matrix because of an intervening oxide film and its associated thin layer of air; the particles are bonded to the matrix with atomic perfection, having grown atom by atom from the liquid.

The difference in the bonding of an in situ generated MMC based on  $\text{TiB}_2$  particles in an Al alloy matrix and Duralcan (a good-quality extrinsically generated MMC based on SiC particles) was shown clearly in work by Emany and Campbell (1995). A non-fed casting, designed to create a reduced internal pressure, possibly a slightly negative pressure (corresponding to a hydrostatic tensile stress), was seen to cause significant dispersed microporosity in Duralcan, but very little in the in situ MMC. The difference between the relatively poor bond and the perfect bond was clear.

Hadian (2009) studies the system Al–Mg<sub>2</sub>Si, and the refinement of its Mg<sub>2</sub>Si particles by more rapid freezing and by the addition of Li. Although the Mg<sub>2</sub>Si particles are usually regarded as brittle, this study is notable for its image of an Mg<sub>2</sub>Si particle cracked (one assumes by the presence of a central bifilm on which it formed) but plastically peeled open, revealing the particle to be impressively ductile (Figure 6.22). This is expected to be a universal feature of in situ MMCs; all the hard, strong particles will probably deposit on a bifilm, and thus all will be expected to possess an in situ crack, despite the intrinsic strength and crack resistance that they would be assumed to possess.

The common Al–Si system similarly behaves as an in situ MMC in which the silicon particles act as the hard, strengthening phase in the ductile Al matrix. Once again the presence of central cracks in the Si is attributed to the formation of the Si particles onto bifilms in suspension in the melt. It is known that clean melts cannot form Si particles in this way, with the result that the Si is forced to precipitate at a lower temperature and a different form, as a finely spaced eutectic, which we call a ‘modified’ Al–Si eutectic. The addition of such elements as Sr and Na similarly acts to inhibit precipitation on the oxide bifilms, thus encouraging the modified structure (Campbell 2009). When the Si phase forms in this way it can now no longer be regarded as separate particles, even though this is its appearance on a polished micrographic section. The Si has the form of a continuous branching growth known as a coral form. This form of the Al–Si MMC can be particularly strong and tough if bifilms are somehow removed by careful processing, since the development of the MMC structure now no longer depends on their presence (see Section 6.3.5).

---

## 14.6 REMELTING PROCESSES

In the quest for really clean steels, so-called secondary remelting processes have been developed in which steel is prepared in the form of an electrode which is re-melted and re-solidified into a new ingot. Although many forms of melting have been employed from time to time, including plasma and electron beam, the two main processes used world-wide are vacuum arc remelting and electro-slag remelting processes, sometimes called refining processes.

### 14.6.1 Vacuum arc remelting (VAR)

The process consists of remelting the electrode in a vacuum, striking an arc between the electrode and the water-cooled base of the mold, and melting off the electrode drop by drop to form the new ingot (Figure 14.5). All this takes place in a water-cooled mold.

The selection of vacuum for the process was clearly to reduce re-oxidation of components of the melt, which it does successfully. It was probably also selected with the intention of reducing hydrogen content of the steel even though for ingots up to 400 mm diameter much hydrogen is lost during a 10-hour homogenizing type of heat treatment, and more is lost if the ingot is reduced in section by hot working. Thus except for the very largest ingots out of which hydrogen has too far to diffuse in a reasonable time, hydrogen is not a problem, and VAR is unnecessary.

Other major problems with this process include the casting of the electrode, which is often top-poured into a slim, tall ingot mold, and thus having an awful structure, full of oxide laps (actually bifilms of course). Thus the process has a serious challenge with extremely poor starting material. The

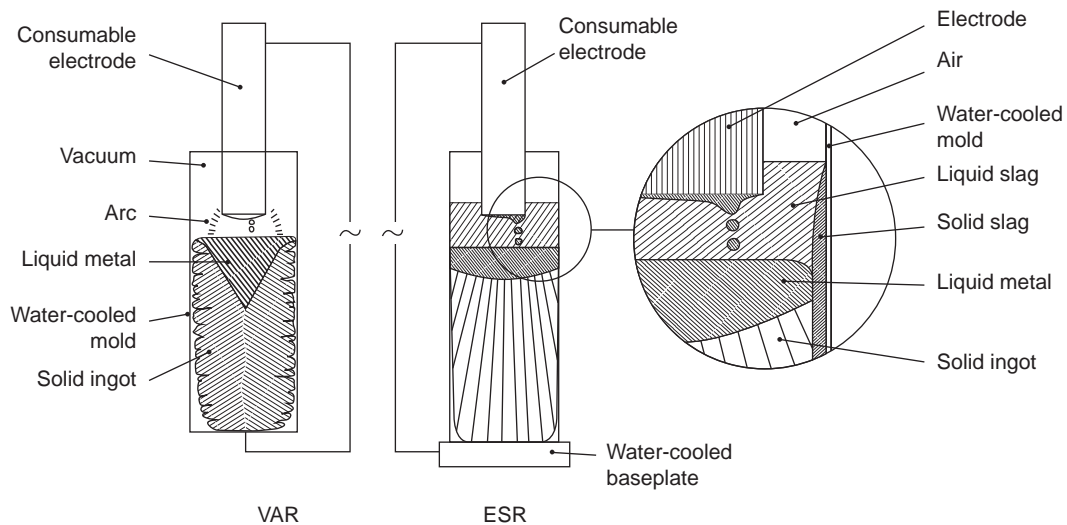


**FIGURE 14.5**

Comparison of the two major ferrous alloy refining systems.

aspect for which I personally would never choose this process is the poor structure of the final remelted ingot. This is also full of oxide laps caused by the irregular arrival of liquid metal from the arc, and the relatively poor vacuum, creating the ingot by a series of ‘pancakes’. The pancakes appear to be more or less welded in their central areas, but act as bifilm cracks that have to be machined off prior to forging, otherwise the cracks simply open up. This requirement for ‘peeling’ prior to working involves a large loss of yield.

### 14.6.2 Electro-slag remelting (ESR)

The heat source in this process is the resistance heating of the layer of liquid slag between the electrode and the ingot (Figure 14.5). The slag also freezes, creating a thin protective layer on the water-cooled wall of the mold, so that the melt is not in direct contact with the mold. Thus the melt is not strongly chilled against the cold wall, and laps are avoided. As a result, it is well known that the difficult Ni-base alloy, Waspalloy, requires considerable peeling of the VAR ingot surface otherwise it is not forgeable without cracking, whereas an ESR ingot of Waspalloy forges like butter.

Although it was generally assumed that the melt was cleaned from inclusions by dissolution of inclusions in the slag layer as droplets of the melt passed through the slag, a study of a cross-section of an electrode taken out of the slag and sectioned down its centerline clearly shows that all of the inclusions go into solution at the very high temperatures before melting occurs. The subsequent relatively clean structure of the ingot, displaying only extremely fine dispersed inclusions if any, is the result of the relatively rapid solidification encouraged by the water cooling of the mold and its baseplate.

It has always seemed to me that VAR has enjoyed an unearned reputation as a refining or secondary melting process, whereas ESR in general provides a superior product.

Figure 10.2 illustrates the complexity of the casting industry by the wide variety of its molds. The rapid freezing giving castings with good mechanical properties in permanent metal molds brings with it the penalty of having to wait for the casting to freeze prior to the opening of the mold and the ejection of the casting. For molds manufactured each time from aggregates, the cooling is slower usually giving poorer properties to the casting, but there is no waiting time for solidification. Productivity is now governed by the speed at which molds can be made. This can be impressively high for highly productive green sand plants; a mold every 10 seconds is possible. Furthermore it is common for the mold to contain more than one impression.

This broad-brush description requires much, very much, qualification as is attempted in this chapter.

---

## 15.1 INERT MOLDS AND CORES

As mentioned in Section 4.1 Very few molds and cores are really inert towards the material being cast into them. However, some are very nearly so, especially at lower temperatures.

Metal molds have the great advantage that they are relatively inert towards the liquid metal. They are usually used warm and dry, so their intrinsic hydrogen content is low, in sharp comparison to the various aggregate molds that contain sufficient moisture and other volatile and reactive components to make copious and generous contributions to the cast metal.

The usefulness of a relatively inert mold is emphasized by the work of Stolarczyk (1960), who measured approximately 0.5% porosity in gunmetal casting into steel-lined molds, compared with 4.5% porosity for identical test bars cast in greensand molds.

For light alloys and lower-temperature casting materials, investment molds are largely inert. Interestingly, dry sand molds (i.e. greensand molds that have been dried in an oven) have been found to be largely inert, as shown by Locke and Ashbrook (1950).

Carbon-based and graphite dies have been found useful for zinc alloys. However, their lives are short for the casting of aluminum alloys because of the degradation of the carbon by oxidation. All the more impressive therefore is the use of graphite molds for steel, used for the casting of millions of railroad wheels by the Griffin Process. Carbon-based molds are used for the casting of titanium alloys in vacuum. Oxidation of the mold is reduced by the vacuum environment, but the contamination of the surface of the titanium casting with carbon is severe, promoting the formation of an outer layer of the alloy where the titanium alloy alpha-phase is stabilized. This surface layer is known in titanium castings as *the alpha-case*. It usually has to be removed by machining or chemical dissolution.

### 15.1.1 Permanent metal molds (dies)

The use of a mold that is permanent has always been attractive to founders ever since the use of hollowed out pieces of stone used to cast multiple copies of bronze axes and arrow heads.

The concept remains popular because usually the customer will pay for it, and once paid for, the mold then costs little more in service, provided no catastrophe overtakes it. Unfortunately, it has to be noted, catastrophic failure, often as a result of thermal fatigue aided by internal stress from its heat treatment, is not uncommon.

The practice of using permanent molds is, with some significant exceptions that will be listed below, usually confined to low-melting-point alloys; aluminum alloys being the most common. Other cast materials include alloys of magnesium, zinc, and lead. Only rarely are permanent molds used for the higher-temperature alloys such as brasses and bronzes, and cast iron.

The major metallurgical benefit of a metal mold, compared to an aggregate mold, is the relatively rapid freezing, conferring higher mechanical properties. Moreover, the liquid metal and mold are practically inert towards each other, so that there are no significant chemical reactions. This is an additional and significant metallurgical benefit of metal molds that is often overlooked.

The major challenge provided by permanent molds is that the mold has to be designed to disassemble to release the casting. This obvious point is not to be underestimated, since for many castings this presents major limitations to both the casting and the filling and feeding systems. Sand castings have no such problem since the mold is destroyed to release the casting, thus allowing geometries of almost any complexity or sophistication.

#### Gravity and low-pressure die-casting dies (permanent molds)

For dies filled simply by pouring under gravity, they are not surprisingly called *gravity dies* (known in the USA, also not surprisingly, as *permanent molds*). The service conditions for a gravity die are not too severe because the die is to some extent protected from direct contact with the melt by the application of a die coat. More details are given in Chapter 16 'Casting'.

Low-pressure die casting dies are extremely similar; being made from iron or steel, depending on the service requirements, and once again enjoy the protection of a ceramic die coating applied as a wash by painting or spraying.

One of the most notable high-temperature developments of low-pressure die casting is the famous Griffin Process for steel railway rolling stock. In this case the dies are machined from graphite. Although a successful process has been built on this process, the machining of graphite is always a somewhat messy and dirty occupation. There seems little doubt that the process might have been operated with greensand with practically no loss of accuracy and no loss of performance of the steel casting. It would be interesting to see a comparative evaluation of the two types of mold for this high-volume product.

#### High-pressure die-casting dies

High-pressure die casting is known in the USA, confusingly, as die casting.

Dies for pressure die casting are hardly inert, partly because of the gradual dissolution of the unprotected steel die, but mainly because of the overwhelming effect of the evaporation of the die-dressing material. This may be an oil- or water-based suspension of graphite sprayed onto the surface of the die, and designed to cool and lubricate the die between shots. The gases found in pores in



pressure die castings have been found to be mainly products of decomposition of the die lubrication, and the volume of gases found trapped in the casting has been found to correspond on occasions to nearly the volume of the die cavity.

A little-known problem is the boiling of residual coolant trapped inside joints of the die. Thus as liquid metal is introduced into the die, the coolant, especially if water-based, will boil. If there is no route for the vapor to escape via the back of the die, vapor may be forced into the liquid metal as bubbles. If this happens it is likely that at least some of these bubbles will be permanently trapped as blow holes (note the *correct* and rather rare use of the term ‘blow hole’ in this instance) in the casting. This problem is common in pressure die and squeeze casting processes.

The recent development in pressure die casting to separate the functions of (i) cooling of the die and (ii) its lubrication, is seen as a positive step toward solving this problem. The approach is to use more effective cooling by built-in cooling channels, whereas lubrication is achieved by the application of minute additions of waxes or other materials to the shot sleeve.

When used for its common purpose of casting aluminum or magnesium alloys the dies are necessarily made from good-quality hot work tool steel, H13. In this case gray iron would not have the adequate surface integrity because of the presence of graphite flakes in the material, and would not have the strength or fatigue resistance. No protective coating is applied to the surfaces of the die. The result is an excellent surface finish. The danger of cold laps is reduced by extremely rapid filling, and by high pressure that is subsequently applied to ensure faithful reproduction of the profile of the mold. Even so, of course, the high speed of filling causes other serious problems that we shall consider later.

Like all dies, however, it is regrettable that they are not really permanent. An aluminum casting weighing up to 1 kg might be produced tolerably well for up to 80 000 or 100 000 shots before the die will require to be refurbished as a result of heat checking (cracks due to thermal fatigue of the die surface that produce a network of unsightly raised fins on the cast surface).

Magnesium alloy high-pressure die castings are much kinder to dies, giving perhaps five times or more life. This is partly the result of the lower heat content of Mg alloys, and partly because of the low solubility of iron in liquid magnesium that reduces its action to dissolve the die surface. In contrast, liquid Al has a relatively high solubility of iron, resulting in a phenomenon known as ‘soldering’ of the casting to the die. This action is particularly destructive to dies. It is countered to some extent by the addition of high levels of iron to high-pressure die-casting alloys, thus pre-saturating the liquid metal with iron and so greatly reducing the tendency for the melt to dissolve the die.

Attempts have been made to cast molten stainless steels by high-pressure die casting. In this case the only die material capable of withstanding the rigors of this process was an alloy of molybdenum. Even these ‘moly’ dies suffered early degradation by thermal fatigue cracking, threatening the commercial viability of the process. So far as the author is aware, partially solid (inaccurately called ‘semi-solid’) stainless steels have not been extensively trialed. These cooler mixtures that have already given up practically half of their latent and specific heat during freezing would greatly benefit die life. The commercial viability of the somewhat more expensive mixture would remain a potential show-stopper of course.

Because of the very high pressures involved in HPDC internal cavities are usually limited to those formable by straight withdrawable steel cores. If the core cannot be withdrawn then the usual alternatives such as sand cores are totally unsuitable because they are penetrated by the liquid metal. One of the very few options to make undrawable cavities in HPDCs are salt cores described below.

### 15.1.2 Salt cores

Salt cores are a class of components that once again can be extremely dry and can be used hot. Provided the salts are mainly chlorides and fluorides these highly stable compounds have very little reaction with most molten metals.

They are useful to provide the undercuts and other difficult-to-mold features in permanent mold and in high-pressure die casting (HPDC) of Al alloy parts, where simple two-parted dies are preferred for robustness and mechanical simplicity. The core is subsequently dissolved out by immersion in water. They are also occasionally used in permanent molds, for instance for the oil cooling channel in Al alloy pistons.

Loper and colleagues (1985) review how salt has been used in various ways to make cores in Al alloy and gray iron castings. They describe many different mixtures of salts, including NaCl, KCl, and CaCl<sub>2</sub>. The only problem they reported was the loss of some mechanical properties of the cores during periods of high humidity. The cores were dissolved out by simple immersion in cold water, but faster in hot water, and faster still by pressurized water jet.

- (i) Solid salt cores have been made by the casting of molten salt using a gravity die (permanent mold) process.
- (ii) Solid salt cores can be made by pressure die casting. Their successful use for internal combustion engines includes such achievements as closed deck cylinder blocks, as demonstrated by the Mercury Marine company in the USA since 1976. The heat content of the salt is sufficiently low that the dies have never been observed to suffer from any heat checking (cracking) problem. The cores are used almost immediately, being ejected from the first machine and loaded into a second pressure die-casting machine standing nearby to make an Al casting. The cores may be subjected to a temperature equilibration treatment in an oven, the high coefficient of thermal expansion of the salt allowing an adjustment of size of the core if necessary.

One of the major advantages of the salt core technique in HPDC is its flexibility. It allows expensive tooling to be adapted, simply changing the salt core dies to revise the inner features of the casting, for a fraction of the cost of complete new tooling. With changes to cylinder bore diameter, or iron sleeves, etc., a block can be refurbished quickly and at minimal expense, compared to conventional HPDC tooling. Also, of course, the cores can provide much more complex internal detail. Major complex parts for small engines such as closed deck cylinder blocks could not be made without the use of such cores.

The cores are characterized by excellent surface finish and accuracy. Core breakage problems appear to be practically unknown. Furthermore, the salt casting is optimized for internal porosity simply by holding it against a light, since it is translucent. No costly X-ray radiography is required.

Although to make a HPDC it is first necessary to make 'a second HPDC' tool for the core, the salt casting costs only about one-quarter or one-fifth of the cost of the Al die casting so the economics are not discouraging. The rate of production of cores matches the rate of production of Al castings, and the rate of washing out is twice this rate.

- (i) Aggregates bonded with salt have sometimes been used. The aggregates have been alumina, iron oxide, or silica sand and up to 40% by volume of salt has been used.
- (ii) A mixture of grains of an inert aggregate with grains of salt both bonded with a resin binder. The best solution rates were achieved using a similar size of sand and aggregate grains since this

maximized the permeability of the core. The production technique has the benefit of being a cold process using normal core production techniques.

Salt cores have been used for many years world-wide for the production of oil galleries in Al alloy gravity cast pistons. There is still interest in Japan on improving these core materials still further (Yaokawa 2007).

These versatile molding materials probably deserve wider use throughout the industry.

### 15.1.3 Ceramic molds and cores

The other category of inert molds is the ceramic molds. Thus lost wax molds are fired at high temperature (usually 1000°C or above) and thus are especially dry. In addition, of course, ceramic molds can be used at high temperature, so there is a greatly reduced chance for reactions with volatile mold components.

Ceramic molds are such a specialized technology that only an outline can be given here. A tremendous and unique advantage is the freedom to select an appropriate mold temperature for casting. Ceramic molds are usually fired to a relatively high temperature prior to casting. Thus they are generally free from outgassing and reactivity problems with melts. Ceramic molds for light metals are often preheated to a temperature in excess of the freezing point of the melts so that there are no problems of fluidity – if a sufficiently long fluidity test could be devised the melt would run for ever! For Ni- and Co-based superalloys for single crystal turbine blades, the molds are similarly held above the freezing point of the melts during filling, and only slowly withdrawn into a cooling zone to grow the crystal under conditions of controlled speed and temperature gradient.

#### Investment shell (lost wax) molds

As a monarch might be *invested* in the *vestments* of royalty, the verb *to invest* means *to coat, cloak, or enrobe* and thus nicely enshrines the concept of the making of an *investment coating* around a wax pattern, which is *invested* (i.e. *coated* by dipping) in successive layers of a slurry of finely powdered mineral, most commonly zircon or aluminum silicate (mullite), and binder (typically a very fine dispersion (a sol) of silicic acid). A coarser mineral (stucco) is applied to each layer of slurry before drying, so as to gradually build up a shell. The investing process is the special feature that confers the admirable surface finish and fine detail that investment castings enjoy. After drying, the shell is steam heated, typically in an autoclave to melt out the wax, giving the process its other well-known name, the *lost wax* process. Having lost its wax, the shell is then fired to (i) burn out any residual carbon remaining from traces of wax, and (ii) develop the full strength of the shell. Strength development during firing comes about as a result of the silicic acid losing its water and being converted to a ceramic substance (cristobalite). Sometimes the shells are cooled to room temperature once again and checked for cracks which are then repaired. Otherwise, the shells are taken directly at the firing temperature and filled with metal.

When the casting has cooled to room temperature the shell has to be removed. This can present a problem. Many shells are stronger than the light alloy castings they contain, so that mechanically breaking off the shell can easily damage the casting. Analogously, the Ni-based single crystals are vulnerable, since any impact damage can cause a recrystallization event during the subsequent heat treatment, thereby scrapping the blade.

Other disadvantages with the lost wax process include high unit cost, high energy consumption and the fact that the spent shells are not reclaimed, although work is in progress to improve the latter. It should also be noted that it is difficult and expensive both to make cores for investment casting and to remove them afterwards. One common approach is to prepare a core by injecting a slurry of ceramic and wax into a core box cavity, cooling the resultant product and then firing it. The core can be removed from the casting mechanically or by washing with caustic soda solution, techniques which are only feasible for ferrous metal castings.

Yet more potential problems should be highlighted: accuracy starts to be a significant problem for larger investment castings. This mainly results from distortions that occur in the wax, prior to investment. For this reason the provision of costly jigs and fixtures to straighten wax patterns is sometimes essential to guarantee accuracy.

Graphite-based investment shells have been used, particularly for very reactive metals such as titanium and zirconium (Howe 1965).

A number of recent developments are promising to revolutionize the lost wax process. These include new, low-cost aggregate systems, new binder systems, techniques enabling shells and cores to be made far more quickly and cheaply and shells and cores that can be removed by washing with water after casting. This may lead to a growth in the popularity of lost wax investment casting, particularly for light metals.

#### Investment two-part block molds (Shaw Process)

The investment block molds, originally called the Shaw Process, originated in England by two British scientists, Clifford and Noel Shaw, in 1938, the year of my birth.

Although the process has generally fallen into disuse because of the apparent economy of simply making a lightweight shell, it has interesting strengths and advantages. For instance a key difference between the shell and the block processes is that the block mold is made up as a cope and drag by the use of normal patternwork (not a wax pattern).

Ceramic slurry is prepared as a colloidal suspension of silica in alcohol, to which are added various ceramic fillers to make a smooth cream. The slurry is poured (invested) over a pattern, filling up to the top of a surrounding frame. After the mold is nearly set, but retains some flexibility as a gel, it is stripped from the pattern and placed on a board to dry and develop its green strength. At this stage the alcohol is flamed off, causing the surface of the mold to develop its characteristic micro-crazed structure, conferring essential permeability and thermal shock resistance to the mold. In this way a drag half of a mold can be made. The cope half is made similarly. The two halves are then assembled, fired and cast. The cope and drag technique for mold assembly allows cores to be placed. Errors from the distortion of the wax pattern are also avoided. Lubalin and Christensen (1960) give a good description of the process and the wide range of castings that can be made.

One can envisage a more modern variant of this process in which the mold halves are injection molded, and thus produced rapidly for volume production with a fully robotized process. This concept seems ripe for re-examination and fuller exploitation.

#### Plaster investment block molds

Plaster of Paris ( $\text{CaSO}_4 \cdot \frac{1}{2}\text{H}_2\text{O}$ ) is used as a mold material to make block molds by a variant of the lost wax investment process. Plaster formulations contain 15–25% plaster of Paris, the remainder being inert fillers such as quartz and cristobalite and often Portland cement.

After energetic mixing of the powder mixture with water to make a paste, the mixture can be subjected to a vacuum and mechanical vibration to encourage the detrainment of bubbles, after which the mixture is poured around the wax pattern. The plaster takes up water of crystallization, converting to gypsum ( $\text{CaSO}_4 \cdot 2\text{H}_2\text{O}$ ) and turns solid. Controlled slow drying follows, then de-waxing, and final firing at about  $700^\circ\text{C}$  (any higher temperature would cause the gypsum to lose its water of crystallization and break down to a powder once again). In this way a one-piece block mold is made by a variant of the lost wax process.

The combination of this process with the application of a reduced pressure applied to the base of the permeable molds (the steel box is open at its base) is the principle of the vacuum-assisted casting, allowing the pouring in air of extremely thin-walled castings only a fraction of a millimeter in wall thickness (Figure 16.29). The natural high fluidity noted in this process arises because of the high temperature of the mold (above the freezing point of the alloy, so that 'fluidity' in terms of flow distance is effectively infinite) and its extremely low thermal diffusivity. The process is ideal for aluminum and magnesium alloys, but can also produce some copper-based products if the castings are not too heavy.

The castings can be de-molded by placing the molds in water, causing the mold material to spall, pieces jumping off in a series of energetic and noisy explosions. The final traces of wet mold are brushed or washed away.

#### 15.1.4 Magnetic molding

The concept of holding a mold of fine steel shot together as a rigid mold by the application of a magnetic field has an alluring attraction. This apparently attractive process was invented in 1971 (Wittmoser 1971, 1972, 1975) but never seems to have come into general use. Steel shot is 'frozen' into position around the pattern by the application of a magnetic field. After the casting is poured and solidified, the magnetic field is switched off, allowing the mold to disintegrate and the casting to be removed.

The reality, however, may be something else. Since Wittmoser first publicized his work in Germany relating to magnetic molding in 1975, little has been done to extend and confirm this early sign of promise, and this early failure to develop the process has never been explained. Wittmoser poured cast iron into lost foam molds surrounded by steel shot in an Al alloy molding box, the shot being held in place by a powerful magnetic field. This early work was almost certainly undermined to some extent by the mold material exceeding the Curie temperature of mild steel at approximately  $900^\circ\text{C}$ . Above this temperature the ferromagnetic property is lost, so that parts of the mold would have become effectively non-magnetic. This may have explained some of the difficulties with the original experiments. Later workers (Geffroy et al. 2006) trialed Al alloys. At this lower casting temperature the process might have been expected to have achieved more success. However, all these early trials continued to use a lost foam pattern as a starting point. This starting point may have been necessary to support the steel shot, but the process appears never to have been tested without this support, so remains unclear. If the magnetically held mold did not require the foam pattern for support it would have been valuable to know.

A further important disadvantage, apparently never mentioned in print, would be the cost of maintaining the powerful magnetic field that would have been required. In times gone by this would only have been possible with the use of powerful electromagnets, thus consuming significant amounts

of power for all the time the mold is made, assembled and cast. A hold-up on the casting line would have been particularly expensive. Nowadays a sufficiently powerful field may be available with modern permanent magnets, such as the neodymium–iron–boron types. As with all permanent magnets, such devices can be effectively switched on or off by the use of keepers. This possible option appears never to have been tested.

Although claims have been made that the technology combines the benefits of sand molding with the rapidity of freezing of metal mold Geffroy finds this to be largely untrue. The solidification rate is much nearer to that of sand molds. This follows from the reduced contact between steel particles and the lower overall bulk density of the packing of the steel.

This process might be significantly more attractive if freed from the lost foam approach. The ability to make conventional ‘lost air’ magnetically molded castings in copes and drags may yet hold promise. However, finally, we have to conclude that we all remain in the dark about the viability and economic value of this technology.

---

## 15.2 AGGREGATE MOLDING MATERIALS

Ken Harris (2008) has passed on to me a useful little formula due to Dr Robert Sparks (2000). It is approximately:

$$\text{AFS number} \times \text{micrometers} = 15\,000$$

Thus the widely quoted AFS fineness number for aggregates, particularly sands, can be approximately converted quickly into average grain diameters. Thus we obtain some rough equivalents that are useful to commit to memory:

$$\text{AFS } 50 = 300 \mu\text{m}$$

$$\text{AFS } 75 = 200 \mu\text{m}$$

$$\text{AFS } 100 = 150 \mu\text{m}$$

$$\text{AFS } 150 = 100 \mu\text{m}$$

$$\text{AFS } 200 = 75 \mu\text{m}$$

When the molten metal enters an aggregate mold, the mold can react violently. Frenzied activity crowds into this brief moment of the birth of the casting: buckling, outgassing, pressurization, cracking, explosions, disintegration, and chemical attack. After all these possibilities the survival of a saleable casting should perhaps be a matter for surprise. In this section we examine the options for the casting engineer to ensure that the molding and casting processes are appropriate, economic, and under control.

Non-permanent molds made from particulate materials that are designed to be broken up to release the casting after it has solidified are commonly known as sand molds. However, there are now so many options for aggregates that are no longer really ‘sands’ that it hardly seems appropriate to continue to call them sand molds. We should be calling them aggregated molds (but the reader will notice occasional lapses by the author).

The many aggregates that can serve as adequate molding sands have been reviewed many times. The reader who would like more detail is referred to reviews by Middleton (1964), Garner (1977), Rassenfoss (1977), and Harris (2005).

The nature of aggregate molds is nicely illustrated by the observation that patterns transferred from old jolt-squeeze machines to new high-pressure molding machines produced castings that were undersize (simply because the molds were harder and did not yield a little, becoming oversize, under the weight of the melt, or the pressure generated by the graphite precipitation when casting iron).

### 15.2.1 Silica sand

Naturally, the most common aggregate still in use is silica sand due to its world-wide availability, appropriate particle size and distribution, and high melting point. Even so, the situation is undergoing rapid change as a result of the danger of breathing in silica dust leading to the danger of silicosis, an incurable and sometimes deadly affliction. At the time of writing, silica sand in foundries is already banned in New South Wales, Australia.

In addition, the alpha quartz to beta quartz transition at around 530°C is accompanied by a total volume expansion of about 2.5% leading to length changes in the mold of around 1.5%. This is a serious volume change and gives the founder many problems of mold failure and loss of control over casting accuracy. For instance, in a mold 600 mm long with a delicate central core, when surrounded by liquid aluminum at 700°C, the core would easily exceed 530°C, but the mold would only achieve less than half of this increase, making a differential expansion of the order of 1.0%. Thus the core would expand relative to the mold by  $600 \times 1/100 = 6$  mm. For a modern light-weight casting with walls at each end of the casting only 4 mm thick, the walls might be only 1 mm thick if the expansion were symmetrical. If not, the wall thickness could easily be 2 mm at one end and 0 mm at the other. It is understandable that customers are resistant to the offer of windows in their castings in exchange for walls.

The problem of the large and non-linear expansion of silica sand is even worse in ferrous castings, particularly where castings are made with new sand. However, repeated reuse (recycling) of silica sand can reduce the problem, since the proportion of more stable forms of silica such as cristobalite tends to increase each time the sand is heated to higher temperatures. Light-alloy foundries do not generally heat enough of the sand sufficiently to gain this benefit, although light-metal foundries that use thermal sand reclamation methods may do so.

It is also worth noting that the thermal shock responsible for the change of crystalline form of silica leads to increased fracture of the sand grains. This will cause a good-quality, round-grained silica sand to become steadily more angular in shape, thereby increasing binder demand for the same sieve analysis, impairing surface finish of the castings, and wearing out tooling and plant at an enhanced rate (as witnessed by the huge accumulation of iron filings on the magnet in the sand recycling system).

There are other natural sands that do not share all of these problems. These include zircon (zirconium silicate, a white, yellow, or orange sand mainly produced in Florida and Australia, and rather expensive because of its rarity). Another is chromite, usually available as a crushed mineral, black in color. The other common crushed molding aggregate is olivine (that derives its name from its olive color when new, although it turns brown after use for casting) and widely used in steel casting to reduce both expansion and metal-sand interactions. These three products contain little or no free silica and have relatively low and linear thermal expansion coefficients.

Finally, it is of interest that some silica sands, such as those produced in Sweden, contain quantities of feldspars (up to 25–30%) that help to reduce the deleterious effects of silica expansion. These feldspars work in two ways: (a) by virtue of their lower, more linear expansion, and (b) because some melt at lower temperatures than silica, thus counteracting the general expansion of the mold or core from which they are made. These facts do, however, argue against these sands being used for high-temperature work, e.g. large ferrous and steel castings.

Some suppliers offer additives that can be mixed in various proportions with silica sand to reduce the effects of the expansion caused by the change in crystalline structure. Common to many of these is a content of iron oxide (Naro 2000). These would appear to function in a similar way to the naturally occurring feldspar/silica sands described above; however, they may have a role to play where such sands are not locally available. A novel approach showing much promise uses additions of sodium bicarbonate to a urethane-bonded sand. The approach appears to work by generating a foam structure in the bond material which allows the core sufficient plasticity to avoid cracking (Schrey 2007).

### 15.2.2 Chromite sand

Chromite is a widely used aggregate valued for its relatively low thermal expansion and good chilling power, particularly for steel castings.

However, the general problem with chromite is only found in steel casting operations where it is commonly employed as a facing sand for silica molds. Here the surface of the casting can become coated in so-called ‘chromite glaze’, the result of chromite being fluxed by silica or clay, or simply by the decomposition of chromite as discussed below. This is difficult to remove and results in a poor finish to the casting (Petro and Flinn 1978).

The chromite glaze problem has been assumed to be the formation of fayalite (ferrous orthosilicate  $\text{Fe}_2\text{SiO}_4$  with a melting point of  $1205^\circ\text{C}$ ) as the reaction product between silica and chromite. Fayalite is not magnetic and so cannot be separated from the sand magnetically. During the recycling of the sand this low-melting-point constituent therefore builds up, lowering the refractoriness of the molding aggregate. It seems likely that another ferrous silicate, grunerite ( $\text{FeSiO}_3$ ), also non-magnetic, with a melting point of about  $1150^\circ\text{C}$  may also contribute to the impairment of the foundry sand for ferrous castings. These issues have yet to be properly researched and clarified.

An additional problem with chromite is that it is not particularly stable at steel casting temperatures. In oxidizing conditions it slowly oxidizes to  $\text{Fe}_2\text{O}_3$  and  $\text{Cr}_2\text{O}_3$  but in the presence of carbon from organic binders its iron oxide constituent can reduce to liquid iron. Drops of liquid iron form microscopic beads on the surfaces of the sand grains (Scheffer 1975, Biel et al. 1980) causing the sand to become highly magnetic (as quickly tested by the reader with a hand-held magnet). The reducing conditions are of course avoided by the use of carbon-free inorganic binders such as silicates. Whether oxidized or reduced, the weakened grains subsequently crumble to fragments.

Most chromite sand is derived from crushed ore, and so as well as being therefore rather angular, dust is created during conveyance which in turn increases the risk of reaction with silica sand. In general, it is estimated that 20–30% of chromite sand is lost each time that the sand is reused.

### 15.2.3 Olivine sand

Olivine sand is sometimes used as an alternative to silica, primarily by foundries that cast high-alloy steels. Olivine possesses a number of advantages compared to silica, the most important being a lower



and more uniform thermal expansion and inertness towards certain difficult alloys, notably manganese steels. As olivine does not react with chromite, unlike silica, it can be tolerated at far higher levels in reclaimed chromite sand, and vice versa. Furthermore olivine with low loss on ignition (LOI), having a low serpentine content, is not regarded as being hazardous to health. Olivine sand does not react with alkaline binders. Some foundries use a 'dead-burnt' serpentine/olivine which is brown in color and behaves similarly to ordinary olivine.

In spite of these valuable advantages, olivine is not widely used for two main reasons. The most important is that it is incompatible with the common binder system, furan no-bake (FNB), and requires specially formulated phenol-urethane no-bake (PUNB) binders. This means that olivine is used almost solely with alkaline binders and this leads to low sand reclamation rates with conventional equipment. A secondary disadvantage suffered by olivine sand is that it is, like chromite, made from crushed rock and thus possesses an angular grain shape that causes dusting during conveying and mixing. Finally, the refractoriness of olivine is related to its iron content, which for steel casting should not be greater than 8% and for certain goods, e.g. large carbon steel castings, maximum 6%.

#### 15.2.4 Zircon sand

Zircon sand is a light color, and generally in the form of fine rounded grains. Its extremely low and linear coefficient of expansion allows it to make extremely accurate cores and even whole molds. Its high bulk density almost exactly matches the density of liquid aluminum, so that cores have close to neutral buoyancy, which makes zircon the ideal aggregate for delicate and poorly supported cores in Al alloy castings.

Zircon has a fairly high thermal diffusivity compared to silica, giving it greater chilling power and faster freezing of castings. However, this effect is not great, and in any case, greater chilling power is a two-edged sword; although conferring slightly improved properties for the casting, the achievement of thin-walled sections is made more difficult.

The high density of zircon (nearly double that of silica sand) leads to significantly greater mechanical handling challenges in the foundry. Robots for conventional sand molds will usually find zircon molds too heavy to lift, and sand silos require strengthening. Vibrating equipment and pneumatic conveying systems require twice the energy.

The rate of wear of patternwork and tooling is a serious consideration when using denser molding materials. Zircon in particular is found to be especially abrasive towards tooling as a result of its hardness and its high density thus requiring high blow pressures on core blowing machines to fill core boxes. As the percentage of broken zircon grains increases with cycling around the sand system, the increasing number of sharp edges greatly increases the rate at which it can inflict wear damage on the core boxes and other expensive tooling and plant. Although foundries that use zircon complain about its high cost, the real hidden cost is the rate of destruction of the tooling.

#### 15.2.5 Other minerals

There seems no shortage of minerals that would make good molding materials (Ramrattan et al. 1996). Of growing interest is the possibility of using quite new minerals for molding that could be available as fines, the unwanted by-products of crushed aggregates for other purposes such as road making, and thus in plentiful supply and at relatively low cost. One such material is Norite. Another might be anorthosite. When it is realized that there are probably 10 or 20 local quarries for every foundry,

supplies of such materials seem virtually unlimited (Harris 2005). In addition, the relative closeness could mean considerable savings for some casting operations that are hundreds of kilometers from a source of the more traditional sands, and for whom the transport cost of the sand is the major part of the mold costs.

From time to time investigators have reported the benefits of molding in various kinds of bonded metal shot. For instance, Al shot has been used for the casting of Al alloys, and steel shot is commonly used for many alloys. The rusting corrosion of these metals is a source of trouble that prevents the easy recycling of the material. Also, of course, for steel shot the molding material is heavy, and requires strengthened storage silos, and expensive, heavy-duty cranes and mold handling equipment.

There has been a long-standing interest in molding with hollow ceramic spheres that originate as a component of flue-gas dust from fuel-fired power stations. The particles are occasionally known as cenospheres. They are extraordinarily light and insulating, and have a melting point in the region of 1400°C. Because of their extremely low thermal diffusivity metals tend to run twice or three times as far in such molds. They have wide uses for the casting of many metals up to the melting point of cast irons (Showman 2005, 2007). Their suitability for re-cycling at a reasonable rate is questionable however, because the spheres are relatively easily broken during mold compaction or possibly by the thermal shock of casting.

### 15.2.6 Carbon

Carbon has been used for molds in a variety of ways. Investment molds have been mentioned above. However, its use as an aggregate represents a major application.

The aggregate particles can be round, fine grains that can be bonded with clay and water mixes (Saia and Edelman 1968) or enhanced with syrups (Kihlstedius 1988) to make a 'greensand'. Alternatively they can be bonded simply with a resin binder (Clausen 1992). The light weight of graphite does not provide it with much thermal capacity, but its excellent thermal conductivity can be useful. Its stability of dimensions is the result of its extremely low coefficient of thermal expansion, and its chemical stability has found good use in the casting of the extremely reactive Mg–Li alloys (Saia and Edelman 1968), copper-based alloys (Clausen 1992), titanium alloys (Pulkonik 1967), and uranium (Edelman and Saia 1968). Practically, of course, in the foundry environment it is welcome as a result of its light weight, greatly easing the handling of molds and cores.

For ferrous alloys the carbon sand has uncomfortably high sulfur content, sometimes as high as 7 wt% (Gentry 1966). This can contaminate the surface layers of steel castings, and lead to loss of nodularity in the surface layers of nodular cast irons. The sulfur content can be reduced during the manufacture of the sand, boiling off the sulfur at treatment temperatures in the region of 1000°C.

Another major use of carbon is in permanent molds, machined from solid blocks of graphite. Mihaichuk (1986) describes the successful use for the casting of ZA (zinc–aluminum) alloys. The process is also highly successful for the casting of steel rail road wheels as seen in the Griffin Process.

The author has only one experience of attempting to introduce the large-scale use of carbon in the foundry. This was a trial using carbon fibers for reinforcing delicate water jacket cores for high-performance cylinder heads. The fibers flew about in the atmosphere, were trodden and crushed underfoot and reduced to powder at several other stages of manufacture. After a week or so, the powder eventually found its way into our numerous electric motors and other equipment around the plant and shorted these out, bringing the plant to a stop. The trial was immediately discontinued and never repeated.

---

## 15.3 BINDERS

Aggregate molds such as sand molds require the individual particles to be held together with some kind of binder. There are very many binders from which to choose but the broad categories are listed below.

### 15.3.1 Greensand

Greensand is perhaps the most widely used molding medium, consisting of the aggregate, bonded with a mixture of mainly clay and water.

Greensand can be almost any color including brown, red, or black, but I have never known it to be green. It should be written as one word, 'greensand', not as 'green sand'. Its 'greenness' refers to its weak, plastic condition in contrast to that of dried molds which are extremely hard and rigid. The greenness concept is common to other industries such as ceramics where a ceramic component has only green strength until it is fired to melt the glaze bond after which it becomes as hard and brittle as glass. The origin of the concept of greenness almost certainly lies in forestry and timberwork, where the wood is green and flexible when full of sap, unseasoned, prior to drying.

Greensand always has been and remains one of the most important and common binder systems. It is low cost, environmentally friendly (since there can be minimal toxic additions) and recyclable. However, most important of all, it is extremely fast. Compared to chemically bonded molds which can be produced at perhaps 60–100 per hour, modern greensand plants can produce 600 molds per hour. These awesome rates follow from simple fundamentals: once all the grains are evenly coated with the clay/water binder, the bond is formed simply by forcing the grains together. Thus the bond is formed instantly simply by pressure. No other process can compete for speed of molding. Busby (1996) gives a good review of greensand versus other molding processes.

The disadvantages are that the mold is somewhat plastic (i.e. remains rather 'green') so that if the aggregate is not particularly well consolidated, the mold can distort, producing an inaccurate casting. For instance the mold can sag under the weight of heavy cores, or the weight of the casting, or soft-spots can yield under the pressure of liquid metal leading to local swells on the casting (the pressure can be high from the depth of metal in a tall casting, and from the expansion of graphite in cast irons).

These disadvantages are now countered rather successfully by modern molding plants that in addition to their high speed give a mold that is impressively well consolidated. Whereas a mold compacted by hand could show a complete hand print (including the finger prints on all fingers), a really strong mold made on a modern automatic greensand molding plant is so hard that a rather limited thumb print is all that the average person can easily make.

The limit to the hardness of greensand molds is set by the pressure at which the whole mold and its steel molding box will distort elastically, causing the mold to spring into a new shape on being stripped from the pattern. This limit seems to be about 1.0 MPa (150 psi). It creates problems for the founder because such elastically distorted mold halves do not close properly. The faces of the mold bow elastically into a convex form, causing the two mold halves to impinge in their central areas, causing features such as sharp edges in the center of the mold face to break off. This effect is generally controlled by the relief of the tooling to give the region adjacent to such edges sufficient clearance to

avoid direct contact, but not sufficient for the metal to penetrate to cause expensive flash. Such clearance is generally in the region of 0.1 mm and 5–10 mm wide.

Cores may absorb water from the greensand, particularly if a delay happens between coring up and casting, as when a stoppage on the line occurs. Similarly, condensation may occur on metal chills. Condensation occurs even in rather dry resin-bonded sand molds if left closed overnight. This is because the molds cool during the night, but during their re-heating in the morning vapors are driven inwards by the inward flow of heat, thus condensing the volatiles onto the interior metal chills, still cold from their overnight cool. If cored-up molds are required to be stored overnight they should be left open. Condensation problems are then avoided.

There is a strong move nowadays to reducing or eliminating the organic additions to greensands (Grehorst and Crepez 2005). Organics heat up, and pyrolyze or burn, often giving off unhealthy emissions. Thus the motivation is to return to inorganic mixes based on simpler clay/water binders. This subject is too extensive to be reviewed in this work. The interested reader is referred to the important series of researches published over a number of years by Heine and Green (1989 to 1992).

Nearly all the important engineering metals continue to be made in greensand, including Al, cast iron, and steel.

For a small number of hand-molded castings, oil is mixed with the clay instead of water. Oil-bonded greensand is a traditional molding material still popular with model-makers as a result of its plasticity, conferring easy molding and yielding a good surface finish of the castings. The oil/clay/sand mix has such good flowability that it is appropriate for small parts, but, as a result of it being generally ‘greener’ than water-based greensands, it is not suitable for castings weighing more than about 1 kg (Butler and Lund 2003).

### 15.3.2 Dry sand

Dried greensand cores were one of the traditional solutions to the unsuitability of greensand as a core material. The drying process increased the strength enormously, and reduced the outgassing from the relatively high water content (often in the region of 2–4 wt%) of greensand. The cores had to be supported in their green state on cradles called ‘driers’ during being transferred to drying ovens. The process was akin to that used for linseed-oil-bonded cores. Naturally, the drying process was lengthy and energy-intensive. Furthermore, the hardening ‘out of the box’ meant that core distortion was a common problem despite the hundreds or thousands of ‘driers’ that were in use at any one time.

Dry sand cores and oil-baked cores have now been practically entirely superseded by the various chemical binder systems. These later processes harden cores in the core box, thus enjoying the benefit of a huge increase in accuracy. The appellation ‘No-Bake’ applied to many of the modern binder systems is a reminder of the slower, less-convenient binders dating from earlier days, based on oils that required baking in a core oven for many hours.

### 15.3.3 Chemical binders

There are now so many chemical binder systems that it is not possible to review the field here. For those wanting to review the first efforts to use a variety of vegetable and mineral oils and resins the review by Middleton (1965) is interesting. Later reviews of more modern binder systems are provided by Webster (1980) and by Archibald and Smith (1988).

A perfect binder would have low viscosity so that the aggregate mix had good fluidity, and in its cured form was strong, so that little addition was needed, retaining the void content of the aggregate to maximize permeability. It should also react minimally with the melt. However, of course, the chemical interactions increase in number and severity with increasing temperature, so that whereas aluminum may not suffer too much, irons and steels can be significantly damaged by interactions with the mold. The reactions occur with both the mold surface and with the atmosphere formed in the mold during filling with the hot metal. Working our way up the temperature spectrum of casting alloys we have:

- (i) Low-melting-point lead and zinc alloy liquids generally cast at temperatures up to 500°C are too cool to cause significant reactions.
- (ii) Magnesium and aluminum have casting temperatures commonly up to 750°C. They react with water vapor and various organics to produce the solid oxide skin and free hydrogen that can diffuse into the melt. These reactions continue for some time after solidification and during cooling. This source of hydrogen is likely to be important in growing pores that are located just under the casting surface. Subsurface porosity, particularly in Al alloys, is described at several points in Chapters 6 and 7. Despite this reactivity at the surface of the liquid metal, it is worth noting that the temperature at which light alloys are cast does not lead to extensive breakdown of the chemical constituents of the mold, as is clear from Figures 2.1 and 2.4. Thus light alloys have the widest free choice of binder systems.
- (iii) Copper-based melts up to 1300°C take part in several important reactions as will be described later.
- (iv) Irons and steels (including Ni- and Co-base alloys) in the range 1400–1600°C are especially reactive in many ways. Aggregates and binders start to be a problem, greatly constraining the choice of materials for the steel caster. We shall devote some space to adequate solutions.
- (v) Titanium and zirconium in the range 1600–1700°C are so reactive that they are problematic to cast into molds of any type. Reactions with most molding materials cause the formation of the troublesome alpha-case on titanium alloys, in which the alpha-titanium phase is stabilized by interstitial elements (oxygen and/or carbon) absorbed from the breakdown of the mold. The alpha-case usually has to be removed by machining or chemical dissolution.

There are many different types of chemical binders. They divide into two main types: organic and inorganic. The molecular chemistry for keen chemists is described in detail in the work edited by Webster (1980). We can only give an outline here, concentrating on their practical application in foundries.

### 15.3.3.1 *Furans*

Sulfonic acid cured furan no-bake (FNB) binders are based upon furfuryl alcohol (2-furylmethanol) and are very widely used in ferrous casting since they provide excellent mold and core strength, cure rapidly and allow the sand with which they are used to be reclaimed at fairly high yields, generally 75–80% where due allowance is made for the need to keep total sulfur content below 0.1%. In passing it may be noted that furan foundries generally exceed this sulfur level in order to minimize sand consumption and accept poorer surface properties of the casting! Foundries that wish to reduce the sulfur content of a conventionally reclaimed furan-bonded sand do have a number of alternatives to using a sulfonic acid, and both phosphoric and lactic acid are sometimes used for this purpose. These are, however, weaker acids and will cure furan resins more slowly than the sulfonic acids, lactic acid particularly so. The use of phosphoric acid may necessitate a lower reclaim rate.

Furan binders are more or less anhydrous and commonly used at a rate of about 1% on (silica) sand. Experience shows that properly reclaimed furan-bonded sand that contains less than 0.1% total sulfur can be used with phenol–urethane no-bake (PUNB) binders.

The use of furan binders is, however, associated with a number of casting defects, the most serious being sulfur damage, which leads to poor surface finish in some steels, and destruction of near-surface graphite spheroids in ductile irons. The presence of urea-based polymers in some types of furan binders may also lead to nitrogen damage. As mentioned elsewhere, furan binders appear also to reduce chromite sand, forming iron metal.

Finally, and giving rise to most concern, furan binders have been found to be carcinogenic and decompose at casting temperatures with the emission of toxic gases; they contribute significantly to air pollution and the general blackening of the foundry environment, particularly the windows, thus further contributing to our dungeon-like furan foundries.

### **15.3.3.2 Alkaline phenolics**

Alkaline phenolic (A-P), also called phenolic ester, binders are fairly widely used in non-ferrous and steel casting, particularly where the use of furans can lead to difficulties, e.g. where alloys are cast that are sensitive to nitrogen or sulfur compounds and where hot tearing is prevalent. A-P binders contain about 50% water and are typically used at an addition rate of about 1.3% on silica sand. A-P binders are typically cured by the addition of an ester, such as di- or tristearin, by injecting methyl formate gas.

A-P-bonded sand is more difficult to reclaim conventionally than furan-bonded sand; reclaim rates being typically 70–75%, leading to higher volumes of waste per ton cast. Reclaim rates are somewhat lower with silica sand than with olivine, since the alkali in the binder reacts with the silica to form a surface film of sodium silicate that is highly resistant to attrition during conventional processing. Alkaline residues in the sand make it difficult to use reclaimed A-P-bonded sand with PUNB or FNB binders. Like furans, alkaline phenolic binders may also cause deterioration of chromite sand and both the binders and their pyrolysis products are considered to be toxic.

### **15.3.3.3 Phenol–urethane (PU) (cold box)**

At the time of writing this binder system is probably the most widely used in the non-ferrous casting industry.

It can be used in an ‘air hardening’ form (the curing process has in fact nothing to do with air) in which its excellent bench life, followed by a sudden and rapid curing, is convenient for molders, and the timing is widely adjustable by varying the catalyst addition at the mixer.

It is also important as a core binder in which the resin is hardened by an amine gas. The gassing time is usually a few seconds, but is required to be followed by an air purge that can last several times longer. The whole cycle for the production of an average core weighing a kilogram or so would be in the range of 30–60 seconds. This rapidity of production, together with its high strength, requiring low resin additions, has promoted this system to number one choice at this time. The reek of amine gas is tenacious, however, and can be unpopular on arrival home at the end of the day. The amines in the exhausted gases need to be removed by washing with dilute acid, which adds to costs.

### **15.3.3.4 Sodium silicates (waterglass)**

The inorganic types are typified by one of the earliest of the chemical binders, sodium silicate, or waterglass. A number of good reviews are available (Srinagesh 1979, Harris 2004). This substance

can be 'cured' (better: 'set') by passing carbon dioxide gas through the mold to precipitate silica. For this reason the process is widely referred to as *the CO<sub>2</sub> Process*. However, many foundries prefer to use esters such as di- and tristearin to accomplish this. Ester curing is easier to control and more uniform, although slower and more expensive than CO<sub>2</sub>. The fact that sodium silicate binders are not thermally degraded and may indeed melt during casting can cause molds and cores made with these binders to be difficult to break down after casting, so it is often difficult to remove the casting from the mold and even more difficult to remove the core from the casting. Many Al-alloy castings have been scrapped as a result of internal cores that are rock hard, and impossible to dislodge.

These properties also make silicate-bonded sand difficult to reclaim at high yield by conventional mechanical methods, whilst thermal reclamation is more or less useless. A typical reclamation yield for a standard shake-out + screening operation may be as low as 50%.

It has been such historical difficulties that have forced the ferrous casters away from silicates to organic binders. The main reason for the change appears to be the difficulties associated with core removal and sand reclamation, particularly when the older silicate systems that required additions of 4–6% of binder were used. However, the newer systems provide in most cases more than adequate strength and are typically used at the rate of 2.5–3%.

Silicate binders are inorganic bulk products, not based on oil, and are thus very much cheaper both per ton and per ton of metal cast than the other binders considered here.

Silicate binders possess a number of technical advantages, including greater resistance to hot tearing of the casting, almost complete lack of emissions, a considerable chill effect that can make the use of chromite facing sand unnecessary for steel casting and yield castings having an excellent surface finish. Silicate binders can also be formulated to cure as rapidly as furans, although the silicate process is better described as 'setting' rather than 'curing'.

However, even with the modern silicate systems, silicate-bonded sand is still difficult to reclaim. Furthermore, the presence of alkaline binder residues means that conventionally reclaimed silicate-bonded sand cannot be used with FNB or PUNB binders. The limited bond strength of silicate binders may restrict the size of boxless molds that can be lifted and moved.

More recently, however, there have been considerable advances in the use of sodium silicate, allowing it to become the binder of choice for both light alloy and steel castings. The use of hot air to dry the binder has the effect of providing a uniform set of the binder without limiting its bench life. It has the great benefit of environmental friendliness, low cost, and low gas evolution on casting. Heating of the cores to about 300°C removes the remaining water of crystallization, making the cores virtually inert, free from outgassing problems. This is a massive benefit, allowing the use of core designs impossible in other processes. In addition, the binder can be made soluble in water, allowing the molds and cores to be removed easily after casting.

Other recent developments in inorganic binder systems include the use of mixtures of silicates with phosphates and even borates. The sodium polyphosphate glass binder deserves special mention, simply requiring warm air to remove excess water to cure the bond. This process is attractive for difficult-to-vent cores because of its extremely low gas evolution on casting (Armbruster and Dodd 1993). However, many inorganics do not enjoy this benefit; they require caution because of their significant water of crystallization, which has the potential to give problems with core blows. Silicate binders contain about 60–65% water. Some others contain more. Even so, careful use of these recent inorganic materials promises a revolution in casting techniques.

Concerns about the costs and environmental aspects of organic binders and thermal reclamation have led some of our major light-metal foundries to devote a growing amount of attention to silicate binders and advanced mechanical reclaim systems. Inorganic silicate binders are commonly used in ferrous and particularly steel casting because of their low cost and excellent casting properties. However, the major growth area for these binders is light-metal casting. The benefits will be enhanced if foundries were to use non-silica sands. Since many such sands have a rather angular grain shape, it may be a good idea to use a grain-rounding attrition process, in order to minimize binder consumption and improve the surface finish of cast parts.

Cores made with silicate binders for ferrous casting can, if necessary, be removed in the dry state by vibration, although this might damage light metal parts, in which case a water-soluble core system might be preferred. New technology is becoming available that promises to provide rapid manufacture of cores with minimal gas development during casting, minimal environmental impact and that can be removed from the finished casting by washing out with water.

#### **15.3.3.5 Hot box and warm box processes**

The hot box and warm box processes use a liquid thermosetting resin binder. The mix is blown into a heated steel core box and allowed to cure for 10–30 seconds prior to ejection. Some post-curing may be needed outside the box, aided by the exothermic heat provided by the chemical reaction. The process has enjoyed wide popularity for the production of water jacket cores for such castings as automotive cylinder heads and blocks as a result of the strength of the cores and their relatively low volatile content, reducing blow problems.

#### **15.3.3.6 Croning shell process**

This process, often known simply as the *Shell Process*, patented in Germany by Johannes Croning in 1943, for making molds or cores, was based on a thermosetting resin. Mariotto (1994) gives a good review of the development of the process. The sand grains are pre-coated with the resin, which can then be handled as dry, free-flowing sand. The sand is put into contact with a heated metal pattern, against which the resin melts and sets after about 30 seconds. The remainder of the unheated sand further away from the pattern can be poured away to leave the shell to complete its hardening process, after which it can be ejected from the hot pattern. Mold halves can be made in this way, or hollow cores can be made if there is a print sufficiently large that can be used to pour out the unreacted sand. If there is no large core print the core can be produced solid, at additional cost of material, and introducing the possibility of core blows if the core cannot be vented in some other way. Taft (1968) describes how the process was used with great success in his family foundry using 100% zircon sand, and specializing in hydraulic castings in gray iron. These castings benefited by improved dimensional accuracy, soundness and more easily cleared coreways eliminating the risk of the contamination of hydraulic circuits.

When molds are made by putting together two mold halves, this shell mold can be cast with its parting line oriented vertically. For such orientation a good filling system can be provided that runs around the parting line; even a good pouring basin design can also be incorporated. The problem with vertical orientation is that the mold halves require to be supported by backing up with steel shot or other technique. If shot is used it is usually consolidated by vibration although too much vibration can crush the mold. The mold back-up requires some engineering and associated cost, but has the potential for making excellent castings.



If the two shell halves are put together to make a horizontal mold the filling system now becomes problematic to the point that I normally recommend owners of such lines to shut them down. The sprue is now necessarily wrongly tapered and no pouring basin of any respectable design can be incorporated. Thus the castings are necessarily at significant risk from entrainment defects. Such defects are therefore common in horizontal shell-molded castings. Some reduction of defects can be made by such means as the provision of filters at the base of the sprue or at the entrance to the runner, so as to assist the sprue to back-fill as effectively as possible. Overall, however, despite its relatively wide use and evident surface finish advantages, the horizontal shell casting process is not a casting system to be recommended.

#### 15.3.4 Effset process (ice binder)

The Effset process was invented by Fred Hoult in the 1970s, together with the H-Process. Impressively, this double achievement was made after his retirement at the age of 60 (I am encouraged that there may be hope for me yet). Silica sand mixed with a little clay (2–5%) and selected amounts of water allowed molds to be made by consolidating in a core box. The molds had sufficient green strength to be stripped from the box and laid out on a specially profiled support like a cradle. The mold on its support was transferred into a cryogenic chamber where liquid nitrogen was rained on to the molds. Only sufficient nitrogen was applied to freeze the surface of the molds, which were then extracted from the cryogenic chamber, assembled (usually in a stack) and cast. I have happy memories of a conference in which Fred was projecting an image of his process onto the screen. The image was of a stack of molds that had just been filled with liquid iron, revealing hoar frost still over parts of the mold, and gentle clouds of white steam rising from other disintegrating parts. In his characterful English accent, Fred announced with tremendous enthusiasm, to the entertainment of all, ‘You can *see* it doesn’t smell!’

The process was used in Fred’s Rotherham foundry for many years, giving excellent surface finish and showing no problems of chill (i.e. white iron) in his iron castings (Hoult 1979). However, the Effset process has never been taken up in volume production. It seems the high energy cost involved in the use of liquid nitrogen inhibits its use. An effort at re-examination of ice as a binder was provided by Abbas and colleagues (1993). Even so, as energy costs and cryogenic gas availability change, the environmental benefits of this process suggest it should be kept under review.

#### 15.3.5 Loam

Loam is a kind of mud. It is a mix of sand, clay, and water, plus on occasions time-honored fiber-strengthening additions such as manure from horses fed with a high diet of straw (horses chew the straw, chopping the fibers into exactly the right lengths, whereas cow manure is of no use since the fiber content, fiber length, and strength based on grass is not helpful). The sticky and sloppy mix is usually applied by hand to build up a mold or core, and is particularly useful for the forming of molds for bells which are formed to final shape by a sweep, a kind of strickling action made by a shaped blade rotated around a central axis. Additionally, the loam surface is conducive to finishing by sleeking with a wet brush. At that stage letters and ornamentation can be carefully impressed into the surface for the insignia and decoration of the casting. The shape is then transferred to an oven where it is subjected to a careful and thorough drying treatment taking typically several days. This is not a process designed for high production.

An interesting historical account of John Wilkinson, an English iron master from the seventeenth century, describes how his iron cannons outperformed all other cannons. His were cast solid and the

bore machined afterwards, compared to the normal manufacturing route in which cannons were cast with a loam core to form the bore. To the solidification scientist this may have been surprising because the long freezing time of the solid casting should have yielded a coarser and weaker structure. However, this expectation overlooks the casting problems associated with loam cores. The core would probably have been formed around an iron rod for strength, then wrapped with rope to provide some permeability and allow gases to escape, and finally sleeved with loam and dried. The drying process could never be complete, because the clay itself would contain a significant volume of water in its crystal structure overwhelming the ability of the rope to convey away the volume of gases. Thus the core would be expected to outgas violently, causing the melt to boil and thereby creating a mass of entrained defects that would have greatly weakened the casting.

The long and slender aspect ratio of the cannon core meant that its narrow rope vent was hopelessly inadequate. The bell survives because its loam core is usually made hollow, on a perforated steel former of large area, and outgases easily via its large base.

### 15.3.6 Cement

The mixture of sand, cement, and water forms an extremely hard mold capable of withstanding the loads imposed by very large castings, particularly ships' propellers, in the days when one of the only alternative mold materials was greensand which was far too weak for such products (Menzel 1937). Later work summarized much earlier studies and investigated improved mixes and enhanced breakdown after casting (Wallace and Hrusovsky 1979). The process is still in use for large heavy castings such as propellers in Ni/Al bronze and 40-ton ductile iron gears.

### 15.3.7 Fluid (castable) sand

Castable sand was invented in Russia in the 1960s by Liass and Borsuk (Liass 1968). A small amount of wetting agent added to the sand caused a foaming action during mixing. The special feature of the process was the low liquid content, the fluid properties of the mix being achieved by suspending the sand in an air/liquid foam, reducing the friction between sand grains and allowing the sand mix to flow rather like water. As such it could be poured into a molding box, where the kinetic energy of the fall would provide the necessary compaction. The mix had a fluid life of around one minute, and would subsequently harden by a chemical reaction. The process was analogous to the forming of light-weight concretes, and similar to the production of foamed plaster molds.

Setting mixtures such as sodium silicate and dicalcium silicate were originally used, later superseded by various cement mixes. The process attracted world attention in the early days because of its contribution towards a cleaner foundry environment, reduced labor requirement, and high productivity. Mixing a 250-kg batch would take around 4 minutes, and could be discharged into a mold or core box, building up large molds or cores in layers (with nearly undetectable joints between the layers) or could of course be discharged into a rapid succession of smaller boxes. The application of a wax parting agent to the pattern-work was necessary (Hassell 1980).

But the use of foam caused the molding material to have relatively poor resistance to metal penetration resulting in poor surface finish to the castings (Brown 1970, Nicholas 1972). Later developments using no wetting agent improved on this problem (Tsuruya 1974). Even so, the process seems only ever to have been applied to simple-shaped castings. These include ingot molds, slag

ladles, and machine bases, but has on occasions been extended to the production of medium to heavy cores for large valve castings using a furane resin binder (Hassell 1980).

Despite the enthusiasm that accompanied its launch, fluid sand is probably no longer used today.

---

## 15.4 OTHER AGGREGATE MOLD PROCESSES

### 15.4.1 Precision core assembly

The use of hard cores hardened 'in the box' has led to the possibilities of highly accurate cores and molds that can be assembled with extreme precision, often measured in micrometers. Thus the name 'precision core assembly' arose to describe this new standard of achievement. The castings from this process were some of the first to team up successfully with robotized pick-up and machining systems, although this achievement is now shared by many of the high-pressure greensand lines, and, of course, by products of the various forms of high-pressure die casting.

### 15.4.2 Machined-to-form

This process is not a molding process at all. A rigid block of chemically bonded sand is simply machined by a programmed robot or machining center. In this way a mold can be shaped with tolerable accuracy and with tolerable surface finish. It is a technique for rapid prototyping, in which the digital model sitting in the computer memory is used to produce a mold directly, eliminating the lengthy intermediate stage of the production of dies or patterns. The process can of course also be used for the production of a limited series of parts. Critics of the process complain that the robot or machining center wears out rapidly (despite the best protective measures) as a result of the creation of fine abrasive ceramic dust that the cost of replacement of the machining facilities should form a major component of the cost of the mold, but is frequently overlooked. Advocates of the process say this problem is now solved.

### 15.4.3 Unbonded aggregate molds

Both the lost foam process and the V process use unbonded aggregates. These molding processes are integrally defined together with the casting process. As a result, they are dealt with in Chapter 16.

---

## 15.5 RUBBER MOLDS

I am reluctant to describe rubber as an engineering material for molds. Even so, for a relatively few zinc alloy castings it can be excellent. A liquid silicone rubber is poured around the pattern, contained within a frame, and compressed between platens. After curing, a knife is used to slice into the rubber, opening up a cut sufficiently wide that the rubber can be peeled back to release the pattern. The mold is closed and replaced between the platens, constraining the mold to retain its overall shape. The low-melting-point alloy can be poured directly into the rubber, with surprisingly faithful accuracy for the casting. Usually, the process seems confined to castings of up to 100 g, although reports of castings up to 1 kg are not unknown.

As an alternative to using cast rubber form as a mold, many foundries instead use the cast rubber shape as a pattern, and produce from it a plaster mold. Such molds are used, for instance, to cast millions of Al alloy turbocharger impellers per year, since for these small 100-g castings the patterns can be withdrawn vertically from the cured plaster (the complex helical shape of some blades cannot be perfectly withdrawn even if the pattern were twisted on withdrawal) creating accurate castings with excellent surface finish.

---

## 15.6 RECLAMATION AND RECYCLING OF AGGREGATES

The greensand system, based essentially on a clay–water bond, has enjoyed the attention of enormous development, with the result that whole books are devoted to this important technology. We shall not attempt to reproduce this extensive fund of knowledge.

The reclamation and recycling of greensand has always been a major factor in the success of this molding system. The burning out of a percentage of the clay in ferrous foundries has been dealt with by the dumping of a similar percentage and top up with new sand and binder. New sand introduced via cores, if any, can provide all or part of the top-up. Even so, despite its enormous importance, it has to be admitted that the recycling of greensand has the problems of being both capital-intensive, requiring large plant and equipment for major foundries, and energy-intensive, as a result of the energy of crushing, sieving, and re-mixing (the word ‘mulling’ is often used, the process being carried out in a ‘muller’. The word ‘mull’ being the German word for ‘mill’ as used by millers for milling grain to make flour.)

One of the dangers of the reclamation of greensand has been the addition of uncontrolled water make-up; if this has contained chlorides, as is common in drinking water, the gradual build-up of chlorides in the recycled sand seriously reduced the strength of the bond. Boenisch (1988) was the first to point out this problem, which was quickly confirmed in independent tests by Hold and co-workers (1989).

Turning now to those foundries using chemical binders, the recycling of chemically bonded sands has provided new challenges to the industry. In this section we shall confine ourselves to the complexities of foundries with a variety of chemical-bonding processes which in general have so far not been treated in foundry textbooks.

### 15.6.1 Aggregate reclamation in an Al foundry

Most sand reclamation equipment is designed to target a low *loss on ignition* (LOI). The LOI of the sand consists of four components: (i) char; (ii) partially degraded binder films; (iii) undegraded binder films; and (iv) carbon as a thin film around the sand. Attrition processes remove components (i) and (ii) efficiently, but is less effective with (iii). Component (iv) is not removed and is in fact a desirable component in the sand! Thermal reclaim removes, of course, all four of these components, but could be regarded as an overkill.

Grain attrition processes appear to work well enough for binders that are brittle after casting, such as furans. These binders spall off as shell-like fragments forming a light dust, allowing much of the binder to be removed via the dust extraction system. However, attrition can be difficult to use with binders that remain in an elastic or plastic state after use because such binders can become soft during grain compaction and redistribute themselves, smearing onto other sand grains.

The rather low casting temperatures in an Al foundry mean that the residual binder adhering to the PU-bonded sand grains risks still being non-brittle. This means that it cannot easily be removed by the attrition forces that are encountered during the lump reduction and screening processes (so-called primary attrition) widely used. For this reason, many light metal foundries that use PU binders have chosen to reclaim their sand thermally.

Thermal reclamation naturally yields a sand with a low, practically zero, LOI. However, these units are expensive to install and operate. Perhaps counter-intuitively, they tend to lead to a deterioration in grain shape not because of thermal shock (which is negligible) but simply because the grains suffer fragmentation over time, and the percentage of fractured grains simply increase. In addition, the fluid bed de-dusters that often accompany thermal reclaim can also be difficult to run optimally, particularly if loading rate or sand quality varies. For instance if little sand is being processed the fluid bed level will fall a little, increasing the air flow and causing the increased loss of good sand into the extraction system. If sand loading on the bed increases, the bed will fluidize less energetically with the result that too few fines will be eliminated. The result is that actual thermal reclaim rates are typically of the order of 92–94%.

After the reduction of the sand to grain size, secondary attrition ('scrubbing') can expose the sand particles to higher energy processing. Grain impact techniques throw particles against a fixed target or against other particles (particle-on-particle, 'POP', attrition). POP attrition appears to be capable of running at high attrition energies with little or no grain fracture because the sand grains experience multiple glancing collisions, rather than single direct impacts when using a fixed target. The POP attrition seems efficient at removing brittle and partly embrittled binder films. Additionally, it rounds off the grains with reduced risk of fracturing or crushing them or of binder adhering again to their surface.

If the secondary attrition is followed by an efficient classifier such as a modern air cross-flow type (rather than a fluid bed for instance) then dust, fines, and oversize particles can be nicely divided into separate bins, allowing the foundry to optimize the particle size distribution of the sand.

Embrittlement of PU binders starts at about 200°C but proceeds rapidly at over 350°C. The reclaim rate for sand processed by secondary attrition will therefore, for a given LOI (or more accurately that large proportion of the LOI that derives from undegraded binder), depend upon the sand's thermal history, which in turn is a function of sand-to-metal ratio. Since the heat capacities of aluminum and silica are roughly similar on a kg for kg basis, this suggests that PU binder would be sufficiently embrittled at sand-to-metal ratios of up to about 4 to be removed, allowing the achievement of rates of sand reclamation characteristic of thermal processing.

In some foundries a useful compromise is reached by using thermal reclaim together with POP secondary attrition to maintain sand LOI at an acceptable level. This would entail reclaiming all sand by POP but using a small thermal unit to provide sufficient sand for cores only. In other words, cores would be based entirely on sand that had been both mechanically and thermally reclaimed whilst molds would be based upon a mixture of mechanically reclaimed sand plus enough new sand to make up for losses during reclaim and otherwise in the foundry. Sand used in molds will then consist of perhaps 12% new sand (from approximately 7% reclaim loss + 5% general losses in the foundry) and 88% mechanically reclaimed sand. If we assume that 10% of the total sand in circulation is core sand, the mold sand will consist of 12% new sand, 10% sand with low LOI from cores, and 78% reclaimed mold sand. Provided the foundry runs at sand-to-metal ratios lower than about 8 this should reduce LOI sufficiently to allow molds to be made without problems.

### Traditional mechanical processing

A conventional sand reclamation line will typically consist of a shake-out unit coupled with a vibrating sieve that functions as a low-energy lump crusher. Some foundries employ a mill to break down small lumps to individual grains and remove binder residues. The sieved sand can then be passed through a sand cooler, often a fluid bed that also functions as a deduster.

This system works satisfactorily with sand bonded with organic binders as long as the binder is fully thermally degraded, which is normally the case for steel cast at low sand/metal ratios. However, conventional reclamation imparts relatively little attrition energy and cannot efficiently remove binder residues that are only partly degraded; it has relatively little effect on alkaline binder residues that are fused onto the surface of the sand grains.

Furthermore the fluid bed deduster is sensitive to variations in both feed rate and particle size distribution and both these factors need to be carefully controlled if the system is to function optimally. Most foundries that use fluid bed equipment tend to set the air speed for average or even worst case conditions, leading to excessive loss of useful sand if the feed should contain more fines or is processed at higher rates.

### Impact attrition

Impact attrition systems accelerate the sand particles to high speed, using compressed air or a rotating disc. The grains are impacted onto a stationary steel target to dislodge the binder. Sand processed by air attrition will almost always suffer a disproportionate loss of the largest particles. A further limitation is the size of the individual units, typically 0.5–2 tons h<sup>-1</sup> (TPH), so that several must be mounted in parallel if a higher capacity is needed. Naturally, the system is self-destructing, particularly if high air speeds are employed to remove recalcitrant binder residues, and it is not uncommon for parts to be replaced every 1 or 2 months. Use of a fluid bed deduster additionally results in loss of useful sand from the bed because of fluctuating conditions.

### Particle-on-particle (POP) attrition and classification

Attrition by particle-on-particle collision can be nicely controlled, giving a scrubbing action to the grains. Binder residues are stripped from the sand as small flakes, up to 0.2 mm in size, as well as dust. The process will yield reclaim rates of around 90% or more with all chemically bonded sand systems. The quality of sand processed in the equipment is steadily improved, becoming steadily more rounded and will generally be better than new sand, especially for crushed aggregates.

Attrition requires to be followed by a classification process. A cross-flow air classifier using laminar air flow is excellent for separating useful sand from fines, flakes, and oversized particles. The design has been demonstrated to be robust and tolerates far wider variations in feed rate and particle size distribution than a fluid bed deduster.

At the time of writing, there are clear moves towards (i) mechanical as opposed to thermal reclaim and (ii) inorganic as opposed to organic binders. There are a number of good reasons for preferring mechanical reclaim; perhaps the most important being:

1. Mechanical systems are more flexible as regards feed and can be used to reclaim sand bonded with organic, alkaline phenolic and inorganic binders.
2. When used with sand bonded with organic binders, POP mechanical systems will provide yields of high-quality sand similar to that provided by thermal reclaim, i.e. reclaimed sand that can replace new sand.

3. Thermal systems are ineffectual for reclaiming inorganic bonded sand and do not offer particularly good yields.
4. POP mechanical systems improve the sand's grain shape and particle size distribution, allowing binder consumption to be reduced and improving the surface finish of cast parts; this is particularly valuable for foundries located in areas having poor-quality local sand.
5. Mechanical systems are far cheaper to install and operate than thermal systems.

### 15.6.2 Aggregate reclamation in a ductile iron foundry

As an example of the complexities of some real foundries it is worth considering the problems of reclamation of core sand in a ductile iron foundry using greensand and furan-bonded sand for molds and furan- and PU-bonded sands for cores.

This mix of bonding processes arises from fundamental considerations: a greensand line cannot, of course, use cores made in greensand since the material is relatively weak, and contains up to 10 vol% of binder in the form of moist clay, filling most of the voids between the sand grains and so making the mix nearly impermeable; its high water content then leading to insoluble outgassing problems from cores.

Thus cores for greensand lines are typically chemically bonded. The high strength of the chemical binders means that only a relatively small percentage addition of binder is required (often approximately 1 wt%, corresponding to approximately 3 vol%), which, together with a larger and closer grading of sand particle sizes, gives tolerable permeability, allowing outgassing to occur more easily via the core prints.

Alongside the greensand system, a POP-type secondary reclaim system together with an efficient cross-flow air classifier can reclaim up to 94% of organically bonded mold and core sand from iron casting. The reclaimed sand can have a low LOI and more importantly a low total sulfur content ( $\leq 0.12\%$ ). Once loose char, dust, and fines are removed from the sand, total sulfur is also reduced, and constitutes the prime determining factor for making good ductile iron castings with this binder system and for using reclaimed furan-bonded sand with PU binders.

Experience shows that a foundry using such a reclaim system to make sand for PU-bonded cores (and molds) from reclaimed (furan-bonded) sand experiences the following benefits:

- (a) Lower scrap rate because of lower thermal expansion of reclaimed sand compared to new sand.
- (b) Lower binder consumption than with standard reclaimed sand, since the POP system will provide sand with better grain shape and optimized particle size distribution (giving higher bulk density but with better gas permeability).
- (c) Minimized sand consumption and dumpsite costs. Of course, the energy consumption, which for a small plant is about 3.5 kWh per tonne processed, is far lower than a thermal unit (approximately 200 kWh per tonne).
- (d) A better working environment.

A suggested optimization of the foundry reclaim system might be:

1. All chemically bonded sand to be reduced to grain size through primary attrition, then mixed with the required amount of new make-up sand to replace losses, and finally put through secondary attrition (preferably POP type).

2. This sand (so-called 'unit' sand) is then used for *all* cores, i.e. those used in both greensand and chemically bonded sand molds. Reclaimed sand has a lower thermal expansion than new sand and will have a grain shape and particle size distribution that is as good as or better than new sand. Furthermore, the addition of new sand to this unit sand will reduce LOI to well below any level that might cause problems for ductile iron chemistry.
3. New sand is used for chemically bonded molds, although of course reclaimed sand could be used here too.

An example known to the author was a furan/PU foundry that ran a POP attrition plant, reclaiming 94% of the furan sand and using this to make their PU-bonded cores without any problems arising (something that they had been unable to do prior to the POP unit). Although a maximum 1% LOI for reclaimed furan sand was traditionally thought to be the limit when using PU binders, the LOI was found to fall from about 3.5% to only 2.6% (i.e. by about a third), but, somewhat surprisingly, was observed to cause no problems. On closer examination it was found that the total sulfur content had fallen from more than 0.3% to 0.12% (i.e. by almost two-thirds), almost certainly accounting for the improved behavior.

LOI on its own can, of course, be misleading; for example the presence of the carbon film around the sand grains (which shows up as LOI) can be beneficial, effectively insulating the grain from chemical attack by the metal and its vapors.

### 15.6.3 Aggregate reclamation with soluble inorganic binders

The use of inorganic binders that are soluble in water has great attraction in the foundry. The chemicals are without smell, clean and mostly free from any toxicity problems.

The most widely successful of the inorganic binder systems have been based on sodium silicate. The curing action has traditionally been effected by carbon dioxide gas. The 'CO<sub>2</sub>' process, as it has become known, has a long history. It can deliver hard molds tolerably quickly. One of its major drawbacks is the tendency of the silicate binder to melt at casting temperatures, fritting like a glass to make cores extremely problematic to remove.

Alternatively for light alloy casting, the mold can be cured simply by drying. This approach has the great advantage that the binder remains soluble in water. Thus after casting, the mold can be ablated (i.e. eroded off by water jets) off the casting without damage to the casting. This is especially valuable in an Al alloy foundry in which the castings are relatively weak and soft, and so easily damaged, when breaking out the molds. The ablation casting process, patented by Alotech in about 2006, takes advantage of the solubility, removing the mold while the casting is still at least partially molten, hence greatly enhancing the rate of solidification.

By removing the mold by jets of water, the atmosphere of the foundry is freed from dust, eliminating the huge and expensive dust extraction systems. The elimination of fume means that operators enjoy clean conditions, in contrast to most resin-bonded binder systems in which the pungent fumes unpleasantly cling to skin and permeate fabrics.

Not all inorganic salts are suitable as binders. For instance many have relatively large quantities of water of crystallization that is released when heated by contact with the hot metal, causing blow defects in the castings. An example is MgSO<sub>4</sub> that contains five molecules of water for each molecule of magnesium sulfate. Although common salt, NaCl, has no such combined water, it has not so far been found to have useful binding properties.



Sodium silicate does contain some combined water, but this does not seem to create significant problems for Al castings. Measured gas evolution from silicate-bonded cores has been found to be low (Wolff and Steinhauser 2004). For steel casting the release of water vapor at the higher temperature seems a positive advantage, since its evaporation conveys heat away from the casting, causing silica sand to achieve the chilling power of chromite sand. A number of steel foundries have abandoned the use of chromite as a facing sand, adopting instead a simpler and less-costly one-piece mold bonded with a sodium silicate binder.

Traditionally the reasons for the inhibition of the widespread adoption of silicate binders in foundries include the following:

1. Shake-out difficulty for cores. This problem has been addressed by (a) organic additions to the silicate, and (b) in quite separate developments avoiding carbon dioxide, using drying in air.
2. Long cycle times for curing by drying have meant that a core weighing a kg or so may require several minutes to be dried sufficiently to be usable. This contrasts with PU binder systems, currently the norm in the industry, that require perhaps only 5 seconds' cure by an amine vapor, followed by 30 seconds or so of purge air to remove the vapor, giving a total cycle time in the core machine of approximately 40 seconds. However, developments are taking place to reduce the cycle time for the drying of silicates by using higher temperature and faster air flows, together with reduced sand thickness using shell techniques.
3. Large energy requirement of curing by evaporation of water. It is true that the energy required to evaporate water is unusually high ( $2.26 \text{ MJ kg}^{-1}$ ). However, most of the water from recycled sand can be eliminated by simple draining, or possibly centrifuging which is not energy intensive, leaving only a percent or two to be removed by evaporation. Each percentage of moisture per tonne of sand requires approximately  $6.4 \text{ kWh}$  to convert it to vapor, so that a maximum of about  $12 \text{ kWh tonne}^{-1}$  would be needed for 2% of residual moisture. (This compares with the energy requirement of at least  $200 \text{ kWh tonne}^{-1}$  for thermal reclamation at  $700^\circ\text{C}$ .) Furthermore, since the binder to be added to the reclaimed sand is water-based, not all the residual moisture need be removed, since the added binder can be concentrated, achieving the correct mix when diluted with the residual moisture already present in the returning sand.

Thus it can be seen that inorganic binders appear to be addressing the issues that originally prevented their use. It is expected that they will become progressively more important in the casting industry during the next few years.

#### 15.6.4 Facing and backing sands

Occasional foundries using chemical binders have simplified their operations to the point that only a single sand, sometimes called a 'unit sand', is used for both molds and cores, together with a single binder system. This unusual achievement has clear benefits to the economics and management of the foundry.

However, a number of ferrous foundries, particularly those making larger castings in relatively low numbers, will often use a facing sand and a backing sand. Chromite and zircon sands have been commonly used to face molds and cores for two reasons: (i) they act as a chill and help to stop penetration by molten metal and (ii) they act as a barrier to stop silica backing sand coming into contact with the molten metal. This latter point is especially useful when casting high-manganese

steel, since silica reacts with manganese steel to form a low-melting-point manganese silicate, causing a severe burn-on problem. In contrast, olivine is perhaps the most resistant of all aggregates to attack by manganese steel.

When chromite is used as a facing sand in silica sand molds, or in cores, silica and chromite become unfortunately mixed during the recycling of the sand. Although fluid bed separation has been reported (Perbet 1988) the more usual magnetic separation represents a significant investment in the recycling system. Chromite is slightly magnetic so that 50–75% can be separated out as a roughly 80–85% rich fraction (Sontz 1972). Normally two magnets are required; the first to remove unwanted iron and steel (it is always amazing how much iron and steel gets into sand-recycling plants) and the second a more powerful (and more expensive) rare-earth magnet that is required to remove the magnetically weaker chromite. If the chromite and silica are not effectively separated during recycling, the sand becomes practically unusable for steel casting, as discussed in the section above on chromite.

Steel foundries have used zircon for facing because they wish to employ a silica sand backing. They have shied away from chromite to avoid the risk of (what is assumed to be) fayalite formation and the hassle, cost and uncertainty of magnetic separation. Zircon cannot be reclaimed separately, and thus is lost into the backing sand after recycling. The rising cost of zircon as world supplies diminish is now closing this option.

The recycling of the silica backing sand can be carried out at or better than 90% efficiency (particularly for alkali phenolic-bonded sand) with modern reclaim systems that can simultaneously improve the grain shape by a progressive rounding action during each cycle. However, the effects from any build-up of low-melting-point phases when using chromite with improved reclaim systems do not appear to be known at this time.

An interesting potential solution for steel foundries is to continue with chromite for facing but replace their silica backing sand with olivine, operating a single-stage magnetic separation. This completely avoids the risk of iron silicate formation and will allow foundries to increase their recycle yields of both chromite (no longer lost as an iron silicate) and olivine (because of lower binder residues). In summary, a facing sand of typically 80% chromite will not be degraded by reaction with its 20% content of olivine since this mixture is effectively inert (in contrast to an 80/20 chromite/silica mixture). Also, of course, the chromite content of the olivine backing sand is not damaging.

Silica–zircon foundries could change to olivine–chromite and need only invest in a simple magnetic separation stage. These are relatively modest investments that would be repaid rapidly. The more expensive olivine is envisaged to be more than offset by the higher rates of reclamation that are offered by POP recycling systems.

Finally, we should note that the benefits of the unit sand concept are enjoyed by some steel foundries who have found a facing sand to be unnecessary. They have discovered that by using a silicate-based binder they are able to avoid using the chromite facing sand. The reason for this seems to be the significant chill effect provided by the silicate binder; its free water together with its water of crystallization is driven off; the superheated steam carrying with it a huge transfer of latent heat into the depths of the mold, as discussed in Chapter 4 on evaporation and condensation zones.

The casting process is the point in manufacture when most of the defects are introduced into the cast part. It is true that the melt might be the wrong composition, and the mold might be the wrong shape or fall apart, but these misfortunes are unusual, and they are usually modest compared to the damage that is inflicted by most filling system designs. Anyway, we shall hope that the earlier chapters in this book have been observed so far as possible, such that these problems are minimized.

In the description of Rule 2 the problems of pouring by gravity were emphasized, leading to solutions for gravity pouring which could only be described as damage limitation exercises. This contrasted with the process that minimizes the effect of gravity, tilt casting, and the elimination of gravity in ‘Level Transfer’ and ‘Counter-Gravity’ filling systems. Only tilt, level transfer and counter-gravity can produce ideal transfer of metal into the mold, thus manufacturing the best quality of casting. These points are so fundamental that they will arise time after time as we examine the various casting systems. No apology is offered for repetition.

---

## 16.1 GRAVITY CASTING

Today’s technology for the production of most castings involves gravity pouring. If this were not bad enough in itself, the design of the filling systems usually makes this bad situation much worse. This requires to be kept in mind. Only relatively rarely are castings produced with filling system designs using the principles set out in this book. Naturally, we all hope this poor situation will improve.

### 16.1.1 Gravity pouring of open molds

Most castings require a mold to be formed in two parts: the bottom part (*the drag*) forms the base of the casting, and the top half (*the cope*) forms the top of the casting. I remember these names because the drag can sometimes be moved by being dragged along the floor. The cope is reminiscent of coping stone, the stone topping the wall, or from the bishop’s cape, the name for his cloak.

Some castings require no shaping of the top surface. In this case only a drag is required. The absence of a cope means that the mold cavity is open, so that metal can be poured directly in. The foundryman can therefore direct the flow of metal around the mold using his skill during pouring (Figure 11.1).

Such open top molds represent a successful and economical technique for the production of aluminum or bronze wall plaques and plates in cast iron, which do not require a well-formed back surface. The first great engineering structure, the Iron Bridge built across the River Severn by the great English ironmaster Abraham Darby in 1779, had all its main spars cast in this way. This spectacular feat is not to be underestimated, with its main structural members over 23 m long cast in open top sand

molds; it heralded the dawn of the modern concept of the structural engineering casting and still stands to this day.

Other viscous and poorly fluid materials are cast similarly, such as hydraulic cements, concretes, and organic resins and resin/aggregate mixtures to form 'resin concretes'. Molten ceramics such as liquid basalt are poured in the same way, as witnessed by the cast basalt curb stones outside the house where I once lived, which have lined the edge of the road for more than one hundred years and whose maker's name is still as sharply defined as the day it was cast.

The remainder of this section concentrates on the complex problem of designing filling systems for castings in which all the surfaces are molded, i.e. the mold is closed. In all such circumstances, a *bottom-gated* system is adopted (i.e. the melt enters the mold cavity from one or more gates located at the lowest point, or if more than one low point, at each lowest point).

### 16.1.2 Gravity pouring of closed molds

The series of funnels, pipes, and channels to guide the metal from the ladle into the mold constitutes our liquid metal 'plumbing', and is known as the *filling system* or *running system*. Its design is crucial; so crucial, that the design of the filling system is by far the most important section of this book.

In addition to them being categorized as pressurized, naturally pressurized, and non-pressurized, filling systems are commonly also categorized as top-gated, gated at the mold joint, or bottom-gated. It will by now be clear that in this book the only pressurization recommended is natural pressurization, and the only gate location recommended is bottom gated.

However, the reader needs to keep in mind that the elimination of a running system by simply pouring into the top of the mold (down an open feeder, for instance) may be a reasonable solution for the filling of a closed mold in some cases. Although apparently counter to much of the teaching in this book, there is no doubt that a top-poured option has often been demonstrated to be preferable to some poorly designed running systems, especially poorly designed bottom-gated systems. There are fundamental reasons for this that are worth examining right away.

In top pouring via, for instance, a feeder, the plunge of a jet into a liquid is accompanied by relatively low shear forces in the liquid, since the liquid surrounding the jet will move with the jet, reducing the shearing action. Thus although damage is always done by top pouring, in some circumstances it may not be too bad, and may be preferable to a costly, difficult, or poor bottom-gated system.

In poor filling system designs, velocities in the channels can be significantly higher than the free-fall velocities. What is worse, the walls of the channels are stationary, and so maximize the shearing action, encouraging surface turbulence and the consequential damage from the shredding and entraining of bubbles and bifilms.

Ultimately, however, a bottom-gated system, if designed well, has the greatest potential for success.

It is all the more disappointing therefore that many of our horizontally parted molds produced on automatic molding systems practically dictate the use of a poor filling system, resulting in the high-rate production of poor castings to the extent that Al alloy casting cannot generally be produced on automatic greensand molding lines. These current designs of automated molding plants are better designed to produce scrap than produce castings. Iron casting is fortunately more tolerant of such abuse of casting principles. The manufacturers of such systems will often deny this assertion, pointing out that a conical basin is not necessarily the only option, and that a 3-D milling machine could cut an

offset step basin while the cope was upside down. Similarly, a tapered sprue could be cut or molded at the same time. However, the author has not yet seen such solutions put into practice. This would be a welcome development.

### Shrouded pouring

The problem of the voluminous entrainment of air by the conical pouring basin has often been tackled by the provision of a shroud. This can be a steel or refractory cylinder that surrounds the outlet from a bottom-poured ladle, and nests in the funnel-shaped pouring basin. By this means the inward flow of air into the conical funnel is reduced. However, even if the shroud were 90% efficient, which would be a surprisingly high efficiency, the remaining 10% of entrained air would still be a serious problem.

Some shrouds have an inert gas piped into them in an additional effort to protect the metal stream. This is clearly helpful, but once again inefficient. Plenty of air will still find its way into the metal stream. In any case, the bursting of bubbles of inert gas will still create some turbulence and splashing in the metal rising in the mold cavity, with consequent creation of defects.

In conclusion, shrouds reduce entrainment problems, but are inefficient. I avoid such unsatisfactory solutions.

### Contact pouring

The sitting of the bottom-pour ladle directly on its mold, so as to align the ladle nozzle and the entrance to the down-sprue of the casting, then raising the stopper to allow the ladle to drain, filling the casting, is the ultimate technique to eliminate the entrainment of air. It is simple, uses no costly inert gas, and is 100% efficient. For shaped casting production the technique has the added advantage that a pouring basin is eliminated. These are all powerful advantages.

Jeancolas and co-workers (1962) draw attention to the importance of the exclusion of entrained air from filling systems, and use contact pouring to achieve this. Schilling and Riethmann (1992) describe the benefits of the process when applied to Al alloy cylinder blocks and head production in sand molds. The molds are offered up to the outlet nozzle from the base of a launder, and the stopper is raised, allowing the melt to descend into the sprue.

The author has used the technique to excellent effect for a 50-ton steel casting that proved to be essentially free from defects as a result of zero air entrainment in the filling system (Kang et al. 2005).

### Automatic bottom pouring (ABP)

The automatic bottom pouring technique (see Section 14.1.5) refers specifically to the use of a crucible with a hole in its base, through which the melt is poured when it is finally molten, the technique as practiced to this day tends to employ only low-cost, one-shot consumable crucibles, often made from simple bonded silica sand or from light-weight ceramic fiber. A specially shaped slug of metal which is a close fit in the crucible is melted extremely rapidly, usually within approximately 60 seconds. The base of the charge melts last, so the melt pours automatically precisely when the last metal is melted. Sometimes the process is used with a penny-shaped metal disc in the exit nozzle of the crucible, so that the superheat at which the melt is poured can be controlled by the thickness of the disc.

The mold is placed, of course, under the crucible. This simple in-line arrangement involves no moving parts, and thus can provide extremely low-cost melting and casting systems, especially for vacuum melting and casting. The cylindrical vacuum chamber can be a fiberglass-resin tube, allowing

the induction coil to be placed outside, once again simplifying the design by avoiding electrical connections through the wall of the chamber. The rather poor vacuum held by the fiberglass tube seems to be no problem for the melting and casting of most alloys. The process continues to be used, being highly productive for the casting of Ni-base superalloys for turbocharger wheels, and iron and steel castings, but has been used for magnesium.

Although attractively simple, it is a pity that it is a *pouring* process, consequently demonstrating a constantly varying proportion of scrap from turbulently filled molds. We really need to get away from *pouring* metals.

### Direct pour

This name was chosen by the Foseco company to describe the use of a ceramic fiber sleeve, fitted with a ceramic foam filter in its base, placed directly onto and in contact with the casting as a substitute for a filling and feeding system. As such, of course, it could be convenient and highly economical (Sandford 1993). However, despite a number of notable successes, the system has not always yielded good results.

This technique has been researched. The results are summarized in Figure 12.50, showing that the technique is mainly effective for relatively small falls after the filter in stabilizing and making reproducible the casting conditions (the filtering action is insignificant). Because the stable regime promoted by the system may not yield a good casting, this means that if the first trial location for the direct pour sleeve on the casting is not good, all castings are likely to be unacceptable. Conversely, if the first trial location does yield a good result, all results are likely to be good.

### Gravity dies (permanent molds)

For dies filled simply by pouring under gravity, they are not surprisingly called *gravity dies* (known in the USA as *permanent molds*).

As stated in Section 15.1, the fact that the mold is hot and extremely dry means that the liquid aluminum and mold are practically inert towards each other. This is a significant benefit of hot dry metal molds that is often overlooked. For this reason subsurface porosity as a result of high hydrogen levels is rarely seen in casting from metal molds. The use of permanent molds is usually confined to low-melting-point metals (e.g. Zn, Pb) and the light alloys (Mg and Al). Only relatively rarely are permanent molds used for the higher-temperature alloys such as brasses and bronzes, and cast iron, although even for these metals, metal molds can be valuable and successful.

The benefit of high temperature of the mold introduces a challenge for the control of the temperature, of course. Thus the die temperature falls when the casting cycle is interrupted by the fairly common occurrence of metal becoming trapped in the die, or coating repair, or sometimes even the arrival of a new batch of cores that have to be signed for and wheeled into place.

Cast iron or steel molds used in gravity die casting (permanent molding) or low-pressure die casting (low-pressure permanent molding) of aluminum are coated with an oxide wash of rather variable thickness, in the range 0.5–2 mm thick, infringing on the accuracy of the casting. Its purpose is to reduce the thermal shock to the die, and by thus reducing the rate of heat transfer, allow the die to fill without premature freezing. Without the die coat it would be difficult if not impossible to fill the die without the formation of cold laps.

Because the die coat reduces the severity of the thermal loading, the die material can sometimes be gray cast iron. This is welcome because of the ease of obtaining a block of starting material, suitably

shaped with a contoured back if necessary, and because of its excellent and easy machining. It has to be admitted that gray iron has limited strength and limited fatigue resistance. Thermal fatigue usually sets in after thousands of casts. This limit to die life can be an important threat to surface finish as the die ages, developing multiple small cracks, often called checks, or occasional large cracks resulting in sudden catastrophic failure. Such failures have disastrous effects on production, because dies take time to replace. Such failure is commonly associated with heavy sections of the casting, such as a heavy boss. The iron or steel die in this region suffers from repeated transformation to austenite and back again. The large-volume change accompanying this reaction corresponds to a massive plastic strain of several percent, so that steel, and more particularly cast iron, suffers thermal fatigue. The severe strains of thermal fatigue often lead to failure after relatively few cycles.

For dies that are subject to the rigors of volume production and where total reliability is required, the dies are machined from steel. Usually a special grade of hot work die steel, commonly an H13 grade containing 4%Cr, is chosen, which is preferably characterized by an especially fine grain size.

For the production of simple two-parted castings, gravity dies are usually constructed with a vertical split line. The moving die half (if only one half moves) is usually arranged to retain the casting. Thus the action of opening the die causes the casting to impact on the ejector pins and so release the casting from the moving side. The casting may be caught on a tray and swung out from between the die halves. Alternatively, it may be simply picked up from where it has fallen. I only once saw a die arranged wrongly by mistake, with the casting retained in the fixed die half. It was an embarrassment to the die designer and a constant source of problems for the die operator until the die could be turned around.

Complex dies such as for automotive cylinder heads are usually provided with vacuum connections to the backs of core prints so as to suck gases out of difficult-to-vent cores such as water jacket cores. The vents usually block by the condensation of tars and other volatiles after 15–25 castings, depending on the casting. Sometimes knock-out vents are employed to allow the vents to be cleaned out by drilling. The stopping of production to clean out the vents is a non-trivial hindrance to production rates using gravity dies. The campaign life of a die is usually dictated by the cleaning-out of vents rather than the maintenance and repair of the die coat. If vents are not maintained fully operational, blows from cores increase to become a major source of scrap.

More recently there is hope that difficult-to-vent cores might become producible with the new generation of silicate binders that do not create condensable outgassing products.

Binders that do not create fume on casting are very much to be desired. Fume in the immediate environment of operators is a problem in gravity die operations. The opening of a die containing cores is usually accompanied by a cloud of fume, most of which avoids the fume extraction hood because of side draughts. Sand castings tend to avoid the worst of such fume emissions because the casting and cores remain in the mold for longer and are cooler by the time the mold is opened. In any case, the sand mold is opened in a completely closed environment so that operators can work in a cleaner atmosphere.

The provision of a small steel mesh filter, of approximately 2 mm mesh opening, is often usefully incorporated into the runner. This can be extracted from the runner while the metal is still hot, so is not recycled with the foundry returns, and thus avoids contaminating the metal with iron.

Turning to the possibility of the casting of cast irons in cast iron dies, the subject is studied at some length by Jones et al. (1974). These authors used gray iron dies coated only with acetylene soot (although the author is aware of other foundries that also coat with an oxide wash, in addition to the application of a fresh layer of soot after the ejection of each casting). They found good results for gray

iron castings at slightly hypereutectic composition, well inoculated, poured close to 1350°C and with mold temperatures up to 300°C. It was also important that the molds were of good quality, avoiding flash. In this way carbide formation in the iron could be avoided. They claimed dimensional reproducibility, surface finish and strength properties were consistently superior to comparable aggregate-molded castings.

These authors went on to check ductile irons. The greater tendency for these irons to solidify with carbides required a higher mold temperature up to 450°C. Even so, conditions for achieving ductile irons completely free from carbide were not found, but the heat treatment to eliminate the carbides was relatively short because of the fine structure.

The production of malleable irons, cast originally of course as white irons, was not considered attractive mainly because of the problem of achieving sound castings without the use of large feeders.

Carbon-based and graphite dies have been found useful for zinc alloys. However, for aluminum alloys their lives are short because of the degradation of the carbon by oxidation. (All the more impressive therefore is the use of graphite molds for steel, used for the casting of millions of railroad wheels by the Griffin Process, described in the next section.) Graphite is often used as a molding material for titanium, but any benefits of inertness are lost by the reaction to form the so-called alpha case. The details are described in Chapter 6 under the various cast metals.

### 16.1.3 Two-stage filling (priming techniques)

There have been a number of attempts over the years to reduce some of the problems of gravity filling by the introduction of a two-stage filling process. The first stage consists of filling the sprue, after which a second stage of filling is started in which the runner and gates, etc., are allowed to fill.

The technique is described in detail in Section 12.4.19 on Priming Techniques in which various sections of the running system are blocked by valves, which are opened only after a second or two delay to allow bubbles and oxides to detrain.

A fascinating major benefit of the two-stage filling of the down-sprue is that no matter how dreadful the design of the down-sprue, once primed during the first stage of filling, it tends to remain full, operating perfectly with zero entrainment of air. This can easily be demonstrated by a water model.

A second completely different incarnation of the two-stage filling concept is the *bottom-pour ladle*. This is illustrated in Figure 12.3 and 12.35c. The device is used mainly in the aluminum casting industry, but would with benefit extend to other casting industries. Instead of transferring metal from a furnace via a ladle or spoon of some kind, and pouring into a pouring basin connected to a sprue, the ladle dips into the melt, and can be filled uphill via the bottom nozzle. The ladle nozzle is then closed by a stopper and the ladle transferred to the mold. The stopper is raised, and can deliver the contents of the ladle into a conventional pouring basin. Preferably, however, it can be lowered onto and seated on the mold, aligning precisely with the entrance to the sprue, and thus delivering the melt directly in the sprue by the *contact pour* technique. This technique is strongly recommended in place of pouring into a pouring basin.

Alternatively again, if the ladle is equipped with an extension (Figure 12.35d), converting it to a *snorkel ladle*, the nose of the snorkel can be lowered down through the mold to reach and engage with the runner. Only then is its stopper raised and the melt delivered to the start of the running system with



minimal surface turbulence. The two-stage fill appears to have attractive potential and thus warrants further development.

#### 16.1.4 Vertical stack molding

The stacking of identical aggregate molds and pouring into the top has been used for a number of products, for instance for cast iron piston rings. Although cast iron has a relatively low susceptibility to entrainment problems compared to many other metals, such mistreatment ensures that even this metal does not survive unscathed. Bubbles and oxides are necessarily entrained during the tumbling of the melt down the necessarily non-tapered irregular sprue (Figure 12.34c), and these defects find their way randomly into castings, requiring much subsequent testing and sorting. This awful process cannot be recommended. It throws all the principles of good filling design to the wind. Both the castings and the profitability of the foundry suffer lamentably.

#### 16.1.5 Horizontal stack molding (H process)

Foundries that are set up based on the H process (another of Fred Hoult's inventions; Hoult 1979) have a pleasing simplicity. The molding section of the foundry consists of relatively small core machines making the molds by blowing into a corebox that forms both the front and back surfaces of the casting (Figure 12.34b). The use of identical cores forming both the front and back surfaces of the mold in this way effectively doubles the rate of production of molds. The molds are stacked vertically in a frame, and then clamped, and the frame is turned horizontally and transferred to the casting area. After casting and cooling, the sand can be mainly recycled, and the castings separated from the running system by simply breaking them off.

The overflow of metal from one mold to the next necessarily involves a fall inside the mold cavity. This fundamental problem leads to the entrainment of severe defects if the fall is much over 200 mm, explaining the fact that H process castings are normally limited in height to about 200 mm and may additionally explain why the process appears to be also limited to cast iron, which has least sensitivity to entrainment problems. The one good feature of the fall of metal in the mold is that the fall distance is also minimized (as opposed to castings poured from above the mold via a conical basin, where velocities can become very high) so that the entrainment damage is limited. The production of Al alloy castings by this process would be expected to be problematic.

A computer study by Xiao (1998) shows that if the mold stack is perfectly horizontal, the melt dribbles into more distant cavities, possibly spoiling these castings. If the mold stack is tilted by about  $7^\circ$ , causing the melt to progress upwards from one cavity to the next, this problem is reduced. Furthermore, if the runner linking the cavities has a flat base, as opposed to being of a circular section, that also helps.

#### 16.1.6 Postscript to gravity filling

Later we consider below an appraisal of counter-gravity filling of molds, but it is salutary to consider why anyone would go to this trouble when gravity filling appears to be so easy.

There are some advantages to the use of gravity to action the filling of molds by simply pouring metal. It is simple, low cost and completely reliable, since gravity has never been known to suffer a power failure. It is with regret, however, that the advantages finish here, and the disadvantages start. Furthermore, the disadvantages are serious.

Nearly all the problems of gravity pouring arise as a result of the velocity of the fall. After a trivial fall distance corresponding to the few millimeters of the critical fall height, gravity accelerates the melt to its critical velocity. Beyond this point the continued acceleration of gravity results in the metal going too fast and having too much energy. Thus the danger of entrainment defects grows alarmingly with the increasing distance of the fall. Because the critical fall distance is so small, nearly all actual falls exceed this limit. In other words the energy content of the melt, when allowed to fall even only relatively small distances under gravity, is nearly always sufficiently high to cause the break-up of the liquid surface. (It is of little comfort at this time to know that foundries on the moon would fare a little better.)

These high speeds result in gravity filling systems being hypersensitive to small errors. For instance a tiny mismatch of a millimeter or so in the sprue can easily lead to the creation of volumes of entrainment defects.

A second fundamental drawback of gravity filling is the fact that at the start of pouring, at the time the melt is first entering the ingates, the narrowest part of the mold cross-section where volume flow rate should be slowest, unfortunately, the speed of flow by gravity is highest. Conversely, at a late stage of filling, when the melt is at its coldest and approaching the top of the mold cavity the speed of filling is slowest, endangering the casting because of cold laps and misruns. Thus filling by gravity gives a completely inappropriate filling profile.

Thus to some extent, there are always problems to be expected with castings poured by gravity. The long section on filling system design in this book is all about reducing this damage as far as possible. It is a tribute to the dogged determination of the casting fraternity that gravity pouring, despite its severe shortcomings, has achieved the level of success that it currently enjoys.

Even so, there is no shortage of viable alternative processes that do not suffer these disadvantages. These are described below, and are recommended. The good-natured behavior of a number of these processes, including some tilt processes and counter-gravity systems that use low filling speeds, errors of mismatch of flow channels and sharp, unradiused corners, etc. are irrelevant.

---

## 16.2 HORIZONTAL TRANSFER CASTING

The quest to avoid the gravity pouring of liquid metals has led to systems employing horizontal transfer and counter-gravity transfer. These solutions to avoid pouring are clearly seen to be key developments; both seem capable of giving competitive casting processes that offer products of unexcelled quality. The major approaches to the first approach, horizontal transfer, are described below.

### 16.2.1 Level pour (side pour)

The *level pour* technique was invented by Erik Laid (1978). At that time this clever technique delivered castings of unexcelled quality. It seems a pity that the process is not more generally used. This has partly occurred as the result of the process remaining commercially confidential for much of its history, so that relatively little has been published concerning the operational details that might assist a new user to achieve success. Also, the technique is limited to the type of castings, being applied easily only to plate-, box-, or cylinder-type castings where a long slot ingate can be provided up the complete

height of the casting. In addition, of course, a fairly complex casting station over a deep floor pit is required.

The arrangement to achieve the so-called level filling of the mold is shown in Figure 16.1. An insulated pouring basin connects to a horizontal insulated trough that surrounds three of the four sides of the mold (a distribution system reminiscent of a Roman aqueduct). The melt enters the mold cavity via slot gates that extend vertically from the drag to the cope. Either side of each slot gate are guide plates that contain the melt between sliding seals as it flows out of the (stationary) trough and into the (descending) mold.

Casting starts with the mold sitting on the fully raised mold platform, so that the trough provides its first metal at the lowest level of the drag. The mold platform is then slowly lowered whilst pouring continues. The rate of withdrawal of the mold is such that the metal in the slot gate has time to solidify against a water-cooled chill positioned underneath the melt entrance. Thus the melt in the open slot is frozen before it emerges, sliding out below the level of the trough.

In one of the rare descriptions of the use of the process by Bossing (1982) the large area of melt contained in the pouring basin and distribution trough is claimed to smooth the rate of flow from the point of pour to delivery into the mold, despite variations in the rate of pour into the launder system from the ladle. Also in this description is an additional complicated distribution system inside the mold, in which tiers of runners are provided to minimize feeding distances and maximize temperature gradients. In general, such sophistication would not be expected to be necessary for most products.

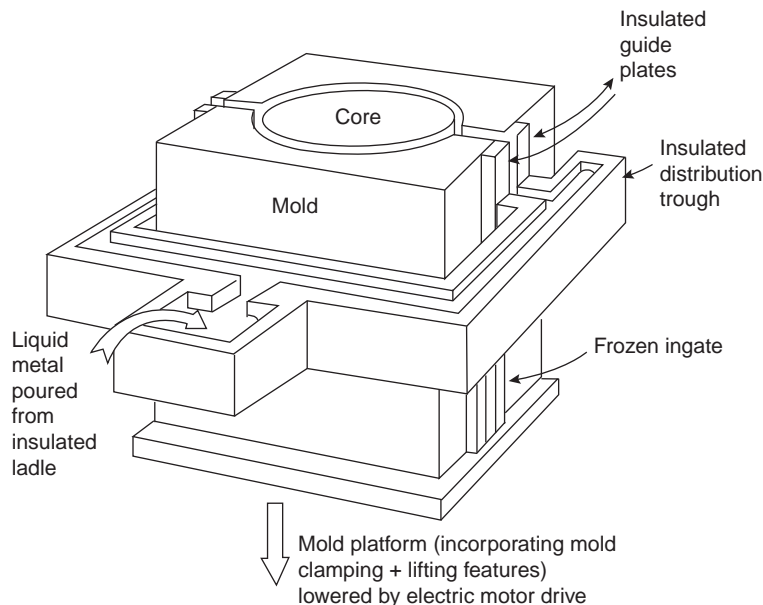


**FIGURE 16.1**

Level pour technique.

### 16.2.2 Controlled tilt casting

It seems that foundrymen have been fascinated by the intuition that tilt casting might be a solution to the obvious problems of gravity pouring. The result has been that the patent literature is littered with re-inventions of the process decade after decade. Even now, the industry has many completely different varieties of tilt process, so the reader needs to be cautious about exactly what tilt process is being referred to.

Furthermore, the deceptive simplicity of the process conceals some fundamental pitfalls for the unwary. The piles of scrap seen from time to time in tilt-pour foundries are silent testimony to these hidden dangers. Generally, however, the dangers can be avoided, as will be discussed in this section.

#### Durville casting

The most common form of tilt casting is a process with the unique feature that, in principle, liquid metal can be transferred into a mold by simple mechanical means under the action of gravity, but without surface turbulence. It therefore has the potential to produce very high-quality castings. This was understood by Durville in France in the 1800s and applied by him for the casting of aluminum bronze in an effort to reduce surface defects in French coinage.

The various stages of liquid metal transfer in the Durville process are schematically illustrated in Figure 16.2a. A melting crucible and a mold are fixed opposite each other on a rotatable platform. A short channel section connects the two. The crucible is heated, charged with metal, and skimmed clear of dross, and the platform is rotated. Some operators of this process have melted elsewhere and transferred the melt to the Durville unit, pouring the melt into the crucible, thus introducing damage. In the process as originally conceived by Durville, the metal is melted in the crucible fixed in the tilt machine. No pouring under gravity takes place at all. Also, since he was casting large ingots in open-ended molds for subsequent working, he was able to look into the crucible and into the mold, observing the transfer of the melt as the rotation of the mold progressed. In this way he could ensure that the rate of rotation was correct, carefully adjusting it all the time, to avoid any disturbance of the surface of the liquid. During the whole process of the transfer, careful control ensured that the melt progressed by 'rolling' in its skin of oxide, like inside a rubber sack, avoiding any folding of its skin by disturbances such as waves. The most sensitive part of the transfer was at the tilt angle close to the horizontal. In this condition the melt front progresses by expanding its skin of oxide, whilst its top surface at all times remains horizontal and tranquil. At this critical stage of metal flow the rate of rotation must be a minimum. If this stage is not kept under good control, the metal surges into the mold as a wave, splashes upwards against the rear face of the mold, and is damaged during its fall by entraining oxides.

Clearly Durville understood what he was doing. He avoided any pouring action to fill the crucible or ladle, and he controlled the rate of rotation of the assembly to ensure horizontal transfer. Few that have followed have understood these critical aspects.

The running system for tilt castings, if any, does not necessarily follow the design rules for gravity casting, since gravity is only marginally influential in this process. The rate of filling of the casting is under the control of the rate of tilt, not necessarily the channels of the filling system. Furthermore, of course, after the mold is filled the filling channels can be used as feeding channels, and thus be sized appropriately. All this is quite different to the design procedure for a gravity-filled mold.

In the USA, Stahl (1961) popularized the concept of 'tilt pouring' for aluminum alloys into shaped permanent mold castings. The gating designs and the advantages of tilt pouring over gravity top

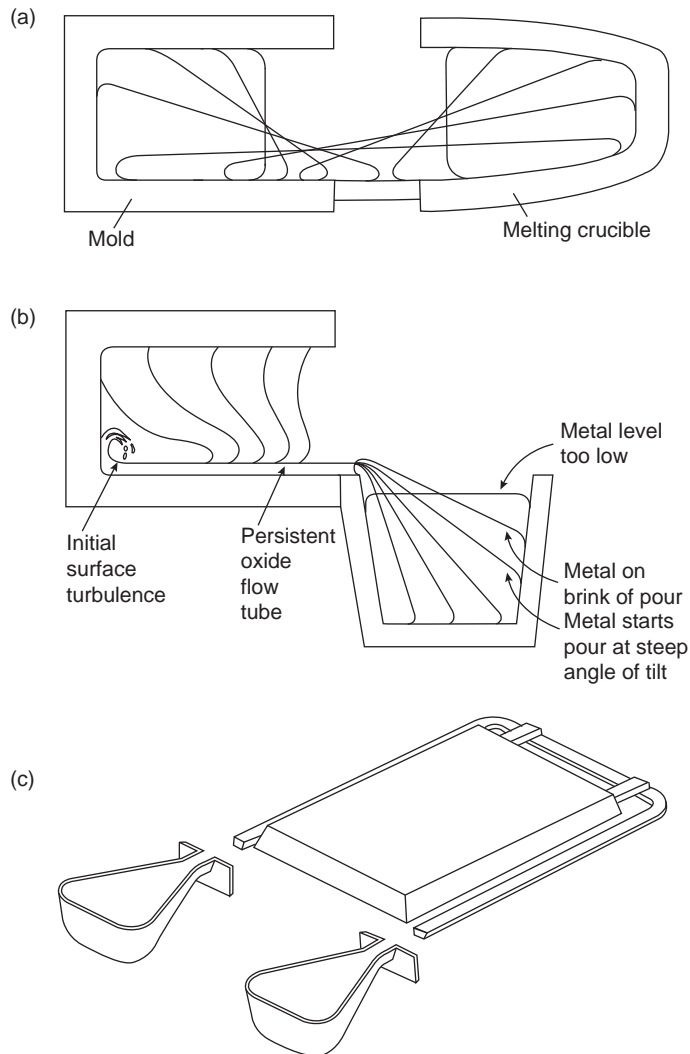


**FIGURE 16.2**

Tilt casting process: (a) Durville; (b) semi-Durville; (c) twin-poured tilting die (adapted from Nyamekye 1994) and (d) outline of tilt running system at the critical moment that metal reaches the far end of the 'sprue' after the melt has effectively fallen height  $h_2$ , unfortunately encouraging damage by surface turbulence.

pouring have been reviewed and summarized in several papers from this source (Stahl 1963, 1986, 1989). These benefits include:

1. The control over the rate of filling helps to control flash. This is because the rate of increase of pressure due to the head of metal is rather slow, starting from zero, in contrast to normal

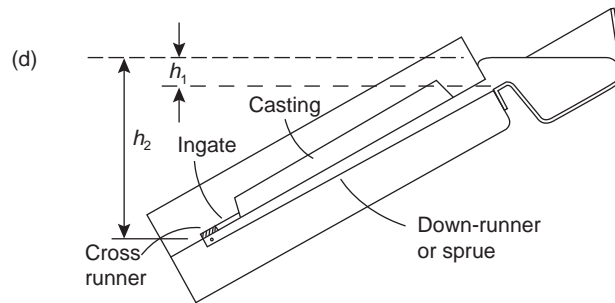


FIGURE 16.2 (continued).

gravity-poured castings, where there are high dynamic pressures and a high rate of attaining the full hydrostatic pressure. The reduced flash is important for castings such as gratings and grills that are otherwise difficult to dress. (This advantage is, of course, available to other gravity-casting techniques, provided a gentle fill is employed; it is less easy to achieve in any of the injection or low-pressure techniques, where the driving force is high, and generally under poorer control.)

2. Automated casting can be arranged relatively easily, with the benefit of consistent results.
3. Two cups can be filled consecutively by one operator, or, alternatively, large cups can be filled by successive charges from a ladle that can be handled by one person. Thus very large castings can be easily produced by one caster. This seems to be a unique benefit for tilt casting, making for considerable economies compared to normal gravity-poured molds, where several casters may be required at one time, pouring simultaneously, or in an unbroken succession, possibly into several down-sprues.
4. The setting of cores has the flexibility of being carried out in either the horizontal or vertical attitude, or even in some intermediate position, depending on the requirements of the cores.
5. For the ejection of the casting the operator similarly has the option of carrying this out vertically or horizontally.

A useful 'bottom-gated' tilt arrangement is shown in Figure 16.2c. Here the sprue is in the drag, and the remainder of the running and gating system, and the mold cavity, is in the cope. Care needs to be taken with a tilt die to ensure that the remaining pockets of air in the die can vent freely to atmosphere. Also, the die side that retains the casting has to contain the ejectors if they are needed.

Dies made for the Stahl casting method feature a tapered sprue carrying metal down to a gate near its base. A typical arrangement is shown in Figure 16.2(c) and (d). Effectively, the running systems are of the bottom-gated type, which give less good temperature gradients, or side-gated, which is some improvement. Figure 16.3 shows a die with side gates, but arranged so as to allow the melt to fall inside the mold cavity. The transfer of the mold cavity into the top half of the die would have eliminated this relatively small defect (but whose consequences are not easily predicted, and might therefore be serious).

Occasionally the metal will be poured directly into the mold cavity, eliminating runners entirely and giving the best temperature gradient but poorest filling. It is significant that Stahl reports the

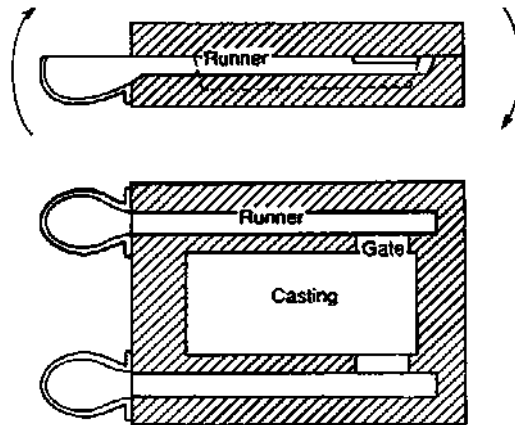


**FIGURE 16.3**

Tilt pour system that would have benefited from the mold cavity mainly in the upper half of the die, avoiding the fall of metal from the gate. Vents would then have been necessary.

disadvantage of the appearance of the flow path down the face of the casting in this case, outlined by streaks of oxide. Such features are a concern since they indicate the presence of flow tubes, thus possibly constituting serious defects. This is a symptom of poor downhill filling, not employing the controlled horizontal fill approach.

In an effort to understand the process in some depth, Nguyen (1986) simulated tilt casting using a water model of liquid metal flow, and King and Hong (1995) carried out some of the first computer simulations of the tilt casting process. They found that a combination of gravity, centrifugal, and Coriolis forces govern tilt-driven flow. However, for the slow rates of rotation such as are used in most tilt casting operations, centrifugal and Coriolis effects contribute less than 10% of the effects due to gravitational forces, and could therefore normally be neglected. The angular velocity of the rotating mold also made some contribution to the linear velocity of the liquid front, but this again was usually negligible because the axis of rotation was often not far from the center of the mold.

However, despite these studies, and despite its evident potential, the process has continued to be perfectly capable of producing copious volumes of scrap castings.

The first detailed study of tilt casting using the recently introduced concepts of critical velocity and surface turbulence was carried out in the author's laboratory by Mi (2000). In addition to the benefits of working within the new conceptual framework, he had available powerful experimental techniques. He used a computer-controlled, programmable casting wheel onto which sand molds could be fixed to produce castings in an Al-4.5%Cu alloy. The flow of the metal during the filling of the mold was recorded using video X-ray radiography, and the consequential reliability of the castings was checked by Weibull statistics.

Armed with these techniques, Mi found that at the slow rotation speeds used in his work the mechanical effect of surface tension and/or surface films on the liquid meniscus could not be neglected. For all starting conditions, the flow at low tilt speeds is significantly affected by surface

tension (most probably aided by the effect of a strong oxide film). Thus below a speed of rotation of approximately  $7^\circ$  per second the speed of the melt arriving at the end of the runner is reduced in a rather erratic way. Gravity only takes control after tilting through a sufficiently large angle.

As with all casting processes, if carried out too slowly, premature freezing will lead to misrun castings. One interesting case was found in which the melt was transferred so slowly into the runner that frozen metal in the mouth of the runner acted as an obstructing 'ski jump' to the remaining flow, significantly impairing the casting. At higher speeds, however, although ski jumps could be avoided, the considerable danger of surface turbulence increased.

The radiographic recordings revealed that the molten metal could exhibit tranquil or chaotic flow into the mold during tilt casting, depending on (i) the angle of tilt of the mold at the start of casting and (ii) the tilting speed. The quality of the castings (assessed by the scatter in mechanical properties) could be linked directly to the quality of the flow into the mold.

We can follow the progress of the melt during the tilt casting process. Initially, the pouring basin at the mouth of the runner is filled. Only then is the tilting of the mold activated. Three starting positions were investigated:

- (i) If the mold starts from some position in which it is already tilted downward, once the metal enters the sprue it is immediately unstable, and runs downhill. The melt accelerates under gravity, hitting the far end of the runner at a speed sufficient to cause splashing. The splash action entrains the melt surface. Castings of poor reliability are the result.
- (ii) If the mold starts from a horizontal position, the metal in the basin is not usually filled to the brim, and therefore does not start to overflow the brim of the basin and enter the runner until a significant tilt angle has been reached. At this stage the vertical fall distance between the start and the far end of the runner is likely to be greater than the critical fall distance. Thus although slightly better castings can be made, the danger of poor reliability remains. This unsatisfactory mode of transfer typifies many tilt casting arrangements as seen in Figure 16.2d and particularly in the so-called semi-Durville type process shown in Figure 16.2b. The oxide flow tube from the downhill flow of the stream, plus the entrainment from the splash at the end of the runner, can be serious defects. Durville would not have liked to see his name associated with this awful process.
- (iii) If, however, the mold is initially tilted slightly uphill during the filling of the basin, there is a chance that by the time the change of angle becomes sufficient to start the overflow of melt from the basin, the angle of the runner is still somewhat above the horizontal (Figure 16.4). The nature of the liquid metal transfer is now quite different. At the start of the filling of the runner the meniscus is effectively climbing a slight upward slope. Thus its progress is totally stable, its forward motion being controlled by additional tilt. If the mold is not tilted further the melt will not advance. By extremely careful control of the rate of tilt it is possible in principle to cause the melt to arrive at the base of the runner at zero velocity if required. (Such drastic reductions in speed would, of course, more than likely be counter-productive, involving too great a loss of heat, and are therefore not recommended.) Even at quite high tilting speeds of  $30^\circ$  per second as used by Mi in his experimental mold, the velocity of the melt at the end of the runner did not exceed the critical value  $0.5 \text{ m s}^{-1}$ , and thus produced sound and repeatable castings.



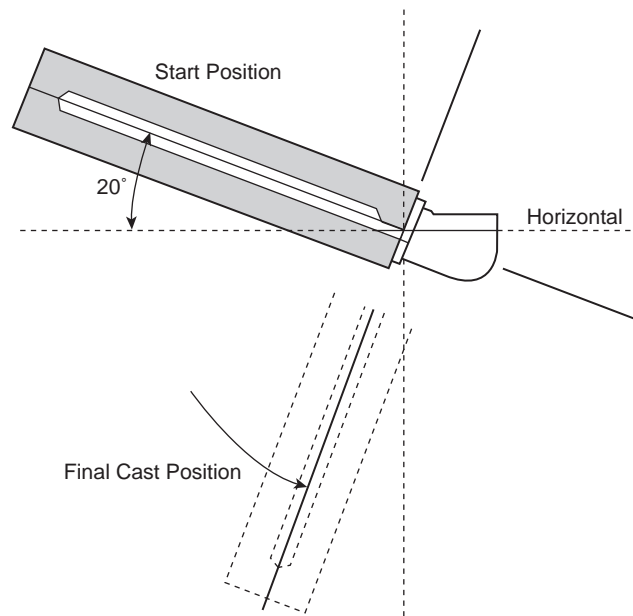


**FIGURE 16.4**

A tilt pour die starting at a  $20^\circ$  positive tilt, designed to encourage the 'runner' to fill uphill (this is a convenient optical illusion), ensuring that the melt reaches the far end of the runner at a controlled speed.

The unique feature of the transfer when started above the horizontal in this way (mode (iii) above) is that the surface of the liquid metal is close to *horizontal* at all times during the transfer process. Thus in contrast to all other types of gravity pouring, this condition of tilt casting does not involve pouring (i.e. a free *vertical* fall) at all. It is a *horizontal* transfer process. It will be seen that in the critical region of tilt near to the horizontal, the liquid transfer occurs essentially horizontally. Durville would have approved.

Thus the optimum operational mode for tilt casting is the condition of horizontal transfer. Horizontal transfer requires the correct choice of starting angle above the horizontal, and the correct tilting speed as found by Cox and Harding (2007). These authors noted that a really accurately controlled tilt speed increased the two-parameter Weibull modulus (the reliability) of Al alloy castings from 2 to 55, an enormous increase. Conversely, a poor choice of rotation parameters created significant surface turbulence.

An operational map can be constructed (Figure 16.5), revealing for the first time an operational window for the production of reliable castings. It is recognized that the conditions defined by the window are to some extent dependent on the geometry of the mold that is chosen. However, the mold in Mi's experiments was designed to be close to the size and shape of many industrial castings, particularly those for automotive applications. Thus although the numerical conclusions would require some adaptation for other geometries, the principles are of general significance and are clear: there are conditions, possibly narrowly restricted, but in which horizontal transfer of the melt is possible, and gives excellent castings.

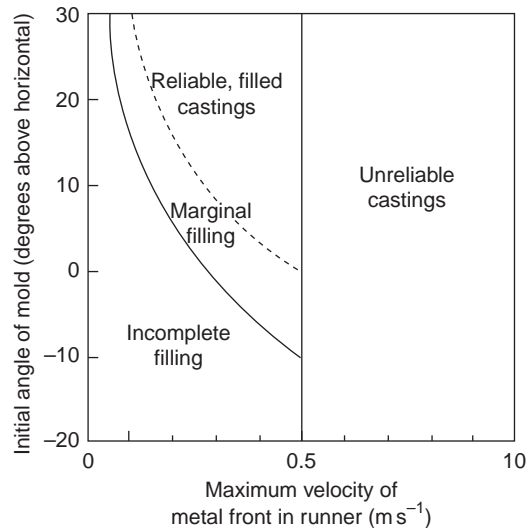


**FIGURE 16.5**

Map of variables for tilt pouring, showing the operational window for good castings (Mi et al. 2002).

The problem of horizontal transfer is that it is slow, sometimes resulting in the freezing of the ‘ski jump’ at the entrance to the runner, or even the non-filling of the mold. This can usually be solved by increasing the rate of tilt *after* the runner is primed. This is the reason for the extended threshold, increasing the range of possible filling conditions on the left-hand side of the window shown on the process map (Figure 16.5). A constant tilt rate (as is common for most tilt machines at this time) cannot achieve this useful extension of the filling conditions to achieve good castings. Programmable tilt rates are required to achieve this solution.

A final danger should be mentioned. At certain critical rates of rise of the melt against an inclined surface, the development of the transverse traveling waves seems to occur to give lap problems on the cope surface of castings (Figure 13.3). In principle, such problems could be included as an additional threshold to be avoided on the operational window map (Figures 16.5). Fortunately, this does not seem to be a common fault. Thus in the meantime, the laps can probably be avoided by increasing the rate of tilt during this part of the filling of the mold. Once again, the benefits of a programmable tilt rate are clear.

In summary, the conclusions for tilt casting are:

1. If tilt casting is initiated from a tilt orientation at, or (even more especially) below, the horizontal, during the priming of the runner the liquid metal accelerates downhill at a rate out of the control of the operator. The metal runs as a narrow jet, forming a persistent oxide flow tube. In addition, the velocity of the liquid at the far end of the runner is almost certain to exceed the critical condition for surface turbulence. Once the mold is initially inclined by more than  $10^\circ$  below the horizontal at the initiation of flow, Mi found that it was no longer possible to produce reliable castings by the tilt casting process.
2. Tilt casting operations benefit from using a sufficiently positive starting angle that the melt advances into an upward sloping runner. In this way its advance is stable and controlled. This

mode of filling is characterized by horizontal liquid metal transfer, promoting a mold filling condition free from surface turbulence.

3. Tilt filling is preferably slow at the early stages of filling to avoid the high velocities at the far end of the running system. However, after the running system is primed, speeding up the rate of rotation of the mold greatly helps to prevent any consequential non-filling of the castings.

### 16.2.3 Roll-over as a casting process

There are casting processes in which the mold is planted upside-down over the mouth of a small melting unit, usually a small induction furnace, and the whole assembly is rotated swiftly through  $180^\circ$ . This technique is widely used in investment casting. However, it is not a process that appears to enjoy much control. It is in reality a kind of dump process for liquid metal. The procedure might not be so bad with a carefully designed filling system in the mold, but this is rarely provided at this time; the melt simply tumbles down the filling system. There is little to commend with this approach.

The InvoCast method by Butler (1980) provides an interesting development, which has similarities to the Stahl tilt-pouring method, in that the first action is to fill a pouring cup, and the next is the rotation of the die, which causes the die cavity to fill. It is shown in Figure 16.6. However, there is an important improvement in that the metal does not necessarily run downhill (this will vary somewhat from casting to casting) but fills the cavity progressively as rotation proceeds. Finally, the feeder is sited on top where it can feed most effectively. The preheating of the running system adds to the effectiveness of its action when it reverts to become the feeding system.

#### Rotacast process

The Rotacast process, first used for the production of Al alloy cylinder heads by the Mandl and Berger company, Austria, is another casting process executed by a roll-over transfer. It is described by

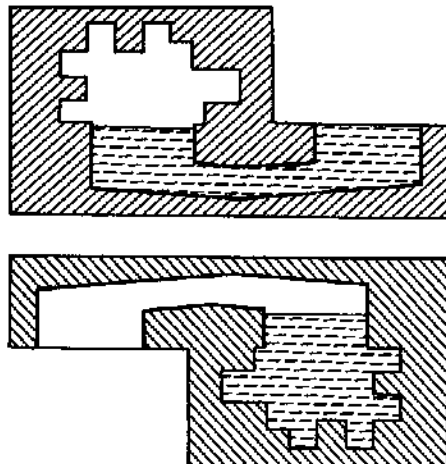


**FIGURE 16.6**

Inversion casting of a gravity die, showing the start and finish stages (after Butler 1980).

Grunenberg et al. (1999). A cylindrical ladle is filled with metal (by pouring, of course, so some defects will be added by this initial action) and is then offered up to a permanent mold (Figure 16.7). The mold is then rotated about its longitudinal axis, transferring the melt from the ladle into the mold. Because the ladle and mold are a pressure-tight system pressure can be applied during the freezing of the casting. This is said to reduce the feeder size in the sand top core, even though pressure timing and magnitude have to be carefully controlled to avoid metal penetration of the sand cores.

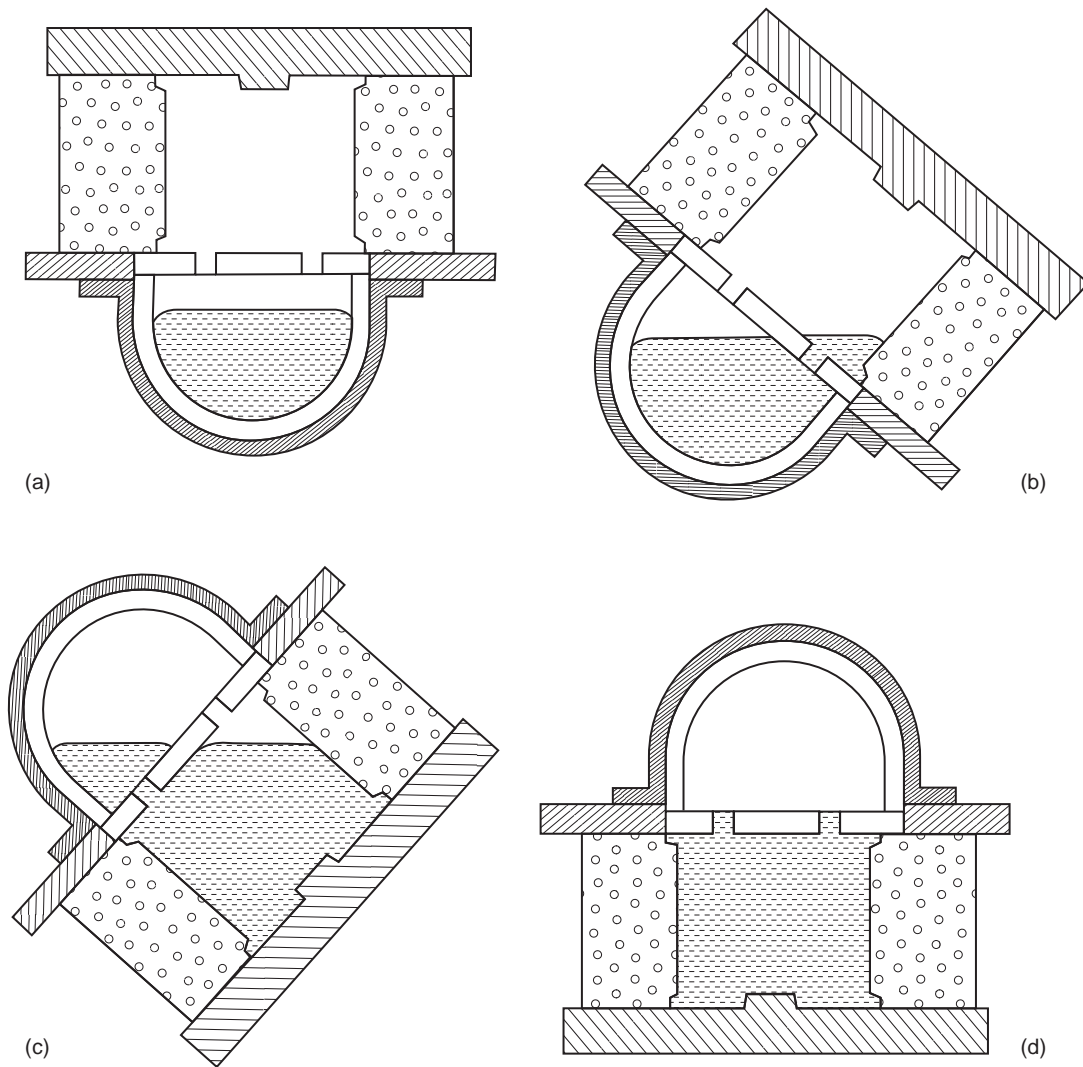


**FIGURE 16.7**

Rotacast process used for automotive cylinder heads and blocks. The roll-over action takes about 10 s (after Schneider 2006).

In this same report these authors go on to describe a second (unnamed) process which they seem to consider at the time to be an improvement on the simple Rotacast process. The system employs a permanent mold with a top sand core to contain the feeders. This is a variety of the semi-Durville process (Figure 16.8), and shares its same problems; the serious limitations of this incomplete application of Durville's technique are clearly seen in Figure 16.8 in which the degree of filling of the ladle, varying from time to time, dictates a varying angle at which the pour can start, resulting in the initial downhill flow of the melt, often at a steep angle, achieving high and damaging velocities. A further feature is the use of pressurization after filling in an effort to reduce feeder size. This need for this complication reveals the poor metal quality, requiring bifilms to be kept closed during freezing. It would surely be better to opt for a technique to improve metal quality and improve filling. I am not aware of this process still being used. Perhaps the users finally had second thoughts about the reality of its capabilities.

#### 16.2.4 Roll-over after casting (sometimes called inversion casting)

Inversion casting is not tilt casting. In fact it might better be described as a solidification control process rather than a casting process, since the pouring action is carried out as a normal gravity fill. It is only after the mold is filled that the whole assembly is rotated through  $180^\circ$  to encourage solidification under improved temperature gradients, and so aid the feeding of the casting.

Batty in 1935 was probably the first to describe simple inversion casting. He gives the example of a heavy-walled cylinder casting that was cast standing upright as shown in Figure 16.6. The gating system was a classical bottom-run method for optimum filling. This would normally result, of course,

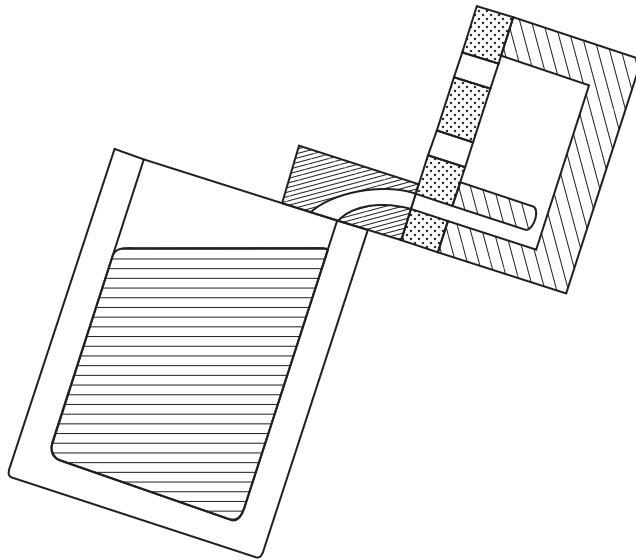


**FIGURE 16.8**

A tilt-casting process in which the ladle connects directly to a permanent mold with a sand top core containing the feeders (Grunenberg, Escherle, and Sturm 1999). The danger of some downhill flow inside the mold can be seen.

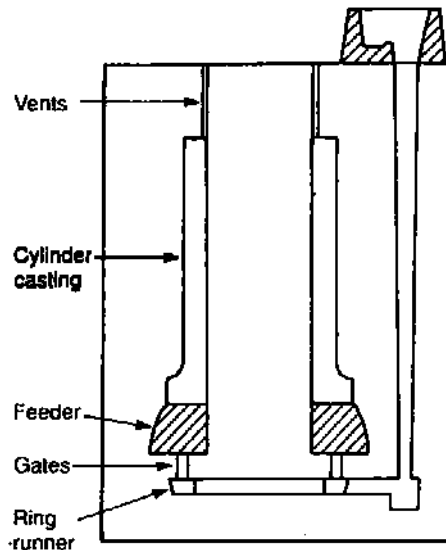


**FIGURE 16.9**

Cylinder casting arranged for inversion casting. Adapted from Batty (1935), but core and mold assembly details omitted for clarity.

in a temperature regime in which the highest temperature was at the base of the casting, and any top feeders would be too cold to be effective. He solves this problem at a stroke by simply turning the whole mold over immediately after casting. The runner is then the feeder (and may need to be somewhat larger than normal to fulfill this additional role) and acts effectively because it is preheated, and because the temperature gradients in the casting are all favorably directional towards the feeder.

Let us review this worthy effort by Batty. We now know that the well at the base of the sprue would have introduced significant entrainment defects; thus this should be eliminated. Personally, I would have eliminated all this fussy runner and ingate complication at the base of the casting, simply turning the sprue and entering the casting tangentially, thus spinning the metal up inside the casting. Finally, Batty's favorable temperature gradients for feeding after roll-over would only be obtained if especially slow pouring was used, thus threatening the formation of cold laps or unfilled castings. In this case, because of the relatively heavy wall section of this casting I would not have employed a roll-over. I would have allowed the casting to have inverted its temperature gradient by itself, simply by the natural action of convection. The feeder then should have been located at the top of the stationary (non-roll-over) casting.

### Cosworth process

After the counter-gravity filling of the mold, the Cosworth process uses the inversion concept whilst keeping the liquid metal under pressure from the pump during the roll-over. In addition to the feeding of the casting being improved by the filling system becoming the feeding system, the mold can be immediately disconnected from the pump, and moved on to a cooling conveyer before freezing is complete. The casting station is then released for the production of further castings. The

technique therefore allows a major improvement in productivity (Smith 1986). Green (2005) draws attention to the importance of maintaining the pressure on the melt during the roll-over because otherwise the metallostatic pressure due to depth alone (particularly when, during rotation, the mold is sideways and so generating a much reduced head pressure) may be insufficient to hold expanding gases in cores, therefore leading to the possibility of core blows. Processes that employ roll-over but which are not capable of maintaining the pressurization of the liquid are therefore at risk.

The so-called *Core-Package System (CPS)*, with an inappropriately widely encompassing name, is in fact a rather specialized form of precision sand core assembly process involving the filling of the sprue by contact pouring by offering up the mold assembly to the underside of a launder (Schneider 2006). The stopper sealing the nozzle in the bottom of the launder is raised and the mold is filled. This works well. After the mold is filled it is lowered to disengage with the launder, and a small arm automatically closes the sprue with a cap to prevent it emptying during the roll-over. The mold is then rolled over so that the reservoir under the casting is brought to the top to act as a feeder. However, during filling, the emptying of the high-velocity metal into feeder volume creates major problems because the constraint over the liquid is lost, allowing the melt to jet and ricochet throughout the volume, entraining major defects (Figure 16.10). This otherwise

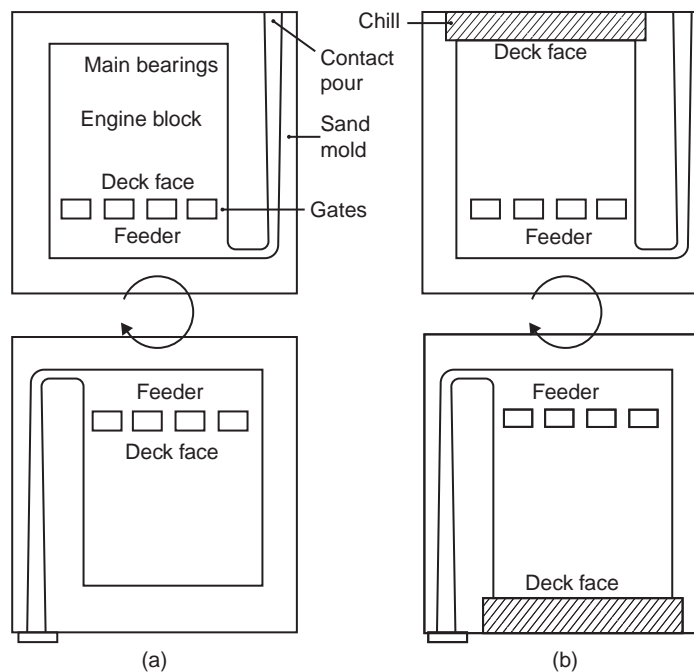


**FIGURE 16.10**

The so-called core-package system (CPS) for engine blocks uses good filling via contact pour, and roll-over for feeding, but the high-velocity flow into the volume of the feeder can cause major problems. The feeder operates via the ingates, and optional cooling can be applied to locally increase properties as necessary (after Schneider 2006).

good casting process contrasts of course with the true counter-gravity filling of the feeder volume which is gentle and controlled, and has the potential to avoid the creation of any defects.

Figure 16.10 does illustrate the other important aspect of the roll-over processes, that chills can be used to good effect to enhance temperature gradients and so enhance feeding. As the figure illustrates, the use of chills dictates which way up the casting is filled; for cylinder heads the chill is desired on the combustion face, and specifically between exhaust valve seats in 4-valve per cylinder engines. For cylinder blocks, the fire face is relatively lightly loaded compared to the main bearings, whose fatigue performance greatly benefits from being chilled.

The roll-over principle, when used appropriately, either as a casting process or post-casting process, seems to be a powerful solution to some of the problems of filling and/or feeding castings. It strongly deserves to be more widely used.

---

### 16.3 COUNTER-GRAVITY

My toes curl when I hear the counter-gravity process called ‘counter-gravity pouring’. Pouring it is not. Furthermore, such inaccuracy undermines the thinking that is fundamental to the whole concept of the avoidance of pouring. The word pouring requires to be eliminated from the vocabulary of those rational souls employing the counter-gravity process. In its place we need the appropriate and heart-warming phrases ‘counter-gravity filling’ or ‘counter-gravity casting’.

Over the last 100 years and more, the fundamental problems of gravity filling have prompted casting engineers to dream up and develop counter-gravity systems.

Numerous systems have arisen. The most common is *low-pressure casting*, in which air or an inert gas is used to pressurize an enclosed furnace, forcing the melt up a riser tube and into the casting (Figure 16.11). Other systems use a partial vacuum to draw up the metal. Yet others use various forms of pumps, including direct displacement by a piston, by gas pressure (pneumatic pumps), and by various types of electromagnetic action.

The fundamental action at the heart of the counter-gravity concept is that the liquid meniscus can be made to rise at a rate at which its oxide is pinned against the mold walls, the oxide becoming the skin of the casting. The oxide on the surface of the advancing meniscus never becomes entrained into the bulk of the melt, creating defects in the casting. Only perfectly executed horizontal filling can match this extraordinary perfection of filling control. Counter-gravity is among the few (the very few) filling processes that can produce uniquely perfect castings.

Clearly, with a good counter-gravity system, it is possible to envisage the filling of the mold at velocities that never exceed the critical velocity, so that the air in the mold is pushed ahead of the metal, and no surface entrainment occurs. The filling can start gently through the ingates, speed up during the filling of the main part of the mold cavity, and finally slow down and stop as the mold is filled. The final deceleration is useful to avoid any final impact at the instant the mold is filled. If not controlled in this way, the transient pressure pulse resulting from the sudden loss of momentum of the melt can cause the liquid to penetrate any sand cores, and can open mold joints to produce flash, and generally impair surface finish.

When using a good counter-gravity system, good filling conditions are not difficult to achieve. In fact, in comparison with gravity pouring where it is sometimes difficult to achieve a good casting,



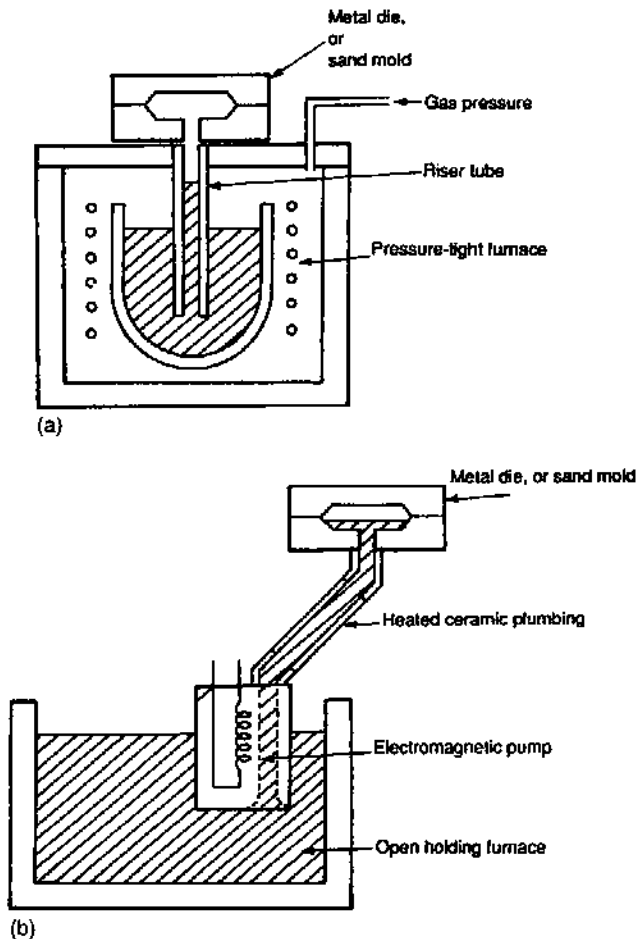


**FIGURE 16.11**

Counter-gravity castings by (a) conventional low-pressure casting machined using a sealed pressure vessel; (b) electromagnetic pump in an open furnace.

counter-gravity is such a robust technique that it is often difficult to make a bad casting. This fundamental difference between gravity and counter-gravity filling is not widely appreciated. In general, those who are familiar with gravity filling but have finally accepted a change to counter-gravity are suddenly amazed by the powerful benefits.

A counter-gravity filled investment casting method that crams a hundred or more steel castings on one wax assembly makes millions of automotive rocker arm castings per year. These show a reject rate in the fractions of a part per million parts, illustrating the astonishing reliability that can be achieved by counter-gravity. Interestingly, however, this mode of casting was devised by Chandley

(1976) not initially for its high reliability but because of its low costs. Further developments of this process by the Hitchener Company into aero engine turbine components among other markets have been impressive. They were reviewed by Shendye and Gilles in 2009. Griffiths (2007) confirms that counter-gravity filling of a low-alloy steel produced castings with a higher Weibull modulus (higher reliability) than even well-designed gravity filling systems. A vertical stack of aggregate molds filled with nodular or highly alloyed cast irons produced high volumes of castings with reliable 2.8-mm-thickness walls (Purdom 1992). Brasses are cast into permanent molds to produce dense, leak-free domestic plumbing fittings required to take a high polish and faultless chromium plate (Lansdown 1997).

That is not to say that the counter-gravity technique is not sometimes used badly. A common poor practice is a failure to keep the metal velocity under proper control. Entering the mold too quickly, even with a counter-gravity system, can make impressively bad castings. However, in principle the technique *can* be controlled, in contrast to gravity pouring where, in principle, control is often difficult or impossible.

A concern often expressed about counter-gravity is that the adoption of filling speeds below the critical speed of approximately  $0.5 \text{ m s}^{-1}$  will slow the production rate. Such fears are groundless. For instance if the casting is 0.5 meters tall (a tall casting) it can, in principle, be filled in 1 second. This would be a challenge!

In fact the unfounded fear of the use of low velocities of the melt leading to a sacrifice of production rate follows from the confusion of (i) flow velocity (usually measured in  $\text{m s}^{-1}$ ) and (ii) melt volume flow rate (usually measured in  $\text{m}^3 \text{ s}^{-1}$ ). For instance the filling time can be kept short by retaining the slow filling velocity but increasing the volume flow rate simply by increasing the areas of the flow channels. Worked examples to emphasize and clarify this point further are given in Chapter 13 dealing with the calculation of the filling system.

The other problems relate to the remainder of the melting and melt handling systems in the foundry, which are often poor, involving multiple pouring operations from melt furnaces to ladles and then into the counter-gravity holding vessel. A widespread re-charging technique for a low-pressure casting unit is illustrated in Figure 16.12; much of the entrainment damage suffered in such processes usually cannot be blamed on the counter-gravity system itself.

The lesson is that only limited success can be expected from a foundry that has added a counter-gravity system on to the end of a badly designed melting and melt-handling system which generates defect-laden metal. There is no substitute for an integrated approach to the whole production system. Some of the very few systems to achieve this so far have been the processes that the author has assisted to develop; the Cosworth process and, perhaps at some future date, in the Alotech ablation processes. In these processes, when properly implemented, the liquid metal is allowed to settle to eliminate a proportion of its defects in suspension, and subsequently is never poured, never flows downhill, and is finally transferred into the mold without surface turbulence. It is not difficult to arrange these highly beneficial features of a melt system.

Finally, the concept of an integrated approach necessarily involves dealing with convection during the solidification of the casting. The problem is highlighted by the author as Casting Rule 7. This serious problem is usually completely overlooked. It has been the death of many otherwise good counter-gravity systems, but is specifically addressed in the Cosworth process by roll-over after casting and in the ablation process by the application of steep temperature gradient provided by ablation cooling.

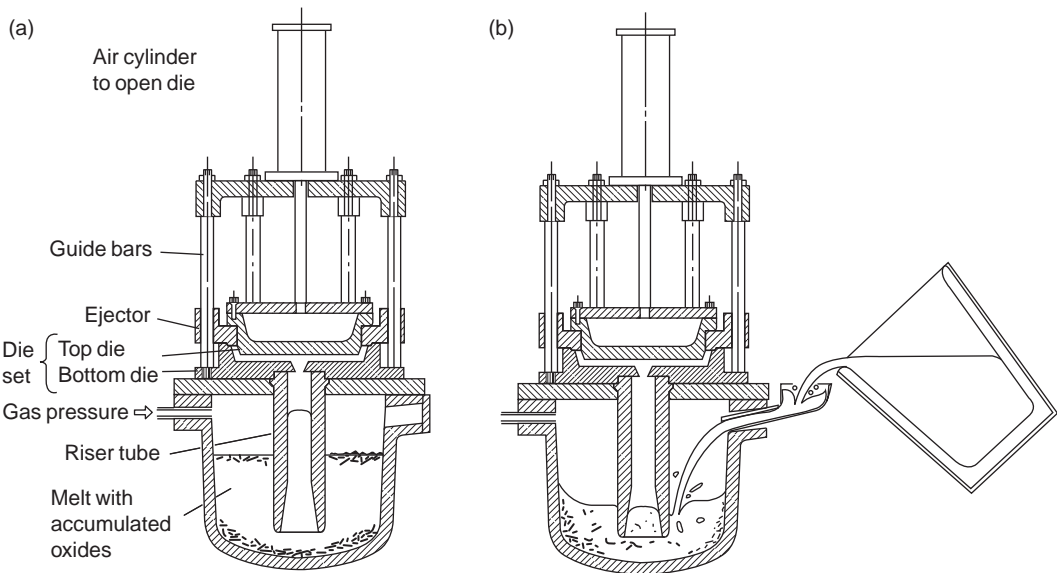


**FIGURE 16.12**

Low-pressure casting unit showing (a) sink and float of oxide; and (b) the conventional poor filling technique that re-entrains debris.

### 16.3.1 Low-pressure casting

#### Low-pressure die casting

The low-pressure die casting (low-pressure permanent mold) process is widely used for the casting of automotive parts such as wheels and cylinder heads which require good integrity and, for wheels, good integrity and good cosmetic appearance when finely machined or polished.

Its name arises from its relatively low pressure (perhaps 0.3–0.5 bar) required to lift the metal into the mold (note that 1 bar will raise the melt approximately 4.5 m) followed sometimes by the application of a higher-pressure stage to reduce any porosity in the casting. During this stage the pressure might be raised to 1 bar. Even these highest pressures are typically only about 1% of the pressures used in high-pressure die casting.

The process enjoys a number of advantages, including ease of automation, so that despite its cycle time being longer than that of gravity permanent mold systems, one man can usually control a number of machines. In addition, in common with most counter-gravity systems, it has metallic yields in the range 80–95%, compared to 50–75% for gravity-poured systems that require oversized feeders as a result of the damage that their filling systems introduce. In common with gravity pouring, sand cores are not a problem provided the applied pressure is under good control (otherwise, with overpressure being sometimes applied to prevent bifilm opening to create microporosity, sand cores can become impregnated with metal. Clearly, if the melt is of good quality, overpressure to suppress porosity is not required).

Low-pressure die casting dies can be made from cast iron or steel, depending on the service requirements, and enjoy the protection of a ceramic die coating applied by spray.

In most low-pressure permanent mold casting the die is split horizontally, with the casting retained in the upper half (ejectors cannot usually be placed in the lower half because of the presence of the furnace under the die). As the upper half is raised after the freezing of the casting, the ejectors impinge against the stripping plate to eject the casting. In this case the casting is usually caught on a tray swung under the upper die as it is raised. The tray and casting are then swung clear, presenting the casting outside the machine for onward processing.

The dies are often water-cooled by internally drilled water channels. Cooled dies are expensive and complicated, but hold the record for productivity of certain types of casting such as automotive wheels. An uncooled die for a wheel might have a cycle time of 5 minutes, whereas a cooled die can be under 2 minutes. For larger castings such as some cylinder blocks a cycle time of 15 minutes may be usual.

One of the most notable high-temperature developments of low-pressure die casting is the famous *Griffin process* for steel railway rolling stock (Figure 16.13), described by Hursen (1955). It makes

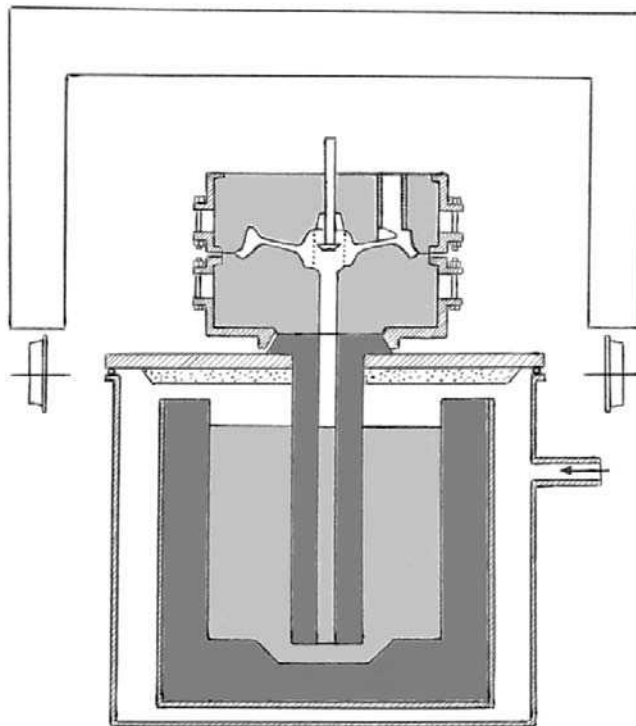


**FIGURE 16.13**

The counter-gravity casting of steel railroad wheels by Griffin process. The mold transfer car (transporting frame shown in outline) carries the mold along the production track, and houses all the gear for lowering, raising and clamping down of the mold and operating the stopper (after Hursen 1955).

an interesting comparison to the use of the process for Al alloys. The insulated ladle in the pressure vessel can hold up to 7 tons of liquid carbon steel. The large density difference between the steel and buoyant defects such as bubbles, bubble trails, and other entrained oxides encourages such materials to float out relatively quickly, so that the topping-up of the furnace does not necessarily introduce permanent damage; after the metal has been poured into the pressurized vessel the entrained defects quickly float away from the bottom of the melt where the intake to the riser tube is located. In addition little or no sediment is to be expected. Thus a good quality of steel has had the chance to develop at this location prior to the filling of the next casting. In this way a high-integrity safety-critical product can be routinely produced. Even so, one can imagine that the deoxidation practice, leaving different amounts of Si, Mn, and Al, plus others such as Ca, could influence the flotation time significantly.

In practice, the process is impressively automated and productive. Molds arrive automatically on a transfer car rolling on a track, and are indexed automatically into place on the casting unit. The filling of the mold with steel at 1620°C is registered by observing the top of one of the three or four sand-lined feeders. When the metal arrives at the top the filling is stopped and the timing of other operations is started (the somewhat variable filling time arises because of the falling level of the melt in the holding furnace). After filling, no waiting is required for solidification because the graphite stopper is lowered to seal off the mold (Figure 16.13) and the mold is automatically indexed to the cooling line. The furnace can cast about 20 wheels before being returned to the melting furnace where its remaining metal is returned and the holder can be topped up. The center of the casting containing the stopper (shown as dotted lines in Figure 16.13) is removed by flame cutting. Only this central bore is machined. The remainder of the casting, including the tread of the wheel that runs directly on the rail, remains cast-to-size. The cast wheels at least equal if not exceed the reliability of forged and rolled steel wheels. I find all this a deeply impressive achievement.

Unfortunately, in spite of its excellent potential, the low-pressure process has some fundamental problems that can produce significant amounts of scrap. The problems arise from a number of sources.

It is necessary to take stock of the many problems associated with low-pressure casting:

- (i) The re-filling of the pressurized furnace with metal (Figure 16.12) is usually a major source of entrainment defects that causes all the usual problems of fine scattered porosity often suffered by the process.

There is one variety of low-pressure casting unit that goes some way towards solving the problem of the massive damage introduced by the conventional topping-up operation. It has a separate crucible and furnace assembly that can be detached from the casting machine. This is usually achieved by the pressurized furnace assembly containing the crucible being indexed out from under the machine. Up to three such assemblies are required per casting machine so that one can be melting, another treating the melt by, for instance, rotary degassing and passive holding, and the third is in place in the machine making castings. This system is clearly a significant improvement on re-filling of the pressurized vessel by gravity pouring through a port in its side.

- (ii) In the past, many low-pressure die-casting machines have been so poorly controlled on flow rate that the speed of entry into the die could greatly exceed the critical velocity, thus negating one of the most important potential benefits of the low-pressure system. Oxide bifilms and possibly

bubbles are generated inside the mold, having little or no time to separate from the casting. Fortunately, most modern machines have significantly improved control so this is no longer a problem.

I recall an instance in the Cosworth foundry when the melt was pumped too quickly into the mold by mistake. The result was disaster, with the X-ray radiograph displaying hot tears, gas bubbles, apparent shrinkage porosity, and sand inclusions. This contrasted with normally defect-free castings when the ingate velocity was correctly controlled below the critical velocity of  $0.5 \text{ m s}^{-1}$ .

- (iii) The melt is usually allowed to fall down the riser tube after the solidification of each casting. This fall leaves a skin of oxide on the inside of the riser tube, which can detach and spoil the subsequent casting, although a filter of some kind at the mouth of the mold is usually in place to help to reduce this problem. Pechiney, France, was probably the first in an attempt to address this issue by providing an inert gas environment for the top of the riser tube (Charbonnier 1983). However, the problem is best solved by keeping the riser tube filled to within a few millimeters of the top, with the melt ready to enter the next casting. Unfortunately there is significant resistance within the industry to keep pressurized furnaces pressurized to achieve this mode of operation, said to be a concern of safety. However, processes using EM pumps achieve this maintenance of the level without difficulty and thereby avoid unnecessary oxide generation.
- (iv) The other serious feature of the sudden release of pressure is fall of the melt in the rise tube creating the consequential 'whoosh' of melt issuing from its base, efficiently stirring up all those oxides that have settled to the floor of the furnace since the last casting. Thus defects in suspension in the melt are never allowed to settle quiescently on the floor of the furnace; inclusions are re-stirred into suspension between every casting. A controlled, gradual release of pressure would easily solve this problem.
- (v) New riser tubes offering longer life might now create conditions in which the sediment now has time to reach depths for which entrainment of the sediment in the casting becomes unavoidable.
- (vi) Convection of melt up the riser tube and into the mold, delaying the freezing of the casting, can be a serious contributor to poor productivity and poor solidification structure in the casting. I recall an operator who related to me that he timed the freezing of his cylinder head casting, then degassed the melt with an inert gas. On re-checking the freezing time it was found to have increased. He concluded the reduced hydrogen affected the freezing behavior. He degassed again and the freezing increased again. This happened three or four times (I forget exactly how many). Clearly, the variations in hydrogen content could not explain these results. I concluded that his original melt convected very little because of its high viscosity resulting from its content of oxide bifilms in suspension. This slurry would move only sluggishly in the rather narrow riser tube. After 'degassing', which would have removed a significant proportion of oxides, the higher fluidity of the melt, as a 'thinned' slurry, would have led to increased thermal convection in the riser tube, conveying heat from the melt in the furnace, up the riser tube and into the casting, delaying its solidification. The progressive cleaning of the melt and progressively worsening productivity illustrated the influence exerted by two powerful factors normally overlooked in casting operations: oxide bifilms and thermal convection.

Riser tubes that deliver the melt directly into the mold cavity (rather than turning some right angle corners in a distribution system) are particularly at risk from this problem. The use of a filter at the top of the riser tube is a further help, but usually does not completely cure the problem. Muller and Feikus (1996) in an excellent article describe the use of a new design of spreader pin sited at the top exit of the riser tube. This device helped to remove some heat from the casting at the top of the riser tube, assisting to control the convective flow of hot metal into the casting at this point, and thus increasing casting quality and productivity.

As a result of all these problems, many of which are not addressed as suggested above, the performance of many low-pressure casting operations is often disappointing. For serious operators, the optimization suggestions by Muller and Feikus (1996) are recommended reading.

#### Medium-pressure (MP) die-casting process

A potentially interesting variant of the low-pressure process has been described as the medium-pressure casting process by Eigenfeld (1988). Essentially the mold is filled exactly as the low-pressure process, but after the mold is filled and the casting partly solidified, the casting is pressurized by one or more small pistons, well known in HPDC as squeeze pins, that collapse the casting surface locally. The internal pressurization of the melt in this way will reduce the 'air gap' around the casting and thus increase the freezing rate. The process is claimed to give better properties than conventional LP die casting for this reason.

#### Counter-pressure casting (CPC) process

A complication of the usual low-pressure die-casting process has been introduced as the *counter-pressure casting process*, in which a pressurized chamber is lowered over the die to apply pressure counter to the pressure in the furnace chamber, so that only the differential pressure raises the melt up the riser tube (Balewsky and Dimov 1965). The counter-pressure, usually between 3–10 bar, acts on the liquid during mold filling and solidification to help to suppress the formation of porosity. The lowering of the counter-pressure chamber and its pressurization with gas would be expected to slow the production cycle, but Wurker and Zeuner (2004, 2006) claim otherwise. The development is clearly devised as a logical approach to reduce the problems arising from current poor melt practice. However, if the cast metal had a reasonable quality, free from oxide bifilms, no porosity could be generated, so that no applied pressure would be needed.

#### VRC/PRC

*Vacuum riserless casting and/or pressure riserless casting* is a process using permanent water cooled metal molds filled by vacuum and/or pressure, so that a riser (i.e. feeder) is not required (Spada 2004).

This author has to admit to being biased; he cannot get to like this process. It seems to him to be unnecessarily and unbelievably complicated. The permanent mold, possibly sprayed with release agent between every cast, is filled partly or entirely by the application of a vacuum to the mold, drawing metal up from the furnace sited below the mold. Any leakage of the riser tube(s) will introduce air bubbles into the casting. The melt may rise up more than one riser tube, introducing the danger of convection between the tubes (melt rising up one and descending down another, the heat thus transferred from the furnace delaying the solidification of the casting, and impairing

structure) although fortunately the strong water cooling of the metal mold will reduce this danger. Having filled the mold, additional pressure can now be applied from below to help to suppress pore formation and increase cooling rate by pressurizing the casting against the mold. When releasing the pressure, the residual melt in the riser tubes falls back into the furnace, potentially increasing oxide, but certainly re-stirring up-settled oxides, maintaining them in suspension. Fortunately, the process can be used with pre-treated melts with exchangeable furnaces, or better still with furnaces kept full from a heated launder distribution system (Spada 2004, 2005).

The control problems are daunting, involving vacuum cycles, pressure cycles, and complex water cooling, in addition to the normal cycles involving opening and closing the die, etc. The capital and maintenance costs must also be daunting. The castings can be excellent of course, but the workforce has to be unusually diligent and well above average capability to succeed with this system. They have my best wishes.

### T-Mag process

A recent interpretation of the tilt casting process for Mg alloy castings named *T-Mag* (T presumably for tilt and Mag for magnesium) has been demonstrated by CSIRO in Australia (Nguyen et al. 2006) using a permanent mold connected to the melting furnace via a heated transfer tube (Figure 16.14). When tilting the assembly, the melt enters the die via a bottom gate, thus having the potential to fill the cavity smoothly. It is therefore better described as a counter-gravity process. After solidification the assembly is rotated back to its vertical position, lowering the melt gently in the riser tube (in contrast to most low-pressure units), the die is opened, and the casting ejected. The casting has the short ‘carrot’ ingate typical of low-pressure castings, and thus enjoys a good metallic yield in addition to its reasonably high quality. At this time the direct addition of ingots or foundry returns to the melt introduces the oxide skins of these charge materials, which are almost certainly troublesome with respect to the attainment of the highest and most reproducible properties (Wang et al. 2011). Thus although at this time performing better than most Mg casting processes, it seems the process is in its early days of development and it is to be hoped that the process will receive further development to achieve its full potential.

## 16.3.2 Liquid metal pumps

A pump can be an excellent way to transfer metal into a mold. There are many varieties of pump, but as with all pumps, they are characterized by their particular characteristic curves. These are graphs of the relation between head height and volume flow rate as shown in Figure 16.15. The characteristic curves require to be treated with some caution; they show the *potential* of the pump. When programming the pump to fill some odd-shaped volume, such as a casting, the setting of the pump power to achieve a certain metal height at a certain time will not, in general, deliver metal at that height at that time. This is simply because it takes *time* for the melt to be accelerated by the pump and *time* for the mold cavity to fill the part of the casting volume up to that level. This wide misunderstanding of the necessary lag between the programmed and achieved conditions is easily dealt with by the computer, which can apply Newton’s laws of motion to the metal without difficulty or complaint, and get the programming exactly right first time. Alternatively, the problem is dealt with, within the limits of the power of the pump, by feedback control as described in Section 16.3.5.



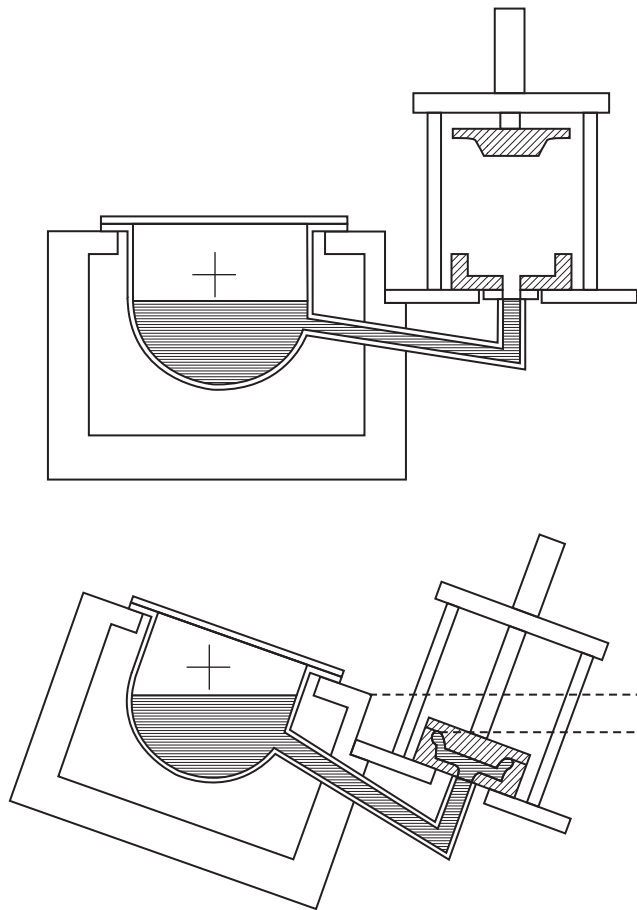


**FIGURE 16.14**

The 'counter-gravity' casting of Mg alloys using the tilting furnace of the T-Mag technique. The figure shows a permanent mold, but would be expected to work perfectly well with a sand mold, particularly if convection were controlled. Solidification occurs under pressure  $\Delta P$ . The unit reverts to its upright mode to open the die and eject the casting.

We shall consider the main pump options for use in foundries below.

### Centrifugal pumps

A brief history of centrifugal pumps is given by Sweeney (1964). He described the first pumps for molten aluminum in Cleveland, Ohio, in 1945.

Centrifugal pumps usually have carbon-based rotors, and can have high volumetric capacity, although the characteristic curves shown in Figure 16.15a show the output of a rather small pump with similar characteristic curves to the electromagnetic pump PG450 used for making castings

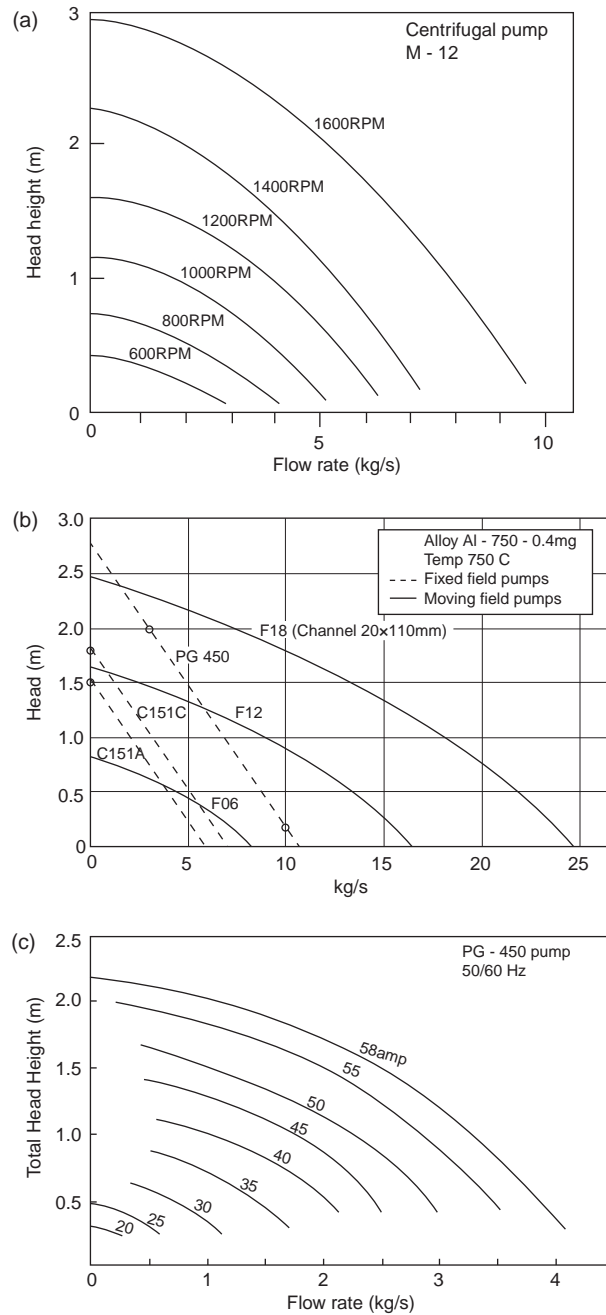


FIGURE 16.15

Characteristic curves for the performance of (a) centrifugal pump; (b) three sizes of two different varieties of electromagnetic pump at full power; (c) a single phase electromagnetic pump at various power levels.

(Figure 16.15c). Much larger centrifugal pumps are available for transferring tonnage quantities of melts between furnaces since they can transfer Al at up to  $100 \text{ kg s}^{-1}$  and up to 7 m high. However, in general it has been concluded that these pumps are not well suited to filling molds, since the filling rate is rather variable as a result of the wear of the rotors and the variable speed of the usual drive, an air motor powered by the compressed air supply in the plant.

Although the centrifugal pump cannot at this time claim the finesse of control enjoyed by EM pumps it might be useful low cost option for really large Al alloy castings. Such a possibility seems never to have been evaluated. There lies a challenge for someone.

### Electromagnetic (EM) pumps

The great benefit of EM pumps is that they contain no moving parts, and their life in a melt can usually be measured in months. Their relatively high initial costs are usually offset by good reliability and relatively modest maintenance and running costs. Their use in the relatively non-aggressive environments for low-melting-point metals tin and lead is easily understood. Use for liquid Mg has been more problematic since only ferritic stainless-type steels can withstand immersion in Mg and the parts out of the melt can withstand oxidation at these higher temperatures for long periods. The ferromagnetism of the alloys does hamper the transfer of magnetic fields to act as driver to the melt. Thus there are plenty of fundamental problems for Mg. However, liquid aluminum alloys, although not easy, have practical engineering solutions, making the use of EM pumps for Al now relatively well established.

There are two main types of EM pumps; both rely on the principles of induction.

- (a) The 3-phase moving field pump. This simple design has at its heart a straight ceramic tube containing the melt. The tube is surrounded by a series of electromagnets, each magnetic coil connected in turn to a single phase of the three-phase electricity supply, with the phases connected to the magnets in the order 1, 2, 3, 1, 2, 3, etc. along the length of the tube. As the phases cycle, so the magnetic field progresses along the length of the tube dragging the liquid metal with it (Figure 16.16). In common with all pumps, the performance of EM pumps is described quantitatively by a characteristic curve giving its rate of delivery at various heights. Thus its maximum rate is delivered at zero height, but its rate of delivery falls to zero at its maximum delivery height. At this height the melt is working hard to just support the column of liquid metal in a kind of stalled mode (Figure 16.15b). An increase in electrical current to the coils will increase performance, moving the characteristic curve out to higher rates and greater heights. Thus a family of curves can normally be generated for a series of different currents. This particular set of curves was generated by placing pumps in series. The curves F16, F12, and F18 correspond to one, two or three pump modules assembled together, end to end. Clearly the volume capacity of the moving field pumps is vastly greater than is required for casting production, being mainly intended for transfer of melts between furnaces. However, the pumps are easily downgraded by the use of a smaller cross-section central tube. The overheating that might occur during their use in a 'stalled' condition, retaining power input to continue holding metal in a mold that is already full, but taking time to solidify, is relatively easily overcome by additional cooling (otherwise the melt, now stationary, in the moving field becomes highly overheated and might melt parts of the pump).

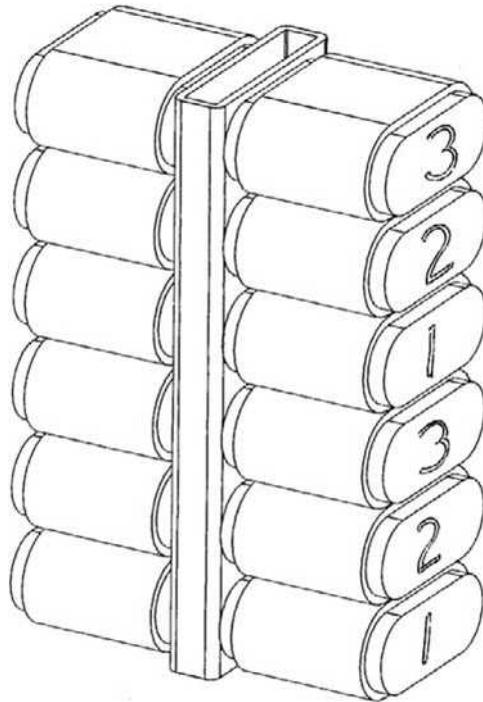


**FIGURE 16.16**

The moving field EM pump with simple ceramic tube delivery system.

**(b)** The AC (alternating current) single phase stationary field pump (Figure 16.17). This pump is a clever but complex design, involving more sophisticated and costly maintenance. It relies on the inductive principle enshrined in Faraday's left-hand motor rule. (The mutual relation between the 3 vectors at right angles is given by the thumb and principal two fingers on the left hand held out at right angles, denoting 'First finger = field; second finger = current; thumb = motion.) Thus the interaction of the magnetic field vector at right angles to the electrical current vector produces a force vector in the liquid at right angles to both (Figure 16.17).

To understand the AC design it is perhaps helpful first to consider what an equivalent DC design might look like. In Figure 16.17 the DC pump has a permanent magnet to give a field vector across the working volume of the liquid metal. Electrodes placed either side are connected to a continuous direct current to give the current vector at right angles to the magnetic field. The liquid in the working volume now experiences a body force, moving it upwards. In principle, as the current was increased the flow would similarly respond. Unfortunately, such a simple incarnation of the EM pump would work excellently for about half an hour if we were lucky, after which the electrodes would be destroyed, having dissolved away in the liquid Al.

The AC pump design avoids any contact by a clever design. It similarly uses an electromagnetic field across the working volume, conducted down to this level via soft magnetic armatures, and at the

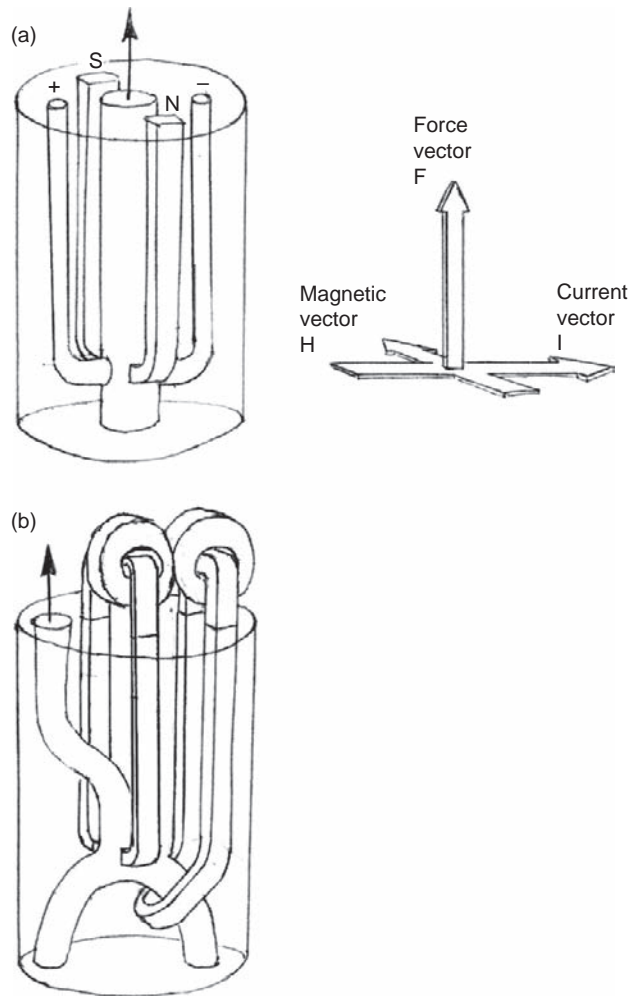


**FIGURE 16.17**

The fixed field pump built from castable refractory blocks designed for part-way immersion in the melt for periods of months: (a) the principle of employing three vectors at right angles; (b) a simplified model of a real pump.

same time induces a current in a loop of liquid metal (once again conducting a field down to the loop via soft magnetic links) that connects outside of the pump via the bulk melt, this providing the electrical current at right angles to the magnetic field. The current in the liquid metal loop is effectively a single turn transformer, linked magnetically to the multi-turn coil above. The motion of the melt is at right angles to both current and field vectors, and is taken up a vertical channel, taking its supply from the arms of the loop which connect to the melt. Since the magnetic and current vectors are in phase,

they both reverse at the same time, fortunately (as you can demonstrate to yourself with the Left Hand Rule) maintaining the force in the same direction. (Physicists will know that multiplying two negative vectors gives a positive vector.) The pulsating force is smoothed by the mass of metal that is moved, although the 60 Hz electrical supply in the USA gives noticeably better performance than the 50 Hz available in the UK. Typical characteristic curves for three of these pumps working at maximum output are also shown in Figure 16.15b. The operation of one of the pumps at variable current is shown in Figure 16.15c. These pumps are ideally suited in the pressure and flow rate range for making automotive and aerospace castings, and have therefore been in use for variants of the Cosworth process since about 1980.

Given reasonably clean metal, the pumps continue to work in the melt for at least 6 months (one pump the author used lasted 15 months!). However, rotary degassing with chlorine at some stage prior to the pump has caused pumps to block with a mixture of liquid chlorides and solid oxides within 10 days (Sokolwski et al. 2003).

### Cosworth process

In 1978 the Cosworth process was the first to use an EM pump for a production plant. It was funded by Cosworth Engineering to provide the cylinder heads and blocks for their highly successful Formula 1 racing engines, although later diversified its achievements to aerospace castings. Initially the process used zircon for its precision sand core assembly process, although silica was later used successfully by licensees. The first form of the process shown in Figure 16.18a ran into severe difficulties because of convection problems that prevented the freezing of the castings and nearly brought the company to a stop. The later variant of the process shown in Figure 16.18b used a roll-over technique after filling the mold. This cured the convection problems and simultaneously increased production from one casting in a mold every 5 minutes to two castings per mold every 45 seconds. The roll-over was the breakthrough that projected the process into a world leading position for making V-shaped cylinder blocks. The process continues to be used in the UK and in Windsor, Ontario, Canada, originally by Ford, now taken over by Nematik.

The Cosworth process was the inspiration for many subsequent plants. Rover (UK) used the process in two plants, one using the moving field pump and the other using the stationary field pump. They named this the *LPS* (low-pressure sand) system. The unfortunate lack of roll-over for these plants meant that casting soundness was never under proper control, with the result that 100% impregnation of castings was necessary. Even so, the process was successful to produce the challenging castings required for the K-series engine, a lightweight thin-walled design that was years ahead of its time, and for which no other process was at that time capable.

### 16.3.3 Direct vertical injection

#### Direct-acting piston displacement pump

Direct-acting piston pumps for lead and zinc appear to be successful. However, their attempted use for liquid Al alloys has so far not resulted in success. Although such wear-resistant and Al-resistant materials as SiC can be finely and accurately ground to make cylinders and pistons, the disruption caused by particles of alumina ensures that the pumps quickly wear and fail. Sweeney (1964) describes how attempts to produce cylinder and piston pumps were rapidly abandoned because of oxide problems. Valves such as the ball check type similarly proved unreliable because of oxides. Such failure is

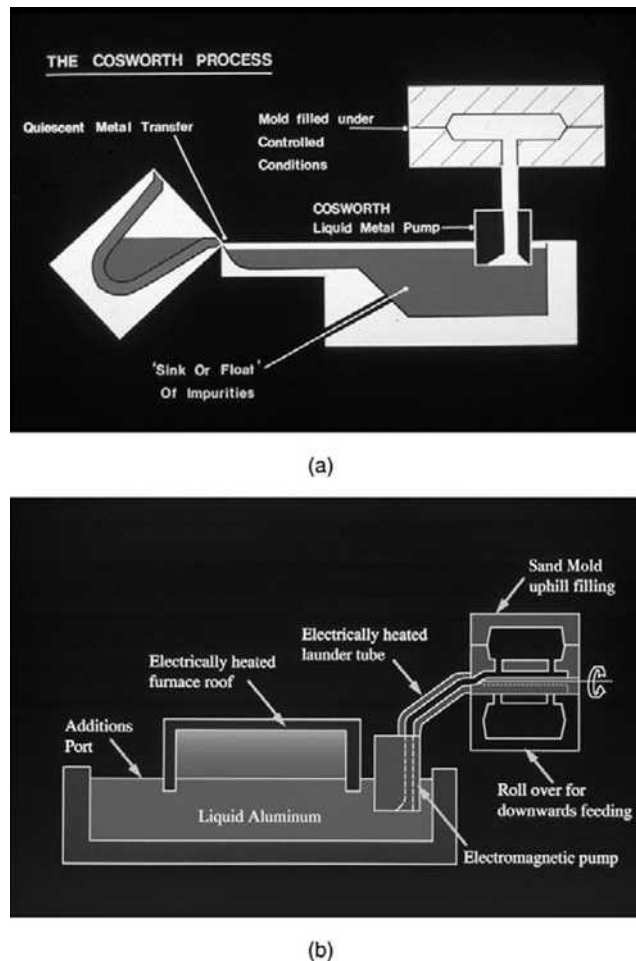


**FIGURE 16.18**

(a) Cosworth Mk I process which was almost unworkable as a result of convection problems; (b) Cosworth Mk II process solving convection and productivity by roll-over after mold filling.

hardly surprising. Films of alumina of thickness measured in nanometers will probably always be present in alloys of liquid Al, and will easily find their way into the most accurately fitting parts, leading inevitably to scoring and wear.

#### Lost crucible technique

A rather different type of direct-acting displacement approach started development under the name *Rimlock* (Rapid Induction Melting Lost Crucible process) as described by Bird and Savage (1996). Commercial changes caused the same project to be continued under a new name, *Crimson* (Jolly

2008). This curious acronym represents ‘Constrained Rapid Induction Melted Single shot Net shape casting process’. Despite its name, the process appears to have good potential, representing a significant departure from conventional foundry thinking. In its original form it uses a one-shot ceramic fiber crucible, into which is placed a pre-cast cylindrical slug of metal as a charge (Figure 16.19). The charge material is a sawn-off log from continuously cast billet, and thus is of reasonable quality. The induction melting is then carried out at high speed, taking perhaps 60 seconds, the idea being to subject the melt to minimum time for hydrogen pick-up, or oxidation of alloying elements. When up to casting temperature a piston pushes up the base of the fiber crucible, pushing out the base, and continues to

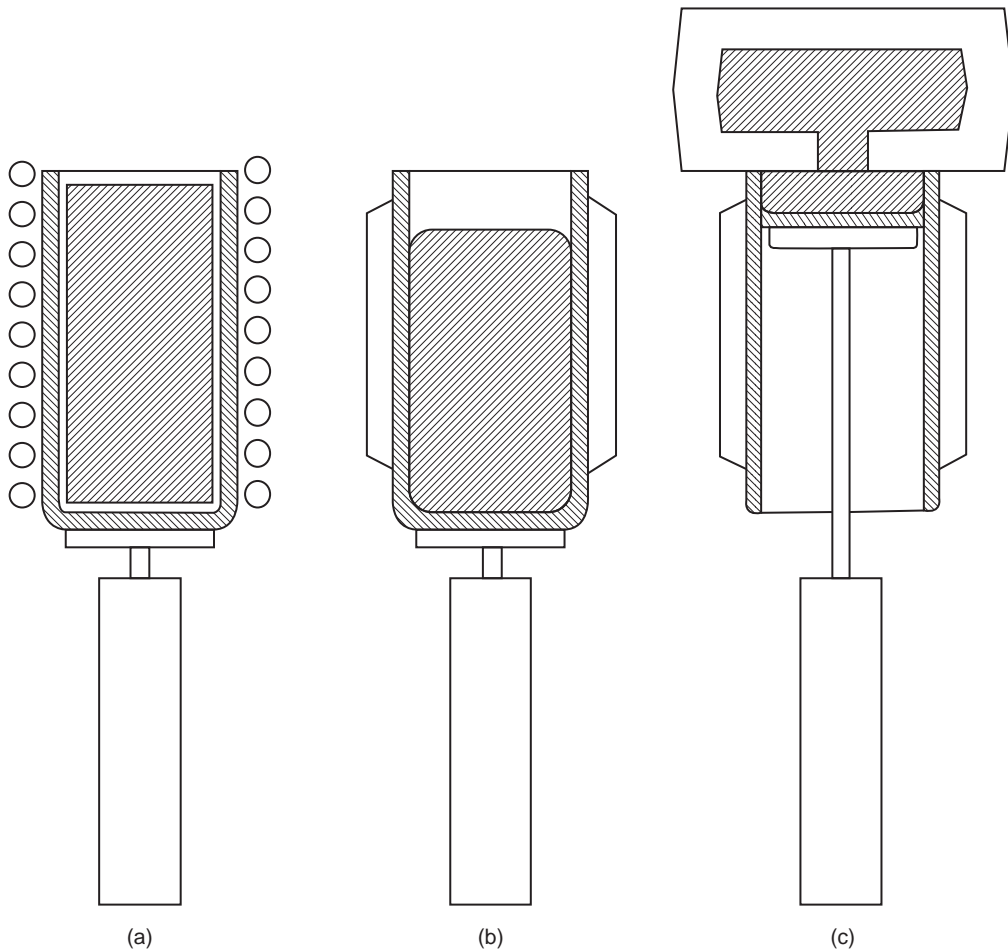


**FIGURE 16.19**

Counter-gravity with a sacrificial fiber crucible showing (a) rapid melting; (b) clamping to support crucible; (c) casting by pushing up the base of the crucible. After the mold is filled the whole assembly can be rotated through  $180^\circ$  to use the residual melt in the crucible as a feeder.



rise, pushing the melt upwards and into the mold cavity sited on the top of the crucible. When the mold is full the whole crucible, piston and mold assembly can be rotated through  $180^\circ$ . The temperature gradient in the mold is now favorable for feeding, which can be maintained under pressure from the piston if necessary.

This is a process enjoying numerous advantages that clearly demands greater attention. One such advantage is the very directness of injection, so that feedback control from sensing the melt level in the mold is unnecessary. The piston position gives it exactly. Thus a piston actuator driven electrically (by rack and pinion or by screw, etc., rather than indirectly by air or hydraulics) can be linked directly to computer control. A modern development is targeting the use of reusable ceramic crucibles with a sliding base.

The technique seems ideal for light metals, particularly magnesium alloys, since the inventory of liquid metal in the foundry is minimized, being a just-in-time melt preparation procedure. This would be an important and welcome safety feature in Mg casting facilities.

#### 16.3.4 Programmable control

The varying cross-sectional areas of the metal as it rises in the mold pose a problem if the fill rate through the bottom gate is fixed (as is approximately true for many counter-gravity filling systems that lack any sophistication of programmable control). Naturally, the melt may become too slow if the area of the mold increases greatly, leading to a danger of cold laps or oxide laps. Alternatively, if the local velocity is increased above the critical velocity through a narrow part of the mold, the metal may jet, causing entrainment defects.

Counter-gravity filling is unique in having the potential to address this difficulty. In principle, the melt can be speeded up or slowed down as required at each stage of filling. Even so, such programming of the fill rate is not easily achieved. In most molds there is no way to determine where the melt level is at any time during filling. Thus if the pre-programmed filling sequence (called here the filling profile) gets out of step, its phases occurring either early or late, the filling can become worse than that offered by a constant rate system. The mis-timing problems can easily arise from splashes that happen to start timers early, or from blockage in the pump or melt delivery system causing the time of arrival of the melt to be late.

#### 16.3.5 Feedback control

The only sure way to avoid the difficulties of the driving signal and actual metal level getting out of synchronization is to provide feedback control from a knowledge of the height of the metal. This involves a system to monitor the height of metal in the mold, and to feed this signal back to the delivery system, to force the system to adhere to a pre-programmed fill pattern. Good feedback control solves many of the filling problems associated with casting production.

Although Lin and Shih (2003) describe a closed-loop control system for a low-pressure casting machine, they monitor the pressure response in the low-pressure furnace chamber, using this as feedback to control the level of their pressurization profile. This is a useful approach for monitoring and compensating for the changes of level in the holding furnace, which is otherwise difficult to monitor accurately; clearly, as castings are produced and the level falls, increasing pressure will be required to fill the castings. Although improvements to their castings were reported, the *rate* of rise of

the melt is still unknown and uncontrolled; it will be variable with (i) different castings, (ii) different dies with (iii) different amounts of leakage of pressurized air from the furnace leading to different back-pressure during filling, and (iv) possible blockages to the flow path, especially if a filter is used at the base of the riser tube.

A related system for the monitoring of height is the sensing of the pressure of the melt in the melt delivery system. This has been attempted by the provision of a pocket of a few cubic centimeters of inert gas above the melt contained in the permanent plumbing of the liquid metal delivery system close to the pump, and connected to a pressure transducer via a capillary. The system appears to be no longer used, as a result of practical difficulties associated with the blockage of the capillary.

A non-contact system used by the Cosworth sand casting process senses the change in electrical capacitance between the melt and the mold clamp plate when the two are connected as a parallel plate condenser. This system has been used successfully for many years. However, it is not necessarily recommended since capacitance is powerfully affected by moisture. The Cosworth system with relatively dry molds countered this problem by zeroing the signal at the instant the melt entered the mold. This was set as the start point for the remainder of the fill profile.

Probably, the use of inductance to monitor the rising of the melt, using an inductive loop above the mold, might have given a more reliable signal since inductance is not affected by moisture. To the author's knowledge this has never been tested.

The author has demonstrated that archeological ground-penetrating radar will penetrate aggregate molds, and will deliver a signal indicating the progress of the metal as it rises in the mold. However, a higher-frequency system might be beneficial to increase accuracy; an accuracy of defining the level of the melt to at least  $\pm 10$  mm is really required.

However, it is a pity that feedback control is little used at this time. The lack of proper control in counter-gravity leads to unsatisfactory modes of filling that explains many of the problems with this otherwise excellent technique.

### 16.3.6 Failure modes of low-pressure casting

Most counter-gravity systems are quite safe, particularly the direct piston action filling, and filling by EM pumps.

I am often asked the question about the danger of leakages from the mold when using an EM pump. I always recall the experience of walking past the casting machine and seeing a gentle flow of liquid aluminum emerging from the base of the mold and spreading over the casting table. I pointed this out to Trevor, our casting man, who was sitting reading the newspaper at the time. He carefully folded his newspaper, got out from his chair, walked to the stack of ingots to be melted, brought one back, and placed it against the mold to freeze the stream. He then sat down and continued reading his newspaper.

The purpose of this story is to show how relaxed and safe counter-gravity casting can be. The pressures in the mold are only those that would have been experienced with conventional gravity casting – otherwise in a sand mold penetration of the mold by metal would occur.

Even in permanent mold low-pressure casting with pressure intensification, pressures are only approximately 1 bar. Pressures in compressed air systems used extensively around the foundry are usually seven times this value.

Even the most significant danger with a low-pressure system for casting Al or Mg is rather tame; it occurs if the melt level in the furnace becomes too low. A bubble escaping up the riser tube expands as it rises, and can eject metal from the top. However, any danger is avoided because the furnace is only pressurized when the mold is in place, thus the ejected metal, plus air, is easily contained by the strong metal mold. The only item that suffers from this event is the casting.

With dense alloys based on Cu or Fe the situation can be different. As a result of the greater density of these melts the pressures required are nearly three times those required for light alloys. This is still not a problem for those processes that use a relatively hard pneumatic system to drive the casting process. Such processes are akin to that used by the Griffin process for the low-pressure casting of steel railroad wheels. In this process the metal is contained in a ladle which is a relatively close fit in its pressurized container. Thus the process is under relatively good control because relatively little air is required to change the pressure in the container.

It is a mistake to place the steel melting furnace in a large pit, pressurizing the pit to force the melt up the riser tube. In this situation at least ten times the volume of air is required to pressurize the furnace. This introduces significant delay in the response of the casting process, making the control 'spongy' and uncertain. Furthermore, this uncertainty in the control of pressure is worsened because cold air introduced to deliver a certain amount of pressure is subjected to significant heating and further uncontrolled expansion in the vicinity of the furnace and the liquid metal. The heating of the gas might increase its pressure by a further factor of 2 or more. Thus the energy contained in the pressurized gas will be between 30 and 60 times that required for a light-alloy casting. If the furnace level now becomes too low, so that air escapes up the riser tube, the expansion of this highly compressed air will eject metal and destroy a sand mold, taking the foundry roof with it. At least one such event has happened in a UK development facility.

This danger is avoided for steel castings by reducing the volume of pressurized air. The building of special induction furnaces with pressurized steel shells is expected to be extremely safe. Furthermore, the control of the melt is improved, being a hard pneumatic system giving more immediate casting process response. Such pressurized furnaces would revolutionize steel foundries. No ladles would be needed, and few would ever see any liquid metal. They might read their newspapers while the casting was made.

---

## 16.4 CENTRIFUGAL CASTING

### Centrifuge casting

Casting on a rotating centrifuge table is commonly used for alloys based on Ti and Nb. The melting furnace and rotating table are enclosed in a vacuum chamber. Molds to make shaped castings are placed around the periphery of the centrifuge, and are connected by a spider of radial runners to a central sprue. This is perhaps usefully called centrifuge casting.

Centrifuge casting is used for the casting of high-melting-point metals melted in a water-cooled copper crucible (the 'cold crucible' technique) since, it is considered, the superheat is too low for simple gravity casting, so the mold is required to be filled as quickly as possible. This dubious logic has led to the universal occurrence of entrainment defects in all titanium castings, requiring them all to be subjected to an expensive HIPping (hot isostatic pressing) process to close up voids. Fortunately for Ti and its alloys, oxygen is soluble in Ti with the result that the HIP process not only closes defects, but

encourages them to go into solution. We can be grateful that poor Ti casting technology can nevertheless result in a good (if expensive) product.

Guo (2001) studied the filling of automotive exhaust valves with TiAl alloy by this technique, showing that the radial runner only fills along one side with a thin jet, leading to severe turbulence. Other researchers (Changyun 2006, Jakumeit 2007) also show that the direct siting of the radial runner (equivalent to top gating) onto the casting results in very poor filling. Somewhat improved filling is obtained by the equivalent of bottom gating into the mold cavity, in which the runner bypasses the mold and turns back, entering the mold from its outer-most side. Even in this case the results were still impressively turbulent because the velocities are so high. Once again, as is common for castings of all types, the filling systems are greatly oversized, and thus have only a small proportion of their area conveying any liquid metal, allowing a disappointing degree of turbulence from unconstrained flow of the melt. The design of a radial runner of a size to completely fill with liquid along its length, in which the melt is subject to increasing acceleration as it progresses outwards, represents an interesting challenge. The channels can be predicted to be of extreme thinness, and experience extreme drag forces from the walls, whose roughness will be of a similar scale to the dimensions of the channel. Thus there are plenty of unknowns to be explored. Perhaps the answer is that centrifuge casting cannot be optimized. Perhaps it should be abandoned. Alternatively, perhaps we shall have to live with centrifuge casting together with its defects and the expense of HIPping.

Jewelry is similarly produced by centrifuge casting to overcome the capillary repulsion experienced by melts when attempting to fill such narrow channels and fine detail. This process is better engineered because the melt, being at the end of the long rotating arm, travels along only a short radial runner into the mold. It seems, with good reason, both casters and wearers are content with the process as it is.

#### 16.4.2 True centrifugal casting

What I call ‘true’ centrifugal casting uses the centrifugal action to hold the melt against the wall of a rotating mold. For interested readers, there is much to be learned from the practical and entertaining account given in an article by one of the leading UK companies (Gibson 2010), which contrasts with the practical but sober descriptions by the Americans Zuehlke (1943) and Janco (1988).

Rings, hollow cylinders, tubes, pipes, and large motor housings are often cast using the centrifugal casting process for a number of reasons. There is no central core required and the wall thickness can therefore be controlled simply by controlling the volume of metal poured. Neither running system nor feeders are required so the metallic yield can be close to 100%. Rollers or bushings have high concentricity, straightness and uniform wall thickness. Rolls are often cast using a double pour, in which the outer working surface of the roll is composed of a hard-wearing alloy, or corrosion-resistant alloy, whereas the interior backing alloy is a lower-cost cast iron or steel. Centrifugally cast rolls are used in the paper, printing, plastics, foil, and textile industries.

The centrifugal action exerts an acceleration  $v^2/r$  on the metal whilst it solidifies, where  $v$  is the linear velocity of the metal and  $r$  is the radial distance from the axis of rotation. This acceleration can be 100 or more times the acceleration due to gravity  $g$ . Thus contact with the wall of the rotating die is good, and the strong temperature gradient which results assists the feeding under the enhanced  $g$  force. The inward advance of the solidification front can push remaining defects

(particularly oxide films that may not have centrifuged to the center as a result of their high drag and consequential low Stokes velocity) concentrating them in the inner bore, which is often cleaned up by machining.

However, the pouring of metal into spinning molds usually involves considerable surface turbulence as the metal surges into the mold and is then whisked up to speed. In horizontally spun castings the melt may slip for some time, delaying its acceleration up to the mold speed, and so will rain from the upper parts of the mold. If this problem continues until the casting is nearly solid laps and oxide defects are created. Gray cast iron pipes are relatively free from any substantial problems which result from this trauma. This is less true for ductile iron pipes because of the presence of magnesium. It becomes a major problem for higher-temperature materials such as stainless steels, where deep laps are sometimes seen. These form spiral patterns on the outside of spun-cast tubes. The problem is worst in relatively thin-walled tubes which solidify quickly. In thicker-walled tubes the problem seems to disappear, probably as a result of the extra time available for the re-resolution of some of the less stable constituents of the surface film, or possibly the washing away of the film from the surface. If the film is mechanically removed in this way then it will be expected to be centrifuged to the inner surface of the casting to join and be assimilated with the other low-density impurities such as slags, inclusions, and bubbles, which is one of the well-known valuable features of the spin-casting process.

The surface turbulence generated during the pouring of centrifugal castings of all types seems to be a general major fault of centrifugal casting, and seems to be generally ignored. This is surely a mistake. The process spends all of its efforts on centrifuging out those defects that should never have been put in. Worse still, not all of the defects introduced by the pour are eliminated by the centrifugal action. The melt delivery spout might be modified to greatly reduce these problems. Some actions expected to reduce turbulence are:

1. It should be shaped to deliver a ribbon of melt parallel to the rotating surface and as close as possible to this surface, reducing unwanted excess fall distance of the stream.
2. It should guide the flow directly onto the walls in the direction of rotation.
3. It should match the velocity of delivery of the metal (see Equation 13.2) to the speed of travel of the wall. Wall speeds are typically in the range  $2\text{--}5\text{ m s}^{-1}$ , and so are easily matched by velocities from a good filling system.
4. The conical basin delivery into the filling system requires to be abandoned, together with other aspects of the launder and spout design, so as to fulfill the requirements of a good naturally pressurized filling system. In this way only metal will be delivered via the filling system, not a mix of metal and air. However, even natural pressurization might have to be abandoned, since at high delivery speeds the delivery system may require to be highly pressurized, reducing the final orifice area, to speed up the flow (of air-free metal) to match the linear wall speed.

When fully up to speed the liquid in a vertical axis mold takes up a paraboloidal shape, with the result that the wall at the base of the cylinder is thicker than that at the top. Figure 16.20 shows experimentally measured profiles for different speeds by Donoho in 1944, and Figure 16.21c shows the effect as more commonly seen. We can calculate the extra machining allowance,  $b$ , which is needed to produce a parallel bore. The attempted solution to this problem in *Castings* 1st Edition (1991) resulted

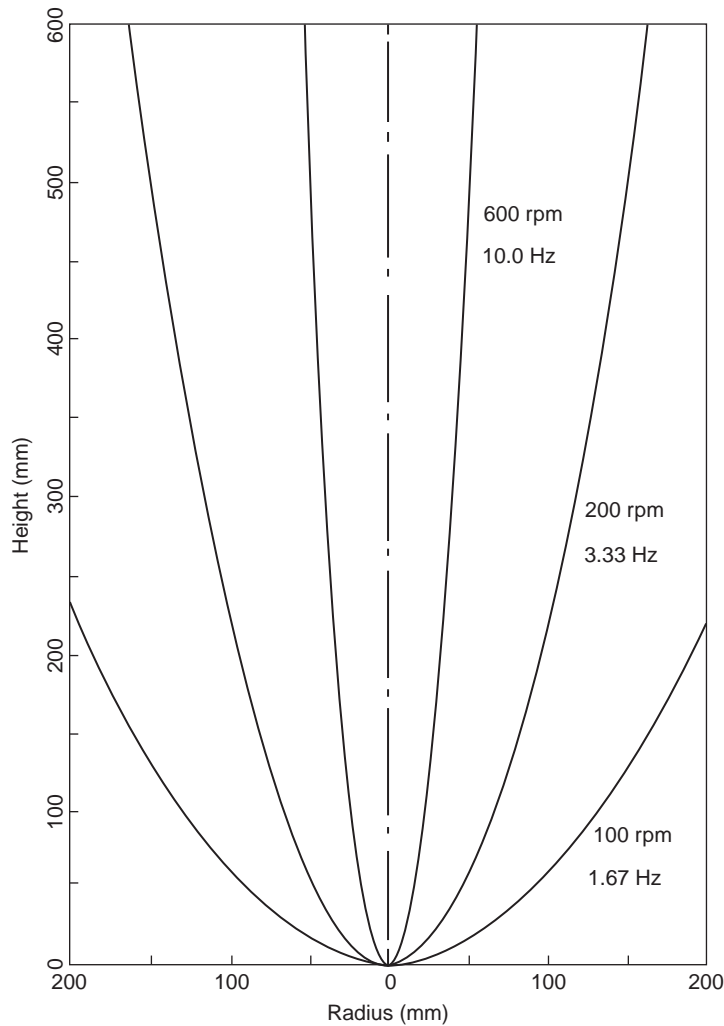


**FIGURE 16.20**

Profiles of spinning melts found experimentally by Donoho (1944).

in equations of the correct form, but whose constant term was regrettably in error. I am happy to confirm that the version below is correct, and further corroborated by comparison with the valuable experimental data discovered in the work recorded by Donoho.

When the liquid surface is in balance, it experiences the simultaneous accelerations of gravity  $g$  downwards, and the centrifugal acceleration  $v^2/r$  inwards towards the rotation axis, where  $v$  is the linear speed of the surface at that point, and  $r$  is the radial distance from the axis. The liquid takes up a parabolic form. The equation of the curve given by Donoho is:

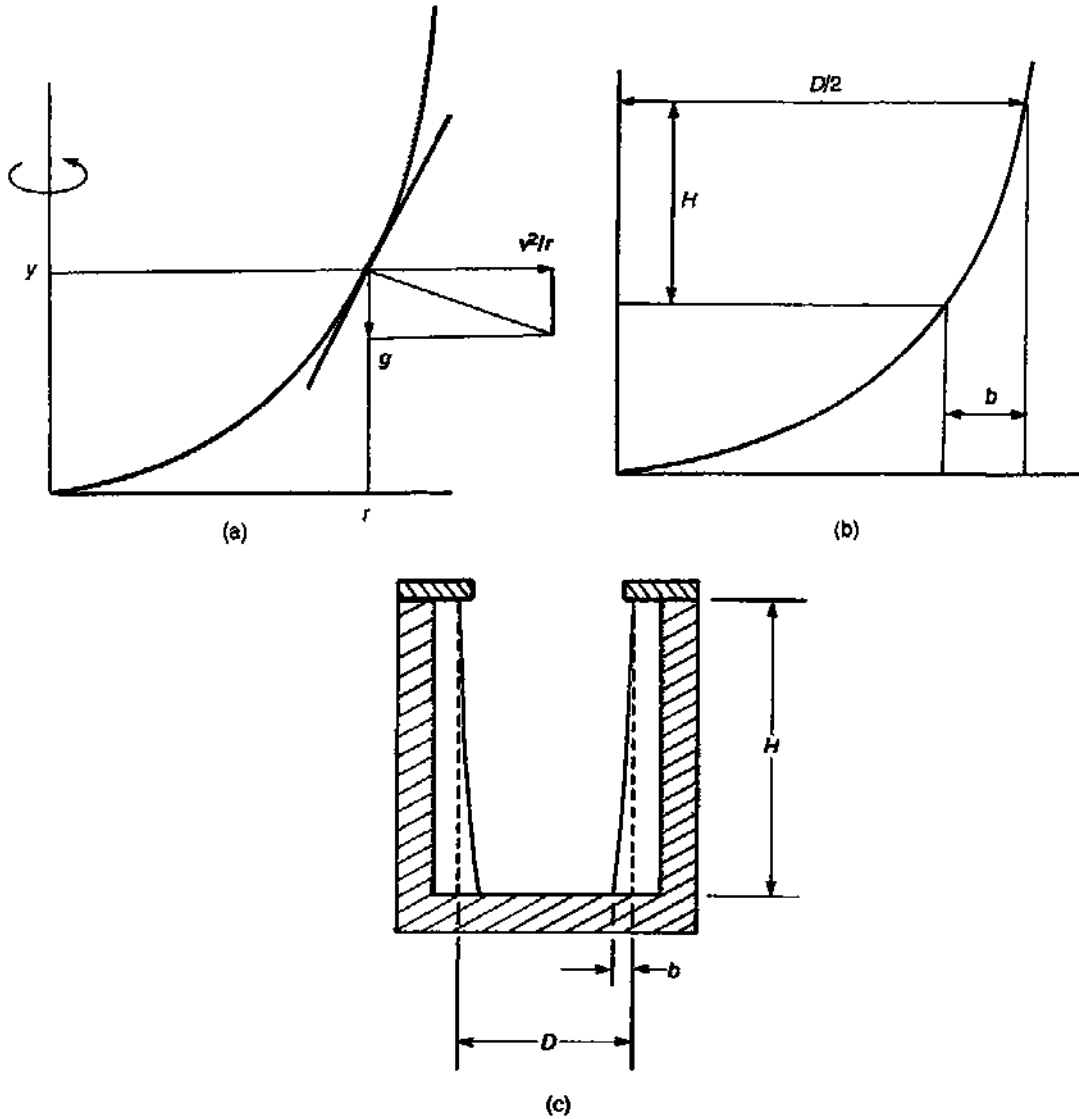


**FIGURE 16.21**

Vertical axis spinning: (a, b) generation of parabola; (c) consequential additional machining allowance required on the internal bore of a spun-cast tube.

$$h = 0.0000142N^2r^2$$

where  $N$  is in rotations per minute (rpm) and  $r$  is in inches. This equation is translated below into SI units (and, incidentally, thereby takes up the pleasing simplicity of equations and parameters that can be usually enjoyed in the SI system)

$$h = 2N^2r^2 \quad (16.1)$$

where  $h$  is the distance up the vertical axis in meters and  $N$  is the rate of rotation in revolutions per second. We can integrate to obtain the relation between  $h$  and  $r$  as:

$$h_t - h_b = 2N^2(r_t^2 - r_b^2)$$

Furthermore,  $h_t - h_b = H$ , the height of the cylindrical casting, and  $(r_t^2 - r_b^2)$  can be rewritten in terms of its factors  $(r_t + r_b)(r_t - r_b)$ . This in turn can be written to a close approximation if the machining thickness  $b \ll r$

$$(r_t + r_b) = 2R = D$$

where  $R$  is accurately the average radius, but is closely similar in size to the radius at the top of the cylinder, where, of course,  $2R$  is the diameter  $D$ . Furthermore

$$(r_t - r_b) = b$$

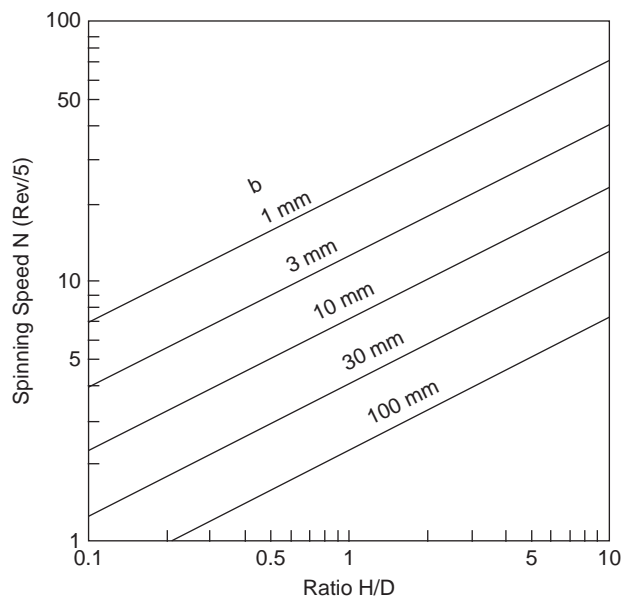


FIGURE 16.22

Machining allowance  $b$  from Equation 16.2 in terms of speed and height/diameter ratio.



in terms of the extra machining  $b$  which will be required to make the bore parallel. Approximating again if  $b \ll D$  we obtain an explicit relation for  $b$

$$b = (1/2N^2)(H/D) \quad (16.2)$$

Thus it is clear that when calculating the extra machining  $b$  required for a vertically spun tube, the only important parameters are  $N$  (which is, of course, intuitively obvious!) and the ratio  $H/D$ , which greatly simplifies predictions. The approximate Equation 16.2 is the basis of Figure 16.22. The figure illustrates the regime at the top of the figure where machining allowance is less than 1 mm, so that extra machining allowance is practically negligible, and the products have virtually parallel bores. For the regime below the 10 mm line, the extra machining for those alloys which are difficult to machine may become so severe that other routes such as horizontal spinning or conventional static casting using an internal core may have to be considered.

The centrifuging of the drosses caused by pouring into the bore of the part represent loss of metal and increased difficulties of machining, increasing the amount of metal suggested by the calculation of the machining allowance  $b$ . The provision of better pouring systems promises better products at lower cost.

---

## 16.5 PRESSURE-ASSISTED CASTING

The application of pressure during the solidification of a casting has, in line with natural expectations, generally been beneficial to soundness and mechanical properties.

In terms of the classical theory of the formation of pores, whether of gas or shrinkage origin, the application of pressure suppresses porosity as described in Chapter 7. In practical detail, it seems that the main reason for the suppression of porosity is probably the effect of pressure to keep bifilms firmly closed, thus negating the action of the various mechanisms that would drive them to open. The maintenance of the population of bifilms in their compact form maintains the reasonably high soundness and properties of the casting. This is the action of hot isostatic pressing (Section 19.3).

A second indirect but additive effect may be the action of pressure to maintain better contact between the casting and the wall of the mold, so facilitating heat transfer. Once again, this is an effect that results in the bifilms being frozen in their compact form, before they have much chance to unfurl.

These benefits of the application of pressure have been widely explored and widely reported, as seen for instance in the work of Berry and colleagues (1999, 2005). These authors survey the long history of the use of pressure back to 1922, although they note that Whitworth patented the process in the 1850s. In particular they list the benefits of pressure applied to sand castings of steel and aluminum by solidification in autoclaves, or pressurization of the casting simply by pressurizing the metal in the feeder. Both techniques work, but pressurization of the feeder would be expected to be especially effective because of its additional actions (i) to establish a pressure gradient to aid feeding, and (ii) pressurizing the casting internally to suppress the formation of any surface-initiated porosity. The benefit of avoiding surface-initiated porosity is not enjoyed by most other general applications of pressure that act both on the outside and inside of the casting.

However, the application of pressure to a feeder noted in earlier work by Berry and Watmough (1961) required caution, since an application too early or too severe would result in swelling of the casting and penetration of the sand mold by metal (the pressurization in an autoclave would not give this problem). A delayed application of pressure would allow the build-up of a strong oxide film, and possibly some surface solidification, resisting the penetration of the liquid metal into the mold. Interestingly, only modest pressures of up to 1 atmosphere were found to be effective in greatly reducing porosity and improving properties.

The use of pressure to suppress pore formation is common to the Counter-Pressure Casting (CPC) system in which an overpressure of up to 6 bar is applied during the counter-gravity filling. Filling occurs by a relatively small differential pressure (Wurker and Zeuner 2004).

Experiments are regularly reported in which the application of pressure during solidification is found to benefit castings, but the experiments are often fundamentally flawed. For instance Mufti et al. (1995) describe solidification of Al alloy casting in a chamber pressurized to 20 bar (2 MPa) that is found to suppress porosity. However, unfortunately, the pouring of the melt from a height of about a meter creates the very problems that the pressure freezing has subsequently to attempt to cure. It is probable that careful mold filling without the application of any pressure would have resulted in a better casting.

The application of pressure in the case of high-pressure die casting is a similar matter; the vicious turbulence of the filling cycle generates massive defects in the form of bifilms and bubbles. In this case the action of pressure is the attempt to reduce the size and deleterious action of these defects. Squeeze casting and counter-pressure casting processes are not so disadvantaged; their tolerable or even good filling retains whatever quality of the melt has already been achieved, so that the pressure is able to act in a fully positive way. These processes are discussed below.

### 16.5.1 High-pressure die casting (HPDC)

The reader is recommended to the excellent book by Arthur Street (2nd edition, 1986) for a mass of historical and technical details. In this short account we can only highlight the fundamental issues.

As readers will be well aware, high-pressure die castings are characterized by excellent surface finish and accuracy (at least when the die is new). Although the tooling is expensive the productivity is high and part price is thereby modest. As such the process is highly popular, so that over 50% of all Al alloy castings are produced by HPDC.

Turning now to the process itself, there are two main varieties of HPDC; hot chamber and cold chamber. The hot chamber machines are normally used to cast zinc and magnesium alloys, whereas the cold chamber machines mostly make aluminum alloy castings. There are numerous texts describing the technical details of the machinery involved. In fact, the dominance of the machinery aspects of the work dictate that most operators of HPDC do not consider themselves foundry people at all; they consider themselves engineers. The rift between the attitudes of the personnel involved in these two casting industries has been unhelpful in the past. After all, what do HPDC engineers need to know about sands, binders, insulated feeders, and the like? However, there are signs of improved relations with developments such as indirect squeeze casting, etc., proving the benefits of cross-fertilization of ideas between the two technologies. Long may this continue and prosper.

High-pressure die casting is an injection casting technique. The usual design of cold-chamber machines has a horizontal-stroke injection (Figure 16.23) which is programmed to pressurize the melt as shown in Figure 16.24. However, it is regrettable that optimally controlled filling has proved elusive in this particular mode of injection. In fact, in the past, most high-pressure die-casting machines have used injection strokes that cause much damage to the integrity of the finished casting. Typically the metal stream jets or sprays to the far end of the die cavity, and then ricochets and splashes backwards down the walls, sealing off routes for the venting of gases from the die cavity, and so entrapping the residual air inside the casting. Not only the air in the cavity is entrained, but also the vapors boiling off from the die lubricant and/or coolant.

The result is a casting which exhibits the typical ‘Aero chocolate’ structure – a tolerably good skin but full of air bubbles just beneath the surface (Figure 16.25). So much air is entrained in most pressure die castings that Hangai and co-workers (2010) remelt scrap castings as an optimum charge material to make Al alloy foam. In detail, it seems that the average high-pressure casting probably has two populations of bifilm defects. These will be (i) oxide flow tubes that have formed around the incoming jets, separating the casting into longitudinal isolated zones as is clear in Figure 2.31; and (ii) compact convoluted bifilms resulting from less organized turbulence during filling. The fact that the flow tubes are likely to be often aligned parallel to stresses explains the good performance of some castings. However, the unpredictability of turbulence and consequential bifilms would normally make the application of HPDC to safety-critical parts an unacceptable risk.

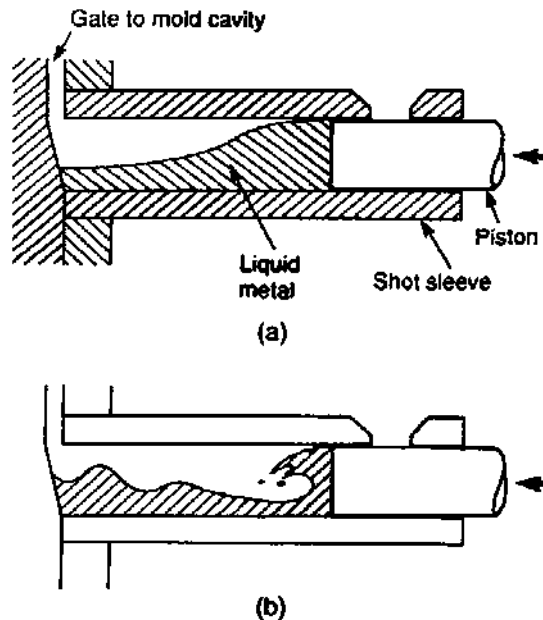


**FIGURE 16.23**

Injection of metal in a horizontal shot sleeve of a cold chamber die-casting machine comparing (a) controlled and (b) uncontrolled first stages of injection.

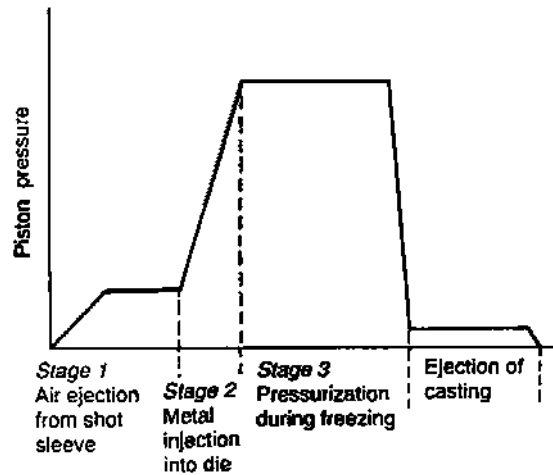


**FIGURE 16.24**

Typical injection stages during pressure die casting.

Koster and Goehring (1941) have demonstrated the filling action by injecting Wood's metal into transparent dies. They confirm that the spread of the liquid metal around the cavity causes the vents to be sealed first, so that the high pressures are merely required to compress the entrapped gases. The castings have a structure which is full of discontinuities which result from the surrounding of the initial spray of oxidized and already frozen droplets by liquid metal which arrives and freezes subsequently, as can be discerned from interesting micrographs by Bonsack (1962).

For these reasons, pressure die castings have to be treated differently to most other types of castings. For instance:

1. Pressure die castings cannot be solution heat treated because the reduced strength and creep resistance of the metal at high temperature allows the entrapped gases to expand, causing blisters on the surface, or even gross distortion of the casting. The use of pressure die castings for structural parts is therefore restricted because not only are the castings limited in strength by high internal porosity, and planes of additional weakness caused by bifilms, but also the presence of these defects in turn prevents any subsequent strength benefit from heat treatment.
2. Pressure die castings should not be machined at all if possible. Even light machining cuts are likely to penetrate the relatively sound skin (which is actually not particularly sound), encountering the unsatisfactory structure beneath. Deep cuts or drilled holes should be expected, therefore, to connect with the internal network of porosity and so cause leakage of fluids via distant points on the casting.
3. Subsequent chemical treatments in aqueous media, such as electroplating or anodizing, are made less easy because of penetration of the aggressive liquids into pores or laps through the relatively sound skin, and the subsequent unsightly spots of corrosion which are caused by the liquid slowly leaking out over a long period of time.

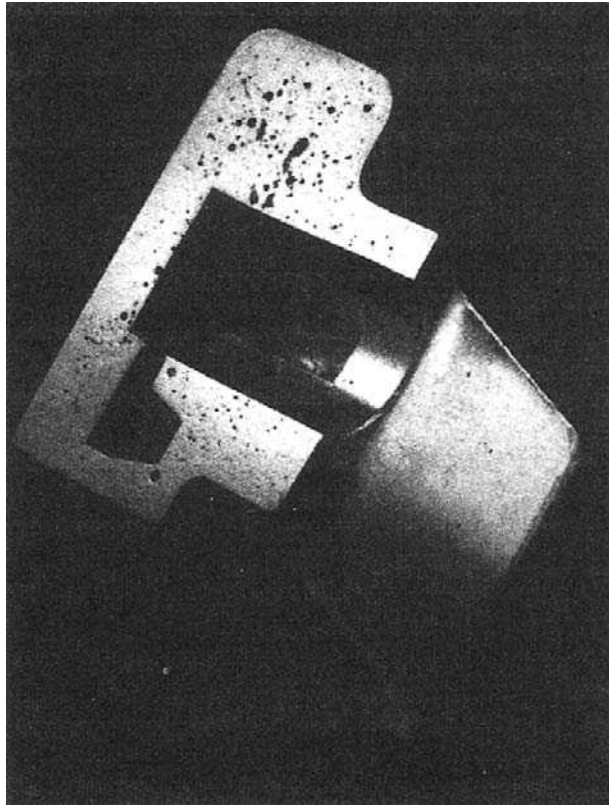


**FIGURE 16.25**

A pressure die casting in Zn-27Al alloy showing a polished section through a heavy section.

4. Pressure die castings cannot be welded; in any such attempt the weld pool excels itself in an energetic imitation of Mount Etna!

In view of this apparently damning list of shortcomings it is nothing short of amazing that pressure die casting has achieved such an important place in manufacturing. In the Western world aluminum alloy pressure die castings make up over half of the tonnage of all aluminum alloy castings. The great success of pressure die castings derives from the advantages of accuracy, surface finish, and the ability to reproduce detail, all at low cost and reasonable production rates. It is not surprising, therefore, that much effort has been expended on attempts to overcome the important disadvantages of the process.

A first attempt to improve on the filling of the die came with the adoption of three-stage injection (Figure 16.24). The stages are:

1. A controlled acceleration of the piston to cause a wave of liquid metal in the shot sleeve to expel the air ahead (not trap a bubble of air which was then injected at a part-full stage) as shown in Figure 16.23.

2. A more rapid fill of the die.
3. A high-pressure consolidation.

This three-stage technique, whilst being a great step forward in avoiding air injection during the first stage, was still far from perfect during the second stage; the high entrapment of air required high consolidation pressures during the final stage.

Recently, much work has been carried out in an attempt to optimize gating designs and fill rates to promote the progressive filling of the die, to expel air ahead of the metal. In addition entrapment of vapor from coolant sprayed onto the die can be reduced by providing the die with internal cooling passages. Furthermore, there is some move away from water-borne graphite-sprayed lubricant towards less volatile substances such as waxes. Substantial progress has also been made using computer simulation to ensure that the pattern of mold filling avoids entrapping major volumes of entrapped gases.

A novel design of runner for HPDC uses a significantly smaller cross-sectional area, and has been reported to improve casting soundness (Gunasegaram 2007). It seems to me to be likely to be the result of improved priming and exclusion of air from the shot sleeve, thus sparing the casting from massive defects that subsequent filling and pressurization attempts to heal. The action of improvement is unlikely to be any reproducible mechanism within the mold cavity itself since conditions are so dramatically turbulent; one can envisage that the narrower runner will occasionally but not always benefit the filling of the mold, even though there may be additional beneficial effects from a refined structure, such structural benefits to strength and performance are likely to be small (see Section 9.4).

Fundamentally, the Weber numbers are so far from optimum (see Chapter 2) that it is difficult to see how a really satisfactory filling solution can be achieved. The production of high-quality castings by the use of horizontal shot sleeves for the injection of metal into dies remains a largely unsolved quest. Nevertheless, the huge market tells us that these castings are adequate, if not more than adequate, for the purposes of most customers. Having said this, significant efforts continue in an attempt to improve HPDC further as noted below.

### Squeeze pins

Pressure die castings can be made more sound in local areas by the use of squeeze pins. Such techniques are in the category of keeping the customer happy by appearing to provide a sounder casting. It is doubtful if strength is improved, but leak tightness would, of course, benefit. When investigating the technique for Al–Si–Cu alloys Wan and colleagues (2002) found that the Cu was squeezed out from the highly pressurized region, reducing in concentration from 2.6 to 1.6% Cu, and was segregated to the surface regions around the pin.

### ‘Pore-free’ process

The filling of the die with oxygen prior to the injection of the liquid metal greatly reduces the entrained porosity as a result of the entrapped oxygen reacting with the metal to produce a compact solid oxide. The technique has been mainly used for Al casting, but is also reported for Zn and Pb alloys. However, of course, the oxygen is an additional cost, and productivity is reduced because of the additional time taken to flush with oxygen. Furthermore, bifilms might be expected to be made worse, impairing both mechanical properties and machining although I could find no report of this.

The process was useful in the early days of its invention prior to computer simulation and vacuum techniques, but is much less used today. A good summary of the process is given by Arthur Street (1986).

### Vacuum processes

One of the many systems for evacuating the shot sleeve and die is shown in Figure 16.26. The evacuation of the die leads to the melt being drawn up from the holding furnace and filling the shot sleeve. In itself, the counter-gravity filling of the shot sleeve probably significantly reduces defects in the casting. The movement of the piston cuts off the supply of metal from the holder and fills the cavity in the usual way. Naturally, porosity is significantly reduced. Some users claim that the castings are sufficiently sound to be heat-treated and welded, although some users have been less than satisfied. Progress probably continues on this issue.

## 16.5.2 Squeeze casting

There are two varieties of squeeze casting. Both subject the solidifying casting to a high pressure partly to suppress the formation of porosity, and partly to achieve good thermal contact between the casting and the die to achieve rapid solidification in the quest of good properties and good productivity.

### Indirect squeeze casting

The indirect squeeze casting process uses a high-pressure die-casting machine, but oriented with a vertical shot tube so that the die can be filled via a bottom gate by a kind of counter-gravity process. The machine, in common with conventional high-pressure die-casting machines, is complex and capital-intensive. Installation costs and general difficulty of maintenance are non-trivial matters since its height usually requires it to be set in a deep pit. (The machine contrasts sharply with the simplicity of the forge required for direct squeeze casting discussed below.)

Even so, the indirect process enjoys the important benefit of a counter-gravity filling technique that solves at a stroke many of the problems of the direct process. The simplicity of the filling process makes for easy and precise control. The melt is transferred upwards into the closed die by the vertical displacement of the piston in the shot sleeve. Pressure during freezing is applied directly by the piston. Generation of oxide defects during filling are avoided by keeping the ingate velocity lower than the critical  $0.5 \text{ m s}^{-1}$ . This critical velocity has been confirmed by many investigators (for instance Xue and Thorpe 1995, Itamura 2002). This is aided by increasing the area of the gate to such a size that the gate requires to be cut off by sawing rather than simply fracturing or clipping (shearing) as is usual for conventional HPDC. The size of the gate means that metallic yield is often only about 50% for this process.

The counter-gravity filling ensures that the oxide on the liquid meniscus is laid out against the surface of the die as the melt rises, thus protecting the die from direct contact with the metal. For this reason no welding or 'soldering' occurs, so that low-Fe high-performance alloys can be cast (in contrast to HPDC). In addition, the absence of the momentum impact at the end of the filling stroke gives better dimensional control; no die 'bounce', no pushing back of pins, no flash, allowing greater tolerance for tool fits, encouraging the use of moving parts in the die including squeeze pins. Even so, naturally, such tooling is expensive.

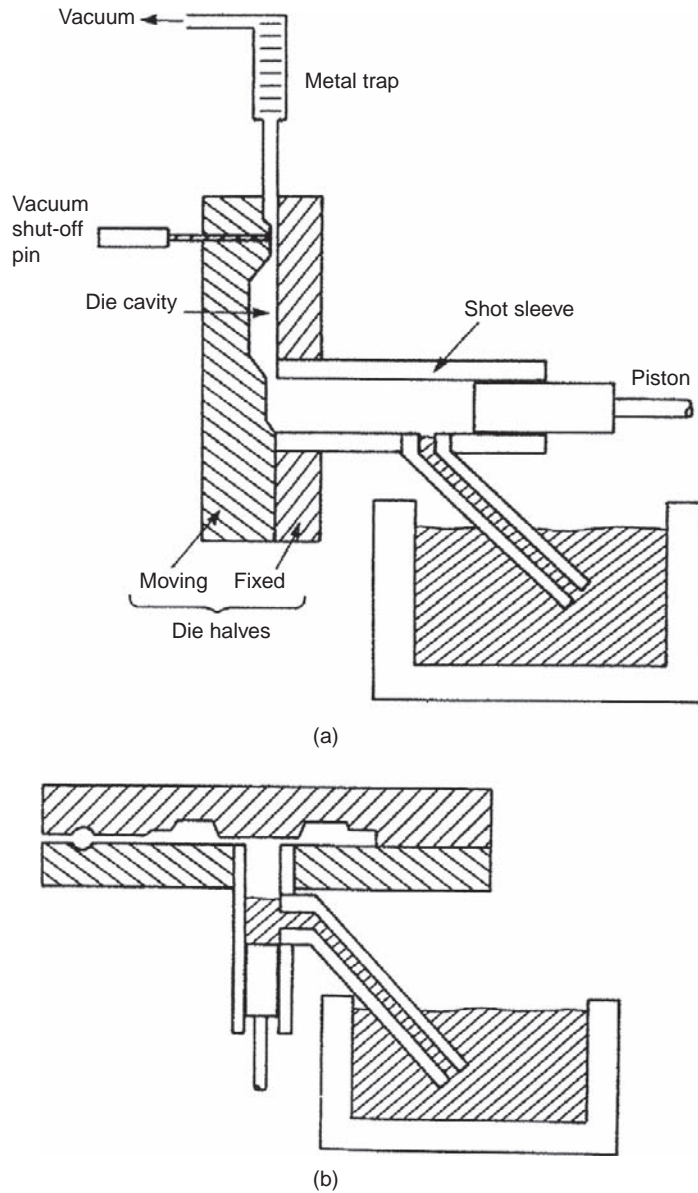


**FIGURE 16.26**

Vacuum delivery systems to the shot sleeves of pressure die-casting machines (a) horizontal cold chamber; (b) vertical injection type machine.



Modest problems reported from time to time include criticism that (i) the narrowest walls are limited to perhaps 4 mm thickness, and (ii) the machines are slower than conventional high-pressure die-casting machines. Although some of the slowness is clearly attributable to the wait required for the heavier to freeze, some is probably due to the heavier sections of the castings, and cannot therefore be claimed as a justified criticism; any permanent mold process would have suffered a similar disadvantage. Overall, these seem to me to be reasonable penalties if the customer's priorities are the reliability of the casting.

However, it has to be reported that the process has suffered some lack of reliability of its castings as a result of the entrainment of oxide bifilms during the pouring of the melt into the shot sleeve. This fall of only 50–100 mm entrains bubbles (and unseen bifilms of course) which appear on the cope surface, and were originally tolerated by using the drag as the best surface, or providing more machining allowance to the cope. These unsatisfactory solutions have finally been bravely tackled by the counter-gravity filling of the shot sleeve itself via a side port as illustrated schematically in Figure 16.26b (Okada et al. 1982). The connecting up of furnaces and casting machines in this way is known to be difficult, and in practice it is not known how successful this technique has been in the years subsequent to its introduction.

### Direct squeeze casting

When shaping a solid piece of metal by closed die forging, the die is initially open. The workpiece is placed in the lower die half, and the top die is then brought down to engage with the workpiece. The application of pressure between the slowly closing die halves causes the solid to flow plastically within the constraints of the die, being displaced to fill the outer sections of the die cavity.

There are a number of casting processes that have much in common with this shaping technique. Their common features are the loading of the liquid metal into the bottom half of an open die or mold, and the subsequent closing of the die or mold so as to displace the liquid into the extremities of the cavity (Figure 16.27).

This process for the 'forging' of liquid metal has a long and complicated history. It was first suggested by Chervov in 1878 but appears to have been first used prior to 1930 under the name of Cothias process in the UK (Chambers 1980) although Welter in Germany was studying the effect of pressure on solidifying metals in 1931. However, it was in Russia during the 1960s and 1970s under the name of extrusion casting (Plyatskii 1965) that the bulk of the early work to develop the process was carried out.

In general, no running system is required. Furthermore, because the liquid displacements are rather limited, no great flow distances are involved, so that fluidity, which is normally such an advantage for normal casting alloys, is no longer required. For this reason squeeze casting, as it has become known, has the unique advantage over all other casting processes of being not limited to casting alloys. In fact, it can operate very satisfactorily with wrought alloy compositions and so benefit from the considerably higher strengths that are attainable with these materials. The users of the process sometimes emphasize this fundamental difference by avoiding the description 'squeeze casting' and instead calling the process 'squeeze forming'.

Additional benefits to the metallurgical structure of squeeze-cast material result from the high pressure that is applied during the freezing of the casting. The rate of cooling of gravity and other die castings is normally slowed by the presence of an air gap which forms between the casting and the die

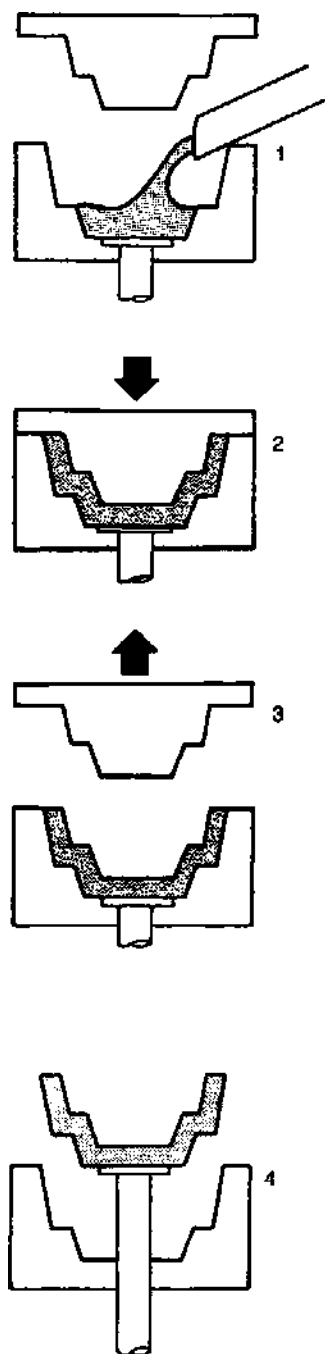


**FIGURE 16.27**

Squeeze casting.

as the casting cools and contracts away from the die. This does not occur to such an extent in squeeze casting and the consequent improved cooling rate results in a significantly finer cast structure. Figure 5.8 shows how the freezing rate is twice that of an equivalent gravity die casting, and nearly ten times faster than conventional sand castings. The application of the high pressure during solidification also tends to suppress the formation of porosity. Squeeze castings are probably more sound than most types of casting.

As always, however, freedom from defects is not infallibly guaranteed. For instance, lap defects are easily formed if the displacement velocity is not correct, especially if a waterfall effect occurs during the displacement of the liquid during die closure. Hong (2000) investigates some of these problems. Even porosity is possible in a heavy section, especially if it is surrounded by thin sections that solidify first, holding the die halves apart, and thus prevent the application of the full die closure pressure to the heavy section during its later solidification.

Interestingly, Herrera and the author (1997), when studying the mechanical properties of direct squeeze forming of copper alloys compared with forgings, the squeeze castings were highly variable and unreliable. The poor results were thought to reflect the inability of the process to close up serious oxide bifilm defects introduced by the poor filling of the die. This result would not be expected to be confined to copper alloys, but would be expected to be a general result applying to squeeze cast alloys of all metals; it reflects the problems introduced by poor filling of the die.

Furthermore, the very high temperature gradient generated by the pressurization of the casting against the face of the die leads to dendritic segregation (inverse segregation) as described in Section 5.3.3. Even worse, the eutectic can be squeezed out of the alloy, appearing as an unsightly exudate on the surface of the casting. Although this effect is accentuated with strongly segregating solutes, such as the element Cu in Al alloys, the effect can be so pronounced when using high squeeze pressures that it even occurs in alloys that usually show no segregation problems such as the normally well-behaved Al-7Si-0.4Mg alloy (Britnell and Neailey 2003).

Squeeze casting, in common with other die processes, has generally been limited to relatively low-melting-point materials such as zinc-, magnesium-, and aluminum-based alloys. Although gravity die casting has been extended to cast iron to a limited degree, such an extension is difficult to envisage for squeeze casting, where the enhanced rate of heat transfer would almost certainly result in rapid deterioration of the die.

The direct squeeze process uses a forging press to make castings. A forge is a simple machine costing a fraction of the capital investment of the indirect squeeze forming machine. Even so, the advantages probably finish at that point. This is because in general, despite the enormous potential of the process as described above, its performance in a production environment is often deeply disappointing. It seems that scrap arises from a number of causes that are not easily overcome. These include:

1. Poor melt control prior to casting (clearly this is not the fault of the casting process!).
2. Poor transfer into the die, creating oxide dross in the casting (a bottom-stoppered transfer ladle is recommended to deliver melt into the bottom of the die, preferably into a pocket in the base of the die so that the melt can be constrained during the initial spurt on transfer, and general turbulence in the die can be suppressed).
3. Boiling of mold dressing/lubricant in die joints (recommended to provide generous vents out of the back of the die, or ensure nearby cooling water channels to prevent boiling).

4. Relatively thick-walled castings (compared to HPDC) because of the time required to close the die.
5. Dosing weight requires reasonable control to ensure control of casting thickness.

The great simplicity of the process cries out for it to be properly developed to achieve its full potential.

### Press casting

The forging technique has been extended to sand castings, but not for the purpose of applying high pressure during freezing, which would, of course, only lead to metal penetration into the sand, but simply to move the two halves of the mold together immediately after casting so that a thinner section can be cast.

In this way cast iron gutters were cast in the UK for over 50 years (Chadwick and Yue 1989). For more sophisticated Al alloy products, Miller (1967) describes a Boeing development that demonstrated how aircraft castings of large surface area could be cast at 0.5 mm thickness. The method is, of course, limited to configurations where the thin-wall portions of the casting lie in nearly horizontal planes that do not overlap. High pouring temperatures were required, and excess melt was expelled into feeders and reversed in the filling system during closure of the mold. This movement of high-temperature metal was claimed to remelt sufficient solidified skin to permit the full closure of the mold to obtain success in achieving the thinnest sections.

Terashima et al. (2008) outline a further development of this concept, using greensand molds. The open mold receives the melt which is poured into the drag, and the cope is then lowered into place. The process specifically avoids pressurizing the melt to any significant extent to reduce sand penetrated by the metal and the impairment of surface finish (Tasaki et al. 2008).

The forging approach to the filling of a sand casting does appear to be an interesting process since fluidity problems are reduced as a result of the only limited displacement of the melt into outer regions of the mold at extremely gentle speeds. This clearly contrasts with conventional filling systems in which flow has to take place through long filling channels and then enter the mold cavity at relatively high speed via limited locations. The complete absence of a filling system (and a feeding system if the wall thickness is relatively small and uniform) is another powerful advantage. The press casting technique promises great potential.

### Cast pre-forms for forging

There are possibly good reasons for the casting of a material such as ductile cast iron and subjecting this material to hot rolling or forging as described by Neumeier and colleagues (1976). Such a product would have properties that would not be easily achievable by any other process route.

However, I have come across a number of applications of Al alloy castings as part of development projects loudly heralded as being 'the way forward', in which the castings were used as pre-forms for a subsequent forming process in a closed die forging operation. Such developments have never succeeded. The reason is that the casting defects are typically oxide bifilms introduced by the poor casting technique. These defects are not repairable by forging, with the result that the final parts inherit the variable and often poor mechanical properties of the casting.

The cast + forge production route is in any case fundamentally illogical. If the casting had been made without defects it would have been reliably strong, making a forging step unnecessary since the

properties could not have been further improved (the work hardening involved in such simple forging steps is relatively trivial).

---

## 16.6 LOST WAX AND OTHER CERAMIC MOLD CASTING PROCESSES

In the molding section it was mentioned that at the time of writing, the investment casting industry and its customers suffer from the use of probably the worst mold filling systems anywhere in the casting industry, seemingly devised to deliver the most defective castings possible.

This regrettable fact arises from the conventional way a wax tree is assembled, usually with a central conical pouring basin. As explained earlier in this work, the conical basin is one of the worst possible features. Moreover, the filling channels are nearly always vastly oversized because they have been built to maintain the strength of the wax assembly rather than designed for control of flow during filling. (In fact it is not so difficult to devise designs that are mechanically strong and combine good filling designs as illustrated in this work.)

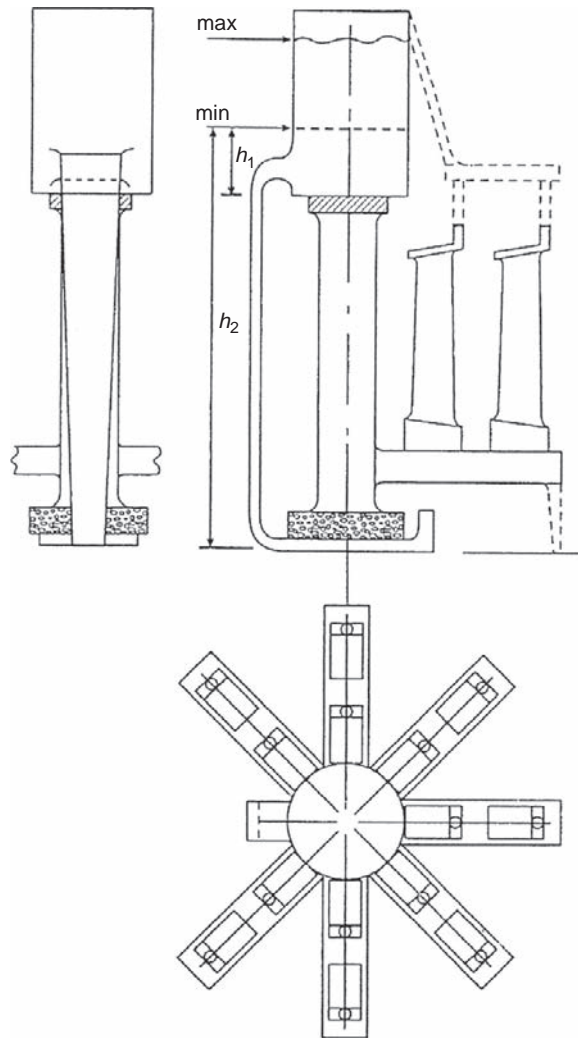
The cases of poor filling are maximized for vacuum casting, where the melting furnace is typically a meter or more above the mold, creating masses of entrained oxide bifilms as a result of the severe surface turbulence when falling from this height. (This point is covered in Section 16.10.)

Furthermore, convection is common in investment shell castings, creating heterogeneous, irregular structures, containing both fine and coarse regions in adjacent regions of the same casting. Those regions with coarse structures being expected to exhibit poorer properties of course, but in any case often failing customer specifications for grain size, even though the grain size may have little effect on properties.

The one good feature of current filling system designs, that happens by chance to prevent lost wax castings from being worse than they are, is the use of small-sized ingates. Ingates of small area do not permit large bifilms to enter, especially those strong oxide films formed by certain stainless steels as found in the work by Cox et al. (2000). The effect is analogous to the blocking of flow into flash by the bridging of oxide films at the entrance to the thinner section. The effect explains why melts of Al alloys recently grain refined with Ti+B additions, leaving a clean melt because of the sedimentation of bifilms, suffer significantly increased metal flash on the castings, and increased dressing costs.

In summary, the beautiful surface finish and fine detail of lost wax castings presents an allure in common with high-pressure die castings, in that the surface appearance often covers a poor internal structure with properties much less good than could be achieved. It might be unjust to call these products 'whited sepulchres', but what can be said is that most lost wax castings have some considerable way to go to become properly reliable.

Figures 16.28a and b illustrate a type of casting cluster which is commonly used, but whose central post is no longer the sprue. The sprue has become a slim piece of sheet wax, cut with a knife to its calculated tapered profile. The vents off the top of the molds do not connect with the pouring basin so that melt cannot spill down the vents and into the mold, nor can a convective loop be set up to delay the freezing of the casting. Thus these connections have to be plugged at some point to prevent the flow of metal (an offshoot will allow the escape of air if necessary). Figure 16.28a shows the concepts of minimum depths in the pouring basin that require to be met

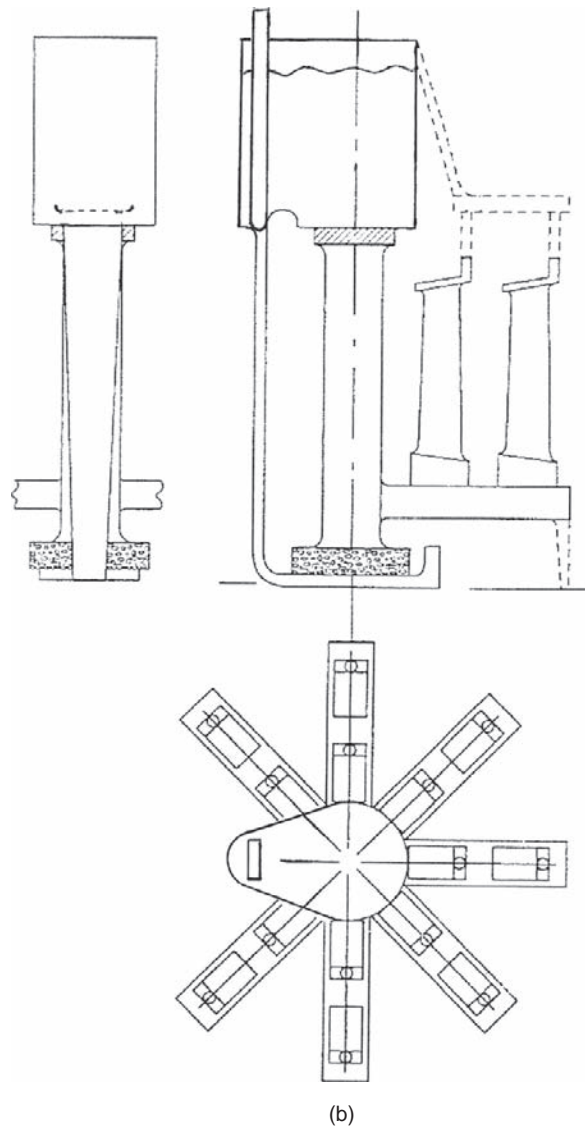


*Investment casting, design methodology.*

(a)

**FIGURE 16.28**

Investment mold using (a) an offset basin, natural pressurization and bottom gating; and (b) an improved design using a stopper, with a basin preferably sufficiently large to make the whole casting without top-up of the basin.



(b)

**FIGURE 16.28** (continued).

to ensure the pressurization of the filling system. Figure 16.28b shows an improved system in which the accessible entrance to the sprue can be sealed with a stopper until the basin is filled and some seconds of delay are imposed prior to allowing the metal to fill the casting. If this basin can be sized to hold the entire volume of melt required to fill the casting so much the better.

With some notable exceptions, including probably vacuum investment casting which would require a quite different design of vacuum furnace, these advances are often neither difficult nor costly to make, and promise a better future for both producers and users.

#### Shaw process (two-part block mold)

Shaw process molds are made by pouring a ceramic slurry into fairly conventional core boxes or patternwork. Thus a cope and drag can be made. The process is described in Section 15.1.3.

The cope and drag technique for mold assembly has advantages in that cores, filters, and chills are easily placed. Conventional filling system designs can usually be implemented, for instance the placement of a runner around a horizontal joint line. The fact that the mold can be placed horizontally usually means that the velocities in the filling system are relatively low, especially from lip-poured hand-held crucibles, so that relatively little damage is introduced compared to vacuum-cast investment molds where the fall heights of the melt are a disaster. The development of the process as a relatively thin shell rather than a block mold has improved the economics (Ball 1991, 1998). There is no record that the process has ever used a good design of pouring basin, but with very small castings, particularly if poured rather slowly, require such narrow sprues that a conical basin may be acceptable, because surface tension will assist to keep air out of the sprue. Finally, the casting is relatively easily extracted by separating the mold halves after solidification.

#### 16.6.2 Plaster investment (integral block molds)

The combination of this process with the application of a reduced pressure applied to the base of the permeable molds (the steel box containing the plaster mold is open at its base) is the principle of the *vacuum-assisted casting process* (see Section 3.9), allowing the pouring in air of extremely thin-walled castings only a fraction of a millimeter in wall thickness.

From the point of view of achieving high properties from castings made by vacuum assistance in plaster molds there is a concern that the extremely thin walls fill by a curiously deleterious process I have called micro-jetting. This was first observed by Evans (1997) in plaster molds and seems to arise because of the small dimensions of the advancing meniscus, having an area of oxide that is beginning to be too small to contain serious defects. Thus this relatively strong oxide film resists the advance of the melt, building up a back-pressure. When the back-pressure builds up sufficiently, the film bursts, allowing a jet of melt to shoot forward. This happens repeatedly, with the melt not advancing in the conventional way by the smooth progression of a smoothly curved meniscus, but by a tangled mass of jets, all surrounded by their tube of oxide. The creation of masses of oxides in this way was thought to be the reason for the low reliability (in terms of Weibull modulus) of cast test pieces in this work.

Clearly, more research is required on the phenomenon of micro-jetting. It is not certain whether this is a fundamental limitation to the attainment of good properties in casting sections thinner than a few mm. Also, it is not clear at this time whether the phenomenon is limited to plaster molds or is a feature common to thin sections of any mold. If true, this would be a serious threat to the attainment of high reliabilities in such parts as turbine blades. Although these parts currently have good properties, it may be that even higher properties might be attainable if micro-jetting could be avoided.



---

## 16.7 LOST FOAM CASTING

The lost foam technique is a clever and intriguing process for the production of castings, first announced by Wittmoser in 1968. However, whereas precision sand (otherwise known as core assembly) casting is evidently straightforward, the apparent simplicity of the lost foam casting process is misleading. Furthermore, lost foam casting is not without its own special, and serious, problems.

The starting point is the production of polystyrene beads, which are blown into tooling (the patternwork) and expanded in situ by steam to fill the tooling. Heat is then extracted, cooling the expanded foam and causing it to gain strength so that it can be ejected from the tooling. Naturally the tooling has to have high thermal conductivity to maintain a good rate of production when oscillating between the hot and cold parts of its cycle. It is therefore usually made of aluminum alloy, and is sculpted on its reverse side to reduce its thickness as far as possible. The foam pattern is a replica of the finished casting. By gluing together separately produced foam components, complex geometries can be assembled which can be difficult to reproduce by conventional casting techniques. The assembly is then attached to its filling system and dipped into (or poured over by) a refractory wash.

After coating (investing) the foam pattern with the ceramic slurry, the coat takes time to dry. When dry the assembly is ready to cast. Clearly the thin invested shell around the foam will not support the weight of the metal pouring into the foam, so it is backed up with an aggregate. Thus the purpose of the aggregate in this case is mainly to support the ceramic shell and to conduct heat away from the casting.

Early problems of the lost foam production of cylinder heads and other castings requiring some degree of precision were found to be associated with silica sand used for backing, since the alpha/beta quartz transition at around 570°C created unacceptable distortions. Manufacturers therefore changed to artificial ceramic beads based on alumina or mullite ceramics that have a much reduced and uniform coefficient of expansion. This move has been rewarded by an immediate improvement in casting accuracy and reproducibility.

A further advantage of the ceramic beads is that their spherical shape allows them to flow easily, filling all parts of the pattern, sometimes required to be uphill into blind holes, usually with some encouragement from carefully controlled vibration of the mold. The upper surface of the pouring cup attached to the filling system is arranged to remain clear above the aggregate. The cup is then filled with liquid metal, which proceeds to vaporize the foam, progressively replacing it as it advances, thus forming the casting. The final benefit of using an unbonded aggregate is seen after the castings have solidified, when the casting is removed from its mold simply by releasing the bottom doors on the box, or by turning the mold box over and tipping everything out. The casting is caught on a grid, and the aggregate pours through the grid to start its recycling process.

A nice paper by Walling and Dantzig (1994) suggests that in the case of the casting of Al alloys, the foam melts and collapses but very little breakdown of the polystyrene occurs. The rate of pattern elimination at 60–80 mm s<sup>-1</sup> controls the rate of advance of the liquid metal. The more rapid melting and collapsing of the foam during the casting of iron, plus much greater breakdown of the polystyrene to produce volumes of styrene vapor, lead to significantly greater cooling of the iron, but allow its filling rate to be controlled by the filling system.

The volumes of gaseous products evolved from the foam must contain a significant proportion of air, since the foam itself contains a high percentage of air, which in turn will expand further when heated by the melt. This large volume of gases requires to be vented through the ceramic coating, which is why the permeability of the coating appears to be of great importance for the control of the process.

With respect to the competition between castings produced by lost foam processes and other conventional 'lost air' processes there are a number of issues. These are not easily compared because all processes are operated rather differently by different manufacturers, with different degrees of competence and with different overhead costs, giving different apparently final costs. However, even allowing for this, there are a number of differences which are fundamental, and these are discussed below.

Tooling for lost foam process used to be regarded as complicated as a result of the back of the tool having to be sculpted to reduce overall thickness so that heat could be transferred from the foam at the maximum rate to maintain productivity of the foam patterns. The wide use of CAD/CAM has reduced this problem. The tooling is typically machined from aluminum alloy, and so is relatively light in weight. It also has a long life, because the polystyrene beads exact almost no wear. Even so, in appearance, the tooling is a mass of tubing for steam and water supplies, in addition to pull-backs and other motions now beautifully engineered with various varieties of linear actuators using roller bearing sleeves and similar bearings as a result of its life in a light engineering, rather than a foundry, environment.

Conversely, tooling for nearly every other casting process does suffer wear. Most other tooling suffers either sand or hot metal or both, in addition to foundry personnel! The conventional practice is to introduce hardened steel wear plates into core box tooling which can be replaced from time to time as necessary. However, as designs of core blowing machines improve the fluidization of sand prior to blowing, the problem is gradually being reduced. Ultimately, although wear remains a potential threat to accuracy an adequate standard of casting can be achieved with the application of SPC techniques for the dimensions of the casting.

The lost foam process is renowned for the accuracy with which it can maintain wall thickness. Also, for small castings, particularly bracketry, the ability to cast bolt holes and to work with zero draft angles so that machining of some faces can be avoided altogether is a further powerful advantage.

However, for larger castings, the slow drift in dimensions of the foam due to loss of pentane during the ageing of the beads after the pre-expansion is a constant threat to overall accuracy. Assembly of foam patterns can also introduce errors. Small scale errors include the glue bead which is particularly unwelcome to the designers of such features as aerodynamic ports in cylinder heads. An additional well-known problem contributing to large scale dimensional control and distortion is the problem of maintaining the shape and size of the flimsy polystyrene pattern during the time it is being covered with about half a ton of sand. It is practically inconceivable that the application of the backing aggregate, no matter how well controlled, can be accomplished without some distortion.

For certain applications the absence of a parting line in the mold can be a great advantage (the parting line on the polystyrene pattern still exists of course, but this can be well controlled and so is not usually a problem).

Turning to the issue of surface finish, although the industry has made great strides in improving finish of lost foam castings over recent years, there remains from time to time on the patterns an area of poorly consolidated beads, giving a strong 'orange peel' effect on patches of the casting. These impressed patterns in the surface have been the subject of widespread discussion for many years. There has been talk of the roots of such impressions being sites for fatigue initiation but I am not aware of this ever having been demonstrated. Nevertheless the possibility remains a concern.

The real problem with the re-entrant pockets in the surface is their content of refractory wash and possibly entrapped sand grains. If these are released into water and oil ways of castings during service this is clearly a serious matter. This problem is especially acute at the junction of glued patterns, where a local absence of glue will allow the ingress of the refractory slurry, resulting in a casting defect of some kind, depending whether the fin of refractory remains in place to penetrate the wall, or whether it is washed off into the liquid metal to appear elsewhere as an inclusion.

Conventional core assembly also suffers cores with occasional poorly compacted sand, resulting in localized areas which may exhibit metal penetration and retained grains of sand in the surface. There seems to be relatively little to choose between the processes on these grounds.

The minimum wall thickness of lost foam castings is typically about 3.5 mm, being dictated by the ability to blow and consolidate the polystyrene beads; a minimum section is said to be about three bead diameters. However, the wall thickness is also dictated to some extent by the fluidity of the metal to fill the section. This appears to be reduced by the evaporation of the polystyrene which is endothermic (requires heat) and thus chills the liquid metal. The permeability of the pattern coating also influences the resistance offered by the pattern to the advancing liquid.

Worse still, the resistance offered by the foam to the advance of the metal will result in the metal taking different routes into the mold on different occasions depending on the precise density of different parts of the pattern. This may result in the serious situation that entrapment of the foam may occur, enclosing foam decomposition products in the casting. Such defects are not uncommon in lost foam products. Even without wholesale entrapment of decomposition products, the advancing surface of the liquid metal seems to have a considerable thickness of a film, of somewhat uncertain composition, but probably mostly oxide, which, on meeting other liquid fronts in a confluence of fronts, results in a serious lap defect known generally within the industry as a 'fold'. It is effectively a highly visible and serious bifilm defect.

The appearance of dispersed gas porosity, entrained decomposition products, and film/lap defects is to be expected in lost foam castings. These are serious defects which exceed those to be found in most competitive casting processes.

The development of foams which give less undesirable reaction products is reported from time to time. Nevertheless, the majority of the industry appears to be still working with polystyrene as a pattern material which is known to give these serious problems. Furthermore, the integration of the process with pressurization of the metal immediately after casting is a further treatment that improves the reliability of lost foam products, although coming at the expense of additional processing complexity and cost (Garat 1987, 1991). Although this technique clearly improves the castings a little its effectiveness is necessarily limited, and cannot achieve the properties achieved by well-made 'lost air' castings.

From observations of the filling of lost foam castings by X-ray radiography it is clear that a high proportion of damage to the melt comes from the initial fall down the foam-filled sprue. This is

particularly chaotic, with liquid metal fighting its way downwards in fragmenting and turbulent masses against the turbulent pockets of liquid styrene and vapor powering and meandering upwards. If the sprue is narrowed, as in conventional 'lost air' casting to reduce turbulence, the foam extracts so much heat from the advancing front that the melt freezes, never reaching the base of the sprue. This emphasizes the nature of fluidity in lost foam molds: the front advances by fresh melt arriving at the front by its momentum as illustrated in Figures 3.24a and 5.24b. This important mode of flow requires plenty of space, with generous-sized filling systems, so that constrained systems such as the naturally pressurized filling designs recommended elsewhere in this book do not work for lost foam castings.

There are numerous studies to illustrate that all attempts to fill lost foam molds by any kind of gravity pouring technique introduce masses of defects into castings. For Al alloy castings Kata-shima (1989) uses a silica window in the mold, revealing horrifyingly messy filling conditions in which islands of foam fragments are surrounded by metal. Bennett (2000) and Tschopp (2000) illustrate micrographs and fractographs of clear fold type defects (i.e. bifilms) and blisters on the surfaces of the castings (again double oxide defects inflated probably by outgassing vapors). Similarly Carlson (1989) and Shivkumar (1989) report oxide films and black films, with diameters sometimes measured in centimeters, on fracture surfaces. For iron castings Gallois (1987) identifies lustrous carbon films. Metallurgically, therefore, lost foam castings poured by gravity usually contain large numbers of serious defects. The author has to admit he has not earned himself popularity for drawing attention to this relatively lamentable performance over many years (Campbell 1991).

Counter-gravity filling of lost foam molds immediately suggests itself as a possible remedy, as actually confirmed by X-ray radiographic studies. However, even this route is not without its challenges since Ainsworth and Griffith (2006) show that a rate of advance of the front of only  $5 \text{ mm s}^{-1}$  in an Al-10Si alloy is the maximum velocity that can be tolerated before the front advances irregularly and entrains foam and its degradation products. Moreover, this velocity was found to be too low to allow the complete filling of their test mold. Furthermore, Weibull analyses of the mechanical properties indicated that even at such low filling speeds the reliability of the castings did not reach those of normal 'lost air' castings.

Fan and Ji (2005) used counter-gravity filling of Mg alloy AZ91E, but found rather indifferent properties, which they considered a good result, since the properties were as good as their indifferent 'lost air' castings.

Clearly, the production of lost foam castings cannot yet achieve the quality that reasonable quality conventional 'lost air' castings can achieve, even when produced at glacially slow filling rates that threaten the filling of the mold, or even when subjected to a variety of post-casting HIPping process. Clearly, the process is not yet fully out of serious problems. Perhaps further development to solve its problems may be successful.

In the meantime, admittedly, not all castings require perfection, and quality needs to be appropriate to the product. With all its faults, lost foam remains highly appropriate for such castings as motor housings equipped with closely spaced cooling fins where dressing of flash (extensively required for instance at the parting line of greensand molded castings) is not easily accomplished between each fin, and does not exist for lost foam products. Other products having long, complex internal passageways may lend themselves to lost foam, whereas to provide such passages by the use of cores might be practically impossible.

Even so, the launch of this process onto an unsuspecting foundry industry prior to its full development into a reliable process is a charge often heard. The charge can be countered, however, since, clearly, the buyer should have carried out his due diligence, and this would not have been difficult. Sadly, many lost foam operations have struggled and finally shut down their operations as a result of these failures. To close a disappointing chapter in the history of the casting industry it would be good to think that lost foam might one day emerge to become the reliable process we all would like it to be.

As a postscript to this less than flattering account, based perhaps on my expectations and aspirations that might be set rather high, if not too high, the reader might wish to see the excellent account given by Donahue and Anderson (2008), which is much less pessimistic, and does not regard lost foam defects so negatively. The company they work for has a successful lost foam production line which incorporates pressurization immediately after casting.

### Replicast

Replicast is a process in which the invested coating of the foam is built up rather more thickly so that although it can remain fragile it can be self-supporting. The foam pattern with its thickened ceramic shell is then fired to burn out the foam. The shell is immersed in an unbonded aggregate to support the shell during casting, and the shell can then be filled with liquid metal (Ashton 1991). Naturally, the process has many of the benefits of lost foam, plus many of its disadvantages. The major benefit is the elimination of foam, eliminating the major defects that characterize lost foam castings. As a kind of investment casting process, the process has traditionally suffered from the problem typical of most investment casting processes; the provision of a poor filling system. This is, of course, probably not endemic to the process but appears not to have been explored at the time of writing. Developments here are awaited with interest.

---

## 16.8 VACUUM MOLDING (V PROCESS)

The vacuum molding process, or V process, is an interesting hard sand molding process not requiring control over materials of imprecise chemistry such as resins, to maintain the bonding and rigidity of the mold. It was invented in Japan in 1972 (Akita 1972) and immediately attracted world-wide interest.

In summary, it uses a dry, unbonded, free-flowing aggregate, usually silica sand. The mold is made in a special molding box, sealed on the top and bottom surfaces by a plastic film, and the dry, unbonded, free-flowing sand is consolidated by the application of a vacuum (actually a partial vacuum in the region of 0.5 atm). It is significantly different from other molding processes, and thus possesses a number of unique advantages plus, of course, unique disadvantages.

In practice, a plastic film is heated by overhead radiant heaters to soften the film, making it more stretchable. It is then drawn down onto the pattern by the application of a vacuum, drawing air through vents planted in the surface of the pattern. The vents connect through to a hollow base plate through which the vacuum is drawn. In particular, vents on the pattern need to be sited at the bottoms of recesses, or in sharp corners to ensure that the film sucks completely down, faithfully reproducing the contours of the pattern.

The film is subsequently coated by spraying with a ceramic coat. In the move from alcohol to water-based coatings the drying time has become a significant disadvantage. When the coating is dry, a molding box is lowered onto the pattern, and dry sand is poured into the box, being consolidated against the plastic film by vibration. A second plastic film is applied, covering and sealing the top of the mold, and a vacuum is drawn through the walls of the molding box. The mold then becomes impressively hard. So long as the vacuum is connected to the box the mold can be handled like any other mold. A major disadvantage of some interpretations of the process is the flexible connection to the mold. The floor of the foundry can resemble a snake pit of trip hazards. Fortunately, some good engineering designs for automated plants avoid this problem. Others have valves on the mold that can be turned off to allow the mold to be disconnected from the vacuum line, but this introduces the risk that small leaks in the film or elsewhere will cause the mold to collapse as the vacuum is gradually lost. If this happens during the handling of the mold the event can be a hazard.

The mold enjoys the benefits of other hard sand processes such as the core assembly process, in claiming to produce among the most dimensionally accurate castings.

A remarkable and useful feature of the V process is that because of the presence of the plastic film, which confers a glossy, slippery, almost sensuous smoothness, to the mold surface, molds can be stripped from patterns with almost zero force without the aid of any taper or draft. Even slight negative draft of a few degrees can be tolerated, since the mold can spring back elastically if the deformation is not too severe. The positioning of cores is also delightful, since the core slides into place into zero-clearance prints and is gripped by the mold in a unique way. The puncturing of the plastic film at the base of the core print prior to the insertion of the core ensures that the core can vent, otherwise the core is sealed from the outside world so that core blows could become a serious possibility. (Small holes in the plastic films appear to be harmless to the process while the vacuum continues to be drawn.)

There seems to be little problem with the silica sand aggregate, but although the *molds* are of excellent accuracy, the *casting* can suffer distortion as a result of the heating up of the sand and its expansion because of the alpha/beta quartz transition. I am not aware of anyone using a non-silica sand for this process, even though the process would be ideally suited to an improved aggregate.

The use of an unbonded sand eliminates, of course, the cost of a binder, which is particularly valuable for large castings requiring only a modest rate of production. For this reason the process has achieved good success for the production of iron castings for piano frames, and counter-weights for forklift trucks.

During the filling of the mold with cast iron, the hot metal radiates heat ahead to vaporize the film prior to its arrival, the vapor recondensing in the nearby cool surface grains of the aggregate to create a temporary binder to that localized region, and thus assisting to avoid the collapse of the surface during the few seconds that the support of the film + vacuum combination is lost. Any film that survives evaporation is submerged by the iron usually without problem as a result of the high density and high surface tension of iron, although Schmied (1988) draws attention to occasional blow holes and spatter from the vaporization of the film.

These problems are significantly more acute for Al alloys. Negligible heat is radiated ahead by the advancing Al front, so that the plastic film is always over-run by the liquid metal. The film boils and the vapors easily penetrate the metal as oxidizing bubbles, forming bubble trails and laminations right

through the cast section. The consequential oxide films and bubble trail defects are often misinterpreted as entrained plastic film.

The spray coating of the mold is a significant disadvantage of the process. It seems to be generally required to prevent collapse of the mold during the pouring of the liquid metal. Since the coating is applied to the plastic film on its sand side, away from the pattern, the coating does not affect accuracy. It acts to maintain the surface finish of the casting, reducing metal penetration by the suction of the vacuum. It also supports the maintenance of the vacuum, and hence the integrity of the mold, during the early stages of the filling of the mold. A coating is a significant disadvantage of course, because it costs money, requires drying time thus requires floor space and affects production rate; all these resources are usually at a premium.

The 15–20% slower cooling rate of evacuated molds is an advantage for the running of thin sections such as bath tubs (Clark 1989), but a disadvantage for those products requiring high mechanical properties.

Whereas the molding of bath tubs does not present undue challenges, there are a large number of cases in which the process will not mold for what appears to be a trivial but enormously frustrating reason. If two upstanding features on the pattern stand nearer together than the depth between them, then the plastic film bridging the upstanding features has difficulty to stretch to reach the bottom of this hollow, the elongation being required is 200% (i.e. stretching to a distance of three times its original length). The film will usually tear, and the mold is spoiled. It is surprising how often this troublesome issue of 1-to-1 spacing-to-depth ratio occurs. Apparently innocent shapes on the pattern can bring the process to a stop.

Another concern about the process generally overlooked is the presence of the partial vacuum inside the mold cavity itself. In principle, the mold cavity should not be at a reduced pressure. In fact, if it has feeders open at the top, it will originally be at atmospheric pressure. However, as a result of small leaks in the film, parts of the mold will have air sucked out. Thus as the melt reaches these parts, and if the filling metal cuts off connections to the atmosphere, the melt will accelerate, possibly becoming locally turbulent. Thus the advantages of a nicely designed filling system are potentially lost, the control over the flow being lost in randomly different regions of the mold on different occasions, leading to inconsistent quality of the products.

The vacuum pumps work in an environment full of abrasive silica dust, so that pumps are usually of the water-ring-seal variety, avoiding rubbing sealing surfaces. Even so, maintenance of the pumps seems to be a significant process cost.

After pouring and solidification, the casting is released from the mold simply by turning off the vacuum and releasing air into the mold. The mold collapses onto a grid, freeing the casting from its mold with minimum effort.

The sand falls through the grid for recycling. Only 1–2% sand losses are reported (Engels and Schneider 1986), although this figure seems low in view of the dust nuisance reported at shake-out. The dust may result from sand fracture at the higher temperature of iron and steel castings, plus the reversion of the coating to powder when dry, all carried aloft by the strong convection of the air around hot castings.

While the dust ascends skywards, accompanied by a small mushroom cloud of unpleasant smoke and fume from the incomplete burning and pyrolysis of the film, the residual plastic film from the outer areas of the mold remains in a heap on the grid. The film is partly blackened and sticky, with adhering aggregate and remains of broken cores as a tangled, dusty and gritty

mess requiring disposal. It is a messy conclusion to an otherwise elegant and relatively clean process.

## 16.9 VACUUM-ASSISTED CASTING

Molds poured in air may be assisted to fill by the application of vacuum at some part of the mold.

A common use is in plaster block molds. These are formed in steel boxes with open tops and open bases. The open top exposes the sprue entrance for the gravity pour, plus any vents or feeders. The open base is placed on a manifold connected to a vacuum line, and roughly sealed to prevent excessive leakage of air into the vacuum line. Air is drawn through the permeable mold, so that after pouring, the metal is assisted in its flow, effectively being pulled through the mold into all the finest features and corners (Figure 16.29). The technique achieves the filling of extremely narrow sections in the region of 0.5 mm.

Similarly, a sand mold filled by a bottom-gated gravity system may have problems to fill completely; the net head for filling decreasing as the melt level builds up in the mold cavity. Some bosses or ears at the top of the casting may have problems to fill. The application of a gentle suction from a domestic vacuum cleaner, applied locally to the top of the sand mold in the region of the unfilled features, will greatly assist the filling. This technique has the benefit of not affecting the filling of the main portion of the mold, which is probably filling satisfactorily. The effect is only felt by the metal as it nears the source of suction, so that the ever-decreasing volume above the melt experiences a concentration of the suction effect, accelerating the melt into these remaining volumes.

The great power of a modest amount of suction to transform the filling of molds is easily explained. For instance for a perfect vacuum of 1.0 atmosphere, as every reader should know, this would be capable of sucking up 760 mm height of mercury (whose density is  $13\,500\text{ kg m}^{-3}$ ). For liquid aluminum of density only  $2400\text{ kg m}^{-3}$  this level of suction could raise the level of aluminum by the huge height of 4.2 m. Thus to make a few centimeters difference to the height of an Al casting we need

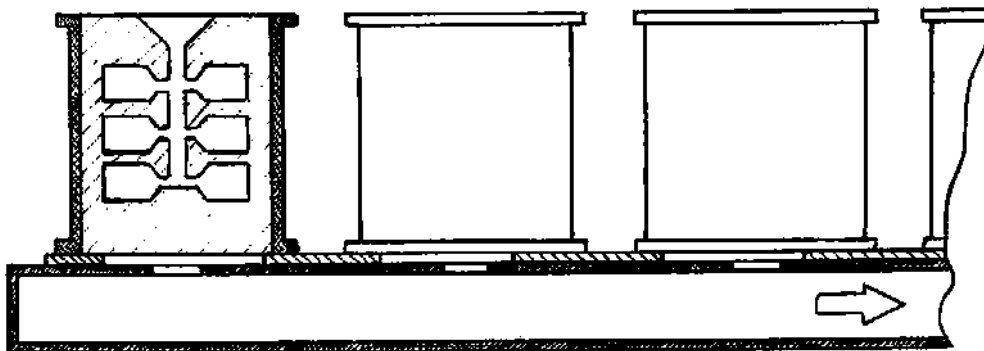


FIGURE 16.29

Vacuum-assisted casting, showing plaster molds sitting on a vacuum manifold lined up for pouring.



a maximum of only 0.1 atmosphere (1.5 psi); even this tiny pressure difference can raise the liquid height by an impressive 420 mm.

For the ferrous metals and copper-based alloys whose densities are in the region of 7000 or 8000 kg m<sup>3</sup> an atmosphere corresponds to a height of approximately 1.3 m.

Vacuum-assisted casting is often misleadingly called vacuum casting, implying the assumed benefits of low gas content and an expensive production process. Buyer beware.

---

## 16.10 VACUUM MELTING AND CASTING

In the shaped casting industry although some melting and casting of Ti and Nb alloys is carried out in vacuum chambers, often under an inert gas atmosphere, the majority of the melting and casting under vacuum (or inert atmosphere) is carried out by the Ni- and Co-based superalloy casters. This section and following sections deals mainly with this industry.

When melting under vacuum, the melt attempts to equilibrate with the vacuum environment, thus losing its volatile content, such as volatile alloys and gases. The volatile metals re-condense as dust over the internal surfaces of the vacuum chamber, occasionally flaring off, burning to their oxides when the vacuum is released and the door is opened to let in air. Vacuum chambers therefore become very dirty environments, coated in black dust. From time to time this requires to be completely fired to become a relatively inert oxide, and then be carefully cleaned off with a suction cleaner.

The loss of alloying elements sometimes has to be compensated by alloy additions, although some losses (such as heavy element contaminants including Pb, As, etc.) are of course usually beneficial.

The reduction of gases such as hydrogen, nitrogen and oxygen (often as carbon monoxide, thus simultaneously removing carbon which may need to be replaced) is also generally desirable. Mainly, these are removed by the alloy manufacturer who mixes the alloy, melts it in a large induction furnace to achieve a homogeneous melt, then casts it into convenient 'sticks' of various diameters for remelting and casting by foundries.

The fundamental problem with the 'vacuum' is that it is far from perfect. It seems best to view it as 'dilute air'. The residual oxygen and nitrogen in the dilute air is effectively 'gettered' by the active elements Al and Cr which are universally in high temperature alloys based on Ni and Co. The pouring of the melt in the dilute air entrains bifilms into the melt in generous amounts. The entrained bifilms are rich in very stable oxides, alumina, chromia and titania. The evidence for this behavior is compelling. It is set out in Section 6.72.

At the stage of the production of the alloy by the alloy producer, mixing pure liquid nickel with the alloying elements, massive damage is done to the alloy by the unfortunate way the alloy is cast into sticks. This is carried out by pouring from the tilting furnace into a series of launders, the melt falling from launder to launder, and finally falling into tall steel tubes. These pouring events, totaling probably several meters, entrain quantities of oxide films, plus probably nitride films. Thus the alloy arrives at the foundry already in a poor condition before being remelted by the foundry and poured for the final time to make shaped castings.

Even if the Ni-base alloy producer and caster were to improve his casting process, the producers of the shaped casting are, at this time, unfortunately likely to undo any good that the

alloy caster could provide. This disappointing situation follows because of the geometry of conventional vacuum melting and casting furnaces used in foundries, since the melting crucible is typically a meter or more above the mold. Figure 16.30 shows the problem in the form of the fall distance ' $h$ '. Metal entry velocities into the filling system are therefore often in the region of 4 or  $5 \text{ m s}^{-1}$ . The entrance into the filling system is always a conical funnel, concentrating and accelerating the melt, together with its entrained vacuum, even further, so that damage from turbulence is practically guaranteed. This is the regrettable situation for the current manufacture of nearly all of the world's Ni- and Co-base alloy turbine blades for aircraft engines. For single crystal turbine blades, the melt suffers a similar traumatic filling mode, but molds are held above the freezing point of the melts during filling, and only slowly withdrawn into a cooling zone to grow the crystal under conditions of controlled speed and temperature gradient. The holding of the melt for this relatively long period probably helps to float out a large proportion (but clearly not all) of the oxide bifilms entrained during the pour. As well, the directional solidification will push oxides ahead rather than entraining them in the solid. Thus there are good reasons why the single crystals blades appear to be more free from bifilm failures than polycrystalline blades.

There is an interesting situation with the Ni-base alloys containing hafnium (Hf). It seems that when these alloys are cast, a curious unexplained glassy surface defect appears on the blades that runs down the casting surface like a congealed river. If a filter is placed in the filling system the defect does not occur. It seems likely that this represents an attack of the ceramic mold by HfO generated by turbulence. The HfO will most likely form a low-melting-point oxide mixture with the components of the mold, often mainly  $\text{Al}_2\text{O}_3$ . If the filter is present, any HfO already present

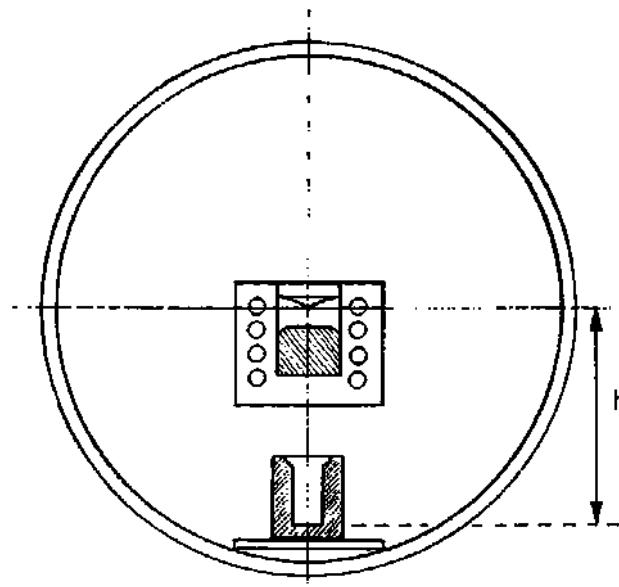


**FIGURE 16.30**

The unfavorable pouring geometry of a typical vacuum melting and casting furnace.

will be reduced by filtering out, and the reduced turbulence after the filter will not generate more HfO.

Clearly, this is an industry that is very much in need of improved melt handling technology, and would greatly benefit from a transition to better mold filling techniques. These are already well proven and demonstrated for aerospace high-temperature alloys in the case of gravity systems that reduce defects by approximately a factor of 10 (Li 2004) and better still, counter-gravity systems (Shendye and Gilles 2009).

This page intentionally left blank

# Controlled solidification techniques

# 17

## 17.1 CONVENTIONAL-SHAPED CASTINGS

Most castings will solidify from the outside, and will grow grains that will finally merge and consolidate in the center of the casting. Central regions that form hot spots not in communication with a source of feed metal will cause some local shrinkage that may take the form of internal porosity if the porosity can be initiated, meaning in practice that bifilms will be required to be present. Alternatively, in the absence of bifilms (i.e. very clean metal) local shrinkage may create external porosity in the shape of surface sinks.

Although many foundry texts recommend the provision of a feeder to counter this problem, my personal approach is to avoid the provision of a feeder if at all possible. I prefer to use some kind of chill. This may take the form of a substantial block of cold metal forming part of the mold, or might even be an internal chill around which the melt freezes. More usually, however, I opt for the provision of cooling fins.

Cooling fins work excellently for high-conductivity alloys such as Al and Mg alloys, and some Cu-based alloys (although not particularly for aluminum bronzes). Unfortunately, the concept works so poorly for steels that fins cannot be recommended. For gray cast irons the situation is somewhat intermediate, with fins often working sufficiently well to strike back white iron locally into the casting; such an effect has been used historically for the tips of cams on camshafts for automotive engines, although there seems to have been a move away from this technique to the placing of shaped chills in the interests of greater reproducibility and control. More recently still, there is interest in the production of wear faces on cams not by solidification control but by subsequent heat treatment of the casting by local application of rapid induction heating.

In the special case of conventionally poured and solidified polycrystalline turbine blades, the fundamental problem in the casting of these alloys in a conventional vacuum induction furnace is seen in Figure 16.30. The height ' $h$ ' of the fall of metal into the mold, followed by freezing from all directions, means that bifilms created by the fall have little chance to escape, but become trapped in the casting. As a result of them being pushed by advancing dendrites they naturally finish up in grain boundaries. As a result, during creep or other tensile failure modes the castings fail by 'cavitation' at the boundaries, the growing cavities gradually joining to lead to complete rupture. This explains the relatively poor properties of polycrystalline equiaxed turbine blades compared to other grain structures (Figure 17.1) as described in the following sections.

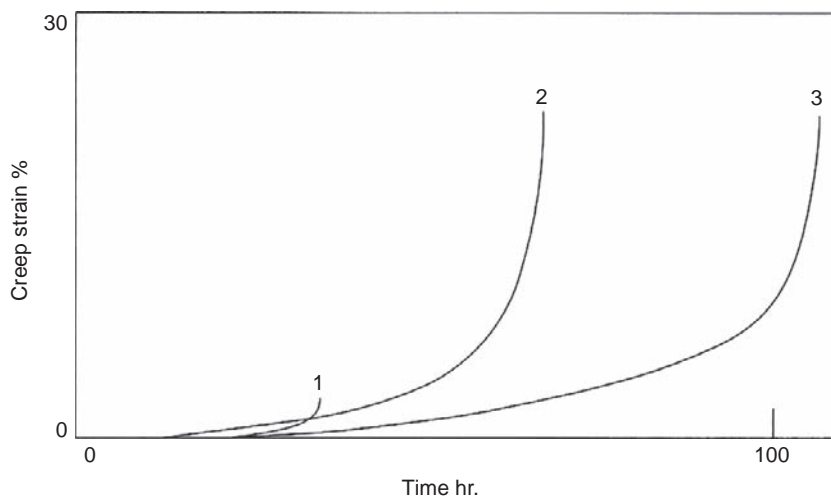


**FIGURE 17.1**

Creep behavior of Ni-base alloy Mar M200 at 980°C and 207 MPa cast as (1) conventional equiaxed structure; (2) directionally solidified (DS) columnar structure; (3) single crystal (after Versnyder and Shank 1970).

## 17.2 DIRECTIONAL SOLIDIFICATION (DS)

The unidirectional solidification of castings has a long history, promoted initially by the desire to obtain high soundness; the high temperature gradient shortening the pasty zone so that feeding could occur to the roots of the dendrites with greater efficiency. Directional solidification (DS) is mostly used to imply unidirectional solidification. It has been used for permanent magnet manufacture, but its main use has been for turbine blades for jet engines.

In practice, DS has nearly always been carried out vertically in an upward direction. It was not suspected that this particular mode of freezing would yield an additional important effect; a significant reduction in the bifilm population. This occurs partly (i) by the vertically directed freezing allowing bifilms to float upward, away from the freezing front, and (ii) because of the unusually long time available for this flotation because of the relatively slow rate of advance of the front during DS, and (iii) any residual bifilms will have the best chance to be pushed ahead of the advancing solidification front, thereby keeping the solid relatively free from serious defects.

Work at MIT first published in 1965 for steel castings, by various combinations of the authors Nereo, Polich, and Flemings, quickly showed benefits to the strength, toughness, and fatigue-resistance revealed by directional solidification. Later work (Flemings and Mehrabian 1970, Hurtuk and Tzavaras 1975) has further confirmed the beneficial effects of DS for steel castings. The melting and pouring in this work was all carried out in air into relatively simple molds (Figure 17.2a) approximately 100 mm diameter and 230 mm tall so that significant oxidation and bifilm contamination of the melt would be expected, particularly during the final pour into the molds.

Significantly, the benefits to properties were a strong function of DAS in non-directionally solidified castings but *not* for DS castings. This result is difficult to explain unless one assumes that

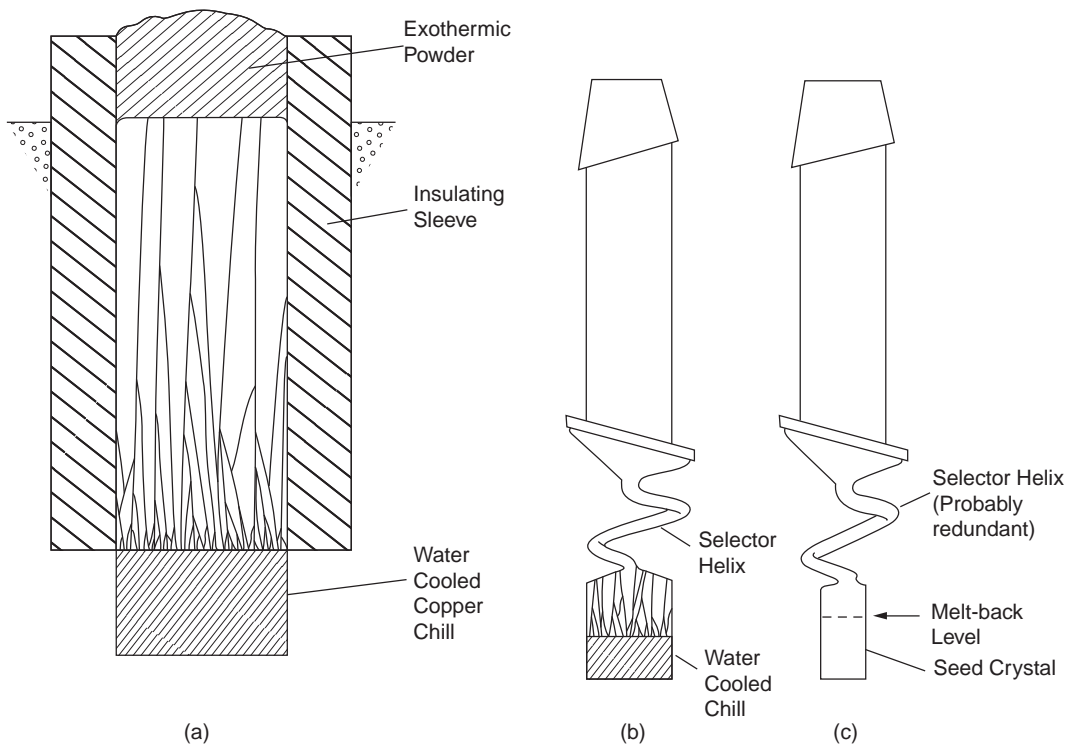


**FIGURE 17.2**

(a) Directional vertical solidification of a steel casting (after Polich and Flemings 1965); (b) single crystal by selection from a chilled DS base; (c) single crystal grown from a seed and therefore accurately oriented.

bifilms are trapped amongst grains during equiaxed freezing but not in DS material. Thus for the relatively clean DS material the properties are not affected by DAS as seen in Figure 9.26 confirming that mechanical properties are a function of bifilms; the *apparent* strong effect of DAS in most castings and many alloys is the result of the presence of unfurling bifilms.

This work on steels coincided with a technically analogous, but, as it turned out, far more important and exciting breakthrough in Ni-base superalloys. Versnyder and Shank (1970) review the early development of DS and single crystals for blades and vanes for use in aircraft turbine engines. Their world-famous summary of their creep behavior is seen in Figure 17.1. These early studies also indicated that DS polycrystal castings possessed up to 10 or 100 times greater fatigue life compared to equiaxed polycrystal castings (Leverant and Gell 1969). Despite this spectacular advance, Zhou and Volek (2007) draw attention to the fact that performance, particularly in creep, remained limited by crack formation along both the longitudinal and transverse grain boundaries of the DS castings, although the failure of transverse boundaries is most usually cited as the driving force for the development of single crystals, in which, of course, all grain boundaries were eliminated. Since, of course, grain boundaries are enormously strong, it seems most likely that these grain boundary failures were not the result of failures of the grain boundaries themselves but the result of bifilms segregated to the boundaries by dendrite

pushing. This seems especially likely in view of the extreme turbulence associated with the manufacture of these vacuum cast blades, so that the presence of bifilms is guaranteed. They are such serious defects that it is reasonable to suppose they will have a major effect on properties.

If, as seems reasonable and logical, it is accepted that grain boundaries are strong, the Versnyder and Shank result shown in Figure 17.1 cannot be explained by conventional metallurgy. The DS and single crystal technology for turbine blades in jet engines is, perhaps, the best evidence yet for the profound effect of bifilms in castings. If true, similar amazing improvements are to be expected in most other alloy systems as bifilm populations are reduced.

---

## 17.3 SINGLE CRYSTAL SOLIDIFICATION

The benefits of DS are brought to complete fruition in single crystal growth.

By the provision of a crystal selector such as a helical channel (known as the 'pig tail'), a single grain orientation can be selected close to the  $\langle 001 \rangle$  favored dendrite growth direction. Grains growing in other directions impinge on the walls of the helix and are eliminated (Figure 17.2b). Alternatively, the provision of a seed crystal allows any direction of growth to be selected, effectively making the pig tail redundant, even though to this date the pig tail seems to have survived for no good reason that anyone can think of (Figure 17.2c).

After the melting and pouring of the metal into the mold, the mold is withdrawn slowly from a hot zone at a temperature above the melting point of the alloy, into a cold zone. The two zones are separated by a baffle designed to fit around the mold as closely as possible to maintain the temperature gradient as high as possible. Withdrawal for an average turbine blade might take up to 2 hours.

By the production of a single crystal, grain boundaries (thought to be the weak features of the structure) could be eliminated. In addition, the alloy could be developed for maximum properties such as strength and oxidation resistance because the absence of grain boundaries meant that complications of the control of grain boundary precipitates were avoided. Thus turbine blades and vanes for aircraft engines took a further leap forward, beyond the attainments of the DS castings (Figure 17.1), and are now used for the most demanding locations in turbines, withstanding extremes of stress and temperature, justifying their name 'superalloys'.

It is a pity that at this time the casting of these excellent materials has to suffer casting conditions that risk the introduction of defects. The risk is significant because of the huge fall in properties that is clearly possible as illustrated in Figure 17.1 (interpreting the figure as illustrating the effects of bifilm rather than the effects of grain boundaries). Current vacuum furnace designs with the melting crucible approximately a meter above the mold, and the mold having a funnel-shaped entrance to its filling system (despite its attempts to control problems with the incorporation of a filter) together spell problems for the proper control of both structure and properties (Figure 16.30).

The target to achieve a single crystal is often undermined by the growth of various kinds of secondary or stray crystals. Carney and Beech (1997) found oxides at the root of most such misaligned crystals as might be expected if bifilms were present, simply because crystals would not, in general, be expected to grow through bifilms. Although the directional growth of single crystals would be expected to push many bifilms ahead, thus clearing the casting of many if not most defects, some bifilms that stretch into or across the casting section will be expected to be attached to the mold walls, and thus be immovable. Such barriers to growth will lead to the undercooling of the melt on the far side



of the barrier as the mold continues to be withdrawn into the cool zone of the furnace. Eventually, the undercooling will become sufficient to nucleate a new grain having no necessary orientation relation to the original growth direction. This stray crystal would probably cause the casting to be rejected.

It is important to note that the bifilm barriers may not only be oxides. Ford and Wallbank (1998) found that all castings with additions of nitrogen to the melt formed stray crystals, suggesting the existence of nitride-based bifilms.

In passing, we should note that the seed crystal is covered with an oxide film which appears to be no problem to the orientation of the seeded growth. This is probably as a result of the oxide on the seed being an old, thick oxide and/or nitride that grew in the solid state. It would be expected to be highly fractured and porous, unlike most bifilms which would be only micrometers or nanometers thick, and probably, like most thin films in their early phase of growth, rather perfect.

Other factors emerge to erode the perfection of growth of the single crystal.

- (i) While the advance of the front drives the solidification of the dendrites in a vertical direction these long stalks of solid grow relatively true to their  $\langle 001 \rangle$  direction. However, when they arrive at a point in the casting where they have to grow sideways, the cantilevered weight of the dendrite (denser than the liquid by only a few percent of course) can be supported for a limited distance. Beyond this the bending moment at the root of the dendrite causes the sideways arm to hinge at the root, until it falls, its fall arrested by the mold or other dendrites. In this way low angle boundaries are created (Newell et al. 2009). The situation is analogous to the formation of the branched columnar zone in steel ingots.
- (ii) The microsegregation between dendrite arms accumulates near the roots of the advancing array. If this is denser than the matrix alloy this liquid tends to flow to the edges of the mold, creating a convex front. If the segregated liquid is lighter than the bulk alloy, the situation is unstable, and plumes of segregated liquid can ascend through the mesh, dissolving the mesh as it goes, forming a channel segregate. The dendrite arms that are melted off tumble into new orientations in the channel, giving the name ‘freckle defect’ when studied in the etched condition. Ever since McDonald and Hunt uncovered the mechanism for the formation of the channel segregate in 1969, there has been a huge amount of work on this subject, particularly in relation to superalloys (for instance Purvis 1994) and more generally reviewed by Beckermann (2002). A key parameter now included so far as possible in new alloy designs is the balancing of elements in an attempt to make the interdendritic liquid as near neutral buoyancy as possible.

Although the Ni-base superalloys have excellent resistance to oxidation at high temperature, their resistance requires to be enhanced further for the highest temperature applications. This is achieved by various kinds of coatings, often by a kind of aluminizing process, in which aluminum is diffused into the surface of the casting and then subjected to oxidizing conditions to generate a strong protective layer of alumina. The beauty of such a coating is that it is mainly metallic, having some ductility and thus resistant to damage such as spalling experienced by brittle or poorly adherent coatings. Also, because of its reserve of aluminum in depth, it is self-healing if damaged.

We need to note, however, that in their studies of the protection of Rene 80 with an aluminide coating, Rahmani and Nategh (2010) observed that cracks in the casting associated with grain boundaries and carbides (features strongly suggesting the presence of bifilms) unfortunately overwhelmed the effects of the coating, since the cracks from the matrix extended through the coating. Once again, it seems that bifilms are likely to be responsible for this major potential failure mode of an

otherwise excellent technology, making improved casting technology an urgent issue for superalloy castings.

If it is true that single crystal blades derive their extraordinary properties mainly by the adventitious reduction of bifilms, it follows that there are almost certainly much cheaper ways to obtain bifilm-free alloys by sensible melting and casting techniques. Thus polycrystalline blades, produced quickly and cheaply, could in principle equal the creep properties of single crystals, although they would not have the unique directional properties of single crystals which are exploited in some blade designs to improve stiffness and vibrational response of course.

Alternatively, of course, an improved melting and casting approach could bring further benefits to single crystals, eliminate the current risks to integrity, providing manufacturing economies and possibly further improving properties to give extended times between service inspections of engines.

---

## 17.4 RAPID SOLIDIFICATION CASTING

The use of the term rapid solidification (RS) has traditionally been attributed to such processes as splat cooling of perhaps a gram of material between cold anvils, or the production of ribbon off a rapidly rotating wheel. These processes give cooling rates in the region of millions of degrees per second, but the product is hardly a shaped casting; more a heap of bits or ribbons requiring some other process for consolidation.

Here we shall content ourselves with more limited rates of cooling, at rates in the region of perhaps a hundred degrees per second. These more modest rates are still capable of delivering excellent if not astonishing properties, but at the same time, of course, can directly deliver engineering products such as shaped castings.

### Sophia and Hero processes

During freezing of a conventional-shaped casting, the casting contracts away from the mold, and the mold expands, opening the so-called 'air gap' between the casting and the mold. This gap, possibly containing a variety of gases except air, is a major barrier to the rate of escape of heat from the casting. Thus the air gap, above nearly all other contributors to cooling, controls the rate of cooling. The metallurgist will be concerned about the fineness of the microstructure, particularly the DAS, but as we have seen the mechanical properties of castings seem mainly dependent on the unfurling of bifilms.

Some Al alloy investment castings are subjected to a more rapid solidification by being immersed in a coolant immediately after the mold is filled with liquid metal. The Sophia process is known to involve quenching the mold and its liquid metal contents into a soluble oil. At the same time a pressure is applied to close porosity so far as possible. These actions significantly increase the properties of casting, and make any further enhancement by, for instance, HIPping, to be unnecessary.

The Hero process used by Tital in Germany is thought to be similar. Even though the claimed original patent is now likely to be nearly or actually expired the details of the process remain closely guarded.

The quenching of the complete investment mold and its liquid metal into a cooling liquid certainly raises properties, but is clearly a messy process. Furthermore, of course, the efficiency of heat transfer is also limited by the presence of the investment shell that remains in place during freezing. These issues are largely solved by the following aggregate mold process, even though, of course, an aggregate mold process cannot match the surface finish enjoyed by the investment casting.

### Ablation casting

I first came across the word ‘ablation’ in relation to the NASA shuttle space vehicle re-entering the earth’s atmosphere. To avoid the vehicle heating up and being destroyed, its leading surface was covered with ceramic tiles that were designed to heat up and vaporize, the vapor carrying away and leaving behind the frictional heat generated by the atmosphere so that the space craft itself did not heat up. Thus the term ablation denotes an eroding away and carrying away process.

Ablation casting is a new approach to the making of an aggregate molded casting in which the fundamental limitation to heat flow presented by the air gap is removed by the application of coolant direct onto the surface of the solidifying casting. As a necessary prior step the mold is removed to allow direct access of coolant. This is achieved by the application of a solute directed onto the mold, but with the mold aggregate bonded with a binder soluble in the coolant. The mold is thereby dissolved away and removed in the flow of the coolant. Thus, unlike Sophia or Hero, in ablation casting the mold does not obstruct cooling.

In practice, therefore, the liquid metal is poured into an aggregate mold bonded with a water-soluble binder. While the metal is still molten, the mold is ablated away by water jets (Figure 17.3a). Because the mold is progressively removed, disappearing steadily as ablation advances along its length, the water is enabled to contact the metal casting directly. A high-temperature gradient is progressed through the casting, assisting to eliminate porosity especially in thick sections. The outcome is solidification of a shaped casting under (i) an unprecedented temperature gradient and (ii) solidification speeds. A unique microstructure characterized by extreme soundness and fineness of the last phases to solidify is thereby produced. Porosity can be controlled to be extremely low or effectively zero even in such features as isolated bosses. This is because freezing conditions are now no longer under the control of the mold, but under independent control from ablative cooling.

The solidification can be directed to a final corner of the casting where a feeder is located, possibly planted off the casting on a short extension, as an extended feeder neck. Because the freezing front arrives at this point fairly quickly, the feeder can be arranged to drain almost completely, its final form being only a metal skin like an empty paper cup. Feeding can therefore be extremely efficient, so that metal yields can be high.

At the completion of ablation, the mold has been completely removed and the casting sits on the ablation station clean and cold, ready to be picked up immediately for further processing (Figure 17.3b).

The mechanical properties achieved by the process are equal to or surpass the best competitive processes such as squeeze casting. This is perhaps not so surprising because the pouring conditions for most squeeze products are poor, introducing defects. In addition, cooling conditions for most squeeze castings are heterogeneous, with only parts of the casting feeling the compressive force holding the casting and mold in contact. Ablation casting can use any form of filling, with the current gravity filling processes naturally suffering defects. Nevertheless, despite the general use of gravity filling during this early stage of development of the process, rapid solidification freezes in bifilms in their compact state so that properties remain good. Also, it is worth noting that the company, Alotech Limited, generally applies filling systems that conform to the principles of this book, which has to be a further significant advantage over most competition at this time. Even so, the properties are *surprisingly* good, leading one to suspect some additional factor. It seems likely that the unusually powerful temperature gradient of the process may be efficient in assisting the freezing front to push bifilms ahead, effectively cleaning large areas of the casting. When the process is further developed, perhaps introducing a filling process



(a)



(b)

**FIGURE 17.3**

Ablation casting of an Al alloy: (a) eroding the mold away and cooling the casting; (b) the final casting, cold and clean.

such as counter-gravity, properties from ablation should give yet further improvement, even though, of course, competitive processes should also improve if provided with such advantageous filling systems.

Additional advantages for ablated castings appear to be their highly competitive cost. This arises mainly because the silicate-based binder is much less costly than competitive resin-based binders, but also benefits from the relatively low cost of capital equipment and modest cost of tooling. Further benefits arise as a result of the water-based technology. The process produces no smell, no fume, no

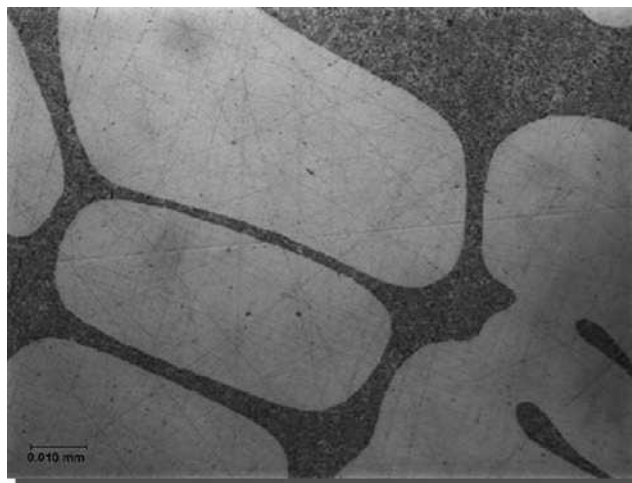
dust (the recycled aggregate is mostly either wet or damp), saving the installation of costly fume and dust extraction equipment.

The optical microstructure of an Al-7Si-0.4Mg test casting that was allowed to solidify without ablation is shown in Figure 6.9a, and is typical of a non-modified Al-Si eutectic. Typical ablation-cooled structures are shown in Figures 17.4 and 17.5 illustrating the extreme fineness of the eutectic spacing that is difficult to resolve even at 1000 $\times$  magnification in the optical microscope (but only limited regions of the dendrite spacing that have been refined). The Si inter-particle spacing is under 1  $\mu\text{m}$  in this structure. Note that no Na or Sr has been added to achieve this apparently well-modified structure.

Figure 17.5 illustrates the extent of freezing that has taken place before the ablation cooling has had time to reach these regions. Thus the secondary dendrite arm spacing (DAS) is in general rather coarse, and typical of a sand casting of that section thickness. In some instances, particularly in the centers of sections, it is at first sight curiously perverse that the DAS is fine (normally fine structures as a result of rapid cooling are limited to the outer skin of the casting). The fine central regions are of course the result of ablation arriving in time to limit dendrite arm coarsening in these regions. Furthermore, such regions would often contain porosity, thus weakening the structure, whereas ablation tends to yield sound and fine-grained interiors that would be expected to have enhanced properties.

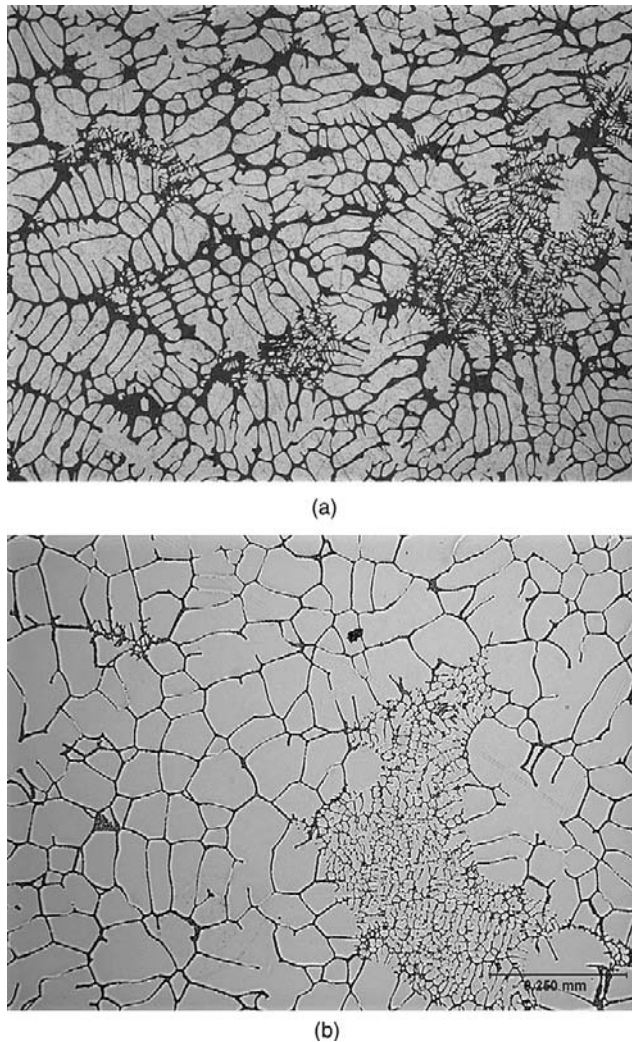
It is extremely significant that the improved properties are clearly not directly related to DAS, which in general is not improved. Improved properties appear to be a result only from improved control of the solidification of the eutectic. The current preoccupation focussing on the achievement of a fine DAS is therefore seen in general to be an error (although of course it is correct that DAS indicates the freezing time of the dendrites).

Alloys that are traditionally difficult to cast because of hot tearing problems such as the Al-4.5Cu series alloys prove to be relatively straightforward with ablation, although the rapid and directional



**FIGURE 17.4**

Structure of an Al-7Si-0.4Mg alloy achieved by ablation, without added modifiers such as Sr or Na. In the optical microscope the dendrites are seen to be coarse, but the Al-Si eutectic is hardly resolvable even at 1000 $\times$ .

**FIGURE 17.5**

The dual dendrite structure often observed in ablation-cooled castings of Al alloys as a result of natural cooling finally caught up by ablation cooling: (a) in an Al-7Si-0.4Mg alloy containing significant eutectic phase; (b) in an Al-4.5Cu solid solution alloy exhibiting no significant eutectic phase.

solidification requires to be carefully controlled to avoid dendritic segregation problems (inverse segregation). Furthermore, the wrought alloys including the 6000 and 7000 series have been demonstrated to be capable of being made into shaped castings. Much of this success with otherwise difficult casting alloys arises because the casting does not build up long-range stresses during casting: the casting ahead of the freezing front remains molten and can therefore effortlessly accommodate strain without causing stress.

Perhaps surprisingly, ablation has produced excellent Mg alloy castings which have displayed properties well in excess of those of any other competing Mg casting process at this time.

At the time of writing the process is protected by a number of patents, and is, in common with many new processes, probably somewhat more difficult than it looks, even though its difficulties are clearly worth overcoming. It is still undergoing rapid development, and at this time is just starting its first series production of castings.

For the future of ablation, a combination of the molding and solidification technology with good filling, possibly via a counter-gravity process, promises to be a powerful process for both Mg- and Al-based castings. It is not known at this time whether the process can be extended to encompass higher-melting-point copper and ferrous alloys. As we continue to note in this book, there remains no shortage of future challenges.

This page intentionally left blank



# Dimensional accuracy

# 18

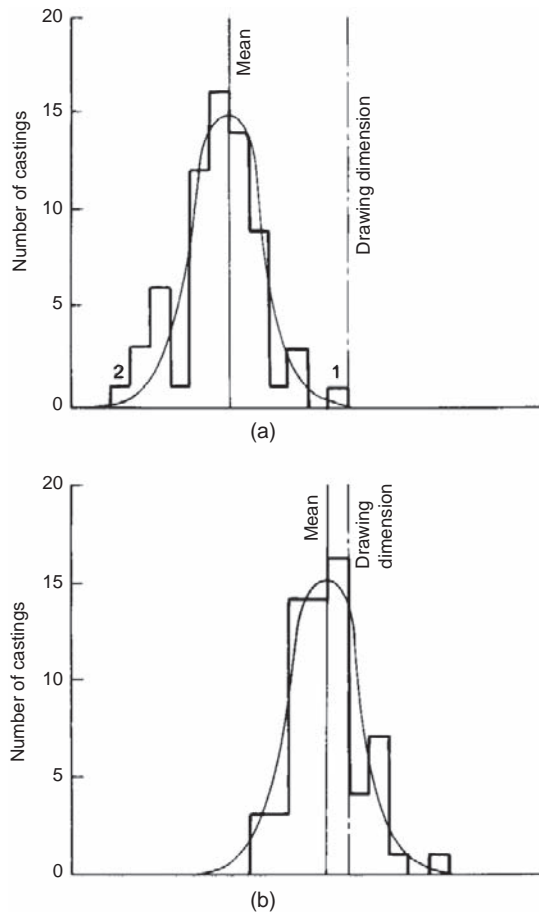
The casting which we make is, of course, never quite perfect in terms of size and shape. To allow for this, tolerances are quoted on engineering drawings. So long as the casting is within tolerance, it will be acceptable.

Some reasons for the casting being out of tolerance include elementary mistakes like the patternmaker planting the boss in the wrong place. This leads to an obvious systematic error in the casting, and is easily recognized and dealt with by correcting the pattern. It is an example of those errors which can be put right after the first sample batch of castings is made and checked. (Even in this simple case, care may be needed if great accuracy is required, as is explained a little later below.)

Another common systematic error in castings is the wrong choice of patternmaker's contraction allowance. The contraction of the casting during cooling in the mold is often of the order of 1 or 2%. However, it depends on a number of factors, particularly strongly on the strength of the mold and the cores. For instance, in an extreme case, a perfectly rigid mold will fix the casting size; in such a situation the casting simply would have to stretch during cooling since it would be prevented from taking its natural course of contracting. Such a situation is common for thin wall castings made in steel molds. However, there is often uncertainty. The choice of contraction allowance prior to the making of the first casting sometimes has to be decided in the absence of previous similar castings that would have provided a guide. Thus the chosen value for contraction is often not exactly right. This point is taken up at length in Section 18.1, with recommendations on how to live with the problem.

Other errors are less easily dealt with. These are random errors. No two castings are precisely alike. The same is true for any product, including precision-machined parts. The ISO (International Standards Organisation) Standard (1984) for casting tolerances indicates that although different casting processes have different capabilities for precision, in general the inaccuracies of castings grow with increasing casting size, and the standard therefore specifies increasing linear tolerances as linear dimensions increase. (Nevertheless it is worth pointing out that the corresponding percentage tolerance actually falls as casting size increases.) Although other work on the tolerancing of castings suggests that the ISO standard has considerable potential for further improvement (Reddy et al. 1988), it is the only European standard at this time. This also has to be lived with.

Because of the effects of random errors being superimposed on systematic errors, where great precision is required, it is of course risky to move the boss into an apparently correct location simply after the production of the first trial casting. Figure 18.1 illustrates that the random scatter in positions might mean that the boss appeared to be in the correct place first time if the casting happened to be casting 1 in Figure 18.1, or might have been over twice as far out of place, compared to its average position, if the first casting had been number 2 in Figure 18.1. A sample of at least two or three castings is really needed, and preferably ten or a hundred. The mean boss location and its standard deviation from the mean position can then be known accurately and the appropriate actions taken.

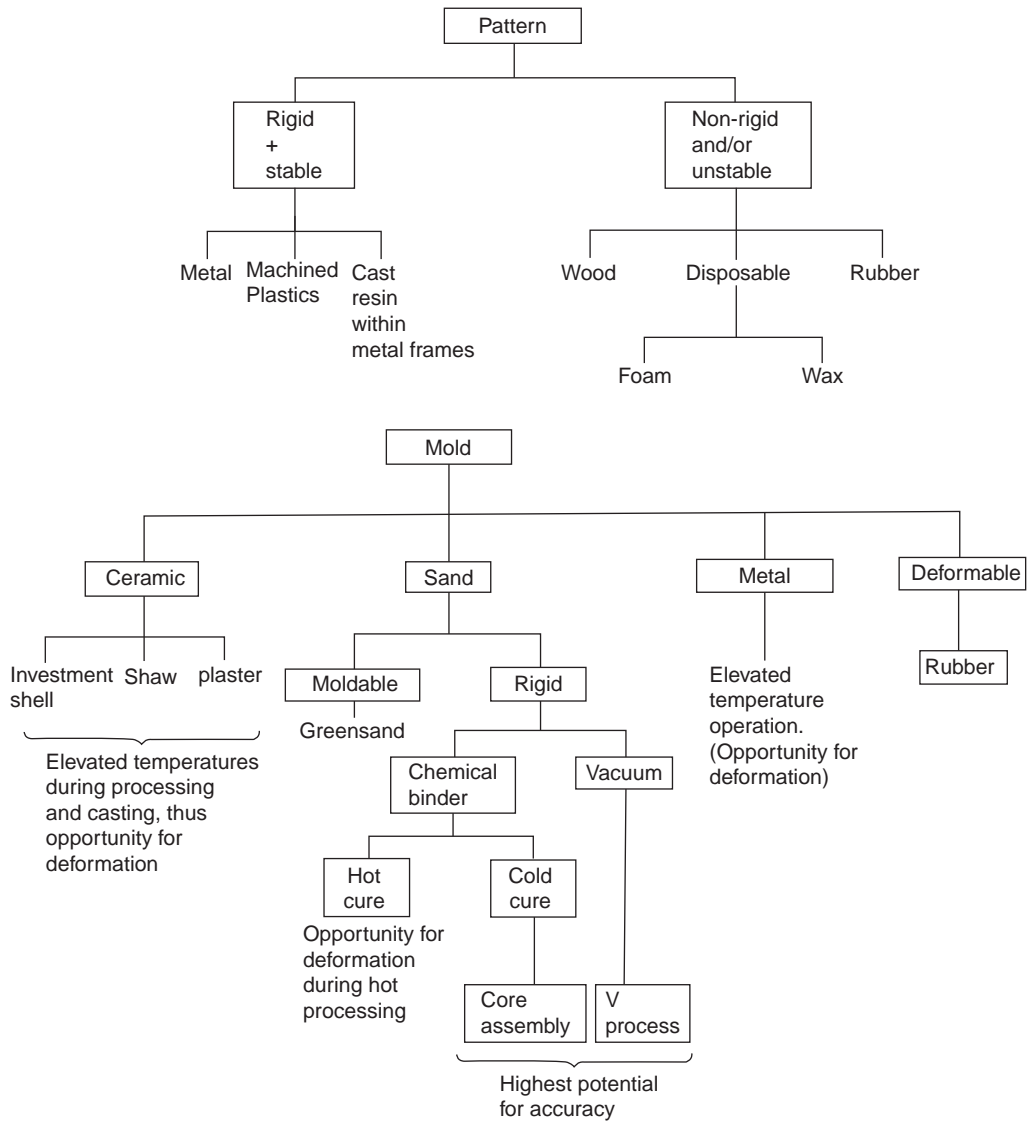
**FIGURE 18.1**

Statistical distribution of casting dimensions (a) before and (b) after pattern development. Based on Osborn (1979).

At the present time it will be of little surprise to note that such exemplary action is not common in the industry. This is because companies are not generally equipped with a sufficient number of fast, automated three-coordinate measuring machines. As such standards of measurement become more common, so the attainments in terms of accuracy of castings will increase. However, it is a pleasure to note that advances in metrology are occurring fast and furiously. In particular, the use of lasers and computers has revolutionized measurement of the exterior features of castings. For those fortunate enough to be able to afford it, a similar revolution has happened in X-ray radiographic tomography, so that three-dimensional views of the interiors of castings can now be measured with confidence to ensure that hidden wall thicknesses are correct, and that interior cores have not moved or distorted during casting.

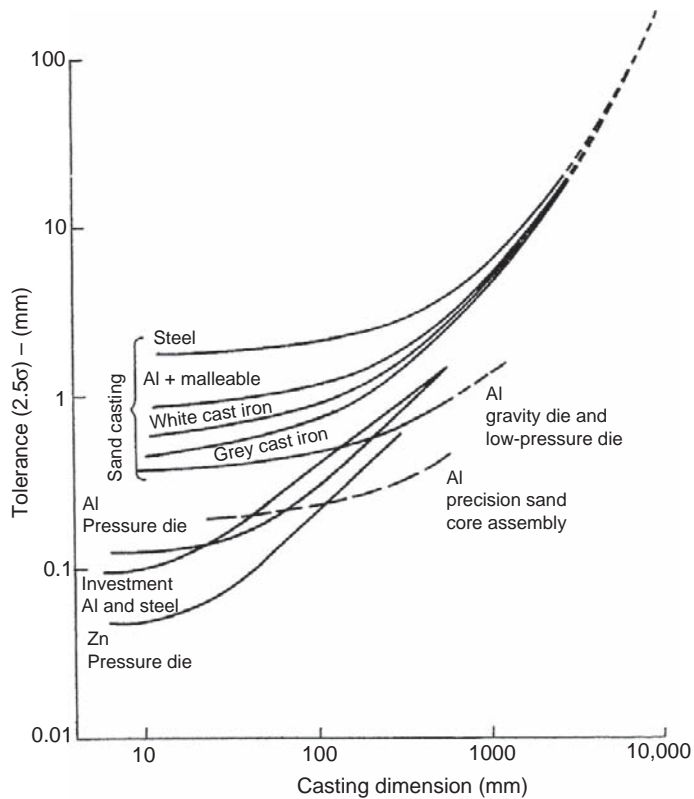
Turning now to the accuracy of castings themselves: one of the fundamental requirements for an accurate casting is an accurate rigid pattern and an accurate rigid mold. This may seem self-evident, but it is comparatively rarely achieved.

Figure 10.2 shows a number of process routes for the manufacture of castings, but in Figure 18.2 they are assessed in terms of their potential for accuracy, and this potential is quantified in Figure 18.3.

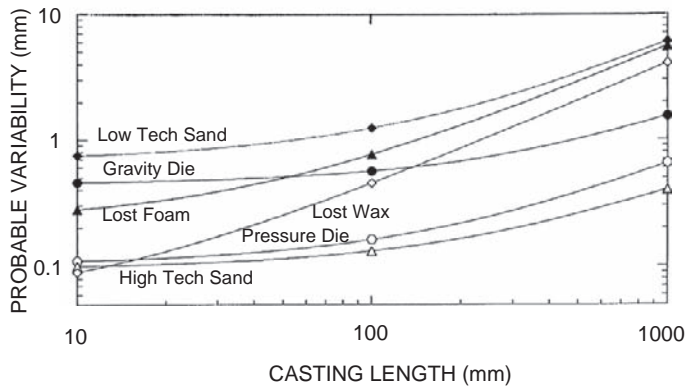


**FIGURE 18.2**

Patterns and molds categorized according to their potential for accuracy.



(a)



(b)

**FIGURE 18.3**

The average tolerance (taken as  $2.5\sigma$ ) exhibited by various casting processes (sand, and gravity and low-pressure die from IEE TS71; investment from BICTA 1990; pressure die from ZDA 1990; sand core assembly data are tentative, from early production experience).

In principle, only the rigid patterns in combination with the hard aggregate mold routes (core assembly and V process) meet all the requirements of accuracy, rigidity, room temperature operation, and formation of the mold against the patternwork.

This is not to say that other processes are inappropriate. Some will be adequate in accuracy and have the benefit of low cost. Others will be available locally to the customer and the foundry may have the capacity to accept the order at that time. There are many factors that influence the choice of an appropriate manufacturing route and choice of manufacturer.

The ISO standard for casting accuracy gives the general trend of increase in the size of random errors as casting size increases. However, the casting designer and engineer require much more detailed knowledge of the sources of individual contributions to the final total error. The remainder of this chapter is an examination of these contributions. The reduction of these errors allows the production of castings which can considerably exceed the minimum accuracy requirements specified in the ISO.

The use of computers has of course greatly aided the quest for more accurate and reproducible tooling production and replication. CAD/CAM (computer-aided design/computer-aided manufacture) has itself benefited from the rationalization and standardization of data transfer in the form of Standard Triangulation Language (STL), International Graphical Exchange Standard (IGES), and Standard for Exchange of Product Information (STEP). The world-wide adoption of such standards has allowed tool sourcing to become a world-wide activity.

---

## 18.1 THE CONCEPT OF NET SHAPE

A 'net shape' product is one whose shape requires no further modification, and thus is ready for use. The concept is one which is usually applied only to parts which are required to assemble and fit closely with other parts.

Most soft plastic toys are made net shape, but the shape is often not critical, and the concept has no relevance. However, it is critical in the case of components such as Lego, where each injection-molded part is required to fit accurately into other parts without any further processing; clearly, in this case, no machining can be contemplated on grounds of cost. The component must be net shape.

For many metal components, with perhaps the exception of some powder-forming routes, the part can rarely be finished exactly to the required final tolerance in a single forming operation. Thus, in general, a forming operation such as forging or casting is carried out to produce a 'near-net-shape' product, which is subsequently brought into the required tolerance by a finishing operation of some kind.

If we try to evaluate the various casting processes for their capability in the production of net or near-net shape products the problem resolves to 'what accuracy can the various casting processes achieve?'

Answers to this question are a task not easily limited to a manageable scale. For instance, accuracy is required in terms of straightness, flatness, concentricity, etc. Here we shall consider only the ability to reproduce a length.

Sources of error come in various forms: (i) random errors as a result of variations in processing and (ii) systematic errors of many types, including the boss in the wrong place, and more general problems that apply uniformly to parts or to the whole of the product. For instance, these sources include such important features as the mismatch between mold halves. Also included in this category are features like the thickness of a mold coating when applied uniformly (well or badly) to the whole or part of

a mold by spraying or dipping. Systematic errors occur due to expansion or contraction during processing, and which are thus a function of the size of the component.

There is also the fundamental difficulty associated with the fact that an intrinsically poor processing route could be carried out with extreme care by one manufacturer, giving a satisfactory product in spite of the technology. This contrasts with the situation where an intrinsically reproducible process is carried out with ineptitude or even crass irresponsibility by another, therefore giving an unacceptable product. Thus although in this study the fundamental capability of the process will be emphasized, the ability of the manufacturer to overcome deficiencies in the process by intelligent and diligent effort must not be underestimated. Even so, the view is taken here that processes which are intrinsically reproducible are to be favored over those which are not. Also, some attempt will be made to place limits on the achievements of both good and bad practice to assess the extent of the tolerance problem.

The only previous comparative study of the accuracy of the various casting processes has been carried out by the author (Campbell 2000). However, because of the paucity of data on the accuracy of castings produced by different processes (notwithstanding the existence of the ISO 1984 standard and one notable experimental attempt, IBF 1979), he found himself driven to making estimates of accuracy of the different processes based merely on his own experience. This, clearly, is hardly satisfactory, but is judged to be better than nothing at this stage, and therefore comes with no apologies. This section considering the problems of net shape is based on the original paper, and is offered as a preliminary study, outlining the concepts involved, and providing a framework in which the mechanics of the problem can be understood, and into which better data can be fitted as they become available.

### 18.1.1 Effect of casting process

Inaccuracy can be introduced into the product at several stages of the casting process, which typically usually involves the sequential production of a series of shapes, one formed intimately against the other, thus producing a series of positive and negative forms which finally give the desired positive shape. As the number of steps increases there is an increasing chance to introduce error. The main processes are considered in order of increasing complexity, and by implication, vulnerability to error, below.

#### Exterior shapes

Die casting is the most direct of the casting processes. Here, a metal mold (a near-net-negative of the required shape) is filled with liquid metal which is allowed to solidify to give the final desired positive form. Pressure die casting involves the injection of the metal at high speed and high pressure into the die cavity, whereas low-pressure die casting and gravity die casting use similar cast iron or steel dies which are covered with a protective refractory coating, and which are filled relatively quiescently.

Sand casting involves the additional step of having a positive pattern which is used to produce a negative sand mold to produce the positive cast form. Two main types of sand mold are used, (i) greensand and (ii) chemically bonded sand. Although sand has a poor image, and is in fact often used badly and under poor control, the fact is that it has considerable potential for reproducibility. It often does not require a protective mold coat and thus retains the accuracy of the pattern. Because the pattern never contacts the liquid metal it can be long-lived if it suffers little wear, retaining its original accuracy for up to ten times longer than die-casting processes.

Lost wax (i.e. investment) casting involves a further additional step, because a negative die is required, usually accurately machined from an aluminum alloy. This die to form the wax pattern is

long-lived and retains its accuracy well. The die is filled with liquid wax to make a positive pattern. A ceramic shell mold is formed around this, and the wax melted out, to produce a negative into which metal is finally poured to create the final positive shape. Significant scope for variability exists in (i) the expansion and/or distortion of the wax pattern; (ii) the stresses of the dewaxing operation; (iii) the firing of the shell where sintering and shrinkage of the shell occurs; (iv) the expansion and phase changes in the shell which occur on casting (particularly when pouring high-temperature alloys and steels); and (v) the variable restraint of the mold on cooling as a result of the prior variations in chemistry and sintering of the ceramic shell.

Lost foam casting is in some ways similar to lost wax, but where the disposable positive pattern is formed from polystyrene expanded inside a machined aluminum die. Again, the die is accurate and the least subject to errors of wear compared to all the casting processes. The foam pattern may be subject up to 0.8% shrinkage (depending on the type of foam (Brown 1992)) and may require to be assembled and glued together from individual foam parts. The whole is then coated with a ceramic slurry which is allowed to dry. The assembly is finally placed in a box, loose dry sand is vibrated into place around the pattern to support it during casting, and extract the heat during freezing. This action of pouring and vibrating sand into place in this way usually introduces measurable distortion of the flimsy polystyrene pattern. The metal is poured into the foam, displacing it to form the final positive shape. The mold may, of course, distort during the casting and cooling process.

### Interior shapes

Hollow parts of castings, which can be formed by simple withdrawable shapes, can be introduced into die castings. In this case the core is a permanent feature of the die tooling and is usually made from steel, and is sometimes water-cooled. Pressure die cast engine blocks are among the most ambitious aluminum alloy castings made by this process.

More complex interior shapes cannot be withdrawn, and thus require to be formed by disposable cores. The most common type is the resin-bonded sand core, in which the resin is designed to break down after casting, allowing the sand to flow out of the cored cavity. Alternatively, in a few instances, cores can be dissolved out (such as salt core by water, or silica core by hydrofluoric acid in the case of Ni-base turbine blades).

The core is supported inside the mold cavity by its prints. These are (positive) core extensions which locate in (negative) print locations in the mold or die. For sand casting the location of the core can be precise because assembly is all at room temperature, and because the core-to-mold interface is usually kept clear of uncertainties such as a variable thickness of core coating. For gravity die casting, the sand core is often poorly located because the thermal distortion of the die causes the print negatives to be out of location. In addition, the die has a variable thickness of die coat which has been sprayed on, some of which finds its way onto the print locations, causing further deterioration of their precision. Worse still, especially if core loading of the die is lengthy or is delayed, the heat of the die can sometimes soften, or even cause to break down, the resin binder in the sand core, causing the core prints to disintegrate and the core to sag.

Once surrounded by liquid metal the core will be subject to buoyancy forces which will tend to make it float. This is not so bad in liquid magnesium where the density difference with silica sand is near zero. Similar neutral buoyancy applies for the aluminum/zircon sand system. Buoyancy becomes increasingly problematic for the common systems such as aluminum/silica sand and liquid iron (or other dense metals such as copper and steel) and silica. The latter systems more particularly so

because of the higher casting temperatures involved. Flotation forces have to be withstood by adequate mechanical support of the core, usually by good print design and location, or, often less desirably, by internal steel reinforcement or metallic supports (chaplets) which are cast-in to the product as permanent features. To ensure good fusion between the insert and the casting is not always easy. Sometimes such features are subsequently machined out.

### 18.1.2 Effect of expansion and contraction

In greensand molding systems the sand is bonded automatically by the compaction of the sand. However, at compaction pressures above about 1 MPa (10 bar) the sand mold deforms elastically, and, on withdrawing the pattern, is subject to 'spring back'. This general distortion of the mold leads to numerous difficulties relating to core assembly and mold closure. This, to the author's knowledge, is the only common molding system exhibiting distortion due to stress. Most distortions in casting processes arise because of thermal expansion as is discussed below.

When the metal first enters the mold, the mold, and more particularly the cores, heat up and expand. Thus the mold cavity enlarges and will probably suffer some distortion. This is reasonably reproducible in sand molds because the pouring temperature is normally under good control (usually  $\pm 10^\circ\text{C}$  or better) and the molding sand is always close to room temperature. Thus the starting conditions are usually reproducible. This is less true for the various processes using metal molds, where the die temperature of perhaps 300 or 400°C is often poorly controlled, varying by as much as  $\pm 100^\circ\text{C}$  or more.

As the casting cools it contracts, with the result that some parts of the casting are subject to tensile extension or compression because of geometrical constraint of the mold. The constraints exerted by the disposable sand mold are perhaps less severe than those of the metal die, but in general the casting stays in the sand mold longer and the constraint therefore operates for longer.

Although an attempt will be made to estimate these expansions and contractions, the final result corresponds to the Patternmaker's Contraction Allowance. This is the value based on hundreds of years of experience by patternmakers and toolmakers, and is the allowance they have to provide, making the pattern a little larger than the final casting. Unfortunately the factor is sensitive to geometry of the casting, and mistakes are often made in the correct choice of the allowance, which can vary between 0 and 1.3% for aluminum castings and up to 2.4% for steel castings. Some recent work in the author's laboratory has highlighted the uncertainties of this factor for cast aluminum and cast irons (Nyichomba 1998). Estimates of this allowance are made in Section 18.5.

In the pressure die-casting process, the casting is normally thin-walled and thus rather weak. As it cools in the rigid steel die, contracting onto projections of the geometry, it is therefore forced to stretch plastically. The size of the casting is thus mainly controlled by the time to ejection.

The hot casting is cooled to room temperature in a variety of ways. This may occur as a series of individual castings on a cooling conveyor, as a heap in a bin, or by an immediate quench into water. These post casting operations are likely to create different patterns of distortion. Likewise, heat treatment, even natural aging, affects many products, particularly heat-treatable aluminum alloys. These grow slightly (of the order of 0.05%, i.e. 0.5 mm per meter) as hardening precipitates form.

### 18.1.3 Effect of cast alloy

*Zinc castings* are most commonly supplied as pressure die castings. As we have seen earlier, the thermal distortions of both die and casting are the least of any of the casting processes because



(i) the casting temperatures are low, creating low expansion problems for the die and minor contraction problems for the casting; (ii) the dies are accurately machined from steel, (iii) the dies use no protective die coating; and (iii) are supported in a close-fitting and rigid steel bolster. Thus zinc pressure die castings are intrinsically capable of meeting many net shape requirements. This is a clear-cut example of near-automatic achievement of net shape by zinc pressure die castings.

The *light alloys* based on magnesium and aluminum can be cast in molds of all types. For HPDC the dies are steel, and no protective mold coat is used, so maximizing accuracy. For low-pressure and gravity die castings the die is cast iron or steel but is protected by a ceramic die coat. The thickness of the coating is not easily controlled, thus limiting accuracy. The dies are also often subject to gross distortion partly because the die is free-standing (i.e. not supported by a surrounding steel bolster as in the case of dies for pressure die casting). For sand castings the molds can be used without a protective coating, and thus retain their dimensions.

*Cast iron* is most commonly poured into greensand molds with no protective coating. Chemically bonded sand molds and cores on the other hand usually require a refractory wash coat to obtain an acceptable surface finish. Although cast iron dies are possible for cast iron, their use in Western Europe is limited to specialized casting operations, where, again, a die coat is required. At this time the process is more widely used in Eastern Europe.

*Steel* is cast into aggregate molds. For modest sizes of products greensand is widely used without a mold coat. Increasingly often, however, steel is being cast into chemically bonded sand molds with a protective mold coat to achieve an acceptable finish. The coating ranges in thickness from 0.2–0.6 mm, being usually  $0.3 \pm 0.1$  mm. The high temperature of steel casting leads to considerable interaction of the surface of the casting with its environment, leading to sand burn-on and oxidation, although much of these problems would be solved immediately by the application of a good mold filling system. Many large steel castings lose up to 0.8 mm or more of their surface during heat treatment because of the flaking off of oxide from the outside surface of the casting, and approximately 0.4 mm from interior surfaces. Because of these interactions, plus the application of mold coatings, steel castings are normally the furthest removed from the net shape concept. On top of this, the rough-and-ready patterns often seen in the cast steel industry clearly do not help the attainment of accuracy. For steel components weighing up to a few kg the favored route for near net shape is therefore lost wax casting in vacuum.

## 18.2 MOLD DESIGN

### 18.2.1 General issues

The problem for the casting engineer is to achieve a successful design of the mold. This problem is not to be underestimated, since it requires the simultaneous solving of a list of issues including:

- (i) The design of the mold and core assembly can be a problem in itself. It is not uncommon to find that it is impossible to assemble the cores because some shape feature of neighboring cores has been overlooked. It is all too easy to stumble into such pitfalls in a complex core assembly. When the first set of cores is made from the new patternwork, with its shining new varnish and paintwork, the discovery of such ‘passing problems’, where one core will not pass another and so fit into the assembly, are greeted with embarrassment and dismay.

The other common problem for the casting engineer and toolmaker is the design of the assembly so that cores fit, in logical order, only into the drag if possible (Figure 18.4). Cores in the cope are not usually an option for horizontally parted greensand molds, since, if the sand strength is not high, they are in danger of falling out of their prints when the cope is turned over and closed onto the drag prior to casting. Gluing cores into the cope is possible in the case of strong chemically bonded sand molds. However, gluing takes time and is therefore costly, and introduces the danger that any excess glue that exudes out of the join may cause a blow hole defect in the casting if it contacts the metal. In addition, glue applied to a core print may prevent the core from venting, leading to a blow defect from the core. The use of glues should therefore be avoided if at all possible.

It is common for complex core assemblies to be assembled at a separate station sited off the mold assembly line. Core assembly can then be accurate since the assembly is built up in a jig. The cores

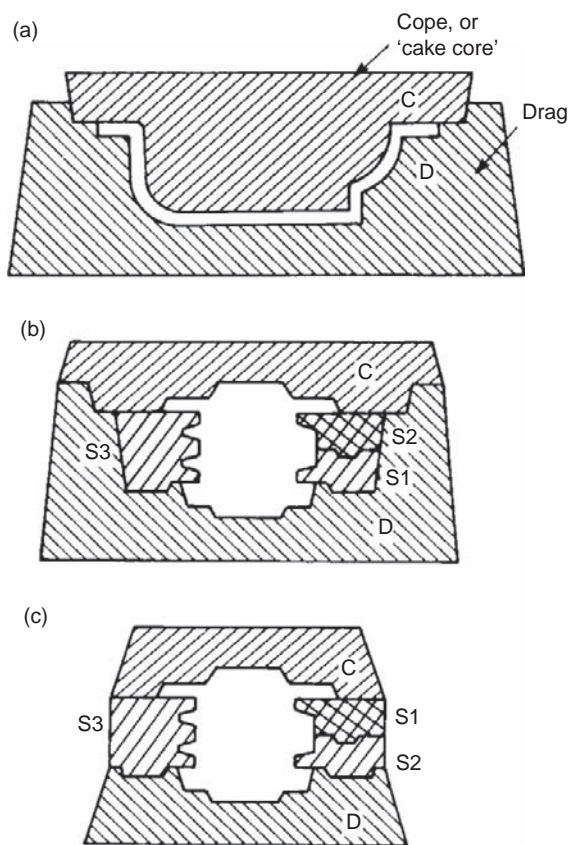


**FIGURE 18.4**

(a) A simple cake core and drag assembly; and (b) a cope and drag with side cores, all located in the drag; (c) an apparently lower-cost alternative to (b), but resulting in loss of dimensional control.

are designed to be lifted by the jig, transferring from the assembly station and lowered into the mold as a complete package. Castings that require lengthy core assembly times are not thereby allowed to slow the cycle time of the molding line.

- (ii) The filling system. The provision of a good filling system, and its integration with the rest of the mold and core system is sometimes not easy, and in some cases the additional trouble or expense to provide a good filling system is by-passed. (The minefield of poor castings and high scrap rates is always entered for apparently good reasons.) The filling system design forms a major part of this book. It is mandatory reading. Its rules are strongly recommended to be followed in all cases.
- (iii) The feeding system. Naturally, following the first rule for feeding, it is clearly best if feeders can be completely avoided. However, if they are considered to be necessary, it is usually not a problem to place feeders high on a casting. Thus the provision of feeders rarely involves difficulties of mold design. One of the key issues is to place the feeders so that they are easy to cut off or machine away subsequently.
- (iv) The avoidance of infringement of any of the 10 Rules. For instance, convection considerations might force the issue of rotating the mold through 180° after filling. This action usually confers other benefits and makes the integration of the filling and feeding systems powerfully effective and economic. It is a strategy to be recommended, although it is essential to observe the precautions listed in the section on rollover systems.

However, sometimes the solution to all these issues is not straightforward. For instance much time may be spent attempting to solve the issues with the casting oriented in one direction, only to realize that such an orientation involves insoluble problems. The casting is then turned upside-down and the exercise is repeated in the hope of a better outcome. Such experiences are the day-to-day routine of the casting engineer.

Furthermore, the complexity of the issues is not easily solved at this time by computer. There have been many such attempts, but it is fair to say at this stage that such efforts have not been developed to such a degree that the professional casting expert is offered any significant help. However, of course, we can look forward to the day when the computer is sufficiently capable to provide useful solutions.

### 18.2.2 Assembly methods

The design of the mold assembly often simply involves two parts; a cope and a drag; such maximum simplicity makes for maximum accuracy. But for more complex castings the mold assembly can be complicated, requiring many parts, and requiring much discussion between the pattern shop, foundry, and casting designer to find an appropriate solution. Accuracy can now become illusive and troublesome.

The simplest form of construction of molds, which was popular with many foundrymen, consisted of a drag with a cope in the form of a 'cake core' as shown in Figure 18.4a. This simple construction did not allow for the placement of any useful bottom-gated running system, and the top pouring which had to be accepted as a consequence was generally acceptable for gray iron castings in greensand molds. It did not give good results for the majority of casting alloys. The arrangement would, however, have been excellent for a counter-gravity filling technique.

As a general rule, it is useful to ensure that even in the most complicated of mold assemblies, the design of the assembly consists principally of a drag and a cope, and that all parts are interrelated via a single mold part, which will normally be the drag (Figure 18.4b). In this case the assembly of cores will be in the drag, with each core located separately, and the final operation will simply consist of

closing with the cope (sometimes called 'a cake core'). The cope also should have features which contact and locate directly on the drag as the key mold part.

Such simple rules are easily forgotten. One can see many ambitious castings which have failed to achieve dimensional acceptability because the mold assembly has resembled a random heap of assorted shapes: one layer of cores tottering upon another, with finally the cope perched precariously on top (Figure 18.4c). Clearly, the details of the casting formed in the drag will bear no constant relation to the details formed in the cope.

Figure 18.4b shows a simple type of cope–drag arrangement with side cores, all located in the drag, apart from side core S2, which rests on S1. It was judged that the small accumulation of errors in the positioning of S2 would be acceptable in this case. If the positioning of S2 had been critical, it could still have been located in the drag by stepping the contour of the drag appropriately.

Figure 18.4c shows how it would have been easy to save some sand by abandoning the deep drag construction, and having a core assembly which consists simply of a pile of cores, rather than a proper cope and drag. The overall accuracy of the casting now suffers from the accumulation of errors introduced by the intermediate side cores S1, S2, and S3, providing a poor match between the top and bottom features of the casting.

The dimensional problems which arise in setting cores are examined by Skarbinski (1971). In general it needs to be said about the accurate printing of cores that the core print should be designed assuming that the core will be produced with errors in its size and shape, and will have to fit into a mold which will also have suffered some distortion during its manufacture. The print also sometimes has to restrict the movement of the core during mold filling because of buoyancy, and yet may also have to allow the relative movement of the core in its print to permit the thermal expansion of the core. All this is a seemingly impossible task to achieve accurately. However, it is usually solvable by applying the following simple rules:

1. The print requires *tolerance* where it needs to fit (i.e. must not be made size-for-size, that would have produced an interference fit. The only exception to this is the heights of cores where cores are stacked one on top of the other, since in this case the accumulation of errors requires to be kept to a minimum.)
2. The print requires *clearance* where it is not required to fit, and where expansion clearance is required.
3. The number of cores should be reduced to a *minimum*, molding as much as possible directly in the cope and drag.

Rules often appear pedantic or even pedestrian when they are spelled out! However, the application of the rules involves much work which, unfortunately, is often neglected during the urgency involved in the design of patternwork. Although some prints are easily designed, others require much thought, and compromises have to be carefully assessed. Every print requires individual detailed design. It is attention to details such as these that makes the difference between the inadequate and the excellent casting.

Nevertheless, these problems are eliminated if the use of the core can be avoided altogether, as suggested by following the useful Rule Number 3. Not only does the application of this principle reduce dimensional errors, but also the addition of each core involves considerable extra tooling cost, and an additional cost in the production of the casting, sometimes approaching the cost of the production of a cope or drag; it is effectively the third piece of sand to be added to the two original mold halves; thus the costs at this stage may increase by 50% for the addition of the first core. At other

times a small core can save money by avoiding extra complexity of the tooling. Each case needs separate evaluation.

The perhaps unexpectedly high addition to total casting costs resulting from the use of cores arises from the accumulation of a number of minor operations, most of which are usually overlooked. For instance, the core needs to be scheduled, made, perhaps on a capital-intensive core-making machine, stored, de-flashed, retrieved from storage, transported to the molding line, and then correctly assembled into the mold. Errors arise as a result of the incorrect core being made or transferred, or sufficient are broken in storage or transit to cause the whole process to be repeated, or its assembly into the mold gets forgotten at the last moment! Cores are therefore almost certainly more expensive than most foundry accounting systems are aware of. (The costs of chills, and of scrapped castings, are similarly illusive and therefore generally underestimated or completely overlooked.)

A further use of cores, in addition to their obvious purpose in providing detail which cannot be molded directly, is that the running system can often be integrated behind and underneath them, the main runner and gates being located beneath side or end core(s). This is a valuable facility offered by the use of a core and should not be overlooked. In a number of castings the addition of a core may be for the sole purpose of providing a good running system. Such a core is often money well spent!

Where a complex array of internal cores has to be loaded into a drag, as in the case of the assembly of an automotive crankcase for instance, it is common to arrange for the cores to be preassembled in an assembly jig, and for the complete core package to be lowered into the drag. This saves time on the assembly line.

The problem with the automation of core-assembly systems is finding the core again after it has been put down on, for instance, a conveyor or a storage rack. This is a difficult job for a robot, since extreme accuracy is required, and the cores are often of extreme delicacy. Although this problem is being increasingly well addressed by vision systems and improved robots, clearly, one method of solving this problem is never to put the cores down in the first instance. This simple solution is powerful.

Schilling (1987) has succeeded in developing this concept with a unique system of making and assembling cores in which the cores are not released from one half of the opened core-box until the other half of the core has already been located in the core-assembly package. In this way the cores are assembled completely automatically and with unbelievable precision. Cores are located to better than 0.03 mm, allowing them to be assembled with clearances which are so small that the cores could not be assembled by hand. In fact the cores are sprung into place with interference fits. The rigorous application of this technique means that castings need to be designed for the process, since the assembly of each core is by vertical placement over the previous core. For instance, any threading of cores through holes in the sides of other cores, such as often occurs with port cores through the water jacket core of a cylinder head casting, is not possible. This disadvantage will limit the technique to partial application, loading some but not all cores of a cylinder head, for instance. Even this would be an important advance.

The fundamental objection to this super-accuracy technique is the requirement for the plant to run with sufficient reliability. Because the cores are never released, but always under the control of a core box, there can be no buffer stock of cores between operations. A typical core assembly system involving this principle might involve at least 30 or 40 machines including core blowers and robots, etc. Even if the machines were of excellent reliability, each having an up-time of 95–98%, the multiplication of all those values results in an overall reliability for the whole operation of usually less than 50%. This is a serious disadvantage that requires an order of magnitude increase in maintenance effort and skill to reduce this drawback.

A final note in this section relates to cope-to-drag location. This is, of course, of primary importance. Failure to achieve good location results in a mismatch defect. For the case of precision core packages, the sand mold is not contained in a box, and thus is located directly with a sand-to-sand location. Since this is defined from the pattern-work, the location relates perfectly to the casting details, and mismatch is therefore not possible.

In foundries using molds contained in molding boxes, however, mismatch is unfortunately all too common and is usually the result of the use of worn pins and bushes which are used to locate the boxes. Southam (1987) analyzes the effect of the errors involved in the pin and bush location system. These are numerous and serious. The pin to bush clearance is typically 0.25 mm, and given an apparently acceptable additional wear of 0.35 mm, he finds that the total possible mismatch between cope and drag molds is as much as 1.5 mm. (Mismatch is a lateral location error, and not to be confused with the vertical precision with which cope and drag meet, which is normally of the order of  $\pm 0.1$  mm.)

He proposes, therefore, a completely different system, in which mold closure is carried out in a special station, where the cope and drag boxes are simply guided by wear blocks fixed to the outside edges of the box. These slide against two guides on the long side of the box, and one guide against the narrow side of the box during molding and closing operations. The boxes are held against the guides by light pressure from springs or pneumatic cylinders. The system appears deceptively simple, but actually requires a certain amount of good engineering to ensure that it operates correctly on mold closure, as Southam describes. Although Southam calls his method the three-point registration system, it is in reality a classical six-point location system, since he uses a further three points to locate the drag in a parallel plane to the cope during closure (the six-point location system is discussed in relation of casting datums as Good Casting Rule Number 10).

The ability to locate cope to drag with negligible error has a number of benefits, which Southam lists. The maintenance and replacement of worn pins and bushings is a foundry chore and expense which is eliminated. Instead, only three guides on the closer and three each on the cope and drag pattern need to be checked, and the effect of wear of these parts on mismatch is minimal because the resultant displacement is largely self-compensating. In addition, the foundry will be capable of producing castings with thinner walls, reduced dressing, reduced machining, and improved appearance.

---

## 18.3 MOLD ACCURACY

### 18.3.1 Aggregate molds

Buyers of castings have been traditionally prejudiced against sand castings as opposed to the various varieties of metal molded castings because they have long memories. They recall, or perhaps imagine they recall, the time when most sand castings were made individually by a bench molder or floor molder, equipped with a wheelbarrow, watering can and shovel to produce his greensand mix, together with a wood pattern that had usually seen better days. Working practices encouraged additional variability, for example by rapping or vibrating the pattern to ease its withdrawal from the mold. Lifting off by hand or crane produced similar inaccuracies, as did errors in draft angle from hand-made patterns. All these variations would usually result in an oversized mold. The addition of mold and core washes would add further variation.

A typical problem in hand-molded castings was the variability of core location. This arose because a core laid in a print on the main cope/drag joint would usually be a poor fit. If it sat proud of the

surface, then on the closing of the mold the core would be forced to settle, by deforming either the cope or the drag. Depending on which happens to have been more densely rammed that day, the core would be accommodated more in the drag or the cope, so that detail on the casting would vary up or down from day to day, and from casting to casting.

Originally most sand molds were made using greensand. This is a mixture of sand, clay, and water, often in the form in which it was dug out of the local hillside. As such it would be termed a natural greensand. Such natural products were a pleasure to work with, but its variable content of clay, and variability in the type of clay, together with variations in water content, necessarily resulted in rather variable castings.

Later, more controlled greensand mixtures were created by the use of clean, washed silica sands that were mixed with selected clays and other additives to form synthetic greensands. These dough-like mixtures were rammed around the pattern to form the mold. The synthetic sands could give rather harder and more reproducible molds. Additionally, developments away from hand compaction to small-scale automation, such as jolt-squeeze compaction, have slowly given way to massive, fully automated plants with sophisticated high-rate compacting mechanisms, which produce very-high-density molds of impressive rigidity. Such molding methods produce the highest accuracy yet achieved by the greensand route.

Studies like those of Bates and Wallace (1966) show how the greensand mold deforms less during casting as the mold density increases, while those of Rao and Roshan (1988) confirm that the final castings improve in accuracy as the compaction is improved.

Naturally, the use of a well-controlled synthetic greensand, with a metal pattern, and the mold reproduced by an automated molding process yielding uniformly hard molds, was a substantial step forward. Such systems continue to be widely used today for large-volume production with the highest rates of production and highly competitive economics. Despite these benefits, it may be no surprise that the high-pressure molding process has brought its own crop of new problems in the quest for accuracy. These include distortion of tooling if not adequately constructed, and of spring-back of the mold because of the elastic behavior of the highly compacted and highly stressed sand mold.

One of the consequences of requiring an accurate pattern and accurate mold is the requirement for *room temperature operation*. Clearly for all those pattern and molding processes that have to operate at high temperature raise the danger of (i) distortion of the tooling and (ii) poor temperature control leading to temperature variation, leading in turn to dimensional changes.

A further step in the production of accurate, very hard molds has been developed in recent years. This involves the use of chemically bonded sand. The ability to cure the binder at room temperature has had a further important benefit; the tooling remains accurate, suffering neither expansion nor distortion by significant changes in temperature. In fact, providing the tooling is made from metal and/or resin, the tooling never deviates by more than a few degrees from the temperature at which the toolmaker made it. This, together with the fact that the mold or core can cure while in contact with the tooling, are the two vital keys in the construction of accurate molds. They have revolutionized the concept of the production of accurate castings.

One of the major advantages for accuracy enjoyed by the aggregate mold is not only its reproducible temperature during its formation, but also its reproducible temperature at casting. This is always reasonably close to room temperature. A temperature variation of 20°C will produce a change in length of approximately 0.02%, or 0.1 mm in 500 mm. This is a useful stable base from which to start, and contrasts with the problems suffered by metal dies that are not easily controlled to this

precision. In fact a variation of die temperature of 100–200°C would not be uncommon, with a consequent change of size of up to 0.2%, or 1 mm in 500 mm. This represents a serious error in a casting that is required to maintain a wall thickness of 2.0 mm. Figure 18.2 is a brief summary of the competing processes.

Nowadays the hard sand core assembly technique is perhaps the most accurate of all the casting processes, especially for castings exceeding 100 mm in size (Figure 18.3).

Such statements are not easily justified, however, because individual foundries differ widely in their capability, often simply because of attention to detail. Also, individual castings suit some processes and not others. Moreover, as a result of the new standards set by precision sand processes the competitive processes have improved markedly. Thus although it is true to say that sand casting has come a long way in recent years, so have all the others!

Thus although our castings buyer no longer has any justification for rejecting aggregate molded castings, he might still be justified to select a permanent mold of some kind. The phrase ‘metal die’ continues to have an *aura* of engineering excellence, and ‘pressure die casting’ has the *impression* of having an advantage of consolidation by pressure. Producers of sand castings clearly need to market their new achievements.

Core making has gone through a similar revolution. The two main original processes for making cores employed dry sand (i.e. dried greensand) and linseed-oil-bonded sands. Both processes had in common the transfer of the core from the corebox in its green, or soft, state directly into a specially shaped cradle or carrier, often called, rather confusingly, a ‘drier’. The core at this stage was so weak that it would deform at the touch of a finger. It was then hardened by drying in an oven for an hour or more. Naturally, the opportunities for loss of accuracy were plentiful. Neither process is much used today, to the relief of most casting engineers.

A great improvement in accuracy came with the development of chemical binders that would allow the core to be hardened in the core box. In this way cores of very precise form could be guaranteed and are nowadays commonplace in the industry.

The original chemical-binder process used sodium silicate that was cured by carbon dioxide gas, often known as ‘the CO<sub>2</sub> process’ for short. This process was useful for molds, but never popular for cores for the casting of Al and iron alloys because the heat of casting fused the silicate bond to the sand grains, producing a glassy bond of such strength that the core could not be subsequently removed from the casting. Its strength resembled that of concrete, and for many aluminum alloy castings the heat-treated core exceeded the strength of the casting. Attempts to remove the core therefore often led to the destruction of the casting!

The Croning shell process, often known for short simply as the shell process, was another step forward. Here the binder was a phenolic resin, pre-coated onto the sand grains and solidified as a dry coating, thus allowing the sand to be blown or dumped in a dry, free-flowing state onto the pattern. The pattern had to be heated to melt and cure the resin in the thin shell of sand in contact with the pattern. Because of the use of heat for curing there was the danger of distortion of the tooling, and the biscuit-like core was sufficiently thin that it too was subject to distortion if not carefully handled and stored. For aluminum alloy castings the heat input from modern thin-walled castings is starting to give problems because of the incomplete breakdown of the resin after casting, with the result that de-coring is returning as a problem, although developments continue in an attempt to overcome this.

The hot-box process again involves the curing of the core inside the box, and in general gives much improved de-coring performance. However, the problems of heating and controlling the temperature of



core boxes, and the distortion of tooling, and the rate of diffusion of heat into sand, all remain to limit the size of core which it is feasible to produce by this technique. It remains a useful and economical process for cores where such limits are acceptable.

The various cold (or more accurately room temperature) curing processes are not subject to the same limitations. Large products can be produced so that not only internal cores for castings, but also whole molds, can be manufactured by these processes. This has allowed the opportunity for the creation of the 'core-assembly' technique for the production of a mold. Because the tooling and the mold are all at room temperature, no thermal expansion or distortions arise to impair accuracy. For this reason the core-assembly technique is probably the most accurate molding process in use today, and can produce the most accurate aggregate mold castings. The process rivals the accuracy of other near-net-shape processes such as investment casting and high-pressure die casting (Figure 18.3).

The control problem faced by users of chemically bonded sands is that of controlling the strength of the cured sand. Continuous mixers are notoriously difficult to control; the quantities of sand and resin that are processed through the mixer change erratically, so that the quality of mixed sand is often not reproducible from time to time during the day. This will, of course, alter the strength of the molds and cores, resulting in changes to the size and shape of the casting. Some progress is being made in using continuous monitoring and feedback control on the mixers. However, the problem is resolved to a certain extent by the use of batch mixers, where ingredients can be weighed into a mixing bowl. This still leaves the problem that the chemistry of the components of the binder themselves needs to be controlled within close limits. This is an area of continuing concern, since organic resins are not easily characterized nor the chemical processing by the resin supplier controlled to the degree a founder might wish. The problem may already be limiting the accuracy of castings produced by this process route.

One interesting hard sand molding process not requiring control over materials of imprecise chemistry such as resins is the vacuum film molding process, or V process, in which the mold is sealed on all sides by a plastic film, and the sand is consolidated by the application of a vacuum. An investigation by Grote (1982) into the reproducibility of greensand, cold set, and V process confirmed that cold set (a room-temperature-cured resin binder) and V process had similarly good reproducibility, and both were better than greensand, although his version of greensand was probably less than optimum!

A final problem remaining for the sand mold is that of retaining its accuracy when subjected to the shock of being filled with molten metal. This problem includes phenomena such as the thermal distortion of the mold, its deformation under the weight of metal pressing against its walls, and the tendency for cores to float. All these matters are now usually controllable within close limits, particularly for a wide variety of non-silica aggregates and binders. For silica sand, however, we cannot avoid the 1.5% linear expansion at 570°C as it experiences its alpha to beta quartz transition. This is a major factor affecting the accuracy and reproducibility of castings, as illustrated, for instance, in the work by Jennings (2001) in which castings enjoy a standard deviation ten times less when cast in zircon sand which suffers no such phase change.

### 18.3.2 Ceramic molds

Ceramic molds as used in investment casting have enjoyed the reputation of being the most accurate of all the various mold types available. This is a curious perception, which may be the result of the process being for many years limited to the production of rather small castings where dimensional problems were naturally too small to be of concern. It probably also relates to the wonderful

appearance of investment castings, with such excellent surface finish and sharp, fine detail, giving the comforting impression of accuracy.

However, when ceramic molds are produced in sizes similar to those of other casting processes, such as precision sand core assembly processes, the dimensional problems of investment castings are seen to be non-trivial. This is hardly surprising in view of the multiple operations involved in the production of a ceramic mold, each of which can introduce errors. These include the injection of the wax into the aluminum die; the temperature of both the wax and the die affect the size of the wax pattern. The temperatures of the slurry tank and the drying room will similarly contribute an effect during the building up of the shell. The firing of the ceramic involves a certain amount of contraction of the ceramic as the bond is created, and the temperatures of the mold and the metal at the time of casting are other key influences. During the time that the molten metal is in the mold, the mold suffers creep as it sinters and softens, often leading to swelling or other distortions of the casting.

Beeley (1972) shows how the expansion characteristics of different ceramic shell materials are strongly affected by how much silica is contained. He also quotes Carter who showed that a Co–Cr alloy in an investment mold shrinks by 1.6% when the mold is at room temperature, but less than 0.3% when heated to 1000°C. Clegg and Das (1987) evaluate similar problems with Shaw process molds, finding that the linear dimensions of the mold are greatly affected by the time and temperature used for firing, by the composition of the ceramic, and by the size of casting which is produced.

To summarize the dimensional problems of ceramic molds, it seems a tribute to the dedication and perseverance of the industry, rather than to the intrinsic merits of the process, that all of these problems are held within tolerance sufficiently well that an acceptable product can usually be made.

### 18.3.3 Metal molds (dies)

Castings produced in zinc-based alloys by the pressure die-casting process represent a level of accuracy which is hard to beat (Figure 18.3), representing one of the casting industry's most accurate products. This is because of the low temperatures involved. The metal die is accurate, and distorts very little, and the casting itself contracts little during its limited cooling to room temperature. (By extension of this reasoning, plastic injection moldings are similarly highly precise.)

For higher-melting-point materials, however, the problems mount rapidly. Table 18.1 shows how metal dies suffer increasing problems with thermal shock and fatigue as the temperature of the casting alloy increases. The difficulties are such that although Mo dies have been tried for a stainless steel, the results were not satisfactory and so far as is known no-one now uses the process. Even for lower-temperature materials such as Al alloys, the degradation of the surface of the die by the development first of fine cracks, leading to general crazing, and finally resulting in major disintegration of parts of the surface, leads to inaccurate and roughened products long before the die becomes so bad that the decision to abandon or rework it becomes unavoidable. These problems are common in long-running aluminum alloy castings made by HPDC and gravity die (permanent mold) casting. Total failure of the die by catastrophic cracking is also sometimes suffered.

Magnesium presents less of a problem when cast into metal molds because the heat content of magnesium is significantly lower than that of aluminum, resulting in reduced thermal shock to the die. In addition magnesium dissolves iron less readily than aluminum, so that 'soldering' to the die, a localized welding effect, with the consequent gradual removal of die surface, is reduced. The attempt to solve the soldering problem in aluminum alloys by increasing the iron content of the alloys to

**Table 18.1** Die life for different die materials

Alloy base	Rubber	Graphite	Cast iron	Steel			
			Gravity (permanent mold)	Gravity (permanent mold)	Low pressure	High pressure	Squeeze
Zn	Good	Good	Excellent	Excellent	Excellent	Excellent	Excellent
Mg	—	—	Good	Excellent	Excellent	Excellent	Excellent
Al	Limited	Limited	Good	Satisfactory	Satisfactory	Tolerable	Excellent
Cu	—	—	Tolerable	Tolerable	Tolerable	Rare	Tolerable
Cast iron	—	—	Tolerable	Tolerable	Rare	—	—
Stainless steel	—	—	—	—	—	Mo-based die	—
Steel	—	Griffin only	—	—	—	—	—

near-saturation levels is only partially successful since some sticking of the casting together with erosion of the die can be experienced.

The standard of construction of dies for HPDC is necessarily extremely high. This is a consequence of the requirement for the die to fit into, and be operated within, the massive (and expensive) machine tool that is the HPDC machine. The accuracy of fit between the various parts of the die also needs to be excellent to prevent the penetration of liquid metal at the high pressures used for injection. Between each shot the die is sprayed with a coolant and lubricant and/or parting agent. The parting agent gives minimal build-up problems on the die, contributing significantly to the ability of HPDC to maintain the accuracy of its products (unlike, for instance, gravity die casting, where a rather thick die coat is used).

In fact it seems that for HPDC one of the most significant variables affecting the size of castings is the temperature at which the castings are ejected from the die. This is because if ejected early, the casting is hotter, and thus cools and contracts over a greater temperature range without the constraint of the die, thus finishing smaller. A casting ejected late cools more in the die, so its contraction is restrained by the rigidity of the die; the casting is stretched plastically, as by medieval torture on a rack, thus finishing larger.

In low-pressure and gravity die casting the standard of die construction is considerably lower. This is because the die does not need to be fitted into a precise machine, but is usually serviced by simple bolt-on actions such as rack and pinion, or simple hydraulic cylinders, which actuate opening and closing of the die. The gravity die-casting industry is therefore less capital-intensive, and grows more easily in a piecemeal manner. It is more labor-intensive than the HPDC industry. The two processes are not often mixed in the same foundry.

The lower rates of filling of the die under gravity require the die to be coated with an insulating ceramic layer known as a die coat. This is usually sprayed on at the start of a shift, and cleaned off by grit blasting prior to renewal. The coating may become damaged during the production of a run of castings and might require running repairs by the operator. The die coat is therefore a major variable in the size of gravity and low-pressure die castings. Its thickness of application will vary from day to day because the spray techniques for its application are not easily controlled. Also, parts of the coating on faces with minimal relief or draw will wear during the production run, giving slowly increasing sizes of castings.

The die itself is subject to wear in many ways. In particular, the working face will be slowly eroded by repeated cleaning and recoating, in addition to any thermal damage it may be suffering. The moving parts of the die include slides and other mating components which are subject to general sliding and abrasive wear, particularly if sand cores are used in the mold.

Table 18.1 indicates some of the different materials used for dies. For HPDC dies the construction material is usually a special hot-work-tool steel containing chromium for greater strength and hardness, oxidation resistance and good response to nitriding. It is usually heat-treated to achieve its optimum strength and toughness, and finally nitrided to give an extremely hard-wearing surface. Gray iron would not be adequate for pressure dies because it lacks strength and fatigue resistance. Furthermore, its graphite flakes would tend to open up by oxidation, degrading the integrity of surface which would be needed against the penetrating action of liquid metals at high pressure.

Gray iron is, however, widely used for gravity and low-pressure dies. This is because the filling of molds under gravity or low pressure introduces only gentle pressurization of the surface by the melt, and the surface is protected by the ceramic die coat. Also, the iron is highly castable, allowing the

rough die parts to be produced quickly and usually without problems of porosity or other unsoundness; the castings are easily machined to final size and shape; the material has good thermal conductivity and fair resistance to thermal shock. Weight is easily reduced by sculpting the back of the die to give a mold of even thickness.

Graphite is occasionally chosen as a die material. It is easily machined, and is not wetted or attacked by most metals (magnesium would be a spectacular exception!). For zinc alloys, therefore, it has been used with success, although care is required in longer runs to avoid damaging the die by mishandling, since its strength is low. The material is not useful for aluminum alloys, because the graphite oxidizes increasingly rapidly at temperatures above about 350°C. After two or three casts of aluminum alloy, the die is unusable. Treatment of the surface by a protective silicate wash extends the die life a little.

This experience makes the use of graphite as a die material in the Griffin process all the more impressive. Here, railway wheels are cast in steel that is displaced into the die by low pressure. The wheels are produced closely to net shape, so that they require little machining (Kotzin 1981).

---

## 18.4 TOOLING ACCURACY

Tooling is taken to include the pattern and its core boxes, or the die, and any measuring or checking jigs and gauges.

The problem of constructing the pattern, allowing correctly for the contraction and distortion of the casting, has already been discussed and will not be dealt with here.

The wear of patterns used in sand casting causes the casting to become undersize, whereas the wear of dies used in die casting causes the casting to become gradually oversize. An effect opposite to wear happens as a result of build-up problems on the tooling. Patterns for sand casting are subject to the deposition of small amounts of sand and binder, and the gradual accumulation of release agents. Dies may accumulate layers of die coat.

Distortion is another problem. Wood is a useful and pleasant material for pattern construction. It is easily worked, light to handle, and easily and quickly repaired or modified as necessary. Even so, it is not a contender for accurate work because of its tendency to warp and shrink. A good patternmaker will attempt to reduce such movement to a minimum by the careful use of ply, taking care to join layers to cross grain where possible, and affixing strengthening battens. The use of various stabilized woods and simulated wood-like materials has also helped considerably (Barrett 1967). Nevertheless the ultimate stability in tooling is only achieved with the use of metal or cast resin in metal frames.

Cast-resin patterns, which are backed with wood frames, are less reliable; the warpage of the wood distorts the internal resin shape, usually within a month or so. After a year the tooling is seriously inaccurate, so that cores will not assemble properly. In contrast, resin patterns cast into aluminum alloy frames for strength and rigidity are usually extremely reliable. However, some resin systems such as polyurethanes tend to suffer from the absorption of solvents from the chemical binders in the sand, and so can suffer swelling and degradation (Gouwens 1967).

The working temperature of tooling affects the casting size directly; a warm pattern will give a slightly larger casting. If we consider an epoxy resin corebox cast into an aluminum alloy frame, the box will largely take its size from the temperature of the metal frame (i.e. not the internal lining of epoxy resin) which has a coefficient of expansion of  $20 \times 10^{-6} \text{ K}^{-1}$ . If the temperature at the start of the

Monday morning shift is 10°C, and if the returning sand creeps up to 30°C by the end of the morning, then for a 500 mm long casting the 20°C temperature rise will cause the castings to grow by  $20 \times 20 \times 10^{-6} \times 500 = 0.2$  mm. This is not large in itself, but when it is added to other random variables the uncertainty in the final casting length becomes increasingly out of control.

Anderson (1987) has emphasized the important requirement that for the most accurate work the pattern or die should be utilized as an adaptive control element in production. Thus it needs to be built in such a way that it can be modified to produce the required size and shape of the casting. The use of patterns split transversely across their major length is common. The prior insertion of a spacer in this split allows the spacer to be removed and replaced by shims thinner or thicker as necessary. Such simple techniques involve only modest extra expense during the construction of the pattern but are a reassurance against the possibility of major expensive rebuilds later.

---

## 18.5 CASTING ACCURACY

For a good general review of accuracy, precision, and tolerance concepts in casting manufacture the interested reader is recommended to the paper by Anderson (1987). We shall rely on some of the major points Anderson raises in this section.

### 18.5.1 Uniform contraction

This section is an examination of the various effects that follow from the strains and consequent stresses in the casting/mold system as a result of the linear contraction of the solid casting as it cools. Uniform contraction and distortion are considered separately. A distorted casting can usually be straightened, whereas a casting that is uniformly oversize or undersize is scrap.

Following Figure 7.1, when the contraction in the liquid state and most of the contraction on freezing will have been completed, the casting has cooled sufficiently to develop some coherence as a solid. Further cooling in the solid state will cause the casting to contract as a whole.

The point at which the casting develops its solid-like character is different for long- and short-freezing-range alloys. For short-freezing-range material the point is reached when the casting has developed a solid skin. For the case of long-freezing-range alloys, the point is marked by the development of a coherent skeleton of solid dendrites.

At this stage of freezing, since the casting fits the mold rather well, having been poured in as a liquid (and therefore at that earlier stage fitting perfectly!), as it cools further and contracts, something has to give.

It is not the case that either the casting or the mold will yield. Both yield. The action of the casting on the mold causes an equal and opposite action of the mold on the casting. The degree of yielding of the casting and mold depends on the relative strengths of each. Naturally, this varies greatly from one casting/mold system to another.

The contraction of the casting from its freezing temperature to room temperature can cause the patternmaker sleepless nights. This is because the pattern must be made oversize by an amount known as the contraction allowance (or patternmaker's shrinkage allowance) so that the casting will finally finish at the correct size at room temperature. However, the patternmaker often does not know exactly what allowance to use when he starts to construct the pattern.

This was not so important in the ‘bad old days’ (perhaps ‘the good old days’?) when castings were regarded only as ‘rough castings’ having plenty of machining allowance. However, now that greater accuracy is being sought in the quest for a ‘near net shape’ product, the problem has become serious; the patternmaker risks finding that the wrong allowance was chosen only after the first casting is made! This is the emergency scenario when the tooling has to be modified or remade, but the tooling budget has already been spent, and the deadline for delivery is about to be passed. The contents of this small chapter are recommended to the reader as the only procedure known to the author to avoid this disaster.

The Imperial System of measurements gave us a vast legacy of choice of presentation of this data. For instance, for simple and heavy aluminum alloy castings many are made using an addition of ‘5/32 inch per foot’ to all the linear sizes. This corresponds to the widely used contraction allowance of ‘1 in 77’. The author has given up these various units and ratios in favor of a simple percentage, in this case 1.30%.

For other aluminum alloy castings with larger internal cores, such as cylinder blocks, the allowance is only 1/8 inch per foot, or 1 in 96, or, as recommended here, 1.04%.

Other aluminum alloy castings such as sumps (oil pans) and thin-walled pipes contract even less. A contraction of 0.60% is common.

Whereas the patternmaker would originally have chosen a special wooden rule whose scale was expanded by the correct amount so that he could read the dimensions directly, without conversion problems, this clearly limited him to specific contraction values. Nowadays, the greater accuracy requires that intermediate values must be chosen, such as 1.15, or 1.20%, etc. for different castings. These are now easy to apply with the use of electronic and digital measuring instruments, which can be programmed for any value of contraction. In fact, a virtual solid model developed in the computer should be capable of allowing for three different contractions along each of the three perpendicular axes.

The different contractions are the result of different degrees of constraint by the mold during cooling. For instance, in the case of zero constraint, a casting such as a straight bar will contract freely to its maximum extent. We can therefore calculate this rather easily, assuming an average linear contraction. For instance, for Al–Si alloys the coefficient of thermal expansion is close to  $20.5 \times 10^{-6} \text{ }^\circ\text{C}^{-1}$  and the total cooling from  $660^\circ\text{C}$  to  $25^\circ\text{C}$ . From this we can predict the contraction as  $20.5 \times 10^{-6} \times 635 = 0.0130$  or 1.30%, in exact agreement with practice.

Turning now to the case of high mold constraint, it is possible to envisage an ideal case in which a large box casting with thin walls was cast around a large, rigid sand core. If the wall thickness of the casting is imagined to be vanishingly thin, like a sheet of paper, then its strength will be negligible and the mold not compressed at all. Thus the casting will not be allowed to contract; its paper-thin walls will be forced to stretch. We can therefore envisage in principle the case of infinite constraint in which the casting contraction is zero.

In practice, of course, the real world is filled with casting/mold combinations that lie intermediate between the case of zero and infinite constraint; i.e. part way between 0 and 1.30% contraction in the case of aluminum alloy castings.

How can we obtain an estimate of the degree of constraint, so as to be able to predict the contraction allowance exactly? This is the patternmaker’s problem. It is a difficult question, to which there is no accurate answer at this time. However, we can obtain a useful estimate by the following procedure, which, fortunately, is good enough for many purposes.

In the case of the straight parallel-sided bar casting made in a sand mold, the casting suffers no constraint. We can define this as being a fully dense metal casting, in the case of aluminum having a density of about  $2700 \text{ kg m}^{-3}$ . This casting will contract the maximum amount, which for aluminum contracting from its melting point is 1.30%. In contrast, our thin-walled box casting has maximum constraint, contains maximum sand, and has (when cast and finally emptied of sand) a density of practically  $0 \text{ kg m}^{-3}$ . This simple theory gives us the two extreme points on our calibration curve given in Figure 18.5.

Intermediate points are found from measurements on actual castings, taking the volume of the casting divided by the overall volume occupied by the envelope of the casting (Figure 18.5). The envelope is the shape given by a tight-fitting rubber balloon stretched over the casting. This gives

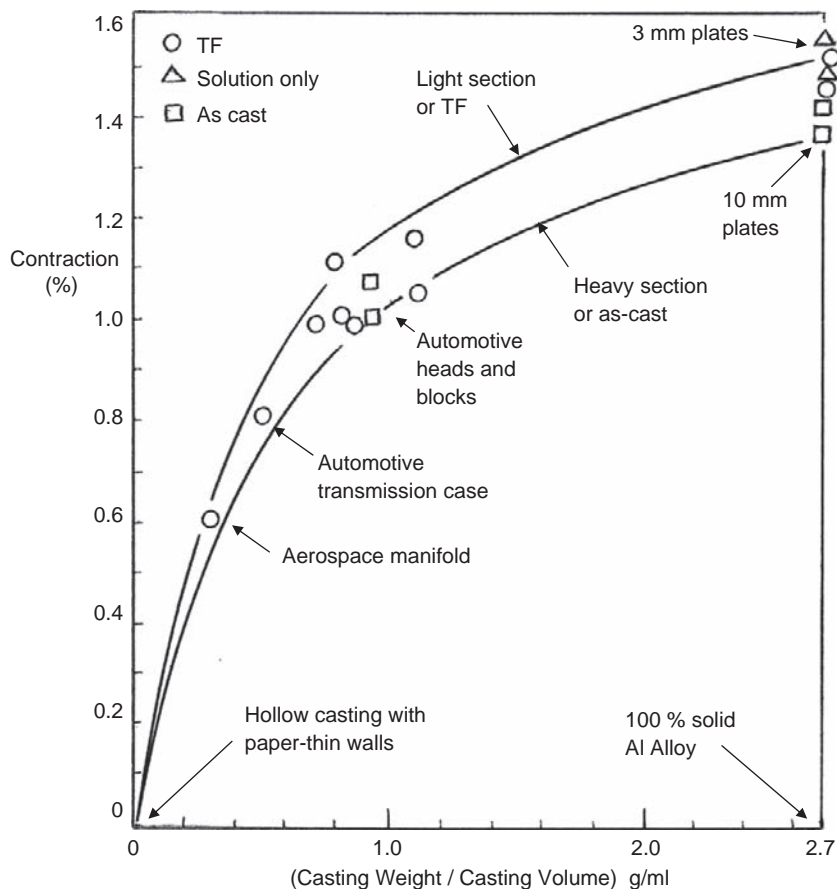


**FIGURE 18.5**

An experimental result from an automotive and aerospace foundry showing how some castings hardly shrink in size at all when cast, whereas other shrink almost the full theoretical amount of the solid metal. The resistance to shrinkage provided by core and mold geometry accounts for the difference.



a measure of the amount of restraining sand it contains, compared with the amount of metal in the casting. Working this out for one or two castings quickly conveys the principle.

When this is carried out accurately, it is found that different varieties of casting are found to lie on a family of approximately parallel curves, all starting and finishing at our theoretical points. Thus the procedure is not absolute, it does not yield a single universal curve. Nevertheless it is a helpful guide in the absence of any better alternative at the present time.

In the case of steel castings the famous result shown in Figure 18.6 can be explained for the first time. Following the procedure that was outlined for aluminum: for the straight bar, the average thermal contraction of steel is around  $16 \times 10^{-6} \text{ }^\circ\text{C}^{-1}$  and the cooling range from freezing point to room temperature is close to  $1500^\circ\text{C}$ . Thus the contraction is  $16 \times 10^{-6} \times 1500$ , which is 2.4%, in agreement with the measured value (Figure 18.6). We can plot this at the full density of steel of approximately  $7850 \text{ kg m}^{-3}$  to define our theoretical point, coincident with our measured point, to define the zero constraint condition. The other theoretical point is, of course, the origin (zero contraction at zero envelope density) as before. Working out the area of the sand mold envelopes of the dumb-bell and H shapes in Figure 18.6, and dividing by the area of the casting, allows us to plot the two remaining points, giving the nearly linear relation in Figure 18.7.

Until better methods become available, it seems reasonable to suppose that each foundry will have to determine for itself an equivalent of Figures 18.5 and 18.7 for each of its processes. For instance, it is well known that the values of contraction allowance for greensand are dependent on the hardness of ramming. Similarly the percentage of binder in chemically bonded sands significantly affects the contraction of the casting. A standard trick to reduce the constraint provided by a central core is to reduce its binder level, or to make it hollow.

These relations for sand molds and sand cores are not expected to apply accurately to metal dies. Here the casting is subject to high mold constraint up to the time of ejection. Clearly the casting contracts freely after this instant.

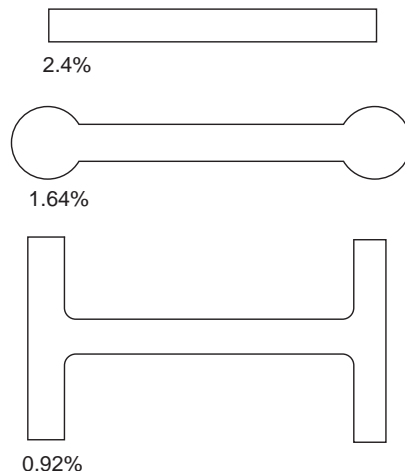


**FIGURE 18.6**

Contraction of steel greensand castings, showing widely different contractions (*Steel Castings Handbook* 1970).

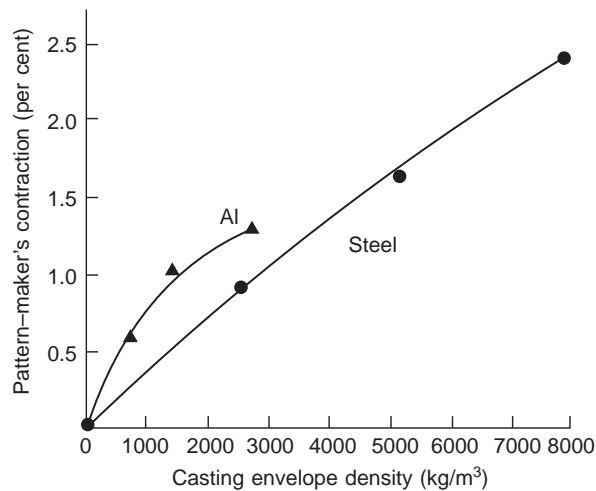


**FIGURE 18.7**

Contraction allowance for aluminum and steel castings as a function of mold constraint.

For Al–Si alloys cast in gravity and low-pressure dies the contraction varies between 0.75% for low-silicon alloys, and 0.5% for eutectic (approximately Al–11Si) alloys (Street 1977), although much of the industry seems to work generally at 0.6%. These low values reflect the high resistance of the die to the contraction of the casting. However, much lower contractions, effectively zero, are occasionally found for thin boxes and window-frame-type castings.

For pressure die casting in magnesium the contraction allowance is 0.7%, whereas for aluminum alloys it is close to 0.5%. The value is at the lower end of the range for gravity and low-pressure dies, indicating the even greater constraint in high-pressure die design.

These figures for the contraction allowance of die castings are the result of the prior expansion of the die from room temperature to its working temperature, and the subsequent contraction of the casting after its ejection out of the die (we shall assume that its contraction whilst in the die is negligible). We can estimate this quantitatively, taking the die working temperature as roughly 350°C on average (the hot face will be nearer 450°C, but the interior of the die may be water-cooled), ambient temperature as 25°C, and the temperature of the casting at ejection approximately 500°C, we have:

$$\begin{aligned}
 \text{Total casting contraction} &= \text{Die expansion} - \text{Casting contraction after ejection} \\
 &= (350 - 25) \times 11.7 \times 10^{-6} - (500 - 25) \times 20.5 \times 10^{-6} \\
 &= 0.60\%
 \end{aligned}$$

Using these rough assumptions and simple logic the answer is seen to be precisely correct. Furthermore, it is clear, as confirmed by experience, that the size of pressure die castings is controlled by the time of ejection of the casting from the die.

For lost-wax castings the problem is compounded by having to take account of the expansion of the aluminum die into which the hot wax is injected, the contraction of the wax pattern, the expansion of the ceramic shell, and the final contraction of the casting itself. This complicated equation is a major source of uncertainty in the accuracy of what is known as 'precision casting'. Regrettably, it is the reason why many so-called precision castings suffer dimensional out-of-tolerance problems.

It is important to note that the pattern contraction allowance can often be different in different directions, because of different geometrical constraints offered by the casting. Thus each of the  $x$ ,  $y$ , and  $z$  axes may require a different value.

It is also important to remember that the casting contraction can be greatly affected by the precipitation of gas during solidification. Girshovich et al. (1963) draw attention to this problem in aluminum-, copper-, and ferrous-based alloys. The author has sobering and unforgettable experience of a major pick-up of hydrogen gas in a 1000-kg holding furnace after the addition of Sr to an Al-7Si-0.4Mg alloy. Over the next 3 days the castings suffered up to 3 vol% porosity, therefore growing linearly by 1% (the 500-mm-long castings growing by 5 mm!). The castings were all outside their machining allowance and were consequently scrapped. Strontium addition was immediately discontinued at that time! The subsequent introduction of better degassing techniques has allowed the question of Sr addition to be revisited. In a related experience with steels, Schurmann (1965) describes how rimming steel ingots that failed to develop any significant rimming action tended to grow a solid crust over the ingot top. The internal pressure in the ingot could not then be relieved by the escape of gas, so the ingot swelled.

Finally, the reader would be forgiven for assuming that the size of the casting was fixed when at last it reached room temperature. However, this is rarely true. For instance, Figure 18.8 shows how the common zinc pressure die-casting alloys continue to shrink in size for the first 6 months or so. Alloy A is then fairly stable for the next few decades. Alloy B, on the other hand, starts to reverse its shrinkage after about the first year. At 100°C these changes can be accelerated by about a factor of 250, effectively compressing years into days, as the time axis shows.

The zinc die-casting alloy ZA27 (Zn-27%Al) shrinks only about one-tenth of the amount of the lower-aluminum zinc alloys (8 and 12%Al), but its expansion is greater, as seen in Figure 18.9. (Incidentally, Figures 18.8 and 18.9 are calculated assuming a factor of 2 increase in reaction rate for every 10°C rise in temperature.)

Aluminum alloy castings also show size changes. For instance, Al-7Si-0.5Mg alloy contracts by 0.1-0.2% after solution treatment and quenching as alloying elements are taken into solution. The castings grow by 0.05-0.15% during aging as the alloying elements precipitate once again (Hunsicker 1980). Gloria (2000) find that Al-8Si-3.3Cu-0.2Mg expands during solution treatment as the CuAl2 phase dissolves.

Figure 18.10 shows the Al-17Si alloy used for wear-resistant applications exhibiting considerable growth at temperatures high enough to allow silicon to precipitate. This growth in service can be reduced by a pre-age at a minimum of 230°C for 8 hours (but a treatment of 260°C for 1 hour would be closely equivalent, using our 10°C rule equivalent to doubling the reaction speed).

Even higher percentage growths are exhibited by white cast irons. At high temperatures, above approximately 900°C, the breakdown of the metastable cementite to stable graphite takes several days. During this period the linear dimensions of the casting will grow by up to 1.6% (Johnson and Nohr 1970). Gray irons will also grow at temperatures down to 350°C, and growth can be catastrophic if the

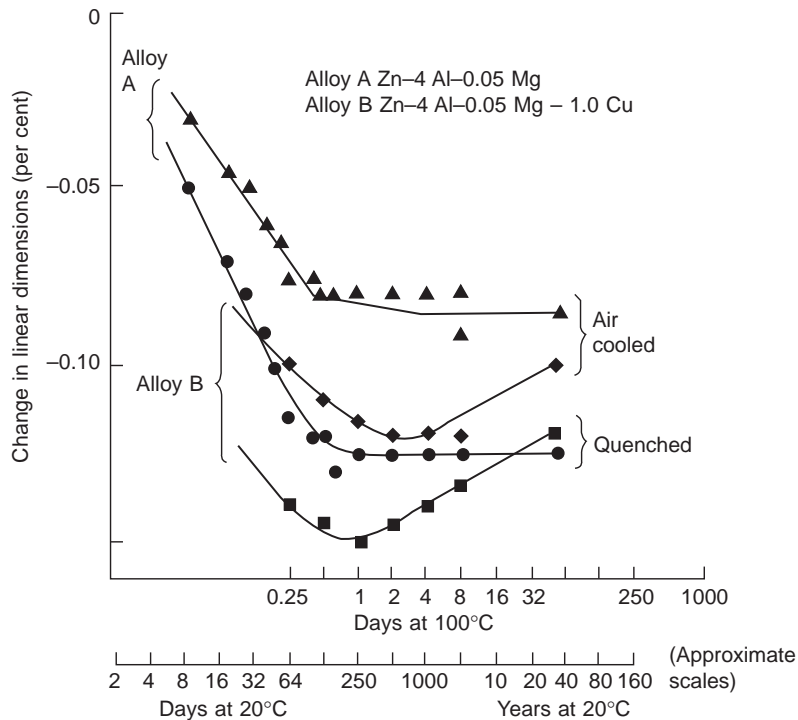


**FIGURE 18.8**

Zinc pressure die-casting alloys (Zn-4Al) showing accelerated aging at 100°C, or slow shrinkage followed by expansion in alloy B taking place in decades at 20°C (data from Street 1977).

iron is cycled repeatedly through the ferrite/austenite phase change. Walton (1971) observed a growth of 3.5% in only 500 hours in a gray iron subjected to cyclic heating to 800°C. Growth can be further enhanced by the internal oxidation of the material. Angus (1976) gives more details of the growth of cast iron at elevated temperatures, and the means by which it can be controlled by control of structure and chemical composition of the iron.

These are just a few examples of the growth and/or shrinkage of castings that can occur in the solid state because of microstructural changes occurring within the alloy. The casting engineer needs to be on guard against such problems.

The changes cause the patternmaker problems when attempting to decide what contraction allowance to use when constructing the pattern. His decision may be right or wrong, depending on whether the foundry check the dimensions of the casting before or (more correctly) after heat treatment, and will depend on the service conditions.

If the allowance was chosen wrongly, giving an undersized casting in gray cast iron, then a heat treatment may save the day by growing the casting by up to 1% or so. However, such good fortune is rare. The choice of contraction allowance prior to making the casting will remain a difficult and risky decision, and will become more difficult as demands on casting accuracy increase.

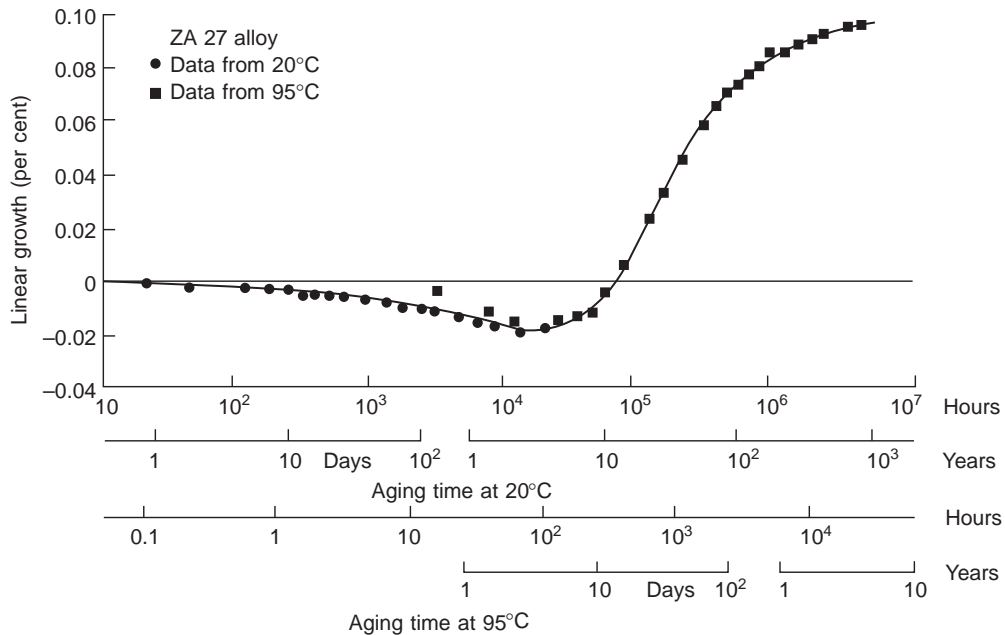


**FIGURE 18.9**

Zn-27Al alloy dimensional changes with time (data from Fakes and Wall 1982).

### 18.5.2 Non-uniform contraction (distortion)

If the casting was cooled at a uniform rate and with a uniform constraint acting at all points over its surface, then it would reach room temperature perfectly in proportion, perhaps a little large, or a little small, but not distorted.

In practice, of course, this utopia is never realized. Usually the casting is somewhat large, or somewhat small, and is not as accurate a shape as a discerning customer would prefer. Occasionally it may be very seriously distorted. We shall examine the reasons for these factors and see to what extent they can be controlled.

#### Mold constraint

Again, wishing ourselves into utopia, we can envisage that if the constraint by the mold were either zero or infinite, in both cases the casting would be of predictable size and correct shape.

In reality of course, different parts of the casting experience different degrees of constraint by the mold. One of the most common examples of this problem is a simple five-sided box with its sixth side remaining open, as shown in Figure 18.11. The closed face wishes to contract as a straight length, whereas the vertical sides have maximum constraint. The result is a compromise, with the straight side shortening with an effective contraction allowance of perhaps 1.2% in the case of an aluminum alloy casting. The vertical sides will be restrained from pulling inwards, and so have an effective contraction allowance of perhaps only 0.9%, or perhaps as low as zero if the walls are very thin. During cooling the

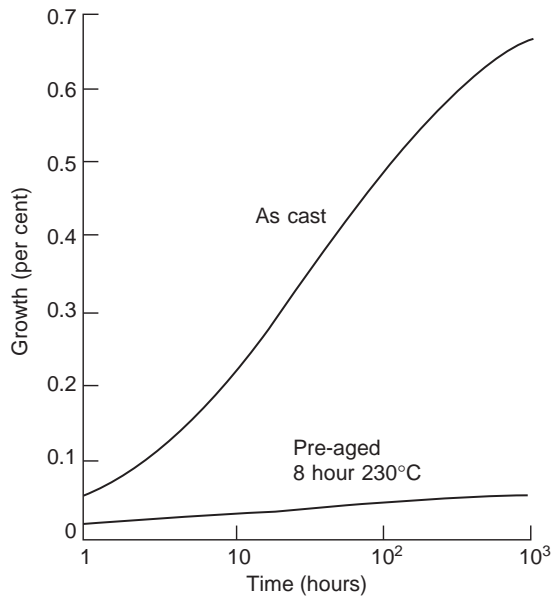


**FIGURE 18.10**

Permanent growth of A390 (Al-17Si alloy) at 165°C with time (Jorstad 1971).

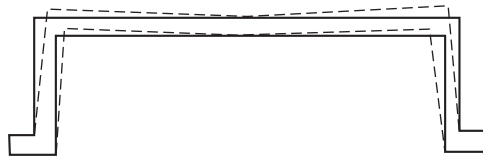


**FIGURE 18.11**

Distortion of an open-sided box casting during cooling as a result of uneven mold constraint.

casting therefore develops a bowed shape. For a hard, chemically bonded sand mold the camber will be approximately 1 mm in the center of the long side of an open box  $500 \times 100 \times 100$  mm with walls 4 mm thick.

The box casting may be cast somewhat straighter by a number of techniques well known to the foundry technologist:

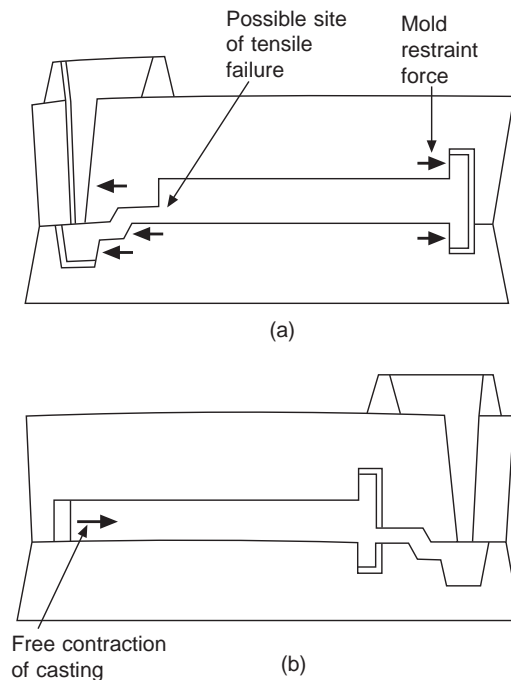
1. The center core can be made weaker, reducing its constraint on the contraction of the casting. This is achieved either by reducing the percentage addition of binder, or, usually more conveniently, by hollowing out the center core. The thin shell of sand thereby becomes hotter, giving greater breakdown of the binder in the case of an organic binder, and so allowing the core to collapse earlier.
2. Tie bars can be connected across the open side of the box, thereby holding the walls in place, and balancing the effect of the contraction of the closed side. The tie bar need not be a separate device. It can be the running system of the casting, carefully sized so as to carry out its two jobs effectively.

This raises the important issue of the influence of the running and feeding system. Unfortunately these appendages to the casting cannot be neglected. They can be used positively to resist casting distortion as above. Alternatively they can cause distortion and even tensile failure as shown in the simple case in Figure 18.12a. Alternatively, if this casting is fed at the flange end, leaving the plate free to contract along its length as shown in Figure 18.12b, the problem is solved. However, note the important point that whether or not casting 'a' has suffered any tensile failure, it will measure somewhat longer than casting 'b'. Thus different pattern contraction allowances are appropriate for these two different constraint modes.

In more complex castings the effect of geometry can be hard to predict, and harder to rectify if the casting is particularly badly out of shape. Especially for large, thin-walled castings requiring close dimensional tolerance it may be wise to include for a straightening jig in the tooling price. This will be an expensive piece of tooling, usually resisted by the customer.

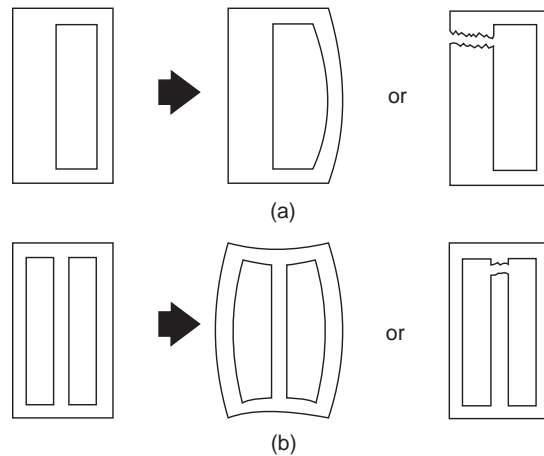
### Casting constraint

Even if the casting were subjected to no constraint at all from the mold, it would certainly suffer internally generated constraints as a result of uneven cooling. The famous example is the mixed-section casting shown in Figure 18.13a. If a failure occurs it always happens in the thicker section. This may at first sight be surprising. The explanation for this behavior requires careful reasoning, as follows.



**FIGURE 18.12**

(a) Effect of the filling and feeding systems imposing constraint on the contraction of a casting. (b) Applying the filling system to the opposite end of the casting eliminates the problem, permitting the casting to contract freely.

**FIGURE 18.13**

(a) Thick-/thin-section casting showing tensile stress in the thick section; (b) even-walled casting showing internal tensile stress.

First, the thin section solidifies and cools. Its contraction along its length is easily accommodated by the heavier section, which simply contracts under the compressive load since it is hot, and therefore plastic, if not actually still molten. Later, however, when the thin section has practically finished contracting, the heavier section starts to contract. It is now unable to squash the thin section significantly, which has by now become rigid and strong. The result is the possible bending of the thin section as tension builds up in the thick section. Under its tensile stress the thick section might therefore stretch plastically, or hot tear, or cold crack.

The example shown in Figure 18.13b is another common failure mode. The internal walls of a casting remain hot for longest even though the casting may have been designed with even wall sections. This is, of course, simply the result of the internal sections being surrounded by other hot sections. The reasoning is therefore the same as that for the thick-/thin-section casting above. The outer walls become cool and rigid, and the internal walls of the casting suffer tension at a late stage of cooling. This tension may be retained as a residual stress in the finished casting, or may be sufficiently high to cause catastrophic failure by tearing or cracking.

The same reasoning applies to the case of a single-component heavy-section casting such as a solid ingot, billet, or slab, and especially when these are cast in steel, because of its poor thermal conductivity. The inner parts of the casting solidify and contract last, putting the internal parts of the casting into tension (notice it is always the inside of the casting that suffers the tension; the outside being in compression). Because of the low yield point of the hot metal, extensive plastic yielding occurs at high temperature. However, as the temperature falls, the stress cannot be relieved by plastic flow, so that increasing amounts of stress are built up and retained.

An example shown in Figure 18.14 shows the kind of distortion to be expected from a box section casting with uneven walls. The late contraction of the thicker walls collapses the box asymmetrically (the casting is at risk from tensile failure in the thicker walls, but we shall assume that neither tearing



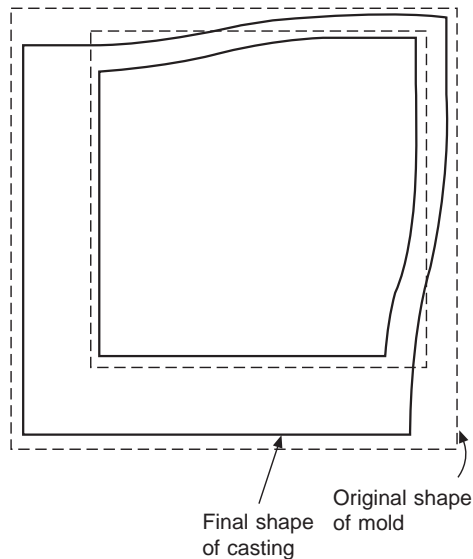


**FIGURE 18.14**

Distortion in an uneven box section casting because of combined casting and core constraint.

nor cracking occurs in this case). There is clearly some strong additional effect from mold constraint. If the central core were less rigid, then the casting would contract more evenly, remaining more square.

There is an important kind of distortion seen in plate-shaped castings which have heavy ribs adjoining the edges of the plate, or whose faces are reinforced by heavy-section ribs. It is often seen in thin-section boxes that have reinforcing ribs around the edges of the box faces. The general argument is the same as before: the thin, flat faces cool first, and the subsequent contraction of the heavier ribs causes the face to buckle, springing inwards or outwards. This is known as 'oil-can distortion'; an apt name which describes the exasperating nature of this defect, as any attempts to straighten the face cause it to buckle in the opposite direction, taking up its new reversed curvature. It can be flipped backwards and forwards indefinitely, but not straightened permanently. Once a casting exhibits oil-can distortion it is practically impossible to cure. The effect is more often seen after quenching from heat treatment, where, of course, the rate of cooling is greater than in the mold, and where the casting does not have the benefit of the support of the mold.

Oil-can distortion may be preventable by careful design of ribs, to ensure that their geometrical modulus (i.e. their cooling rate) is similar to, or less than, that of the thinner flat face. Alternatively, the cooling rate from the quench needs to be equalized better, possibly by the use of polymer quenchant and/or the masking of the more rapidly cooling areas.

In ductile iron castings that exhibit expansion on solidification due to graphite precipitation, the expansion can be used to good effect to reduce or eliminate the necessity for feeders, particularly if the casting cools uniformly. Tafazzoli and Kondic (1977) draw attention to the problem created if the cooling is not uniform. The freezing of sections that freeze first leads to mold dilation in those regions that solidify last. Although these authors attribute this behavior to the mismatch between the timing of

the graphite expansion and the austenite contraction, it seems more likely to be the result of the pressure within the casting being less easily withstood by those portions of the mold that contain the heavier sections of the casting. This follows from the effect of casting modulus on mold dilation; the lighter sections are cooler and stronger, and the thicker sections are hotter and thus more plastic. Any internal pressure will therefore transfer material from those sections able to withstand the pressure to those that cannot. The thinner sections will retain their size while the thicker sections will swell. Tafazzoli and Kondic recommend the use of chills or other devices to encourage uniformity.

In a classic series of papers, Longden (1931–32, 1939–40, 1947–48, 1948) published the results of measurements that he carried out on gray iron lathe beds and other machine beds. The curvature of a casting up to 10 m long could result in a maximum out-of-line deviation (camber) of 50 mm or more. Longden summarized his findings in a nomogram that allowed him to make a prediction of the camber to be expected on any new casting. The reverse camber was then constructed into the mold to give a straight casting. Although Longden's nomogram is probably somewhat specific to his type of machine tool bases, it is presented in Figure 18.15 as an example of what can be achieved in the prediction of casting distortion. It is to be expected that castings of other types will exhibit a similar relationship.

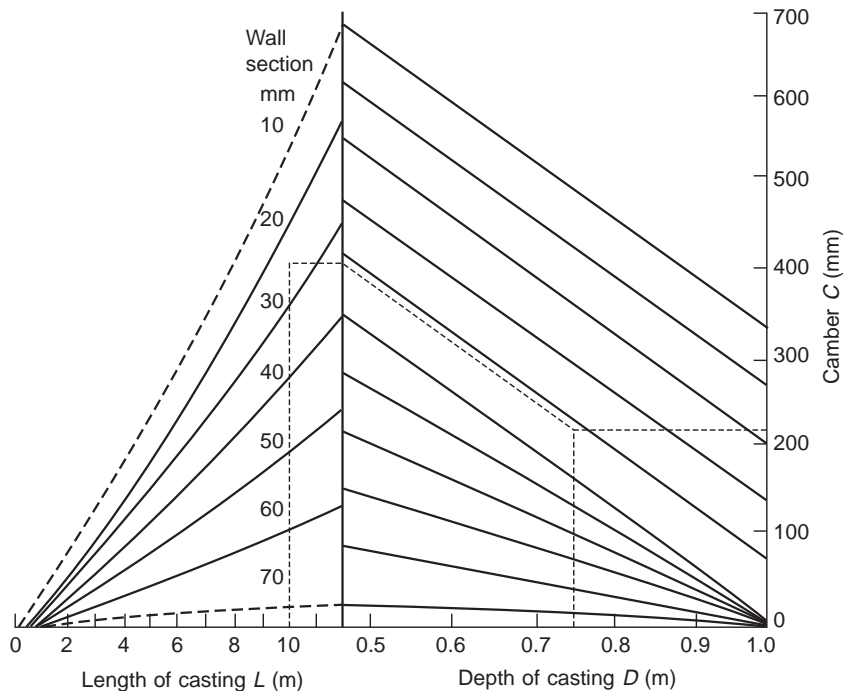


**FIGURE 18.15**

Camber nomogram based on data from Longden (1948) for machine tool bed castings in gray iron. A 10-m-long casting with 25-mm-thick side walls, 750 mm depth will show approximately 210 mm camber (deviation from straight).

We can convert Longden's qualitative summary into a quantitative form, where length  $L$  and depth  $D$  are in meters, and wall section thickness  $w$  and camber  $c$  are in mm. Simplifying Longden's nomogram within the limits of accuracy of the original data, and making the further approximation that the slight curved lines on the left-hand side are straight lines through the value  $L = 1.5$  m, then with perhaps about 10% accuracy for wall thickness  $w$  from 10–40 mm the camber is given by:

$$c = (L - 1.5)(7.62 - 1.073w) - 660D + 310$$

and for wall thickness  $w$  from 40–70 mm:

$$c = (L - 1.5)(144 - 2.03w)(1 - D)$$

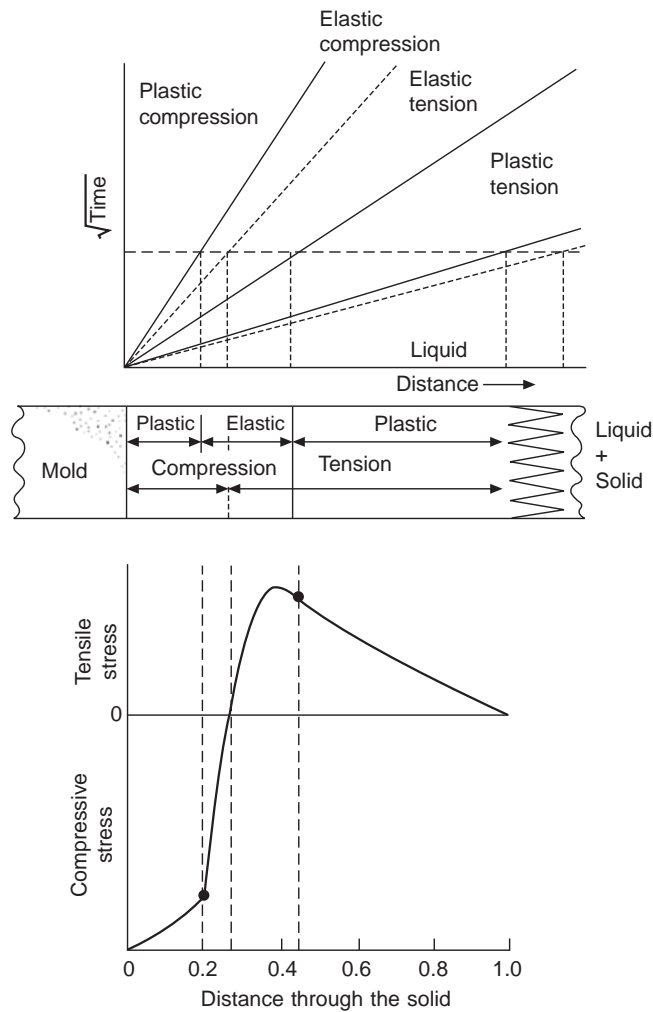
We now move on to a further type of internal constraint that appears to be universal in castings of all sizes and shapes, and which is rarely recognized, but was investigated by Weiner and Boley (1963) in a theoretical study of a simple slab casting. They assumed elastic–plastic behavior of the solid, and that the yield point of the solid was zero at the melting point (not quite true, but a reasonable working approximation) and increased as the casting cooled. They found that plastic flow of the solid occurs at the very beginning of solidification. The stress history of a given particle was found to be as follows. On freezing, the particle is subject to tension, and since the yield stress is initially zero, its behavior is at first plastic. As it cools, the tensile stress on it increases and remains equal to the yield stress corresponding to its temperature until such time as the rate of increase of stress upon it is less than the rate of increase of its yield stress. It then starts to behave elastically. Soon after, unloading begins, the stress on the particle decreasing rapidly, becoming compressive, and finally reaching the yield stress in the opposite direction. Its behavior remains plastic thereafter. Weiner and Boley's analytical predictions have been accurately confirmed in a later numerical study by Thomas and Parkman (1998).

To sum up their findings, in a solidifying material there will be various deformation regimes. These are: (1) a plastic zone in tension at the solidification front, since the strength of the solid is low; (2) a central region where the stresses are in the elastic range; and (3) a zone at the surface of the casting where there is plastic flow in compression. The overall scheme is illustrated in Figure 18.16.

The propagation of the tensile plastic region, the central elastic zone, and the compressive plastic zone are reminiscent of the propagation of the various transformation zones through the sand mold. These waves of strain and stress spread through the newly solidified casting, remaining parallel to the solidification front and remaining at the same relative distances, as illustrated in Figure 18.16.

If the yield stress were not assumed to be zero at the freezing point, but were to be given some small finite value, then the analysis would be expected to be modified only very slightly, with a narrow elastic zone appearing at the solidification front on the right-hand side of Figure 18.16.

The analysis will be fundamentally modified for materials that undergo certain phase changes during cooling. If the crystallographic rearrangement involves a large enough shear strain, or change of volume, as is common in steels cooling through the  $\gamma$  to  $\alpha$  transition for instance, then the material will be locally strained well above its yield point, adding an additional plastic front which will propagate through the material. The phenomenon is known as *transformation-induced plasticity* (TRIP). This additional opportunity for the plastic relief of stress will fundamentally alter the distribution of stress as predicted in Figure 18.16. However, the prediction is expected to be reasonably accurate for many other metals such as zinc-, aluminum-, magnesium-, copper-, and nickel-based alloys, and for those steels that remain single phase from solidification to room temperature.

**FIGURE 18.16**

Elastic-plastic regimes in a simple slab casting (after Weiner and Boley 1963).

The high internal tensions predicted by this analysis will be independent of, and will be superimposed on, stresses that arise as a result of other mold and/or casting constraints as we have discussed above. It is not surprising, therefore, to note that on occasions castings fail whilst cooling after solidification.

Drezet and co-workers (2000) showed that the elastic-plastic model would not be fundamentally altered if creep flow behavior were assumed instead of the elastic-plastic flow behavior with yield stress a function of temperature. They found that such simulations were insensitive to the rheological model employed, but that the deformation was mainly a simple function of the thermal contraction and the conditions for continuity.

Richmond and Tien (1971) and Tien and Richmond (1982) criticize the model by Weiner and Boley on the grounds that they do not take account of the friction at the casting–mold interface. When Richmond and Tien include this they find that the casting–mold interface is no longer in compression but in tension. This is almost certainly true for large castings in metal molds such as steel ingots in cast iron ingot molds, where the pressure between the mold and casting is high, the friction is high, and the mold is rigid. These authors explain the occurrence of surface cracks in steel ingots in this way. However, Weiner and Boley are likely to be more nearly correct for smaller castings in sand molds. Here the interfacial pressure will be less, and the surface more accommodating, and the air gap ensuring that the casting and mold are not in contact in some places. All these factors will reduce the restraint due to friction. Thus their analysis remains probably the most appropriate for medium-sized shaped castings.

### 18.5.3 Process comparison

It is not easy making a comparison between the various casting processes to ascertain their comparative capabilities in terms of accuracy, or possibly reproducibility. There are many separate factors that influence the capabilities of different processes, to the extent that it may seem rather surprising that a casting achieves any approach to accuracy at all. However, it is a pleasure to note that the majority of casting processes do rather well, and some excellently. That is not to exclude the certainty that most could probably do better!

There have been a number of studies attempting to quantify what tolerances are achieved in practice. Useful researches were carried out in Sweden by Villner (1969, 1974) and in the UK by the Institute of British Foundrymen (IBF Technical Subcommittee T571, 1969, 1971, 1976, 1979). These workers took production castings from a number of foundries, covering a wide variety of different metals and different processes. Linear measurements taken from a large number of castings were subjected to multiple regression analysis, a statistical technique used to assess quantitatively the effects of a large number of factors simultaneously. The technique identified the following factors as important:

1. The total area of cores projected in the plane of the mold joint.
2. The wall thickness; indicating that thinner-walled castings were in general more accurate.
3. The mold joint was generally closed accurately to within approximately 0.1 mm showing that the main mold joint was usually one of the most accurate of the mating interfaces within the mold assembly, contributing only a small error to any final dimension across this joint. (Note that lateral error, known as mismatch across the joint, was a separate problem. Mismatch could often be more than ten times the closing error, and could easily scrap castings.)
4. The great value of keeping critical dimensions or reference points all within one half of the mold, or totally within one core was demonstrated. This was a large factor reducing variability.

Apart from the three continuous variables, ‘drawing dimension’, ‘projected area of core’, and ‘general wall thickness’, there were additional factors contributing to variation such as metal type, pattern and mold distortions, temperature variations, coating thickness, etc.

Regardless of these numerous effects, the main result was that the standard deviation  $\sigma$  increased with size of the dimension. Although the regression equation derived by these investigators indicated that  $\sigma$  increases linearly with the dimension, this was only, of course, the result of the regression

analysis itself being carried out assuming linearity, although the assumption of linearity was probably not too bad as a working approximation at this stage.

Taking therefore an example of a hollow casting 5 mm wall thickness, of overall size approximately  $250 \times 200 \times 200$  mm, containing a large body core, Figure 18.3a shows the result for  $2.5\sigma$  where  $\sigma$  is the expected standard deviation ( $2.5\sigma$  encloses 99% of all expected results) (*Castings* 1991). A second study by me in 2000 considered only probable variation in the length of a simple solid casting using  $\sigma$  as a measure. The results of this rather different casting are shown in Figure 18.3b. The similarities between the two plots are probably significant because not only length is seen to dominate.

In fact, from Figure 18.3b it is clear that the variability of processes such as gravity die casting are dominated by factors which are not functions of length, and probably include such variable factors as die coating. This contrasts with processes such as lost foam, and more particularly lost wax, whose variability increases with casting size, reflecting the importance of thermal expansion problems in these processes. Thus lost wax can retain its common name 'precision casting process' only for very small castings. For large castings the accuracy of the process becomes no better than low-technology sand casting (although it retains its excellent surface finish and definition of course).

The processes which shine out as having intrinsically repeatable dimensions are pressure die casting and high-technology sand casting. There are good reasons for this. Pressure die casting is a simple, direct process, operated in a rigidly supported steel die, and which uses no die coat. Sand casting involves more steps, but all the steps are carried out at room temperature so that no significant expansion errors accumulate.

The position of gravity die being systematically below that of the variability of low-technology sand casting was one of the major reasons for the historical choice of 'die casting' as opposed to sand casting for many automotive applications. Now, interestingly, recent advances in sand molding, both in greensand and chemically bonded sands, have overtaken the accuracy possible in gravity die. Even so, the poor image of sand casting lives on in the engineering profession, whereas 'die casting' has the image of cleanness and precision! It is clear that a re-education of the engineering profession, along with ourselves as founders, will take a generation or more.

From Figures 18.3a, b the increase in accuracy for a 500-mm-long aluminum alloy casting when changing from gravity die to a precision sand process is a factor of between 2 and 4. This is roughly in line with measurements carried out on production runs of cylinder heads by Ford of America who found on average that an accurate sand process yielded castings more than twice as accurate as their standard supplies of gravity die castings. This was a critical finding which led to the adoption of aggregate molds using the Cosworth process in North America instead of their previous reliance on permanent molded castings.

In conclusion, pressure die casting and high-technology sand casting are the processes with the greatest capability for reproducibility of dimensions. The lost wax process is accurate for small components, but as the casting size increases it becomes rapidly poorer, eventually becoming as bad as low-technology sand casting at large sizes. Gravity die casting and lost foam casting show intermediate performance.

A word of warning about Figures 18.3a and b is probably necessary. Such comparative diagrams are intended to give a general overview of the capability of the various processes, and to this extent they are useful and fair. In particular instances, though, certain foundries may achieve much better results than the norm and, regrettably, some much worse! Also, some castings of regular shape are

more easily kept to close tolerance, whereas flimsy or complex shapes may prove very difficult. Thus figures such as Figure 18.3 require to be treated with some caution.

Finally, we need to remind ourselves that cast products are not bought simply for their dimensional reproducibility. Surface finish, internal integrity and many other factors, not least cost, are important. This section has been aimed at clarifying and quantifying so far as possible only the ability of a process to achieve a level of dimensional control.

### 18.5.4 General summary

The main factors which control the accuracy of the final casting are briefly listed as a summary:

1. Pattern (or tooling) inaccuracy.
2. Mold inaccuracy.
3. Mold expansion and/or contraction because of temperature or pressure.
4. Casting expansion because of precipitation of less-dense phases such as graphite or gases.
5. Casting contraction on freezing (solidification shrinkage) causing local sinks.
6. Casting contraction on cooling leading to (a) different overall casting size, depending on the constraint by the mold, and (b) distortion if unevenly constrained or unevenly cooled.
7. Casting overall change of size on heat treatment or on slow aging at room temperature.
8. Casting distortion if unevenly cooled by an inappropriate quenchant or too rapid quench from heat-treatment temperature.
9. Casting distortion caused by shot blasting. The compressive stresses introduced into the surface by a peening effect can lead to the distortion of the casting as outlined in Chapter 19.

---

## 18.6 METROLOGY

The technology of metrology has advanced so far over recent years, and continues to advance, such that I seriously thought that this section should be abandoned. However, not all of us have the benefits of modern, computer-controlled, remote scanning laser techniques that operate as 3-D coordinate measuring machines. Thus in this transitional period, while many of us struggle with our traditional systems, there is perhaps room for this section for a year or two more. Those with laser systems are permitted to skip this section.

Even if it were possible to produce an absolutely accurate casting, it would not be possible to prove it! This apparently curious statement is the consequence of errors which occur during measurement. Inexact measuring of the casting will cause the random deviations in the measurements, causing dimensions of the casting to appear too large or too small. Svensson and Villner (1974) point out this problem, and work out the influence of measuring accuracy on the apparent dimensional accuracy of the casting.

It is clear that even if the casting has dimensions which are perfectly correct, even careful measurement will introduce a certain amount of apparent error, and careless measurement will, of course, introduce even more. The more recent introduction of large-size three-dimensional coordinate-measuring machines has significantly reduced these errors, which have been such a traditional problem within the industry.

Even so, problems will remain. For instance, the Swedish workers point out that for small dimensions, and where high accuracy is required, the surface roughness will influence the apparent accuracy of the casting. Thus a change in the surface finish from 75  $\mu\text{m}$  to 200  $\mu\text{m}$  will give an increase of one tolerance grade in the ISO system.

The surface finish influences the measurement and location processes in other ways. For instance, the modern touch probes, which locate dimensions on the casting with the most delicate of contact pressure, effectively only measure to high spots, thus biasing the measurements in one direction: exterior dimensions on the casting are measured oversize, and cored holes appear undersize.

Results from mark-out equipment using a mark-out table and a mechanically scribed line tend to give more averaged results, since minor surface irregularities are cut through.

Similarly, when castings are clamped on to their location points, the small area of the contact points, typically 5 mm diameter, and the high loads which can be exerted by the clamps, ensure that the locating jig point actually indents the surface of the casting by up to 0.25 mm for some aluminum alloy sand castings. Harder materials such as cast irons will, of course, indent less. All surface irregularities are effectively locally smoothed and averaged in this operation. The indentation effect sets an upper limit to the accuracy and repeatability with which castings can be picked up for measurement or machining.

A traditional method of checking the profile of a casting is by the use of template gauges. These are typically sheets of metal which have been cut to the correct contour. On applying them to the casting, the contour on the casting can be seen to be correct or not, depending on the clearance which can be seen between the two. This is an analog technique which can no longer be recommended in these modern times. The gauges are expensive to make. They are also subject to wear, and thus need to be checked regularly, and occasionally replaced. However, what is much more serious, they are difficult to use in any effective way. This is because in practice the contours never match exactly. The problem for the user then is how inaccurate can the contour of the casting be allowed to become before remedial action must be taken?

The use of 'go/no go' gauges removes the matter of judgment. However, the gauges are again subject to wear, and thus require the cost and complexity of a calibration system. More fundamentally, their use is similarly not helpful in terms of providing useful data to assist process control.

All these difficulties can be removed by the use of a much simpler technique: the use of simple goalpost fixtures which straddle the casting and which are equipped with one or more spring-contact probes, such as dial gauges. The readings from the gauges are read and recorded. The operation becomes even simpler with the use of digital read-out devices (Figure 18.17). Linear transducers are easily fitted and operated, and give an immediate numerical signal of the degree of inaccuracy. Laser techniques give an even faster and contactless benefit involving no wear.

The goalpost would be calibrated and stored on a standard casting, and thereby always be seen to be in calibration by being set to zero in this position. (For calibration away from the zero, other readings can be obtained by the insertion of slip gauges under the probe.)

The use of digital electronic read-out in this way allows its incorporation into data-logging and quality-monitoring systems, such as statistical process control. By watching the trends on a daily or weekly basis, the gradual drifts in casting dimensions can be used to predict, for instance, that tooling wear will reach a level which will require the tooling to be replaced in 3 months' time. Such prior warning allows the appropriate action to be planned well in advance.



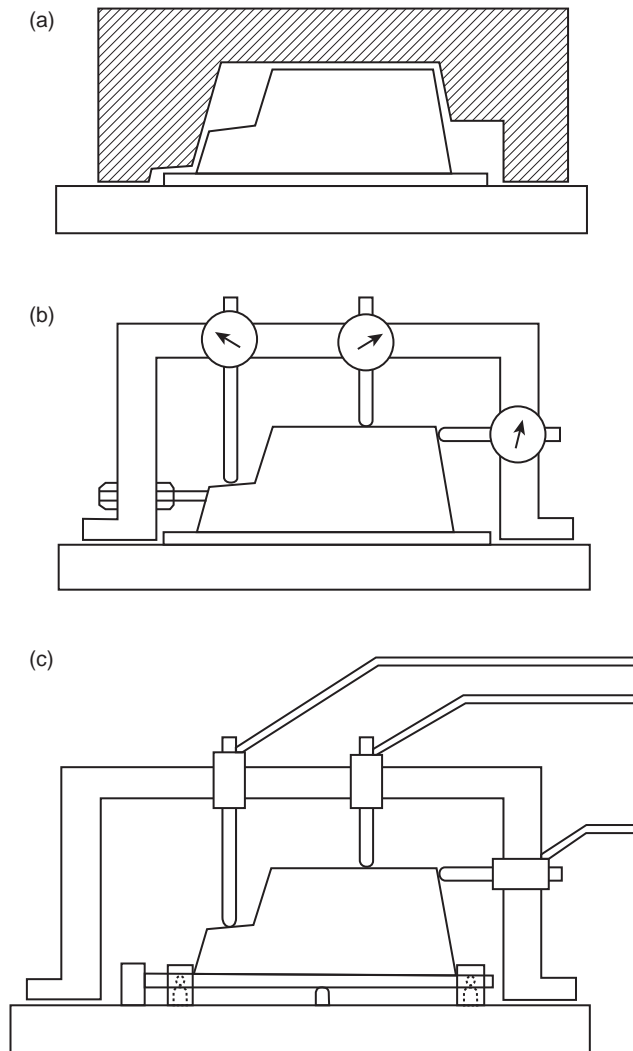


**FIGURE 18.17**

Checking techniques for size and shape of castings: (a) template; (b) analog quantification using dial gauges; (c) digital quantification using linear displacement transducers with the casting on a six-point jig. Modern equivalents are laser non-contacting techniques.

Even the use of goalpost systems is outdated by modern digital laser-reading systems, in which the contour is held as a virtual contour inside the computer. Even complex free-form surfaces typical of aerofoils can now be modeled remotely on a screen; the products scanned and checked for conformity within seconds; and the results immediately forwarded electronically to the customer in any part of the world.

Very large castings benefit particularly, since the handling of mechanical gauges several meters long, while attempting to measure to fractions of millimeters, become difficult if not impossible. The use of a remote laser technique is quick, easy for the operator, and amazingly accurate. Parts of up to 4 m in size can be measured to within 0.03 mm (Tigges 2010).

Digital techniques have introduced a new level of capability in terms of the accurate measurement of castings. This has raised the stakes for the founder, who now is challenged to improve casting accuracy yet further.

# Post-casting processing

# 19

The cutting off of gates and feeders is a chore, significantly aided by not having feeders, or even running systems, if possible.

Zinc castings are special because they can be cleaned from flash by cryogenic tumbling as a result of embrittlement of the alloy by cooling to  $-196^{\circ}\text{C}$  in liquid nitrogen, or possibly using a thermal deburring operation in which the castings are momentarily heated to  $3000^{\circ}\text{C}$  in a sealed chamber in which a mix of natural gas and oxygen is ignited to burn off flash and melt corners (Birch 2000).

High-pressure die castings of Zn, Mg, and Al alloys can be clipped as a result of (i) their high accuracy and (ii) their cleanness. The clipping of sand castings might be expected to result in a very blunt clipping tool, bringing the press to a full stop. However, these disadvantages cannot be too great since the process is currently being promoted for aluminum and iron sand castings (SERF 2002, Ricken 2009). The process is highly productive, taking seconds (not minutes by grinding for instance). Clean clippings are efficiently remelted, again contrasting with grindings. Operator problems such as white finger are also avoided.

Other alloy systems are much less easy. Feeder heads on steel castings can sometimes be removed by a powerful hammer blow, or with hydraulic wedges, although I suspect these fracturing processes are successful because of the density of bifilms, created by the poor filling technique, concentrating high up in the casting, particularly in the region of the feeder neck. The impact or wedge-removal technique would probably not be possible with well-made castings. Alternatively, large steel feeder heads are most often removed by flame cutting. The troublesome cracks generated by the process are avoided if the filling system is improved so as to avoid oxide entrainment (founders are amazed and delighted that the cracks no longer appear after a good naturally pressurized filling system is applied to the casting!).

The removal of cores can be a challenge. Mechanical shock and vibration systems are widely used, as are high-pressure water systems. Donohue (2006) describes a novel high-velocity jet of liquid nitrogen, of similar density to water, as being highly effective for the removal of residual shell and core material from ceramic investment-molded castings.

Having completed de-molding, de-gating, de-flashing, and removing feeders, there is often still much to do to get the casting into the condition the customer has ordered (working in a foundry is a challenge).

This final chapter deals with these final issues. When these are complete, it is always a pleasure to see the castings going out of the door. (However, it is worth bearing in mind that finally getting paid for them is more certain if the castings are good.)

## 19.1 SURFACE CLEANING

A common treatment for the cleaning of castings of all types was *sand blasting*, in which particles of sand are entrained in a powerful blast of air directed at the casting. The process is now almost universally unused as a result of the concern about the generation of harmful silica dust.

Treatments nowadays include *shot blasting* in which steel or iron shot is used, centrifuged to high speed by spinning wheels in so-called airless blasting. Stainless steel shot is, naturally, significantly more expensive than conventional carbon steel shot, but has the advantage for aluminum castings that they remain bright and free from rust stains. Other treatments include *grit blasting* in which the grit is commonly a silica-free hard mineral such as alumina. The many other blast media include glass beads, plastic particles, walnut shells; almost anything seems to be used.

The particular benefit of blasting with a heavy shot such as steel is that the surface of the casting is deformed by the impact of each particle, generating a localized compressive stress at the site of impact. This is a peening process. Fathallah (2000) finds 100% coverage of the surface is optimum to improve the fatigue resistance of a steel, whereas at 1000% coverage the overlaps and scaling of the surface damage reduces the fatigue resistance once more.

Many other studies have confirmed that the compressive stresses in the surface of shot-blasted or shot-peened castings enjoy an improved fatigue performance as a result of the inhibition of the growth of surface cracks when subject to compressive stress. Improvements to alloy Al-7Si-0.5Mg were shown by Pitcher and Forsyth (1982); Ji (2002) showed the benefits for ductile iron; Naro and Wallace (1967) improved steel castings. These experimental demonstrations have been supported by some excellent theoretical models by Fathallah (1998) and Evans (2002).

Although the improvement of fatigue resistance following shot peening is perhaps to be expected, the effect of grit blasting is less easy to predict, because the fine notch effect from the indentations of the grit particles would impair, whereas the induced compressive stresses would enhance fatigue life. From tests on aluminum alloys, Myllymaki (1987) finds that these opposing effects are in fact tolerably balanced, so that grit blasting has little net effect on fatigue behavior.

Kasch and Mikelonis (1969) noticed that the compressive stresses introduced into the surface by the peening effect caused significant movement of the casting on machining. Mroz and Goodrich (2006) found for both gray and ductile irons the depth of cold work and the residual stress did not change significantly after the first shot blast cycle.

However, the distortion effect is used to good effect in the sheet metal industry to induce the controlled forming of curved surfaces; aircraft wing panels are formed from flat sheets in this way; the flat product gradually curls up, becoming convex towards the direction of the impingement of the shot. The distortion effect of the peening treatment is controlled by the use of Almen strips. These are small strips placed alongside the article to be peened, and the curvature of the strips (measured as the arc height) is measured as a function of processing time (Cao et al. 1995). It seems that the use of controlled peening to adjust or vary the shapes of castings seems, so far as I am aware, not used at this time, but might be a useful technique to generate subtle curves on castings that might be difficult to mold.

Sand retention on as-cast surfaces of sand castings can be a problem. Figure 19.1 shows such a surface for an Al alloy cast in a zircon sand mold. A 10-kg cylinder head casting might have 0.5–1 g of sand retained on its surface. This compares with values of up to 0.05 g for a permanently molded cylinder head which would have relatively few sand cores.

After a blasting treatment, the surface of the casting will have achieved some degree of uniformity of appearance and texture. For sand castings, however, not all of the sand particles are removed; a significant percentage of adhering particles are pounded into the surface, thus becoming even more attached by the plastic flow of metal around and over them. This residual adhering sand is not important and not noticed for most applications. It might even be slightly beneficial for applications

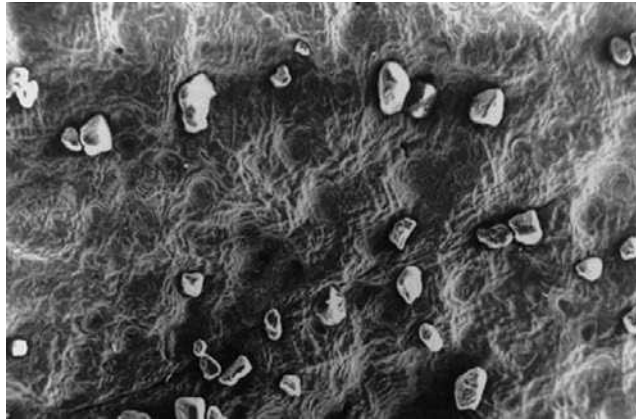


**FIGURE 19.1**

Surface of an Al alloy sand casting, showing adhering sand.

requiring paint adherence. However, it does affect the rate of wear of machine cutting tools if extensive machining of the surface is required.

The elimination of such sand from Al alloy sand castings can be achieved by a caustic etch. This seems to release most of the particles, and improves machinability. However, of course, such chemical treatments are to be avoided if at all possible for environmental reasons.

For the cast of grit blasting of Al alloy castings, whether sand castings or permanent mold castings, residual grit is always found to be embedded in the surface. Simply picking up the casting and dropping it on to a cast iron surface table will reveal a ghostly outline of the casting on the table delineated by the grit that has been shaken out by the impact of the fall.

Little research appears to have been carried out on the prevention or reduction of sand retention on castings. We may speculate that, as suggested in Section 9.12 on surface finish, any process that thickens the oxide on the advancing melt would be beneficial. Thus slower filling will allow the oxide to grow thicker, and the surface will experience a slower build-up of pressure, delaying mold penetration while the surface oxide thickens further. Chemical additions to the alloy may also help, as suggested for Sr addition to Al–Si alloys. Finally, of course, the final overpressure applied by counter-gravity filling systems also requires to be reduced so far as possible.

---

## 19.2 HEAT TREATMENT

The heat treatment of castings is one of the most expensive of all the post casting operations. Furthermore, high-temperature treatments are, of course, the most expensive of these. The high-temperature treatments include: (i) stress relieving followed by a slow cool, and (ii) solution or homogenization treatments followed by a quench. In addition to the high costs, the treatments requiring a quench are significant dangers to the integrity and accuracy of the casting as we shall discuss. There are both considerable economic and technical incentives to avoid these processes if at all possible.

The heat treatment of ferrous castings is a huge subject that cannot be covered here. In relation to castings, it is worth mentioning that alloy steel castings require to be homogenized at a temperature of at least 1300°C (Flemings 1974). These are challenging temperatures, requiring highly specialized furnaces with vacuum or protective atmosphere, and specialized quenching facilities.

Similarly for light alloys, the solution treatment is also expensive. It is performed at temperatures as near as possible to the melting temperature of the alloy, generally in the region of 500–550°C followed by a quench to retain solutes in solution.

The high temperature is a risk from the possibly incipient melting (or worse, wholesale melting). The quench is risky from the point of view of introducing a number of problems including residual stress and distortion. We shall devote some space to considering the important questions as to how these risks can be reduced or avoided.

### 19.2.1 Homogenization and solution treatments

For a single-phase alloy, Flemings (1974) describes a simple and elegant model of the microsegregation, or coring, present in the dendrites, and how it can be reduced by a high-temperature heat treatment termed homogenization. He defines a useful parameter that he calls the index of residual microsegregation,  $\delta$ , as:

$$\delta = \frac{C_M - C_m}{C_M^O - C_m^O} \quad (19.1)$$

where  $C_M$  = maximum solute concentration of element (in interdendritic spaces) at time  $t$ ,  $C_m$  = minimum solute concentration of element (in center of dendrite arms) at time  $t$ ,  $C_M^O$  = maximum initial concentration of element, and  $C_m^O$  = minimum initial concentration of element.

The parameter  $\delta$  is precisely unity prior to any homogenization treatment. If homogenization could be carried out to perfection, then  $\delta$  would become precisely zero. After any real homogenization treatment,  $\delta$  would have some intermediate value that depends on the dimensionless group of variables  $Dt/l^2$ . Here  $D$  is the coefficient of diffusion of the homogenizing element,  $t$  is the time spent at the homogenizing temperature, and  $l$  is the diffusion distance, of the order of the DAS. Assuming a sinusoidal distribution of the concentration of the element across the dendrite, Flemings finds the solution, approximately, as:

$$\delta = \exp(-\pi^2 Dt/l_0^2) \quad (19.2)$$

where  $l_0 = (DAS)/2$ . Equation 19.2 is useful for the approximate prediction of times and temperatures required to homogenize a given cast structure. Flemings shows that for a low-alloy steel, carbon is always homogenized by the time that the steel is heated to about 900°C for all normal values of DAS because of its high value for  $D$  (see Figure 1.4c). However, for the substitutional elements manganese and nickel, little homogenization occurs below 1100°C, and for homogenization to be about 95% complete ( $\delta = 0.05$ ) requires 1 hour at 1350°C if  $DAS = 50 \mu\text{m}$ . The fine DAS value is obtained by ensuring that such critical parts of the casting are within 6 mm of a chill. If no chill is used and the  $DAS = 200 \mu\text{m}$  or more, then practically no homogenization is achieved ( $\delta = 0.95$ ) at this time and temperature.

Flemings emphasizes that the normal so-called homogenization treatments for steels based on temperatures of 1100°C achieve only the homogenization of carbon. The more recent use of vacuum

heat-treatment furnaces capable of 1350°C and above has produced very large improvements in the mechanical properties of cast steels.

The term *homogenization treatment* is reserved for treatments designed to smooth out concentration gradients within a single-phase alloy.

The term *solution treatment* applies to those treatments designed to take into solution (i.e. dissolve) one or more second phases. These are also discussed by Flemings (1974). His presentation is summarized below.

Flemings considers a binary alloy containing a non-equilibrium eutectic. The dendrites are again assumed to be cored, having a sinusoidal distribution of solute as before, but containing interdendritic plates of divorced eutectic; for instance, in the case of the Al–4.5Cu alloy, a single plate of CuAl<sub>2</sub> phase separates the cored aluminum-rich dendrites. Dissolution of the interdendritic second phase is assumed to be limited by diffusion in the  $\alpha$ -phase. If  $f$  and  $f_0$  are the volume fractions of eutectic at times  $t$  and  $t_0$  respectively, then the answer is similar to that seen in Equation 9.2, approximately:

$$f/f_0 = \exp(-2.5Dt/l_0^2) \quad (19.3)$$

If the DAS is 100  $\mu\text{m}$ , and if impurity levels in the alloys are kept low, so that solution temperatures within 10 or 20°C of the melting point can be employed without danger of melting the alloy, then a 10-hour solution treatment is needed to dissolve all the second phase. This large DAS is easily reduced to below 30  $\mu\text{m}$  by chilling the casting, so that times under 1 hour are easily attained.

Experimental tests of the theory show good agreement, particularly at short times (Figure 19.2). At long times the dissolution of the last traces of segregate require more time than the simple theory predicts. This is because more segregate exists between primary arms than between secondary arms, and so the last remnant of solute must diffuse over larger distances than simply the secondary DAS.

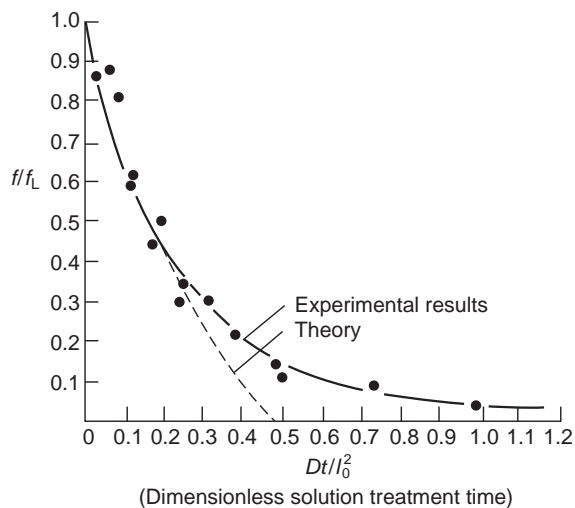


**FIGURE 19.2**

Rate of solution of eutectic in Al–4.5Cu alloy as a function of (dimensionless) time. (Data from Singh et al. 1970.)

### 19.2.2 Heat treatment reduction and/or elimination

There is strong motivation to abandon or significantly modify the high temperature solution treatment for Al alloys. This has taken three different options:

- (i) The total avoidance of any artificial heat treatment, using those alloys that exhibit natural aging at ambient temperatures such the 7xx alloys based on the Al–Zn–Mg series (Sigworth 2006). At room temperatures the development of properties is particularly slow, taking days or months, but only an hour or less at economic aging temperatures in the region of 100°C.
- (ii) Avoidance of solution heat treatment and quenching, but using heat treatments that involve only aging at temperatures in the region of only 150–250°C. These treatments often take several hours, although I personally aim to get the treatment over within an hour at most by opting for higher temperatures.
- (iii) Using only minimal solution treatment times and temperatures, followed by quenching and minimal aging. For instance a typical solution heat treatment for the common structural engineering alloy Al–7Si–0.4Mg might be 6–12 hours at 530°C followed by quenching and finally aging for up to 12 hours at 160°C. Personally, I always aim for a treatment not longer than 1 hour on the grounds that if cast well, the alloy will display more than adequate properties to pass all specifications. The various ways to reduce these excessive treatment times (optimized by metallurgists in an age of plentiful and low-cost energy, and now completely inappropriate) are discussed below. In the meantime, as an instance, the treatment described above would give nearly equivalent results at 1 hour at 540 or 545°C if possible, and 1 hour at 200°C. Examples of such developments discussed in Section 10.9 are summarized in Figure 10.57.

The use of the 10°C rise rule, leading to a doubling of reaction rates, is illustrated in Figure 18.8 and 18.9. The curves of strength versus time all collapse onto a single curve if allowance is made for the 10°C rule. It is strongly recommended that all heat treatment results are presented in this way. Occasionally the curves will not precisely superimpose, but this effect is easily distinguished by a fanning outwards of the curves, or the generation of a set of curves that are clearly part of a family, and so largely parallel or uniformly diverging. As an example the treatment of an Al alloy at 180°C for 4 hours is more or less exactly equivalent to a treatment at 190°C for 2 hours, or 200°C for 1 hour. These are all effectively *equivalent* treatments. One would expect an identical microstructure and identical properties from all of these treatments, since they are *equivalent*. Although, of course, there is a limit to how far this translation of the treatment can be pushed to higher temperatures and shorter times, for most practical purposes on the shop floor, it is often surprisingly effective over many iterations.

From time to time various stepped solution treatments are proposed. From the point of view of achieving the very best properties such treatments are probably necessary. For instance Gauthier and Samuel describe solutionizing at 515°C for 12 hours followed by 540°C for a further 12 hours which gives excellent strength and ductility for the common automotive alloy 319.2 (Al–6Si–3.5Cu). Their optimum aging treatment is 155°C for 12 hours. However, such a daunting high-cost treatment for such a low-cost alloy can hardly be recommended. For instance the aging treatment can be seen to be approximately equivalent to 1 h at 200°C. By contrast, Rometsch (2001) studied the solution treatment of 356 alloy (Al–7Si–0.4Mg), finding with a DAS of 40 µm that the alloy can be solution-treated at 540°C in a time somewhere between 4 and 15 minutes.



For those alloys produced by HPDC that would blister and distort with even my kind of reduced treatment, Mehta (2008) reports that treatments as short as 10–15 minutes at temperatures of only 430–490°C, followed by quenching into water, result in useful properties when combined with aging treatment for T4 condition (22°C), T6 (150°C) and T7 (200°C).

Thus the conventional wisdom that HPDC material cannot be heat treated would be normally true for conventional HPDC and conventional solution heat treatments, but it seems it may be possible to develop a useful degree of improvement as outlined above. In addition, the improvements in HPDC involving evacuation of the die and careful control of the shot stroke all contribute to increasing the soundness and reduced bifilm content of HPDC material, further allowing the benefit of some kind of solution treatment if necessary.

Another related aside might usefully be introduced here. It is unhelpful to see heat treatment results plotted on a linear time scale, since the short times are necessarily too compressed to be properly discernible. I find a logarithmic plot based on the factor of 2 extremely convenient for the plotting of heat treatment results. Thus the time axis has equal divisions labeled 1 s, 2 s, 4 s, 8 s, 15 s, 30 s, 1 m, 2 m, 4 m, 8 m, 15 m, 30 m, 1 h, 2 h, 4 h, 8 h, 16 h, 32 h, etc. The small error introduced by using 15 instead of 16 in this series can easily be shown to be quite negligible in relation to the other inevitable experimental inaccuracies that will be naturally present in the plots. Another useful approximate log base 2 scale I sometimes use is 1, 2, 4, 8, 16, 32, 64, 125, 500, 1000, 2000, 4000, etc. Figure 18.8 shows an example of this kind of plot, combined with the 10°C effect of the doubling of reaction rates, allowing all of the different temperature results to be collapsed, with acceptable accuracy, onto a single curve. This technique for recording all kinds of diffusion-rate-limited reactions is warmly recommended.

### 19.2.3 Blister formation

A further problem can occur for those alloys cast turbulently, such as by HPDC. The hydrogen absorbed from the atmosphere of the heat treatment furnace can diffuse into the part, inflating internal bifilms. Thus blisters can occur (a localized distortion) if the bifilm is close to the surface, whereas if the inflated bifilms are deeper inside the casting, distortion of the whole casting can occur. Figure 19.3 shows blisters developed on a rolled product produced from a defective cast ingot. Blisters are common on plaster-molded castings of Al alloys produced from relatively dirty metal, and are even seen on the surface of premium-quality forgings produced from less-than-well-cast performs.

In the past, of course, the essential role of the bifilm was not appreciated, all attention being focussed on the role of hydrogen. This is understandable since the introduction of a little NaBF<sub>4</sub> in the furnace atmosphere completely eliminates the problem (Dorward 2001). This illustrates that some kind of absorption mechanism is taking place in which the absorption of hydrogen at the casting surface is inhibited by some kind of passivating action of the fluoride. In similar work, Zurecki (1996) finds that low levels of sulfur hexafluoride gas (SF<sub>6</sub>) suppress blister formation during the heat treatment of Al–Mg alloys. Other halogen gases (those containing Cl and/or F) would also be expected to be effective to different extents. These solutions to blister problems are unwelcome because of the toxicity of the chlorides and fluorides.

As a personal experience of these problems, Al alloy castings produced by counter-gravity casting never displayed blisters from heat treatment even in atmospheres containing high levels of water vapor (the work basket was unfortunately constructed from square tubular steel, with the result that

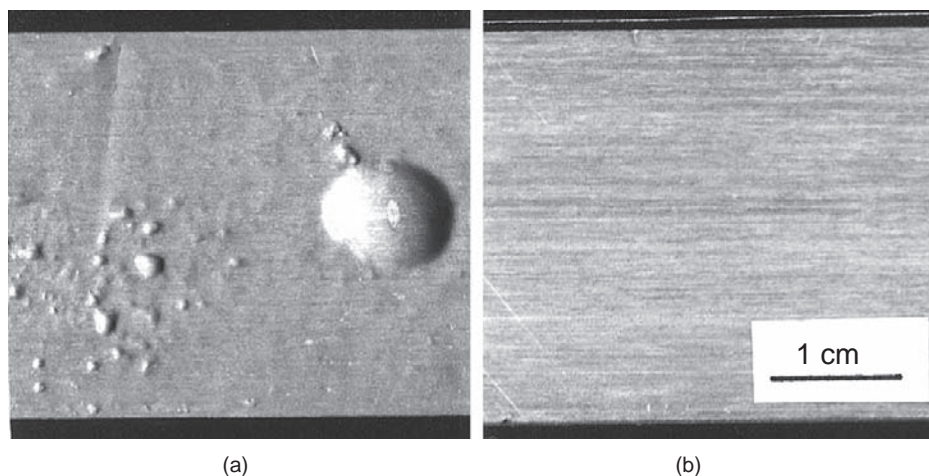


**FIGURE 19.3**

Surfaces of stretched sheet of 7475 (Al-Zn-Mg-Cu) alloy heated to 515°C (a) in air atmosphere; (b) with  $\text{NaBF}_4$  in furnace atmosphere (Dorward 2001).

the tubes filled with water during the quench, but boiled off when returned into the furnace, giving a nearly pure steam atmosphere). However, gravity-poured products treated in the same furnace, even after heavy forging, would, on occasions, produce crops of unsightly blisters, causing the parts to be scrapped.

Blister defects in rolled products are likely to be the consequence of the decoherence of near-surface films, often aided by the precipitation of hydrogen into such ready-made fissures. Celik and Bennett (1979) have shown that inclusions are implicated, and filtering of the melt prior to casting is an effective way to control the blistering behavior of the rolled product. This observation is further confirmation that rolling is not especially effective in bonding or welding such defects to render them harmless.

### 19.2.4 Incipient melting

The use of solution treatment temperatures as high as possible, taking advantage of the general rule that an increase of 10°C will double the rate of reaction, is of course limited to the temperature at which the alloy will melt. The sight of the castings flowing out from under the door of the heat treatment furnace is to be avoided if at all possible.

However, well before the castings become too hot to melt entirely, they can suffer from overheating; a phenomenon known as 'incipient melting'. This phenomenon was a puzzle in the sense that on heating above some low-melting-point constituents of the alloy, which might constitute only 1 or 2 vol% of the alloy, these constituents would clearly melt. However, on subsequent cooling they should re-solidify so as to result in no net effect. However, this was untrue for most alloys and most castings. Their mechanical properties, particularly ductility, would be significantly impaired by overheating.

An exception known to me was the early Cosworth castings, which were exceptionally clean, and did not suffer loss of properties if heated above the melting point of some phases, but were in fact

observed to continue to improve in properties. Researchers have occasionally reported (for instance Zhan 1998) that temperatures up to 560°C have been perfectly acceptable for Al–7Si–0.4Mg alloy in contrast to most of the industry that works at a maximum temperature of 540 or perhaps 545°C, in view of the known melting points of Fe-rich phases in the region of 550–555°C. This gave a clue that the presence of bifilms, as an uncontrolled influence, may be a factor contributing to the permanent degradation of properties when overheated. In confirmation of this suspicion, the author has proposed a mechanism that appears to fit the facts (Campbell 2009). This is outlined below.

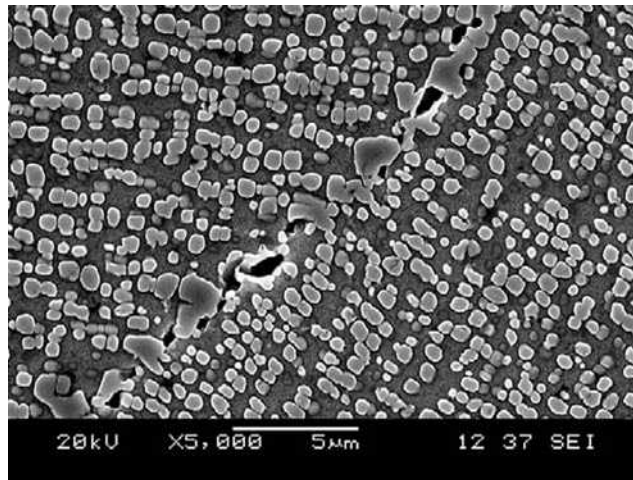
On heating over the melting point of some of the low-melting-point grain boundary constituents, these phases will liquefy, and so expand in volume. This expansion is not easily contained since both the newly arrived liquid phase and the surrounding solid are both effectively incompressible, resulting in the plastic deformation of the surrounding solid matrix. These millions of tiny expansions will result in a tiny growth of the whole casting. The resulting high-compression stress around the melting phases will ensure that any bifilm on which the phases formed will remain tightly shut. However, on subsequent cooling and solidification, the previously melted phase will now occupy less volume as a result of natural solidification shrinkage. The overall plastic growth of the casting is not reversed because the nearby bifilm accommodates this reversed stress by simply opening (since there is no bonding between its internal surfaces). This is vastly easier than the problem of reversing all the plastic flow. Thus the alloy now suffers from grain boundary porosity in the form of expanded bifilms.

The presence of bifilms at the sites of incipient melting is strongly indicated by Ni-base alloys, and is common in heat-affected zones (HAZ) of welds that experience temperatures not only in the incipient melting range but naturally up into the complete melting region. Figure 19.4 shows instances of incipient melting in the HAZ of welded 738LC Ni-base superalloy (Sidhu 2005). In the case of example (a) the bifilm is thin and symmetrical, suggesting it is a rapidly entrained alumina type; the  $M_{23}C_6$  particle has cracked through its center, and grain boundary  $\gamma'$  particles also contain traces of cracks. In contrast, example (b) shows MC carbides on only one side of the crack, suggesting the originating bifilm to be asymmetrical, perhaps an alumina plus a spinel? Figure 19.4c shows a typical convoluted bifilm, opened by the melting of the grain boundary phase in the heat affected zone of the weld.

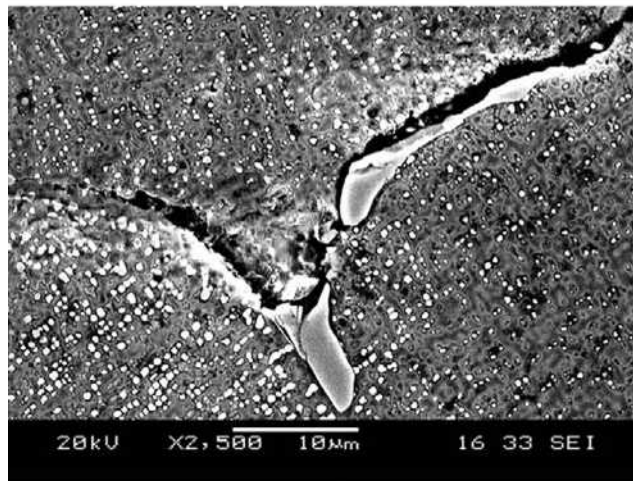
### 19.2.5 Fluid beds

Over recent years there has been significant interest in the use of fluidized beds for heat treatment, particularly for Al alloys (Chaudhury and Apelian 2006). The advantages include extreme uniformity of temperature (a muffle furnace with circulating air often has a problem to achieve the uniformity required for demanding work, in which all nine checked points – the eight corners and the center – of the furnace are required to be within 2.5°C) and good heat transfer leading to rapid heat-up of parts. However, when used for quenching, the rate of cooling is only about half that of a water quench. A slower quench is almost certainly a benefit for some castings, where the water quench is sufficiently fast to create severe residual stress problems. In fact the relevant question is, ‘is the quench slow enough?’ In general, the loss of properties as a result of a slower quench is relatively minor compared to the overall benefit to the product, which can be extremely valuable.

For those who want to know the response of properties to differing quench rate the technique described by Dolan and colleagues (2005) is recommended. These researchers used a variant of the



(a)

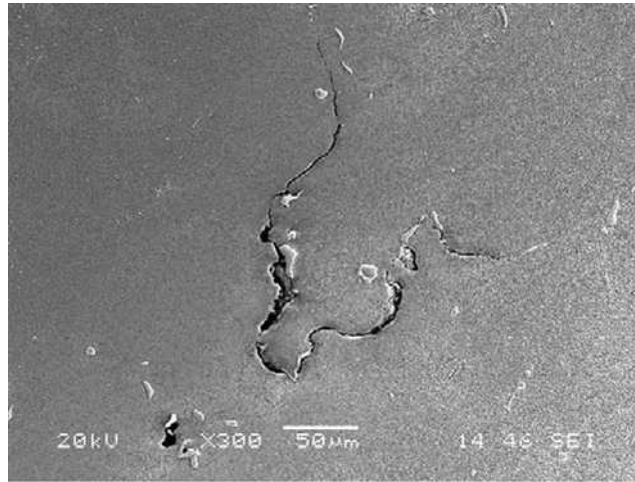


(b)

**FIGURE 19.4**

Grain boundary melting phenomena in the HAZ of welded Ni-base alloy 738LC showing (a) cracked and decohered grain boundary carbides; (b) asymmetric features of the crack and melted regions suggestive of an asymmetric bifilm; (c) a convoluted crack reminiscent of an opened bifilm (Sidhu 2005).

Jominy end quench technique, usually reserved for the investigation of steel heat treatments, in which water is jetted on to the end of a pre-heated 25-mm-diameter bar of the alloy to be tested. Thermocouples are inserted in holes drilled at intervals of 2, 38, and 78 mm along the length of the bar to ascertain the spectrum of cooling rates with increasing distance. These are correlated with hardness measurements at 2-mm intervals along flats machined on both sides of the bar.



(c)

FIGURE 19.4 (continued).

## 19.3 HOT ISOSTATIC PRESSING

In his history of HIPping, Mashl (2008) describes how pressing from all directions on a component, using a gas at high pressure, was found to densify ceramics as early as the 1950s. In 1970 it was first used on Al alloy castings, and within 5 years had started to become widely used for light-alloy aerospace castings. In a significant historical paper, Coble and Flemings (1971) confirmed that pores, if sufficiently fine, and in a fine-grained matrix, would gradually disappear given a few tens of hours and a temperature high enough for a ‘sintering reaction’ to occur. They found that the application of modest pressure, about 20 atmospheres, greatly assisted the process. The development of hot isostatic pressing (HIPping) was the outcome. Much higher pressures were employed, usually nearer 1000 atmospheres (100 MPa), and temperatures as near the melting point as was practical. The optimum conditions for HIP have been defined in an elegant study by Arzt, Ashby, and Easterling (1983) in which they characterize tool steel, superalloys, alumina, and ice.

The significant improvement in mechanical properties, particularly average fatigue life, reported for certain alloys after HIPping is probably at least in part due to the contribution towards the deactivation of entrained double oxide film defects (bifilms) as fatigue crack initiators. We shall evaluate the evidence here for HIPping as a solid-state process for the closing of pores and bifilms.

When a cast Al–7Si–0.3Mg alloy with oxide film defects, like that shown in Figure 19.5a, is subjected to HIPping treatment, the applied pressure at temperature close to its melting temperature induces a substantial plastic deformation in the casting causing the defects to collapse and their surfaces to be forced into contact (Figure 19.5b). This plastic collapse phase occurs almost immediately, probably requiring only a few seconds or a few minutes. The slightly extended time may be required for the residual air to be reacted to form oxides and nitrides. At this stage the pores and cracks are closed but, of course, not necessarily bonded. Thus only a modest, if any, benefit from HIPping may be expected at this early stage. Also noticeable in Figure 19.5b are residual pores among the collapsed oxide bifilms that appear to have

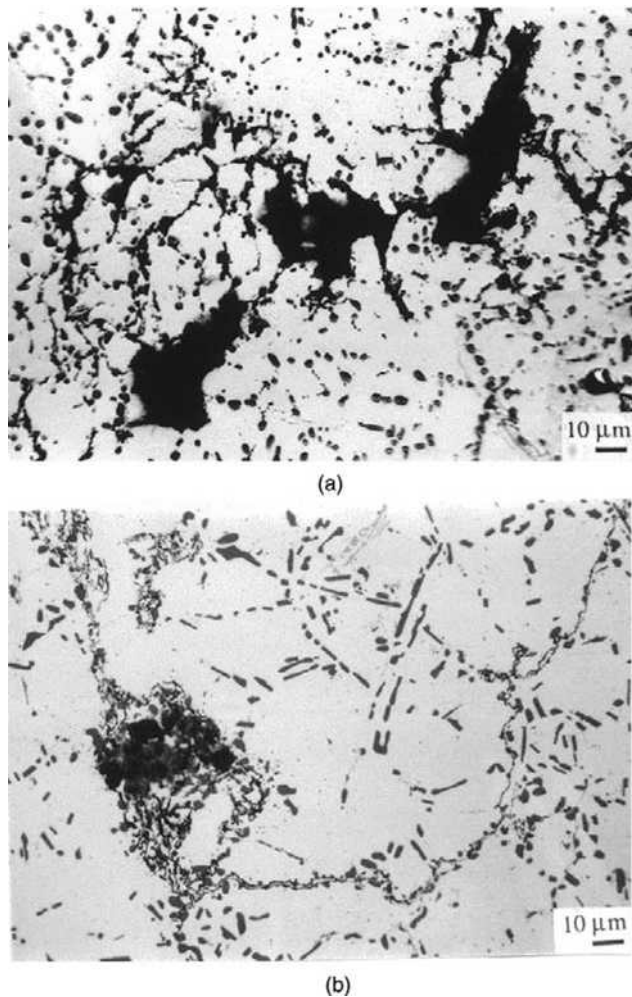


**FIGURE 19.5**

Optical micrograph of an Al-7Si-0.4Mg alloy showing (a) a network of oxide films and associated pores in the as-cast condition; (b) the network of films and collapsed pore in the HIPped condition (Nyahumwa et al. 2000).

survived the complete HIP process. It seems likely they contain the insoluble 1% argon constituent from the air. Such pores are never expected to close, but will contain the argon at the huge pressure experienced during the HIP process, and will pressurize most of their associated bifilm, and thus will expand again if the temperature is raised sufficiently. Such pores might be expected to re-grow to some extent, triggering failure during such processes as creep or super plastic forming.

For those Al alloys containing no Mg for which the oxide is the very stable ceramic, alumina,  $\text{Al}_2\text{O}_3$ , there is little or no benefit to be expected from extending the HIP cycle. Similarly, for those alloys containing over approximately 1%Mg, once again the oxide is extremely stable, being pure

magnesia, MgO. For such alloys no bonding is expected to develop between the extremely stable ceramic surfaces dividing the central interface of the bifilm.

The situation is interestingly different for many aluminum alloys of intermediate Mg content in the range of perhaps 0.05–0.5%, as for instance typified by Al–7Si–0.4Mg alloy. For such alloys an alumina ( $\text{Al}_2\text{O}_3$ ) film is first formed during the rapid entrainment process. However, after an incubation period that is a function of time and temperature, the entrained film transforms to magnesium aluminate spinel,  $\text{MgAl}_2\text{O}_4$  (Aryafar 2010). This involves a volume change and atomic re-arrangement of the crystal structure that would be expected to encourage diffusion bonding across any oxide–oxide interface that happened to be in contact. Analysis of bifilms that have acted as fatigue crack initiation sites have confirmed their conversion to a spinel and confirms that fatigue properties are improved by HIPping (Nyahumwa 1998, 2000). A further positive finding from this work was that compared to filtered castings, the unfiltered but HIPped castings exhibited higher fatigue performance, despite larger maximum defect sizes, implying some degree of bonding across the crack. The application of HIP to castings shown in Figure 9.34a resulted in fatigue test samples that did not fail; the run-outs at the stress 150 MPa reached nearly  $10^8$  cycles (not shown). At the higher stress of 240 MPa improved fatigue lives were still recorded (Figure 9.34b), although it is of interest that in all failures, with the possible exception of the most resistant specimen, the fatigue failures still occurred from oxides, being probably healed or partly healed bifilms.

The liquid-state healing mechanism as described in Section 2.4, and the HIP solid-state healing mechanism are suggested to be analogous. However, there are interesting differences. In the liquid state, where bifilms are floating freely in the melt, the healing mechanism operates at high temperature (i.e. approximately  $700^\circ\text{C}$  for an aluminum alloy) and with only the moderate external applied pressure ( $<0.1$  MPa) due to depth in the liquid. When the casting has solidified, the solid-state healing process due to HIP operates at lower temperature but very much higher pressure (i.e. 100 MPa at  $500^\circ\text{C}$  for Al–7Si–Mg alloy). In both the liquid and solid conditions pressure inside the bifilm will be expected to fall as the oxidation reaction proceeds. When all the oxygen is consumed, the nitrogen is subsequently consumed to form nitrides (Raizadeh and Griffith 2008).

Whether bifilms are actually ‘healed’ (i.e. effectively welded) clearly relates to the chemistry of the alloy and its films. Some bifilms appear to heal as we have seen above, whereas others are resistant. These important factors are not well researched at this time. Thus HIPping has limitations that do not appear to be widely known or understood. However, evidence for possible mechanisms is discussed below.

In contrast to this beneficial action of HIPping found by Nyahumwa and others as described above, Wakefield and Sharp (1992) observed HIPping to have no beneficial effect on the fatigue properties of Al–10Mg alloy castings, despite the closure of pores and cracks. The inference is that the bifilms in this alloy proved impossible to de-activate, resisting effective welding. To restate and expand on the phenomenon, this is attributed to the magnesia (MgO) film formed during oxidation of Al–10Mg and entrained during casting. The magnesia film is (i) thicker, and (ii) has a stable structure that does not transform during HIPping (Nyahumwa 1998, 2000). This lack of any substantial atomic movement explains the inert nature of the highly stable MgO compound. (Similarly, again, as discussed above, it would be expected that Al alloys with very low Mg content, that would be expected to contain entrained alumina films would be similarly resistant to HIPping because of the great stability of alumina in the absence of sufficient Mg to convert it to a spinel structure.)

A further sobering example from failed attempts to hip Ni-base superalloys is an object lesson. During the early development of the Pegasus engine for the Harrier Jump Jet, 25 polycrystalline Ni-based alloy

turbine blades that had previously been scrapped because of their content of porosity were subjected to HIPping, and were fitted to a test engine alongside sound blades to evaluate whether HIPping might be a satisfactory reclamation technique for blades. The HIPped blades failed within a few hours, damaging the engine and forcing a rapid shut down of the test. The failures had occurred by creep cavitation at the grain boundaries of recrystallized regions in the center of the castings. Almost certainly the original porosity would be caused by bifilms, probably of aluminum and/or chromium oxides entrained by the severe turbulence that is usual during the vacuum casting process. (The vacuum is known to contain plenty of residual air to ensure the creation of surface films.) The great stability of the films, formed at the high casting temperature, would ensure that they were resistant to any re-bonding action. The recrystallization would have happened because of the large plastic strains that were a necessary feature of the collapse of the porosity. However, the subsequent grain growth would expand grains up to local barriers such as bifilms. Thus the bifilms, effectively unbonded, and so acting as efficient cracks, were automatically located at the grain boundaries from where the failures were seen to occur.

The closure of internal cavities usually causes negligible changes to the overall dimensions of the casting if the pores are small and/or deep-seated. For large or near-surface pores, however, the collapse of the surface of the casting in the form of a localized sink may scrap the casting if the depression exceeds the machining allowance. In a severe case, the surface may puncture, opening up the internal cavity to the surface (Zeitler 1984).

Naturally, HIPping cannot work if the pores are already connected to the outer surface of the casting. Such pores will never heal. Unfortunately this is all too common. The existence of the various forms of surface-connected porosity is well known to those who HIP castings. In particular, pressure die castings are woefully resistant to the benefits of HIPping because of their many surface-connected bifilms (traversing the so-called 'dense' outer layers of the casting). However, many gravity-filled and even counter-gravity-filled castings exhibit surface-connected pores as a result of bifilms intersecting the surface.

In addition, although an excellent start, even good filling of the castings will not guarantee a satisfactory response to HIP treatment if the alloy has a long freezing range and is poorly fed. As we have seen in Section 7.1.5 poor feeding in a long-freezing-range alloy can easily lead to conditions in which residual liquid is sucked away from the surface of the casting, subsequently expanding as shrinkage porosity inside the casting, to create surface-connected porosity.

For reliable HIP response, the surface of the casting must be sound.

Finally therefore, although the mechanical properties of castings usually exhibit an improvement, in the sense that their *average* properties are raised, the Weibull modulus most often *falls*. This is a direct result of the closure and welding of some defects, improving the properties of some castings, but leaving some castings unaffected, for the various reasons we have seen. Thus the *scatter* of properties is increased. Regrettably, this is one of the greatest disadvantages of HIPping, often overlooked.

---

## 19.4 MACHINING

There are numerous textbooks on machining, so we shall limit our attention to only a few of those aspects of relevance to castings.

An early experience of mine taught me that casting defects can have a profound effect on the difficulties experienced by the machinist. An Ni-base superalloy turbine blade for a land turbine was



top-poured through the root of the blade, creating oxide flow tube defects that opened into vertical cracks when grinding the 'fir tree' roots. The founder asserted the problem was the result of severe grinding, the heat of grinding producing grinding cracks. However, in fact, even the lightest grinding had difficulty to eliminate the problem (Figure 10.5).

Turning to the wide field of cast irons, Teague and Richards (2010) review the information on the age strengthening of gray irons, finding that aging for 5 days at room temperature greatly improves tool life. Apparently the effect is the result of the precipitation of nitrides. They report an investigation that attempted to reduce this time by aging at 271°C for 75 minutes which yielded no clear result. It seems to me this attempted treatment was way over the top. Taking the 5 days at room temperature as 120 hours at 20°C, and using the useful approximation that a 10°C rise in temperature will double the rate of reaction, this gives equivalent treatments at 60 hours for 30°C, 30 hours for 40°C, etc., finally indicating 1 hour at 90°C. This extrapolation of times and temperatures makes no claim to be more than an approximation, but I have often found it to be impressively accurate. It seems more modest times and temperatures have not yet been tested.

Machining of gray cast iron can pose additional difficulties (Hoff and Anderson 1968) because the skin typically contains:

- (i) no graphite but only fine pearlite (equivalent to a hard steel);
- (ii) oxides;
- (iii) sand grains.

For this reason machinists are usually keen to ensure that the first machining cut is taken well under the casting skin. This is not always possible, however, and the effects of decarburization and inclusions are noted below.

Rickards (1975) has researched the problems of poor machinability as a result of the formation of graphite-free surface layers on gray iron castings made in greensand molds. It seems the problem is affected by section size and the carbon content of the sand. For instance for 300 mm section thickness the graphite-free layer can reach 1 mm. He found 5% coal additions to the sand to roughly halve the problem, and additions up to 10% would control the problem in thin-walled castings, but could cause a carburized layer in castings with heavy sections up to 100 mm thick.

The author recalls those working in a machine shop drilling ductile iron crankshafts who could tell the difference between those castings made with good and bad filling system designs simply by listening as they walked among the machines. Those that were cast with significant surface turbulence contained inclusions rich in magnesium oxide, creating the characteristic high-pitched singing noise that the machinists knew signaled a poor finish and short tool life.

The effect of oxides in castings is well known to machinists. The alumina inclusions in light alloys and mixed oxides in iron and steel castings are all known to cause defects on the machined surface by dragging out, leaving unsightly grooves. Worse still, the cutting edge of the tool is often chipped or blunted by encounters with such hard particles, which are in general vastly harder than the cast alloy, and even harder, in many cases, than the tool tip.

For sand castings of all types, but particularly the softer light-alloy castings, and particularly when turbulently filled, the presence of residual sand on the surface of the casting is often a problem. For iron castings it is widely appreciated that the first cut should be sufficiently deep to get below the glassy surface inclusions.

In light alloys cast in sand the complete removal of all sand is practically impossible short of dissolving away part of the surface in an acid or alkaline bath. Normally, some residual surface grains are broken and hammered into the surface by the so-called cleaning processes such as shot blasting. Grit blasting can be even worse, since particles of grit (often hard, angular, abrasive grains of alumina) remain embedded in the surface.

Because of this residual surface aggregate problem, the slightly impaired machinability of sand castings of all types, ferrous and non-ferrous, compared to die (permanent mold) castings is one of the very few potential disadvantages of sand castings. This disadvantage seems little known and publicized, but needs to be acknowledged and accepted by all the parties in the casting supply chain to save future heartache and canceled orders.

It is worth emphasizing once again benefits of gentle uphill filling of mold cavities. The beautiful glossy shine that iron castings exhibit when filled by non-turbulent bottom-gated systems illustrates the protection provided by the lustrous carbon film acting as a mechanical barrier between the liquid metal and the mold. Because the liquid metal now no longer comes into contact with the sand mold, the surface of the casting should be completely free from embedded sand grains, and should exhibit excellent machinability. Similar benefits are achieved for most casting alloys by the insulating action of the oxide film when carefully uphill filling molds. At this time I am not sure that this prediction has ever been tested.

For Al alloys, the machining of high-Si alloys (in the range approximately 10–20%Si) is well known to require diamond-tipped tools. However, what is less well known is that even the lower-Si alloys present some degree of tool wear. Armstrong and Martin (1974) draw attention to the excellent machinability of the 7%Zn alloy (771.0) that requires only a low-temperature age (180°C for about 4 hours) followed by an air cool (not a quench), resulting in a highly stable casting with low internal stress that maintained its highly accurate dimensions after machining, and enjoyed tool lives up to 20 times longer than the normal Si-containing alloys, plus machining speeds up to 5 times faster.

Dasch (2009) describes investigations into the dry machining of Al alloys which would have significant environmental benefits compared to current wet machining methods, but has been prevented by the build-up of hot Al on tool tips. He finds only 0.15%Sn addition to an Al alloy achieved a 1000-fold increase in tool life, in addition to the ability to machine dry. Higher cutting speeds enhanced the effect, such that faster drilling worked better than low-speed drilling.

For the future, the advent of other machining techniques will become increasingly important. These include machining or cutting by fluid bed, water jet, flame, plasma, oxygen, laser, spark, and abrasive finishing. The smoothing of complex internal passageways in castings is sometimes accomplished by forcing through abrasive mixtures of SiC in silicone putty. Even so, our current cutting technology based mainly on single-point or multipoint cutting tools is likely to be with us for a long time yet.

As an interesting and potentially important aside, designers of light-alloy castings often despair at the inability of threaded holes in castings to avoid stripping out of the threads when subjected to large loads. Thus, relatively expensive heli-coil inserts are specified. These strong steel inserts spread the pull-out load and significantly strengthen the fastener. However, these are costly and inefficient solutions. The author has experience of M8 self-tapping bolts (thread-rolling type rather than the thread-cutting type) in an Al alloy casting that enjoyed no cost to machine the thread, and the better thread engagement and work hardening of the surrounding matrix resulted in 8 times greater pull-out load. The benefits of thread-forming fasteners (TFFs) in net-shape cast holes of light alloys has been further researched by Paxton (2006). The work-hardened region around the fastener acts as its own

integral heli-coil, spreading the pull-out load. Furthermore, the avoidance of a second metal minimizes the potential for corrosion problems.

Although cast holes can be envisaged for HPDC, small-diameter cast holes are not attractive for aggregate-molded castings because the small sand projections on cores and mold would be vulnerable to being slightly ill-formed or even broken off. Thus for sand castings it would be preferable to machine the tapping sized holes in the casting. This seems a relatively small penalty, still enjoying the benefit of avoiding tapping, and still achieving a greatly superior engineering feature which may be particularly important for certain critical castings.

## 19.5 PAINTING

For those painting processes where the paint is cured by heat, such as powder coating, the curing cycle is usually integrated with the heat treatment requirements for the casting, and thus constitutes the final heat treatment stage (the aging) of the product. Aluminum alloy wheels for cars are usually heat-treated and painted in this combined process.

However, problems arise if the casting exhibits any surface-connected porosity. This can cause a defect in the smooth surface of the paint known as a paint crater.

Prior to painting, the surface of the casting is usually machined to a bright finish, and may be further mechanically polished and subsequently subjected to cleaning with a solvent. The paint powder is usually applied electrostatically to achieve a tolerably uniform deposit on a complex shape. During the heating of the casting for the baking cycle, the powder melts and slowly cures, while air expands from surface-connected cavities in the casting. At this stage of the process the liquid paint is continuously blown away from the pore to form a succession of bubble-like blisters; the collapsing walls of the blister at a later stage when the paint becomes viscous tend to remain 'frozen' in place, becoming the crater wall (Figure 19.6a). Micks and Zabek (1973) investigated paint craters originally assuming them to be faults in the paint application process. However, they found that the craters were invariably linked to surface-connected porosity. The central hole in the crater was always connected to an internal cavity which was found to remain free from paint (Figure 19.6b).

Unfortunately, such craters are a serious source of scrap for aluminum alloy road wheels for cars, and kitchen utensils, since the cosmetic requirement for such castings from the car owner and the cook is simply perfection.

For Mg alloy castings, particularly those for aerospace applications, the special surface coatings to protect the casting from corrosion are a significant contribution to the cost of the product, and, since Mg alloys are so light, even make a contribution to its weight. The maintenance of the coating, often requiring replacement after weld repair or other disturbance, represent further discouraging costs to the selection of these otherwise attractive alloys.

## 19.6 PLASTIC WORKING (FORGING, ROLLING, EXTRUSION)

It seems curiously perverse that most metallurgical texts continue to foster the erroneous assumption that working eliminates casting defects. Usually, the strains involved in most working operations are too low to effect any significant welding of faults. Bifilms in general are merely pushed around, if anything,

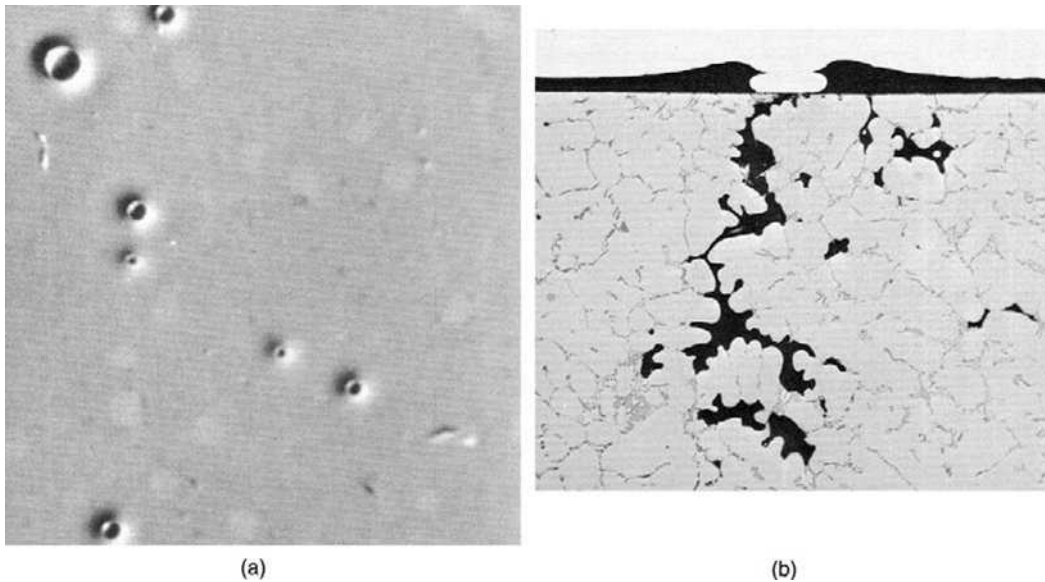


**FIGURE 19.6**

(a) Paint craters of varying sizes on the surface of an Al-5Si-0.5Mg alloy casting, acrylic powder coated and baked at 230°C. (b) Optical micrograph of a section through a crater, showing its connection into surface-connected porosity (Micks and Zabek 1973).

growing worse before (if ever) getting better. The growth of casting defects by plastic working is well known to those who work in the forging industry. There are good reasons for this behavior.

During the working of cast material, for instance by rolling, it is to be expected that the defects will be elongated in the direction of working. The elongation of the defect necessarily rotates it, aligning the defect along the rolling direction. This is clearly seen in the lengthening of graphite nodules during the rolling and forging of ductile iron (Neumeier 1976).

In addition, of course, elongation of the work piece increases the area of its defect. The newly extended surfaces in the bifilm would necessarily be oxidized by the remnant of air entrained in the defect. The entrapped air would be contained partly amid the microscopic pores between the crystals of the oxide, and partly in reservoirs formed by folds and in expanded regions constituted by those bubbles entrained as part of the bifilm. During rolling, the continued oxidation of the expanding surfaces would hinder the welding of the interfaces that were being newly created, and by this means assisting the defect to grow as a crack, possibly to many times its initial size. The great effectiveness of the creation of this newly oxidized extension to the crack would be a consequence of the small oxygen requirement; the oxide would grow to a thickness of only nanometers at the hot working temperature (which is, naturally, much lower than the temperature at which the film was first formed on the melt). In other words, the entrained residual oxygen is highly efficient at these temperatures to continue the oxidation of new area as it is formed.

Miyagi et al. (1985) used ultrasonics to observe this increased area of cavities in 5083 alloy (Al-Mg type) during the early stages of hot rolling. Micro-cavities near the surface of the rolled plate seemed to close early, but those nearer the center were long-lived. Micro-examination revealed that

they were smooth sided, and appeared to have opened and expanded along grain boundaries. (The association with grain boundaries is, of course, a feature to be expected of bifilms.) They were seen to reduce in size only after reductions of over 50%.

Later, if the extension were sufficiently large to consume the remaining air, further extension would result in the welding up of new extensions to the crack. It seems likely that normal forging and rolling do not reach this stage for most alloys, and so do little to heal defects, simply extending and re-aligning them as described above. Processes such as extrusion and multi-pass rolling may sometimes account for a more complete elimination of the casting defects because of the much greater strains that can be involved. Even so, it seems that many defects remain, as indicated, for instance, by the evidence from corrosion (see Section 9.10).

Work by Harper (1966) on the hot rolling of wire-bar copper showed that rounded bubbles of gas are collapsed asymmetrically, becoming pinched off, and forming what appear to be trails of minute beads on a string, the beads being microscopic bubbles only 30–40 nm diameter. It is hard to avoid the conclusion that the bubbles are the residual insoluble argon sitting in the collapsed bifilm, or even the collapsed bubble trail, resembling a string on the two-dimensional polished section.

Many bifilms will be already linked to the surface. Alternatively, during working operations such as rolling, they can become linked to the air by local plastic failure of ligaments of sound material separating the defect from the outside world. Thus a corroding environment is expected to penetrate most near-surface entrainment defect cracks in cast, forged, rolled, and even extruded materials as is seen in Section 9.10.

The huge amount of work on the behavior of inclusions in steels during working cannot be covered in this short account. However, the early work by Wojcik et al. (1967) was notable since they were able to show that their steels, destined for piercing to make tubes, contained a distribution of inclusions that they found to be log normal. This finding allowed them to extrapolate their inclusion counts from relatively few microsections to assess the probability of the presence in the billets of a small number of inclusions sufficiently large to cause wall defects in the tubes.

Charles and Uchiyama (1969) and Wardle and Billington (1983) studied the plasticity of inclusions in steels as a function of composition and temperature, showing the regimes in which the inclusions would either flow, thereby elongating, or fracture, so forming chains of fragments. Leduc and co-workers (1980) checked the density of cast low-carbon steels during hot rolling, but did not find any evidence for a fall in density during the early stages of rolling similar to that found for the non-ferrous materials. They found a progressive increase in density, becoming fully dense at about 75% reduction. Examination of the microstructure indicated that all the pores were eliminated at that stage. This is probably understandable in view of the low residual levels of Al in the steels (0.02–0.04%) and absence of other strong oxide-forming elements. Any surface oxide would therefore have been expected to be a liquid iron–manganese silicate, and so any bifilms, if present, would have been easily welded shut.

---

## 19.7 IMPREGNATION

The impregnation process is a sealing technique, designed to seal porosity and eliminate leakage problems in castings.

Clearly, good casting processes do not need impregnation – however, many do.

For instance high-pressure die castings are highly prone to leakage problems because of their high content of bifilms and inflated bubble trails. Similarly, low-pressure castings that have not had the benefit of the roll-over action following the filling of the mold are sometimes prone to an interconnected type of shrinkage porosity as a result of convection problems.

Although some casting operations use impregnation only to seal those castings that are shown to leak, others do not carry out an initial sorting test, but simply apply impregnation to all castings. Although, like heat treatment, impregnation is often carried out by specialist off-site operators at a price usually based on the weight of the casting, it is sometimes installed as an integral part of the foundry operation.

The impregnation process involves the placing of the casting in a vessel from which the air is evacuated. The casting is then lowered into the sealing liquid. When fully immersed, air is re-introduced into the vessel to restore atmospheric pressure. In this way the liquid is forced into the evacuated pores in the casting. The casting is then raised out of the liquid and is left to drain. Excess sealant is then washed off and the sealant is cured.

There are two main curing processes based on two different sealing systems. These are (i) sodium silicate cured with the addition of a catalyst to the liquid; and (ii) a thermosetting resin hardened by a subsequent low-temperature heat treatment.

A recent development is the streamlining of the process by the use of special sealants, allowing the process to be carried out in a single vessel with only a short treatment time (Young 2002).

In a small percentage of cases leakage of the casting is not cured by the first impregnation. Some casters and their buyers allow two or even three such attempts. Usually, if the casting still leaks after repeated attempts to seal it, it is finally scrapped.

---

## 19.8 NON-DESTRUCTIVE TESTING

Although destructive testing is the most discriminating and reliable way to determine the suitability of a casting for service, the destroyed casting is somewhat unfit for service. Clearly, it is essential to have reliable tests that do not involve destroying the product. Naturally, this criterion puts severe limitations on the appropriateness of the various approaches to the solution to this problem.

### 19.8.1 X-ray radiography

Radiography is a powerful technique for checking the presence of severe defects such as open cracks, porosity, or foreign (entrained) inclusions. The traditional radiographic limit to detection has been approximately 2% of the section thickness, although modern techniques are providing ever greater sensitivity of detection. If 1% could be achieved this would be 100  $\mu\text{m}$  in a 10-mm section. This is a substantial defect, especially if it is a crack. In general, however, a crack can usually only be detected if it is aligned with the viewing direction. Even then, if the crack is tightly closed, the crack can remain undetected. Thus it has to be concluded that radiography cannot offer reliability for the detection of cracks.

It is well to remember that the features noted on radiographs generally appear to be shrinkage; porosity is nearly always *not* shrinkage, but clusters of bifilms together with their entrained internal air. Rounded pores generally identified as 'gas' are also most often entrained air bubbles. The reader needs

to be aware that at the time of writing practically all radiographic inspections are diagnosed incorrectly. The accurate diagnosis of radiographs cannot be expected for many years.

The powerful new technique of three-dimensional radiographic examination by tomography can be attractive if the cost and the significant time required are available. Although the technique is clearly capable of identifying serious defects, the additional capability to assess inaccessible wall thickness deep inside complex castings, or the presence of residual core material in an inaccessible passageway, are major potential advantages.

### 19.8.2 Dye-penetrant inspection (DPI)

DPI is a sensitive technique for surface-connected defects such as porosity and cracks. In this process the casting is bathed or immersed in a dye, a liquid designed to be highly wetting so as to penetrate small holes and fissures rapidly. The casting is withdrawn from the die, washed, and coated with a 'developer' in the form of a fine white powder that can absorb the dye by capillary attraction as a blotting paper, sucking the die out of its crevice and into the developer layer where it can be seen. The most sensitive dyes fluoresce in ultraviolet light, and are therefore viewed in a darkened area.

The DPI approach is of course limited to the detection of surface-connected defects; any internal defects, which may be major faults, remain undetectable.

### 19.8.3 Leak testing

Section 9.11 describes how the leakage of castings is almost never from 'porosity' due to shrinkage or gas. Section 10.5 illustrates how leaks can result from core blows that have effectively punched holes through the walls of the casting, creating serious leaks. In general, however, leaks appear to be mainly the result of the presence of bifilms. Figure 19.7 shows an approximately 20 mm long bifilm in an Al alloy casting which clearly had no problem to bridge the 5 mm wall thickness even though the path was long and meandering.

The finding of such leaks by leak testing is a costly and time-consuming activity, which those counter-gravity operations that do not make leaky castings have the good fortune to avoid. Interestingly, the leak shown in Figure 19.7 was discovered not by leak testing but by a resonance test which is far quicker and easier, besides, of course, also discovering any other seriously deleterious features from which the casting may be suffering. This indicates an interesting future direction for the general testing of castings.

However, for those casters that need to conduct a leak test the many techniques are listed in some detail in Section 9.11. By far the commonest system is the time-honored bubble test by pressurization of the casting with air while immersing the casting in water. However, the test is easier described than done. Leakages from seals as a result of imperfect dressing of prints can give plenty of additional bubbles that boil to the surface of the water, obscuring any observation of the relatively tiny leaks that the test was designed to find.

Another aspect of the test which gives cause for some concern is the procedure that sets aside any failed casting, for instance an aluminum cylinder head, with a view to repeat the test on the following day. Often, the casting will pass the test on the following day, almost certainly as a result of the leak path being sealed by corrosion products. The rapidity of the corrosive action is likely to result from the association of intermetallic particles that have precipitated on the bifilm, creating efficient corrosion

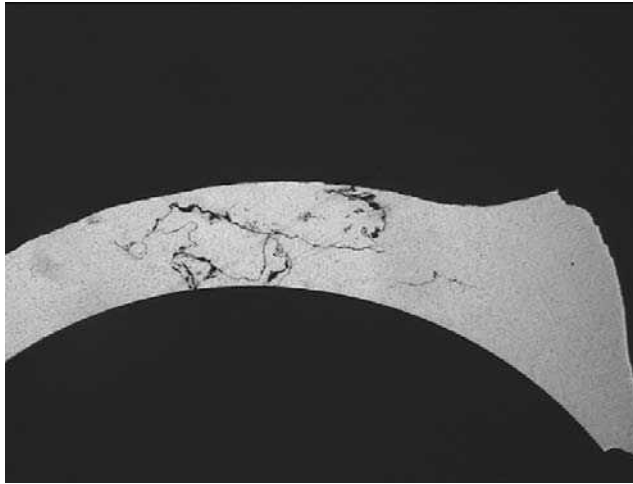


**FIGURE 19.7**

A leak path formed by an oxide bifilm, causing the master brake cylinder to be rejected (courtesy of Magnaflux Quasar).

couples. Having reflected for some years on the honesty of this procedure I find I have never been aware of any failures of these castings in service. Thus it seems a proven technique for the rescue of expensive and valuable products. Perhaps the procedure would be less acceptable for products that had to withstand high pressures.

Overall, however, the shop floor experience that counter-gravity operations with good quality melts do not suffer leakage problems is powerful evidence that the leaks are mainly the result of bifilms. The clear message is that these features are avoidable using good filling technology as described in this book, and leak testing could, with relief, be yet another foundry chore consigned to the rubbish bin of history.

#### 19.8.4 Resonant frequency testing

Parts have been tested by checking their resonant frequency for many years. From time to time various forms of the ‘ding it and listen’ method, sometimes enhanced with electronic equipment, have been tried but have not in general been demonstrated to be sufficiently discriminating for testing the serviceability of castings. The normal variations within castings often changed the ‘ringing frequency’ more than unacceptable changes in material or structural integrity.

It is worth devoting some space to one particular development of the resonance test that has become available over recent years to illustrate the degree of sophistication that has been necessary to evolve a useful and powerfully discriminating test. The technique is outlined below.

A casting is subjected to a swept spectrum of vibrational frequencies and its response is recorded as a frequency spectrum. Among the thousands of resonance peaks observed in the spectrum, about 50 prominent and recognizable peaks are selected as potentially useful for further analysis. These 50 frequencies are recorded for each casting in a sample ‘teaching’ set of 100 or more castings, some of



which are normal, acceptable castings and some of which have been rejected for various reasons. These samples provide the resonant frequency information to ‘teach’ the system to accept changes in frequencies that are the result of normal process changes (such as slight changes in size or shape, chemical composition, etc.), which do not affect its serviceability. The software selects and analyzes about six resonant frequencies to incorporate the possible variations into one comprehensive ‘pattern’ that can encompass all the acceptable variations.

The presence of the unacceptable castings in the sample set is to ascertain whether the frequency pattern that accepts all the good parts is in fact capable of rejecting all of the castings in which there is a known defect. If defects are present, the frequency pattern of the unacceptable casting will change in ways that are different from those for normal castings. The amount of change is usually a measure of the seriousness of the defect. This concept relies on the quality assurance teaching phase defining as ‘acceptable’ those parts that are structurally acceptable, as measured by metallurgical, destructive, and non-destructive testing. An iterative ‘teaching’ process is undertaken, so that suitable frequency patterns are progressively identified and confirmed by separate testing as useful indicators. Because of the number of castings required for this setting-up phase, the technique is limited to long series production parts, but achieves zero or near-zero false acceptance errors in millions of components. Typical production testing time is a few seconds per casting in a fully automated, computer-controlled sorting operation.

A typical distribution chart of testing for leaking master brake cylinders is shown in Figure 19.8. ‘Perfect’ castings would be expected to fall on the 45° line for which observed and predicted vibration frequency pattern are identical. However, a spread of vibration pattern (i) within the region defined by the ellipse and (ii) to the left of a second criterion is found to deliver acceptable products. Frequencies outside these two boundaries, ‘the acceptance window’, were always found to have some serious fault, although many had been accepted by X-ray and liquid dye-penetrant inspection. Figure 19.8 shows only two discriminating frequency boundaries as a simplifying example, whereas in fact the technique

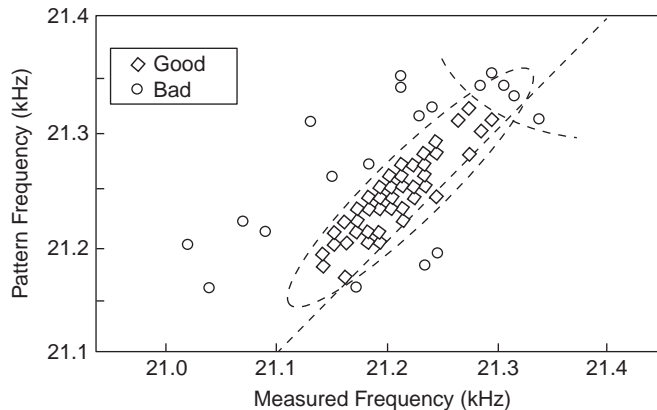


**FIGURE 19.8**

A representation of a sophisticated resonant frequency sorting technique, here illustrating a two-dimensional elliptical and a curved boundary, separating good parts from bad. In practice multi-dimensional criteria are used (data courtesy of Magnaflux Quasar).

always uses a pattern combining about six resonances analyzed by sophisticated software. In view of the ability of the technique to allow for the harmless changes caused by slight process variations, it has been called 'process compensated resonance testing' (PCRT).

Current developments include the exploration of computer models of the component under test, to ascertain whether the 'teaching' stage, and the exploration of the effects of different kinds and sizes of defects and other changes, may be carried out in the computer.

Castings with structural weakness (previously accepted because the major defects were effectively invisible bifilms that gave little or no classical NDT indications) are rejected. Conversely, castings that would have been rejected for negative NDT indications are accepted if they are assessed to be structurally acceptable.

A further interesting capability of the technique, known as resonant ultrasound spectrometry, is the accurate measurement of the elastic (Young's) modulus, as well as other elastic properties such as shear modulus and Poisson's ratio. The elastic moduli are reduced if there are a large population of small bifilms present in the casting. The casting can be rejected if the elastic moduli fall sufficiently to indicate a serious concentration of bifilms that would, for instance, impair the ductility and toughness of the alloy. The ability of the technique to assess ductility and toughness without resort to the expense and delay involved with a destructive tensile test is a further impressive advantage.

The concept provides a quality assurance method that predicts the structural performance of the casting, reduces false reject scrap, and reduces testing costs. This new, fast and low-cost technique appears to outperform our existing NDT techniques, and promises to be powerful for future high production and safety-critical products.

# Appendix I

## THE 1.5 FACTOR

Experimental results for side-gated 99.8 Al plate castings plotted in Figure A1 show that casting time  $t_c$  may be estimated for the plates and other castings from an equation:

$$t_c = 1.5 \times \text{Casting volume}/\text{Initial casting rate} \quad (1)$$

This is equivalent to:

$$\text{Initial fill rate}/\text{Average fill rate} = 1.5 \quad (2)$$

These experimental results gives support to the value of 1.5 chosen by previous authors, particularly those of the British Non-Ferrous Research Association (now no longer with us) researching for the UK Admiralty (Ship Department 1975).

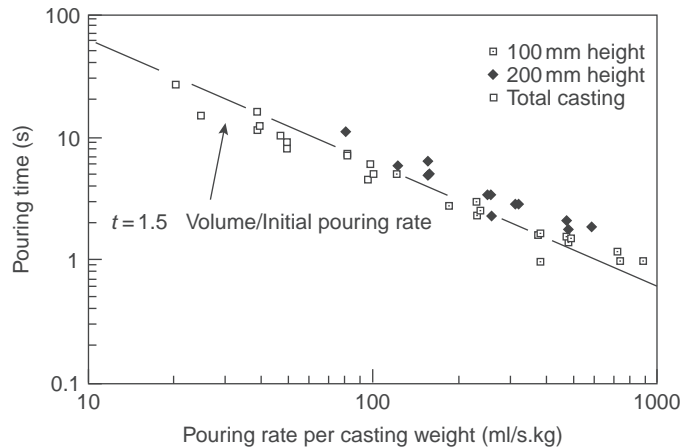
Exploring the 1.5 factor further by a theoretical approach is not quite so straightforward, but an attempt is outlined below.

Considering Figure A2, the velocity at the base of the sprue is given by:

$$V_2 = (2gH)^{0.5}$$

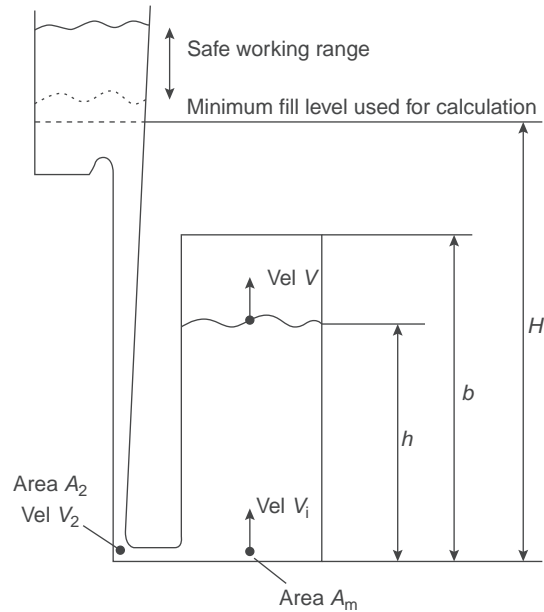
If the area of the base of the sprue is  $A_2$  and the mold cavity is of uniform area  $A_C$  the initial velocity of rise in the mold will be given by

$$V_i = (A_C/A_2) \cdot (2gH)^{0.5}$$



**FIGURE A1**

Experimental demonstration of the relation between initial and average filling rates (data from Runyoro and Campbell 1992).

**FIGURE A2**

Schematic view of the filling of a uniform section casting.

Similarly, at some later instant, when the melt has reached height  $h$ , the net head driving the filling is now reduced to  $(H - h)$  so that the rate of rise is now:

$$V = (A_c/A_2) \cdot (2g(H - h))^{0.5}$$

Substituting  $dh/dt$  for the rate of rise  $V$ , rearranging and integrating between the limits of time  $t = 0$  at  $h = 0$ , and  $t = t_c$  at  $h = b$ , we find the casting time (the time to fill the mold)  $t_c$  is given by:

$$t_c = (A_m/A_2) \cdot (2/g)^{0.5} [(H^{0.5} - (H - b)^{0.5})]$$

Now writing simple definitions of the initial rate of castings  $Q_i$  and the average rate of casting  $Q_{av}$  in such units as volume of liquid per second, defined by the appropriate velocity times the area, we have:

$$Q_i = A_2 \cdot (2gH)^{0.5}$$

$$Q_{av} = A_m \cdot b/t_c$$

It follows that:

$$Q_i/Q_{av} = 2H^{0.5} [(H^{0.5} - (H - b)^{0.5})]/b$$

This solution to the filling problem is interesting. There are various combinations of  $H$  and  $b$  that can fulfill the conditions defined by the equation. For instance, if  $H = b$ , then  $Q_i/Q_{av} = 2$ , which is actually an obvious result meaning simply that the average is half of the start and finishing rates.

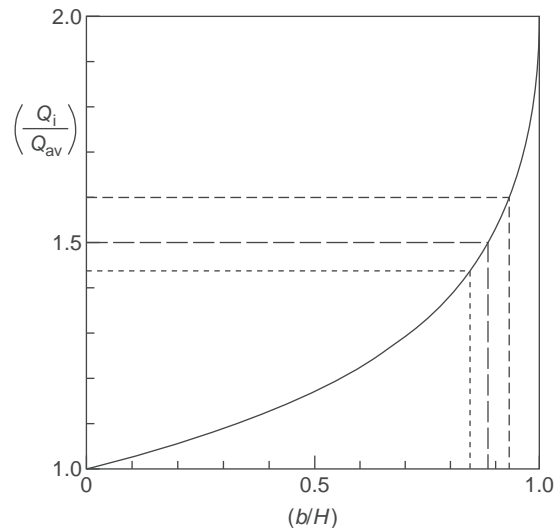


**FIGURE A3**

The relation between the initial and average fill rates for a uniform section casting as a function of the relative heights of the casting and the pouring basin.

On the other hand,  $Q_i/Q_{av} = 1.5$  only when  $b = 0.89H$ . This represents an intriguing result, indicating that for most castings the top of the pouring basin is on average only about 10% higher than the height of the casting. Thus it seems the factor 1.5 is quite fortuitous, and results simply from the geometry we happen to select for most of the castings we make. If, in general, we were to raise (or lower) our pouring basins in relation to the tops of our castings, the factor would have to be revised.

However, all is not so bad as it seems. Figure A3 shows that the factor 1.5 does not change rapidly with changes in relative height of basin, varying over reasonable changes in basin height of  $b/H$  from 85% to 95% from roughly 1.55 to 1.60. These changes are of the same order as errors arising from other factors such as frictional losses, etc., and so can be neglected for most practical purposes.

This page intentionally left blank

# Appendix II

## THE BERNOULLI EQUATION

Daniel Bernoulli represents the revered name in flow. He published his equation in 1738 in one of the first books on fluid flow. This magnificent result is the one used for all descriptions of flow in pipes and channels. Whole books are devoted to its application.

There are, of course, excellent examples of the power of Bernoulli's equation. Sutton (2002) has made good use of the equation to describe the pressures along a long runner, explaining the early partial filling of gates at different positions along the runner, and thus resulting in part-filled castings. He used the equation in its simplest form, derived from a statement of conservation of energy along a flow tube as illustrated schematically in Figure A4:

$$p_1/\rho g + v_1^2/2g + z_1 = p_2/\rho g + v_2^2/2g + z_2 = \text{constant}$$

where all the component terms of this equation have units of length, conveniently meters. For this reason each term can be regarded as a 'head'. Thus  $p/\rho g$  = pressure head,  $v^2/2g$  = kinetic or velocity head, and  $z$  = potential or elevation head.

In application to the running system used by Sutton (Figure A5) at location 1 the height above the centerline of the runner is 0.5 m, the kinetic head at this point is zero because the melt has zero downwards velocity, and the elevation head  $z$  is considered zero because the runner is horizontal. At point 2, the pressure head requires to be known, since this is the pressure raising the melt level in the vertical ingate. The elevation is zero once again, and the velocity head is close to 0.25 m, easily deduced from the total fall height and allowing for a small loss factor of 0.70 (probably overestimated, since I think this should be more like 0.80 or even 0.85) as a result of the turn at the base of the sprue. Thus the Bernoulli equation becomes:

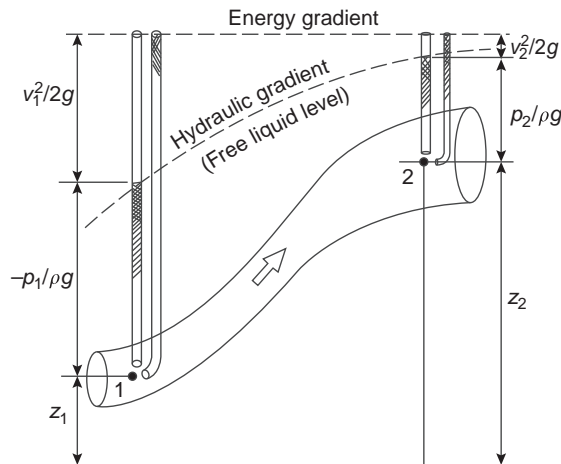


**FIGURE A4**

A pictorial representation of the factors in the Bernoulli equation.

$$0.5 + 0 + 0 = p_2/\rho g + 0.25 + 0$$

Thus:

$$p_2/\rho g = 0.25 \text{ meter}$$

It is not necessary to find  $p_2$  alone; the whole term is the height distance. Thus this answer would be the same for aluminum or iron.

Sutton found that because of this kinetic head, ingates were filling before the runner was fully filled. The first impression in his multi-impression mold was only about 200 mm above the runner so that metal entered the mold cavity under only about 50 mm net head. The result was a premature dribble into the cavity that quickly froze. The arrival of melt at the intended full flow rate a few seconds later was too late to remelt and thus assimilate the frozen droplets. An apparently mis-run casting was the result.

In general, however, the application of the Bernoulli equation to filling systems is not quite so straightforward as has sometimes been assumed. There are various reasons for this.

1. In general, Bernoulli's equation relates to steady state flow. However, of course, in filling systems most of the interest necessarily lies in the priming of the flow channels. In this situation the surface tension of the advancing meniscus can be important, as enshrined in the Weber number. If the priming is not carried out well, the casting is likely to suffer severely.
2. The surface tension of liquid metals is over ten times higher than that of water, and even higher still compared to most organic liquids. Thus pressures due to surface tension have been neglected and

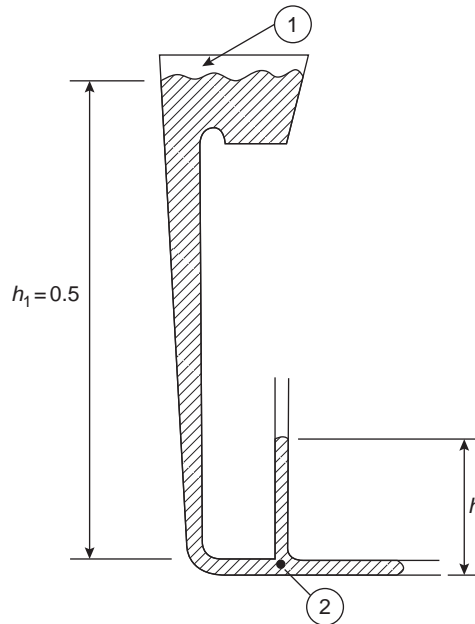


**FIGURE A5**

An example of the use of the Bernoulli equation by Sutton (2002) to calculate the rise of metal in a vertical gate.



are neglectable for such common room temperature liquids on which most flow research has been conducted. The additional pressure generated because of the curvature of the meniscus at the flow front, and the curvature at the sides of a flow stream, affect the behavior of metals in many examples involved in the filling of molds. For instance at the critical velocity that is targeted in mold filling, the effects of surface tension and flow forces are equal. At velocities lower than this, surface tension dominates.

3. The presence of the oxide (or other thin, solid film) on the surface of an advancing liquid is a further complication, and is not easily allowed for. The flow adopts a stick-slip motion as the film breaks and re-forms. The advance of the unzipping wave is a classic instance that could not be predicted by a purely liquid model such as that described by Bernoulli.
4. The frictional losses during flow, which can be explicitly cited in Bernoulli's equation, are known to be important. However, in general, although they are assumed to be known, they have been little researched in the case of the flow of liquid metals. Furthermore, it is unfortunate that most of the research to date in this field has used such poor designs of filling systems that the existing figures are almost certainly misleading. The losses need to be confirmed by new, careful, accurate studies, supplemented by accurate computer simulation together with video X-ray radiography of real flows.
5. The presence of oxide films floating about in suspension is another uncertainty that can cause problems. The density of such defects can easily reach levels at which the effective viscosity of the mixture can be very much increased (although it is to be noted that viscosity does not appear explicitly in the Bernoulli equation). The suppression of convection in such contaminated liquids is common. Flow out of thick sections and into very thin sections can be prevented completely by blockage of the entrance into the thin section.

From the above list it is clear that the application of Bernoulli is more accurate for thicker section flows where surface effects and internal defects in the liquid are less dominant. As filling systems are progressively slimmed, and casting sections are thinned, Bernoulli's equation has to be used with greater caution.

As a result of the problems of the application of Bernoulli to the priming of the filling system, it has been relatively little used in this book because the concentration of effort has focussed on the control of the priming of the system. The subsequent flow of the system when completely filled, as nicely described by Bernoulli, is, with the greatest respect to the Great Man and his magnificent equation, much less important.

This page intentionally left blank

# Appendix III

The recording of the lists of choices when drafting up a new methoding design for a casting requires to be carefully recorded. If there is found to be any problem with the first design, a second iteration can be worked out in the light of what appears to be needed (for instance the casting may be required to fill a little faster). Table A1 can be used as a hard copy, allowing up to four iterations for a new filling system design. Alternatively, of course, the table can form the basis of a computer spreadsheet, so that iterations can be performed rapidly and recorded digitally.

Table A1 Running system record			Design 1	Design 2	Design 3	Design 4
Casting name			Signature	Signature	Signature	Signature
Part number						
Customer			Date	Date	Date	Date
Alloy						
Casting weight	$M_C$	kg				
Rigging weight	$M_R$	kg				
Total pour weight	$M_C + M_R = M$	kg				
Fill time selected	$t$	s				
Average flow rate	$M/t$	$\text{kg s}^{-1}$				
Design flow rate	$2 M/t$	$\text{kg s}^{-1}$				
Volume flow rate	$Q = 2M/\rho t$	$\text{m}^3 \text{s}^{-1}$				
Height in basin	$h$	m				
Working basin depth	$h$ to $2h$	m				
Velocity into sprue	$V_1 = (2gh)^{1/2}$	$\text{m s}^{-1}$				
Area sprue top	$A_1 = Q/V_1$	$\text{m}^2$				
Velocity exit sprue	$V_2 = (2gH)^{1/2}$	$\text{m s}^{-1}$				
Area sprue exit	$A_2 = Q/V_2$	$\text{m}^2$				
Radius to runners	$R = A_2^{1/2}$	m				
Number of runners	$n$					
Area of each runner	$A_2/n$	$\text{m}^2$				
Select critical velocity	$V_C = 0.5-1.0$	$\text{m s}^{-1}$				
Total gate area	$A_3 = A_2(V_2/V_C)$	$\text{m}^2$				
Basin volume (1 second)	$Q$	$\text{m}^3$				

### RATE OF POUR OF STEEL CASTINGS FROM A BOTTOM-POUR LADLE

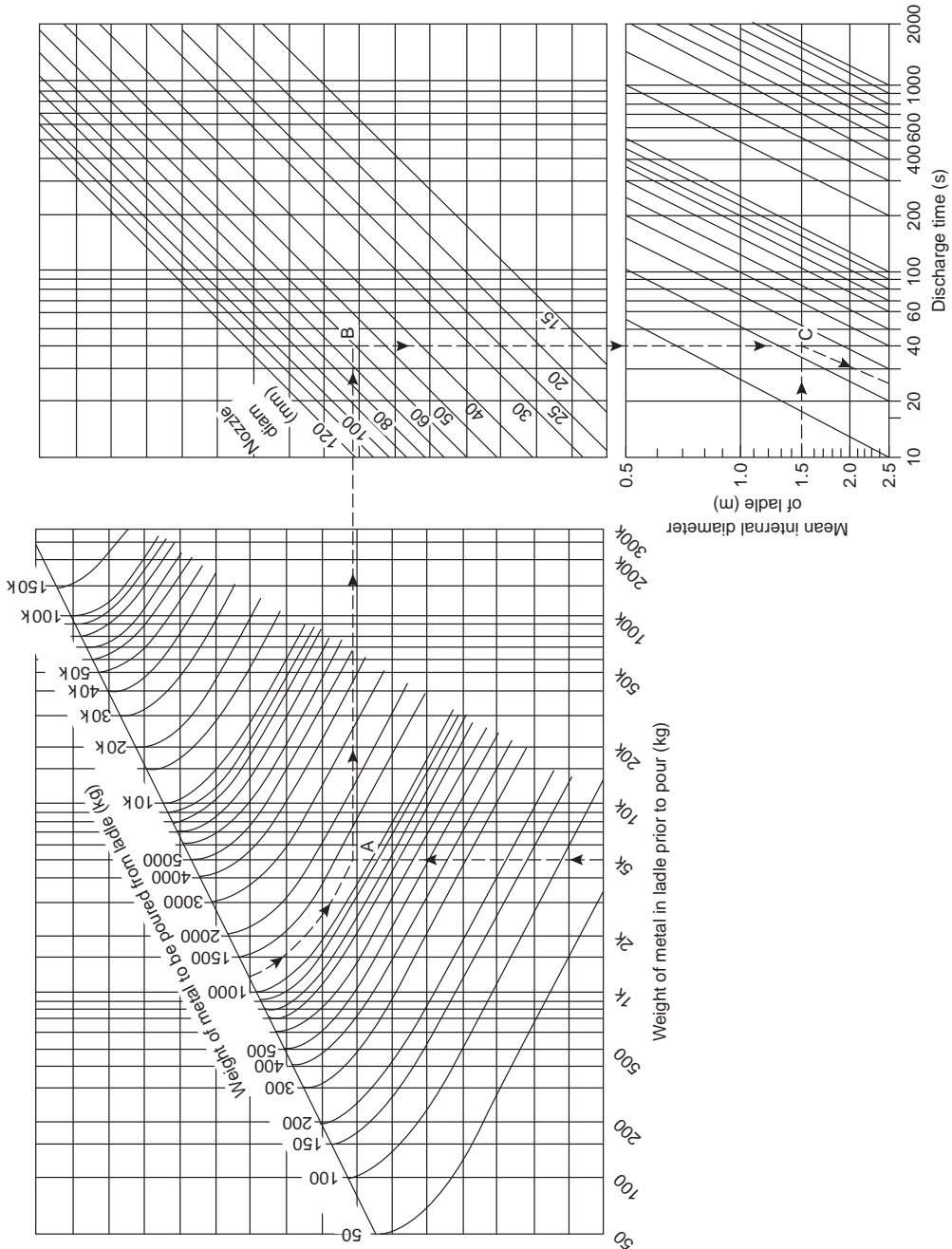


**FIGURE A6**

Rate of delivery of metal from a bottom-pour ladle.

## RATE OF DELIVERY OF STEEL FROM A BOTTOM-POUR LADLE

The following is an example of how the nomogram is used.

A ladle contains 5000 kg of steel, from which we wish to pour a casting of total weight 1250 kg. Thus we follow the arrows from the start point to junction A. From here a horizontal line connects to the next figure, where we select a pouring nozzle for the ladle of 60 mm diameter. At this junction B we drop a vertical line down to intersect with the line denoting that our ladle is about 1.5 m internal diameter. From this junction C we continue with a parallel line to the family of sloping lines, to find that our casting will pour in approximately 23 seconds.

Interestingly, the reader can check that the next 1250 kg casting in line (now starting with a ladle of  $5000 - 1250 = 3750$  kg) will be found to pour in about 29 seconds, and the next in 34 seconds, and the next in 77 seconds, as the ladle progressively empties.

This page intentionally left blank

# Index

- 1.5 factor (initial/average fill rates), 1091–3
- 10 rules for good castings, *see* Rules
- 10 test bar mold, 500–2

## A

- Ablation casting (RS), 1019–23
- Accuracy, *see* dimensional accuracy
- Acetylene black and fluidity, 132
- Active feeding, 687–8
- Additions to melts, 901
- ADI, *see* austenitic ductile iron
- 'Aero chocolate structure' (zinc alloys), 987
- Aerofoil fluidity tests for investment casting, 138
- Aerospace applications:
  - aluminium alloys, 612
  - castings and quenching, 712
  - location points, 729
- AFS fitness number for aggregates, 918
- Ag<sub>3</sub>Sn (intermetallic), 255
- Aggregate molding materials:
  - AFS fitness number, 918
  - carbon, 922
  - chromite sand, 920
  - description, 939
  - hollow ceramic spheres, 922
  - minerals, 921–2
  - olivine, 919–21
  - silica sand, 919–20
  - zircon sand, 919–21
- Aggregate molds:
  - coatings, 183–4
  - Cosworth Process, 1062
  - mold accuracy, 1038–1041
  - residual stress, 707
  - steels and dimensional accuracy, 1039
- Aided flotation and detrainment, 897
- Aided sedimentation and detrainment, 897–9
- Air:
  - entrainment, 780, 941
  - gap and metal–mold interface, 191–8

- melting and casting of nickel alloys, 383
- quenching, 719
- 'Air gap' and rapid solidification, 1018–1023
- 'Air inclusion', term, 827
- Air lock*, 849
- Alcan, 433, 906, 908
- Alkaline phenolic (A-P) binders, 926, 934
- Allan, Alec, 882
- Alotech, 887, 897
- Alumina:
  - bifilms, 89, 373–4, 894
  - bismuth, 88
  - furling and unfurling, 84–5
  - inclusions, 518
  - liquid aluminium, 21
  - liquid steel, 37
  - slag and flux inclusions, 32
  - stringers, 37–8
  - vertical filling of casts, 59
  - zinc alloys, 258
  - γ-alumina, 271
- Aluminides (titanium alloys), 227, 275, 387–90, 449
- Aluminium:
  - aluminium inserts, 211
  - bifilms, 528, 535
  - bubble trails analysis, 73
  - contact pouring, 761–762
  - critical velocity, 48–9, 617
  - crucible melting, 881–2
  - diffusion coefficients, 12
  - ductility, 535
  - expansion and contraction, 1032
  - fcc structure, 543
  - feeders, 66, 660–1, 674–5
  - filtration, 899–900
  - fins, 213–14, 215–16
  - fluidity, 135
  - freezing range, 666
  - hexachlorethane degassing, 892
  - holding, 885
  - HPDC, 986
  - hydrogen, 6–7, 306–9, 895, 902
  - L-junctions, 213–14
  - magnesium alloys, 266
  - melting, 879

- melts, 4
- mold gases, 165
- Ni-base alloys, 382–6
- oxides, 28, 263–5, 904
- reclamation and recycling of
  - aggregates, 932–5
- residual stress (quenching), 712
- rotary degassing, 893–6
- rotary furnaces, 881
- shot, 922
- shot blasting, 1068
- siphons, 888
- solidification, 398
- strength of castings, 617
- strontium, 1051
- structure, 3
- surface tension, 756, 760
- T-junctions, 213–14
- thermal conductivity, 881
- vapor zones in greensand mold, 159–60
- wall plaques, 939
- water vapor, 9
- zinc alloys, 255–60
- see also* liquid aluminium
- Aluminium alloys:
  - 7000 series, 378, 496, 713
  - 7050 high strength, 559
  - ablation casting, 1019–23
  - accuracy, 1073
  - active feeding, 687–8
  - aerospace, 612
  - alumina films, 593
  - aluminium bronze
    - chills and fins, 217–19
    - critical velocity, 49–50
    - Durville casting, 948–55
    - feeder neck constriction, 674–5
    - feeding distance, 676–9
    - hydrogen solubility, 8
    - leaks, 1087
    - penetration barriers, 177
    - pouring, 54
    - surface films, 15
  - Al–0.2Cu porosity/interdendritic segregation, 240–1
  - Al–1Cu equiaxed grains, 485–6
  - Al–1Si–1Cu slip band direction, 547

Aluminium alloys: (*Continued*)

- Al–1Sn hot tear, 470
- Al–3Cu–5Si modulus, 131
- Al–3Mg grain size, 543
- Al–4Mg oxidation and corrosion resistance, 578–9
- Al–4.5Cu
  - ablation casting, 1019–20
  - CuAl<sub>2</sub>, 304
  - DAS, grain size and T<sub>f</sub>, 236–7
  - elongation to fracture, 537–8
  - eutectic and time, 1071
  - furling and unfurling, 82–5
  - grain refinement, 542–5
  - inclusions, 517
  - macrosegregation, 705
  - quality indices, 594–7
  - tilt casting, 957
- Al–4.5Cu–0.7Ag tear initiation, 475–6
- Al–4.5Cu–1.5Mg ductility, 534, 536, 554–5
- Al–4.5Mg bifilms, 91
- Al–4.5–0.4Mg elongation v. yield strength, 538
- Al–4.8Cu dendritic segregation, 249
- Al–5Mg
  - deactivation of entrained films, 88
  - freezing range, 666
  - oxidation, 263–5
- Al–5Si, penetration barriers, 177
- Al–5Si–3Cu
  - chills, 207
  - residual stress, 574–5
- Al–6Zn–2.7Mg–1.7Cu aging time, 538–9
- Al–6.6Cu hot tear, 467–86
- Al–7Si
  - cellular growth, 282, 287
  - chills, 207–8
  - magnesium, 655
  - modulus, 131
  - oxide bifilms, 227–8
  - phenolic-urethane binders, 654
  - superheat and fluidity, 132–3
  - thermal analysis, 305–6
- Al–7Si–0.3Mg
  - channel defects, 253
  - external chills, 249
  - gas porosity, 443
  - gravity segregation, 711
  - macrosegregation, 706
  - viscosity, 128
- Al–7Si–0.4Mg
  - ablation casting, 1019–23
  - bifilms, 98, 609–11
  - bubble trails, 73
  - deactivation of entrained films, 88–92
  - engineering, 270
  - flow channel behaviour, 220–3
  - fluidity, 110
  - furling and unfurling, 77–8
  - grain refinement, 542–5
  - heat treatment, 1072–73
  - HIPping, 1077–80
  - hot tear, 466
  - hydrogen porosity, 453–7
  - incipient melting, 1075
  - β-iron, 548–9
  - mechanical properties, 86–7
  - micro-blows, 654–5
  - microjetting, 66
  - pore initiation on bifilms, 433
  - pouring, 902–5
  - reduced pressure tests, 95–6
  - sand inclusions, 40–1
  - squeeze casting, 995
  - strontium, 273
  - surface films, 26–7, 32–5
  - uniform contraction, 1046–53
- Al–7Si–0.4Mg–0.4Fe eutectic phase, 553–4
- Al–7Si–0.5Mg
  - fatigue/fracture, 560–1
  - shot blasting, 1068
  - uniform contraction, 1046–53
- Al–7Si–0.6Mg fracture toughness, 557
- Al–7Si–Mg
  - 10 test bar mold, 500–2
  - elongation to fracture, 537–8
  - fatigue, 564–5
  - quality indices, 595
- Al–8Si–3.3Cu–0.2Mg uniform contraction, 1051
- Al–9Si–4Mg oxide skin, 320–1
- Al–10Mg
  - batch melting, 879–80
  - beryllium, 272
  - hipping, 1079
- Al–10Si lost foam castings, 1004
- Al–11Si
  - dendritic segregation, 247–50
  - surface films, 32, 34
- Al–11.5Mg layer porosity, 441–2
- Al–11.5Si bifilms evidence, 95
- Al–12Si
  - feeder size, 400–1
  - freezing range, 666
  - oxide bifilms, 299–300
  - shrinkage porosity, 414, 416–17
- Al–17Si
  - engine blocks, 136
  - uniform contraction, 1051, 1054
- Al–21Cu channel segregation, 252
- Al–Ag bonding, 210
- Al–Cd hot tear, 470
- Al–Cu
  - casting, 270
  - channel segregation, 252
  - continuous fluidity, 152–3
  - gravity segregation, 250–2
  - hot tearing, 465–6, 480–1, 483
  - hydrostatic tension, 409–10
  - silicon, 304
  - stress concentration, 473–4
  - susceptibility prediction of hot tearing, 479–81, 483
- Al–Cu–Fe/Mg alloying and hot tears, 492
- Al–Cu–Si fluidity and latent heat, 122–3, 136
- Al–Li elastic modulus, 573
- Al–Mg
  - barriers to diffusion, 461
  - beryllium, 93, 272
  - blister formation, 1073–4
  - casting, 270
  - eutectics and interdendritic feeding, 408–9
  - hot rolling, 1084–5
  - intergranular corrosion, 585–6
  - properties, 263–6
  - surface films, 13, 15
  - susceptibility prediction of hot tearing, 479–83
- Al–Mg<sub>2</sub>Si system, 303, 909
- Al–Pb hot tear, 470
- Al–Si
  - bifilms, 77–8, 227, 298, 332, 609–10



- casting, 270
- chills, 203
- continuous fluidity, 151–3
- CSC parameters, 482
- eutectic Si, 279–98
- extended fluidity, 148–9
- feeding theory, 690
- filter contamination, 851
- flowability, 142
- fluidity, 110–1
- furling and unfurling, 77–88
- gates, 815
- Hall-Petch relation, 540
- hot tear, 466
- interdendritic phases, 548
- iron-rich intermetallics, 299
- latent heat and fluidity, 134–7
- machining, 1081–2
- magnesium, 272, 655
- micrographs, 347
- microjetting, 66
- modulus, 131
- mold explosions, 166–7
- nucleation, 227–8, 284
- phase diagram, 287–90
- phosphorus, 283
- sand blasting, 1067–9
- shrinkage porosity initiation, 418–36
- silicon particles, 228, 280–1, 284
- in situ MMC, 908–9
- sodium, 273
- strontium, 260, 273, 302, 1051
- susceptibility prediction of hot tearing, 479–83
- tensile properties, 501, 529–30
- titanium, 277–8, 304
- uniform contraction, 1047, 1050
- Al–Si–0.4Mg reverberatory furnaces, 880–1
- Al–Si–3.5Cu heat treatment, 1072
- Al–Si–Mg ductility, 538
- Al–Sn fluidity, 115–16
- Al–Ti phase diagram, 275–6
- Al–TiB<sub>2</sub> metal/matrix composite, 30
- Al–Zn
  - AZ91, 262–3, 266, 267–9
  - fluidity, 116–18
  - superheat, 116–18
- Al–Zn–Mg–Cu
  - ductility, 538
  - surface, 1074
- argon, 886
- automatic greensand molding, 940
- automotive systems, 520–1, 657
- beryllium, 93
- bifilms
  - Al–Si, 531, 538, 610
  - bismuth, 88
  - evidence, 94–100
  - furling and unfurling, 77–88
  - hydrogen precipitation, 79–80, 296
  - intermetallics in Al–Si alloys, 82
  - mechanism, 339
  - melting, 887
  - oxides, 82–5
  - pouring and turbulence, 271
  - shrinkage, 70, 80
- binders, 923–32
- bismuth, 88
- borides, 518
- boron, 918
- bubble trails, 72, 75–6
- bubbles, 70
- carbides, 518
- carbon black (thin-walled parts), 144
- castings, 192–5, 269–71
- ‘cell count/size’, 240–1
- ceramic foam filters, 839
- chills, 203–4
- ‘Chinese script’, 303
- clamping points, 736
- confluence welds, 57–8, 63–4
- contact pouring, 941
- contraction, 887
- corrosion, 518, 541, 575–87
- counter-gravity casting, 1073–4
- cracks, 46–7, 497
- critical fall heights, 741
- crucible melting, 881–2
- cylinder heads, 955–6
- datums, 729–30
- deactivation of entrained films, 88–9
- degassing, 888–96
- delivery, 879–80
- dendrite arm spacing, 86–7, 278–9
- dendrites, 229, 231–2, 235
- detrainment, 896, 901
- dies, 912–13
- direct chill, 378
- dry hearth furnaces, 53, 612, 883–5
- entrained inclusions, 273–4
- expansion and contraction, 1032
- external chills, 204–6
- feeding, 663, 667
- filtration, 899–901
- fins, 1013
- flow, 108–153
- fluidized beds, 1075
- furling and unfurling, 77–88
- grain refinement, 182–3, 228, 274–8, 542–5
- gravity die castings, 882
- grit blasting, 1068–9, 1082
- growth restriction parameter, 275–8
- Hall-Petch relation, 540–1
- heat pipes, 219
- heat treatment, 719–20
- high-volume, 762
- hot isostatic pressing, 1077–80
- HPDC, 913–14, 986–7, 1033, 1042, 1044
- hydrogen, 5–9, 13–16, 306–9, 454, 457, 894
- hydrostatic tensions, 396–9, 404–5, 412
- inclusions, 3–5, 9, 273–4, 607
- internal chills, 207–10
- iron-rich metallics, 298–303
- liquid, 271, 273, 880, 888
- liquid fluxes, 38, 93
- long-freezing-range (feeding distance), 677
- lost foam casting, 1001–5
- lost-wax casting, 1051
- magnetic molding, 917–18
- markets, 270–1
- melting, 879–910
- melts, 879, 882, 886–98, 901–2, 909
- metal/matrix composites, 29, 39
- Mitsubishi, 256, 258
- mushy state testing, 489
- non-feeding role of feeders, 695–6
- oxide bifilms, 892–7, 900, 909
- oxides, 53, 64, 261, 271–2
- painting, 1083
- pouring, 54–7
- quenching, 712
- rapid solidification, 1018–9
- residual stress, 707–14, 720–5
- reverberatory furnaces, 880

- Aluminium alloys: (*Continued*)  
 rolling waves, 108  
 rotary degassing, 893–6  
 rubber molds, 931–2  
 salt cores, 914–15  
 sand castings, 61  
 sedimentation, 94  
 shrinkage porosity, 69  
 SiC MMC, 908  
 Sn addition, 1082  
 solid feeding, 412–18  
 steel  
   gauze filters, 852  
   titanium inserts, 210  
 strength, 719–22, 839  
 strontium, 272, 593, 1051  
 structure, 3  
 superplastic forming, 576–8  
 surface-tension-controlled filling,  
   751–6  
 surfaces, 19, 24, 25–7, 32–3, 32–5,  
   53, 56–7  
 temperature distribution in  
   greensand mold, 159–60  
 thermal analysis, 305–6  
 Ti-Rich grain refiners, 612  
 ‘tilt pouring’, 948, 954  
 titanium, 275, 543, 979  
 ultimate tensile strength, 553–5  
 ultra-clean, 612  
 ultrasonics, 4, 98, 541, 608  
 unzipping waves, 109  
 vacuum molding, 1005–8  
 yield strength, 539–48  
 zircon sand molds, 1068–9
- Aluminium carbide in magnesium  
 alloys, 267
- Aluminium nitride, 370, 894
- Aluminium phosphide (AIP), 280–7,  
 290, 295, 298–9, 303
- Aluminium silicate (mullite), 915
- Ammonia and nitrogen porosity, 460–1
- Anorthosite (aggregate molding  
 materials), 921
- AOD (argon-oxygen-  
 decarburization),  
 889–91, 896
- Area ratios in pressurized/  
 unpressurized filling,  
 861
- ‘Areal pore density’ (parameter),  
 433–4
- Argon:  
 aluminium alloys, 886  
 degassing, 886  
 inert gas shroud, 902–3  
 magnesium alloys, 262–3  
 Asarco-type furnace, 884  
 ASTM radiographic standards, 518  
 Asymmetric films, 57  
 Austenite:  
   cast iron, 315–62  
   matrix structure, 224  
   pearlite transformation, 382  
   residual stress, 707  
   steels, 203, 379  
 Austenitic ductile iron (ADI), 359  
 Automatic bottom pouring (ABP),  
   882–3, 941–2  
 Automotive cylinder heads:  
   accuracy, 1062  
   air quenching, 719  
   Cosworth process, 974  
   die casting, 963–4  
   gravity dies, 942–3  
   residual stress, 707–14  
   strength reduction by heat  
     treatment, 720–2  
 ‘Avoid bubble damage’ rule:  
   bubble damage  
     counter-gravity systems,  
       634–5  
     description, 658  
     gravity filling systems, 633–4  
   bubble trail, 631  
 ‘Avoid convection damage’ rule:  
   academic background, 696–7  
   convection  
     countering, 704  
     damage and casting section  
       thickness, 701–4  
   engineering imperatives, 697–701  
 ‘Avoid core blows’ rule:  
   background, 635–47  
   core blow model study, 653  
   micro-blows, 654–5  
   outgassing pressure in cores,  
     647–53  
   prevention of blows, 655–9  
 ‘Avoid laminar entrainment of the  
 surface film’ rule:  
   hesitation and reversal, 629–30  
   horizontal stream flow, 627–8  
   meniscus, 623–5  
   oxide lap defects, 630  
   waterfall: oxide flow tube, 625–7  
 ‘Avoid shrinkage damage’ rule:  
   definitions/background, 659–60  
   feeding to avoid shrinkage  
     problems, 660–1  
   seven feeding rules, 661–88  
 ‘Avoid turbulent entrainment’  
   (critical velocity) rule:  
   introduction, 614–15  
   maximum velocity requirement,  
     615–19  
   ‘no-fall’, 619–22
- ## B
- Back-diffusion and microsegregation,  
 245
- Backing sands, 937–8
- Base for sprue, 781–2
- Batch melting (liquid metals),  
 879–83
- Bcc, *see* body-centered-cube
- Bells and loam, 929–30
- Bernoulli, Daniel, 1095–7
- Bernoulli equation, 1095–7
- Berthelot’s experiment, 397
- Beryllium:  
 aluminium alloys, 93  
 Al–Mg alloys, 272  
 iron-rich metallics, 298–303
- ‘Bifilm crack’, 26
- Bifilms:  
 alumina, 368, 894  
 aluminium, 528, 535  
 aluminium alloys, 886, 899–900,  
   905, 907  
 blister formation, 1073–4  
 bubbles, 29–32, 72, 99, 892  
 buoyancy, 28  
 castings, 255  
 chills, 204  
 copper alloys, 314–15  
 corrosion, 581  
 Cosworth Process, 102  
 cracks, 910  
 creep, 576  
 DAS and tensile properties, 550–3  
 deactivation of entrained films,  
   88–92  
 defects in magnesium alloys, 261  
 density, 27–8  
 description, 24–8

- detrainment, 94  
 directional solidification, 1014–6  
 double  
   entrainment defects, 24–42  
   evidence for bifilms, 94–100  
   furling and unfurling, 77–88  
   gray iron, 321  
   oxide flow tubes defects, 57, 65  
   surface flooding, 57  
   term, 21  
 ductile iron, 322–4  
 ductility, 533–9, 551  
 elastic modulus, 573–4  
 entrainment, 24–8, 51, 84, 86, 91, 98  
 flow regimes, 52  
 flux and slag inclusions, 32  
 furling and unfurling, 77–88  
 gold, 99–100  
 grain refinement, 274–5, 544  
 graphite, 339–43  
 gray iron, 320–322  
 Griffith's cracks, 103  
 heat treatment of Al alloys, 727  
 HIPping, 1077  
 hot tearing, 493  
 hydrogen, 713–14  
 importance, 100–3  
 initiation of porosity, 418–26  
 iron, 904–5  
 leaks, 1086–8  
 magnesium alloys, 268  
 melts, 608–12, 655  
 microstructure, 542  
 Ni-base alloys, 386  
 nitride, 325–6, 352  
 non-destructive testing, 103  
 pitting corrosion, 582  
 pore initiation, 433–6  
 pronunciation, 24  
 reduced pressure test, 95–7  
 residual stress, 713  
 scanning electron microscopy, 95, 99  
 shrinkage, 80  
 silicon, 279  
 single crystal solidification, 1016–8  
 steels, 380, 562, 586, 904–5  
 tear growth, 476–9  
 titanium alloys, 389  
 ultrasonics, 4, 98, 608  
 viscosity, 128  
 waterfall effect, 625  
 white iron, 359  
 X-rays, 1086  
 zinc alloys, 258–60  
*see also* aluminium alloys; double films;  
 oxide bifilms  
 Bimodal distribution, 506–7  
 Binary alloys, 230–1, 275–6  
 Binders:  
   alkaline phenolics, 926  
   cement, 930  
   chemical, 924–5  
   Croning shell process, 928–9  
   dry sand, 924  
   Effset process, 929  
   fluid (castable) sand, 930–1  
   furans, 925–6  
   gravity dies, 943  
   greensand, 923–4  
   hot box and warm box processes, 928  
   light-metal casting, 928  
   loam, 929–30  
   phenol-urethane, 926  
   silicates, 926–9, 937, 1040  
   sodium polyphosphate glass, 927  
   sodium silicate, 926–9, 937, 1040  
 Bismuth, 88, 232  
 Blind casters, 680–1  
 Blind feeders, 669, 680–2  
 Blister formation, 1073–4  
*Blow defect*, 635, 637  
 Blow holes and gas porosity, 445  
*Blow* term, 636  
*Blow-hole* term, 635  
*Blowhole* term, 635  
 Blows, *see* core blows  
 Body-centered-cube (bcc) structure, 224, 301, 497, 544  
 Boron, 183  
 Boron nitride and Mg–Zr alloys, 268  
 Bottom-gating:  
   filling system, 750–1, 757–8  
   gravity pouring of open molds, 940  
   molds, 619  
 Bottom-pour ladle, 767–9, 944, 1100–1  
 Box shaped castings, 749  
 Branched columnar zone, 238  
 Brasses, 309–12  
 Briefcase handles (zinc alloys), 259  
 Bronze:  
   bubble trails, 75  
   cannon, 654  
   description, 302  
   foundries, 178  
   'Freedom Bell', 627–8  
   grain refinement, 544–5  
   'skeins of geese', 74  
   wall plaques, 939  
   *see also* aluminium alloys:  
   aluminium bronze  
 Bubble damage:  
   'avoid bubble damage' rule, 631–5  
   copper, 74–5  
   description, 72  
   entrapment of small bubbles, 69–70  
   inclusion control, 826–7  
   leaks, 1086  
   radiography, 70–1  
   runner, 791  
   shrinkage porosity, 69  
   surface turbulence in filling system, 636–8  
   *see also* Rule 4 for good castings  
*Bubble damage* term, 69, 72, 827  
 Bubble trails, 1085–6  
   aluminium alloys, 72  
   aluminium and X-ray video, 68, 73  
   'avoid bubble damage' rule, 631–2  
   bifilms, 99  
   cast iron, 639–40  
   castings in vacuum, 76–7  
   collapse, 68  
   copper, 74–5  
   core blows, 639–40  
   description, 67  
   iron, 68–9, 75  
   length, 76  
   low-pressure casting, 75  
   structure, 67  
 Bubble traps, 835, 843  
 Bubbles:  
   bifilms, 29–32, 892  
   collapse, 31  
   core blows, 636–9  
   degassing, 891–3  
   detachment, 636, 639, 643–4  
   entrainment, 616, 775  
   gray iron, 639, 641–2  
   large, 28–9  
   leaks, 589  
   outgassing of cores, 636–9

- Bubbles: (*Continued*)  
 shape, 32  
 small, 28, 69–70  
 trail, 28–9
- Buoyancy forces and liquid metals,  
 1031–2
- Burst feeding (shrinkage porosity),  
 409–12
- Bypass designs (surge control),  
 819–20
- C**
- ‘Cake core’ (mold design), 1034–6
- Calcium cyanamide and steels,  
 379–80
- Calcium in magnesium alloys, 263
- Calcium silicide, 334, 369
- Capillary attraction, 753
- Capillary repulsion, 753
- Carbon:  
 aggregate molding, 922  
 black and casting thin-walled parts,  
 144  
 cast iron, 315–16  
 ferrous alloys, 922  
 metal surface reactions (pick up and  
 loss), 179–81  
 steels, 362–3, 367, 484, 497
- ‘Carbon boil’, 362
- Carbon dioxide in magnesium alloys,  
 262
- Carbon equivalent* (CE), 316
- Carbon equivalent value* (CEV), 316,  
 335
- Carbon films (lustrous carbon),  
 170–1, 326–31
- Carbon monoxide:  
 cast iron, 317  
 gas porosity, 447–8  
 pressure in steel castings, 451
- Carbon tetrachloride and tensile  
 strength, 397
- Carbon-based filters for steels, 852
- Carburization in low-carbon steels,  
 180
- Cast iron:  
 bubble trails, 68–9, 75–6, 639–40  
 carbon, 315–16  
 carbon monoxide, 317  
 carbonyl, 172  
 CaSi, 613  
 chills, 207
- chunky graphite, 357–9
- core blows, 640–2
- decarburization, 180–1
- dies, 943–4
- dimensional accuracy, 1033
- Ellingham diagram, 318–19
- expansion and contraction, 1032
- Fe–C and graphite films, 330–1
- flake graphite iron and inoculation,  
 334–43
- gases, 316–18
- graphite flakes, 228
- gravity dies, 942–4
- holders, 886
- machining, 1080–3
- microstructures  
 eutectic growth graphite/  
 austenite, 345–7  
 flake graphite iron, 334–43  
 graphite, 333–4  
 introduction, 332–3  
 nucleation and austenite mix,  
 343–5
- nitrogen, 317–18
- nodularity, 922
- pressure requirement (feeding),  
 685–7
- pressurized systems, 857–60
- sand mold penetration, 176
- solidification, 190–1
- spheroidal graphite iron, 347–52
- structure hypothesis summary,  
 360–2
- surface films  
 bifilms in ductile iron, 322–4  
 carbon films, 326–31  
 introduction, 318  
 nitride bifilms, 325–6  
 oxide bifilms in gray iron,  
 320–2  
 oxides, 318–20  
 plate fracture defect in ductile  
 iron, 324–5  
 temperature, 60  
 white iron, 359–60
- Cast material:  
 just-in-time slurry production,  
 906–7  
 liquid metal, 905  
 metal/matrix composites, 907–8  
 Mg alloy slurry production from  
 granules, 907
- partially solid mixtures, 905–6
- rheocasting, 906
- strain induced melt activation, 907
- thixocasting, 906
- Cast pre-forms for forging, 996–7
- Cast-on fins, 219
- Cast-resin patterns, 1045
- Casting:  
 centrifugal, 980–5  
 constraint, 1055–61  
 counter-gravity, 960–79  
 dimensions statistics, 1025–6  
 gravity, 939–46  
 horizontal transfer, 947–60  
 industry structure, 600–2  
 lost foam, 1001–5  
 lost wax/ceramic mold processes,  
 997–1001  
 manufacture, 600–2  
 pressure assisted, 985–97  
 vacuum melting and casting,  
 1009–11  
 vacuum molding, 1005–8  
 vacuum-assisted, 1008–9
- Casting accuracy:  
 non-uniform contraction, 1053–61  
 process comparison, 1061–3  
 shrinkage, 1048  
 summary, 1063  
 uniform contraction, 1046–52
- Casting alloys:  
 aluminium, 269–309  
 cast iron, 315–62  
 copper, 309–15  
 introduction, 255  
 magnesium, 260–9  
 nickel, 382–6  
 steels, 362–82  
 titanium, 386–90  
 zinc, 255–60
- Casting rules, *see* rules
- Cavitation description, 684
- ‘Cavitation’ (superelastic forming),  
 576
- ‘Cell count’, 241
- ‘Cell size’, 241
- ‘Cell’ term, 241
- Cellular front growth, 229–30, 282
- Cement binders, 930
- Cementite (carbide), 360
- Central versus external systems (gates  
 and filling), 814–15

- Centrifugal casting, 979–85  
 Centrifugal pumps for liquid metals, 969–70  
 Centrifuge casting, 980  
 Ceramic block filters, 838–40, 851  
 Ceramic foam filters, 838–9, 841–2, 851  
 Ceramic molds accuracy, 1041–2  
 Ceramic molds and cores:  
   investment shell (lost-wax) molds, 915–17  
   investment two-part block molds, 916  
   magnetic molding, 917–18  
   plaster investment block molds, 916–17  
   properties, 915  
 CFD, *see* computational fluid dynamics  
 CGI, *see* compacted graphite iron  
 Channel segregation in aluminium alloys, 252  
 Chaplets, 210, 1032  
 “Chattanooga Choo Choo”, 334  
 Chemical binders, 924–5  
 Chills:  
   benefits, 203–4  
   bifilms, 204  
   chaplets, 210  
   copper, 206–7  
   external, 204–7  
   feeding, 692  
   fins comparison, 215–18  
   heat transfer, 202–3  
   internal, 209–11  
   iron, 207  
   relative diffusivities, 206  
   thermal conductivity, 219  
   thickness, 219  
 ‘Chinese script’, 268, 303  
 Choke in pressurized/unpressurized systems, 857–62  
 Chromite sand (molding aggregate), 919, 920–1, 937–8  
 Chunky graphite (CHG), 357–9  
 Chvorinov’s rule, 130, 200–2, 663, 671, 689  
 Clamping points for machining, 736  
 Close packed cubic symmetries (fcc, bcc), 301  
 Cloth filters siting, 834–6  
 CO<sub>2</sub> process (cores), 1040  
 Coal pyrolysis, 169  
 Cobalt:  
   aluminate and grain refinement, 182  
   Co-base alloys, 382–4, 613  
   ceramic molds and cores, 915–17  
   vacuum casting, 1009  
   molds, 183  
 COD, *see* crack opening displacement  
 Cold cracking:  
   crack growth, 497  
   crack initiation, 496–7  
   nucleation, 496  
*Cold cracking*, term, 495–7  
 ‘Cold crucible’ technique, 979  
 Cold lap defects, 628  
 Columnar dendrites, 232  
 Columnar-to-equiaxed transition and solidification, 238  
 Compacted graphite iron (CGI), 355–7, 359  
 Computational fluid dynamics (CFD), 148–9  
 Computer simulation:  
   convection, 694  
   feeding, 694  
   filling systems, 853, 856  
   molds and cores, 658–9  
   solidification of castings, 663  
 Cone test for hot tearing, 487–8  
 Confluence welds:  
   aluminium alloys, 63–4  
   Cosworth Process, 60  
   ductile iron casts, 64  
   filling instability, 61  
   mechanism, 62  
   surface films, 62–3  
 Conical basin:  
   pouring, 757–72  
   sprue, 785–6  
 Connective loops and convection, 704  
 Constitutional undercooling, 230, 232  
 Contact pouring, 761–2, 941  
*Continuous fluidity*, 152  
 Continuous melting, 883–5  
*Continuous-Fluidity Length*, 111, 151  
 Contraction:  
   allowance, 392, 1050  
   dimensional accuracy, 1032  
   *see also* uniform contraction  
 Controlled solidification:  
   conventional-shaped castings, 1013–4  
   cooling fins, 1013  
   directional solidification, 1014–6  
   rapid solidification casting, 1018–23  
   single crystal solidification, 1016–8  
 Controlled tilt casting (Durville method):  
   description, 947  
   summary, 954–5  
 Convection:  
   connective loops, 704  
   Cosworth Process, 802  
   countering, 704  
   damage and casting section thickness, 701–4  
   heat transfer, 219–20  
   *see also* rule 7 for good castings  
 Conventional-shaped castings (controlled solidification), 1013–4  
 Cooling of castings, 1013, 1059  
 Cope surface evaporation, 163–4  
 Cope term, 939  
 Cope–drag arrangement, 1036, 1039  
 Copper:  
   Asarco-type furnace, 884  
   bubble damage, 74–5  
   chills, 206–7  
   diffusion coefficients, 12  
   ductility, 517, 533  
   hot rolling, 1085  
 Copper alloys:  
   Aluminium bronze modulus, 664  
   bifilms, 314–15  
   brass, 309, 311–12  
   chills, 203  
   Cu–10Al  
     critical velocity, 46–8, 618  
     hydrogen porosity, 453  
   Cu–10Sn porosity, 406  
   Cu–Ni carbon, 457  
   Cu–Zn vaporization, 16  
   ductility and grain refinement, 545  
   Ellingham diagram, 313  
   gas porosity, 457  
   gases, 310–15  
   grain refinement, 315  
   granulated charcoal, 313–14  
   gunmetal, 309–10  
   lead, 17, 310  
   melting, 313–14  
   ounce metal, 310

- Copper alloys: (*Continued*)  
 penetration barriers, 177  
 phosphorus, 313  
 Reduced Pressure Test, 314  
*steam reaction*, 311  
 sub-surface pinholes, 314  
 surface films, 310  
 zinc, 312  
*see also* bronze
- Core blows:  
 bubble trails, 639  
 bubbles, 636–9  
 cast iron, 640–1  
 condensation, 646  
 gas porosity, 647  
 gray iron, 639, 641–2  
 metal chills, 646  
 molds, 641  
 prevention, 655–9  
 steel boxes, 647  
*see also* rule 5 for good casting
- Core blows and gas porosity, 522–3
- Core-Package System (CPS), 959–60
- Cores:  
 assembly, 1037  
 dimensional problems, 1036  
 making, 1040  
 running system, 1054  
*see also* molds and cores
- Cosworth Process:  
 accuracy and aggregate molds, 1062  
 bifilms, 102  
 bubble damage in counter-gravity systems, 634  
 confluence welds, 60  
 convection, 698  
 critical velocity, 618  
 electro-magnetic pumps, 971  
 entrainment of bubbles, 634  
 grain size in aluminium alloys, 541  
 incipient melting, 1074–5  
 ingates, 802  
 leak elimination, 1085  
 leaks, 591  
 liquid aluminium alloys, 886  
 location points, 730–6  
 pouring (Al alloys), 904  
 roll-over after casting, 502, 958–60  
 tensile strength, 553
- Cothias process (squeeze casting), 993
- Counter-gravity casting:  
 10 test bar mold, 502  
 aluminium alloys, 1073–4  
 counter-pressure, 967  
 description, 960–4  
 direct vertical injection, 976–7  
 failure modes for low-pressure casting, 979–80  
 feedback control for counter-gravity casting, 978–9  
 filling system design, 741  
 gravity problems, 745  
 liquid metal pumps, 970–6  
 low-pressure casting, 964–70  
 medium pressure die-casting, 967–8  
 programmable control, 977–8  
 surface turbulence, 747  
 T-Mag process, 968–9  
 terms, 960–1  
 VRC/PRC, 967–968
- Counter-gravity filling:  
 bubble damage, 634–5  
 filling defects, 628  
 Griffin Process, 905, 911–12, 922  
 lost foam castings, 1004  
 magnesium alloys, 986
- Counter-pressure casting (CPC), 967
- CPS, *see* Core-Package System
- Crack opening displacement (COD), 559
- 'Cracking' term, 495
- Cracks and tears, 465–95, 495–9
- Creep, 575–6, 577–8
- Cristobalite and investment shell molds, 915
- Critical fall heights:  
 aluminium alloys, 744  
 filling systems, 745  
 liquids, 46, 54–7
- Critical velocities:  
 aluminium, 48–9  
 aluminium bronze, 49–50  
 copper alloys, 46  
 equations, 43–4  
 filling systems, 745  
 good casting, 614–18, 618–19  
 liquid aluminium, 45–6, 52  
 liquids, 46  
 metals, 616  
 summary, 618–19  
 Weber Number, 48–50
- Croning, Johannes, 928
- Croning shell process, 1040
- Crucible melting (electric resistance/gas heated), 881–2
- Cryolite (flux), 35
- CSC (cracking susceptibility coefficient) for hot tearing, 480–3
- Cupola shaft furnace for iron, 883–4
- Cylindrical systems and location points, 734–5
- C–Cr steels and microsegregation, 246–7
- ## D
- Darby, Abraham, 939
- DAS, *see* dendrite arm spacing
- Datums and location points, 729–30
- Deactivation of entrained films, 88–92
- Decarburization of iron castings, 180–1
- Defects:  
 alloys, 101  
 blow, 635, 637  
 castings  
 bifilms, 526–7, 527–9  
 gas porosity, 520–4  
 inclusion types and diagnosis, 516–20  
 introduction, 516–17  
 quantification, 3  
 shrinkage porosity, 525–6  
 tears, cracks and bifilms, 526–7  
 cold lap, 628  
 'dents', 654  
 dross, 638, 640  
 entrainment, 309, 929, 980  
 exfoliation, 636  
 melts, 607  
 oxide lap, 628, 630–1  
 pouring, 741–5
- Degassing (melts):  
 aluminium alloys, 892–6  
 bubbles, 871–3  
 gaseous argon shield, 890  
 liquid argon shield, 889–890  
 passive, 889  
 vacuum degassing, 896
- Dendrite arm spacing (DAS):  
 ablation casting, 1019–23  
 aluminium alloys, 86, 278–9

- cast materials, 3, 88  
 chills, 203  
 defects, 516  
 directional solidification, 1010  
 grain size, 236–7, 240  
 growth, 234–7  
 homogenization and solution treatments, 1070–1  
 nucleation, 228  
 pore initiation on bifilms, 433–6  
 solidification structure, 187  
 yield strength  
   bifilms, 550–3  
   description, 539, 545–6  
   heat treatment, 550  
   interdendritic spaces, restricted growth, 548–50  
   residual Hall-Petch hardening, 546–7  
   zinc alloys, 259
- Dendrites:**  
 aluminium nitride, 370  
 columnar, 232  
 grains, 232, 235  
 graphite, 345  
 growth, 229–30, 232–4, 238  
 hot tears, 467  
 instability condition, 231  
 $\delta$ -iron, 380, 382  
 microsegregation, 245–7  
 segregation, 247–9, 705–6
- Dendrites*, term, 229
- Dendritic segregation, 247–9, 995
- 'Dent' defects, 654
- Detrainment (cleaning):**  
 aided flotation, 897  
 aided sedimentation, 897–8  
 description, 92–4  
 filters, 900–1  
 filtration, 94, 899–900  
 natural flotation and sedimentation, 896–7  
 packed beds, 900  
 practical aspects, 901  
 rotary degassing, 94  
 sedimentation, 94
- Diamond films, 331
- Die-casting:**  
 contraction allowance, 1050  
 expansion and contraction, 1032  
 exterior shapes, 1030–1  
 interior shapes, 1031–2
- low-pressure, 964–7  
 maximum velocity requirement, 615–19  
 medium pressure, 967  
 zinc alloys, 1045
- Differentiation of solid (grain multiplication), 236–41
- 'Diffraction mottle', 542
- 'Diffuser' term (runner), 793
- Diffusion coefficients of elements, 10–12
- Digital laser-reading systems (metrology), 1065
- 'Dilute air' (vacuum), 76
- Dimensional accuracy of castings:  
 accuracy, 1046–63  
 alloys, 1032–3  
 description, 1025–9  
 expansion and contraction, 1032  
 ISO, 1025, 1029  
 metrology, 1063–6  
 molds, 1033–8, 1038–45  
 net shape concept, 1029–33  
 non-uniform contraction, 1053–61  
 tolerances, 1028  
 tooling, 1045–6
- Direct chill (DC):  
 aluminium alloys, 378, 593  
 casting, 93  
 grain refinement, 898  
 packed beds, 900  
 residual stress, 710
- Direct gates, 771, 795–6
- Direct pour casting, 942
- Direct pour filters, 845, 850–1
- Direct squeeze casting, 993–6
- Direct vertical injection, 974–7
- Direct-acting piston displacement pump, 974–5
- Directional solidification (DS), 1014–6
- Distortion, *see* non-uniform contraction
- Distortion and residual stress, 722
- Division of sprue, 780–1
- Double bifilms* term, 24
- Down-runner, *see* sprue
- DPI, *see* dye penetrant inspection
- Drag* term, 939
- Dross defects, 638, 640
- 'Dross stringers' in ductile iron, 322–4
- Dross trap (slag trap), 820, 827–8
- Dry coatings for molds and cores, 186
- Dry hearth furnaces, 53–4, 612, 884–5
- DS, *see* directional solidification
- Ductile iron:**  
 brittleness, 352  
 casting, 320  
 confluence welds, 64  
 critical velocity, 46–8  
 distortion, 1056–8  
 'dross stringers', 322–4  
 ductility, 360  
 feeding, 670  
 fluidity, 134  
 gas porosity, 459  
 gravity casting, 939–46  
 gravity dies, 942–4  
 growth, 344  
 machining, 1080–1  
 melts, 613  
 oxidation, 579–80  
 plate fracture defect, 324–5  
 pouring, 54  
 pyrolysis, 168  
 reclamation and recycling of aggregates, 932–8  
 strength and filters, 839  
 stringers, 322–4  
 sulfur, 181  
 surface films, 15  
 vaporization, 17  
*see also* spheroidal graphite iron
- Ductility:**  
 bifilms, 528, 535, 551  
 copper, 517, 533  
 failure, 533, 535  
 freezing of castings, 536  
 layer porosity, 554  
 pores and cracks, 537  
*Duplex stainless steels*, 363
- Duralcan, 908
- Durville casting (controlled tilt), 948–55
- Dye-penetrant inspection (DPI), 383, 386, 1087
- E**
- Ease of removal (castings), 747
- ECAP, *see* equal channel angular pressing
- Effset process (ice binder), 929

- Elastic modulus*, 573
- Elastic stiffness (Young's modulus):  
 damping capacity, 573–4  
 Mitsubishi alloys, 258  
 residual stress from casting, 708–12  
 resonant ultrasound spectrometry, 1090
- Elastic-plastic model, 1060
- Electrical conductivity inclusions, 608
- Electro-magnetic (EM) pumps for liquid metals, 971–4
- Electro-slag remelting (ESR), 204, 910
- Ellingham diagram:  
 cast iron, 318–19  
 copper, 313  
 oxides, 13–16, 272
- EM, *see* electro-magnetic
- Entrained inclusions:  
 aluminium alloys, 273–4  
 aluminium nitride, 370  
 description, 367–8  
 liquid surface oxide films, 369  
 partly liquid surface oxide films, 369  
 pourings, 519–20  
 solid oxide surface films, 368–9
- Entrainment:  
 air, 979, 941  
 air bubbles and gas porosity, 521–2
- defects  
 bifilms, 24–8, 51, 617  
 bubbles, 28–32, 616, 827  
 Cosworth process, 958–60  
 critical heights, 741  
 extrinsic inclusions, 32–41  
 gravity filling, 945–6  
 liquid surface, 616
- description, 24–8
- filling, 20
- films  
 elimination, 15–16  
 oxide, 21–2, 32, 38–40  
 viscosity, 128–30
- oxide films, 621
- processes  
 bifilms evidence, 94–100  
 bifilms importance, 100–3  
 bubble trails, 67–77
- deactivation of entrained films, 88–92
- detrainment, 92–4
- furling and unfurling, 77–88
- microjetting, 65–7
- oxide flow tube, 64–5
- oxide lap defects  
 confluence weld, 60–4  
 surface flooding, 57–60
- oxide skins from melt charge materials, 52–4
- pouring, 54–7
- soluble, transient films, 92
- summary, 42
- surface turbulence, 42–52
- surface films, 5, 15–16, 22, 42–3  
*see also* rules 2, 3 for good castings
- Equal channel angular pressing (ECAP), 907
- Equilibrium gas pressure concept, 7–9
- ESR, *see* electro-slag remelting
- Eutectic Si in aluminium alloys:  
 Al–Si  
 hypereutectic, 280  
 hypoeutectic, 280–3  
 phase diagram, 287–90
- introduction, 279
- mechanical properties, 291–2
- non-chemical modification, 298
- nucleation of Si, 284–7
- Sr modification  
 application, 290–1  
 porosity, 292–5, 295–6  
 summary, 297–8
- Eutectics:  
 fluidity, 118–22, 125–6  
 growth of graphite/austenite, 345–7  
 interdendritic feeding, 407–9  
 latent heat, 134  
 superheat, 118, 120  
 temperature, 118, 120
- Evaporation, 161–4
- Exfoliation defect*, 636
- Expanded runner, 793–5
- Expansion and dimensional accuracy, 1032
- Exploded nodular graphite, 353–5
- Extended fluidity, 148–51
- External chills, 204–7, 250
- External porosity (surface links), 420–1
- External running system, 789
- Extrinsic inclusions:  
 flux and slag, 32–8  
 old oxides, 38–40  
 sand, 40–2
- Eye-dropper ladle*, *see* Snorkel ladle
- ## F
- Face-centered-cube (fcc) structure, 224, 544, 600
- Facing sands, 937–8
- Fatigue:  
 high cycle  
 defects, 563–9  
 initiation, 561–3  
 performance, 569–71  
 steel solidification, 562  
 low cycle and thermal, 571–3
- Fayalite (ferrous orthosilicate), 920
- Fcc, *see* face-centered cube
- Fe<sub>3</sub>Al (intermetallic) and tensile properties, 578
- Fe–3.25Si steel, 380
- FeCr powder and steels, 379–80
- Fe/Si competition for sites (intermetallics), 302–3
- Feed path requirement:  
 criteria functions, 679  
 directional solidification towards feeder, 673–6  
 feeding distance, 676–9  
 introduction, 672–3  
 minimum temperature gradient requirement, 676
- Feedback control for counter-gravity casting, 977–8
- Feeders:  
 absence, 660  
 blind, 669, 680–2  
 neck constriction, 674–5  
 non-feeding role, 695–6  
 reverse taper, 667  
 theory, 666  
 thin-walled castings, 661–3  
 volume, 668–9
- Feeding:  
 blind feeders, 669  
 computer modeling, 694  
 criteria and shrinkage porosity, 399–402, 680  
 definition, 659–60  
 ductile iron, 667–70  
 five mechanisms, 692–4



- freeze volume, 668–1
- freezing systems design, 692
- graphite, 669–70
- Heuvers circles, 673
- new logic, 688–92
- non-feeding role of feeders, 695–6
- padding, 673–4
- random perturbations, 694–5
- reverse tapered feeder, 667
- rule 1: ‘do not feed’ (unless necessary), 662–3
- rule 2: heat transfer requirement, 663–4
- rule 3: mass transfer (volume) requirement, 664–70
- rule 4: junction requirement, 670–1
- rule 5: feed path requirement, 672–9
- rule 6: pressure gradient requirement, 680–3
- rule 7: pressure requirement, 683–8
- rules, introduction, 661–2
- solid feeding, 693–4
- summary, 696
- system, 1035, 1054
- thin-walled castings, 662–3
- Feldspars and silica sand, 920
- Feliu, S, 111, 151–3
- Ferrite:
  - matrix structure (bcc), 224
  - residual stress, 710
  - Schoefer diagram, 363–4
  - titanium, 379
- ‘Ferrite Potential’ (FP), 378
- Ferromanganese (liquid), 36–7
- Ferrosilicon (FeSi), 335–8, 613
- Ferrous alloys:
  - carbon, 922
  - oxide films, 618
  - residual stress, 710
  - silica sand, 919–20
- Ferrous castings, heat treatment, 1070
- Filiform corrosion, 584–5
- Filing system design, records, 1000
- Fillability and surface tension, 141–2
- Filling:
  - bubble damage and surface turbulence, 636
  - definition, 659
  - entrainment elimination, 15–16
  - flow channel structure, 221–2
  - molds, 614–15
- Filling system components:
  - filters, 833–52, 846–8
  - gates, 795–819
  - inclusion control: filters and traps, 826–32
  - pouring basin, 757–72
  - runner, 787–95
  - sprue, 772–87
  - surge control system, 819–23
  - vortex systems, 823–6
- Filling system design:
  - bottom gating, 748, 750
  - casting constraint, 1055–61
  - description, 939
  - down-runner, 771
  - ease of removal, 747
  - economy of size, 747
  - filling speed, 747
  - gating at joint line, 775
  - gravity pouring
    - closed molds, 940–4
    - ‘no fall’ conflict, 741–5
  - introduction, 741
  - liquid metal and mold cavity, 746–7
  - maximum fluidity, 110–48
  - maximum velocity requirement, 741
  - mold design, 1033–8
  - pouring speed, 744
  - practice
    - fill rate, 866–7
    - gates, 873, 875
    - introduction, 852
    - layout, 854
    - methoding approach, 854
    - pouring basin, 867
    - pouring time, 862–5, 872
    - pressurized/unpressurized, 857–62
    - runner, 871–3
    - sprue, 867–71
    - thin sections and slow filling, 865–6
    - weight and volume estimate, 854–7
  - reduction/elimination of gravity problems, 745–51
  - surface turbulence elimination, 745
  - surface-tension-controlled filling, 751–6
  - targets, 791
  - top-gating, 742
- turbulence, 744
- vacuum-assisted, 754–5
- Filters:
  - bubble traps, 843
  - ceramic block, 838–40, 851
  - detrainment, 896–901
  - direct pour, 845, 850–1
  - flow control, 838–9
  - gravity dies, 943
  - leakage control, 840–6
  - runner systems, 787
  - running systems, 846–8
  - siting, 842, 847
  - sprue, 844
  - strainers, 833–4
  - summary, 852
  - tangential placement, 848–50
  - woven cloth or mesh, 834–7
- Filtration and detrainment, 94, 896–7
- Fins:
  - cast-on, 217
  - chills comparison, 217–18
  - cooling, 1013
  - description, 203–4
  - feeding, 692
  - junctions, 211–12
  - L-junctions, 213–14
  - length, 214–15
  - T-junctions, 211–13
  - thermal conductivity, 217, 219
  - thickness, 215–16
- Fischer, R.B., 314, 454
- Flake graphite iron and inoculation:
  - eutectic grain, 345
  - graphite growth, 339–41
  - history, 334–5
  - mechanism, 335–9
  - practical experience, 341–3
- Flemings, Merton C.:
  - fluidity, 112, 114
  - gravity segregation, 696
  - growth of solid, 232
  - heat transfer, 187–223
  - homogenization and solution treatments, 1070–1
  - resistance and heat transfer, 189–91
  - rheocasting, 906
  - solidification
    - metals, 225
    - mode, 113
    - time, 130

- Flow:
- channel structure
    - gates, 810–1
    - heat transfer, 221–4
  - control and filters, 838–9
  - introduction, 105
  - maximum fluidity (unrestricted flow), 110–48
  - microjetting, 105
  - surface forms and filling, 105–6
    - rolling waves, 106–8
- Flow-off device, 819
- Flowability and heat transfer, 141–2
- Fluid beds, 1075–7
- Fluid (castable) sand binders, 930–1
- Fluidity:
- acetylene black, 132
  - advantages, 137
  - alloys, 125
  - critical length, 111
  - definition, 111
  - eutectics, 118–22
  - extended, 148–50
  - freezing, 126
  - intermetallics, 121–2
  - phosphorus, 125–6
  - solidification, 110–16
- Fluidity*, term, 110
- Fluidity:
- tests
    - comparison, 144–8
    - description, 144
    - spiral, 144–7
    - superheat data, 142, 145–7
    - VK strip, 141, 144–7*see also* maximum fluidity
- Fluidity to modulus* ratio, 131–2
- Fluorides (flux), 35
- Fluxes:
- inclusions, 32–8, 518
  - liquids, 37–8, 93–4
  - melt cleaning, 895
- FNB, *see* furan no bake
- Forrest, Reginald, 334
- Foseco Porotec test (France), 95
- FP, *see* 'Ferrite Potential'
- Fracture pressure of liquids, 398–9
- Fracture toughness:
- applied stress/critical defect size, 559, 561
  - description, 555–60
  - yield strength, 559–60
- Frankel Alloys Limited, 449
- 'Freckle defects', 252
- 'Freckles' in Ni-base superalloys, 223
- Free energy of formation (surface films), 13–14
- 'Freedom Bell', Washington DC, US, 627–8
- Freezing:
- description, 393
  - ductility of castings, 536
  - fluidity, 126
  - ice cubes, 393
  - mild steel liquid, 210
  - plate-shaped castings (alloys), 200–1
  - skins, 113
  - systems design for feeding, 692–4
  - times for pouring, 864
- Freight wheel market in US, 905
- Froude Number (Fr), 50–1
- Furan no bake (FNB) binders, 921, 925–6
- Furane resin in molds, 181–2
- Furane/sulfonic acid (FS), 654
- Furans binders, 925–6
- Furfuryl alcohol, 925
- Furling and unfurling of bifilms, 77–85, 85–8
- Furnaces:
- dry hearth, 53–4, 612, 884–5
  - holding, 897
  - iron cupola shaft, 883–4
  - liquid aluminium, 273
  - reverberatory, 880–1
  - rotary, 881
- G**
- 'Gas inclusion', term, 827
- 'Gas' porosity:
- blow holes, 445
  - castings
    - core blows, 522–3
    - entrained air bubbles, 521–2
    - gas precipitated from solution, 520–1
  - core blows, 647
  - diagnosis, 461
  - entrained (external) pores, 443–5
  - initiated in situ
    - barriers to diffusion, 461
    - carbon, oxygen and nitrogen, 457–60
    - description, 445–53
    - hydrogen, 453–7
    - layer porosity, 523–4
    - molds, 647
- Gases:
- cast iron, 315–18
  - Cu alloys, 310–15
- Gates (filling system):
- central versus external systems, 814–15
  - design, 873–5
  - direct, 795–6, 809
  - flow channel structure, 810–11
  - gating ratio, 797–8
  - horizontal velocity in the mold, 799–800
  - horn, 806, 809
  - indirect gating, 795–6, 811–15
  - junction effect, 800–3
  - knife, 805
  - L-junction, 802
  - multiple, 798
  - pencil, 806
  - premature filling problem via early gates, 798–9
  - priming, 817–19
  - sequential, 815–17
  - siting, 795
  - slot, 802, 812–15
  - summary, 800
  - T-junction, 800–2
  - theory, 802
  - total area, 796–7
  - touch, 803–5
  - vertical, 809
  - vortex, 824–5
- Gating:
- joint line, 619, 742–3
  - ratio for filling system, 897–8
  - ratios, 860–2
- Gauges (metrology), 1064, 1066
- Geffroy (metal mold), 918
- Glass cloth filters, 834, 837
- Glissile (gliding) drops, 44, 616
- 'Go/no go' gauges, 1064
- Gold, 3, 99–100
- Good fluidity*, 111
- Grain boundary wetting by liquid (hot tearing), 469–70

- Grain refinement:  
 aluminium alloys, 274–8  
 amplitude/frequency of vibration, 232, 236  
 bifilms, 544  
 copper alloys, 315  
 direct chill, 900  
 Hall-Petch relation, 542  
 hot tearing control, 492  
 magnesium alloys, 266–7  
 mass feeding, 406–7  
 melt cleaning, 278  
 metal surface reactions, 182–3  
 mold coats, 238  
 nucleation of solid, 225–8  
 porosity, 406  
 rotary degassing, 898  
 steels, 379, 380  
 titanium in Al alloys, 275–7  
 zirconium, 267
- Grain size:  
 dendrite arm spacing, 232–6  
 hot tearing, 493–4  
 vibration, 238–9  
 yield strength, 539, 541–5
- Granulated charcoal and copper alloys, 313–14
- Graphite:  
 bifilms, 342–3  
 cast iron, 332–4  
 dies, 963, 1045  
 feeding, 669–70  
 films in Fe–C alloys, 330–1  
 growth mechanisms, 360  
 nodule structure, 347–50  
 nucleation, 355  
 oxide bifilms, 342  
 titanium, 944  
*see also* flake graphite iron
- Gravity casting:  
 dies, 173, 657, 790, 912, 1044  
 dies (permanent molds), 942–4  
 gravity pouring  
 closed molds, 940–4  
 open molds, 939–40  
 horizontal stack molding, 945  
 postscript to gravity filling, 945–6  
 sand, 745  
 two-stage filling, 944–5  
 vertical stack molding, 945
- Gravity filling:  
 disadvantages, 945–6  
 horizontal, 58, 65  
 segregation, 249–53, 703
- Gravity pouring of closed molds:  
 automatic bottom pouring, 941–2  
 contact pouring, 941  
 description, 940–1  
 direct pour, 942  
 gravity dies, 942–4  
 shrouded pouring, 941
- Gravity pouring of open molds, 939–40
- Gray iron:  
 bubble trails, 75–6  
 carbides, 360  
 carbon films, 327–8  
 casting, 320  
 cooling fins, 1013  
 core blows and bubbles, 639, 641–3  
 cylinder blocks, 75  
 decarburization, 180  
 distortion, 1057–8  
 eutectic grain, 346  
 flake graphite iron, 342  
 fluidity, 125–6, 134  
 gas porosity, 461  
 graphite flakes, 339–40  
 gravity dies, 942–4  
 Industrial Revolution, 315  
 machining, 1080–3  
 magnesium oxide surface film, 594  
 mold accuracy, 1044–5  
 nitrogen, 181  
 oxide bifilms, 320–2  
 permanent molds, 185  
 phosphorus, 125–6, 316  
 pressurized versus unpressurized filling, 857–62  
 pyrolysis, 168–9  
 residual stress, 710  
 ‘rosettes’ (cells), 240  
 runner, 787–95  
 salt cores, 914–15  
 silica, 177  
 silicon, 316  
 steel inserts, 210  
 stress relief, 725–7  
 uniform contraction, 1046–52
- Great Paul bell, 573
- Greensand molds:  
 accuracy, 1039  
 active feeding, 687–8  
 binders, 923–4  
 high-pressure molding, 176  
 inert property, 911  
 iron castings, 175  
 mold penetration, 176  
 pyrolysis, 168–9  
 residual stress, 707  
 steels, 165  
 structure, 156, 158  
 vapor zones, 159–60
- Greensand* spelling, 923–4
- Griffin Process (steel railway stock):  
 carbon, 922  
 graphite dies, 1045  
 gravity dies, 942–4  
 inert molds and cores, 911–18  
 low-pressure casting, 963–8, 978–9  
 production, 905
- Griffith’s cracks, 103
- Grit blasting, 562, 1068–9
- Growth:  
 aluminium alloys, 263–5, 275–8, 282, 287  
 atoms, 225  
 cellular front in solids, 229–30  
 dendrites, 229–30, 232–4, 238  
 ductile iron, 344  
 morphology of graphite, 334  
 solid in alloys, 229–30  
 transparent organic alloys, 232, 234
- Growth restriction parameter (Q)*, 275–8
- Gumbel distribution, 516, 570
- Gunmetal alloys:  
 castings, 417  
 description, 309–10  
 grain refinement, 542–5  
 phosphorus and porosity, 458
- ## H
- ‘H Process’ (sequential filling), 816–17
- H14 hot work steel, 985
- Hadfield Manganese steel, 721
- Hafnium in Ni-base alloys, 382, 1010–1
- Hall-Petch relation:  
 aluminium alloys, 543  
 dendrite arm spacing, 545–6, 546–8  
 grain refinement, 542  
 magnesium alloys, 266, 543  
 residual hardening, 546–7  
 yield strength, 540

- Harris, Ken, 918  
 HAZ, *see* heat-affected zones  
 Heat pipes, 219  
 Heat transfer coefficient (HTC):  
   casting–chill interface, 189  
   description, 231  
   die coatings, 198  
   fluidity, 132  
   light alloys, 198  
   metal–mold interface, 192  
   quenching, 712  
   review, 196  
 Heat transfer requirement rule  
   (feeding), 663–4  
 Heat transfer and solidification:  
   convection, 219  
   external chills, 204–7  
   flow channel structure, 220–3  
   increased heat transfer, 202–19  
   remelting, 219–20  
   resistances, 187–9  
 Heat treatment:  
   homogenization and solution  
     treatments, 1069–70  
   post-casting processing, 1069–70  
   reduction and/or elimination, 1070  
   residual stress, 707–8, 722, 724,  
     725  
 Heat-affected zones (HAZ), 1075  
 Hero process (RS), 1018  
 Hesitation and reversal (laminar  
   entrainment of surface  
   films), 629–30  
 Heuvers circles (feeding), 673  
 Hexachlorethane (aluminium  
   degassing), 892  
 Hexagonal close-packed structure  
   (hcp) in magnesium  
   alloys, 266  
 High pressure die-casting (HPDC):  
   impregnation, 1083  
   leaks, 1087–8  
*High temperature alloy* term, 382  
 High-alloy steel castings and gravity  
   segregation, 252  
 High-pressure die-casting (HPDC):  
   aluminium alloys, 986–7, 1042  
   blister formation, 1073–4  
   cold chamber, 986–7  
   description, 993  
   dies, 912–14  
   heat treatment, 1073  
   hot chamber, 986  
   metal molds, 1042–5  
   MP die-casting, 967  
   ‘pore free process’, 990–1  
   post-casting processing, 1067  
   salt cores, 914–15  
   solid mixtures, 905  
   squeeze pins, 990  
   vacuum processes, 991  
   zinc alloys, 255, 258, 260  
 High-strength low-alloy (HSLA)  
   steels, 369  
 High-temperature tensile properties,  
   575–8  
 High-volume Al alloys and pouring  
   basin, 762  
 HIPping, *see* hot isostatic pressing  
 Hipping of solid castings, 91  
 Hiratsuka, S. et al, 148–50  
 Hitchener Company, 962  
 Holder failure (melting), 887–8  
 Holding furnaces, 897  
 Holding, transfer and distribution  
   (melting):  
   description, 885–7  
   holder failure, 887–8  
   transfer and distribution, 888  
 Hollow castings, 637–9, 714  
 Hollow ceramic spheres, 922  
 Homogeneous nucleation  
   temperature, 226  
 Homogenization and solution  
   treatments,  
   1070–1  
*Homogenization treatment* term,  
   1070  
 ‘Horizontal’ stack molding, 816  
 Horizontal stack molding (H  
   process), 945  
 Horizontal stream flow, 627–8  
 Horizontal transfer casting:  
   controlled tilt, 948–55  
   level pour, 946–7  
   roll-over, 945–7  
   roll-over after casting, 957–60  
 Horizontal transfer (‘level pour’), 745  
 Horizontal velocity in the mold,  
   799–800  
 Horizontal vortex well, 824–5  
 Horn gates, 806, 809  
 Hot isostatic pressing (HIPping):  
   bi-Weibull analysis, 512, 1077–80  
   centrifugal casting, 980  
   post-casting, 1077–80  
   rapid solidification, 1018  
 Hot tearing:  
   characteristics, 466–9  
   control  
     alloying, 492–3  
     brackets, 491  
     castings, 489–90, 492  
     chilling, 490  
     contracting length, 493  
     grain refinement, 492  
     improved mold filling, 489  
     reduced constraint, 490–1  
   cracks, 484  
   CSC model, 482  
   filling system, 465  
   grain boundary wetting by liquid,  
     469–70  
   initiation, 474–6  
   opposed cones test, 487–8  
   porosity summary, 493–4  
   pre-tear extension, 470–2  
   predictive techniques, 495  
   ring die test, 482, 487  
   stainless steels, 494–5  
   strain concentration, 472–3  
   stress concentration, 473–4  
   susceptibility prediction, 479–83  
   tear growth, 476–9  
   tear initiation, 474–6  
   testing methods, 483–9  
 Hot-box process, 928, 1040–1  
 Hoult, Fred, 929, 945  
*Hydraulic lock*, 849  
 Hydrogen:  
   aluminium, 892, 894  
   aluminium alloys, 616, 894  
     description, 306–8  
     pick-up, 308–9  
     rotary degassing, 308  
     solubility, 6–8  
   bifilms, 713  
   binders, 923–31  
   magnesium, 896  
   magnesium alloys, 896  
   porosity, 453–7  
   steel melts, 612–13  
   steels, 900  
 Hydrostatic tensions in liquids, 395  
 Hypereutectic alloys, 280, 332  
 Hypoeutectic alloys, 280–3, 332

- I**
- I-beam ('dog-bone') test for hot tearing, 484–6
- Ice cubes and freezing, 393
- IDECO test (Germany), 95
- 'If in doubt, visualize water' concept, 746
- Impregnation of castings, 1085–6
- Incipient melting, 1074–5
- 'Inclusion', term, 826
- Inclusion control: filters and traps:
  - dross trap, 827–8
  - introduction, 826–7
  - slag pockets, 828–9
  - swirl trap, 829–32
- 'Inclusion shape control', 93
- Inclusions:
  - aluminium alloys, 4–5, 273–4, 608
  - electrical conductivity, 608
  - liquid aluminium, 3–4
  - steels, 365–7, 374
- Increased heat transfer:
  - chills and fins, 202–4
  - external chills, 204–7
  - fins, 203–4, 211–19
  - internal chills, 207–11
- Indirect gates, 795–6, 803–4
- Indirect gating (into up-runner/riser), 811–14
- Indirect squeeze casting, 991–3
- Induction melting, 882
- Industrial Revolution and gray iron, 315
- Inert gas cloud (pouring basin), 757–8
- Inert gas shroud (steels), 902–3
- Inert molds and cores:
  - ceramic molds and cores, 915–17
  - description, 911–12
  - permanent metal molds, 911–13
  - salt cores, 914–15
- 'Ingates', *see* gates
- Interdendritic feeding, 407–9, 494
- Intergranular corrosion, 585–6
- Intermetallics:
  - Ag<sub>3</sub>Sn, 255
  - Al–Si alloys, 82
  - brittle behavior, 578
  - CuAl<sub>2</sub>, 304
  - Fe<sub>3</sub>Al, 578
  - FeSi, 335
  - fluidity, 121–2
  - iron-rich aluminium alloys, 298–303
  - Mg<sub>17</sub>Al<sub>12</sub>, 268–9
  - Ti-rich, 304
  - TiAl, 387–90, 449, 980
  - TiAl<sub>3</sub>, 228, 275, 544, 898
- Internal chills, 207–11
- Internal porosity by surface initiation, 418–20
- Internal running system, 789
- International Magnesium Association, 262
- International Meehanite Metal Corporation (IMMCO), 335
- International Nickel Company, New York, 907
- International Standards Organization, *see* ISO
- International Zinc Association, 256
- 'Interrupted pouring', 817
- Interstitial diffusion, 10
- 'Inverse chill' in cast iron, 202
- Inverse segregation*, *see* Dendritic segregation
- Invest* term, 915
- Investment mold, 1000
- Investment shell (lost-wax) molds, 915–16
- Investment two-part block molds (Shaw Process), 916
- Invocast method (roll-over casting), 955
- Iron:**
  - bifilms, 904–5
  - binders, 923–32
  - casting, 941
  - cupola furnace, 883–4
  - diffusion coefficients, 13
  - flux and slag inclusions, 32–8
  - 'inverse chill', 202
  - liquid, 9, 377
  - residual stress, 707–14
  - structure, 224
  - surface films, 15
  - Type A/C, 341
  - Type D/E, 346–7
  - see also* cast iron; ductile iron; gray iron
  - α-iron, 224, 298
  - β-iron:
    - Al–7Si–0.4mg alloy, 548–9, 553–4
  - bifilms, 82
  - iron-rich intermetallics, 298–302
- δ-iron, 377, 380, 382
- Iron alloys:
  - crack growth in bcc structure, 497
  - ferro (liquid), 36–7
  - Fe–3Si, TiB<sub>2</sub>, 228
  - Fe–C
    - eutectics, 280
    - eutectics and interdendritic feeding, 408
    - fluidity, 122, 124
    - freezing, 393–4
    - micrographs, 347
    - phase diagram, 332
    - white iron, 359
  - Fe–C–Mn porosity, 246
  - Fe–O–Si inclusions, 371–2, 374–5
  - filters, 839
  - see also* steels
- Iron Bridge, UK, 741
- Iron carbide, 334, 360
- Iron-rich intermetallics (aluminium alloys), 298–302
- ISO (International Standards Organisation)
  - accuracy, 1025, 1029, 1064
- J**
- Jewelry and centrifuge casting, 980
- Jorstad, John, 136
- Junction effect and gates (filling system), 800–3
- Junction requirement rule (feeding), 670–1
- Just-in-time slurry production, 906–7
- K**
- K-mold test (evaluation of melt cleanliness), 502–3
- Killed steels, 245, 251
- Kirkcaldie alloy, 255
- Kiss gate, *see* touch gate
- Krypton gas and leaks, 590–1
- L**
- L-junctions:
  - feeding, 671
  - fins, 213–14
  - gates, 802

- Laid, Erik, 946
- Lap-type defects and rolling waves, 106–8
- Large bubbles and entrainment, 28–9
- Latent heat (H) and solidification time, 134–7
- Layer porosity:
  - Al–Mg alloys, 408–9
  - ductility, 554
  - gas porosity, 520–1
  - shrinkage pore structure, 436–43
  - yield strength, 540
- Layout and filling system design, 854
- Lead alloys:
  - binders, 923–31
  - brasses/bronzes, 310
  - copper, 310
  - Pb–Sb resistance and heat transfer, 189
  - Pb–Sn alloys
    - fluidity, 117, 119
    - shrinkage pores, 436
- Lead distribution, 888
- Lead-bronze and vapor transport, 178
- ‘Leaded gunmetal’, 309
- Leak testing of castings:
  - description, 1087–8
  - detection, 1100–1
- Leak tightness, 587–91, 590–1
- Leakage control and filters, 840–6
- Ledeburite (iron carbide eutectic), 360
- LEFM, *see* linear elastic fracture mechanics
- Lego and net shape concept, 1029
- Level pour (side pour) casting, 745, 946–7
- Liberty Bell, *see* ‘Freedom Bell’
- ‘Light Alloys2006’, 387
- Light alloys:
  - dimensional accuracy, 1033
  - machining, 1081
  - woven cloth or mesh filters, 834
- LiMCA (Liquid Metal Cleaness Analyzer), 4, 608–9
- Linear elastic fracture mechanics (LEFM), 558–9
- Liquid aluminium:
  - alloys, 273, 879
  - bubble trail, 76
  - critical velocity, 45–51, 54
  - density, 921
  - furnaces, 273
  - gravity dies, 942–4
  - holding, 887
  - hydrogen, 306–7
  - mold gas explosions, 166–8
  - ‘no-fall’ requirement, 619
  - oxides, 26, 271
  - oxygen, 9
  - packed beds, 900
  - strength-related defects, 3
  - surface films, 21
  - thermal conductivity, 881
  - velocity, 46
  - zircon sand, 921
- Liquid basalt, 940
- Liquid cast iron, 318–31
- Liquid copper packed beds, 900
- Liquid ferro-alloys granulation, 36–7
- Liquid ferromanganese granulation, 36–7
- Liquid gold, 3
- Liquid iron, 9, 377, 880
- Liquid magnesium, 179, 625
- Liquid metals:
  - ablation casting, 1019–23
  - advancement, 623
  - air, 617
  - aluminium, 881
  - aluminium alloys, 880
  - batch melting, 879–83
  - buoyancy forces, 1031
  - cast material, 905–9
  - Cosworth Process, 541
  - critical velocities, 616
  - dry hearth furnaces, 885
  - expansion, 623
  - filling systems design, 741, 745–6
  - gas precipitated from solution, 525
  - greensand, 923–4
  - maximum velocity requirement, 615–16
  - melts, 607
  - microjetting, 66
  - models, 3
  - primary inclusions, 373
  - pumps
    - centrifugal, 969–71
    - Cosworth Process, 974
    - electro-magnetic, 969–71
  - sand cores, 635
  - slot gates, 815
  - surface turbulence, 42–3
  - tensile strength, 397
- Liquid silver, 15
- Liquid steel, 37, 210, 377
- Liquid titanium, 386
- Liquids:
  - bubble detachment, 636, 639
  - critical heights/velocities, 46
  - feeding (shrinkage porosity), 403–18
  - flow behavior, 52
  - fluxes, 37–8, 93–4
  - fracture pressure, 398–9
  - maximum heights supported by one atmosphere, 682
  - penetration: surface tension and pressure, 173–6
  - surface and entrainment, 616
  - velocities, 46
- Loam, 806, 929–30
- Location points:
  - clamping points, 733
  - cylindrical systems, 734–5
  - datums, 729–30
  - description, 731
  - integrated manufacture, 736
  - jigs, 736
  - metrology, 1063–6
  - rectilinear systems, 732–4
  - six-point system, 732
  - thin-walled boxes, 735–6
  - triangular systems, 735
- ‘Location Points’ term, 730–6
- Long-freezing-range alloys:
  - 85Cu–5Sn–5Zn–5Pb, 408
  - bubble damage, 636–8
  - freezing distance, 677–9
  - layer porosity, 438
  - porosity, 412
- Longden, E., 1059
- Loss on ignition (LOI), 652, 921, 932, 935–6
- ‘Lost air’ castings, 1004
- Lost crucible technique, 977
- Lost foam casting:
  - description, 1001–5
  - exterior shapes, 1030–1
  - Replicast, 1005
- Lost-foam castings, 165–6, 329
- Lost-wax casting, 915, 1030, 1051

- Lost-wax* process, 915  
 Lost-wax/ceramic mold casting processes:  
     description, 997–9  
     plaster investment, 1000  
     Shaw process, 1000  
 ‘Low nitrogen’ binders, 460  
 Low-alloy steels:  
     cooling, 380  
     crack growth, 497  
     DAS and bifilms, 551  
     entrained inclusions, 367  
     growth, 232–3  
     microsegregation, 245  
     superheat/fluidity, 132–3  
 Low-carbon steels:  
     carburization, 180  
     cooling, 380  
     crack growth, 497  
     grain evolution, 380–1  
 Low-pressure casting:  
     counter-gravity, 961, 964  
     failure modes, 978  
 Low-pressure die casting, mold accuracy, 1044  
 Low-pressure filling, 617  
*LPS* (low-pressure sand) system, 974  
 Lustrous carbon, *see* carbon films
- M**  
 Machined-to-form mold process, 931  
 Macrosegregation, 257, 705  
 Magnesium:  
     aluminium alloys, 272–3, 655  
     critical velocity, 48  
     hydrogen, 896  
     liquid, 179, 625  
     melting, 9  
     metal molds, 1042–3  
     oxidation, 178  
     oxide bifilms, 347, 351–3, 355–8  
     plaster molds, 178  
     sulfur hexafluoride, 179  
 Magnesium alloys:  
     ablation casting, 1019  
     aided sedimentation, 898  
     aluminium, 266  
     aluminium carbide, 267  
     argon, 262–3  
     AZ91E counter-gravity filling, 1004  
     bifilms, 268–9  
     binders, 925  
     calcium, 272  
     carbon black, 144  
     carbon dioxide, 262  
     chills, 203  
     ‘Chinese Script’, 268  
     detrainment, 896  
     dies, 912–13  
     films, 261–6  
     fins, 1013  
     flow channel structure, 810–1  
     grain refinement, 266–7, 542  
     Hall-Petch relation, 266, 543  
     hexagonal close-packed structure, 266  
     high-pressure die-casting, 913  
     HPDC (hot chamber), 987  
     hydrogen, 896  
     lost crucible technique, 975–6  
     magnesium aluminate, 263–5  
     manganese, 271  
     melting, 879  
     metal surface reactions, 178  
     metallurgy, 261  
     Mg–9Al–1Zn corrosion resistance, 261  
     Mg–Al, 267, 268–9, 481  
     Mg–Li carbon, 922  
     Mg–Zn  
         hot tearing, 481  
         shrinkage porosity, 409, 439  
         TS and elongation, 524, 554  
     Mg–Zr description, 267–8  
     microstructure, 268–9  
     multiple sprue, 780  
     oxidation, 261–2  
     potassium borofluoride, 461  
     protective atmospheres, 261–6  
     recycling, 260–1  
     slurry production from granules, 907  
     strengthening, 266–7  
     sulfur hexafluoride, 261  
     superplastic forming, 576–7  
     surface films, 15  
     surface turbulence, 263  
     susceptibility prediction of hot tearing, 481  
     T-Mag process, 968  
     uniform contraction, 1050  
     vaporization, 17  
     ZE41A–T5 574 elastic modulus, 574  
     zinc, 266  
     *see also* casting alloys  
 Magnesium aluminate, 263–5, 1079  
 Magnesium carbide, 267  
 Magnesium oxide, 261–2, 272, 347  
 Magnesium silicate (dross ‘stringers’), 324  
 Magnetic molding, 917–18  
 Major, Fred, 433  
 Mandl and Berger, Austria, 955  
 Manganese:  
     evaporation, 17, 172–3  
     magnesium alloys, 266  
     steels, 17, 362, 718  
 Martensitic stainless steel, 810  
 Mass feeding (shrinkage porosity), 406–7  
 Master brake cylinders and leakage, 1089  
 Matrix structure:  
     differentiation of solid, 237–41  
     general, 224–5  
     growth of solid, 229–37  
     nucleation of solid, 225–9  
 Maximum Fluidity Length, 111, 151  
 Maximum fluidity (unrestricted flow):  
     extended fluidity, 148–50  
     fluidity tests, 144–8  
     introduction, 110–13  
     running system, 110  
     solidification, 113–26  
     solidification time  $t_f$ , 130–40  
     surface tension, 140–2  
     unstable substrates, 143–4  
     velocity, 126–8  
     viscosity, 128–30  
 Maximum velocity requirement, 45–7, 615–19, 741  
 Medium pressure (MP) die-casting, 967  
 Meehan, Gus, 334–5  
 ‘Meehanite’, 334  
 ‘Meehanite Metal’, 334  
 Meehanite Metal Corporation, 334  
 Melt treatments:  
     additions, 901–2  
     cast material, 905–9  
     degassing, 888–93

- Melt treatments: (*Continued*)  
 detrainment, 896–901  
 pouring, 902–5  
 remelting processes, 909–10
- Melting:  
 automatic bottom pouring, 882–3  
 continuous, 883–5  
 crucible melting, 881–2  
 induction, 882  
 introduction, 887  
 melt treatments, 888–905  
 reverberatory furnaces, 880–1  
 titanium alloys, 389–90
- Melting process:  
 batch, 879–83  
 cast material, 905–9  
 continuous melting, 883–5  
 holding, transfer and distribution, 885–8  
 melt treatments, 888–905  
 remelting, 909–10
- Melts:  
 aluminium, 4  
 bifilms, 655  
 cleaning and grain refinement, 278  
 combustion, 6  
 description, 3–5  
 environment, 5–9  
 oxide films, 13–14, 21, 28, 633  
 pressurized filtration tests, 5  
 Reduced Pressure Test, 5, 609–11  
 surface films, 13–16  
 tilt casting, 952–3  
 transfer, 619–20  
 transport of gases, 9–13  
 ultrasonic reflections, 4  
 vaporization, 16–17  
*see also* rule 1 for good casting
- Meniscus (laminar entrainment), 623, 624–5
- Mercury Marine Company, US, 914
- Mercury tensile strength, 397–8
- Metal molds (dies), 911  
 accuracy, 1042  
 die life, 1043
- Metal surface reactions:  
 boron, 183  
 carbon (pickup and loss), 179–81  
 grain refinement, 182–3  
 nitrogen, 181  
 oxidation, 178–9  
 phosphorus, 181–2
- sulfur, 181  
 surface alloying, 182  
 tellurium, 183  
 water vapor, 178
- Metal/matrix composites (MMCs):  
 air exclusion from sprue, 817  
 aluminium alloys, Al–Si, 39, 271, 904  
 Al–Mg<sub>2</sub>Si, 302–3  
 Al–TiB<sub>2</sub>, 30  
 cast material, 905, 906  
 description, 22–3  
 in situ, 908–9  
 viscosity, 128  
 vortex technique, 39
- Metals:  
 bifilms, 608–12  
 chills, 185–6  
 defects, 607  
 dendrite arm spacing, 3  
 fins and thermal conductivity, 217, 219  
 growth of solid, 228–36  
 hydrogen solubility, 6–7  
 liquids, metal molds, 911  
 shrinkage rates, 391–443  
 solidification shrinkage, 393  
 strength-related properties, 3, 607  
*see also* liquid metals
- Metal–mold interface:  
 heat-transfer coefficient, 196–8  
 resistance and heat transfer  
 air gap, 191–6  
 description, 187  
 heat transfer coefficient, 196–8  
 sequential gating, 816
- Metal–mold reactions:  
 magnesium alloys, 461  
 nitrogen, 460
- Methane and combustion of melts, 6
- 'Metallic inclusions' term, 826
- Methoding approach (filling system design), 854
- Metrology:  
 description, 1063–4  
 digital laser-reading systems, 1065  
 gauges, 1064, 1066
- Mg<sub>2</sub>Si ('Chinese script') in  
 magnesium alloys, 268–9
- Mg<sub>17</sub>Al<sub>12</sub> and magnesium alloys, 262
- Micro-blows, 654–5
- Microjetting:  
 entrainment, 65–7, 621  
 flow, 105  
 mechanical properties of casts, 66  
 mechanism, 66  
 plaster investment molds, 1000  
 surface-tension-controlled filling, 751–6  
 touch gates, 803–5
- Microsegregation, 245–7, 257, 705–7  
 single crystal solidification, 1016–8
- Microstructure and bifilms, 542
- Mild steel liquid and freezing, 210
- Miller, Glen, 334
- Mitsubishi aluminium alloys, 258
- MMCs, *see* metal/matrix composites
- Modulus:  
 definition, 660  
 dimensions, 663  
 feeder, 663–4  
 gradient technique, 673  
 ratio, 661, 663  
 solidification, 673  
 solidification time, 130–40
- Mold accuracy:  
 aggregate molds, 1038–41  
 ceramic molds, 1041–2  
 metal molds (dies), 1042–5  
 process routes, 1027
- Mold atmosphere:  
 composition, 164–6  
 explosions, 166–8
- Mold cavity:  
 conical basin, 756, 771  
 filling system design, 745  
 gates, 743, 795, 815  
 sprue, 774
- Mold coatings:  
 aggregate molds, 183–5  
 dry coatings, 186  
 grain refinement, 228  
 permanent molds and metal chills, 185–6
- Mold constraint, 1053–5
- Mold contamination:  
 gravity die casters, 173  
 iron carbonyl, 172  
 manganese evaporation, 172
- Mold design:  
 assembly methods, 1035–8



- 'cake core', 1034–6
- cope-to-drag location, 1038
- dimensional accuracy, description, 1033
- infringement of 10 Rules, 1035
- Mold penetration:
  - chemical interactions, 177–8
  - liquids penetration: surface tension and pressure, 173–6
  - penetration barriers, 176–7
  - temperature and time dependence, 177
  - vapor transport, 178
- Mold processes:
  - machined-to-form, 931
  - precision core assembly, 931
  - unbonded aggregate molds, 931
- Mold surface reactions:
  - lustrous carbon film, 170–1
  - mold contamination, 171–3
  - mold penetration, 173–8
  - pyrolysis, 168–70
  - sand reactions, 171
- Molding:
  - aggregate molding materials, 918–22
  - binders, 923–31
  - casting industry, 911
  - inert molds and cores, 911–18
  - reclamation and recycling of aggregates, 932–8
- Molds:
  - blows, 641, 643–4, 646–7
  - filling, 614–15
  - gating, 619
  - investment, 1000
  - resistance and heat transfer, 198–202
  - rubber, 931–2
  - temperature and solidification time, 137–40
  - wall movement, 192–3
- Molds and cores:
  - computer simulation, 658–9
  - evaporation and condensation zones, 159–64
  - gas evolution rates, 155–6
  - greensand mold structure, 156, 158
  - metal surface reactions, 178–83
  - molds
    - atmosphere, 164–8
    - coatings, 183–6
    - gases composition, 157, 159
    - inert or reactive, 155–6
    - surface reactions, 168–78
    - transformation zones, 156–9
  - Multiple gates for filling system, 798
  - Multiple sprue, 778–80
- N**
- Naturally pressurized* system
  - concept, 787, 860
- 'Navy Gun Metal', 309
- NDT, *see* non-destructive testing
- 'Near-net-shape' concept, 1029, 1041
- Negatively tapered sprue, 777
- Net shape concept:
  - casting process, 1030, 1031–2
  - description, 1038
- Ni-base alloys:
  - air melting and casting, 383
  - automatic bottom pouring, 882–3
  - bifilms, 385, 1075
  - ceramic molds and cores, 915–17
  - cobalt aluminate, 183
  - convection, 699
  - description, 382–6
  - dye-penetrant inspection, 383, 386
  - furling and unfurling, 85–6
  - gravity segregation, 252
  - hafnium, 1010
  - heat-affected zones, 1075
  - incipient melting, 1074–5
  - layer porosity, 415, 438
  - melts, 613
  - modulus, 664
  - oxidizable elements, 382
  - porosity, 413–15
  - production, 613
  - steel inserts, 211
  - turbine blades, 383, 613, 699–700
  - ultrasonic reflections, 4
  - vacuum melting and casting, 383–6, 1010
  - Waspalloy, 910
- Ni-base superalloys:
  - aerofoil test, 138–9
  - ceramic molds and cores, 915–17
  - dendrites, 238
  - directional solidification (DS), 1014–6
  - flow channels, 220–3
  - flowability and fillability, 139, 141–2
  - 'freckles', 223
- HIPping, 1079–80
- machining, 1080–3
- mold temperature and solidification time, 137–40
- nitrogen, 384
- nucleation, 228
- oxide flow tubes, 65
- oxides in melts, 613
- single crystal solidification, 1016–8
- vacuum casting, 77
- waterfall flow, 625–7
- white iron, 359–60
- Nitride bifilms, 325–6, 352
- Nitrogen:
  - binders and pyrolysis, 169
  - cast iron, 317–18
  - metal surface reactions, 181
  - nucleation, 459–60
  - porosity, 460–1
- 'No-Fall' requirement (casting), 619–22, 813
- Noble metals (gold, platinum and iridium) and surface films, 14
- Nodular iron, *see* ductile iron
- Non-classical initiation of pores:
  - high-energy radiation, 429–31
  - pore initiation on bifilms, 433–6
  - pre-existing suspension of bubbles, 431–3
- Non-destructive testing (NDT):
  - bifilms, 103
  - dye penetrant inspection, 1087, 1089
  - leak testing, 1087–8
  - resonant frequency testing, 1088–90
  - X-rays, 1086–7
- Non-ferrous casting, 884–5, 926
- 'Non-metallic inclusion' term, 827
- Non-uniform contraction (distortion):
  - casting constraint, 1055–61
  - ductile iron, 1057, 1068
  - elastic-plastic model, 1059
  - gray iron, 1058
  - mold constraint, 1053–5
  - plate-shaped castings, 1057
- Non-uniform* elongation, 538
- Norit (aggregate molding materials), 921

## Nucleation:

- austenite mix, 343–5
- burst feeding and shrinkage porosity, 410–12
- cast iron, 343–5, 377–80
- cold cracking, 496
- graphite, 333–4, 355, 360
- internal porosity
  - heterogeneous, 423–6
  - homologous, 421–3
  - shrinkage pores, 426–9
- nitrogen, 459–60
- oxygen, 458
- primary inclusions, 372–3
- silicon, 284–7
- solids and grain refinement, 228, 274–8

*Nucleation*, term, 225

**O**

- Offset sprue, 825–6
- Offset step (weir) basin, 501, 770–5, 762–9, 852
- ‘Oil-can’ distortion, 1057
- Olivine sand (molding aggregate), 920–1, 938
- ‘One pass filling’ (OPF) designs, 621–2, 746
- Ounce metal*, 310
- Outgassing:
  - loss of ignition, 652
  - pressure in cores, 647–53
- Oxidation:
  - magnesium, 179
  - magnesium alloys, 261–2
  - metal surface reactions, 178
- Oxidation and corrosion resistance:
  - corrosion, 579–82
  - filiform corrosion, 584–5
  - intergranular corrosion, 585–6
  - internal oxidation, 578–9
  - pitting corrosion, 582–4
  - stress corrosion cracking, 586–7
- ‘Oxidation index’, 459
- Oxide bifilms:
  - Al-12Si alloys, 299–300
  - aluminium, 895
  - aluminium alloys, 269–71, 897
  - carbides, 362
  - crack initiation, 496–7
  - direct chill aluminium alloys, 378

- graphite, 342
- gray iron, 320–2
- magnesium, 347, 352, 355–7
- stainless steels, 363–5
- ‘Oxide crack’, 26
- Oxide films:
  - aluminium, 28
  - aluminium alloys, 271–3
  - cast iron, 318–20
  - down-runner, 750
  - entrainment, 21–2, 24–8, 38–40, 621
  - ferrous alloys, 618
  - flow, 115
  - flux and slag inclusions, 32–48
  - furling and unfurling, 83–5
  - inclusion control, 826–7
  - leaks, 1088
  - melts, 13, 22, 30, 630
  - microjetting, 66
  - old oxide, 39
  - sand inclusions, 40–2
- Oxide flow tubes:
  - double bifilms, 65
  - laminar entrainment of surface films, 625–7
  - pouring, 54
  - waterfall flow, 625–7
- Oxide lap defects:
  - entrainment, 57–60, 60–4
  - surface films, 628–30
- Oxides:
  - aluminium alloys, 263–5
  - flow tubes, 54, 64–5
  - lap-defects
    - confluence welds, 60–4
    - surface flooding, 57–60
  - machining, 1081–3
  - sedimentation, 898
  - single crystal solidification, 1016–8
  - skins
    - bubble damage, 70
    - melt charge materials, 52–4
- Oxygen:
  - liquid aluminium, 9
  - nucleation, 458
  - steels, 897

**P**

- Packed beds and detrainment, 896
- Padding and feeding, 673–4
- Painting of castings, 1083

- Paris-Erdogan equation, 570
- Partially solid mixtures (casting), 905–6
- Particle on particle (‘POP’) attrition, 933–6
- Passive degassing, 889
- Pasty zones:
  - freezing (mode of solidification), 113
  - hot tears, 485–7
  - shrinkage porosity, 440
- Patternmaker’s Contraction Allowance, 392, 1032
- Patterns and accuracy, 1027
- PCRT, *see* ‘process compensated resonance testing’
- PDPC, *see* counter-pressure casting
- ‘Peeling’ process (heat transfer), 204
- Pegasus engine, Harrier Jump Jet, 1079
- Pencil gates, 806
- Permanent metal molds (dies):
  - description, 912
  - gravity/low pressure die-casting dies, 912
  - high-pressure die-casting dies, 912–13
- Permanent mold casting (US), 185–6, 745
- Phenol-urethane no bake (PUNB) binders, 921, 926
- Phenol-urethane (PU) binders, 926, 933, 935–6
- Phenolic-urethane (PF) binders:
  - aluminium alloys, 654
  - carbon (pick up and loss), 179–81
  - isocyanate, 460
  - pyrolysis, 166
  - resins, 454, 456
  - strength, 47
- Phosphoric acid and mold surface reactions, 170
- Phosphorus:
  - Al-Si alloys, 285–6
  - copper alloys, 313
  - gray iron, 125–6, 316
  - gunmetal, 458
  - metal surface reactions, 178–83
- Pilling–Bedworth ratio, 261

- Pitting corrosion, 582–4
- Pitting Resistance Equivalent (PRE)  
for stainless steels,  
363–5
- Planar front:  
growth in solids, 228–36  
hypo-eutectic Al–Si alloys, 280–4  
segregation, 242–5, 705–7
- Plaster investment (integral block  
molds), 1000
- Plaster investment block molds,  
916–17
- Plaster of Paris, 916
- Plastic working (forging, rolling,  
extrusion),  
1083–5
- Plate fracture defect in ductile iron,  
324–5
- Plate-shaped castings distortion, 1057
- PoDFA tests, 3, 608, 894
- Poisson's ratio, 1090
- Polymer quenching, 716–19
- 'Pore free process' (HPDC), 990–1
- Pore initiation on bifilms, 433–6
- Porosity:  
ablation casting, 1019–23  
aluminium alloys, 609  
diagnosis  
gas porosity, 461  
shrinkage, 461–4  
summary, 461–2  
Fe–C–Mn alloys, 246  
fin length, 214–16  
gas, 443–65  
hot tearing summary, 493–4  
leak testing, 1087–8  
nitrogen, 460–1  
shrinkage, 391–443  
steels, 459–61  
surface pinhole, 459
- Positive segregation, 707
- Post casting processing:  
blister formation, 1073–4  
description, 1095  
fluid beds, 1075–7  
heat treatment, 1069–77  
reduction and/or elimination,  
1072–3  
hot isostatic pressing, 1077–80  
impregnation, 1085–6  
incipient melting, 1074–5  
machining, 1080–3  
non-destructive testing, 1086–90  
painting, 1083  
plastic working, 1083–5  
surface cleaning, 1067–9
- Potassium borofluoride (Mg alloys),  
461
- Pour rate of steels, 1100–1
- Pouring:  
contact, 761–2, 941  
critical fall height, 54–7  
defects, 741  
entrained inclusions, 519–20  
entrainment, 54–7  
filling systems  
speed, 744  
time, 862–5  
melt treatments, 907  
oxide films, 56  
oxide flow tubes, 54  
problems, 602  
shrouded, 941  
sprue, 904  
steels, 883, 904
- Pouring basin:  
conical basin, 757–60  
contact pouring, 761–2  
design, 867  
inert gas cloud, 760–1  
offset step (weir) basin, 762–3, 786  
sharp cornered/undercut basin,  
769–70  
stoppers, 771–2
- PRC, *see* pressure riserless casting
- PRE, *see* Pitting Resistance  
Equivalent
- Pre-tear extension, 470–2
- Precision core assembly mold  
process, 931
- PREFIL tests, 3, 608
- Premature filling problem via early  
gates, 798–9
- Press casting, 996
- Pressure assisted casting:  
description, 985  
high-pressure die-casting, 986–91  
squeeze casting, 991–7
- Pressure die-casting:  
dimensional accuracy, 1033  
magnesium and uniform  
contraction, 1050  
oxide flow tubes, 625–7  
precautions, 989  
rotary degassing and leakage, 895  
surface finish, 592–3  
surface-centered-control filling,  
756  
zinc alloys, 76, 140
- Pressure requirement (feeding),  
680–8  
active feeding, 687–8  
cast iron, 685–7
- Pressure riserless casting (PRC), 968
- Pressurized filtration tests, 5, 609
- Pressurized versus unpressurized  
(filling system  
design):  
choke, 859–60  
gating ratios, 860–2  
introduction, 857–9
- Primary inclusions, 370–4
- Priming of gates (filling system),  
817–19
- Principles of Magnesium Technology*,  
261, 268
- Process comparison (casting  
accuracy), 1061–3
- 'Process compensated resonance  
testing' (PCRT), 1090
- Process routes for castings  
manufacture, 602,  
1027–8,  
1061–3
- 'Product Design and Development for  
Magnesium Die  
Castings', 261
- Programmable control for counter-  
gravity casting, 977
- Properties of castings:  
defects, 516–29  
Elastic (Young's modulus) and  
damping capacity,  
573–4  
fatigue, 561–73  
fracture toughness, 555–61  
gas porosity, 520–4  
high-temperature tensile properties,  
575–8  
leak tightness, 587–91  
oxidation and corrosion resistance,  
578–87  
quality indices, 594–7  
residual stress, 574–5  
statistics of failure, 504–16  
surface finish, 591–4

Properties of castings: (*Continued*)  
 tears, cracks and bifilms, 526–9  
 tensile properties, 529–55  
 test bars, 499–503

PU, *see* phenol-urethane

Pyrolysis:

coal, 169  
 description, 168  
 nitrogen containing binders, 169

## Q

'Quality Assurance' (QA), 102–3

'Quality Control' (QC), 102

Quality indices, 594–7

Quartz transition, 919

Quenching:

polymers and other quenchant,  
 716–17  
 quench factor analysis, 720  
 residual stress, 708–12  
 stress relief, 725–7

## R

RA, *see* reduction in area

Radial choke for sprue, 785

Radius of sprue/runner junction,  
 785–7

Railroad wheels, 911, 922

Rapid solidification (RS) casting:

ablation casting, 1019–23  
 Sophia and Hero processes, 1018

Rappaz, M., 465, 467, 482, 494

Re-oxidation inclusions, 519

Reclamation and recycling of

aggregates:

aluminium foundry, 932–5  
 ductile iron, 935–6  
 facing and backing sands, 937–8  
 impact attrition, 934  
 POP attrition and classification,  
 934–5  
 soluble inorganic binders, 936–7  
 thermal reclamation, 932  
 traditional mechanical processes,  
 934

Rectilinear systems and location

points, 732–4

'Reduce residual stress' rule:

beneficial residual stress, 724  
 controlled quenching, 716–19  
 distortion, 722–3  
 epilogue, 728

heat treatment developments,  
 722–4

introduction, 707–8

quenching, air, 719

residual stress, 707–8, 712–16

strength reduction by heat  
 treatment, 720–2

stress relief, 725–7

'Reduce segregation damage' rule:

gravity segregation, 704  
 introduction, 707–8  
 macrosegregation, 705  
 microsegregation, 705  
 planar front segregation, 706–7

Reduced Pressure Test (RPT):

bifilms, 78, 82–3, 95–7  
 copper alloys, 314  
 feeding of castings, 400  
 gas porosity in situ, 449, 451  
 inclusions, 609, 611  
 melts, 5, 608–11, 895–6

Reduction in area (RA) and ductility,  
 538

Relative diffusivities and chills, 206

Remelting process:

electro-slag, 910  
 heat transfer, 220–1  
 vacuum arc, 909–10

Replicast, lost foam casting, 1005

Residual stress:

beneficial, 724  
 castings, 707–8, 708–12  
 description, 574–5  
 distortion, 722  
 quenching, 712–16, 716–19, 719

'Resin concretes', 940

Resistance and heat transfer:

castings, 189–91  
 heat-transfer coefficient, 196–8  
 metal–mold interface, 191–6,  
 191–8  
 molds, 198–202  
 summary, 187–9

Resonant frequency testing, 1088–90

Resonant ultrasound spectrometry,  
 1090

Reveratory furnaces, melting, 880–1

Reverse tapered feeder, 667

Reverse tapered sprue, 785

Reynold's number (Re), 51–2, 77, 88,  
 750

Rheocasting (cast material), 906

Ribs and liquid distribution, 622

Riley, Percy, 448–9

Rimming steel ingots and  
 segregation, 243–4

Ring die test for hot tearing, 482, 487

Riser (up-runner):

flow channel structure, 223  
 indirect gating, 811–14  
 rotary surge, 821

'Rock candy structure', 370

'Rodding' of castings, 411

Rohatgi, Pradeep, 907

Roll-over:

casting process, 957–8  
 convection, 704  
 Cosworth Process, 974–5

Roll-over after casting (inversion):

Cosworth Process, 502, 959–60  
 description, 502, 958–9

Rolled steels, 37–8

Rolling waves, 105, 106–8

Room temperature operation and

mold accuracy, 1039,  
 1041

Rosettes (cells):

flake graphite, 345  
 gray cast iron, 240

Ross Meehan Foundry, Chattanooga,  
 US, 334

Rotacast process (roll-over casting),  
 955–7

Rotary degassing:

aluminium alloys, 308, 893–6  
 detrainment, 94  
 grain refinement, 898

Rotary furnaces, 881

Rotary surge risers, 821

Rover (UK), 974

RS, *see* rapid solidification

Rubber molds, 931–2

Rules for good castings:

- 1: 'use a good quality melt',  
 607–13, 827
- 2: 'avoid turbulent entrainment',  
 614–22, 741–2, 749,  
 756, 941
- 3: 'avoid laminar entrainment of the  
 surface film',  
 623–30, 1040
- 4: 'avoid bubble damage', 631–5,  
 748
- 5: 'avoid core blows', 635–59

- 6: 'avoid shrinkage damage', 659–96
- 7: 'avoid convection damage', 696–704, 966
- 8: 'reduce segregation damage', 705–6
- 9: 'reduce residual stress', 707–28
- 10: 'provide location points', 728–37, 1038
- summary, 605–6
- Runner:
- bubble damage, 791
  - description, 787
  - design, 771–3
  - 'diffuser', 793
  - expanded, 809
  - external system, 789
  - filters, 791
  - internal system, 790
  - slot, 789, 791, 870
  - speed, 790
  - tapered, 792–3
  - vortex, 825–6
- Running system, *see* Filling system
- ## S
- St. Paul's Cathedral, London, 573
- Salt cores, 914–15
- Sand:
- casting, 329, 700, 943, 1030
  - cores composition, 652
  - inclusions, 40–2
  - machining, 1080–3
  - molds
    - 10 test bar, 500
    - magnesium alloys, 263
    - penetration, 176
    - resin binders, 155, 157
  - reactions, 171
  - silica, 919–20
- Sand blasting, 1067
- Sb–Cd/Pb alloys and fluidity, 116, 119
- Scanning electron microscopy (SEM):
- bifilms, 95, 99
  - bubble trails, 69, 71, 73
  - compact graphite iron, 355–6, 360–1
  - ductile iron, 579
  - gas porosity in situ, 445
  - graphite spherule, 349
  - hot tears, 466
  - intermetallics, 303–4
  - lustrous carbon film, 329–31
  - Mg–Zr alloys, 267–8
  - Ni-base superalloy, 384–6
  - stress corrosion cracking, 586–7
  - superplastic forming, 576–8
  - vapor transport in molds, 178
  - zinc alloys, 76
- Schoefer diagram for stainless steels, 363–4
- Sealing of castings (impregnation), 1085–6
- Seawater corrosion, 581–4, 586
- Secondary dendrite arm spacing, *see* dendrite arm spacing
- Sedimentation and detrainment, 94
- Segregation:
- definition, 241–2
  - dendritic, 247–8, 995
  - gravity, 250–3
  - microsegregation, 245–7
  - planar front, 242–5
  - positive, 707
  - ratio, 245–6
  - solidification, 241–53
  - see also* rule 8 for good castings
- Semi-killed steels, 244
- Sequential gates, 815–17
- Sessile (sitting) drops:
- critical fall height, 54, 741
  - critical velocity, 614, 616, 618, 741–2
  - entrainment, 616–18
  - surface flooding, 57
  - vapor transport, 178
- Seven feeding rules, *see* feeding
- Sharp cornered/undercut basin and pouring, 769–71
- Shaw, Clifford, 916
- Shaw, Noel, 916
- Shaw process (two-part block mold), 1000
- Shear modulus, 1090
- Shell Process*, 928
- Short-freezing-range alloys (shrinkage cavity), 438
- Shot blasting, 1068
- Shower nucleation, 239
- Shrinkage cavity or pipe, 436–38
- Shrinkage damage, *see* Rule 6 for good castings
- Shrinkage porosity:
- computer simulated, 418, 420
  - defects in castings
    - macroshrinkage, 525–6
    - microshrinkage, 525
  - description, 391–2
  - diagnosis, 461–4
  - feeding criteria, 399–401, 402–3, 679
  - feeding mechanisms
    - burst feeding, 409–12
    - interdendritic feeding, 407–9
    - introduction, 403–4
    - liquid feeding, 404–6
    - mass feeding, 406–7
    - solid feeding, 412–18
  - initiation
    - external porosity (surface links), 420–1
    - growth of shrinkage pores, 436
    - internal porosity by surface initiation, 418–20
    - non-classical initiation of pores, 429–36
    - nucleation of internal porosity, 421–9
  - pore structure
    - cavity or pipe, 436–8
    - layer porosity, 438–43
  - reduction, 396
  - solidification shrinkage, 392–9
  - types, 395–6
- Shrouded pouring, 941
- Si/Fe competition for sites (intermetallics), 302–3
- Siemens' open hearth furnace, 880
- Sievert's law (gas concentration and pressure), 6
- Silica:
- molds and cores, 158
  - sand, 919–20, 1041–2
  - thermal shock, 919
- Silicate, sodium, 926–8, 936–7, 1040, 1086
- Silicic acid (binder), 915
- Silicon:
- bifilms, 286
  - fluidity, 34–7
  - gray iron, 315–16
  - latent heat, 123, 134–6
  - nucleation, 284–6

- Silicon carbide, 337  
 Silicosis, 919  
 SIMA, *see* strain induced melt activation  
 Single crystal solidification, 1016–8  
 Siphons and aluminium, 888  
 Siting:  
   filters, 845  
   gates, 795  
 Six-point location system, 730–2  
 ‘Skeins of geese’ (bronzes), 74  
 Skin-freezing, 113  
 Slag:  
   inclusions, 32–8  
   pockets, 828–9  
 Slot:  
   gates, 801, 812, 813  
   runner, 794, 795, 870  
   sprue, 794, 870  
 Small bubbles, 28, 69–70  
 Smalley, Oliver, 334–5  
 Smith, C.S., 469  
 Snorkel ladle, 818, 947  
 Sodium:  
   aluminium alloys, 273  
   latent heat, 135  
   vaporization, 16–17  
 Sodium polyphosphate glass binder, 927  
 Sodium silicate, impregnation, 1086  
 Sodium silicate binder, 926–8, 937, 1040  
 Solid feeding:  
   dangers, 693–4  
   shrinkage porosity, 412–18  
 Solid surface film and surface finish, 593–4  
 Solidification:  
   alloys, 238  
   castings and computer simulation, 663  
   controlled, 1013–23  
   fatigue in steel, 562  
   fluidity, 113–26  
   heat transfer, 185–224  
   matrix structure, 224–7  
   modulus, 673  
   segregation, 241–53  
   times, 640–2  
 Solidification shrinkage:  
   hydrostatic tensions in liquids, 396–9  
   metals, 391  
   pores, 395–6  
   sphere model, 395  
 Solidification time (tf):  
   DAS and grain size, 236–7  
   heat transfer coefficient, 132  
   latent heat, 134–7  
   maximum fluidity, 130–40  
   modulus, 130–2  
   mold temperature, 137–40  
   superheat, 132  
 Soluble inorganic binders and aggregate reclamation, 936–7  
 Soluble, transient films, 92  
*Solution treatment* term, 1070–1  
 Sophia process (RS), 1018  
 Southern bentonite (clay), 165  
 Sparks, Robert, 918  
 SPC, *see* statistical process control  
 Speed of filling systems, 745, 750, 790  
 Spherical wax castings and feeding behavior, 413–15  
 Spheroidal graphite iron (SGI) (ductile iron):  
   description, 347–52  
   exploded nodular graphite, 353–5  
   mis-shapen spheroids, 352–3  
   *see also* ductile iron  
   ‘Spiking’ in fracture surfaces, 325  
 Spinels, 33, 272–3, 898  
 Spiral tests for fluidity, 144–6  
*Spraying time*, 849  
 Sprue (down-runner):  
   base, 781–2  
   design, 772  
   division, 780–1  
   expanding runner, 793–5  
   filling systems design, 743, 745, 750–1, 867–8  
   filters, 843  
   gravity filled systems, 621  
   multiple, 778–80  
   negatively tapered, 779  
   ‘no fall requirement’, 619  
   offset, 825–6  
   pouring, 904  
   priming of gates, 817–19  
   radial choke, 785  
   radius of runner junction, 785–7  
   reverse tapered, 776  
   slot, 794, 870  
   stoppers, 772  
   straight tapered, 775, 777  
   surge control, 821  
   tapered, 501, 775  
   tilt casting, 952  
   vortex, 787, 823–4  
   well, 782–5  
   zero tapered, 777  
 Sprue/runner junction:  
   description, 785  
   radius, 785–7  
 Squeeze casting:  
   ablation casting, 1019–23  
   cast pre-forms for forging, 996–7  
   direct, 993–6  
   indirect, 991–3  
   press casting, 996  
   ‘*Squeeze casting*’ term, 993  
   ‘*Squeeze forming*’ term, 993  
 Squeeze pins (HPDC), 991  
 Stainless steels:  
   ferrite, 363–4  
   hot tearing, 494–5  
   martensitic, 362  
   oxide bifilms, 363  
   Pitting Resistance Equivalent, 363–5  
   pouring, 54  
   radiography, 74–5  
   Schoefer diagram, 363–4, 377  
   shot, 1068  
   superheat and fluidity, 132, 133  
    $\sigma$  phase, 364  
 Statistical process control (SPC), 695  
 Statistics and casting dimensions, 1026  
 Statistics of failure:  
   accuracy limits, 514–16  
   bimodal distribution, 506–7  
   extreme value distributions, 516  
   introduction, 504–7  
   Weibull analysis, 507–14  
*Steam reaction* in copper alloys, 310–1  
 Steel boxes and core blows, 647  
 Steel Foundry Society of America (SFSA), 903  
 Steels:  
   1.5Cr–1C, segregation damage, 705  
   aluminium nitride, 370

austenitic, 203, 379  
 automatic bottom pouring, 882–3  
 bcc structure, 544  
 bifilms, 380, 904–5  
 binders, 925  
 calcium cyanamide, 379–80  
 carbon, 362–3, 367, 484, 497  
 carbon-based filters, 852  
 casting into ingots, 244  
 chaplets, 1032  
 chromite sand, 937–8  
 cold mild and freezing, 209  
 columnar grains, 238  
 contraction, 1049  
 cooling, 1059  
 cracks, 496  
 creep, 575–6  
 CSC model, 482  
 C–Cr microsegregation, 246–7  
 dimensional accuracy, 1025  
 directional solidification (DS),  
     1014–6  
 dross defects, 636  
 entrained inclusions, 367–70  
 expansion and contraction, 1032  
 fatigue and solidification, 562  
 feeders, 666–7, 674  
 feeding distance, 676–9  
 Fe–3%25Si, 380  
 films and deoxidation, 60  
 filters, 839  
 fins, 1013  
 fluidity, 111–13, 126  
 flux and slag inclusions, 35  
 freezing times of plate-shaped  
     castings, 200–1  
 gases, 459  
 grain refinement, 379, 380, 544  
 gravity dies, 942–3  
 gravity segregation, 250–1, 706  
 greensand molds, 165  
 heat pipes, 219  
 high-alloy castings and gravity  
     segregation, 252  
 high-strength low-alloy, 369  
 hot work H14, 1044  
 hydrogen, 891  
 hydrogen in melts, 611  
 inclusions, 365–7, 374  
 inert gas shroud, 902–3  
 ingots and gravity segregation,  
     250–3

inserts and gray iron, 210–11  
 introduction, 367  
 investment casting, 180  
 killed, 244–5  
 layer porosity, 438–43  
 liquid, 37, 377  
 low-alloy, 132–3, 232–3, 245  
 low-carbon, 177–80  
 magnetic molding, 917–18  
 manganese, 17  
 melting, 363  
 melts, 896  
 microsegregation, 245–7  
 nucleation, 225–8, 377–80  
 olivine, 919–21, 938  
 oxygen, 889, 891  
 permanent molds, 185  
 phase changes in cooling, 240  
 pitting corrosion, 582–4  
 plasticity of inclusions, 1085  
 porosity, 391–464  
 pour rate, 1100–1  
 pouring, 864, 902–5  
 primary inclusions, 370–4  
 railway stock, *see* Griffin process  
 residual stress from quenching,  
     712–13, 714  
 rimming ingots and segregation,  
     242–5  
 rolled, 37–8, 520  
 rolling waves, 108–9  
 secondary inclusions and second  
     phases, 374–7  
 semi-killed, 244  
 shot, 913, 917, 922  
 Siemens' open hearth furnace,  
     879–80  
 strength reduction by heat  
     treatment, 720–2  
 structure development in solid,  
     380–2  
 surface, 1073  
     films, 5, 14–15  
     finish, 591–4  
     tension, 751–6  
 ultrasonics, 4, 89, 98  
 unzipping waves, 105, 107–9  
 welding, 382  
 yield point, 539  
 zircon sand, 921  
*see also* Stainless steels  
 Stokes velocity, 93–4, 321

Stoppers for pouring basin, 775–6  
 Straight-tapered sprue, 776, 779  
 Strain concentration (hot tearing),  
     472–3  
 Strain induced melt activation  
     (SIMA), 907  
 Strainers (filling system), 833–4  
 Straube-Pfeiffer test, 95, 449  
 Street, Arthur, 255, 986  
 Stress concentration (hot tearing),  
     473–4  
 Stress corrosion cracking (SCC),  
     586–7  
 Stress relief:  
     alloys, 725–6  
     elongation failure and quenching,  
         727  
     sub-resonance, 727  
 Stringers:  
     alumina, 37–8  
     dross, 322–4  
     ductile iron, 322–4  
 Strontium (Sr):  
     aluminium, 902  
     aluminium alloys, 1051  
     Al–Si alloys, 273, 290–3, 302, 1069  
     zinc alloys, 266  
 Structure development in solid  
     (steeels), 380–2  
 Substitutional diffusion, 10  
 Subsurface:  
     pinholes in copper alloys, 314  
     pores, 459  
     porosity, 521, 942  
 Sulfides, 375–7, 625–6  
 Sulfonic acids pyrolysis, 169–70  
 Sulfur hexafluoride, 179, 261–2  
 Sulfur and metal surface reactions,  
     181  
 Sump (oil pan) casting:  
     datums, 729–30  
     gravity filling, 58  
     leak tightness, 587–91  
     leakage, 1088  
     runner system, 787–8  
     thin-walled boxes, 736  
*Superalloy* term, 382  
 'Superalloys', 1015  
 Superheat and fluidity, 132–4  
 Superplastic forming, 576–8  
 Surface alloying, 182  
 Surface cleaning (castings), 1067–9

- Surface films:  
 aluminium, 21  
 aluminium alloys, 15, 25, 35  
 confluence welds, 60–4  
 copper alloys, 310, 313  
 entrainment, 15–16, 21, 35–6  
 free energy of formation, 13  
 gates, 815  
 laminar entrainment, 623–30  
 liquid cast iron, 318–31  
   bifilms, 320–2, 322–4, 325–6  
   carbon films, 326–31  
   oxide films, 318–20  
   plate fracture defect, 324–5  
 magnesium alloys, 15  
 melts, 13–16  
 noble metals, 14  
 oxides, 13–15  
 speed of growth, 22  
 steels, 14–15  
 surface finish, 593–4  
 titanium alloys, 390  
 Surface finish, 591–3, 593–4, 1064  
 Surface flooding, 57–60  
 Surface forms on filling:  
   rolling waves, 105, 106–8  
   surface tension, 105–6  
   unzipping waves, 105, 107–10  
 Surface lap defects in confluence  
   welds, 60–4  
 Surface pinhole porosity, 459  
 Surface tension:  
   core blows, 636  
   flow, 105–6  
   maximum fluidity, 140–2  
   surface finish, 591–3  
   thin walled castings, 622  
 Surface turbulence:  
   counter-gravity casting, 748  
   critical heights/velocities, 46–8  
   elimination in filling systems, 748,  
     758  
   Froude Number (Fr), 50–1  
   liquid metal, 42–3  
   machining, 1080–3  
   magnesium alloys, 263  
   oxide lap defects, 630  
   physics, 43–5  
   Reynolds number (Re), 51–2  
   Weber Number, 48–50  
 Surface-tension-controlled filling:  
   aluminium, 754, 755  
   filling systems design, 751  
   steels, 755  
 Surge control system (filling), 819–22  
 Susceptibility prediction of hot  
   tearing, 479–83  
 Swirl traps, 829–32
- T**
- T-junctions:  
   feeding, 671, 672–3  
   fins, 211–13  
   gates, 800–3  
 T-Mag process for counter-gravity  
   casting, 968  
 Tangential placement of filters,  
   848–50  
 Taper and sprue, 777  
 Tapered runner, 791–3  
 Tear, *see* hot tear  
 ‘*Tearing*’ term, 494  
 Tears, cracks and bifilms (defects in  
   castings), 526–9  
 Tellurium and metal surface  
   reactions, 183  
 Temperature and tooling, 1045–6  
 Template gauges, 1064  
 Tensile properties:  
   ductility, 533–9  
   microstructural failure, 529–33  
   strength in liquids, 397  
   ultimate tensile strength, 553–5  
   yield strength, 539–53  
 Test bars for castings:  
   10 test bar mold, 500–2  
   history, 499–500  
   K-mold test, 502–3  
 ‘The breaking of the surface oxide’  
   concept, 22  
 ‘The breaking of the surface tension’  
   concept, 22  
 ‘The Diecasting Book’, 255  
 Thermal analysis of aluminium  
   alloys, 305–6  
 Thermal conductivity and chills/fins,  
   217, 219  
 Thermal fatigue, 571–3  
 Thick section castings, 695  
 Thin section castings, 694, 865–6  
 Thin-walled castings:  
   carbon black, 144  
   feeders, 662  
   surface tension, 622  
 Thixocasting (cast material), 906  
 Thread forming fasteners (TTFs),  
   1082  
 Three-bar frame castings and residual  
   stress, 708  
 Ti-rich intermetallics, 304  
 Tilt casting and convection, 704  
 ‘Tilt pouring’ concept, 951  
 Time (pouring), 862–5  
 Tin and iron castings, 210  
 Tin (Sn) addition to aluminium  
   alloys, 1083  
 Tin-bronze:  
   dendritic segregation, 247–50  
   description, 324  
   vapor transport, 178  
 Tiryakioğlu, Ergin, 688, 690  
 Tiryakioğlu, M.  
   bi-Weibull distributions, 512–16  
   fatigue, 567–8, 570  
   feeder rules, 399, 402  
   feeding logic, 689  
   freezing time of casting, 202  
   quality indices, 594–7  
   tensile properties, 529–33  
 Tital, Germany, 1018  
 Titanium:  
   aluminium alloys, 275, 543–4, 1001  
   Al–Si alloys, 277–8, 304  
   binders, 923  
   ferrite, 379  
   grain refinement of aluminium,  
     275–7  
   graphite, 944  
   liquid, 386  
   metal surface reactions, 179  
   nickel alloys, 382  
   properties, 388  
   TiAl<sub>3</sub> 228, 275, 544, 898  
 Titanium alloys:  
   ‘ $\alpha$  case’, 179, 911  
   aluminides, 227, 275, 387–90, 449  
   bifilms, 389  
   CaO crucible, 388  
   carbon (pickup and loss), 179  
   description, 387  
   hipping, 387  
   inert molds and cores, 911  
   melting and casting, 387–9  
   metal surface reactions, 179  
   mold materials, 388–9  
   soluble, transient films, 92



- surface films, 389–90  
 Ti–5Al–2.5Sn, 387  
 Ti–6Al–4V, 387  
 Ti–22Al–26Nb, 390  
   Tungsten droplets, 826–7  
 Titanium aluminide (TiAl, Ti<sub>3</sub>Al),  
   387–90, 449, 980  
 Titanium diboride (TiB<sub>2</sub>), 39, 227,  
   229, 275, 898  
 Titanium oxide and vertical filling of  
   casts, 59  
 Tolerances (dimensional accuracy),  
   1028, 1061–3  
 Tooling, 1045–6  
 Tooling Point (TP), 731  
 Top-gating, 806  
 Touch gates, 803–5  
 Tower (shaft) furnaces, 883–4  
 Transfer and distribution (melting),  
   888  
*Transformation-induced plasticity*  
   (TRIP), 1059  
 Transmission electron microscopy  
   (TEM), 275, 284–5,  
   288  
 Transparent organic alloys (growth),  
   232, 234  
 Transport of gases in melts, 9–13  
 Transverse wave effects, 107  
 Triangular systems and location  
   points, 735  
 True centrifugal casting, 980  
 ‘True gas porosity’, 520  
 TS, *see* ultimate tensile strength  
 TTFs, *see* thread forming fasteners  
 Turbine blades:  
   ceramic molds and cores, 915–17  
   conventional-shaped castings, 1013  
   lost wax assembly, 699–700  
   machining, 1080–1  
   Pegasus engine, Harrier Jump Jet,  
     1079–80  
   single crystal solidification, 1016–17  
   titanium, 386  
   vacuum melting and casting, 383  
   waterfall flow, 625  
 Turbulence and filling systems, 745–6  
 Two-stage filling (priming) for  
   gravity casting, 945–6  
 ‘Two-stage pour’, 818, 944  
 Type A/C iron, 341  
 Type D/E iron, 346–7
- U**  
 Ultimate tensile strength (TS), 553–5  
 Ultra-clean aluminium alloys, 612  
 Ultrasonics:  
   aluminium alloys, 4, 98, 541, 608  
   bifilms, 4, 98, 608  
   reflections, 4, 608  
 Unbonded aggregate molds process,  
   931  
*Under-feeder shrinkage porosity*,  
   401, 670  
*Underside shrinkage* in zinc alloys,  
   260  
 Uniform contraction and casting  
   accuracy, 1046–52  
*Uniform* elongation, 538  
*Unimpeded flow*, 111  
 Unstable substrates and maximum  
   fluidity, 143–4  
 Unzipping waves, 105, 107–10  
 Up-runner, *see* riser  
 ‘Use a good quality melt’ rule, 607–13
- V**  
 Vacuum arc remelting (VAR), 204,  
   587, 909–10  
 Vacuum castings, 65, 76–7, 449,  
   753  
 Vacuum degassing of melts, 896  
*Vacuum lock*, 849  
 Vacuum melting and casting, 383–6,  
   941–2,  
   1009–11  
 Vacuum molding (V process),  
   1005–8, 1041  
 Vacuum processes (HPDC), 991–2  
 Vacuum riserless casting (VRC),  
   967  
 Vacuum-assisted casting, 1008–9  
 Vacuum-assisted filling, 754  
 Vapor pressure, 312  
 Vapor zones:  
   greensand molds, 159–60  
   transport, 162–4, 178  
   water content, 161  
 Vaporization:  
   alloys melted in vacuum, 17  
   copper alloys with lead, 17  
   ductile iron, 17  
   magnesium alloys, 17  
   manganese steels, 17  
   melts, 16–17  
   sodium, 16  
   zinc, 16  
 VAR, *see* vacuum arc remelting  
 Velocity:  
   flow channels, 221–2  
   maximum fluidity, 126–8  
 Vertical filling of casts, 59  
 Vertical gates, 809, 815, 848  
 Vertical stack molding, 945  
 Vibration, 233, 236, 238–9  
 Viscosity and maximum fluidity,  
   128–30  
 VK (Voya Kondic) Fluidity Strip Test,  
   141, 144–7  
 Volatile organic compounds (VOCs),  
   184  
 Volume criterion, *see* feeding, rule 3  
 Vortex:  
   base, 785, 787  
   gates, 824–5  
   MMCs, 39  
   runner, 785, 787  
   runner (offset sprue), 825–6  
   sprue, 787, 823–4, 825–6  
   well, 824–5  
 VRC, *see* vacuum riserless casting
- W**  
 Wall plaques, 939–40  
 Warm box processes (binders), 928  
 Waspalloy (Ni-base), 910  
 Water:  
   flow, 746  
   hammer (momentum effect) test  
     piece, 175  
   tensile strength, 397  
 Water vapor:  
   aluminium, 9  
   cores, 644–6  
   metal surface reactions, 178  
   zinc alloys, 9, 255  
 Waterfall effect, 64, 625–7  
 Weber Number (We):  
   critical velocities, 48–51  
   HPDC, 991  
 Wedge trap, 820, 828  
 Weibull analysis:  
   background, 507–10  
   bi-Weibull, 512–14  
   description, 504–6  
   extreme value distributions, 516  
   runner system, 826

- Weibull analysis: (*Continued*)  
 sample number, 516  
 three-parameter, 511–12  
 tilt casting, 952  
 two-parameter, 510–11  
 two-stage filling, 945
- Weight and volume estimate (filling system), 854–7
- Welders in foundries, 368
- Welding steels, 382
- Wells for sprue, 783
- Western bentonite (clay), 165
- White iron (iron carbide), 359–60
- Wilkinson, John, 929–30
- 'Will the metal fill the mold'? 110
- Wood and tooling, 1045
- Woolley, J.W. and Woodbury, K.A. (heat-transfer coefficients), 198
- Woven cloth or mesh filters, 834–7
- Wright, George, 60
- X**
- X-ray studies:  
 bubble traps, 840  
 filling systems, 741  
 horizontal transfer casting, 953  
 lost foam casting, 1004  
 low-pressure die-casting, 967  
 non-destructive testing, 1086–7, 1089  
 pressurized/unpressurized systems, 857–9, 860  
 radiography of turbine blades, 383  
 runner, 787–8  
 sprue, 778, 783  
 tangential placement of filters, 848–50  
 tomography, 1026
- video technique for bubble trails in  
 aluminium  
 castings, 73
- Y**
- Yield strength ( $\sigma_y$ )  
 dendrite arm spacing, 540, 545–53  
 grain size, 541–5  
 Hall-Petch relation, 540, 546–7  
 layer porosity, 540  
 magnesium alloys, 266
- Yielding fracture mechanics (YFM), 559
- Young's modulus (elastic stiffness), 258, 573–4, 708, 1090
- Z**
- Zero tapered sprue, 775–6
- Zildjian cymbals, 574
- Zinc:  
 boiling point, 312  
 copper alloys, 312  
 distribution, 888  
 Mg–Zn alloys, 266, 409, 439  
 mold coats, 184  
 post-casting processing, 1067  
 vapor, 457  
 vapor pressure, 312  
 vaporization, 16–17
- Zinc alloys:  
 accuracy, 1029, 1033  
 aging, 258  
 alumina, 258  
 aluminium, 256–60  
 bifilms, 258–60  
 binders, 925  
 blisters, 259  
 carbon-based dies, 911  
 casting, 256–7  
 creep resistance, 258  
 dendrite arm spacing, 259  
 dimensional accuracy, 1031  
 failure, 259  
 graphite dies, 911, 1045  
 gravity dies, 944  
 gunmetal, 309  
 heavy metal castings, 259–60  
 high-pressure die-casting, 255, 258, 260  
 HPDC (hot chamber), 987  
 macrosegregation, 257  
 microsegregation, 257  
 oxides, 259  
 pressure die casting, 76, 137  
 rubber molds, 931–2  
 strontium, 260  
*underside shrinkage*, 260  
 water vapor, 9  
 ZA series, 137, 259, 260, 618, 922  
 ZA27, 144, 259–60, 1051  
 ZAMAK series, 256  
 zinc flare, 311  
 Zn–4Al, 202, 1052  
 Zn–27Al, 141, 989  
 Zn–Al phase diagram, 257  
 Zn–Cu–Al, 137  
*see also* casting alloys
- Zip fasteners (zinc alloys), 259
- Zircon sand (zirconium silicate), 915, 919, 921, 928, 937
- Zirconium:  
 binders, 925  
 grain refinement, 268–9, 544–5  
 Zr–Cu alloys and vapor transport, 178

# References – Volume II

- Adams, A. (2001). *Modern Castings*, 91(3), 34–36.
- Ainsworth, M. J., & Griffiths, W. D. (2006). *TAFS*, 114, 965–977.
- Akita, K. K. (10 April 1972). U.K. *Patent 1,397,821 filed*.
- Ali, S., Mutharasan, R., & Apelian, D. (1985). *Metallurgical Transactions*, 16B, 725–742.
- Allen, A. G. (25 January 1968). *Foundry Trade Journal*, 159–161.
- Allen, A. G., Howard, J. C., Howard, J. F., & Neenan, P. A. U.K. *Patent Specification 1,013,851*. Application date 31st January 1963.
- Anderson, G. R. (1985). *Patt-Tech 85 Conference*, Oxford, UK.
- Anderson, G. R. (1987). *TAFS*, 95, 203–210.
- Anderson, S. H., Foss, J. W., Nagen, R. M., & Jhala, B. S. (1989). *TAFS*, 97, 709–722.
- Armstrong, G. L., & Martin, W. (1974). *TAFS*, 82, 253–255.
- Aryafar, M., Raiszadeh, R., & Shalbazadeh, A. (2010). *Journal of Material Science*, 45, 3041–3051.
- Ashton, M. C. (January 1991). *Metals and Materials*, 12–17.
- Badia, F. A. (1971). *TAFS*, 79, 347–350.
- Badia, F. A., & Rohatgi, P. (1969). *TAFS*, 77, 402–406.
- Balewsky, A. T., & Dimov, T. (1965). *British Foundryman*, 78(7), 280–283.
- Ball, R. (May 1998). *Foundryman*, 175, 157–160.
- Ball, R., & Hardcastle, P. (January 1991). *Foundry Trade Journal* (11/25), 52–53.
- Barrett, L. G. (1967). *TAFS*, 75, 326–329.
- Bates, C., & Wallace, J. F. (1966). *TAFS*, 74, 174–185.
- Bhaumik, S., Moles, V., Gottstein, G., Heering, C., & Hirt, G. (2010). *Advanced Engineering Materials*, 12(3), 127–130.
- Beck, A., Schmidt, W. (1928). Schreiber 0. U.S. *Patent 1,788,185*.
- Beckermann, C. (2002). *International Materials Reviews*, 47(5), 243–261.
- Beeley, P. R. (1972). *Foundry Technology*, London: Butterworths.
- Beeley, P. R., & Smart, R. F. (2009). ‘Investment Casting’ published by Maney Materials Science.
- Bennett, S., Moody, T., Vrieze, A., Jackson, M., Askeland, D. R., & Ransay, C. W. (2000). *TAFS*, 108, 795–803.
- Berry, J. T., Luck, R., Taylor, R. P. (2005). In M. Tiryakioglu, & P. N. Crepeau (Eds.), *Shape Casting: The John Campbell Symposium* (pp. 113–122). TMS.
- Berry, J. T., & Taylor, R. P. (1999). *TAFS*, 107, 203–206.
- Berry, J. T., & Watmough, T. (1961). *TAFS*, 69, 11–22.
- Bex, T. (1991). *Modern Casting* (November) 56.
- Birch, J. (2000). *Diecasting World*, 174 (March) 35.
- Bird, P., & Savage, W. (1996). *TAFS*, 104, 321–324.
- Bird, P. G. (1989 1 March). Examination of the factors controlling the flow rate of aluminium through DYPUR units. *Foseco Technical Service Report MMP1.89*.
- Biswas, P. K., Rohatgi, P. K., & Dwarakadasa, E. S. (1985). *British Foundryman*, 78, 511–516.
- Bishop, H. F., Myskowski, E. T., & Pellini, W. S. (1955). *TAFS*, 63, 271–281.
- Bossing, E. (1982). *TAFS*, 90, 33–38.
- Bradley, F. J., Hooper, J. A., Kannan, S., Balakrishna, J. V., & Heinemann, S. (1992). *TAFS*, 100, 917–923.
- Bracale, G. (1962). *TAFS*, 70, 228–252.
- Britney, D. J., & Neailey, K. (2003). *Journal of Materials Processing Technology*, 138, 306–310.
- Bromfield, G. (July 1991). *The Foundryman*, 261–265.
- Brown, N., & Rastall, D. (1986). *European Patent Application No 87111549.9 filed 10.08.87*, p. 9.
- Busby, A. D. (1996). *TAFS*, 104, 957–968.

## RII-2 References

- Campbell, J. published (1991). *Castings*. Butterworth Heinemann (now Elsevier).
- Campbell, J. (1991 September). *Metals and Materials*, 575.
- Campbell, J. (2008). *Materials Science and Technology*, 24(7), 875–881.
- Campbell, J. (2009). *Metallurgical & Materials Transactions A* 40A (May) 1009–1010. Discussion of ‘Effect of Sr and P on Eutectic Al-Si Nucleation and Formation of beta-Al<sub>5</sub>FeSi in Hypoeutectic Al-Si Foundry Alloys’.
- Campbell, J. (2009). Incipient grain boundary melting. *Materials Science & Technology*, 25(1), 125–126.
- Campbell, J., & Caton, P. D. (1977). In *Institute of Metals Conference on Solidification Sheffield, UK*, pp. 208–217.
- Campbell, J., & Isawa, T. (1994). U.K. *Patent GB 2,284,168 B (filed 04-02-1994)*.
- Cao, W., Fathallah, R., & Castex, L. (1995). *Materials Science & Technology*, 11(9), 967–973.
- Carlson, B. E., & Pehlke. (1989). *TAFS*, 97, 903–914.
- Carlson, C., & Beckermann, C. (2009). *Metallurgical Materials Transactions A*, 40A, 163–175, and pp. 3054–3055.
- Carney, C. A., & Beech, J. (1997). In J. Beech, & H. Jones (Eds.), *Solidification Processing* (pp. 33–36). UK: Sheffield University.
- Chadwick, G. A., & Yue, T. M. (January 1989). *Metals and Materials*, 6–12.
- Chambers, L., W. (April 24, 1980). *Foundry Trade Journal*, 802.
- Chandley, G. D. (1976). *TAFS*, 84, 37–42.
- Changyun, L., Shiping, W., Jingjie, G., & Hengzhi, F. (2006). *International Journal of Cast Metals Research*, 19(4), 237–240.
- Charbonnier, J., & Perrier, J. J. (January 1983). *Giesserei*, 70(2), 50–55.
- Chaudhury, S. K., & Apelian, D. (2006). *International Journal of Cast Metals Research*, 19(6), 361–369.
- Chen, T. J., Ma, Y., Li, Y. D., Lu, G. X., & Hao, Y. (2010). *Materials Science & Technology*, 26(10), 1197–1206.
- Chen, X. G., Klinkenberg, F. J., Ellerbrok, R., & Engler, S. (1994). *TAFS*, 102, 191–197.
- Chernov, D. K. (December 1878). *Reports of the Imperial Russian Metallurgical Society* (see *Russkoe Metalurgicheskoe Obshchestvo* 1, 1915).
- Chu, M. G. (2002). *Light Metals*, 899–907.
- Chvorinov, N. (1940). *Giesserei*, 27, 177–186, 201–208, 222–225.
- Clark, J. C. (April 1989). *BCIRA Report Number 1769*, 181–193.
- Clegg, A. L., & Das, A. A. (1987). *British Foundryman*, 80, 137–144.
- Cook, R. Kearns, M. A., & Cooper, P. S. (1997). In R. Huglen (Eds.), *Light Metals (TMS)* (pp. 809–814).
- Cox, M., & Harding, R. A. (2007). *Materials Science & Technology*, 23(2), 214–224.
- Cox, M., Wickins, M., Kuang, J. P., Harding, R. A., & Campbell, J. (November–December 2000). *Materials Science & Technology*, 16, 1445–1452.
- Creese, R. C., & Safaraz, A. (1987). *TAFS*, 95, 689–692.
- Creese, R. C., & Safaraz, A. (1988). *TAFS*, 96, 705–714.
- Creese, R. C., & Xia, Y. (1991). *TAFS*, 99, 717–727.
- Czerwinski, F. (November 2008). *Journal of Metals*, 82–86.
- Dai, X., Yang, X., Campbell, J. & Wood, J. (2003). *Materials Science and Engineering A*.
- Das, A. A., & Chatterjee, S. (1981). *The Metallurgist and Materials Technologist*, 13(3), 137–142.
- Dasch, J. M., Ang, C. C., Wong, C. A., & Waldo, R. A. (2009). *Journal of Material Process Technology*, 209, 4638–4644.
- Datta, N., & Sandford, P. (1995). *3rd AFS International Permanent Mold Casting of Aluminum Conference paper* 3, p. 19.
- Davis, K. G. (March 1977). *AFS International Cast Metals Journal*, 23–27.
- Davis, K. G., & Magny, J.-G. (1977). *TAFS*, 85, 227–236.

- Daybell, E. (1953). *Proceedings of the Institute of British Foundryman*, 46, B46–B54.
- D'Errico, F., Rivolta, B., Gerosa, R., & Perricone, G. (November 2008). *Journal of Metals*, 70–75.
- Din, T., & Campbell, J. (1994). University of Birmingham, UK: unpublished work.
- Din, T., Kendrick, R., & Campbell, J. (2003). *TAFS*, 111 (paper 03-017), 91–100.
- Disa Industries. (July 2002). *Foundry Trade Journal*, 27.
- Dolan, G. P., Flynn, R. J., Tanner, D. A., & Robinson, J. S. (2005). *Material Science Technology*, 21(6), 687–692.
- Donahue, J. (June 2006). *Incast* 11.
- Donahue, R., & Anderson, K. (2008). *ASM Handbook Casting, Volume 15*, 640–645.
- Donoho, C. K. (1944). *Transactions of American Foundry Association*, 52, 313–332.
- Dorward, R. C. (2001). *Oxidation of Metals*, 55(1/2), 69–74.
- Doutre, D. A., Hay, G., & Wales, P. (July 26 2000). European Patent 20000951137 filed.
- Durville, P. H. G. (1913). *British Patent*, 23, 719.
- Eastwood, L. W. (1951). *AFS Symposium on Principles of Gating*, pp. 25–30.
- Eigenfeld, K. (1988). 8th Europe Kolloquium der ne. Metallgiesserei im CAEF. Paris.
- Elliott, H. E., & Mezoff, J. G. (1947). *TAFS*, 55, 241–253.
- Elliott, H. E., & Mezoff, J. G. (1948). *TAFS*, 56, 223–245, 279–285.
- Emamy, M., Abbasi, R., Kaboli, S., & Campbell, J. (2009). *International Journal of Cast Metals Research*, 22(6), 430–437.
- Emamy, M., & Campbell, J. (1995). *Cast Metals*, 8(2), 115–122.
- Emamy, M., Taghiabadi, R., Mahmudi, M., & Campbell, J. (October 2002). *Statistical Study of Tensile Properties of A356 Aluminum Alloy, using a New Casting Design* (ASM 2nd ed). Columbus Ohio: Internat Al Casting Technology Symposium. 7–10.
- Engels, G., & Schneider, G. (1986). *Casting Plant & Technology*, (2), 12–20.
- Evans, J., Runyoro, J., & Campbell, J. (1997). In *SP97 4th Decennial International Conference on Solidification Processing*, Sheffield: pp. 74–78.
- Evans, R. W. (August 2002). *Materials Science & Technology*, 18, 831–839.
- Fan, Z., Ji, S., Fang, X., Liu, G., Patel, J., & Das, A. (2007). In P. N. Crepeau, M. Tiryakioglu, J. Campbell, (Eds.), *Shape Casting: The 2nd International Symposium* (pp. 299–306). TMS 2007.
- Fan, Z.-T., & Ji, S. (2005). *Materials Science & Technology*, 21(6), 727–734.
- Fathallah, R., Inglebert, G., & Castex, L. (1998). *Materials Science & Technology*, 14, 631–639.
- Fathallah, R., Sidham, H., Braham, C., & Castex, L. (August 2000). *Materials Science & Technology*, 19, 1050–1056.
- Flemings, M. C., & Mehrabian, R. (1970). *TAFS*, 78, 388–394.
- Fletcher, A. J., & Griffiths, W. D. (1995). *Materials Science & Technology*, 11(3), 322–326.
- Forslund, S. H. C. (1954). *21st International Foundry Congress, Florence*: paper 15.
- Fruehling, J. W., & Hanawalt, J. D. (1969). *TAFS*, 77, 159–164.
- Gallois, B., Behi, M., & Panchal, J. M. (1987). *TAFS*, 95, 579–590.
- Gammelsaeter, R., Beck, K., & Johansen, S. T. (1997). *Light Metals (Conference)*, 1007–1011.
- Garat, M. (16 November 1987). *European Patent Application 0,274,964 filed 16* in French.
- Garat, M., Guy, S., & Thomas, J. (1991). *The Foundryman*, 84(1), 29–34.
- Gauthier, J., & Samuel, F. H. (1995). *TAFS*, 103, 849–857.
- Gauthier, J., Louchez, P. R., & Samuel, F. H. (1995). *Cast Metals*, 8(2), 91–106.
- Gebelin, J.-C., & Jolly, M. R. (2002). *TAFS*, 110, 109–119.
- Gebelin, J.-C., & Jolly, M. R. (2003). *Modeling of Casting, Welding and Solidification Processing Conference X*, Destin, USA.
- Gebelin, J.-C., Jolly, M. R., & Hsu, F.-Y. (2005). In M. Tiryakioglu, & P. N. Crepeau (Eds.) *Shape Casting: The John Campbell Symposium* (pp. 355–364). TMS.

## R11-4 References

- Gebelin, J.-C., Jolly, M. R., & Hsu, F.-Y. (2006). *International Journal of Cast Metals Research*, 19(1), 18–25.
- Gebelin, J.-C., Jolly, M. R., & Jones, S. *INCAST*, 13(11) (Dec), 22–27.
- Geffroy, P.-M., Lakehal, M., Goni, J., Beugnon, E., Heintz, J.-M., & Silvain, J.-F. (2006). *Metallurgical & Materials Transactions A*, 37A, 441–447.
- Geffroy, P.-M., Pena, X., Lakehal, M., Goni, J., Egizabal, P., & Silvain, J.-F. (February 2006). *Fonderie Fondateur d'aujourd'hui*, 252, 8–19.
- Geskin, F. S., Ling, E., & Weinstein, M. I. (1986). *TAFS*, 94, 155–158.
- Gloria, D., Hernandez, F., Valtierra, S., & Cisneros, M. A. (October 2000). *20th ASM Heat Treating Society Conference Proceedings* (pp. 674–679). St Louis, MO.
- Goad, P. W. (1959). *TAFS*, 67, 436–448.
- Gouwens, P. R. (1967). *TAFS*, 75, 401–407.
- Granath, O., Wessen, M., & Cao, H. (2008). *International Journal of Cast Metals Research*, 21(5), 349–356.
- Grassi, J. R., & Campbell, J. (2009). Patent Application as a Continuation in Part.
- Green, N. R., Tomkinson, A. M., Wright, T. C., Evans, J. P., Fuchs, U., & Tschegg, S. (2005). In M. Tiryakioglu, & P. N. Crepeau, (Eds.), *Shape Casting: The John Campbell Symposium*. TMS.
- Griffiths, W. D., Cox, M., Campbell, J., & Scholl, G. (2007). *Materials Science & Technology*, 23(2), 137–144.
- Grube, K. R., & Kura, J. G. (1955). *TAFS*, 63, 35–48.
- Grunengerg, N., Escherle, E., & Sturm, J. C. (1999). *TAFS*, 107, 153–159.
- Grupke, C. C., Hunter, L. J., Leonard, C., Nath, R. H., & Weaver, G. J. (2011). Quality Assurance with Process Compensated Resonant Testing (paper 11-036). *TAFS*.
- Gunasegaram, D., Givord, M., O'Donnell, R., & Finnin, B. (December 2007). *Foundry Trade Journal*, 362–365.
- Guo, J., Sheng, W., Su, Y., Ding, H., & Jia, J. (January 2001). *International Journal of Cast Metals*. Research submitted.
- Grote, R. E. (1982). *TAFS*, 90, 93–102.
- Gupta, N., & Satyanarayana, K. G. (2006). The solidification processing of metal-matrix composites: The Rohatgi Symposium. *JOM: Journal of the Minerals, Metals and Materials Society (ISSN 1047-4838)*, 58(11), 92–94.
- Hadian, R., Emamy, M., & Campbell, J. (2009). *Metallurgical & Materials Transactions B*, 40(6), 822–832.
- Hairy, P., Longa, Y., & Laguerre, C., et al. (2003). *Fonderie Fondateur d'aujourd'hui. ALFED catalogue C/27918*. No. 226 (June/July) 20–30.
- Hammond, D. E. (August 1989). *Modern Castings*, 29–33.
- Hangai, Y., Kato, H., Utsunomiya, T., & Kitahara, S. (2010). *Metallurgical Materials Transactions A*, 41A, 1883–1886.
- Hansen, P. N., & Rasmussen, N. W. (1994). *BCIRA International Conference*. UK: University of Warwick.
- Hansen, P. N., & Sahm, P. R. (1988). Modelling of casting, welding and advanced solidification processes IV. In A. F. Giamei, & G. J. Abbaschian, (Eds.), *The Mineral, Metals and Materials Society*.
- Harrison Steel (1999). Personal communication.
- Hashemi, H. R., Ashoori, H., & Davami, P. (2001). *Materials Science & Technology*, 17, 639–644.
- Haugland, E., & Engh, T. A. (1997). *Light Metals (TMS Conference)*, 997–1005.
- Hayes, K. D., Barlow, J. O., Stefanescu, D. M., & Piwonka, T. S. (1998). *TAFS*, 106, 769–776.
- Hedjazi, D., Bennett, G. H. J., & Kondic, V. (1975). *British Foundryman*, 68, 305–309.
- Heine, R. W. (1982). *TAFS*, 90, 147–158.
- Heine, R. W., & Uicker, J. J. (1983). *TAFS*, 91, 127–136.
- Hendricks, M. J., Wang, P., & Bijvoet, M. (2005). *British Investment Casters' Association Bulletin*, 47, 4–5.
- Herrera, A., & Campbell, J. (1997). *TAFS*, 105, 5–11.
- Hess, K. (March 1974). *AFS Cast Metals Research Journal*, 6–14.
- Heyn, E. (1914). *Journal Institute of Metals*, 12, 3.

- Hillis, J. E. (November 2002). *International Conference on SF6 and the Environment*.
- Hiratsuka, S., Niyama, E., Anzai, K., Horie, H., & Kowata, T. (1966). *4th Asian Foundry Congress*, 525–531.
- Hirt, C. W. (2003). [www.flow3d.com](http://www.flow3d.com)
- Hong, C. P., Shen, H. F., & Lee, S. M. (2000). *Metallurgical & Materials Transactions B*, 31B, 297–305.
- Hoover, W. R. (1991). In N. Hansen, et al. (Eds.). *Proceedings 12th Riso International Symposium Materials Science: Metal Matrix Composites – Processing, Microstructure and Properties* (pp. 387–392).
- Hoult, F. H. (1979). *TAFS*, 87, 237–240.
- Hoult, F. H. (1979). *TAFS*, 87, 241–244.
- Hsu, W., Jolly, M. R., & Campbell, J. ‘Vortex gate’ to be published 2003.
- Hu, Z. C., Zhang, E. L., & Zeng, S. Y. (2008). *Materials Science and Technology*, 24(11), 1304–1308.
- Huang, H., Lodhia, A. V., & Berry, J. T. (1990). *TAFS*, 98, 547–552.
- Hurtuk, D. J., & Tzavaras, A. A. (1975). *TAFS*, 83, 423–428.
- Hutchins, M. (2007). *Foundry Trade Journal*, 181 (3645), 195.
- IBF Technical Subcommittee T571. (1969). *British Foundryman*, 62, 179–196.
- IBF Technical Subcommittee TS71. (1971). *British Foundryman*, 64, 364–379.
- IBF Technical Subcommittee T571. (1976). *British Foundryman*, 69, 53–60.
- IBF Technical Subcommittee T571. (1979). *British Foundryman*, 72, 46–52.
- Isawa, T. (1993). *The control of the initial fall of liquid metal in gravity filled casting systems*. [PhD Thesis]. University of Birmingham Department of Metallurgy and Materials Science.
- Isawa, T., & Campbell, J. (November 1994). *Transactions Japan Foundrymen’s Society*, 13, 38–49.
- ISO Standard 8062. (1984). *Castings – System of Dimensional Tolerances*.
- Itamura, M., Murakami, K., Harada, T., Tanaka, M., & Yamamoto, N. (2002). *International Journal Cast Metals Research*, 15(3), 167–172.
- Itamura, M., Yamamoto, N., Niyama, E., & Anzai, K. (1995). In Z. H. Lee, C. P. Hong, & M. H. Kim, (Eds.), *Proceedings 3rd Asian Foundry Congress* (pp. 371–378).
- Jacob, S., & Drouzy, M. (1974). *International Foundry Congress*. 41 Liege, Belgium: Paper 6.
- Jakumeit, J., Laqua, R., Hecht, U., Goodheart, K., & Peric, M. (2007). In H. Jones (Ed.), *SP07 Proceedings 5th Decennial International Conference Solidification Processing* (pp. 292–296).
- Jeancolas, M., Cohen de Lara, G., & Hanf, H. (1962). *TAFS*, 70, 503–512.
- Jeancolas, M., & Devaux, H. (1969). *Fonderie*, 285, 487–499.
- Jeancolas, M., Devaux, H., & Graham, G. (1971). *British Foundryman*, 64, 141–154.
- Jennings, J. M., Griffin, J. A., & Bates, C. E. (2001). *TAFS*, 109, 177–186.
- Ji, S., Roberts, K., & Fan, Z. (February 2002). *Materials Science & Technology*, 18, 193–197.
- Jirsa, J. (October 1982). *Foundry Trade Journal*, 7, 520–527.
- Johnson, S. B., & Loper, C. R. (1969). *TAFS*, 77, 360–367.
- Johnson, W. H., & Baker, W. O. (1948). *TAFS*, 56, 389–397.
- Johnson, W. H., Bishop, H. F., & Pellini, W. S. (1954). *Foundry*, 102–107, and 271–272.
- Jolly, M. J. (2008). *Engineering School*. UK: University of Birmingham. Personal communication.
- Jolly, M. J., Lo, H. S. H., Turan, M., Campbell, J., & Yang, X. (2000). In P. R. Sahn, P. N. Hansen, & J. G. Conley (Eds.), *Modeling of Casting, Welding and Advanced Solidification Processing IX Aachen*.
- Jones, C. A., Fisher, J. C., & Bates, C. E. (1974). *TAFS*, 82, 547–559.
- Jones, Samantha (2005). *Foundry Trade Journal*, 179(June), 156–157.
- Jones, Samantha (2006). *Foundry Trade Journal*, 180(October 3638), 267–270.
- Jones, Samantha (2006). *Incast*(April), 18–21.
- Kahn, P. R., Su, W. M., Kim, H. S., Kang, J. W., & Wallace, J. F. (1987). *TAFS*, 95, 105–116.
- Kang, X., Li, D-Z., Xia, L., & Campbell, J., Li, Y. Y. (2005). In M. Tiryakioglu, & P. N. Crepeau (Eds.), *Shape Casting: The John Campbell Symposium* (pp. 377–384). TMS.

## R11-6 References

- Kasch, F. E., & Mikelonis, P. J. (1969). *TAFS*, 77, 77–89.
- Katashima, S., Tashima, S., & Yang, R.-S. (1989). *TAFS*, 97, 545–552.
- Karsay, S. I. (1992). *Ductile Iron Production I; state of the art 1992. QIT Fer et Titane Inc. and 'Ductile Iron; the essentials of gating and risering system design'* revised 2000 published by Rio Tinto Iron & Titanium Inc.
- Kasch, F. E., & Mikeloms, P. J. (1969). *TAFS*, 77, 77–89.
- Kim, M. H., Moon, J. T., Kang, C. S., & Loper, C. R. (1993). *TAFS*, 101, 991–998.
- Kim, M. H., Loper, C. R., & Kang, C. S. (1985). *TAFS*, 93, 463–474.
- Kim, S. B., & Hong, C. P. (1995). Modeling of casting, welding and advanced solidification processes VII. *TMS* 155–162.
- Kono, R., & Miura, T. (1975). *British Foundryman*, 69, 70–78.
- Khorasani, A. N. (1995). *TAFS*, 103, 515–519; *Modern Castings* (1996) 86, 36–38
- Kotschi, T. P., & Kleist, O. F. (1979). *AFS International Cast Metals Journal*, 4(3), 29–38.
- Kotzin, E. L. (1981). *Metalcasting and Molding Processes*. Des Plaines, Illinois, USA: American Foundrymen's Soc.
- Kubo, K., & Pehlke, R. D. (1985). *Metallurgical Transactions*, 16B, 359–366.
- Kunes, J., Chaloupka, L., Trkovsky, V., Schneller, J., & Zuzanak, A. (1990). *TAFS*, 98, 559–563.
- Kuyucak, S. (2002). *TAFS*, 110, 2002.
- Laid, E. (1978). U.S. *Patent Application 16 February 1978 Number 878,309*.
- Lansdow, P. Personal communication 1997 regarding casting plant from KWC, Unterkulm, Switzerland, seen at Maynal Castings Limited, Wolverhampton, UK.
- Lashkari, O., & Ghomashchi, R. (April 2007). *Materials Science Engineering A*, 454–455, 30–36.
- Laslaz, G., & Laty, P. (1991). *TAFS*, 99, 83–90.
- Latimer, K. G., & Read, P. J. (1976). *British Foundryman*, 69, 44–52.
- Lawrence, M. (February 1990). *Modern Castings*, 51–53.
- Lee, J.-K., & Kim, S. K. (2007). *Materials Science Engineering A* (March), 449–451, 680–683.
- Lerner, Y., & Aubrey, L. S. (2000). *TAFS*, 108, 219–226.
- Leverant, G. R., & Gell, M. (1969). *TAIME*, 245, 1157–1172.
- Li, D. Z., Campbell, J., & Li, Y. Y. (2004). *Journal of Processing Technology*, 148(3), 310–316.
- Lin, D.-Y., & Shih, M. C. (2003). *International Journal of Cast Metals Research*, 16(6), 537–540.
- Lin, H. J., & Hwang, W.-S. (1988). *TAFS*, 96, 447–458.
- Lo, H., & Campbell, J. (2000). In P. R. Sahm, P. N. Hansen, & J. G. Conley (Eds.), *Modeling of Casting, Welding and Advanced Solidification Processes IX*, pp. 373–380.
- Loper, C. R., Javaid, A., & Hitchings, J. R. (1996). *TAFS*, 104, 57–65.
- Lynch, R. F., Olley, R. P., & Gallagher, P. C. J. (1977). *AFS International Cast Metals Journal* (March), 61–86.
- Maeda, Y., Nomura, H., Otsuka, Y., Tomishige, H., & Mori, Y. (2002). *International Journal Cast Metals Research*, 15, 441–444.
- Mampaey, F., & Xu, Z. A. (1999). *TAFS*, 107, 529–536.
- Manzari, M. T., Lewis, R. W., Gethin, D. T. (2000). Optimum design of chills in sand casting process. In *Proceedings IMECE 2000 International Mechanical Engineering Congress Florida, USA: DETC98/DAC-1234 ASME* (p. 8).
- Martin, L. C. B., Keller, C. T., & Shivkumar, S. (1992). In *AFS 3rd International Conference on Molten Aluminum Processing* (pp. 79–91). Orlando: Florida.
- Mashl, S. J. (2008). Casting. *ASM Handbook*, Vol. 15, pp. 408–416.
- Mbuya, T. O., Oduari, M. F., Rading, G. O., & Wekesa, M. S. (2006). *International Journal of Cast Metals Research*, 19(6), 357–360.
- McDavid, R. M., & Dantzig, J. (1998). *Metallurgical & Materials Transactions*, 29B, 679–690.
- McDonald, R. J., & Hunt, J. D. (1969). *Transactions AIME*, 245, 1993–1997.



- McKim, P. E., & Livingstone, K. E. (1977). *TAFS*, 85, 491–498.
- Mertz, J. M., & Heine, R. W. (1973). *TAFS*, 81, 493–495.
- Mi, J., Harding, R. A., & Campbell, J. (2002). *International Journal Cast Metals Research*, 14(6), 325–334.
- Micks, F. W., & Zabek, V. J. (1973). *TAFS*, 81, 38–42.
- Midea, A. C. (2001). *TAFS*, 109, 41–50; *Foundryman* (March) 2003, 60–63.
- Midson, S. P. (September 2008). *Die Casting Engineer*.
- Mikkola, P. H., & Heine, R. W. (1970). *TAFS*, 78, 265–268.
- Miles, G. W. (1956). *Proceedings Institute British Foundryman*, 49, A201–A210.
- Miller, G. F. (1967). *Foundry*, 95, 104–107.
- Momchilov, E. (1993). *Journal of Materials Science and Technology, Institute for Metal Science*. Sofia: Bulgarian Academy of Sciences. 1(1), 5–12.
- Morthland, T. E., Byrne, P. E., Tortorelli, D. A., & Dantzig, J. A. (1995). *Metallurgical & Materials Transactions B*, 26B, 871–885.
- Mroz, S. S., & Goodrich, G. M. (2006). *TAFS*, 114, 493–505.
- Mufti, N. A., Webster, P. D., & Dean, T. A. (1995). *Materials Science & Technology*, 11(8), 803–809.
- Muller, W., & Feikus, F. J. (1996). *TAFS*, 104, 1111–1117.
- Mutharasan, R., Apelian, D., & Romanowski, C. (1981). *Journal Metals*, 83(12), 12–18.
- Myllymaki, R. (1987). In W. B. Young (Eds.), *Conference on Residual Stress in Design, Process and Materials Selection* (pp. 137–141). ASM.
- Nadell, R., Eskin, D., & Katgerman, L. (2007). *Material Science & Technology*, 23(11), 1327–1335.
- Nath, R. H., Grupke, C. C., Leonard, C., & Johnson, M. K. (2011). In P. Crepeau et al. (Eds.), *Shape Casting, The John Berry Honorary Symposium*. San Diego: TMS.
- Navisi, S. (2010). *Modern Castings*, 100(9), 35–38.
- Nereo, G. E., Polch, R. F., & Flemings, M. C. (1965). *TAFS*, 73, 1–13.
- Neumeier, L. A., Betts, B. A., & Crosby, R. L. (1976). *TAFS*, 84, 437–448.
- Nguyen, T., & Carrig, J. F. (1986). *TAFS*, 94, 519–528.
- Nguyen, T., de Loose, G., Carrig, J., Nguyen, V., & Cowley, B. (2006). *TAFS*, 114, 695–706.
- Nikolai, M. F. (1996). *TAFS*, 104, 1017–1029.
- Noguchi, T., Kano, J., Noguchi, K., Horikawa, N., & Nakamura, T. (2001). *International Journal of Cast Metals Research*, 13, 363–371.
- Nyamekye, K., An, Y.-K., Bain, R., Cunningham, M., Askeland, D., & Ramsay, C. (1994). *TAFS*, 102, 127–131.
- O'Hara, P. (February 1990). *Engineering*, 41–42.
- Ohnaka. (2003). Mould coat doubles the back-pressure in moulds.
- Okada, Y., Fujii, N., Goto, A., Morimoto, S., & Yusuda, Y. (1982). *TAFS*, 90, 135–146.
- Osborn, D. A. (1979). *British Foundryman*, 72, 157–161.
- Pattyn, R. (1967). *34th International Foundry Congress*. Paris: paper 26.
- Paxton, D. M., Dudder, G. J., Reynolds, J., Charron, W., & Cleaver, T. (2006). *TMS Annual Meeting Light Metals Division Session III*.
- Pechiney Aluminium. (April 26 1977). *British Patent*, 1,574,321.
- Pellini, W. S. (1953). *TAFS*, 61, 61–80, and 302–308.
- Peters, T. M., & Twarog, D. L. (1992). *TAFS*, 100, 1005–1023.
- Pillai, R. M., Mallya, V. D., & Panchanathan, V. (1976). *TAFS*, 84, 615–620.
- Plyatskii, V. M. (1965). *Extrusion Casting*. New York, USA: Primary Sources.
- Polich, R. F., & Flemings, M. C. (1965). *TAFS*, 73, 28–33.
- Pouly, P., & Wuilloud, E. (1997). *Light Metals (TMS Conference)*, 829–835.
- Prakash, M., Cleary, P., & Grandfield, J. (2009). *Journal of Materials Processing Technology*, 209(7), 3396–3407.
- Prodhon, A., Carpenter, M., & Campbell, J. (1999). *CIATF Technical Forum*.

## R11-8 References

- Puhakka, R. (2009). Personal Communication.
- Puhakka, R. (2011). *TMS Annual Meeting*. San Diego, CA: 'Shape Casting; The John Berry Honorary Symposium'.
- Puhakka, R., & Campbell, J. (June 2009). *Modern Castings*, 27–29.
- Purdum, P. (March 1992). *Metals and Materials*, 169.
- Purvis, A. L., Hanslits, C. R., & Diehm, R. S. (1994). *TAFS*, 102, 637–644.
- Rabinovich, A. (March 1969). *AFS Cast Metals Research Journal*, 19–24.
- Rahmani, Kh., & Nategh, S. (2010). *Metallurgical & Materials Transactions A*, 41A(1), 125–137.
- Raiszadeh, R., & Griffiths, W. D. (2008). *Metallurgical & Materials Transactions B*, 39B, 298–303.
- Rao, G. V. K., & Panchanathan, V. (1973). *Cast Metals Research Journal*, 19(3), 135–138.
- Rao, T. S. V., & Md, Roshan H. (1988). *TAFS*, 96, 37–46.
- Rashid, A. K. M. B., & Campbell, J. (2002). Casting defects in vacuum-investment-cast Ni-base turbine blades. Research at the University of Birmingham, to be published.
- Reddy, D. C., Murty, S. S. N., & Chakravorty, P. N. (1988). *TAFS*, 96, 839–844.
- Rezvani, M., Yang, X., & Campbell, J. (1999). *TAFS*, 107, 181–188.
- Richins, D. S., & Wetmore, W. O. (1951). *AFS Symposium on Principles of Gating*, 1–24.
- Ricken, H., Ostermeier, M., Hoffmann, H., & Fent, A. (2009). *Casting Plant and Technology*, (1), 30–32.
- Roedter, H. (September 1986). *Foundry Trade Journal International*, 6.
- Rohatgi, P. (1990). *Advanced Materials and Processes*, 2, 39–44.
- Rogers, K. P., & Heathcock, C. J. (1990). U.S. Patent 5,316,070 date 31 May 1994.
- Romero, J. M., Smith, R. W., & Sahoo, M. (1991). *TAFS*, 99, 465–468.
- Rometsch, P. A., Schaffer, G. B., & Taylor, J. A. (2001). *International Journal of Cast Metals Research*, 14(1), 59–69.
- Runyoro, J. (1992). PhD Thesis 'Design of the Gating System'. University of Birmingham.
- Runyoro, J., Boutorabi, S. M. A., & Campbell, J. (1992). *TAFS*, 100, 225–234.
- Safaraz, A. R., & Creese, R. C. (1989). *TAFS*, 97, 863–870.
- Sandford, P. (March 1988). *The Foundryman*, 110–118.
- Sandford, P. (1993). *TAFS*, 101, 817–824.
- Sarazin, J. R., & Hellowell, A. (1987). Solidification Processing. In J. Beech, & H. Jones (Eds.) (pp. 94–97). UK: Sheffield University.
- Schaffer, P. L., & Dahle, A. K. (2009). *Metallurgical & Materials Transactions A*, 40A(2), 481–485.
- Schaffer, P. L., Dahle, A. K., & Zindel, J. W. (2004). *Light Metals*, 821–826.
- Schilling, H. (1987). Patent PCT WO 87/07543.
- Schilling, H., & Reithmann, M. (1992). *Casting Plant + Technology*, (3), 12–14.
- Schmidt, D. G., & Jacobson, A. E. (1970). *TAFS*, 78, 332–337.
- Schmied, H.-J. (1988). *Giessereitechnik*, 34(4), 133–135.
- Schneider, W. (2006). *Casting Plant and Technology*, (1), 30–37.
- Sciama, G. (1974). *TAFS*, 82, 39–44.
- Sciama, G. (1975). *TAFS*, 83, 127–140.
- Sciama, G. (1993). *TAFS*, 101, 643–651.
- SERF. (June 2002). *Foundry Trade Journal*, 34.
- Sexton, A. H., & Primrose, J. S. G. (1911). *The Principles of Ironfounding*. London: The Technical Publishing Co.
- SFSA. (May 2000). (Steel Founders Society of America). *Foundry Trade Journal*, 40–41.
- Shendye, S. B., & Gilles, D. J. (2009). *TAFS*, 117, 305–311.
- Ship Department Publication 18. (1975). 'Design & Manufacture of Nickel-Aluminium-Bronze Sand Castings'. Foxhill, Bath, UK: Ministry of Defence (Procurement Executive).

- Shivkumar, S., Wang, L., & Steenhoff, B. (1989). *TAFS*, 97, 825–836.
- Showman, R. E., Aufderheide, R. C., & Yeomans, N. P. (2006). *TAFS*, 114, 391–399.
- Sidhu, R. K., Richards, N. L., & Chaturvedi, M. C. (2005). *Material Science Technology*, 21(10), 1119–1131.
- Sieurin, S. I. (June 1974). *Foundry*, 94, and following.
- Sieurin, S. I. (March 1975). 8th Soc Die Casting Engineers International Congress. Detroit MI: paper G-T75-045 (4 pages).
- Sigworth, G. K., Howell, J., Rios, O., & Kaufman, M. J. (2006). *International Journal of Cast Metals Research*, 19(2), 123–129.
- Sikorski, S., & Groteke, D. E. (October 2005). *AFS International Conference High Integrity Light Metal Castings*.
- Simensesn, C. (1981). *Journal of Metallurgical Transactions*, 12B, 733–743.
- Sirrell, B., & Campbell, J. (1997). *TAFS*, 105, 645–654.
- Skarbinski, M. (1971). *British Foundryman*, 44, 126–140.
- Sokolowski, J. H., Kierkus, C. A., Brosnan, B., & Evans, W. J. (2003). *Modern Castings*, 93(1), 39–42.
- Southam, D. L. (1987). *Foundry Management and Technology*, 7, 34–38.
- Spada, A. T. (2004). *Modern Casting*, 94 (Feb) 20–24, 2004 (June), p. 48 only; 2005 (July), pp. 18–22.
- Spenser, D., Mehrabian, R., & Flemings, M. C. (1972). *Metallurgical Transactions*, 3, 1925.
- Srimanosaowapak, S., & O'Reilly Keyna. (2005). *Shape Casting: The John Campbell Symposium* (pp. 41–50). In M. Tiryakioglu, & P. N. Crepeau (Eds.), TMS.
- Stahl, G. W. (1961). *TAFS*, 69, 476–469.
- Stahl, G. W. (1963). *TAFS*, 71, 216–220.
- Stahl, G. W. (1986). *TAFS*, 94, 793–796.
- Stahl, G. W. (1989). The gravity tilt pour process; *Proceeding AFS International Conference: Permanent Mold Castings*, Miami. Paper 2.
- Starobin, A., Goetsch, D., & Walker, M. (2010). *AFS International Journal of Metalcastings*.
- Steel Founders Society of America (Anon). (May 2000). *Foundry Trade Journal*, 40–41.
- Stefanescu, D. M., Giese, S. R., Piwonka, T. S., Lane, A. M., Barlow, J., & Patabhi, R. (1996). *TAFS*, 104, 1233–1264.
- Stratton, P. (June 2010). *Materials World*, 28–29.
- Street, A. C. (1986). *The Diecasting Book*, pp. 635–646 (2nd ed.). Portcullis Press.
- Sullivan, E. J., Adams, C. M., & Taylor, H. F. (1957). *TAFS*, 65, 394–401.
- Sun, L., & Campbell, J. (2003). *TAFS*. Paper 03-018.
- Sutton, T. (June 2002). *The Foundryman*, 95(6), 223–231.
- Suzuki, K., Nishikawa, K., & Watakabe, S. (1996). *Materials Transactions Japan Institute of Metals*, 37(12), 1793–1801.
- Suzuki, S. (October 1989). *Modern Castings*, 38–40.
- Svensson, I. L., & Dioszegi, A. (2000). *Modelling of casting, welding and advanced solidification processes IX* (pp. 102–109). In P. Sahm, P. Hansen, & Conley (Eds.).
- Svensson, I., & Villner, L. (1974). *British Foundryman*, 67, 277–287.
- Sweeney, V. D. (1964). *TAFS*, 72, 911–913.
- Swift, R. E., Jackson, J. H., & Eastwood, L. W. (1949). *TAFS*, 57, 76–88.
- Swing, E. (1962). *TAFS*, 70, 364–373.
- Tasaki, R., Noda, Y., Terashima, K., & Hashimoto, K. (February 2008). *Proceeding 28th World Foundry Congress*. Chennai India, pp. 121–126.
- Taylor, K. C., & Baier, A. (2003).  *Casting Plant + Technology International*, 123(2), 36–46.
- Taylor, C. M., Jr., & Taylor, H. F. (1953). Fundamentals of Riser Behavior. *AFS Transactions*, 686–693.
- Teague, J., & Richards, V. (2010). *AFS International Journal Metalcasting*, 4(2), 45–57.

## R11-10 References

- Terashima, K., Noda, Y., et al. (February 2008). *Proceedings 28th World Foundry Congress*, 113–119, Chennai India, pp. 121–126.
- Tian, C., Irons, G. A., & Wilkinson, D. S. (1999). *Metallurgical & Materials Transactions B*, 30B(2), 241–252.
- Tigges, U. (December 2010). *Foundry Trade Journal*, 310–311.
- Tiryakioğlu, E. (1964). 'A Study of the Dimensioning of Feeders for Sand Castings'. *Ph.D. Thesis*. UK: University of Birmingham.
- Tiryakioğlu, M., Tiryakioğlu, E., & Askeland, D. A. (1997a). *International Journal Cast Metals Research*, 9, 259–267.
- Tiryakioğlu, M., Tiryakioğlu, E., & Askeland, D. A. (1997b). *TAFS*, 907–915.
- Trojan, P. K., Guichelaar, P. J., & Flinn, R. A. (1966). *TAFS*, 74, 462–469.
- Tschopp, M. A., Ramsay, C. W., & Askeland, D. R. (2000). *TAFS*, 108, 609–614.
- Turner, G. L. (1965). *British Foundryman*, 58, 504–505.
- Turner, A., & Owen, F. (1964). *British Foundryman*, 57, 55–61, and 355–356.
- Versnyder, F. I., & Shank, M. E. (1970). *Materials Science & Technology*, 6(4), 213–247.
- Villner, L. (1969). *British Foundryman*, 62, 458–468; Also published in *Giesserei* (1970), 57(27), 837–844; and *Cast Metals Research Journal* (1970), 6(3), 137–142.
- Wall, A. J., & Cocks, D. L. (1980). *British Foundryman*, 73, 292–300.
- Wan, L., Nakashima, T., Kato, E., & Nomura, H. (2002). *International Journal of Cast Metals Research*, 15, 187–192.
- Wang, L., Lett, R., Felicelli, S. D., & Berry, J. T. (2011). *TAFS*. In press.
- Ward, C. W., & Jacobs, I. C. (1962). *TAFS*, 70, 332–337.
- Webster, P. D. (1967). *British Foundryman*, 60, 314–319.
- Wells, M. B., & Oleka, J. T. (1988). *TAFS*, 96, 913–918.
- Welter, V. G. (1931). *Zeitschrift für Metallkunde*, 23.
- Wen, S., W., Jolly, M. R., & Campbell, J. (1997). In J. Beech, & H. Jones (Eds.), *Proceedings 4th Decennial International Conference on Solidification Processing* (pp. 66–69), Sheffield.
- West, T. D. (1882). *American Foundry Practice* (11th ed.) (p. 107). Wiley NY: Chapman & Hall, London, 1910.
- Wieser, P. F., & Dutta, I. (1986). *TAFS*, 94, 85–92.
- Weiss, D. J., & Rose, D. (1993). *TAFS*, 101, 1065–1066.
- Wildermuth, J. W., Lutz, R. H., & Loper, C. R. (1968). *TAFS*, 76, 258–263.
- Wittmoser, A. (1975). *TAFS*, 83, 63–72.
- Wittmoser, A., & Hofmann, R. (1968). *35th Foundry Congress*, Kyoto, Japan.
- Wright, T. C., & Campbell, J. (1997). *TAFS*, 105, 639–644; and *Modern Castings*, June 1997; see also Dimmick, T. (March 2001). *Modern Castings*, 91(3), 31–33.
- Wuilloud, E. (1994). *Light Metals*, 1079–1082.
- Wurker, L., & Zeuner, Th. (2004). *Aluminium*, 80(11), 1207–1213.
- Wurker, L., & Zeuner, Th. (2006).  *Casting Plant and Technology*, (1), 38–42.
- Xiao, B., Wang, Q. G., Jadhav, P., & Li, K. (2010). *Journal of Materials Processing Technology*, 210, 2023–2028.
- Xiao, L., Anzai, K., Niyama, E., Kimura, T., & Kubo, H. (1998). *International Journal of Cast Metals Research*, 11(2), 71–81.
- Xu, Z. A., & Mampaey, F. (1994). *TAFS*, 102, 181–190.
- Xu, Z. A., & Mampaey, F. (1997). *TAFS*, 105, 853–860.
- Xue, X., & Thorpe, R. (1995). *TAFS*, 103, 743–747.
- Yang, X., & Campbell, J. (1998). Pouring basin. *International Journal Cast Metals Research*, 10, 239–253.
- Yang, X., Din, T., & Campbell, J. (1998). Offset sprue. *International Journal Cast Metals Research*, 11, 1–12.
- Yang, X., Jolly, M. R., & Campbell, J. (2000). Vortex flow runner. *Aluminum Transactions*, 2(1) 67–80 and *Modelling of casting, welding and advanced solidification processing IX*. (2000). In P. Sahm, P. Hansen, & Conley (Eds.), pp. 420–427.

- Yurko, J. A., Martinez, R. A., & Flemings, M. C. (June 2003). *Metallurgical Science & Technology (Teksid Aluminum)*, 21. Number 1.
- Zadeh, A. H., & Campbell, J. (2002). *TAFS*, 02–020.
- Zhang, C., Mucciardi, F., Gruzleski, J., Burke, P., & Hart, M. (2003). *AFS Transactions*, paper 010-03.
- Zhang, D. L., Zheng, L. H., & StJohn, D. H. (1998). *Materials Science & Technology*, 14(7), 619–625.
- Zhou, Y. Z., & Volek, A. (2007). *Materials Science & Technology*, 23(3), 297–302.
- Zuehlke, H. B. (1943). *Transactions of the American Foundry Association*, 51, 773–797.
- Zurecki, Z. (1996). In D. Saha (Eds.), *Gas Interactions in Nonferrous Metals Processing* (pp. 79–93). TMS.
- Zurecki, Z., & Best, R. C. (1996). *TAFS*, 104, 859–864.

This page intentionally left blank